CHROMATOGRAPHIA

Vol. 24 (1987)

11th International Symposium on Column Liquid Chromatography

Amsterdam, 28 June-3 July 1987

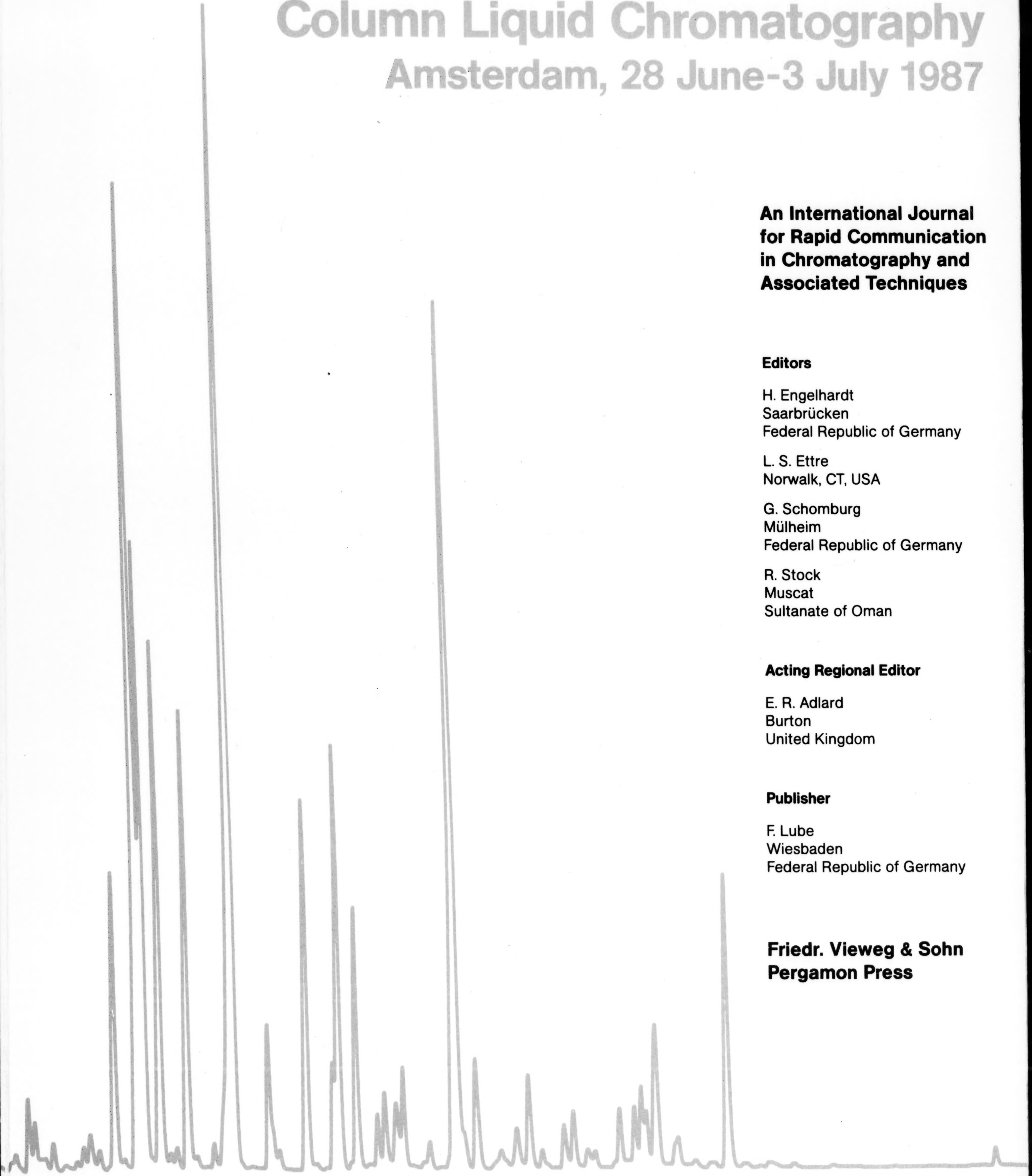

An International Journal
for Rapid Communication
in Chromatography and
Associated Techniques

Editors

H. Engelhardt
Saarbrücken
Federal Republic of Germany

L. S. Ettre
Norwalk, CT, USA

G. Schomburg
Mülheim
Federal Republic of Germany

R. Stock
Muscat
Sultanate of Oman

Acting Regional Editor

E. R. Adlard
Burton
United Kingdom

Publisher

F. Lube
Wiesbaden
Federal Republic of Germany

Friedr. Vieweg & Sohn
Pergamon Press

CHROMATOGRAPHIA

Fusica™

320 μm I.D. capillary
HPLC columns

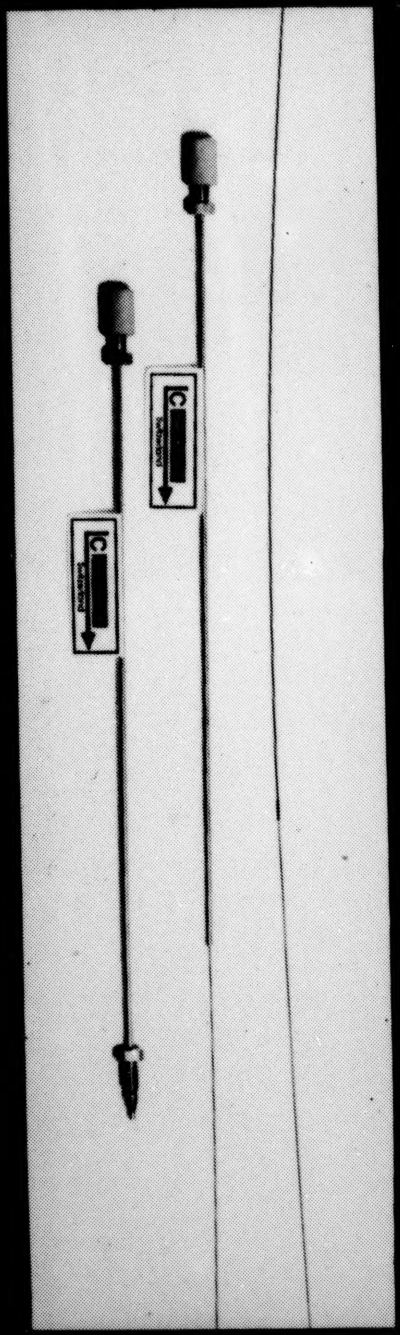

The answer to success in micro-LC and ancillary techniques

LC PACKINGS
Switzerland

CH: Dufourstr. 30, 8008 Zürich, Tel. 01/252 21 58
Telex 816 193
US: Union Street 1717, San Francisco, CA 94123
Tel. (415) 474 84 20, Telex 281 247 (NGTV UR)

CHROMATOGRAPHIA

An International Journal for Rapid Communication in Chromatography and Associated Techniques

Volume 24 (1987)

Editors

H. Engelhardt
Angewandte Physikalische Chemie
Universität des Saarlandes
D-6600 Saarbrücken, FRG

L. S. Ettre
P.O.Box 21 75
Belden Avenue Station
Norwalk, CT 06852, USA

G. Schomburg
Max-Planck-Institut für Kohlenforschung
Kaiser-Wilhelm-Platz 1
D-4330 Mülheim/Ruhr, FRG

R. Stock
Department of Chemistry
Sultan Qaboos University
Muscat, Oman

Acting Regional Editor

E. R. Adlard
Delryn, Vicarage Lane
Burton L64 5TJ, UK

Editorial Advisory Board

E. Bayer, Tübingen, FRG
F. Bruner, Urbino, Italy
C. A. Cramers, Eindhoven, NL
D. R. Deans, Wilton, UK
P. Devaux, Romainville, France
F. Erni, Basle, Switzerland
R. W. Frei, Amsterdam, NL
F. Geiss, Ispra, Italy
G. Guiochon, Knoxville, TN, USA
E. Grushka, Jerusalem, Israel
J. F. K. Huber, Vienna, Austria
D. B. Jack, Birmingham, UK
K. Jinno, Toyohashi, Japan
B. Karger, Boston, MA, USA
M. L. Lee, Provo, UT, USA
P. C. Lu, Dalian, P. R. China
M. Martin, Palaiseau, France
M. V. Novotny, Bloomington, IN, USA
C. S. G. Phillips, Oxford, UK
L. Rohrschneider, Marl, FRG
K. I. Sakodynskii, Moscow, USSR
P. A. Sewell, Liverpool, UK
R. E. Sievers, Boulder, CO, USA
W. Simon, Zurich, Switzerland
C. F. Simpson, London, UK
L. Szepesy, Budapest, Hungary
D. Westerlund, Uppsala, Sweden
W. L. Yu, Lanchow, Kansu, P. R. China
A. Zlatkis, Houston, TX, USA

Honorary Editorial Board

C. Cremer, Innsbruck, Austria
G. Hesse, Erlangen, FRG
G. Machata, Vienna, Austria
R. L. Munier, Paris, France
H. M. McNair, Blacksburg, VA, USA
G. Schay, Budapest, Hungary
E. Smolková-Keulemansová, Prague, CSSR
K. Tesarik, Brno, CSSR
G. Widmark, Stockholm, Sweden
A. A. Zhukhovitskii, Moscow, USSR

Editorial Office Manager

A. A. Weis, Friedr. Vieweg & Sohn Verlagsgesellschaft mbH,
P.O. Box 5829, D-6200 Wiesbaden 1, FRG
Tel. (06121) 160247 or 160222; Telex 4 18 69 28 vwv

Publisher

F. Lube, Friedr. Vieweg & Sohn Verlagsgesellschaft mbH,
P.O. Box 5829, D-6200 Wiesbaden 1, FRG

Advertising Representatives

Friedr. Vieweg & Sohn Verlagsgesellschaft mbH
P.O.Box 5829
D-6200 Wiesbaden 1
Tel. (06121) 308021
Telex 4 186 928 vwv

USA

Trade Media International
424 Madison Avenue
New York, NY 10017, U.S.A.
Tel. (212) 421-1229

United Kingdom

Pergamon Press Ltd.
Headington Hill Hall
Oxford OX3 OBW
United Kingdom
Tel. (865) 64-881 / Telex 831 77

Distribution in the USA

CHROMATOGRAPHIA (USPS 374 810) is distributed by German Language Publications, Inc., 560 Sylvan Avenue, Englewood Cliffs, NJ 07632. Second class postage is paid at Englewood, NJ 07631.

Postmaster: Send address changes to CHROMATOGRAPHIA/German Language Publications, Inc., 560 Sylvan Avenue, Englewood Cliffs, NJ 07632.

Submission of Papers

1 Original and 2 copies of manuscripts in English or German should be sent to the address of the Editorial Office Manager.

For articles intended for the *green pages* or for review-type articles, an outline of the proposed article should first be forwarded to one of the editors for preliminary discussion, prior to preparation.

CHROMATOGRAPHIA was founded by R.E. Kaiser in 1968.

Subscription Rates

CHROMATOGRAPHIA is published monthly. Up to three volumes may be published per year.

Vols. 25 + 26 (1988)	DM 798,–	US $ 478.00
Single copy	DM 40,–	US $ 24.00

For individual subscribers who will certify that CHROMATOGRAPHIA is for their personal use only (to be ordered directly from the Publisher):

Vols. 25 + 26 (1988)	DM 399,–	US $ 239.00

All prices postage included.

Unless the subscription is recalled with notice three months before the end of the year its validity is automatically extended by one year.

Copyright

On publication of a manuscript the exclusive copyright for every language and country passes over to the Publisher. In the USA permission to photocopy for internal or personal use or the internal or personal use of specific clients is granted by the Publisher for libraries and other users registered with the Copyright Clearance Center (CCC), provided that the stated fee per copy is paid directly to the CCC, 21 Congress Street, Salem, MA 01970. Special requests should be addressed to the Publisher.

The use of general descriptive names, trade names, trademarks, etc., in this publication, even if the former are not especially identified, is not to be taken as a sign that such names, as understood by the Trade Marks and Merchandise Marks Act, may accordingly be used freely by anyone.

While the advice and information of this book is believed to be true and accurate at the date of going to press, neither the authors nor the editors nor the publisher can accept any legal responsibility for any errors or omissions that may be made. The publisher makes no warranty, express or implied, with respect to the material contained herein.

Vieweg is a subsidiary company of the Bertelsmann Publishing Group.

© Friedr. Vieweg & Sohn Verlagsgesellschaft mbH,
Braunschweig 1987

Printed in the Federal Republic of Germany

ISSN 0009-5893

Chromatogram on front page: Gas chromatographic separation of gasoline hydrocarbons (selected section of chromatogram) with glass capillary column.

Enclosure / Beilagenhinweis
Enclosed in this issue is an information leaflet of
ict-Handels GmbH
Diese Ausgabe enthält eine Beilage der Firma
ict-Handels GmbH, Antoniterstr. 36, 6230 Frankfurt/Main 80

Foreword

The Eleventh International Symposium on Column Liquid Chromatography, promoted as HPLC 87, was held from June 28th to July 3rd 1987 in the RAI Congress Centre in Amsterdam, The Netherlands. The choice of this venue by the Permanent Scientific Committee of this series has been much appreciated by the Dutch chromatographic community and has been considered as very appropriate because of the significant contributions to the field of instrumental chromatography originating in this country. Some of the history on this was discussed by dr. J.J. van Deemter in his opening lecture.

The growing importance and broadness of HPLC methods were again reflected in the size of the meeting: more than 1100 active participants could gather new information from 450 scientific presentations. Among these were 9 review lectures, which enabled participants to keep abreast of the contemporary developments in largely diverging fields, and keynote lectures that were selected by the scientific committee for their large significance.

The appreciation among participants for this schedule was generally very good, and the organizers express their gratitude to all invited speakers who all performed their allotted tasks so well.

On the exhibition more than 60 manufactures and suppliers exhibited their newest equipments and materials, and there is no doubt that this event contributed very much to the effectiveness of the time spent by participants in Amsterdam.

As a chairman of HPLC 87, I wish to express my sincere appreciation to all individuals and organizations whose efforts were essential for the final good results. In the first place this applies to the people of the OBA organization bureau with their professional skills, and to the numerous sponsors, whose donations enable the organizers to provide participants with various services (including the receipt of this volume!) free of charge. It also applies to the exhibiting firms that responded so actively, to the sponsoring scientific organizations listed overleaf that helped with the publicity, and – last but not least – to all the delegates, both presenters and not presenters, who actively participated and made the meeting as a whole work as it should.

The present volume of Chromatographia contains the accepted papers presented at HPLC 87. The said amount also forces me to express my gratitude to the Journal and its editorial board for the successful completion of their huge task.

Lastly, I express the hope that the material gathered in this issue will constitute a valuable and lasting contribution to the progress in HPLC.

On behalf of the local committees
of HPLC 87

H. Poppe, symposium chairman

HPLC 87
Amsterdam

Sponsoring Scientific Organizations

Arbeitskreis Chromatographie der Gesellschaft Deutscher Chemiker
Chromatographic Society (UK)
Chromatography Forum of the Delaware Valley
Groupement pour l'Avancement des Méthodes Spectroscopiques et Physico-Chimiques d'Analyse (GAMS)
Koninklijke Nederlandse Chemische Vereniging (KNCV)
Sectie voor Analytische Chemie, KNCV
Österreichische Gesellschaft für Mikrochemie und Analytische Chemie
Schweizerischer Chemiker-Verband
Società Italiana di Biochimica Clinica
Svenska Kemistsamfundet Analytiska Sektionen (Sweden)

CHROMATOGRAPHIA

An International Journal for Rapid Communication in Chromatography and Associated Techniques

Contents Vol. 24, 1987

Foreword 3

High-Performance Capillary Electrophoresis Using Open Tubes and Gels 15
A. S. Cohen / A. Paulus / B. L. Karger

Spectrometers and High Performance Liquid Chromatography 25
H. Poppe

Solvent-Strength Selectivity in Reversed-Phase HPLC 33
L. R. Snyder / M. A. Quarry / J. L. Glajch

Advantages and Limitations of HPLC in Environmental Analysis 45
J. F. Lawrence

Effects of the Column Pressure Drop in Packed-Column Supercritical-Fluid Chromatography 51
P. J. Schoenmakers / L. G. M. Uunk

Liquid Phase Separation Methods: HPLC, FFF, Electrophoresis 58
J. J. Kirkland / R. M. McCormick

Prediction of the Detection Ranges for HPLC-Peroxyoxalate Chemiluminescence Detection System of Fluorescent Compounds 77
K. Imai / A. Nishitani / Y. Tsukamoto

A Simplified Description of HPLC Separation under Overload Conditions. A Synthesis and Extension of Two Recent Approaches 82
L. R. Snyder / G. B. Cox / P. E. Antle

Recent Development in HPLC Enantioseparation — A Selected Review 97
W. Lindner

The Determination of Starting Conditions for Modifier Optimization in Reversed-Phase HPLC 108
L. de Galan / D. P. Herman / H. A. H. Billiet

Influence of the Peak Height Distribution on Separation Performances: Discrimination Factor and Effective Peak Capacity 115
M. Z. El Fallah / M. Martin

Anion Chromatography in Open Tubular Capillary Columns with Indirect Fluorometric Detection 123
W. D. Pfeffer / T. Takeuchi / E. S. Yeung

Data Handling in HPLC-Diode Array UV-Spectrometry 127
B. G. M. Vandeginste / G. Kateman / J. K. Strasters / H. A. H. Billiet / L. de Galan

CHROMATOGRAPHIA

An International Journal for Rapid Communication in Chromatography and Associated Techniques

Miniaturisation in Pressure and Electroendosmotically Driven Liquid Chromatography: Some Theoretical Considerations 135
J. H. Knox / I. H. Grant

Packings and Stationary Phases for Biopolymer Separations by HPLC 144
K. K. Unger / R. Janzen / G. Jilge

Direct Injection of Plasma into Column Liquid Chromatographic Systems 155
D. Westerlund

Preparative Liquid Chromatography 165
G. Guiochon / Anita Katti

A Review of Reaction Detection in HPLC 190
U. A. Th. Brinkman

Automation and Validation of HPLC-Systems 201
F. Erni / W. Steuer / H. Bosshardt

Multivariate Analysis of Non-Homogeneous Peaks in Liquid Chromatography 208
G. G. R. Seaton / A. F. Fell

Developments in Detection Methods for Ion Chromatography 217
P. R. Haddad

The Use of Derivatives for Establishing Integration Limits of Chromatographic Peaks 226
Eli Grushka / I. Atamna

Open Tubular Columns and Non-Porous Packings in Copolymer HPLC Analysis 233
G. Glöckner / J. H. M. van den Berg

HPLC of Biological Macromolecules: The First Decade 241
F. E. Regnier

Indirect Detection in Liquid Chromatography
I. Response Models for Reversed-Phase Ion-Pairing Systems 252
J. Crommen / G. Schill / D. Westerlund / L. Hackzell

Computer Simulation as a Means of Developing an Optimized Reversed-Phase Gradient-Elution Separation 261
J. W. Dolan / L. R. Snyder / M. A. Quarry

Study of Biologically Relevant Physical-Chemical Properties of Bile Salts by Reverse-Phase Liquid Chromatography 277
A. Cantafora / A. Di Biase / M. Angelico / D. Alvaro

Measurement of Concentrations of a New H_2-Receptor Antagonist (SK&F 93574) in Plasma, Urine and Bile 282
V. S. Picot / E. Doyle / L. J. Read / R. M. Lee

CHROMATOGRAPHIA

An International Journal for Rapid Communication in Chromatography and Associated Techniques

High-Performance Liquid Chromatographic Analysis of Cyclizine and its Metabolite, Norcyclizine in Biological Fluids Using Solid-Phase Extraction 287
R. Walker / I. Kanfer

Peak Height Determination in Analysis of Chlortetracycline in Animal Feeds 291
S. E. Hudson / M. E. Cohen / D. L. Hudson / B. Gump

Column Purification and HPLC Determination of Teicoplanin and A40926 295
E. Riva / M. Zanol / E. Selva / A. Borghi

On the Polarity of Stationary Phases in Straight-Phase LC 302
M. Verzele / F. Van Damme / C. Dewaele / M. Ghijs

Miniaturized RPLC for the Rapid Determination of Total Tryptophan in Pediatric Plasma Samples 309
Linda C. Peterson / M. E. Dwyer / P. R. Brown

Simple and Practicable High-Performance Liquid Chromatographic Assay of Some Tricyclic Drugs, Haloperidol, Diltiazem, Verapamil, Propafenone and Amiodarone 313
G. Mazzi

Chromatographic Separation and Identification of Human Urine Components 317
Y. Nagata / Y. Matsushima / H. Ugai / M. Kikuchi / N. Takai

Determination of Phenol in Raw and Potable Waters by HPLC Multi-Electrode Electrochemical Detection 319
P. J. Rennie / S. F. Mitchell

Influence of Silica Gel Pretreatment and Bonding Technique on PAH Selectivity of Octadecyl Bonded Phases 324
P. J. van den Driest / H. J. Ritchie

HPLC Quantification of rDNA Polypeptides Like Insulin Precursors Produced in Yeast 329
L. Snel / U. Damgaard / I. Mollerup

Preparative HPLC for Analysis of Mineralocorticoids in Human Plasma 333
C. Lejeune-Lenain / S. Kina / D. Bosson

Determination of α-Aminonitriles, α-Amino Acid Amides and α-Amino Acids by Means of HPLC, Post-Column Reaction and Fluorescence Detection 339
A. L. L. Duchateau / M. G. Crombach

Simple and Rapid Analysis of Nitrofurazone from Blood, Milk, Urine and Meat Samples 344
T. Suortti / K. Heinonen

High-Performance Liquid Chromatographic Determination of Major Organic Acids in Apple Juices and Ciders 347
D. Blanco Gomis / M. J. Moran Gutierrez / M. D. Gutierrez Alvarez / A. Sanz Medel

Application of a New Capsule-Type Silica Gel Coated with Hydrophobic Polymer to Preparative Liquid Chromatography on an Industrial Scale 351
Y. Ohtsu / O. Shirota / T. Ogawa / I. Tanaka / T. Ohta / O. Nakata / Y. Fujiyama

CHROMATOGRAPHIA

An International Journal for Rapid Communication in Chromatography and Associated Techniques

Direct HPLC Resolution of Beta-Aminoalcohol (Tazifylline, Ranolazine, Sotalol) Enantiomers 357
E. Delée / L. Le Garrec / I. Jullien / S. Béranger / J. C. Pascal / H. Pinhas

HPLC Determination of Plasma Taurine 360
P. A. Biondi / F. Manca / A. Negri / C. Lucarelli

Development and Performance of an Automated HPLC-Analyzer for Catecholamines 363
K.-S. Boos / B. Wilmers / R. Sauerbrey / E. Schlimme

Quantitative Reversed Phase HPLC Analysis of L-Ascorbic Acid (Vitamin C) and Identification of its Degradation Products 371
Linda L. Lloyd / F. P. Warner / C. A. White / J. F. Kennedy

Highly Sensitive Measurement of Mepindolol in Biological Fluids Using HPLC and Electrochemical Detection 377
L. Millerioux / L. Ntzanis / B. Julian / J. Girault / M. A. Lefebvre / A. Mignot / J. B. Fourtillan

Structures and Chromatographic Characteristics of Capsule-Type Silica Gels Coated with Hydrophobic Polymers in Reversed-Phase Liquid Chromatography 380
Y. Ohtsu / H. Fukui / T. Kanda / K. Nakamura / M. Nakano / O. Nakata / Y. Fujiyama

Novel Method for the Preparation of Chemically Bonded Phases and Studies of their Chromatographic Performance 385
T. M. Khong / C. F. Simpson

A Post-Column Extraction System for the Determination of Tertiary Amines by Liquid Chromatography with Chemiluminescence Detection 395
P. J. M. Kwakman / U. A. Th. Brinkman / R. W. Frei / G. J. de Jong / F. J. Spruit / N. G. F. M. Lammers / J. H. M. van den Berg

A New Polymer Supported Packing Material as a Substitute of Hydroxylapatite: Purification of Topoisomerases 400
K. Majumder / N. Ramesh

Determination of DEHP in Blood Products Stored in Plastic Bags by HPLC 403
I. Gerlai / J. Pintér / J. Pick

Assay of Urinary Free Catecholamines: Routine Use in a Clinical Chemistry Laboratory 407
E. Baraldi / D. Cavani / S. Seghedoni / G. Chiossi / L. Roli / A. T. Scacchetti / G. F. Baraghini

Quantification of a Positive Inotropic Agent in Plasma: Towards Total Automation 411
G. S. Murkitt / J. C. Pearce / R. D. McDowall

Packed Capillary Columns for Liquid Chromatography 416
S. Hoffmann / L. Blomberg

HPLC of Porphyrinogens with Electrochemical Detection 421
Famei Li / C. K. Lim / T. J. Peters

An Improved Approach for the Determination of Plasma-Free Catecholamines by HPLC-ED: Application to Normal and Hypertensive Patients 423
C. Lucarelli / P. Betto / G. Ricciarello / M. Giambenedetti / F. Sciarra / C. Tosti Croce / P. L. Mottironi

CHROMATOGRAPHIA

An International Journal for Rapid Communication in Chromatography and Associated Techniques

Study on Optimal Packing Materials for High-Performance Hydrophobic-Interaction Chromatography of Proteins 427
T. Ueda / Y. Yasui / Y. Ishida

Separation of Polypeptide Antibiotics by Reversed-Phase High-Performance Liquid Chromatography 433
H.-P. Fiedler / T. Hörner / A. Wörn

HPLC Assay of Enzymatic Activities 439
P. Pietta / P. Mauri / M. Pace

Theoretical Considerations for Zone Electrophoretic Sample Treatment in Liquid Chromatography 442
W. Th. Kok

A Micropreparative Chromatographic Strategy for the Purification and Sequence Analysis of Murine Granulocyte-Colony Stimulating Factor (mG-CSF) 449
E. C. Nice / R. J. Simpson / N. A. Nicola

Assessment of Semi-Automated Catecholamine Assay by HPLC: Choice of Reverse Phase C18 or Cation-Exchange Columns 455
M. Beschi / M. Castellano / E. Agabiti-Rosei / D. Rizzoni / P. Rossini / G. Muiesan

Indirect Detection in Reversed-Phase Liquid Chromatography: Ion-Pair Retention Models for Cations on Polystyrene Polymers 460
E. Arvidsson / J. Crommen / G. Schill / D. Westerlund

Improved Cleanup Method for the Multiresidue Analysis of N-Methylcarbamates in Grains, Fruit and Vegetables by Means of HPLC with Postcolumn Reaction and Fluorescence Detection 469
A. de Kok / M. Hiemstra / C. P. Vreeker

Determination of the Enantiomeric Composition of Chiral Carboxylic Acids Using Chiral Derivatization and HPLC 477
L. Ladányi / I. Sztruhár / P. Slégel / G. Vereczekey-Donáth

Improved High-Performance Liquid Chromatographic Determination of Amanitins with Electrochemical Detection 482
F. Tagliaro / S. Chiminazzo / S. Maschio / F. Alberton / M. Marigo

Approaches to the Liquid Chromatographic Determination of Carboxylic Acids Using Potentiometric Detection with a Metallic Copper Electrode 487
P. R. Haddad / P. W. Alexander / M. Y. Croft / D. F. Hilton

Tests for Liquid Chromatographs 492
M. J. Rehman / K. P. Evans / A. J. Handley / P. R. Massey

Simultaneous Determination of CGP 22848 and its Major Metabolite (Free Carboxylic Acid) CGP 35652 in Plasma by HPLC 501
A. Sioufi / F. Leroux / J. P. Dubois / C. Mondadori / W. Froestl

New HPLC-Chiral Stationary Phases for Enantiomeric Resolution of Sulfoxides and Selenoxides 505
G. Gargaro / F. Gasparrini / D. Misiti / G. Palmieri / M. Pierini / C. Villani

CHROMATOGRAPHIA

An International Journal for Rapid Communication in Chromatography and Associated Techniques

Fast LC Analysis of the α-Acid Content of "Fresh" and "Aged" Hops 510
J. T. Hann

The System Evaluation Strategy in Practice, Allowing Direct Estimation of Peak Heights and Limits of Detection in HPLC 513
Pamela J. Naish / M. J. Keesman

High-Performance Liquid Chromatographic Analysis of Ginsenosides in *Panax Ginseng* Extracts Using Glass-ODS Column 517
H. Kanazawa / Y. Nagata / Y. Matsushima / M. Tomoda / N. Takai

Relationship Between Enantioselectivity and Solute Structure on a Chiral α_1-Acid Glycoprotein Column 520
J. Hermansson / Kerstin Ström / R. Sandberg

High Voltage Capillary Zone Electrophoresis: Operating Parameters Effects on Electroendosmotic Flows and Electrophoretic Mobilities 527
K. D. Altria / C. F. Simpson

Sequential Simplex Optimization and Multichannel Detection in HPLC: Application to Method Development 533
A. G. Wright / A. F. Fell / J. C. Berridge

Group Separation of PCDDs, PCDFs, PACs and Aliphatic Compounds on an Amino Bonded Stationary Phase for HPLC 541
A. L. Colmsjö / Y. U. Zebühr / Conny E. Östman

Liquid Chromatographic Characterization of the Deoxyribonucleoside-5'-Phosphates and Deoxyribonucleoside-3',5'-Bisphosphates Obtained by ^{32}P-Postlabeling of DNA 545
M. W. Dietrich / W. E. Hopkins II / Karen J. Asbury / W. P. Ridley

Hysteretic Effect of the Coating Solvent on Chiral Recognition by Cellulose Derivative 552
T. Shibata / T. Sei / H. Nishimura / K. Deguchi

Fluorescence Enhancement for Aflatoxins in HPLC by Post-Column Split-Flow Iodine Addition from a Solid-Phase Iodine Reservoir 555
H. Jansen / R. Jansen / U. A. Th. Brinkman / R. W. Frei

Determination of Chlorproguanil and Metabolites in Biological Fluids 560
R. B. Taylor / R. R. Moody / N. A. Ochekepe / B. Law

Optimization of Peptide Separations in Reversed-Phase HPLC: Isocratic Versus Gradient Elution 565
C. T. Mant / T. W. Lorne Burke / R. S. Hodges

Study on the Structure of Chemically Bonded C_{18} Phase for HPLC 573
B. Buszewski / Z. Suprynowicz

Criteria for Judging the Quality of Separation in Chromatograms Containing Solvent Peaks 579
P. J. Schoenmakers / P. J. Naish / R. J. Hunt

HPLC Determination of Non-Ionic Surfactants Used in Tertiary Oil Recovery 588
P. L. Desbène / B. Desmazières / J. J. Basselier / L. Minssieux

CHROMATOGRAPHIA

An International Journal for Rapid Communication in Chromatography and Associated Techniques

Automated Preparative HPLC of Prostanoids 593
J. Veisserik / T. Somer / M. Lohmus / Y. Lille

High-Performance Liquid Chromatographic Analysis of Isoxazolylpenicillins in Plasma and Urine Samples 597
U. R. Tjaden / H. Lingeman / R. A. M. van der Hoeven / J. A. C. Bierman / H. J. E. M. Reeuwijk / J. van der Greef

Surface Treatment and Porosity Control of Porous Silica Microspheres 602
R. W. Stout / G. B. Cox / T. J. Odiorne

Determination of Priority Pollutant Phenols by Isocratic HPLC 613
P. Alarcón / A. Bustos / B. Cañas / M. D. Andrés / L. M. Polo

The Application of Porous Silica Layers in Open Tubular Columns for Liquid Chromatography 617
P. P. H. Tock / G. Stegeman / R. Peerboom / H. Poppe / J. C. Kraak / K. K. Unger

New Detection Modes for the Determination of Cephalosporins and Their Decomposition Products 625
M. D. Blanchin / W. Th. Kok / H. Fabre

High Performance Liquid Chromatography with Post-Column Photolysis of Pesticides for Generation of Fluorophores 628
C. J. Miles / H. Anson Moye

Effect of Draining of Macromolecules on the Results of Size-Exclusion Chromatography Measurements 633
L. Z. Vilenchik / T. P. Zhmakina / V. P. Sklizkova / V. V. Kudriavtsev / T. B. Tennikova / N. G. Belnikevich / B. G. Belenkii / S. Ya. Frenkel / M. M. Koton

Solid Phase Extraction and Direct HPLC Separation of Bilirubin and its Conjugates in Plasma 637
Fami Li / C. K. Lim / T. J. Peters

Some Aspects of the Preparative Separation of Enantiomers on Chiral Stationary Phases 639
Veronika R. Meyer

Protein Surface Area and Retention in Hydrophobic Interaction Chromatography 646
A. Katti / Y.-F. Maa / Cs. Horváth

Biomonitoring of Workers Exposed to Aromatic Amines in Rubber Vulcanization 651
I. Pavan / F. Belliardo / E. Buglione / M. M. Massiccio

L-N-(3,5-Dimethoxybenzoyl)isoleucine Chiral Stationary Phase for Separation of Enantiomers by HPLC 655
W. J. Vloon / C. Siekerman / J. C. Kraak

Recognizing Chromatographic Peaks with Pattern Recognition Methods III. Application of the Algorithm for Peak Recognition in Trace Analysis 659
G. Reich

Analysis of Enhanced Oil Recovery Formulations 666
Y. L. Hofman / H. P. Angstadt

CHROMATOGRAPHIA

An International Journal for Rapid Communication in Chromatography and Associated Techniques

Chiral Stationary Phases Based on Cinchona Alkaloids for the HPLC Resolution of Racemates 671
C. Rosini / C. Bertucci / D. Pini / P. Altemura / P. Salvadori

Attempts for the Chromatographic Separation of D- and L-Penicillamine Enantiomers 677
Katalin Kovács-Hadady / Ilona T. Kiss

Determination of 2′-Acetyl Erythromycin and Erythromycin in Plasma by HPLC Using Manual and Robotic Sample Preparation 680
P. Kokkonen / H. Haataja / S. Välttilä

Chromatographic Properties of Mixed Cyano/ODS Chemically Bonded Phases for HPLC 683
A. Colmsjö / Monica W. Ericsson

Measurement of Polyunsaturated Fatty Acids of Myocardial Lipids by High Performance Liquid Chromatography 687
G. A. Cordis / M. Renuka Prasad / H. Otani / R. M. Engelman / D. K. Das

An Expert System for Eluent Optimisation in Liquid Chromatography with Photodiode Array Detection 691
T. P. Bridge / M. H. Williams / G. G. R. Seaton / A. F. Fell

Automated Two-Dimensional HPLC Residue Procedure for Glyphosate on Cereals and Vegetables with Postcolumn Fluoregenic Labelling 696
L. G. M. Th. Tuinstra / P. G. M. Kienhuis

Characteristics of a New HPLC Column Packed with Octadecyl-Bonded Polymer Gel 701
Y. Yanagihara / K. Yasukawa / U. Tamura / T. Uchida / K. Noguchi

On-Line Extraction of Metal Ions Using Liquid-Liquid Segmentation and a Membrane Type Phase Separator for Fluorescence Detection 705
B. D. Karcher / I. S. Krull / R. G. Schleicher / S. B. Smith, Jr.

Use of Unmodified Silica with Buffered Aqueous Mobile Phase Mixtures for Selective Chromatography of Basic Drugs 713
R. W. Schmid / Ch. Wolf

Liquid Chromatographic Method for the Simultaneous Determination of Sulphasalazine and its Main Metabolites in Biological Fluids 720
K. Róna / V. Winkler / T. Riesz / B. Gachályi

Enantiomeric Resolution of N-Methyl-α-Amino Acids and α-Alkyl-α-Amino Acids by Ligand-Exchange Chromatography 725
H. Brückner

The Application of Immobilized Liquids for Open Tubular Liquid Chromatography 739
O. van Berkel / H. Poppe / J. C. Kraak

Analytical and Preparative Methods for β-Exotoxin from *Bacillus Thuringensis* 745
T. Suortti / L. Ylinen / P. Kärppä

CHROMATOGRAPHIA

An International Journal for Rapid Communication in Chromatography and Associated Techniques

Multidimensional Ion-Pair HPLC for the Purification of Aminoglycoside Antibiotics with Refractive Index Detection 748
D. Samain / P. Dupin / P. Delrieu / G. Inchauspe

Effects of Modifiers on the Chromatographic Behaviour of Propafenone and its Major Metabolites 753
B. Marchesini / L. Tomasi

Narrow-Bore Liquid Chromatography with Multichannel Detection in Paediatric Biochemistry: Analysis of Phenylalanine and Tyrosine in Phenylketonuria 759
Elaine M. Kirk / B. J. Clark / A. F. Fell

A Rapid Method for the Determination of an Unstable Metabolic Intermediate. The Metabolic Formation of Benzamide and Benzoic Acid via Diacyl Amine Intermediate 766
M. Pálfi-Ledniczky / I. Weisz / G. Dénes / K. Ujszászy

High-Performance Liquid Chromatography of Amino Acid Peptides and Proteins 769
M. T. W. Hearn / A. N. Hodder / P. G. Stanton / M. I. Aguilar

Determination of Hydrophobic Parameters by Reversed-Phase High-Performance Liquid Chromatography. Effect of Stationary Phase 777
Th. Braumann / H.-G. Genieser / C. Lüllmann / B. Jastorff

An Experimental Verification of the Electrostatic Theory for Ion Pair Chromatography 783
J. Ståhlberg / A. Furängen

Size-Exclusion High-Performance Liquid Chromatography of Integral Membrane Proteins; Effect of Detergents on Immunological Activity 790
G. W. Welling / B. Kazemier / S. Welling-Wester

HPLC of 9-Fluorenylmethylchloroformate-Polyamine Derivatives with Fluorescence Detection 795
J. R. Price / P. A. Metz / H. Veening

Selectivity in a Liquid-Solid Chromatographic System 800
S. M. Petrović / S. Lomić / I. Šefer

Monitoring Free Silanols on Reversed-Phase Supports with Peptide Standards 805
C. T. Mant / R. S. Hodges

Synthesis of an N-butylpyrrolidine Phase Using the Allyl Bonded Stationary Phase as an Intermediate 815
J. J. Pesek / E. L. Tarver / A. Lange

A Quantitative Evaluation of the Electrostatic Theory for Ion Pair Chromatography 820
J. Ståhlberg

Determination of Acetylcholine and Choline in the Femtomole Range by Means of HPLC, a Post-Column Enzyme Reactor, and Electrochemical Detection 827
G. Damsma / D. Lammerts van Bueren / B. H. C. Westerink / A. S. Horn

CHROMATOGRAPHIA

An International Journal for Rapid Communication in Chromatography and Associated Techniques

A Practical Approach to the Preparative Purification of Peptides using Analytical Instrumentation with Analytical and Semipreparative Columns 832
J. M. Robert Parker / C. T. Mant / R. S. Hodges

RP-HPLC Assay for 1,2-5,6-Dianhydro-3,4-Disuccinyl-Galactitol and Its Metabolites in Blood Plasma and Liver 839
Gy. Szókán / I. Elekes / E. Táborhegyi / Gy. Csanádi / J. Bencze

A Fully Automated Catecholamines Analyzer Based on Cartridge Extraction and HPLC Separation 842
G. Grossi / A. Bargossi / A. Lippi / R. Battistoni

Separation of Urea and other Polar Compounds by HPLC 847
M. Pálfi-Ledniczky / G. Dénes / K. Ujszászy

Study of the Selective Retention of Fluorinated Compounds on Perfluorinated Stationary Phases 849
I. de Miguel / S. Exbrayat / D. Samain

HPLC and RIA Procedure for Cyclosporine A Determination Compared with Clinical Background 854
J. Klima / R. Petrásek / V. Kočandrle / J. Kašlik

Analysis of Non-Ionic Surfactants Used in Tertiary Oil Recovery. Optimisation of Stationary Phase in Normal Phase Partition Chromatography 857
P. L. Desbène / B. Desmazières / V. Even / J. J. Basselier / L. Minssieux

High-Performance Liquid Chromatographic Analysis of Azlocillin in Serum 862
T. Valenza / P. Rosselli

Determination of Organic Colorants in Cosmetic Products by High-Performance Liquid Chromatography 865
J. W. Wegener / J. C. Klamer / H. Govers / U. A. Th. Brinkman

Determination of CGP 6140 and its N-Oxide Metabolite, CGP 13231, in Plasma and Urine by Columns or Cartridge Switching HPLC 876
J. B. Lecaillon / A. Sioufi / C. Souppart / J. P. Dubois

High Performance Displacement Chromatography of Proteins: Separation of β-Lactoglobulins A and B 881
A. W. Liao / Z. El Rassi / D. M. LeMaster / Cs. Horváth

Sensitive and Selective Bioanalytical Assay for the Determination of Dobutamine in Rat Plasma Samples 886
H. Lingeman / J. A. Haverhals / H. J. E. M. Reeuwijk / U. R. Tjaden / J. van der Greef

Classification of Chromatographic Data Using Multidimensional Polynomials 891
M. E. Cohen / D. L. Hudson

Quantitative Determination of Terbutaline in Human Plasma After Administration of Bambuterol Using Coupled Columns and Electrochemical Detection 895
B.-M. Kennedy / A. Blomgren / L.-E. Edholm / C. Roos

High-Performance Capillary Electrophoresis Using Open Tubes and Gels

A. S. Cohen / A. Paulus / B. L. Karger*

Barnett Institute and Department of Chemistry, Northeastern University, Boston, Massachusetts 02115, USA

Key Words

Capillary electrophoresis
Capillary gelelectrophoresis
Micropreparative electrophoresis

Summary

This paper overviews several aspects of high performance capillary electrophoresis (HPCE), a promising new method of analytical and micropreparative separation of biochemically important samples. The basic migration equations of electrophoresis are first presented and the benefit of high fields for rapid analysis and high performance emphasized. Since power is generated with high voltages, Joule heating results and this heat must be dissipated. The use of capillary columns is shown to be important in efficient heat removal and in minimizing the temperature differences within the column. The various factors influencing band broadening are next described, and it is shown how plate counts close to 10^6 can be achieved. Various results from our laboratory on open tube and gel columns are then presented to illustrate the potential of this method. Chiral resolution of dansylated amino acids using a chiral metal chelate micelle in open tube HPCE is shown. With the gel columns, the baseline separation of a 2-chain variant from methionine growth hormone (met-hGH) under non-denaturing conditions at fields close to 1000 V/cm is presented. Finally, the micropreparative purification of a 20-mer oligonucleotide using the gel column is described.

Introduction

Currently, electrophoresis is one of the most important tools available for separation and analysis. Among the various significant applications of this method are DNA sequencing [1], purity assessment *via* 2-dimensional electrophoresis [1], and protein characterization *via* SDS polyacrylamide gel electrophoresis [2] and isoelectric focusing [3]. Many of the applications of electrophoresis involve problems of biological interest.

In the past, chromatographers and electrophoresis workers have generally had limited overlap in their research efforts. This is surprising, given the similarities of both methods, as was clearly pointed out by Giddings many years ago [4]. This lack of overlap is rapidly changing today as the fields come together, driven by developments in biotechnology [5]. In addition, electrophoresis is becoming more automated, and the relationship to chromatography from an instrumentation point of view has become clearer.

Today, electrophoresis is predominantly conducted by means of slab or open bed operation. However, in its earliest devleopments in moving boundary electrophoresis [6] or the initial studies with anticonvective media involving polyacrylamide gels [7], columns were frequently used. Indeed, even today microcolumns are employed in some forms of 2-dimensional electrophoresis, in which a separation is first obtained within a column, and the gel is extruded for further development on a slab [8].

Column operation began with tube diameters of 3–6 mm and over a period of time decreased to the present use of capillary dimensions of roughly 100 μm or lower. Particularly noteworthy in this development are the work of Hjerten in the late 60's using 2 mm ID tubing [7], Everaerts and co-workers on capillary isotachophoresis [9] and Jorgensen and co-workers [10] on capillary electroosmotic separation. At the present time there is a great deal of interest in capillary electrophoresis and a number of workers worldwide are active (e.g. [11–18]).

Capillary electrophoresis is an important development in that high performance operation (high speed/high efficiency) is readily attainable. Fig. 1 shows a separation of fluorescamine labeled peptides obtained from tryptic digest of chicken ovalbumin. In some published examples close to 1,000,000 theoretical plates have been achieved [16]. Such high performance is a consequence in part of the ability of capillaries to operate with high fields without resultant loss in performance due to thermal and convective gradients. These gradients are caused by the Joule heating

0009-5893/87 0015-10 $03.00/0

© 1987 Friedr. Vieweg & Sohn Verlagsgesellschaft mbH

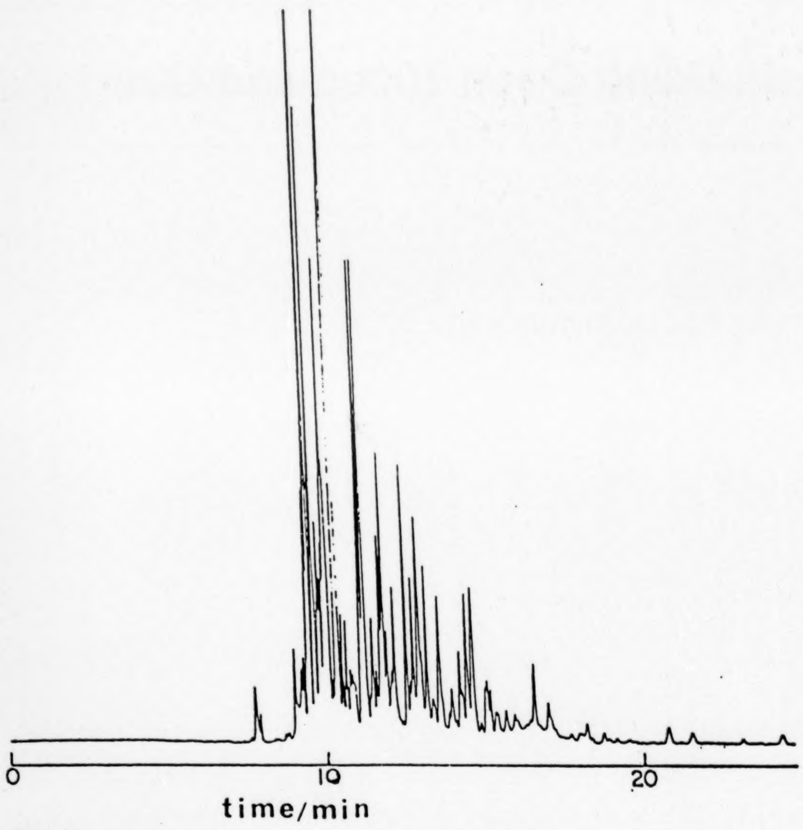

Fig. 1
Electropherogram of fluorescamine labeled peptides obtained from a tryptic digest of chicken ovalbumin (see Ref. [21]).

at high power levels (see later). In addition, on-column injection and detection capabilities allow the possibility for an automated instrumental approach to electrophoresis. Finally, a single instrument can potentially be used for a wide variety of electrophoretic procedures including: free zone electrophoresis with and without electroosmotic bulk flow, gel electrophoresis, isoelectric focusing and isotachophoresis. Each procedure generates its own selectivity, while affinity agents can also be added for biospecific manipulation of selectivity [19].

As a consequence of the above characteristics, high performance capillary electrophoresis has significant potential to become an important tool of the analytical biochemist. Commercially, only capillary isotachophoretic instruments are currently available, but it can be anticipated that several other capillary electrophoretic instruments will be on the market within the next year.

Fig. 2 shows a simple schematic of a basic capillary electrophoretic instrument consisting of a power supply, column and on-line detection. Injection can be accomplished either electrophoretically [12], or by siphoning [11] or valving [20]. A simple, automated, well-constructed injector would be desirable. On-column detection can easily be accomplished with fused silica, in which the polyamide coating is burned off and the exposed quartz tubing placed in a micro HPLC-UV detection cell. Other detectors include fluorescence [21], conductivity [22], electrochemical [17] and laser induced fluorescence [14]. Recently, efforts have been devoted toward coupling to mass spectrometry [23]. Returning to Fig. 2, the capillary ends are placed in buffer reservoirs of several mL's, and platinum electrodes in the reservoirs complete the circuit. A stable power supply of 10 kV or greater is used to drive the ions through the capillary. In micropreparative operation a fraction collector is employed and either the ions can be directly collected in vials of solvent or with a make-up flow after the column [24].

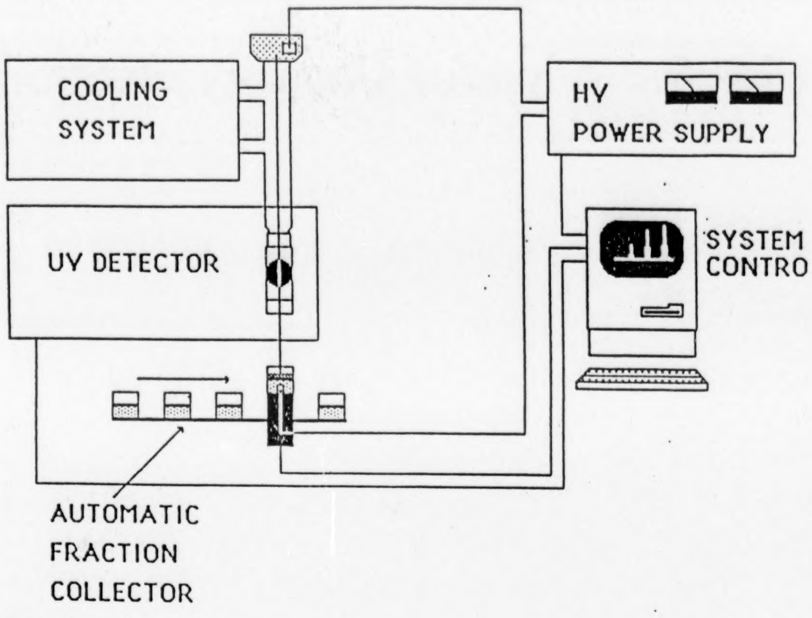

Fig. 2
A simple schematic diagram of a basic capillary electrophoretic instrument.

In this paper we shall present the fundamentals of capillary electrophoresis, especially pointing to the beneficial use of narrow diameter tubes. Then, we shall illustrate several aspects of the power of the method from results of our laboratory. Both open tube and polyacrlyamide gel columns will be illustrated.

Fundamentals

Migration

Electrophoresis is the migration of charged species by the action of an electric field. The fundamental parameter characterizing this migration is the electrophoretic mobility μ_e which has units of $cm^2 \cdot sec^{-1} \cdot V^{-1}$. The mobility thus represents the distance a solute molecule travels in a given time period for a given field (and buffer system). For column operation with on-column detection one can write,

$$\mu_e = \frac{\ell}{tE} = \frac{\ell L}{tV} \tag{1}$$

where ℓ = distance from injection to the detector, t = time for species to migrate the distance, E = electric field = V/L, V = voltage and L = distance between two electrodes. The velocity of migration v_e is equal to ℓ/t, and Eq. (1) can be rearranged to

$$v_e = \mu_e E \tag{2}$$

Thus, high fields and high mobilities lead to fast analyses.

The mobility of a species in an open tube can be approximated as

$$\mu_e = \frac{\epsilon \xi}{\eta} \tag{3}$$

where ϵ = dielectric constant of the medium, ζ = zeta potential of the species and η = viscosity of the medium. Migration velocity is thus a function of the given species and medium, as well as E. With respect to the species, for a given mass, the greater the surface charge, the greater will be the ζ potential. On the other hand for a fixed charge, the greater the mass the lower will be the ζ potential. Hence, large species will in general migrate slower in a given buffer medium. In addition, the mobility is temperature dependent, increasing at the rate of roughly 2 %/°C [25]. Thus, for good reproducibility in electrophoresis, as well as good performance, temperature control is important (see below).

In analogy to Eq. (2), when electroosmosis occurs, the bulk flow velocity v_0 can be written as

$$v_0 = \mu_0^* E \tag{4}$$

where μ_0^* is the apparent mobility of the medium undergoing electroosmotic flow

$$\mu_0^* = \frac{-\epsilon \xi_w}{\eta} \tag{5}$$

where ζ_w = the zeta potential on the walls. The velocity of a species now becomes

$$v = v_0 + v_e = (\mu_0^* + \mu_e) E. \tag{6}$$

If fused silica tubes are used, the charge on the walls will be negative, and bulk flow will occur towards the negatively charged electrode. If the separation of negatively charged solutes is considered, then, if $|\mu_e| < |\mu_0^*|$, these species will move toward the negative electrode with a velocity slower than v_0 and elution will be in the order of increasing electrophoretic mobility. Note also, if $|\mu_e| > |\mu_0^*|$, the net migration of the species will be toward the positive electrode.

Based on this argument, positive species should elute faster than v_0 in fused silica tubing under electroosmotic flow. Because of this, it would seem that both positive and negative species can be made to migrate in the same direction and detected at a common point. However, since the wall surface is negatively charged, adsorption of cationic species on the walls is possible [10]. Adsorption on the walls can not only increase retention, but can be quite detrimental to band efficiency and symmetry through slow desorption kinetics. Various approaches have been taken to reduce this problem while maintaining electroosmosis: diol bonded phase coverage, pH buffer manipulation [16] and increased buffer concentration. Several of these approaches reduce the ζ potential on the walls, thus slowing separation. An alternative approach is to minimize as completely as possible electroosmosis by coating the walls with a neutral hydrophilic polymeric viscous thin layer such as cross-linked methyl cellulose [7] or acrylamide [26]. In this case, free zone electrophoreis will occur with no bulk flow, and wall adsorption will be minimized. Of course, positive and negatively charged species will migrate in opposite directions. Nevertheless, as for electroosmosis, the method is characterized by high efficiency and speed [26].

Returning to the general topic of migration in an open capillary, Terabe and co-workers recently introduced an important development in the use of micelles to manipulate separation of neutral species in free zone electrophoresis with electroosmosis [13]. Using sodium dodecyl sulfate (SDS) micelles (i.e. SDS concentrations in the buffer above the critical micelle concentration, CMC), high performance separation of neutral species are possible, Fig. 3B. The SDS micelle, having a high charge density, possesses a high value of μ_e, of opposite sign to μ_0^*. Since $|\mu_e| < |\mu_0^*|$, Eq. (6) shows that the SDS micelles will move slowly toward the negative electrode, see Fig. 3A.

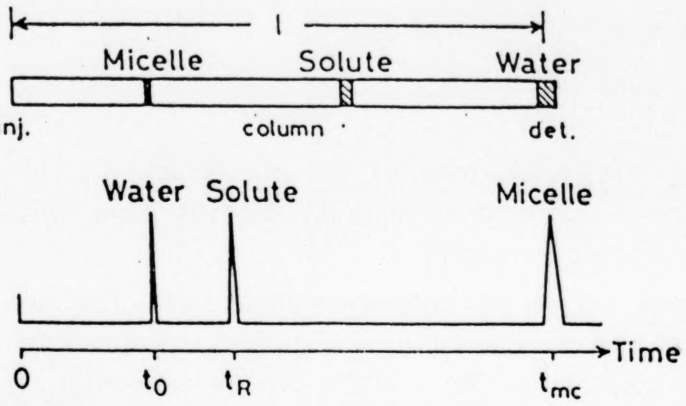

Fig. 3A

Schematic illustration of zones separate in the tube (1) and chromatogram (2) of the hypothetical mixture of water, solute and micelle (see Ref. [13]).

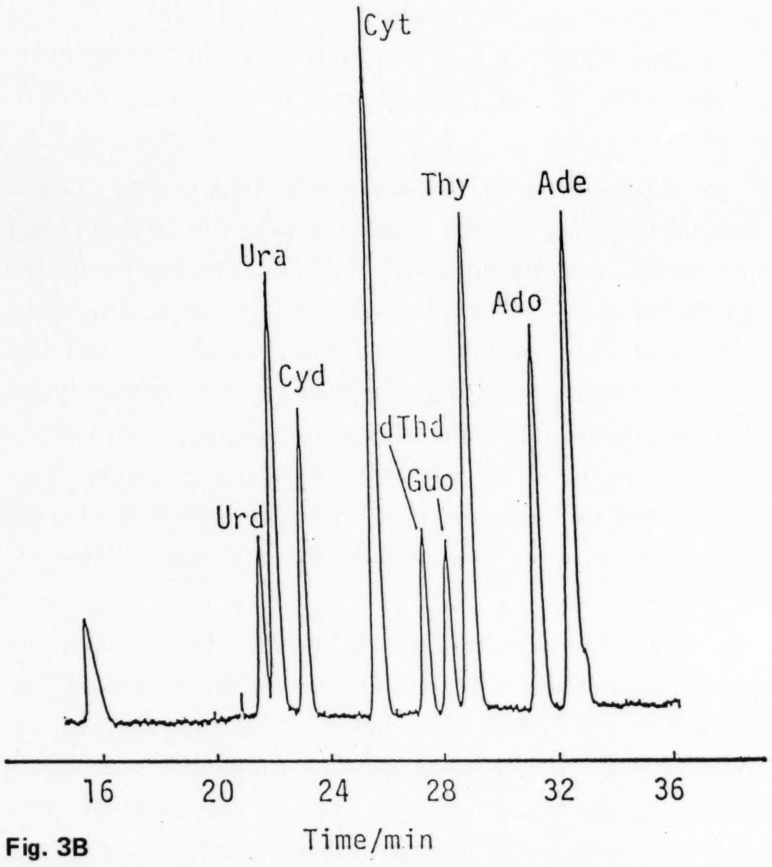

Fig. 3B

Separation of bases and nucleosides: (1) Ura, (2) Cyt, (3) Thy, (4) Ade, (5) Urd, (6) Cyd, (7) dThd, (8) Guo, (9) Ado (see end of paper for observations).

Buffer: 0.025 M sodium fetraborate, 0.05 M sodium dihydrogen phosphate, 0.1 M SDS, pH = 7.

Capillary, 600 mm × 0,05 mm I.D., effective length 800 mm, detection wavelength 210 nm; applied voltage 14 kV, 50 μA (see Ref. [11]).

Bases →
Ura — uracil
Cyt — cytosine
Thy — thymine
Ade — ademine

Nucleosides →
Urd — uridine
Cyd — cytidine
dThd — deoxythymidine
Guo — guanosine
Ado — adenosine

Neutral species will partition within the interior of a micelle according to their hydrophobicity (the phase within the micelle consists mainly of C-12 alkyl chains). When inside the micelle, the species will migrate with the mobility of the micelle, whereas in free solution the species will migrate with the bulk flow. Retention will then depend on the capacity factor of the species

$$k' = \frac{n_{mc}}{n_{aq}} = K\frac{Vmc}{Vaq} \qquad (7)$$

where n = moles of solute, K = partition coefficient between the micellar (mc), and aqueous (aq) phases and V = volume of the given phase. The retention time t_R is then (13)

$$t_R = \frac{1 + k'}{1 + (t_0/t_{mc})\,k'}\,t_0 \qquad (8)$$

where t_{mc} = retention time of the micelle and t_0 = unretained time, i.e. the time a neutral non-partitioning solute takes to travel the distance ℓ.

Qualitatively, we see that capillary electrophoresis has been transposed into a type of liquid-liquid chromatographic separation procedure. The micelle can be considered as the "stationary" phase which migrates at a constant, fixed rate through the "mobile" phase. Separation is then based on partition differences between the micellar and aqueous phases. The high efficiency is in part a consequence of the rapid formation and dissociation of the micelles [11]. The method thus employs the selectivity of chromatography with the high efficiency potential of capillary electrophoresis.

Another approach is to employ the surface of the micelle for separation [11]. In this case, it is possible to add metal ions to a solution containing SDS micelles. The high negative charge density of the micellar surface will electrostatically attract metal ions, leading to a surface which is available for metal complexation. Fig. 4 shows an electropherogram of olgonucleotides in which separation is based on differential complexation with the metal-micelle surface. This approach can be considered a type of ligand exchange chromatography. We shall discuss this method further in a later section.

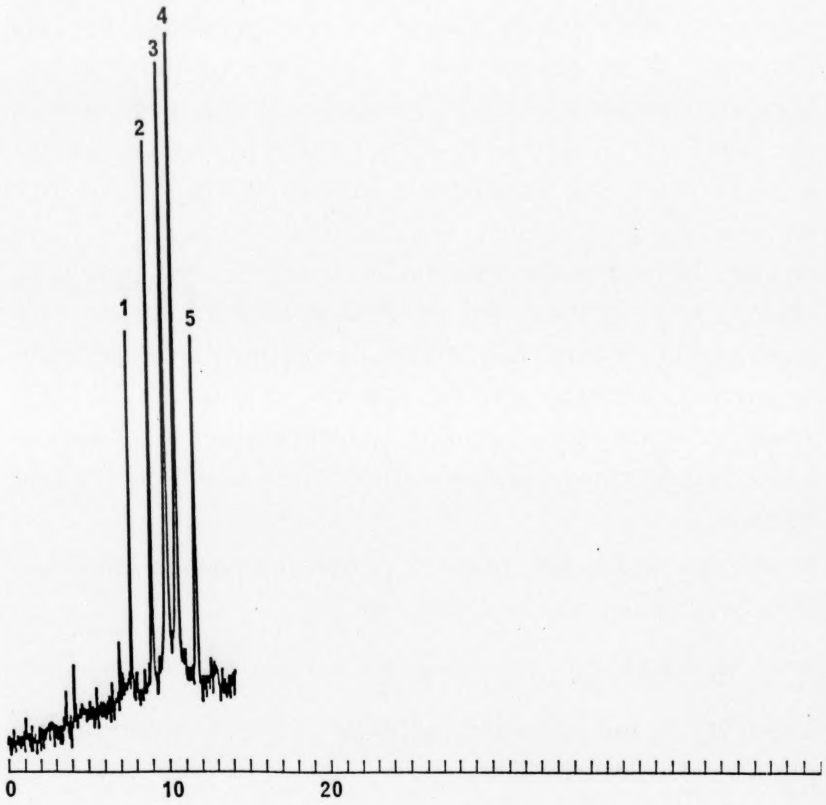

Fig. 4

Capillary zone electrophoretic separation of oligonucleotides using SDS micelles: 1 = 9 bases; 2 = 12 bases; 3 = 15 bases; 4 = 18 bases; 5 = 21 bases.

Buffer: 2 M urea, 50 mM SDS, 5 mM Tris – Na_2HPO_4, pH = 7.4; 3 mM Zn (II).
Capillary, 650 mm X 0.05 mm I.D., effective length 450 mm, applied voltage 20 kV (12 μA), detection wavelength 260 nm thermostated at 25 °C.

Up to now, unrestricted migration has been assumed. However, separations are often conducted in porous gel media. When the pores of a gel such as polyacrylamide are comparable to the size of the molecule, restricted migration takes place, leading to a decrease of the mobility. Indeed, using gels with a gradient in pore size, focusing takes place, in which a band concentrates in a relatively sharp zone at a particular position (i.e. pore size) in the slab gel. The pore size of the gel can be manipulated by the relative composition of monomer to cross-linking agent in the polymerization mixture [2]. A variety of separations in electrophoresis can thus either be partially or totally based on size differences. For example, the separation of oligonucleotides beyond ~ 10 bases is determined predominantly by size differences, since each additional base adds the same amount of mass and charge (the molecular shape is assumed to remain constant) [2]. Also, in the case of SDS-PAGE (sodium dodecyl sulfate – polyacrylamide gel electrophoresis), reduced proteins yield a common shape in the presence of an excess of SDS. Moreover, a constant amount of SDS is adsorbed per unit weight of protein (~ 1.4 g/g), and hence similar charge densities are obtained. Elution is then proportional to log MW and is strictly size related. As discussed later, SDS-PAGE can be readily achieved in polyacrylamide capillary gel columns [12].

Fields and Currents

One form of Ohm's Law is

$$E = \frac{J}{\sigma} \qquad (9)$$

where the current density $J = I/\pi r^2$, r = capillary tube radius and σ = specific conductivity. Eq. (9) can then be rearranged to yield:

$$I = \pi r^2 \sigma E \qquad (10)$$

The specific conductivity can be written as

$$\sigma = \mathscr{F}\sum_i c_i\,\mu_i \qquad (11)$$

where $\mathscr{F}$ = Faraday constant and c_i = molar concentration and μ_i = mobility of species i. Substituting eq. (3) into eq. (11) and then into eq. (10) yields

$$I = \pi r^2 E \sum_i c_i |z_i| \lambda_i = \frac{\pi r^2 \epsilon E c_i \zeta_i}{\eta} \qquad (12)$$

where z_i = charge and λ_i = equivalent conductivity of i-th ion. In this equation $z_i \lambda_i$ has been substituted for the zeta potential of the i-th ions.

Eq. (12) provides an important relationship between I and E. Generally, E is controlled by a power supply and the current I results according to eq. (12). Thus, for a given E and buffer system, wider tubes yield higher current. In addition, a higher buffer concentration or the use of a more conducting buffer yields a higher current. Finally, a more viscous solution produces a lower current. Therefore, for a given field, tube radius and buffer, gel columns produce lower current than open tube columns since the former are much more viscous.

Eq. (1) reveals that higher fields result in faster separations. However, such high fields create concerns with regard to the generated power W

$$W = I^2 R = IV \tag{13}$$

This power creates Joule heating which, if not dissipated, results in a temperature difference ΔT between the center of the tube and the walls [25]

$$\Delta T = \frac{0.24\, Wr^2}{4k} \tag{14}$$

where k = thermal conductivity of the medium. Such temperature differences affect viscosity η (η decreases exponentially with T) and thus mobility, see eq. (3). Therefore, if radial diffusion is slow, the solute molecules near the center of the tube axis will migrate faster than those near the wall leading to band broadening. Also, nonelectrophoretic convective migration can take place since the solvent density will differ at the different temperatures along the tube radius. On another point, when chemical equilibria are superimposed on the electrophoretic migration, temperature variation can affect retention and separation. If the heat is not well dissipated, the temperature difference ΔT at the high fields can be extensive, $> 50\,^\circ$C or more, leading in some cases to tube drying [27].

The need for narrow capillaries is clearly seen in eq. (14), as ΔT is proportional to r^2. In addition, viscous drag on the walls provides an anticonvective effect, and the narrower the capillaries, the greater the surface area of the wall to tube volume ratio. Workers today in general operate with tube diameters in the range of 25–200 μm.

While qualitative separations can be successfully run on capillaries exposed to room temperature, reproducible operation requires temperature control, particularly at higher current levels. In addition, judicious selection of buffers and buffer concentrations is required, along with tube diameter. Note also that short columns need more attention with respect to heat dissipation relative to long columns, since in the former case higher fields result and the surface area over which dissipation can take place is lower.

Efficiency and Resolution

As in chromatography, chromatographic performance can be indexed to H, the height equivalent to a theoretical plate

$$H = \frac{\sum_i \sigma_{x,i}^2}{L} = \frac{L}{N} \tag{15}$$

where σ_x^2 = the length-based variance and N = theoretical plates. This equation assumes that the total plate count is made up of a series of "i" independent band broadening mechanisms, each contributing a variance to the total variance. Since capillaries are employed, the influence of extra column effects on column efficiency are of concern. Terabe has recently performed a careful analysis of this problem in electroosmotic flow [28]. Low nL injection volumes yield high performance conditions. In addition, multiphasic buffer focusing can aid in introducing narrow bands [29]. Indeed, even using water as the injection solvent (or a lower conducting buffer than the operating buffer), some focusing is achieved [2]. With respect to on-column detection, the length of the slit through which the source light travels is important in terms of the total cell volume. Small cell volumes are required for capillary operation. Moreover, the width of the slit should be approximately equal to the internal diameter of the capillary. For high efficiency and fast separations, the response time of the detector must also be considered.

In chromatographic operation, laminar flow results in a parabolic flow profile and the rate of diffusional (or convective) mixing between the various velocities across the tube greatly influences band broadening. In the case of capillary electrophoresis this term is small or nonexistent since electroosmosis creates plug flow [13] and ion mobility is constant in an open tube. This, of course, presumes temperature effects are negligible. If convective phenomena occur as a result of thermal effects, extra broadening will be observed; hence, as already stated, control of current and good heat dissipation at high fields is important.

The Joule heating effect can be considered a form of thermal overloading. Sample overloading is also possible. If the conductivities of the sample and the buffer components are different, then band broadness and asymmetry will result when overloading occurs [18]. In general, ng or lower sample sizes are used in capillary electrophoresis and high performance is achieved. The importance of low detection limits from the detection device is thus emphasized, in order to obtain a wide linear dynamic range of concentration.

Assuming no thermal or sample overloading, extra column effects, or adsorption on the column walls, band broadening in open-tube operation will be controlled by axial diffusion. H in an open tube can then be expressed as

$$H = \frac{2D}{\mu_e E} = \frac{2DL}{\mu_e V} \tag{16}$$

or

$$N = \frac{\mu_e V}{2D} \tag{17}$$

In this "ideal" case, N does not appear to depend on L. Higher voltages would yield more plates and from eq. (1) faster analyses. This double benefit indeed does take place [10]; however, there are limits. Higher voltages ultimately cause Joule heating and lower N. Similarly, shorter columns, as already noted, may also result in thermal overloading. Thus, as pointed out by Jorgenson and co-workers [30], there is an optimum column length or field for a given system.

Nevertheless, even with these limits, impressive performance is possible. For example, for proteins, one can predict from eq. (17) that in the "ideal" case, over 2,000,000 plates could be generated. As we have noted, close to 1,000,000 have already been achieved [16]. In that same example, roughly 1500 plates per second were found for protein separations.

In the case of gel columns, other factors can influence band broadening e.g. eddy diffusion, solute sorption on the gel matrix and restricted migration [12]. While lower efficiency than the open tube can be expected, nevertheless, high performance can still be achieved (see later). Moreover, selective separations based on size differences are possible. It is a combination of efficiency and selectivity which accomplishes separation.

As in chromatography, we can define resolution as

$$R_s = \frac{\Delta t}{4\sigma_t} = \left(\frac{\Delta\mu_e}{4\bar{\mu}_e}\right) N^{1/2} \tag{18}$$

where $\Delta\mu_e$ = difference in mobilities of two components and $\bar{\mu}_e$ = average mobility of the two components. It has been emphasized many times in the chromatographic literature that as Δt becomes smaller, the required number of theoretical plates increases dramatically [31]. In addition, as zones become very sharp at high plate counts, the challenges in terms of retention and separation reproducibility significantly increase [32]. Thus, in practice capillary gas chromatographic columns often contain approximately 50,000 theoretical plates. For very high resolution columns up to 250,000 are frequently employed. It is self evident that when the number of components of a mixture is limited, manipulation of selectivity, $\Delta\mu_e$, is mandatory. Indeed, the power of electrophoresis is in part due to this ability, e.g. isoelectric focusing with immobilized pH gradients [33]. Moreover, when complex mixtures are to be resolved, 2-dimensional electrophoresis on slabs are more powerful than a 1-dimensional column [1–2]. These arguments provide some lessening of the need for excessively large plate counts in capillary electrophoresis. Nevertheless, the convenient and practical use of 100,000–200,000 plates which are rapidly generated would appear to be of real value. In addition, quantitative analysis is possible in the capillary system by the oncolumn approach, whereas on the slab, it is problematical, particularly when using trace staining procedures [34].

From this overview of the fundamentals, we can appreciate some of the power of capillary electrophoresis as an analytical and micropreparative tool. Impressive high performance results are possible, if care is taken in the operation of the system. As already noted, we can expect automated systems to be commercially available in the near future. In the next sections we present some of our recent results in this area using both open tube and gel columns in order to demonstrate the power of the method.

Experimental

Apparatus

Capillary electrophoresis was performed in fused silica tubings 50–200 μm I.D. (Scientific Glass Engineering, Austin, TX, USA) with various column lengths from 250–850 mm, depending on the experiment. A high voltage dc power supply, Model LG-30R-5 (Glassman, Whitehouse Station, NJ, USA) which could deliver high voltage up to 30 kV was used to produce the potential across the capillary. A UV detector, modified as previously described (5–6), was employed (Soma S-3702, IR & D, Kingston, MA, USA) at a wavelength of 260 or 280 nm. The tubing and detector were cooled using a thermostated air bath or a liquid cooling system (Lexacal Model Ex-100DD) with FTC-350 (Neslab Instruments, Inc., Portsmouth, NH, USA). An analog/digital interface (Nelson Analytical, Cupertino, CA, USA) attached to an IBM PC/XT was used to record the results and process the data.

Materials

Samples of oligonucleotides were a kind gift of Dr. John Smith, Massachusetts General Hospital (Boston, USA), and human growth hormone samples were a kind gift of Dr. Bill Hancock, Genentech (South San Francisco, CA, USA). Dns-amino acids were purchased from Sigma (St. Louis, MO, USA). The other reagents were of protein research grade (Schwartz/Mann Biotech, Cambridge, MA, USA). The water was deionized and triply distilled. All buffer solutions were filtered through a Nylon 66 filter unit of 0.2 μm pore size (Schleicher and Schuell, Keene, NH, USA). The samples were kept frozen at −20 °C and working sample solutions were stored at 4 °C. Before use, every buffer solution was carefully vacuum degassed.

Procedure-open tube HPCE: The open tube capillaries were filled with the desired buffer using a 100 μL gas-tight syringe (Hamilton Co., Reno, NV, USA). Both ends of the tube were dipped into separate 5 mL reservoirs filled with the same buffer. The end in which samples were introduced was connected with a platinum electrode to the positive high voltage. The reservoir at the detector end was connected with a platinum electrode to ground. Samples were introduced by electroinjection.

Polyacrylamide gel HPCE: As previously, acrylamide polymerization was accomplished within the capillary, in the presence of the desired buffer, using the appropriate amount of monomer and bis-acrylamide cross-linking reagent, with ammonium persulfate and N,N,N′,N′-tetramethylenediamine (TEMED) as free-radical initiator and catalyst, respectively [1–2]. After polymerization, as in open tube HPCE, both ends of the capillary tube were dipped into separate 5 mL reservoirs, filled with the desired buffer. The reservoir at the injection end contained a platinum electrode attached to the negative side of the power supply, and at the detector end the platinum electrode was attached to the positive side. Samples were electrophoretically introduced into the gel capillary.

Results and Discussion

In a previous paper [11], we have shown the value of high-performance micelle capillary electrophoresis with bulk flow electroosmosis. We illustrated this approach for separation of neutral species: bases and nucleosides via partition within the micelle (see Fig. 3). Advantage was taken of solute partition into the interior of a micelle. An anionic surfactant, SDS, was used to form the micelle, and the elution order was based on increasing hydrophobicity of the solute. As we have noted, since the interior of the SDS micelle is hydrophobic, the more hydrophobic the species the greater will be its partition into the micelle.

Separation of negatively charged species such as oligonucleotides using SDS micelles is problematic since both species are negatively charged and carry a high charge density. On the other hand, metals e.g. Cu(II), Zn(II), Mg(II) and others are known to complex with oligonucleotides with either the phosphate groups and/or the bases [35]. These metals are known to adsorb electrostatically to the surface of anionic micelles [36], and a metal surface is thus created where complexation of oligonucleotides can take place. Fig. 4 shows the power of this approach in the separation of oligonucleotides with 9–21 bases.

As in the case of neutral species partitioning within the interior of the micelle, the attachment of nucleotide to the micelle results in a reduction in the migration velocity of the solute due to the SDS – metal (II) – oligonucleotide complexation. The moving "stationary" phase in this case is the metal-SDS micelle surface. As in ligand-exchange chromatography, different selectivities can be obtained by variation of the metal [11]. In addition, the high efficiency is result of the rapid decomplexation kinetics as well as the rapid dissociation of the micelle. The power of this approach was shown in a previous paper where 14 of 18 oligonucleotide 8-mers were separated in 30 min [11].

Not only is high performance achieved, but retention is reproducible. Table I shows retention time results for a series of oligothymidines using SDS-Mg (II). It can be seen that reproducibility from run to run is better than 1 % relative standard deviation. It was further found that the relative standard deviation was better than 3 % from day to day. The key to this constancy in retention is proper washing of the capillary walls. Eq. (5) shows that the bulk flow depends on the zeta of potential on the tube walls. In order to maintain a constant zeta potential, we purged the capillaries after each run with 100 μL of 0.1 M NaOH, followed by 250 μL of triply distilled water. Care was taken to equilibrate the tubing with buffer prior to the next run. The total time between runs was 3–5 min. It is to be noted that neither in free zone electrophoresis without electroosmotic flow nor in gel electrophoresis is it necessary to control the zeta potential on the walls by washing.

Table I. Reproducibility of Retention in High Performance Capillary Electrophoresis

Solute	t_R min 1	2	3
2-mer	5.87	5.87	5.87
3-mer	8.39	8.43	8.39
4-mer	8.92	8.88	8.88
6-mer	9.72	9.79	9.72
10-mer	10.58	10.58	10.51

Mixture of Oligothymidines
Column: L = 650 mm, ℓ = 400 mm, 50 μm ID fused silica
Conditions: 20 kV, 24 μA
Buffer: 20 mM Tris, 50 mM SDS, 7 M urea, 5 mM Mg (II)

Returning to the metal system, it is well-known in ligand-exchange chromatography that chiral separations are possible if the metal is attached to a chiral ligand. We tested the feasibility of this approach by employing a chiral chelate detergent, didecyl-L-alanine. Solubilization of this reagent in an aqueous solution was possible only in the presence of SDS, and, as a result, it is presumed that mixed micelles are formed in solution. The reagent is incorporated into the micelle in such a way that the hydrophilic chiral centers of L-Ala are on the surface, while the hydrophobic tail is in the interior. It is to be noted that use of mixtures of detergents to form micelles may allow manipulation of the micelle surface that could prove useful in controlling the distance between ligand-exchange chiral centers [37].

Fig. 5 shows the chiral separation of dansylated amino acids using this mixed micelle system. While the system has not been optimized, the validity of the approach is clearly demonstrated. Other workers have used chiral buffers [14] and chiral chelates for separation [38]. There are obviously a variety of strategies that can be used for chiral separation, and there is no doubt that other schemes will be devised in the future.

Another area where capillary electrophoresis will play an important future role is in polyacrylamide gel systems. As we have noted, it is possible to separate both proteins and oligonucleotides based on size differences with properly designed gels. Indeed, these approaches are widely used to characterize and separate proteins, and it is the conventional method for oligonucleotide separation (e.g. DNA sequencing) [39].

Previously, we have demonstrated the use of polyacrylamide gel capillary columns for molecular weight determination by SDS-PAGE [12]. By means of Ferguson plots, we were able to show that true size separations were occurring with these columns. The method is rapid (10–20 min) and on-line detection at the ng level or lower can be achieved. The problems inherent in staining in slabs – reproducibility, quantitation and speed – are removed.

In this paper we present some recent results under non-denaturing conditions (i.e. no SDS, no urea added to the gel). In the production of genetically engineered human growth hormone (Met-hGH: methionine added to the

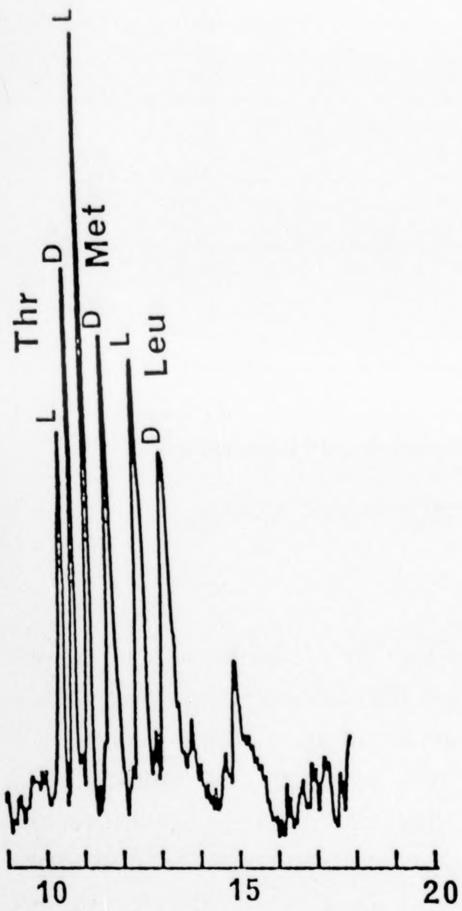

Fig. 5

Resolution of three DL-DNS-amino acids (DL-DNS-Thr, DL-DNS-Met, DL-DNS-Leu) using a mixed chiral micelle.
Buffer: 10 mM sodium acetate 20 mM SDS, 5 mM N,N Didecyl L-Ala, 25 mM Cu (II) 10 % v/v glycerol. Capillary: 800 MM × 0.075 mm I.D., effective length 600 mm, applied voltage 25 kV (20 μA), detection wavelength 260 nm, thermostated at 25 °C.

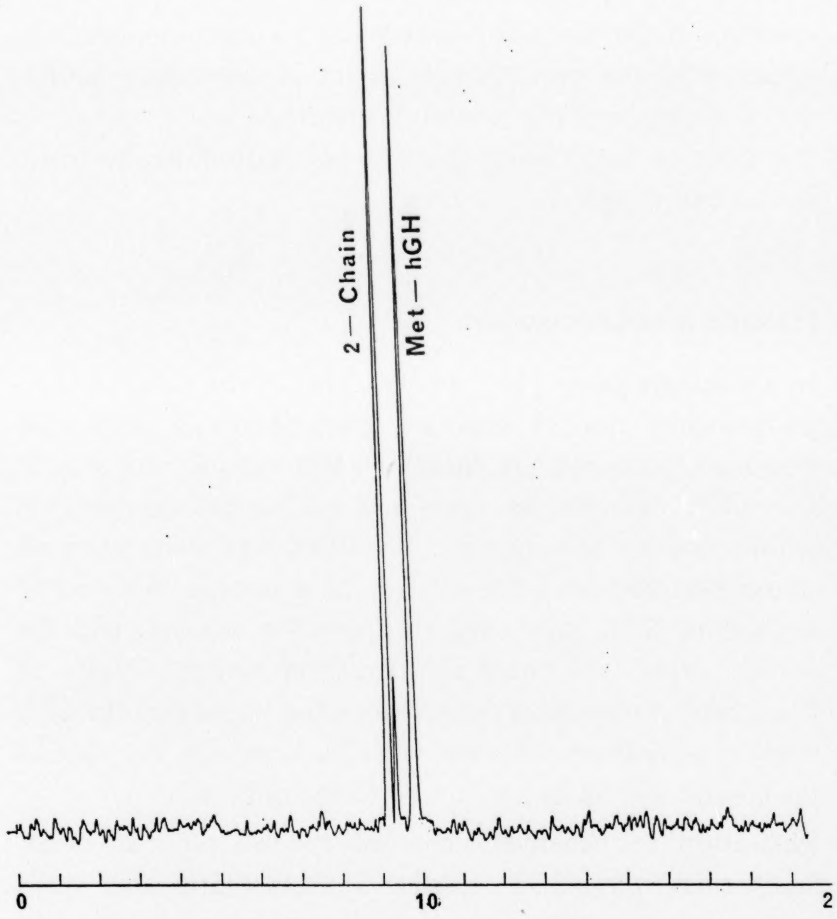

Fig. 6

High-performance capillary polyacrylamide gel separation: (1) two chain (2) met-hGH.
Buffer: 0.1 mM Tris-borate pH = 7.8.
Conditions: 930 V/cm 12 μA, 25 °C; T = 10 %, C = 3.3 %, 270 mm × 0.075 mm, effective length 150 mm.

N-terminal amino acid of growth hormone), a minor product is often found – so-called two chain. This product has a proteolytic enzymatic cleavage (clip) between Thr 142 and Tyr 143 [40]. Disulfide bonds keep the two chains together, and thus the only difference between the 192 amino acid hormone and its impurity is a proteolytic single clip.

Fig. 6 demonstrates the baseline separation in 10 minutes of the two related components with essentially the same molecular weight and a small pI difference [41]. Sharp peaks are obtained at field strengths of 926 V/cm. In our previous work on SDS-PAGE, the field strength did not go above 400 V/cm in the higher conductivity buffer containing 0.1 % SDS. It is interesting to note that on slab gels with Coomassie blue staining, only when the 2-chain is at least 5 % of the main product is it possible to detect these species in the mixture. In Fig. 6, less than 0.1 % of the impurity would be easily observed. The results demonstrate that high performance separation are possible in capillary gel columns under non-denaturing conditions.

With respect to trace analysis, crescormon, a wild type of human growth hormone (hGH), often has a minor product of a dimer of hGH. Fig. 7B shows an electropherogram of crescormon by SDS-PAGE under non-reducing conditions. A single peak is observed for the sample injected with a trace signal for a late peak. Increasing the injected amount to ~ 400 ng clearly shows the latter peak which is presumably the dimer. Note that while the main peak is overloaded, the extent of distortion is limited. One could simply quantitate the two peaks in a single run by operating at a relatively insensitive UV wavelength for the main peak and a sensitive wavelength for the trace species.

Finally, Fig. 8 illustrates the potential of capillary electrophoresis in micropreparative purification. Using a 200 μm column with 8 % T and 3.3 % C and 7M urea in the buffer, Fig. 8A shows the analytical separation of a crude 20-mer oligonucleotide with a sample size of ~ 100 ng. Fig. 8B presents the separation when ~ 800 ng was injected. The major component was collected, and Fig. 8C shows the reinjection of this fraction, illustrating the extent of purification. Full details on micropreparative collection will be published separately.

These few examples illustrate the potential of open tube and gel capillary columns. The method is rapid, efficient and will ultimately be automated. Relative to slab gel operation, trace level quantitative analysis is possible. Of course, slabs have the ability to run many samples simultaneously for high throughput, and 2-dimension electrophoresis is a higher resolving tool than capillary electrophoresis. Thus, both slab and capillary operation complement each other and both will be widely used. We can anticipate the use of capillary electrophoresis in many diverse applications.

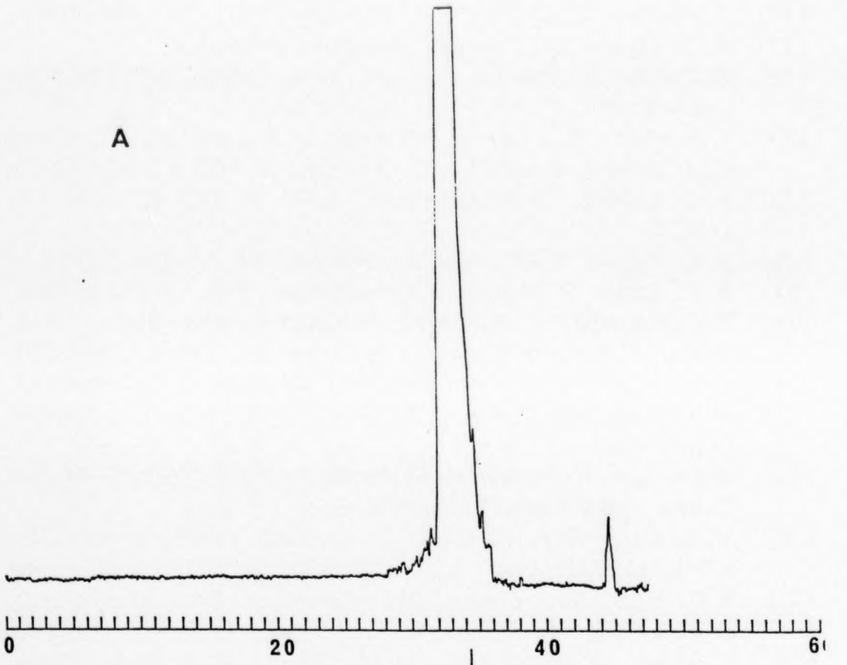

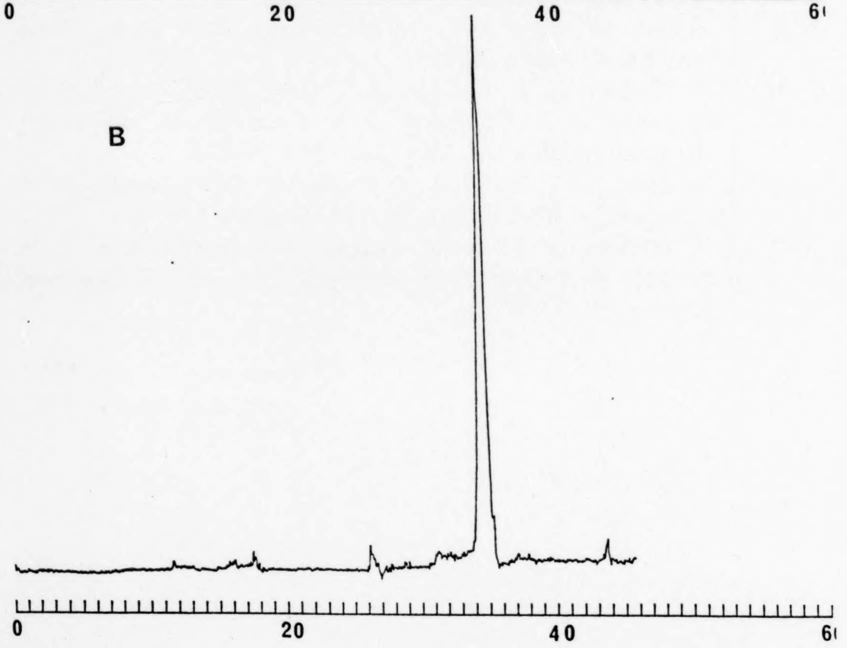

Fig. 7A

Gel capillary electrophoresis of crescormon, a wild type human growth hormone.

Buffer 0.1 M Tris – borate, 0.1 % SDS, 7 M urea. Polyacrylamide gel: T = 10 %, C = 3.3 %; Capillary: 400 mm × 0.075 mm I.D., effective length 200 mm, applied field 200 V/cm, 7 μA; injected amount (estimated) 50 ng.

Fig. 7B

Conditions same as Fig. 7A except the injected amount ~ 400 ng.

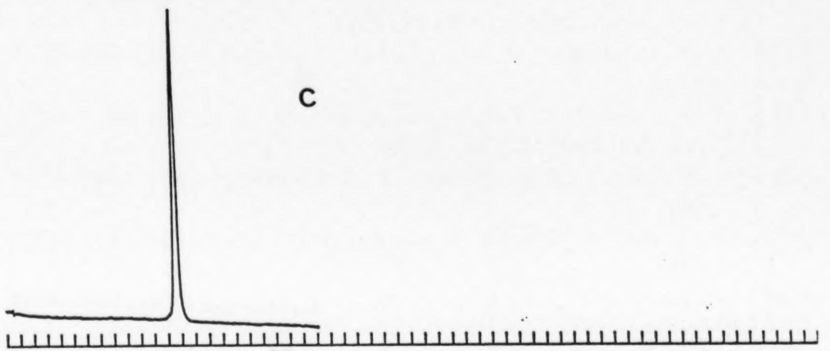

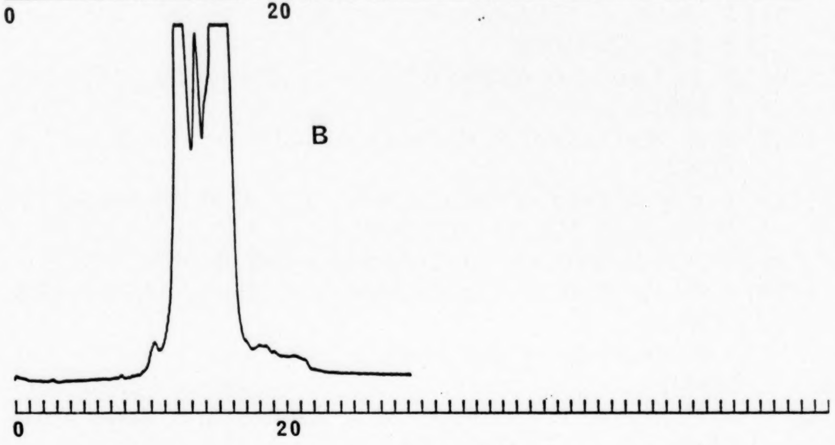

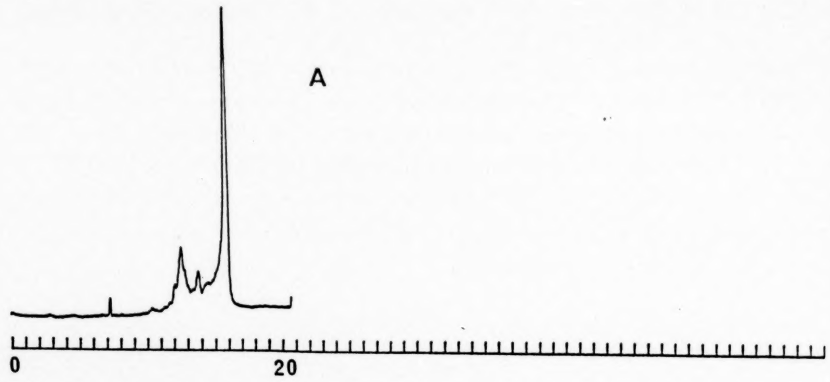

Fig. 8A

High-performance capillary gel electrophoresis of a crude mixture of an 20-mer oligonucleotide.

Buffer: 0.1 M Tris – borate pH 8.6, 8 M urea. Polyacrylamide gel T = 8 %, C = 3.3 %. Capillary: 300 mm × 0.1 mm I.D., effective length 150 mm, applied field 500 V/cm, 30 μA, detection wavelength 260 nm thermostated at 25 °C, injected amount ~ 100 ng.

Fig. 8B

Conditions same as Fig. 8A except the injected amount ~ 800 ng.

Fig. 8C

Reinjection of pure 23-mer oligonucleotide. Conditions same as Fig. 8A.

Acknowledgements

B. L. Karger gratefully acknowledges support from the James L. Waters Chair in Analytical Chemistry, the National Science Foundation and the Dow Chemical Company. A. Paulus acknowledges the NATO Science Council and the DAAD, Bonn FRG, for fellowship support. The authors thank Prof. J. A. Smith from MGH for the crude sample of oligonucleotide, Dr. W. Hancock from Genentech for the sample of human growth hormone and Dr. N. Grinberg for stimulating discussions on chiral separations and for the synthesis of the didecyl-L-alanine. Contribution No. 332 from the Barnett Institute.

References

[1] DNA Sequencing: Laboratory Techniques in Biochemistry and Molecular Biology; *T. S. Work, R. H. Burdon* (Editors); Elsevier Biomedical Press: Amsterdam, New York, Oxford (1986).
[2] Gel Electrophoresis of Proteins: A Practical Approach; *B. D. Hames, D. Rirkwood* (Editors); IRL Press, Washington, D.C. 1983.
[3] Isoelectric Focusing. Theory, Methodology and Application, *P. G. Righetti* (ed.), Elsevier Biomedical Press, New York, (1983).
[4] *J. C. Giddings,* Sep. Sci. **4**, 181–189 (1969).
[5] *S. Bowman,* Anal. Chem. **59**, 969A (1987).
[6] *J. C. Bennett,* Methods in Enzymology, Vol. XI, S. P. Colowick and N. O. Kaplan (Editors), Academic Press, New York 330 (1967).

[7] *S. Raymond, L. Weintraub,* Science, **130**, 711 (1959).

[8] *V. Neuhoff,* Electrophoresis **5**, 251 (1984).

[9] *F. E. P. Mikkers, F. M. Everaerts, T. P. E. M. Verheggen,* J. Chromatogr. **169**, 11–20 (1979).

[10] *J. W. Jorgenson, K. D., Lukacs,* Science **222**, 266–272 (1983).

[11] *A. S. Cohen, S. Terabe, J. A. Smith, B. L. Karger,* Anal. Chem. **59**, 1021–1028 (1987).

[12] *A. S. Cohen, B. L. Karger,* J. Chromatogr. **397**, 409–417 (1987).

[13] *S. Terabe, K. Otsuka, T. Ando,* Anal. Chem. **57**, 834–841 (1985).

[14] *E. Gassmann, J. E. Kno, R. N. Zare,* Science **230**, 813–814 (1985).

[15] *T. Tsuda, G. Hakagawa, M. Tato, K. Yagi,* J. Appl. Biochem. **5**, 330–336 (1983).

[16] *H. H. Lauer, D. McManigill,* Anal. Chem. **58**, 166–170 (1986).

[17] *R. A. Wallingford, A. G. Ewing,* Anal. Chem. **59**, 1762–1766 (1987).

[18] *F. E. P. Mikkers, F. M. Everaerts, T. P. E. M. Verheggen,* J. Chromatogr. **169**, 11–20 (1979).

[19] *V. Horejsi, J. Tickam,* J. Chromatogr. **376**, 49–67 (1986).

[20] *T. Tsuda, T. Mizuno, J. Akiama,* Anal. Chem. **59**, 799–800 (1987).

[21] *J. W. Jorgenson, K. D. Lukacs,* J. Chromatogr. **218**, 209–216 (1981).

[22] *X. H. Huang, T. K. J. Pang, M. J. Gordon, R. N. Zare,* Anal. Chem., **59**, 2747–2749 (1987).

[23] *J. A. Olivares, N. T. Nguyen, C. R. Yonker, R. D. Smith,* Anal. Chem. **59**, 1232–1236 (1987).

[24] *S. Hjerten, D. M. Zhu,* J. Chromatogr. **327**, 151–164 (1985).

[25] *R. J. Wierne,* Chromatography: A Laboratory Handbook of Chromatography and Electrophoresis Methods, 3rd, ed., Heftmann, E. (Editor), Van Norstrand: New York (1975).

[26] *S. Hjerten, M. D. Zhu,* J. Chromatogr. **347**, 191–198 (1985).

[27] *A. S. Cohen, B. L. Karger,* unpublished results.

[28] *S. Terabe, K. Otsuka, T. Ando,* Anal. Chem., submitted for publication.

[29] *S. Hjerten, K. Elbering, F. Kilar, J. L. Liao, A. J. C. Chen, C. J. Siebert, M. D. Zhu,* J. Chromatogr. **403**, 47–61 (1987).

[30] *K. D. Lukacs, J. W. Jorgenson,* HRC & CC **8**, 407, 411 (1985).

[31] *B. L. Karger, R. W. Giese,* Anal. Chem., **50**, 1048A (1978).

[32] *B. L. Karger, P. Vouros,* J. Chromatogr., **323**, 13–32 (1985).

[33] *P. G. Righetti, E. Gianazza,* Electrophoresis 1981, *R. C. Allen, P. Arnand* (Editor), de Gruyther, Berlin, 655–665.

[34] New Directions in Electrophoresis Methods, *J. W. Jorgenson, M. Phillips* (eds.), American Chemical Society, Washington, D.C. (1987).

[35] *Metal Ion in Biological Systems, H. Sigel* (Editor), Marcel Dekker: New York (1979), Vol. 9.

[36] *M. V. Oko, R. L. Venable,* J. Colloid. Interface. Sci. **35**, 53–59 (1971).

[37] *B. Feibush, M. J. Cohen, B. L. Karger,* J. Chromatogr. **282**, 3–26 (1983).

[38] *P. Gozel, E. Gassmann, H. Michelsen, R. N. Zare,* Anal. Chem. **59**, 44–49 (1987).

[39] *J. M. Prober, G. L. Trainor, R. J. Dam, F. W. Hobbs, C. W. Robertson, R. J. Zagursky, A. J. Cocuzza, M. A. Jensen, K. Baumeister,* Science, **238**, 336–341 (1987).

[40] *V. J. Lewis, J. T. Dunn, L. F. Benewald, B. K. Seavey, W. P. Vanderlaan,* J. Biol. Chem. **263**, 2679–2687 (1987).

[41] *A. E. Wilhelmi,* Hormone Drugs, *J. L. Guerigriam, E. D. Bransonk, A. S. Outskoern* (Editors), 369–381, Convection, Rockville, MD 1982.

Received: Nov. 6, 1987
Accepted: Nov. 9, 1987
F

Spectrometers and High Performance Liquid Chromatography

H. Poppe

Laboratory for Analytical Chemistry, University of Amsterdam, Nieuwe Achtergracht 166, 1018 WV Amsterdam,
The Netherlands

Key Words

Mass spectrometry
UV spectrometry
Fluorescence spectrometry
Fourier transform infrared
Nuclear magnetic resonance
Supersonically cooled jet
HPLC-coupling
Hyphenated techniques

Summary

The coupling of HPLC to a spectrometer is considered from a general point of view. Dynamic adaptation of the two systems, in terms of volume or time effects with respect to the preservation of sensitivity and resolving power, is discussed. It is shown that this problem, and the large amounts needed for obtaining certain sorts of spectra, in some cases points to a reconsideration of off-line approaches. A number of spectrometric methods is discussed in more detail from the point of view of HPLC coupling.

Introduction

It is the purpose of this paper to give a general discussion of the present and future analytical possibilities regarding the coupling of HPLC separations to spectrometric techniques. The discussion will be organized with on-line coupling, often involving the use of a spectrometric cell as a flow cell, in mind; however, it is evident that on many occasions it will also be necessary to devote attention to off-line coupling, involving the use of HPLC as a (micro-) preparative device, with subsequent spectrometric investigation of the obtained fractions. For some techniques, and indeed, for some scientific experts this view has a general value; the off-line technique is the more logical choice. This may be the case, as both HPLC and spectrometry are methods that work at the limits of what is physically, chemically and technically possible, with little room for adaptation and compromise. The result is that mutual adaptation of the separation and spectrometric stages in the analysis may bring about an inacceptable loss in the performance of one or both of these techniques.

Despite the validity of such views there is great and vigorous interest in on-line HPLC (or in general chromatography) spectrometry coupling. This interest may partly be caused by the enormous success of the GC-MS combination as an analytical tool in various fields of analysis, but the advantage of the coupling approach is of fundamental and general validity, as will be discussed below. Presently many spectrometric techniques are utilized for their suitability for HPLC coupling, and therefore the present general discussion may be of some use.

The above-defined purpose of the paper is indeed a very ambitious one. The complete fulfillment of this task would require deep insight into the physical limitations of chromatography and its analytical use, as well as knowledge of the limitations of all the different spectrometric techniques; a combination of gifts and education that is very difficult to find. Thus it would be fair, both to the readers and to the author, to make clear what the pretentions of this paper are.

On-line HPLC-spectrometer coupling is already implemented on a routine basis for two types of spectrometry: UV absorption and mass spectrometry. Each of these coupled techniques are so widespread and bring about so many fundamental and practical questions, that each already deserves a regular review paper on their own. Therefore, in the first place, this paper does not pay much attention to these techniques; rather its subject is the future or non-future of other combinations.

In the second place this paper is written by an author who, though is partly specialized in detectors and therefore aware of some of the aspects of spectrometry, feels basically at ease only in chromatographic-analytical questions and who, for the present paper, would have preferred to have a number of spectrometric experts as his coauthors. The paper will therefore doubtless be deficient in the spectrometric aspects and hardly will scratch the surface in this respect. However, as such it may serve partly as a challenge

0009-5893/87 0025-08 $03.00/0

© 1987 Friedr. Vieweg & Sohn Verlagsgesellschaft mbH

to better experts in these fields to consider the problems stated along the same lines. If this target is hit, the paper has served its purpose.

The Benefits of Spectrometer Coupling

During the last decade it has been recognized that the increase in performance in chromatographic separations and spectrometry alike is subject to the law of diminishing returns. The increase in magnet strength in NMR and the decrease in particle size in HPLC are comparable in the respect that the attainment of the technological standard of today has brought orders of magnitude in performance. However, at the same time we realize now that there is no room left for an additional gain of some factors of ten in one-dimensional resolution. Still, the problems posed by analytical, day-to day practice do ask for more and the multidimensional approach is rapidly gaining ground in spectrometry and chromatography alike. MS-MS, 2D-NMR, and chromatographic multicolumn operation may be classified as "homo-technique" coupling. The "hetero-technique" approaches (GC-MS as the first example, LC-MS, LC-UV, GC-FTIR, etc.), encompass the subject of this paper, and they have some very attractive features:

Information content: Each two-dimensional technique leads to a leap in the rate of information production. However, the two dimensions are less rewarding when there is correlation between the two axes. Because of the dissimilarity of the techniques, this is less likely to occur in HPLC-spectrometry, and the gain in information production is therefore in general very large.

The more spectrometric resolution ("peak capacity", range of the spectrum divided by the peak width of the average peak) present in both techniques, the more information will be produced by the combination.

Interpretation: One peak is one component in chromatography, an enormous advantage in the interpretation.

Interfacing with routine chromatographic analysis: This is exemplified by the numerous cases where compounds are routinely assayed with a simple low investment chromatograph with single channel detection, but where method development and validation, peak confirmation, etc. are done with a coupled spectrometer (GC-MS, LC-UV).

From a analytical, chromatographic-analytical point of view this leads to the following possibilities:

Confirmation of the identity of a peak: Badly needed in view of the limited efficiency of an HPLC (e.g. compared to GC where peak confusion is much less likely) by comparison of the spectrum with the standard.

Identification of unknown peaks by library search techniques in a file of known spectra: Of course this is highly dependent on what is indicated as "portability of spectra": dependence of the spectra on the experimental conditions, especially solvent composition, but also spectrometer type and maybe even its serial number. Obviously, the solvent composition problem is the most severe. With some techniques a phase transformation is necessary (MS, some modes of FTIR, supersonic jet fluorescence); the resulting awkward experimental complication is partly compensated by the disappearance of the influence of the solvent.

Structure elucidation of unknown and unfiled components in the chromatogram: Here the ease of interpretation in the sort of spectrometry at hand is crucial, with probably NMR as the absolute winner and UV-absorption as a poor performer.

This paper will discuss the coupling of HPLC to the spectrometric techniques listed in the first column of Table I.

Some techniques that are well accepted (although seldomly applied) as structure elucidation techniques are missing: electron spin resonance, microwave (rotation), near infrared, and such modern laser techniques as, for instance, Coherent Anti-Stokes Raman Scattering. This is the result of the rather subjective opinion of the author that such techniques either have a too limited application field, or are too far removed from the stage where coupling to HPLC could even be considered, and therefore their inclusion would unnecessarily complicate the present overview.

The second column in the table lists the order of magnitude of the "peak capacities" of the various sorts of spectrometry, often indicated as "resolution" by spectrometrists, a term we want to avoid for obvious reasons. The larger the peak capacity, the more attractive the combination with HPLC is. However, this should not be over-emphasized, Even a moderate spectrometric peak capacity of ten potentially multiplies the information production of an HPLC

Table I

Spectrometry	"peak capacity" (spectrometric) resolution)	amount for decent spectrum, MIQ (S/N = 5)	increase of quantitation MIQ with volume of cell		portability of spectra
Mass spectrometry QP	3 000	100 pg	?	–	+
Mass spectrometry MS	100 000	100 pg	?	–	+
UV-absorption	10	1 ng	V 1/2	+	–
UV-fluorescence	10	10 pg (?)	V 1/2 ?	+	–
Fourier Tr. infrared	1 000	100 ng	V 1/2	+	+ –
Nuclear magnetic resonance	30 000	30 μg	–	+ (?)	+
Supersonic jet UV-fluorescence	3 000	ng range?	na	?	+

? = not known or depending on conditions
na = not applicable
QP = quadrupole

MS = magnetic sector
UV = UV-visible

with that number. Depending on price, detection limit or minimum identifiable quantity (MIQ-listed in the third column), and quantitative reliability (fourth column), this can be of enormous potential, as has been shown by the development of HPLC-diode-array spectrometry.

The Essential Stumbling Blocks

The attractiveness of the two-dimensional approach leads to the question of what the impediments for the application of the combinations listed in Table I are. The main impediments include:

Detection limit in amount, or minimum amount needed for an identifiable spectrum, indicated as MIQ. Table I displays the order in which this difficulty is the most pronounced: UV, NMR, FTIR. Analytical practice unfortunately shows that identification or structure elucidation problems (apart from pure chemical research situations) more often than not occur with amounts in the (low) nanogram level. Nanogram amounts of an unknown compound may be a ppb constituent of a blood sample, of which one does not have much more then a few milliliters, or a ppt constituent in an environmental sample, of which one is not able to process more then 1 kg.

Interfacing, or better: What does the spectrometer with the solvent? The selective response of UV-detection and spectrometry has been mentioned in the past as a significant limitation. However, the fact that is does not "see" a large variety of solvents and other retention moderators has been of very large practical importance. In retrospect, one can only guess where HPLC would be now if the UV detector had not allowed us to measure a significant number of compounds of interest at nanogram level while at the same time, numerous solvents without UV absorption and of greatly varying polarity could be used for tuning the chromatographic selectivity (cf. the relative poor success of the refractometer detector in HPLC). The more universal techniques, such as MS, FTIR and NMR respond to the solvents as well, but make us pay dearly for this advantage in the form of "interfacing problems" that force us to devise moving belts and on-line solvents extractors, etc., in order to get rid of the few responses we do not want (those of the mobile phase) and which would saturate our measuring system.

Mutual Dynamic Adaptation of HPLC and Spectrometry

In many types of spectrometry (MS is the most impressive exception), signal to noise ratio ("sensitivity", or detection limit, minimum identifiable amount, etc.) becomes the main obstacle when it comes to coupling to HPLC. The small peak volumes and the high rate of elution of peaks in HPLC aggravate this problem. It is useful to try and discuss such problems from a general point of view.

The first problem encountered concerns the time scale of data acquisition in HPLC and the spectrometry at hand. Development of HPLC in the last decades has been focussed on increased speed of separation. In effect, the emphasis on speed has been much larger than that on separation performance (plate number) per se; despite efforts [1–3] to develop long micro-columns and open tubular columns with plate numbers in excess of 20 000, up to about $1 \cdot 10^6$, the plate number applied in analytical work is still between 2000 and 10 000. Figure 1 shows the dependence of the peak width at a given plate number of 10 000, expressed as the standard deviation in seconds, as a function of the parameter which best reflects the technical progress in HPLC, the particle size, calculated according to standard theory [4].

The rate at which the spectrometer has to produce, handle and store new information (spectra) has to keep pace with this. The acquisition of spectra with a time interval of Δ_t corresponds to the discretization of the chromatogram, as normally applied in digital data processing for chromatography. It is known that a time interval of slightly less than one standard deviation σ_T [5] suffices to produce a faithful representation of the chromatogram:

$$\Delta_t < \sigma_t \qquad (1)$$

This requirement puts a large burden on the technical implementation of some sorts of spectrometry, because with present HPLC technology the acquisition interval should be smaller than 0.3 seconds, as is shown by Fig. 1. However, this holds for the unretained compound. For retained peaks, compromising with respect to this require-

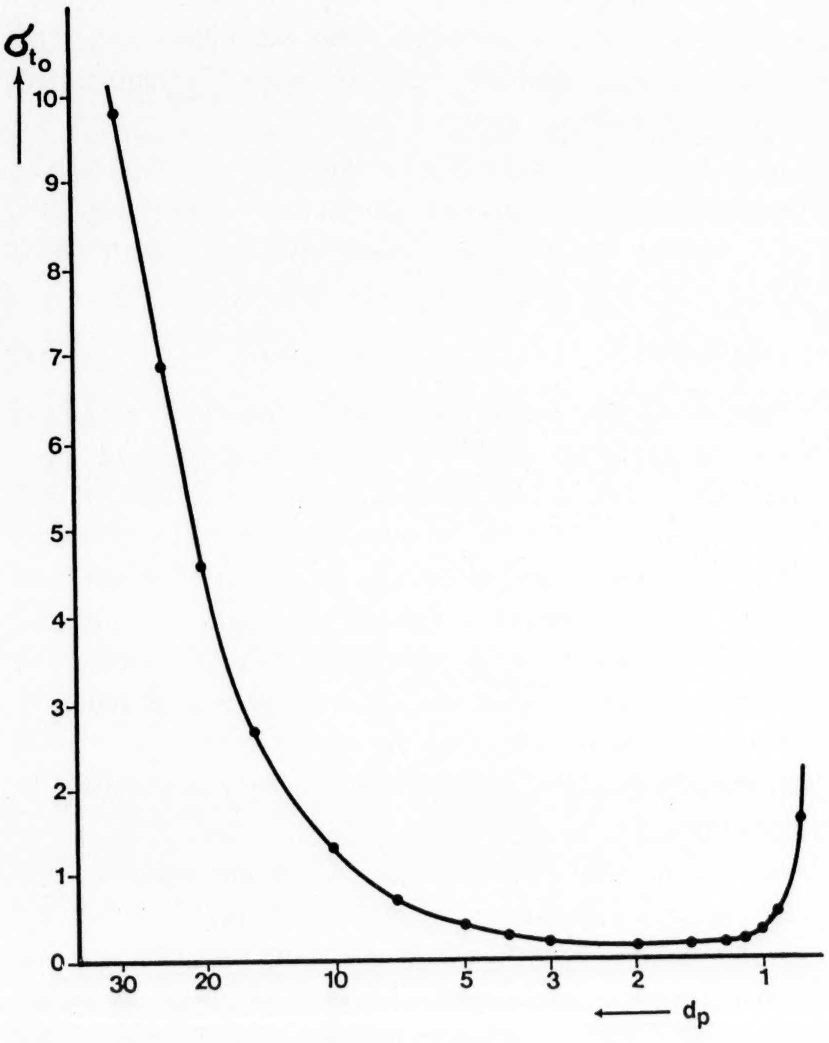

Fig. 1

Peak width expressed as standard deviation for a time optimized column in HPLC as a function of particle size. Parameters: $D_{im} = 10^{-9}\ m^2\ s^{-1}$, $\eta = 10^{-3}\ kg\ m^{-1}\ s^{-1}$, $\Delta p = 3 \cdot 10^7$ Pa, $N = 10^4$, $\Phi = 10^3$.

Plate height equation $h = 1.5/\nu + 1.5 + 0.1\ \nu$.

ment is often admissible, especially as the enormous increase of information production when spectrometers are coupled more then offsets the slight loss of information in the beginning of the chromatogram. Moreover, it is comforting to know that most probably the decrease in chromatographic peak width in time as a result of the the ongoing developments in HPLC has more or less come to an end: Reduction of particle size to values smaller than about 2 μm is not likely [4], except for high molecular weight solutes that will give slower peaks anyhow.

A few years ago, the requirement of a 0.3–1 second acquisition time still presented problems with respect to data storage. However, present cheap computer technology has freed us of most of these worries and the physical limitations are now more important. Moving mechanical parts occasionally may form the bottleneck, e.g. in UV instruments where a grating or mirror is rotated. Electrically-scanned instruments, such as diode arrays or quadrupole mass spectrometers, do not present any problems, no more than highly sophisticated feed-back controlled mechanical movements of mirrors in FTIR-spectrometry [6].

The requirement regarding acquisition time is easily met by mass spectrometry (except for some time lag effects that may occur in more complicated interfaces, such as moving wire/belt, with or without on-line extraction into a more friendly solvent), by UV-diode array spectrometry, by future simultaneous multiwavelength fluorescence technique, and by Fourier transform infrared spectrometry. However, in some of these techniques the short measuring time available interferes with the requirement to improve the signal to noise ratio.

The situation is more tricky with NMR coupling [7]. Depending on the required spectrometric resolution, the time needed for data acquisition in a FT experiment is 0.1 to 10 seconds according to the Nyquist criterion:

$$\Delta t > 2/\Delta f, \qquad (2)$$

where Δt is the acquisition interval, which is of course equal to or larger than the acquisition time, and Δf is the peak width in the spectrum. The latter can be well below 1 Hz in NMR. It follows that with state-of-the-art HPLC-instruments and NMR, the coupling of the methods nearly always leads to a loss of resolution in either the chromatographic time or the NMR frequency axis. The necessity, depending on the physical system at hand, to allow for a relaxation time for the spin to return to its equilibrium position after excitation, may aggravate this situation.

Apart from the time effects on chromatographic and spectrometric resolution discussed above, one has to handle volume effects, which e.g. dominate the external contribution to peak width in classicial HPLC detectors such as UV- and refractive index detectors. Studies in this field have revealed that in most cases, this contribution to peak width is adequately described by the expression

$$\sigma_{V,\mathrm{det}} = \alpha \cdot V_{\mathrm{cell}} \qquad (3)$$

where $\sigma_{V,\mathrm{det}}$ is the volume standard deviation of the detector and V_{cell} is the volume of the measuring cell. The numerical factor α depends on the flow geometry, and under suitable design conditions it normally is not far from 1.

From the rule of additivity of variances

$$\sigma^2_{V,\mathrm{tot}} = \sigma^2_{V,\mathrm{col}} + \sigma^2_{V,\mathrm{det}} + \sigma^2_{V,\mathrm{inj}} \qquad (4)$$

it is easily derived that a noticeable increase in chromatographic peak width (and corresponding loss in the chromatographic resolution) can be avoided when the cell volume V_{cell} suffices

$$V_{\mathrm{cell}} < 0.3 \cdot \sigma_{V,\mathrm{col}}. \qquad (5)$$

This is beautiful theory. However, it is not easy to know what practical conclusion can be derived there from. Should one decrease the cell volume, or increase the column volume in order to satisfy Eq. (5)? It is noteworthy that in the literature, this choice seems to be dictated most by the field of specialization of the researcher, i.e., a chromatographer using a FTIR is inclined to change the column, while the IR specialist might rather construct another "light pipe". The problem should be handled with extreme care, because both approaches have their effect on the performance of the system in terms of sensitivity, which is crucial.

The first thing to note is that the numbers for "the minimum amounts for a decent spectrum", or minimum identifiable quantity, MIQ [5] as, e.g., quoted in Table I, are nearly always dependent on the volume of the measurement cell. Of course, the more diluted the amount is (with a solvent, gas or vacuum), the smaller a S/N ratio one can expect (the opposite case would never occur; one could then simply use post-column dilution to circumvent this!). For instance, in UV absorption a 1 ng amount would give a worse S/N in a large cell than in a small cell, because the larger volume available in the first case cannot, for optical reasons, be used for just increasing the length and thus obtaining the same absorbance. For several techniques (UV, FTIR, NMR), the MIQ will go up with the cell volume. Therefore, at first sight it would seem appropriate to choose the smallest cell that is technically feasible or is available. Next, dilution in the chromatograph can be minimized by choosing the column diameter such that the peak standard deviation $\sigma_{V,\mathrm{col}}$ satisfies Eq. (5). Fortunately, the choise of column diameter does not have much influence on the separation characteristics of HPLC columns.

The following equations then give the amount, M_{cell}, of material in the cell:

$$M_{\mathrm{cell}} = M_{\mathrm{sample}} \cdot V_{\mathrm{cell}}/(\sqrt{2\pi} \cdot \sigma_{V,c}) \quad \text{(dilution)} \qquad (6)$$

$$\sigma_{V,c} = 3 \cdot V_{\mathrm{cell}} \quad \text{(adaptation of column; Eq. (5))}$$

$$\therefore M_{\mathrm{cell}} = 0.3 \cdot M_{\mathrm{sample}}. \qquad (7)$$

Independent of other conditions, one can always arrange the column diameter such that about one-third of the injected sample is present in the cell at the moment of spectrum acquisition at the elution of the peak crest. As small cell volumes generally give the smallest MIQ values, this is the rationale for using microbore columns, e.g. in HPLC-FTIR.

Unfortunately this often does not lead to a system of any practical analytical performance. The reason is that the MIQ is very close to the maximum loadability of the column M_{max}, and the system only works properly with samples in which every peak has about the same intensity, a rare situation indeed. The philosophy concerning spectrometer coupling should somehow take into account that the crucial point in analytical practice is the characterization of minor and often of trace constituents. The ability to do this is adequately expressed by the ratio of maximum load on the column and the value of the MIQ, in short the dynamic range, D, of the compound system:

$$D = M_{max}/MIQ \tag{8}$$

This approach is of course dependent on the availability of sufficient sample to "fill" the system with an amount M_{max} (this value stands for the amount of the major constituents appearing in the chromtogram, that would be just at the limit of column overload). As argued at length on other occasions, quite often this is not a limitation.

M_{max} can, other things such as plate number, particle size, phase system, etc., being equal, be safely assumed to be proportional to the size of the column; it is therefore also proportional to its volume standard deviation $\sigma_{V,c}$.

It follows that the dynamic range is a function of the size of the system as described by $\sigma_{V,c}$ (or by V_{cell}, or column volume, because all of these vary in the same manner under our assumptions) of the following form:

$$D = \frac{\text{constant} \cdot \sigma_{V,c}}{F\,(V_{cell})} = \frac{\text{constant} \cdot V_{cell}}{F\,(V_{cell})}, \tag{9}$$

where F is some function which describe the dependence of the MIQ on the available cell volume. For UV, F would approximately be equal to $V_{cell}^{1/2}$ and the dynamic range goes up with the size of the system. For FTIR, the form of F may be quite complicated (see discussion by Griffiths, ref. [5]), but the increase of MIQ with V_{cell} will be weaker than proportional and the larger systems should do better. For NMR, the cell volume does not matter too much, as long as it fits into the sample coil, and therefore larger systems should be definitely superior. Indeed Albert et al. [6a] experimented with a semi-preparative column.

Summarizing this discussion: The MIQ values as stated in Table I give some indication of what the system can do. However, for fine tuning, the relationship of MIQ to cell volume (the size of the system), should be taken into account. If MIQ goes up with the cell volume with a power smaller than one, it is advantageous to use the biggest system practically feasible and for which enough sample is available.

The Various Sorts of Spectrometry

UV spectrometry has now become commonplace and the technical aspects are more or less standardized. The solid state diode array multichannel photoreceptor allows acquisition of spectra many times a second. Cell volumes are in the range of 5–10 μl. A common misconception is that a diode array would be at some disadvantage in detection limit compared to single wavelength UV-schemes, because of suspected compromises in the system. However, there is no reason to believe that this is the case; in both systems the physics of the measurement is the same as is the available measuring time. If some non-simultaneous UV's have a small edge in terms of minimum absorbance per cm compared to some diode array instruments, this has in all likelihood to do with another compromise with respect to cell volume that has been drawn in the design.

Although the peak capacity of UV is low – not instrumentally but effectively because of the broad UV absorption profiles – the analytical utility is boosted by the quantitative reliability of the absorption profiles. With this all sorts of linear data-reduction techniques become applicable, about which not much has to be said in this paper because others treat the field in this same volume [8].

A point of discussion is the suitability of identification and library search techniques; the dependence of the spectra on the mobile phase composition is a matter of concern. Hopefully chemometric techniques can bring improvements here.

Mass spectrometry is also separately treated in this issue [9]. This field is highly confused because of the various solutions to the interfacing problem, each of which have strong effects on all the other characteristics of the system. The point of information production is important: Many interfacing solutions preclude the exploitation of fragmentation, and the sole occurrence of the molecular ion detracts very much from the potential information production. The increased use of thermospray interface reinforces this. Efforts to improve this situation, either the smart way by adapting the interfacing, or the brute force approach by using LC-MS-MS, are studied intensively.

The strength of MS of course also resides in the low MIQ values, which allow coupling to high resolution capillary GC, a technique generally applicable only to samples of a microgram or less, while still maintaining a resonable dynamic range. Although such low- and sub-picogram sensitivities cannot normally be obtained with HPLC-coupling, the MS is still the most sensitive spectrometer that can be considered for HPLC-coupling.

The above two techniques are accessible for routine analysis and are commercially supported on a reasonable scale. The remaining techniques are still in the research stage and require more discussion.

Fluorescence detectors hold the second place in popularity in HPLC, and a multiwavelength (excitation or emission, or both: a 4-D plot would be required to represent the data!) would seem to be a very valuable asset. However, relatively few compounds are fluorescent. As in unknown mixtures (and that's where spectrometry coupling is likely to be the most valuable), it is difficult to guess in advance whether the unknowns will or not fluoresce (much more difficult than it is to predict an UV-absorbance); the analytical applicability is probably rather limited. In the estimation of the future of a HPLC-fluorescence spectrometry combination, it should also be realized that the popularity of the single channel fluorimeter is largely connected to the use of derivatization schemes, carried out either pre- or post-column. It is not to be expected that the spectra of such derivatives would be as informative on identity (let alone structure) of the analyte as are spectra of native fluorescence or UV-absorbers.

There are also some instrumental problems. At the emission side one can imagine a photodiode array as is used in UV-absorption. However, although the diodes of the array are as good as single photoreceptors (solid state or vaccum photodiodes, and photomultipliers) for the measurement of high radiation level, they fall significantly short of the performance of multipliers when it comes to the detection of small amounts of light. For instance, multipliers can easily detect a few photons per second, a performance that is out of the question with solid state photodiodes, at least at the present stage of technology. The use of multipliers, however, would inevitably lead to the necessity of moving gratings or similar devices, with fast, but in principle *sequential* measurements, in contrast to the diode array which works *simultaneously*. Optical image intensifying devices such as channel plates are available, but still very expensive.

For the measurement of excitation spectra (that would in principle yield similar information), it is in any case difficult to imagine how one could avoid the moving parts and the sequential measurement. Apart from the disadvantage of the mechanical complexity, this approach has the fundamental drawback of shorter measuring times available for every spectral element and the connected lower S/N ratios.

The conclusion from the above may seem rather dim with respect to the future of the HPLC-fluorescence spectrometry combination. However, it remains difficult to make predictions; technical optical breakthroughs cannot be foreseen, and it has also been shown by the widespread introduction of FTIR spectrometers that very complicated mechanical-optical systems can be made to work on a routine basis.

Fourier transform infrared spectrometry is presently being introduced in commercial instruments for GC-FTIR cpupling. The spectra display a high peak capacity, and the information produced fills the gap that left by MS in the distinction and determination of isomers, especially geometric isomers, and is therefore very much welcomed by many scientists.

Sensitivity is the main problem in the development of the technique; the MIQ values are unattractive. The measurement is predominantly limited in sensitivity (MIQ) by thermal noise in the radiation receptor, now that digitization noise has become less important with the availability of more powerful A–D converters and increased computer capacities (word length, speed). This type of noise condition leads to a significant influence of measuring time on S/N ratio; the larger the number of scans that can be co-added, the better S/N is attainable. Such a situation is not favourable for on-line coupling, as little time is available for the acquisition of a spectrum.

The sensitivity problem dominates the literature on HPLC-FTIR coupling. In addition, one has to handle the absorbance by the solvent. Normal LC-solvents, with the exception of carbon tetrachloride and some other non-polar chlorinated alkanes, leave only relatively small "windows" open for observing the analytes. (Fortunately the solvent signals do not saturate the spectrometer, as may be the case in e.g. NMR; the measurement is in absorption and the most intense signal corresponds to zero light level!)

First experiments on HPLC-FTIR have therefore been carried out in normal phase adsorption systems with such mobile phases, contrary to the prevailing trend in HPLC towards reversed-phase systems with more polar and aqueous mobile phases. With the latter interesting spectral areas are inaccessible. A number of solvent elimination techniques have been investigated, and these have been reviewed very recently by Griffith and Conroy [10].

When normal cell (light pipe) measurements are performed, the most obvious approach is to extract the analytes form the reversed-phase mobile phase in an on-line flow through extractor, e.g. into carbon tetrachloride, as was demonstrated by Hellgeth and Taylor [11]. Other schemes use different measuring conditions. For instance, Diffuse Reflectance (DRIFT) measurements of the analystes deposited on alkalihalogenide powder were carried out by Kuehl and Griffiths [12] after the mobile phase was evaporated. However, this technique precludes the use of aqueous solvents necessary in the reversed phase mode, unless the water that would dissolve the halogenide is eliminated by reaction with 2,2-dimethoxypropane in a post column reactor, as demonstrated by Kalasinsky et al. [13]. A similar approach has been used by Gagel and Biemann [14], where the effluent was sprayed onto an aluminium disk and measured in reflectance-absorbance.

Such complicated schemes, together with the sensitivity problem, aggravated by the short measuring time available, indeed raise the question whether it would not be much better to work off-line in a (semi) preparative way, in relatively fat columns, with collection of the relevant peaks, subsequent concentration and transfer to a suitable matrix or solvent, which would allow one to devote the available time on the expensive spectrometer to the few specific peaks that are of interest. The two deposition techniques mentioned above are already partly aimed in this direction, as it is possible to spend more measuring time on interesting peaks in the measuring process (this is not necessarily carried out in real time).

In this context it is useful to mention the development in GC-coupling of an interface advertized as the Cryolect [15], where the GC-column effluent is frozen as a trace on a cryogenic matrix and scanned by FTIR more or less off-line. The matrix isolation technique brings the additional advantage of much narrower and much more intensive absorption lines. It is interesting to observe possible future developments of this principle for HPLC coupling.

Nuclear magnetic resonance, in combination with HPLC, has been studied less intensively than FTIR, but still a number of interesting papers have appeared on this subject. The problems are similar, sensitivity (MIQ) being the most severe one, even considerably more unfavourable than in FTIR. Proton NMR (e.g. [16–19]) is relatively in the best position in this respect, but the universally present solvent protons generate signals that not only obscure interesting areas of the spectrum, but also tend to saturate the measuring system. As in FTIR, all authors agree that any system of practical significance cannot be limited to solvents like carbon tetrachloride. Pulse presaturation techniques and additional instrumental efforts (dynamic range, A–D range, word length) can circumvent the saturation problem, but not that of the blind parts in the spectrum.

The sensitivity of an NMR in terms of amount is practically independent of the cell volume, as long as the cell fits into the cavity. The latter are fairly large in comparison to HPLC dimensions (Laude and Wilkins [16] even advovate the use of columns "in bore", i.e. in the magnetic field, a rather confusing statement for a chromatographer!). Therefore, there is much reason to use rather fat columns that are able to transport as much material as possible to the spectrometer. Indeed Albert et al. [19], who courageously investigated 13C NMR-HPLC coupling (where the sensitivity problem is even an order of magnitude larger) used semi-preparative HPLC columns.

This is in sharp contrast to the speculations by Laude and Wilkins [16] about the use of microbore-HPLC, which would have the advantage that proton-free (deuterated) solvents could be used at acceptable running costs. It appears to the author that the loss in concentration sensitivity would be insurmountable.

For NMR the balance between off-line and on-line coupling undoubtedly is more in favour of the former than is the case for FTIR: The sensitivity is worse. Moreover, as the spectrometers (at least the high field types that are suitable for this kind of work) are much more expensive, it is in general not likely that connection of an NMR for hours to an HPLC can be justified economically. Also, in many cases the necessity of a high spectral acquisition rate in HPLC deteriorates spectral resolution, as has been discussed in a previous section. Therefore, it appears to the author that in general the off-line mode is preferable. It is quite likely that such off-line techniques, although not formally described in literature, are in fact already very widely applied, as semi-preparative purification by HPLC is an accepted technique in chemical synthesis and in some branches of biochemistry, and NMR spectra are a regular part of following synthetic and purification routes.

The last technique to be discussed is a relative newcomer: the measurement of fluorescence in supersonical jets that are cooled by the occurring expansion in a vacuum. The jets are obtained by pressing the analyte molecules, together with large amounts of an inert gas like argon, through a narrow orifice into a vacuum region. Because of the effective cooling (down to a few degrees Kelvin), organic molecules are frozen into a state of low or zero vibrational and rotational energy. As a result, electronic absorption and emission bands narrow down appreciably, with a corresponding increase in peak intensity [20, 21]. From the analytical point of view this brings two important advantages, that of the S/N ratio (MIQ-value!) and that of the much greater spectral peak capacity (information!). Such potentialities warrant further intensive research efforts, despite the obvious drawbacks of the technique: it is expensive because a tunable dye laser is used for measurement of excitation spectra and a large vacuum system is required, and the application range is limited as is always the case with fluorimetry. Stiller and Johnston [20] demonstrated the GC-coupling and obtained 50 pg detection limits. Quite recently Ishibashi and collaborators [21] showed that similar results can be obtained from a methanolic solution. They showed impressively fine-structured spectra and reported a 50 ng detection limit from a 0.2 ml/minute methanol flow, which was mixed post column with the argon gas. It is presently not known to the author whether a larger number of compounds are likely to respond at these low temperatures than at room temperature in solution.

Conclusion

Presently numerous efforts are being undertaken to interface various sorts of spectrometry to HPLC. In view of the limited resolution of HPLC and of the complicated mixtures that analytical practice presents, such efforts are highly indicated.

With universally applicable methods, such as MS, NMR and IR, a main problem is that of solvent response. Numerous methods, involving phase separations such as extraction and evaporation have been devised. They are inelegant and endanger quantitative reliability, but presently they appear to constitute the only possible choice.

Some of the more informative methods, especially FTIR and NMR, suffer from a sensitivity problem. A reconsideration of high capacity columns, and their interfacing to these spectrometries, appears to be indicated.

With all methods one should constantly keep the balance between on-line and off-line approaches in mind. A narrow focussing on on-line work, in all likelihood due to the success of the GC-MS combination, is possibly not the appropriate attritude in HPLC, where the manipulation of fractions of the eluate is much easier than is the case in (capillary) GC. The advantages off off-line work are by no means negligible.

The new technique of supersonically cooled jet spectrometry is most promising, from the point of view of sensitivity as well as that of information content.

References

[1] *J. C. Kraak, F. Smedes, H. Poppe,* J. Chromatogr. **122,** 147 (1976).

[2] *R. P. W. Scott, E. Kucera,* J. Chromatogr. **169,** 51 (1979).

[3] *J. H. Knox, M. T. Gilbert,* J. Chromatogr. **186,** 421 (1979).

[4] *J. H. Knox, M. Saleem,* J. Chromatogr. Sci. **7,** 614 (1969).

[5] *P. R. Griffiths,* Applied Spectroscopy **31,** 284 (1977).

[6] *A. J. Barnes, W. J. Orville-Thomas,* (ed.), Vibrational Spectroscopy – Modern Trends, Elsevier, Amsterdan, 1977.

[7] *R. R. Ernst, G. Bodenhausen, A. Wokaun,* Principles of Nuclear Magnetic Resonance in One and Two Dimensions, Clarendon Press, Oxford, 1987.

[8] *B. Vandeginste,* This issue of Chromatographia **24,** 127 (1987).

[9] *D. E. Games*, to be published in Chromatographia.
[10] *P. R. Griffith, C. M. Conroy*, in J. C. Giddings et al., eds. Advances in Chromatography, Vol. 34, Marcel Dekker, New York, 1987.
[11] *J. W. Hellgeth, L. R. Taylor,* Anal. Chem. **59,** 295 (1987).
[12] *D. T. Kuehl, P. R. Griffiths,* Anal. Chem. **52,** 1394 (1980).
[13] *K. Kalasinsky, J. A. S. Smith, V. F. Kalasinsky,* Anal. Chem. **57,** 1969 (1985).
[14] *J. J. Gagel, K. Biemann,* Anal. Chem. **58,** 2184 (1986).
[15] Mattson Instruments Inc., Madison WI, USA.
[16] *D. A. Laude, Jr., C. L. Wilkins,* Anal. Chem. **59,** 546 (1987).
[17] *D. A. Laude, Jr., C. L. Wilkins,* Trends Anal. Chem. **5,** 230 (1986).
[18] *D. L. Rabenstein, S. Fan,* Anal. Chem. **58,** 3178 (1986).
[19] *K. Albert, M. Nieder, E. Bayer, M. Spraul,* J. Chromatogr. **346,** 17 (1985).
[20] *S. W. Stiller, M. V. Johnston,* Anal. Chem. **59,** 567 (1987).
[21] *T. Imasaka, N. Yamaga, N. Ishibashi,* Anal. Chem. **59,** 419 (1987).

Received: Aug. 3, 1987
Accepted: Aug. 20, 1987
F

Solvent-Strength Selectivity in Reversed-Phase HPLC

L. R. Snyder*

LC Resources Inc., 26. Silverwood Ct., Orinda, CA 94563, USA

M. A. Quarry / J. L. Glajch

E. I. du Pont de Nemours and Company, Medical Products and Central Research and Development Departments,
Experimental Station, Wilmington, DE 19898, USA

Key Words

Retention optimization
Solvent-strength selectivity

Summary

Solvent-strength selectivity refers to the variation of band spacing by changing the %-organic in the mobile phase (ion-pair or reversed-phase HPLC). A review of the literature has been combined with new experimental data to illustrate the general potential of this approach for HPLC optimization. It appears that most samples exhibit significant changes in band spacing method development based on solvent-strength optimization plus computer simulation (DryLab software) are given for illustration. For relatively simple mixtures (10 or fewer components), it appears that solvent-strength optimization compares favorably with other methods such as mapping the organic-solvent selectivity of methanol, acetonitrile, tetrahydrofuran, and water.

Introduction

Method development is of broad interest for separations by reversed-phase HPLC. Several different approaches have been described for optimizing such separations [1–4], most of which emphasize the control of band spacing or selectivity. Separation selectivity can be systematically varied in several ways, but the most popular procedure is some form of optimization based on the use of different solvents or secondary-equilibria. Solvent-type optimization refers to the mapping of retention as a function of the composition of mobile phases composed of methanol, acetonitrile, tetrahydrofuran and water [5]. The optimization of secondary-equilibria can be carried out in similar fashion, by varying pH and/or the concentration of an ion-pair reagent [6]. Either approach is widely accepted as a powerful technique for improving the resolution of most samples.

A change in solvent strength (% organic in an aqueous-organic mobile phase) while other variables are held constant has not been considered useful for varying band spacing (e.g., discussion of [7]). Nevertheless a few workers have successfully used this approach for developing an isocratic HPLC method [8–10]. For the purpose of varying band spacing, a change in %-organic in isocratic HPLC is equivalent to changing the steepness of the gradient in gradient elution. Several recent papers have reported significant changes in band spacing as a result of changing gradient steepness [11–13]. In addition to these examples where changes in solvent strength (or gradient steepness) have been deliberately used to vary selectivity, the literature shows numerous "accidental" examples where changes in solvent strength lead to changes in band spacing and reversals of elution order ([14, 15] for ion-pair HPLC, [16–20] for reversed-phase separation).

We will refer to the intentional use of changes in %-organic to alter band spacing as solvent-strength optimization (SSO). This paper explores this alternative to traditional solvent-type optimization for HPLC method development, and attempts to show when it is most promising. We also present a substantial data base – gathered from both the literature and our own laboratories – to substantiate our belief that SSO is a broadly applicable and often preferable means for carrying out HPLC method development. A few comparisons of the use of SSO vs solvent-type optimization are presented, as well as the combined use of solvent-strength plus solvent-type optimization. Finally, the most effective application of SSO and related procedures is favored by the use of computer simulation for minimizing experimental runs and presenting results in an easily interpreted format. We will illustrate this here, using commercially-available software (DryLab I from LC Resources).

0009-5893/87 0033-12 $03.00/0

© 1987 Friedr. Vieweg & Sohn Verlagsgesellschaft mbH

Experimental

HPLC Equipment and Conditions

Du Pont 8800 liquid chromatographs were used to collect the data reported here. Experimental details and a description of samples and materials have been given elsewhere [9]. For further information on various procedures and calculations, see Refs. [7, 21, 22].

Samples

The various hydrocarbon and nitro-compound samples were the gift of M. Rigney (Dept. of Chemistry, University of Minnesota). The steroid samples have been described previously [7]. The herbicide samples consisted of both common herbicides and proprietary compounds obtained from the Agricultural Chemicals Department of Du Pont (Wilmington, DE, USA); the exact chemical structures of these latter compounds were not disclosed in all cases.

Computer Simulations

DryLab I and DryLab G software (LC Resources, San Jose, CA, 95125, USA) was used with an IBM-XT personal computer for performing calculations related to solvent-strength optimization. Previously described software [23] was used for the solvent-type optimization studies reported here.

Precision of Measured S-values

Previous reports [12, 22] have shown that values of $S = d(\log k')/d\Phi$ can be measured from gradient elution runs with an accuracy of ± 5–10% (see Glossary of terms at end of paper). In the present paper we are primarily concerned with the determination of differences in S-values for adjacent bands in a typical sample, using DryLab I or DryLab G software (the algorithm for measuring S-values is the same in each program). The accuracy required in such S-value differences is ± 1–2%. The approach used here mimics what a chromatographer would do during method development based on computer simulations with this software; values of S were obtained from two experimental runs (different gradient times) for a total sample. Differences in these S-values will be more accurate than individual S-values, because of the cancellation of certain measurement errors [24, 25]. We attempted to assess the reliability of data reported here as follows.

A sample of 22 o-phthaldehyde derivatives of the common amino acids had been separated [26] using gradient elution with different gradient times (25 cm, 5 μm C18 column, acetonitrile/water gradients). Raw experimental data from these runs were kindly supplied to us by the authors. DryLab I was used to measure S-values for each compound, using two different run-pairs: 14 and 46 min gradient times, and 11 and 27 min gradient times. The agreement between S-value differences for the same adjacent band-pairs was equivalent to ± 0.8% in S (1σ).

In a second comparison, we determined values of S for 16 polyaromatic hydrocarbons as described here – using gradient times of 20 and 60 min. This determination was

Table I. Summary of S-value Measurements from the Literature Plus Data Reported Here. Average values of $(\delta S/\bar{S})$ are reported and are corrected for any correlation of S with solute retention (see text).

Compound type	Ref.	n*	Organic solvent**	Avg. $(\delta S/\bar{S})$	Comment ***
Alkyl benzenes	27	11	MeOH	±0.1%	correlates
Polyaromatic hydrocarbons	34	16	MeOH	±2 %	correlates
Polyaromatic hydrocarbons****	*****	16	ACN	±4 %	correlates
(Table V)		16	MeOH	±4 %	correlates
Chlorobenzenes	27	12	MeOH	±0.5%	correlates
Chlorotoluenes	27	9	MeOH	±0.4%	correlates
Chloronaphthalenes	27	16	MeOH	±1.9%	correlates
Chlorobiphenyls	27	65	MeOH	±1.4%	correlates
o-Phthaldehyde derivatives of amino acids	26	22	ACN	±1.5%	correlates
Miscellaneous substituted organics	30	31	MeOH	±6 %	correlates
			ACN	±14 %	
			THF	±12 %	correlates
Nitrocompounds	*****	10	MeOH	±9 %	correlates
(Table II)			ACN	±9	
			THF	±8	
Steroids	*****	6	MeOH	±5	
(Table III)			ACN	±4	correlates
			THF	±3	
	38	12	MeOH	±3	
			ACN	±5	
			THF	±3	
			PrOH	±4	
			MeEtOH	±5	
			MeEtOAc	±4	
	39	5	MeOH	±8	
			ACN	±2	
Herbicides	*****	15	MeOH	±10	
(Table IV)			ACN	±10	
			THF	±4	correlates
Herbicides	31				
phenylureas		10	MeOH	±2 %	correlates
		10	ACN	±5 %	
s-triazines		6	MeOH	±1 %	correlates
phenoxycarbonic acids		7	MeOH	±2 %	correlates
phenoxycarbonic esters		7	MeOH	±2 %	correlates
Peptides, proteins					
IL2-muteins	12	30	ACN	±7 %	correlates
nuclease muteins	40	13	ACN	±2 %	
lysozyme digest	11	17	ACN	±10	
myoglobin digest	11	–	ACN	±12	
Dansyl amides	41	18	MeOH	±3	correlates
			EtOH	±6	

* number of solutes

** MeOH, methanol; ACN, acetonitrile; THF, tetrahydrofuran; PrOH, propanol; MeEtOH, 2-methoxyethanol; MeEtOAc, 2-methoxy ethylacetate

*** correlates indicates dependence of S on sample retention; values of $(\delta S/\bar{S})$ are corrected for this dependence – that is, values of δS are measured vs the best-fit correlation curve; see text for discussion

**** a polymeric bonded phase was used in these studies; such columns give different selectivity vs monomeric phases

***** present study

Table II. Summary of retention parameters for reversed-phase separation of nitro-compound sample. Column, 25 X 0.46cm, 5μm Zorbax C8; mobile phase, 5–100% organic/water in 15 and 45 min, at 2 ml/min; 35°C.

Compound	values of S*			values of log k_W		
	MeOH	ACN	THF	MeOH	ACN	THF
nitrobenzene	3.02	3.12	4.28	2.05	1.86	2.57
2,6-dinitrotoluene	3.62	3.65	4.70	2.51	2.28	2.34
benzene	2.72	2.87	3.91	2.03	1.85	2.81
2-nitrotoluene	3.51	3.37	4.71**	2.58	2.19	2.33**
4-nitrotoluene	3.50	3.35	4.71**	2.60	2.20	2.33**
3-nitrotoluene	3.51	3.35	4.68	2.64	2.22	2.35
toluene	3.34	3.12	4.99	2.67	2.21	2.20
2-nitro-1,3-xylene	4.03	3.49**	4.82	3.09	2.46**	2.28
4-nitro-1,3-xylene	3.85	3.49**	4.40	3.02	2.46**	2.50
1,3-xylene	3.79	3.21	4.62	3.18	2.47	2.38

* for different organic solvents; MeOH, methanol; ACN, acetonitrile; THF, tetrahydrofuran; averages for duplicate determinations

** approximate values because two bands are overlapped in each gradient run

repeated with a different column, and it was found that S-value differences agreed between the two determinations within ± 1.2% (1σ).

In a final comparison, four repeat gradients each (8 runs) were carried out (15 and 45min, 5–100% methanol/water) for the nitro-compound sample of Table II. The repeatability of values of S and differences in S (adjacent bands) was as follows: S, ± 4% (1σ); δS, ± 1.2% (1σ). We have also previously shown [9] that resolution as a function of mobile-phase %-organic (which depends on these differences in S) can be accurately and reproducibly predicted when appropriate procedures are followed.

Background and Theory

An example of changes in band spacing that result from a change in solvent strength is shown in Fig. 1, for a 10-component mixture of some aromatic compounds and their nitrated derivatives. All 10 bands are resolved in the chromatogram of Fig. 1a, for 30% methanol/water as mobile phase, but the run time is an unacceptable 160min. Upon changing to 50% methanol/water, bands #2 and 3 coalesce (arrow), and bands #8 and 9 reverse positions (arrows). With 70% methanol/water bands #8 and 9 have moved further apart, band #6 has merged with #8 (arrow), and bands #3 and 4 have also combined (arrow). The most practical separation of this sample occurs for 55% methanol/water (Fig. 2), where adequate resolution (R_S = 1.3) is achieved within a reasonable run time (17min).

The effect of solvent strength on band spacing is further illustrated in the hypothetical example of Fig. 3. Here log k′ is plotted vs the volume-fraction Φ of organic in the mobile phase. This example assumes the relationship

$$\log k' = \log k_w - S\Phi\,, \qquad (1)$$

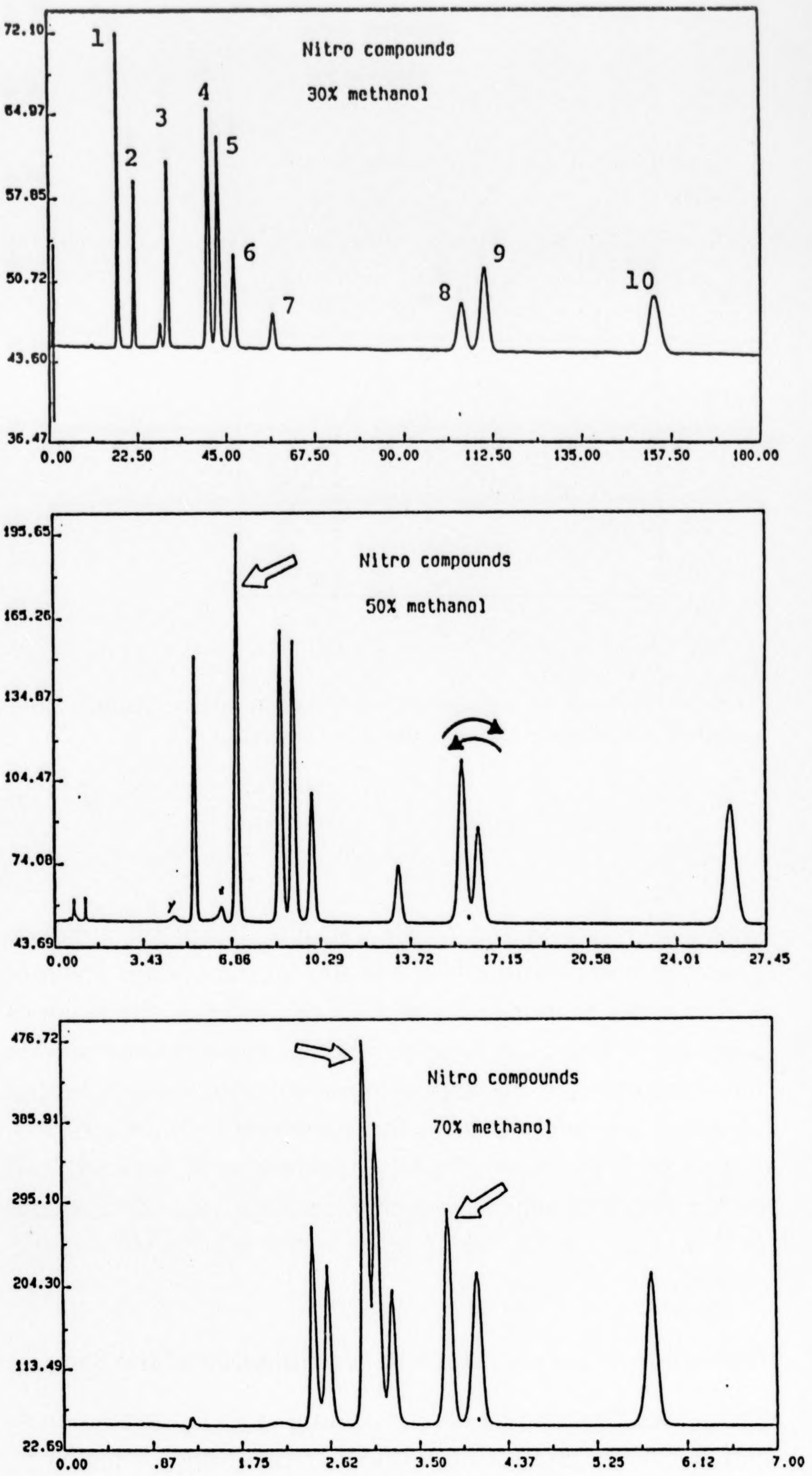

Fig. 1

Isocratic separation of nitro-compound sample. Conditions as in Table II except for mobile-phase composition. (a) 30% methanol/water; (b) 50% methanol/water; (c) 70% methanol/water.

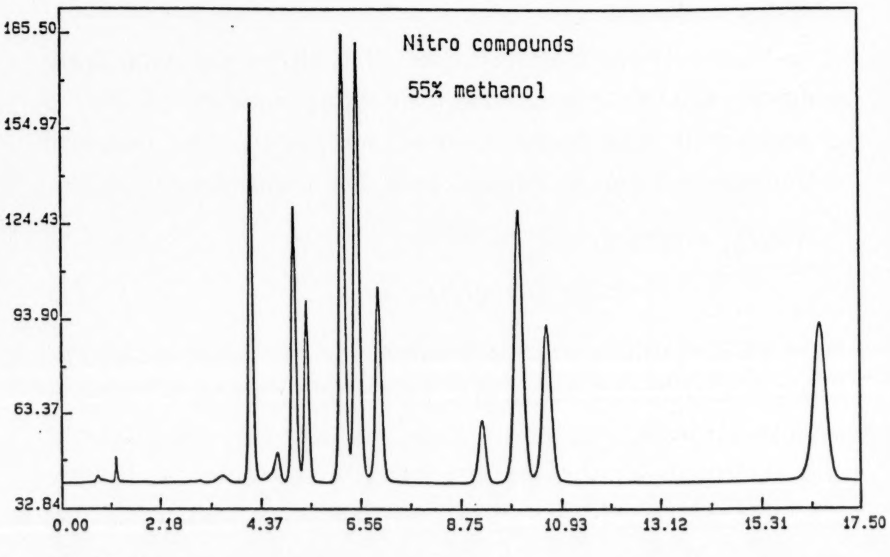

Fig. 2

Best isocratic separation of nitro-compound sample. Conditions as in Table II except mobile phase is 55% methanol/water.

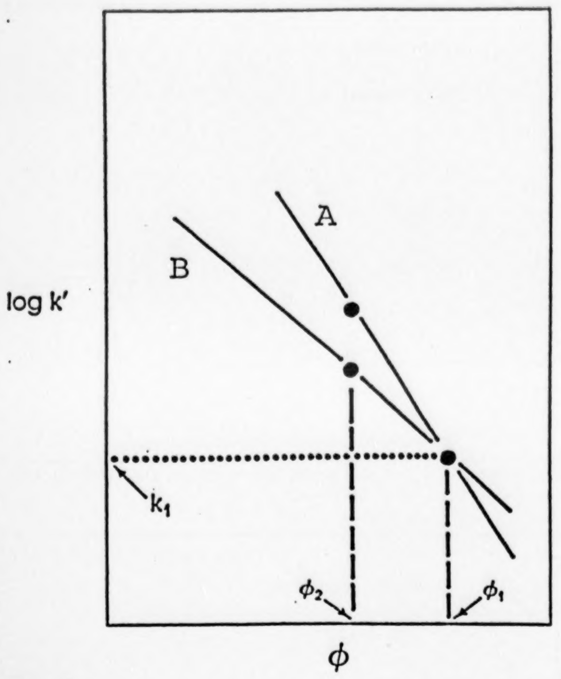

Fig. 3
Theoretical basis of solvent-strength optimization. Sample composed of compounds A and B; see text for details.

where k' refers to the solute capacity factor for a mobile phase of composition Φ, k_w is the (extrapolated) value of k' for water as mobile phase ($\Phi = 0$), and S is the slope of plots as in Fig. 3. A large number of experimental studies have documented the approximate validity of eq. 1, several of which are referred to in the subsequent discussion [27]. Values of S are approximately constant as Φ is varied, but each compound will have a characteristic value of S; values of S may also differ for changes in the organic solvent and column.

Resolution vs Solvent Strength as a Function of the Sample

For a mobile phase of composition $\Phi = \Phi_1$, compounds A and B of Fig. 3 co-elute with no separation. Changing Φ to a value Φ_2, however, results in different values of k' for each compound. That is, a change in solvent strength (Φ) leads to a change in the separation factor α. These changes in band spacing require that the S-values for the two compounds differ. It is therefore of interest to know the relative probability of such differences in S; this is one goal of the present paper.

It is not sufficient that values of S differ for two compounds; this difference must be large enough so that a change in Φ will result in their resolution. The required difference in S can be derived as in the Appendix:

$$(\delta S/\bar{S}) = (8/2.3)\,\Delta R_s\,N^{-0.5}\,[(1+k')/k']/[\log(20\,k_a/k_z)]\,. \tag{2}$$

Here δS is the difference in S-values for two adjacent bands, $\bar{S}$ is their average S-value, ΔR_s refers to a necessary increase in resolution R_s, k_a refers to k' for the first-eluted band and k_z equals k' for the last band. Eq. 2 provides insight into the use of SSO for HPLC method development. First, we see that it is not the absolute difference in solute S-values that is important, but their relative difference ($\delta S/\bar{S}$ rather than δS).

Second, the applicability of SSO is limited by the retention range of the sample (k_a/k_z). Acceptable solvent strengths (values of Φ) will position all sample bands so that $1 < k' < 20$. When the ratio of k'-values for the last band vs the first (k_z/k_a) approaches a value of 20, the choice of Φ becomes fixed by the need to avoid $k' < 1$ or $k' > 20$; the required value of $\delta S/S$ therefore becomes large. Consequently, for this case Φ cannot be varied to improve band spacing (SSO). SSO becomes more useful as the retention range of the sample becomes smaller, because then a larger range of Φ-values can be explored. This limitation does not apply to gradient elution, which suggests the use of gradient elution as an alternative to isocratic separation in solvent-strength optimization, for samples with a wide spread in k'-values. For gradient elution, eq. 2 applies with $k_z/k_a = 1$.

As an example of the application of eq. 2, assume an improvement in resolution such that $\Delta R_s = 1.0$ is required. This might be the case for two bands that are initially totally overlapped ($R_s = 0$). Further assume a value of $N = 10{,}000$, $k' = 5$ (average case), and $k_z/k_a = 10$. Then, from eq. 10 $(\delta S/S) = 0.14$. That is, about a 14% difference in S-values will be required for the resolution of the two bands using SSO.

The latter example is somewhat pessimistic, however. First, k_z/k_a is often less than 10, and for gradient elution (discussed later) it equals about one for every sample. Second, the initial band-pair will rarely have $R_s = 0$; in general, R_s will lie between 0 and .6 for a pair of apparently overlapping bands. In many cases, an increase in R_s of $\Delta R_s = 0.5$ will make the difference between poor and adequate resolution. Inserting the latter values into eq. 10 gives a (best case) value of $(\delta S/\bar{S}) = 0.02$. So if SSO is to prove useful, the required difference in S-values for two bands will vary from about 2 to 15%, depending on the particular situation. This means that $(\delta S/\bar{S})$ values of as little as 2% can be useful in some cases, while for values of $(\delta S/\bar{S}) = 5\%$ the sample can usually be separated by means of solvent-strength optimization.

S as a Function of Solute Structure

The first detailed discussion of S as a function of solute structure was that of Geng and Regnier [28, 29], who showed that values of S can vary widely with the structure of the solute molecule; e.g., $2 < S < 150$. These authors postulated a displacement model for reversed-phase retention, in which a sorbing solute molecule releases some number Z previously retained solute molecules from the stationary phase. Z is proportional to the contact area of the solute molecule, and is therefore often proportional to solute molecular weight. It can be shown [12] that S and Z are related as

$$S = 2.3\Phi Z\,, \tag{3}$$

where Φ refers to an average value (Φ) during the elution of the sample from the column. We have seen (eq. 1) that relative rather than absolute values of S are of interest in SSO: we can therefore (approximately) equate values of S and Z in the following discussion.

S vs solute molecular weight and retention. The preceding discussion suggests that values of S will increase regularly with the size of the solute molecule, and this is generally observed [27–29]. Additionally it has been found in several (but not all) studies that S tends to increase with solute retention [27, 30, 31]. Usually this relationship is reported in the form

$$S = a(\log k_w) + b\,, \qquad (4)$$

where a and b are constants for a given HPLC system. Since there is a general trend of increasing retention in reversed-phase HPLC as solute molecular size increases, an increase in S with retention is not unexpected. However other factors also affect solute retention, which explains the frequent exceptions to this relationship. One study [30] found that S correlated strongly with solute retention for methanol/water as mobile phase but not for acetonitrile/water; other workers [31] have found (for different solutes) comparable correlations of S with retention for both organic solvents. A previous discussion [9] has shown that changes in S (δS) that correlate with retention are not very useful for carrying out SSO. To be of value in assessing the general applicability of SSO, values of ($\delta S/\bar{S}$) must be corrected (reduced) for any dependence on solute retention [4]. Values of ($\delta S/\bar{S}$) reported here are so corrected (see discussion of Fig. 4).

S vs solute functionality. Values of S for solutes of similar size and/or retention are observed to vary somewhat with the nature (and number) of polar substituent groups on the solute molecule. Thus one study [9] showed S increasing for the following compound types (benzene derivatives):

> anilines < alkyl benzenes < chlorobenzenes < ethers < aldehydes, ketones < nitriles < unsubstituted polyaromatics < nitro compounds < phthalates < phenyl alkanols.

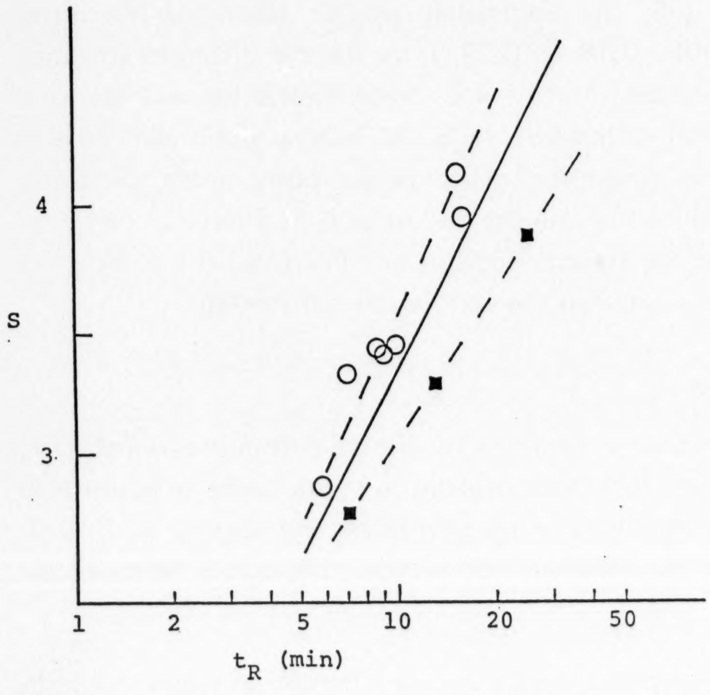

Fig. 4
Correlation of solute S-values with retention for nitro-compound sample of Table II; methanol as organic solvent. ○ = nitro-compounds; ■ = parent hydrocarbons.

When these changes in S are corrected for the contact area of the molecule, it appears that there is a tendency for more polar molecules to exhibit smaller values of S, other factors equal. Likewise another study [31] showed different values of S for herbicides of different functionality, after correcting for the dependence of S on retention.

S vs solute molecular shape and conformation. If the displacement model for reversed-phase retention [28, 29] is correct, S should be determined by the contact area required for adsorption of the solute molecule. Therefore S should vary with molecular shape and conformation. By analogy with related effects that determine the temperature-dependence of retention in reversed-phase HPLC, it might also be expected that "more compact" molecules will exhibit differences in S that arise from corresponding changes in entropy upon retention [32].

Consider first the shape of small, nonpolar solute molecules, specifically aliphatic and aromatic hydrocarbons. The molecular shape of these compounds can be characterized as either "extended" or "compact". Generally it is found (other factors equal) that compact molecules have smaller S-values. One study [33] shows this for the reversed-phase separation of several hydrocarbons with methanol/water mobile-phases: cyclo-octane and hexamethylbenzene (compact) have smaller S-values than extended molecules such as p-terphenyl, n-octane, various primary alkynes, phenylhexane and 1,4-diphenyl-butane. As a result, these compact molecules become more retained vs extended molecules, as the %-organic in the mobile phase increases.

Another study reports S-values for various fused-ring aromatic hydrocarbons with methanol/water as mobile phase [34]. It can be shown for these data that S-values correlate with sample retention (as in other studies):

$$S = 1.109\,(\log k_w) - 0.0265\,(\log k_w)^2\,. \qquad (5)$$

The quantity k_w refers to the value of k' for water as mobile phase. After correcting for the dependence of S on sample retention (eq. 5), it is found that "extended" benzologs such as naphthalene, phenanthrene, chrysene, etc. have larger S-values by an average of 0.8%, while more highly condensed ("compact") structures such as acenanphthylene, pyrene and perylene have smaller S-values by an average of 0.8%. These S-value differences are small, but we will see in a later section that they can play a significant role in solvent-strength optimization.

The conformation of large molecules such as synthetic polymers and proteins would be expected to have an important effect on values of S. Thus native proteins in aqueous mobile phases, or synthetic polymers in "poor" solvents, will have a compact, globular conformation and smaller contact areas. Denatured proteins or synthetic polymers that are well solvated by the mobile phase will have more extended conformations and larger contact areas. Therefore we expect values of S to be smaller (for the same compound) in the former case (compact conformation) vs the latter (extended, random-coil conformation). Likewise the dependence of S on solute molecular weight should vary for these two cases. Compounds having an extended conformation should show S increasing in proportion to solute molecular weight. Compounds with a more compact conformation should show S increasing with some fractional power of molecular weight (e.g., roughly 2/3 power for spherical shapes, such as native, globular proteins).

In agreement with this picture, it was found for several proteins that Z (and S) increase in proportion to solute molecular weight, for a mobile phase (propanol/formic acid/water) that is highly denaturing [28]. For less denaturing mobile phases (acetonitrile/water) and other proteins, values of S were found to increase approximately as the half-power of molecular weight [35], suggesting some retention of 3-dimensional structure in this case. Likewise S-values for polystyrenes of varying molecular weight [36] show a one-half-power dependence on molecular weight in the poor-solvent system THF/water. Finally, another study found 3-fold differences in S for proteins of the same molecular weight (interleukin-2 muteins), and showed that higher S-values appear to correlate with easier (more complete) denaturation of the protein.

Values of S from the Literature

A review of the literature reveals a number of studies that describe the measurement of S-values for various compounds in the usual reversed-phase systems. Several such compilations have been summarized and extended by Johnson et al. [37] and by Opperhuizen et al. [27]. To be useful for the purpose of inferring values of $(\delta S/\overline{S})$ for different sample types, it is necessary that special care be taken in the measurement of these data (see discussion of Experimental section). Many of these studies involve compounds of similar structure — generally less-polar hydrocarbons and/or simple mono-functional derivatives based on common functional groups ($-NO_2$, -OH, -CHO, etc.). Table I summarizes some results from selected studies. Since the systems of Table I cover a wide range in solute structure and solvent type, and include data for about 600 individual S-values, these results can be used to draw general conclusions about the variability of S and the prospects for solvent-strength optimization. In many cases (Table I) it is apparent that the average values of $\delta S/\overline{S}$ is large enough to make SSO quite promising. In other examples (e.g., certain of the herbicides of ref. [31]), the sample appears to exhibit neglible changes in band spacing as Φ is varied.

Results and Discussion

Values of S were measured for several groups of related compounds (nitro-compounds, steroids, herbicides, polyaromatic hydrocarbons), using three different solvent systems (methanol, acetonitrile or THF plus water). These studies were expected to answer some questions concerning solvent-strength optimization, and are summarized in Table I.

Nitro-Compounds

Gradient elution runs were used to derive values of S for the compounds of Table II, using the DryLab I program based on the treatment of Ref. [22] and further described in Ref. [9]. Resulting values of S are tabulated in Table II for each solvent system: methanol, acetonitrile and THF. Significant band-to-band variations in S are noted, as illustrated in Fig. 4 where S for each compound is plotted vs isocratic retention time (50% methanol/water, predicted from DryLab I). Deviations of the data-points in Fig. 4 from the best straight line (solid curve) are an indication of potential changes in band-spacing during SSO. The average deviation of all points equals 0.22 units, which is equivalent to 6% in S[1]. This suggests that SSO should be promising for this sample. We note also in Fig. 4 that individual compound classes (aromatic hydrocarbons, nitrobenzene derivatives) show less deviation of S-values from the best curves (dashed lines) through these data. However variations in S for the nitrobenzene derivatives are still large enough to permit some band-spacing changes using SSO. Fig. 4 also shows a clear correlation between S and solute retention for this system.

Values of S for the nitro-compound sample show a somewhat similar dependence on solute structure for each of the three solvent-systems. This is seen in Fig. 5, where values of S for acetonitrile (a) and tetrahydrofuran (b) as organic solvent are plotted vs corresponding values for methanol. Values of S for the three nitrotoluene isomers of Table I are identical within experimental error for all three solvents. This suggests that SSO will be less advantageous for compounds of closely similar structure. However the differences in S for the two nitroxylene isomers (bands #8 and 9 of Fig. 1a) are large enough to allow an SSO procedure for their resolution. This can be seen in the examples (previously discussed) of Fig. 1.

Steroids

Values of S were obtained for the 6 steroids of Table III, for each of the three organic solvents (same procedure as for Table I). There is no significant correlation of S with retention for these compounds, except with acetonitrile as solvent (the latter data show S decreasing with increasing retention). The band-to-band variations in S for these steroids (δS) are somewhat smaller than for the nitro-compounds: 0.15 to 0.19 units for the different solvents, or an average $(\delta S/\overline{S}) = 4\%$. Nevertheless we will see that these small differences in S can play a significant role in SSO. The structures of these six compounds are fairly similar, differing only in one or two hydroxyl or carbonyl groups in the steroid ring-system. There is little correlation of S-values between the various solvent systems.

Herbicides

Values of S were obtained for the 15 herbicides of Table IV, for each of the three organic solvents (same procedure as in Table I). There is no significant correlation of S with retention for methanol or acetonitrile, but S tends to in-

---

[1] We can also estimate the average difference in values of S from the band-to-band values, equal to ± 0.33 units (uncorrected for the correlation of S with retention). However the latter value overstates the significance of variations in S for this sample, so far as solvent-strength optimization is concerned.

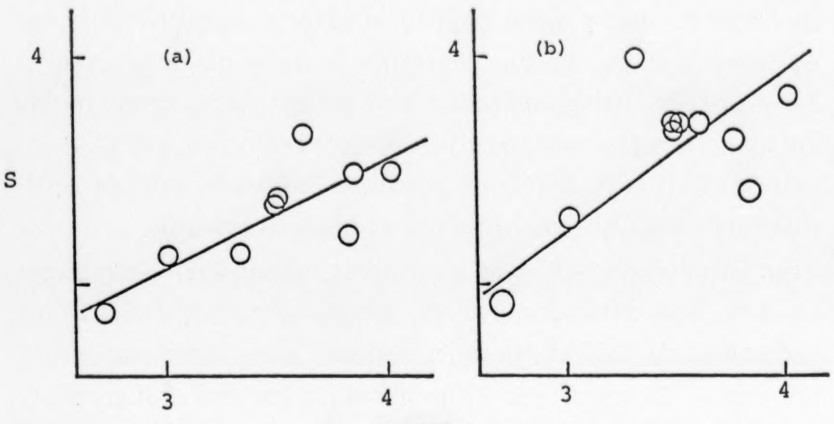

Fig. 5

Correlation of solute S-values for nitro-compound sample; (a) S-values for acetonitrile vs methanol; (b) S-values for THF vs methanol; data of Table II.

Table III. Summary of retention parameters for reversed-phase separation of steroid sample. Column, 25 X 46cm, 5μm Zorbax C8; mobile phase, 5–100% organic/water in 15 and 45min, at 2ml/min; 35°C.

Compound	values of S*			values of log k_W		
	MeOH	ACN	THF	MeOH	ACN	THF
prednisone	5.24	6.30**	6.10	3.17	2.41**	1.98
cortisone	5.22	6.19	5.93	3.20	2.43	2.00
hydrocortisone	4.88	6.30**	6.15	3.13	2.41**	2.14
dexamethasone	5.15	5.95	6.39	3.51	2.59	2.52
corticosterone	4.83	5.24	6.20	3.40	2.51	2.32
cortexolone	5.03	5.27	6.11	3.57	2.57	2.40

* for different organic solvents, as in Table II.

** approximate values because two bands are overlapped in each gradient run

Table IV. Summary of retention parameters for reversed-phase separation of herbicide sample. Column, 15 X 0.46cm, 5μm Zorbax C8; mobile phase, 10–80% organic/water in 15 and 30min, at 1.5ml/min; 40°C.

Compound*	values of S**			values of log k_W		
	MeOH	ACN	THF	MeOH	ACN	THF
N-methyl benzyl amine	4.35	***	***	1.38	***	***
A	3.64	***	***	1.25	***	***
B	3.29	***	***	1.21	***	***
C	3.75	***	***	1.48	***	***
D	4.02	4.03	3.60	2.13	1.93	1.51
E	3.30	3.53	3.43	2.28	1.94	1.79
F	4.65	4.61	4.58	2.89	2.30	1.95
G	4.39	4.35	4.90	2.84	2.29	2.11
benzaniline	3.76	3.74	4.81	2.61	2.30	2.43
H	4.38	4.21	4.81	2.88	2.30	2.00
phenyl sulfone	4.18	3.71	4.84	2.86	2.42	2.29
I	4.37	4.36	4.89	2.95	2.39	2.27
J	3.85	4.11	5.02	2.71	2.22	1.78
K	3.88	3.67	5.43	3.09	2.56	2.81
L	–	3.55	5.51	–	3.11	3.54

* These are in most cases proprietary compounds (see Experimental section)

** For different organic solvents, as in Table II.

*** Compounds elute too early in the gradient for reliable S-value determinations

Table V. Summary of retention parameters for reversed-phase separation of polyaromatic-hydrocarbon sample. Column, 15 X 0.46cm, 5μm Supelcosil LC-PAH; mobile phase 5–100% organic/water in 20 and 60min, at 2ml/min; 35üC.

Compound	values of S*		values of log k_W	
	MeOH	ACN	MeOH	ACN
naphthalene	4.07	5.33	3.03	2.60
acenaphthylene	4.39	5.51	3.36	2.84
acenaphthene	4.33	5.19	3.57	2.94
fluorene	4.46	5.40	3.74	2.80
phenanthrene	4.65	5.37	3.95	3.17
anthracene	4.61	5.19	4.05	3.21
fluoranthene	4.73	5.15	4.25	3.31
pyrene	4.64	4.89	4.25	3.25
benz(a)anthracene	4.85	4.78	4.74	3.50
chrysene	4.70	4.60	4.69	3.44
benzo(b)fluoranthene	4.82	4.42	4.97	3.55
benzo(k)fluoranthene	4.73	4.27	5.01	3.57
benzo(a)pyrene	4.56	4.04	4.91	3.49
dibenz(a,h)anthracene	4.44	4.20	4.96	3.77
benzo(g,h,i)perylene	4.69	3.92	5.24	3.59
indeno(1,2,3-cd)pyrene	4.29	3.64	4.94	3.73

* for different organic solvents, as in Talbe II

crease with retention for THF. The band-to-band values of $(\delta S/\bar{S})$ average about 10% for methanol and acetonitrile, and 4% for THF. Therefore there are excellent prospects for the use of SSO to achieve resolution of various mixtures of these compounds, especially for methanol and acetonitrile. Values of S show a rough correlation between methanol and THF.

Polyaromatic Hydrocarbons

The 16 compounds of Table V were separated on a polymeric alkyl-phase column (Supelcosil LC-PAH) using 5–100% gradients of both acetonitrile/water and methanol/water. Values of S and log k_w for each compound and organic solvent are listed in Table V. There is a moderate correlation of values of S with retention (ACN data); interestingly, S decreases with increasing retention and molecular weight (the opposite of the behavior of these compounds on monomeric alkyl-phase columns; [34]). Separations of this sample using THF/water gradients gave badly bunched chromatograms with much poorer resolution than for the other two organic solvents. No attempt was made to derive values of S from these latter runs (which would have been difficult).

Solvent-Strength Optimization for Achieving the Separation of the Samples of Tables II–V

The compounds of Tables II–V allow us to examine the practical application of SSO to typical samples composed of mixtures of related compounds. We have used the entire compound-set of Tables II or III, since each of these samples can be separated isocratically. We have divided the compounds of Table IV into two 6-component samples, since the retention range of this compound-set is somewhat wide for the isocratic separation of the entire mixture: group #1, compounds D, E, F, G, benzaniline and H;

group 2, compounds G, H, phenyl sulfone, I, J and K. We have also examined SSO for the entire sample of Tables IV and V, using gradient elution for the final procedure. This is described in an accompanying paper [21].

Acetonitrile/water mobile phases. It is generally recommended when using SSO for the development of an HPLC method to begin with acetonitrile as organic solvent. The UV-transparency of this solvent extends to lower wavelengths, and acetonitrile/water mobile phases are less viscous (lower column pressures). Two experimental gradient runs were carried out initially (with two different values of t_G, as in Tables II–V). The resulting retention data were entered into the DryLab I program, allowing trial-and-error computer simulations to be carried out in place of further experimental runs. A more efficient use of the DryLab I software, however, is to (a) request the k′-range as a function of %-organic, then (b) ask for a relative resolution map (RRM) over the %-organic range that corresponds to $1 < k' < 20$ for the sample in question (a relative-resolution map is a plot of minimum or worst resolution as a function of %-organic in the mobile phase, for a column of specified plate-number). This procedure was followed in the present case for those samples that could be separated isocratically (see Ref. [21] for a similar discussion of the gradient separation of the herbicide and polyaromatic hydrocarbon samples).

In the case of the nitro-compound sample (Table II, ACN column), it was found that the same two compounds (#8, 9) overlapped in each experimental gradient run. This was also observed for bands #1 and 3 of the steroid sample (Table III, ACN column). This means that SSO cannot provide the resolution of these two samples, using acetonitrile/water mixtures as mobile phase. This was not the case for the two herbicide samples (Table IV) or the polyaromatic hydrocarbon sample (PAH, Table V). The RRM's for the two herbicide samples are shown in Fig. 6. Here it is seen (for a 10,000-plate column) that a resolution of $R_s > 2$ can be achieved for each sample, using an appropriate value of %-acetonitrile in the mobile phase. "Best" values of %-organic for each sample are summarized in Table VI, along with other pertinent information.

Combination of SSO with solvent-type optimization. When SSO is found not to work with one organic solvent (acetonitrile in the above examples), two additional gradient runs can be obtained with a second organic solvent (methanol or THF), and SSO can be repeated using the DryLab I software. Likewise, if it is found that separation is possible with the first organic solvent, but greater resolution is desired, SSO can also be repeated with a second organic solvent. This approach was carried out for the four "isocratic" samples of Tables II–IV (methanol as organic solvent), with the resulting resolution maps shown in Fig. 7. It is seen that separation can be achieved for each of these four samples. It was also found that methanol provides better resolution for the PAH sample, compared with acetonitrile.

Best values of %-methanol for each sample are summarized in Table VI as before. For the two herbicide samples, we see that the maximum resolution attained with acetontrile as organic solvent (Figs. 6a, b) is greater than with methanol as solvent (Figs. 7c, d). Therefore there is no advantage to be gained by using methanol instead of acetonitrile. In the case of the nitro-compound and steroid samples, a maximum resolution of $R_s > 1.5$ is possible for each sample with methanol (but not acetonitrile) as organic solvent.

The latter approach was continued, using THF as organic solvent. The nitro-compound sample was found to be inseparable by SSO with this solvent (the same two compounds – #4 and 5 – overlap in each experimental gradient run), but RRM's for the remaining three samples are shown

Table VI. Summary of conditions for optimum separation of the samples of Tables II–IV using different organic solvents.

Solvent	Sample	Optimum %-organic	Minimum R_s	k′-range
ACN	nitro	–	0.0	–
	steroid	–	0.0	–
	herb #1	27	3.1	7–20
	herb #2	35	1.8	6–19
MeOH	nitro	55	1.3	2–13
	steroid	50	2.2	3–11
	herb #1	48*	1.5	2–6
	herb #2	66%	0.8	1–3
THF	nitro	–	0.0	–
	steroids	24	2.9	3–10
	herb #1	34	1.1	2–6
	herb #2	32	1.6	1–12

* other %-organic values give higher R_s, but k′-values are not in the range of 1–20

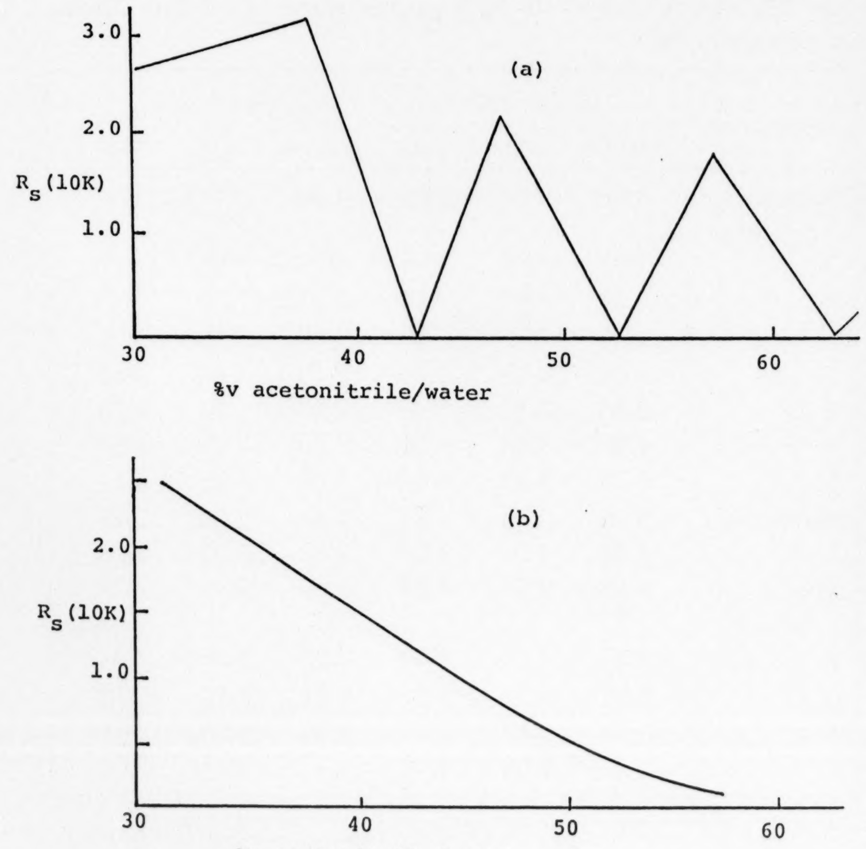

Fig. 6

Relative resolution maps (minimum resolution for 10,000-plate column) for acetonitrile/water mobile phases and isocratic separation. (a) herbicide sample #1; (b) herbicide sample #2.

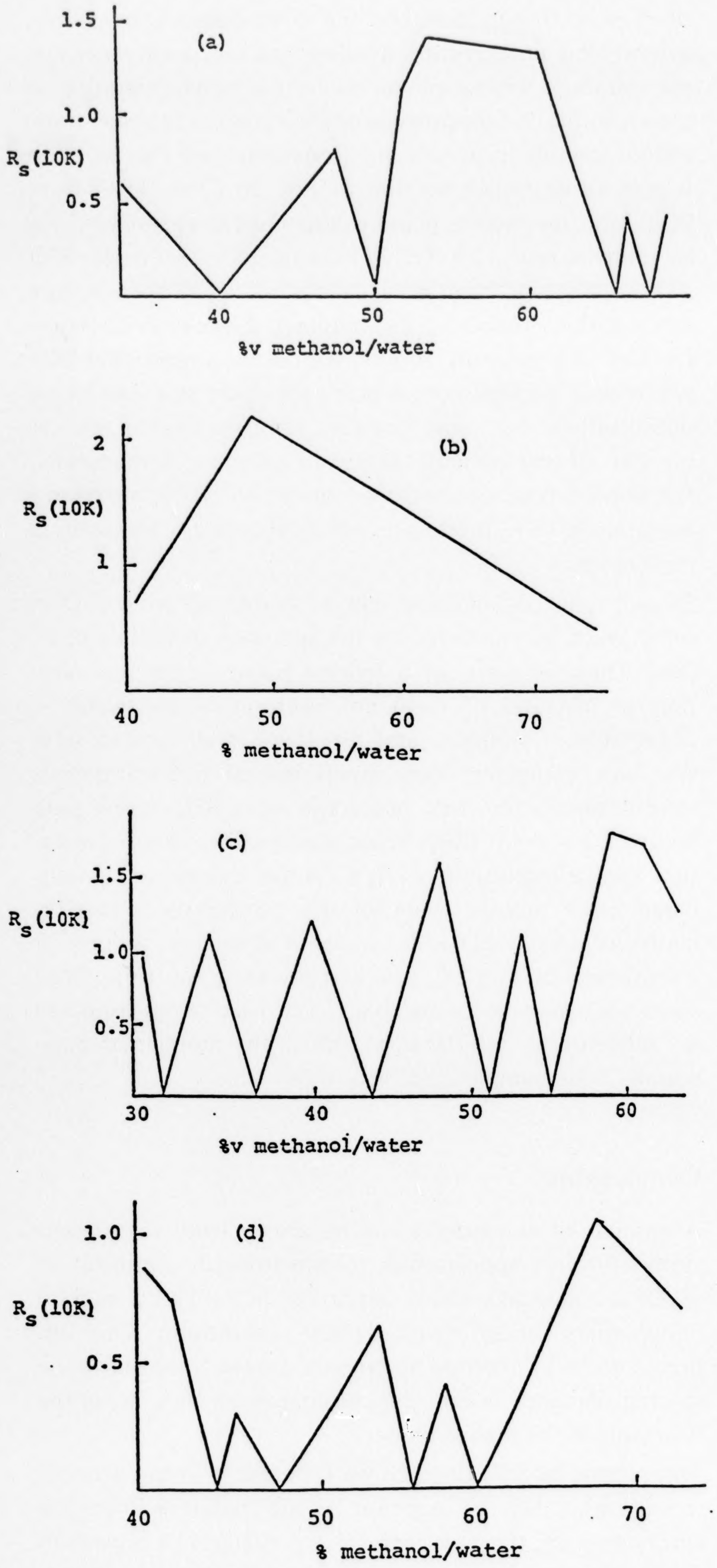

Fig. 7

Relative resolution maps for methanol/water mobile phases and isocratic separation. (a) nitro-compound sample; (b), steroid sample; (c) herbicide sample #1; (d) herbicide sample #2.

in Fig. 8. The maximum resolution for the steroid sample (Fig. 8a) exceeds that obtainable using methanol as organic solvent (Fig. 7b), but the maximum resolution for each herbicide sample (Figs. 8b, c) is less than can be obtained with acetonitrile as organic solvent (Figs. 6a, b). The conditions for maximum sample resolution with THF as organic solvent are summarized in Table VI.

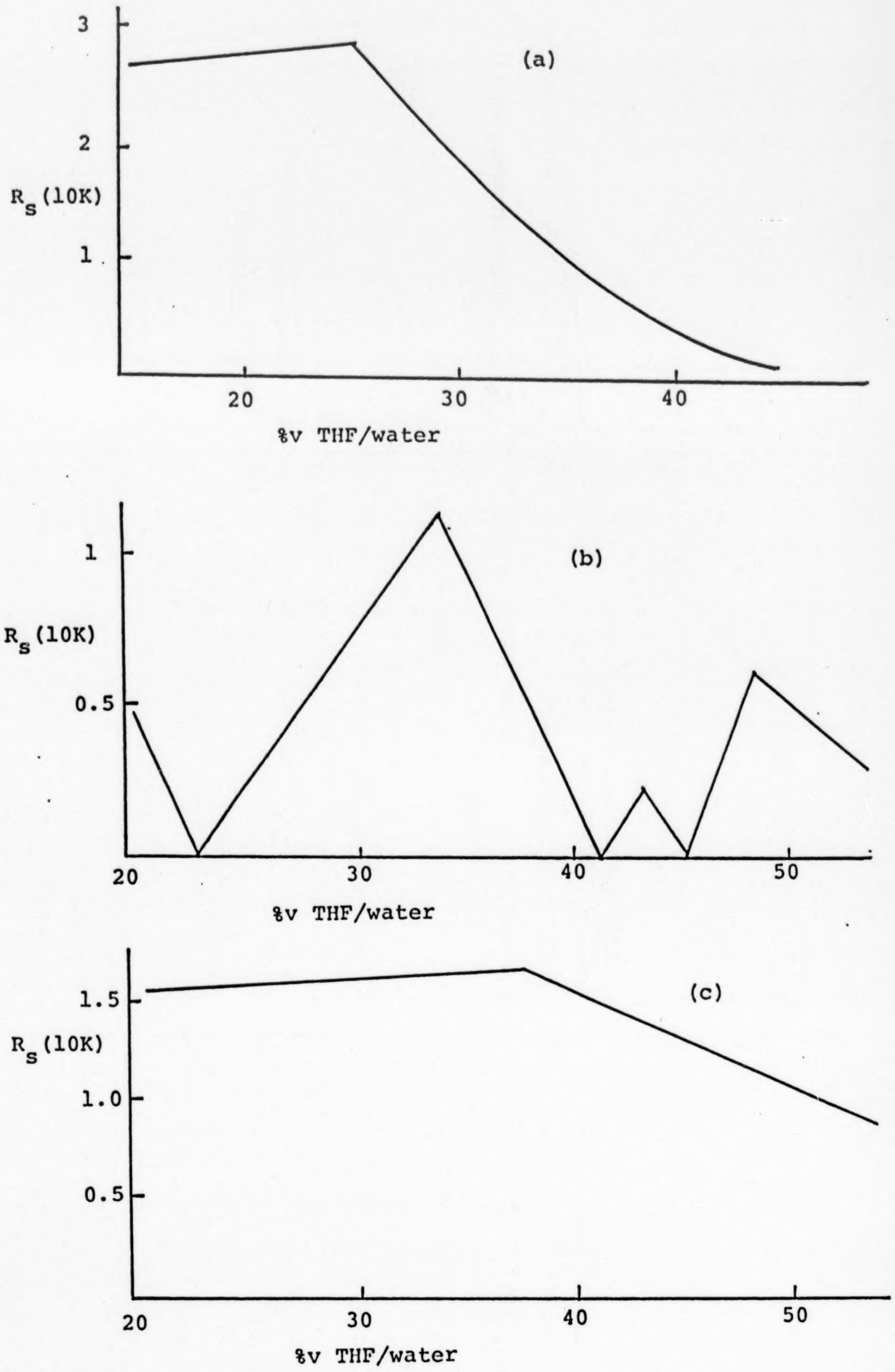

Fig. 8

Relative resolution maps for THF/water mobile phases and isocratic separation. (a) steroid sample; (b) herbicide sample #1; (c) herbicide sample #2.

Experimental isocratic separations. The information of Table VI for each sample was next used to predict optimum isocratic separation, and some of these runs were confirmed experimentally, as shown in Fig. 2 and 9. Fig. 2 shows the best separation of the nitro-compound sample, with 55% methanol/water. Figs. 9a, b show the optimized isocratic separations of the steroid sample, using either methanol or THF respectively. The THF-separation (Fig. 9b) is clearly better, as predicted by the resolution maps of Fig. 7b and 8a. These results could have been further improved by optimizing column length, particle size and flowrate, however we chose not to do this.

Comparisons of Solvent-Strength Optimization (SSO) vs Solvent-Type Optimization

The present examples have demonstrated the potential power of SSO. It is possible to combine the advantages of SSO and solvent-type optimization in various ways, and to compare the results with either individual approach. The

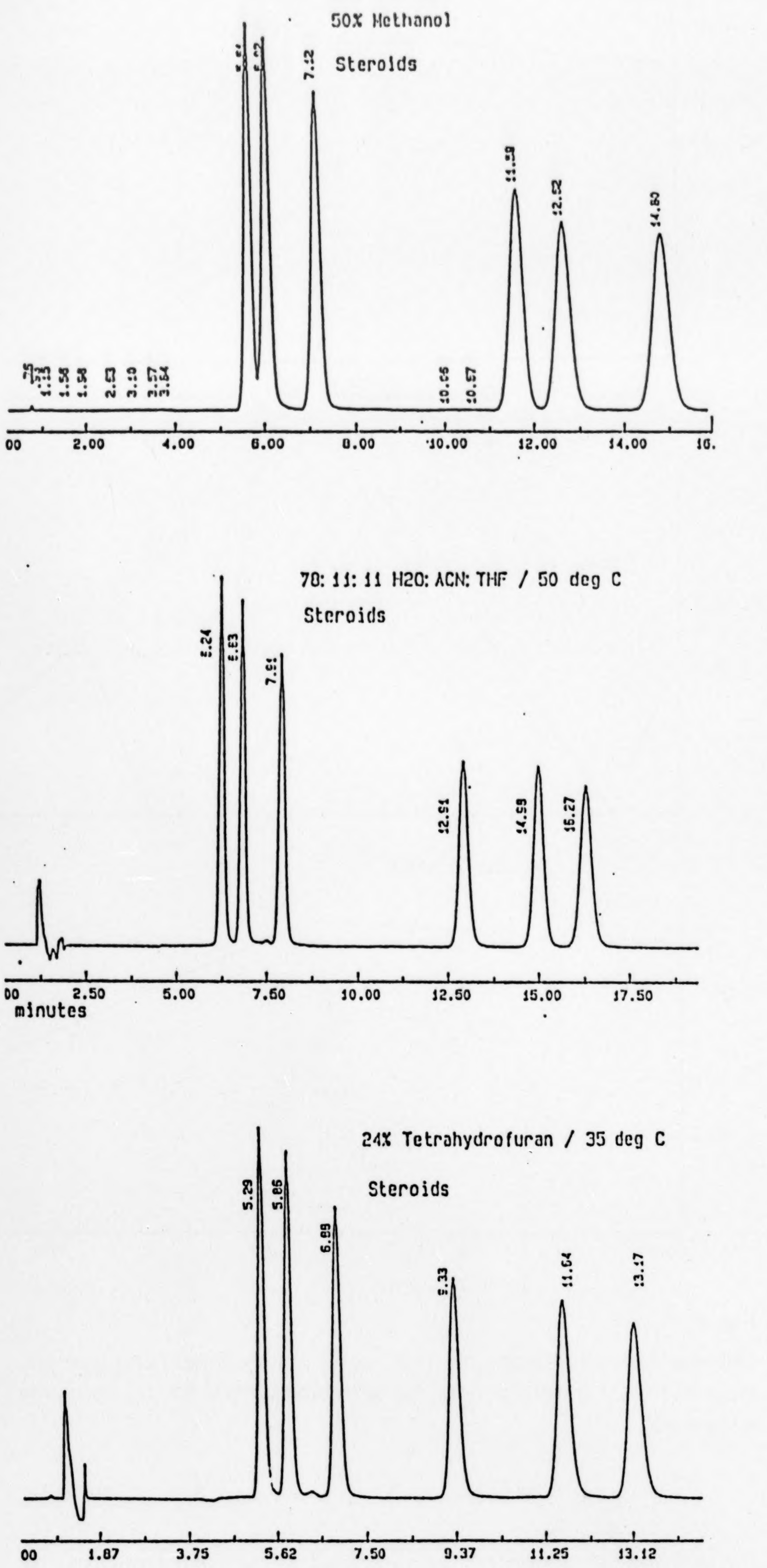

Fig. 9

Optimized isocratic separations of steroid sample. Conditions of Table III except as noted. (a) 50% methanol/water; (b) 24%/THF water; (c) 11% acetonitrile plus 12% THF/water (solvent optimization result).

simplest procedure, in our opinion, is to use SSO as illustrated in the examples of Fig. 6–8. This means starting with acetonitrile as organic solvent, carrying out SSO with that solvent, and then continuing with other solvents (repeating SSO each time) if previous separations are inadequate. This procedure works for each of the samples of Tables II–V (shown here or in Ref. [21]).

An alternative is to use solvent-type optimization from the start, as described by Glajch et al. [5]. We carried out this approach for the nitro-compound and steroid samples of Tables II and III. For the nitro-compound sample, solvent-type optimization showed that methanol/water was the optimum mobile phase, giving the same separation as shown in Fig. 2. Solvent-type optimization in the case of the steroid sample provided the separation of Fig. 9c. This is seen to be similar to that of Fig. 9b (24% THF, from SSO), and the mobile phase is also somewhat similar (11% acetonitrile plus 12% THF). Thus in these two cases, SSO gives essentially the same results as from solvent-type optimization. However, the number of experimental runs for SSO will generally be less. We do not expect that SSO will always provide comparable resolution vs solvent-type optimization. For more complex samples, having a larger number of components (e.g., 10 or more compounds), full solvent-type optimization (mapping of all methanol/acetonitrile/THF mixtures) will probably be required in most cases.

Solvent-type optimization can be combined with SSO in other ways, as illustrated by the approach of Smilde et al. [39]. These workers use a scheme based on the optimization of mixtures of methanol, acetonitrile and water — where solvent strength (and run time) is allowed to vary. We have compared their separation of a 5-component steroid sample by this procedure with SSO, using data reported by them [39]. Their predicted optimum separation has a resolution of $R_s = 2.4$ (vs 2.3 experimental), based on a mobile phase of 4% acetonitrile plus 67% methanol. Using SSO with methanol as solvent, we predict a resolution of $R_s = 2.2$, in about the same run time. Thus again SSO appears comparable to various alternatives based on solvent-type optimization, when the number of compounds in the sample is not too large.

Conclusions

A number of conclusions can be drawn from the present study. First, it appears that solvent-strength optimization (SSO) is a generally viable option for initial HPLC method development under reversed-phase conditions. This approach to HPLC method development seeks to optimize the spacing of bands within the chromatogram by varying the %-organic in the mobile phase.

The success of SSO depends on differences in the S-values ($S = d[\log k']/d\Phi$) of adjacent solute bands within the chromatogram. If a change in solvent strength (% organic in the mobile phase) is to lead to the resolution of an initially-overlapped bandpair, the S-values of the two bands must differ by at least 2% (most favorable case), but preferably by 5% or more. The present study (47 solutes of widely varying structure, 3 mobile-phase systems) shows an average difference in S between adjacent bands of 6% for samples of "related" compounds; i.e., typical samples for HPLC separation. Other studies involving a wide range of sample types (Table I) show comparable variability in S. We therefore conclude that there is a general tendency toward variation in S for adjacent chromatographic bands, sufficient to make SSO a broadly useful technique. However some samples show negligible variations in S and therefore require another method-development approach.

Second, the applicability of SSO depends on the retention range of the sample. SSO for isocratic HPLC methods will be most promising for samples whose components have generally similar k′-values; e.g., a k′-range of 2 to 4-fold. Samples with a k′-range of 10–20-fold will be less likely to undergo substantial changes in band spacing for allowable changes in solvent strength, because the possible change in %-organic will be less, if all sample bands are to elute with $1 < k' < 20$. However, SSO can be applied to samples of wider retention range if gradient elution is used for the final method. This also applies to samples where $1 < k' < 20$ for all sample bands; that is, such samples are normally separated isocratically, but their separation by gradient elution allows the more effective use of SSO.

Third, the present study provides further insight into the effect of solute molecular structure on S. It appears that S varies in a major way with differences in solute molecular weight, functionality (or polarity), and conformation (in the case of peptides and proteins). Smaller differences in S can arise from subtle variations in the shape of the solute molecule, as illustrated here by various polycyclic aromatic hydrocarbons. Small but sometimes significant differences in S are found also for isomeric compounds (e.g., nitroxylenes of Table II). Finally, S-values for a particular solute vary significantly from one solvent system to another; e.g., methanol, acetonitrile or THF as organic solvent in reversed-phase mobile phases. Little useful variation in values of S was observed for non-polar compounds of closely related structure (e.g., alkyl or chlorobenzenes, Table I).

Fourth, it is recommended that the SSO approach to HPLC method development be started with acetonitrile/water as mobile phase. However if SSO is unsuccessful with acetonitrile as organic solvent, the same procedure can be repeated with either methanol or THF. In the present study several different samples were used to evaluate this approach. Initial method development using SSO with acetonitrile resulted in the successful separation of two herbicide samples, but was unsuccessful for the case of a nitrocompound sample and a steroid mixture. Repeating SSO with methanol as solvent gave good separations of the steroid and nitro-compound mixtures, but did not improve the herbicide separations obtained with acetonitrile. Finally, the use of SSO with THF improved the steroid separation, but did not enhance the separation of the other three samples.

In the latter example it was found that acetonitrile was best for two samples, methanol was best for one sample, and THF was best for the remaining sample. This general approach to HPLC method development (repeated use of SSO with different organic solvents) represents a combination of SSO and a simplified form of solvent-type optimization as introduced by Glajch, Kirkland et al. [4]. A comparison of SSO with solvent-type optimization for two samples did not show a significantly better separation using either approach. However solvent-type optimization is expected to be preferable for more complex samples (containing more than 10 components), but the number of experimental runs will be larger.

Finally, the use of SSO for HPLC method development is considerably enhanced by the use of commercially available computer programs for both isocratic (DryLab I) and gradient (DryLab G) procedures. Some illustrations of this are described here.

Glossary of Terms

a, b	constants (eq. 12)
F	mobile-phase flowrate (ml/min)
k'	capacity factor (Ref. [7])
k_a, k_z	k′-values for first and last bands in chromatogram
k_w	value of k′ for water as mobile phase
k_{wa}, k_{wb}	values of k_w for solutes A and B
k_1, k_2	k′-values for solute in mobile phases with $\Phi = \Phi_1$ and Φ_2 (Fig. 3)
N	column plate number (Ref. [7])
P	see eq. i-4
R_s	resolution (Ref. [7])
S	$d(\log k')/d\Phi$ (eq. 1)
$\bar{S}$	average value of S for two adjacent bands
S_a, S_b	value of S for compounds A and B
SSO	solvent-strength optimization
t_G	gradient time (min)
Z	number of organic-solvent molecules displaced by solute molecule upon retention (eq. 11)
α	separation factor (Ref. [7])
α_1, α_2	α-values in mobile phases 1 and 2 for bands A and B; ($\alpha = k_b/k_a$)
δS	difference in S-values for two adjacent bands A and B
ΔR_s	some required increase in R_s, to achieve adequate final resolution of adjacent bands A and B
Φ	volume-fraction of organic solvent in mobile phase
Φ_1, Φ_2	values of Φ for mobile phases 1 and 2 (Fig. 3)

Appendix. Derivation of eq. 2.

We will assume solutes A and B plus mobile phases 1 and 2 as in Fig. 3. Let S_a and S_b refer to S-values for solutes A and B, with subscripts a, b, 1, 2 referring to solutes A and B and mobile phases 1 and 2, respectively. Values of α can be defined for each mobile phase, equal to (k_b/k_a), where k_a and k_b refer to k′ for A and B, respectively. Then from eq. 1

$$\log\alpha_1 = \log(k_{wb}/k_{wa}) - (S_b - S_a)\,\Phi_1 \qquad \text{(i-1)}$$

and

$$\log\alpha_2 = \log(k_{wb}/k_{wa}) - (S_b - S_a)\,\Phi_2\,. \qquad \text{(i-2)}$$

We are interested in the change in α $(\alpha_2-\alpha_1)$ that will result from some change in Φ equal to $(\Phi_2-\Phi_1)$. From eqs. i-1, 2 this is

$$\log\alpha_2-\log\alpha_1=-(S_a-S_b)(\Phi_2-\Phi_1). \qquad \text{(i-3)}$$

The allowable change in Φ is determined by the k'-range of the sample and the average value of S for the two compounds. Thus if the k'-values of the first and last bands in the sample are k_a and k_z, and if $1<k'<20$ for all bands, then the maximum allowable change in k' for the sample is a factor P equal to

$$P=20/(k_z/k_a)=20\,k_a/k_z\,. \qquad \text{(i-4)}$$

For example, if k'-values range from 2 to 10 for mobile phase #1, the average value of P is 20 (2/10) = 4. Thus a k' range of either 1 to 5 or 4 to 20 is allowable (for P = 4). This assumes that a given change in Φ will affect all k'-values by the same factor, which is the case if values of S for the initial and final bands are roughly the same. We will see that this is generally a good approximation. For a given sample, values of P can vary from about 1 to 20, assuming that the sample can be separated isocratically. The average (as opposed to the maximum) change in k' is then $\sqrt{P}$.

The average allowable change in Φ, given a value of P, is

$$\Phi_2-\Phi_1=(\log P)/2\bar{S}\,, \qquad \text{(i-5)}$$

where $\bar{S}$ is the average value for the sample. This value of $(\Phi_2-\Phi_1)$ assumes either $k_a=1$ or $k_z=20$. Now the change in α from eqs. 4 and 6 is given by

$$\begin{aligned}\log\alpha_2-\log\alpha_1 &= [(S_a-S_b)(\log P)]/2\bar{S}\\ \log(\alpha_2/\alpha_1) &= (1/2)\,\delta S/\bar{S}\,(\log P)\,. \qquad \text{(1-6)}\end{aligned}$$

Here $(\delta S/\bar{S})$ is the difference in solute S-values for A and B expressed as a fraction of the average S-value $\bar{S}$ for the two bands.

Eq. 7 can be used to estimate the required difference in S-values for two adjacent bands that will allow SSO to achieve their resolution, assuming that the two bands are initially totally overlapped ($\alpha=1$). From the resolution eq. (7)

$$R_s=(1/4)\,(\alpha-1)\,N^{0.5}\,[k'/(1+k')]\,, \qquad \text{(i-7)}$$

we can write that a change in resolution ΔR_s resulting from a change in α (equal to $\alpha_2-\alpha_1$) is equal to

$$\Delta R_s=(1/4)\,(\alpha_2-\alpha_1)\,N^{0.5}\,[k'/(1+k,)\,.^{*} \qquad \text{(i-8)}$$

The required change in α for a separation with some necessary change in resolution ΔR_s can be written for the case of α_2 and α_1 small (the case of usual interest) as

$$\begin{aligned}(\alpha_2-\alpha_1) &= 2.3\,\log(\alpha_2/\alpha_1)\\ &= 4\,R_s\,N^{-0.5}\,[(k'+1)/k']\,. \qquad \text{(i-9)}\end{aligned}$$

Eqs. i-5, i-7, i-9 give eq. 2.

---

* R_s will change also as a result of a change in k' that is associated with this change in α; however, the change in k' can be either favorable (larger) or unfavorable (smaller). In the general case we will not know whether k' must be increased or decreased in order to increase α and resolution.

References

[1] *J. L. Glajch, J. J. Kirkland*, Anal. Chem. **55**, 319 A (1983).

[2] *J. C. Berridge*, "Techniques for the Automated Optimization of HPLC Separations", Wiley-Interscience, New York, 1985.

[3] *P. J. Schoenmakers*, "Optimization of Chromatographic Selectivity", Elsevier, Amsterdam, 1986.

[4] *L. R. Snyder, J. L. Glajch, J. J. Kirkland*, "Practical HPLC Method Development", Wiley-Interscience, New York, 1988.

[5] *J. L. Glajch, J. J. Kirkland, K. M. Squire, J. M. Minor*, J. Chromatogr. **199**, 57 (1980).

[6] *A. P. Goldberg, E. Nowakowska, P. E. Antle, L. R. Snyder*, J. Chromatogr. **316**, 241 (1984).

[7] *L. R. Snyder, J. J. Kirkland*, "Introduction to Modern Liquid Chromatography, 2nd edn.", Wiley-Interscience, New York, 1979, pp. 49–56.

[8] *A.-J. Hsu, R. J. Laub, S. J. Madden*, J. Liquid Chromatogr. **7**, 615 (1984).

[9] *M. A. Quarry, R. L. Grob, L. R. Snyder, J. W. Dolan, M. P. Rigney*, J. Chromatogr. **384**, 163 (1987).

[10] *L.-Y. Lin, W. T. Cooper*, J. Chromatogr. **390**, 285 (1987).

[11] *J. L. Glajch, M. A. Quarry, J. F. Vasta, L. R. Snyder*, Anal. Chem. **58**, 280 (1986).

[12] *M. Kunitani, D. Johnson, L. Snyder*, J. Chromatogr. **371**, 313 (1986).

[13] *J. W. Dolan, L. R. Snyder*, Chromatography Mag. **2**, 49 (1987).

[14] *S. O. Jansson, S. Johansson*, J. Chromatogr. **242**, 41 (1982).

[15] *D. S. Lu, J. Vialle, H. Tralongo, R. Longeray*, J. Chromatogr. **268**, 1 (1983).

[16] *F. de Croo, W. van den Bossche, P. de Moerloose*, J. Chromatogr. **325**, 395 (1985).

[17] *P. Lehtonen*, J. Chromatogr. **314**, 141 (1984).

[18] *J. Wynants, B. Petrov, J. Nijhof, H. van Belle*, J. Chromatogr. **386**, 297 (1987).

[19] *G. J.-L. Lee, R. M. K. Carlson, S. Kushinsky*, J. Chromatogr. **212**, 108 (1981).

[20] *P. Jandera, J. Churacek*, "Gradient Elution in Column Liquid Chromatography," Elsevier, Amsterdam, 1985, p. 36.

[21] *J. W. Dolan, L. R. Snyder, M. A. Quarry*, Chromatographia, this symposium issue.

[22] *M. A. Quarry, R. L. Grob, L. R. Snyder*, Anal. Chem. **58**, 907 (1986).

[23] *J. L. Glajch, J. J. Kirkland, J. M. Minor*, J. Liq. Chromatogr., **10**, 1727 (1987).

[24] *M. A. Quarry, R. L. Grob, L. R. Synder*, J. Chromatogr. **285**, 1 (1984).

[25] *M. A. Quarry, R. L. Grob, L. R. Snyder*, J. Chromatogr. **285**, 19 (1984).

[26] *M. Eslami, J. D. Stuart, K. A. Cohen*, J. Chromatogr., submitted for publication.

[27] *A. Opperhuizen, T. L. Sinnige, J. M. D. van der Steen, O. Hutzinger*, J. Chromatogr. **388**, 51 (1987).

[28] *X. Geng, F. E. Regnier*, J. Chromatogr. **296**, 15 (1984).

[29] *X. Geng, F. E. Regnier*, J. Chromatogr. **332**, 147 (1985).

[30] *P. J. Schoenmakers, H. A. H. Billiet, L. de Galan*, J. Chromatogr. **185**, 179 (1979).

[31] *T. Braumann, G. Weber, H. Grimme*, J. Chromatogr. **261**, 329 (1983).

[32] *L. R. Snyder*, J. Chromatogr. **179**, 167 (1979).

[33] *H. J. Mockel, F. Hofler, H. Melzer*, J. Chromatogr. **388**, 285 (1987).

[34] *K. Jinno, M. Kuwajima*, Chromatographia **22**, 13 (1986).

[35] *M. A. Stadalius, H. S. Gold, L. R. Snyder*, J. Chromatogr. **296**, 31 (1984).

[36] *M. A. Stadalius, M. A. Quarry, T. H. Mourey, L. R. Snyder*, J. Chromatogr. **358**, 17 (1986).

[37] *B. P. Johnson, M. G. Khaledi, J. G. Dorsey*, Anal. Chem. **58**, 2354 (1986).

[38] *S. D. West*, J. Chromatogr. Sci. **25**, 122 (1987).

[39] *A. K. Smilde, C. H. P. Bruins, D. A. Dornbos*, J. Chromatogr., in press.

[40] *J. C. Ford, J. A. Smith*, J. Chromatogr. **390**, 307 (1987).

[41] *P. Lehtonen*, J. Chromatogr. **314**, 141 (1984).

Received: June 29, 1987
Accepted: Sep. 9, 1987
F

Advantages and Limitations of HPLC in Environmental Analysis

J. F. Lawrence

Food Research Division, Health Protection Branch, Ottawa, Ontario, Canada K1A 0L2

Key Words

HPLC
PAH (polycyclic aromatic hydrocarbons)
Mycotoxins
Organo-metallics
Sulfite
Headspace-HPLC

Summary

The application of HPLC to environmental analysis is often hindered by difficulty not experienced in other areas of analysis. Usually the components being determined are at parts per million levels or less and are usually in sample matrices that can yield many interferences. In order to develop successful methodology the prime requirements for an HPLC system are column efficiency and the sensitivity and selectivity of the detection system. In this presentation, examples are given to illustrate how HPLC can be used to advantage by comparing it to gas chromatographic (GC) methods and even TLC methods. For many classes of compounds, such as halogenated hydrocarbons (pesticides, PCB's, dioxins), the GC methods may be preferred. However, for polycyclic aromatic hydrocarbons (PAH) HPLC with fluorescence detection has proven to be excellent for trace environmental analysis. Comparisons of HPLC with TLC for aflatoxins and with bioassays for paralytic shellfish toxins are made. Novel combinations such as headspace-HPLC analyses for SO_2 and HPLC-AA for organometallic compounds are discussed.

Introduction

High performance liquid chromatography (HPLC) has become a widely used technique for the analysis of many substances including both organic and inorganic compounds in a large variety of sample types. Environmental analyses, however, often require special HPLC conditions. The concentrations to be determined are often in the parts per million range or less. At these levels, the detector characteristics become very important. Both sensitivity and selectivity are required. The refractive index detector, for example, is widely used for HPLC applications where extremely low level detection is not required. This detector is unsuitable for trace environmental analysis.

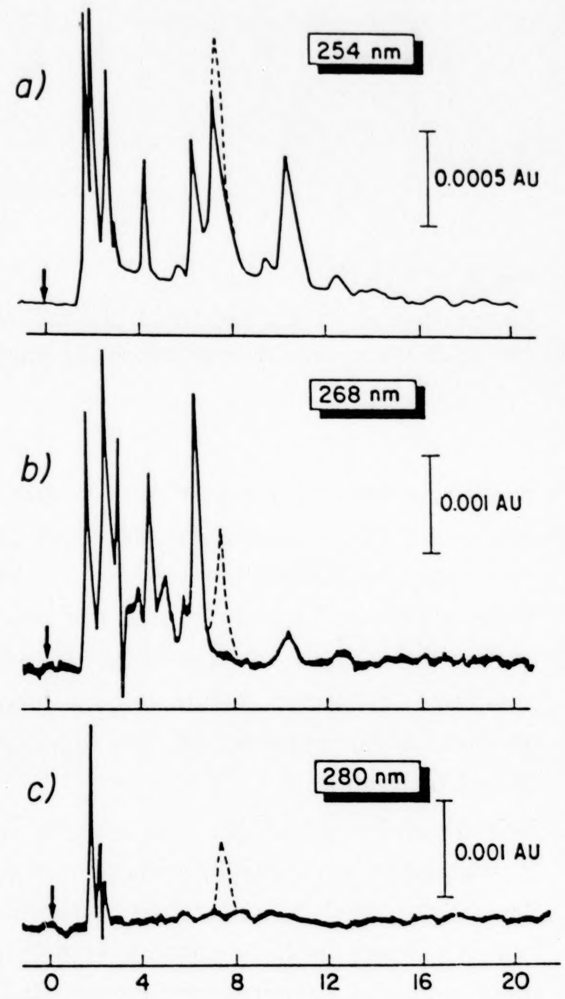

Fig. 1
Chromatograms of asulam in whole wheat flour extract (at 1.0μg/g) with different detector wavelengths.

Sensitivity and Selectivity

Sensitivity alone may not be enough to enable a determination to be made. Fig. 1 shows chromatograms of a pesticide, asulam, in a food extract at 1.0ppm run at different UV absorption wavelengths [1]. Although the compound is detectable at all three wavelengths it can be seen that at 254nm the selectivity is poor resulting in interferences from the food matrix. At the wavelength maxima for asulam, 268nm, the chromatogram has improved. However, best selectivity was found at 280nm, and, in fact, would be the wavelength of choice for routine analysis.

In a comparison to gas chromatography (GC) for the herbicide, metoxuron [2], (Fig. 2) it can be seen that only

0009-5893/87 0045-06 $03.00/0
© 1987 Friedr. Vieweg & Sohn Verlagsgesellschaft mbH

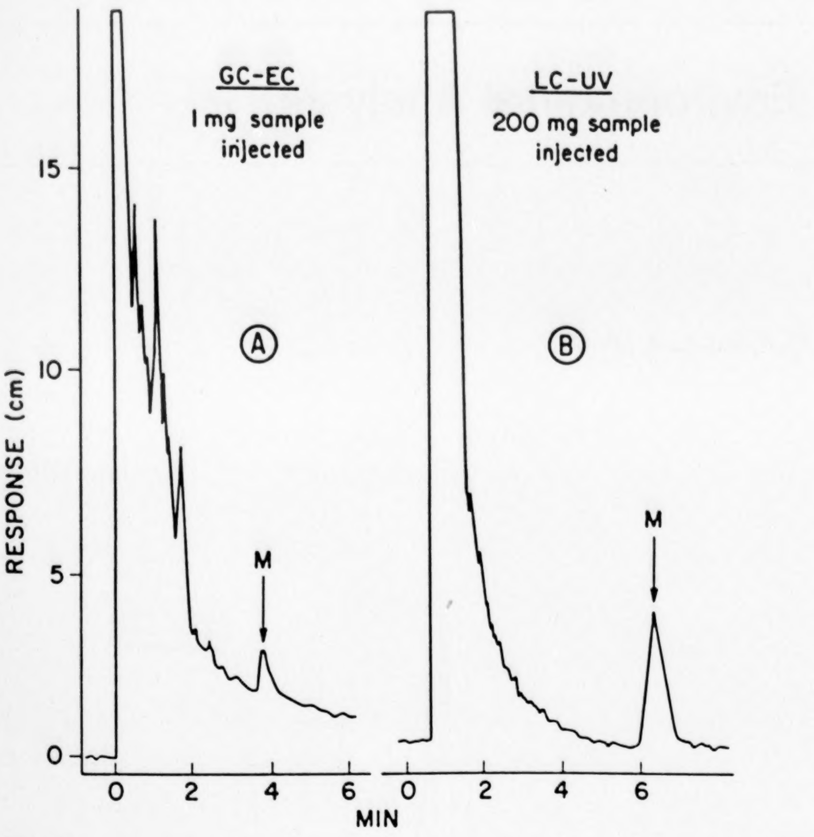

Fig. 2

Comparison of GC-EC and HPLC-UV for the determination of the herbicide, metoxuron in a soil extract (1.0µg/g).

the equivalent of 1 mg of sample was injected for the GC analysis (which employed an electron capture detector) compared to 200 mg required for the HPLC-UV absorption determination. This illustrates the much better sensitivity of the GC system compared to the HPLC one. However, the latter provided better results based on signal: background ratio, because of the superior selectivity of the detection system.

The disadvantage of poor sensitivity with good selectivity is that large amounts of sample extract must be injected which can lead to shortened column life. Normally it is best to inject as little sample as possible while using the most sensitive detector setting that still gives a good baseline.

Applications

There are many areas in environmental analytical chemistry where HPLC is less suited than, for example, capillary GC. The latter uses columns (30 m) which can have efficiencies of around 100,000 theoretical plates whereas commonly used HPLC columns have only about 10,000 plates or less. For compounds such as halogenated hydrocarbons (pesticides, PCB's, dioxins) which are thermally stable, the high separation efficiencies and sensitive detection by electron-capture or mass spectrometry make capillary GC the method of choice.

However, in other areas, HPLC is clearly advantageous. It is particularly suited to the determination of polycyclic aromatic hydrocarbons. Many of these compounds have intense native fluorescence and can be readily detected in the picogram range [3]. Fig. 3 shows a separation of eight PAH standards. Some of these compounds could be easily detected at 20 pg. Table I compares detection limits obtained by HPLC-fluorescence with GC-MS with selected ion monitoring. It can be seen that the HPLC method is somewhat more sensitive. Fig. 4 shows chromatographic results using HPLC-fluorescence for several food types. It can be seen that for some samples many unidentified peaks appear. From the sample preparation procedure and the HPLC conditions it is likely that these substances are other PAH related compounds because of their non-polar nature and from the fact that they fluoresce.

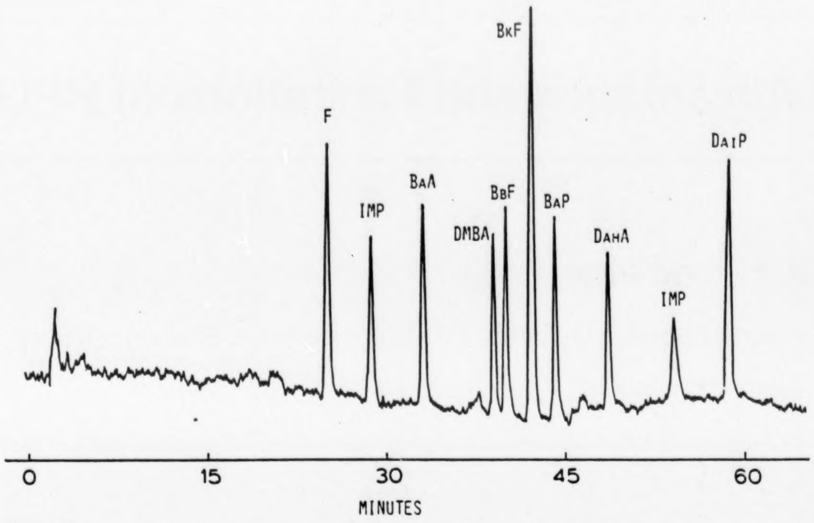

Fig. 3

Chromatograms of eight PAH standards by HPLC-fluorescence. 130 pg of each injected (except D(ai)P, 2.8 ng). IMP = impurity, F = fluoranthene, BaA = benz(a)anthracene, DMBA = dimethylbenz(a)anthracene, BbF = benz(b)fluoranthene, BkF = benz(k)fluoranthene, BaP = benz(a)pyrene, DahA = dibenz(ah)anthracene, DaiP = dibenz(ai)pyrene.

Table I. Detection limits of eight PAH by HPLC-fluorescence and GC-MS/SIM analysis.

PAH	Detection Limits (PG)	
	HPLC-Fluor.	GC-MS/SIM
F	18	30
BaA	14	30
DMBA	12	30
B(b)F	12	30
B(k)F	5	–
B(a)P	13	60
D(a,h)A	16	60
D(ai)P	264	300

Another example of the use of HPLC with fluorescence detection is for the determination of aflatoxins in foods. These fungal mycotoxins are strong carcinogens and thus methods must be available to detect them in contaminated foods, (usually nuts and grain type products) at low ng/g levels. Fig. 5 shows HPLC results of work done by Tartar et al. [4] of the Canadian Health Protection Branch for four aflatoxins spiked in peanuts. The chromatogram represents aflatoxin levels of 0.5 and 1.0 ng/g in shelled peanuts. Aflatoxins B_1 and G_1 must be derivatized to B_{2a} and G_{2a} in order to have adequate fluorescence. While the HPLC detection limits are very good it should be pointed out that this technique is not necessary for rapid screening since direct TLC methods are equally as sensitive capable of detecting sub ng/g levels of these toxins without the use of expensive instrumentation. The HPLC method of course would be preferred for quantitation.

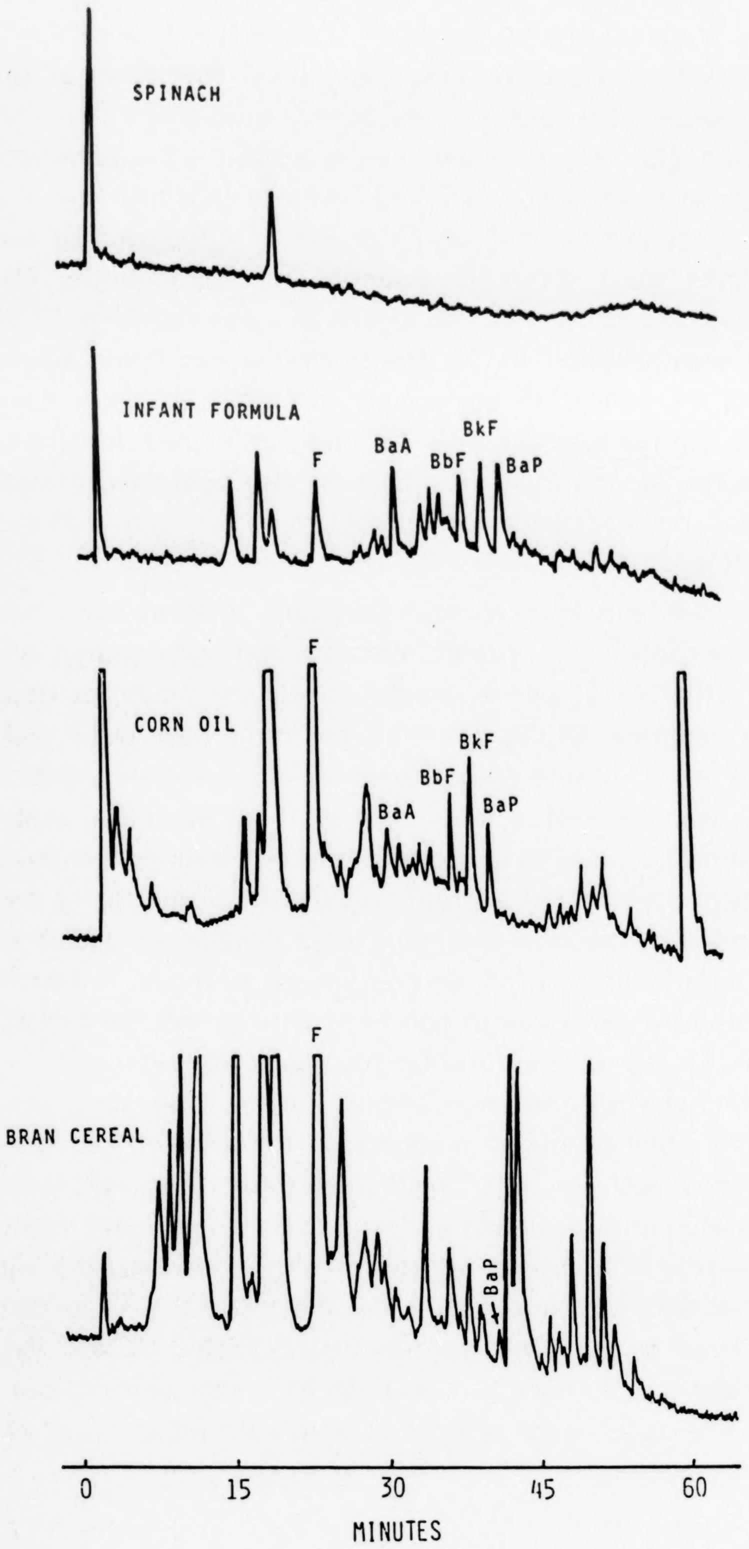

Fig. 4

Chromatograms of four food extracts for PAH determinations. PAH abbreviations as in figure 3.

HPLC has proven to be very useful for the determination of toxins associated with paralytic shellfish poisoning (PSP). These chemicals are some of the most potent neurotoxins known and are accumulated by shellfish which feed on certain microscopic dinoflagellates. Human consumption of contaminated shellfish can lead to poisonings and in extreme cases death. The lethal oral human dose is estimated to be about 1 mg of the toxins [5]. The most commonly used method for determination of PSP toxins is the mouse bioassay which has a number of drawbacks including a precision of ± 20%, interference from NaCl, and the need for a continuous supply of mice. The HPLC methods are preferred because of better precision, much better detection limits, the ability to quantitate any of the 18 different PSP toxins presently identified and no requirement for a supply of mice. The HPLC technique involves separation of the individual toxins followed by post-column oxidation and fluorescence detection. Fig. 6 shows the general structure of these toxins. The oxidation creates an aromatic system producting the fluorescence. Fig. 7 shows a schematic of the apparatus [6] and Fig. 8 shows an analysis of a non-toxic mussel extract and a clam extract containing about 1 ppm total toxins [7]. The selectivity of the system can be easily seen.

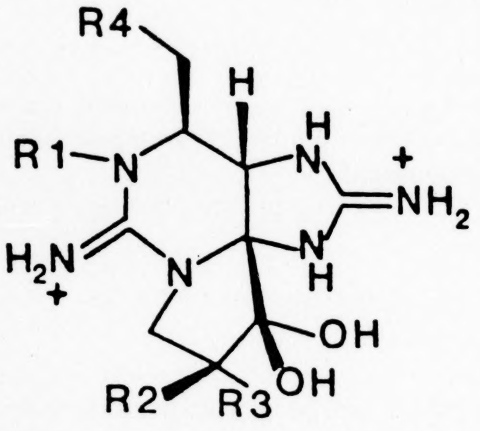

Fig. 6

General structure of PSP toxins. R_1, R_2 and R_3 are either –H, –OH or $-OSO_3$. R_4 is –OH, NH_2COO-, or $-O_3SONCOO-$.

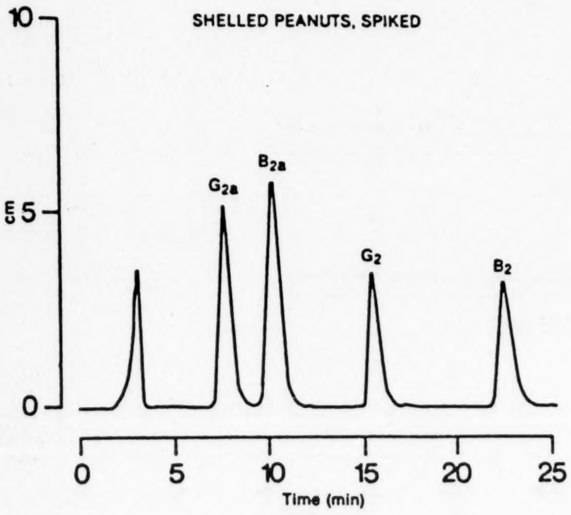

Fig. 5

Chromatogram of an extract of shelled peanuts spiked with 1 ng/g aflatoxins B_1 and G_1 and 0.5 ng/g aflatoxins B_2 and G_2 (from ref. [4] with permission of the Association of Official Analytical Chemists).

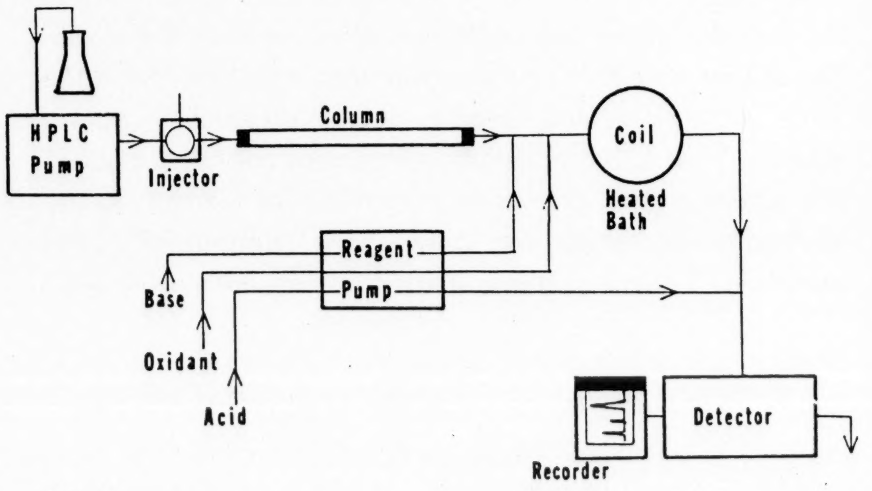

Fig. 7

Schematic of the HPLC system for the determination of PSP toxins in shellfish (from ref. [6] with permission of the Association of Official Analytical Chemists).

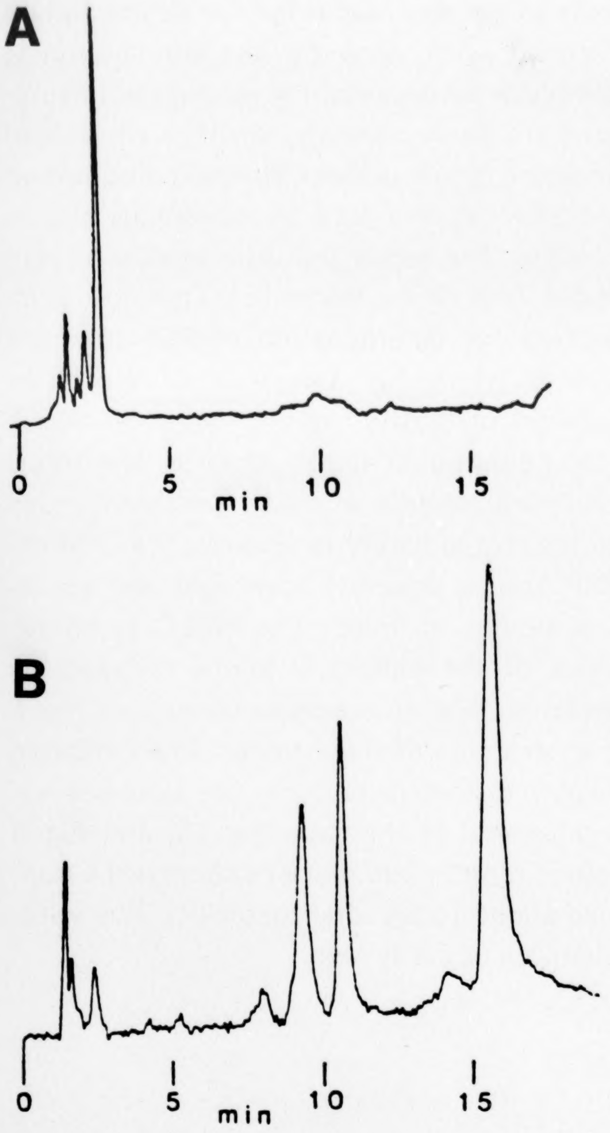

Fig. 8
Chromatograms of PSP toxins in: A. non-toxic mussels and B. clams containing about 1 ppm total toxins (from ref. [7] with permission of the Institute of Food Technologists).

HPLC-Atomic Absorption

One of the areas where HPLC has particular promise is in trace element speciation. Most health assessments of environmental samples, particularly foods, are made on the basis of total metal content of a food. Lead, cadmium and arsenic, for example, are usually determined after acid digestion and atomic absorption analysis to yield total element concentrations. However, it has been known for many years that the form of the element can greatly affect its toxicity. There are significant differences in the toxicities of inorganic lead versus organo-lead compounds and the same with inorganic arsenic versus organically bound arsenic. Thus a better health assessment could be made if the actual organic or inorganic form of the element in the environmental sample was known. It is here that HPLC has potential. Table II outlines a problem we are having with high levels of arsenic in certain marine fish. Our attempts at solving the problem involved HPLC speciation of the organoarsenicals with off-line atomic absorption (AA) detection [8]. Fig. 9 shows reconstructed chromatograms prepared from analysing 0.5 ml fractions collected from the HPLC. It can be seen that extracts of different fish and shellfish yield different organoarsenic compounds. The compounds shown in the figure are arsenobetaine (AB) and arsenocholine (AC). Arsenobetaine was found to account for almost all the arsenic in most fish species analysed. Shrimp was the only fish that contained detectable amounts of arsenocholine. Salmon also contained an unknown organoarsenic compound which we have not yet identified.

Table II. Organoarsenic compounds in fish.

1. Some marine fish species have high concentrations of arsenic.
2. It appears to be mainly organically bound.
3. Problem: to identify the organoarsenic compounds.

A simpler approach to organometallic analysis would be to incorporate the atomic absorption detection step online with the HPLC separation. Such combinations have been reported in the literature but none have been evaluated on a routine basis. However, GC-AA combinations have been somewhat more successful for volatile organometallics particularly for organolead compounds. We have recently constructed a promising GC-AA interface for the detection of volatile organometallics capable of detecting sub ng/g levels of alkyllead compounds in foods. Research is presently underway to construct an interface for HPLC. Some of the inherent problems associated with this are the limitations on solvent composition and flow rate. These are the same problems encountered for other HPLC combinations such as HPLC-mass spectrometry or HPLC-inductively coupled plasma emission spectrometry and might be overcome by using microbore HPLC. However, the big advantage of coupling with AA is the cost. An AA spectrometer can be purchased for less than $15,000 US and the interface and furnace can be built for a few hundred dollars. The total price is right in line with other types of HPLC detectors.

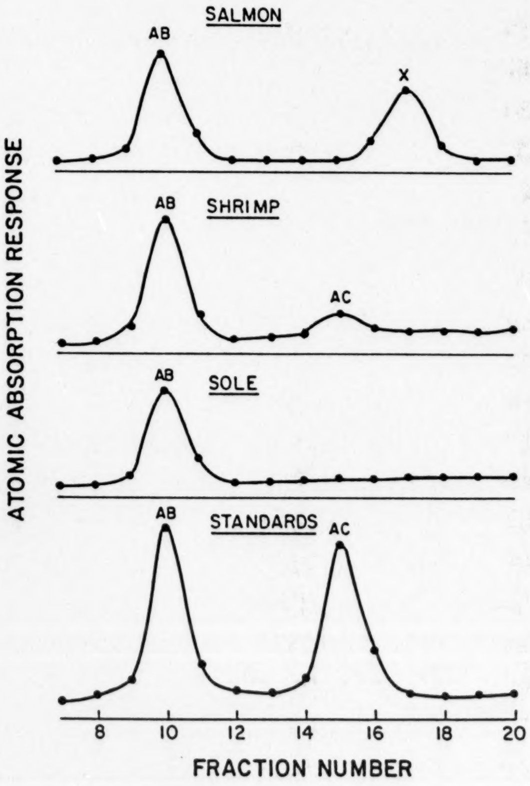

Fig. 9
Chromatograms of three fish extracts. AB = arsenobetaine, AC = arsenocholine, X = unknown.

Headspace-HPLC

Headspace-HPLC is another approach which may have potential in environmental analysis. The technique is similar to headspace-GC except that a trapping solution is present in the headspace sampling syringe. Fig. 10 shows the setup for the determination of sulfite in foods. The sample slurry is placed in the vial which is then sealed. A 3ml volume of 50% phosphoric acid is injected into the vial and the contents mixed for 10min. Four millilitres of headspace are removed into a syringe containing 0.5ml of HPLC mobile phase (pH 11, 0.03*M* methane sulfonate). The syringe is locked and shaken for 30sec. Then an aliquot of the trapping solution is analysed by HPLC. Fig. 11 shows typical results for the determination of sulfite in treated and untreated raisins. This same approach could be useful for other volatiles such as CO_2 and NH_3, as well as organics. In this same area HPLC has proven to be particularly ad-

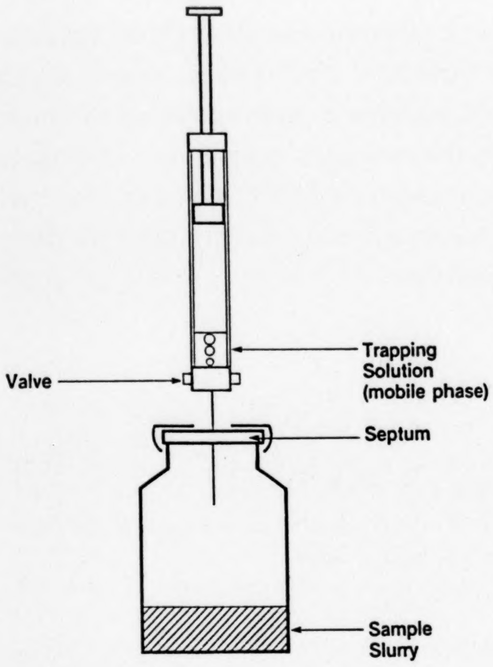

Fig. 10
Headspace sampling for the HPLC determination of sulfite in foods.

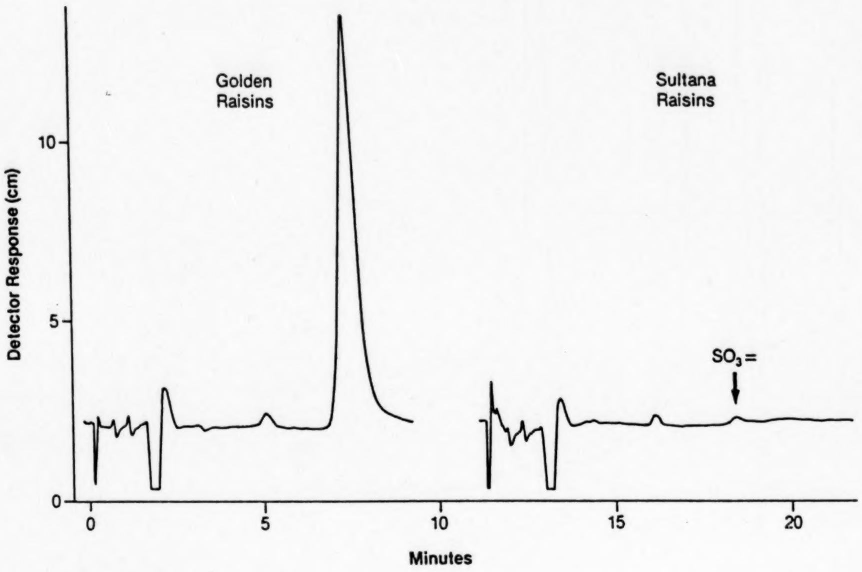

Fig. 11
Chromatograms of sulfited golden raisins containing 157ppm sulfite, and unsulfited sultana raisins. Ion chromatography with oxidative amperometric detection.

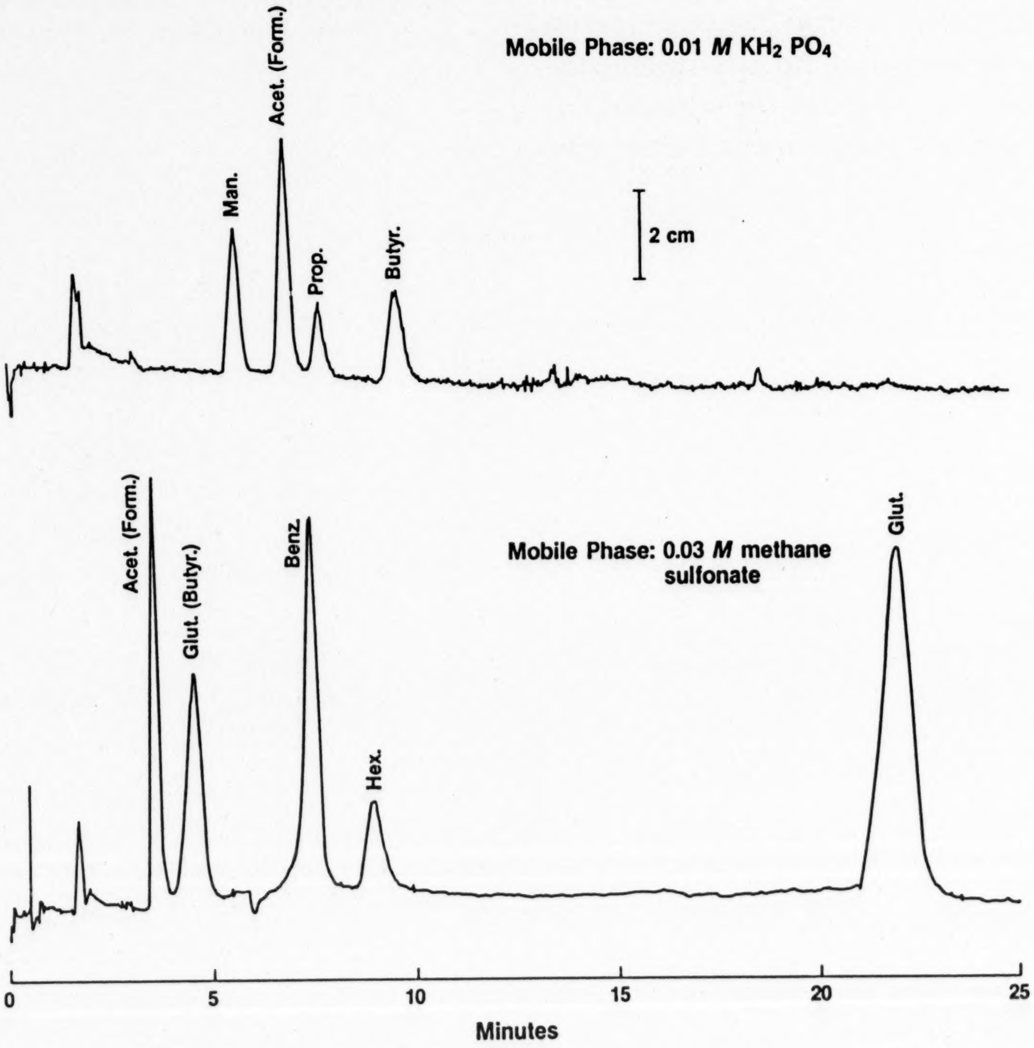

Fig. 12
Chromatogram of aldehyde-sulfite adducts using ion chromatography with amperometric detection.

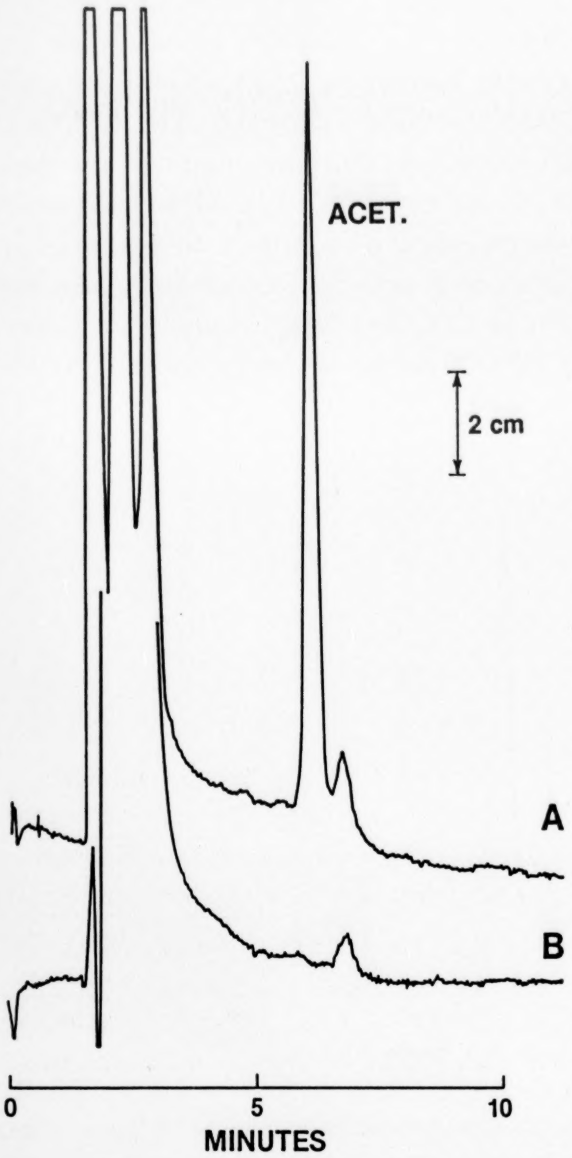

Fig. 13

Direct analysis of wine by ion chromatography with amperometric detection. A = before H_2O_2 treatment. B = after treatment.

vantages because it is possible to speciate the bound forms of sulfite in biological matrices, which no other methodology is able to accomplish. Fig. 12 shows the separation of several aldehyde-sulfite adducts using ion chromatography with amperometric detection. Fig. 13 shows the direct analysis of a wine sample containing acetaldehyde-sulfite adduct with confirmation by treatment with H_2O_2. The particular adduct accounted for about 80% of the total sulfite content of the sample.

Conclusion

HPLC clearly has a useful place in environmental analysis. It is advantageous for the determination of large numbers of compounds which cannot be easily analysed by GC. Also, HPLC combinations with atomic absorption spectrometry and other spectrometric techniques offers much potential for trace determinations in environmental samples, particularly in speciating the different organic and inorganic forms of toxic elements. Headspace-HPLC also has potential as a simple but efficient sample cleanup technique for both organic and inorganic volatiles.

References

[1] *J. F. Lawrence, L. G. Panopio, H. A. McLeod*, J. Agric. Food Chem. **28**, 1323 (1980).
[2] *J. F. Lawrence, C. Van Buuren, U. A. T. Brinkman, R. W. Frei*, J. Agric. Food Chem. **28**, 630 (1980).
[3] *J. F. Lawrence, B. S. Das*, Int. J. Environ. Anal. Chem. **24**, 113 (1986).
[4] *E. J. Tarter, J. P. Hanchay, P. M. Scott*, J. Assoc. Offic. Anal. Chem. **67**, 597 (1984).
[5] *H. A. Bates, H. Rapoport*, J. Agric. Food Chem. **23**, 237 (1975).
[6] *J. J. Sullivan, W. T. Iwaoka*, J. Assoc. Offic. Anal. Chem. **66**, 297 (1983).
[7] *J. J. Sullivan, M. M. Wekell, L. L. Kentala*, J. Food Sci. **50**, 26 (1985).
[8] *J. F. Lawrence, P. Michalik, G. Tam, H. B. S. Conacher*, J. Agric. Food Chem. **34**, 315 (1986).

Received: June 29, 1987
Accepted: July 23, 1987
F

Effects of the Column Pressure Drop in Packed-Column Supercritical-Fluid Chromatography

P. J. Schoenmakers* / L. G. M. Uunk

Philips Research Laboratories, P.O. Box 80000, 5600 JA Eindhoven, The Netherlands

Key Words

Supercritical-fluid chromatography
Packed columns
Pressure drop

Summary

Columns packed with small particles (*i.e.* 3 to 10μm) may be used for fast separations in supercritical-fluid chromatography (SFC). The analysis times required for such packed columns are typically an order of magnitude smaller than what may be achieved with contemporary open-tubular (capillary) columns (25 to 100μm i.d.).

However, packed columns give rise to much higher pressure drops over the column. The maximum allowable pressure drop will determine how many plates can be achieved with packed columns. In this paper the effects are described of the pressure drop on retention (capacity factor) and efficiency (number of plates) for packed columns of various lengths and internal diameters, packed with three different octadecylsilica materials. Carbon dioxide has been used as the mobile phase under several different sets of pressure and temperature conditions.

Introduction

One key issue in a comparison between the potential applicability of packed columns and open-tubular (capillary) columns for supercritical-fluid chromatography (SFC) is the speed of analysis, which can be described by [1]

$$t_\omega = \frac{N_{ne} h d^2}{\nu \mathbf{D}_m}(1 + k_\omega), \quad (1)$$

where t_ω is the retention time of the (last) peak with capacity factor k_ω, N_{ne} is the required number of theoretical plates, h is the reduced plate height ($h = H/d$, where H is the plate height in length units), ν is the reduced linear velocity (related to the linear velocity u by $\nu = ud/\mathbf{D}_m$), $\mathbf{D}_m$ is the diffusion coefficient of the solute in the mobile phase, and d is the characteristic dimension (the column diameter d_c for capillary columns or the particle diameter d_p for packed columns). For a given separation (*i.e.* for a given combination of a mobile and a stationary phase, with a given phase ratio and at a given pressure and temperature) the parameters N_{ne}, $\mathbf{D}_m$, and k_ω are constants, independent of the type (packed or open) and dimensions of the column. In that case we find

$$t_R = C\frac{hd^2}{\nu}, \quad (2)$$

where C is a proportionality factor. In eq. (2), the factor hd^2/ν represents the effect of the column on the required analysis time. We will refer to it below as the retention time factor and express it in units of μm^2.

Packed columns are typically used at or around $\nu = 10$, where for a good column $h = 3$. Assuming particle sizes to be in the range of 3 to 10μm, we find retention time factors between about 3 and 30. If we consider the operation of packed columns at the minimum in the *H vs. u* curve, where the analysis time is longer, but the required pressure drop is lower, then we find $\nu = 3$, $h = 2$, and values for hd_p^2/ν between about 7 and 67. If we operate open-tubular SFC columns at high flow rates in order to increase the speed of analysis (*e.g.* $\nu = 45$, $h = 4.5$), then we find for the contemporary columns with d_c of 50 or 100μm retention time factors between 250 and 1000. For columns with d_c = 25μm this factor would be 62.5. From this we may conclude that the fastest separation that may currently be achieved with open-tubular (capillary) SFC is roughly comparable with the slowest separation ($\nu = \nu_{opt}$) on a packed column with 10μm particles. However, in most cases packed columns are at least an order of magnitude faster than contemporary open-tubular columns.

The above simple analysis of the required analysis time in SFC using either packed or open-tubular columns relies on a number of implicit and explicit assumptions, which will be reviewed below.

The stationary and mobile phase, as well as the phase ratio and the operating conditions (pressure and temperature) have been assumed to be identical on the different columns.

0009-5893/87 0051-07 $03.00/0

© 1987 Friedr. Vieweg & Sohn Verlagsgesellschaft mbH

This is certainly not correct for the different columns currently in use. In packed-column SFC the stationary phase is typically a chemically bonded monolayer on a silica support. In open-tubular SFC the stationary phase is a film of a cross-linked polymer, which usually requires a relatively high operating temperature. In current practice, packed columns may require a higher density (or solvating power) of the mobile phase. However, this may not always be true, especially since it is desirable to use thicker films of stationary phases in open columns [1]. Therefore, it is not unreasonable to assume the diffusion coefficient $\mathbf{D}_m$ to be independent of the physical characteristics of the column. The same can be said regarding the capacity factor, because both packed columns and open-tubular columns will be operated with capacity factors roughly in the optimum range (*i.e.* $1 < k < 5$).

The required number of theoretical plates (N_{ne}) is determined by the selectivity of the phase system (mobile and stationary phase). For simple chromatograms in which there are a limited number of peaks to be separated, N_{ne} can be readily calculated from the capacity factors of the critical pair of peaks, *i.e.* the pair of solutes i and j that is least separated in the chromatogram (see Ref. [2] chapter 4):

$$N_{ne} = 4\left[\frac{2+k_j+k_i}{k_j-k_i}\right]^2 = \frac{4}{S^2_{min}}, \tag{3}$$

where S is the separation factor between the two components, and where the subscript min indicates that i and j are the least separated peaks (lowest value for S) in the chromatogram.

For complex chromatograms, with very large numbers of peaks, N_{ne} cannot be defined exactly. In these cases N_{ne} can be seen as a desired number of plates, *i.e.* as the result of a compromise between the required input (column length, analysis time, pressure drop) and the desired output (resolution). For complex chromatograms the required (or desired) number of plates is usually high.

Selectivity of phase systems in SFC is a largely unexplored area. Although some studies have been reported in the literature (*e.g.* Ref. [3, 4]), little is known about the selection of selective phase systems. Certainly, there is no reason to assume that the selectivity will be systematically better on open columns than on packed columns, or *vice versa.*

Clearly, since there is no reason to assume that either $\mathbf{D}_m$, or k_ω, or N_{ne} will be significantly different if the type (packed or open) or dimensions of the column are varied, eq. (1) facilitates a comparison of the required analysis times for different columns in SFC.

Effects of Column Pressure Drop

So far it has been tacitly assumed that the required number of plates can be realized by using a column of the required length, *i.e.*

$$L_{ne} = N_{ne}H = N_{ne}hd. \tag{4}$$

The pressure drop over such a column (Δp) can be found from the Darcy equation, if we neglect the expansion of the mobile phase along the length of the column. Under conditions outside the immediate vicinity of the critical point the density of the mobile phase does not vary considerably along the column length [5] and we may assume an average linear velocity $\bar{u} = L/t_0$, where t_0 is the hold-up time of the column (elution time for an unretained solute). The Darcy equation now reads

$$\Delta p = B^0 \eta L \bar{u} = B^0 \eta N_{ne} h \bar{\nu} \mathbf{D}_m. \tag{5}$$

If Δp is in Pa, then the viscosity (η) of the mobile phase may be expressed in Pa.s, the column length (L) in m and the velocity (u) in m/s. B^0 is the specific permeability coefficient (m^{-2}), which for open columns equals

$$B^0 = 32/d_c^2. \tag{6}$$

For packed columns B^0 can only be approximated. A conservative (high), but common estimate is

$$B^0 \simeq 1000/d_p^2. \tag{6a}$$

From eq. (5) and (6a) we can derive an equation for the maximum number of plates that can be obtained from a packed column, *i.e.*

$$N_{max} = \frac{\Delta p_{max}}{B^0 \eta h \bar{\nu} \mathbf{D}_m} = \frac{\Delta p_{max} d_p^2}{1000\, \eta h \bar{\nu} \mathbf{D}_m}. \tag{7}$$

With $\mathbf{D}_m = 2.10^{-8}$ m^2/s and $\eta = 5.10^{-5}$ Pa.s as reasonable estimates [1] we find

$$N_{max} = \frac{\Delta p_{max} d_p^2 10^9}{h\bar{\nu}} \tag{8}$$

with Δp_{max} in Pa and d_p in m, or

$$N_{max} = \frac{100 \Delta p_{max} d_p^2}{h\bar{\nu}} \tag{8a}$$

with Δp_{max} in bar and d_p in μm. At $\bar{\nu} = 10$, $h = 3$ we find for 5μm particles and a maximum allowable column pressure drop of 25 bar a maximum number of about 2000 theoretical plates. At the optimum in the h–$\bar{\nu}$ curve (*i.e.* $\bar{\nu} = 3$, $h = 2$) this figure would be 5 times higher. It would also be 4 times higher for 10μm particles, but almost 3 times lower for 3μm particles. The operating conditions (pressure and temperature) do not have a dramatic effect because changes in η will be compensated to some extent by changes in $\mathbf{D}_m$. For open-tubular columns the maximum number of plates is about 100 to 500 times higher in current practice. Even if the diameter of the open column is reduced sufficiently to yield comparable analysis times as packed columns, open-tubular columns may provide a 15 times higher maximum number of plates [1]. Therefore, capillary columns will need to be used if N_{ne} is high, *e.g.* for recording chromatograms of very complex samples with large numbers of peaks.

The one parameter for which no reasonable estimate can be given is the maximum allowable pressure drop over the column. Because supercritical fluids are compressible, a significant pressure drop over the column will imply variations in the mobile phase density, and hence in the solvent strength, viscosity and diffusivity along the length of the column. In a previous publication [6] we have shown that the pressure drop over the column does affect the observed capacity factors. Gere *et al.* [7] have used columns with very small particles (down to 3μm) with very high pressure drops over the column (up to 184 bar). They observed efficiencies in agreement with theoretical values ($h \simeq 2$) even at the highest flow rates. Schwartz, in a recent comparison of packed and open-tubular columns for SFC [8], stated that "The inherently higher pressure drop in packed columns ... should not be a deterrent to most applications".

The present paper reports on a systematic study of the effects of the column pressure drop on capacity factors and efficiency (plate numbers) in packed-column SFC, in order to evaluate whether or not this last statement is correct.

Experimental

The instrument used for this study was a modified liquid chromatograph from Philips Analytical (Cambridge, U.K.), the details of which have been described elsewhere [6, 9, 10]. Slight changes were made to the connections and to the detector-cell design in order to minimize the extra-column pressure drop. This resulted in an increased contribution of the instrumentation to the observed peak widths, as was especially evident when using narrow-bore columns.

One remarkable result of our efforts to reduce the extra-column pressure drop was that the marked decrease in capacity factors upon increasing the flow rate at very low pressure drops [6] could no longer be observed. Capacity factors are expected to increase with decreasing overall pressures over the column, hence to increase with increasing pressure drop. Therefore, the observations in the range of very low flow rates in the present study are more likely to be correct. However, the fact that changes in instrumentation (particularly in the size of the entrance and exit ports of the detector flow cell) may affect the observed capacity factors is in itself reason for concern. Similar effects might occur in pressure restrictors which are purposely positioned in the flow stream prior to atmospheric (*e.g.* flame ionization) detectors.

Flow control in the present system was realized either by using a needle valve [6, 9] or by a combination of a mass-flow controller and a mass-flow meter connected in series at the outlet of the system (*i.e.* after the detection). The mass-flow of carbon dioxide was measured at low pressures with a Hi-Tec (Ruurlo, The Netherlands) F-121 flow meter. This signal was used to control the valve of the mass-flow controller (also from Hi-Tec). Teflon parts were found to yield the best compromise between leakages through the valve and reliability of operation.

In this study the pressure drop over the column was varied by changing the outlet pressure (measured after the detector), while keeping the inlet pressure (before the injector) constant. Pressures were measured using low-dead-volume flow-through pressure gauges (Chrompack, Middelburg, The Netherlands).

Columns with three different octadecylsilica packings were used in this study. CP-spher and Chromspher columns were obtained from Chrompack and Rosil-C18 columns were obtained from Alltech (Eke, Belgium). The columns used in this study and the identification codes used in the text are listed in Table I.

Table I. Columns used in this study. All packing materials are ODS silicas.

Code	Packing Material	Particle size μm	Length mm	Diameter mm
CS 5-15	Chromspher	5	150	4.6
CP 8-10	CP-spher	8	100	4.6
CP 8-25	CP-spher	8	250	4.6
Ro 5-25	Rosil	5	250	4.6
Ro 5-15	Rosil	5	150	4.6
Ro 5-15nb	Rosil	5	150	2.1

A dilute solution of naphthalene, ethylbenzene and biphenyl in dichloromethane was used as a test sample. Variations in the size (volume and concentration) of the sample did not affect the results. Retention times were measured at the peak maximum. The observed efficiency (number of theoretical plates) was calculated from the peak width at half the maximum height.

Results and Discussion

The results obtained on the variation of the efficiency (N) and the retention (k) are summarized in Table II. Fig. 1 shows an example of a plot of the number of theoretical plates as a function of the column pressure drop for the 25 cm long column with 8 μm particles. A plot of N *vs.* Δp is similar to the more conventional H-$\bar{u}$ plot. The former type of figure has been preferred in this work, because of the great variations observed in N (see below), and because Δp is a directly controllable parameter in SFC, whereas $\bar{u}$ usually is not.

Fig. 1 shows a maximum number of theoretical plates (N_{max}) at a pressure drop of about 20 bar for all three test solutes. The corresponding minimum reduced plate height ($h_{min} = L/N_{max}d_p$), optimum pressure drop (Δp_{opt}), and optimum (average) linear velocity ($\bar{u}_{opt}$, calculated from the elution time of dichloromethane at $\Delta p = \Delta p_{opt}$) are all listed in Table II for each solute.

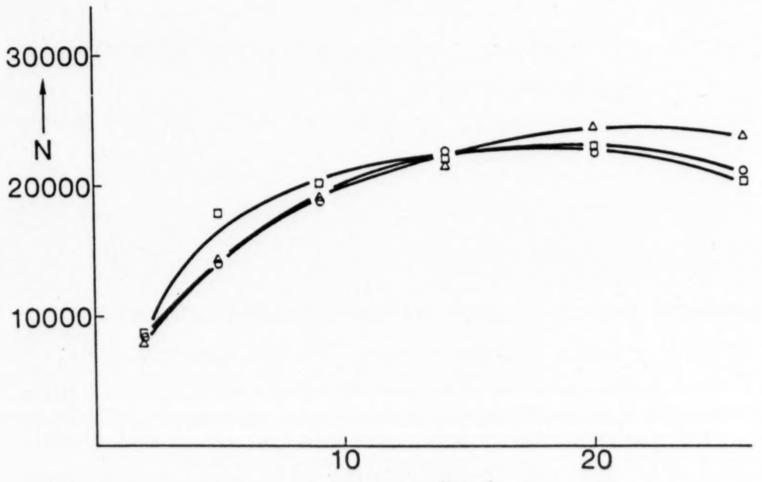

Fig. 1

Example of a plot of efficiency (N) *vs.* column pressure drop (Δp). Column: CP 8-25. Temperature: 40°C. Inlet pressure: 122 bar. Solutes: ○ = ethylbenzene, △ = naphthalene, □ = biphenyl.

Table II. Summary of the results obtained for measurements of efficiency (N) and capacity factors (k) as a function of column pressure drop. Solutes: E = ethylbenzene, N = naphthalene, B = biphenyl. Δp_{opt} is the pressure drop at which $N = N_{\mathrm{max}}$ and $\bar{u}_{\mathrm{opt}}$ is the corresponding (average) linear velocity. $\Delta k/k_0$ is the increase in the capacity factor at $\Delta p = \Delta p_{\mathrm{opt}}$ relative to the extrapolated value (k_0) at $\Delta p = 0$.

Column	T °C	p_{in} bar	Solute	N_{max} X 10^3	h_{min}	Δp_{opt} bar	$\bar{u}_{\mathrm{opt}}$ mm/s	k_0	$\Delta k/k_0$ %
CP 8-25	40	122	E	23	1.4	18	3.4	0.13	23
			N	23	1.4	22	3.9	0.74	22
			B	23	1.4	20	3.7	1.18	20
CP 8-25	50	122	E	18	1.7	14	2.6	0.23	40
			N	18	1.7	9	2.0	1.27	10
			B	20	1.6	9	1.9	2.10	13
CP 8-25	50	153	E	23	1.4	18	3.1	0.14	7
			N	22	1.4	20	3.4	0.75	10
			B	26	1.2	20	3.4	1.14	12
Ro 5-25	40	122	E	16	3.1	18	2.5	0.51	8
			N	18	2.8	14	1.9	1.96	7
			B	17	2.9	16	2.3	2.74	10
Ro 5-25	50	122	E	16	3.1	12	1.9	0.74	5
			N	12	4.2	9	1.5	2.76	15
			B	13	3.8	8	1.4	4.18	15
Ro 5-25	50	153	E	17	2.9	20	2.6	0.47	6
			N	17	2.9	20	2.6	1.76	12
			B	16	3.1	17	2.2	2.40	13
CS 5-15	40	123	E	14	2.1	15	4.6	0.22	9
			N	16	1.9	14	4.3	0.75	5
			B	17	1.8	13	4.0	0.91	9
Ro 5-15	40	122	E	12	2.5	12	2.1	0.29	2
			N	12	2.4	14	2.3	1.03	3
			B	13	2.3	16	2.5	1.30	3
CS 5-15	50	122	E	9	3.3	17	5.3	0.26	12
			N	11	2.7	15	4.8	0.86	26
			B	11	2.7	11	3.6	1.10	19
CS 5-15	50	152	E	11	2.7	14	4.4	0.20	10
			N	13	2.3	15	4.6	0.68	9
			B	13	2.3	18	5.2	0.84	16
CS 5-15	60	122	E	9	3.3	10	3.8	0.51	27
			N	7	4.3	9	3.5	2.2	18
			B	8	3.8	8	3.2	3.2	20
Ro 5-15 (nb)	40	122	E	–[1]	–	4[2]	3.5	0.23	1
			N	–	–	14[2]	3.9	0.86	6
			B	–	–	16[2]	4.6	1.09	9
Ro 5-15 (nb)	50	122	E	–	–	21	8.1	0.28	64
			N	–	–	16	6.1	1.38	15
			B	–	–	11	3.9	1.88	6
Ro 5-15 (nb)	50	152	E	–	–	5	1.6	0.22	0
			N	–	–	6	1.9	0.79	1
			B	–	–	7	2.1	0.98	2

[1] Efficiency values on narrow-bore columns were not obtained because of excessive extra-column band broadening.

[2] Value assumed to be identical to the one obtained on a 4.6 mm i.d. column.

The capacity factor of each solute was measured as a function of the column pressure drop. As an example, Fig. 2 shows the variation of the capacity factor of biphenyl on a 15 cm long column with 5 μm particles at different (inlet) pressures (Fig. 2a) and temperatures (Fig. 2b). Apart from the region where Δp is close to zero (see Experimental), the results are similar to those reported earlier [6]. The variation of k with Δp is seen to be greatest in conditions where k is known to be a strong function of p [11]. With carbon dioxide as a mobile phase at 35 °C, k decreases rather abruptly if p is increased from about 70 to about 80 bar. At 40 °C, the decrease is slightly less abrupt and takes place between about 70 and about 90 bar. At 50 °C, a much more gradual decrease is observed between 70 and 110 bar. Above a certain value for the pressure, k is virtually independent of the pressure. As long as the column outlet pressure remains above this value, the pressure drop may be high. Hence, Δp may be higher if p_{m} is higher, or if T is lower.

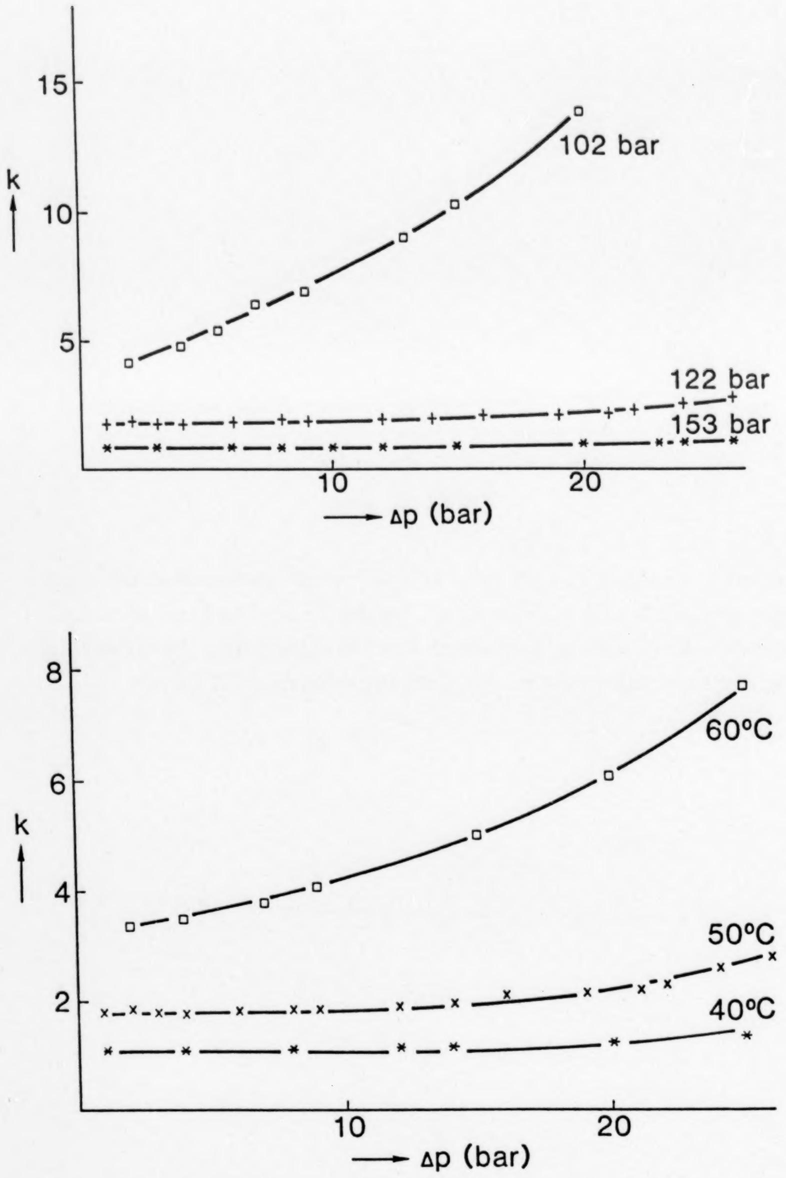

Fig. 2

Variation of the capacity factor (k) with the column pressure drop (Δp) for biphenyl on the CS 5-15 column at different temperatures and pressures. **a.** Temperature: 50°C. Inlet pressures: 102, 122 and 153 bar. **b.** Inlet pressure: 122 bar. Temperatures: 40, 50 and 60°C.

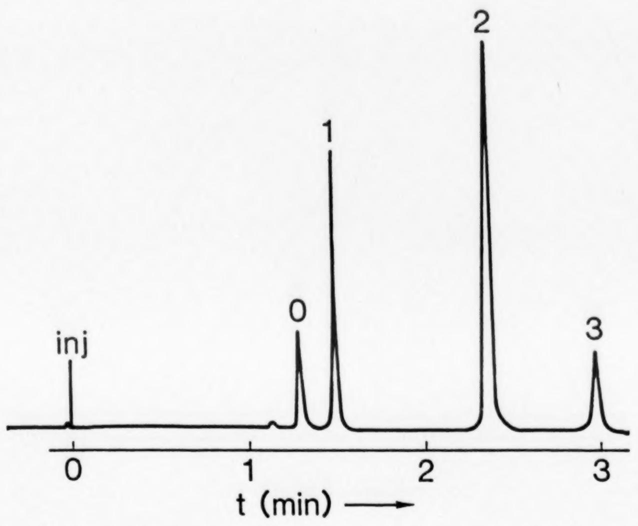

Fig. 3

Chromatogram of the three test solutes obtained with the CP 8-25 column at T = 50°C and p_{in} = 153 bar. UV detection at 210nm, 1.28 AUFS. Solutes: 0 = dichloromethane (solvent), **1** = ethylbenzene, **2** = naphthalene, **3** = biphenyl. $N \simeq 23{,}000$.

It is seen in Fig. 2a that at 50°C, little variation in k is observed if p_{m} is 153 bar. Under these conditions carbon dioxide behaves essentially as a liquid. At 122 bar inlet pressure, the variation in k becomes significant at higher pressure drops, *i.e.* when the column outlet pressure approaches 100 bar. At 102 bar inlet pressure k is a strong function of Δp even at low pressure drops. In general, when the absolute pressure increases, the variation of k with Δp becomes less.

Fig. 2b shows that at 40°C the variation of k with Δp, with $p_{\text{in}} = 120$ bar is seen to be much smaller than at 50°C and at 60°C at the same pressure. At 40°C and pressures above 100 bar liquid-like conditions are approached. At 60°C and 100 bar carbon dioxide is a highly compressible fluid. At this pressure, the variation of k with Δp is stronger at higher temperatures.

The efficiencies observed on the CP 8–25 column (see Fig. 1) are excellent. Reduced plate heights of between 1.2 and 1.7 can be found in Table I. The value of h_{min} was calculated on the basis of the manufacturer's information on the particle size. If this is indeed 8μm, then the observed plate counts are remarkably good. Fig. 3 shows a chromatogram in which more than 20,000 theoretical plates are obtained in a few minutes. Clearly, it is possible to realize very fast and very efficient separations by packed-column SFC.

When 5μm instead of 8μm particles are used, a further increase in the observed number of plates is expected. However, the results for the Ro 5–25 column in Table II shown that the contrary is true in SFC. Only between 12 and 17 thousand plates are observed, with reduced plate heights of 3 or 4. Also, the optimum linear velocities, which, for non-compressible fluids, would be expected to be about 60% higher than on the column packed with 8μm particles, actually turn out to be significantly lower. The difference between the observed efficiencies for these two columns is not due to differences between the different packing materials, because the CS 5–15 and Ro 5–15 columns yield comparable results (see Table II).

A much more likely explanation is that the required pressure drop is too high for the Ro 5–25 column. This is supported by the fact that the optimum pressure drops are about the same for CP 8–25 and the Ro 5–25 columns at equal inlet pressures and temperatures. Once $\Delta p > \Delta p_{\text{opt}}$, the observed number of plates starts to fall off very rapidly on the Ro 5–25 column. At the same time, the capacity factors start to increase rapidly. It appears that the column outlet pressure becomes too low for SFC to be performed successfully.

Fig. 4 shows a dramatic example of an N *vs.* Δp plot, in which N falls off very rapidly above a certain pressure drop. The pressures at the column outlet at which N starts to fall off are in reasonable agreement with the upper limit of the range in which k varies strongly with p, as described above. It appears, therefore, that the column outlet pressure is the limiting factor for what may be achieved with a certain column, under given conditions in SFC. In practice, it may be possible to maintain the outlet pressure at a constant value and to increase the flow rate by increasing the column inlet pressure.

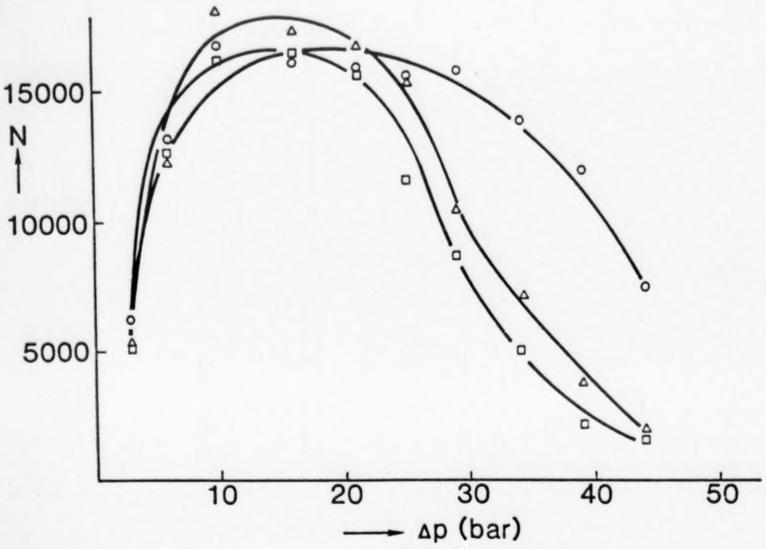

Fig. 4

Plot of the efficiency (N) *vs.* column pressure drop (Δp) for the Ro 5-25 column. Temperature: 40°C. Inlet pressure: 122 bar. Solutes: ○ = ethylbenzene, △ = naphthalene, □ = biphenyl.

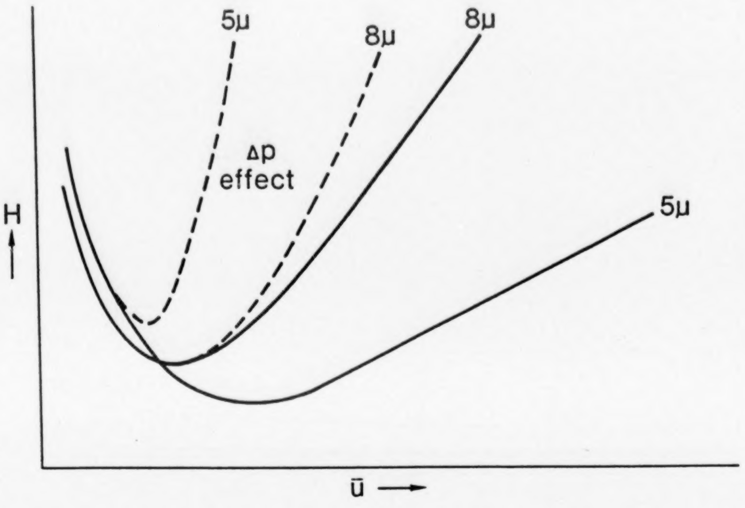

Fig. 5

Schematic explanation of the efficiency *vs.* pressure drop curves shown in Fig. 1 and 4. Figure applies to 25cm long columns under conditions as in Table II. Dashed lines illustrate the detrimental effects of a too large pressure drop on the observed efficiency.

With the Ro 5–25 column, under the conditions shown in Table II, the column outlet pressure becomes too low and N starts to fall off well before the optimum linear flow rate in the H-$\bar{u}$ curve is reached. The plate height is determined by the longitudinal diffusion (B) term, and the observed efficiencies are low. Before the plate height can reach its minimum value, N starts to fall off because the solubility of the solute in the mobile phase under the conditions at the column outlet becomes the limiting factor. This is schematically illustrated in Fig. 5. In this figure, the detrimental effect of the column pressure drop is indicated by the dashed line. According to eq. (5) and (6a), the pressure drop over a column packed with 5μm particles is 2.5 times higher than with 8μm particles for the same value of $\bar{u}$. Therefore, the dashed line starts much earlier and is much steeper with the smaller particles, for which u_{opt} is also higher.

If this explanation is correct, then at much higher values of p_{in} a higher pressure drop over the column is possible and the Ro 5–25 column may be useful. However, the required value for p_{in} is mainly determined by the solutes to be eluted from the column. With the present test solutes, very low k values would be obtained at higher column inlet pressures. Nevertheless, it is true that higher pressure drops are permissible at higher densities. For example, we found that the efficiency of the Ro 5–25 column did not fall off at 40°C and $p_{\text{in}} = 153$ for pressure drops up to 70 bar. For the present test solutes, on columns of 25cm length, 8μm particles appear to be optimal. For solutes of higher molecular weight, which require mobile phases with higher densities, much higher pressure drops are allowed and the optimum particle size will be lower.

It is seen in Table II that better results are obtained on 15cm long columns packed with 5μm particles. On the CS 5–15 column, the optimum value for the (average) linear velocity is significantly higher than on the CP 8–25 column, as expected. Together with the reduction in the column length and a small decrease in k values, this leads to elution times that are roughly a factor of three less on the CS 5–15 column, but N_{max} (and h_{min}) values are never quite as good as on the CP 8–25 column. The pressure drop required to reach the minimum in the H-$\bar{u}$ curve is expected to be in between the values for the CP 8–25 and the Ro 5–25 columns. However, the values for Δp_{opt} are all lower on the CS 5–15 column than on the CP 8–25 column. This, together with the values for $\bar{u}_{\text{opt}}$, suggests that the CS 5–15 columns has a much higher specific permeability than the CP 8–25 column.

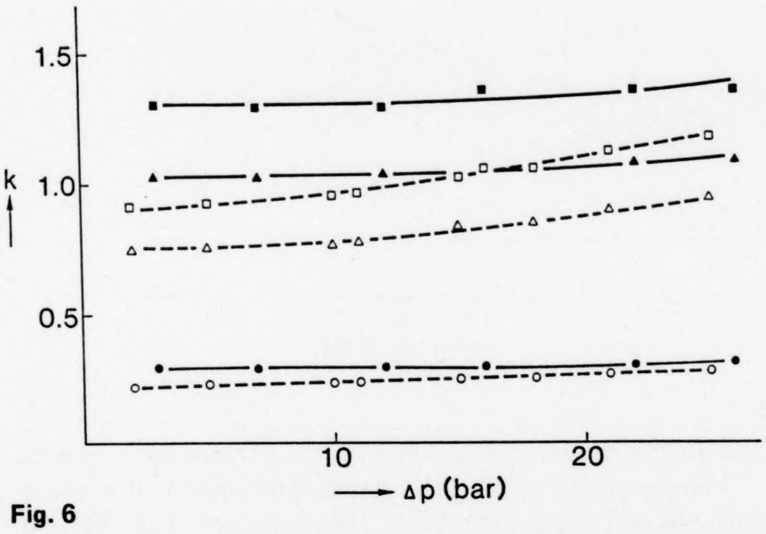

Fig. 6

Variation of k with Δp for the Ro 5-15 (drawn lines, heavy symbols) and CS 5-15 (dashed lines, open symbols) columns at T = 40°C and $p_{\text{in}} \simeq 122$ bar. Solutes: ○,● = ethylbenzene, △,▲ = naphthalene, □,■ = biphenyl.

Fig. 6 illustrates that nominally identical columns may behave quite differently in SFC, not only in terms of the capacity factors, but also in their variation as a function of the column pressure drop. The N *vs.* Δp curves for the two columns also reveal differences. The CP 5–15 column shows good efficiencies (N_{max} = 14–17,000), but a rather sharp maximum. At $\Delta p = 24$ atm, the efficiency is reduced to about 12,000. The Ro 5-15 columns show much shallower curves, which moreover are virtually identical for the three test solutes. On this column, at $\Delta p = 24$ atm, which in this case is about twice the optimum value, $N \simeq 11{,}000$, *i.e.* only 10% of the plates have been lost. The permeabil-

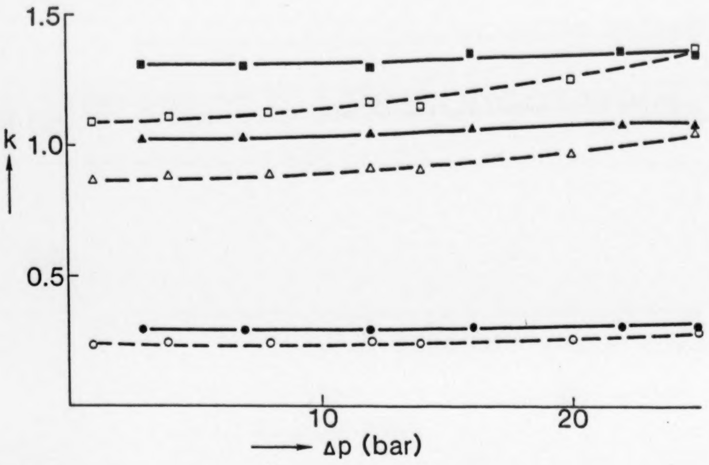

Fig. 7

Variation of k with Δp for the Ro 5-15 (drawn lines, heavy symbols) and Ro 5-15nb (dashed lines, open symbols) columns at T = 40°C and $p_{in} \simeq 122$ bar. Solutes: ○,● = ethylbenzene, △,▲ = naphthalene, □,■ = biphenyl.

ity between the two columns was also different. In order to achieve the same linear velocity, a considerably higher pressure drop was required on the Ro 5-15 column than on the CS 5-15 column.

Consequently, the results of the present study cannot be used to predict the optimum operation conditions on any given column. Thus, it is to be recommended that the physical suitability (*i.e.* diameters of the column and particles) of a given column for a given application of SFC should be tested by measuring N as a function of Δp at the required pressure and temperature. The results of this study may be of help for the initial selection of the column.

Fig. 7 illustrates the variation of k with Δp for a column of conventional diameter (4.6 mm i.d.) in comparison with a narrow-bore column (2 mm i.d.). Quite comparable results were obtained on the two columns, indicating that lack of thermal equilibrium is unlikely to be a serious problem in packed-column SFC. Efficiency measurements were not possible on narrow-bore columns with the present instrumentation.

Conclusions

1. This study has shown that the performance of packed-column SFC is limited by the maximum allowable pressure drop over the column.
2. By selecting suitable dimensions for particles and columns, it is possible to achieve fairly large numbers of theoretical plates ($N > 20{,}000$) within a few minutes.
3. However, when the mobile phase density (at the outlet of the column) becomes too low, the observed efficiency may decrease dramatically. The (physical) suitability of a given column for a given application of SFC can easily be established by characterizing its efficiency as a function of the column pressure drop. If N falls off prematurely, then larger particles or a shorter column should be used.
4. When the required density is low, the pressure drop over the column must not be too high. Therefore, relatively large particles (*e.g.* 8 or 10 μm) should be selected. The optimum particle diameter will be smaller for larger solute molecules (higher molecular weight), requiring higher mobile-phase densities.
5. Nominally identical columns (*e.g.* from different manufacturers) may behave differently in SFC, not only in terms of retention and efficiency, but also in the variations of these parameters with the column pressure drop. Columns with a high permeability have very considerable advantages for SFC.
6. Capillary (open) columns appear to be most attractive when either the required density is very low, or the required number of plates is very high.

References

[1] *P. J. Schoenmakers* in: P. Sandra (ed.), Proceed. 8th Int. Symp. Cap. Chromatogr., Riva del Garda, May 1987, pp. 942–954.

[2] *P. J. Schoenmakers*, The Optimization of Chromatographic Selectivity, A Guide to Method Development, Elsevier, Amsterdam (1986).

[3] *L. G. Randall*, Hewlett-Packard Technical Paper No. **102**, (1983).

[4] *F. Erni, J. P. Chervet, M. Schindler*, 8th Int. Symp. on Column Liq. Chromatogr., New York, Mar 20–25 (1984).

[5] *P. J. Schoenmakers, P. E. Rothfusz, F. C. C. J. G. Verhoeven*, J. Chromatogr. **395**, 91 (1987).

[6] *P. J. Schoenmakers, F. C. C. J. G. Verhoeven*, J. Chromatogr. **352**, 315 (1986).

[7] *D. E. Gere, R. D. Board, D. McManigill*, Anal. Chem. **54**, 736 (1982).

[8] *H. E. Schwartz*, LC-GC Magazine **5**, 14 (1987).

[9] *P. J. Schoenmakers, F. C. C. J. G. Verhoeven*, J. Chromatogr. **371**, 121 (1986).

[10] *P. J. Schoenmakers, F. C. C. J. G. Verhoeven*, Trends Anal. Chem. **6**, 10 (1987).

[11] *P. J. Schoenmakers*, J. Chromatogr. **315**, 1 (1984).

Received: June 29, 1987
Revised manuscript
received: Aug. 10, 1987
Accepted: Aug. 12, 1987
F

Liquid Phase Separation Methods: HPLC, FFF, Electrophoresis

J. J. Kirkland*/R. M. McCormick

E. I. DuPont de Nemours & Co., Central Research and Development Dept., Experimental Station, B-228, Wilmington, DE, 19898, USA

Key Words

Column liquid chromatography
Macromolecular separations
Overview
Field flow fractionation
Electrophoresis

Summary

Recent research in separations has been directed towards extending the molecular weight range for these high-resolution methods, while at the same time improving reproducibility and convenience of operation. This overview summarizes some of these developments and provides insights into the inherent resolution, range, speed, and limitations of these methods.

Important advances in HPLC include the development of better siliceous supports, as well as fresh approaches for producing both covalently-bonded and crosslinked, mechanically-immobilized organic stationary phases that provide a new level of reproducibility and stability for separations. Very wide-pore packings now permit separations of species with molecular weights up to about 10^7 daltons, and columns of particles in the 1–2 μm range allow rapid separations of macromolecules.

New results in sedimentation and thermal field flow fractionation (FFF) demonstrate the power of these methods to separate species with high resolution in molecular weight ranges that cannot be accessed by either HPLC or electrophoresis. Of special interest is the use of sedimentation FFF for isolating soluble, high-molecular-weight molecules and particulates such as sub-cellular components. Recent studies have confirmed that thermal FFF is a powerful method for determining the molecular-weight distribution of fragile, high-molecular-weight synthetic polymers with good accuracy and reproducibility.

Capillary electrophoresis techniques give promise of very fast, high-resolution separations of ionic macromolecules; on-line detection affords high sensitivity, and quantitation is readily achievable. Special agarose gel electrophoretic techniques now permit excellent DNA separations for species up to 5×10^6 base pairs, and 2D electrophoretic methods provide resolution of more than 10^4 components in coupled sequential separations of protein mixtures.

I Introduction

Recent research in separation science often has involved the development of better high-resolution methods for the separation of large organic molecules. Although problems in polymer chemistry and related fields have originated some new approaches, pressing needs in the biological sciences largely have been the catalyst for these studies. Many knowledgeable workers now consider the area of macromolecular separations to be the most important frontier in separation science.

Because each has the ability to provide unique information about macromolecular systems, three different separation methods have received the most attention by researchers: (1) high performance liquid chromatography (HPLC), (2) field flow fractionation (FFF), and, (3) electrophoresis. The level of activity in these fields is illustrated in Fig. 1, as measured by the number of articles listing these techniques in the abstracts or key words of publications since 1967. Clearly, HPLC and electrophoresis have been applied most for needed separations. The data in Fig. 1 further suggest that activity with electrophoresis has leveled off in the past half-dozen years, whereas a linear growth in the use of HPLC is suggested for that period. Fig. 1 also indicates that the FFF methods are just beginning to make substantial contributions to the separation science of large species; fewer than two hundred papers have been published on this subject to date.

0009-5893/87 0058-19 $03.00/0

© 1987 Friedr. Vieweg & Sohn Verlagsgesellschaft mbH

These three separation methods are based on diverse principles; each can provide distinctly different data for various samples of interest. As suggested in Fig. 2, these methods overlap considerably in the range of molecular weights to which they can be applied. However, the three separation techniques generally are not competitive; each has the potential for providing important complementary information. Certain forms of HPLC and electrophoresis utilize unique chemical properties in the separation process; other variations of these methods allow separations based on size or molecular weight. In contrast, separation by the FFF methods is based solely on physical differences between sample components.

Table I compares various aspects of the high-resolution separation methods under discussion. Data are given on (specific) resolution, peak capacity, dynamic range of separation, and other properties that have been experimentally demonstrated for these methods. From these results, some areas of applicability of the various methods can be determined. For example, the greatest range of molecular weight (MW) access is generally obtainable with methods that involve some form of programming during the run (e.g, the programmed FFF methods). Highest resolution has been demonstrated with reversed-phase chromatography (RPC) and pulsed-field electrophoresis. The separation of very complex mixtures of proteins is best approached with 2D electrophoresis since this method has by far the highest potential peak capacity. RPC also has relatively high peak capacity, and might be a favored method for separation of complex mixtures of compounds by non-ionic interactions. Capillary electrophoresis is the most efficient separation method (in terms of plates/sec), with RPC a distant second. Size-exclusion chromatography (SEC) has the most desirable properties for isolating purified fractions from samples because of speed, low potential for degrading the sample, high yield, and ease of scale-up. In contrast, the FFF methods are slightly downgraded in

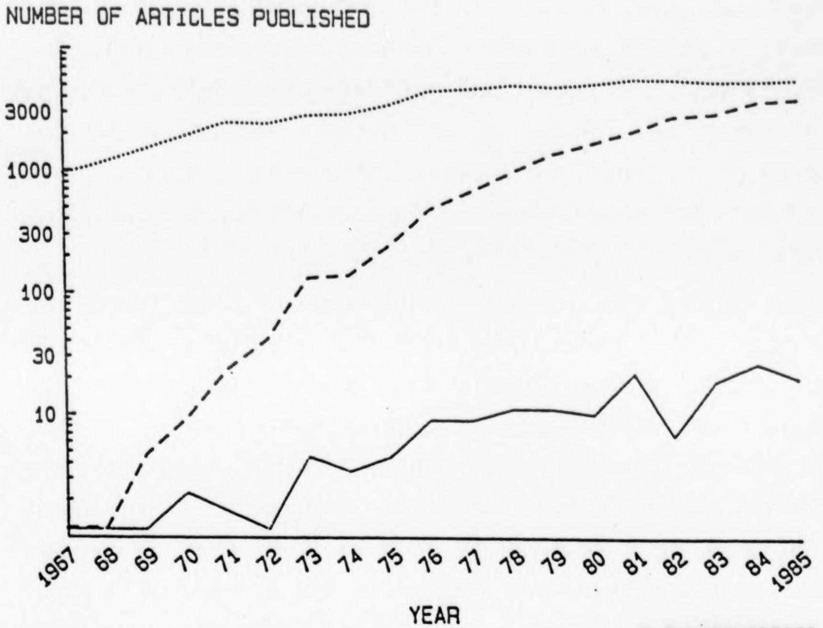

Fig. 1
Number of Publications, 1967–1985.

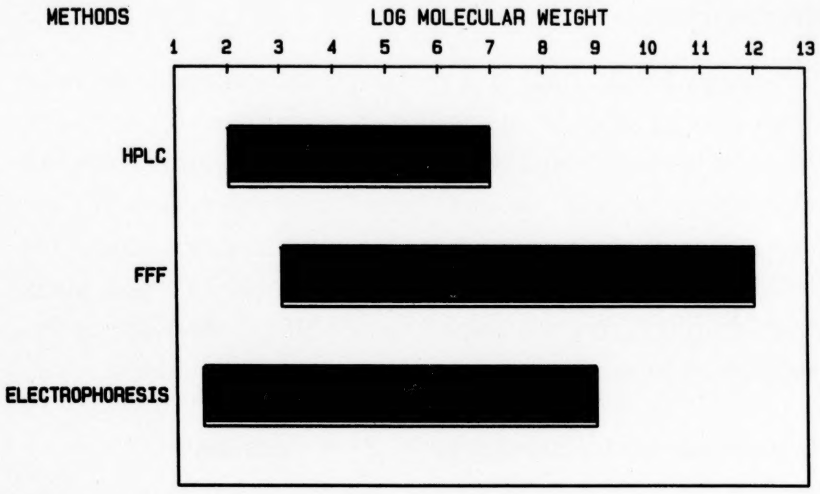

Fig. 2
Molecular Weight Range for Separation Methods.

Table I. Comparison of High-Resolution Separation Methods for Macromolcules. (Estimated from Best Available Separations.)

Method[a]	Separation Basis	MW Range[b]	Dynamic[c] Range	Specific[d] Resolution	Discrimination[e] Capacity	Peak[f] Capacity	Plates[g] Per Sec	Isolation Capability	Typical Separation Time, Hrs.
HPLC									
SEC	Size	10^2–10^7	10^5	0.2	0.9	7	30	++++	0.25
RPC	Hydrophobicity	10^3–2×10^5	2×10^2	1.2	0.15	38	60	+++	0.10
FFF									
TDE-SdFFF	Mass	10^5–10^{10}	10^5	0.3	0.7	22	0.05	+++	2
TDE-TFFF	Mass	10^3–5×10^7	5×10^4	0.3	1.0	16	0.06	+++	1
CF-TFFF	Mass	5×10^3–3×10^5	60	0.4	0.5	10	0.20	+++	0.5
Electrophoresis									
2D	Charge, Mass	10^4–2×10^5	20	–––	–––	$>10^4$	–––	+	80
Pulsed-Field	Mass	10^6–3×10^9	40	3	0.25	50	0.01	+	32
Capillary	Mass/Charge	10–10^5	10^4	–––	–––	>100	>1500	–	0.5

[a] SEC – size exclusion chromatography; RPC – reversed phase chromatography; TDE-SdFFF – time-delayed exponential decay sedimentation field flow fractionation; TDE-TFFF – time-delay exponential-decay thermal FFF; CF-TFFF – constant-field TFFF; 2D – two dimensional. [b] Approximate MW separation range for one experiment. [c] Ratio of largest to smallest MW separable in a single run. [d] Resolution found for a 20% difference in mass. [e] Fractional difference in MW separated with unit resolution. [f] Maximum number of R_s = 1 peaks obtained within a dynamic range. [g] Plate number per second. See Ref. [1] for theory and background of calculations.

this category because of the increased dilution of the sample during separation, as well as scale-up difficulty. Preparative electrophoretic methods generally involve more problems, but are still useful for certain isolations. Finally, separation times are least for the HPLC methods and greatest for electrophoretic separations (exception: capillary).

This report will provide an overview of some recent advances within these three areas that have been selected as the most important or that have the greatest potential for separating macromolecular components. As it is not possible to cover all technology within these fields, we have chosen to emphasize advances that provide the most distinctive new information, or those that provide solutions to important problems that were not achievable by previously-existing separation technology. The focus will be on advances in those areas in which we have the most familiarity, or on techniques with which we are actively conducting research.

II HPLC

Introduction

Although HPLC now is a maturing technology after more than two decades of use, research in this area is continuing to produce important advances. Particularly interesting are developments that permit faster, more convenient, and more reproducible separations of biomacromolecules. The following sections describe some advances in these areas, with emphasis on the expansion of HPLC methods to the separation of very-high molecular-weight components.

Separations with Columns of < 2-μm Particles

In the early 1960's, theoretical predictions by Giddings [2a], Knox and Saleem [2b], and others indicated that separations in liquid chromatography could be greatly accelerated by using columns packed with very small particles. As a result, developments in column technology have lead to the widespread use of ~ 5-μm particles. Recently, columns of 3–4 μm particles exhibiting even faster separations have become commercially available. However, columns of < 3-μm particles have largely been neglected, even though theory clearly indicates that very small particles will yield even faster separations [3]. Very small particles are especially useful for separating macromolecules having relatively poor diffusion characteristics that limit the efficiency (and speed) of HPLC separations.

Three major reasons are suggested for the relative neglect of < 3-μm particles: (1) Earlier HPLC equipment generally exhibited extra-column band broadening effects that significantly degraded the very high efficiencies (very sharp peaks) that are characteristic of such columns; (2) < 3-μm particles were difficult to make and were not generally available; < 3-μm particles with the large pores (e.g., > 100 Å) needed for separation of macromolecules had not been reported; and, (3) potential applications that could be solved by columns of very small particles were not clearly defined. Each of these limitations has now been largely overcome. Commercial HPLC apparatus is now available for carrying out separations with columns (e.g., "microbore") that produce peaks with very small volumes. Such apparatus is designed with small extra-column dead volumes, including injection valve and detector cell volumes of 0.5 μL or less. This equipment often can be used with columns of 2-μm particles with satisfactory results. Gradient elution capability also is available in certain apparatus for carrying out separations that require this technique (e.g., mixtures of proteins). Nevertheless, to take full advantage of the capabilities of columns with 1–2 μm particles, further developments in HPLC equipment may be required to accommodate the extremely sharp peaks that are generated. Especially important is the need for a variety of sensitive, fast-response detectors with sub-microliter dead volumes. Much promise has been exhibited by optical detection methods based on laser technology [4] and by certain electrochemical approaches [5].

The preparation of < 3-μm particles of different forms has been reported by several workers. Unger *et al.* [6] have presented data on columns made with irregular, unmodified, small-pore silica and alumina particles in the 1.8–2.8 μm range. Dewaele and Verzele [7] described reversed-phase columns packed with irregular, small-pore, 2-μm silica particles. Unger and coworkers [8–10] have used 1–2-μm non-porous microspheres of silica. (See Ref. [11] for similar particles formed by the hydrolysis of ethyl-orthosilicate.) These particles have been utilized for several forms of chromatography, including adsorption, reversed-phase, and affinity separations. Fast reversed-phase separations of proteins were reported using solid microparticles surface-modified with a hydrophobic silane stationary phase [8]. Columns of one form of these particles are now commercially available from E. Merck.

A similar approach has been used by Horvath and Kalghatgi [12] to prepare micropellicular sorbents composed of solid silica particles with a molecular "fur" of n-octyl chains covalently bonded to the surface. These spherical micropellicular packings exhibited good stability at high operating temperatures, which allowed relatively high flow velocities of hydro-organic mobile phases for very fast separations at practical operating pressures. Fig. 3 shows chromatograms of protein tryptic digests obtained in 1 and 3 minutes with a column of this packing material.

A different strategy was used by Danielson and Kirkland [13] to prepare totally-porous 1.5–2 μm microspheres. These particles were produced with 200 Å pores to permit access of proteins and other macromolecules to the internal surface. To prepare these particles, a silica sol of known size was coacervated into porous spheres of relatively narrow size distribution. These particles were then surface-derivatized with a C_4 – silane to prepare a column packing suitable for the very fast separation of proteins and other macromolecules by reversed-phase chromatography. Fig. 4 shows the gradient elution separation of a mixture of proteins with molecular weights up to 100,000 on a column of 2-μm particles. Because of the larger surface area, these porous particles exhibit a higher level of loadability compared to nonporous particles of the same size. The coacervation method also has been used to prepare porous ultramicrospheres as small as 0.5 μm [14]. For example, Fig. 5 shows a scanning electron micrograph of ~0.7 μm microparticles with 75 Å pores prepared by this method.

Applications for the very rapid separation of macromolecules afforded by columns of <3-μm particles have also been identified. In addition to speeding up the usual analytical separations, very fast separations provide the possibility for the rapid control of manufacturing processes using large molecules, and for the analysis of systems requiring a very rapid sampling rate, such as in certain kinetic studies. Also, since the residence time of the sample on the column is reduced in these rapid separations, the yield of biologically active sample components is enhanced for preparative chromatography. Finally, the very short analysis time makes feasible the significant acceleration of operations such as protein sequencing, for which the rate-limiting step is often the separation analysis.

Separations With Very Wide-Pore Packings

The molecular-weight capability of HPLC has been steadily increasing, largely as a result of the development of particles with very wide pores. Large pores are required to permit access of macromolecules to the internal surface or internal volume of the particles so that the desired chromatographic interaction may take place. Small particles with very large pores were first developed in the mid-1970's for use in the size-exclusion chromatography (SEC) of organic-soluble polymers with molecular weights up to about 10^7 (e.g., see [15, 16]). More recently, however, particles have been

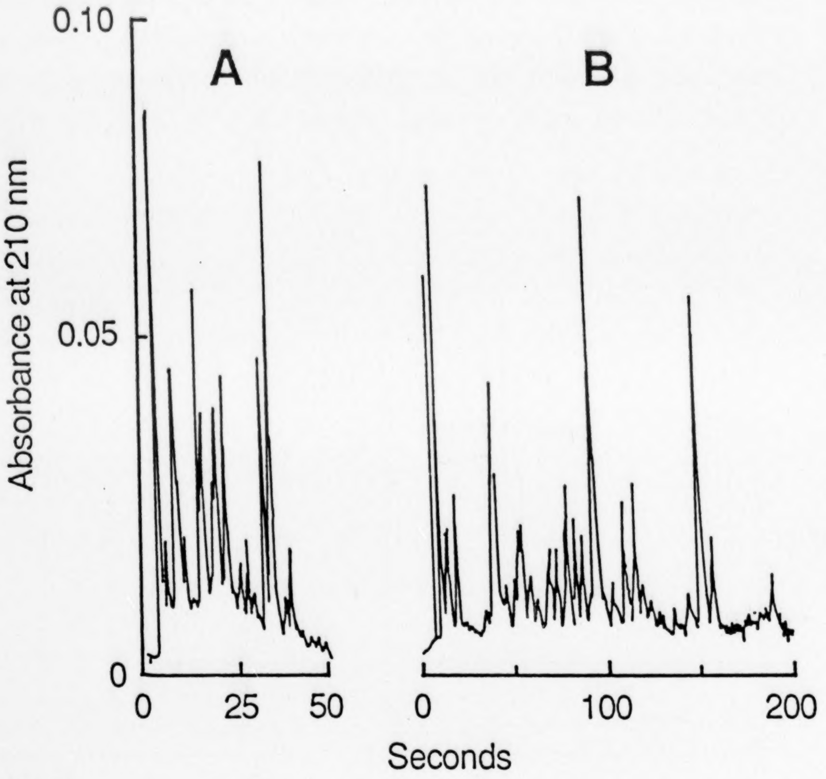

Fig. 3

Chromatographic Profiles of Tryptic Digests.

(A) β-lactoglobulin A; (B) methionyl human growth hormone. Column: 30 × 4.6 mm, 2-μm non-porous, spherical silica with covalently-bound n-octyl groups; linear gradient from 0 to 95% (v/v) acetonitrile in water with 0.1% trifluoroacetic acid, (A) in 2 min at 5 mL/min, and (B) in 6 min at 4 mL/min; temperature, 80 °C; detection at 210 nm; each sample corresponds to 5 μg of protein incubated with 1% (w/w) trypsin in a solution of 100 mM sodium acetate, 10 mM Tris, 0.1 mM calcium chloride, pH 8.3, at 37 °C for 4 hrs. Reprinted with permission from Ref. [12].

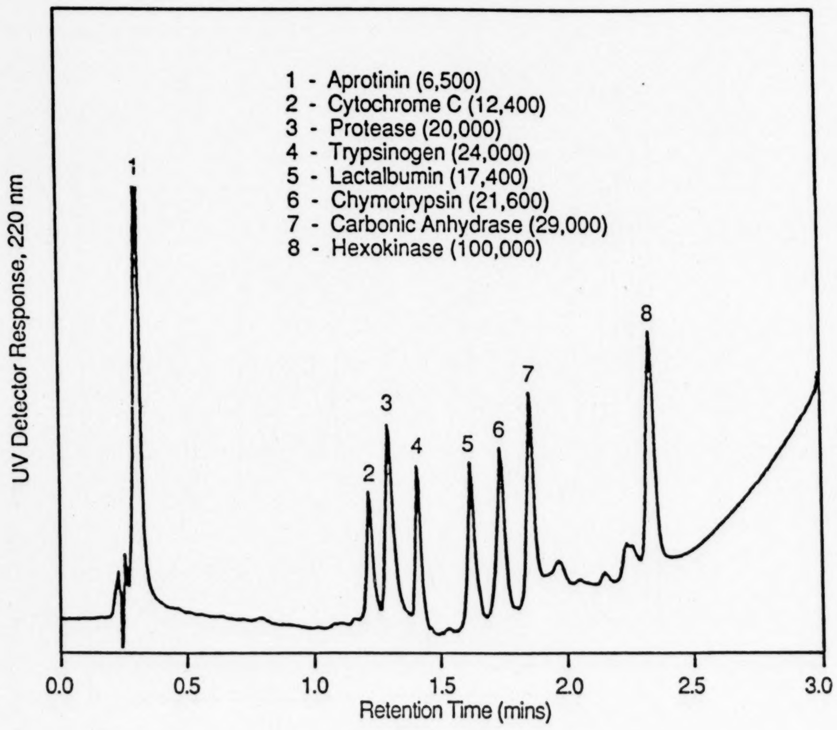

Fig. 4

Separation of Protein Mixture with Porous 2-μm Silica Particles.

Column: 3.3 × 0.62 cm, C_4-modified 2-μm silica microspheres, 200 Å pores; mobile phase, 25:75 acetonitrile/water to 100% acetonitrile (both with 0.1% trifluoroacetic acid); gradient time, 3.0 min; flow rate, 3.0 mL/min; sample, 0.5 μL, 1 μg of each protein; detection, 260 nm; pressure, 260 bar. Reprinted with permission from Ref. [13].

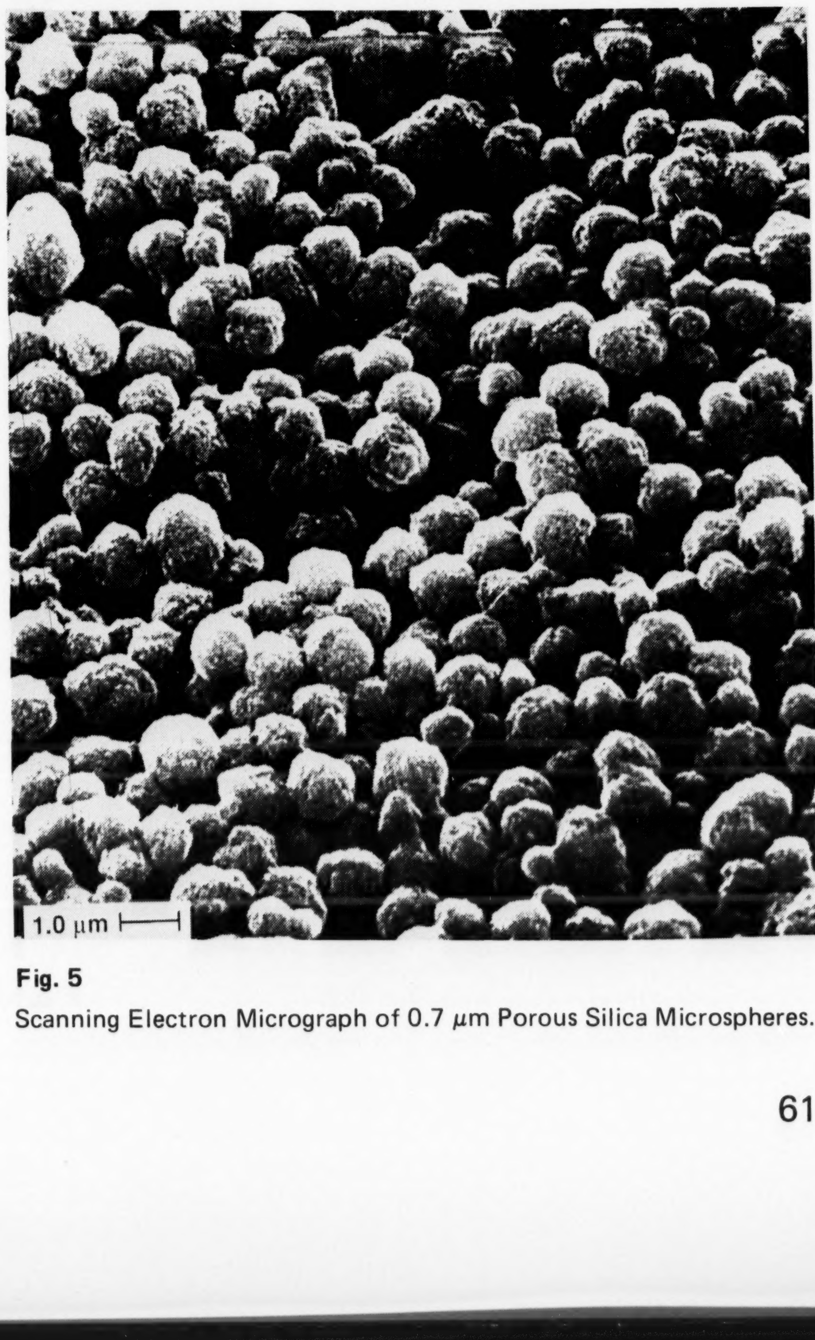

Fig. 5

Scanning Electron Micrograph of 0.7 μm Porous Silica Microspheres.

developed for separating water-soluble biomacromolecules in the same molecular weight range. These particles have been surface-modified to permit both SEC and separations based on other HPLC methods.

Wide-pore silica-based microspheres surface-modified with a thin, hydrophilic polymer coating, as well as porous particles of hydrophilic polymers, have been successfully used for separating a wide variety of very large components by SEC. For example, TSK G PW-series columns (Toyo Soda) have been utilized for separating DNA's [17], polysaccharides and serum proteins [18–20], and viruses [21]. Very wide-pore columns of this series (TSK G5000 PW and G6000 PW, presumably 5000 and 6000 Å pores) have exhibited excellent SEC separations of biological particulates such as vesicles and viruses [22]. Fig. 6 shows chromatograms of two viruses with hydrodynamic diameters of more than 100 nm that were obtained with these columns.

Very wide-pore packings for other forms of HPLC have also been used to carry out separations of biomacromolecules. For example, a 17-μm silica-based anion exchanger with 4000 Å pores has been utilized to separate high-molecular-weight nucleic acids and their fragments [23]. As shown in Fig. 7, a DNA insert was separated from its plasmid vector by this approach; separations were performed in both analytical and preparative modes [24]. This HPLC method apparently does not degrade these components, and, at the same time, provides high resolution, good sample capacity, and relatively short separation times.

Wide-pore silica-based packings with weakly-hydrophobic bonded phases also have been developed for the separation of large macromolecules by hydrophobic interaction chromatography (HIC) [25–29]. This is a gentle separation method that often allows high-resolution separation of relatively labile species in their natural state with excellent recoveries. Fig. 8 shows the separation of t-RNA's using a linear salt gradient on an HIC column prepared with a poly(ethyleneglycol) bonded phase [30]. It is likely that

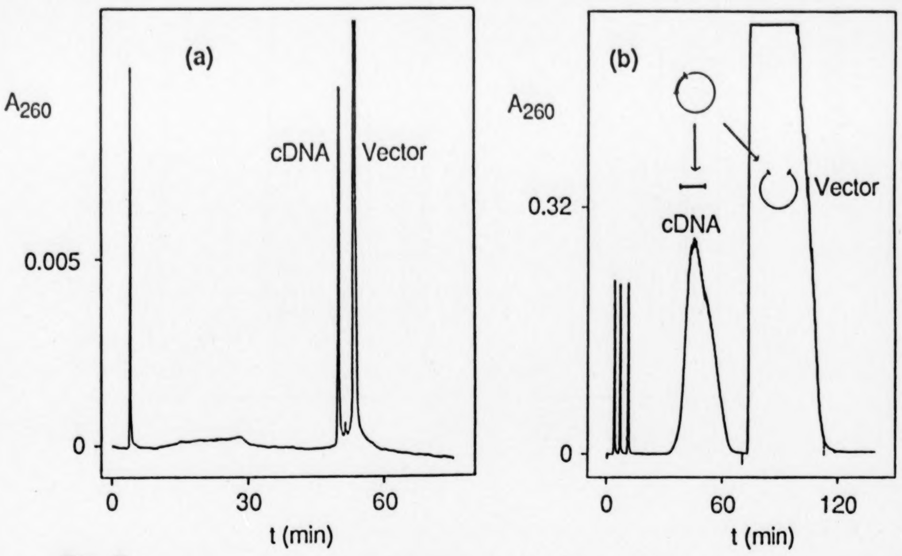

Fig. 7

Ion-exchange Separation of a DNA Insert from its Plasmid Vector.

The cleavage of plasmid pRH 101 with the restriction enzyme *Bam HI* resulted in the cDNA of PSTV (358 bp) and the plasmid vector pVH 27 (3739 bp).

(a) analytical chromatogram: 5 μg DNA; column, Nucleogen-DEAE 4000-10, 125 × 10 mm; flow rate, 2 mL/min; pressure, 27 bar; temperature, 23 °C; linear gradient, 500 mM to 1200 mM potassium chloride in 70 min (10 mM/min) in 6M urea-20 mM potassium phosphate (pH 6.7).

(b) preparative chromatogram: 7 mg DNA; column as in (a); flow rate, 2.25 mL/min; pressure, 24 bar; temperature, 23 °C; linear gradient, 840 mM to 1200 mM potassium chloride in 360 min (1 mM/min) in 6M urea-20 mM potassium phosphate (pH 6.7). Reprinted with permission from Ref. [24].

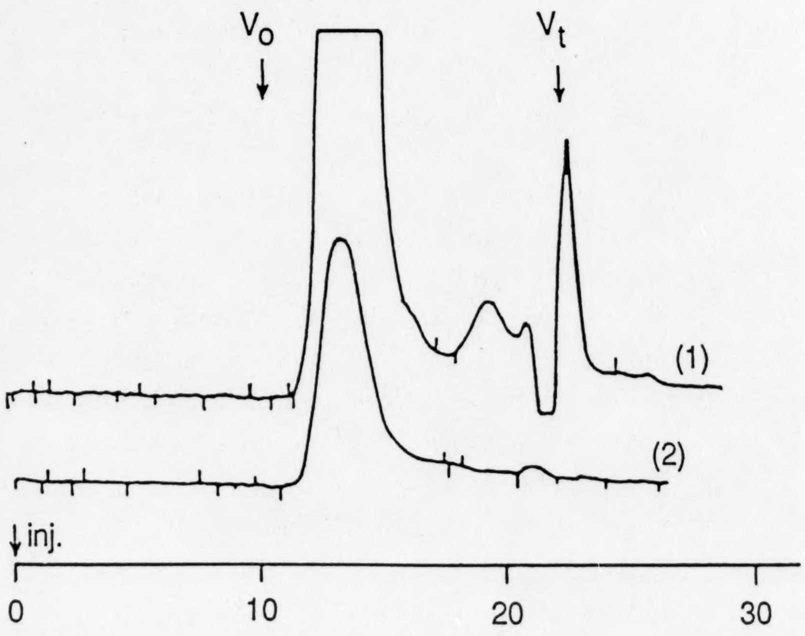

Fig. 6

SEC Elution Profiles of Viruses.

(1) adenovirus; (2) vesicular stomatitus virus; columns, one ea. of 30 × 0.75 cm, 17 μm, TSK G5000PW and G6000PW; mobile phase, 145 mM sodium chloride, 10 mM Na-HEPES (4-(2-hydroxyethyl)-1-piperazine ethanesulfonic acid), pH 7.4, 0.02% sodium azide; flow rate, 0.27 mL/min; sample volume, 50 μL; detector, 254 nm. Reprinted with permission from Ref. [22].

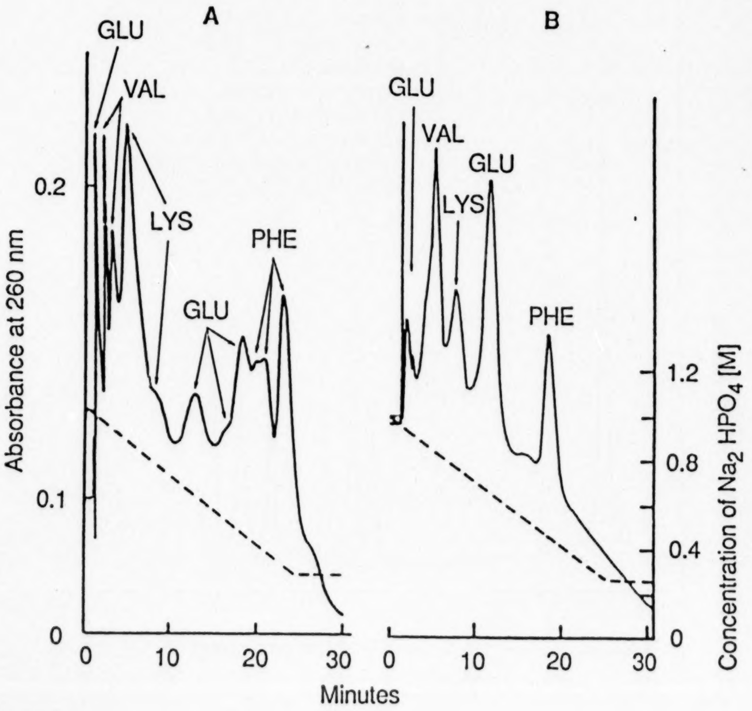

Fig. 8

Hydrodynamic Interaction Chromatography Separation of t-RNA's. Column, 100 × 4.6 mm, (A) poly(ethylene glycol) 400 and (B) poly(ethylene glycol) 4000; flow rate, 1 mL/min; temperature, 25 °C; linear gradient in 25 min from 1.0 to 0.25M phosphate buffer, pH 6.3. Three-letter code represents the amino acid transferred by the particular t-RNA. Reprinted with permission from Ref. [30].

HIC separations can be extended to much larger molecules by using supports with wider pores. HIC may be a preferred HPLC method for separating very large biomacromolecules that need a relatively gentle interactive retention process.

Trends in Particle Technology

What is the ultimate limit of molecular weight range that might be attained with HPLC separations? What is the limit of the particle sizes that can be used to speed up separations of macromolecules – 2 μm, 1 μm, 0.5 μm? And, what is the magnitude of the problems associated with such effects as shear degradation of the macromolecule, mobile phase disturbances that influence retention, packing bed irregularities, extra-column effects, column and detector plugging, etc.? Several practical considerations pertaining to the SEC of synthetic polymers have been discussed by Engelhardt and Ahr [31]. Initially, many workers believed that columns of < 3-μm particles might not be usable for practical separations because of difficulties in packing columns, problems with column blockage during use, changes in column performance, etc. However, recent work with columns of very small particles has shown that with proper experimental care, these problems are not difficult to overcome. It can be predicted that columns of < 3-μm particles will become relatively commonplace as experience and particle availability increases.

Theoretical aspects of some of the above questions have also been addressed for bioseparations [3, 32]. Separations of certain materials (e.g., globular proteins) up to at least 10^6 molecular weight may be accomplished with particles as small as 0.5 μm without encountering serious problems with operating conditions (although separations of compounds with molecular weights of $< 10^5$ on these columns would probably not be practical because of pressure limitations encountered when operating the column at the high flow rate required). In terms of shear degradation, it has been calculated that random-coil macromolecules at least as large as 2×10^6 MW might be successfully separated with columns of 0.5 μm particles without serious difficulty [3]. However, the shear imposed by flow in packed columns ultimately will limit the upper molecular weight separation range of fragile macromolecules, and other separation methods will be required for these species.

The trend toward using smaller porous particles for faster separation of macromolecules is also ultimately limited by the fact that, with shrinking particle sizes, the pore diameter becomes a significant fraction of the particle diameter. Useful silica-based packings with particle/pore diameter ratios of about 17 have been reported [16]. These 6-μm particles with 3500 Å pores allowed the SEC separation of random-coil polymers with MW up to 10^7. This particle configuration may represent a practical limit for this type of packing material. Porous particles with particle/pore diameter ratios of <15 are not only difficult to prepare, but they also lack the structural integrity to be useful for HPLC applications. In addition, as the pore diameter becomes a significant fraction of the interparticle diameter, convective flow could occur within the particle to produce a change in the basic retention process with changes in column flow rate [3].

Thus, 1-μm particles with ~500 Å pores may be a practical limit for macromolecular separations requiring a porous packing structure (e.g., SEC). In this case, the pore structure would limit access to molecules of no more than about 10^6 molecular weight to the interior of the particle. The solid microparticles discussed in the previous section may be the functional answer to very fast separations with particles of <1-μm diameter. For example, the diameter of interparticle pores formed in a random-packed bed of 1-μm non-porous, spherical particles would be about 5000 Å. Such a bed should have interesting possibilities as a hydrodynamic chromatography column for the rapid separation of both polymers and biomacromolecules – somewhat of a packed bed analogy to the very small capillaries used for hydrodynamic chromatography by Tijssen *et al.* [32a]. In contrast to SEC, the mass-transfer-limiting stagnant mobile phase would not be present in this packed-bed hydrodynamic column; solute bands would be very sharp, so that the signal/noise ratio and solute detectability would be high. Careful and systematic experiments are now required to define the practical limitations presented by molecular weight and by the configurational aspects of biomacromolecules.

New Silica Support and Bonded-Phase Technology

The nature of the silica support used in column HPLC has a strong influence on the quality of separations that can be made. Bonded-phase columns made from certain silicas exhibit especially poor properties for separating basic compounds [33]. These supports strongly retain basic molecules, usually with badly tailing peaks. To use such packings, basic additives or modifiers must be placed in the mobile phase before successful chromatography of these components can be performed. However, other silica supports demonstrate superior properties for the chromatography of basic components, and packings of these supports are especially useful for separating proteins and other macromolecules [34]. The difference between "bad" (Type A) and "good" (Type B) silica supports can be simplistically represented by the structures in Fig. 9. Spectroscopic and chromatographic evidence suggest that Type A silicas have a relatively high concentration of free or non-hydrogen-bonded surface silanol (Si-OH) groups. These Si-OH groups exhibit the acidic characteristics that are deleterious to the chromatography of basic substances [33]. This effect is heightened by an incomplete hydroxylation of the silica with surface silanol concentrations of less than the theoretical 8 μmol/m^2. The inhomogeneous distribution of the silanol groups on the silica surface also may contribute to undesirable chromatographic properties [33].

On the other hand, Type B silicas exhibit excellent properties for the separation of basic compounds. Such silicas are characterized by a large surface population of homogeneously-dispersed, hydrogen-bonded silanols, with few free or unbonded silanols in evidence [33]. Type B silicas are fully hydroxylated to a surface population of 8 μmol silanol groups/m^2. Some Type B silicas can be converted into

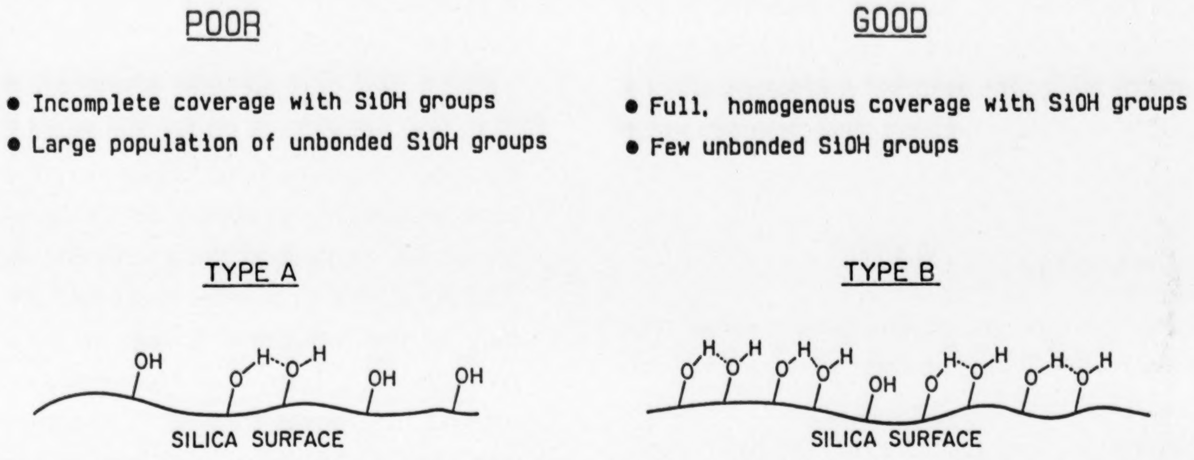
POOR
• Incomplete coverage with SiOH groups
• Large population of unbonded SiOH groups
GOOD
• Full, homogenous coverage with SiOH groups
• Few unbonded SiOH groups
TYPE A
OH
O
H
O
H
OH
OH
SILICA SURFACE
TYPE B
O
H
O
H
OH
SILICA SURFACE

Fig. 9
Surface of Silica Chromatographic Supports.

"bad" Type A silicas by heating at high temperatures [33]. More importantly, however, Type A silica that has been prepared with a high-temperature procedure can be transformed into the desirable Type B silica by rehydroxylation with certain activators [35]. These transformed silicas maintain the advantage of structural strength resulting from high-temperature sintering. Another feature of Type B silicas is the improved stability of reversed-phase packings made from these supports compared to the analogous packings made from more acidic Type A materials [33,35]. This increased stability is especially important in separations where aggressive mobile phases are used (e.g., separation of proteins in mobile phases with 0.1% trifluoroacetic acid, pH 2).

Even with Type B silicas as supports, the widely utilized monomeric bonded-phase packings for reversed-phase chromatography are not stable in certain chromatographic environments. For example, Fig. 10 shows the decrease in k' for tryptophan on a column of dimethyloctylsilane-modified silica packing over the course of 13 hours operated at 50 °C with a methanol/pH 2.1 phosphoric acid (40:60) mobile phase [37]. The decrease in k' from an initial value of 7.1 to a final value of 6.2 is unacceptable for many practical analyses. With use, especially in aqueous mobile phases at pH <3, such reversed-phase packings often undergo significant hydrolytic degradation, with loss of a significant fraction of the bonded phase from the column and a simultaneous decrease in retention and separation efficiency [36]. A particularly undesirable feature is that the degradation products elute from the column to complicate detection and to contaminate any fractions collected from the separation (the latter being particularly undesirable in preparative chromatography).

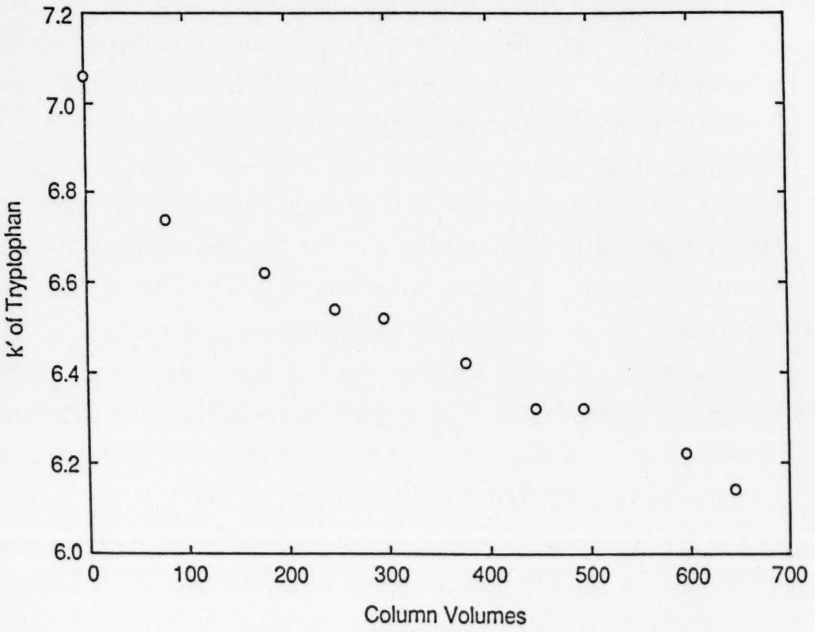

Fig. 10
Degradation of C_8 Reversed-Phase Column with Use.
Loss of k' for tryptophan; column, 25 × 0.46 cm; mobile phase, methanol-pH 2.1 phosphoric acid (40:60); temperature, 50 °C; flow rate, 2.0 mL/min. Reprinted with permission from Ref. [37].

As a result of such problems, other methods of preparing more stable, efficient bonded-phase packings now have been developed. In addition to the widely-used monomeric dimethylsilane reactions with silica (Fig. 11A), reversed-phase packings have been prepared with thin, polymerized stationary phases. These polymerized phases can be covalently attached to the substrate particle (Fig. 11B) or mechanically held in place around the particle by extensive cross-linking (Fig. 11C) [38]. Such packings often exhibit good column efficiency, but sometimes lack the level of stability that is desired for long-term, reproducible separations, particularly when aggressive mobile phases and higher operating temperatures are used. Retention times be may relatively stable with some polymerized phases because renewed ligand surfaces form as hydrolytic degradation proceeds at the outer layer of the multilayered polymer structure. However, degradation products may still elute from the column and contaminate collected fractions.

To address the shortcomings of existing packings, new silane chemistry has been developed to produce very stable, efficient, covalently-bound stationary phases for all forms of HPLC. Two different approaches have been devised: (1) use of "bidentate" silanes [39, 40], and, (2) sterically protecting the labile silane-silica covalent bond with a special functionality [41, 42]. The chemistry of the bidentate silanes is illustrated in Fig. 12A. A bidentate silane containing at least two silicon atoms bridged by spacer groups is attached to the fully hydroxylated silica.

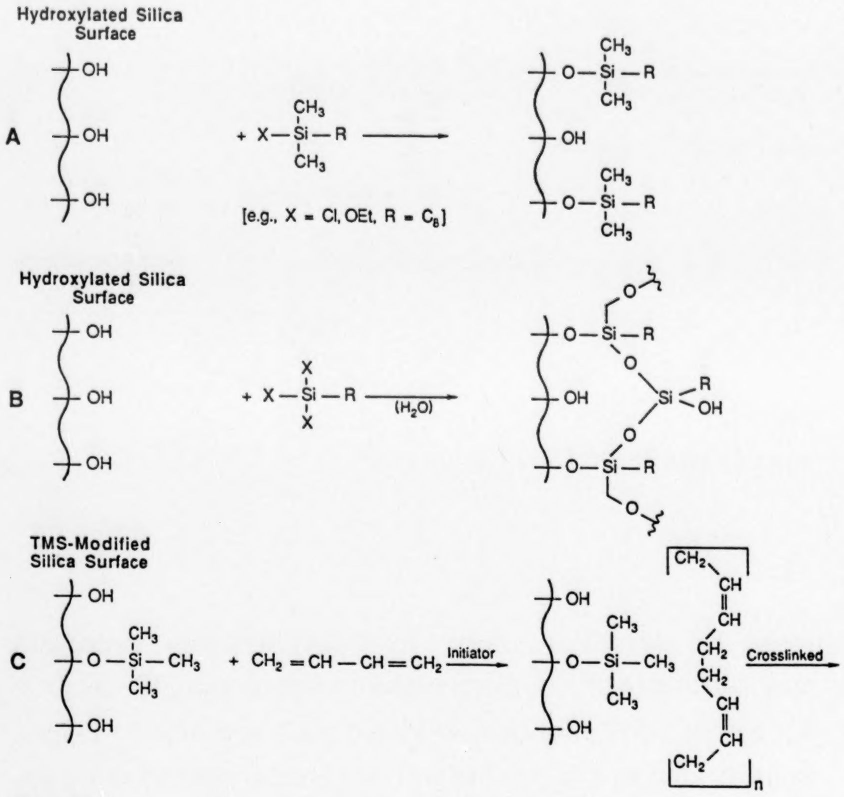
Hydroxylated Silica Surface
A
[e.g., X = Cl, OEt, R = C$_8$]
Hydroxylated Silica Surface
B
(H$_2$O)
TMS-Modified Silica Surface
C
Initiator
Crosslinked

Fig. 11

Preparation of Stationary Phases on Silica Support.

(A) Reaction of dimethylsilanes with silanols to form monofunctional bonded phase.

(B) Reaction of lightly polymerized tri- (and/or di-) functional silanes with silanols.

(C) Polymerization of alkenes on trimethylsilyl-modified silica surface.

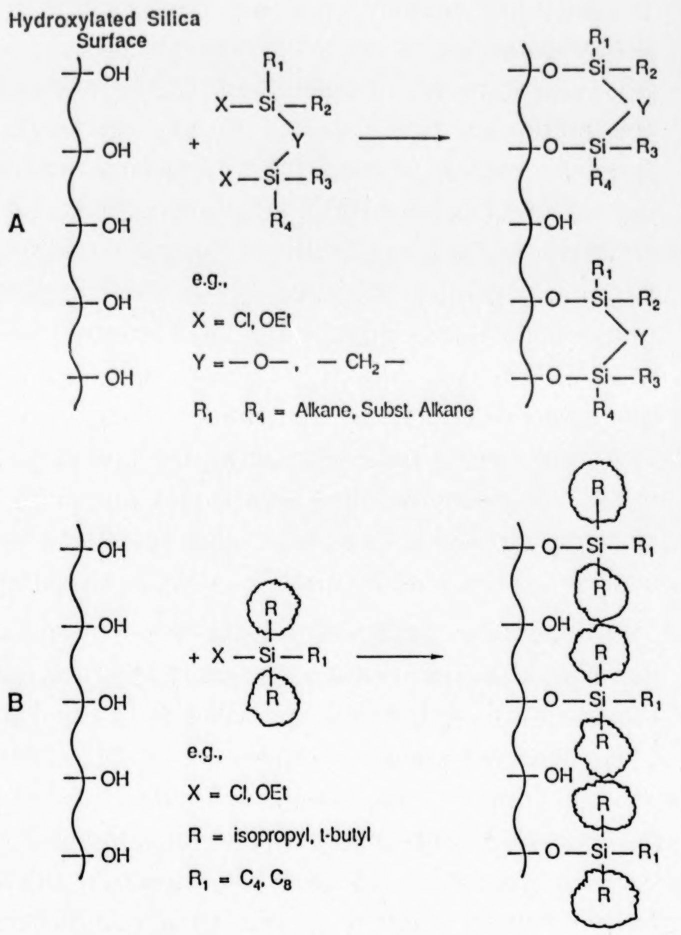

Fig. 12

Preparation of Stable Bonded Phases.

This bidentate silane requires that at least a seven-membered ring system be formed by the silane and the atoms to which it is covalently attached on the substrate surface. The bridge functionality (Y) and the R-groups (Fig. 12A) of the structure can assume a wide range of structures depending on the use of the bonded phase. By properly selecting the bridge group (Y), the distance between the reactive groups (X) on the bidentate silane can be adjusted to closely match the distance between reactive groups on the substrate surface. This feature permits a higher level of coverage (based on carbon content) by the bidentate silane than is achievable with analogous monomeric silanes. Without sacrificing chromatographic efficiency, this bidentate attachment provides substantially improved stability of bonded phases compared to those prepared by conventional monofunctional silane reactions.

A second approach for stabilizing bonded phase packings involves the use of a covalently-bonded monofunctional silane that contains sterically-protecting groups attached to the silicon atom of the silane. An example of this chemistry is shown in Fig. 12B. In this case the monofunctional silane contains two sterically-protecting groups, R, and a group, R$_1$, that imparts the desired chromatographic qualities to the bonded phase. The tightly-compacted, relatively bulky R groups effectively shield the hydrolytically-labile linkage that connects the silane to the support (e.g., -Si-O-Si-, when covalently bonded to silica), creating a stationary phase that is substantially more resistant to hydrolytic degradation than are stationary phases prepared from monofunctional silanes.

The increased stability of packings made by these new silane bonding chemistries is illustrated by the data in Fig. 13. To obtain these data, k′ measurements were made on columns over a four-day test period with a neutral com-

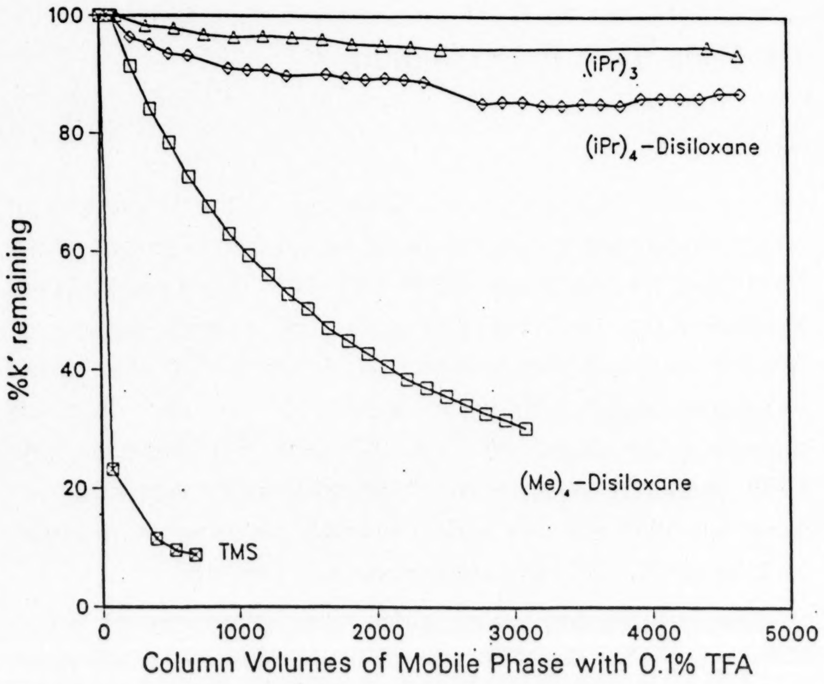

Fig. 13

Degradation of Bonded-Phase Packings.

Columns, 15 × 0.46 cm; k′ measurements with phenylheptane, using mobile phase of 1:1 acetonitrile/water with 0.1% trifluoroacetic acid, pH ~2; sample, 10 μL containing 1 μg of phenylheptane; with alternate gradient elution runs from 0–100% acetonitrile (with 0.1% TFA) in 80 min, followed by re-equilibration.

pound (phenylheptane) using a mobile phase of 1:1 acetonitrile-water with 0.1% trifluoroacetic acid (TFA) (pH ~2). Phenylheptane was chosen to probe the hydrophobicity of the stationary phase caused by the immobilized silanes. Between each k′ measurement, a gradient elution run was carried out from 0–100% acetonitrile (with 0.1% TFA) to simulate the harsher conditions typically used for separating peptide or protein mixtures. Under these aggressive mobile phase conditions, the column of trimethylsilane-modified silica (TMS) was quickly degraded, as noted by the sharp decrease in the % of remaining k′ for phenylheptane retention on the packing. (Under the test conditions used, the k′ for phenylheptane approaches zero with no organic stationary phase.) This result also correlated with carbon analyses of the packing material prior to and after the tests.

The bidentate tetramethyldisiloxane column in Fig. 13 demonstrated significantly increased stability, even though the trimethyl ligand was the same as in the TMS packing. This increased stability results solely from the bidentate configuration of the silane. A column of tetraisopropyldisiloxane demonstrated a further large increase in stability, showing almost no change in retention over the test period. This increased stability is due to a combination of two effects: bidentate attachment and steric protection from the bulky isopropyl groups.

However, data on the triisopropylsilane column in Fig. 13 clearly show that the larger contribution to stability for the tetraisopropyldisiloxane packing is the steric protection provided by the isopropyl groups, since the triisopropylsilane ligand has no bidentate configuration. These and other data strongly suggest that appropriate steric protection is a very effective means of improving the stability of bonded-phase packings for chromatography (and for other uses), without compromising the performance or the convenience of familiar silane technology.

III Field Flow Fractionation

Background

In the mid-1960's, Prof. J.C. Giddings of the University of Utah introduced a new family of separation methods called field flow fractionation (FFF) [43, 44]. These methods are applicable to the characterization of a wide variety of soluble macromolecules and particulates in the broad molecular weight range of about 10^3 to 10^{12} (particle diameters of about 10^{-2} to $10^2\,\mu$m). Furthermore, the FFF methods permit the high-resolution separation of materials that are not easily handled by other techniques, such as HPLC, GC, and electrophoresis [45, 46].

In the intervening years since the inception of FFF, development of the FFF methods has been relatively slow. This slow development has variously been due to the lack of commercial equipment for the methods, to difficult technical problems, and, perhaps most important, to a relatively poor understanding of the ultimate potential of the methods. However, in recent years, interest has heightened, and several laboratories have begun to develop research activities and to demonstrate important applications for FFF, as reviewed in references [47–50].

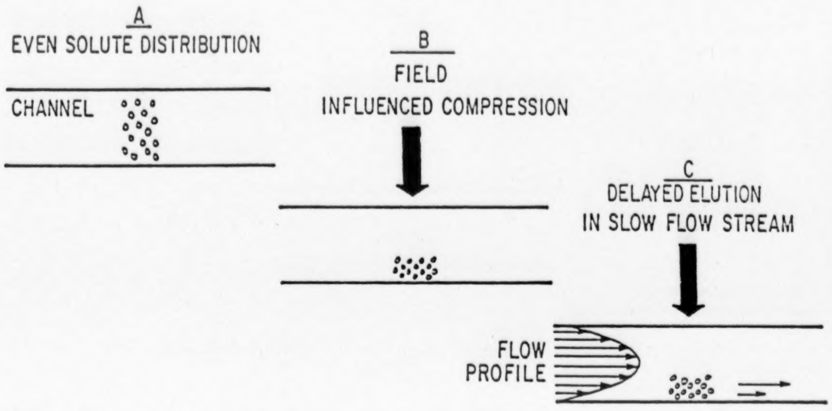

Fig. 14
Basic Steps of Field Flow Fractionation.

All of the FFF methods are based on a common principle, as illustrated in Fig. 14. Separations are performed in a thin, open channel. Upon injection, sample components are evenly distributed across the narrow, rectangular cross-section (Fig. 14A). Application of a force field (of many possible types) perpendicular to the channel causes these sample components to crowd towards one wall (Fig. 14B). Differential retention results from the redistribution of the sample components between fast and slow moving streams of the laminar flow profile generated across the liquid mobile phase flowing through the channel. Solvent and other low molecular weight components unaffected by the force field move downstream in the channel at the average velocity of the laminar flow stream. In contrast, larger sample components are forced close to the wall by the external force field and are carried downstream by the slower-moving streams near the wall; they lag behind and elute after the solvent (Fig. 14C).

To date, sedimentation-FFF (SdFFF) and thermal-FFF (TFFF) have received the most research attention, as suggested by the number of publications on various FFF methods (Fig. 15). Work on SdFFF has led the way,

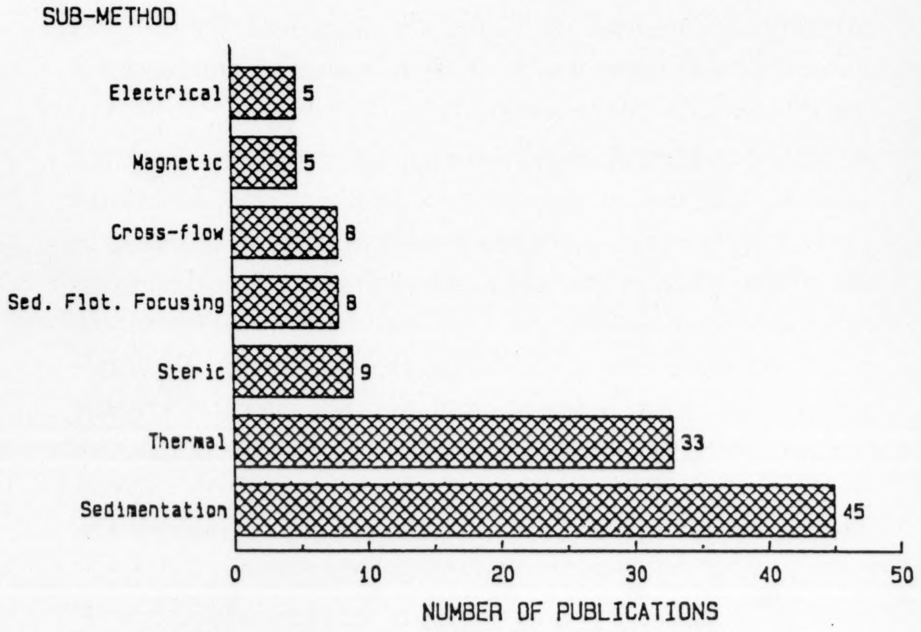

Fig. 15
FFF Publications by Subject.

primarily because of the high resolution of this method (Table I), the wide range of applicability (about 10^5 to 10^{10} molecular weight), and the total predictability of retention from the physical parameters of the sample components and the experimental conditions. TFFF has also received considerable attention, because of the relatively simple nature of the equipment, the high resolution, and the ability of the method to provide molecular weight information on fragile, high-molecular-weight polymers.

Sedimentation Field Flow Fractionation (SdFFF)

Progress in the development of FFF equipment and techniques has been most rapid for SdFFF. Equipment with force fields up to 100,000 gravities has now been developed [51], and force-field programming with computer software has been devised to assist in conveniently and accurately characterizing a wide variety of particulates and soluble macromolecules [52]. Commercial SdFFF equipment of this type is now available (DuPont), and this analytical method is positioned to make the level of impact that was originally predicted by Prof. Giddings.

For separations based on SdFFF, samples are injected into a thin, ribbon-like channel suspended in a centrifuge (Fig. 16A). With the mobile phase flow turned off, the channel is rotated in the centrifuge for a relaxation or pre-equilibration period, allowing sample species to be forced towards the wall regions. Sample particles that have a density greater than the mobile phase are forced towards the outer wall. Diffusion in opposition to the external force field causes the particles to establish a specific mean-layer thickness near the wall as a function of particle mass. In Fig. 16b, liquid mobile phase is then flowed continuously through the channel with a characteristic bullet-shaped or parabolic velocity profile. Movement of the larger particles towards the wall places them in regions of slower flow. Solvent and very small particles that are not influenced by the external force field are engaged by all flow streams and elute from the channel first (at one channel volume) as indicated in Fig. 16c. The mobile phase carries retained sample components at smaller average velocities through the channel for detection at the outlet (Fig. 16d). The resulting fractogram provides information on the masses of sample constituents via quantitative relationships describing SdFFF retention [53].

Early applications of SdFFF were largely concerned with particulate and colloidal systems (e.g., polymer latices, pigments, ceramics, etc.) that were difficult or impossible to characterize by other methods. With the newer SdFFF techniques and equipment, the quantitative particle-size distribution of particulates in the 0.005–1 µm range can be accurately and reproducibly determined. For example, Fig. 17 shows the particle-size analysis of a diamond dust sample by a time-delayed exponential-decay (TDE-SdFFF) procedure [52]. (In TDE-SdFFF, mobile-phase flow is initiated following sample injection and the initial force field is maintained constant for a time equal to tau. After this delay, the force field is allowed to decay exponentially with a time constant equal to tau. In the TDE-SdFFF mode of operation, a simple log-linear relationship is obtained

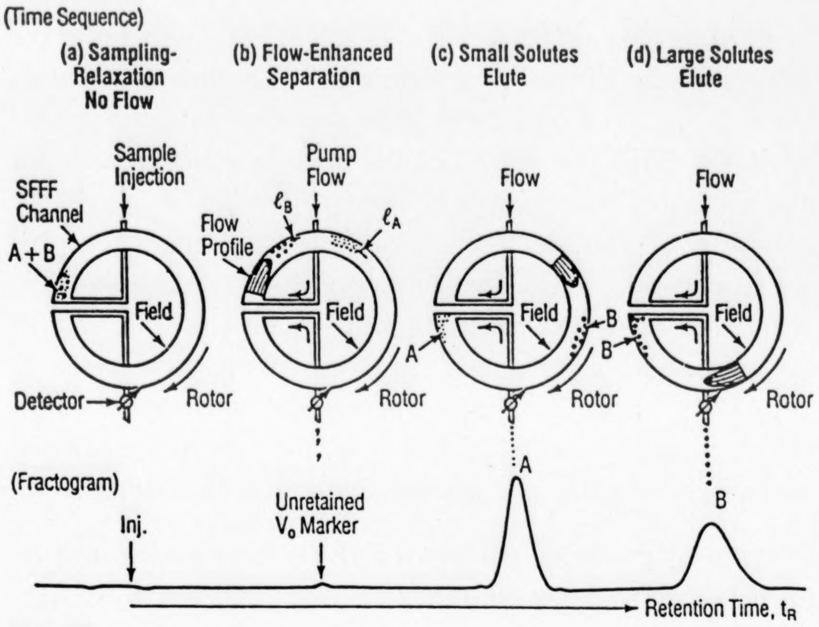

Fig. 16

Development of Sedimentation FFF Separation.

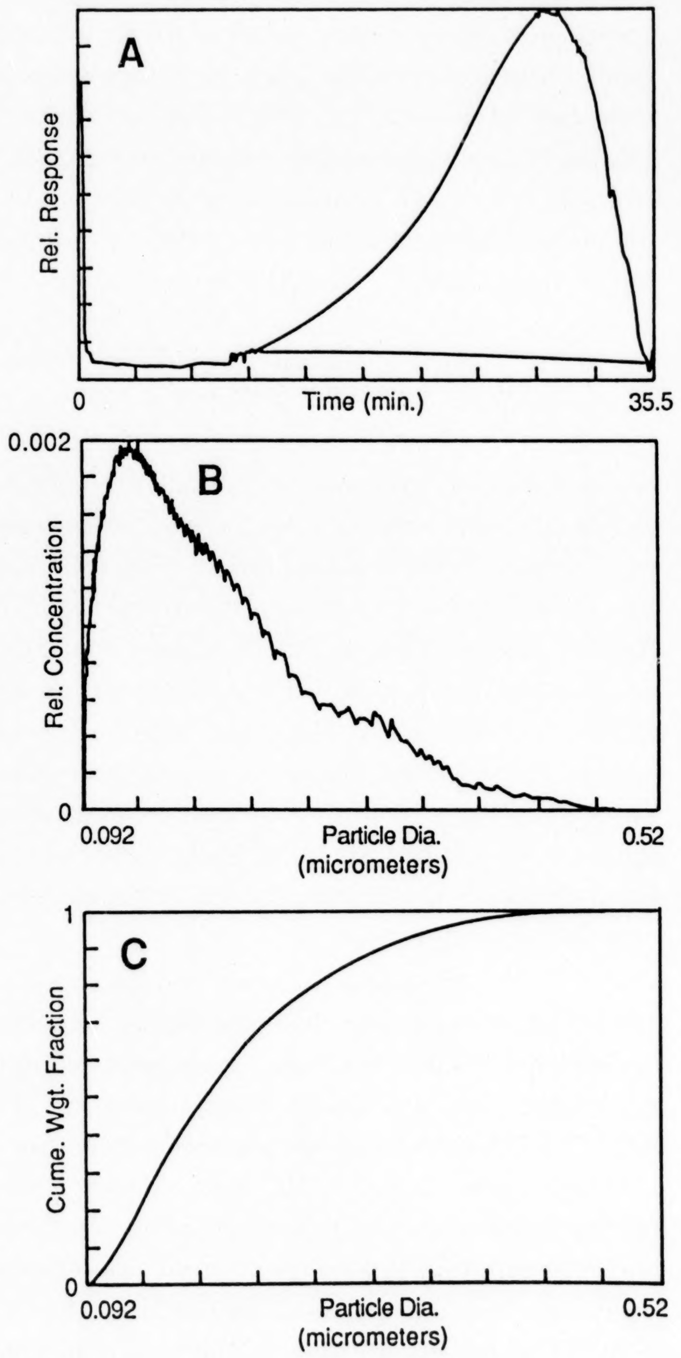

PARTICLE SIZE AVERAGES
(Micrometers)

Number	0.142	Weight	0.200
Surface	0.148	Volume	0.157
Sp Surface	0.175	Turbidity	0.229
		Median	0.182

Fig. 17

Particle-Size Distribution of Diamond Dust by TDE-SdFFF.

Channel, 254 µm; mobile phase, 0.1 % "Micro" detergent; flow rate, 6.0 mL/min; initial rotor speed, 2200 rpm; delay-decay constant, tau, 6.0 min; sample, 250 µL, of 0.1% solids in mobile phase; turbidimetric detector, 700 nm.

with both particle mass and size versus retention time; the programming of the force field allows samples with a very wide range of particle sizes to be analyzed in a convenient time [54, 55].) The output of the turbidimetric detector for the diamond dust sample is shown in Fig. 17A. Since the response of this detector is particle-size dependent, this signal can be transformed with known, quantitative light-scattering relationships to produce a plot of the relative concentration as a linear function of particle-diameter (Fig. 17B). Fig. 17C shows the cumulative-weight fraction vs. particle-diameter plot. Given at the left of Fig. 17 are various particle size averages calculated for this sample.

In spite of the great utility of SdFFF for a wide range of particle-size analyses of industrial interest, the most important applications for this method undoubtedly will be for the isolation and characterization of bioparticulates and large biomacromolecules. Many areas of biotechnology can use the inherent advantages of SdFFF: high resolution and speed, with the gentleness required for structurally-sensitive, labile biologicals ranging from very large proteins to whole cells (see review in Ref. [49]). The utility of SdFFF for soluble biomacromolecules is shown in Fig. 18A for a lysate from *E. coli* V517 containing various plasmids and other materials. This separation was carried out with an constant initial force field (~ 78,000 gravities) to first elute lower molecular weight proteins and RNA's. Various plasmids of increasing molecular weight then eluted in the molecular weight range of $1.5-2.9 \times 10^6$. After 225 minutes into the separation, the force field was exponentially decayed with a tau of 8 minutes to conveniently elute the highest molecular-weight plasmid in the sample. Gel electrophoresis of collected fractions from this separation (Fig. 18B) substantiated the identification and the purity of the isolated plasmids. Results such as those in Fig. 18 suggest that SdFFF can be quite useful for a wide variety of separation problems involving nucleic acids (e.g., the selective isolation of a desired recombinant vector of a particular size from the various products of a plasmid ligation experiment). Under optimum conditions, baseline resolution of non-interacting, equal-density components can be achieved that differ by only 20% in solute mass.

Many types of bioparticulates are also well-suited for SdFFF separation. For example, recent experiments with bovine and rabbit cartilage proteoglycans indicate that these materials are easily fractionated by TDE-SdFFF [56, 57]. The fern-like glycoprotein structure associated with aggregates ($0.2-2 \times 10^8$ daltons) that are responsible for the shock-absorbing properties of cartilage is completely unchanged during SdFFF separation. These aggregates are easily resolved and isolated from monomers ($2-4 \times 10^6$) (Fig. 19) whose concentrations increase with animal age or arthritic involvement.

SdFFF also shows promise as a superior method for fractionating and isolating subcellular organelles from both plants and animals. For example, subcellular fractions have been isolated by SdFFF from corn roots [58]. The various organelle components in a microsomal pellet (105,000 gravities for 1 hr.) from rat liver also have been fractionated, as shown in Fig. 20. The elution maxima for various components in this sample were identified by the SdFFF analysis of "purified" fractions obtained from a density-gradient centrifugation separation performed on a like sample [59]. In spite of the fact that the microsomal pellet is a very heterogeneous mixture of constituents (with densities ranging from about 0.8–1.3 g/cc and molecular weights of about 10^6-10^9), the survey SdFFF separation of Fig. 20 was performed with a resolution that is significantly higher than currently-used methods. The gentle nature of SdFFF separations is coupled with the ability to conveniently isolate high-purity components with excellent recovery. Such fractions often are ready for use without further treatment. These and other advantages make possible the prediction that SdFFF will find extensive use in the solution of certain biochemical problems for which there now are no answers. Additional research on the bioapplications of SdFFF are required to define the full potential and limitations of the method.

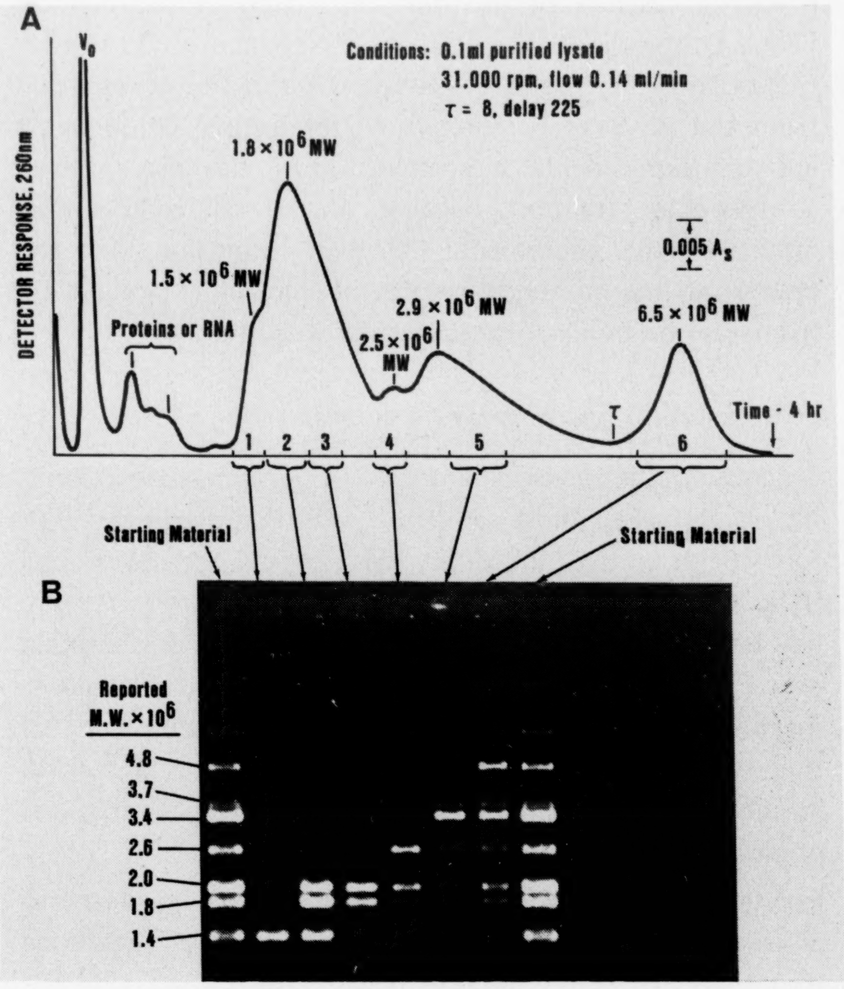

Fig. 18

SdFFF Separation of Plasmids from *E. Coli* V517.

Channel, 254 μm; 100 μL of purified lysate; mobile phase, 0.01 M Tris-0.01 M sodium chloride, pH 7.6; flow rate, 0.14 mL/min; initial rotor speed, 31,000 rpm; relax, 5.0 min; delay, 225 min; tau decay, 8.0 min. A: SdFFF fractogram; B: gel electrophoresis of collected fractions.

Thermal Field Flow Fractionation (TFFF)

As indicated in Fig. 15, TFFF has been the second most-researched of the FFF methods. This form of FFF has primarily been directed toward the characterization of synthetic, organic-soluble polymers (e.g., see [60, 61]), but the method also has potential for fractionating certain macromolecules in totally aqueous systems [62].

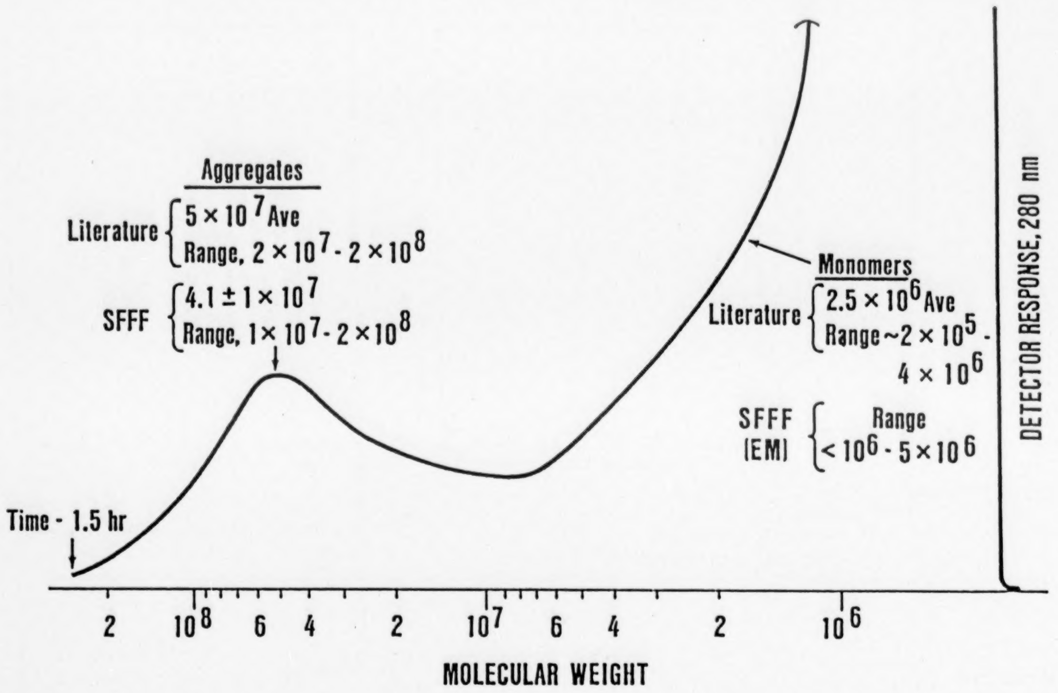

Fig. 19

TDE-SdFFF of Proteoglycans from Calf Cartilage.

Channel, 254 µm; sample, 500 µL of isolated suspension in mobile phase; mobile phase, 0.05 M sodium acetate–0.15 M sodium chloride; flow rate, 0.5 mL/min; initial rotor speed, 32,000 rpm; relax, 20 min; delay, 20.0 min; exponential decay constant tau, 12.0 min; detector, 280 nm.

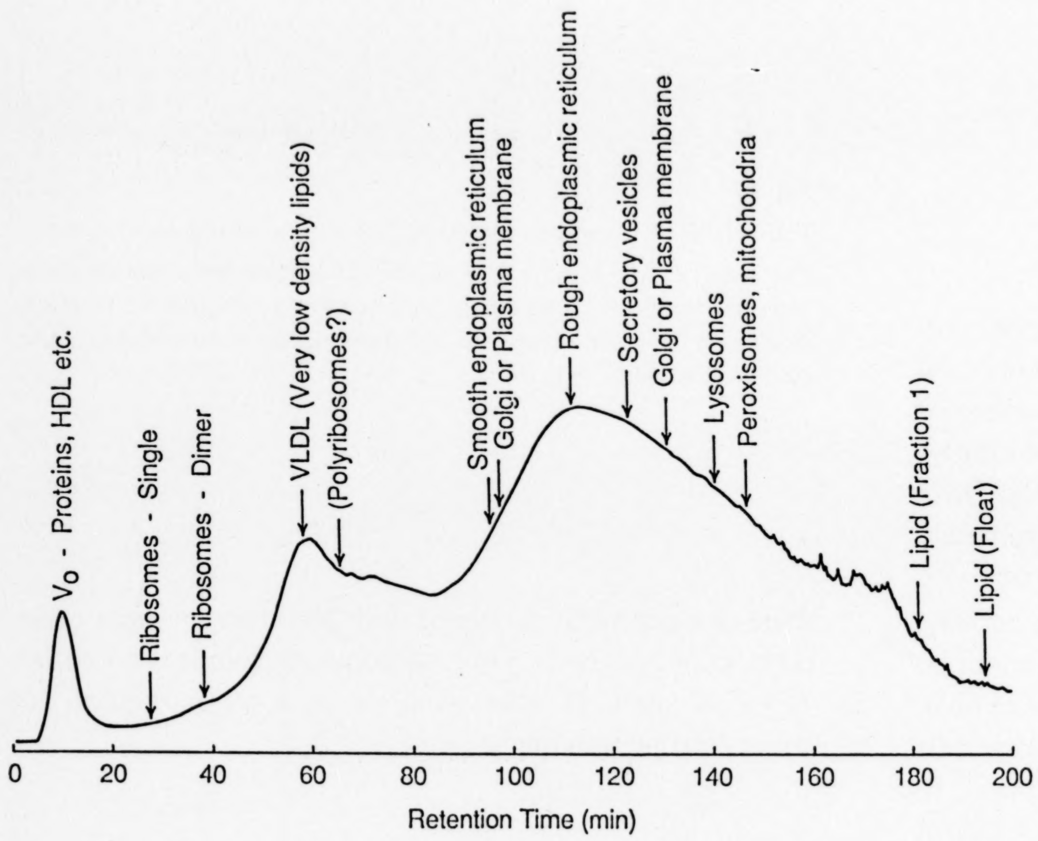

Fig. 20

TDE-SdFFF of Organelles in Microsomal Pellet from Rat Liver.

Channel, 254 µm; 50 µL of pellet re-suspended in mobile phase; mobile phase, 1 mM Tris, 0.25 M sucrose; flow rate, 0.2 mL/min; initial rotor speed, 32,000 rpm; relax, 20.0 min; delay-decay constant, tau, 15.0 min; detector, 280 nm, 0.1 AUFS.

In TFFF, analogous to SdFFF, separations are performed with a mobile phase flowing through a thin, highly-regular, open channel. However, with TFFF, retention of components results from applying a large thermal gradient across flat, parallel plates [63]. Although this method is thought to be based on the principle of thermal diffusion, the separation mechanism associated with this technique is not well understood. Therefore, the dependence of retention on polymer type is not yet predictable. Nevertheless, the unique characteristics of TFFF suggest that this method possesses several important features applicable to polymer characterization.

First, with time-delay, exponential-decay programming (TDE-TFFF), a plot of log MW vs. retention time is a linear relationship that provides a convenient and accurate calibration for molecular-weight-distribution measurements over a wide MW range [61]. Second, TFFF is capable of high resolution, under optimum conditions, this resolution can be five-fold greater than that of most size-exclusion (SEC or GPC) separations. Because of this higher resolution, the accuracy of molecular weight measurements is significantly improved; corrections for instrumental band broadening are usually unnecessary. With presently-available equipment, operating techniques, and hardware, polymer molecular-weight measurements with reproducibilities of 3% (1σ) or better have been demonstrated over long periods without the need for recalibration [64]. Fig. 21 shows the resolution of three poly(methylmethacrylate) standards in a TDE-TFFF separation used as part of a calibration procedure for this polymer. Resolution of each component is compromised in this programmed mode to permit a wide MW range to be covered in a single separation. Nevertheless, unit resolution can be achieved for about a 3-fold difference in MW under these particular operating conditions.

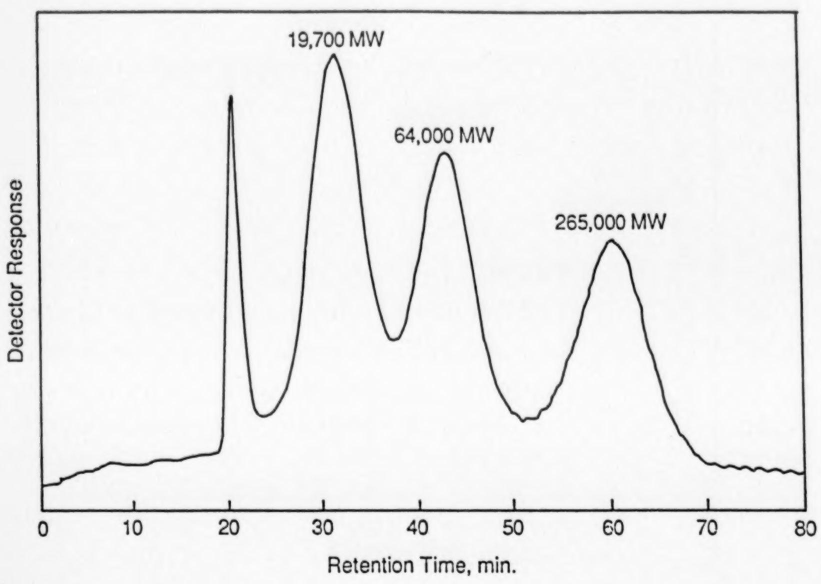

Fig. 21

TDE-TFFF Separation of Poly(methyl methacrylate) Standards. Channel, 127 μm; sample, 25 μL of 1 mg/mL ea. in dioxane, mobile phase, dioxane; flow rate, 0.10 mL/min; initial hot block, 90 °C; final hot block, 20 °C; cold block, 20 °C; delay-decay time constant, tau, 20.0 min; detector 215 nm.

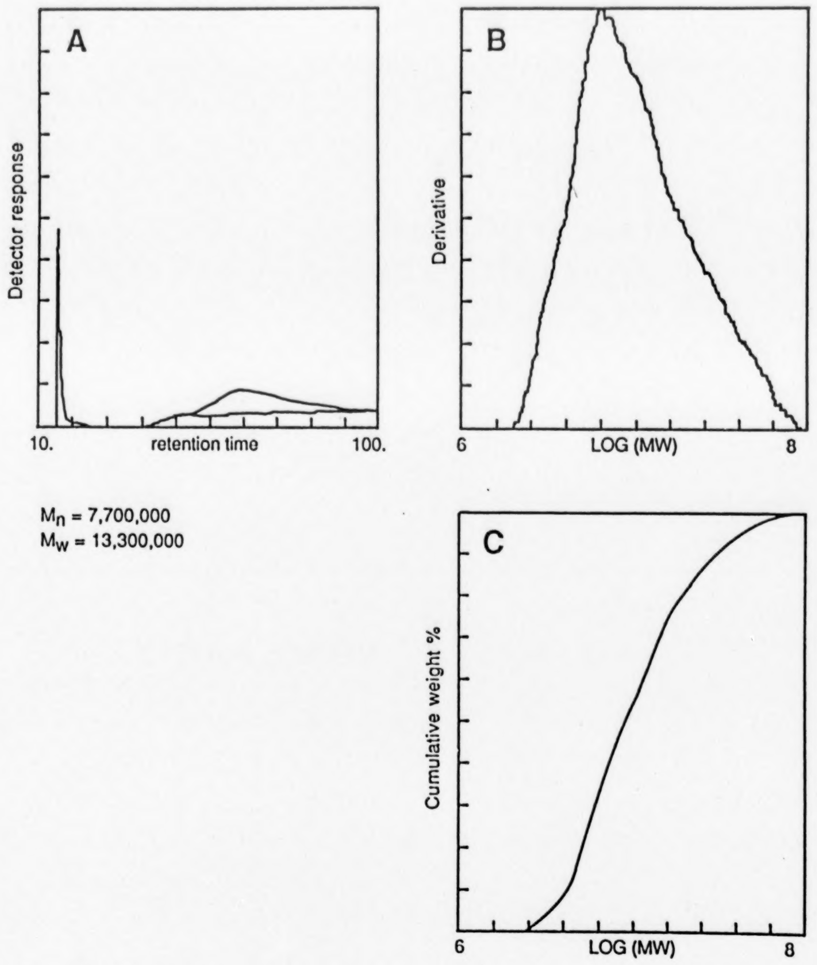

Fig. 22

TDE-TFFF of Very High Molecular Weight Experimental Polymer. Channel, 127 μm; sample, 100 μL, 0.0125% in heptane; mobile phase, heptane; flow rate, 0.15 mL/min; initial hot block, 50 °C; final hot block, 25 °C; cold block, 25 °C; delay-decay time constant, tau, 20.0 min; detector, RI.

The accuracy of the TDE-TFFF method basically is limited by the accuracy of MW values for the standards that are used for calibrating each polymer system. Good correlations between TDE-TFFF results and those attained by SEC and other methods have been found for a variety of commercial polymers. The results of these quantitative molecular-weight-distribution studies suggest that, with improved equipment, the TDE-TFFF method is ultimately capable of MW measurements with reproducibilities of 1–2%.

Finally, the TFFF method is well-suited for characterizing very high-molecular-weight, fragile polymers that cannot be analyzed accurately by existing methods. For example, Fig. 22 shows the fractogram of a very high-molecular-weight, fragile, experimental polymer. Attempts to characterize this polymer by SEC were unsuccessful because of total exclusion of a fraction of the sample from a column packing with the largest pores available, severe problems with shear of the polymer in the SEC columns also were experienced. Some samples of this polymer have exhibited weight-average molecular weight values in excess of 15×10^6, with high-molecular weight "tails" eluting at greater than 50×10^6 MW.

As a result of the inherent advantages of this FFF method, an obvious question is: "Will TFFF ultimately supplant SEC as the prime method for characterizing polymer molecular weights?" The proposed answer is that both methods will be used; the better method will be utilized for the specific problem. Low MW polymers will likely require SEC; TFFF generally is less suited because of difficulties in resolving lightly-retained, low MW materials from the channel dead-volume (V_0) peak. Conversely, TFFF is especially suited for characterizing high-MW polymers; SEC has severe problems in this area because of difficulties in preparing column packings with pores large enough to allow the required permeation by the polymer. In addition, there are potential problems with the shear of large molecules in packed beds. Thus, based on its unique capabilities, TFFF is likely to take its place as a major method for characterizing polymers.

IV Electrophoresis

Introduction

As surmised from the introduction, conventional electrophoresis has become a mature technology. Typically, electrophoretic separations are characterized as slow, labor-intensive techniques. However, several developing technologies promise to increase the utility of electrophoresis by making the technique more instrument-oriented, by extending the molecular weight range of separations, and by increasing the peak capacity to values that could never be achieved in chromatographic separations. These new electrophoretic methods will be discussed below.

2D Electrophoresis

Because of the need to separate the components of very complex biological mixtures, bioscientists have developed multidimensional electrophoretic separations with very high peak capacities to accommodate the large number of proteins in such mixtures. Numerous two-dimensional (2D) electrophoretic separation techniques, including 2D SDS-PAGE (sodium dodecyl sulfate – polyacrylamide gel electrophoresis) [65] separations, have been reported. However, the most powerful multidimensional method, which uses two electrophoretic techniques that separate proteins by fundamentally different mechanisms, combines an isoelectric focusing (IEF) first-dimension separation with SDS-PAGE for the second-dimension separation [66]. The first-dimension separates the proteins on the basis of isoelectric point (pI) values; the separation is carried out in a pH gradient (e.g., pH 3 to 10) which has been established by carrier ampholytes in a high porosity gel, where sieving effects in the pores are minimal and thus the separation is based solely on the charge on the proteins. After the separation, the IEF gel (usually a tube gel) is placed in the "application well" of an SDS-PAGE slab gel. This second gel may be of a constant or gradient acrylamide concentration, the latter providing a pore-size gradient in the gel and thus improving separation when proteins of a wide MW range are to be resolved. The second-dimension gel usually contains the surfactant SDS, and the sample in the first-dimension gel is usually treated with this surfactant prior to the second-dimension separation. SDS interacts with proteins in a constant ratio (~ 1.4 g SDS per g protein), and imparts a constant negative charge per mass of protein. Thus, charge differences between various types of proteins are minimized and separation in the second dimension can occur solely on the basis of molecular weight due to sieving through the pores of the gel. After the second-dimension separation, the bands are visualized by staining the proteins, or by autoradiography (if the proteins were radiolabeled prior to separation).

Several problems have been addressed to make 2D electrophoresis useful for practicing researchers. The major obstacle that confronted users of the technique in the early days was a lack of reproducibility in the separations, not only between workers in different laboratories, but also day-to-day variations in the same lab. This lack of reproducibility arose from the fact that execution of a 2D separation is complex, requiring a large number of tedious, labor-intensive manipulations and a large number of chemical reagents. Anderson and Anderson [67, 68] recognized these difficulties and made significant progress toward standardization of separations by developing the ISO-DALT system, which permits simultaneous casting and running of 20 IEF gels or 10 SDS-PAGE gradient gels. Other sources of variability, including the quality of ampholytes, SDS, and acrylamide used in gel preparation, still plague 2D separations.

Another major obstacle was the detection of the protein bands once the separation had been achieved. The difficulty lies in the fact that for complex samples of biological interest, proteins are present in relative concentrations that differ by several orders of magnitude. Thus, if sufficient sample is applied to the gel to permit easy visualization of the minor components, the gel is overloaded by the major components in the sample. It is not possible to visualize all of the components of a complex mixture in a single detection step. Staining of the proteins with Coomassie Blue dye visualizes only the major components of a complex biological matrix. Even the most sensitive detection method (autoradiography) requires several exposures of the gel since the dynamic range of x-ray film does not cover the orders of magnitude necessary to quantitate all of the protein bands. (In addition, this detection method requires that the proteins be radioactive.) Development of silver-staining techniques [69], whereby protein bands are visualized by adsorption and reduction of silver ions, has somewhat alleviated these difficulties. Detection limits have been lowered to the subnanogram range, though the dynamic range of the technique is still somewhat limited. Once the proteins have been visualized, computerized gel scanners [70] which locate, quantitate, identify, and compare protein bands on the gel, greatly facilitate the application of 2D electrophoresis.

Numerous applications of 2D electrophoresis have been reported. The first applications were for analysis of protein patterns in bacteria [66] (Fig. 23). Other applications include screening for marker proteins for diagnosis of genetic diseases [71, 72]. Perhaps the most ambitious program is the development of the Human Protein Index as part of the Molecular Anatomy Program of Anderson and Anderson [73]. The program proposes to catalogue the bands arising from the 30,000–50,000 proteins in the

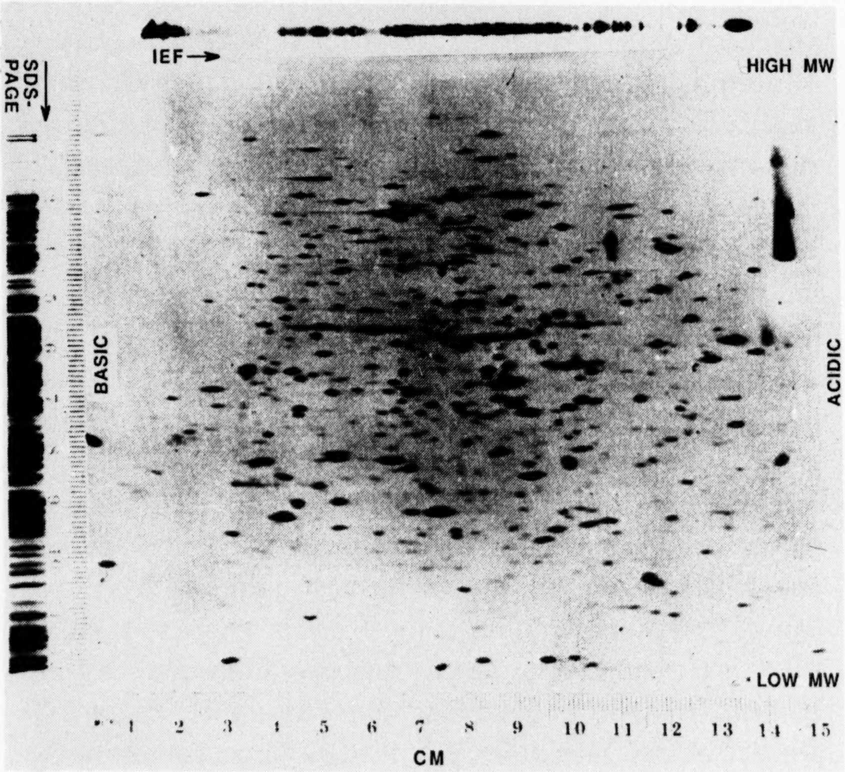

Fig. 23

2D Electrophoretic Separation of *Escherichia coli* Proteins.

E. coli was grown in a broth of ^{14}C amino acids, lysed by sonication, and treated with DNase and RNase. Twenty-five microliters of sample (180,000 counts per minute) containing 10 μg of protein were loaded onto the IEF tube gel (first dimension) and run at 400 V for 12 hr followed by 800 V for 1 hr. The first-dimension IEF separation was then treated for 30 minutes with SDS denaturation buffer prior to loading into the slot in the second-dimension SDS-PAGE gel. The second-dimension gel was a 10.0–14.0% exponential acrylamide gradient gel. The second-dimension separation was run at a constant current of 20 mA for 5 hr. Following visualization of the major bands by Coomassie staining, the gel was then dried and autoradiographed to visualize the separation shown. Adapted from Reference [66] with permission.

human body to facilitate computerized disease diagnosis by matching location, intensity, and variation of the protein bands on 2D gels with specific disease states in the human organism.

Pulsed-Field DNA Electrophoresis

With the increased activity in the fields of molecular biology and genetics, the study of the composition and structure of the genomic DNA of organisms has been increased substantially. Since genomic DNA is a large, fragile polymer (e.g., human genomic DNA consists of ~300 million base pairs) of essentially constant composition, separation of large fragments of DNA has been difficult to achieve.

Separation of DNA fragments has conventionally been carried out in agarose gels, where fragments of DNA ranging from 0.10 to 50 kilobase (Kbp) pairs long can be separated on gels of 0.3 to 2.0% agarose. However, resolution of the larger fragments (20–50 Kbp) is poor because of the log dependence of electrophoretic mobility on molecular weight). Fragments (up to 750 Kbp) can be only partially resolved on very porous (0.1 to 0.5% agarose) gels at very low voltages for long periods of time [74]. Very large fragments (> 750 Kbp) cannot be separated at all because the sieving properties of the agarose gel become unimportant once the size of the molecule exceeds the size of the largest gel pores.

The loss of resolution for the larger DNA fragments arises from the fact that when subjected to an electric field, DNA fragments relax from their normally supercoiled structure to form elongated linear strands (Fig. 24). These elongated strands then migrate through the pores of the agarose gels by a mechanism called reptation [75], analogous to a snake moving through tall grass. For migration governed by this mechanism, mobility of the DNA fragments is essentially independent of molecular weight, and fragments of different sizes travel with the same velocity.

This limitation, which presents an obstacle to separation of biologically important fragments of DNA (e.g., intact chromosomes), has been overcome by introducing a secondary phenomenon that reinstates the size dependence to the separation. This phenomenon is derived from a viscoelastic technique [76], in which the size of DNA fragments can be determined by imposing an electric field to elongate them and then measuring the time required for relaxation of the DNA to its original supercoiled structure. The rate of elongation and relaxation is dependent upon the size of the DNA molecule. This size-dependent phenomenon was introduced into the separation of large fragments of DNA; separations are based on the rate at which DNA molecules alter their shape inside the matrix of the gel. To accomplish this, instead of imposing a constant electric field across the gel (as in conventional electrophoresis), the electric field is pulsed; voltage is applied across the gel for a period of time and then the field is switched off, allowing the elongated strands of DNA to partially relax to a semi-supercoiled structure (Fig. 24).

Alternatively, instead of using one set of electrodes as in conventional electrophoresis, two pairs of electrodes oriented at different angles across the gel can be used. The applied voltage is then alternated between these two pairs of electrodes at a predetermined frequency by a time-programmed power supply. Numerous arrangements of the electrodes are possible, with complementary electrode pairs being 90°, 120°, or 180° apart. (In the latter case, a single pair of electrodes is used and the imposed field is varied by inverting the voltage applied across these two electrodes.) Under these conditions, the mechanism underlying separation may be more complicated than the simplistic description given in Fig. 24, since the DNA molecules are forced to periodically alter their direction of travel through the gel when two pairs of electrodes are used.

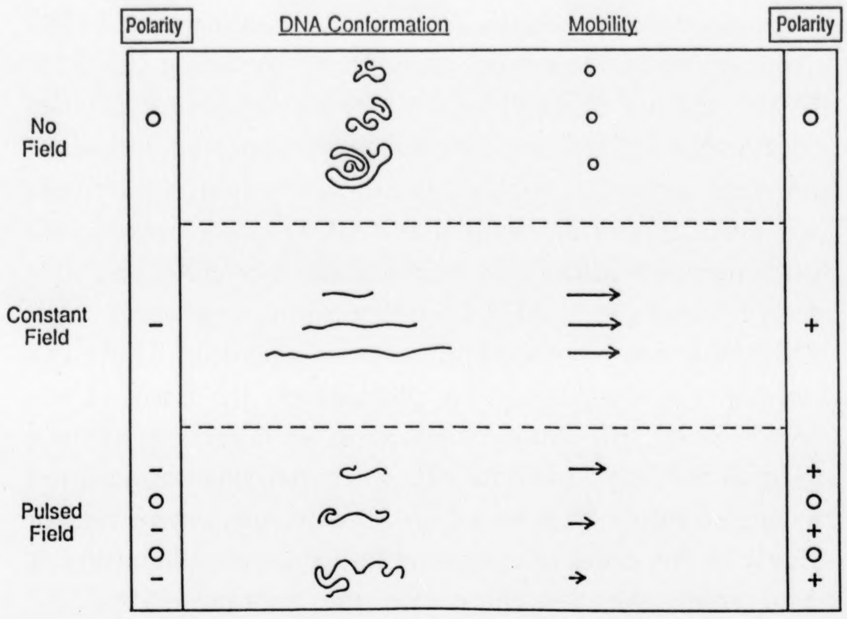

Fig. 24
Mechanism of DNA Separation in Pulsed-Field Electrophoresis.

The critical parameters in these pulsed-field techniques are the duration of the pulses applied at the electrodes and the time period allowed for DNA relaxation between pulses; if the actual relaxation time of the DNA is much greater than the time period allowed for relaxation (i.e., no field), the DNA molecules cease to respond to the variation in the electric field and the shape of the DNA becomes independent of molecular weight; no separation is achieved. However, if the time period approximates the relaxation time of the DNA molecule, the mobilities of the DNA's vary with molecular weight and separation can be obtained. Thus, under any given set of experimental conditions, a "window" of optimized resolution is attained for a group of similarly-sized DNA fragments; fragments much larger or smaller than these are not as well resolved as the fragments whose relaxation times approximate the time period when no field is applied to the gel. This limitation can be overcome to some extent by varying the length of the relaxation period during the course of the separation, so that the frequency of field alternation is comparable to the relaxation time for each size of DNA fragment during some portion of the separation; optimum differential migration then occurs for each DNA fragment during some time period in the separation.

Using these techniques, it has been possible to extend the separation range of DNA fragments up to 5000 Kbp. With the development of ancillary sample preparation techniques, it is now possible to separate and identify the chromosomes of many lower eukaryotic organisms. For example, direct analysis of yeast chromosomes has been achieved [77]. Resolution of intact chromosomes up to 2000 Kbp pairs was attained; no shearing of the DNA was observed because the DNA was protected by embedding the yeast cells in agarose prior to cell lysis. Since the chromosomes of lower eukaryotes do not condense and thus they cannot be visualized by the classical karyotyping technique using light microscopy, this technique is particularly important for analysis of DNA from such organisms.

This electrophoretic technique is also useful for studying the differentiation of parasites resulting from chromosomal recombination. Many parasites (e.g. *Trypanosoma brucei* [78], which causes sleeping sickness, or *Plasmodium falciparum* [79], which causes malaria) undergo rearrangement of genes in their chromosomes during stages of their development to avoid destruction by the immune system of the infected host. With these new electrophoretic techniques, it is now possible to study directly the translocation, insertion, and deletion of genes by directly analyzing the size of the chromosome and its fragments. Fig. 25 shows the pulse-field electrophoretic separation of chromosomal DNA's from three strains of the parasitic agent responsible for malaria. These electrophoretic techniques may find use in clinical diagnosis of pathogenic organisms by allowing researchers to derive a "fingerprint" of each of the species of an infectious agent from the pattern of its chromosomal DNA. Rapid identification of the particular strain of the organism facilitates treatment of infected individuals.

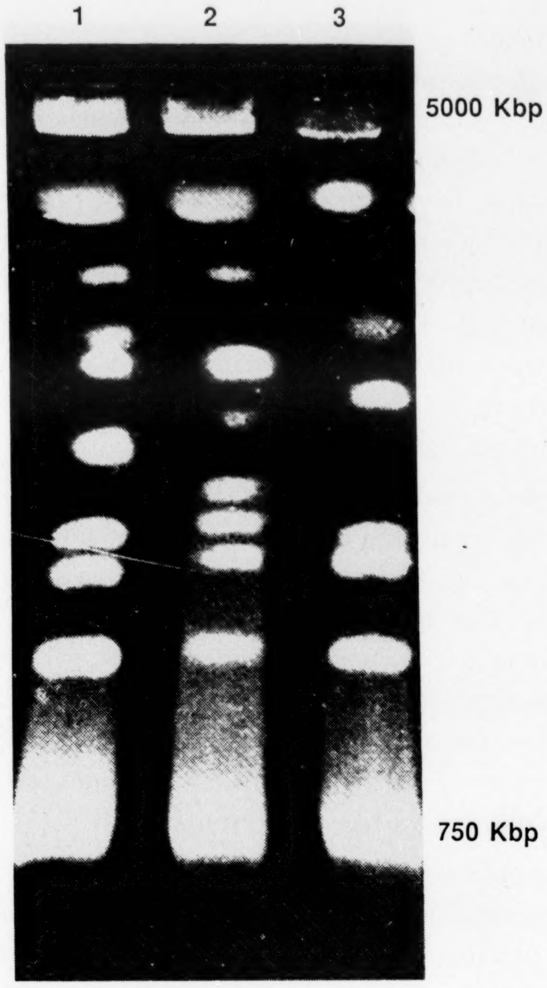

Fig. 25

Chromosomes of 3 Strains of the Malaria Parasite *Plasmodium falciparum*; ranging in size from 750 Kbp to 5 Mbp (MW = 5×10^8 to 3.3×10^9 AMU) separated by pulsed-field gel electrophoresis. Adapted with permission from LKB product literature.

Finally, because of the ability to separate DNA fragments up to 5000 Kbp, these techniques, together with those of classical genetics, molecular cloning, and chromosome linking, should be indispensable in mapping genes on mammalian chromosomes [80, 81]. These techniques should facilitate in assigning the location of specific genes in the chromosome and in identifying genetic defects, and, ultimately, reduce the effort required for the massive task of sequencing the human genome.

Capillary Zone Electrophoresis

Conventionally, electrophoresis is done through a porous matrix which is used to stabilize the solute bands and prevent mixing which could arise from thermal convection. The porous matrix is usually an agarose or acrylamide gel. Though conventional electrophoresis is not technically complicated, it is labor-intensive and time-consuming. Solutions must be prepared and cast into gels, separations are run at relatively low voltages (5–10 V/cm) for long periods of time (8–16 hr), and the gels are stained and destained to visualize the protein bands. Though qualitative information can be readily obtained, quantitation is poor, even when the gel is scanned with a densitometer. Also, barring autoradiographic detection of radiolabeled samples, detection sensitivity is low, with ~0.5 μg and ~0.1 ng of protein detectable with Coomassie and silver stain, respectively.

Capillary zone electrophoresis eliminates many of these limitations. Small fused silica or glass capillaries (50–100 μm id) replace the gel. Capillary forces between the buffer and the walls of the glass stabilize the liquid buffer in which the separation occurs, obviating the need for the semi-rigid gel. In addition, because the capillaries are narrow, high voltages (30 KV) can be employed with small resultant electrical currents; Joule heating is rapidly dissipated from the thin capillary while achieving rapid separations. Furthermore, because electrophoresis occurs through a UV transparent medium, a portion of the capillary can function as an optical flow cell, thereby permitting on-line detection of separated bands by absorption and fluorescence measurements.

Most importantly, separations in a free liquid (as opposed to those in the pores of a gel or those through a packed bed of particles) eliminate many of the band-broadening mechanisms normally encountered in separations through porous media. For example, contributions from eddy diffusion and mass transfer are not present in free-zone electrophoresis; the most significant band-broadening contribution is from longitudinal diffusion. Assuming molecular diffusion as the only source of band broadening, Jorgenson [82] derived an equation relating the important parameters affecting the number of theoretical plates (N) achievable in capillary zone electrophoresis as

$$N = \frac{\mu V}{2D}$$

where V is the applied voltage and D is the diffusion coefficient of a solute with electrophoretic mobility μ. The length of the capillary has no direct bearing on the efficiency of the separation, and thus the conclusion was drawn that one should apply very high voltages across short capillaries to achieve the best separations in the shortest period of time. In practice, as the length of the capillary is decreased, the current through the capillary will increase and the concomitant heating will degrade the separation. Capillaries of 0.5–1.5 meters length with internal diameters ranging from 50–100 μm are found to be the most useful. With these, efficient separations ($N > 10^5$) can easily be achieved in less than 30 minutes.

As a result of the high efficiency of the technique and of the small size of the separation capillary, sample bands are not significantly broadened during separation; detection of minute quantities of solute can be achieved. This aspect makes the technique useful for separations where small quantities of sample are available. (Along these lines, work has been reported on a technique [83] that would allow injection of sub-nanoliter volumes from a total sample volume of a few microliters.)

Applications of capillary zone electrophoresis include separations of fluorophore-labelled amines [84], inorganic ions [85, 86], chiral amino acids [87], oligonucleotides [88], peptides [84], and proteins [89]. Neutral species can also be separated by this technique [90] if a charged complexation agent is added to the electrophoresis buffer. Fig. 26 illustrates the power of this technique for the high-resolution separation of proteins. Fifteen proteins with molecular weights ranging from 11K to 77K and pI values from 4.5 to >11 were separated in 25 minutes in a surface-modified 50 μM fused quartz capillary filled with pH 2 phosphate buffer. Similar protein separations with efficiencies exceeding 10^6 theoretical plates have been achieved in unmodified silica capillaries filled with low pH buffers.

Fig. 26 also suggests some of the problems with the technique that are still to be overcome. A major difficulty is the prevention of sorption of solutes (particularly proteins) onto the surface of the capillary. Several approaches to overcoming this problem have been reported, including chemical deactivation of the surface of the capillary [91] and use of buffer pH to manipulate the surface charge on the protein and on the capillary, to cause electric charge repulsion between the two materials [89]. For the separation in Fig. 26, a low pH (2.0) buffer was used to inhibit surface-sorption problems with the capillary wall. The separation in Fig. 26 also illustrates the limited peak capacity typical of current capillary separations. This problem could be overcome if a pH closer the pI of the proteins to be separated could be used, thereby maximizing the differential mobilities of the proteins. In addition, variation of the pH of the electrophoresis buffer during the separation would be most useful in further extending the peak capacity. Unfortunately, because of the aforementioned problem of protein adsorption onto the capillary, separations at more neutral pH values are not now accessible. Fig. 27 shows the separations of five proteins at two pH values. As the pH of the buffer is increased from 1.4, the difference in mobilities of the proteins increases, as evidenced by the broader time range over which the proteins elute. However, the asymmetry of the bands is much worse for the separation in the buffer of higher pH; band symmetry is poorest for proteins whose pI values are closest to the pH value of the buffer in which the separation occurs.

Another area that needs to be addressed is the development of sensitive, low-volume detectors for capillary electrophoresis. At present, fluorescent detection of the proteins is not practical since labeling of a protein yields a mixture of products due to the large number of reactive groups on

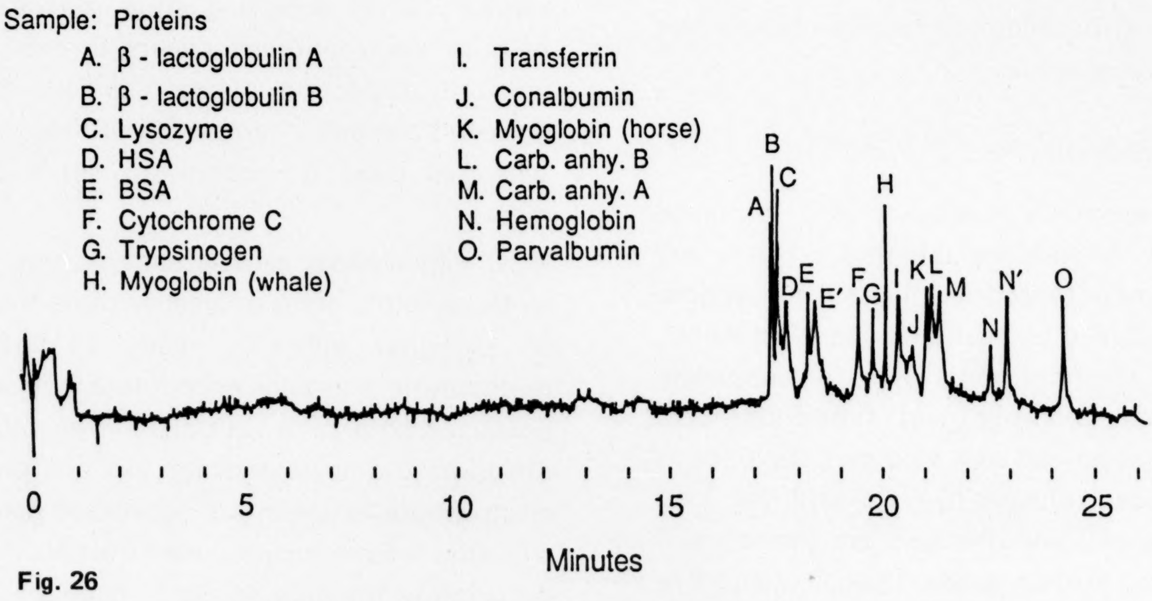

Fig. 26

Separation of a Protein Mixture by Capillary Electrophoresis.

Capillary: 110 cm length of 50 μm id fused silica capillary derivatized with vinyl-pyrollidinone; separation monitored 75 cm from anode; Buffer: 38.5 mH H_3PO_4/20 mH NaH_2PO_4, pH 2.03. Detector: 0.02 AUFS at 190 nm; Injection voltage: 5 sec at 5 KV at anode; Separation voltage: 5–25 KV linear voltage gradient in 300 seconds; Sample Components: A. β-Lactoglobulin B (bovine), B. β-Lactoglobulin A (bovine), C. Lysozyme (chicken egg white), D. Human serum albumin, E. Bovine serum albumin, F. Cytochrome c (horse heart), G. Trypsinogen (bovine pancreas), H. Myoglobin (whale skeletal muscle), I. Transferrin (human), J. Conalbumin (chicken egg white), K. Myoglobin (horse heart), L. Carbonic anhydrase B (bovine), M. Carbonic anhydrase A (bovine), N. Hemoglobin (human), O. Parvalbumin (rabbit muscle).

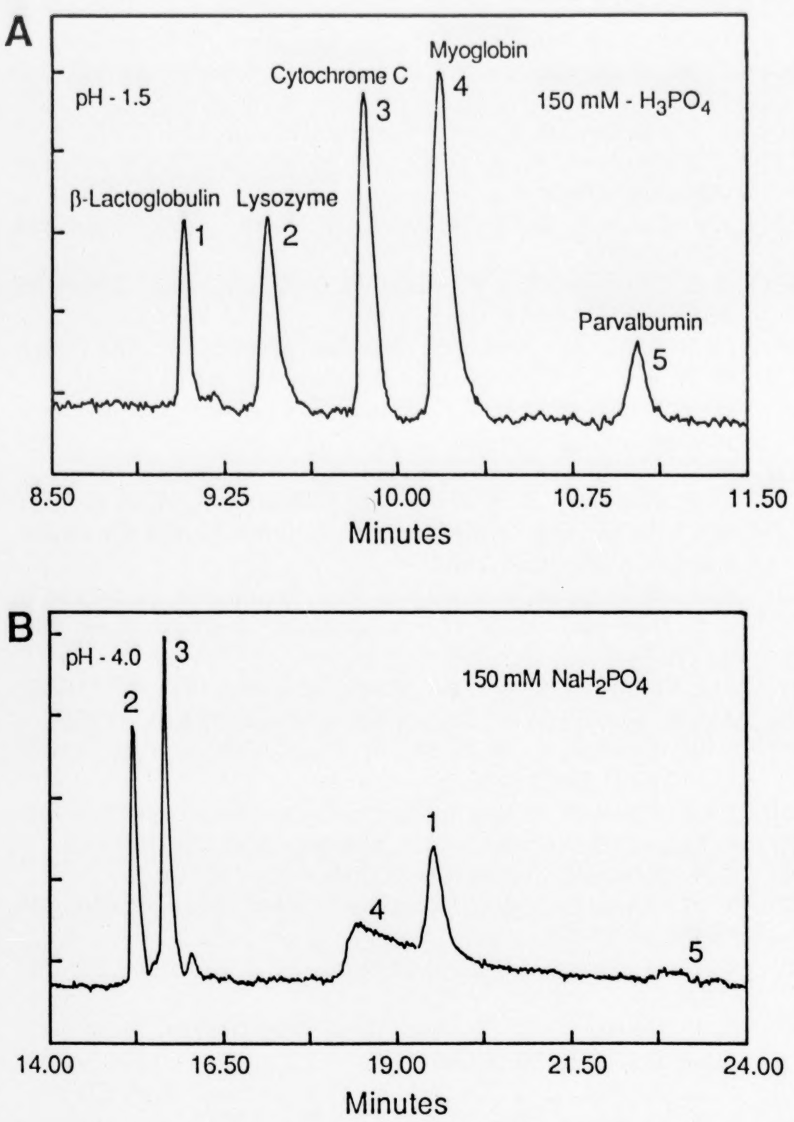

Fig. 27

Effect of pH on Separation in Unmodified Silica Capillary.

Capillary: 110 cm length of 50 μm id fused silica capillary; separation monitored 75 cm from anode. Sample: 1. β-Lactoglobulin A, 2. Lysozyme, 3. Cytochrome c, 4. Myoglobin (horse heart), 5. Parvalbumin. Buffer: A. 150 mM H_3PO_4, pH 1.5; B. 150 mM NaH_2PO_4, pH 4.0.

the protein that can accept the labeling agent [84]. Electrochemical detectors have promise [5], but are not universally applicable. Finally, improvement in sample injection techniques would yield more reproducible introduction of samples into the capillary with a minimum of band-broadening due to the injection volume.

V Conclusions

This overview has focused on some of the new technologies that have been developed to deal with problems associated with the separation and characterization of biomacromolecules. With the application of these new techniques in HPLC, FFF, and electrophoresis, significant advances in the basic understanding of macromolecular systems is foreseen. More importantly, solutions to some of the outstanding problems involving large molecules may now be possible. For example, high-speed HPLC separations with < 2-μm particles will significantly accelerate developments in recombinant technology by permitting very rapid protein sequencing identifications. Important kinetic studies on biological systems will also be accessible with this technology. HPLC separations with very wide-pore particles will allow the isolation and purification of nucleic acids, membrane proteins, and a wide variety of large molecules that are not amenable to current methods. The new HPLC bonded-phase technology will result in efficient, stable columns for the analysis of a wide range of small and large molecules. In addition, development of stable bonded phases signals a new level of potential for preparative isolations with greatly-reduced contamination of the isolated fractions because of diminished stationary phase degradation. Very stable bonded phases on optimum silica supports also greatly enhance the potential for high-speed affinity chromatography as well as improved speed and yields in protein sequencing.

The developing SdFFF method not only provides a powerful tool for determining the particle-size distribution of industrially- and environmentally-important colloids, but also affords new potential for separating, isolating, and characterizing bioparticulates and large, soluble biomacromolecules for which current methods are inadequate. TFFF has outstanding potential for characterizing very high MW synthetic polymer molecules, as well as for separating and characterizing copolymers, block polymers, and related systems for which current technology is deficient. The high degree of analytical reproducibility of MW measurements with TFFF makes feasible the delineation of very small differences in polymer characteristics.

The potential impact of new technology in electrophoresis is clear. The 2D technique is uniquely suited for the high-resolution separation of very complex mixtures of clinical and toxicological importance. It is likely that this method will have significant impact in the identification of diseases with a genetic background. The pulsed-field method opens up a whole new area of research with very large nucleic acids and chromosomal-size DNA. The range of applicability for this method somewhat overlaps that of SdFFF, so with the combination of these two new separation methods, unsolved problems involving complex cell chemistry can now be successfully attacked. The small sample requirements, speed, and high resolution capability of capillary electrophoresis will make possible the separation of complex mixtures of proteins. This method also has strong potential for the very rapid separation of the proteins within a single cell.

Acknowledgments

We thank L. E. Schallinger for collaborating with J.J.K. to obtain Figures 18 and 19, and M. P. Reinhart for furnishing the microsomal pellet and assistance in obtaining Figure 20.

References

[1] *W. W. Yau, J. J. Kirkland,* J. Chromatogr. **218,** 217 (1981).
[2a] *J. C. Giddings,* "Dynamics of Chromatography", Marcel Dekker, New York, 1965, Chap. 2.
[2b] *J. H. Knox, M. Saleem,* J. Chromatogr. Sci. **7,** 614 (1969).
[3] *G. Guiochon, M. Martin,* J. Chromatogr. **326,** 3 (1985).
[4] *E. S. Yeung, R. E. Synovec,* Anal. Chem. **58,** 1237A (1986).

[5] *J. G. White, R. L. St. Claire III, J. W. Jorgenson,* Anal. Chem. **58**, 293 (1986).

[6] *K. K. Unger, W. Messer, K. F. Krebs,* J. Chromatogr. **149**, 1 (1978).

[7] *C. Dewaele, M. Verzele,* J. Chromatogr. **282**, 341 (1983).

[8] *K. K. Unger, G. Jilge, J. N. Kinkel, M. T. W. Hearn,* J. Chromatogr. **359**, 61 (1986).

[9] *K. K. Unger, G. Jilge, R. Janzen, H. Giesche, J. N. Kinkel,* Chromatographia **22**, 379 (1986).

[10] *K. K. Unger, H. Giesche,* Ger. Pat., 3534143 (1987).

[11] *W. Stober, A. Fink, E. Bohn,* J. Colloid Interface Sci. **26**, 62 (1968).

[12] *K. Kalghatgi, C. Horvath,* J. Chromatogr. **398**, 335 (1987).

[13] *N. D. Danielson, J. J. Kirkland,* manuscript accepted for publication. Anal. Chem., Oct., 1987 (proposed).

[14] *J. J. Kirkland,* E.I. duPont de Nemours & Co., Wilmington, DE, unpublished result, 1977.

[15] *K. Unger, J. Schick-Kalb, K.-F. Krebs,* J. Chromatogr. **83**, 5 (1973).

[16] *J. J. Kirkland,* J. Chromatogr. **125**, 231 (1976).

[17] *Y. Kato, Y. Yamasaki, T. Hashimoto, T. Murotsu, S. Fukushige, K. Matsubara,* J. Chromatogr. **320**, 440 (1985).

[18] *I. Hara, M. Okazaki, Y. Ohno,* J. Biochem. **87**, 1863 (1980).

[19] *P. M. Young, J. E. Brown,* J. Chromatogr. Biomed. Appl. **311**, 79 (1984).

[20] *C. T. Wehr, R. L. Cunico, G. S. Ott, V. G. Shore,* Anal. Biochem. **125**, 386 (1982).

[21] *M. E. Himmel, P. G. Squire,* J. Chromatogr. **210**, 443 (1981).

[22] *M. Ollivon, A. Walter, R. Blumenthal,* Anal. Biochem. **152**, 262 (1986).

[23] *M. Colpan, D. Riesner,* J. Chromatogr. **296**, 339 (1984).

[24] *R. Hecker, M. Colpan, D. Riesner,* J. Chromatogr. **326**, 251 (1985).

[25] *Y. Kato, T. Kitamura, T. Hashimoto,* J. Chromatogr. **266**, 341 (1983).

[26] *J. D. Pearson, M. Mitchell, F. E. Regnier,* J. Liq. Chromatogr. **6**, 1441 (1983).

[27] *D. L. Gooding, M. N. Schmuck, K. M. Gooding,* J. Chromatogr. **296**, 107 (1984).

[28] *N. T. Miller, B. Feibush, B. L. Karger,* J. Chromatogr. **316**, 519 (1984).

[29] *J.-P. Chang, Z. El Rassi, C. Horvath,* J. Chromatogr. **319**, 396 (1985).

[30] *Z. El Rassi, C. Horvath,* J. Liq. Chromatogr. **9**, 3245 (1986).

[31] *H. Engelhardt, G. Ahr,* J. Chromatogr. **282**, 385 (1983).

[32] *J. C. Giddings,* Advan. Chromatogr. **20**, 217 (1982).

[32a] *R. Tijssen, J. Bos, M. E. van Kreveld,* Anal. Chem. **58**, 3036 (1986).

[33] *J. Kohler, D. B. Chase, R. D. Farlee, A. J. Vega, J. J. Kirkland,* J. Chromatogr. **352**, 275 (1986).

[34] *J. D. Pearson, N. T. Lin, F. E. Regnier,* Anal. Biochem. **124**, 217 (1982).

[35] *J. Kohler, J. J. Kirkland,* J. Chromatogr. **385**, 125 (1987).

[36] *J. L. Glajch, J. J. Kirkland, J. Kohler,* J. Chromatogr. **384**, 81 (1987).

[37] *J. L. Glajch, J. C. Gluckman, J. G. Charikofsky, J. M. Minor, J. J. Kirkland,* J. Chromatogr. **318**, 23 (1985).

[38] *H. Figge, A. Deege, J. Kohler, G. Schomburg,* J. Chromatogr. **351**, 393 (1986).

[39] *J. L. Glajch, J. J. Kirkland,* patent applied for, 1986.

[40] *J. L. Glajch, J. J. Kirkland,* manuscript submitted for publication.

[41] *J. J. Kirkland, J. L. Glajch,* U.S. Patent allowed, 1987.

[42] *J. J. Kirkland, J. L. Glajch,* manuscript submitted for publication.

[43] *J. C. Giddings,* Sep. Sci. **1**, 123 (1966).

[44] *G. H. Thompson, M. N. Myers, J. C. Giddings,* Sep. Sci. **2**, 797 (1967).

[45] *J. C. Giddings, S. R. Fisher, M. N. Myers,* Am. Lab. (Fairfield, Conn.) **10**, 15 (1978).

[46] *J. C. Giddings, M. N. Myers, K. D. Caldwell, S. R. Fisher,* Methods Biochem. Anal. **26**, 79 (1980).

[47] *J. C. Giddings,* Sep. Sci. **19**, 831 (1984).

[48] *K. D. Caldwell,* in "Chemical Analysis; Modern Methods of Particle Size Analysis", Vol. 73, New York, 1984, p. 211.

[49] *L. E. Schallinger, L. A. Kaminski,* Biotechniques, **3**, 124 (1985).

[50] *L. J. Mathias, R. Vaidya,* Polymer News **9**, 115 (1984).

[51] *J. J. Kirkland, C. H. Dilks, Jr., W. W. Yau,* J. Chromatogr. **255**, 255 (1983).

[52] *J. J. Kirkland, S. W. Rementer, W. W. Yau,* Anal. Chem. **53**, 1730 (1981).

[53] *J. C. Giddings, F. J. F. Yang, M. N. Myers,* Anal. Chem. **46**, 1917 (1974).

[54] *W. W. Yau, J. J. Kirkland,* Sep. Sci. Technol. **16**, 577 (1981).

[55] *W. W. Yau, J. J. Kirkland,* US Patent 4 285 810 (1981).

[56] *L. E. Schallinger, J. J. Kirkland, E. C. Arner,* manuscript in preparation.

[57] *E. C. Arner, J. J. Kirkland,* manuscript in preparation.

[58] *K. D. Caldwell, S. H. Mozersky, J. Magahaski, R. A. Barford,* 8th International Symposium on Column Liquid Chromatography, 1984, paper 3aG4.

[59] *E. H. Harrison, W. E. Bowers,* J. Biol. Chem. **258**, 7134 (1983).

[60] *J. C. Giddings, M. N. Myers, J. Janca,* J. Chromatogr. **186**, 37 (1979).

[61] *J. J. Kirkland, W. W. Yau,* Macromolecules **18**, 2305 (1985).

[62] *J. J. Kirkland, W. W. Yau,* J. Chromatogr. **353**, 95 (1986).

[63] *G. H. Thompson, M. N. Myers, J. C. Giddings,* Anal. Chem. **41**, 1219 (1969).

[64] *J. J. Kirkland, W. W. Yau,* manuscript submitted for publication.

[65] *P. Tijssen, E. Kurstak,* Anal. Biochem. **128**, 26 (1983).

[66] *P. H. O'Farrell,* J. Biol. Chem. **250**, 4007 (1975).

[67] *N. G. Anderson, N. L. Anderson,* Anal. Biochem. **85**, 331 (1978).

[68] *N. G. Anderson, N. L. Anderson,* Anal. Biochem. **85**, 341 (1978).

[69] *C. R. Merril, R. C. Switzer, M. L. Van Deuren,* Proc. Natl. Acad. Sci. USA. **76**, 4335 (1979).

[70] *N. L. Anderson, J. Taylor, A. E. Scandora, B. P. Coulter, N. G. Anderson,* Clin. Chem. **27**, 1807 (1981).

[71] *A. H. M. Burghes, M. J. Dunn, H. E. Statham, V. Dubowitz,* in "Electrophoresis '81" (New York: Walter de Gruyter and Co., 1981), p. 295.

[72] *S. E. Bustos, L. Fung,* in "Electrophoresis '81" (New York: Walter de Gruyter and Co., 1981), p. 317 ff.

[73] *N. G. Anderson, L. Anderson,* Clin. Chem. **28** (4), 739 (1982).

[74] *W. L. Fangman,* Nucl. Acid Res. **5**, 653 (1978).

[75] *P. G. deGennes,* J. Chem. Phys. **55**, 572 (1971).

[76] *L. C. Klotz, B. H. Zimm,* Macromolecules **5**, 471 (1972).

[77] *G. F. Carle, M. V. Olson,* Proc. Natl. Acad. Sci. USA **82**, 3756 (1985).

[78] *L. H. T. Van der Ploeg, D. C. Schwartz, C. R. Cantor, P. Borst,* Cell **37**, 77 (1984).

[79] *L. H. T. Van der Ploeg, M. Smits, T. Ponnudurai, A. Vermeulen, J. H. E. T. Meuwissen, G. Langsley,* Science **229**, 658 (1985).

[80] *W. R. A. Brown, A. P. Bird,* Nature **322**, 477 (1986).

[81] *S. K. Lawrance, C. L. Smith, R. Srivastava, C. R. Cantor, S. M. Weissman,* Science **235**, 1387 (1987).

[82] *J. W. Jorgenson, K. D. Lukacs,* Clin. Chem. **27** (9), 1551 (1981).

[83] *R. A. Wallingford, A. G. Ewing,* Anal. Chem. **59**, 678 (1987).

[84] *J. W. Jorgenson, K. D. Lukacs,* Science **222**, 266 (1983).

[85] *T. Tsuda, K. Nomura, G. Nakagawa,* J. Chromatogr. **264**, 385 (1983).

[86] *P. Gebauer, M. Deml, P. Bocek, J. Janak,* J. Chromatogr. **267**, 455 (1983).

[87] *E. Gassmann, J. E. Kuo, R. N. Zare,* Science **230**, 813 (1985).

[88] *A. S. Cohen, S. Terabe, J. A. Smith, B. L. Karger,* Anal. Chem. **59**, 1021 (1987).

[89] *H. H. Lauer, D. McManigill,* Anal. Chem. **58**, 166 (1986).

[90] *Y. Walbroehl, J. W. Jorgenson,* Anal. Chem. **58**, 479 (1986).

[91] *S. Hjerten,* J. Chromatogr. **347**, 191 (1985).

Received: June 29, 1987
Accepted: July 15, 1987
F

Prediction of the Detection Ranges for HPLC-Peroxyoxalate Chemiluminescence Detection System of Fluorescent Compounds

K. Imai*/A. Nishitani/Y. Tsukamoto

Branch Hospital Pharmacy, University of Tokyo, 3-28-6 Mejirodai, Bunkyo-ku, Tokyo 112, Japan

Key Words

Column liquid chromatography
Chemiluminescence detection
Determination of limits of detection

Summary

A manual method for predicting the detection ranges of fluorescent compounds for the HPLC-peroxyoxalate chemiluminescence detection system is presented utilizing bis(4-nitro-2-(3,6,9-trioxadecyloxycarbonyl)phenyl) oxalate (TDPO) as a chemilumigenic reagent. The generated chemiluminescence decay curves were measured on a photomultiplier and extrapolated to zero time based on the first part of the decay curve. Dipyridamole, perylene, DNS-Ser, Rose Bengal, DNS-Asp, Trp-P-1, pyrenecarboxylic acid methyl ester, perfenazine, alimemazine, oxypertine, Glu-P-2, benzydamine and doxorubicin gave chemiluminescence intensity (Icl) values of 3.2×10^6, 2.8×10^6, 2.3×10^5, 2.1×10^5, 1.9×10^5, 1.4×10^5, 9.4×10^3, 6.2×10^3, 4.2×10^3, 3.3×10^3, 2.3×10^3, 9.7×10^2 and 3.1×10^2, respectively. The reaction conditions for the HPLC-CL detection system were investigated and optimum conditions obtained.

Introduction

The peroxyoxalate chemiluminescence (CL) reaction developed by Rauhut et al. [1] has been used in HPLC for the detection of fluorescent compounds such as DNS-amino acids [2–6], DNS-catecholamines [3], DNS-drugs [7, 8], DNS-amines [9], NBD-amines [9], OPA-amines [9], fluoresceamine-catecholamines [10], DCA-carboxylic acids [11], polycyclic aromatic hydrocarbons [12, 13], polycyclic aromatic amines [14, 15] and nitropolycyclic aromatic hydrocarbons [16]. Certain easily oxidizable compounds such as sulphite and anilines [17], and substrates (acetylcholine and choline) for enzymes (acetylcholine hydrolase and choline oxidase) [18] have also been detected. A picomol to subfemtomol range of detection of these compounds has been achieved [19].

The detectability (detection limit) for analytes in the peroxyoxalate CL detection system is dependent on the total CL intensity (Icl) generated; high Icl results in high detectability. Icl is defined as:

$$Icl = k1 \times D \times Ydf \times Yf \times F \quad [20]$$

where

k1 = a constant
D = the concentration of the intermediates
Ydf = fluorescence quantum yield
F = concentration of the fluorescent compound.

Ydf has been reported to correlate well with the oxidation potentials of the fluorescent compounds [14, 21, 22]. Although the relative Icl value of a certain analyte for a fixed fluorescent compound can be estimated by measuring values for those parameters (relative Ydf and Yf) under a fixed reaction condition, it is not a easy task to measure these values.

In practice, the relative Icl for a certain analyte is available by calculating the Icl extrapolated to the zero time of the reaction using the decay curve obtained by a manual method. If these apparent Icl values correlate well with the detection limits, it should be possible to predict the detection limit for a certain analyte by measuring its apparent Icl.

The other parameter to affect the final detection limit in the HPLC-peroxyoxalate CL detection system is the performance of the detection system. There are many parameters which affect the performance: purity of the reagents and solvents, solvent delivery system, CL reaction condition, mixing of the solution, timing the detection of CL light, types of detector cell and photo-detector, etc. The effect of some of these parameters have been extensively studied [2, 3, 7, 12, 15, 23–27]. In this work, the reaction condition has been re-investigated to enhance the detectability.

We propose, in this paper, an easy way to find the detection limit of a certain analyte for the HPLC-peroxyoxalate CL detection system utilizing bis(4-nitro-2-(3,6,9-trioxadecyloxycarbonyl)phenyl) oxalate (TDPO) [28, 29] – hydrogen peroxide reaction by a modified manual method described in previous papers [21–23, 28].

0009-5893/87 0077-05 $03.00/0

© 1987 Friedr. Vieweg & Sohn Verlagsgesellschaft mbH

Experimental

Chemicals

Bis(4-nitro-2-(3,6,9-trioxadecyloxycarbonyl)phenyl) oxalate (TDPO) and Rose Bengal were purchased from Wako Pure Chemical Industry (Tokyo, Japan). Dansyl (DNS)-amino acids, dipyridamole and perylene were from Sigma (St. Louis, MO, USA). Alimemazine tartrate, benzydamin hydrochloride and oxypertine were donated from Daiichi Seiyaku Co. (Tokyo, Japan). Perfenazine, doxorubicin hydrochloride and carbocromen hydrochloride were donated from Kanebo Yakuhin Co. (Tokyo, Japan), Kyowa Hakko Kogyo Co. (Tokyo, Japan) and Takeda Chemical Industries (Osaka, Japan), respectively. Pyrenecarboxylic acid methyl ester [30] was a gift from Drs. T. Nambara and J. Goto, the Tohoku University, and Trp-P-2 and Glu-P-1 [31] were from Drs. K. Shudo and Y. Hashimoto, the Universisty of Tokyo. 30% Hydrogen peroxide was purchased from Mitsubishi Gas Kagaku (Tokyo, Japan). Imidazole (Merck, Darmstadt, FRG) was used after crystallizing once from diethyl ether [6]. Distilled water (HPLC grade), acetonitrile (HPLC grade), ethyl acetate (HPLC grade) and hydrochloric acid (volumetric analytical grade) were from Wako. All other chemicals were of reagent grade.

CL Reaction Time of Fluorescent Compounds Utilizing the TDPO-Hydrogen Peroxide System

A 10 μl volume of a 0.05 to 20 μM fluorescent compound in acetonitrile or methanol and 5 μl 0.05 M imidazole-nitrate (pH 6.1) were pre-mixed in a borosilicate glass tube (50×6 mm i.d.) with a vortex mixer for several seconds, then 250 μl of a mixture of 0.5 mM TDPO and 12.5 mM hydrogen peroxide in acetonitrile were added with a microsyringe. The tube was immediately placed inside a Chem-Glow photometer (Aminco, Baltimore, MD, USA) and the variation of the intensity with time was recorded after adding TDPO solution. From the results obtained the Icl, extrapolated to zero time from the first part of the decay curve, was calculated.

HPLC-Chemiluminescence Detection System

A schematic diagram for the system is shown in Fig. 1. The pumps used were a KHP-011 (Kyowa Seimitsu Co., Tokyo, Japan) for the eluent and a LC-5A (Shimadzu Seisakusho Co., Tokyo, Japan) for the reagent solution. The injection valve (Rheodyne, Cotati, CA, USA) with a 20 μl loop was from Shimadzu, an analytical column (TSK ODS 80Tm, 150×4.6 mm i.d., 5 μm), a dummy column for the eluent (TSK TMS-250, 100×4.6 mm, i.d., 5 μm), a dummy column for the reagent solution (TSK ODS-120A, 150×4.6 mm i.d., 5 μm) were from Toyo Soda Manufacturing Co. (Tokyo, Japan). A photon counting type chemiluminescence monitor, LC-30-DPC 10LC (JEOL, Tokyo, Japan) with a 70 μl spiral type flow cell and a recorder (Technicorder Type 3047, Yokogawa Denki, Tokyo, Japan) were used. A 25 μl rotating mixing device (Kyowa Seimitsu Co., Tokyo, Japan) was heated at 35 °C in a water-bath. The flow line (PTFE tubing, 50×0.5 mm i.d. and 50×0.8 mm i.d.) was connected to the detector after the mixing device. The eluent for perylene and carbocromen was 0.1M imidazole nitrate (pH 7.0) – acetonitrile (10:90, v/v). Similar eluents with different ratios of the buffer and acetonitrile were used for the other fluorescent compounds (20:80 for doxorubicin, oxypertine, perylene and pyrenecarboxylic acid methyl ester, 50:50 for dipyridamole and benzydamine, 70:30 for Trp-P-1 and 80:20 for DNS-Ser). Flow rates varied from 0.6 to 1.5 ml/min. The reagent solution was a 1:1 (v/v) mixture of 0.05, 0.1, 0.25, 0.5 or 1.0 mM TDPO in acetonitrile – ethyl acetate (1:1, v/v) and 0.5 to 1000 mM hydrogen peroxide in acetonitrile – ethyl acetate (1:1, v/v). Since the pre-mixed reagent solution of TDPO and hydrogen peroxide in the mixture of ethyl acetate and acetonitrile retained its activity for 6hrs [28], we used, in this experiment, TDPO instead of TCPO which is usually used. The flow rates were varied from 1.0 to 3.0 ml/min. Both solutions were mixed just prior to use. The stock solutions of the fluorescent compounds in acetonitrile or methanol were diluted with the same solvents to appropriate concentrations, and a 20 μl aliquot was subjected to HPLC analysis.

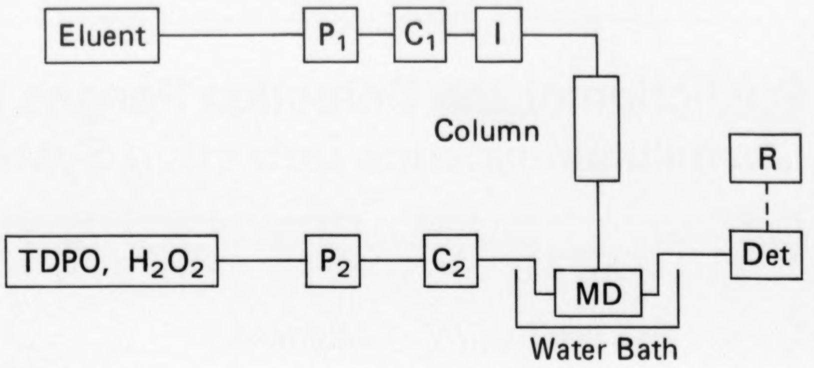

Fig. 1

Flow Diagram for the HPLC-Peroxyoxalate Chemiluminescence Detection System.

Eluent 0.05M imidazole-nitrate (pH 7.0)-acetonitrile (10:90 to 90:10, v/v); P_1 pump for eluent, KHP-011, P_2 pump for reagent, LC-5A; reagent solution was a mixture of 0.5 mM TDPO and 50 mM hydrogen peroxide in ethyl acetate-acetonitrile (1:1, v/v); I injector; C_1 TSK TMS-250; C_2 TSK ODS-120A; column TSK ODS-80Tm; MD rotating flow mixing device; D chemiluminescence monitor; R recorder.

Results and Discussion

For easy handling of the assay system in a manual method for measuring the CL reaction curves we modified the solvent composition for the system reported previously [21, 22, 28], to give reaction conditions similar to the reaction conditions in the detection system of the HPLC but the ratio of hydrogen peroxide and the oxalate was reduced (12.5 mM/0.5 mM) to give a longer half life of the CL light. The experimental procedure, outlined, is shown in Fig. 1. In this system [0.05M imidazole-nitrate (pH 6.1)-acetonitrile, 5:95 (v/v)], various compounds which were thought to have fluorescence properties from their chemical structures were arbitrary taken and investigated. As shown in Fig. 2, some fluorescent compounds gave high CL intensities while others gave lower intensities. The CL

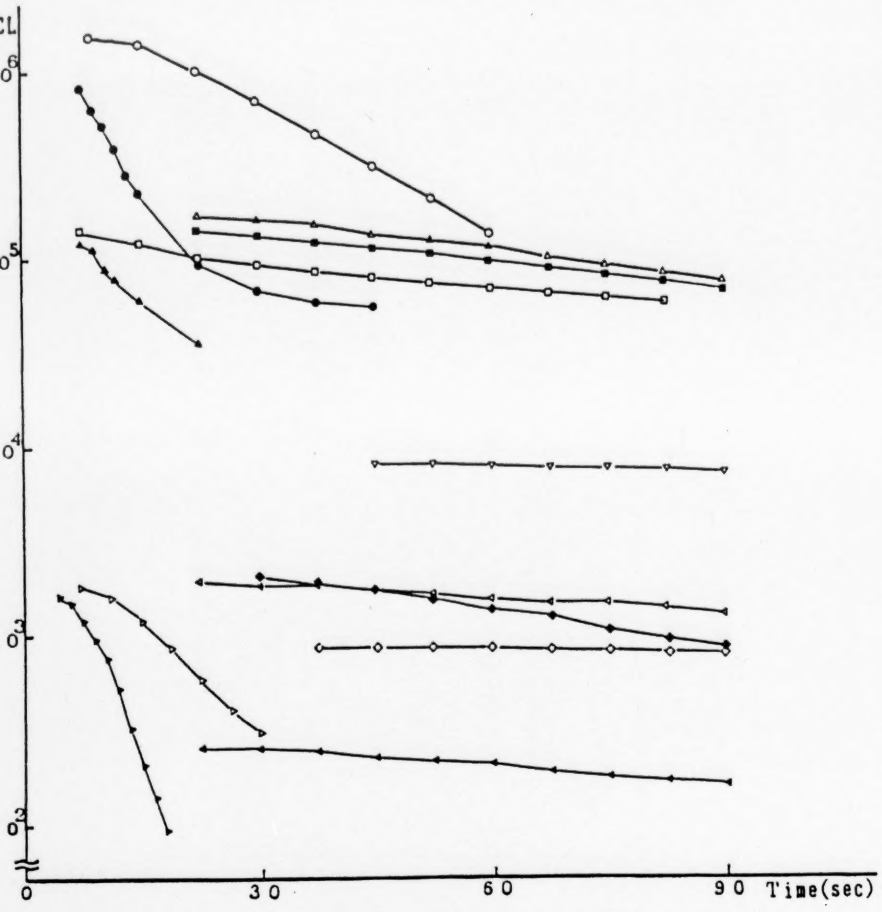

Fig. 2

Time Courses of Peroxyoxalate Chemiluminescence Reaction with Different Fluorescent Compounds.

●——● dipyridamole ○——○ perylene △——△ DNS-Ser
▲——▲ Rose Bengal ■——■ DNS-Asp □——□ Trp-P-1
▽——▽ pyrenecarboxylic acid methyl ester ▶——▶ perfenazine
▷——▷ alimemazine ◆——◆ oxypertine ◁——◁ Glu-P-2
◇——◇ benzydamine ◀——▶ doxorubicin

Table I. Relative chemiluminescence intensities obtained by the manual method.

Fluorescent compounds	Icl
dipyridamole	3.2×10^6
perylene	2.8×10^6
DNS-Ser	2.3×10^5
Rose Bengal	2.1×10^3
DNS-Asp	1.9×10^5
Trp-P-1	1.4×10^5
pyrenecarboxylic acid methyl ester	9.4×10^3
perfenazine	6.2×10^3
alimemazine	4.2×10^3
oxypertine	3.3×10^3
Glu-P-2	2.3×10^3
benzydamine	9.7×10^2
doxorubicin	3.1×10^2

Icl: relative chemiluminescence intensities, extrapolated to zero time;
DNS: 5-N,N-dimethylaminonaphthalenesulfonyl;
Trp-P-1: 2-amino-1-methyl-5H-pyrido[4,3-b]indole;
Glu-P-2: 2-amino-6-methyldipyrido[1,2-a:3′,2′-d]imidazole.

intensities obtained after extraporation to zero time based on the first part of the decay curves were measured (Table I). The results were similar to those reported by others which showed a variety of CL responses in case of polycyclic aromatic hydrocarbons and other fluorescent compounds [12, 22].

Compared to the intensity of dipyridamole (3.2×10^6) or perylene (2.8×10^6), DNS-Ser (2.3×10^5) and benzydamine (9.7×10^2) gave intensities by 1 to 4 orders of magnitude lower. The data suggest that the structure of pyrimidopyrimidine (dipyridamole) appeared to be the best for the CL reaction detector, in addition to perylene which has been the best reported so far [12, 22] but the molecular weight of the latter is rather large for its use as derivatization reagent [22]. In this respect, fluorogenic reagents retaining the structure of pyrimidopyrimidine would be suitable for the peroxyoxalate CL reaction detector in HPLC. We are currently investigating modifications to the structure of dipyridamole for appropriate CL tags.

Before investigating the detection limits for HPLC-CL detection system we optimized the conditions for the reaction detector using dipyridamole as a standard. The eluent composition and flow rate were fixed at 0.05M imidazole-nitrate (pH 7.0) – acetonitrile (50:50, v/v) and 1.5 ml/min, respectively and the reagent composition and flow rate were changed. The molar ratios of hydrogen peroxide and TDPO (0.5 mM) were changed from 50:1 to 100:1 to 200:1. The resulting signals (peak height) for dipyridamole were in the ratios of 1.0:0.8:0.5 with a constant noise level. The molar ratio of hydrogen peroxide and TDPO was selected as 100:1 for the rest of our work.

Next, the concentration of TDPO was varied from 0.1, 0.5 to 1 mM. The relative peak heights for dipyridamole were 0.86, 1.0 and 0.36. Thus, from this experiment, 0.5 mM concentration of TDPO was adopted. The data suggest that the liberated phenol (4-nitrosalicylic acid) quenched the CL intensity with the increment of TDPO concentration in this HPLC-CL detection system. This appears to contradict the results in a previous paper in which the increased concentration of TDPO in proportion to the concentration of hydrogen peroxide resulted in an increase of chemiluminescence intensity [29]. However, the molar ratio of hydrogen peroxide and TDPO fixed at 1 in these experiments [29] resulted in only a small amount of the liberated phenol which might not be large enough to quench the CL. The present data revealed this disadvantage of TDPO although its great solubility in aprotic solvents such as acetonitrile (1 M) would afford better results in capillary liquid chromatography in which a concentrated oxalate is required in the original reagent solution [11]. In this respect, other compounds of similar structure with ϵ values than 4-nitrosalicylic acid ($\epsilon = 9.52 \times 10^3$ at 316 nm in phosphate buffer, pH 6.86 and $\epsilon = 1.08 \times 10^4$ at 333 nm in ethanol) are now required to avoid the quenching.

The ratios of the flow rates for the eluent and the reagent are also important to get a high signal/noise ratio (S/N). Therefore, at the fixed flow rate of the eluent, the reagent flow rates were varied from 1.5, 2.0, 2.3, 2.5, 2.8 and 3.0 ml/min. The relative S/N values for dipyridamole were 0.24, 0.27, 0.16, 0.16, 0.17 and 0.17 femtomol, respectively. Finally, we fixed the following conditions for further experiments: TDPO, 0.5 mM; hydrogen peroxide, 50 mM; flow rate for the eluent, 1.5 ml/min, and for the reagent, 2.5 ml/min; reaction time 0.5 sec at 35 °C.

We took several of these fluorescent compounds to obtain their detection limits in an HPLC-CL detection system. Since the water content in the reaction medium affected the Icl [18], the eluents containing similar water content would be preferable for the comparison of detection limits obtained by the manual method. However, the range of detection limits appeared to be not greatly affected by the final water content for several DNS-amino acids by gradient elution chromatography, where the water contents were changed from 18.17% to 12.4% [6]. Therefore, in this experiment, with isocratic elution, we selected 0.05M imidazole-nitrate (pH 7.0)-acetonitrile as a basic elution solution and changed the ratio of the buffer and acetonitrile from 80:20 to 10:90 (v/v) in order to get the k' values less than about 6. Thus, the final water contents in the reaction detector were changed from 30 to 7.5%.

The detection limits based on peak height (S/N=2) for dipyridamole (Fig. 3b), perylene, DNS-Ser, DNS-Asp, Trp-P-1, alimemazine, pyrenecarboxylic acid methyl ester, oxypertine, Glu-P-2, benzydamine, doxorubicine (Fig. 3a) and carbocromene were 0.16, 0.18, 2.4, 5.0, 5.9, 95, 110, 280, 800, 880, 1600, and 16,000 femtomol, respectively. These values were plotted against the Icl values obtained by the manual method. Fig. 4 shows the correlation between the two sets of data. (The Icl for carbocromen was not obtained in this experiment because of its low concentration, 20 μM). Since the peak height for a certain analyte is dependent on the retention time and reaction conditions for CL, some variations might occur with variation of the eluent composition, but still good correlation between log of the Icl intensities and log of the values of the detection limits existed. These data suggest that the detection limit for a certain analyte might be predicted by estimation of the Icl value provided that the detection limit for a fixed analyte is taken as standard, for example, with dipyridamole as 0.16 femtomol or DNS-Ser as 2.4 femtomol. Although a further proof with other fluorescent compounds is required, the proposed manual method for the prediction of the detection range for the fluorescent compounds for the HPLC-peroxyoxalate CL detection system should be useful from a practical point of view.

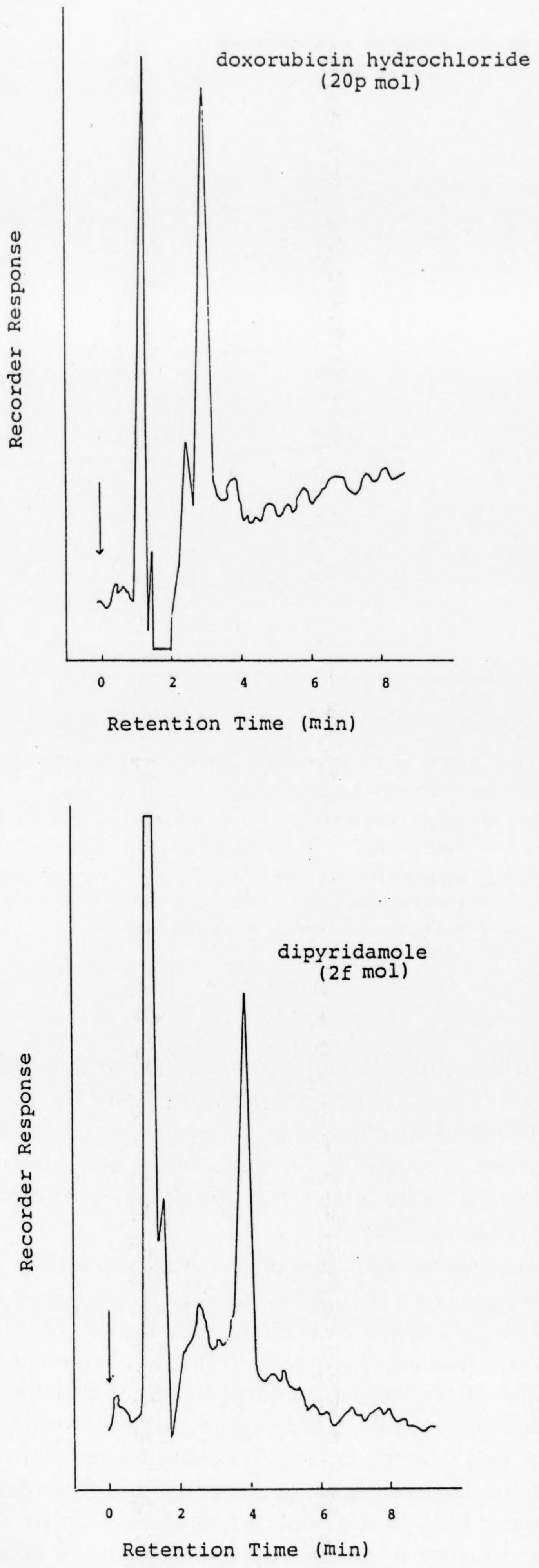

Fig. 3

Chromatograms of dipyridamole and doxorubicin obtained by the HPLC-Peroxyoxalate Chemiluminescence Detection system.

a) doxorubicin (20 picomol), b) dipyridamole (2 femtomol)

Conditions are described in the text.

Acknowledgement

The authors wish to thank Drs. T. Nambara, and J. Goto, the Tohoku University, and Drs. K. Shudo and Y. Hashimoto, the University of Tokyo, for their generous gift of standard samples. They also wish to thank to K. Aoki, R. Yamane and C. Tajima for their technical assistance and Toyo Soda Manufacturing Co. for the gift of TSK columns, Kyowa Seimitsu Co. for the use of a pump, Daiichi Seiyaku Co., Kyowa Hakko Kogyo Co. and Takeda Chemical Industries for the gift of various drugs.

Abbreviations

DNS: 5-N,N-dimethylaminonaphthalenesulfonyl;
NBD: 4-nitrobenzo-2-oxa-1,3-diazolyl;
DCA: 4-(7-N,N-diethylamino-4-methyl-2-coumaryl)aminocarbonylmethyl;
Trp-P-1: 2-amino-1-methyl-5H-pyrido[4,3-b]indole;
Glu-P-2: 2-amino-6-methyldipyrido[1,2-a:3',2'-d]imidazole.

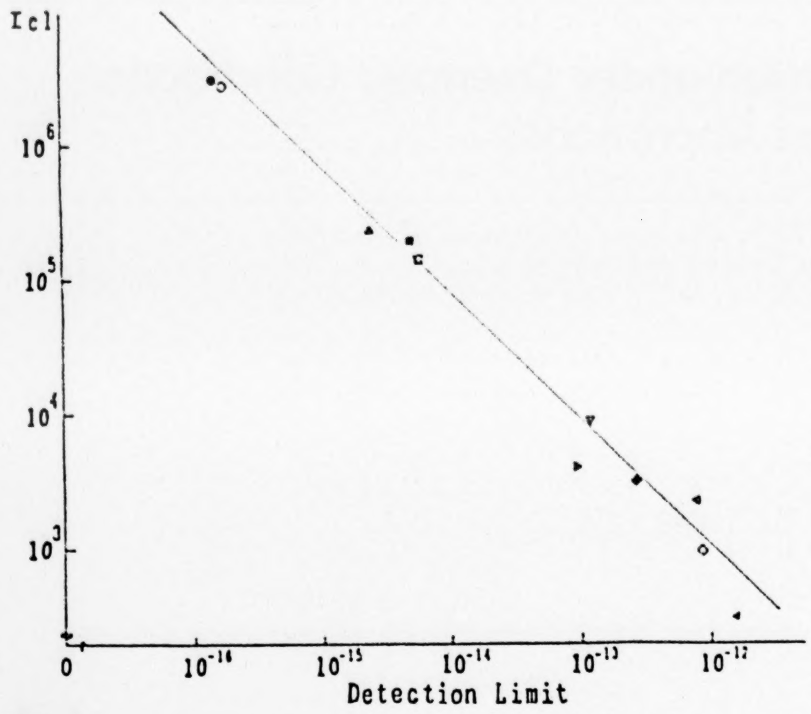

Fig. 4

Relationship between Chemiluminescence Intensities obtained by the Manual Method and Detection Limits obtained by the HPLC-Peroxyoxalate Chemiluminescence Detection System.

● dipyridamole ○ perylene △ DNS-Ser ■ DNS-Asp □ Trp-P-1
▽ pyrenecarboxylic acid methyl ester ▷ alimemazine
◆ oxypertine ◁ Glu-P-2 ◇ benzydamine ◀ doxorubicin

References

[1] *M. M. Rauhut, L. J. Bollyky, B. G. Roberts, M. Loy, R. H. Whitman, A. V. Iannotta, A. M. Semsel, R. A. Clarke,* J. Amer. Chem. Soc. **89,** 6515 (1967).

[2] *K. Kobayashi, K. Imai,* Anal. Chem. **52,** 424 (1980).

[3] *G. Mellbin,* J. Liq. Chromatogr. **6,** 1603 (1983).

[4] *K. Miyaguchi, K. Honda, K. Imai,* J. Chromatogr. **316,** 501 (1984).

[5] *K. Miyaguchi, K. Honda, K. Imai,* J. Chromatogr. **303,** 173 (1984).

[6] *K. Miyaguchi, K. Honda, T. Toyo'oka, K. Imai,* J. Chromatogr. **352,** 255 (1986).

[7] *G. J. de Jong, N. Lammers, F. J. Spruit, U. A. Th. Brinkman, R. W. Frei,* Chromatographia **18,** 129 (1984).

[8] *T. Koziol, M. L. Grayeski, R. Weinberger,* J. Chromatogr. **317,** 355 (1984).

[9] *G. Mellbin, B. E. F. Smith,* J. Chromatogr. **312,** 203 (1984).

[10] *K. Kobayashi, J. Sekino, K. Honda, K. Imai,* Anal. Biochem. **112,** 99 (1981).

[11] *M. L. Grayeski, J. K. De Vasto,* Anal. Chem. **59,** 1203 (1987).

[12] *K. W. Sigvardson, J. W. Birks,* Anal. Chem. **55,** 432 (1983).

[13] *M. L. Grayeski, A. J. Weber,* Anal. Lett. **17,** 1539 (1984).

[14] *K. W. Sigvardson, J. M. Kennish, J. W. Birks,* Anal. Chem. **56,** 1096 (1984).

[15] *R. Weinberger, C. A. Mannan, M. Cerchio, M. L. Grayeski,* J. Chromatogr. **288,** 445 (1984).

[16] *K. W. Sigvardson, J. W. Birks,* J. Chromatogr. **316,** 507 (1984).

[17] *P. van Zoonen, D. A. Kamminga, C. Gooijer, N. H. Velthorst, R. W. Frei, G. Gubitz,* Anal. Chem. **58,** 1248 (1986).

[18] *K. Honda, K. Miyaguchi, H. Nishino, H. Tanaka, T. Yao, K. Imai,* Anal. Biochem. **153,** 445 (1984).

[19] *K. Imai,* in: "Methods in Enzymology" (*M. A. DeLuca* and *W. D. McElroy,* ed.), Vol. **133,** p. 435, Academic Press, New York, 1986.

[20] *M. M. Rauhut, B. G. Roberts, D. R. Maulding, W. Bergmark, R. Coleman,* J. Org. Chem. **40,** 330 (1975).

[21] *K. Imai, K. Honda, K. Miyaguchi,* in: "Bioluminescence and Chemiluminescence: Instrumentations and Applications" (*K. Van Dyke,* ed.), Vol. **2,** p. 65. CRC Press, Boca Raton, Florida, 1985.

[22] *K. Honda, K. Miyaguchi, K. Imai,* Anal. Chim, Acta **177,** 111 (1985).

[23] *K. Honda, J. Sekino, K. Imai,* Anal. Chem. **55,** 940 (1983).

[24] *R. Weinberger,* J. Chromatogr. **314,** 155 (1984).

[25] *G. J. de Jong, N. Lammers, F. J. Spruit, R. W. Frei, U. A. Th. Brinkman,* J. Chromatogr. **353,** 249 (1986).

[26] *A. J. Weber, M. L. Grayeski,* Anal. Chem. **59,** 1452 (1987).

[27] *G. J. de Jong, N. Lammers, F. J. Spruit, C. Dewaele, M. Verzele,* Anal. Chem. **59,** 1458 (1987).

[28] *K. Imai, Y. Tsukamoto, A. Nishitani,* J. Chromatogr. **400,** 169 (1987).

[29] *K. Imai, H. Nawa, M. Tanaka, H. Ogata,* Analyst **111,** 209 (1986).

[30] *A. Berg,* Acta Chem. Scand. **10,** 1362 (1956).

[31] *Y. Hashimoto, K. Shudo, T. Okamoto,* Acc. Chem. Res. **17,** 403 (1987).

Received: June 29, 1987
Accepted: July 29, 1987
F

A Simplified Description of HPLC Separation under Overload Conditions. A Synthesis and Extension of Two Recent Approaches

L. R. Snyder*

LC Resources Inc., 26 Silverwood Ct., Orinda, CA 94563, USA

G. B. Cox / P. E. Antle

Medical Products Dept., E. I. Du Pont de Nemours Inc., Wilmington, DE 19898, USA

Key Words

Preparative HPLC
Sample size effects
Reversed-phase HPLC

Summary

Knox and Pyper [1] have recently proposed a simplified model of HPLC separation in an overload mode. We have now compared certain predictions of their model with experimental data reported by us earlier [2]. The Knox/Pyper model shows quantitative agreement with this data base, over a broad range in sample size and other experimental conditions. The neglect by Knox and Pyper of mixed-isotherm effects seems generally unimportant, except for the case where two adjacent bands begin to overlap appreciably at elution. The Knox/Pyper model and other treatments based upon a two-term expansion as an approximation to the sorption isotherm appear unreliable when the mass of any solute exceeds 5–10 % of the column saturation capacity.

We have combined certain features of the Knox/Pyper model with our own model of preparative HPLC, so as to allow convenient and reliable computer simulations to be carried out under conditions of mass-overload. The use of this program (PREPSIMX) in conjunction with the Knox/Pyper model has made it possible to draw a number of general conclusions relating to optimum conditions for preparative HPLC.

Introduction

The past year or so has seen significant advances in our theoretical understanding of HPLC separation in an overload mode. Three somewhat different approaches to this subject can be recognized at this point, as represented in Table I by the treatments of Knox et al. [1], Eble et al. [2], and Guiochon et al. [3, 4]. For convenience, we will refer to these as the models of Knox, Eble or Guiochon. These individual descriptions of preparative HPLC mainly reflect varying degrees of simplification in the final treatment, rather than fundamental differences in approach or assumptions. As we progress from the Knox model to the Eble model to that of Guiochon, there is a transition from general predictions based on explicit algebraic relationships to numerical calculations that require an increasing amount of computer effort. Each model can be useful in creating a picture of how preparative HPLC works, and in helping practical chromatographers develop a preparative HPLC method.

In this paper we will explore a combination of the Knox and Eble models in an effort to obtain a treatment that is able to provide both general and specific predictions concerning preparative HPLC separation. From this starting point, we will see that it is possible to derive simple algebraic relationships that describe the general effects of different variables on separation. It is also possible to carry out detailed predictions for individual separations, requiring only a few minutes on a personal computer. Finally, a comparison of certain features of these two models will provide insight into the accuracy and reliability of each.

Theory and its Experimental Confirmation

A quantitative understanding of HPLC separation under overload conditions is most easily arrived at if we consider only one solute at a time. The separation of multicomponent samples can then be approximated by the superimposed elution bands of individual components, ignoring the interaction of adjacent bands as they migrate through the column. We will refer to this as the "1-solute case". We will see that this approximation is not a bad one; more

0009-5893/87 0082-15 $03.00/0

© 1987 Friedr. Vieweg & Sohn Verlagsgesellschaft mbH

Table I. Three models that describe preparative HPLC separation.

Model	Description
Knox [1]	Assumes Langmuir isotherm and approximates band shape by "nested right triangles"; ignores mixed-isotherm effects (changes in one band due to the presence of another, for multi-component samples)
	Bandwidth is derived as a function of sample mass and the small-sample column plate-number N_0; effect of sample volume on bandwidth is treated
	No computer calculations are required; all relationships can be derived algebraically
	Little attempt made to verify quantitative accuracy of final predictions using experimental data – model so far used for approximate predictions of a general nature
Eble [2]	Uses relationships obtained from Craig-distribution computer-modeling of preparative HPLC; modifies these relationships empirically to agree with a large experimental data base; assumes Langmuir isotherm; takes mixed-isotherm effects into account
	Separation of 2-component samples is predictable, given values of k_0 and N_0 for each compound in the sample, plus sample weights w_i and column saturation-capacity values w_s for each solute
	Predictions carried out on a personal computer (about 1 min per run)
	Extensive experimental verification of final computer model
Guiochon [3, 4]	Based on numerical solution of mass-balance equations for mass-overload HPLC; convex or concave isotherms can be treated, as long as the isotherm is representable by a two-term expansion; takes mixed-isotherm effects into account
	Separation of 2-component samples is predictable, given information on individual solute isotherms plus plate number of column for small sample
	Predictions carried out on a large computer (about 20 min per run)
	Considerable experimental verification of final computer model

importantly, it is possible using the 1-solute approximation to derive general relationships that describe the major features of preparative HPLC.

When more accurate and detailed predictions for a preparative HPLC separation are desired for a specific sample and defined experimental conditions, it becomes necessary to recognize solute/solute interaction effects ("mixed-isotherm" contributions). The 1-solute case is a useful starting point for building a more complete theory of these separations. The following discussion begins with the 1-solute case and progresses to a discussion of mixed-isotherm effects.

Knox Model: 1-Solute Samples

The Knox model is central to the following discussion; therefore we will review some its main features. According to this treatment, as the mass of a sample is increased, the shape of the resulting elution band changes from Gaussian to triangular. A series of overlapped bands (from separate runs) where only sample mass has been varied will resemble the "nested right-triangles" example shown in Fig. 1. A similar result is shown schematically in Fig. 2; bands 2a–c

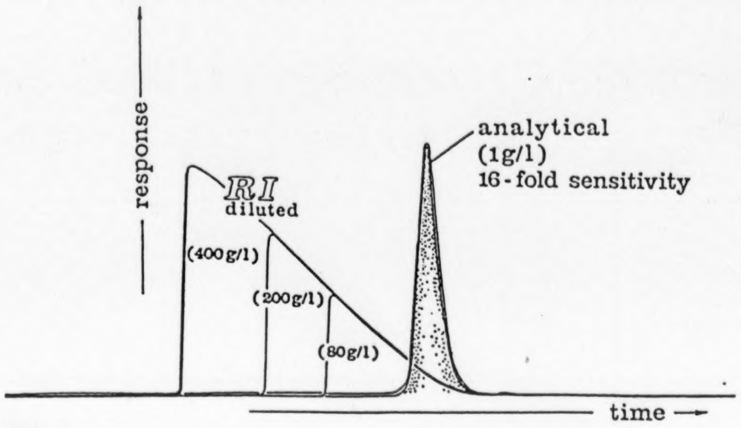

Fig. 1

Illustration of mass-overloaded bands from Eisenbeiss et al. [5]. Diethylphthalate solute, silica column.

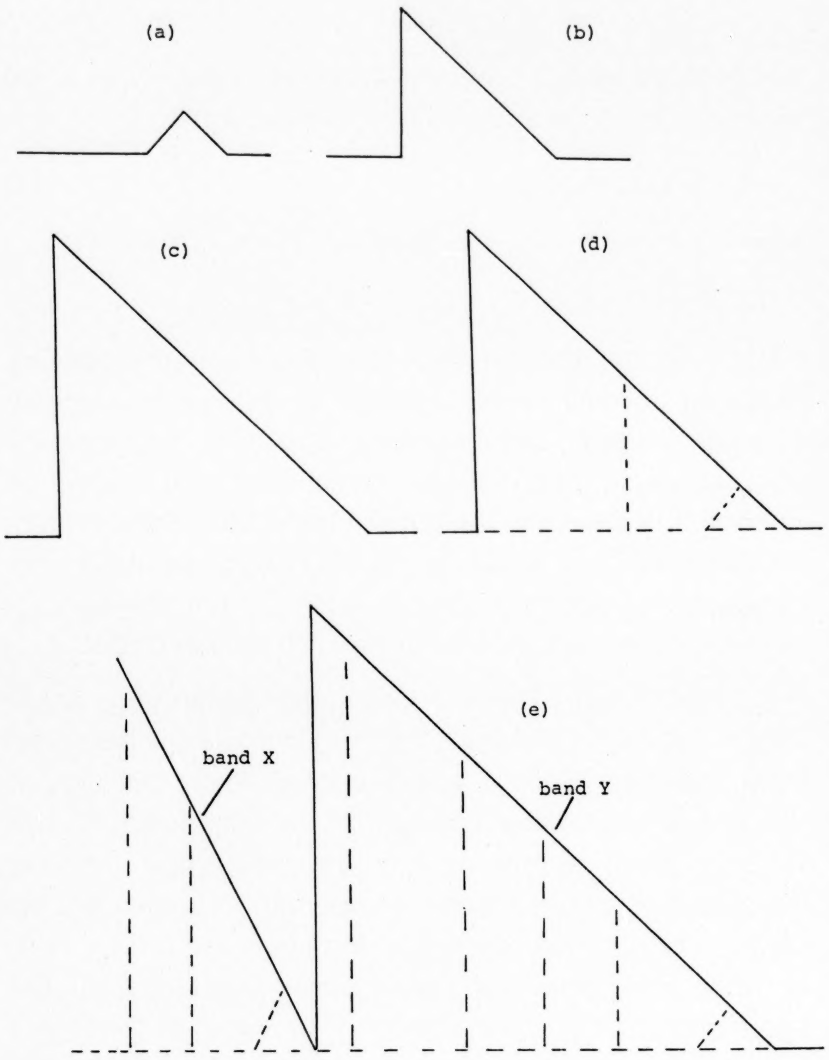

Fig. 2

Schematic representation of nested right-triangles as an approximation to mass-overloaded solute bands.

corresponding to increasing sample mass are simultaneously displayed (overlapped) in Fig. 2d. Experimental results similar to those of Figs. 1 or 2d are often encountered [3, 5–7]. Chromatographic behavior of this type (nested right-triangles) is a direct result of the applicability of Langmuir-isotherm behavior in a given HPLC system (see pp. 10–13 of Ref. [1]), when the solute mass is not too large. Other studies [8, 9] suggest for the case of small sample molecules (mol. wt. <500) that the sorption isotherm is often of the Langmuir type.

Fig. 3 provides some definitions with respect to bands that have a right-triangle shape. Retention time can be defined variously from the band maximum t_R^{max}, the first moment or 50%-elution value (so-called "cumulative" value in Ref. [8]) t_R^{cum}, or the band maximum for a small sample t_R^0. It

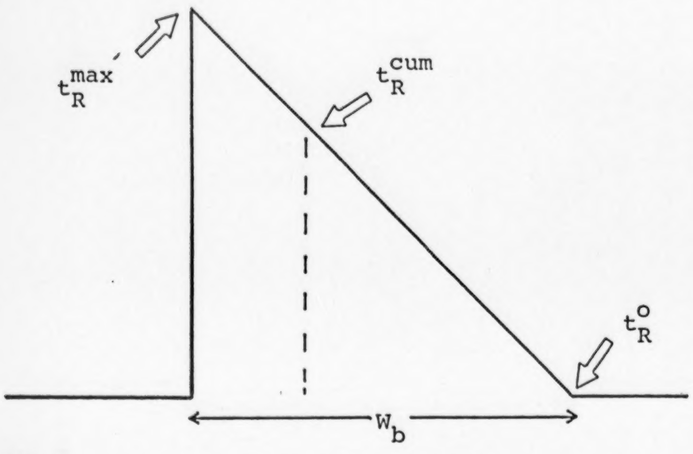

Fig. 3
Definition of retention and width parameters for right-triangle band shape.

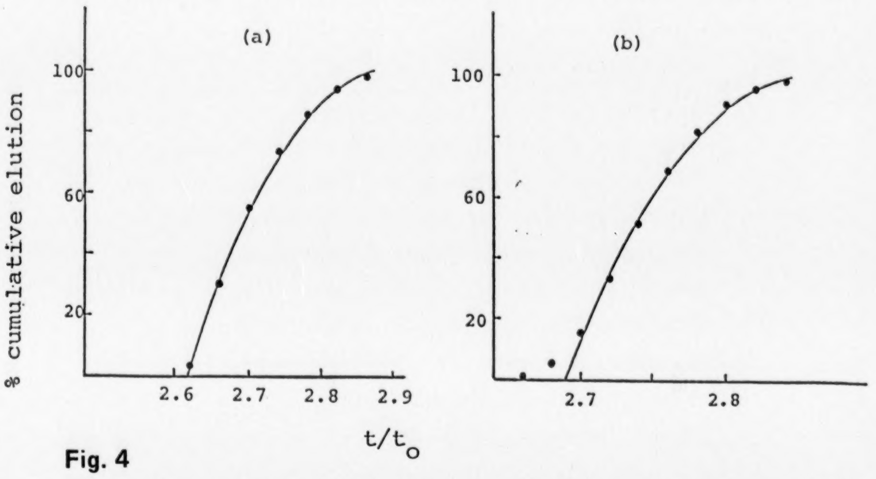

Fig. 4
Comparison of cumulative-elution curves for a given case as calculated by the Knox [1] or Eble [2] models. Conditions correspond to HPLC runs for solute HET as described in Ref. [2]. $N_0 = 5750$, $k_0 = 1.85$, $w_s = 240$ mg. Eble model, ●; Right-triangles, ——. PREPSIMX calculations, with appropriate modification. (a) $w_{xn} = 6$, $N/N_0 = 0.30$; (b) $w_{xn} = 0.6$, $N/N_0 = 0.82$.

has been claimed [1] that the appropriate definition of the plate number N involves the use of the quantity t_R^0:

$$N = 16(t_R^0/W_b)^2\ , \tag{1}$$

where

$$t_R^0 = t_0(1+k_0)\ . \tag{2}$$

Here t_0 is the column dead-time and k_0 is the capacity factor for a small sample. Because of the simple geometry of a right triangle, and the proportionality of band area and injected solute mass, various relationships that we will be interested in are easily derived. Thus the 50%-elution retention-time t_R^{cum} is equal to $(t_R^0 - 0.71 W_b)$. Similarly, the bandwidth at half-height equals $0.5 W_b$, while the cumulative (2σ) bandwidth defined in Ref. [10] equals $0.52 W_b$[1].

Adequacy of right triangles as an approximation to actual sample bands. Fig. 1 suggests that a right triangle is a rather good approximation to a solute band when the mass of injected sample is large enough. On the other hand, for sufficiently small samples the solute band-shape becomes Gaussian and a right-triangle representation is then less accurate. The question thus arises: as sample size is decreased, at what point does the right-triangle approximation fail significantly? The Eble model [10] uses an empirical description of band shape (cumulative-elution curves), which accurately reflects the transition of solute bands from Gaussian to triangular shapes as sample mass is increased[2]. It is therefore of interest to compare predictions of band shape by the Eble model with corresponding right-triangle bands, for the case of smaller samples. Fig. 4 shows such a comparison, for two different sample sizes: (a) $w_{xn} = 6$, corresponding to $(N/N_0) = 0.30$; (b) $w_{xn} = 0.6$, corresponding to $(N/N_0) = 0.82$. N_0 refers to the N-value for a small sample, and the loading function w_{xn}

$$w_{xn} = N_0[k_0/(1+k_0)]^2\ (w_x/w_s) \tag{3}$$

is related to N/N_0 as

$$N/N_0 = f\{w_{xn}\}\ . \tag{4}$$

Here f { } refers to "a function of", w_x is the mass of compound X injected, and w_s is the saturation-capacity of the column [8, 10].

It is seen in Fig. 4 that cumulative-elution plots for right-triangle bands closely track the plots predicted by the Eble model (which in turn agree closely with experimental data), for this range of column overload. A value of (N/N_0) equal to 0.82 (Fig. 4b) represents a rather minor overloading of the column, suggesting that the right-triangle approximation of the Knox model is valid for samples sizes such that $w_{xn} > 1$. Preparative HPLC for the most part will involve values of $w_{xn} \gg 1$. Note that the examples of Fig. 4 involve large values of N_0 ($N_0 = 5750$); the agreement between experimental bands and those of right-triangle shape becomes poorer as the value of N_0 is decreased, due to a rounding of the ends of bands that approximate right-triangles for small values of N_0.

Band width: sample-mass effects. Band width as a function of sample mass is central to any discussion of overloaded HPLC separation. Knox and Pyper [1] begin with the relationship

$$H_{total} = H_0 + H_{th}\ . \tag{5}$$

Here H_{total} refers to the plate-height of the (mass-overloaded) band,

$$H_{total} = L/N\ , \tag{6}$$

with an experimental value of N obtained using eq. (1); L is column length. H_0 is the value of H_{total} for a small sample, and H_{th} reflects the contribution from "thermodynamic" or mass-overload effects. We can obtain a value of H_0 from an experimental measurement (for a small sample, $H_0 = H_{total}$). A value of H_{th} can be derived as follows.

---

[1] This also means that N values reported by us in Refs. [2, 8] must be multiplied by $[(0.52/0.50)\ (1+k_0)/(1+k')]^2$ in order to obtain N-values defined by eq. (1). All N-values reported on here have been recalculated on this basis.

[2] The algorithm described in Appendix II of Ref. [10] for the prediction of cumulative-elution profiles for mass-overloaded bands has since been found to be less accurate for very large sample sizes; e.g., corresponding to w_{xn} values $\gg 25$.

Knox and Pyper [1] give a relationship for H_{th} which can be rewritten as[3]

$$H_{th} = (L/4)\,[k_0/(1+k_0]^2\,(w_x/w_s)\,. \qquad (7)$$

Eq. (4), (5) give

$$N = L/(H_0 + H_{th})\,, \qquad (8)$$

and the plate number N_0 for a small sample ($H_{th} = 0$) is similarly given as

$$N_0 = L/H_0\,. \qquad (9)$$

Combination of Eqs. (7)–(9) then yields

$$N/N_0 = 1/[1+(p/4)\,w_{xn}]\,, \qquad (10)$$

where w_{xn} is defined by eq. (3). The parameter p of eq. (10) is an empirical correction factor (introduced by us) that takes into account various approximations in the above treatment; p is ignored (i.e., set equal to one, in Ref. [1]. Note that bandwidth W_b can be obtained from a value of N and retention time t_R^0 (eq. (1)). Eqs. (3), (10) therefore allow the prediction of values of W_b as a function of k_0, N_0, sample size w_x and column capacity w_s. Values of k_0 and N_0 can be determined from a single small-sample run, and w_s can be obtained from two runs, one with a small sample and one with a larger sample [2].

Eq. (10) can be compared with eq. (4) of the Eble model; it is seen that these two relationships are of the same form. Eq. (10) with a best-fit value of $p = 1.5$[4]

$$N/N_0 = 1/[1+(3/8)\,w_{xn}]\,. \qquad (11)$$

is found to accurately predict experimental data reported by Eble et al. [2] and others [3]. This is illustrated in Fig. 5, where the solid curve is eq. (11), and the various data points are experimental values for selected samples and experimental conditions. Fig. 6 similarly shows a comparison of experimental and calculated values of N for the entire data-set (150 values of N) reported in Ref. [2, 8]. For a range of $70 \leqslant N \leqslant 20{,}000$, values of N are predicted by eq. (11) within ±20% (1 SD). This corresponds to only ±10% error in bandwiths W_b.

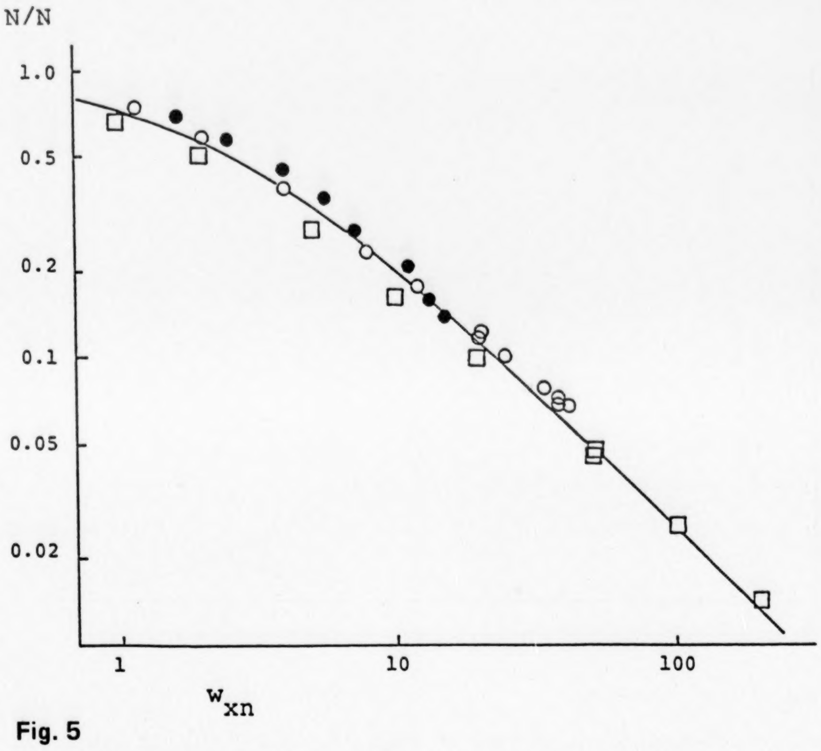

Fig. 5

Dependence of (N/N_0) on loading function w_{xn}. Solid curve is predicted by eq. (11). Data points are taken from the previous literature: ○, benzyl alcohol as solute, 5 × 0.46cm Zorbax C18 column, 40% methanol/water, 1 ml/min (2); ●, benzyl alcohol as solute, C18 column, 17% methanol/water, 20 °C (1); □, HPT as solute, 15 × 0.46cm Zorbax C8 column, 25% (methanol+acetonitrile)/water mobile phase [2]. Experimental values of N recalculated using eq. (1).

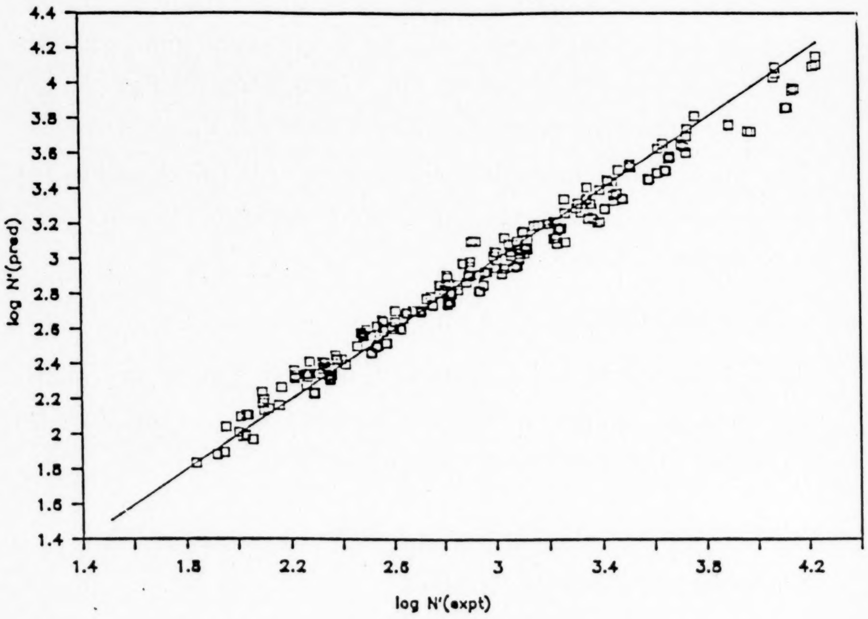

Fig. 6

Comparison of experimental mass-overloaded plate numbers with values predicted by eq. (11). N defined by eq. (1), data of Ref. [2, 8].

Band width: sample-volume effects. According to Knox and Pyper [1], the effect of a larger sample volume V_s will only be noticable when V_s exceeds one-half the volume of the (mass-overloaded) sample band V_b for a small sample-volume ($V_b = W_b\,F$, where F is flowrate). This generalization is tested in Fig. 7, using Craig-simulations as in Ref. [2] for a typical case. The solid curve in Fig. 7 is for a small sample-volume and a large sample mass ($w_x/w_s = 0.15$). The resulting band is seen to tail badly, and to roughly approximate a right-triangle shape. The volume V_b of this band is approximately equal to $0.6\,V_m$ (V_m is the column dead-volume). The open circles are for the same sample mass, but a larger sample volume: sample volume $V_s = (0.20\,V_m) = (0.33\,V_b)$. There is no significant change in band width or shape as a result of the larger volume. For $V_s = (0.30\,V_m) = (0.50\,V_b)$ (solid squares) there is a perceptible change in band shape and a slight increase in band width. For a still larger sample volume ($V_s = 0.50\,V_m = 0.8$

---

[3] Knox and Pyper [1] do not refer to the saturation capacity w_s of a particular column, but rather to the corresponding value (C_s^∞) for a column of unit cross-sectional area and unit volume.

[4] The discrepancy of 1.5 in eq. (11) (i.e., the value of p) corresponds to a 1.5-fold difference in values of w_s derived from measurements of k' vs N. For a further discussion of values of w_s derived from k'-values as a function of sample mass, see the discussion of Appendix I.

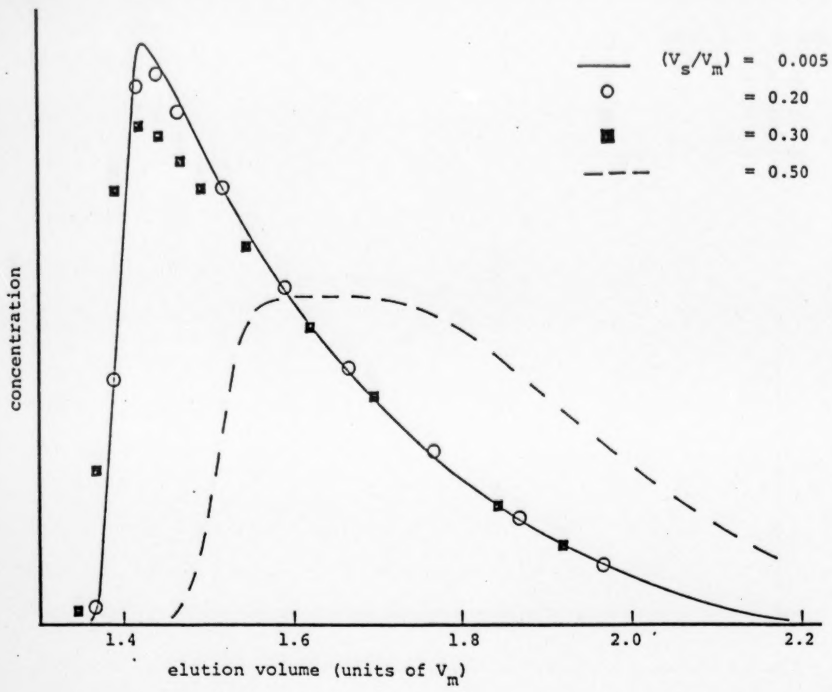

Fig. 7

Effect of sample volume on a mass-overloaded elution band, as illustrated by Craig-simulations (as in Ref. [2]). Number of Craig stages n_c = 200, k_0 = 1, w_x/w_s = 0.15. Sample volume varies as shown in figure.

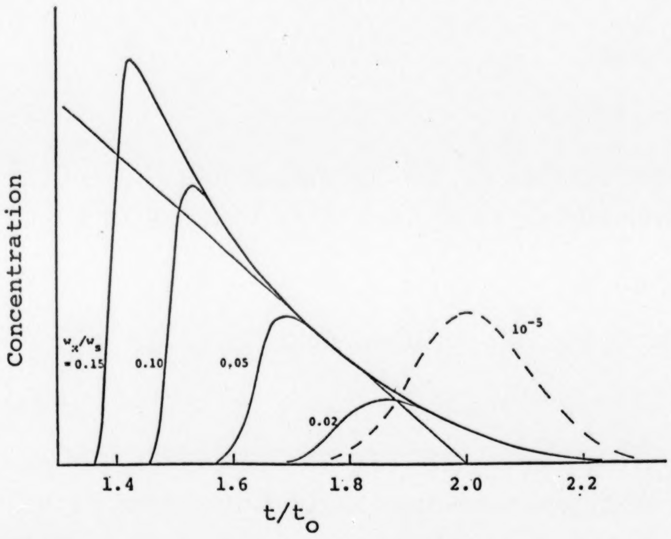

Fig. 8

Craig-model simulations of band-shape as a function of solute mass (w_x/w_s), obtained as in Ref. [2]. Assumes k_0 = 1, 200 transfer stages, and therefore N_0 = 400. Solid curves for $(w_x/w_s) > 0.01$ are plotted on same scale.

V_b), there is a marked deterioration of band shape combined with considerable band broadening (dashed curve). Thus these simulations confirm the accuracy of Knox and Pyper's generalization: the sample volume does not affect separation, until it exceeds one half the band volume for the same sample-mass injected in a small volume. The effect on band width and shape of a relatively small increase in sample volume (from 0.3 V_m to 0.5 V_m in Fig. 7) can be quite dramatic, when V_s just exceeds 0.5 V_b.

The maximum allowable volume of sample (dissolved in the mobile phase), if no volume-related reduction in resolution is to occur, is given as

$$V_s = (1/2)\ (k_{oy} - k_{ox})\ V_m \qquad (11a)$$

for the case of R_s = 1 (see definition of R_s below: eq. (12)). For smaller values of R_s, this volume (eq. (11a)) can be increased in proportion to sample weight.

Knox Model: 2-Solute Samples

The Knox model ignores interaction effects between different sample bands. That is, each sample band is assumed to migrate through the column independently of other sample components. The Eble model takes such mixed-isotherm phenomena into account [2], in terms of what has been referred to as "blockage". The presence of a more strongly retained band Y leads to the more rapid elution of an adjacent band X, and a decrease in the bandwidth of X. These two effects work together to improve the overall separation — vs the separation predicted by superimposing the bands from two single-solute separations (other conditions the same). A significant question therefore is: to what extent will the Knox model be in error because of its omission of mixed-isotherm effects? We will return to this in a later section.

Failure of Knox and Other Models for Large Samples

The Knox and Guiochon models of Table I assume that a Langmuir isotherm can be approximated by a two-term expansion. When (w_x/w_s) becomes large enough, this approximation is no longer valid. The general effect of a continued increase in sample size can be seen in the simulated (overlapped) bands of Fig. 8, obtained from the Craig model described in Ref. [10] (cf. similar plots of Fig. 1). These results are for k_0 = 1 and a 400-plate column. The general nested-right-triangle pattern that we expect for a Langmuir-isotherm system is apparent[5], but it is also seen that the bands tend to become narrower and taller for larger values of (w_x/w_s), vs the case of bands with a true right-triangle shape (indicated by the straight line that intersects the x-axis at t/t_0 = 2).

Fig. 8 suggests that the Knox and Guiochon models will begin to fail when (w_x/w_s) approaches a value of 0.10. For larger samples, the shape of the elution band should depart from a right-triangle, as in Fig. 8, and the experimental plate number should be greater than the value predicted by a right-triangle, as in Fig. 8, and the experimental plate number should be greater than the value predicted by eq. (11). This is illustrated by data reported in Ref. [2] for 7-β-hydroxylpropyltheophyline (HPT), where sample size was varied from 1 μg to 25 mg for a 25 cm column with w_s = 240 mg. For samples of 10 mg or smaller, band-shape is well approximated by a right triangle as shown in Fig. 9. However a larger sample (25 mg, $[w_x/w_s]$ = 0.10) yields a band-shape similar to those of Fig. 8 for $(w_x/w_s) > 0.05$. Likewise, when (w_x/w_s) is large, values of N from this study show the expected trend to larger values of N/N_0 vs values from eq. (11). This is summarized in Table II. Unacceptable errors in calculated values of N and band-width occur when (w_x/w_s) is much greater than 0.05. It may be possible to correct for these errors empirically, but this is a topic for examination at a later time.

---

[5] The use of a larger value of N_o in this simulation would lead to a closer fit to the right-triangle model in the vicinity of t/t_o = 2; see previous discussion.

Table II. Failure of the Knox model for larger sample sizes. Data for 7-β-hydroxypropyltheophyline (HPT) as solute, Zorbax C8 15 X 0.46 cm column, and other conditions of Ref. [2]; $k_0 = 3.15$, $N_0 = 5750$.

w_s (mg)	w_x/w_s	N/N_0		
		expt.	eq. (11)	error
0.001	4×10^{-6}	1.00	1.00	
0.3	0.0013	0.36	0.39	+11%
1.0	0.0042	0.14	0.16	+14
2.5	0.0104	0.077	0.072	− 9%
10	0.042	0.025	0.019	−24
25	0.104	0.014	0.0076	−46

General Relationships Derivable from the Knox Model (Ignoring Blockage)

The simplicity of the Knox model suggests its application to various general questions that arise during preparative HPLC; e.g., the effect of sample volume on bandwidth discussed above. Knox and Pyper [1] recommend that separation conditions (including sample size) be adjusted so as to cause two bands of interest to just touch – as in Fig. 1e. We will define resolution R_s in such a way that $R_s = 1$ for this case:

$$R_s = (t_{y0} - t_{x0})/W_y \,. \tag{12}$$

Here t_{x0} and t_{y0} refer to the t_R^0-values (small sample) for bands X and Y, and W_y refers to the W_b-value for band Y.

Maximum Sample Size for $R_s = 1$. Fig. 1e suggests that the mass of solute Y determines at what point bands X and Y will touch, so that $R_s = 1$. That is, the mass of compound X is unimportant.[6] We can determine this mass of band Y (w_y) as follows.

The retention times t_{x0} and t_{y0} are given as

$$t_{y0} = t_0(1 + k_{0x}) \tag{13}$$

and

$$t_{y0} = t_0(1 + k_{0y}) \,, \tag{13a}$$

where k_{0x} and k_{0y} are k_0-values for X and Y. Likewise the bandwidth W_y is equal to

$$(R_s = 1) \qquad W_y = t_0(k_{0y} - k_{0x}) \,. \tag{14}$$

The value of N for band Y is then given by eq. (1), (13a) and (14):

$$(R_s = 1) \qquad N_y = 16[(1 + k_{0y})/(k_{0y} - k_{0x})]^2 \,. \tag{15}$$

Combination of eq. (11) $(N = N_y)$ with eq. (3) (rewritten for band Y; i.e., w_y replaces w_x) and eq. (15) finally yields

$$(R_s = 1) \qquad (w_y/w_s) = (1/6)[(\alpha - 1)/\alpha]^2 (1 - [N_y/N_{0y}]) \tag{16}$$

$$= (1/6)[(\alpha - 1)/\alpha]^2 (1 - [1/q]) \,. \tag{16a}$$

Here α is defined as (k_{0y}/k_{0x}), the separation factor for bands X and Y when the sample is small. The factor q is equal to N_{0y}/N_y.

According to eq. (16), the maximum sample size w_y for $R_s = 1$ is determined by α (small sample) and the ratio (N_y/N_{0y}) for band Y. Knox and Pyper [1] have proposed that an optimum value of = q is about 3[7], which is seen to reduce the maximum sample size by 1/3, relative to the case of a large value of N_{0y}:

$$(\text{large } N_{0y}) \qquad (w_y/w_s) = (1/6)[(\alpha - 1)/\alpha]^2 \,. \tag{17}$$

Eq. (17) suggests that the maximum possible value of (w_y/w_s) is equal to 1/6. However, for very large values of α and k_{0y} it should be possible to separate a sample size such that $w_y = w_s$; i.e., 6 times greater than predicted by eq. (17). In the latter case, pure X would elute from the column until Y completely saturates the column (for $w_y = w_s$). This 6-fold discrepancy arises from the fact that right-triangle bands are only predicted for moderate loading of the column; i.e., over a (limited) sample-size range where a two-term expansion of the Langmuir isotherm is a good approximation (see eq. (17)–(25) of Ref. [1]). This approximation is no longer valid for very large sample sizes, as we have seen (Figs. 8, 9; Table II).

Best values of N_0 and k_0 for $R_s = 1$. Given some desired value of $q = (N_{0y}/N_y)$, eq. (15) can be expressed as

$$(R_s = 1) \qquad N_{0y} = 16q\{[(1/k_{0x}) + \alpha]/(\alpha - 1)\}^2 \,. \tag{18}$$

Often α is not very sensitive to changes in k_{0x}, so that α can be assumed constant as solvent strength (and k_{0x}) is varied. Thus to obtain some value of (w_y/w_s) given by eq. (16a), various combinations of N_{0y} and k_{0x} are possible – a smaller value of k_0 requires a larger value of N_0, and vice versa.

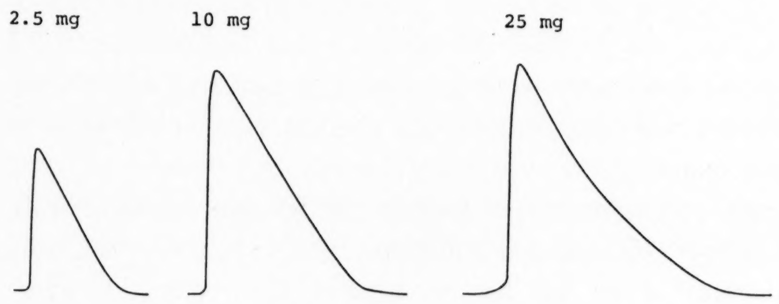

Fig. 9

Experimental elution bands for 7-β-hydroxypropyltheophyline and a Zorbax C8 column (25 X 0.46 cm, w_s = 240 mg). Detector attenuations differ for each band; reprinted from Ref. [2].

---

[6] This ignores effects due to the "blockage" of band Y by band X. Except for the case of a severely oberloaded column, however, we can usually ignore the blockage of Y by X (see later discussion). A relatively large value of N_o is also assumed, since small N_0-values lead to a rounding of the ends of mass-overload bands.

[7] In Appendix II we derive an optimum value of q = 2.5, which is similar to the value of Knox et al. [1]. The exact value of q is determined by the dependence of N_o on flowrate F (d N_o/d F), which varies with the reduced flowrate.

An optimum trade-off depends on the cost of increasing N_0 vs the benefit (in terms of throughput) of stronger mobile phases and resulting lower values of k_{0x}. We will explore this in a later section.

Effect of sample size on recovery and purity of separated fractions. As long as $R_s > 1$, it is possible to obtain 100% recovery and purity of both X and Y (assuming right-triangle bands). The situation that results for larger samples and $R_s < 1$ is illustrated in Fig. 10. A cutpoint at time t_c can be selected (Fig. 10b) that will furnish a fraction containing either X or Y of any desired purity. The yield of the solute in question will decrease as sample size is increased and/or the required purity of the recovered fraction is greater. The geometrical relationships implied by Fig. 10b allow us to (easily) calculate yield as a function of purity and sample size.

Fig. 11 summarizes one such calculation, for the case of two bands of equal mass and equal band widths. This is a good approximation for the case of samples with equal concentrations of X and Y, when the k_0-values for X and Y are not very different (meaning small values of α). Sample size in Fig. 11 is expressed as (wt. Y)/(wt. Y for $R_s = 1$). It is seen that the yield of purified X will generally be greater than that of purified Y, because of the way the bands overlap in Fig. 10b; i.e., the yield of X is relatively insensitive to changes in the required purity, because as t_c is increased, much more Y than X is added to the fraction of purified X.

Fig. 11 is of qualitative value in obtaining an idea of how yield and purity vary with sample size and cutpoint. However, not too much should be made of this particular example, because blockage effects (which are ignored here) play a role in the interdependence of yield, purity and sample size. We must also keep in mind the errors associated with larger samples, as summarized in Table II.

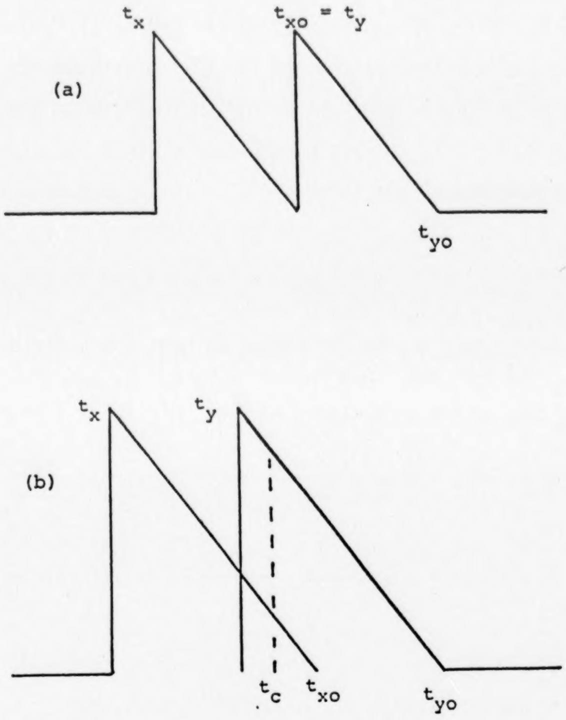

Fig. 10

Illustration of recovery and purity as a function of band overlap in preparative HPLC (see text).

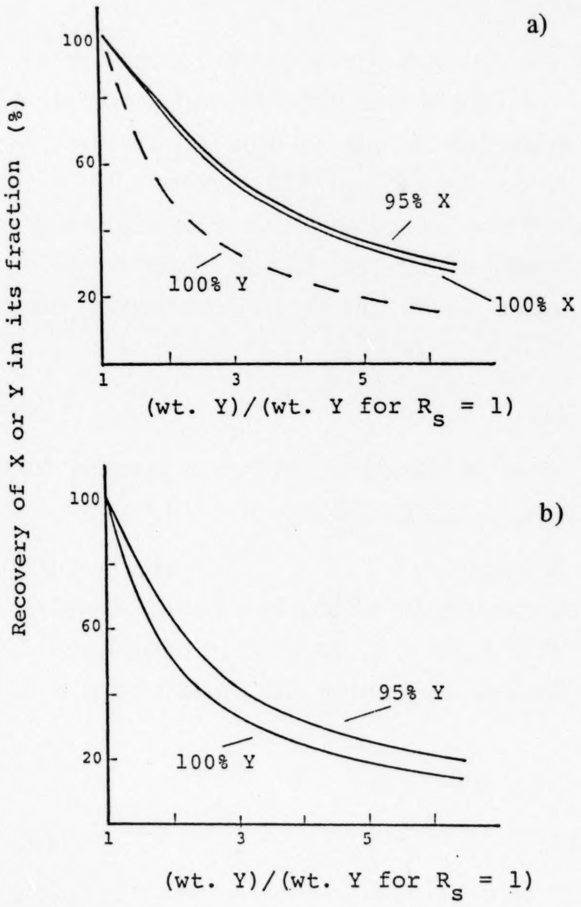

Fig. 11

Recovery of solute X or Y as a function of sample size. Blockage effects ignored (see text).

A Composite Theory Based on the Knox and Eble Models (PREPSIMX)

The Knox model is surprisingly accurate in some respects, and simple enough to provide a picture of what will happen when certain changes in separation conditions are made; e.g., variation of k_0, α, N_0 and sample size. Its main limitations appear to be (a) the neglect of blockage effects arising from the presence of two or more compounds in the sample, and (b) its eventual failure as $(w_y/w_s) \rightarrow 1$. Predictions by the Knox model may therefore be significantly in error, particularly when we attempt to predict yield and purity as a function of sample size for overlapping bands, as in Figs. 10b and 11. The Knox model also becomes more complicated to use for predictions as in Fig. 11, when samples containing different proportions of two solutes X and Y are of interest.

We have previously described a simple computer-model to simulate the separation of 2-solute mixtures under mass-overload conditions [2, 8, 10]. We have since improved this program by incorporating two features of the Knox model: (a) the use of right-triangle band-shapes for larger sample sizes ($w_{xn} > 3$), and (b) the use of eqs. (1), (11) to calculate band widths. The resulting program for IBM-compatible personal computers is called PREPSIMX. We have shown that this model can provide reliable predictions of the separation of sample mixtures that contain two or more components.[8] As also pointed out previously, we are less confident of the predictions of our present model (and PREPSIMX) for the case of very large samples ($w_y/w_x >> 0.05$) combined with extensive band-overlap ($R_s << 1$).

---

[8] A previous comparison of experiment with our model used an earlier version of PREPSIMX [2]; both versions of this software provide similar (good) correlations with experimental data reported here and previously.

In the remainder of this paper we will describe our results from the application of the PREPSIMX program to various representative situations. These data plus the general relationships derived from the Knox model will provide further insight into the significance of different operating parameters encountered in preparative HPLC.

Results and Discussion

The use of computer simulations based on the present model (PREPSIMX) allow us to explore certain questions which were raised in the preceding section. Once these issues are resolved, we can then apply what we have learned to the design of preparative HPLC separations.

Blockage Effects

So far we have overlooked errors that arise from our neglect of other solutes in the sample (mixed-isotherm interactions). Because blockage results in the displacement of the first band X away from the second band Y, blockage should result in improved resolution, or an increase in the allowable sample mass for some specified resolution; e.g., $R_s = 1$. This effect is examined in Table III, where the allowable value of (w_y/w_s) is shown as a function of the separation factor α. The result of taking blockage into account (PREPSIMX) is a modest increase in the allowable sample size, from 1% for $\alpha = 1.2$ to 14% for $\alpha = 3$. That is, blockage is more important for larger values of α because this corresponds to larger sample sizes for $R_s = 1$ (and correspondingly larger blockage effects; see discussion of Ref. [11]). However, the net effect of blockage in all of these examples is small enough to suggest that the generalizations arrived at in the preceding section (where blockage was ignored) are not seriously in error. It should also be noted that larger samples (with $R_s < 1$) may involve values of (w_y/w_s) that are large enough to be in error for other reasons (see discussion of Table II). That is, for those cases where blockage is likely to constitute a major contribution to separation, the Knox/Eble model begins to break down for other reasons.

Table III. Effect of mixed-isotherm effects (blockage) on the allowable sample size (w_y/w_s) for a resolution of $R_s = 1$. Assumes $k_{0x} = 1$, N_{0y} large ($q = \infty$); prepsimx simulations.

α	(w_y/w_s) for $R_s = 1$ no blockage*	(w_y/w_s) for $R_s = 1$ with blockage	increase in (w_y/w_s)**
1.2	0.0046	0.00465	+ 1%
1.5	0.0185	0.0210	11
2.0	0.042	0.048	14
3.0	0.074	0.082	14

* values from eq. (17)

** increase in sample size (for $R_s = 1$) as a result of blockage

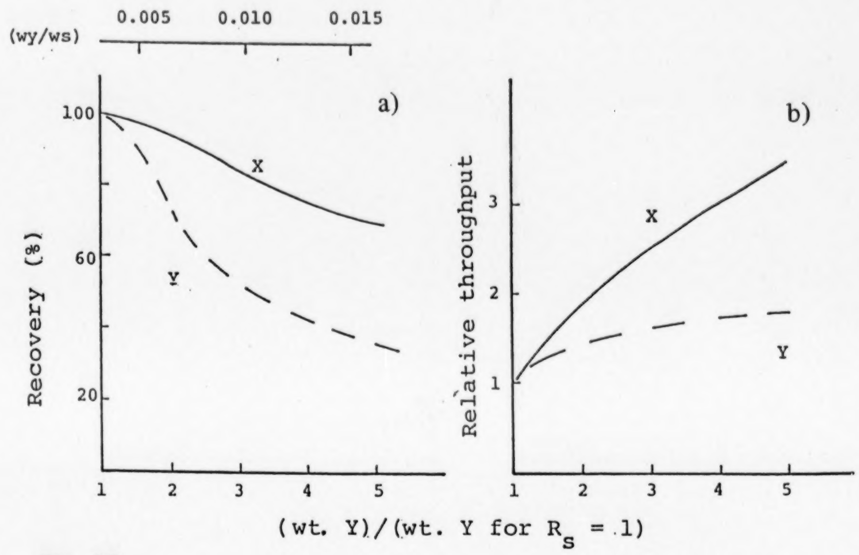

Fig. 12

Recovery of 99%-pure material as a function of sample size; equal concentrations of X and Y in sample, $\alpha = 1.2$. PREPSIMX simulations with $N_0 = 5800$ ($q = 3$), $k_0 = 1$; (w_y/w_s) for $R_s = 1$ equals 0.0032. ——, band X; – – –, band Y.

Throughput as a Function of Sample Size

A major question in any preparative HPLC separation is: what sample size is optimum for a given set of other conditions (column, mobile phase, etc.)? Knox and Pyper [1] have assumed that an optimum sample size corresponds to a value of (w_y/w_s) that gives $R_s = 1$. This is a useful first approximation, but most chromatographers intuitively believe that larger sample sizes are advantageous if the yield of purified product (grams per run) is to be maximized. We can now examine this question using PREPSIMX simulations for representative cases.

Equal concentrations of X and Y. Consider first a sample which has equal concentrations of X and Y so that the injected sample-masses w_x and w_y are equal. PREPSIMX simulations for this case are shown in Fig. 12a, for an α-value of 1.2 (a fairly difficult separation for preparative HPLC) and recovered material of 99% purity. The general pattern seen in Fig. 12a is similar to that observed in Fig. 11. The yield of purified X is always greater than of purified Y, for reasons that have been discussed. Similar plots are shown in Fig. 13a for the case of $\alpha = 3$. Here the yield of pure X drops more rapidly with increasing sample size, because the widths of the two bands are no longer approximately equal as in Figs. 11 and 12a. That is, proportionate increases in W_b for both bands result in a more rapid overlapping of band X by Y. Other features of Figs. 12a and 13a can be similarly rationalized with our preceding discussions of preparative HPLC.

Also shown in Figs. 12b and 13b is the relative throughput of each system. Here we define relative throughput as the yield of purified product relative to the yield for $R_s = 1$. A maximum relative throughput is desired, since this corresponds to the maximum yield of purified material per run (or per unit time). In Fig. 12b (for $\alpha = 1.2$) it is seen that relative throughput continues to increase with increase in sample size, beyound the value of w_y for $R_s = 1$. This is particularly pronounced for the case of solute X, and throughput can be increased (relative to a sample size for

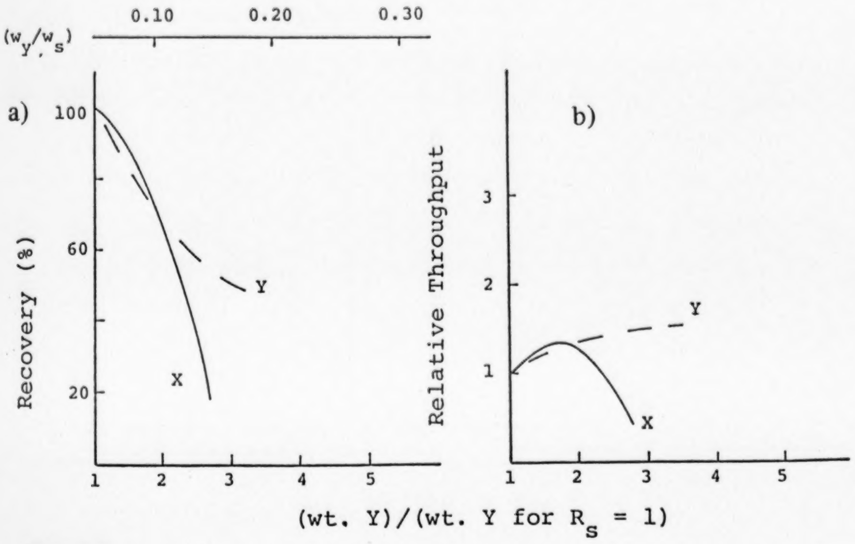

Fig. 13

Recovery of 99%-pure material as a function of sample size; equal concentrations of X and Y in sample, $\alpha = 3$. Same conditions as in Fig. 12, except $N_0 = 192$ ($q = 3$) and (w_y/w_s) for $R_s = 1$ equals 0.055.

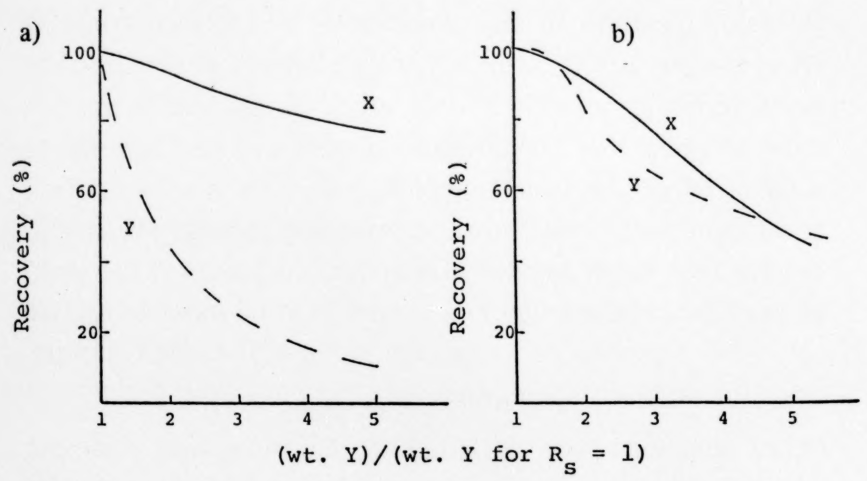

Fig. 14

Recovery of 99%-pure material as a function of sample size and composition; $\alpha = 1.2$. Same conditions as Fig. 12 except ratio of weights of X and Y in sample varies. (a) $w_X = 3\,w_Y$; (b) $w_Y = 3\,w_X$.

$R_s = 1$) by a factor of over three, simply by charging a 4-fold greater sample to the column. The corresponding advantage for recovery of pure Y is not as large; however, the relative throughput of Y can be increased by almost 2-fold vs the case where $R_s = 1$ (if larger samples are injected).

When the value of α is larger, as in Fig. 13b ($\alpha = 3$), the advantage of increasing sample size beyond $R_s = 1$ is similar for solute y, but not for solute X. It is possible in this case to obtain a reduced relative throughput for solute X by injecting too large a sample. This suggests a more cautious approach when increasing sample size for maximum throughput, particularly if α is larger and solute X is of interest.

Different concentrations of X and Y. Generally it is more difficult to achieve a high recovery of some compound i when the concentration of i in the sample is relatively small. Fig. 13 examines this case for samples where there is a 3-fold difference in the concentrations of X and Y (other conditions the same as in Fig. 12, with $\alpha = 1.2$). In Fig. 13a, X is present in 3-fold higher concentration, and in Fig. 13b Y is present in 3-fold higher concentration. When X is present in higher concentration (Fig. 14a), its recovery is improved vs the case where X and Y are present in equal concentrations (Fig. 12a). Likewise, when Y is present in higher concentration (Fig. 14b), the reverse is true for X. In both cases, however, the throughput of X increases for larger sample sizes. This is not always the case for compound Y when it is the lower-concentration component of the sample.

Throughput as a Function of k_0

In analytical-scale HPLC, where two compounds are to be separated, there is an advantage in having k′-values fall in the range of 2–5 [12]. The question then arises: is there an optimum range of k′-values for separation in an overload mode, and what is this range? This question is not an easy one to answer in general terms, but specific examples based on computer simulation can prove enlightening.

Effect of k_0 on recovery as a function of sample size. Consider first the question of how the recovery of 99%-pure material varies with the choice of k_{0x}, assuming that α is independent of k_{0x}. As before we have assumed a value of $q = 3$, and have carried out simulations for k_{0x} equal 1 or 3, with α equal either 1.2 or 3. The results of these PREPSIMX calculations are summarized in Table IV. In general we find little difference between the recoveries of X or Y for different values of k_{0x}; smaller values of k_{0x} lead to somewhat higher recoveries in a few cases.

Effect of k_0 on throughput. In view of the results of Table IV, we will ignore changes in (wt. Y)/(wt. Y for $R_s = 1$) so far as the question of throughput vs k_{0x}. That is, we assume a value of $R_s = 1$ for different values of k_{0x}, and evaluate throughput as a function of k_{0x}. Table V summarizes some results that are relevant to this issue. Our approach was to first determine the value of N_0 required for different values of k_{0x}, assuming $q = 3$ and $\alpha = 1.2$ (eq. (18)). Then computer simulation with DryLab I software (LC Resources Inc.) was used to determine the conditions required for these different values of N_0 vs k_{0x}. Here we assumed that 25 × 2.3cm C8 columns were available, and that these could be connected in series to achieve different values of N_0. Variation in flowrate was also allowed

Table IV. Effect of value of k_{0x} on recovery of 99%-pure material. PREPSIMX simulations, $q = 3$.

(wt. Y)/(wt. Y)	recovery of 99%-pure material							
	$\alpha = 1.2$				$\alpha = 3$			
for $R_s = 1$)	X		Y		X		Y	
k_{0x} =	1	3	1	3	1	3	1	3
1.5	98%	95%	92%	78%	89%	87%	83%	83%
2.0	94	90	73	65	65	59	83	83
2.5					34	25	58	59
3.0	84	83	53	48				
5.0	70	69	36	34				

in order to fine-tune the final value of N_0. The DryLab I program recognizes the dependence of plate number on k′, solute molecular weight, mobile phase viscosity, and other factors; see Ref. [13, 14] for a review of the basis of DryLab I computer simulations.

Table V summarizes the resulting simulations that allow throughput to be determined as a function of the value of k_{0x} assumed. Pressure was not normalized (set equal to a constant value) in these simulations, but the final pressures varied only between 660–1500 psi, which has little effect on the final conclusions. We see in Table V that throughput (equal to wy divided by run-time) is not much affected by k_{0x} values between 0.5 and 1.5, but throughput decreases for higher k_{0x}-values. This suggests that the choice of k_{0x} for an optimized preparative-HPLC separation is arbitrary (for $0.5 > k_{0x} > 1.5$), and can be subordinated to other considerations; e.g., the column size (and N_0-value) available, etc.

Throughput as a Function of Column-packing Particle Size

Knox and Pyper [1] have provided a general analysis of the role of particle size as it affects throughput in preparative HPLC. These authors' conclusion is that particle size is not a critical parameter in this regard; they find that column length can be varied to achieve a given value of N_0 with any particle size in the usual range of values (5–100μm diameters). There are a number of important assumptions in this treatment, however, and it is not obvious that packings of different particle size are equivalent in terms of throughput for all preparative-HPLC application.

We cannot hope to resolve this complex question here. However, the application of computer simulation to another representative example may be helpful in forming an initial opinion. We have used the same system described in Table V, with k_{0x} held constant at 1.5, and particle size varied. The results in Table VI show throughput increasing in this case for larger particles, with a 50% increase in throughput occurring as particle size is increased from 5 to 50μm. This comparison is similar to that of Knox and Pyper, in terms of how different-size particles are treated.

It is also of interest to consider the throughput (mg/min) per unit column-volume, shown in the last column of Table VI. Expressed in these terms, throughput decreases sharply as particle size is increased. It is premature to speculate on whether larger or smaller particles are generally advantageous, since this involves a detailed economic analysis of various differences between corresponding large-particle and small-particle separations. We will consider this matter further in a later communication.

Table V. The effect of values of k_{0x} on throughput in a representative case. Column length and mobile-phase flowrate varied to achieve the required value of N_0, with DryLab I software used to calculate N_0. Column: lengths of 25 X 2.3cm, 10μm Zorbax C8 assumed, joined together in series to achieve various overall lengths; mobile phase: 50% methanol/water; 25 C; mol. wt. of sample equal 400; w_s equal 7300mg and w_y equal 22.5mg (per 25cm column).

k_{0x}	k_{0y}	N_0*	column length**	flowrate (ml/min)	pressure (psi)	run time (min)	throughput (mg/min)
0.5	0.6	12,300	100cm	16.6	1520	21.4	4.2
1.0	1.2	5,800	50	19.3	880	12.7	3.5
1.5	1.8	4,200	50	33	1510	9.4	4.8
3.0	3.6	2,800	25	29	1663	8.8	2.6

* value from eq. (18) column length and flowrate adjusted to provide this value

** 100cm column = 4 25cm columns in series, etc.

Table VI. The effect of column-packing particle size d_p on throughput in a representative case. Column length and mobile-phase flowrate varied to achieve the required value of N_0, with DryLab I software used to calculate N_0. Column: lengths of 25 X 2.3cm of Zorbax C8 assumed (except 15cm for 5μm particles), joined together in series as needed for a given length; other conditions as in Table V. N_0 equal 4200.

d_p (μm)	column length	flowrate (ml/min)	pressure (psi)	run-time (min)	throughput	
					(mg/min	(mg/min) per V_m*
5	15cm	28	1540	3.3	4.1	(1.0)
10	50	33	1510	9.4	4.8	0.4
20	200	40	1830	31	5.8	0.1
50	1100	40	1610	170	5.8	0.02

Choosing Conditions for a Preparative-scale Separation

It is possible to use the conclusions presented here in combination with our basic understanding of HPLC [15–19] to create a general approach to method development for preparative separations. This approach is summarized in Table VII and is further discussed below. Here we assume that the purification of compound Y is desired, where contaminants X and Z surround the band of interest. Several of the steps of Table VII can be omitted, particularly when only a small amount of purified Y is required, or where the separation of Y from X and Z is relatively easy.

Develop an analytical separation. Previous references [15–17, 19] have discussed the variation of experimental conditions so as to maximize resolution under analytical conditions. The composition of the mobile phase, the nature of the column packing and/or separation temperature can be adjusted to optimize values of α for individual band-pairs of interest. In general, a similar approach is followed in developing a preparative-scale separation. For the case of a single major compound which is to be purified (Y), we desire that the α-values for the band-pairs X/Y and Y/Z be as large as possible, since this determines how much sample can be charged to a given column (eq. (16)).

Depending on the relative concentrations of X, Y and Z in the sample, it will be desirable to place band-Y closer to either X or Z, assuming that we can vary the relative position of band-Y between bands X and Z. When the concentration of Y is large (the usual case in prep-HPLC purification), it is desirable to maximize α for bands X and Y, which means that α for bands Y and Z is less important. In this case, band Y will overload the column more quickly, and in turn overlap band X. At the same time, the smaller mass of Z will less quickly lead to band broadening with resulting overlap onto band Y.

Table VII. A systematic approach for developing a preparative HPLC separation.

Step	Comment
1. develop corresponding analytical-scale separation	choose best conditions for suitable values of k_0 for components of interest
2. carry out a preliminary assessment of desired preparative conditions	use simple relationships derived here plus DryLab I simulations; anticipate possible problems
3. confirm separation and/or modify conditions for actual column-packing to be used in preparative run	use appropriate column length with 0.46 cm diameter (analytical scale)
4. measure the column capacity w_s	use measurement of bandwidth W_b as described in text
5. determine optimum sample load and value of N_0	use simple relationships derived here; confirm with actual sample size
determine optimum cutpoints	cutpoints estimated by analysis of fractions
6 scale up the separation to final sample size	determine best combination of column dimensions and mobile-phase flowrate using DryLab I simulations

Preliminary assessment of preparative conditions. The initial experimental runs provide us with values of k_0 and N_0 for compounds X, Y and Z in our preliminary system. We can use eq. (16) (assume q = 3) to estimate corresponding values of w_y/w_s and w_z/w_s for this system (assume $R_s = 1$). At this point it can be assumed that w_s (mg) = 0.5 × (surface area in m^2) for the column. A 10 nm-pore packing will have a surface area of about 200 m^2/g, which means that a 25 × 0.46 cm column will have $w_s \approx 350$ mg. Figs. 12–14 then allow preliminary estimates of throughput as a function of sample size for this column. Given the required amount of purified Y, we can estimate the column-size required for the purification of this amount of sample.

Consider the following example:

Compound	k_0	α	fractional wt. in spl.	wt. spl. w_i/w_s*	($R_s = 1$) w_i	max. wt. (Figs. 12–14)
X	1.5		20%	–		
Y	3.0	2.0	60	0.028	9.8 mg	20 mg**
Z	4.2	1.4	20	0.009	3.2	

* from eq. (16a) with q = 3

** assumes 30 mg of Y charged to column (Fig. 14)

We see for $R_s = 1$ that we can charge either 9.8 mg of Y or 3.2 mg of Z to the column. Since a sample that contains 9.8 mg of Y will contain 3.3 mg of Z, there is no problem with overloading the column with Z[9]. Fig. 14 suggests that if we charge 3-times this amount of sample, our throughput will increase about 2-x, corresponding to obtaining 20 mg of sample per run, using the 25 × 0.46 cm column. This throughput-enhancement factor (2x) will require verification in Step #5. At this point, a factor of 2-x is simply a rough estimate of possible sample size and throughput.

Based on how much purified Y is desired, and how many repetitive runs are practical, the final column size can now be estimated. For example, if 5 grams of material are required, and we want to carry out the separation in a single run, the column volume must be (5000/20) = 250-times larger. This could correspond, for example, to a 50 × 5 cm column. The amount of sample charge would then equal 250 × 30 = 7500 mg of Y. Often we have a limited choice of column sizes, which may dictate the use of repetitive runs with pooling of purified Y from each run.

Knowing the sample weight, the maximum sample-volume can be obtained from eq. (11a). It should be determined at this point whether there will be any problem in dissolving the sample in this volume of mobile phase. Often this is a major consideration in designing a final separation; it may be necessary to consider other solvents (in place of the mobile phase) for dissolving the sample; see discussion of Fig. 15.11 of Ref. [15].

---

[9] If compound Z overloads first in this situation (smaller value of w; as above), then this could limit the total amount of sample that can be injected. The use of programs similar to PREPSIMX allows a quantitative evaluation of this situation.

Given the required value of N_0 for this separation (eq. (18)) and the necessary column volume V_m (determined by the necessary sample size, as above), we can carry out computer simulations with the DryLab I software to estimate the best conditions (column length and diameter, particle size, flowrate); see the example of Table VI. These calculations should be for an analytical-scale column (0.46cm diameter). Here we are constrained by the operating conditions that are possible: available column sizes and pump flowrates, maximum pressure, etc.

Confirm separation for final column packing. If preliminary work has been carried out on an analytical column, step #2 may indicate that a different column-packing particle-diameter will be preferred. In this case, we need to confirm the original separation with the exact column packing to be used for the final preparative separation. Alternatively, when the probable final packing material is known at the beginning of method development, a high-plate-number column ($N_0 > 2000$) packed with this identical material can be used in Step #1.

Measure the column capacity w_s. Previously we have described how w_s can be measured from two runs, using measurements of retention (k') as a function of sample mass [2]. We now feel that a better approach is to measure N for two runs, corresponding to (a) a small-sample run (N_0) and (b) a mass-overloaded run (N) where $(N/N_0) < 0.5$. Eq. (11) can then be used to determine w_{xn} for the mass-overloaded separation, and eq. (3) can in turn be used to determine w_s.

If w_s is much less than $0.3 mg/m^2$, it suggests that column-packing silanol effects are limiting the potential capacity of the column [8]. This is often the case for solutes that are acidic or basic. It may be possible to significantly increase w_s (and the amount of sample that can be purified per run) by suppressing the silanols: addition of salt or amine modifiers to the mobile phase, operating at a lower pH, etc. [19]. Many workers prefer to avoid non-volatile mobile-phase modifiers, but this can be a mistake. These additives are easily and quickly removed in a subsequent gradient separation carried out without mobile-phase additives [20].

Determine optimum sample size and value of N_0. First repeat the procedure of Step 2 to determine the approximate sample size that will be charged to the 0.46cm column. Next obtain a value of N_0 for $R_s = 1$ (eq. (18)). The latter value can be reduced by the factor (wt. Y for $R_s = 1$)/(wt. Y in final separation), to give the N_0-value required for the final separation[10]. Adjust column conditions (length, flowrate) to obtain this value of N_0 and inject the sample.

This trial separation can be evaluated either by visual appearance of the chromatogram, or by collecting fractions for analysis. Depending on the results of this run, changes in the weight of sample charged may be indicated. If conditions for $R_s < 1$ are chosen (for higher throughput), fraction-analysis is recommended at this stage to confirm that the recovery and purity of compound Y are adequate. Information on optimum cutpoints can also be obtained.

Scala-up. The separation that has been confirmed in Step 5 can now be repeated with a larger column. Separation on the large and small columns should be identical, as long as values of k_0 and N_0 are the same for each band in the two runs, and values of (w_i/w_s) are maintained constant by injecting a proportionally larger sample to the large column. It is necessary to maintain the same column packing and mobile phase, so that k_0-values for individual compounds do not change. It is also required that N_0 for the large column be the same as for the small column used in Step 5; the adjustment of conditions for equal N_0-values has already been illustrated in the examples of Table VI, using the DryLab I software.

In carrying out the final separation, cut-points determined in Step 6 can be used. However it is safer (especially when $R_s < 1$) to collect fractions, analyze them, and pool purified material.

Conclusions

Knox and Pyper [1] have reported a description of preparative HPLC separations, based upon Langmuir-isotherm retention and certain simplifying assumptions. This approach allows many aspects of preparative HPLC to be described in terms of explicit mathematical relationships. In the present paper we have examined possible limitations in this approach by comparing it to a related model we have recently described [2]. It appears that the conclusions of Knox and Pyper [1] are in general agreement with experimental data reported previously by us [2]. Specifically, band-shape data reported by us for moderately to heavily overloaded separations ($0.8 > N/N_0 > 0.02$) agree well with the right-triangle shapes assumed by Knox and Pyper. Plate numbers and bandwidths are also accurately predicted by the Knox/Pyper model over this same range of column overload. We have confirmed their finding that sample volume plays no role in affecting resolution in preparative HPLC, as long as sample volume is less than one-half the volume of the eluted (overloaded) band.

The Knox/Pyper model assumes that the mass-overloaded separation of multi-component samples can be approximated by the independent elution of each solute (mixed-isotherm effects ignored). This appears to be a good approximation as long as adjacent bands do not overlap appreciably (errors of only 1–15% in the sample mass that gives rise to a given separation). The Knox/Pyper model begins to fail appreciably, however, whenever the mass of any sample component exceeds about 5% of the column capacity w_s.

It has been found advantageous to combine certain features of the Knox/Pyper model with a semi-empirical description of preparative HPLC reported by us previously [2].

---

[10] This calculation of N_0 is based on the approximate proportionality between N and $1/w_x$ (eq. (11)) for a large sample.

This has resulted in our development of a personal-computer program that can simulate separations carried out in a mass-overload mode (PREPSIMX). We have applied this program in the present study to obtain a better general understanding of preparative HPLC.

Because of the general accuracy of the Knox/Pyper model for a broad range of conditions that are appropriate for preparative HPLC, it is worthwhile using this model to uncover insights into certain general features of such separations. Several such relationships are presented here, augmented in certain cases by computer simulations using our own model (PREPSIMX) for computer simulations of preparative HPLC separation. Our conclusions include the following:

1. The weight of sample that can be charged to a column depends mainly on the separation factor α of the critical band-pair, and to a lesser extent on the plate number of the column for a small sample (N_0) (eq. 16).
2. A change in solvent strength and related solute k'-values affects the optimum value of N_0 for the separation, but has little affect on throughput (maximum quantity of purified solute per run) when k_0 for the first band is between 0.5 and 1.5. Throughput decreases for larger k_0-values ($k_0 > 1.5$ for the first band).
3. Throughput can be increased in some (but not all cases) by charging larger samples than correspond to the case of two bands of interest just touching ($R_s = 1$).
4. The effect of particle size on throughput is complex and there is currently no single "rule of thumb" to guide its choice. Because of this complexity, the optimum particle size for any given case can best be determined only from a knowledge of the exact circumstances surrounding the separation.

Based upon the present model of HPLC separation in a mass-overload mode, we have proposed a systematic approach to the development of these separations.

Glossary of Terms

f { }	a function of
F	mobile-phase flowrate (ml/min)
H_0	value of H_{total} for a small sample (eq. 5)
H_{total}	plate height (eq. 6)
H_{th}	contribution to H_{total} as a result of column overload (eq. 5)
k'	solute capacity factor
k_0	value of k' for a small sample
k_{0x}, k_{0y}	value of k_0 for band X or Y
L	column length (cm)
N	plate number of a band calculated from the baseline width W (eq. 1 and Fig. 3)
N_0	value of N for a small sample
N_{0y}	value of N_0 for band Y
p	correction factor (equal to 1.5) used in eq. 10; also (Appendix II), an arbitrary factor
q	equal to N_0/N (eq. 16a)
R_s	resolution function defined for preparative HPLC by eq. 12
t	time required for a separation; equal to t_R^0 for last-eluted band
t_0	column dead-time (min)
t_R^0	retention time measured at end of band (Fig. 3); also equal to retention time t_R for small-sample band (eq. 2) (min)
t_R^{cum}	retention time measured at 50% elution of band (Fig. 3) (min)
t_R^{max}	retention time (min) measured at band maximum (Fig. 3) (min)
t_{x0}, t_{y0}	value of t_R^0 (small sample) for bands X and Y
V_b	baseline volume of a band when it elutes (ml) (equal to F W_b)
V_m	column dead-volume; equal to t_0 times flowrate (ml)
W_b	baseline bandwidth (Fig. 3)
w_i, w_x, w_y, w_z	mass of injected solutes i, X, Y, Z (mg)
w_s	column saturation capacity; equal to maximum sample-mass that the column can hold (mg)
w_{xn}	loading function defined by eq. 3
W_{by}	value of W for band Y
X, Y, Z	sample components; X elutes first, Z last
α	separation factor (small sample), equal to k_{0y}/k_{0x} for bands X and y
σ	1 standard deviation

Appendix I

Relation of Values of k' to Sample Load

This relationship has been derived semi-empirically [2, 10]. A more rigorous derivation has since been achieved as described here. Originally, the loading function w_{xk} was defined:

$$w_{xk} = N^{1/2} [k_0/(1+k_0)] \ (w_x/w_s) \qquad \text{(i-1)}$$

with

$$k'/k_0 = f \ \{w_{xk}\}. \qquad \text{(i-2)}$$

An empirical relationship between eq. (i–2) and experimental data reported in Ref. [2] can be obtained:

$$w_{xk} = [1-(k'/k_0)]/1.4 \qquad \text{(i-3)}$$

A value of w_s results by combination of eq. (i–1), (i–3):

$$w_s = 1.4 w\, N^{1/2} [k_0/(1+k_0)] [k_0/(k_0/(k_0-k')] . \qquad \text{(i-4)}$$

We assume a Langmuir isotherm, which can be expressed as [10]

$$\phi_x = K\, N_x/(1+K\, N_x) . \qquad \text{(i-5)}$$

The following approximations can be made (see Appendix I of Ref. [10]):

$\phi_x = w_{xs}/w_s$, $N_x = C_x$, and $k_0 = w_{xs}/(V_m C_x)$. The phase ratio can also be defined:

$$\psi = w_s/V_m \, . \tag{i-6}$$

With these approximations and definitions, eq. (i–5) becomes

$$w_{xs} = w_s K C_x/(1+K C_x) \, . \tag{i-7}$$

The distribution coefficient K is given as

$$K \;= k_0 V_m/w_s \, . \tag{i-8}$$

The quantity of solute in the mobile phase is given as $q_m = w_x/(1+k')$, and the volume within the column in which this is contained can be estimated as follows. We assume that the average peak volume is equal to the peak volume as it reaches the column midpoint. The solute concentration is then

$$C_x \;= w_x (2N)^{1/2}/(1+k')\, V_m \, . \tag{i-9}$$

Since the solute capacity factor is equal to w_{wx}/q_m, eq. (i–7) can be written

$$\begin{aligned} w_{xs}/C_x V_m = k' &= (w_s K/V_m)/(1+K C_x) \\ &= k_0/(1+KC_x) \, . \end{aligned} \tag{i-10}$$

Eq. (i–1) then yields

$$w_s = (2N)^{1/2} w_x [k'/(1+k')]/[(k_0-k')/k_0] \, , \tag{i-11}$$

which is similar to eq. (i–4), except that $[k'/(1+k')]$ replaces $[k_0/(1+k_0)]$.

It is interesting to compare eq. (i–11) with the result from the approximate form of the Langmuir isotherm. For small C_x, eq. (2) can be written

$$w_{xs} = w_s K C_x - w_s (K C_x)^2 \, , \tag{i-12}$$

which yields (as in the derivation of eq. (11))

$$w_s = (2N)^{1/2} w_x [k_0/(1+k')]/[k_0-k')/k_0] \, . \tag{i-13}$$

Fig. i–1 shows a typical plot of w_s-values derived from the three equations above: (i–4), (i–11) and (i–13) (benzyl alcohol solute, 3µm C8 column). Eq. (i–4) and (i–12) show close agreement, and reasonably constant values of w_s for $(k'/k_0) < 0.95$ (as expected). Eq. (i–13) gives values that deviate to higher values of w_s for $(k'/k_0) < 0.85$. This is a reflection of the point at which the approximation to the Langmuir isotherm (eq. (i–4)) breaks down.

It is of interest in the present situation to note that when efficiency is defined in terms of eq. 1, all three equations become identical. This is probably the reason that the Knox model, although it is based on the two-term approximation to the Langmuir isotherm, fits data to loads significantly in excess of those required to reduce k'/k_0' below 0.85. The Eble model, which uses eq. (i–4), is also therefore a reasonable approximation to the full Langmuirian isotherm behaviour (for predictions of k′, but not W_b).

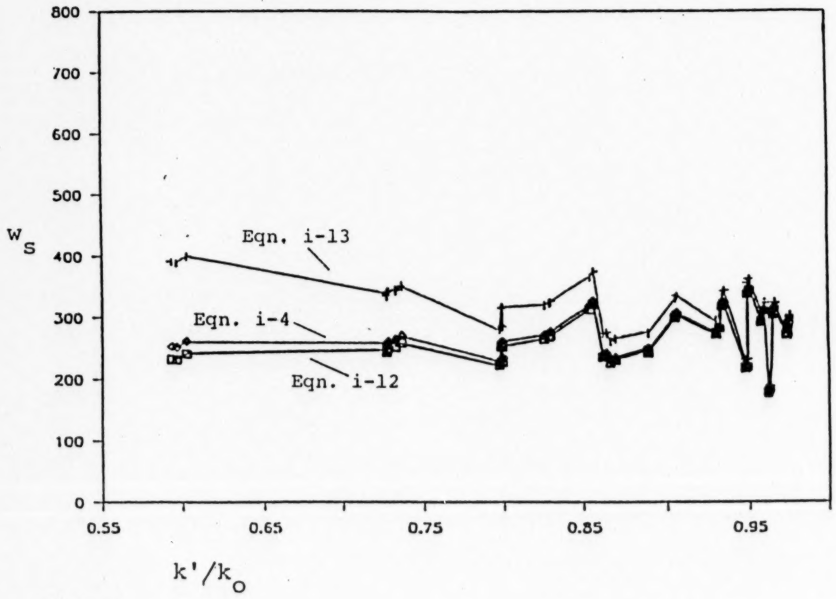

Fig. i–1

Dependence of w_s on (k'/k_0) using different ways of calculating w_s. Column, 15 × 0.46 cm, 3µm Zorbax C8; mobile phase, 30% methanol/water, 1.0 ml/min; temperature, 21°C; benzyl alcohol solute.

Appendix II

Derivation of an Optimum Value of N_{0y}/N_0

Let the weight of Y in the sample be wy and the time to complete the separation be t ($t = t_{y0}$). Further assume $R_s = 1$ (bands of X and Y just touch, as in Fig. 2e). We desire a maximum throughput per unit time,

$$w_y/t = \text{maximum} \, , \tag{ii-1}$$

without increasing column pressure beyond some upper limit. Let N_y initially equal N_{0y} (q = 1), and then allow N_{0y} to increase with pressure held constant by simultaneously (a) increasing column length L by some factor p and (b) decreasing flowrate F by the same factor p. The quantity q can then be approximated as

$$q = N_{0y}/N = p^{3/2} \, . \tag{ii-2}$$

Thus N increases in proportion to L (by the factor p), while N also increases with decrease in flowrate – usually by a factor that lies between 1 and 1/F ($\sim F^{1/2}$) for reasonable flowrates. Eq. (16a) allows us to write

$$w_y = (1/6)\,[(\alpha-1)/\alpha]^2\,(1-[1/q])\, w_s \, , \tag{ii-3}$$

so that (eq. (1))

$$w_y/t = (\text{constant})\;(1-1/q])\; w_s/t = \text{maximum} \, . \tag{ii-4}$$

Since w_s is proportional to column length and therefore p, while t is proportional to p^2, we have

$$\begin{aligned} w_y/t &= (\text{constant})\;(1-p^{-3/2})\, p/p^2 \\ &= (\text{constant})\;(1/p)\;(1-p^{-3/2}) \, . \end{aligned} \tag{ii-5}$$

Setting $\partial\,(w_y/t)/\partial\, p = 0$, we have

$$p = (5/2)^{3/2}$$

and therefore (eq. (i–2))

$$q = 5/2 \, . \tag{ii-6}$$

References

[1] *J. H. Knox, H. M. Pyper*, J. Chromatogr. **363**, 1 (1986).

[2] *J. E. Eble, R. L. Grob, P. E. Antle, G. B. Cox, L. R. Snyder*, J. Chromatogr., **405**, 31 (1987).

[3] *A. Jaulmes, C. Vidal-Madjar, H. Colin, G. Guiochon*, J. Phys. Chem. **90**, 207 (1986).

[4] *G. Guiochon, S. Ghodbane, S. Golshan-Shiraze*, presented at the 3rd Washington Symposium on Preparative Scale Liquid Chromatography, Washington DC, May 4–5, 1987

[5] *F. Eisenbeiss, S. Ehlevding, A. Wehrli, J. F. K. Huber*, Chromatographia **20**, 657 (1985).

[6] *M. J. Gonsalez, A. Jaulmes, P. Valentin, C. Vidal-Madjar*, J. Chromatogr. **386**, 333 (1987).

[7] *A. Tambute, P. Gareil, M. Caude, R. Rosset*, J. Chromatogr. **363**, 93 (1986).

[8] *J. E. Eble, R. L. Grob, L. R. Snyder*, J. Chromatogr. **384**, 25 (1987).

[9] *Cs. Horvath, G. Guiochon*, personal communications

[10] *J. E. Eble, R. L. Grob, L. R. Snyder*, J. Chromatogr. **384**, 1 (1987).

[11] *J. E. Eble, R. L. Grob, L. R. Snyder*, J. Chromatogr., **405**, 1 (1987).

[12] *L. R. Snyder*, J. Chromatogr. Sci. **7**, 352 (1969).

[13] *R. W. Stout, J. J. DeStefano, L. R. Snyder*, J. Chromatogr. **282**, 297 (1983).

[14] *L. R. Snyder, P. E. Antle*, LC/GC Mag. **3**, 98 (1985).

[15] *L. R. Snyder, J. J. Kirkland*, Introduction to Modern Liquid Chromatography, 2nd edn., Wiley-Interscience, New York, 1979

[16] *J. C. Berridge*, Techniques for the Automated Optimization of HPLC Separations, Wiley-Interscience, New York, 1985

[17] *P. J. Schoenmakers*, Optimization of Chomatographic Selectivity, Elsevier, Amsterdam, 1986

[18] *M. Verzele, C. Dewaele*, Preparative High Performance Liquid Chromatography. A Practical Guideline, TEC, Ghent, 1986

[19] *L. R. Snyder, J. L. Glajch, J. J. Kirkland*, Practical HPLC Method Development, Wiley-Interscience, New York, 1988

[20] *J. Rivier, R. McClintock, R. Galyean, H. Anderson*, J. Chromatogr. **288**, 303 (1984).

Received: June 30, 1987
Accepted: Sept. 9, 1987
F

Recent Development in HPLC Enantioseparation – A Selected Review

W. Lindner

Institute of Pharmaceutical Chemistry, University of Graz, A-8010 Graz, Austria

Key Words

Enantioseparations by HPLC
Separation of optical isomers

Summary

Recent developments in the field of separating optical isomers by HPLC are discussed in this brief review. In particular it is focussed on various techniques for direct enantioseparation, the interpretation of possible enantioselective separation mechanisms, and the advantages and limitations of the diverse methods. This goal is supported by representative and selected examples of chiral separations.

1. Introduction

The preparation of and the demand for optically pure compounds are of rapidly growing interest, especially in life science applications, such as in biochemical and pharmaceutical research.

In biological systems, looked upon at a molecular level, asymmetry and optical activity dominate in nature, as shown in sugars, proteins, encymes, receptors, etc. It is not surprising that drugs having chiral centers will be recognized by biological systems stereochemically or stereospecifically. As a consequence, the stereoisomers of the drug might react biologically different due to these phenomena.

In many cases the optical isomers of chiral bioactive compounds show great differences not only in their activity, but also in the metabolic pathways described in their pharmacokinetic, pharmacodynamic and toxicologic patterns. There is a large number of examples where one isomer of a chiral racemic drug has therapeutically different or unwanted side effects, which could be largely eliminated via exclusion [1].

There is no doubt from a scientific point of view that many chiral drugs administered or introduced today as racemic mixtures should be given as optically pure isomers; however, such ethical thinking cannot be completely isolated from commercial aspects. The synthesis of optically pure compounds is usually quite expensive, and up until now often a compromise has been made between the "biological and economical activity" of a chiral (racemic) drug. Nevertheless, the future trend is clearly foreseeable: the preparation of enantiomers via commercially acceptable routes presents a challenge for chemists in the field of enantioselective synthesis (including biotechnological approaches) as well as in various fields of separation sciences. Such preparation includes fractional crystallization of diastereomeric salts and covalently formed diastereoisomers, as well as diverse liquid chromatographic resolution techniques of enantiomers. Principally speaking the synthetic and the resolution approach generating optically pure compounds (drugs) are complementary and vary from compound to compound; and the amount of optically pure substances needed defines the technique to be chosen. Each class of chiral compounds has its own unique chemical characteristics.

However, in all cases analytical tools are needed in order to control the enantiomeric excess and the optical purity of the chiral precursors or of the final products produced preparatively, and in many cases the chiral LC and GC have already proven their great potential.

The gas and the liquid chromatographic separation of enantiomers has, besides some earlier examples, been successfully applied since the 1960s. Particularly in GC, the development of chiral amid containing GC phases has led to broadly applicable chiral GC capillary columns [2]. Parallel to the development of highly efficient HPLC columns (use of small particles) in the 1970s, the search for chiral stationary phases began and has been booming in the last years. Several review articles covering the development of enantioselective HPLC in broad terms, as well as articles focussed particularly on chiral stationary phases, have been published over the years [3–14]. Therefore, to avoid

0009-5893/87 0097-11 $03.00/0

© 1987 Friedr. Vieweg & Sohn Verlagsgesellschaft mbH

unneccessary overlapping, primarily recent literature dealing with the development and application of new chiral HPLC systems have been considered here for citation; however, this should not stop the reader from looking up "older", very relevant publications on this subject.

In order to discriminate enantiomers (selectands, Sa) chemically as well as physico-chemically from each other, it is necessary to provide a chiral source (chiral handle, chiral selector, So) as a contact point and to form diastereomeric molecule associates (See reaction scheme 1).

To form such stable Sa-So molecule complexes, simultaneously acting intermolecular binding forces are needed to keep the molecules of the associate spatially oriented. According to Dalgliesh and Pirkle's viewpoint, for this purpose at least three binding forces are necessary, where one of them has to be stereospecific and can be repulsive or attractive. However, a controversy exists among various researches on this simplified binding model, depicted in Fig. 1.

Some researchers are of the opinion that only one or two interactions are needed in order to attain sufficient discrimination between the diastereomeric molecule complexes. When viewed at the molecular level and considering a one-to-one complex, this seems rather unlikely. However, in liquid or gas chromatography, one deals more with clusters or layers of (solvated) chiral selectors, in which the enantiomeric mixture of an analyte (selectand, Sa) have become imbedded. An enantioselective multipoint attachment between several selector molecules and one Sa molecule could therefore theoretically also be discussed, including the formation of (semi-)structured chiral cavities or structured aggregates of the So molecules. For chiral GC phases, such models have been proposed [15] and transferred to peptide phases used in LC [16], but generally it seems more difficult to prove the evidence of such postulates, due to solvation effects of the chiral stationary phase caused by mobile phase components.

However, in many cases the three point binding model proved to be an excellent tool for studying and designing diastereomeric molecule associates in connection with intermolecular steric attraction or repulsion (steric fit). The development of the so-called Pirkle type phases, and in particular the chiral N-naphthylaminoacid ester phase, clearly demonstrates the advantages of such a way of looking at things and interpreting the results [16, 17]. Via NMR experiments, the binding model depicted in Fig. 9 has been postulated and subsequently proved experimentally by separating a great number of specifically functionalized

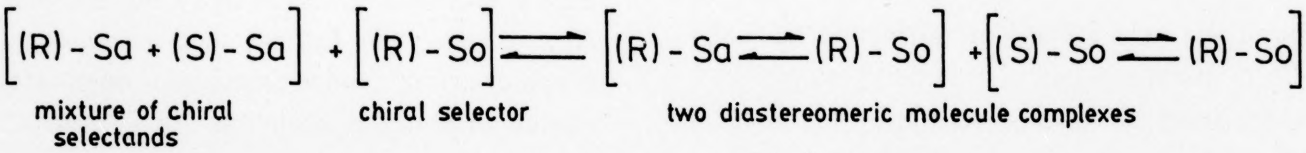
[(R) - Sa + (S) - Sa] + [(R) - So] ⇌ [(R) - Sa ⇌ (R) - So] + [(S) - So ⇌ (R) - So]
mixture of chiral selectands
chiral selector
two diastereomeric molecule complexes

Scheme 1

Reaction scheme of the formation of diastereomeric molecule associates.

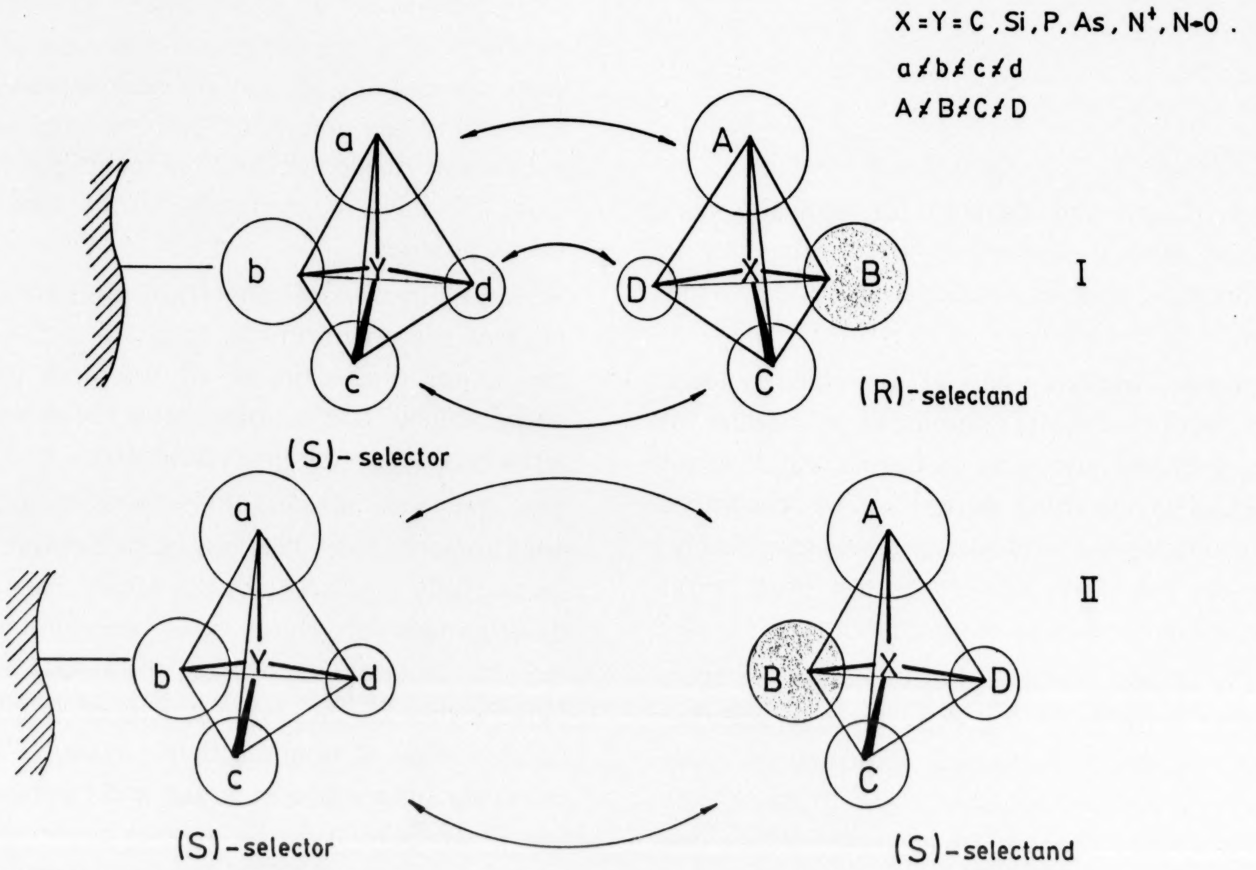

Fig. 1

Stereoselective binding model between chiral selector and racemic selectand molecules; I represents ideal, II nonideal fit.

chiral Sa molecules. This success was based on the systematic investigations made with N-dinitrobenzoyl amino acid amide phases [9] and was due to the reciprocity of chiral recognition, which means that Sa and So can be exchanged (assuming the chiral recognition model is correct).

Another approach for explaining and predicting enantioseparation has recently been developed by Armstrong et al. [18] via computer, where possible fits between a β-cyclodextrin macro molecule and (R)- and (S)-propranolol were calculated (see Fig. 2).

Together with computer projections of x-ray crystal structures, some very helpful information might be gained in terms of understanding intermolecular bindings or fits that lead to chromatographic enantioseparation. For simple molecule structures, this computerized approach seems feasible to date, but it becomes quite complicated if one thinks about the proteins as chiral selectors (discussed later), their tertiary structures and the receptor like interactions with chiral selectands. It should not be forgotten that in chromatography one deals with solvated Sa and So molecules, something not usually taken into consideration in computer modeling.

Given these two examples, it should be briefly noted that there is a definite need for conceptual models to explain mechanistically observed enantioseparations and consequently to predict the resolvability of a given pair of enantiomers on diverse chiral HPLC systems.

As pointed out earlier, the key to direct enantioseparation is the formation of discriminatory and more or less stable, but reversible, diastereomeric molecule associates. Techniques using such principles are termed "direct", in contrast to, enantioseparation techniques, which involve the covalent formation of diastereomeric molecules using an optically active derivatizing reagent (CDR) as the chiral selector, termed "indirect" approaches (see Scheme 2). Such pairs of formed diastereoisomers are physically different and are therefore conventionally (e. g. crystallographically) resolvable, including non-chiral chromatographic systems. This approach has recently been reviewed [19], and for that reason it will only be briefly covered in this paper (see paragraph 4).

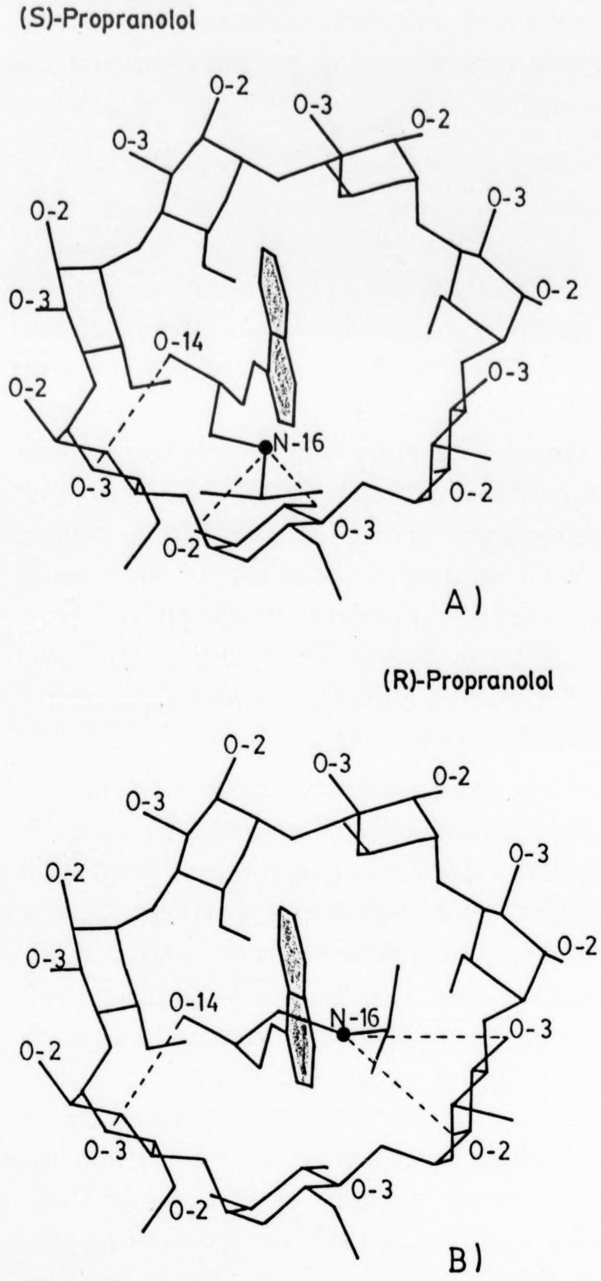

Fig. 2

Computer projection of inclusion complexes of A) (S)-propranolol and B) (R)-propranolol in β-cyclodextrin, from x-ray crystallographic data (reprinted with permission from ref. [18]).

2. Direct Enantioseparation

Over the last years a broad spectrum of chiral selectors with quite different chemical structures have been investigated in order to generate enantioselectivity. Three principal ways have been exploited: 1) The approach of using biopolymers, modified biopolymers and synthetic polymers, plain or coated onto silica gel particles; 2) the synthesis of covalently-bonded chiral stationary phases (CDRs); 3) the method of adding a chiral selector to the mobile phase, thus creating dynamically coated chiral stationary phases.

2.1 Chiral Stationary Phases Using Polymers as Chiral Selectors

The collective name "chiral polymers", covering compounds not clearly defined in their chemical structure and molecular weight, can be applied to large peptides or

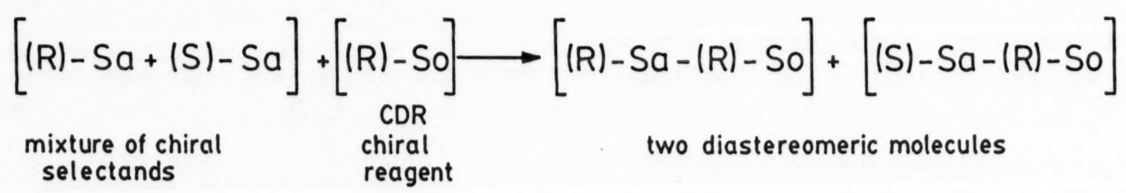
[(R)-Sa + (S)-Sa] + [(R)-So] → [(R)-Sa-(R)-So] + [(S)-Sa-(R)-So]
mixture of chiral selectands
CDR chiral reagent
two diastereomeric molecules

Scheme 2

Reaction scheme of the formation of diastereoisomers via derivatization with optically active derivatizing reagents.

proteins, polysaccharides and derivatized polysaccharides, as well as synthetic polymers (e.g. polyacrylamides) and polystyrene type resins.

2.1.1 Chiral stationary phases based on polysaccharides

Historical, naturally-occurring biopolymers have been considered first as possible chiral selectors for enantioseparations. It was Hesse and Hagel [20] who soon realized the possible usefulness of microcrystalline triacetylcellulose as a chiral support. These authors also created the term "chiral inclusion" chromatography. From todays perspective, this term should describe the phenomena linear polymers might orient themselves in such a way that aggregates with a tertiary structure (which might be helical) are formed. But such aggregates could also be oriented in such a way as to create chiral cavities which, on their part, could be enantioselective due to their special sizes and shapes, capable of including chiral guest molecules (selectands) via stereospecific interactions.

Based on Hesse's early work, Mannschreck and co-workers [21], parallel to the companies of Merck and Macherey & Nagel, have developed enantioselective columns filled with plain microcrystalline triacetylcellulose particles in the range of 15 μm (and larger) suitable for HPLC applications. This working group, as well as others like Blaschke [22], were able to separate great series of racemic chiral compounds with such columns, in particular pharmaceutical drugs, including substances having chiral axis, chiral plains or helicity rather than a chiral center as a chiral element. This is of particular interest, as such "rare" types of enantiomers are usually only separated via chiral inclusion phenomena rather than via 1:1 molecular association principle (see the following).

However, in the last years it has become evident that for high efficient HPLC columns only pressure stable small particles (< 10 μm) are suitable. As a consequence, approaches have been developed to coat large pore-size silica gel particles with chiral polymers, rather than to use them plain and in small-size particles, in order to get around the swellability and pressure instability of organic polymers. Shibata et al. [23], as well as Y. Okomoto and coworkers [24], have successfully developed such SiO_2 particles coated with differently derivatized polysaccharides. They examined cellulose triesters, e.g. acetate (CTA), benzoate (CTB) [25], phenylcarbamate (CTPc) [26], cinnamate (CTCi), nitrate, methylcarbamate, propionate, as well as tribenzylether (CTE). The abbreviations refer to chiral columns (Chiralcel, OA, OB, OP, OK and OE) offered by Daicel.

The separation factors of the enantiomers (α-value) obtained on these diverse phases can be quite different as well as strongly influenced by the type of mobile phases used. Predictions as to whether or not resolution is observable, and as to which conformer elutes first, seem at present difficult to make, mainly due to the lack of knowledge regarding the exact enantioselective separation mechanism. It should also be noted that the microcrystalline particles usually have a different enantioselectivity than the polymeric coated silica gel particles.

Cyclic polysaccharides (α-, β-, or γ-cyclodextrins which consist of 6, 7 or 8 sugar moieties) are chemically better defined than the relatively high molecular weight polysaccharide derivatives mentioned above. As pointed out earlier, these cyclic molecules (see also Fig. 2) have a very defined size and shape, and enantioselective inclusion phenomena can occur. Armstrong [27] immobilized these cyclic saccharides onto silica gel (the chemistry of immobilization was not described); such phases are commercially available from Advanced Separation Technologies. The columns show unique stereoselectivity, mainly based on the Sa molecular size for various applications. Although the computer modeling approach discussed by Armstrong has not been successfully adapted to many real life samples, it is clearly a good starting point and the structure of the chiral selector is relatively well known.

2.1.2 Chiral stationary phases based on polyacrylamides

Since the mid – 1970s Blaschke and co-workers [21, 27] have published several papers about the stereoselectivity of chiral polyacrylamide or polymethacrylamide gels used as stationary phases in liquid chromatography. These gels were polymerization products of chiral monomers, as depicted in Fig. 3. They showed remarkable stereoselectivity for many pharmaceutical drugs that contained an aromatic system, amide and/or ester, and/or basic functional groups. Unfortunately, these gels were soft and therefore only suitable for preparative separations in low pressure LC systems.

However, recently, Blaschke and co-workers [26] performed an in situ linear polymerization of chiral acrylamides adsorptively bonded on polar modified silica gel particles, thus generating HPLC particles (10 μm and smaller). The HPLC particles show nearly the same enantioselectivity as the soft polyacrylamide gels of the same structure, but with great improvement in terms of efficiency.

Examples of the performance and selectivity of such new columns are given in Fig. 4.

The enantioselectivity of these systems is hardly predictable. It is also not clear whether linear polymers, having multiple chiral centers derived from the chiral monomer, orient themselves in a somewhat helical structure, whereby these chains might additionally agglomerate with the neighbor chains in such a way as to create chiral cavities.

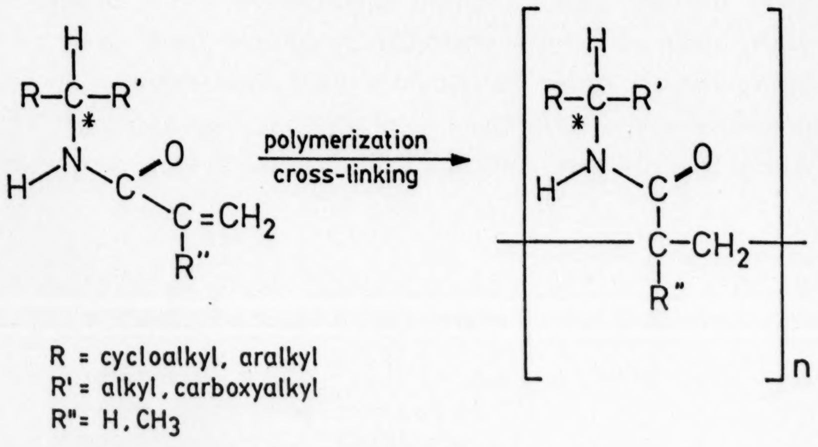

Fig. 3

Reaction scheme for the synthesis of chiral polyacrylamides.

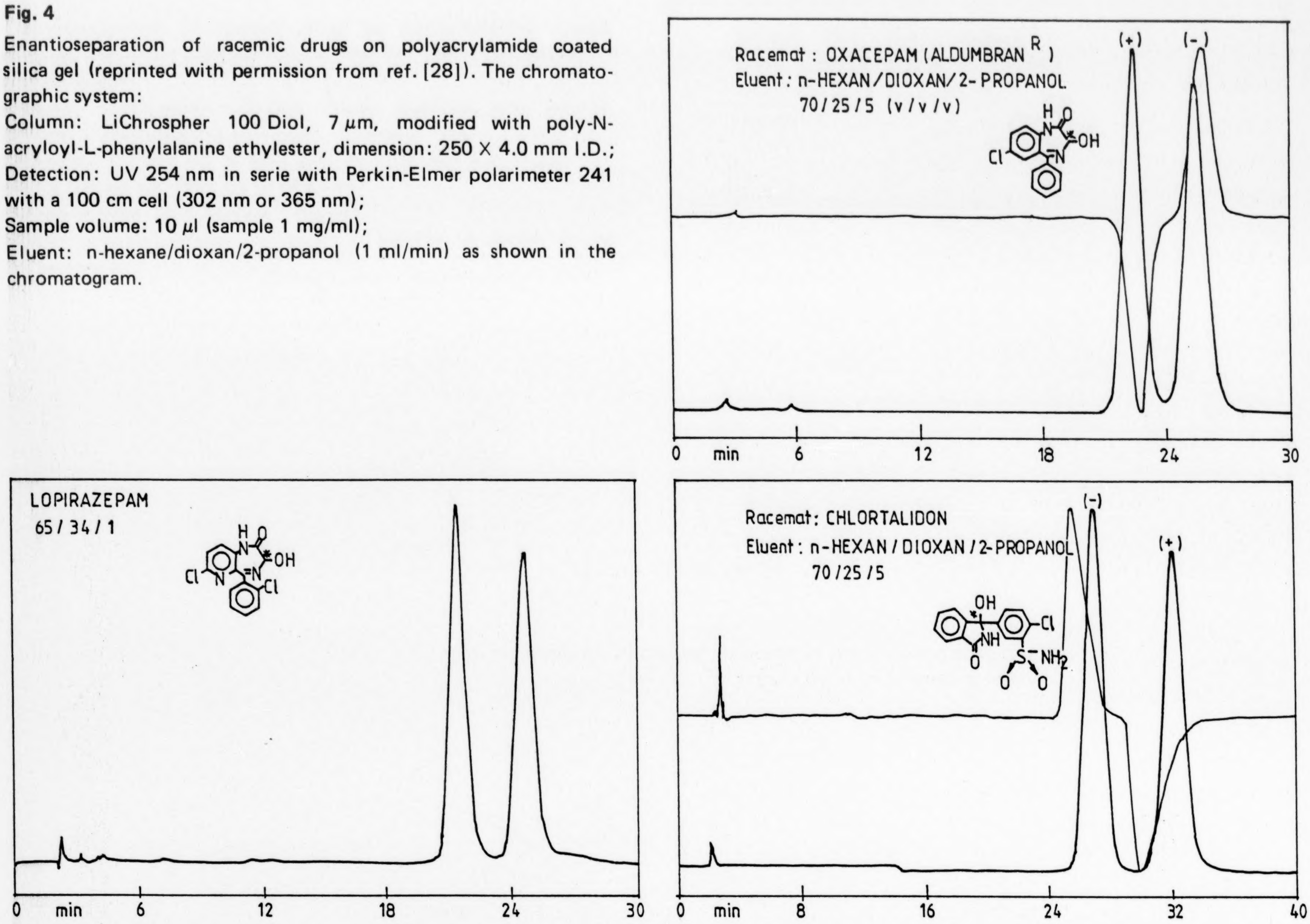

Fig. 4

Enantioseparation of racemic drugs on polyacrylamide coated silica gel (reprinted with permission from ref. [28]). The chromatographic system:
Column: LiChrospher 100 Diol, 7 μm, modified with poly-N-acryloyl-L-phenylalanine ethylester, dimension: 250 X 4.0 mm I.D.;
Detection: UV 254 nm in serie with Perkin-Elmer polarimeter 241 with a 100 cm cell (302 nm or 365 nm);
Sample volume: 10 μl (sample 1 mg/ml);
Eluent: n-hexane/dioxan/2-propanol (1 ml/min) as shown in the chromatogram.

2.1.3 Poly (triphenyl methacrylate) phase

The idea behind the phases invented by Y. Okomoto and coworkers [29, 30] was the synthesis of optically active polymers, whose chirality is caused only by helicity, as opposed to the Blaschke-type polyacrylamides. The chiral (+) polymer is generated using a chiral anionic initiator, such as (−)-sparteine-butyllithium [29]. The reaction scheme is shown in Fig. 5. These resins also showed remarkable stereoselectivity used as chiral supports; however, the full power of these helical polymers was apparent only after the development of weakly and heavily polymer-coated HPLC silica particles had progressed. Such chiral phases and columns are available from Daicel as Chiralpak OT (+). Numerous applications have been made with Chiralpak OT, and many different types of stereoisomers (having chiral centers, axis, plains, etc.) can be resolved, primarily due to steric fit and charge transfer interactions between the triphenylmethyl whorl and the π-electrons of the chiral selectands. There is no theory in the literature to help formulate a prediction for a successful resolution.

Since the diverse coating techniques of chiral polymers (cellulose derivatives, polyacrylamides, etc.) onto silica gel particles have been explored more extensively, this type of polymer particle "fits for good into the modern HPLC society".

In the near future, the prediction of different and new polymeric phases will begin to appear in the literature and subsequently on the market, and will be more widely used, even if an obvious problem with the polymeric phases is not yet solved. The efficiency of such phases is rather poor compared to "simple", "brush type" chiral phases and particularly when compared to non-chiral systems. There is a lack of a deeper understanding of the separation mechanism involved and therefore of approaches to influence and control the (stereo)specifity and high performance (efficiency) modern HPLC columns must have.

2.1.4 Imprinted chiral stationary phases

Conceptual, organic polymers are formed from chiral monomers consisting of a chiral template, on which polymerizable substituents are linked via cleavable functional groups. Following the three-dimensional polymerization, the chiral templates are removed (e.g. by hydrolization) and washed out, leaving behind a polymer with chiral footprints and cavities based on the size and structure of the chiral templates. Wulff and co-workers have pursued this concept for a long time and recently developed an imprinted chiral polymer involving functionalized HPLC silica gel particles in order to avoid the drawbacks of soft

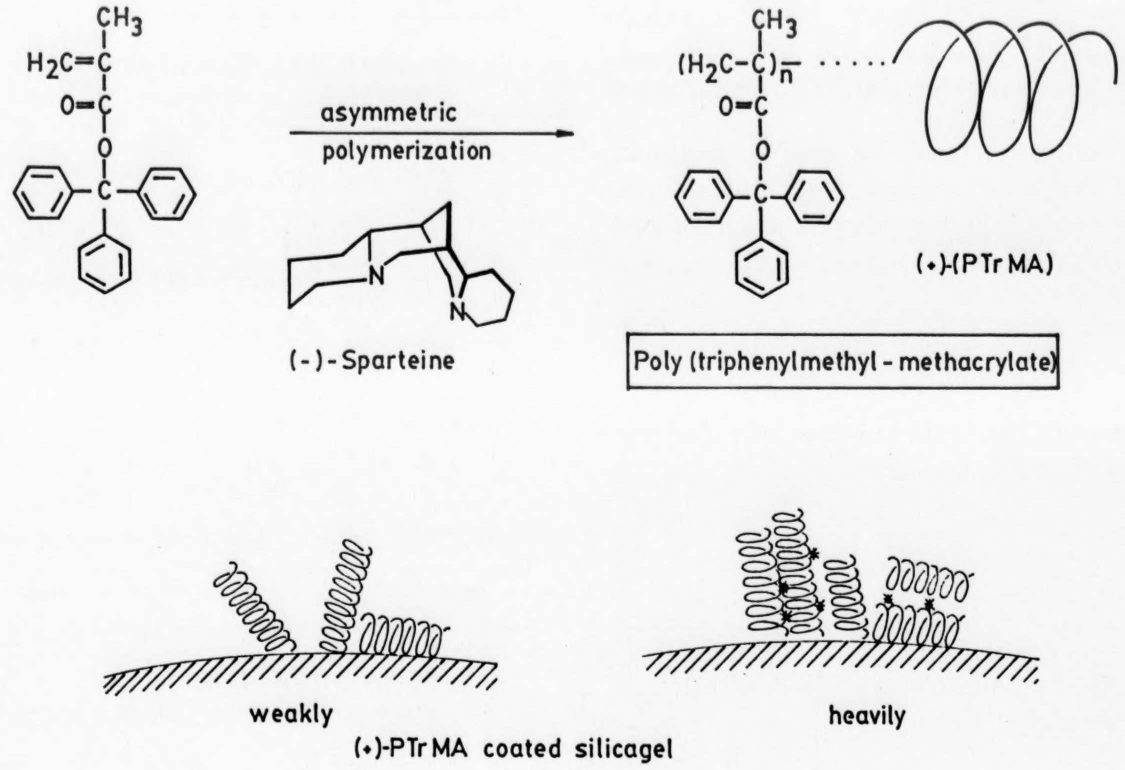

asymmetric
polymerization
(-)-Sparteine
(+)-(PTrMA)
Poly (triphenylmethyl - methacrylate)
weakly
heavily
(+)-PTrMA coated silicagel

Fig. 5
Reaction schema for the synthesis of chiral poly (triphenyl methacrylate) phases and silica gel coating.

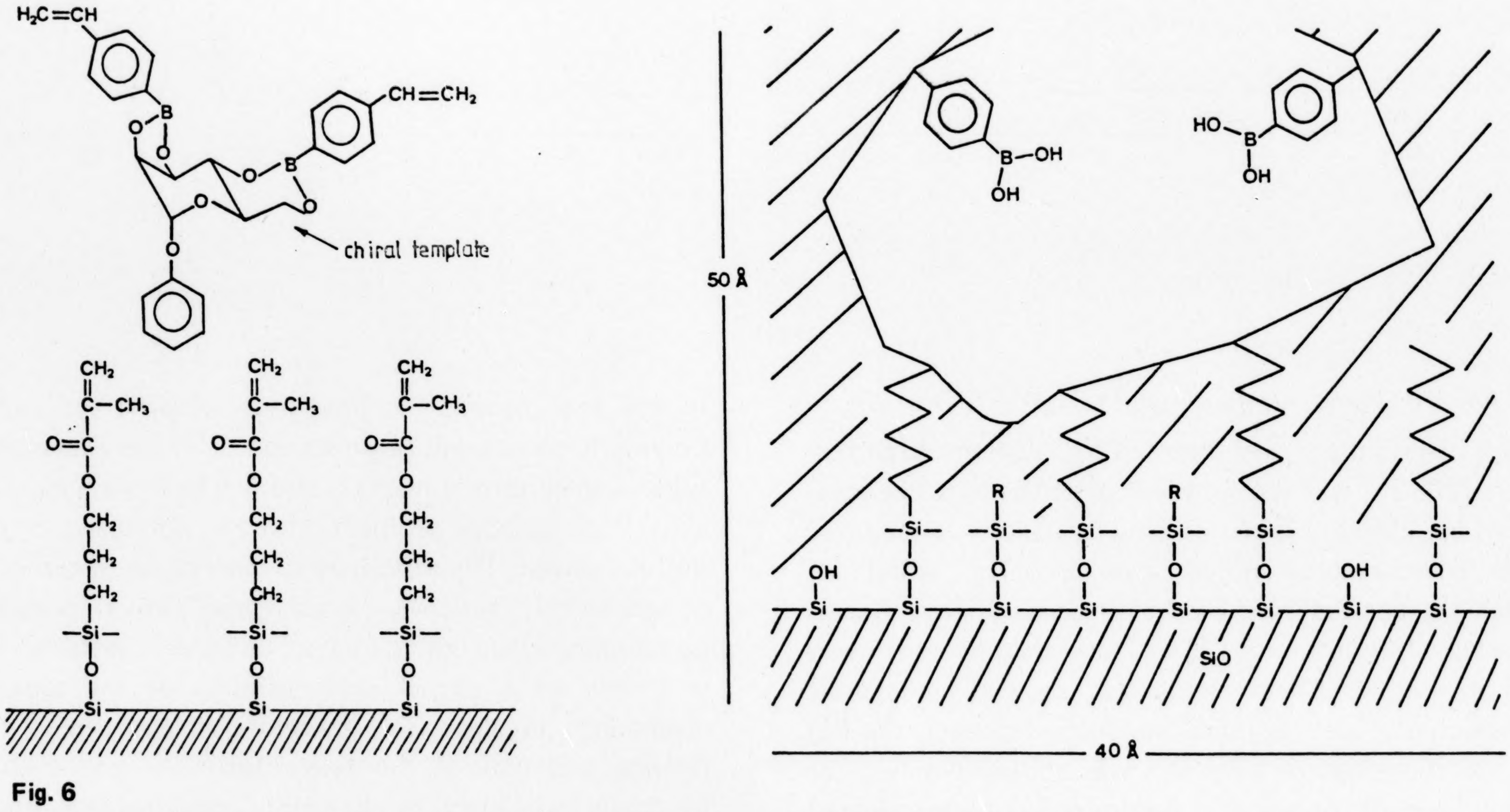

chiral template
50 Å
40 Å
SiO

Fig. 6
Reaction scheme of synthesizing imprinted chiral polymers (reprinted with permission from ref. [31]).

gels [31]. The relatively low chromatographic efficiency of such phases (see Fig. 6) is still a serious limitation, but the hope that this will be bypassed in the future remains.

2.1.5 Chiral stationary phases using proteins (peptides) as chiral selectors

These types of natural biopolymers have unique primary, secondary and tertiary structures, depending on the sequence of the amino acids linked together, as well as on the degree of glycosylation. In particular the tertiary structure, and the folding and unfolding of the protein chains forming lipophilic and hydrophilic "pockets", might be responsible for the stereospecific recognition of such biopolymers for small chiral molecules. Covalently immobilized protein LC phases (on the basis of silica gel) were originally developed by Allenmark [32] and Hermansson [33], using bovine serum albumin and α_1-acid glycoprotein, respectively. Due to the bonding procedure, the proteins might become partially denatured. However, there are still regions of the folded proteins that are capable of forming enantioselective pockets for many different types of molecules, in particular, pharmaceutical drugs and compounds having acidic, basic, amide and hydroxy group functions. The selectivity of these phases can be "tuned" to some extent by varying pH and the ionic strength of the buffer, as well as by adding small amounts of ionic organic modifier and organic solvent to the aqueous mobile phase. Several useful applications in pharmaceutical analysis are described in the recent literature [34, 35].

There seems to be a serious limitation with such LC phases as their poor loadability restricts them to analytical applicability only. Two protein type columns on the market are sold by Machery & Nagel and LKB.

Recently it was also demonstrated [36] that proteins can be dynamically adsorbed onto silica gel, forming stable protein LC phases. This simple approach could be of particular interest to the study of different proteins and/or digested proteins (peptides of the parent proteins) in order to elucidate protein sequences responsible for chromatographic stereoselectivity of, for example, drugs, which might in turn also provide some hints for studying potential receptor structures.

2.2 Chiral Stationary Phases Using Small Molecules as Chiral Selectors

A large number of different chiral molecules has been covalently immobilized onto silica gel particles. Most of these phases show a more restricted spectrum of enantioselectivity for the usually-tested racemates (drugs, amino acids and derivatives thereof, alcohols, amines, amides, etc.) compared to the diverse polymeric chiral phases discussed earlier. But, and this can sometimes be of great value, these "brush type" chiral phases (a) usually show better efficiency and (b) give us the opportunity to study an enantioselective separation mechanism on the basis of a simplified one-to-one molecule association model, as depicted in Fig. 1. This model drawing should simulate the attraction (binding) of complementary Sa and So molecules via non-specified binding forces, whereby the upper diastereomeric molecule complex "fits" better (due to the stereospecific orientation of the chiral substituents to each other) compared to the other diastereomeric molecule complex. As a result, the association and dissociation constants of the two diastereomeric complexes are (slightly) different from each other, which consequently leads to resolution in an enantioselective chromatographic system. Coulomb attraction, π-π-interaction, dipol-dipol and hydrogen bonding, as well as hydrophobic attraction, are effective as intermolecular binding forces. But, as mentioned earlier, this binding model represents a simplified point of view and does not consider other effects such as solvation, aggregation, etc.

However, the consequent use of such binding models can lead to the design of HPLC systems and stereospecific So-Sa interactions, resulting in remarkable enantioselectivity and α-values ($>$ 100), as demonstrated by Pirkle [37].

Correlations between elution order and absolute configuration based on such one-to-one models have also been found for some examples (and homologous series), which can be of value in stereochemistry [9].

2.2.1 *Chiral phases based on hydrogen bonding*

Since the 1960s hydrogen bonding between Sa and So molecules has been tested to effect chiral separations in GC [2]. In HPLC, this type of chiral phase has rarely been used in comparison to others, but recently Hara et al [38] and Oi and co-workers [39] presented comprehensive results on this matter, working with chiral amides and ureas as selectors and analytes showing primary amid groups. The stereoselectivity of these systems is, however, somewhat small, and a large plate number N might be required to get baseline resolution for a pair of enantiomers.

An interesting example of separating closely related species has been described by Feibush et al. [40], who designed and synthesized a chiral complementary selector to imide-type selectand compounds, as can be seen in Fig. 7.

It should be noted that barbiturates and hydantoins can also easily be separated by other systems (chiral polymers, ligand exchange, etc.) but this is not the point. The example should only demonstrate the extremes of designing enantioselective systems: on one side the way to approach a very specific phase is described by such an example, as compared to the usual for very broadly applicable chiral phases.

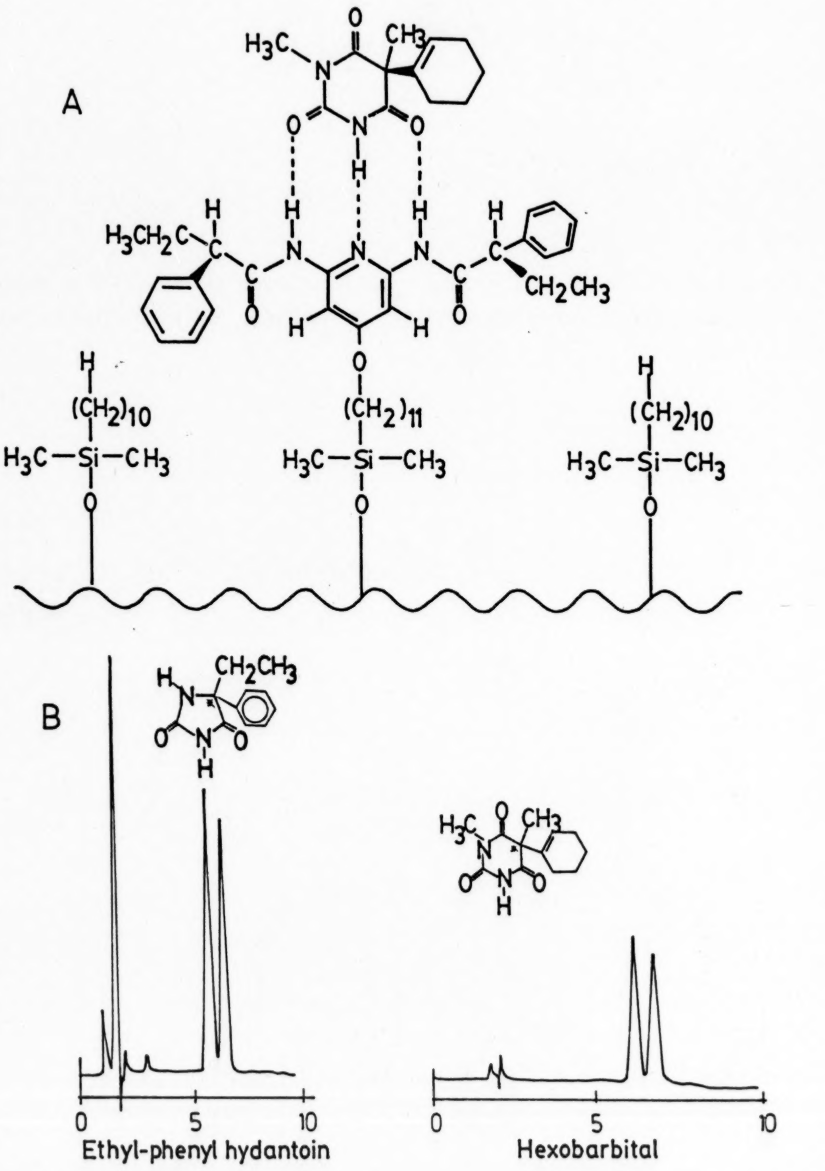

Fig. 7

A) Structure of the molecule complex between chiral stationary phase and imide type solute based on hydrogen bonding;
B) chromatographic examples (reprinted with permission from ref. [40]).

2.2.2 *Chiral phases involving π-π-interactions*

Over the years a considerable number of chiral π-π active "brush type" HPLC phases have been described [11–14, 41–45], but are led by the so-called Pirkle phases [41, 17] (see Fig. 8) that are commercially available and most wide spread. In order to activate π-π interactions, the selectand molecules must have a π-base system complementary to the π-acid (dinitrobenzoyl group) of the chiral selector or vice-versa. Additionally, hydrogen bonding and dipol-dipol interaction (stacking) need to be activated between the So and Sa molecules to fulfill the requirements of the postulated three point binding model. Numerous chiral compounds, often derivatized (functionalized) to fit into the binding model, could be resolved on these columns. During the last years in Pirkle's group several π-π active chiral phases have been developed and described [45]; recently a new and promising chiral "Pirkle phase" [17], somewhat complementary to the old one [41], entered the market [47] (structure see Fig. 8) and Fig. 9). Once the chiral selectands can be functionalized with an π-acid (DNB- and DNAn, see Fig. 9), a great possibility exists for resolving these species efficiently. Besides the popular Pirkle phases, the π-π active chiral supports developed by Oi and co-workers [39] should also be mentioned, as well as the investigations of diverse other working groups; the results are described by Meyer et al. [12], Armstrong [14] and Lindner and Pettersson [13].

In summary, most of these chiral π-π binding phases show good to reasonable chromatographic efficiency and have proved their usefulness in numerous applications published by diverse authors. These phases can be used on preparative scale separations (if affordable) and they are usually run with organic mobile phases (e.g. hexane/isopropanol mixtures). Under aqueous conditions the enantioselectivity drops significantly and most often diminishes.

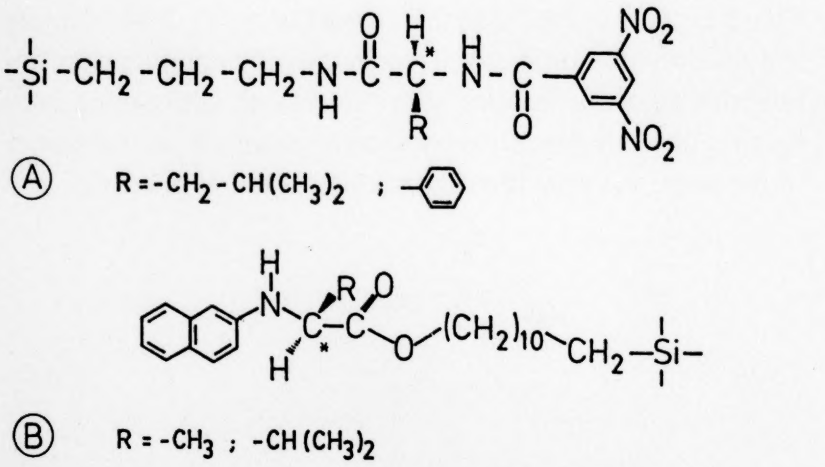

Fig. 8

Structure of chiral π-π interacting stationary phases: A) π-acid, dinitrobenzoylamino acid amides; B) π-base, N-2-naphthylamino acid ester.

2.2.3 *Chiral phases involving metal chelation*

Historically seen, these systems have been addressed since the early 1970s after Davankov et al. [46] published their first paper on this subject, known as "chiral ligand exchange chromatography".

The enantioselective separation mechanism involves the formation of a mixed and therefore diastereomer chelate complex, consisting of the immobilized, chiral selector ligand, the selectand molecule and the central transition metal ion. The stability of such a formed pair of diastereomeric chelates is different due to stereochemical interactions (attraction or repulsion) between the chiral substituents on So and Sa. Subsequently, by transferring this physical principle to a chromatographic system, effective enantioseparations can eventually be achieved, choosing appropriate mobile phase conditions and components which can act as weak but competing complexing agents.

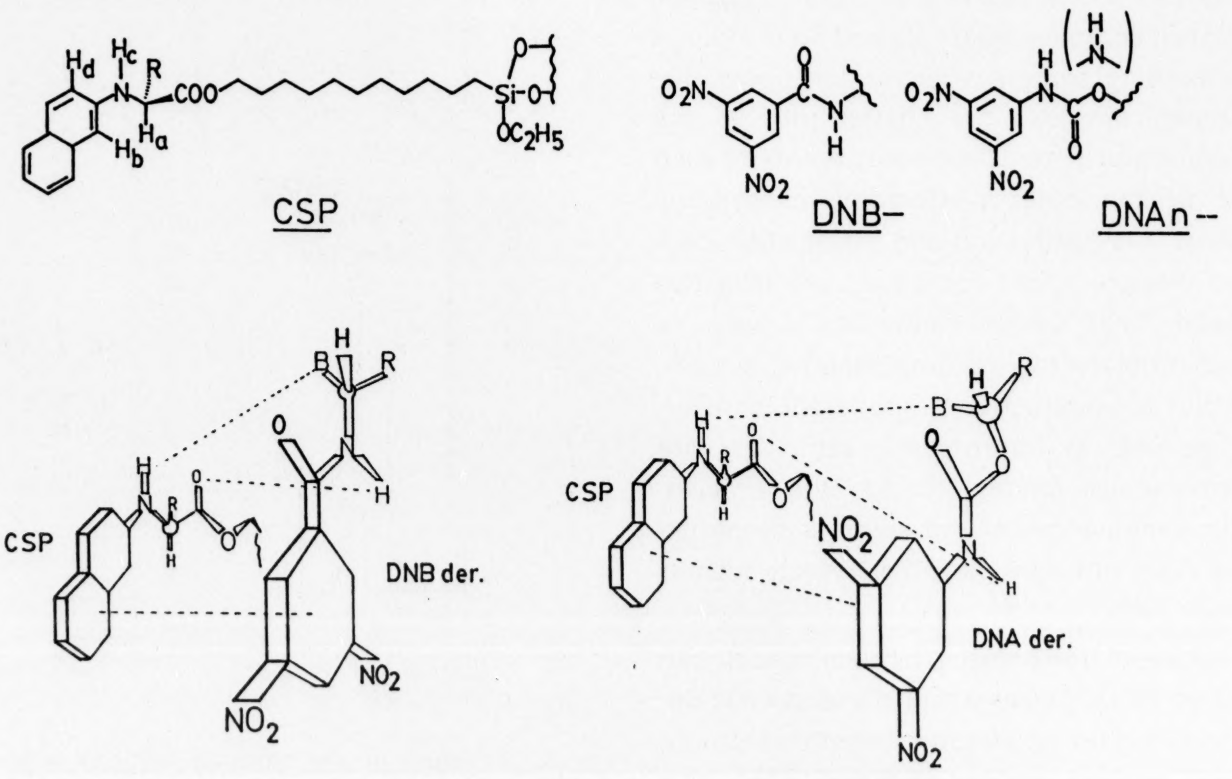

Fig. 9

Generalized chiral recognition model between chiral stationary phase (CSP) and derivatized selectands (reprinted with permission from ref. [17]).

However, it is a must that the selector and the selectand show chelating properties with transition metal ions (e.g. Cu II, Zn II, Cd II, etc.); consequently, these structure characteristics also strongly limit the type of compounds fulfilling such requirements. α-Amino acids and derivatives, as well as α-hydroxycarbocylic acids and compounds with an imide structure, fit the above-made requirements very well and consequently can be resolved by this technique. Buffered and ph-controlled aqueous (organic) mobile phases are usually used in chiral ligand exchange chromatography; appropriate columns are sold by Macherey & Nagel and Loba Feinchemie. (For more details and applications see the reviews [5, 11, 13] and their citations.)

2.3 Enantioseparations Via Chiral Mobile Phase Additives

Conceptual, conventional achiral LC columns run in a reversed or straight phase mode can be dynamically coated with diverse chiral selectors added to the mobile phase. Such systems have to be in equilibrium and carefully controlled (type of achiral stationary phase, chiral selector content, pH, ionic strength, temperature, organic modifier and water content of the mobile phase) in order to achieve the separation of suitable racemic compounds in a reproducible way. Depending on the type of chiral compound added to the mobile phase, and consequently on the responding chiral separation mechanism chosen, diverse enantioselective HPLC systems can be created: a) Via chiral chelating agents in general, and α-amino acids and derivatives thereof in particular, added to the mobile phase together with, e.g., Cu II ions, chiral ligand exchange systems can be generated which are fairly selective for α- and β-amino acids and derivatives, but also other chelating compounds (see paragraph 2.2.2). This type of chiral HPLC was first described by W. Lindner et al. [47] and later approached by many others [13, 48]; b) via chiral ion pairing agents like acids (e.g. camphorsulfonic acid, N-benzoxycarbonyl-α-amino acids and dipeptides) or amines (e.g. quinine), dynamically formed ion exchanger can be developed. Such chiral systems were first described by Pettersson and Schill [49], followed by several papers of this working group [13, 50, 51]; c) via the addition of cyclodextrins to an aqueous mobile phase, which was first demonstrated by Sybilska's group [52] and G. Szepesi and co-workers [53], chiral inclusion type chromatography also seems possible. This simple but effective approach is best demonstrated by recent examples [54, 56]. For illustrative reasons it is worthy to note that with the β-cyclodextrin additive mode, chiral hydantoins can also be separated [56], as is possible with a ligand exchange approach [57], but also via the hydrogen bonding base pair mechanism [40] (see 2.2.1).

Several enantioselective resolution principles lead to the same goal. It is not only a question of which technique to apply, but it is also important to consider the sample matrix and solvent (aqueous or non-aqueous).

As can be seen from the above statement and classification, the mobile phase additive approach is quite diversified and is also relatively simple to perform. However, the direct separation of common and uncommon α-amino acids via reversed phase chiral ligand exchange systems still seems to be one of the most popular approaches [45, 58]. No doubt, there are advantages to working with this technique (e.g. flexibility due to easily feasible mobile phase changes, etc.), but also drawbacks, the most obvious of which is its restriction to analytical applications.

An interesting and thus far barely – explored method of enantioseparation via mobile phase composition (chiral additive) is enantioselective distribution and extraction between two immiscible phases using a chiral extractand. There are a few examples in the literature that adapt this principle to HPLC systems [59, 60], but this technique could have more potential in the future, considering droplet counter-current chromatographic techniques as well. A practical example has recently been published [61].

3. Enantioseparations Via Indirect Method

This technique deals in principle with the formation of covalently-formed diastereoisomers by derivatising the (racemic) mixture of selectands with an optically pure chiral derivatising reagent (CDR) (see also reaction scheme 2). Depending on the derivatizable functional group, the type of CDR is selected with the goal of performing a 100% reaction with no noticeable racemization of the chiral centers in either the So or in the CDR molecules. Diastereomeric amides, carbamides and ureas usually show better chromatographic diastereoselectivity (greater α-values) than esters do, which deal with hydrogen bonding and dipol-dipol interaction between the polar stationary phase (e.g. silica gel) and the diastereomeric solute, together with the particular intramolecular arrangement (position) of the chiral substituents to each other. The same pair of diastereoisomers resolvable on SiO_2 may also be separated on a reversed phase system, but in this case mainly due to lipophilicity differences. Therefore, the elution order of the diastereoisomeric pair could be reversed for both systems. Such considerations have been confirmed experimentally [62].

In this particular example, the very small α-values of simple diastereomeric esters usually found can be significantly enhanced if there are additional intermolecular bindings activatable in order to form relatively rigid diastereoisomers, which are usually physically more different from each other than freely rotatable structures [13, 19, 62].

Many chiral reagents (CDRs) have been synthesized and described [19]; however, steadily new CDRs with better selectivity and/or sensitivity have appeared in the literature and on the market and have proven to be of value, especially in the enantioselective bioanalytical field (e.g. enantioselective drug monitoring, drug metabolism, amino acid analysis [63], etc.).

The indirect method of enantioseparation seems less elegant and more restricted than the direct approach [19], but for certain applications (for instance monitoring the enantiomeric composition in a complex matrix) it is often much faster and more appreciable than the direct mode, especially in terms of method development.

4. Final Remarks

This paper has stressed the fact that most chiral columns (except ligand exchange systems and the cyclodextrin phases) show better enantioselectivity when run with pure organic mobile phases. Also, the sample loading per gram stationary phase should always be minimal in order to ensure free and unhindered accessability of the chiral selectors by the selectand to form diastereoselective molecule associates.

The chiral inclusion columns are less sensitive to overloading effects than the π-π hydrogen bonding and the protein phases. Thus, upscaling from analytical separation to (semi)preparative resolutions usually causes some problems and disappointment. The isolation of grams of optically pure compounds can become quite costly since the chiral stationary phases are still expensive and also the mobile phase consumption is not to be neglected. It is questionable whether preparative chiral columns will ever be of widespread importance (special examples excluded) since this technique is in heavy competition with stereospecific synthesis.

The most important domain of chiral chromatography will remain in the analytical field, supported by a broad spectrum of commercially available columns for a diversified selection of chiral compounds (see list of manufacturers [12]). Besides the "classical" methods, enantioselective subcritical fluid HPLC approaches will also be of some interest in the future, as has recently been demonstrated by certain researchers [64, 65]. Enantioselective coupled column chromatography (column switching) has hardly been investigated thus far; it should become more important in the future, especially in the bioanalytical field.

Even if many successful chromatographic resolutions (of model compounds as well as of real life substances) have been performed; however, important questions concerning the better understanding of the diverse separation mechanisms, including the prediction of resolvability of given selectands, are waiting for an answer, not only from a scientific point of view, but also for many practical reasons. There is still a demand for new broadly as well as specifically selective chiral straight phase and reversed phase HPLC systems to be developed challenged and judged by analytical chemists working in diversified areas.

References

[1] *E. Ariens,* Medicinal Research Reviews, **6/4**, 451 (1986).

[2] *V. Schurig,* in Asymmetric Synthesis, Volume 1, Analytical Methods, ed. *J. D. Morrison,* (Academic Press, New York, 1983).

[3] *R. Audebert,* J. Liqu. Chromatogr. **2**, 1063 (1979).

[4] *G. Blaschke,* Angew. Chem. Int. Ed. Engl., **19**, 13 (1980).

[5] *V. Davankov,* Adv. Chromatogr., **18**, 139 (1980).

[6] *W. Lindner,* Chimia, **35**, 294 (1981).

[7] *W. Lindner,* in Chemical Derivatization in Analytical Chemistry, Volume 2, *J. F. Lawrence* and *R. W. Frei,* eds. (Plenum Press, New York, 1982) 145.

[8] *W. Lindner,* Österr. Chemie Zeitschr. 163 (1983).

[9] *W. Pirkle, J. Finn,* in Asymmetric Synthesis, Volume 1, Analytical Methods, ed. *J. D. Morrison,* (Academic Press, New York, 1983) 87.

[10] *S. Allenmark,* J. Biomed. Biophys. Meth., **9**, 1 (1984).

[11] *G. Gübitz,* GIT Fachz. Lab., Suppl. Chromtogr., **4**/85, 6 (1985).

[12] *R. Däppen, H. Arm, V. Meyer,* J. Chromatogr., **373**, 1 (1986).

[13] *W. Lindner, C. Pettersson,* in Liquid Chromatography in Pharmaceutical Development, *J. W. Wainer,* ed. (Aster Publ. Corp., Springfield, USA, 1985) 63.

[14] *D. Armstrong,* Anal. Chem. **59**, 84A (1987).

[15] *H. Frank, G. Nicholson, E. Bayer,* Angew. Chem., **90**, 396 (1978).

[16] *K. Lipkowitz, J. Landwer, T. Darden,* Anal. Chem., **58**, 1611 (1986).

[17] *W. Pirkle, T. Pochapsky, G. Mahler, D. Corey, D. Reno, D. Alessis,* J. Org. Chem., **51**, 4991 (1986).

[18] *D. W. Armstrong, T. Ward, R. D. Armstrong, T. Beesley,* Science, **232**, 1132 (1986).

[19] *W. Lindner,* in Chromatographic Chiral Separations, *L. Crane* and *B. Zief,* eds. (Marcel Dekker, New York, 1987) 91.

[20] *G. Hesse, R. Hagel,* Chromatographia, **6**, 277 (1973).

[21] *A. Mannschreck, H. Kolber, R. Wernicke,* Kontakte (E. Merck, Darmstadt, FRG, 1985) 40 and citations therein.

[22] *G. Blaschke,* J. Liq. Chromatogr., **9**, 341 (1986) and citations therein.

[23] *T. Shibata, J. Okamoto, K. Ischii,* J. Liq. Chromatogr., **9**, 313 (1986) and citations therein.

[24] *Y. Okamoto, M. Kawashima, K. Hatada,* J. Am. Chem. Soc., **106**, 5357 (1984).

[25] *Y. Okamoto, R. Aburatani, K. Hatada,* J. Chromatogr., **389**, 95 (1987).

[26] *Y. Okamoto, M. Kawashima, K. Hatada,* J. Chromatogr., **363**, 173 (1986).

[27] *G. Blaschke, J. Maibaum,* J. Chromatogr., **366**, 329 (1986).

[28] *G. Blaschke, W. Frankel, J. Kinkel,* Kontakte (Merck, Darmstadt, FRG, 1987) 3.

[29] *Y. Okamoto, K. Suzuki, K. Ohta, K. Hatada, H. Yuki,* J. Am. Chem. Soc., **101**, 4769 (1979).

[30] *Y. Okamoto, K. Hatada,* J. Liq. Chromatogr., **9**, 369 (1986) and citations therein.

[31] *G. Wulff, H. G. Poll, M. Minárik,* J. Liq. Chromatogr., **9**, 385 (1986) and citations therein.

[32] *S. Allenmark, B. Bomgren, H. Borén,* J. Chromatogr., **237**, 473 (1982).

[33] *J. Hermansson,* J. Chromatogr., **269**, 71 (1983).

[34] *S. Allenmark,* J. Liq. Chromatogr., **9**, 425 (1986).

[35] *G. Schill, I. Wainer, S. Barkan,* J. Liq. Chromatogr., **9**, 641 (1986) and J. Chromatogr., **365**, 73 (1986).

[36] *P. Erlandsson, L. Hansson, R. Isaksson,* J. Chromatogr., **370**, 475 (1986).

[37] *W. Pirkle, T. Pochapsky,* J. Chromatogr., **369**, 175 (1986).

[38] *A. Dobashi, Y. Dobashi, S. Hara,* J. Liq. Chromatogr., **9**, 243 (1986).

[39] *N.ôi, H. Kitahara,* J. Liq. Chromatogr., **9**, 511 (1986).

[40] *B. Feibush, A. Figueroa, R. Charles, K. Onan, P. Feibush, B. L. Karger,* J. Am. Chem. Soc., **108**, 3310 (1986).

[41] *W. Pirkle, J. Finn, J. Schreiner, B. Hamper,* J. Am. Chem. Soc., **103**, 3964 (1981).

[42] *R. Däppen, V. Meyer, H. Arm,* J. Chromatogr., **361**, 93 (1986).

[43] *M. J. Lloyd,* J. Chromatogr., **351**, 219 (1986).

[44] *J. Kip, P. VanHaperer, J. Kraak,* J. Chromatogr., **356**, 423 (1986).

[45] *W. Pirkle, G. Mahler, H. Hyun,* J. Chromatogr., **9**, 443 (1986) and citations therein.

[46] *S. Rogazhin, V. Davankov,* Chem. Commun., 490 (1971).

[47] *W. Lindner, J. LePage, G. Davies, D. Seitz, B. L. Karger,* J. Chromatogr., **185**, 323 (1979).

[48] *J. Wagner, E. Wolf, B. Heintzelmann, C. Gaget,* J. Chromatogr., **392**, 211 (1987).

[49] *C. Pettersson, G. Schill,* J. Chromatogr., **204**, 179 (1981).

[50] *C. Pettersson, G. Schill,* J. Liq. Chromatogr., **9**, 269 (1986).

[51] *C. Pettersson, M. Josefsson,* Chromatographia, **21**, 321 (1986).

[52] *D. Sybilska, J. Zukowski, J. Bojarski,* J. Liq. Chromatogr., **9**, 591 (1986) and citations therein.

[53] *M. Gazdag, G. Szepesi, L. Huszár,* J. Chromatogr., **351**, 128 (1986).

[54] *K. Feitzma, B. Drenth, R. Dezeeuw,* J. Chromatogr., **387**, 447 (1987).

[55] *T. Takeuchi, H. Asai, K. Ischii,* J. Chromatogr., **357**, 409 (1986).
[56] *J. Maguire,* J. Chromatogr., **387**, 453 (1987).
[57] *S. Fritz, W. Lindner, J. Roots, B. Frey, A. Küpfer,* J. Pharmacol. Exp. Ther., (1987) in print.
[58] *S. Lam, A. Karmen,* J. Liq. Chromatogr., **9**, 291 (1986).
[59] *V. Prelog, Z. Stojanac, K. Kovacevic,* Hebr. Chim. Acta, **65**, 377 (1982).
[60] *C. Pettersson, H. Sturman,* J. Chromatogr. Sci., **22**, 441 (1984).
[61] *S. Oya, J. Snyder,* J. Chromatogr., **370**, 333 (1986).
[62] *W. Lindner, C. Leitner, G. Uray,* J. Chromatogr., **316**, 605 (1984).
[63] *S. Einarsson, B. Josefsson, P. Möller, D. Sanchez,* Anal. Chem., **59**, 1191 (1987).
[64] *S. Hara, A. Dobashi, K. Kinoshita, T. Hondo, M. Saito, M. Senda,* J. Chromatogr., **371**, 153 (1986).
[65] *P. Macaudiere, A. Tambute, M. Caude, R. Rosset, M. Alembik, I. Wainer,* J. Chromatogr., **371**, 177 (1986).

Received: July 1, 1987
Accepted: July 21, 1987
F

The Determination of Starting Conditions for Modifier Optimization in Reversed-Phase HPLC

L. de Galan / D. P. Herman / H. A. H. Billiet*

Laboratorium voor Analytische Chemie, Technische Universiteit Delft, De Vries van Heystplantsoen 2, NL-2628 RZ Delft, The Netherlands

Key Words

Reversed-phase HPLC
Optimization
Transfer rules
Starting conditions

Summary

After a brief introduction of the subject, the paper focusses on the first step in any optimization procedure: the delineation of the parameter space, wherein the global optimum is to be found. For organic modifier optimization in reversed-phase liquid chromatography it is shown that the necessary information can be derived from a single water-methanol gradient. It first yields an estimate of the total number of solutes in the sample, which is vital to define the peak capacity needed to achieve separation at a certain confidence level. Next, the gradient allows the prediction of suitable isocratic methanol binary solvents, and transfer rules formulate the iso-eluotropic composition of the common binary solvents (tetrahydrofuran and acetonitrile). Because all predictions are based on a statistical analysis of a limited data base, attention is given to the practical situation where an actual sample deviates from the average solute behaviour. Such deviations are revealed in the first isocratic run and can be used to arrive at a better estimate of solute retention.

Introduction

There is no need to stress the importance of method development, especially for HPLC, where the modest plate count makes it mandatory to make optimal use of the available separation power and selectivity of the phase systems. Whether such method development is done by an analyst using his experience and intuition or by a computer-based "expert system", a complete optimization scheme involves three steps:

a) The choice of the parameters and the ranges over which they are allowed to vary; together these define the parameter space;
b) the selection of a suitable optimization criterion that will guide the procedure towards the desired separation;
c) a strategy that will find the highest value of the criterion (the global optimum) in an accurate and efficient way.

During the past ten years several research groups have devoted much attention to the latter two aspects in an attempt to design computer algorithms and relieve the chromatographist of this task [1].

The optimization criterion selected by the chromatographer should meet the practical demand that it is easily derived from an experimental chromatogram. It should further retain a useful (but low) value in the case of severely overlapping solutes, because this unfortunate situation will frequently be encountered in the initial stage of the optimization process, and the procedure should rapidly move into more promising areas of the parameter space. Above all, the criterion should quantitatively express the desired separation. It is not enough to want "a decent separation within a reasonable analysis time". We must specify whether we want to separate all solutes or only a few key components; whether the analysis time must be at a minimum or restricted to a certain upper value, etc. Once the goal of the optimization has been defined, it is almost always possible to express it in a corresponding criterion. Most criteria revolve around resolution, either focussing on the least resolved peak pair or accounting for the resolution (product) of all adjacent solutes.

There is at present no single preferred strategy to find the global optimum. *Sequential* procedures, of which the Simplex is the main representative, are flexible because the next chromatogram is based upon the results of previous data. These procedures are guided directly by the optimization criterion selected and, therefore, need no knowledge about the sample, but may encounter problems in locating the global optimum in complex response surfaces containing many (secondary) maxima. *Experimental designs* are more rigid in that they work with a fixed pat-

0009-5893/87 0108-07 $ 03.00/0

© 1987 Friedr. Vieweg & Sohn Verlagsgesellschaft mbH

tern of chromatograms. Again no knowledge of the sample is needed in grid searches, but their disadvantage is the large number of chromatograms needed to cover the entire parameter space in sufficient detail. A much more efficient alternative is provided by *regression designs* that work indirectly through the retention surfaces of the solutes, but this alternative requires an adequate model for retention behaviour and peak tracking in consecutive chromatograms. An intermediate strategy is the *iterative regression design*, developed in the author's laboratory [2, 3], that can adapt to irregularities in retention behaviour, but still requires peak tracking.

Fortunately, the previous condition that peak tracking must rely on the separate injection of all solutes is rapidly vanishing. With the advent of photo-diode-array detectors, sophisticated mathematical techniques have been developed to extract reliable spectra from overlapping band systems that can then be used to match solutes in consecutive chromatograms. Because the techniques are equally applicable to other detectors that provide full spectra, the present limitation that the solutes must be UV-active will vanish when infrared or mass spectrometers become routinely coupled to liquid chromatographs [4].

The concentrated efforts of many research groups to develop such computer-assisted strategies have been documented in review papers [5–7] and collected in recent books by Berridge [8], Jandera [9], Schoenmakers [1]. And yet, little of this effort has penetrated the market or convinced the average chromatographer of its utility. One reason may be that the software provided is somewhat less than user-friendly. More important is the complaint that despite the software, users still do not obtain a good separation. It is of little use to explain that it is not the software that is to blame, but it is the chromatography that is incapable of separating the mixture at hand. For example, even the best software will fail to separate two enantiomers if the phase system does not entail some chiral activity. However, the user's complaint must still be taken seriously. It is not enough that a well-designed optimization schema provides the *best possible* separation within the constraints of the phase system, or in the proper vernacular, that it finds the global optimum in the parameter space. It should also predict the chances of obtaining an *acceptable* separation, and warn the user that the system has exhausted its possibilities and that a change in chromatography is needed.

Choice of Parameters

It is customary to divide the variables in a chromatographic system in two broad categories: continuously variable parameters such as temperature, flow rate and mobile phase composition, and discontinuous parameters such as column length and stationary phase. Apparently, the distinction is based more on practicality than on principle. With these parameters we wish to manipulate the retention of the solutes in the sample in two ways. First, we want *sufficient* retention; not too much, for reasons of impatience and detectability, but certainly not too little. Because retention relies on residence in the stationary phase, the main parameter is the nature of the stationary phase, which is responsible for the classification of LC-systems in various modes: straight phase, reversed phase, ion exchange, size exclusion. Once the stationary phase has been chosen, the overall retention of the sample is determined by the composition of the mobile phase and expressed in a tautological quantity known as solvent strength. Decisive parameters are the organic modifier content, the pH, and ionic strength.

However, continuously variable parameters, notably the mobile phase composition, serve an important second purpose, namely in fine-tuning the selectivity between the solutes of the sample. It would be highly desirable if we had parameters at our disposal that could position each solute anywhere in the chromatogram. If this were possible, the peak capacity of a column would mean just that: it would by definition describe the number of solutes that the sample may contain to be completely separated on that column. Practical systems fall very short of the ideal. It is relatively easy to vary the retention of any particular solute, but we have only limited control over the mutual position of component pairs. For example, in ion (exchange) chromatography the pH is very effective in determining the total duration of the separation, but rarely interchanges the position of two eluting ions of the same charge. As will be shown below (cf. Fig. 2), even in reversed-phase LC we are lucky if we can separate a number of solutes equal to one-quarter of the maximum obtainable peak capacity. This limitation justifies the search for more efficient columns, because the plate count appears in the equation for the peak capacity:

$$Nc \approx 1 + (1/4)\sqrt{N}\,\ln\frac{1 + k_\omega}{1 + k_\alpha} \qquad (1)$$

where k_α and k_ω are the capacity ratios of the first and the last peak in the chromatogram, respectively, N is the plate count, and the constant 4 in the denominator indicates that we want all peaks separated with unit resolution. Once we have fixed the plate count by the column length, the particle size and the flow rate, the expression indicates that the positions of the first and the last eluting solutes determine the peak capacity. The mobile phase composition is our major tool to vary these positions and to manipulate the position of the solutes within this range.

Not all constituents of the mobile phase are equally effective for all samples. A change in the organic modifier (tetrahydrofuran, acetonitrile or methanol) may produce large changes in selectivity for some solutes and hardly any for others. Likewise, the pH exerts a large influence on the retention of weak acids and bases, but has no effect on neutral solutes. The choice of the mobile phase parameters, therefore, depends upon the composition of the sample to be separated. If we know that our sample contains ionized solutes, then the pH or an ion-pairing reagent immediately becomes of interest. If we know little about the sample, then the potential effect of various mobile phase constituents must be verified.

In a simple situation where the parameters act independently, each one can be tested separately at two levels. As a hypothetical example let us consider two isoeluotropic solvents, one containing 50% methanol, the other 38%

acetonitrile, neither of which produces a sufficiently resolved chromatogram. When the *same* solute-pair overlaps and, hence, the two chromatograms are virtually identical, it is unlikely that a ternary mixture of the two binary solvents will produce a well-separated chromatogram. If, on the other hand, *different* solutes overlap in the two binaries, then exploration of the full ternary range becomes profitable. Of course, in either situation it is advisable to test a third modifier (e.g. tetrahydrofuran).

However, the situation may well be more complex. If a chromatogram run at pH = 2 differs significantly from another chromatogram run at pH = 5, it is highly probable that the sample contains weak acids and the pH becomes a potential optimization parameter. Alternatively, an anion-pairing reagent could be considered, but its influence will be vastly different at either pH: when tested at high pH = 5, where many acids are dissociated, the cationic-pairing reagent would be observed to effectuate major changes in their retention; but at low pH = 2, the dissociation of all acids may be suppressed to such an extent that the addition of the reagent produces no effect. Such situations call for a factorial design, where the parameters are tested simultaneously to reveal their separate influence as well as their interdependence.

Once we have selected the most suitable mobile phase parameters, preferably in order of interest, it becomes important to narrow their variation down to the range where they exert their largest effect. The reason is that on the one hand we do not want to waste valuable time in exploring unprofitable areas of the parameter space, while on the other hand we wish to retain sufficient peak capacity and selectivity. In other words, we must define the ranges of the parameters such that we can expect all solutes of interest to become separated.

For the optimization of the organic modifier content in isocratic reversed-phase LC, it will now be shown that such a delineation of the parameter space can be achieved by answering the following three questions:

1. What is the total number of solutes in the sample?
2. Which peak capacity do we need to be reasonably assured of a successful separation?
3. How can we realize this peak capacity with the parameters selected?

Determining the Total Number of Solutes

As will be shown in connection to the third question formulated above, it is recommended to start modifier optimization in isocratic reversed-phase LC with a water-methanol gradient. Obviously, a lower estimate of the total number of solutes in the sample, M, can be obtained by simply counting the number of peak maxima, p_{max}, in the gradient run. Because the possibility of peak overlap is quite real, a better estimate can be extracted from an expression derived by Davis and Giddings based on Poisson statistics [10]:

$$M = P_{max} \cdot \exp[M/2Nc] \qquad (2)$$

which is easily solved by iteration starting with equating M to p_{max}. For isocratic elution Nc is given by eq. (1), but for gradient elution the expression must be adapted according to Snyder [11]:

$$Nc = \frac{\Delta t \cdot \sqrt{N}}{t_0 \cdot G \cdot [1 + k_a/(2.3 \cdot k_a \cdot b + 1)]} \qquad (3)$$

where t_0 is the void time, Δt the difference in gradient retention times between the first and the last peak, G a band compression factor, b the gradient steepness parameter for a linear solvent strength gradient and k_a the average capacity factor of the mixture at the beginning of the gradient. These factors can all be derived from the gradient run. For UV-absorbing solutes a still better estimate of the number of solutes contributing to an overlapping band system can be derived from a mathematical analysis of photodiode-array spectra taken during the gradient run. From the gradually changing spectra the number of contributing factors can be extracted by such techniques as Principal Component Analysis or Iterative Target Testing [4]. In combination, the three estimates put a lower and upper limit on the probable number of solutes in the sample. As will be seen in the next section, this is sufficient.

The Necessary Peak Capacity

In a previous study we addressed the question concerning what peak capacity is needed in RPLC to be reasonably confident of a successful separation. The answer was found in a statistical analysis of computer simulated optimizations for samples containing an arbitrary number of solutes taken from a data base of 32 solutes [12]. The following conclusions are taken from that analysis.

Whether we want to separate all solutes in the sample or only a few key components, in either case the overriding quantity is the total number of solutes. The actual composition of the sample also plays an important, but secondary role. As an example, Fig. 1 shows the probability of achieving a complete separation of all solutes with at least unit resolution after optimization in ternary mixtures containing water, methanol and tetrahydrofuran. The sigmoid curve drawn for a given number of solutes indicates that some easily manipulated samples can be separated with low peak capacity, whereas other, more complex samples require a much higher peak capacity. Conversely, in a *random* sample containing 9 solutes we have a 10% chance of achieving acceptable separation with a peak capacity of Nc = 20, but a higher peak capacity of Nc = 40 is required to be 90% confident of complete separation in a water, methanol, tetrahydrofuran ternary mixture. With an increasing number of solutes the curves shift to the right, indicating that higher peak capacities are needed to expect separation with a certain probability.

This is further demonstrated in Fig. 2, where peak capacities are presented for separating samples of increasing complexity at the 50% confidence level. The two extreme curves in this figure refer to the ideal situation of complete control over retention and to the unhappy situation where we rely on chance alone [10]. The intermediate position of

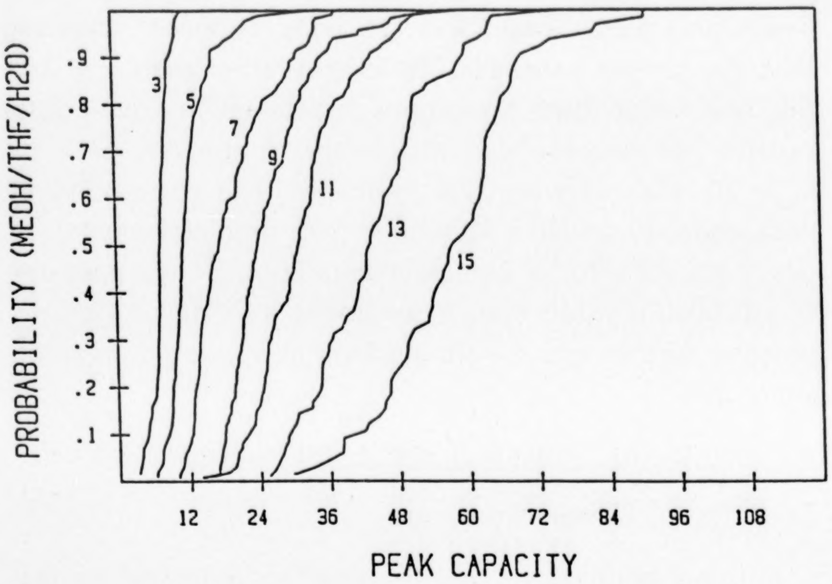

Fig. 1

Probability of achieving complete separation in dependence on the peak capacity for samples containing an increasing number of solutes (reprinted from ref. [12] by permission of *Analytical Chemistry*).

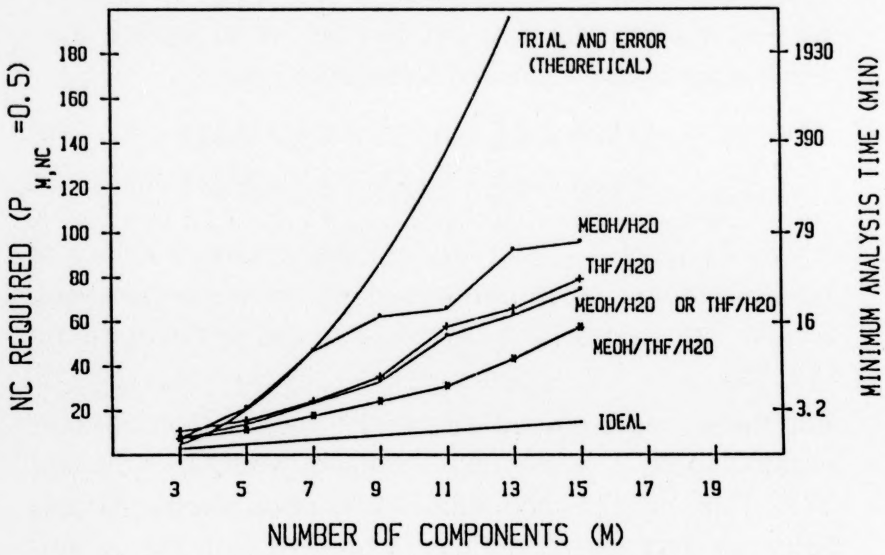

Fig. 2

Peak capacities needed for complete separation of an increasing number of solutes at the 50% confidence level. The curve labelled "ideal" refers to the situation where one has complete control over the retention of each solute, whereas the "trial and error" curve presents the random situation of no control at all [10]. The intermediate curves refer to the practical situations of binary and ternary optimization in water-methanol-tetrahydrofuran. (Reprinted from ref. [12] by permission of *Analytical Chemistry*).

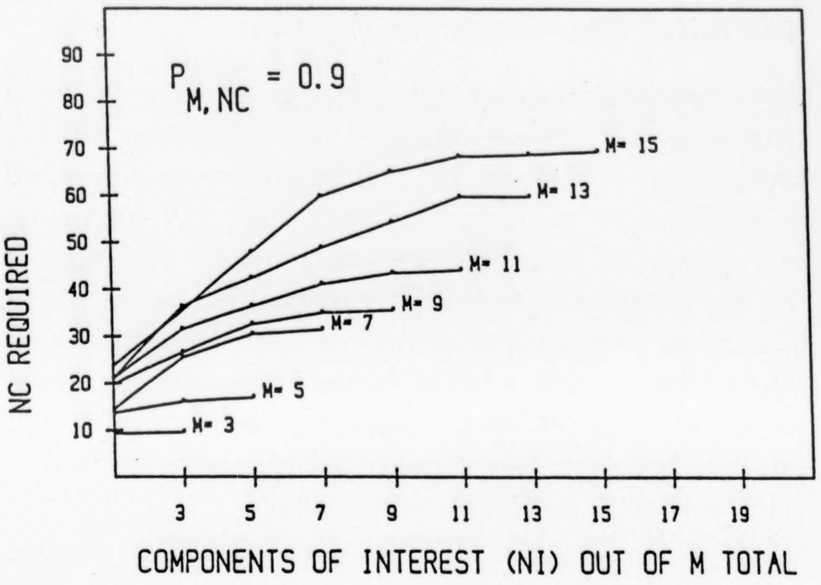

Fig. 3

Peak capacities required for separating a number of key components, NI, smaller than or equal to the total number of solutes in the sample, M. The figure refers to ternary optimization in water-methanol-tetrahydrofuran at the 90% confidence level. (Reprinted from ref. [12] by permission of *Analytical Chemistry*).

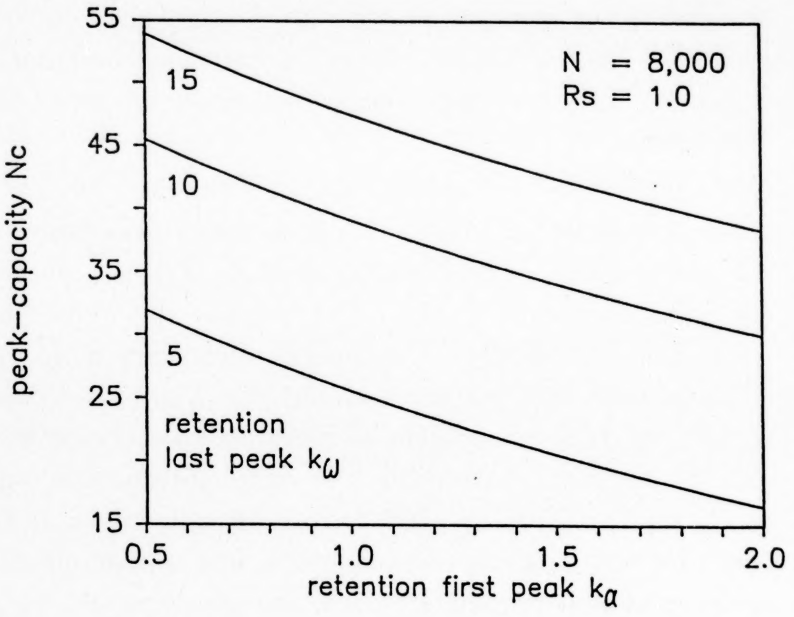

Fig. 4

Peak capacities calculated from eq. (1) for a plate count of 8000 as a function of the initial capacity factor, k_α, for various values of the final capacity factor, k_ω.

the other curves indicates that mobile phase manipulation supplies significant, but certainly not complete control over selectivity. For complex samples, ternary mixtures of water, methanol and tetrahydrofuran are more effective than either binary alone.

If we are no longer interested in separating all solutes, but only in a smaller number of key components, the result is not different in principle, but quantitatively more attractive, as long as the number of solutes of interest is less than half the total number in the sample (Fig. 3). The question then becomes what peak capacity we can realize in RPLC. The answer is provided by eq. (1). Assuming that a well-packed column of 15cm yields a plate count of 8000, the peak capacity is completely determined by the capacity range over which our sample elutes. As is shown by Fig. 4, the capacity factor of the first eluting solute, k_α, has such a pronounced influence that it is virtually impossible to realize high peak capacities within a reasonable analysis time, unless the first solute elutes close to the dead volume of the column. Allowing for a solvent peak at $k = 0$, we should aim at a lower capacity factor of $k_\alpha = 0.5$, while maintaining the freedom to expand the higher capacity factor, k_ω, to the value dictated by the required peak capacity. Whether this can be achieved depends on the composition of our sample. It is thus important that we relate the capacity range over which the sample components elute to the organic modifier content of the solvents. The necessary information is derived from an initial water-methanol gradient and from transfer rules formulated by Schoenmakers et al. [13].

The Initial Water-Methanol Gradient

Fig. 5 presents isocratic capacity factors of a solute in methanol-water binary mixtures as a function of the retention time observed for that solute during a standard 0–100% water-methanol gradient [13]. Of particular interest are the retention times observed for the first and the last solute to elute from the gradient run. A horizontal line at any binary composition intersects the vertical lines through the gradient retention times at two distinct values for k_α and k_ω; in combination with eq. (1), these two values provide the peak capacity achieved with this water-methanol binary for this particular sample.

In the example shown in Fig. 5, the first and the last solutes elute at 6 and 11 minutes net gradient retention time, respectively, and, hence, in an isocratic solvent containing 43% methanol, their respective capacity factors are predicted to be $k_\alpha = 1$ and $k_\omega = 7$. When substituted in eq. (1), these values yield a peak capacity of 30 for a plate count of $N = 8000$. This would be sufficient to expect a complete separation of 5 solutes with more than 90% probability in a binary methanol-water solvent [12]. A lower peak capacity of $Nc = 22$ is obtained with 56% methanol, which would provide a faster chromatogram ($k_\omega = 3$), but only 70% chance of success for separating all 5 solutes.

Obviously, these probabilities decrease rapidly with an increasing number of solutes. Suppose that a peak count of the gradient run in combination with eq. (2) had revealed the presence not of 5, but of 11 solutes, still eluting between 6 and 11 minutes. The lower peak capacity of $Nc = 22$ obtained with 56% methanol would then yield a probability of only 10% to separate all eleven solutes. To be 90% sure of complete separation, the methanol content must be lowered to 27% to yield a peak capacity of 45 at the cost of a long analysis time, $k_\omega = 20$. In the example of a one-dimensional parameter space, the advise would be to vary the methanol content between 27% and 56% to arrive at the highest methanol content and, hence, the shortest analysis time, where the solutes are just separated.

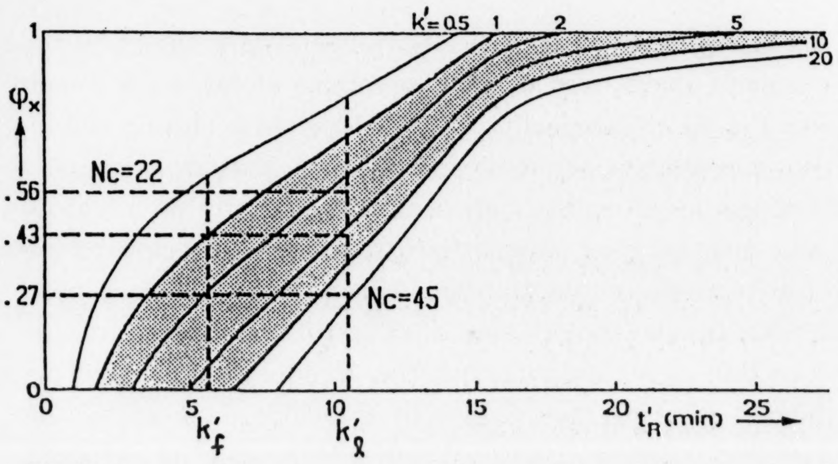

Fig. 5

Curves relating the isocratic composition, $\Phi_{methanol}$, to gradient net retention time, t'_R, calculated for various isocratic capacity factors. The dotted lines refer to a sample eluting from the gradient between 6 and 11 minutes and the peak capacities obtained in various methanol fractions have been calculated from eq. (1). (Reprinted from ref. [13] by permission of *Journal of Chromatography*).

These may all be acceptable solutions. Suppose, however, that the sample contained 15 solutes rather than 5 or 11. Suppose further that, for reasons of detectability, we would restrict the isocratic capacity factor of the last peak to $k_\omega = 20$, realized with 27% methanol. The corresponding peak capacity of $Nc = 45$ would then predict a chance of less than 20% for a complete separation. If we consider this probability too low, it would be a waste of time to proceed further and we should look at a chromatographic alternative.

Transfer to Other Modifiers

Within the confines of organic modifier optimization the obvious alternative is an extension to other modifiers, because fig. 2 shows that ternary mobile phases provide more selectivity than a binary methanol-water mobile phase. In order to maintain the desired peak capacity, the ternary solvent should be a mixture of two *iso-eluotropic* binary solvents that yield – on average – the same capacityctors. For the two most relevant alternatives, tetrahydrofuran and acetonitrile, transfer rules from methanol were first formulated by Schoenmakers et al. [13]. Reexamination of the original data set has led us to replace their expressions by the following cubic equations:

$$\Phi_{THF} = -0.420 \times \Phi_M^3 + 0.702 \times \Phi_M^2 + 0.423 \times \Phi_M \quad (4)$$

$$\Phi_{ACN} = -0.490 \times \Phi_M^3 + 0.953 \times \Phi_M^2 + 0.447 \times \Phi_M \quad (5)$$

where Φ_{THF}, Φ_{ACN} and Φ_M are the volume fractions of tetrahydrofuran, acetonitrile and methanol, respectively. Similar expressions have been formulated in the literature [14, 15].

For the example quoted above, the volume fractions corresponding to 27% and 56% methanol would be 16% and 38% THF or 17% and 46% ACN, respectively. At this point we have several options to proceed with the optimization.

1. We can explore ternary and quaternary solvents mixed from the iso-eluotropic binaries 56% MeOH, 38% THF and 46% ACN, which should all yield a peak capacity of $Nc = 22$ and the last solute eluting at $k_\omega = 3$.
2. Similarly, we can explore a parameter space confined within the boundaries of 27% MeOH, 16% THF and 17% ACN to yield a higher peak capacity of $Nc = 45$ and, hence, a greater probability of success at the cost of a longer analysis time, $k_\omega = 20$.
3. Alternatively, we might explore an even broader parameter space by allowing the solvent strength and, hence, the peak capacity to vary between the above two limits in an effort to obtain an acceptable separation at the shortest possible analysis time.

It is important to stress that the above parameter ranges are all derived from *a single water-methanol gradient*. From the gradient we first derive an estimate of the total number of solutes in the sample. Together with the number of solutes we wish to separate, Figs. 1 and 3 provide us with the peak capacity needed for a separation at a preselected confidence level. To arrive at the isocratic binary methanol-water solvents that achieve this peak capacity, the gradient run is consulted again in connection with Fig. 5. Finally, eqs. (4) and (5) predict the iso-eluotropic THF and ACN binaries. At the end of the exercise the parameter space has been defined and we can begin the search for the global optimum within this space.

Samples that Deviate from Average Behaviour

The guidelines formulated in the previous paragraphs to help define the starting conditions of the eluent optimization procedure in isocratic RPLC have all been derived from a statistical analysis of a single data base of 32 solutes [12]. Consequently, the probability curves in Figs. 1 and 3, the correspondence between isocratic methanol-water binaries and gradient retention times in Fig. 5, and the transfer rules expressed by eqs. (4) and (5) refer to an *average* solute from this data base. In practice, therefore, deviations can be encountered, especially for a solute not included in the data base. Indeed, it is not uncommon to observe differences up to a factor of two between the isocratic capacity factors predicted from Fig. 5 or expected from eqs. (4) and (5), and the values observed in practice, for a particular solute. Since the capacity factors of the first and the last eluting solute, k_α and k_ω, respectively, determine the peak capacity, Nc, and therefore the probability of success, such deviations can have a serious impact on the results of the optimization. Fortunately, the start-up procedure can be easily modified to correct for observed differences. For Table I we used net retention times observed for some solutes during a thirty minute water-methanol gradient. From a figure analogous to Fig. 5 it is possible to derive the methanol content needed to achieve a certain isocratic capacity factor. The table shows the predictions for target values of k = 2 and k = 10, respectively. When the isocratic chromatogram in a consecutive experiment is recorded, then the target values are immediately verified or falsified. In many cases the observed capacity factors, k_{exp}, agree reasonably well with the target values; occasionally large deviations can be seen (e.g., the last two solutes in the table). If the operator is not satisfied with the observed capacity factor, he now has another experimental value at his disposal that he can use to correct the initial prediction made on the basis of a gradient run only. As can be seen from the right hand side of the table, the methanol contents corrected for these deviations yield capacity factors that are very close to the target values. In the rare instance that even this second prediction fails, the operator has *two* isocratic retention data at two different methanol concentrations. These two data suffice to derive capacity factors at any methanol content over the range where the logarithmic capacity factor is a linear function of the volume fraction of methanol.

There are two reasons why it is not advisable to always run two different isocratic methanol binaries. First, without a preliminary gradient it is difficult to select suitable binaries for a novel sample. And secondly, serious deviations from average behaviour are rare enough not to waste time on unnecessary additional measurements.

In a similar way, the operator is warned of erroneous predictions from the transfer rules (eqs. (4) and (5)) when the advised THF and ACN binaries are run. Again, unacceptably large deviations can be used to correct the initial estimate and arrive at more accurate values. Some examples are presented in Table II. Reference values for the capacity factors at a certain methanol fraction are shown in the second column after the solute names. When the volume fraction of methanol is entered into eqs. (4) and (5), we

Table I. Predicted methanol-water binary eluents and verification of the target capacity values (k = 2 and k = 10)

Solute	Gradient scan procedure				Corrected with isocratic value			
	Φ_M (k = 2)	k_{exp}	Φ_M (k = 10)	k_{exp}	Φ_M (k = 2)	k_{exp}	Φ_M (k = 10)	k_{exp}
Benzaldehyde	0.443	1.74	0.130	13.06	0.418	2.04	0.156	11.05
Benzylalcohol	0.520	1.67	0.235	12.37	0.495	1.99	0.253	10.89
m-Dinitrobenzene	0.556	1.85	0.285	10.94	0.548	1.96	0.291	10.58
Dimethylphtalate	0.577	1.23	0.314	15.28	0.530	1.92	0.347	11.09
Prednisone	0.620	0.96	0.373	19.17	0.555	2.10	0.429	9.66
Hydrocortisone	0.648	0.97	0.411	17.62	0.595	1.85	0.456	10.15

Table II. Transfer between iso-eluotropic binary solvents

Solute	Methanol		Acetonitrile				Tetrahydrofuran			
	Φ_M	k_M	Φ (eq. 5)	k_{exp}	Φ_c	k_c	Φ (eq. 4)	k_{exp}	Φ_c	k_c
Benzaldehyde	0.20	4.7	0.124	4.0	0.106	4.8	0.109	2.9	0.068	4.0
	0.30	2.5	0.207	1.8	0.166	2.6	0.179	1.8	0.142	2.3
m-Dinitrobenzene	0.20	10.6	0.124	19.4	0.223	8.7	0.109	22.6	0.211	10.8
	0.40	3.1	0.300	4.8	0.379	2.7	0.255	7.6	0.353	3.3
Prednisone	0.40	9.9	0.300	1.7	0.178	14.9	0.255	1.8	0.139	10.9
	0.50	3.0	0.401	0.3	0.216	7.6	0.335	0.8	0.234	2.3
Hydrocortisone	0.40	9.7	0.300	1.9	0.181	14.6	0.255	2.0	0.144	10.3
	0.50	3.1	0.401	0.3	0.217	7.8	0.335	0.9	0.241	2.4

obtain the "average" volume fractions of ACN and THF. However, for the particular solutes in the table, the experimentally-observed capacity factors deviate appreciably from the methanol reference values. When these deviations are used to compute corrected volume fractions, Φ_c, the capacity factors, k_c, agree much better.

As an illustration of the entire procedure, we shall discuss a practical example. An unknown sample was eluted from the thirty minute water-methanol gradient between 17 and 26 min and was found to contain nine solutes. Because we wanted a separation of all nine solutes at the 0.75 probability level, the necessary peak capacity was $Nc = 30$. The gradient retention times predicted that this could be obtained with a binary solvent containing 57% methanol and that the isocratic capacity factors of the first and last solute would be $k_\alpha = 1.95$ and $k_\omega = 14.2$, respectively. When run, the observed values were 2.29 and 12.2. Not only were these sufficiently close, but the probability of success calculated for this slightly restricted range was still 0.73, which was considered fully acceptable. From eq. (4) the corresponding THF fraction was calculated as 39%, but in this solvent the first and last solutes actually eluted at $k_\alpha = 1.79$ and $k_\omega = 8.10$, respectively, which lowered the peak capacity to such an extent that the probability of success decreased to 0.58. This was no longer acceptable, but the retention data observed in 39% THF immediately allowed a better estimate of 34% THF, in which binary the first and last solutes eluted at $k_\alpha = 2.48$ and $k_\omega = 12.9$, respectively, very close to the values observed in 57% methanol. In a similar way the initial advise of 47% ACN (eq. (5)) was updated to 38% via the correction procedure. The capacity factors were now found to be $k_\alpha = 3.36$ and $k_\omega = 16.4$. Although these values still deviate somewhat from the values observed in 57% methanol, the resulting peak capacity was similar and, therefore most importantly, the probability of a successful separation was equally high: 0.72.

In summary then, after running one gradient and five isocratic chromatograms the parameter space for a better than 70% probability of complete separation was defined as a triangle located between 57% methanol, 34% tetrahydrofuran and 38% acetonitrile. Thereafter one can begin a ternary eluent optimization along the sides of the triangle or quaternary optimization over the entire triangle.

Acknowledgement

The financial support of Millipore Waters Chromatography Division, Milford, Mass. USA, throughout the course of this work is gratefully acknowledged.

References

[1] *P. J. Schoenmakers*, "Optimization of chromatographic selectivity, a guide to method development" (J. Chromatogr. Library Vol. 35) Elsevier, Amsterdam, 1986.

[2] *P. J. Schoenmakers, A. C. J. H. Drouen, H. A. H. Billiet, L. de Galan*, Chromatographia, **15**, 688 (1982).

[3] *A. C. J. H. Drouen, H. A. H. Billiet, P. J. Schoenmakers, L. de Galan*, Chromatographia, **16**, 48 (1982).

[4] *J. K. Strasters, H. A. H. Billiet, L. de Galan, B. G. M. Vandeginste, G. Kateman*, J. Chromatogr. **385**, 181 (1987).

[5] *S. N. Deming, J. C. Bower, K. D. Bower*, in "Advances in Chromatography", *J. C. Giddings, E. Grushka, J. Cazes, Ph. Brown*, ed., Marcel Dekker, Inc. New York, 1984; Vol. **24**, p.35.

[6] *H. J. Issaq*, in "Advances in Chromatography", *J. C. Giddings, E. Grushka, J. Cazes, Ph. Brown*, ed., Marcel Dekker, Inc. New York, 1984; Vol. **24**, p. 55.

[7] *L. de Galan, H. A. H. Billiet*, in "Advances in Chromatography", *J. C. Giddings, E. Grushka, J. Cazes, Ph. Brown*, ed., Marcel Dekker, Inc. New York, 1986; Vol. **25**, p. 63.

[8] *J. C. Berridge*, "Techniques for the Automated Optimization of HPLC Separations", John Wiley and Sons, New York, 1986.

[9] *P. Jandera, J. Churácek*, "Gradient elution in column liquid chromatography" (J. Chromatogr. Library Vol. 31), Elsevier, Amsterdam, 1985. Chapt. 7, p. 157.

[10] *J. M. Davis, J. C. Giddings*, Anal. Chem. **55**, 418 (1983).

[11] *L. R. Snyder, J. W. Dolan, J. R. Grant*, J. of Chromatogr. **165**, 3 (1979).

[12] *D. P. Herman, H. A. H. Billiet, L. de Galan*, Anal. Chem. **58**, 2999 (1986).

[13] *P. J. Schoenmakers, H. A. H. Billiet, L. de Galan*, J. Chromatogr. **205**, 13 (1981).

[14] *M. DeSmet, G. Hoogewijs, M. Puttemans, D. L. Massart*, Anal. Chem. **56**, 2662 (1984).

[15] *H. B. Patel, T. M. Jefferies*, J. of Chromatogr. **389**, 21 (1987).

[16] *J. L. Glajch, J. J. Kirkland, K. M. Squire, J. M. Minor*, J. of Chromatogr. **199**, 57 (1980).

Received: July 10, 1987
Accepted: July 27, 1987
F

Influence of the Peak Height Distribution on Separation Performances: Discrimination Factor and Effective Peak Capacity

M. Z. El Fallah / M. Martin*

Laboratoire de Chimie Analytique Physique, Ecole Polytechnique, F-91128 Palaiseau, France

Key Words

Gas chromatography
Liquid chromatography
Separation performances
Statistical theory
Peak height distribution

Summary

A new index of performance of the chromatographic separation between two adjacent peaks, the discrimination factor, d_0, is defined. It is normalized between 0 and 1 and is directly and easily determined from the chromatogram. It does not depend on any assumption regarding peak shape, except that the peak profiles of individual sample components have a single mode. Its value depends on the relative heights of the two peaks as well as on their separation.

The separation power of a chromatographic system is classically measured by its peak capacity, defined on the basis of constant resolution between adjacent peaks. A previously developed statistical theory of the composition of mixtures makes it possible to extend the concept of peak capacity by taking into account the peak height distribution in typical average chromatograms. A new parameter, the effective peak capacity, is defined for this purpose on the basis of a constant discrimination factor between adjacent peaks. It allows to take into account the distribution of peak heights in statistical theories of the evaluation of complex chromatograms and in the measurement of the limit of determination in quantitative analysis.

The characteristics of the two new parameters, the discrimination factor and effective peak capacity, are discussed and compared with those of their classical homologs, resolution and peak capacity, in the case of gaussian component peaks of equal widths.

Introduction

In the past few years, statistical models of component peak overlap in chromatography have been developed [1–5]. All these models basically recognize that the peaks observed in a chromatogram may not correspond to single individual sample components, but that several components may interfere within a chromatographic peak. They allow the estimation of such quantities as the probability that a peak corresponds to a single component, the probability that all the sample components are separated, the number of components contained in the sample and its probability distribution. Some of these models require the knowledge of the separation power of the chromatographic system, conveniently expressed by the peak capacity, n_c. The peak capacity is the maximum number of peaks which can be accommodated within a given retention interval with a constant resolution factor between adjacent peaks. This resolution factor was originally taken equal to 1 [6], that is, it corresponds to a 4σ separation between adjacent peaks, where σ is the average standard deviation of the two peaks. But the definition of the peak capacity can easily be extended to any value of the resolution, that is to any value, x_0, of the separation between adjacent peaks.

One of the major difficulties encountered when applying the peak overlap statistical models that are based on the knowledge of the peak capacity is to precisely define the value of x_0. In fact, since these statistical models also require counting the number of observed peaks in a chromatogram, the value of x_0 must be coherent with the means used to scrutinize the chromatogram and to count the number of peaks. For instance, if, as frequently done when using an integrator or when visually looking at the chromatogram, a peak is counted each time a maximum appears on the chromatogram, it is felt that x_0 should be close to 2σ. Indeed, it can easily be shown that two maxima are obtained by the addition of two equal height and equal width gaussian curves when the distance between their apices exceeds 2σ. However, this minimum distance increases when the two peak heights become increasingly different. The correct value of x_0 to be used for the cal-

0009-5893/87 0115-08 $03.00/0

© 1987 Friedr. Vieweg & Sohn Verlagsgesellschaft mbH

culation of the peak capacity therefore depends on the peak height distribution in the analyzed sample, which is closely related to the concentration distribution of the sample components. This distribution is generally not known and, in fact, one of the major objectives of chromatographic separation is to determine the concentrations of the sample components. However, use can be made of a recently developed statistical theory of the composition of mixtures [7] to determine the average concentration distribution of a large number of mixtures.

In the following, we address the problem of the determination of the x_0 value to be used in the statistical models of peak overlap. In this regard we define a new parameter measuring the separation power of a chromatographic system, taking into account the peak height distribution in a chromatogram, the effective peak capacity, $n_{c, \text{eff}}$. This requires the use of a criterion of merit of the separation between two adjacent peaks, which also takes into account the relative heights of the two peaks. Because the widely-used resolution factor is inadequate for this purpose, we first define another new parameter characterizing the quality of a two-peak separation, the discrimination factor, d_0.

The Discrimination Factor

The resolution factor, R_s, has certainly, for nearly three decades, been the most used index of merit of the quality of the separation of two peaks. It is defined as the ratio of the difference of the retention times of the two peaks to their average baseline width, which for gaussian peaks is equal to twice the sum of their standard deviations [8]:

$$R_s = 2(t_{R2} - t_{R1})/(w_1 + w_2) \qquad (1)$$

where t_{R1} and t_{R2} are the retention times, and w_1 and w_2 the baseline widths, respectively, of the two peaks. This definition has the advantage of simplicity and relates the resolution factor to the basic peaks parameters, plate number, retention factor and selectivity. The corresponding relationship can be considered as one of the most important equations in chromatography since it allows the prediction of the influence of various operating parameters on the value of R_s. However, the precise determination of R_s requires injecting the two adjacent peaks seperately. Indeed, in principle, the resolution factor cannot be determined from the chromatogram when the two adjacent peaks interfere, since, even for gaussian peaks, the retention times of the peak maxima on the chromatogram are not exactly equal to the retention times of the individual peaks, and their baseline widths are affected by their degree of interference [9]. Moreover, the major disadvantage of the resolution factor is that it does not take into account the relative height of the two peaks. Therefore, R_s may reach values as large as 1.5, which is frequently considered as reflecting an excellent separation, while only one peak maximum is observed if the two peak heights are sufficiently different. This is well demonstrated in Figures 2 to 7 of reference [10]. For this reason, the use of the resolution factor does not appear appropriate when the influence of peak height variation on the peak capacity of a chromatographic system should be taken into account.

Other criteria of merit of a two peak separation have been proposed in the past. Kaiser has used the f/g factor, sometimes expressed as a percentage, variously called "Auflösung" [11, 12], "Auftrennung" [13] or "Trennvermögen" [14] and translated as "peak separation" [15]. This factor is easily determined from the geometrical construction of Fig. 1. f and g are distances measured on the vertical passing through the valley between the two peaks from the intersection point of this vertical with the line joining the two peak maxima, to the depth of the valley and to the baseline, respectively. This parameter takes values between 0, when the valley disappears, and 1, for baseline separation. The determination of f and g becomes, however, relatively imprecise when the peak height ratio increases because the two lines needed for the geometrical construction become progressively parallel. This determination is not possible if the maximum of the major peak exceeds the scale of the recorder. Christophe uses the valley to peak ratio, defined as the ratio of the minimum height between the two peaks (i.e., height of the valley, h_v) to the height of one of the peaks [16]. This factor does not need a geometrical construction for its determination, but, in addition to the fact that two such parameters can be defined for one given pair of peaks, the valley to peak ratio has the disadvantage that it decreases when the separation improves.

The Kaiser and Christophe factors have clearly an advantage over the resolution factor in that their values depend both on the relative heights of the two adjacent peaks and on their separation. In addition, they can be determined for gaussian as well as non-gaussian, possibly tailing, peaks. In order to remove some of their limitations or disadvantages, we have defined a new parameter for the purpose of characterizing the separation between two adjacent peaks, the discrimination factor, d_0, as:

$$d_0 = (h_p - h_v)/h_p \qquad (2)$$

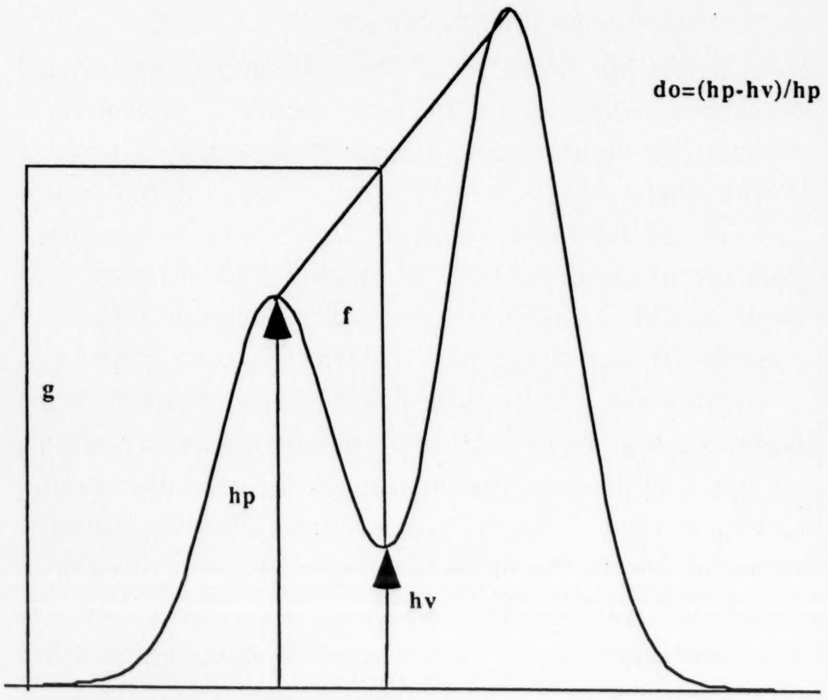

Fig. 1
Definitions of the Kaiser f/g factor and of the discrimination factor, d_0.

where, as shown on Fig. 1, h_v and h_p are the height of the valley and the height of the smallest of the two peaks, respectively. d_0 is unique for a given pair of peaks and easily determined without a geometrical construction, for tailing peaks as well as for symmetrical ones, even when the maximum of the major peak is out of scale, which sometimes occurs in trace analysis. It increases when increasing the separation between the peaks, which is desirable for a criterion of merit of the separation, and conveniently takes values between 0, when the valley disappears, and 1, when the signal goes back to the baseline between the two peaks. When it is close to 1, which means the separation is nearly complete, a further increase in the separation between the peaks proportionally increases the resolution factor and significantly increases the analysis time, while it does not significantly change d_0. Therefore, the use of d_0 in the response function of optimization procedures appears more desirable than that of R_s.

One of the main drawbacks of the discrimination factor is that it cannot be determined when there is no valley between two adjacent peaks, while the resolution has a non-zero value. While there is some possibility to extend the definition of d_0 to this case [17], one should note that our present definition is basically coherent with the postulate that the elution profiles of individual sample components have a single mode. Accordingly, if two maxima appear in the chromatogram, two components are at least present in the sample. This postulate is generally assumed. It implies, firstly, that the elution concentration profile of a component is unimodal and, secondly, that the detector response function is monotonous, i.e. that the detector signal increases, even if not linearly, with the solute concentration. Deviations from this last assumption are rare, but have sometimes been encountered, for instance, with the thermal conductivity detector in gas chromatography [18].

The discrimination factor is somewhat closely related to the Kaiser and Christophe parameters. It becomes equal to the f/g Kaiser factor for equal height peaks, and it is equal to the complement of 1 of the Christophe valley to peak ratio if this ratio is defined on the basis of the observed height (not on the height of the parent peak as occasionally implied in Christophe's publication) of the smallest of the two peaks [19].

Discrimination Factor and Resolution Factor

Because of the very wide use of the resolution factor, it is interesting to compare the d_0 and R_s values. In the following, the numerical calculations are done assuming gaussian peaks of equal standard deviations. This assumption is generally found to be approximately correct all over the chromatogram in programmed analysis (temperature programmation in gas chromatography and gradient elution in liquid chromatography) or in a more restricted retention interval in isotherm and isocratic analysis. In such conditions, the resolution factor is directly proportional to the difference, Δt, of the retention times of the two peaks:

$$\Delta t/\sigma = 4 R_s \tag{3}$$

For a given ratio of the two individual parent peak heights, a_{rp}, there is a minimum resolution value below which only one peak appears in the chromatogram of a two-component mixture. In Fig. 2, this critical resolution, R_s^*, which corresponds to the limiting value $d_0 = 0$, is plotted versus the parent peak height amplitude, a_{rp}. Of course, the critical resolution increases when this ratio increases. However, the variation is relatively the largest for small values of a_{rp}. The critical resolution increases from 0.5 to 0.75, then to 1.0 and to 1.25 when a_{rp} changes from 1 to 4.2, then to 73 and to 4100, respectively.

Similarly, one can compute the R_s value required to ensure a given discrimination factor as a function of the observed peak height amplitude, a_r. Such curves are plotted on Fig. 3 for different values of d_0. They are seen to have about the same shape as Fig. 2. Clearly, these curves show that one cannot state that a separation is satisfactory because the resolution factor is relatively large without taking into account the relative peak height. It should be noted that a_r, which measures the height of the higher peak relative to that of the lower one, can directly be determined from the chromatogram, in contradiction to a_{rp}. Figure 4 shows the relationship between R_s and d_0 for constant a_r values. It can be seen that R_s increases first relatively rapidly, then roughly linearly with increasing d_0 values before increasing asymptotically to infinity as d_0 approaches 1. It appears that even when the height of the small peak is as much as 10,000 lower than that of the large peak, a resolution factor close to 2 is large enough to insure that the signal between the two peaks does not exceed 2% of the height of the small peak ($d_0 = 0.98$). Because the analysis of samples containing components giving a_r values as large as

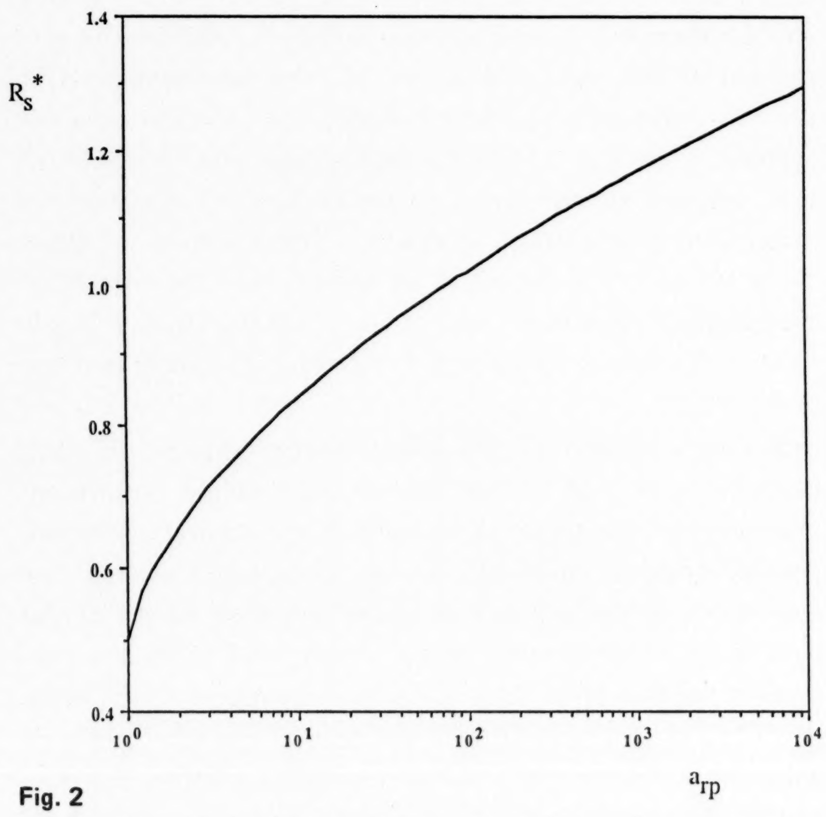

Fig. 2

Plot of the critical resolution factor, R_s^*, for observing a valley between two adjacent peaks (resolution factor corresponding to $d_0 = 0$) *vs* the relative peak height amplitude, a_{rp}, of the two parent peaks (a_{rp} is the ratio of the parent peak heights, i.e. the ratio of the two peak heights which would be observed if the two components were injected separately).

10,000 is difficult and very rare, it is useless to look for a resolution factor larger than 2, even in trace analysis. Figures 3 and 4 are useful as they allow the determination of the non-measurable resolution factor from d_0 and a_r, which are very easily measured from the chromatogram. Alternatively, one can try to determine an analytical relationship between the three parameters. By least-mean square regression analysis of the data, one obtains the coefficients of the second-order Taylor development of $1/R_s$ as a function of d_0 and $1/\sqrt{a_r}$:

$$1/R_s = f(d_0) + g(d_0)/\sqrt{a_r} + h(d_0)/a_r \tag{4}$$

with:

$$f(d_0) = f_1 + f_2 d_0 + f_3 d_0^2 \tag{5}$$

$$g(d_0) = g_1 + g_2 d_0 + g_3 d_0^2 \tag{6}$$

$$h(d_0) = h_1 + h_2 d_0 + h_3 d_0^2 \tag{7}$$

The values of the coefficients depend on the range of d_0 investigated:

for: $d_0 \leqslant 0.05$,

$f_1 = 0.9212$ $f_2 = -1.0987$ $f_3 = 5.9286$
$g_1 = 0.6865$ $g_2 = 1.8826$ $g_3 = -16.143$
$h_1 = 0.3923$ $h_2 = -14.792$ $h_3 = 203.195$

for: $0.05 < d_0 \leqslant 0.7$,

$f_1 = 0.8940$ $f_2 = -0.3512$ $f_3 = 0.0828$
$g_1 = 0.7548$ $g_2 = -0.1313$ $g_3 = -0.3567$
$h_1 = 0.1349$ $h_2 = -1.0251$ $h_3 = 0.9007$

for: $0.7 < d_0 < 1.0$,

$f_1 = -0.0666$ $f_2 = 2.1726$ $f_3 = -1.5896$
$g_1 = -0.3016$ $g_2 = 2.5401$ $g_3 = -2.0303$
$h_1 = 0.3662$ $h_2 = -1.3886$ $h_3 = 0.9265$

Eqs (4) to (7) can be found useful since, from the very easily measured d_0 and a_r parameters, they allow the estimation of the resolution factor. As the dependence of R_s on the operating parameters of the chromatographic system is generally known, appropriate modifications of the relevant parameters can be performed in order to improve the separation as desired. The accuracy of equations (4) to (7) is found to be better than 2% in most of the range of d_0 and a_r, except for small d_0 ($d_0 < 0.1$) and a_r ($a_r < 5$) values for which the error may reach as much as 5%.

The determination of the discrimination factor, in combination with that of the relative peak height amplitude, may greatly help the improvement of the accuracy of quantitative analysis. Indeed, one can compute the error associated with the measure of either the peak height or the peak area as a function of d_0 and a_r and bring the correction for this error into the analytical report. Such computations have been made in the case of gaussian peaks of equal peak widths [22]. Alternatively, this offers the possibility of significantly reducing the analysis time, which concomitantly decreases the resolution, without sacrificing the accuracy of the quantitative determination.

The discrimination factor, like the Kaiser and the Christophe factors, may be found useful for the characterization of the separation when using non-linear detectors, such as the flame photometric detector in the sulfur mode in GC or the evaporative light scattering detector in LC. In these cases indeed, the resolution factor cannot be correctly measured [23].

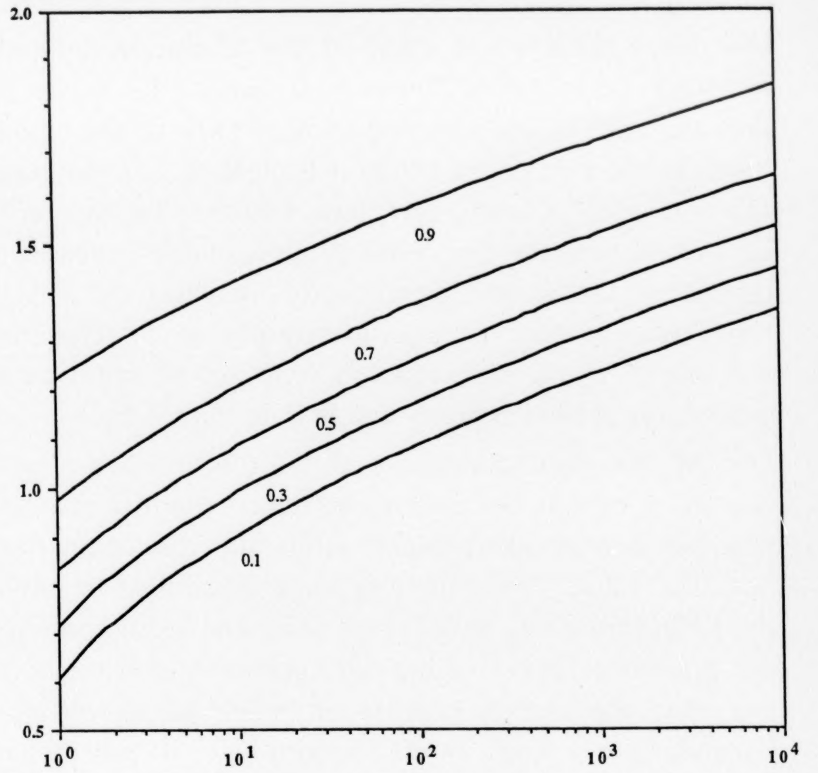

Fig. 3
Plot of the resolution factor, R_s, *vs* the relative peak amplitude a_r at various constant d_0 values. The values of the discrimination factor are indicated on the curves. a_r, which is the ratio of the two peak heights observed on the chromatogram, is directly measurable from the chromatogram.

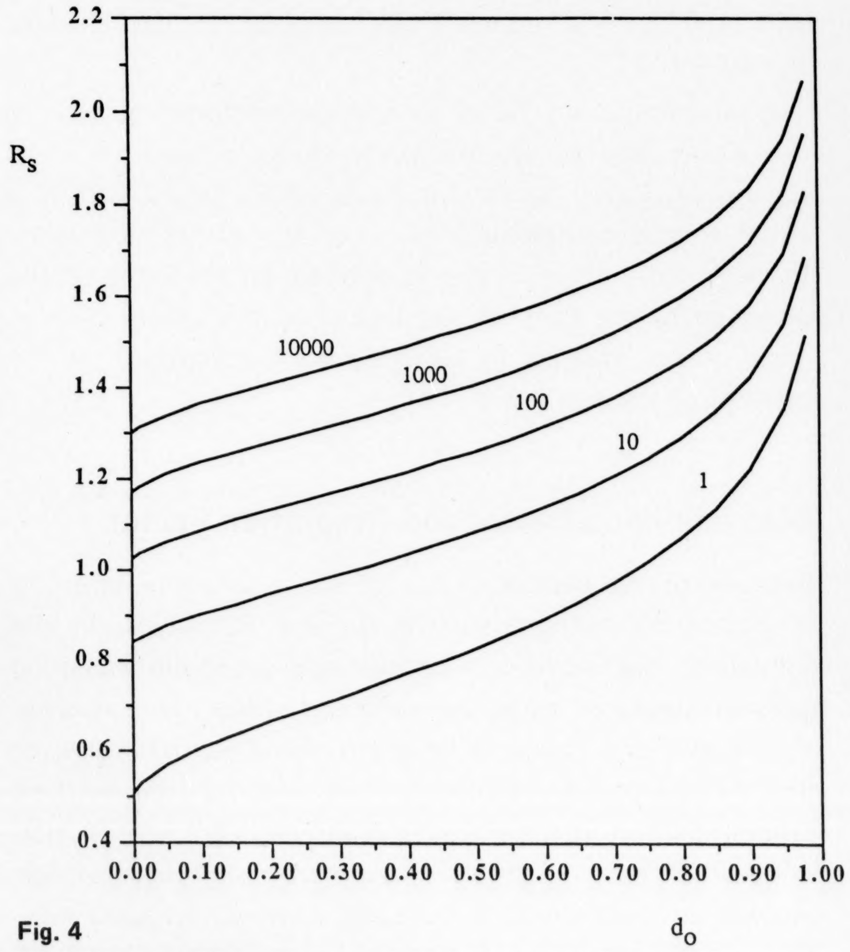

Fig. 4
Plot of the resolution factor, R_s, *vs* the discrimination factor, d_0, for different constant values of the relative peak height amplitude, a_r, indicated on the curves.

The Effective Peak Capacity

In the context of this paper, we are mainly concerned with the influence of the peak height distribution on the overall resolving power of the chromatographic system. For this purpose, one defines, by analogy with the classical definition of the peak capacity, n_c [6], a new parameter, called the effective peak capacity, $n_{c,eff}$, as the maximum number of peaks which can be accommodated within a fixed retention interval with a given constant discrimination factor between adjacent peaks. Clearly, since, in order to achieve a given d_0 value, the distance between the apices of two adjacent peaks, which is proportional to the resolution, depends on the relative peak height amplitude, the effective peak capacity will depend on the peak height distribution in the chromatogram, as well as on the elution order of the sample components. Consequently, in order to compute the effective peak capacity, one must specify these two characteristics.

Let us first address the peak height distribution. In order to simplify the computational process, one assumes the sample components all have a gaussian elution profile with a constant standard deviation, σ. As discussed above, this assumption is most likely to be valid in programmed analysis (temperature programmation in GC and gradient elution in LC). In these conditions, the distribution of the peak heights observed on the chromatogram is identical to the distribution of the concentrations of the components of the injected sample, provided that the detector signal is proportional to the solute concentration in the mobile phase and that the response factor is the same for all components. This last assumption is almost never valid in LC, but one nevertheless assumes that the peak height distribution is similar to the distribution of the sample component concentrations, i.e. that convoluting the concentration distribution by the response factor distribution does not change the shape of the concentration distribution. There are reasons to think that this should be approximately correct in chromatography [3]. A statistical theory of the composition of mixtures has recently been developed [7]. It shows that, in the limiting case of complex mixtures, the relative number of sample constituents having a molar fraction smaller than a given value x increases exponentially with increasing x. In other words, the normalized cumulative frequency probability function of the peak height is exponentially distributed. In the calculations, the peak height distribution of the individual component peaks is therefore chosen so as to be exponential.

Once this distribution is known, the sequence of the elution of the components with various peak heights has to be specified in order to determine the effective peak capacity, since the distance between two consecutive peaks required to obtain a given d_0 value is a function of their relative peak height amplitude. The length of the retention interval required to accommodate m peaks with a constant d_0 value between adjacent peaks is comprised between a minimum and a maximum distance, for which the sequences of elution are specified so as to globally minimize or maximize, respectively, the relative peak height amplitude between adjacent peaks. In Fig. 5, the number of components, m, is plotted versus the length of the retention interval in σ units, $\Delta T/\sigma$, for these two extreme sequences, the discrimination factor between each pair of adjacent peaks being equal to 0.5. For a given ΔT value, m represents the effective peak capacity of the corresponding sequence. For the sake of simplification, these sequences are, in the following, referred to as the minimum or maximum configurations, respectively. The minimum configuration is obtained when the peaks are eluted in order of increasing (or decreasing, which is equivalent since the peaks are assumed symmetrical) peak height. The maximum configuration is assumed to be that obtained when placing the highest peak in the center of the chromatogram, then the two lowest peaks adjacent to it, then the second highest peak adjacent to the lowest peak and the third highest peak adjacent to the second lowest peak, and so on. While we have no absolute proof that this should lead to the maximum ΔT value, we have always found that randomly chosen sequences give lower ΔT values than that obtained with the configuration described above. Figure 5 shows that, for both configurations, the effective peak capacity increases nearly linearly with increasing $\Delta T/\sigma$, as expected on a primary basis.

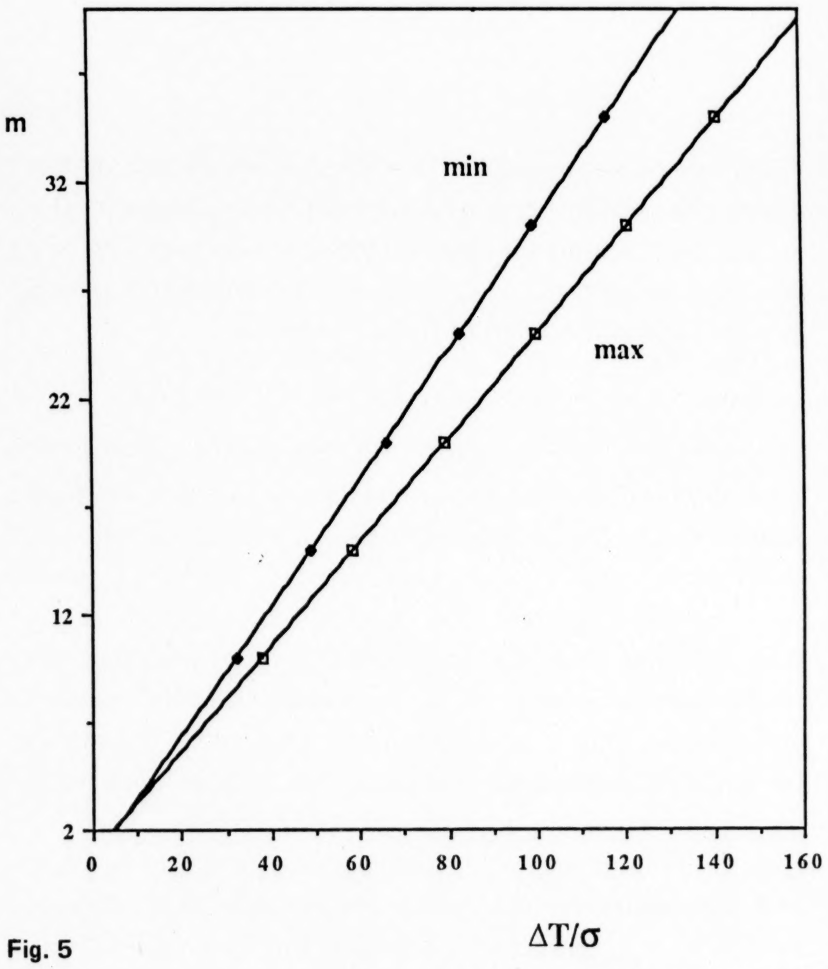

Fig. 5

Plot of the number of gaussian peaks, m, with an exponential peak height distribution, which can be accommodated within an interval ΔT *vs* the length of that interval, $\Delta T/\sigma$, where σ is the standard deviation of the peaks, with a constant discrimination factor, $d_0 = 0.5$, between adjacent peaks. m is called the effective peak capacity, $n_{c,eff}$. ΔT represents the time difference between the apices of the last and first peaks.

The upper and lower curves correspond to the sequences of elution of the various peaks leading to the minimum and maximum ΔT values for a given m value, respectively (see text).

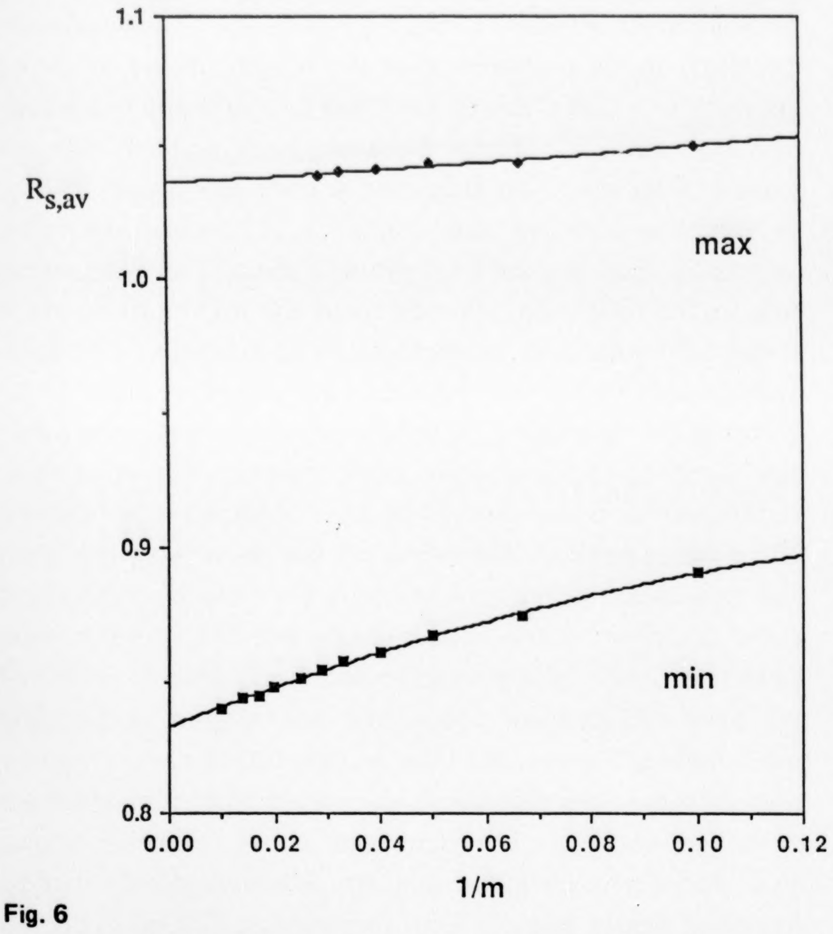

Fig. 6

Average resolution factor, $R_{s,av}$, in a chromatogram with a constant discrimination factor, $d_0 = 0.5$, between adjacent, equal width, gaussian peaks with an exponential peak height distribution *vs* the reciprocal of the number of peaks. The upper and lower curves correspond to the so-called maximum and minimum configurations, respectively (see text).

Figure 6, however, shows that this is not exactly correct. Here, the average resolution in the chromatogram, $R_{s,av}$, is plotted instead of the effective peak capacity. $R_{s,av}$ is easily related to $n_{c,eff}$, i.e. to the number m of components accommodated in the ΔT interval:

$$R_{s,av} = (\Delta T/4\sigma)/(n_{c,eff} - 1) = (\Delta T/4\sigma)/(m - 1) \qquad (8)$$

According to this equation, ΔT represents, as usual, the time interval between the apices of the first and last peaks, assuming all the component peaks are of equal width. If m were linearly proportional to ΔT, then $R_{s,av}$ would be a constant. In fact, Fig. 6, which corresponds to $d_0 = 0.5$, indicates that, for both the minimum and the maximum configurations, $R_{s,av}$ decreases slightly with increasing m. This is due to the fact that when the number of sample components increases, the relative peak height amplitude between adjacent peaks decreases. Therefore, their minimum distance for reaching a given d_0 value, and, consequently, the resolution between them decrease. In Fig. 6, $R_{s,av}$ is plotted, not versus m, but versus 1/m in order to show that the intercept of a least-mean square fit of the computed data to a quadratic expression can give a reasonably good estimate of the limiting value of $R_{s,av}$ for a very large number of components. The change of $R_{s,av}$ with m is more important for the minimum configuration than for the maximum one.

Obviously, the average resolution depends on the fixed d_0 value and decreases as d_0 is lowered. This is reflected in Fig. 7, where the average resolution is plotted versus d_0 for the minimum (lower points) and maximum (higher points) configurations, as well as for the mean (intermediate points) of 50 randomly chosen sequences of elution, all having the same exponential peak height distribution. The data are given for 10-component configurations (white figures) and 20-component configurations (black figures). For the purpose of comparison, the curve of variations with d_0 of the resolution of two equal peak height components, which is classically used for the determination of the peak capacity n_c, is also shown on this Figure (solid line). It can be seen that the discrepancy between the 10- and 20-component configurations is the largest, although still relatively small, for the minimum configuration. The curves for the mean configurations are of particular interest since they correspond to the typical elution sequence which may be encountered in chromatograms. It should be noted that they are nearly independent of component number. The curves are shown to be closer to the maximum configuration than to the minimum configuration data. This is to be expected, as it is more likely to find a random configuration closer to the maximum one, which is somewhat disordered, rather than

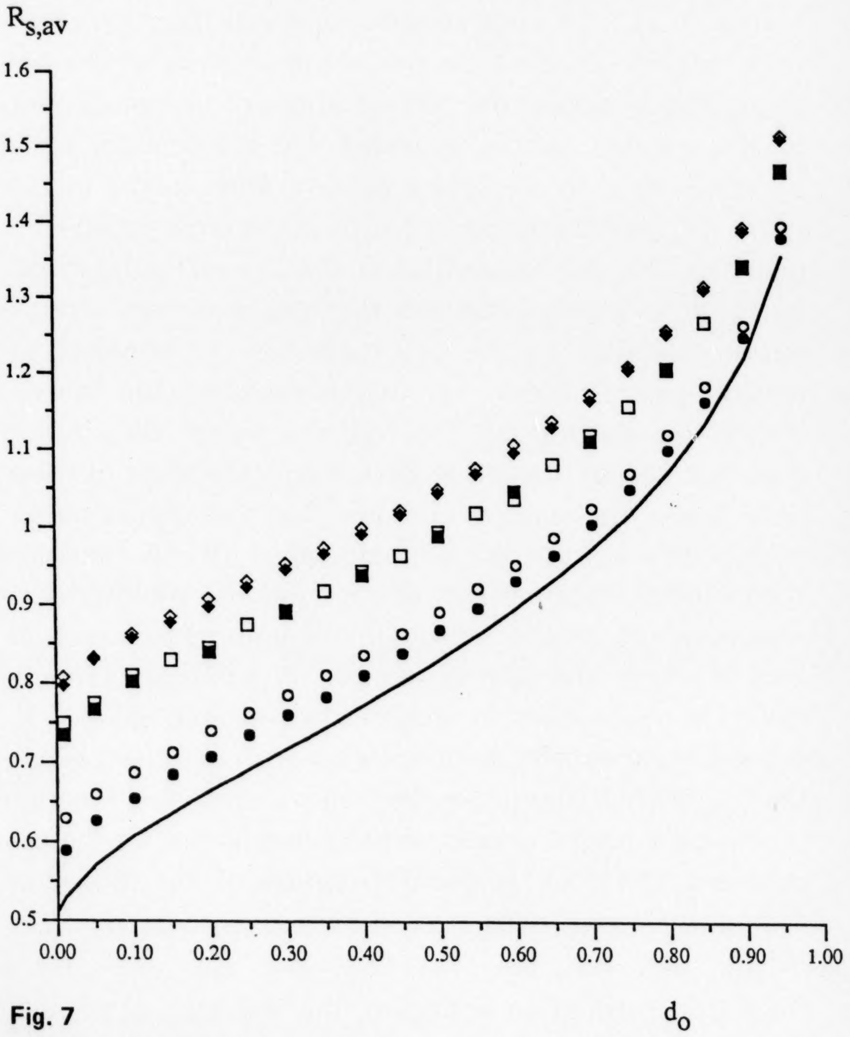

Fig. 7

Average resolution factor, $R_{s,av}$, in a chromatogram constructed from a given number of equal width, gaussian peaks with an exponential peak height distribution such as the discrimination factor, d_0, between adjacent peaks is constant *vs* d_0. The circles and lozenges correspond to the so-called minimum and maximum configurations, respectively (see text). The squares correspond to the mean values from fifty chromatograms with a randomly chosen sequence of elution (mean configuration).

The white and black figures are obtained from chromatograms with 10 and 20 components, respectively. For the purpose of comparison, the resolution of two equal gaussian peaks is plotted versus d_0 (solid line).

to the minimum one, which is perfectly ordered. As an average over the d_0 scale, it was found that, for a given d_0, they are located at a distance from the maximum configuration data equal to 37 ± 3% and 30 ± 2% of the gap between the maximum and minimum configurations, for 10 and 20 components, respectively. The standard deviation of the fifty $R_{s,av}$ (mean, 20) simulation data, i.e. of the average resolution determinations when randomly permuting 50 times the order of elution of 20 components with an exponential peak height distribution, is found to have very little dependence on the d_0 value and to decrease from 0.017 to 0.013 when d_0 increases from 0.05 to 0.95. This corresponds to a relative standard deviation ranging approximately between 2.2 and 0.9%, which is rather small.

The limiting $R_{s,av}(\infty)$ values, i.e. the average resolution values obtained for an infinite number of components and estimated from interpolation of the data such as those of Figure 6 to $1/m = 0$, are plotted on Fig. 8 for the minimum and maximum configurations. It is interesting to note that the curve for the minimum configuration is strictly identical to the curve which would be obtained when determining, according to eq. (8), the average resolution of an infinite number of equal height components. Indeed, the relative peak height amplitude of two adjacent peaks in the minimum configuration comes closer and closer to 1 as the total number of components increases. Consequently, the average distance required to have a given d_0 value between two adjacent peaks becomes equal to that required when the two peaks have the same height. Figure 8 shows that the gap between the two extreme configurations decreases as d_0 increases, which can be explained by the fact that interferences between non-adjacent peaks decrease as d_0 increases. It can be expected that, as d_0 comes closer and closer to 1, the gap between the two curves vanishes. Of particular interest are the critical average resolution values for the minimum and maximum configurations corresponding to $d_0 = 0$, $R^*_{s,av}(\min, \infty)$ and $R^*_{s,av}(\max, \infty)$, respectively. A regression analysis of the simulation data shows that they are equal to:

$$R^*_{s,av}(\min, \infty) = 0.536 \tag{9}$$

and

$$R^*_{s,av}(\max, \infty) = 0.796 \tag{10}$$

while the data of Fig. 7, and the above-indicated average location of the mean configuration relative to the minimum and maximum ones, indicate that the corresponding value for the mean distribution is approximately equal to:

$$R^*_{s,av}(\text{mean}, \infty) = 0.71 \pm 0.01 \tag{11}$$

It may appear surprising that the $R^*_{s,av}(\min, \infty)$ found in eq. (9) is not exactly equal to 0.5, the resolution corresponding to the appearance (or disappearance) of a valley between two equal height peaks. This is due to the fact that, even for equal height peaks, the minimum distance required for the appearance of a valley between a pair of adjacent peaks is affected by interferences with peaks located on both sides of the pair. This distance is found equal to 2.14σ.

Eq. (11) provides the answer to the question raised in the Introduction section, regarding the value of the distance between adjacent peaks to be taken in the calculation of the peak capacity for application of the statistical models of component peak overlap in chromatography. This distance, which is equal to $4\sigma R^*_{s,av}$ (mean, ∞), i.e. $2.84\,\sigma$, is shown to be significantly larger than the minimum distance, 2σ, required to produce two maxima for equal height and equal width peaks. It must be kept in mind that this value is obtained under the assumption that the peaks are gaussian and have the same variance. Work is in progress to address the case of non-gaussian peaks as well as to improve the statistical models of peak overlap by using this value to take the peak height distribution into account. Furthermore, $R^*_{s,av}$ (mean, ∞) corresponds to the critical value $d_0 = 0$ (actually, it is computed for $d_0 = 10^{-4}$), which assumes a perfectly noise-free detector signal. The baseline noise can be taken into account by using a non-zero critical d_0 value for the appearance of two peaks.

It is interesting to note that the value of $R^*_{s,av}$ (mean, ∞) is relatively close to the critical resolution, $R^*_s = 0.8$, empirically selected by Creten and Nagels in their simulations of the determination limit in multicomponent chromatograms [24]. It can be emphasized that their approach to critical resolution, based on the experimentally-observed peak height distribution in plant extract chromatograms [25], and our approach, based on a statistical theory of the composition of mixtures, are quite complementary. The similarity between the two results gives us some confidence about the general validity of this theory. It is not surprising that Creten and Nagels found a slightly

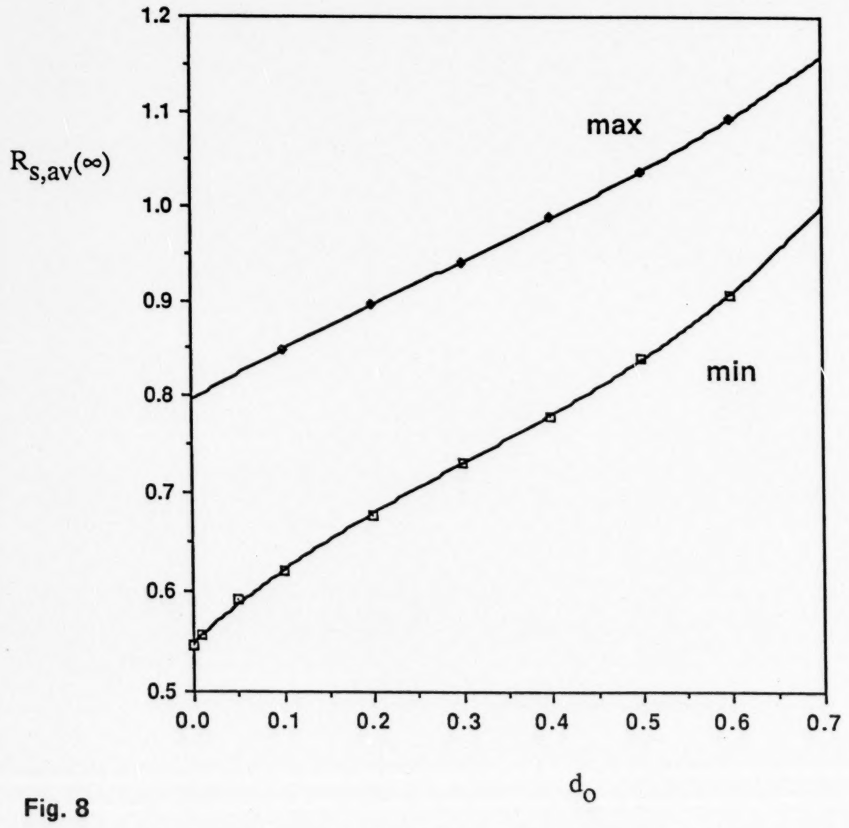

Fig. 8

Extrapolated average resolution factor, $R_{s,av}(\infty)$, in chromatograms constructed from an infinite number of equal width, gaussian peaks with an exponential peak height distribution such as the discrimination factor, d_0, between adjacent peaks is constant *vs* d_0. The upper and lower curves correspond to the so-called maximum and minimum configurations, respectively (see text).

larger R_s^* value than $R_{s,av}^*$(mean, ∞). Indeed, they simulated random chromatograms and looked for the one producing the largest number of peaks to estimate the peak capacity [24]. However, in spite of the very large number of simulated chromatograms (more than 120,000) and even for the smallest number of detected peaks [30], there is only a very small probability that one of these chromatograms will have the right retention and peak height configuration so as to provide the well-ordered configuration which leads to the determination of the peak capacity. Therefore, it is likely that the use of $R_{s,av}^*$ (mean, ∞) in the simulations should somewhat improve the accuracy of the estimation of the limit of determination due to matrix interferences.

References

[1] *D. Rosenthal*, Anal. Chem. **54**, 63 (1982).

[2] *J. M. Davis, J. C. Giddings*, Anal. Chem. **55**, 418 (1983).

[3] *M. Martin, G. Guiochon*, Anal. Chem. **57**, 289 (1985).

[4] *J. M. Davis, J. C. Giddings*, Anal. Chem. **57**, 2168 (1985).

[5] *M. Martin, D. P. Herman, G. Guiochon*, Anal. Chem. **58**, 2200 (1986).

[6] *J. C. Giddings*, Anal. Chem. **39**, 1027 (1967).

[7] *M. Martin, G. Guiochon*, "Statistical theory of the composition of mixtures. Application to the estimation of the number of theoretically detectable components by chromatography", Communication presented at the 9th International Symposium on Column Liquid Chromatography, Edinburgh, July 1–5, 1985.

[8] *D. Ambrose, A. T. James, A. I. M. Keulemans, E. Kovats, H. Röck, C. Rouit, F. H. Stross*, in "Gas Chromatography 1960", *R. P. W. Scott*, ed., Butterworths, London, 1960; p. 423.

[9] *E. Grushka*, Anal. Chem. **44**, 1733 (1972).

[10] *L. R. Snyder*, J. Chrom. Sci. **10**, 200 (1972).

[11] *R. Kaiser*, "Chromatographie in der Gas Phase. I. Gas-Chromatographie", Bibliographisches Institut, Mannheim, 1960; p. 16 and 35.

[12] *R. Kaiser*, "Chromatographie in der Gas Phase. III. Tabellen", Bibliographisches Institut, Mannheim, 1962; p. 148.

[13] *R. Kaiser*, "Chromatographie in der Gas Phase. II. Kapillar-Chromatographie", Bibliographisches Institut, Mannheim, 1961; p. 32.

[14] *R. Kaiser*, "Gas Chromatographie", Akademische Verlagsgesellschaft Geest & Portig K.-G., Leipzig, 1960; p. 33.

[15] *L. S. Ettre*, J. Gas Chromatogr., **1**, 36 (1963).

[16] *A. B. Christophe*, Chromatographia, **4**, 455 (1971).

[17] *M. Martin, M. Z. El Fallah*, unpublished work.

[18] *A. I. M. Keulemans, A. Kwantes, G. W. A. Rijnders*, Anal. Chim. Acta, **16**, 29 (1957).

[19] Since the beginning of this work and the submission of a related abstract for communication to a symposium [20], we have been informed that a criterion very similar to d_0 has been independently suggested by *Schoenmakers* [21].

[20] *M. Z. El Fallah, M. Martin*, "Extension des concepts de résolution et de capacité de pics en chromatographie", Communication presented at the 4th Congress of Analytical Chemistry — 36th Congress of GAMS, Paris, December 8–13, 1986.

[21] *P. J. Schoenmakers*, "Optimization of chromatographic selectivity", Journal of Chromatography Library, Vol. 35, Elsevier, Amsterdam, 1986; p. 121–123.

[22] *M. Z. El Fallah, M. Martin*, submitted to publication.

[23] *A. Stolyhwo, H. Colin, M. Martin, G. Guiochon*, J. Chromatog. **288**, 253 (1984).

[24] *W. L. Creten, L. J. Nagels*, Anal. Chem. **59**, 822 (1987).

[25] *L. J. Nagels, W. L. Creten, P. M. Vanpeperstraete*, Anal. Chem. **55**, 216 (1983).

Received: June 29, 1987
Accepted: Oct. 19, 1987
F

Anion Chromatography in Open Tubular Capillary Columns with Indirect Fluorometric Detection

W. D. Pfeffer/T. Takeuchi/E. S. Yeung*

Ames Laboratory-USDOE and Department of Chemistry, Iowa State University, Ames, Iowa 50011, USA

Key Words

Capillary liquid chromatography
Anion chromatography
Fluorometric detection

Summary

A C_8 reversed-phase open tubular capillary column is dynamically modified with cetylpyridinium chloride to provide anion-exchange sites. Sodium salicylate is used as the eluent at the micromolar concentration range. The low capacity of the dynamically modified column allows the elution of common anions with k′ values similar to those in conventional ion chromatography. The reduced salicylate concentration allows good detectability in the indirect fluorescence mode, even though the baseline noise increased because the fluorescence intensity is lower. The noise level is equivalent to one picogram of non-fluorescing anions.

Introduction

Recently, there has been a lot of interest in the use of microcolumns in HPLC [1]. The main advantages are the enhanced mass detectability and the reduction of the amounts of mobile phase and stationary phase used. The former is particularly important when the sample size is limited, such as in natal or prenatal body fluids, or in analysis at the cellular level. The latter allows designs of special separation modes, such as chiral phases or affinity phases, or the use of unique detection schemes. Very efficient separations have been obtained in microcolumns [2]. It is predicted that optimum open-tubular capillary liquid chromatographic (LC) columns can generate in excess of 10^6 theoretical plates [3, 4]. The internal volume of such a column is around or less than 10 nl. Therefore, injection and detection volumes should be substantially reduced compared with conventional LC so that they do not degrade column efficiency. Injection of small volumes of sample can be readily achieved by split injection techniques, while detection has been a more difficult problem in open-tubular capillary LC.

Ion chromatography (IC) has become an important analytical method as a result of research efforts in the last few years [5–7]. Much attention has been given to nonsuppressed ion chromatography, because of the potential for minimizing band broadening. Most of the detectors have very similar limits of detection (LOD), which are in the nanogram range for typical ions. Since these detectors have already been utilized to their full potential, additional improvements in LOD can only come if new detection principles are introduced.

In conventional liquid chromatography (LC), the lowest LOD's have been reported for the fluorescence detector [7]. For ions that fluoresce, one can thus expect improved LOD in IC as well. However, the number of ions that inherently show fluorescence is very small. Recently, several indirect detection methods for LC have been demonstrated [8, 9]. Indirect fluorescence detection [10–12] is particularly interesting. Briefly, a fluorescing eluting ion is used in the nonsuppressed IC mode. So, there is a constant background signal generated at the detector when no analytes are present. When the analyte ion elutes, it displaces an equal amount of the eluting ion at the detector. Even though the detector does not respond to the analyte, the lower eluent concentration at the detector causes a decrease in signal. The analyte can then be monitored as a negative signal, i. e., indirectly.

There is an important feature in indirect fluorescence detection versus indirect photometry [8]. As the volume of the detector decreases, such as in moving to microcolumns, the sensitivity of absorption methods will decrease to the point where they are no longer suitable for indirect detection. The background level cannot be maintained high enough to observe the negative signal. In fluorescence, especially if lasers are used for excitation, there is adequate sensitivity even if pathlengths are small or if the concentration of the eluting ion is low. In this paper, we report the use of open-tubular capillary column for ion chromatography. Indirect fluorescence allows detection of non-fluorescing anions at very low levels.

0009-5893/87 0123-04 $ 03.00/0

© 1987 Friedr. Vieweg & Sohn Verlagsgesellschaft mbH

Experimental

Apparatus

Fig. 1 shows a diagram of the chromatographic system employed in this work. A syringe pump (ISCO, Lincoln, NE, Model 2600) was used as a pump and was operated in the constant-pressure mode. A line filter SSI 05-0105 (0.5 μm, supplied by Alltech, Deerfield, IL) was connected before the injector. A Rheodyne Model 7520 (1 μl, Cotati, CA) was employed as a sample injector and the split ratio was regulated by an SSI two-way valve (Alltech) and stainless-steel tubing of 2 m x 0.1 mm I.D. (Japan Spectroscopic, Tokyo, Japan). An SB-OCTYL-50 (n-octylmethylpolysiloxane, 50% n-octyl groups) open-tubular fused-silica capillary column (10 m x 50 μm I.D. and 0.5 μm thickness) was commercially available from Lee Scientific (Salt Lake City, UT). The capillary column was directly connected to the sample injector through a T-joint (0.75 mm bore; Valco, Houston, TX). A linearly polarized 325-nm UV beam of a HeCd laser (Liconix, Sunnyvale, CA, Model 4240NB) at about 7 mW is used as an excitation source. The polarization of the beam is modulated at 100 kHz by an electrooptic modulator (Lasermetric, Inc., Teaneck, NJ, Model 3030), which is driven by a high-frequency modulator driver (Conoptics, Inc., Danbury, CT, Model 25). Unipolar positive-going square waves (0 to + 1.0 V) from a wave generator (Wavetek, San Diego, CA, Model 162) are in turn applied to the modulator. A calcite beam displacer (Karl Lambrecht Corp., Chicago, IL, MBDA10) splits the polarization-modulated beam into two separate beams. The perpendicularly polarized beam continues straight through while the horizontally polarized beam goes through the calcite at 6°. The horizontally polarized beam emerges displaced 3.3 mm apart from the first, and parallel to it. The two beams are directed to the centers of the sample and reference flow cells, respectively.

Two parallel 1-mm i.d. x 2-mm o.d. quartz tubes are held 3.3 mm apart. A 50-cm focal length quartz lens is used to collimate the laser beam into the modulator. A 4.5-cm focal length quartz lens is placed before the calcite displacer in order to focus the 1.2-mm diameter laser beam down to 54 μm at the flow cells. The fluorescence from each cell is collected by separate optical fibers similar to the arrangement in Ref. [13]. Both fibers are directed to a single photomultiplier tube (Hamamatsu, Bridgewater, NJ, R928) after passing through three filters (Corning Glass, Corning, NY, 0-52 and 3-75 and Schott Glass, Duryea, PA, K-5). The photomultiplier tube output is directed to a lock-in amplifier with a 1-s time constant (EG & G, PAR, Princeton, NJ, Model 5202) through a 100x amplifier (Hewlett Packard, Palo Alto, CA, Model 420). Initially the fluorescence signals from the sample and reference cells are maximized and balanced (during the two half-cycles of the modulation) by adjusting the distance of each fiber to the irradiated zones. This then provides a null output at the lock-in amplifier when eluent is present. The reference cell contains identical eluent flowing at approximately the same rate in a conventional gravity-induced flow system. A typical flow rate is 2 μl/min.

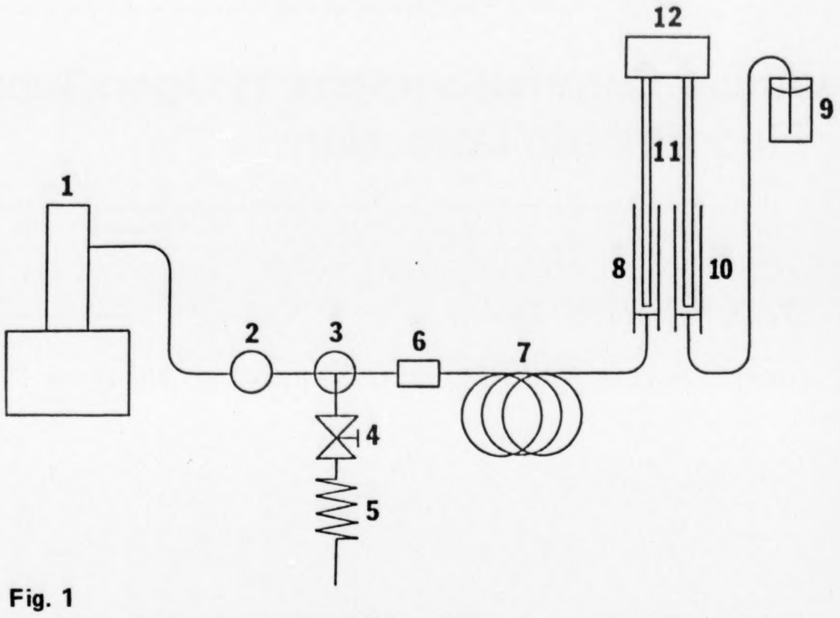

Fig. 1
Diagram of the chromatographic system. **1** = pump; **2** = injector; **3** = T-joint; **4** = two-way valve; **5** = restrictor; **6** = 1/16 in. x 1/32 in. reducing union; **7** = capillary column; **8** = sample flow cell; **9** = gravity flow system; **10** = reference flow cell; **11** = optical fibers; **12** = photomultiplier tube.

Reagents

HPCL-grade methanol was supplied by Fisher Scientific (Fair Lawn, NJ). Water employed in this work was pure water prepared with the Barnstead Nanopure II system (Barnstead, Division of Sybron, Boston, MA). Cetylpyridinium Chloride monohydrate (CPC) was supplied by Aldrich (Milwaukee, WI). The other reagents used in this work were reagent grade and supplied by Fisher Scientific, unless otherwise noted. The mobile phase was degassed in an ultrasonic bath under vacuum. The reference solution for fluorometric detection was degassed the same way and then filtered with a disposable Nylon 66 filter (Alltech, 0.2 μm). The samples were dissolved in the eluent.

Preparation of the Column

The quaternary ammonium salt (50 mM) was dissolved in 2% methanol. The prepared reagent solution was passed through the column for 6 h, followed by washing with water for 30 min. After the above dynamic modification, the sodium salicylate aqueous solution used as the eluent was passed through the dynamically modified column. In order to wash out the modified reagent from the column, methanol was passed through the column at least for 1 h.

Results and Discussions

In the indirect detection method, the dynamic reserve (which is defined as the ratio between the background signal and its noise level), the concentration of the visualization reagent, and the displacement ratio (which is defined in this work as the number of visualization ions which are transferred by one analyte ion) all play important roles in the sensitivity that can be achieved. The concentration detectability (C_{lim}) at the detector is given by these parameters as follows.

$$C_{lim} = C_m/RD \qquad (1)$$

where C_m is the concentration of the visualization reagent, R is the displacement ratio, and D is the dynamic reserve. The dynamic reserves for fluorescence and for absorption vary differently with the magnitude of the background signal. While the former maintains a 5×10^3 level until the concentration of the visualization reagent falls below 10^{-7} M [10], the latter is proportional to the concentration when the background absorption is below 1.0 a.u. The displacement ratio for monovalent ions is expected to be unity in ion-exchange chromatography (independent of the mobile phase concentration). Ion-exchange columns having very low capacities are required to demonstrate the separation of ions using a mobile phase with low concentrations of visualization reagent.

To produce an open-tubular capillary column that allows low concentrations of eluting ions to be used, one needs a low capacity. This can be achieved by dynamic modification. The column generation procedure is similar to earlier reports [12, 14]. The limited surface area of the open tube automatically lends itself to a low capacity mode. We found that common anions can be separated by elution with salicylate ions at the micromolar range. This is two to three orders of magnitude lower than those typically used for analytical scale nonsuppressed IC. According to eq. (1), this is favorable for detection.

Fig. 2 shows a chromatogram of anion-exchange chromatography using such a dynamically modified column. The conditions there have been optimized for the detection of the two anions Cl^- and NO_3^-. Salicylate at 2.5×10^{-6} M is used as the eluent. At higher salicylate concentrations, the elution strength does not allow separation of the two ions. At lower salicylate concentrations, the retention times become too long, and the peak heights decrease proportionately. The 50 µm i.d. of the open-tubular column is not optimal for LC. Ideally, one wants to use i.d. of the order of 1–3 µm, [4]. Our choice is limited by the commercial availability of such columns. Another advantage is that a smaller column will improve mass detectability even further because of the reduced peak volume.

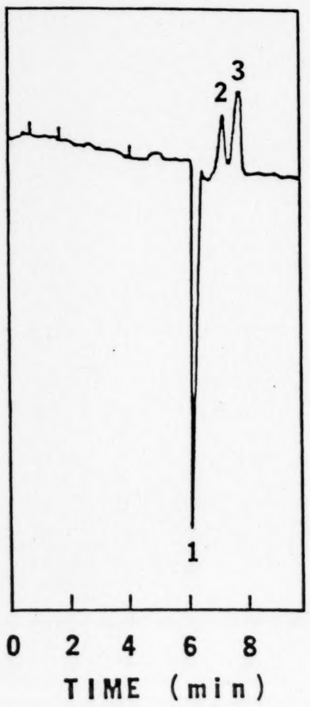

Fig. 2

Indirect fluorescence chromatogram of anions. **1** = salicylate (system peak); **2** = chloride; **3** = nitrate. Random spikes before the salicylate peak are due to microbubbles in the effluent. Flow rate = 2 µl/min. 0.5 pmol of each ion was injected.

The magnitudes of the signals can be compared to those predicted from the displacement of the eluting ions by the analyte ions on a per equivalent basis. The background fluorescence signal, as determined by irradiating only the sample flow cell, was 14.4 mV measured by the lock-in amplifier. The peak heights of chloride and nitrate in Figure 2 corresponded to 0.50 mV and 0.70 mV, respectively. So, the signals at the peaks corresponded to decreases of roughly 1/29 and 1/21 of the total fluorescence, or a displacement of 8.6×10^{-8} N and 1.2×10^{-7} N of salicylate ions, respectively. Now 5×10^{-13} mol of each of the two ions were injected, and these were diluted to peak volumes (fwhm) of 0.4 µL each. The actual concentrations of the analyte ions at the peaks are then 1.2×10^{-6} N. This is 10 times larger than the signal levels would indicate, since an ion-exchange mechanism for separation and a displacement mechanism at the detector (due to electroneutrality) must be responsible for the observed chromatogram. In previous work [10], a one-to-one correspondence was observed. The present results indicate that stray light is dominating over the fluorescence at this low a concentration of salicylate. If stray light can be further reduced, one would expect even better detectability for the anions. Possible contributors to stray light include Raman scattering of the solvent, fluorescent impurities in the eluent, and fluorescence from both the quartz tube and the optical fiber that is coupled to the phototube. We have independently confirmed the contribution of stray light in this arrangement by measuring the phototube current while water alone is passed through the flow cell.

The peak height of the nitrate ion is about 0.7 mV. So, the noise level in the chromatogram corresponds to 1 pg of NO_3^- injected. This is substantially better than previous results in detection in IC [6, 10]. This is due to the small peak volumes in open-tubular capillary LC. The noise level corresponds to 4.5×10^{-8} N of ion present at the detector. This is similar to those in standard detectors for nonsuppressed IC. Because of stray light and the lower fluorescence intensity, the dynamic reserve here is lower than that in Ref. [10]. However, the eluent concentration here is lower. According to eq. (1), the two balance out and the concentration detectability did not change.

Future improvements in this system should be possible. These can include better stray light rejection, better coupling between the capillary column and the detection cell, the use of smaller i.d. capillary columns, still lower concentrations of the eluent by further reducing the capacity of the column, and a higher degree of intensity stability from the laser. Still, the present system provides one of best mass detectabilities of non-fluorescing anions separated by IC.

Acknowledgements

Ames Laboratory is operated for the U.S. Department of Energy by Iowa State University under contract No. W-7405-Eng-82. This work was supported by the Director for Energy Research, Office of Basic Energy Sciences.

References

[1] *M. Novotny,* Ed., "Microcolumn Separations", Elsevier, Amsterdam, 1985.

[2] *H. G. Menet, P. C. Gareil, R. H. Rosset,* Anal. Chem. **56**, 1770 (1984).

[3] *J. H. Knox, M. T. Gilbert,* J. Chromatogr. **186**, 405, (1979).

[4] *J. W. Jorgenson, E. J. Guthrie,* J. Chromatogr. **255**, 355 (1983).

[5] *H. Small,* in "Trace Analysis", *J. F. Lawrence,* Ed., Academic Press, New York, Vol. I., 1982, p. 267.

[6] *J. S. Fritz, D. T. Gjerde, C. Pohlandt,* "Ion Chromatography", Hüthig, New York, 1982.

[7] *H. Small,* Anal. Chem. **55**, 235A (1983).

[8] *H. Small, T. E. Miller,* Anal. Chem. **54**, 462 (1982).

[9] *D. R. Bobbit, E. S. Yeung,* Anal. Chem. **56**, 1577 (1984).

[10] *S. I. Mho, E. S. Yeung,* Anal. Chem. **57**, 2253 (1985).

[11] *T. Takeuchi, E. S. Yeung,* J. Chromatogr. **366**, 145 (1986).

[12] *T. Takeuchi, E. S. Yeung,* J. Chromatogr. **370**, 83 (1986).

[13] *M. J. Sepaniak, E. S. Yeung,* J. Chromatogr. **190**, 377 (1980).

[14] *R. M. Cassidy, S. Elchuk,* Anal. Chem. **54**, 1558 (1982).

Received: June 30, 1987
Accepted: July 17, 1987
F

Data Handling in HPLC-Diode Array UV-Spectrometry

B. G. M. Vandeginste* / G. Kateman

Laboratorium voor Analytische Scheikunde, Katholieke Universiteit Toernooiveld, 6525 ED Nijmegen, The Netherlands

J. K. Strasters / H. A. H. Billiet / L. de Galan

Laboratorium voor Analytische Scheikunde, Technische Universiteit, De Vries van Heystplantsoen 2, 2628 RZ Delft, The Netherlands

Key Words

Column liquid chromatography
Factor analysis
Curve resolution
Iterative target transformation factor analysis
Diode array detector

Summary

The mathematical resolution of overlapped chromatographic peaks obtained in HPLC with a diode array UV detector has received considerable attention recently. The purpose of the proposed methods is the quantitation and identification of unknown solutes in complex mixtures by an efficient use of all available data.

Basically two approaches have been proposed: the first one resolves the concentration profiles and calculates the pure spectra by applying a minimal number of assumptions, which is denoted self-modeling-curve resolution. The second one is based on a match of pure spectra available in a spectral library with the measured mixture spectra.

In this paper both approaches are evaluated with respect to their performance to provide the pure spectra and an accurate quantitation of the concentrations.

Introduction

Giddings and Davis [1] and later Herman et al. [2] have shown that the peak capacity of a liquid chromatographic system should largely exceed the number of compounds one wants to separate in order to be more than 90% confident that the compounds of interest will appear as isolated peaks. Although this required peak capacity can be diminished by optimizing the conditions of the separation for a given criterion, the problem of overlapping peaks is a nearly universal concern in the practice of analytical separations [3]. When using a single wavelength detector, qualitative and quantitative information has to be derived from the obtained chromatogram: namely the retention times of the compounds and the heights or areas of the recorded peaks. The accurate determination of these parameters requires a certain minimal resolution. One of the available so called univariate methods for the resolution of overlapping peaks and the subsequent determination of the peak areas or heights is curve fitting [4]. Each peak is described by a mathematical model, e.g. a Gaussian function. The parameters of that model, peak height, peak position and peak width are calculated by a nonlinear regression procedure that minimizes the squared differences between the model and the measured overall concentration profile. A critical evaluation of the performance of curve fitting by Vandeginste [4] and later by Maddams [5] has shown that the allowable peak overlap is limited also in case that the model describes the peak shape exactly.

A rule of thumb is that the peak areas become inaccurate when the resolution is to small to detect the peaks by the second derivative: i.e. the number of negative areas in the second derivative should be equal to the number of peaks. Fig. 1 shows the detectability of overlapping Gaussian peaks as a function of the ratio of peak heights, peak widths and peak separation. On the average, peaks become undetectable by the second derivative when the resolution drops below $R = 0.7$. In practice however, matters are worse as the peak shape and model may deviate, because of a lack of suitable models to describe peak asymmetry or tailing. The required resolution is therefore somewhat higher than is read from Fig. I.

The determination of peak purity is of course limited because one can hardly decide whether a peak is skewed because of an underlying second component or because of peak tailing. Evidently the information content of the retention time to identify the compounds is very limited.

0009-5893/87 0127-08 $03.00/0

© 1987 Friedr. Vieweg & Sohn Verlagsgesellschaft mbH

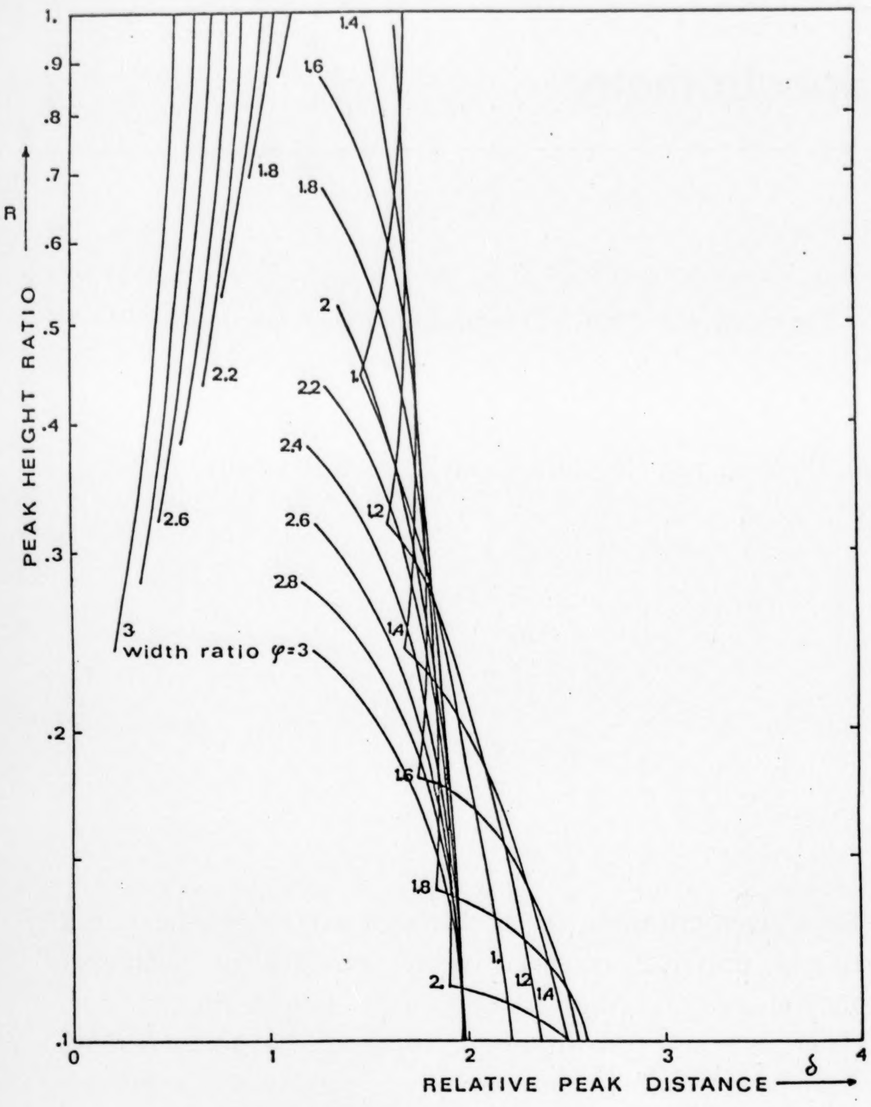

Fig. 1

Detectability of two overlapping Gaussian peaks with unequal halfband withs: model is exact

$\varphi = (w_{\frac{1}{2}})_1/(w_{\frac{1}{2}})_2$

$R = h_2/h_1$

$\delta = \left[\frac{1}{(w_{\frac{1}{2}})_1} + \frac{1}{(w_{\frac{1}{2}})_2}\right] \Delta t \sqrt{\ln 2}$

Reprinted with permission from the American Chemical Society.

When using a dual wavelength detector the determination of peak purity by evaluating a ratiogram is less sensitive for overlap and peak shape [6].

When using a diode array detector one obtains several chromatograms, measured at several wavelengths and several spectra measured at short time intervals. The type of data is similar to the one generated by GC-MS or other type of hyphenated method. During a typical run one spectrum is measured every 0.1 sec over 80 wavelengths (resolution 2 nm) in the Uv-vis region. Of course when all compounds are well separated the data are in optimal shape to extract the quantitative and qualitative information. The time axis (Fig. 2) contains the qualitative information whereas the wavelength axis provides the qualitative information. Although at a first sight this should not provoke serious problems, it appears that the identification of the pure spectra by means of a spectrum library is not trivial at all [7]. Because of a large influence of the type of diode array detector and of the used solvent on the shape (resolution, sensitivity) of the spectra, some considerable care is required in establishing the spectral library.

Matters become even more complicated when the peaks are not completely resolved. In that case a specific data treatment should preceed quantitation and identification. The type of data treatment to be applied depends on the availability and completeness of a spectrum library.

In this paper an overview is given of the available algorithms to handle various situations. Furthermore the performance and limitations of these algorithms are discussed.

Experimental

Instrumentation and Software

A description of the software, equipment, chromatographic conditions and data used in the various experiments can be found in the referenced publications.

Methods and Discussion

It has probably not to be argued that the algorithms for the data handling of a measured data matrix will originate from multivariate statistics. The reason is very obvious: all

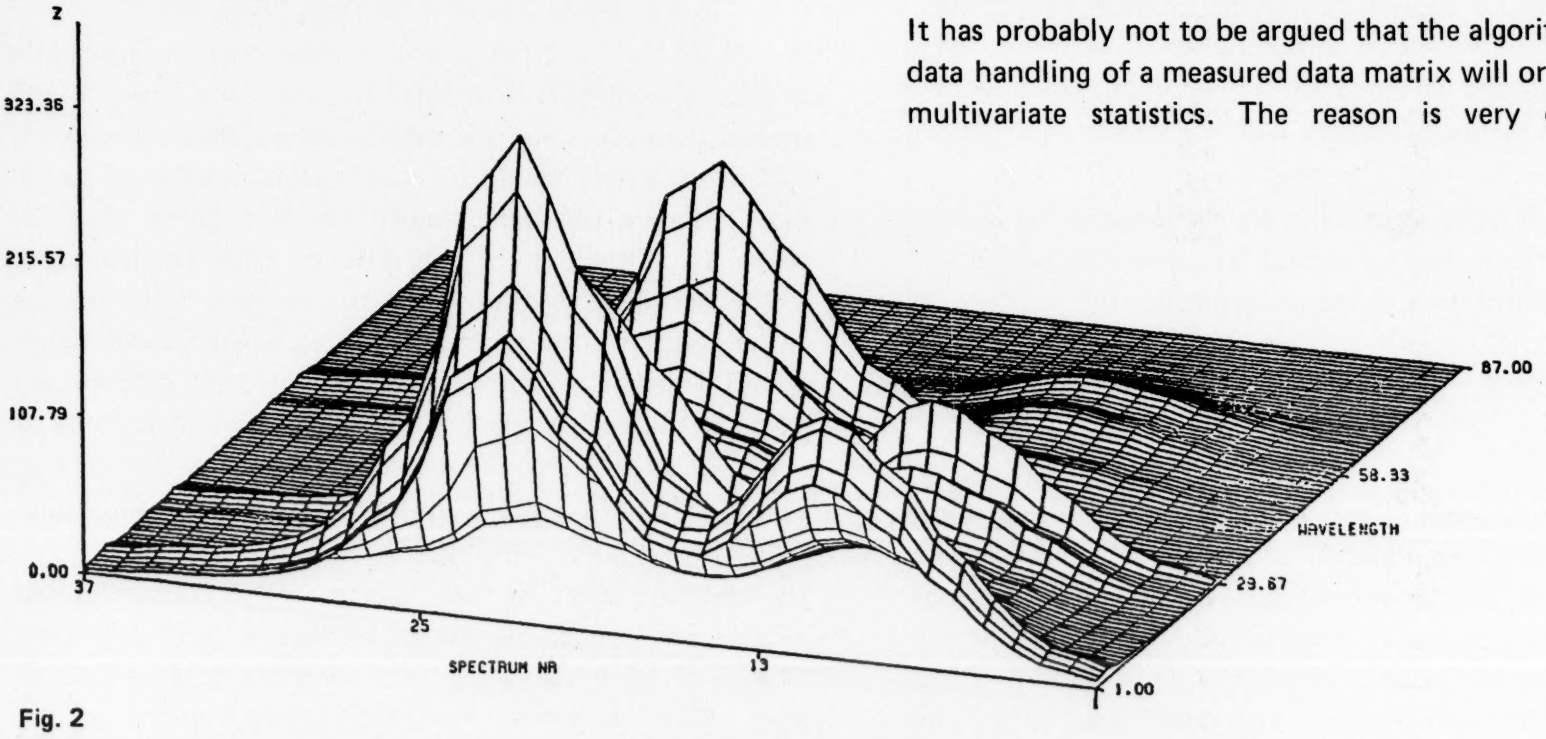

Fig. 2

A 3-d representation of the measurements in HPLC with diode array detector.

measured spectra are related because of the smoothly evolving concentration profiles of the eluted compounds. An overview of the various situations which are encountered in chromatography with the respective data handling methods is given in Table I. It should be borne in mind that all situations refer to unresolved peaks.

Methods with a Spectral Library

The simplest situation is met when a library is available with pure spectra. If the library is large enough to contain all solutes (i.e. analytes and interferents) which are coeluting, one can apply a multicomponent analysis (MCA). The algorithm of MCA is well described and can be found in many textbooks [8].

One should however be very aware of some important limitations of MCA.

- spectra of all components should be available: i.e. not only of the analytes but also of all interferents, including a model for an eventual drifting baseline.
- there is an error propagation (amplification) of the spectral error into the calculated concentration profiles [8]. This error propagation is larger with an increasing overdetermination of the considered system. This is illustrated by the results obtained from an MCA carried out on a two-component system of chlorinated phenols by a two-component analysis and by an eight-component analysis (Fig. 3a, b). It becomes clearly unpractical to perform an MCA with a large library.
- deviations of the spectra (e.g. small shifts) caused by solvent effects propagate into the calculated concentration profiles as well, and may render the results useless. This is illustrated by the results obtained for an eight-component analysis carried out on a two-component system of chlorinated phenols (Fig. 4a). The spectra were recorded in THF : water = 35:65 mobile phase whereas the spectra used for the MCA were measured in ACN : THF : water = 17,5:17,5:65 (Fig. 4b).

As a consequence the use of a large external database for peak identification and subsequent quantitation of unresolved peaks is unpractical as it would require that a database is available of the compounds in a large variety of solvents.

In many cases the available database will be incomplete and subsequently inhibit to carry out a multicomponent analysis. It should be kept in mind that as the peaks are not resolved, all measured spectra will be mixture spectra and can not be identified by some sort of spectrum retrieval system. Several algorithms have been proposed to tackle the problem of identifying the compounds present in mixture spectra by using a database with pure spectra. Some of these algorithms

Table I.

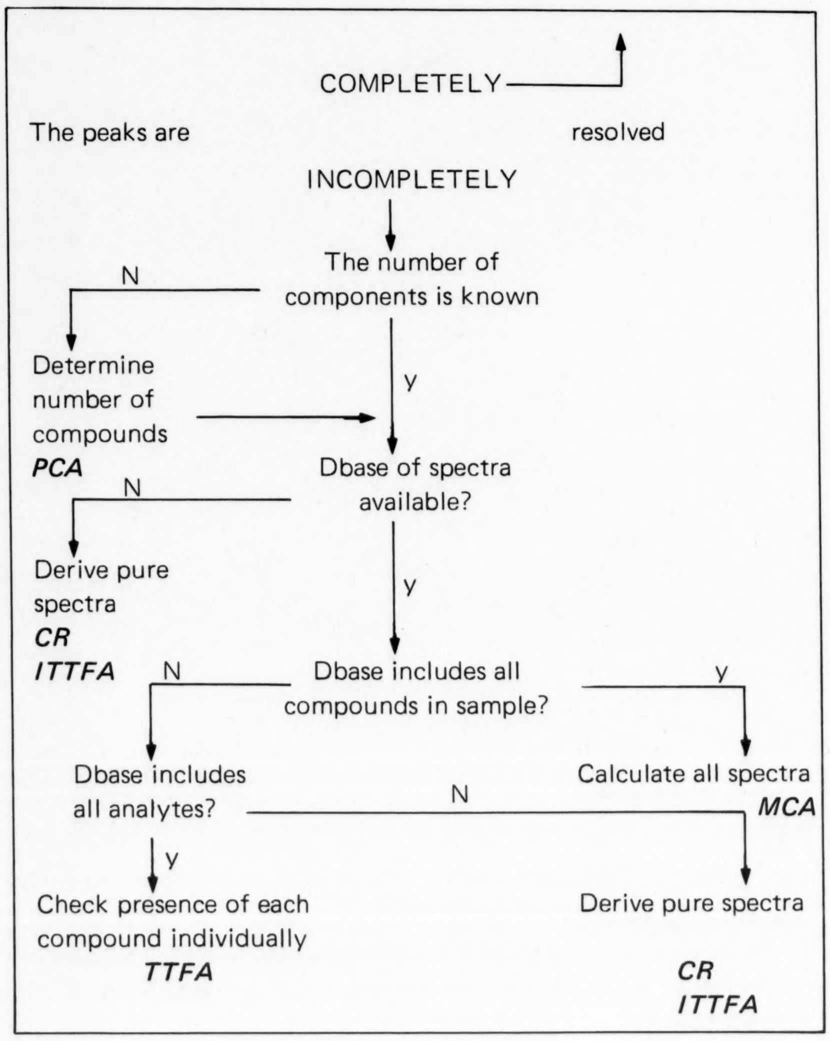
COMPLETELY
The peaks are
resolved
INCOMPLETELY
N
The number of components is known
Determine number of compounds
PCA
y
N
Dbase of spectra available?
Derive pure spectra
CR
ITTFA
y
N
Dbase includes all compounds in sample?
y
Dbase includes all analytes?
N
Calculate all spectra
MCA
y
Check presence of each compound individually
TTFA
Derive pure spectra
CR
ITTFA

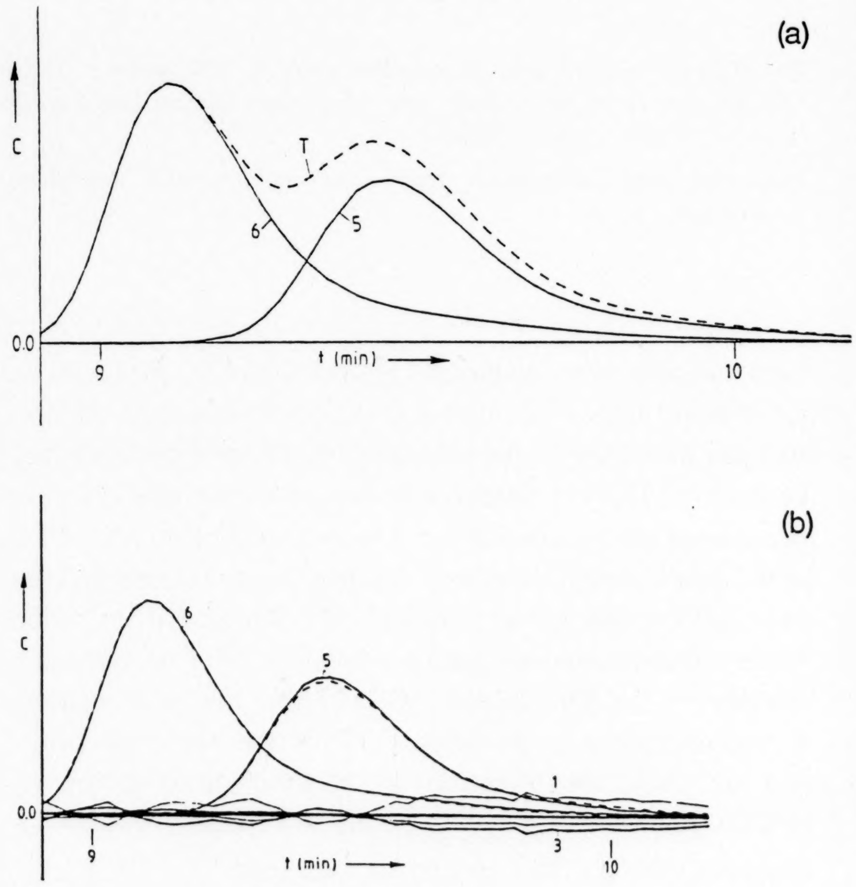

Fig. 3a

The recorded chromatogram, T, of a mixture of 3,5-dichlorophenol and 2,4-dichloro-5-methylphenol, and the individual component profiles calculated by means of MCA, using the correct pure component spectra.

3b Results of MCA, using eight pure component spectra (p-chloro-o-cresol, 2,5-dichlorophenol, p-chloro-m-cresol, 2,3-dichlorophenol, 3,5-dichlorophenol, 2,4-dichloro-5-methylphenol, p-chlorophenol, o-chlorophenol). Reprinted with permission from Elsevier Scientific Publishers Amsterdam.

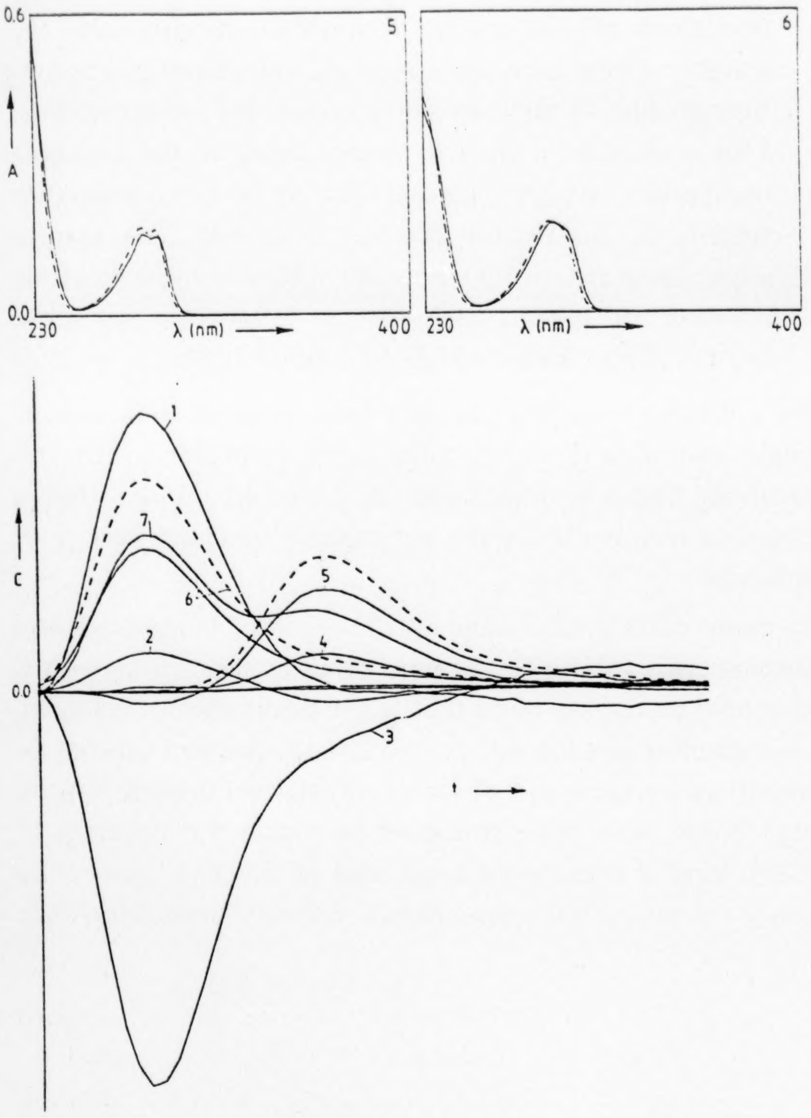

Fig. 4a

The pure spectra of 3,5-dichlorophenol and 2,4-dichloro-5-methylphenol in aceto-nitrile-water (35:65)(-----) and in tetrahydrofuran-water (35:65)(—).

4b MCA of mixture spectra recorded in ACN:THF:water = 17,5: 17,5:65 and fitted with eight pure component spectra (see Fig. 3) recorded in THF:water = 35:65.

Reprinted with permission from Elsevier Scientific Publishers Amsterdam.

have initially been developed to tackle similar problems in GC-MS and GC-IR [9]. There are basically three approaches: two are based on factor analysis [10–12] and one on fuzzy clustering [13, 14]. Methods based on factor analysis have been extensively studied on their applicability in HPLC with diode array detector, whereas fuzzy clustering has been introduced quite recently [14]. An algorithm called Target Transformation Factor Analysis (TTFA) has been introduced by Malinowski [15, 16] and has been studied at the laboratory of de Galan [17] for the particular problem of peak identification in method optimization in HPLC.

Basically the algorithm consists of two steps:

(1) the determination of the number of components in the mixture by a Principal Components Analysis (PCA)

(2) An individual test of each spectrum (called target) in the spectral library on its presence in the mixture spectra

Without going into the mathematical details, a short description of both steps is given below.

The Determination of the Number of Components by PCA

Principal components analysis (PCA) is a technique from linear algebra that has been well described in literature [18, 8] and is available in most general statistical packages for mainframe computer and microcomputer. PCA considers the data as a datamatrix, with rows being the spectra and columns being the chromatograms. It actually calculates the minimal number of uncorrelated spectra (these are spectra with a cross product equal to zero) with which all measured mixture spectra in the datamatrix can be reproduced. These uncorrelated spectra are calculated in a particular sequence: namely, the first spectrum describes as much variation in the spectra as possible. The second spectrum is selected in such a way that linear combinations of the first and second spectrum improve the fit of all measured spectra as much as possible and so on. The procedure is continued until all spectra can be described within the spectral noise. This procedure is schematically shown in Fig. 5. It should be stressed at this point that the calculated uncorrelated spectra are not the true spectra. They are called abstract factors or abstract spectra. For example all spectra of a three-component mixture of polynuclear aromatic hydrocarbons can be reproduced by a linear combination of the three abstract spectra shown in

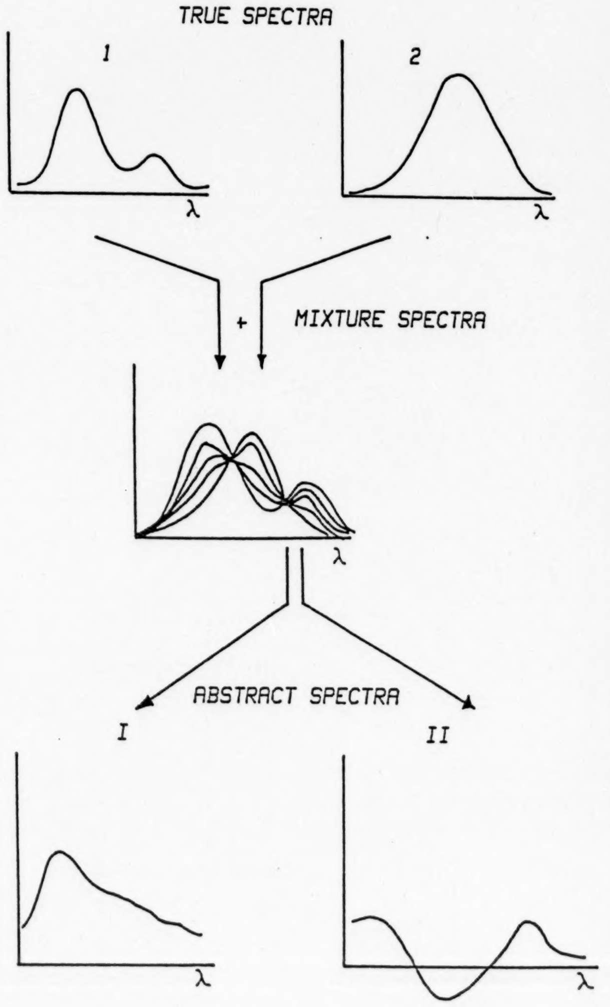

Fig. 5

The measured mixture spectra are linear combinations of the (unknown) true spectra 1 and 2.

By PCA the mixture spectra are decomposed in two abstract spectra (I) and (II). All measured spectra are linear combinations of the abstract spectra I and II.

Fig. 6. Mathematically these abstract spectra are the eigenvectors of the variance-covariance matrix of the datamatrix [18, 8]. The number of abstract spectra corresponds with the number of concentration profiles or chemical species.

An important feature of PCA is the detectability of an impurity. This depends on several factors: the noise level, stability of the baseline, spectral similarity of the compounds, sensitivity, chromatographic overlap, nonlinearities and matrix effects or solute interactions. The determination of the number of components from a PCA is not a trivial matter. Several methods have been proposed to that purpose [15, 19] giving sometimes diverging results. Main reason is that most methods rely on statistical assumptions with regard to the distribution of the noise. In HPLC with diode array detector one can safely state that impurities below 5% (in signal units) can be detected down to a chromatographic resolution of R = 0.3 (Fig. 7) in the presence of 0.1% noise.

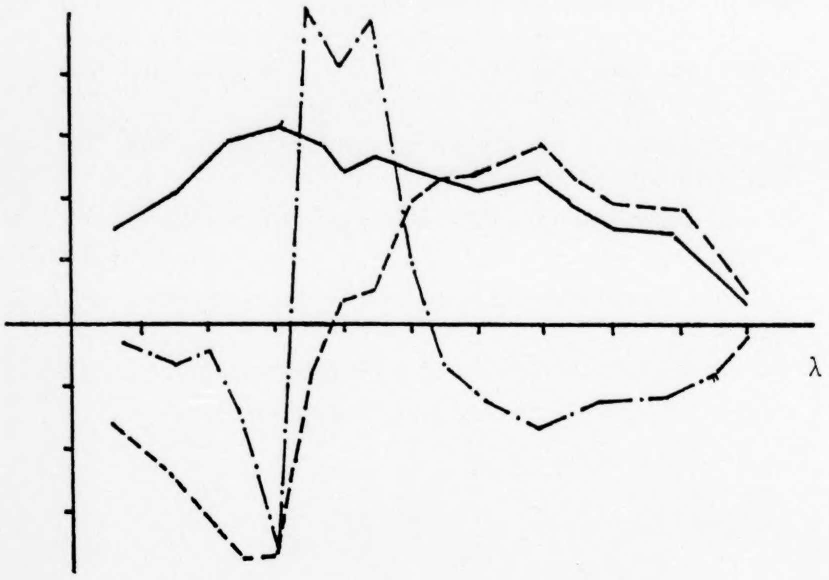

Fig. 6

Abstract spectra found for a three component mixture of polynuclear aromatic hydrocarbons (PAH).

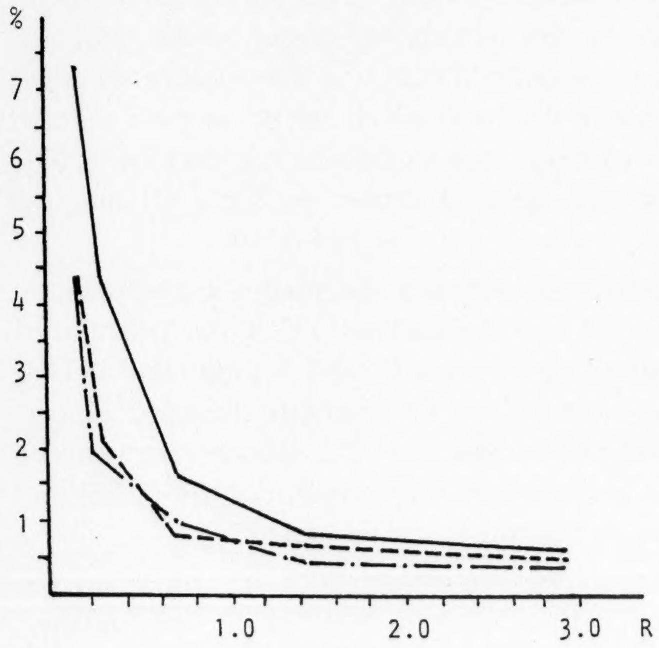

Fig. 7

Peak purity check by PCA. Lowest detectable amount of an impurity (% of total area) as a function of the chromatographic resolution ($R = \delta t/w_{\frac{1}{2}}$). Signal to noise ratio is 1000:1. Similarity (correlation): —— 0.85, ----- 0.53, .—.—. 0.45.

An alternative PCA method looks for the minimal number of uncorrelated concentration profiles necessary to reproduce all chromatograms in the datamatrix. Both methods are equivalent.

Test of a Library Spectrum on its Presence in a Set of Mixture Spectra

The test whether the mixture spectra contain a particular test spectrum (here: a spectrum of a library) is based on a relatively simple principle: From a PCA analysis carried out on the measured datamatrix, one obtains a number of abstract spectra, with which each of the measured mixture spectra can be reconstructed by a simple multicomponent analysis. It is therefore plausible that also the pure spectra of which the mixture spectra are constituted can be reconstructed with the same set of abstract spectra. This is the principle of Target Transformation Factor Analysis (TTFA). The test consists of two steps:

(1) a multicomponent analysis is carried out with the abstract spectra on the spectrum being tested. This gives that linear combination of the abstract spectra with which the tested spectrum is reconstructed the best as possible (Fig. 8). By taking that linear combination, one recalculates thereafter the target, which is called the estimated target.

(2) the test fails when tested and estimated target differ to a larger extent than is expected from noise level considerations. Otherwise the test passes (Fig. 8).

TTFA has been extensively evaluated by Malinowski [16] for GC/MS and later by de Galan and coworkers in HPLC with diode array detector [17]. The overall conclusion is that when the test spectra are exact (no solvent effects)

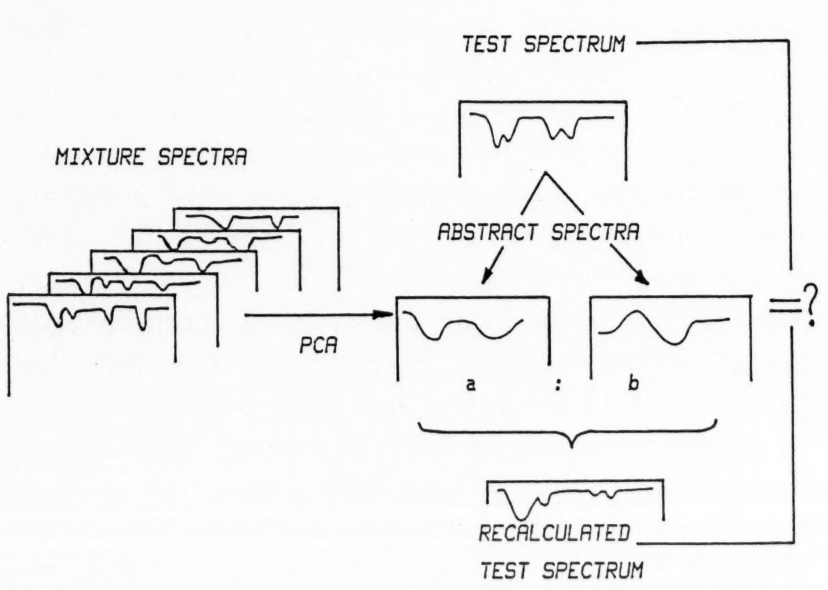

Fig. 8

Schematic representation of Target Transformation Factor Analysis.

the test will indicate the right components for resolutions down to R = 0.006 (lowest measured value) also when the spectra are very similar.

When the test spectra are distorted as indicated in Fig. 4 a resolution down to R = 0.1 still provides good results. It may happen that one is not able to identify all components in the mixture, because of the incompleteness of the library. The extreme case of course is that no spectra are available at all. To cope with these problems one has to derive the pure spectra from the abstract spectra by curve resolution (CR) or Iterative Target Transformation Factor Analysis (ITTFA) which are discussed below.

Methods without Library

When no spectra are available, one has to derive the pure spectra directly from the measured datamatrix. Solutions to this problem have been proposed first by Lawton and Sylvestre [20]. By the increased interest caused by the introduction of GC/MS and HPLC with diode array detector, these methods have been adapted and evaluated resulting in readily available software tools [21, 22].

PCA is the starting point of these algorithms as it provides the number of components, and the abstract spectra or abstract concentration profiles with which all spectra respectively all chromatograms can be reconstructed.

In the first instance, methods have been developed to extrapolate the uncorrelated (abstract) spectra into true spectra. In 1982, Kowalski [9] proposed a method that works fine for binary mixtures, and is commercially available for the HP1040A diode array detector. In 1985 Vandeginste [23] extended this method to ternary profiles. All methods have in common that they apply constraints to find the solution: e.g. nonnegativity of spectra and concentration profiles. By extrapolating abstract chromatograms instead of abstract spectra a constraint can be applied which looks for the solution with the sharpest concentration profiles [23]. It has been demonstrated that this latter method gives the best overall performance for binary and ternary mixtures. No methods based on this principle of extrapolation have been reported for four and more component mixtures. Generally one refers to this method as self-modeling-curve resolution, as it does not use a priori information on the shape of the elution profiles. From Table II it can been seen that, depending on the spectral overlap one may expect to obtain the concentration profiles within an accuracy of 5% (relative). Moreover the obtained spectra are of a good quality (Fig. 9).

Recently the limitation on the number of coeluting compounds has been removed. Independently from each other, Gemperline [11] and Vandeginste et al. [12] have developed an iterative version of TTFA to calculate the concentration profiles. Instead of submitting spectra from a library as a target, one tests concentration profiles. Because the concentration profile of a component is unknown, one starts with testing a pulse (Fig. 10). Of course it will be impossible to reconstruct this pulse as a linear combination of the abstract concentration profiles calculated from the measured chromatograms at the various wavelengths. As a consequence the test will fail. However one obtains a linear combination of the abstract elution profiles that matches the best the target (here a pulse). Looking to that linear combination one observes that it is a better estimation of the true elution profile. Resubmission of that profile as a new target has no sense as the TTFA test will always pass, because here a linear combination of the abstract concentration profiles is tested. One way to get the procedure iterated is to modify the recalculated target before resubmission. This is not a difficult matter as the recalculated target will have negative side lobes which can be removed to force the target to converge to a true concentration profile. The procedure is schematically shown in Table III and the course of the iteration is depicted in Fig. 10.

Table II. Relative accuracy (%) of peak areas in 3-component ITTFA and CR. Adapted from Ref. [27] with permission from Wiley.

factor	1	2	3	4	5	6	7	8
A	+	+	+	+	–	–	–	–
B	+	+	–	–	+	+	–	–
C	+	–	+	–	+	–	+	–
CR3	8.0	5.5	6.2	2.7	5.1	2.1	4.0	1.5
ITTFA3	1.6	0.6	0.8	0.2	0.7	0.3	1.2	0.2
The factor levels are:					+		–	
factor A: area of elution profiles					1:1:1		0.2:1:0.2	
factor B: resolution				R_{12}	0.25		0.37	
				R_{23}	0.5		0.37	
factor C: similarity of spectra					0.99		0.36–0.76	

The factor levels are visualized in Fig. 12.

Table III. Iterative target factor analysis.

Submit any CONCENTRATION PROFILE as a TARGET to be checked on its presence in the chromatograms

A target passes the test if the recalculated and tested target are equal within the noise

A recalculated target is a BETTER target than the submitted target

MODIFY the recalculated target (remove negative values) and RESUBMIT

The procedure CONVERGES to a TRUE concentration profile

REPEAT this procedure until ALL profiles are found

The main difference between the methods proposed by Vandeginste [12] and Gemperline [11] is the selection of the initial targets to be iterated. Table II shows that ITTFA performs better than the CR-methods discussed before, and that good results (less than 2% relative error) can be expected for systems with a low resolution (R = 0.25) and high similarity of the compound spectra [27].

Recently Maeder [24] has developed a method, known as evolving factor analysis, which will not be discussed further. A comparison of this method with ITTFA by our laboratory has shown that both methods perform equally. Strasters [25] has successfully applied a combination of TTFA and ITTFA for an unambiguous peak identification during the optimization of the separation.

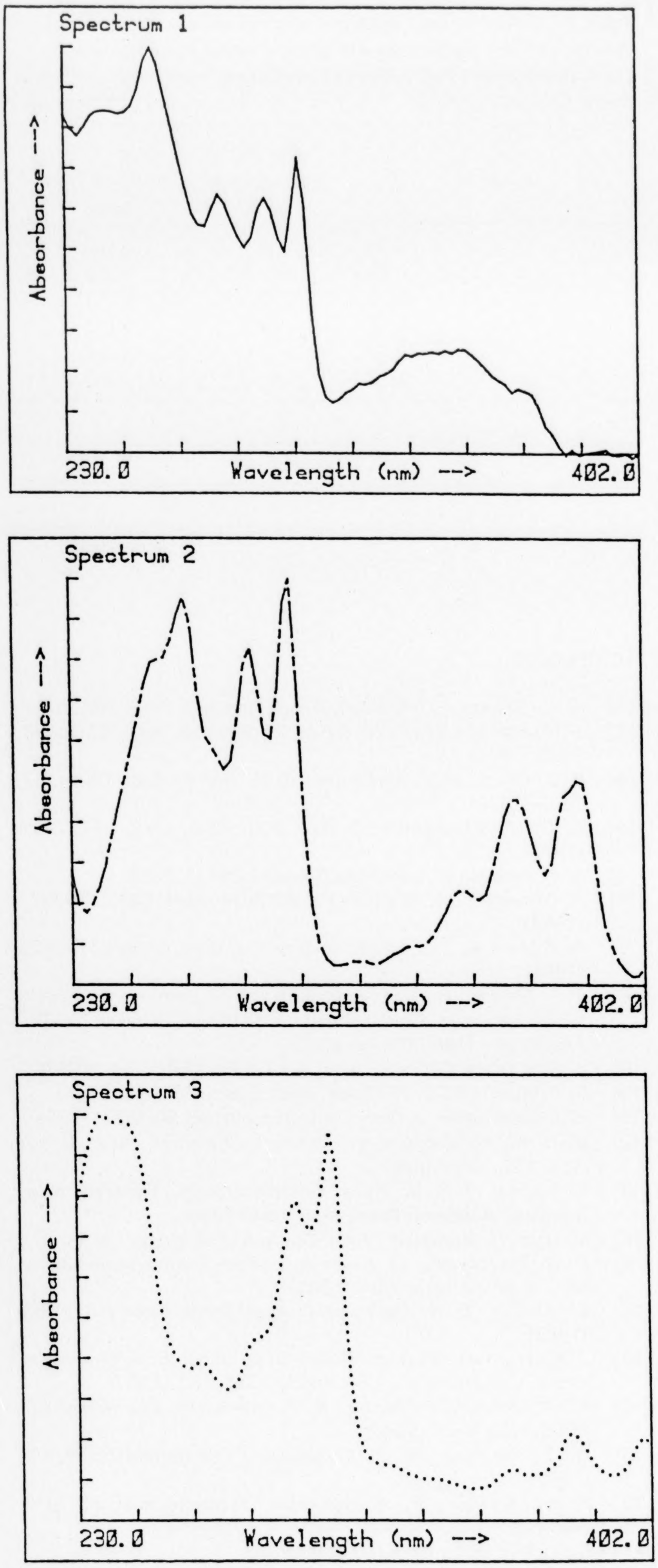

Fig. 9

Results of three component curve resolution on a mixture of polynuclear aromatic hydrocarbons.

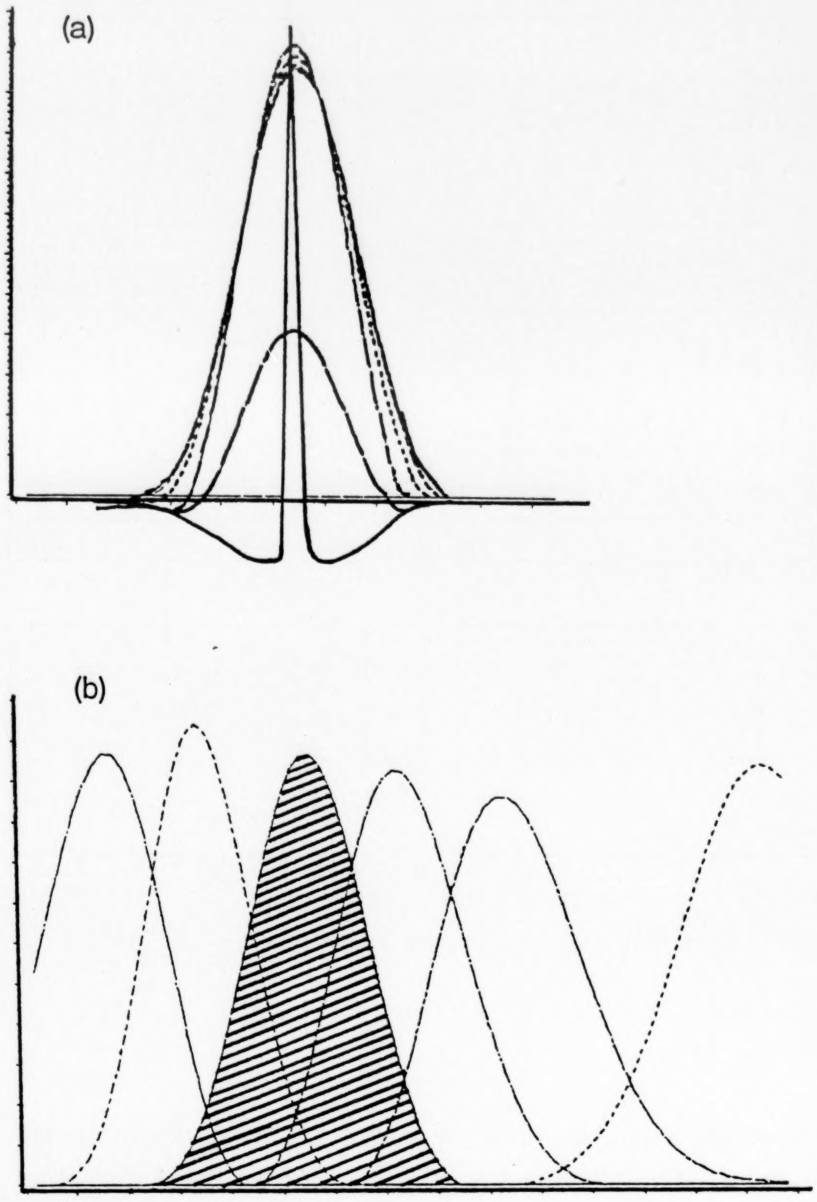

Fig. 10

Iterative Target Transformation Factor Analysis.

a. First target is a pulse. Next targets are the recalculated targets with negative values set to zero.

b. Result of ITTFA for peak 3 in a 6 component mixture of PAH's.

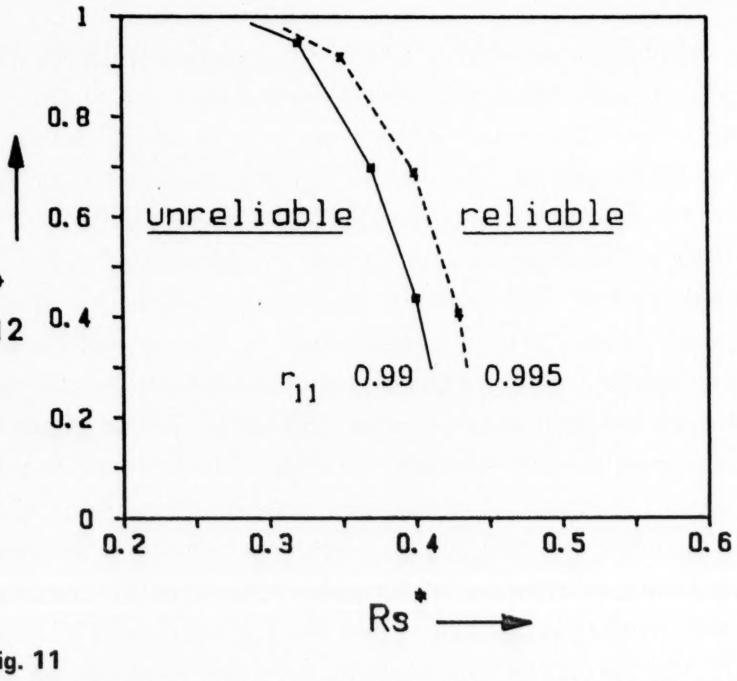

Fig. 11

Performance of ITTFA for peak identification as a function of the resolution of the calculated concentration profiles (R_s^*), and the correlation coefficient of the calculated spectra (r^*_{12}) for a two component mixture. r_{11} is the correlation coefficient between the spectra obtained by ITTFA and the true spectra (quality criterion).

In the context of this paper the discussion of ITTFA is limited to the presentation of a criterion which allows a quick judgement of the results obtained by ITTFA on binary mixture peaks with comparable peak areas. This criterion is based on the observed resolution between the calculated concentration profiles and the observed similar-

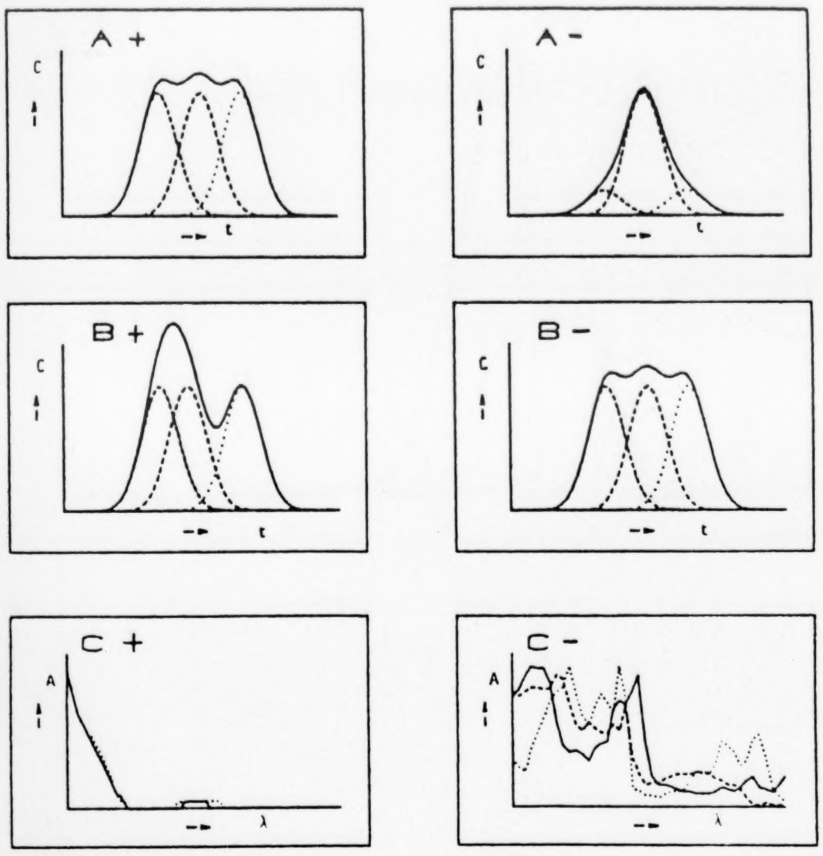

Fig. 12
Factor levels of the systems given in Table II.

ity of the calculated spectra (expressed in correlation coefficient). This criterion has been derived from a comparison of the obtained spectra of a large number of simulated peak systems. It shows that reliable results (less than 1% error) can be expected down to a resolution R = 0.4 (Fig. 11). Gemperline [26] evaluated the performance of ITTFA for several degrees of peak skewness, noise levels and chromatographic resolution (Table IV). The noise level appears to be a dominant factor, which should not exceed 1% of the peak maximum.

Conclusions

The application of methods from multivariate statistics can greatly improve the ability to obtain qualitative and quantitative information from HPLC with a diode array detector under conditions of poor resolution. By the lower requirements for resolution analysis speed can be augmented without loss of accuracy which can be an important point in process control. The weakest part of the procedure which certainly needs further investigation is the determination of the number of components in a concentration profile. Moreover the influence of other components than concentration profiles (e.g. drifting baseline, interactions) is still not clear. The ability to identify unknown compounds is not restricted by the accuracy of the calculated spectra, but by the low intrinsic information content of the spectra. It is therefore to be expected that the application of ITTFA in GC/MS or GC/IR will become an even more powerful tool to identify the compounds in complex mixtures, also when resolution is not complete.

Table IV. Effect of peak skew and random noise on accuracy of results of ITTFA applied on a mixture of adenylic and guanylic acid (adapted from Ref. [26] with permission from the Amer. Chem. Soc.).

S/N	skew	R_s	error (%) of adenylic peak area[a]	error (%) of gyanylic peak area[a]
	1.2	0.43	0.4	0.3
	1.3	0.39	1.9	1.8
	1.45	0.32	7.7	7.4
1000:1		0.42	0.7	0.3
100:1		0.42	3.0	0.8
20:1		0.42	30.0	14.0

[a] ratio of peak areas is 1:1

References

[1] *G. C. Giddings, J. H. Davis*, Anal. Chem. **57**, 2168 (1985).
[2] *D. P. Herman, H. A. H. Billiet, L. de Galan*, Anal. Chem. **58**, 2999 (1986).
[3] *S. D. Frans, M. L. McConnell, J. M. Harris*, Anal. Chem. **57**, 1552 (1985).
[4] *B. G. M. Vandeginste, L. de Galan*, Anal. Chem. **47**, 2124 (1975).
[5] *W. F. Maddams*, Appl. Spectroscopy **245** (1980).
[6] *A. Drouen, H. A. H. Billiet, L. de Galan*, Anal. Chem. **56**, 971 (1984).
[7] *A. F. Fell, B. J. Clark, H. P. Scott*, J. Chromatogr. **316**, 423 (1984).
[8] *D. L. Massart, B. G. M. Vandeginste, S. N. Deming, Y. Michotte, L. Kaufman*, Chemometrics, a textbook, Elsevier Sc. Pu, Amsterdam (1987), in press.
[9] *B. R. Kowalski, M. A. Sharaf*, Anal. Chem. **54**, 1291 (1982).
[10] *B. R. Kowalski, D. W. Osten*, Anal. Chem. **56**, 991 (1984).
[11] *P. J. Gemperline*, J. Chem. Inf. Comput. Sci **24**, 206 (1984).
[12] *B. G. M. Vandeginste, W. Derks, G. Kateman*, Anal. Chim. Acta **173**, 253 (1986).
[13] *D. Dubois, H. Prade*, Fuzzy sets and systems: Theory and application, Academic Press, New York, 1980.
[14] *M. Otto, H. Bandemer*, Anal. Chim. Acta in press.
[15] *E. R. Malinowski, D. G. Howery*, Factor Analysis in Chemistry, J. Wiley, New York (1980).
[16] *M. McCue, E. R. Malinowski*, Appl. Spectroscopy **37**, 463 (1983).
[17] *J. K. Strasters, H. A. H. Billiet, L. de Galan, B. G. M. Vandeginste, G. Kateman*, J. Chromatogr. **385**, 181 (1987).
[18] *M. A. Sharaf, D. Illman, B. R. Kowalski*, Chemometrics, Wiley, New York (1986).
[19] *H. T. Eastman, W. J. Krzanouski*, Technometrics **24**, 73 (1982).
[20] *W. H. Lawton, E. A. Sylvestre*, Technometrics **13**, 617 (1971).
[21] QuickRes, Infometrix Inc. (1983).
[22] CR-3, B.G.M. Vandeginste (1985)
[23] *B. G. M. Vandeginste, R. Essers, T. Bosman, J. Reijnen, G. Kateman*, Anal. Chem. **57**, 971 (1985).
[24] *M. Maeder*, Anal. Chim. Acta **181**, 287 (1986).
[25] *J. Strasters, H. A. H. Billiet, L. de Galan*, submitted for publication.
[26] *P. J. Gemperline*, Anal. Chem. **58**, 2658 (1986).
[27] *B. G. M. Vandeginste, F. Leijten, M. Gerritsen, J. W. Noor, G. Kateman, J. Frank*, J. of Chemometrics **1**, 57 (1987).

Received: July 22, 1987
Accepted: Aug. 5, 1987
F

Miniaturisation in Pressure and Electroendosmotically Driven Liquid Chromatography: Some Theoretical Considerations

J. H. Knox*/I. H. Grant

Department of Chemistry, University of Edinburgh, West Mains Road, Edinburgh EH9 3JJ,
UK

Key Words

Electrochromatography
Miniaturisation in HPLC
Capillary zone electrophoresis
Electroendosmotic chromatography
Micro-HPLC

Summary

In electrochromatography, electrolyte is driven along a narrow bore chromatographic column at typical HPLC linear velocities by applying a potential gradient of around 50,000 V m^{-1}. Contrasting with pressure driven LC, the tube bore is limited to not more than 200 μm by self heating. Thus miniaturisation is mandatory in electrochromatography whereas it is optional in pressure driven LC unless very small particles (e.g. 1 μm diameter) are used. Because the velocity profile in open tubular electrochromatography is close to that of perfect plug flow, contrasting with the parabolic flow profile in pressure driven LC, open tube electrochromatography provides plate efficiencies limited only by axial diffusion, and comparable to those obtainable in open tubular gas chromatography. Contrasting with pressure driven open tubular LC there is no requirement for the tube bore to be very small (e.g. $< 10\,\mu$m). Although pure electrophoresis is applicable only to ionised solutes, and is not strictly a chromatographic method, neutral species can be chromatographed by partitioning them between two phases which move at different rates, for example by using micellar solutions or colloidal sols as the moving fluid, thereby retaining the high plate efficiency of electrophoresis. With packed tubes electrochromatographic separations of high efficiency can be obtained with 5 μm particles and extremely high efficiencies should be obtainable without sacrifice of eluent velocity by using submicron particles. In principle, electrochromatographic methods can provide a wide range of partitioning methods of extremely high plate efficiency, and will, in future, undoubtedly rival conventional HPLC.

Introduction

It is possible to drive a liquid through an open tube or packed bed either by the application of a hydrostatic pressure or by the application of a potential difference across the length of the column. Both methods may be used in what are essentially chromatographic techniques of separation, but the different drive methods have properties which differ in important ways. While the factors which determine the optimum conditions for pressure drive LC have been considered in detail elsewhere [1–3], those determining optimum conditions for electically driven LC separations have received little attention. The motion of liquid under pressure results from a balance between the applied pressure gradient and the viscous resistance of the column. The motion of liquid under electro-drive arises in the electrical double layer at the liquid-solid interface, and is called electroendosmosis. It arises from a balance between the electrical forces on the excess ions on the solution side of the double layer, and the viscous drag of the liquid in the layer.

There are a number of distinct separation methods in which the flow is driven by electroendosmosis and we propose that all such methods should be grouped under the general name ELECTROCHROMATOGRAPHY. In the current practice of electrochromatography a voltage of 10–50 kV is applied across a column 0.5–1.5 m long and 50–100 μm in bore. The column (which may be packed or open) contains an electrolyte whose concentrations is in the range 0.001 to 0.1 M. With appropriate selection of the operating parameters, electronendosmotic velocities of around 1 mm/s can be achieved. As in normal chromatography, the solutes are introduced as a narrow band at the upstream end of the column and are detected by a suitable miniaturised detector near the outlet. On-column detection is widely used to preserve the chromatographic integrity of separated solute peaks. The electrolyte which follows the sample as it migrates along the column in electrochromatography, is the same as the electrolyte which preceds it. In this respect electrochromatography contrasts with isotachophoresis [4] where the follower electrolyte must contain a follower ion with a lower electrophoretic mobility than any of the ions in the sample; isotachophoresis is analogous to the pressure driven method of displacement chromatography. In electrochromatography as in normal HPLC a series of peaks is obtained,

0009-5893/87 0135-09 $ 03.00/0

© 1987 Friedr. Vieweg & Sohn Verlagsgesellschaft mbH

one for each separated solute, whereas in isotachophoresis and displacement chromatography the bands of separated solute components are contiguous, with each band displacing the one ahead of it. In HPLC and electrochromatography relative retention times (or k-values) characterise the eluted solutes, whereas in isotachophoresis and displacement chromatography the concentrations of bands characterise the solutes.

Forms of Electrochromatography

At the present stage, five forms of electrochromatography may be distinguished.

1. **Capillary Electrophoresis** [5–9]

The sample to be separated is a mixture of ionised solutes and the separation depends upon differences in their electrophoretic mobilities. There is no partitioning between separate phases and strictly this is not a chromatographic method. However in terms of the form of equipment used, the output produced, and the mechanisms of peak broadening, the concepts of chromatography apply. Capillary electrophoresis could be thought of as analogous to size exclusion chromatography, where again there is no partitioning between physically distinct phases. A representative separation by this method due to Jorgenson and Lukacs [8] is shown in Fig. 1. Plate counts of 500,000 are regularly obtained by this method in times of around 30 minutes.

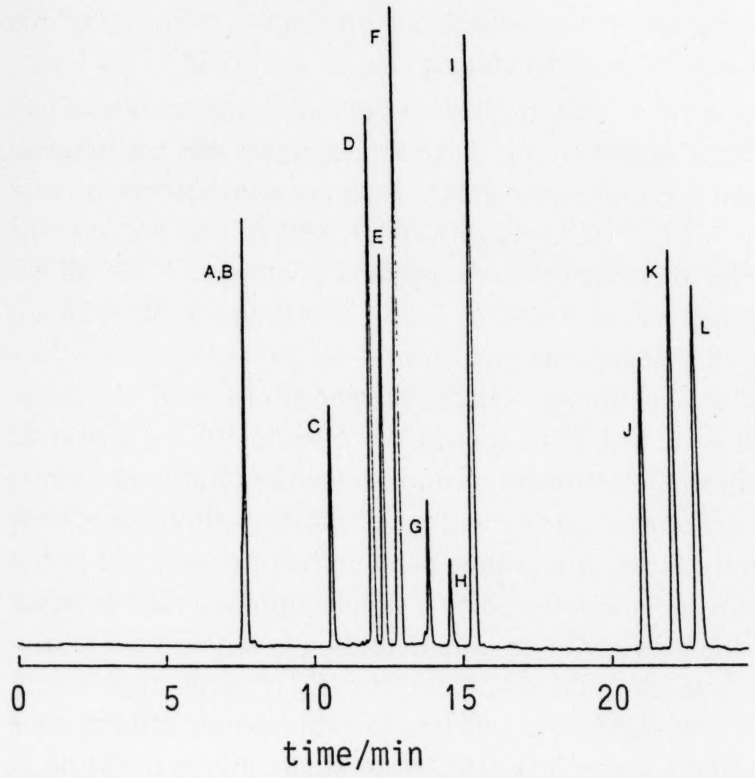

Fig. 1

High voltage electrophoretic separation of dansyl amino acids: **A** = unkn., **B** = ϵ-labelled lysine, **C** = di-labelled lysine, **D** = leucine, **E** = serine, **F** = glycine, **G, H** = unkn., **I** = dilabelled cystine, **J** = glutamic acid, **K** = aspartic acid, **L** = cysteic acid. Column 1000 mm X 75 μm; voltage 30 kV; eluent 0.05 M phosphate buffer pH 7. (Reprinted by permission from Science **222**, 266–272, (1981), ref [8], copyright 1983 by the AAAS)

2. Micellar Electrochromatography or Capillary Electrophoresis in Micellar Solutions [10–12]

This method, developed by Terabe and coworkers [10, 11], is closely related to electrophoresis but uses a micellar solution as the moving fluid. Since the micelles are themselves charged they move relative to the eluent surrounding them. Partitioning of solutes occurs between the micelles and the surrounding eluent, so that the migration velocity of any solute lies between that of the eluent (k = o) and that of the micelles (k = ∞). The solutes need not be ionised. This is a true chromatographic method since differential migration rates depend upon the different partition ratios of the solutes between two phases which move at different velocities. A representative separation by this method is shown in Fig. 2 taken from the work of Terabe et al [10] illustrates the extremely high plate efficiency of around 300,000 obtained. The use of a micellar solution does not result in any loss of plate efficiency since mass transfer in and out of the micelles is extremely fast.

3. **Electroendosmotic Chromatography** [13, 6]

In this method, which is a close analog of ordinary chromatography, a packed column is used, but the eluent is driven by electroendosmosis rather than by pressure. Partitioning of solutes between the mobile and stationary phases occurs in the normal way. Electro-drive does however introduce

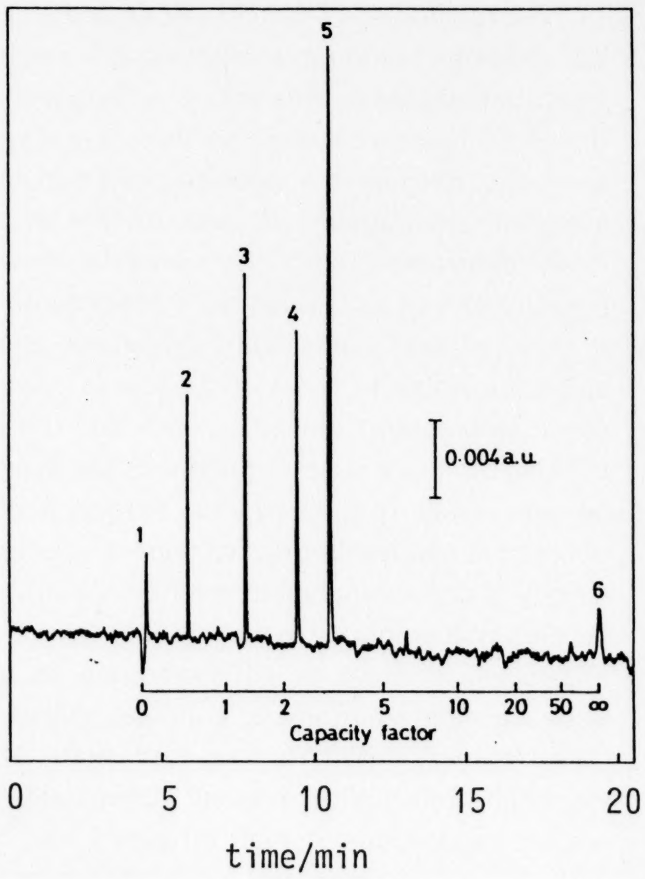

Fig. 2

Micellar electrophoretic separation of neutral solutes. **1** = methanol, **2** = phenol, **3** = 2-cresol, **4** = 2,6 xylenol, **5** = 3-ethyl phenol, **6** = Sudan III. Column 650 mm X 50 μm, Voltage 15 kV, current 33 μa, Detection u.v. 220 nm, eluent 0.1 M borate 0.05 M phosphate at pH 7 containing 0.05 M sodium dodecyl sulphate. (Reprinted by permission from Analyt. Chem. **56** 111–113 (1984), ref. [10]).

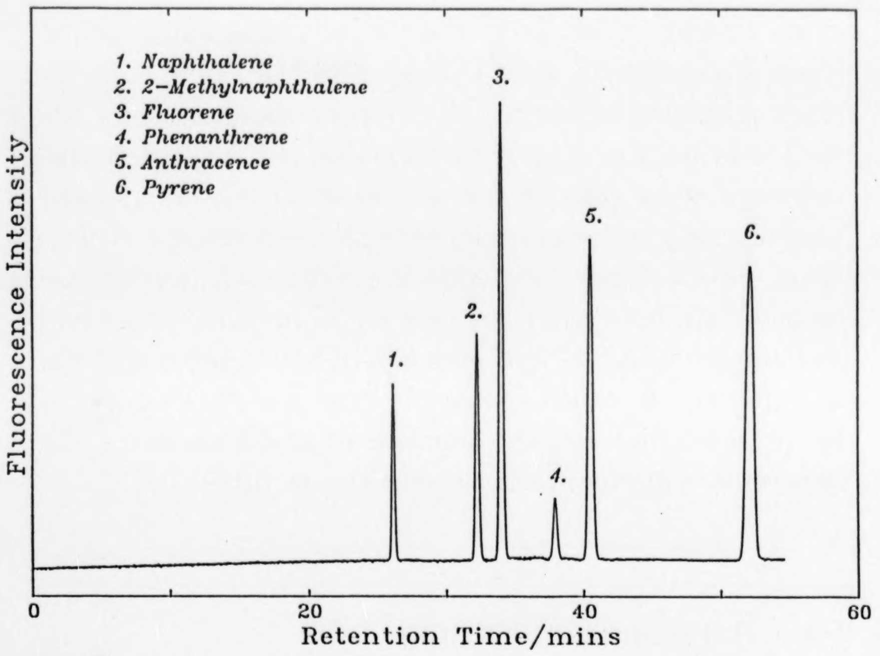

Fig. 3

Electroendosmotic chromatography of polynuclear aromatic hydrocarbons. Solutes as shown. Column: drawn packed capillary 600 mm X 50 μm packed with 5 μm Hypersil ODS-bonded in situ. Field 32 kV/m. Plate number 69,000. Eluent methanol:water (70:30) containing 0.002 M sodium dihydrogen phosphate.

some novel possibilities which are discussed below. A recent separation using 5 μm particles in a 650 mm long drawn packed capillary is shown in Fig. 3. The reduced plate height for this separation is below 2, comparing more than favourably with the efficiency obtainable in pressure driven HPLC using a similar column.

4. Colloidal Sol Electrochromatography or Capillary Electrophoresis in Colloidal Sols

This method, not yet realised experimentally, is a hybrid of methods two and three. A colloidal sol is used as the moving fluid. As in micellar electrochromatography, the colloidal particles are charged and move relative to the eluent surrounding them. Partitioning can again occur between two phases which move at different speeds. It should be possible, using this method, to reproduce the wide variety of partitioning modes which are currently exploited in pressure driven chromatography.

5. Complexation Electrophoresis [14, 15]

Accounts are beginning to appear of electrochromatographic separations of neutral solutes where differential migration results from the formation of weak complexes between a component of eluent with a finite electrophoretic mobility (a host species) and the solute species. Examples of the "host" species are β-cyclodextrins [14], and tetraalkyl ammonium ions [15]. As in methods (1) to (3), the high efficiency of electrophoresis is maintained.

It is clear that there are now exists a considerable range of electrochromatographic methods, and there is every chance this range will be further extended. The basic technique possesses great versatility and it must be scheduled to become one of the major separation fields of the future.

Pressure driven systems: parabolic flow

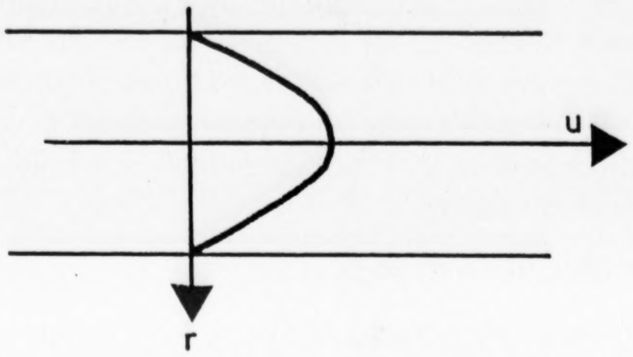

Electroendosmotically driven systems: plug flow

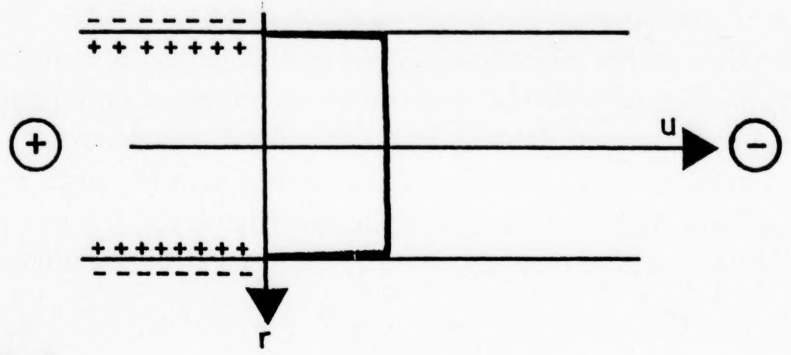

Fig. 4

Flow profiles in open tubes under pressure driven flow (upper) and electroendosmotically driven flow (lower).

Flow Profiles and Dispersion in Open Tubes

There are important differences in the flow and thermal properties of pressure driven and electrically driven chromatographic systems. These influence the geometical configurations of the columns and ancillary equipment, and profoundly affect their overall performance.

Fig. 4 compares the flow profiles across an open tube under pressure-drive and electro-drive. With pressure-drive, the flow profile is parabolic, the flow velocity at the wall being zero and in the centre being twice the mean flow rate (normally designated by u in chromatography). With electrodrive, the flow originates within the electrical double layer which exists at all surfaces. Surfaces such as those of silica, ODS bonded silica and graphite, bear fixed negative charges, while the solution in contact with them contains an excess of positively charged ions. This excess positive charge is located very close to the surface (typically within about 10 nm) and forms what amounts to a charged sheath around a core of uncharged liquid. When a potential gradient is applied across the length of the tube, shear develops within the sheath, and thereby propels the core along with it towards the negative electrode. As there is no charge imbalance within the core, the flow profile within the core is flat. Furthermore, since the sheath itself is very thin, the flow within the tube as a whole is near perfect plug flow.

These differences in flow profile have important consequences for separations in open tubes. In pressure driven systems, even when a solute is unretained, the flow variation across the tube disperses the solute. This is counteracted by transverse molecular diffusion. The resulting net dispersion is given by the Taylor equation [16]. With the dispersion from axial diffusion added in, we obtain the well known HETP equ. (1) for an unretained solute in an open tube (mathematical symbols are defined in the glossary at the end of this paper).

$$H = 2\,D_m/u + u\,d_c^2/96\,D_m \qquad (1)$$

The minimum plate height is then $H \simeq d_c/7$, and occurs at an eluent velocity of $u \simeq D_m/14\,d_c$. It is widely recognised [2] that to obtain the highest performance at high speed with conventional pressure drops in open tubular HPLC, d_c must be around 1 µm. Achievement of successful chromatography in such narrow tubes imposes formidable constraints on the injection and detection systems. Consequently open tubular HPLC systems are to be found only in advanced research laboratories [17–20]. With electro-drive systems the second term in eq. (1) is absent [6] since the velocity profile is flat and there is no tendency for an unretained solute to be dispersed by the flow. Thus we obtain

$$H = 2\,D_m/u \qquad (2)$$

The tube diameter no longer enters into the HETP equation so that, within limits discussed below, any tube diameter can be used without sacrifice of performance. The plate number is now given by eq. (3).

$$N = L\,u/2\,D_m \qquad (3)$$

For typical values of $L = 1.0$ m, $u = 1$ mm/s, $D_m = 10^{-9}\ m^2\,s^{-1}$, we obtain $N = 500{,}000$. As shown in the examples of Fig. 1 and 2 such values can be obtained in relatively wide tubes of up to 100 µm bore. However, as soon as a solute is retained, transcolumn equilibration becomes necessary and the plate height equation contains a diameter-dependent mass transfer term, and there is a catastrophic loss in performance. The reappearance of the mass transfer term reimposes the requirement to use very narrow tubes if high speeds and efficiencies are to be obtained. The separation of proteins by electrophoresis presented serious problems for this very reason until Lauer and McManigill [9] showed that by proper adjustment of pH to make the proteins negatively charged so that they were repelled by the negatively charged walls of the tube, high efficiencies could be regained. It may be noted that since D_m appears in the denominator of eq. (3) electrophoresis will provide higher efficiencies the higher the molecular weight of the solute. This is in complete contrast to other chromatographic methods where the reverse is always true.

The relevant eq. (4) and (5) for retained solutes in pressure and electro-drive systems are due to Golay [21] and Aris [22] respectively:

Pressure drive

$$H = 2\,D_m/u + \{1 + 6\,k + 11\,k^2)/96\,(1 + k)^2\}\,\{d_c^2\,u/D_m\} \qquad (4)$$

Electro-drive

$$H = 2\,D_m/u + \{k/(1 + k)^2\}\,\{d_c^2\,u/D_m\} \qquad (5)$$

Evidently, as soon as one tries to carry out genuine chromatography in an electrodrive system the problem of slow mass transfer arises as it does in pressure-drive systems. Thus in practice, if one is using a 100 µm bore tube for electrophoretic separation of unretained solutes, there will be a catastrophic drop in performance if the slightest wall retention takes place. A full discussion of the dispersion of retained solutes in electrophoretic chromatography in open tubes, which allows for electrical double layer overlap (see below), has been given by Martin, Guiochon, Walbroehl and Jorgenson [23, 24]. There are, however, other options, as noted above, which enable the mass transfer problem to be circumvented without sacrifice of performance or the requirement to move to extremely narrow tubes.

Flow Rates and Self Heating

The linear flow rates in pressure and electro-drive are given by eq. (6) and (7):

Pressure drive

$$u = (d^2/\phi\,\eta)\,(\Delta p/L) \qquad (6)$$

Electro drive

$$\begin{aligned} u &= (\epsilon_0\epsilon_r\,\zeta)\,(V/L) \qquad (7)\\ &= \epsilon_0\epsilon_r\,\zeta\,E \end{aligned}$$

(where $E = V/L$ is the potential gradient along the length of the tube). Under pressure-drive the velocity, u, is proportional to d^2 where d is the tube bore in the case of an open tube and the particle diameter in the case of a packed tube. Under electro-drive, d does not enter the flow equation, and the elution velocity is apparently independent of the tube or particle diameter. It is therefore possible with electro-drive, subject to limits discussed below, to maintain the elution velocity as the tube or particle diameter is reduced without any increase in the potential gradient across the tube. While the use of extremely narrow tubes is not attractive, the use of small particles in packed tubes has distinct advantages since H-values are generally lowered by lowering d_p. The possibility thus exists for conducting electrochromatography in packed tubes with extremely high efficiency by using very small particles. The serious limitation of pressure-drive systems which results in an optimum particle diameter for any desired plate count [1] does not affect electro-drive systems.

While the above considerations suggest that electro-drive possesses some remarkable advantages over pressure-drive, the attainment of the highest performance is limited by the much greater self heating which occurs in electro-drive systems. Poppe et al. [25, 26] considered in detail the effects of homogeneous heat release arising from viscous drag in packed columns. Although their equations are general and complex, they lead to a simple asymptotic result (readily derived independently) for the case of an infinitely long cylinder within which heat is generated homogeneously and lost by conduction through the walls. The temperature difference between the centre of such a cylinder and its walls is given by eq. (8).

$$\Delta T = Q\,d_c^2/16\,K \qquad (8)$$

where Q is the rate of heat generation per unit volume within the cylinder and K is the thermal conductivity of the medium. For water $K = 0.6\ W\ m^{-1}\ K^{-1}$ and for methanol $0.2\ W^{-1}\ m^{-1}\ K^{-1}$. A typical value of $0.4\ W\ m^{-1}\ K^{-1}$ will therefore be used for specimen calculations.

In pressure driven LC, Q is obtained from the frictional work dissipated in the column, and is given by $\Delta p\ u\ \epsilon/L$. u is given by eq. (6), resulting in eq. (9) for Q.

$$Q = (\epsilon\, d_p^2/\phi\, \eta)\ (\Delta p/L)^2 \tag{9}$$

Combining eq. (8) and (9) then gives the temperature excess at the centre of the tube:

$$\Delta T = (\epsilon/(16\ K\ \phi \eta))\ ((d_p d_c)^2(\Delta p/L)^2 \tag{10}$$

Taking typical values for conventional LC columns $\epsilon = 0.75$, $\Delta p = 100$ bar, $d_p = 5\ \mu m$, $d_c = 5$ mm, $L = 100$ mm, $K = 0.4\ W\ m^{-1}\ K^{-1}$, $\phi = 1000$, $\eta = 10^{-3}\ N\ s\ m^{-2}$, we obtain.

$$Q = 0.2\ W\ cm^{-3}, \text{ and } \Delta T = 0.7\ K$$

This temperature variation will result in a corresponding variation in eluent viscosity and so flow rate. Typically the viscosities of water and methanol decrease by about 2.6 % per degree at 20 °C. Thus in normal pressure-drive chromatography with a 5 mm bore column we expect a velocity variation of 1 of 2 % across the column. When peaks are retained there will be an additional effect on the band velocity from the dependence of k upon temperature which will normally accentuate the effect from the velocity profile. In a 5 mm bore column the adverse effects of internal self heating will not be removed by transverse molecular diffusion and so will result directly in additonal band spreading and distortion. It may be noted that if an eluted band has a standard deviation of 1 % of its elution distance, the column will be equivalent to 10,000 plates, and if 2 %, 2500 plates. Thus even quite small temperature inequalities in 5 mm bore packed columns may have serious effects on column efficiency. Very wide columns operate under what are effectively adiabatic conditions, that is the frictional heat is removed simply by flow of heated eluate from the outlet of the column. In this case the temperature difference between the entry and exit of the column is given by eq. (11)

$$\Delta T = \Delta p/C_v \tag{11}$$

where C_v is the differential heat capacity per unit volume of the eluate. The temperature variation across the column is then flat, except very close to the walls.

Eq. (10) appears to show that ΔT will decrease as d_p is reduced. This, in fact, is true only if the pressure gradient, $\Delta p/L$, is kept constant. Under normal chromatographic conditions, if one is to operate at a fixed reduced velocity in order to maintain peak performance, $\Delta p/L$ must be altered in proportion to d_p^{-3}. ΔT is then proportional to d_p^{-4}, and so becomes rapidly larger as the particle size is reduced. In order to maintain ΔT constant under optimum operating conditions it is necessary in pressure driven LC to reduce d_c in proportion to the d_p^2. Miniaturisation of the column bore to say 100 μm is therefore forced when the particle diameter is reduced to a values in the region of 1 μm, and some reduction in column bore below 5 mm is undoubtedly desirable whenever the particle diameter falls below 5 μm.

The situation is strikingly different with electro-drive systems. Here the heat generation arises from the flow of current through the electrolyte filling the tube and is given by V^2/R where V is the voltage across the tube and R its resistance. Introducing the equivalent conductivity λ, and replacing $(1/R)$ by $(\lambda\ c\ A/L)$ we obtain Q according to eq. (12).

$$Q = E^2\, \lambda\, c\, \epsilon \tag{12}$$

The excess temperature at the centre of the tube is then obtained by applying eq. (8) and is given by eq. (13)

$$\Delta T = E^2\, \lambda\, c\, \epsilon\, d_c^2/16\ K \tag{13}$$

Taking typical values; $E = 50{,}000\ V\ m^{-1}$, $\lambda = 150\ cm^2 mol^{-1}\ \Omega^{-1} = 0.015\ m^2 mol^{-1} \Omega^{-1}$, $c = 10^{-2}\ M = 10\ mol\ m^{-3}$, $\epsilon = 0.75$, $d_c = 100\ \mu m$, and $K = 0.4\ W\ m^{-1}\ K^{-1}$, gives:

$$Q = 280\ W\ cm^{-2}, \text{ and } \Delta T = 0.44\ K$$

The heat release per unit volume is about 1500 times larger for electro-drive than for pressure-drive under typical operating conditions: the tube diameter which must be used to avoid excessive temperature gradients is therefore very much smaller. Miniaturisation is mandatory when electrodrive is used, whether with open or packed tubes: miniaturisation is necessary with pressure driven packed tubes only when the particle diameter becomes very small. It has to be admitted that this conclusion is hardly new and has long been recognised in isotachophoresis and thin-layer electrophoresis [4].

Although self heating can have deleterious effects on performance in both pressure- and electro-drive systems, there is an important difference between the overall effects in the two cases. In pressure drive systems, which use fairly wide tubes, the dispersive effects of self heating cannot be removed by transverse molecular diffusion. In electro-drive systems which uses much narrower tubes, dispersive effects of self heating can rather easily be removed by molecular diffusion. In a packed tube the parabolic temperature profile across the tube results in a corresponding parabolic velocity profile which is superimposed upon the main flow velocity of the eluent within the column. The dispersive effect of this velocity profile may be treated, using a slight modification of the Taylor equation for dispersion in an open tube. The velocity excess at the centre of the column is denoted by $2\ \Delta u$ and the velocity of the main band by u. To analyse this situation, we imagine an observer moving at a velocity u with the main band. He will observe a situation similar to a stationary observer monitoring the flow in an open tube: he will see a band moving slowly along the tube, but at a mean velocity Δu rather than u. During the movement of the band along the whole column length, L, the moving observer will see a band which appears to move a distance $(\Delta u/u)L$. The Taylor equation can then be applied to obtain the dispersion arising from this effect namely:

$$\sigma_L^2/\{(\Delta u/u)L\} = d_c^2\, \Delta u/(96\ D_m) \tag{14}$$

The HETP is then given as:

$$H \equiv \sigma_L^2/L = (d_c^2\ u/96\ D_m)\ (\Delta u/u)^2 \tag{15}$$

The velocity spread Δu which arises from the self heating can be expressed as

$$\begin{aligned} 2\,(\Delta u/u) &= (\eta_{\mathrm{wall}} - \eta_{\mathrm{centre}}/\pi_{\mathrm{wall}} \qquad (16)\\ &= \Delta\eta/\eta \\ &= 0.026\,\Delta T \quad (\text{with } \Delta T \text{ in K}) \end{aligned}$$

whence

$$(\Delta u/u) = 0.013\,\Delta T$$

We can therefore substitute (16) for $(\Delta u/u)$, (13) for ΔT and (7) for u to give the final expression for H:

$$\begin{aligned} H &= \frac{d_c^2}{96\,Dm}\,\frac{\epsilon_r \epsilon_0 E \zeta}{\eta}\left\{\frac{0.013\,E^2 \lambda c \epsilon d_c^2}{16\,K}\right\}^2 \qquad (17)\\ &= \frac{7 \times 10^{-9}\,\epsilon_r \epsilon_0 \zeta \lambda^2 \epsilon^2 d_c^6 E^5 c^2}{D_m \eta K^2} \end{aligned}$$

Using the representative values: $\zeta = 50$ mV, $\lambda = 0.015\ \mathrm{m^{-2}\,mol^{-1}\,\Omega^{-1}}$, $d_c = 100\ \mu$m, $E = 50000\ \mathrm{V\,m^{-1}}$, $c = 10\ \mathrm{mol\,m^{-3}} = 0.01$ M, $D_m = 10^{-9}\ \mathrm{m^2\,s^{-1}}$, $\eta = 10^{-3}\ \mathrm{N\,s\,m^{-2}}$, and $K = 0.4\ \mathrm{W\,m^{-1}\,K^{-1}}$ gives

$$H = 6 \times 10^{-9}\ \mathrm{m} = 0.006\ \mu\mathrm{m} \qquad (18)$$

Clearly this value is very small and in practice negligible when compared to typical HETPs of 5 to 10 μm. However one notes that H is proportional to $d_c^6 \times E^5 \times c^2$. Thus quite small changes in column diameter, potential gradient and electrolyte concentration can have dramatic effects on the contrbution to H arising from the self heating. For example if the column diameter is increased to 200 μm ΔT is increased 4 times to 1.8 K and H rises 64 times to 0.4 μm. If, in addition, E were to be doubled H would rise to the unacceptable value of 12 μm, but reduction of c to 0.002 M (from 0.01 M) would bring H down again to 0.5 μm. It is thus clear that careful consideration has to be given to the interconnected parameters, column diameter, potential gradient and electrolyte concentration if adverse effects from self heating are to be avoided. With the currently used conditions where E does not exceed about 50000 $\mathrm{V\,m^{-1}}$, columns bores of 200 μm can safely be used with electrolyte concentrations up to 0.01 M.

Current and Power Requirements in Electrochromatography

In the specification of equipment for electrochromatography it is important to be aware of the power requirements for the high voltage power supply to be employed. The current which will be used in any system is readily calculated from eq. (19).

$$i = E \lambda c \pi \epsilon d_c^2/4 \qquad (19)$$

Table I lists some typical values for practical systems.

Table I. Typical currents and power requirements for electrochromatography.

Assumed parameters: $E = 50000\ \mathrm{V\,m^{-1}}$, $\lambda = 0.15\ \mathrm{m^2\,mol^{-1}\,\Omega^{-1}}$; $\epsilon = 1.0$, L = 0.5 m			
d_c/μm	c/M	i/μa	Power/W
50	10^{-3}	1	0.025
	10^{-2}	10	0.25
	10^{-1}	100	2.5
100	10^{-4}	0.4	0.01
	10^{-3}	4	0.1
	10^{-2}	40	1.0
200	10^{-4}	1.6	0.04
	10^{-3}	16	0.4
	10^{-2}	160	4

The Electrical Double Layer and Zeta Potential

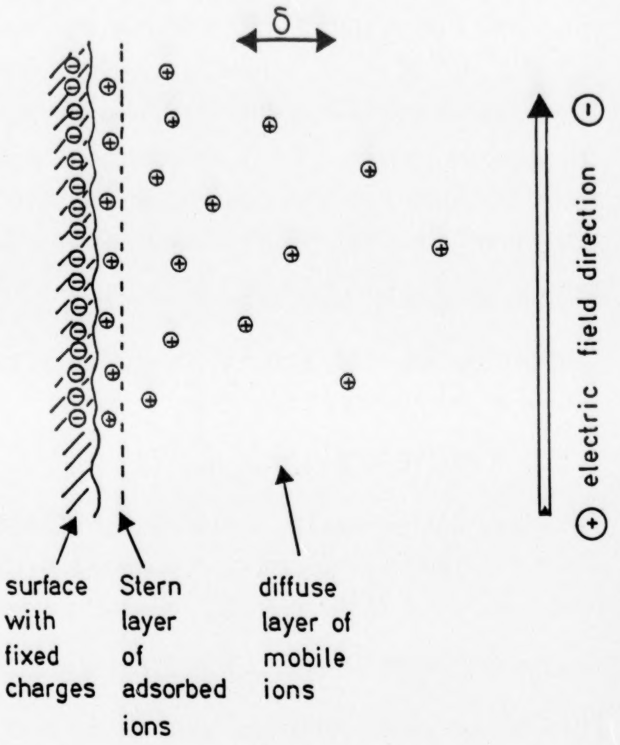
δ
−
electric field direction
+
surface with fixed charges
Stern layer of adsorbed ions
diffuse layer of mobile ions

Fig. 5
The electrical double layer, showing the magnitude of the thickness parameter, δ.

In electrochromatography the eluent flows along the column as a result of a potential gradient parallel to the surface of the electrical double layer. The electrical double layer, illustrated diagramatically in Fig. 5, is a feature of all surfaces immersed in a liquid. The typical surfaces of silica, hydrocarbon bonded silicas, and graphite possess fixed negative charges. With silica these charges arise from partially ionised acidic silanol groups on the surface. When such a surface is in contact with a solution there is a slight excess of positive charge in the solution to balance the fixed negative charges on the surface. Some of these charges may be ions firmly held on the surface by adsorption: these constitute the so-called Stern layer. The remaining excess ions further from the surface are solvated, and behave in a field like any of the other ions in the adjacent solution. The excess charge density associated with these ions falls off rapidly with distance from the surface, along with the associated electric potential which is proportional to the charge density. The potential at the boundary between the Stern layer and the start of the diffuse part of the double layer is called the zeta potential, denoted by ζ, and is typically between 0 and 100 mV. The fall-off in electrical potential with distance from the surface is roughly exponential. The distance, δ, over which z falls by a factor e (= 2.718) is called the thickness of the electrical double layer. For a 1 : 1

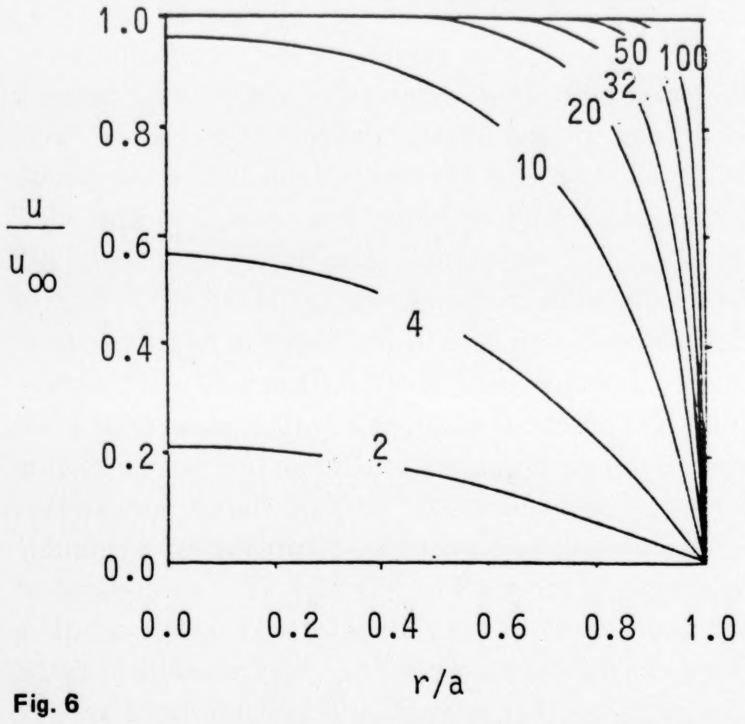

Fig. 6

Velocity profiles from Rice and Whitehead [27] where double layer overlap occurs: r/a = fractional distance from centre of tube (r/a = 0 at centre, r/a 2 1 at wall); the ratio d/δ is given on each line.

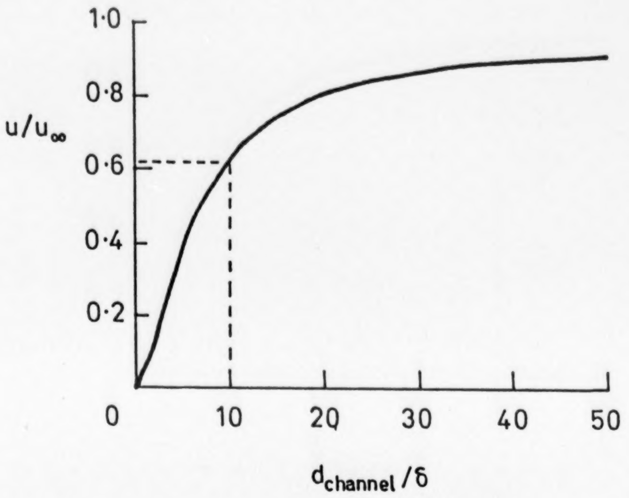

Fig. 7

The effect of "double layer overlap" on the electroendosmotic velocity in an open tube after Rice and Whitehead [27]; u/u_∞ is the ratio of the velocity in a tube of a given diameter to that in a tube of infinite diameter.

electrolyte such as sodium chloride, δ according to the Stern-Gouy-Chapman theory is given by eq. (20) which is the same as found in the Debye-Huckel theory.

$$\delta = \{\epsilon_r \epsilon_0 RT/2cF^2\}^{1/2} \qquad (20)$$

For a concentration of $c = 1\ \text{mol m}^{-3} = 0.001$ M, with water as solvent (for which the relative dielectric constant is $\epsilon_r = 80$), eq. (20) gives the thickness of the double layer, δ, as 10 nm.

When a potential gradient, E, is applied across the length of the column the excess ions within the double layer, or at least those of them that are not firmly adsorbed in the Stern layer, move towards the appropriately charged electrode carrying any enclosed liquid along with them. Shearing of the solution occurs only within the diffuse part of the double layer resulting in the plug-flow profile already shown in Fig. 1 when the tube diameter is much larger than δ. The mean flow velocity under these conditions is given by eq. (7). Typically with a zeta potential, ζ, of about 50 mV, and a potential gradient of $50000\ \text{V m}^{-1}$, the electroendosmotic flow velocity in water is calculated to be about $1.8\ \text{mm s}^{-1}$, a typical of flow rate in HPLC. This linear velocity corresponds to $u/E = 0.036\ \text{mm}^2\,\text{V}^{-1}\,\text{s}^{-1}$. The independence of u upon d_c, however, holds only when the tube diameter is much greater than the double layer thickness. When d approaches δ, double layer overlap occurs, as shown in Fig. 6, and eventually when d is of the same order as δ, the flow velocity is much reduced and the velocity profile approaches parabolic. Rice and Whitehead [27] analysed the situation in detail. Fig. 7, redrawn from their paper, shows how u/u_∞ declines as the ratio d/δ falls. A significant decline from u_∞ is noted when $d/\delta \leqslant 50$, and particularly when $d/\delta \leqslant 10$. As a rule of thumb, we propose that the electroendosmotic velocity is acceptable when $u/u_\infty \geqslant 0.6$, that is when d_c exceeds 10 δ. For packed tubes the mean channel diameter has to take the place of the open-tube diameter. This is significantly smaller than the particle diameter, and may be estimated from the ratio of the φ-values for a bed of random packed impermeable spheres ($\phi \simeq 500$) to the value for an open tube ($\phi = 32$). We thereby obtain:

$$\text{Mean Channel Diameter/Particle Diameter} = (32/500)^{1/2} = 0.25 \qquad (21)$$

Accordingly with slurry-packed columns (SPC's), we expect a significant loss in electroendosmotic flow rate when $d_p \leqslant 40\ \delta$. For drawn packed capillary columns [28] (DPC's), where $\phi = 120$, the corresponding condition is $d_p \leqslant 20\ \delta$. Table II lists a number of representative cases for different ionic strengths when the eluent is water.

Table II shows that with eluents typically used in electrochromatography, which have ionic strengths from 0.001 M to 0.01 M, there should be little sacrifice in electroendosmotic velocity even when the particle size is as low as 0.4 μm. If this conclusion is substantiated by experiment it will be possible to obtain extremely high column efficiencies in electrochromatography by using columns packed with submicron particles. Indeed it should be possible to approach a plate height which is given only by the diffusion term $2D_m/u$ as in open tubular electrochromatography. Because of the plug nature of the flow under electrodrive we may

Table II. Particle and tube diameters at which significant loss of electroendosmotic velocity will occur. Condition $u/u_\infty = 0.6$ with a 1 : 1 electrolyte.

c / mol m^{-3}	c / mol dm^{-3}	δ / nm	Minimum tube of particle diameter/μm		
			OTC $d_c = 10\ \delta$	DPC $d_p = 20\ \delta$	SPC $d_p = 40\ \delta$
10^{-2}	10^{-5}	100	1.0	2.0	4.0
10^{-1}	10^{-4}	31	0.3	0.6	1.2
1	10^{-3}	10	0.1	0.2	0.4
10	10^{-2}	3	0.03	0.06	0.12
100	10^{-1}	1	0.01	0.02	0.04

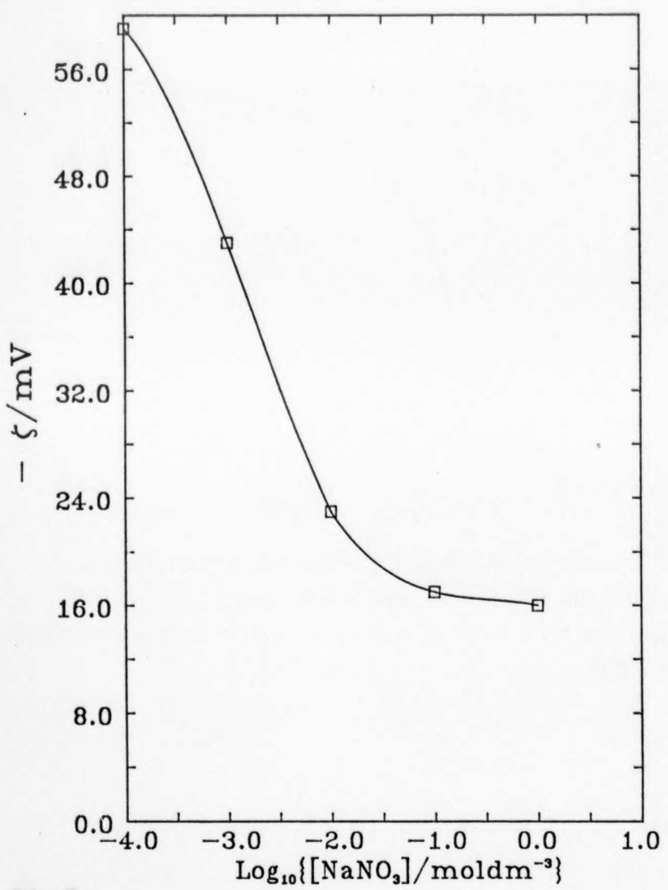

Fig. 8

The effect of electrolyte concentration on the zeta potential with 5 μm ODS Hypersil. Data taken from Knox, Kaliszan and Kennedy [29].

expect that the structure dependent A-term in the plate height equation will be lower under electro-drive than under pressure drive, leading to further enhancement of performance in electroendosmotic chromatography.

A second important consideration in electrochromatography is the dependence of zeta potential upon electrolyte concentration, since u is directly proportional to ζ. There is no doubt that ζ decreases with electrolyte concentration. Knox, Kaliszan and Kennedy [29], for example, measured ζ as a function of $[NaNO_3]$ and pH using particles of ODS Hypersil, a typical ODS bonded silica gel. Some of their results are replotted in Fig. 8. At pH > 6 with 0.005 acetate buffer $\zeta = 50$ mV but decreases to zero more or less linearly as the pH drops from 5 down to 2. With dilute $NaNO_3$ ζ is about 50 mV but in 0.001 M solution it has a value of 45 mv and in 0.01 M solution it has fallen to 25 mV. Thus the concentration range 0.001 to 0.01 M appears to be acceptable both from the point of view of double layer thickness and from the point of view of zeta potential. Eluents with concentrations in the range 0.0001 to 0.001 M would be better in regard to zeta potential but the double layer thickness would now limit the minimum particle size to 1 or 2 μm. Ionic strength buffering would also begin to be a problem if solutes were ionised. This problem has been considered in detail by Everaerts et al [30].

Experimental evidence on the effects of particle diameter and electrolyte concentration on electroendosmotic velocity is regrettably conflicting. Stevens and Cortes [31] measured electroendosmotic velocities in 20 mm X 1 mm bore plastic tubes for several silica gels, namely Bio-sil-A (d_p = 100 μm), Corasil II (d_p = 50 μm) and Partisil 10 (d_p = 10 μm). They first used four salt-free liquids: water, methanol:water (85:15), methanol and acetonitrile, and found that u/E decreased more or less linearly towards zero as d_p fell from 50 μm. Since they used non-electrolytes where the double layer thickness would be large, this result was not unexpected. When KCl was added, with water as solvent, u/E rose until the ionic strength reached about 10^{-4} M, and then fell to near zero at 0.01 M. With the larger particles, maximum u/E values were about 0.03 $mm^2 V^{-1} s^{-1}$ consistent with zeta potential of about 80 mV (see eq. (7)), while with the 10 μm particles, the maximum u/E value was only 0.003 $mm^2 s^{-1}$ even with 10^{-4} M KCl. Cortes and Stevens explained the small u/E values for 10 μm Partisil by double layer overlap and the fall in u/E above 10^{-4} by collapse of the zeta potential. While the u/E values were clearly sensitive to particle size the electrical conductivities were also affected. Thus the conductivities with 50 and 100 μm particles were about 1/3rd those in an open tube, and with the 10 μm particles about 1/10th. It seems most likely that the low u/E values and the low electrical conductivity with 10 μm Partisil were directly connected and probably not the result of double layer overlap as suggested. By contrast our own results, as illustrated in Fig. 3, show no fall in electroendosmotic velocity with particles as small as 5 μm. There is clearly room for further experimental work to resolve these discrepancies.

Conclusions

1. HPLC systems can be operated using either pressure-drive or electro-drive. A typical potential gradient in electrochromatography would be 50000 V m^{-1}.
2. In electrochromatography miniaturisation of the bore is mandatory to avoid self heating effects. Typical bores are 50 to 100 μm.
3. Fast electrochromatography can be carried out in 50—100 μm bore open tubes with extremely high efficiencies (similar to those of capillary gas chromatography) provided that there is no wall retention.
4. Wall retention is avoided in four of the electrochromatographic methods: capillary electrophoresis (for ionised solutes), micellar capillary electrophoresis (for neutral and ionised solutes), colloidal sol capillary electrophoresis (for neutral and ionised solutes), and in complexation electrophoresis (for neutral and ionised solutes).
5. With packed tubes, very efficient electroendosmotic chromatography should be possible using submicron particles since the electroendosmotic flow velocity for a given potential gradient should not fall appreciably until the particle diameter is below 1 μm.
6. It may be confidently expected that there will be a massive growth of effort into the development and application of electrochromatographic methods over the next few years.

Glossary of Symbols

A	Cross sectional area of column
c	Molar concentration of electrolyte
C_v	Differential heat capacity per unit volume
d	Particle diameter or column bore
d_c	Column bore
d_p	Particle diameter
D_m	Diffusion coefficient of solute in eluent: typical value $10^{-9}\ m^2\,s^{-1}$
E	Electric field strength
F	Faraday constant = 96500 c mol^{-1}
H	Height equivalent to a theoretical plate, HETP
i	Electric current
k	Capacity factor for a solute (often written k')
K	Thermal conductivity: typical value 0.4 $W\,m^{-1}\,K^{-1}$
L	Column length
N	Number of theoretical plates to which a column is equivalent
Δp	Pressure drop across column
Q	Rate of heat release per unit volume of column bed
R	Universal gas constant = 8.314 $J\,K^{-1}\,mol^{-1}$
T	Temperature
ΔT	Temperature excees at centre of column
u	Linear velocity of eluent
u_∞	Linear velocity of eluent in electroendosmotic flow when column bore is large compared to thickness of double layer
Δu	Mean velocity excess in column when self-heating present: velocity excess at centre = 2 Δu
V	Voltage drop across column
δ	Thickness of electrical double layer
ϵ	Porosity (total) of packed bed
ϵ_0	Permittivity of a vacuum = $8.85 \times 10^{-12}\ C^2\,N^{-1}\,m^{-2}$
ϵ_r	Relative permittivity or dielectric constant: typical value 80
ϕ	Pressure resistance factor for packed columns
η	Viscosity: typical value 0.001 $N\,s\,m^{-2}$
λ	Equivalent (or molar) conductivity: typical value 0.015 $m^2\,\Omega^{-1}\,mol^{-1}$
σ_L	Standard deviation of a chromatographic band in length units.
ζ	Zeta potential

References

[1] *J. H. Knox, M. Saleem,* J. Chromatogr. Sci., **7**, 614–622 (1969).

[2] *J. H. Knox, M. T. Gilbert,* J. Chromatogr., **186**, 405–418 (1979).

[3] *J. H. Knox,* J. Chromatogr. Sci., **18**, 453–461 (1980).

[4] *F. M. Everaerts, J. L. Beckers, Th. P. E. M. Verheggen,* "Isotachophoresis" J. Chromatogr. Library, Vol 6, Elsevier Science Publishers, Amsterdam, 1976.

[5] *F. E. P. Mikkers, F. M. Everaerts, Th. P. E. M. Verheggen,* J. Chromatogr., **169**, 11–20 (1979).

[6] *J. W. Jorgenson, K. D. Lukacs,* J. Chromatogr., **218**, 209–216 (1981).

[7] *J. W. Jorgenson, K. D. Lukacs,* Analyt. Chem., **53**, 1298–1302 (1981).

[8] *J. W. Jorgenson, K. D. Lukacs,* Science, **222**, 266–272 (1983).

[9] *H. H. Lauer, D. McManigill,* Analyt. Chem., **58**, 166–171 (1985).

[10] *S. Terabe, K. Otsuka, K. Ichikawa, A. Tsuchiya, T. Ando,* Analyt. Chem., **56**, 111–113 (1984).

[11] *S. Terabe, K. Otsuka, T. Ando,* Analyt. Chem., **57**, 834–841 (1985).

[12] *M. J. Sepaniak, R. O. Cole,* Analyt. Chem., **57**, 834–841 (1985).

[13] *V. Pretorius, B. J. Hopkins, J. D. Schieke,* J. Chromatogr., **99**, 23–30 (1974).

[14] *S. Terabe, H. Ozaki, K. Otsuka, T. Ando.* J. Chromatogr., **332**, 211–217 (1985).

[15] *Y. Walbroehl, J. W. Jorgenson,* Analyt. Chem., **58**, 479–481 (1986).

[16] *Sir G. I. Taylor,* Proc. Roy. Soc. (Lond), **A219**, 186, (1953).

[17] *T. Tsuda, G. Nakagawa,* J. Chromatogr., **268**, 369–374 (1983).

[18] *E. J. Guthrie, J. Jorgenson,* Analyt. Chem., **56**, 483–486 (1984).

[19] *S. Folestad, L. Johnson, B. Josefsson,* Analyt. Chem. **54**, 925–929 (1984).

[20] *R. Tijssen, J. Bos, E. Van Kreveld,* Analyt. Chem., **58**, 3036–3044 (1986).

[21] *M. J. E. Golay,* in "Gas Chromatography 1958", Ed. D. H. Desty, Publ. Butterworths, London, 1959, p. 36.

[22] *R. Aris,* Proc. Roy Soc. (Lond), **A235**, 67 (1953).

[23] *M. Martin, G. Guiochon,* Analyt. Chem., **56**, 614–620(1984).

[24] *M. Martin, G. Guiochon, Y. Walbroehl, J. W. Jorgenson,* Analyt. Chem., **57**, 559–561 (1985).

[25] *H. Poppe, J. C. Kraak,* J. Chromatogr., **282**, 399–412 (1983).

[26] *H. Poppe, J. C. Kraak, J. F. K. Huber, J. H. M. Van den Berg,* Chromatographia **9**, 515–523 (1981).

[27] *C. L. Rice, R. Whitehead,* J. Phys. Chem. **69**, 4017–4024, (1965).

[28] *T. Tsuda, I. Tanaka, G. Nakagawa,* Analyt. Chem., **45**, 1249–1252 (1984).

[29] *J. H. Knox, R. Kaliszan, G. J. Kennedy,* Faraday Discussions of Royal Society of Chemistry **15**, 113–125 (1980).

[30] *F. E. P. Mikkers, F. M. Everaerts, Th. P. E. M. Verheggen,* J. Chromatogr., **169**, 1–10 (1979).

[31] *T. S. Stevens, H. J. Cortes,* Analyt. Chem., **55**, 1365–1370 (1983).

Received: July 27, 1987
Accepted: Aug. 3, 1987
F

Packings and Stationary Phases for Biopolymer Separations by HPLC

K. K. Unger* / R. Janzen / G. Jilge

Institut für Anorganische Chemie und Analytische Chemie, Johannes Gutenberg-Universität, D-6500 Mainz, FRG

Key Words

Column liquid chromatography
Biopolymer separation
Stationary phases and packings
Properties
Stationary/mobile phase combination and selection

Summary

Packings and stationary phases applied to high resolution separations of proteins, enzymes, and nucleic acids must satisfy a series of distinct criteria that are different from those usually required by HPLC of low molecular weight non-biologically active analytes. These requirements have been met through substantial improvements in classical gel media together with novel developments in silica supports, and have led to a family of products with tailor-made and reproducible properties. Supports consisting of cross-linked organic gels, and inorganic materials (mostly silicas) are now available with graduated particle sizes, pore sizes, porosities and surface areas as well as non-porous beads. A whole range of stationary phases, such as reversed phase, hydrophobic interaction, ion exchanger and affinity packings, were designed for application as chemical sensors for biopolymer recognition in adsorptive chromatography. The phase systems are operated in the gradient mode, giving high resolution and high peak capacities. In addition, aqueous liquid-liquid partitioning systems have been developed for the fractionation of proteins and nucleic acids. Size exclusion media complete the set of HPLC variants enabling a discrimination of proteins according to their size and shape in an isocratic elution mode. Basically, protein purification and isolation is a multistage process whereby the HPLC variants are combined in a logistic sequence, utilizing the different selectivities of the phase systems and thus maximising resolution, speed and throughput.

I Introduction

In recent years, the separation and isolation of biopolymers has become substantially impacted by High Performance Column Liquid Chromatography (HPLC). This development was brought about by the combined efforts in two highly innovative areas: first in biotechnology, biochemistry and gene technology where highly selective and biocompatible separation methods are required; and second, in HPLC which has grown to become a versatile and effective means in pharmaceutical and environmental analysis, as well as in purity control of industrial chemicals and products.

Initially it was assumed that the pool of methods and information accumulated in HPLC separations of low molecular weight analytes could be easily transferred to the high resolution separation of biopolymers. However, it soon became apparent that the handling of these substances in HPLC under particular conditions in which they maintain their biological activity requires a careful choice and control of the separation conditions. Moreover, it became apparent that novel concepts and strategies should be developed to gain resolution.

To adapt HPLC to its new application, so-called wide pore packings of 30 nm of nominal pore size were marketed, compared to 6 to 15 nm pore size packings traditionally employed in HPLC of low molecular weight analytes. This approach merely satisfies one of many important aspects, namely, to provide sufficient accessibility of the stationary phase. With time and experience major emphasis was placed on the stationary phase chemistry of packings and on appropriate eluent compositions to utilize and match the different solute-surface interactions encountered in biopolymer separation by adsorptive chromatography. A thorough examination of the retention phenomena, together with studies on the conformational behaviour of biopolymers in chromatographic separation processes, revealed that the phase system, the column dimension and configuration, and the operation conditions have to

0009-5893/87 0144-11 $03.00/0

© 1987 Friedr. Vieweg & Sohn Verlagsgesellschaft mbH

be tailored for each specific separation and purification case. Furthermore, biocompatible HPLC instruments were designed that avoided many of the problems related to heavy metal contamination, reduced yield, denaturation and loss of biological activity [1].

This paper aims to survey the current situation in LC packings and phase systems under the aspects mentioned above and provides an outlook on future developments. The first part addresses several of the issues associated with the synthesis of appropriate packings (such as choice of support, pore size and particle size, bonding chemistry) and evaluates the available commercial packings. The second part discusses the characteristic features of the various LC phase systems relevant to biopolymer separations.

II Criteria, Key Phenomena and Properties of Stationary Phases, Packings, and Columns in Biopolymer Separations

In order to achieve a fast and high resolution as well as an efficient isolation of biopolymers in HPLC, a number of distinct criteria to be met by stationary phases, packings, and columns can be listed. These include:

- high selectivity and specificity;
- high flexibility to accomodate a variety of analytes;
- preservation of biological activity together with high mass recovery;
- high bed stability and low flow resistance;
- high chemical stability during use and storage to tolerate aqueous eluents;
- adequate efficiency;
- fast and complete regeneration and re-equilibration;
- minimum fouling;
- lot-to-lot and column-to-column consistency;
- availability of graduated particle sizes in order to scale up a separation.

The design of a phase system suitable for this purpose is dictated by the specific chemical structure of a given biopolymer, by its solvation and by the resulting solute-surface interactions. Biopolymers such as proteins, enzymes, and nucleic acids have molecular weights ranging from 10,000 to 1,000,00 with viruses and plasmids up to tens of millions. The structure is built by linked hydrophobic, hydrophilic and charged entities exhibiting a secondary, tertiary and often quaternany structure. Thus, exposure and accessibility to the active sites is controlled by the conformation of biopolymers. Reversible adsorption of a biopolymer requires a hydrophilic and homogeneous surface with a chemical functionality that imitates the solute structure. Heterogeneously polar or strongly hydrophobic surfaces will consequently lead to irreversible adsorption and to denaturation. As pointed out by El Rassi and Horvath [2], the surface should be soft, generating low free energies of adsorption through non-convalent bonds. As solute-surface interactions involve multisite attachment of the biopolymeric solute to the surface, time is needed to bring the molecule into its "right" position. This results in a much slower kinetic of the adsorption and desorption than is observed for low molecular weight analytes. Of the functional groups of a biopolymeric molecule, only those take part in surface interactions that are sufficiently exposed at the surface and spaced from each other to accomodate the active functional sites at the stationary surface. Apart from these considerations, a number of additional aspects have to be taken into account. Biopolymers undergo protonation/deprotonation when the pH alters, which often substantially changes their charge and charge distribution. Solvation of the biopolymer, as well as of the stationary phase, is significantly influenced by the eluent composition and hence affects the adsorptive interactions. Complexes can be formed between the analyte and constituents of the eluent, e.g. with metal ions, ion-pair reagents etc. Protein-protein aggregation, multimer-monomer association and sol-gel transitions might occur in chromatographic elution [3]. In conclusion, the retention of a biopolymer solute in HPLC is extremely sensitive to changes in the stationary phase structure as well as in the eluent composition.

Because of their large size, biopolymeric solutes have low free diffusivities in the order of 10^{-10} to 10^{-11} m^2/s [4]. These are further decreased by the diffusion into and out of the pores of the packings (so-called pore diffusion). When the ratio of molecular diameter to pore diameter of packing exceeds about 0.2, the diffusion becomes restricted and the solute is unable to access the total stationary surface. To overcome the obstacle of slow mass transfer kinetics in porous media, the pores should be sufficiently wide and the particles should be small. Small spherical particles with a narrow size distribution arranged in a homogeneous dense and stable column bed are a prerequisite for minimizing the contribution of eddy diffusion to the peak dispersion. Conformational interconversions of the biopolymer are known to occur at the stationary surface as well as in the mobile phase [3]. The corresponding equilibria are controlled by kinetics, i.e. by their rate constants. Thus, as biopolymers are sensitive to conformational changes and to losses of biological activity they should only spend a short time in the column. Although the fundamental phenomena occuring in protein-surface interactions are not yet completely clear, some important directives can be derived with regard to the properties of packings and stationary phases.

In the classical period of column liquid chromatography of biopolymers, the soft gels, such as agarose, cellulose and polyamides maintained a premier position as separation media. Porous glasses and silicas even when modified attracted very little attention. The situation changed considerably when pressure stable microparticulate packings were needed for fast and high resolution separations. Nowadays highly crosslinked synthetic polymers and agarose gels are manufactured as beads in small particle sizes. Yet these polymers still possess a remaining swelling porosity and thus a limited pressure resistance. Inorganic media such as silica exhibit a permanent porosity and excellent mechanical stability. Both types of packings can be surface functionalized by well-established methods to obtain, suitable stationary phases for the various HPLC branches. However, all types of media still exhibit residual matrix effects in chromatographic separation that can be masked to some extent by adding modifiers to the eluent and by other manipulations. In polymers hydrophobic or charged entities of the backbone often create problems. In bonded silica phases the remaining hydroxyl groups cause unwanted residual adsorptivity. The adjustment of an appropriate pore size, particularly in the macro-pore range is performed in the course of the synthesis of polymers and silicas. While polymers tolerate a wide pH range, bonded silicas are restricted to applications between pH 2 and 8. Attempts were made to improve the pH stability of silica and to achieve a more complete and dense coverage by depositing layers and coatings. The most promising route is to first bond a dense sublayer and then to bind the desired functional groups of the top layer. In terms of stability and matrix effects, the future packings of HPLC are most probably inorganic packings with organic coatings, thus combining the favourable mechanical properties of silica with the favourable chemistry and chemical stability of polymers.

Packings are marketed with different physical structure parameters detailed in Fig. 1 [5]. Regarding the particle shape, beads are favoured over angular particles as they provide a more dense, homogenous and stable column bed. But this must be paid for with a tenfold higher price. The particle size of packing ranges from 3 to several hundred μm. Packings of 3 to 5 μm are applied in fast separations using short columns. Analytical separations are typically carried out with 5 to 10 μm particles. Packings with a particle size between 15 to 60 μm are employed in preparative isolation. Large particles mainly serve for up-scale separations.

Packings are manufactured in graduated pore size from 6 to 400 nm. Macroporous silicas and synthetic organic gels have nominal pore size of pd > 50 nm. The majority of so-called wide-pore packings span a range of $30 < pd < 50$ nm. To circumvent all the problems associated with pore diffusion, non-porous beads of up of 2–7 μm appear to be the packings of choice. Some products are already commercially available (Bio-Rad, Merck, Toyo Soda) allowing fast separations of proteins within a few minutes [6–8]. They resemble the classical superficially porous packings that have an impermeable core and a thin porous layer.

A bewildering number of products for adsorptive chromatography exist as surface functionalized media including polymers and bondes silicas [9]. As most of the functionalization procedures of commercial media remain proprietary, it becomes rather difficult to discriminate between their types. To enlighten the situation, functionalized or bonded phases are grouped in three common aspects: type, size and topography (Fig. 2a/b/c). A surface can carry a dense monolayer, a cross-linked layer, a multilayer (sub- and toplayer) or a coating. Most of the chromatographic packings fall into these categories, although there is some mutual overlapping.

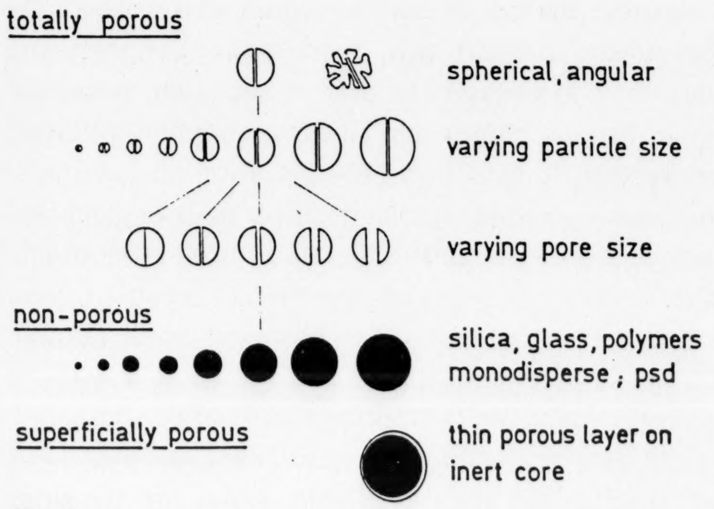
totally porous
spherical, angular
varying particle size
varying pore size
non-porous
silica, glass, polymers
monodisperse ; psd
superficially porous
thin porous layer on
inert core

Fig. 1

Types of packings according to their physical structure parameters: particle morphology, particle size, and pore size (psd = particle size distribution) (from ref. [5] with permission of Elsevier, Amsterdam).

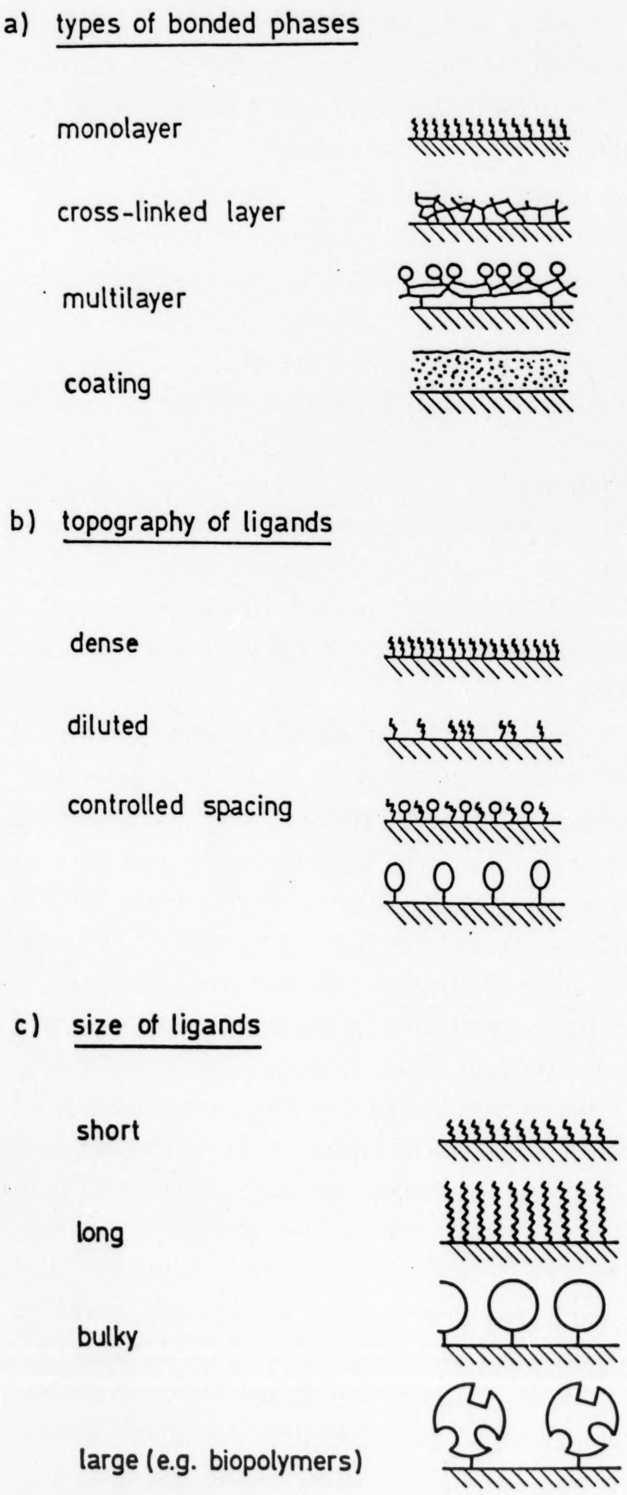
a) types of bonded phases
monolayer
cross-linked layer
multilayer
coating
b) topography of ligands
dense
diluted
controlled spacing
c) size of ligands
short
long
bulky
large (e.g. biopolymers)

Fig. 2

Survey of types of bonded stationary phases (from ref. [5] with permission of Elsevier, Amsterdam).

Of fundamental importance is the topography of ligands or functional groups, i.e. their distribution across the stationary surface. Three main cases can be distinguished: dense, diluted and controlled spacing. The topography of functional groups can be further changed by solvation as known in reversed phase silicas. In addition, functional groups may differ substantially in size and volume. Large ligands are bonded to the surface of activated affinity media.

III Survey of Commercial Packings and Stationary Phases

A Size Exclusion Packings (Table I)

The classical soft gels first introduced by Porath and Flodin [10, 11] have been replaced to a very large extent today by microparticulate cross-linked hydrophilic gels such as agarose and vinyl copolymers, and by hydrophilic bonded silicas [9, 12] (s. Table I). SEC media are marketed in graduated pore sizes or molecular weight exclusion limits and cover a molecular weight fractionation range between 10 to 2,000 kilodalton. Yau et al. [13] developed clear directives on what an ideal SEC packing should look like in terms of porosity, pore size and pore size distribution to match a wide fractionation range and to achieve an acceptable linearity of the calibration curve. In spite of these recommendations, some of the commercial SEC media exhibit an inhomogenous pore structure and a multimodal pore size distribution, resulting in a pronounced sigmoidal shape of the calibration curve. For high resolution analytical separations, SEC media have mean particle sizes between 3 to 13 μm whereas for preparative work larger particles are preferred. Depending on the particle size and the porosity of SEC media marked differences in the chromatographic resolution were observed [12, 14].

Table I. Size exclusion packings

Trade name	Supplier	Type of packing
Aquapore OH-100, -300, -500, -1000, -4000	Brownlee	silica, bonded diol
Zorbax GF 250 GF 450	Dupont	zirconia stabilized silica, bonded diol
LiChrosorb Diol LiChrospher 100, 500, 1000, 4000 Diol	Merck	silica, bonded diol
μ-Bondagel E-125, E-500, E-1000, E-high, E-linear Protein-Pak 60, 125, 300 SW	Millipore/Waters	silica, hydrophilic polymer
Superose 6 and 12	Pharmacia	cross-linked agarose
Si 60, 100, 300, 500 Polyol SP (Daltosil Polyol) 75, 150, 300, 500, 1200, 3000	Serva	silica, bonded diol
Shim-pack Diol-150 Diol-300	Shimadzu	silica, bonded diol
SynChropak GPC 100, 300, 500, 1000, 4000	SynChrom	silica, bonded diol
TSK-Gel SW type 2000, 3000, 4000 TSK-Gel PW type 2000, 2500, 3000, 4000, 5000, 6000 TSK-Gel-GDNA-PW	Toyo Soda	silica, hydrophilic polymer vinyl polymer

According to their bulk composition, packings are grouped into organic and silica-based types. Representatives of the first type are cross-linked agarose (Superose 6 and 12 of Pharmacia, Sweden) and the TSK-Gel PW series, cross-linked hydrophilic vinyl polymer. Both products are available in analytical and preparative size grades. The organic gels do not allow the application of high pressures because of their swelling porosity. Silica-based SEC media possess superior mechanical stability although the highly porous large pore size silicas do not withstand pressures exceeding 40 MPa [15]. A more severe problem is the modification of the silica surfaces in such a way that matrix effects are minimized, and the surface becomes homogeneously hydrophilic and less succeptible to dissolution. Commercial SEC silica packings have bonded monomeric or polymeric diol groups. Another approach is to coat the silica with hydrophilic polymers such as in TSK-Gels SW of Toyo Soda, Japan, the μ-Bondagel of Millipore/Waters, USA, and the Si Polyol series of Serva, West Germany. Du Pont offers two diol bonded phases on zirconia stabilized silicas, providing a hydrolytic stability towards buffered eluents up to pH 9.0 (Zorbax GF 250 and 450) [16]. CAA-HIC of Beckman, USA, a polyether bonded silica designed for HIC can also be employed as SEC packing.

B Reversed-Phase Packings (Table II)

Reverse phase gradient HPLC employing acidic, low ionic strength eluents has become as widely established technique in the purification, isolation and structure elucidation of proteins [17–20]. Due to the size of proteins wide-pore packings of about 30 nm nominal pore size are favoured but larger pore size materials up to 400 nm are also available. With a few exceptions (Poly F, Du Pont, USA, Macrophase MP-1, Interaction Chemicals, USA, and PLRP-S 300, Polymer Laboratories, UK), the majority of reversed phase packings are silanized silicas. The chemistry of silanization is treated in depth in ref. [9]. The most common bonded hydrophobic groups are n-octadecyl, n-octyl, n-butyl and phenyl. Very hydrophobic proteins were chromatographed on cyano-propyl bonded silicas. Among the phases are monolayer and multilayer (polymeric) types, endcapped products and those carrying two distinct types of ligands, e.g. Pep RPC (Pharmacia Sweden, C2/C18) and Pro RPC (also Pharmacia C1/C8). Reversed-phase silica possess a dynamic structure in the solvated state which is determined by the solvent composition and the temperature.

Table II. Wide-pore Reversed Phase packings of nominal pore diameter pd $\geqslant$ 30 nm

Trade name	Supplier	Matrix
Bakerbond Butyl, Octyl, Octadecyl, Diphenyl	Baker	silica
Ultrapore C8	Beckman	silica
Hi-Pore RP-304 (butyl) Hi-Pore RP-318 (octadecyl)	Bio-Rad	silica
Aquapore Butyl Bu-300, Octyl RP-300, RPC 18, RP-300, Phenyl, PH-300	Brownlee	silica
Poly F	DuPont	fluororganic polymer
Chromegabond TMS, C3, C4, M-C8, M-C18, AP DP, Gamma-C18 phase	ES Industries	silica
Macrophase MP-1	Interaction	St-DVB copolymer
Isco MP C4, MP C18	Isco	silica
Nucleosil 300 C18, 300 C_6H_5, 500 C4, 500 C8, 500 C 18, 500 C_6H_5, 1000 C4, 1000 C18, 1000 C_6H_5, 4000 C4, 4000 C18, 4000 C_6H_5, 300 C4, 300 C8	Macherey-Nagel	silica
LiChrospher 500 RP8, 1000 RP18, 4000 RP8	Merck	silica
Monospher RP8, RP18		silica, non-porous
Pro RPC HR 5/2, HR 5/10	Pharmacia	silica
PLRP-S 300	Polymer Lab's	St-DVB copolymer
Vydac 201 TPB, 214 TPB, 218 TPB, 219 TPB, RPC C8	Separations Group	silica
Serva Butyl = Si 300 Polyol, Butyl = Si 500 Polyol, Octyl = Si 300 Polyol, Octyl = Si 500 Polyol, Octadecyl = Si 300 Polyol, Octadecyl = Si 500 Polyol, Diphenyl = Si 300 Polyol, Octyl = SP 500, Octadecyl = SP 500, Phenyl = Sp 500	Serva	silica
WP-300, WP-300 Octyl	Shandon	silica
Supelcosil LC-304, LC-308, PLC-318, PLC-8, PLC-18	Supelco	silica
SynChropak RP-PC 1, RP-PC 4, RP-PC 8, RP-PC 18	SynChrom	silica
TSK-Gel Octadecyl-NPR	Toyo Soda	polymer, non-porous
Protesil 300 Octyl, 300 Phenyl	Whatman	silica

The structure ranges from bristle-like, over blanket-like to a collapsed droplet-like. Long chain n-alkyl bonded silicas e.g. n-octodecyl are known to undergo phase transitions with rising column temperature [9]. Chain length and structure of the ligand appears to play a minor role in retention as the proteins are less capable of intercalating the chains. For instance the retention times of proteins on a column of 35 X 8 mm packed with non-porous silicas of dp = 1.5 μm with bonded C4, C8, C18 and phenyl groups were scarcely affected by the type of ligand [21]. A more critical feature is the preservation of the biological activity of proteins in RPC. First due to the strongly hydrophobic surface, irreversible adsorption, unfolding and loss of bioactivity might occur. Second, the harsh elution condition e.g. acidic pH and the high content of organic solvent may operate in the same direction. For instance the biological activity of horseradish peroxidase diminished with increasing chain length of the reversed phase silica in the sequence C2 < phenyl < C4–C8 < C18 at otherwise constant gradient conditions [22]. The commercial wide-pore reversed phase packings are listed in Table II.

C Packing for Hydrophobic Interaction Chromatography, HIC (Table III)

As opposed to Reversed Phase Chromatography HIC is carried out on weakly hydrophobic stationary phases with eluents of pH 6 to 8 with a descending salt gradient [23–26]. Supports are organic (cross-linked agarose, e.g. Superose 12, vinyl polymers e.g. TSK-PW and Fractogel) and wide-pore silicas. The hydrophobic ligands are phenyl, pentyl, neopentyl, butyl, propyl, hydroxypropyl, ethyl

Table III. Packings for Hydrophobic Interaction Chromatography (HIC)

Trade name	Supplier	Matrix hydrophobic spacer
WP-Hi-Propyl	Baker	silica, propyl
CAA-HIC	Beckman	silica, polyether
Butyl-Fractogel	Merck	vinyl polymer, butyl
Phenyl-Superose HR 5/5, HR 10/10 Alkyl-Superose HR 5/5, HR 10/10	Pharmacia	cross-linked agarose phenyl neopentyl
W-Porex	Phenomex	silica, butyl
Poly Propyl A Ethyl A Methyl A	Poly LC	silica, polypeptide coating propyl, ethyl, methyl
SynChropak SynChroprep	SynChrom	silica,
Methyl		methyl
Propyl		propyl
Hydroxypropyl		hydroxypropyl
Benzyl		benzyl
Pentyl		pentyl
TSK-Phenyl-5 PW	Toyo Soda	vinyl polymer, phenyl

and methyl bonded at a low density. Other types are Poly Methyl A, -Ethyl A and -Propyl A, carrying a hydrophobic ligand on a polypeptide sublayer coated on a wide-pore silica (Poly LC, USA) and CAA-HIC (Beckman, USA), a bonded polyether silica. The products are listed in Table III.

D **Ion Exchangers** (Table IV)

According to their net charge and charge distribution, proteins and nucleic acids begin to be retained on ion exchangers when the pH is +/− 0.5–1.0 units apart from the isoelectric point of the biopolymer [27]. Depending on the isoelectric point strong and weak anion, as well as cation exchangers were employed with salt or pH gradient. The latter method was advocated by Pharmacia, Sweden as Chromatofocusing. Supports were wide-pore synthetic polymers (hydrophilic copolymers, styrene-divinylbenzene copolymers) and wide-pore silicas of a mean pore diameter between 30 and 400 nm. For fast separations non-porous beads (e.g. Tuff-beads of Bio-Rad, USA) were recently introduced [10, 11]. Silica-based ion exchangers (s. Table IV) differ in the bonding chemistry by which the surface is functionalized (s. ref. [9] for details). DuPont, USA uses a zirconia stabilized wide-pore silica as base material to introduce ionic groups (Zorbax 300-SCX, -WCX, -SAX, -WAX). A large amount of work was done by Regnier's group on the synthesis of silica-based ion exchangers by polyethylene (PEI) coating crosslinked with polyglycidether [28, 29]. Further reactions of the PEI layer with reagents yield strong anion exchangers and also hydrophobic stationary phases. The method was also adopted in the synthesis of cation exchangers [30]. The PEI coating is not restricted to silica and can be applied to non-siliceous inorganic and to organic supports [31]. Another route was followed by Alpert in coating a gamma-aminopropyl silica

Table IV. Wide-pore ion exchange packings of nominal pore diameter pd ⩾ 30 nm

Trade name	Supplier	Matrix type of exchanger
Bakerbond	Baker	silica,
PEI		WAX
Quat		SAX
Carboxyethyl		WCX
Carboxy-Sulfon		SCX
AB_x		WAX, WCX
MAb		WAX
Ultrasil AX	Beckman	silica, SAX
Tuff-Beads	Bio-Rad	hydrophilic polymer, WAX
Aquapore	Brownlee	silica,
AX 300, AX 1000		WAX
CX 300		WCX
Zorbax	DuPont	zirconia stabilized silica,
300-SCX		SCX
300-WCX		WCX
300-SAX		SAX
300-WAX		WAX
P-SCX, A-SCX	Es Industries	silica, SCX
P-WCX, A-WCX		WCX
SAX		SAX
QMA-Spherosil	IBF	silica, SAX
DEA-Spherosil		WAX
C-Spherosil		WCX
S-Spherosil		SCX
Mp DEA	Isco	silica, WAX
Mp CM		WCX
Nucleogen DEAE 50, 500, 4000	Macherey-Nagel	silica, WAX
Accell QMA	Millipore/Waters	silica, SAX
CM		WCX
Mono Q	Pharmacia	hydrophilic polymer, SAX
Mono S		SCX
PolyCat A	Poly LC	silica, poly-peptide coating, WCX
PolyWAX LP		WAX
PolySulfoethyl-SCX		SCX
PL-SAX	Polymer Lab's	St-DVB copolymer, SAX
Aminohexyl SP 500	Serva	silica, WAX
Aminophenyl SP 500		WAX
Aminopropyl SP 500		WAX
Carboxymethyl SP 500		WCX
Carboxypentyl SP 500		WCX
DEAE SP 500		WAX
Si 300 Polyol		WCX
DEAE 300 Polyol		WAX
DEAE 500 Polyol		WAX
Shim-pack WAX-2	Shimadzu	silica, WAX
Shim-pack WCX-2		WCX
Supelcosil 3 SCX	Supelco	silica, SCX
3 SAX		SAX
SynChropak CM 300	SynChrom	silica, SCX
S 300		WCX
SynChropak AX 300		WAX
AX 500, AX 1000		
SynChropak Q 300		SAX
SynChrosorb CM		WCX
AX		WAX
Q		SAX
TSK-Gel	Toyo Soda	silica,
CM-2 SW, CM 3 SW		WCX
DEAE-2 SW, DEAE-3 SW		WAX
SP-5 PW		vinyl polymer, SCX
DEAE-5 PW		WAX
TSK-Gel DEAE-NPR		polymer, nonporous
TSK-Gel HA-1000		hydroxyapatite

with a poly (aspartic acid) coating [32]. In this way WCX (Poly CATA), WAX (Poly WAX LP) and a SCX (Polysulfoethyl), all of Poly LC, USA, were synthesized. Baker has successfully introduced two ion exchangers AB_x a mixed WAX, WCX and MAb a WAX that were widely used in the separation and isolation of monoclonal antibodies. The commercial ion exchangers not only differ in the type of ionic functional group, but also in their ion-exchange capacity. The ionic capacity measured with monovalent ions is less significant. More relevant is the protein binding capacity. It is well worth emphasizing first that the utility of this capacity is a function of the pore size relative to the size of protein and second that the dynamic capacity achieved at chromatographic conditions is often much less than the static capacity.

Among the ion-exchangers, Mono Q and Mono S of Pharmacia, Sweden composed of monodisperse polymer beads have gained wide-spread application. Attempts were also made to utilize the ion exchange properties of hydroxyapatite, as in TSK-Gel HA-1000 (s. also reference [33, 34].

E Liquid-Liquid Partition Systems (Table V)

Albertson pioneered aqueous poly(ethyleneglycol)-dextran phases to separate cells and cell fragments [35]. Mueller [36–38] has adopted this partition system in order to develop an efficient chromatographic method for the resolution of proteins and nucleic acids. He used hydrophilic vinyl polymers (Fractogel, Merck, Darmstadt) or diol bonded silicas (Lichrospher Diol also Merck) as supports and grafted a polyacrylamide layer at the surface (see Fig. 3). The polyacrylamide layer immobilizes the dextran-rich phase, e.g. composed of 2.2 % W/W of PEG 4000 and 16.7 % W/W of dextran T 70 (Fig. 3). The loaded support is then equilibrated with poly(ethyleneglycol)-rich phase as mobile phase. Polyacrylamide coated hydrophilic vinyl polymers are marketed in two versions as LiPar Gel 650 and 750 (s. Table V). LiPar Gel 650 has an exclusion limit of about 5,000 kdalton and is designed for proteins and RNA's, LiPar Gel 750 has an exclusion limit of about 50,000 kdalton and fractionates DNA restriction fragments and larger RNA's. The products can be obtained either immobilized with the dextran-rich phase (LiPar Gel coated) or without (LiPar Gel uncoated). Correspondingly, the stationary liquid phase LiPar Solv staph (Dx 40/PEG 6000) and the mobile liquid phase LiPar Solv moph (Dx 40/PEG 6000) are available. The former contains 1.6 % W/W of PEG 6000 and 18.3 % of Dx 40, the latter 9.3 % W/W of PEG 6000 and 1.2 % (W/W) of Dx 40.

Table V. Packings for Liquid-Liquid Partition Chromatography

Trade name	Supplier	Matrix, ligand
LiParGel	Merck	vinyl polymer, polyacrylamid

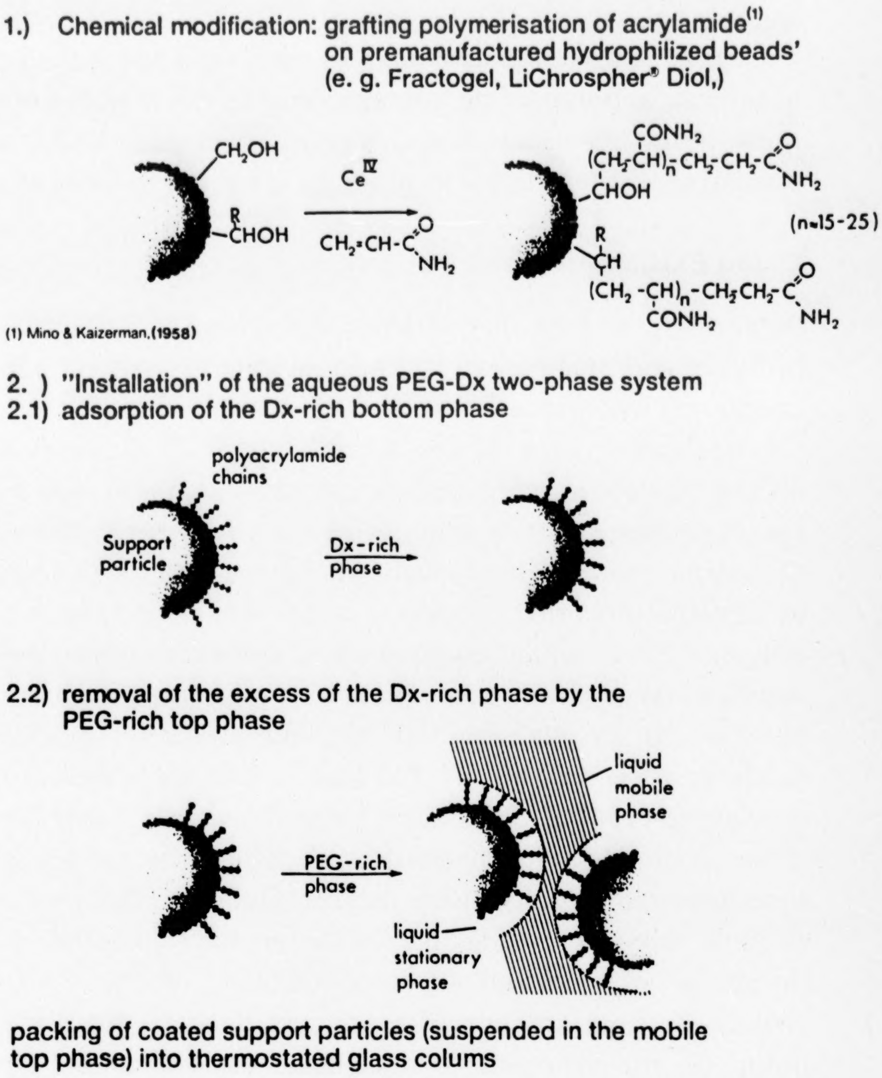
1.) Chemical modification: grafting polymerisation of acrylamide(1)
on premanufactured hydrophilized beads'
(e. g. Fractogel, LiChrospher® Diol,)
CH₂OH
R
CHOH
Ce IV
CH₂=CH-C=O NH₂
CONH₂
(CH₂-CH)ₙ-CH₂-CH₂-C=O NH₂
CHOH
(n=15-25)
R
CH
(CH₂-CH)ₙ-CH₂CH₂-C=O NH₂
CONH₂
(1) Mino & Kaizerman.(1958)
2.) "Installation" of the aqueous PEG-Dx two-phase system
2.1) adsorption of the Dx-rich bottom phase
polyacrylamide chains
Support particle
Dx-rich phase
2.2) removal of the excess of the Dx-rich phase by the PEG-rich top phase
PEG-rich phase
liquid mobile phase
liquid stationary phase
packing of coated support particles (suspended in the mobile top phase) into thermostated glass colums

Fig. 3

Preparation of supports for partition chromatography in the aqueous poly (ethyleneglycol)-dextran two phase system (courtesy of W. Müller, E. Merck, Darmstadt).

IV Characteristic Features of LC Phase Systems Applied to Biopolymer Separations

A Size Exclusion Systems

The major target quantities in SEC of biopolymers are defined as [9]:

- predictable and reproducible elution volumes;
- minimum slope and a wide linear range of calibration curve;
- low peak dispersion of solutes;
- optimum chromatographic resolution in an acceptable analysis time;
- high peak capacity;
- high mass reocery and maintenance of biological activity;
- extended column life-time.

The quantities listed are controlled by the physical and chemical properties of the SEC packings, by the column characteristics and by the operating conditions [39]. The primary choice is made by selecting a SEC column that matches the desired molecular weight range. Usually two columns of 10 and 50 nm pore size span a fractionation range between 10 to 2,000 kdalton. Column dimensions are about 300 mm length and 10 mm inner diameter. Next, the calibration curve is assessed with standard proteins. Eluents are 50 to 100 mM buffer (phosphate, Tris HCL etc.) of pH 5 to 8 adjusted to an ionic strength $\mu > 0.2$ aiding salts (NaCl, Na_2SO_4, NH_4HCO_3, NH_4 acetate). Furthermore, traces of reagents such as sodium azide are added to prevent microbial contamination. To mark the separation range the elution volume of a totally excluded solute (V_0) and a totally permeating solute (V_m) is measured. Elution volumes V_E of proteins that are larger than V_m indicate that solute-surface interactions take place in addition to size exclusion. This can be corrected by changing the eluent composition. Recoveries of proteins are in the range of 80 to 100 % with sample loads from 0.1 to 10 mg (maximum) per column (300 × 10 mm). The use of guard columns is suggested to protect the SEC columns. A column of described dimension should be operated at a flow rate of 20 µl/min (10 µm particles) or 50 µml/min (5 µm particles) to gain the highest plate number and lowest peak dispersion. Such low flow rates, however, extend the analysis time to several hours. Consequently, a compromise has to be made between resolution and analysis time. Fig. 4 shows separation of a protein mixture on a Zorbax GF 250 column in 23 minutes at a plate count of about 30,000 [9]. SEC can also be carried out under denaturing conditions employing sodium dodecyl sulphonate, 6 M area or 6 M guanidine hydrochloride solutions. Denaturation increases the size of proteins compared to native solutes and thus the molecular weight fractionation range decreases correspondingly.

In conclusion, SEC has the merits of eluting proteins according to their size in a short and predictable volume interval at isocratic conditions. Drawbacks are the low selectivity, small peak capacity and low mass loadability.

B Reversed-Phase Systems

As opposed to SEC, RPC of proteins is operated in the gradient elution mode, generating much higher peak capacities in the order of 100 and higher, depending on the gradient time. The starting eluent is a 10 mM acid, e.g. trifluoracetic acid, phosphoric acid, perchloric acid, and hepta-fluorobutyric acid of pH 2 to 5. The displacing eluent contains an organic solvent such as methanol, acetonitril, 1- or 2-propanol. Linear gradients are run up to 70 % (W/W) of the organic solvent within 20 to 60 minutes. Typically, flow rates are about 2.0 ml/min with changes of the organic modifier of 0.2 to 1 % min. With increasing solvent strength the retention of protein decreases as exemplified by the plot of the logarithm of the capacity factor against the content of organic solvent in the eluent (Fig. 5). Retention is further regulated by the ionic strength employing buffers such as triethylammonium phosphate, ammonium acetate and pyridinium acetate and by ion pairing reagents [17–19].

Elution of proteins on reversed phase columns is often associated with losses of biological activity. Studies of the changes of the biological activity of proteins in RPC are reviewed in ref. [9]. Furthermore, mass recovery may be less than 100 % due to irreversible adsorption at the frits, column tube materials and at the bonded phase.

On analytical columns of 250 × 4 mm packed with 5 or 10 µm particles the mass loadability often exceeds 50 mg per g of support.

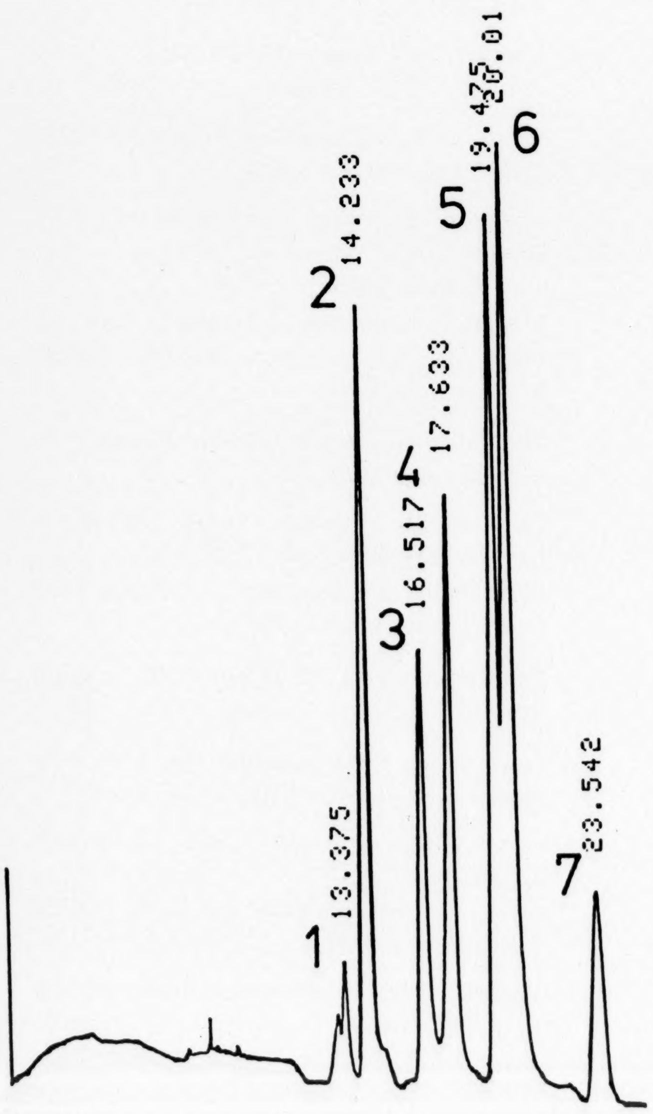

Fig. 4

Separation of a protein mixture on a Zorbax Bio-Series GF 250 column 250 × 9.4 mm, eluent: 0.2 M phosphate buffer pH 7.0 + 0.3 M KCl, F = 0.5 ml/min^1 UV detector

elution sequence: **1** = ferritine, **2** = aldolase, **3** = bovine albumin, **4** = ovalbumin, **5** = carbanhydrase, **6** = trypsin inhibitor, **7** = lactalbumin.

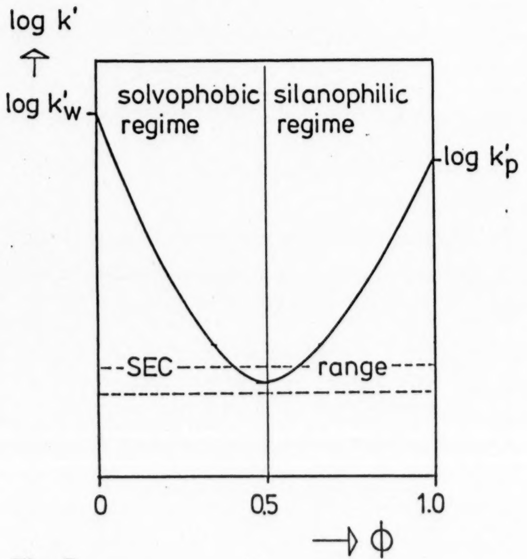

Fig. 5

Retention scheme of a protein in reversed phase gradient HPLC (k'_p capacity factor in pure organic solvent, k'_w capacity factor in pure water, ϕ volume fraction of organic solvent in the hydro-organic eluent).

Table VI. List of suppliers

Baker	J. T. Baker, Research Products, 222 Red School. Lane Phillipsburgh, NJ 08865, USA Baker Chemikalien, Postfach 1661, D-6080 Groß-Gerau, FRG
Beckman	Beckman Instruments Inc., 2350 Camino Ramon, P.O. Box 5101, San Ramon, CA, USA Beckman Instruments GmbH, Frankfurter Ring 115, D-8000 München 40, FRG
Bio-Rad	Bio-Rad Laboratories, 2200 Wright Avenue, Richmond, CA 94804, USA Bio-Rad Laboratories GmbH, Dachauerstraße 364, D-8000 München 50, FRG
Bischoff	Bischoff Analysentechnik und -geräte GmbH, Ulmerstraße 2, D-7250 Leonberg, FRG
Brownlee	Brownlee Labs Inc., 2045 Martin Ave, Santa Clara, CA 95050, USA
Chrompack	Chrompack Inc., P.O. Box 6795, Bridgewater, NJ 08807-0795, USA Chrompack Deutschland GmbH, Nürnbergerstraße 14–15, D-1000 Berlin 30, FRG
DuPont	DuPont Company, Analytical Instruments Division, McKean Bldg.-Concord Plaza, Wilmington, DE 19801, USA DuPont GmbH, Postfach 1509, Dieselstraße 18, D-6350 Bad Nauheim 1, FRG
ES Industries	ES Industries, 8 South Maple Ave, Marlton, NJ 08053, USA
HP Chemicals	HP Chemicals Inc., 4221 Forest Park Blvd., St. Louis, Missouri 63108, USA
hplc	HPLC Technology-Phenomex, 405 Via Corta, Palos Verdes, CA 90274, USA
IBF	Reactifs IBF – Societe Chimique Pointet-Girard, 35, avenue Jean-Jaures, 92390 Villeneuve-La-Garenne, France
ICN Biomedicals	ICN Biomedicals GmbH, Postfach 369, D-3440 Eschwege, FRG
Interaction	Interaction Chemicals, Inc., 1615 Plymouth Streat, Mountain View, CA 94043, USA
ISCO	ISCO Inc., P.O. Box 5347, Lincoln, Nebraska 68505, USA
Macherey-Nagel	Macherey-Nagel, Neumann-Neander-Straße 6–8, Postfach 307, D-5160 Düren, FRG
Manville	Manville, Filtration and Minerals, P.O. Box 5108, Denver, Colorado 80217, USA
Merck	E. Merck, Frankfurter Straße 250, D-6100 Darmstadt, FRG E. M. Science, 111 Woodcrest Road, P.O. Box 5018, Cherry Hill, N.J. 08034-0395, USA
Micromeritics	Micromeritics Instrument Corp, One Micromeritics Drive, Norcross, GA 30093-1877, USA
Millipore-Waters	Millipore, Waters Associates, Milford, MA 01757, USA Millipore, Waters Chromatographie, Hauptstraße 71–79, D-6236 Eschborn, FRG
Orpegen	Orpegen, Czernyring 22, D-6900 Heidelberg, FRG
Pharmacia	Pharmacia Fine Chemicals AB, Box 175, S-75104 Uppsala 1, Sweden Deutsche Pharmacia GmbH, Bereich Biotechnologie, Munzinger Straße 9, D-7800 Freiburg, FRG
Phase Separations	Phase Separations Ltd., Deeside Industrial Estate, Queensferry, CLWYD CH5 2LR, GB
Pierce	Pierce Chemical Company, P.O. Box 117, Rockford, IL USA Pierce GmbH, Daimlerstraße 15–17, D-6054 Rodgau 6, Weiskirchen, FRG
Poly LC	Poly LC, 9052 Bellwart Way, Columbia, MD 21045, USA
Polymer Lab's	Polymer Laboratories Ltd., Essex Road, Church Stretton, Shropshire SY6 6AX, UK
Reichelt	Reichelt Chemie Technik, Euglerstraße 18, D-6900 Heidelberg 1, FRG
Scientific Systems	Scientific Systems Inc., Marketing Department, 1120 W. College Ave, State College, PA 16801, USA
Separations Group (Vydac)	Separations Group, 17434 Mojare Street, P.O. Box 867, Hesperia, CA 92345, USA
Serva	Serva, Carl-Benz-Straße 7, Postfach 105260, D-6900 Heidelberg, FRG
Shandon	Shandon Southern Instruments Inc., 515 Broad Street Draw 43, Sewickley, PA 15143-0043, USA Shandon Labortechnik GmbH, Karl von Prais Str. 18, Postfach 501029, D-6000 Frankfurt 50, FRG
Shimadzu	Shimadzu (Europa) GmbH, Ackerstr. 11, D-4000 Düsseldorf, FRG
Supelco	Supelco Inc., Supelco Park, Bellefonte, PA 16823-0048, USA Supelchem, Am Laubach 3, Postfach 1127, D-6231 Sulzbach/Taunus, FRG
SynChrom	SynChrom Inc., P.O. Box 110, Linden, IN 47955, USA
Toyo Soda	Toyo Soda, Manufacturing Co. Ltd. 1-7-7 Akasaka, Minato-Ku, Tokyo 107, Japan
Varian	Varian, 220 Humbolt Court, Sunnyvale, CA 94089, USA Varian GmbH, Alsfelder Straße 6, D-6100 Darmstadt 11, FRG
Whatman	Whatman Inc., 9 Bridgewell Place, Clifton, NJ 07014, USA

Fast protein separations within a few minutes can be performed on columns (35 X 8 mm) packed with non-porous monodisperse 1.5 μm n-alkyl silicas on conventional HPLC equipment [21]. Such columns also exhibit a high sensivity in detection attributed to the high efficiency and low column volume [8].

In conclusion, RPC is the method of choice when proteins should be separated that do not denature at the harsh elution conditions or might renature after a certain incubation time [22]. Elution sequence is with increasing hydrophobicity. Loadability of RP columns is exceedingly high.

C Hydrophobic Interaction Systems

Eluents in HIC are 10–100 mM buffers such as phosphate of pH 5 to 8. Displacing solvents are salts such as ammonium sulphate. Linear descending gradients are run with salt concentrations from 1.0 to 3.0 M down to OM within 20 to 180 minutes. Proteins are eluted according to their hydrophobic character under mild conditions mostly preserving their biological activity. Peak capacity of HIC columns is usually less than for RP columns by a factor of 2 to 3. Mass loadability of columns is comparable to RP columns and comparable to RP columns and decreases with the size of the hydrophobic ligand [33]. For instance, mass loadability on a Phenyl-Superose column of 100 X 10 mm is about 80 mg.

Fast HIC separations within a few minutes were reported on columns (35 X 8 mm) packed with non-porous monodisperse 1.5 μm acetamido bonded silicas [41].

D Ion-Exchange Systems

To establish an optimum ion-exchange system for protein separation, it is extremly useful to know or to assess the so-called retention map of proteins [27] where the retention volume is plotted against the pH of the eluent. Retention of a protein is proportional to the ion exchange capacity of an ion exchanger. In most cases WAX or SAX is employed with starting eluents containing 10 to 20 mM buffer of pH 5 to 8 e.g. phosphate or Tris HCl buffer. The displacing eluent is a 0.5 to 1.0 M salt solution (NaCl). Linear ascending salt gradients are run in 20 to 60 minutes at a flow rate of 0.5 to 2.0 ml/min.

A powerful method called chromatofocusing is to apply a pH gradient instead of a salt gradient with a polybuffer [42–44]. Ion exchangers exhibit a very high mass loadability in the order of 50 to 200 mg per g of support.

E Liquid-Liquid Partition Systems

As opposed to aqueous/organic phases employed in LLPC of low molecular weight compounds aqueous/aqueous systems based on poly(ethyleneglycol) and dextran have been found to be highly suitable phase systems for the separation of nucleic acids (DNA, RNA restriction fragments), nucleic-acid protein complexes, proteins, multienzyme complexes and hormone receptors [36–38]. The supports are large pore size polyacylamide coated hydrophilic vinyl polymers (LiPar Gel s. Table V) or diol modified silicas that selectively immobilize the dextran rich phase. The biopolymers distribute between the two phases according to their size, nature of surface and net charge. Retention and selectivity are controlled by the type of salt, the salt concentration, the pH, the temperature and the molecular weight of the two constituents poly(ethyleneglycol) and dextran. The conditions for a given separation problem can be established through microscale partition measurements, measuring the partition coefficients. Chromatographic separation are carried out in the gradient elution mode on columns of about 200 X 10 mm of a flow rate of < 0.5 ml/min [36]. Column loadability is dependent on the molecular weight of analytes and varies between 2 mg per cm^2 of column cross-section (200 mm length) for a 80 kdalton protein, and 0.5 mg/cm^2 for DNA fragments of 1.300 to 2.000 kdalton [37].

V Conclusions and Future Prospects

In this article the various aspects of the design and the properties of packings and stationary phases as well as the characteristic features of phase systems for HPLC biopolymer separations were discussed. A survey of commercial packings and phase systems reveals that highly selective and fast separations can be accomplished. Particular emphasis was placed on systems that enable the resolution of large biopolymers exceeding 500 kilodalton. Activities in academic and industrial research clearly indicate that an increasing number of improved packings and phases will be brought on the market within the next five years, which will very much extend the present separation capabilities. Progress will come from a number of novel developments.

First, packings of more defined pore characteristics and surface chemistry with greater chemical stability will be available. Efforts are centered on synthesizing silicas with improved surface properties (forinstance s. ref. [45]) and cross-linked organic polymers (s. ref. [46]). The remaining polar adsoprtion properties of silica and the remaining hydrophobic character of organic polymers seem to be best shielded by an organic polymeric coating. Based on the immobilization of various kinds of oligomers in GC fused-silica-columns, Schomburg's group adopted these techniques to coat silicas and other inorganic supports with a dense hydrophobic (polyorganosiloxane) or hydrophilic (polyvinylpyrolidone) oligomeric layer [47, 48]. Bayer and Rapp successfully graftet long poly(ethylene) chains on the surface of macroporous cross-linked polystyrene packings [46]. The PEI coating technique was also applied to cross-linked St-DVB copolymers to obtain anion exchangers [49].

Substantial interest has been placed on non-porous organic and inorganic particles with a desired bonding or coating for fast separations in all branches of HPLC of biopolymers except SEC.

Second, polytpic and mixed stationary phases have gained widespread interest because of their flexibility in separation. For instance phases with hydrophobic/ionic ligands, anionic, and cationic groups were synthesized and tested. Packings with hydrophobic ligands can be employed both in SEC and HIC e.g. CAA HIC of Beckman depending on the eluent composition. An alternative to those polytypic stationary phases is the use of a sequence of HPLC branches in the course of a biopolymer separations e.g. IEC followed by RPC and SEC, AC followed by IEC and RPC. Systems offering a high column loadability are chosen at the initial stage of separation. Furthermore, a typical feature of HPLC is that several modes are applicable to a separation problem, as demonstrated for membrane proteins [50, 51] and nucleic acids [52, 53].

References

[1] *L. A. Haff,* Chromatography **2,** 25–34 (1987).

[2] *Z. El Rassi, Cs. Horvath,* Chromatographia **19,** 9 (1984).

[3] *M. T. W. Hearn, A. N. Hodder, M.-I. Aguilar,* J. Chromatogr. **327,** 47–66 (1985).

[4] *G. Guiochon, M. Martin,* J. Chromatogr. **326,** 3–32 (1985).

[5] *K. K. Unger, B. Anspach,* Trends in Analytical Chemistry **6,** 121–125 (1987).

[6] *D. J. Burke, J. K. Duncan, L. C. Dunn, L. Cummings, C. J. Siebert, G. S. Ott,* J. Chromatogr. **353,** 425–437 (1986).

[7] *D. J. Burke, J. K. Duncan, G. S. Ott,* J. Chromatogr. **359,** 553–540 (1986).

[8] *K. K. Unger, G. Jilge, J. N. Kinkel, M. T. W. Hearn,* J. Chromatographia **359,** 61 (1986).

[9] *K. K. Unger, B. Anspach, R. Janzen, G. Jilge, K. D. Lork,* Bondes Silica Phases for the Separation of Biopolymers by Means of Column Liquid Chromatography, in: *Cs. Horvath* (editor), HPLC: Advances and Perspectives, Vol. 5, Academic Press, New York, in print.

[10] *J. Porath, P. Flodin,* Nature **183,** 1657 (1959).

[11] *J. C. Janson,* Chromatographia **23,** 361–369 (1987).

[12] *K. K. Unger, J. N. Kinkel,* Native and Bonded Silicas in Aqueous SEC, in: *P. Dubin* (editor), Journal of Chromatogr. Libr. Series, Elsevier, Amsterdam, in print.

[13] *W. W. Yau, C. R. Ginnard, J. J. Kirkland,* J. Chromatogr. **149,** 465 (1979).

[14] *G. W. Welling, K. Slopsema, S. Welling-Wester,* J. Chromatogr. **359,** 307–314 (1986).

[15] *B. Anspach,* Ph. D. thesis, Johannes Gutenberg-Universität, 1987.

[16] *R. W. Stout, J. J. De Stefano,* J. Chromatogr. **326,** 63 (1985).

[17] *M. T. W. Hearn,* in: *J. C. Giddings, E. Grushka, J. Cases, Ph. Brown* (editors), Advances in Chromatography Vol. 20, pp. 87–155, 1982, Academic Press, London.

[18] *M. T. W. Hearn,* in: *Cs. Horvath* (editor), HPLC: Advances and Perspectives Vol. 3, pp. 87–155, 1983, Academic Press, New York.

[19] *M. T. W. Hearn,* in: *W. B. Jakoby* (editor), Methods in Enzymology Vol. 104, Enzyme Purification and Related Techniques, Part C, pp. 190–212, 1984, Academic Press, New York.

[20] *F. Lottspeich,* Chromatographia **22,** 407–410 (1986).

[21] *G. Jilge, R. Janzen, J. Giesche, K. K. Unger, J. N. Kinkel, M. T. W. Hearn,* J. Chromatogr. **397**, 71–80 (1987).

[22] *R. Janzen, K. K. Unger, H. Giesche, J. N. Kinkel, M. T. W. Hearn,* J. Chromatogr. **397**, 81–89 (1987).

[23] *Y. Kato, T. Kitamura, T. Hashimoto,* J. Liquid Chromatogr. **9,** 3209 (1986).

[24] *H. Engelhardt, U. Schön,* J. Liquid Chromatogr. **9,** 3225 (1986).

[25] *Z. El Rassi, C. Horvath,* J. Liquid Chromatogr. **9,** 3245 (1986).

[26] *N. T. Miller, C. H. Shieh,* J. Liquid Chromatogr. **9,** 3269 (1986).

[27] *F. E. Regnier,* in: *W. B. Jakoby* (editor), Methods in Enzymology Vol. 104, Enzyme Purification and Related Techniques, Part C, pp. 170–189, 1984, Academic Press, London.

[28] *A. J. Alpert, F. E. Regnier,* J. Chromatogr. **185,** 375 (1979).

[29] *J. D. Pearson, F. E. Regnier,* J. Chromatogr. **255,** 137 (1983).

[30] *W. Kopoaciewicz, F. E. Regnier,* in print.

[31] *R. M. Chicz, Z. Shi, F. E. Regnier,* J. Chromatogr. **359,** 121–130 (1986).

[32] *A. J. Alpert,* J. Chromatogr. **266,** 23 (1983).

[33] *T. Kawasaki, S. Takahaski, K. Ikeda,* Eur. J. Biochem. **152,** 361 (1985).

[34] *T. Kawasaki, K. Ikeda, S. Takahaski, Y. Kuboki,* Eur. J. Biochem. **155,** 249 (1986).

[35] *P. A. Albertsson,* Partition of cell particles and macromolecules, Almquist Z. Wichsell, Stockholm, 1971.

[36] *W. Mueller,* Eur. J. Biochem. **155,** 213–222 (1986).

[37] *W. Mueller,* Kontakte (Darmstadt) **3,** 3–11 (1986).

[38] *W. Mueller,* Kontakte (Darmstadt) **1,** 45–56 (1987).

[39] *K. K. Unger,* in: *W. B. Jakoby* (editor), Methods in Enzymology Vol. 104, Enzyme Purification and Related Techniques, Part C, pp. 154–169, 1984, Academic Press, New York.

[40] *M. N. Schmuck, K. M. Gooding,* LC Magazine **3,** 814–816 (1985).

[41] *R. Janzen, K. K. Unger, H. Giesche, J. N. Kinkel, M. T. W. Hearn,* J. Chromatogr. **397,** 91–97 (1987).

[42] *L. A. E. Sluyterman, J. Wijdenes,* J. Chromatogr. **150,** 31 (1978).

[43] *L. A. E. Sluyterman, J. Wijdenes,* J. Chromatogr. **206,** 429 (1981).

[44] *L. A. E. Sluyterman, J. Wijdenes,* J. Chromatogr. **206,** 441 (1981).

[45] *J. Köhler, J. J. Kirkland,* J. Chromatogr. **385,** 125–150 (1987).

[46] *E. Bayer,* Xth International Symposium on Column Liquid Chromatography, San Francisco, CA, May 1986, paper 507.

[47] *G. Schomburg, A. Deege, J. Köhler, U. Bien-Vogelsang,* J. Chromatogr. **282,** 27–39 (1983).

[48] *G. Schomburg, H. Czisch, A. Deege, J. Köhler,* Xth International Symposium on Column Liquid Chromatography, San Francisco, CA, May 1986, paper 2502.

[49] *F. E. Regnier,* to be published.

[50] *G. W. R. Welling, S. van der Zee, S. Welling-Wester,* Trends in Analytical Chemistry **9,** 255f. (1986).

[51] *R. S. Matson, St. C. Cohen,* LC/GC Magazine **4,** 624–635 (1986).

[52] *Th. Floyd, J. B. Crowther, R. Hartwick,* LC Magazine **3,** 508–520 (1985).

[53] *L. W. Mc Laughlin,* Trends in Analytical Chemistry **8,** 215–219 (1986).

Received: July 27, 1987
Accepted: Aug. 31, 1987
F

Direct Injection of Plasma into Column Liquid Chromatographic Systems

D. Westerlund

Dept. of Analytical Pharmaceutical Chemistry, Uppsala University Biomedical Center, P.O. Box 574, S-751 23 Uppsala, Sweden

Key Words

Reversed-phase liquid chromatography
Bioanalytical techniques
Drugs
Biological fluids

Summary

Since the late 1970's several techniques involving the direct injection of biological fluids, like plasma and serum have been published. Most of the systems presented utilize a precolumn for the reception of the biological fluids, trace enrichment and preliminary clean-up before the analyte fraction is transferred to the separation column. The most common solid phase for the precolumn is silanized silica, but many other types have been used. One was especially designed for the purpose of direct injections of biological fluids: the Internal Surface Reversed Phase support.

The main problem with direct injections is the development of column instabilities due to the denaturation and precipitation of plasma proteins on the support. It has, however, been possible to design systems which can handle the injection of 25 ml total plasma volume without the need to exchange precolumn. The most promising techiques in this respect are the so called "pre-column" venting plug technique and the use of micellar mobile phases.

Losses of analytes may be a problem when protein-binding extends 95%. However, remedies are available, such as the use of more hydrophobic solid phases, the addition of competitive binders and pH adjustments of injected solutions.

Introduction

Methods developed for assays of drugs and related compounds in biological fluids have traditionally included steps for preliminary sample work-up, such as protein-precipitation, liquid/liquid extraction, liquid/solid distribution, re-extraction, evaporation, etc. Such procedures are time-consuming and require heavy, repetitive work; they constitute in many applications the main share of the total bioanalytical method. For laboratories with a large number of routine samples for chemical analysis, this means that a lot of time must be devoted to sample work-up procedures. This is largely the reason why much effort has been put into the development of liquid chromatographic systems that can tolerate the direct injection of biological fluids.

The most difficult and demanding fluids in such techniques are those that contain a large fraction of proteins – mainly blood, plasma and serum. Cerebrospinal and interstitial fluids, as well as urine, are in general more compatible with liquid chromatographic systems, due to their low protein content.

Besides the *reduced time for analysis* and the consequent increased sample throughput, there are two further important advantages in utilizing direct injection techniques; namely, an *improved accuracy* in the quantifications, due to minimized risks of chemical changes in the analytes because of the reduced number of steps necessary in the analytical methodology. The fewer steps needed in methods utilizing direct injection techniques as compared to traditional methodologies will also provide conditions precedent for *improved precision*.

The first papers written about this kind of system with modern liquid chromatographic techniques were published in the late 1970's [1], and the present paper will give an overview of the different principles that have been utilized for direct injections since that time. The first applications involved the injection of very small volumes ($\leqslant 3 \mu l$) of the biological fluid directly onto the analytical column packed with modified hydrophobic silica [2]. This simple procedure has in recent years been extended by the use of micellar mobile phases [3] in which the proteins do not precipitate.

However, soon after the presentation of this first system, the inclusion of a pre-column in systems of this kind became the standard technique. The pre-columns can be used in two principally different ways: in the foreflush or backflush mode. A Japanese group has found that a pretreatment of the solid phase with plasma proteins, mainly albumin, increased the useful lifetime of the pre-column significantly [4]. An interesting approach is the technique developed by Pinkerton and co-workers, which involves the treatment of the solid phase so that the surface within the pores has different properties compared to the external surface [5]. Finally, some uncommon pre-columns have been used, each in only one or a few papers: the well-known polystyrene divinylbenzene polymer, XAD-2 [6],

0009-5893/87 0155-10 $ 03.00/0

© 1987 Friedr. Vieweg & Sohn Verlagsgesellschaft mbH

size-exclusion supports [7], anion exhange [8], phenylboronate [9] and polyclonal antibodies [10]. All systems described thus far were based on pre-column affinities for the anylates; one deviating principle involved the design of a pre-column which retained proteins by hydrophobic forces, while the analytes were transferred directly to the separation column [11].

Silanized Silica

System Without a Pre-Column

In some early applications of direct injection techniques, the biological fluid was introduced directly into silanized silica solumns. In most cases, very small volumes, 1–3μl, were injected, and the applications were aimed at therapeutic drug monitoring of compounds that were present in rather high concentrations ($\geqslant 1\mu$g/ml) in the biological fluid. Manno et al. [2] claimed in 1979 that the final presentation of their methodology had been delayed for three years because of the nonacceptance, by journal editors, of the concept of direct injection onto LC columns.

Mobile phases in these early papers were typically neat buffer [12] or buffers containing small amounts of acetonitrile [13, 14]. Solid phases were mainly octadecyl-modified silica in long columns (300 × 4mm), and the column lifetimes extended to the injection of (in total) between 0.6–4ml serum or plasma. It was pointed out [14] that columns last longer by using small injection volumes, large packing volumes and large total volume mobile phase through the column. Theophylline [1, 14], acetaminophen [13], cytarabine and uracil arabinoside [12] were the analytes.

Systems with a Precolumn

Foreflush Mode

The limited lifetime of silica-based analytical columns after direct injections of biological fluids stimulated the development of systems including precolumns. However, already in 1978 Popovich et al. [1] developed a system for the analysis of theophylline in serum. The precolumn (2 × 7.1mm) contained pellicular ODS-coated silica particles coupled on-line to the analytical column packed with Partisil-ODS-2 (10μm). A 10μl sample was followed by an 10μl internal standard solution at the injection of a large volume loop, thus eliminating the need for mixing. 30 serum samples could be run before the guard column needed replacement, while the analytical column was effectively protected – after every 120 to 130 serum samples, 60ml of methanol were run through the Partisil-ODS-2 column in order to remove impurities.

The use of large particles in a precolumn in line with the analytical column may decrease the efficiency of the system, which made Wahlund design systems with small particle precolumns [15]. The surface of small porous silica particles is much larger than pellicular ones, and the risk for denaturing the proteins by surface contact is highly increased in this kind of system. Great care was therefore taken regarding the composition of the mobile phase in order to keep the endogenous proteins solubilized during chromatography. Most importantly, the concentration of the organic modifier should be kept as low as possible, preferably < 10%.

This principle has been further developed, mainly by Wahlund and coworkers, first by the introduction of the so-called precolumn venting technique [16]. A three-port valve separates the precolumn (10 × 3.2mm) from the analytical column (100 × 4.6mm) (Fig. 1). The precolumn here serves the dual function of acting as a guard column similar to the simpler system above, as well as effecting a preseparation of the analytes from the biological fluid matrix. It was found that under optimal conditions, the lifetime of the analytical column was so high that several hundred injections (10μl) could be performed without loss of stability. It was further found that only matrix components that elute early from the precolumn destroy the analytical column under nonventing conditions. It is assumed that these components are macromolecules that are excluded from the pores in the silica-based solid phase. The stability of the analytical column was further influenced by the content of organic modifier in the mobile phase, decreasing concentration increased the column lifetime. A larger particle diameter in the precolumn increases its lifetime, and a moderate flow rate involves the highest possible stability, indicating a kinetic factor in the denaturating of the proteins in systems of this kind.

The precolumn venting technique was applied for assays of theophylline [17] and to some antiepileptic drugs [18].

A further development of the foreflush mode was aimed at reducing the influence of the organic modifier, since as low a content as possible of this component in the mobile phase was essential for optimal stability of the dual column system. The system resulting from these efforts is called the precolumn venting plug technique [19] (see Fig. 2). The difference between this and the earlier technique is simply a second injection valve with a large loop containing 2ml

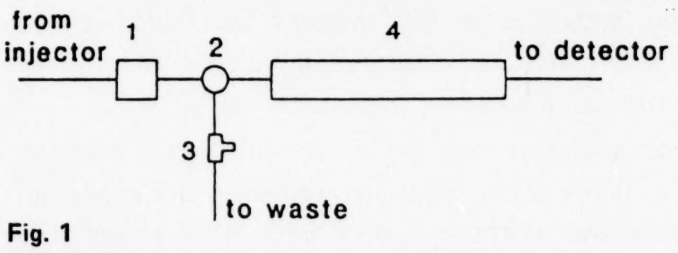

Fig. 1

Pre-column venting system. **1** = Pre-column, 10 × 3.2mm i.d.; **2** = Threeport valve; **3** = Pressure regulator; **4** = Separation column, 100 × 4.6mm i.d. [16].

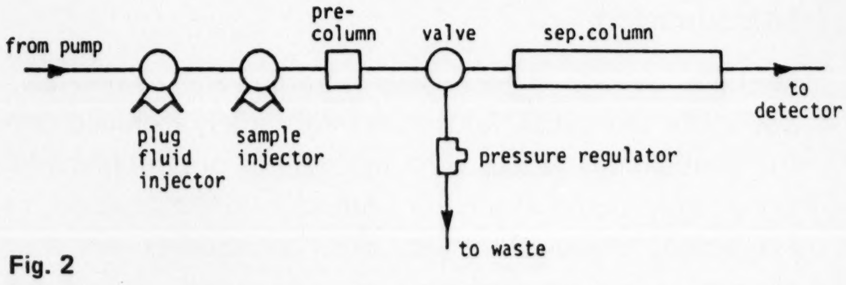

Fig. 2

Pre-column venting plug system. Plug fluid injector is 2ml; sample injector c:a 100μl [19].

buffer. The sample, in the second loop, is injected in the center of this buffer. In this way, the matrix proteins will not come in contact with the organic modifier. An acidic (pH 2) phosphate buffer was found to be the best fluid regarding column stability, which was greatly prolonged by this principle. It was also found, as has been pointed out by other groups, that screens should be used instead of frits at the precolumn top. An optimally designed system was stable up to the injection of ~ 25 ml plasma total volume, making the system useful for routine applications of a large number of samples, i.e. ~ 500 × 50 μl, before the precolumn had to be exchanged. The lifetime of the analytical column could not be measured since it was hardly affected at all. The principle was applied in a system for the quantification of lidocain and its two main metabolites in plasma [20], producing inter-assay precisions $<2\%$ for therapeutic concentrations of the compounds.

The stability index used in these series of studies was defined as the number of injections (corresponding to a certain total volume of plasma) that reduced the chromatographic efficiency, or alternatively increased the pressure by 10%. The two criteria rather often coincided. It was further found that a strong drug protein binding may result in losses of the analyte from a short precolumn [21]. There are, however, several possible remedies for this: increasing the precolumn length and/or its hydrophobicity, alternatively diluting or changing the pH of the sample solution. The results indicated that losses of analytes in this kind of system due to protein binding only occur when the binding degree is $>95\%$.

Miniaturization

A miniaturized pre-column has been designed for direct injection of biological fluids on narrow-bore (1 mm) columns [22], an improvement over earlier work [23] where the extra column effect was large. The principle of the new design was to insert the pre-column in a switching valve, resulting in the dimensions 4.5 × 1 mm. It was packed manually with 40 μm particles (octylsilica) with a syringe. The analytical column was 200 × 1 mm and contained octadecylsilica, 3 μm particles, and was inserted directly into the switching valve in close contact with the pre-column. The complete setup (Fig. 3) also contained a sample loop and two pumps. Typically 100 μl plasma was injected onto the pre-column, followed by a wash with water. The valve was switched and the enriched sample was foreflushed into the analytical column by a mobile phase containing an organic modifier for efficient desorption from the pre-column. The detection limits increased by about 40% compared to an injection directly on the analytical column, indicating continued problems with extra column effects, some certainly originating from dispersion on the pre-column that contained large particles.

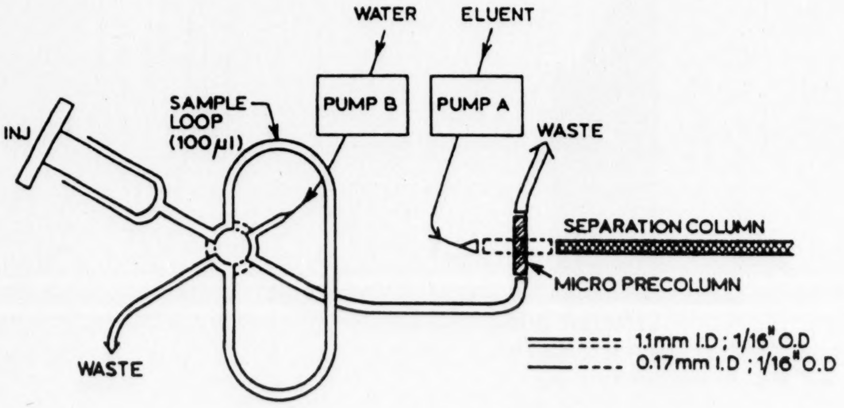

Fig. 3

Miniaturized system for direct plasma injections. Pre-column: 4.5 × 1 mm i.d., 40 μm octylsilanized silica; separation column: 200 × 1 mm i.d., 3 μm Spherisorb ODS-2 [22].

Backflush Mode

A paper by Roth et al. [24] on "Fully Automated High-Performance Liquid Chromatography" involved a breakthrough for the application of direct injection techniques for routine analyses of drugs and related compounds in biological fluids. The system (Fig. 4) consisted of two precolumns, one analytical column and two pumps connected via two valves and an autosampler. The most attractive feature, besides the possibility of injecting biological fluids directly without pretreatment, was the so-called "alternating pre-column sample enrichment technique". This involved an efficient and time-saving operation of the analytical column — the sample was injected and loaded on

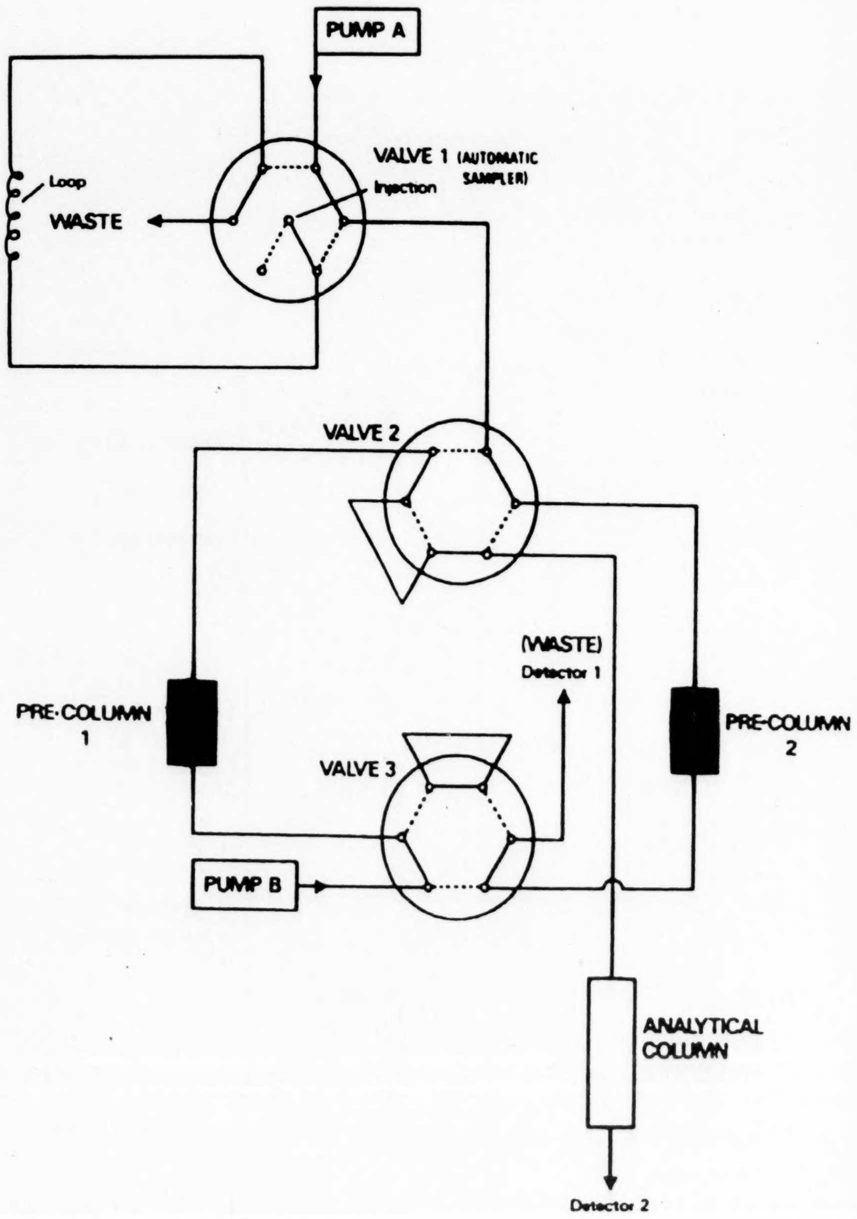

Fig. 4

Alternating pre-column switching system for sample enrichment and backflush [24].

one of the precolumns and after a purge phase, the analytes were backflushed to the analytical column. During the purge phase a new sample was injected, and while the first sample was eluted on the analytical column, the next sample was backflushed onto the same analytical column from the second pre-column. The procedure was automatically operated under microprocessor control. The pre-columns contained large (37–50μm) hydrophobic (C_{18}) silica particles, and the analytical column octadecylsilanized 5μm silica. The analytes were enriched on the top of the precolumn. By applying the backflush mode in the transfer of the compounds to the separation column, no decrease in the chromatographic efficiency due to the large particles resulted. A drawback to the backflush technique is that the column packing in the precolumn can be disturbed by applying mobile phases alternately in opposite directions.

This principle has been applied in many papers with slight modifications in design and use of alternative solid phases; only a few will be mentioned here. Jeurgens [25] elaborated the methodology for routine assays of the most common antiepileptics. Precolumn lifetime extended approximately to the injection of 400 samples of 50μl each, while the analytical column lasted for 1400 injections. The technique has also been modified for studies on drug metabolism [26–28].

A modification of the principle involved the design of a three-column system [29], see Fig. 5. The sample is injected onto a large particulate precolumn (RP-2) and then transferred to the analytical column (RP-8). In many cases this technique involves a very efficient clean-up of biological samples.

This principle was developed into a fully automated fashion through a so-called boxcar configuration [30]. This involves the injection of samples to the maximal frequency permitted by the resolution on the separation column. An example of chromatograms resulting from such a system elaborated for antiepileptic drugs (Fig. 6) has the appearance of a recording from flow injection analysis; 40 samples per hour could be analyzed.

Protein-Coated Silica

In 1982 a Japanese group [4, 31] introduced a technique which involved the pre-treatment of small pore silica with plasma. The biological fluid was injected in a total volume

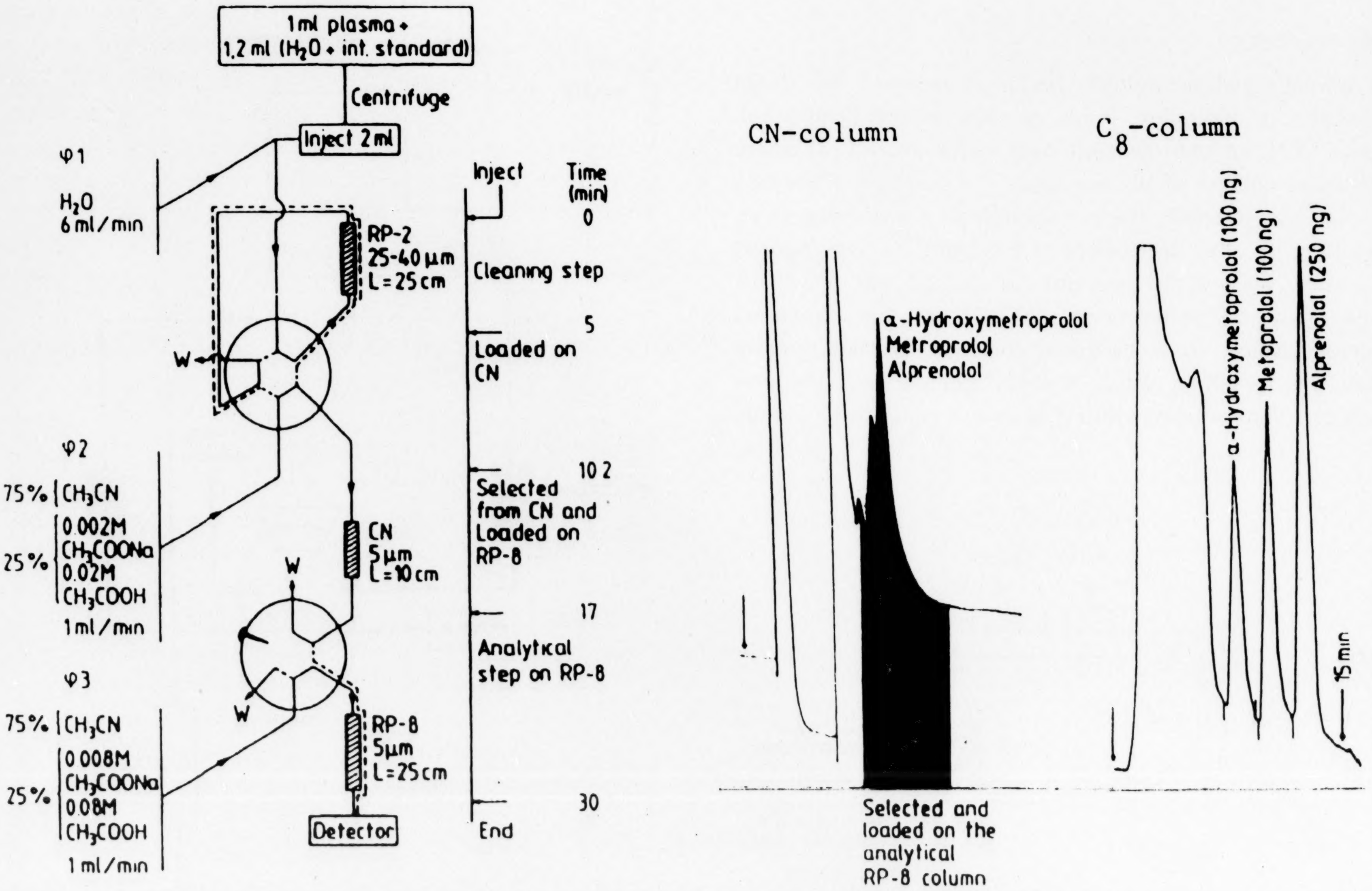
1 ml plasma +
1.2 ml (H₂O + int. standard)
Centrifuge
Inject 2 ml
φ1
H₂O
6 ml/min
RP-2
25-40 µm
L=25cm
W
φ2
75% CH₃CN
25% 0.002M CH₃COONa 0.02M CH₃COOH
1 ml/min
CN
5µm
L=10cm
W
W
φ3
75% CH₃CN
25% 0.008M CH₃COONa 0.08M CH₃COOH
1 ml/min
RP-8
5µm
L=25cm
Detector
Inject
Time (min)
0
Cleaning step
5
Loaded on CN
10 2
Selected from CN and Loaded on RP-8
17
Analytical step on RP-8
30
End
CN-column
C₈-column
a-Hydroxymetroprolol
Metroprolol
Alprenolol
Selected and loaded on the analytical RP-8 column
α-Hydroxymetoprolol (100 ng)
Metoprolol (100 ng)
Alprenolol (250 ng)
15 min

Fig. 5

Column switching with backflush, heartcut and separation [29]. A. System set-up.

B. Chromatograms after heartcut (CN-column) and separation (C_8-column)

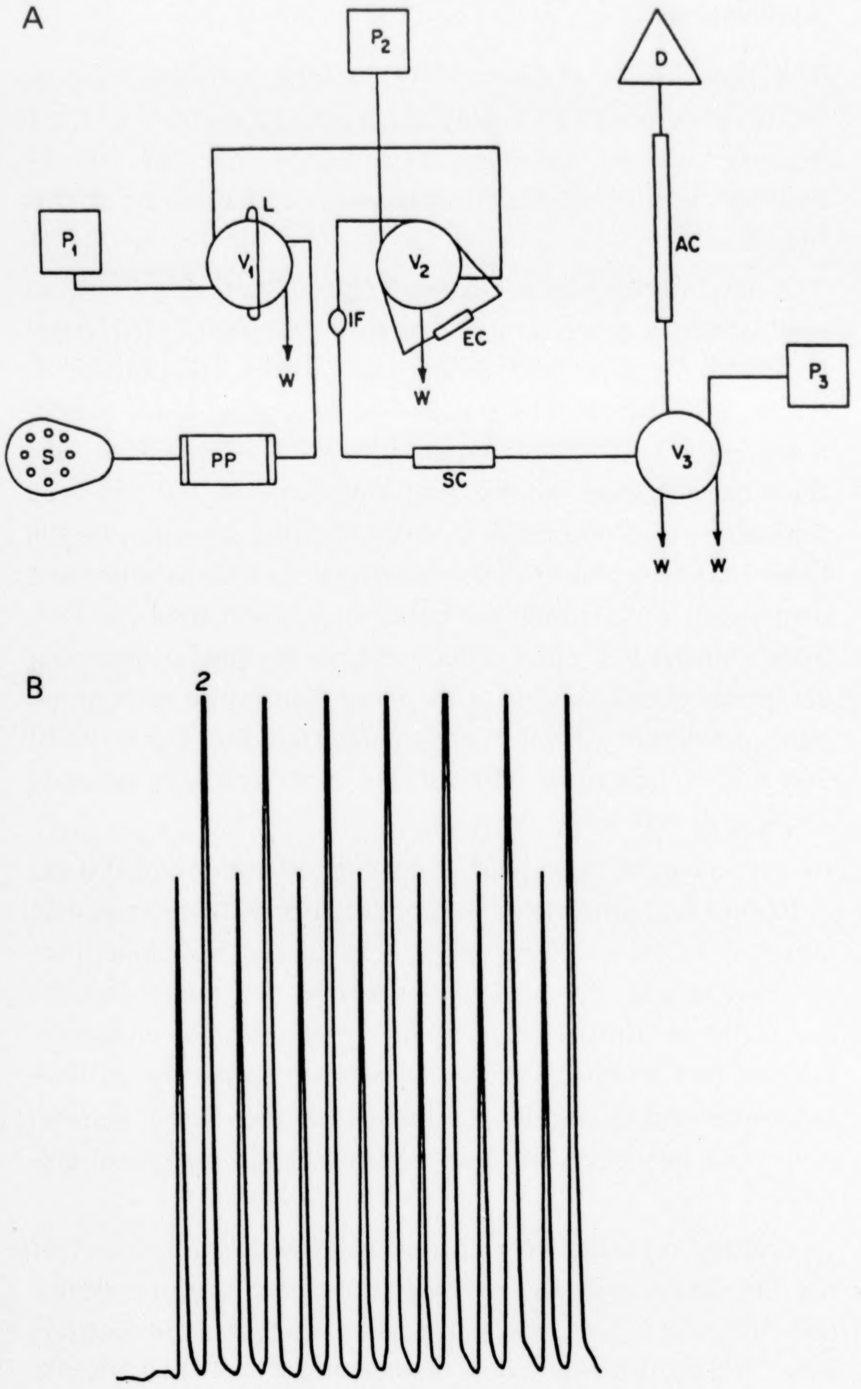

Fig. 6

Fully automated LC-system in boxcar configuration [30].

A S = autosampler, PP = peristaltic pump, L = sample loop, V_1, V_2 and V_3 = six-port switching valves, W = waste, P_2 and P_3 = mobile phase pumps, P_1 = wash pump, EC = pre-column, SC = short column, AC = analytical column, IF = in-line filter, D = detector.

B Chromatograms on analysis of primidone (1) and phenobarbital (2) in serum at a rate of 40 samples per hour.

of 300µl into a short column (40–50 × 4mm), and it was found that quantitative recoveries of different kinds of drugs were obtained after direct injection of plasma samples on such pretreated columns. The drugs included compounds that were both weakly (e.g. procainamide, 6-mercaptopurine) and strongly (e.g. propranolol) bound to plasma proteins. Later, the pre-treatment procedure was modified to start by the injection of bovine serum albumin (BSA), complemented by injecting 100µl of the plasma protein fraction of dialyzed rabbit plasma. The treatment was repeated until quantitative recoveries of the proteins were obtained [32]. It was found that the specific area of the solid phase, as measured according to the BET method, as well as the specific pore volume were unaffected by the treatment. The pores are so small that the plasma proteins will not penetrate, and it is assumed that the macromolecules are adsorbed only onto the external surface of the particles, leaving the largest part of the surface area in its native state. Capacity ratios of the small drug compounds are largely unaffected by the treatment supporting this hypothesis. However, the efficiency of the small molecules decreases by 20–60% [33], probably due to the fact that the adsorbed macromolecules will disturb the diffusion of the small molecules into the pores.

The columns seem to be very stable; laboratory uses over several months have been reported [32].

Internal Surface Reversed-Phase Silica Supports

A new concept in LC packing materials for bioanalytical purposes was introduced in 1985 by Thomas C. Pinkerton and coworkers [5]. The basic idea was to develop a material that eliminated the risk of denaturing the proteins, but still retained the small molecules like drugs and related compounds. This was accomplished by producing a solid phase that exposed a hydrophilic external surface towards the large biomolecules, and, simultaneously, a rather hydrophobic internal surface towards the small molecules. In the technique for developing such supports, the large differences in molecular magnitude between drugs and macromolecules were exploited: The starting material was a small pore diameter silica (~ 70 Å) in order to exclude the biomolecules from the pores. The solid phase was initially modified into a glycerylpropylbonded support, then activated with carbonyldiimidazole and derivatized with a di- or tripeptide, e.g. Gly-L-Phe or Gly-L-Phe-L-Phe. This modified silica was then treated with an enzyme, carboxypeptidase A, which is too large to have access to the pores. Consequently only the peptide bonded to the external surface will be cleaved off, leaving a solid phase with a hydrophilic external surface, glycerylbonded, and a moderately hydrophobic internal surface, di- or tri-peptide bonded. When a biological fluid like serum or plasma is injected directly onto a column packed with this solid phase, the macromolecules will only come into contact with the hydrophilic external surface, while the small analyte molecules will also penetrate into the pores and be retained there by the bonded peptide-phase.

The new concept of packing materials was named internal surface reversed-phase (ISRP), and it is quite obvious that an almost unlimited number of different supports may be produced according to this basic principle. An alternative prototype ISRP-material was later proposed by Hagestam and Pinkerton [34], involving an initial attachment of an amine phase by reacting silica supports with o-aminobutyldimethylmethoxysilane, followed by the bonding of Boc-L-Phe with 1,1-ethyl-3-(3-diaminopropyl)carbodiimide as the coupling catalyst. The removal of the peptide-phase from the external phase was performed by α-chymotrypsin; finally, the residual amine phase on this external surface was capped with glycidol (2,3-epoxyl-1-propanol) to yield glycerol groups. Both low and high-performance supports were starting materials: large particulate (37–74µm) silica with a nominal pore diameter of 40 or 87 Å, and Hypersil 5μm, respectively.

Characterization of ISRP Supports

The success of ISRP packings is determined by following properties: their ability to exclude proteins from the pores with a negligible adsorption of the macromolecules to the external surface; their capacity and ability to retain small analytes; their selectivity and efficiency.

The adsorption tendencies of proteins are closely related to the coverage of the solid phase with hydrophilic ligands and the accessability of the pores. A monolayer coverage of the glycolphase corresponds to 2μmol/m^2 of the support. It was found that the coverage was strongly dependent on the pore size [35] – an initial pore size of $\sim$ 100 Å was essential in order to get a coverage $>$ 1μmol/m^2. The interpretation of the result is that steric hindrance of the silanizing reagent into the small pore silicas is at work. The pore sizes, determined as median pore diameters from pore volume access distributions by inverse size-exclusion chromatography [35], were found to decrease by 17–43 Å for different silicas when modified into ISRP supports. The enzyme carboxypeptidase A has an effective sphere radius of 31 Å, and thereby access to 11–26% of different supports [35]. Since the most abundant plasma protein, albumin, has an effective radius of 40 Å, the risk for adsorption to the solid phase would be very small. This was also indicated in practical experiments of running plasma samples on underivatized, nonenzyme-treated and enzyme-treated solid phases. The tailing of the front peaks were eliminated in the ISRP packings [5, 34].

The coverage of the peptide-phases was found to be very different for the two types presented so far: the Boc-L-Phe gave a much higher coverage – 330μmol/g compared to only about 55μmol/g for the Gly-L-Phe-L-Phe type of support, indicating the importance of attaching a spacer to the support before attachment of the peptide phase [5, 34]. Some common anticonvulsant drugs have been used to characterize the retention properties of the supports. The Gly-L-Phe-L-Phe phase was demonstrated to produce about the same retention of phenytoin as a phenyl-bonded phase, but smaller than C_8 and C_{18} materials. The Boc-L-Phe phase gave a higher retention, partly due to the higher coverage [34]. Studies on the former phase show that the retention in principle was proportional to the surface area of the silica starting material [35].

The enzymatic cleavage of the tripeptide phase gave highly varying results from the different supports, ranging from 7–43% cleavage [35], indicating very wide variations in the pore accessability of the enzyme.

Investigations on the dependence of plate height on flow rate revealed a deviating and disadvantageous behaviour for one commercially available support (Zorbax) used as starting material. The results indicated problems with the mass transfer term and were interpreted to be due to the fact that this special support has a small pore volume and a small median pore diameter [35].

Applications

The possibilities of using ISRP packing materials have so far been demonstrated only for a limited number of compounds, and no complete bioanalytical method, i.e. including method validation, has yet been presented in the literature.

The low performance material (37–74μm, Gly-Phe-Phe) was used as a precolumn for retaining phenytoin [5]. After directing proteins and other fast eluting compounds to waste, the analyte was transferred to a small trace enrichment column (C_{18}) placed in a loop. The phenytoin was then back-flushed to the analytical column for the final separation and detection by UV. A direct injection of the three anticonvulsants (phenobarbital, carbamazepin and phenytoin) onto a high performance support (Gly-Phe-Phe, 5μm) showed a good selectivity, with the endogenous components only visible at the front. 5μm silica with initial pore diameters of 80 ± 30 Å permitted the injection of 240 × 20μl injections without any problems with pressure increase or efficiency decrease.

In a commercial note [36], a small guard column (3.0 (i.d.) × 10mm) was introduced for combination with an analytical column, 5, 15 or 25cm long. After about 500 injections of 10μl serum, the back pressure over the guard column was 3250 psi (initial value 50 psi). However, the analytical column had retained its original back pressure. The authors recommended a regular exchange of the guard column after 120 injections in order to protect the analytical column.

In a study on selectivity optimization with the support of the Snyder triangle [37], it was found that serum proteins did not precipitate in water-organic solvent combinations when tetrahydrofuran, isopropanol or acetonitrile contents were less than 10%, 20% and 25%, respectively. The analytes were oxyphenbutazone, phenylbutazone and furosemide.

Micellar Chromatography

Micellar chromatography was initially studied by Armstrong et al. [38–41]. A retention model was developed, taking into account the partitioning of the solute between a stationary phase, a mobile aqueous phase and a mobile micellar phase. This model has been extensively applied in later studies and seems to be rather useful and valid for different solid phases, micelleformers and mobile phases. More detailed studies by a French group, involving the determination of amounts of sodium decylsulfate (SDS) and cetyltrimetylammoniumbromide (CTAB) adsorbed on several different solid phases, as well as retention data for solutes of different characters with mobile phases of different properties [42–44], demonstrated that the retention behaviour largely followed the original model.

The surfactants are, below the critical micelle concentration (cmc), adsorbed according to a Langmuir-model on alkyl-bonded supports [42]. After cmc the adsorption is either constant or very slowly increasing with increasing concentration of the surfactant. A micellar chromatographic system thus offers an eluite several possibilities for interaction: with the original solid phase, with the adsorbed surfactant, with the aqueous mobile phase, and with the micelles in the mobile phase. In general, with the increasing concentration of surfactant above cmc, the retention decreases, due to an increasing distribution of the eluite to the micellar phase. Charged eluites are normally repelled electrostatically from surfactants with the same charge, or attracted to oppositely charged surfactants, both when these are adsorbed to the solid phase and as micelles. However, there are some exceptions to this rule; when the eluites posess surfactant properties, they may behave as binding compounds even with equi-charged micelleformers [43]. Micellar chromatographic systems obviously offer a multitude of possible parameters for regulation and fine-tuning of retention and selectivity, demonstrated efficiently by Cline Love et al. [45] with both an- and cationic surfactants (Fig. 7).

Further, surfactants have the ability to solvate macromolecules like proteins in aqueous solutions. This property has been utilized in applications for the analysis of biological fluids by Cline Love et al. [3, 46, 47]. Anionic, like SDS, and nonionic, like Brij-35 (polyoxyethylene(23)dodecyl), surfactants have been utilized. However, with cationic, like CTAB, the proteins will be denaturated, and this kind of surfactant can obviously not be used for direct injections of biological fluids.

Neat aqueous phases with a dissolved surfactant have the drawback of producing rather low chromatographic efficiencies. However, the addition of small amounts of an organic modifier, like propanol, improves the efficiency dramatically [3].

The chromatographic systems used in these applications comprise a pre-column located between the pump and the injector and packed with silica gel (25–30μm) in order to saturate the mobile phase with silic acid and to increase the lifetime of the analytical column. Silica gel modified with CN or C_{18}-groups were used in the separation columns. They were found to be stable with no increase in pressure after the injection of $250 \times 20\mu l$ serum directly onto the analytical column [46].

The first studies utilizing micellar chromatography for direct injections of serum involved the use of SDS as the surfactant. However, nonionic compounds, like Brij-35, have the advantage of giving simpler and more predictable interactions with most solutes because of reduction of the electrostatic forces. This compound was shown to produce systems as stable in bioanalytical applications as with SDS as the surfactant [47]. The separation of the diastereomers quinine and quinidine added to human serum is demonstrated in Fig. 8. The addition of propanol (10%) was necessary to achieve the separation, and with neat aqueous SDS solutions, the compounds co-eluted.

Micellar chromatography may have other advantages, like the possibility for achieving rapid gradient capabilities [48]. No re-equilibration is necessary after a micelle gradient since the concentration of monomer (i.e., the species distributed to the solid phase) in the aqueous phase changes very little with increasing micell-concentration. Another

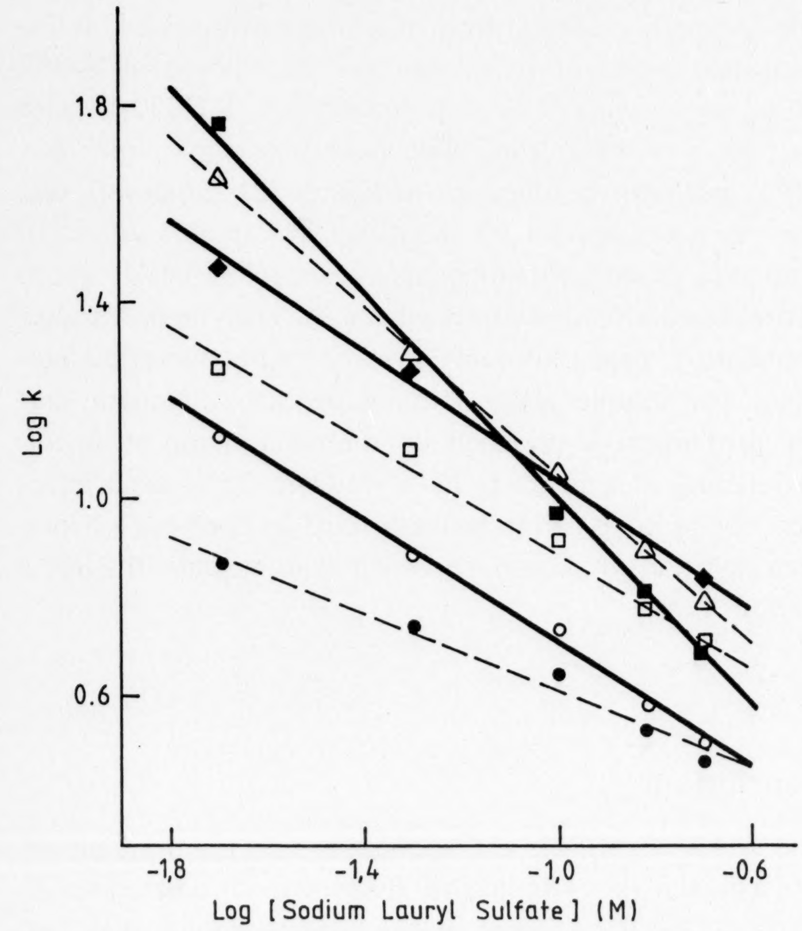

Fig. 7

Effect of sodium laurylsulfate concentration on retention.

● phenol, ○ p-nitro-aniline, □ benzene, ♦ nitrobenzene, ▲ toluene, ■ 2-naphtol [45].

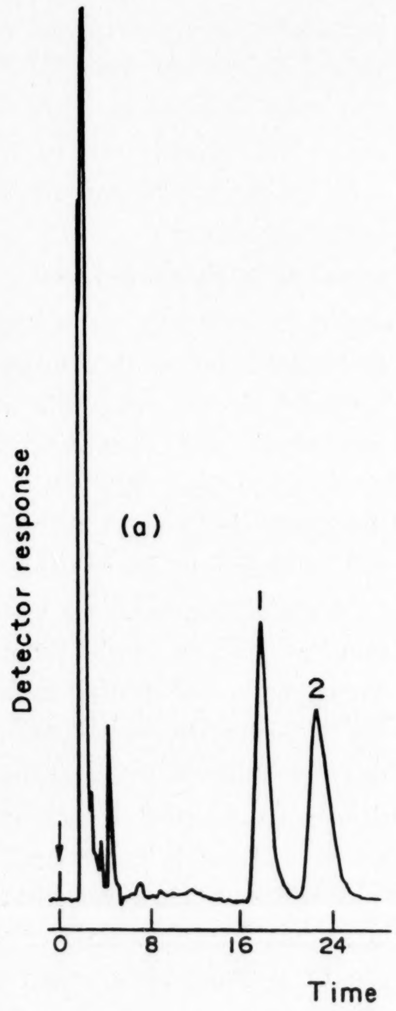

Fig. 8

Micellar chromatography on serum spiked with quinine (1) and quinidine (2).

Column: Supelcosil CN (25cm); mobile phase: 0.08 M aqueous Brij-35 with 10% propanol. Fluorescence detection [47].

phenomenon that could be exploited is the fact that certain compounds get an enhanced fluorescence (in some cases even the appearance of room temperature phosphorescence) when present in a more hydrophobic environment compared to an aqueous solution [49].

Odd Pre-Columns

In a carefully designed study, Cantwell et al. [6] investigated the possibilities of using the copolymer of polystyrene and divinylbenzene, XAD-2, as a pre-column for direct injection of plasma. The short, 20 × 2 mm, column was packed with 37–44 μm large particles and connected via the back-flush principle to the analytical column, LiChrosorb RP 18. The main advantage of using XAD-2 is due to the possibility of using a mobile phase with a high pH. It was pointed out that most plasma proteins have isoelectric points below 7, which makes using a higher pH for the precolumn (here 9.3) advantageous, since then their solubility in the aqueous phase is high. Large plasma volumes could be applied ($\leqslant$ 4 ml, most frequently 0.5 ml) and the analyte, the rather nonpolar drug metaqualone, was transferred to the analytical column by acetonitrile (30%) in citrate buffer pH 5.4. The precolumn lasted for about two weeks, while the analytical column could be used for more than 6 months.

Theophylline is beyond doubt the most frequently studied drug for direct injection techniques. In an uncommon approach, a size exclusion column (Waters I-125) was used for precolumn in front of the analytical reversed phase (Ultrasphere ODS) column [7]. A heartcut for 2 minutes after the macromolecular front, eluted by a buffer pH 7, was taken and transferred to the second column for elution with an acetate buffer pH 5 containing methanol (7%) and tetrahydrofuran (1%). 70 samples of buffer-diluted plasma could by analyzed per day.

An anion-exchange solid phase, based on a polyacrylamide gel substituted with aminoethyl-groups, was used for the isolation of homovanillic acid (HVA) and 5-hydroxy-indole-acetic acid (5-HIAA) from biological fluids (plasma, urine and CSF) [8]. During the direct injection of the biological fluid (200 μl), the mobile phase was buffer pH 5.5. A step-gradient to buffer pH 2.5 was then generated to transfer the acids to a short (20 × 3.8 mm) enrichment column packed with octadecylsilica. A backflush with the acidic buffer diluted with methanol (18%), and containing N,N-dimethyl-N-octylamine (DMOA, 0.5 mM), transferred the acids to the analytical column (Spherisorb ODS-2, 3 μm), 10 cm long. It was emphasized that silica gel-based anion exchangers could not be used due to unstable retention volumes. However, the polyacrylamide-based material is somewhat compressible, and an essential feature is the use of a short enrichment column in order to keep the backpressure low during the transfer of the acids. The presence of the tertiary aliphatic amine DMOA was necessary in order to receive a fast and quantitative recovery of the acids from the enrichment column. The detection was performed by a coulometric detector.

A related technique was applied for the quantification of catecholamines in plasma and urine [9]. A polyacrylamide gel substituted with phenylboronate, that selectively couples with catecholamines, was used in the precolumn (10 × 4.6 mm), with a slightly alkaline mobile phase. The complex is dissociated with phosphoric acid, which transfers the catecholamines to an enrichment octadecylsilica column (3 μm in 20 × 4.6 mm) conditioned by decylsulphate in a pH 5 buffer. The catecholamines are trapped as ion-pairs on the enrichment column top, and then transferred to the analytical column (octadecylsilica, 3 μl, 75 × 4.6 mm) by backflush with a mobile phase containing 25% of methanol. The adrenalines were detected fluorimetrically after coulometric oxidation and alkaline rearrangement to trihydroxyindole-derivatives post-column (Fig. 9). Similar to the application of the polyacrylamide anion exchanger, in this case a low backpressure over the first column is also essential and is achieved by using a very short enrichment column. Large plasma-volumes ($\leqslant$ 2 ml) could be applied automatically, even unattended over-night, and the lifetime of the phenylboronate gel was seemingly infinite.

A different kind of affinity packing material was recently introduced for the determination of phenytoin in plasma: an immobilized polyclonal immunoglobulin [10]. Silica was used as the basic solid phase, and the antibody was covalently attached to an organic silane derivative on the surface. A short pre-column (50 × 4 mm) was combined with an octadecylsilica (240 × 3.9 mm). 25 μl plasma was loaded onto the immunosorbent with phosphate buffer pH 7.4 as mobile phase. The complexed phenytoin was then transferred by backflush to the analytical column by a buffer-methanol (6+4 v/v) mixture. The pre-column continued to be stable even after three months' use.

An approach deviating from the others involves an on-line deproteinization of serum samples for analysis of hydrophilic compounds [11]. A polyvinylresin, BT 650-M, with particle size 44–88 μm, wide pore (exclusion limit: 5×10^6), and with butylgroups as ligands (850 μmol/ml), was used as a pre-column for the direct injection of serum. In a mobile phase containing perchloric acid (0.4%), serum proteins are effectively trapped and the analyte, in this case gentamicin, passes through directly to the analytical column. The mobile phase contains pentanesulphonate, and the gentamicin is enriched on the column top as an ion pair before elution starts by a gradient. After each injection, the proteins had to be washed off by applying a strong urea solution, a procedure which will increase the total analysis time.

Conclusion

The numerous studies and applications on the principle of direct injections of biological fluids into chromatographic systems clearly demonstrate that the technique now has matured to a stage where it can be used routinely in bioanalytical laboratories for the automated analysis of a large number of samples originating from, e.g., pharmacokinetic, toxicological and clinical studies.

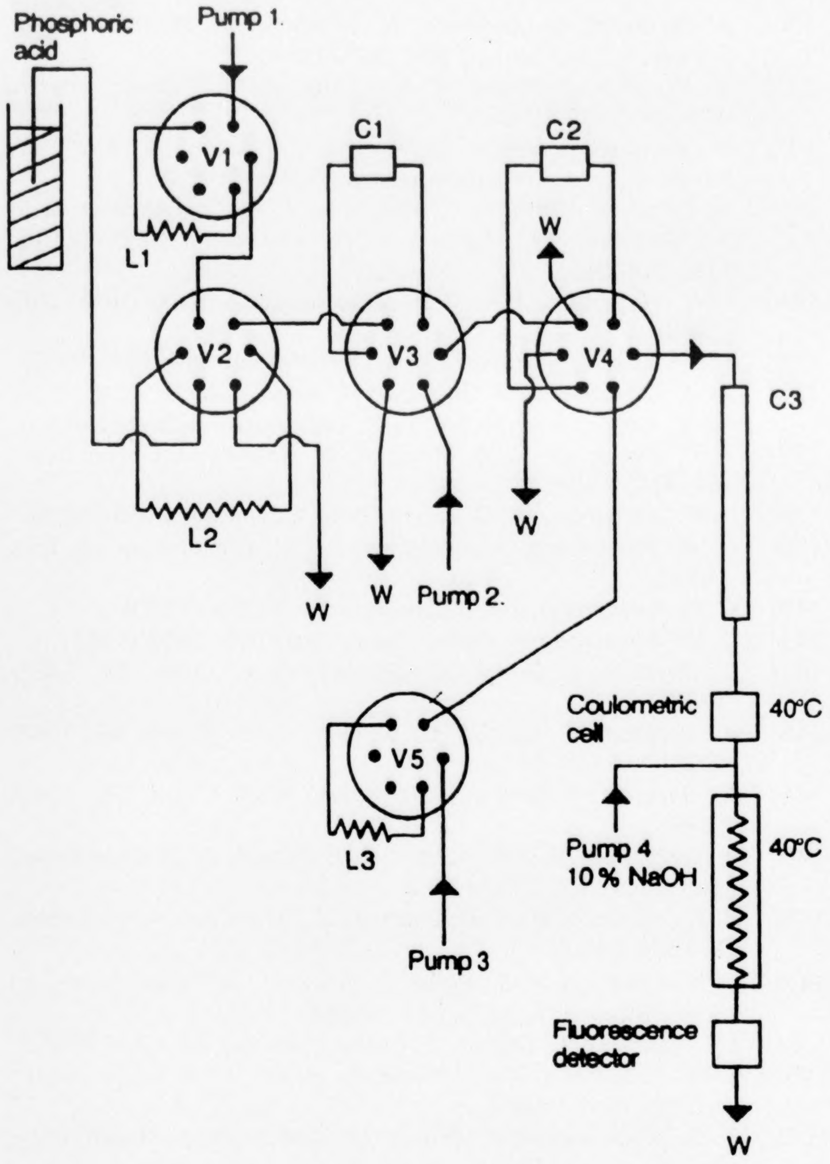

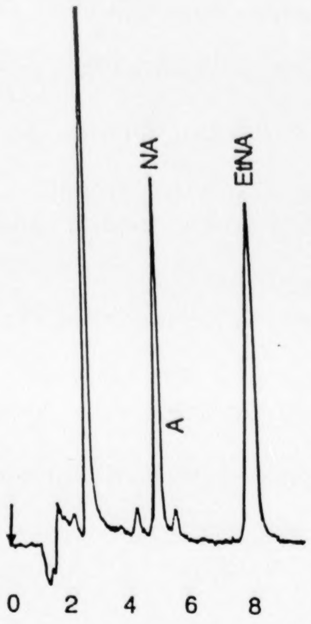

Fig. 9

Column-switching and post-column derivatization system for assay of catecholamines in plasma [9].

A C1 = phenylboronate column, C2 = enrichment column (C_{18}), C3 = analytical column (C_{18}), L1 = sample loop (1 ml), L2 = loop for phosphoric acid, L3 = loop for direct injection to analytical column, V_1-V_5 = 6-port switching valves.

B Chromatograms on catecholamines after direct injection of 1 ml plasma. NA = noradrenaline, A = adrenaline, EtNA = ethylnoradrenaline (internal standard).

Many different kinds of solid phases have been used, from simple silanized silica or hydrophobic polymers in broad applications, to supports with immobilized antibodies for highly selective isolations on the pre-column. An important feature of the technique of direct injection is that since the same pre-column can be used for all assays in a series of specimens, the risk for non-reproducibility of the solid phase, by within and between batch variations, is largely eliminated. This is in contrast to the case with off-line procedures [50], where a new pre-column is used for each sample.

The main problem with direct injection of biological fluids is the risk for protein-denaturation and -precipitation. There are two techniques that have thus far proved to be the most promising and useful in order to render as long a lifetime as possible to the pre-column: the so-called *"pre-column venting plug technique"* [19], where the injected sample is surrounded by an aqueous buffer in order to reduce the contact time between the plasma proteins and the organic modifier in the mobile phase; and *micellar chromatographic systems* [3], where the surfactants serve to solubilize the plasma proteins. The so-called "Internal Surface Reversed Phase" supports [5] also seem to be interesting alternatives. However, such systems have so far not been adequately tested for column stabilities in bioanalytical applications.

There are, however, also occasions where direct injection principles are unsuitable: when the analytes are chemically or biochemically transformed in the biological fluid, it may be necessary to rapidly transfer them to a non-biological environment by a liquid/liquid or liquid/solid distribution. Obviously, if only a single specimen has to be analysed, it can be directly injected into a suitable chromatographic system; the problem arises when there is a series of samples with unstable analytes that are to be analysed. However, in some cases it may be possible to stabilize the analytes by the addition of antioxidantia and/or enzyme inhibitors, and in this way make it possible to apply direct injections of the biological fluid.

The development of chromatographic systems aimed at the direct injection of biological fluids may take a longer time compared to off-line procedures. However, in routine bioanalytical laboratories with several thousands of specimens for the same assays, this initial eventual time loss is easily compensated by the more rapid final bioanalytical method based on the direct injection principle.

References

[1] *D. J. Popovitch, E. T. Batts, C. J. Lancaster*, J. Liq. Chromatogr. **1**, 469 (1978).

[2] *B. R. Manno, J. E. Manno, B. C. Hilman*, J. Anal. Toxicol. **3**, 81 (1979).

[3] *M. Arunyanart, L. J. Cline Love*, J. Chromatogr. Biomed. Appl. **342**, 293 (1985).

[4] *H. Yoshida, I. Morita, T. Masujima, H. Imai*, Chem. Pharm. Bull **30**, 2287 (1982).

[5] *I. H. Hagestam, T. C. Pinkerton*, Anal. Chem. **57**, 1757 (1985).

[6] *R. A. Hux, H. Y. Mohammed, F. F. Cantwell*, Anal. Chem. **54**, 113 (1982).

[7] *S. F. Chang, T. M. Welscher, R. E. Ober*, J. Pharm. Sci. **72**, 236 (1983).

[8] *P. O. Edlund*, J. Pharm. Biomed. Anal. **4**, 641 (1986).

[9] *P. O. Edlund, D. Westerlund*, J. Pharm. Biomed. Anal. **2**, 315 (1984).

[10] *B. Johansson*, J. Chromatogr. **381**, 107 (1986).

[11] *G. Tamai, H. Imai, H. Yoshida*, Chromatographia **21**, 519 (1986).

[12] *H. Breithaupt, J. Schick*, J. Chromatogr. **225**, 99 (1981).

[13] *B. R. Manno, J. E. Manno, C. A. Dempsey, M. A. Wood*, J. Anal. Toxicol. **5**, 24 (1981).

[14] *M. Riedmann, R. Schuster*, Hewlett Packard Application Note AN 232 (1983).

[15] *K.-G. Wahlund*, J. Chromatogr. **218**, 671 (1981).

[16] *T. Arvidsson, K.-G. Wahlund, N. Daoud*, J. Chromatogr. **317**, 213 (1984).

[17] *N. Daoud, T. Arvidsson, K.-G. Wahlund*, J. Pharm. Biomed. Anal. **4**, 253 (1986).

[18] *N. Daoud, T. Arvidsson, K.-G. Wahlund*, Acta Pharm. Suec. **23**, 65 (1986).

[19] *N. Daoud, T. Arvidsson, K.-G. Wahlund*, J. Chromatogr. **385**, 311 (1987).

[20] *N. Daoud, T. Arvidsson, K.-G. Wahlund*, J. Pharm. Biomed. Anal. Submitted for publication.

[21] *T. Arvidsson*, J. Chromatogr. Submitted for publication.

[22] *M. W. F. Nielen, R. C. A. Koordes, R. W. Frei, U. A. Th. Brinkman*, J. Chromatogr. **330**, 113 (1985).

[23] *M. W. F. Nielen, E. Sol, R. W. Frei, U. A. Th. Brinkman*, J. Liq. Chromatogr. **8**, 1053 (1985).

[24] *W. Roth, K. Beschke, R. Jauch, A. Zimmer, F. W. Koss*, J. Chromatogr. **222**, 13 (1981).

[25] *U. Juergens*, J. Chromatogr. **310**, 97 (1984).

[26] *W. Voelter, T. Kronbach, K. Zech, R. Huber*, J. Chromatogr. **239**, 475 (1982).

[27] *R. Huber, K. Zech, M. Wörz, Th. Kronbach, W. Voelter*, Chromatographia **16**, 233 (1982).

[28] *W. Roth*, J. Chromatogr. **278**, 347 (1983).

[29] *J. B. Lecaillon, C. Souppart, F. Abadie*, Chromatographia **16**, 158 (1982).

[30] *A. Nazareth, L. Jaramillo, B. L. Karger, R. W. Giese, L. R. Snyder*, J. Chromatogr. **309**, 357 (1984).

[31] *H. Yoshida, I. Morita, T. Masujima, H. Imai*, Chem. Pharm. Bull. **30**, 3827 (1982).

[32] *H. Yoshida, I. Morita, G. Tamai, T. Masujima, T. Tsuru, N. Takai, H. Imai*, Chromatographia **19**, 466 (1984).

[33] *H. Imai, H. Yoshida, T. Masujima, I. Morita, K. Matsuura, A. Nakamuru, K. Katayama, H. Matsuo*, Anal. Lett. **16**, 1109 (1983).

[34] *I. H. Hagestam, T. C. Pinkerton*, J. Chromatogr. **351**, 239 (1986).

[35] *S. E. Cook, T. C. Pinkerton*, J. Chromatogr. **368**, 233 (1986).

[36] *T. J. Szczerba, L. J. Glunz, J. D. Rateike, S. R. Patel, J. A. Perry*, Report from Regis Chem. Co., Morton Grove (1986).

[37] *T. C. Pinkerton, J. A. Perry, J. D. Rateike*, J. Chromatogr. **367**, 412 (1986).

[38] *D. W. Armstrong, R. Q. Terrill*, Anal. Chem. **51**, 2160 (1979).

[39] *D. W. Armstrong, S. J. Henry*, J. Liq. Chromatogr. **3**, 657 (1980).

[40] *D. W. Armstrong*, J. Liq. Chromatogr. **3**, 895 (1980).

[41] *D. W. Armstrong, F. Nome*, Anal. Chem. **53**, 1662 (1981).

[42] *A. Berthod, I. Girard, C. Gonnet*, Anal. Chem. **58**, 1356 (1986).

[43] *A. Berthod, E. Girard, C. Gonnet*, Anal. Chem. **58**, 1359 (1986).

[44] *A. Berthod, I. Girard, C. Gonnet*, Anal. Chem. **58**, 1362 (1986).

[45] *P. Yarmchuk, R. Weinberger, R. F. Hirsch, L. J. Cline Love*, Anal. Chem. **54**, 2233 (1982).

[46] *F. J. DeLuccia, M. Arunyanart, L. J. Cline Love*, Anal. Chem. **57**, 1564 (1985).

[47] *L. J. Cline Love, S. Zibas, J. Noroski, M. Arunyanart*, J. Pharm. Biomed. Appl. **3**, 511 (1985).

[48] *J. S. Landy, J. G. Dorsey*, J. Chromatogr. Sci 22, 68 (1984).

[49] *D. W. Armstrong, W. L. Hinze, K. H. Bui, H. N. Singh*, Anal. Lett. **14**, 1659 (1981).

[50] *R. D. McDowall, J. C. Pearce, G. S. Murkitt*, J. Pharm. Biomed. Anal. **4**, 3 (1986).

Received: Aug. 2, 1987
Accepted: Aug. 27, 1987
F

Preparative Liquid Chromatography

G. Guiochon* / Anita Katti

University of Tennessee, Chemistry Department, Knoxville, TN, 37996-1600, and
Oak Ridge National Laboratory, Analytical Chemistry Division, Bldg 4500 South, M.S. 120, P.O. Box X,
Oak Ridge, TN, 37831, USA

Key Words

Column liquid chromatography
Preparative scale
Operating parameters
Optimization

Summary

Historically, liquid chromatography has been a preparative technique. Its applications have been limited, however, until a decade ago. The needs of modern chemical, pharmaceutical and biochemical industries have motivated this period of phenomenal growth which is being witnessed now.

Novel packing materials, new packing technologies, and advancements in instrumentation and process technologies have appeared in rapid succession. Instruments using columns with diameters ranging from a few inches to a few feet, can be packed with efficiencies comparable or better than analytical columns having the same packing material. This permits the development of new applications covering a wide variety of problems.

The empirical approach, followed until recently for the development of new applications, is being improved by insights derived from a better understanding of the theory of large concentration chromatography. With increased computer power and a greater comprehension of the theoretical aspects, a fundamental approach to design and optimization of the operating parameters is being developed. Investigation of the components of the cost of industrial production is also in its early stages.

Historical trends, theoretical treatments, column technologies, operating modes and guidelines for optimization will be discussed and reviewed.

I Introduction and Scope

By its very principle, chromatography is a preparative technique. For in the early days of chromatography where modern electronic detectors were not available: the column effluent had to be collected and then analyzed. Thus, in order to gain information about the sample composition, a "preparative" separation was performed and subsequent analysis of the fractions provided information on the sample purity. In the sixties, major advances in instrumentation technology allowed analysts to circumvent the preparative operation and continuously monitor the column effluent. Then, analytical chromatography made its debut and the field has since flourished, leaving preparative liquid chromatography by the wayside. The growth of biotechnology and recombinant DNA techniques have demanded the development of nontraditional separation methods to purify the delicate bioproducts on the laboratory, as well as the industrial, scale. Therefore, preparative chromatography is being revisited, but, now, it is essential to rethink and transcend the procedures generated for analytical chromatography to solve the new problems with new approaches.

The basic difference between analytical and preparative chromatography is not the quantity of sample to be separated, but the purpose of the separation and the nature of the information obtained. There are four major categories by which the nature of the separation can be distingushed, with many intermediate possibilities:

1. – In analytical chromatography, as it is classically pursued, we need information regarding the composition of the mixture. We do not need to collect the separated components to a specific degree of purity. Although chromatography separates the components of the analyzed mixture, providing pure compounds diluted in the mobile phase, the eluent and the eluites are promptly considered as waste. Thus, the cost of the separation is measured in terms of dollars per analysis or per bit of information, not in terms of dollars per pound of product prepared. Chromatography is used because it is fast, powerful, convenient and flexible, not because it prepares pure compounds. The information, that is the detector signal, is the highly valued product of the analysis and we will fight for shorter time constants, smaller detector cells, lower signal noise and lower detection limits. The design of the waste line is usually irrelevant, except in one case: post-column reaction detectors, in which case again information is looked for, this time through chemical reaction. This introduces the second type of application.

0009-5893/87 0165-25 $03.00/0

© 1987 Friedr. Vieweg & Sohn Verlagsgesellschaft mbH

2. — In a number of applications, covering analytical as well as preparative chromatography, the chemist is not finished after the compounds have been eluted. Further identification is needed, and spectrometric analyses or chemical reactions have to be performed on the purified components, or, at least, on some of them. There is a fine separation between (i) on-line LC/MS, where the eluent is immediately sprayed in the MS source, (ii) reaction detectors, which are chemical reactors placed on-line with the chromatographic column but where the solutes may stay several minutes before the reaction is complete, (iii) on-line LC/FTIR, where the eluate is sprayed on a rotation disk, the eluent vaporized and the solute transferred to the spectrometer, (iv) on-line NMR, where elution is interrupted to let the sample stay in the probe long enough to permit the acquisition of the requested number of scans, and (v) off-line NMR, where the appropriate fractions are collected and run as separate samples. Here again, the cost of the separation is related to the information obtained and this depends essentially on the time spent by the investigators, which has to be minimized.

3. — Whereas the previous two categories covered preoccupations which are essentially analytical in nature, there are many applications where information is needed about the physical, chemical or biological properties of the chemicals contained in the sample. However, this requires important subsequent manipulations and possibly the preparation of rather large amounts of these products. This occurs, for example, in the development of new drugs where data on the toxicity and the efficiency of the new product is urgently needed. Money is rarely of primary importance: the cost of the separation has to be compared to the value of the time saved by the company. Until quite recently, preparative HPLC was used to prepare the products needed for research and development. This is why there is such a large number of applications in this area, and why little attention has been paid to process optimization, in the chemical engineering sense of the term. Other processes, sometimes involving completely different synthetic routes, were developed for industrial production.

4. — Finally, HPLC can be used to prepare products for sale. Then the cost of the product is an essential component of the "bottom line". Maximum production per unit time must be achieved in order to save on investment and running costs. The experimental conditions selected will be quite different from those used for the applications described in the previous sections, since the assumptions are different. The chemical engineer becomes the architect of the process, not the chromatographer we know. In fact we may not even recognize the apparatus.

Recent trends in HPLC have involved the development of industrial processes for the preparation of new products requiring the use of preparative HPLC to purify or extract the component(s) of interest. This explains the attention paid to new approaches such as *overloaded elution chromatography* and *displacement chromatography*, which will be discussed extensively later in this review. The current theoretical framework is not adequate yet, as it deals with linear chromatography. Optimization procedures are not available since most of the previous work has centered around maximizing the amount of information obtained, not the amount of product prepared. Instrumentation, often designed by analytical chromatographers, has many shortcomings. The packing materials have never been studied with preparative HPLC applications in mind; we do not even know what parameters control or even enhance loading capacity. Few descriptions of large scale applications have been published so far, because the conditions under which the chemists work who produce chemicals are far different from those under which analysts work. Although information collected by both groups is often confidential, the latter may speak much more freely than the former about the way they have obtained this information.

Many papers published in the scientific literature discussing preparative liquid chromatography deal with the problems encountered in categories 2 and 3 described above, that is preparative applications in the analytical laboratory or for development applications. In the last case, the work is often entrusted to the analyst "who knows what chromatography is all about", and brings his prejudices at the same time as his expertise. Sometimes, a chemical engineer who has never heard of chromatography before is in charge. He comes with his ignorance as well as with the time proven methods of his art. As a result, the field looks very much like a collection of exercises in chemical engineering, carried out by excellent organic and/or analytical chemists. The book recently published by Verzele [1] is an excellent review of this work. Its reading is strongly recommended to anyone interested in problems involving most aspects of preparative HPLC. On the other hand, the book published by Wankat [2] illustrates well the advantages and prejudices of the chemical engineering viewpoint. The fact that the conventional modes of operation of a chromatographic column, elution or displacement, are batch modes and that continuous operation is nearly impossible as noted by the latter author, is certainly a serious drawback. However, it does not make the process impractical for industrial scale applications.

The field of preparative scale HPLC is now very large. A computer search of the literature has produced more than 700 references by the end of 1986. Within the time and space allowed, it would have been difficult to review the whole subject properly. Therefore, we have focused our work on industrial process problems, where it is important to address issues dealing with the theory of the process, the properties of the packing materials, the performance of the separation units and the physical properties of the products involved. This review includes a discussion of the theoretical aspects of column liquid chromatography, optimization, column technology and instrument development and presents a few applications.

II History

Column liquid chromatography (LC) was discovered at the beginning of the century by Tswett, while studying the composition of plant pigments [1, 3, 4]. Because of the nature of analytical chemistry at the time, all separations had to be preparative in nature. There was no detector to place on line to monitor the composition of the effluent. Accordingly, Tswett realized the potential of chromatography as a preparative technique. He even discussed in 1910 the processes of elution and displacement [5]. Unfortunately, with a few exceptions [6–8], Tswett's insights were resisted strongly and the field remained dormant for several decades.

The work of Lederer, Kuhn and Winterstein [9–11] demonstrated the usefulness of chromatography as a preparative method which led to numerous applications. Among many important early contributions, we must note the clear and systematic definition by Tiselius of the three modes by which one can operate a chromatographic column, namely, elution, frontal analysis and displacement [12]. Until the early forties, however, LC was mostly used for the purification of compounds in the fields of organic chemistry and biochemistry. The progressive realization that adsorption chromatography could provide a high selectivity few other separation techniques could offer paved the way for several large scale applications in the mid-forties, such as the isolation of oxides of rare earth elements for nuclear applications and the purification of petroleum products [13].

The development of large scale purification schemes for the separation of rare earth metals stemmed from the demands of physicists who became interested in their unusual nuclear properties in the early fortis [16]. These investigations were carried out under the auspices of the Manhattan project. Purification of the rare earth elements by ion-exchange chromatography was primarily conducted by Spedding et al. [14–19], who were able to separate various oxides by displacement chromatography. Fig. 1 presents a chromatogram whereby they separate Samarium, Neodymium and Praseodymium on Aberlite IR-100, using a 22 mm i.d., 120 cm long column. Numerous investigations on the effects of the various operating parameters were carried out. A pilot plant involving sixty eight 4- and 6-inch diameter columns, in a four step cascade was developed to achieve high purity products in large quantities [15–18].

In the late forties and early fifties, the American Petroleum Institute used preparative LC to fractionate samples of virgin crude oil and petroleum distillates to determine their content of paraffins, naphthenes, olefins and aromatics and to isolate many pure compounds which were identified for the first time in crude oil or crude oil extracts [20]. In addition to working on the laboratory scale, a team led by Rossini [21–23] assembled and tested a 3/4" i.d., 52.4 foot long column, a schematic of which is shown in Fig. 2. The column was packed with 3.7 kg of 200–235 mesh silica gel. It was operated in the displacement mode, using isopropanol as displacer. The composition profile of the column eluent is reproduced in Fig. 3.

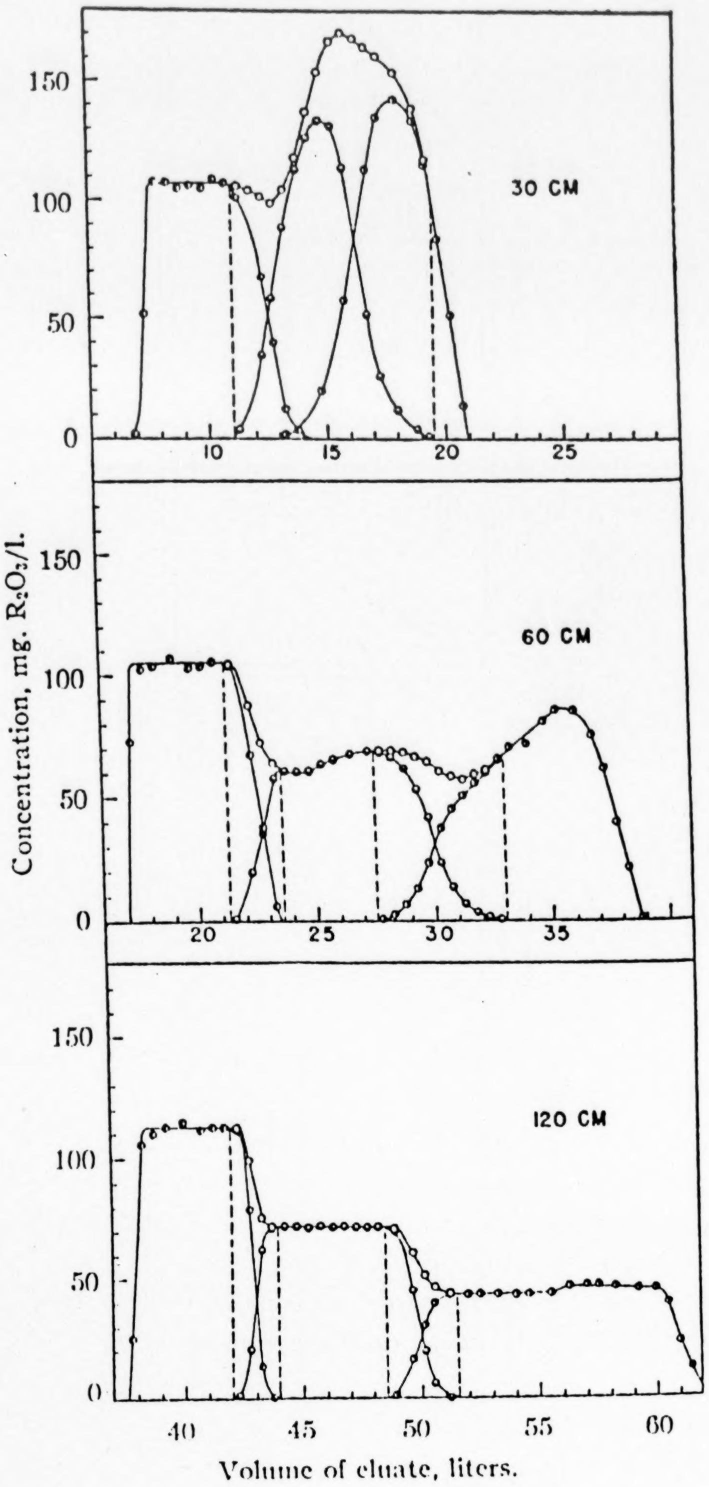

Fig. 1

Separation of Sm203, Nd203 and Pr6011 by displacement chromatography with a 0.01% citrate solution, pH 5.3, as the displacer.

Column: 22 mm i.d., 30, 60, and 120 cm long, packed with Amberlite IR-100 resin.

Reproduced from *F.H. Spedding, E.I. Fulmer, T.A. Butler,* and *J.E. Powell,* J. Am. Chem. Soc. **72,** 2349 (1950), by courtesy of the American Chemical Society.

In the early seventies, Union Oil developed and patented a chromatographic system based on the principle of a simulated moving bed [24]. Plants have been built and are operated for the fractionation of various petroleum distillates, for example, the selective separation of p-xylene, o-xylene and ethylbenzene from the C7-C8 aromatic fraction, the separation of olefins from paraffins in feed mixtures of hydrocarbons having ten to fourteen carbon atoms and for the separation of fructose and dextrose from corn syrup. It has been shown that chromatography, which is normally a batch process in both the elution and the displacement mode, could be turned into a continuous process if the stationary phase were forced to move along the column, Physically moving the stationary phase bed is impractical. However, the moving bed operation can be

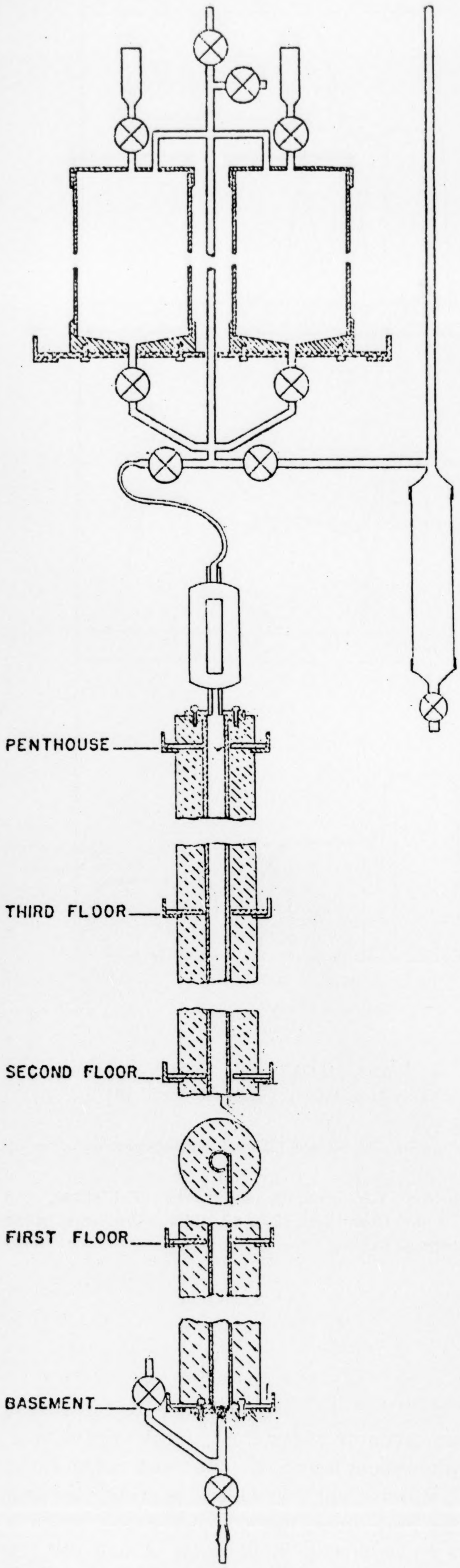

Fig. 2

Assembly of a 52 foot Adsorption column.

Reproduced from *B.D. Mair, A.L. Gaboriault,* and *F.D. Rossini,* Ind. Eng. Chem. **39**, 1072 (1947), by courtesy of the American Chemical Society.

simulated, which is accomplished in the Union Oil process by the use of a number of columns placed on-line and connected to a rotary valve, as shown in Fig. 4. The position of the desorbent, extract, feed and raffinate can be switched in a practical way permitting continuous operation of the plant.

In the late seventies, Elf developed a process to extract a large proportion of the n-pentane contained in light petroleum distillates to prepare high octane gasoline. This process is based on the injection of large pulses of feed on a Molecular Sieve column. The branched pentanes and hexanes are not retained and elute as a large unretained pulse. In this process, n-pentane is strongly retained and elutes as a very wide band. In practice, when feed pulses are injected sequentially at sufficiently high a frequency, the eluent contains a constant concentration of n-pentane, which is given by the product of the n-pentane concentration in the feed and the ratio of the pulse duration to the pulse period. The elution bands of isoparaffins are collected as a high octane gasoline. With this gas chromatographic process, it is easy to decrease the n-pentane concentration in the gasoline by about half. The plans to build a 100,000 tons per year plant were cancelled due to local difficulties independent of the economics of the process.

Several attempts at operating continuously the chromatographic process by moving the column relatively to the feed injector and the fraction collector were made in the seventies. Barker used a rectangular cross-section column, with an open side sliding along a plate pierced by several holes for the feed injection and the collection of a "retained" (i.e., moving backward, in the same direction as the column) and an "unretained" (i.e., moving forward, in the same direction as the carrier gas) fraction [25]. Scott et al. used a rotating, annular column [26]. The feed is injected in a fixed point. The solutes follow helicoidal paths in the annular column and exit at fixed places were are placed the fraction collected. Although this process is continuous, only a fraction of the column volume does work at any given time. These processes are complex. Either because of excessive complexity and non-competitive performance, or because they were early for the times they have not been accepted.

In conclusion, it is interesting to note that the early applications of preparative LC involved operating in the displacement mode, where by definition chromatography is performed in non-linear conditions. Nowadays, the approach to preparative scale chromatography is somewhat different. Twenty years of successful applications of LC to analytical separations, where column "overloading" is scrupulously avoided, have made people extremely reluctant to perform separations under conditions which deviate strongly from analytical practice. The present trend seems to be toward the use of large diameter columns operated in the elution mode, with the injection of rather large volumes of dilute solutions, in order to achieve "volume overloading", with only moderate "concentration overloading". We are of the opinion that, in most cases, this is an economical non-sense. We should learn again the properties of non-linear chromatography.

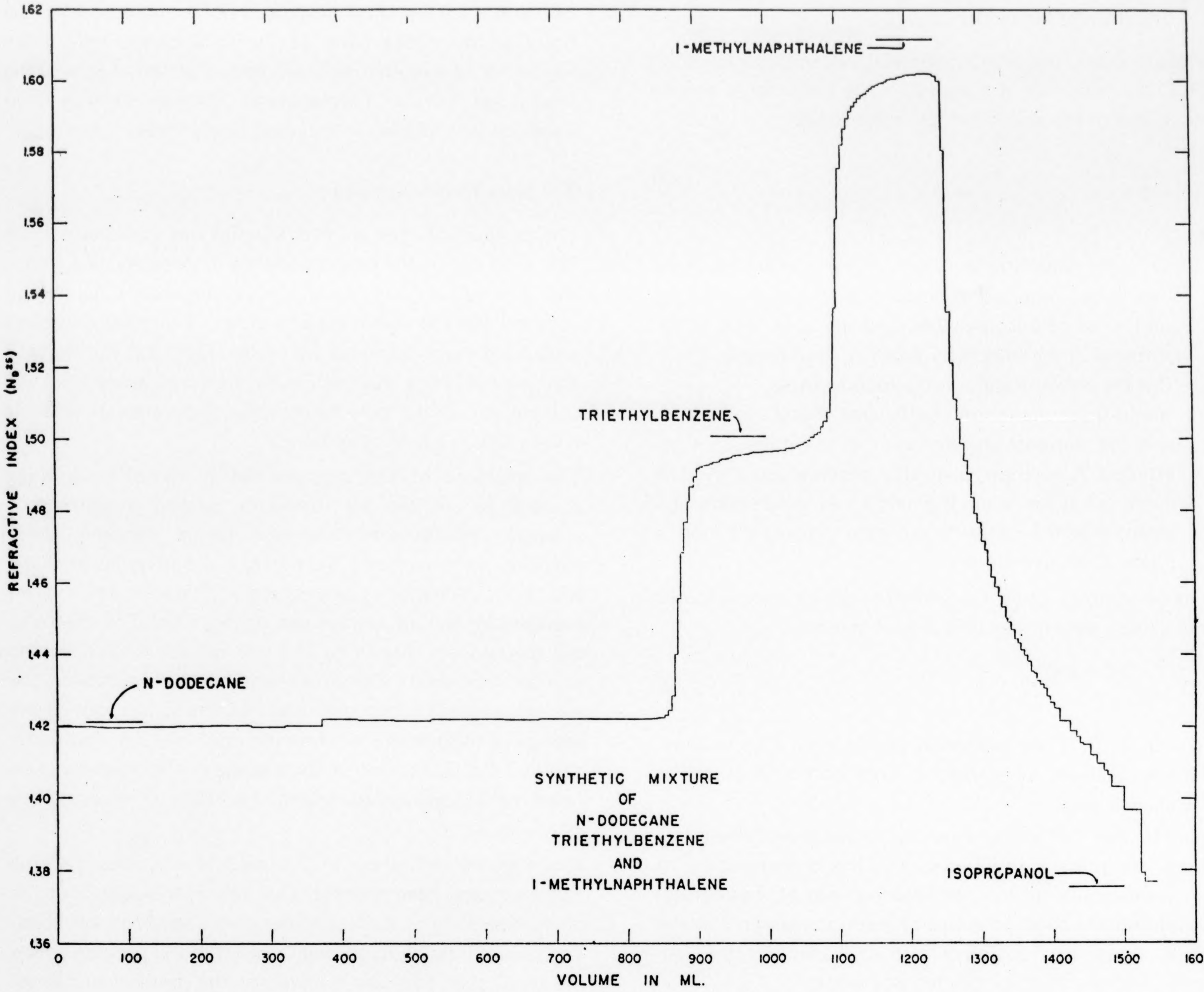

Fig. 3

Separation of a synthetic mixture of n-dodecane, triethylbenzene, 1-methylnaphalene with isopropanol as the displacer on a 3/4″ i.d., 52.4′ column packed with silica gel.

Reproduced from *B.D. Mair, A.L. Gaboriault,* and *F.D. Rossini,* Ind. Eng. Chem. **39**, 1073 (1947), by courtesy of the American Chemical Society.

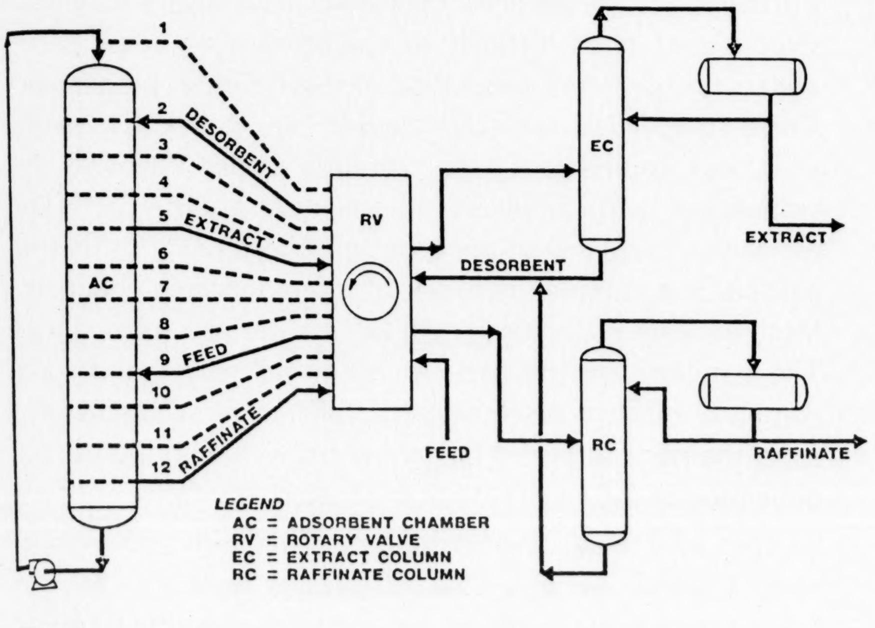
1
2
3
4
5
6
7
8
9
10
11
12
DESORBENT
EXTRACT
FEED
RAFFINATE
AC
RV
EC
RC
DESORBENT
EXTRACT
FEED
RAFFINATE
LEGEND
AC = ADSORBENT CHAMBER
RV = ROTARY VALVE
EC = EXTRACT COLUMN
RC = RAFFINATE COLUMN

Fig. 4

Chromatographic system based on a simulated moving bed.

Reproduced from *D.B. Broughton,* Sep. Sci. Tech. **19,** 723 (1984), by courtesy of M. Dekker, Inc.

III Theory of Non-linear Chromatography

The chromatographic problem is to relate the concentration profile of the band at the outlet of the column to the equilibrium isotherm, the mass transfer kinetics and the profile of the injection band.

The classical approach to the solution of these problems in chemical engineering is to write the mass balance equations of the chemical species involved, the mass transfer kinetics and to solve the system of partial differential equations obtained. This is a task of major importance and has not been successfully completed, due to the enormous difficulties arising from the mathematical properties of the system obtained. These problems have been reviewed in detail [27, 28]. Some excellent results have been reached for simplified problems derived by using different sets of additional assumptions. We review here the present state of the problem.

A – Equilibrium Isotherms

In many cases, the compounds and systems considered in HPLC are such that a Langmuir type isotherm is a good description of the experimental isotherm [29]:

$$Q = \frac{aC}{1 + bC} \tag{1}$$

where:

- Q is the concentration (bulk or surface or "apparent bulk", i.e., reported as amount of sorbed material per unit mass of adsorbent)material per unit mass of adsorbent) in the stationary phase at equilibrium,
- C is the concentration in the mobile phase,
- a and b are numerical coefficients. Both are positive. a is the slope of the isotherm at the origin (the coefficient K in linear, analytical chromatography). The curvature at the origin is given by –ab, where the – sign means that the isotherm is curved towards the mobile phase concentration axis.

In more complex cases, the isotherm can be approximated satisfactorily by a higher polynomial quotient:

$$Q = \frac{aC + a'C^2}{1 + bC + b'C^2} \tag{2}$$

where a, a', b, b' are numerical coefficients. This relationship may account for Langmuir type isotherms as well as for S-shaped ones.

Eqs. (1) and (2) apply to pure compounds. When two solutes are present simultaneously, the concentration of each component in the stationary phase at equilibrium depends on the concentrations of both components in the mobile phase. In the simple case of Langmuir type isotherms, we have the two coupled isotherms:

$$Q_1 = \frac{a_1 C_1}{1 + b_1 C_1 + b_2 C_2} \tag{3}$$

$$Q_2 = \frac{a_2 C_2}{1 + b_1 C_1 + b_2 C_2} \tag{4}$$

where:

- Q_1 and Q_2 are the concentration of the two components, 1 and 2, in the stationary phase, at equilibrium,
- C_1 and C_2 are their concentrations in the mobile phase,
- a_1, a_2, b_1, b_2 are numerical coefficients. The ratio a_1/a_2 is equal to the relative retention of the two compounds in analytical chromatography.

When the adsorption isotherms are more complex, it is possible to generalize eq. (2) for the case of a binary mixture. When a mixture with more than two components is studied, a system of equations, with as many equations as there are compounds, similar to eqs. (3) and (4) for the two components system can be written. Nevertheless, the solution of the two component problem is sufficient to explain the mechanism of separation in chromatography. It is probable that the solution of a three component problem is all that is needed to calculate the elution band profiles of complex mixtures: interaction between closely eluted components are strong enough to lead to the onset of the displacement effect at moderate concentrations; but the formation of the displacement train is prevented by the finite width of the band of the third compound, which results in its eventual collapse into a series of interfering overloaded bands. Displacement usually involves two components and their interaction, rarely three.

B – Mass Transfer Kinetics

The problem of mass transfer kinetics was discussed for the first time within the context of chromatography by Lapidus and Amundson [30]. Various equations were suggested to account for the radial mass transfer. The most complete ones have been discussed by Huber [31] and by Horvath and Lin [32]. The main difficulty, however, arises from the complexity of the chromatographic phenomenon when it takes place in a packed column.

The structure of the column bed is complex. A huge number of particles are irregularly packed. A pattern of strongly anastomozed channels forms between these particles. In most cases the particles are irregular in shape and their dimensions are crudely characterized by an average size and an average size distribution. The choice of the method for measuring the size influences directly the number obtained. For irregularly shaped particles, the average dimension (optical methods), the square root of the average of the diameter squared (permeability, i.e., hydraulic data) or the cubic root of the average of the diameter cube (mass or volume measurement, i.e., Coulter counter) are different.

Whatever the definition of the particle size, most packing materials used have a rather wide size distribution, but the random packing of these particles gives a heterogeneous bed. The stream lines going through regions in the packing where the density of particles is lower, or the particles are larger than average, move much faster than those going through other regions where the particle density is larger than average and their size smaller. This generates regions in the column cross-section where the average velocity is larger than in others and increases the time required for the achievement of radial equilibrium by diffusion inside the band. Thus, it contributes much to band broadening.

Furthermore, the particles themselves have a very complex structure which is difficult to characterize by a few parameters for use in the calculation of mass transfer properties. These properties, already studied in connection with analytical applications, are currently under intensive investigations with emphasis on the mass transfer of large molecules (proteins) at high concentrations [33]. Inside the particle is a complex network of interconnected channels. Most packing materials for HPLC are derived from silica. The structure of the particles seems to correspond to a complex, random assemblage of spheres of all diameters, from the silica ion up. This model fits well with the fractal dimension of 2.8 reported for this material [34].

Be that as it may, it is possible to distinguish two mobile phase fractions, interparticle and intraparticule. The former flows between the particles and occupies a volume fraction of the column equal to the external porosity. The latter is stagnant and fills the inner porosity of the packing. In the flowing solvent, mass transfer is by molecular diffusion across the streamlines and across the eddies which form between the particles. Molecules at the center of the streamlines drift a long time before entering a particle. Eddies, however, contributes also to mass transfer, by tearing the streamline pattern. In the stagnant solvent, mass transfer is entirely by molecular diffusion. It is slowed down by the complex structure of the interconnected network of channels inside the particles and by their tortuosity. The transfer across the boundary between stagnant and flowing mobile phase is not instantaneous either. Finally, the kinetics of adsorption – desorption may be important in some cases. Whereas there are plenty of papers dealing with band broadening in analytical chromatography [35], there has been little theoretical or experimental study on the influence of kinetics on band profiles at large concentrations. On the other hand, the influence of the rate of complex dissociation in affinity chromatography on the elution band shape has been pointed out by Carr [36].

In the general case, the kinetic equation relates the concentration of the solute in the mobile and stationary phase, and may be written:

$$\frac{dq}{dt} = k_a (S_o - q) - k_d q \tag{5}$$

where:

- q is the concentration of solute in the stationary phase, at time t,
- S_o is the concentration of binding sites (liquid solid or affinity chromatography),
- k_a and k_d are the rate constants for adsorption and desorption, respectively.

The complexity of the kinetic equations derived in the general case is such that the theoretical problem of chromatography can be solved only for linear isotherms. The result is a Gaussian profile at zero solute concentration, a case of limited interest in preparative experimental parameters, and from this mode the plate height equation is derived [37]. Recently, Carr et al. [36] has derived a solution for a finite concentration band, with a slow Langmuir kinetics of complex dissociation (affinity chromatography). Previous work in this field has been done by Giddings [38] and by Villermaux [39]. The calculated profiles are in striking agreement with the experimental ones. The general problem, finite mass transfer kinetics and non-linear isotherms, does not have an analytical solution and still awaits an algorithm for the calculation of a correct numerical solution.

Most other authors have assumed infinitely fast mass transfer kinetics and negligibly small axial diffusion, which means an infinite column efficiency [40]. This is the classical assumption of ideal, non-linear chromatography. It is not a realistic model, but it offers the advantage of singling out the thermodynamic effect, i.e., the influence of the non-linearity of the isotherm on the band profile.

Another popular approach assumes that the kinetics of mass transfer is independent of the concentration. Although this would not be valid under the experimental conditions studied by Carr, it is a very reasonable assumption in most cases where preparative HPLC is carried out. Then, the kinetics of mass transfer are essentially controlled by diffusion. It is well known that diffusion coefficients vary quite slowly with the concentration, at least in the concentration range experienced in HPLC, where it rarely exceeds a few percents at the column exit and 10–15% at the inlet. It may, then be assumed that the kinetics of mass transfer is accounted for by an apparent diffusion coefficient, which is directly related to the column HETP at zero concentration. This approach has been used by Houghton [41], Jaulmes et al. [42, 43], Guiochon et al. [44]. The apparent diffusion coefficient is equal to the molecular diffusion coefficient of a solute which would give the same Gaussian concentration distribution in a simple diffusion experiment lasting a time equal to the retention time, where an infinitely narrow plug (Dirac delta function) is placed at time zero, in a motionless fluid. After time t, the concentration profile is Gaussian, with a variance given by the Einstein relationship:

$$[\sigma]^2 = 2\,Dt \tag{6}$$

where:

- $[\sigma]$ is the standard deviation of the Gaussian profile,
- D is the apparent diffusion coefficient,
- t is the time.

The variance of a Gaussian band profile in chromatography (linear isotherm or zero concentration) is related to the column length and HETP by the classical relationship [45]:

$$[\sigma]^2 = H\,L \tag{7}$$

where:

- H is the column HETP,
- L is the column length.

Thus:

$$D = \frac{HL}{2\,t_R} \tag{8}$$

where:

- t_R is the retention time of the studied compound, under analytical conditions (very small sample size).

C – Injection Function

The injection function constitutes the boundary condition for integration of the system of partial differential equations describing the chromatographic problem (see next section). This system describes the propagation of the input profile and its progressive change of shape arising from the fact that a velocity is associated with the concentration of the profile and this velocity is a function of the concentration [27, 46, 47].

The major types of input functions are:

- a rectangle for elution and overloaded elution. Depending on the size of the rectangle, it is possible to distinguish between volume overload (broad shallow rectangular injection, linear chromatography, see ref. [48] and [49] and concentration overload (i.e., non-linear chromatography).
- a rectangular step input as in frontal analysis. This step may originate from a previous step in concentration

(typical situation in the determination of isotherms) or from the pure eluent.

- a rectangular injection followed by a step of a more strongly retained compound: these are the conditions for displacement chromatography. This method has been traditionally studied using the H-transform [50, 51] and an equivalent theory by Rhee and Amundson [52], which is an approximate solution to the chromatographic problem, within the frame of the ideal model.

Other types of input functions should be possible. In practice, a rectangular injection is the ideal goal, while the experimental result is often an exponential rising front, followed by an exponential decay. As long as the time constant for this decay is small compared to the band width of the Gaussian profile obtained under the same experimental conditions, but with a very low concentration of sample, the influence of this decay on the final band profile will remain negligible [53].

D – Mass Balance Equations

The mass balance equation for one solute is given by:

$$\frac{d}{dt}(C_s + C_m) + \frac{d(uC_m)}{dz} = D\frac{d^2 C_m}{dz^2} \qquad (9)$$

where:

- C_s and C_m are the concentrations of solute in the stationary and the mobile phase, respectively,
- u is the mobile phase average velocity,
- z is the absissa along the column,
- t is the time,
- D is the molecular diffusion coefficient (the term in the RHS of eq. (9) accounts for axial diffusion).

It is important to realize that the concentrations C_s and C_m in eq. (9) are not related by the isotherm equation (eqs. (1) to (4)). The relationship between these two concentrations is given by the kinetics equation (eq. (5)). Combination of this equation with eq. (9) gives the system of partial differential equations which makes the classical chemical engineering model of chromatography.

Before discussing the methods used to solve this problem, two remarks are in order. First, for the sake of simplicity, eq. (9) is written neglecting the phase ratio, i.e., the relationship between concentrations in the two phases and actual amounts of compounds. The proper coefficients must be introduced in the equation to that effect. Secondly, no equation has been written for the mass balance of the mobile phase. This is again a simplifying assumption, which is arguable. It originates in part in the confusions associated with the definition of concentrations in an adsorption system [54]. It is assumed here that the mobile phase is not sorbed. This is not true, of course. The error can be serious in some cases of reverse phase chromatography, when strong organic solvents are used. This assumption should be revisited some time.

E – Approximate Solutions of the System

The system of equations obtained for the model is intractable. There is no analytical solution, and numerical solutions have proven impossible to program so far. This is not only due to the complexity and length of the computation, not a completely negligible problem (see below), but is due to the mathematical properties of the system [28]. Programs written without careful study of the numerical analysis involved give unacceptable solutions, due to the numerical instabilities of conventional algorithms in this case.

Simplifications are in order. The first one regards the kinetics equation. Three approaches have been used:

- keep the kinetic equation, but assume a linear isotherm. This will apply to problems encountered in analytical chromatography, where the kinetics of adsorption – desorption are slow, or in analytical affinity chromatography at low or moderate concentrations [38, 39]. In the case where the concentration is small and the kinetics are essentially controlled by diffusion, the problem has an exact analytical solution, a Gaussian profile, and an HETP equation is derived [31, 32].
- keep the kineticequation and calculate an approximate analytical solution. The results obtained for the elution profile of a single, pure compound with a non-linear isotherm and slow reaction kinetics are discussed in the first subsection below [36].
- assume a constant apparent diffusion coefficient, i.e., neglect the kinetic equation, assume that the concentration in the stationary phase, in eq. (9) is related to the concentration in the mobile phase by the isotherm equation, and assume that the concentration is small enough and the isotherm can be approximated by a parabola (two term expansion of eqs. (1) or (2)). If we let:

  $$k' = \frac{dC_m}{dC_s} \qquad (10)$$

  (this is an extension of the analytical definition, where k' is constant), we can rewrite eq. (9) as:

  $$\frac{dC}{dt} + \frac{u}{1+k'}\frac{dC}{dz} = D\frac{d^2C}{d^2z} \qquad (11)$$

  where C stands for the concentration in the mobile phase.

  The problem has an approximate analytical solution, the properties of which have been studied by Houghton [41] and Jaulmes [42, 43].
- entirely neglect the kinetic problem, and assume that the column has an infinite efficiency. Eq. (10) (with the RHS term equals to 0, since the axial molecular diffusion coefficient becomes null in the ideal model of chromatography) can now be programmed, using a finite difference method and following the Godunov algorithm [28, 52].

We now discuss some of the results obtained.

1. Non-linear isotherm, finite kinetics

Using complex mathematical operations, including a Thomas transform of the system of eqs. (5) and (9) and a two-dimensional Laplace transform, Carr derived an approximate solution for the peak profile, involving the zeroth and first order modified Bessel functions of the first kind and an integral of the former Bessel function [36]. This profile depends on four parameters, the slope and curvature of the isotherm at the origin, a kinetic parameter and the sample size. A study of the behavior of the first three normalized moments as a function of the column overload was also undertaken as a means of checking the validity of the numerical results.

The band profiles calculated for various sets of numerical values of the different parameters involved give profiles which look very familiar to the chromatographer. Thermodynamic and kinetic constants can be derived from the recorded profiles for the elution of a large sample of a pure compound by curve fitting. Systematic use of this model in affinity chromatography permits the study of binding site heterogeneity. This could permit the rapid design of efficient preparative HPLC purification strategies when this mode is used by letting the values of the relevant thermodynamic and kinetic parameters be determined accurately and rapidly, from the elution signal of a single, large concentration injection.

It does not seem possible, however, to extend the approach to the solution of the binary mixture problem, when two compounds compete, with different thermodynamic and kinetic parameters for adsorption on the active binding sites. This situation is not uncommon, however, when proteins are manufactured by forcing bacteria to express a cloned gene, with a high yield. Then a number of transcription errors take place, and some faulty amino acids are incorporated in various positions. When this takes place not too close to the active site, the separation of the related protein becomes very difficult by affinity chromatography. The mathematical model now incorporates two mass balance equations and two kinetics equations, which makes it extremely difficult to solve by the same method as used for a single compound [36].

2. Low concentrations

When the sample size is small, the isotherm may be replaced by a two term expansion, a simple approximate solution of eq. (11) can be obtained, assuming that the diffusion coefficient D is constant and equal to the apparent diffusion coefficient (eq. (8)). A simple equation is obtained which accounts very well for experimental results obtained in many typical situations encountered in HPLC, when columns are moderately overloaded [41,43]. The results are valid in a range of concentrations which depends, of course, on the curvature of the isotherm at the origin (zero sample size), but in practice goes from 0 to about 10 millimolar [43].

The integration of eq. (11) gives the following equation for the concentration profile:

$$C = \frac{2}{[\lambda]U}\left(\frac{D'}{[\pi]t}\right)^{1/2} \frac{\mathrm{Exp}\left(-\frac{[t_R-t]^2}{2[\sigma]t^2}\right)}{\coth\left(\frac{[\mu]}{2}\right) + \mathrm{erf}\left(\frac{[t_R-t]}{V_2[\sigma]t}\right)} \qquad (12)$$

where:

- t_R is the retention time of a zero concentration sample, corresponding to the slope of the isotherm at the origin.
- $[\sigma]t$ is the standard deviation (time unit) of the zero concentration band, from which is defined the apparent diffusion coefficient (eq. (6)).
- $D' = D/(1 + k'o)$, where D is the apparent diffusion coefficient (eq. (8)).
- $U=u/(1+k'o)$, where u is the mobile phase velocity.
- $[\lambda]=2(K_2C_v-K_1)/(K_1+V_g/V_1)C_v$.
- $[\mu]=\frac{[\lambda]U}{2D'}\ \frac{m}{S}$, where m is the mass of solute injected (mole), and S the cross section area of the column available to the gas phase.
- C is the solute concentration at time t, at the outlet of the column.

Eq. (12) permits the prediction of the band profile, knowing the various parameters which control the band profile: the sample size, the coefficients of the isotherm expansion, the apparent diffusion coefficient, the average gas velocity and the average column pressure. Experimental results confirm the validity of this approach, at concentrations which are usually much lower than those used in preparative HPLC. Thus we shall not discuss the results in detail [43].

3. Integration of the ideal model and numerical diffusion

Study of the properties of the differential equation which is related to the Burgers equation [55], permitted the selection of proper conditions for numerical calculation of its solutions. A condition relating the integration steps in the space domain (along the column) and in the time domain must be satisfied. This leaves an indetermination regarding the selection of one of these increments [44]. We have found that choosing the space increment equal to the column HETP permits an exact coincidence of the (Gaussian) profiles calculated and measured at very low concentrations.

The numerical results obtained with large concentration pulses of pure components for which the isotherms have been measured are in excellent agreement with those recorded [56]. Furthermore, we have shown that it is possible to derive the parameters of the isotherm from one single injection of a large sample size, if the isotherm is of the Langmuir type. Then, calculations performed on the elution profile of a single, large injection permit the accurate prediction of the elution profile of a smaller sample, and a good prediction of the elution profile of larger samples [56].

One great advantage of this method is that its extension to the problem of the two- or three-component mixture is straightforward. Calculations performed with two components having an interactive equilibrium isotherm of the type described by eqs. (3) and (4) give results in excellent qualitative agreement with the observations reported in the literature [57]. Proper tests of the accuracy of the prediction of the model require the determination of ternary isotherms, a task currently under way.

Especially important, in the case of Langmuir type isotherms, is the onset of displacement of the lesser retained compound by the more retained one, when the concentration of the second compound is important [57]. A sharp boundary exists between the two band profiles, although the signal does not demonstrate a good resolution in the analytical chromatography sense. By proper selection of the time when the fraction collection valves are actuated, it is possible to recover a large and very pure fraction of the first component. The steepness of the tail of the first component elution profile depend strongly on the column efficiency, in a concentration range where the degree of column overload achieved is such that the width of the profiles of either pure component would not be greatly affected by a change in the column efficiency. This explains conflicting reports regarding the usefulness of column efficiency [58]. On the other hand, the profile of the first component tails under the profile of the second one, and it may be difficult to recover a large fraction of this second component if the purity required is large. When the concentration of the second compound is small compared to that of the first one, a different phenomenon takes place and the first compound drags forward the second one. In this case heavy concentration overload would prove adverse to high production rate.

F – Conclusion

Significant progress has been made toward the general solution of partial differential equations describing the chromatographic process. The approximate solutions which have been proposed can be divided into groups. In the first group, solutions are available for the prediction of profiles of elution bands of pure compounds, when the isotherm is non-linear and the kinetics of mass transfer is slow. This solution is not applicable to the study of the separation between two compounds. In the second group, solutions are available for the quasi-ideal problem, for a two component mixture, and it could easily be extended to as many components as required. The kinetics of mass transfer must be rapid, as it is in most applications of HPLC, independent of the concentration, and must be accounted for by an apparent diffusion coefficient.

It should be emphasized that the solution of the problem discussed above, solving eqs. (9) or (11) with the proper set of boundary conditions, is not the exact solution to the chromatographic problem. These equations assume that the mobile phase is not retained, which, in fact, is not true. Adsorption is a competitive process, and this has to be taken into account. The recent work by Riedo and Kovats [59], which followed the pioneering work by Schay [60], points in the right direction. Finally, we have also assumed that the chromatographic phenomenon is isothermal. This is not so, since in many instances the retention time depends on the column temperature. It does not appear, however, that neglecting the enthalpy balance results in serious errors.

Further work will most probably result soon in a complete solution of the general problem, at least under the form of a numerical algorithm and a computer program [61].

IV Instrumentation

For process scale liquid chromatography, the chromatographic instrument must be entirely redesigned. Thusfar, advancements have centered on the design of improved column technology; however, sample introduction and distribution on the column top, detection and automation of the process have also been intensely studied. Dedicated instruments covering a wide range of throughputs are available from different manufacturers in what seems to be a very competitive market.

A – Column Technology

The column is the heart of the process and accordingly deserves the attention of the process designer. Although considerable controversy has raged over the importance of column efficiency in preparative HPLC and the question has yet to be settled, there is agreement that a minimum efficiency is needed to achieve a reasonable throughput. For a given packing material (i.e., using particles of a given average size), the efficiency depends essentially on the method for packing the column and on the column length. Accordingly, any improvement in the packing method will result in the achievement of the required efficiency with a shorter column. This means important savings on both investment and running costs.

In a recent publication, Lightfoot has criticized the use of a particle bed in chromatography, on the grounds of the excessive hydraulic resistance, which is a valid point, and has suggested the use of parallel capillary tubes [62]. This issue has not escaped the attention of chromatographers. It has been discussed by analysts and several attempts at the preparation of LC columns using optical fiber technology have been made [63]. Two approaches have been tried, preparing hollow fibers, or packing tightly solid core fibers. In both cases, advantage is taken of the ability of industry to manufacture optical fibers which have virtually constant diameter. It does not seem that these efforts have been even partly successful, due to very stringent requirements regarding the tube diameters, lengths and active surface areas, stemming from the need to achieve a very narrow distribution of the average residence times of all solutes on all the open tubular columns of the bunch. We are of the opinion that conventional packed columns will stay with us for a long time.

The column efficiency, measured by the HETP of the peak for the injection of a very small sample of a pure compound, should be as high as the efficiency of an analytical column packed with the same material. The packing technique should also be reproducible and give columns having a HETP proportional to the average particle size. This permits the process engineer a choice of the final column performance by adjusting the particle size, the column length and the inlet pressure. The use of coarse particle packing material tends to be favored because it permits operation of the column at a low inlet pressure and, thus, requires the purchase of a low cost pump. Often the use of coarse particles results in the use of long columns (to achieve a certain degree of resolution), high mobile phase velocities (to keep retention times short and throughput high) and, as a consequence, moderate or small number of effective plates. Although that kind of performance seems satisfactory in the development of various separations, it is certain that the use of columns packed with finer particles and run at about the same velocity would permit the achievement of a better resolution (same column length) or shorter analysis times (same efficiency) and, in both cases a larger throughput. This improvement is obtained at the cost of a much higher pressure, which requires the use of a more expensive pump and of thicker, stronger, more expensive column tubings.

Thus, packing technology is very important in preparative HPLC, just as important as it is for analytical separations, since a good method will permit the preparation of better columns which have the same permeability. The quality of a packing method may be characterized by the reduced plate height (ratio of the plate height to the average particle size) achieved, the reproducibility of this reduced plate height and the stability of the columns obtained. Reduced plate heights below 2.3 are very good, below 3 they are satisfactory, above 4 they are poor, but sometimes they have to be accepted. The problems related to the optimization of column design and operation parameters will be discussed in more detail in the next section. Since the packing technology currently employed in the laboratory is difficult to apply to large diameter columns, various methods of compressing the packing have been developed and will also be discussed.

1. Packing technology

There are two types of methods for packing chromatographic columns, dry and slurry methods. The first method is easier to implement, but the latter affords more efficient columns, especially when small particles are used.

a) Dry packing: The first preparative columns were prepared by dry packing [9, 10]. In this technique the column is vibrated, rotated, tapped along its wall and/or dropped repeatedly on the floor while the packing material is slowly poured into the tube. Besides the average particle size, the factors which influence the column efficiency are the column diameter and the rate at which the packing is poured [64].

The main advantage of this procedure is its simplicity. It is easy to perform, does not require sophisticated equipment nor skilled manpower. There are important drawbacks, however. The column efficiency is not reproducible and is often poor, with reduced plate heights often well in excess of 10; the method does not work for particles smaller than about 30 um. Much better results may be obtained by strongly vibrating the column and rotating it around its axis, but this requires expensive, complex equipment and does not apply well to small particle packing [65].

After the column is packed, a steady stream of mobile phase is circulated through the column, typically for a few hours, at a flow rate as large as permitted by the column tubing or the pump capacity. This has the effect of compressing the packing. Therefore, afterwards, the top of the column must be refilled in order to avoid, a dramatic loss of efficiency associated with the existence of a void of packing material. This operation may have to be repeated.

Applied to particles with an average particle size between 30 and 60 um, this method permits the inexpensive preparation of low or medium pressure columns having good reduced plate heights. Although they have to be operated well above the flow velocity corresponding to the maximum efficiency, for the sake of reasonable elution times and acceptable throughputs, such columns allow the production of gram size amounts of pure products when the separation is not very difficult. This method is used in academic laboratories when low production costs are necessary, but when time is not important. In the assessment of true production costs, it should not be forgotten that chromatography is a dilution process, and that the extent of dilution increases with increasing elution time and decreasing column efficiency. The cost of concentrating the collected fractions and recovering the products desired is always a significant part of the total cost of the preparative LC process. It may become very important when long, low efficiency columns are used, a fact often overlooked in academic research, where utilities are usually free.

In order to improve the column efficiency, packing materials with smaller average particle sizes and narrow size distributions must be used. The width of the size distribution is more important in preparative than in analytical chromatography, because the column diameter is much larger. It is important to avoid the local accumulation of large particles or small particles in any part of the column. If there are regions where this accumulation occurs, the permeability will be different from the average and so will the local velocity of the mobile phase. A radial velocity gradient is a very important source of band broadening, especially since radial diffusion is much too slow to relax the concentration gradient caused by the difference in velocity over the column section.

Fine particles, below ca 25 to 30 um average diameter, are nearly impossible to dry pack, because electrostatic interactions between particles with a high surface to mass ratio result in attraction forces which become large compared to their mechanical inertia. Stable agglomerates are formed, so that dry packing results in the formation of a bed which has the flow resistance of small particles and the efficiency corresponding to agglomerated particles, clearly an unacceptable situation. Slurry methods must be employed in order to weaken the forces of interaction and disperse the particles in the solvent.

b) Slurry packing: The packing of fine particle stationary phases can be carried out easily, with excellent results, by using slurry packing techniques. The presence of the solvent drastically reduces the interaction energy between particles and this circumvents the problem just described [66, 67]. Several variants have been described in the literature: packing at constant flow rate and packing at constant pressure. In the former, the flow rate at which the pump operates is adjusted to the maximum value the pump can sustain through the fully packed column and the inlet pressure rises progressively during the packing. This method seems to be preferred over the latter one where the pump is set at its maximum flow rate, then the flow rate decreases during packing while the pressure increases rapidly. In the latter case, the column tends to be denser at the bottom than at the top, where the column is packed at a lower flow velocity. In both cases, the final pressure may be as high as

500 to 700 atm. Air driven pumps are generally used, since they supply high pressures and large flow rates at relatively low cost; the pressure pulsations do not seem to have a harmful effect. It appears that the exact procedure employed must be adapted to the specific packing material used, especially as far as the preparation of a stable suspension is concerned.

In the slurry methods, the incoming particles are thrown against the top of the rising bed by their momentum and forced into place by the drag force generated by the viscous flow. This force, F, is given by Stokes law, and the ratio of the drag force to the particle weight, P, is:

$$\frac{F}{P} = \frac{18\,[\eta]\,u}{d^2\,[\rho]\,g} \tag{13}$$

where:

- $[\eta]$ is the fluid viscosity.
- u, the fluid flow velocity,
- d, the particle diameter,
- $[\rho]$, the apparent density of the particle,
- g, the gravity.

For a solvent velocity of 10 cm/s, which is typical of packing conditions for conventional analytical columns, this ratio is about 7,400 for 5 um particles ($[\rho]=1$, $[\eta] = 1$ cP). This explains why slurry packing is so much more efficient than dry packing. The drag force applied on a particle exceeds its weight by almost four orders of magnitude. The force is applied to each particle, which must sit in the most stable position in the rising bed. We note in passing that if different solvents are used at constant pressure, for example, the maximum pressure which the pump can deliver, the drag force depends only on the fluid density. The effect of the solvent viscosity is cancelling out. Slurry packing produces very dense, very hard column beds and the hardness of the bed at the column end is often comparable to that of limestone.

Slurry methods can be divided further, according to the mechanism by which the particles are suspended: balance density (the liquid is a mixture of halogenated solvents having the same density as the solid of the particles, i.e., 2.4 for silica), high viscosity (the particles falls slowly during the column packing operation, which is usually short, 10 to 15 min), electrostatic dispersion (an ionizing solvent is used, at a pH such that the surface of the packing material is ionized and the particles carry all charges of the same sign), or low density, low viscosity fluid, strongly agitated to keep the particles in suspension during the operation [66, 68]. The goal is to prevent selective sedimentation of the stationary phase, with large particles accumulating in some areas and small ones in another, and to increase the probability of radial homogeneity of the packing.

Slurry packing was originally developed for analytical columns, but, now, is applied successfully to the prepration of high efficiency preparative columns. Basically the same procedure developed for analytical columns is used. The maximum pressure which may be applied is limited, however, by the mechanical resistance of the column wall and of the fittings. Moreover, when the column diameter increases it becomes more difficult and expensive to find a pump capable of delivering a fluid at the same high velocity used to pack analytical columns. Hence, the maximum flow velocity at which columns can be packed tends to decrease with increasing column diameter. For example, compression fittings used to seal columns can hold 10,000 psi for a 0.5″ i.d. column, but only about 2,000 psi for a 2″ i.d. column [69]. For larger diameter columns, flanged-end fittings are used. They are either bolted or fastened with special collars that can withstand the very high pressures required [70]. The column tubing and the flanges are thick and have to be made of high tensile strength alloys which are heavy and expensive. Thusfar, a good solution to the second problem has not been proposed, since the issue comes down to the level of pump technology.

Outstanding performances has been achieved with, for example, 6″ i.d. columns packed with 10 um particles, resulting in minimum plate heights around 18 um (i.e., reduced plate heights below 2.0) [69]. We can conclude from this remarkable result that apart from the requirements of a hoist and a large workshop, it is easier to pack high efficency large diameter columns than conventional ones. We are of the opinion that this paradoxical result is explained by the fact that when the column diameter increases, it becomes easier to develop and operate a sampling system and a detector whose dead volume contribution to the apparent column performance is negligible.

The same reason which limits the maximum inlet pressure which can be used during column packing also limits the maximum column length. When columns longer than 50 cm are required they have to be packed in several sections, later connected by the appropriate fittings.

In summary, dry packing is widely used in the academic laboratories and when high performance is not demanded or is not affordable and when time is available. Satisfactory results are obtained with large size particles. Slurry packing is more difficult to carry out, since this technique requires large volumes of expensive solvents which are costly to recycle. It is not commonly used in academic laboratories, but is the preferred method of companies selling packed columns. This explains the relatively small number of papers dealing with systematic or comprehensive investigations of the influence of the design and operating parameters on the performance of these columns. Nevertheless, the bottom line is that the technology works and columns are available on the market with efficiencies equal to or very close to those typical of analytical columns.

With the slurry packing method, however, the column tubing and end fittings must withstand the pressure required for making a homogeneous, dense packing, which is much larger than the pressure at which the column will be operated during its use. This results in a large cost for these parts. The cost increases very rapidly with the column diameter, faster than the cross-section area. New methods for packing columns have been developed to meet the demand for large diameter, high efficiency columns.

2. Compression technology

Compression technology has been developed to solve the problems encountered in the preparation and operation of preparative chromatographic columns. One of the major difficulties encountered in this area is the lack of long term stability of columns. This problem is especially vexing because it has not been explained yet, nor related to any identified factor of the packing process. Due to the complexitiy of the phenomena involved and the lack of systematic studies, there are several points of confusion. It seems that a zone of low density packing forms slowly at the column inlet, leading to the formation of a void at the top of the column. Eddies which form in this void are irregularly shaped and cause considerable back mixing. This results in a sharp drop in the column performance.

The origin of this phenomenon is unclear. It takes place too rapidly, a hole developing sometimes within a few hours, to be explained by the slow dissolution of the packing material in the solvent used as mobile phase. The hole may form after a few hours under the slow flow rate used during normal column operation, while the column has just been packed and percolated at high flow velocity for a couple of hours. Could it be explained by a consequence of the Bernouilli effect [71]?

Slow dissolution of the stationary phase explains the long term appearance of a hole on top of the column. The phenomenon is much more dramatic in reversed phase liquid chromatography (RPLC) than in normal phase chromatogrpahy. Silica is much more soluble in the high polarity solvents used in RPLC (mixtures of water, methanol and acetonitrile) than in the organic solvents used in normal phase chromatography (heptane, toluene, chloroform, etc). Even protected by the organic groups bound to it, silica dissolves slowly, as shown by the results of performed by Slavin and Atwood [72]. A simple calculation shows that unless the solvent is saturated with silica by percolation through a bed of cheap, large particle size silica prior to reaching the sampling system, the amount dissolved may correspond to the size of the void observed after long term operation. For example, if a 4.3 mm i.d. RPLC column is operated continuously, 24 hours a day, with a flow rate of 1 mL/min, the solubility of silica in water/acetonitrile mixtures (pH ca 10.7) being of the order of 1 ppm, 1.4 mg are dissolved each day. After a month, the loss is ca 0.042 g, leaving a void of about 0.1 mL or 0.7 cm long. Since preparative columns are operated continuously, the problem tends to be more serious than under analytical conditions. The solubility of silica in RPLC mobile phases has been demonstrated by the observation of deposits on LC/MS interfaces and by reports that products purified by RPLC have a significant amount of ash, unless the silica is eliminated.

a) Radial compression: Radial compression was developed by Little et al. in the mid-seventies [73]. Flexible-walled cartridges (30 × 5.7 cm) filled with silica or other packing material for liquid chromatography are placed in a chamber arranged so that the cartridge is connected to the pump with a sampling system at one end and a detector and fraction collecting device at the other end. The space between the chamber inner wall and the cartridge can be pressurized with nitrogen (500 psi). Compression takes about 1 minute [74]. The flexible wall shrinks around the prepacked bed, resulting in a tight, rather homogeneous packing bed having a high efficiency. The drawback of the system is that cartridges are factory sealed, they cannot be packed with material prepared in the laboratory, and they cannot be reused. The material presently being used is coarse, about 40 to 60 um average size. so the absolute performance can only be fair.

b) Axial compression: Axial compression was developed by Godbille and Devaux [75] at about the same time that radial compression was invented at Waters. Axial compression has been employed in numerous chromatographs incorporating columns with inner diameters between 2 and 60 cm and lengths between 30 and 120 cm [70].

The column design consists of a cylinder which is approximately three times longer than the column length desired and a sliding piston with appropriate fittings to prevent leaks between the piston and the barrel. In order to prepare a column, the cylinder is first filled with a slurry of the packing material in a suitable solvent. The density of the packing in the slurry is about 30% of the density of the particles in a conventional packed column. When the column is filled with slurry, the top end-fitting is fastened and the piston is slowly raised forcing the solvent out of the cylinder through a frit placed in the top end-fitting which retains the packing particles. The column is formed as a filtration bed. Eventually the particles are compressed between the piston and the frit and a consolidated bed is formed. The maximum pressure applied to the bed in order to obtain a good quality packing is between 5 and 20 atm depending on the size of the packing material used and on the flow rate desired. When the process of compression is complete, the cylinder can be locked into position to prevent it from being pushed back if the mobile phase inlet pressure exceeds the pressure the cylinder applies to the packed bed [74]. A floating piston, pressed against the column bed by the pressure differential created by a piece of tubing, can also be used to guarantee constant positive compression of the column bed.

The process of preparing highly efficient columns takes about 10 minutes [76]. For columns with 8 and 18 mm i.d., the reduced plate height achieved was 4.0 and 2.3; respectively. For columns larger than 4″ in inner diameter the reduced plate heights of about 2.0 are regularly achieved [75]. Voids formed by the eventual dissolution of silica in the mobile phase are easily removed by stopping the flow of mobile phase, unlocking the cylinder and applying a proper pressure to press the packing bed against the metal frit. Carrying out this operation periodically prevents loss of efficiency due to bed instability.

The advantage of this procedure is that the bed remains very stable, that excellent column performance is achieved reproducibly and that moderate pressures, barely larger than the pressure required to achieve the desired mobile phase flow rate, is required to pack the column. Axial compression seems preferable to radial compression, because it does not require the use of plastic cartridges which must be precisely molded to ensure leak-proof connections at both ends and which must be changed every time the column has to be disconnected from the instrument. The axial compression syringe is expensive but flexible. It can be used easily with any kind of packing material including proprietary ones. The column length can be adjusted as desired over a large range. Furthermore, the piston can be used to remove rapidly the packing, in a clean and easy way. Finally, in axial compression gradients of particle size and density, i.e. permeability, are axial while in radial compression they are radial. The former type of gradient has a much smaller effect on column performance than the latter which influences the radial velocity profile of the mobile phase.

c) Other types of compression: In 1985, Rainin developed and marketed a column which is packed using the conventional slurry packing method and then fitted at both ends with a cap which can be screwed, compressing the packing material. Periodically, when the column performance shows signs of deterioration, the caps are tightened, which compresses the packing and fills the void volume which may have developed at the column inlet. With this system, columns may be operated in both directions, which is unsafe with conventional columns. This design permits an easy elimination of the voids which progressively appears in reverse phase applications, but does not provide the other advantages of axial compression. It is best applied to columns between 1/2 and 2 inch diameters, but would be difficult to use with larger columns because of the stress applied to the column tube.

In 1987, Separation Technology developed another procedure for packing columns [77]. A conical rod which has a small angle and an average diameter of about 1/2″ for a 1 1/2″ inner diameter column is inserted along the column axis. The column is packed as a conventional column, although, obviously dry packing is much easier. Then endfittings are placed on the column, which hold the rod and permit it the same time axial and radial compression. In principle, this procedure appears to have the potential to permit the use of dry packing followed by filling the column with an appropriate solvent to decrease the interaction energy between particles and then tightening the rod to achieve a dense, homogeneous packing, without submitting the column tubing to extreme mechanical stress. The slow formation of a void at the column inlet could be remedied by periodic tightening of the inner rod, in the same fashion as with the Rainin column. Very little data is available yet on this device.

B – Sample Injection and Distribution

The introduction of the infinite diameter effect in the late sixties by Knox and Parcher [78] has considerably influenced the development of procedures for the injection of the sample and its distribution over the column cross-section. The original publication is based on the phenomenon, obvious in thin layer chromatography, that if a very narrow band is injected on a column it will spread in all the directions in the chromatographic column, the direction of flow as well as the perpendicular direction. Furthermore, it was observed in the early work that the column packing was not homogeneous, but that the region close to the wall had a different permeability from the core. Thus, if it were possible to inject a point like band at the column inlet on a column sufficiently short and wide for the band not to spread radially over the entire cross-section before it reaches the exit, the band would not experience elution through the irregularly packed area along the walls and, as a result, would not be subjected to additional contributions to band broadening.

There is no doubt that a point-like band injected at the column inlet spreads in the radial direction as well as the axial direction. Thin layer chromatograms demonstrate this clearly. Experimental results obtained with a dual polarograph detector have confirmed the reality of this phenomenon [79]. The effect seems to have been more adverse in the late sixties when column packings were less homogeneous than they are now. The problem is now the reverse, at least for preparative applications. The question is how can we spread the injected band over the entire column cross-section in order to minimize axial dispersion and the consequences of local overloading. Two issues arise: First, should a sampling valve be used with a sample loop (with an empty or a packed loop) or should we pump the feed (with the same pump as used for the mobile phase or with an auxiliary pump)? Second, how should we distribute the incoming mixture of feed and mobile phase on the column top to avoid an additional surce of band spreading resulting from unequal path length for molecules entering at the column center or along the wall? These issues have been seriously studied and acceptable solutions have been found.

1. Sampling

Injection of the feed through a sampling loop is reserved to cases when small samples are involved and there is no pump avaialble to handle such small samples. This involves the use of analytical or "semi-preparative" columns. Sampling loops with a volume exceeding 1 mL should be avoided. Such loops should be filled with non-porous particles having a diameter not exceeding two or three times the size of the particles used to pack the column. It has been shown that because of the Poiseuille radial velocity profile in empty tubes, there is a strong broadening of the injected band. The solution which is placed in the center of the tube reaches the column much before the solution which is at the wall [80]. When an empty loop is used, the column efficiency is often better if the loop is placed off-line after one loop volume of mobile phase has swept it. But then, only part of the solution filling the loop has been injected. Packing the loop transforms it into a narrow LC column, with no retention, and greatly reduces the band broadening due to uneven radial flow velocity distribution.

Pump injection can be carried out using either the same pump which is used for the pumping of the mobile phase, or an auxiliary pump. In the first case, the feed can be completely mixed with the mobile phase and the injection can be carried out over the entire column cross-section. Very well behaved injection profiles are easily achieved this way. It is necessary to dilute the feed in the mobile phase rather than in another solvent in order to avoid precipitation of feed components at the column top. In all cases, the solubility of the feed in the mobile phase limits the amount of sample injected by limiting the concentration at the column inlet. Samples with concentrations close to saturation may be injected, however. The maximum concentration of such bands falls very quickly during the beginning of the elution and the band broadens rapidly, so excessive concentration overload might be limited to the column entrance. Nonetheless, an auxiliary pump permits more flexibility. If the main pump is kept on, it is possible to carry out simultaneously the concentric injection of the sample in the center of the column and that of pure mobile phase along the wall. If the main pump is switched off, it is possible to achieve the injection of a dilute feed at a flow rate lower than the one used for the mobile phase, which may be useful with viscous samples.

Automation of a preparative LC instrument should provide the possibility to perform feed injection through the main pump, which is the preferred method, as long as the feed volume exceeds a few piston stoke volumes. In many instruments which do not provide this function, it is possible to perform injection with the main pump by making provisions for step gradients or for gradient elution.

2. Sample distribution

It is important that the injected band be distributed regularly over the entire column cross-section. If the molecules moving along the wall take more time to enter the column than those moving in the center, because the path length is longer and/or the average velocity slower, the band may broaden considerably. To avoid this phenomenon, the column should be covered with a metal frit having a permeability lower than that of the column, and the mobile phase inlet should be distributed over the entire cross-section of the column [81]. The hydrodynamics of the problem is complex and contradictory results have been reported.

Coq et al. [81] have calculated that an abrupt change in the cross-sectional area at the column inlet could be extremely detrimental to the efficiency. Their model seems to describe the worst possible set of experimental conditions since the experimental results reported have never been as bad as suggested by the theoretical results derived by these authors. Further calculations show that the use of a low permeability frit at column inlet, preceded by a very thin empty zone on top of this frit, considerably alleviate the situation.

Godbille et al. [76] have compared the results obtained using central injection (injection carried out in a point-like fashion at the exact center of the column) and cross-sectional injection (injection carried out in such a way that the eluate entering the column is always homogeneous radially). An 18 mm i.d. axial compression column was employed and data were measured at reduced velocities between 1 and 10. At low sample concentrations, the HETP is lower for central injection than for cross-sectional injection; however, as the sample volume injected increases, the HETP increases at a faster rate for the former compared to the later. Thus, at high volume loading, central injection gives larger HETP value as seen in Table I. This result is reasonable as the narrower the cross-sectional area over which the injection is effectively spread, the longer the part of the column occupied by a given injected volume.

Table I. Comparison of the sample volume injected for cross-sectional injection and central injection with the HETP (Ref. [76]).

Injection type	Sample volume Injected (ml)	HETP (μm)
Cross-Sectional	0.1	34.5
	0.2	33.5
	0.5	31.0
	1.0	40.5
	2.0	49.5
Central	0.1	24.5
	0.2	25
	0.5	30
	1.0	58
	2.0	290

DeJong et al. [82] investigated the performance obtained with three different distributor designs, (i) central injection, (ii) conical injection and (iii) flow separated by a conical disperser (FSCD). The experimental results show that peak symmetry increases when going from the first to the second to the third distributor.

Coq et al. have investigated a number of distributors which can be placed in four different categories, (i) central injection, (ii) sample injected at five different points regularly distributed across the column top, (iii) conical injection, and (iv) split stream injection [83]. Compared to the other methods, split stream injection seemed to allow the largest increase in the sample volume without deformation of the injected plug and to permit the highest recovery yield of purified product . These results deal with experimental conditions which are only marginally relevant to preparative chromatography, since "concentration overload" is carefully avoided.

C – Detection

Two types of detection problems may arise in PLC. First, the detector should not be easily saturated. Second, it is necessary to follow the elution of individual compounds in order to control the valves required for fraction collection.

The detection problems in preparative LC arise from the large eluite concentration often observed. If conventional analytical LC detectors are used, the response may be saturated. Typically, a conventional UV photometric detector might become blind during the elution of the main components, preventing the use of the signal to monitor the chromatograph.

Special cells with short path lengths (e.g., 0.25 mm) are being employed to alleviate the problem [84]. Alternately, an aliquot of the main stream of eluate may be diluted in a stream of scavenger mobile phase before entering a standard detector cell. Some authors have used UV spectrophotometric detectors at wavelengths where the compounds of interest have a weak or low absorptivity. This is valid only if the spectrum derivative, $dA/d[\lambda]$, is small; otherwise marked deviation from Beer's law may be anticipated.

In order to maximize the production rate, it is crucial to cut the fractions at the appropriate time. This is especially important when there is significant peak overlap. In order to operate the valves, it is necessary to know the individual elution profiles of the compounds. The best method for monitoring the eluent is by on-line analysis where an analytical HPLC is employed to sample the effluent of the PLC. The separations required are often simple and can be carried out very rapidly. The operation of this auxiliary chromatograph should be controlled by the same computer as the PLC.

D – Automation

Automation in preparative LC is a major issue since repetitive processes are often involved in order to collect the desired quantiy of product. In most cases it is not economical to build a big chromatograph and inject samples which are of the order of the monthly or the yearly production. It is better to design a separation unit capable of processing the necessary raw materials by operating on a daily production schedule. The unit size will be smaller, the instrument simpler, easier and cheaper to purchase, operate and maintain. Additionally, optimization of the experimental conditions is justifiable and could lead to better yields and to recovery of the product at higher concentrations. Automatic instruments are thus necessary.

Recent developments of computer controlled instrumentation makes automation easy, providing unattended 24-hour operation if needed, increased reproducibility of results by exact repetition of tedious manual operations and elimination of the need for costly, unskilled manpower.

The early instruments were controlled by timers which would switch pneumatic actuated valves or pumps, in order to alter the flow path of the eluent and the feed [85, 86]. This type of system allows repetition of well-defined cycles until the desired amount of product is collected [87,88]. Reproducibility of experimental conditions is not guarenteed, however, and flexibility is limited. The next step in automation was the design of electronic circuitry to monitor the intensity of the detector signal so that it could be compared with specific threshold limits for sample selection and fraction collection [89–91].

More advanced systems permit peak detection and feed-back control. The use of the first derivative of the detector signal eliminates the need to run a standard solution profile in order to set the threshold values for fraction collection [92, 93]. Flexibility to adjust the program to slow drifts of the chromatographic conditions is provided by the software which can smoothly adjust the event times within some range defined by the operator, e.g. the times when valves open or close. to begin and end fraction collection or to direct the effluent, as deemed necessary by the operator.

Computer control permits new modes of operation such as the "back and forth" procedure suggested by Colin, whereby production of a purified compound is increased by reversing the direction of mobile phase flow at the end of the elution and by injecting a new feed load at the same time [94]. Proper timing permits doubling the production, while the early eluted impurities of the new injection are collected in the waste tank in the same time as the late eluted impurities of the previous injection.

An algorithm has been developed for programing the chromatograph which can collect in separate fractions all the resolved bands in the chromatogram of an unknown mixture [94]. Fractions are cut at the base line between or at each valley between partly resolved peaks. Combined with gradient elution, this procedure offers the organic chemist the possibility to separate synthetic mixtures or extract natural substances in a number of fractions without much prior understanding of chromatography. The use of the second derivative to determine the time when the switching valves should be actuated to control access of the eluate to the fraction collection tanks has been proposed by Grushka [108]. The results seem to be in rather close agreement with the predictions of more complex calculations [57].

V Optimization

A – Aim of Production Liquid Chromatography

As stated in the introduction, the aim of PLC is not the resolution of the band profiles, but the production of the compound(s) of interest at a specified purity level, at an acceptable production rate and at a cost which is economically feasible. Consequently, most concepts popular in analytical chromatography must be abandoned, since their use would be seriously misleading.

Especially pernicious is the fascination that production LC (PLC) must be carried out under experimental conditions such that the behavior of the chromatographic column is linear. Many authors have published excellent discussions on the optimization of the performance of linear PLC, which seems to us to be a contradiction of terms. Although non-linear preparative liquid chromatography is not well understood, we know that we have to grossly overload preparative columns. We observe, and all practitioners know, that the production continues to increase with increasing amount injected until very large values are reached, at which point band interference is extremely serious and the column behavior is grossly non-linear [57,69]. Thus, the linear requirement is an unrealistic condition, whose only justification seems to be the fear of a poorly understood phenomenon.

Resolution, efficiency, and peak symmetry are irrelevant as optimization tools. Only cost is meaningful. To a certain extent, in view of the difficulties associated with the calculation of production costs and because some accounting procedures are arbitrary, production can be substituted by another parameter. Thus, we agree partly with Knox [95]: "optimization of performance in preparative LC implies seeking conditions which provide the maximum [...] throughput of material with specified purity and at a specified yield, but under the restriction of a limited pressure drop across the length of the column". We do not accept the restriction of a specified yield, however, and certainly not that of a total yield. All processes in the chemical industry are accompanied by some loss. Without discussing the issue, Knox, in an otherwise profound and perceptive discussion of the theory of PLC optimization, assumes that the yield must be unity [95]. Accordingly, he has to assume that the bands of the compounds of interest must be completely resolved. This yield requirement is quite arbitrary and unrealistic, however. A yield less than 100% is quite acceptable provided that the loss is compensated by a large increase in production or that the production requirements are met within the financial constraints. This is especially true if the products which do not find their way to the pure component tanks are not wasted, but recycled.

An illustration of the possibilities offered by the injection of very large feed pulses, which correspond to local concentrations at which the equilibrium isotherm is not linear, is given by displacement chromatography. In fact, the jury is still out deciding whether the most economical production can be achieved in elution or displacement chromatography, or some hybrid in between.

B – Choice of Mode: Elution or Displacement

Displacement, although widely used in the thirties and forties for preparative applications [14–23], had been abandoned until the early eighties when it was revived by the work of Horvath [96, 109–111]. Its development was impaired by the lack of high efficiency columns, by the lack of an understanding of the phenomenon, by practical difficulties encountered in the selection of a proper displacer and by the fear of not being able to regenerate the column. On the other hand, the use of elution chromatography for preparative separations is rapidly gaining acceptance due to the current popularity of and familiarity with analytical HPLC. Currently, the use of frontal chromatography lags behind both elution and displacement, as it does not appear well suited to the preparation of pure compounds.

The selection of the mode of operation depends in a large part on the nature of the sample, the purity required, and the production rate expected. In the following sections we hope to review some of the strengths and drawbacks of the different approaches.

1. Elution

In elution chromatography, a sample plug is injected and eluted by a stream of mobile phase. The bands of the different sample components migrate at a rate depending on the equilibrium isotherm of the compounds between mobile and stationary phase. Then, the bands broaden while they separate progressively.

Two elution modes may be distinguished, linear elution and non-linear or overloaded elution. In the former, the maximum concentration of each band is such that it is possible to assume that the equilibrium isotherm is linear; in the latter the concentrations are too large and this is not possible. The advantages of the elution mode are related to the ease with which data obtained with an analytical column can be used in the scale-up and the design of a preparative column. A preparative column of similar length and efficiency, using the same mobile and stationary phases, will give a chromatogram very similar to the one obtained with the analytical column. The drawbacks result from the poor utilization of the expensive stationary phase employed and from the dilution of the sample components under the influence of the strong concentration gradients which form at the band boundaries.

Scaling-up from analytical to preparative scale is not different in linear and non-linear elution chromatography. Although a better use of the stationary phase is made in overloaded elution than in linear elution, and dilution of the compounds recovered is less, the differences are of degree rather than of nature. This can be contrasted with the fact that analytical, elution chromatography is not as useful in the scale-up of operations in the displacement mode.

2. Displacement

In displacement chromatography, the column is equilibrated with the carrier, the sample is pumped or injected onto the column, and then the displacer, which is a solution containg a compound more strongly adsorbed than any component in the feed, is pumped as a constant stream into the column. The displacer moves at the same velocity as the carrier, and thus it forces the feed components to compete for adsorption sites, through a complex dynamic process, until a series of adjacent bands are formed where the feed components are arranged in the order of decreasing adsorption. The adjacent bands which form are called the displacement train.

Since the bands all move at the same velocity, their maximum concentration depends on the concentration of the displacer and on the adsorption isotherm of the considered compound. It does not depend on the concentration of this compound in the feed. Accordingly, since the band area is proportional to the concentration of the compound in the feed and its height is constant, the width of the band is proportional to the amound injected. Although band boundaries are sharp, however, they are not vertical; their shape depends on the column efficiency and consequently the degree of mixing between the zones.

The advantages of this technique are that the products are concentrated, large throughputs are achieved and yields can be enhanced by increasing the amount of feed injected, as well as the column length, to widen the bands and reduce the relative importance of the interfering zones between the bands. The drawbacks of displacement chromatography are the need to select a proper displacer and adjust its concentration, the need to purge the column of the displacer before separating a second batch of feed and the method development time required to determine the optimum conditions for the formation of an isotachic displacement train.

The basic mass balance equation is the same for all modes of chromatography, eq. (11), for which there is no exact solution available yet. The difference is merely in the selection of the boundary conditions. Complex mathematical manipulations have lead Helferich and Klein to derive a method of calculating the position of the bands in the displacement train, with the assumption of ideal chromatography, i.e., infinite column efficiency [50]. This method is very complicated, however, and gives no information regarding the extent of the intermediate, mixed zones between bands, nor the influence of the parameters which control the importance of these mixed zones.

C – Volume or Concentration Overload

There are many papers dealing with optimization of PLC which discuss the issue of column overload. It seems that it has been half-heartedly recognized by the community of chromatographers that in PLC columns must be overloaded in order to achieve a reasonable throughput. However, a compromise is being desperately sought between resolution or efficiency and production, much in the same way as in analytical chromatography a compromise is looked for between analysis time and resolution: a 10 or 20% loss in plate number would be traded for a certain throughput. Unfortunately, the rules of the game are not the same as for analytical chromatography and column efficiency, peak resolution or band symmetry have no place in PLC. The bottom line is throughput, yield and production cost.

The various issues regarding column overload will be addressed; however, it is the opinion of the authors that the only reasonable choice, at present, is between displacement and heavily overloaded elution, with feed pulses large enough to cause strong interference between successive bands.

1. Linear chromatography and volume overload

In this model, the sample concentration is kept constant and is sufficiently low for operation in the linear region of the isotherm. Then, the volume is increased until the resolution between successive bands is around unity. For rectangular injection pulses of constant height and increasing width, the elution band becomes higher and broader. The response of the chromatographic column to the injection of a concentration step (Riemann problem) is an erf function. In the general case, the elution profile obtained as a response to the injection of a wide rectangular pulse of a low concentration solution is given by the product of the inverse of the pulse width and the difference between the responses to the Riemann problems corresponding to the front and tail of the rectangular injection [48, 49]. In this model, the front and rear parts of the elution profile of a very wide band can be described by the error function. As a consequence, the band broadens rapidly when the injection plug becomes of the same order as the standard deviation and a plateau appears when the width exceeds about 8 standard deviations [95]. The concentration of this plateau is equal to that of the feed.

Several authors have discussed models relating the feed volume injected [97–99], the volume of the fractions collected, the concentration of the sample components, the recovery ratio and the resolution between analytical size samples (zero mass Dirac pulse). These models are fairly simple and the calculations are made directly from the classical resolution equation. Introduction of the plate number, necessary to perform a certain separation and achieve a certain resolution between the mixture components, permits the calculation of the column dimensions, the recovery rate and the purity of the products.

Calculations and experiments show that the band front is eluted at a constant retention time (elution time of the front is defined by its inflection point) [49], while the retention time of the rear part of the profile increases with the pulse width. Conclusions regarding the column design and operating parameters lead to the recommendation of the use of a very high flow velocity [100]. Accordingly, a rather long column should be used, which will have a low permeability. The optimum column is thus long, packed with rather coarse particles, and delivers the required plate number (ca twice the necessary plate number for a resolution of unity) at the maximum inlet pressure acceptable. The excess resolution is sacrificed to production by injecting a wide pulse, as described above.

Although these recommendations regarding the column design are reasonable, the fascination in considering that the column must be operated in the linear mode, results in very low production rates. Furthermore, there is a certain degree of self-contradiction in this approach. Because chromatography is a dilution process, the maximum concentration of the band increases rapidly with the sample volume at first: as long as we are in the linear mode, the band remains symmetrical, while the sample amount increases. If, as is often recommended, the concentration is adjusted so that the efficiency for a narrow plug is approximately 10 or 20% larger than for an infinitely dilute plug, significant concentration overloading will take place on the plateau of a wide pulse. This effect lead more than a few people to surreptitiously achieve both volume and concentration overload, without actually realizing the latter situation.

2. Non-linear chromatography and band interaction

When a column is operated under conditions of "concentration overload", we must take into account the fact that the equilibrium isotherm of the feed components between the mobile and stationary phases is not linear. The band profile broadens and becomes unsymmetrical, even if there is no volume overload. For Langmuir type isotherms the profile becomes triangular, with an almost vertical front and a slanted tail [55, 56, 95]. For anti-Langmuir or S-shaped isotherms, the profile also becomes triangular, with a slanted front and a vertical tail [56]. For S-shape isotherms, beyond the inflection point, more complex profiles are observed [56], but similar conclusions may be reached.

At moderate overload, it is still possible to use the concept of height equivalent to a theoretical plate; however, under these conditions the HETP is the sum of both kinetic and thermodynamic contributions [95]. The kinetic contribution is constant and equal to that observed for a very small sample size. The thermodynamic contribution is a function of the concentration at the band maximum and of the curvature of the isotherm. This concept allows the extension of the HETP to concentration overload and application of the classical theory of analytical HPLC [95].

This approach permits some simple, but correct, conclusions backed by experimental results [95]. We can compare, for example, two columns using the same phase system, but packed with particles of different size, so that the first column, packed with smaller particles, is more efficient than the second one, packed with coarser material. When the sample size is increased, the effect of the thermodynamic overload will be relatively more important on the former, more efficient column. This column will appear to become overloaded with smaller sample sizes than the second one, although it will always remain more efficient [58, 95, 100].

Since the resolution between closely eluted bands is a function of the column HETP; which is itself, the sum of two contributions, kinetic and thermodynamic; it is legitimate in the optimization of the experimental parameters to select conditions where the kinetic contribution is of the same order as the thermodynamic one [95]. This means that rather coarse particle material will be used to pack the column which will be operated at a greater flow velocity than the one giving the maximum efficiency (minimum kinetic contribution to the plate height). These conclusions are parallel to those derived from the volume overload approach, but the numerical values calculated are quite different.

3. Comparison

It has been shown by Knox, in an excellent discussion of the problem of PLC optimization, that concentration overload always results in a production larger than the one which can be achieved by volume overload [95]. A similar result has been predicted by Gareil et al., who even suggested a ratio of 10 between the maximum production in volume and concentration overload [101].

There should be no doubt, that PLC columns should be both concentration and volume overloaded. The real qustion is to what extent. Implicit in the discussion by Knox [95], is the assumption that the resolution between closely eluted bands should be of the order of unity or better, so that there is almost no cross-contamination between these bands when they are collected. Also, the fraction cuts are made at the bottom of the valleys between the resolved bands. This ensures a yield close to unity.

We submit that this is an unnecessary and arbitrary condition. In fact, it is observed that when the size of the feed sample injected is increased beyond the limit corresponding to the one postulated by Knox, the yield decreases only slowly, but the production continues to increase until the two bands have merged and a valley is hardly discernible [57, 58, 69]. The reason for this phenomenon is that the compounds involved interact. Adsorption is a competitive process. In the presence of the more strongly adsorbed compound, the lesser adsorbed one is forced out of the interface and back into the solution. In other words, the less strongly adsorbed compounds becomes less retained in the presence of the more strongly adsorbed compound. This is, indeed, the same phenomenon that takes place in displacement chromatography. When the column is so seriously overloaded that the bands interfere during their entire elution and are not fully resolved at the column exit, conditions where the second eluted compound displaces the first one may arise [57]. The build-up of a fully developed displacement train is not possible, however, because the band of the most retained compound, the pseudo-displacer, is too narrow to sustain isotachic migration. Nevertheless, the front of a later eluted component may act very much as a displacer for the less strongly adsorbed components of the mixture, provided its velocity and its concentration are large enough [57].

In practice, it is extremely difficult to predict the optimum extent of overloading which should be achieved. This largely depends on the yield which is required, if any. The phenomenon of partial displacement used is not symmetrical. In the case of a Langmuir isotherm, the less retained components are displaced by the more retained ones. The yield is larger for the former compounds. It increases with the ratio of the concentration of the less retained components to that of the most retained ones. Recycling is costly, especially if the recycled fraction has a composition which is different from the feed, and its recycling requires somewhat different experimental conditions. Finally, the characteristics of the mixed equilibrium isotherm, which describes the nature of the interaction between the two compounds in the sorbed phase, is important. In the ideal case, the ternary isotherm will be a Langmuir type isotherm (see eqs. (3) and (4)). in some cases, positive or negative interaction energy may appear and very complex situations may, at least conceivably, arise.

Figs. 5, 6 and 7 compare the results of separations simulated for the same mixture of two compounds, using volume overload, concentration overload and displacement chromatography. In the conditions selected, the productions achieved in concentration overload and in displacement are 25 times larger than the one obtained in volume overload, but, admitedly, none of the three separations have been optimized.

Much further research work will be required in order to clarify these complex issues.

D — Semi-Empirical Models

In addition to the various models derived from the assumptions discussed in the previous sections, some semi-empirical models have been suggested. The most important is the one derived by Snyder et al. [102–104], using the Craig machine analogy. Calculations based on this model have allowed a reasonable representation of the elution band of a pure compound. Optimization methods based on the characteristics of this profile may be derived [104].

The method is useful to predict the band broadening observed for different amounts of the same compound injected on different columns, prepared with various packing materials, but using the same chromatographic system (same surface chemistry and solvent composition), from a single overloaded chromatogram. The difficulty arises, once more, from the inadequacy of the approach to the actual problem. In order to optimize a PLC separation, one must consider at least two different compounds. As we have seen above, when their bands interfere a prediction of the

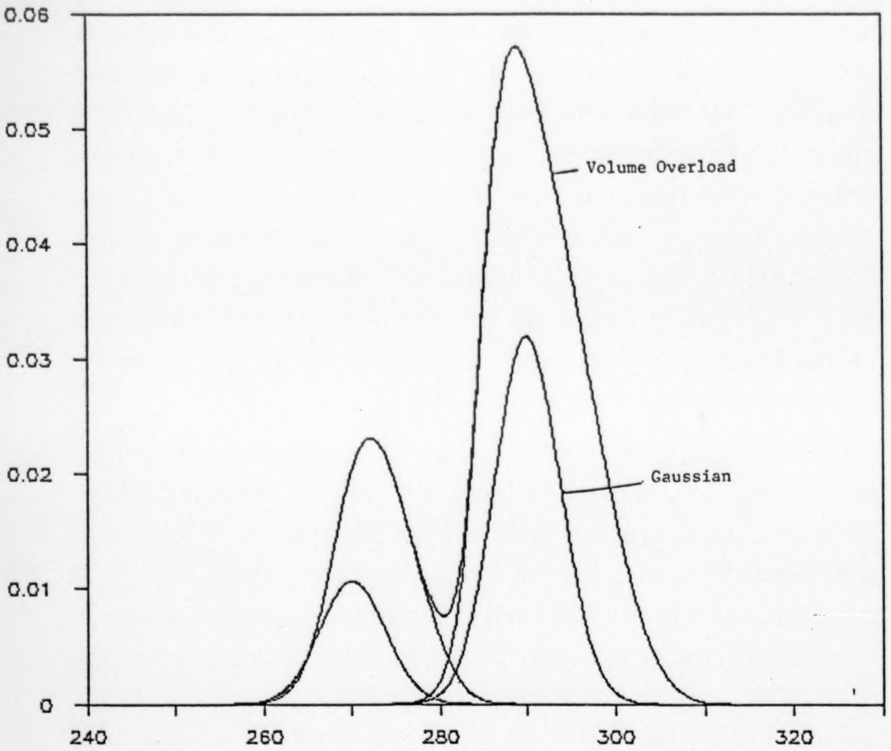

Fig. 5

Peak profiles of a two component mixture under volume overload (volume injected, 2 standard deviations) compared with the peak profiles of a Gaussian peak.

Note: the profiles of the Gaussian peaks have been magnified for illustrative purposes.

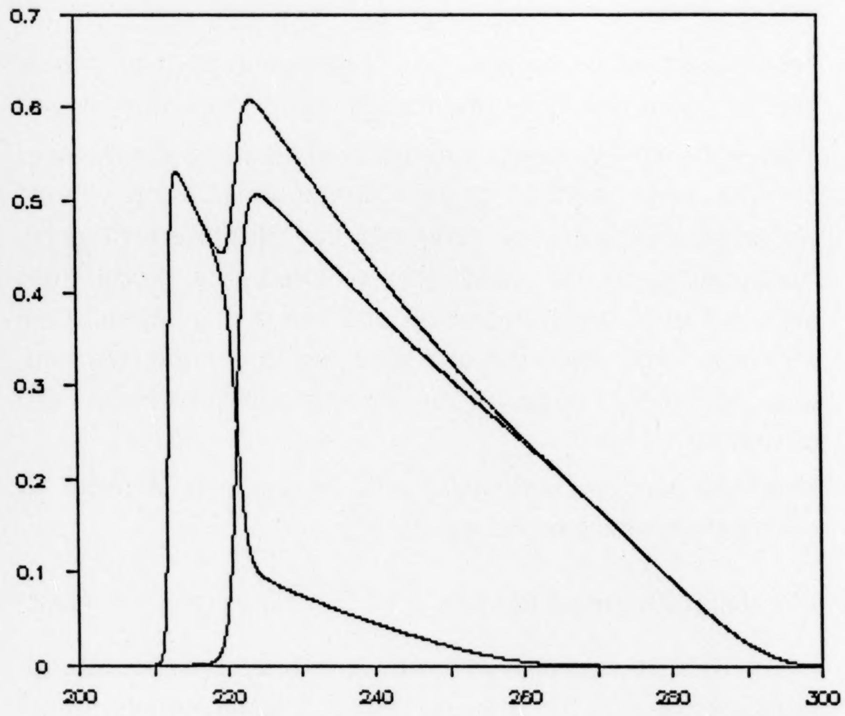

Fig. 6

Elution profiles simulated for a two component separation, separation factor 1.09, under conditions of mass overload. Binary Langmuir isotherm.

For details see ref. [57].

elution profile of each compound must take their interaction into account.

E – Practical Rules

In summary, a few convenient rules can be derived from the extensive body of literature discussing the problem of PLC optimization. They deal with the selection of the components of the phase system, the column design and the flow velocity used.

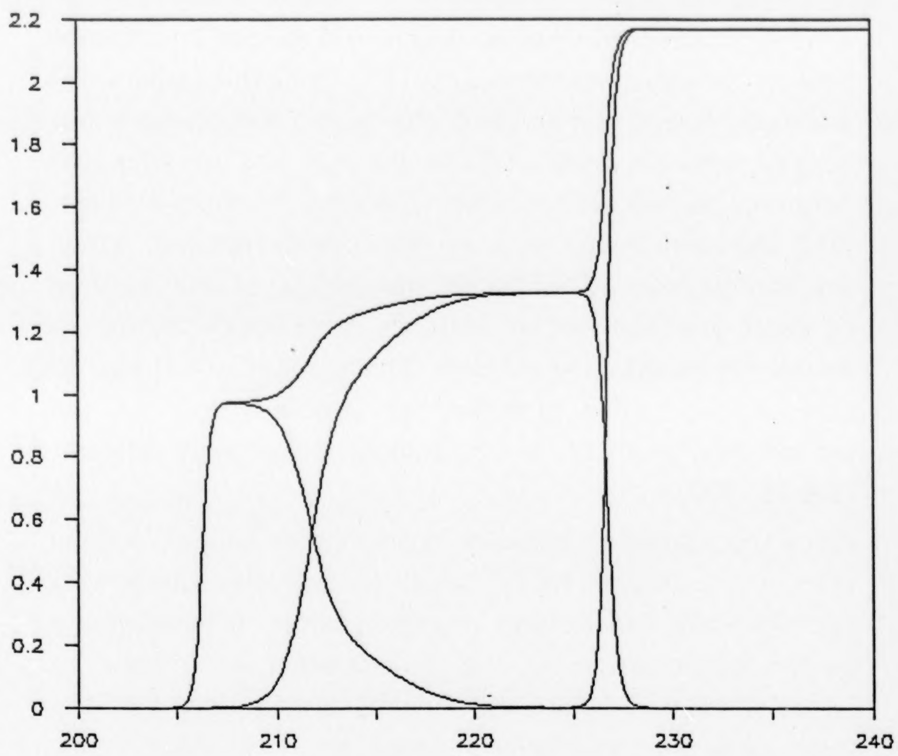

Fig. 7

Displacement chromatogram of a two component separation having the same mass injected as in Fig. 6, for the same compounds, having the same competitive isotherm. The relative retention between the second component and the displacer is 1.2.

See details in ref. [112].

1. Choice of the phase system

The phase system must be selected with more care than for analytical applications. It is important to have a large relative retention between the components of importance in the feed and those from which they must be separated. This has been the obvious conclusion arrived at by all those who have discussed models based on the analytical resolution equation. The relative retention of the compounds to be separated is only one important characteristic, however, another one is the curvature of the isotherm.

It is our observation that for a given compound, on closely related adsorbents, using the same mobile phase, equilibrium isotherms may have similar slopes and markedly different curvatures. For example, isotherms may form a slowly divergent crescent, that is the isotherm with the larger slope is also associated with the larger curvature radius, or isotherms may cross, that is the isotherm with a larger slope is associated with the lower curvature radius. Correlations between the slope and the curvature are not obvious. Clearly, the larger radius of curvature will correspond to the larger column loadability and should be preferred. The situation, where the isotherm has an inflection point placed at the origin could provide an extended concentration range in which the isotherm is close to a straight line, i.e., a larger column loadability. Unfortunately, we do not know well yet how to manipulate the composition of the mobile phase to modify at will the characteristics of the equilibrium isotherms.

It has been reported in at least one instance, that the equilibrium isotherms of two closely related compounds cross each other [105]. These isotherms are single component isotherms, however, and do not explain the behavior of the ternary solution. However, this reference discusses elution profiles of mixtures at high concentration and points to possible complications in their separation. Complex situations may arise if, for example, sorbed compounds interact more strongly in the sorbed layer than in solution, through dipolar forces, hydrogen bonding, charge transfer complexation, etc. Such forces can be used to enhance separation in PLC, but, also, their possible negative influence must be recognized so that their occurence may be avoided.

2. Choice of column

Although the column length, the particle size and the flow velocity control the column efficiency, the requirements of PLC optimization lead one to choose the flow velocity and the column efficiency first, then to design the column. Column efficiency is not the first parameter in PLC. Nevertheless, it is always good to have an efficient column, because the efficiency can be traded off for something useful. In the present case, we may trade efficiency for elution time, by accepting a large flow velocity, or for additional sample load.

It has been reported [57] that although the width of elution bands observed in concentration overload tends to become independent of the column efficiency, in the case of the elution of a binary mixture, the slope of the tail of the first peak and the front of the second one depend strongly on the column efficiency. This is very important as these two slopes determine the width of the interfering zone, the amount of the intermediate fraction to be recycled and the yield of the operation. In this case, the column efficiency is important. This conclusion, based on theoretical calculations, is confirmed by independent measurements [58].

a. Efficiency: Column efficiency can be defined through the height equivalent to a theoretical plate, H. In analytical chromatography, H is both equal to the column length divided by the square of the standard deviation of the elution peak and the sum of the contributions due to molecular, axial diffusion and to resistance to mass transfer. In PLC, due to the thermodynamic contribution to the HETP, the value of the plate number will be different if derived from the two definitions. There appears to be much confusion in the literature surrounding the issue of efficiency and sample loading. Although the peaks broaden with increasing sample loading, and the resolution between closely eluted peaks decreases, the column efficiency as measured from the resistance to mass transfers in and between the mobile and the stationary phases remains constant. Perhaps the former definition which includes kinetic and thermodynamic contributions should be called the apparent efficiency and the later definition the true efficiency of the column.

The importance of column efficiency in PLC is that it provides high resolution between the low concentration bands of the compounds to be separated. By increasing the flow velocity or increasing the sample loading, at the cost of peak overlap, i.e. by accepting a reduction of the apparent efficiency, the production rate can be maximized. The maximum efficiency required for operation in process-scale chromatography is not known; however, the efficiency required will be intimately linked with the flow velocity, the pressure drop, the relative retention of the compounds involved, the curvature of their isotherms and the particle size.

b. Particle size: The particle size directly influences the efficiency, the loading capacity and the pressure drop in PLC. Its effect on efficiency and pressure drop has been extensively studied for applications in analytical chromatography while its effect on sample loading [106] is not as well understood. Optimization of the particle size for large production rates is in its infancy. There appear to be two schools of thought in determining the optimal particle size in PLC. One approach is to use small particles, which yield high efficiency columns. The other approach is to use large particles, but either sacrifice efficiency or increase the column length to generate the same column efficiency obtained for small particles.

The advantage of small particle columns is the high resolution obtainable for difficult separations. The disadvantage is the large pressure drop and the high cost of the particle; although it has been questioned that if the stationary phase is long lasting, the price of the particles compared to the total cost of operating a plant could be small [107]. In contrast, large particles are considered inexpensive and allow for higher throughputs. However, the optimal particle size that should be employed in order to obtain adequate resolution is still not well defined. The throughput can be high, but if the recovery ratio is too low, the process will dot be feasible. Morever, in PLC, the bottom line is the production rate and not the throughput. The chromatographic process leads to a severe dilution of the injected sample, and the lower the column plate height, the lower the concentration of the eluate.

c. Column length: In overloaded elution chromatography, the column length is a parameter that needs to be optimized along with the efficiency, the flow velocity and the particle size. There is a minimum column length, below which the resolution between the bands is not sufficient to permit production of pure enough products. However, there is a maximum length for which it is possible to obtain a homogeneously packed bed. For small particles, it is difficult to pack columns greater than 50 cm in length and for large particles, although they are easier to pack, there will also be a length beyond which the column efficiency does not increase linearly with increasing column length, due to the inhomogeneity of the packed bed. The second parameter which puts an upper limit on the column length is the capacity of the pumping system. Additional parameters which would contribute to optimization of the column length will be the production rate desired, the product purity and the number of recycling steps.

In displacement chromatography, the optimal column length is defined as the length where no further improvement in the separation occurs. This is the distance required for the formation of the displacement train after which the components move at constant velocity, i.e. isotachic conditions. It must be emphasized that an improvement in the separation will not occur for columns

Table II. Applications.

Name of Compound	Column	Column Dimension	Sample Size	Prod. Rate*	Sample Source	Ref #
		i.d. X L cm	mg	mg/min		
adenosine	C18	0.46 X 25	48	0.34	synth. mix.	96
an antibiotic	C18	1 X 50 15 X 60	200 60000	0.12 –	semi-syn. antibiot.	116
aromatase cytochrome P-450	IE mono Q	0.5 X 5	27.7	0.14#	human placenta	123
aromatase cytochrome P-450	size exclus.	0.75 X 30	5.64	0.03#	human placenta	123
$[^{35}S]$ Calmodulin	phenyl	0.4 X 30	0.035-3	<0.2	cell extract	113
cephalosporin	C18	20 X 60	270000	4200	commercial	114
cerebrosides	homemade	2.5 X 40	10	0.08	brain extract	115
catechol	C18	0.46 X 50	160	1.28#	synth.mix	110
3-dihydroxyphenyl acetic acid	C18	0.46 X 25	110	0.11#	synth. mix	96
dipeptide mixture	C18	0.46 X 50	80	4.8 #	synth. mix	96
fibrinonectin domains	Biogel P60	5 X 100	500	–	human plasma fibrinectin	117
gonadotropin releasing hormone	C18	5 X 30	1200	0.93; 0.21	crude syn. product	118
glycopeptides I II III	C18	2.5 X 50	2000	0.13# 0.08# 0.08#	crude antibiotic extract	119
glycopeptides I II III	C18	4.5 X 50	2000	2.0 # 0.93# 0.74#	purified antibiotic	119
glycopeptides I II III	C18	4.8 X 50	25000	13.3 # 11.3 # 8.6 #	crude antibiotic complex	119
glycopeptides I II III	C18	4.8 X 50	50000	27.5 # 25.0 # 24.2 #	crude antibiotic complex	119
4-hydroxyphenyl acetic acid	C18	0.46 X 25	110	0.12	synth. mix	96
2-hydroxyphenyl acetic acid	C18	0.46 X 25	110	0.14	synth. mix	96
jaborosalactone D	silica	0.46 X 25	0.1	0.0001	leaf extr.	120
jaborasalactone A	silica	0.46 X 25	0.1	0.0001	leaf extr.	120
(1E, 3Z) & (1E, 3E)-m-[4-(5,6,7,8 tetrahydro-8,8 di-methyl-2, naphthyl)-1,3-pentadienyl]phenols	silica	1.3 X 50	64	0.26; 0.98	reaction product	121
hydroxyethyl-flurazepam	C18	4.8 X 50	3500	8.8	urine extract	122
human pancreatic grown hormone releasing factor	C18	5 X 30	2100	I 0.9 II 4.9 III 2.0	crude peptide synthesis	118
1 & 4-hydroxy 1,2,3, 4-tetrahydrophenanthrene	silica	5.7 X 30	10000	340 130	synthetic mixture	73
inosine	C18	0.46 X 25	48	0.3#	synthetic mixture	96
L-lactate dehydrogenase	homemade affinity	15 X 200	1800	1.62	rabbit muscle extract	124
lipids	polymer	0.75 X 30	300	22.5	ppb pcb's	125
7α-7β methyl 17β acetoxy-3-oxoandrost-4-enes	30 g C18	4.0 i.d.	700	13.3	reaction product	126
7α-7β methoxycarbonyl methyl steroids	μporasil	5.7 X 30	50	5	from derivatives	127
methyl 2E,4E,6Z & methyl 2E,4E, 6E-3-methyl-7-(5,6,7,8) tetrahydro-8,8dimethyl-2,naphtyl, 2,4,6-octatrichoates	silica	1.3 X 50	50	0.33 0.6	reaction product	121
(4-methoxy-1-naphthyl±methyl phosphine oxide	homemade chiral phase	8 X 22	1000-500	4.0	enantiomers of terpine oxides	128
methyl-(E)-p-[2-(5,6,7,8-tetrahydro-8,8-dimethyl 2-naphthyl)propenyl benzoate	silica	1.3 X 50	53	0.13 0.1	reaction product	121
monoclonal antibodies	IE mono Q	0.5 X 5	25	0.45	ascitic fluid	129
monoclonal antibodies	IE	0.75 X 7.5	10	<0.16	in murine ascites	130

Name of Compound	Column	Column Dimension	Sample Size	Prod. Rate*	Sample Source	Ref #
		i.d. X L cm	mg	mg/min		
neurofilament proteins	C4	1.0 X 25	75	0.13	fibrillary acid	131
oligosaccharrides	amino	0.4 X 25	4.2	0.004 0.002 0.005 0.0073	hydrazinalysis of hen ovomucoid	132
oxazepam	C18	0.94 X 10	40	2.6	semi-purif. urine extract	122
glucuronide	C18	5.7 X 30	3000	7.5		
peptide	C18	5.7 X 30	2.5	0.06	synth. mixture	133
polychlorobiphenols congeners	C18	2.1 X 20	20	0.1	reaction product	134
polyenic antibiotic	C8	1.3 X 47	550	3.0	ferm. product	135
recorcinol	C18	0.46 X 50	160	0.74#	synth. mixture	110
30S ribosomal proteins	IE TSK-SP5	2.1 X 15	100	0.0002	Mix of 21 Proteins	136
50S ribosomal proteins	IE TSK-SP5	2.1 X 15	100	0.0003	Mix of 25 Proteins	136
sinapoylglucose	C18	1.6 X 25	–	2.5	plant extract	137
terpines (oxygenated)	silica gel	2.0 X 50	2110	–	hydrocarbons	138
thrombin	1-arginyl methylester mod. polystyrene	1.0 X 20	–	0.003#	human plasma fraction	139
try-34b PTH amide	polyacrylamide	2.0 X 100	86.5	0.5#	solid ph. syn. mixture	140
withaferin A	silica	0.46 X 25	0.15	0.0001	leaf extract	120
withanolides A	silica	0.46 X 25	0.15	0.0001	leaf extract	120

*Production rate estimated from data supplied in corresponding reference. Some of the values are very approximate due to the limited amount of information published.

#Excluding time to regenerate the column as in displacement chromatography or reequilibrate the column during gradient operation.

of greater length. Therefore, the column length is of primary importance in the design of a column for prepapartive displacement separations. This length is a function of the amount of the feed stock, however, which provides some flexibility in the selection of operating conditions.

d. Flow velocity: The maximum flow velocity is determined by the particle size, column dimensions and pump capacity. Although initially it seems favorable to operate at high flow velocity to obtain large production rates, it is not clear that operating with maximum throughput is optimal. Again, there are tradeoffs and there are limitations. Since the HETP increases with increasing flow velocity, thus increasing the peak overlap, there is a tradeoff between throughput and resolution. Additionally, solvent consumption increases with increasing flow velocity at a point the cost will exceed the benefit. There is a need for systematic studies for the optimization of the flow rate in PLC, but this must be done in combination with the other parameters.

F – Unsolved Issues

As we have shown in this section there is still considerable uncertainty regarding the basis of an optimization theory of PLC. The issues dealing with column overloading and some of the issues dealing with column design are far from solved. Research is very active in these area, however, and a solution should be reached in a rather short time. There are, however, several issues which have been hardly investigated so far. One of them deals with the optimum number of recycling steps. In many complex cases, it is not possible to achieve the required purity during the first step. The fractions prepared during this first step must be reprocessed. It would be useful to find methods to predict the number of steps necessary and the order in which these several steps must be carried out.

Finally, we have not discussed the problems asociated with the use of gradient elution. The discussion of band profiles and of the separation between bands in isocratic chromatography is complex enough. In spite of its practical importance, the theory of gradient PLC, which seems formidable to discuss, will take a long time to unravel.

VI Applications

Hundreds of applications employing preparative liquid chromatography have been published with the goal of isolating various compounds. Although these applications are concerned with finding elution conditions in order to obtain a specific quantity of product, many do not discuss their results in quantitative terms. However, many do not discuss their results in quantitative terms. However, it is important to consider the applications within the context of preparative liquid chromatography and in terms of the production rate, throughput, yield, and product purity. In order to summarize various applications, Table II presents a brief list of compounds in alphabetical order which have been isolated along with the stationary phase employed, the column dimensions, the sample size, the sample source, and an estimated production rate. The list was not intended to be comprehensive and excludes many papers where it was not possible to calculate a production rate from the published data.

The production rate is calculated as the amount of pure compound produced per unit time, that is the product of the throughput, the concentration of the corresponding component in the feed and the yield as estimated from the experimental data presented in the respective papers. When the chromatography was conducted under conditions where regeneration or reequilibration of the column was required, for example, when displacement chromatography or gradient elution is employed, the production rate estimated excludes the time needed for these processes.

References

[1] *M. Verzele, C. Dewaele,* "Preparative High Performance Liquid Chromatography, A Practical Guideline", TEC, Gent, Belgium, 1985.

[2] *P. C. Wankat,* "Large-Scale Adsorption and Chromatography", Vol. 1 and 2, CRC Press, Boca Raton, Fl, 1986.

[3] *M.S. Tswett,* Ber. Deutsch. Botan. Ges. **24,** 316 (1906).

[4] *M.S. Tswett,* Ber. Deutsch. Botan. Ges. **24,** 384 (1906).

[5] *M.S. Tswett,* "Khromofilly v Rastitel'nom Zhivotnom Mire" [Chromophylls in the Plant and Animal World] Izd. Karbasnikov, Warzaw, Poland, 1910. (Partly reprinted in 1946 by the publishing house of the Soviet Academy of Science, *A.A. Rikhter* and *T.A. Krasnosel'skaya* (Eds.)).

[6] *C. Dhere, W. Rogowski,* C.R. Acad. Sci., Paris, France, **155,** 653 (1912).

[7] *C. Dhere, G. Vegezzi,* C.R. Acad. Sci., Paris, France, **163,** 399 (1916).

[8] *L.S. Palmer, C. Eckles,* J. Biol. Chem. **17,** 191 (1914).

[9] *R. Kuhn, E. Lederer,* Naturwissenschaften **19,** 306 (1931).

[10] *R. Kuhn, A. Winterstein, E. Lederer,* Z. Physiol. Chem. **197,** 141 (1931).

[11] *R. Kuhn, E. Lederer,* Bericht. **64,** 1349 (1931).

[12] *A. Tiselius, S. Claeson,* Arkiv Kemi Mineral Geol. **16A,** 18 (1943).

[13] *L.S. Ettre,* in "High Performance Liquid Chromatography: Advances and Perspectives", *C. Horvath* (Ed.), Academic Press, New York, NY, Vol. 1, 1980, p. 25.

[14] *F.H. Spedding, A.F. Voigth, N.R. Sleight, J.E. Powel, J.M. Wright, T.A. Butler, P. Figard,* J. Am. Chem. Soc. **69,** 2746 (1947).

[15] *F.H. Spedding, E.I. Fulmer, J.E. Powel, T.A. Butler,* J. Am. Chem. Soc. **72,** 2349 (1950).

[16] *F.H. Spedding, J.E. Powel,* J. Am. Chem. Soc. **76,** 2545 (1954).

[17] *F.H. Spedding, J.E. Powel,* J. Am. Chem. Soc. **76,** 2550 (1954).

[18] *F.H. Spedding, J.E. Powel, H.J. Svec,* J. Am. Chem. Soc. **77,** 6125 (1955).

[19] *F.H. Spedding, J.E. Powel,* in "Ion-Exchange Technology", *F.C. Nachod* and *J. Schubert* (Eds.), Academic Press, New York, NY, 1956, p. 359.

[20] *D.L. Camin, A.J. Raymond,* J. Chromatogr. Sci. **11,** 625 (1973).

[21] *B.J. Mair, A.L. Gaboriault, F.D. Rossini,* Ind. Eng. Chem. **39,** 1072 (1947).

[22] *B.J. Mair, A.J. Sweetman, F.D. Rossini,* Ind. Eng. Chen. **41,** 2224 (1949).

[23] *B.J. Mair, J.W. Westhaver, F.D. Rossini,* Ind. Eng. Chem. **42,** 1279 (1950).

[24] *D.B. Broughton,* Sep. Sci. Tech. **19,** 723 (1984).

[25] *P.E. Barker, R.E. Deeble,* Chromatographia **8,** 67 (1975).

[26] *C.D. Scott, R.D. Spence, W.G. Sisson,* J. Chromatogr. **126,** 381, (1976).

[27] *L. Jacob, G. Guiochon,* Chromatogr. Rev. **14,** 77 (1971).

[28] *P. Rouchon, M. Schonauer, P. Valentin, G. Guiochon,* in "The Science of Chromatography", *F. Bruner* (Ed.), Elsevier, Amsterdam, NL, 1985, p. 131.

[29] *J. Jacobson, J. Frenz, C. Horvath,* J. Chromatogr. **316,** 53 (1984).

[30] *L. Lapidus, N.R. Amundson,* J. Phys. Chem. **56,** 984 (1952).

[31] *J.F.K. Huber,* Ber. Bunsenges. Phys. Chem. **77,** 179 (1973).

[32] *C. Horvath, H.J. Lin,* J. Chromatogr. **149,** 43 (1978).

[33] *K. Unger,* 3rd Symp. Preparative Liquid Chromatogr., Washington, DC, 1987.

[34] *D. Forin, S. Peleg, D. Yavin, D. Avnir,* Langmuir **1,** 399 (1985).

[35] *G. Guiochon,* in "High Performance Liquid Chromatography. Advances and Perspective", *C. Horvath* (Ed.), Academic Press, New York, NY, 1980, p. 1.

[36] *J.L. Wade, A.F. Bergolde, P.W. Carr,* Anal. Chem. **59,** 1286 (1987).

[37] *J.C. Giddings,* "Dynamics of Chromatography", M. Dekker, New York, NY, 1965.

[38] *J.C. Giddings,* J. Chem. Phys. **26,** 169 (1957).

[39] *J. Villermaux,* J. Chromatogr. **83,** 205 (1973).

[40] *D. De Vault,* J. Amer. Chem. Soc. **65,** 532 (1943).

[41] *G. Houghton,* J. Phys. Chem. **67,** 84 (1963).

[42] *A. Jaulmes, C. Vidal-Madjar, A. Ladurelli, G. Guiochon,* J. Phys. Chem. **88,** 5379 (1984).

[43] *A. Jaulmes, C. Vidal-Madjar, H. Colin, G. Guiochon,* J. Phys. Chem. **90,** 207 (1986).

[44] *G. Guiochon, S. Golshan-Shirazi,* in preparation.

[45] *J.C. Giddings,* in "Chromatography", *E. Heftmann* (Ed.), Van Nostrand, New Yor, NY, 1975, p. 27.

[46] *H. Poppe, J.C. Kraak,* J. Chromatogr. **255,** 395 (1983).

[47] *G. Guiochon, H. Colin,* Chromatography Forum **1,** xxxx (1986).

[48] *C.N. Reilley, G.P. Hildebrand, J.W. Ashley,* Anal. Chem. **34,** 1198 (1962).

[49] *von E. Wicke,* Ber. Bunsenges. Phys. Chem. **69,** 761 (1965).

[50] *F. Helfferich, G. Klein,* "Multicomponent Chromatography, Theory of Interference", M. Dekker, New York, NY, 1970.

[51] *J. Frenz,* PhD Thesis, Yale University, New Haven, CT, 1983.

[52] *H.K. Rhee, R. Aris, N. Amundson,* Trans. Roy. Soc. **A267,** 419 (1970).

[53] *J.C. Sternberg,* in "Advances in Chromatography", *J.C. Giddings* and *R.A. Keller* (Eds.), M. Dekker, New York, NY, **2,** 205 (1966).

[54] *E. sz Kovats,* in "The Science of Chromatography", *F. Bruner* (Ed.), Elsevier, Amsterdam, NL, 1985, p. 205.

[55] *P. Rouchon, M. Schonauer, P. Valentin, G. Guiochon,* Separation Science **22** (1987), to be published.

[56] *G. Guiochon, S. Golshan-Shirazi,* unpublished data. 1986.

[57] *G. Guiochon, S. Ghodbane,* unpublished data, 1986.

[58] *J. Newburger, L. Liebes, H. Colin, G. Guiochon,* Separation Science, to be published, 1987.

[59] *F. Riedo, E. sz Kovats,* Anal. Chem., J. Chromatogr. **239,** 1 (1982).

[60] *I. Dekany, L.G. Nagy, G. Schay,* J. Colloid and Interface Science, **66,** 197 (1978).

[61] *B.C. Lin, S. Golshan-Shirazi, G. Guiochon,* unpublished data, 1987.

[62] *S.J. Gibbs, E.N. Lightfoot,* Ind. Eng. Chem. Fundam. **25,** 49 (1986).

[63] *R.F. Meyer, P.B. Champlin, R.A. Hartwick,* J. Chromatogr. Sci. **21,** 433 (1983).

[64] *M. Kaminski, J. Klawiter, J.S. Kowalszyk,* J. Chromatogr. **243,** 207 (1982).

[65] *M. Verzele, E. Geeraert,* J. Chromatogr. **18,** 559 (1980).

[66] *M. Kaminski, J. Klawiter, J.S. Kowalszyk,* J. Chromatogr. **243,** 225 (1982).

[67] *P.A. Bristow, P.N. Brittain, C.M. Riley, B.F. Williamson,* J. Chromatogr. **131,** 57 (1977).

[68] *M. Martin, G. Guiochon,* Chromatographia **10,** 194 (1971).

[69] *H. Colin,* Prochrom, Nancy, France, Private Communication, 1987.

[70] *P. Hilaireau,* Prochrom, Nancy, France, Private Communication, 1986.

[71] *R.B. Bird, W.E. Stewart, E.N. Lightfoot,* "Transport Phenomena", Wiley, New York, NY, 1960.

[72] *J.G. Atwood, G.J. Schmidt, W. Slavin,* J. Chromatogr. **171,** 109 (1979).
[73] *J.W. Little, R.L. Cotton, J.A. Pendergast, P.D. McDonald,* J. Chromatogr. **126,** 439 (1976).
[74] *D.E. Nettleton,* J. Liq. Chromatogr. **4,** 359 (1981).
[75] *E. Godbille, P. Devaux,* J. Chromatogr. Sci. **12,** 565 (1974).
[76] *E. Godbille, P. Devaux,* J. Chromatogr. **122,** 317 (1976).
[77] *P. Jennings,* 1987 Pittsburgh Conf. Anal. Chem., paper No. 174.
[78] *J.H. Knox, J.F. Parcher,* Anal. Chem. **41,** 1599 (1969).
[79] *J.H. Knox, G.R. Laird, P.A. Raven,* J. Chromatogr. **122,** 129 (1976).
[80] *J.G. Atwood, M.J.E. Golay,* J. Chromatogr. **218,** 97 (1981).
[81] *B. Coq, G. Cretier, J.L. Rocca, R. Kastner,* J. Chromatogr. **178,** 41 (1979).
[82] *A.W.J. DeJong, H. Poppe, J.C. Kraak,* J. Chromatogr. **148,** 127 (1978).
[83] *C. Coq, C. Cretier, C. Rocca,* J. Chromatogr. **186,** 457 (1979).
[84] *A. Joraczko, D. Jenota, L. Wojt,* J. High Resolut. Chromatogr. Chrom. Commun. **9,** 255 (1986).
[85] *W.H. Pirkle, R.W. Anderson,* J. Org. Chem. **39,** 3901 (1974).
[86] *A.Y. Tehrani,* Am. Lab., February 1985, p. 43.
[87] *S.M. Cramer, Cs. Horvath,* in press.
[88] *Z. El-Rassi, Cs. Horvath,* J. Chromatogr. **266,** 319 (1983).
[89] *D. Beger, B. Gilliaud,* J. Chromatogr. **210,** 33 (1981).
[90] *A.F. Hatfield, R.N. Dreyer, A.C. Sartorelli,* J. Chromatogr. **257,** 1 (1983).
[91] *D.A. Kohler, M.J. Telepchak,* Am. Lab. January 1979, p. 75.
[92] *F.R. Sugnaux, C. Djerassi,* J. Chromatogr. **248,** 373 (1982).
[93] *P.A. Bristow,* J. Chromatogr. **122,** 277 (1976).
[94] *H. Colin, G. Lowy, J. Cazes,* Am. Biotechnol. Lab. **3,** 36 (1985).
[95] *J.H. Knox, H.M. Pyper,* J. Chromatogr. **363,** 1 (1986).
[96] *Cs. Horvath, J. Frenz, Z. El-Rassi,* J. Chromatogr. **255,** 273 (1983).
[97] *R.P.W. Scott, P. Kucera,* J. Chromatogr. **119,** 461 (1976).
[98] *B. Coq, G. Cretier, C. Gonnet, J.L. Rocca,* Chromatographia **12,** 139 (1979).
[99] *L. Personnaz, P. Gareil,* Sep. Sci. and Tech. **16,** 135 (1981).
[100] *H. Colin,* Eastern Analytical Symposium, New Yor, NY, 1986.
[101] *Gareil,* PhD. Thesis, Universite Pierre et Marie Curie, Paris, 1983.
[102] *J.E. Eble, R.L. Grob, P.E. Antle, L.R. Snyder,* J. Chromatogr. **384,** 25 (1987).
[103] *J.E. Eble, R.L. Grob, P.E. Antle, L.R. Snyder,* J. Chromatogr. **384,** 45 (1987).
[104] *J.E. Eble, R.L. Grob, P. E. Antle, L.R. Snyder,* J. Chromatogr., to be published, 1987.
[105] *M.J. Gonzales, A. Jaulmes, P. Valentin, C. Vidal-Madjar,* J. Chromatogr. **386,** 333 (1987).
[106] *H. Colin, G. Guiochon,* in preparation.
[107] *H. Colin,* to be published, Chromatographia, 1988. (Lecture presented to HPLC'87.)
[108] *E. Grushka,* 3rd Symposium on Preparative HPLC, Washington, DC, May 1987.
[109] *J. Frenz, Ph. Van der Schrieck, Cs. Horvath,* J. Chromatogr. **330,** 1 (1985).
[110] *Cs. Horvath, A. Nahum, J. Frenz,* J. Chromatogr. **218,** 365 (1981).
[111] *J. Frenz, Cs. Horvath,* AIChE J. **31,** 400 (1985).
[112] *A. Katti, G. Guiochon,* unpublished results, 1987.
[113] *A.S. Manalan, D.L. Newton, C.B. Klee,* J. Chromatogr. **326,** 387 (1985).
[114] *A.M. Cantwell, R. Calderone, M. Sienko,* J. Chromatogr. **316,** 133 (1984).
[115] *K. Kant, R.M. Hallen,* Anal. Biochem. **147,** 455 (1985).
[116] *C.K. Shih, C.M. Snavely, T.E. Molnar, J.L. Meyer, W.B. Caldwell, E.L. Paul,* Chem. Eng. Prog. **79,** 53 (1983).
[117] *K. Majumdar, P.K. Latha, S.K. Brahmadien,* J. Chromatogr. **355,** 328 (1986).
[118] *J. Rivier, R. McClintock, R. Galyenn, H. Anderson,* J. Chromatogr. **288,** 303 (1984).
[119] *R.D. Sitrin, G. Chan, P. DePhillips, J. Dingerdissin,* in Purfication of Fermentation Products, ACS Symposium Series (1985).
[120] *G. Burton, A.S. Veleiro, E.G. Gros,* J. Chromatogr. **248,** 472 (1982).
[121] *S. Mohanraj,* J. Liq. Chromatogr. **7,** 1455 (1984).
[122] *R. Dixon, R. Evans, T. Crews,* J. Liq. Chromatogr. **7,** 177 (1984).
[123] *N. Muto, L. Tan,* J. Chromatogr. **326,** 137 (1985).
[124] *Y.D. Clonis, K. Jones, C.R. Lowe,* J. Chromatogr. **363,** 31 (1986).
[125] *M.P. Seymour, T.M. Jefferies, L.J. Notarianni,* Analyst (London) **111,** 1203 (1986).
[126] *F. Gasparrini, S. Cacchi, L. Caglioti, D. Misiti, M. Giovannoli,* J. Chromatogr. **194,** 239 (1980).
[127] *B. Charpentier, A. Dingas, D. Duval, R. Emiliozzi,* J. Chromatogr. **355,** 427 (1986).
[128] *A. Tambute, P. Gariel, M. Caude, R. Rosset,* J. Chromatogr. **363,** 81 (1986).
[129] *J.P. Mahieu, B. Sebille, M. Gosselet, M.C. Garet, Y. Bewzard,* J. Chromatogr. **359,** 461 (1986).
[130] *M.P. Strickler, M.J. Gemski,* J. Liq. Chromatogr. **9,** 1655 (1986).
[131] *K.-S. Hui, M. Hui, F.-C. Chiu, M. Baney-Schwartz, T. Deguzman, R.S. Sacchi, A. Lajtha,* Anal. Biochem. **153,** 230 (1986).
[132] *J.P. Parente, G. Strecker, Y. Leroy, J. Montreuil, B. Fournet,* J. Chromatogr. **249,** 199 (1982).
[133] *D.R. Knighton, D.R.K. Harding, J.R. Napier, W.S. Hancock,* J. Chromatogr. **249,** 193 (1982).
[134] *J.D. McCurry, G.D. Davies,* Anal. Chem. **58,** 2785 (1986).
[135] *P. Gariel, G. Salinier, M. Caude, R. Rosset,* J. Chromatogr. **208,** 365 (1981).
[136] *M. Capel, D. Datta, C.R. Nierras, G.R. Craven,* Anal. Biochem. **158,** 179 (1986).
[137] *W. Brandl, K. Herrmann,* J. Chromatogr. **260,** 447 (1983).
[138] *T. Yamasaki, M. Sakai, T. Kanamori, M. Sogo,* Chromatographia **21,** 478 (1986).
[139] *A.M. Fisher, X.J. Yu, J.-T. Bretaudiere, D. Muller, A. Bros, J. Jozefonvicz,* J. Chromatogr. **376,** 429 (1986).
[140] *A. Tyler, M. Rosenblatt,* J. Chromatogr. **266,** 313 (1983).

Received: Aug 6, 1987
Accepted: Aug 24, 1987
F

A Review of Reaction Detection in HPLC

U. A. Th. Brinkman

Free University, Dept. of Analytical Chemistry, De Boelelaan 1083, 1081 HV Amsterdam, The Netherlands

Key Words

Post-column reaction detection
Photochemical reactors
Solid-phase reactors
Chemiluminescence detection
Fluorescence detection

Summary

In the past decade, reaction detection has rapidly gained importance as a means to improve the sensitivity and selectivity of detection in HPLC. Today, most attention is being paid to post-column reaction detection with final analysis via fluorescence monitoring. Novel developments involve the use of solid-phase reactors for reagent addition or catalysis (ion-exchange resins, immobilized enzymes), and the increasing use of systems based on peroxyoxalate chemiluminescence detection. The rapidly growing number of reported applications indicates that commercialization of reaction-detection equipment is urgently needed.

Introduction

In the past few years, a large number of papers, reviews and books has been published on the use of reaction detection as a powerful means to improve the sensitivity and selectivity of detection in HPLC. A series of selected references, some of which contain exhaustive bibliographies, are included in the list of references to this paper [1–6].

In order to understand the rapidly increasing popularity of reaction detection, one should realize that in modern trace-level analysis – which, in a large majority of cases, is concerned with the determination of organic constituents in complex mixtures of biomedical, pharmaceutical or environmental, etc. origin – chromatographic techniques play a predominant role. They are employed to create an efficient separation prior to the actual measurement, i.e., detection step. Unfortunately, however, even the combined force of an efficient separation and a sophisticated mode of detection does not always create sufficient selectivity and/or sensitivity for the final goal to be reached – quantitation of sample constituents typically present at the low ppm to low ppt (ca. 10^{-5}–10^{-11} g/ml) range. In such cases, special attention has to be devoted to sample pretreatment (for trace enrichment and clean-up) – which will *not* be discussed in the present overview – and pre- or post-separation derivatization or conversion of the analyte(s) of interest. The latter topic will be discussed in some detail below. Special attention will be given to the main selection criteria for proper reaction detection chemistry, reaction detection chemistry itself, and the discussion of a few illustrative real-life examples.

Reaction Detection: General Aspects

Pre- and Post-Column Reactors

In principle, chemical derivatization or conversion of trace-level analytes can be carried out in a pre-column or post-column mode. The main advantages of post-column reactions are:

- the analytes are separated in their original form, which often permits the adoption of published separation procedures
- artefact formation plays a minor role, which is in distinct contrast with derivatization or conversion prior to separation
- the reaction does not need to be complete and the reaction products need not be stable; the only requirement is reproducibility.

Disadvantages of post-column reaction detection are (i) the need to add reagent(s) or reagent solution(s) which generally will require the use of additional pumps, (ii) the extra-column band broadening caused by the reactor, which may well mar the chromatographic resolution, and (iii) the presence of excess reagent which can interfere with the signal of the reaction products. Means to reduce these disadvantages will be included in the examples given below.

0009-5893/87 0190-11 $03.00/0

© 1987 Friedr. Vieweg & Sohn Verlagsgesellschaft mbH

For the rest, one should realize that post-column reaction detection is invariably carried out in an on-line mode, which makes the technique well suited for use in automated systems, i.e., for the processing of large series of samples. Pre-column techniques, on the other hand, are most often employed in an off-line mode. For that reason, they are in a way outside the field of reaction detection, as it is usually defined. In the present paper, attention will therefore mainly be focussed on the potential and limitations of post-column reaction detection. Interesting recent developments in the area of (semi) on-line pre-column reaction detection will be mentioned briefly.

HPLC-Reaction Detection Systems

A typical — though neither the simplest nor the most sophisticated (cf. below) — schematic of an HPLC system with reaction detector is shown in Fig. 1. Pump 1 is used to deliver the eluent. After the separation — which is generally carried out on a chemically bonded phase or on an ion exchanger — a reagent solution is added by means of the, preferably pulseless (post-column situation!), pump 2 via a low-dead-volume mixing tee. The post-column reactor provides the desired hold-up time for the reaction. Finally, the combined streams are passed through the detector. Several remarks should be made here.

Reactor. Three main types of reactors are generally distinguished, their choice being primarily dependent on the kinetics of the reaction involved: open-tubular reactors, packed-bed reactors and segmented-stream reactors.

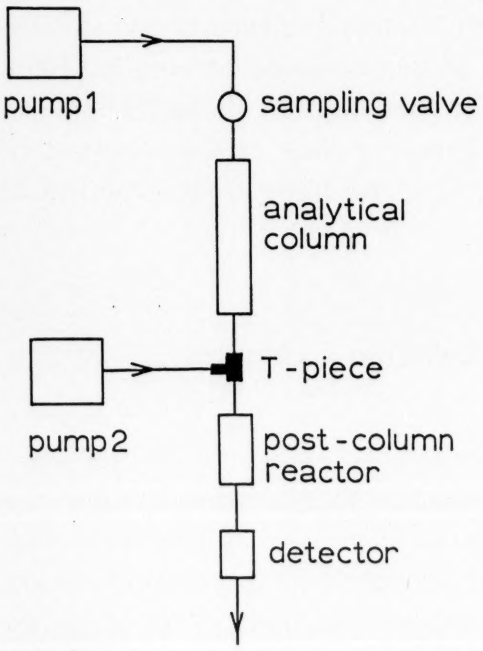

Fig. 1

Typical schematic of an HPLC system with reaction detector. For details, see text.

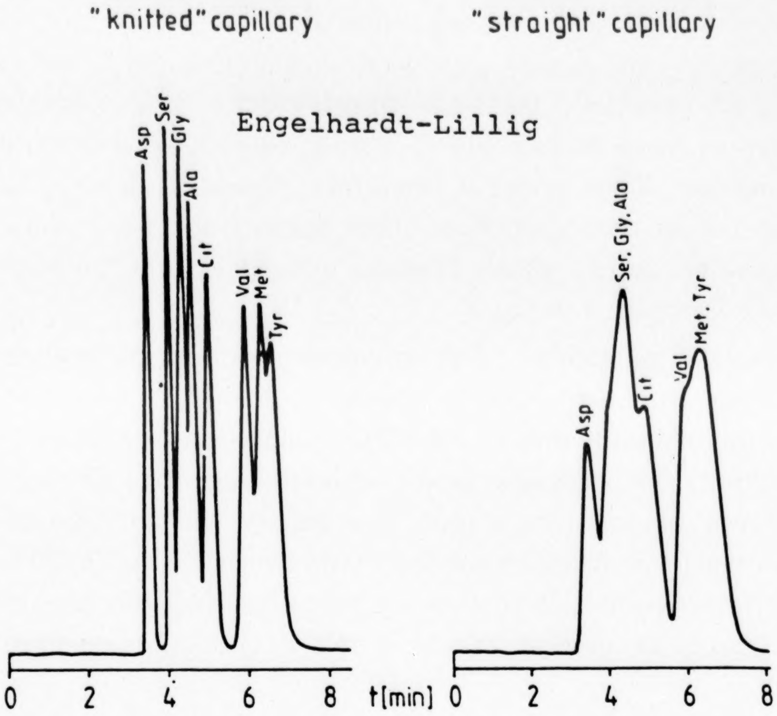

Fig. 2

The effect of replacing a knitted by a straight capillary on resolution. HPLC separation of derivatized amino acids under otherwise identical conditions [9].

The open-tubular reactor is the post-column reactor that it is the most simple to construct. It is a straight, coiled or knitted piece of stainless-steel, glass or PTFE tubing, and its dimensions are mainly determined by the hold-up time required for the reactions being used. Coiling or knitting is recommended because it effects a relative decrease in band broadening due to secondary-flow phenomena [7–9]. The effect of replacing a knitted by a straight capillary on resolution, is nicely demonstrated in Fig. 2 using a critical HPLC separation — and otherwise identical conditions — as example [9]. Open-tubular reactors are preferably used for reactions with fast kinetics, i.e., for residence times of up to 30–60sec.

Initially, packed-bed reactors were stainless-steel or glass columns packed with small (typically, 10–15μm particle diameter), inert, non-porous glass beads. Such reactors were shown to have favourable characteristics with regard to mixing and band broadening for reactions with intermediate reaction times of about 0.5–4min [7, 10], and also for use with narrow-bore (1mm i.d.) columns [11]. Today, however, such reactors are more often packed with active instead of inert materials. These so-called solid-phase reactors are increasingly used for catalytic (ion-exchange resins, immobilized enzymes) as well as stoichiometric (redox reagents, finely divided metals) reactions. Examples will be included in the relevant sections below.

Segmented-stream tubular reactors are especially useful in the case of reactions with slow kinetics which require reactor residence times of 4–5min or more. The segmented-stream technique is based on segmenting the HPLC column effluent with either air bubbles or non-miscible solvent plugs. If leakage from one solvent segment to another is prevented by means of a proper choice of the reactor tubing material and if the size of the individual segments is sufficiently small, axial dispersion is efficiently reduced [12]. As a consequence, additional band broadening is negligible even for residence times of, e.g., some 20min [13]. Working with a segmented-stream system is relatively complex in that it requires debubbling (air segmentation) or phase separation (solvent segmentation) prior to the actual detection step. In practice, the debubbler or phase separator make rather large contributions to band broadening [14, 15] as can, for example, be read from the data in Table I:

even though the capillary dimensions – and, thus, the residence time – vary considerably, the measured σ_t values remain essentially the same. In other words, the contribution to band broadening is mainly caused by the phase separator. Much effort is, therefore, nowadays devoted to the proper construction of these parts. One recent phase separator design which features a dead volume of 40μl only, is depicted in Fig. 3.

Reaction principles. Any chemical reaction or analyte conversion which can be carried out under conditions compatible with that of the HPLC separation – with compatibility, if necessary, being achieved by means of post-column pH or temperature changes, or the addition of another (non-miscible) solvent – and which yields 40–50% or more product formation within several minutes can, in principle, be used as the basis of a post-column reaction detection system. Reaction principles which have been applied extensively in the literature and which will, therefore, be discussed in this paper include:

- chemical derivatization, which includes conventional derivatization reactions with, e.g., dansyl chloride or o-phthalaldehyde (OPA) as well as ion-pair formation and ligand exchange – with the latter two principles being typical examples of rather rapid and relatively slow reactions, respectively
- UV irradiation which effects the conversion of the analyte(s) of interest into products that display a strongly improved detectability in, e.g., fluorescence or electrochemical detection; since most compounds are decomposed to different extents if subjected to UV irradiation, this reaction principle may be expected to provide high selectivity
- solid-phase reactions which include catalytic as well as stoichiometric principles (cf. above) and which have the inherent advantage that the catalytic action or reagent supply occurs on-line without the use of an additional pump
- chemiluminescence, a reaction principle which is rapidly gaining in popularity and which, if combined with an HPLC separation, is almost invariably based on the highly efficient and versatile peroxyoxalate system; its essentials are explained in Fig. 17 (cf. [17]) below.

Detection step. Next to reaction, reaction detection of course also requires detection itself. According to literature surveys and the experience of experts, in HPLC generally, over 80% of all detection is done by means of UV-vis absorption measurement, with a further 5–7% for fluorescence and electrochemical detection each. In the field of reaction detection, the situation is substantially different. The high selectivity and sensitivity aimed at in this area strongly favours the use of fluorescence as the detection mode. UV-vis absorption is a distinctly less attractive choice; however, it possesses the advantage of general availability and, besides, is often a satisfactory alternative in cases where detector selectivity is relatively unimportant because of extensive clean-up via sample pretreatment. Surprisingly little attention has been devoted to electrochemical detection which displays a selectivity and sensitivity comparable to that of luminescence techniques. Here, the main barriers no doubt are an often unusually high loss in performance when analyzing real samples instead of standard solutions [18], and the insufficient expertise of many analytical chemists.

Table I. Influence of length and internal diameter of PTFE capillaries on band broadening [15].

Conditions: segmentation liquid, hexane; flow-rates, eluent at 0.88 ml/min, hexane at 0.32 ml/min, flow via phase separator through flow-cell, 0.53 ml/min; injection, 20μl of $NaNO_3$ solution.

Capillary L (m)	i.d. (mm)	σt (sec) with eluent: water	water-MeOH (1:1)	Residence time (sec)
1	0.5	2.4	2.4	9
5	0.5	2.2	2.2	45
1	0.8	2.3	2.5	20
5	0.8	2.3	2.4	97
10	0.8	2.4	2.6	265

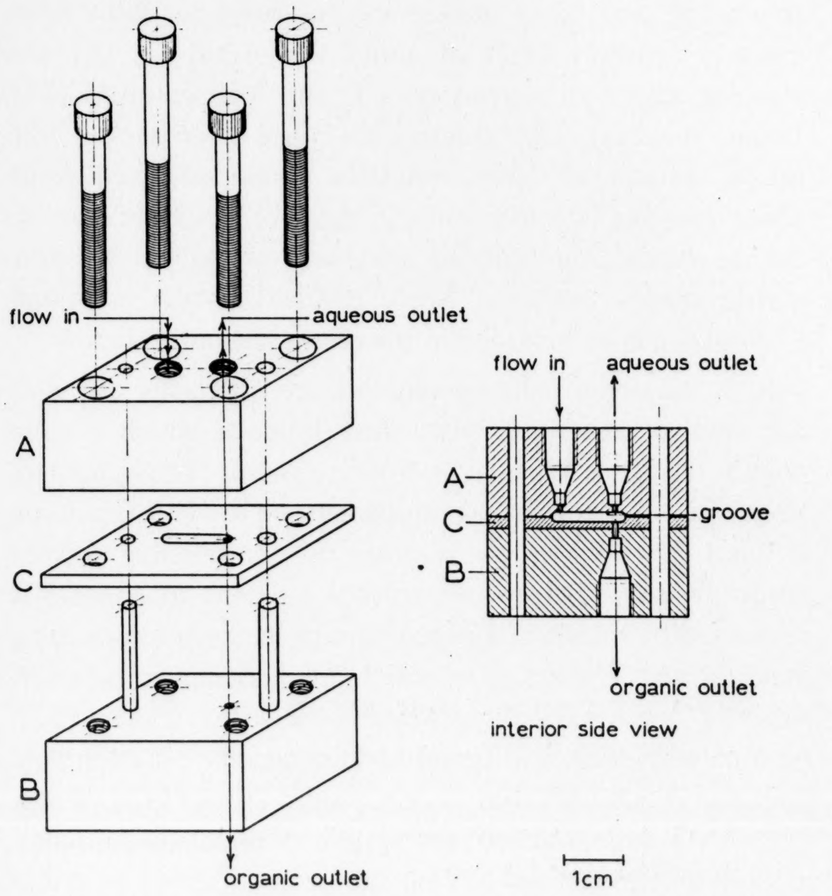

Fig. 3

Sandwich-type phase separator with about 40μl internal volume (groove). Parts A and B constructed of stainless steel; part C constructed of PTFE. Phase separation is based on the wetting principle [16].

Reaction Detection: Selected Examples

Photochemical Reactors

Next to the solid-phase reactors to be discussed below, the photochemical reactor is an example of a pumpless reaction unit: in the simplest case, photons are the only reagent added. If we limit ourselves to the area of detection by means of fluorescence monitoring, the irradiation with UV light converts the weakly or non-fluorescing analytes into reaction products which are highly fluorescent. Photochemical reactors for use with HPLC systems are not commercially available. The laboratory-made reactors all essentially consist of a medium- or high-power mercury or xenon-mercury light source, a PTFE reaction coil – which shows an efficient light transmission in the 200–300nm region comparable to that of quartz, which is more expensive and less easy to handle – and a reactor housing which allows good temperature control. The temperature should be kept rigidly constant, because fluctuations will affect the HPLC eluent flow-rate as well as the reaction kinetics and/or pathways and, consequently, will mar the optimization procedure.

Most photochemical reactions utilized to yield fluorescent products for HPLC analyses require reactor residence times of some 5–60sec only. That is, an open-tubular reactor is the best choice, especially if it is either coiled or knitted. Uihlein and Schwab [19] used an elegant knitted reactor with the UV light source mounted on a sledge so that it could be moved easily further into or out of the reactor proper in order to vary the irradiation time. Nieder and Jaeger [20] have recently described a reactor having a PTFE capillary coiled around two light sources; they demonstrate that band broadening is clearly less with a non-helical as compared to a helical coil.

A number of applications of HPLC with on-line photochemical conversion and fluorescence detection is presented in Table II. Most of these are for urine, blood and/or surface water samples. The detection limits often are 50–500pg and, according to expectation, the selectivity is high. As an example, the determination of the anti-anxiety drug clobazam and its metabolite desmethylclobazam in serum is shown in Fig. 4 [23, 24]. Neither of the two compounds displays native fluorescence, but an optimum irradiation time of 15sec suffices to identify them with detection limits of 20pg and 50pg, respectively.

Table II. Applications of HPLC with on-line photochemical reaction detection*

Cannabinol	Demoxepam	Methotrexate
Chlorophenols	Desmethylclobazam	Phenothiazines
Ciprofloxacin	Diethylstilbestrol	Phenylureas
Clobazam	LSD	Tamoxifen
Clomiphene	Metal ions	Vitamin K_1

* For references, see especially [21, 22]. Some applications also deal with metabolite determination.

The use of a photochemical reaction followed by electrochemical detection has been studied extensively by Krull and his co-workers [25, 26], and they have published pertinent analytical data for a wide variety of organic nitro compounds. For all of these, photolysis releases inorganic nitrite which can easily be detected under oxidative electrochemical conditions. Fig. 5 shows single-electrode chromatograms for a standard mixture of three nitro-containing explosives, both in the lamp-off and lamp-on mode.

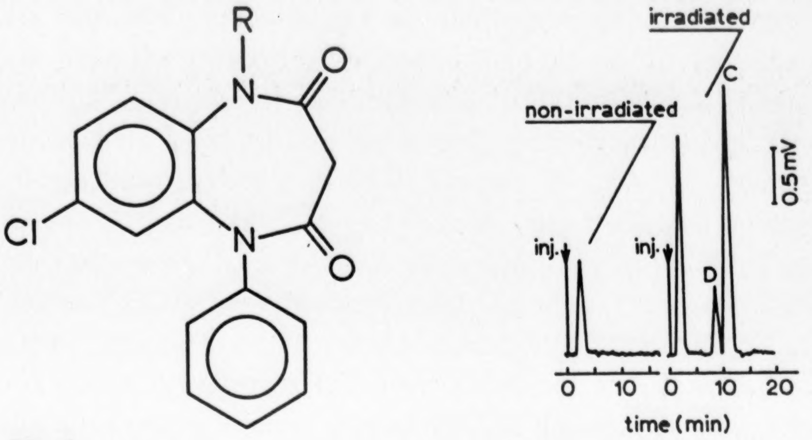

Fig. 4

Structure of clobazam (C; R = CH_3) and desmethylclobazam (D; R = H) and their determination in human serum (0.7ppm each) using a C18/methanol-water (1:1) HPLC system. Fluorescence detection without (left) and with (right) 15sec UV irradiation time is shown [23, 24].

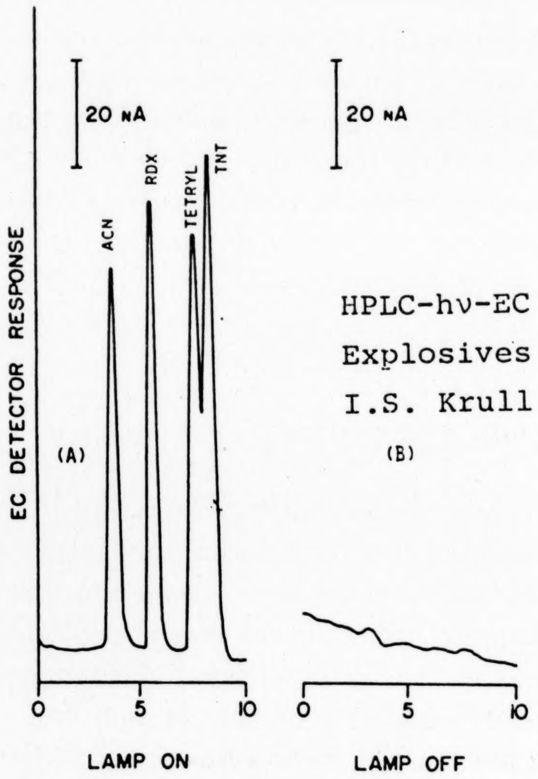

Fig. 5

HPLC-hν-electrochemical (+1.0 V) detection of the explosives RDX, Tetryl and TNT using a C8/methanol-0.1 M NaCl (1:1) HPLC system. The 'lamp off' and 'lamp on' situations are compared [25].

Ion-Pair Formation

As has been outlined above, the selection of a fast reaction will, in principle, allow the use of a simple, open-tubular reactor and will cause a small contribution to band broadening only. An elegant method to achieve this end is the utilization of ion-pair formation. Unfortunately, however, ion-pair formation always requires a simultaneous extraction step, as will be explained below. Consequently, despite the fast kinetics, a solvent-segmented tubular reactor has to be substituted for the open-tubular reactor!

Ion-pair formation has been used for basic and acidic analytes. These are first separated under the proper pH conditions and, next, a solution containing a highly fluorescent (or: UV-absorbing or electroactive) counter ion is added by means of a reagent pump. The main problem is that the counter ion is the active principle, i.e., the large excess of the counter ion contributes dramatically to the total fluorescence signal and has, therefore, to be separated from the analyte ion-pair to be detected. This can be achieved by an on-line extraction procedure effected via rapid segmentation of the HPLC effluent with a non-miscible solvent. The general set-up for basic analytes is shown in Fig. 6, where 9,10-dimethoxyanthracene-2-sulphonate (DAS) is used as counter ion which is added as an aqueous solution of its sodium salt; an halogenated hydrocarbon such as tetrachloroethane (TCE) serves as extraction/segmentation solvent. The non-polar analyte ion pair is extracted into TCE, while the excess of the polar sodium salt of DAS largely remains in the aqueous phase. After phase separation in, for example, a device such as that shown in Fig. 3, the TCE stream passes through the fluorescence detector (Flu) and is monitored there; the aqueous stream goes to waste.

Interesting biomedical applications include the trace-level determination of pheniramines in urine [27], and of secoverine, remoxipride and a pancuronium-type compound in serum and plasma [28–30]. In environmental analysis, the detergent ditallowdimethylammonium chloride [31] and a number of C10-C18 linear alkylsulphonates and related sulphates [32] have been determined in surface water. In the latter case, the highly fluorescent acridiniumH^+ was the counter ion, and the HPLC separation was achieved by means of a linear acetone-to-water gradient. As an illustration, the determination of the selective dopamine antagonist remoxipride in plasma is shown in Fig. 7. The detection limit was 1 ng/ml plasma, the recovery 88%, and the repeatability 3.5% RSD at the 200 ng/ml level.

True Chemical Derivatization

A reagent excess can be tolerated without difficulty if it is only the reaction product formed – and not the reagent itself – which is sensed by the detector. This condition will never hold true in ion-pair formation (cf. above) and, unfortunately, only seldom in any other case. A pleasant exception to this rather negative statement is o-phthalaldehyde (OPA) which has the additional advantage that the pertinent reaction kinetics are rather fast, so that a coiled stainless-steel open-tubular reactor can be used. The general reaction scheme for an OPA derivatization is shown in Fig. 8: in alkaline solution and in the presence of a reducing agent such as 2-mercaptoethanol, non-fluorescent OPA reacts with primary amino groups to yield highly fluorescent derivatives. The reagent is best known [33] for the determination of amino acids in biological fluids at the picomole level, and for the determination of various types of therapeutics agents. Here, we will not discuss this relatively simple and straightforward system any further. Instead, we shall combine it with the use of another, viz. a solid-phase reactor.

Dual-reactor approach. In the field of environmental trace-level analysis, there is a distinct need for the sensitive and selective monitoring of N-methylcarbamates such as carbaryl, aldicarb and methomyl. Several workers [34, 35] recommend, firstly, an HPLC separation of the carbamates, next, a base-catalyzed hydrolysis using a solution of NaOH as catalyst and a coiled capillary kept at 80°C as a reactor and, finally, reaction of the methylamine formed with OPA.

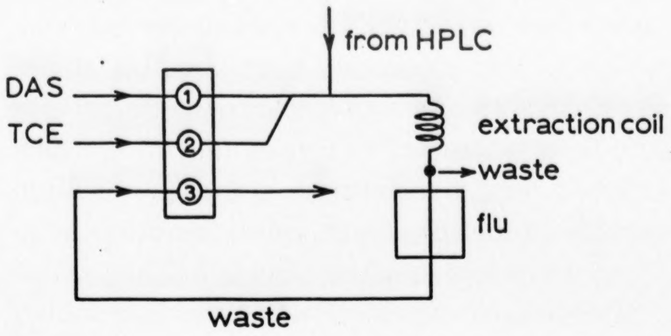

Fig. 6

General set-up of chemically bonded stationary phase/partly aqueous eluent HPLC system with post-column ion-pair formation plus extraction, and fluorescence detection. For explanation, see text.

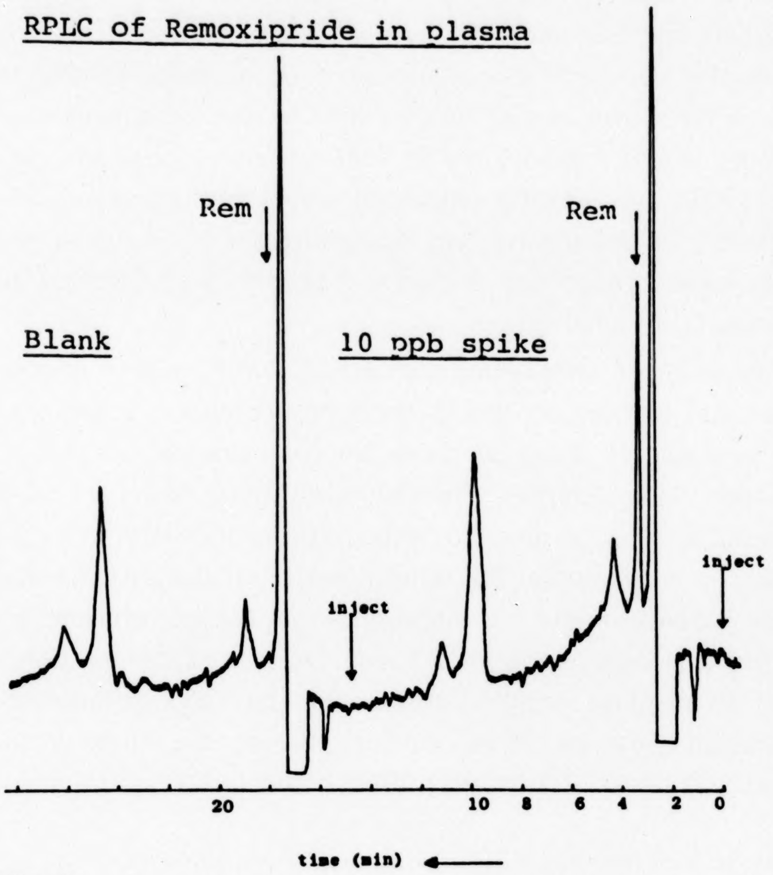

Fig. 7

HPLC-DAS ion pairing/extraction-fluorescence detection of remoxipride in plasma using a cetrimide-based ion-pair separation. Analysis of a blank and a 10 ppb spiked sample is shown [29].

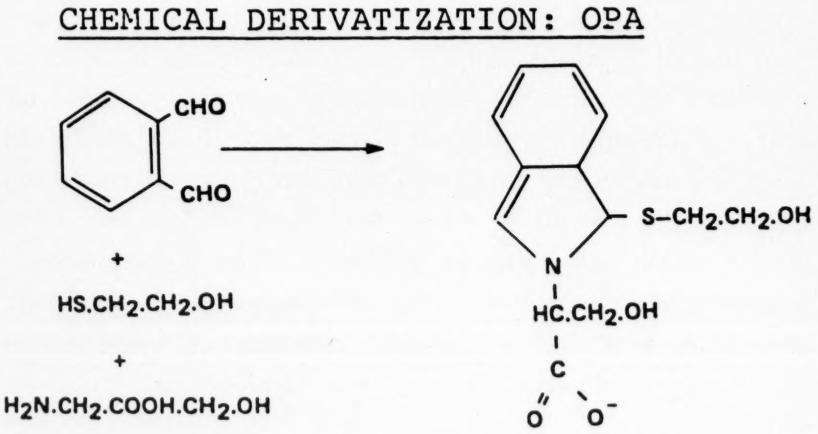

Fig. 8

General reaction scheme for the OPA derivatization of a primary amino group. Reactions are typically carried out using a borate buffer of pH = 9.

Obviously, the introduction of heterogeneous catalysis can, in principle, considerably simplify the reaction detection unit and improve sensitivity by reducing extra-column band broadening. A more recent study [36], therefore, advocates reversed-phase HPLC with, subsequently, on-line hydrolysis in a relatively short — typically, 4–6 cm × 4.6 mm i.d. — stainless-steel column packed with an anion-exchange resin such as Aminex A-28 and heated at a temperature of about 100°C. The total set-up is shown in Fig. 9; the system yielded detection limits of between 0.1 and 1 ng for the six carbamates tested. For ultra-trace-level analysis, the method has been combined with on-line precolumn trace enrichment [37]. Using a 20 ml surface water sample spiked with carbaryl, a detection limit of about 20 ppt can then be obtained (cf. Fig. 10).

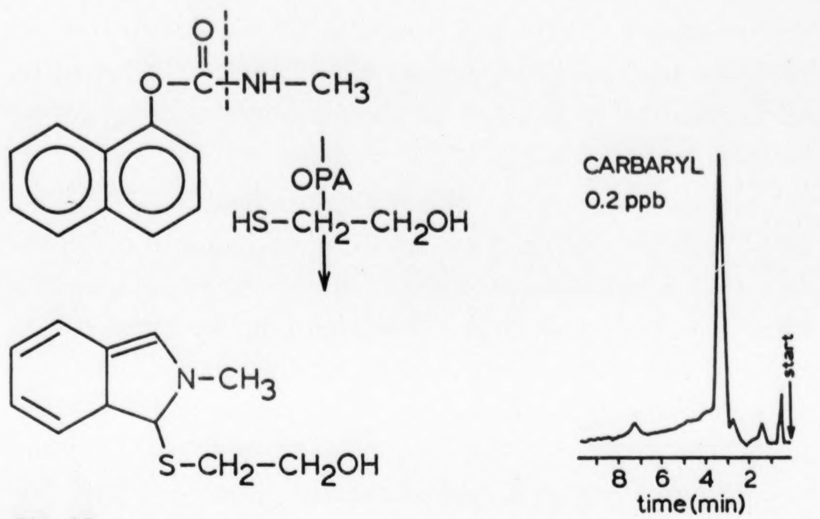

Fig. 10

Catalytic hydrolysis of the N-methylcarbamate carbaryl, its reaction with OPA, and the determination of 0.2 ppb of carbaryl in a 20 ml surface water sample [37].

Optical-resolution studies

An interesting extension of the use of the OPA derivatization principle is in the area of optical resolution of amino acid enantiomers [38, 39]. Buck and Krummen [38] use a laboratory-built automated precolumn derivatization device which is integrated on-line into the total HPLC system. The fluorescent diastereoisomers of the amino acid enantiomers are formed by rapid reaction with OPA and Boc-L-cysteine (instead of 2-mercaptoethanol) at ambient temperature. Gradient elution yields complete resolution for the enantiomers of some 20 amino acids, and the (fluorimetric) detection limits are in the low picomol range. Nimura and Kinoshita [39] use N-acetyl-L-cysteine rather than Boc-L-cysteine as chiral derivatization agent. They utilize both (off-line) precolumn and (on-line) post-column reaction techniques. In the latter case, diastereoisomer recognition can only be achieved by introducing a chiral separation. As an example, Fig. 11 shows the HPLC chromatogram obtained for the amino acids — as their diastereoisomers — present in a bovine serum albumin hydrolysate.

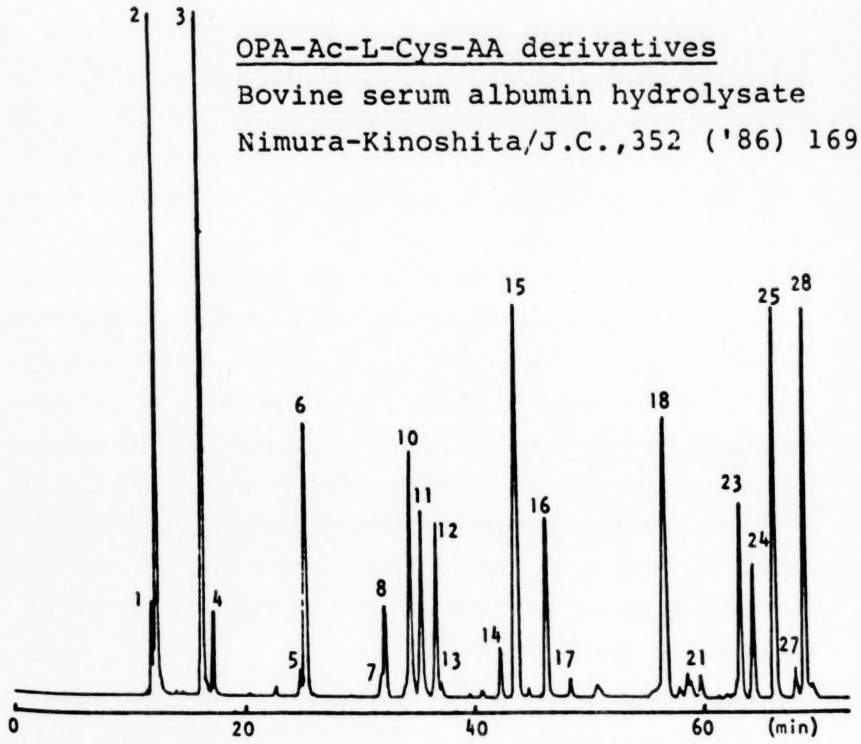

Fig. 11

HPLC of OPA-acetylcysteine derivatives of amino acids present in a bovine serum albumin hydrolysate, using a C18/acetate buffer-methanol gradient system. Peaks: **1** = D-Asp; **2** = L-Asp; **3** = L-Glu; **4** = D-Glu; **5** = D-Ser; **6** = L-Ser; **7** = D-Thr; **8** = L-His; **10** = L-Thr; **11** = Gly; **12** = L-Arg; **13** = D-Arg; **14** = D-Ala; **15** = L-Ala; **16** = L-Tyr; **17** = D-Tyr; **18** = L-Val; **21** = D-Val; **23** = L-Phe; **24** = L-Ile; **25** = D,L-Lys; **27** = D-Leu; **28** = L-Leu [39].

Solid-Phase Reactors

Until recently, very little work had been done in the area of heterogeneous derivatization as a means to expand the scope of post-column reaction detection. Today, this situation is rapidly changing, and a growing number of workers is paying attention to this promising field (e.g., cf. [5, 6]). One way to classify solid-phase reactors (SPRs) for use in HPLC systems is by means of the underlying reaction principle, viz. as catalytic or stoichiomeric reactors. As for the catalytic systems, a study dealing with base-catalyzed hydrolysis [36] has already been quoted above. The acid-catalyzed decomposition of sugars to allow the sensitive detection of non-reducing oligosaccharides [40] is another example. The use of SPRs to achieve a much desired post-column pH change, and the high potential of systems involving the utilization of immobilized enzymes will be exemplified below.

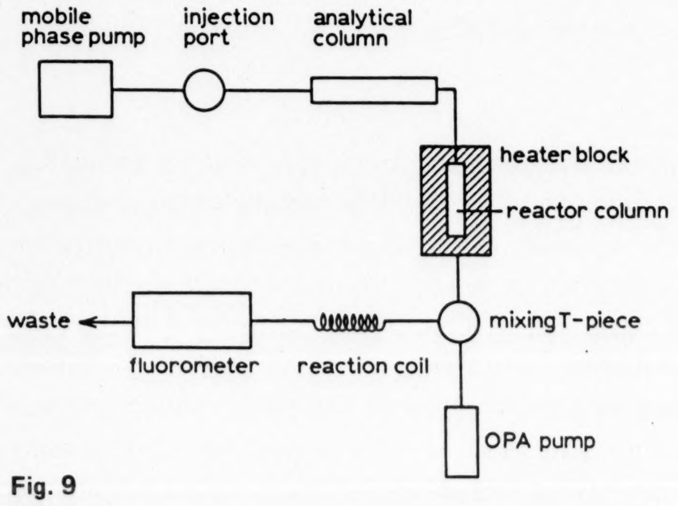

Fig. 9

Schematic of system used for the HPLC determination of N-methylcarbamates with on-line catalytic hydrolysis and OPA derivatization [36].

Stoichiometric SPRs are generally of the derivatization/complex formation, reductive or oxidative type. Recently, an application in the area of chemiluminescence detection has been reported [41].

Studebaker [42] was among the first to apply SPRs in an HPLC system. He used a reactor containing a thiol-Sepharose that is reacted with a chromophore or fluorophore to form a mixed disulphide. Thiols eluting from the HPLC column can form a disulphide which incorporates this active moiety. Disulphides are firstly cleaved in a reactor containing only thiol-Sepharose to form thiolate anions which then react in a second reactor which contains the chromophore or fluorophore. Irth et al. [43] have published an application based on complex formation of dithiocarbamates and other similar compounds with finely divided metallic copper. A 2–4 mm × 2.1 mm i.d. reactor suffices for the quantitative conversion, and determination, of thiram (in surface water) and disulfiram (in urine). Final detection is by visible absorption measurement at 435 nm.

SPRs based on reduction reactions include systems employing borohydride held on a silica, alumina or polymer support [44]. A large variety of organic compounds can be reduced if proper reaction conditions are selected, and the SPR can be employed in both the pre- and post-column mode. Powdered zinc has been used by Lankmayr et al. [45] for the determination of iodinated thyronines in blood serum. Sigvardson and Birks [46] have used zinc reduction – combined with fluorescence or chemiluminescence detection – for the determination of nitro-containing polycyclic aromatic hydrocarbons. On-line reduction is carried out either in the pre- or post-column mode yielding, self-evidently, two different chromatograms (Fig. 12). The detection limits of the amino compounds formed are typically between 0.1 and 10 pg if peroxyoxalate chemiluminescence detection is used.

Oxidation-type SPRs can be based on, e.g., reactions involving an ion-exchange resin in its permanganate form [47], or oxidations with solid PbO_2 (for manganese and chromium) [48] or MnO_2 adsorbed on silica (for catecholamines) [49]. Recently, a parallel-column technique, which had earlier been reported for post-column pH adaptation in barbiturate analysis [50], has been applied for the post-column iodination/oxidation of aflatoxins [51]. The set-up is shown in Fig. 13. Mobile phase splitting prior to HPLC analysis eliminates the need for an additional pumping system, and the split flow dissolves sufficient iodine from the parallel column to achieve the desired goal, viz. conversion of the aflatoxins B_1 and G_1 into highly fluorescent products of partly unknown structure. The latter reaction is rapid and can conveniently be carried out in a coiled PTFE capillary (40 sec residence time; 60°C). One should realize that neither the dimensions of the parallel reactor column nor the particle size of the solid iodine are of major importance: the parallel set-up prevents any contribution to band broadening. The low-ppb level determination of the quoted aflatoxins as well as the native-fluorescent aflatoxins B_2 and G_2 in peanut butter is shown in Fig. 14.

Immobilized enzymes. In the field of catalytic reaction detection, by far the most attention is devoted to the use of immobilized enzymes. In principle, the same considerations apply when working with immobilized-enzyme reactors (IMERs) as when employing more conventional types of SPRs. In practice, however, there are many distinct differences because of, e.g., enzyme bonding and enzyme stability problems, enzyme selectivity, and the – often rather limited – compatibility of the HPLC eluent and the immobilized enzyme. Because it is impossible to treat even the major aspects of IMERs in sufficient detail within the scope of the present review, only a brief discussion of some relevant topics will be given together with an outline of

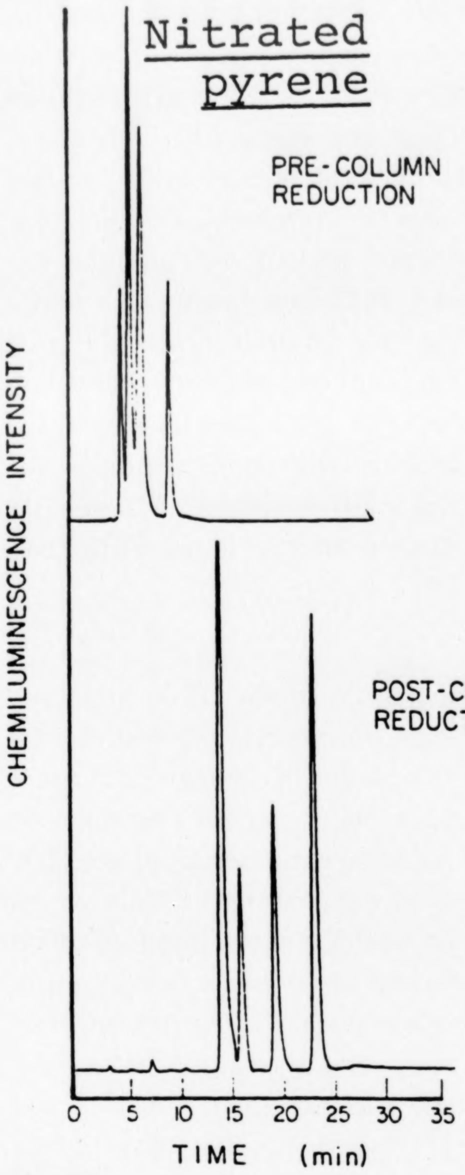

Fig. 12

HPLC of a nitrated pyrene sample using pre- or post-column zinc reduction and chemiluminescence detection [46].

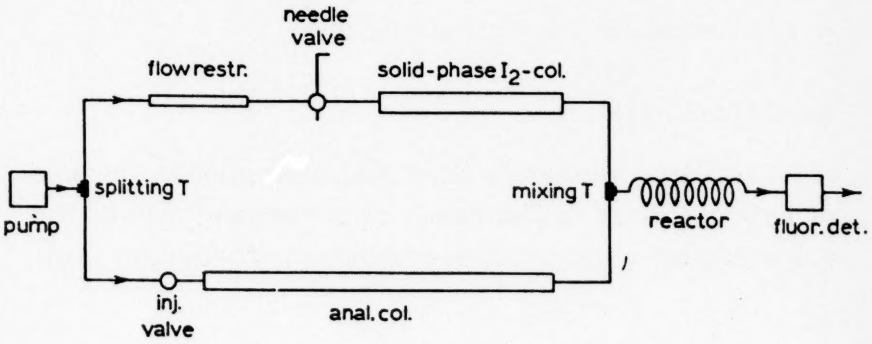

Fig. 13

Schematic of the HPLC-post-column reaction detection system with a parallel-column set-up used for aflatoxin determination. For further details, see text and [51].

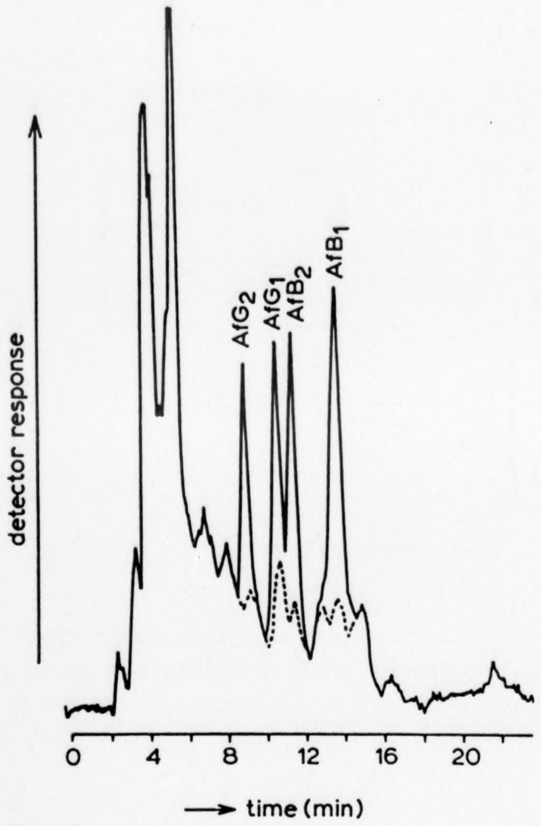

Fig. 14

HPLC of an extract of non-spiked (-----) and aflatoxins-spiked (——, 4–8 ppb each) peanut buffer in a C18/water-methanol-acetonitrile (15:6:4) system using post-column reaction detection according to Fig. 13.

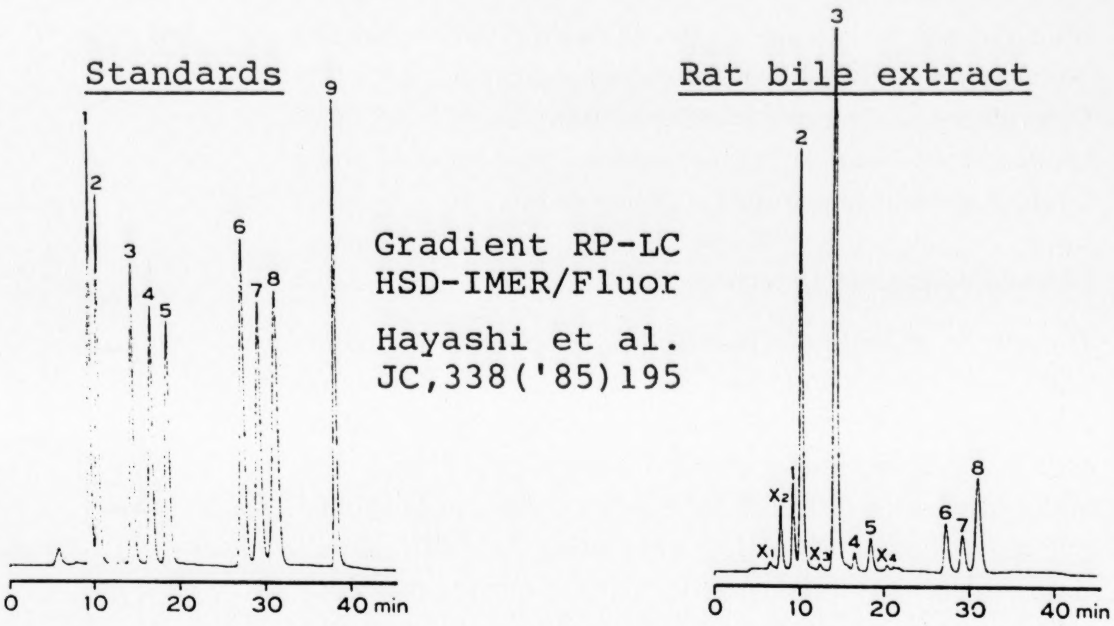

Gradient RP-LC
HSD-IMER/Fluor

Hayashi et al.
JC,338('85)195

Fig. 15

HPLC-3α-hydroxysteroid dehydrogenase IMER-fluorescence detection of (left) standard bile acids and (right) bile acids extracted from normal rat bile. A C8/phosphate buffer-acetonitrile gradient system was used for separation. Peaks: **1** = α-muricholic acid; **2** = β-muricholic acid; **3** = cholic acid; **4** = ursodeoxycholic acid; **5** = hyodeoxycholic acid; **6** = chenodeoxycholic acid; **7** = deoxycholic acid; **8** = internal standard; **9** = lithocholic acid; x1-x4, unknowns [55].

interesting applications. For a good general introduction to the field of IMER reaction detection, the reader should consult ref. [52].

An on-line pre-column IMER application is the use of the enzyme β-glucuronidase to cleave the glucuronic acid moiety from compounds such as steroids and drugs. Bowers and his group have, for example, determined steroids and morphine [53, 54] using either gradient elution or column switching to avoid exposure of the enzyme to a solvent system it can not tolerate.

In post-column IMER studies, the enzymes are often immobilized by covalent attachment. In the case of silica as support material, this will generally involve activation with, e.g. γ-aminopropyldichlorosilane, further activation with glutaraldehyde and, finally, coupling of the enzyme to the activated matrix. Amongst the enzymes which have been used with success in HPLC-IMER systems are those mentioned in Table III. In each case, a single relevant reference has been added. It is interesting to add that with several of these IMER systems as well as with many other enzyme-based reactions which appear, in principle, useful for IMER development, the compound finally produced and measured is H_2O_2 or NADH. That is, both fluorescence (NADH), chemiluminescence (H_2O_2) and electrochemical (H_2O_2) detection can be used for sensitive and selective monitoring.

Table III. Enzymes used in HPLC-IMER systems.

Enzyme	Reference
3α-Hydroxysteroid dehydrogenase	55
Glycosidase	56
Urease	57
Phosphatase	58
L-Amino acid oxidase	59
Choline oxidase/cholinesterase	60
Xanthine oxidase	61

The enzyme 3α-hydroxysteroid dehydrogenase has been used most often in HPLC-IMER systems, viz. for the determination of bile acids in biological fluids. To quote one example, Hayashi et al. [55] report a reversed-phase HPLC separation involving an aqueous phosphate buffer (pH 6.8)—acetonitrile gradient. Resolution of the limited number of bile acids studied is good, and the detection limits are in the order of 1 ng (fluorescence detection of NADH). The IMER could be used for at least 200 analyses without a significant loss of repeatability. Fig. 15 shows the separation of a standard bile acid mixture as well as a bile acid extract from normal rat bile. The reader is also referred to a paper by Ishii et al. [62] who use a miniaturized HPLC system which includes a precolumn for on-line clean-up and trace enrichment of the bile acids.

Several authors have published papers on the use of a combined choline oxidase/cholinesterase IMER for the determination of choline and acetylcholine. After HPLC separation on a cation exchanger or in the reversed-phase mode, the mixed-enzyme reactor serves to hydrolyze acetylcholine to acetate and choline, and to convert choline into betaine and H_2O_2. Meek and his group [60, 63] and Damsma and coworkers [64, 65] use electrochemical detection, with the latter group claiming a 50 femtomol detection limit. Van Zoonen et al. [41, 66] apply peroxyoxalate-based chemiluminescence as a detection principle. Since such a detection system tends to become rather expensive because of the two additional pumps which are required (for aryl oxalate and fluorophore addition; cf. below), the authors have devised an elegant dual-bed reactor which contains both solid bis-(2,4,6-trichlorophenyl)oxalate and the fluorophore 3-aminofluoranthene immobilized on glass beads. As an example, the analysis of a non-spiked and a 20 pmol spiked urine sample is shown in Fig. 16.

Chemiluminescence Detection

The use of chemiluminescence measurement as the detection step in HPLC with post-column reaction detection has already been referred to in earlier sections when dealing with the zinc reduction of nitro aromatics [46] and with the utilization of an IMER for the determination of choline and acetylcholine via H_2O_2 monitoring [41, 66]. A full discussion of chemiluminescence (CL) is outside the scope of the present review, and attention will only be given to a few relevant aspects of HPLC with CL detection. For a recent general introduction into HPLC-CL the reader is referred to reference 17.

The peroxyoxalate reaction is probably the most versatile and efficient CL system available today. The mechanism generally proposed for the peroxyoxalate reaction is shown in Fig. 17, and briefly explained in the legend; bis-(2,4,6-trichlorophenyl)oxalate and bis-(2,4-dinitrophenyl)oxalate are the aryl oxalates generally used. Aspects of major importance in, and also typical for, HPLC-CL systems are (i) the half-life of the CL signal, which is dependent on many system parameters, and which mainly determines the dead volume that should be present between the mixing tee (HPLC eluent, H_2O_2 and aryl oxalate streams) and the CL flow-cell; (ii) the proper solvent selection — especially for the aryl oxalates — with solubility, stability and miscibility being the chief parameters; and (iii) effective light collection, where the use of 2π steradian mirror devices and the positioning of the flow-cell in close proximity to the photomultiplier are promising alternatives. The interesting possibility of simplifying the conventional — and rather expensive — three-pump HPLC-CL systems to two-pump and, occasionally, even one-pump systems has already been referred to above [41].

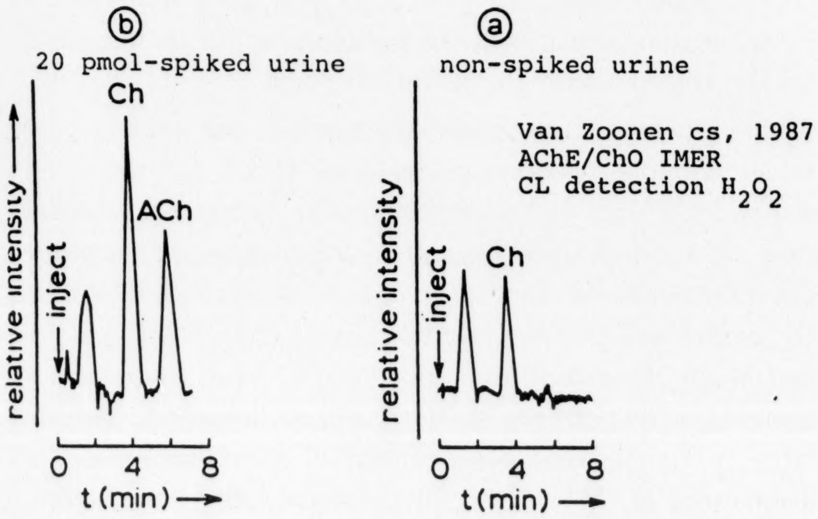

Fig. 16

HPLC-choline oxidase/cholinesterase IMER-chemiluminescence detection of (a) a non-spiked urine sample, and (b) a 20 pmol spiked urine sample [41, 66].

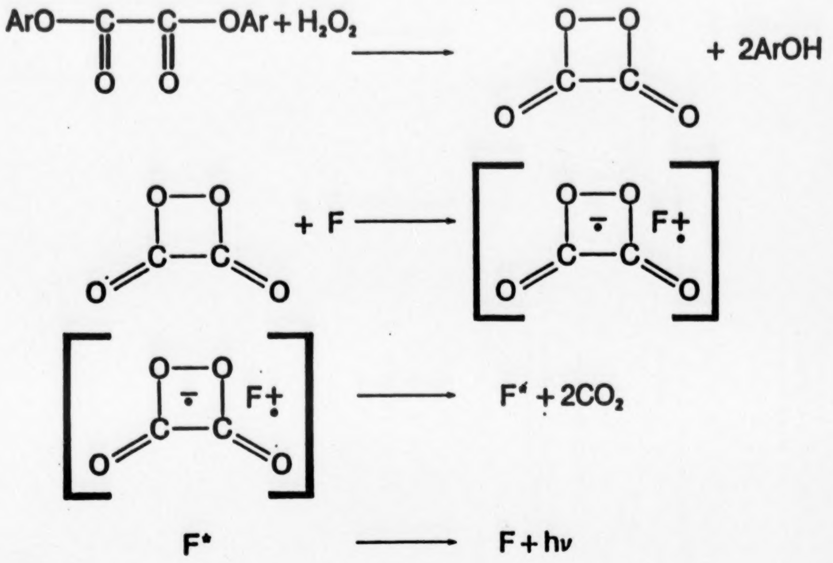

Fig. 17

Peroxyoxalate CL reaction scheme. An energy-rich intermediate, generated by the reaction between an aryl oxalate and H_2O_2, excites a fluorophore F, which returns to the ground state via emission of light.

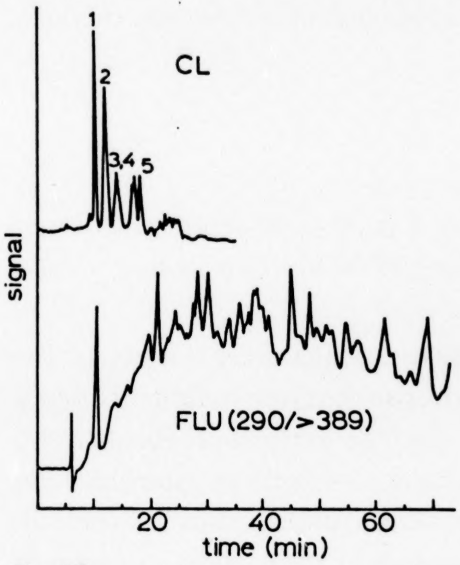

Fig. 18

HPLC of fractionated shale oil extract with CL and fluorescence detection. Peaks: **1** = aminonaphthalenes; **2** = C1-aminonaphthalenes; **3** = aminophenanthrenes; **4** = aminoanthracenes; **5** = aminopyrenes. Separation was done in a C18/acetonitrile-water (3:1) system [71].

The potential of the peroxyoxalate system for HPLC-CL has been widely demonstrated for dansylated amino acids [67–69] and other dansyl derivatives [70]. Amino-substituted aromatics are among the analytes that are most sensitively detected by CL. This has been shown for the trace-level determination of this class of compounds in a shale oil extract, comparing CL with fluorescence detection (Fig. 18, [71]), for nitro aromatics after suitable reduction (Fig. 12) as well as for carboxylic acids [72] or aldehydes and ketones [73] derivatized with an amino-containing aromatic label. Finally, in the presence of an excess of fluorophore, the peroxyoxalate CL system has been used to determine trace-level amounts of H_2O_2 produced in either HPLC-IMER systems (Fig. 16 and [74]) or present in rain water samples [41].

Conclusion

A decade ago, the use of reaction detection in HPLC systems was virtually unknown. Today, the potential of this technique for improved detection sensitivity and selectivity is fully recognized. A wide variety of (physico)-chemical principles has been applied and trace-level constituents have been determined successfully in many divergent types of samples. Unfortunately, there is a lack of commercially available equipment as well as of thoroughly evaluated application notes. Obviously, this is an area where substantial progress should be made in the near future.

As regards the post-column reactors proper, the open-tubular, inert or active packed-bed and air- or solvent-segmented stream reactors appear to offer sufficient flexibility for almost all applications. So far, miniaturization has not been a particularly important issue, but scaling down to a size which makes the reactors compatible with narrow-bore HPLC has been shown to yield no major problems [11, 50]. Miniaturization has especially attracted attention in HPLC-CL systems (cf. [17]). On-line pre-column derivatization or analyte conversion is gradually becoming a worthwhile alternative to post-column techniques [38, 46, 52]. Automated pre-column derivatization units for amino acid analysis are available from Hewlett Packard (APDS) and Varian (Amino Tag).

An overview of the chemistry utilized today for post-column reaction detection shows a surprisingly large variety of reaction types involved. Close scrutiny of one's chemistry and physical-chemistry textbook will no doubt reveal still more possibilities to improve the HPLC detection performance. Heterogeneous catalysis – and, especially, IMER systems – and CL detection – which is often stated to be 10-25-fold more sensitive and/or more selective than fluorescence measurement – will no doubt be favoured research topics in years to come.

After suitable post-column reaction, much final detection is done by means of fluorescence measurement. This is, no doubt, a highly sensitive and selective method of detection, for which many excellent labelling and photoconversion procedures are available. Besides, in the near future its performance may well be improved still further when laser-induced fluorescence becomes a less expensive and more versatile tool. This certainly does not imply that UV-vis absorption, electrochemical, CL or mass spectrometric [75] detection should be neglected. They all have their specific advantages and special fields of application. It does mean, however, that the competition will be fierce and that, as a result, improved reaction detection systems will be elaborated. In other words, in the past decade new developments in the area of reaction detection have become manifest each year; this dynamic situation will undoubtedly continue in the near future.

References

[1] *J. F. Lawrence, R. W. Frei*, Chemical Derivatization in Liquid Chromatography, Elsevier, Amsterdam, 1976.

[2] *K. Blau, G. S. King*, Handbook of Derivatives for Chromatography, Heyden, London, 1977.

[3] *G. Schwedt*, Chemische Reaktionsdetektoren für die schnelle Flüssigkeitschromatographie, Hüthig, Heidelberg, 1980.

[4] Chemical Derivatization in Analytical Chemistry, Vols. 1–2, *R. W. Frei, J. F. Lawrence*, eds., Plenum Press, New York, 1981–1982.

[5] Reaction Detection in Liquid Chromatography, *I. S. Krull*, ed., Marcel Dekker, New York, 1986.

[6] *R. W. Frei, H. Jansen, U. A. Th. Brinkman*, Anal. Chem. **57**, A357 (1985).

[7] *R. S. Deelder, M. G. F. Kroll, A. J. B. Beeren, J. H. M. van den Berg*, J. Chromatogr. **149**, 669 (1978).

[8] *R. Tijssen*, Sep. Sci. Technol. **13**, 681 (1978).

[9] *B. Lillig, H. Engelhardt*, in: Reaction Detection in Liquid Chromatography, I. S. Krull, ed., Marcel Dekker, New York, Ch. 1, 1986.

[10] *K. M. Jonker, H. Poppe, J. F. K. Huber*, Z. Anal. Chem. **279**, 154 (1976).

[11] *J. A. Apffel, U. A. Th. Brinkman, R. W. Frei*, Chromatographia **17**, 125 (1983).

[12] *A. H. M. T. Scholten, U. A. Th. Brinkman, R. W. Frei*, Anal. Chem. **54**, 1932 (1982).

[13] *C. E. Werkhoven-Goewie, W. M. A. Niessen, U. A. Th. Brinkman, R. W. Frei*, J. Chromatogr. **203**, 165 (1981).

[14] *R. W. Deelder, A. T. J. M. Kuypers, J. H. M. van den Berg*, J. Chromatogr. **255**, 545 (1983).

[15] *A. H. M. T. Scholten, U. A. Th. Brinkman, R. W. Frei*, J. Chromatogr. **205**, 229 (1981).

[16] *C. de Ruiter, J. H. Wolf, U. A. Th. Brinkman, R. W. Frei*, Anal. Chim. Acta, **192**, 267 (1987).

[17] *U. A. Th. Brinkman, G. J. de Jong, C. Gooijer*, Pure Appl. Chem. **59**, 625 (1987).

[18] *W. Th. Kok*, Thesis, Free University, Amsterdam, 1986.

[19] *M. Uihlein, E. Schwab*, Chromatographia **15**, 140 (1982).

[20] *M. Nieder, H. Jaeger*, J. Chromatogr. **413**, 207 (1987).

[21] *J. W. Birks, R. W. Frei*, Trends Anal. Chem. **1**, 361 (1982).

[22] *I. S. Krull, W. R. LaCourse*, in: Reaction Detection in Liquid Chromatography, I. S. Krull, ed., Marcel Dekker, New York, Ch. 7, 1986.

[23] *A. H. M. T. Scholten, U. A. Th. Brinkman, R. W. Frei*, Anal. Chim. Acta **114**, 137 (1980).

[24] *A. H. M. T. Scholten, P. L. M. Welling, U. A. Th. Brinkman, R. W. Frei*, J. Chromatogr. **199**, 239 (1980).

[25] *I. S. Krull, C. Selavka, X.-D. Ding, K. Bratin, G. Forcier*, Bioanalytical Systems' Current Separations **5**, 57 (1984).

[26] *X.-D. Ding, I. S. Krull*, J. Agr. Food Chem. **32**, 622 (1984).

[27] *R. W. Frei, J. F. Lawrence, U. A. Th. Brinkman, I. Honigberg*, J. High Res. Chromatogr., Chromatogr. Commun. **1**, 11 (1979).

[28] *R. J. Reddingius, G. J. de Jong, U. A. Th. Brinkman, R. W. Frei*, J. Chromatogr. **205**, 77 (1981).

[29] *C. de Ruiter, U. A. Th. Brinkman, R. W. Frei*, J. Liq. Chromatogr., 1987, in press.

[30] *J. H. Wolf, C. de Ruiter, U. A. Th. Brinkman, R. W. Frei*, J. Pharm. Biomed. Anal. **4**, 523 (1986).

[31] *C. de Ruiter, J. Hefkens, U. A. Th. Brinkman, R. W. Frei*, in preparation.

[32] *F. Smedes, J. C. Kraak, C. E. Werkhoven-Goewie, U. A. Th. Brinkman, R. W. Frei*, J. Chromatogr. **247**, 123 (1982).

[33] *A. T. Rhys Williams*, Fluorescence Detection in LC, Perkin-Elmer, Beaconsfield, UK, 1980.

[34] *H. A. Moye, S. J. Scherer, P. A. St. John*, Anal. Lett. **10**, 1049 (1977).

[35] *R. T. Krause*, J. Chromatogr. Sci. **16**, 281 (1978).

[36] *L. Nondek, R. W. Frei, U. A. Th. Brinkman*, J. Chromatogr. **282**, 141 (1983).

[37] *K. S. Low, U. A. Th. Brinkman, R. W. Frei*, Anal. Lett. **17**, 915 (1984).

[38] *R. H. Buck, K. Krummen*, J. Chromatogr. **315**, 279 (1984).

[39] *N. Nimura, T. Kinoshita*, J. Chromatogr. **352**, 169 (1986).

[40] *P. Vrátny, R. W. Frei, U. A. Th. Brinkman, M. W. F. Nielen*, J. Chromatogr. **295**, 355 (1984).

[41] *P. van Zoonen*, Thesis, Free University, Amsterdam, 1987.

[42] *J. F. Studebaker*, J. Chromatogr. **185**, 497 (1979).

[43] *H. Irth, G. J. de Jong, U. A. Th. Brinkman, R. W. Frei*, J. Chromatogr. **370**, 439 (1986).

[44] *I. S. Krull, S. Colgan, K.-H. Xie, U. Neue, R. King, B. Bidlingmeyer*, J. Liq. Chromatogr. **6**, 1015 (1983).

[45] *E. P. Lankmayr, B. Maichin, G. Knapp, F. Nachtmann*, J. Chromatogr. **244**, 239 (1981).

[46] *K. W. Sigvardson, J. W. Birks*, J. Chromatogr. **316**, 507 (1984).

[47] *K.-H. Xie, C. T. Santasania, I. S. Krull, U. Neue, B. Bidlingmeyer, A. Newhart*, J. Liq. Chromatogr. **6**, 2109 (1983).

[48] *J. Rüter, B. Neidhart*, Mikrochim. Acta (1984 I) 271.

[49] *J. Rüter, U. P. Kurz, B. Neidhart*, J. Liq. Chromatogr. **8**, 2475 (1985).

[50] *H. Jansen, C. J. M. Vermunt, U. A. Th. Brinkman, R. W. Frei*, J. Chromatogr. **366**, 135 (1986).

[51] *H. Jansen, R. Jansen, U. A. Th. Brinkman, R. W. Frei*, 1987, submitted for publication.

[52] *L. D. Bowers*, in: Reaction Detection in Liquid Chromatography, I. S. Krull, ed., Marcel Dekker, New York, Ch. 4, 1986.

[53] *L. D. Bowers, P. R. Johnson*, Clin. Chem. **27**, 1554 (1981).

[54] *P. R. Johnson, L. D. Bowers*, Anal. Chem. **54**, 2247 (1982).

[55] *M. Hayashi, Y. Imai, Y. Minami, S. Kawata, Y. Matsuzawa, S. Tarui*, J. Chromatogr. **338**, 195 (1985).

[56] *L. Dalgaard, L. Brimer*, J. Chromatogr. **303**, 67 (1984).

[57] *H. Jansen, R. W. Frei, U. A. Th. Brinkman, R. S. Deelder, R. P. J. Stellings*, J. Chromatogr. **325**, 255 (1985).

[58] *J. L. Meek, F. Nicoletti*, J. Chromatogr. **351**, 303 (1986).

[59] *N. Kiba, M. Kaneko*, J. Chromatogr. **303**, 396 (1984).

[60] *C. Eva, M. Hadjiconstantinou, N. H. Neff, J. L. Meek*, Anal. Biochem. **143**, 320 (1984).

[61] *M. Kito, R. Tawa, S. Takeshima, S. Hirose*, J. Chromatogr. **278**, 35 (1983).

[62] *D. Ishii, S. Murata, T. Takeuchi*, J. Chromatogr. **282**, 569 (1983).

[63] *J. L. Meek, C. Eva*, J. Chromatogr. **317**, 343 (1984).

[64] *G. Damsma, B. H. C. Westerink, A. S. Horn*, J. Neurochem. **45**, 1649 (1985).

[65] *G. Damsma, D. Lammerts van Bueren, B. H. C. Westerink, A. S. Horn*, Chromatographia, 1987, in press.

[66] *P. van Zoonen, D. A. Kamminga, C. Gooijer, N. H. Velthorst, R. W. Frei*, J. Liq. Chromatogr. **10**, 819 (1987).

[67] *S. Kobayashi, K. Imai*, Anal. Chem. **52**, 424 (1980).

[68] *K. Honda, J. Sekino, K. Imai*, Anal. Chem. **55**, 940 (1983).

[69] *K. Miyaguchi, K. Honda, K. Imai*, J. Chromatogr. **316**, 501 (1984).

[70] *T. Koziol, M. L. Grayeski, R. Weinberger*, J. Chromatogr. **317**, 355 (1984).

[71] *K. W. Sigvardson, J. M. Kennish, J. W. Birks*, Anal. Chem. **56**, 1096 (1984).

[72] *K. Honda, K. Miyaguchi, K. Imai*, Anal. Chim. Acta **177**, 111 (1985).

[73] *B. Mann, M. L. Grayeski*, J. Chromatogr. **386**, 187 (1987).

[74] *K. Honda, K. Miyaguchi, H. Nishimo, H. Tanaka, T. Yao, K. Imai*, Anal. Biochem. **153**, 50 (1986).

[75] *J. A. Apffel, U. A. Th. Brinkman, R. W. Frei*, J. Chromatogr. **312**, 153 (1984).

Received: Aug. 28, 1987
Accepted: Sep. 11, 1987
F

Automation and Validation of HPLC-Systems

F. Erni* /W. Steuer/H. Bosshardt

Analytical Research and Development, Pharma Division, Sandoz Ltd., Basle, Switzerland

Key Words

Automation
Validation column liquid chromatography
System suitability test ruggedness
Method transfer

Summary

The automation of chromatographic systems is of increasing interest to industry and research laboratories in routine applications. Besides potentially saving time or making better use of available instrumentation, automation also improves the quality of results by producing more precise and more reproducible HPLC data. The need for the validation of methods and qualification of instruments is increasingly recognised in order to ensure compliance with legal requirements (e.g. in the pharmaceutical industry) and to ensure the reliability of analytical results. Possibilities and requirements for automated HPLC systems are elaborated. Emphasis is placed on defining the goals of validation and on discussing different aspects of the validation of LC methods, system suitability tests, ruggedness of methods and the transfer of LC methods from laboratory to laboratory. Adequate strategies of HPLC method development provide very useful information on the validation and ruggedness of LC methods.

Introduction

During the last ten years, HPLC emerged as a generally accepted analytical tool for very broad areas of application. A prerequisite for such a breakthrough was the possibility of automating HPLC systems. Automated HPLC systems are used worldwide for routine applications at universities, in industry and in governmental laboratories. Wherever HPLC is used as a quality control tool, e.g. for release analysis of pharmaceutical preparations, the validation of HPLC methods is absolutely necessary. Validation is not only necessary for fulfilling governmental regulations, but is a vital task in serious analytical laboratories, where high quality work in research, development and quality assurance is performed. This paper will discuss applications of automated HPLC, its possibilities and limitations, as well as trends for future development. It will also discuss validation and show that validation is not just an administrative necessity performed for regulatory agencies, but is an extremely demanding scientific task for all chromatographers.

Automation

The goals of automation are:

- to save labour, time and money;
- to make better use of expensive instrumentation during nights and weekends;
- to achieve higher analysis output;
- to achieve higher quality results compared to manually operated HPLC systems.

Automation can be achieved by the mechanisation of sample handling and by data acquisition and processing via computer systems.

Mechanisation: Very early in the development of HPLC instrumentation, manual injectors were replaced by automatic sample injectors to allow for unattended operation and to achieve a higher potential for reproducibility of the injection process. Modern autosamplers can inject even small sample volumes without significant loss, with good precision and adequate reproducibility. More sophisticated samplers are able to inject variable amounts, dilute the sample prior to injection and even perform precolumn derivatisation [1]. In the past, autosamplers were successfully connected to continous flow systems (autoanalyser) [2] for online sample preparation. More complex sample handling can be done by laboratory robots [3]. The possibilities for utilizing laboratory robots for sample preparation in HPLC are collected in Table I. There are, however, some limita-

Table I. Unit operation of laboratory robots

Possibilities of Laboratory Robots for sample preparation in HPLC
Unit operations
inject into HPLC
dillute
add solvents/reagents
solvent extractions
filtration
weighing

0009-5893/87 0201-07 $03.00/0

© 1987 Friedr. Vieweg & Sohn Verlagsgesellschaft mbH

tions to be considered in the application of currently available robot systems:

- They are rather slow in operation;
- method development and the change from one method to another can be very time consuming;
- they use an enormous amount of laboratory space;
- there are still some limitations in the processing of powder samples;
- the installation cost of presently available robot systems is rather high, and the versatility and flexibility of the systems should be further improved.

Mechanisation is not always easy and probably has reached its limits. In the future, integrated approaches may prove to be more elegant. There are some simple solutions for dedicated tasks, such as the sample processer system for derivatisation of amino acids [1] and approaches for serum sample processing with special columns [4] or multidimensional HPLC systems [5].

Data Processing: Computers play an increasingly important part in the automation of HPLC systems. Table II shows the different steps and levels of HPLC data processing. Modern data systems can do more than just integrate peak areas. More and more, efficient tools are used in the evaluation and documentation of HPLC results. Graphic presentation of chromatogrammes is much more suitable for human data interpretation than huge tables of numeric data. A few good modern chromatography data systems help to routinely determine column characteristics (plate numbers, tailing factors, resolution of peaks and H/u-curves). Laboratory Information and Management Systems (LIMS) help in the documentation of chromatogrammes and in the establishment of huge data bases for optimal storage and retrieval. There is an increasing need for the integration of chromatographic data processing systems with widely-used spread sheet programmes like Lotus 123 [6] and RS/1 [7], with statistical packages like SAS [8], and with word processing systems for report generation. Hopefully it will soon be possible to really integrate text, tables, chromatogrammes, other graphical figures (like spectra) and chemical structures and reactions in a single computer system for the preparation of manuscripts or reports [9].

Trends and future developments: Expert systems will play an increasing role in HPLC laboratories. They help to optimally design experiments (Expert system for experimental design [10]); they automatically develop HPLC methods [11]; they simulate HPLC runs with modified experimental conditions (DryLab 1–5 [12]); and they even help locate origins of instrument failures (HPLC DOCTOR is an expert system for trouble shooting in HPLC [13]).

The presently available hardware for automated HPLC systems provides nearly unlimited possibilities for automation if one is willing to pay the price. There is, however, much room for improvement and there is a real need for it. Compared to spectroscopic analytical instruments, the current HPLC systems still have a very unsatisfactory mean time of failure. Reliability should be improved. On-line diagnoses could be built into sophisticated HPLC systems so that the proper function could be documented. Under routine conditions the precision of autosamplers can be a problem. Very often the specifications of the instruments are only fulfilled with test mixtures under ideal conditions. Thereafter reproducibility becomes more difficult. The speed of laboratory data systems is far from optimal. HPLC is a very fast chromatographic method and will be even faster in the future [14] with the introduction of shorter columns and smaller column packing materials. However, what is the use of achieving a chromatographic separation within a couple of seconds if you have to wait minutes thereafter for data processing and report generation? A very important weakness of current instrumentation in big laboratories is the lack of communication standards for the integration of laboratory data systems in LIMS computer systems and corporate EDP. Experience has shown that the more intelligent the HPLC systems are, the more problems one will have to communicate with LIMS. Unfortunately there is little hope for fast improvement in the standardisation of data communication interfaces.

Table II. Possibilities of EDP in automation

Data Processing in HPLC
Raw data collection
Peak identification
Calibration/Standardisation
Report generation
Documentation
Evaluation
Graphic Presentation
Laboratory information management

Validation

Many laboratory managers associate validation with increased workload in the laboratory, increased paperwork and missing capacity. However, validation is basically nothing new. Since the development of analytical methods, data have been elaborated to prove the reliability and precision of these methods. New to present validation processes is the consequent planning of validation and systematic documentation of all the experiments. What is validation?

> VALIDATION IS THE PROCEDURE USED TO PROVE THAT A TEST METHOD CONSISTENTLY YIELDS WHAT IT IS EXPECTED AND REQUIRED TO DO WITH ADEQUATE ACCURACY AND PRECISION

Validation consits of three important parts:

- planning
- experimentation
- documentation.

Planning experiments well can significantly reduce the number of experiments needed and can improve the quality of the results. Good documentation of the validation results helps in the transfer of methods from user to user and from laboratory to laboratory.

For HPLC a typical set of validation criteria for assay and purity determination is shown in Table III. The number of parameters that must be studied depends on the goal of the

Table III. Validation criteria for HPLC tests

Typical Validation criteria for HPLC
• LINEARITY of the analytical function • Origin of the analytical function • Detection limit/limit of quantification • Precision • Accuracy • Selectivity • Specificity • Column to column variability

analytical method. For assay methods, the linearity of the analytical function is tested (Fig. 2). The origin should be within the confidence limits of the regression line, and the correlation coefficient should usually be greater than 0.99, except for trace analysis where lower correlation coefficients often must be tolerated. The precision of the HPLC determinations is measured by assaying the same sample several times, including all the sample preparation steps. The standard deviation of these independent determinations provides a good estimate of the precision of the HPLC assay. The accuracy of HPLC assays is much more complicated to prove. It has to be shown that no interfering compounds mimic overly high assay values of the compound of interest. Adequate specificity of the detection and selectivity of the separation have to be demonstrated. Like many other separation methods and spectroscopic quantitative assays, it is very time consuming and not at all trivial to show specificity and selectivity. Davis and Giddings [15], as well as Martin, Hermann and Guiochon [16], investigated the problems of peak distribution in chromatogrammes with a statistical approach. As shown in Table IV, the minimal peak capacity and the theoretical plates necessary for separation with a probability of only 90 per cent are excessive if more than 10 compounds are present in the sample. This demonstrates clearly that separation of multicomponent samples is not feasible with only plate numbers.

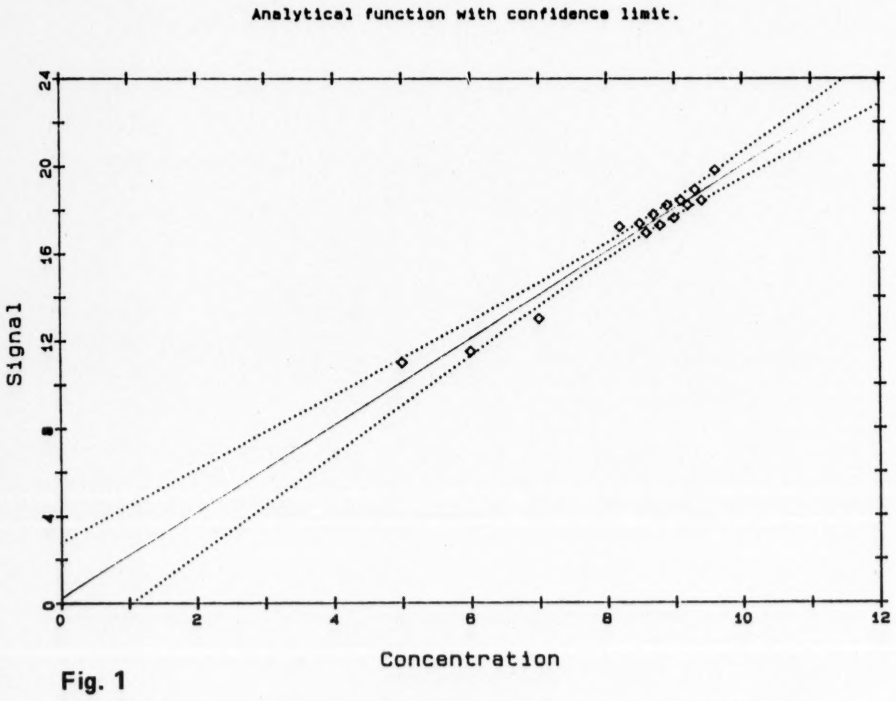

Fig. 1

Analytical Function of HPLC Assay: Linear Regression with confidence limits.

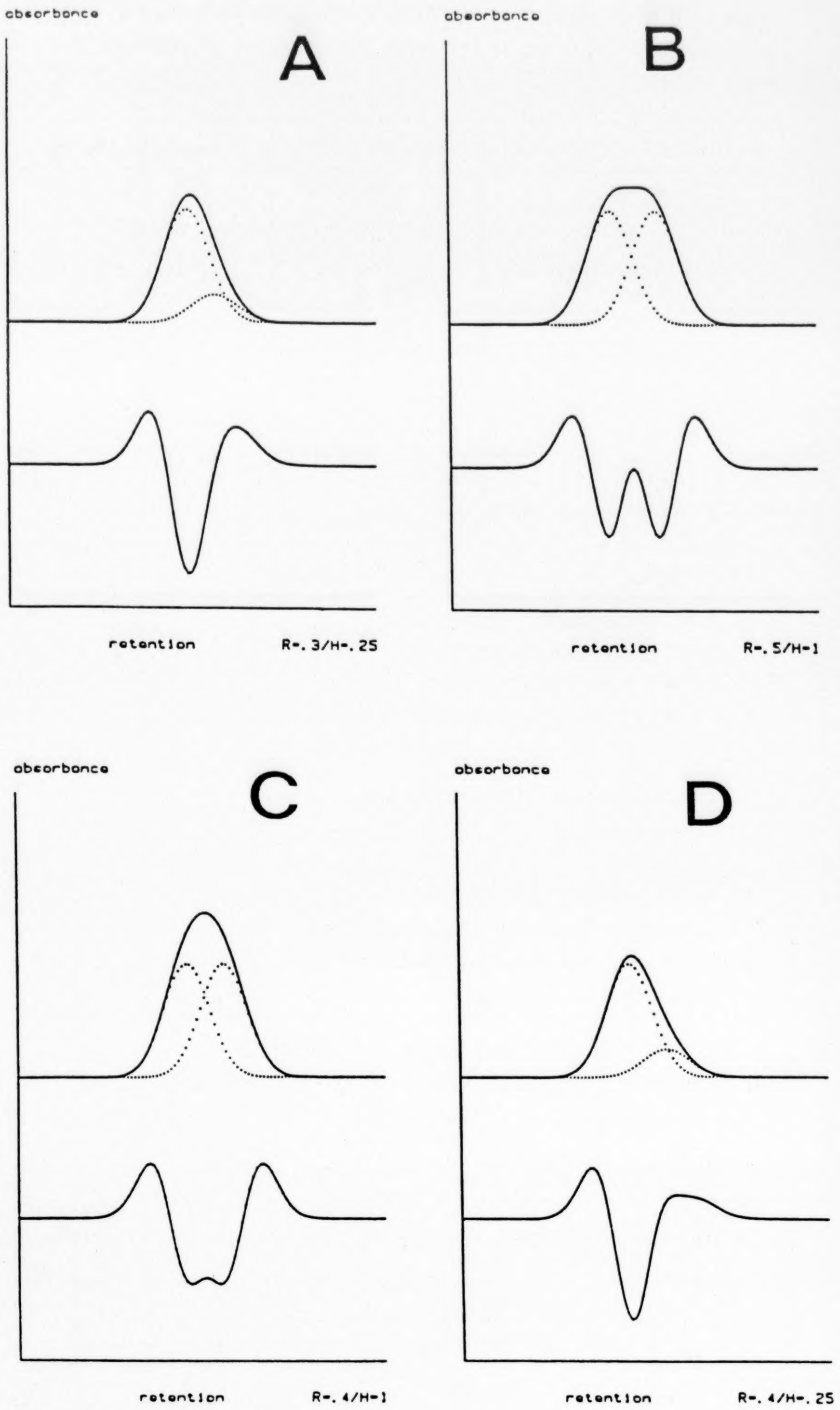

Fig. 2

Use of derivatives of chromatogrammes for the detection of overlapping peaks.

upper curve: simulated overlapping chromatographic peaks with Resolution R and peak high ratio H.

lower curve: second derivative.

Method optimisation usually is one of the ways to overcome this problem by adjusting the selectivity of the separation and perhaps the selectivity of the detection system as well [17]. However, the risk of interferences always remains [18]. This risk can be minimised by several methods (Table V). Using chromatographic means, the peak capacity can be enlarged either by using a more efficient column (with more theoretical plates) or by using multi-dimensional HPLC, where the overall peak capacity of independent chromatographic steps can be multiplied [19]. The selectivity of the system can be improved by systematic solvent optimisation. On the other hand, the selectivity of the detection and data processing can be improved. Broad peaks and tailing peaks indicate possible interferences [18]. This can be more easily detected by using derivatives of the chromato-

Table IV. Peak capacities and theoretical plates necessary to separate statistically distributed peaks with 90 per cent confidence with a single injection [15]

number of compounds	peak capacity	theoretical plates
3	21	1900
4	59	15000
8	402	6.8×10^5
16	2013	1.7×10^7
20	3254	4.4×10^7

Table V. Peak purity tests

Peak purity

A. Chromatographic Approaches
- higher peak capacity
  - more plates
  - multidimensional HPLC
- systematic method optimisation

B. Detection and Signal processing
- peak width
- tailing
- derivates of chromatograms
- dual wave length detection
- diodearray detection (LC-UV)
- LC-MS

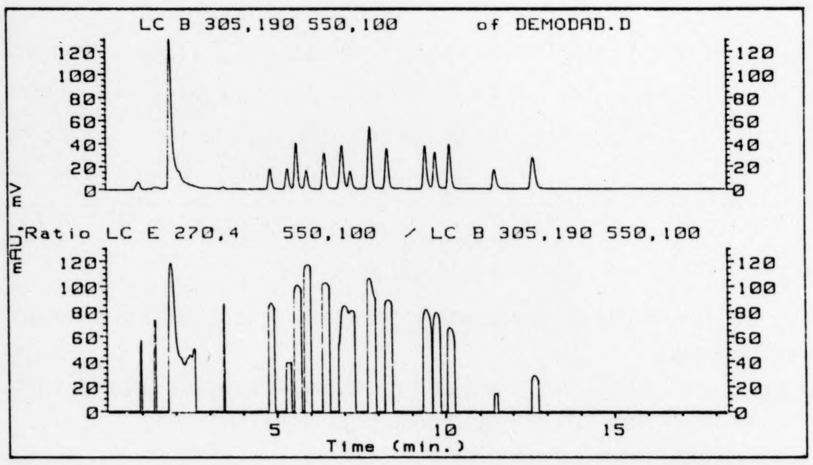

Fig. 3
Detection of peak overlapp by wavelength Ratio Chromatogrammes.

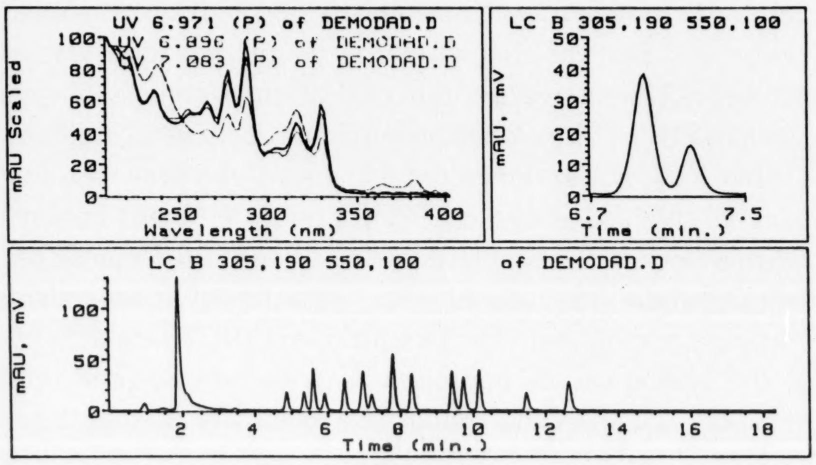

Fig. 4
LC-UV.

gramme [20, 21], as shown in Fig. 2. Dual wavelength detection [22] can give indications of overlapping peaks by examining the ratio of two or more wavelengths (see Fig. 3). Multi-dimensional detection, like LC-UV with diodearray detection (see Fig. 4) or LC-MS [23, 24] (see Fig. 5) gives additional information about the peak purity. Unfortunately, the general impression is that only a few of these methods are used in routine laboratories. Software tools to perform these methods efficiently on a routine basis are perhaps not available. The problem of interference is also related to the type of standardisation. Table VI shows the advantages and disadvantages of internal and external standardisation. Internal standards clearly have the advantage of not being sensitive to complex sample preparation, not even to sample losses during the sample preparation. On the other hand, the internal standard is an additional peak in the chromatogramme to be separated and there are additional possibilities for interferences. Generally, according to error addition rules, internal standardisation gives a higher standard deviation because of the two measurements. Table VII shows the advantages and disadvantages of peak height versus peak area evaluation. Practical experiences have shown that for gradient analysis, peak area measurements are to be preferred.

In the context of validation, method optimisation is of importance for two reasons. As mentioned, the problem of

Table VI. Advantages and disadvantages of internal and external standardisation

	internal Standard	external Standard
advantage	– not sensitive to loss during complex sample preparation	– simple – fast – more accurate for simple separations
disadvantage	– error addition – 2 possible interferences	– reliability of injection

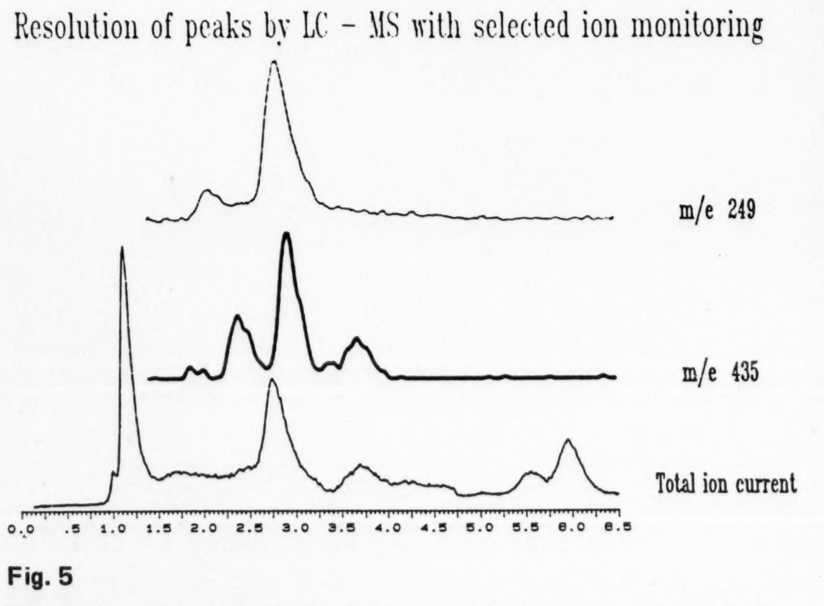

Fig. 5
Resolution of unresolved peaks by specific detection using LC-MS.

peak purity can be addressed by a good optimisation strategy. The second reason is that a good optimisation strategy produces excellent input for the validation of an HPLC method. Systematic evaluation of separation parameters ultimately provides the answer to what parameters are important, not important or critical. This information is useful for the transfer of HPLC methods from one laboratory to another. Good experimental design and reasonable documentation significantly improve the acceptance of an HPLC method in another laboratory and may even overcome the 'NIH-Syndrome' (Not invented here).

Ruggedness

The result of the optimisation also gives valuable information about the ruggedness of the method. Fig. 6 shows a contour-plot of an optimisation function with two parameters, where the maximum of the optimisation response is close to a steep slope. Under routine conditions it may be wise not to operate in the overall maximum, but in a flat region near the maximum. Such an operating condition is much more resistant to fluctuation in parameters and therefore more rugged. Many optimisation strategies are described in the literature, but from the point of view of validation only those methods that lead to a global survey of the response surface are valuable. For example, simplex optimisation does not produce a general survey and may be stuck in local maxima. In this respect the method described by Lankmeyer and Wegscheider [17] is very interesting because – at every step of the optimisation – it provides information on the expected global maxima, as well as on the region of the hyperplane, where more experiments are necessary in order to minimise the uncertainty of the global hyperplane.

Table VII. Peak height versus peak area for quantitation of HPLC

Peak Height or Peak Area
peak height
• not sensitive to flow variation
• sensitive to solvent composition
• sensitiv to temperature (k')
• sensitive to column degradation
• less sensitive to interferences than area
peak area
• sensitive to flow variation
• not sensitive to solvent composition, temperature, and retention
• not sensitive to column degradation
• preferred for gradient analysis

System Suitability Test (SST)

The goal of the system suitability test is to demonstrate adequate performance of the HPLC system prior to the use of the HPLC test. A prerequisite is a validated HPLC method. In HPLC usually the plate number, k'-factors and/or retention times, the detection limit, selectivities of critical pairs of peaks, peak tailing and the relative standard deviation of a number of standard injections are checked. Many pharmacopoea like the USP give detailed information about what is required for GC and HPLC system suitability tests. Fig. 7 demonstrates the importance of the SST and shows how bad column-to-column reproducibility may be (25). Nominally identical HPLC reversed phase columns RP18 (from the same manufacturer but from different batches) produce significantly different retention and selectivity. It may be necessary to discard such a column for this specific separation and look for another more adequate separation column. For this reason the system suitability test should contain limits and minimal requirements for the performance of the separation.

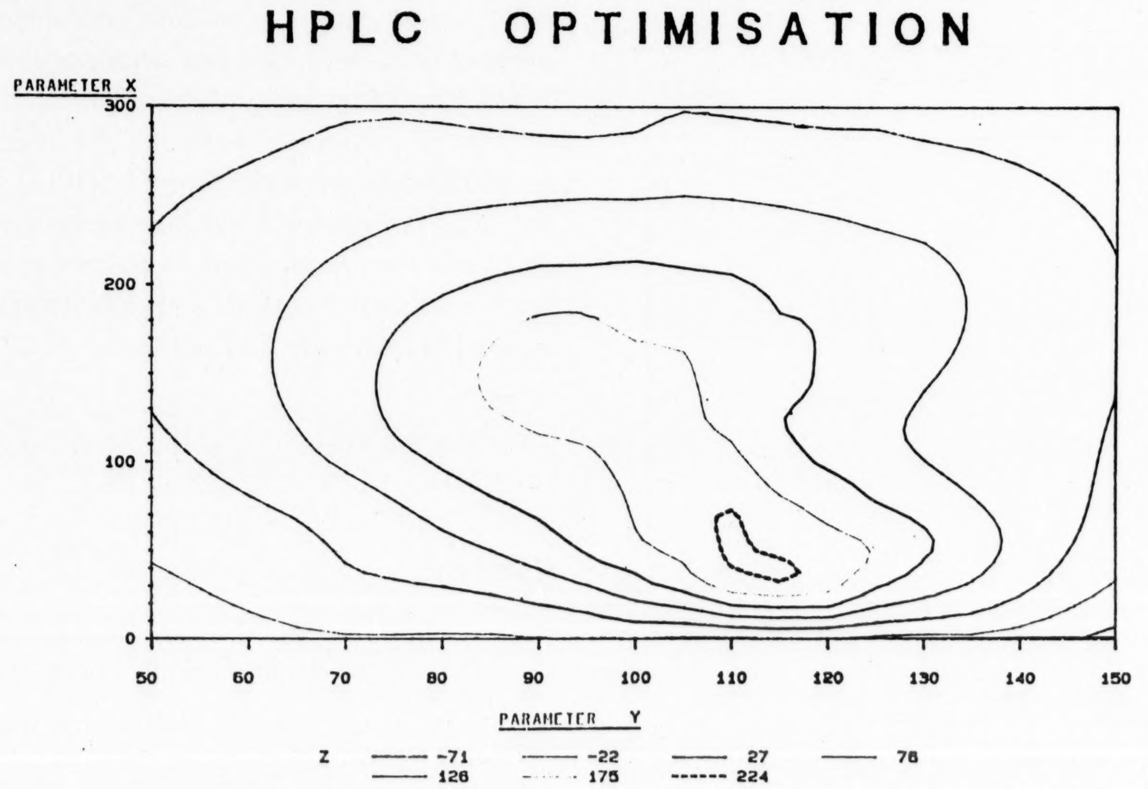

Fig. 6

Contour-plot of an optimisation function.

Qualifications of Instruments

It is obvious that HPLC instruments must work properly in order to insure reliable and valid results. This should be checked from time to time. This validation of instruments is called **QUALIFICATION.** Practical experience in our laboratory has shown that qualification in regular intervals is necessary. Many automatic injectors show excellent reproducibility of the injection volume when they are new. After a couple of months, however, this reproducibility can diminish. It is very important that a malfunction in the instrumentation is identified as early as possible. Qualification of instruments is also important if HPLC methods have to be transferred from laboratory to laboratory, especially for the transfer of gradient elution HPLC methods. Fig. 8 shows that the gradient delay-volume, as well as the gradient mixing-volume, of the HPLC instruments is important for the gradient characteristic. If either of these parameters is very different from the original HPLC instrument, significant differences in the retention times and even in the selectivity of separation may occur, especially if a gradient method has to be transferred from a high pressure gradient HPLC instrument to a low pressure side-gradient mixing instrument. Usually the low pressure mixing instruments have much higher delay- and mixing-volumes. In cases of very short columns with small inner diameters, the operation with a low pressure-side gradient instrument may be impossible.

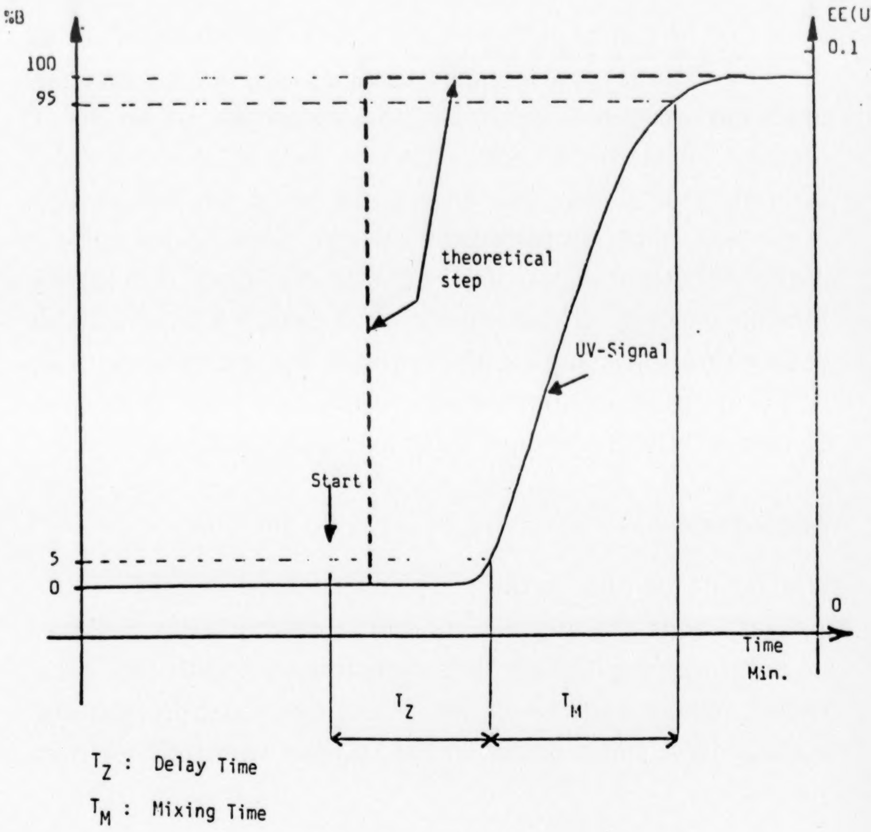

Fig. 8

Gradient characteristics: Delay volume and Mixing volume.

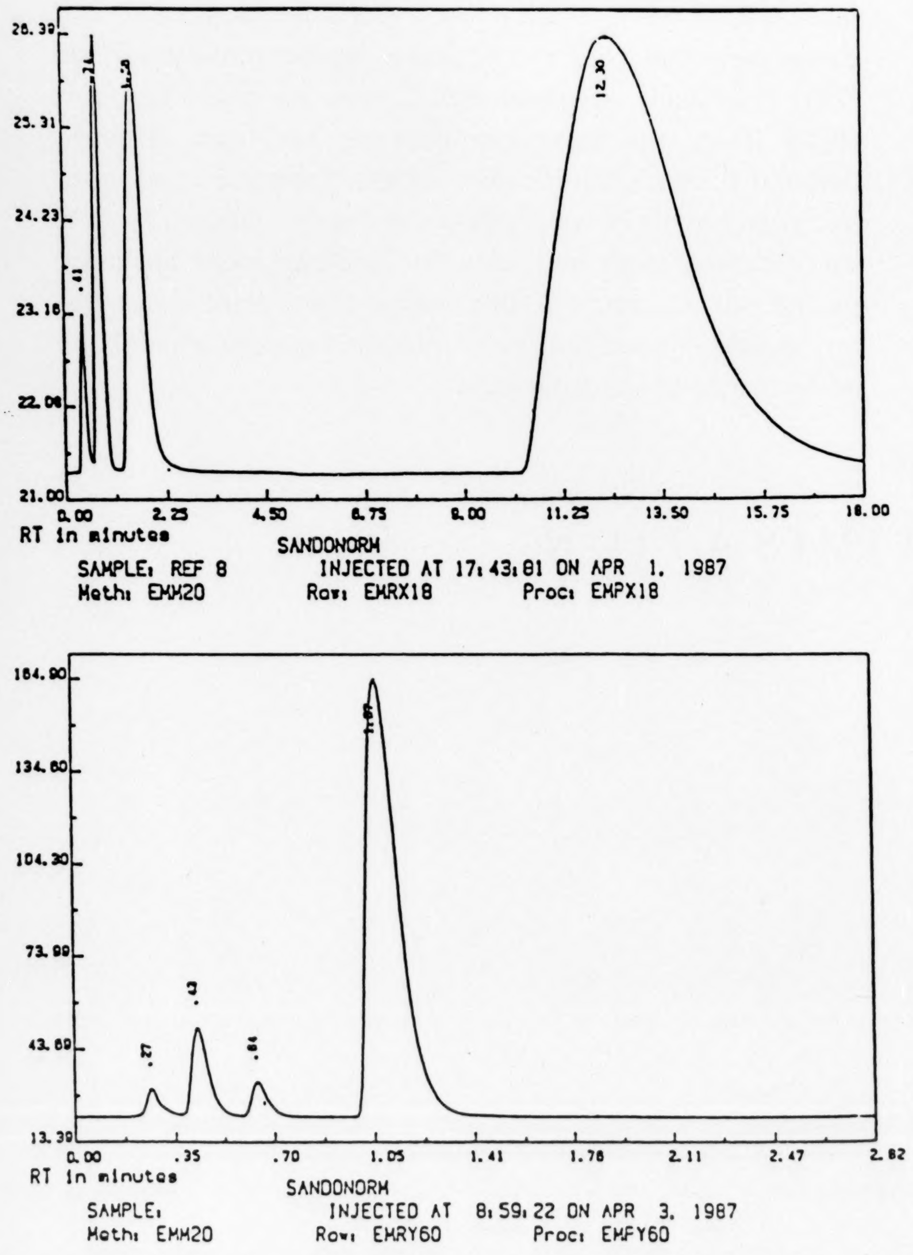

Fig. 7

Differences of retention and selectivities by column to column variability.

Conclusions

It has been shown that automation of HPLC systems was successful in routine applications. Mechanisation and laboratory robots make even complex sample preparations with unattended operation and high reproducibility possible. In the future, computer systems will also expand in areas of documentation and laboratory information management. Expert systems will soon help handle routine problems efficiently, without replacing the human expert. It was emphasised that the validation of HPLC methods, especially the proof of peak purity, is extremely demanding scientifically and may never come to an end. It was also shown that system suitability tests and qualification of instruments assure the reliability and validity of HPLC results.

References

[1] *R. Schuster, W. Haecker,* Application Note "Automated Precolumn Sample Preparation System", Hewlett-Packard, Waldbronn, GFR.

[2] *J. M. Huen, J. P. Thevenin,* Chromatographia **12**, 6, 405–407 (1979).

[3] *R. Vivilecchia,* LC/GC Magazine **4**, 94–106 (1986) .

[4] *St. E. Cook, Th. C. Pinkerton,* J. of Chromatography **368**, 233–248 (1986).

[5] *F. Erni, H. P. Keller, C. Morin, M. Schmitt,* J. of Chromatography, **204,** 65–67 (1981).

[6] Lotus Development Corp., Cambridge, Ma., USA.

[7] RS/1: BBN Research Systems, Cambridge, Ma, USA.

[8] SAS:SAS Institute Inc., Cary, North Carolina, USA.

[9] Chem Text, Molecular Design, Ltd., San Leandro, Ca., USA.

[10] Experimental Design, Statistical Programmes, Houston TX, USA.

[11] *J. Karnicky, T. Schlabach, Sj. Van der Wal, S. Abbott,* 8th International Symposium on Column Liquid Chromatography, New York 1984.

[12] *L. R. Snyder, J. W. Dolan,* DryLab: LC Resources Inc., San Jose, Ca., USA.

[13] Pi Technologies; Orinda, Ca. USA, "The HPLC Doctor"

[14] *F. Erni,* J. of Chromatography **282,** 371–383 (1983).

[15] *J. M. Davis, J. C. Giddings,* Anal. Chem. **55,** 418–424 (1983).

[16] *M. Martin, D. P. Herman, G. Guiochon,* Anal. Chem. **58,** 2200–2207 (1986).

[17] *W. Wegscheider, E. P. Lankmayr, M. Otto,* Anal. Chimica Acta **150,** 87–103 (1983).

[18] *S. Ebel,* Chromatographia **22,** 7–12, 373–378 (1986).

[19] *F. Erni, R. W. Frei,* J. of Chromatography **149,** 561–569 (1978).

[20] *K. Jost,* Dissertation 1985, Saarbrücken.

[21] *A. F. Fell, H. P. Scott, R. Gill, A. C. Moffont,* J. of Chromatography **273,** 3 (1983).

[22] *A. C. J. H. Drouen, H. A. H. Billiet, L. De Galaan,* Anal. Chem. **56,** 971 (1984).

[23] *F. Erni,* J. of Chromatography **251,** 141–151 (1982).

[24] *K. Schellenberg, M. Linder, A. Groeppelin, F. Erni,* J. of Chromatography **394,** 239–251 (1987).

[25] *A. P. Goldberg,* Anal. Chem. **54,** 342–345 (1982).

Received: June 30, 1987
Accepted: July 22, 1987
F

Multivariate Analysis of Non-Homogeneous Peaks in Liquid Chromatography

G. G. R. Seaton / A. F. Fell*

Department of Pharmaceutical Chemistry, University of Bradford, Bradford, BD7 1DP, UK

Key Words

Linear diode array detectors (LDA, DAD)
Deconvolution
Iterative target testing factor analysis (ITT-FA)
Multicomponent analysis (MCA)
Analysis of variance (ANOVAR)

Summary

The effects of concentration, separation and spectral similarity as factors influencing the accuracy of iterative target testing factor analysis (ITT-FA) are investigated for three component systems by the application of analysis of variance (ANOVAR). ANOVAR is applied over a range of peak separations to map the changing effects of the three factors with increasing overlap. Two error responses were measured and analysed, (a) Relative cluster error (RCE) a measure of the error over all peaks in a cluster and (b) Relative peak error (RPE) the error of an individual peak. Multicomponent analysis (MCA) a method requiring *a priori* spectral information, is used as a referee method for ITT-FA.

Introduction

The multivariate data sets generated by linear diode array detectors (LDA) in the form of spectrochromatograms, have resulted in the development of a number of mathematical techniques which take advantage of the extra information in the wavelength domain [1]. These techniques can deconvolute from spectrochromatographic data matrices, representing nonhomogeneous peak clusters, estimations of the spectral profiles and/or elution profiles of the pure components present. These include multicomponent analysis (MCA) [2], curve resolution (CR) [3], iterative target testing factor analysis (ITT-FA) [4, 5] and, most recently, evolving factor analysis (EFA) [6]. Only the first of these methods requires *a priori* information on all components in the peak cluster.

The application of these methods may be for one of two main reasons. Firstly as a tool in the optimisation procedure, automated or otherwise, by assisting in the tasks of determining the number of pure components present in a peak cluster, and the estimation of their respective resolutions and identities (peak tracking). Secondly, in cases where further optimisation of peak separation is impractical, as a method to improve peak quantitation and identification by direct estimation of pure elution profiles and spectra.

The aim of this work was to analyse the errors propagated by ITT-FA with respect to the three main factors considered to affect multivariate deconvolution techniques, namely: separation (resolution), absorbance contribution (concentration) and spectral similarity of the components present in a nonhomogeneous peak cluster. This involves giving an estimation of the magnitude of the errors produced by a specific set of compounds, whose similarity is expressed as a correlation coefficient, for a defined range of absorbance contributions and separations. Analysis of variance (ANOVAR) is used to indicate how the effect of the factors involved may change with decreasing peak resolution. The analysis of the errors produced by ITT-FA, where no prior knowledge is known about the system, is compared with the results from MCA (least squares deconvolution), where the spectral information for all components is known. MCA is therefore used here as a referee method for ITT-FA.

Theory

A spectrochromatogram D (t by w) can be conceived as either a matrix of t rows of linear combinations of pure spectra (at w wavelengths) or as w columns of linear combinations of pure elution profiles (at t elution times). A spectrochromatogram matrix D can be simulated by the product of two matrices; C, a (t by n) matrix of n pure component column vector elution profiles, and S, a (n by w) matrix of spectra of the corresponding n pure components held as row vectors (Figs 1–4):

$$D = C \cdot S \qquad (1)$$

0009-5893/87 0208-09 $03.00/0

© 1987 Friedr. Vieweg & Sohn Verlagsgesellschaft mbH

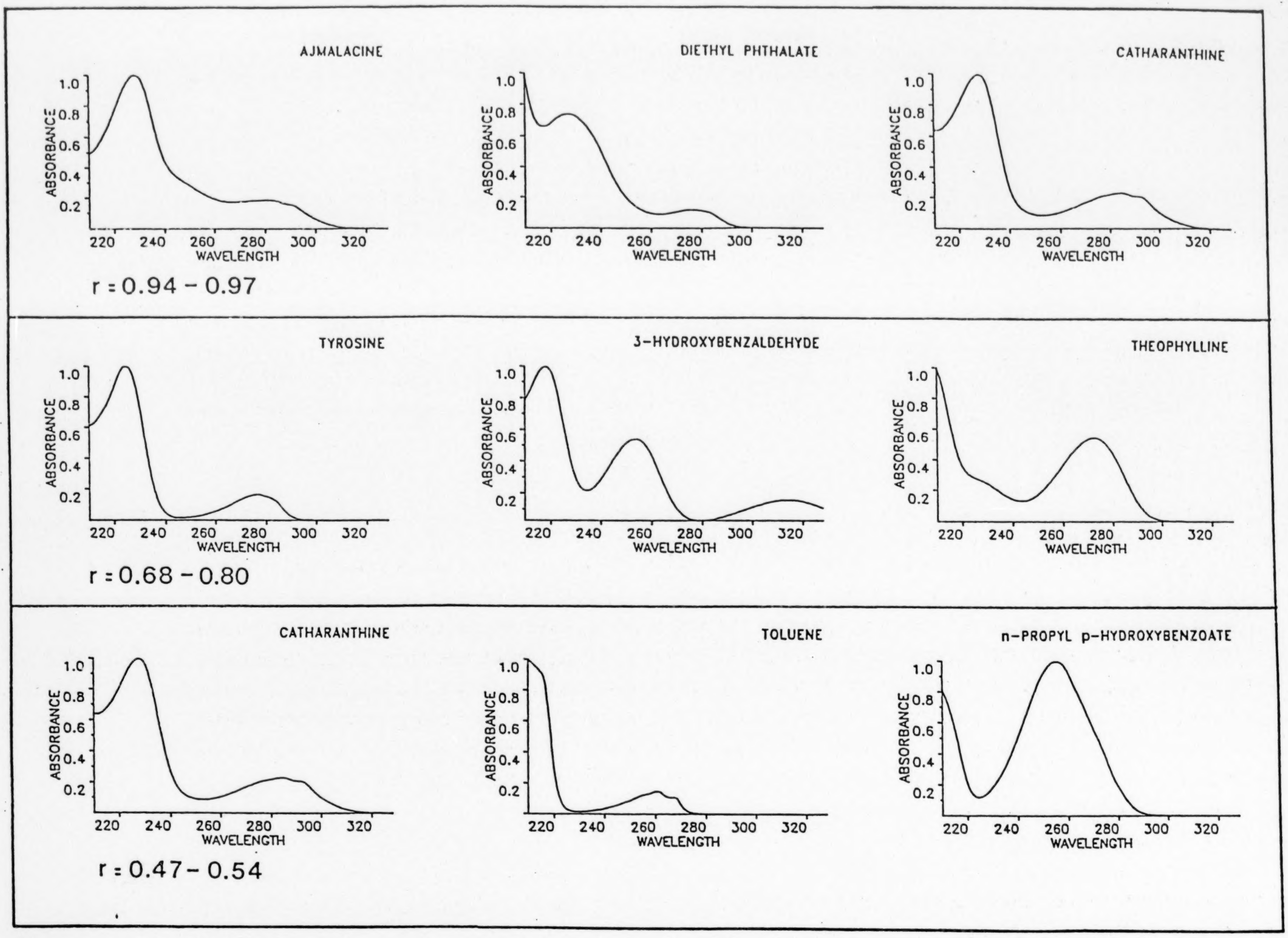

Fig. 1

Three sets of normalised UV spectra used for three-component nonhomogeneous peak cluster simulation. Each set represents one level of the factorial similarity factor (factor 3) as measured by the correlation coefficient range: Top r = 0.94–0.97; Middle r = 0.68–0.8; Bottom r = 0.47–0.54.

This noiseless simulation is made more realistic by the addition of random, normally distributed error with a mean of zero and a standard deviation similar to that produced by a real system (e.g. 0.12 mAU).

The simulations of the pure elution profiles are based on the Gaussian (normal) distribution:

$$y(x) = e^{-x^2/2} \qquad (2)$$

although in practice this function may be convoluted with a single sided exponential decay function to simulate peak tailing [7]. The pure spectra used in this work are the digitised spectra of various real compounds.

Deconvolution therefore is the reverse process where, from the spectrochromatogram data matrix D, estimations of the pure chromatographic and spectral matrices (C and S) are made. The mathematical estimations of C and S will henceforth be identified as E and A (Elution and Absorbance matrices), respectively, to denote that they are not formally equivalent although they may be highly similar.

One technique which requires no prior knowledge of the components present in a nonhomogeneous chromatographic peak is iterative target testing factor analysis (ITT-FA).

Iterative Target Testing Factor Analysis

The first step in ITT-FA is the extraction of the abstract and mutually orthogonal chromatographic eigenvectors of the covariance matrix,

$$D \cdot D^T \quad (t \text{ by } t) \qquad (3)$$

and the determination of the number (n) of significant eigenvectors that account for the variance in D, excluding noise, and hence the number of chemical components present. This work utilised Householder's tridiagonalisation of the real symmetric covariance matrix, followed by the QL algorithm to derive the full set of t eigenvectors. The determination of n has been discussed by Malinowski and Howery [8] and by Wold [9]. In the present work n is known from the simulation.

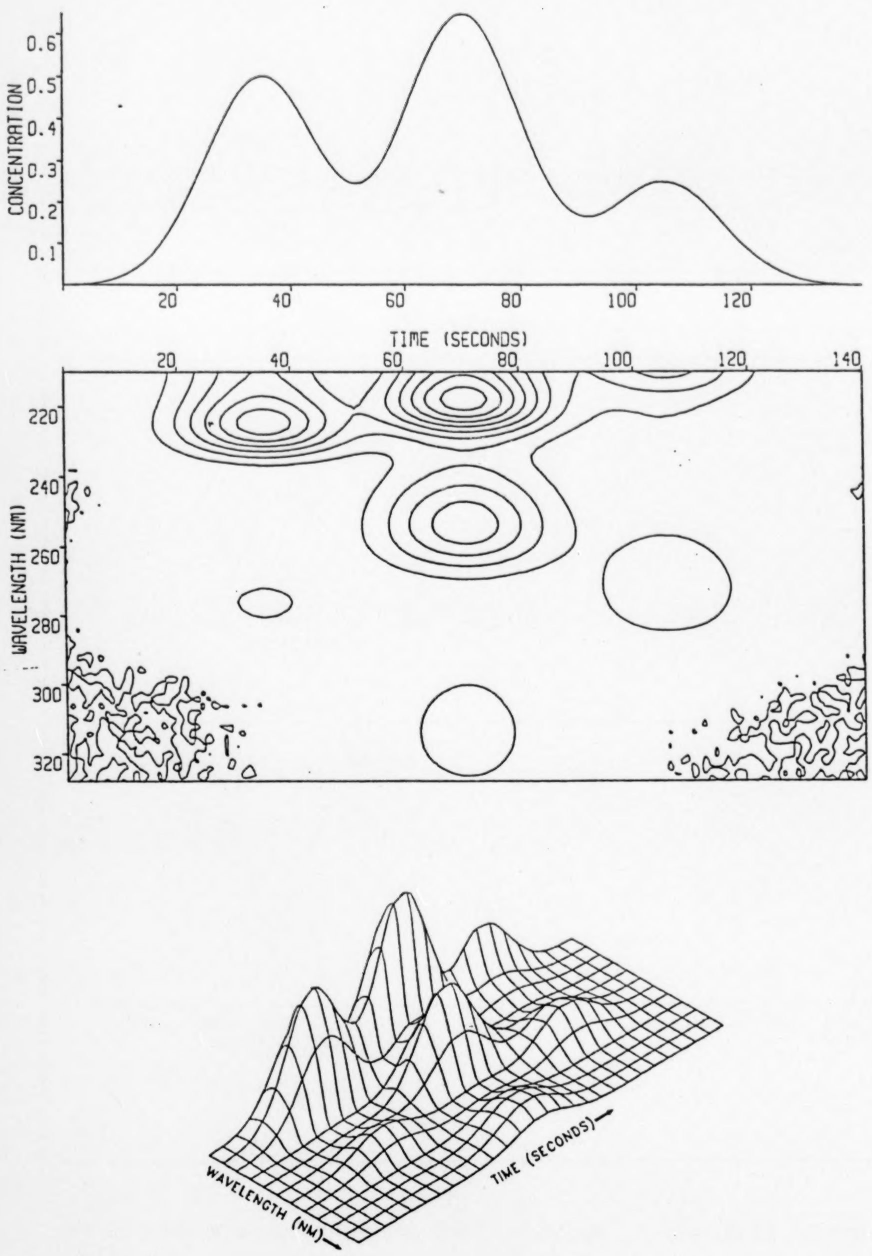

Fig. 2

Simulated concentration profile, contour plot and spectrochromatogram for a set of three overlapping components defined by: similarity range r = 0.68 – 0.80; adjacent peak separation Δt = 0.3; relative peak heights 1 : 1.3 : 0.5.

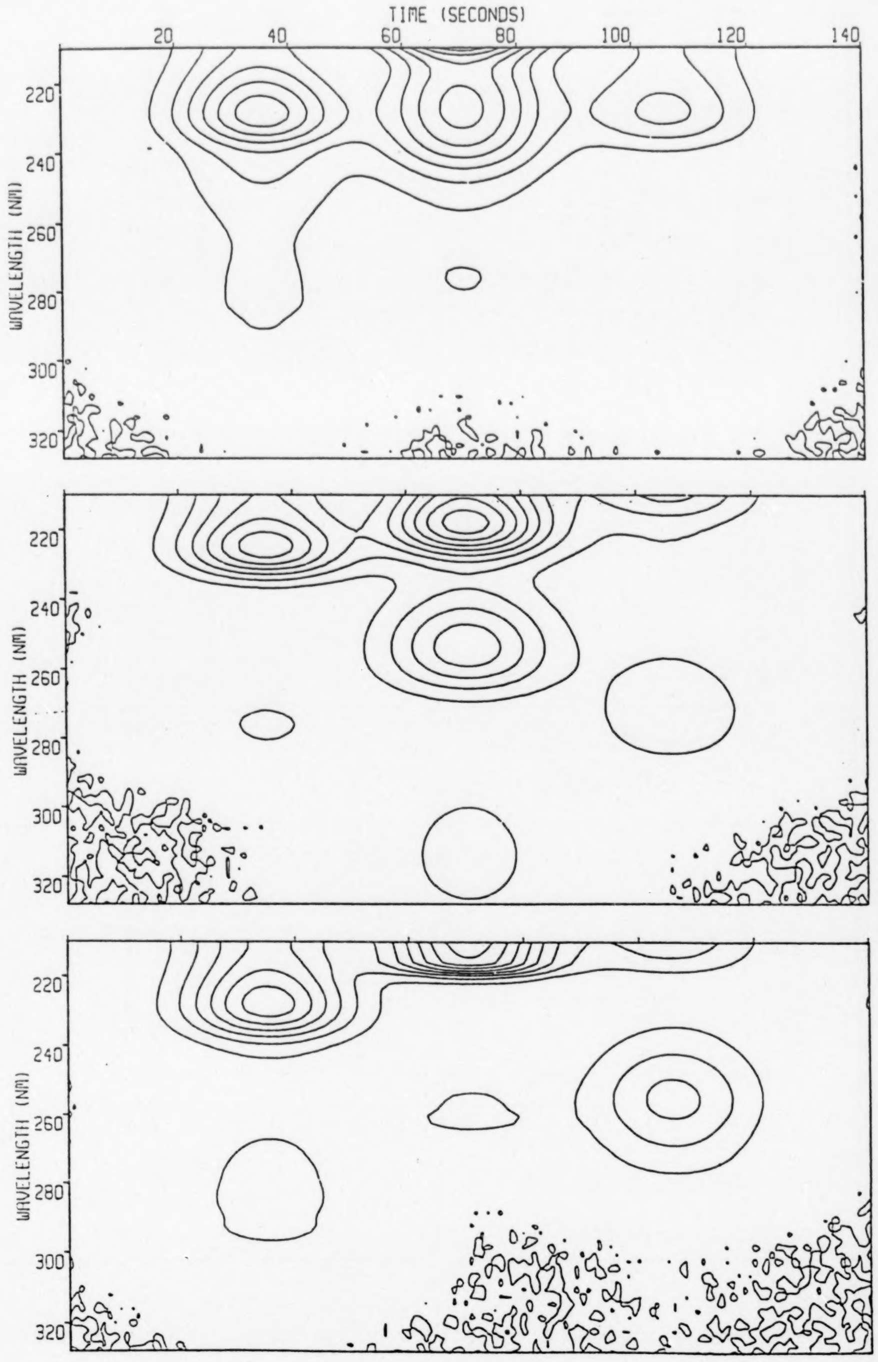

Fig. 3

Three simulated three component spectrochromatograms presented as contour plots. Each plot represents one level of the factorial similarity factor (factor 3) as measured by the correlation coefficient range: Top r = 0.94–0.97; Middle r = 0.68–0.8; Bottom r = 0.47–0.54. All three plots are further defined by adjacent peak separations of Δt = 0.3 with relative peak heights 1 : 1.3 : 0.5.

Vandeginste *et al.* [5] suggested the use of the VARIMAX [10] method of factor rotation of the normalised n abstract eigenvectors (matrix E) for estimation of the initial targets used for subsequent iterative improvement. VARIMAX, as the name suggests, maximises the sum of the variance (s^2) of all vectors according to the equation:

$$s^2 = \frac{1}{t}\sum_{i=1}^{n}\sum_{j=1}^{t} e_{ji}^4 - \frac{1}{t^2}\sum_{i=1}^{n}\left(\sum_{j=1}^{t} e_{ji}^2\right)^2 \tag{4}$$

where e_{ji} is the j^th^ loading on the i^th^ factor (column vector) in E.

Iterative target testing is now utilised to improve the VARIMAX result from which an estimation of the apex position of each pure elution profile is derived. The initial test vector T (t by 1) for each component is simply 1.0 at the maximum value of the vector chosen for iterative improvement; all remaining values are set to zero.

The rotation vector R (n by 1), which results in the least squares approximation to the target T is calculated by:

$$R = (E^T \cdot E)^{-1} \cdot E^T \cdot T \tag{5}$$

T_2, the approximation to T, is a linear combination of the vectors defining the factor space calculated by:

$$T_2 = E \cdot R \tag{6}$$

T_2 is adjusted for re-submission as T, in eq. (5), by the removal of any secondary maxima to maintain the unimodal nature of a pure peak and setting to zero any values below 0.005. Iteration stops when no noticeable improvement occurs, that is when the similarity between T and T_2 exceeds a threshold, typically 0.99, as measured by the correlation coefficient r.

This process is repeated for all vectors until finally matrix E holds n column vectors, each one of which is an estimate

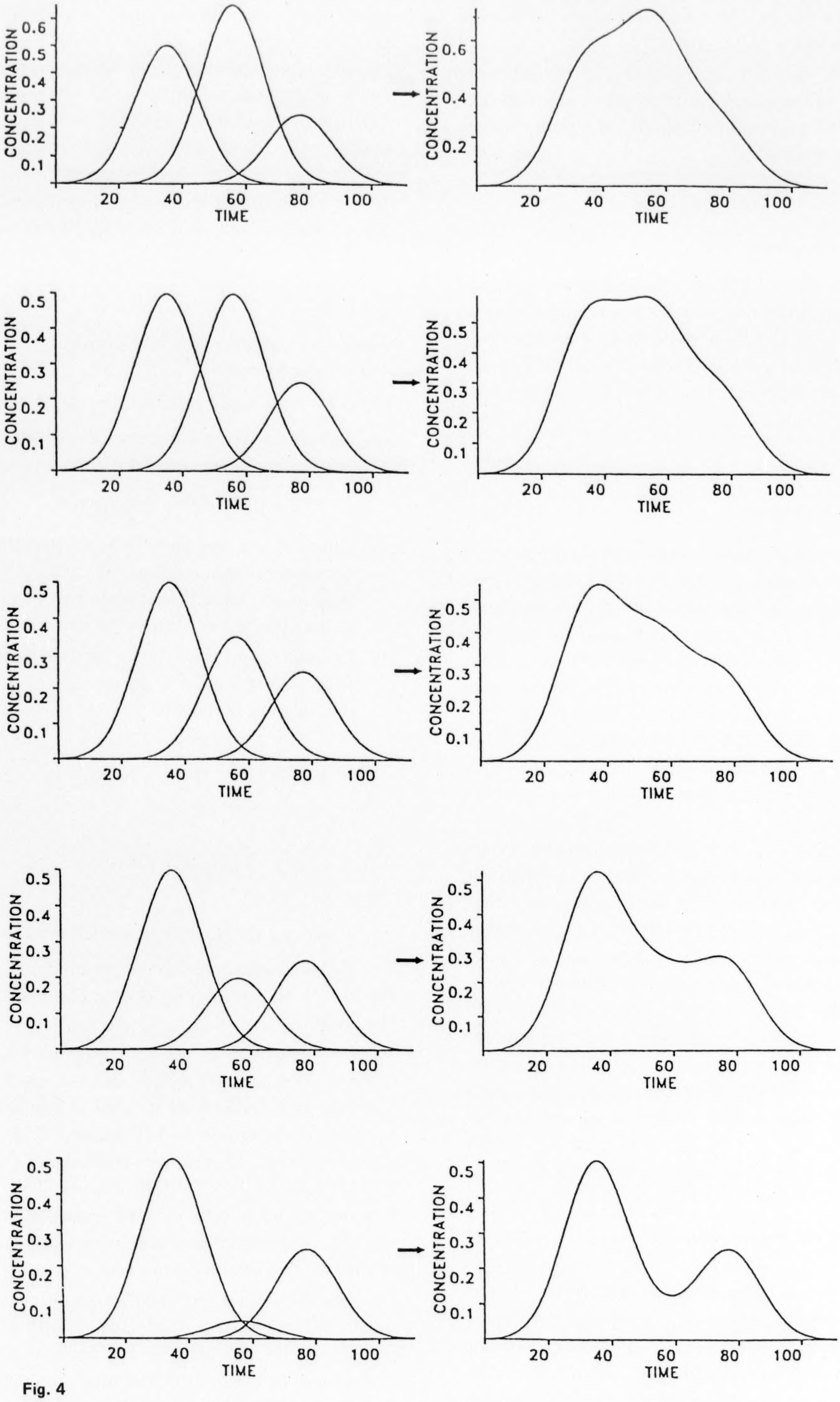

Fig. 4

The five relative concentration (factor 1) levels. On the left, individual peak concentration profiles, on the right total concentration profile. Peak 1 and 3 are kept constant at concentrations 0.5 and 0.25, respectively. The concentration of peak 2 is decreased from top to bottom: 0.65; 0.5; 0.35; 0.2; 0.05.

of a true pure elution profile, which represents the sharpest solution possible in the factor space.

The final step is the least squares fitting of the estimated elution profiles to the spectrochromatogram D thus deriving estimations of the spectral identities of the n pure chemical components in matrix A:

$$A = (E^T \cdot E)^{-1} \cdot E^T \cdot D \qquad (7)$$

Multicomponent Analysis

Multicomponent analysis [2], in this case where the pure spectra are known from the simulation and are held as row vectors in matrix S, can be considered as the converse of eq. (7). The matrix of estimated elution profiles, E, is calculated by the least squares fitting of S to D:

$$E = D \cdot S^T \cdot (S \cdot S^T)^{-1} \qquad (8)$$

Hardware and Software

Pure component spectra with a resolution of 2nm in the range 210–328nm were extracted from spectrochromatographic data captured and stored on 5.25 inch floppy discs. The diode array detection system used for data capture was based on the Hewlett-Packard HP85 microcomputer/controller with input/output, plotter/printer, mass storage and advanced programming ROMs installed, connected by HP-IB (IEEE 488) interface bus to a 82901M dual disc drive and a 1040A rapid scanning spectrophotometer, fitted with a 4.5μl flow cell (Hewlett-Packard, Waldbronn, FRG).

The extracted spectra were transferred manually to the CDC Cyber 180/830 mainframe installation at Bradford University (Control Data Corporation, Minneapolis, USA). General programming in FORTRAN 77 for simulations, ITT-FA, MCA and data analysis was performed by the authors. The VARIMAX routine was programmed from an original description by Kaiser [10]. Procedures for the inversion of a real matrix, Householder's tridiagonalisation and the QL algorithm for extraction of all eigenvectors from a real symmetric matrix were translated from those of Wilkinson and Reinsch [11]. Graphical output was produced by the Simpleplot (Version 2.8) graphical library (Bradford University Software Services, Bradford, UK).

Materials

Catharanthine sulphate, ajmalacine (Gedeon Richter Chemical Works, Budapest, Hungary), tyrosine, 3-hydroxybenzaldehyde, theophylline, n-propyl p-hydroxybenzoate (Sigma, Poole, UK), diethyl phthalate (May and Baker, Dagenham, UK) and toluene (BDH, Poole, UK) spectra (Fig. 1) were measured at concentrations in solution corresponding to absorbance values in the range 0.1–0.3 AU, in the HP1040 diode array detector cell.

Methods

The data sets generated were based on 8 real spectra normalised to their respective spectral maxima (Fig. 1) and, combined in the time domain according to the assumed Gaussian model of an elution profile. The spectrochromatograms and contour plots representing the matrix of (A, λ, t) data can be visualised as indicated in Figs 2 and 3. Each plot represents a cluster of three peaks, with defined overlap ($\Delta t = 0.5$) and defined relative concentration (1:1.3:0.5). In Fig. 3 each cluster differs with respect to the range of correlation coefficients between the three spectra involved, which is calculated from the equation:

$$r = \frac{\Sigma xy - (\Sigma x)\,(\Sigma y)/n}{[(\Sigma x^2 - (\Sigma x)^2/n) \cdot (\Sigma y^2 - (\Sigma y)^2/n)]^{1/2}} \qquad (9)$$

where n represents the dimensionality of the vectors x and y being correlated.

The error responses measured after deconvolution were:

(a) Relative peak height error of a single peak, RPE, expressed as a percentage of the model peak height:

$$RPE = [|Hin - Hout|/Hin] \cdot 100 \qquad (10)$$

where Hin is the known model peak height of a pure component measured at its spectral maximum and Hout is the peak height after deconvolution measured at the same wavelength in the same units.

(b) Relative peak height error of the three peak cluster, RCE, expressed as a percentage of the sum of the simulated peak heights:

$$RCE = \left\{ \left(\sum_{c=1}^{n} [H_c in - H_c out]^2 \right)^{1/2} \Big/ \sum_{c=1}^{n} H_c in \right\} \cdot 100 \qquad (11)$$

where n is the number of components in the cluster.

The factors under investigation are absorbance contribution (factor 1), peak separation (factor 2) and spectral similarity (factor 3).

The dimensionality of the total error matrices recorded for both ITT-FA and MCA was defined by 5 concentration levels (peak 2, 0.05–0.65 stepped at intervals 0.15; Fig. 4), by 10 separations (0.1–1.0 stepped 0.1), by 3 spectral similarity levels (correlation coefficients for each cluster $r_{1:2:3} \approx 0.55$, ≈ 0.75, ≈ 0.95; Fig. 1). This was replicated 3 times giving a total of 450 simulated spectrochromatograms, deconvolutions and error calculations for each of the two deconvolution techniques.

To determine how the relative importance of the three factors affecting error may change with decreasing peak separation, the data used for the analyses of variance were submatrices ($5 \times 3 \times 3$) of the total data sets ($5 \times 10 \times 3$). The first ANOVAR therefore is a 5×3^2 factorial design over peak separations 1.0–0.8, the next ANOVAR analyses the data included in the separation submatrix 0.9–0.7. This is repeated until eight analyses are completed ranging from totally separated (1.0–0.8) to highly overlapped (0.3–0.1) three-component systems.

The resulting F values for the three main factors are adjusted by dividing them by the tabulated F value at the 1% significance level for the appropriate numbers of degrees of freedom. The 8 ANOVAR separation sets of adjusted F values are subsequently plotted against the ANOVAR separation factor median levels, (e.g. if factor 2 has the range 0.6–0.4 then the adjusted F values are plotted versus 0.5) resulting in a 'factorial plot'. This is repeated for both deconvolution techniques for both RCE and RPE (Figs 5–8).

Results and Discussion

Figure 5 represents the effect of concentration, peak separation and similarity on the relative cluster error generated by ITT-FA, and how the effects of the factors change with decreasing separation.

The first two ANOVAR results covering peak separations 1.0–0.8 and 0.9–0.7 indicate that only the similarity and concentration factors have significant effects on the RCE of ITT-FA, although the latter effect of the concentration factor is only marginal.

Over the separation range 0.8–0.5 the influence of the similarity and concentration factors remains essentially constant, although a gradual increase in the importance of the concentration factor is detectable. Over the same range the effect of peak separation as a factor in ITT-FA increases rapidly, first showing an effect intermediate to the other two factors, and subsequently becoming dominant.

The rank of all three factors remains stable over peak separations 0.6–0.1, with separation the dominant factor affecting the RCE of ITT-FA followed by relative concentration and lastly spectral similarity. The magnitude of the effects of the three factors however, increases dramatically.

The plot of factor influence on the RCE of MCA (Fig. 6) indicates that, as expected, the effects of the three factors

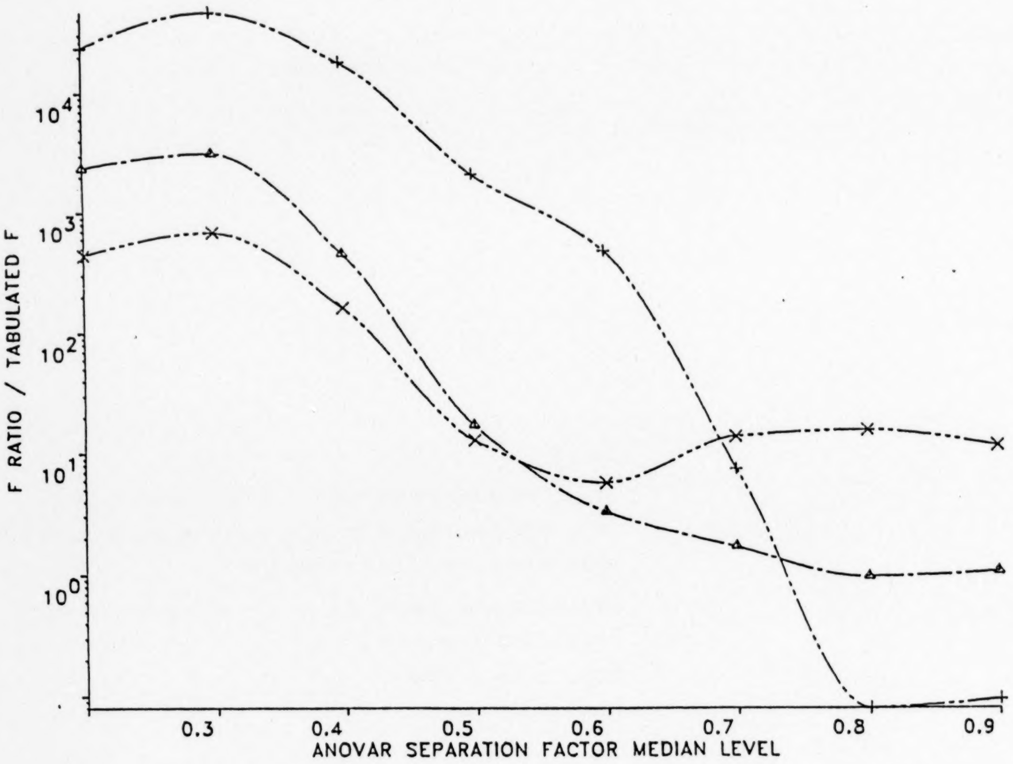

Fig. 5

Changing main factor effects on the relative cluster error (RCE) in ITT-FA, with respect to decreasing peak separation. The factors are:

Concentration (factor 1) ——–——Δ——–——;
Separation (factor 2) ——–—–—+——–——;
Spectral similarity (factor 3) ——–––—X—–––—.

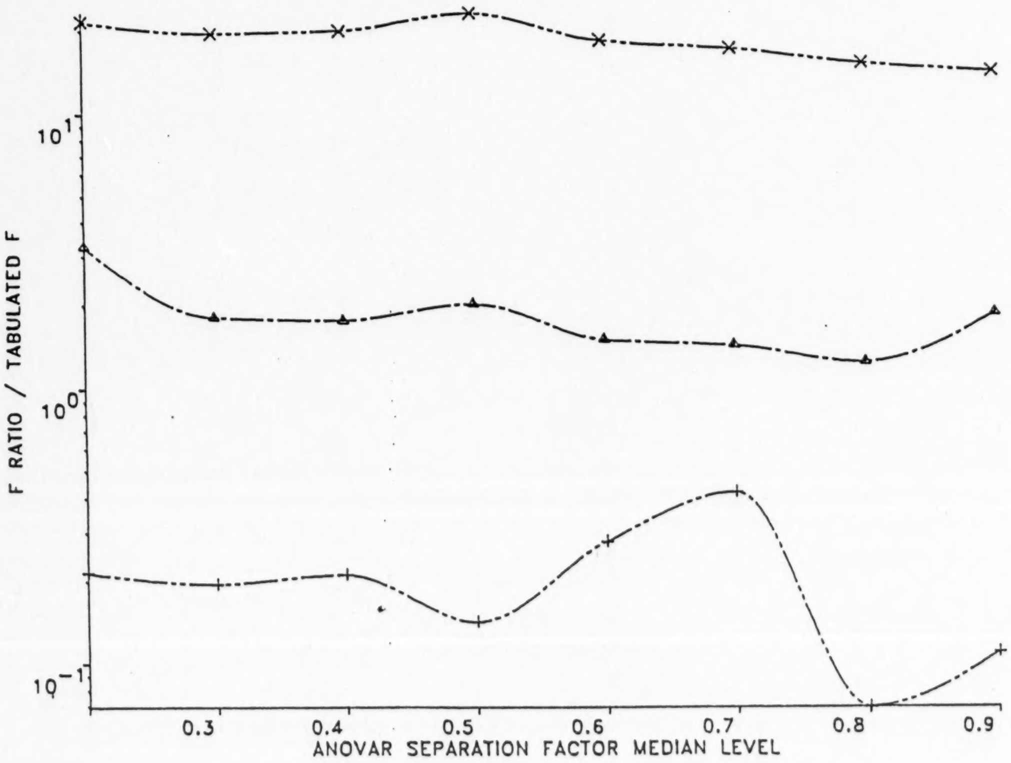

Fig. 6

Changing main factor effects on the relative cluster error (RCE) in MCA, with respect to decreasing peak separation. The factors are:

Concentration (factor 1) ——–——Δ——–——;
Separation (factor 2) ——–—–—+——–——;
Spectral similarity (factor 3) ——–––—X—–––—.

remains relatively constant over the entire separation range, with spectral similarity dominating, concentration having a marginal effect and peak separation having no significant effect on the relative cluster error.

Comparing the above analyses it can be seen that over the separation range 1.0–0.7, the two data sets being 1.0–0.8, 0.9–0.7, all three factors elicit effects on the RCE of ITT-FA that are almost identical to those of the RCE of MCA. The effects of the concentration and similarity factors remain comparable in both techniques down to a separation of ≈ 0.5. At separations less than 0.5 all factors affect ITT-FA to a far greater extent than MCA. As the final step of ITT-FA represents a least-squares fit of the estimated elution profiles to the spectrochromatogram matrix (*cf.* MCA), any errors produced by ITT-FA can be explained by its inability to make *accurate* estimations of the true elution profiles.

The simulation experiments were designed so that only the concentration of the middle peak of a three component peak cluster was varied, thus allowing comparison of the factorial analysis of the relative peak error (RPE) of this peak alone with that of the relative cluster error (RCE).

Figure 7 represents the effect of concentration, peak separation and similarity on the relative peak error (RPE) generated by MCA, and how the effects of the factors change with decreasing separation. Note that although, like the factorial plot of the RCE of MCA (Fig. 6), separation is an insignificant factor, concentration exerts a greater influence than similarity. This indicates that when RCE is the measure of error, it *underestimates* the importance of relative concentration as a factor affecting the ability of MCA to estimate the true concentration of an individual peak.

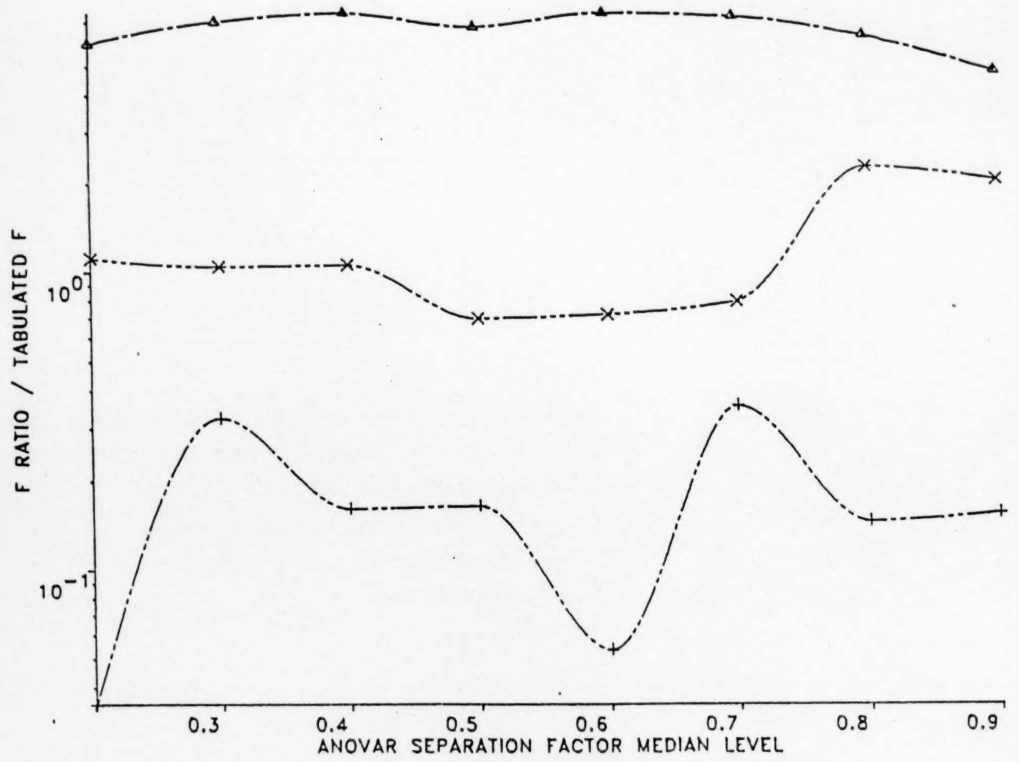

Fig. 7

Changing main factor effects on the relative peak error (RPE) in MCA, with respect to decreasing peak separation. The factors are:

Concentration (factor 1) ——-——Δ——-——;
Separation (factor 2) ——-——+——-——;
Spectral similarity (factor 3) ——-——X——-——.

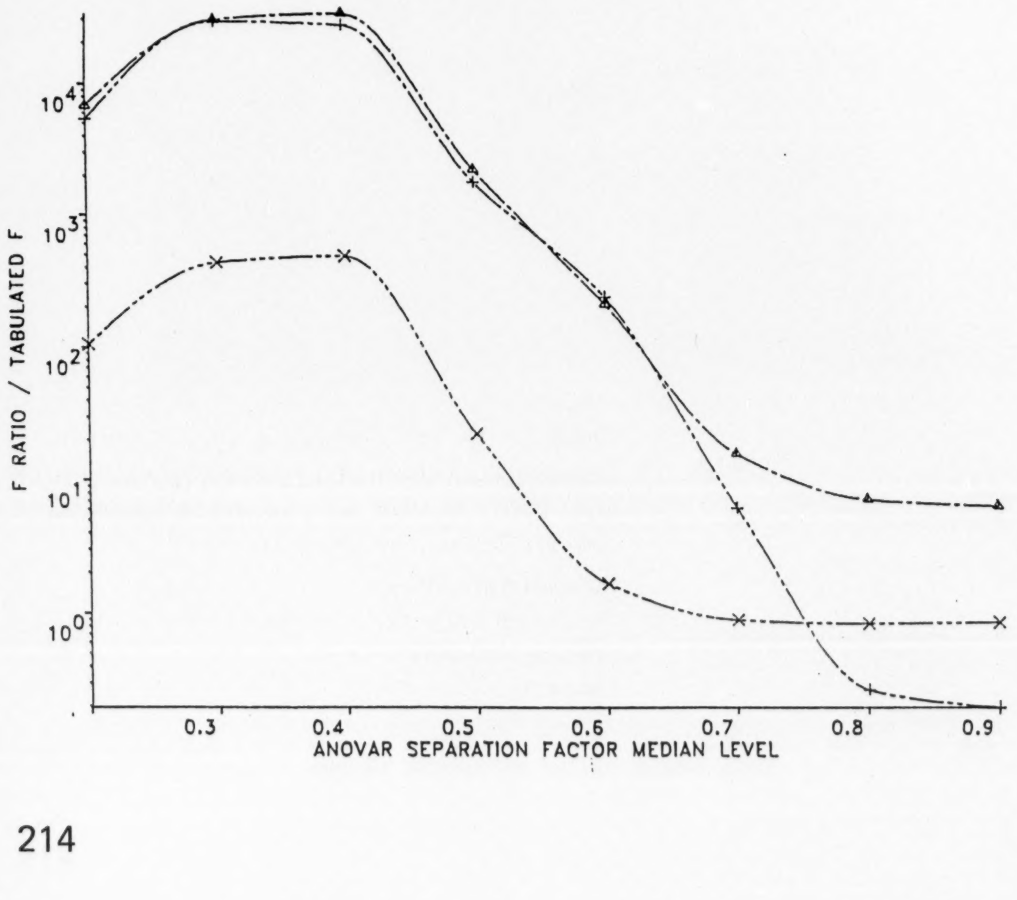

Fig. 8

Changing main factor effects on the relative peak error (RPE) in ITT-FA, with respect to decreasing peak separation. The factors are:

Concentration (factor 1) ——-——Δ——-——;
Separation (factor 2) ——-——+——-——;
Spectral similarity (factor 3) ——-——X——-——.

This point is confirmed in Fig. 8, which is the equivalent factorial plot for the RPE of ITT-FA. Here both separation and spectral similarity exert comparable effects on ITT-FA, as they do on the RCE of ITT-FA (Fig. 5). Relative concentration, however, now closely follows separation as a major influence on ITT-FA error and, appears to be marginally more important.

Clearly when considering peak height as a factor affecting ITT-FA, the highest peak error is found when a low concentration component is flanked on both sides by high concentration peaks. The most extreme example of this situation in the present data set, occurs when peak 1 concentration = 0.5, peak 2 = 0.05 and peak 3 = 0.25. Although the *relative* peak error of the second peak expressed as a percentage can be high e.g. 5.3% (Figure 9a), the *absolute* peak height error (5.3% of 0.05) is in fact low when compared with the concentrations of the flanking peaks. As the calculation of RCE essentially expresses the sum of the absolute errors as a percentage of the sum of the peak heights, it is understandable that the relatively high error of a single low concentration component can be masked by surrounding high concentration — low error peaks (Fig. 9b).

Conclusions

The accurate quantitation of unresolved chromatographic peaks in HPLC-LDA can be achieved by the application of ITT-FA, within its limitations, to nonhomogeneous peak clusters. As already suggested [12], ITT-FA should ideally be limited to resolutions where not more than two components in a cluster overlap at any one time i.e. at separations ⩾ 0.5, and when the absorbance contributions of all components are within an order of magnitude.

The 'factorial plots' in Figs 5 and 8 demonstrate that, as separation decreases, when the ANOVAR data window

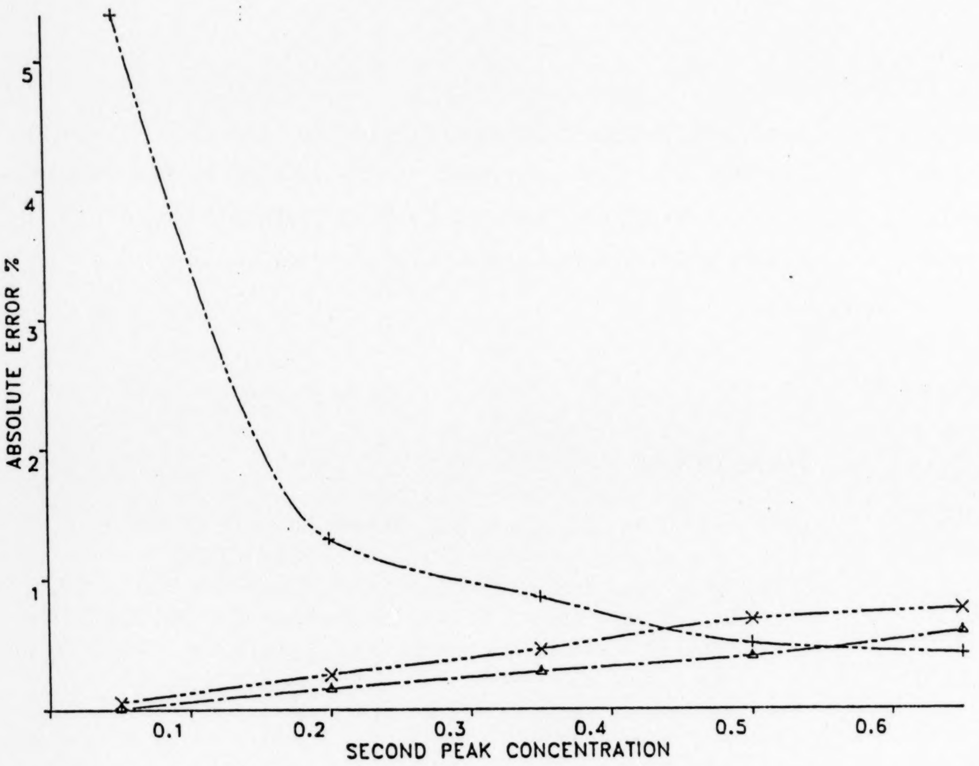

Fig. 9a

ITT-FA relative peak error (RPE) for each peak in three-component clusters is plotted as a function of second peak concentration. Adjacent peak separation $\Delta t = 0.4$, spectral similarity range r = 0.94–0.97.

First Peak ——— Δ ———;
Second Peak ——— + ———;
Third Peak ——— X ———.

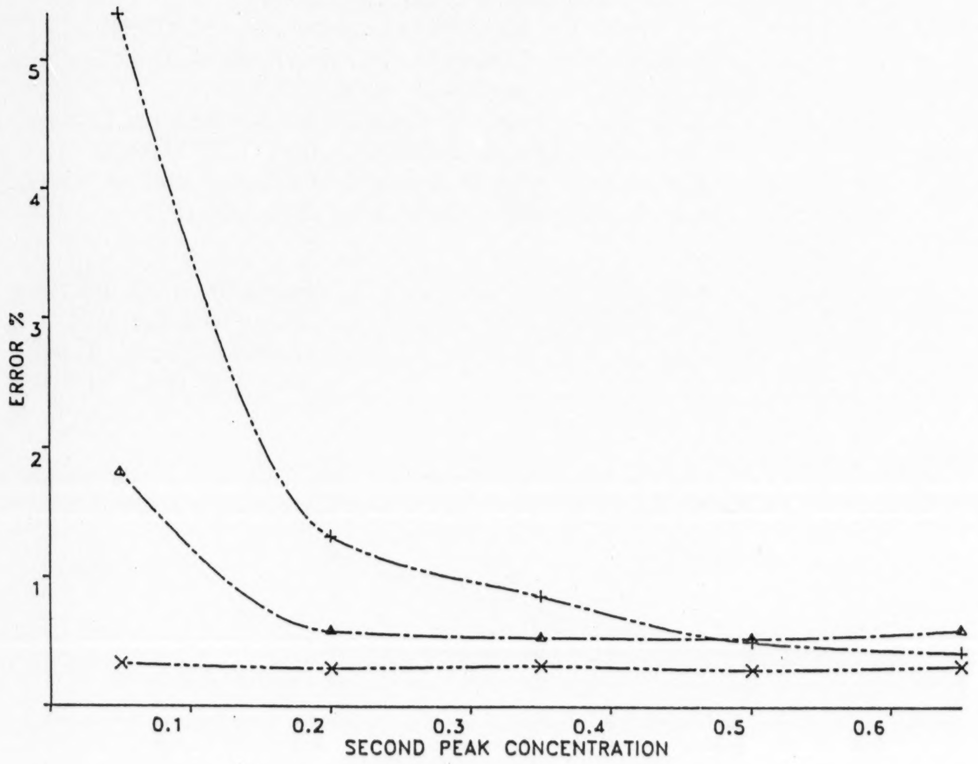

Fig. 9b

Three ITT-FA three-component peak height error responses are plotted as a function of second peak concentration. Adjacent peak separation $\Delta t = 0.4$, spectral similarity range r = 0.94–0.97.

Cluster mean relative peak error ——— Δ ———;
Second peak relative error ——— + ———;
Relative cluster error ——— X ———.

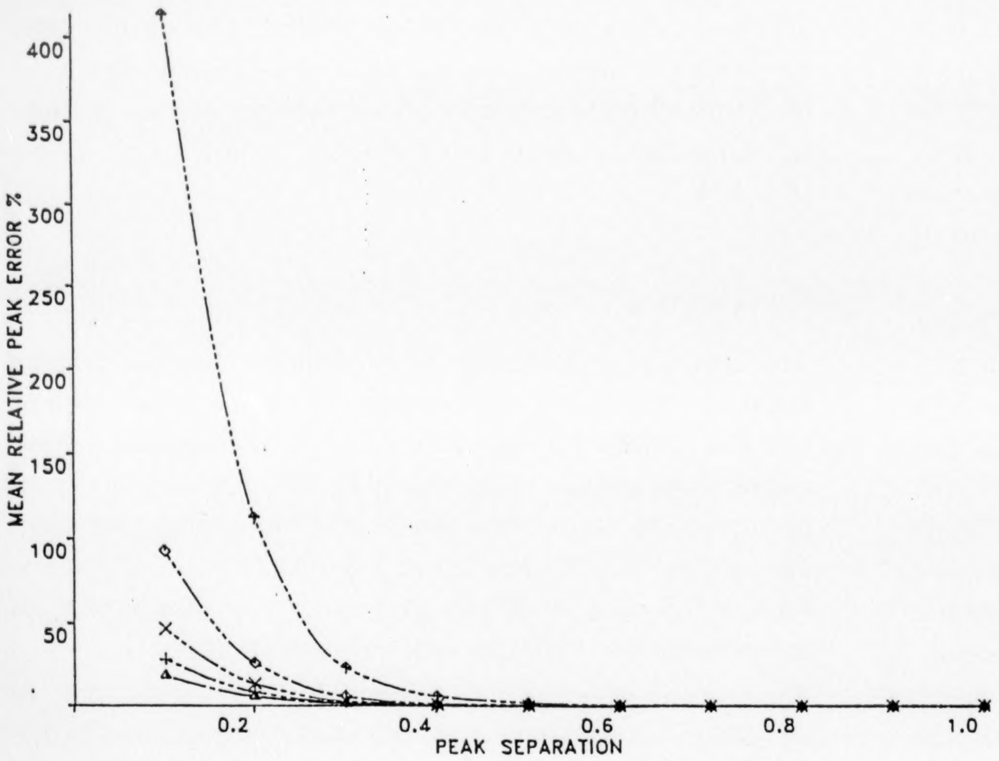

Fig. 10

ITT-FA second peak mean relative peak error curves are plotted against peak separation. The mean RPE is taken as average over all similarity levels (r ≈ 0.95; 0.75; 0.55) and replications.

Peak 2 concentration 0.65 ———Δ——— ;
Peak 2 concentration 0.5 ——+—— ;
Peak 2 concentration 0.35 ——X—— ;
Peak 2 concentration 0.2 ------◇------ ;
Peak 2 concentration 0.05 ------Δ------ .

includes the data at separation 0.6, the errors associated with the three factors in ITT-FA deviate, from those of MCA, although not greatly. As separation decreases below the limiting value of 0.6, all factors have increasingly greater effects on the accuracy of ITT-FA.

This is supported by the relative peak error (RPE) curves (Fig. 10) where the RPE of the second peak at concentration 0.05 (0.1 of largest peak concentration), taken as a mean over the three similarity levels and all replications at a separation of 0.5, equals 2.14%. Below this separation as the peaks become increasingly overlapped, RPE increases steeply. If however a larger error margin is acceptable, e.g. in the region of 10%, ITT-FA can be applied to peak clusters with a minimum separation of ≈ 0.4 and possibly as low as 0.35.

Clearly ITT-FA produces errors greater than MCA at separations less than 0.6. MCA however, requires prior spectral information for at least all components in the non-homogeneous peak cluster and, to be accurate, the spectra should be recorded in a mobile phase identical to that of the mixture under analysis [13].

As a method requiring no *a priori* information iterative target testing factor analysis is a powerful tool for deconvoluting from spectrochromatographic data, estimations of true elution profiles.

Acknowledgements

The Authors thank the Trustees of the Analytical Chemistry Trust Fund of the Royal Society of Chemistry for the award of an SAC Research Studentship to one of us (G.G.R. Seaton). Thanks are also expressed to colleagues in the Pharmaceutical Analysis Research Unit at Bradford University for kindly providing real spectra for this work.

References

[1] *A. F. Fell, B. J. Clark*, Eur. Chrom. News. **1**, 6 (1987).
[2] *J. A. Blackburn*, Anal. Chem. **37**, 1000 (1965).
[3] *M. A. Sharaf, B. R. Kowalski*, Anal. Chem. **54**, 1291 (1982).
[4] *P. J. Gemperline*, J. Chem. Inf. Comput. Sci. **24**, 206 (1984).
[5] *B. G. M. Vandeginste, W. Derks, G. Kateman*, Anal. Chim. Acta. **173**, 253 (1985).
[6] *M. Maeder*, Anal. Chem. **59**, 530 (1987).
[7] *F. J. Knorr, H. R. Thorsheim, J. M. Harris*, Anal. Chem. **53**, 821 (1981).
[8] *E. R. Malinowski, D. G. Howery*, Factor Analysis in Chemistry, Wiley, New York, 1980.
[9] *S. Wold*, Technometrics. **20**, 397 (1978).
[10] *H. F. Kaiser*, Ed. Psych. Measurement. **19**, 413 (1959).
[11] *J. H. Wilkinson, C. Reinsch*, Handbook for Automatic Computation II, Springer-Verlag, Berlin, 1971.
[12] *B. G. M. Vandeginste, F. Leyten, M. Gerritsen, J. W. Noor, G. Kateman, J. Frank*, J. Chemometrics. **1**, 57 (1987).
[13] *J. K. Strasters, H. A. H. Billiet, L. De Galan, B. G. M. Vandeginste, G. Kateman*, J. Chromatogr. **385**, 181 (1987).

Received: June 30, 1987
Revised manuscript
received: Oct. 9, 1987
Accepted: Oct. 20, 1987
F

Developments in Detection Methods for Ion Chromatography

P. R. Haddad

Department of Analytical Chemistry, University of New South Wales, P. O. Box 1, Kensington, N.S.W. 2033, Australia

Key Words

Ion chromatography
Electrochemical detection
Indirect UV absorption

Summary

Recent advances in detection methods for ion chromatography are reviewed, with particular emphasis on conductimetric, amperometric, potentiometric and indirect UV absorption methods. It is shown that a wide variety of detection methods now exists and this has decreased the dependence of ion chromatography on conductivity detection.

Introduction

The development of sensitive and reliable detection methods has been a dominant factor in the progress of ion chromatography as an extension of classical open column ion-exchange chromatography. Many properties of inorganic ions have formed the basis of detection methods, including conductance, UV absorbance, redox properties, complexing abilities and refractive index. A number of reviews and books on ion chromatography [1–5] provide ample coverage of the theory and application of these detection methods, however this paper will highlight some of the more recent developments in this field.

Fig. 1 depicts a classification of detection methods in ion chromatography, and shows that the major types can be described as electrochemical, spectroscopic and post-column reaction. It is also noteworthy that each detection method can be applied in a direct or indirect mode. The meanings of these terms can be seen by reference to typical anion and cation-exchange equilibria, as given below; for simplicity only univalent species are considered:

$$\text{Anion-exchange: Resin-NR}_3^+\text{E}^- + \text{A}^- \Rightarrow \text{Resin-NR}_3^+\text{A}^- + \text{E}^- \qquad (1)$$

$$\text{Cation-exchange: Resin-SO}_3^-\text{E}^+ + \text{C}^+ \Rightarrow \text{Resin-SO}_3^-\text{C}^+ + \text{E}^+ \qquad (2)$$

Here the ion-exchange resin contains either a quaternary ammonium group (anion-exchanger) or a sulphonic acid group (cation-exchanger) and the eluent contains an appropriate competing ion, depicted as E^- or E^+, respectively. Eqns (1) and (2) illustrate the manner in which the solute ions A^- and C^+ are retained on the column. The eluent ions are able to achieve elution by virtue of either a stronger affinity for the resin or a concentration advantage in comparison with the solute ions. When solute ions elute from the ion-exchange column they replace in the eluent an equivalent number of eluent ions so that electroneutrality is maintained. It follows that if a property of the eluent is monitored by the detector, then changes in detector signal will occur upon elution of a solute ion which has a different value of that same property. This method is satisfactory provided there is a large enough difference in the values of the measured property between the eluent and solute ions. For the purposes of this paper a further distinction will be made, that is, methods where the eluent ion has a *lower* value of the measured property than the solute ion will be described as *direct* detection methods, whereas methods in which the eluent ion has a *higher* value of the measured property will be described as *indirect* detection methods.

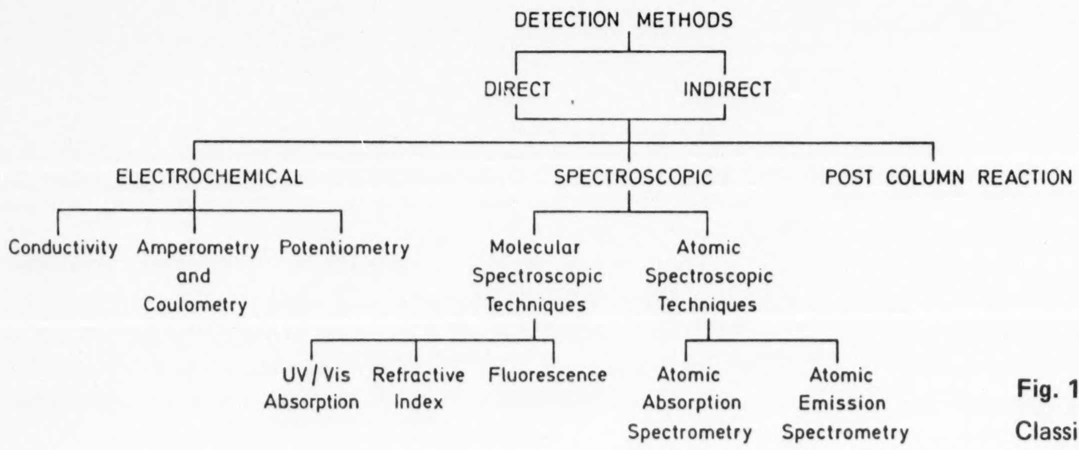
DETECTION METHODS
DIRECT
INDIRECT
ELECTROCHEMICAL
SPECTROSCOPIC
POST COLUMN REACTION
Conductivity
Amperometry and Coulometry
Potentiometry
Molecular Spectroscopic Techniques
Atomic Spectroscopic Techniques
UV/Vis Absorption
Refractive Index
Fluorescence
Atomic Absorption Spectrometry
Atomic Emission Spectrometry

Fig. 1
Classification of detection methods for ion chromatography

0009-5893/87 0217-09 $03.00/0

© 1987 Friedr. Vieweg & Sohn Verlagsgesellschaft mbH

Electrochemical Methods of Detection

Conductivity Detection

Conductivity detection has long been the mainstay of detection methods for ion chromatography and has the advantages of universal response to ionic species and simplicity of operation. The principle of operation of a conductivity detector in ion-exchange chromatography can be illustrated by considering the conductance of a typical eluent prior to and during the elution of a solute ion. In its simplest form, the detector response equation (in this case for an anion-exchange system) is:

$$\Delta G = \frac{(\lambda_{S^-} - \lambda_{E^-})\, C_S}{10^{-3} K} \qquad (3)$$

where ΔG is the conductance signal, λ_{S^-} and λ_{E^-} are the limiting equivalent ionic conductances of the solute and eluent anions, respectively, C_S is the concentration of the solute anion and K is a constant (called the *cell constant*) with units cm^{-1} which takes into account the physical dimensions of the cell.

This equation shows that if a conductivity detector is used to monitor the effluent from an ion-exchange column, the signal observed when a solute ion elutes is proportional to the solute concentration and to the difference in limiting equivalent ionic conductances between the eluent and solute ions. A similar relationship has been derived for the conductimetric detection of cations after ion-exchange separation [6]. These relationships show that sensitive detection can result as long as there is a considerable difference in the limiting equivalent ionic conductances of the solute and eluent ions. This difference can be positive or negative, depending on whether the eluent ion is strongly or weakly conducting, as illustrated schematically in Fig. 2. Table I shows values of the limiting equivalent ionic conductances of some common inorganic anions and cations.

Widely used eluents in which the limiting equivalent ionic conductance of the eluent ion is low include solutions of phthalate [7], benzoate [8] and other aromatic acid salts and these usually give direct detection (in terms of the definition given earlier) of eluted solute ions, that is, an increase in conductance occurs when the solute enters the detection cell. An alternative is to use a highly conducting eluent and to monitor the decrease in conductivity which accompanies the elution of a solute ion. This is an indirect detection mode and has been applied to the detection of anions in an aqueous potassium hydroxide eluent [9], alkali metal cations in a dilute nitric acid eluent [4] (Fig. 3), and transition metal and alkaline earth cations

Table I. Limiting equivalent ionic conductances of some common ions

Cations	λ_+	Anions	λ_-
H^+	350	OH^-	198
Li^+	39	F^-	54
Na^+	50	Cl^-	76
K^+	74	Br^-	78
NH_4^+	74	NO_3^-	71
Anilinium	5	Benzoate	32
Benzylammonium	32	Phthalate	38

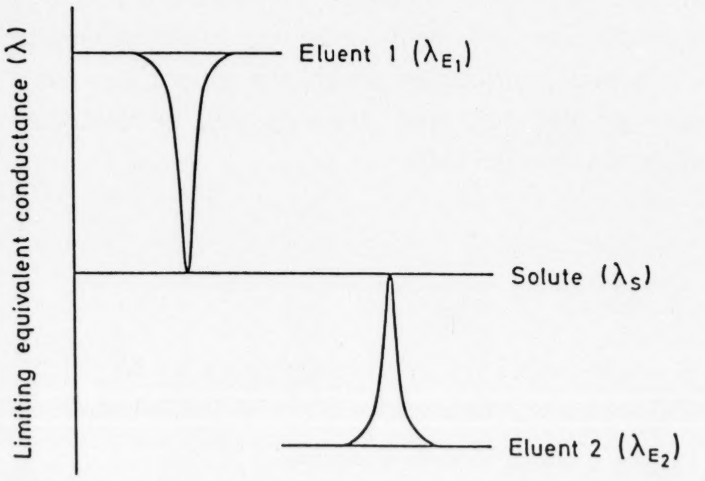
Limiting equivalent conductance (λ)
Eluent 1 (λ_{E_1})
Solute (λ_S)
Eluent 2 (λ_{E_2})

Fig. 2

Schematic representation of indirect (negative peak) and direct (positive peak) conductivity detection using eluent with high (eluent 1) or low (eluent 2) limiting equivalent ionic conductance. Reproduced with permission from Ref. [11].

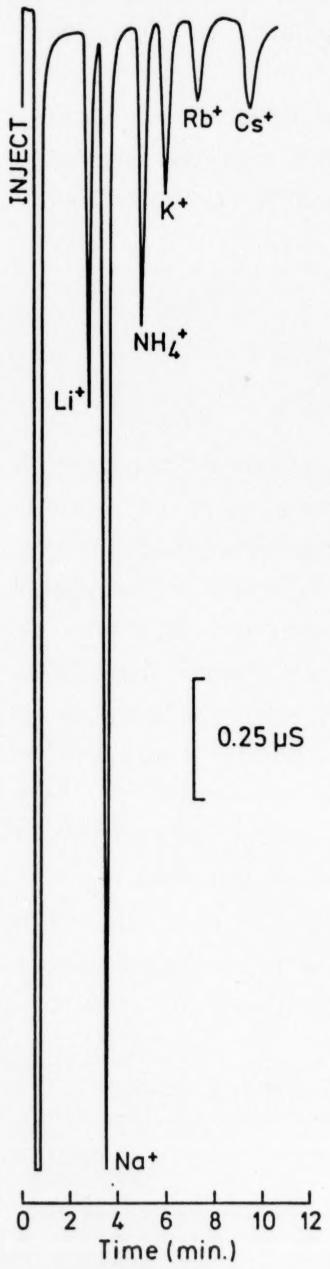

Fig. 3

Indirect conductivity detection of cations in non-suppressed ion chromatography using eluent with high background conductance. Column: Waters Associates IC PAK C. Eluent: 1.0mM nitric acid. Solute concentrations: 10^{-5}M in each species, except for sodium which has twice this concentration. Reproduced with permission from Ref. [11].

using ethylenediamine/tartrate solutions [10]. Each of the eluents used in these examples provides excellent detector response because of the very high limiting equivalent ionic conductances of the hydroxide, hydrogen and ethylenediammonium ions.

Despite the widespread success of indirect conductivity detection of anions using aromatic acid solutions as eluents, the same approach has only recently been adapted for detection of cations using aromatic bases as eluents [11]. One of the main problems encountered when such eluent solutions are used is interference by hydrogen ions present under the acidic conditions used to ensure that the eluent base is protonated. The eluent therefore contains two different eluting species, the protonated base cation and the hydrogen ion, both of which produce conductivity changes of opposite direction. An *increase* in conductivity occurs when a base cation of low limiting equivalent ionic conductance is responsible for elution, whereas a *decrease* in conductivity occurs when a highly conducting hydrogen ion is responsible for elution. This is illustrated in Fig. 2. A combination of both effects can lead to peaks of either direction or complete absence of a peak: these effects have been observed in practice [11]. Provided the base has a pKa value high enough to permit protonation in the neutral to alkaline region, then direct conductivity detection of cations is possible; for example, the separation and detection of alkali metals using 2,6-dimethylpyridine at pH 6.35 [12], as shown in Fig. 4.

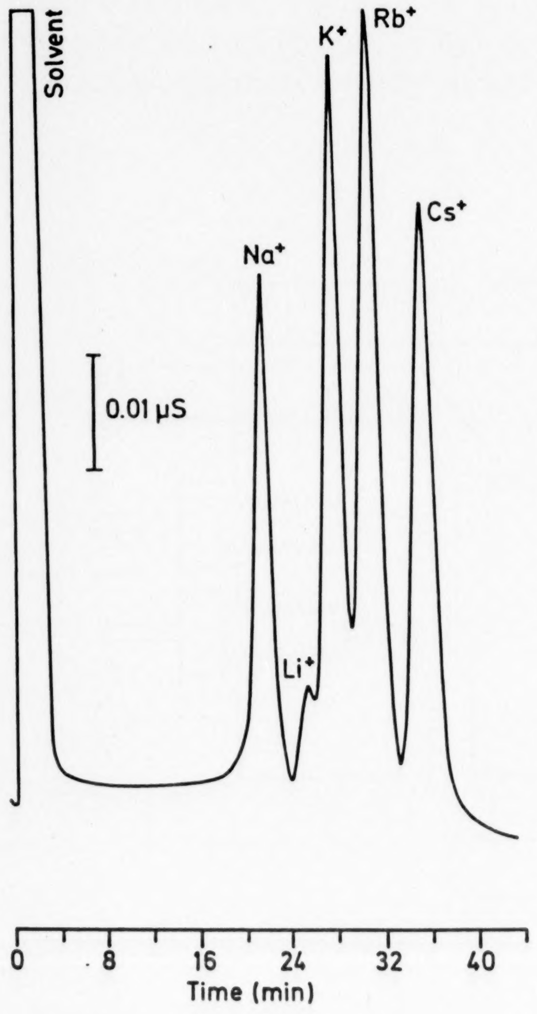

Fig. 4

Direct conductivity detection of alkali metal cations using an aromatic base as eluent. Column: Waters Associates IC PAK C. Eluent: 0.2 mM 2,6-dimethylpyridine pH 6.35. Solute concentrations: 0.14–2.66 ppm.

When non-suppressed ion chromatography is used with a fully ionised eluent solution, it is possible to estimate solute concentrations without the use of standards [13]. This procedure is based on eqn (3) above and involves the measurement of detector response using first an eluent with a high limiting equivalent ionic conductance and then an eluent with a low limiting equivalent ionic conductance. Two equations of the form of eqn (3) are then obtained which are used to solve for the two unknowns C_S (the solute concentration) and λ_S (the limiting equivalent ionic conductance of the solute ion). Indeed, it is also possible to calibrate the detector response by measuring the peak areas of each of the two eluting ions using the other as an eluent at a known concentration; when this is done, it is no longer necessary to determine the cell constant or any physical properties of the eluent. The individual charges of the solute ions can be deduced from a study of adjusted retention times, so that molar concentrations of solutes can be determined.

It has recently been shown [14] that electrically neutral carbohydrates can be detected by conductivity measurements provided boric acid is included as a component of the eluent. These carbohydrates form anionic borate complexes which are separated by ion-exclusion chromatography. Differential conductivity detection, which involves measurement of the difference in conductivity between a sample and a reference stream, has been applied to the simultaneous detection of anions and cations using lithium hydrogen phthalate solution as the eluent [15].

In suppressed ion chromatography, the relatively recent availability of high capacity membrane suppressors has led to the possibility of using concentration gradients to achieve rapid elution of strongly retained solutes whilst at the same time retaining resolution of weakly retained solutes. The eluents used for such gradients have included hydroxide [16] and zwitterionic species such as 3-(N-cyclohexylamino)-1-propanesulphonate [17].

Amperometric Detection

Over the last few years there has been an increase of interest in the usage of amperometric methods in ion chromatography, especially where high selectivity and sensitivity are required. It has only recently been shown that the amperometric detection of inorganic ions can be improved through the use of electrode materials which mediate or participate directly in the electrode reaction. Silver is one such material for which the following electrode reactions can be postulated

$$L^- + Ag \Rightarrow AgL + e^- \qquad (4)$$

$$X^- + Ag \Rightarrow AgX + e^- \qquad (5)$$

where either complexes (AgL) or precipitates (AgX) are formed, for example, iodide, cyanide and sulphite may be sensitively detected using a silver electrode polarised at small positive potentials [4]. Sulphite, which does not exhibit the same complexing ability as cyanide or iodide, has to be oxidised directly at a higher potential and the sensitivity of detection is diminished in comparison to the complexing anions. These observations suggest some mediating role of silver, even for the oxidation of sulphite, and for this reason silver is the most widely used electrode material for the detection of inorganic anions.

A series-configured, dual-electrode amperometric detector has been shown to be effective in achieving selective detection of iodide in the presence of other electroactive species such as thiosulphate [18]. Here the iodide is oxidised at the first electrode and then reduced at the second. An alternative approach for iodide detection has involved modification of a platinum electrode by soaking it for a long time in a solution of iodide ions [19], which produces a chemisorbed layer of iodide on the electrode surface. This layer of iodide has been shown to be essential for satisfactory electrode performance. Amperometric detection of Co(II) and Mn(II) in tartrate media has been reported [20] and the high sensitivity of the method (0.3ng Co(II) in a 100μl injection) has been attributed to the electrocatalytic effect.

Considerable attention has been directed to the development of an indirect amperometric detection method for ion chromatography. In one successful attempt [21], 1 mM salicylate was used as eluent and it was shown that the electroactive component of the eluent need be pesent at only a very low concentration, suggesting that other eluent components could be added to improve resolution. A further indirect method has been reported [22] in which pyrrolidinedithiocarbamate was added as a post-column reagent in the cation-exchange separation of metal ions, using amperometric detection at oxidative potential to monitor the dithiocarbamate concentration. Reaction of the dithiocarbamate with eluted metal ions to produce electrochemically inactive complexes formed the basis of the indirect detection method.

Potentiometric Detection

In potentiometry, the potential of an indicator electrode varies with the concentration of a particular ion in the solution in contact with the indicator electrode, in accordance with the Nernst equation, giving a logarithmic relationship between electrode potential and solute concentration. The most familiar potentiometric devices are glass electrodes for the measurement of pH and ion-selective electrodes for the determination of inorganic anions and cations. Whilst these devices are usually used for measurements in static solutions, they are also adaptable to measurements in flowing solutions such as the effluent from an ion chromatograph. In such cases, a suitable flow-cell must be designed to accomodate the indicator and reference electrodes whilst keeping the cell volume to a level where solute dispersion in the cell is not excessive.

The main drawbacks of potentiometric detectors (particularly ion-selective electrodes) in ion chromatography are the slow response of many electrodes and the fact that they respond at best to only a few different species. This inherent selectivity arises both from the nature of the indicator electrode and also from the presence of an ion-selective barrier which separates the indicator electrode from the surrounding solution. This barrier is deliberately chosen to be as selective as possible and therefore naturally restricts the ions which are detected by the indicator electrode. Such selectivity is advantageous when the electrode is required to respond to one ion in the presence of others, but is particularly disadvantageous in chromatographic applications where a broader range of electrode response is desired.

On account of the above considerations, it is not surprising that potentiometry with ion-selective electrodes has found few applications in ion chromatography and these have generally involved those indicator electrodes which show relatively general potentiometric response. Examples include a silver/silver chloride electrode for the detection of halides [23], a silver/silver salicylate electrode for the detection of halides and thiocyanate [24], a silver sulphide membrane electrode for the detection of sulphide and cyanide [25] and an iodide electrode for the detection of iodide, thiocyanate and thiosulphate [26].

The only general purpose potentiometric detector capable of sensitive detection of a wide range of solute species is based on the use of a metallic copper wire or tube as the indicator electrode [27–37]. Detector response arises from changes in the concentration of cuprous or cupric ions at the electrode surface which occur when a solute species comes into contact with the electrode. The main strength of the metallic copper electrode detector is the fact that it provides a certain degree of selectivity yet can respond in a variety of different modes to a wide range of species. It is this latter capability which differentiates the copper electrode detector from previously reported potentiometric sensors.

The cell design reported [29] for the copper electrode detector is shown in Fig. 5. The eluent passes over a copper wire housed in a flow cell of 2μl volume which also contains a silver/silver chloride reference electrode. An auxiliary

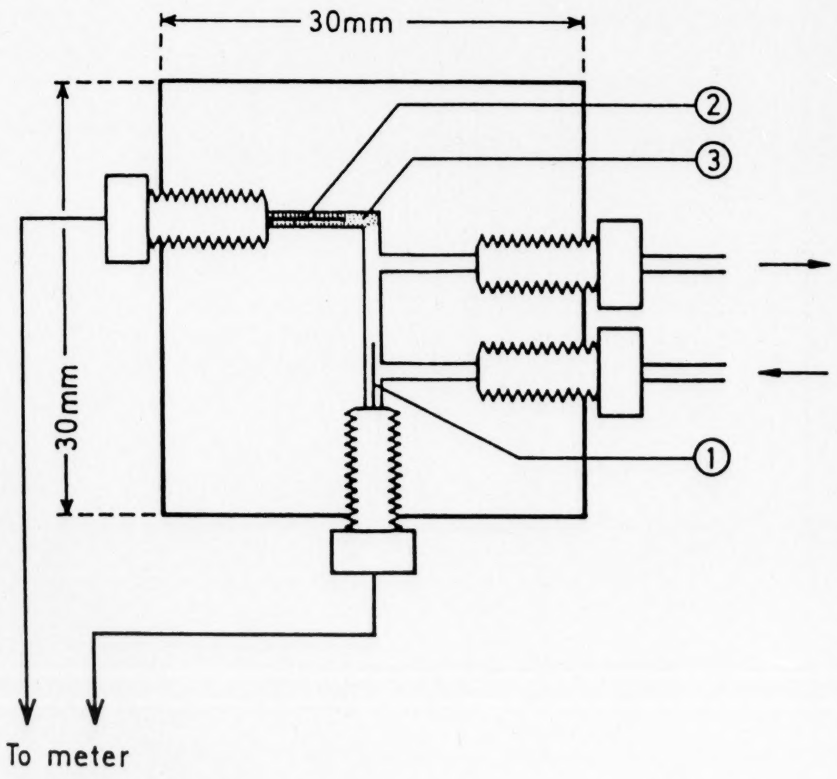

Fig. 5

Flow-cell for potentiometric detector based on metallic copper indicator electrode. (1) Copper wire indicator electrode, (2) Ag/AgCl reference electrode, (3) agar gel. Reproduced with permission from Ref. [29].

electrode constructed of platinum is also included to enable the cell to be used in an amperometric mode. The potential of the copper electrode in a flowing stream will be dependent on the concentration of copper ion (cuprous and cupric) at the electrode surface, which in turn will be governed by the complexation properties of the eluent components. When a solute ion elutes, the detector voltage may change, depending on the characteristics of that particular solute. The possible detection modes which can therefore result are summarised below.

(1) If the eluted solute forms a more stable complex with copper ions than does the eluent ion, a local decrease in copper ion concentration will occur at the electrode surface, leading to a decrease in the electrode potential.

(2) If the eluted solute forms a less stable complex with copper ions than does the eluent ion, a local increase in the copper ion concentration will occur at the electrode surface, leading to an increase in the electrode potential. This process assumes that an ion-exchange separation is being employed so that solute ions replace an equivalent number of eluent ions in the mobile phase at the time of elution.

(3) If the eluted solutes are strong oxidants and are able to oxidise the surface of the metallic copper electrode, a local increase in copper ion concentration will occur and the electrode potential will increase. Reducing solutes can also be detected by reducing cupric ions to cuprous and this will also result in an increase of the electrode potential due to the higher standard electrode potential of the Cu^+/Cu^0 couple (+0.520 V) compared to the Cu^{2+}/Cu^0 couple (+0.337 V).

The first and last detection modes can be classified as direct, whereas the second is indirect. Each of these detection mechanisms has been realised in practice and Table II gives a summary of the applications of the metallic copper electrode detector to ion chromatography. Provided the potential change measured at the copper electrode is restricted to less than a few millivolts (the exact potential range depends on the sample type and the response mode employed), then detector response is observed to be linear with respect to solute concentration. This behaviour is illustrated in Fig. 6 which also shows that the expected Nernstian response is observed at higher concentrations of the solute. Linear detector response can be explained by appropriate mathematical manipulation of the response equation.

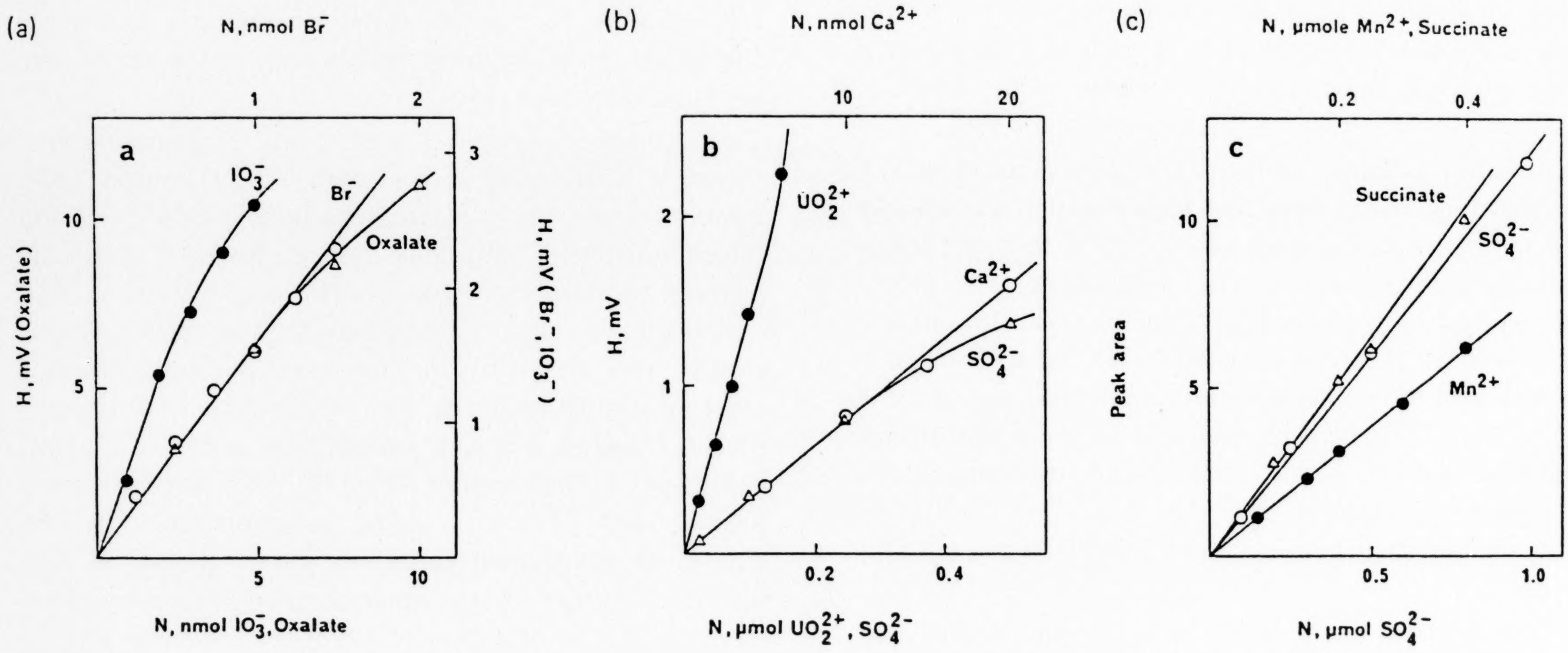

Fig. 6

Examples of calibration plots for direct (a) and indirect (b, c) detection with metallic copper electrode. Chromatographic conditions as Refs [31–37]. Reproduced with permission from Ref. [35].

Table II. Some ion chromatographic applications of potentiometric detection using a metallic copper electrode

Solute ions	Eluent	Detection mode	Ref.
Mg^{2+}, Ca^{2+}, Sr^{2+} and Ba^{2+}	tartrate + diethylenetriamine	indirect	31
Organic acids	phthalate, phosphate or citrate	direct and indirect	32
CN^-, Cl^-, Br^-, I^- and SCN^-	tartrate	direct	33
IO_3^-, BrO_3^- and ClO_3^-	tartrate	direct	33
NO_2^-, NO_3^- and SO_4^{2-}	tartrate	indirect	33
Transition metal ions	tartrate or citrate + ethylenediamine	direct and indirect	34, 36
Ascorbate, hydrazine and hydroxylamine	tartrate, citrate + ethylenediamine	direct	37

Spectroscopic Methods of Detection

Molecular Spectroscopic Techniques

The detector response equation for an anion-exchange system coupled with a UV absorption detector is [4]:

$$\Delta A = (\epsilon_{S^-} - \epsilon_{E^-}) \cdot C_S \cdot 1 \qquad (5)$$

where ΔA is the absorbance change caused by the elution of a solute, ϵ_{E^-} and ϵ_{S^-} are the molar absorptivities of the eluent and solute anions, respectively, C_S is the solute concentration and 1 is the path length. Eqn (5) shows that the detector absorbance depends on the solute concentration, the detector cell path length and the difference in molar absorptivities between the solute and eluent anions.

In the simplest case, the solute ion absorbs more strongly than the eluent ion, resulting in direct detection. This method has been widely applied to anions such as nitrate, nitrate, bromide, bromate, iodide, iodate, periodate, thiocyanate and thiosulphate. Some anions, such as chloride, fluoride, sulphate, phosphate, perchlorate and cyanide do not show appreciable absorption of UV radiation except at very short wavelengths. Some degree of detection selectivity therefore exists which enables common sources of interference such as high levels of chloride or sulphate ions in samples to be minimised or even eliminated. Alternatively, choice of a short wavelength such as 190nm permits direct UV absorption to be used as a more general detection mode and this has been applied to the detection of common anions in atmospheric precipitation [38].

In a recent application of direct UV absorbance detection, UV absorbing anions have been determined simultaneously with metal cations using a wavelength of 210nm and anion-exchange chromatography with ethylenediaminetetraacetic acid (H_4EDTA) as eluent [39]. Under these conditions, the metal ions (M^{2+}) form anionic $MEDTA^{2-}$ complexes which are separated by ion-exchange with $HEDTA^{3-}$ acting as the eluting anion. The metal complexes show strong absorbance at 210nm and the eluent is only weakly absorbing at this wavelength, so sensitive detection is achieved. Detection limits for metal ions ranged from 5.0–70.0ng in a 100μl sample.

Eqn (5) suggests that indirect detection will result when the eluent ion absorbs more strongly than the solute ion. This has developed into one of the most widely used detection methods in ion chromatography, and has been called "indirect photometric chromatography [40]" and "vacancy detection". Here, the eluent ions are chosen to have have high molar absorptivities in the UV region and if the background absorbance of the eluent is monitored at a suitable wavelength, a change in absorbance will occur on elution of a solute ion which has a molar absorptivity different to that of the eluent. This is illustrated schematically in Fig. 7.

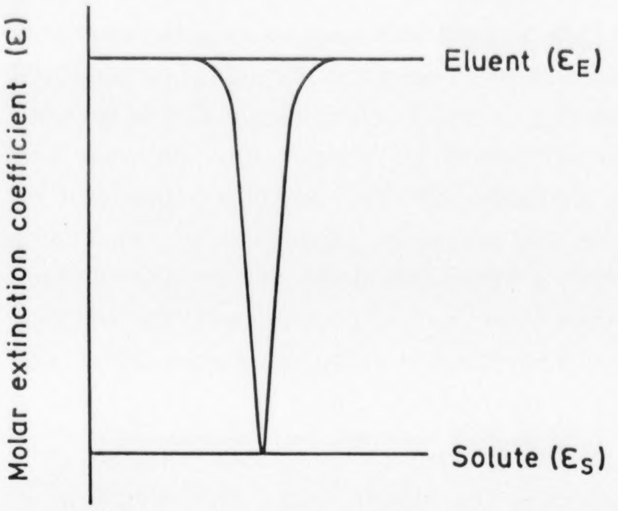

Fig. 7
Schematic representation of indirect UV absorption detection using eluent ion having higher molar absorptivity at detection wavelength than solute ion. Reproduced with permission from Ref. [11].

The sensitivity attainable with this method will depend on a number of factors. In the first place, it is clear from eqn (5) that if the molar absorptivity of the eluent is maximised by selection of the wavelength of maximum absorption, the absorbance change accompanying solute elution is also maximised. However, this can create problems by providing such a high eluent background absorbance that the detector signal is incapable of being reduced to zero. Furthermore, photometric error is reduced if the detector is operated in the approximate absorbance range 0.2–0.8, so it is desirable that the background absorbance be maintained within this range. A further factor is that the detector baseline noise increases with the eluent concentration, so that the signal-to-noise ratio (and hence the sensitivity of the method) improves as the eluent concentration is reduced [40].

The technique is very well established for anion chromatography, with eluents such as phthalate [41], nitrate [42], sulphobenzoate [43], benzenetricarboxylate [41, 44] and toluenesulphonate [45] being typical. Recently, the same method has been used with iron(II) phenanthroline [46], molybdate [5] and 2,4-dihydroxybenzoic acid [47] as eluents. This success has inspired research into the development of similar methods for the detection of cations. Eluents based on inorganic cations such as copper(II) [40] and more recently cerium(III) [48] have achieved some success, with Ce(III) providing detection limits at least 100 times lower than Cu(II). It might appear at first sight that aromatic bases would serve as ideal eluents for the indirect UV detection of cations, since these are the cationic equivalents of the aromatic acid eluents which have proved so successful in anion-exchange chromatography. When such eluents are used in practice, interference is encountered from hydrogen ions, similar to those discussed earlier for direct conductivity detection of cations using aromatic bases. With careful attention to the type of base used as eluent and the operating pH, very successful separation and detection is possible. For example, benzyltrimethylammonium has been used for the determination of organic bases [49], 2,6-dimethylpyridine for alkali metal ions [12] (see Fig. 8) and phenethylamine for alkaline earth ions [12].

Indirect UV absorption detection has been successfully applied to the simultaneous independent determination of anions and cations using a single detector [50]. A dual column system comprising an anion-exchange column and a cation-exchange column connected in series was used

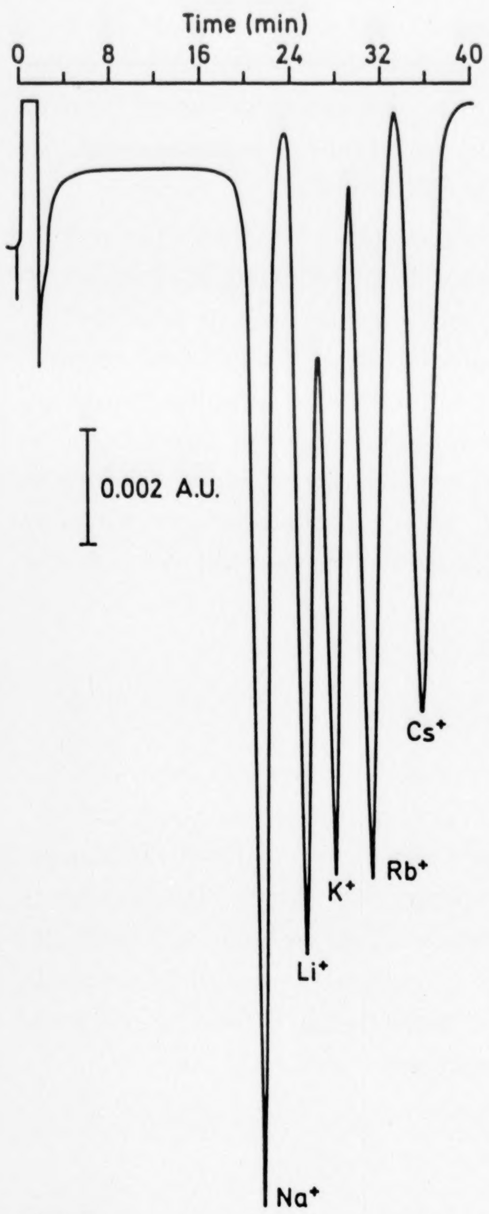

Fig. 8
Indirect UV absorption detection of alkali metal cations using aromatic base as eluent. Conditions as Fig. 4, except that absorption at 269nm used.

and the eluent was 2.5×10^{-4} M copper o-sulphobenzoate. This eluent was selected because both the anion and cation components could exhibit appreciable elution power in an ion-exchange mode and both also showed significant UV absorbance. A desirable feature of this technique is for the eluent anion and cation to have absorption maxima at different wavelengths and for each species to be transparent at the absorption wavelength of the other species. This is not possible with the copper o-sulphobenzoate eluent, so it is necessary to monitor the absorbance at two wavelengths and to apply ratioing and scaling techniques to obtain independent chromatograms of solute anions and cations. A dual, variable-wavelength detector with ratioing capability is therefore required.

An unusual feature of some chromatograms obtained with indirect UV detection is the appearance of a slowly eluting peak which is not directly attributable to any injected ion. This peak, which is generally called a "system" peak, is most prevalent when partly dissociated aromatic acid eluents are used in the separation of anions. The system peak can be very large and often represents a major interference in the quantitation of later eluting solute ions. Several studies have been directed towards elucidation of the nature of the system peak in both ion-exchange and ion-interaction chromatographic systems [51–53].

Indirect detection is also applicable to refractive index and fluorescence detectors. In the former case, anions can be detected after ion-exchange separation by monitoring the refractive index of an eluent containing an aromatic acid such as phthalate [54]. In this detection mode, the background refractive index of the eluent is not restricted (unlike the indirect UV detection mode) since measurements are conventionally made by comparison of the column effluent with pure eluent contained in a reference cell. Sensitivity is therefore limited only by the performance of the detector used. A further distinction between the indirect UV and refractive index detection modes is that the latter can be used with quite concentrated eluents and is therefore suitable for use with columns of relatively high ion-exchange capacities.

An indirect fluorescence detection procedure for ion chromatography has been devised [55, 56] in an attempt to utilise the high sensitivity of fluorometric measurements. Here, sodium salicylate was used as a fluorescent eluting ion for anion-exchange chromatography and decreases in the background fluorescence were used to detect eluted solute anions. A modulated double-beam, laser-excited fluorometric detector was designed in an attempt to overcome the inherent flicker noise of the laser source. The detection sensitivity for anions was at the sub-nanogram level.

Atomic Spectroscopic Techniques

Some detection methods based on atomic spectroscopic techniques have been reported for ion chromatography. These incorporate selective detection methods such as atomic absorption spectroscopy and atomic emission spectroscopy, with a variety of excitation sources being applied in the latter technique.

In the case of atomic absorption (AAS) linked with ion chromatography, some advantage may be gained in the speciation of solutes; for example, a range of arsenic species has been separated and detected in this manner [57] and free chromate has been determined in the presence of chromium(III) [58]. Direct and indirect detection by AAS has been reported [59] using lithium nitrate as the eluent for the direct detection of cations, and the copper-EDTA complex as the eluent for indirect detection of anions. In this work, water was added to the column effluent via a post-column reactor in order to match the eluent flow with the aspiration rate of the AAS instrument.

Atomic emission spectroscopy has been used in a new detection scheme called replacement ion chromatography [60], which is reported to have the potential for very low detection limits and universal applicability. Here the counter cation associated with an eluted anion is stoichiometrically replaced in a cation-exchange column by a cation which shows good flame photometric response (e.g. lithium). The replacement column is situated after the separation column and the eluent from the replacement column is directed into a flame photometer. The resulting signal observed for lithium emission at 670nm provides an indirect but quantitative measure of the eluting anion concentration. Similarly, the concentrations of eluted cations can be determined after their replacement in the eluent with lithium. The detection limits attainable with this technique are in the micromolar region and are comparable or superior to those of conventional conductivity detection.

Detection Using Post-Column Reactions

Post column reactions involving colour formation have found some application to ion chromatography. The ideal characteristics of colour forming reactions and the hardware suitable for their use have been studied [61] and it has been shown that very fast reactions are preferable in order to eliminate the requirement for inclusion of a reaction coil into the system because of the band broadening which necessarily results from the use of such devices. The mixing apparatus in which the reactant stream is merged with the column effluent is crucial to the sensitivity and resolution achieved with the post-column reactor. If the colour forming reaction is fast, a simple mixing tee giving 90° impingement of the flowing streams can be satisfactory [62]. The ideal angle of impingement is a matter of some contention and it has been suggested that a Y type device yields superior results [25]. Annular membrane and screen-tee reactors have been compared as post-column mixing devices and both were found to give almost perfect mixing [63]. Packed-bed reactors can also be of great value for some post-column reactions and these devices eliminate the need for both a pump to deliver the post-column reactant and a mixing chamber for reaction to occur. The band broadening introduced when a packed-bed reactor is used has been shown to be minimal [64]. A packed-bed reactor for the detection of sulphate in industrial wastewaters has been described [65], in which the indirect colorimetric method based on reaction of sulphate with barium chloroanilate is employed. Sulphate reacts with barium chloroanilate to produce insoluble barium sulphate (which remains in the post-column reactor) and highly coloured acid chloroanilate ions.

A simple detector designed specifically for the detection of cations after post-column reaction with PAR has recently been described [62]. This device is miniature (approximately 25mm in length) and incorporates an LED light source and a photocell, both of which are mounted directly onto the ends of the detector flow-cell. The detector was found to give minimal contribution to band broadening and provided sensitivities of about $10\,\mathrm{ng\,ml^{-1}}$ for transition metal ions.

Post-column reactions have been much more widely applied to the detection of cations than is the case for anions; indeed it is fair to say that there is no better method for the detection of transition metals and lanthanides. The colour forming reagent should give a low background absorbance, together with high molar absorptivities for as large a range of cations as possible. Many reagents have been evaluated for their suitability as colour forming reagents in post-column reaction detection and these include broad spectrum reagents such as dithizone, Eriochrome Black T, 4-(2-pyridylazo)-resorcinol (PAR), xylenol orange and Arsenazo dyes. The most widely applicable reagents are PAR and Arsenazo I or Arsenazo III which together provide rapid colour reactions with most elements of interest [66]. One example is the detection of lanthanides after separation by ion-exchange using methyllactic acid as eluent, and post-column reaction with Arsenazo I, using detection at 600nm [25].

A post-column fluorescence detection method for nitrite, thiosulphate and iodide has been reported [67] in which these anions are reacted with cerium(IV) to produce the fluorescent species cerium(II) in a packed-bed reactor. Nitrate and nitrite may be determined simultaneously by including into the system a post-column copperised reductor which reduces nitrate to nitrite, prior to further reaction with cerium(IV) in the packed-bed reactor. The detection limits attainable with this method were in the low ppb range.

Conclusions

Many significant developments in detection methods for ion chromatography have occurred in recent years, primarily in the areas of amperometric, potentiometric and indirect UV absorption detection. These developments have enabled sensitive detection to be achieved with detectors commonly found in chromatographic laboratories and have diminished the dependence of ion chromatography on conductivity detection.

References

[1] *D. T. Gjerde, J. S. Fritz*, Ion Chromatography, 2nd Edn., Huthig, Heidelberg, 1987.

[2] *J. G. Tarter* (Ed.), Ion Chromatography, Marcel Dekker, New York, 1986.

[3] *F. C. Smith Jr., R. C. Chang*, The Practice of Ion Chromatography, Wiley-Interscience, New York, 1983.

[4] *P. R. Haddad, A. L. Heckenberg*, J. Chromatogr., **300**, 357 (1984).

[5] *J. S. Fritz*, Anal. Chem. **59**, 335A (1987).

[6] *J. S. Fritz, D. T. Gjerde, R. M. Becker*, Anal. Chem., **52**, 1519 (1980).

[7] *D. T. Gjerde, J. S. Fritz, G. Schmuckler*, J. Chromatogr., **186**, 509 (1979).

[8] *J. E. Girard, J. E. Glatz*, Amer. Lab., **13**, 26 (1981).

[9] *T. Okada, T. Kuwamoto*, Anal. Chem., **55**, 1001 (1983).

[10] *G. J. Sevenich, J. S. Fritz*, Anal. Chem., **55**, 12 (1983).

[11] *R. C. L. Foley, P. R. Haddad*, J. Chromatogr., **366**, 13 (1986).

[12] *R. C. L. Foley, P. R. Haddad*, Proceedings 9th Australian Symposium on Analytical Chemistry, Vol 2, Sydney, 1987 p. 589.

[13] *S. A. Wilson, E. S. Yeung, D. R. Bobbitt*, Anal. Chem., **56**, 1457 (1984).

[14] *T. Okada, T. Kuwamoto*, Anal. Chem., **58**, 1375 (1986).

[15] *J. G. Tarter*, J. Chromatogr., **367**, 191 (1986).

[16] *R. D. Rocklin, C. A. Pohl*, 37th Pittsburgh Conference on Analytical Chemistry and Applied Spectroscopy, Atlantic City, NJ (1986) Abstract 585.

[17] *K. Irgum*, Anal. Chem., **59**, 363 (1987).

[18] *M. Lookabaugh, I. S. Krull, W. R. LaCourse*, J. Chromatogr., **387**, 301 (1987).

[19] *K. Han, W. F. Koch, K. W. Pratt*, Anal. Chem., **59**, 731 (1987).

[20] *J. R. Heuser, J. E. Girard*, Anal. Chem., **57**, 2847 (1985).

[21] *G. Horvai, J. Fekete, Zs. Niegreisz, K. Toth, E. Pungor*, J. Chromatogr., **385**, 25 (1987).

[22] *H. Hojabri, A. G. Lavin, G. G. Wallace, J. M. Riviello*, Anal. Chem., **59**, 54 (1987).

[23] *M. C. Franks, D. L. Pullen*, Analyst (London), **99**, 503 (1974).

[24] *H. Hershcovitz, C. Yarnitzky, G. Schmuckler*, J. Chromatogr., **252**, 113 (1982).

[25] *Wang-nang Wang, Yeong-jgi Chen, Mon-tai Wu*, Analyst (London), **109**, 281 (1984).
[26] *E. C. V. Butler, R. M. Gershey*, Anal. Chim. Acta, **164**, 153 (1984).
[27] *P. W. Alexander, C. Maitra*, Anal. Chem., **53**, 1590 (1981).
[28] *P. W. Alexander, P. R. Haddad, G. K.-C. Low, C. Maitra*, J. Chromatogr., **209**, 29 (1981).
[29] *P. W. Alexander, M. Trojanowicz, P. R. Haddad*, Anal. Lett., **17** (A4), 309 (1984).
[30] *P. W. Alexander, P. R. Haddad, M. Trojanowicz*, Anal. Chem., **56**, 2417 (1984).
[31] *P. R. Haddad, P. W. Alexander, M. Trojanowicz*, J. Chromatogr., **294**, 397 (1984).
[32] *P. R. Haddad, P. W. Alexander, M. Trojanowicz*, J. Chromatogr., **315**, 261 (1984).
[33] *P. R. Haddad, P. W. Alexander, M. Trojanowicz*, J. Chromatogr., **321**, 363 (1985).
[34] *P. R. Haddad, P. W. Alexander, M. Trojanowicz*, J. Chromatogr., **324**, 319 (1985).
[35] *P. W. Alexander, P. R. Haddad, M. Trojanowicz*, Chromatographia, **20**, 179 (1985).
[36] *P. W. Alexander, P. R. Haddad, M. Trojanowicz*, Anal. Chim. Acta, **177**, 183 (1985).
[37] *P. R. Haddad, P. W. Alexander, M. Trojanowicz*, J. Liq. Chromatogr., **9**, 777 (1986).
[38] *G. P. Ayers, R. W. Gillett*, J. Chromatogr., **284**, 510 (1984).
[39] *S. Matsushita*, J. Chromatogr., **312**, 327 (1984).
[40] *H. Small, T. E. Miller, Jr.*, Anal. Chem., **54**, 462 (1982).
[41] *P. R. Haddad, A. L. Heckenberg*, J. Chromatogr., **252**, 177 (1982).
[42] *A. Laurent, R. Bourdon*, Ann. Pharm. Fr., **36**, 453 (1978).
[43] *C. A. Hordijk, C. P. C. M. Hagenaars, Th. E. Cappenberg*, J. Microbiol. Methods, **2**, 49 (1984).
[44] *A. Diop, A. Jardy, M. Caude, R. Rossey*, Analusis, **14**, 67 (1986).
[45] *J. Andrasko*, J. Chromatogr., **314**, 429 (1984).
[46] *P. G. Rigas, D. J. Pietrzyk*, Anal. Chem., **58**, 2226 (1986).
[47] *R. Golombek, G. Schwedt*, J. Chromatogr., **367**, 69 (1986).
[48] *J. H. Sherman, N. D. Danielson*, Anal. Chem., **59**, 490 (1987).
[49] *D. L. McAleese*, Anal. Chem., **59**, 541 (1987).
[50] *Z. Iskandarani, T. E. Miller, Jr.*, Anal. Chem., **57**, 1591 (1985).
[51] *P. E. Jackson, P. R. Haddad*, J. Chromatogr., **346**, 125 (1985).
[52] *W. E. Hammers, C. N. M. Aussems, M. Janssen*, J. Chromatogr., **360**, 1 (1986).
[53] *R. M. Cassidy, M. Fraser*, Chromatographia, **18**, 369 (1984).
[54] *P. R. Haddad, A. L. Heckenberg*, J. Chromatogr., **252**, 177 (1982).
[55] *T. Takeuchi, E. S. Yeung*, J. Chromatogr., **366**, 145 (1986).
[56] *T. Takeuchi, E. S. Yeung*, J. Chromatogr., **370**, 83 (1986).
[57] *E. A. Woolson, N. Aharonson*, J. Assoc. Off. Anal. Chem., **63**, 523 (1980).
[58] *J. M. Pettersen*, Anal. Chim. Acta, **160**, 263 (1984).
[59] *S. Maketon, E. S. Otterson, J. G. Tarter*, J. Chromatogr., **368**, 395 (1986).
[60] *S. W. Downey, G. M. Hieftje*, Anal. Chim. Acta, **153**, 1 (1983).
[61] *J. P. Sickafoose*, Ph.D. Dissertation, Iowa State University, Ames, Iowa (1971).
[62] *G. J. Schmidt, R. P. W. Scott*, Analyst (London), **109**, 997 (1984).
[63] *R. M. Cassidy, S. Elchuk, P. K. Dasgupta*, Anal. Chem., **59**, 85 (1987).
[64] *L. Nondek, U. A. Th. Brinkman, R. W. Frei*, Anal. Chem., **55**, 1466 (1983).
[65] *K. Brunt*, Anal. Chem., **57**, 1338 (1985).
[66] *Y. Hirai, N. Yoza, S. Ohashi*, J. Chromatogr., **206**, 501 (1981).
[67] *S. H. Lee, L. R. Field*, Anal. Chem., **56**, 2647 (1984).

Received: June 28, 1987
Accepted: July 20, 1987
F

The Use of Derivatives for Establishing Integration Limits of Chromatographic Peaks

Eli Grushka* / I. Atamna

Department of Inorganic and Analytical Chemistry, The Hebrew University, Jerusalem, Israel

Key Words

Composite peaks
Low peak resolution
Peak integration
Integration limits
Use of derivatives

Summary

The paper deals with composite peaks in which the resolution is not sufficient to allow simple area determinations with conventional integrator procedures. It is proposed to use the second derivatives of composite peaks, since the derivatives accentuate envelope perturbations due to overlapped peaks. In particular, when there are two solutes in the composite, and when the peak separation is between 2 and 4σ, the second derivative of the composite has two minima and three maxima. The second maximum is indicative of the cross point of the two solutes. This point can be used to initiate and/or terminate the integration of the components in the composite. Similarly, the second minimum occurs at a point close to the true maximum of the second peak in the composite. This point can also be used for the quantitative determination of the second component in the composite. The second derivative traces can also be integrated, but their utility in quantitative analysis of the peaks is questionable. An inversion procedure is given in which the second derivative trace is inverted to yield a trace similar to the conventional chromatograms but with better apparent resolution. In special circumstances, the inverted derivatives can be used for integration purposes.

Introduction

The use of (mathematical) derivatives in analytical chemistry is well known. In UV-VIS spectroscopy, in fact, the derivatives are used routinely [1], and all but the lower price spectrophotometers offer the capability of obtaining the derivatives of the spectra. The use of the derivatives in IR spectroscopy has also been reported [2]. Perhaps the most common usage of the derivatives is in electrochemistry for the purpose of estimating the end points of titrations. The derivatives offer some attractive possibilities in signal treatment due to their ability to accentuate small perturbation on top of a major signal (or lack thereof). It is because of this property that the derivatives are used, by digital integrators, to sense the beginning and end of a detector signal, as well as its extreme position. The recent book by Sharaf et al. [3] gives a short up-to-date discussion on derivatives and their application to signal manipulation.

Derivatives are exploited in chromatography to a much lesser extent. The number of papers dealing with the application of derivatives in chromatography is rather small. Ashley and Reilly [4] described the use of electronic differentiation in order to sharpen gas chromatographic peaks and, thus, electronically deconvoluting them. Grushka [5, 6] used derivatives to discern the existence of multiple components under a single envelope. Zelt and his coworkers [7] as well as Traveset and his colleagues [8] have coupled HPLC and TLC, respectively, to spectrometric detectors capable of obtaining derivatives. Berridge [9] used the second derivatives to obtain information about the quality of the optimum mobile phase during a simplex optimization process. Fell and his co-workers, in a series of papers [10–13], discussed the utilization of the derivatives in conjunction with diode array detectors. They have shown that better qualitative and quantitative information can be obtained from the use of the derivatives. Gerow and Rutan [14] employed first derivatives in conjunction with Kalman filtering in order to remove background noises from TLC chromatograms. Grant and Bhattacharyya [15] used the derivatives to develop a strategy for the determination of the purity of chromatographic peaks. Ebel [16] described, briefly, the use of derivatives for deconvolution purposes.

These papers demonstrate very well the usefulness and the versatility of the derivatives. The paucity of application is, therefore, surprising. While most spectrometers are equipped with software for differentiating data, very few, if any, chromatographic detectors posses this capability. Perhaps even more surprising is the fact that only a few of the available chromatographic integrators provide this capability on a routine basis.

The purpose of the present communication is to further demonstrate the usefulness of the derivatives in chromatography. In particular, we will show the application of second derivatives to the quantitation of components in badly overlapped peaks, when the usual integration techni-

0009-5893/87 0226-07 $03.00/0

© 1987 Friedr. Vieweg & Sohn Verlagsgesellschaft mbH

ques cannot cope with the situation. This paper will lay the theoretical background by demonstrating, with the aid of simulated chromatograms, that the second derivative of the chromatogram can be used to establish the points of integration initiation (and if desired, of termination). We will discuss two strategies for that purpose. They will be compared to each other and to the expected results based on the model used. Other possible applications, based on these strategies, will be described at the end of the paper.

Theoretical Background

For the initial purposes of demonstrating the possible role of the derivatives in integration, we will assume a Gaussian model. Thus, a composite peak of two components is described by:

$$Y = Y_1 + Y_2 = A\exp[-(x-x_0)^2/2\sigma^2] + \\ + B\exp[-(x-x_0-d)^2/2\sigma^2] \quad (1)$$

Y_1 and Y_2 represent the two individual peaks, A and B are the heights of the first and second component, x_0 is the position of the maximum of the first peak, d is the separation between them and σ is the standard deviation of the Gaussians. It will be assumed here that the widths of the two peaks are identical. This is a reasonable assumption when the two peaks elute very close to one another, which is precisely the situation in which we are interested.

The second derivative of the signal described in eq. (1) is given by:

$$Y'' = Y_1[(x-x_0)^2/\sigma^4 - 1/\sigma^2] + \\ + Y_2[(x-x_0-d)^2/\sigma^4 - 1/\sigma^2] \quad (2)$$

When the separation between the peaks, d, is larger than 4σ, then the components are fairly well resolved (in fact, the resolution, Rs is greater than unity) and, barring extreme differences in the amounts or in the detectable properties of the two solutes, the integration could proceed without any difficulties. Under such conditions, the contribution of one component to the area of the other is small. Since the peaks at 4σ separation are not baseline resolved, the second derivative of the composite will have two minima and three maxima. Fig. 1 shows this case; Fig. 1a is the chromatogram of the two peaks with 4.5σ separation and 1b is the second derivative. The second derivative trace shows three maxima and two minima. The position of the two minima coincide closely with the position of the maxima of the two peaks. Since the peaks in the composite are symmetrical and of equal height, the second maximum of the derivative trace indicates the point of minimum overlap between the two solutes. To be more exact, this is the point where the two profiles cross each other.

When the separation is greater than 6σ, the "peak" is not a composite any more and the chromatogram shows two well resolved peaks. The second derivative trace in this case will show four maxima and two minima, as expected from two different peaks.

However, if $d < 4\sigma$, difficulties can arise. Fig. 2a shows a composite when $B = 0.4A$ and $d = 2.5\sigma$ ($Rs = 0.625$). Although the existence of two components under the

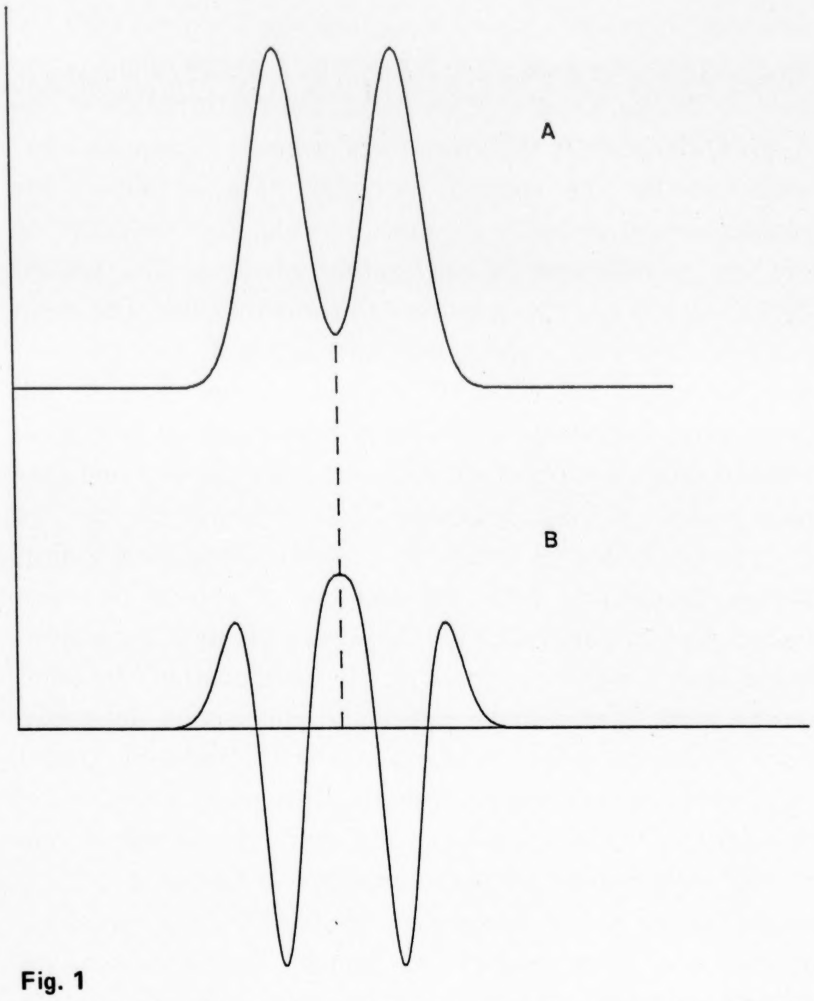

Fig. 1

A) Two Gaussians of equal heights at 4.5σ separation. **B)** The second derivative of the composite.

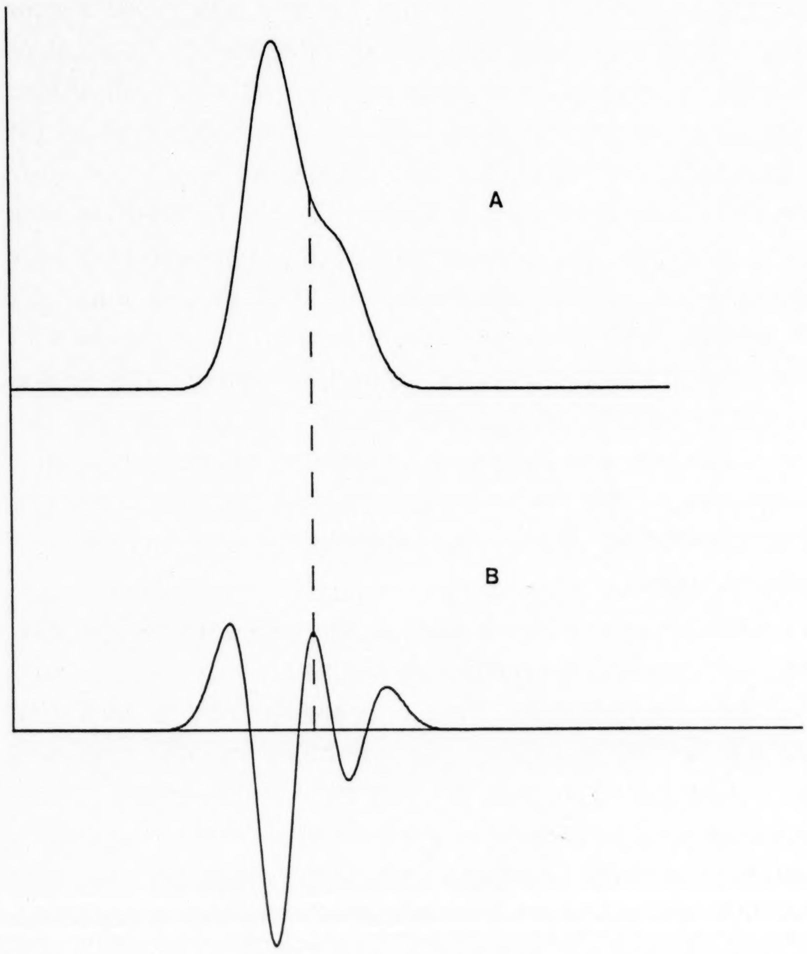

Fig. 2

A) A composite of two Gaussians at 2.5σ separation. The second component is 0.4 the height of the first. **B)** The second derivative of the composite. The dashed line connects the second maximum of the second derivative trace with composite. This is the point of integration initiation and/or termination.

envelope is visually clear, the integration process may fail to recognize the peak as a composite, and the quantitation will be wrong. On the other hand, the perturbation in the descending part of the composite is easily recognized and amplified by the second derivative. Fig. 2b shows the second derivative of the composite in Fig. 2a. The existence of two components is now rather obvious. The second derivative still has two minima and three maxima. The minima positions give a good, but not an exact, indication of the maximum positions of the two components in the composite. Similarly, the middle maximum gives a good indication of the point of minimum overlap between the two peaks in the composite. This information can be utilized in order to establish a valid integration point. Before proceeding with the analysis, it should be mentioned that this approach will fail when the peak separation is less than 2 sigma. In this case of severe overlap, the composite appears as a single peak, and the second derivative trace shows only two maxima and one minimum. Under these conditions, slope analysis [5, 6] is more appropriate. In addition, for $2\sigma \leqslant d \leqslant 6\sigma$ the method will fail if one of the components in the composite is below a critical height so as to be completely masked by the presence of the other component. The smaller d, the higher will be that critical peak height.

The second derivative trace, as depicted in Fig. 2b, allows two approaches to the problem of quantitation of strongly overlapped peaks. In one approach, the second maximum can be used as the point of integration stop for the measurement of the area of the first peak in the composite, and of integration initiation for the area determination of the second component. The reason for this was stated above: the second maximum provides an estimate of the point of minimum overlap or of peak profiles crossing. All that is needed is an algorithm to find the time coordinate of the second maximum in the second derivative of the composite. Once that time is known, it can be used to stop and/or trigger the integration in the conventional time domain i.e. in the chromatogram. The second approach is similar, with the exception that the time coordinate of the second minimum in the second derivative curve is used as the integration initiation criterion. The rationale for this approach was also indicated above; the second minimum is indicative of the maximum position of the second peak in the composite. These two approaches will be analyzed and compared.

In addition to the integration of the conventional chromatographic peaks, the second derivative curve is also available for data manipulation. Thus, since areas of the derivative curves can be integrated, the usefulness of this approach was investigated as well. In this part of the study, it was advantageous to transform the second derivative to a form which resembles conventional chromatograms. In this fashion, the integration of the second derivative trace can proceed in a more familiar manner. Moreover, this procedure has the added advantage of yielding "chromatograms" with better apparent resolutions.

Calculations

Software Used

The simulations of the chromatograms and their derivatives were obtained either on a CDC mainframe computer or on an IBM PC/XT microcomputer. Programs ran on the mainframe were written in Fortran. Programs written for the microcomputer were written in Asyst (Macmillan Software Co, NY, USA). Asyst is a high level programming language designed especially for scientific applications. It allows for rapid and efficient numerical manipulations of large arrays of numerical data and for interactive graphics. For this reason all initial explorative studies were made with the aid of Asyst.

Methods of Establishing Integration Limits

The differentiation of the simulated chromatograms was accomplished either analytically via equation (2), or, with Asyst, numerically using interpolating polynomials. The agreement between the two methods was excellent.

Area integration was carried out using the 1/3 Simpsons rule.

For the purpose of the study, composite peaks were simulated by combining two Gaussian peaks at different separations and different height ratios. The second derivatives were calculated, and the appropriate minimum or maximum were found. The abscissa positions of the extrema were determined and these were used as the integration initiation points.

The areas under the second derivative traces were also calculated using the methods mentioned above. To avoid problems with negative areas, the second derivative was squared and then integrated.

Second Derivative Inversions

The negative peaks of the second derivative curves were inverted using the following procedure. A straight line connecting the first and second maxima of the second derivative curve was calculated using the regression analysis procedure of Asyst. Then, the negative peak of the second derivative was reflected about that line. The procedure was repeated with the second negative peak as well. Fig. 3 shows the inversion in a schematic manner. The inverted second derivative has two inflections on the up-swing and on the down-swing parts of the curve. Savitzky-Golay smoothing can used to minimize these perturbations.

Results and Discussions

To prove the validity of the proposed approach, it is necessary to show that the information obtained is directly related to the quantities injected. This will be accomplished by correlating the areas calculated with the aid of the second derivative points to the height ratios of the components in the composite. Initially, we will discuss the

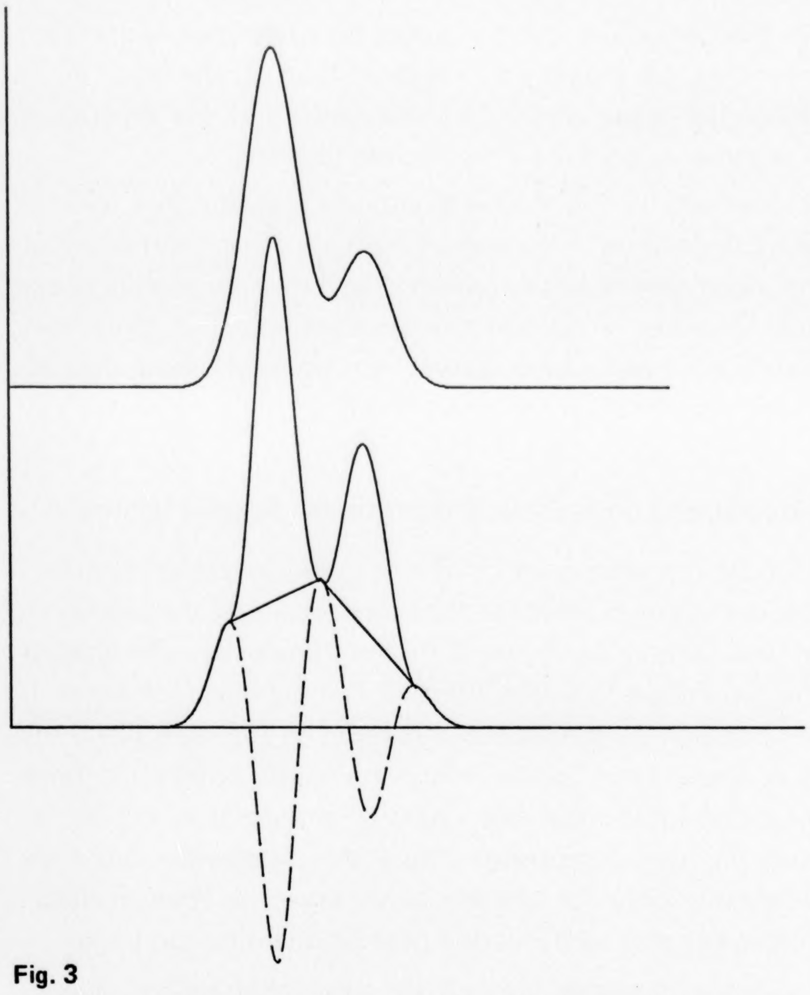

Fig. 3

The procedure used for the inversion of the second derivative. The upper trace shows a composite of two Gaussians. The bottom dashed line is the usual second derivative of the top composite. The bottom solid trace is the inverted derivative. The inversion is done by reflection about the lines, also shown in the figure, connecting the maxima in the second derivative.

results obtained from integration limits established from the second maximum in the second derivative trace. Then, the results obtained using the second minimum of the second derivative will be analyzed.

Integration Limits Established from the Second Maximum

Fig. 4 shows plots of the area of the second component versus the height ratio of the two peaks in the composite. The initiation of the integration was determined from the time coordinate of the second maximum in the second derivative of the composite (see Fig. 2). In the present communication we examined height ratios between 0.1 to 1. The behavior of the area of the second component is shown in Fig. 4 for several separation values. There are several points to note in the figure. The first point is that, within the height ratios and separations studied here, the values of the second peak areas are a linear function of the height ratios. Since the heights of the peaks in these simulated chromatograms are directly proportional to the areas of the peaks and, therefore, to the concentration of the injected solutes, it can be stated that the areas measured are a linear function of the amount of the solutes. Thus, calibration lines can be established, and the quantitation which can be achieved is rather good.

The second point to note is that when the two peaks in the composite are of equal, or nearly equal, width, the areas determined with the aid of the second derivative initiation point is only a weak function of the separation of the components. As expected, the greatest variation in the areas measured occur at the low height ratios; i.e., when the first component is in excess. For example, at the height ratio of .2, the difference in the areas of the second component is about 20%. On the other hand, when the two peaks are of identical height, the measured areas are completely independent of the separation. This will be true as long as the two peaks in the composite are of identical width and symmetrical. Only under these conditions will the portion of the second peak lost up to the point of integration initiation be compensated by the added portion of the first peak included in the integration due to the overlap.

The third point to note is that the line corresponding to the 2σ separation starts from a height ratio of 0.2 since the second derivative of the composite fails to show three maxima and two minima below that value. The conventional methods of determining the point of integration initiation would have failed long before that separation. In fact, the case of two sigma separation cannot be handled at all by conventional means. At the separation of 2.75σ, the perpendicular drop approach, in which the areas are determined on both sides of a perpendicular line dropped from the valley point of the composite to the baseline, is incapable of recognizing the two components when the height ratio is less than 0.5. In such cases, the analyst can use techniques such as "skimming" procedures. However, due to the switching of the integration methods, the calibration line for the solute is not a continuous one, a fact which makes the quantitation susceptible to errors. On the other hand, the second derivative method allows one to establish continuous and monotonic calibration curves over a wide range of separations and concentration ratios.

Since the height of the first peak in the composite remains constant throughout the entire domain shown in Fig. 4, its area should, ideally, remain the same for every composite. In general, this was found to be the case. For each

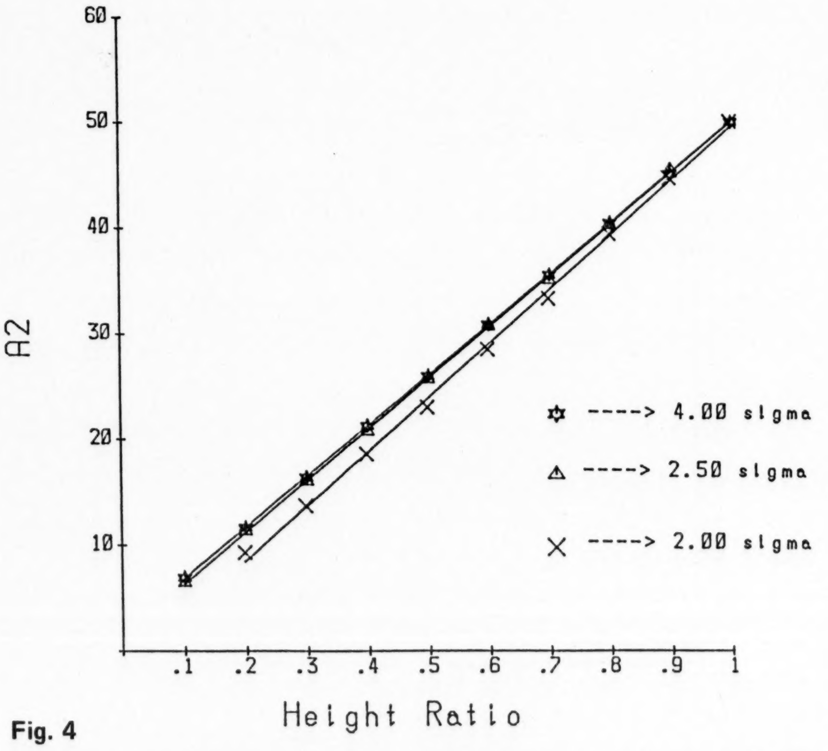

Fig. 4

The areas of the second component in the composite as a function of the height ratio of the solutes. The behavior is shown for several separations. The integration limit was chosen from the time position of the second maximum of the second derivative.

separation, the area of the first peak was about 4% smaller than the theoretical value when the height ratio was 0.1. As the height of the second peak in the composite increased, the error in the area of the first peak decreased. When the two peaks were of equal height, the areas of both were within few tenth of a percent of the theoretical value. This point, again, is of great importance in ensuring the quantitative fidelity of the approach.

Foley [17] recently discussed in detail the possible errors involved in the integration of overlapped peaks. He showed that in cases of tailing peaks the difference between the measured areas and the true values can be rather large. The errors would be much less when the two peaks in the composite are symmetrical, as in the present case. Fig. 5 shows plots of the relative error in the areas of the second component versus the height ratio. The relative error was computed by dividing the difference between the measured area of the second peak and the true area of that peak by the true area. The behavior of the relative error is given in the figure for several separations. The unique feature of the figure lies in the fact that the error is *decreased* as the separation between the peaks diminishes. The reason for this behavior is due to fact that as the separation between the two peaks decreases, the contribution of the first component to the area of the second increases at the same time. The true area of the second peak, for a given height, remains constant. Although the integration initiation point varies with the separation, the change is such that the contribution of the first peak compensates progressively more and more for the second peak area which is truncated by the integration. However, were the plots extended to even greater separations, the errors would have started to diminish again, as the peaks disentangle completely.

As the height ratio is decreased the error worsens. This is expected since the contribution of the first component in the composite can be proportionately more significant. However, for height ratios greater than .3, the error in the measured areas is $< \pm 7\%$ independent of the separation. For equal heights the error is close to zero.

The results in Fig. 4 and 5 indicate that the true areas of the components in the composite are, perhaps, not essential, provided that a linear relation can be established between the measured areas and the amounts injected. Only then meaningful calibration curves can be established, and accurate quantitation can be attained.

Integration Limits Established from the Second Minimum

The second minimum in the second derivative plot corresponds, *grosso modo,* to the true position of the maximum of the second component in the composite. The greater the separation between the two components, the closer is the position of the second minimum to the position of the peak maximum. To use this point as an integration limit means an intentional loss (gain) of area for the last (early) peak in the composite. Thus, this approach might be acceptable only for the last peak since the error in determining the area of the earlier peak(s) might be too large.

Fig. 6 shows several plots of the area of the second peak in the composite, as determined from the second minimum of the second derivative, versus the height ratio of the peaks. Each line in the figure corresponds to a different separation between the two peaks. Several points of interest should be discussed here. In the first place, the ordinate values are much smaller here than in the previous figure. The reason is obvious: the integration started here much later than in the previous procedure. The second point is that unlike the behavior depicted in Fig. 3, the separation between the components has much more influence on areas measured. This is the result of the fact that as the separation between the peaks decrease, the position of the second

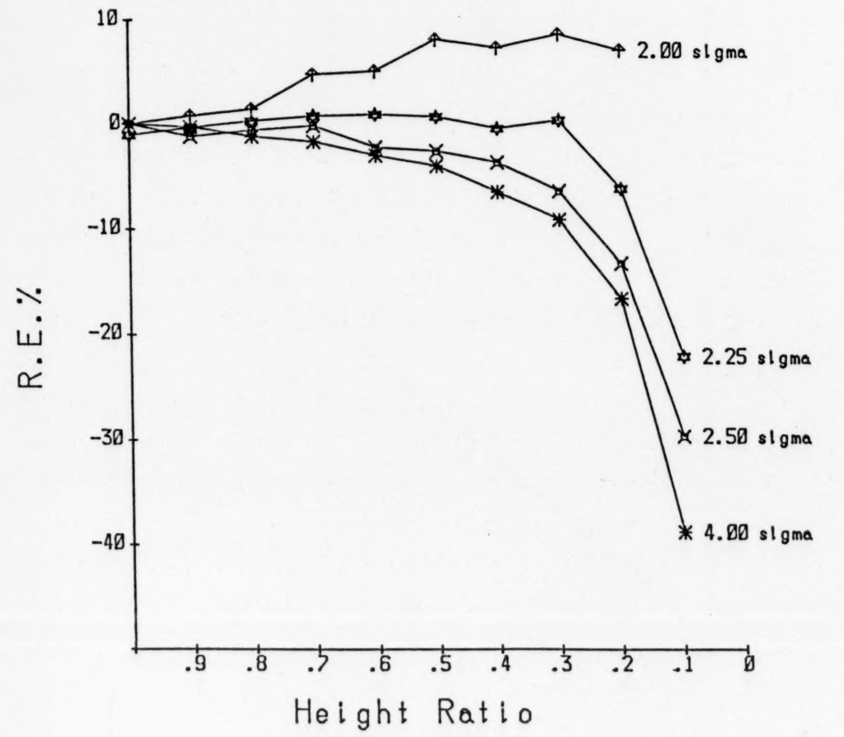

Fig. 5

The relative errors in the integration of the second component versus the height ratio. The integration limit was chosen from the time position of the second maximum of the second derivative.

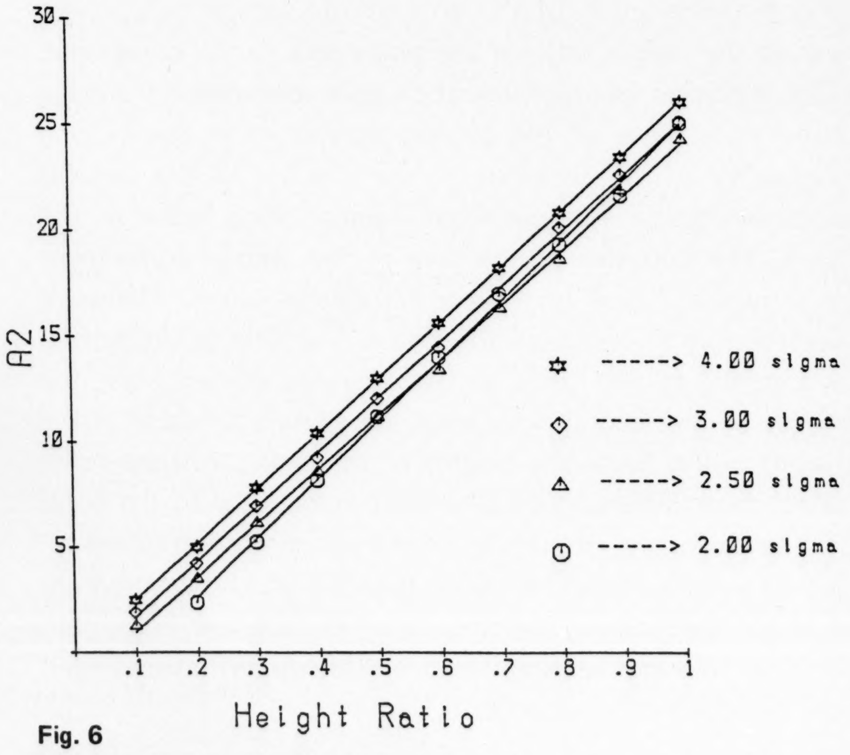

Fig. 6

The areas of the second component in the composite as a function of the height ratio of the solutes. The behavior is shown for several separations. The integration limit was chosen from the time position of the second minimum of the second derivative.

minimum in the second derivative does not shift to the same extent as does the peak maximum. Therefore, the integration initiation is proportionately later in the peak. At the same time, for separations greater than 2.5σ, the contribution of the first peak to the measured area of the second peak is small. The net result is an increase in the areas measured as the separation decreases from 4 to 2.5σ. At 2σ separation, especially for large height ratios, the contribution of the first component is more significant, and the measured areas increase. A related observation to the above discussion is, with the exception of the 2σ line, the parallel nature of the lines in Fig. 6.

The third point to observe in Fig. 6 is perhaps the most important. All the lines in Fig. 6 are straight lines with correlation coefficients in the 0.999 range. Therefore, this mode of operation can be also used in quantitative determination. The fact that a part of the peak area is lost is of no consequence, providing that the location of the second minimum of the second derivative curve is done with sufficient precision. The drawback of the approach is due to the necessity to change the integration methods for the various peaks in the composite since the area lost from the last peak cannot be included in any of the determinations of the other areas.

Unlike the previous case, an error analysis is meaningless since part of the area was intentionally neglected. This fact should not deter from the potential usefulness of the approach.

Areas Under the Second Derivative Curve

Eq. (2) shows that the second derivative is a function of the concentration of the solutes in the composite. During the study it became apparent that the second derivative of the composite can be integrated directly. This possibility was investigated in the present study. For that purpose, the integration limits discussed above were used here as well: the second maximum in the second derivative was used as the integration termination for the first peak and as the integration initiation for the last peak in the composite. Fig. 7 shows the results of such integration.

The most prominent feature of Fig. 7 is the great dependence of the areas on the separation of the solutes. This effect can be deleterious to accurate quantitative analysis, since small variations in the resolution render the calibration curves useless. The dependence on the separation is especially noticeable in cases when the two peaks are roughly equal in height. This means that the chromatographic conditions must be rigorously adhered to in order to be able to obtained meaning full data.

Another feature of Fig. 7 is the nonlinear dependence of the area on the height ratio of the solutes in the composite. While the behavior in the case of 4σ separation is suitable for quantitative analysis, the linearity of the line deteriorates as the separation decreases. Thus, when the separation is 2σ, the areas of the second component cannot be quantified in cases with height ratios less than 0.4.

Not shown in Fig. 7 is the behavior of the area due to the first component in the composite. It was mentioned before that when the integration was performed on the conventional chromatogram, using the position of the second maximum of the second derivative, the area of the first peak was, to a good approximation, independent of the height ratios and of the separations. This was not the case with the derivative area of the first component. It was found that, depending on the separation, the area due to the first peak can vary between 5% to 40% as the height ratio changes from 0.1 to 1. Moreover, the change in the area can be either in the positive or negative direction, depending upon the separation.

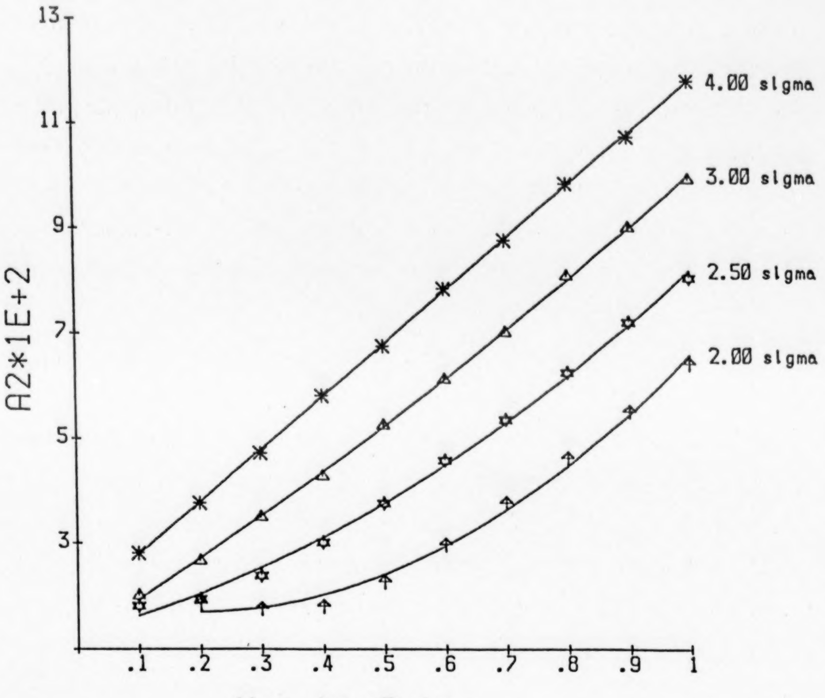

Fig. 7

The area of the second component, as determined directly from the second derivative curve, versus the height ratio of the solutes. The behavior is shown for several separations.

These results indicate that the derivative trace is not suitable for precise determination of areas, in cases where there is overlap between the solutes to be quantified.

The Inversion of the Second Derivative Curve

Fig. 3 shows that the second derivative can be inverted in such a way as to make it appear similar to a conventional chromatogram. The characteristics of the inverted second derivative trace is that its upper part is narrower than the true peaks, while the base of the inverted trace is wider. This results in "bumps" which appear on the front and back parts of the inverted second derivative of the composite. The "bumps" can be greatly reduced using smoothing techniques such as Savitzky-Golay moving average or Fourier filtering. The resulting trace is a conventional looking chromatogram with better apparent resolution than the original detector signal. It should be stressed that the resolution improvement is due to mathematical manipulation only. The inherent resolving power of the chromatographic system was not changed at all as a result of the inversion process.

The inverted chromatogram can also be subjected to integration. The possible use of the integration of the inverted second derivative trace was examined by using the perpendicular drop method. Fig. 8 shows the behavior of

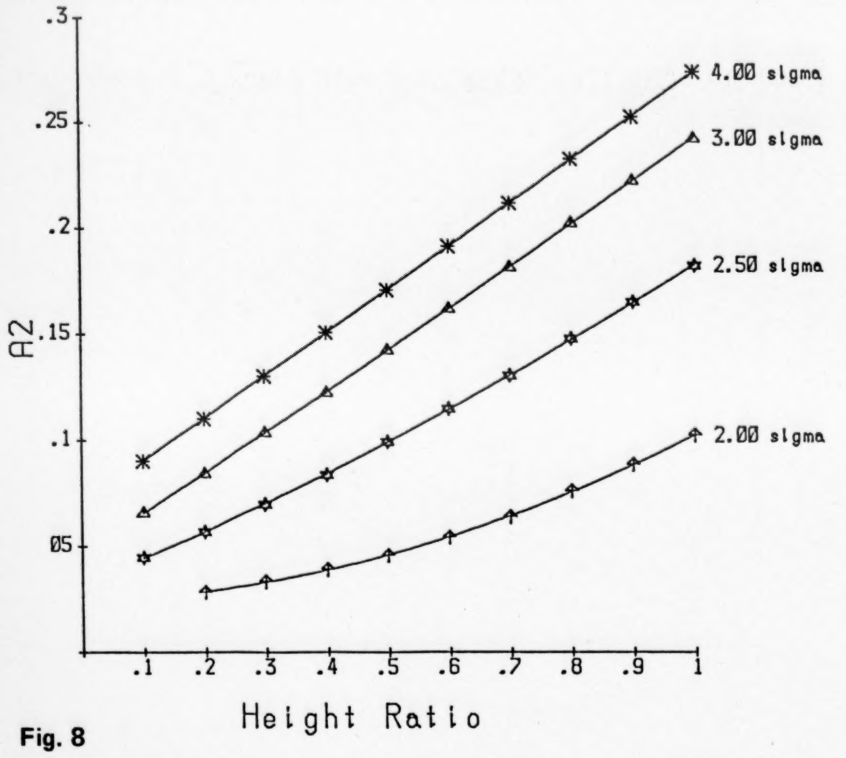

Fig. 8

The area of the second component, as determined directly from the inverted second derivative curve, versus the height ratio of the solutes. The behavior is shown for several separations.

the second peak area as a function of the height ratio of the two components (the height ratios refer to the ratio of the solutes' concentrations in the injected mixture). Several levels of peak separations are given in the figure. The areas seem to be linearly dependent on the height ratio; even at 2σ separation a straight line can describe the behavior of the area rather well. There is, however, still a large dependence of the area, at a given height ratio, on the separation. The dependence is not linear, being stronger at low resolutions. Fig. 8 implies that the quantitative determination of the second component can be accomplished from the inverted second derivative, provided that the chromatographic conditions are rigorously controlled so that the resolution does not vary greatly over the course of the analysis time. In fact, since the linearity of the lines in Fig. 8 are much better than those in Fig. 7, the range of the usefulness of the inverted form of the second derivative is much greater, especially at low resolutions and small height ratios, than that of the conventional second derivative trace.

Unfortunately, as with the untreated second derivative curve, the area of the first peak of the inverted second derivative curve is a strong function of both the height ratio (at a given separation) and of the resolution (at a given height ratio). This fact limits greatly the analytical utility of the inverted curve: while the quantitation of the second component in the composite can be made, under certain conditions, the accurate determination of the first component is virtually impossible. The inverted derivative approach is best suited to numerically improve the resolution, so as to make the recognition of composite peaks much easier for the users of chromatography – the inverted signal is much easier to interpret than the usual second derivative curve.

Conclusions

The derivative of the chromatographic signal can be used to extend the useful range of electronic integrators. This is accomplished by utilizing the fact that the differentiation process narrows the peak width. Composite peaks with low resolutions, in which the existence of the components is recognizable by perturbations on the overall envelope, cannot be easily quantified by conventional integrators. The differentiation accentuates these perturbations and makes it easier to decide on logical points of peaks' beginnings and ends. These points can then be used to initiate and terminate the integration of the components in the composite.

When the composite is made of two components, the best strategy for deciding the limits of integration seems to be at the abscissa position of the second maximum in the second derivative curve. This point, to a first approximation, marks the point of minimum overlap (or crossing) of the two components. At this point the integration of the first peak should end, and that of the second peak should start.

It seems to us that, with the current digital integrators, the implementation of derivative manipulation is fairly straight forward. It is recommended that an option be included, by the makers of integrators, that allows for area integration based on the second derivative behavior.

References

[1] *T. C. O'Haver, G. L. Green*, Anal. Chem., **48**, 312–318 (1976).
[2] *B. G. M. Vandegiste, L. de Galan*, Anal. Chem., **47**, 2124–2132 (1975).
[3] *M. Sharaf, D. L. Illman, B. R. Kowalski*, Chemometrics, John Wiley & Sons, N. Y., 1986.
[4] *J. W. Ashley, Jr., C. N. Reilley*, Anal. Chem., **37**, 626–627 (1965).
[5] *E. Grushka, G. C. Monacelli*, Anal. Chem., **44**, 484–489 (1972).
[6] *E. Grushka*, Anal. Chem., **44**, 1733–1738 (1972).
[7] *D. T. Zelt, J. A. Owen, G. S. Marks*, J. Chromatogr., **189**, 209–216 (1980).
[8] *J. Traveset, V. Such, R. Golzalo, E. Gelpi*, J. Chromatogr., **204**, 51–58 (1981).
[9] *J. C. Berridge*, chromatographia, **16**, 172–174 (1982).
[10] *A. F. Fell, H. P. Scott, R. Gill, A. C. Moffat*, Chromatographia, **16**, 69–78 (1982).
[11] *A. F. Fell, H. P. Scott, R. Gill, A. C. Moffat*, J. Chromatogr., **273**, 3–17 (1983).
[12] *A. F. Fell, H. P. Scott, R. Gill, A. C. Moffat*, ibid, **282**, 123–140 (1983).
[13] *B. J. Clark, A. F. Fell, H. P. Scott, D. Westerlund*, ibid, **286**, 261–273 (1984).
[14] *D. D. Gerow, S. C. Rutan*, Anal. Chim. Acta, **184**, 53–64 (1986).
[15] *A. Grant, P. K. Bhattacharyya*, J. Chromatogr., **347**, 219–235 (1985).
[16] *S. Ebel*, Chromatographia, **22**, 373–378 (1986).
[17] *J. P. Foley*, J. Chromatogr., **384**, 301–313 (1987).

Received: Aug. 3, 1987
Accepted: Aug. 11, 1987
F

Open Tubular Columns and Non-Porous Packings in Copolymer HPLC Analysis

G. Glöckner

Dresden University of Technology, Department of Chemistry, Mommsenstraße 13, DDR-8027 Dresden, GDR

J. H. M. van den Berg[1]

DSM Research, P. O. Box 18, 6160 MD Geleen, The Netherlands

Key Words

Column liquid chromatography
High molecular weight polymers
Gradient elution
Open tubular columns
Packed columns

Summary

The separation of poly(styrene-co-acrylonitrile) is presented in open tubular stainless steel columns and columns packed with non-porous glass beads. Furthermore separation on a short silica packed column proved to be better than on a similar longer column. A definition of the term high performance precipitation liquid chromatography is suggested for gradient elution with sample injection into a starting eluent which is a nonsolvent for the copolymer under investigation. The choice of a suitable solvent-nonsolvent combination is of essential importance.

Introduction

In gradient elution chromatography, the quality of the mobile phase is varied from an initial low to a final high elution strength. This can be done by gradual transition from a weak eluent, A, to a strong one, B. The absolute requirements of the nature of A and B are that B is a chromatographically stronger solvent than A, and that A and B are miscible. For reversed-phase (RP) HPLC, the first condition means that B is less polar than A, whereas in normal-phase (NP) HPLC, B must be more polar than A. Gradient HPLC provides faster elution of strongly retained constituents than isocratic elution does, and yields narrower bandwiths. These are the main reasons for its application in low-molecular mass HPLC, where the samples are usually dissolved in a portion of the starting eluent. Neither the starting eluent nor the final one need be a pure liquid. Mixtures of A and B with a higher content of B in the final eluent are also suitable. Ternary or even more complex gradients may also be of advantage in certain cases.

Gradient elution is of decisive importance in polymer HPLC. RP separation of proteins is a typical example. Here, the starting eluent is usually water and the final one the mixture of water and on organic liquid, the "modifier". Certain additives, e.g., trifluoroacetic acid, may also be substantial components of the eluent.

The relationship between the capacity factor k' and the volume fraction φ of the modifier for isocratic elution (eq. 1) is well known and has been verified extensively.

$$\log k' = \log k'_0 - S\varphi \qquad (1)$$

In eq. (1) k'_0 is the capacity factor in pure solvent A. If eq. (1) is applied to gradient elution, k'_0 stands for the capacity factor in the starting eluent. The slope factor S is influenced by several factors including the molecular size of the sample substances. For low molecular weight samples, typical values are in the range between 1 and 5, whereas with polymers S values can be 30 to 100-fold larger [1]. This means that in polymer gradient chromatography very small differences in eluent composition can cause dramatic changes in elution behaviour. Thus, a polystyrene standard of molecular mass 50,000 daltons was eluted without retention from a 30 nm RP C18 column with water/THF (13/87 v/v) whereas no elution occurred with a 17/83 v/v mixture within a reasonable time [2].

The capacity factor k' represents the mass distribution of a component between the stationary and the mobile phase:

$$k' = m_{stat}/m_{mob} \qquad (2)$$

At the same time it can be expressed as the probability ratio for a given solute to be either adsorbed or moving.

---

[1] Present address: Duphar B. V., Research Laboratories, Analytical Development Department, P. O. Box 2, 1380 AA Weesp, The Netherlands.

0009-5893/87 0233-08 $03.00/0

© 1987 Friedr. Vieweg & Sohn Verlagsgesellschaft mbH

With the probability p of being adsorbed, the probability of being non-adsorbed is $(1-p)$ and

$$k' = p/(1-p) \quad (3)$$

This holds for each solute molecule and, since polymer chromatography is governed by the same principles as low-molecular mass chromatography, for each structural unit of a flexible macromolecule.

Polymer coils are adsorbed via trains of repeat units while other parts of the coil protrude into the solution as tails and loops. Assuming independent adsorption/desorption equilibrium for each unit of a train, we can express the mobility conditions of a macromolecule by the product of the corresponding probabilities of the units, $(1-p_u)$.

For an adsorbed train of n units we have:

$$(1-p_{total}) = (1-p_u)^n \quad (4)$$

or, with eq. (3) and k'_{total} as the capacity factor of the macromolecule:

$$k'_{total} = (k'_u + 1)^n - 1 \quad (5)$$

(Note that the logarithmic form of eq. (5) is essentially equivalent to the Martin rule for the members of a homologous series with carbon number n).

For illustration, let us assume adsorption of 100 repeat units which may be representative of a macromolecule. Then from eq. (5), if $k'_{total} = 10$ (which is an arbitrarily chosen reasonable upper value of k' for sufficient mobility), $k'_u = 0.024$, and if $k'_{total} = 1$ (which is about the lower limit), $k'_u = 0.007$.

The eluent quality determines (in combination with other factors, naturally) the k'_u values. The latter only has to decrease from 0.024 to 0.007 in order to change the behaviour of the macromolecule from high to almost no retention. Thus, the large effect of small changes in eluent composition on polymer retention is plausible.

Since $(k'_u + 1)^n \gg 1$, the combination of eqs. (1) and (5) yields (with $k' = k'_u$ in eq. (1)):

$$S_{total} = S_u * n \quad (6)$$

This increase of S with n has been established experimentally with polystyrene (PS) oligomers [2, 3].

Strict adherence to the Martin equation cannot be expected for high molecular weight polymers since (i) cooperative effects will influence the probabilities of repeat units in longer trains and (ii) increasing molecular mass will affect the ratio of trains to loops and tails. Nevertheless, increase of $\log k'_{total}$ with molecular mass has been found experimentally for PS including a sample with $n = 470$ (corresponding to 50,000 daltons) [2].

In addition to separation of proteins and nucleic acids, the analysis of synthetic polymers with respect to compositional and structural heterogeneities is another application of polymer non-exclusion HPLC. In particular the evaluation of chemical composition distribution is a common task [4].

Synthetic polymers are normally insoluble in water. Hence, gradient HPLC is better performed with A and B as organic solvents. Normal-phase separations have been carried out on polar columns with mixtures of iso-octane (A) and THF (B) (e.g. [5]). Reversed-phase separations on C18 or C8 columns have been carried out with methanol/dichloromethane [6, 7] or methanol/THF mixtures [8] e.g. With synthetic polymers, most of the successful separations have been performed with combinations of non-solvents (A) and solvents (B). With poly(styrene-co-acrylonitrile) samples (SAN), the combination of iso-octane as non-solvent with THF as solvent performed equally well with normal and reversed-phase columns. The latter combination of a normal-phase gradient with a reversed-phase column is strange and will not work in low-molecular mass separations. Together with the observations (i) that the elution characteristic of SAN is almost identical with the solubility characteristic in the respective system [9] and (ii) that the effect of molecular mass on HPLC elution matches that of solubility [10], we concluded that retention was due to precipitation of the samples.

Recently we found that copolymers from styrene and methyl methacrylate can be separated by composition if normal-phase gradients are applied on normal-phase columns. The unusual combination mentioned above of a normal-phase gradient and an RP C18 column only yielded retention graded by composition but no separation of a standard mixture [11, 12]. In addition to this, the separation characteristics on silica were well above the solubility characteristics of this system (i.e. in the solution area). Thus, adsorption was necessary for these separations.

However, precipitation phenomena would still seem to be of importance. One observation is the parallel orientation of solubility and elution characteristics [12], another even more general observation is the fact that polymer HPLC differs from low-molecular mass gradient HPLC in sample application. The limited solubility of polymers usually does not allow the preparation of a homogeneous sample solution in a liquid with the quality which is necessary for retaining the polymer in a column. Thus, to the best of our knowledge, synthetic polymers are always injected as solutions in a thermodynamically better solvent than the starting eluent. This means that the polymer will be precipitated on injection by the starting eluent.

Stating this, we are well aware of the fact that most protein separations are performed differently, i.e., with water as the sample solvent as well as the starting eluent. But samples of poor solubility, e.g. membrane proteins or collagen, must be dissolved in a liquid of higher dissolving strength than the starting eluent [13–15]. Here, intermediate precipitation has also been observed.

This paper has two objectives. The first one is an attempt to find out more about the separation mechanism in polymer HPLC. By using non-porous packings and open tubular columns we hope to learn whether a single of a multistep mechanism is present.

The second one deals with the influence of column length on gradient HPLC of synthetic polymers. It has been found experimentally that column length has little effect on gradient separation of proteins [16]. These findings gave rise to the "pop-off" proposal, which assumes (i) that a solute is retained at the top of the column until the eluting strength of the gradient mixture suffices and (ii) that the molecule, if movable, is not re-adsorbed on its way through the column. It has been shown that this mechanism as well as the multi-site retention discussed above can be understood as logical extensions of normal chromatography [1, 18]. Recently evidence has been given that reversed-phase separation of proteins occurs with higher resolution on a 6.3 x 4.6 mm I.D. column than on a 45 x 4.6 mm I.D. one, especially if steep gradients and low flow rates are applied [19].

Experimental

HPLC Apparatus

Liquid chromatograph model HP 1090, Series A, (Hewlett Packard, Waldbronn, FRG) with auto-injector and auto-sampler, ternary DR 5 pump, built-in diode array detector HP 1040 and data processing unit HP 3392, connected to a thinkjet printer HP 2225A, a flexible disk drive HP 9121 D and a graphic plotter HP 7470 A and an additional analog recording device. A personal computer HP-85 was used as a system controller.

Columns

1: Cartridge column 60 x 4 mm I.D., packed with ground glass, 10 μm fraction.
2: Cartridge column 60 x 4 mm I.D., (Knauer, Bad Homburg, FRG), packed with silica Nucleosil 50, particle size 5 μm (Macherey & Nagel, Düren, FRG).
3: 150 x 4.6 mm I.D., packed with Polygosil 60-5, particle size 5 μm (Macherey & Nagel, Düren, FRG).
4: 55 x 4.6 mm I.D., packed with Polygosil 60-5, particle size 5 μm.
5: Open tube, stainless steel SS316, 11,000 x 0.5 mm I.D.
6: Open tube, stainless steel SS316, 7,800 x 0.25 mm I.D.

HPLC Conditions

The eluent components were continuously purged with nitrogen or helium, the column thermostated at 50°C. The gradient programs are listed in Table I. The sample solvent was THF p.a. quality, stabilized with 0.025 % butylated hydroxy toluene. The chromatograms were monitored at 259 nm.

Samples

The poly(styrene-co-acrylonitrile) specimens were prepared by radical polymerization under conditions ensuring a narrow range of chemical composition. Table II lists some properties of these copolymers. The polystyrene samples were commercial standards for size exclusion chromatography calibration. They have narrow molecular-mass distribution. The average value is given (in kdaltons) by the figures added.

Table I. Survey of gradient programs used in this investigation

No. 30/1984:

t, min	i-octane v/v	THF v/v	Methanol	Flow, ml/min
0	90	10		1
1	90	10		
1.2	85	15		
1.8	55	45		
2	50	50		
22	0	100		
23	0	100		
24	10	90		
24.1	90	10		
25.9				1
26				2
28				2
28.1	90	10		1

No. 84

t, min	i-octane v/v	THF v/v	Methanol	Flow, ml/min
0	90	8	2	0.5
8	40	58	2	
10	0	100	0	0.5
10.5				2
11	0	0	100	
12	0	100	0	
13	90	8	2	
13.5				2
14	90	8	2	0.5

No. 85

t, min	i-octane v/v	THF v/v	Methanol	Flow, ml/min
0	80	18	2	0.5
1	50	48	2	
11	0	98	2	
13	0	98	2	0.5
13.5				2
14	0	80	20	
15	0	98	2	
16	80	18	2	
16.5				2
17	80	18	2	0.5

Solvents

THF was used in gradient HPLC without a stabilizer. It was cleaned as described elsewhere [12, 20] and kept throughout under a nitrogen blanket. Iso-octane (2,2,4-trimethylpentane) was purchased from Fluka (Buchs, Switzerland) or from Merck (Darmstadt, FRG; HPLC quality LiChrosolv). Methanol of the same quality also came from Merck.

Table II. Specification of poly(styrene-co-acrylonitrile) samples investigated

Sample code	A	B	C	D	E
Acrylonitrile, mass %	16.1	23.0	29.1	36.4	42.5
Styrene, mol %	72.6	63.0	55.4	47.1	40.6
Molecular mass (osmometric), 1000 daltons	325	480	510	380	340
Presence in mixture M1, %	17.1	19.5	17.1	26.8	19.5
Presence in mixture M2, %	11.5	22.5	17.7	26.1	22.2

Mixture M3 is composed of 36.8 % TSK 37 Polystyrene
31.6 % TSK 110 Polystyrene
31.6 % TSK 1260 Polystyrene

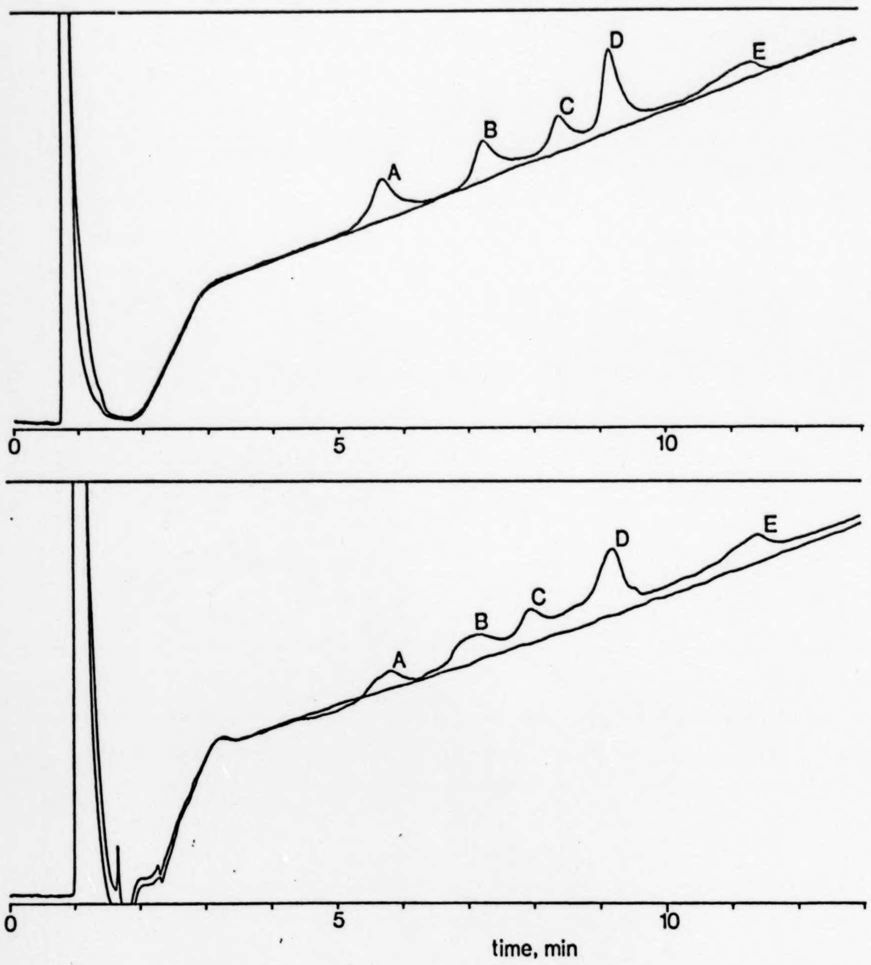

Fig. 1
Gradient elution of five SAN copolymers on 60 x 4 mm I.D. columns packed either with impervious glass particles (column no. 1, upper trace, 1081/85) or silica Nucleosil 50 (column no. 2, lower trace, 1071/85). Injection of 8.2 µg of mixture M1, V_0 = 20 µl. Gradient no. 85, 30 mAU full scale.

Results

Separation of SAN Mixture on Non-Porous Glass Particles

Fig. 1 shows the elution pattern obtained with a column packed with non-porous particles of ground glass (upper trace) and with a column packed with silica Nucleosil 50 (lower trace), which was porous, of course. The dimensions of both columns, the gradient program and the brand of eluent components as well as the sample solution were identical (both analyses were performed on the same day with less than five hours difference in injection time). Both chromatograms were plotted with the same position of time scale although the gradient breakthrough would indicate a backward shift of the upper trace by about 0.1 min. To a first approximation, correspondence of both chromatograms can be assumed. Closer examination, however, shows that the specimens B, C and D are obviously eluted later from the glass particles than from the porous silica. The peak shape in the chromatogram from the non-porous packing is even better than that obtained with the silica column although the latter was packed with 5 µm spheres whereas the glass powder was a 10 µm sieve fraction.

The chromatogram shown in Fig. 1 was obtained from the 6th repetitive injection of the sample. Fig. 2 shows this chromatogram once more in the uppermost trace, but this time plotted with the patterns of all the preceeding runs. The bottom trace with the experimental baseline is from the first injection on the brand-new column. There is obviously an increase in signal height from one injection to

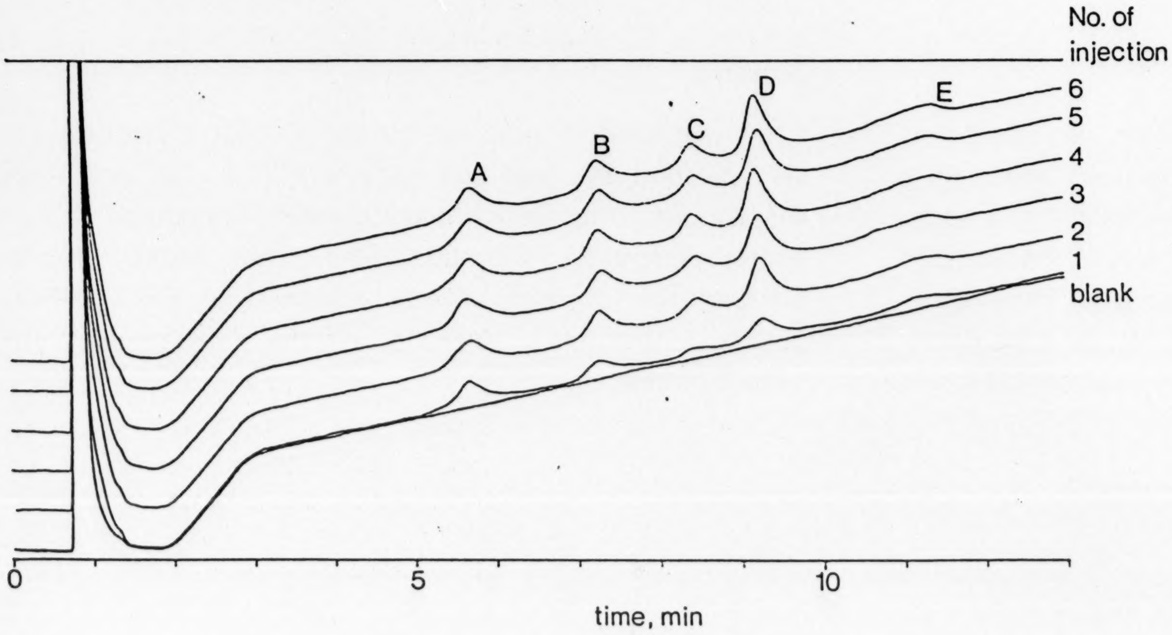

Fig. 2
Repeated injections and gradient elution of SAN mixture M1 on column no. 1. The bottom trace is from the very first injection (1076/85) on the new column. The traces from the subsequent injections are plotted with an increment of 8 % in zero position. 50 mAU full scale, conditions see Fig. 1.

the next, which is comparable to the "conditioning period" sometimes observed with a new column in protein separation, e.g., in hydrophobic interaction chromatography on ether-bonded phases [21].

Separation of SAN Mixture in an Open Tube

Fig. 3 shows the elution pattern obtained after the injection of 63 μg of mixture M2 dissolved in 30 μl THF. The five components are eluted according to increasing acrylonitrile concentration, i.e., in the normal order, and form clearly visible bands. With regard to sample, gradient, and solvents used, the chromatogram can be compared with those shown in Figs. 5 and 6.

A short comment on the "spikes" might be necessary. The tube had been used before as post-column reactor for detection of low-molecular mass substances and solid particles had adhered to the inner surface of the tube. Unfortunately, these particles could not be removed by the rinsing procedures, but tended to leave the column after the polymer injection especially in an eluent composition with a high THF content. Later experiments with a fresh tube proved that the spikes did not indeed belong to the sample polymer.

With regard to the quality of the separation it must be noted that it is much behind the resolution which can be obtained by packed column, see Figs. 5 and 6. The remaining question was whether the "surface modification", which was responsible for the spikes, gave rise, at the same time, to the surprising separation effect.

The results from a new SS column presented in Fig. 4 are arguments in favour of the separating power for SAN copolymers of a clean steel tube.

Elution of the Mixture of Three Polystyrene Samples from a Stainless-Steel Open Tube

Although the SAN peaks in Fig. 3 occurred in regular order and position, the spikes lead us to doubt whether the possibly modified surface of the steel tube might have provoked unexpected influences. Hence we had been eager to perform similar experiments with a brand-new steel tube.

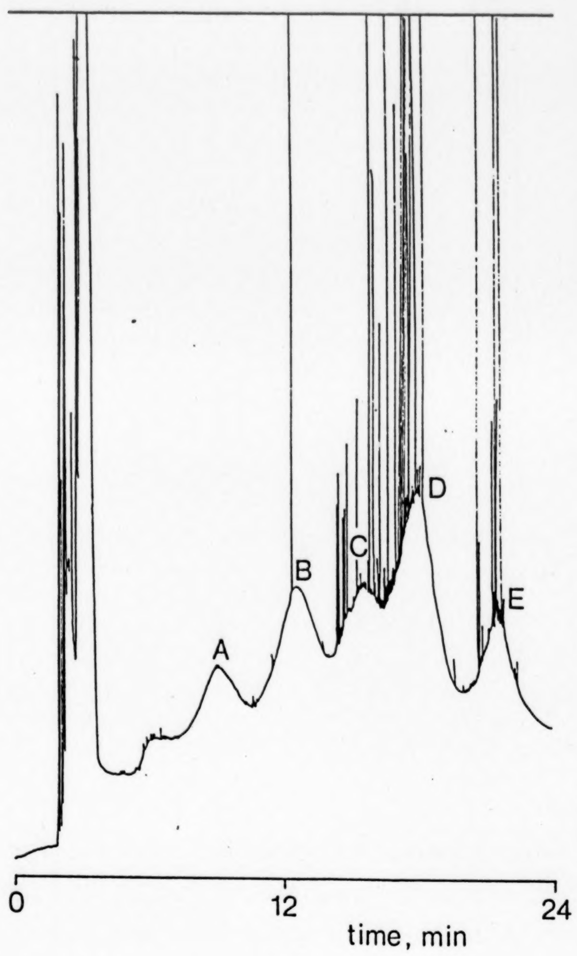

Fig. 3

Gradient elution of SAN mixture M2 after injection into an open tube 11,000 x 0.5 mm I.D. made of 316 stainless steel, column No. 5, (162/84). $m_0 = 62.7\,\mu g$, $V_0 = 30\,\mu l$, gradient no. 30/1984, 20 mAU full scale.

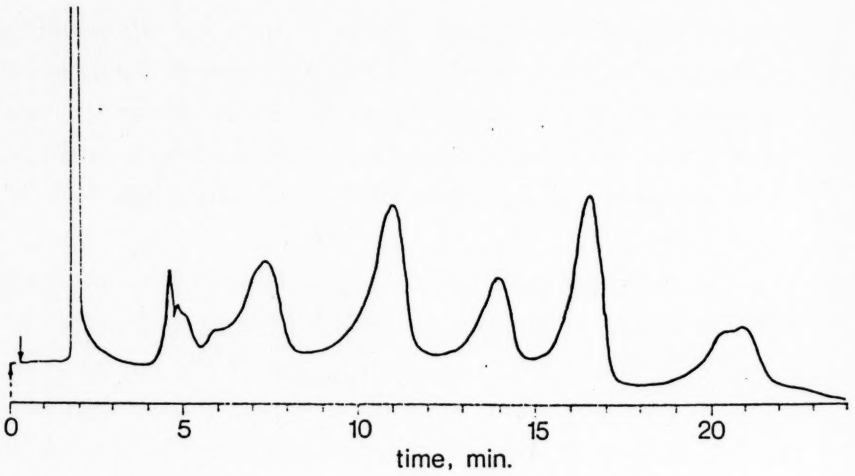

Fig. 5

Gradient elution of SAN mixture M2 after injection 131/84 of 62.7 μg in $V_0 = 30\,\mu l$, gradient no. 30/1984, 25 mAU full scale, column no. 3, 150 x 4.6 mm I.D.

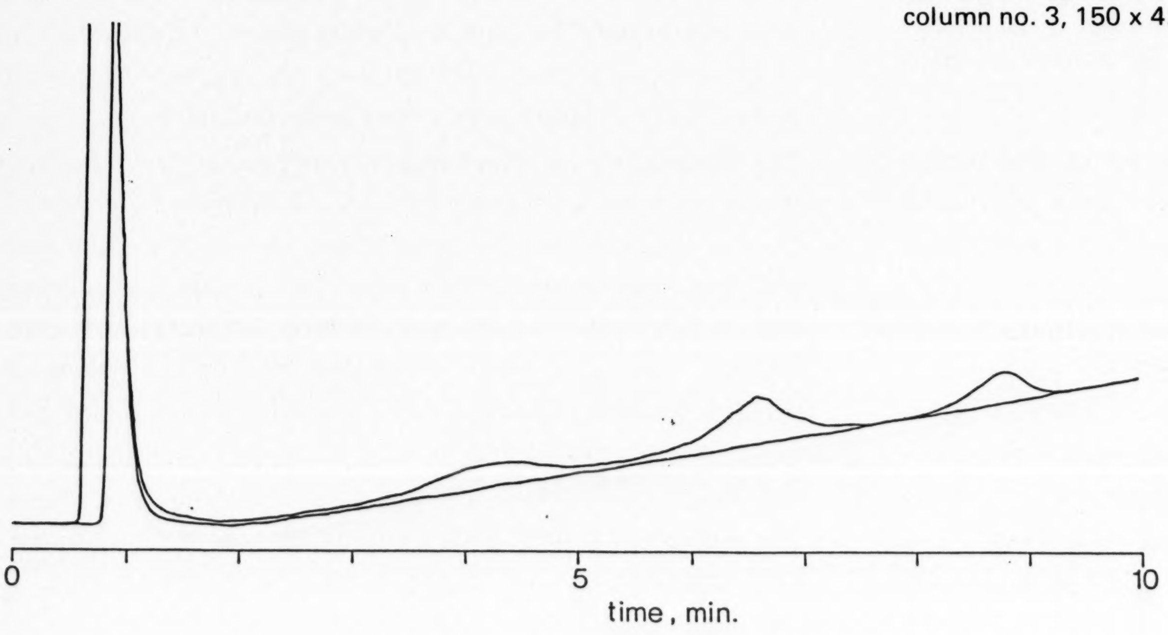

Fig. 4

Gradient elution of mixture M3 composed of three polystyrene standards with molecular masses 37,000, 110,000 and 1,260,000 daltons (in the order of elution) after injection into a new open tube 7,800 x 0.25 mm I.D. made from 316 stainless steel (column no. 6, 1048/85). $m_0 = 3\,\mu g$, $V_0 = 7.5\,\mu l$, gradient no. 84, 50 mAU full scale.

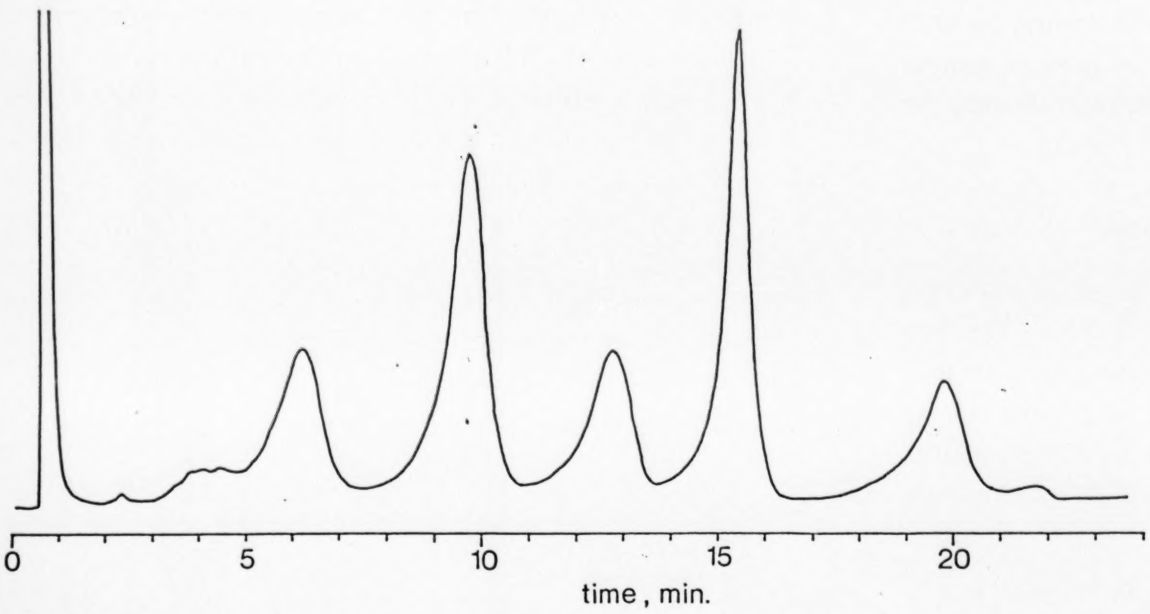

Fig. 6
Conditions as in Fig. 5, but column length 55 mm (column no. 4, 134/84), 30 mAU full scale.

This oppertunity presented itself during the investigation of PS standards by gradient HPLC. The higher the molecular mass of this homopolymers, the longer they are retained. Separation by molecular mass could be performed on polar columns though NP gradients as well as on nonpolar columns through RP gradients [22].

Fig. 4 shows the elution pattern obtained on injection of 3 μg containing 36.8 % of a standard with molecular mass 37,000 and 31.6 % each of standards with 110,000 and 1,260,000 daltons. The gradient was iso-octane with 2 % methanol constant and THF increasing from 8 to 58 % in 8 min. Three bands can be observed which are reproducible and belong to the samples mentioned above in the order of increasing molecular mass. Before the PS injection, the new column had only been rinsed with the starting eluent and three gradient cycles were performed with injection of 7.5 μl THF.

The result shows that the unused surface of stainless steel 316 has a separation activity similar to that of a polar column. This was found with a mixture of PS samples. We think it can be concluded from this result that a surface of this quality is also capable of retaining SAN samples according to polarity. Thus, the separation of a SAN mixture shown in Fig. 3 is scarcely influenced by the previous use of that tube.

Influence of Column Length on the Separation of SAN Samples on Silica

In the experiments shown in Figs. 5 and 6, the sample solution, the gradient program and the brands of eluents were the same as in the experiment with the open tube shown in Fig. 3.

Fig. 5 shows the separation of SANs by acrylonitrile content achieved on a 150 x 4.6 mm I.D. column packed with silica Polygosil 60-5 which is a small-pore material (pore diameter = 6 nm) of grain size 5 μm. The result is definitely better than that obtained with the steel tube.

Fig. 6 shows the chromatogram of the same sample (62.7 μg of mixture M2 in 30 μl solution with THF as a solvent) which was monitored three hours later in an experiment under identical conditions of eluent quality and gradient program. The only difference was the column length which, in this latter case, amounted to 55 mm only. The packing material and packing technique for this and the previously used longer column were also identical. Without doubt, the chromatogram obtained with the shorter column is superior.

Discussion

The higher resolving power of a 55 mm column compared to that of a 150 mm one in the separation of SAN copolymers is in line with recent findings in protein separation [19]. We suppose that the diffusion of the eluent components, which is definitely faster than the diffusion of the high-molecular sample, may cause band broadening. This effect should be especially pronounced if steep gradients are employed in combination with low flow rates. This tendency can be seen in the data of Moore and Walters [19].

The retention and separation of SAN copolymers by their acrylonitrile content on impervious glass particles and stainless steel is caused by the polar sites on these materials. As expected, impervious RP8 particles did not separate the mixture of SAN copolymers when normal-phase gradients were employed. The high separation power of these packings in protein separation [23] parallels the activity of ground glass in normal-phase separations described here.

The chromatographic activity of non-porous polar surfaces shows that the separation of SAN copolymers by composition is also effected by adsorption. Hence, the statement that the mechanism of this separation is just precipitation and redissolution needs qualification although this conception was once more suggested by the similarity of chromatograms obtained with a given normal-phase gradient on columns with a variety of porous packings (Si50, Si300, CN, C18, μ-Bondapak) [12].

The elution of a given SAN sample occurs in the iso-octane/THF gradient always in the same eluent composition irrespective of the kind of porous packing materials. Table 3 lists data from a previous publication and those estimated from the results of the experiments presented here. The critical points of these calculations are (i) the limited precision of gradient lag-times and (ii) the question which elution volume is representative of a broad band. The data in Ref. [5] and, consequently those in Table III as well, were estimated from the peak maxima. The first moments of the bands would be more accurate, but this would be of minor influence on the final conclusion.

The separation by composition of poly(styrene-co-methylmethacrylate) samples occurs on polar columns with an elution characteristic, which is parallel to the solubility characteristic and located in the range of homogeneous solutions [12]. The excess of the polar solvent THF indicates the adsorption contribution.

The corresponding separation of SAN copolymers with alkane hydrocarbon/THF gradients occurs on polar and porous nonpolar columns with a characteristic which represents retention and solubility as well. The results of the present paper show (i) that adsorption phenomena are effective also in these separations and (ii) from the influence of column length, that the "pop-off" model seems to be adequate for copolymers.

As mentioned in the Introduction, in gradient HPLC of synthetic polymers the starting eluent is mostly a nonsolvent that has not enough dissolving power for the samples under investigation. Consequently, sample solutions cannot be prepared by using the starting eluent. A solvent is required which must be better with respect to thermodynamic quality. On injection, the polymer samples, whose solubility is generally much more limited than that of low-molecular substances, are precipitated by the eluent.

Effective gradients are, in addition to other requirements, suitable combinations of solvents and precipitants.

Hence, we suggest the term high-performance precipitation liquid chromatography (HPPLC) for gradient elution with sample injection into a starting eluent which is a nonsolvent (precipitant) for the sample under investigation. This definition of HPPLC does not ignore the contribution of adsorption which is essential in some cases. The hypothesis of the combined action of precipitation and adsorption proved a guiding principle in the search for methods for the separation by composition of copolymers from styrene and ethyl methacrylate (SEMA) [20], from styrene and methoxyethyl methacrylate [24] and from styrene and t-butyl methacrylate [25] and showed itself reliable even for normal- and reversed-phase elution of SEMA mixtures with reversal of elution order [8].

Acknowledgement

One of the authors (GG) is indebted to the Sonderforschungsbereich 41 at the Johannes-Gutenberg Universität Mainz, FRG, for having given him the oppertunity of performing HPLC investigations. Part of the work was carried out with an instrument that the Dutch branch of the Hewlett Packard company put at our disposal at DSM Research, Geleen, The Netherlands. We appreciate the support given by both institutions.

Furthermore, we are indebted to Prof. Dr. H. Engelhardt, Universität des Saarlandes, FRG, for grinding and sieving the glass particles and to Dr. H. Knauer, Berlin, FRG, for packing this material in such a way that comparison of the results from column 1 and 2 was possible.

References

[1] *L. R. Snyder, M. A. Stadalius, M. A. Quarry,* Anal. Chem., **55**, 1412A (1983).
[2] *J. P. Larmann, J. J. De Stefano, A.P. Goldberg, R. W. Stout, L. R. Snyder, M. A. Stadalius,* J. Chromatogr., **255**, 163 (1983).
[3] *S.-T. Lai, L. Sangermano, D. C. Locke,* J. Chromatogr., **312**, 313 (1984).
[4] *G. Glöckner,* Advances in Polymer Science, **79**, 159 (1986) (Springer-Verlag, Heidelberg, FRG).
[5] *G. Glöckner, J. H. M. van den Berg,* Chromatographia, **19**, 55 (1984).

Table III. Solvent composition at peak apex (volume percent of eluent component B)

Column	Poly(styrene-co-acrylonitrile) sample					Reference, remarks
	A	B	C	D	E	
LiChrosorb Si4000 RP 18, d_p 10 μm, 150 × 4.6 mm ID	58.1	66.8	74.1	80.7	91.2	5, mixture M2
Polygosil 60-5 C18, d_p 5 μm, 150 × 4.6 mm ID	57.0	66.5	74.0	80.7	90.4	5, M2
μ-Bondagel E-1000, d_p 10 μm, 300 × 4 mm ID	57.1	66.3	73.8	80.3	88.5	5, M2
Nucleosil 5 CN, d_p 5 μm, 150 × 4.6 mm ID	57.7	66.7	74.1	80.6	89.1 91.3	5, M2
Column no. 3 Polygosil 60-5, d_p 5 μm, 150 × 4.6 mm ID	57.2	66.3	73.8	80.3	91.1	5 & Fig. 5 of the present paper, M2
Column no. 4 Polygosil 60-5, d_p 5 μm, 55 × 4.6 mm ID	57.1	66.1	73.5	80.4	91.1	5 & Fig. 6 of the present paper, M2
Average from the porous packings:	57.4[a]	66.5[a]	73.9[a]	80.5[a]	90.4[a]	
Column no. 1 ground glass, d_p 10 μm, 60 × 4 mm ID	61.3[b]	69.2[b]	74.9[b]	78.8[b]	89.6[b]	Fig. 1, mixture M1
Column no. 2 Nucleosil 50, d_p 5 μm, 60 × 4 mm ID	60.8[b]	67.6[b]	71.5[b]	77.7[b]	88.8[b]	Fig. 1, M1
Open tube no. 5, SS316, 11,000 × 0.5 mm ID	58.6[a]	64.8[a]	75.1[a]	81.3[a]	90.1[a]	Fig. 3, M2

[a] THF with 10 % methanol added (v/v).
[b] 2 % methanol constant throughout the analysis.

[6] *D.W.Armstrong, K.H.Bui,* Anal. Chem., **54**, 706 (1982).
[7] *D. W. Armstrong, K. H. Bui, R. E. Boehm,* J. Liq. Chromatogr., **6**, 1 (1983).
[8] *G. Glöckner,* J. Chromatogr., **403**, 280 (1987).
[9] *G. Glöckner, H. Kroschwitz, Ch. Meissner,* Acta Polymerica, **33**, 614 (1982).
[10] *G. Glöckner, J. H. M. van den Berg, N. L. J. Meijerink, T. G. Scholte, R. Koningsveld,* Macromolecules, **17**, 962 (1984).
[11] *G. Glöckner, J. H. M. van den Berg,* J. Chromatogr., **352**, 511 (1986).
[12] *G. Glöckner, J. H. M. van den Berg,* J. Chromatogr., **384**, 135 (1987).
[13] *A. K. Taneja, S. Y. M. Lau, R. S. Hodges,* J. Chromatogr., **317**, 1 (1984).
[14] *S. M. J. Skinner, B. Grego, M. T. W. Hearn, G. C. Liggins,* J. Chromatogr., **308**, 111 (1984).
[15] *K. A. Smolenski, A. Fallon, N. Light,* J. Chromatogr., **287**, 29 (1984).
[16] *F. E. Regnier,* Science, **222**, 245 (1983).
[17] *G. Lindgren, B. Lundström, I. Källman, K.-A. Hansson,* J. Chromatogr., **296**, 83 (1984).
[18] *M. A. Quarry, M. A. Stadalius, T. H. Mourey, L. R. Snyder,* J. Chromatogr., **358**, 1 (1986).
[19] *R. M. Moore, R. W. Walters,* J. Chromatogr., **317**, 119 (1984).
[20] *G. Glöckner, M. Stickler, W. Wunderlich,* Fresenius Z. Anal. Chem., **328**, 76 (1987).
[21] *N. T. Miller, B. Freibush, B. L. Karger,* J. Chromatogr., **316**, 519 (1984).
[22] *G. Glöckner,* unpublished results.
[23] *K. K. Unger, G. Jilge, J. N. Kinkel, M. T. W. Hearn,* J. Chromatogr., **359**, 61 (1986).
[24] *G. Glöckner, P. Steijskal, P. Kratochvil,* In preparation.
[25] *G. Glöckner, A. Müller,* In preparation.

Received: June 28, 1987
Accepted: Aug. 10, 1987
F

HPLC of Biological Macromolecules: The First Decade

F. E. Regnier*

Department of Biochemistry, Purdue University, Lafayette, Indiana, 47907, USA

Key Words

Size exclusion
Ion-exchange
Hydrophobic interaction
Bioaffinity
Molecular structure
Histones
Proteins

Summary

During the past decade, HPLC has developed into a powerful new technique for the analysis of complex mixtures of biological macromolecules. Through the use of microparticulate supports of vastly improved mechanican strength, superior stationary phase chemistry, and advanced instrumentation, it is now possible to separate biological macromolecules more than 10 times faster and with greater resolution than in the classical SEC, IEC, HIC, bioaffinity, and hydroxyapetite chromatography columns. Additionally, the introduction of new separation modes such as RPC and metal chelate make it possible to carry out separations that were not possible with the classical gel-type media. It is anticipated that 1) expanded use of non-porous media, 2) development of new stationary phases for carbohydrates, 3) greater throughput and resolution in preparative separations, and 4) better understanding of retention mechanisms are a few of the areas of macromolecular separations in which advances can be expected in the next few years.

Introduction

The potential value of microparticulate chromatographic media was first recognized by A. J. P. Martin in 1941 [1] when he noted that the stagnant mobile phase mass transfer contribution to band-spreading was inverseley related to solute diffusivity and that the time required for mass transfer could be reduced with small particle sorbents. Martin pointed out that microparticulate column packings would be most valuable in the separation of macromolecules because their diffusion coefficients are so low. At that time methods for producing and packing macroporous, microparticulate media did not exist and high performance liquid chromatography did not emerge for another two decades.

Chromatography of proteins began in 1958 with the observation that proteins could be adsorbed on a bed of diethylaminoethyl (DEAE) derivatized cellulose and then differentially eluted with an ionic strength gradient [2]. This was followed closely by the development of carboxymethyl (CM) cellulose ion exchange sorbents [3] and dextran based size exclusion gels for the separation of both nucleic acids proteins [4]. The poor mechanical strength of these gel-type media made them unsuitable for HPLC.

A breakthrough came when Tsuji and Robertson found that porous microparticulate silica derivatized with alkyl silanes could be used in fractionating bacitracin [5]. Through the use of an acidic mobile phase containing an organic solvent, several structural forms of this small peptide antibiotic were resolved by a reversed phase chromatography (RPC) column in less than 30min. This was followed by reports that macroporous silica derivatized with hydrophilic organic polymers could be used in high performance size exclusion (SEC) [6] and ion exchange chromatography (IEC) [7] of proteins with almost quantitative recovery and retention of biological activity. These high performance media retained the selectivity and resolution of their soft-gel counterparts at 60 times greater mobile phase velocity. High performance bioaffinity media were subsequently prepared by attaching either antibodies or biomimetic ligands to the surface of rigid media [8]. These four early papers established that 1) macromolecules could be separated quickly with high resolution, 2) the pressure and turbulance generated in an HPLC column did not alter the biological activity of proteins, 3) high performance and gel-type columns have very similar selectivity when they have identical stationary phases, and 4) most of the separations achieved on gel-type sorbents could be accomplished at much higher speed and resolution with mechanically stable, high performance media. In the ensuring decade an avalanche of papers appeared describing both the preparation and use of high performance media in the separation of biological macromolecules. This review will focus on the essential elements of HPLC media for the separation of biological macromolecules, selection of mobile phases, and advances in biopolymer fractionation that have accrued by HPLC.

0009-5893/87 0241-11 $03.00/0

© 1987 Friedr. Vieweg & Sohn Verlagsgesellschaft mbH

Columns and Media

Supports

The development of microparticulate, macroporous silica supports [9] was a pivotal factor in the emergence of HPLC media for the separation of biological macromolecules. Although both controlled pore glass and silica were used in early HPLC columns for proteins, silica quickly became the support of choice because it was easy to derivatize and was commercially available in spherical particles ranging in size from 5 to 20μm and pore diameter from 100 to 1000 A. Organic resin based sorbents for HPLC developed much more slowly. Other than the polymethacrylate based Spheron media [10], the first organic resin based packings widely available commercially were the Pharmacia monobead materials [11]. Through the use of a charged hydrophilic surface layer on a macroporous polystyrene support, Pharmacia was able to prepare strong anion and cation exchange sorbents which showed none of the hydrophobic characteristics of the classical styrene-divinyl benzene ion exchange materials. Recent work has shown that organic resin and silica based sorbents of identical stationary phase, porosity, and particle size, are almost identical in chromatographic behavior [12].

Very small ($<3\mu$m) non-porous supports provide another advance in the fractionation of proteins [13]. In the past two years, there has been growing interest in these non-porous media because the absence of support pores eliminates the problem of stagnant mobile phase mass transfer. This in turn allows higher separation speed. Both ion exchange [14] and reversed phase separations [15] of 100μg protein samples have now been achieved in less than 60sec. with non-porous sorbents. Such high speed separations will probably be of greatest value in the process control environment and high throughput analytical laboratories. The disadvantages of very small particle diameter media are that they have a greater tendency to plug and are of low capacity.

Size Exclusion Media

Silica based media have been by far the most successful in size exclusion chromatography (SEC). This stems from the fact that silica based supports generally provide greater pore volume, and are less hydrophobic [16]. This allows the construction of SEC columns with a greater number of theoretical plates, greater peak capacity, and fewer hydrophobically induced deviations from ideal size exclusion behavior. Unfortunately, silica based SEC media have two limitations. The first is that columns are not stable with alkaline mobile phases and the second is that derivatization of the silica surface seldom sequesters all surface silanols [17]. These residual silanols function as exchangers of cations and either partially or totally adsorb basic proteins [18].

Before they may be used in SEC, porous silica supports must be derivatized with a hydrophilic organic phase. The glycerolpropyl silane (or "diol") phase [19] has been popular but suffers from poor chemical stability. Stabilization of the diol phase by first cladding the silica sorbent with zirconia greatly extends the lifetime of the organosilane bonded phase [20]. Although most commercial SEC columns are proprietary, it is likely that polymers such as polyvinyl alcohol are also used to create hydrophilic surface layers on silica. The motivation for using polymers would be to enhance the stability of the surface coating.

At the present there are several purely organic SEC media. Superose is an agarose based material from Pharmacia which shows little electrostatic interaction with proteins [21]. However, it does interact hydrophobically with some proteins above 0.5 M salt. Apparently hydrophobicity is introduced into Superose during crosslinking. Methacrylate based media are even more hydrophobic in addition to showing cation exchange properties [22]. The absence of a quantitatively evaluation of the hydrophobic and electrostatic properties of polyvinyl alcohol based SEC columns makes an assessment their utility impossible.

Ion Exchange Media

As noted above, there is little difference in the separation of biological macromolecules on silica in stationary phase composition, surface charge density, and physical properties. However, the method of preparing ion exchange media can vary greatly.

Occasionally, the properties of an ion exchange chromatography (IEC) sorbent are dictated by some physical of chemical property of the solute, as in the case of polynucleotides.

IEC sorbents for the separation of polynucleotides must be of greater than 500 A pore diameter to allow penetration of the larger members of this family without diffusion limitations [23]. A dimethylaminoethyl (DMAE) stationary phase coupled through siloxane bonding to the surface of 4000 A pore diameter microparticulate silica has proven very effective in the separation of polynucleotides. The fact that this sorbent is of low ligand density may also be an advantage.

Simple organosilanes have also been used in the preparation of ion exchange media for proteins on zirconyl clad silica sorbents [24]. As in the case of SEC media, the objective in zirconyl cladding is to stabilize both the stationary phase and sorbent matrix against erosion.

A second approach to matrix stabilization is the use of polymeric organic films on the support which are bonded to the surface by either covalent [25–26] or electrostatic coupling [27]. In the case of covalent bonding, active groups on either the organic polymer [25] or organosilane coupling agent [26] graft the polymer to the support at multiple sites. Electrostatically bonded stationary phases, in contrast, are prepared by adsorbing small positively charged polymers to the negatively charged silica surface and subsequently crosslinking them into a continuous film [27]. There is evidence that when these adsorbed films are tightly crosslinked they diminish the erosion of silica supports under basic conditions.

Ion exchanging stationary phases are attached to methacrylate based resins through ester bonds [28]. These materials are of much broader pH stability than silica but extended exposure to very strong acids or bases will cleave these esters. Acrylate supports could also be used as supports. Presumably the BioRad non-porous organic resins are based on an acrylate matrix to which polyethyleneimine has been attached with an amide linkage [29]. Such materials would be of good stability in the pH range from 2 to 12 but the amide linkages can also slowly hydrolyze under very acidic or basic conditions. The authors experience with the organic based ion exchange media from ToyaSoda would suggest that they are based on either an acrylate or methacrylate support. Unfortunately, the ToyaSoda resins are of proprietary composition. The Pharmacia monobead ion exchange media are based on a polystyrene-divinyl benzene matrix to which a hydrophilic surface coating has been added that masks the hydrophobic character of the aromatic support.

Variables such as pore diameter, loading capacity, and type of stationary phase must also be considered in the selection of ion exchange columns. Pore diameter is an indirect determinant of mass loadability [30]. Since more than 95% of the surface area of a porous sorbent is within the pore matrix, pores must be sufficiently large to give macromolecules access to the interior. A pore diameter of 300 to 500 A is optimum for proteins of 30 to 100kD [31] while materials of 800 to 1000 A pore diameter function well for proteins that exceed 100kD. The larger pore diameter materials have lower mass loadability with small proteins, but are very good in analytical columns because they show little resistance to mass transfer over a broad range of molecular weight. As noted above, non-porous media have the lowest capacity and lowest resistance to mass transfer.

The question of whether to choose a strong or weak ion exchange sorbent is not easily answered. Charge density on weak ion exchange media is variable and a function of stationary phase pK_a. The pK_a of some weak ion exchange sorbents can extend over more than 4pH units [27]. Since the degree of ionization of both the sorbent and protein change as a function of pH, it is more difficult to optimize separations on weak ion exchange media. The fact that strong ion exchange media retain almost constant charge density across a broad pH range is very useful in optimization because the only charge density variable is from the protein. However, ease of optimization has no relationship to selectivity. There are cases where the resolution of a weak ion exchange sorbent is superior to that of a strong ion exchange material based on selectivity [32]. Apparently, slight differences in ligand density and matrix hydrophobicity can make important contributions to selectivity in weak ion exchange media.

Reversed Phase Media

Alkyl silane derivatized silica media have been the overwhelming favorite for reversed phase chromatography of biological macromolecules although both silica and organic resins have been used. At least five variable must be considered in the selection of a silica based RPC column for polypeptide separations. First there is alkyl chain length. Longer alkyl chain lengths (C_8 to C_{18}) seem to be more effective with small peptides whereas shorter (C_4 to C_8) derivatives are prefered for large peptides and proteins [33]. Electrostatic interaction of amino groups with surface silanols is also a consideration in sorbent selection. Exhaustively silylated and end capped sorbents present the fewest problems, particularly when the polypeptide mixture contains very basic proteins. Pore diameter is another variable. When separating polypeptides of greater than 10 kD it is desirable to use 300 to 1000 A pore diameter materials to insure adequate mass transfer [33]. In the purely analytical mode, it is also acceptable to use non-porous media. It is interesting that silicas of the same particle size and pore diameter are not all equally suitable as supports for RPC of polypeptides. Very poor recovery of large hydrophobic cyanogen bromide cleavage fragments has been experienced from some silica supports [34]. Since manufacturers are aware of this problem, supports have been specially selected in commercial columns that are designated by the supplier for protein and peptide separations. The fifth variable is sorbent particle size. It is generally the practice in analytical separations to use particles of 5μm or less to achieve maximum resolution. In the case of preparative separations, 10 to 20μm media are often used because the resolution of 5μm sorbents decays quickly when they are overloaded.

Selection of columns for RPC of nucleic acids requires much less rigor than with polypeptides. Other than the obvious need for large pore diameter with large polynucleotides, there are few reports of media problems.

Macroporous polystyrene-divinylbenzene based RPC sorbents have also been used in protein separations [35]. One of their advantages is that they can be used at extremes of Ph. It remains to be determine how the selectivity of these aromatic matrices compares to the alkyl silane derivatized silica materials.

Hydrophobic Interaction Media

It was recognized during the development of gel-type media for bioaffinity chromatography that the hexamethylene spacer used to couple ligands to the support matrix was capable of interacting with proteins in the absence of a biomimetic ligand. Protein adsorption was shown to be due to weak interactions between external hydrophobic groups on the protein and the hexamethylene spacer of the chromatographic support [36]. This type of separation has come to be known as hydrophobic interaction chromatography (HIC) [37]. These weak hydrophobic interactions are enhanced by increasing the concentration of special salts that elevate mobile phase surface tension [38]. The most effective salts are of a high molal salting out coefficient, generally do not denature proteins at high ionic strength, and allow proteins to easily come back into solution when their ionic strength is decreased. These same characteristics are used in describing the ideal salt for salting proteins out of solution. There is in fact, considerable similarity between fractionation by ammonium sulfate precipitation and HIC.

Hydrophobic interactions are so strong on RPC sorbents that organic solvents must be used to elute nucleic acids and polypeptides. Alterations in the quaternary and tertiary structure of proteins which occur under these conditions are undesirable because it is difficult to renature proteins and regain their biological activity. In contrast, HIC media are of much lower surface hydrophobicity. Hydrophobic interactions between proteins and HIC sorbents are so weak that most proteins only adsorb at high concentrations of salt. Under these conditions the three-dimensional structure of most proteins is not irreversibly disturbed [39]. Subsequent elution in a descending ionic strength gradient is also sufficiently gentle that the biological activity of most proteins is maintained.

The weak hydrophobicity of HIC relative to RPC media is the result of either reducing alkyl ligand density or chain length. Hydrophobicity can be reduced even further by coupling alkyl chains to an underlying hydrophilic matrix. As in SEC and IEC columns, both silica and organic resins have been used as support matrices. Silica based HIC sorbents have been prepared by bonding the stationary phase through either a simple organosilane coupling agent or attachment to a hydrophilic polymer film on the silica surface. N-acyl [40] and alkoxy diethylene glycol [41] ligands which have been coupled to silica through a propyl silane linker are examples of simple organosilane bonding. In contrast, polymeric films are prepared by first bonding a hydrophilic organic polymer layer to the silica surface followed by either alkylation or acylation of the polymer [42]. Polyamide layers have been the most popular of these polymeric HIC media.

A variety of silica based HIC columns of gradually increasing hydrophobicity and pore diameter are commercially available. Guidelines for the selection of an HIC column are generally provided by manufacturers when they supply multiple HIC columns.

All of the organic resin based HIC materials are of proprietary composition. However, the fact that they have some anionic character would suggest that the supports are prepared from either acrylate or methacrylate monomers. Both polyether and phenyl stationary phases are available. The phenyl sorbent is the more hydrophobic of the two and should be used with very hydrophilic proteins that are not retained on the polyether columns.

Bioaffinity Media

One of the disadvantages of bioaffinity chromatography is that a different stationary phase must be used for almost every separation. This often means that columns must be prepared by the user. Although numerous procedures for coupling ligands to support materials have been published, the reticence of many chromatographers to become involved in bonding chemistry has slowed the progress of bioaffinity chromatography. The recent introduction of preactivated high performance columns that couple ligands upon contact has simplified column preparation. At present columns which have been activated with epoxy [43], N-hydroxysuccinimide [44], or diazonium salts [44] are commercially available. Other preactivated sorbents are in development and should be introduced in the next 12 months. Protein A and concanavalin A sorbents [44] are also available. Immobilized protein A binds to the F_c region of many antibodies and has been used in the fractionation of both monoclonal antibodies and immunoglobulin G subclasses. Protein A sorbents have also been used in antibody immobilization [45]. Subsequent to adsorption, the protein A-antibody complex is crosslinked with a protein crosslinking agent to permanently fix it to the support. This process covalently immobilizes antibodies with the antigen binding sites directed away from the sorbent surface.

Concanavalin A and a variety of other plant lectins adsorb molecules which contain specific carbohydrate groups [46]. For example, Concanavalin A columns adsorb gycopeptides, glycoproteins, and glycolipids which contain either glucose or glucose amine [47].

Metal Chelate Affinity Media

High performance metal chelate columns are generally prepared by coupling iminodiacetic acid to a silica support through a simple organosilane [48–49]. One synthetic route is to derivatize silica with glycidoxysilane and then add iminodiacetic acid to the oxirane [48]. The second route is to silylate the support with an organosilane which already contains the iminodiacetic groups [49]. Organic resins have also been used as supports for iminodiacetic acid [50]. The nature of the matrix and bonding chemistry is proprietary in the case of the organic resin. These columns must be loaded with the desired metal before use. Two types of elution protocol have been used in metal chelate-interaction chromatography (MCIC). In one protocol, adsorbed proteins were eluted with an ascending salt gradient. Retention is based primarily on the interaction of the metal chelate with amino acids in the protein in this case. Histidine and glycine act as competing ligands and reduce retention. Different selectivity is achieved when these columns are loaded with protein in concentrated ammonium sulfate and eluted with a descending salt gradient. Elution in this case is based more on hydrophobic interactions than chelation.

Mobile Phases

Many achievements in the separation of biological macromolecules are do as much to developments in mobile phase selection as advances in column technology.

Protein Solubilization

Limited solubility is often a problem in the chromatography of proteins. For example, some membrane and viral coat proteins are of such low solubility that they could not be fractionated by RPC before the observation that 5–60% formic acid greatly increased their solubility and recovery [51–52]. Although 60% formic acid is reported to slowly hydrolyze polypeptides at certain labile bonds, the addition of small quantities of organic solvent to formic acid greatly diminishes hydrolysis [53]. Even 0.1% trifluoroacetic acid increases the solubility of some proteins and peptides in RPC.

Protein solubility can also be a problem in IEC. Nonionic and zwitterionic detergents have been very effective in solubilizing proteins for IEC [54]. Six molar urea can also be an effective solubilizing and dissociating agent in protein systems which show a tendency to aggregate [55]. Even organic solvents such as ethylene glycol, alcholols, and ethyl acetate, have found application as solubilizing agents in IEC [56]. None of these agents seriously change retention in the ion exchange mode unless they alter protein structure.

Sodium dodecylsulfate (SDS) at 0.01% concentration is also an effective solubilizing agent which reduces the three-dimensional structure of non-disulfide crosslinked proteins to a random coil. Following reduction, even disulfide bridged polypeptides assume a random coil structure in SDS. This reagent is also widely used in SEC to reduce shape differences between species [57]. The very large amount of SDS that polypeptides adsorb in effect gives them all the same charge to mass ratio and precludes IEC. The presence of adsorbed SDS also presents problems in RPC. Guanidinum hydrochloride, ethylene glycol, urea, and organic acids have also been used a solubilizing agents in SEC [58].

Elevated column temperature can also be effective in increasing both solubility and resolution when thermolability is not a problem [59]. Thermolability presents a problem in IEC, SEC, and HIC where structural changes are often associated with loss of biological activity, resolution, and even recovery. In contrast, complete denaturation in RPC systems can be an advantage by eliminating the possibility of multiple comformational states which give multiple peaks.

Ion Exchange Chromatography

Control of selectivity is an important part of optimizing any separation. In ion exchange chromatography, both mobile phase pH and type of displacing ion influence selectivity. The fact that proteins vary widely in number of charged amino acids, ratio of charged amino acids, and charge distribution within the molecule means that both net charge and electrostatic potential at any point in the structure can vary widely among proteins. Based on these variables, it is possible that two proteins with very similar electrostatic properties at one pH will vary at another. This is the basis of pH optimization.

Polypeptides are generally retained on anion exchange sorbents above their pI and cation exchange sorbents below their pI [60]. To achieve any significant degree of retention, it is usually necessary to be at least one pH unit away from the pI. As mobile phase pH is moved further away from the pI, retention generally increases to a plateau 2–3 pH units away from the pI. Plots of retention versus pH are unique for most proteins. The problem in optimization is to find the pH at which these unique differences are maximum. Unless retention maps for all the components in the mixture are available, pH optimization will be achieved by trial-and-error.

Dramatic differences in selectivity have also been noted with different types of displacing ions [61]. Mobile phase salt can influence matrix hydrophobicity, protein hydration, protein structure, and double layer thickness, all of which play a role in ion exchange retention. The role of salts in ion exchange is very complex and does not have a fundamental explanation at present. It is disturbing that the ions which give maximum selectivity occassionally diminish recovery by destabilizing or altering protein structure. As in the case of pH, optimization is achieved by trial-and-error.

Hydrophobic Interaction Chromatography

Mobile phase salts and pH are equally important in determining HIC selectivity [62]. Retention behavior can be a function of the type of salt with some proteins [63]. When incremental changes in retention as a function of salt concentration are different there is the opportunity for optimization of selectivity. These differences in retention are either due to salt specific alterations of protein structure or differential hydration of the sorbent and protein surfaces. Bivalent metal ions are the most likely to change selectivity [64]. Unfortunately they are also most likely to destabilize protein structure. Salts such as ammonium and sodium sulfate have been shown to be very effective in HIC [65]. However, sodium sulfate precipitates in the pumps and column at less than 2 M, depending on ambiant temperature. Pump seal life is diminished with sodium sulfate, presumably because of salt precipitation on the pistons.

Retention of most proteins is minimal at their pI and maximum at acidic pH [66]. Changes in retention in the pH range from five to eight are generally due to the ionization of histidine residues [64]. It is even possible to determine the pK_a of a histidine in the contact surface area with pH retention mapping. Again, changes in retention increments as a function of pH varies between proteins and presents the opportunity for optimization. The specific pH where selectivity will be greatest is found by pH retention mapping.

Reversed Phase Chromatography

It has been found that mobile phase components such as acetonitrile, methanol, ethanol, propanol and isopropanol contribute little to selectivity in RPC proteins [67, 68]. Selection of an organic solvent for RPC of proteins is based more on solubility and viscosity [69]. When there is a solubility problem, isopropanol is generally used because it is a better solvent. When solubility is not a problem, solvent selection is based on minimizing mobile phase viscosity, i.e. maximizing resolution. Acetonitrile is the solvent of choice in this case.

Acidic and basic components of the mobile phase have a major impact on selectivity because they act both as ion pairing agents and suppress electrostatic interactions of polypeptides with RPC columns [70]. Mineral acids, such as phosphoric and perchloric acid, form hydrophilic ion pairs with amines and decrease retention in proportion to amine content [71]. In contrast, trifluoroacetic acid and heptafluorobutyric acid form hydrophobic ion pairs with amines which increase retention in proportion to the number of amino groups in the polypeptide [72]. Triethylamine phosphate is an interesting mobile phase additive because it forms ion pairs with both carboxyl and amino groups [73]. With this array of pairing agents it is apparent that retention and concomitantly, selectivity may be varied easily in RPC of polypeptides based on both their hydrophobic and electrostatic characteristics. In fact, purification of peptide hormones has been greatly simplified by using different pairing agents in sequential preparative separations on the same column [74].

It has been noted above that mobile phase acids suppress electrostatic interactions with sorbent silanols. The importance of this is that polypeptide peaks are much sharper and the recovery higher at acidic pH, particularly with basic proteins.

Bioaffinity Chromatography

Solute elution in bioaffinity is achieved either by specific methods which involve some type of specific displacement or by non-specific methods which alter the solute binding constant. The most familiar specific methods are substrate displacement of an enzyme from a pseudo-substrate ligand [75], displacement of an enzyme from a psuedo-cofactor ligand by a cofactor [76], antigen displacement of an antibody from an immobilized antigen [77], or displacement of a glycoprotein from an immobilized lection by a simple carbohydrate [78]. The great advantage of biospecific displacement is that polypeptides are usually eluted in their nature state. Unfortunately, these exquisitely selective displacement methods often suffer from poor displacement knetics. Complete solute displacement from concanavalin A can take up to 8 min [79].

Less common biospecific methods of elution are displacement by inhibitors which compete with the biospecific ligand for the active site of the protein and desorption with allosteric effectors [80]. The natural function of an allosteric effector is to control the biological activity of a protein by altering it's structure at the active site. Initiation of elution from a bioaffinity column is the result of the effector diminishing the affinity of the adsorbed protein for the immobilized ligand. Desorption kinetics could also be a problem with these biospecific elution methods. Chemical cleavage of the ligand-support complex is another specific elution method [81]. Although not biospecific, it is based on the cleavage of a disulfide bond which couples the ligand to the sorbent.

The fact that desorption kinetics may be poor in the specific displacement methods is really not as serious as it might seem. Adsorption specificity is often so great that little additional fractionation is achieved by selective desorption. For this reason, multiple non-specific methods have been applied which alter the affinity of the polypeptide for the sorbent. A common non-specific elution method is to use a mobile phase pH which is four to five units away from physiological conditions [82]. Under these conditions there is a sufficient change in protein structure and concomitantly binding affinity that elution is easily achieved. Acidic conditions are more commonly used but alkaline conditions can also be effective. Separations have been achieved in minutes using pH desorption [83]. This indicates that the rate at which a proteins can be denatured and eluted from an affinity column can be faster than specific displacement. When refolding is easily achieved, this method is very effective. In those cases where the protein is renatured with difficulty, the method is unsuitable.

Ethylene glycol, urea, thiocyanate, and high concentrations of salt have all been used to non-specifically elute proteins from bioaffinity columns [84]. Each of these reagents is effect in specific cases where altering some combination of electrostatic and van der Waals forces diminishes interactions in the ligand-protein complex sufficiently to cause elution.

Molecular Structure

One of the most distinguishing features of biological macromolecules is their structural complexity. Based on their primary structure, biopolymers assume a unique three dimensional structure which is maintained by a combination of electrostatic, hydrophobic, and hydrogen bonds. This is particularly significant because these are the same forces by which biological macromolecules are adsorbed to chromatographic sorbents. This means that the internal forces in the polymer which maintain it's three dimensional structure are in competition with forces at the surface of the column pulling the molecule down against the surface. When forces at the sorbent surface are stronger than the internal forces maintaining molecular structure, a biopoymer can denature. Through judicious selction of both the sorbent and non-destabilizing mobile phases this problem can be avoided.

Evidence is accumulating that chromatographic retention is strongly influenced by the three-dimensional structure of biological macromolecules [85]. Early work on peptides of less than 20 residues showed that chromatographic retention in RPC columns could be predicted from amino acid composition [86]. This contrasts with the finding in larger peptides were there is little relationship between amino acid composition and chromatographic retention [87]. These finding are interpreted to mean that formation of three-dimensional structure in larger peptides precludes simultaneous contact of all residues with the sorbent surface [88]. Similar behavior has been reported with oligonucleotides of greater than 10–15 residues which have accumulated sufficient three-dimensional structure to sterically limit adsorption [89]. When complex three-dimensional structures does exist, as in the case of proteins, it has been found that chromatographic retention is determined by a relatively small number of groups which can be localized in a defined region on the polypeptide surface [90–92].

Some understanding of molecular retention at surfaces may be gained by comparing solute dimensions to the distance that attractive forces extend into solution from the sorbent surface. Biological macromolecules are often 20 A or more in diameter whereas forces extending from sorbent surfaces become very weak beyond 5 A. This means that only a fraction of the residues in a semirigid macromolecule can simultaneously experience adsorptive forces. Furthermore, amino acid distribution at the surface of a protein is often assymetric. When a disproportionate number of the amino acids involved in the retention process are accumulated in one portion of the protein surface, that region can dominate chromatographic retention.

It has been observed in all of the surface mediated separation modes that conformers of the same macromolecule can give different chromatographic retention [93–95]. There is even evidence that the amino acid composition in the contact region between these conformers and the sorbent surface is different [96]. This is very important because the conformation of a protein is environmentally dependent and conformational transformations can be promoted in a column. Both the rate of conformer transformation and the ratio of conformers has been shown to be column and mobile phase specific in RPC [97]. Organic solvent components of the mobile phase, alkyl residues on the column and the very acidic mobile phases used in RPC of proteins act in concert to alter the quaternary and tertiary structure of proteins [98]. When the rate of conformer interconversion approaches elution time, it is possible to observe the various conformers and calculate the rate of their interconversion on the column [99].

Advances in Biopolymer Separations

There is considerable similarity between high performance columns and the older gel-type columns in both retention mechanism and selectivity. However, there are also large differences. Superior mechanical strength and a wider variety of stationary phases enable high performance media to achieve separations that are not possible on the conventional gel-type columns. Some of these advances will be discussed below.

Resolution of Peptides

HPLC has made a unique contribution to protein chemistry in the resolution of peptides derived from polypeptide fragmentation, solid phase synthesis, and natural sources. Peptide mapping is widely used in the determination of product purity by both biotechnology firms and regulatory agencies. However, peptide mapping has limits. Tryptic digests of large polypeptides are so complex that RPC columns can not resolve all of the fragments [100]. Two-dimensional chromatographic systems for peptide mapping may be a solution to this problem. IEC can be used in one dimension and RPC in the other. The problem with 2-dimensional chromatography is that it is labor intensive. This problem has recently been addressed by the construction of an automated tandem HPLC system for the separation of very complex peptide mixtures [101]. The peptide mixture was separated in the first dimension on an IEC column and effluent fractions transferred directly to an RPC column for separation in the second dimension. Stepwise gradient elution of the ion exchange column, eluent transfer, gradient elution of the reversed phase column, and generation of 2-dimensional maps were all under computer control.

Histones

This family of small basic proteins is found in nature associated with the DNA of eucaryotic cells. The role of histones is to assist in maintaining the structure of nucleosomes. Histones range in molecular weight from 11 to slightly over 20 kD and contain approximately 25% basic amino acids. The very basic character of these proteins seriously diminishes resolution and recovery on any column showing anionic character [102]. Effective RPC of histones is only seen when columns are end-capped and eluted with an acidic mobile phase such as 0.1% TFA. It is no suprise that there are major differences in the utility of various commercial columns [103]. On a given support, the C_{18} bonded phase is the most suitable although C_8 and CN columns give reasonable results. Through column switching, histones of whole *Drosophila* nuclei were separated into five fractions [104]. Purification of histones will allow their structure determination.

Ribosomal Proteins

Ribosomes serve as the site where messenger RNA, ribosomal RNA, transfer RNA's and some 50–60 proteins come together to carry out polypeptide synthesis in cells. The *C. coli* microbial ribosome is composed of two parts, a smaller 30S component carrying 21 proteins and a larger 50S component with 33 associated proteins. Both the fractionation and reconstitution of ribosomes is an important endeavor in determining quantitatively how the system is constituted and the mechanism by which proteins are synthesized. Fractionation of ribosomal proteins may be achieved on any of the macroporous RPC columns which have been designed for protein separations [105–107]. Alkyl chain length is not critical as critical as the mobile phase. TFA is the most common mobile phase pairing agent. Isopropanol is the organic solvent of choice because it gives higher recoveries and allows less protein complex formation than acetonitrile. Four of the 21 proteins from the microbial 30S subunit have been purified to homogeneity by RPC while an additional 15 were purified to a high degree [108]. Twenty three of the 33 proteins from the 50S subunit were purified [109]. Recovery ranged from 27 to 91% with the average being 70%.

Cation exchange chromatography has also been effect in the fractionation of ribosomal proteins when 5M urea is used to dissociate the components of the system. Both weak carboxymethyl [110] and strong sulfonylpropyl columns [111] resolved, at least partially, 18 of the 21 proteins from the 30S microbial subunit with an average recovery of 90%. In the case of the 50S subunit, 19 of 32 proteins were partially or totally purified.

Membrane Proteins

Proteins of cellular membranes are of three types; peripheral membrane proteins which are adsorbed at the internal or external surface of the membrane, transmembrane proteins which span the membrane and are exposed on either side, and integral membrane proteins which are embedded in the lipid of the membrane. Peripheral membrane proteins are generally released from the membrane with salt or EDTA and are soluble in aqueous mobile phases. Chromatography of the peripheral membrane proteins is similar to that of most cytosolic proteins. In contrast, transmembrane and integral membrane proteins are much more difficult to chromatograph.

Membrane disruption is required as a prerequisite for solubilizing transmembrane and integral membrane proteins because at least a portion of their structure is embedded with the membrane. In addition, those portions of membrane proteins embedded within the membrane are generally very hydrophobic and associated with membrane lipids. Additives such as sodium dodecyl sulfate (SDS), guanidinium hydrochloride, and non-ionic detergents have been effective in both disrupting membranes and solubilizing membrane proteins. The only problem with the use of solubilizing agents is that they occassionally preclude some types of chromatography.

Most solubilizing agents may be used in SEC as noted above [57, 58]. However, SEC is of such limited resolving power that it is only used as an analytical tool in monitoring extraction optimization or purification by some other method. IEC and RPC are much greater utility.

IEC of integral membrane proteins is only possible when an additive such as the zwitterionic CHAPS or a non-ionic detergent is used to maintain solubility [112]. Polyethylene glycol alkyl ethers of varying alkyl chain length and number of glycol residues [113] and n-octyl-glucopyranoside [114] are some of the non-ionic detergents that have been effective. Unfortunately, the optimum additive in terms of both resolution and solubilizing power is protein specific. This means that additive selection is a trial-and-error process.

The very hydrophobic character of membrane proteins also presents a problem in RPC. Recovery of membrane proteins from RPC columns can be much lower than with water soluble proteins. This problem has partially been overcome with the use of 5–60% formic acid in the mobile phase [115, 116]. Bacteriorhodopsin, cytochrome b_5 and cytochrome b_5 reductase are several microbial membrane proteins which could only be chrromatographed with formic acid [115]. Poliovirus coat proteins are another example [116]. The principle limitation of formic acid is that it will slowly cleave the alkyl bonded phase from the support.

The separation of human plasma membrane proteins of cultured human fibroblasts has been achieved by affinity chromatography on microparticulate silica derivatized with an affinity ligand [117]. Both Procion Orange and mannan columns successfully retained and released plasma membrane proteins as determined by SDS-PAGE.

Cereal Proteins

A large portion of the proteins consumed in cereals are of limited water solubility. This may be attributed to their relatively high content of hydrophobic amino acids, extensive intermolecular disulfide bridging, and hydrogen bonding. Through the use of extremes in pH, detergents, denaturants, reducing agents and alkylating agents, many of these proteins can be solubilized. Chromatographic analyses of endosperm proteins are providing cereal chemists and geneticists with a new set of markers for assessing functional and nutritional quality in cereal products and genetically improving cereal producing plants. At the present time, RPC has been applied to the identification of wheat varieties [118], prediction of bread quality [119], genetic studies of wheat [120], and analysis of corn proteins [121].

RPC is by far the most successful of the HPLC modes for the separation of cereal proteins [122]. Through the use of TFA, column temperatures ranging up to 70°C, and high flow rates it is possible to resolve 36 of the 46 low molecular gliadin components seen by two-dimensional gel electrophoresis. The water soluble albumins and globulins have been successfully examined by high performance IEC [123].

Hemoglobins

There is great interest in hemoglobins because of their association with disease states in humans. Structural variants of hemoglobin produced both by mutation and post-synthetic chemical modification either cause or reflect serious health problems. Hemoglobin variants have been determine chromatographically in three ways; direct separation and identification of the intact protein, resolution and identification of the globin chains, and analysis of globin chain tryptic digests. Since the analysis of peptide fragments has been discussed above, the discussion here will be limited to the separation in intact proteins.

It is not suprising that IEC is very effective in the resolution of variant hemoglobins. Most of the known variants were identified by either IEC or electrophoresis and are known to be the result of either eliminating a charge, adding a charge, or switching the sign of a charged group in the hemoglobin through mutations. With high performance cation exchange chromatography alone it is possible to differentiate between normal individuals and those that have hemoglobin Bart's sickle cell trait, sickle cell disease, hemoglobin E trait, hemoglobin D Los Angeles disease, sickle cell hemoglobin D disease, hemoglobin C trait, hemoglobin C disease, hemoglobin G Philadelphia disease, hemoglobin Winnipeg disease, hemoglobin Sealy disease, and sickle cell-hemoglobin G Philadelphia disease [124]. Anion exchange chromatography has also been widely used in the separation of variant hemoglobins [125–127] and is comparable to cation exchange chromatography in separation speed, recovery, ease of sample manipulation and column lifetime. However, cation ion exchange chromatography seems to discriminates between more variant hemoglobins.

Hemoglobin variants can also be formed in the red blood cell during it's 120 day life in the circulatory system. Amino groups in hemoglobin are slowly glycosylated by serum glucose to produce several glycated hemoglobins; one of the more abundant being HbA_{1c}. Since the concentration of AbA_{1c} is proportional to the average serum glucose level during the life of the red blood cell, it is useful in monitoring glucose regulation in patients under treatment for diabetes. Cation exchange chromatography is by far the most suitable for HbA_{1c}. HbA_{1c} can be determined chromatographically in the presence of HbF, HbA_{1a}, HbA_{1b} and HbA_2 with a cycle time of 15 min, i.e. 4 samples/hr [128].

Immunoglobulins

High performance size exclusion, anion exchange, cation exchange, hydrophobic interaction, hydroxyapatite, protein-A affinity, and dye columns have all been used in the fractionation of immunoglobulins. The five major classes of antibodies of interest today are immunoglobulin A (IgA), immunoglobulin D (IgD), immunoglobulin E (IgE), immunoglobulin G (IgG), and immunoglobulin M (IgM).

SEC has been used in three ways in the purification and characterization of immunoglobulins. The first is in the fractionation of the immunoglobulins themselves [129]. The five major immunoglobulin classes are separated into three fractions by SEC. IgM (950 kD) elutes first, followed next by IgA (300 kD), and finally a mixture of the other three immunoglobulins. The second major used of SEC is for the removal of serum albumin and transferrin in the purification of IgG [130]. It is very difficult to remove these two proteins from some IgG subclasses by IEC. The third major use for SEC is in the fractionation of immunoglobulin cleavage fragments [131]. Reduction of IgG with mercaptoethanol in the presence of 6 M urea produces heavy and light chains which differ three fold in molecular weight. Resolution by size is simple and quick. The F_{ab} and F_c fragments produced by papain cleavage of IgG may also be resolved by SEC.

IEC has been far more widely used in immunoglobulin fractionation. Monoclonal antibodies which have been subjected to an initial ammonium sulfate precipitation are purified to near homogeneity in a single pass through a high performance anion exchange column [132]. Even the salt precipitation step can be eliminated by a combination of either anion exchange and cation exchange chromatography [133] or anion exchange and hydrophobic interaction chromatography [134]. Partial fractionation of the IgG subclasses has also been achieve by anion exchange chromatography [135–136].

Protein A affinity chromatography is the second most widely used technique for the purification of IgG. Protein-A is known to bind to the F_c region of a variety of antibodies [137]. Protein-A columns separate both IgG subclasses and many monoclonal antibodies when eluted with a pH gradient ranging from 8 to 2 [138]. The principal limitation of protein-A columns are that they do not bind all antibodies.

Hydroxyapatite columns have been used in the purification of antibodies where they generally give greater than 75% recovery of antibodies [139]. The selectivity of hydroxyapatite is uniquely different than any other type of column. The disadvantage of these columns is that they have a much shorter life than other sorbents.

HIC and dye ligand columns have seen relatively little use in the fractionation of immunoglobulins. HIC works well and has been a valuable supplement to IEC in antibody purification [132]. When HIC has been used successfully in more cases as the primary purification technique it will be easier to assess it's true utility in antibody fractionation. Dye ligand columns are used indirectly in antibody purification, i.e. they adsorb impurities such as serum albumin [132]. Sorbents used in this way can be very useful but must be used in conjunction with other columns to produce antibodies of high purity.

Lipoproteins

HPLC has been used more in the examination of plasma lipoproteins than any other group of lipoproteins. Plasma lipoproteins are classified according to their density and composed of very low density lipoproteins (VLDL), low density lipoproteins (LDL), and high density lipoproteins (HLP). In addition to lipoproteins, plasma contains chylomicrons.

SEC is the only high performance chromatographic technique that has been applied to plasma lipoproteins. The molecular weight range of these lipoproteins is sufficiently wide that tandem SEC columns of different pore diameter provide optimum resolution of the mixture [140–141]. A three column set composed of G5000PW+G3000SW+G3000SW columns from ToyaSoda resolve the plasma lipoproteins into three fractions. Chylomicrons and VLDL elute first as a mixture followed by LDL in the second peak and HDL_2 and HDL_3 in a partially resolved third peak. Although resolution is incomplete, quantitative data obtained from this separation has clinical significance. The separation of apolipoproteins by SEC and IEC has also proven to be effective [142–144].

References

[1] *A. J. P. Martin, R. L. M. Synge*, Biochem. J. **35**, 1358 (1941).
[2] *H. A. Sober, E. A. Peterson*, J. Am. Chem. Soc. **76**, 1711 (1954).
[3] *E. A. Peterson*, "Cellulosic Ion-Exchangers", Amsterdam (1970).
[4] *J. Porath, P. Flodin*, Nature, **183**, 1657 (1959).
[5] *K. Tsuji, J. H. Robinson*, J. Chromatogr. **112**, 663 (1976).
[6] *F. E. Regnier, R. Noel*, J. Chromatogr. Sci. **14**, 316 (1976).
[7] *S. H. Chang, K. M. Gooding, F. E. Regnier*, J. Chromatogr. **125**, 103 (1976).
[8] *S. Ohlson, L. Hansson, P. O. Larsson, K. Mosbach*, FEBS Lett. **93**, 5 (1978).
[9] *K. Unger, J. Schick-Kalb, K.-F. Krebs*, J. Chromatogr. **83**, 5 (1973).
[10] *O. Mikes, P. Strop, J. Zbrozek, J. Coupek*, J. Chromatogr. **119**, 339 (1976).
[11] *J. Richie*, Amer. Lab. Oct. 104 (1982).
[12] *M. A. Rounds, W. D. Rounds, F. E. Regnier*, J. Chromatogr. **397**, 25 (1987).
[13] *K. K. Unger, G. Jilge J. N. Kinkel, M. T. W. Hearn*, J. Chromatogr. **359**, 61 (1986).
[14] *M. A. Rounds, F. E. Regnier*, J. Chromatogr. In press.
[15] *G. Jilge, R. Janzen, H. Giesche, K. K. Unger, J. N. Kinkel, M. T. W. Hearn*, J. Chromatogr. **397**, 71 (1987).
[16] *E. Pfannkoch, K. C. Lu, F. E. Regnier, H. Barth*, J. Chromatogr. **18**, 430 (1980).
[17] *P. Roumeliotis, K. K. Unger*, J. Chromatogr. **149**, 211 (1978).
[18] *H. Engelhardt, D. Mathes*, J. Chromatogr. **142**, 311 (1977).
[19] *F. E. Regnier*, U.S. Patent, 3,983,299 (1976).
[20] *R. W. Stout J. J. DeStefano*, J. Chromatogr. **326**, 63 (1985).
[21] *L. Hagel, T. Andersson*, J. Chromatogr. **285**, 295 (1984).
[22] *O. Mikes, P. Strop, J. Sedlachova*, J. Chromatogr. **148**, 237 (1978).
[23] *M. Colpan, D. Riesner*, J. Chromatogr. **296**, 339 (1984).
[24] *R. W. Stout, S. I. Sivakoff, R. D. Ricker, H. C. Palmer, M. A. Jackson, T. J. Odiorne*, J. Chromatogr. **352**, 381 (1986).
[25] *S. H. Chang R. Noel, F. E. Regnier*, Anal. Chem. **48**, 1839 (1976).
[26] Japanese Patent, 80 05, 941 (1980).
[27] *A. J. Alpert, F. E. Regnier*, J. Chromatogr. **185**, 375 (1979).
[28] *O. Mikes, P. Strop, J. Zbrozek, J. Coupek*, J. Chromatogr. **180**, 17 (1979).
[29] *D. J. Burke, J. K. Duncan, L. C. Dunn, L. Cummings, C. J. Siebert, G. S. Ott*, J. Chromatogr. **353**, 425 (1986).

[30] *F. E. Regnier, S. H. Chang, K. M. Gooding*, "Contemporary Topics in Analytical and Clinical Chemistry", Plenum Press (1977).

[31] *M. A. Rounds, W. Kopaciewicz, F. E. Regnier*, J. Chromatogr. **362**, 187 (1986).

[32] *W. Kopaciewicz, F. E. Regnier*, Anal. Biochem. **133**, 251 (1983).

[33] *R. V. Lewis, A. Fallon, S. Stein, K. D. Gibson, S. Udenfriend*, Anal. Biochem. **104**, 153 (1981).

[34] *J. Pearson, W. C. Mahoney, M. A. Hermodson, F. E. Regnier*, J. Chromatogr. **207**, 325 (1981).

[35] *K. A. Tweeten, T. N. Tweeten*, J. Chromatogr. **359**, 111 (1986).

[36] *S. Shaltiel, Z. Er-el*, Proc. Natl. Acad. Sci., USA. **70**, 778 (1973).

[37] *S. Hjerten*, J. Chromatogr. **87**, 325 (1973).

[38] *W. Melander, C. Horvath*, Arch. Biochem Biophys. **183**, 200 (1977).

[39] *C. Tanford*, "The Hydrophobic Effect", John Wiley, New York (1973).

[40] *H. Engelhardt, D. Mathes*, J. Chromatogr. **142**, 311 (1977).

[41] *K. Benedek, S. Dong, B. L. Karger*, J. Chromatogr. **317**, 227 (1984).

[42] *A. J. Alpert*, J. Chromatogr. **359**, 85 (1986).

[43] Beckman Instruments, Berkeley, California. "Epoxy" High Performance Affinity Column.

[44] Pierce Chemical Company, Rockford, Illinois. N-hydroxy Succinimide Affinity Column.

[45] *T. M. Phillips N. S. More, W. D. Queen, A. M. Thompson*, J. Chromatogr. **327**, 213 (1985).

[46] *C. A. K. Borrebaeck, J. Soares, B. Mattiasson*, J. Chromatogr. **284**, 187 (1984).

[47] *A. J. Muller, P. W. Carr*, J. Chromatogr. **294**, 235 (1984).

[48] *Z. Rassi C. Horvath*, J. Chromatogr. **359**, 241 (1986).

[49] *L. Fanou-Ayi, M. Vijayalakshmi*, Ann. N.Y. Acad. Sci. USA. **413**, 300 (1983).

[50] *E. S. Hemdan, J. Porath*, J. Chromatogr. **323**, 255 (1985).

[51] *H. G. Khorana, G. E. Gerber, W. C. Herlihy, R. J. Anderegg, C. P. Gray, K. Hibei, K. Biemann*, Proc. Natl. Acad. Sci. USA, **76**, 5046 (1979).

[52] *Y. Takagaki, G. E. Gerber, K. Nihei, H. G. Khorana*, B. Biol. Chem. **255**, 1536 (1980).

[53] *J. Heukeshoven, R. Dernick*, J. Chromatogr. **252**, 241 (1982).

[54] *P. Karsnas, J. M. Lopez, T. Kristiansen*, J. Chromatogr. **266**, 643 (1983).

[55] *Y. Kato, K. Komiya, H. Sasaki, T. Hashimoto*, J. Chromatogr. **193**, 29 (1980).

[56] *N. E. Tandy, R. A. Dilley, F. E. Regnier*, J. Chromatogr. **266**, 643 (1983).

[57] *Y. Kato, K. Komiya, H. Sasaki, T. Hashimoto*, J. Chromatogr. **193**, 458 (1980).

[58] *R. Pabst, T. Nawroth, K. Dose*, J. Chromatogr. **285**, 333 (1984).

[59] *J. A. Bietz, L. A. Cobb*, Cereal Foods World, **29**, 506 (1984).

[60] *W. Kopaciewicz, M. A. Rounds, J. Fausnaugh, F. E. Regnier*, J. Chromatogr. **266**, 3 (1983).

[61] *W. Kopaciewicz, F. E. Regnier*, Anal. Biochem. **133**, 251 (1983).

[62] *S. Hierten, K. Yao, K. O. Eriksson, B. Johansson*, J. Chromatogr. **359**, 99 (1986).

[63] *Z. El Rassi, C. Horvath*, Chromatographia, **19**, 9 (1985).

[64] *J. Fausnaugh, F. E. Regnier*, J. Chromatogr. **359**, 131 (1986).

[65] *S. M. Hyder, N. Sato, J. L. Wittliff*, J. Chromatogr. **397**, 251 (1987).

[66] *H. Englehardt, U. Schonn*, J. Liq. Chromatogr. **9**, 3225 (1986).

[67] *M. J. O'Hare, E. C. Nice*, J. Chromatogr. **171**, 209 (1979).

[68] *S. D. Powers, M. A. Lochrie, R. O. Poyton*, J. Chromatogr. **266**, 585 (1983).

[69] *M. Rubenstein*, Anal. Biochem. **98**, 1 (1979).

[70] *M. E. F. Biemond, W. A. Sipman, J. Olivie*, J. Liq. Chromatogr. **2**, 1407 (1979).

[71] *M. T. W. Hearn, W. S. Hancock*, TIBS, **4**, 58 (1979).

[72] *H. P. J. Bennett, C. A. Browne, S. Soloman*, J. Liq. Chromatogr. **3**, 1353 (1980).

[73] *J. Riviers*, J. Liq. Chromatogr. **1**, 343 (1978).

[74] *J. Riviers, R. Burgus*, J. Chromatogr. Sci. **10**, 147 (1979).

[75] *G. S. J. Rao, M. S. Savithri, S. Seethalakshmi, N. A. Rao*, Anal. Biochem. **95**, 401 (1979).

[76] *Y. D. Clonis, M. J. Goldfinch, C. R. Lowe*, Biochem. J. **197**, 203 (1981).

[77] *C. J. van Oss, D. R. Abolsom, A. W. Neumann, W. Zingg*, Biochim. Biophys. Acta, **670**, 64 (1981).

[78] *D. Josic, W. Hofmann, R. Habermann, A. Becker, W. Reutter*, J. Chromatogr. **397**, 39 (1987).

[79] *A. J. Muller, P. W. Carr*, J. Chromatogr. **284**, 33 (1984).

[80] *R. K. Sharma, S. W. Tam, D. M. Waisman, J. H. Wang*, J. Biol. Chem. **255**, 11102 (1980).

[81] *P. Singh, S. D. Lewis, J. A. Shafer*, Arch. Biochem. Biophys. **203**, 776 (1980).

[82] *K. Yamamoto, L. J. DeGroot*, J. Biochem. (Tokoyo), **91**, 775 (1982).

[83] *R. W. Walters*, J. Chromatogr. **249**, 19 (1982).

[84] *D. R. Absolom*, Sep. Purif. Methods, **10**, 239 (1981).

[85] *R. A. Houghten, J. M. Ostresh*, Biochromatogr. **1**, 437 (1987).

[86] *J. Meek, Z. L. Rossetti*, J. Chromatogr. **211**, 15 (1981).

[87] *M. Kunitani, D. Johnson, L. R. Snyder*, J. Chromatogr. **371**, 313 (1986).

[88] *F. E. Regnier*, Science, **238**, 319 (1987).

[89] *R. Drager, F. E. Regnier*, J. Chromatogr. **359**, 147 (1986).

[90] *R. Drager, F. E. Regnier*, J. Chromatogr. In press.

[91] *J. L. Fausnaugh, F. E. Regnier*, J. Chromatogr. **359**, 131 (1986).

[92] *M. T. W. Hearn, M. I. Aguilar*, J. Chromatogr. **397**, 47 (1987).

[93] *M. T. W. Hearn, A. N. Hodder, M.-I. Aguilar*, J. Chromatogr. **327**, 47 (1985).

[94] *S. A. Cohen, K. Benedek, Y. Tapuhi, J. C. Ford, B. L. Karger*, Anal. Biochem. **144**, 275 (1985).

[95] *X. M. Lu, K. Benedek, B. L. Karger*, J. Chromatogr. **359**, 19 (1986).

[96] *X. M. Lu, A. Figueroa, B. L. Karger*, J. Chromatogr. In press.

[97] *E. S. Parente, D. B. Wetalufer*, J. Chromatogr. **314**, 327 (1984).

[98] *S. A. Cohen, Y. Tapuhi, J. C. Ford, B. L. Karger*, Anal. Biochem. **56**, 217 (1984).

[99] *A. Light, J. N. Higaki*, Biochemistry, **26**, 5556 (1987).

[100] *N. Takahashi, N. Ishioka, Y. Takahashi, F. W. Putnam*, J. Chromatogr. **326**, 407 (1985).

[101] *N. Takahashi, Y. Takahashi, N. Ishioka, B. S. Blumberg, F. W. Putnam*, J. Chromatogr. **359**, 181 (1986).

[102] *L. R. Gurley, D. A. Prentice, J. G. Valdez, W. D. Spall*, J. Chromatogr. **266**, 609 (1983).

[103] *L. R. Gurley, J. A. D'Anna, M. Blumenfeld, J. G. Valdez, R. J. Sebring, P. R. Donahue, D. A. Prentice, W. D. Spall*, J. Chromatogr. **297**, 147 (1984).

[104] *J. A. D'Anna, M. M. Thayer, R. A. Tobey, L. R. Gurley*, Biochemistry **24**, 2005 (1985).

[105] *A. R. Kerlavage, C. J. Weitzmann, T. Hasan, B. S. Cooperman*, J. Chromatogr. **266**, 225 (1983).

[106] *N. P. Nick. R. E. H. Wettenhal, M. T. Hearn, F. J. Morgan*, Anal. Biochem. **148**, 93 (1985).

[107] *A. R. Kerlavage, L. Kahan, B. S. Cooperman*, Anal. Biochem. **123**, 342 (1982).

[108] *R. M. Kamp, A. Bosserhoff, D. Kemp, B. W. Liebold*, J. Chromatogr. **317**, 181 (1984).

[109] *A. R. Kerlavage, C. J. Weitzman, B. S. Cooperman*, J. Chromatogr. **317**, 201 (1984).

[110] *P. J. Flanion, J. P. Scheiber*, Anal. Biochem. **147**, 458 (1985).

[111] *M. Capel, D. Datta, C. R. Nierras, G. R. Craven*, Anal. Biochem. **158**, 179 (1986).

[112] *D. Josic, W. Hofmann, B. Wieland, R. Nuck, W. Reutter*, J. Chromatogr. **359**, 315 (1986).

[113] *H. Ikigai, R. Nakae, Y. Kato*, J. Chromatogr. **322**, 212 (1985).

[114] *P. Lundahl, E. Greijer, H. Lindblom, L. G. Fagerstam*, J. Chromatogr. **297**, 129 (1984).

[115] *Y. Takagaki, G. E. Gerber, K. Nihei, H. G. Khorana*, J. Biol. Chem. **255**, 1536 (1980).

[116] *J. Heukeshoven, R. Dernick*, J. Chromatogr. **326**, 91 (1985).

[117] *J. N. Kinkel, B. Anspack, K. K. Unger, R. Wieser, G. Brunner*, J. Chromatogr. **297**, 167 (1984).

[118] *T. Burnouf, J. A. Bietz*, J. Cereal Sci. **2**, 3 (1984).

[119] *F. R. Heubner, J. A. Bietz*, Cereal Chem. **61**, 544 (1984).

[120] *T. Burnouf, J. A. Bietz*, J. Chromatogr. **299**, 185 (1984).

[121] *B. A. Marchylo, J. F. Kruger*, Cereal Chem. **61**, 295 (1984).

[122] *J. A. Bietz*, Cereal Chem. **62**, 201 (1985).

[123] *J. A. Bietz, L. A. Cobb*, Cereal Foods World **29**, 506 (1984).

[124] *C. N. Ou, G. J. Buffone, G. L. Reimer, A. J. Alpert*, J. Chromatogr. **266**, 197 (1983).
[125] *M. B. Gardiner, J. Carver, B. Abraham, J. B. Wilson, T. H. J. Huisman*, Hemoglobin. **6**, 1 (1982).
[126] *S. M. Hanash, D. N. Shapiro*, Hemoglobin. **5**, 165 (1981).
[127] *K. M. Gooding, K. C. Lu, F. E. Regnier*, J. Chromatogr. **164**, 506 (1979).
[128] *U. H. Stenman, K. Pesonen, K. Ylinen, M. L. Huhtala, K. Teramo*, J. Chromatogr. **297**, 327 (1984).
[129] *M. J. F. Schmerr, K. R. Goodwin, H. D. Lehmkuhl, R. C. Cutlip*, J. Chromatogr. **326**, 225 (1985).
[130] *S. Goheen, R. S. Matson*, J. Chromatogr. **326**, 235 (1985).
[131] *S. W. Burchiel*, Meth. Enzymol. **121**, 596 (1986).
[132] *B. Pavlu, U. Johansson, C. Nyhlen, A. Wichman*, J. Chromatogr. **359**, 449 (1986).
[133] *E. H. Cooper, E. A. Johns, Y. Itoh, J. R. Webb*, J. Chromatogr. **327**, 179 (1985).
[134] *D. Josic, W. Schutt, J. V. Renswoude, B. Rutter*, J. Chromatogr. **353**, 13 (1986).
[135] *P. Clezardin, J. L. McGregor, M. Manach, H. Boukerche, M. Dechavanne*, J. Chromatogr. **319**, 67 (1985).
[136] *P. Gallo, O. Olsson, A. Siden*, J. Chromatogr. **327**, 293 (1985).
[137] *T. M. Phillips, N. S. More, W. D. Queen, A. M. Thompson*, J. Chromatogr. **327**, 205 (1985).
[138] *P. L. Ey, S. J. Prowse, C. R. Jenkin*, Immunochem. **15**, 429 (1978).
[139] *J. Salinas, G. S. Ott, J.-C. Chen, T. J. Brooks, L. H. Stanker*, Meth. Enzymol. **21**, 58 615 (1986).
[140] *M. Okazaki, Y. Ohno, I. Hara*, J. Chromatogr. **221**, 257 (1980).
[141] *R. Vercaemst, M. Rosseneu, J. P. Van Viervliet*, J. Chromatogr. **276**, 174 (1983).
[142] *D. Polacek, C. Edelstein, A. M. Scanu*, Lipids **16**, 927 (1981).
[143] *G. S. Ott, V. G. Shore*, J. Chromatogr. **231**, 1 (1982).
[144] *P. Schwandt, W. O. Richter, V. Heinemann, P. Weisweiler*, J. Chromatogr. **345**, 145 (1985).

Received: Sept. 14, 1987
Accepted: Sep. 17, 1987
F

Indirect Detection in Liquid Chromatography
I. Response Models for Reversed-Phase Ion-Pairing Systems

J. Crommen[1] * / G. Schill[2] / D. Westerlund[2] / L. Hackzell[2a]

1 Department of Analytical Chemistry, Institute of Pharmacy, University of Liège, rue Fusch, 5, B-4000 Liège, Belgium
2 Department of Analytical Pharmaceutical Chemistry, Biomedical Center, University of Uppsala, Box 574, S-751 23 Uppsala, Sweden

Key Words

Reversed-phase ion-pair chromatography
Indirect detection
Response models
Non-absorbing organic ions
Non-absorbing neutrals

Summary

Ionic compounds without inherent detectable properties show good response in reversed phase ion-pairing systems containing a detectable ionic compound (probe) in the mobile phase. The basis for the indirect detection is the common interaction effect for solutes and probe caused by the limited binding capacity of the adsorbent. Quantitative models for solutes and probe with the same or opposite charges show a simple dependence of the response on the retention of the solute and the coverage of the binding surface by the probe. Applications of the models have shown good agreement between calculated and found response. The binding to sites of different kinds on the adsorbent and possibly ion-pair formation in the mobile phase have an influence on the indirect response. Uncharged solutes give low response in such systems owing to low binding to the competitive sites.

Introduction

Ion-pair extraction with ultraviolet-absorbing counter ions has been commonly used as a means for quantitative determination of ionic compounds without inherent absorptivity. The same indirect quantitation principle has been applied in liquid-liquid chromatography with an organic mobile phase and the detectable counter ion in the aqueous stationary phase [1].

Indirect detection based on the ion-pair distribution principle can also be used in reversed-phase systems. A detectable ion is included in the aqueous mobile phase and distributed to the hydrophobic adsorbent used as stationary phase. Injected solutes affect the distribution of the detectable ion by binding or displacement in such a way that a detector response is obtained also for solutes that are devoid of inherent detectable properties.

The indirect detection effect in reversed phase ion-pairing systems has mainly been applied to cationic and anionic organic compounds [2–10] but there are also several publications on the application to inorganic ions [11–13] and uncharged solutes [5, 8, 14]. The technique is furthermore applicable to ion-exchange systems, as has been discussed in a series of papers (cf. [15]), as well as to reversed-phase nonionic systems by use of an uncharged compound as the detectable component [16, 17]. The detection has been based on UV absorbance in most cases but fluorescence [5] and electrochemical detection [18] have also been used.

The background to the indirect response for ionic compounds has so far mainly been presented in general terms but it has formed an adequat basis for qualitative conclusions about the dependence of the response pattern and the detection sensitivity on the properties of the solute and the chromatographic system.

The injection of a sample gives rise to two kinds of peaks: one for each of the injected solutes and one or several additional peaks that are characteristic for the system. These so called system peaks appear with the same retention whenever an injection is made but the direction of the peaks depends on the properties of the sample. Solute peaks are positive before the system peak and negative after when the solute is uncharged or has the same charge as the detectable mobile phase ion (the probe). The response pattern is reversed when the solute and the probe have opposite charges: negative peaks before the system peak and positive after. The magnitude of the response is proportional to the amount of the solute but it is independent of the properties and the amount of other sample components.

The detection sensitivity changes with the retention of the solute relative to the system peak and it has a maximum when the capacity ratios of the two peaks are about the same [4]. The response is also dependent on the loading of the probe on the adsorbent, which can be regulated by e.g. the probe concentration in the mobile phase [9]. The addition of a hydrophilic modifier e.g. methanol to the mobile phase may decrease the detection sensitivity since it decreases the loading of probe on the adsorbent [9].

---

[a] Present address: Aco Läkemedel AB, S-171 03 Solna 3, Sweden

0009-5893/87 0252-09 $ 03.00/0

© 1987 Friedr. Vieweg & Sohn Verlagsgesellschaft mbH

The equilibrium disturbances that occur when a solute is injected in a chromatographic system have been extensively treated by Helfferich [19] and the theoretical background has recently been elucidated by Kovats et al. [20] and Poppe [21]. It is shown that the disturbances are due to the fact that the distribution of the solute and the components in the chromatographic system are coupled by a common interaction. On this basis expressions can be derived that give the possibility of calculating the changes in the concentrations of mobile phase components in the eluted solute peak.

The present paper gives expressions for quantitative calculations of the indirect response for ionic compounds in reversed phase ion-pairing systems containing a probe with the same or the opposite charge. The expression are applied to the estimation of the indirect response for organic cations and anions in two systems containing an anionic and a cationic probe, respectively. The validity of the equations is demonstrated by a comparison of calculated and found response.

Experimental

Apparatus

The detectors were an LDC UV-III-Monitor and an LDC Spectromonitor III. The pump was an Altex 100 A and the injector a Rheodyne 17–25 with a loop volume of 15.5μl.

The columns (100 × 3.2 mm i.d.) were made of stainless steel with polished inner surface, equipped with modified Swagelok connectors and Altex 250-21 filters. The spectrophotometric measurements were made with a Zeiss PMQ II Spektralphotometer.

Chemicals and Reagents

Sodium naphthalene-2-sulphonate (NS) was obtained from Eastman-Kodak (Rochester, NY, USA) and recrystallized from water before use. 1-Phenethyl-2-picolinium bromide (PEP) (Eastman-Kodak) was converted into the hydroxide by use of an anion exchanger in the hydroxide form and freed from UV absorbing impurities by repeated extractions with methylene chloride.

Chromatographic System

μBondapak Phenyl (10μm) (Waters Assoc., Milford, MA, USA) was used as the solid phase. The columns were packed by a slurry technique using water-ethanol (58+42) as the suspending medium. They were washed with 200 ml of water-methanol (1+4) before use. Column testing was carried out with water-methanol (2+3) as mobile phase and toluene and mesitylene as retained samples, giving capacity ratios (k′) of about 1 and 4 respectively. Columns that gave reduced plate heights of less than 10 were accepted.

The mobile phases were aqueous solution of NS or PEP containing buffering compounds.

Chromatographic Technique

The eluent reservoir, injector, column and connecting tubes were thermostated at 25.0±0.1 °C in a water-bath. The detection wavelength was 254 nm.

The mobile phase flow rate was 0.50 ml/min. Equilibrium was obtained after passage of about 50 ml of the mobile phase. The samples were injected dissolved in mobile phase. The volume of mobile phase in the column, V_M, was obtained from the front peak of the chromatogram. Peak areas were determined by planimetry.

Response Models

In reversed-phase chromatography ionic solutes and mobile phase components are distributed to the solid phase as ion pairs with counter ions present in the mobile phase. If several ionic components in the mobile phase take part in such processes, rather complex distribution expressions are obtained which will make the theoretical treatment of indirect detection effects difficult. The development of the basic response models is therefore made for a system containing a hydrophobic adsorbent and an aqueous mobile phase with three components: a cation, Q^+, which is the detectable component (the probe), an anion, X^-, and a third, cationic, component, B^+, which is so hydrophilic that its distribution to the adsorbent is negligible.

The injection of a solute in this chromatographic system gives rise to a change of the distribution in the injection zone of Q^+ and X^- if their distribution equilibria are coupled to that of the solute by a common interaction effect such as competition for the binding capacity of the absorbent.

In analytical applications the concentration disturbances caused by solute injection are so small that it is possible to linearize the description of the distribution behaviour. The changes in the different concentrations can be expressed by

$$\Delta C_{i,S} = C_{i,S} - C^{\circ}_{i,S} = \sum_{j=1}^{n} a_{i,j} \cdot \Delta C_{j,M} \tag{1}$$

where $\Delta C_{i,S}$ is the change in the concentration of a compound i in the stationary phase and the corresponding change in the mobile phase is $\Delta C_{i,M}$. $C_{i,S}$ is here defined as the quotient of the amount of i in the stationary phase to the volume of the mobile phase in the column. C° is the initial concentration and

$$a_{i,j} = \frac{\partial C_{i,S}}{\partial C_{j,M}} \tag{2}$$

$a_{i,j}$ for each solute and mobile phase component is evaluated for the starting concentration in the mobile phase reservoir, i.e. zero for the solute and different from zero for the mobile phase components. The distribution of the major mobile phase constituent, the solvent, is not taken into account. A relationship such as eq. (1) is valid for each compound (solute or mobile phase component) which means that for n compounds n^2 $a_{i,j}$ terms are obtained. They represent in fact the elements of a quadratic matrix.

Solute and Probe with the Same Charge

When the solute is a cation, HA^+, which competes for the binding capacity of a homogeneous surface according to a Langmuir model, the following expressions are obtained for the concentrations of solute and probe on the solid phase:

$$C_{HA,S} = \frac{A \cdot K_{HA} \cdot C_{HA,M} \cdot C_{X,M}}{N_1} \tag{3}$$

$$C_{Q,S} = \frac{A \cdot K_Q \cdot C_{Q,M} \cdot C_{X,M}}{N_1} \tag{4}$$

where

$$N_1 = 1 + (K_{HA} \cdot C_{HA,M} + K_Q \cdot C_{Q,M}) \cdot C_{X,M} \tag{5}$$

$A = K^\circ \cdot W_s/V_M$, i.e. the product of the binding capacity of the solid phase and the phase-volume ratio in the column, expressed in mol/l. K_Q and K_{HA} are ion-pair distribution constants defined as follows:

$$K_Q = \frac{C_{Q,S}}{C_{Q,M} \cdot C_{X,M} \cdot C_{A,S}} \tag{6}$$

$$K_{HA} = \frac{C_{HA,S}}{C_{HA,M} \cdot C_{X,M} \cdot C_{A,S}} \tag{7}$$

where $C_{A,S}$ = concentration of available binding sites in mol/l.

It is the interaction between the solute and the probe that is of main interest in the present discussion and $C_{X,M}$ can be substituted for in eqs. (3)–(5) as shown in the following expression based on the electroneutrality in the system:

$$C_{X,M} = C_{HA,M} + C_{Q,M} + C_{B,M} \tag{8}$$

The partial derivatives for the probe, Q^+, and the solute, HA^+, are

$$\frac{\partial C_{HA,S}}{\partial C_{HA,M}} = a_{HA,HA} = A \cdot K_{HA} \cdot (1-\Theta_Q)(C_{Q,M} + C_{B,M}) = \\ = k'_{HA} \tag{9}$$

where Θ_Q is the fractional coverage of the solid phase by Q^+, defined by:

$$\Theta_Q = \frac{C_{Q,S}}{A} = \frac{K_{Q,M} \cdot C_{Q,M} \cdot C_{X,M}}{1 + K_Q \cdot C_{Q,M} \cdot C_{X,M}} \tag{10}$$

and

$$(1-\Theta_Q) = \frac{1}{1 + K_Q \cdot C_{Q,M} \cdot C_{X,M}} \tag{11}$$

$$\frac{\partial C_{HA,S}}{\partial C_{Q,M}} = a_{HA,Q} = 0 \tag{12}$$

$$\frac{\partial C_{Q,S}}{\partial C_{Q,M}} = a_{Q,Q} = A \cdot K_Q \cdot (1-\Theta_Q)^2 \cdot (2C_{Q,M} + C_{B,M}) = \\ = k'_Q \tag{13}$$

$$\frac{\partial C_{Q,S}}{\partial C_{HA,M}} = a_{Q,HA} = -k'_{HA} \cdot \Theta_Q + \frac{k'_Q \cdot C_{Q,M}}{2C_{Q,M} + C_{B,M}} \tag{14}$$

These coupled expressions for the chromatographic distribution can be treated as an eigenvalue problem. The matrix is triangular and the eigenvalues are the diagonal elements, $a_{HA,HA}$ and $a_{Q,Q}$, which correspond to the capacity ratios of the solute, HA^+, and the probe, Q^+, respectively. The latter gives the so called system peak.

The relative changes of the concentrations of HA^+ and Q^+ in the eluted solute peak are given by the corresponding eigenvector that can be derived from the matrix. The eigenvector for $k'_{HA} \neq 0$ and $k'_{HA} \neq k'_Q$ gives:

$$\frac{\Delta C_Q}{\Delta C_{HA}} = L_1 - M \quad \text{(relative response)} \tag{15}$$

where

$$L_1 = \frac{\alpha_S}{1-\alpha_S} \cdot \Theta_Q \quad \text{(loading term)} \tag{16}$$

$$M = \frac{1}{1-\alpha_S} \cdot \frac{C_{Q,M}}{2C_{Q,M} + C_{B,M}} \quad \text{(mobile phase term)} \tag{17}$$

$$\alpha_S = \frac{k'_{HA}}{k'_Q} \quad \text{(relative retention)} \tag{18}$$

M is negligible when $C_{B,M}$ is much larger than $C_{Q,M}$. M also decreases with increasing relative retention of the solute, α_S. The loading term, L_1, increases with the fractional coverage, Θ_Q. The increase can be achieved by increasing the mobile phase concentrations of Q^+ or the counter ion, X^- (cf. eq. (10)). L_1 has a maximum when α_S is close to unity, i.e. when the solute and the system peak have about the same retention.

When the response is monitored with a UV detector and quantified by measurement of the peak area, it is possible to calculate an apparent molar absorptivity, ϵ^x, which is the peak area per mole of solute. Since

$$\frac{\epsilon^x_{HA}}{\epsilon_Q} = \frac{\Delta C_Q}{\Delta C_{HA}} \tag{19}$$

the relative response can be expressed by the quotient of the apparent molar absorptivity to the molar absorptivity of the probe.

Solute and Probe with Opposite Charges

When an anionic solute, Y^-, is applied in the same chromatographic system, the following expressions are valid:

$$C_{Y,S} = \frac{A \cdot K_Y \cdot C_{Y,M} \cdot C_{Q,M}}{N_2} \tag{20}$$

$$C_{Q,S} = \frac{A \cdot K_Y \cdot C_{Q,M} \cdot C_{Y,M} + A \cdot K_Q \cdot C_{Q,M} \cdot C_{X,M}}{N_2} \tag{21}$$

where

$$N_2 = 1 + (K_Y \cdot C_{Y,M} + K_Q \cdot C_{X,M}) \cdot C_{Q,M} \tag{22}$$

$$K_Y = \frac{C_{Y,S}}{C_{Y,M} \cdot C_{Q,M} \cdot C_{A,S}} \tag{23}$$

After replacement of $C_{X,M}$ by:

$$C_{X,M} = C_{Q,M} + C_{B,M} - C_{Y,M} \tag{24}$$

the following partial derivatives are obtained for the solute and the probe:

$$a_{Y,Y} = A \cdot K_Y \cdot C_{Q,M} \cdot (1-\Theta_Q) = k'_Y \tag{25}$$

$$a_{Q,Y} = k'_Y \cdot (1-\Theta_Q) - \frac{k'_Q \cdot C_{Q,M}}{2C_{Q,M} + C_{B,M}} \tag{26}$$

$a_{Q,Q}$ is given by eq. 13; $a_{Y,Q} = 0$.

The eigenvector for $k'_Y \neq 0$ and $k'_Y \neq k'_Q$ gives:

$$\frac{\Delta C_Q}{\Delta C_Y} = \frac{\epsilon^x_Y}{\epsilon_Q} = -(L_2 - M) \tag{27}$$

where

$$L_2 = \frac{\alpha_S}{1-\alpha_S} \cdot (1-\Theta_Q) \tag{28}$$

and M is given by eq. (17).

An increase of the fractional loading, Θ_Q, decreases the loading term, L_2, and also the magnitude of the relative response, when the conditions are such that the M term is negligible. This means that the effect of increasing the fractional loading is opposite to the case where the solute and the probe have the same charge.

Systems with Ion Exchange Properties

When the fractional coverage of the solid phase by the probe is high, the expressions for the concentration of the solute in the stationary phase can be simplified. Eq. (3), which is valid when the solute and the probe have the same charge, can then be changed to:

$$C_{HA,S} = \frac{A \cdot K_{HA} \cdot C_{HA,M}}{K_Q \cdot C_{Q,M}} \tag{29}$$

If the probe, Q^+, is the only mobile phase component with the same charge as the solute to be distributed to the solid phase, $C_{Q,S}$ approaches A, and Θ is almost unity (cf. eq. (10)). The capacity ratio of the system peak will then approach zero (cf. eq. (13)) and $\alpha_S/(1-\alpha_S)$ approaches -1. This means that the expressions for the relative response (eqs. (15) and (19)) are simplified to:

$$\frac{\epsilon^x_{HA}}{\epsilon_Q} \approx -1 \tag{30}$$

The solutes will under these conditions only give negative peaks and the apparent molar absorptivity is approximately the same as that of the probe and independent of the solute retention. This is in accordance with the observations made in ion-exchange chromatography (cf. [15]). The large positive peak which appear at the front in all such chromatograms, is obviously the system peak.

Adsorbent with Two Kinds of Binding Sites

The models developed above are valid for adsorbents with only one kind of binding sites. They cannot be applied to such chromatographic conditions as ion-pair distribution to hydrophobized silica, since retention studies have shown that the adsorbent then has two kinds of binding sites [22, 23].

The principles given above can, however, be applied to a two-site adsorbent, if the sites are treated separately with different values for the binding capacities and ion pair distribution constants. The partial derivatives then consist of two elements with analogous forms.

When the solute and the probe have the same charge, the partial derivatives are obtained from eqs. (9) and (12)–(14) and from the eigenvector for k'_{HA} the following expression can be derived when the M term is negligible:

$$\frac{\epsilon^x_{HA}}{\epsilon_Q} = \left(\frac{k'_{HA,1} \cdot \Theta_{Q,1}}{k'_{HA}} + \frac{k'_{HA,2} \cdot \Theta_{Q,2}}{k'_{HA}}\right) \cdot \frac{\alpha_S}{1-\alpha_S} \tag{31}$$

The retention and the fractional coverage on the two sites are expressed by $k'_{HA,1}$, $\Theta_{Q,1}$ and $k'_{HA,2}$, $\Theta_{Q,2}$, respectively.

When the solute and the probe have opposite charges, the partial derivatives are obtained from eqs. (12)–(13) and (25)–(26) and the eigenvector expression for k'_Y has the following form if the M term is negligible:

$$\frac{\epsilon^x_Y}{\epsilon_Q} = -\left(\frac{k'_{Y,1} \cdot (1-\Theta_{Q,1})}{k'_Y} + \frac{k'_{Y,2} \cdot (1-\Theta_{Q,2})}{k'_Y}\right) \cdot \frac{\alpha_S}{1-\alpha_S} \tag{32}$$

The expressions above show that the general response pattern is the same as on single site adsorbents with opposite directions of the solute peaks before and after the system peak. However, the magnitude of the response can only be estimated if the fractional coverage and the capacity ratios on the separate sites are known.

Ion-Pair Formation in the Mobile Phase

If the solute and the probe have opposite charges and, beside being distributed to the solid phase as an ion pair, also have the ability to form ion pairs in the mobile phase to a significant extent, the capacity ratio of the solute has the following form (cf. eq. (25)):

$$k'_Y = \frac{A \cdot K_Y \cdot C_{Q,M} \cdot (1-\Theta_Q)}{1 + K_c \cdot C_{Q,M}} \tag{33}$$

where K_c is the formation constant of the ion pair QY defined by:

$$K_c = \frac{C_{QY,M}}{C_{Q,M} \cdot C_{Y,M}} \tag{34}$$

$a_{Q,Q}$ is given by eq. (13) and an expression analogous to eq. (26) is obtained for $a_{Q,Y}$, the only difference being that now the first term is equal to $k'_Y \cdot (1-\Theta_Q) \cdot (1 + K_c \cdot C_{Q,M})$. Calculation of the eigenvector for k'_Y gives (cf. eqs. (27)–(28)):

$$\frac{\epsilon^x_Y}{\epsilon_Q} = -\left[(1-\Theta_Q) \cdot (1 + K_c \cdot C_{Q,M}) \cdot \frac{\alpha_S}{1-\alpha_S}\right] + M \tag{35}$$

An increase of the concentration of the probe, Q^+, gives rise to an increase of the fractional coverage, Θ_Q. From the equation follows that this will have a decreasing effect on the magnitude of the relative response but it is counteracted by an increase of the ion-pair formation in the mobile phase.

Results and Discussion

The response studies were made in reversed-phase systems with 1-phenethyl-2-picolinium (PEP) or naphthalene-2-sulfonate (NS) as the detectable mobile phase component. The solvent was water containing hydrophilic buffers. Phenyl bonded silica (μBondapak Phenyl) was used as the solid phase. A chromatogram is given in Fig. 1. The response pattern for the charged solutes is in accordance with the principles presented in several previous papers (cf. [4]). When the solute and the probe have the same charge, the solute peaks are positive before the system peak and negative after; when the solute and the probe have opposite charges the response pattern is reversed.

Cationic Probe

As a test of the validity of the response models presented above, some quantitative results with the cation PEP as probe are presented in Table I. It gives the relative retention, α_S, the observed relative response, ϵ^x/ϵ, and the calculated values of the mobile phase term, M (eq. (17)) at a PEP conc. of $3 \cdot 10^{-4}$ M. The evaluation of M was based on the assumption that H^+ is not distributed to the solid phase and corresponds to B^+ in eq. (17). The cationic solutes and probe were distributed to the solid phase with acetate as counter ion. Anionic solutes were distributed as ion pairs with the probe.

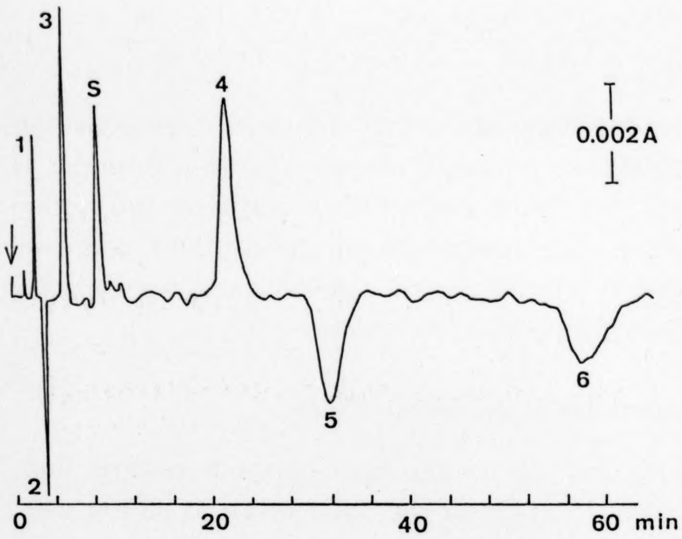

Fig. 1

Indirect detection of anions and cations

Solid phase: μBondapak Phenyl.

Mobile phase: naphthalene-2-sulfonate $4 \cdot 10^{-4}$ M in phosphoric acid 0.05 M. Sample: **1** = butyl sulfate; **2** = pentylamine; **3** = hexanesulfonate; **4** = heptylamine; **5** = octanesulfonate; **6** = octylsulfate; **S**: system peak.

Table I. Response and retention with 1-phenethyl-2-picolinium as probe. Solid phase: μBondapak Phenyl. Mobile Phase: 1-phenethyl-2-picolinium $3 \cdot 10^{-4}$ M in acetic acid 0.1 M ($CH^+ = 1.3 \cdot 10^{-3}$); $k'_Q = 4.3$; $\epsilon_Q = 3.03 \cdot 10^3$

No.	Solute	α_S	ϵ^x/ϵ	M	$L_1; -L_2$
1	Dibutylamine	0.28	0.031	0.22	0.25
2	Tripropylamine	0.38	0.091	0.26	0.35
3	Octylamine	1.27	−1.48	−0.59	−2.07
4	Nonylamine	3.70	−0.52	−0.06	−0.58
5	Decylamine	10.4	−0.53	−0.02	−0.55
6	Methylsulfate	0.41	−0.11	0.27	−0.38
7	Propylsulfate	0.84	−1.41	0.99	−2.40
8	Butylsulfate	1.74	0.95	−0.21	1.16
9	Pentanesulfonate	2.47	0.55	−0.11	0.66
10	Hexanesulfonate	5.3	0.57	−0.04	0.61

Cations: $\epsilon^x/\epsilon + M = L_1$; Anions: $\epsilon^x/\epsilon - M = -L_2$; M calculated by eq. (17)

The Table shows that M is rather large in this system when α_S is lower than 2. From eq. (17) follows that M reaches a maximum value when α_S is close to unity and decreases rapidly with higher α_S. M is also expected to decrease with increasing excess of the non-distributed cation B^+ over the concentration of the probe.

The values of the loading term (L_1 or $-L_2$) in the Table have been obtained as the sum or the difference of the observed relative response, ϵ^x/ϵ, and the calculated M value (cf. eqs. (15) and (27)). L_1, $-L_2$ and M change from positive to negative values simultaneously since they depend on $(1-\alpha_S)$ in the same way (cf. eqs. (16), (17) and (28)). The sign of ϵ^x/ϵ, i.e. the direction of the solute peak, then depends on the relative magnitudes of the L and M terms. In the experiments presented in Table I the L values are larger than M and a normal response pattern is obtained with change of the direction of the solute peaks at $\alpha_S = 1$. This change of direction might not occur if M has a high value, which is the case when the non-distributed B^+ is absent or present in very low concentration. A behaviour of this kind has been observed when the mobile phase contains only a salt of the probe and no buffer or other additive [5].

It should furthermore be noted that the apparent molar absorptivity, ϵ^x, can be higher than the molar absorptivity of the probe. Octylamine and propylsulfate are examples of this kind in Table I.

A graphical presentation of the results is given in Fig. 2. It is based on eq. (16) for cations and eq. (28) for anions, L_1 or $-L_2$, respectively, being plotted versus $\alpha_S/(1-\alpha_S)$. With plots of this kind the fractional coverage of the solid phase by the probe can be obtained directly from the slope. Straight linear relationships are obtained with intercepts close to zero, which supports the validity of the models. The positive slope obtained for the cationic solutes, which should correspond to the fractional coverage, Θ_Q, is equal to 0.46. The slope of the line for the anionic solutes, which should give $-(1-\Theta_Q)$ is equal to −0.46, corresponding to $\Theta_Q = 0.54$. Possible reasons for this deviation are discussed below.

The computed values of the fractional loading and the mobile phase term, M, can be used for calculating the relationships between the relative response and the relative retention α_S (cf. eqs. (15)–(19), (27)–(28)). The results are given as dotted lines in Fig. 3 together with the experimental values. The expressions used give a good illustration of the response pattern for cationic and anionic solutes when the probe is cationic. It should be noted that a reversal of the response pattern is predicted at very low α_S values.

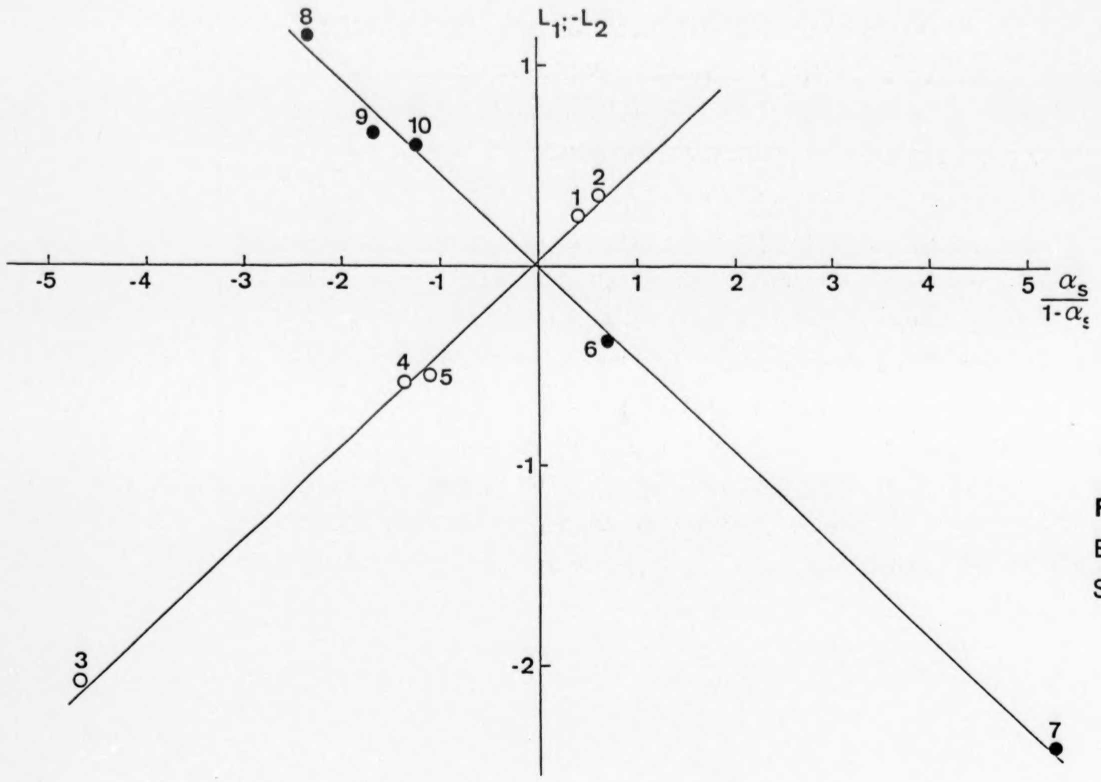

Fig. 2
Estimation of fractional coverage with PEP as probe.
System and solutes: see Table I.

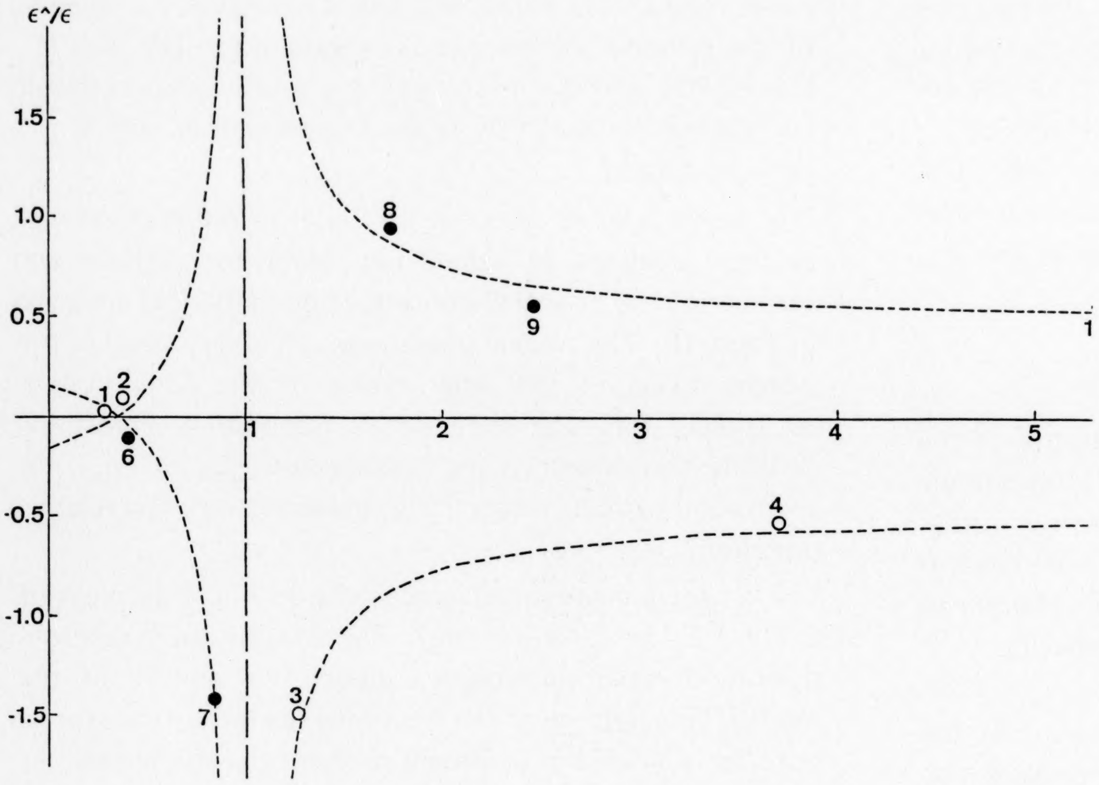

Fig. 3
Response dependence on relative retention.
System and solutes: see Table I.
Dotted lines: calculated values.

Estimation of Solid Phase Coverage

The computation of the fractional coverage was based on expressions that are valid when the solid phase has only one kind of binding sites. Binding studies based on retention have shown that the chromatographic system behaves as having one site with strong competition and one site with very weak competition when the solutes are distributed as ion pairs. If part of the binding in the actual PEP concentration range, $(1\text{–}6)\cdot 10^{-4}$ M, is due to a site without competition it is obvious that the slopes in Fig. 2 do not give a correct value of Θ_Q. An illustration can be based on the expressions for binding to an adsorbent with two kinds of sites. For a solute with the opposite charge to the probe, eq. (32) can be reduced to:

$$\frac{\epsilon_Y^x}{\epsilon_Q} = -\left(\frac{k'_{Y,1}\cdot(1-\Theta_Q)}{k'_Y}\right)\cdot\frac{\alpha_S}{1-\alpha_S} \qquad (36)$$

A similar reduction can be applied to the equation for solutes with the same charge as the probe (eq. (31)). If the plot in Fig. 2 is based on an equation analogous to eq. (36), the slope of the line will give $-(q-q\cdot\Theta_Q)$ where $q = k'_{Y,1}/k'_Y$. A plot for cationic solutes according to the same principle will have a slope of $q\cdot\Theta_Q$, where now q is equal to $k'_{HA,1}/k'_{HA}$. The value of q should be less than unity, and an application of this approach to Fig. 2 shows that there is a good agreement between the fractional coverages obtained from the two lines if it is assumed that $q = 0.9$.

The estimation of the fractional coverage may also be influenced by the formation of ion pairs between the solute and the probe in the mobile phase. The effect is demonstrated by eq. (35). It is obvious that it can only appear when the solute and the probe have opposite charges, and in the plots shown in Fig. 2, the slope of the line for anions

Table II. Influence of probe concentration on the response. Solid phase: μBondapak Phenyl. Mobile phase: 1-phenethyl-2-picolinium (Q) in acetic acid 0.1 M.

Solute	$C_Q \cdot 10^4$	α_S	ϵ^x/ϵ	M	$L_1; -L_2$	Θ_Q
Nonylamine	1.0	3.3	−0.58	−0.03	−0.61	0.43
	2.1	3.6	−0.72	−0.05	−0.77	0.56
	3.1	3.4	−0.64	−0.07	−0.71	0.50
	4.1	3.4	−0.62	−0.08	−0.70	0.49
	5.9	3.0	−0.71	−0.12	−0.83	0.55
Hexanesulfonate	1.0	2.4	0.67	−0.05	0.72	0.59
	2.1	4.9	0.76	−0.03	0.79	0.37
	3.1	6.5	0.60	−0.03	0.63	0.47
	4.1	8.4	0.57	−0.03	0.60	0.47
	5.9	10.7	0.66	−0.02	0.68	0.38

Θ_Q calutated by eq. (16) (cations) and eq. (28) (anions).

should be equal to $-(1-\Theta_Q) \cdot (1 + K_c \cdot C_{Q,M})$, i.e. the ion-pair formation in the mobile phase should increase the negative value of the slope. If it is assumed that the line for cationic solutes gives a correct value of $\Theta_Q = 0.46$, the anionic solutes should give a line with a slope of $-(1-\Theta_Q) = -0.54$. The observed slope is, however, only -0.46. Obviously ion pair formation in the mobile phase cannot be the main reason for the observed deviations in the Θ_Q values calculated from the two lines in this case.

Probe Concentration and Solid Phase Coverage

The effect of a change of the probe concentration in the mobile phase on the response has been studied with cationic and anionic solutes. The results obtained with two rather highly retained compounds, nonylamine and hexanesulfonate, are given in Table II. The separation column was not the same as that used in Table I and the capacity ratios are somewhat different.

The relative response, ϵ^x/ϵ, is affected only slightly by the increase of the probe concentration. The fractional coverage, Θ_Q, calculated for a single-site adsorbent by eqs. (15)–(19) for the cation and eqs. (27)–(28) for the anion shows no significant trend to change with the probe concentration. However, it is known from break-through experiments that the loading increases with the probe concentration in the mobile phase. The explanation of this discrepancy might be the existence of two kinds of binding sites and a change of the binding ratio to the two sites with the probe loading. However, the anionic solute gives in most cases lower values of Θ_Q than the cationic solute, which might be an indication of ion-pair formation in the mobile phase according to eq. (35).

Anionic Probe

The response model has also been tested with naphthalene-2-sulfonate (NS) as the probe. Phosphoric acid 0.05 M was used as the mobile phase solvent and the calculations were based on the assumption that $H_2PO_4^-$ was not distributed to the solid phase. All the expressions in the section "Response model" can be applied after a change of the meaning of the symbols for the ions: Q should mean NS, X is H^+, B is $H_2PO_4^-$ and the meaning of the solute symbols should be reversed so that HA is an anionic solute and Y is a cationic solute.

The found relative response and relative retention as well as the calculated M values (eq. (17)) for cationic and anionic solutes at an NS concentration of 10^{-4} M are given in Table III. The mobile phase term, M, is very small in this system owing to the large excess of the non-distributed $H_2PO_4^-$ ion, and the relative response is almost exclusively dependent on the loading term, L_1 or $-L_2$, for anions and cations, respectively, except at very low relative retention.

The results are presented graphically in Fig. 4 by plots of L_1 or $-L_2$ versus $\alpha_S/(1-\alpha_S)$. The straight linear relationships with small intercepts support the validity of the models. Calculations of the fractional loading by the expressions for a single site adsorbent gives for the anionic solutes $\Theta_Q = 0.18$ (eq. (16)) and for the cations $\Theta_Q = 0.65$ (eq. (28)). The deviation between the Θ_Q values is large and calculations based on the assumption of two kinds of binding sites, analogous to those made for eq. (36), give $k'_{Y,1}/k'_Y = 0.5$, i.e. the site with strong competition only

Table III. Response and retention with naphthalene-2-sulfonate as probe. Solid phase: μBondapak Phenyl. Mobile Phase: sodium naphthalene-2-sulfonate (NS) $1.0 \cdot 10^{-4}$ in phosphoric acid 0.05M ($C_{H_2PO_4^-} = 2.2 \cdot 10^{-2}$); $k'_{NS} = 11.2$; $\epsilon_{NS} = 3.02 \cdot 10^3$

No.	Solute	α_S	ϵ^x/ϵ	M	$L_1; -L_2$
1	Hexanesulfonate	0.44	0.127	0.008	0.135
2	Octanesulfonate	3.89	−0.250	−0.002	−0.252
3	Diisopropylamine	0.08	−0.017	0.005	−0.022
4	Triethylamine	0.10	−0.019	0.005	−0.024
5	Hexylamine	0.26	−0.110	0.006	−0.116
6	Tripropylamine	0.71	−0.851	0.016	−0.851

Anions: $\epsilon^x/\epsilon + M = L_1$; Cations: $\epsilon^x/\epsilon - M = -L_2$

Table IV. Influence of probe concentration on the response. Solid phase: μBondapak Phenyl. Mobile phase: sodium naphthalene-2-sulfonate in phosphoric acid 0.05 M.

Solute	$C_{NS}\cdot 10^4$	α_S	ϵ^x/ϵ	M	$L_1;-L_2$	Θ_Q
Octane-sulfonate	1.0	3.89	−0.250	−0.002	−0.25	0.19
	2.0	3.75	−0.315	−0.003	−0.32	0.23
	3.7	4.02	−0.405	−0.005	−0.41	0.31
	5.6	4.22	−0.420	−0.007	−0.43	0.33
Tripropylamine	1.0	0.71	−0.835	0.016	−0.85	0.65
	2.0	1.47	0.890	−0.019	0.91	0.71
	3.7	2.34	0.801	−0.012	0.81	0.54
	5.6	3.41	0.505	−0.010	0.52	0.63

Θ_Q calculated by eq. (16) (anions) and eq. (28) (cations)

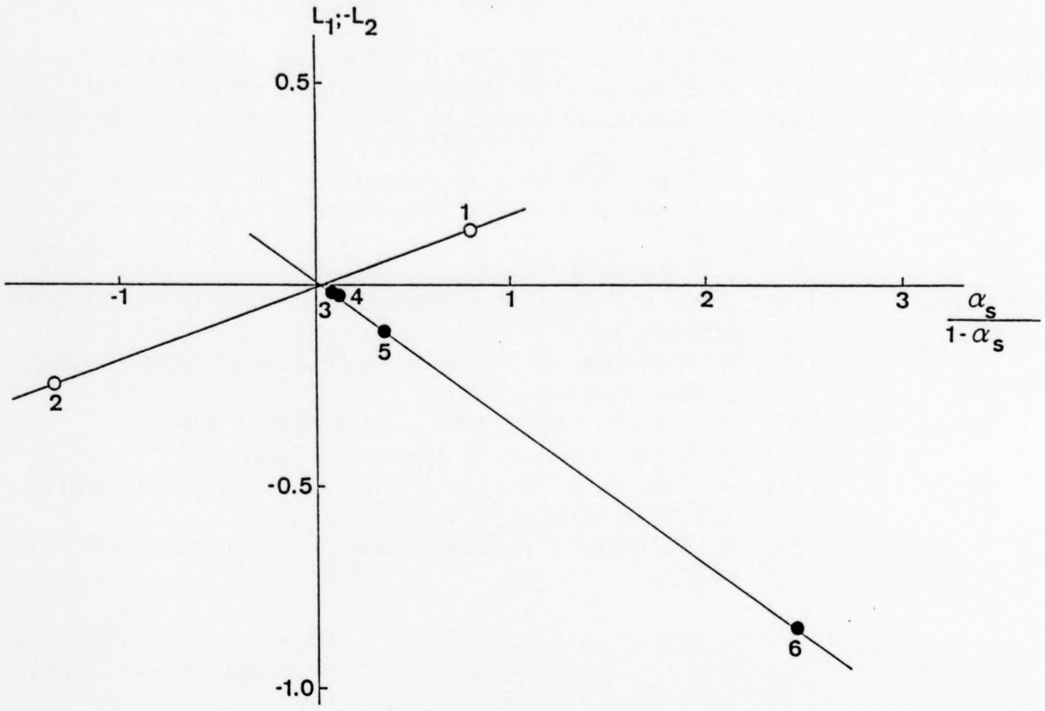

Fig. 4
Estimation of fractional coverage with NS as probe. System and solutes: see Table III.

Table V. Response of uncharged solutes with naphthalene-2-sulfonate as probe. Solid phase: μBondapak Phenyl. Mobile phase: sodium naphthalene-2-sulfonate $2\cdot 10^{-4}$ M in phosphoric acid 0.05 M; $k'_{NS} = 8.3$; $\epsilon_{NS} = 3.00\cdot 10^3$

No.	Solute	α_S	ϵ^x/ϵ	F
1	Butanol	0.20	0.005	0.020
2	Pentanol	0.55	0.043	0.035
3	Methylisobutyl ketone	1.15	−0.069	0.009
4	Caproic acid	1.41	−0.057	0.017
5	Hexanol	1.61	−0.038	0.014
6	Butyl acetate	1.93	−0.019	0.009
7	Heptanoic acid	3.97	−0.028	0.021
8	Octanesulfonate	3.72	−0.279	0.205

$F = \epsilon^x/\epsilon \cdot (1-\alpha_S)/\alpha_S$

gives rise to about 50% of the retention. It should, however, be mentioned that significantly larger values of $k'_{Y,1}/k'_Y$ have been obtained with another column of the same brand but the same mobile phase and solutes.

The effect of a change of the concentration of the probe in the mobile phase is demonstrated in Table IV. The changes in the calculated values of Θ_Q are rather small and the observed changes of the relative response depend mainly on the differences in relative retention.

Uncharged Solutes

Uncharged compounds can also be indirectly detected in systems containing a charged probe and the response pattern is the same as for solutes with the same charge as the probe. However, the magnitude of the relative response is much lower.

Results obtained with uncharged solutes of different kinds are given in Table V. A comparison between the uncharged heptanoic acid and the anion octane sulfonate, which have about the same retention, shows that the relative response of the uncharged solute is about 10 times lower. Butyl acetate and methyl isobutyl ketone have inherent absorptivity at the detection wavelength (254 nm) but the negative detector response shows that the indirect detection effect dominates.

The background to the low response of the uncharged solutes seems to be in accordance with the assumption of two kinds of binding sites on the adsorbent made previously. The solute is distributed to the two sites but competition, which is the common interaction effect that gives rise to the indirect response, occurs mainly on one of these sites. The uncharged solutes seem to be mainly distributed to the sites without competition and only a minor part of the retention is due to the binding to the site with competition.

A quantitative comparison of the influence of the competitive sites on the response of uncharged and charged solutes can be based on eq. (31). Assuming that site 2 is negligible, the product of the fractional coverage and the fractional retention for site 1 can be calculated:

$$\frac{k'_{HA,1} \cdot \Theta_{Q,1}}{k'_{HA}} = \frac{\epsilon^{x}_{HA}}{\epsilon_{Q}} \cdot \frac{1-\alpha_S}{\alpha_S} = F \qquad (37)$$

The results in Table V show that the F values for the uncharged solutes are only about 10% of the value obtained for an anionic solute. It indicates that only a few percent of the retention of the uncharged solutes is due to the competitive sites. The lower F values of butyl acetate and methylisobutyl ketone is due to the inherent absorptivity of these compounds which counteracts the indirect response.

Acknowledgements

The authors are very grateful to Professor H. Poppe (University of Amsterdam, The Netherlands) and to Dr. B. Kågström (University of Umeå, Sweden) for helpful discussions.

References

[1] *G. Schill, D. Westerlund*, in Chemical Derivatization in Analytical Chemistry, R. W. Frei and J. F. Lawrence, eds., Vol. 2, Plenum, New York, 1982, p. 43.
[2] *N. Parris*, Anal. Biochem. **100**, 260 (1979).
[3] *B. A. Bidlingmeyer*, J. Chromatogr. Sci. **18**, 525 (1980).
[4] *M. Denkert, L. Hackzell, G. Schill, E. Sjögren*, J. Chromatogr. **218**, 31 (1981).
[5] *L. Hackzell, G. Schill*, Chromatographia **15**, 437 (1982).
[6] *B. A. Bidlingmeyer, F. V. Warren*, Anal. Chem. **54**, 2351 (1982).
[7] *L. Hackzell, T. Rydberg, G. Schill*, J. Chromatogr. **282**, 179 (1983).
[8] *J. Crommen*, J. Pharm. Biomed. Anal. **1**, 549 (1983).
[9] *J. Crommen, P. Herné*, J. Pharm. Biomed. Anal. **2**, 241 (1984).
[10] *E. Gruschka, S. Levin*, Anal. Chem. **57**, 1830 (1985).
[11] *M. Dreux, M. Lafosse, M. Pequignot*, Chromatographia **15**, 653 (1982).
[12] *W. E. Barber, P. W. Carr*, J. Chromatogr. **260**, 89 (1983).
[13] *W. E. Barber, P. W. Carr*, J. Chromatogr. **301**, 25 (1984).
[14] *T. Gnanasambandan, H. Freiser*, Anal. Chem. **54**, 1282 (1982).
[15] *H. Small, T. E. Miller Jr.*, Anal. Chem. **54**, 462 (1982).
[16] *P. Herné, M. Renson, J. Crommen*, Chromatographia **19**, 274 (1984).
[17] *J. E. Parkin*, J. Chromatogr. **287**, 457 (1984).
[18] *J. Ye, R. P. Baldwin, K. Ravichandran*, Anal. Chem. **58**, 2337 (1986).
[19] *F. Helfferich, G. Klein*, Multicomponent Chromatography, Dekker, New York, 1970.
[20] *F. Riedo, E. Kovats*, J. Chromatogr. **239**, 1 (1982).
[21] *H. Poppe*, University of Amsterdam, 1984.
[22] *A. Tilly Melin, M. Ljungcrantz, G. Schill*, J. Chromatogr. **185**, 225 (1979).
[23] *A. Sokolowski, K.-G. Wahlund*, J. Chromatogr. **189**, 299 (1980).

Received: July 2, 1987
Accepted: July 11, 1987
F

Computer Simulation as a Means of Developing an Optimized Reversed-Phase Gradient-Elution Separation

J. W. Dolan / L. R. Snyder*

LC Resources Inc., 3182C Old Tunnel Rd, Lafayette, CA 94549, USA

M. A. Quarry

Medical Products Dept., E. I. Du Pont de Nemours & Co., Wilmington, DE 19898, USA

Key Words

Gradient elution
Reversed-phase
Method development
Computer simulation
Retention prediction

Summary

A personal-computer program (DryLab G) is described for the simulation of reversed-phase gradient-elution separations. After two experimental gradient runs are carried out initially, this program allows the user to develop a final separation by varying gradient conditions (gradient time, initial and final %-organic in the mobile phase, gradient shape), column dimensions, flowrate and particle size. This approach takes advantage of "solvent-strength selectivity", as reported recently [28] for isocratic separations. Method development using this procedure can result in better separations with much less effort. Examples of its validation and application are presented.

Introduction

Gradient elution is useful for the HPLC analysis of many samples. Mixtures with a wide retention range cannot be handled effectively by isocratic separation, but the use of gradient elution is not restricted to such cases. Sometimes a sample with a limited retention range can be eluted under isocratic conditions, but will nevertheless be better separated by gradient elution. In the past, for various reasons, many workers have been reluctant to accept gradient elution methods. However this situation is now changing, and in the future gradient elution is expected to be used routinely in most laboratories.

The general principles required for developing and optimizing a gradient elution method are now well known [1–4]. However it is doubtful that the full potential of gradient elution is very often realized in practice. The technique is inherently complex, and many different separation variables are involved. As a result, changes in separation conditions not infrequently lead to surprising results and a need for additional experiments. Samples that require gradient elution often contain a larger number of individual components, and this also adds to the difficulty of systematic method development. Finally, the effective use of gradient elution should take advantage of changes in band spacing (variations in α) that can result from a change in gradient conditions (apart from other changes in the HPLC system [4–8]).

A rigorous mathematical description of gradient-elution retention as a function of separation conditions has been available for some time [2–4]. Bandwidth in gradient elution can also be predicted for the various HPLC methods (reversed-phase, ion-exchange, etc.) for different separation conditions, including the nature of the sample and the type of column used [2–4, 9–11]. In principle, it is therefore possible to predict the resolution obtainable in a given separation as a function of such variables as gradient time, initial and final mobile phase composition, flowrate, column dimensions, etc. For a given HPLC system, however, it is necessary to first measure the dependence of isocratic retention on mobile phase composition, for each solute in the sample.

The latter approach presumes the use of a computer in carrying out the necessary calculations for each simulated run (with some change in conditions). Several examples of this type have been reported [12–15]. So far, however, these cases have involved the application of computer-simulation to specific problems. No effort has been made to develop an overall strategy built around computer-simulation as the main tool for developing a gradient-elution method. Also, previous examples of the prediction of separation in gradient elution often lack the accuracy required for method development.

0009-5893/87 0261-16 $03.00/0

© 1987 Friedr. Vieweg & Sohn Verlagsgesellschaft mbH

Commercial software (DryLab G) has recently become available for predicting separation as a function of experimental conditions in reversed-phase HPLC carried out in a gradient mode. Here we describe some preliminary examples which illustrate the potential of this approach for developing and optimizing a final gradient-elution method. We will also explore some possible problems that can arise during computer simulation, especially for the case of unknown samples that contain a large number of components.

Theory

Resolution in both isocratic and gradient elution is given as

$$R_s = 2(t_2 - t_1)/(W_1 + W_2). \qquad (1)$$

Here t_1 and t_2 refer to the retention times t_g of adjacent bands 1 and 2 (sec), and W_1 and W_2 are their baseline bandwidths W (sec). A prediction of resolution therefore requires values of t_g and W for each band in the sample.

Prediction of Retention Times t_g

Retention time in gradient elution is given as (2)

$$\int_0^{t_g} F\,dt/[V_m(1 + k')] = 1 \qquad (2)$$

Here F is the mobile-phase flowrate, V_m is the column dead-volume (equal to F t_0), and k' is the capacity factor of the solute at time t during the gradient. For the case of more complex gradients, those composed of several segments (including pre-elution by the initial mobile phase and post-elution by the final mobile phase), values of t_g can be determined by applying an alternative form of eq. (2) to each gradient segment (pp. 135–42 of Ref. [3]) and combining the results.

The preceding procedure is greatly simplified if an explicit relationship is assumed between capacity factor values k' and mobile phase composition. Numerous studies (see discussion of Ref. [16, 17]) have confirmed that values of k' in reversed-phase HPLC are related approximately to the volume-fraction of organic solvent in the mobile phase (ϕ) as

$$\log k' = \log k_w - S\,\phi. \qquad (3)$$

Here, S is a constant for a given solute, and k_w is the value of k' for $\phi = 0$. This relationship is assumed here as a first approximation, but predicted values of t_g can be corrected for small curvature of plots of $\log k'$ vs ϕ [18].

Estimates of values of k_w and S. Previous attempts to use eq. (1) for the purpose of predicting values of t_g in gradient elution usually assume that values of k' vs ϕ have been determined experimentally from isocratic measurements. However this is experimentally inconvenient, because samples that require gradient elution are not easily studied by isocratic elution. A better approach is to carry out two initial gradient runs and use these to obtain values of $\bar{k}$ and S as described previously [19] for the prediction of isocratic retention as a function of ϕ. This same procedure can be used for predicting t_g values in gradient elution as a function of experimental conditions.

When pre-elution and post-elution of the solute in gradient elution can be ignored, values of $\bar{k}$ and S can be obtained from the numerical solution of two simultaneous equations [19]:

$$(t_g)_i = (t_0/b_i)\log(2.3k_0 b_i + 1) + t_0 + t_D \qquad (4a)$$

and

$$(t_g)_j = (t_0/b_j)\log(2.3k_0 b_j + 1) + t_0 + t_D. \qquad (4b)$$

Here $(t_g)_i$ and $(t_g)_j$ are experimental retention times for a given solute obtained from runs i and j with linear gradients of different steepness: $b = b_i$ and b_j. The quantity t_D is the dwell-time of the HPLC gradient equipment, equal to the time it takes the gradient to move from the mixer to the column inlet. The gradient steepness parameter b is given as

$$b = V_m\,\Delta\phi\,S/t_G\,F, \qquad (5)$$

where $\Delta\phi$ refers to the change in ϕ during the gradient, t_G is gradient time, and S is given by eq. (3). The quantity k_0 refers to the original value of k' at the start of the gradient; it is given by

$$\log k_0 = \log k_w - S\phi_0, \qquad (6)$$

where ϕ_0 is the value of ϕ at the start of the gradient.

The above procedure becomes more complicated when the initial gradient runs are affected by pre-elution of the sample, as can occur when the dwell time t_D is fairly large, and values of k_0 are small (see discussion of Ref. [20]). In principle this problem could be handled by techniques for the numerical solution of eq. (1) as applied to the combined gradient, which includes pre-elution followed by gradient elution. An example of this approach is suggested by the work of Parente and Wetlaufer [21], for the prediction of corresponding isocratic parameters in ion exchange. However this procedure can be complex as well as time consuming; we wanted a method that would yield final values of k_w and S within short run-times on a personal computer such as the IBM PC. We were able to achieve this by an iterative solution based on the fact that S-values obtained from eqs. (4a, b) are relatively insensitive to pre-elution. This procedure is incorporated into the DryLab G software used in the present study.

Prediction of Bandwidth W

Elsewhere [4] it has been shown that bandwidth in gradient elution is given as

$$W = t_0(1 + k_f)\,J\,G\,N^{-1/2}, \qquad (7)$$

where k_f is the value of k' at the time the band leaves the column, N is the column plate number, G is a gradient "compression factor" and J is a correction factor that accounts for an anomalous broadening of bands in gradient elution when the gradient is quite steep [9]. If experimental values of J are multiplied by calculated values of G, it is found that the product

$$JG \approx 1.1 \pm 0.1 \tag{8}$$

over the entire range of values of b. This allows eq. (7) to be restated approximately as

$$W = 1.1 t_0 (1 + k_f) N^{-1/2}. \tag{9}$$

Eq. (9) has been found by others [3] to be in approximate agreement with experimental data from a number of gradient HPLC systems. The value of k' when a band leaves the column during gradient elution is given as [2]

$$k_f = 1/[2.3b + (1/k_0)]. \tag{10}$$

Value of N in gradient elution. The quantity N in eq. (9) is the plate number measured in a "corresponding" isocratic system, where the effective value of k' in gradient elution ($\bar{k}$, equal to k' when the band is at the column midpoint) is equal to k' in isocratic elution for the same column and similar other conditions. Values of N can be predicted as described elsewhere [4, 22, 23], when the chromatographic conditions are specified and the molecular weight of each solute can be estimated.

Control of Resolution in Gradient Elution

Resolution in gradient elution can be expressed as a function of the same factors that are used to control resolution in isocratic separation; i.e., capacity factor k', plate number N and separation factor α:

$$R_s = (1/4)\ (\alpha - 1)\ N^{1/2}\ [\bar{k}/(1 + \bar{k})]. \tag{11}$$

Previous discussions of resolution in gradient elution [1, 2, 4, 24, 25] have emphasized the importance of the column plate-number N and the effective capacity factor $\bar{k}$. Systematic changes in gradient conditions that affect N and $\bar{k}$ can be used to increase the peak capacity of a gradient separation and maximize overall resolution.

We believe that changes in band spacing (values of α) are of equal importance in optimizing separations by gradient elution. All the separation variables used to control values of α in isocratic elution can be used in the same way for gradient elution: a change in the organic solvent, changes in pH or temperature, a change in the column stationary phase, etc. (1, and see specific examples of Ref. [14, 15, 26] for gradient elution).

During the initial phase of method development for gradient elution, we have found that changes in α are conveniently achieved by varying gradient conditions so as to vary $\bar{k}$ [5, 8], which is given as

$$\bar{k} = 1/1.15b. \tag{12}$$

Corresponding changes in band spacing are also observed in isocratic elution as k' or ϕ is varied ([27, 28], and see especially discussion of Ref. [29]). Previously we have shown that it is possible to systematically vary gradient-elution band-spacing in this way by changing either flow-rate or gradient time. Here we will show that similar changes in band spacing can also result from changes in ϕ or the use of complex gradients (linear segments of different steepness). This in turn provides a basis for a considerable control over band spacing in gradient elution.

Experimental

Equipment, Materials and Procedures

The HPLC system was a DuPont 8800 liquid chromatograph equipped with a Model 860 fixed-wavelength (254 nm) detector and column oven. Procedures and solvents are described in Ref. [20].

Samples. The polyaromatic hydrocarbon mixture was supplied by Supelco Inc. (Bellefont, PA). The herbicide mixture was obtained from the Agricultural Chemicals Dept. of DuPont (Wilmington, DE, USA), and is described further in Ref. [29]; several of these compounds are proprietary in nature, and their exact composition was not disclosed to us.

Computer Simulations

All simulations were carried out on an IBM XT personal computer, using DryLab G software (LC Resources Inc., Lafayette, CA, USA).

Results and Discussion

The application of a somewhat complex scheme for the computer simulation of gradient-elution separation first requires validation of the overall procedure. Then a systematic approach based on computer simulation must be designed for the development of optimized gradient elution methods. This approach will differ from that used in experimental trial-and-error procedures (the traditional way in which gradient methods have been developed), for reasons that will become apparent. Next, possible problems that can arise in the computer-simulation approach should be considered, and remedies to these problems must be found. Finally, actual applications of the overall scheme to real samples are required – as a practical demonstration of the value of such an approach. The present paper will address each of these areas.

Accuracy in the Prediction of Retention in Gradient Elution

Previous studies [2–4, 30, 31] have reported on the accuracy of predictions of gradient retention t_g as a function of values of k_w and S obtained from corresponding isocratic runs. Here we are interested in the accuracy of t_g-values predicted from k_w and S values derived from initial gradient runs. Because these data are to be used mainly for predictions of resolution (eq. (1)), the accuracy of relative retention $(t_2 - t_1)$ is of greater interest than the accuracy of individual t_g-values. The present software (DryLab G) is also designed to correct for pre-elution effects in (a) the gradient data from which values of k_w and S are initially derived and (b) t_g-values that are to be predicted by computer-simulation. We have therefore tested these specific cases. Suitable data for the present validation of the DryLab G software were either (a) obtained from the literature or (b) measured by us as reported here.

Phthalate ester sample. Gradient retention data have been reported [31] for five C_1–C_5 dialkylphthalates under various conditions. DryLab G requires starting data for two runs carried out with different t_G values; gradient times of 20 and 80 min were selected for this purpose from the data of Ref. [31] (other conditions the same). In selecting values of t_G for the two starting gradient runs, it is advisable that these t_G-values differ by a factor of 3 or more for maximum accuracy in the resulting predictions of t_g for other gradient conditions [19]. With these two experimental runs as input to DryLab G, computer simulation was then carried out for other gradient times, as summarized in Table I.

The experimental test of computer-simulation summarized in Table I corresponds to near-ideal experimental conditions. All bands (except one solute in one run) elute during the gradient, with negligible contribution of pre-elution effects during initial elution. Furthermore, special care was taken in this study to evaluate the usual contributions of equipment and other factors to non-ideal gradient behavior (see discussion of [20, 31]). As a result, we should see good agreement between the experimental and calculated values of t_g in Table I. Maximum accuracy in such predictions will occur for interpolated conditions ($20 < t_G < 80$ min), and for this case (Table I, $t_G = 40$ min) we see that both retention time and resolution (R_s is proportional to $[t_2 - t_1]$) are predicted within about ± 1% (1 SD). For other values of t_G (5, 10, 160, 320 min), the prediction of retention time is accurate within an average error of ± 6% (1 SD), while resolution is accurate within ± 5%. This is adequate for the purposes of using computer-simulation in lieu of actual gradient runs during method development.

The agreement between experimental and computer-simulated values of t_g and resolution in Table I is superior to that found for corresponding isocratic values predicted from the same experimental gradient data [19]. That is, experimental gradient data seem better suited for predicting t_g values in gradient elution, than for predicting isocratic retention as a function of ϕ. We have seen other instances where both this and the converse are true (i.e., isocratic data are better suited for predicting isocratic retention as a function of ϕ). From a practical standpoint, when the highest accuracy in computer-simulated retention or resolution data are required, it suggests using experimental runs that are matched to the same technique as assumed for the computer simulations (isocratic/isocratic or gradient/gradient).

Steroid sample. Gradient separations were carried out with a 6-component steroid sample, varying both gradient time and range. Separations for a 5–100% methanol/water gradient and t_G-values of 30 and 90 min are shown in Fig. 1, with retention data superimposed on these plots. Additional runs were carried out, varying not only gradient time but the initial and final ϕ-values for the gradient. This provides an additional test of the DryLab G software for retention predictions when substantial pre-elution of the solute occurs (see Table II).

It is seen in Table II that retention times t_g are predicted with an average error of ± 3% (1 SD), while resolution (values of $t_2 - t_1$) are accurate with an average error of ± 7% (1 SD). This is adequate for purposes of method development. The data of Fig. 1 and Table II can also

Table I. Comparison of experimental and computer-simulation values of t_g in the gradient separation of five dialkyl-phthalates. Experimental data of Ref. [31], computer simulations using DryLab G. 25-cm column of Zorbax® ODS (6-nm pore), 10–100% acetonitrile/water gradients, 35°C, dwell volume $V_D = 5.5$ mL, data for $t_G = 20$ and 80 min used as inputs to DryLab G.

$t_G = 5$ min

Solute	t_g (min) expt.	t_g (min) calc.	$(t_2 - t_1)$ (min) expt.	$(t_2 - t_1)$ (min) calc.	% error t_g	% error $(t_2 - t_1)$
C_1	6.88	6.78	0.78	0.74	−2	−5
C_2	7.66	7.52	0.28	0.29	−2	+3
C_3	7.94	7.81	1.13	1.02	−2	−10
C_4	9.07	8.83	0.68	0.45*	−3	–
C_5	9.75	9.28*			–	
				avg error (1 SD)	−2 ± 0	−4 ± 8

Solute	t_g for indicated value of t_G: $t_G = 10$ min expt.	$t_G = 10$ min calc.	$t_G = 40$ min expt.	$t_G = 40$ min calc.	$t_G = 160$ min expt.	$t_G = 160$ min calc.	$t_G = 320$ min expt.	$t_G = 320$ min calc.
C_1	8.82	8.71	16.20	16.41	32.0	30.9	43.8	39.7
C_2	10.31	10.17	21.72	21.94	51.7	50.1	79.8	72.7
C_3	10.92	10.79	24.45	24.65	62.9	61.3	102.1	94.5
C_4	12.83	12.75	31.76	31.92	89.7	87.8	153.5	144.3
C_5	13.74	13.68	35.80	35.86	105.4	104.2	183.6	177.5
error (1 SD)								
t_g	−1 ± 0%		+1 ± 0%		−3 ± 3%		−7 ± 3%	
$(t_2 - t_1)$	0 ± 2		−1 ± 1		0 ± 3		+0 ± 8	

* DryLab G indicated that this band elutes after the gradient is over; while DryLab G corrects for such post-elution, the rounding of the gradient near its end is quite severe for small values of t_G (see discussion of Ref. [18, 30]), leading to greater error in the final value of t_g predicted by computer-simulation

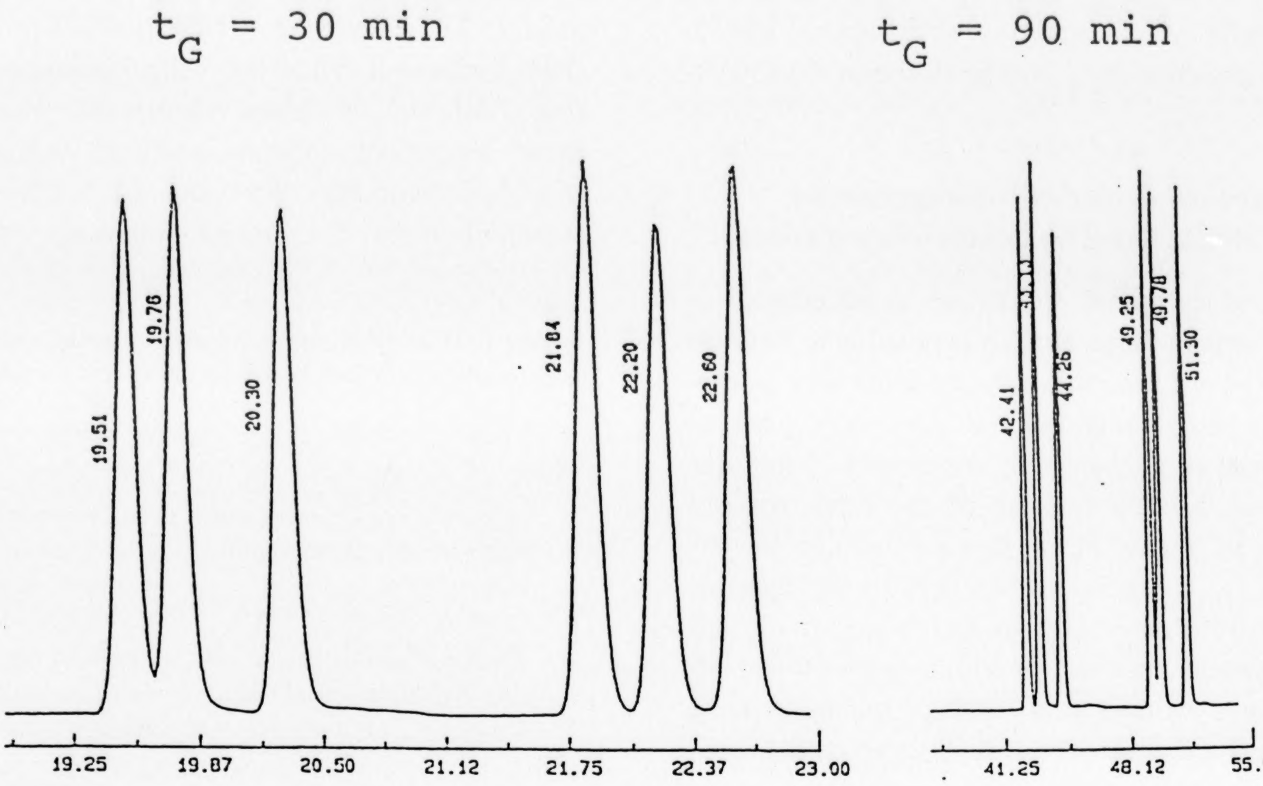

Fig. 1

Gradient separations of a steroid sample with two different values of t_G. Data used for calculations of Table II. Column, 25 X 0.46-cm Zorbax® ODS; 5–100% methanol/water gradients; flowrate, 2 mL/min; 35°C, dwell volume V_D = 5.5 mL. Sample components, in order of elution (#1–6 of Table II): prednisone (band 1), cortisone (2), hydrocortisone (3), dexamethasone (4), corticosterone (5), cortexolone (6)

Table II. Comparison of experimental and computer-simulation values of t_g in the gradient separation of six steroids. Experimental runs of Fig. 1 used as input to DryLab G. Other conditions the same, except for gradient time t_g and gradient range.

	t_g for indicated values of t_g and gradient range (min)							
Solute*	t_g = 15 min 5–100% MeOH**		t_g = 45 min 5–100% MeOH**		t_g = 30 min 35–75% MeOH**		t_g = 15 min 55–75% MeOH**	
	expt.	calc.	expt.	calc.	expt.	calc.	expt.	calc.
1	12.71	12.62	25.83	25.75	13.51	13.85	3.86	3.46#
2	12.84	12.75	26.20	26.12	14.04	14.38	4.08	3.70#
3	13.18	13.07	26.82	26.84	15.05	15.38	4.71	4.43##
4	13.89	13.80	29.29	29.22	18.72	18.96	6.44	6.37##
5	14.13	14.04	29.72	29.66	19.23	19.52	7.00	6.99##
6	14.29	14.20	30.38	30.32	20.33	20.58	7.56	7.60##
error (1 SD)								
t_g	+ 1 ± 0%		0 ± 0%		− 2 ± 1%		+ 5 ± 5%	
$(t_2 - t_1)$	+ 1 ± 5		+ 1 ± 5		+ 3 ± 6		+ 8 ± 9	

* numbered in order of elution; see Figure 1 for identity (no band reversals)

** MeOH refers to methanol

# these bands elute isocratically in 55% MeOH/water (before start of gradient)

## these bands exhibit pre-elution; fractional migration in initial mobile phase (55% MeOH) is: band #3, 79%; band #4, 46%; band #5, 40%; band #6, 35%; i.e., band #3 migrates 79% through the column before the initial gradient reaches it.

be used to illustrate another practical point. Generally it is advantageous to use larger values of t_g (or $\bar{k}$) in the experimental runs used for computer simulation. Thus, if the 15 and 45-min runs of Table II are used as input for computer simulation, the resulting errors in predicted resolution (for the remaining runs of Fig. 1 and Table II) are significantly larger: ± 11% (1 SD), or 50% greater error than for the predicted values of Table II[1]. This is discussed in a later section.

---

[1] In this case (15/45-min runs) the predicted values of t_g are in error by only ± 2% (1 SD), which is misleading if considered in isolation. That is, accuracy in values of $(t_2 - t_1)$ is of major concern, since this determines the accuracy of predictions of resolution for various experimental conditions.

Additional examples of the accuracy of computer simulation for predicting values of t_g will be found in the following discussion.

A Systematic Approach to Method Development for Gradient-elution HPLC, Based on Computer-simulations

With the advent of computer simulation as an alternative to trial-and-error experimental runs, it is possible to develop and improve a gradient separation in the same way as previously — where actual experimental runs were used to evaluate separation vs a change in conditions. Computer simulation requires a small fraction of the time required for actual runs, so many more possibilities can be explored. However a computer offers additional features that we will illustrate here. This in turn suggests the approach to systematic method development outlined in Table III, which has evolved as a result of our experience with the DryLab G program. We will illustrate this procedure with several examples.

Mixture of OPA-Amino Acids

Eslami et al. [32] have reported data for the separation of 22 o-phthaldehyde (OPA) amino acids by reversed-phase HPLC (17–55% acetonitrile/water linear gradients). These data (32 runs involving different t_G values and 5 different column lengths) were made available to us for evaluation using DryLab G. In the following example, we have assumed that an optimum method is to be developed, and have used those data that were appropriate to this goal. We will follow the 6 steps of Table III.

Step 1. Two gradients were run initially, with the results shown in Figs. 2a, b. The gradient times are (a) $t_G = 15$ min and (b) $t_G = 35$ min. It is seen that there are 22 distinct bands in each chromatogram; i.e., no unresolved band pairs. DryLab G requires that each band in the second run (b) be numbered to correspond to band-sequence in the first run; i.e., the band labeled #1 must be the same compound in each run, even if there are band reversals between the two runs. We will discuss this further in a following section. It is seen that there are no band reversals in run (b), so retention times for each run are entered in sequence.

Step 2. These retention data and other separation conditions (see Fig. 2) were entered into the computer, and a relative-resolution map (RRM) was requested, as shown in Fig. 3. A RRM is a plot of the resolution of the poorest-resolved band-pair in the sample vs gradient time t_G, assuming a 10,000-plate column (N = 10,000) [27, 28]. It allows a quick conclusion as to the optimum gradient time for a given separation. Note that the poorest-resolved band-pair is indicated on the RRM; this is seen to be bands #9/10 for $t_G < 5$ min, and bands #6/7 for $t_G > 5$ min. The maximum resolution possible for this sample, using the same column and flowrate, is about $R_s = 1$ for a 10,000-plate column. That is, this is a fairly difficult separation. We also see that there are no band-reversals as t_G is varied; i.e., there is little change in separation selectivity as a function of t_G or $\bar{k}$. This is somewhat unusual, as will be seen from later examples.

Step 3. The resolution of bands #6/7 in Fig. 2a is about 0.94, estimated from the valley between the two bands (see Table IV). A plate number for the column under these conditions (15 min gradient) was next requested. DryLab G estimates this value of N (N = 11,600 in this example) from the known retention times and resolu-

Table III. Recommended approach to HPLC method development using gradient elution, based on computer simulation with DryLab G.

Step	Goal
1. carry out two experimental runs with 5–100% organic/water gradients, and t_g values of 30 and 90 min*	input retention data into computer to allow predictions of separation as a function of varying conditions
2. request a relative-resolution map (RRM) as a function of t_g	determine feasibility of sample separation with present HPLC system**; determine optimum t_G-value (preliminary)
3. adjust resolution to match one of initial experimental runs (optional)***	obtain exact resolution values for computer simulations with original column and flowrate
4. determine optimum gradient range	minimize run time
5. fine-tune band-spacing and resolution, by (a) varying initial %-organic in gradient, (b) using segmented (non-linear) gradient	optimize final gradient for resolution and run time
6. vary column conditions while holding gradient conditions fixed	retain optimized band spacing from steps #2–5, while optimizing plate number N; finalize method for adequate resolution, acceptable pressure and minimum run time

* the choice of t_G-values is arbitrary; the two values should differ by a factor of 3 to 4 for accurate predictions, columns with large N-values are preferred (e.g., 25-cm, 5-μm), and flowrates should be 1–2 mL/min

** for the successful development of a final gradient method, the RRM should show $R_s > 1$ for some value of t_G

*** this option is mainly useful when column length, particle size and flowrate are to be held constant; for this situation, simulations as a function of gradient conditions will more closely match experimental runs

Table IV. Estimating resolution from the valley between two overlapping bands. Calculated for Gaussian bands.

Valley*	R_s for indicated ratio of band sizes				
	1/1	2/1	4/1	8/1	16/1
3%	1.46	1.50			
5	1.35	1.42	1.48	1.52	
8	1.26	1.33	1.40	1.45	1.50
10	1.22	1.29	1.35	1.41	1.47
15	1.14	1.21	1.27	1.33	1.39
20	1.07	1.15	1.21	1.27	1.33
30	0.97	1.06	1.12	1.19	1.24
40	0.90	0.98	1.06	1.12	1.18
50	0.83	0.92	1.00	1.07	1.12
60	0.78	0.87	0.95	1.02	1.08
80	0.68	0.78	0.86	0.93	0.99

* Measured as height of valley from baseline divided by height of smaller band; see Ref. [1], pp. 46–7 for details

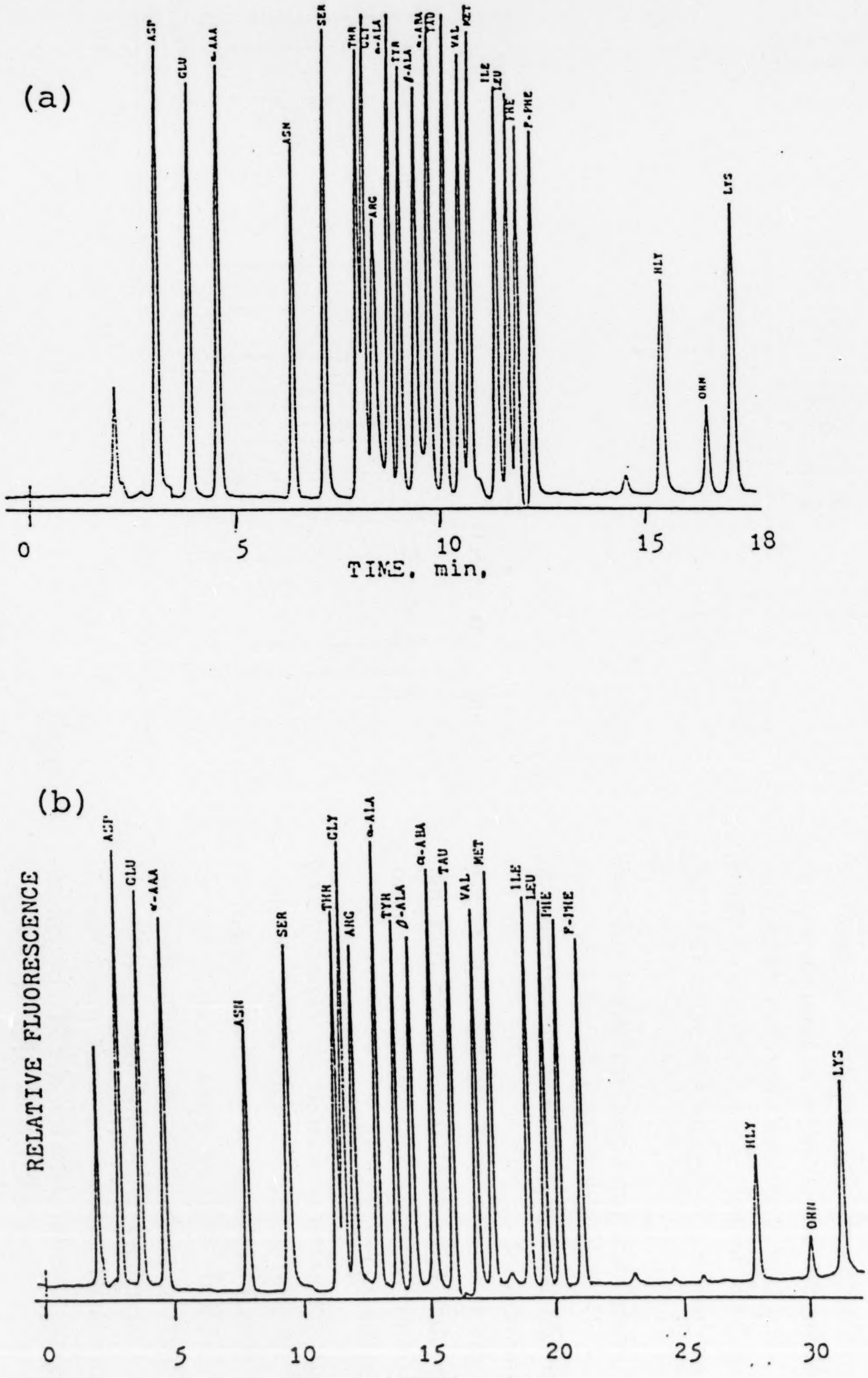

Fig. 2

Gradient separations of a mixture of 22 OPA-derivatives of the common amino acids. Data used for calculations discussed in text and shown in Figs. 6 and 7. Column, 15 × 0.46-cm IBM C18; 17–55 % acetonitrile/water gradients; flow-rate, 0,8 mL/min; 22°C; system dwell-volume equal to 0.0 mL. Sample

(c)

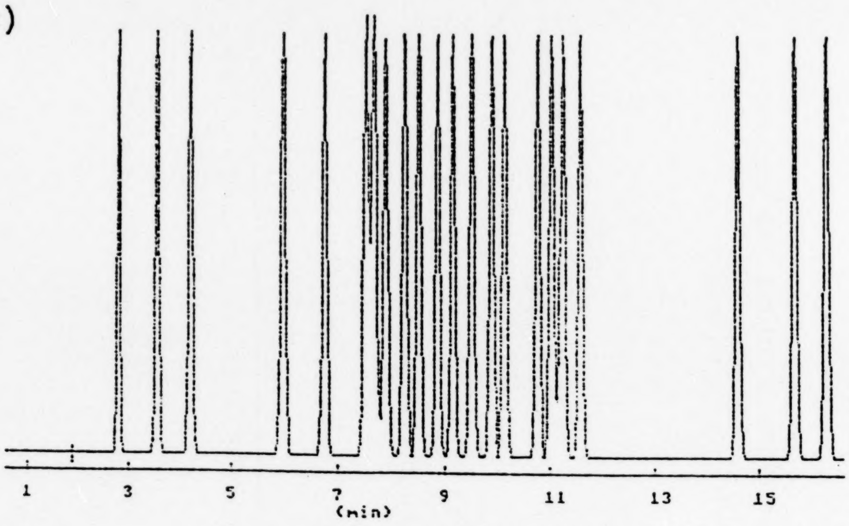

(d)

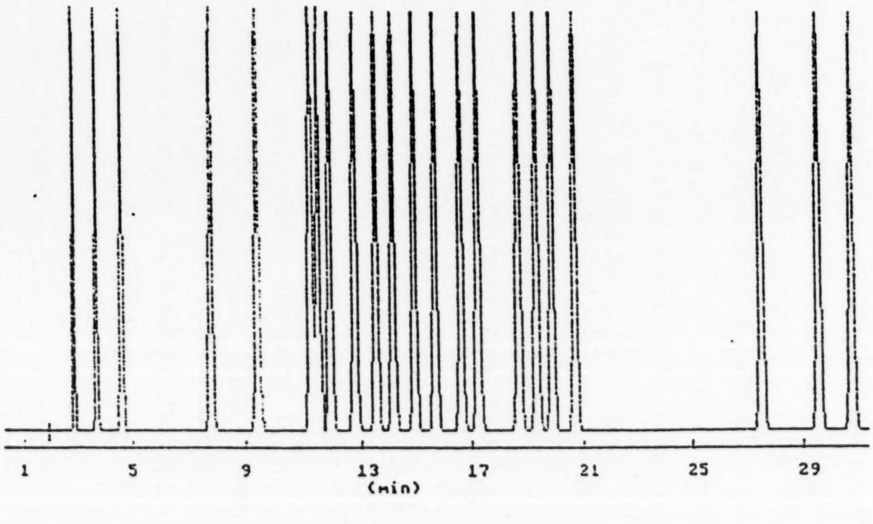

components identified in chromatograms. (a) experimental chromatogram, t_G = 15 min; (b) experimental chromatogram, t_G = 35 min; (c) simulated chromatogram, t_G = 15 min; (d) simulated chromatogram, t_G = 35 min.

tion. Selecting this DryLab G option automatically adjusts all resolution calculations for the actual plate number of the column, rather than for an N-value of 10,000 as in Fig. 3. At this point we have the option of simulating the starting runs (Figs. 2a, b), and these simulations are shown in Figs. 2c, d for comparison with the experimental runs (Figs. 2a, b). Good agreement between computer-simulated and actual runs is observed. Returning to Fig. 3, we see that resolution reaches a maximum for $t_G = 25$–30 min. Under these conditions, the shortest gradient time is desirable, and a value of $t_G = 27.5$ min was selected.

Step 4. The gradient range (initial and final %-organic in the mobile phase) was next adjusted. The computer will recommend an approximately optimum range if requested: 15–59% acetonitrile/water was predicted in this case. This range is slightly different from that used initially (17–55%), but not significantly so. In this case we opted to keep the original range (17–55%) because experimental data were not available for other ranges.

Step 5. Changes in ϕ_0 or gradient shape were not considered useful in the present example, because of the minimal change in selectivity (band spacing) as t_G and $\overline{k}$ are varied. Trial-and-error changes in these parameters, using computer simulation, confirmed that this was the case.

Step 6. Computer simulations were continued by varying column conditions. DryLab G allows variation of column dimensions, particle size and flowrate. Since only columns of varying length were available in the present data set, a longer column (25 cm) was tried. When column size or flowrate is changed in gradient elution (eq. (5)), the effective gradient steepness b changes also. Since Steps 1–5 are intended to optimize b and sample retention, it is undesirable to vary b when optimizing column conditions. DryLab G therefore automatically adjusts the gradient time t_G to compensate for any changes in column size or flowrate (so as to keep b and relative retention constant). In this case, the use of a longer column (25 cm vs 15 cm to start) requires an increase in t_G by the ratio (25/15), or a final t_G-value of 46 min.

The simulated chromatogram predicted for these gradient conditions is shown in Fig. 4a. Band-pair #6/7 is least resolved, with a predicted $R_s = 1.36$. The actual chromatogram for these conditions is shown in Fig. 4b; the experimental resolution for bands #6/7 is $R_s = 1.5$ (Table III). This is reasonable agreement, considering that different columns (15 cm) were used to generate the computer simulation for the 25-cm column.

Retention data for computer-simulated vs experimental runs. Comparison of the simulated and actual chromatograms of Fig. 4 shows an error in predicted retention times of $-2 \pm 1\%$ (1 SD), and an error in $(t_2 - t_1)$ of $3 \pm 9\%$ (1 SD). This compares favorably with the data of Tables I and II, especially when the use of different columns for experimental input and final prediction is considered. When experimental data for the 25-cm column were used for computer simulation (14 and 46-min gradients), similar errors in predicted t_g-values was found for experimental runs with other gradient times:

t_G	error in t_g (1 SD)
8 min	$2 \pm 4\%$
10	$2 \pm 2\%$
18	$-1 \pm 1\%$
26	$-1 \pm 1\%$
34	$-1 \pm 1\%$

This example therefore confirms the accuracy of these DryLab G simulations.

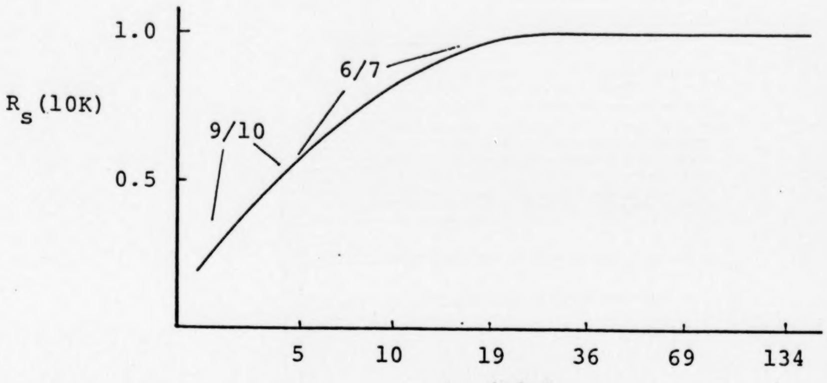

Fig. 3

Relative-resolution Map for OPA-amino acid separations of Fig. 2. Calculated by DryLab G.

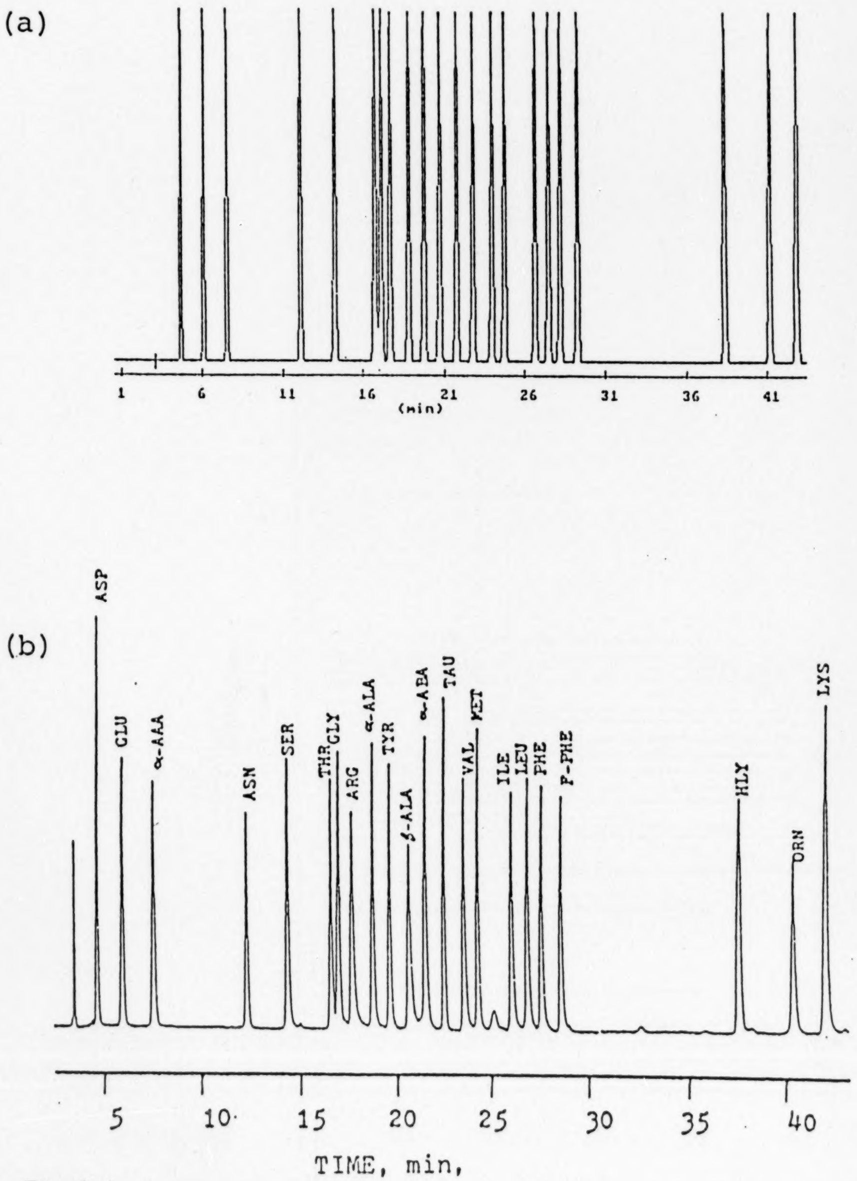

Fig. 4

Optimized separation of OPA-amino acids. Column, 25-cm; gradient time, 46 min; other conditions as in Fig. 2. (a) DryLab G simulation; (b) experimental run.

Mixture of Polyaromatic Hydrocarbons

A sample containing 16 priority pollutants (polyaromatic hydrocarbons, PAHs) required analysis, using reversed-phase gradient elution. Previously a method had been developed for this mixture, using the conventional trial-and-error approach based on experimental runs. The best separation that could be achieved required 17 min for elution of the last band, with a resolution of $R_s = 0.94$ for the poorest-resolved band-pair. Typically the development of such a method would require a minimum of half a dozen runs, and 3 to 5 days of work in the laboratory (depending on the experience of the chromatographer). The design of the DryLab G software makes rapid method development less dependent on operator skill, because each trial-and-error run can be carried out in 2–5% of the time required for an actual run. Computer simulation was next used to repeat the development of this method, using the same column and flowrate employed in the original procedure.

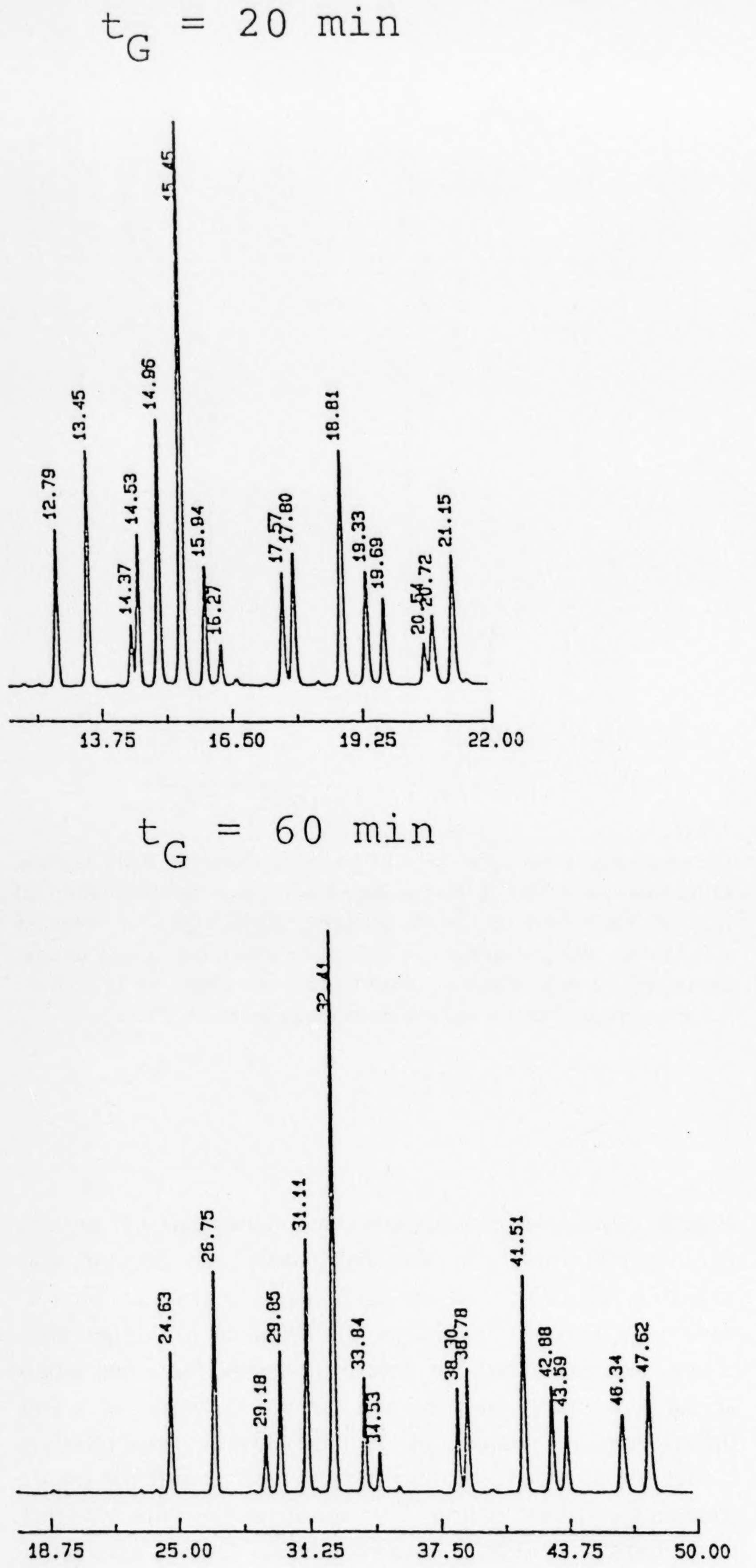

Fig. 5

Gradient separations of a polyaromatic-hydrocarbon sample with two different values of t_G. Data used for calculations discussed in text and shown in Figs. 6 and 7. Column, 15 × 0.46-cm Supelcosil® LC-PAH; 5–100% acetonitrile/water gradients; flowrate, 2 mL/min; 35°C; system dwell-volume equal 5.5 mL. Sample components in order of elution (#1–16) are: naphthalene (1), acenaphthylene (2), acenaphthene (3), fluorene (4), phenanthrene (5), anthracene (6), fluoranthene (7), pyrene (8), benz(a)anthracene (9), chrysene (10), benzo(b)fluoranthene (11), benzo(k)fluoranthene (12), benzo(a)-pyrene (13), dibenz(a,h)anthracene (14), benzo(g,h,i)perylene (15), indeno(1,2,30cd)pyrene (16).

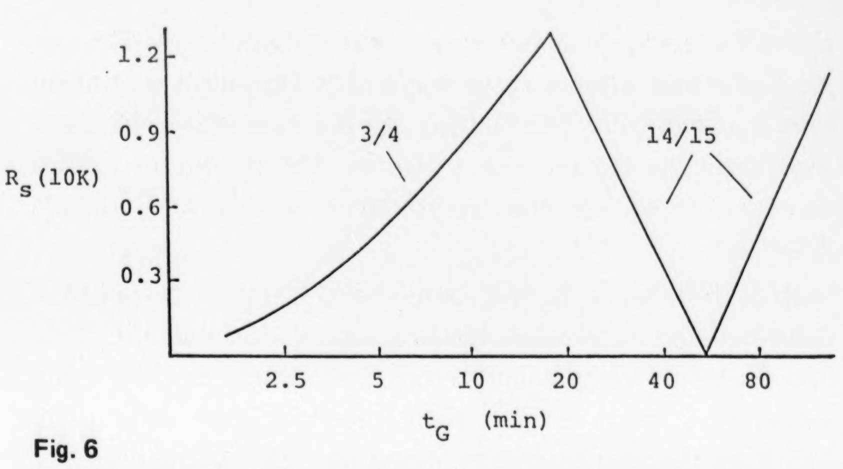

Fig. 6

Relative-resolution Map for PAH separations of Fig. 5. Calculated by DryLab G.

Steps 1 and 2 (Table III). Two gradients were carried out initially, with the results shown in Fig. 5 (step 1). Sixteen bands can be seen in the 20-min gradient run, and 15 bands are present in the 60-min run; bands #14/15 appear to have fused together in the 60-min run. These retention data were entered into the computer, and a relative-resolution map was requested, shown in Fig. 6 (step 2). It appears that a resolution of about $R_s = 1.3$ can be achieved with a 10,000-plate column, so it should be possible to achieve adequate separation of this sample within a reasonable run-time. Band-pair #3/4 limits resolution for $t_G < 20$ min, while band-pair #14/15 limits resolution for $t_G > 20$ min. Bands #3/4 move apart (increase in α) as t_G increases, while bands #14/15 move together with increase in t_G.

Step 3. The resolution of bands #14/15 in the 20-min run of Fig. 5 is about 1.03, estimated from Table IV. A plate number for the column under these conditions was next requested, along with an automatic adjustment of all resolution calculations for a column having this value of N (N = 7142). The optimum gradient time from Fig. 6 is about 20 min; a more precise value for this number was next obtained by asking for a summary of R_s vs t_G for $15 \leqslant t \leqslant 27$ min. The best value of t_G determined in this way was $t_G = 19$ min, with a minimum resolution (bands #14/15) of 1.05. This run compares favorably with the original method (slightly better resolution, $R_s = 1.05$ vs 0.94; the run times are essentially the same, 17 vs 19 min.

Step 4. The gradient range was next optimized. Entering a t_G-value of 19 min into the computer, a gradient range of

44–94% acetonitrile/water was recommended by DryLab G. These values were accepted, and an optimum separation was automatically determined by the computer: 44–94% acetonitrile/water with $t_G = 10$ min. The minimum resolution predicted by the computer was $R_s = 1.11$ (bands #14/15).

Step 5. Finally, a further attempt was made to improve run-time and resolution by fine-tuning the gradient. This can be done by trial-and-error; e.g., simply try different values of ϕ, or investigate segmented-gradients. Often it is useful at the end of step 4 to examine the whole chromatogram as a function of a change in t_G. When this was done for the present sample, it was found that bands #3/4 and 14/15 limit resolution as t_G is varied (as in Fig. 6):

t_G	R_s (3/4)	R_s (14/15)
5 min	0.89	1.39
10	1.29	1.11
20	1.47	0.72

These data suggest the use of a 2-step gradient; i.e., a shallow gradient-step (larger $t_G/\Delta\phi$) for the initial separation of bands #3/4 and a steep gradient-step (smaller $t_G/\Delta\phi$) for the final separation of bands #14/15.

Various 2-step gradients were next examined by computer simulation. The first step was selected from 44% acetonitrile starting to a value of 55–70%, ending in a time of 4–8 min. The second step was from 55–70% acetonitrile to a value of 100%[2] in a time of 1–4 min. The best choice of gradient, on the basis of these simulations was a gradient from 44–60% acetonitrile in 7 min, followed by a gradient of 60–100% in 2 min (total $t_G = 9$ min).

The resulting computer simulation for this optimum gradient (44/60/100%, 0/7/9 min) showed a minimum resolution of 1.26 and a run time of 13 min. The computer-simulated chromatogram is shown in Fig. 7b. The conditions for the original method (25/35/100%, 0/2/16 min) were also entered into the computer, giving the chromatogram of Fig. 7a. It is seen that the optimum separation of Fig. 7b is faster (13 vs 17 min) and resolution is better ($R_s = 1.26$ vs 1.00 calculated[3]).

More significantly, perhaps, only a half-day of work has been required to this point, including about 30 min of computer simulations. Finally, the PAH mixture was run using the final, optimum conditions (44/60/100%, 0/7/9 min), with the result shown in Fig. 7c. There is reasonably close agreement between the simulated run of Fig. 7b and the actual run of Fig. 7c, as summarized in the following section.

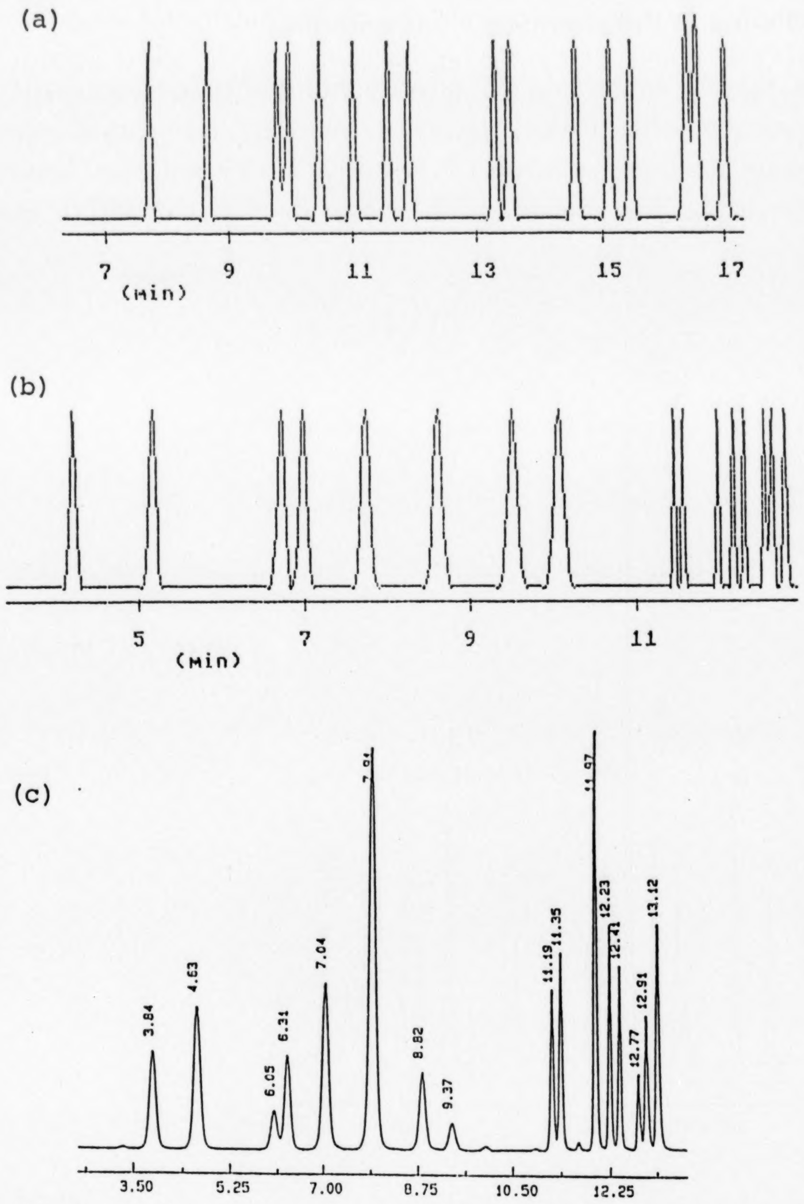

Fig. 7

Chromatograms for gradient-elution separations of PAH sample. Conditions as in Fig. 5, unless stated otherwise. (a) simulation of original PAH method: 2-step gradient, 35/35/100% in times of 0/2/16 min; (b) simulation of optimum separation predicted by computer: 2-step gradient, 44/60/100% in times of 0/7/9 min; (c) actual separation for same conditions as in (b).

Step 6. Computer simulations were continued by varying column conditions. In this case, only one column was available, so only flowrate variation was studied. Significant improvement in R_s, at the expense of longer run-times, was predicted for lower flowrates. However when actual separations were carried out for flowrates of 1 and 0.5 mL/min (t_G values of 18 and 36 min, respectively), it was found that resolution became poorer and the bands showed significant tailing. This abnormal behavior was not predicted by DryLab G, and may be an artifact associated with the use of the polymeric bonded phase used in these columns.

Data for computer-simulated vs experimental runs of Fig. 7. A detailed comparison was made between the runs of Figs. 7b, c in terms of retention, bandwidth, and resolution. Our purpose was mainly to verify the accuracy of computer-simulation for complex gradients – in this case a 2-step gradient with significant pre-elution of early bands. The overall agreement between these two runs was satisfactory, but not as good as observed earlier for

[2] It might seem logical to end the gradient at the value of 94% acetonitrile initially recommended by the computer. Because the second step is steep, however, it was considered advisable to increase the gradient range as much as possible, in order to minimize effects from the rounding of the gradient by the equipment [20].

[3] The calculated value of $R_s = 1.00$ for the original method can be compared with a value of $R_s = 0.94$ from the actual chromatogram (not shown).

simple linear gradients. One reason for this is that rounding of the gradient by the equipment [20] is more serious for the case of segmented gradients (vs linear gradients), and is not taken into account by the present version of DryLab G. Errors in the predicted values of various quantities were as follows (averages for 16 bands): retention time t_g, $-4 \pm 3\%$ (1SD); $(t_2 - t_1)$, $10 \pm 11\%$ (1SD); bandwidth, $10 \pm 17\%$ (1SD); resolution, $0 \pm 21\%$ (1SD). Note that the combination of an 11% error in $(t_2 - t_1)$ with a 17% error in bandwidth should yield a 20% error in resolution; this agrees with the observed value (± 21%).

Mixture of Herbicides

A sample containing 15 herbicide compounds was to be analyzed by reversed-phase HPLC. Unlike the preceding two samples, which are comprised of mixtures of structurally similar compounds, these herbicides represent a number of different compound types. It was therefore anticipated that band-spacing changes as a function of gradient time t_G would be more pronounced.

Steps 1 and 2 (Table I). Two gradient runs were carried out initially, as shown in Fig. 8. Fifteen distinct bands can be observed in each run, but it is seen that the sequence of bands in the two runs is not identical; bands #8 and 9 reverse their positions in the chromatogram as t_G is changed from 30 to 90min. These retention data (after assignment of the correct band position for each compound) were entered into the computer, and a relative-resolution map was requested (Fig. 9). The RRM of Fig. 9 indicates a much more complex dependence of relative retention on gradient time (and $\overline{k}$) than was found in the previous examples of Figs. 3 and 6. There are four band-reversals as t_G is increased from 5min to 100min. This is illustrated further in the chromatograms of Fig. 10; bands #6 and 8 overlap in the 15-min run, bands #8 and 9 overlap in the 60-min gradient, and bands #2 and 3 are unresolved in the 120-min gradient. Other changes in band position can also be observed in the runs of Figs. 8 and 10.

Step 3. The marginal resolution observed in the RRM of Fig. 9 suggests that we will have to optimize column conditions for a satisfactory final separation. Therefore the empirical adjustment of resolution at this step was omitted. The resolution map of Fig. 9 suggests that an optimum t_G-value (for this gradient range) is about 20min.

Step 4. The gradient range was next optimized. Entering a t_G-value of 20min into the computer, a gradient range of 17–77% acetonitrile/water in a gradient time of 16min was recommended. Resolution ($R_s = 1.1$ min) and run time (16min vs 21min for 5–100% run) were not much improved, however. This simulated run is shown in Fig. 11a.

Step 5. Various attempts were next made to improve the separation by varying the starting %-organic (ϕ_0) and/or using multi-step gradients. The DryLab G software allows a rapid assessment of the value of changes in ϕ_0, accompanied by optimization of t_G. Following a change in ϕ_0, a RRM can be requested so as to optimize t_G. This is illustrated in Fig. 12, for ϕ_0-values of 5, 10, 15 and 20%. Significant changes in resolution are observed as ϕ_0 is varied; the major effect is an increase in R_s for larger t_G-values ($100 < t_G < 250$ min) as ϕ_0 is increased. A R_s-value of 1.7 can be obtained with a 20–100% acetonitrile gradient, for a gradient time of 250min. However we found that a better approach was to use a t_G-value corresponding to about 20min in Fig. 9, then optimize column conditions (column length and flowrate). The actual (starting) gradient

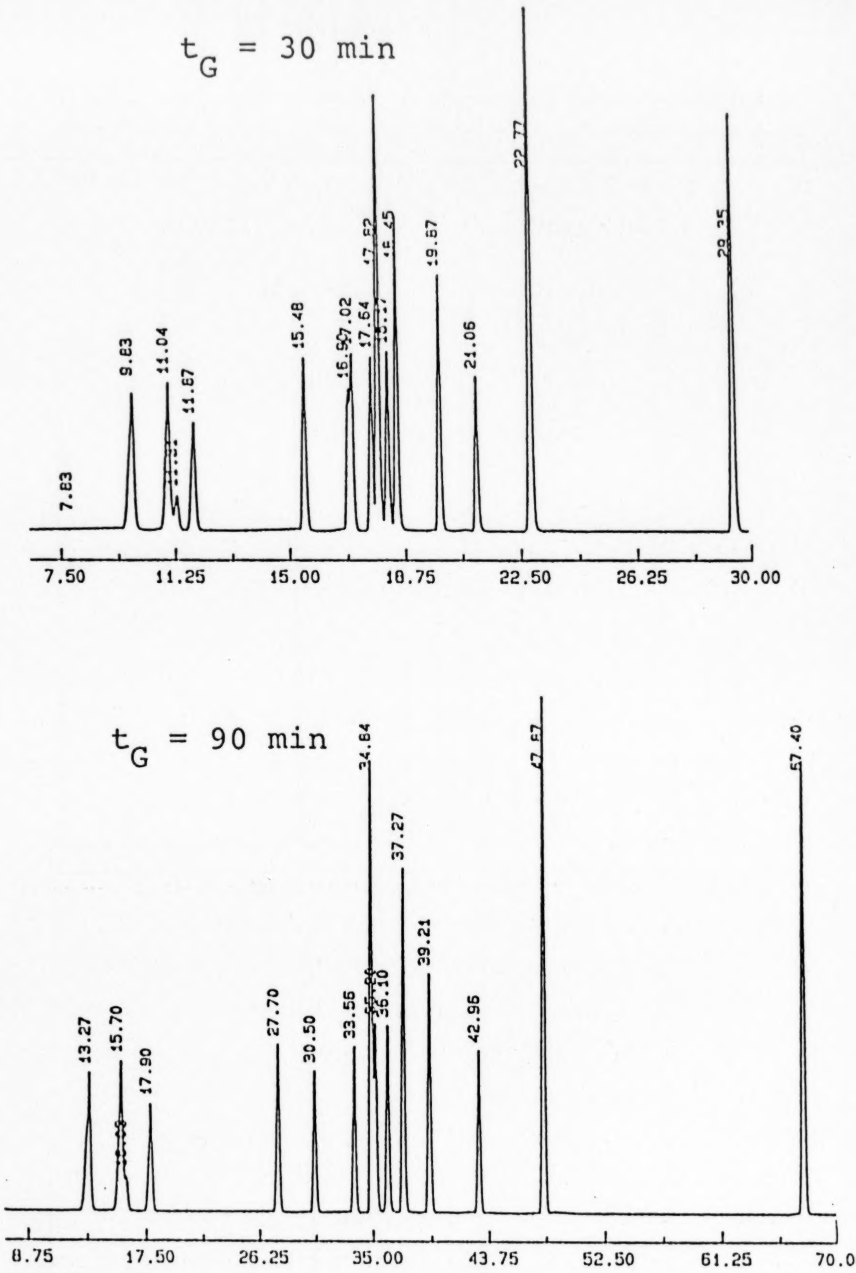

Fig. 8

Gradient separation of a mixture of 15 herbicides with two different values of t_G. Data used for calculations discussed in text and shown in Figs. 9, 11 and 12. Column, 25 X 0.46-cm Zorbax® C8; 5–100% acetonitrile/water gradients; flowrate, 2mL/min; 35°C; system dwell-volume 5.5mL. Sample components described in Ref. [28].

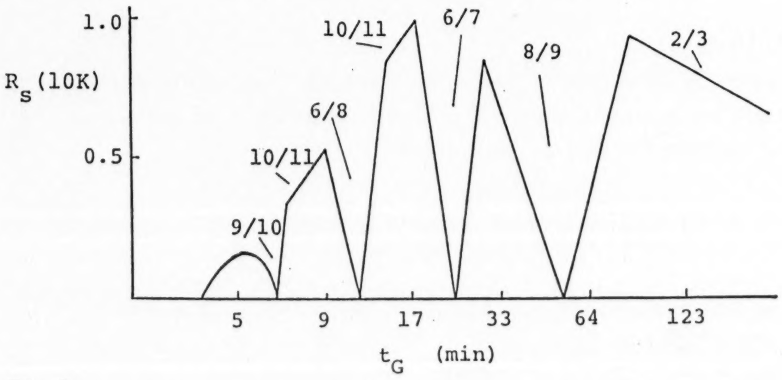

Fig. 9

Relative-resolution map for herbicide separation of Fig. 8. Calculated by DryLab G.

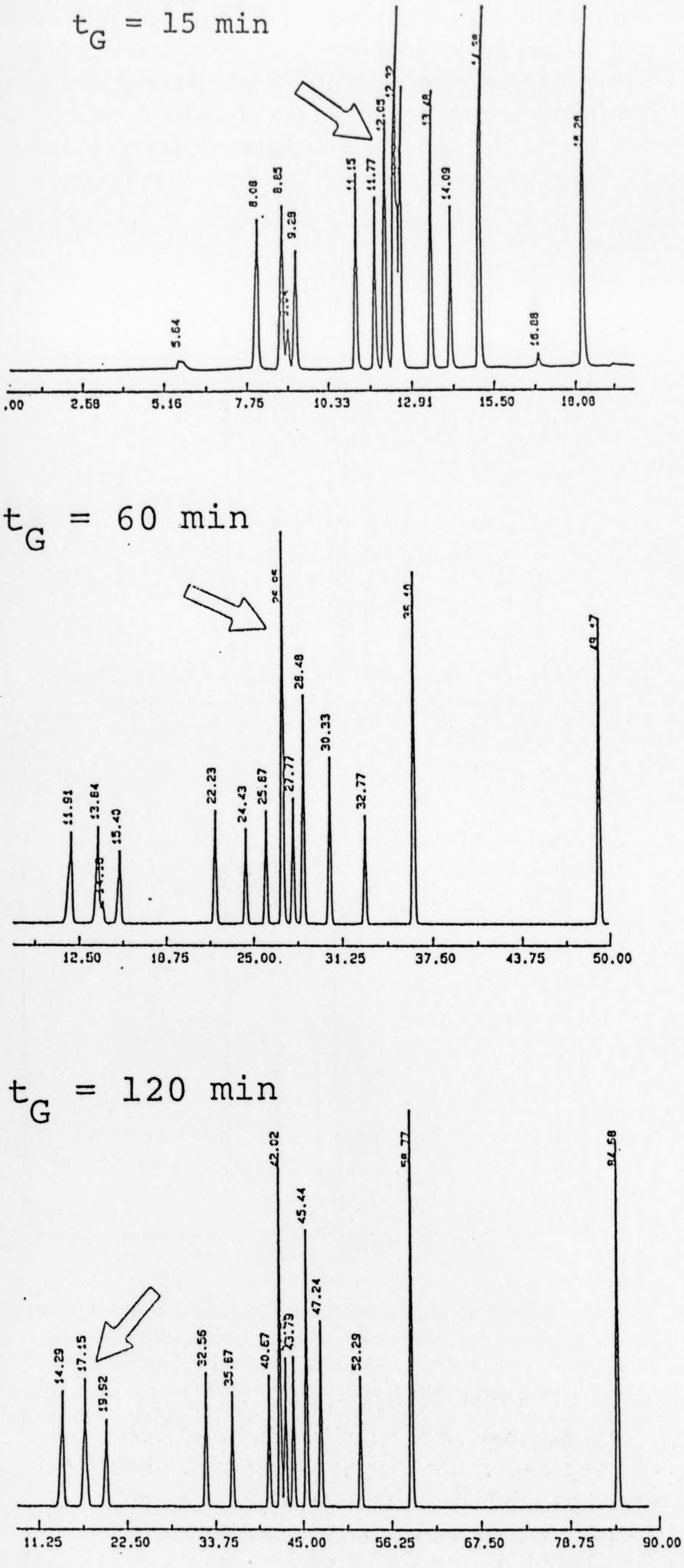

Fig. 10

Gradient separations of herbicide mixture. Conditions as in Fig. 8, except for gradient time (15, 60 and 120min – as indicated). Arrows indicate unresolved band-pairs.

used in Step #6 was a 10–100% acetonitrile gradient with t_G equal 20min.

Multi-step gradients were also studied by computer simulation, but these did not appear to improve resolution significantly. The problem is that bands #6–11 (Fig. 8a) are crowded together in the center of the chromatogram, and exhibit marked changes in band spacing as gradient shape or ϕ_0 are varied. Under these circumstances it is usually preferable to increase the peak capacity of the separation, by increasing the column plate number N.

Step 6. Computer simulations were continued by varying column length and flowrate, using the 10–100% gradient and a gradient time of 20min as starting point (25-cm column, 2mL/min flowrate). An increase in column length by 2-fold (to 50cm) combined with a decrease in flowrate to 1mL/min (from 2mL/min) gave the predicted chromatogram of Fig. 12b (N = 29,900). This was deemed acceptable, and an experimental run was carried out (Fig. 12c). The final chromatogram of Fig. 12c shows good

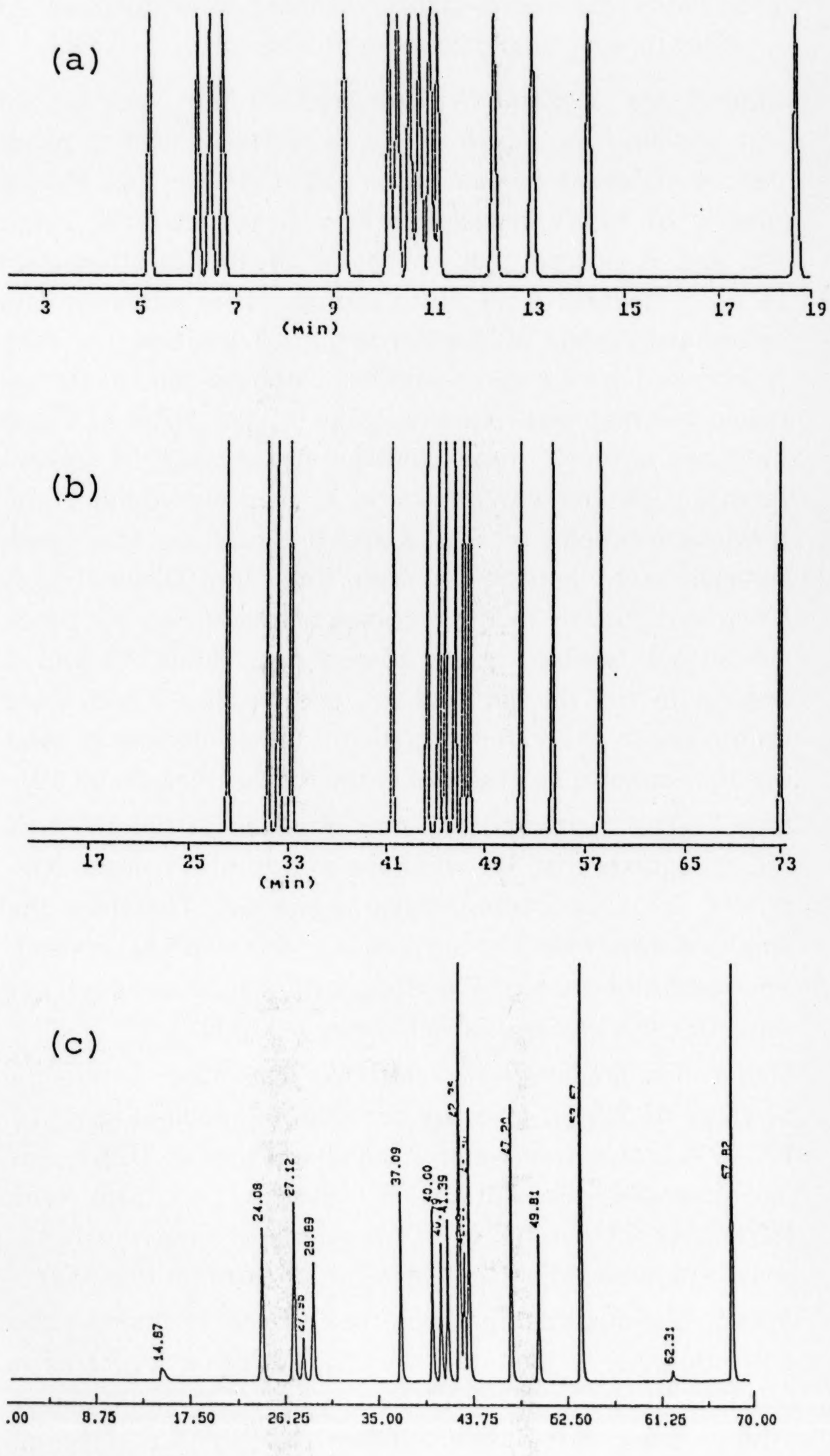

Fig. 11

Optimized separations of herbicide sample. Conditions as in Fig. 8 except where noted otherwise. (a) simulated run for t_G = 16min, gradient range equal 17–77% acetonitrile; (b) simulated run for t_G = 80min; gradient range = 10–100% acetonitrile, 50-cm column and 1mL/min; (c) experimental run corresponding to (b).

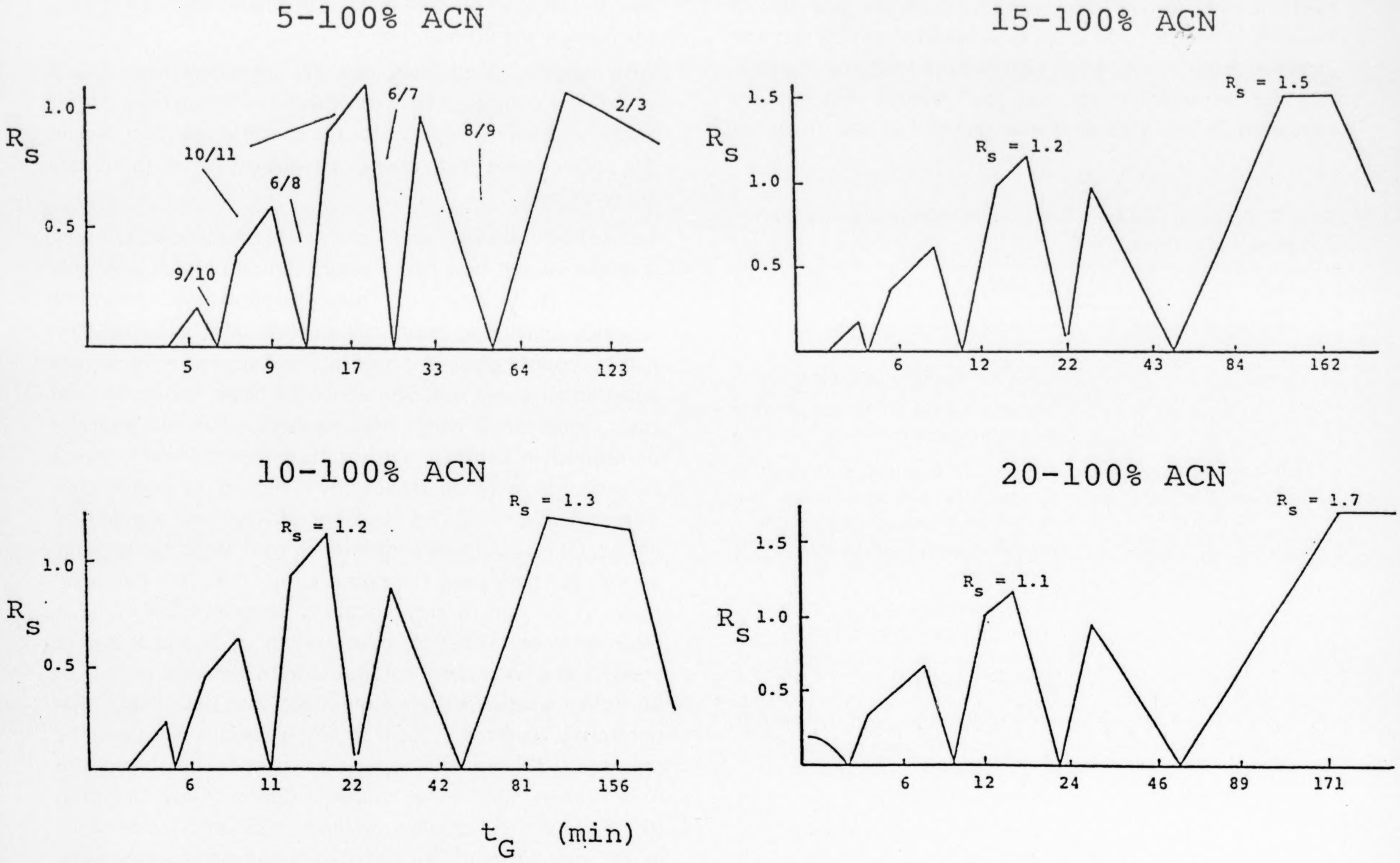

Fig. 12
Resolution maps (N = 11,900) for herbicide sample, using different gradient ranges (indicated in figure).

resolution of all band-pairs and agrees well with the computer simulation of Fig. 12b.

Data for computer-simulated vs experimental runs of Figs. 10 and 12. For the chromatograms of Fig. 10, errors (1 SD) in values of t_g and $(t_2 - t_1)$ were as follows: 15-min run, −2 ± 0% (t_g) and −4 ± 4% $(t_2 - t_1)$; 60-min run, +1 ± 1% (t_g), and +2 ± 11% $(t_2 - t_1)$; 120-min run, −1 ± 1% (t_g), and −1 ± 2% $(t_2 - t_1)$.

The corresponding comparison for the experimental run of Fig. 12c is: +3 ± 1% (1 SD) error in t_g; +2 ± 11 (1 SD) error in $(t_2 - t_1)$. The average baseline-bandwidth value for this run was 0.36 min vs 0.32 min predicted. A similar comparison was made for a 10–100% acetonitrile gradient in a time of 20 min, with a 25-cm column and a flowrate of 2 mL/min (original column conditions of Fig. 8); the average bandwidth was 0.15 min (expt) vs a simulated value of 0.14 min.

These various results for the herbicide sample compare favorably with the accuracy of predicted values of retention, bandwidth and resolution presented earlier.

Possible Pitfalls in the Use of Computer Simulation for Predicting Gradient Separation

Gradient elution is often used to separate complex, unknown mixtures which contain numerous components (e.g., 20 or more compounds) of widely varying concentration. This is particularly true for samples of biological origin, such as protein digests, fermentation broths, etc. The use of computer simulation with such samples requires special care if useful results are to be obtained. Other samples of less complexity can also give problems when computer simulation is used for method development. Table V summarizes some specific situations that can contribute to unreliable predictions using DryLab G or similar software.

Mismatched bands. We have noted that each band in the second experimental run used as input for computer simulation must be matched to a corresponding band in the first run. For example, in Fig. 8, band #8 in the 30-min run corresponds to band #9 in the 90-min run. This particular assignment is relatively easy, based on a visual matching of bands according to retention and peak size. In other cases, a similar attempt at matching bands between two runs may result in ambiguous assignments – particularly when several bands of similar size are found in one part of the chromatogram. In these cases, the best approach is usually to run a third experimental run, with a gradient time intermediate between the two t_G-values initially selected. Often a visual examination of the three chromatograms will remove any doubts concerning band assignment. Additionally, DryLab G with the original peak assignments can be used to predict retention times for the third run, and these can be compared with the values actually found. We will illustrate this using the two runs of Figure 8 as inputs to DryLab G, assuming both correct and incorrect band assignments. Resulting predictions of retention for an intermediate run (t_G = 60min, Fig. 10) are compared in Table VI with experimental values. It can be seen in this example that bands #8/9 have reversed between the 30-min and 90-min runs.

Table V. Potential problems in the use of computer simulation for predicting gradient separation

Problem	Remedy
1. mismatched bands between two chromatograms	run additional run(s) with different t_g; verify that retention times are correctly predicted; measure %-areas for various bands to confirm peak matching
2. unresolved bands in complex samples (unknown)	run additional runs with different t_g; verify that number of bands in each chromatogram is correctly predicted, along with their retention times increase peak capacity by using longer, more efficient columns, slower flowrates, and/or longer gradient times
3. errors in retention time for poorly resolved bands	run additional runs with different t_g; confirm that same resolution vs t_g is predicted using different run-pairs with DryLab G increase peak capacity as above (#2)
4. errors in experimental gradients or estimate of dwell volume	check gradient shape by running analog gradient avoid early and late-eluting bands in initial (experimental) gradient runs by using broad gradient-range predictions for segmented gradients may be less accurate
5. curved plots of log k′ vs ϕ	less important as a contribution to error in predicted results for R_S; t_g-values may be less accurate for extrapolated simulations

Table VI. Matching bands between two runs used as input for computer simulation. Bands #6–11 of herbicide sample of Figs. 8 and 10.

Band position*	area-% t_g = 30	t_g = 90	retention for t_g = 60min expt.	simulated correct**	incorrect**
6	3.6	4.0	24.4	24.6	24.6
7	5.1	4.5	25.9	26.0	26.0
8	4.8	11.9	27.0***	27.2	27.0
9	12.2	5.0		27.2	27.3
10	5.0	5.1	27.8	27.9	27.9
11	8.8	9.1	28.5	28.6	28.6

* elution order in each run

** the correct assignment: band #8 (t_g = 30) is the same as band #9 (t_g = 90); the incorrect assignment assumes that peak order is the same in the two runs

*** peaks #8 and 9 fuse in the actual 60-min run; this is predicted by computer simulation with the correct assignments of bands in the two starting runs; the incorrect assignment predicts R_S = 0.9 for bands #8/9 in the 60-min run (cf. Fig. 10)

Alternatively, band-areas can be converted into area-% values and compared between the two starting runs. This is also illustrated in Table VI for the bands in question. Again, the correct peak assignments are obvious when these data are examined.

Unresolved (missing) bands. In the case of unknown samples, it is not known how many bands should be seen when the sample is fully resolved. Therefore we cannot determine whether unresolved bands are present in a chromatogram just by counting peaks. This problem becomes more serious when small bands are overlapped by larger bands. In such cases, some small bands may be resolved in one run and unresolved in another, and resolved (but different) bands in each run may be mistakenly assumed to match each other. Problems of this type are usually best avoided by either (a) carrying out additional runs with t_G varying, and/or (b) increasing the space within the chromatogram so as to be able to accomodate a larger number of fully-resolved bands. That is, when values of N and $\overline{k}$ are increased (by increasing column length, flowrate or t_G, or by using smaller-particle columns), it is less likely that unresolved bands will occur in any given run. Studies to be reported [33] on the separation of ribosomal proteins have shown that long columns (25cm), low flowrates (0.7mL/min) and shallow gradients (25–45% acetonitrile in 60 and 240min) are required to properly apply computer simulation. This problem is further discussed in Ref. [5].

Retention-time errors. If values of t_g for the two input runs for computer simulation are in error, errors in the resulting predictions by computer simulation can be even larger. Usually retention times can be measured experimentally with adequate precision. However when two bands are partly resolved, errors in the resulting values of t_g can occur (see discussion of Ref. [1], pp. 43–44). This problem is especially critical when the bands in question exhibit only minor changes in band-spacing as t_G is varied. In these cases, predicted resolution values can have a large relative error. This problem can also be mitigated by increasing the peak capacity of the system (longer column, lower flowrate, etc.). If doubt exists as to the reliability of starting t_G-values, additional experimental runs should be carried out and used for independent simulations. Simulated separations based on the two different sets of starting experimental runs should agree with each other, for prediction of a given separation.

Errors in the gradient. DryLab G assumes that the HPLC equipment is capable of providing gradients which are in close agreement with the desired shape. Computer simulation also requires an accurate measurement of the gradient dwell volume V_D. Both questions can be resolved by measuring the gradient shape, as described in Ref. [18]. A UV-absorber is added to the second solvent of the gradient system, so that a tracing of the gradient shape results when a gradient is run without sample injection and with the column removed.

Curvature in plots of log k' vs ϕ. Eq. (3) is often not an exact description of experimental plots of k' vs ϕ, although resulting errors are of marginal practical importance [18]. It is possible to correct for these effects as described in Ref. [18]. These corrections will be incorporated into the DryLab G software shortly, but the present examples are not corrected.

Conclusions

Computer simulation provides an alternative to trial-and-error experimental runs for the purpose of improving separations by gradient elution. A simulated run can be carried out in less than a minute, saving more than 90% of the time required for an actual gradient-elution separation. At the same time the computer can present the results of many possible experiments as convenient plots of sample resolution vs gradient time (relative-resolution map). A computer can also facilitate systematic method development by holding relative retention fixed while column conditions (column length and diameter, particle size and flowrate) are varied for further improvement of separation. These various factors can result in the faster development of better methods, even by chromatographers having little experience with gradient elution.

The present study has analyzed the performance of commercial software (DryLab G) for carrying out computer simulations for reversed-phase gradient elution. Two experimental gradient separations of the sample of interest are run initially, followed by computer simulation. For several different samples, it is shown that retention predicted in this way agrees closely with experimental results. A systematic approach to method development for reversed-phase gradient elution is also presented, and its application to several samples is shown. This approach relies strongly on "solvent-strength optimization", based on band-spacing changes that result when gradient conditions are changed so as to change relative sample retention during elution through the column. Several examples of this effect can be seen in the present examples.

Acknowledgements

We are grateful to Dr. Roy Eksteen of Supelco., for giving us the column for the PAH separations. We also thank Drs. K. A. Cohen (Boehringer-Ingelheim) and J. D. Stuart (Univ. of Connecticut) for providing the raw data cited in Ref. [32].

Glossary of Terms

b	gradient steepness parameter (eq. 5)
b_i, b_j	values of b (for a given solute) in runs i and j differing only in t (eqs. 4a, b)
F	mobile-phase flowrate (mL/min)
G	gradient compression factor; see Ref. [1]
J	anomalous band-broadening factor in gradient elution; see Ref. [7]
k'	solute capacity factor; also instantaneous value in gradient elution at a given time (eq. 2)
$\overline{k}$	value of k' for a band in gradient elution when the band has migrated halfway through the column
k_f	value of k' for a band as it leaves the column during gradient elution (eq. 10)
k_0	value of k' for a given solute at the beginning of the gradient (for $\phi = \phi_0$)
k_w	value of k' for water as mobile phase (eq. 3)
N	plate number in corresponding isocratic separation where k' (isocratic) = $\overline{k}$ (gradient)
PAH	polyaromatic hydrocarbon
RRM	relative-resolution map (see Figs. 3, 6, 9)
R_s	resolution of two adjacent bands (eqs. 1, 11)
S	$d(\log k')/d\phi$ (eq. 3, isocratic elution)
SD	standard deviation
t	time (min) after sample injection and start of gradient
t_D	dwell time for a given HPLC system (min); equal to V_D/F
t_g	retention time (min) in gradient elution
t_G	gradient time (min)
$(t_g)_i$, $(t_g)_j$	values of t_g for a given solute in runs i and j, differing only in t_G (min)
t_0	column dead-time (min)
t_R	retention time (min) in isocratic elution
t_1, t_2	values of t_g for first and second (adjacent) bands (min)
V_D	dwell volume for a given HPLC system (mL)
V_m	column dead-volume (mL), equal to (t_0 F)
W	baseline bandwidth (min)
W_1, W_2	values of W for first and second (adjacent) bands (min)
α	separation factor (eq. 11)
ϕ	volume-fraction of organic solvent in mobile phase
ϕ_0	initial value of ϕ for a gradient
$\Delta\phi$	change in ϕ during the gradient

References

[1] *L. R. Snyder, J. J. Kirkland*, Introduction to Modern Liquid Chromatography, 2nd edn., Wiley-Interscience, New York 1979, Chap. 16.

[2] *L. R. Snyder*, in High-performance Liquid Chromatography. Advances and Perspectives, Vol. 1, *Cs. Horváth*, ed., Academic Press, New York, 1980, p. 207.

[3] *P. Jandera, J. Churacek*, Gradient Elution in Column Liquid Chromatography, Theory and Practice, Elsevier, Amsterdam, 1985.

[4] *L. R. Snyder, M. A. Stadalius*, in High-performance Liquid Chromatography. Advances and Perspectives, Vol. 4, *Cs. Horváth*, ed., Academic Press, New York, 1986, p. 195.

[5] *J. L. Glajch, M. A. Quarry, J. F. Vasta, L. R. Snyder*, Anal. Chem., **58**, 280 (1986).

[6] *P. Jandera, M. Spacek*, J. Chromatogr., **366**, 107 (1986).

[7] *M. Kunitani, D. Johnson, L. R. Snyder*, J. Chromatogr., **371**, 313 (1986).

[8] *J. W. Dolan, L. R. Snyder*, Chromatography Mag., **2**, 49 (1987).

[9] *M. A. Stadalius, H. S. Gold, L. R. Snyder*, J. Chromatogr., **327**, 27 (1985).

[10] *A. J. Banes, G. W. Link, L. R. Snyder*, J. Chromatogr., **326**, 419 (1985).

[11] *R. W. Stout, S. I. Sivakoff, R. D. Ricker, L. R. Snyder*, J. Chromatogr., **353**, 439 (1986).

[12] *Y. Baba, N. Yoza, S. Ohashi*, J. Chromatogr., **350**, 461 (1985).

[13] *S. Tomellini, S.-H. Hsu, R. A. Hartwick*, Anal. Chem., **58**, 904 (1986).

[13a] *Z. El Rassi, Y.-F. Maa, F. D. Antia, Cs. Horváth*, presented at the 10th Intern. Symp. on Col. Liq. Chromatography, San Francisco, May 18–23, 1986.

[14] *J. L. Glajch, JJ. Kirkland*, J. Chromatogr., **255**, 27 (1983).

[15] *J. L. Glajch, J. J. Kirkland*, J. Chromatogr. Sci., **25**, 4 (1987).

[16] *W. R. Melander, Cs. Horváth*, in High-performance Liquid Chromatography. Advances and Perspectives, Vol. 2, *Cs. Horváth*, ed., Academic Press, New York, 1980, p. 114.

[17] *L. R. Snyder, J. W. Dolan, J. R. Gant*, J. Chromatogr., **165**, 3 (1979).

[18] *L. R. Snyder, M. A. Quarry*, J. Liq. Chromatogr., in press.

[19] *M. A. Quarry, R. L. Grob, L. R. Snyder*, Anal. Chem., **58**, 907 (1986).

[20] *M. A. Quarry, R. L. Grob, L. R. Snyder*, J. Chromatogr., **285**, 1 (1984).

[21] *E. S. Parente, D. B. Wetlaufer*, J. Chromatogr., **355**, 29 (1986).

[22] *R. W. Stout, J. J. DeStefano, L. R. Snyder*, J. Chromatogr., **282**, 263 (1983).

[23] *L. R. Snyder, P. E. Antle*, LC, Liq. Chromatogr. HPLC Mag., **3**, 98 (1985).

[24] *M. A. Stadalius, M. A. Quarry, L. R. Snyder*, J. Chromatogr., **327**, 93 (1985).

[25] *L. R. Snyder, M. A. Stadalius, M. A. Quarry*, Anal. Chem., **55**, 1412A (1983).

[26] *P. Jandera, J. Chruacek, H. Colin*, J. Chromatogr., **214**, 35 (1981).

[27] *L. R. Snyder, J. W. Dolan*, LC/GC Mag., **4**, 921 (1986).

[28] *M. A. Quarry, R. L. Grob, L. R. Snyder, J. W. Dolan, M. Rigney*, J. Chromatogr., **384**, 163 (1987).

[29] *L. R. Snyder, M. A. Quarry, J. L. Glaijch*, Chromatographia, **24**, 33 (1987).

[30] *M. A. Stadalius, H. S. Gold, L. R. Snyder*, J. Chromatogr., **296**, 31 (1984).

[31] *M. A. Quarry, R. L. Grob, L. R. Snyder*, J. Chromatogr., **285**, 19 (1984).

[32] *M. Eslami, J. D. Stuart, K. A. Cohen*, J. Chromatogr., in press.

[33] *B. F. D. Ghrist, B. S. Cooperman, L. R. Snyder*, J. Chromatogr., to be submitted.

Received: June 29, 1987
Accepted: Sept. 9, 1987
F

Study of Biologically Relevant Physical-Chemical Properties of Bile Salts by Reverse-Phase Liquid Chromatography

A. Cantafora* / A. Di Biase

Istituto Superiore di Sanita', Viale Regina Elena 299, 00161 Rome, Italy

M. Angelico / D. Alvaro

II Cattedra di Gastroenterologia, Universita' "La Sapienza", Rome, Italy

Key Words

Bile salts
Octanol-water partition coefficient
Micellar cholesterol-solubilizing capacity
Critical micellar concentration
Dissociation constant

Summary

The study of chromatographic behaviour of bile salts with reverse-phase HPLC columns (C18 and C8) and buffered water – methanol eluent systems indicated that the octanol-water partition coefficient and the micellar cholesterol-solubilizing capacity are linearly correlated with the chromatographic mobilities if eluents with pH > 7 and 0.154 M saline concentration are used (correlation coefficients 0.98 and 0.86 respectively). The critical micellar concentration was poorly correlated with the chromatographic mobility under the various conditions tested. The pKa values of bile salts were determined by the changes of mobility with the pH of eluent. Values in the range 4.92–5.06 and 4.27–4.47 were found respectively for unconjugated and glycine-conjugated bile salt, in agreement with previous estimates. Values in the range 0.74–1.02 represent the first direct evaluation for taurine-conjugates.

Introduction

The high performance liquid chromatographic (HPLC) mobility of a substance is easily evaluated by the capacity factor (K′). This explains the interest in correlating K′ to physical-chemical properties requiring complex procedures of determination. The octanol/water partition coefficient (Pow), for instance, may be estimated from reverse-phase HPLC (RP-HPLC) mobility in the case of apolar, non-ionizable solutes [1, 2]. Bile salts (BS) which are polar, amphiphilic and ionogenic substances show complex correlations Pow-K′ as the mechanisms of chromatographic process are influenced not only by solute structure but also by chromatographic conditions [3, 4]. In spite of these theoretical difficulties the RP-HPLC mobility of BS has been correlated to the equilibrium micellar cholesterol-solubilizing capacity (ChM) [5], a biologically relevant physical-chemical property. It has been proposed furthermore that values of K′ of BS are related to an empirical scale, the so-called hydrophilic-hydrophobic balance, which bears important relationships with other relevant properties [6]. On the other side, some authors deny the existence of simple relationships between chromatographic mobility and properties or structure of BS [7, 8].

This led us to study the effect of changes of chromatographic conditions on the retention behavior of BS in order to find the proper conditions for correlating K′ with some biologically relevant physical-chemical properties as Pow, ChM and critical micellar concentration (cmc).

Experimental

Chemicals

The sodium salts of following bile acids were purchased from Calbiochem-Behring (La Jolla, CA, USA): Ursodeoxycholic acid (UDCA), cholic acid (CA), chenodeoxycholic acid (CDCA), deoxycholic acid (DCA), plus respective glycine conjugates (GUDCA, GCA, GCDCA, GDCA), taurine conjugates (TUDCA, TCA, TCDCA, TDCA) and tauro 7α,12α-dihydroxy-5β-cholanic acid, used as internal standard (9). HPLC-grade solvents were obtained from Carlo Erba (Milan, Italy).

Apparatus and Conditions

The chromatographic apparatus (Gilson Medical Electronics, Middleton, WI, USA) was equipped with a spectrophotometric UV detector set at 205 nm, a computerized

0009-5893/87 0277-05 $03.00/0

© 1987 Friedr. Vieweg & Sohn Verlagsgesellschaft mbH

data station and a Clar 055 electronic thermostat for columns (Violet, Rome, Italy) set at 37°C. Two different types of columns were used: Spherisorb ODS-2 (5μ) and Spherisorb C8 (5μ) supplied by Lab. Service (Bologna, Italy).

The mobile phases were made with mixtures methanol/20 mM phosphate buffer adjusted at different values of ionic strength (IS) (by addition of sodium chloride), apparent pH (by glass electrode) and ratio methanol/water. The range of variation was 20–154 mM, 2.5–8.0, 50:50–75:25, v/v respectively. The flow rate was of 1 ml/min in all experiments.

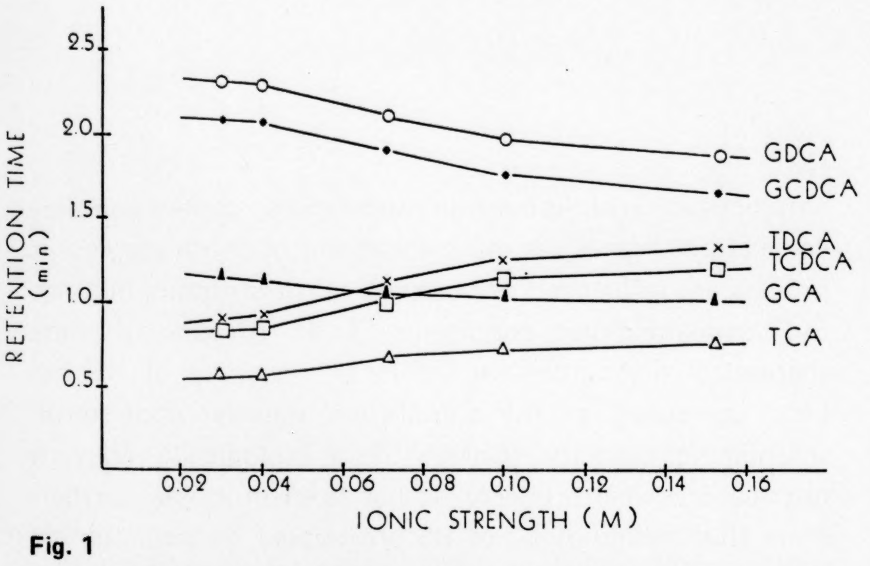

Fig. 1

Effect of the ionic strength in the mobile phase on the retention time of glycine and taurine conjugates of some common bile salts. Column spherisorb ODS-2, 5μ, 3 × 0.47 cm i.d., used at the temperature of 37°C with mobile phases made with methanol/potassium phosphate buffer (20 mM, pH 4 plus sodium chloride as ionic strength adjustor) mixture (70:30, by vol.) at the flow rate of 1 ml/min.

Results and Discussion

The analytical HPLC fractionation of BS is usually obtained with ODS columns and mobile phases containing high concentration of methanol (60–70%), low IS (20–40 mM) and acidic pH (3–5). Under these conditions, the chromatographic pattern shows in the order taurine conjugates, glycine conjugates and unconjugated BS. Due to this behavior the taurine conjugates are generally considered more hydrophylic than glycine conjugates.

Using ODS stationary phases the elution order is altered by variations of IS, pH and, in a lesser extent, of water content, as shown in Fig. 1, 2 and 3 respectively. We have observed a similar behavior in an other set of experiments with the C8 stationary phase (data not shown). As expected for ionizable compounds, these observations suggest that the profile obtained under analytical conditions can be dramatically altered by combined changes in mobile phase composition. This would be the case, for example, of an eluent with IS 154 mM, pH 7 and 100% water which can be considered "physiological". This eluent even if not suitable for chromatographic purposes should be of interest for studying the interactions of BS with the hydrophobic environment of biological membranes. The verifiability of this supposition requires the extrapolation of the experimental data to higher content of water in the mobile phase. Both linear [10] and parabolic [11] relationships between log K′ and water content have been proposed for methanol-water systems but extrapolation of data from low methanol content to the total absence of organic modifier could be misleading in both cases. We found a perfect linear relationship in the experiments with mobile phases adjusted at pH 7, IS 154 mM and water content ranging from 25 to 50% (Table I) thus the linear extrapolation of these data appeared the simplest way for evaluating log K′ values of the "physiological" eluent.

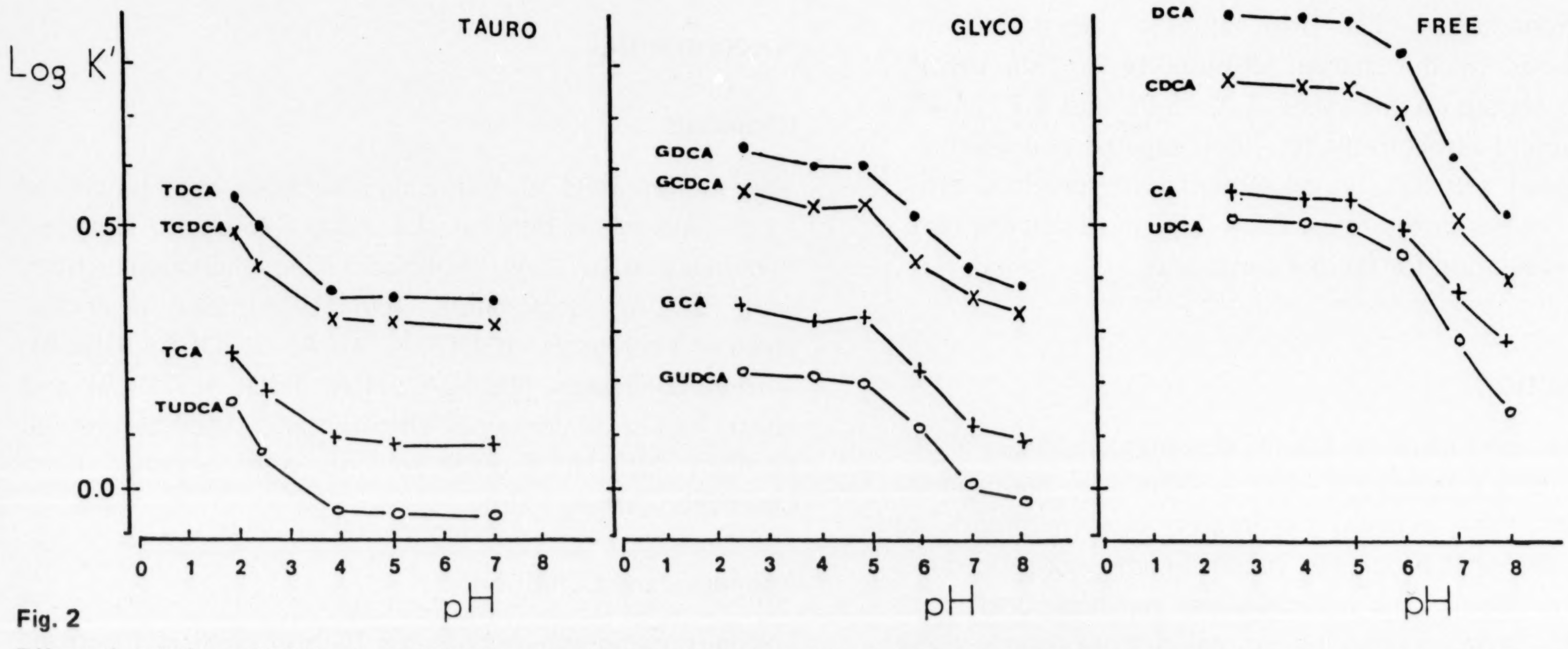

Fig. 2

Effect of variations of pH in the mobile phase on the retention time of free, glycine and taurine conjugates of some common bile salts. Column as in Fig. 1. Mobile phase: methanol/potassium phosphate buffer (40 mM IS, pH adjusted in the range 2.5–8.0) mixture (70:30, by vol.) at the flow rate of 1 ml/min.

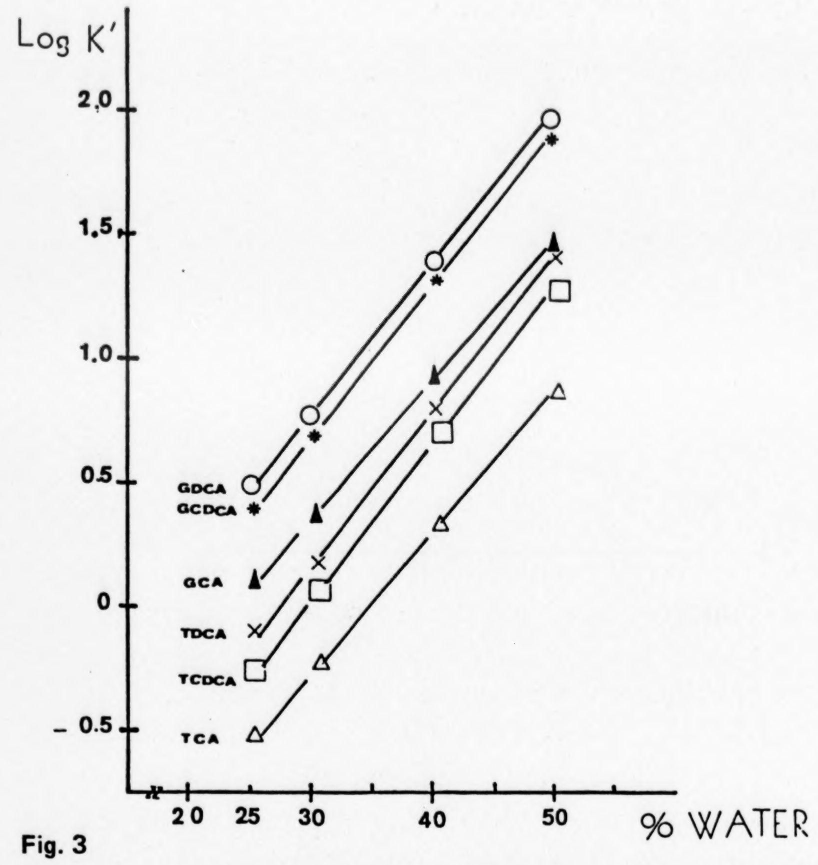

Fig. 3

Effect of variations of water content in the mobile phase on mobility of glycine and taurine conjugates of some common bile salts. Column as in Fig. 1. Mobile phase: methanol/potassium phosphate buffer (pH 4, 20 mM IS) mixture (in ratios ranging from 80:20 to 50:50, by vol.) at the flow rate of 1 ml/min.

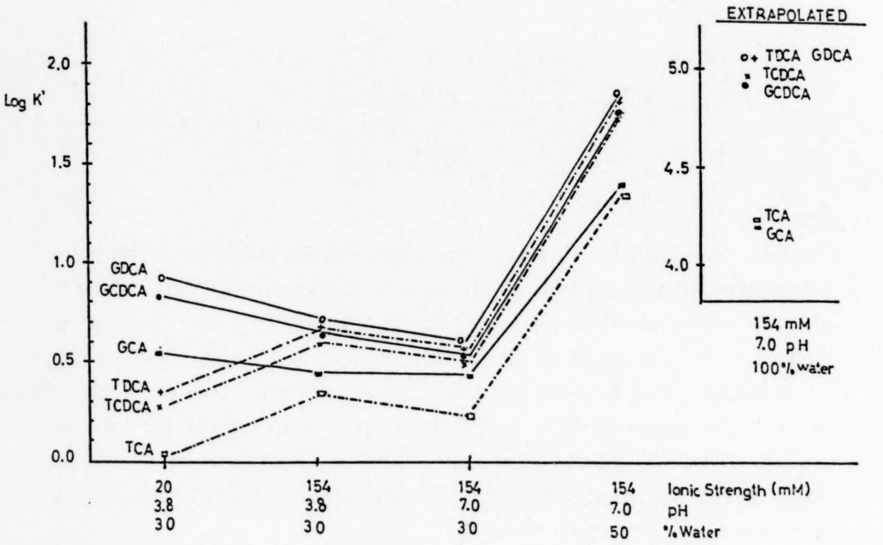

Fig. 4

Combined effects of changes in mobile phase composition on the elution order and capacity coefficients of some common bile salt conjugates. Column: octyl, 5μl, 3 × 0.47 cm, temperature 37°C.

Table I. Values of linear regression coefficients of six common bile salts obtained from the equation: log K' = A · (% water in mobile phase) + B in the case of octadecyl (C18) and octyl (C8) stationary phase. The mobile phases used were made with methanol/aqueous buffer 9 pH 7, 154mM IS) mixtures in various ratios.

BS	A Coefficient		B Coefficient		Correlation Coeff.	
	(C18)	(C8)	(C18)	(C8)	(C18)	(C8)
TCA	0.057	0.057	–1.52	–1.74	0.998	0.999
TCDCA	0.064	0.065	–1.45	–1.76	0.998	0.999
TDCA	0.065	0.066	–1.44	–1.72	0.999	0.999
GCA	0.055	0.057	–1.42	–1.73	0.998	0.999
GCDCA	0.063	0.065	–1.36	–1.72	0.997	0.999
GDCA	0.064	0.066	–1.34	–1.69	0.998	0.999

Experimental and extrapolated values of K' are shown in the pattern of Fig. 4 which indicates the changes of elution order of BS going from "analytical" to "physiological" conditions. It is interesting to note that: (i) glycine conjugates can be eluted before or very close to their correspondent taurine conjugates; (ii) elution order within each class of BS is determined by the number and orientation of the nuclear hydroxyls and not by mobile phase changes (sequence: 3α-7β-dihydroxy, 3α,7α,12α-trihydroxy, 3α,7α-dihydroxy and 3α,12α-dihydroxy).

The correlation of chromatographic mobility, at different experimental conditions, with Pow, ChM and cmc was the next step in the study. Fig. 5 shows the results of linear

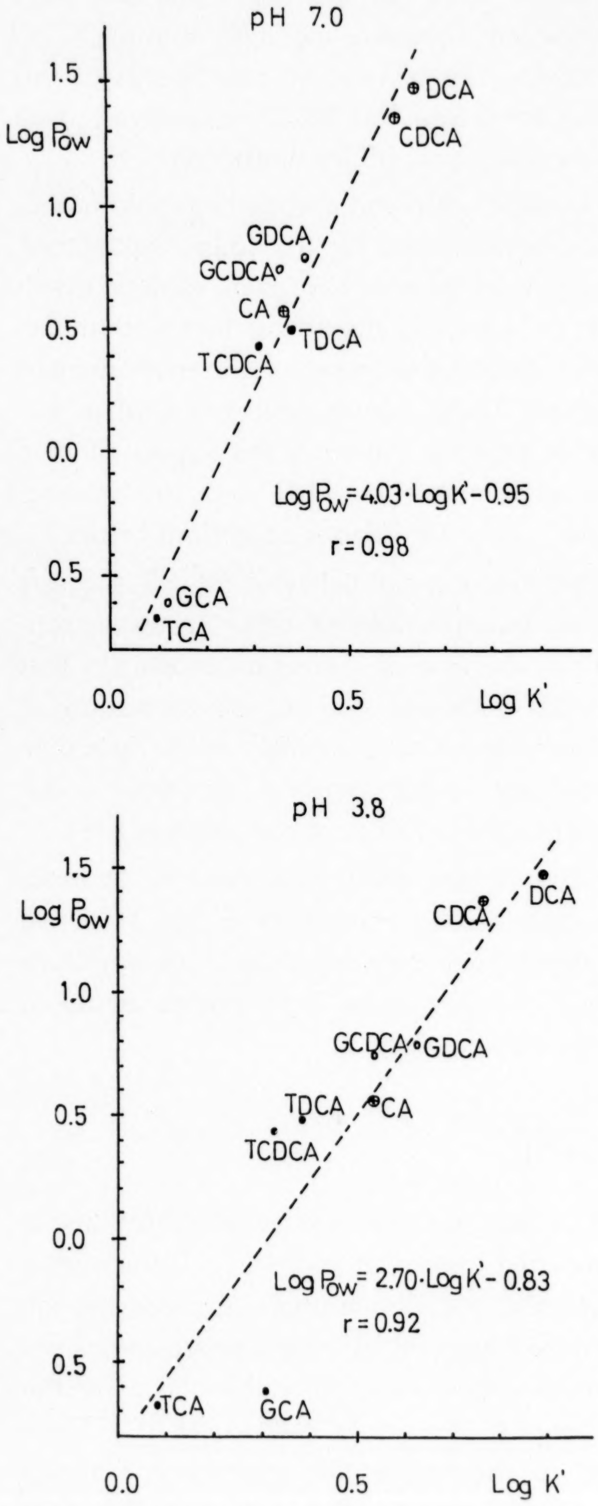

Fig. 5

Double logarithmic plots of partition coefficients water/octanol (log Pow) versus capacity factors (log K') measured with the octyl column and mobile phases made with methanol/aqueous buffer (154 mM IS and pH values of 3.8 and 7.0). The linear regression curves and equations are reported on the same plot. The values of correlation coefficient (r) indicate a poorer correlation at the acidic pH.

regression log Pow versus log K′ using the column C8 and two mobile phases at IS 154 mM, 70% of methanol and pH adjusted at 7 and 3.8 respectively. The values of log Pow were determined by us in the case of conjugated BS and derived from the literature in the other case [12]. The correlation coefficient is higher at neutral pH and physiological IS (the same used in the determination of partition coefficient). Similar results obtained at higher pH (pH = 8, R = 0.98) showed that a good linear correlation between log Pow and log K′ exists when mobile phases with pH ⩾7 and IS 154 mM are used.

The values of ChM reported by Armstrong et al. [5] are plotted in Fig. 6 against values of log K′ obtained with mobile phases at IS 154 mM, 70% methanol and acidic or alkaline pH (3.8 and 8.0 respectively). At the lower pH there is a linear correlation among the free, glycine and taurine conjugates of each BS. At the higher pH there is a linear correlation between log ChM and log K′ of all the BS considered. The correlation coefficients of this general correlation are 0.860 and 0.975 respectively if all BS or only the dihydroxylated BS are considered.

The correlation between cmc and chromatographic mobility of BS appears complicated by the following factors: 1) contrasting evaluations of cmc have been obtained with different methods [13] and; 2) the driving forces for micellar aggregation are ineffective in the alcoholic environement of the mobile phase. These factors probably explain our failure in the attempt of correlating the values of cmc determined by a reliable method [14] with the chromatographic mobilities, under the various conditions tested.

The study of chromatographic behavior of BS suggests new possibilities of determination of other relevant properties of BS. This is the case of ionization properties that are determined with difficulty due to the formation of micelles or to the presence of a strongly acidic group in taurine conjugates by potentiometric titration under equilibrium conditions [15] or in alcoholic solution [16].

It is possible, following the theory of mobility of ionogenic substances described by Harváth et al. [3], to derive the value of the dissociation constant (Ka) from variations of K′ with mobile phases ranging from highly acidic to neutral pH by using the equation:

$$K' = K_0 - \frac{(K' - K_{-1}) \cdot K_a}{[H^+]_m}$$

where K_0 and K_{-1} represent the values of K′ for undissociated and dissociated molecules and $[H^+]_m$ is the hydrogenion concentration in the mobile phase. Considering the value of K′ determined at pH 8 of mobile phase equivalent to K_{-1}, it is possible to obtain the value of Ka by the slope of linear curve K′ versus $(K' \leftarrow K_{-1})/[H^+]_m$. These values are related to the methanolic environment of the mobile phase but can be extrapolated to pure aqueous solution as previously described [16].

The results obtained by this approach are given in Table II. The comparison with values of pKa found in literature evidences a close resemblance of the present data with that obtained by potentiometric titration in methanolic solution [16]. As concerns the glycine conjugates only few data obtained by equilibrium titration in water are reported [15]: these values are influenced by micellar interactions in water solution and vary even with concentration of BS itself. The magnitude of pKa values of the glycine conjugates, given by Carey [17], is comprised between 4 and 5 in agreement with our data. Because even 10 M hydrochloric acid cannot titrate sulfonic acids to completion [18] the pKa values of taurine-conjugates have been estimated to fall in the range from −1.5 to +1.5, on the base of experimental estimates for taurine [19]. Our data for taurine-conjugates fall within this large interval and are the only so far known measurement of ionization properties of these compounds.

The above described applications of reverse-phase HPLC confirm the potentiality of this technique in determining some relevant physical-chemical properties of BS.

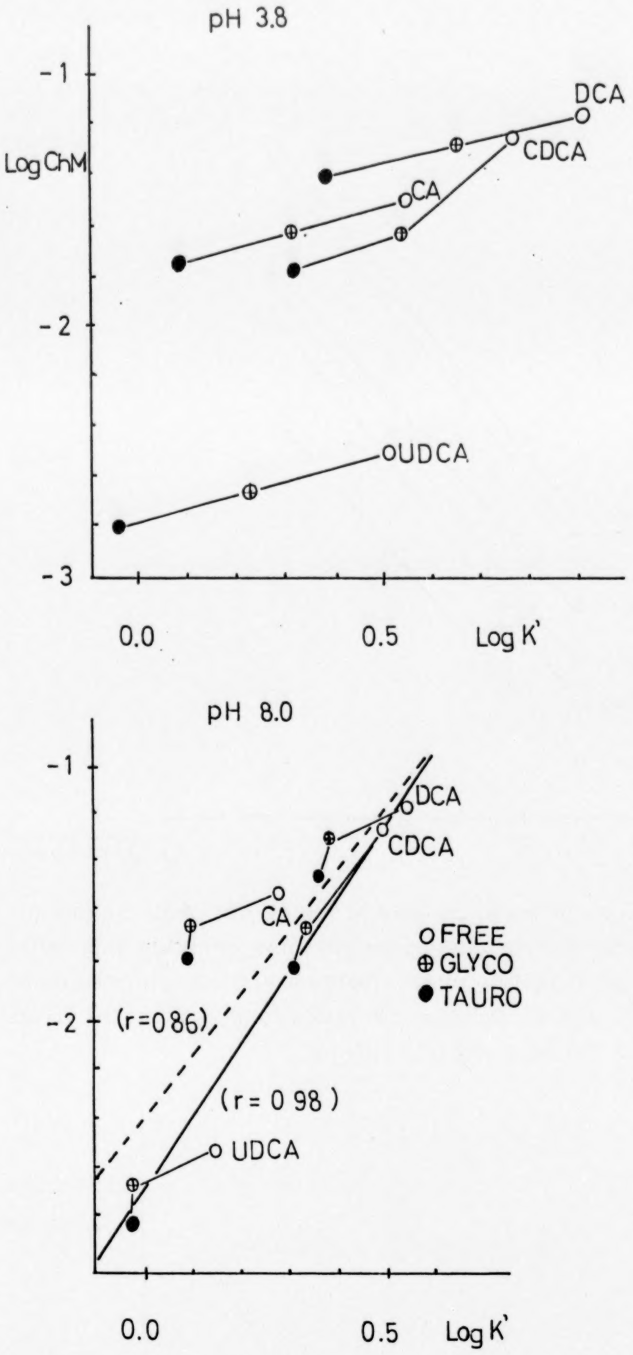

Fig. 6

Double logarithmic plots of the equilibrium micellar cholesterol-solubilizing capacity (log ChM) versus the capacity factor (log K′) of four types of bile salts in the forms free, glycine and taurine conjugates. The values of K′ were determined with the ODS column and mobile phases made with methanol/aqueous buffer (154 mM IS and pH values of 3.8 and 8.0) in the ratio 70:30, by vol. The linear regression curves and equations are reported at the higher value of pH for all the bile salts (solid line) and for the dihydroxylated bile salts only (dotted line).

Table II. Values of pKa of some bile salts calculated according the equation of Horváth [3] using values of capacity factor obtained with octyl stationary phase and mobile phases made with methanol/aqueous buffer (154 mM IS, pH adjusted in the range 2.5–8.0) 70:30, v/v.

Bile Acid	pKa (found in Methanol/ water	pKa (extra-pol.) in water^1	pKa (literature)	
			(a)	(b)
UDCA	6.57	5.04	5.08	5.97
CA	6.58	5.05	5.08	–
CDCA	6.59	5.06	5.07	6.44
DCA	6.45	4.92	5.02	–
GUDCA	6.00	4.47		4.92
GCA	5.87	4.34		–
GCDCA	5.80	4.27		4.60
GDCA	5.81	4.28		
TUDCA	2.35	0.94		
TCA	2.15	0.74		
TCDCA	2.35	0.94		
TDCA	2.34	1.02		

(a) Values obtained by potentiometric titration in methanolic solution and extrapolated to water solution [16].

(b) Values obtained by equilibrium titration in 0.154 M saline at 20 mM concentration of the bile salt [15].

1) Calculated from the equation pKa (water) = pKa(MeOH/water) –3.4 X MeOH according reference [16].

References

[1] *C. V. Eadsforth, P. Moser*, Chemosphere **12**, 1459 (1983).
[2] *J. E. Haky, A. M. Young*, J. Liquid Chromatogr. **7**, 675 (1984).
[3] *C. Horváth, W. Melander, I. Molnar*, Anal. Chem. **49**, 142 (1977).
[4] *M. C. Hennion, C. Picard, C. Combellas, M. Caude, R. Rosset*, J. Chromatogr. **210**, 211 (1981).
[5] *M. J. Armstrong, M. C. Carey*, J. Lipid Res. **23**, 70 (1982).
[6] *M. C. Carey*, Hepatol. **4**, 138S (1984).
[7] *A. F. Hoffman, A. Roda*, J. Lipid Res. **25**, 1477 (1984).
[8] *R. Show, M. Rivetna, W. M. Elliot*, J. Chromatogr. **21**, 347 (1980).
[9] *A. Cantafora, A. Di Biase, D. Alvaro, M. Angelico*, J. Chromatogr. **386**, 367 (1987).
[10] *G. Salvioli, R. Lugli, J. M. Pradelli, G. Gigliotti*, FEBS **187**, 272 (1985).
[11] *M. C. Hennion, C. Picard, C. Combellas, M. Caude, R. Rosset*, J. Chromatogr. **210**, 211 (1981).
[12] *P. J. Shoenmakers, H. A. H. Billiet, L. de Galan*, J. Chromatogr. **185**, 179 (1979).
[13] *M. C. Carey*, in "Bile acids in gastroenterology", L. Barbara, R. H. Dowling, A. F. Hoffman and E. Roda Eds., MTP Press Ltd., Lancaster (UK), 1983, p. 19.
[14] *A. Roda, A. F. Hoffman, K. J. Mysels*, J. Biol. Chem. **258**, 6362 (1983).
[15] *H. Igimi, M. C. Carey*, J. Lipid Res. **21**, 72 (1980).
[16] *A. Roda, A. Fini*, Hepatol. **4**, 72S (1984).
[17] *M. C. Carey*, Hepatol. **4**, 66S (1984).
[18] *D. M. Small*, in "The bile acids", P. P. Nair and D. Kritchevsky, Vol. 1, Plenum Press, N. Y., 1971, p. 249.
[19] *R. J. Huxtable*, in "Taurine in nutrition and neurology", R. J. Huxtable and H. Pasantes-Morales, Plenum Press, N. Y., 1982, p. 1.

Received: June 30, 1987
Revised manuscript
received: Sep. 21, 1987
Accepted: Sep. 22, 1987
F

Measurement of Concentrations of a New H_2-Receptor Antagonist (SK&F 93574) in Plasma, Urine and Bile

V. S. Picot/E. Doyle*/L. J. Read/R. M. Lee

Smith Kline and French Research Limited, The Frythe, Welwyn, Hertfordshire, AL6 9AR, UK

Key Words

Reversed-phase HPLC
H_2-receptor antagonist
Measurement in biological fluids
Solid phase extraction

Summary

An assay for the measurement of SK&F 93574, a new H_2-receptor antagonist, in plasma, urine and bile is described. The assay uses solid-phase extraction, reversed phase HPLC and UV detection at 229 nm. A strongly retaining extraction column and three different solvent washes, which involve pH changes and an aqueous/organic wash, ensure that there is no interference from endogenous material without significant loss of drug. The assay is sufficiently sensitive to measure concentrations of 20 nm ml^{-1} SK&F 93574 in plasma and 0.2 μg ml^{-1} SK&F 93574 in urine and bile. The assay is reproducible from day to day and therefore can be used to define the pharmacokinetics of SK&F 93574.

Introduction

SK&F 93574, 5-(1,2-dihydro-2-oxo-pyrid-4-ylmethyl)-2-[2-[5-(dimethylaminomethyl)furanylmethylthio] ethylamino]pyrimidin-4(IH)-one, is a potent and specific histamine H_2-receptor antagonist in animals and humans. It is an analogue of the previously described long acting histamine H_2-receptor antagonist SK&F 93479 [1]. However, it is more hydrophilic than SK&F 93479.

The possible utility of SK&F 93574 has been discussed by Burland et al. [2], but until now it has not been possible to follow the kinetics of this compound during the period of pharmacological activity, because of the absence of a suitable analytical method.

This paper describes a reversed phase HPLC/UV assay for SK&F 93574 in plasma, urine and bile, which has been developed for use in pharmacokinetic studies.

Materials and Methods

Materials

Sodium acetate trihydrate and anhydrous sodium carbonate, both AnalaR grade, were supplied by BDH Chemicals, Poole, Dorset, UK. Glacial acetic acid (Pronalys) was supplied by May and Baker Ltd, Dagenham, UK.

Bond-Elut solid phase extraction columns (1 ml capacity, containing 100 mg of sorbent), and associated Vac-Elut equipment were manufactured by Analytichem International (Harbor City, CA, USA) and supplied by Jones Chromatography Ltd, Llanbradach, UK.

Additional equipment was obtained through local suppliers.

SK&F 93574 was synthesised by Smith Kline and French, Tonbridge, UK and was > 99 % pure by HPLC analysis.

SK&F 93924, 5-(1,2-dihydro-2-oxo-pyrid-4-ylmethyl)-2-[2-[5-(dimethylaminomethyl) thienylmethylthio] ethylamino]-pyrimidin-4(IH)-one trihydrochloride hydrate (the internal standard) was synthesised by The Department of Synthetic and Isotope Chemistry, Smith Kline and French, Welwyn, UK and was > 99 % pure by HPLC analysis.

Structures of SK&F 93574 and SK&F 93924 are shown in Fig. 1.

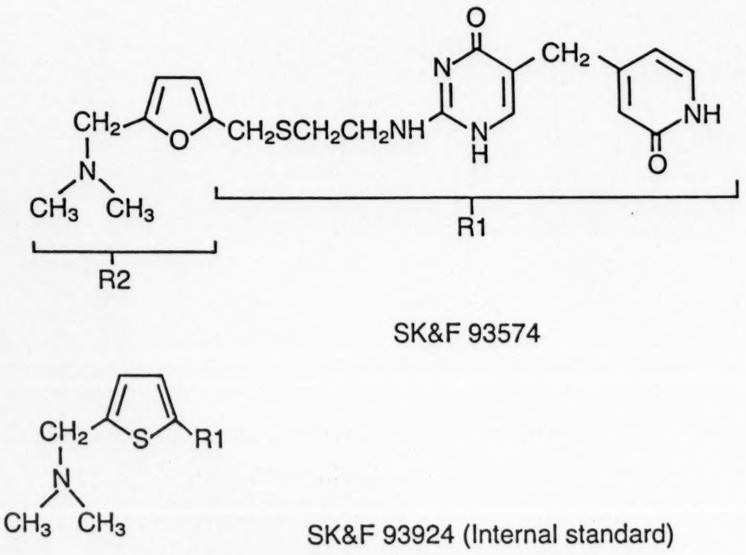

SK&F 93574

SK&F 93924 (Internal standard)

Fig. 1
Structures of SK&F 93574 and Internal Standard.

0009-5893/87 0282-05 $ 03.00/0

© 1987 Friedr. Vieweg & Sohn Verlagsgesellschaft mbH

HPLC Apparatus for Plasma and Urine Assays

The HPLC equipment consisted of a Waters Associate Model M6000A or 590 pump (Millipore (UK) Ltd, Harrow, UK), a Waters Wisp 710B autosampler, and a Kratos Spectroflow 783 variable wavelength detector (Severn Analytical Gloucester, UK), monitoring at 229 nm. Chromatographic recordings and integrations were performed on an LDC 301 recording integrator (Laboratory Data Control, Stone, Staffordshire, UK).

The reversed phase analytical column was prepacked with Ultrasphere^{TM} ODS, particle size 5 μm (Altex 15 cm x 4.6 mm I.D.; supplied by Beckman-RIIC Ltd, High Wycombe, UK), and it was maintained at 40 °C by using a DuPont 8800 column oven.

Methanol and acetonitrile, both HPLC grade, were supplied by Rathburn Chemicals Ltd, Peebleshire, Scotland. Filtered, HPLC grade water was obtained daily from a Milli-Q water purification system (Millipore (UK) Ltd, Harrow, UK). AnalaR grade potassium dihydrogen orthophosphate and orthophosphoric acid were both supplied by BDH Chemicals, Poole, Dorset, UK.

Mobile Phase

The mobile phase was a mixture (70:20:10 v/v) of 0.01 M potassium dihydrogen orthophosphate, (adjusted to pH 4.0 by addition of 1.0 M orthophosphoric acid) : methanol : acetonitrile. Prior to use, the organic solvents were filtered through 0.50 μm membrane filters, type FH, and the phosphate buffer through 0.45 μm membrane filters, type HA (Millipore (UK) Ltd, Harrow, UK). The flow rate was 1.0 ml min^{-1} and any dissolved gases were removed by sparging with helium before and during use.

HPLC Apparatus for Bile Assay

A Hewlett-Packard HP1090 LC system equiped with an automatic sample injector, HP85B microcomputer, HP3392A integrator and HP9121 disk drive (Hewlett-Packard Ltd, Winnersh, UK) was used. Alternatively, the system used for the assay of SK&F 93574 in plasma and urine can be used for bile, but without gradient facility no column clean-up can be performed between samples, as described below.

Mobile Phase

The mobile phase was 0.05 M phosphate buffer pH 4.0 mixed (2:1 v/v) with a mixture of methanol : acetonitrile mix (80:20 v/v). The flow rate was 1.5 ml min^{-1} and the column was kept at 40 °C.

Following an isocratic run time of 10 minutes, integration was suppressed and the percentage of methanol : acetonitrile mix increased over 1 minute from 20% to 50%. This combination was maintained for 5 minutes after which time the original conditions were re-established. An equilibration delay of 10 minutes was allowed before injection of the next sample. In this way the amount of endogenous biliary material remaining on column was kept to a minimum.

Preparation and Storage of Stock Solutions

Stock solutions of SK&F 93574 (base) and SK&F 93924 (trihydrochloride) were both prepared by dissolving the required weight of compound in a minimal volume of methanol, and diluting with distilled water to a concentration of 100 μg ml^{-1}. The SK&F 93574 stock solution prepared in this manner may be stored at 4 °C for 4 weeks, and the SK&F 93924 stock solution for 2 weeks. Working solutions of SK&F 93574 produced by dilution of stock solution with distilled water may also be stored for up to 4 weeks at 4 °C, but working solutions of SK&F 93924 should be made up daily.

Collection and Storage of Samples

Blood was drawn into tubes containing lithium heparin as anticoagulant. The plasma was separated by centrifugation at 1500 x g for 10 minutes at 4 °C, transferred to non-heparinised tubes and stored at − 20 °C. No deterioration was observed in plasma samples stored under these conditions for 24 weeks, and urine samples stored for 12 weeks. No storage information is available for bile.

Extraction from Plasma

80 μl of internal standard solution (SF&K 93924, 5 μg ml^{-1}), 100 μl water and 1 ml 0.2 M acetate buffer (pH 4.5) were added to 1 ml plasma samples in 12 ml polypropylene centrifuge tubes. The water was added so that the volume extracted would be consistent with that of the calibration standards which were made by adding aqueous solutions of SK&F 93574 to drug free plasma. The samples were vortex mixed, and then centrifuged at approximately 3000 x g for 10 minutes to remove precipitated plasma proteins.

1 ml Bond-Elut columns containing 100 mg of C_{18} sorbent, were pretreated with 1 ml methanol, followed by 1 ml water, drawn through under vacuum supply to a Vac-Elut assembly. 3 ml reservoirs were fitted to the Bond-Elut columns and the mixture of sample plus buffer carefully poured into each. A vacuum of 18 kPa was applied, so that the samples were slowly drawn through the sorbent. As soon as all of the samples had been drawn through, any residual droplets were removed by increasing the negative pressure to approximately 50 kPa. The columns were then washed with 1 ml 0.1 M sodium carbonate, two separate 1 ml measures of distilled water, and finally with 1 ml of a methanol: water mixture (35:65 v/v). This was drawn through at approximately 50 kPa until all of the columns appeared to be dry. The wash was not allowed to remain on the Bond-Elut for longer than necessary, as failure to remove the solvent quickly resulted in low recoveries of SF&F 93574 and internal standard.

The column outlets were wiped with a non-fibrous tissue, and the catchment tray containing 1.5 ml microcentrifugate tubes was placed in position. Samples were eluted from the columns with 250 μl of a mixture of methanol:water (80:20 v/v), and transferred to low volume autosampler vials. 25 μl injections were made for HPLC analysis.

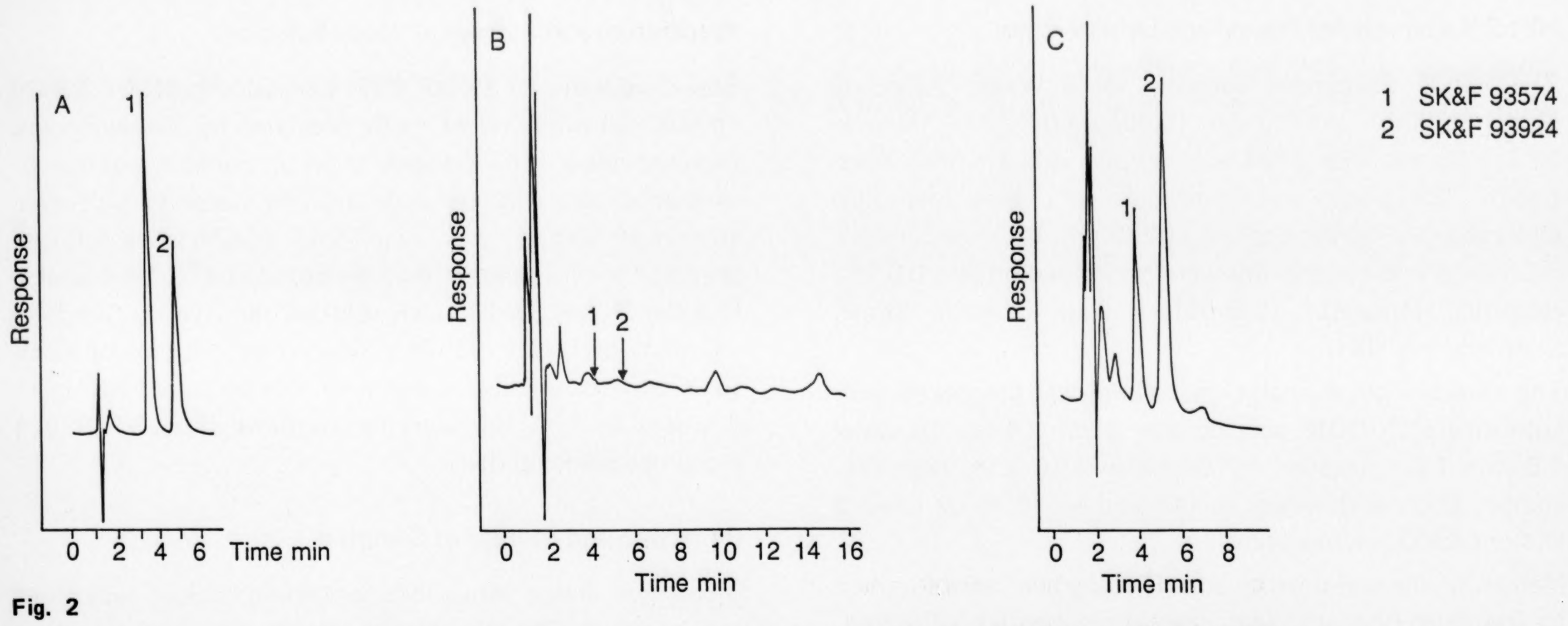

Fig. 2

A: The chromatogram obtained following injection of an aqueous solution containing SK&F 93574 and SK&F 93924 both at concentrations of 5 $\mu g\ ml^{-1}$.

B: A typical chromatogram of extracted control (drug-free) human plasma, containing no peaks that interfere with the method.

C: A typical chromatogram of extracted plasma from a human volunteer following intravenous infusion of SK&F 93574 at a dose of 35 $\mu g\ kg^{-1}$.

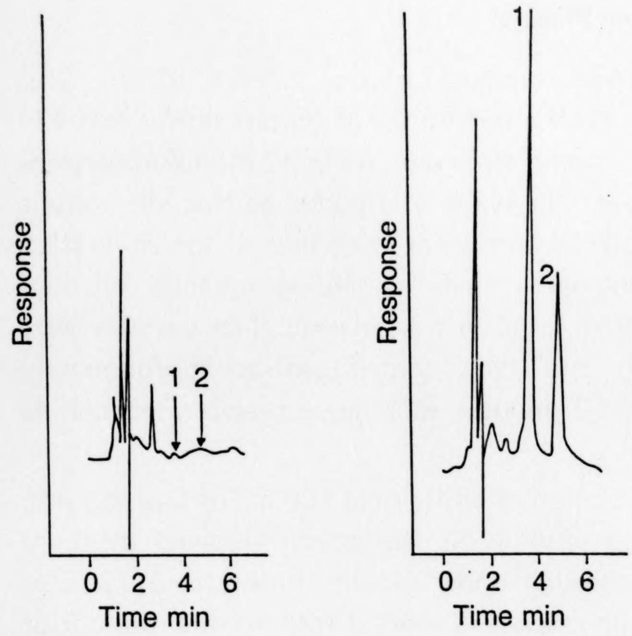

Fig. 3

A: A typical chromatogram of extracted control human urine.

B: A typical chromatogram of extracted urine from a human volunteer following intravenous infusion of SK&F 93574. 0–4 h urine sample containing 3.4 $\mu g\ ml^{-1}$ SK&F 93574.

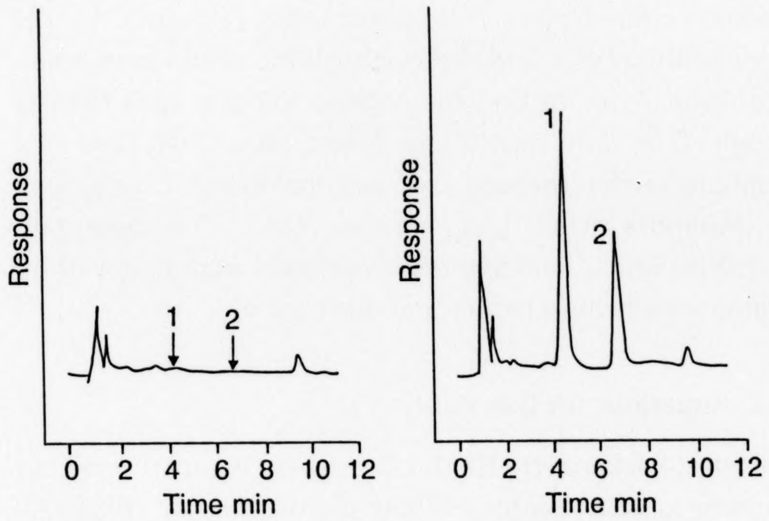

Fig. 4

A: A typical chromatogram of control human bile.

B: A typical chromatogram of human bile spiked with 2 $\mu g\ ml^{-1}$ SK&F 93574 and 1 $\mu g\ ml^{-1}$ SK&F 93924.

Extraction from Urine

100 μl of internal standard solution (10 $\mu g\ ml^{-1}$ SK&F 93924), 200 μl water and 0.5 ml 0.2 M acetate buffer pH 4.5 were added to 0.5 ml urine samples in 1.5 ml polypropylene microcentrigue tubes, and thoroughly vortex mixed. The samples were extracted by the same method detailed for plasma, except that 3 ml reservoirs were not required, and 10 μl aliquots of the final eluent were injected onto the HPLC column for analysis.

Acid hydrolysis of urine samples prior to extraction has been performed using 0.5 ml hydrochloric acid (2.0 M) to 0.5 ml urine, heated at 100 °C for 30 minutes. No acetate buffer was added before extraction.

Extraction from Bile

1 ml bile samples were mixed with 50 μl water in 5 ml polypropylene tubes, so that the total volume extracted was consistent with calibration standards. A constant amount of ammonium sulphate (approximately 0.4 g) was added. The tubes were vortex-mixed and left to stand for approximately 10 minutes, before pouring the contents into 1.5 ml microcentrifuge tubes. They were then centrifuged at 14930 $\times$ g for 4.5 minutes. The oily top layers which formed were gently removed using glass pasteur pipettes so that 1 ml of each bile supernatant could be transferred to a 12 ml polypropylene tube. 100 μl of internal standard (10 $\mu g\ ml^{-1}$) and 2 ml citrate buffer

(0.1 M) were added to each tube. The tubes were vortex-mixed and the collected supernatant extracted by the method described for plasma. 30 μl aliquots of the final eluent were injected onto the HPLC column for analysis.

Acid hydrolysis of the bile prior to addition of ammonium sulphate, using 1.0 ml 2 M hydrochloric acid to 1.0 ml bile, has also been performed and does not result in any interference from endogenous material.

Preparation of Calibration Lines

Calibration lines were constructed by plotting the peak height, or peak area, ratio of SK&F 93574 to internal standard, against known concentrations of SK&F 93574 added to drug-free plasma, urine or bile.

A calibration line was constructed by two-variable linear regression analysis, and the concentration of SK&F 93574, quantified by relating the respective peak height (area) ratio to the line.

Results and Discussion

Chromatography

Under the conditions described, the retention time of SK&F 93574 was approximately 4 minutes, and that for SK&F 93924 was 5.1 minutes. These times varied slightly if column or mobile phase were changed, but not so that the analytical results were affected.

Precision and Accuracy

The precision of the method was calculated as the coefficient of variation of replicate assays of standards containing SK&F 93574 at concentrations of between 0.02 and 1.0 μg ml^{-1} for plasma and between 0.2 and 4.0 μg ml^{-1} for the urine and bile data. Replicates at each concentration were performed on three different days, and by different analysts, so that the coefficients of variation reported in Table 1 include day to day and inter-individual variation.

The accuracy of the method was assessed by re-fitting the ratios from standards used to assess precision into the regression equation derived from these data, and calculating the bias, Table 1.

Recovery

To assess the recoveries of SK&F 93574 and SK&F 93924 from plasma, urine and bile, the HPLC responses of these compounds in extracted standards were compared with the responses of known amounts on column. Recovery of SK&F 93574 was assessed at three different concentrations, Table 2.

Stability of SK&F 93574 in Biological Samples

Control plasma to which SK&F 93574 had been added was analysed immediately and after storage at − 20 °C throughout a 24 week period. Urine samples from human volunteers following an intravenous dose of SK&F 93574 were

Table I. Precision and bias of the assay for SK&F 93574 in plasma, urine and bile

Amount of SK&F 93574 added in 1 ml plasma (ng)	Number of replicates	Mean estimated (ng ml^{-1})	CV %	Bias (%)
20	17	20.0	26	< 1
60	9	57.6	13	4
100	9	98.6	7	1
200	9	201	6	< 1
400	9	381	13	5
700	9	686	8	2
1000	17	998	6	< 1
Amount of SK&F 93574 added in 1 ml urine (μg)	**Number of replicates**	**Mean estimated (μg ml^{-1})**	**CV %**	**Bias (%)**
0.20	18	0.21	18	5
0.50	9	0.50	11	< 1
1.00	9	0.99	5	1
2.00	8	1.98	2	1
3.00	9	3.00	3	< 1
4.00	15	4.00	2	< 1
Amount of SK&F 93574 added in 1 ml bile (μg)	**Number of replicates**	**Mean estimated (μg ml^{-1})**	**CV %**	**Bias (%)**
0.20	17	0.21	20	5
0.50	9	0.45	13	10
1.00	8	1.02	15	2
2.00	8	1.90	10	5
3.00	9	3.00	9	< 1
4.00	17	4.22	9	6

CV = coefficient of variation

Table II. Recovery of SK&F 93574 and internal standards from plasma, urine and bile

Fluid	Amount of SK&F 93574 added in 1 ml (ng)	Relative Counts ± CV %		Recovery (%)
		Extracted	Non-extracted	
Plasma	20	164 ± 10 (n = 4)	181 ± 12 (n = 4)	91
	100	726 ± 8 (n = 3)	679 ± 8 (n = 3)	105
	250	1698 ± 8 (n = 6)	1804 ± 10 (n = 6)	94
Urine	200	18977 ± 5 (n = 6)	27004 ± 5 (n = 6)	70
	1000	97249 ± 4 (n = 3)	132723 ± 1 (n = 3)	73
	4000	390119 ± 3 (n = 6)	553198 ± 1 (n = 6)	71
Bile	200	99504 ± 14 (n = 5)	111747 ± 1 (n = 6)	89
	1000	378645 ± <1 (n = 2)	562138 ± 1 (n = 6)	67
	4000	1897075 ± 8 (n = 4)	2268167 ± 1 (n = 6)	84

Fluid	Amount of SK&F 93924 added in 1 ml (ng)	Relative Counts ± CV %		Recovery (%)
		Extracted	Non-ectracted	
Plasma	400	1463 ± 11 (n = 15)	1397 ± 11 (n = 16)	105
Urine	2000	158666 ± 5 (n = 15)	206671 ± 5 (n = 33)	77
Bile	2000	591675 ± 7 (n = 11)	622251 ± 1 (n = 18)	95

n = number of replicates
CV = coefficient of variation

analysed immediately after collection and after storage at − 20 °C over a 12 week period. The stability of SK&F 93574 in plasma and urine over 26 hours when maintained at 25 °C was investigated in similar manner.

Samples of plasma and urine, when stored at − 20 °C for 24 and 12 weeks respectively, did not give peaks that would interfere with the measurement of SK&F 93574 and internal standard. There was no appreciable loss of SK&F 93574 from the samples when stored under these conditions, or when maintained at 25 °C for 26 hours.

No storage stability studies were performed for bile samples.

Conclusion

This method demonstates good application of solid-phase extraction to provide a simple and robust assay for the measurement of SK&F 93574 in biological fluids. The strongly retaining extraction column and the series of washes, which involve pH changes and an aquous/organic wash, were effective in removing endogenous material without significant loss of drug. The assay can therefore be used to measure concentrations of 20 ng ml^{-1} SK&F 93574 and above in plasma, and 0.2 μg ml^{-1} and above in urine and bile. It is sufficiently reproducible from day to day and has been used in the authors' laboratory for one year by different analysts. The demonstrated reproducibility and sensitivity of this assay make it suitable for the definition of the pharmacokinetics of SK&F 93574.

References

[1] *R. C. Blakemore, T. H. Brown, R. J. Chenery, G. J. Durant, C. R. Ganellin, M. E. Parsons, A. C. Rasmussen,* D. A. Rawlings, SK&F 93574 A Potent and Long Acting Histamine H_2-Receptor Antagonist for Intravenous Administration. Br. J. Pharmacol. 1985, 86 (Suppl), 570P.

[2] *W. L. Burland, J. G. Mills, L. Richardson, K. Wareham,* SK&F 93574 – Preliminary Evaluation of a Potent and Long-Acting parenteral H_2-Receptor Antagonist In Man. Gut 1985, 26, A1107, Abstr P15.

Received: July 3, 1987
Accepted: July 28, 1987
F

High-Performance Liquid Chromatographic Analysis of Cyclizine and its Metabolite, Norcyclizine in Biological Fluids Using solid Phase Extraction

R. Walker/I. Kanfer*

School of Pharmaceutical Sciences, Rhodes University, Grahamstown, 6140, South Africa

Key Words

Column liquid chromatography
Solid-phase extraction
Cyclizine
Norcyclizine
Serum
Urine

Summary

A high-performance liquid chromatographic analysis of cyclizine and its metabolite, norcyclizine in biological fluids using protryptiline hydrochloride as internal standard is described. The drug and metabolite were extracted from the relevant biological matrix using a solid-phase extraction procedure combined with a simple phase separation step prior to chromatographic analysis. The separation was achieved on a reversed-phase C_{18} column (10 μm) using acetonitrile – 0.05 M (pH = 3) phosphate buffer (40 : 60), as the mobile phase with UV detection at 200 nm. Calibration curves were linear over the entire concentration range 5–100 ng/ml for cyclizine in serum and urine and for norcyclizine in urine. Precise quantitative analysis with relative standard deviations of < 5 % was achieved.

Introduction

Cyclizine is an antihistaminic compound used mainly for its antiemetic action in the prevention of motion sickness. In spite of its popularity and availability as an over-the-counter product little has been published regarding its absorption and disposition kinetics. The absence of such data can be attributed to the lack of suitable analytical methods capable of measuring the low concentrations of cyclizine found in human serum and urine following administration of the drug.

A method for determining cyclizine in plasma and urine involving gas-liquid chromatography using nitrogen selective detection has previously been published [1] whilst a similar system was recently applied to determine blood and urine concentrations of the drug [2]. Previous methods for measuring cyclizine in biological fluids with methyl orange [3] or derivitization with tritiated acetic anhydride [4] were non-specific and relatively inaccurate at the low concentrations found following cyclizine administration.

The high-performance liquid chromatographic (HPLC) method described below, which employs UV detection at 200 nm is capable of measuring cyclizine in serum as well as the demethylated metabolite, norcyclizine (Fig. 1), in urine and has the necessary sensitivity and precision for application in pharmacokinetic and bioavailability studies.

Experimental

Chromatography Systems

Analysis was performed with a modular high-performance liquid chromatograph consisting of an M6000A pump (Waters Assoc.), an automated sample injector (WISP 710B, Waters Assoc.), a variable wavelength UV absorbance detector (Spectra-Physics, Model SP 8480 XR) and a strip chart recorder (Model 561 Perkin-Elmer Corp, USA). The column was maintained at 30 °C with a Model LC-22 temperature controller (Bioanalytical Systems, USA).

Reagents

All reagents were of analytical grade. The acetonitrile was distilled-in-glass UV grade (Burdick and Jackson, USA). The water used in the mobile phase was of HPLC grade, purified through a Milli-Q system (Millipore, USA).

Cyclizine hydrochloride was obtained from Wellcome (Pty) Limited, South Africa, norcyclizine from the Wellcome Foundation Ltd, United Kingdom and protryptiline hydrochloride from MSD Laboratories, South Africa.

Techsil (HPLC Technology, UK) 10 μm octadecylsilane (C_{18}) material was used as the stationary phase.

0009-5893/87 0287-04 $03.00/0

© 1987 Friedr. Vieweg & Sohn Verlagsgesellschaft mbH

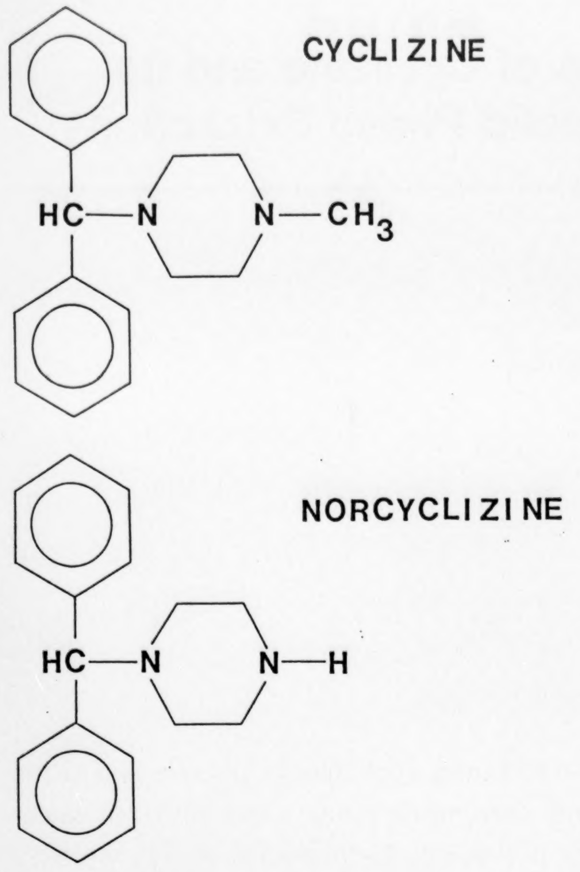

Fig. 1

Molecular structures of cyclizine and its demethylated metabolite, norcyclizine.

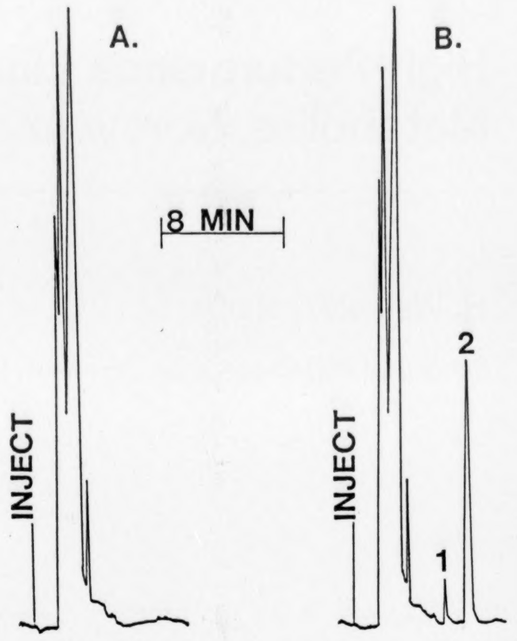

Fig. 2

HPLC chromatogram of cyclizine in human serum.

Peaks: **1** = cyclizine; **2** = internal standard (protryptiline)
A = blank serum extract; **B** = serum extract containing cyclizine (5 ng/ml)

Conditions: Column Techsil C_{18} (10 μm); length 250 mm; I. D 4.1 mm; Eluent acetonitrile – 0.05 M (pH 3) phosphate buffer (40:60); flow rate 1 ml min^{-1}; pressure 7 X 10^6 Nm^{-2}; wavelength 200 nm; temperature 30°C.

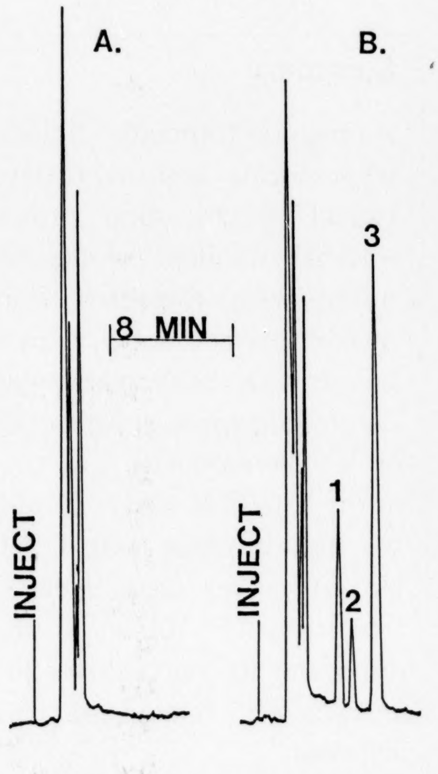

Fig. 3

HPCL chromatogram of cyclizine and norcyclizine in human urine.

Peaks: **1** = norcyclizine; **2** = cyclizine; **3** = internal standard (protryptiline); **A** = blank urine extract; **B** = urine extract containing norcyclizine (50 ng/ml) and cyclizine (10 ng/ml).

Conditions: Column Techsil C_{18} (10 μm); length 250 mm; I. D 4.1 mm; eluent acetonitrile – 0.05 M (pH 3) phosphate buffer (40:60); flow rate 1 ml min^{-1}; pressure 7 X 10^6 Nm^{-2}; wavelength 200 nm; temperature 30 °C.

All solvents were filtered and degassed prior to use. The mobile phase was constantly degassed using an in-line vacuum degassing unit (Model ERC-3510, Erma Optical Works, Japan).

Typical chromatograms are depicted in Fig. 2 and 3 together with the chromatographic conditions used.

Extraction Procedure

One millilitre aliquots of either serum or urine were deproteinized by mixing with 1 ml of acetonitrile, vortexing for 30 seconds and then centrifuging for 5 minutes at 3000 r.p.m. The resulting supernatant was transferred to a culture tube containing 4 ml of water and 100 ng of internal standard (protryptiline hydrochloride). One millilitre disposable extraction columns packed with octodecylsilane (Analytichem International) that had been pre-washed were used. The wash sequence involved a 5 ml acetonitrile wash, followed by a 5 ml acetonitrile – 0.05 M (pH = 3) phosphate buffer (70: 30) wash and finally a 5 ml water wash. Care was taken to ensure that the columns did not dry out between washes. The sample was then loaded onto the pre-treated column with the aid of a 15 ml reservoir. After loading, the column was washed with 5 ml water and then 5 ml acetonitrile-water (70:30). At this stage the columns were kept under vacuum until dry. Cyclizine (serum) and cyclizine and its metabolite, norcyclizine, (urine) were eluted into 3 ml glass tapered collection tubes, with three 500 μl aliquots of acetonitrile – 0.05 M (pH = 3) phosphate buffer (70 : 30). The samples were then evaporated to dryness in a rotary vacuum centrifuge (Savant Instruments, USA). The residue was reconstituted in 20 μl of water and vortexed for 1 minute. On addition of 30 μl of acetonitrile two layers formed. The samples were then vortexed for a further minute and centrifuged at 3000 rpm for 30 seconds. All samples were kept sealed so as to prevent excessive loss of acetonitrile. The top layer was transferred to a WISP insert (Waters Assoc.) using a 100 µl microsyringe. Ten microlitre aliquots were injected onto the column. Typical chromatograms are depicted in Fig. 2 and 3.

Results and Discussion

Linearity

Serum samples spiked with cyclizine hydrochloride were extracted at six different concentrations and a calibration curve was obtained by plotting the ratio of the peak height of cyclizine hydrochloride to that of the internal standard versus the concentration of cyclizine hydrochloride. Calibration curves were linear over the entire range studied. The calibration curve (5–100 ng/ml) had a slope of 0.0206 and a y-intercept of 0.1019 with a correlation coefficient of 0.9981.

Urine samples spiked with cyclizine hydrochloride and norcyclizine were extracted at six different concentrations and calibration curves obtained for each compound. The calibration curve for cyclizine hydrochloride (5–100 ng/ml) had a slope of 0.00614 and a y-intercept of 0.01608 with a correlation coefficient of 0.9970 while the calibration curve for norcyclizine (5–100 ng/ml) had a slope of 0.00794 and a y-intercept of 0.01502 with a correlation coefficient of 0.9960.

Precision and Accuracy

Precision was determined by extracting five of each of the serum and urine samples at each of the six concentrations studied. The results are shown in Table I. In all cases the percent relative standard deviation was < 5 %.

Extraction Efficiency

Serum and urine samples were assayed in quadruplicate at two different concentrations within the range studied. The samples were extracted as described except that the top layer of acetonitrile was transferred to another glass collection tube containing 100 ng of internal standard. This was then evaporated to dryness and reconstituted with 20 µl water and 30 µl of acetonitrile. A 10 µl aliquot was injected onto the HPLC column. The ratio of peak heights of cyclizine hydrchloride (serium and urine) and norcyclizine (urine) to internal standard were compared to ratios obtained from the evaporation to dryness of aqueous samples containing the same amount of drug and reconstituted in the same way. The mean recovery values obtained for cyclizine hydrochloride were 83 % (serum) and 84 % (urine) whilst the recovery of norcyclizine from urine was 83 %.

Stability

Spiked samples at two different concentrations, containing cyclizine hydrochloride in serum and urine and norcyclizine in urine were stored at 4 °C and − 10 °C for 1, 2 and 4 weeks. The cyclizine hydrochloride samples in serum and urine were stable for 4 weeks at both temperatures. The norcyclizine samples were stable at − 10 °C for 4 weeks but at 4 °C for only 2 weeks after which a reduction in the concentration of norcyclizine was observed.

Table I. Accuracy and precision of the method for the determination of cyclizine and its metabolite, norcyclizine in biological fluids. (n = 5)

Cyclizine/Norcyclizine added (ng/ml)		Cyclizine/Norcyclizine found (ng/ml)	R.S.D. (%)
Serum	5.05	4.68 ± 0.24	5.0
	10.10	8.55 ± 0.31	3.6
	25.25	25.32 ± 1.01	4.0
	50.50	52.78 ± 2.90	4.8
	75.75	74.25 ± 3.07	4.1
	101.00	100.70 ± 0.98	1.0
Urine	5.27	6.08 ± 0.29	5.0
(Cyclizine)	10.54	11.54 ± 0.48	4.2
	26.35	25.71 ± 1.04	4.2
	52.70	54.17 ± 1.25	2.3
	79.05	75.83 ± 1.68	2.2
	105.40	105.39 ± 1.75	2.6
(Norcyclizine)	5.27	6.84 ± 0.54	4.9
	10.54	11.67 ± 0.52	4.5
	26.35	25.78 ± 1.04	4.0
	52.70	49.29 ± 2.08	4.2
	79.05	76.54 ± 2.04	2.7
	105.40	108.92 ± 5.68	3.0

Pilot Trial

The method described was used to assay samples obtained from a human volunteer after the administration of a single 50 mg oral dose of cyclizine hydrochloride. A peak serum cyclizine concentration of 57 ng/ml was obtained (Fig. 4A). Urine samples were found to contain both cyclizine and norcyclizine in approximately ten times higher concentrations than previously reported using a gas-liquid chromatographic method [2]. (Fig. 4B)

Discussion

Very few analytical methods for the quantitative analysis of cyclizine and norcyclizine in biological fluids have been reported [1–4], none of them involving HPLC. This can be partially attributed to the fact that both cyclizine and norcyclizine have relatively poor UV absorptivities at the wavelengths normaly used to detect compounds separated by HPLC ($>$ 220 nm or more commonly, 254 nm). This detection difficulty was overcome by employing a highly selective solid-phase extraction technique in conjunction with a final phase-separation step.

A review of the literature revealed that protryptiline and other similar tricyclic anti-depressant drugs can be successfully extracted from biological fluids using cyano packed disposable extraction columns. Since protryptiline was currently used as the internal standard, attempts were made to develop a method using cyano columns. Contaminants which interfered with the detection of cyclizine and nor-

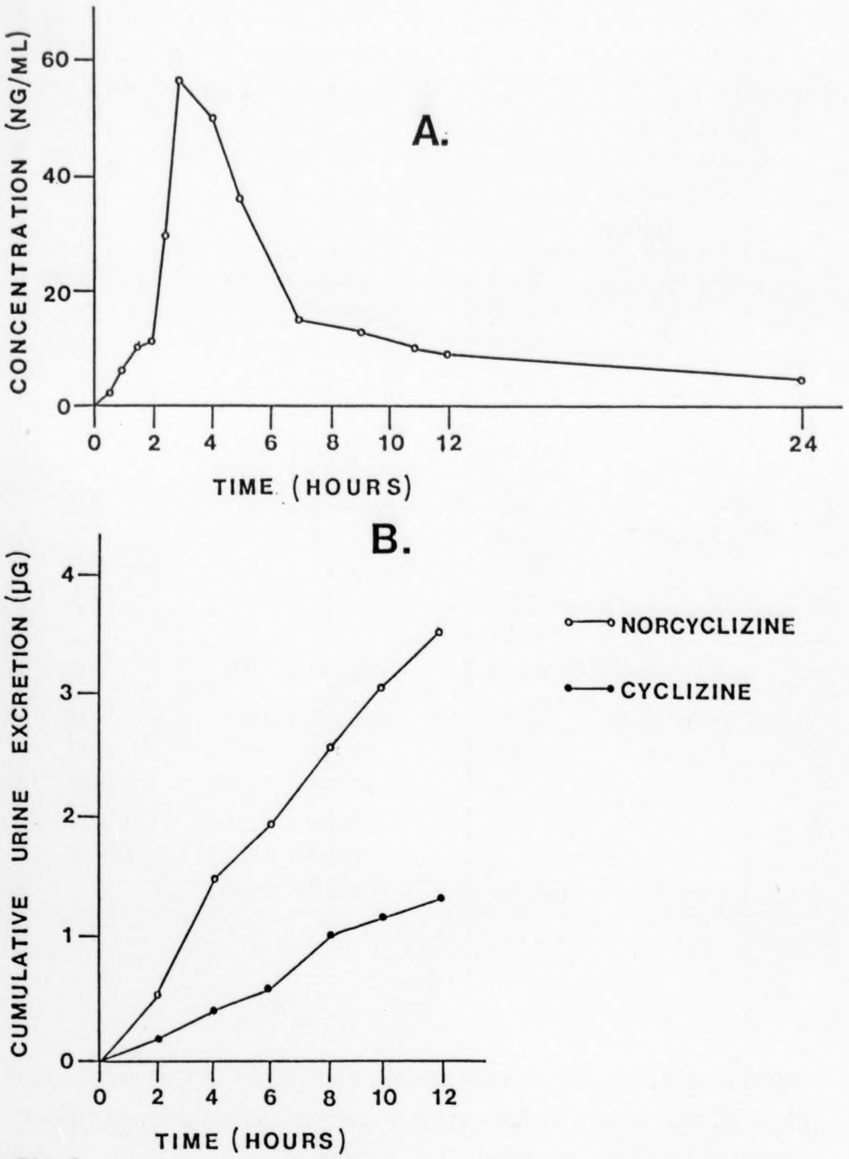

Fig. 4

A: Cyclizine serum concentration-time profile in a human subject after the administration of a single 50 mg oral dose.

B: Urinary excretion plot of cyclizine after the administration of a single 50 mg oral dose.

cyclizine were unfortunately extremely prevalent. On the basis of results obtained in our laboratory with macrolide antibiotics, where C_{18} extraction columns were used to extract erythromycin from serum and urine [5], C_{18} extraction columns were thus adopted for use. Modification of the above method resulted in a procedure which allowed unhindered quantitative analysis of the relevant compounds using low wavelength UV detection at 200 nm, a region where usually a great deal of interference is encountered.

Conclusions

The success of the method reported was largely due to the efficiency of the solid-phase extraction procedure followed by a simple phase separation step. This enabled the rapid and precise quantitative determination of cyclizine in serum and cyclizine together with norcyclizine in urine and should prove extremely useful for the pharmacokinetic characterization of this drug in human subjects.

References

[1] *G. Land, K. Dean, A. Bye,* J. Chromatogr. **222,** 135 (1981).
[2] *D. S. Griffin, R. C. Basselt,* J. Anal. Toxicol. **8,** 97 (1984).
[3] *R. Kuntzman, A. Klutch, I. Tsai, J. J. Burns,* J. Pharmacol. Exp. Therap. **149,** 29 (1965).
[4] *R. Kuntzman, I. Tsai, J. J. Burns,* J. Pharmacol. Exp. Therap. **158,** 332 (1967).
[5] *C. Stubbs, J. M. Haigh, I. Kanfer,* J. Pharm. Sci. **74,** 1126 (1985).

Received: June 29, 1987
Accepted: July 13, 1987
F

Peak Height Determination in Analysis of Chlortetracycline in Animal Feeds

S. E. Hudson*

Department of Chemistry, University of California, Santa Cruz, CA 95064, USA

M. E. Cohen

Department of Mathematics, California State University, Fresno, CA 93740, USA

D. L. Hudson

Section on Medical Information Science, University of California, San Francisco, 2615 East Clinton Avenue, Fresno, CA 93703, USA

B. Gump

California State University, Fresno, CA 93740, USA

Key Words

Peak height determination
Chlortetracycline
Curve fitting
Orthogonal polynomials
Antibiotic determination

Summary

In an HPLC method for the analysis of chlortetracacline (CTC) in animal feed, a problem arose with the presence of peaks which did not return to baseline before the occurrence of a subsequent peak. Two methods were used to determine the peak height. In the first method, a perpendicular was dropped from the maximum of the second peak. A linear function was then fitted to the descending slope on the first peak. The point of intersection was taken as the baseline point. In the second approach, a polynomial fit was used instead. Results show excellent agreement with analysis obtained by established methodology. This approach provides a practical method for determination of chlortetracycline in animal feeds allowing up to six samples to be analyzed within 8 hours.

Introduction

The original three members of the tetracycline family were isolated from substrates of various streptomyces bacteria from 1948 to 1952 [1]. The first to be isolated was 7-chlortetracycline (CTC) in 1948. In acid solution (0.1 N HCl) it procudes ultraviolet absorption maxima at 230, 262.5 and 367.5 nm.

Chlortetracycline has been used in animal feed preparations since shortly after its isolation. It is used primarily in swine, poultry and bovine feed preparations at levels ranging from 5 g/ton to 200 g/ton [2].

The traditional assay method for CTC in animal feeds has been the microbiological cylinder plate method [3, 4]. This method has been satisfactory for most applications, but it does exhibit some limitations. Some of the limitations of this method are interferences from other antibiotics that may be present in the feed and certain cations, for example, magnesium, calcium, iron, copper, manganese, zinc, and cobalt in the form of soluble salts or oxides. CTC is a strong complex forming ligand and these complexes inhibit the biological activity. Quantitation of a sample of unknown concentration is difficult and laborious. The assay itself takes up to several days to complete and only a modest number of samples may be assayed at any one time.

Fluorometric [5, 6] and colorimetric [7] methods have been developed. These methods entail conversion of the drug to various isomers (isochlorotetracycline and anhydrochlorotetracycline) and are difficult to control. Other methods developed have been alternating current polarography [8] and thin-layer chromatography [9].

Several high-performance liquid chromatographic (HPLC) methods have been developed for CTC in other matrices [10]. Other researchers [11, 12] have reported HPLC methods for CTC in premixes.

HPLC seems to be the best alternative to the microbiological methods as it offers the best options for dealing with the interferences and is much more rapid in dealing with large numbers of samples.

0009-5893/87 0291-04 $03.00/0

© 1987 Friedr. Vieweg & Sohn Verlagsgesellschaft mbH

In the above method, a problem arose with the presence of peaks which did not return to baseline before the occurrence of a subsequent peak. Two methods were used for the determination of peak height. In the first method, peak heights were arrived at by extrapolating a tangent to the side of a neighboring peak that was not quite resolved from the CTC peak. This appears to give the height of the maximum CTC absorbance and the minimum absorbance of that nearest neighbor. The second approach involved curve fitting using a new orthogonal polynomial obtained by Cohen. These methods are illustrated below.

The method described in this paper for the HPLC analysis of chlortetracycline provides a rapid and efficient method for industrial analysis of this compound, as an alternative to the previous time-consuming standard method.

Methodology

Apparatus

The apparatus consisted of an Altex model 110A pump, a Waters Model U6K injector, a pellicular C-18 guard column, a Waters μ-Bondpak C-18 25 cm long column with 10-μm C-18 reversed-phase particles, a Waters Model 440 UV detector and a recorder capable of 10 mV input.

Typical operating conditions were: chart speed, 20 cm/hr; flow rate, 0.6 ml/min; temperature constant in the range of 20–45 °C; Detector wavelength, 365 nm; sensitivity 0.005 AUFS (Absorbance Units Full Scale); injection volume, 29 μl.

Reagents

The extraction solvent consisted of 1:13:6; 4N HCl, acetone (ACS), deionized water. The mobile phase consisted of water – dimethylformamide (DMF) (75:25, V/V) containing 0.001 M EDTA, 0.05 M citric acid, 0.013 M sodium citrate and 0.1 M KNO_3. The mobile phase was filtered (0.45 μm membrane) and degassed. The CTC stock solution was 50 mg CTC/100 ml acid-acetone extracting solvent. Working standards were 1, 2, 4, 5 ml aliquots of the stock solution per 100 ml volumes.

Lab Equipment

The following are required: a wrist-action shaker, syringe filter, Gelman alpha-metrical membrane filters or equivalent, and a centrifuge capable of at least 200 rpm.

Determination

Enough sample was weighed into a 250 ml glass stoppered flask to give an estimated concentration of 100 μg/ml. Acid-acetone (100 ml) was pipetted into the flask and the mixture was shaken on a wrist-action shaker for one hour. The sample was then cooled in a refrigerator for 30 min after which it is centrifuged for 20 min at 2000 rpm. It was then gravity-filtered through Whatman # 42 or equivalent followed by syringe filtration through 0.45 μm alpha-metrical membrane filters.

The sample were then chromatographed on the previously described HPLC system using 20 μl injection volumes. A fresh working standard was prepared and injected with each set of samples.

Enough internal standard (ortho-nitrophenol, ONP) was added to the unextracted feed to provide a concentration of 6 g/ml. The sample was then carried through the extraction and filtration procedure. A second sample of feed was extracted and filtered. Then an amount of ONP was added to provide a concentration of 6 g/ml. The ratios of the peak heights of CTC and ONP for each sample were compared. These procedures were repeated multiple times and a t-test was applied.

Peak Height Determination

Two methods were used for peak height determination of peaks which were not fully resolved from neighboring peaks. The first method is illustrated in Fig. 1. In this method, a perpendicular is dropped from the maximum value of the CTC peak. A tangent line is then drawn to the neighboring peak. The point of intersection yields the baseline point for determination of the peak height of the CTC peak. This method is necessary to compensate for the drifting baseline.

A second method was implemented as an independent check on the above method. A polynomial fit was used to closely approximate the shape of the CTC curve if there had not been interference from a neighboring curve. This method is illustrated in Fig. 2. The function used for the fit was a new orthogonal polynomial developed by Cohen. The function takes the form

$$F(\lambda, a_t; x) = \sum_{k=0}^{n} \frac{\prod_{i=0}^{n-1} (\lambda + a_i + a_k)\, x^{a}k\_}{\prod_{j=0}^{k-1} (a_j - a_k) \prod_{s=1}^{n-k} (a_{k+s} - a_k)}$$

where

$$\prod_{j=0}^{k-1} (a_j - a_k) = (a_0 - a_k)(a_1 - a_k) \ldots (a_{k-1} - a_k) \qquad k \geqq 1$$
$$= 1 \qquad k = 0$$

$$\prod_{s=1}^{n-k} (a_{k+s} - a_k) = (a_{k+1} - a_k)(a_{k+2} - a_k) \ldots (a_n - a_K) \qquad n \geqq l$$
$$= 1 \qquad n = l$$

Results from the above methods showed excellent agreement with traditional methods of CTC analysis.

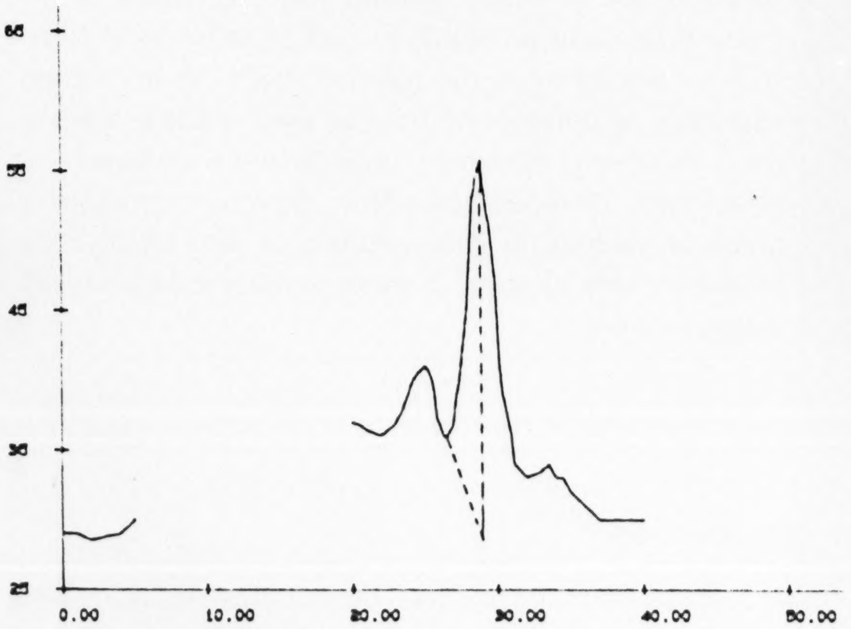

Fig. 1 Peak height determination by tangential method

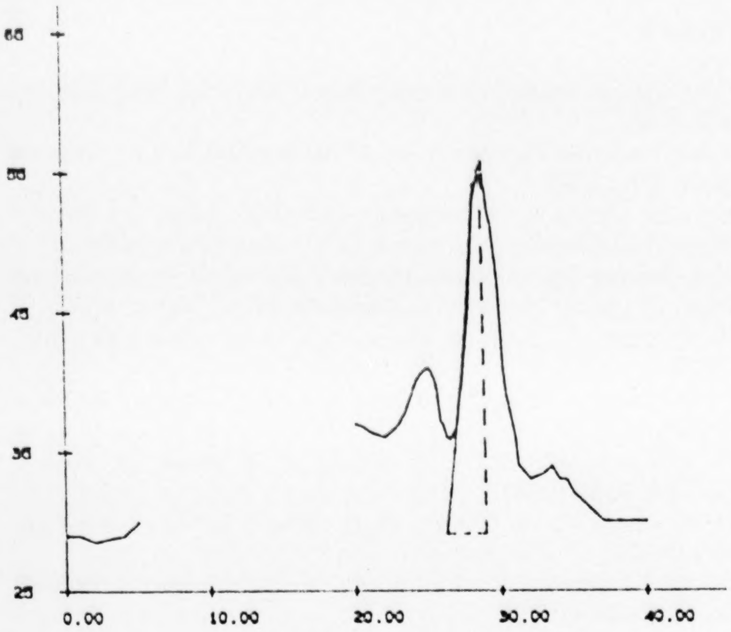

Fig. 2 Peak height determination by curve fitting

Results

A retention time of 19 minutes was found for one column after several were tested. A detection limit of 0.01 μg was obtained after successive dilutions. Several dilutions were chromatographed and it was determined that the response was linear over the range of concentration interest.

The optimum percentage of the organic modifier (DMF) in the mobile phase was determined by studying the elution characteristics of CTC and an internal standard (ortho-nitrophenol). From these studies, an optimum concentration of 25% DMF was determined. The separation of the two peaks was about 2.5 minutes at this point. It allowed close comparison without the two peaks merging. A quantity of ground corn was prepared with CTC premix to a concentration of 100 g/ton. Triplicate chromatograms gave a recovery of 101.9 g/ton. Quantitation was by the method of peak heights.

The acid-acetone solution was cooled after extraction to help prevent evaporation and alteration of the concentration of drug. The solution was gravity-filtered for two reasons. First, vacuum-filtration caused observable evaporation and hence change in concentration. Secondly, gravty-filtration prevented plugging of the subsequent membrane-filtration.

The mobile phase was decided on for several reasons. The DMF concentration of 25% gave optimal separation and more normal peaks than for instance acetonitrile. The EDTA was included to complex various metal ions which may have been present in the feed. The citric acid-sodium citrate maintained a buffer of pH 3 at which CTC is stable. The KNO_3 was added to further normalize the peaks and adjust the ionic strength of the solution.

Duplicate assays were performed on 19 feed samples and the results were compared with assays performed on the same sample by an outside laboratory using the official A.O.A.C. method. The results are tabulated in Table I. A t-test was performed on the data with very satisfactory results. A t-value of 0.25 was obtained, which was compared to the t-value of 2.093 for the 95% confidence level. Ortho-nitrophenol (ONP) was added to one of the samples before extraction and just before final clarification, then chromatographed. Nine replicates of this procedure were performed and the peak height ratios of each procedure were compared. The t-test gave a value of 0.165. When compared with the value of 2.306 for the 95% confidence level, it indicates very little drug was lost during extraction and clarification. The results are shown in Table II.

The work here provides a rapid, accurate method of analysis for CTC in animal feeds. Six samples can be easily assayed in an 8 hour day.

Table I. Comparison of HPLC samples with outside laboratory results obtained on the same samples using the cylinder plate method

Sample number	A g/ton	B g/ton	C g/ton	Mean	Outside Lab	Guar. g/ton	Feed type
70	82.4	75.7		79.1	79.7	100	Swine
71	72.7	73.3		73.1	73.4	100	Swine
72	73.2	72.5	75.9	73.9	73.0	100	Cattle
74	67.7	71.5		69.6	70.5	100	Swine
77	89.6	88.8		89.2	92	100	Swine
78	72.0	70.0		71.1	71	100	Swine
79	128.7	114.5		121.6	122	100	Swine
80	85.3	92		88.6	85.9	100	Swine
81	86.1	89.8		88.0	87.7	100	Swine
82	74.6	75.5		75.1	76.5	100	Swine
83	200.6	190.2		195.4	194	200	Poultry
84	16.1	16.0		16.1	14.7	5	Dairy
85	15.5	16.4		16.0	14.5	100	Horse
86	16.0	15.5		15.8	14.9	100	Poultry
87	264	281		272	284	400	Swine
88	38.2	35.5		36.8	32.4	25	Swine
90	79.2	84.1		81.6	77.5	100	Beef
94	172	168		170	173	170	Sheep
96	39.0	46.2		42.6	42.1	100	Swine

Table II. Comparison of peak height ratios of duplicate samples

83A	83B
0.820	0.847
0.879	0.846
0.824	0.838
0.822	0.832
0.798	0.827
0.843	0.815
0.852	0.796
0.892	0.847
0.830	0.892

The column sample 83A represents peak height ratios for CTC vs. an internal standard (ONP) added before the extraction process had begun. The column for 83B represents peak height ratios obtained after the internal standard was added prior to final filtration.

References

[1] The Merck Index, 10th Ed., Merck and Co., Inc., Rahway, NJ, 1983.

[2] Feed Additive Compendium, Miller Publishing Co., Minneapolis, MN, 1984.

[3] Official Methods of Analysis, 13th Ed., Assoc. of Official Analytical Chemists, Arlington, VA, 1980; 42.211-42.214.

[4] The United States Pharmacopeia, 20th Ed., United States Pharmacopeial Convention, Rockville, MD, 1980; p. 81.

[5] *S. E. Katz, J. Spock,* J. Assoc. Off. Anal. Chem., **47**, 1157 (1964).

[6] *S. E. Katz, J. Spock,* J. Assoc. Off. Anal. Chem., **47**, 203 (1964).

[7] *F. S. Chiccarelli, M. H. Woolford, M. E. Avery,* J. Pharm. Sci., **54**, 694 (1959).

[8] *M. E. Caplis, H. S. Ragheb, E. D. Schall,* J. Pharm. Sci., **54**, 694 (1965).

[9] *A. A. Fernancez, V. T. Noceda, E. S. Carrera,* J. Pharm. Sci., **58**, 443 (1969).

[10] *J. H. Knox, J. Jurand,* J. Chromatogr., **186**, 763 (1979).

[11] *H. R. Howell, L. L. Rhodig, A. D. Sigler,* J. Assoc. Off. Anal. Chem. **67**, 572 (1984).

[12] *F. Barbatschi, R. A. Leese,* 97th Annual International Meeting, Assoc. Official Anal. Chemists, Poster Session, Washington, D.C., 1983.

Received: June 30, 1987
Accepted: July 28, 1987
F

Column Purification and HPLC Determination of Teicoplanin and A40926

E. Riva* / M. Zanol / E. Selva / A. Borghi

Merrell Dow Research Institute, Lepetit Research Center, Via R. Lepetit 34, 21040 Gerenzano
(VA), Italy.

Key Words

Affinity chromatography
Column liquid chromatography
Glycopeptide antibiotics
Purification and determination

Summary

A simple HPLC method for quali- and quantitative determination of teicoplanin and A40926 in fermentation broths and in biological fluids is described. The sample is purified on affinity chromatography and then analyzed on a reverse phase column using a gradient phosphate buffer-acetonitrile as mobile phase and UV detection at 254 nm. No interference from endogenous sources has been observed. The analytical method, with partial modifications, was also used to isolate on semipreparative scale the single components of these antibiotics, in order to investigate their structure and their biological activity.

Introduction

The increased frequency of multiply antibiotic-resistant gram-positive bacteria has led to a renewed interest in the clinical use of glycopeptide antibiotics, which are strongly effective against gram-positive bacteria; moreover, resistance phenomena have not emerged.

Glycopeptide antibiotics are naturally produced in fermentation broths as mixtures of chemically related substances. Among them, teicoplanin [1], produced by Actinoplanes teichomyceticus nov. sp. ATCC 31121, is active against streptococci and staphylococci, including multiresistant strains [2]. A40926, recently discovered in our laboratories, produced by Actionomadura strain ATCC 39727, presents an interesting antibacterial activity against Neisseria gonorrhoeae, a gram-negative coccus [3]. Due to its favourable pharmacokinetics profile, it can be considered as a possible candidate for therapeutic agent in gonorrhoea treatment.

These antibiotics inhibit the cell wall biosynthesis by binding to the D-alanyl-D-alanine portion of nascent peptidoglycan. The specific binding of these antibiotics has been utilized also in their extraction and purification from broths and biological fluids. An affinity resin was in fact developed [4] by attaching D-alanyl-D-alanine to a matrix, such as sepharose or cellulose, through a spacer arm formed by 6-aminocaproic acid.

Furthermore, as the biological and chemical characterization of the single components is required for the complete knowledge of the complex, a HPLC method able to identify the mixture and to isolate suitable amounts of the components is needed.

In the present paper a reliable method to purify A40926 and teicoplanin by affinity chromatography is described. A HPLC method on reverse phase in analytical and semipreparative scale is also reported for the successive identification and for the isolation of the single components in sufficient amount for structure elucidation.

Experimental

Drugs and Reagents

Teicoplanin and A40926 analytical reference substances were prepared in our laboratories.

Acetonitrile (Carlo Erba, Milan, Italy) was HPLC grade, while all other reagents were of analytical grade.

Affinity Chromatography

Prepacked columns (0.5 ml of resin volume) of D-Alanyl-D-Alanine-aminocaproyl Sepharose CL-6B were used as affinity resin and were available in our labs. The columns were equilibrated by percolating 10 ml of buffer A (0.05 M sodium dihydrogen phosphate – 0.2 M sodium chloride adjusted to pH 7.5 with 1 N sodium hydroxide).

An appropriate volume of sample (filtered fermentation broths or biological fluids) is loaded on the column and the eluates discharged. After washing the column with 3 ml of buffer A, the antibiotics, selectively adsorbed, are eluted with three 0.75 ml volumes of 1.5 % ammonium hydroxide.

0009-5893/87 0295-07 $ 03.00/0

© 1987 Friedr. Vieweg & Sohn Verlagsgesellschaft mbH

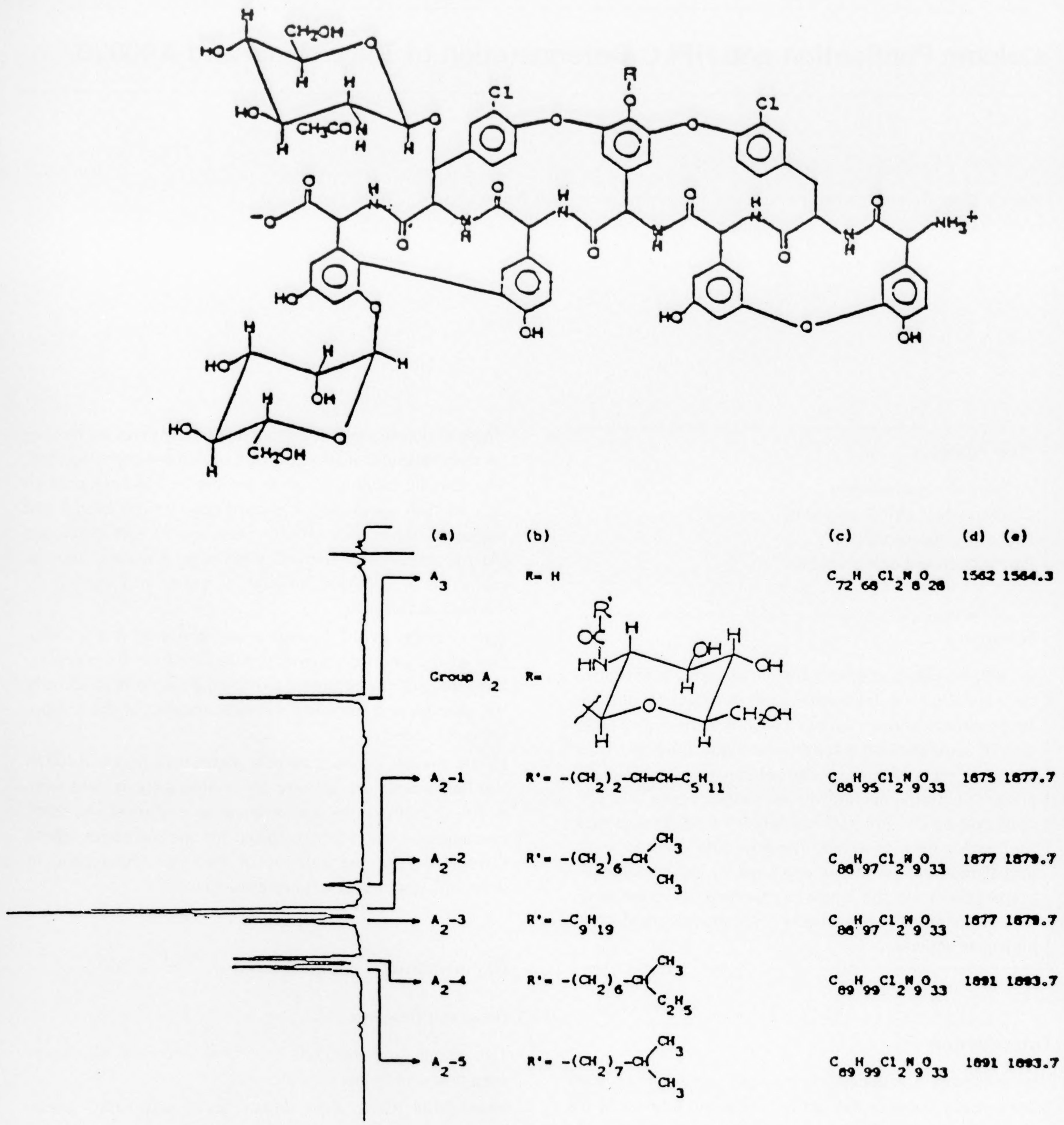

(a)	(b)	(c)	(d)	(e)
A_3	R= H	$C_{72}H_{68}Cl_2N_8O_{28}$	1562	1564.3
Group A_2	R=			
A_2-1	R'= $-(CH_2)_2-CH{=}CH-C_5H_{11}$	$C_{88}H_{95}Cl_2N_9O_{33}$	1675	1677.7
A_2-2	R'= $-(CH_2)_6-CH(CH_3)_2$	$C_{88}H_{97}Cl_2N_9O_{33}$	1677	1679.7
A_2-3	R'= $-C_9H_{19}$	$C_{88}H_{97}Cl_2N_9O_{33}$	1677	1679.7
A_2-4	R'= $-(CH_2)_6-CH(CH_3)(C_2H_5)$	$C_{89}H_{99}Cl_2N_9O_{33}$	1891	1893.7
A_2-5	R'= $-(CH_2)_7-CH(CH_3)_2$	$C_{89}H_{99}Cl_2N_9O_{33}$	1891	1893.7

Fig. 1

Structures of the teicoplanin components and relationship to the HPLC chromatogram.
a = component name; **b** = structural formula; **c** = molecular formula; **d** = molecular weight by mass spectrometry; **e** = calculated relative molecular weight.

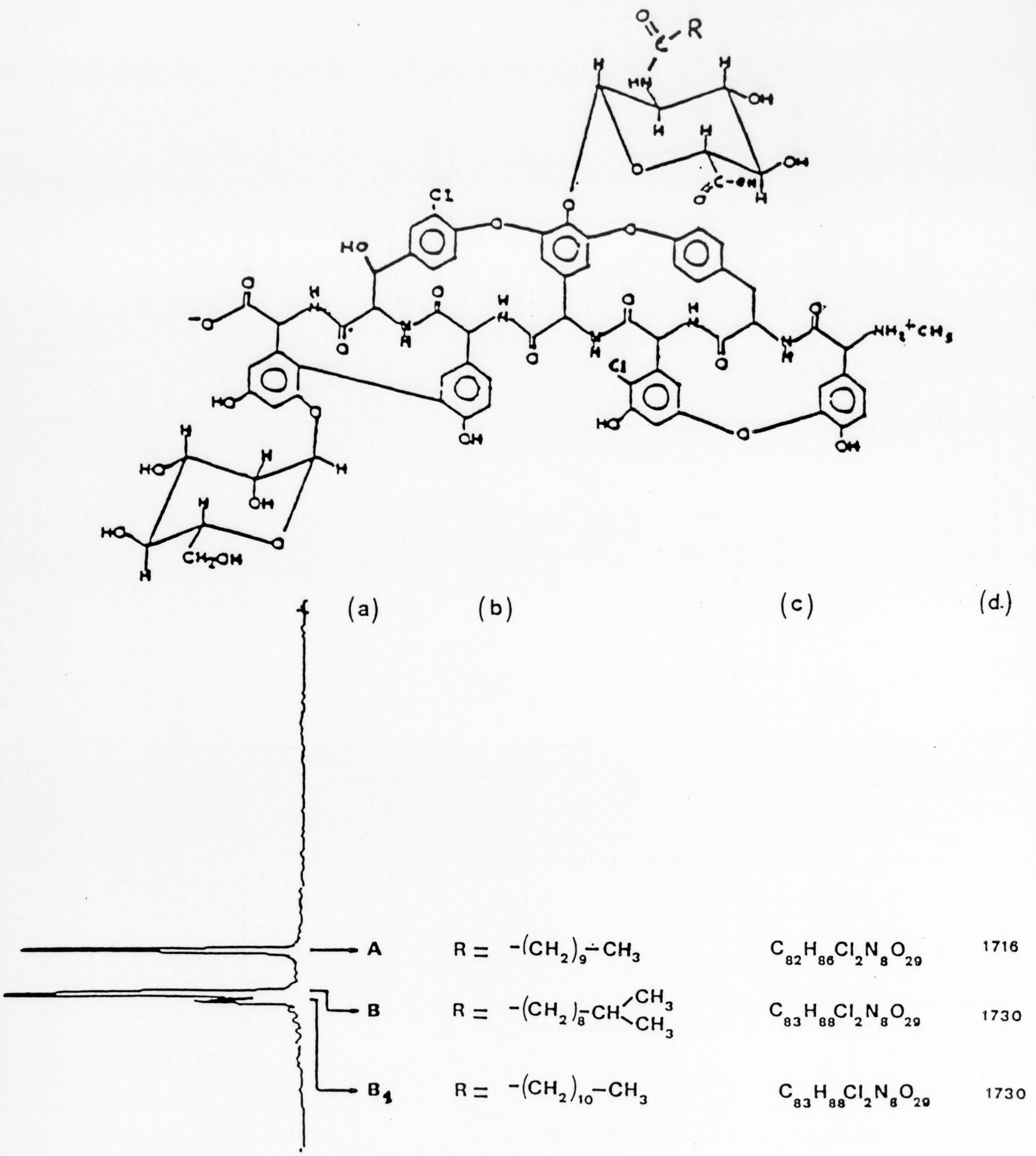

(a)	(b)	(c)	(d.)
A	R = $-(CH_2)_9-CH_3$	$C_{82}H_{86}Cl_2N_8O_{29}$	1716
B	R = $-(CH_2)_8-CH\begin{smallmatrix}CH_3\\CH_3\end{smallmatrix}$	$C_{83}H_{88}Cl_2N_8O_{29}$	1730
B_1	R = $-(CH_2)_{10}-CH_3$	$C_{83}H_{88}Cl_2N_8O_{29}$	1730

Fig. 2

Structures of the A40926 components and relationship to the HPLC chromatogram.
a = component name; **b** = structural formula; **c** = molecular formula; **d** = molecular weight.

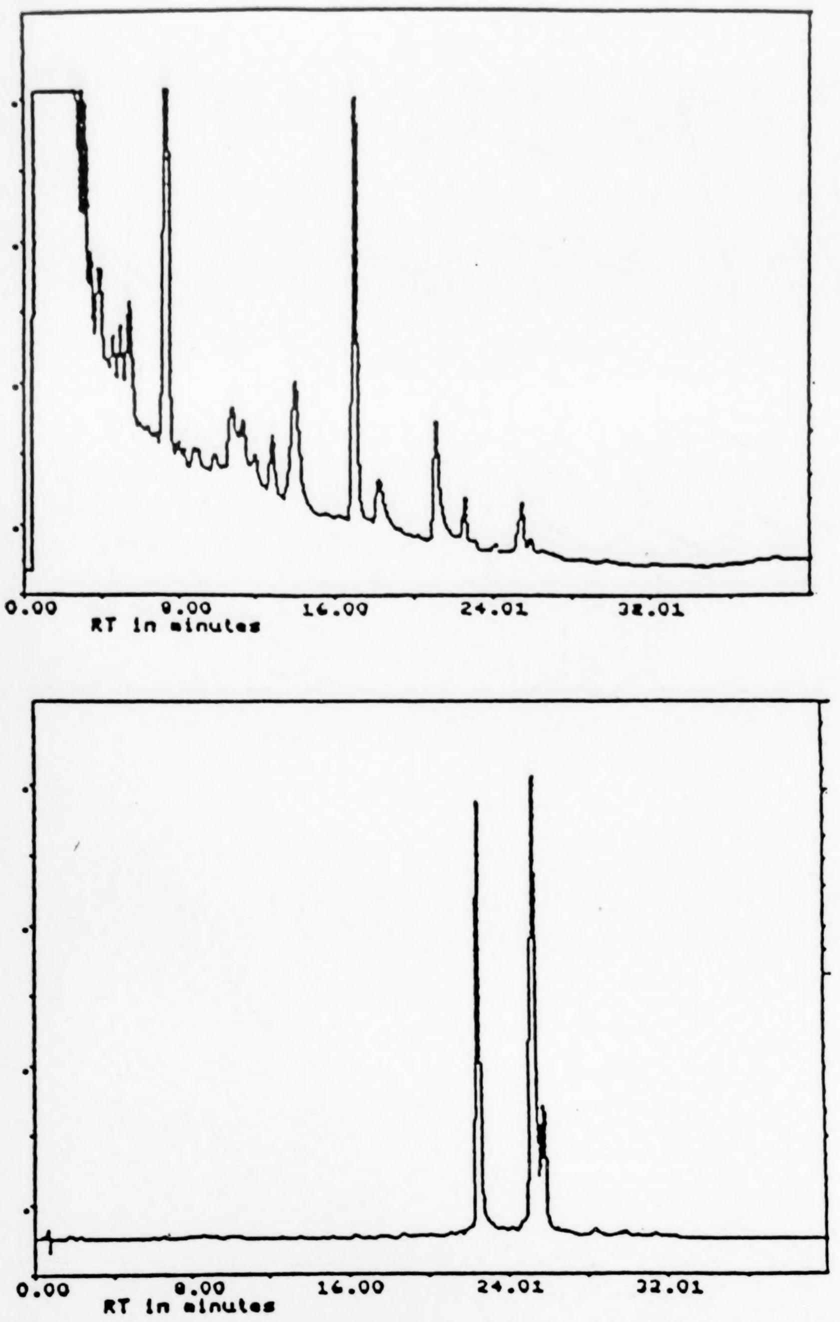

Fig. 3

HPLC profile of a typical fermentation broth of antibiotic A40926. A: after treatment at pH 12 with NaOH; B: after affinity chromatography.

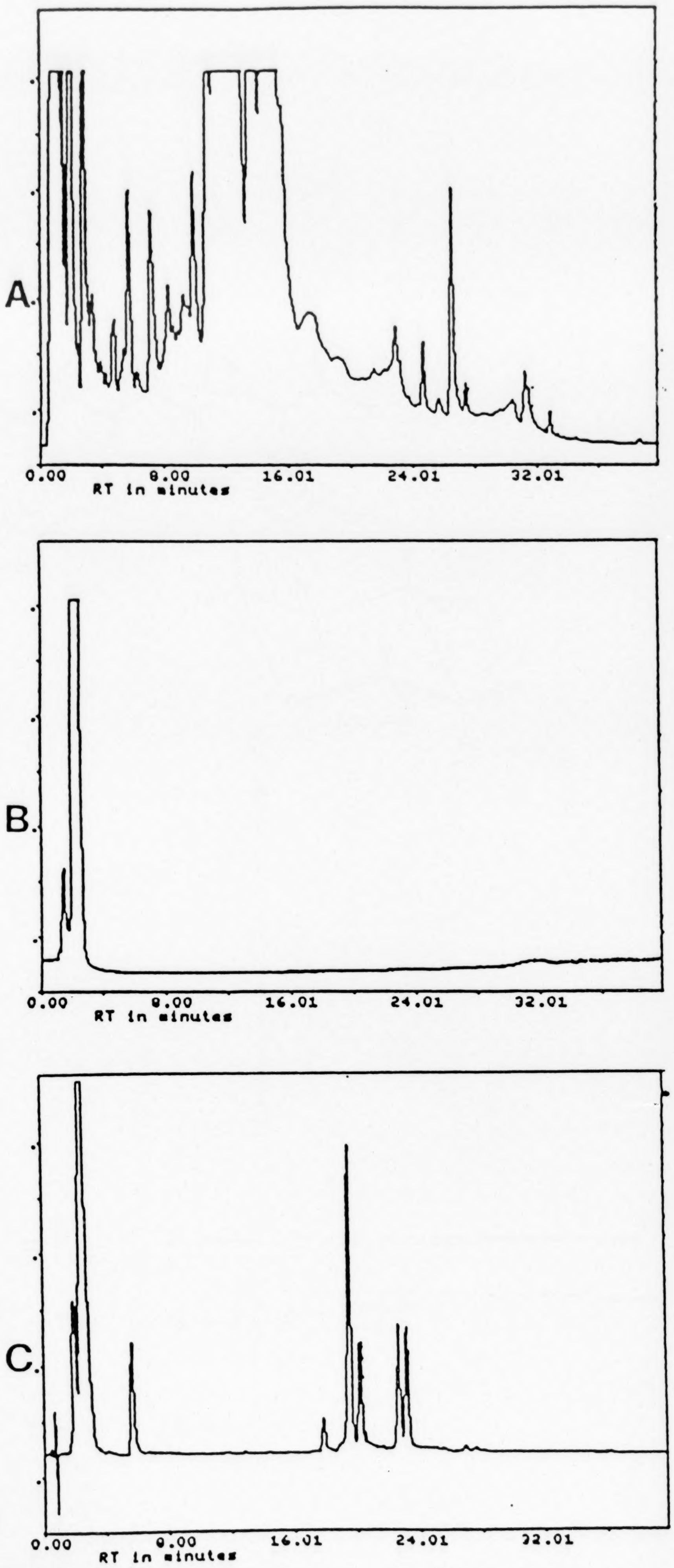

Fig. 4

A: Plasma, centrifuged and injected into the LC;
B: Plasma, centrifuged, adsorbed to the affinity resin, eluted and injected into the LC;
C: Plasma fortified with teicoplanin, treatet as in B, and injected into the LC.

The eluates, collected in 2 ml conical tubes and taken to neutrality by adding 0.1 ml of 18 % hydrochloric acid, are assayed on HPLC.

Analytical HPLC

Apparatus: Chromatograph mod. 1084 (Hewlett Packard)
Detector: UV 254 nm
Column: Ultrasphere ODS 5 μm 250 X 4.6 mm (Beckman)
Precolumn: RP-18 5 μm 50 X 4.6 mm (Brownlee)
Eluent: A) 0.018 M sodium dihydrogen phosphate – acetonitrile 90/10 pH 6
b) 0.018 M sodium dihydrogen phosphate – acetonitrile 30/70 pH 6
Gradient: From 5 % B to 60 % B in 40 min
Flow: 1.6 ml/min

Calculation: The concentration of antibiotics was determined by using the external standard procedure. The response to the detector was assumed to be the same for each component, because the chromophore responsible for the absorbance at 254 nm is the same. The amount of total antibiotic present in the sample was therefore calculated as follows:

$$\text{antibiotic conc. } (\mu g/ml) = \frac{As \times C \times Vstd}{Astd \times Vs}$$

where:

As = sum of the areas of the peaks of the antibiotic in the sample
C = concentration (μg/ml) of the standard
Astd = sum of the areas of the peaks of the antibiotic in the standard
Vstd = volume of the standard or of the enforced biological sample
Vs = volume of the sample

Semipreparative HPLC

Apparatus: Chromatograph mod. 1084 (Hewlett Packard)
Detector: UV 254 nm
Column: Lichrosorb RP-18/7 μm/250 X 10 mm (Merck)
Eluent: A) 0.02 M ammonium formiate — acetonitrile 95/5
A) 0.02 M ammonium formiate — acetonitrile 25/75
Gradient: linear, from 10 to 40 % B in 40 min
Flow: 5 ml/min

Results and Discussion

The chromatograms and the structure of teicoplanin and A40926 are reported in Fig. 1 and 2 respectively. As it can be seen, the components of each mixture differ for the length and the ramification of the chain attached to the glucosamine, while the peptidic backbone of the molecules is unchanged. Such difference however is sufficient, in our HPLC system, to separate them with good resolution.

In Fig. 3 the chromatograms of the fermentation broths of A40926 before and after affinity chromatography are reported. It appears that the D-alanyl-D-alanine columns are efficient both in purification and in enrichment.

With the case of teicoplanin [5] the same method gives good results also in biological fluids, as can be seen in Fig. 4 for plasma and Fig. 5 for urine respectively.

In Fig. 6 the chromatogram after elution through a semipreparative column of teicoplanin is reported on the top. The collected fractions are indicated. On the bottom the chromatograms at the analytical conditions are reported.

In Fig. 7 the same chromatograms of A40926 are shown.

Conclusions

The described methods are relatively simple and very effective. The HPLC semipreparative method gives well resolved chromatograms and, even starting from small quantities of materials, allows to isolate highly pure components, in sufficient amounts for structure elucidation.

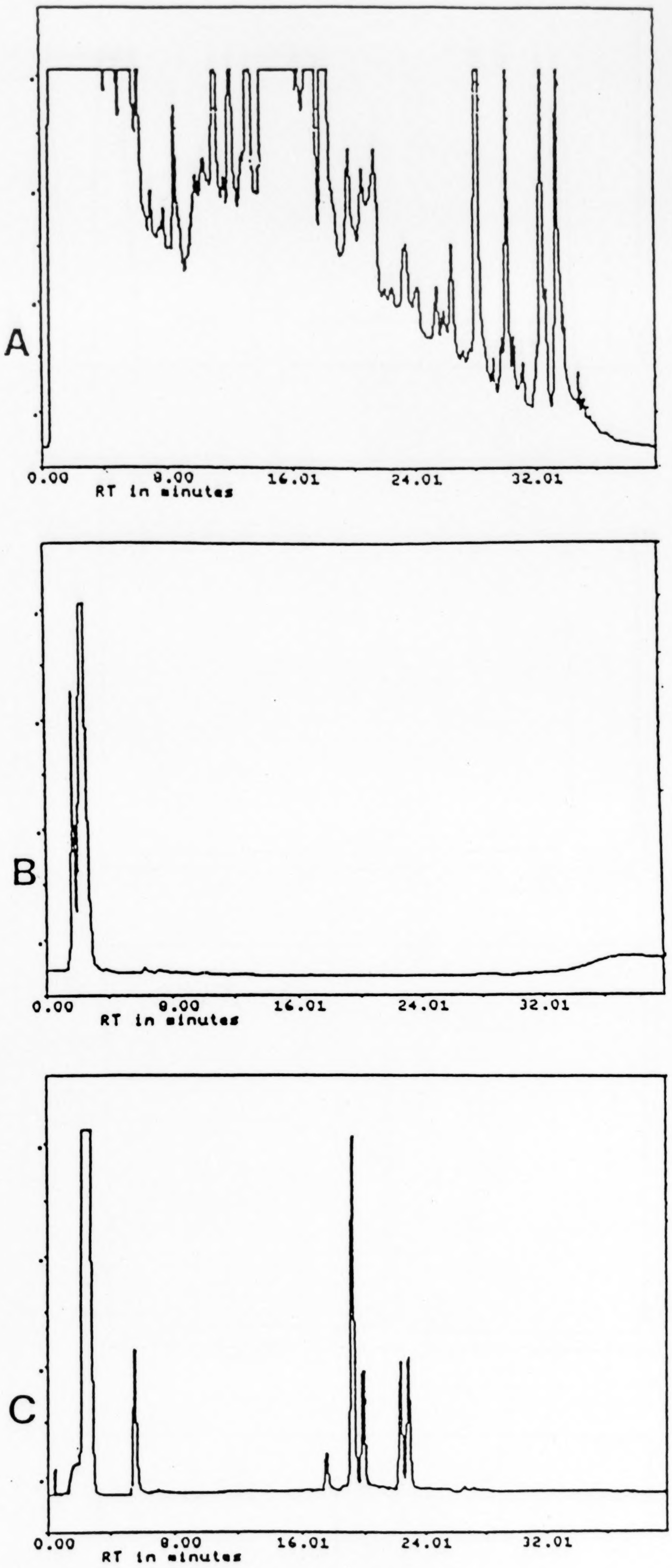

Fig. 5

A: Urine, filtered on Gelman Acrodisc and injected into the LC;
B: Urine, filtered on Gelman Acrodisc, adsorbed to the affinity resin, eluted and injected into the LC;
C: Urine fortified with teicoplanin, treated as in B, and injected into the LC.

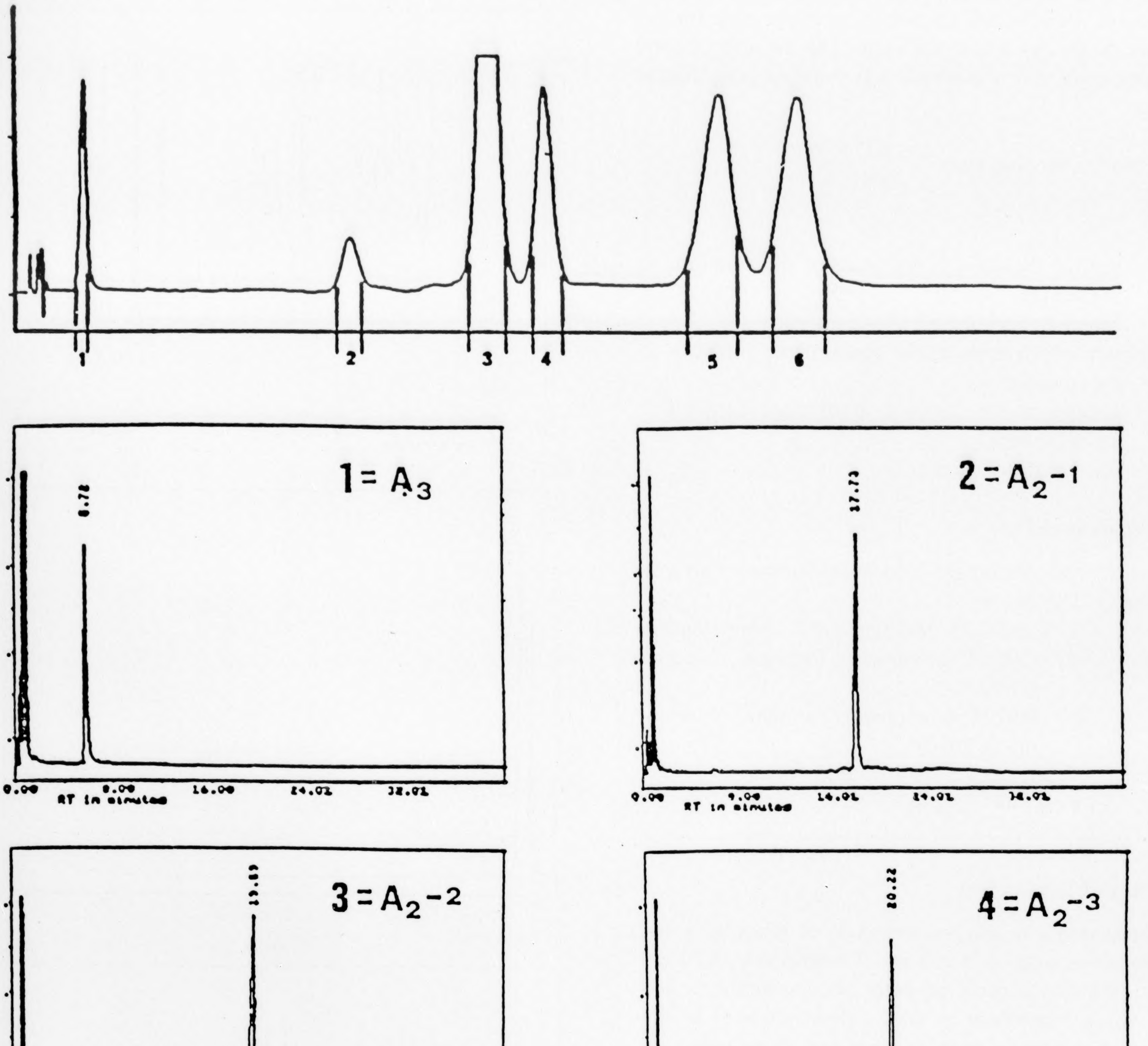

Fig. 6

Semipreparative HPLC of teicoplanin and relative analytical HPLC chromatograms of the isolate components.

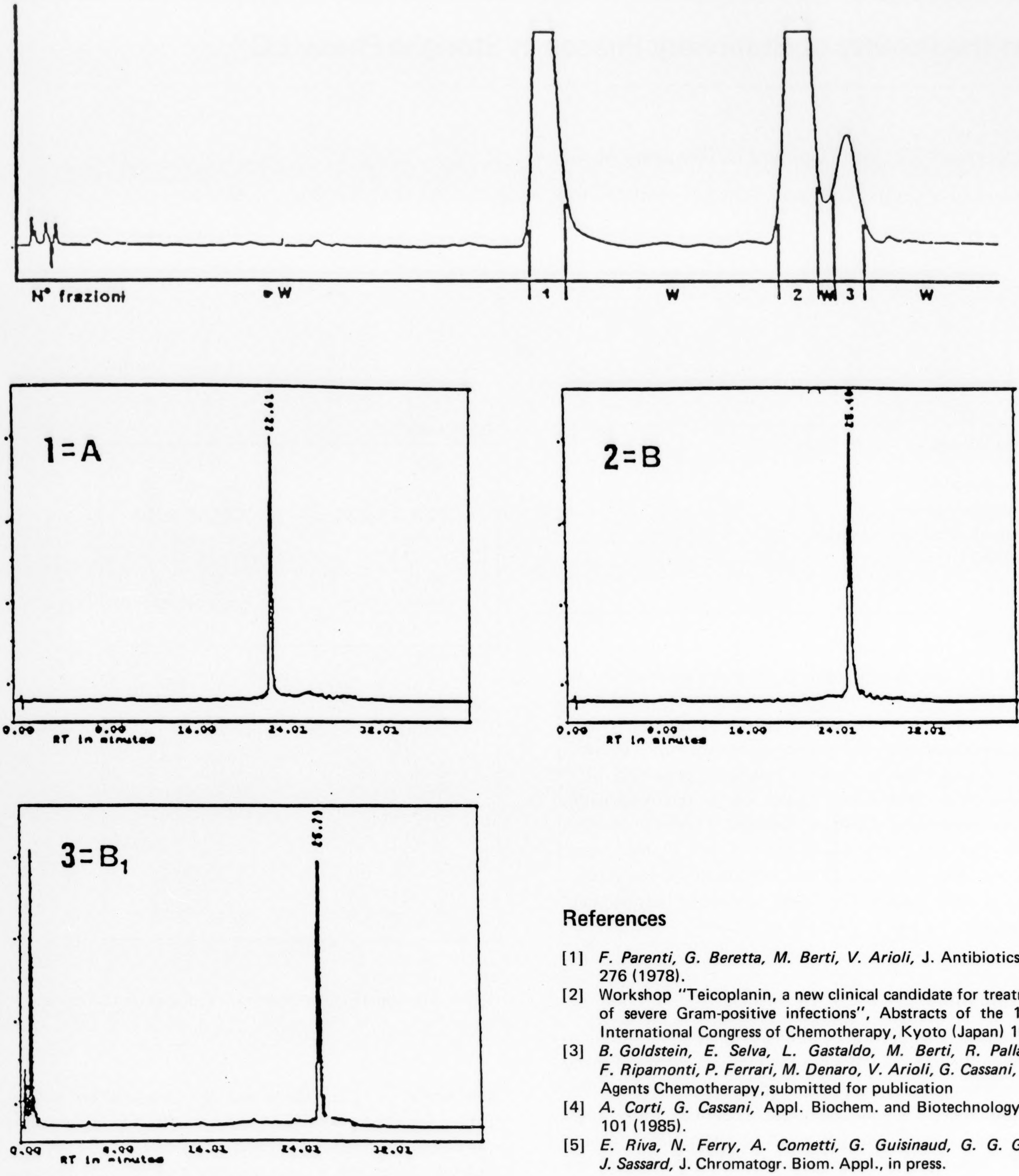

Fig. 7

Semipreparative HPLC of A40926 and relative analytical HPLC chromatograms of the isolate components.

References

[1] *F. Parenti, G. Beretta, M. Berti, V. Arioli,* J. Antibiotics, **31**, 276 (1978).

[2] Workshop "Teicoplanin, a new clinical candidate for treatment of severe Gram-positive infections", Abstracts of the 14the International Congress of Chemotherapy, Kyoto (Japan) 1985

[3] *B. Goldstein, E. Selva, L. Gastaldo, M. Berti, R. Pallanza, F. Ripamonti, P. Ferrari, M. Denaro, V. Arioli, G. Cassani,* Ant. Agents Chemotherapy, submitted for publication

[4] *A. Corti, G. Cassani,* Appl. Biochem. and Biotechnology, **11**, 101 (1985).

[5] *E. Riva, N. Ferry, A. Cometti, G. Guisinaud, G. G. Gallo, J. Sassard,* J. Chromatogr. Biom. Appl., in press.

Received: June 30, 1987
Accepted: July 22, 1987
F

On the Polarity of Stationary Phases in Straight-Phase LC[1)]

M. Verzele* / F. Van Damme / C. Dewaele / M. Ghijs

Laboratory of Organic Chemistry, State University of Ghent, Krijgslaan, 281 (S.4), B-9000 Gent, Belgium

Key Words

Straight-phase LC
Stationary phases
Non-displacement retention
Polarity factor

Summary

The LC retention strenght of non-bonded silica gel is compared with that of seventeen derivatized silica gels and polystyrenes in straight-phase conditions with hexane-dioxan and hexane-tetrahydrofuran mobile phases. For this purpose a polarity mixture containing UV-active polar compounds is used. Larger retention with dioxan containing eluents is observed. This is an indication that non-displacement H-bond and dipole interactions with adsorbed dioxan contribute to the retention of polar solutes. The linear correlation between log k′ and lox Xs was verified for all phases.

Introduction

The characterization of stationary phases for straight-phase chromatography has been the subject matter of many papers. Hara et al. [1, 2] compared the retentivity of silica gel with that of cyano- and aminopropyl derivatized silica gels, using steroids and protected oligopeptides as probes [3–7]. Linear correlations between the logarithm of the capacity ratio (log k′) and the logarithm of the mole fraction of the stronger eluent in binary solvent systems (log Xs) were observed.

$$\log k' = c - n \log Xs \qquad (1)$$

The Snyder-Soczewinski displacement model [8–10] and the sorption model of Scott and Kucera [8, 11] explain solvent composition effects in Liquid-Solid Chromatography (LSC). Both lead also to an equation of the form above (eq. 1). A simple representation of displacement and sorption is shown in Fig. 1.

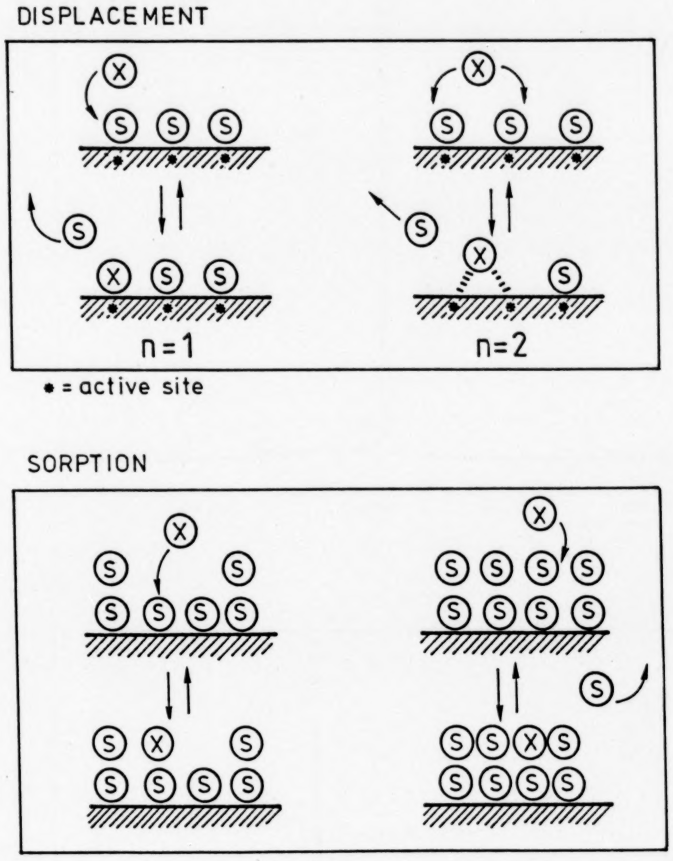

Fig. 1
Pictural representation of displacement and sorption LSC models.

Hennion et al. [12] developed the displacement model further for amino-bonded phases and the role of solvation was discussed. Snyder [13] and Hurtubise et al. [14] also observed linear log k′, log Xs relations for aminopropyl silica gel. The characterization of polyphenol-derivatized silica gel (RSiL-Polyphenol) [15] and polyol-derivatized silica gel (RSil-Polyol) [16] has been reported by us. These new polar phases too follow equation 1 and the correlation coefficients on these phases were even better than on bare silica [17]. That this can be the case has been reported previously [18]. Soczewinski and Dzido [19] proposed the possibility of H-bond formation between solute molecules and adsorbed dioxan molecules (they call this co-adsorption) thus contributing to retention in LSC without displacement. This was confirmed by relative stronger adsorption in hexane-dioxan versus hexane-isopropanol solvent systems for H-donor solutes. These ideas were further

---

1 Presented in part at HPLC-87 in Amsterdam.

0009-5893/87 0302-07 $ 03.00/0

© 1987 Friedr. Vieweg & Sohn Verlagsgesellschaft mbH

developed recently by the same authors [20, 21]. Apparently, displacement and sorption occur together, to varying degrees according to the precise conditions of a particular experimental LSC situation.

In the present paper, seventeen stationary phases (amino-, cyano-, diol-, polyol-, polyphenol- I and II, nitro-, sulfonic acid, polyoxiran coated silica gels, polystyrene and polyoxiran coated polystyrenes) are compared with bare silica gel as standard. A "polarity mixture" (anisole, nitrobenzene, diethylphthalate, anthraquinone, benzhydrol, benzoic acid and benzanilide) is used with dioxan and tetrahydrofuran (THF) containing mobile phases to evaluate the stationary phases.

Experimental

The chromatographic system consisted of a Varian 5020-LC pump, a Varian UV-50 detector, a Linear recorder and a 7000 psi 15μl Valco sample loop injector. Columns were Lichroma tubes (25 × 4.1 cm i.d. and 25 × 0.46 cm i.d.) provided with Valco fittings. Except for the LiChrosorb-DIOL phase (Merck) [22, 23], all silica gel derived packing materials were based on 10μm RSiL (irregularly shaped silica gel from RSL-Alltech Europe, Eke-Belgium). This silica gel has a specific surface area of about 350 m^2 and a mean pore diameter of 8–10 nm. The amount of organic material bonded to the silica gel surface in the different phases was determined by Thermal Gravimetric Analysis (TGA). The % bonded material found in this way is: RSiL-NH_2: 7%, RSiL-CN: 8%, RSiL-Polyol: 14%, RSiL-Polyphenol: 15%, RSiL-NO_2: 12%, RSiL-Cat: 12%, LiChrosorb-DIOL: 14%, Polyoxiran coated RSiL: 6, 14 and 20%.

The polystyrene packing materials were based on RoGeL (a rigid polystyrene-divinylbenzene packing material of RSL-Alltech Europe, Eke, Belgium). The RoGeL we used had 7μm particle size, 450 m^2/g for 7 nm pore size and 250 m^2/g for 30 nm pore size respectively.

Amino-, cyano- and sulfonic acid-bonded silica gel (RSiL-NH_2, RSiL-CN and RSiL-Cat) [24] are commonly used and require no further comment. RSiL-Polyol is obtained by bonding an organic moiety bearing a large number of hydroxyl groups. The nitro-phase (RSiL-Nitro) is synthesized by nitration of phenyl-bonded silica gel [25]. RSiL-Polyphenol is obtained by bonding tannic acid to silica gel. This phase is therefore a polyphenol but also a polyester. As such it is sensitive to low and high pH media and can hydrolyse and solvolyse in any medium containing OH or NH functions. To avoid this, two approaches were considered. The solvent can be composed with no or a minimum of solvolytically active components. This is what we have done in the present paper. Another approach is cross-linking of the aromatic rings with terephthaldicarboxaldehyde. This indeed leeds to a more stable polyphenol-phase, but the retention strenght or "polarity" is decreased considerably. Polyoxiran coating of silica gel and of polystyrene was carried out by a proprietary process.

All columns were filled by slurry packing techniques. 3–5 g of the various stationary phases was suspended in 20 ml of solvent and pumped downwards in the columns with a Haskel Air Driven Fluid Pump at a pressure of 300–600 bar. The silica gel, polyol-, nitro- and sulfonic acid-bonded phases were suspended in carbontetrachloride and pressurized with iso-octane. Polyphenol-, amino-, cyano-, diol-bonded and polyoxiran coated silica's were suspended in methanol-water (90-10) and pressurized with the same solvent. The polystyrene phases were packed downward in a methanol slurry as above, but only 300 bar pressure was applied.

All experiments were at ambient temperature. The column dead volume was determined by injection of nonane, producing a solvent negative dip. Capacity factors were determined from the formula $k' = tr/to - 1$. The solvents hexane, dioxan and THF (Alltech-Associates) were LC-grade and not especially dried before use. The compounds of the "polarity mixture" were obtained from various chemical suppliers and were used as received.

Results and Discussion

Elution Order-Selectivity

Fig. 2 presents the capacity factors of the "polarity mixture" on most of the silica gel based phases, with as eluting phase the same mixture of hexane-dioxan. On all columns anisole is eluted first followed by nitrobenzene which is most strongly retained on the nitro-phase ($k' = 2.1$). Diethylphthalate and anthraquinone have similar k'-values on the various phases based on silica gel and their resolution is not so easy. This couple is not separated on the amino-, sulfonic- and cross-linked polyphenol-phase. Their resolution is best on RSiL-Polyphenol. The strong hydrogen bond forming capacity of alcohols (benzhydrol) is expressed in higher capacity ratios. The highest k' is reached on RSiL-Polyol ($k' = 3.8$). Benzoic acid is strongly retained on polyol- and polyphenol-phases ($k' = 7.0$ and 8.7 resp.). On the cyano- and sulfonic acid-phase, benzoic acid is eluted before benzhydrol. Benzoic acid did not elute from the amino-column despite the acidic mobile phase. The resolution of benzoic acid and benzhydrol is obviously very variable. Capacity ratios and selectivity factors for these two solutes are presented in Table I. This pair is selected out of all other possibilities because it is most strongly influenced by stationary phase changes. The retention of benzoic acid being so variable for reasons which are unclear to us, it seems better not to include this acid in the probe mixture for determining the "Polarity Factor". In similar stationary phase evaluating studies, often acids and bases are chosen as probes (see e.g. reference [21]). Benzanilide, with an amide function, is the most polar of all references.

Here H-bonds are possible through the acceptor character on the highly polarized carbonyl function and the donor character of the N-H bond. This results in high k'-values on most phases. The eluting sequence of the probes is similar on all phases and apparently follows H-bond forming capacity with the stationary phase. From the k'-values in Fig. 2

Table I. Retention and selectivity data for benzhydrol and benzoic acid on different polar phases (hexane/dioxan – 85/15)

Phase	RSiL	NH_2	CN	Pol	Pp1	Pp2	NO_2	SO_3H	DIOL
k'a	2.2	3.0	2.1	3.8	3.1	2.7	2.3	2.3	2.0
k'b	2.3	–	1.9	7.0	8.7	5.7	2.7	2.1	3.0
α	1.1	–	0.9	1.9	2.8	2.1	1.2	0.9	1.5

k'a = k' benzhydrol; k'b = k' benzoic acid; α = k'a/k'b

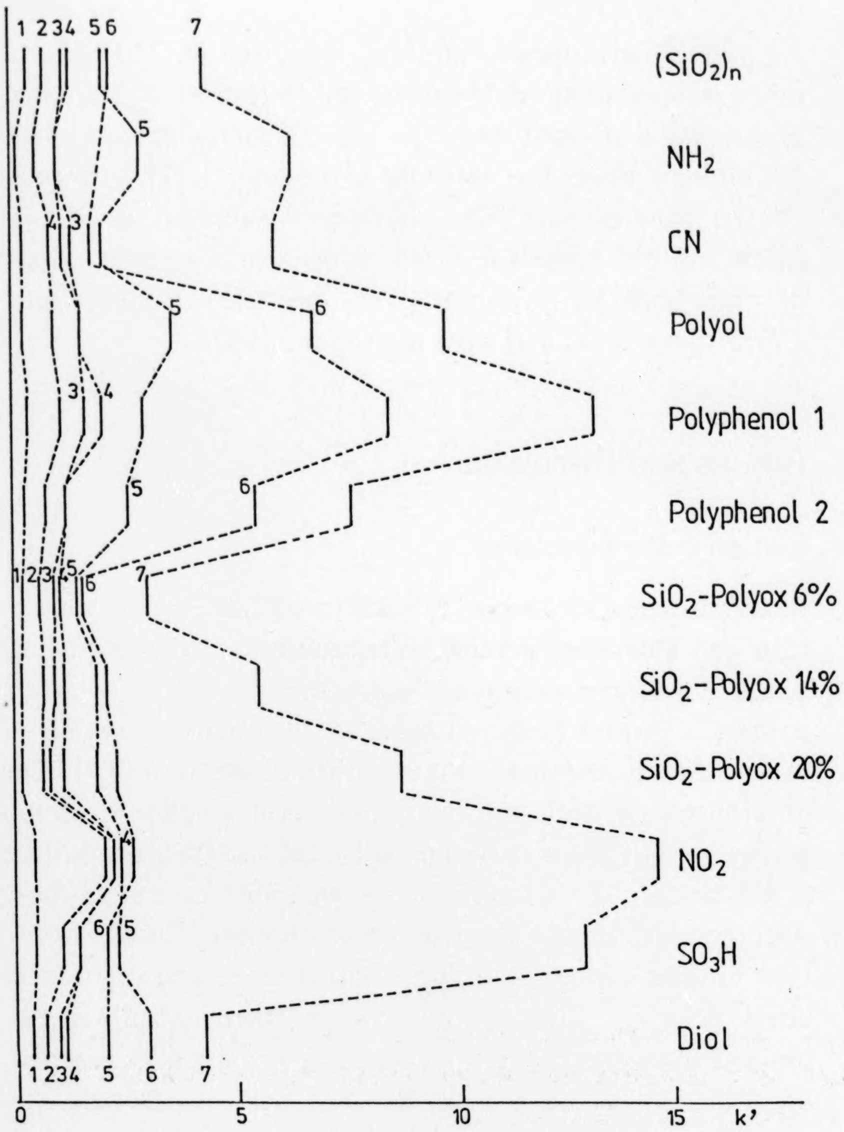

Fig. 2

Capacity factors (k') for anisole (1), nitrobenzene (2), diethylphthalate (3), anthraquinone (4), benzhydrol (5), benzoic acid (6) and benzanilide (7) on nine stationary phases. $(SiO_2)_n$ = silica gel, $-NH_2$ = aminopropyl silica gel, -CN = cyanopropyl silica gel, POLYOL = RSiL-Polyol, POLYPHENOL = RSiL-Polyphenol, POLYPHENOL-II = cross-linked RSiL-Polyphenol, $-NO_2$ = nitrophenyl-bonded silica gel, $-SO_3H$ = sulfonic acid silica gel, DIOL = LiChrosorb-DIOL.

Columns: 25 × 0.41 cm i.d. filled with the above materials in 10 μm particle size. Eluent: hexane-dioxan (85 – 15 + 0.1 % citric acid). Detection: UV 254 nm.

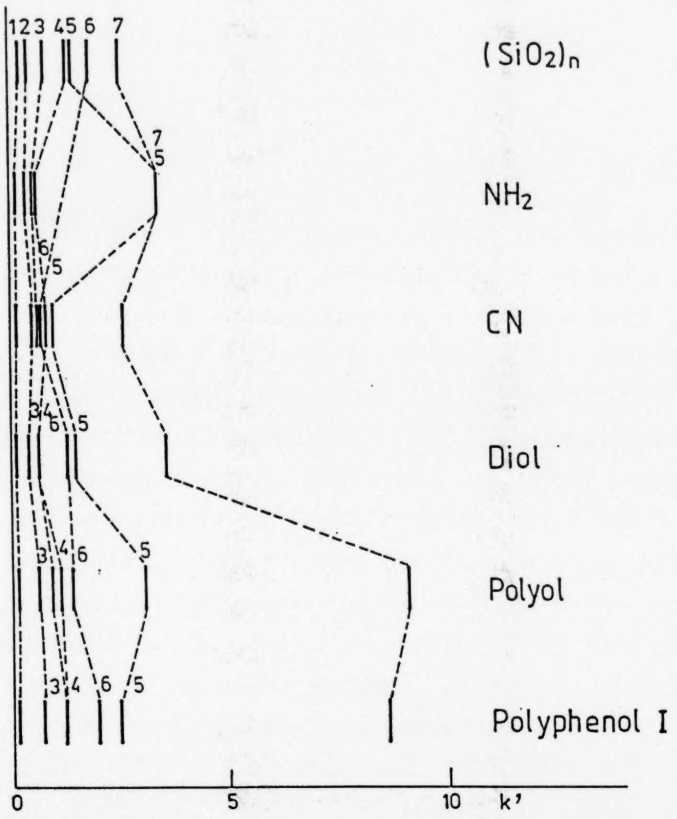

Fig. 3

Capacity factors of the polarity references as under Fig. 2, now with hexane-THF mobile phase (85-15 + 0.1 % citric acid).

it is clear that RSiL-Polyphenol, RSiL-Polyol, RSiL-Nitro and RSiL-Cat have the highest retention strenght or "polarity". The cross-linked polyphenol-phase shows a decreased retention and thus a lower "polarity".

Fig. 3 presents the capacity factors on six silica gel based phases now with hexane-THF as mobile phase. Retention times are shorter for each reference with this solvent combination, without exception. This is rather surprising because dioxan and tetrahydrofuran have about the same solvent strength (P' = 4.8 and 4.0; ϵ° 0.56 and 0.57 for dioxan and THF resp.) [26]. Only the dielectric constant (ϵ = 2.2 and 7.6 for dioxan and THF resp.) differs greatly. As Soczewinski has shown, the explanation of the stronger retention with dioxan containing solvents is that the second ether function of dioxan is directed towards the bulk mobile phase and contributes through strong H-bond formation to the retention of polar compounds in hexane-dioxan systems. Dzido and Soczewinski [19] present their data in plots of the log k' in dioxan (log k'D) versus the log k' values in THF (log k'T). Figs. 4a–c show such plots for five different phases. These illustrate again the stronger retention in dioxan containing solvents and also, that benzoic acid is most heavily influenced by this effect. This is consistent with the strong hydrogen bond forming capability of this acid.

Selectivity is different with the hexane-THF binary system. Anthraquinone is now eluted before or together with diethylphthalate on the different phases. This is reversed

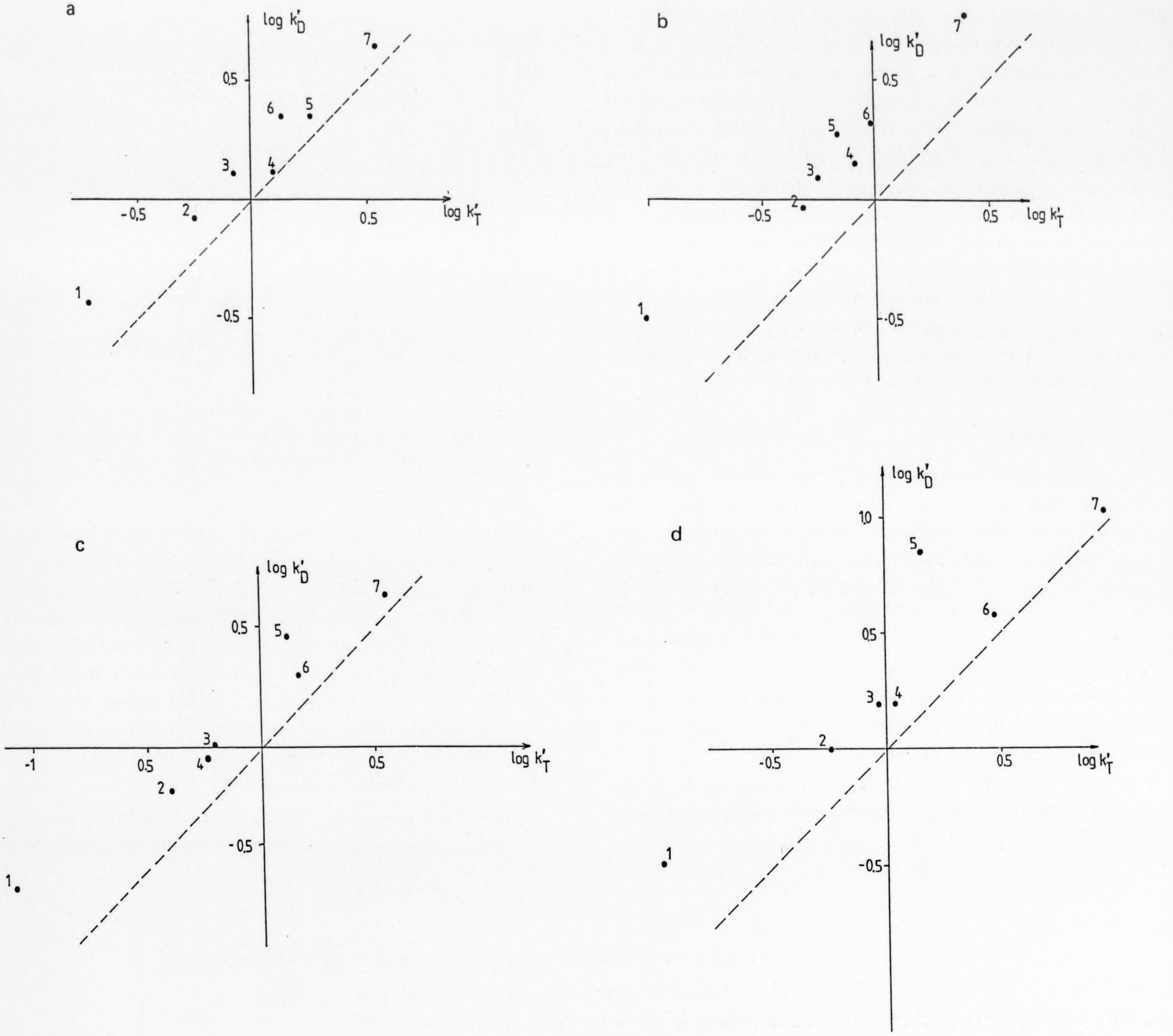

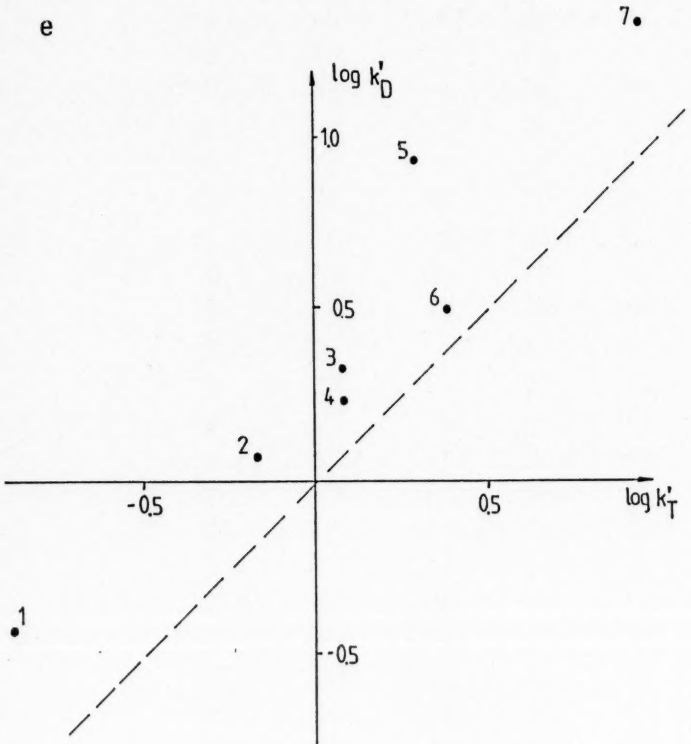

Fig. 4

Correlation of logk' obtained for hexane-dioxan (85-15) (logk'D) versus the logk' obtained for hexane-THF (85-15) (logk'T).

1 = anisole; **2** = nitrobenzene; **3** = anthraquinone; **4** = diethylphthalate; **5** = benzoic acid; **6** = benzhydrol; **7** = benzanilide.

Stationary phase: (a) silica gel (RSiL), (b) RSiL-CN, (c) Lichrosorb-DIOL, (d) RSiL-Polyol, (e) RSiL-Polyphenol.

in comparison with dioxan containing mobile phases. Benzoic acid and benzhydrol can also change elution sequence, with changing solvents. While the retention strength or "polarity" of the phases under discussion is very different, the elution sequence of the chromatographed compounds, as long as the eluting solvent is not changed, is remarkably similar. A possible explanation could be that all phases are covered by a layer of the polar solvent on which chromatography actually occurs. This layer "hides" the phase surface. All surfaces become more similar through this phenomenon. For this reason it is easier to change selectivity by changing the mobile phase than by changing the stationary phase! Dzido and Soczewinski [21] show examples also illustrating this point. The above picture of LSC in dioxan containing solvents on polar columns is closest to the sorption model of Fig. 1.

Fig. 5 presents capacity factors in the same way as Fig. 2 and 3, but now for polystyrene and polyoxiran coated polystyrene phases. The solvent system is hexane/dioxan 85/15 like in Fig. 2. Benzanilide elutes again last, but the retention sequence for the other compounds is very different than on silica gel based phases. Polystyrene is least "polar" of all phases, as expected, while the degree of coating determines the retention strength of the polyoxiran coated polystyrenes. Anthraquinone is most selectively retarded by the polystyrene phases. This results in easy separation of this compound from diethylphthalate, something which was impossible on any silica gel phase.

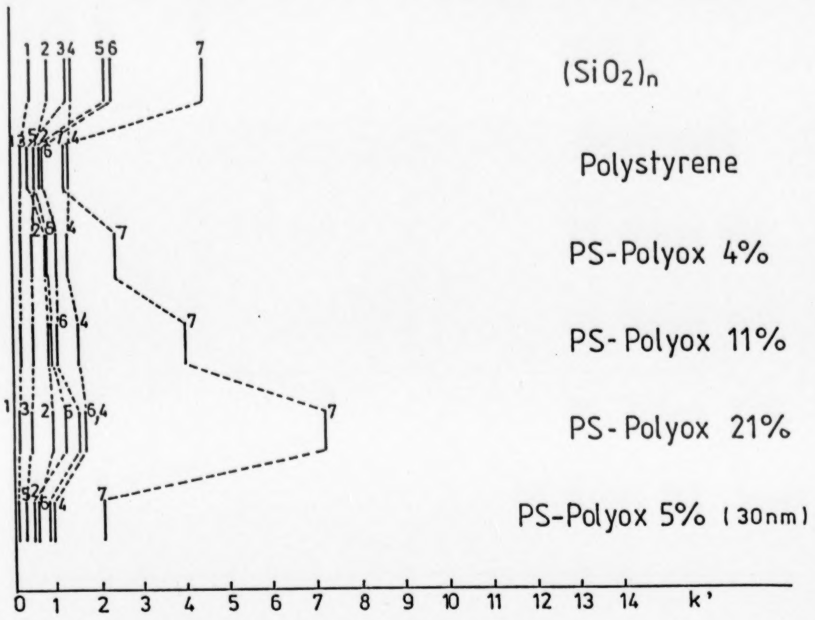

Fig. 5

Capacity factors of the polarity references as under Fig. 2, now on polystyrene and polyoxiran coated polystyrene phases, with hexane-dioxan (85-15 + 0.1 % citric acid).

Capacity Factor versus Xs

For eight solutes the $\log k'$ was plotted against the log of the mole fraction of the stronger eluent (dioxan) in the binary system hexane-dioxan. For each reference, k' and $\log k'$ were calculated for varying percentages of dioxan in the mobile phase (15, 20, 25, 30, 35, 40, 50% of p-dioxan in n-hexane giving molar fractions of −0.654, −0.541, −0.455, −0.387, −0.322, −0.285, −0.209 resp.). Slope, intercept and correlation coefficient of the best fitting straight lines were then calculated with the method of least squares. The values of n (slope), c (intercept) and r (corr. coeff.) are presented in Table II.

The low r-values for anisole are probably caused by small retention time variations which for this early compound lead to large errors in the k'-values. Correlation coefficients are in general higher than 0.98, except on the silica gel column. A possible explanation is the more difficult equilibration of bare silica gel. Equilibration is generally faster and easier on bonded-phases. This makes them more attractive than silica gel for straight-phase LC. The best values are reached on polyol- and polyphenol bonded silica gels. Perhaps more voluminous bonded phases shield the silica gel surface better and make the non-derivatized silanol functions more difficult to approach. A more rapid equilibration could be a logical consequence.

The excellent correlation coefficients of Table II show that all bonded phases follow the same mathematical relation-

Table II. Slopes (n), intercepts (c) and correlation coefficients (r) of the polarity references on the different phases in hexane-dioxan.

Phase		SiO_2	NH_2	CN	Po	Pp	Pp'	NO_2	SO_3H	DIOL
Anisole	n	.84	.14	.69	.60	.58	.70	.49	.57	.54
	c	.88	.81	.84	.83	.83	.91	.72	.81	.83
	r	.74	.38	.81	.87	.94	.95	.41	.96	.64
Nitrobenzene	n	1.25	.81	1.12	1.25	1.25	.89	1.13	.95	.88
	c	.81	.74	.72	.79	.74	.62	.40	.61	.66
	r	.90	.98	.97	.99	.99	.97	.98	.96	.85
Diethylphthalate	n	1.65	1.22	1.47	1.67	1.65	1.45	1.54	1.39	1.32
	c	.88	.82	.77	.88	.85	.81	.65	.74	.80
	r	.95	.98	.99	.99	.99	.99	.99	.93	.92
Anthraquinone	n	1.44	1.09	1.38	1.51	1.55	1.38	1.46	1.30	1.22
	c	.72	.70	.73	.76	.67	.76	.54	.68	.71
	r	.94	.98	.97	.99	.99	.98	.98	.99	.93
Acetophenone	n	1.20	.69	1.16	1.16	1.21	1.02	1.01	1.02	.86
	c	.73	.66	.69	.74	.67	.69	.39	.62	.66
	r	.90	.96	.98	.99	.99	.98	.98	.99	.88
Benzhydrol	n	1.88	.49	1.95	2.14	1.98	1.85	1.62	1.50	1.68
	c	.81	.95	.90	.84	.80	.78	.65	.62	.74
	r	.97	.99	.99	.99	.99	.99	.98	.99	.97
Benzoic acid	n	1.88	–	1.72	2.63	3.79	2.29	1.74	1.56	1.77
	c	.81	–	.80	.87	1.52	.75	.65	.66	.64
	r	.97	–	.99	.98	.99	.99	.99	.98	.98
Benzanilide	n	2.31	2.24	2.19	2.55	2.60	2.30	2.06	2.34	2.07
	c	.77	.66	.61	.64	.59	.60	.14	.48	.62
	r	.98	.99	.99	.99	.99	.99	.99	.99	.97

Table III. Slopes (n), intercepts (c) and correlation coefficients (r) of the polarity references on the different phases in hexane-tetrahydrofuran.

Phase		SiO_2	NH_2	CN	DIOL	Po	Pf
Anisole	n	1.17	.89	1.05	1.66	.48	.80
	c	1.50	1.52	1.66	1.97	1.29	1.40
	r	.98	.62	.66	.74	.91	.88
Nitrobenzene	n	1.53	1.04	1.87	1.29	1.34	1.84
	c	1.26	1.07	1.47	1.19	1.11	1.33
	r	.95	.94	.97	.98	.99	.93
Diethylphthalate	n	2.57	1.57	1.95	1.68	1.92	1.94
	c	1.50	1.16	1.31	1.25	1.20	1.15
	r	.97	.95	.98	.99	.99	.99
Anthraquinone	n	1.83	1.11	1.74	1.73	1.65	1.74
	c	1.22	.95	1.33	1.26	1.10	1.02
	r	.97	.94	.96	.95	.99	.99
Acetophenone	n	1.68	1.23	1.49	1.74	1.53	1.40
	c	1.18	1.12	1.22	1.42	1.19	1.02
	r	.98	.97	.99	.93	.99	.98
Benzhydrol	n	2.48	3.11	2.10	2.10	2.49	2.13
	c	1.40	1.40	1.33	1.14	1.15	1.03
	r	.98	.98	.97	.98	.99	.99
Benzoic acid	n	2.71	–	2.30	1.73	1.54	1.83
	c	1.51	–	1.61	.99	.84	.96
	r	.99	–	.97	.99	.99	.99
Benzanilide	n	2.44	2.37	2.44	2.43	2.67	2.50
	c	1.02	.85	1.13	.99	.81	.75
	r	.99	.95	.98	.99	.99	.99

The excellent correlation coefficient of Table II show that all bonded phases follow the same mathematical relationship and that a same retention mechanism occurs. Because retention is related to H-bonding capacity this H-bond must be a leading interaction in the adsorption-desorption equilibrium at the adsorbent surface.

Table III presents the n, c and r-values of the references on six stationary phases now with hexane-THF mobile phases. The r-values of the straight lines are not so good with this mobile phase combination. The slopes of the various compounds are in general higher in hexane-THF systems (vs. hexane-dioxan). Only three exceptions occur: benzoic acid on LiChrosorb-DIOL (1.8 vs. 1.7 in dioxan and THF resp.), on RSiL-Polyol (2.6 vs. 1.5) and on RSiL-Polyphenol (3.8 vs. 1.8). These larger slopes in THF containing eluents are difficult to explain. A possibility could be that dioxan forms two H-bonds with vicinal silanol functions or polar functional groups of the bonded phase (flat adsorption). This is not possible with the monofunctional THF which is probably adsorbed vertically. A bifunctional solute could thus displace two THF molecules, and only one dioxan molecule if this is "flat" adsorbed. Detailed correlation of the n values with the number of solvent molecules displaced was attempted. Attempts were also made to "reduce" the n values by dividing them by the n value for silica gel, like we [17] and Hara [2] have already done. We feel that the results of these calculations were too speculative and unsatisfactory to be presented.

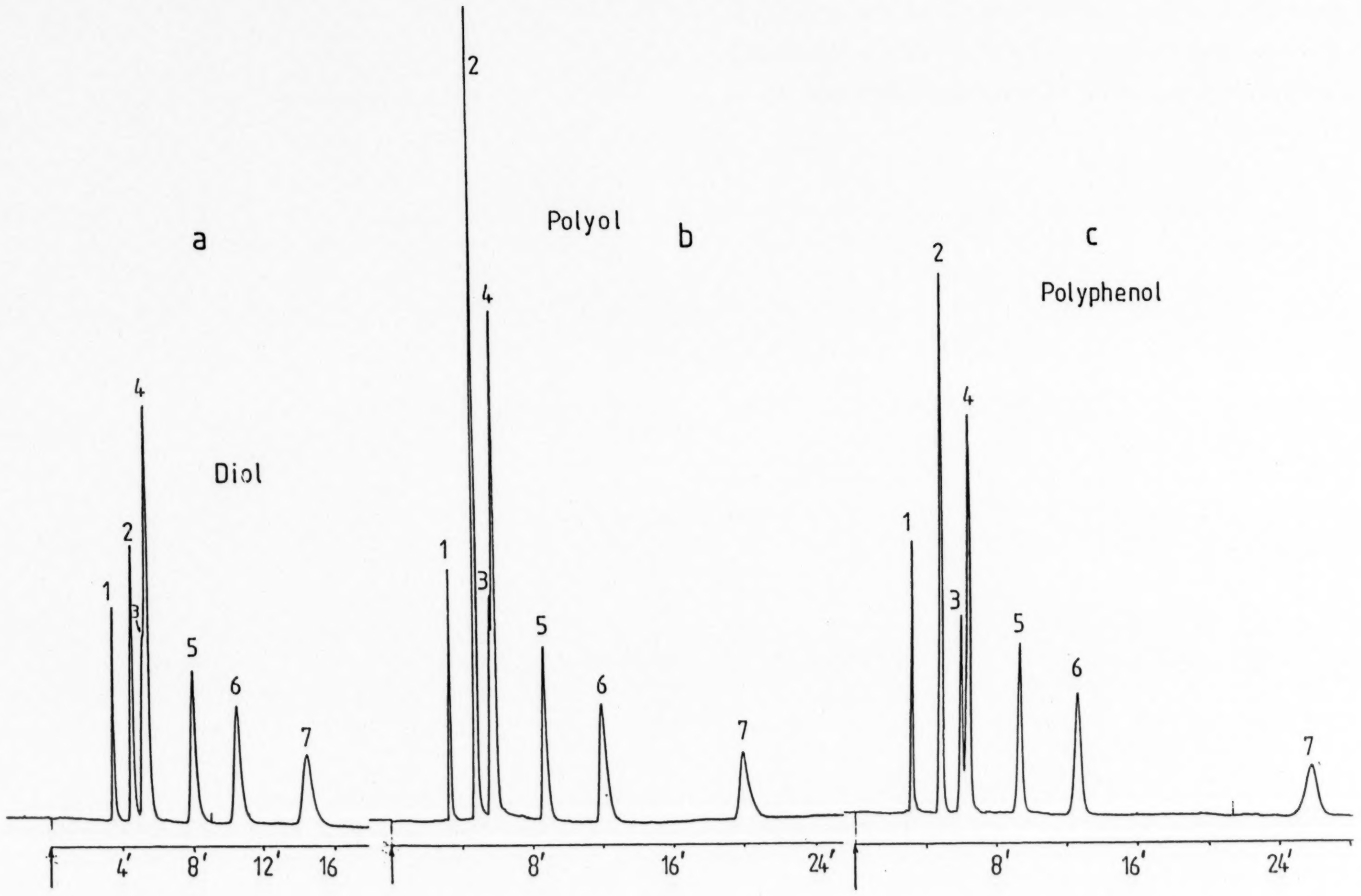

Fig. 6

Chromatograms of anisole (1), nitrobenzene (2), diethylphthalate (3), anthraquinone (4), benzhydrol (5), benzoic acid (6) and benzanilide (7). (a) on 10µm Lichrosorb-DIOL, (b) on 10µm RSiL-Polyol, (c) on 10µm RSiL-Polyphenol. Columns 15 X 0.46cm. Hexane-Dioxan (85-15 + 0.1 % citric acid) at 1 ml/min.

Figures 6a–c show the chromatograms of the polarity references on three hydroxyl-group containing stationary phases. The lower polarity of LiChrosorb-DIOL is well reflected by lower retention strenght for the probes in comparison with RSiL-Polyol and RSiL-Polyphenol. The improved resolution on the latter phases could be correlated to the longer retention times.

Conclusions

The solvent layer adsorbed on the surface neutralizes stationary phase differences and equalizes elution sequence for the same solvent on various chemically derivatised phases. Selectivity changes can therefore be induced more easily by changing the mobile phase than by changing the stationary phase or stationary phase bonding chemistry.

The linearity of $\log k'$ with $\log X_s$ is confirmed for a number of new phases.

H-bond formation seems to be the most important interaction for polar solutes in LSC with hexane-dioxan as solvent. Silica gel has a medium retention strenght when compared to the other phases mentioned in this paper.

Acknowledgements

We are grateful to the "Ministerie voor Wetenschapsbeleid", the "Instituut tot Aanmoediging van het Wetenschappelijk Onderzoek in Nijverheid en Landbouw – IWONL", the "Nationaal Fonds voor Wetenschappelijk Onderzoek – NFWO" for financial help to the Laboratory.

This text has been elaborated within the framework of the Belgian Programme for the reinforcement of the scientific potential in the new technologies – PREST (Prime Minister's Office for Science Policy). The scientific responsability is assumed by its authors.

References

[1] *S. Hara, S. Ohnishi*, J. Liq. Chromatog. **7**(1), 59 (1984).
[2] *S. Hara, S. Ohnishi*, J. Liq. Chromatog. **7**(1), 69 (1984).
[3] *S. Hara, S. Ohnishi*, J. Chromatog. **200**, 85 (1980).
[4] *S. Hara, S. Miyamoto*, Anal. Chem. **53**, 1365 (1981).
[5] *S. Hara, N. Yamaguchi, C. Nakae, S. Sakai*, Anal. Chem. **52**, 33 (1980).
[6] *K. Oka, S. Hara*, J. Chromatog. **202**, 187 (1980).
[7] *S. Hara, K. Kunihiro, H. Soczewinski*, J. Chromatog. **239**, 687 (1982).
[8] *L. Snyder, H. Poppe*, J. Chromatog. **184**, 363 (1980).
[9] *E. Soczewinski*, Anal. Chem. **41**, 179 (1969).
[10] *L. Snyder*, Anal. Chem. **46**, 1384 (1974).
[11] *R. P. W. Scott, P. Kucera*, J. Chromatog. **171**, 37 (1979).
[12] *M. Hennion, C. Picard, C. Combellas, M. Clause, R. Rosset*, J. Chromatog. **210**, 211 (1981).
[13] *L. Snyder, T. Schunk*, Anal. Chem. **54**, 1734 (1982).
[14] *R. Hurtubise, A. Hussain, H. Silver*, Anal. Chem. **53**, 1993 (1981). *E. Soczewinski, T. Dzido*, Chromatographia **22**, 25 (1986).
[15] *F. Van Damme, M. Verzele*, J. Chromatog. **351**, 506 (1986).
[16] *M. Verzele, f. Van Damme*, J. Chromatog. **362**, 23 (1986).
[17] *M. Verzele, F. Van Damme*, J. Chromatog. **393**, 25 (1987).
[18] *L. Snyder*, "High Performance Liquid Chromatography", Academic Press, New York, 1983, Vol. 3, p. 157.
[19] *E. Soczewinski, T. Dzido*, Chromatographia, **22**, 25 (1986).
[20] *E. Soczewinski*, J. Chromatog., **388**, 91 (1987).
[21] *T. Dzido, E. Soczewinski*, J. Chromatog., **388**, 99 (1987).
[22] *N. Becker, K. Unger*, Chromatographia, **12**, 539 (1979).
[23] *C. Brons, C. Olieman*, J. Chromatog., **259**, 79 (1983).
[24] *C. Kientz, A. Verweij, H. Boter*, J. Chromatog., **282**, 643 (1983).
[25] *M. Verzele, P. Mussche, S. Qureshi*, J. Chromatog. **172**, 493 (1979).
[26] *L. Snyder, J. Kirkland*, "Introduction to Modern Liquid Chromatography", John Wiley and Sons, Inc., New York, 1979, p. 249.

Received: July 1, 1987
Accepted: July 16, 1987
F

Miniaturized RPLC for the Rapid Determination of Total Tryptophan in Pediatric Plasma Samples

Linda C. Peterson / M. E. Dwyer[1] / P. R. Brown*

Department of Chemistry, University of Rhode Island, Kingston, R.I. 02881, USA

Key Words

RPLC of tryptophan
Rapid assay
Pediatric plasma

Summary

A 8.3cm column packed with 3μm C_{18} particles was used for the quantitative analysis of total tryptophan in plasma. The plasma samples were deproteinized with cold perchloric acid and 5–20μl of the plasma extract were injected into the RPLC column The tryptophan was readily separated from other plasma components in 5 minutes using isocratic elution. Thus the method can be readily automated. The minimum detection limit was 5pmoles using UV detection, and 1pmole using fluorescence detection. Since low concentrations of total tryptophan in small volumes ($\leqslant 500\mu$l) of plasma can be determined reproducibly and rapidly, this fast RPLC method can be used in pharmaceutical and clinical laboratories for newborn, and infant and pediatric samples.

Introduction

Tryptophan, an aromatic amino acid which can be found free or bound to serum albumin in blood fluids [1, 2], is essential for optimal growth in infants and for nitrogen equilibrium in human adults. Levels of tryptophan and its metabolites in blood fluids, urine and cerebrospinal fluids have been determined in nutritional investigations as well as in studies of disease states. Altered levels of free and total tryptophan have been found in subjects with migraine headaches [3], hepatic coma [4], chronic renal failure [5], breast and bladder cancer [6–9], Parkinson's disease [10, 11] and mental depression [12].

HPLC has become a routine tool in the separation and quantitation of amino acids in physiological fluids. Ion exchange methods or reverse-phase separations of tryptophan with or without pre- or post column derivatization have been reported [14, 15]. However these separations require time consuming sample preparation and chromatographic procedures. In addition they lack selectivity.

With the availability of high speed columns, a rapid HPLC method for the determination of tryptophan in biological matrices is now possible. In this paper, we report on the development of a rapid method for the direct quantitation of total tryptophan in plasma. Using UV detection at the absorbance maximum of tryptophan (280nm) coupled with fluorescence detection (excitation 280nm, emission 340nm cutoff), reproducible, sensitive and selective results were obtained.

Materials and Methods

Apparatus

A Perkin-Elmer Series 3B liquid chromatograph (Perkin-Elmer Corp., Norwalk, CT, USA) was used. Detection of the UV absorbing compounds at 280nm was accomplished by means of a Perkin-Elmer LC95 UV-visible detector equipped with a 4.5μl flowcell. Native fluorescence was measured with a FS 970 LC Fluorometer (Schoeffel Instruments Corp., Westwood, NJ, USA). Injections were made via a Micromeritics Model 725 Autoinjector with a 5μl loop (Micromeritics, Norcross, GA, USA). Peak heights were recorded with a dual-channel strip chart Omniscribe recorder (Houston Instruments, Austin, TX, USA). Peak areas were electronically integrated with a Perkin-Elmer 3600 Data Station using CHROM2 software.

Centrifugations were performed with a Damon/IEC Division refrigerated centrifuge (Needham Heights, MA, USA) at a maximum speed of 4375 RPM. Samples were vortexed on a Vortex Genie K 550-G (Scientific Industries, Springfield, MA, USA).

Column

All separations were performed on a Pecosphere 8.3cm × 4.6mm, 3μm C18 column (Perkin-Elmer Corp., Norwalk, CT, USA). A guard column packed with pellicular C18 (Perkin-Elmer) was used to protect the analytical column. The guard column was repacked after every 20 injections of deproteinized plasma.

Chemicals and Supplies

Potassium dihydrogen phosphate was obtained from Fisher Scientific (Fair Lawn, NJ, USA). HPLC grade distilled in

---

[1] Present address, Water Assoc. Division of Millipore Corp., Milford, MA.

0009-5893/87 0309-04 $03.00/0

© 1987 Friedr. Vieweg & Sohn Verlagsgesellschaft mbH

glass methanol was purchased from Borden & Remington (Fall River, MA, USA). Mobile phases were prepared with doubly distilled deionized water and filtered through a 0.45μm Millipore membrane filter (Millipore Corp., Bedford, MA, USA). The tryptophan reference compound and the tryptophanase (E.C. 4.1.991) were of the highest purity available (Sigma Chemical Co., St. Louis, MO, USA).

Green-top Vacutainer tubes containing sodium heparin as anticoagulant for plasma collection were purchased from Fisher Scientific (Fair Lawn, NJ, USA).

Sample Preparation and Chromatographic Conditions

For the determination of total tryptophan, blood was drawn into evacuated blood collection tubes containing sodium heparin as anticoagulant. The samples were centrifuged for 15 minutes at high speed after which the plasma (supernatant) was removed from the blood cells. To 500μl of plasma, 500μl of a cold perchloric acid solution (3.5% w/v) was added. The sample was then vortexed vigorously for 1 minute. Precipitated protein was removed by centrifuging for 10 minutes. To neutralize the extract, 500μl of 3.5% KOH and then 500μl of the mobile phase were added to the neutralized supernatant.

The samples were assayed isocratically using a flow rate of 1.0 ml/min and a mobile phase of 90% 0.02 M KH_2PO_4/ 10% MeOH (v:v) which was adjusted to pH 5.7 with dilute KOH.

Peak Identification

The tryptophan peak was tentatively identified by retention time, co-chromatography with a standard tryptophan solution, and by the fluorescence signal. The peak was unambiguously identified by the enzyme peak shift technique using tryptophanase.

Results and Discussion

Acid precipitation is routinely used to remove proteins from plasma or to break the bonds of substances bound to proteins. Normally proteins are precipitated with the addition of strong acid such as purchloric acid (PCA) or trichloracetic acid (TCA) to a measured quantity of plasma, followed by neutralization with strong base or buffer [16, 17]. However, when only very small volumes of plasma are available as in newborn or pediatric samples, it is desirable to minimize the number of steps in the preparation of the sample and the dilution of the volume.

Therefore we investigated the possibility of injecting directly the acidic plasma supernatant onto the analytical column, without performing a neutralization step. Although reproducible results were obtained, the strongly acid samples caused a shortened life-time of the column. Therefore for the second group of samples we neutralized the samples with KOH.

Because we employed short columns (8.3cm) filled with very small particles (3μm), we used small injection volumes; 5μl with the acidic samples and 20μl with the neutralized samples. Periodic washes with 100% methanol helped maintain the performance and the lifetime of the column.

Identification of tryptophan in the plasma samples was based on retention time, and co-chromatography with standards, fluorescence signal, and the enzyme peak shift with tryptophanase. In the enzyme peak shift, the tryptophan peak at 5 minutes was shifted to a peak at 9 minutes which is tentatively identified as indole (Fig. 1) [18].

Retention times and peak areas and peak shapes are reproducible, as indicated in Table I. Peak shapes remained the same throughout the study. Fig. 2 shows the UV and fluorescence chromatograms of an adult plasma sample and Fig. 3 that of a pediatric sample. Tryptophan elutes in less than 4 minutes and is well removed from any possible interferences. Calibration curves were linear over the concentration range investigated with sensitivities of 5 picomole of tryptophan with UV detection and 1 pmole with the fluorescence detection.

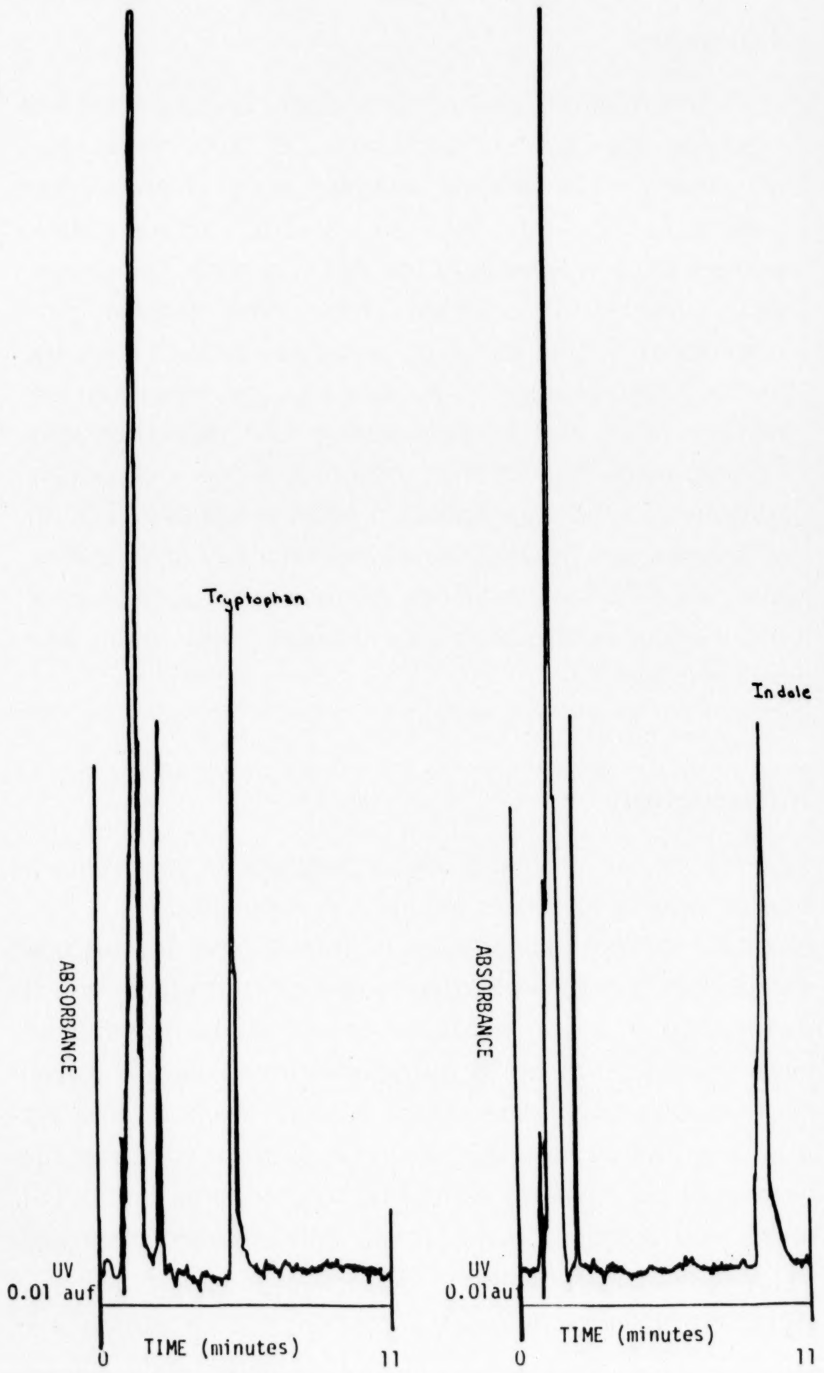

Fig. 1

Enzyme peak shift using tryptophanase: Chromatogram A without tryptophanase, chromatogram B with tryptophanase.
Column: Pecosphere^{TM} 8.3cm, 3μm C18.
Mobile Phase: 90% 0.02M KH_2PO_4, 10% Methanol (v:v), pH 5.7.
Flow Rate: 1.0ml/min.
Trace: U.V. detection at 280nm, detector response 500msec, range 0.01 aufs.

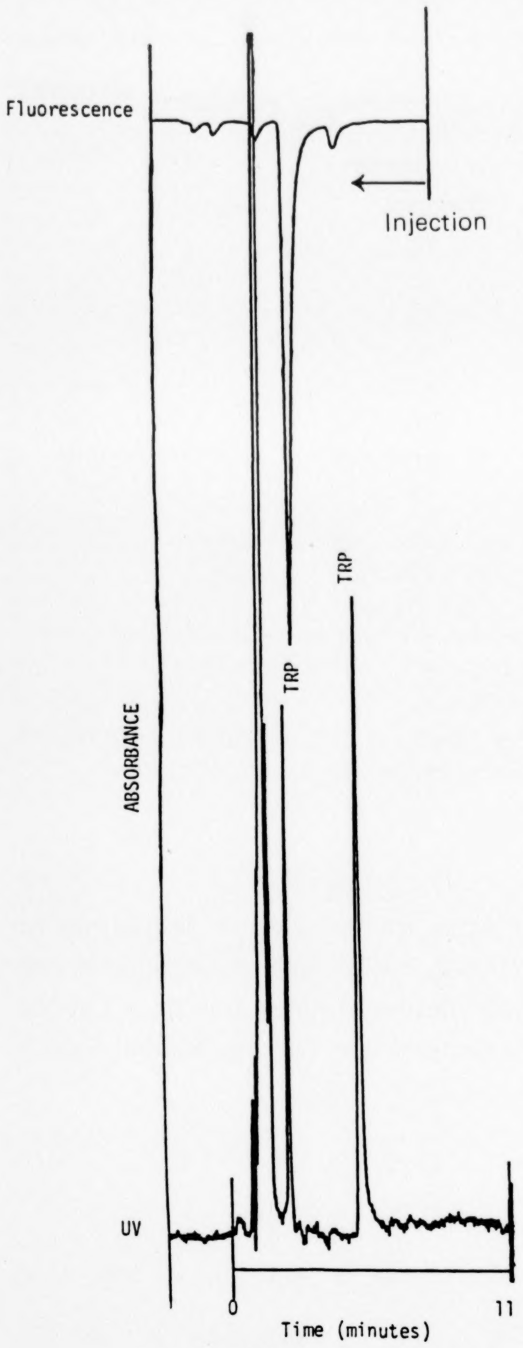

Fig. 2

Chromatographic separation of acidic plasma supernatant, adult.

Injection volume: 5μl

Column: Pecosphere^{TM} 8.3cm, 3μm C18

Mobile Phase: 90% 0.02M KH_2PO_4, pH 10% Methanol (v:v), pH 5.7.

Flow Rate: 1.0ml/min.

Lower Trace: UV detection at 280nm, response time 100msec, range 0.01 aufs.

Upper Trace: Fluorescence detection (excitation 280nm, emission 340nm cutoff filter), time constant 6sec, range 10.0μAmps.

Note: The fluorescence peak is smaller in this chromatogram than in that of Fig. 3 because a different attenuation was used to "scale down" the size of the peak.

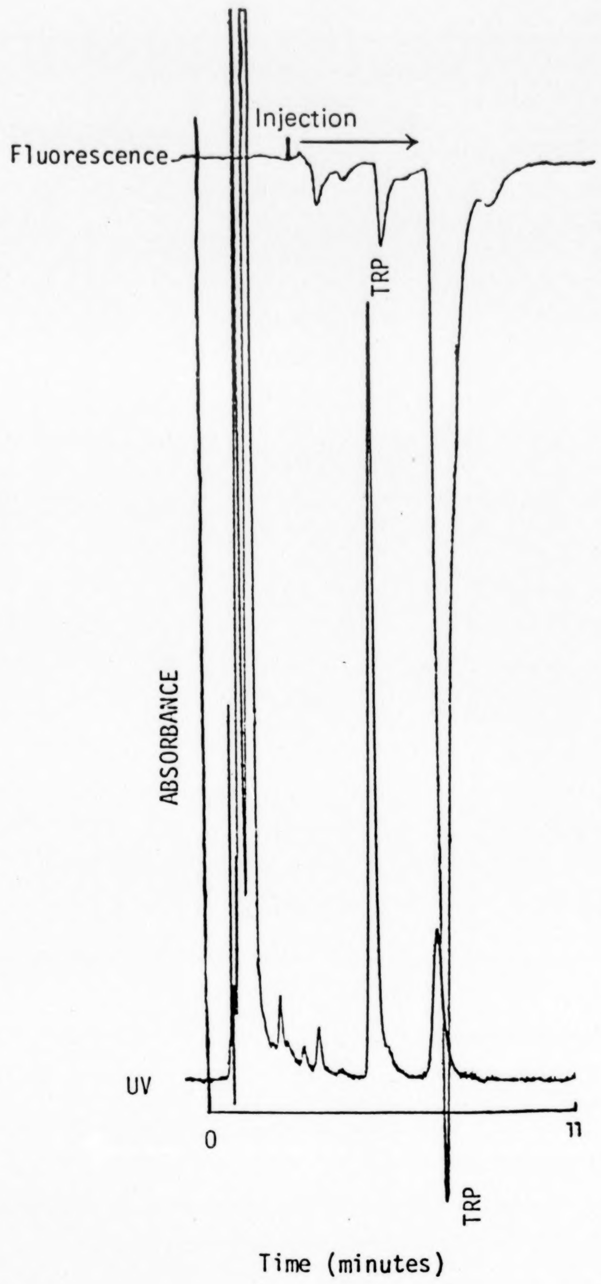

Fig. 3

Chromatographic separation of acidic plasma supernatant of pediatric sample.

Column: Pecosphere^{TM} 8.3cm, 3μm C18.

Mobile Phase: 90% 0.02M KH_2PO_4, 10% Methanol (v:v), pH 5.7.

Flow Rate: 1.5ml/min.

Lower Trace: UV detection at 280nm, detector response time 100msec, range 0.01 aufs.

Upper Trace: Fluorescence detection (excitation 280nm, emission 340nm cutoff filter), time constant 6sec, range 1.00μAmps.

Both pediatric and adult samples gave results in the established clinical range (Table II and III). The range of the concentrations of total tryptophan for the pediatric samples was 47.5–92.2μM compared to the literature range of 41–91μM [19]. Each value listed in the Tables is the average of three successive injections of the same sample. With data collected for adult plasma samples, the range of values we obtained was 45.6–54.2μM compared to 20–61 μM as reported in the literature [19]. We also compared the results we obtained with the results on the same samples obtained by a manual fluorometric method done in another laboratory [20]. Using a T-Test analysis where P was equal to 0.50, our mean value of 73.9 ± 88.8μM showed no significant difference from theirs of 71.1 ± 7.0μM.

Table I. Reproducibility Data*.

	Retention Time	Peak Area
	5.25	77533
	5.23	64653
	5.23	68466
	5.23	71260
	5.23	69674
	5.24	73977
	5.25	74777
	5.25	69695
	5.25	69216
	5.25	71201
Average	5.24 ± 0.01	71045 ± 3000
RSD	0.20%	4.22%

* Based on ten, 5μl injections of 2.50 X 10-4M solution of tryptophan

Table II. Concentration of total tryptophan in pediatric plasma samples.

Sample**	Concentration (μM) of tryptophan*	%RSD
1	74.9	2.5
2	59.9	1.0
3	71.0	0.7
4	57.8	1.0
5	58.3	0.3
6	72.9	3.0
7	92.2	1.7
8	74.8	1.3
9	90.6	1.6
10	62.7	8.3
11	59.3	4.3
12	74.2	4.6
13	64.6	9.8
14	63.7	5.4
15	67.5	4.8
16	44.3	2.0
17	69.2	0.6
18	47.5	0.4
19	72.3	1.0
20	52.8	4.0
21	63.6	2.0
22	72.7	3.0
23	79.5	0.6
24	76.7	0.4
Average	73.9	8.8
Average obtained by Manuel Fluorometric method	71.1	7.0

Range 47.2–92.2μM

Literature Range 41–91μM [19] for children ages 6 months to 3 years old, obtained by ion exchange chromatography

(* Average of three injections)

(** Samples 1–12 were acidic and samples 13–24 were neutralized)

Table III. Concentration of total tryptophan in adult plasma samples.

Sample	Concentration (μM) of tryptophan**	%RSD
1	51.2	0.7
2	52.0	1.7
3	51.0	1.3
4	51.0	1.0
5	50.0	1.1
6	52.0	0.9
7	45.6	0.4
8	54.2	0.8
9	49.2	0.7
10	53.5	2.0
Our Range*	45.6–54.2μM	
Literature Range***	20–61μM	

* Ages of adults: 26–31 years

** Average of three injections

*** Range as given in the literature [19] for adults, ages 18–77, obtained by ion exchange chromatography.

Conclusions

In conclusion, our RPLC method for the determination of total tryptophan in plasma samples has several advantages. Very small sample volumes of plasma can be used. Sample preparation time and sample dilution are minimized and detectable limits of 1 picomole have been established. Our method is rapid and reproducible with tryptophan eluting in less than 5 minutes. Since isocratic elution is used, there is no turn around or equilibration time; thus the method can be readily automated. In addition the method is cost effective with savings in column costs and solvent consumption. The method therefore is well suited for the determination of tryptophan levels in newborn, infant and pediatric samples in clinical, pharmaceutical, nutritional or biomedical research laboratories.

Acknowledgements

The authors thank Dr. Pamela Perrone and Dr. J. Russel Gant of the Perkin Elmer Corporation for their technical assistance, the Perkin Elmer Corporation for the analytical column used in this study and for the fellowship for M.E.D. We also thank Teknor Apex for the summer fellowship for L.C.P. University of Rhode Island Health Services is acknowledged for the adult plasma samples and Ross Laboratories for the pediatric samples and for the manual fluorometric analysis.

References

[1] *R. H. McMenamy, J. L. Oncley*, J. Biol. Chem., **233**, 1436 (1958).

[2] *R. H. McMenamy, C. C. Lund, J. Van Marcke, J. L. Oncley*, Arch. Biochem. Biophys., **93**, 135 (1961).

[3] *S. Salmon, M. Fanciullacci, M. Bonciani, F. Sicuteri*, Headache, **17**, 238 (1978).

[4] *D. G. Hutson, J. Ono, R. S. Dombro, J. U. Levi, A. Livingstone, R. Zeppa*, Am. J. Surg., **137**, 235 (1979).

[5] *A. L. Barnett, H. Veening*, Clin. Chem., **31** (1), 127 (1985).

[6] *H. L. Davis, Jr., R. R. Brown, J. Leklem, I. H. Carlson*, Cancer, **31**, 1061 (1973).

[7] *D. P. Rose*, Clin. Chim. Acta, **18**, 221 (1967).

[8] *R. R. Brown, G. A. Friedall, J. E. Leklem*, Am. Ind. Hyg. Assoc. J., **33**, 217 (1972).

[9] *G. T. Bryan*, J. Clin. Nutr., **24**, 841 (1971).

[10] *J. Lehman*, Acta Med. Scand., **194**, 181 (1973).

[11] *C. D. Hall, E. A. Weiss, C. E. Morris, A. J. Prange*, Neurology, **22**, 231 (1972).

[12] *K. Wood, A. Copper*, Neuropharmacology, **17**, 428 (1978).

[13] *A. M. Krstulovic, P. R. Brown, D. M. Rosie, P. B. Champlin*, Clin. Chem., **23**, 1984 (1977).

[14] *R. F. Pfeifer, D. W. Hill*, in "Advances in Chromatography". **22**, 37, *J. C. Giddings, E. Grushka, J. Cazes, P. R. Brown*, (editors), Marcel Dekker, Inc., NY (1983).

[15] *M. T. W. Hearn*, in "Advances in Chromatography", **20**, 1, *J. C. Giddings, E. Grushka, J. Cazes, P. R. Brown*, (editors), Marcel Dekker, Inc., NY (1982).

[16] *J. X. Khym*, Clin. Chem., **21**, 1245 (1975).

[17] *D. A. Van Haverbeke, P. R. Brown*, J. Liq. Chromatogr., **1** (4), 507 (1978).

[18] *P. R. Brown*, J. Chromatogr., **52**, 257 (1970).

[19] *S. Meites*, (editor in chief), Pediatric Clinical Chemistry 2nd edition, American Association for Clinical Chemistry, Inc., Washington, D.C., (1981).

[20] *L. M. Janas, T. A. Picone, H. Churella, T. Daniels, K. Ponto*, Fed. Proc., **46**, 896 (1987).

Received: June 29, 1987
Accepted: Aug. 5, 1987
F

Simple and Practicable High-Performance Liquid Chromatographic Assay of Some Tricyclic Drugs, Haloperidol, Diltiazem, Verapamil, Propafenone and Amiodarone

G. Mazzi

Laboratorio di Chimica Clinica e di Ematologia, Istituti Ospitalieri, I-37126 Verona, Italy

Key Words

Column liquid chromatography
Tricyclics
Antiarrhytmics
Haloperidol
Diltiazem
Verapamil

Summary

A rapid, practicable and versatile high-performance liquid chromatographic method is described, which applies to different therapeutic drug-monitorings. Using the same extraction procedure with 500 μl of serum and 250 μl of extracting mixture, the same column and the same mobile phase, the following drugs were separated from endogenous molecules: amitriptyline with nortriptyline, imipramine with desipramine, chlomipramine, haloperidol, diltiazem, verapamil, amiodarone and desethylamiodarone.

Introduction

Due to various individualized therapeutic reactions, to the need for utilizing the lowest efficacious dosage of drugs that can have negative side-effects in patients receiving them on a chronic basis, and due to the risk of exceeding therapeutic ranges, extensive knowledge of drug concentrations in the blood (plasma or serum) for individual treatments is required. For particular patients, moreover, e.g. mental or elderly heart patients, it may be necessary to evaluate the actual intake of prescribed drugs. For all these reasons, the clinical laboratory is asked to make assays of several different drugs in a short amount of time.

Among the various analytical methodologies, high-performance liquid chromatography (HPLC) has been shown to be a sensitive, specific and versatile technique, responding to such needs [1, 2]. Unfortunately, most of the methods of drug dosage by HPLC are too time-consuming to be performed routinely.

This study tries to demonstrate that a new HPLC method may be at hand for dosing different drugs by the same column and mobile phase, and the same purifying procedure, reduced to extremely simple steps that every laboratory can use. Of course, this is possible because drugs are molecules that are not normally present in biological fluids. With minimal organization it is possible, along with the test request, to acquire a list of the prescribed drugs (or those which the patient is suspected of consuming) and to ascertain possible interferences with the analysis. If the chemical behaviour of other consumed drugs is not known, and these molecules may be suspected to overlap the tested drug in the chromatogram, the interference is easily checked by utilizing a specimen of the drug(s) in question.

Using this method we evaluated some tricyclic antidepressant drugs: amitriptyline and its metabolite nortriptyline; imipramine and its metabolite desipramine; chlomipramine; as well as haloperidol, an antipsychotic drug; diltiazem, a calcium-channel blocking agent; verapamil, a coronary vaso-dilatator; and an antiarrhytmic agent, propafenone. Amiodarone and its metabolite desethylamiodarone have also been assayed by this method; the results, obtained by a similar procedure, were previously published [3]. In most published methods sample preparation for HPLC is achieved by liquid-liquid extraction, followed by evaporation of solvent [4–9] or by reextraction by acid [10–13]; others use column extraction [14]; and simple protein precipitation with acetonitrile is also used followed by the injection of the supernatant itself [15]. The analytical column used in published methods is usually reversed-phase [10–16], but silica [5, 6] or polar-bonded [3, 4, 7, 17] are also used.

According to our experience, simple extraction of serum by a suitable extraction mixture has shown itself to be more convenient, because, with a small volume, a high recovery and drug concentration is attained. In the stationary phase containing bonded nitrile groups we found the core of the analytical separation of these molecules. Because of the complex nature of its retention [18], this stationary phase selectively retains these drugs, letting go of the endogenous biological substances.

0009-5893/87 0313-04 $ 03.00/0

© 1987 Friedr. Vieweg & Sohn Verlagsgesellschaft mbH

Reagents and Standards

Di-iso-propylether (RPE), n-buthyl alcohol (RS per HPLC), acetonitrile (RS per HPLC), phosphoric acid (RPE-ACS) and ammoniumhydroxide (RPE) were from Carlo Erba (Milan, Italy). Tetrahydrofuran for chromatography was from Merck (Darmstadt, FRG). Imipramine hydrochloride, desipramine hydrochloride, amitriptyline hydrochloride, verapamil hydrochloride, diltiazem hydrochloride and haloperidol were from Sigma. Chlomipramine hydrochloride was from Ciba-Geigy (Saronno, Italy). Nortriptyline hydrochloride was supplied by Eli Lilly Italia S.p.a. (Sesto Fiorentino, Italy). Propafenone hydrochloride was supplied by Knoll AG (Ludwigshafen, FRG). Amiodarone hydrochloride, desethylamiodarone hydrochloride, L-8040 and minaprine hydrochloride were supplied by Midy (Milan, Italy).

The extracting mixture was prepared by mixing 70ml of di-iso-propylether with 30ml of n-buthyl alcohol. Ammonium formate 2.0M, pH 4.0 was prepared, adding ammonium hydroxide to formic acid. The mobile phase was prepared by mixing 700ml of acetonitrile with 100ml of tetrahydrofuran, 195ml of water and 5ml of 2.0M ammonium formate. Stock solutions of each drug were prepared in methanol at a concentration of 5mg/ml and stored at −20 °C. Diluted methanolic solutions at drugs concentrations of 2.00 to 10.00 μg/ml were used for preparation of calibration standards. Calibration standards, with appropriate concentrations, were prepared by adding drug-free pooled sera to evaporated methanolic drug solutions. L-8040 was used as the internal standard, which elutes after all drugs; minaprine, which elutes before all drugs, was used as the control of L-8040, but it is not indispensable. Both were dissolved in the extracting mixture at concentrations of 1600ng/ml for L-8040 and 800ng/ml for minaprine (800 and 400, respectively, for the assay of haloperidol and verapamil).

Apparatus

A Beckman HPLC isocratic system with a 114 solvent delivery module, a 165 variable wavelength detector, a 450 data system, and an omniscribe d-5000 recorder was used. A sample injector Gilson model 401/231 was used. The analytical polar-bonded phase column was an Altex ultrasphere cyano 5 μm, 4,6 × 250mm (Beckman), preceded by a cyano spheri-5, 5 μm, 4.6 × 30mm guard column (Brownlee labs).

Analytical Procedure

A 500 μl aliquot of the sample or standard was pipetted into a 5ml polypropylene tube, and 250 μl of the extracting mixture, containing L-8040 and minaprine, were added. The tubes were then centrifuged for 2 minutes and, after a manual shake to disrupte the pellet at the interface between organic and acqueous phases, recentrifuged for 5 minutes. A 50 μl aliquot of the top organic layer was injected onto the analytical column, kept at a temperature of 20 °C. The flow-rate was 1.5 ml/min. The absorbance was measured at 235 nm for verapamil (Fig. 1); at 240 nm for amitriptyline, nortriptyline (Fig. 2), haloperidol (Fig. 3) and diltiazem (Fig. 4); at 248 nm for imipramine, desipramine and chlomipramine (Fig. 5), as well as for propafenone, amiodarone and desethylamiodarone (Fig. 6). For amiodarone, however, and its metabolite, the maximum absorbance was 242 nm.

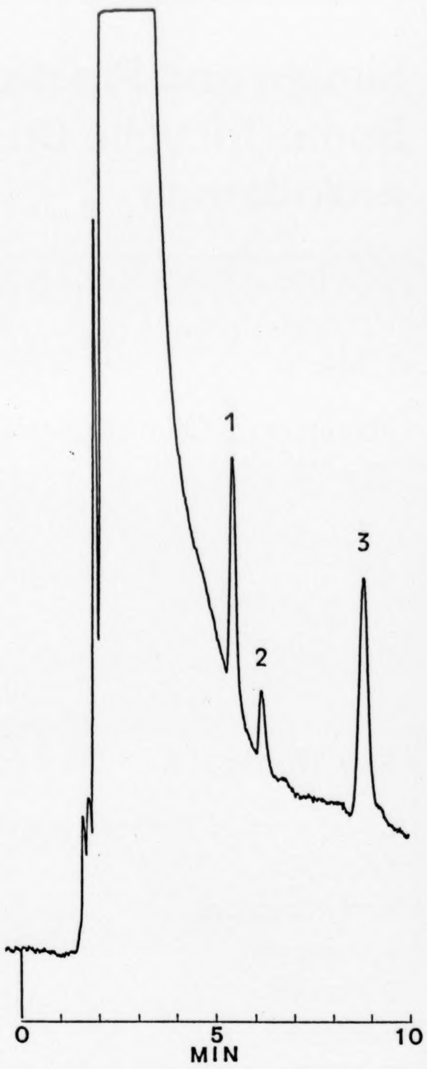

Fig. 1

Chromatogram of pooled sera with concentrations of 200 ng/ml minaprine (**1**), 100 ng/ml verapamil (**2**), and 400 ng/ml L-8040 (**3**).

Sensitivity was regulated at 0.02 a.u.f.s. Chromatograms were recorded at a chart speed of 1 cm/min and at 10 mV f.s. The peaks were acquired by computer and calculated by height.

Results and Discussion

Assay precision was evaluated with repeated measurements of a pool of drug-free sera brought to the given concentrations. Within-run precision was assessed from ten measurements. The day-to-day precision was calculated from data obtained from ten duplicate measurements taken over one month. The mean concentration and coefficient of variation for within-run and between-run variances are shown in Table I.

The absolute recovery of each drug was calculated by height, comparing measurements of precision study with triplicate measurements of a standard solution of the drug in the extracting mixture. No significant differences were found between high and low values. Absolute recovery was 100% for amitriptyline and nortriptyline, 98% for chlomipramine, 93% for imipramine, desipramine and verapamil,

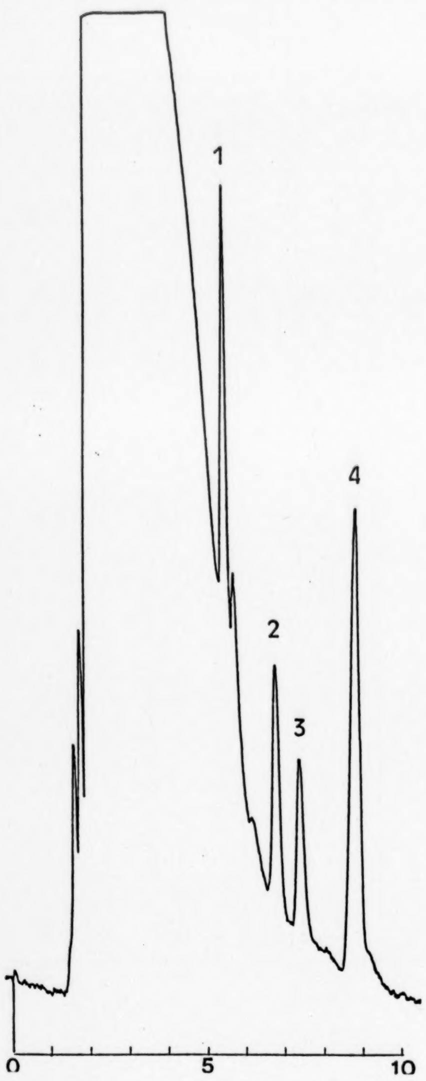

Fig. 2

Chromatogram of patient's serum with concentrations of 400 ng/ml minaprine (1), 261 ng/ml nortriptyline (2), 207 ng/ml amitriptyline (3), and 800 ng/ml L-8040 (4).

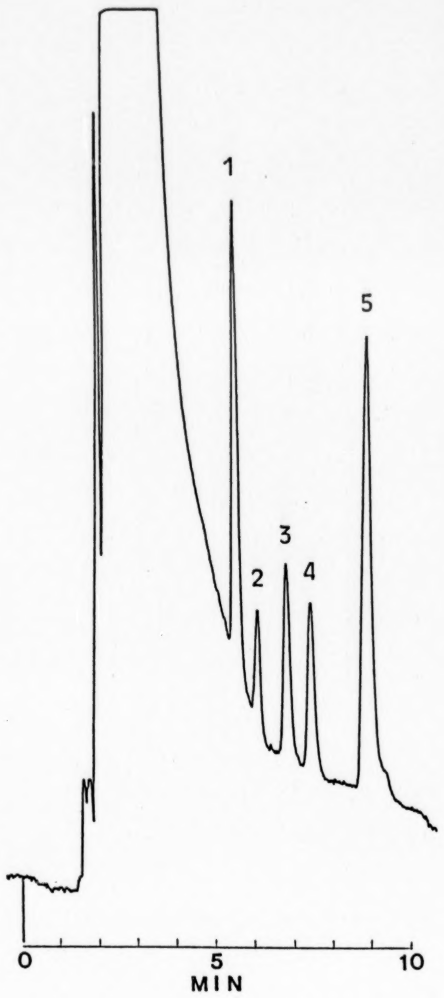

Fig. 4

Chromatogram of pooled sera with concentrations of 400 ng/ml minaprine (1), 100 ng/ml diltiazem (2), 200 ng/ml nortriptyline (3), 200 ng/ml amitriptyline (4), and 800 ng/ml L-8040 (5).

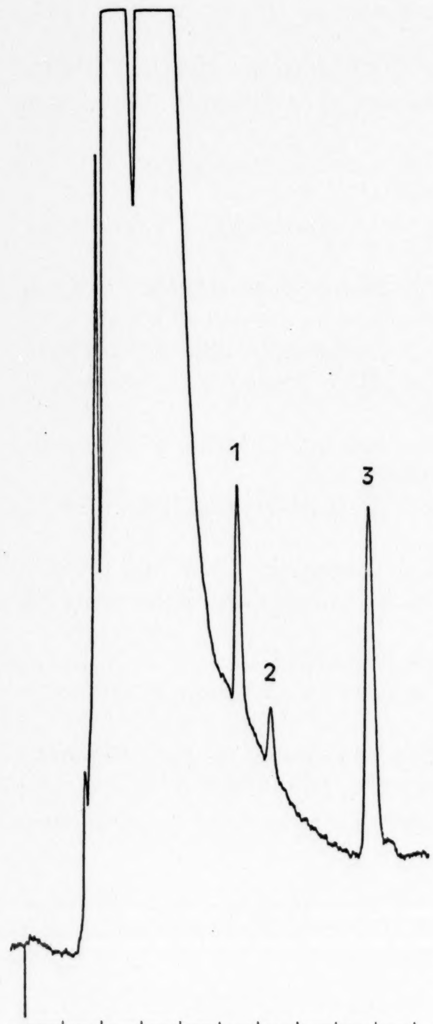

Fig. 3

Chromatogram of pooled sera with concentrations of 200 ng/ml minaprine (1), 100 ng/ml haloperidol (2), and 400 ng/ml L-8040 (3).

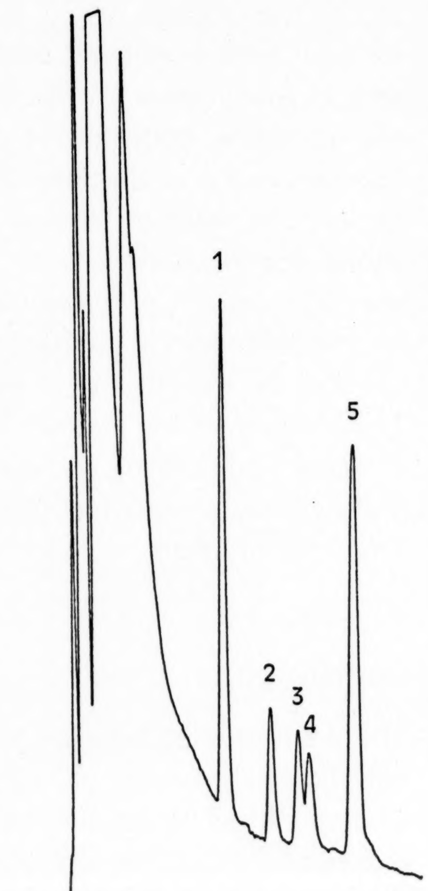

Fig. 5

Chromatogram of pooled sera with concentrations of 400 ng/ml minaprine (1), 200 ng/ml desipramine (2), 200 ng/ml imipramine (3), 200 ng/ml chlomipramine (4), and 800 ng/ml L-8040 (5).

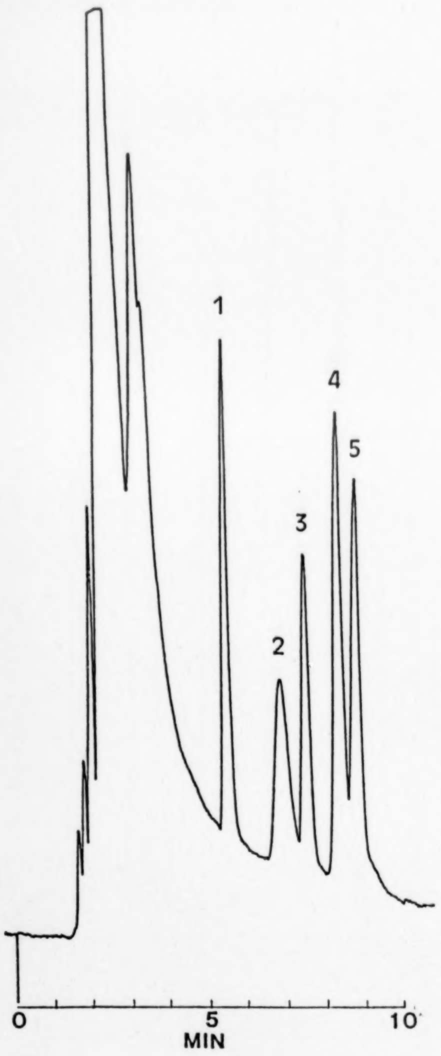

Fig. 6

Chromatogram of pooled sera with concentrations of 400 ng/ml minaprine (**1**), 1000 ng/ml propafenone (**2**), 500 ng/ml desethylamiodarone (**3**), 1000 ng/ml amiodarone (**4**), and 800 ng/ml L-8040 (**5**).

Table I. Precision study

	Within-run (n = 10)		Between-run (n = 10)	
	means ng/ml	CV%	means ng/ml	CV%
Amitriptyline	100	3.0	101	5.6
	502	4.6		
Nortriptyline	98	2.9	99	5.0
	495	5.2		
Imipramine	104	4.5	101	7.7
	500	4.3		
Desipramine	103	2.8	102	7.7
	498	4.3		
Chlomipramine	98	3.6	101	7.3
	494	1.6		
Haloperidol	58	6.7		
	200	4.3	196	6.0
Diltiazem	47	6.5		
	201	2.3	195	5.9
Verapamil	51	8.8		
	202	2.6	198	5.1
Propafenone	200	3.2		
	995	2.6	984	5.2

88% for haloperidol and propafenone, and 83% for diltiazem. It is an "apparent recovery", as during extraction the organic phase undergoes a certain reduction in volume. The sensitivity of the method depends on the light-power of the UV detector. In our case it was rather low, but allows the measurement of serum concentrations lower than 50 ng/ml for propafenone, amiodarone, desethylamiodarone, and lower than 20 ng/ml for all the other drugs. It can also be increased by injecting 100 μl of organic layer. The linearity of the method for each drug, on pools of sera at scalar concentrations, was checked up to 5 mg/l for profafenone, amiodarone, desethylamiodarone, and up to 1 mg/l for all others.

Conclusion

The drugs studied here are those used by the clinicians of our hospital, above all cardiologists and neurologists; however, other drugs may be dosed by this method, employed as such or after trivial modifications.

References

[1] *B. A. Scoggins, K. P. Maguire, T. R. Norman, G. D. Burrows,* Clin. Chem. **26/1,** 5 (1980).

[2] *T. R. Norman, K. P. Maguire,* J. Chromatogr. **340,** 173 (1985).

[3] *G. Mazzi, M. Miguidi, A. Gallo,* G. Ital. Chim. Clin. **11** (1), 61 (1986).

[4] *R. Terlinden H. O. Borbe,* J. Chromatogr. **382,** 372 (1986).

[5] *F. L. Vandemark, R. F. Adams, G. J. Schmidt,* Clin. Chem. **24/1,** 87 (1978).

[6] *M. Bliss, M. Mayersohn, P. Nolan,* J. Chromatogr. **381,** 179 (1986).

[7] *A. Hutchings, B. P. Spragg, P. A. Routledge,* J. Chromatogr. **382,** 389 (1986).

[8] *K. T. Muir, K. A. Kook, C. Stern, K. M. Gardner,* J. Chromatogr. **374,** 394 (1986).

[9] *C. D. Kinney, J. G. Kelly,* J. Chromatogr. **382,** 377 (1986).

[10] *J. S. Kiel, R. K. Abramson, C. S. Smith, S. L. Morgan,* J. Chromatogr. **383,** 119 (1986).

[11] *P. P. Rop, T. Conquy, F. Gouezo, A. Viala, F. Grimaldi,* J. Chromatogr. **375,** 339 (1986).

[12] *H. F. Proelss, H. J. Lohmann, D. G. Miles,* Clin. Chem. **24/11,** 1948 (1978).

[13] *R. L. Miller, C. L. Devane,* J. Chromatogr. **374,** 405 (1986).

[14] *F. Susanto, S. Humfeld, H. Reinauer,* Chromatographia **22,** 135 (1986).

[15] *S. Lam,* J. Chromatogr. **381,** 175 (1986).

[16] *D. A. Breutzmann, L. D. Bowers,* Clin. Chem. **27/10,** 1907 (1981).

[17] *C. Verghese, M. S. Smith, L. Aanonsen, E. L. C. Pritchett, D. G. Shand,* J. Chromatogr. **272,** 149 (1983).

[18] *S. M. Staroverov, G. V. Lisichkin, E. L. Styskin,* Chromatographia **21,** 165 (1986).

Received: June 30, 1987
Accepted: Aug. 5, 1987
F

Chromatographic Separation and Identification of Human Urine Components

Y. Nagata[1]/Y. Matsushima[1]*/H. Ugai[1]/M. Kikuchi[1]/N. Takai[2]

[1] Kyoritsu College of Pharmacy, Shibakoen 1-5-30, Minato-ku, Tokyo 105 Japan
[2] Institute of Industrial Science, University of Tokyo, Roppongi 7-22-1, Minato-ku, Tokyo 106, Japan

Key Words

Large scale column liquid chromatography
Human urine
Uric acid
Strongly basic anion-exchange resin

Summary

Ultraviolet-absorbing components of human urine were separated by HPLC with a large scale column (250 X 28 mm I.D. stainless-steel) containing a macroreticular type strongly basic anion-exchange resin. The sample was eluted with a linear gradient of 0.006 M to 6.0 M ammonium acetate buffer (pH 4.40) and different fractions were collected. The identification of one compound using ultraviolet, infrared and mass spectral data is illustrated; it was found to be uric acid.

We reported previously the analysis of ultraviolet (UV)-absorbing compounds in human urine by means of high-performance liquid chromatography using a column containing macroreticular anion-exchange resin (Diaion CDR-10) maintained at 60 °C [1].

Reproducible chromatograms with 69 well-resolved peaks were obtained. The method is expected to find its place among the routine analytical methods of human urine applicable to diagnostic purpose. In the study, the chromatographic peaks were identified by comparing the retention times with standards. However, for further confirmation, the identification of some of the urine components is required. For this purpose, fractions were collected from a large-scale column and subjected to identification by physico-chemical methods. The present paper outlines these investigations and the result of the investigation of one fraction is illustrated here.

For the chromatographic separation of the fractions, a Hitachi Model 655 high-performance liquid chromatograph equipped with a Hitachi solvent programming system (a Model 655 proportioning valve and a Model 655-66 controller) and a Rheodyne Model 7125 injector was used. The chromatograph was coupled to a Hitachi Model 150-20 double-beam spectrophotometer operated at 260 nm with a flow cell.

The macroreticular-type strongly basic anion-exchange resin, Diaion CDR-10, obtained from Mitsubishi Chemical Industries, Tokyo, Japan, was packed into the main column (250 X 28 mm I.D., stainless-steel) and a pre-column (50 X 8 mm I.D.). The temperature of the main column was controlled within ± 0.2 °C with help of a Shimadzu Model CTO-2A thermostat, at 60 °C.

A urine sample obtained from a healthy person was filtered with a 0.45-μm filter, refrigerated, completely frozen and stored at -20 °C. Before fractionation, it was thawed, filtered, pretreated with Hitachi-gel #3019 and concentrated. The concentrate was dissolved in water and a 6-ml portion of the solution, which corresponded to a 8-ml volume of the urine, was injected into the chromatograph. The sample was eluted with a linear gradient of 0.006 M to 6.0 M ammonium acetate buffer (pH 4.40) [2] (see Table I). Fig. 1 shows the chromatogram. Several fractions of UV-absorbing compounds were collected.

A portion of each fraction was analyzed by reversed-phase HPLC. Two sets of a Shimadzu Model LC-6A pump were controlled by a Shimadzu SLC-6A system controller. A Shimadzu SPD-6A UV-monitor and an octadecylsilica column (TSK-gel ODS-120A, Toyo Soda; 250 X 4.6 mm I.D.) were used. The sample was eluted with a linear gradient of 0.1 M potassium dihydrogen phosphate (pH 2.12) to 0.1 M potassium dihydrogen phosphate-acetonitrile (1:1) at 0-60 min and 0.1 M potassium dihydrogen phosphate-acetonitrile (1:1) at 60-80 min with a flow rate of 0.8 ml/min and monitored at 254 nm [3]. Fig. 2 shows the chromatogram of fraction A in Fig. 1.

The fractions which contained a single UV-absorbing peak were treated with a cation-exchange resin (Dowex 50W-X8, 100-200 mesh), recrystallized, if necessary, and freeze-dried.

Table I. Elution program

Time (min)	Flow rate (ml/min)	Mobile phase (%) 0.006-M buffer	6.0-M buffer (%)
0	5.3	100	0
15	4.5	100	0
150		80	20
300		50	50
380		0	100
450		0	100
460		100	0

0009-5893/87 0317-02 $03.00/0
© 1987 Friedr. Vieweg & Sohn Verlagsgesellschaft mbH

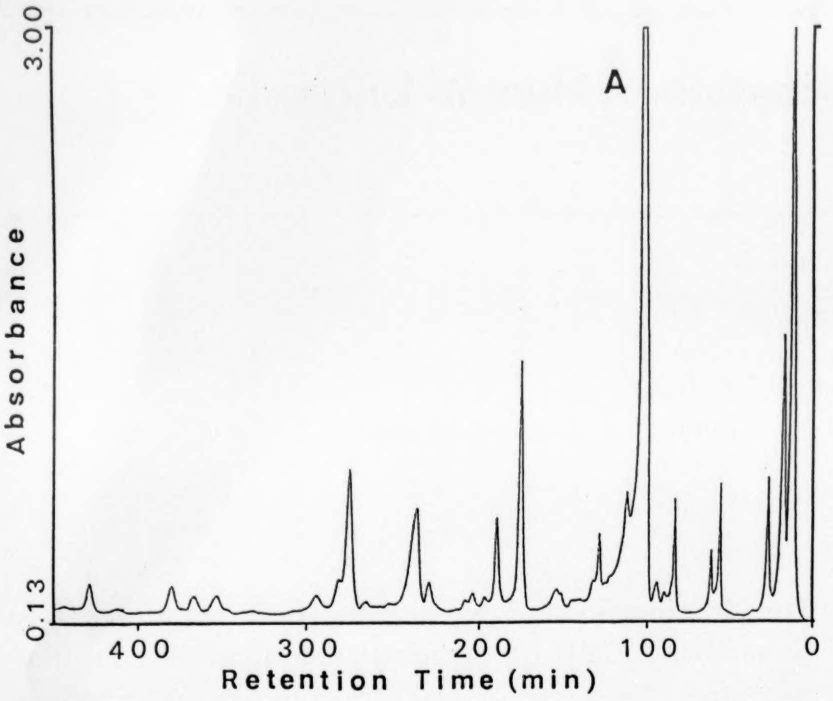

Fig. 1

Chromatogram of a human urine sample using a column (250 X 28 mm I.D.) containing a macroreticular type strongly basic anion-exchange resin. For the chromatographic conditions see the text.

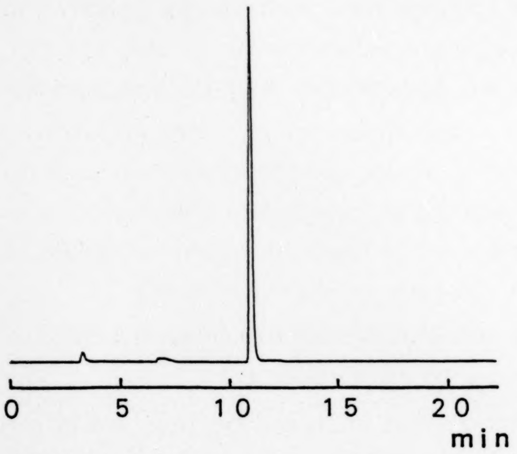

Fig. 2

Reversed-phase liquid chromatogram of fraction A in Fig. 1. For the chromatographic conditions see the text.

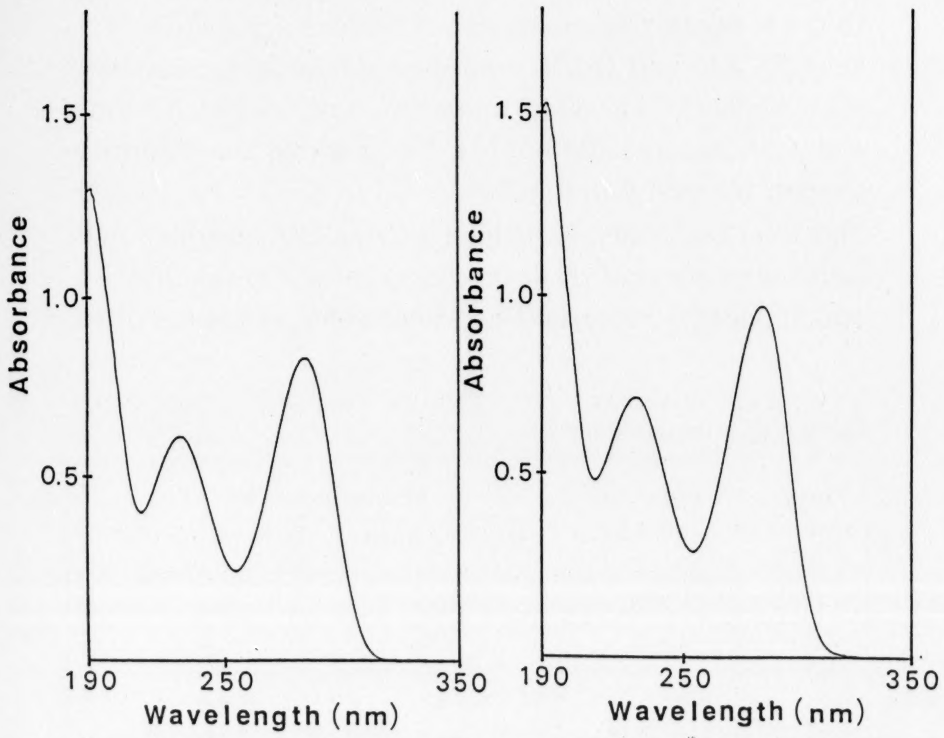

Fig. 3

Ultraviolet absorption spectra of uric acid (left) and the compound purified from fraction A (right).

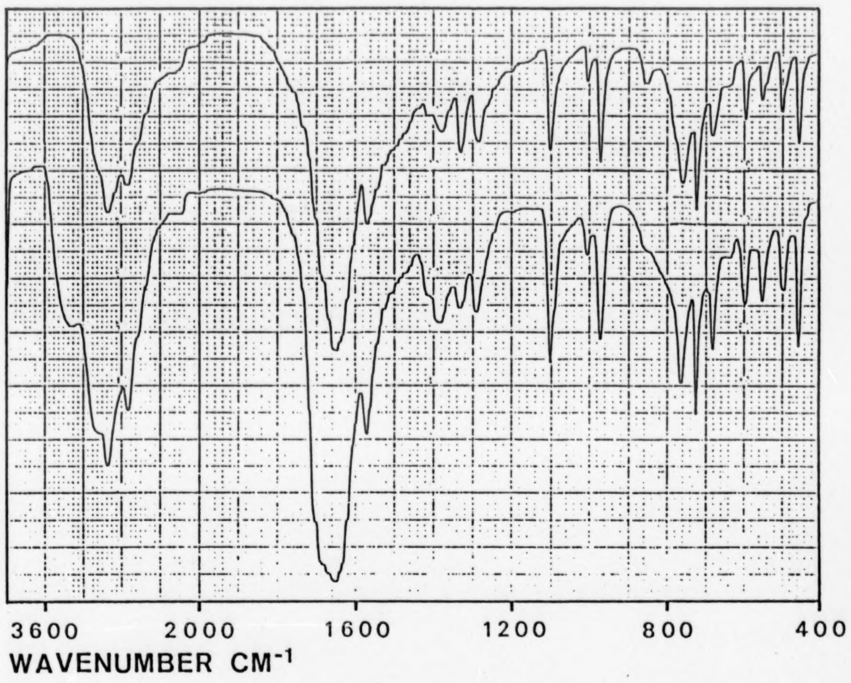

Fig. 4

Infrared spectra of uric acid (upper curve) and the compound purified from fraction A (lower curve).

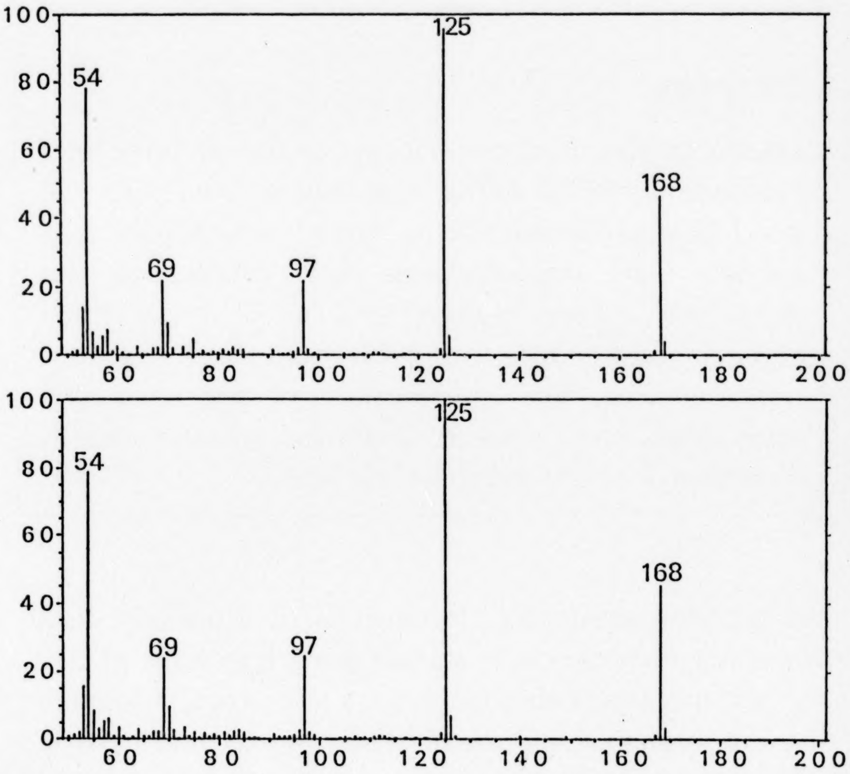

Fig. 5

Mass spectra of uric acid (upper) and the compound purified from fraction A (lower).

The compounds thus purified are then subjected to UV, infrared (IR) and mass spectral (MS) studies. We show here the results for the compound purified from peak A. Figs. 3-5 illustrate that its UV, IR and MS data were almost identical to those of a standard uric acid sample. Thus, the compound in fraction A can be identified as uric acid, investigations of other fraction are in progress.

References

[1] *Y. Nagata, Y. Yokoyama, S. Nagura, S. Sugata, T. Fujie, Y. Matsushima, N. Takai, J. Liq. Chromatogr., in press.*

[2] *K. Seta, M. Washitake, T. Anmo, N. Takai, T. Okuyama,* Bunseki Kagaku, **27**, 73 (1978).

[3] *Y. Nagata, M. Uchida, M. Koyanagi, Y. Matsushima, N. Takai, M. Umino,* J. Life Support Technology Soc., **1**, 86 (1987).

Received: Juli 1, 1987
Accepted: July 31, 1987
F

Determination of Phenol in Raw and Potable Waters by HPLC Multi-Electrode Electrochemical Detection

P. J. Rennie*

North West Water Authority, Huntington W.T.W., Chester CH3 6EA, UK

S. F. Mitchell

Severn Analytical, 36 Brunswick Rd., Gloucester GL1 1JJ, UK

Key Words

Column liquid chromatography
Phenol determination
Water
Coulometric
Electrochemical

Summary

A method is proposed for the determination of phenol in raw and potable waters using multi-electrode electrochemical detection HPLC. The coulometric efficiency of the electrochemical cell together with an ability to 'screen out' other electrochemically active species precludes the need for trace enrichment concentration techniques. The development work leading up to the proposed method is discussed with reference to selection of solvent pH and electrode potentials. The method has a limit of detection of 0.034μgl^{-1} phenol and a total standard deviation of 0.083μgl^{-1} phenol at a phenol concentration of 1.048μgl^{-1} phenol in river water.

Introduction

Present E.E.C. legislation [1] requires that 'the maximum admissable concentration of phenol in water intended for human consumption is 0.5μgl^{-1}'. It is therefore essential that the water-supply analyst is capable of detecting phenol at this level. Although electron capture gas chromatography [2, 3] is capable of satisfying the detection criteria, HPLC was investigated as a possible technique which would lend itself to automation, a necessary prerequisite, as a trace phenol analyser was required for use in an unmanned laboratory monitoring river water quality. It was a result of developing HPLC (U.V. detection/trace enrichment) for this application, that electrochemistry was first considered, although initial method development has been confined to a manual laboratory method.

A dual electrode electrochemical detector (ESA Coulochem 5100A) was chosen for evaluation. The first electrode of this system could be set below the potential required for oxidation of the analyte thus reducing matrix interferences associated with direct aqueous injections at the sensitivity required to achieve sub-microgram per litre detection limits. This detector also had the advantage of coupling a high-surface area coulometrically efficient electrode with a high efficiency amperometric electrode.

Selection of Solvent and Electrode Potentials

Selection of solvent and electrode potentials was by construction of hydrodynamic voltammograms (C-V or Current-Voltage curves). These were used in preference to cyclic voltammograms as no X-Y plotter was available and difficulties can be exhibited from impurities present in the compound of interest. C-V curves were constructed for phenol using a 5μgml^{-1} solution of phenol, a 10μl sample loop, 25cm 10μ Lichrosorb RP18 analytical column and mobile phases buffered to pH 3.3, 6.0 & 9.2. See Fig. 1.

Mobile Phase I: From the C-V curves obtained pH 3.3 was ruled out as the potentials required for the electrochemical oxidation of phenol would be 1100 mV+ exceeding the efficient range for the detector.

Mobile Phase II: Using this mobile phase at pH 6.0 problems were encountered with potentials $>$600 mV with a reduction in current possibly being due to bubble formation on the electrode.

Mobile Phase III: Mobile phase III gave a C-V curve with an oxidation potential for phenol of $<$800 mV and was chosen for further development. After examining the voltammograms the potentials on the electrodes were set at 250 mV for electrode 1 (for the screening out of other electrochemical compounds with half-wave potentials $<$250 mV) and 650 mV for electrode 2. Mechanisms for the anodic oxidation of phenol can be found in the literature [7, 8, 9].

0009-5893/87 0319-05 $03.00/0

© 1987 Friedr. Vieweg & Sohn Verlagsgesellschaft mbH

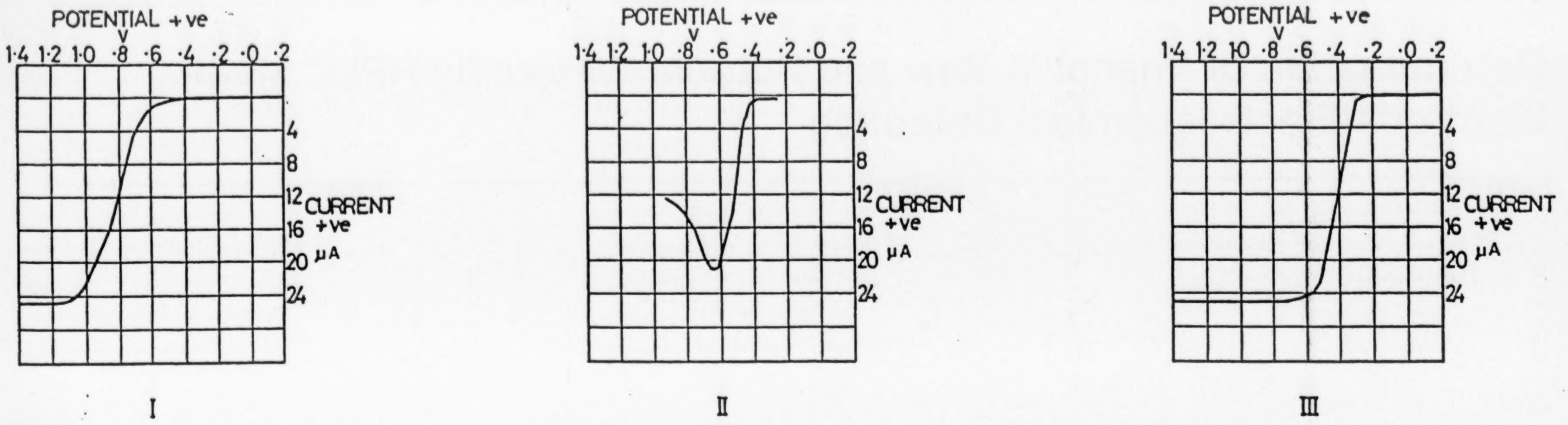

Fig. 1

I. 2gl^{-1} potassium nitrate + 0.05gl^{-1} sulphuric acid in 60/40 methanol/water: pH = 3.3 [4]; II. 6.3gl^{-1} citric acid + 2.27gl^{-1} sodium acetate + 2.0gl^{-1} sodium hydroxide in 55/45 acetonitrile/water: pH 6.0 [5]; III. 1.065gl^{-1} (10mM) dibasic sodium phosphate in 25/75 acetonitrile/water: pH 9.2 [6].

In order to remove electrochemically active contaminants present in the mobile phase the guard cell potential was set at 800 mV and all mobile phase was continuously recycled. The concentration of water in the mobile phase was decreased to 50% in order to decrease retention time and a 15cm 5μ polystyrene/divinylbenzene copolymer column used instead of the Lichrosorb RP18 column as dissolution of silica would occur at the high pH used. Using these selected parameters a method was proposed for the analysis of phenol. This method was subjected to an analytical quality control exercise to ascertain precision of standards, samples and spiking recoveries.

Proposed Analytical Method

Apparatus

HPLC Pump: A pulse free HPLC pump is required capable of delivering up to 1.0ml min^{-1}. A dual reciprocating pump is preferable. A Kontron 420 LC pump was used fitted with a microbore head and flow-through Bourdon Tube type pulse damper.

Electrochemical Detector: An ESA Coulochem 5100A detector together with a model 5011 Analytical cell and model 5020 Guard cell.

Injector: Rheodyne 7125 injector fitted with a 100μl sample loop.

Syringes: 250μl Rheodyne syringe (Hamilton 725SNR) and 2ml syringe with Luer tip fitted with a 7125 needle port cleaner.

LC Column: A 15cm 5μ reverse phase styrene/divinylbenzene copolymer column. Prior to this analytical column a 5 × 3mm styrene/divinylbenzene copolymer guard column must be fitted.

Computing Integrator: A Spectra Physics SP4270 integrator was used.

In-line Filters: 0.5μ stainless steel filter, 2 × 0.2μ ESA Graphite filters and filter holders.

The apparatus was configured as in Fig. 2.

Reagents

All reagents must be of sufficient purity that they do not give rise to interfering peaks in the analysis. All solvents used for the mobile phase should be of HPLC grade. Solvents and standards should be stored in all-glass vessels and have no contact with organic matter, e.g., plastics.

Water used for standard and blank preparation should have a phenol content which is negligible compared with the smallest concentration of phenol to be determined in the samples. Unchlorinated borehole water was found to be the most satisfactory.

Dibasic sodium phosphate, 10mM: Dissolve dibasic sodium sulphate (1.420 ± 0.005g) in HPLC grade water (1000 ± 1 ml).

Acetonitrile/dibasic sodium phosphate mobile phase: Add 10mM dibasic phosphate solution (1000 ± 1 ml) to Acetonitrile (1000 ± 1 ml).

Phenol stock standard solution: 1000mgl-1. Stable for 3 months.

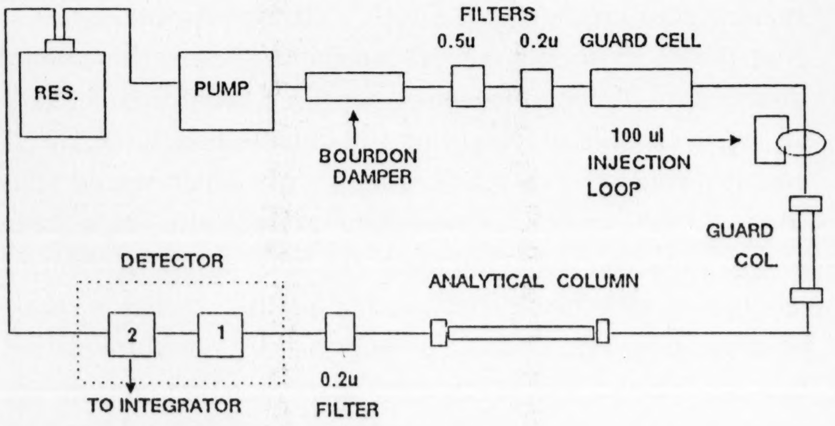

Fig. 2

Suggested HPLC/Electrochemical detector configuration.

Working phenol standards: Dilute the phenol stock standard solution, as appropriate, to produce standards for calibration of the same order as the expected concentration of phenol in the sample (the method is linear up to 1000μg l^{-1} phenol). Note: Standards $< 5 \mu g l^{-1}$ should be prepared within 1 hour of use.

Copper sulphate, 10% m/V: Store in a glass bottle (stable for at least 1 year).

Phosphoric acid, sp. gr. 1.6 @ 20°C.

Sample Collection and Preservation

The samples must be collected in borosilicate glass bottles (250 ml) fitted with ground glass stoppers, previously cleaned by standing overnight in chromic acid and thoroughly rinsed. After filling the bottle with the sample, the stopper must be replaced immediately after sampling ensuring that no air bubbles are present.

For direct injection of samples onto the HPLC no preservative is used and thus samples must be kept as cool as possible, preferably below 4°C and analysed as soon as possible. Fig. 3 shows the effect of biodegradation on a sample of river water spiked with phenol and stored with and without cooling after sampling. The graphs clearly illustrate the need for care with the sample storage temperature and time. At temperatures below 4°C degradation can be seen to be negligible.

If analysis is not to be carried out shortly after sampling then the addition of preserving agents is essential. To preserve a sample, phosphoric acid (0.34 ± 0.02 ml) and copper sulphate solution (2.5 ± 0.01 ml) are added to the sample (250 ml) immediately after sampling and the stopper replaced ensuring that no air bubbles are present. The sample should be stored at 4°C and analysed as soon as possible and no later than 24 hours after sampling. The preservative must be removed before the sample is injected.

Procedure

The HPLC system and detector should be set up according to the manufacturers instructions and the previously discussed configuration and voltage settings.

Analysis is carried out by direct injection of sample (unpreserved and unfiltered) and standards. The injection loop should be flushed out with phenol-free water between injections. The standards are used to construct a calibration graph or linear regression used to find the coefficient (m) and constant (c) of a $y = mx + c$ where y is the concentration of phenol in $\mu g l^{-1}$ and x is the peak area of the phenol peak.

Samples that have been preserved must have the preservatives removed using the following procedure (on no account inject sample containing preservative directly on to the column):

Place the sample (100 ± 1 ml) in a 250 ml round-bottomed flask containing a few anti-bumping granules. Connect the flask to a suitable distillation apparatus and collect 90 ml of distillate. Add phenol free water (10 ± 0.02 ml) to the distillation flask and continue the distillation until 100 ml of distillate has been collected. This distillate can now be injected directly onto the column as an unpreserved sample would be.

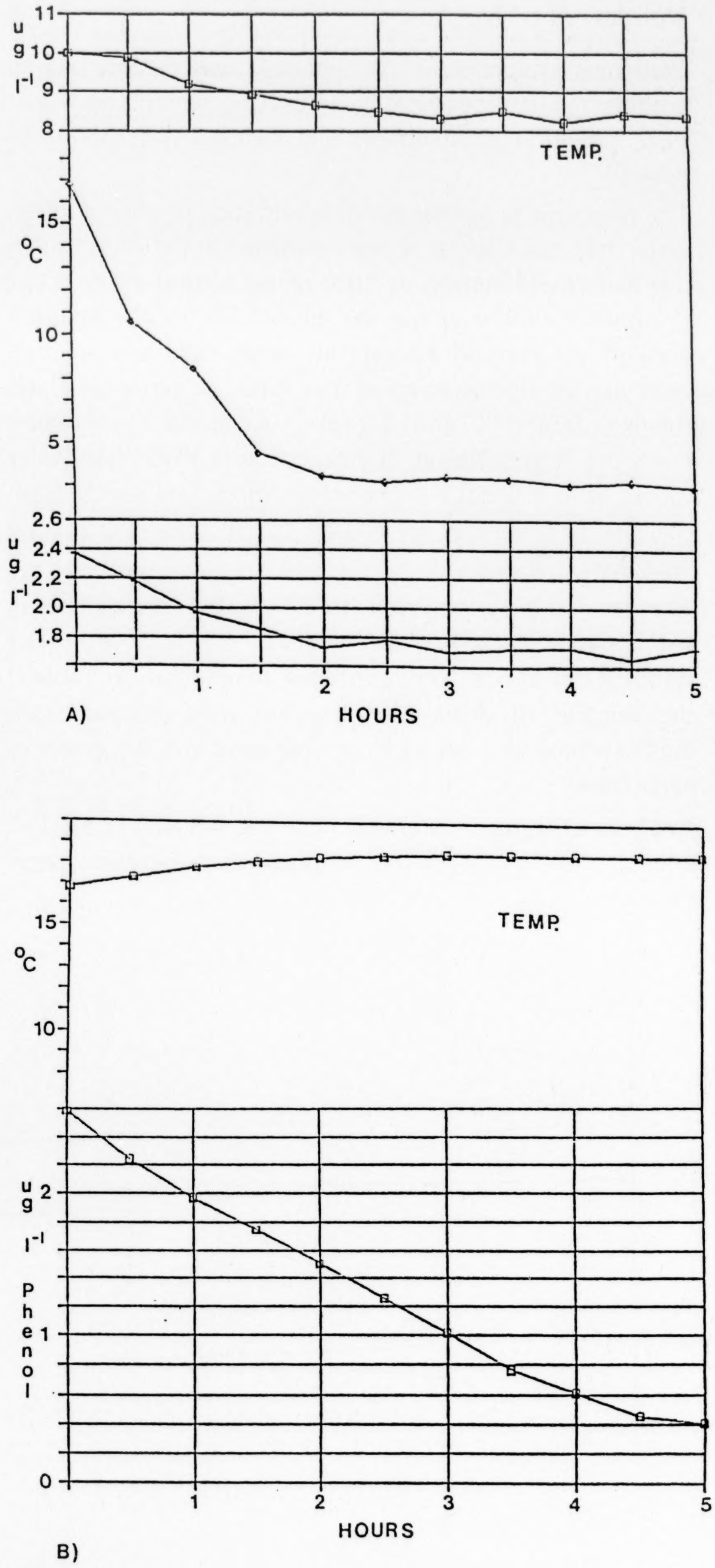

Fig. 3

Biodegradation of phenol. Graph A) represents phenol concentrations found in river water spiked with $10 \mu g l^{-1}$ phenol (top) and river water spiked with $2.5 \mu g l^{-1}$ (bottom) analysed every 30 m. The sample is cooled to below 4°C after sampling. Graph B) represents phenol concentrations found in river water spiked with $2.5 \mu g l^{-1}$ and analysed every 30 m. This sample was stored at room temperature.

Fig. 4 shows an example of a chromatogram obtained for a raw river water spiked with $1.0 \mu g l^{-1}$ phenol.

Validation of Method

Statistical evaluation of the method was carried out according to the procedures given by Cheeseman and Wilson (viz., precision of standards and samples and spiking recovery).

The precision target for the determination of phenol in raw water had been set at a total standard deviation of an individual determination of 10% of concentration or $0.1 \mu g\, l^{-1}$ phenol whichever was the greater. To test the performance of the method against this target duplicate analyses were carried out on each of five days, of borehole water (blank), $0.5 \mu g l^{-1}$ and $1.0 \mu g l^{-1}$ standards, river water from the River Dee at Huntington and River Dee water spiked with a $1.0 \mu g l^{-1}$ phenol addition. The results from the last two samples were used to calculate the spiking recovery.

The results were analysed to derive the corresponding within-batch (s_w), between batch (s_b) and total (s_t) standard deviations. The results are summarised in Table I; the number of degrees of freedom were derived from duplicate analyses on each of five days and are given in parentheses.

Analysis of variance showed that the 0.5 and $1.0 \mu g l^{-1}$ phenol standards showed no significant between-batch variability.

A limit of detection of $0.034 \mu g l^{-1}$ of phenol was calculated by using the formula $2t\sqrt{2}(s_w)$, where t is Student's single sided t for a probability of 0.10 and s_w is the within-batch standard deviation of the blanks. This satisfies a target of $0.05 \mu g l^{-1}$ of phenol in raw and potable water determinations.

The spiking recovery of 102.4% was considered satisfactory. The method was found to have a linear range up to $100 \mu g l^{-1}$ phenol.

Scope of Method

Although validation is only given for monohydric unsubstituted phenol many other compounds can be determined by this method as is shown by the chromatogram (Fig. 5) obtained for a mixture of phenols and chlorophenols under the previously stated conditions.

Development of System for On-line Use

It is envisaged that development of the system for on line use will entail replacing the existing injector (Rheodyne 7125) with a pneumatically or electronically activated injector (Rheodyne 7010). River water would be pumped continuously through the sample loop and the injector switched to inject the river water onto the column. After the peaks of interest have been eluted the injector would

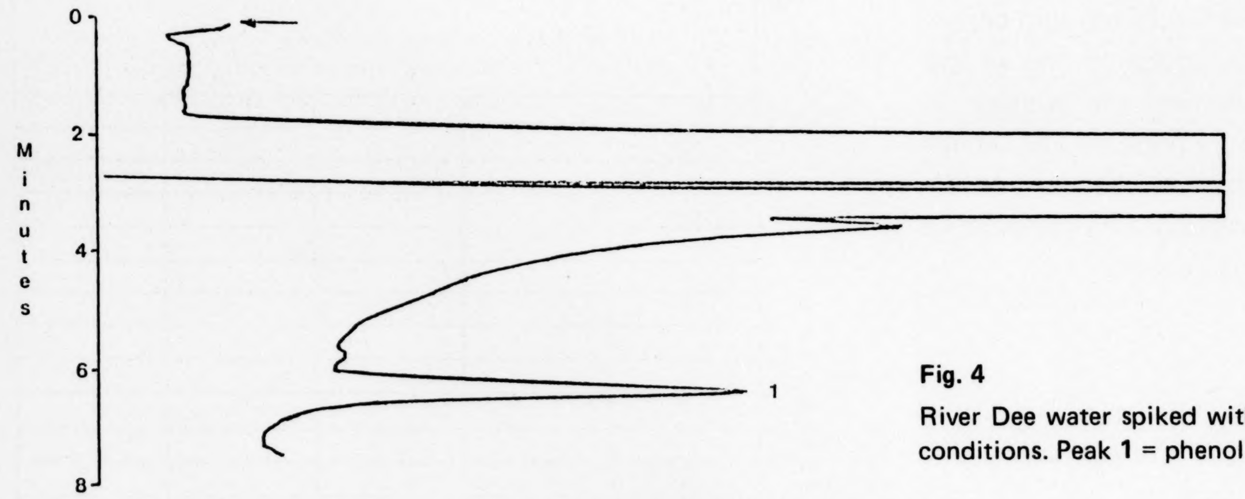

Fig. 4

River Dee water spiked with $1.0 \mu g l^{-1}$ phenol run under the stated conditions. Peak **1** = phenol.

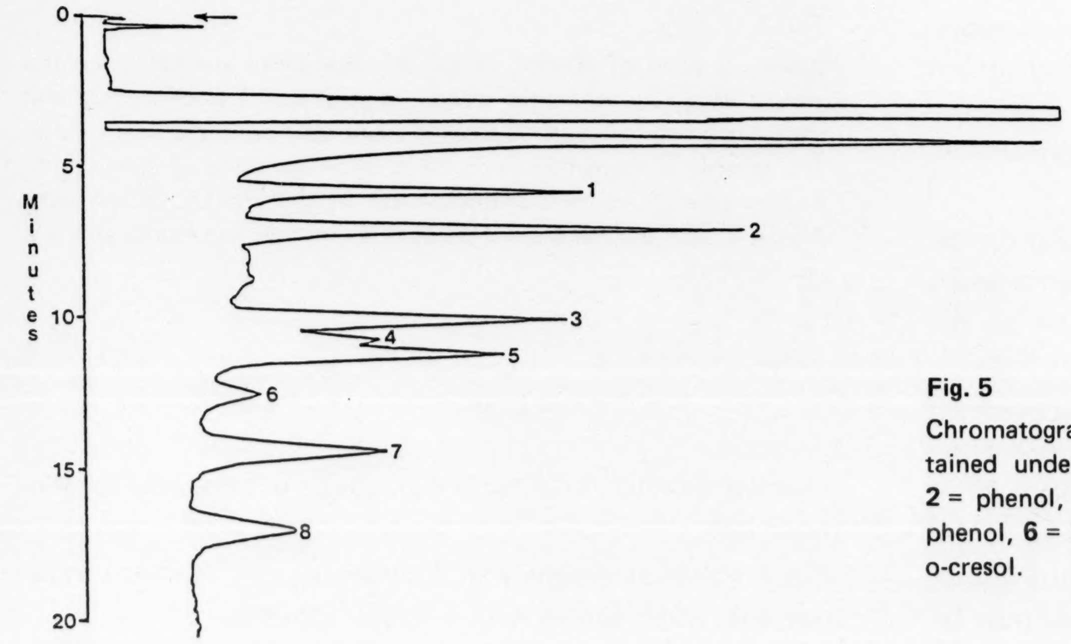

Fig. 5

Chromatogram of river water 'spiked' with phenols ($5 \mu g l^{-1}$) obtained under described conditions. Peaks **1** = 2,6-dichlorophenol, **2** = phenol, **3** = 2-chlorophenol, **4** = 4-chlorophenol, **5** = 3-chlorophenol, **6** = 2,4-dichlorophenol, **7** = 4-chloro-m-cresol, **8** = 4-chloro-o-cresol.

Table I. Precision of Analytical Results

Solution	Standard deviation*/μg l^{-1} phenol			Mean concn. found μg l^{-1} phenol
	s_w	s_b	s_t	
Blank (Borehole water)	0.006(5)	–	–	0.022
0.50μg l^{-1} phenol	0.019(5)	N.S. (4)	0.023(6)	0.483
1.00μg l^{-1} phenol	0.034(5)	N.S. (4)	0.038(6)	1.000
R. Dee water	0.012(5)	0.021(4)	0.025(4)	0.023
Dee + 1.00μg l^{-1} phenol	0.063(5)	0.054(4)	0.083(7)	1.048

* Figures in parentheses are the degrees of freedom. N.S. indicates that the result is not statistically significant.

be switched back to the load position. Baseline drift normally associated with electrochemical detectors was hardly evident in manual laboratory use and the only problems the authors can foresee with the automation of the system is blockage of columns and guard cartridges with particulate matter present in the river water.

Conclusions

The proposed method is simple, rapid and with satisfactory precision and detection limit. The method is economical on running costs and requires the minimum of maintenance.

The method has been used to good effect in the monitoring of phenols and cresols following pollution incidents in tributaries of the River Dee, enabling a more comprehensive analysis profile of the pollution than would otherwise have been possible. It has the potential for the determination of many other compounds and for use in an automated role.

Acknowledgements

The authors would like to thank Mr. J. B. Oldfield, Chief Executive of the North West Water Authority for permission to present this paper and to Mr. A. M. Sumner, Mr. S. Rodham and Miss J. P. Edwards for useful discussions and support.

References

[1] Council Directive on the Quality of Water Intended for Human Consumption, Off. J. Eur. Commun., August 1980, No. L229/11 (80/778/EEC).

[2] *P. J. Rennie*, Analyst, **107**, 327 (1982).

[3] *E. Lindley, P. J. Rennie*, "Phenolic Compounds in Potable Water Treatment-Effects and Analytical Review", paper presented to the Scientific Section of the Institute of Water Engineers and Scientists, Matlock, Derbyshire, September 9th (1981).

[4] *J. V. Geil, J. Schaefer, H. Kraenzler*, Gewässerschutz, Wasser, Abwasser, **67**, 229 (1983).

[5] EDT Research, Lab. Equip. Dig., April (1985).

[6] *S. F. Mitchell, P. J. Rennie*, Chromat. Intern., **19**, 35 (1986).

[7] *U. Palmquist, A. Ronlan, V. D. Parker*, Acta Chem. Scand. Ser. B., **24**, 267 (1974).

[8] *A. Ronlan, V. D. Parker*, J. Chem. Soc., **19**, 3214 (1971).

[9] *A. Capon, R. Parsons*, J. Electroanal. Chem., **65**, 285 (1975).

Received: June 30, 1987
Accepted: July 23, 1987
F

Influence of Silica Gel Pretreatment and Bonding Technique on PAH Selectivity of Octadecyl Bonded Phases

P. J. van den Driest* / H. J. Ritchie

Chrompack International, Research and Development Department, P. O. Box 8033, NL-4330 EA Middelburg, The Netherlands

Key Words

Column liquid chromatography
Silica gel pretreatment
Octadecyl bonded phase
Polycyclic aromatic hydrocarbons

Summary

The effect of silica gel pretreatment and of different bonding techniques, on the chromatographic properties of octadecyl bonded phases is described. The experiments show that a monomeric octadecyl bonded phase, prepared from silica gel that has not been treated before bonding, has a poor selectivity towards polycyclic aromatic hydrocarbons (PAHs) and shows high adsorption of basic components. Silica gel treatment before the bonding of the monofunctional silane does not give a substantial improvement. Polymeric phases on the other hand show a much better PAH selectivity and a lower adsorptivity towards basic components. Further improvement can be achieved with the polymeric modification if silica gel treatment is carried out before bonding.

Introduction

The properties of silica gel alkyl bonded phases depend on many variables including surface area, pore size, pore structure and pore volume [1, 2]. The particle shape, size and size distribution also have influence on the behaviour of the bonded phase [3]. Besides these physical parameters the chromatographic performance is undoubtedly affected by the chemical composition of the silica gel. Multiple interactions, due to the presence of accessible residual silanol groups and trace impurities, can lead to poor chromatographic peak shapes, which become more obvious with polar basic components [4]. Removal of the impurities by boiling with hydrochloric acid can result in improved properties of the silica gel bonded phase [5]. Treatment of the silica gel with aqueous acids and bases prior to bonding is also observed to result in changes in the chromatographic behaviour of the bonded phase [1, 6].

On the dry and fully hydroxylated silica surface, the hydroxyl groups are present as isolated silanol groups, vicinal or associated silanol groups and geminal silanols. There may also be physically bound water present on the surface. The different hydroxyl groups are not all equivalent in their behaviour in adsorption or in chemical reactivity [7]. It is believed that unfavourable adsorption of basic components and low hydrolytic stability of alkyl bonded phases is due to the presence of isolated silanol groups [8]. Silica supports, containing the highest possible concentration of homogeneously distributed associated silanol groups, can result in bonded phase packings with higher hydrolytic stability and substantially lower adsorptivity towards basic components. These silica supports can be obtained by dehydroxylation of the silica followed by rehydroxylation in water or basic or acidic aqueous solutions [9].

Besides the properties of the silica base material the properties of the bonded phase are strongly dependent on the type of silane used and the bonding technique. These determine the carbon loading, surface coverage and the number of accessible residual silanol groups [1, 10–12].

Endcapping of the residual silanol groups can have the effect of improving the chromatographic properties [13].

The chromatographic performance of the bonded phase is ultimately dependent on the conditions under which it is evaluated [14–16]. In this work we examined the effect of silica gel pretreatments in combination with different bonding techniques, which result either in monomeric or polymeric octadecyl bonded phases. The silica gels before and after treatment were characterised with nitrogen adsorption measurements and ^{29}Si cross-polarization magic-angle-spinning nuclear magnetic resonance spectroscopy. The bonded phases were evaluated by carbon analysis and chromatographic tests with polycyclic aromatic hydrocarbons and organic bases.

Experimental

Reagents

An experimental silica gel was used in this study (5μm spherical particles) from Chrompack International, Middelburg, The Netherlands. Dimethyloctadecyldimethylaminosilane was purchased from EPFL, Lausanne, Switzerland. Octadecyltrichlorosilane, trimethylchlorosilane, hydrofluor-

0009-5893/87 0324-05 $03.00/0

© 1987 Friedr. Vieweg & Sohn Verlagsgesellschaft mbH

ic acid (48%) and all the HPLC-grade solvents used in syntheses and chromatographic separations were obtained from Merck, Darmstadt, F.R.G.. Solvents used in syntheses were dried on molecular sieves from B.D.H. Chemicals, Poole, England, which were activated before use by heating at 350°C under dry nitrogen. Mixtures of 16 PAHs were prepared from dilute solutions of the pure components in methanol obtained from Chem Service, West Chester, England. Pyridine and N,N-diethylaniline were supplied by Aldrich-Chemie, Steinheim, West-Germany.

Silica Gel Pretreatment

The silica gel was dehydroxylated by heating at 450°C under dry nitrogen. The temperature at which complete removal of silanol groups is achieved can cause a change in the morphology of the silica gel. Therefore, the dehydroxylation temperature was held below that at which sintering would occur. This dehydroxylation was carried out for a fixed time (5 hours); heating for longer periods was shown to have no effect. After cooling to room temperature, the silica sample was refluxed in an aqueous hydrofluoric acid solution for 3 days. The concentration of the acid has an optimum range. If the concentration is too low the effect of pretreatment is negligible. At too high a concentration ($>$ 0.2%) a change in surface morphology is observed, resulting in a decrease in surface area of the silica gel support. After the rehydroxylation the suspension was allowed to cool to room temperature and the treated silica gel was filtered, washed with water to neutrality and finally washed with acetone and dried at 120°C for 16 hours.

Bonded Phase Syntheses

Before bonding, each silica gel sample was dried at 120°C for 16 hours to remove most of the physically adsorbed water. At the temperature required to remove all physically adsorbed water, some loss of silanol groups would occur. Monomeric phases with a maximum achievable surface coverage were prepared by reaction with dimethyloctadecyldimethylaminosilane. The polymeric phases were prepared using octadecyltrichlorosilane in a two stage reaction. The first stage was carried out in the absence of water, creating a monolayer on the silica surface. In the second stage water was added, leading to the formation of a polymeric phase. The procedures, which have been described [17], resulted in phases with reproducible phase loadings. Some phases were endcapped by refluxing (3g) in a mixture of trimethylchlorosilane (20ml) and dry toluene (30ml) over a period of 5 hours. Before endcapping the polymeric phases, any remaining chlorine atoms were hydrolysed with water, after which the phases were well dried at 120°C.

Chromatographic Experiments

All phases prepared were packed in 100 × 3mm ChromSep columns (Chrompack International, Middelburg, The Netherlands) using high pressure slurry-packing methods [18].

The chromatographic evaluations were performed with a liquid chromatograph consisting of a Spectra Physics SP 8700 solvent delivery system, 10μl Valco loop injector and a Perkin Elmer LC95 spectrophotometric detector operated at 254nm. Data were collected on-line and analyzed by a Trivector data acquisition computer system. All columns were thermostated at 25°C and mobile phases were carefully degassed by helium before use.

Freshly prepared columns were initially tested using acetonitrile-water (70-30%) at a flow of 0.4ml/min. Columns with platenumbers above 70000 plates/m calculated for fluoranthene were used for further study.

The column selectivity was determined using a mixture of the 16 PAHs on the U.S. Environmental Protection Agency's priority polutant list [19]. This mixture was chromatographed isocratically using acetonitrile-water (78-22%) at a flowrate of 1.0ml/min.

The adsorptivity towards basic components was tested with pyridine and N,N-diethylaniline. Toluene was added to this test mixture in order to check the column efficiency during the evaluation of the column. The eluent used was acetonitrile-water (70-30%) with a flow of 1.0ml/min.

Physical and Chemical Characterization

^{29}Si cross-polarization magic-angle-spinning NMR (^{29}Si-CP-MAS NMR) was used to determine the amount of different silanol groups before and after silica gel pretreatment. Spectra were obtained on a Bruker CXP-300 NMR spectrometer. The physical properties of the silica gel samples before and after pretreatment as well as the resultant bonded phases were measured using nitrogen adsorption methods. The data were obtained with a DigiSorb 2500 analyser from Micromeritics. From the BET isotherm the surface area, the total pore volume and the mean pore diameter were calculated.

Each of the synthesized bonded phases was also characterized by carbon analysis, which was performed on a Perkin Elmer 240C analyser.

Results and Discussion

The results of the physical and chemical characterisation of the silica gel samples are summarised in Table I. This data shows that the pretreatment does not significantly change the physical properties of the silica gel. However, due to

Table I. Properties of the silica gel before and after pretreatment.

Silica gel*	BET surface area (m^2/g)	Total pore volume (cm^3/g)	Mean pore diameter (nm)	Relative % silanol	
				≡SiOH	=Si(OH)$_2$
A	180	0.61	12	99	1
B	172	0.61	14	90	10

* Silica gel A: untreated silica gel
Silica gel B: pretreated silica gel A

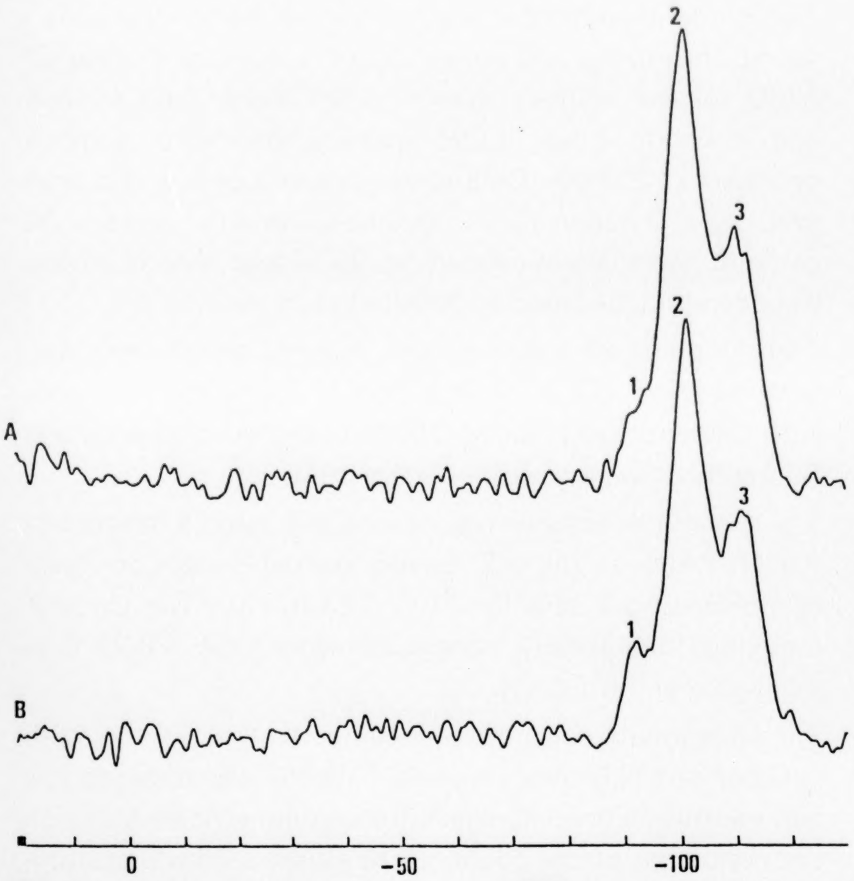

Fig. 1
^{29}Si-CP-MAS NMR spectrum of untreated silica gel (A) and pretreated silica gel (B); peak 1 := $Si(OH)_2$; peak 2 :≡ SiOH; peak 3 = $Si(OSi)_4$.

the pretreatment, the chemical properties of the gel have been altered. The results of the ^{29}Si-CP-MAS NMR spectroscopy indicate that the pretreatment has altered the relative silanol concentration on the gel surface. The NMR spectra (Fig. 1) show that the total concentration of silanol groups is not changed after pretreatment, while the geminal hydroxyl to single hydroxyl ratio is increased. In Table II the surface area, pore volume and mean pore diameter of the bonded phases prepared are given. As expected, the values of these properties are all lower than those of the unmodified silica gels. In each phase the percentage of carbon was independent of the method of bonding. Endcapping did not increase the carbon loading on any of the phases.

The evaluation of the prepared phases shows that the differences in the properties of the silica supports and the resulting bonded phases were reflected in the chromatographic performance. Under the isocratic chromatographic conditions employed, three pairs of PAHs were partially or completely unresolved on the monomeric phases. In Fig. 2A and 2B the poor resolution of acenaphthene and fluorene (peaks 3 and 4), benz(a)anthracene and chrysene (peaks 9 and 10) and benzo(ghi)-perylene and indeno-(1,2,3-cd)pyrene (peaks 15 and 16) is shown. This is in agreement with the observations of Sander and Wise [17]. The polymeric phases were found to be more selective towards the PAH probes (Fig. 2C and 2D). In contrast to the monomeric phases, further improvement in selectivity was seen when the silica gel was given pretreatment as described.

All the phases prepared showed different adsorptivity towards basic components. The monomeric phases (Fig. 3A and 3B) gave poor peaks for both pyridine and N,N-diethylaniline. Some improvement for these components was seen when pretreatment was carried out prior to bonding. The improvement was more pronounced for N,N-diethylaniline. Both basic test solutes showed substantially lower adsorptivity on the polymeric phases (Fig. 3C and 3D). The best peak shapes were observed when the polymeric bonded phase was prepared from pretreated silica gel. The retention mechanism which completely describes the selectivity of PAH solutes on alkyl bonded phases undoubtedly contains contributions from several factors [12, 20]. The primary retention mechanism for these components is assumed to be solvophobic interactions between the solutes, the mobile phase and the stationary phase [14]. From the observations made with the monomeric phases, it is clear that the retentive capacity and selectivity towards PAHs is not affected by pretreatment. However the adsorptivity towards basic solutes was decreased as a result of pretreatment. This effect was more pronounced for the larger, and therefore more sterically hindered N,N-diethylaniline.

The hydroxyl groups on the bare silica surface are present as isolated silanol groups, vicinal or associated silanol groups and geminal silanols [7]. Geminal silanol groups are believed to be more reactive towards the silane reagent [9]. The pretreatment of the silica gel has been seen to in-

Table II. Properties of the octadecyl bonded phases.

Bonded phase	Silica gel* used	Phase type	BET surface area (m^2/g)	Total pore volume (cm^2/g)	Mean pore diameter (nm)	% Carbon
1	A	monomeric	90	0.30	10	12.9
2	A	monomeric, endcapped				13.0
3	B	monomeric	90	0.31	10	12.5
4	A	polymeric	100	0.31	10	12.1
5	B	polymeric	99	0.30	9	12.8
6	B	polymeric, endcapped				12.8

* Silica gel A: untreated silica gel
Silica gel B: pretreated silica gel A

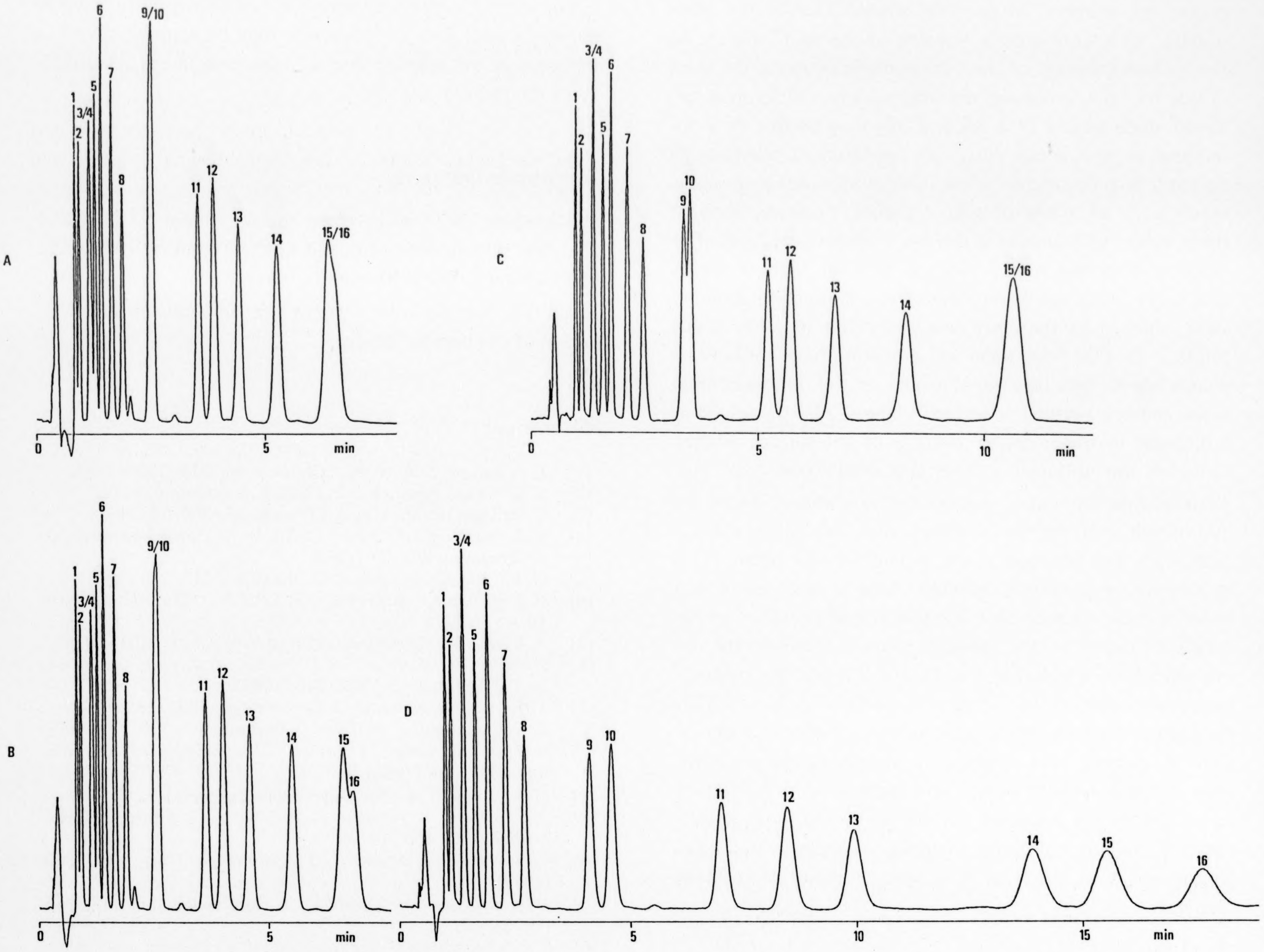

Fig. 2

PAH separation on the octadecyl bonded phases. A: monomeric phase on untreated silica gel; B: monomeric phase on pretreated silica gel; C: polymeric phase on untreated silica gel; D: polymeric phase on pretreated silica gel. Peak identification: **1** = Naphthalene; **2** = Acenaphthylene; **3** = Acenaphthene; **4** = Fluorene; **5** = Phenanthrene; **6** = Anthracene; **7** = Fluoranthene; **8** = Pyrene; **9** = Benz(a)anthracene; **10** = Chrysene; **11** = Benzo(b)fluoranthene; **12** = Benzo(k)fluoranthene; **13** = Benzo(a)pyrene; **14** = Dibenzo(a,h)anthracene; **15** = Benzo(ghi)perylene; **16** = Indeno-(1,2,3-cd)pyrene.

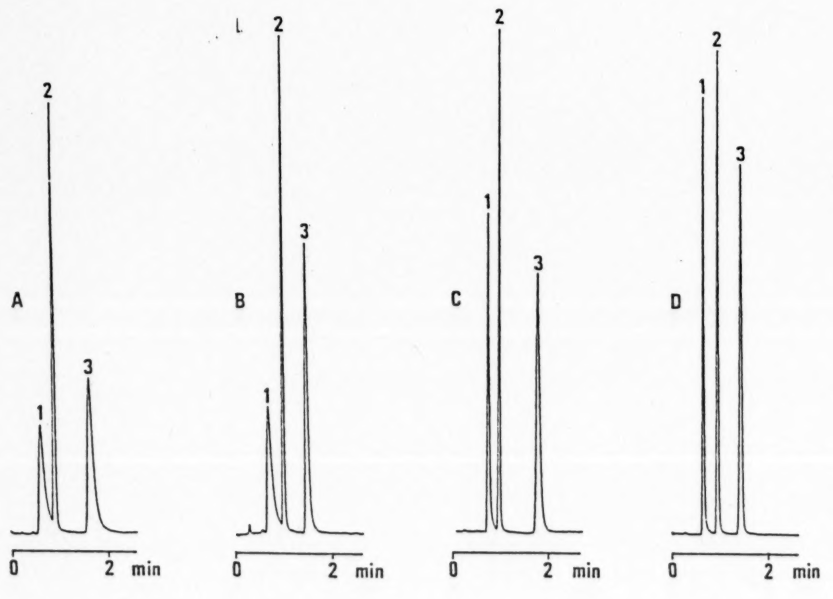

Fig. 3

Separation of pyridine (peak 1), toluene (peak 2) and N,N-diethylaniline (peak 3) on octadecyl bonded phases; A: monomeric phase on untreated silica gel; B: monomeric phase on pretreated silica gel; C: polymeric phase on untreated silica gel; D: polymeric phase on pretreated silica gel.

crease the number of geminal silanols, while the total number of silanol groups remains unaltered (Table I). As the surface coverage of both monomeric phases is the same (Table II), the observed chromatographic difference between these phases (Fig. 3A and 3B) may be due to a difference in the accessibility of the residual silanols. In bonding the pretreated silica, the monofunctional silane reacts with all types of silanol groups, however, each of these types will possess a different reactivity [2, 8]. The reaction with the highly reactive geminal silanols results in a single hydroxyl being located very close to the bonded alkyl chain, and therefore less accessible to larger basic solutes. In the first stage of preparation of polymeric phases one or two functional groups of the polyfunctional silane can react with the surface silanols [2]. This results in a decrease in the primary coverage of the surface relative to that of the monomeric phases discussed above.

After adding the water, the remaining chlorine atoms are hydrolysed and further reaction with the silica surface hydroxyls and between silane molecules will occur [17]. In this way a polymeric bonded phase is built up with a lower number of accessible residual silanol groups. The reduced influence of the residual silanols is shown by the improved PAH selectivity (Fig. 2C and 2D) and the substantially lower adsorptivity of organic bases (Fig. 3C and 3D). Pretreatment of the silica gel, creating a higher number of geminal silanols, was effective in improving the performance of the polymeric phase. This improvement is thought to be due to the increased number of bifunctional attachments of the polyfunctional silane to the adjacent hydroxyl groups and thus resulting in a lower number of residual silanols.

Conclusions

The chromatographic performance of octadecyl bonded phases is strongly influenced by both the properties of the silica gel support and the bonding method.

The surface of the silica gel studied was seen to have a higher number of geminal silanol groups after acidic treatment. Bonding a polyfunctional ligand onto these supports was seen to give both a unique selectivity towards polycyclic aromatic hydrocarbons and less adsorptivity towards organic bases. This improvement may be associated with a decrease of the number and or a decrease in the accessibility of the residual silanols.

Acknowledgements

H. Claessens, Dr. J. W. de Haan and M. Hetem for the NMR analyses, which were obtained at the Technical University of Eindhoven, The Netherlands.

J. van Gils for his assistance in the preparation and evaluation of the bonded phases.

References

[1] *L. C. Sander, S. A. Wise*, J. Chromatogr., **316**, 163 (1984).
[2] *K. K. Unger*, Porous Silica, Elsevier, Amsterdam, 1979.
[3] *C. Dewaele, M. Verzele*, J. Chromatogr., **260**, 13 (1983).
[4] *G. Schomburg, A. Deege, J. Köhler, U. Bien-Vogelsang*, J. Chromatogr., **282**, 27 (1983).
[5] *M. Verzele, C. Dewaele*, J. Chromatogr., **217**, 399 (1981).
[6] *H. Engelhardt, B. Dreyer, H. Schmidt*, Chromatographia, **16**, 11 (1982).
[7] *R. K. Iler*, The Chemistry of Silica, Wiley, New York, 1979.
[8] *J. Köhler, D. B. Chase, R. D. Farlee, A. J. Vega, J. J. Kirkland*, J. Chromatogr., **352**, 275 (1986).
[9] *J. Köhler, J. J. Kirkland*, J. Chromatogr., **385**, 125 (1987).
[10] *G. E. Berendsen, L. de Galan*, J. Chromatogr., **196**, 21 (1980).
[11] *H. Figge, A. Deege, J. Köhler, G. Schomburg*, J. Chromatogr., **351**, 393 (1986).
[12] *L. C. Sander, S. A. Wise*, Anal. Chem., in press.
[13] *C. J. Little, J. A. Whatley, A. D. Dale, M. B. Evans*, J. Chromatogr., **171**, 435 (1979).
[14] *C. Horvath, W. Melander*, J. Chromatogr. Sci., **15**, 393 (1977).
[15] *J. Chmielowiec, H. Sawatzky*, J. Chromatogr. Sci., **17**, 245 (1979).
[16] *P. J. Schoenmakers*, Optimization of chromatographic selectivity, Elsevier, Amsterdam, 1986.
[17] *L. C. Sander, S. A. Wise*, Anal. Chem., **56**, 504 (1984).
[18] *J. H. Knox*, High Performance Liquid Chromatography, Edinburgh University Press, Edinburgh, 1978; p. 148.
[19] *R. Amos*, J. Chromatogr., **204**, 469 (1981).
[20] *S. A. Wise, W. J. Bonnett, F. R. Guenther, W. E. May*, J. Chromatogr. Sci., **19**, 457 (1981).

Received: June 30, 1987
Revised manuscript
received: Aug. 10, 1987
Accepted: Aug. 12, 1987
F

HPLC Quantification of rDNA Polypeptides Like Insulin Precursors Produced in Yeast

L. Snel* / U. Damgaard / I. Mollerup

Novo Research Institute, Novo Alle, DK-2880 Bagsvaerd, Denmark

Key Words

Reversed-phase HPLC
Insulin precursor
Yeast fermentation broth
Peptide quantification

Summary

A reversed-phase HPLC system for the quantification of recombinant DNA insulin precursors in yeast fermentation broth is described. HPLC monitoring of the polypeptide can be achieved without interference from substrate components or proteins stemming from the host cell, thus serving to determine the optimum harvesting time. Furthermore, it is demonstrated how different amino acid links of the insulin A- and B-chains affect the chromatographic behaviour of the insulin precursor making it possible to identify each precursor by its retention on the reversed phase support.

Introduction

Human insulin precursors can be produced from strains of Saccharomyces cerevisiae using recombinant DNA technology [1, 2].

The expression levels were originally determined by radioimmunoassay (RIA) of immunoreactive insulin [3] exported into the fermentation broth. This RIA method encountered the problem of estimating not only correctly folded and processed insulin precursors but also insulin-like components, e.g. unprocessed insulin precursors and insulin precursor derivatives, thus overestimating the expression level. Therefore the aim of the present study was to develop an HPLC method capable of quantifying and identifying insulin precursors directly in the fermentation broth. Since the first separation of porcine and bovine insulin by reversed phase HPLC [4], numerous reports have described HPLC of insulin and insulin-related substances (reviews, see [5, 6]), but HPLC quantification of insulin or insulin precursors in a fermentation medium has not been reported.

Experimental

Yeast Fermentation

The yeast strains containing plasmids encoding 7 different single-chain insulin precursors (see Fig. 1) were grown on a YPD medium at 30°C [7]. Cells were spun down and the supernatant subjected to RIA and HPLC analyses.

Radioimmunoassay

RIA for immunoreactive insulin was performed as described [3] using semisynthetic human insulin as a standard (Novo Industri A/S).

Reversed-Phase HPLC

The HPLC equipment (Waters Associates) consisted of two M510 pumps, a WISP 710B, a M440 UV detector equipped with a 214 nm extended wavelength module and a 840 chromatography control station. Column dimensions were 4 × 250 mm packed with LiChrosorb RP-18, 5 μm particles

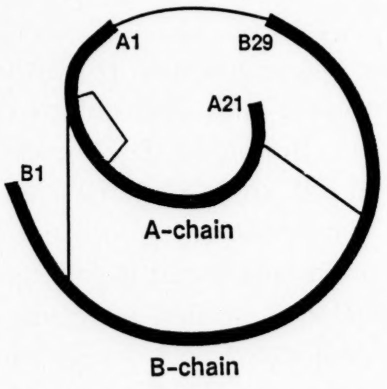

Fig. 1

Insulin precursors (mini proinsulins) with different links between residue B29 and residue A1.

Precursor 1. B ——————A;
Precursor 2. B —SerLys— A;
Precursor 3. B–ThrArgArg–A;
Precursor 4. B–ThrLysArg–A;
Precursor 5. B–ThrArgLys–A;
Precursor 6. B–ThrLysLys–A;
Precursor 7. B–AlaAlaLys–A.

0009-5893/87 0329-04 $03.00/0

© 1987 Friedr. Vieweg & Sohn Verlagsgesellschaft mbH

(Merck) or with Nucleosil RP-18, 5μm particles (Macherey-Nagel). The guard column was a 4 × 30mm Hibar steel column (Merck) packed with Nucleosil RP-18, 10μm particles (Macherey-Nagel).

Column temperature was 50–54°C (guard column ambient temperature) and the flow rate 1.0ml/min.

Two solvent systems were used.

Mobile phase system 1:

A. 0.25M ammonium sulphate, 10% acetonitrile, pH adjusted to 2.5 with sulphuric acid.

B. 50% acetonitrile.

Mobile phase system 2:

A. 0.04M phosphoric acid, 0.2M sodium sulphate, 10% acetonitrile, pH adjusted to 2.5 with ethanolamine.

B. 50% acetonitrile.

HPLC analysis of the yeast fermentation broth was performed by loading cell-free supernatant onto the RP-column and eluting isocratically at 58% A/42% B. These conditions ensured a k' of approximately 10.

Calibration of the peak area was achieved by running 10μl samples of a standard solution (0.918mg/ml) of porcine monocomponent insulin (Novo Industri A/S) under the isocratic conditions of 52% A/48% B.

Reproducibility was checked by pooling 17 duplicate runs of the insulin standard and calculating the standard deviation of the peak area response.

Recovery analyses were carried out in two ways:

1. Injection of 5μl of insulin standard solution onto a LiChrosorb RP-18 column followed by an injection of the same amount of insulin onto an empty column and comparison of the peak areas obtained (injection noise excluded).
2. Spiking of a fermentation supernatant containing a known amount of insulin precursor with a standard solution (0.1mg/ml in 0.01M formic acid) of the same insulin precursor in a highly purified form.

Electrophoresis and Immunoblotting

SDS-PAGE was performed according to Laemmli [8] with 10–20% acrylamide gradient. Proteins were electroblotted onto nitrocellulose sheets (0.2μm, Schleicher & Schuell) in 0.02M phosphate buffer pH 8.0 containing 10% 2-propanol for 2 hours at 40V. Immunodetection was performed using either polyclonal antibodies raised in rabbits against yeast proteins or monoclonal antibodies against insulin. Horseradish peroxidase conjugated goat antirabbit and goat antimouse IgG serum (TAGO Inc., USA) was used as a detecting antibody.

Chemicals

All chemicals used were of analytical or HPLC grade. Water was of Milli-Q quality (Millipore).

Results and Discussion

Quantification of Insulin Precursors

Two reversed phase separation systems have been tested. The first one having ammoniumsulphate in the mobile phase is commonly used [5] whereas the second RP-HPLC system was originally developed in our laboratory and has been routinely used for HPLC analysis of insulin, glucagon and related substances.

Yeast fermentation broth was subjected to both HPLC systems. Fig. 2 shows that identical peak shape and peak area of the insulin precursor were obtained.

A relatively high column temperature was chosen, because it was observed that the retention of the insulin precursor increased with increasing temperature, whereas retention of fermentation components decreased. The high column temperature helped to mediate a $k' > 5$ for the precursor peak which was necessary to avoid overshaddowing by the strong UV absorbing fermentation components eluting during the first 10 minutes (see Fig. 2).

The HPLC chromatograms of Fig. 3 show how overlapping substrate and insulin precursor peaks can be separated by changing the column temperature, thus facilitating the quantitation of the insulin precursor. A demonstration of the absence of yeast proteins in the insulin precursor peak is given in Fig. 4. Using the immunoblotting technique after SDS polyacrylamide electrophoresis the insulin precursor isolated from the HPLC analysis of the fermentation broth is shown to contain no detectable yeast proteins (Fig. 4, lane 2).

These results show that by choosing the appropriate HPLC conditions quantification of the expression levels of insulin precursor is achieved without interference from substrate components or proteins stemming from the yeast cell.

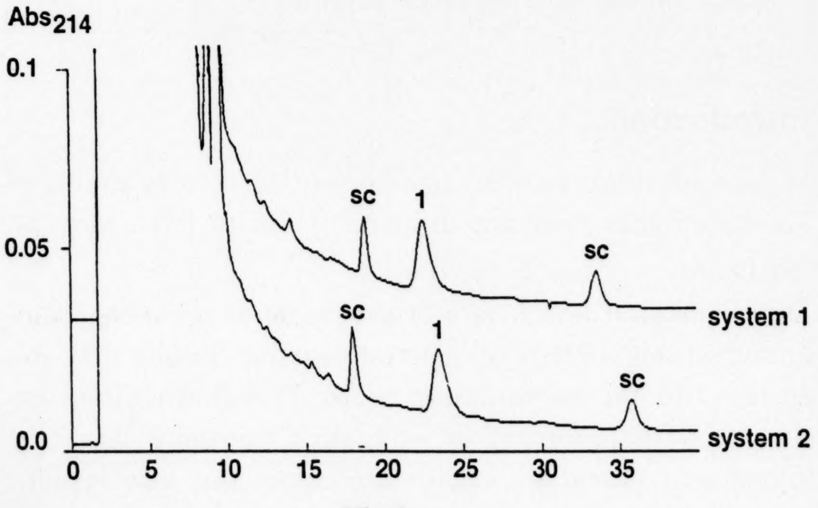

Fig. 2

HPLC chromatograms of yeast fermentation broth on LiChrosorb RP-18.

Isocratic elution at 26.8% acetonitrile (58% A/42% B) with mobile phase system 1 containing ammonium sulphate (upper track) and mobile phase system 2 containing sodium sulphate and ethanolamine (lower track). Column temperature: 50°C. 150μl of fermentation supernatant injected. Peaks: **1** = insulin precursor 1; **SC** = substrate component.

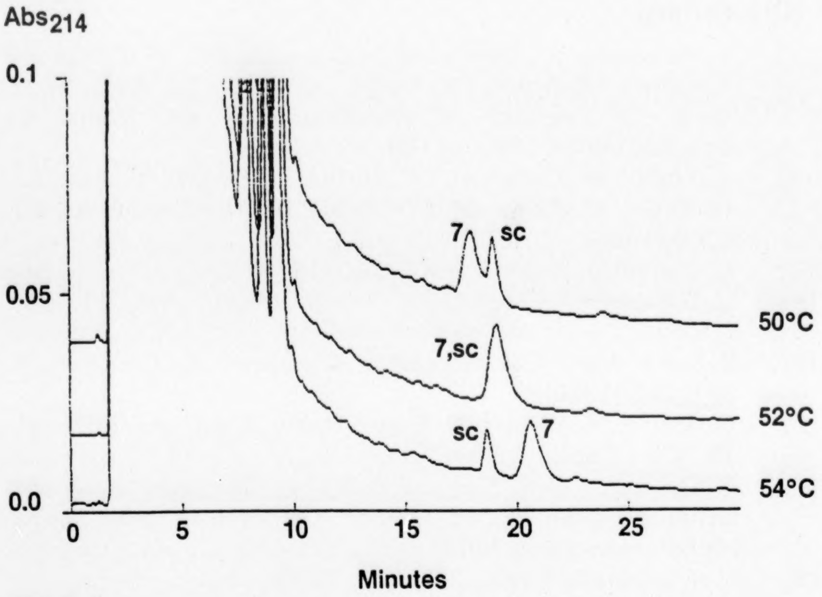

Fig. 3

Influence of column temperature on the retention of insulin precursor 7 and a substrate component during RP-HPLC of yeast fermentation broth.

Column: LiChrosorb RP-18, 5μm. Isocratic elution at 26.8% acetonitrile (58% A/42% B) with mobile phase system 2 containing sodium sulphate and ethanolamine. Column temperatures 50°, 52° and 54°C as indicated. 150μl of fermentation supernatant injected. Peaks: **7** = insulin precursor 7; **SC** = substrate component.

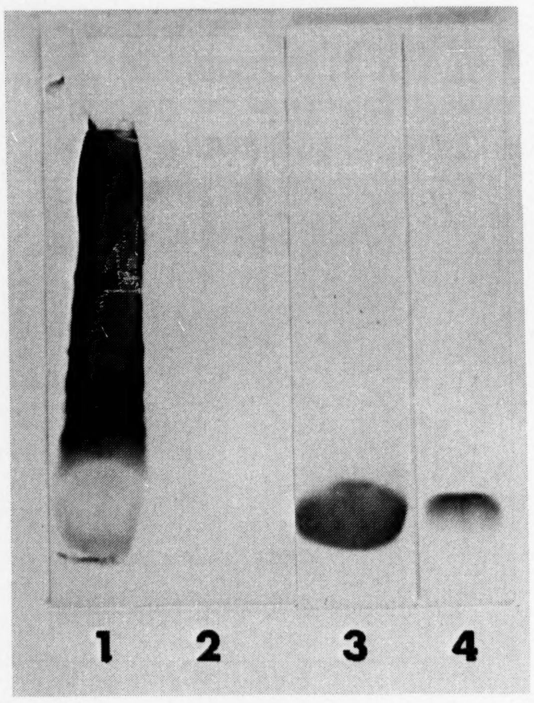

Fig. 4

Immunoblotting after SDS-PAGE.

Samples containing insulin precursor 7: Lane **1** Fermentation broth, load 40μl; Lane **2** Isolated precursor peak from HPLC, load 10μg; Lane **3** Same as lane 1; Lane **4** Pure precursor 7, load 0.25μg. Lanes **1** and **2** detected with polyclonal rabbit antibodies against yeast proteins. Lanes **3** and **4** detected with monoclonal antibody against insulin.

Consequently HPLC monitoring of the production level during fermentation can serve to determine the optimum harvesting time.

Recovery of the HPLC analysis is 99% and reproducibility is better than 99%. The detection limit is 0.3–0.5 mg insulin precursor per litre fermentation broth depending on the sample volume injected.

RIA analyses of fermentation broth showed strong dilution effects and the correlation of RIA and HPLC results indicated that RIA overestimated the expression level of insulin precursor by a factor of approximately 2.5 (data not shown). Therefore it is preferred to use the faster and more precise HPLC analysis for precursor expression levels above 0.3 mg per litre fermentation broth, whereas the extremely high sensitivity of RIA is useful for the determination of very low expression levels.

Separation of Insulin Precursors

The chromatographic behaviour of 4 different insulin precursors on two RP-columns from different manufacturers are shown in Fig. 5. It can be seen that the Nucleosil RP-18 column does not resolve insulin precursors 1 and 4, whereas the LiChrosorb RP-18 column separates all 4 insulin precursors. In fact, the LiChrosorb column separated all 7 insulin precursors in the following order of hydrophobicity (precursor 1 being the most hydrophobic): $k' = 10.0$ (precursor 1), $k' = 9.0$ (precursor 2), $k' = 8.8$ (precursor 3), $k' = 8.5$ (precursor 4), $k' = 8.2$ (precursor 5), $k' = 7.8$ (precursor 6) and $k' = 6.5$ (precursor 7).

The difference in hydrophobicity makes it possible to identify each precursor by its retention time. This is ex-

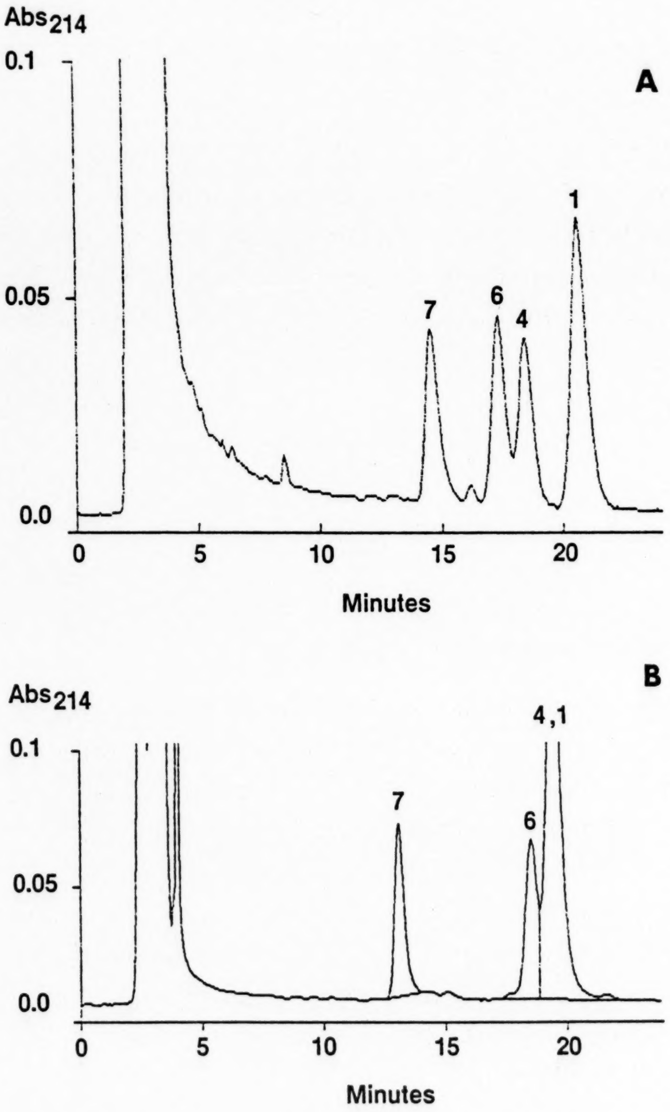

Fig. 5

HPLC separation of various insulin precursors on LiChrosorb RP-18 (panel A) and Nucleosil RP-18 (panel B).

Isocratic elution at 27.2% acetonitrile with mobile phase system 2 (57% A/43% B). Sample: Mixture of 1 μg insulin precursor 7 (peak **7**), 1 μg insulin precursor 6 (peak **6**), 1 μg insulin precursor 4 (peak **4**) and 2 μg insulin precursor 1 (peak **1**). Column temperature: 50°C.

tremely useful for the study of expression levels of yeast strains containing plasmid constructions encoding two different insulin precursor genes.

Furthermore, the HPLC quantitation and identification method described in this study might be applicable for studying expression levels of rDNA polypeptides similar to the insulin precursor, simply by adjusting the mobile phase composition.

Acknowledgements

We wish to thank Ms. Lis Gotfred and Ms. Anne-Marie Skov Sørensen for skilful technical assistance and Ms. Suzanne Pichard for the preparation of the manuscript.

References

[1] *J. Markussen, U. Damgaard, I. Diers, N. Fiil, M. T. Hansen, P. Larsen, F. Norris, K. Norris, O. Schou, L. Snel, H. O. Voigt*, in 'Peptides' (*D. Theodoropoulos*, ed.) Walter de Gruyter, Berlin, 1986; p. 189.

[2] *L. Thim, M. T. Hansen, K. Norris, I. Hoegh, E. Boel, J. Forstrom, G. Ammerer, N. P. Fiil*, Proc. Natl. Acad. Sci. **83**, 6766 (1986).

[3] *L. G. Heding*, Diabetologia **8**, 260 (1972).

[4] *U. Damgaard, J. Markussen*, Horm. Metab. Res. **11**, 580 (1979).

[5] *B. S. Welinder, H. H. Sørensen, B. Hansen*, J. Chromatogr. **361**, 357 (1986).

[6] *G. Seipke, H. Müllner, U. Grau*, Angew. Chem. Int. Ed. Engl. **25**, 535 (1986).

[7] *F. Sherman, G. R. Fink, J. B. Hicks*, 'Methods in Yeast Genetics', Cold Spring Harbor Laboratory, Cold Spring Harbor, New York, 1981.

[8] *U. K. Laemmli*, Nature **227**, 680 (1970).

Received: June 29, 1987
Accepted: Aug. 5, 1987
F

Preparative HPLC for Analysis of Mineralocorticoids in Human Plasma

C. Lejeune-Lenain* / S. Kina / D. Bosson

Chimie Médicale, Hôpital Saint-Pierre, Université Libre de Bruxelles, rue Haute, 322, 1000 Bruxelles, Belgium

Key Words

HPLC-RIA
Mineralocorticoids
Glucocorticoids
Adrenal steroids

Summary

A method has been developed to measure simultaneously in human plasma the mineralocorticoids and glucocorticoids involved in mineralocorticoid excess.

Briefly: plasma extracts were chromatographied in a fully-automated procedure on a lichrospher-diol column using a hexane:isopropanol:triethylamine gradient. Eluates were collected on a preprogrammed fraction collector. Final quantification was achieved by RIA on the selected fractions.

This procedure allowed: 1) the separation of each measured steroid from plasma contaminants; 2) precise collection; 3) quantification of mineralocorticoids with a precision and sensitivity equivalent to that of direct methods; and 4) improved specificity.

Introduction

The differential diagnosis of mineralocorticoid disorders requires the simultaneous estimation of various steroids in plasma. Unfortunately, their plasmatic concentrations, except for cortisol, are very low and direct measurements are only possible with very highly specific antibodies that are not readily available. This process entails the use of purification steps before final immunological quantification.

Numerous methods have previously been reported. All procedures, however, are too time-consuming to fit the requirements of a clinical laboratory. Only the method described by Schönshöfer in 1981 [1], involving a high performance liquid chromatography (HPLC) step prior to RIA, is suitable for complete automation. But Schönshöfer's technique allowed one to handle only one sample per hour with very high water blanks.

The aim of this work was to develop a fast, automated procedure capable of estimating, with high specificity and sensitivity on a single plasma sample, the major steroids involved in mineralocorticoid disorders: 11-deoxycorticosterone (DOC), 11-deoxycortisol (S), corticosterone (B), aldosterone (ALDO) and 18-hydroxycorticosterone (18-OHB). Simultaneous determination of progesterone (PRO) was designed to detect a possible block in 17-hydroxylase activity; estimation of F provided a reference for the overall glucocorticoids secretion.

Methods

Experimental Procedure

Equipment: The HPLC was a 5500 Varian (Wolnut Creek, CA 94598, USA), equipped with an autosampler and a Vista 402 computer loaded with a programme allowing complete automation of chromatography and fractions collection. The collector was a FRAC-300 (Pharmacia, Upsala, Sweden). The HPLC column (Lichrospher-100 Diol, from Merck, Darmstadt, Germany) had the following characteristics: length 250 mm; internal diameter 4 mm; particule diameter 5 μm.

Reagents: The organic solvents hexane (H), ethylacetate (EA), isopropanol (IP) and ethanol were of chromatographic analysis quality (Lichrosolv, Merck) and not further purified. Triethylamine (TEA) originated from Merck. The borate buffer (TBA) pH 8.2, used in the RIA, contained 2 g/l of bovine serum albumin (BSA) provided by Armour Pharmaceutical (Eastbourne, England). Albumin coated charcoal was 1.5 g/l of neutral norit (Fisher, New Jersey 07410, USA). Tritiated steroids (1,2,6,7)-^{3}H PRO, (1,2)-^{3}H DOC, (2,4,6,7)-^{3}H Estradiol, (1,2,6,7)-^{3}H B, (1,2,-6,7)-^{3}H ALDO, (1,2,6,7)-^{3}H F and (1,2)-^{3}H 180HB were obtained from Amersham (Little Chalfont, HP7 9NA, England) at a specific activity ranging from 50 to 100 Ci/mmoles. (1,2)-^{3}H S was provided by New England Nuclear (Dreieich 6072, West Germany) at an activity averaging 50 Ci/mmoles. They were repurified every month by the HPLC. Pure steroids were purchased from Steraloids (PO Box 310, Wilton, NH 03086, USA) and stored in ethanol containing 0.1% TEA. Antisera against PRO were obtained from Steranti (St. Albans, Herfs, England), against DOC and S from Radioassay System Laboratories (Carson, CA 90746), against ALDO from Diagnostic Product Corporation (DPC, Los Angeles, CA 90045), and against B

Correspondence: C. Lejeune-Lenain, I.R.I.B.H.N., Faculty of Medicine, Université Libre de Bruxelles, Campus Erasme, bât. C, 808, route de Lennik, 1070 Brussels, Belgium.

0009-5893/87 0333-06 $03.00/0

© 1987 Friedr. Vieweg & Sohn Verlagsgesellschaft mbH

and 18OHB from Endocrine Science (Tarzana, CA 91356). They were used at the dilution required to achieve 30–50% of maximum binding.

Treatment of sera: Sera (1.0 ml) were extracted by 10 ml of a mixture of H:EA:TEA (2:8:0.002) (v:v:v) after the addition of 10,000 CPM tritiated estradiol (E_2) to monitor the procedural losses. The supernatants were evaporated and prepared for the HPLC step; i.e., redissolved in 290 µl eluant mixture, filtered and 200 µl injected into the HPLC system.

The mobile phase was an H:IP gradient increasing from (93:7) to (87:13) (Fig. 1-a). All solvents contained 0.02% TEA. The solvent flow varied from 1.8 to 2.9 ml/min. The column temperature was set at 45°C and the UV detector wavelength at 254 nm. A complete chromatographic run lasted 27 min. For investigations requiring no 18OHB estimations, alternative chromatographic conditions were selected with slight modifications of the gradient, 88-12 to 85-15 (H:IP), and of the flow, 1.5 to 2.2 ml/min, allowing a faster chromatographical run of 17 min (Fig. 1-b).

The collection conditions were established taking into account a possible shift in the retention time due to the tube lengthening. Each new column was calibrated by collecting the mixture of the cold steroids and their radioactive markers added to a plasma at 0.2 min intervals (Fig. 2).

After chromatography and collection, the selected fractions were aliquoted in duplicate and evaporated before the performance of the RIA.

RIA procedure: The extract aliquots were incubated overnight at 4°C with the tritiated steroid and the corresponding antibody, the various amounts ranging from 6000 DPM for 18OHB, 9000 DPM (DOC, S, ALDO) and 14000 DPM (PRO). The bound fraction was isolated by centrifugation at 2°C after the addition, in the cold room, of 1 ml albumin-coated charcoal suspension. Computation of sample concentrations were performed on a Wang 2000, using the logit-log transform with a special RIA software. The individual procedural losses were corrected by measuring the recovery of the tritiated estradiol. Each assay included 7 additional standards, prepared by adding pure steroids to a low-content calf serum and 4 samples of human serum control material. The concentration of the additional standards and control material covered the physiological and pathological plasmatic range.

Cortisol was measured by the "coat-a-count" kit (DPC). The intra- and inter-assay coefficients of variation (CV) were inferior to 5 and 9%, respectively.

Results

Analytical Characteristics of the Various Steroid Assays

The mean performances of the last 12 assays are shown in Table I.

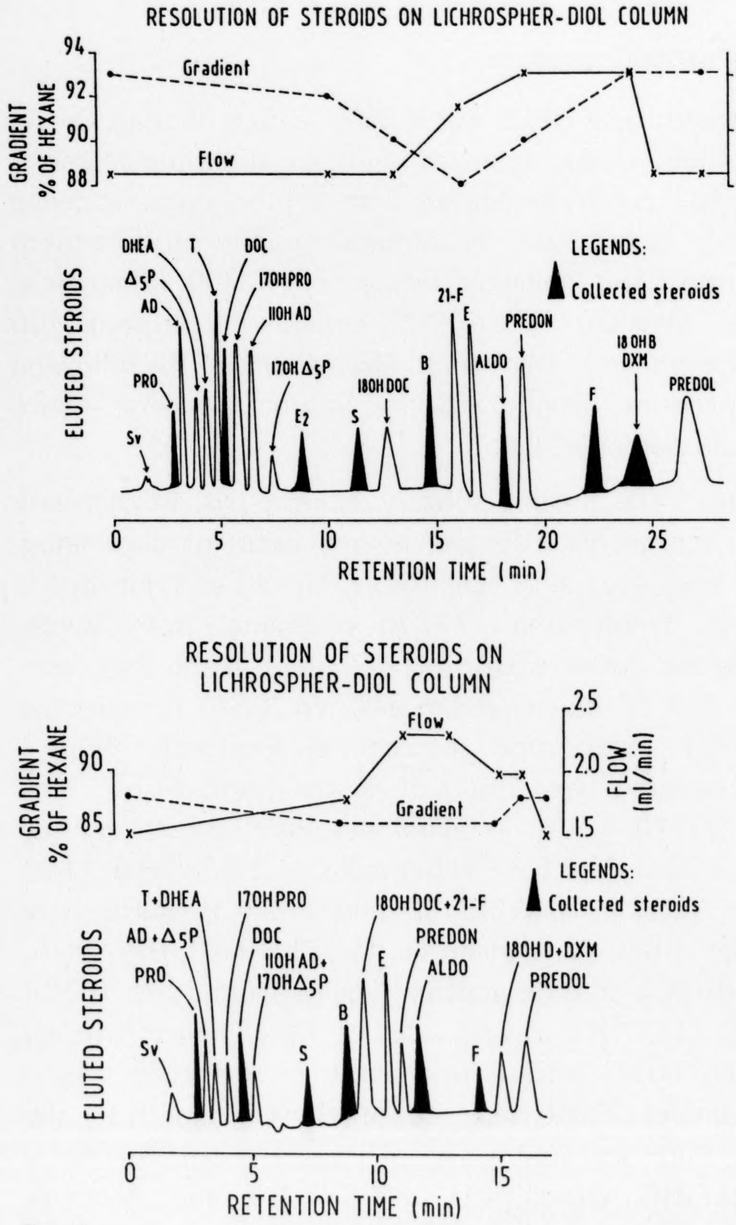

Fig. 1

(a-b) separation of adrenal steroids on a Lichrospher-diol column, using UV detection and 2 different (hexane: 2-propanol) gradients. The gradients in solvent composition and flow are represented on the upper part of the graphs. For abbreviations, see Table II.

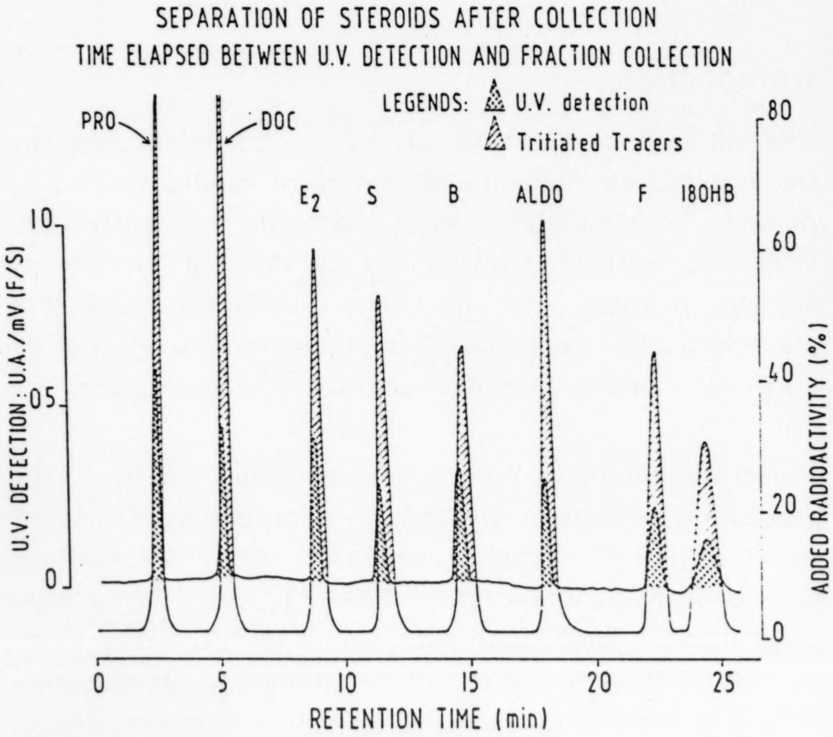

Fig. 2

Profile of a mixture of the eight collected steroids, observed by UV detection and after collection of the radioactive fraction.

1. Efficiency of extraction and recovery of chromatography were estimated as the mean recuperation of tritiated steroids added to a few plasma (n = 5) and submitted to the whole procedure. They were maximal for DOC, about 94%, and the lowest for ALDO and 18OHB, averaging 74%. As part of a daily routine, procedural losses on each estimated plasma sample were checked by using tritiated E_2 as the internal standard and were always found to be inferior to 10%.
2. Stability of the chromatographical parameters, depending upon the automated equipment, was proven by the low variability of the retention times, with interday coefficients of variation always inferior to 2%.
3. Assessment of the RIA:
   - the limit of detection ranged from 0.02 to 4 ng/ml serum, according to the physiological levels of each steroid.
   - reagent blanks were estimated by measuring the content of free-steroid sera and were below the limit of detection.
   - the standard curves, obtained after logit-log transformation of the standard data, were linear in all the required physiological range (ng/ml): 0.012 to 1.6 for PRO, DOC and ALDO; 0.085 to 5.43 for S and 18OHB; 0.27 to 17 for B and 5 to 400 for F. Standard curves with their SEM averaging 5.9 to 9.3% are illustrated in Fig. 3.
4. Reproducibility of the whole procedure was estimated as the intra- and inter-assay coefficients of variation on quality column samples and on the unknown plasma. They ranged from 6.7 to 10.6% and from 10 to 19%, respectively, for concentrations superior to twice the limit of detection.
5. Accuracy was assessed by measuring the recovery of pure steroids added to low-content sera and was between 92 and 107%.

Table I. Analytical characteristics of steroid assays.

Performances of the method	PRO	DOC	S	B	ALDO	F	18OHB
Efficiency of extraction and chromatography (%)	88 ± 4	94 ± 4	89 ± 4	84 ± 2	74 ± 4	87 ± 4	73 ± 3
Retention time (min)	2.69 ± 0.014	4.81 ± 0.023	10.52 ± 0.038	13.39 ± 0.062	17.03 ± 0.034	21.05 ± 0.073	22.87 ± 0.076
Standard error on the logit-log curve (%)	8.0 ± 0.7	8.7 ± 0.6	9.3 ± 1	8.9 ± 0.7	7.6 ± 1	5.9 ± 0.5	7.1 ± 0.5
Limit of detection (ng/ml)	0.1	0.02	0.05	0.2	0.02	4	0.05
Reagents blank (ng/ml)	0.007 ± 0.003	0.003 ± 0.001	0.009 ± 0.002	0.102 ± 0.013	0.008 ± 0.001	1.2 ± 0.46	0.002 ± 0.003
Intra assay error (%)	10.6	8.3	7.4	6.7	8.5	9	9.5
Inter assay error (%)	16	12	13	10	19	10	11
Recovery of added steroids (%)	92 ± 5	106 ± 7	91 ± 6	92 ± 5	107 ± 4	91 ± 5	99 ± 3
Mean ± SEM of 12 Assays							

Table II. Specificity of steroid assays.

	Steroids		% Cross-reactions of antibodies with the main plasma steroids						
			Antibodies against						
Retention time (min)	Trivial name	Identific. on elution pattern	PRO (STER)	DOC (RSL)	S (RSL)	B (E.S.)	ALDO (DPC)	F (DPC)	18OHB (E.S.)
1.18	Solvent	S_v	–	–	–	–	–	–	–
2.69	Progesterone	PRO	100	2.9	0.09	0.6	< 0.01	0.15	0.04
2.94	Androstenedione	AD	1.3	0.10	–	–	< 0.001	–	–
3.35	Pregnenolone	Δ_5-P	0.5	–	–	0.04	–	–	–
3.89	DHEA	DHEA	< 0.1	–	< 0.01	0.03	< 0.001	–	–
4.35	Testosterone	T	0.5	0.16	–	0.1	< 0.01	–	–
4.81	11-Desoxycorticosterone	DOC	1.5	100	1.0	4.6	< 0.01	1.5	0.01
5.11	17OH-Progesterone	17OH PRO	1.5	0.04	15	0.01	< 0.001	< 0.01	–
5.93	11OH-Androstenedione	11OH AD	–	< 0.01	< 0.01	–	–	–	–
6.90	17OH-Pregnenolone	17OH Δ_5P	–	< 0.01	< 0.01	0.01	–	–	–
8.09	Estradiol	E_2	1.5	< 0.01	< 0.01	0.01	–	< 0.03	–
10.52	11-Desoxycortisol	S	< 0.2	0.23	100	0.2	< 0.001	0.25	–
13.39	Corticosterone	B	–	0.5	0.05	100	< 0.001	1.4	0.03
14.97	21-Desoxycortisol	21-F	–	–	< 0.01	< 0.01	–	0.04	–
16.04	Cortisone	E	< 0.1	–	0.04	8.5	< 0.001	0.6	–
17.03	Aldosterone	ALDO	< 1.0	–	< 0.01	0.02	100	0.01	–
17.45	Prednisone	PREDON	–	–	–	0.04	< 0.001	3.1	–
21.05	Cortisol	F	< 1.0	< 0.01	1.7	0.4	< 0.001	100	< 0.01
22.40	Dexamethasone	DXM	–	–	< 0.01	0.05	–	0.53	< 0.001
22.87	18OH-Corticosterone	18OHB	–	–	–	< 0.001	< 0.0001	–	100
25.15	Prednisolone	PREDOL	–	–	–	–	< 0.001	46	< 0.002

STER = Steranti
RSL = Radioassay system laboratory
ES = Endocrine science

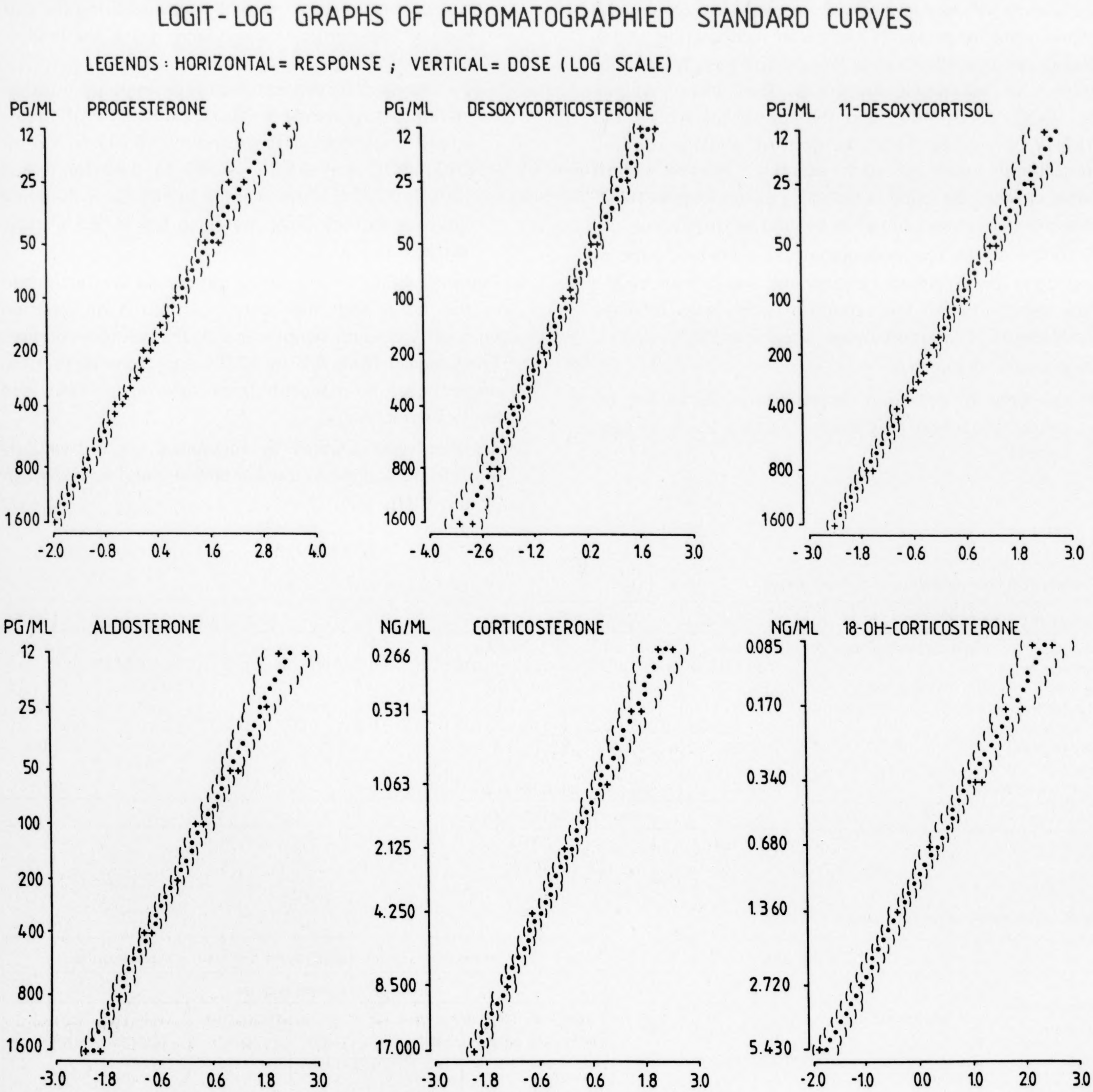

Fig. 3

Logit-log graphs of the standard curves for PRO, DOC, S, B, ALDO and 18OHB, obtained in a routine assay.

Specificity of the Assays

The HPLC procedure allowed a good separation of all steroids to be measured. Fig. 1-a and 1-b illustrate the resolution of the different symmetrical and sharp steroid peaks in the various chromatographical conditions. Between-peak intervals were superior to 2 min, with peak duration inferior to 1.3 min, allowing precise collection. No noticeable shift between UV detection of the steroids and collection of their eluates was observed, as illustrated in Fig. 2.

The cross-reactions of the different anti-sera are listed in Table II. Taking into account the plasma levels of the various steroids eluting with close R_F, the presence of significant interferences can be excluded. In addition, commercial control sera (Radioassay System Labs) were analyzed by this methodology. The steroid content measured (listed in Table III) agreed, for all steroids tested, with the values expected, given by this reference laboratory.

Normal Values

Samples were measured on 19 normal volunteers of both sexes, belonging to the staff of the hospital, aged 25 to 46

Table III. Estimation of commercial control sera.

	Control values (RSL)			Measured values (HPLC-RIA)		
	Range (ng/ml)			Range (ng/ml)		
Steroid	Low	Medium	High	Low	Medium	High
PRO	0.42–0.85	4.7–7.0	18–32	0.50–0.67	3.3–4.0	19–22
DOC	0.018–0.038	0.065–0.135	0.46–0.69	0.012–0.027	0.13–0.18	0.48–0.54
S	1.8–3.9	25–37	85–125	2.2–2.6	20–30	60–110
B	0.37–0.59	1.2–1.8	4.1–6.9	0.34–0.56	0.49–0.87	2.6–4.1
ALDO	0.05–0.11	0.17–0.31	0.42–0.82	0.04–0.07	0.11–0.13	0.45–0.56
F	16–36	48–82	176–230	35–45	62–84	138–190
180HB	–	–	–	undetectable	undetectable	undetectable

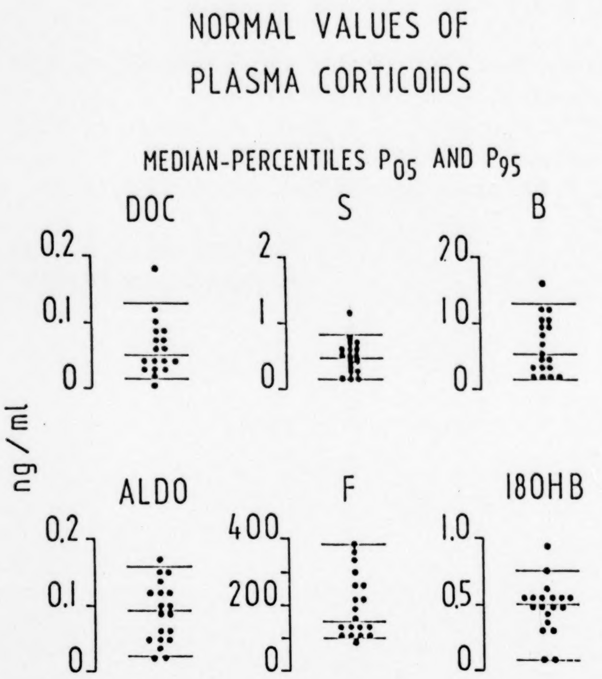

Fig. 4

Values of plasma corticoids in 19 normal adult subjects, in an upright posture.

years. Blood samples were obtained between 7 and 9 a.m. and were immediately centrifuged. The sera were frozen and stored at − 20°C until assayed. Values obtained in an upright standing position and from unrestricted sodium diets are illustrated in Fig. 4. They were similar to the levels generally reported in the literature [2–13]. The median and percentiles 05 and 95 were (ng/ml): 0.050, 0.015–0.13 (DOC); 0.45, 0.15–0.8 (S); 5.0, 0.45–13 (B); 0.095, 0.025–0.16 (ALDO); 150, 100–390 (F); 0.50, 0.15–0.75 (180HB), respectively. PRO was measured on 8 normal subjects (4 females and 4 males), excluding postovulatory women, and ranged from 0.05 to 0.15 ng/ml. Plasma ALDO was also estimated in 10 additional normal subjects, after 2 hours in a recumbent position. The levels were inferior to 0.08 ng/ml and significantly lower, as previously described [14], than those observed in an upright posture.

Discussion

One of the difficulties encountered in the determination of steroid hormones present in the plasma in small concentrations is the presence of larger amounts of closely related steroids, causing a real analytical challenge for their specific and accurate estimation. This feature obliges one to undertake time-consuming purification steps. This is the case for aldosterone and other mineralocorticoids involved in the pathogenesis of hypertension and ion disorders.

Since 1970, the HPLC of steroid hormones has been shown to be a good tool for the separation of steroids present in the biological fluids [16]. However, apart from cortisol [17, 18], photometric quantification of most interesting plasma steroids was hindered by their low plasma levels. It appeared, then, that the conjunction of HPLC efficiency and RIA sensitivity could represent a solution for measuring these hormones [1, 19].

The present work describes an automated HPLC-RIA procedure for the measurement, in low plasma volume, of various steroids involved in mineralocorticoid disorders. This methodology is faster and easier than Schönshöfer's [1] procedure owing to the following improvements:

- The treatment of plasma by a simple organic extraction allows one to obtain extracts cleaned from most polar compounds.
- The addition of triethylamine to all organic solvents prevents the polymerization of 18-hydroxycompounds in the presence of trace of organic acids [20].
- The choice of labelled estradiol as an internal standard avoids the interference of radioactive markers in the various RIA. Indeed, estradiol is completely resoluted from the estimated compounds.
- The use of spherical particules as solid supports coated with silicagel substituted by alkyldiols radicals results in a highly efficient separation system, characterized by well-resoluted compounds with sharp symmetrical peaks. This allows precise collection by a preprogrammed collector and shorter chromatographical runs. Eight steroids were separated and collected in less than 30 min.
- The high stability of the retention times allows one to only check collection conditions infrequently, avoiding the contamination of the eluates by highly concentrated standards. Absence of contamination was demonstrated by undetectable reagent blanks.

- The complete automated chromatographical equipment, including sampling and collection, is designed to be self-operating during 24h, handling about fifty samples, without manual intervention. This robotic ease allows one to include several quality controls in the assay, improving the fiability of steroids measurement.

In conclusion, this procedure is suitable for routine measurements of multiple plasma steroids with a precision and sensitivity equivalent to that of direct methods. Moreover, specificity was improved because it depends more on the complete isolation of the various steroids than on the characteristics of their antisera.

References

[1] *M. Schönshöfer, A. Fenner, H. J. Dulce*, J. Steroid Biochem., **14**, 377 (1981).
[2] *H. H. Newsome Jr., A. S. Clements, E. H. Borum*, J. Clin. Endocrinol. Metab., **34**, 473 (1972).
[3] *R. H. Underwood, G. H. Williams*, J. Lab. Clin. Med., **79**, 848 (1972).
[4] *C. J. Oddie, J. P. Coghlan, B. A. Scoggins*, J. Clin. Endocrinol. Metab., **34**, 1039 (1972).
[5] *C. D. West, D. K. Mahajan, V. J. Chavré, C. J. Nabors, F. H. Tyler*, J. Clin. Endocrinol. Metab., **36**, 1230 (1973).
[6] *P. A. Mason, R. Fraser*, J. Endocrinol., **64**, 277 (1975).
[7] *V. I. Martin, C. R. W. Edwards, E. G. Biglieri, G. P. Vinson, F. C. Bartter*, Steroids, **26**, 591 (1975).
[8] *A. Wilson, P. A. Mason, R. Fraser*, J. Steroid Biochem., **7**, 611 (1976).
[9] *D. C. Anderson, B. R. Hopper, B. L. Lasley, S. S. Yen*, Steroids, **28**, 179 (1976).
[10] *M. Honda, W. Nowaczynski, G. P. Guthrie Jr., F. H. Messerli, G. Tolis, O. Kuchel, J. Genest*, J. Clin. Endocrinol. Metab., **44**, 264 (1977).
[11] *M. Schöneshöfer*, J. Steroid Biochem., **8**, 995 (1977).
[12] *W. G. Sippell, F. Bidlingmaier, H. Becker, T. Brünig, H. Dörr, H. Hahn, W. Golder, G. Hollmann, D. Knorr*, J. Steroid Biochem., **9**, 63 (1978).
[13] *H. Witzgall, S. Hassan-Ali*, J. Clin. Chem. Clin. Biochem., **19**, 387 (1981).
[14] *G. H. Williams, J. P. Cain, R. G. Dluhy, R. H. Underwood*, J. Clin. Invest., **51**, 1731 (1972).
[15] *K. J. Kosunen, A. Pakarinen*, J. Clin. Endocrinol. Metab., **47**, 665 (1978).
[16] *S. Siggia, R. A. Dishman*, Anal. Chem., **42**, 1223 (1970).
[17] *F. K. Trefz, D. J. Byrd, W. Kochen*, J. Chromat., **107**, 181 (1975).
[18] *J. H. M. Van den Berg, Ch. R. Mol, R. S. Deelder, J. H. H. Thijssen*, Clin. Chim. Acta, **78**, 165 (1977).
[19] *N. Imaizumi, S. Morimoto, T. Kigoshi, K. Uchida, H. Hosojima, I. Yamamoto*, J. Chromat., **308**, 295 (1984).
[20] *R. Fraser, C. P. Lantos*, J. Steroid Biochem., **9**, 273 (1978).

Received: July 2, 1987
Accepted: July 19, 1987
F

Determination of α-Aminonitriles, α-Amino Acid Amides and α-Amino Acids by Means of HPLC, Post-Column Reaction and Fluorescence Detection

A. L. L. Duchateau*/M. G. Crombach

DSM Research, P.O. Box 18, NL-6160 MD Geleen, The Netherlands

Key Words

Column liquid chromatography, Post-column derivatization, α-Amino acids, α-Amino acid amides, α-Aminonitriles

Summary

An HPLC method was developed for the simultaneous assay of intermediate (α-aminonitrile and α-amino acid amide) and end products (α-amino acid) in process streams of α-amino acid synthesis. Applications are given for Ala, Val and Leu. α-Aminonitriles were stable in a phosphate buffer pH 3, which was subsequently used for sample handling and chromatography. The α-aminonitrile, the corresponding acid amide and α-amino acid were separated using a buffered ion-pair mobile phase on an RP column and were detected fluorimetrically after post-column reaction with fluorescamine. Linearity and precision of the method are given.

Introduction

Enantiomerically pure amino acids are becoming increasingly important as intermediates for the production of pharmaceuticals, food- and agrochemicals. Production methods include fermentation, asymmetric synthesis and resolution processes. At our Centre an enzymatic process has been developed based upon the stereospecific hydrolysis of α-amino acid amides by aminopeptidases. Both D- and L-amino acids with a high optical purity can be produced under mild reaction conditions, starting from simple raw materials (aldehydes and ketones). α-Aminonitriles, obtained via Strecker reaction of aldehydes, and α-amino acid amides are intermediates in the amino acid synthesis. To obtain information about the efficiency of the reactions in the amino acid synthesis, it is necessary to quantitate the intermediates in the corresponding reactions. The aim of this study was to develop a simultaneous assay method for intermediates (α-aminonitrile and α-amino acid amide) and α-amino acid. Numerous HPLC methods have been developed for the analysis of α-amino acids. For the analysis of α-amino acid amides, HPLC methods are described for the naturally occuring α-amino acid amides, glutamine and asparagine. In the literature only two HPLC methods for the assay of α-aminonitriles have been described [1, 2]. For the separation of a series of peptide compounds, including peptide nitriles and α-aminopropionitrile, an HPLC method has been described on an ion-exchange column using pH 3.25 and pH 5.28 buffers as eluents [1]. Another HPLC method was described for the assay of aminocyclohexanecarbonitriles on a C18 reversed phase column using an acidic methanol-water mobile phase [2]. The aqueous buffer was pH 2.9. Attempts at separations at higher pH levels resulted in poor resolution and peak shape for these compounds. This may indicate that nitrile compounds undergo decomposition reactions during the separation process at pH levels $>$ 2.9.

The decomposition of α-aminonitriles as a result of heat [1, 3, 4] and the pH of aqueous solutions [5] makes instrumental analysis of these compounds difficult.

Aliphatic amino compounds have poor detection properties for sensitive HPLC detectors, like UV-VIS absorbance and fluorescence. The use of chemical derivatization is one possible way to overcome this problem. For aliphatic α-aminonitriles, however, no data are available in the literature for the derivatization of this class of compounds.

In this study, we discuss the use of an HPLC system coupled with post-column derivatization for the quantitative determination of α-aminonitrile, α-amino acid amide and α-amino acid in process streams from the production of three aliphatic α-amino acids.

Experimental

Materials

Alanine (Ala), alanine amide (Ala-NH_2), α-aminopropionitrile (APN), valine (Val), valine amide (Val-NH_2), α-amino-isovaleronitrile (AVN), leucine (Leu), leucine amide (Leu-NH_2, α-amino-isocapronitrile (ACN), α-methylalanine (Me-Ala) and α-methylalanine amide (Me-Ala-NH_2) were synthesized at our Centre and all D, L-compounds were used in

0009-5893/87 0339-05 $03.00/0 ©1987 Friedr. Vieweg & Sohn Verlagsgesellschaft mbH

their racemic form. Fluorescamine and 2-mercapto-ethanol (MCE) were obtained from Fluka. The pairing ion laurylsulphonate and o-phthalaldehyde (OPA) were obtained from Merck. Water was purified by a Milli-Q$^{(TM)}$ system.

HPLC grade propanol-2, ethanol and acetone were obtained from Merck and used as supplied. All other chemicals were of analytical grade.

Instrumentation

The chromatographic system consisted of a Hewlett-Packard model 1081B liquid chromatograph, a Rheodyne 7010 injection valve for manual injection or a Micromeritics model 725 autosampler for automated injection. The injection loop was 25 μl. The column used was a Nucleosil-120-C18 (250 × 4.0 mm i.d., 5 μm) from Marcherey-Nagel. Column temperature was 40 °C.

For reaction detection with fluorescamine, the borate buffer was added to the column effluent by a mixing T, and after passage through a short capillary SS tubing, the fluorescamine reagent was added to the stream by a second mixing T. Post-column addition of buffer and reagent was performed with two Gilson model 302 pumps, both with a flow rate of 1 ml min^{-1}. The fluorescamine reaction was carried out in a coiled capillary SS tube (14 m × 0.35 mm i.d., coil-diameter 12 mm) at ambient temperatures. The fluorophores were monitored with a Waters model 420 fluorescence detector. For excitation a 365 nm band-pass filter was used, and for emission a 415 nm long-pass filter was chosen. Quantitation was performed with a Hewlett Packard 3350 Laboratory Automation System.

Measurement of the fluorescence intensity of the fluorescamine derivates of the amino compounds under different pH reaction conditions was performed with the above-mentioned instrumentation without the use of a column. For the OPA-MCE reaction, the same equipment was used except for the excitation filter (338 nm band-pass filter), and the instrumental part was omitted for the addition of the borate buffer. A Metrohm titroprocessor model 636 was used for pK$_a$-measurement of α-aminonitriles.

Buffer, Eluent, Reagent and Sample Preparation

Sodium phosphate buffer (0.01 M Na$^+$, pH 3.0) was prepared by dissolving sodium hydroxide in water and titrating to the required pH with phosphoric acid. Laurylsulphonate was dissolved in water : propanol-2 (1:1). The eluent was a mixture of sodium phosphate buffer (0.01 M Na$^+$, pH 3.0), laurylsulphonate (0.5 mM) and propanol-2. Sodium borate buffer (0.1M boric acid, 25 mM sodium tetraborate, pH 8.6) was prepared by dissolving boric acid and sodium tetraborate in water. The fluorescamine reagent (1 mM) was prepared by dissolving fluorescamine in acetone. Potassium borate buffer (0.4 M, pH 10.0) was prepared by dissolving boric acid and titrating to the required pH with potassium hydroxide. OPA was dissolved in ethanol. The OPA-MCE reagent was a mixture of potassium borate buffer (0.4 M, pH 10.0), OPA (6 mM), MCE (0.1 %) and ethanol (1.0 %). The buffers used for evaluating the optimum pH for the fluorescamine reaction were prepared by dissolving the appropriate amounts of boric acid and sodium tetraborate in water. The buffers used for testing the stability of the α-aminonitriles were prepared by dissolving phosphoric acid or acetic acid in water and titrating to the required pH with sodium hydroxide. Standards of the amino compounds were dissolved in eluent. Samples of process streams were diluted with phosphoric acid (0.1 M) to pH 3.

Results and Discussion

Stability of α-Aminonitriles

Depending on the pH of the aqueous solution, different equilibria exist between α-aminonitriles and their decompositions products. These equilibria can be summarized as follows [5]:

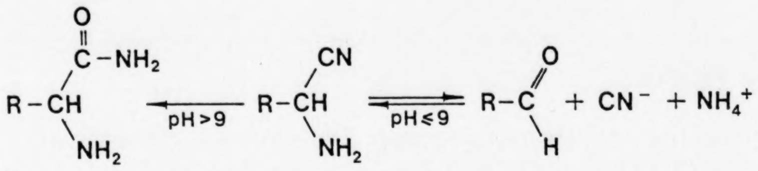

$$R-CH(NH_2)-C(=O)-NH_2 \xleftarrow{pH>9} R-CH(NH_2)-CN \underset{pH\leq 9}{\rightleftharpoons} R-C(=O)H + CN^- + NH_4^+ \quad (1)$$

Our goal was to examine the stability of α-aminonitriles in aqueous solutions within the pH range 2-7. This particular pH range was chosen because these solutions can be used as chromatographic buffers for silica-based columns. The stability of APN, AVN and ACN has been evaluated in buffer solutions at pH 7, pH 5 and pH 3. The influence of the ionic strength on the stability of the nitrile compounds was evaluated by using two buffers with the same pH but different ionic strength. The stability of the three aliphatic α-aminonitriles as a function of time is shown in Fig. 1. For the tested α-aminonitriles degradation occurs at pH 5 and pH 7. At pH 7 the decomposition rate is highest. At pH 3 APN, AVN and ACN are stable for 32 h in 0.1 M as well as in 0.05 M phosphate buffer. The process streams in which α-aminonitriles have to be determined are alkaline. The immediate addition of phosphoric acid to bring the sample solution to pH 3 will stabilize the α-aminonitrile (Fig. 1).

However, the ultimate ionic strength in the sample solution after acidification will vary depending on the process stream from which the sample is taken. In Fig. 1 (pH 3.0) it is shown that a change of the ionic strength does not influence the stability of the α-aminonitriles. Considering the similarity of the stability curves of APN, AVN and ACN, it can be concluded that the kind of alkyl-substituent (methyl, isopropyl or isobutyl) of the α-aminonitrile does not play an important role where the stability of these compounds is concerned.

A possible explanation for the stability of the α-aminonitriles at lower pH values can be found in the low basicity of these compounds. Calculated from [6], the pK$_a$-values of APN, AVN and ACN are 4.7, 4.8 and 4.6, respectively. The pK$_a$-values found by titration differed maximally 0.7 units from the theoretically calculated values. On the basis of the pK$_a$-values found for APN, AVN and ACN, it can be said that at pH $\leqslant 3$, the studied α-aminonitriles mainly appear in the ammonium form, in which form the compounds are unreactive. At pH > 3, the α-aminonitriles will deprotonate towards the amino form because of their weak basicity. The free amino group can easily interfere in degradation reactions in which CN$^-$ can be formed.

Besides sample handling (acidification of the sample to pH 3), the stability of the α-aminonitriles can also be guaranteed during chromatography by choosing a phosphate buffer pH 3 as mobile phase.

Post-Column Derivatization

The most commonly used derivatization reactions for primary amines [7] proceed in a neutral or alkaline medium. Because of the instability of the studied α-aminonitriles in non-acidic media, pre-column derivatization is not suitable as a labelling technique for these compounds. OPA was evaluated as the fluorescence-introducing reagent for post-column derivatization of Ala, Val, Leu and the corresponding intermediates (α-amino acid amide and α-aminonitrile). The molar fluorescence intensities (relative units) obtained for the OPA-MCE derivatives of Ala, Ala-NH$_2$ and APN were 100, 9 and 1.4, respectively. Neither a change in pH of the OPA-MCE reagent (pH 10.0 to pH 8.2), nor a change in reaction temperature (25 °C to 40 °C) altered the molar fluorescence intensity of APN. Due to the low sensitivity to APN after reaction with OPA-MCE, another fluorescence-introducing reagent, i.e. fluorescamine, was evaluated. Molar fluorescence intensities were recorded in reaction media within the pH range 6.8-9.3. The results are shown in Table I.

The α-amino acids (Ala, Val, Leu) yield maximum fluorescence at pH 9.3, with little fluorescence at pH 6.8. These observations for amino acids were also made by others [8]. For the α-amino acid amides (Ala-NH$_2$, Val-NH$_2$, Leu-NH$_2$) maximum fluorescence appears at pH 7.7 and the α-aminonitriles give their highest fluorescence at pH 6.8-7.7. Since the relative fluorescence of individual fluorescamine derivates is constant from pH 4 to 10 [8], the variations depend on the reactivity of each amine at different pH values and on differences in quantum yields for various types of fluorophors.

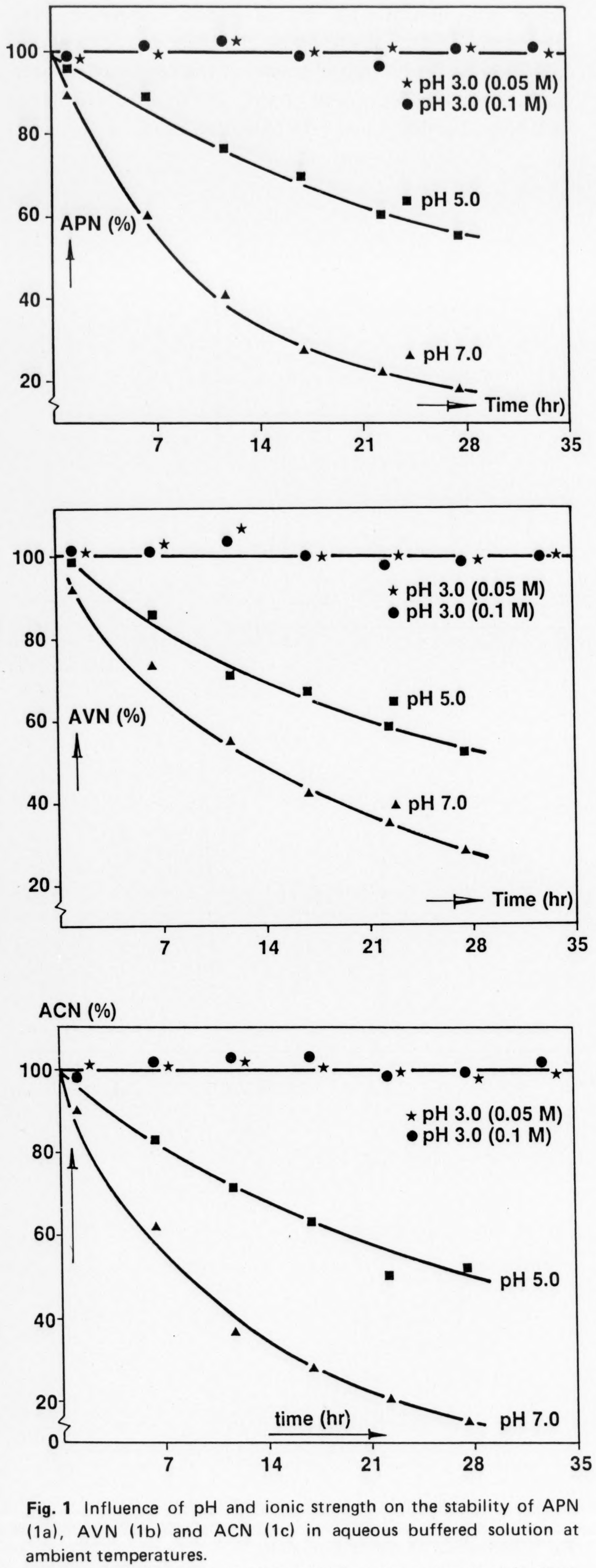

Fig. 1 Influence of pH and ionic strength on the stability of APN (1a), AVN (1b) and ACN (1c) in aqueous buffered solution at ambient temperatures.
Buffers: sodium acetate (0.1 M, pH 5.0), sodium phosphate (0.05 M, pH 3.0; 0.1 M, pH 3.0; 0.1 M, pH 7.0).

Table I Molar fluorescence intensities (relative units) of α-amino acids (Ala, Val, Leu), α-amino acid amides (Ala-NH$_2$, Val-NH$_2$, Leu-NH$_2$) and α-aminonitriles (APN, AVN, ACN) after fluorescamine reaction at different reaction medium pH.

Compound	Fluorescence intensity pH 6.8	pH 7.7	pH 8.6	pH 9.3
Ala	24	252	682	749
Val	3	45	325	473
Leu	13	169	654	706
Ala-NH$_2$	675	941	901	788
Val-NH$_2$	726	935	911	841
Leu-NH$_2$	836	972	923	849
APN	89	88	68	42
AVN	49	50	43	31
ACN	74	74	63	42

The increase in fluorescence intensity of the α-amino acids and α-amino acid amides in the lower part of the studied pH range (Table 1) can be explained in terms of the basicity of these compounds. At pH 6.8 the α-amino acids (Ala, Val, Leu) will be fully in their ammonium form (pK_a Ala 9.7, pK_a Val 9.8, pK_a Leu 9.6), while amino acid amides will mainly appear in the ammonium form (pK_a Ala-NH_2 7.7, pK_a Val-NH_2 7.8, pK_a Leu-NH_2 7.6). An increase in pH will deprotonate both α-amino acids and α-amino acids amides, making these compounds more reactive towards the fluorescamine reagent. As a result derivative formation will increase and a higher fluorescence intensity will be measured. At pH 6.8-7.7 the α-aminonitriles (APN, AVN, ACN) are already fully deprotonated; an increase in pH does not increase their fluorescence intensities (Table I). From Table I it can be seen that α-amino acids and α-amino acid amides reach their maximum fluorescence at $pH \cong pK_a$. Therefore, for α-aminonitriles it is expected that these compounds show their maximum fluorescence at $pH \cong 4.7$. For simultaneous assay of α-amino acid, α-amino acid amide and α-aminonitrile, a buffer pH of 8.6 will be suitable.

A comparison of the fluorescence intensity of APN after OPA-MCE derivatization (pH 8.2-10.0) and fluorescamine derivatization (pH 8.6) showed that the fluorescamine derivative of APN is a factor 5 more sensitive than the corresponding OPA-MCE derivative.

Qualitative Analysis

By varying the concentration of the ion-pairing reagent (laurylsulphonate) and the content of organic solvent (propanol-2) in the mobile phase, optimal separations have been found of α-amino acid, α-amino acid amide, α-aminonitrile and potentially interfering amines. In Fig. 2 the chromatograms are shown for a standard mixture of Ala, Ala-NH_2, APN (Fig. 2a), Val, Val-NH_2, AVN (Fig. 2b) and Leu, Leu-NH_2, ACN (Fig. 2c). In all three standard mixtures a set of potentially interfering amines (Me-Ala, Me-Ala-NH_2, NH_3) has been included. From Fig. 2 it can be seen that, depending on the hydrophobicity of the R-group (isobutyl (Fig. 2c) > isopropyl (Fig. 2b) > methyl (Fig. 2a)), increases in the mobile phase content of propanol-2 can be used to reduce to a minimum the time needed for a given chromatogram. Under certain mobile phase conditions, peak splitting occurred, as can be seen in Fig. 2a for Me-Ala. Probable mechanisms for this phenomenon have been described [9, 10]. A representative chromatogram of a sample from a process stream is given in Fig. 3.

Quantitative Analysis

Quantitative determinations were made by comparing the peak areas of the samples with those of standard solutions using the external standard method. The linearity of the amount-response relation for the studied compounds was established over the range 2-146 nmol (APN, AVN, ACN), 0.1-0.6 nmol (Ala-NH_2, Val-NH_2, Leu-NH_2) and 0.1-8 nmol (Ala, Val, Leu). Linear regression analysis from standard curves indicated that the correlation coefficients for all these compounds were higher than 0.9997. The within-run precision of the assay gave coefficients of variation lower than 2 % (n = 10) for all studied compounds. The detection limits, calculated by doubling the noise ratios, and expressed in terms of pmoles of the compounds injected, were: 115-380 (APN, AVN, ACN), 6-18 (Ala-NH_2, Val-NH_2, Leu-NH_2) and 5-18 (Ala, Val, Leu).

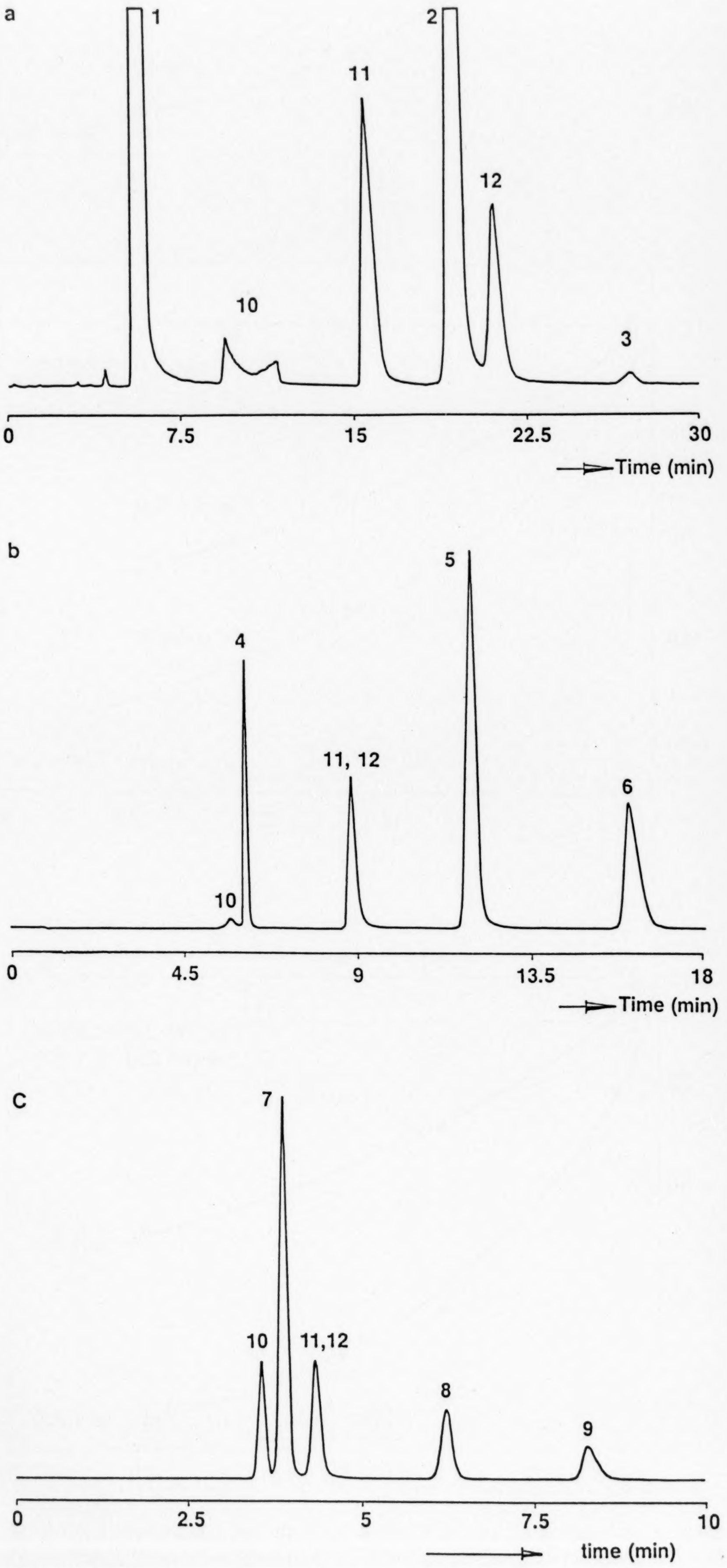

Fig. 2 Separation of standard mixtures.

(a) Flow-rate: 1.5 ml/min. Eluent containing 2 % propanol-2.
(b) Flow-rate: 1.2 ml/min. Eluent containing 15 % propanol-2.
(c) Flow-rate: 1.2 ml/min. Eluent containing 20 % propanol-2.

Remaining conditions — see Experimental. Peaks: **1** = Ala; **2** = Ala-NH_2; **3** = APN; **4** = Val; **5** = Val-NH_2; **6** = AVN; **7** = Leu; **8** = Leu-NH_2; **9** = ACN; **10** = Me-Ala; **11** = NH_3; **12** = Me-Ala-NH_2.

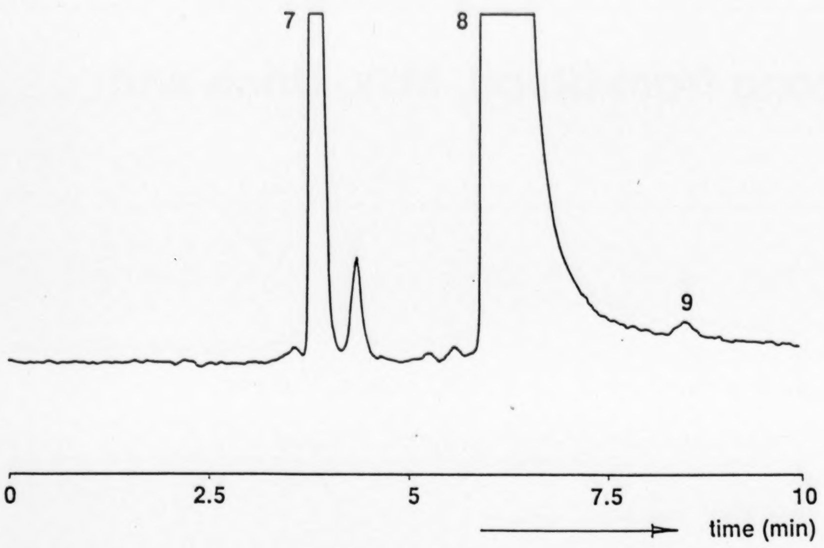

Fig. 3 Chromatogram of a sample from the Leu-NH_2 synthesis. Conditions – see Fig. 2c, Peaks: **7** = Leu; **8** = Leu-NH_2; **9** = ACN.

Conclusions

HPLC coupled with post-column derivatization is a useful technique for the simultaneous assay of aliphatic α-aminonitrile and the corresponding α-amino acid amide and α-amino acid. Decomposition of the α-aminonitrile can be avoided by using pH3 buffer for both sample handling and chromatography. In comparison with OPA-MCE, fluorescamine gives a higher fluorescence yield for the α-aminonitrile derivative. The optimal pH for reaction of fluorescamine with α-aminonitrile, α-amino acid amide and α-amino acid can be deduced from the pK_a of the α-amino group of these compounds.

The HPLC method described can be applied to process stream control in α-amino acid synthesis.

References

[1] *K. Kawashiro, S. Morimoto, H. Yoshida, K. Sugiura,* Origins Life, **8**, 347 (1977).

[2] *G.M. Wall, C.R. Clark,* J. Assoc. Off. Anal. Chem., **64**, 1431 (1981).

[3] *J.R. Ballinger, J. Marshman,* J. Anal. Toxicol., **3**, 158 (1979).

[4] *W.H. Soine, S.C. Vincek, D.T. Agee,* N. Engl. J. Med., **301**, 438 (1979).

[5] *J.C. Jallageas, H. Fradet, K. Bui, M. Maestracci, A. Thiéry, A. Arnaud, P. Galzy,* Analyst, **109**, 1439 (1984).

[6] *D.D. Perrin, B. Dempsey, E.P. Serjeant,* 'pK_a Prediction for Organic Acids and Bases', Chapman and Hall, London, 1981; p. 30.

[7] *H. Lingeman, W.J.M. Underberg, A. Takadate, A. Hulshoff,* J. Liq. Chromatogr., **8**, 789 (1985).

[8] *S. Udenfried, S. Stein, P. Böhlen, W. Dairman, W. Leimgruber, M. Weigele,* Science, **178**, 871 (1972).

[9] *G.K.C. Low, A.M. Duffield, P.R. Haddad,* Chromatographia, **15**, 289 (1982).

[10] *G.K.C. Low, P.R. Haddad,* J. Chromatogr. (Biomed Appl.), **336**, 15 (1984).

Received: July 2, 1987
Revised manuscript
received: July 29, 1987
Accepted: Aug. 3, 1987
F

Simple and Rapid Analysis of Nitrofurazone from Blood, Milk, Urine and Meat Samples

T. Suortti*[1] / K. Heinonen[2]

[1] Technical Research Centre of Finland, Food Research Laboratory, Biologinkuja 1, SF-02150 Espoo, Finland

[2] College of Veterinary Medicine, Department of Obstetrics and Gynecology, SF-04840 Hautjärvi, Finland

Key Words

Nitrofurazone
Dairy cows
Blood and milk
Meat, fat, kidney, liver

Summary

Nitrofurazone is an effective chemotherapeutic drug in the treatment of infections of the urinary tract. In order to study its occurrence and metabolism, a simple and sensitive method was developed.

Introduction

The method consists of the homogenization of the sample with acetonitrile: aqueous buffer, centrifugation, filtration and dilution of the sample with buffer. The analysis is carried out on a reverse phase column. Nitrofurantoin is used as an internal standard and also as a demonstration that degradation of nitrofurazone by the action of light has not occurred. The sensitivity reached by this simple preparation is of the order of 5 μg/kg for most samples, with the exception of liver samples, which very quickly degrade small additions of nitrofurazone and thus make determinations impossible at concentrations below 40 μg/kg.

The method can also applied to the analysis of the other nitrofuranes. Nitrofurazone is an effective chemotherapeutic drug with a wide therapeutic spectra. In some countries, although not in Finland, it may be added to pig and swine feed [1]. Nitrafurazone is used in the local treatment of uterine infections of dairy cows. In order to study its absorption into systemic blood circulation after intrauterine application as well as its residues in edible tissues and milk, a sensitive and simple method was developed.

Several methods have been described for the analysis of nitrofurans, ranging from colorimetry [2], through gas chromatography [3, 4] to high performance liquid chromatography (HPLC) [5–9]. The required sensitivity can be obtained with some HPLC methods [1, 10, 11], but they require tedious sample preparation including extractions, concentrations and column chromatography purifications.

By combining the rather high selectivity of detection attainable at a wavelength of 365 nm with the sensitivity obtained by trace enrichment, a simple sample preparation was developed for the analysis of nitrofurazone in low concentrations at the μg/kg level.

Materials and Methods

The liquid chromatograph consisted of M-6000A pump, M-710B automatic injector, Nova-Pak C_{18} column (8 × 100 mm) in RCM-100 column chamber and M-440 detector monitoring at 365 nm (all from Millipore/Waters). The mobile phase was 23.5/76.5 acetonitrile/20 mM sodium acetate (pH 5.0). The solvents used were of HPLC quality and water was purified using a Milli-Q system. All reagents were of analytical grade. Nitrofurazone and nitrofurantoin stock solutions (600 mg/l) were made in dimethyl sulfoxide and standard solutions were diluted from them in 15/85 acetonitrile/sodium acetate buffer-solution. All the samples were stored in the dark at − 18 °C. The sample preparations were carried out in a room illuminated with incandescent lamps and no fluorescent light or daylight.

Blood and Milk Samples

To a one milliliter sample, 10 μl 10 mg/l nitrofurantoin solution was added as internal standard and one milliliter of acetonitrile. The sample was centrifuged for 25 minutes at 3000 g, and 4 ml 20 mM sodium asetate buffer was added (pH 5.0). The samples were filter through a Millex-HV filter (0.45 μm pores) and 100 ... 400 μl samples were injected into the HPLC instrument.

Meat, Liver and Kidney Samples

Samples were sliced and ground with an ordinary household grinder. A five milligram sample was taken, and a 25 μl 10 mg/l nitrofurantoin solution was mixed into the sample. The sample was then homogenized with 20 ml 30/70 acetonitrile/sodium acetate buffer and centrifuged at

0009-5893/87 0344-03 $ 03.00/0

© 1987 Friedr. Vieweg & Sohn Verlagsgesellschaft mbH

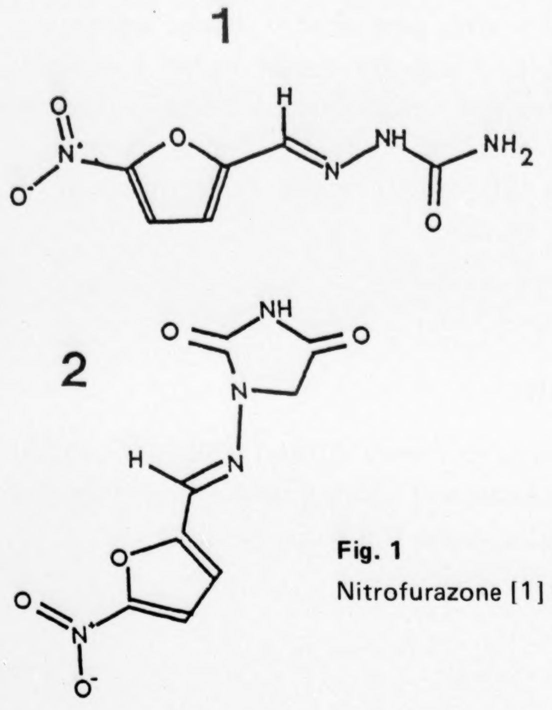

Fig. 1
Nitrofurazone [1] and nitrofurantoin [2].

3000 g for 15 minutes. Five milliliters of this suspension was taken and diluted with 2 ml sodium acetate buffer and centrifuged for 25 minutes at 3000 g. The suspension was then filtered through a Millex-HV filter and injected into the HPLC instrument.

Fat Samples

The sample was ground with an ordinary household grinder and a 5 g sample was taken. 25 μl 10 mg/l nitrofurantoin solution and 6 ml acetonitrile were added and the sample was melted at 60 °C in a water-bath. It was then homogenized concurrently with the addition of 14 ml sodium acetate buffer. After homogenization, the sample was centrifuged for 15 minutes at 3000 g. To five milliliter of this suspension, 2 ml sodium acetate buffer was added before recentrifuging. Prior to injection, the sample was filtered through a Millex HV-filter.

Results and Discussion

Nitrofurantoin was chosen as an internal standard because it is chemically chromatographically and spectrophotometrically suitable and shows a somewaht higher sensitivity to degradation by light (30 % loss cf. 10 % for nitrofurazone after 1.5 h exposure to daylight), which confirms that degradation of nitrofurazone by light during sample manupulation in blank samples had not taken place. The standard curve for nitrofurazone was linear at the concentration range studied (10 ... 3000 μg/l) and went through the origin.

No disturbing peaks at the retention times of nitrofurazone or nitrofurantoin were seen with blank samples. In order to achieve the required sensitivity, trace enrichment was utilized. As can be seen in Fig. 1, if the standard was injected in a solution where the acetonitrile concentration was 8 % less than in the mobile phase, no adverse effect on peak shape was detected with 200 μl injections. However, the sensitivity was twenty-fold in comparison with normal 10 μl injections. A forty-fold increase in sensitivity may be obtained with 400 μl injections. Thus, a simple sample preparation with only an extraction/protein precipitation step and a subsequent sample dilution step could be used (Fig. 2). The recovery for both compounds in blood and milk samples was 98–104 % at the 50 μg/l level and 76 % in other samples. The standard deviation for the determination of nitrofurazone was 6.8 %, and the standard deviation using an internal standard for quantitation was 5.8 %. The sensitivity of the determination was in the range of a few μg/kg for all the other samples except liver. The beef liver samples contained disturbing impurities which limited the sensitivity to about 40 μg/kg (Fig. 3); these samples also necessitated frequent changing of the pre-column. This cannot be regarded as a major drawback of the method, as the alternative would be far more complex sample preparation. Furthermore, the lower sensitivity obtained with liver was less significnat because it was shown during these studies that the freshly frozen beef liver samples, in contrast to normal commercial pig

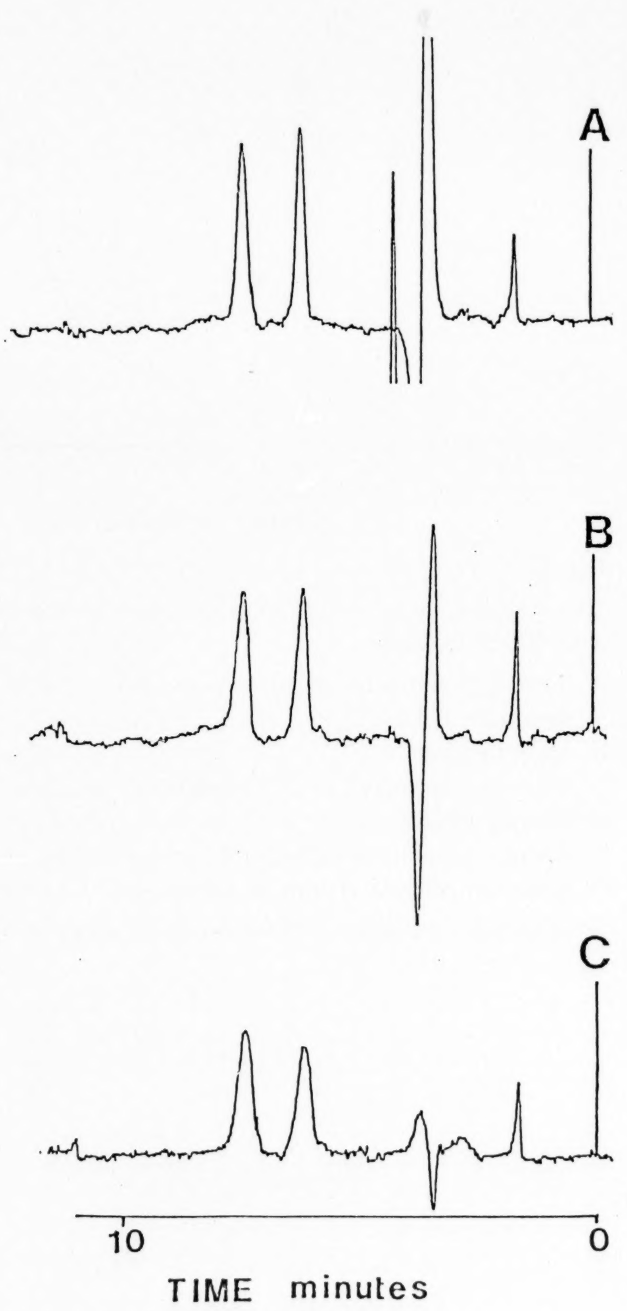

Fig. 2
Effect of sample solvent on chromatography of nitrofurazone [1] and nitrofurantoin [2] with 200 μl injections.
A: 15/85 Acetonitrile/sodium acetate buffer
B: 20/80 Acetonitrile/sodium acetate buffer
C: 25/75 Acetonitrile/sodium acetate buffer
Mobile phase 23.5/66.5 acetonitrile/sodium acetate buffer 1 ml/minutes flow-rate, 0.005 aufs at 365 nm.

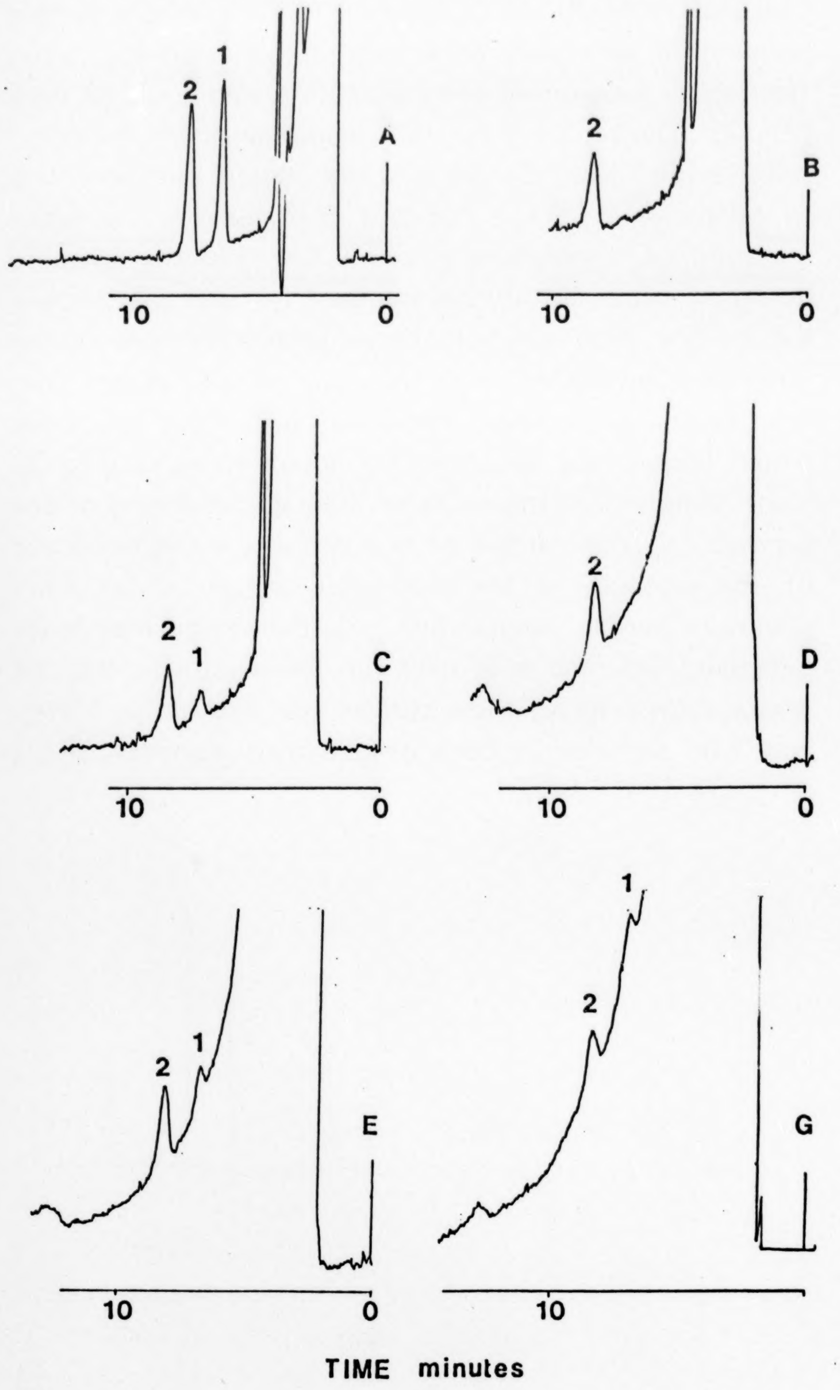

Fig. 3

Chromatography of the samples prepared by the method described with 400 μl injections.

A: 13.4 $\mu g/l$ standard of nitrofuranzone [1] and 13.7 $\mu g/l$ nitrofurantoin [2]
B: Meat sample
C: Meat sample spiked with 20 $\mu g/kg$ nitrifurazone
D: Kidney sample
E: Kidney sample spiked with 20 $\mu g/kg$ nitrofurazone
F: Liver sample spiked with 40 $\mu g/kg$ nitrofurazone

To all samples 50 $\mu g/kg$ nitrofuratoin was added as internal standard.

liver samples (which also gave much cleaner chromatograms), were capable of rapidly decomposing low levels of both nitrofurazone and nitrofurantoin. The small sample requirement of the method made it possible to scale it down for analysis of nitrofurazone concentrations in 150 mg endometrial biopsies.

Acknowledgements

Deepest thanks are due to Hymy, Sirkku, Lysti, Misa, Oili, Valko, Nasta, Orko, Osta and Lirkku, whose contributions by donations of samples made this study possible.

References

[1] *E. A. Sugden, A. I. MacIntosh, A. B. Vilim,* J. Assoc. Off. Anal. Chem. **66,** 874 (1983).
[2] *R. J. Herrett, J. A. Buzard,* Anal. Chem. **32,** 1676 (1960).
[3] *A. R. Ritchie, M. H. Clear, S. R. B. Solly,* N. Z. J. Sci. **20,** 225 (1977).
[4] *U. R. Cieri,* J. Assoc. Off. Anal. Chem. **62,** 168 (1979).
[5] *A. B. Vilim, A. I. MacIntosh,* J. Assoc. Off. Anal. Chem. **62,** 19 (1979).
[6] *V. A. Thorpe,* J. Assoc. Off. Anal. Chem. **63,** 981 (1980).
[7] *M. B. Aufrère, B.-A. Hoener, M. E. Vore,* Clin. Chem. **23,** 2207 (1977).
[8] *H. Roseboom, H. A. Koster,* Anal. Cim. Acta **101,** 359 (1978).
[9] *T. B. Vree, Y. A. Hekster, A. M. Baars, J. E. Damsma, E. van der Klejn,* J. Chromatogr. **162,** 110 (1979).
[10] *M. Petz,* Dtsch. Lebensm.-Rundsch. **78,** 396 (1982).
[11] *R. Malisch,* Z. Lebensm. Unters. Forsch. **183,** 253 (1986).

Received: June 29, 1987
Accepted: Aug. 5, 1987
F

High-Performance Liquid Chromatographic Determination of Major Organic Acids in Apple Juices and Ciders

D. Blanco Gomis* / M. J. Moran Gutierrez / M. D. Gutierrez Alvarez / A. Sanz Medel

Departamento de Quimica Fisica y Analitica, Facultad de Quimica, Universidad de Oviedo, Oviedo, Spain

Key Words

High-performance liquid chromatography
Reversed-phase
Organic acids
Apple juice
Cider

Summary

A reversed-phase high-pressure liquid chromatographic method is presented for the simultaneous separation and determination of malic, citric, lactic, succinic and ascorbic acids in apple juices and ciders. After filtration and/or degasification, the organic acids in the sample are separated on a LiChrosorb/C_{18} column and quantified by using a rapid diode array detector.

The method is considered to be a suitable choice for the accurate and precise determination (C.V. 5%) of these compounds.

Introduction

Among the substances under analysis in apple, apple juice and ciders, organic acids are becoming increasingly important because of their role in maintaining quality and nutritive value in addition to other roles still unknown. These acids directly and indirectly affect the quality of apples and their industrial drinking derivatives. Directly, because they influence the flavour and stability of juices (and may be added to prevent settling of solids or darkening of the juices, or to modify the flavour) and ciders. For example, it is well known that natural malolactic fermentation brings about several consequences: firstly, the acidity of the cider diminishes and secondly, it leads to the replacement of malic acid by lactic acid which has a less marked taste. As a result, a net gustative improvement of ciders is achieved, as the cider becomes lighter. On the other hand, some of the acids, especially malic, are indirectly important because they can be used as indicators of apple maturity. Moreover the determination of the organic acids makes it possible to prove the adulteration of apple beverages, e.g. high citric acid content (because normally in pure apple juice the concentration of citric acid is not more than 10–20mg/100ml although some European countries allow a maximum of 40mg/100ml [1]) or the presence of D-malic acid (because only the L-isomer is present in natural products).

Many analytical methods are reported in the literature for the separation and determination of organic acids. These methods are often time-consuming as a result of the extraction, concentration and/or derivatization procedures necessary depending on different matrices [2–6]. High performance liquid chromatography (HPLC) has simplified the analysis of various food components, including organic acids. Its advantages include rapid analysis of many components in foods and beverages, nearly specific analysis, detection at low levels, and simplified sample preparation. The determination of acids in apple juice included in this paper have been achieved by several ways: (a) ion-exchange [7], a technique preferred by some authors [8] although sorbitol, fructose and malic acid co-elute on hydrogen resin columns, presenting a potential problem in the analysis of organic acids in apple juice, unless detection at the longer wavelengths (220–230nm) is used [8, 9]; (b) ion exclusion [10] or (c) reversed-phase chromatography [11–13].

In this paper a reversed-phase HPLC method for the determination of malic, citric and ascorbic acids in apple juice and malic, lactic and succinic acids in ciders is reported.

Experimental

All reagents were of analytical-reagent grade and were used without further purification. Malic, succinic, citric, lactic and ascorbic acids were purchased from Merck (Darmstadt, FRG) and Sigma (St. Louis, MO, USA). Buffer solutions consisted of 10^{-2}M potassium dihydrogen phosphate (KH_2PO_4), adjusted to different pHs with phosphoric acid (H_3PO_4). The solvents used for the mobile phase were of HPLC grade (Merck) and were employed as supplied.

A LKB (Bromma, Sweden) liquid chromatograph equipped with a Model 2150 pump, a Rheodyne Model 7125 injection valve equipped with a 20-μl loop, a LKB Model 2140

0009-5893/87 0347-04 $03.00/0 © 1987 Friedr. Vieweg & Sohn Verlagsgesellschaft mbH

rapid spectral detector and an IBM data station were used for HPLC analysis.

The HPLC columns were 250 × 4mm i.d. LiChrosorb RP-18 (C_{18}) and RP-8 (C_8) 5-μm particle size.

Processed apple juice and cider samples were purchased from local markets. Before injection all samples were filtered through 0.45μm Millipore filters, and the carbonated ciders were first degassed for 5min in an ultrasonic bath. When acid concentrations were too high, the samples were diluted to 2–5° Brix.

Results and Discussion

The major organic acids found in apple juices are malic and citric acids. As a result of fermentation, the major carboxilic acids present in ciders are succinic and lactic acids, although malic and lactic acids are present in the initial stages of malolactic fermentation. Ascorbic acid – better known as vitamin C – is a natural product of the apple, but it is only present in small quantities. However, it has been used as an antioxidant in apple juices because ascorbic acid has no adverse clinical effects in the quantities used, about 100mg per L. The first pKa of each acid are 3.4 (malic), 3.14 (citric), 4.16 (succinic), 3.86 (lactic) and 4.17 (ascorbic). The observed effect of eluent pH on the total retention time of the five studied acids is shown in Fig. 1. At lower pH values, all of the acids are essentially in the nonionic form and retention of each acid is favoured. Because citric acid retention decreased as the pH was raised (due to dissociation), and in order to avoid possible peak overlapping when ascorbic acid in high concentration is present, an optimum pH = 2.25 was selected for further studies. Lactic and ascorbic acids were coeluted at all pHs tested. This did not present any problem in the analysis of real samples because firstly, lactic acid is a fermentation product and should not be present in apple juices, and secondly, ascorbic acid is not usually a common additive in natural ciders (where lactic acid should be controlled).

In any case, if the acids were all present in the same sample, the diode array detector would minimize the problem because it would allow the acquisition of spectral information within a defined wavelength range during elution, generating a data matrix (Abs, λ, t: spectrochromatogram or λ, t: isogram) for subsequent processing. As can be seen in the two dimensional contour plots (Fig. 2), the overlapping of ascorbic and lactic acids was at a minimum at 206nm. Ascorbic acid can be determined free of interferences at 270nm, while the other acids, in the absence of ascorbic acid, could be determined with more sensitivity (the shorter the wavelength used the more sensitive the corresponding determination, as shown by Fig. 3 at 206nm).

The effect of the ionic strength of the eluent on the retention time of carboxilic acids seems to be slight, but it can be observed that when the ionic strength decreases, the width of the peaks increases and the chromatograms lose resolution.

Investigations on the effects of increasing temperature and mobile phase flow rate show a decrease in analysis time for both, but a parallel decrease in resolution. This fact is in contradiction with the results reported by other authors, who recommended an optimum temperature of 45°C [9].

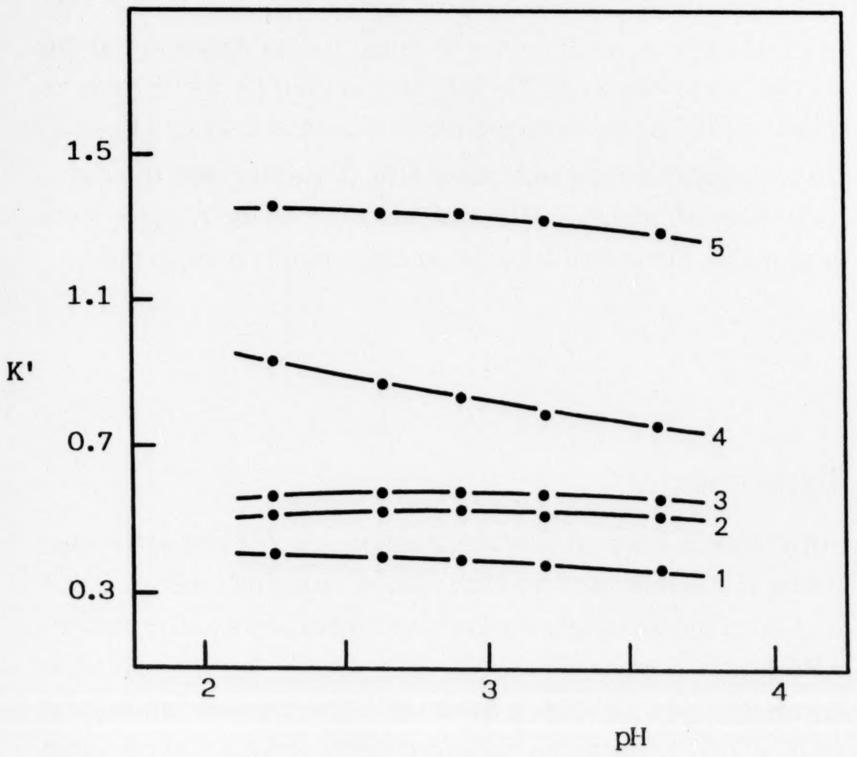

Fig. 1

Effect of eluent pH on the capacity factor of organic acids.

Column, LiChrosorb RP-18, 250 × 4mm i.d. Mobile phase: 0.01M potassium dihydrogen phosphate (KH_2PO_4) adjusted pHs with H_3PO_4; flow-rate, 1.0ml/min; temperature, 26°C. **1** = malic acid; **2** = ascorbic acid; **3** = lactic acid; **4** = citric acid; **5** = succinic acid.

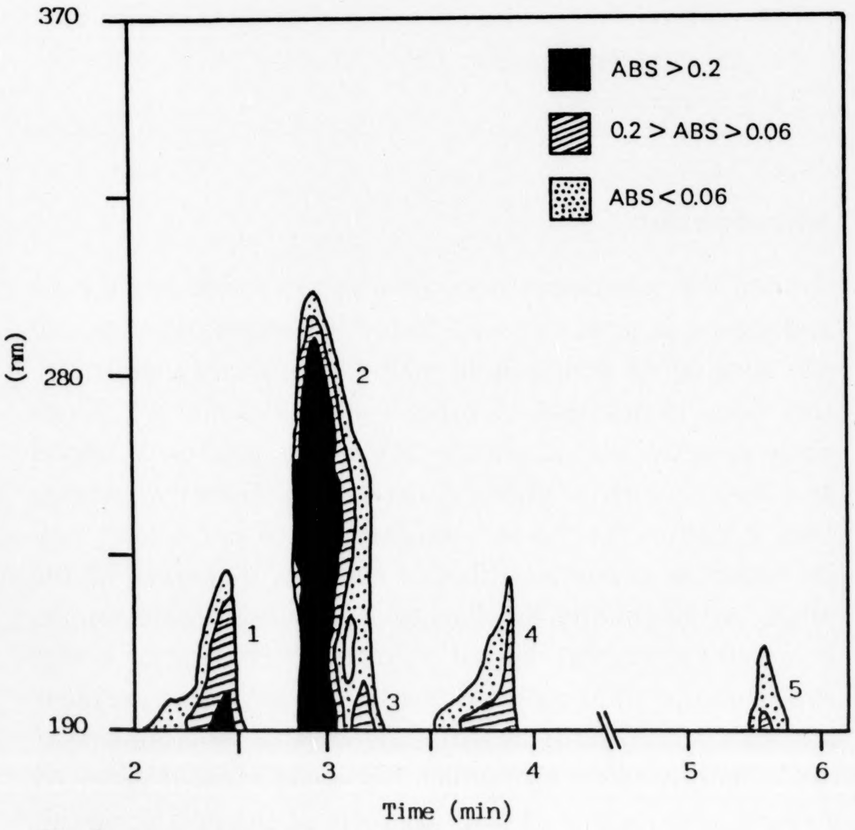

Fig. 2

Isogram of organic acids, showing the isoabsorbance contours plotted in the wavelength-time plane.

Mobile phase pH = 2.25; other conditions as in Fig. 1. **1** = malic acid; **2** = ascorbic acid; **3** = lactic acid; **4** = citric acid; **5** = succinic acid.

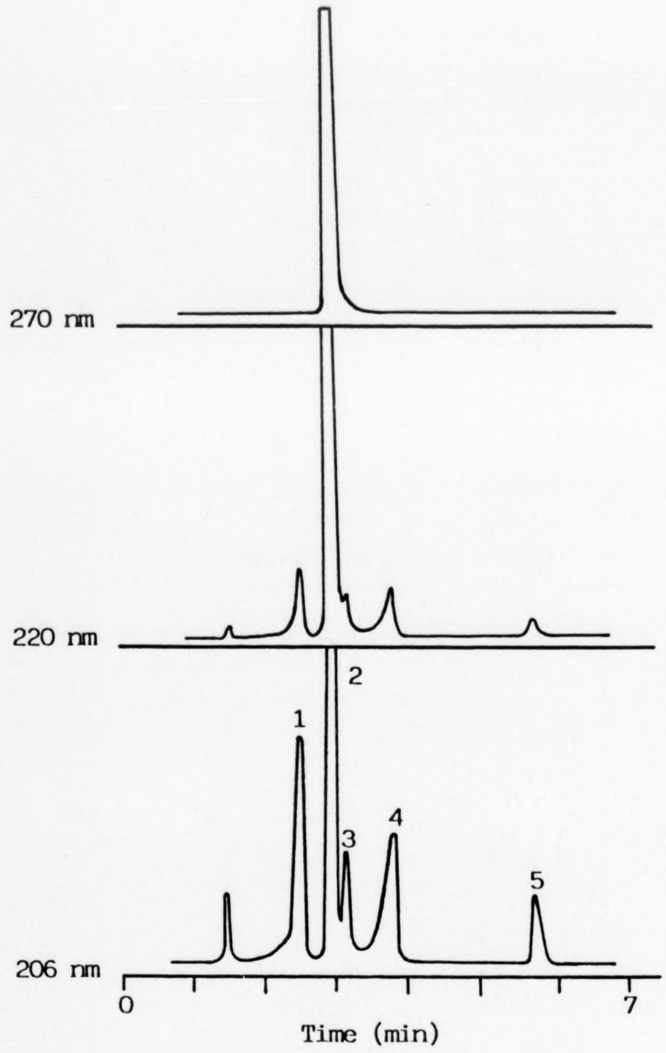

Fig. 3

Multiple wavelength chromatograms of organic acids: post run plots at 206, 220, and 270nm.

Column and chromatographic conditions as in Fig. 2.

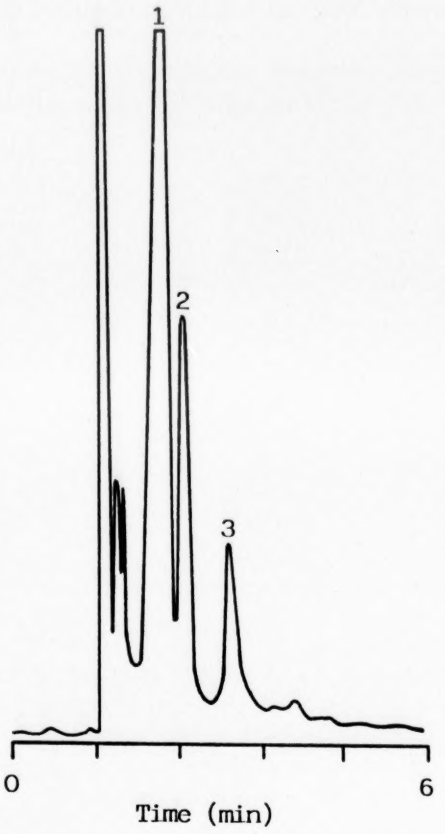

Fig. 4

Typical chromatogram of organic acids in commercial apple juice. Column and chromatographic conditions as in Fig. 2. **1** = malic acid; **2** = ascorbic acid; **3** = citric acid.

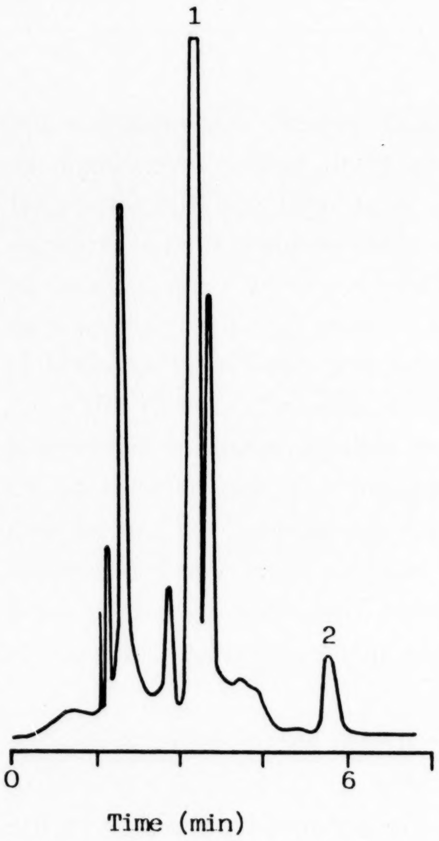

Fig. 5

Typical chromatogram of organic acids in natural cider.

Column and chromatographic conditions as in Fig. 2. **1** = lactic acid; **2** = succinic acid.

Moreover, chromatography of ascorbic acid at elevated column temperatures could not be performed because of chemical degradation.

These studies were developed using two different stationary phases: RP-18 and RP-8. Both columns exhibited similar efficiency in separating these organic acids, but in their practical application in apple juices and ciders, the best results were achieved with the RP-18 column.

As a result of optimization studies the experimental conditions were fixed as: column RP-18, flow rate 1 ml/min, pH 2.25, ionic strength 10^{-2}M and temperature 25°C. Final UV detection was carried out at 206nm.

Quantification and Recovery

Examples of the practical application of the described procedure for the separation and analysis of organic acids in samples of apple juice and cider are shown in Figs. 4 and 5. The quantification of the acids was achieved by using the external standard method. Calibration plots were generated by repeated injections of a fixed volume (20μl) of standard solutions of acids of different concentrations, and the resulting plots (peak area vs. amount injected) were stored in the data module. A volume of 20μl of the samples was then injected and the amount of acids was obtained directly from the data module. The data module calibration was checked regularly with standard solutions.

Recovery studies (Table I) were performed for 4 different apple juices and 4 ciders. Each acid was spiked at three

Table I. Recovery study of organic acids added to apple juices.

Acid	Amount in apple juices (g/l)	Amount added (g/l)	Calc. (g/l)	Found (g/l)	% Recovery
		Spiking Level-1			
Malic	2.4552	0.80	3.2552	3.2732	100.5 ± 1.1
Ascorbic	0.0783	0.03	0.1083	0.1015	93.7 ± 6.7
Citric	0.0911	0.20	0.2911	0.2866	98.5 ± 1.2
		Spiking Level-2			
Malic	2.4552	1.60	4.0552	4.0436	99.7 ± 1.1
Ascorbic	0.0783	0.05	0.1283	0.1247	97.2 ± 7.4
Citric	0.0911	0.40	0.4911	0.5018	102.2 ± 4.3
		Spiking Level-3			
Malic	2.4552	2.40	4.8552	4.7820	98.5 ± 1.1
Ascorbic	0.0783	0.07	0.1483	0.1440	97.1 ± 6.8
Citric	0.0911	0.60	0.6911	0.6840	99.0 ± 4.5

Table II. Recovery study of organic acids added to natural ciders.

Acid	Amount in ciders (g/l)	Amount added (g/l)	Calc. (g/l)	Found (g/l)	% Recovery
		Spiking Level-1			
Lactic	1.6886	0.20	1.8886	1.8921	100.2 ± 0.9
Succinic	0.7191	0.47	1.1891	1.2019	101.1 ± 0.6
		Spiking Level-2			
Lactic	1.6886	0.40	2.0886	2.0576	98.5 ± 0.6
Succinic	0.7191	0.65	1.3691	1.3869	101.3 ± 0.2
		Spiking Level-3			
Lactic	1.6886	0.60	2.2886	2.2516	98.4 ± 1.0
Succinic	0.7191	1.10	1.8191	1.8465	101.5 ± 1.1

different concentrations, and typical recoveries ranging from 97–102% for all acids at all spiking levels were obtained. Some authors [8] have pointed out that some compounds generally present in these samples, such as fructose, may interfere with the determination of the acids if recovery is carried out at a low wavelength (i.e., shorter than 220–230nm). Sugars like fructose possess an appreciable capacity of absorption at the wavelength used in this work and elute near malic acid. In order to check this potential interference, malic acid recovery was also determined by adding 150g/l of fructose to the samples. As can be seen in Table I, the analytical data indicate no interference from sugars at the wavelength used. Similar results were obtained for recovery studies in ciders, as can be seen in Table II.

The coefficients of variation for the three replicates of each sample were generally less than 5%. The viability, reproducibility and accuracy of the proposed procedure in the quantitative analysis of organic acids in apple juices and ciders has thus been demonstrated here.

Conclusions

Reversed-phase chromatography, using acid or buffer in the mobile phase to suppress the ionization of the solutes, is probably the most suitable and simple separation method for carboxylic acids. The use of a linear photodiode array for detection was important in optimizing analyte responses and in avoiding some interferences spectrally. Since it is rapid and simple, the proposed procedure may be useful in monitoring the evolution and transformation of organic acids during apple maturity, as well as during the industrial processing of apple juices and wine-ciders in order to control the organoleptic properties.

Acknowledgement

This work was financially supported by the Comisiòn Asesora para la Investigaciòn Cientifica y Técnica (CAICYT).

References

[1] *Association Francaise* de Normalisation (1978), NFV **76**, 002–006.

[2] *D. A. Heatherbell*, J. Sci. Food Agr., **25**, 1095 (1974).

[3] *D. W. Backer*, J. Assoc. Offic. Anal. Chemist, **56**, 1257 (1973).

[4] *Boehringer*, Mannheim (Germany), (1975/1976).

[5] *H. Rebelein*, Dent. Lebensm. Rundschau, **63**, 327 (1967).

[6] *R. Schwarzenbach*, J. Chromatogr., **251**, 339 (1982).

[7] *V. T. Turkelson, M. Richards*, Anal. Chem., **50**, 1420 (1978).

[8] *A. G. H. Lee, S. J. Smith*, Flüssiges Obst, **52**, 599 (1985).

[9] *R. Bushway, J. Bureau, D. McGann*, J. Food Sci., **49**, 75 (1984).

[10] *R. Andersson, B. Hedlung*, Z. Lebensm. Unters. Forsch., **176**, 440 (1983).

[11] *R. H. Evans, A. W. van Soestberben, K. A. Ristow*, J. Assoc. Off. Anal. Chem., **66** (6), 1517 (1983).

[12] *E. D. Coppola*, Food Technol., **36** (4), 88 (1984).

[13] *H. J. Jeuring, A. Brands, P. van Doorninck*, Z. Lebensm. Unters. Forsch., **168**, 185 (1979).

Received: Aug. 6, 1987
Accepted: Aug. 14, 1987
F

Application of a New Capsule-Type Silica Gel Coated with Hydrophobic Polymer to Preparative Liquid Chromatography on an Industrial Scale

Y. Ohtsu / O. Shirota* / T. Ogawa / I. Tanaka / T. Ohta / O. Nakata / Y. Fujiyama

Shiseido Research Center, 1050 Nippa-cho, Kohoku-ku, Yokohama, Japan 223

Key Words

Reversed-phase liquid chromatography
Preparative liquid chromatography
Silicone polymer-coated silica gel
γ-linolenic acid
Chromatographic purification

Summary

A new type of column packing material designed for preparative liquid chromatography, silicone polymer-coated silica gel modified with octadecyl group (S/S-C_{18}), was applied to chromatographic purification of a lipophilic biotechnological product. Triglycerides containing γ-linolenic acid were separated from the curde oil that consisted of triglycerides, diglycerides, free fatty acids, sterols and other polar substances, using a S/S-C_{18} packed column (150 mm I.D. × 1000 mm). No column deterioration was observed after more than 1500 times of sample introductions.

Introduction

Recent rapid developments in biotechnology have caused considerable interest in the scale-up of the chromatographic technique as a method of purification. A lot of large-scale chromatograph systems have appeared on the market since around 1985. However, the most important factor in introducing large-scale chromatography is the "column packing material" rather than the chromatograph from the point of view of both chromatographic techniques and economics.

We have already developed a new silica-based column packing material (S/S-C_{18}), or "capsule-type silica gel" for analytical reversed-phase liquid chromatography (RPLC). It is obtained by bringing hydrophobic silicone monomers in touch with the silica surface, making them form the polymer film, and thereafter chemically modifying the polymer film with an octadecyl group [1].

It has been proven that S/S-C_{18} has not only high peak resolution and strong pressure resistance (which could be expected in some other silica-based packing materials), but also shows chemical stability against alkaline mobile phases (which seems impossible to expect in conventional ODS-silica gels).

Schomburg et al. first introduced the idea of "polymer coating" and have been reporting good results since 1983 [2–5]. They immobilized various polymers, such as methylpolysiloxane, alkyl-substituted polysiloxane, polybutadiene, etc., to silica, endcapped silica or alumina.

Although several successful results were reported on the techniques of polymer coating, few of their applications to preparative liquid chromatography (PLC) have been reported. In this work, several types of S/S-C_{18} for PLC were prepared and their performances were studied through an actual purification of a lipophilic biotechnological product.

Experimental

For high performance liquid chromatography (HPLC) on an analytical scale, LC-6A (Shimadzu, Japan) was employed and a Differential Refractometer R401 (Waters Associates, USA) was connected to the system.

A semi-preparative HPLC system consisted of a Pump 64 with a maximum flow rate of 50 ml/minute and a Differential Refractometer (Knaur, FRG), Sample Injector EA-25 (Kyoto Chromato, Japan), and UV Detector S-310A (Soma, Japan).

An industrial automatic preparative HPLC system was fabricated by Kyoto Chromato, Japan. Its flow diagram is shown in Fig. 1. The system consists of two flow systems so that two different jobs can be operated simultaneously. These are designed for automated operation controlled by a personal computor. Maximum flow rates are 3.0 liter/minute and 5.0 liter/minute, respectively. Sample injections were carried out by a geared pump at 300 ml sample/minute. All the electric parts were sealed from outer air movements, and valve movements were controlled by pressed air so as to make the whole system antiexplosion-designed.

0009-5893/87 0351-06 $03.00/0

© 1987 Friedr. Vieweg & Sohn Verlagsgesellschaft mbH

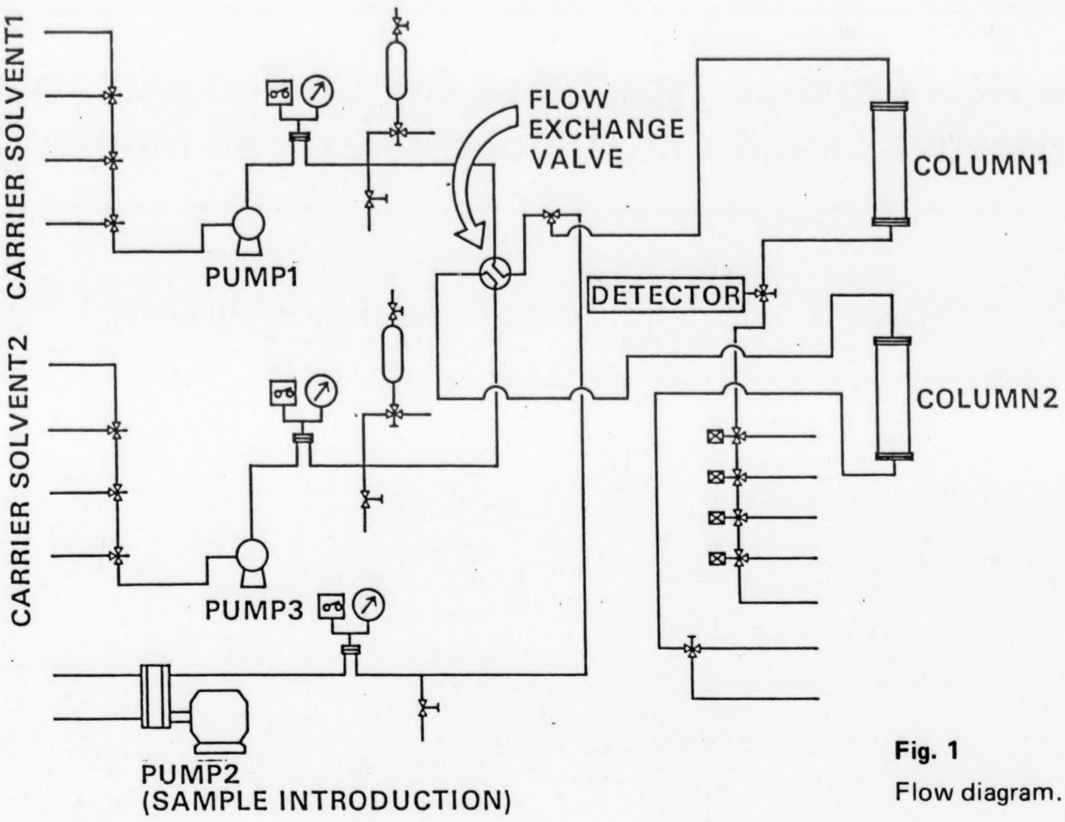

Fig. 1
Flow diagram.

Gas chromatography (GC) for analysis of the whole chemical composition was performed using a packed column (3 mm I.D. × 500 mm) of OV-1, at 100 °C to 340 °C (16 °C/minute), with nitrogen (60 ml/minute) as a carrier gas.

GC analysis of fatty acid composition was performed using a packed column (3 mm I.D. × 2000 mm) with polyethyleneglycol as a liquid phase at 200 °C to 240 °C, with nitrogen (60 ml/minute) as a carrier gas.

A constant-pressure pump of a maximum flow rate of 1.2 liter/minute (Haskel, USA) was used to pack columns by the balanced slurry packing method. High quality standard chemicals were used without further purification. Solvents used in this work were liquid chromatographic grade except for those used in the industrial-scale chromatography.

Results and Discussion

Preparation of Packing Materials

Totally porous silica gels differing in particle size and particle type were treated along the same flow sheet of S/S-C_{18} preparation. After the procedure, it was verified by solid state high resolution nuclear magnetic resonance (NMR) spectrometry that all the packing materials shared the same surface structure.

Roughly speaking, the synthesis of S/S-C_{18} consists of two steps. The first step includes coating a silica surface with silicone polymer so as to make a homogeneous polymer film on the surface. Secondly, the surface of polymer-coated silica gel is chemically modified with an octadecyl group. The density of an octadecyl group of about 4 μmol/m^2 can be estimated from the surface area and weight increase after the second step.

Performance of Packed Column

Columns (20 mm, 50 mm and 100 mm I.D. × 250 mm and 500 mm) for PLC or semi-PLC can be packed with S/S-C_{18} by the balanced slurry method, using a constant-pressure pump (max. flow rate: 1.2 liter/minute) connected to a packer whose volume is more than twice that of the column. Since the initial linear velocity and packed condition are varied according to the particle size of the packing material and the column diameter and length, a slurry solvent of appropriate viscosity must be prepared. A column can be packed using the slurry solvent so that the number of theoretical plates (NTP) corresponding to the average particle size of a packing material and length of column can be attained. Several chromatograms of standard compounds are shown in Figs. 2 and 3.

Fig. 4 shows the relationship between NTP and sample size for two different S/S-C_{18}-packed columns. Measurements were carried out using a semi-preparative column (20 mm I.D. × 250 mm, which seems to be convenient in handling and large enough to make a prediction for scaling-up). As expected, a column of S/S-C_{18} prepared from a silica gel of particle diameter 10–25 μm, spherical (10–25 s) shows a greater NTP in every sample size than that of 25–44 μm, irregular-shaped (25–44 i.s.). The difference in NTP observed here must be due to particle size. Thinking about linear velocity, a flow rate of 19 ml/minute corresponds to 1.0 ml/minute in a column for analytical HPLC (4.6 mm I.D. × 250 mm). This linear velocity is commonly used in analytical LC, but is three or four times greater than that used in large-scale LC. Although an NTP of 25–44 i.s. is much smaller, it can be considerably improved by decreasing the flow rate (plots are shown by white triangles in Fig. 4). The pressure drop of 25–44 i.s. (23 kg/cm^2 at 19 ml/minute) is about a half that of 10–25 s (43 kg/cm^2 at 19 ml/minute).

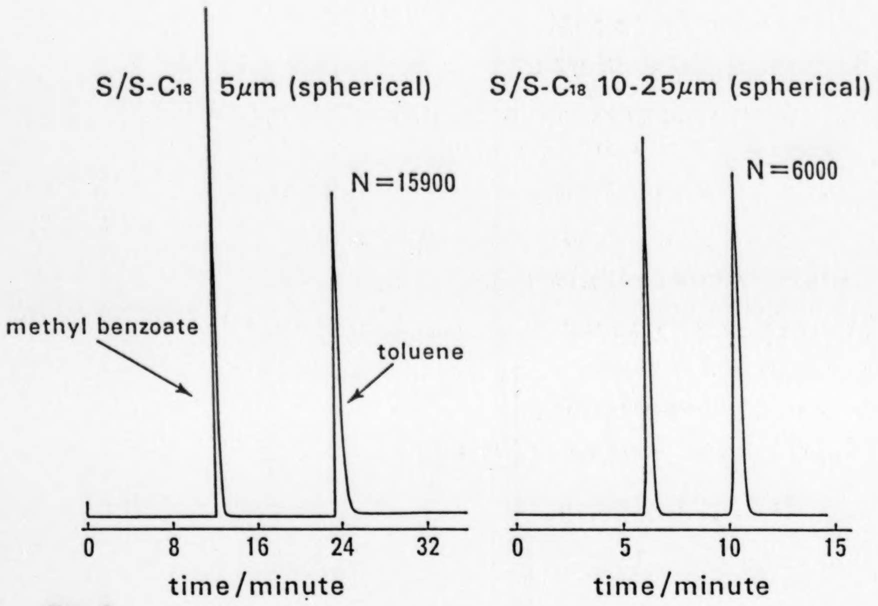

Fig. 2

Chromatograms of standard sample.

column:	20 mm I.D. X 250 mm
mobile phase:	methanol/water (7/3)
flow rate:	9.5 ml/minute
detection:	UV, 254 nm
pressure:	101 kg/cm^2
column:	20 mm I.D. X 250 mm
mobile phase:	methanol/water (7/3)
flow rate:	19 ml/minute
detection:	UV, 254 nm
pressure:	43 kg/cm^2

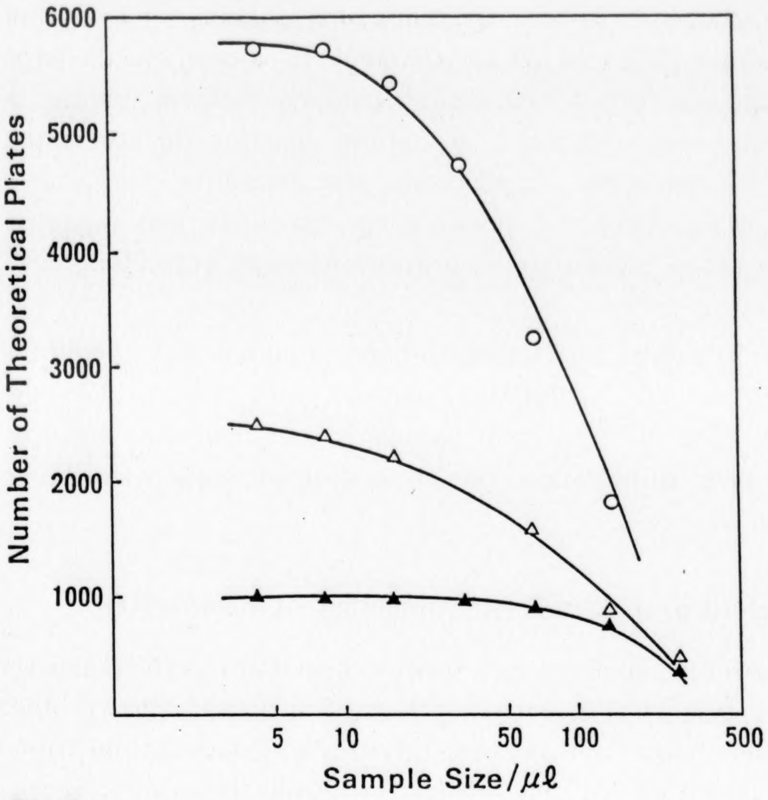

Fig. 4

Relationship between sample size and number of theroetical plates.

column:	20 mm I.D. X 250 mm
mobile phase:	methanol/water (7/3)
sample:	toluene

—○— S/S—C_{18}, 10—25 μm (spherical) flow rate 19 ml/minute
—△— S/S—C_{18}, 25—44 μm (irregular-shaped flow rate 5.0 ml/minute
—▲— S/S—C_{18}, 25—44 μm (irregular-shaped) flow rate 19 ml/minute

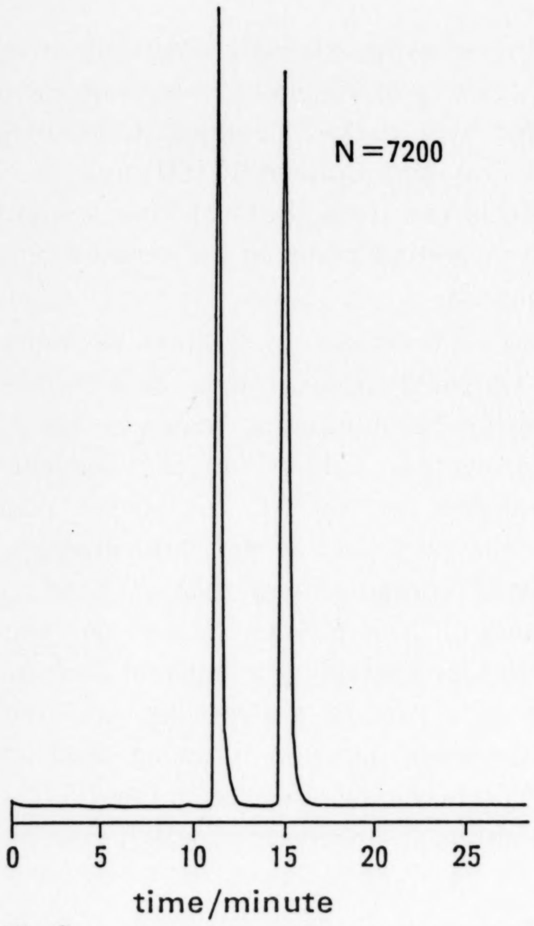

Fig. 3

Chromatogram of standard compounds.

column:	S/S—C_{18}, 10—25 μm (spherical) 50 mm I.D. X 500 mm
flow rate:	90 ml/minute
pressure:	37 kg/cm^2
mobile phase:	methanol/water (85/15)
detection:	UV, 254 nm
sample:	methyl benzoate/toluene = 1/5

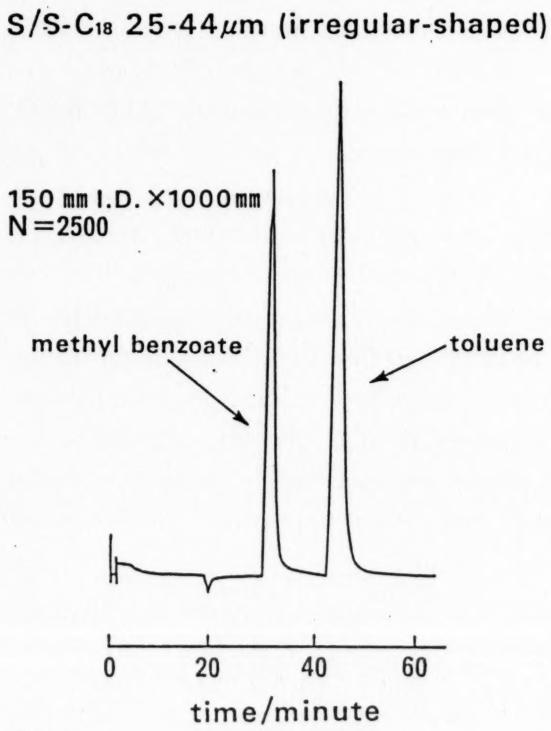

Fig. 5

Chromatogram of standard sample.

mobile phase:	methanol/water (85/15)
flow rate:	500 ml/minute
detection:	RI

A large-sized packer is required for packing an industrial column (150 mm I.D. X 1000 mm or more), but a large packer is hard to handle. A packing method without a packer was considered. A column was directly connected to the above-mentioned pump, and thereafter, the process of introducing and pressurizing the slurry was repeated five times, increasing the pressure stepwise from 20 kg/cm^2 to 70 kg/cm^2.

Fig. 5 shows the standard chromatogram by a column (150 mm I.D. X 1000 mm) packed with S/S-C_{18} (25–44 i.s.). The NTP is 2500, which is sufficient for the preparative purification on an industrial scale mentioned later.

Analysis of the Crude Oil Containing γ-Linolenic Acid

γ-Linolenic acid is a rare substance in nature, which acts as a precursor of a certain group of prostaglandins in the human body. It had been industrially obtained only from the seed oil of an evening primrose. However, recent research by the Chemical Technology Laboratories of the Agency of Industrial Science and Technology, Japan, made it possible to biotechnologically produce fatty oil containing γ-linolenic acid using a mold called "Mortierella Isaberina". Given this technique, fermentation of the mold started and mass-production of this fatty oil required a quick and efficient means of purification. The aim of purification was to obtain triglycerides containing γ-linolenic acid in high triglyceride purity and high γ-linolenic acid content. Attention was also given to PLC. (Hereafter, the fatty oil containing γ-linolenic acid is called "crude oil".)

Retention behavior of crude oil produced by biotechnology was observed using a S/S-C_{18} packed column (spherical, 5 μm, 4.6 mm I.D. X 250 mm) for analytical purposes; its chromatogram is shown in Fig. 6.

Using acetone as a mobile phase, first free fatty acids eluted from the column and diglycerides followed. Triglycerides eluted as the last component in this mixture. The triglycerides consisted of a group of peaks. The experiment using a semi-preparative column (20 mm I.D. X 250 mm) elucidated that the early part of triglycerides corresponds to that containing γ-linolenic acid in a high content (over 23 %), and the corresponding part is indicated in Fig. 6 as "triglycerides containing γ-linolenic acid". It seems that peak distribution of triglycerides in Fig. 6 are caused by a difference in fatty acid combinations forming a certain triglyceride molecule. In addition, the existance of γ-linolenic acid moiety within a triglyceride molecule causes an increase in polarity of the whole molecule and makes its retention time shorter than that of other triglycerides.

The chromatogram in Fig. 6 suggests that the purification of triglycerides involves removing relatively polar substances from this bio-synthesized mixture.

Purification of Triglycerides Containing γ-Linolenic Acid

As previously described, the aim of purification is to obtain triglycerides containing γ-linolenic acid in high triglyceride purity by removing relatively polar impurities from the crude oil. S/S-C_{18} of 25–44 i.s. was chosen as a packing material, and two packed columns, Column A (100 mm I.D. X 500 mm) and Column B (150 mm I. D. X 1000 mm), were used in this study. Both of them showed approximately 2500 theoretical plates in the measurement using standard compounds.

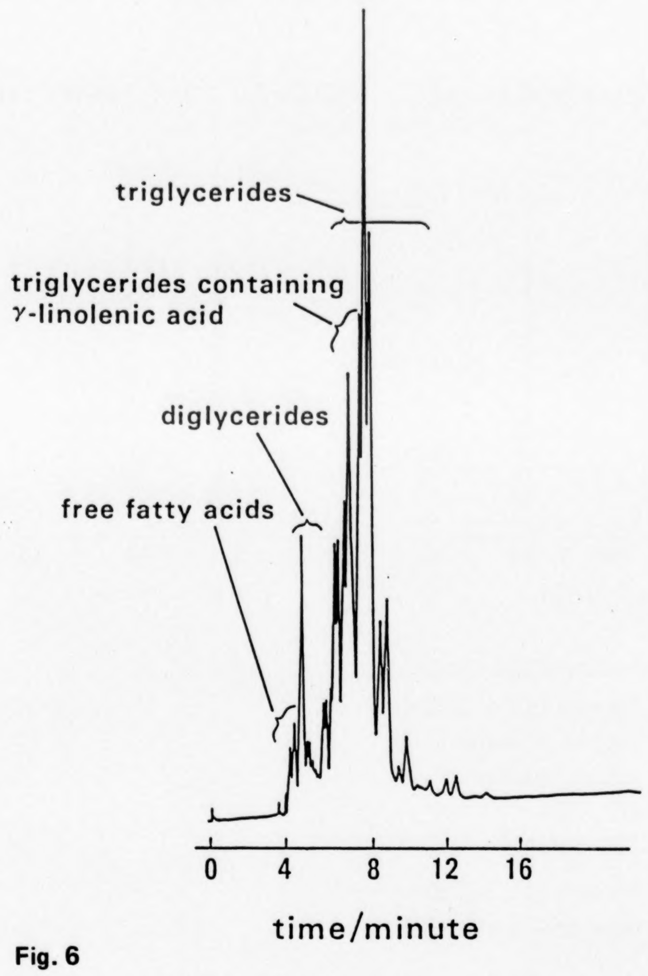

Fig. 6

Separation of the crude oil containing γ-linolenic acid.

column: S/S–C_{18}, 5 μm (spherical) 4.6 mm I.D. X 250 mm
mobile phase: acetone
flow rate: 1.0 ml/minute
detection: RI

60 g of crude oil were introduced to Column A, and a chromatogram was obtained using acetone as a mobile phase at a flow rate of 300 ml/minute, shown in Fig. 7. Fig. 7 also shows percentage composition of γ-linolenic acid of each fractionated part by GC. γ-Linolenic acid content is higher at the early part of the chromatogram, and the fraction No. 3 contains more than 20 % of γ-linolenic acid in crude oil is 7–8 % an the average. This indicates that triglycerides containing γ-linolenic acid are concentrated in the early part of triglycerides, and that the resonable reversed-phase partition is taking place in chromatography using this column as well as in the S/S-C_{18} column for analysis, although a decrease in peak resolution is observed.

For the next step, Column B was connected to the automatically-operated line of the industrial-scale chromatograph (shown in Fig. 1). Scaling-up from Column A to Column B corresponds to an increase of 4.5 folg in column volume. 250 g of crude oil were introduced into the system. Fig. 8 shows a chromatogram obtained by flowing acetone at a rate of 1500 ml/minute. The shaded area weighed 175 g and was evaluated by GC analysis. It

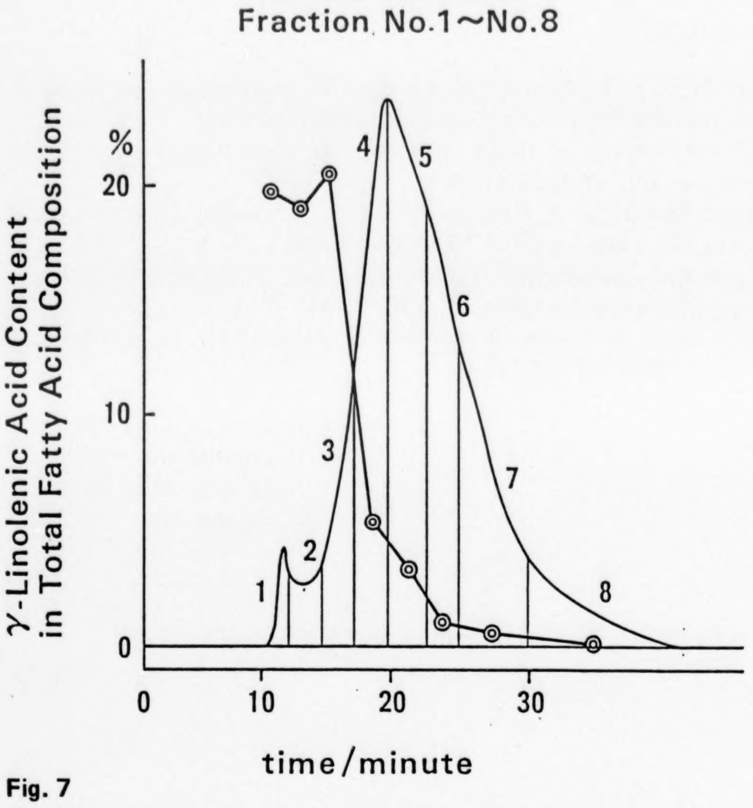

Fig. 7

Relationship between retention time and γ-linolenic acid content.

column: S/S–C_{18}, 25–44 μm (irregular-shaped)
100 mm I.D. × 500 mm
mobile phase: acetone
flow rate: 300 ml/minute
detection: RI
sample size: 60 g

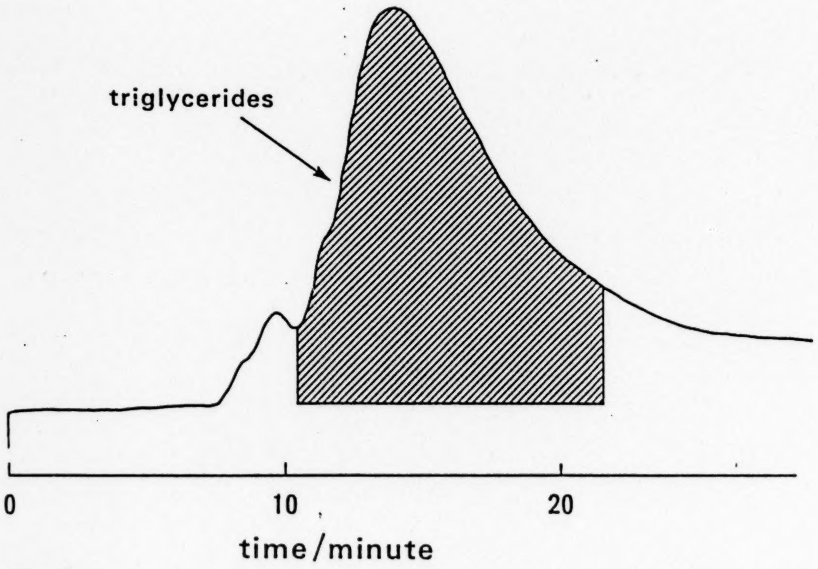

Fig. 8

Chromatogram of crude oil obtained by using the scaled-up column.

column: S/S–C_{18}, 25–44 μm (irregular-shaped)
150 mm I.D. × 1000 mm
mobile phase: acetone
flow rate: 1500 ml/minute
detection: RI
sample size: 250 g

showed a triglyceride purity of 99 %, and an γ-linolenic acid content of 8 %. Fig. 9 shows the comparison in chemical composition before and after purification of crude oil by GC. The shaded area in Fig. 8 corresponds to purified oil. The exclusion of fatty acids, sterols and diglycerides can readily be observed from the chromatogram. Furthermore, it was possible to obtain triglycerides of high γ-linolenic acid content (max. about 20 %) by terminating the collection of the triglyceride fraction at an earlier time. It seems that the reasonable partition is also taking place.

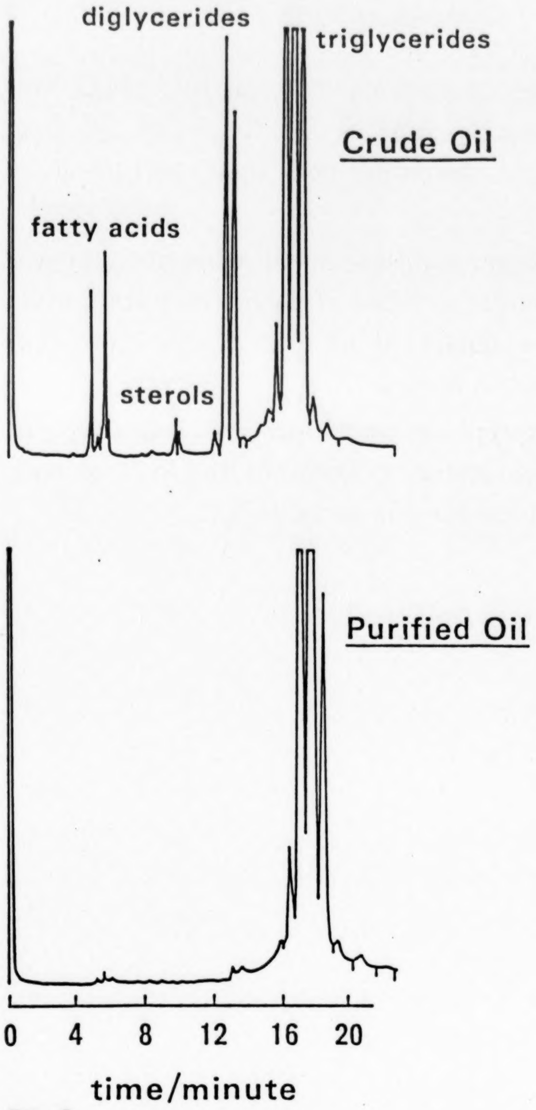

Fig. 9

Gas chromatogram of crude oil and purified oil.

column: Diasolid ZT, 0.5 m
column temperature: 100–350 °C, 16 °C/minute
carrier gas: nitrogen, 60 ml/minute
detection: FID

The last part of the chromatogram in Fig. 8, which is removed in this fractionation, corresponds to triglycerides containing little γ-linolenic acid. In successive sample introductions and fractionations, this part can be overlapped with the part of polar impurities before the triglyceride fraction by means of a time program in order to carry out the separation efficiently.

The purification on an industrial scale has been carried out using Column B. Although more than 1500 times of sample injections (380 kg of crude oil) have been made so far, no drawbacks such as deterioration of column, or change in retention behavior have been observed. Purification is still going on without renewing Column B.

Triglycerides separated in the above-mentioned process were given a final treatment using a large column (200 mm I.D. × 1000 mm) packed with an adsorbent and connected to another line of the chromatograph. Colorless and odorless triglycerides containing γ-linolenic acid were obtained as a final product.

Conclusion

S/S-C_{18}, a new type of packing material for RPLC, was applied to PLC. Several types of S/S-C_{18}- and S/S-C_{18}-packed columns were prepared and their performances were studied.

Using a S/S-C_{18} column, purification of a bio-product was carried out on an industrial scale. Triglycerides containing γ-linolenic acid were separated in high purity from biotechnologically-produced fatty oil.

A reasonable reversed-phase partition was observed in the experiments using scaled-up columns for PLC, as well as in the S/S-C_{18} column for analytical HPLC.

References

[1] *Y. Ohtsu, H. Fukui, T. Kanda, K. Nakamura, M. Nakano, O. Nakata*, Chromatographia **24**, 380 (1987).

[2] *G. Schomburg, A. Deege, J. Kohler, U. Bien-Vogelsang*, J. Chromatography **282**, 27 (1983).

[3] *G. Schomburg, J. Kohler, H. Figge, A. Deege, U. Bien-Vogelsang*, Chromatographia **18**, 265 (1984).

[4] *U. Bien-Vogelsang, A. Deege, H. Figge, J. Kohler, G. Schomburg*, Chromatographia **19**, 170 (1984).

[5] *H. Figge, A. Deege, J. Kohler, G. Schomburg*, J. Chromatography **351**, 393 (1986).

Received: June 29, 1987
Revised manuscript
Received: Aug. 28, 1987
Accepted: Sep. 01, 1987
F

Direct HPLC Resolution of Beta-Aminoalcohol (Tazifylline, Ranolazine, Sotalol) Enantiomers

E. Delée/L. Le Garrec/I. Jullien*/S. Béranger/J. C. Pascal/H. Pinhas

Recherche Syntex France, Leuville-Sur-Orge, 91310 Montlhéry, France

Key Words

Direct HPLC
Enantiomers
Resolution
Beta-aminoalcohols

Summary

A routine chiral analysis has been developed to control the optical purity of chiral drugs and to monitor their asymmetric synthesis. The recent advent of new chiral stationary phases for HPLC enabled us to achieve the direct resolution of chiral drugs without any derivatization.

The factors affecting chiral resolution on a new alpha$_1$-acid glycoprotein column (EnantioPac, LKB) were assessed with three beta-aminoalcohols.

Following chromatographic parameters were measured:

t_R : retention time of each peak (min)

k' : capacity factor $\left(\frac{t_R - t_0}{t_0}\right)$

α : relative retention $\left(\frac{k'_2}{k'_1}\right)$

R_s : resolution factor $\frac{2(t_{R2} - t_{R1})}{\omega_2 + \omega_1}$

The Enantiopac column was a chiral alpha$_1$-acid glycoprotein 100 x 4.0 mm (l x i.d) column (particle size 10 micrometers), developed by Hermansson [1] and now available from LKB, S-161 25 Bromma, Sweden. The matrix is based on a 10 micrometers diethylaminoethyl silica gel onto which a plasma protein (alpha$_1$-acid glycoprotein, orosomucoid) has been immobilized by ionic bonding [2].

Tazifylline and Ranolazine are both piperazines with a 2-hydroxypropyl side chain and their two respective enantiomers could be separated with 2-propanol in phosphate buffer pH = 7 as the mobile phase [1]. To improve resolution, the concentration of 2-propanol and flow rate were adjusted (Table I and Table II).

For Tazifylline, the data generated yielded an optimum eluent composition of 2-propanol/phosphate buffer pH = 7 (15/85 v/v). Phosphate buffer composition = 4 mM NaH_2PO_4 + 4 mM Na_2HPO_4 + 10 mM NaCl. Flow rate = 0.25 ml/min, t° = 20 °C, sample loading = 1 nanomole. See example in Fig. 1.

For Ranolazine, the data generated yielded an optimum eluent composition of 2-propanol/phosphate buffer pH = 7 (4/96 v/v). Phosphate buffer composition was the same as tazifylline buffer. Flow rate was 0.20 ml/min, t° = 20 °C, sample loading = 1 nanomole. See example in Fig. 2.

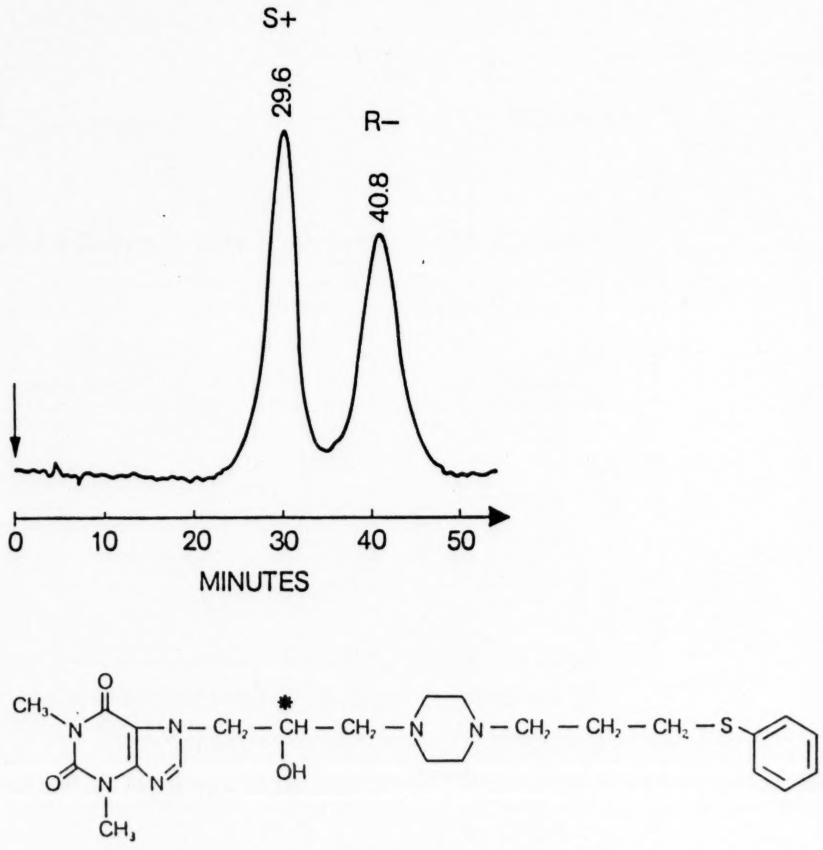

TAZIFYLLINE

Fig. 1

Resolution of R, S Tazifylline with optimum eluent (wavelength = 225 nm).

0009-5893/87 0357-03 $03.00/0

© 1987 Friedr. Vieweg & Sohn Verlagsgesellschaft mbH

Table I. Effect of 2-propanol concentration and flow rate of mobile phase on R, S tazifylline resolution

2-propanol %	14				15	
flow rate ml/min	0.30		0.25		0.25	
enantiomer	S+	R−	S+	R−	S+	R−
t_R (min)	25.5	34.4	30.5	41.7	29.6	40.8
k′	6.8	9.5	6.6	9.4	5.7	8.3
alpha	1.40		1.42		1.45	
Rs	0.89		0.91		1.33	

Table II. Effect of 2-propanol concentration and flow rate of mobile phase on R, S Ranolazine resolution

2-propanol %	3				4	
flow rate ml/min	0.25		0.20		0.20	
enantiomer	S−	R+	S−	R+	S−	R+
t_R (min)	21.7	28.2	27.0	35.2	24.5	32.6
k′	3.8	5.2	3.8	5.2	3.5	4.9
alpha	1.38		1.38		1.42	
Rs	0.88		0.84		1.40	

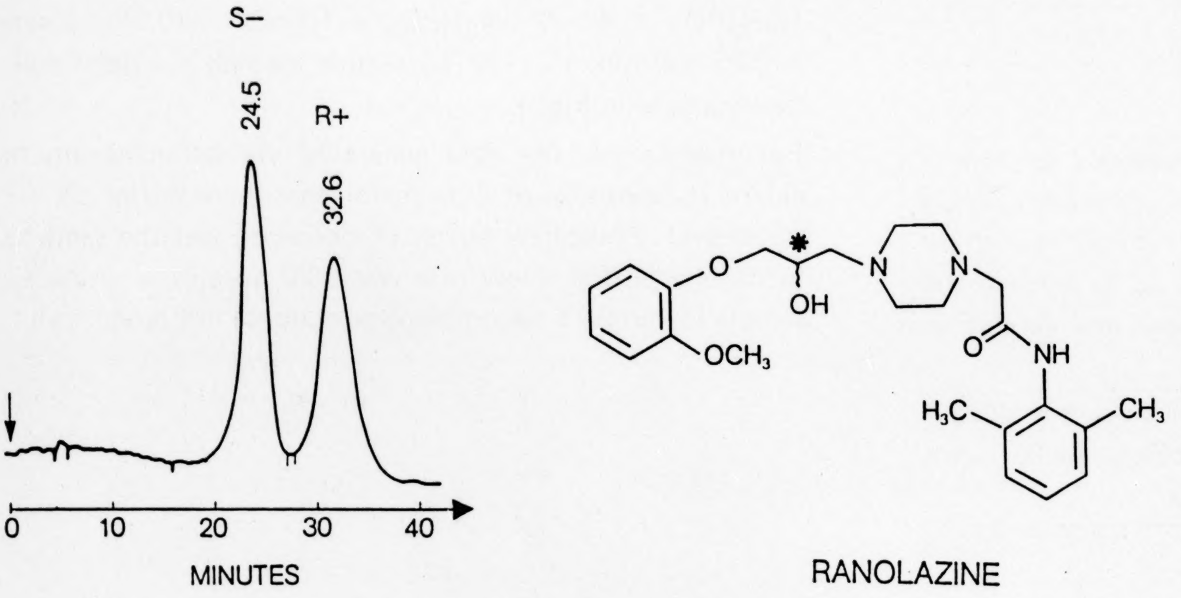

Fig. 2
Resolution of R, S, Ranolazine with optimum eluent (wavelength = 227 nm).

Table III. Effect of nature of anionic modifier on d, l sotalol enantiomer resolution

Acid 0.05 M:	Butyric (C4)		Pentanoic (C5)	Hexanoic (C6)		Heptanoic (C7)		Octanoic (C8)
enantiomer	l (−)	d (+)	one peak	l (−)	d (+)	l (−)	d (+)	one peak
t_R (min)	8.7	9.9	7.0	9.3	12.6	8.6	9.6	9.0
k′	0.6	0.8	–	0.8	1.4	0.6	0.8	–
alpha	1.38		–	1.79		1.29		–
Rs	0.44		–	1.88		0.61		–

Table IV. Effect of concentration of hexanoic acid on d, l sotalol enantiomer resolution (a: retention time t_R and capacity factor k′ of the second eluted enantiomer are given)

	Hexanoic acid concentration								
	0.025 M			0.05 M			0.075 M		
flow rate ml/min	0.15	0.20	0.25	0.15	0.20	0.25	0.15	0.20	0.25
t_R^a (min)	16.5	12.3	9.8	15.9	12.6	9.0	16.2	13.4	8.9
k'^a	2.1	1.7	1.6	1.5	1.4	1.1	1.3	1.5	1.1
alpha	1.49	1.56	1.56	1.62	1.79	1.62	1.64	1.80	1.54
Rs	1.68	1.66	1.36	1.38	1.88	1.40	1.52	1.91	1.16

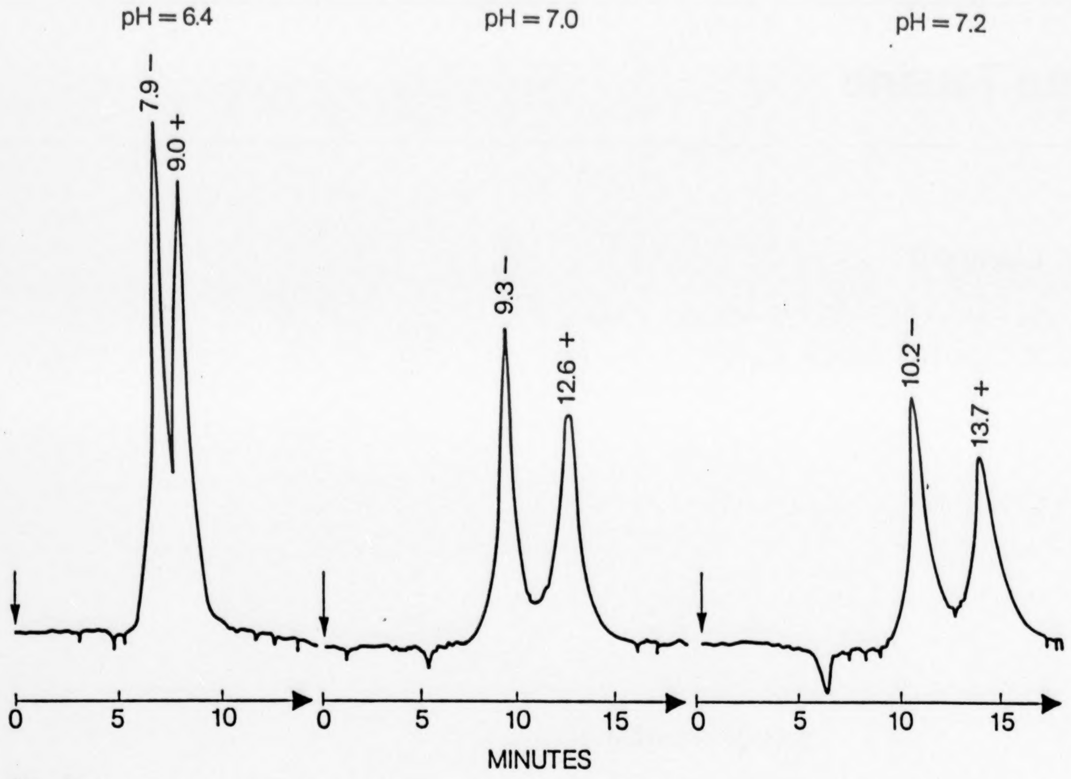

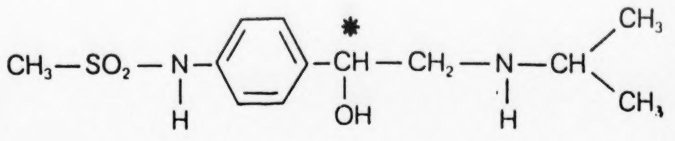

SOTALOL

Fig. 3
Effect of mobile phase pH on resolution of d, l sotalol with optimum eluent (wavelength = 230 nm).

Table V. Effect of pH of mobile phase on d, l sotalol enantiomer resolution

Mobile phase pH	6.4		7.0		7.2	
enantiomer	l(–)	d(+)	l(–)	d(+)	l(–)	d(+)
t_R (min)	7.9	9.0	9.3	12.6	10.2	13.7
k'	0.5	0.7	0.8	1.4	0.9	1.6
alpha	1.48		1.79		1.71	
Rs	1.01		1.88		1.62	

For Sotalol, a beta-aminoalcohol with an aliphatic secondary amine, the same mobile phase as used as above could not resolve the 2 enantiomers. A different organic modifier was necessary and instead of the uncharged 2-propanol modifier, an anionic modifier was added in phosphate buffer [2]. To improve the resolution, the nature of anionic acid modifier, (Table III) its concentration, (Table IV) flow rate of mobile phase, (Table IV) and pH of phosphate buffer, (Table V) were adjusted. Five carboxylic acids (n = 4 to 8) were assayed at 0.05 M and hexanoic acid gave the best resolution with a 0.02 M phosphate buffer pH = 7 as the mobile phase. The concentration of hexanoic acid was adjusted (0.025 M to 0.075 M) as well as the flow rate of the mobile phase (0.15 ml/min to 0.25 ml/min). We also adjusted the pH (6.4 to 7.2).

The data generated yielded the following optimal conditions: mobile phase = 0.05 M hexanoic acid in 0.02 M phosphate buffer (0.01 M NaH_2PO_4 + 0.01 M Na_2HPO_4) pH = 7, flow rate = 0.20 ml/min, t° = 20 °C, sample loading = 1 nanomole. See example of resolution as a function of pH in Fig. 3. Resolution was not improved by adjusting the ionic strength with NaCl.

For all three compounds each enantiomer was identified on the chromatograms with reference to compounds prepared by stereospecific synthesis (Tazifylline and Ranolazine) or differential salt crystallization (Sotalol) [3]. Optical purity above 95 % could be determined with a lower limit of 5 % of each enantiomer.

Two year use of these columns leads us to recommend careful maintenance for maximum column life time. Thermal, physical and chemical shocks should be avoided. Cartridge thermostatting (usually 20 °C) is important. Prolonged equilibration eluent, washing with water and with 2-propanol : water (1 : 1), both at very low flow-rate (0.1 ml/min) are also crucial. With these columns, small changes in pH or concentrations of organic modifiers can substantially improve resolution.

Conclusion

EnantioPac columns permit direct chiral HPLC resolution of new compounds. For each resolution, several factors should be carefully assessed to optimize this useful routine procedure to monitor optical purity during asymmetric synthesis.

References

[1] *J. Hermansson,* J. Chromatogr. **298**, 67–68 (1984).
[2] *G. Schill, I. W. Wainer, S. A. Barkan,* J. Liquid Chromatogr. **9** (2 & 3), 641–666 (1986).
[3] *A. Simon, J. A. Thomis,* Patent No. DE.3.419.067.

Received: July 21, 1987
Accepted: Aug. 5, 1987
F

HPLC Determination of Plasma Taurine

P. A. Biondi*[1] / F. Manca[1] / A. Negri[1] / C. Lucarelli[2]

[1] Istituto di Fisiologia Veterinaria e Biochimica, Via Celoria 10, 20133 Milano, Italy
[2] Istituto Superiore di Sanità, Viale Regina Elena 299, 00161 Roma, Italy

Key Words

Taurine
Column liquid chromatography
Plasma
Ion-pair extraction

Summary

The taurine content in plasma was determined by high performance liquid chromatographic analysis of its dansyl derivative with fluorometric detection. After the reaction with dansyl chloride, the derivative was extracted from an aqueous mixture by using tetrabutylammonium as a counter-ion. The influences of different tetrabutylammonium salts and of the eluent mixture composition were studied. Omotaurine, added as the internal standard to the plasma samples, assured good reproducibility. The procedure was applied to the determination of taurine in specimens from different mammalian species.

Introduction

As pointed out in a recent well-documented review [1], interest in taurine (2-aminoethanesulphonic acid, Tau) studies is continuously increasing. Although its biological role is not yet defined, in different organs the presence of Tau has been related to cell integrity protection. In order to develop a method suitable for the routine analysis of plasmatic Tau content, a rapid and simple procedure is needed. In this regard, high performance liquid chromatography (HPLC) has been shown to be the technique of choice. As an alternative to the unstable o-phthalaldehyde derivatives, we recently introduced the use of 5-dimethylaminonaphtalenesulphonyl-chloride, dansyl-chloride (DNS-Cl) for the analysis of Tau present in formulations [2]. The aim of this work was to test the suitability of the DNS-derivatization for the plasmatic Tau determination in different species. In order to eliminate interferences in the final chromatographic profile, a purification step before the HPLC run was introduced and its parameters studied.

Experimental

Materials

Tau and omotaurine (3-aminopropanesulphonic acid, o-Tau) were supplied by Sigma (St. Louis, MO, USA); DNS-Cl and HPLC-grade methanol by Merck (Darmstadt, FRG); and tetrabutylammonium (TBA) halogenide (TBA-F, TBA-Cl, TBA-Br, TBA-I) by Fluka (Buchs, Switzerland).

Chromatographic Conditions

A Jasco (Tokio, Japan) HPLC system equipped with a GP-A40 gradient programmer, a Familic 300 S pump and a FP-210 fluorometric detector set at 240nm and 520nm (as excitation and emission wavelengths, respectively) were used. The separations were performed on a cartridge (25cm × 4mm i.d.) filled with LiChrosorb RP-8 (7μm), and mounted on a Manu Fix holder. The eluent mixture was changed stepwise during analysis. A methanol-water (30:70) solution containing acetic acid (0.6% v/v) and triethylamine (0.1% v/v) at a flow rate of 1 ml/min was used to elute Tau and o-Tau derivatives; after 20′ from injection the column was washed with methanol for 10′, and reconditioned with the eluent mixture for 10′ before the subsequent injection.

Procedure

All operations were carried out in PTFE-lined screw-capped vials wrapped with aluminium foil in order to protect the samples from photodegradation. Plasma (0.2 ml) was added with 1 mM o-Tau aqueous solution (20μl) and with acetonitrile (0.5 ml) dropwise under vigorous shaking. After centrifugation, the supernatant was added with sodium carbonate buffer 40 mM, pH 9.5, (1 ml) and 2 mg/ml DNS-Cl solution in acetonitrile (0.5 ml). The reaction mixture was kept at 40°C for 20′, washed with dichloromethane (3 ml), added with aqueous 50 mM TBA-Cl (1 ml) and extracted with dichloromethane (3 ml).

The organic phase was filtered on anhydrous sodium sulphate, and evaporated to dryness under a nitrogen stream. The residue was dissolved in the HPLC eluent mixture (0.1 ml) and finally analyzed in HPLC.

0009-5893/87 0360-03 $03.00/0

© 1987 Friedr. Vieweg & Sohn Verlagsgesellschaft mbH

Quantitative Analysis

Different volumes of an aqueous 1 mM Tau solution, containing 5–100 nmoles and a continuously constant volume of aqueous 1 mM o-Tau solution (20 μl), were treated according to the above-described procedure. A calibration graph was obtained by plotting ratios between the peak heights of DNS-Tau and DNS-o-Tau (Rh) versus the amounts of Tau. Tau contents were obtained from the Rh values found in plasma samples.

Recovery Studies

Constant volumes (1.5 ml) withdrawn from an acetonitrile-water reaction mixture, each containing DNS-Tau corresponding to the same amount of Tau (50 nmoles), were added with aqueous solutions of different TBA salts (1 ml) at different concentrations (1–100 mM) and extracted with dichloromethane (3 ml). The resulting separated organic phases were added with constant volumes (0.1 ml) of a dichloromethane solution, each containing DNS-o-Tau corresponding to the same amount of o-Tau (25 nmoles). The Rh from each sample was compared with that obtained from a sample prepared by evaporating the reference dichloromethane solution of DNS-o-Tau and adding to the residue the reference reaction mixture of DNS-Tau that had not been subjected to the extraction step. Recovery yields were calculated from the ratios between the Rhs so obtained.

Results and Discussion

In order to set up a method suitable for a sensitive and selective determination by HPLC of a compound in biological fluids, its structural moyeties are to be exploited. In the case of the small molecule of Tau, amino and sulphonic groups are present. In the described procedure, the first group reacted with DSN-Cl producing a chromogenic product, hence increasing the sensitivity of detection; on the other hand the second group, negatively charged in aqueous solutions, was coupled with a hydrophobic cation and then extracted in an organic solvent, thus increasing the overall selectivity.

As previously stated [2], the DNS-Cl, a well-known amino acid reagent, produces a stable derivative suitable for routinary HPLC determination of Tau.

The chromatographic conditions were slightly different from those we used in formulation analysis, in which we followed a previous experiment on DNS-amino acid derivatives [3]. When the triethylamine content was maintained at 0.008% v/v, the capacity factors (k$'$) of DNS-Tau and DNS-o-Tau extracted with TBA salts increased from TBA-F to TBA-I, as shown in Table I. This is probably due to the fact that the TBA halogenide, extracted into the organic phase and present in the injected sample, allows the less hydrophobic triethylammonium ion of the eluent to be partially split by the TBA ion to an extent dependent on its concentration; in fact with the larger counter ion, the solubility of the corresponding TBA salt in dichloromethane and its amount in the injected sample increases. In view of this situation, the interaction between DNS-Tau and the TBA ion is higher. In order to be independent from the presence of TBA in the final sample, the triethylamine concentration in the eluent mixture was increased to 0.1% v/v. Under these conditions, the DNS-Tau extracted with TBA is eluted with a k$'$ that does not change to any significant extent when a different TBA content is present in the injected sample; in fact the larger amount of triethylamine keeps the interaction between the TBA ion and DNS-Tau at a minimum. Fig. 1 shows two typical HPLC profiles.

The dependence of the recovery of DNS-Tau on the organic solvent from TBA counter ion and TBA salts concentration is shown in Table II. TBA-F and TBA-Cl, less soluble in organic solvents, support, at higher concentrations, a more efficient extraction of DNS-Tau from the aqueous phase, as previously demonstrated in our experiment on a similar compound [4]. As the differences in recovery yields between the two salts are slight, TBA-Cl was chosen for its lower hygroscopicity and cost. The ion-pair extraction of

Table I. Influence of different TBA salts[a] on the capacity factors (k$'$)[b] relative to DNS-Tau.

		counter ion			
	N.E.[c]	F	Cl	Br	I
k$'$	2.55	2.67	3.27	4.17	6.17

a) The concentration of the TBA salt aqueous solutions used for the extraction of DNS-Tau in this experiment was 50 mM, as described in the experimental section.

b) The eluent used for this experiment was a methanol-water (25:75) mixture containing acetic acid (0.6% v/v) and triethylamine (0.008% v/v).

c) Not extracted. This value is relative to a standard sample containing DNS-Tau that has not been subjected to the extraction step.

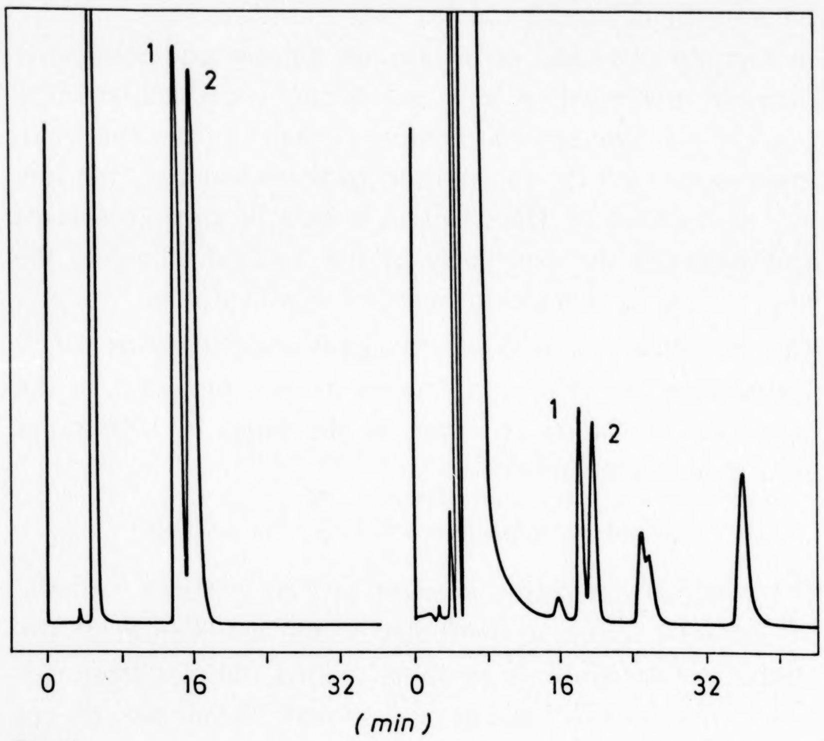

Fig. 1

Typical chromatographic profiles of a standard reaction mixture containing DNS derivatives of Tau and o-Tau (left) and of a sample obtained according the described procedure from a dog plasma specimen (right). Peaks: 1 = Tau; 2 = o-Tau.

Table II. Effect of TBA concentration of DNS-Tau percentage recovery from aqueous solutions of different TBA salts.

Counter ion	TBA concentration (mM)[a]			
	1	10	50	100
F	40.1	46.3	56.2	59.0
Cl	40.4	51.2	58.4	58.9
Br	41.6	52.2	53.1	54.0
I	43.8	49.1	50.6	–[b]

a) Concentrations of aqueous solutions added to the reaction mixtures before ion-pair extraction, according to the procedure described in the experimental section.

b) At this concentration TBA-I is insoluble in water.

Table III. Tau content in plasma samples from different mammalian species.

Species	Sample	Tau content (nmoles/ml)
Dog	1	86
	2	97
	3	90
	4	51
	5	98
Cat	1	138
	2	95
Bovine	1	69
	2	31

an ionic compound from an aqueous phase was shown to be an efficient procedure to help eliminate interferences. In fact, in this case, polar and not anionic compounds remain in the alkaline aqueous phase, while apolar compounds are removed by dichloromethane before the treatment with TBA-Cl. In addition to the selectivity, the ion-pair extraction of DNS-Tau in a volatile organic solvent also increases the sensitivity of the method, allowing the final sample to be concentrated in a small volume.

The relationship between the peak height ratios DNS-Tau/DNS-o-Tau (Rh) and nmoles of Tau subjected to the described procedure is linear, in the range 5–100 nmoles according to the equation:

$$Rh = 0.0444 \cdot \text{nmoles Tau} + 0.178 \quad (r = 0.995)$$

The minimal detectable amount of Tau is about 1 nmole. In Table III, given as examples of the application of the method, Tau contents in some plasma samples from different mammalian species are shown. A sample of cat plasma was analyzed five times, giving a Tau content of 138 ± 6.7 nmole/ml (C.V.: 4.9%). This indicates that the use of o-Tau as the internal standard assures good reproducibility.

In conclusion, the described procedure appears simple, reliable and hence suitable for clinical and nutritional studies where plasmatic Tau analysis is an important biochemical parameter to be considered.

Acknowledgements

This work was supported by a grant from The Ministero della Pubblica Istruzione.

References

[1] *C. E. Wright, H. H. Tallan, Y. Y. Lin, G. E. Gaull,* Ann. Rev. Biochem. **55**, 427 (1986).

[2] *P. A. Biondi, A. Negri, A. Ioppolo,* J. Chromatogr. **369**, 431 (1986).

[3] *Y. Tapuhi, D. E. Schmidt, W. Lindner, B. L. Karger,* Anal. Biochem. **115**, 123 (1981).

[4] *P. A. Biondi, N. F. Gu, C. Secchi,* Clin. Chim. Acta, **121**, 79 (1982).

Received: June 30, 1987
Accepted: Aug. 5, 1987
F

Development and Performance of an Automated HPLC-Analyzer for Catecholamines

K.-S. Boos*[1] / B. Wilmers[1] / R. Sauerbrey[2] / E. Schlimme[3]

1 Laboratorium für Biologische Chemie, Universität, Postfach 16 21, D-4790 Paderborn, FRG
2 E. Merck, Postfach 41 19, D-6100 Darmstadt, FRG
3 Institut für Chemie und Physik, Bundesanstalt für Milchforschung, Postfach 6069, D-2300 Kiel, FRG

Key Words

Column liquid chromatography
Size exclusion and affinity column packing
Column switching
Catecholamines

Summary

An automated, dual-column HPLC method has been developed that can be used routinely to quantify the parent catecholamines in body fluids. The method is based on a new, laboratory-prepared column material with size exclusion and high performance affinity chromatography properties. A microprocessor controlled column-switching technique is used with an optional integrated reaction-system for postcolumn derivatization for fluorescence detection. Natural fluorescence can be used for higher concentration levels.

The commercially available analyzer allows, for the first time, the direct injection (up to 0.5 ml) of an appropriate biological fluid. In its integrated sample-processing mode, it exhibits, chemoselectivity and -specificity, with a detection limit of 2pg, high precision and speed of analysis.

Introduction

The quantitation of catecholamines in physiological fluids is of importance in pathobiochemistry and clinical chemistry as these biogenic amines serve as diagnostic marker molecules for a variety of metabolic and neurological disorders [1, 2].

The availability, therefore, of a rapid and convenient procedure for a routine analysis of these compounds is required. Besides radioenzymatic assays [3], many different analytical methods have been reported ([4, 5] and cited references), especially those using high-performance liquid chromatography [6, 7, 8]. Due to the complexity of biological matrices such as urine, plasma, serum, liquor and tissue homogenates, purely analytical HPLC requires elaborate and labour intensive sample clean-up steps as shown in a comparative study [9]. In common use for such off-line sample pretreatment are liquid-solid phase extractions with aluminium oxide [10] and/or weak cation-exchange resin [11], Sephadex G10 [12], affinity chromatography with boronic acid substituted gels under low-pressure conditions [13] and liquid-liquid extractions by ion-pairing with diphenylborate [14].

These off-line sample clean-up techniques with time-consuming and error-prone washing-, evaporation- and redissolution steps can be overcome by applying column-switching techniques.

For the direct, i.e. on-line HPLC-analysis of the parent catecholamines in urine samples the following dual-column HPLC-methods have been described:

1. a micro-liquid chromatographic system using aluminium oxide as pre-column material, analytical reversed-phase ion pair-chromatography and dual electrochemical detection [15],
2. an aluminium oxide pre-column in combination with a reversed-phase analytical column and fluorimetric detection of the trihydroxyindole derivatives after post-column derivatization with a homogenous [16] or a heterogenous, i.e. solid phase (PbO_2; MnO_2) based, reaction system [17],
3. an affinity pre-column packed with laboratory-prepared phenylboronic acid substituted silica [18] in combination with an analytical cation-exchanger column and amperometric detection [19, 20],
4. a boronic acid affinity- or aluminium oxide pre-column in combination with an analytical ion-exchange or reversed-phase ion-pair partition column and amperometric or natural fluorescence detection [21].

The direct and multidimensional HPLC analysis of catecholamines in proteinaceous fluids such as plasma, serum or tissue homogenates still involves crucial and manually performed deproteinization steps. This off-line sample pretreatment is carried out by ultracentrifugation or acid-precipitation and unspecific adsorption on to aluminium oxide [22–26] and these manipulations diminish the desired analytical precision. Moreover, matrix impurities still present in the particular extracts often interfere with an accurate quantification of trace levels of catecholamines, especially in the case of electrochemical detection. Due to

0009-5893/87 0363-08 $03.00/0
© 1987 Friedr. Vieweg & Sohn Verlagsgesellschaft mbH

the relative instability of electrochemical detectors, when column-switching and changing mobile phase, we decided to use a post-column derivatization method for the routine trace analysis of norepinephrine and epinephrine. To fulfill the demands for high selectivity and sensitivity in method development, we chose the chemospecific generation of highly fluorescent trihydroxyindole derivatives [7, 8, 27–32].

By the preparation of a new bonded phase material (patent pending, [33]) and the application of an optimized post-column derivatization method we have succeeded in developing the first fully automated dual column HPLC-system that can be used routinely to quantify the parent catecholamines (norepinephrine, epinephrine and dopamine) by the direct injection of an appropriate biological fluid.

Experimental

All chemicals used in this study were from E. Merck (Darmstadt, FRG) and of the purest grade available. Buffers were prepared with double glass distilled water and degased by sonication for 10 min. Protein was determined according to the Bio-Rad assay (Bio-Rad Laboratories, Munich, FRG).

For sample preparation native human urine was acidified with 10 M hydrochloric acid to pH 3.0–3.5 and frozen at − 20°C. 24-hr urine was collected in a receiver filled with 20 ml hydrochloric acid (25%), adjusted to pH 3.0–3.5 with 10 M sodium hydroxide and frozen at − 20°C. The frozen urine samples were slowly thawed, centrifuged for 5 min in an Eppendorf desk centrifuge and the supernatant (1 ml) transfered into an autosampler vial.

For plasma analysis 20 μl of a preservative solution (0.16 M EGTA, 0.3 M reduced glutathione, adjusted to pH 7.0 with sodium hydroxide [23]), for serum analysis 10 μl of a preservative solution (0.3 mol/l reduced glutathione adjusted to pH 7.0 with sodium hydroxide) were added per ml of freshly withdrawn blood sample. After preparation of the heparinized plasma or serum fraction by centrifugation the samples were stored at − 20°C. These sampling procedures guarantee a stability of the biogenic amines for at least 12 hours at 4°C on the auto-sampler tray.

Standard stock solutions of norepinephrine, epinephrine and dopamine were prepared with 1 mM hydrochloric acid and photometrically determined at 279 nm using the following extinction coefficients: norepinephrine, $\epsilon = 2.04$; epinephrine, $\epsilon = 2.90$; dopamine, $\epsilon = 2.28$ (μmol^{-1} cm^2). At − 20°C the standard solutions are stabile for one month.

The HPLC-analyzer was built up with modular units from E. Merck (Darmstadt, FRG). As shown in Fig. 1 the apparatus is composed of a LC-controller Model L 5000 (LC-C), two pumps Model 655A-12 (P1, P2), an autosampler Model 655A-40 (AS), an automatic valve switching system Model ELV 7000 (ASV), a fluorescence detector Model F-1100 (FD), an integrator Model D-2000 (I), a pre-column (PC) and an analytical column (AC). For the optional use of post-column derivatization a reaction-system Model 655A-13 (RS) was included.

In order to perform a dual-column switching technique the pre-column and the analytical column were connected via

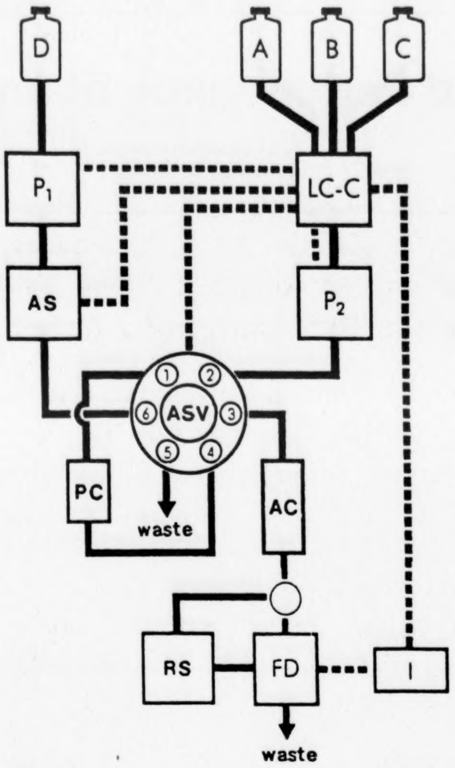

Fig. 1

Apparatus flow-diagram

A, analytical buffer; B, methanol; C, double distilled water; D, pre-column buffer; LC-C, liquid chromatography controller; P1, P2, pumps; AS, autosampler; ASV, automatic switching valve; PC, pre-column; AC, analytical column; FD, fluorescence detector; RS, reaction system; I, integrator.

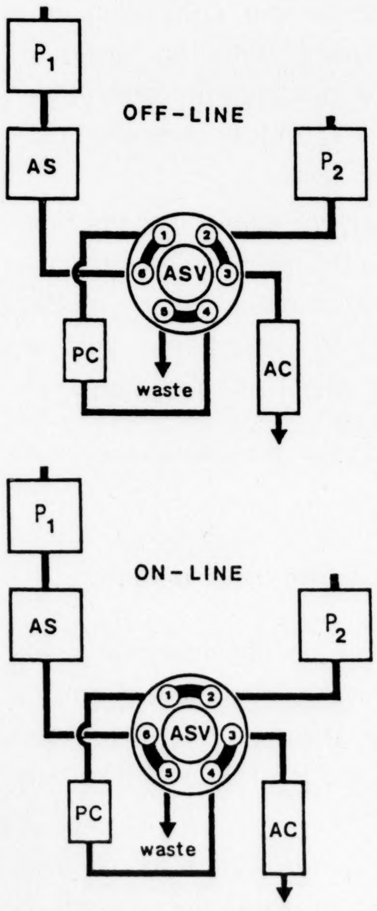

Fig. 2

Valve switching positions

Top: off-line mode; pre-column (PC) and analytical column (AC) can be run separately.

Bottom: on-line mode; pre-column and analytical column are series-connected through valve positions 2-1-4-3.

P1, pump 1; P2, pump 2; AS, autosampler; ASV, automatic switching valve.

an automatic six-port valve, whose configuration is shown in Fig. 2.

This instrumental set-up allows the independent use of the basic HPLC system besides the dual mode. Thus, reliability of the overall system performance can easily be controlled by comparing the off-line (RPLC) analysis of a standard mixture of catecholamines with the on-line (SEC-HPAC/RPLC) analysis of an actual sample (cf. Fig. 9, Table II).

The chromatographic conditions for the on-line analysis of urine samples (100μl) and detection of native fluorescence (excitation, 275nm; emission, 330nm) were as follows:

SEC-HPAC pre-column (binding capacity, 0.18mmol catecholamine per gram dry weight; 30 × 4mm i.d.); pre-column buffer (D), 0.2M diammonium hydrogen phosphate, 10mM EDTA adjusted to pH 8.7 with ammonia (25%); flow-rate, 0.8ml/min; duration, 10min (cf. step 1 and 2 of analysis cycle); analytical column (Hibar LiChrosorb RP-18, 7μm, 250 × 4mm i.d.); analytical buffer (A), 0.1M sodium dihydrogen phosphate, 5mM octane-1-sulfonic acid, 1.5mM sodium azide adjusted to pH 3.0 with phosphoric acid (20%) and methanol (11%, v/v) delivered from eluent reservoir (B); flow-rate, 1.0ml/min; duration, 3min (cf. step 3 of analysis cycle); flow-rate 1.8ml/min; duration 17min (cf. step 4 of analysis cycle).

The chromatographic conditions for the on-line analysis of urine (20μl), plasma or serum (500μl) samples and detection of trihydroxyindole fluorescence were as follows:

Pre-column buffer (D); flow-rate, 0.3ml/min; duration, 10min (cf. step 1 and 2 of analysis cycle); analytical column (LiChrospher RP-18, 5μm, 125 × 4mm i.d.); analytical buffer (A), 0.1M sodium dihydrogen phosphate, 5mM octane-1-sulfonic acid, 1.5mM sodium azide adjusted to pH 3.0 with phosphoric acid (20%) and methanol (11%, v/v) delivered from eluent reservoir (B); flow-rate 1.0ml/min; duration, 5min (cf. step 3 of analysis cycle); flow-rate, 1.0ml/min; duration, 10min (cf. step 4 of analysis cycle). The analytical and pre-column buffers are stable for two weeks at room temperature.

For post-column fluorogenic derivatization of the catecholamines norepinephrine and epinephrine to the corresponding trihydroxyindole derivatives (cf. Fig. 4) a reaction system, which is illustrated in Fig. 3, is placed between the analytical column outlet and the fluorescence detector.

The aromatic catecholamine ring system is stepwise oxidized during 45sec at 40°C in the first knitted reaction coil to the corresponding adrenoquinone (1) and adrenochrome (2) respectively (cf. Fig. 4) by the action of a buffered ferricyanide solution (E) (0.1M sodium dihydrogen phosphate, 0.2M disodium hydrogen phosphate, 2mM potassium hexacyanoferrate (III), pH 7.0), which is delivered by the synchronized pump 1 (SP-1) at a flow-rate of 0.3ml/min.

In order to stabilize the fluorophore generated at the first step as well as to destroy excess ferricyanide a reducing agent (1.5mM ascorbic acid) is added by pump 2 (SP-2) before the alkalization process (cf. Fig. 4). The gradual decomposition of ascorbic acid in the reagent reservoir (F) could be excluded for at least two days by the addition of a stabilizing agent (patent pending).

The intramolecular rearrangement of the adrenochrome is induced by alkali (G) (5M sodium hydroxide) in the third reaction coil. This process generates in 30sec at 40°C stable trihydroxyindole derivatives (3) with a high fluorescence quantum yield at an excitation wavelength of 410nm and an emission wavelength of 520nm.

As the natural concentration proportion is in favour of norepinephrine, the sensitivity for epinephrine was improved by optimization of pH and reagent concentration

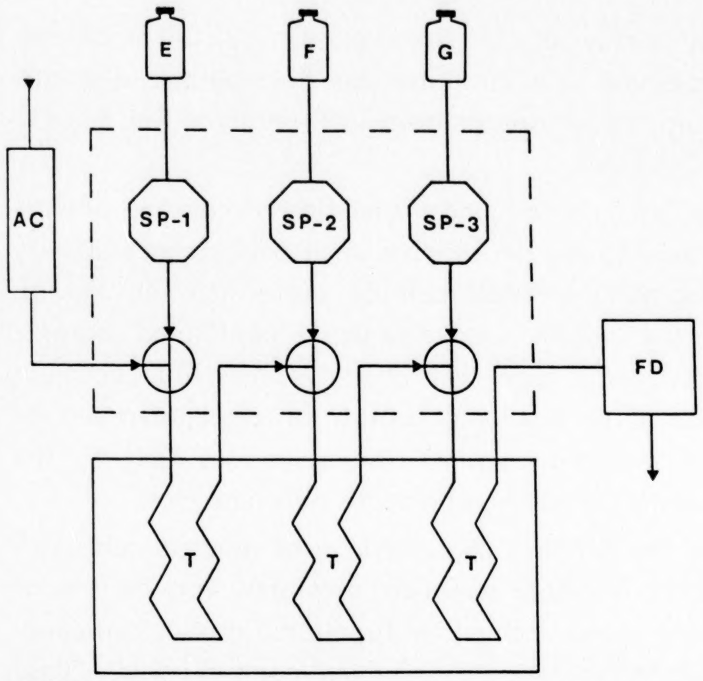

Fig. 3

Chemical reaction-system for post-column derivatization

AC, analytical column; FD, fluorescence detector; SP, synchronized pumps; T, thermostatic reaction coils; E, potassium hexacyanoferrate (III); F, ascorbic acid; G, sodium hydroxide.

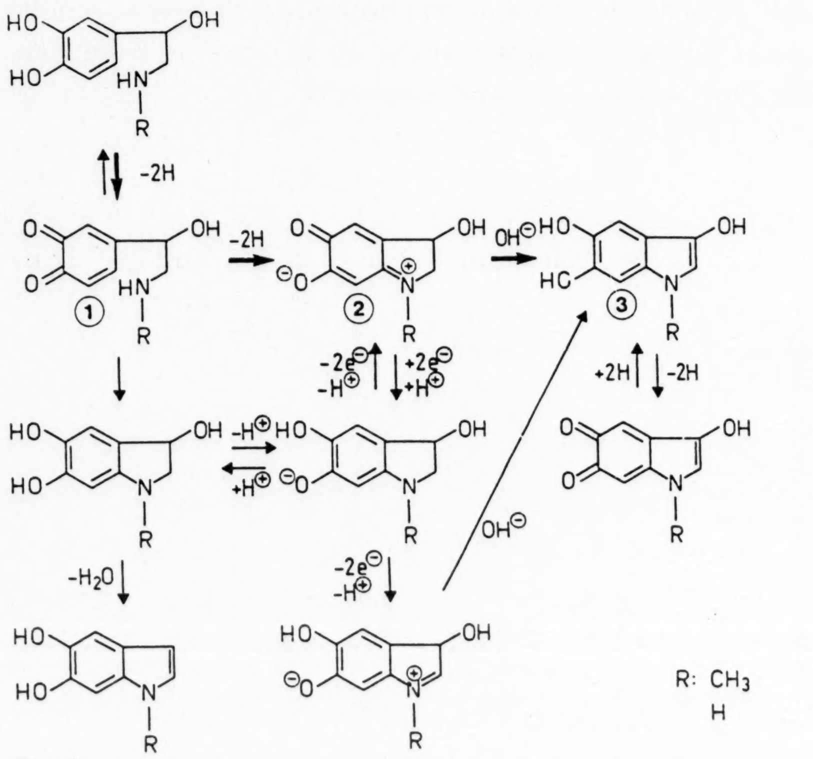

Fig. 4

Reaction-diagram for the generation of trihydroxyindole derivatives (1), adrenoquinone; (2), adrenochrome; (3), trihydroxyindole.

(cf. Fig. 11). Finally, the reaction-system has a low dead-volume of 2.25ml which allows a intimate mixing of the reagents without peak broadening.

Results and Discussion

Fig. 5 shows schematically the chromatographic properties of the newly developed pre-column material for the on-line sample processing of the parent catecholamines. The stationary phase is a chemically modified, semi-rigid gel which tolerates pH-values from 1 to 12 and a back pressure up to 2000 psi. It allows the simultaneous performance of two different modes of high performance liquid chromatography.

First, by virtue of its size-exclusion (SEC) properties, macromolecules (e.g. proteins) can be separated quantitatively from the solute as shown in Table I and Fig. 5 (SEC-step).

Secondly, by immobilizing a specifically modified phenylboronic acid to the gel support, high performance affinity chromatography (HPAC) can be performed (cf. Fig. 5). The affinity ligand, i.e. tetrahedral configured boronic acid, is capable of a pH-controlled, i.e. reversible, covalent interaction with the diol groups of catecholamines or other biomolecules such as ribonucleosides [34] by the chemospecific formation of a cyclic boronate ester.

Although the binding characteristic of boronic acid with vicinal diols is highly selective, secondary interactions of the bonded phase with other functional groups can cause an unspecific retention of sample contaminants. These interactions (hydrogen bonding, charge transfer complexes, ion exchange phenomena, hydrophobic interactions) have been diminished by an optimized buffer composition, molarity and pH value. In order to keep the elution volume of catecholamines from the pre-column at a minimum, i.e. one column bed volume, the acidic elution buffer was optimized with regard to pH value, ionic strength and capacity. In addition, this buffer had to serve as mobile phase for the subsequent analytical separation of the catecholamines under isocratic conditions.

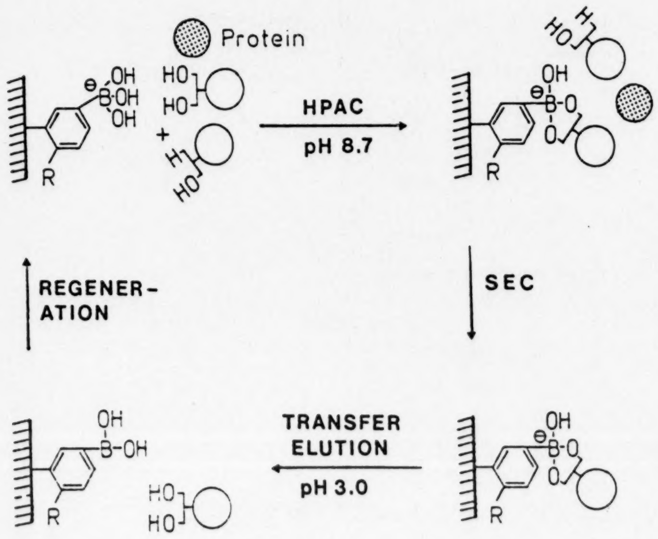

Fig. 5

Chromatographic properties of the pre-column

HPAC, high performance affinity chromatography; SEC, size-exclusion chromatography.

Table I. Size-exclusion-chromatographic properties of the pre-column

Sample	Protein content [mg/ml] Matrix	Protein content [mg/ml] Eluate	Elimination (%)
	x ± SD	x ± SD	x ± SD
Human Albumin	48.3 ± 0.3	48.9 ± 2.3	101.0 ± 4.7
Human Serum	62.9 ± 2.9	61.3 ± 1.5	97.6 ± 2.4

n = 5; x: mean value; SD: standard deviation;

1 ml samples of human albumin in physiological saline or human serum were injected via the autosampler in the valve-configuration "off-line" (cf. Fig. 2) onto the pre-column. Subsequently, the pre-column was washed with 3ml pre-column buffer (D) at a flow-rate of 0.3ml/min and the eluate analysed anew for protein content.

The overall on-line analysis cycle is characterized by five discrete steps:

1. Sample application (10–500μl) via the autosampler in valve-position "off-line" (cf. Fig. 2) followed by chemoselective binding (cf. Fig. 5) as well as enrichment of the catecholamines on the affinity ligand of the pre-column (cf. Fig. 1) under slightly alkaline, i.e. buffer D conditions ("HPAC-STEP", cf. Fig. 5).
2. Simultaneous, quantitative elution of the residual matrix constituents from the pre-column into the waste ("SEC-STEP", cf. Fig. 5, Table I).
3. Microprocessor controlled valve-switching into position "on-line" (cf. Fig. 2). Quantitative, group-selective elution of the catecholamines from the pre-column (cf. Fig. 5) by acidification (buffer A) of the immobilized cyclic boronate ester and simultaneous on-line transfer in a single, narrow elution band through position 2-1-4-3 of the valve to the top of the series-connected analytical column ("TRANSFER-STEP").
4. Automated valve-switching into position "off-line" (cf. Fig. 2) and separation of the catecholamines on the analytical column under isocratic, ion pair and reversed phase chromatographic conditions (SEPARATION-STEP, cf. chromatograms).
5. Replenishing of the tetrahedral trihydroxyboronyl functionality (cf. Fig. 5) for a new extraction cycle during the analytical run with the initial eluent D (REGENERATION-STEP).

Fig. 6 and 7 represent typical chromatograms, which demonstrate that the parent catecholamines can be easily identified and quantitated using the HPLC-analyzer described.

As shown in Fig. 8 no interferences occur with the elution pattern of diol-containing catecholamine metabolites and pharmaceutical catecholamine derivatives.

To assess the accuracy of the analyzer system a comparison of the on-line and off-line analysis of a standard mixture of norepinephrine and epinephrine was performed. It revealed a very good correlation (cf. Fig. 9) and a quantitative on-line recovery, whereby the latter is independent of the amount of catecholamines as well as of the biological matrix (Table II). Thus, this method does not require the addition of an internal standard and calibration can be performed simply with reference samples.

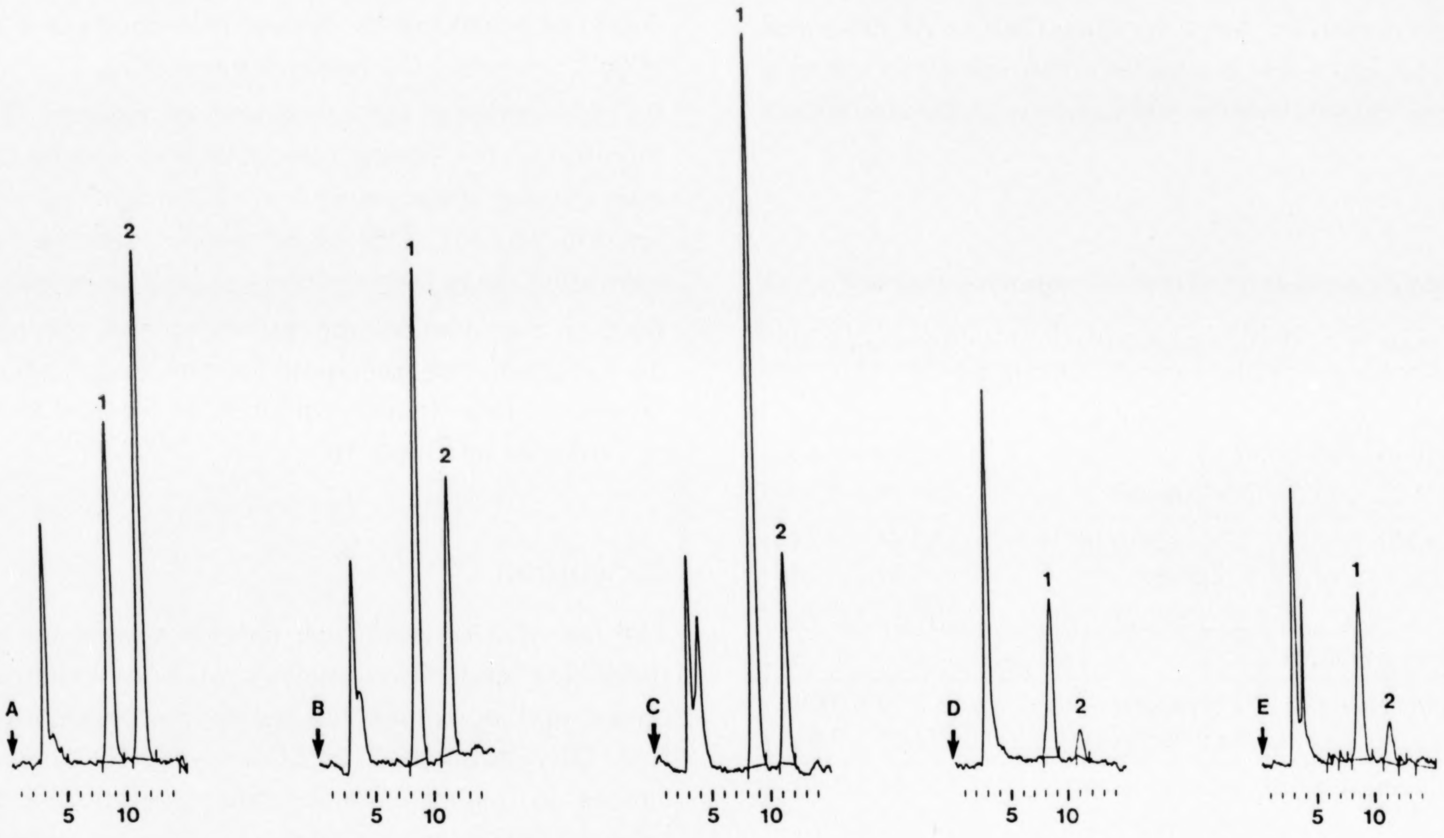

Fig. 6

Automated on-line analysis of urinary catecholamines with natural fluorescence detection

A) Standard, sample-volume 100μl; norepinephrine (1), 0.047nmol; epinephrine (2), 0.016nmol; dopamine (3), 0.130nmol.

B) Native urine, sample-volume 100μl; (1), 0.063nmol; (2), 0.016nmol; (3), 0.250nmol.

C) 24-hr urine, sample-volume 100μl; (1), 0.056nmol; (2), 0.015nmol; (3), 0.343nmol.

D) Pathological urine (phaeochromocytoma), sample-volume 100μl; (1), 0.259nmol; (2), 0.293nmol; (3), 0.161nmol.

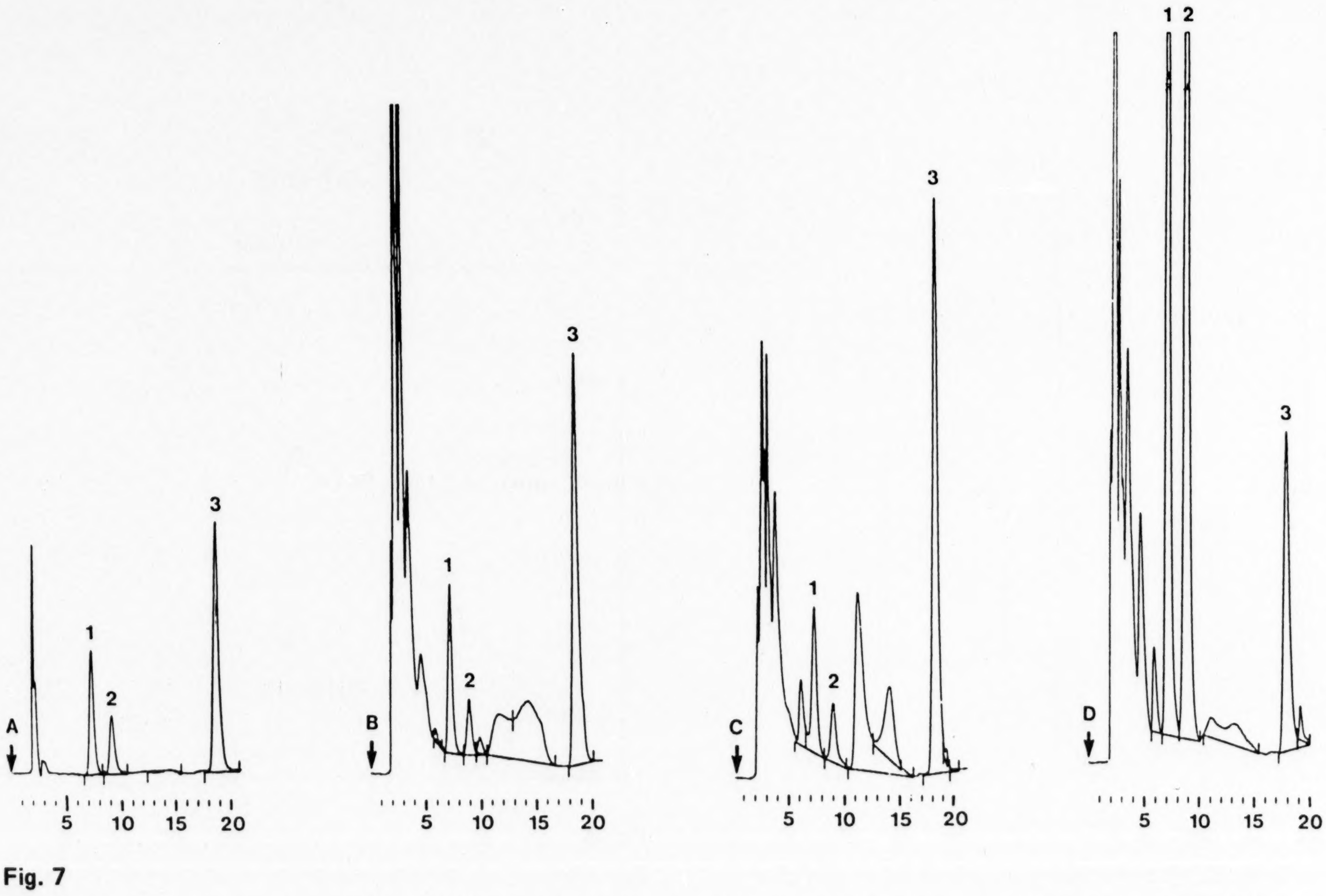

Fig. 7

Automated on-line analysis of urinary, plasma and serum catecholamines with trihydroxyindole fluorescence detection

A) Standard, sample-volume 100μl; norepinephrine (1), 3.78pmol; epinephrine (2), 2.72pmol.

B) Native urine, sample-volume 20μl; (1), 7.25pmol; (2), 1.69pmol.

C) 24-hr urine, sample-volume 20μl; (1), 10.81pmol; (2), 1.24pmol.

D) Plasma, sample-volume 500μl; (1), 1.97pmol; (2), 0.23pmol.

E) Serum, sample-volume 500μl; (1), 1.85pmol; (2), 0.25pmol.

The lower detection limits for quantitation of biological matrices, which were pretreated with alkali to destroy endogenous catecholamines and spiked with standards were found to be 300pg for natural fluorimetry and 2pg for the trihydroxyindole fluorescence monitoring.

Table II. Matrix-dependent and matrix-independent recovery

Urine analysis	Catecholamine	Recovery R(%)
		x ± CV(%)
Standard (n = 20)	Norepinephrine	99.07 ± 1.24
	Epinephrine	96.84 ± 0.93
	Dopamine	97.18 ± 0.07
Urine (n = 20)	Norepinephrine	93.61 ± 4.14
	Epinephrine	95.61 ± 3.25
	Dopamine	99.93 ± 2.26
Plasma, Serum analysis		
Standard (n = 10)	Norepinephrine	99.27 ± 3.99
	Epinephrine	97.05 ± 3.86
Plasma (Serum) (n = 15)	Norepinephrine	103.54 ± 3.89
	Epinephrine	103.18 ± 4.11

x: mean value; CV(%): coefficient of variation; sample-volume: 100µl urine, 500µl plasma, serum;

For measurement of matrix-dependent recovery endogenous catecholamines were destroyed by alkalization prior to the addition of a known amount of catecholamines. Matrix-independent recovery was obtained by repeated injection of standard mixtures in 1mM HCl according to Fig. 9.

Detection: urine, natural fluorescence; plasma, serum, trihydroxyindole fluorescence.

By the optional use of natural or induced fluorescence monitoring the parent catecholamines can be quantitated over a broad linear range from 20fmol/ml up to 3nmol/ml (cf. Fig. 10, 11). This range easily covers the normal concentration range found in physiological samples.

Despite the dual-column switching and the post-column derivatization the precision for the quantitation and the retention times is high for both within-run and between-run analyses (cf. Table III).

Conclusion

The use of a coupled dual column system for the on-line processing and trace analysis of norepinephrine, epinephrine and dopamine has led to the development of the first fully automated HPLC-analyzer for these catecholamines in highly complex and even protein-containing biological matrices.

The dual column technique is based on a newly developed and unique column material for digital chromatography which combines the selectivity of bioaffinity and size-exclusion chromatography with the high resolution and speed of analysis of reversed phase chromatography.

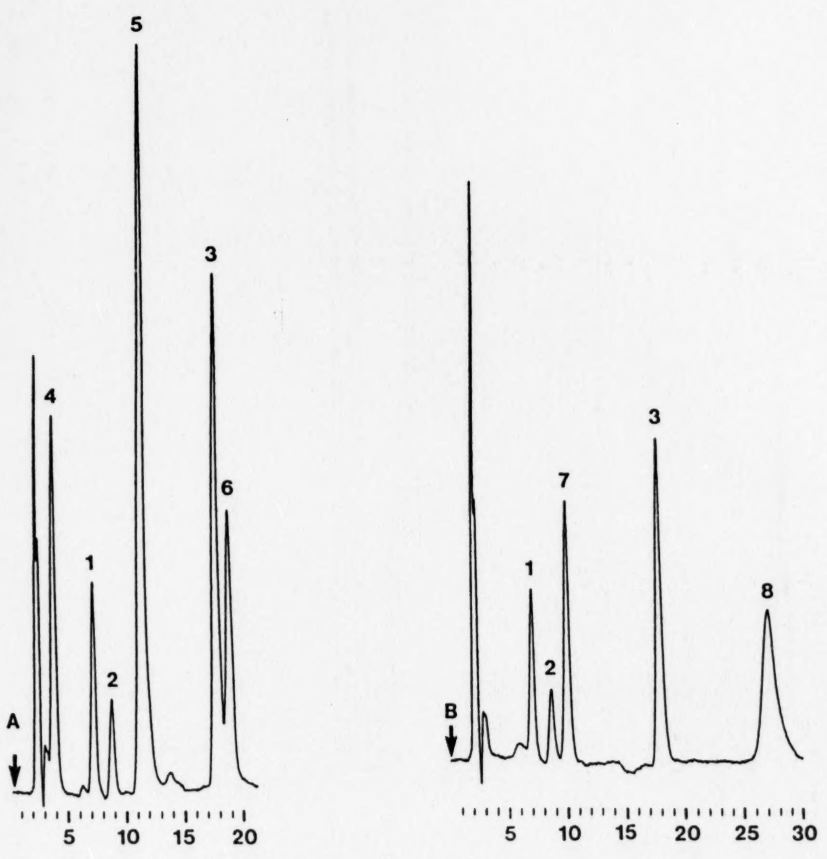

Fig. 8

Automated on-line analysis of catecholamine metabolites and pharmaceutical derivatives with natural fluorescence detection

A) Synthetic mixture of norepinephrine (1), epinephrine (2), dopamine (3) and the metabolites 3,4-dihydroxyphenylglycol (4), 5-hydroxydopamine (5), N-methyldopamine (6).

B) Synthetic mixture of (1), (2), (3) and the pharmaceutical derivatives α-methylnorepinephrine (7), isoproterenol (8).

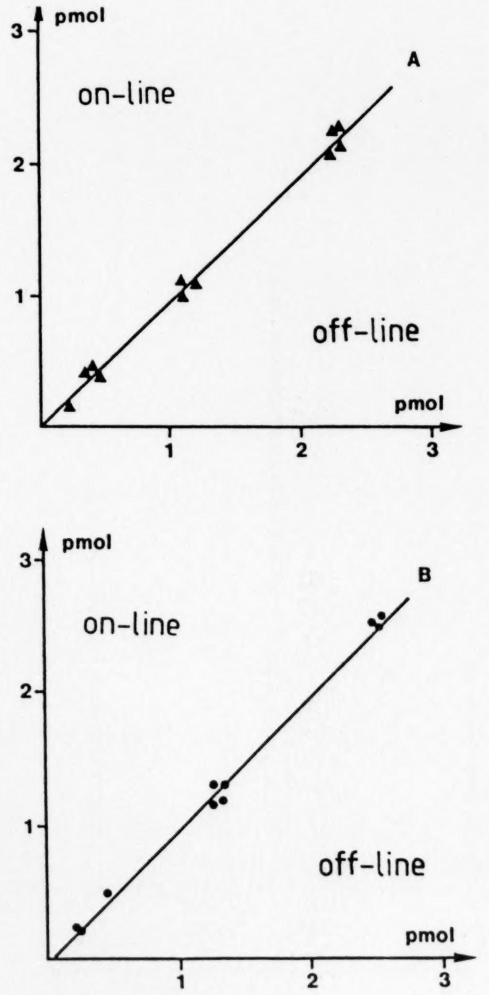

Fig. 9

Comparison of on-line and off-line analysis with trihydroxyindole fluorescence detection

Differently concentrated standard solutions of norepinephrine and epinephrine were applied on to the analytical column (off-line mode) for calibration and analyzed anew in the on-line mode.

A) Norepinephrine, $y = 0.99x - 0.02$, $r = 1.00$

B) Epinephrine, $y = 0.96x$, $r = 1.00$

Table III. Precision and stability

	Concentration		Retention-Time	
	CV_{Serie}(%)	$CV_{Day/Day}$(%)	CV_{Serie}(%)	$CV_{Day/Day}$(%)
Urine analysis				
Standard				
Norepinephrine	2.15	1.89	0.75	1.95
Epinephrine	3.43	0.61	0.96	2.65
Dopamine	3.25	2.75	0.72	2.86
Urine				
Norepinephrine	5.66	–	0.69	–
Epinephrine	6.67	–	0.87	–
Dopamine	2.63	–	0.60	–
Plasma, Serum analysis				
Standard				
Norepinephrine	2.48	3.99	0.66	1.12
Epinephrine	2.77	5.51	0.89	2.22
Plasma (Serum)				
Norepinephrine	4.84	–	0.91	–
Epinephrine	4.63	–	1.28	–

Urine analysis: n = 20, serie; n = 7, day/day; natural fluorescence detection.
Plasma, Serum analysis: n = 10, serie; n = 9, day/day; trihydroxyindole fluorescence monitoring

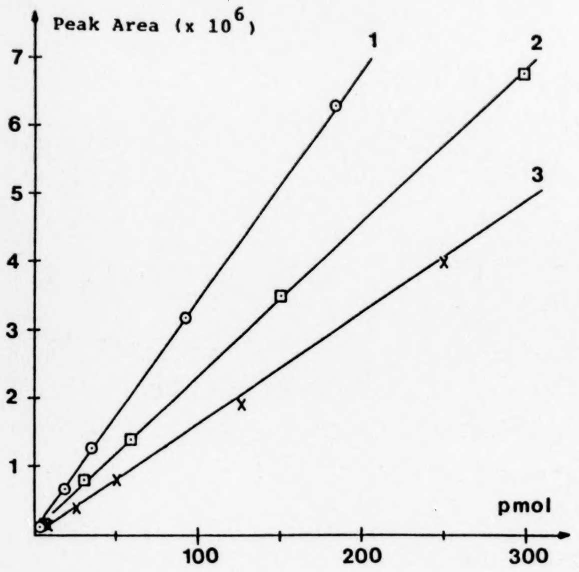

Fig. 10

Linearity between peak area and the catecholamine amount for on-line calibration and natural fluorescence detection

(1) Epinephrine, r = 1.00; (2) Norepinephrine, r = 1.00; (3) Dopamine, r = 0.99; sample-volume, 100 μl.

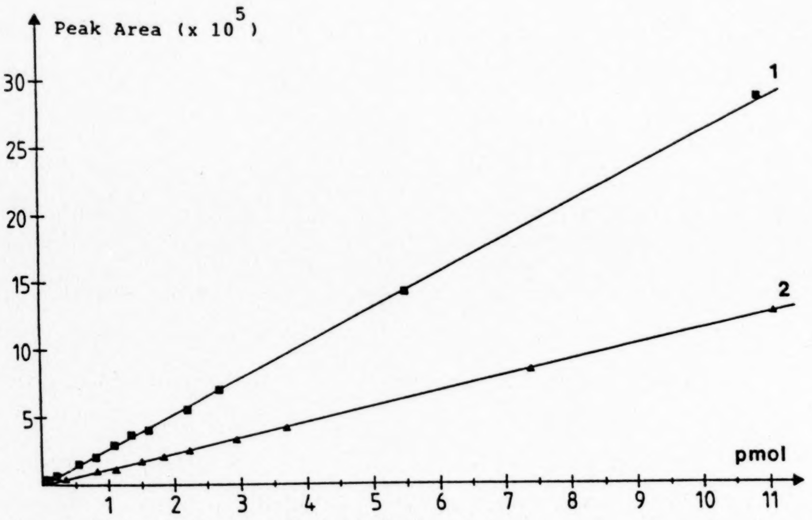

Fig. 11

Linearity between peak area and catecholamine amount for on-line calibration and trihydroxyindole fluorescence detection

(1) Epinephrine, r = 1.00; (2) Norepinephrine, r = 1.00; sample-volume 500 μl.

The optional use of a post-column reaction system provides the required sensitivity by the chemospecific generation of highly fluorescent catecholamine derivatives.

The high precision and excellent long-term stability of the HPLC analyzer is demonstrated by the very low intra- and interassay values of the coefficient of variation for retention times and quantitative results. The wide linear measuring range well covers the concentrations found in normal and pathological samples.

The high accuracy, which primarily is based on the quantitative and matrix-independent recovery of the catecholamines, points to the adoption of this technique as a reference method. The practicability and the commercial availability of the HPLC analyzer render the system attractive for the routine measurement of the parent catecholamines in clinical laboratories.

For the on-line trace analysis of dopamine in protein-containing body fluids a post-column derivatization with o-phthalaldehyde or p-aminobenzoic acid [35] is under investigation.

Acknowledgement

We wish to thank the "Forschungskommission" of the University of Paderborn for financial support and Angelika Boos, Kurwaldklinik, Bad Lippspringe for supplying us with serum and plasma samples.

References

[1] *J. Axelrod, J. Saavedra, E. Usdin*, in "Trace amines and the brain", ed., *Usdin, E., Sander, U.*, New York, (1976); p. 1.
[2] *G. B. Baker, R. T. Coutts*, "Analysis of Biogenic Amines", Elsevier, Amsterdam, 1982.
[3] *G. A. Johnson, R. M. Kupiecki, C. A. Baker*, Metabolism **29**, 1106 (1980).
[4] *M. Quimpere, Y. Volpe*, J. Chromatogr., **294**, 513 (1984).
[5] *J. M. P. Holly, H. L. J. Makin*, Analyt. Biochem., **128**, 257 (1983).
[6] *A. M. Krustulovic*, J. Chromatogr., **229**, 1 (1982).
[7] *S. Allenmark*, J. Liquid Chromatogr., 5, 1 (1982).
[8] *P. Hjemdahl*, Am. J. Physiol., **247**, 13 (1984).
[9] *A. H. B. Wu, T. G. Gornet*, Clin. Chem., **31**, 298 (1985).
[10] *A. H. Anton, D. F. Sayre*, J. Pharmacol. Exp. Ther., **138**, 360 (1962).
[11] *R. M. Riggin, P. T. Kissinger*, Anal. Chem., **49**, 2109 (1977).
[12] *B. H. C. Westerink, F. J. Bosker, J. F. O'Hanlon*, Clin. Chem., **28**, 1745 (1982).
[13] *S. Higa, T. Suzuki, A. Hayashi, I. Tsuge, Y. Yamamura*, Anal. Biochem., **77**, 18 (1977).
[14] *F. Smedes, J. C. Kraak, H. Poppe*, J. Chromatogr., **231**, 25 (1982).
[15] *M. Goto, T. Nakamura, D. Ishii*, J. Chromatogr., **33**, 226 (1981).
[16] *K. P. Kringe, B. Neidhart, Ch. Lippmann* in: *Molnar, I.*, "Practical aspects of modern HPLC", de Gruyter, Berlin, New York, 1982; p. 241.
[17] *B. Neidhart, J. Rüter, Ch. Lippmann, P. Deutschmann, I. Walker*, Fresenius Z. Anal. Chem., **323**, 880 (1986).
[18] *E. Hagemeier, K.-S. Boos, E. Schlimme, K. Lechtenbörger, A. Kettrup*, J. Chromatogr., **268**, 291 (1983).
[19] *K. Kemper, E. Hagemeier, K.-S. Boos, E. Schlimme*, J. Chromatogr., **336**, 374 (1984).
[20] *K. Kemper, E. Hagemeier, D. Ahrens, K.-S. Boos, E. Schlimme*, Chromatographia, **19**, 288 (1984).
[21] *J. De Jong, A. J. F. Point, U. R. Tjaden, S. Beeksma, J. C. Kraak*, J. Chromatogr., **414**, 285 (1987).
[22] *Y. Yui, T. Fujita, T. Yamamoto, Y. Itokawa, C. Kawai*, Clin. Chem., **26**, 194 (1980).
[23] *A. Yamatodani, H. Wada*, Clin. Chem., **27**, 1983 (1981).
[24] *M. Goto, G. Zou, D. Ishii*, J. Chromatogr., **275**, 271 (1983).
[25] *C. D. Kilts, M. D. Gooch, K. D. Knopes*, J. Neurosci. Methods, **11**, 257 (1984).
[26] *D. D. Koch, G. L. Polzin*, J. Chromatogr., **386**, 19 (1987).
[27] *G. Schwedt*, J. Chromatogr., **143**, 463 (1977).
[28] *K.-I. Okamoto, Y. Ishida, K. Asai*, J. Chromatogr., **167**, 205 (1978).
[29] *L. M. Nelson, M. Carruthers*, J. Chromatogr., **183**, 295 (1980).
[30] *Y. Yui, C. Kawai*, J. Chromatogr., **206**, 587 (1981).
[31] *G. M. Anderson, G. Young*, Life Sci., **28**, 507 (1981).
[32] *K. Mori*, J. Chromatogr., **218**, 631 (1981).
[33] *K.-S. Boos, B. Wilmers, R. Sauerbrey, E. Schlimme*, in "8. Königsteiner Chromatographie Tage", ed., *Aigner, H.*, Waters GmbH, Königstein, 1985, p. 219.
[34] *E. Schlimme, K.-S. Boos*, in "Chromatographic and other Analytical Methods in Nucleic Acids Modification Research", ed., *Gehrke, C. W., Kuo, K. C.*, Vol. II: Modified Nucleosides in Cancer, Elsevier, Amsterdam, 1987, in press.
[35] *M. Hamaji, T. Segi*, J. Chromatogr., **163**, 329 (1979).

Received: June 29, 1987
Accepted: July 20, 1987
F

Quantitative Reversed Phase HPLC Analysis of L-Ascorbic Acid (Vitamin C) and Identification of its Degradation Products

Linda L. Lloyd* / F. P. Warner

Polymer Laboratories Ltd, Essex Road, Church Stretton, Shropshire SY6 6AX, UK

C. A. White

Chembiotech Ltd, Institute of Research and Development, University of Birmingham Research Park, Vincent Drive,
Birmingham, B15 2SQ, UK

J. F. Kennedy

Research Laboratory for the Chemistry of Bioactive Carbohydrates and Proteins, Department of Chemistry, University of Birmingham, P.O. Box 363, Birmingham, B15 2TT, UK

Key Words

Ion-suppression RP HPLC
Polymeric reversed-phase adsorbent
L-ascorbic acid/vitamin C
Degradation products

Summary

An isocratic ion suppression reversed phase method is utilized for the qualitative and quantitative determination of L-ascorbic acid in fresh fruit juices – complex sample matrices. The selectivity of the method, when a macroreticular poly(styrene-divinylbenzene) reversed phase adsorbent is used, is sufficient to resolve the isomers L-ascorbic acid and D-erythorbic acid (isoascorbic acid) to baseline in under 8 minutes. L-Ascorbic acid solution stability is monitored using the same analytical conditions with the degradation products sufficiently well resolved not to interfere in the quantification of L-ascorbic acid. By the use of commercial materials and the preparation of the proposed products of the oxidative degradation of L-ascorbic acid the degradation sequence and identification of the products in an aged L-ascorbic acid solution is accomplished.

Introduction

Recently a method has been reported for the qualitative determination of vitamin C in fruit juice [1]. The method utilizes a high surface area, small pore size, polymeric reversed phase adsorbent, PLRP-S 100 Å, with a low pH aqueous mobile phase. The ion suppression reversed phase system is capable of resolving the isomers L-ascorbic acid (vitamin C) and D-erythorbic acid (isoascorbic acid) an isomer which may be added as an antioxidant in some food products and which has been shown to interfere in some previously reported methods for vitamin C determination [2, 3]. A quantitative method for the determination of L-ascorbic acid has been developed and the suitability of the method to the routine quantification of L-ascorbic acid evaluated with reference to freshly extracted fruit juices. A method has been reported for the quantification of this hydrophilic water soluble sugar acid in foods but it was necessary to derivatize the solute of interest prior to the chromatographic separation [4]. The objective of the piece of work reported here was the development of a quantitative determination which required no complex sample pre-treatment, extraction or derivatization prior to a chromatographic separation using a standard HPLC system with spectrophotometric detection.

The qualitative method is also applied to the evaluation of L-ascorbic acid solution stability and the identification of the oxidative degradation products. In a single chromatographic run L-ascorbic acid, solution forms of L-dehydroascorbic acid, 2,3-diketo-L-gulonic acid, oxalic acid and L-threonic acid are resolved and identified.

Experimental

Column

The macroreticular poly(styrene-divinylbenzene) HPLC adsorbent used was the PLRP-S 100 Å with a nominal particle size of 5 μm. The dimensions of the commercially packed column were 250 × 4.6 mm. A guard cartridge system, dimensions of 5 × 3 mm, packed with the same analytical quality material was used to protect the inlet

0009-5893/87 0371-06 $03.00/0

© 1987 Friedr. Vieweg & Sohn Verlagsgesellschaft mbH

of the analytical column from contamination by hydrophobic species (Polymer Laboratories Ltd, Church Stretton, Shropshire, UK). The optimum flow rate as previously determined [1], 0.5 ml/min, was used throughout.

HPLC System

A modular, Knauer, chromatograph consisting of a pump, Model 64; variable wavelength UV detector, Model 87, operated at 220 nm; and twin pen chart recorder was used (Knauer, Berlin, FRG).

A Rheodyne 7125 injection valve, fitted with a 20 μl loop, was used to inject a constant sample volume of 20 μl (suppled by HPLC Technology Ltd, Macclesfield, Cheshire, UK).

Solute retention times, peak heights and areas were obtained from the analogue detector output using a Trilab 2000 computer equipped with an LC/GC data manipulation programme (Trivector Ltd, Sandy, Bedfordshire, UK).

Mobile Phase

The mobile phase, 0.2M NaH_2PO_4, pH 2.14, was prepared using sodium dihydrogen orthophosphate, AR grade and water, HPLC grade. The pH adjustment was carried out using 0.5M hydrochloric acid, volumetric grade (all Fisons Scientific Equipment Division, Loughborough, Leicestershire, UK).

Reagents/Chemicals

DL-homocysteine, L-ascorbic acid (Sigma Chemical Company, Poole, Dorset, UK) and L-dehydroascorbic acid (Aldrich Chemical Company Ltd, Gillingham, Dorset, UK and Fluorochem Ltd, Glossop, Derbyshire, UK) were used as test probes and were of analytical quality. Oxalic acid, AR grade and all other chemicals/reagents, SLR grade, were obtained from Fisons Scientific Equipment Division, Loughborough, Leicestershire, UK).

Results and Discussion

Quantitative Determination of L-Ascorbic Acid

The stability of L-ascorbic acid in 5 and 10 % metaphosphoric acid, 1mM DL-homocysteine, distilled water pH 7.0 and the analytical mobile phase, 0.2M NaH_2PO_4 pH 2.14 was evaluated over a period of 150 minutes. No degradation was shown to occur in either 5 or 10 % metaphosphoric acid, a stabilizing agent for plasma [5], or in 1mM DL-homocysteine. However, with the 1mM DL-homocysteine it was noted that the L-ascorbic acid peak area increased over the first 20 minutes. This is due to the first degradation product L-dehydroascorbic acid being reduced back to L-ascorbic acid by the DL-homocysteine [6]. Therefore by preparing the sample in DL-homocysteine the L-ascorbic acid peak area would be related to total vitamin C activity, L-ascorbic acid present in the sample and L-ascorbic acid produced by the reduction of L-dehydroascorbic acid as both have vitamin C activity. Neither metaphosphoric acid or DL-homocysteine interfere in the chromatographic determination of L-ascorbic acid, both are late eluting peaks under the analytical conditions used. L-Ascorbic acid is rapidly degraded in distilled water pH 7.0 but the rate of degradation is dramatically reduced under low pH/high salt conditions, i.e. in the mobile phase.

For the quantitative determination of L-ascorbic acid in fresh fruit juice the samples were prepared by diluting the freshly extracted juice with the mobile phase in the ratio 1 : 10. The diluted sample was then filtered, (0.45 μm Gelman Acro LC3S Syringe Filter) to remove any suspended fruit debris and the filtrate immediately analysed. No other sample purification prior to the chromatographic determination was necessary. Fig. 1 shows the elution profiles obtained for lemon, orange and grapefruit juices. The calibration graph relating L-ascorbic acid peak area to concentration was produced by sequential dilution of a stock solution and a linear relationship observed over the range 0.02 to 10 μg/ml at a wavelength of 220 nm. From the calibration the concentration of L-ascorbic acid in the diluted samples was determined to be 6 μg/ml in lemon, 2 μg/ml in orange and 6.5 μg/ml in grapefruit, giving concentrations in the freshly extracted juice of 60 mg/litre lemon, 20 mg/litre orange and 65 mg/litre grapefruit.

Solution Degradation of L-Ascorbic Acid

A solution of L-ascorbic acid prepared in the mobile phase was run 24 and 48 hours after preparation, Fig. 2. The solution was stored at ambient temperature and no attempt was made to eliminate oxygen from the system. After 24 hours, Fig. 2a, the L-ascorbic acid peak is reduced in size and this reduction in height is accompanied by the appearance of 3 peaks labelled A, B and G. After 48 hours no L-ascorbic acid peak was detectable, but 6 peaks were apparent: A, B, C, D, E and F. Comparing 2a and 2b peaks A and B are common to both solutions and have increased in height with additional L-ascorbic acid degradation. Y. Kagawa has proposed an oxidative degradation route for L-ascorbic acid [7] as illustrated in Fig. 3. The oxidation to L-dehydroascorbic acid (ii) is reversible, but once the lactone ring is opened to produce 2,3-diketo-L-gulonic acid (iii), the oxidation is not reversible. The final products of this route are oxalic acid (iv) and L-threonic acid (v) which are produced by cleavage of the 2,3-diketo-L-gulonic acid in the presence of oxygen.

Commercially available materials, L-dehydroascorbic acid and oxalic acid or compounds produced by published synthetic methods, 2,3-diketo-L-gulonic acid [7] and L-threonic acid [8] were used to identify the degradation products (ii), (iii), (iv) and (v) in the aged sample of L-ascorbic acid.

Two commercial samples of L-dehydroascorbic acid. Fluka and Aldrich, were prepared in the mobile phase, 1.8 mg/ml, and analysed using the standard chromatographic conditions. In the Aldrich sample, Fig. 4a, 6 peaks are clearly resolved, and in the Fluka sample, Fig. 4b, 5 peaks are evident. Peaks 2, 3, 4, 5 and 7 being common to both samples.

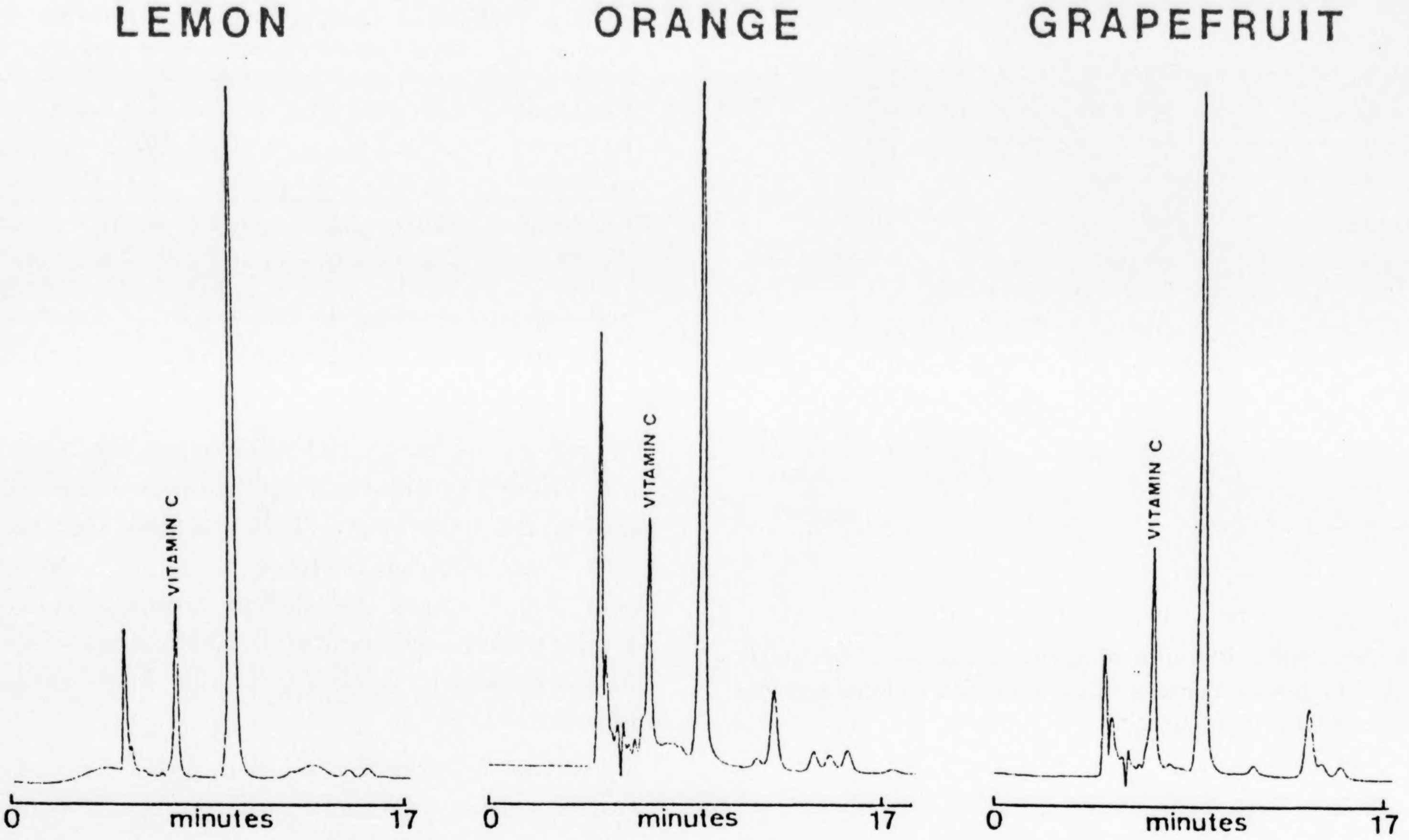

Fig. 1

Elution profiles obtain for the analysis of freshly extracted samples of fruit juice using the standard chromatographic conditions.

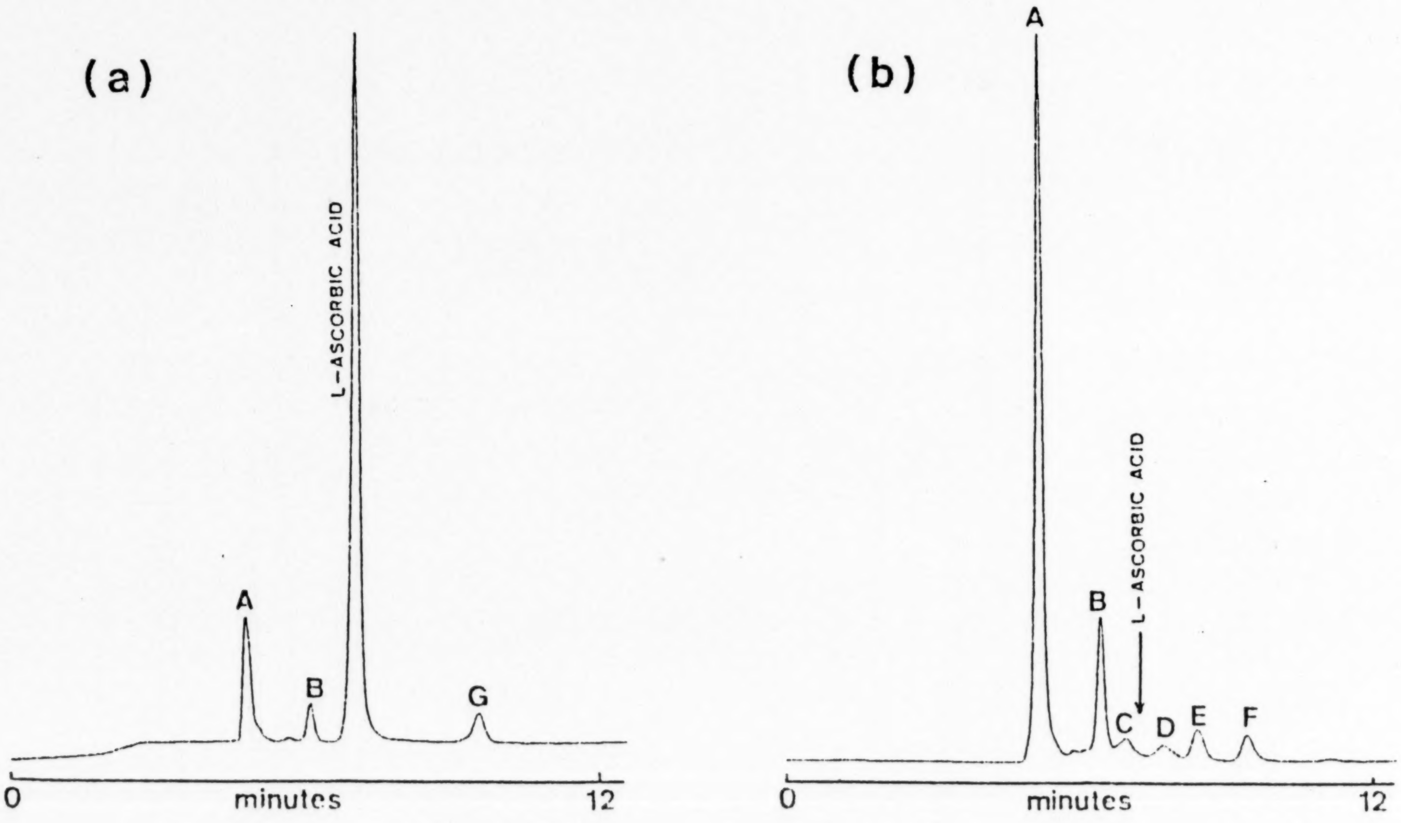

Fig. 2

Elution profiles of a degraded L-ascorbic acid solution prepared in the mobile phase after (a) 24 hours, (b) 48 hours. Peaks A and B being common to both profiles.

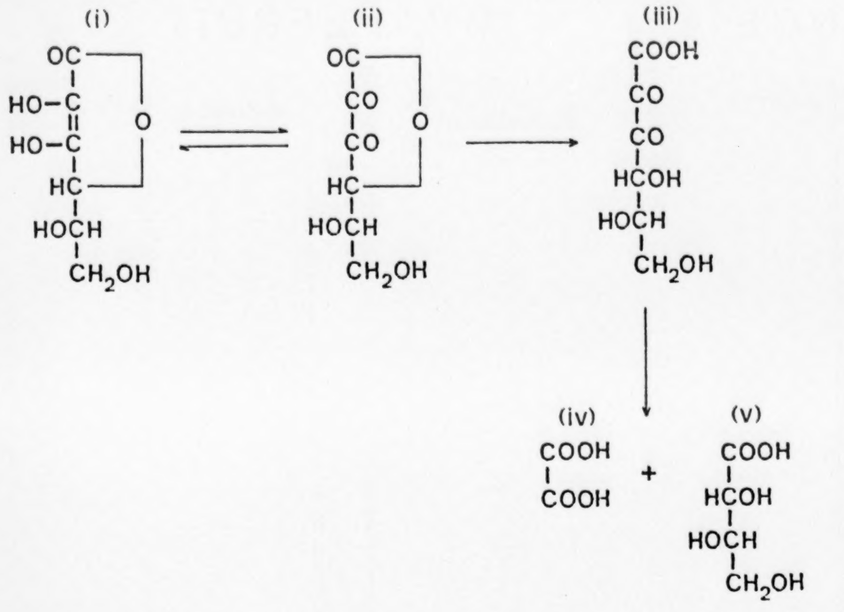

Fig. 3

Oxidative degradation sequence of L-ascorbic acid: (i) L-ascorbic acid, (ii) L-dehydroascorbic acid, (iii) 2,3-diketo-L-gulonic acid, (iv) oxalic acid and (v) L-threonic acid.

Table I. Peak height measurements for the thermal degradation in solution of L-dehydroascorbic acid over a period of 140 minutes.

Solution Time Minutes	Peak Height					
	2	3	4	5	6	7
60	195	228	504	75	104	63
100	312	314	511	46	121	21
140	380	323	494	32	122	12

L-Dehydroascorbic acid is reported to be unstable in aqueous solutions, pH 8 at 37 °C ($t_{1/2}$ = 6 minutes) [5]. Therefore a sample of L-dehydroascorbic acid, Aldrich, was prepared in distilled water pH 8.0 at a concentration of 7.6 mg/ml. The peak heights, 2, 3, 4, 5, 6 and 7, were then monitored over a period of 140 minutes at 40 °C. From Table I it is evident that peaks 2 and 3 increase in height suggesting that they are degradation products of L-dehydroascorbic acid. Peak 6 also increases in height but to a lesser extent. Peak 4 is thermally stable in water pH 8.0 as the height did not change. Both peaks 5 and 7 are unstable as there is a significant decrease in peak height during the experiment. This indicates that both peaks 5 and 7 are possible unstable forms of L-dehydroascorbic acid. Fig. 5 shows the elution profile obtained from the sample solution when run after 100 minutes – the difference in peak heights is clearly visible when compared with Fig. 4a.

To further investigate the L-dehydroascorbic acid (Aldrich) elution profile a DL-homocysteine reduction to L-ascorbic acid was performed. A sample solution, 4.4 mg/ml, was prepared in 1mM DL-homocysteine and filtered under nitrogen after 22 minutes. Peak heights for peaks 2, 3, 4, 5, 6 and 7, were monitored over a period of 225 minutes, Table II. The heights obtained for peaks 2 and 3 are constant over the first 165 minutes after which they start to increase in height, suggesting some oxidation is also occuring. Peak 4 is stable to reduction by DL-homocysteine. The most significant decrease in peak height occurs for peak 7, peak 5 being only slightly reduced. The elution position of L-ascorbic acid corresponds to peak 6. However, peak 6 in

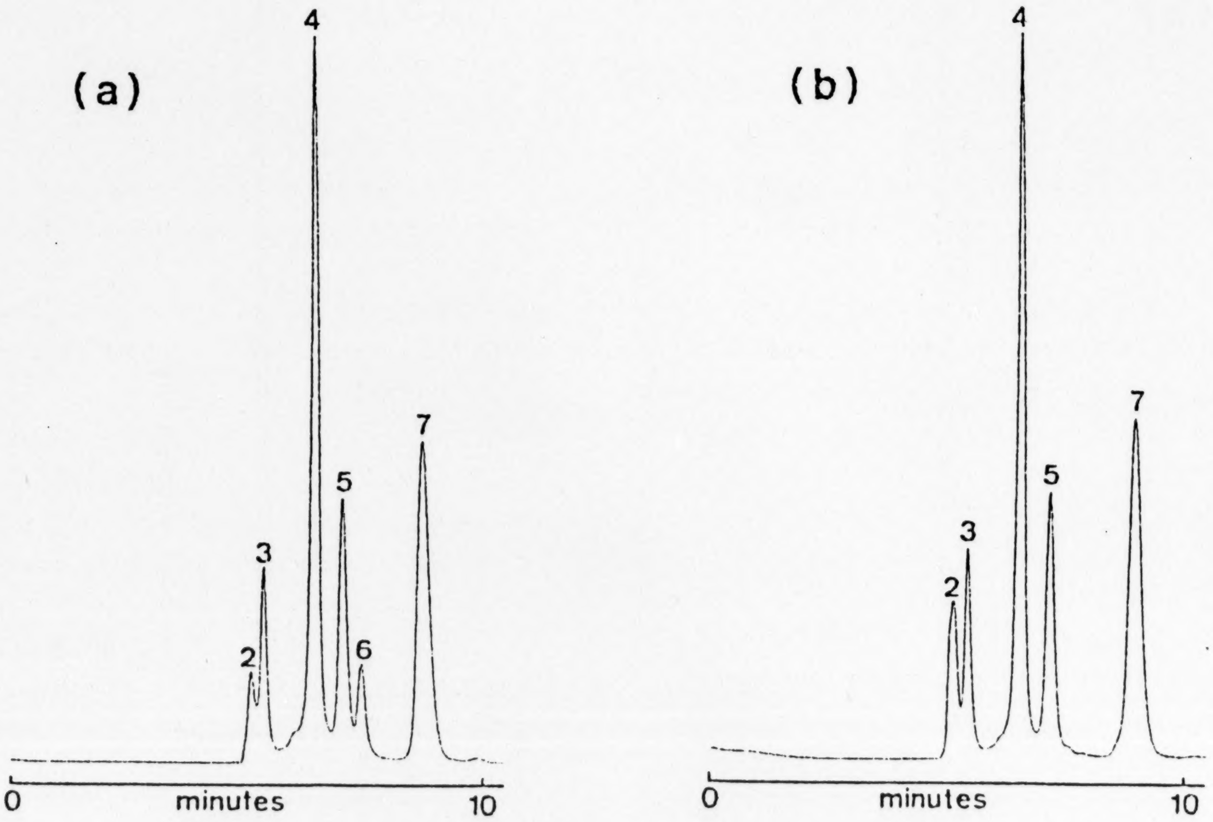

Fig. 4

Elution profiles of two samples of L-dehydroascorbic acid 35 minutes after preparation in the mobile phase, a) sample from Aldrich; b) sample from Fluka.

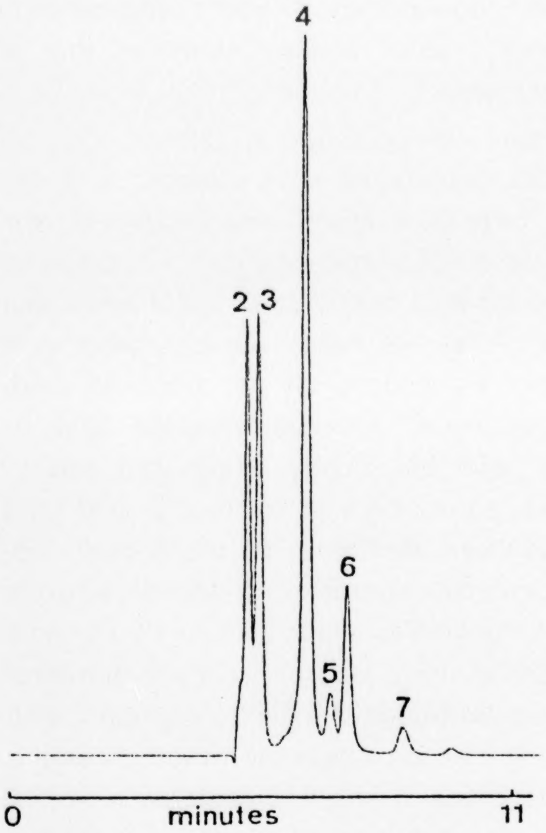

Fig. 5

Elution profile of L-dehydroascorbic acid (Aldrich) after 100 minutes at 40 °C.

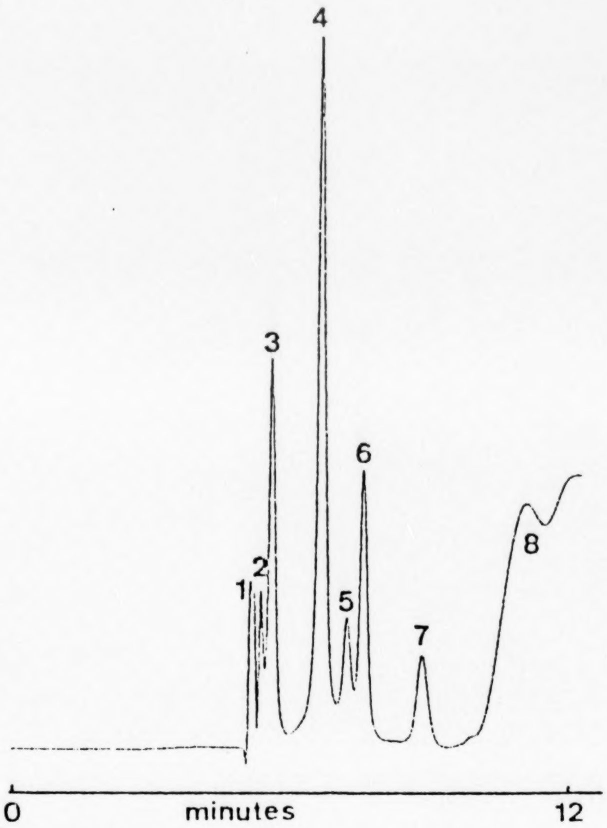

Fig. 6

Elution profile of L-dehydroascorbic acid (Aldrich) after DL-homocysteine reduction of 165 minutes.

Table II. Peak height measurements for the reduction of L-dehydroascorbic acid to L-ascorbic acid by 1mM DL-homocysteine.

Reaction Time Minutes	Peak Height					
	2	3	4	5	6	7
52	–	30	137	31	29	44
80	7	44	138	31	35	37
165	31	77	140	26	54	18
225	53	96	142	20	74	9

the L-dehydroascorbic acid sample is not L-ascorbic acid as it does not increase in height when the detection wavelength is increased to 244 nm, the wavelength maximum for L-ascorbic acid in the phosphate buffer system. Fig. 6 shows the elution profile after 165 minutes, peak 1 is the solvent front and peak 8 is due to the DL-homocysteine. Therefore in the L-dehydroascorbic acid elution profile, Fig. 4a, peaks 2 and 3 are degradation products and peaks 5 and 7 are unstable solution forms of L-dehydroascorbic acid.

A commercial sample of oxalic acid, product (iv), was analysed and a single peak obtained which eluted at the same position as peak 2 in the L-dehydroascorbic acid elution profile, Fig. 4.

Calcium L-threonate, product (v), was prepared by hydrogen peroxide oxidation of calcium ascorbate in aqueous calcium carbonate according to the method of H. S. Isbell and H. L. Frush [8]. A single peak was obtained with an elution position corresponding to peak 3 in the L-dehydroascorbic acid elution profile, Fig. 4.

The method reported by Y. Kagawa [7] for the controlled oxidation of L-ascorbic acid by aqueous potassium iodate was used to prepare a sample of potassium 2,3-diketo-L-gulonate, product (iii) in the degradation sequence. The elution position of this compound was found to be between peaks 3 and 4 in the L-dehydroascorbic acid elution profile. However, as illustrated in Fig. 7, it is possible to resolve oxalic acid, calcium-L-threonate and potassium 2,3-diketo-L-gulonate from peak 4. No peak corresponding to the elution position of the potassium 2,3-diketo-L-gulonate could be seen in either of the samples of L-dehydroascorbic acid or the degraded solution of L-ascorbic acid, although it was found to be stable under the analytical conditions used. Therefore an L-ascorbic acid degradation route which results in the formation of both oxalic acid and L-threonic acid, both of which have been identified in degraded solutions, must exist without the 2,3-diketo-L-gulonic acid intermediate.

By comparing the elution profiles of the L-dehydroascorbic acid samples, Fig. 4, peaks 2–7, and the degraded L-ascorbic acid solutions, Fig. 2, peaks A–F, it is possible to identify the L-ascorbic acid degradation products in the sequence proposed by Kagawa. Peaks 2 and 3, the oxalic acid and L-threonic acid, are identified as peak A in the L-ascorbic acid profile. Peak 4, the component of the L-dehydroascorbic acid samples which is thermally stable in aqueous solution pH 8.0 and not reduced by DL-homocysteine, is a degradation product of L-ascorbic acid and is identified as peak B. Peaks 5 and 7, the unstable solution forms of L-dehydroascorbic acid, are identified as peaks C and E in the degraded L-ascorbic acid elution profile obtained after 48 hours, but are not detected after 24 hours.

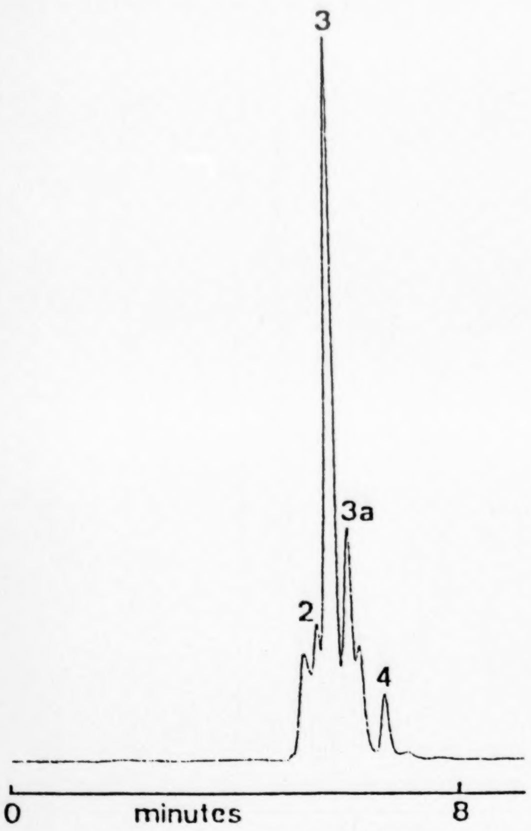

Fig. 7

Elution profile of a mixture of oxalic acid (peak 2), calcium L-threonate (peak 3) and potassium 2,3-diketo-L-gulonate (peak 3a). Peak 4 is the stable component of the commercial L-dehydroascorbic acid samples.

Conclusions

Using the ion suppression reversed phase method with a high performance polymeric column, PLRP-S 100 Å 5 μm, it is possible to quantify the total vitamin C activity and/or the L-ascorbic acid content of complex matrices, such as the fresh fruit juices, on a routine basis with a total run time of approximately 20 minutes. No complex sample pre-treatment or solute derivatization are required to achieve either the necessary resolution or detection limits for fruit juice quantification. Spectrophotometric detection at 220 nm enables concentrations as low as 0.02 μg/ml to be detected.

Using the same system with detection at 220 nm it is possible to monitor the degradation of L-ascorbic acid, the products of which have little absorbance at 244 nm, the λ_{max} of L-ascorbic acid [6]. After 24 hours a decrease in height of the L-ascorbic acid peak occurs and 3 additional peaks are detected. After 48 hours no L-ascorbic acid remains, and 6 peaks are evident. Of the proposed oxidative degradation sequence, L-dehydroascorbic acid to 2,3-diketo-L-gulonic acid and finally oxalic acid and L-threonic acid peaks corresponding to oxalic acid and L-threonic acid have been identified. Of the 5 peaks obtained for the commercial sample of L-dehydroascorbic acid (Fluka), 2 are identified as oxalic acid and L-threonic acid and 3 are evident in the L-ascorbic acid solution after 48 hours degradation. Although 2,3-diketo-L-gulonic acid can be resolved using the ion-suppression method and is stable in the mobile phase it was not detected in either degraded samples of L-ascorbic acid or L-dehydroascorbic acid. This suggests that an alternative degradation route of L-ascorbic acid in solution exists which also produces L-threonic acid and oxalic acid as the final products.

References

[1] *L. L. Lloyd, F. P. Warner, J. F. Kennedy, C. A. White,* Chromatogr. Int. **17,** 6 (1986).
[2] *J. W. Finley, E. Duang,* J. Chromatogr. **207,** 449 (1981).
[3] *W. D. Mason,* Methodol. Anal. Toxicol. **3,** 35 (1985).
[4] *K. Kodaka, S. Inagaki, T. Ujiie, T. Veno, H. Suda,* Bitamin **59** (9), 451 (1985).
[5] *J. Bianchi, R. C. Rose,* J. Micronutrient Anal. **1,** 3 (1985).
[6] *R. C. Rose, D. L. Nahrwold,* Ann. Biochem. **114,** 140 (1981).
[7] *Y. Kagawa,* J. Biochem. **51** (2), 134 (1962).
[8] *H. S. Isbell, H. L. Frush,* Carbohydr. Res. **72,** 301 (1979).

Received: June 30, 1987
Accepted: Aug. 10, 1987
F

Highly Sensitive Measurement of Mepindolol in Biological Fluids Using HPLC and Electrochemical Detection

L. Millerioux / L. Ntzanis / B. Julian / J. Girault / M. A. Lefebvre* / A. Mignot / J. B. Fourtillan

CEPHAC, rue du Haut de la Chaume, F-86280 Saint Benoit, France

Key Words

Column liquid chromatography
Mepindolol
Electrochemical detection
β-Blockers

Summary

Mepindolol, a β-blocker agent, has an indolic structure which can undergo oxidation. A high-performance liquid chromatographic technique has been used to measure mepindolol in biological fluids using pindolol as the internal standard. The chromatography has been combined with electrochemical detection (coulometric detector). This method allows the determination of very low amounts of mepindolol with good precision and accuracy, the limit of quantification being 0.6 ng · ml^{-1}.

Introduction

Electrochemical (amperometric) detection has recently been applied to the analysis of a great variety of drugs, especially for the determination of compounds exhibiting an indolic moiety, such as tryptophan and related compounds [1].

For example, an HPLC assay has been previously published for mepindolol using amperometric detection the estimated limit of detection of which was around 1 ng · ml^{-1} [2].

The method which could be used following oral administration of 20 mg of mepindolol sulphate (mean maximum concentration 45 ng · ml^{-1}) needs to be improved in terms of the limit of detection for measurement of mepindolol following a 5 mg oral administration and/or a 2 mg intravenous administration.

We describe below a new HPLC method using coulometric detection which allows precise and accurate measurement of mepindolol down to 0.6 ng · ml^{-1}.

Material and Methods

Reagents

Mepindolol (Fig. 1-A) and pindolol (Fig. 1-B) were provided by Schering France. Methanol was obtained from Prolabo, pH 9 titrisol buffer, methylene chloride, acetic acid, acetonitrile from Merck. Heptanesulfonic acid (pic B7) was supplied by Waters Assoc. Water was of Milli-Q quality, from Millipore.

Stock Solutions

Stock solutions of mepindolol and pindolol were prepared by dissolving 10 mg of each drug in 20 ml methanol, to get a concentration of 500 μg · ml^{-1}. All the subsequent dilutions were with methanol.

Extraction Procedure

In a 20 ml screw capped tube were successively placed 1 ml plasma, 100 μl methanol, 100 μl of the 1000 ng · ml^{-1} methanolic solution of pindolol (internal standard), 2 ml

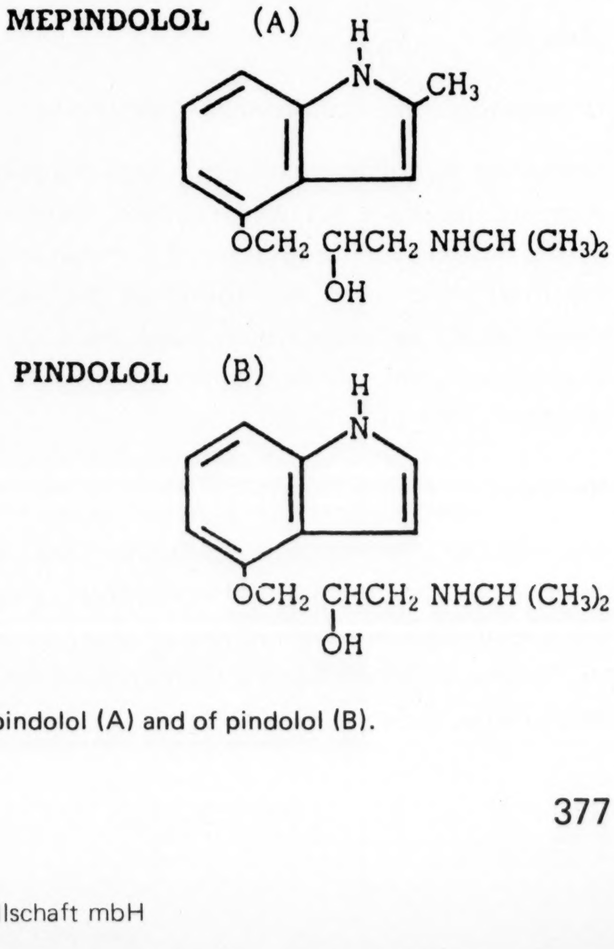

Fig. 1
Formulas of mepindolol (A) and of pindolol (B).

0009-5893/87 0377-03 $03.00/0

© 1987 Friedr. Vieweg & Sohn Verlagsgesellschaft mbH

pH 9 buffer and 10 ml methylene chloride. The tubes were shaken for 10 min and centrifuged for 10 min (3800 RPM). 8 ml of the organic phase were transferred into a 10 ml tube and 250 μl 0.1 M acetic acid added. The mixture was shaken (10 min), then centrifuged (10 min, 3800 RPM). The upper phase (aqueous) was transferred by pipette into an injection cone and an aliquot of 20 to 100 μl was injected into the chromatograph.

Calibration Curves

Plasma: mepindolol calibration curves were constructed by spiking blank plasma with known amounts of mepindolol to get concentrations ranging from 100 ng $\cdot$ ml^{-1} to 0.625 ng $\cdot$ ml^{-1}. The samples were extracted and chromatographed as described below. The standard curves were obtained by plotting the peak area ratio for mepindolol/pindolol against the concentration of mepindolol. Data were processed using a Hewlett Packard loop (HP 3357) with L.A.S. (Laboratory Automation System) software package, on a 7912 Winchester disc drive. The calibration curves were obtained using linear regression by the least squares method.

Urine: mepindolol calibration curves in urines were constructed similarly from 5 to 800 ng $\cdot$ ml^{-1}.

High-Performance Liquid Chromatography

The liquid chromatograph consisted of a M590 pump (Waters Assoc.) coupled with an automated injector Wisp 710B (Waters Assoc.), an electrochemical detector Coulochem model 5100A (ESA) equipped with a guard cell (model 5020) and an analytical cell (model 5011) from ESA, and a chart recorder Omniscribe, Houston Instrument (Waters Assoc.).

The oxidation potential was set at 0.88 V for the guard cell at 0.40 V for the first electrode (screen) and at 0.68 V for the second electrode (working electrode) of the analytical cell.

The sensitivity was fixed at 0.67 μA. The chromatographic column was a μBondapak C18, 10 μm (Waters Assoc.), and the mobile phase was a mixture of acetonitrile, pic B7, acetic acid and water (300/20/3/677 in volumes).

Results

Chromatographic Conditions – Specificity

Under the described conditions, mepindolol and the internal standard pindolol are well resolved, with retention times of 7.5 minutes for pindolol and 9.5 minutes for mepindolol. No interfering peak was found at the retention time of mepindolol. Samples which have been chromatographed without internal standard show no interfering peak at the retention time of pindolol.

Recovery

The recovery of mepindolol which was determined by comparing the mepindolol-to-pindolol peak area ratio calculated after the extraction of a set of plasma samples to the one obtained from a methanolic solution was found to be 75 %.

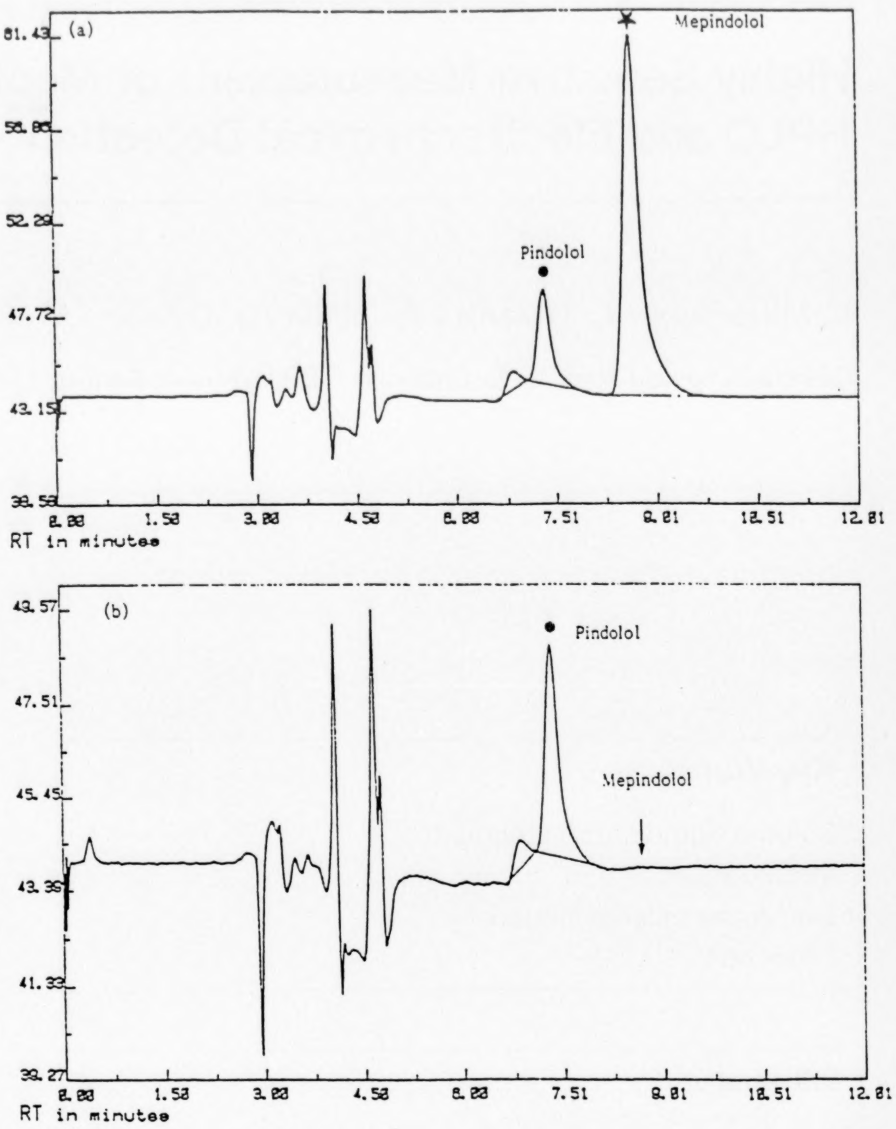

Fig. 2

Specimens of chromatograms corresponding to plasma extracts; acetonitrile, pic B7, acetic acid and water (300/20/677 in volumes); temperature: 20 °C; flow rate: 1 ml $\cdot$ min^{-1}. **a** = plasma extract supplemented with mepindolol (50 ng $\cdot$ ml^{-1}); **b** = blank plasma extract.

Linearity

The linearity of the method was verified from 0 to 100 ng $\cdot$ ml^{-1} for plasma samples and from 0 to 800 ng $\cdot$ ml^{-1} for urine samples.

Reproducibility – Limit of Detection

Precision and accuracy have been calculated from the-same-day repeatability assays using sets of blank plasma spiked with known amounts of mepindolol ranging from 0 to 50 ng $\cdot$ ml^{-1}. The coefficients of variation even at the lower concentration (0.625 ng $\cdot$ ml^{-1}) are less than 5.7 % whereas the corresponding errors are less than 10 % (Table I).

According to the coefficient of variation (5.2 %) and the mean error (− 4.5 %) observed at 0.625 ng $\cdot$ ml^{-1}, this lower concentration can be considered as the limit of detection.

Discussion and Conclusion

Mepindolol is a β-blocking agent, structurally related to pindolol, which is administered in single doses ranging from 2 to 20 mg. The pharmacokinetic profile of this

Table I. Precision and accuracy of the-same-day repeatability assays

Theoretical concentration ng · ml^{-1}	Mean measured concentration ng · ml^{-1}	Number of determination	Standard deviation	Coefficient of variation %	Percentage of error %
50	50.16	10	1.09	2.2	+ 0.3
20	20.16	10	1.14	5.7	+ 0.8
10	10.00	4	0.27	2.7	0
5	4.60	4	0.18	4.0	− 8.0
2.5	2.20	4	0.09	4.1	− 10.1
1.25	1.14	4	0.02	4.6	− 8.9
0.625	0.580	8	0.03	5.2	− 4.5
0	0	10	–	–	–

compound cannot be estimated without a highly sensitive method allowing the quantification of very low concentrations of mepindolol. So we developed a new method using reversed-phase high-performance liquid chromatography, combined with electrochemical detection (LCEC).

LCEC has become a widely accepted technique for the analysis of trace quantities of electroactive compounds. It can be used in a screen mode (first electrode: 0.40 V, second electrode: 0.68 V). When monitoring the current at the second electrode, the contribution of impurities due to the components of the biological extract is drastically reduced (screen effect). Moreover, the background associated with the components of the mobile phase is lowered by the introduction of a guard cell placed between the pump and the injector and set at a high potential (here, 0.88 V).

The described method shows two major advantages: firstly, the limit of detection is improved (0.625 ng · ml^{-1}) compared to the published method. Secondly, the precision of this new assay was demonstrated to be well adapted to kinetic purposes, as the coefficients of variation were always less than 6 % below 5 ng · ml^{-1}.

The method was used to analyse mepindolol in plasma and urine samples collected during a bioavailability study. The analysis of plasma quality control samples along with the study confirms that the precision and accuracy of the method is suitable for pharmacokinetic studies. This is exemplified by the slope (1.010) and the intercept (0.074) of the regression line constructed by plotting theoretical concentrations against found concentrations of quality control samples (Fig. 3).

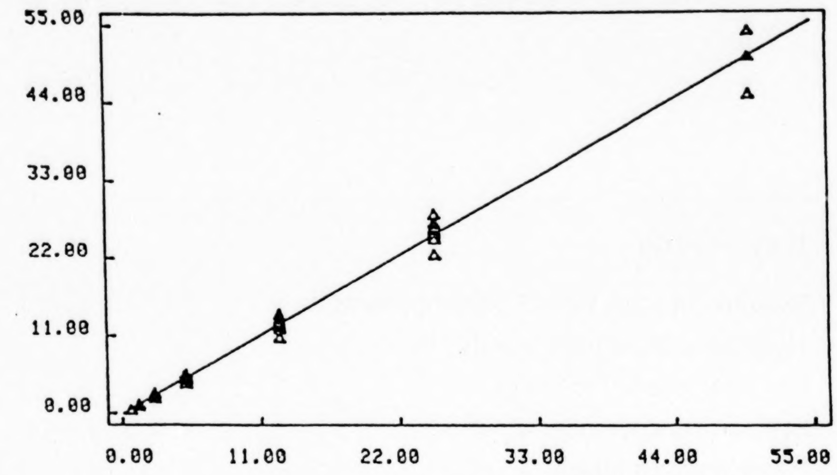

```
----------------------------------------------------------------------
line        slope         intercept          df      coeff. corr.
 1          1.010         -0.074          36.000        0.995
```

Fig. 3

Correlation between theoretical and measured values of plasma quality controls (ng · ml^{-1}).

References

[1] *C. Kim, C. Campanelli, J. M. Khanna,* J. Chromatogr. **282,** 151 (1983).
[2] *W. Krause,* J. Chromatogr. **181,** 67 (1980).
[3] *R. W. Andrews, C. Schubert, J. Morrison, E. W. Zink, W. R. Matson,* Amer. Laboratory, October 1982.

Received: July 27, 1987
Accepted: Aug. 4, 1987
F

Structures and Chromatographic Characteristics of Capsule-Type Silica Gels Coated with Hydrophobic Polymers in Reversed-Phase Liquid Chromatography

Y. Ohtsu* / H. Fukui / T. Kanda / K. Nakamura / M. Nakano / O. Nakata / Y. Fujiyama

Shiseido Research Center, 1050 Nippa-cho, Kohoku-ku, Yokohama, Japan 223

Key Words

Reversed-phase liquid chromatography
Hydrophobic silicone polymer
Polymer-coated silica gel
Separating characteristics
Resistance to alkali

Summary

Silicone polymer-coated silica gels modified with octadecyl and octyl groups (S/S-C_{18}, S/S-C_8), or "capsule-type silica gels" were developed as packing materials for reversed-phase liquid chromatography. They were obtained by coating the surface of totally porous silica gel with a homogeneous silicone polymer film, and thereafter modifying the coating polymer with octadecyl or octyl groups. Retaining the advantages of silica-based packings, they show strong resistance of alkali-like organic porous polymeric materials.

Introduction

Silica-based packing materials, represented by octadecylsilyl silica gel (ODS-silica gel), octylsilyl silica gel etc., have many favorable chromatographic characteristics, such as high peak resolution, applicability in a wide variety of samples and relatively low cost. In addition, it is said that ODS-silica gels amount to more than 80% of all packing materials used in laboratories.

Recent rapid development in biotechnology has increased the necessity for high performance liquid chromatography (HPLC) as a means of separation of peptides, proteins and other biological substances. However, several problems have arisen in the separation using ODS-silica columns, such as limited chemical stability, peak tailings and a decrease in recovery in the case of basic compounds which seem to be caused by irreversible adsorption.

Suppliers of chromatographic columns are trying to overcome these problems by endcapping unreacted silanol groups on the silica surface, for example, with trimethylsilyl group (TMS). This effort works to some extent, but not enough to solve all the problems. Kirkland et al. pointed out that the properties of silica largely affect the chemical stability of bonded phases derived therefrom [1].

Porous polymeric materials, another type of material for reversed-phase liquid chromatography (RPLC), generally endure at a wider pH range and have a greater sample loadability than that of ODS-silica gels. But they have some inevitable problems, such as lower peak resolution, weaker pressure resistance, and swelling or shrinking in certain solvents.

Schomburg et al. introduced an idea, "polymer coating" as a new method of preparation of packing materials for reversed-phase liquid chromatography (RPLC) [2–5]. They immobilized a variety of polymers, such as polysiloxanes, polybutadiene etc., onto silica or alumina supports and have reported good results. For instance, their alumina-based material for RPLC showed adequate stability at pH 12.

Our research has been focused on another process of "polymer coating" for silica support.

The new packing materials, silicone-coated silica gels modified with octadecyl, or octyl groups (S/S-C_{18}, S/S-C_8), or "capsule type silica gels", were obtained by bringing silicone monomers in touch with the surface of totally porous silica gel, polymerizing them, and thereafter attaching alkyl groups (C_{18}, or C_8) to the silicone polymer formed on the surface. This procedure is illustrated in Fig. 1, together with the synthesizing process of conventional chemically-bonded silica gels. This technique is characterized by the following points:

(I) micropores of silica are not filled with the silicone polymer, but a homogeneous polymer film is formed along the wall of micropore;

(II) the thickness of the polymer film is precisely controlled;

0009-5893/87 0380-05 $03.00/0

© 1987 Friedr. Vieweg & Sohn Verlagsgesellschaft mbH

(III) the chemical coating with the silicone polymer provides excellent stability against solvents;

(IV) alkyl groups are attached to the silicone polymer layer by stable chemical bonds.

This polymer coating differs from that of Schomburg et al. in two aspects. For one thing, we deposited silicone monomers on the surface of the silica and forced the monomers to form the polymer afterward, so that the polymer coating is processed right inside the small pores (which is difficult for large polysiloxane molecules). Another difference is that the octadecyl groups were attached to the polysiloxane formed on the surface, while polysiloxane molecules substituted beforehand with alkyl groups are immobilized to silica in their works.

In this paper, structures and chromatographic characteristics of S/S-C_{18}, S/S-C_8 are discussed from various angles.

Experimental

For high performance liquid chromatography (HPLC), a LC-6A (Shimadzu, Japan) was employed and a RC-4A (integrator) was connected to the system.

Micropore distribution, micropore volume and the relative surface area of packing materials were measured by the nitrogen adsorption method using Autosorb-1 (Quantachrom, USA).

GX-270 (JOEL, Japan), equipped with a probe for cross polarization/magic angle spinning (CP/MAS), was employed to obtain solid state ^{13}C- and ^{29}Si-nuclear magnetic resonance (NMR) spectra.

High quality standard chemicals were used without further purification.

All the solvents used in this work were liquid chromatographic grade.

Results and Discussion

Bonding Structure

Fig. 2 shows solid state ^{13}C-NMR spectra of C_{18}-bonded silica gel of carbon content 20%, TMS-endcapped, purchased from Japan-B (a certain anonymous supplier in Japan) and S/S-C_{18}. In the spectrum of the bonded silica gel, signals of methyl groups belonging to octadecyldimethylsilyl and trimethylsilyl groups are observed at 0 to 3ppm. On the other hand, signals of methyl groups belonging to the silicone polymer are observed at -4 to 0ppm, a little upfield. Carbon atoms forming an octadecyl group (No. 1–18 in Fig. 2) show a similar signal pattern in both spectra.

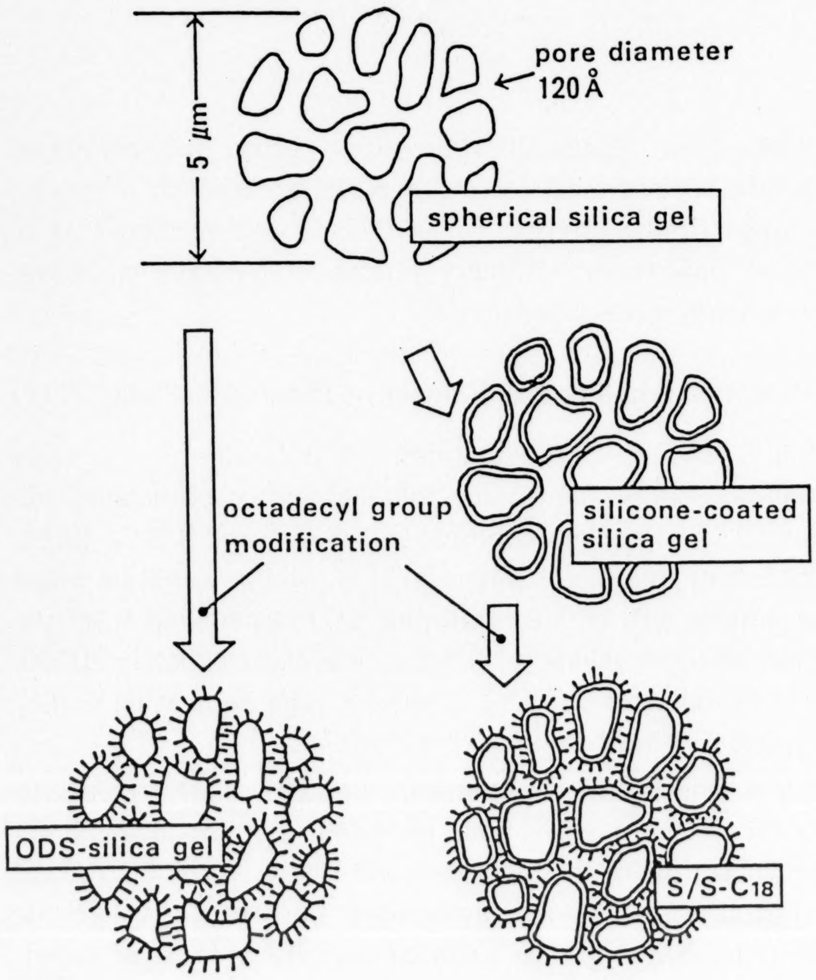

Fig. 1
Illustration of surface structures of C_{18}-packing materials.

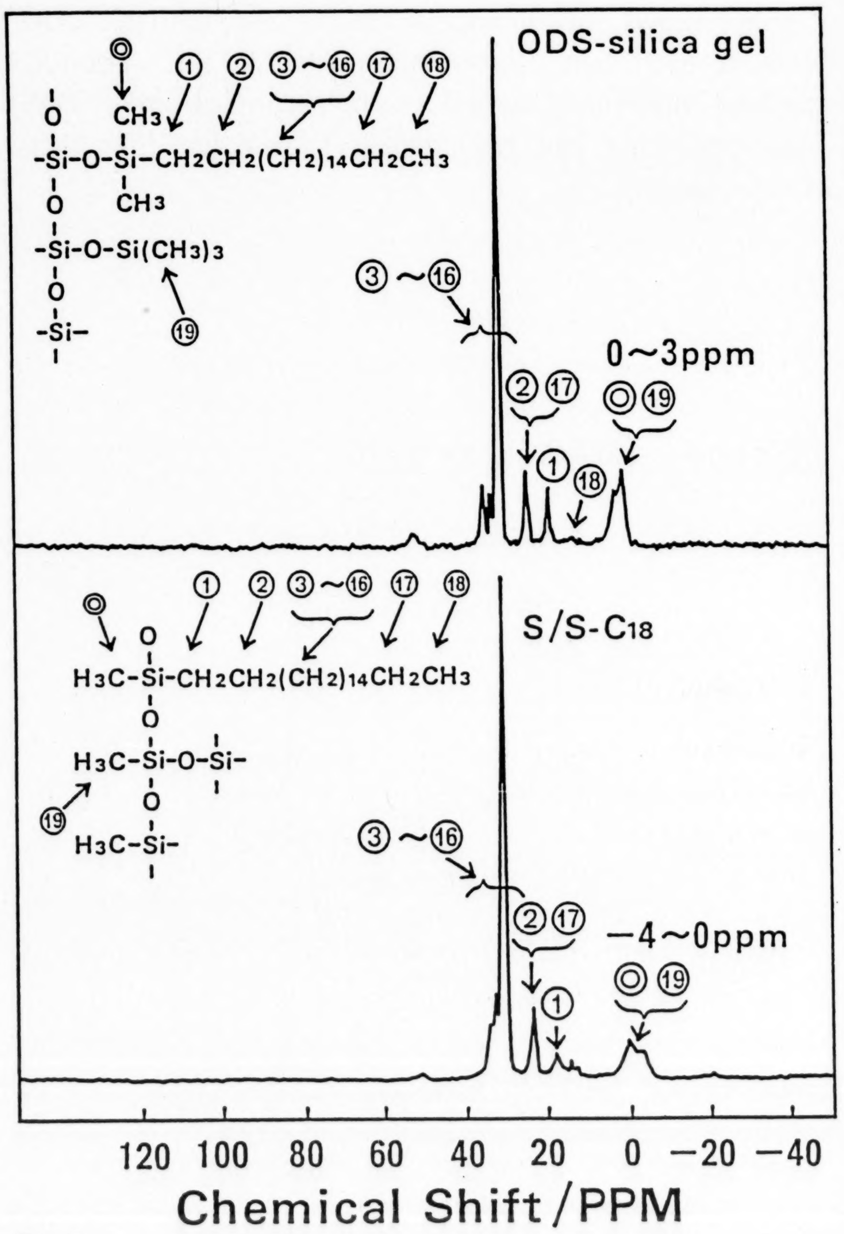

Fig. 2
^{13}C-NMR CP/MAS spectra of C_{18}-packing materials measured with JEOL GX-270.

Fig. 3 shows solid state ^{29}Si-NMR spectra of the silicone polymer-coated silica gel and silica gel. Two peaks at −101 and −91 ppm in the spectrum of silica gel were assigned to two kinds of silanol groups as done by Maciel et al. [6, 7]. These two signals greatly decrease in intensity after the polymer coating, which suggests that part of the silanol groups on the silica gel react with the polymer and make a chemical bond. This chemical bond seems to give S/S-C_{18} and S/S-C_8 high stability in organic solvents, such as hexane, methanol, chloroform, acetone, acetonitrile, tetrahydrofuran etc.

Film Thickness and Micropore

Fig. 4 shows the change in micropore distribution during the following steps: silica gel → silicone polymer-coated silica gel → S/S-C_{18}. The silica gel employed here has an average micropore diameter of 120 Å, average particle diameter of 5 μm with a narrow radius distribution. This silicone polymer coating causes a decrease in micropore radius of 7 Å on the average, which indicates that the homogeneous silicone polymer film of 7 Å in thickness was formed and that it was formed even inside the small micropores, having a pore diameter of 20 to 60 Å.

The introduction of octadecyl groups causes a further decrease in pore radius of 6 Å on the average, which indicates that octadecyl groups are attached to the polymer layer homogeneously.

Table I shows the micropore volume and relative surface area at each step. Corresponding data of a C_{18}-bonded packing material (Japan-B, carbon content 20%, TMS-endcapped) are also tabulated in Table I, and they show similar results.

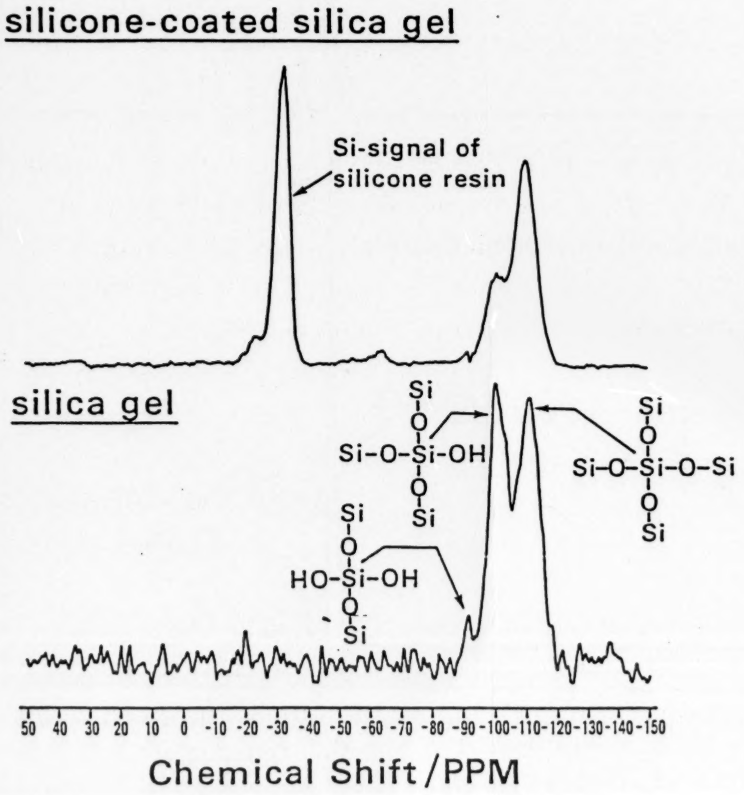

Fig. 3

Comparison by ^{29}Si-NMR CP/MAS spectra between silica gel and silicone-coated silica gel.

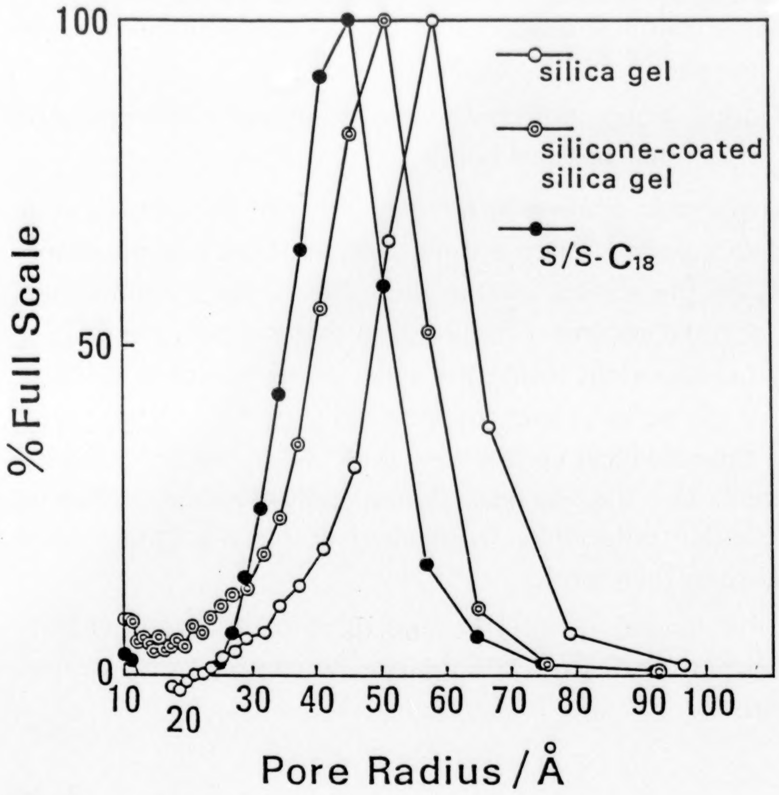

Fig. 4

Micropore radius distribution at each step.

Table I. Characteristic values of micropore.

Sample	Micropore Radius (Å)	Micropore Volume (ml/g)	Surface Area (m^2/g)
Silica gel	58	1.15	335
Silicone-coated Silica gel	51	0.87	245
S/S-C_{18}	43	0.42	130
ODS-silica gel (Japan-B)	43	0.51	140

Performing octadecyl substitution after polymerization on the surface seems to make the orientation of octadecyl groups similar to that of ODS-silicas rather than that of other polymeric stationary phases which have structures extending three-dimentionally.

Retention Property and Number of Theoretical Plates (NTP)

Fig. 5 shows chromatograms of the standard mixture (uracil, methyl benzoate, toluene and naphthalene) obtained using packed columns of S/S-C_{18} and S/S-C_8 (5 μm, spherical). Methanol/water (7/3) is used as a mobile phase at a flow rate of 1.0 ml/minute. NTP, calculated from the peak of naphthalene for S/S-C_{18}, was approximately 20000, which indicates S/S-C_{18} retains a high separating ability typical of silica-based packing materials.

Fig. 6 shows the relationship between log k′ (capacity factor) of anthracene and methanol content in a mobile phase consisting of methanol and water, for S/S-C_{18} and three different chemically-bonded silica gels. As a result, plots for S/S-C_{18} have a similar linearity to those of Japan-B and Japan-C, which seems to be a typical phenomenon of reversed-phase partition.

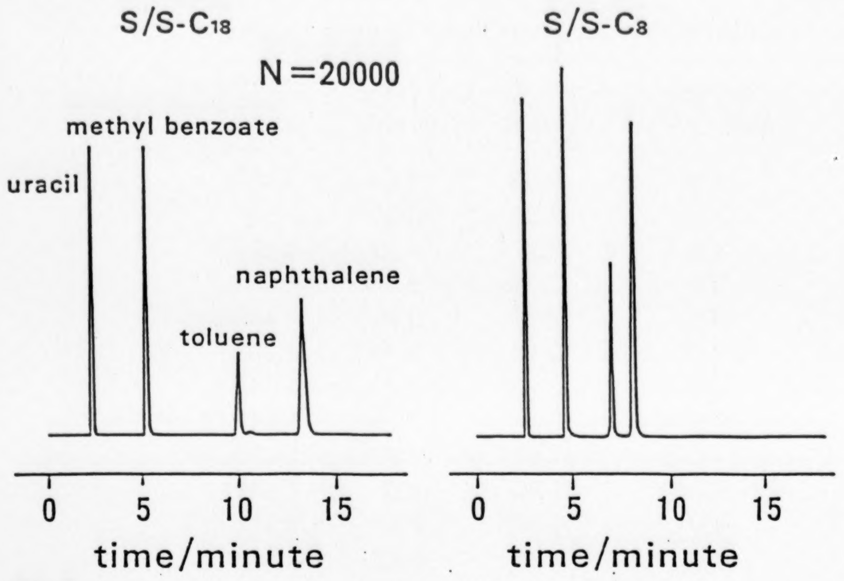

Fig. 5

Chromatograms obtained by using S/S-C_8, -C_{18} packed columns

column:	4.6mm i.d. X 250mm
mobile phase:	methanol/water (7/3)
flow rate:	1 ml/minute
detection:	UV, 254nm

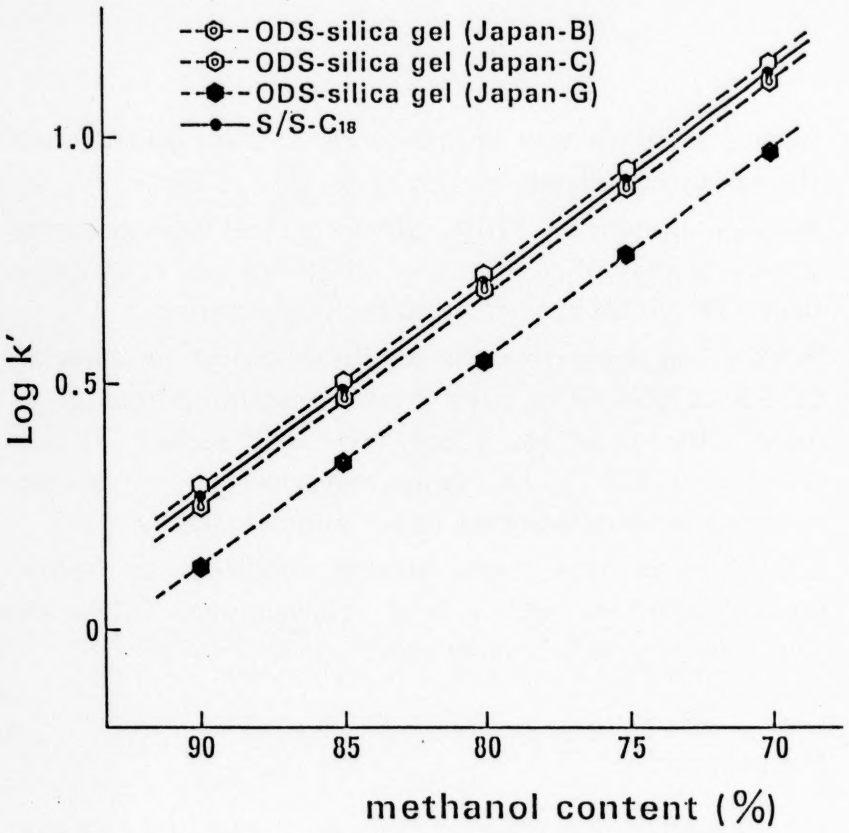

Fig. 6

Capacity factor (k′) of anthrancene in several columns.

Separating Characteristics

It is said that every ODS-silica gel has different separating characteristics, due to brand or lot difference. This seems to indeed be the case, as the polarity and other parameters of packing material can be affected by several factors, such as carbon content (usually, 5–20%), endcapped or not, type of silanizing reagent, or type of silanol groups on silica, as Kirkland et al. pointed out [1].

The authors tried to find out where S/S-C_{18} and S/S-C_8 are ranked among conventional packing materials for RPLC concerning separation property. 13 different chemically-bonded silica gel columns, one organic porous polymer column and S/S-C_{18}, S/S-C_8 packed columns were prepared (4.6mm i.d. × 250mm, or 6.0mm i.d. × 250mm). For each of these, k′ values of methyl benzoate, toluene and naphthalene were measured using methanol/water (7/3) as mobile phase. The k′ ratio was calculated for combinations of toluene/methyl benzoate (T/MB), naphthalene/methyl benzoate (N/MB) and naphthalene/toluene (N/T), shown in Table II.

S/S-C_{18} shows the highest T/MB value (k′ ratio of toluene and methyl benzoate) among all the packing materials prepared, which suggests S/S-C_{18} and S/S-C_8 are extremely non-polar compared with conventional packing materials for RPLC.

The N/T value (naphthalene and toluene) of S/S-C_{18} is near to that of chemically bonded silica gels, while porous polymeric materials generally show high N/T values. Tanaka et al. have studied separation characteristics of planar polynuclear aromatic hydrocarbons (PAHs) for a silica-based stationary phase and organic polymeric phases [8]. S/S-C_{18} turned out to have separating characteristics similar to those of chemically-bonded silica gels rather than those of porous polymeric materials, although it has a polymer surface. The reasons must be that the polymer of S/S-C_{18} or S/S-C_8 does not extend three-dimentionally from the silica surface, but exists as a monolayer and that octadecyl groups are oriented in the same way as they are in monomeric ODS-silicas.

Resistance to Alkali

It has been impossible to use chemically-bonded silica gels under alkaline conditions. This is because silica gel generally dissolves into alkaline solutions, and the siloxane bond connecting the silane to the silica support is easily hydrolyzed at high or low pH in aqueous solutions. Kohler et al. examined stability at low pH of many bonded phases [9].

To study the resistance of S/S-C_{18} to alkali, a test of continuous operation under an alkaline condition was carried out using an automatic LC system. The mobile phases of methanol/water (7/3) adjusted to pH 9 and 10 with Britton Robinson buffer were flown into a S/S-C_{18} column at a flow rate of 1.0ml/minute, at an oven temperature of 40°C. The mixture of uracil, methyl benzoate, toluene and naphthalene was introduced by an autosampler.

S/S-C_{18} endured for 550 hours at pH 9. No change in peak shape or retention time was observed during this time. Fig. 7 shows the chromatograms just after the start and 550 hours later. At pH 10, it endured for 350 hours and a weak peak leading was observed in the chromatogram 350 hours later.

Chemically-bonded silica gels generally deteriorate in 20–40 hours under these conditions. It seems that S/S-C_{18} has made great progress in its resistance to alkali, and that it is as stable at high pH as organic porous polymers.

For further improvements, other supports, such as alumina, might be considered, investigated by Schomburg et al. [4].

Table II. Comparison in retention property among packed columns for reversed-phase liquid chromatography

Packed Columns	Funct. Group	%C	Support	Pore Size (Å)	Surface Area (m^2/g)	α (k'_1/k'_2)		
						T/MB	N/MB	N/T
S/S-C_{18}	18	–	Silica gel	120	320	**2.63**	**3.81**	**1.45**
Japan-A	18	20	Silica gel	100	300	2.35	3.59	1.53
Japan-B	18	20	Silica gel	100	300	2.27	3.37	1.49
Japan-C	18	20	Silica gel	100	300	2.24	3.31	1.48
U.K-D	18	10	Silica gel	100	200	2.23	3.20	1.44
S/S-C_8	8	–	Silica gel	120	320	**2.19**	**2.79**	**1.28**
USA-E	18	12	Silica gel	80	220	2.13	3.28	1.54
USA-F	18	22	Silica gel	80	550	2.04	3.15	1.54
Japan-G	18	–	Silica gel	–	–	1.97	2.90	1.47
FRG-H	18	14	Silica gel	100	300	1.90	2.68	1.54
Japan-A	8	–	Silica gel	100	300	1.86	2.45	1.31
USA-F	8	–	Silica gel	80	550	1.81	2.43	1.34
Japan-B	8	12	Silica gel	100	300	1.76	2.25	1.28
USA-I	18	10	Silica gel	80	400	1.75	2.51	1.43
Japan-J*	18	–	Polyvinyl Alcohol	200	–	1.58	3.93	2.48
FRG-H	8	9	Silica gel	100	300	1.29	1.88	1.45

column size: 4.6mm i.d. X 250mm
mobile phase: Methanol/Water (7/3)
flow rate: 1 ml/min
sample: Toluene (T), Methyl benzoate (MB), Naphthalene (N)
(k': capacity factor)

* 6.0mm i.d. X 150mm

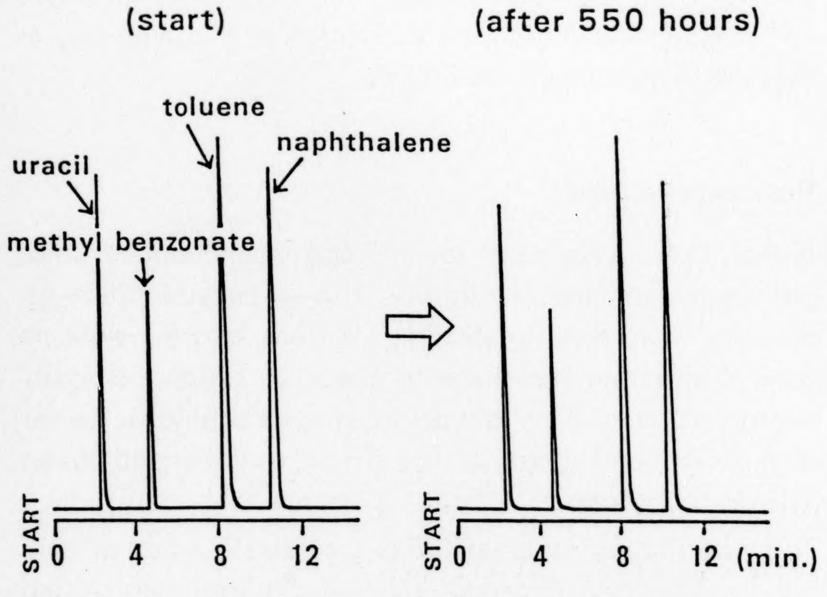

Fig. 7
Stability of S/S-C_{18} packed column under alkaline condition (pH = 9)

column: S/S-C_{18}, 5μm (spherical) 4.6mm i.d. X 250mm
mobile phase: methanol/water (7/3) (pH = 9 with Britton-Robinson buffer.)
flow rate: 1 ml/min
temperature: 40°C
detection: UV, 254nm

Conclusion

The structures of S/S-C_{18} and S/S-C_8, which are obtained by coating silica gel with a silicone polymer film and thereafter chemically modified with alkyl groups, were elucidated by solid state ^{13}C- and ^{29}Si-NMR spectrometry. The measurements of micropore distribution indicated that a homogeneous silicone polymer film (monolayer) is formed along the wall of micropores of silica gel and coats the surface completely.

S/S-C_{18} (spherical, 120 Å) shows a retention property similar to that of conventional ODS-silica gels as well as a high NTP typical of silica-based packing materials.

S/S-C_{18} has separating characteristics similar to those of ODS-silica gels rather than those of organic porous polymers, although it has a polymer-coated surface. It was found that S/S-C_{18} is highly non-polar among packing materials for reversed-phase liquid chromatography.

S/S-C_{18} is as stable under alkaline conditions as organic porous polymers and exceeds conventional ODS-silica gels concerning resistance to alkali.

References

[1] *J. Kohler, D. B. Chase, R. D. Farlee, J. Vega, J. J. Kirkland*, J. Chromatography, **352**, 275 (1986).
[2] *G. Schomburg, A. Deege, J. Kohler, U. Bien-Vogelsang*, J. Chromatography, **282**, 27 (1983).
[3] *G. Schomburg, J. Kohler, H. Figge, A. Deege, U. Bien-Vogelsang*, Chromatographia, **18**, 265 (1984).
[4] *U. Bien-Vogelsang, A. Deege, H. Figge, J. Kohler, G. Schomburg*, Chromatographia, **19**, 170 (1984).
[5] *H. Figge, A. Deege, J. Kohler, G. Schomburg*, J. Chromatography, **351**, 393 (1986).
[6] *G. E. Maciel, D. W. Sindorf*, J. Am. Chem. Soc., **102**, 7606 (1980).
[7] *D. W. Sindorf, G. E. Maciel*, J. Am. Chem. Soc., **103**, 4263 (1981).
[8] *N. Tanaka, K. Hashizume, M. Araki*, J. Chromatography, **400**, 33 (1987).
[9] *J. L. Glajch, J. J. Kirkland, J. Kohler*, J. Chromatography, **384**, 81 (1987).

Received: June 29, 1987
Revised manuscript
received: Aug. 28, 1987
Accepted: Sept. 1, 1987
F

Novel Method for the Preparation of Chemically Bonded Phases and Studies of their Chromatographic Performance

T. M. Khong/C. F. Simpson

Analytical Science Group, Birkbeck College, University of London, 20 Gordon St., London WC1H 0AJ, UK

Key Words

Chemically bonded phases
Fluidised bed technology
Preparative RPLC

Summary

This paper describes a novel process for the production of chemically bonded phases using fluidised bed technology. Hitherto fluidisation of particles with the size range below 50 μm was considered impossible. In this study, particles with sizes as small as 7 μm have been successfully fluidised and subsequently reacted to produce bonded phases. The operating parameters of the fluidised bed system have been studied and their effect on the chromatographic properties of the products have been investigated. Advantages of the process are the *in situ* removal of fines, high batch to batch repeatability and *in situ* chemical post-treatments (end-capping).

Studies of the chromatographic performance of the fluidised bed products show them to possess markedly superior retention characteristics and good peak shapes. Comparisons were made with various C_8 and C_{18} commercially available bonded phases and on bonded phases prepared by conventional method. Mass loading effects were also investigated for preparative HPLC use.

Introduction

For a particular stationary phase, eg. C-18 (ODS) hydrocarbon chain, retention characteristics of RPLC packings vary from manufacturer to manufacturer and even from batch to batch. The differences are invariably due to dissimilar production methods and the variables associated with the reaction such as uneven contact between reagent and silica particles, different types of silica and uneven heat distribution in the solvent. This leads to difficulty in reproducing methodology developed for a given separation and the problem is further exacerbated since commercial RPLC packings with the same functionality, eg. ODS, are available in two forms; either as monomeric phases formed by reaction with monofunctional silanes or polymerised coatings derived from bi- or tri-functional reactants. The nature of the polymeric phases are rigidly determined by the production method.

There are many methods for the preparation of RPLC packings ranging from the laboratory scale to large scale. Typically, for laboratory scale preparation, the apparatus employed is a round-bottom glass flask fitted with a stirrer, reflux condenser attached with drying tube and devices for feeding the modifier reagent and dry nitrogen for outgassing the system. Solvents such as toluene are used and the reaction is initiated by heat. Reaction temperature is maintained constant by stirring the suspension. After conversion the modified product is filtered and washed with different solvents to remove excess reagent. The silica change for this method of modification is usually not greater than 100g.

Fixed bed *in situ* preparation of bonded phases has been studied by Gilpin and co-workers [1, 2]. This procedure involves outgassing of the pre-packed column of silica gel at high temperature in a gas stream to 'activate' the support. Modification is performed by pumping a silane through the Teflon-lined column for a given time. After reaction the excess reagent is washed away by rinsing the column with a range of solvents.

As with all industrial applications, little is known about the large scale preparative processes used by different manufacturers. However, Unger [3] has suggested that slurry reactors are employed. A slurry of the silica gel is agitated by bubbling dry gas through the suspension or by the use of mechanical stirrers. With such a system it is difficult to maintain overall constant reaction temperature because silica gel has low thermal conductivity and the reaction is exothermic. Due to these problems, Unger [3] further suggested that the use of fluidised-bed reactors would overcome the problems of slurry reactors since particles are in continuous motion thereby maintaining a uniform bed temperature.

Fluidisation describes a contact process in which particulate solids are transformed into a fluid-like state by a stream of gas or liquid. This state is achieved by the passage of fluid upwards through a bed of particles to a superficial velocity at which the drag force acting on them equals the gravitational force. At this point the particles move apart and become suspended in the flow. The bed is then referred to as fluidised.

0009-5893/87 0385-10 $03.00/0

© 1987 Friedr. Vieweg & Sohn Verlagsgesellschaft mbH

Whilst the use of fluidised beds in industry is widespread, the fluidisation of cohesive powders, such as silica, and particles of less than 50 μm has been considered impossible [4, 5]. Problems associated with fluidisation of this class of materials are usually channelling of the bed and the low terminal velocity of the particles. Mechanical stirrers have been used to aid fluidisation [6], their use is, however, limited since severe attrition of the particles may occur.

The use of fluidised beds in chromatography has been demonstrated. Aue and Hastings [7] employed a fluidised-bed to effect secondary polymerisation of surface bonded siloxane monomers in moist air. Petsev *et al.* [8] demonstrated a fluidised-bed technique for coating gas-liquid chromatographic stationary phases on a solid support. Recently, its use has been employed in studying chromatographic processes [9]. In all these cases the mean particle size used are in excess of the 50 μm limit.

In this paper, the use of a fluidised bed for the preparation of repeatable and reproducible batches of chemically bonded phases, especially for use in HPLC, is considered. In addition the chromatographic properties of RPLC packings thus prepared are discussed.

Experimental

Materials

Three different types of silica gel of varied particle size and density were used for the preparation of bonded phases.

The alkylchlorosilanes used were 1) dimethylchlorosilane (Fluka), 2) octyldimethylchlorosilane and 3) octadecyldimethylchlorosilane. 2 and 3 were prepared by hydrosilation of appropriate n-alkene with dimethylchlorosilane in the presence of chloroplatinic acid (Johnson Matthey Chemicals). 1-octene & 1-octadecene (Aldrich) were distilled prior to reaction. Pyridine (BDH) was used as received. Toluene (BDH) was dried over sodium.

For the overloading experiments, phenol – AR, benzaldehyde and nitrobenzene (BDH) were used as received.

Fluidising gases used were dried using activated Linde 5A molecular sieve (BDH).

Chromatographic Measurements

The chromatograph employed consisted of a Shimadzu LC-5A pump and a Shimadzu SPD 2Am UV detector operating at 254 nm. A Rheodyne 7120 valve fitted with a 50 μl loop was used for the overloading experiments. A Rheodyne 7143 valve fitted with a 5 μl internal loop was used otherwise. Columns were thermostatted in a water jacket at 20 °C.

Mobile phases were prepared on a volume basis using LC grade solvents. All measurements were performed in a temperature controlled laboratory, 20 °C.

Preparation of Bonded Phases

Liquid phase preparation. Silica gel was dried in an oven at 200 °C overnight before use. The apparatus used was purged with dry nitrogen before reaction and a drying tube of silica gel was fitted. An excess of the appropriate silane reagent was added dropwise to the suspension of silica gel in toluene. About 15 ml of pyridine was added to the reaction vessel. All reactions were refluxed for 6 hr.

After reaction, the product was filtered through a sintered crucible (no. 3 porosity) and washed with THF, n-heptane, THF, methanol and finally THF. It was then vacuum dried in a dessicator overnight before being stored in a dry bottle, ready for column packing.

Fluidised bed preparation. The apparatus used for fluidising is schematically shown in Fig. 1. The fluidised bed was heated with an electrical heater around the reactor and the fluidising nitrogen was preheated prior to passing through the bed.

25 g of silica gel was placed in a fluidising tower (about 45 mm i.d.) to give a bed depth of approximately 50 mm.

For reactions with hydrothermal treatment, the superheated steam was passed up the reactor containing the silica gel for 12 hr. Otherwise dry nitrogen was passed through the bed at 100 ml/min for 3 hours at a bed temperature of 200 °C, until no more water vapour was evolved.

A water condenser was then attached to the top of the fluidising tower. About 35–50 ml of chlorosilane was placed in the vaporiser and heated to near its boiling point. The bed temperature was maintained constant at the required reaction temperature and excess chlorosilane leaving the fluidising tower was recycled.

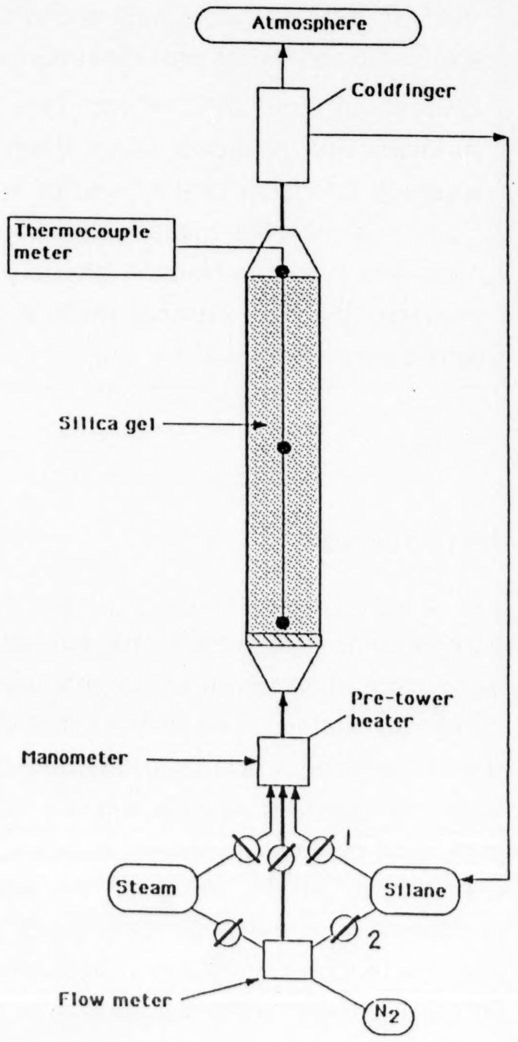

Fig. 1

Schematic diagram of fluidisation reaction

The reaction was stopped after 6 hr and the valves 1 and 2 were closed. Simultaneously, dry nitrogen was allowed to flow to the bed at about 150–200 ml/min, thereby maintaining fluidisation. When no excess reagent was observed to condense from the effluent nitrogen flow, the bed was cooled to room temperature whilst maintaining the nitrogen flow.

Results and Discussion

In this method of preparation, fluidisation is achieved by entrainment by the nitrogen gas and the vapour generated *in situ* by the reaction itself. Depending upon the density of the silica used, different bed distributors are used. The choice of distributor and fluidising gas have an effect on the nature of the fluidisation. For these experiments, sintered glass distributors were used.

Elemental analysis were performed on the prepared bonded phases at the Microanalysis Lab., University College, London. The coverage was calculated using eq. (1) and (2);

$$\text{No. of ligands nm}^{-2} = \frac{\%C \times 0.01 \times A_v}{n_c \times 12 \times S_{BET}} \qquad (1)$$

$$\text{No. of ligands nm}^{-2} = \frac{\%C \times A_v}{((n_c \times 1200) - (\%C(M-1))\,S_{BET}} \qquad (2)$$

where n_c = number of carbon atoms in the chlorosilane,
(10 for octyldimethylchlorosilane)
A_v = Avogadro's number
M = molecular weight of chlorosilane used
S_{BET} = surface area of the silica starting material as measured by nitrogen adsorption, (manufacturers data expressed as nm^2/g).

For expressing the coverage in terms of $\mu mol/m^2$ eq. (1) becomes

$$\mu\text{mol/m}^2 \text{ of ligands} = \frac{\%C \times 10^4}{n_c \times 12 \times S_{BET}} \qquad (3)$$

and similarly eq. (2) becomes

$$\mu\text{mol/m}^2 \text{ of ligands} = \frac{\%C \times 10^6}{((n_c \times 1200) - (\%C(M-1))\,S_{BET}} \qquad (4)$$

where S_{BET} is expressed im m^2/g for both eq. (3) and (4).

Tables I and II list the total coverages for octylsilyl bonded phases prepared on the two different types of silica gel. In both cases it is observed that fluidised bed preparation of the bonded phases yield a more consistent (reproducible and repeatable) material and higher coverage. Hydrothermal treatment to the silica gel also affords a higher degree of activation of the silica and this fact is illustrated by the coverage values in Table II.

Eq. (1) and (3) yield more representative results since the elemental analysis performed gave the %C w/w. The eqs. (2) and (4) proposed by Berendsen and de Galan [3] included the molecular mass of the silane and as such does not correct for the molecular mass of silicon.

The high degree of batch to batch consistency may be attributed to the good control of reaction temperature in the fluidised bed. The reaction temperatures are within ± 1 °C of the set reaction temperature. Temperature measurements at various points, near to the surface, in the middle and at the bottom, of the fluidised bed showed isothermal reaction conditions. Additionally, by hydrothermally treating the silica prior to modification, the surface silanol concentration is maintained at a consistent level for every batch of the same silica used. There is no doubt that this hydrothermal treatment has advantages over the usual method of drying silica gel in an oven prior to modification. Temperature fluctuations may occur and excessive silanols dehydrated. Moreover, transfering of the dehydrated silica to the reation vessel may result in rehydration due to its hygroscopic nature.

Studies by Lochmüller *et al.* [11] have shown that the distribution of surface bound molecules on silica can be quite heterogeneous, although in these studies, steric hindrance, due to the chemical bonding of relatively large molecules, ie. pyrene, may contribute to the apparent heterogeneity of the surface bonded groups. The effect of solvents in the preparation of bonded phases is not known.

Table I. Carbon content and coverage of octylsilyl bonded phase on high density silica gel

			Carbon loading	Coverage			
				no of ligand/nm^2		μmoles/m^2	
Silica gel	Conditions	run no.	%C	equation 1	equation 2	equation 3	equation 4
High density 20 μm	Fluidised with prior steam treatment	1	11.66	1.72	2.15	2.86	3.57
		2	11.45	1.69	2.10	2.81	3.49
		3	13.07	1.93	2.49	3.20	4.13
		4	12.48	1.84	2.34	3.06	3.89
	mean		***12.17***	***1.80***	***2.27***	***2.98***	***3.77***
	std deviation		***0.75***	***0.11***	***0.18***	***0.18***	***0.29***
High density 20 μm	Liquid phase	1	13.67	2.02	2.63	3.35	4.37
		2	6.65	0.98	1.11	1.63	1.84
		3	4.18	0.62	0.66	1.02	1.10
		4	13.59	2.01	2.61	3.33	4.34
	mean		***9.52***	***1.41***	***1.76***	***2.33***	***2.91***
	std deviation		***4.85***	***0.72***	***1.02***	***1.19***	***1.69***

Table II. Carbon content and coverage of octylsilyl bonded phase on low density, 20 μm silica gel

		Carbon loading	Coverage			
			no of ligand/nm^2		μmoles/m^2	
Conditions	run no.	%C	equation 1	equation 2	equation 3	equation 4
Fluidised no prior steam treatment	1	5.31	1.33	1.47	2.21	2.43
	2	5.34	1.34	1.48	2.23	2.45
	3	5.30	1.33	1.46	2.21	2.43
	4	5.48	1.38	1.52	2.28	2.52
mean		***5.36***	***1.34***	***1.48***	***2.23***	***2.46***
std deviation		***0.08***	***0.02***	***0.03***	***0.03***	***0.04***
Fluidised with prior steam treatment	1	6.20	1.56	1.74	2.58	2.89
	2	6.44	1.62	1.82	2.68	3.02
	3	6.25	1.57	1.76	2.60	2.92
	4	6.04	1.52	1.69	2.52	2.81
mean		***6.23***	***1.56***	***1.75***	***2.60***	***2.91***
std deviation		***0.16***	***0.04***	***0.05***	***0.07***	***0.09***
Liquid phase	1	5.30	1.33	1.46	2.21	2.43
	2	4.13	1.04	1.12	1.72	2.43
	3	4.69	1.18	1.28	1.95	2.12
	4	5.23	1.31	1.44	2.18	2.39
mean		***4.84***	***1.21***	***1.32***	***2.02***	***2.20***
std deviation		***0.54***	***0.14***	***0.16***	***0.23***	***0.27***

Table III. Comparison of RPLC for separation of polar compounds

Type	Preparation method	*o*-toluidine			*p*-toluidine		
		As	N	h	As	N	h
Home-made C-8, 20 μm, low density silica	liquid phase			not separated			
Home-made C-8, 20 μm, low density silica	fluidised-bed	1.5	3806	3.3	1.6	2810	4.5
Zorbax C-8, 5 μm commercial		2.2	826	43.2	4	228.9	156

As = peak asymmetry; N = efficiency; h = reduced plate height.

However, it is possible that solvents may lead to the organic moiety being bound so silica surface in clusters, as described by Lochmüller [12]. It is envisaged that in the absence of solvents, improved contact of the reagent and silica will occur, thereby producing a uniform and relatively ordered surface of organic moiety. This may account for the improved retention characteristics of column packings prepared using the fluidised bed method, when compared with that of the liquid phase reacted columns (see Figs. 2, 3, 4, chromatograms of liquid phase and fluidised bed reacted RP).

It is known that the influence of unreacted and unshielded silanol groups can lead to much higher *k′* values [13]. However, the higher *k′* values encountered with the separations of the fluidised prepared column is not due to residual silanols causing mixed retention characteristics. The separation of *o*- and *p*-nitroanilines show no tailing of the peaks, which does occur in the presence of residual silanols. Fig. 4 and Table III illustrate this.

Further evidence suggests that fluidised bed prepared bonded phases have a more homogeneous surface coverage. For nominally the same carbon loading, as with the liquid prepared materials, fluidised bed packings show greater retention. Since the higher *k′* is not due to a mixed retention mechanism, an explanation of this may be a higher degree of homogeneity of the modified surface. Table IV and V (see Figs. 5, 6) shows the *k′* values for C-18 and C-8 columns. In both cases, the hydrothermally pretreated and fluidised reacted packing materials yield a *k′* of approximately 1.45 greater (for the phenetole component) than

Table IV. *k′* values of C-18 RPLC; high density silica gel, small particle size

Silica gel	treatment		Vo	acetone	phenol	p-cresol	2,5-xylenol	phenetole
High density silica small particle size	fluidised hydrothermal pretreatment	retention vol/ml	2.00	3.70	6.50	10.20	18.50	36.20
		k′	0.00	0.85	2.25	4.10	8.25	17.10
Commercially available C-18	endcapped	retention vol/ml	1.80	2.30	4.20	6.50	11.70	23.00
		k′	0.00	0.28	1.33	2.61	5.50	11.78

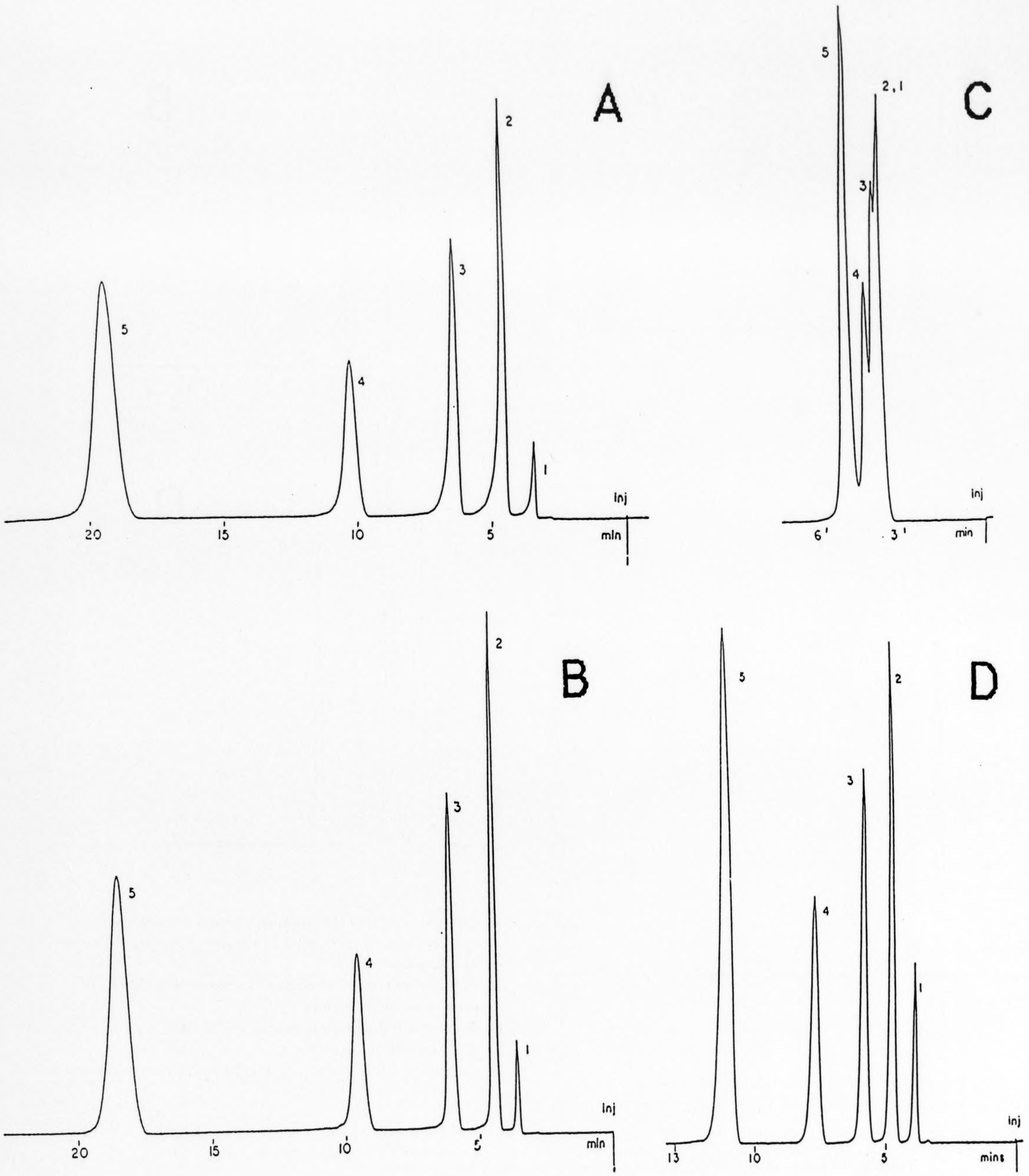

Fig. 2

Separation of acetone, phenol, p-cresol, 2,5-xylenol, and phenetole.
Sample: **1** = acetone; **2** = phenol; **3** = p-cresol; **4** = 2,5-xylenol; **5** = phenetole.

A: Column = Zorbax C-8 uncapped (5 μm; commercial); mobile phase MeOH/H_2O (1:1 v/v); flow-rate = 1 ml/min; temperature = 20 °C.
B: Column = Zorbax C-8 capped (5 μm; commercial); other conditions as in **A.**
C: Column = C-8 liquid phase (20 μm, 30 nm); other conditions as in **A.**
D: Column = C-8 fluidised (20 μm, 30 nm); other conditions as in **A.**

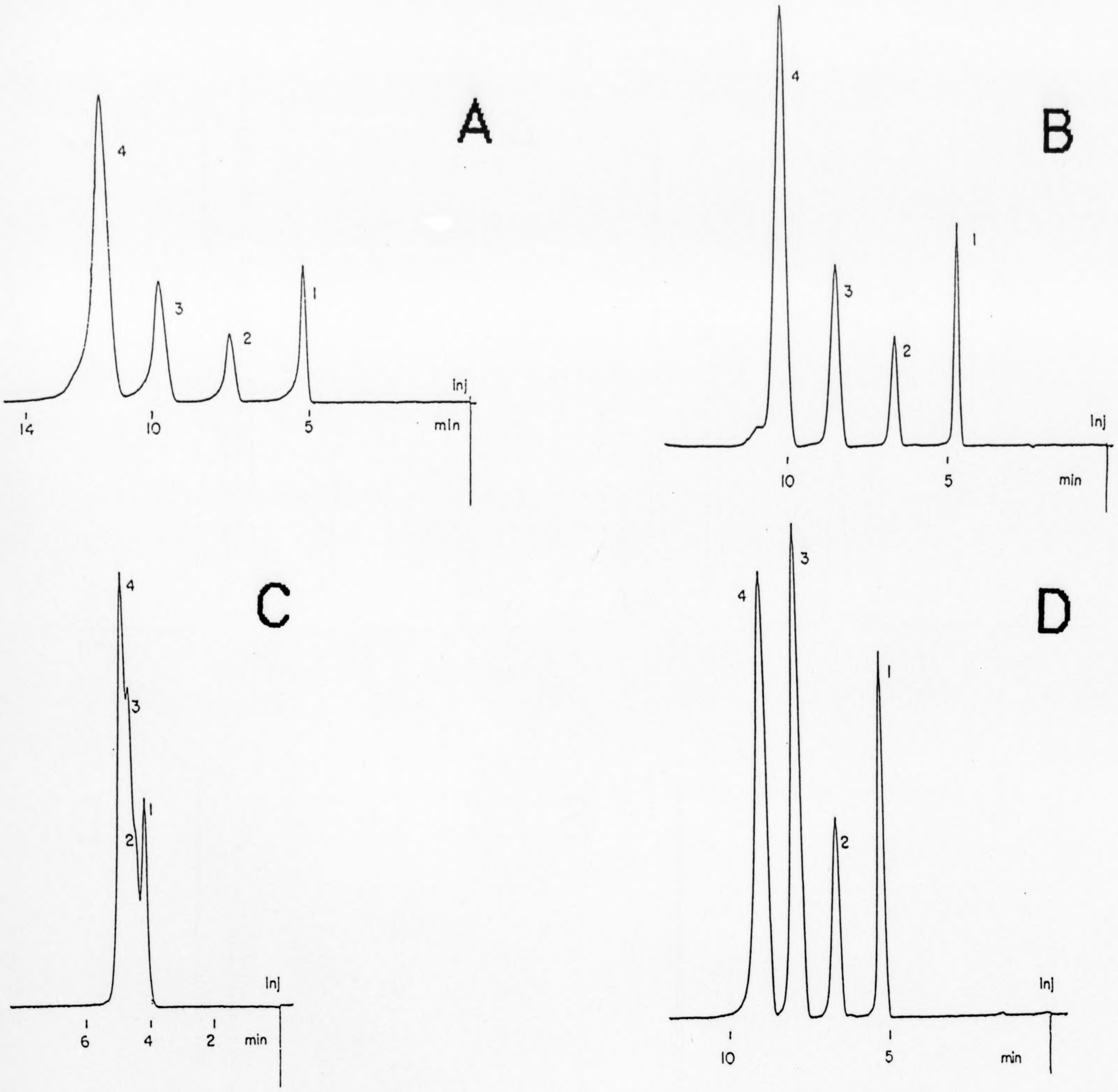

Fig. 3

Separation of PAH's.

Sample: **1** = benzene; **2** = naphthalene; **3** = biphenyl; **4** = phenanthrene.

A: Column = Zorbax C-8 uncapped (5 μm; commercial); mobile phase CH_3CN/H_2O (11:9 v/v); flow-rate = 1 ml/min; temperature = 20 °C.

B: Column = Zorbax C-8 capped (5 μm; commercial); other conditions as in **A.**

C: Column = C-8 liquid phase (20 μm, 30 nm); other conditions as in **A.**

D: Column = C-8 fluidised (20 μm, 30 nm); other conditions as in **A.**

Table V. *k′* values of C-8 RPLC; high density silica gel, small particle size

Silica gel	treatment		Vo	acetone	phenol	p-cresol	2,5-xylenol	phenetole
High density silica small particle size	fluidised no hydro- thermal pretreatment	retention vol/ml *k′*	1.10 0.00	3.75 2.41	4.75 3.32	6.05 4.50	7.95 6.23	11.05 9.05
High density silica small particle size	fluidised hydrothermal pretreatment	retention vol/ml *k′*	1.10 0.00	3.45 2.14	4.80 3.36	6.45 4.86	9.20 7.36	14.75 12.41
Commercially available C-8 equivalent	endcapped	retention vol/ml *k′*	1.05 0.00	2.75 1.62	3.80 2.62	5.05 3.81	7.00 5.67	10.15 8.67

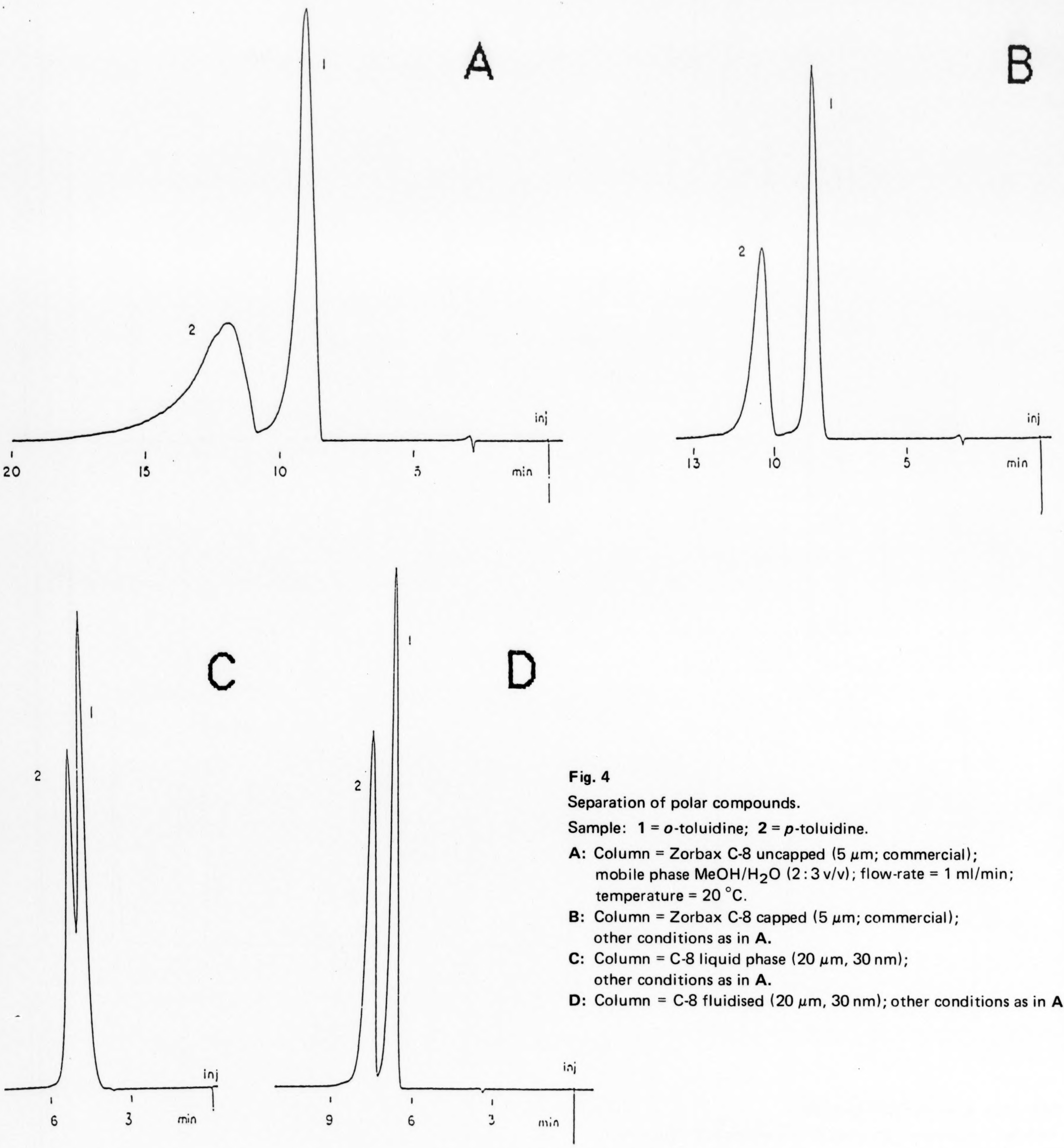

Fig. 4
Separation of polar compounds.
Sample: **1** = *o*-toluidine; **2** = *p*-toluidine.
A: Column = Zorbax C-8 uncapped (5 μm; commercial); mobile phase MeOH/H_2O (2 : 3 v/v); flow-rate = 1 ml/min; temperature = 20 °C.
B: Column = Zorbax C-8 capped (5 μm; commercial); other conditions as in **A.**
C: Column = C-8 liquid phase (20 μm, 30 nm); other conditions as in **A.**
D: Column = C-8 fluidised (20 μm, 30 nm); other conditions as in **A.**

the commercially available counterpart. However, when the silica gel was not pretreated there is virtually no difference in *k′* values (see Table V). This suggests that the activation of silica gel yields a more homogeneous RP surface since the %carbon loading is nominally the same.

An added feature of using fluidised bed technology is that fines, which are deleterious to HPLC columns, are removed in the pretreatment stage prior to reaction. Peak asymmetry at 10% peak height are usually close to unity (see Table VI).

Typically the reagent consumption for a loading of 25 to 30g of silica is in the order of 3 to 5g depending upon the type of silane used. By optimising the flow rate through the system and the cooling of the condenser, consumptions of about 2.5g of octyldimethylchlorosilane for a bed of 25g of silica have been achieved.

Column overloading experiments performed (Fig. 7) show high loadability, about 40mg. Front and back of the peaks were measured at 2/3 peak height. The columns were prepared with prior hydrothermal treatment for 24hr at the appropriate reaction temperatures. The % carbon loading trend shown in Table VII suggests that the silica surface is most activated at 200 °C. The graph of % carbon against temperature of pretreatment and reaction (Fig. 8) shows a linear relationship. This is consistent with the fact that

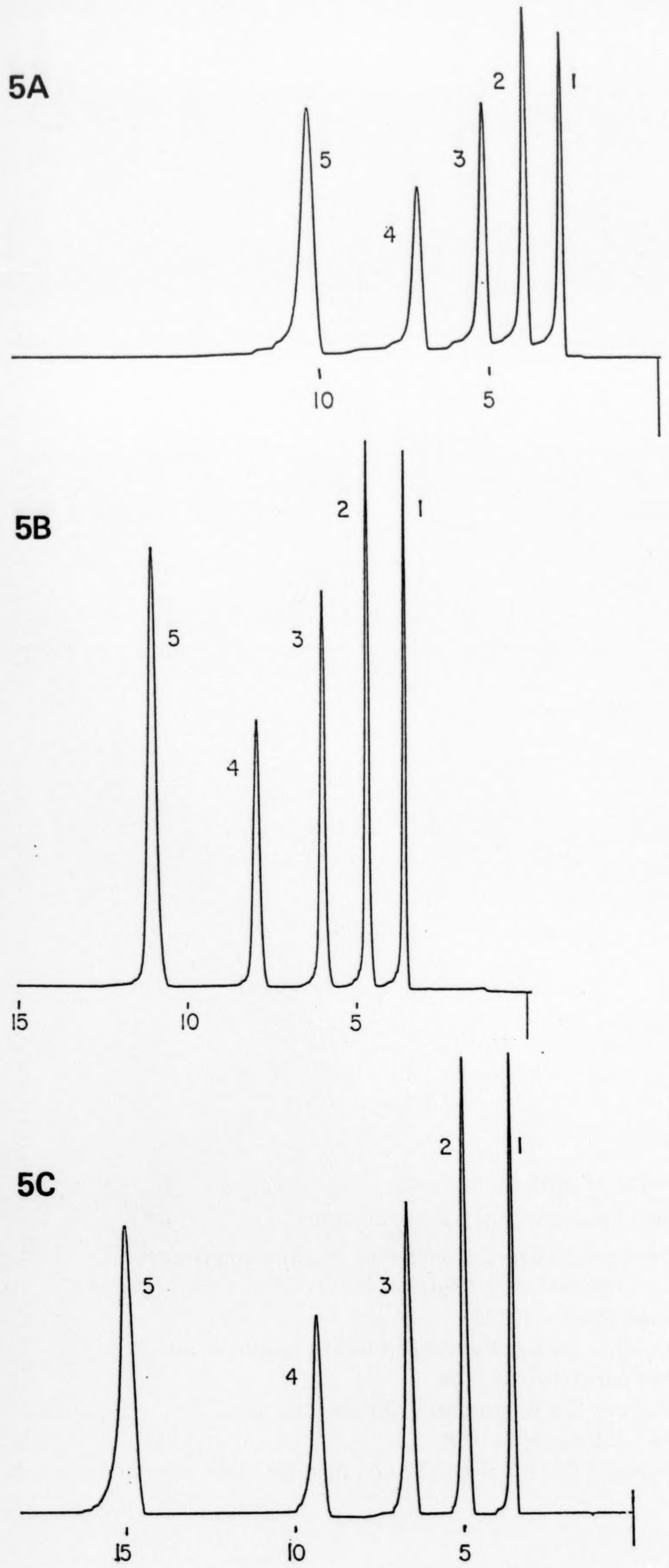

Fig. 5

Separation on 7 μm RPLC packings.

Sample: **1** = acetone; **2** = phenol; **3** = p-cresol; **4** = 2,5-xylenol; **5** = phenetole.

A: Column = Nucleosil C-8/100 Å (commercial); mobile phase MeOH/H_2O (1:1 v/v); flow-rate = 1 ml/min; temperature = 20 °C.

B: Column = Fluidised Nucleosil C-8/100 Å, no steam treatment; other conditions as in **A.**

C: Column = Fluidised Nucleosil C-8/100 Å, with steam treatment; other conditions as in **A.**

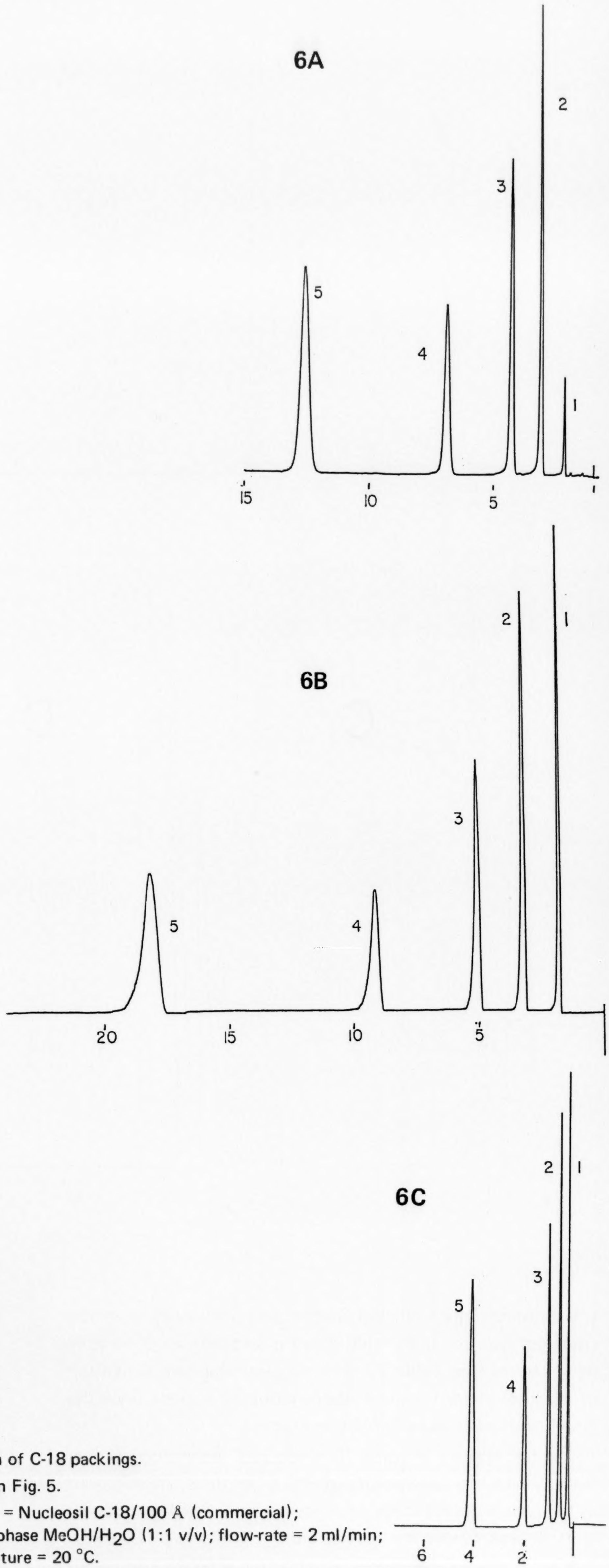

Fig. 6

Comparison of C-18 packings.

Sample as in Fig. 5.

A: Column = Nucleosil C-18/100 Å (commercial); mobile phase MeOH/H_2O (1:1 v/v); flow-rate = 2 ml/min; temperature = 20 °C.

B: Column = Fluidised Nucleosil C-18/100 Å, with steam treatment; other conditions as in **A.**

C: Column = Perkin-Elmer C-18 (3 μm; 3 cm; commercial); other conditions as in **A.**

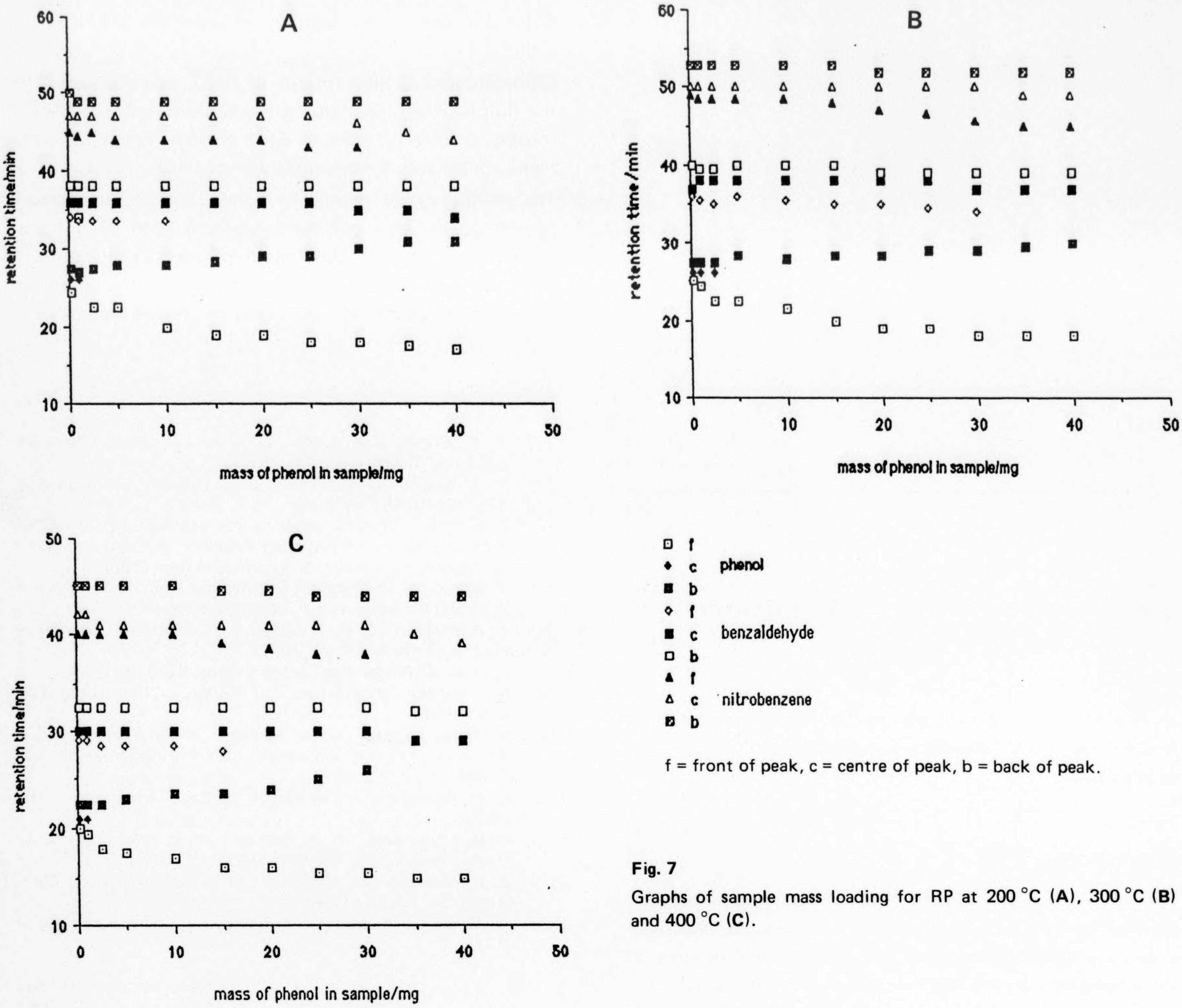

f = front of peak, c = centre of peak, b = back of peak.

Fig. 7

Graphs of sample mass loading for RP at 200 °C (**A**), 300 °C (**B**) and 400 °C (**C**).

Table VI. Comparison of C-8 RPLC highlighting peak tailing

Type	Preparation method	Phenol			Phenetole		
		As	N	h	As	N	h
Home-made C-8, 20 μm, low density silica	liquid phase	not separated from acetone			1.3	2353	5.3
Home-made C-8, 20 μm, low density silica	fluidised-bed	1.1	5444	2.2	1.2	5477	2.2
Zorbax C-8, 5 μm commercial		5	2997	11.9	1.1	2576	13.9

As = peak asymmetry; N = efficiency; h = reduced plate height.

Table VII. Carbon loading and coverage values for C-8 (uncapped) reacted at various temperatures

Silica gel	Temperature of reaction / °C	%C	Coverage no. of ligands/nm (by eq. (1))
high density 20 μm	200	13.07	1.93
	300	11.66	1.72
	400	10.28	1.52

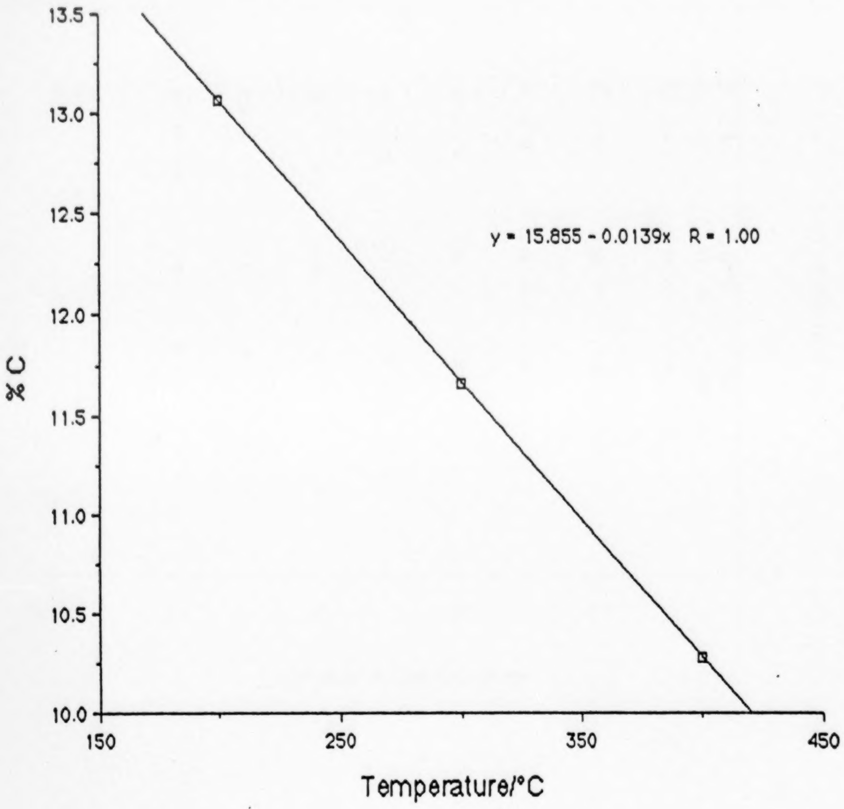

Fig. 8
Graph showing effect of reaction temperature on carbon loading.

surface hydroxyl groups are lost at higher temperature pretreatments and therefore have less silanol groups for modification.

Conclusion

The application of fluidised bed technology to the preparation of chemically bonded phases has been shown to be a viable preparation method. The disadvantages of solvent based reactions are avoided; such as the removal of solvent, washing of bonded phase and other manipulations. Additionally there is no wastage of expensive cholorosilane reagents.

Chromatographic performance of RPLC materials made by the fluidised bed technique is markedly superior to that of solvent prepared products. Furthermore, batch to batch repeatability and reproducibility is very high.

The production of chemically bonded phases for reversed-phased preparative chromatography is seen as a major opportunity for this novel mode of preparation, both in terms of cost savings of the process and the improved chromatographic characteristics of the bonded phases.

References

[1] *R. K. Gilpin, J. A. Korpi, C. A. Janicki,* Anal. Chem. **46,** 1314 (1974).

[2] *R. K. Gilpin, D. J. Camillo, C. A. Janicki,* J. Chromatog. **121,** 13 (1976).

[3] *K. K. Unger,* Porous Silica, J. Chromatog. Libr. **16,** 99 (1979).

[4] 'Characterisation of Fluidised Powders' in Gas Fluidisation Technology by *Geldart, D.,* J. Wiley & Sons (1986).

[5] 'Fluidisation' in Chemical Engineering Vol. II by *Coulson, J. M.* and *Richardson, J. F.,* Pergamon Press (1967).

[6] *R. A. Brekken, E. B. Lancaster, T. D. Wheelock,* Chem. Eng. Prog. Sym. Series **66,** 81 (1970).

[7] *W. Aue, C. R. Hastings,* J. Chromatog. **42,** 319 (1969).

[8] *N. D. Petsev, A. Kostova, P. I. Filchev,* J. Chromatog. **148,** 484 (1978).

[9] *K. I. Sakodynski, S. A. Volkov, K. F. Khalilov, V. I. Reznikov, V. Yu. Zel'venski,* Chromatographia **20**, 538 (1985).

[10] *G. E. Berendsen, L. de Galan,* J. Liq. Chromatog. **1,** 561 (1978).

[11] *C. H. Lochmüller, A. S. Colborn, M. L. Hunnicutt, J. M. Harris,* Anal. Chem. **55,** 1344 (1983).

[12] *D. B. Marshall, K. A. Stutler, C. H. Lochmüller,* J. Chromatog. Sci. **22,** 217 (1984).

[13] *K. Karch, I. Sebestian, I. Halász,* J. Chromatog. **122,** 3 (1976).

Received: July 1, 1987
Accepted: July 23, 1987
F

A Post-Column Extraction System for the Determination of Tertiary Amines by Liquid Chromatography with Chemiluminescence Detection

P. J. M. Kwakman* / U. A. Th. Brinkman / R. W. Frei / G. J. de Jong

Department of Analytical Chemistry, Free University, De Boelelaan 1083, 1081 HV Amsterdam, The Netherlands

F. J. Spruit / N. G. F. M. Lammers / J. H. M. van den Berg

Duphar B.V., P. O. Box 2, 1380 AA Weesp, The Netherlands

Key Words

Column liquid chromatography
Ion-pair extraction detection
Peroxyoxalate chemiluminescence
Chemiluminescent counter ion

Summary

The combination of an ion-pair extraction detection system with peroxyoxalate chemiluminescence detection has been investigated. Ion-pairs of protonated tertiary amines with a chemiluminescent counter ion are on-line post-column extracted to 1,2-dichloroethane containing bis(2,4,6-trichlorophenyl)oxalate (TCPO). Hydrogen peroxide is added to the organic phase by means of a solid-state perhydrit reactor. The influence of the base catalyst (imidazole) on the chemiluminescence reaction in apolar solvents was studied. Some sulfonated chemiluminophores were compared with respect to their chemiluminescence, ion-pairing and extraction properties, and 5-dimethylaminonaphthalene-1-sulfonate was found to be the most suitable reagent. The detection limit of the potential drug secoverine is in the sub-nanogram range.

Introduction

In the last decade peroxyoxalate chemiluminescence (CL) has become one of the most sensitive liquid chromatography (LC) detection systems. This was demonstrated for dansyl derivatives of amino acids [1–4], a steroid [5] and a drug [6], fluorescamine-labelled catecholamines [7], many polycyclic aromatic hydrocarbons [8], a number of labelled alkylamines [9], 3-aminoperylene derivatives of carboxylic acids [10] and, very recently, coumarine derivatives of carboxylic acids [11]. The sensitivity of this detection mode for LC was shown to be often 10–100 times higher than that of conventional fluorescence detection. CL detection, however, is limited to fluorescent analytes with a singlet excitation energy lower than 105 kcal mol^{-1} (λ_{exc} higher than 272 nm) [12] and a low oxidation potential (electron transfer mechanism) [13], or to analytes with the possibility to be labelled with a good chemiluminescent tag. As for the latter aspect, tertiary amines are somewhat problematic due to the lack of derivatization possibilities. However, ion-pair extraction of protonated amines with a negatively charged fluorescent counter ion, like 9,10-dimethoxyanthracene-2-sulfonate (DAS) [14], has been described for LC systems with detection limits in the sub-ng range [15–18]. The counter ion is added to the mobile phase (pre-column), or after separation of the tertiary amines (post-column), and the ion-pair is on-line extracted by segmentation with an organic solvent, like chloroform or 1,2-dichloroethane. After phase separation the detection takes place in the organic phase which usually leads to higher fluorescence quantum yields. Further advantages are the limitation of band-broadening due to segmentation and the easy removal of superfluous counter ion. The CL detection of some tertiary amines with tris(2,2′-bipyridine)ruthenium(III) was shown to be very selective [19]. A yellow-orange light was generated upon mixing an amine and tris(2,2′-bipyridine)ruthenium(III) in an aqueous solution buffered between pH 4 and 7. The sensitivity, however, depended on the modifier content of the mobile phase and ranged from 1 to 47 ng for several trialkylamines.

The aim of this study is to combine ion-pair extraction with peroxyoxalate CL detection. For the optimization of such a system it was necessary to investigate (i) the design of a new chemiluminescent label functioning as a counter ion, (ii) the specific problems of CL in apolar solvents and (iii) the coupling of a post-column ion-pair extraction system with CL detection.

0009-5893/87 0395-05 $03.00/0

© 1987 Friedr. Vieweg & Sohn Verlagsgesellschaft mbH

Experimental

Chemicals

HPLC-grade solvents were purchased from Baker (Deventer, the Netherlands), reagent-grade 1,2-dichloroethane (Baker) was distilled once before use.

Bis(2,4,6-trichlorophenyl)oxalate (TCPO) was synthesized as described [20] with two additional recrystallizations from p.A. benzene. Dansylchloride was purchased from Aldrich (Brussels, Belgium) and Lissamine Rhodamine B sulfonylchloride (larylchloride [21]) from Kodak (Weesp, The Netherlands). The sulfonylchloride groups of these labels were hydrolysed in 40ml acetonitrile-water (1:1, v/v, pH 12; concentration of the sulfonylchloride 10^{-3}M) in order to obtain 5-dimethylaminonaphthalene-1-sulfonate and Lissamine Rhodamine B sulfonate, called dansyl-OH and laryl-OH respectively. Perylene-3-sulfonate was synthesized by P. de Wit (Department of Organic Chemistry, University of Amsterdam, The Netherlands) [22]. 8-Anilinonaphthalene-1-sulfonate was purchased from Kodak (Weesp, The Netherlands), 9,10-dimethoxyanthracene-2-sulfonate (DAS) from Fluka (Buchs, Switzerland). Perhydrit tablets (H_2O_2 on an urea support) were bought from Merck (Darmstadt, F.R.G.). All other chemicals were analytical reagent-grade. The potential drug secoverine (1-cyclohexyl-4-[ethyl(p-methoxy-α-methylphenethyl)amino]-1-butanone hydrochloride; Duphar B.V., Weesp, The Netherlands) was used as a model compound.

High-Performance Liquid Chromatography

A Gilson Model 302 pump (Gilson, Villiers-le-Bel, France) equipped with a Gilson Model 308 manometric module was used to deliver the LC mobile phase. A Valco injection valve with a 25µl (flow injection) or a 100µl (chromatography) loop was used for introduction of samples directly in the detection system or in a 200 × 3.1mm i.d. analytical column, packed by a slurry technique with 10-µm CN-bonded silica (Polygosil 60-10 CN; Macherey, Nagel & Co., Düren, F.R.G.).

Detection System

The scheme of the CL detection system is shown in Fig. 1. The chemiluminescent counter ion was added to the mobile phase prior to the column. The organic flows were delivered by two home-made syringe pumps (Free University Chemistry Workshop). Extraction took place in a 200µl (210 × 1.1mm i.d.) stainless steel capillary. Phase separation was carried out with a new sandwich-type phase separator based on the principles of wetting and gravity [23]. A part of the organic phase was directed to the detector cell by varying the back-pressure via a restriction of the PTFE tubing to the waste outlet of the phase separator. The detector was a Kratos FS 970 fluorimeter (Kratos, Ramsey, NJ, USA) with the excitation lamp off. The fluorimeter was equipped with a commercial 5µl or a home-made 50µl meander-type flow cell [24]. For a suitable CL detection it is necessary to have all the CL components in excess of the extracted ion-pair.

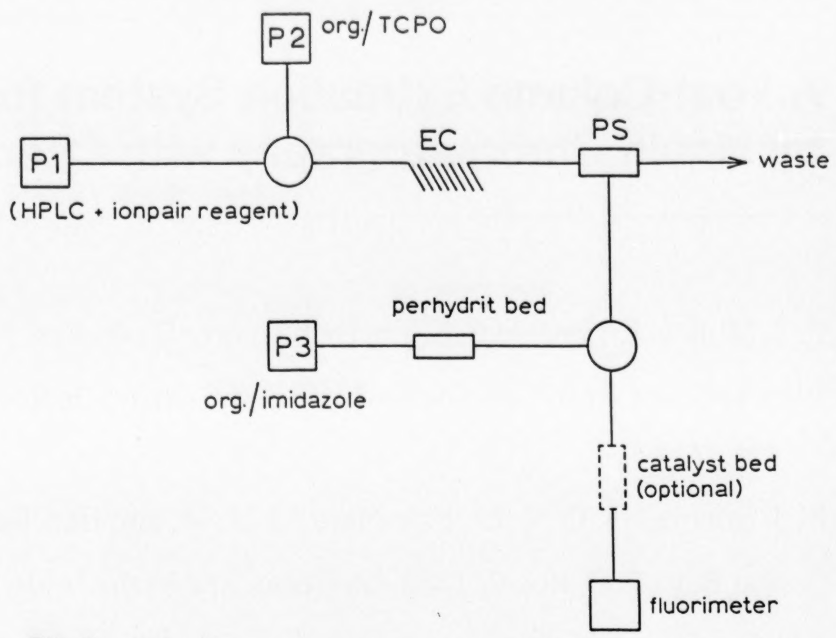

Fig. 1

Scheme of the detection system with post-column extraction and CL detection. P1 = LC pump; P2 and P3 = syringe pumps; EC = extraction coil; PS = phase separator. Flow rates (ml/min): LC, 0.5–0.75; extraction solvent, 0.4; through the perhydrit column, 0.1; through the flow cell, 0.3–0.4.

TCPO (5 × 10^{-3}M) was dissolved in the extraction solvent 1,2-dichloroethane. Imidazole was added as a 5 × 10^{-3}M solution in 1,2-dichloroethane. Alternatively, base catalysis was achieved by a column filled with imidazolin-bonded silica or NH_2-bonded silica. The addition of hydrogen peroxide was performed by using a column (60 × 4.6mm or 150 × 4.6mm i.d.), hand-packed with 0.8 or 2.4g, respectively, of finely ground perhydrit.

Results and Discussion

Combination of Ion-Pair Extraction with CL Detection

In order to be able to change the extraction and CL conditions quickly, the optimization studies were done in the flow injection mode. TCPO was routinely used because of its solubility and stability in organic solvents and the relatively easy control of the CL kinetics. A system with bis(2,4-dinitrophenyl)oxalate (DNPO), for instance, was more difficult to control due to its fast CL kinetics [24] and, furthermore, this oxalate was rapidly hydrolysed as observed by the formation of a yellow colour after addition of the extraction solvent containing DNPO to the aqueous phase. 1,2-Dichloroethane was often found to be the most efficient extraction solvent in earlier reports [16, 25] and, hence, this solvent was used throughout this study.

The problems encountered when combining ion-pair extraction with CL detection were substantial. They included: (1) the dissolving of enough H_2O_2 in an organic phase; (2) the control of the rate of the CL reaction in an organic phase; (3) the choice of a counter ion with good chemiluminescence, ion-pairing and extraction properties. These aspects will now be discussed in detail.

Addition of Hydrogen Peroxide

For the detection of fluorescent compounds with the peroxyoxalate CL system H_2O_2 concentrations in the range of 0.1M [4] to 1.5M [24] are required. Initially, in the flow injection mode, H_2O_2 dissolved in the aqueous phase was co-extracted with the dansyl-secoverine ion-pair into the organic phase by the modifier of the mobile phase. The optimum aqueous phase was acetonitrile-water (50:50, v/v) containing 0.3M H_2O_2, 10^{-2}M phosphate buffer at pH 3.5 and 10^{-3}–10^{-4}M counter ion. A lower acetonitrile content caused too large a decrease of the H_2O_2 concentration in the organic phase and a higher content gave rise to too high a co-extraction of the counter ion as its sodium salt. This system worked reasonably well in spite of the fact that the apolar ion-pair and the polar H_2O_2 had to be simultaneously transferred to the organic phase. The signal-to-noise ratio (S/N) was limited by the co-extraction of the counter ion; the detection limit (S/N of 2) was about 10ng for secoverine.

In order to decrease the co-extraction of the counter ion the percentage modifier was lowered to 10–15%. Furthermore, dioxane was used instead of acetonitrile because according to Reddingius et al. [16] dioxane is the best compromise between acceptable chromatographic retention and low counter ion co-extraction. This meant that the H_2O_2 introduction had to be changed completely since the co-extraction method was no longer possible. It was found that a flow of 100μl/min dichloroethane/acetonitrile (4:1, v/v) through a 60 × 4.6mm i.d. perhydrit column (Fig. 1) dissolved enough perhydrit to establish a concentration of ca. 10^{-2}M H_2O_2 in this solvent mixture. This was calculated from the fact that one-tenth of the perhydrit column volume dissolved in ca. 100ml dichloroethane/acetonitrile (4:1, v/v). Three-fold dilution of the perhydrit column effluent with dichloroethane/acetonitrile (4:1, v/v) and re-using this as H_2O_2 flow did not lower the CL response, which indicates that H_2O_2 is present in sufficient excess. An increase of the concentration acetonitrile or a change to, e.g., acetone in order to increase the H_2O_2 concentration caused precipitation of urea (support of the perhydrit column) in the capillary between the mixing tee and the flow cell. A longer perhydrit column of 150mm instead of 60mm increased the signal by a factor of 2, but the S/N ratio remained about the same.

Base Catalysis and Kinetic Control of the CL Reaction

Using a 5μl flow cell and a 300μl/min flow through the detector, only a very small part of the total CL decay curve is measured; therefore a catalyst is required. Imidazole was chosen for base catalysis because of its favourable solution properties in organic solvents. In order to speed up the reaction rate to a sufficient degree a concentration of at least 10^{-3}–10^{-2}M imidazole in the flow cell is necessary. Imidazole could not be dissolved in the extraction solvent because of precipitation of a reaction product of imidazole and TCPO. Addition to the mobile phase was found not to be feasible either, because at pH 3.5 the base is fully protonated and will only go into the organic phase as an undesirable chemiluminescent ion-pair. However, it was found to be possible to start the CL reaction by a base chemically bonded to silica (Fig. 1, with catalyst column). A simple 10 × 2mm i.d. precolumn was used hand-packed with materials such as 7- or 10-μm NH_2-bonded silica and 10-μm LiChrosorb 100 modified with imidazolinesilan. The results with the imidazolin phase were 10-fold better than with NH_2-bonded silica. However, the CL decay rate was still too low ($t_{1/2}$, ca. 5min) so that more than 98% of the generated light was lost. Addition of 5×10^{-3}M imidazole to the organic solvent led through the perhydrit reactor (cf. previous section) increased the CL rate significantly: the half-life of the CL reaction was now ca. 30s only. A higher concentration of imidazole (up to 5×10^{-2} M) increased the rate but decreased the S/N ratio. This illustrates that a faster CL reaction does not always improve the detection limits because the background increases too. Moreover, in principle, if the reaction becomes too fast a considerable part of the emitted light will be lost prior to the detector.

Replacement of the 5μl flow cell by a home-made 50μl flow cell increased the S/N ratio by a factor of 10. This effect was partly due to the detection of a larger part of the CL decay curve and probably also due to improved mixing in the first section of the 50μl flow cell. The disadvantage of the extra band broadening of the larger flow cell is partly compensated by the so-called chemical band-narrowing effect [6]. For all further experiments the 50μl flow cell was used.

Selection of a Chemiluminescent Counter Ion

Relevant data concerning the characteristics of several counter ions – viz. a series of sulfonated aminonaphthalenes, a sulfonated perylene and a Rhodamine B derivative – are given in Table I. It seemed interesting to include a substituted perylene because of its very high CL quantum yield [10]. Unfortunately, the poor water solubility of the perylene aromatic ring system was only weakly improved by the sulfonate substituent: a very high background extraction prevented the use of perylene-3-sulfonate as a

Table I. Properties of some CL counter ions.

Counter ion	CL intensity	background* extraction	signal-to-noise ratio
5-Aminonaphthalene--1-sulfonate	–	+	–
8-Anilinonaphthalene--1-sulfonate	+	–	–
5-Dimethylamino-naphthalene-1-sulfonate (dansyl-OH)	+	++	++
Perylene-3-sulfonate	++	––	–
Lissamine Rhodamine B sulfonate (laryl-OH)	+	+	+
9,10-Dimethoxyanthracene-2-sulfonate (DAS)	+	+	+

* The background extraction was measured by comparing the base line off set with or without counter ion: –– means high and ++ means low background extraction.

counter ion. More or less the same situation was observed with 8-anilinonaphthalene-1-sulfonate, whereas 5-aminonaphthalene-1-sulfonate combined a relatively low background extraction with a quantum yield of about one-tenth of that of 8-anilinonaphthalene-1-sulfonate (see also ref. [26]).

The best S/N results were obtained with laryl-OH, dansyl-OH and DAS. In comparison with the other ion-pair reagents tested laryl-OH would have been a promising reagent due to its high emission maximum (above 600nm) and, hence, the possibility of removing a large part of the CL background signal (with an emission maximum at about 450nm [27]) with a 550 or a 580nm emission filter. However, the high background extraction of the counter ion itself limited its applicability. Using a 550 or a 580nm filter 95% of the total background signal was caused by laryl-OH itself.

De Ruiter et al. [28] have reported that non-ionic fluorescent by-products are formed during hydrolysis of dansylchloride. These by-products can easily be removed from the aqueous phase by extraction with chloroform. Application of this purification approach to a mobile phase containing 10^{-4}M dansyl-OH lowered the background signal and improved the S/N ratio by a factor of 5. The same procedure with larylchloride did not equally improve the background extraction as with dansylchloride because of the relatively good solubility of the large Rhodamine ring system in organic solvents. The background extraction of purified dansyl-OH is also about 5-fold lower than with DAS and therefore the former reagent was used in further investigations.

With a mobile phase containing 15% dioxane and 10^{-4}M dansyl-OH, the CL background was now 25% of the total background and 75% was still contributed by the counter ion itself. Fig. 2 shows two series of flow injection results under the optimized conditions. The detection limit of secoverine was about 200pg at a S/N of 2, and the linear range at least 3 decades.

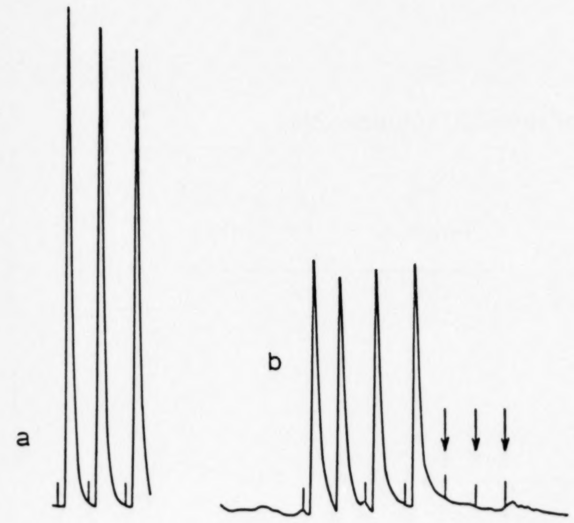

Fig. 2

Flow injection analysis of secoverine standard solutions. (a) 25µl injections of 57ng secoverine (attenuation, 0.1); (b) 25µl injections of 5.7ng secoverine (attenuation, 0.02); blanks indicated as arrows. Carrier stream, 0.1mM dansyl-OH, dioxane-phosphate buffer pH 3.0 (15:85, v/v); extraction phase, 5mM TCPO in dichloroethane; catalyst + hydrogen peroxide, 5mM imidazole in dichloroethane-acetonitrile (4:1, v/v) + 60 × 4.6mm i.d. perhydrit reactor.

See Fig. 1 for experimental details.

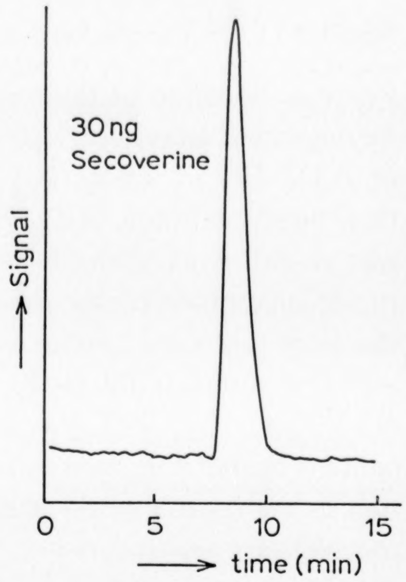

Fig. 3

Chromatogram of 30ng secoverine as its dansyl-OH ion-pair. See Figs. 1 and 2 for experimental conditions. The mobile phase also contained 10mM ethanolamine to suppress peak tailing. LC column: 200 × 3.1mm i.d. 10-µm CN-bonded silica.

Chromatographic System

In order to permit chromatography at a low modifier content of the mobile phase a relatively polar bonded phase was chosen as the stationary phase. A problem encountered with the chromatographic system was the severe tailing of the secoverine peaks. In the literature this problem is solved by adding an alkylamine, e.g. hexylamine, to the mobile phase [29] or by using large amounts of triethylamine in the mobile phase [30]. Both possibilities will give rise to a very high background extraction of the chemiluminescent counter ion. As an alternative ethanolamine was used to improve the peak shape. A concentration of 10^{-2}M ethanolamine improved the peak asymmetry, $A_{0.1}$, from 3.5 to 2.0 while a higher concentration had no further effect. The low chromatographic efficiency still has an unfavourable influence on the detection limit. In Fig. 3 an injection of 30ng secoverine is shown; the detection limit was about 500pg ($k' = 3.5$; $N = 440$).

Conclusions

The post-column extraction chemiluminescence detector described in this paper can be used for the sensitive and selective determination of tertiary amines. The influence of various parameters, such as the way of addition of hydrogen peroxide and the base catalyst, has been studied and much attention has been paid to the proper choice of the ion-pair reagent. The following conditions were found to give the best results: stationary phase, 200 × 3.1mm i.d. 10-µm CN-bonded silica; mobile phase, 0.1mM dansyl-OH in dioxane-10mM phosphate buffer, pH 3.0 (15:85, v/v) containing 10mM ethanolamine; extraction phase, 5mM TCPO in dichloroethane; catalyst, 5mM imidazole in dichloroethane-acetonitrile (4:1, v/v); hydrogen peroxide, 60 × 4.6mm perhydrit reactor. The detection limit for secoverine is now about 500pg which is comparable to results obtained for various compounds in fluorescence-based extraction detection systems; the limiting factor still is the background due to co-extraction of the ion-pair reagent. However, with real samples the CL extraction detection system will probably show a higher selectivity than the fluorescence system as has been demonstrated by the comparison of CL and fluorescence detection for the determination of polycyclic aromatic hydrocarbons in oil [8].

Further research will be directed at a flow cell packed with perhydrit and, possibly, combined with a chemically bonded base catalyst placed in front of the photomultiplier (see also Ref. [31]). The addition of H_2O_2 via a solid-state perhydrit column also seems attractive for CL systems used for detection in normal-phase LC. Current research deals with the use of Lissamine Rhodamine B sulfonylchloride and other substituted Rhodamines as possible prechromatographic derivatization reagents for CL detection. In this case the CL background can be filtered out efficiently by the previously described technique.

References

[1] *S. Kobayashi, K. Imai*, Anal. Chem., **52**, 424 (1980).
[2] *K. Honda, J. Sekino, K. Imai*, Anal. Chem., **55**, 940 (1983).
[3] *G. J. Melbin*, J. Liq. Chromatogr., **6**, 1603 (1983).
[4] *K. Miyaguchi, K. Honda, K. Imai*, J. Chromatogr., **316**, 501 (1984).
[5] *T. Koziol, M. L. Grayeski, R. Weinberger*, J. Chromatogr., **317**, 355 (1984).
[6] *G. J. de Jong, N. Lammers, F. J. Spruit, U. A. Th. Brinkman, R. W. Frei*, Chromatographia, **18**, 129 (1984).
[7] *S. Kobayashi, J. Sekino, K. Honda, K. Imai*, Anal. Biochem., **112**, 99 (1981).
[8] *K. W. Sigvardson, J. M. Kennish, J. W. Birks*, Anal. Chem., **56**, 1096 (1984).
[9] *G. Melbin, B. E. F. Smith*, J. Chromatogr., **312**, 203 (1984).
[10] *K. Honda, K. Miyaguchi, K. Imai*, Anal. Chim. Acta, **177**, 111 (1985).
[11] *M. L. Grayeski, J. K. de Vasto*, Anal. Chem., **59**, 1203 (1987).
[12] *P. Lechtken, N. J. Turro*, Mol. Photochem., **6**, 95 (1974).
[13] *C. L. R. Catherall, T. F. Palmer, R. B. Cundall*, J. Chem. Soc., Faraday Trans. **2**, 80, 837 (1984).
[14] *D. Westerlund, K. O. Borg*, Anal. Chim. Acta, **67**, 89 (1973).
[15] *C. van Buuren, J. F. Lawrence, U. A. Th. Brinkman, R. W. Frei*, Anal. Chem., **52**, 700 (1980).
[16] *R. J. Reddingius, G. J. de Jong, U. A. Th. Brinkman, R. W. Frei*, J. Chromatogr., **205**, 77 (1981).
[17] *J. H. Wolf, C. de Ruiter, U. A. Th. Brinkman, R. W. Frei*, J. Pharm. Biomed. Anal., **4**, 523 (1986).
[18] *C. de Ruiter, U. A. Th. Brinkman, R. W. Frei*, J. Liq. Chromatogr., in press.
[19] *J. B. Hoffsinger, N. D. Danielson*, J. Chromatogr., **388**, 520 (1987).
[20] *A. G. Mohan, N. J. Turro*, J. Chem. Educ., **51**, 528 (1974).
[21] *R. M. Metrione*, J. Chromatogr., **363**, 337 (1986).
[22] *H. Cerfontain, K. Laali, H. J. A. Lambrechts*, Rec. Trav. Chim. Pays-Bas, **102**, 210 (1983).
[23] *C. de Ruiter, J. H. Wolf, U. A. Th. Brinkman, R. W. Frei*, Anal. Chim. Acta, **192**, 267 (1987).
[24] *G. J. de Jong, N. Lammers, F. J. Spruit, R. W. Frei, U. A. Th. Brinkman*, J. Chromatogr., **353**, 249 (1986).
[25] *J. F. Lawrence, U. A. Th. Brinkman, R. W. Frei*, in 'Reaction Detection in Liquid Chromatography', *I. S. Krull*, Ed., Marcel Dekker, New York, 1986, ch. 6.
[26] *A. Tsuji, M. Maeda, H. Arakawa*, in 'Bioluminescence and Chemiluminescence', Vol. 1, *Knox Van Dyke*, Ed., CRC Press, Boca Raton, 1985, p. 185.
[27] *K. W. Sigvardson, J. W. Birks*, Anal. Chem., **55**, 432 (1983).
[28] *C. de Ruiter, R. R. Otten, U. A. Th. Brinkman, R. W. Frei*, in preparation.
[29] *A. Sokolowski, K.-G. Wahlund*, J. Chromatogr., **189**, 299 (1980).
[30] *R. W. Roos, C. A. Lau-Cam*, J. Chromatogr., **370**, 403 (1986).
[31] *P. van Zoonen, D. A. Kamminga, C. Gooijer, N. H. Velthorst, R. W. Frei, G. Gübitz*, Anal. Chim. Acta, **174**, 151 (1985).

Received: July 17, 1987
Accepted: Aug. 5, 1987
F

A New Polymer Supported Packing Material as a Substitute of Hydroxylapatite: Purification of Topoisomerases[1]

K. Majumder* / N. Ramesh

Molecular Biophysics Unit, Indian Institute of Science, Bangalore 560012, India

Key Words

Liquid chromatography
Hydroxylapatite substitute, HAS
Protein purification
Topoisomerases

Summary

Hydroxylapatite (HA), a form of calcium phosphate, finds extensive usages in the fractionation and purification of proteins, enzymes and nucleic acids. However, commercial HA preparations for liquid chromatography (LC) differ from many other LC packing materials in that the former is not polymer supported. We have now developed a substitute packing material which uses Fractosil 200 as the polymer support. Other polymer supports can also be similarly used. Being Fractosil 200 supported, this Hydroxylapatite Substitute (HAS) matrix can be employed for open column LC as well as for HPLC purposes. Although the exact chemical nature of HAS is different from the conventional HA, HAS mimicks the functions of the latter support. Due to the high binding capacity of HA many DNA binding proteins have been partially purified on this support. In the present work HAS has been successfully used in the partial purification of Topoisomerase I and II from wheat germ.

Introduction

Hydroxylapatite (HA) was introduced for protein chromotography by Tiselius et al in 1956 [1]. Since then it has been extensively used for protein and nucleic acid purification [2–4]. HA chromatography often resolves complex mixtures of proteins when all other seperation methods fail. Thus, multiple components are often obtained from the HA analysis of proteins that were shown to be homogeneous by ion-exchange chromotography and/or electrophoresis.

HA used in liquid chromatography differs from many other liquid chromotography (LC) packing materials in that the former is not polymer supported. In order to circumvent one of the major disadvantages of the HA column, namely the fragile nature of its crystals, we have developed a polymer supported matrix which can be used for both open column LC as well as for HPLC column purposes. This substitute packing material which uses Fractosil 200 as the polymer support, mimics the functions of the conventional HA. While HA has been found to be useful in the purification of Topoisomerase II from various sources [5, 6], in the present work we have used the HA substitute or HAS matrix (patent is being applied for) to partially purify Toposiomerase I and II from wheat germ.

Materials and Methods

Reagents

Fractosil 200 was from E. Merck, FRG. Tris; Polymin P; 2-mercaptoethanol (BME) and phenylmethylsulphonylfluoride (PMSF) were from Sigma chemical company, USA. All other reagents used were of analytical grade. Wheat germ was procured form Krishna Flour Mills, Bangalore. Buffer 1 was 50 mM tris HCl pH 7.9, 1 mM ethylenediaminetetraaceticacid, 10 mM BME, 0.1 mM PMSF. Buffer 2 was 100 mM potassium phosphate pH 7.4, 10 mM BME, 0.1 mM PMSF.

Preparation of the HAS Column Matrix (Scheme I)

Fractosil 200 was stored for 24 hrs over saturated LiCl solution. This was then reacted with triethoxyaminopropyl silane when the silanol groups of the silica react with the ethoxy groups and thus develop a long chain spacer arm. The derivatized silica was washed thoroughly with tolune, methanol and 50 % aqueous methanol. It was then shaken overnight with 50 % methanol, filtered and dried. The unreacted silanol groups were silylated with trimethylsilyl chloride [7]. The silylated gel was washed with methanol, solvent ether and dried in vacuo. The dry silica gel was subsequently phosphorylatyed [8] to develop phosphate groups on the amino terminal of the spacer arm. This phosphorylated silica was washed with methylene chloride, methanol, water and then suspended in water. To the

---

[1] Dedicated to Professor Hartmut Seliger on his 50th birthday.

0009-5893/87 0400-03 $ 03.00/0

© 1987 Friedr. Vieweg & Sohn Verlagsgesellschaft mbH

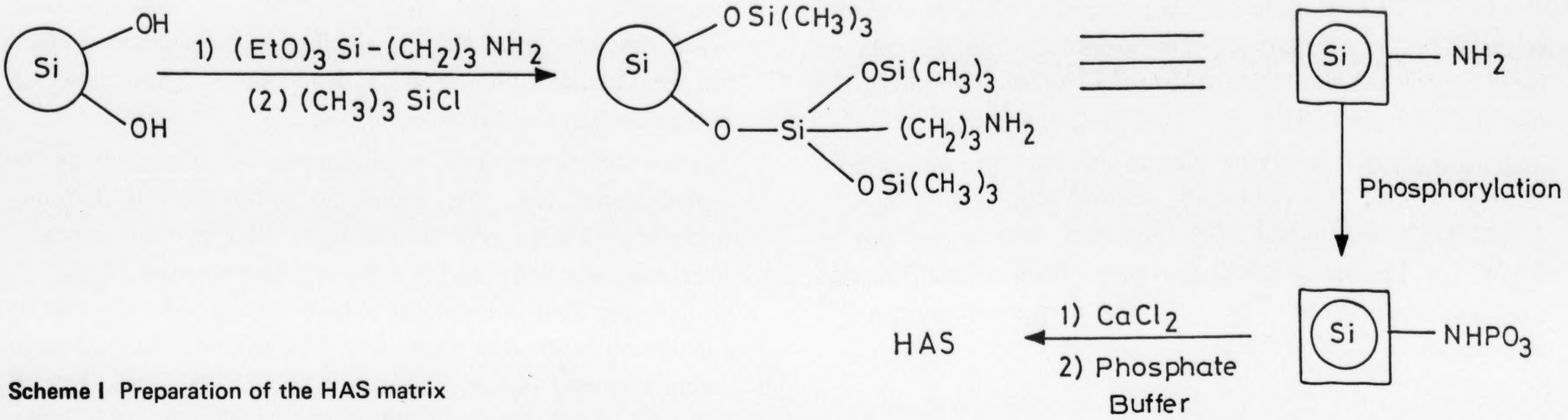

Scheme I Preparation of the HAS matrix

aqueous suspension an equal volume of 2M $CaCl_2$ was added and shaken overnight. The suspension was filtered, washed free of $CaCl_2$ and then washed with water. The support was suspended in 1 M phosphate buffer (pH 7), shaken overnight. The gel was filtered, washed with 10 mM phosphate buffer (pH 7) and stored at 4 °C in 10 mM phosphate buffer containing 0.02 % sodium azide.

Partial Purification of Topoisomerases from Wheat Germ Using the HAS Column

All the steps were carried out at 4 °C. Centrifugation was done on Beckman J2-21M refrigerated centrifuge at 8000 rpm for 15 min in JA 14 rotor. Wheat germ (20 gms) was homogenised in a Waring blender for 2 min in buffer 1 containing 250 mM sucrose, 100 mM sodium chloride. The crude extract was passed through eight layers of cheese cloth. The solution was centrifuged and the pellet (Pel A) saved for the isolation of Topoisomerase II. The supernatent (Sup A) was processed for Topoisomerase I purification following the method of Dynan et al [9]. However, after the second ammonium sulphate precipitation the pellet was suspended in buffer 1 with 10 % glycerol. The solution was dialysed against the same buffer. This was applied to the HAS column and then subsequently washed with 200 mM potassium phosphate buffer (pH 7.4). The enzyme was eluted with a step gradient of 200 mM phosphate buffer (pH 7.4) containing 150 mM KCl. The activity profile of eluted fractions is shown in Fig. 1.

The Pel A was suspended in buffer 1 and blended for 30 sec in Waring blender at high speed, centrifuged and the pellet discarded. Nucleic acids were precipitated from the supernatent using Polymin P. After an 80 % ammonium sulphate precipitation the precipitate was collected, dissolved in buffer 1 and then dialysed against the same buffer. This was then applied to the HAS column. The column was washed with buffer 2 and the enzyme eluted with a step gradient of 200 mM potassium phosphate buffer of pH 7.4 (Fig. 2). The detailed procedure for the purification of Topoisomerase II will be reported elsewhere.

Topoisomerase Assay

Topoisomerase I activity was monitored in a buffer containing 50 mM Tris pH 7.9, 1 mM EDTA, 10 % Glycerol,

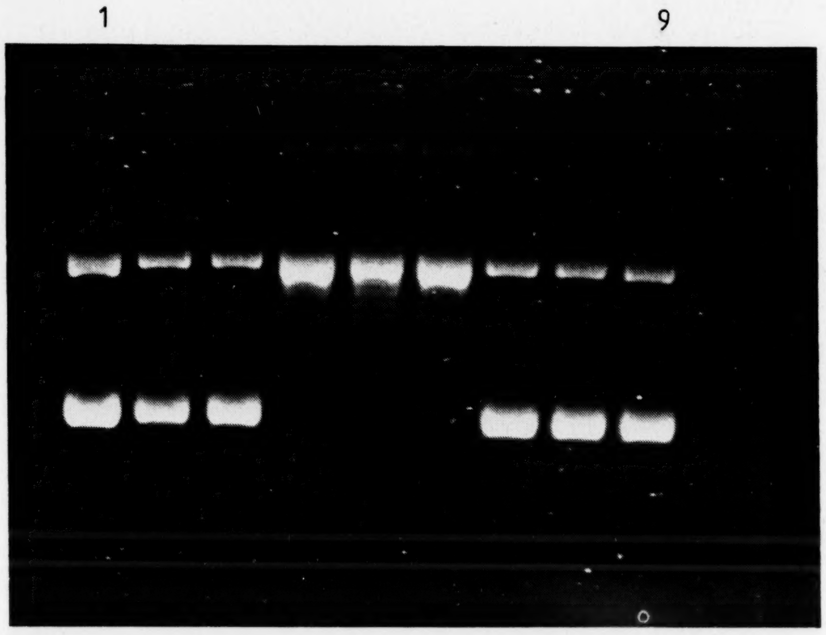

Fig. 1

Topoisomerase I activity of the fractions eluted from the HAS column with 200 mM potassium phosphate buffer (pH 7.4) and 150 mM potassium chloride. Lane 1 (from the left) is the control plasmid pLP332.

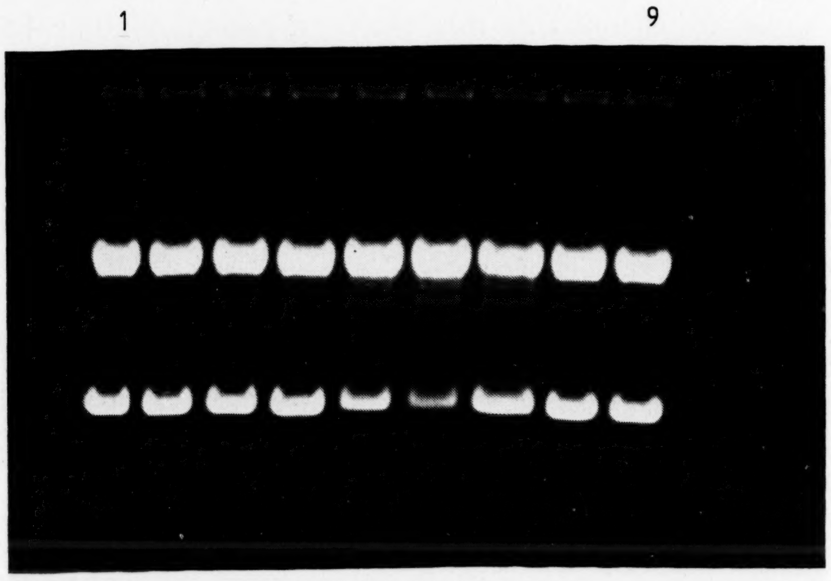

Fig. 2

Topoisomerase II activity of the fractions eluted from the HAS column with 200 mM potassium phosphate buffer (pH 7.4). Lane 1 (from the left) is the control plasmid pLP332.

1 mM DTT, using supercoiled plasmid pLP332 as the substrate. The conversion of the supercoiled to the relaxed form of the plasmid was monitored on a 1 % agarose gel run in TAE buffer [9].

Topoisomerase II activity was monitored in a buffer containing 50 mM Tris (pH 7.9), 15 mM $MgCl_2$, 60 mM KCl, 1 mM DTT, 50 μg/ml BSA. Reaction was carried out at 37 °C for 15 min. The Supercoiled form of pLP332 was used as the substrate. The DNA was then analysed on a 1 % agarose gel in TAE buffer.

Results and Discussion

Hydroxylapatite is one of the most versatile columns that has been in vogue with both protein and nucleic acid biochemists. It has proven itself as a unique tool for the fractionation and purification of proteins, enzymes, nucleic acids, viruses and other macromolecules. Enzymes like Topoisomerases have been purified using HA in one of the steps of their isolation [5, 6]. Dynan et al [9] isolated Topoisomerase I using a combination of ion exchanger and hydrophobic chromatography. Subsequently we modified this method by using a pseudo-affinity Blue Sepharose column in place of the hydrophobic column. However, in order to obtain an enzyme of high specific activity we have now resorted to the new HAS column reported in this communication. The Topoisomerase I isolated was not only highly stable, but also of high specific activity when compared with the preparations using the earlier methods. An ATP independent Topoisomerase II has been partially purified by us using the HAS column. Complete characterisation of this protein will be reported elsewhere.

Although the conventional HA offers unique selectivity, high capacity of binding, low non-specific adsorption, chemical and thermal stability; one of its major disadvantages is its fragile crystalline nature. HA columns need to be handled cautiously as the disintigration of the crystals not only clogs the columns leading to a drastic reduction in flow rate, but also alters the column characteristics. In order to circumvent this major drawback in the HA chromatography we have a developed a silica (Si) based column with similar functional groups. This silica supported column can be used not only in open column Liquid chromatography but also as a HPLC column packing material. It may be pointed out that HA support matrix' for HPLC purposes is available from a few commercial sources. However, to the best of our knowledge these materials are crystalline in nature and thus necessiate careful handling. On the other hand, the present matrix, being silica supported, enjoys the advantages associated with chemically bonded polymer based HPLC supports. Further, the method of preparation of HAS as reported here can be readily adopted for use with other polymer supports as well. This makes our HAS matrix highly versatile. Secondly, the simple chemical processes involved in the preparation of the HAS makes it an easily synthesisable support and thus to the best of our knowledge provides a superior alternative to the HA supports available commercially. However, one of the limitations of the present HAS column is that it can not be used beyond the pH range of 3.5 and 8.5. As this limitation arises basically from the use of silica as the support matrix, we are currently developing other HAS supports which can be used at the extremes of pH.

Since HAS has similar chromatographic properties as the conventional HA, the scope of using HAS is virtually unending. Thus, solid phase assay like protein binding, immunoassay [10] and hormone receptor assay [11, 12] which have been performed with ordinary HA may also be carried out with ease using the HAS matrix. Seperation of single stranded (ss) and double stranded (ds) DNA may be achieved in solution by binding the ds DNA to HAS, filtering or pelleting out the HAS support and later eluting the ds-DNA from the pellet. Various methods employed to remove protein and DNA from polyacrylamide and agarose gels [13–15] may be simplified by using this matrix. Studies to test the utility of this matrix to some of the above mentioned applications are presently in progress.

Acknowledgement

The authors are extremely grateful to Dr. Samir K. Brahmachari for support and interest in this work. Financial assistance from Indian Council of Medical Research, India, through a grant to Dr. Samir K. Brahmachari is acknowledged.

List of Common Abbreviations

ATP – Adenosine-5′-triphosphate
BSA – Bovine serum albumin
DNA – Deoxyribonucleic acid
DTT – Dithiothreitol
EDTA – Ethylenediaminetetraacetic acid
TAE – 40 mM Tris-acetate, 2 mM EDTA
Tris – Tris(hydroxymethyl) aminomethane

References

[1] *A. Tiselius, S. Hjerten, O. Levin,* Arch. Biochem. Biophys., **65,** 132 (1956).
[2] *G. Bernardi,* Nature, **206,** 779 (1965).
[3] *H. G. Martinson,* Biochemistry, **12,** 2731 & 2737 (1973).
[4] *G. Bernardi,* in "Methods in Enzymology", **22,** 325, Academic Press, New York (1971).
[5] *U. Schomburg, F. Grosse,* Eur. J. Biochem. **160,** 451 (1986).
[6] *S. Douc-Rasy, A. Kayser, J-F Riou, G. Riou,* Proc. Natl. Acad. Sci. USA, **83,** 7152 (1986).
[7] *K. Majumder,* Ph. D. Thesis, Indian Institute of Science, Bangalore (1987).
[8] For a review on phosphorylating conditions vide ref [7].
[9] *W. S. Dynan, J. J. Jendrisal, D. A. Hager, R. R. Burgess,* J. Biol. Chem., **256,** 5860 (1961).
[10] *D. J. H. Trafford, P. Ward, A. Ying Foo, H. L. J. Makin,* J. Endocrinology, **65,** 44 (1975).
[11] *E. J. Peck, J. H. Clark,* Endocrinology, **101,** 1034 (1977).
[12] *R. E. Garola, W. L. McGuire,* Cancer Research, **37,** 3329 (1977).
[13] *J. N. Hansen,* Anal. Biochem. **76,** 37 (1976).
[14] *B. Ziola, D. Scraba,* Anal. Biochem., **72,** 366 (1976).
[15] *F. H. Tabak, R. A. Flavell,* Necleic Acids Res. **5,** 2321 (1978).

Received: July 1, 1987
Accepted: July 28, 1987
F

Determination of DEHP in Blood Products Stored in Plastic Bags by HPLC

I. Gerlai*/J. Pintér

National Institute of Haematology and Blood Transfusion, Budapest P.O. Box 44, Hungary H-1502

J. Pick

Institute of Experimental Medicine of the Hungarian Acad. Sci., Budapest P.O. Box 67, Hungary H-1450

Key Words

Column liquid chromatography
Di(2-ethylhexyl) phthalate
Tri(2-ethylhexyl) trimellitate
Plasticizers
Blood product storage

Summary

High-performance liquid chromatography (HPLC) was used for the routine monitoring of the plasticizers di(2-ethylhexyl) phthalate (DEHP) and tri(2-ethylhexyl) trimellitate (TOTM), in blood products. It allows easy sample clean-up, solvent extraction using Celite 545 sorbent, good recoveries and opportunity to inject large number of samples without effect on column performance.

The plasticizer levels were investigated in two types of poly(vinyl chloride) (PVC) bags containing whole blood plasma, platelet concentrates (PCs) during blood taking and storage.

Introduction

During the past 25 years, an exponential increase has occured in the use of plasticized poly(vinyl chloride) (PVC) in nearly every field of medicine.

In blood banking, for example, glass bottles have almost totally been replaced by PVC blood bags.

Poly(vinyl chloride) copolymer plasticized with di(2-ethylhexyl) phthalate (DEHP) provides hemorepellence and protects the red cell membrane to inhibit hemolysis and enhance the *in vitro* survival of erythrocytes [1].

Data from several laboratories have shown that plasticizers leach from blood bags and tubings during collection of blood and storage of various blood components. The concentration reaches a final level and depends on the time and temperature of storage and also on the lipid content of the stored product [2–4].

It is known that during 72 hours of storage, platelets show biochemical and physiological changes which result in decreased viability and survival after transfusion. The new polyolefin bags or PVC bags with tri(2-ethylhexyl) trimellitate (TOTM) plasticizer allow storage of platelets for 5 and 7 days.

We assessed to leaching of DEHP and TOTM to blood products in the case of Draka PVC bags (PSV 3250 cler Medipack, Holland) and Maco-Pharma bags (PSV 3202, 3203 Infufol, France) using HPLC. The separation of these phthalates was achieved on an NH_2 column with hexane-ethyl acetate mixture used as the mobile phase.

Experimental

The HPLC analyses were performed on a Beckman HPLC system, containing a Model 110B pump, and a Model 163 UV detector at 254 nm, 0.01 AUFS and 10 mV output, and an Altex 210 valve with 20-μl loop. The pump-controlling and data handling was provided by the 450 Beckman Data Controller (Beckman Instruments GmbH, Vienna, Austria). The separation of phthalates was carried out on a Nucleosil NH_2 5 μm (Macherey-Nagel, Düren, FRG) column (250 mm × 4.6 mm ID), eluted by hexane-ethyl acetate, 97:3 (v/v), with a flow rate of 1.5 ml/min.

All solvents used for the analyses and extraction procedure were of HPLC grade (E. Merck, Darmstadt, FRG), tested for phthalate content before use. DEHP and TOTM plasticizer standards were obtained from Melle-Bezons (Rue de Villiers, France).

Blood collected from randomly selected normal donors in Draka PVC bags PSV 3250 (cler Medipack, Holland) and in Maco-Pharma bags PSV 3202 (Infufol, France), was stored for 4 weeks.

0009-5893/87 0403-04 $03.00/0

© 1987 Friedr. Vieweg & Sohn Verlagsgesellschaft mbH

The platelet concentrates (PCs) were prepared using standard human platelet-rich plasma banking procedures [5]. PCs of eight donors were stored separately in Maco-Pharma bags PSV 3203 containing both DEHP and TOTM plasticizers. The combined PCs (pooled platelet concentrates by buffy coat method) of four donors were stored in Draka PSV 3250 bags with DEHP softener only.

Aliquots of 0.5 ml of plasma were removed from whole blood bags at intervals of 1, 2, 3 and 4 weeks and analyzed.

In the case of PCs, 8 ml aliquots were taken at 0 and 48 h from Draka bags and at 0 and 5 days from Maco-Pharma bags. The samples were centrifuged and the supernatant and the cells lysed were analyzed separately.

Extraction procedures were carried out as follow: a plasma (0.5 ml aliquot from whole blood or PCs supernatant) or lysed platelet sample was mixed rigorously with 1.0 g of Celite 545 (Johns-Manville Corp., Denver, Colorado, USA), shaken with 10 ml of ethyl acetate for 5 minutes and centrifuged.

The supernatant was evaporated under nitrogen stream. The residue was dissolved in 0.5 ml of the HPLC eluent and 20 μl was injected onto the column.

Results and Discussion

Fig. 1 show the chromatograms obtained after injection of extracts of blank plasma, blank plasma spiked with plasticizer standards and PC supernatant from a sample stored

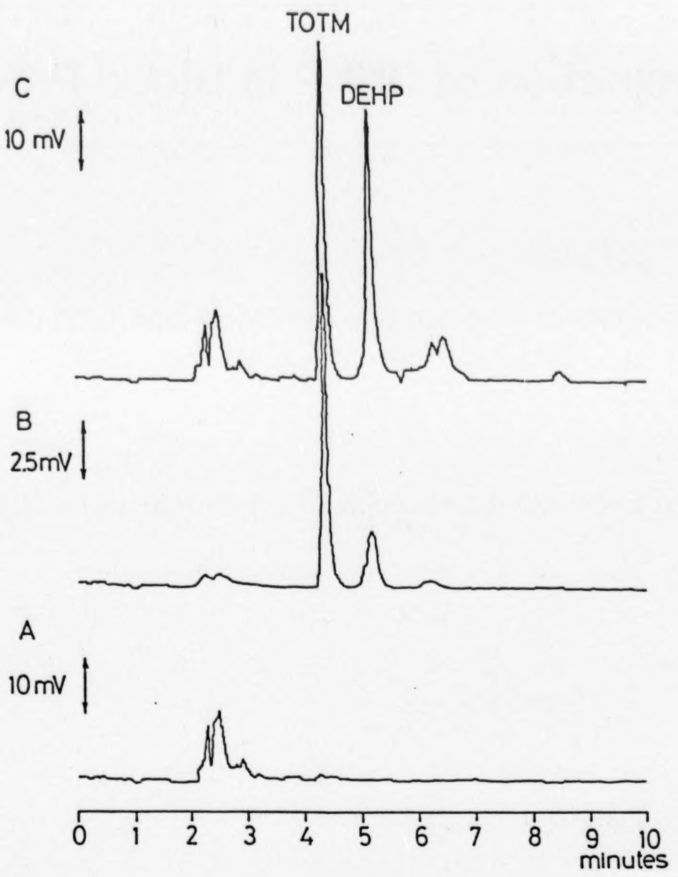

Fig. 1

HPLC chromatograms of the extracts of 0.5 ml supernatant of platelet concentrates: (A) Blank plasma sample; (B) Blank plasma sample spiked with 47.72 μg/ml of DEHP and 47.72 μg/ml of TOTM; (C) Supernatant of platelet-rich plasma stored in Maco-Pharma bag for 5 days containing 43.46 μg/ml of DEHP and 13.15 μg/ml TOTM.

Table I. Precision of assay for DEHP determination in blood extracts*

No.	μg/ml added	μg/ml detected ± SE	n	SD	CV %
1	2.98	2.016 ± 0.011	4	0.105	5.29
2	5.97	5.782 ± 0.021	4	0.147	2.54
3	11.93	12.457 ± 0.018	4	0.133	1.06
4	23.86	24.174 ± 0.217	4	0.466	1.93
5	47.72	46.809 ± 1.693	4	1.301	2.78
6	95.45	92.114 ± 0.251	4	0.501	0.25

* SD – standard deviation
CV – coefficient of variation, %
SE – standard error
n – number of samples extracted.

Table II. Precision of assay for TOTM determination in platelet concentrates*

No.	μg/ml edded	μg/ml detected ± SE	n	SD	CV %
1	2.98	2.812 ± 0.002	5	0.049	1.75
2	5.97	6.157 ± 0.007	5	0.083	1.34
3	11.93	12.439 ± 0.133	5	0.365	2.93
4	23.86	24.199 ± 0.173	5	0.416	1.72
5	47.72	47.032 ± 0.257	5	0.507	1.08
6	95.45	97.925 ± 0.568	5	0.754	0.77

* SD – standard deviation
CV – coefficient of variation, %
SE – standard error
n – number of samples extracted.

for 5 days in Maco-Pharma bag. The retention times are 4.33 min and 5.16 min for TOTM and DEHP, respectively.

The calibration samples were extracted identically to the unknown samples. Calibration curves were prepared on the same day when samples were analyzed to establish the linearity and reproducibility of the assay (Table I and II). Sample standard curves were constructed, for each compound determined, at each run, over the concentration ranges of 2.98–95.45 µg/ml. In each case peak height of each compound was plotted against the concentration of DEHP and TOTM in 1 ml plasma or lysed platelets (Fig. 2 and 3).

The lower detection limit was 40 ng of DEHP and 15 ng of TOTM per injection (S/N = 3).

The extraction procedure described in this paper is rapid and suitable especially for routine monitoring of the plasticizers in blood products, with 60–70% absolute recoveries of DEHP and TOTM. The dried extracts are easily soluble in the eluent and free of visible inpurities. The HPLC analysis on amino-bonded phase indicates no interferences from endogenous materials for DEHP and TOTM.

After storage of whole human blood in PVC bags, there was an accumulation of DEHP in plasma, shown in Fig. 4, with no significant difference in the case of Draka and Maco-Pharma containers.

Fig. 5 and 6 illustrate the leaching of DEHP into PCs during 48 h at 22 °C in Draka bags. According to our data platelets play an important role in the accumulation of DEHP, shown in Fig. 6 and 8, in both cases of storage, which is a lipid-soluble substance able to bind with the bilayer of cell membranes. Fig. 7 shows the removing of plasticizer from Maco-Pharma PSV 3203 bag into PCs supernatant during 5 days of storage.

In the case of PVC containers plasticized by a mixture of two softeners, their ratios are not equivalent in PCs supernatant and lysed platelets (Fig. 9). The reason of the elevated TOTM concentration could be the difference in polarity of the two plasticizers; the higher the apolarity the higher the accumulation of the lipid-soluble compound in the lysed cells.

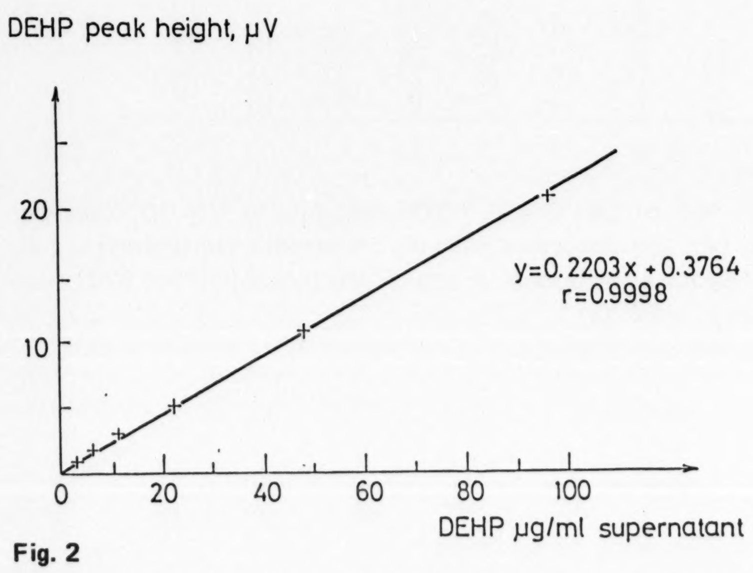

Fig. 2

Standard curve for the determination of DEHP in blood products, achieved by the extraction of 0.5 ml of standard samples.

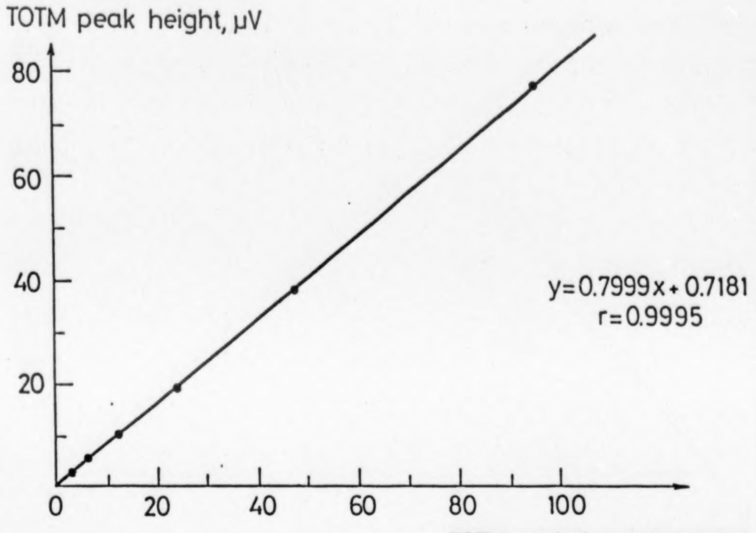

Fig. 3

Standard curve for the determination of TOTM in blood products, achieved by the extraction of 0.5 ml of standard samples.

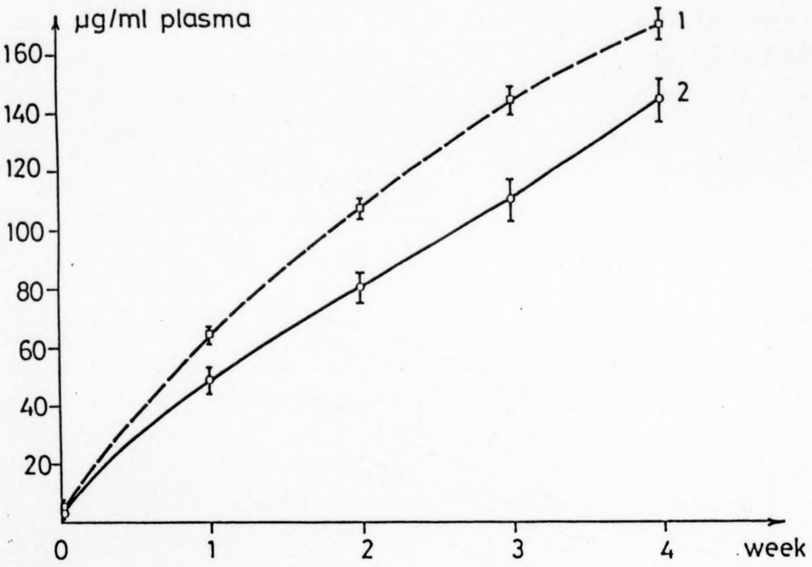

Fig. 4

Correlation between DEHP level (± SD) in whole blood plasma and time. Blood was stored at 4 °C for 4 weeks in Maco-Pharma PSV 3202 (1) and Draka PSV 3250 (2) bags.

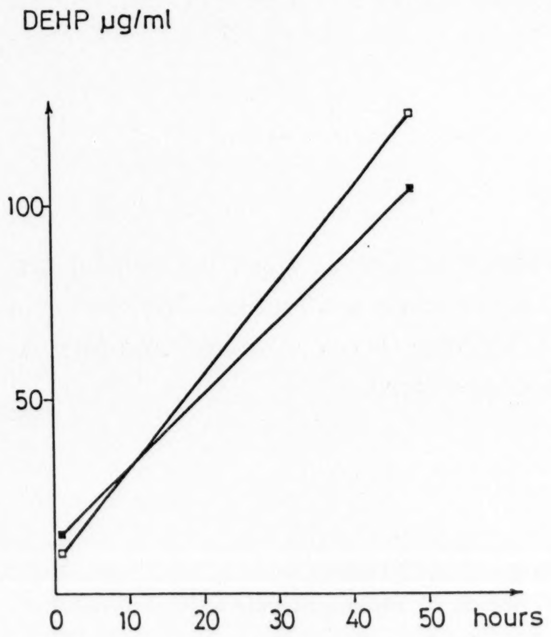

Fig. 5

Aliquots of platelet concentrates were removed from Draka PSV 3250 bags at 1.75 h and 48 h intervals, and the µg DEHP in supernatant measured is plotted as a function of time.

Lines between dots connect studies in the same PC bag during 48 h at 22 °C.

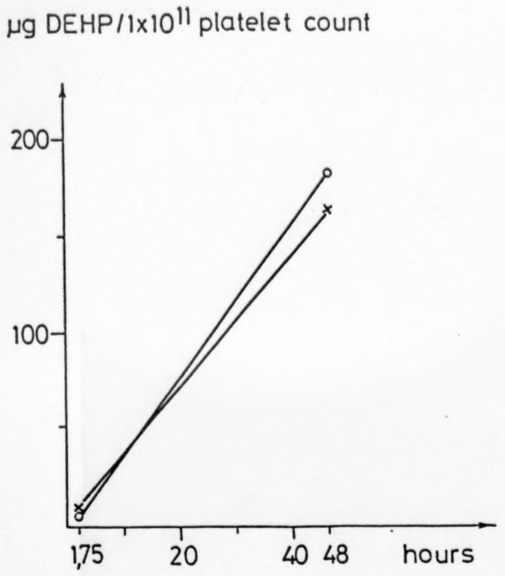

Fig. 6

Aliquots of platelet concentrate were removed from Draka PSV 3250 bags at 1.75 h and 48 h intervals.

The µg DEHP/1 × 10^{11} platelet count measured in lysed platelet concentrates is plotted as a function of time.

Lines between dots connect studies in the same PC bag during 48 h at 22°C.

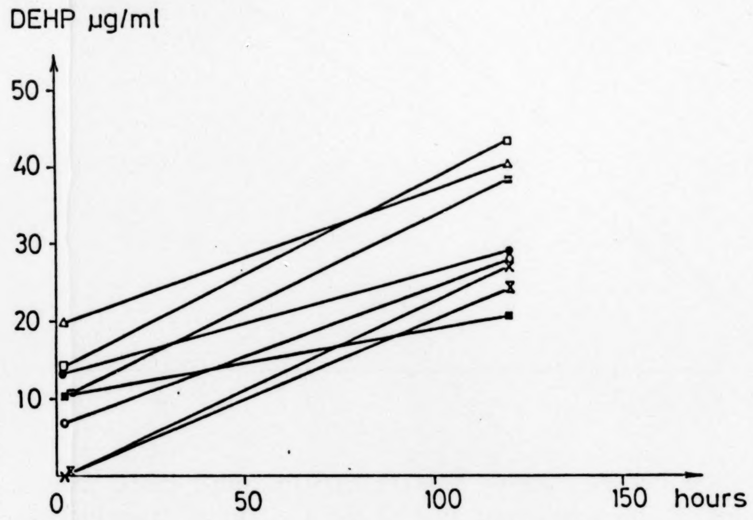

Fig. 7

Aliquots of platelet concentrate were removed from Maco-Pharma PSV 3203 bags at 1.75 h and 120 h intervals, and the µg DEHP in supernatant measured is plotted as a function of time.

Lines between dots connect studies in the same PC bag during 5 days at 22°C.

Acknowledgments

The authors are grateful to Dr. Z. Rácz for helpful discussions on platelet concentrate production. The technical assistance of Mrs. M. Mórotz, Mrs. J. Wendler, and Mrs. A. Jakob is especially acknowledged.

References

[1] *C. Walter,* Vox. Sang., **47**, 318 (1984).
[2] *P. Sjöberg, V. Bondesson, E. Sedin, J. Gustafsson,* Transfusion, **25**, 424 (1985).
[3] *R. Labow, M. Tocchi, G. Rock,* Transfusion, **26**, 351 (1986).
[4] *V. Lovric, G. Archer,* Vox Sang., **49**, 181 (1985).
[5] *Z. Rácz, M. Thék,* Vox Sang., **47**, 108 (1984).

Received: June 30, 1987
Accepted: Aug. 28, 1987
F

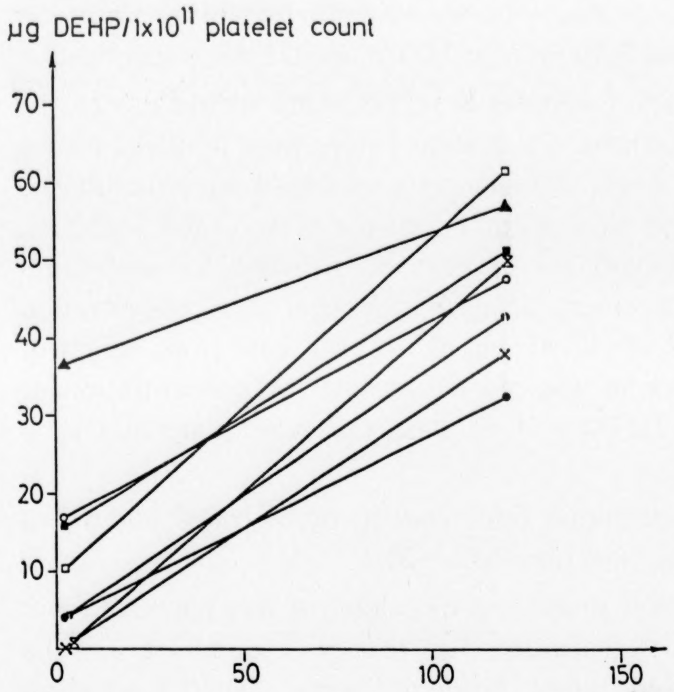

Fig. 8

Aliquots of platelet concentrate were removed from Maco-Pharma PSV 3203 bags at 1.75 h and 120 h intervals.

The µg DEHP/1 × 10^{11} platelet count measured in lysed PCs is plotted as a function of time.

Lines between dots connect studies in the same PC bag during 5 days at 22°C.

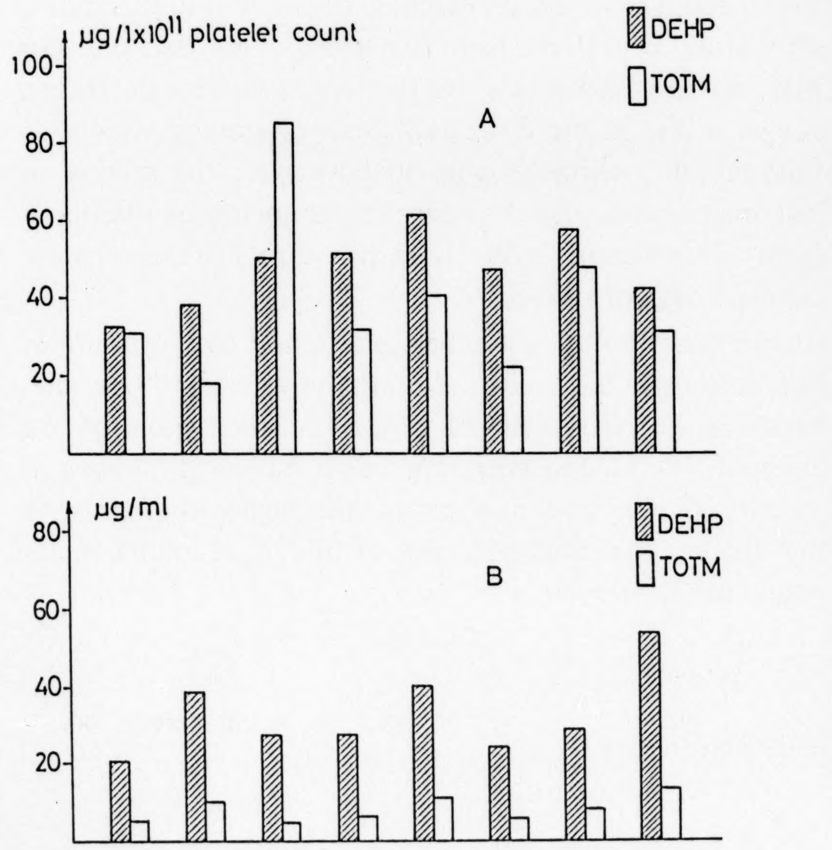

Fig. 9

Comparison of DEHP and TOTM amounts in 1 × 10^{11} platelet count (A) and concentrations (B) in platelet concentrate supernatant from eight donors stored in Maco-Pharma PSV 3203 bags for 5 days at 22°C.

Assay of Urinary Free Catecholamines: Routine Use in a Clinical Chemistry Laboratory

E. Baraldi*/D. Cavani/S. Seghedoni/G. Chiossi/L. Roli/A. T. Scacchetti/G. F. Baraghini

Department of Endocrinology, University of Modena, Via del Pozzo, 71, 1-41100 Modena, Italy

Key Words

Column liquid chromatography
Urinary free catecholamines
Computerized quality control

Summary

The Bio-Rad HPLC method for the assay of urinary free catecholamines was employed during a period of 13 months, on samples of 720 subjects which were all normal but one with a pheochromocytoma diagnosis. The non-parametric reference limits were in accordance with those of other authors.

Preliminary clean-up was carried out both in a standard urine and in the sample urine by means of a disposable micro-cation column prefilled with Bio-Rex 70 and ammonium acetate buffer which retain the weakly basic amines. Next epinephrine (E), norepinephrine (NE), dopamine (DA) and an internal standard (IS, N-methil-dopamine) were removed using ammonium pentaborate, a highly specific eluant. The final eluate was separated by HPLC on a Bio-Rad cation-exchange column, using 5% methanol in 0.06 M phosphate buffer (pH 5.2) as the mobile phase.

Lyphochek normal and abnormal urine controls were elaborated with Lyphline Quality Control Program based on Westgard's rules.

Many amines may be retained on a carboxylic acid resin. However, very few compounds possess a cis-diol structure. In the absence of drug therapy, only three compounds are commonly seen in HPLC chromatograms in addition to E, NE, DA and IS. Two unidentified compounds elute before E.

Alpha-methyldopa (Aldomet TM) is a common anti-hypertensive drug which forms two metabolites closely related to biogenic amines.

Alpha-methylnorepinephrine elutes between E and NE. Alpha-methyldopamine coelutes with dopamine.

The easy and quick method, giving good reproducibility and excellent clinic agreement, is suitable to pheochromocytoma differential diagnosis in clinical chemistry laboratories.

Introduction

Assay of urinary catecholamines and their metabolites is of interest not only for the diagnosis of neural crest tumors but also for the detection of abnormalities in catecholamine metabolism.

For urinary free catecholamines several HPLC procedures have been reported [1, 2], but for none of these are precision and accuracy data available for the entire normal range; also there were no extensive interference studies given. Here we present a routine use assay with high selectivity, precision and accuracy performed by a computerized quality control program, and we characterize the critical steps.

Materials and Methods

Apparatus

We used a Model 1330 Pump, 48-A Autosampler with a 20-μl sample loop, a Model 1340 amperometric detector containing a glassy carbon electrode and Ag/AgCl reference electrode set at a potential of + 0.55 V, 5 nA full scale, a Model 3392A plotting integrator (all from Bio-Rad Laboratories, Richmond, CA, USA). We used a 4.6 mm I.D. x 10 cm weak cation-exchange silica analytical column with a reversed-phase C-18 guard column. The mobile phase, 5% methanol in phosphate buffer (0.06 M, pH 5.2) containing 1 g of disodium EDTA per liter, was passed through a 0.22-μm pore-size filter (Nucleopore Corp., Pleasanton, CA, USA). The vacuum manifold was from Millipore Corp., Bedford, MA, USA.

Urine Collection

We collected 24-h urine specimens in polyethylene containers with 6 M HCl as a preservative. The final pH of the urine was 2 to 3. Samples were stored at 2–8 °C before analysis. Some laboratories have found it useful to run a total creatinine measurement on the samples as a check on complete urine output.

0009-5893/87 0407-04 $03.00/0

© 1987 Friedr. Vieweg & Sohn Verlagsgesellschaft mbH

Controls

We used normal and abnormal lyophilized urine controls (Lyphocheck I and II, Bio-Rad ECS Division, Anaheim, CA, USA) for all determinations.

Procedure

We have used the Bio-Rad "Catecholamines by HPLC" procedure [3] which represents an optimized and highly specific approach to the isolation and detection of epinephrine (E), norepinephrine (NE) and dopamine (DA) in urine, based on a preliminary clean-up on disposable cation exchange columns.

3 mL acidified urine is combined with 5 mL 0.03 M ammonium acetate buffer, pH 7.5 and 200 μL of the internal standard (N-methyl dopamine, IS). The pH is adjusted to 6.0–7.0 with 0.5 M NaOH and checked with pH paper. Then the mixture is poured over a disposable micro-cation column prefilled with Bio-Rex 70. The use of the weak ammonium buffer allows maximum retention of catecholamines, dopamine and the internal standard. Excess urine is washed off with the buffer, raising the column pH to 7.5. Under these conditions, catecholamines will complex readily with borate and can be selectively eluted from the column. 0.04 M ammonium pentaborate (6 mL) is used to maintain a constant pH during the elution process. The entire procedure is complete in about 30 min. Eluates may be stored up to 48 hours prior to injection.

Chromatographic conditions are as follows: injection volume, 20 μL; column temperature, 40 °C; flow rate, 1 mL/min. The unknown catecholamine concentrations were determined by comparing peak heights for unknown urines with those produced by a standard urine containing known amounts of E (96 μg/L), NE (207 μg/L) and DA (270 μg/L). The peak heights were normalized with reference to the internal standard.

Computerized Quality Control

Lyphocheck normal and abnormal urine controls were elaborated with Lyph-line program (Bio-Rad ECS Division, Anaheim, CA, USA), a personal computer program which allows an ease in data preparation, data analysis and a comprehensive set of laboratory reports. These reports include the capability of generating interlaboratory comparison. The Lyph-line software was designed to help maximize laboratory resources by decreasing unnecessary assay rejection and simultaneously increasing sensitivity to error detection. It provides information, with Westgard's criteria [4], about the acceptability of data, but allowing the technologist the final decision. The common practice of regarding any control value ± 2 st. deviations as the basis for test rejection produce a very large rate of false rejection. Lyph-line software is designed to minimize this rate by using any value outside ± 2 st. deviations as a warning signal which causes the software to apply additional decision criteria to the signaled point, and to inspect other control values within the run and those in past test runs. The rules, based on Westgard's work, are sequentially applied to control data after one control value falls outside two standard deviations.

Results

The Bio-Rad HPLC method was employed during a period of 13 months, on samples from 720 subjects which were all normal but one with a pheochromocytoma diagnosis.

We have established our reference limits by means of non-parametric methods. These were:

ephinephrine:	1.7– 22.4 μg/day
norepinephrine:	12.1– 85.5 μg/day
dopamine:	65 –455 μg/day

These values are in accordance with those of ohter authors [5].

Figure 1 shows a typical chromatogram of a standard urine with good resolution, to achieve a better separation, it is possibile to modify the amount of methanol in the mobile phase. If the internal standard is too close to DA, a slight increase in the methanol concentration will improve resolution. Similarly, if the internal standard is too close to NE the methanol concentration may be decreased.

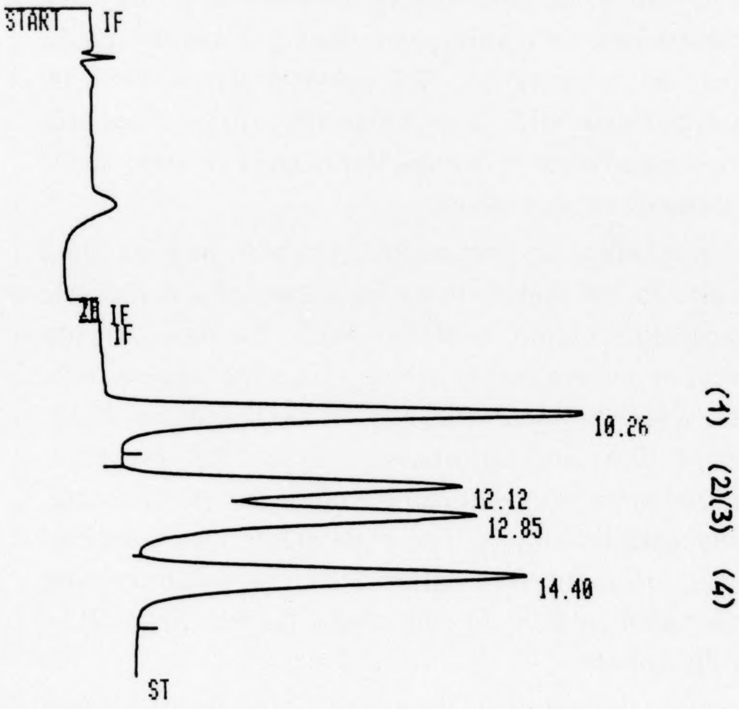

```
RUN #  104                MAY/28/87  11:58:36
WORKFILE ID: B
WORKFILE NAME:

ISTD
  RT        HEIGHT TYPE  CAL #       AMOUNT
 10.26      3982132   BH    1        130.310
 12.12      2756427   HH    2        119.940
 12.85      2860034   HH    3&       200.000
 14.40      3241586   HH    4        137.610


 TOTAL HGHT= 1.2840E+07
 ISTD AMT= 2.0000E+02
 SAMPLE AMT=
 MUL FACTOR= 1.0000E+00
```

Fig. 1

Chromatogram of a standard urine. Analytical conditions: cation-exchange column at 40 °C; mobile phase, 5 % methanol in 0.06 M phosphate buffer, pH 5.2; flow rate, 1 mL/min; injection volume, 20 μL; amperometric detector. Peaks: **1** = epinephrine, **2** = norepinephrine, **3** = internal standard, **4** = dopamine.

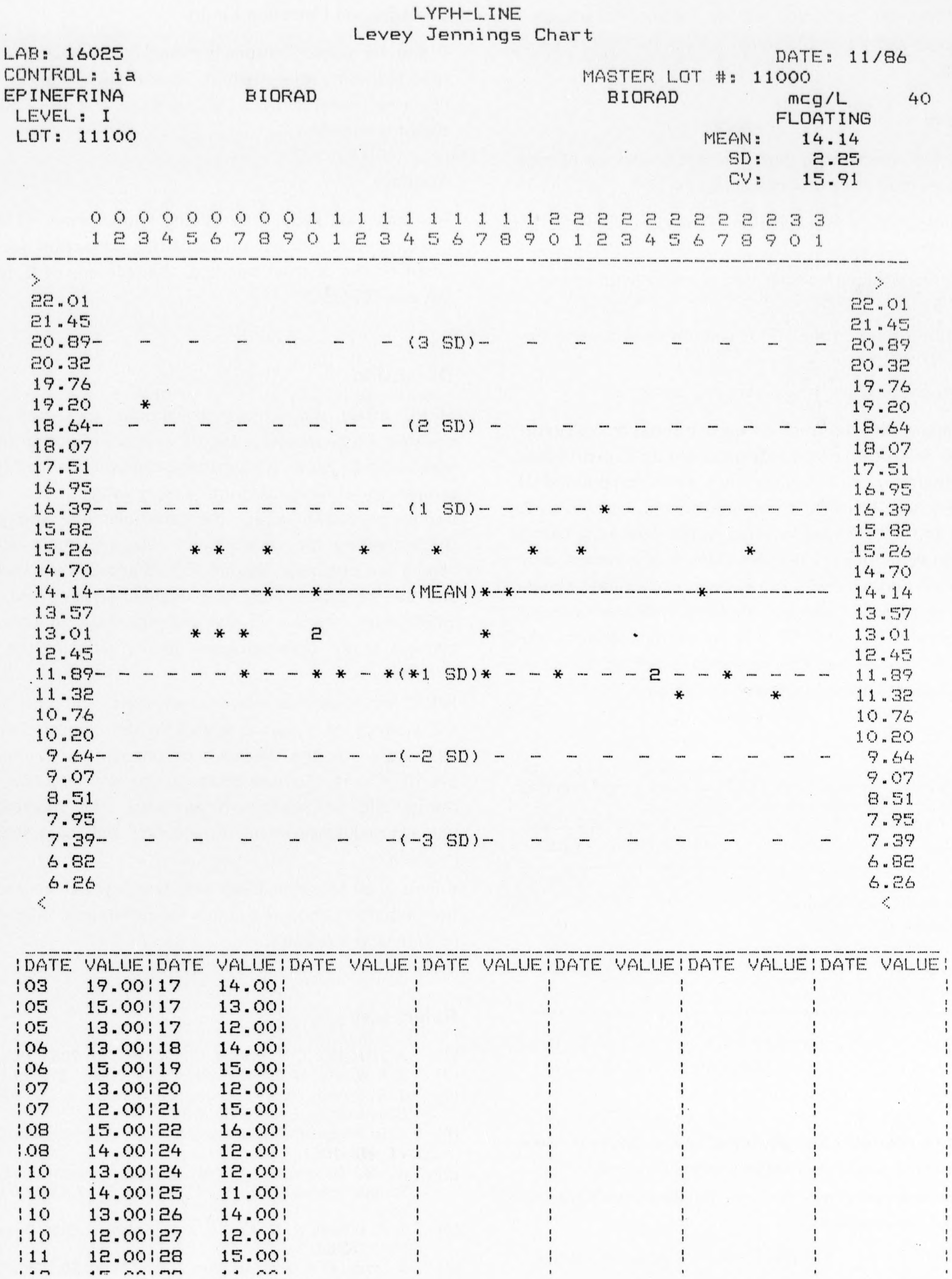

```
                                  LYPH-LINE
                             Levey Jennings Chart
LAB: 16025                                                      DATE: 11/86
CONTROL: ia                                     MASTER LOT #: 11000
EPINEFRINA          BIORAD                        BIORAD         mcg/L     40
 LEVEL: I                                                       FLOATING
 LOT: 11100                                               MEAN:   14.14
                                                            SD:    2.25
                                                            CV:   15.91

        0 0 0 0 0 0 0 0 0 1 1 1 1 1 1 1 1 1 1 2 2 2 2 2 2 2 2 2 2 3 3
        1 2 3 4 5 6 7 8 9 0 1 2 3 4 5 6 7 8 9 0 1 2 3 4 5 6 7 8 9 0 1
---------------------------------------------------------------------------
  >                                                                      >
  22.01                                                                22.01
  21.45                                                                21.45
  20.89-    -   -   -   -   -   - (3 SD)-   -   -   -   -   -   -   -  20.89
  20.32                                                                20.32
  19.76                                                                19.76
  19.20     *                                                          19.20
  18.64-  -  - -  -  -  -  - -  -  (2 SD) -  -  -  -  -  -  -  -  -  -  18.64
  18.07                                                                18.07
  17.51                                                                17.51
  16.95                                                                16.95
  16.39-  - - - - - - - - - - - - (1 SD)- - - - - * - - - - - - - - -  16.39
  15.82                                                                15.82
  15.26         * *   *       *     *       *   *             *        15.26
  14.70                                                                14.70
  14.14---------------*---*-------(MEAN)*-*---------------*----------  14.14
  13.57                                                                13.57
  13.01         * * *     2             *                              13.01
  12.45                                                                12.45
  11.89-  - - - - - * - - * * - *(*1 SD)* - - * - - - 2 - - * - - - -  11.89
  11.32                                                 *       *      11.32
  10.76                                                                10.76
  10.20                                                                10.20
   9.64-   -  -  -  -  -  -  -(-2 SD) -  -  -  -  -  -  -  -  -  -   9.64
   9.07                                                                 9.07
   8.51                                                                 8.51
   7.95                                                                 7.95
   7.39-    -   -   -   -   -   -(-3 SD)-   -   -   -   -   -   -   -   7.39
   6.82                                                                 6.82
   6.26                                                                 6.26
   <                                                                      <

 ----------------------------------------------------------------------------
¦DATE VALUE¦DATE VALUE¦DATE VALUE¦DATE VALUE¦DATE VALUE¦DATE VALUE¦DATE VALUE¦
¦03   19.00¦17   14.00¦          ¦          ¦          ¦          ¦          ¦
¦05   15.00¦17   13.00¦          ¦          ¦          ¦          ¦          ¦
¦05   13.00¦17   12.00¦          ¦          ¦          ¦          ¦          ¦
¦06   13.00¦18   14.00¦          ¦          ¦          ¦          ¦          ¦
¦06   15.00¦19   15.00¦          ¦          ¦          ¦          ¦          ¦
¦07   13.00¦20   12.00¦          ¦          ¦          ¦          ¦          ¦
¦07   12.00¦21   15.00¦          ¦          ¦          ¦          ¦          ¦
¦08   15.00¦22   16.00¦          ¦          ¦          ¦          ¦          ¦
¦08   14.00¦24   12.00¦          ¦          ¦          ¦          ¦          ¦
¦10   13.00¦24   12.00¦          ¦          ¦          ¦          ¦          ¦
¦10   14.00¦25   11.00¦          ¦          ¦          ¦          ¦          ¦
¦10   13.00¦26   14.00¦          ¦          ¦          ¦          ¦          ¦
¦10   12.00¦27   12.00¦          ¦          ¦          ¦          ¦          ¦
¦11   12.00¦28   15.00¦          ¦          ¦          ¦          ¦          ¦
```

Fig. 2

Levey-Jennings control chart for epinephrine.

In addition, the resolution of the metabolites of alpha-methyldopa is excellent in samples from patients receiving this drug.

Specificity

A potential interference with the HPLC analysis of catecholamines must have four characteristics [6]:

1. Retention on a weak cation-exchange column at pH 6.0–7.0.
2. A cis-diol structure which will complex with borate at pH 7.5.
3. Retention time on the HPLC column very close to that of E, NE or IS.
4. Electrochemical activity at very low potential.

Many amines may be retained on a carboxylic acid resin. However, very few compounds possess a cis-diol structure. In the absence of drug therapy, only three compounds are commonly seen in HPLC chromatograms in addition to E, NE, DA and IS. Two unidentified compounds elute before E. Alpha-methyldopa (Aldomet TM) is a common anti-hypertensive drug which forms two metabolites closely related to biogenic amines. Alpha-methylnorepinephrine elutes between E and NE. Alpha-methyldopamine co-elutes with dopamine. The retention times of the compounds discussed above are shown in Table I.

Table I. Relative retention times (RRT) of some amines that may be retained on a carboxylic acid resin

Compund	RRT
Epinephrine	0.79
alpha-Methylnorepinephrine	0.83
Norepinephrine	0.91
n-Methyldopamine (internal standard)	1.00
Dopamine	1.09
alpha-Methyldopamine	1.10

Precision

Lyphocheck normal and abnormal urine controls were elaborated with Lyphline Quality Control Program.

Within-run precision (n = 10) was (in parenthesis the coefficient of variation data):

	Normal urine	Abnormal urine
epinephrine	15 μg/l (4 %)	44 μg/l (3 %)
norepinephrine	43 μg/L (3 %)	173 μg/L (2.8 %)
dopamine	161 μg/L (2.5 %)	480 μg/L (2 %)

Between-run precision was (n = 55):

	Normal urine	Abnormal urine
epinephrine	16.5 μg/L (12 %)	45 μg/L (9.8 %)
norepinephrine	45 μg/L (10 %)	170 μg/L (7.5 %)
dopamine	165 μg/L (7 %)	478 μg/L (6 %)

A Levey-Jennings control chart [7] is shown in Fig. 2.

Linearity and Detection Limits

E and NE concentrations between 2 and 400 μg/l may be reported using this method. Quantitative analysis of epinephrine levels below 5 μg/L is more precise if 50 μL of eluant is injected.

Accuracy

Accuracy was assayed by adding known amounts of catecholamines to normal urines. After correction for losses based on the internal standard, the recovery of E, NE and DA was 102 %.

Discussion

HPLC offers three major advantages to catecholamine analysis. First, recovery can be evaluated with an internal standard (IS) which is a synthetic compound added to each sample in a fixed amount. Losses which occur during extraction equally affect the catecholamines and the IS. By correcting for variability in recovery, more accurate results are obtained. Second, E, NE and DA are separated and can be quantitated in a single analysis. Third, drugs which may interfere in the analysis result in observable changes in the chromatogram greatly reducing the possibility results.

HPLC introduce a new level of selectivity and sensitivity to the analysis of biogenic amines in the clinical chemistry laboratory for the diagnosis of pheochromocytoma and neuroblastoma. Because these tumors are very rare, most results will be normal. Nevertheless, the mortality of undiagnosed cases mandates accurate and rapid screening methods.

For its good reproducibility and excellent clinic agreement the present method is suitable for differential diagnosis in routine laboratory use.

References

[1] *A. H. B. Wu, T. G. Gornet,* Clin. Chem., **31**, 298 (1985).

[2] *S. R. Binder, M. Biaggi, P. Patel,* Clin. Chem., **31**, 957 (1985).

[3] *S. R. Binder,* Nuove Tecnologie in Endocrinologia, Monduzzi Bologna Italy, Ed. (1986), p. 163.

[4] *J. O. Westgard, P. L. Barry, M. Hunt, T. Groth,* Clin. Chem., **27**, 493 (1981).

[5] *W. M. Manger, R. W. Nr. Gifford,* Pheochromocytoma, Springer-Verlag (1977), p. 212, Haber Str. 7, D-6900 Heidelberg.

[6] *S. P. Wilson, P. L. Kamin, J. M. Feldman,* Clin. Chem., **31**, 1093 (1985).

[7] *S. Levey, E. R. Jennings,* Am. J. Clin. Path., **20**, 159 (1950).

Received: Aug. 4, 1987
Accepted: Aug. 15, 1987
F

Quantification of a Positive Inotropic Agent in Plasma: Towards Total Automation

G. S. Murkitt*/ J. C. Pearce/ R. D. McDowall

Department of Drug Analysis, Smith Kline and French Research Ltd, The Frythe, Welwyn, Herts, AL6 9AR, UK

Key Words

Column liquid chromatography
Automation
Gilson-AASP
Liquid-solid extraction
Solid phase extraction
Positive inotropic agent

Summary

An assay for the measurement of SK&F 95654, a new positive inotropic agent in plasma is described. The assay is totally automated, is easy to use and involves minimal human input. It combines solid-phase extraction with reverse phase HPLC and UV detection at 300nm, by the use of a small robotic unit and an AASP LC module. The assay is sufficiently sensitive to measure concentrations of 0.025 mg l^{-1} in dog, rat and mouse plasma, and capable of analysing at least one hundred samples per day. The assay is robust, accurate and precise. The strategy described is widely applicable.

Introduction

SK&F 95654, (5-methyl-6-[4-(4-oxo-1,4-dihydropyridin-1-l) phenyl]-4-5-dihydro-3(2H)-pyridazinone, has been shown to exhibit potent positive inotropic and vasodilatory properties in animals, which suggests that it may be of value in the treatment of congestive heart failure in man.

An analytical method was required in order to follow the kinetics of the drug during pre-clinical and clinical studies. This paper describes a totally automated assay for the quantification of SK&F 95654 concentrations between 0.025 and 2.0 mg l^{-1} in dog, rat, or mouse plasma.

In anticipation of the large numbers of samples for assay, the method was required to be fully automated and have a high sample throughput capability. The approach that was adopted was the integration of the following four areas:

- Liquid handling (using a Gilson 222/401) [1]
- Liquid – solid extraction (using an AASP) [2, 3]
- Separation and measurement of drug and internal standard using reverse phase high performance liquid chromatography and ultra violet detection
- On line data transfer, calculation of results and report generation using LIMS [4, 5]

Experimental

Materials

Analytical grade chemicals were used throughout this study with the following exceptions: methanol and acetonitrile were HPLC grade (Rathburn, Walkerburn, Scotland) and orthophosphoric acid was Aristar grade (B.D.H. Chemicals, Poole, Great Britain). The water used was prepared by deionisation (Milli-Q, Millipore, Molsheim, France) and stored for use in glass containers for a maximum of one week, before being discarded.

Polypropylene centrifuge tubes (1.5 ml) with stoppers were obtained from Sarstedt (Beaumont Leas, Leicestershire, UK) and the AASP C18 cassettes (reference 707005) for sample preparation from Analytichem International (Harbor City, CA, USA).

Supplies of SK&F 95654 and SK&F 94836 (Fig. 1) were obtained from Smith Kline and French Research Ltd, Welwyn and were used without further purification.

Separate standard solutions of SK&F 95654 and SK&F 94836 were prepared as follows: 1.00 mg of compound was accurately weighed into a 500 ml volumetric flask. Water (50 ml) was added to the flask which was left for fifteen minutes immersed within an ultrasonic water bath (Sonicor Instrument Corporation, Copiague, NY, USA). After this time the flask was removed and the volume made up to the mark with water.

Both the stock solutions were stable for at least four weeks provided they were stored at +4 °C when not in use and not exposed to direct sunlight. The working internal standard solution was prepared daily by diluting the stock solution in 1 in 10 with water.

0009-5893/87 0411-05 $03.00/0 © 1987 Friedr. Vieweg & Sohn Verlagsgesellschaft mbH

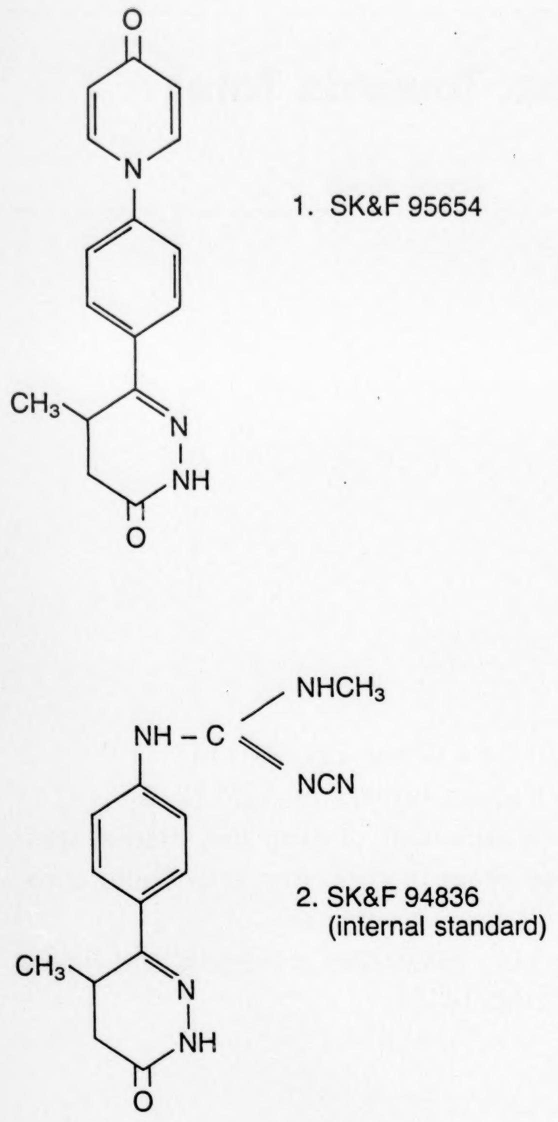

Fig. 1 Structure of SK & F 95654 and SK & F 94836

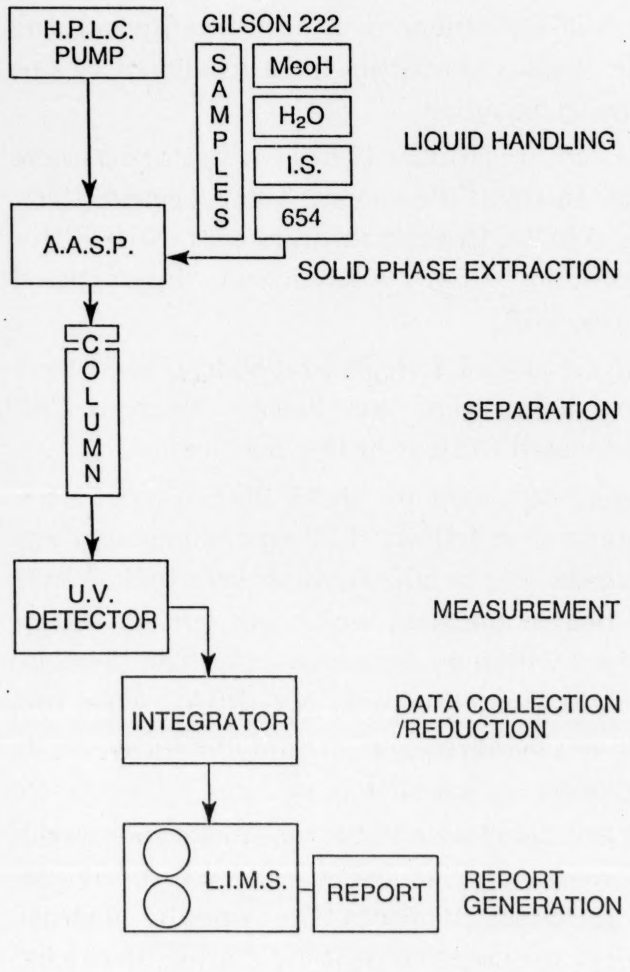

Fig. 2 Schematic of Totally Automated System

Sample Collection

Blood, from animals that had received SK&F 95654, was withdrawn via a cannula or syringe into heparinised containers, mixed and centrifuged. The plasma obtained was transferred to plain tubes, which were quickly frozen over solid carbon dioxide and then kept at −20 °C prior to analysis.

Assay Procedure

Total automation of the assay has been achieved by linking solid phase extraction with HPLC separation and UV detection. This has been accomplished by using a Gilson 222 autosampler with 401 Dilutor (Villiers-le-Bel, France) for sample manipulation, conducting the solid-phase extraction in an AASP LC module, and then at the appropriate time, the HPLC mobile phase is switched through the cartridge allowing elution of the compounds of interest directly onto the analytical column.

The Gilson assumes responsibility as the master controller of the system configuration and communicates with the AASP via a 12 volt interface relay box. In this way the Gilson can remotely start the AASP and advance the cassette at a predetermined time. In addition, switching of the Valco valve is also effected by the controller.

In the only manual part of the procedure, plasma samples for the assay of SK & F 95654 were first thawed at ambient temperatures and microfuged (Beckman microfuge B, California, USA) at 10,000g for 1 minute; to remove the fibrous material that might otherwise block the extraction cartridges. Plasma (100 μl) was transferred to a 1.5 ml polypropylene tube and placed in the Gilson 222 sample rack.

Four software programs were written for the Gilson 222, and used as appropriate:

PURGE — to flush the GILSON/AASP prior to and after use.
STD CVE — to prepare a standard curve, from standard solutions and control plasma.
SAMPLE — to analyse samples.
REPEAT — to repeat analysis of sample, if required.

The method of operation of the SAMPLE program is as follows:

1. Sampling (cycle 1)

Internal standard (400 μl) solution and water (100 μl) are dispensed to sample No. 1 using the probe and the diluted sample mixed by bubbling air through the liquid.

The 401 diluter in conjunction with the 222 then pulls up various liquid phases in reverse order: methanol (1 ml), water (1 ml), diluted sample (0.3 ml), and water (2 ml), into a holding loop with each solution separated by a small air gap (35 μl) (Fig. 3).

Whilst this is taking place the AASP has been instructed to load the first cartridge in line with the 222 injection port which is connected to port 5 on the Valco valve. The HPLC mobile phase at this time is routed to the analytical column.

Fig. 3—Fig. 8 Schematic of Gilson-AASP Automated System

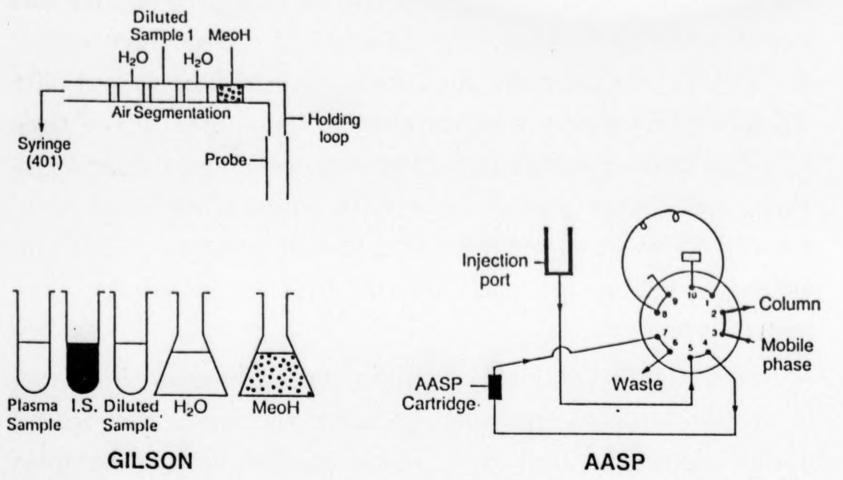
Diluted Sample 1
MeoH
H_2O
H_2O
Air Segmentation
Holding loop
Syringe (401)
Probe
Injection port
Column
Mobile phase
Waste
AASP Cartridge
Plasma Sample
I.S.
Diluted Sample
H_2O
MeoH
GILSON
AASP

Fig. 3 Sampling

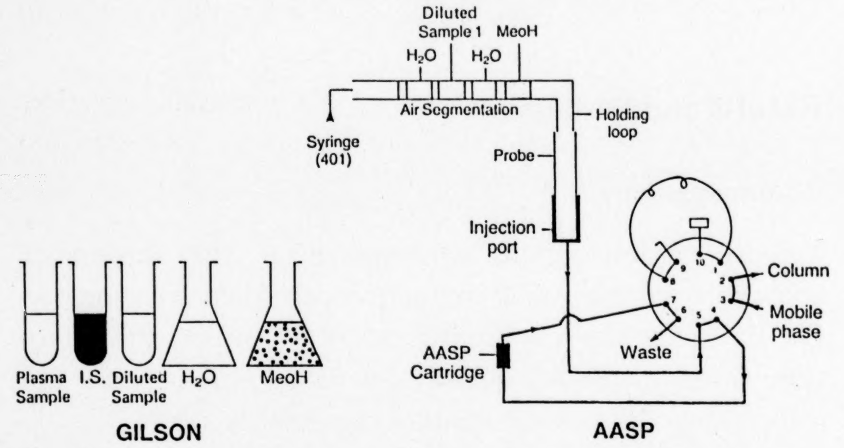
Diluted Sample 1
MeoH
H_2O
H_2O
Air Segmentation
Holding loop
Syringe (401)
Probe
Injection port
Column
Mobile phase
Waste
AASP Cartridge
Plasma Sample
I.S.
Diluted Sample
H_2O
MeoH
GILSON
AASP

Fig. 4 Loading cartridge

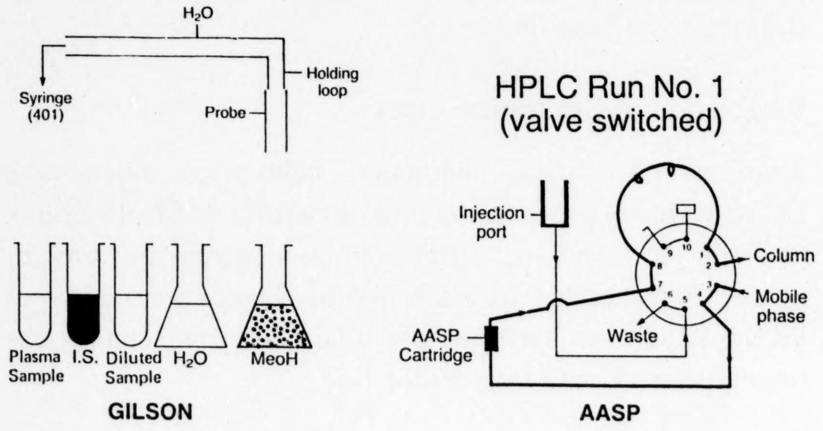
H_2O
Holding loop
Syringe (401)
Probe
HPLC Run No. 1
(valve switched)
Injection port
Column
Mobile phase
Waste
AASP Cartridge
Plasma Sample
I.S.
Diluted Sample
H_2O
MeoH
GILSON
AASP

Fig. 5 Elution

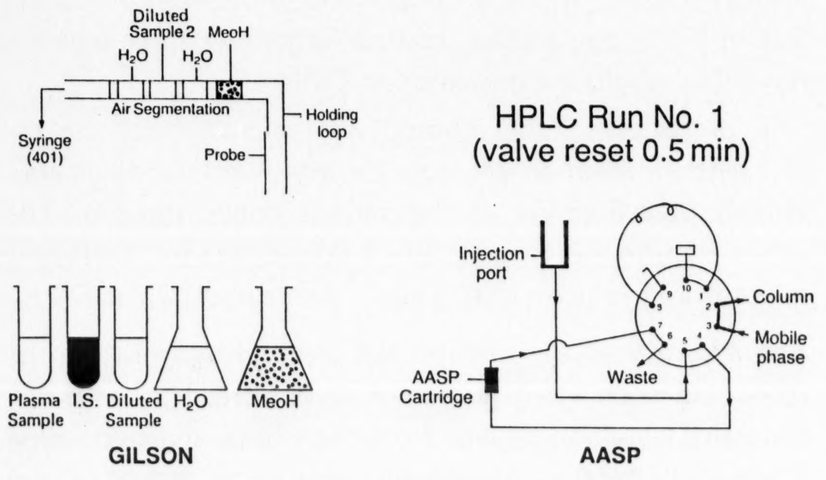
Diluted Sample 2
MeoH
H_2O
H_2O
Air Segmentation
Holding loop
Syringe (401)
Probe
HPLC Run No. 1
(valve reset 0.5 min)
Injection port
Column
Mobile phase
Waste
AASP Cartridge
Plasma Sample
I.S.
Diluted Sample
H_2O
MeoH
GILSON
AASP

Fig. 6 Sampling-HPLC

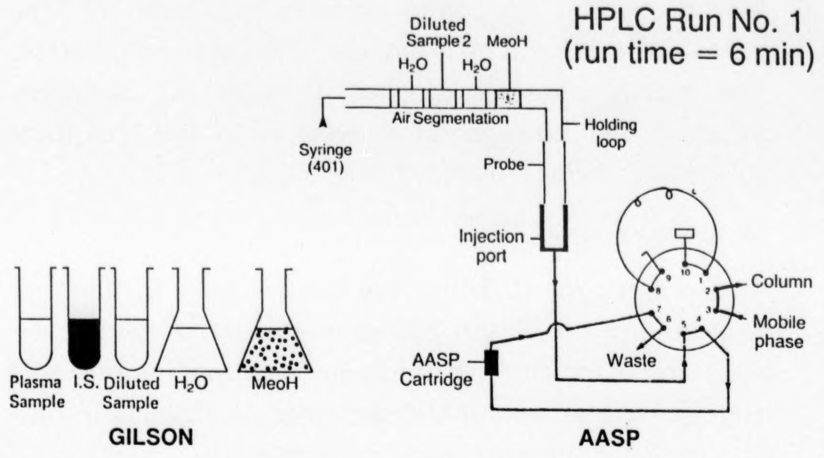
Diluted Sample 2
MeoH
H_2O
H_2O
HPLC Run No. 1
(run time = 6 min)
Air Segmentation
Holding loop
Syringe (401)
Probe
Injection port
Column
Mobile phase
Waste
AASP Cartridge
Plasma Sample
I.S.
Diluted Sample
H_2O
MeoH
GILSON
AASP

Fig. 7 Loading cartridge

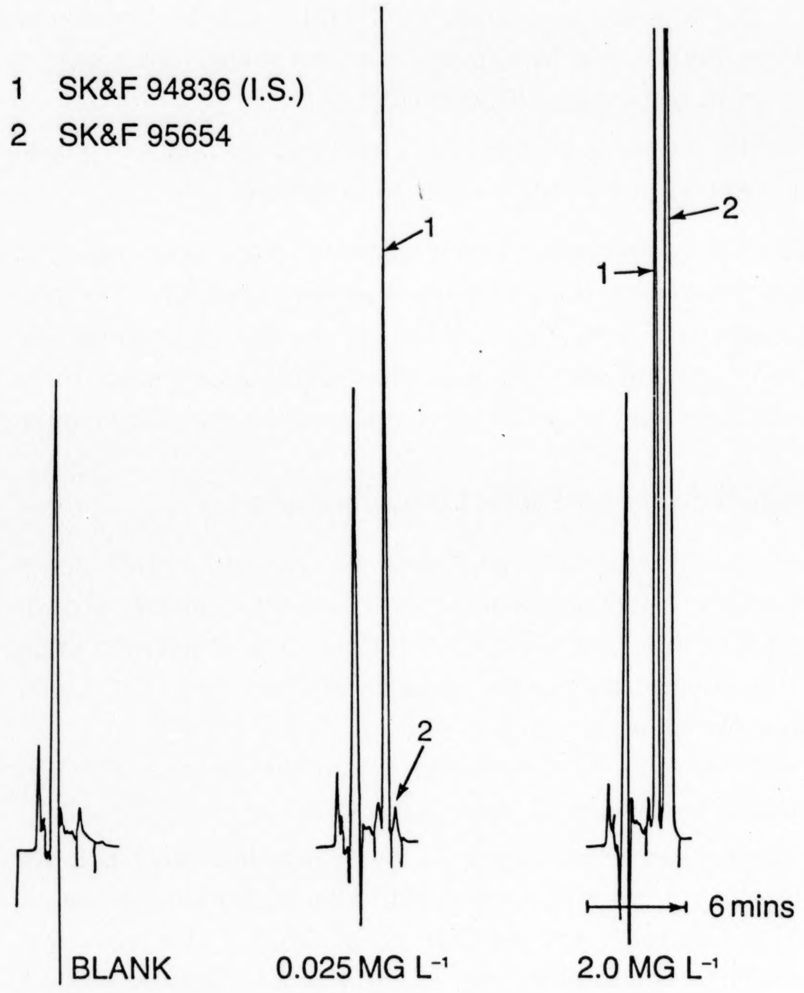

Fig. 8 Typical Chromatograms of Dog Plasma Extracts

2. Loading Cartridge (cycle 1)

The probe moves across to the injection port and the train of liquid is slowly pushed through the C18 AASP cartridge and out to waste (Fig. 4). Thus, in this single operation the bonded sorbent is conditioned with methanol and water, the diluted sample applied and subsequently washed with an additional aliquot of water. (This sequence of course, could be modified to suit the individual analysis, see conclusions.)

3. *Elution (sample 1)*

   With loading now complete, the probe can return to its 'home' position. On command from the Gilson 222 the Valco valve is switched and the integrator run started. The mobile phase is directed through the cartridge, sweeping the analytes of interest onto the analytical column and HPLC run No. 1 is initiated (Fig. 5).

4. *Sampling (sample 2)*

   At a preset time (0.5 min) the valve is reset to the load position and the Gilson 222 proceeds to transfer sample No. 2 and associated liquid phases into the holding loop (Fig. 6). The second AASP cartridge is brought in line with the injection port ready for loading.

5. *Loading Cartridge (cycle 2)*

   The probe, once again, moves across to the injection port and the second sample is processed through the cartridge (Fig. 7). On completion, the probe can return 'home' ready for sample No. 3. HPLC run No. 1 continues to the run end (6 min) and then the valve is again switched to commence HPLC run No. 2.

   This sequence of events will continue until all the plasma samples in the rack have been processed.

The integrator was programmed to store both raw and processed data derived from the UV detector. The processed data sent to a LIMS. for further processing and report generation. This procedure eliminates transcription errors and speeds up the production of the analytical report.

High-Performance Liquid Chromatography

The chromatograph consisted of Model 114M pump (Beckman, Berkeley, California, USA) set to deliver solvent at 1.5 ml min^{-1}, an AASP = LC module with ten port valco valve (Analytichem International, Harbor City, CA, USA) set up as follows:

mode: remote, first cartridge: 1, No. of samples: 99, run time: 0, cycle time: 0, valve reset: 0

The analytes were separated by a stainless steel column 300 mm × 3.9 mm id packed with 10 µm µBondapak-phenyl (Waters Assoc.) and maintained at 35 °C. The analytical column was protected by a Rad-Pak CN (Waters Assoc.) guard column. The column effluent was monitored continuously by a Kratos 773 variable wavelength UV detector set at 300 nm and 0.001 absorbance units full scale. The signal from the detector was fed into a model 301 computing integrator (Laboratory Data Control, Stone, Staffs, UK).

Mobile Phase

The mobile phase was composed of acetonitrile and 0.01 mol l^{-1} ammonium acetate buffer (the pH value of the aqueous buffer was adjusted to 5.0 with the addition of orthophosphoric acid). The solvents were passed through c0.5 µm membrane filters (Millipore type HA and FH for aqueous and organic solvents respectively). Prior to use, the components of the solvent system were mixed (25:75) and a helium sparge was maintained through the solvent reservoir for the duration of the chromatographic analysis.

Standard Curve

At the beginning of any study a standard curve was constructed and run by the Gilson 222 (using the program STD CVE); 100 µl control plasma aliquots were spiked with SK&F 95654 over the concentration range of 0.025–2.0 mg l^{-1}. The curve consisted of 26 points covering six concentrations; one blank sample, one with internal standard only, six replicates at the highest and lowest concentrations and three replicates for each of the four intermediate concentrations.

A set of quality control samples was spiked at the same time the samples for analysis were received, and stored under identical conditions. These quality control samples were processed on each extraction day and any large (> 10%) variation from the known value used to adjust the standard curve.

Results and Discussion

Chromatography

Typical chromatograms observed after the elution of analytes from the AASP extraction cartridges are shown in Fig. 8. Under the conditions described earlier, the retention times of SK&F 94836 and SK&F 95654 were approximately 4.2 and 4.9 minutes respectively.

No endogenous compounds with retention times corresponding to either SK&F 95654 or the internal standard SK&F 94836 have been observed in extracts of samples chromatographed, and therefore the assay was deemed to be specific.

Preparation of Calibration Lines

Two variable linear regression calibration lines were constructed by plotting the peak area ratio of SK&F 95654 to internal standard, against known concentrations of SK&F 95654 added to blank plasma. The concentration of SK&F 95654 in each sample quantified by relating the respective peak area ratio to the line.

Precision and Accuracy

The precision and accuracy of the assay was assessed by spiking and assaying replicate samples of plasma containing known concentrations of SK&F 95654 between 0.025 and 2.0 mg l^{-1} in dog plasma, and performed on three separate days. The results are presented in Table I.

The precision of the method was calculated as the coefficient of variation of replicate assays of standards containing SK&F 95654 at the various concentrations. The values were in the range 0.3 to 1.0%, except for the lowest concentration chosen (0.025 mg l^{-1}) were it was 3.2 to 5.1%.

The accuracy of the method was assessed by re-fitting the ratios from standards used to assess precision into the regression equation derived from these data, and calculating the bias. Generally, the accuracy was better than 2%, and in no case was greater than 5%.

Table I. Accuracy and Precision Data

Concentration ($mg\ l^{-1}$)	Accuracy (Bias %)			Precision (CV%) ±			No. per day
	day 1	day 2	day 3	day 1	day 2	day 3	
0.025	− 5.0(3)	+ 0.4	+ 2.8	5.1 (3)	3.3	3.2	6
0.125	− 2.4	− 1.6	− 3.3	0.7	1.0	0.9	3
0.25	+ 0.4	+ 0.4	− 2.0	1.7	0.8	0.8	3
0.5	+ 0.2	− 0.2	− 2.4	0.5	0.3	0.3	3
1.0	+ 0.5	+ 0.4	− 2.0	0.3	0.6	0.6	3
2.0	− 0.05	− 0.05	− 2.6	0.5	0.6	0.6	6

$$CV = \frac{\text{standard deviation}}{\text{mean calculated concentration}} \times 100\%$$

$$Bias = \frac{(\text{mean calculated concentration} - \text{actual conc.})}{\text{actual concentration}} \times 100\%$$

Conclusions

The assay presented fuses the power attainable with solid-phase sample preparation and the versatility of reverse phase HPLC with UV detection by the use of dedicated robotic units. The method is totally automated, easy to use and involving minimal human input.

It is robust, yet sensitive, accurate and precise, with a high throughput, making it ideal for a busy pharmaceutical laboratory.

Although this paper describes a particular assay, the variables can be altered to suit other compounds. The strategy of linking solid phase extraction with HPLC has wide applicability. One such, could be on-line derivatisation for which a reaction can be conducted either in the holding loop or on the solid phase. Time delays and washes could be introduced to allow any such reaction to proceed, and to remove excess reagent prior to chromatographic analysis. Such approaches are under active consideration.

References

[1] *D. Hawkes, M. Lindsay,* Lab Practice September (1984).

[2] *R. D. McDowall, J. C. Pearce, G. S. Murkitt,* Journal of Pharmaceutical and Biomedical Analysis **4**, 3–21, 1986.

[3] *J. C. Pearce, J. A. Jelly, K. A. Fernandes, W. J. Leavens, R. D. McDowall,* J. Chromatogr. **353**, 371–378, 1986.

[4] Laboratory Information Management Systems, edited by *R. D. McDowall,* Sigma Press, 1987.

[5] *R. D. McDowall, J. C. Pearce, G. S. Murkitt,* Journal of Pharmaceutical and Biomedical Analysis, in press.

Received: July 3, 1987
Accepted: July 25, 1987
F

Packed Capillary Columns for Liquid Chromatography

S. Hoffmann / L. Blomberg*

Department of Analytical Chemistry, University of Stockholm, Arrhenius Laboratory, 106 91 Stockholm, Sweden

Key Words

Liquid chromatography
Capillary columns
Slurry-packing
3 and 2μm particles

Summary

Fused silica capillaries, $\approx 130 \times 0.32$mm have been packed with small reversed phase spherical silica particles, 3 or 2μm, in order to achieve LC-systems giving high plate numbers at relatively low pressure drop in short analysis times. At optimal conditions, columns packed with 3μm particles showed reduced plate heights, h, around 2.5, and the column flow resistance, ϕ, was 335–625. With 2μm particles, a reduced plate height of only 3.7 was achieved, which reflects the difficulty in the packing of such small particles.

Introduction

Relatively low plate numbers are generally obtained with conventional HPLC; the inlet pressure available with current instrumentation seems to be a limiting factor, but with the use of selectively separating systems, most of the present LC-separations can be carried out on columns generating 2000 to 10000 plates. There are, however, a vast number of problems where a high number of plates is required. High plate counts can be achieved with a relatively low pressure drop when using open tubular columns. The low diffusion coefficients with liquids, at least four orders of magnitude lower than those with gases, has led to the use of quite narrow capillaries, ca 5μm. The use of such narrow columns gives extraordinary technological difficulties which, in spite of some recent progress, still await their solution. A reasonable compromise is offered by packed capillary columns, where wall effects are supposed to lead to a reduction in back-pressures. Around 100 000 theoretical plates can be routinely attained when such columns containing 5 or 3μm particles are being used, and when the column length is circa one meter [1–3]. This type of column may, however, often lead to relatively long analysis times.

Besides high plate numbers, a major priority in chromatography is speed of analysis. Speed of analysis can be increased in chromatography by means of three factors. First, the use of selectivity. Second, operation under conditions that minimize resistance to mass transfer as expressed in the Golay equation. This would lead to a moderate increase in a van Deemter plot as the mobile phase velocity increases; such a system could thus be operated at mobile phase velocities which are much higher than optimal without incurring any considerable losses in separation efficiency. Third, by increasing the number of theoretical plate per unit column length. This can be done in packed columns by decreasing packing particle diameter, and in open tubular columns (OTC) by decreasing the column diameter. Further, these steps favour the formation of van Deemter plots that are relatively flat in the C-term region. The small diameters needed for high speed OTC would, however, lead to formidable technical difficulties, and the use of packed columns having a particle size of 1 to 2μm presently seems to be the most realistic approach when a high speed of plate production is desired in LC. The use of 1 and 2μm silica particles in short columns has been demonstrated by Dewaele and Verzele [4, 5]. Unger et al. [6] used 1.8μm alumina particles. Such columns give very low dispersion, and as a result, the extra-column dispersion becomes of decisive importance. Further, since quite rapid chromatographic peaks are obtained here, the detector must have a fast response and the data system used, must offer fast data acquisition. The use of small particles inevitably leads to high column pressure drops; LC-pumps, giving up to 70MPa are, however, available e.g. from Isco and LDC. Micro-injectors are generally limited to 34.5MPa.

The research objective in this work is the development of LC-systems giving high plate numbers in short analysis times. This paper presents the preparation and evaluation of capillary columns, 150×0.32mm, packed with spherical C-18-modified particles, 3 or 2μm.

Experimental

Instrumentation

The system utilized in the column testing consisted of an ISCO μLC-500 syringe pump (ISCO, Lincoln, NE, USA) operated in constant pressure mode and an ISCO μLC-10

0009-5893/87 0416-05 $03.00/0

© 1987 Friedr. Vieweg & Sohn Verlagsgesellschaft mbH

variable wavelength absorbance detector operated at 254nm. The detector cell was modified for on-column detection and the cell volume was 4.4nl. The time constant was set to 0.05sec. Injections were made via a Rheodyne 7520 injector with a 0.2μl loop (Rheodyne, Cotati, CA, USA). The columns were fitted with a vespel ferrule and a 2mm long piece of PTFE tubing (1/16in. o.d. × 0.45mm i.d.) was inserted into the bottom of the injector seat to ensure that the columns were correctly positioned. The PTFE tubing also reduced the void volume at the injector seat.

The packing apparatus consisted of a Gilson 302 piston pump equipped with a Gilson 802 manometer module (Gilson, Villiers Le Bel, France). A slurry reservoir, 60mm long, was constructed from a 1/4in. × 4.6mm column blank. Standard 1/4 × 1/16in. column end fittings were mounted and a 30mm (1/16in. o.d. × 0.5mm i.d.) SS tubing was inserted at the outlet. A 1/16 × 1/16in. union and Vespel ferrules connected the columns to the reservoir. For packing of columns with 2μm particles, a small reservoir, 1ml, containing pure slurry solvent, was attached to the top of the slurry reservoir.

Packing Procedures

Fused silica capillary tubing, 0.45mm o.d. × 0.32mm i.d. (Chrompack, Middelburg, The Netherlands) and 0.20mm o.d. × 0.075mm i.d. (Scientific Glass Engineering, Ringwood, Australia) were used in column preparation. The column end was inserted into a PTFE tubing (1/16in. o.d. × 0.15mm i.d.) that contained a glass wool filter retained by the 0.075mm capillary tubing. Approximately 8mm downstream the filter, the polyimide coating of the fused silica tubing was burnt off to allow for on-column detection.

3μm ODS particles, Spherisorb S3 ODS2 (Phase Separations Ltd., Queensferry, United Kingdom), were suspended in analytical grade tetrachloromethane to give a 2% (w/v) slurry. Downward packing was utilized with acetonitrile/water 6:4 as pumping medium. The packing pressure was kept at 34MPa until at least 100 column volumes of pumping medium had been eluted. The initial packing flow was set to 1ml/min. At higher flow rates, there was a risk that the terminal filter should be blown out. A few columns were packed with 2μm ROSiL-C18-D (obtained from Professor M. Verzele, Rijksuniversiteit-Gent, Belgium). Packing was here performed with a 1.5% slurry in tetrachloromethane, the pumping medium was acetonitrile and the pressure was 34MPa. A small part of the columns was cut off after the packing.

Column Evaluation

The sample used for column evaluation contained nitrobenzene, benzophenone, diphenylamine and phenanthrene dissolved in acetonitrile/water 1/1. A mobile phase of acetonitrile/water 70/30 was used to elute the test solutes. For each column, test chromatograms were obtained at several linear velocities between 0.5mm/sec and 5mm/sec. Values of retention times and peak widths at half peak height were measured five times for each velocity. A PC-based laboratory data system was used for sampling the detector signal at a rate of 18.2 Hz.

Mobile phase viscosities and diffusion coefficients were calculated according to Snyder and Antle [7]. The values of h, ν, E, ϕ, K^0 and ϵ_T were calculated according to Ref. [8].

Results and Discussion

The preparation and evaluation of columns has been the main object of this work. Instrumental factors have been matched to make correct column evaluation possible, although there is room for improvement in the system used here.

Injection was performed by the moving-injection technique [9], i.e. the injection port was rapidly opened and directly closed. Only a small portion of the volume contained in the sample loop was thus injected. In order to further improve the injection, the solutes were dissolved in a polar solvent (without precipitation). A solute focusing effect according to Yang [10, 11] was thereby obtained on the column head.

UV-detection was performed *on-column* according to Yang [10, 11]. Such a system leads to a rather low sensitivity which, of course, limits the split ratio in the injector and the eventual dilution of the test solution.

Aspects of Dead Time Measurement

The retention time of an unretained component, t_M, is an important parameter in column evaluation. Several different methods are available for the measurement of t_M, and under given conditions, these result in somewhat different t_M-values [12, 13]. Bristow and Knox [8] pointed out that compounds similar to the eluent are preferred for t_M-determination; the unretained compound should thus have access to both the interparticle volume and the complete intraparticle pore volume. Acetone is to some slight extent retained on the columns, but it was chosen in this work in order to facilitate comparisons with results of other workers [1, 3].

Temperature Effects

For practical reasons, 65mm of the column is, in our system, situated inside the UV-detector. Since the column is not thermostated, the temperature in this section is circa 33°C. According to Serpinet et al. [14], the C-18 moieties of the packing may go through a phase transition at circa 22°C, which can, of course, influence retentive properties. Further, the viscosity of liquids decreases and the diffusivity increase with temperature.

Halász et al. [15, 16] have proposed that a radial temperature gradient may occur due to viscous friction when small particles are being used. Such heat would be easily dissipated in narrow bore columns.

Column Interparticle Porosity

As pointed out by Verzele et al. [17], dispersion increase with increasing interparticle porosity, ϵ_u. The densest possible packing of spherical particles would result in ϵ_u of 0.26. Typical values of ϵ_u obtained in practice are for Spherisorb S5W, 0.321 [18] and for 5μm Spherisorb ODS, 0.343 [3]. Due to the uncertainty in t_M-values, ϵ_u could not be calculated in a meaningful way in this work.

Packing of conventional columns may be performed at pressures as high as 103 MPa to 172 MPa [19]. For 1 mm i.d. columns, Meyer and Hartwick [20] considered 103 MPa as being the maximum safe pressure; although packing at 145 MPa produced the highest efficiencies, it also caused visual distortion of the packing reservoir. Novotny et al. [3] packed 5μm particles at 46 MPa. Verzele et al. [17] consider 40 MPa as being sufficiently high for 10μm material, but not for smaller particle sizes. These authors thus recommended 60 MPa for packing with 2μm particles [4]. The packing pressure used in this work was 34 MPa, which was reached ca 30 seconds after the packing had been started.

It seems that narrow bore columns can be stable although they are relatively loosely packed. This stability may be a consequence of the supporting effect of the walls [21]. When highest efficiency is desired, however, the packing should be as dense as possible as mentioned above. It is possible that in some cases it could be motivated to trade packing density and column length to advantage.

Conventional and 1 mm i.d. packed columns are reported to have a column flow resistance, ϕ, of 500 to 1000, where $\phi = \Delta p\, t_M\, d_p^2/\eta L^2$ [8, 22, 23]. Borra et al. [3] reported ϕ-values around 700 for columns, 0.25 mm i.d., packed with 5μm particles. Dewaele and Verzele [4] reported ϕ of 980 to 1030 for 2μm particles. In this work 3μm particles resulted in ϕ-values of 336 to 625 for optimal conditions, Table I.

Comparing back pressure of 25 cm long, 4.6 and 0.32 mm i.d. columns, Verzele et al. [24] maintained that with conventional columns, higher backpressures were required than with micro columns. The reasons behind this effect were not explained, but the packing of any bed will undoubtedly be disturbed in the region of the wall [25].

Potential of Small Particles in LC

A clear trend in column technology is the use of smaller particles and shorter columns. Knox and Saleem [26] thus suggested that the use of 2μm particles would be optimal. Halasz et al. [15] proposed that the minimum particle size in HPLC should be 2–1μm. Knox and Gilbert [27] calculated the optimal particle size for slurry packed columns operated under optimal conditions, $h = 2$, $\nu = 4$ and $\phi = 500$. Insertion of typical values of D_m and η for an aqueous eluent and $N = 10000$ and $\Delta p = 200$ bar in equation (1), resulted in $d_{p\,(opt)} = 1.4\,\mu$m.

$$d_{p\,(opt)} = \left[\frac{N\,h\,\nu\,\phi\,\eta\,D_m}{\Delta p}\right]^{1/2} \qquad (1)$$

When a reduced plate height of 2 can be maintained, a 15 cm column would give 7500 plates with 10μm particles, 25000 plates with 3μm particles, 37500 plates with 2μm particles and 75000 plates with 1μm particles. To achieve this, some special conditions must be fulfilled. First, extra column dispersion must be low enough. Second, sensitive detection with a low time constant must be available, and third, it must of course be possible to prepare such super columns. It has been well established that packing becomes exponentially more difficult with a reduction in particle size.

Factors in Column Preparation

Packing with 3μm particles in a dilute slurry in tetrachloromethane resulted in excellent columns, Fig. 1 and 2 and Table I. The separation impedance, E, was for 3μm particles 2300–3600, Table I. This is somewhat higher than reported by Shelly et al. [28], but lower than the values given by Borra et al. [3]. Konishi et al. [29] reported that stable packings were obtained when conditioning the column with water. In this work, conditioning in acetonitrile/water was used to stabilize the columns.

The columns packed with 2μm particles did not show the same low h-values as those packed with 3μm particles, Tables I and II, and Fig. 3. The packing procedure obviously needs to be improved in this case. Moreover, short columns packed with such small particles demand very low extra-column variances.

In Fig. 2, min h occurs at somewhat lower ν than has been observed by others [1, 3, 8]. ν is calculated from the relation $\nu = L d_p/t_M D_m$. Provided d_p is 3μm as indicated by the silica manufacturer, the source of error may here be found in the denominator. As discussed above, the values of t_M obtained with acetone may be somewhat too high,

Table I. Evaluation at optimal conditions of fused silica columns, 0.32 mm i.d., packed with 3μm reversed phase silica particles. Mobile phase: acetonitrile/water 70:30. Capacity factor, k′, for nitrobenzene = 0.45, and for phenanthrene = 3.1; t_M obtained from acetone.

Column length (mm)	Solute	u* (mm/sec)	ν*	h*	E	ϕ	K^0 (mm^2) 10^8	ϵ_T
134	Nitrobenzene	1.15	1.96	2.40	2952	512	1.8	0.62
	Phenanthrene	1.40	3.01	2.58	3614	541	1.7	0.62
125	Nitrobenzene	1.01	1.71	2.79	4566	585	4.1	0.63
	Phenanthrene	1.48	3.19	2.74	4694	625	2.1	0.59
127	Nitrobenzene	0.74	1.26	2.85	2739	336	2.7	0.62
	Phenanthrene	1.17	2.52	2.58	2363	354	2.5	0.63

* Average of five measurements.

Table II. Evaluation at optimal conditions of a fused silica column, 122 × 0.32 mm, Packed with 2 μm reversed phase silica particles. Mobile phase: acetonitrile/water 70:30. Capacity factor, k', for nitrobenzene = 0.50 and for phenanthrene = 3.31; t_M obtained from acetone.

Solute	u* (mm/sec)	ν*	h*	E	ϕ	K^0 (mm^2) 10^9	ϵ_T
Nitrobenzene	1.34	2.82	3.74	8010	573	7.0	0.67
Phenanthrene	1.67	3.59	3.68	7810	575	6.9	0.68

* Average of two measurements.

which partly may account for our low ν-values. The D_m-values have been calculated from a simplified Wilke-Chang equation [7] and they may be in error with ± 50%. Further, part of our columns are at 33°C. Calculated D_m-values for nitrobenzene at 25°C and 33°C were $1.76 \cdot 10^{-5}$ and $2.22 \cdot 10^{-5}$ cm^2/sec respectively. The D_m-values used in our calculations may thus be on the low side.

Conclusions

Packing fused silica capillaries, ≈ 130 × 0.32 mm, with a dilute slurry of 3 μm reversed phase spherical silica particles in tetrachloromethane resulted in highly efficient LC-columns, having a relatively low flow resistance.

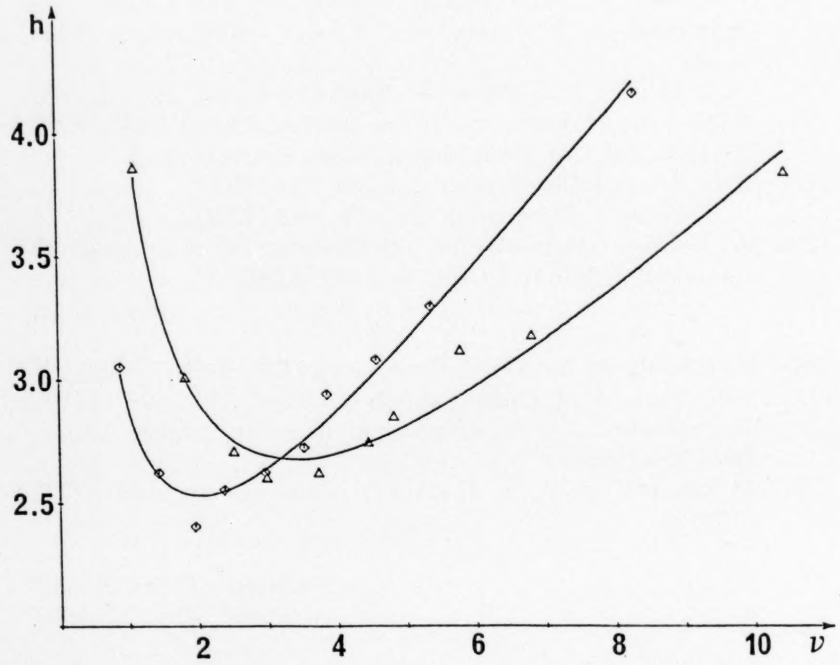

Fig. 1

Reduced plate height versus reduced velocity for nitrobenzene ◇ and phenanthrene △ (k' = 0.45, $D_m = 1.76 \cdot 10^{-5} cm^2$/sec and k' = 3.1, $D_m = 1.39 \cdot 10^{-5} cm^2$/sec respectively). Column: Spherisorb S3 ODS2, d_p = 3 μm, 134 × 0.32 mm. Mobile phase: acetonitrile/water 70:30 (v/v). Detector: Isco μLC-10 (254 nm).

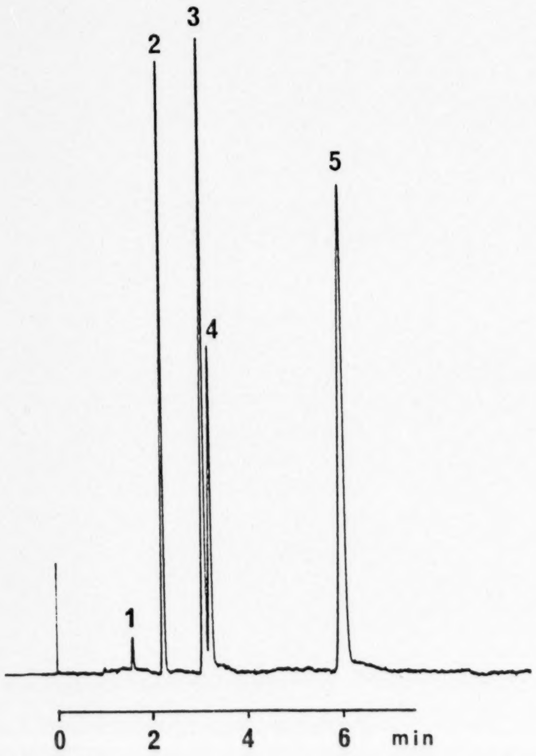

Fig. 2

Test chromatogram for the evaluation of slurry-packed capillary columns. Column: Spherisorb S3 ODS2, d_p = 3 μm, 134 × 0.32 mm. Mobile phase: acetonitrile/water 70:30, at 1.42 mm/sec. Sensitivity: 0.02 Abs. Solutes: **1** = Acetone (k' = 0); **2** = Nitrobenzene (k' = 0.41); **3** = Benzophenone (k' = 0.95); **4** = Diphenylamine (k' = 1.04); **5** = Phenanthrene (k' = 2.83). Detector: ISCO μLC-10 (254 nm).

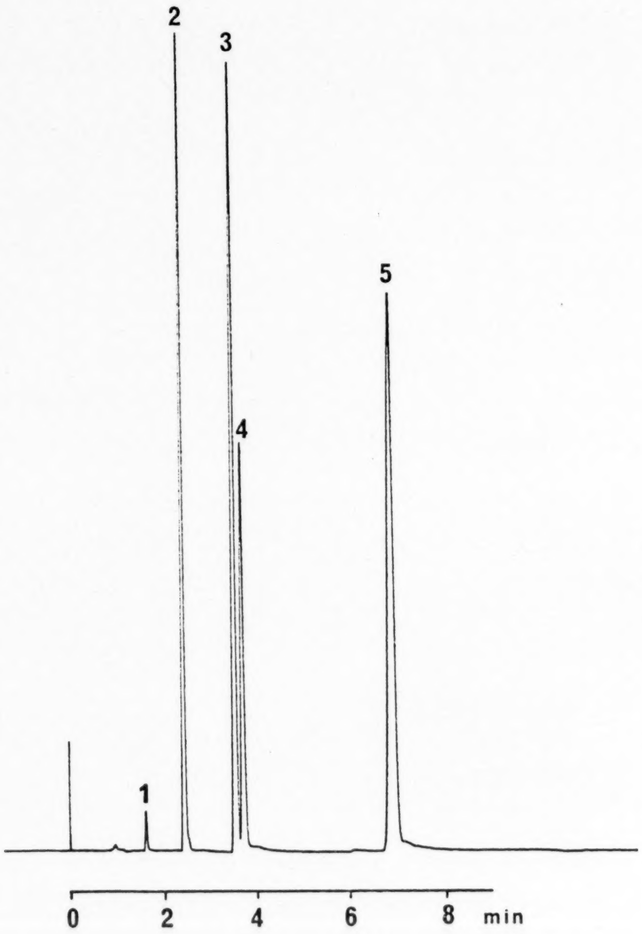

Fig. 3

Test chromatogram for the evaluation of slurry-packed capillary columns. Column: ROSiL-C18-D, d_p = 2 μm, 122 × 0.32 mm. Mobile phase: acetonitrile/water 70:30 at 1.28 mm/sec. Sensitivity: 0.05 Abs. Solutes: **1** = Acetone (k' = 0); **2** = Nitrobenzene (k' = 0.50); **3** = Benzophenone (k' = 1.19); **4** = Diphenylamine (k' = 1.30); **5** = Phenanthrene (k' = 3.31). Detector: ISCO μLC-10 (254 nm).

Columns packed with 2µm particles did not show the same low h-values as those packed with 3µm particles. The packing procedure obviously needs to be improved in this case.

Acknowledgements

This investigation was kindly supported by the Swedish Natural Science Research Council. Silica particles, 2µm ROSiL-C18-D were generously supplied by Professor M. Verzele, Rijksuniversiteit-Gent, Belgium. Thanks are due to B. Holm for reviewing the manuscript.

References

[1] *J. C. Gluckman, A. Hirose, V. L. McGuffin, M. Novotny*, Chromatographia, **17**, 303 (1983).

[2] *Y. Hirata, K. Jinno*, J. High Resolut. Chromatogr. Chromatogr. Commun., **6**, 196 (1983).

[3] *C. Borra, M. Han Soon, M. Novotny*, J. Chromatogr., **385**, 75 (1987).

[4] *C. Dewaele, M. Verzele*, J. Chromatogr., **282**, 341 (1983).

[5] *M. Verzele, C. Dewaele*, in "Science of Chromatography", F. Bruner, ed., Elsevier, Amsterdam, 1985; p. 435.

[6] *K. K. Unger, W. Messer, K. J. Krebs*, J. Chromatogr., **149**, 1 (1978).

[7] *L. R. Snyder, P. E. Antle*, LC Magazine, **3**, 98 (1985).

[8] *P. A. Bristow, J. H. Knox*, Chromatographia, **10**, 279 (1977).

[9] *M. C. Harvey. S. D. Stearns*, J. Chromatogr. Sci., **21**, 473 (1983).

[10] *F. J. Yang*, J. Chromatogr., **236**, 265 (1982).

[11] *F. J. Yang*, J. High Resolut. Chromatogr. Chromatogr. Commun., **6**, 348 (1983).

[12] *R. J. Smith, C. S. Nieass, M. S. Wainwright*, J. Liq. Chromatogr., **9**, 1387 (1986).

[13] *J. H. Knox, R. Kaliszan*, J. Chromatogr., **349**, 211 (1985).

[14] *D. Morel, J. Serpinet*, J. Chromatogr., **200**, 95 (1980).

[15] *I. Halász, R. Endele, J. Asshauer*, J. Chromatogr., **112**, 37 (1975).

[16] *I. Halász, H. Schmidt, P. Vogtel*, J. Chromatogr., **126**, 19 (1976).

[17] *M. Verzele, C. Dewaele, D. Duquet*, J. Chromatogr., **391**, 111 (1987).

[18] *R. Ohmacht, I. Halász*, Chromatographia, **14**, 155 (1981).

[19] *P. Kucera* in "Microcolumn High-Performance Liquid Chromatography", P. Kucera, ed., Elsevier, Amsterdam, 1984; p. 39.

[20] *R. F. Meyer, R. A. Hartwick*, Anal. Chem., **56**, 2211 (1984).

[21] *C. Dewaele*, Comm. Eur. Communities, (REP) EUR, 1986, EUR 10388, Org. Micropollut. Aquat. Environ., p. 3.

[22] *J. H. Knox*, J. Chromatogr. Sci., **15**, 352 (1977).

[23] *J. H. Knox*, J. Chromatogr. Sci., **18**, 453 (1980).

[24] *M. Verzele, M. de Weerdt, C. Dewaele, G. J. de Jong, N. Lammers, F. Spruit*, LC-GC, **4**, 1162 (1986).

[25] *M. Verzele, C. Dewaele*, J. High Resolut. Chromatogr. Chromatogr. Commun., **10**, 280 (1987).

[26] *J. H. Knox, M. Saleem*, J. Chromatogr. Sci., **7**, 614 (1969).

[27] *J. H. Knox, M. T. Gilbert*, J. Chromatogr., **186**, 405 (1979).

[28] *D. C. Shelly, J. C. Gluckman, M. Novotny*, Anal. Chem., **56**, 2990 (1984).

[29] *M. Konishi, Y. Mori, T. Amano*, Anal. Chem., **57**, 2235 (1985).

Received: June 29, 1987
Accepted: Aug. 24, 1987
F

HPLC of Porphyrinogens with Electrochemical Detection

Famei Li/C. K. Lim*/T. J. Peters

Division of Clinical Cell Biology, MRC Clinical Research Centre, Watford Road, Harrow, Middlesex
HAI 3UJ, UK.

Key Words

Column liquid chromatography
Porphyrinogens
Electrochemical detection

Summary

A reversed-phase system is described for the separation of coproporphyrinogen I, II, III, IV isomers, deethylisocoproporphyrinogen and isocoproporphyrinogen. The porphyrinogens are detected electrochemically with high sensitivity. The relative retention of the prophyrinogens is mainly governed by the arrangement of the ethyl and methyl substituents around the macrocycle, although steric effect may also be an important parameter.

Introduction

The porphyrinogens are hexahydroporphyrins. They are intermediates in the biosynthesis of haem, chlorophylls and vitamin B_{12}. It is at the porphyrinogen stage when the side-chain acetic and propionic acid groups of the macrocyclic tetrapyrrole are transformed into the methyl and vinyl groups of protoporphyrinogen IX, the penultimate precursor of haem. The analysis of porphyrins by HPLC is now well established. The separation of porphyrinogens, however, has only been reported recently [1–5]. The present paper describes the HPLC separation and the electrochemical behaviours of porphyrinogens, with coproporphyrinogen I, II, III and IV isomers, deethylisocoproporphyrinogen and isocoproporphyrinogen (Fig. 1) as examples.

Materials and Reagents

Coproporphyrin I, II, III and IV isomers were prepared by decarboxylation of uroporphyrin I, II, III and IV isomers synthesized by polymerization of porphobilinogen in acid [6]. Deethylisocoproporphyrin and isocoproporphyrin were isolated from the faeces of rats treated with hexachlorobenzene by TLC using the method and solvent system described previously [3].

Ammonium acetate, acetic acid, EDTA and KOH were AnalaR grade from BDH Chemicals, Poole, Dorset, UK. Acetonitrile was HPLC grade from Rathburn Chemicals, Walkerburn, Peeblesshire, UK.

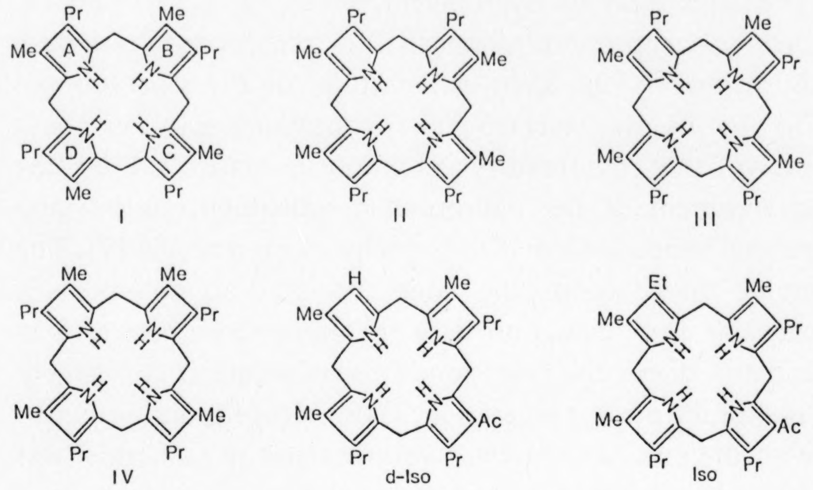

Fig. 1

Structures of coproporphyrinogens. **I** = Coproporphyrinogen I; **II** = coproporphyrinogen II; **III** = coproporphyrinogen III; **IV** = coproporphyrinogen IV; **d-Iso** = deethylisocoproporphyrinogen; **Iso** = isocoproporphyrinogen.

Preparation of Porphyrinogens

The porphyrins were dissolved in 0.01 M KOH (250 μl) and the solution was shaken vigorously with 3 % (w/w) sodium amalgam until no fluorescence was detectable under a UV lamp. The porphyrinogen solution was transferred into a clean vial, flushed with nitrogen, capped and kept on ice in the dark.

HPLC of Porphyrinogens

A Varian Associates (Walnut Creek, CA, USA) model 5000 liquid chromatograph was used with an LCA-15 electrochemical detector (EDT Research, London, UK). The separation was carried out on a 25 cm X 5 mm ODS-Hypersil (5 μm spherical silica chemically bonded with octadecylsilyl groups) from Shandon Southern Products, Runcorn, Cheshire, UK. The mobile phase was 25 % (v/v) acetonitrile in 1 M ammonium acetate, pH 5.16 (adjusted with acetic acid) containing 0.27 mM EDTA. The flow rate was 1 ml/min. The mobile phase was degassed before use and a continuous stream of helium was passed during the separation.

Results and Discussion

The porphyrinogens are colourless compounds with weak UV absorption at the 200–240 nm region. They are easily oxidised by air, particularly in acid solution in the presence of light, to the strongly UV absorbing and fluorescent porphyrins. The ease of oxidation makes these compounds ideal for highly sensitive electrochemical detection by the

0009-5893/87 0421-02 $03.00/0

© 1987 Friedr. Vieweg & Sohn Verlagsgesellschaft mbH

oxidation mode. The electrochemical reaction is shown in Fig. 2. Assuming complete oxidation to porphyrin, the porphyrinogen loses six protons and generates six electrons. Since porphyrins are also electroactive at higher potentials [2], further removal of electron from the macrocycle is possible. The coproporphyrin isomers, deethylisocoproporphyrin and isocoproporphyrin were all shown to be electroactive at + 0.75 V, but only at much higher sample concentrations than the porphyrinogens. They could not be detected at concentrations easily detectable with a fluorescence detector [1].

The separation of coproporphyrinogen I, II, III and IV, deethylisocoproporphyrinogen and isocoproporphyrinogen is shown in Fig. 3. In earlier study of the separation of porphyrins by reversed-phase chromatography we have shown that the relative retention is controlled by the arrangement of the hydrophobic substituents (ethyl and methyl groups) around the porphyrin macrocycle [7]. The closer these groups the larger the hydrophobic surface available for interaction with the stationary phase surface and the longer the retention. This behaviour is still largely true for the present separation. Thus, isocoproporphyrinogen with the ethyl and methyl groups closest to each other was the strongest retaining and the symmetrical coproporphyrinogen I with the methyl groups farthest apart the fastest eluting compound. The relative retention of the other compounds can be similarly explained except for coproporphyrinogen II. This compound is expected to retain longer than coproporphyrinogen III and IV since it has two pairs of adjacent methyl groups and should therefore be more hydrophobic [7, 8]. However, it eluted before coproporphyrinogen III and IV indicating a weaker hydrophobic interaction. It is probable that some of the methyl groups in this molecule are to some extent shielded by the relatively bulky carboxyclic acid groups and thus reducing its ability to interact with the stationary phase. This is possible because the porphyrinogens are flexible compounds in contrast to the rigid porphyrins. The shielding effect has been shown to be an important factor in achieving separation of the heptacarboxylic porphyrinogens [5].

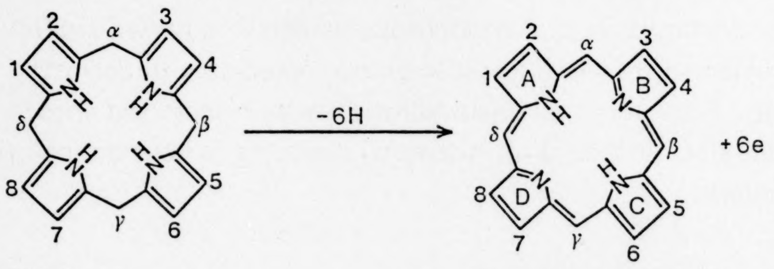

Fig. 2

Electrochemical oxidation of porphyrinogen

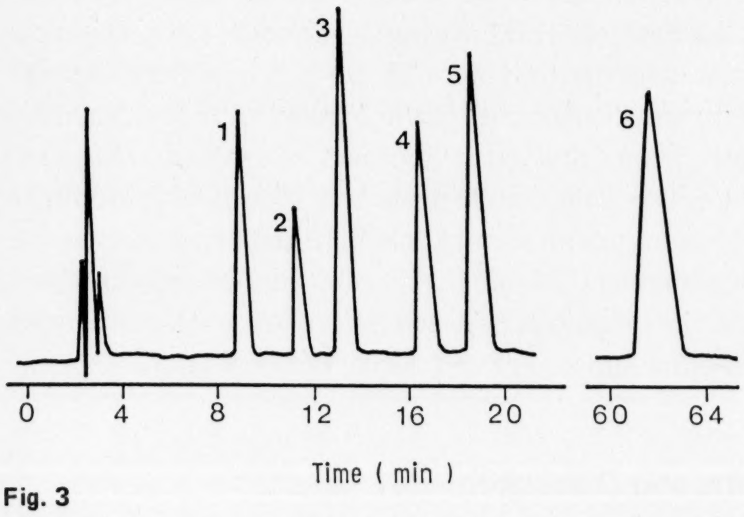

Fig. 3

Separation of coproporphyrinogens. Column, 5 μm ODS-Hypersil (25 cm X 5 mm); eluent, 25 % (v/v) acetonitrile in 1 M ammonium acetate, pH 5.16; flow rate, 1 ml/min; detector, electrochemical, + 0.70 V, 30 nA. Peaks: **1** = coproporporphyrinogen I; **2** = coproporphyrinogen II; **3** = coproporphyrinogen III; **4** = coproporphyrinogen IV; **5** = deethylisocoproporphyrinogen; **6** = isocoproporphyrinogen.

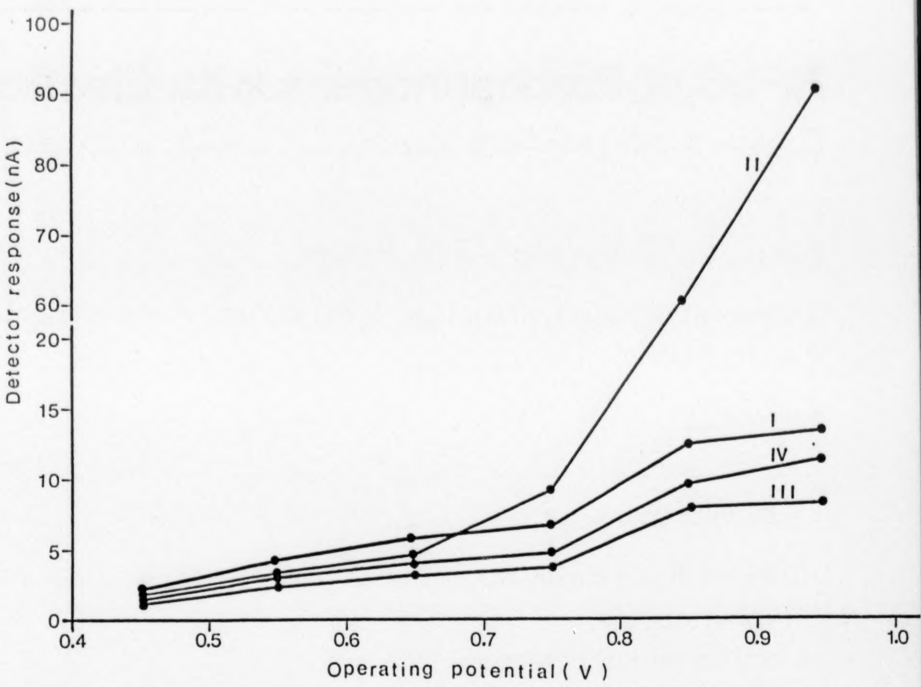

Fig. 4

Voltammograms for coproporphyrinogen I, II, III and IV isomers.

The electrochemical behaviour of porphyrinogens was investigated using the coproporphyrinogen isomers as examples. The voltammograms are shown in Fig. 4. All four isomers were detectable at a potential as low as + 0.45 V. Potentials of between + 0.65 and + 0.75 V were adequate for the sensitive (pmol) detection of the porphyrinogens without significant detector noise levels.

The stability of the porphyrinogens has been studied. Freshly prepared porphyrinogens were stable for at least 3 hours when kept on ice in the dark. The stability can be further improved by flushing the porphyrinogen solution with nitrogen and adding a small quantity of a reducing agent such as dithiothreitol. No significant decreased in peak height was observed when a coproporphyrinogen III solution containing dithiothreitol was analysed after storing in the freezer at − 30 °C for a week.

References

[1] *C. K. Lim, F. Li, T. J. Peters,* Biochem. J. **234,** 629 (1986).
[2] *F. Li, C. K. Lim, T. J. Peters,* Biochem. J. **239,** 481 (1986).
[3] *F. Li, C. K. Lim, T. J. Peters,* Biochem. J. **243,** 621 (1987).
[4] *F. Li, C. K. Lim, T. J. Peters.* Biochem. J. **243,** 863 (1987).
[5] *C. K. Lim, F. Li, T. J. Peters,* Biochem. J. in press (1987).
[6] *D. Mauzerall,* J. Am. Chem. Soc. **82,** 2605 (1960).
[7] *C. K. Lim, J. M. Rideout, D. J. Wright,* J. Chromatogr. **282,** 629 (1983).
[8] *D. J. Wright, J. M. Rideout, C. K. Lim,* Biochem. J. **209,** 553 (1983).

Received: Juni 30, 1987
Accepted: July 28, 1987
F

An Improved Approach for the Determination of Plasma-Free Catecholamines by HPLC-ED: Application to Normal and Hypertensive Patients

C. Lucarelli* / P. Betto / G. Ricciarello / M. Giambenedetti

Istituto Superiore di Sanità, V. le Regina Elena, 299; 00161 Roma, Italy

F. Sciarra / C. Tosti Croce / P. L. Mottironi

V^a Clinica Medica, Università di Roma, 00161 Roma, Italy

Key Words

Column liquid chromatography
Plasma catecholamines
Dual-step prepurification process
Electrochemical detection
Essential hypertension
Physical stress

Summary

A dual-step procedure for the rapid, quantitative isolation of free catecholamines (norepinephrine, epinephrine and dopamine) from plasma, using a little column of CM-Sephadex and alumina adsorption, is described. Sensitive high performance liquid chromatography is also discussed, employing an amperometric detector for the quantitative determination. The recovery of the three catecholamines, and of N-methyldopamine used as the internal standard, was about 70–80%; the detection limits were 2 pg for norepinephrine, 3 pg for epinephrine and 3 pg for dopamine. The combination of the rather specific and easy to handle two-step sample clean-up procedure, the high resolving power of the chromatography and the high sensitivity of electrochemical detection provided a simple method for the determination of free catecholamines in plasma samples of normal and essential hypertensive subjects under different conditions (supine position for 45 min, standing for 5 and 10 min). It was found that a significant increase in epinephrine levels ($P < 0.01$) occurred in hypertensive patients under the three conditions studied.

Introduction

It is well known that urinary levels of catecholamines (CA) and their metabolites are unable do determine fast modifications in Sympathetic Nervous System (SNS) activity produced by various ambiental factors, such as changing body position or other kinds of stress.

Several experimental studies [1–3] have shown good correlation between CA blood level and SNS activity; however, because of a wide variety of individual factors (age, emotional condition, etc.), a clear distinction between pathological and normal CA basal level ranges is sometimes very difficult to determine. In order to verify whether CA plasma level modifications produced by a simple change of body position constituted a clear discrimination between essential hypertensive and normotensive status, the development of a highly sensitive, reliable and inexpensive method for the measurement of CA concentrations in a large sample size was necessary.

The introduction of electrochemical detection coupled with HPLC has made the determination of the low concentration of catecholamines present in plasma possible. A very large number of assay procedures have been published, detailing the use of this methodology. However, there are still some problems associated with the sample clean-up procedure followed by the concentration.

Most commonly, CA's are concentrated and purified by adsorption on alumina and eluted with a small volume of acid [4–6]. The use of a one-step extraction procedure has proven inadequate because it produces chromatograms with extra peaks that interfere with the quantification [7–8]. Extensive purification by adsorption on alumina, combined with cation-exchange resin, has been used [9–13]. Recently, some promising sample clean-up methods have been described, using a complex formation of CA and diphenyl borate at high pH values [14–16]. Not even these methods, however, were selective enough, and an improvement was made through the introduction of a two-stage process of purification on a cationic little column [17–18]. Sample pretreatments have also been carried out, using on-line preconcentration and purification on small columns of alumina [19], cation-exchange [20], reverse-phase [21] and boronic acid-silica [22–23]. The on-line sample pre-treatment required two pumps, and two or more valves, and for the determination of CA in plasma, protein precipitation was necessary before the sample could be introduced into the system [19].

0009-5893/87 0423-04 $ 03.00/0

© 1987 Friedr. Vieweg & Sohn Verlagsgesellschaft mbH

Our aim was to develop a rapid and inexpensive procedure for the isolation of CA from plasma that could produce good recovery and that required relatively simple equipment.

Based on previous investigations [24–25], we evaluated a simultaneous dual-step pre-purification procedure involving the use of a weak-exchange resin and alumina. The weak cation-exchanger was found to be more selective than a strong cation exchanger [23], and alumina could be eluted with a small acid volume obtaining a very good sensitivity. The ion-exchanger Sephadex CM-A25 was particulary suitable, as it showed a very low non-specific adsorption [26]. We also tested the Bio-Rex 70 normally used in this step [27–32], but without very good results under our operative conditions.

Good recovery and reproducibility were obtained working with exact standard operative conditions, and the most important effect was the limited time needed for the two steps of pre-purification.

Samples of normal and untreated essential hypertensive patients obtained in supine (first) and standing (second) positions were subjected to the described dual-step pre-purification procedure and then analyzed by a high performance liquid chromatography coupled with an amperometric detector.

The results presented in this paper also show that a suitable method for revealing, minimum variations of CA plasma levels is indispensable to the further biochemical characterization of essential hypertension.

Experimental

Materials and Reagents

All reference and internal standards were from Sigma (St. Louis, USA). Acetonitrile (HPLC grade) came from C. Erba (Milan, Italy) and 1-Octane sulfonic acid from Fluka (Buchs, Switzerland). All other chemicals were of analytical grade and were obtained from C. Erba (Milan, Italy). Water was purified with a Milli-Q purification system from Millipore (Bedford, USA). The pre-concentration materials were: acid alumina AG-4 from Bio-Rad (Richmond, USA) and CM-Sephadex C-25 from Pharmacia (Uppsala, Sweden). The anticoagulant-antioxidant solution used for sampling was a constitute of EGTA (60 mg/ml) and reduced Glutathione (90 mg/ml), adjusted to a pH 7 with NaOH 0.1 M.

Chromatography

Equipment. HPLC: pump M-45 (Waters, Milford, USA) with Rheodyne 7125; injector and pulse damper Orlita. Detector: Amperometric, model 103 (Chromatofield Châteauneuf-les-Martigues, France) with a glassy-carbon electrode. Potential + 0.7V vs Ag/AgCl reference electrode.

Data acquisition: Computing integrator LCI-100 (Perkin-Elmer, Norwalk, USA)

Column. Nucleosil C_{18} 5 µm, mm 250 × 4 i.d. (Macherey-Nagel, FRG).

Eluent. 0.025 M sodium acetate adjusted to pH 3 with acetic acid, containing 0.2 mM 1-octane sulfonate, 0.3 mM EDTA and 5% (v/v) acetonitrile.

Flow. 1 ml/min.

Temperature. Room temperature.

Sampling Procedure

In order to avoid the CA contribution due to vein puncture stress, a Jelco 20-Gauge Teflon catheter was introduced in to the cubital vein of each one of the monitored patients. The first sample was drawn after 45 min of total relaxation. Two other samples were successively drawn after 5′ and 10 minutes spent in a standing position.

Blood samples were directly placed in tubes containing 20 µl of an EGTA-reduced Glutathion solution for each ml of blood. After immediate centrifugation, plasma was stored at −80 °C until analyzed.

Analytical Procedure

2 ml of plasma were mixed with 8 ml of a 0.1 M phosphate buffer (pH 7.0) and 20 µl of the internal standard solution (224 ng/ml NMDA), and applied to small polypropilene column filled with 2 ml of pre-swollen ion-exchanger Sephadex CM. Before use, the packed column was washed with 10 ml of 0.1 M phosphate (pH 7.0). After the samples had been tested, the column was rinsed with 10 ml of distilled water and 4 ml of 0.1 M perchloric acid.

The catecholamines were eluted with 3 ml of 0.5 M perchloric acid, and the eluate was collected in 15 ml conical tubes. 2 ml of Tris buffer (1.5 M, pH 9.3), containing 0.06 M EDTA and 20 mg of alumina (activated as described by Anton and Sayre [23], were added. The tube was vortex-mixed for 2′. The supernatant was removed by aspiration, and the alumina was washed twice with 2 ml of water, centrifuging between each wash (3000 × g, 3′).

After the second washing, as much water as possible was removed by aspiration and by drying the wall tube with little stripes of filter paper. The catecholamines were eluted from the alumina with 100 µl of 0.1 M acetic acid after vortex-mixing for 2′. After centrifugation, the supernatant was removed and 25 µl were injected into the chromatograph.

Results and Discussion

Side (b) of Fig. 1 shows a chromatogram of a mixture of standards of NE, E, DA and NMDA (internal standard). As can be seen, all compounds are conveniently separated. The isolation of catecholamines from plasma was also complete, as shown in side (a). No detectable interfering substances were observed in the chromatogram.

Linearity response of NE, E and DA was performed by testing the described purification procedure first with acqueous standards, and then by adding known amounts of the compounds to a pooled sample of plasma. In both testing methods, the detector response was linear for all the

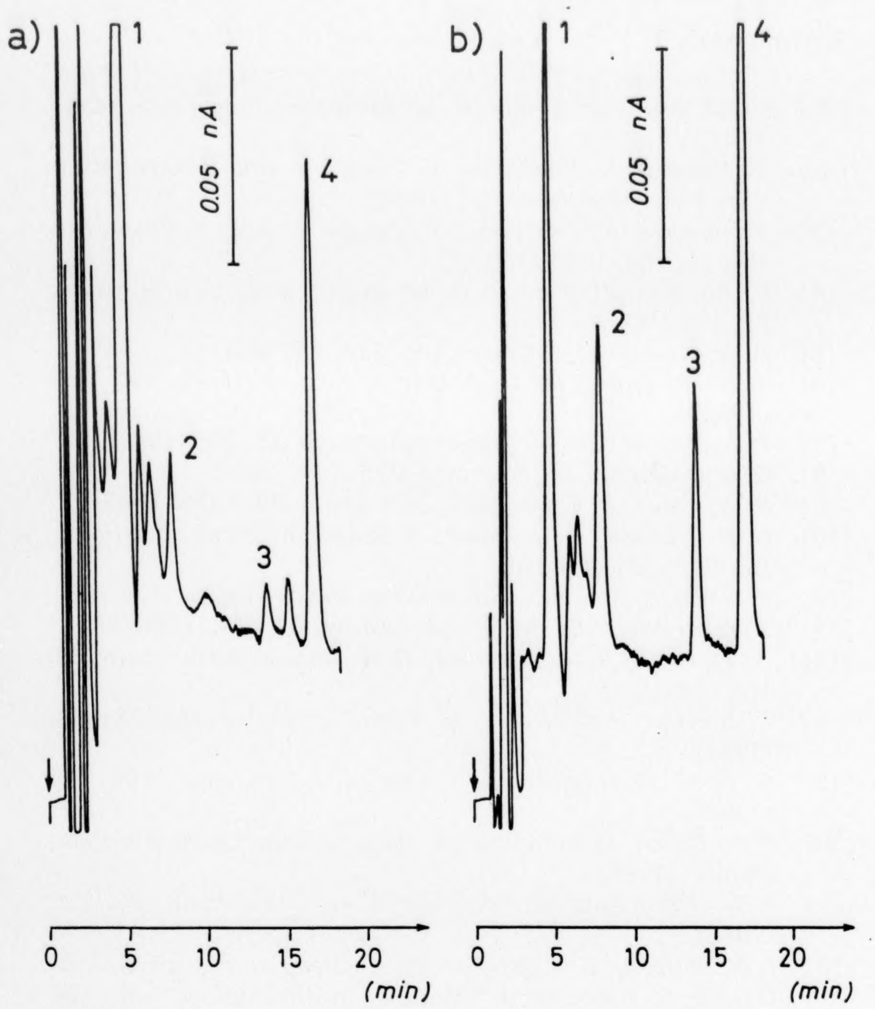

Fig. 1

HPLC analysis of NE, E and DA with electrochemical detector: (a) extract from an essential hypertensive patient sample; (b) synthetic mixture of 85, 102, 73, 402 pg of NE (1), E (2), DA (3), DHBA (4) respectively.

Chromatographic conditions: column, Nucleosil C_{18} 5μm; mobile phase 0.025M sodium acetate adjusted to pH 3 with acetic acid containing 0.2M 1-octane sulfonate, 0.3 mM EDTA and 5% (v/v) acetonitrile; flow rate 1 ml/min; applied potential +0.7 V vs. Ag/AgCl reference electrode.

Tabelle II. Recovery of catecholamines added to plasma pool.

Catecholamine	Catecholamine amount (pg/ml)			Mean recovery (%)
	Plasma	Spike	Plasma + spike (found)	
NE	171	42.5	166.7	78.1
	171	85.0	188.1	77.4
	171	170.0	277.6	81.4
E	86	51.2	111.4	81.2
	86	102.4	156.0	82.8
	86	204.8	228.9	78.7
DA	23	36.8	42.7	71.4
	23	73.5	71.9	71.5
	23	147.0	130.4	76.7
NMDA	–	210.0	161.0	76.7
	–	420.0	324.7	77.3
	–	840.0	637.7	80.2

Each value is the average of three runs

Table III. Reproducibility of the method for the determination of catecholamines in plasma.

Catecholamine	Plasma (pg/ml) n = 6	CV
NE	340.6 ± 11.1	3.2
E	247.8 ± 17.3	7.0
DA	59.4 ± 1.9	3.4
NMDA	294.9 ± 11.8	4.0

compounds. Table I shows the regression lines for the three catecholamines.

After analysing the samples throughout the complete procedure, the recovery of the developed pre-purification protocol was tested by spiking a plasma pool with known amounts of the three catecholamines and with the internal standard (NMDA). The concentrations found were corrected for endogenous concentrations determined in parallel experiments with unspiked plasma. The results are shown in Table II and indicate that the procedure is satisfactory.

The reproducibility of the proposed method was established by the purification of a plasma pool. The catecholamine levels, including the standard deviation, are given in Table III.

The described method has been used for monitoring CA plasma levels of 12 normotensive subjects (n.s.) and 14 essential hypertensive patients* (e.h.p.) in three different situations: after resting in a supine position for 45 min, and after standing for 5 and 10 minutes.

Plasma samples obtained by following the reported procedure were subjected to the described dual-step pre-purification method to be chromatographed under experimental conditions.

Results reported in Fig. 2 show that the behaviour of level variations is different for each of the three CA's.

Table I. Linearity of response of catecholamines as a function of concentration.

Catecholamine	Range tested (pg)	Regression equation		Correlation coefficient	
		Standard	Spiked plasma	Standard	Spiked plasma
NE	21.2–340.0	y = 3.05x + 1.6	y = 2.84x + 27.3	0.9996	0.9984
E	26.5–409.6	y = 9.29x – 2.6	y = 9.61x + 91.1	0.9992	0.9985
DA	18.4–294.0	y = 7.22x + 1.5	y = 7.10x + 5.8	0.9999	0.9485

y = NE, E or DA peak height; x = NE, E or DA amount (pg).

---

* deprived of every anthihypertensive pharmacological theraphy since 20 days at least

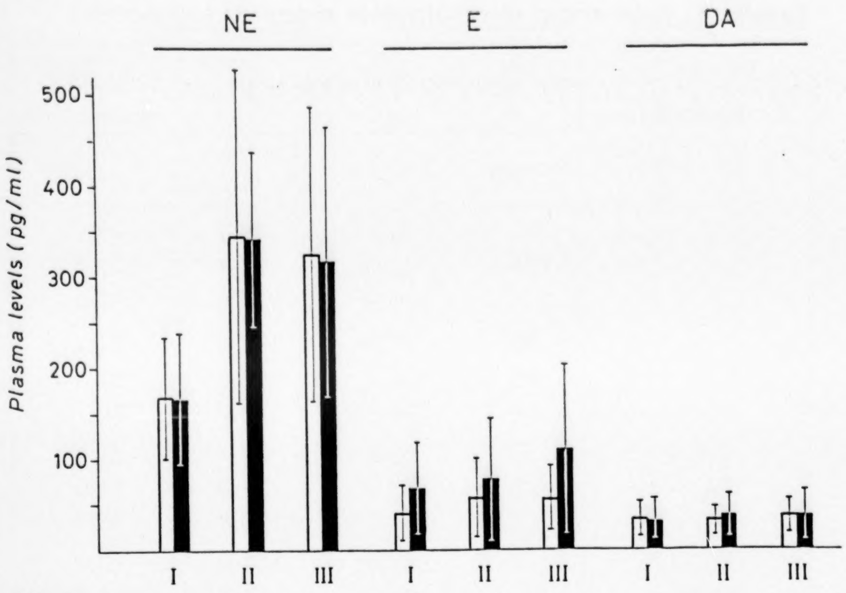

Fig. 2

Behaviour of dopamine (DA), epinephrine (E) and norepinephrine (NE) levels in a supine position (I) and after 5 (II) to 10 (III) minutes of standing in 12 normotensive (white) and 14 hypertensive patients (black). By comparing the different positions it is possible to observe that E is the only catecholamine whose corresponding levels increase differently in the two groups.

In both groups (n.s. and e.h.p.), NE levels show a remarkable increase (105.30% and 106%, respectively, with $P < 0.001$) after 5 min of standing, while DA levels do not increase significantly. In n.s., E levels show a significant increase after 5 min of standing (37% with $P < 0.001$), and only after 10 min of standing in e.h.p. (62% with $P < 0.001$). By comparing corresponding data for n.s. and e.h.p. it is possible to see that NE and DA plasma levels are not substantially different, while E levels are higher in e.h.p. than those in n.s.

Conclusion

The described dual step pre-purification procedure is an essential part of the whole analytical method and appears sufficiently simple, sensitive and reliable to measure CA concentrations in a high number of samples within a reasonable time. This, coupled with a very strict sampling procedure, allows the determination of quick (and sometimes very small) changes in CA plasma levels, even those caused by such little a stress as rising and standing for 5 and 10 min time periods.

Moreover, under the reported experimental conditions, only modifications in levels of E appear capable of discriminating essential hypertensive from normotensive status.

Acknowledgement

We are thankful to Prof. G. P. Cartoni from the Chemistry Department of Rome University for the precious collaboration.

References

[1] *C. Mörlin, G. B. Wallin, B. M. Ericksson*, Acta Fisiol. scand. **119**, 117 (1983).
[2] *Y. Kawano, K. Fukiyama, Y. Takeya, I. Abe, T. Omae*, Clin. Exp. Hypertens. **A6**, 1131 (1984).
[3] *Y. Kawano, K. Fukiyama, Y. Takeya, I. Abe, T. Omae*, Am. Heart J. **104**, 1351 (1982).
[4] *P. Boulaux, D. Perrett, G. M. Besser*, Ann. Clin. Biochem. **22**, 194 (1985).
[5] *A. M. Krstulovic*, J. Chromatog. **229**, 1 (1982).
[6] *J. M. P. Holly, H. L. J. Makin*, Anal. Biochem. **128**, 257 (1983).
[7] *P. F. Maycock, K. N. Frayn*, Clin. Chem. **33**, 286 (1987).
[8] *D. S. Goldstein*, J. Chromatog. **275**, 174 (1983).
[9] *K. N. Frayn, P. F. Maycock*, Clin. Chem. **29**, 1426 (1983).
[10] *G. P. Jackman, C. J. Oddie, H. Skews, A. Bobik*, J. Chromatog. **308**, 301 (1984).
[11] *E. Gerlo, R. Malfait*, J. Chromatog. **343**, 9 (1985).
[12] *A. H. B. Wu, T. G. Gornet*, Clin. Chem. **31**, 298 (1985).
[13] *G. C. Davis, P. T. Kissinger, R. E. Shoup*, Anal. Chem. **53**, 156 (1981).
[14] *F. Smedes, J. C. Kraak, H. Poppe*, J. Chromatog. **231**, 25 (1982).
[15] *G. Rossi, O. Doppieri, A. C. Pessina*, J. Chromatog. **380**, 117 (1986).
[16] *H. J. Bauch, V. Kelsch, W. H. Hauss*, J. Clin. Chem. Biochem. **24**, 651 (1986).
[17] *I. A. Macdonald, D. M. Lake*, J. Neurosci. Meth. **13**, 239 (1985).
[18] *I. N. Mefford, E. J. Caligiuri, R. K. Grady Jr, P. Capella, I. A. Durkin, P. Chevalier* in "Methods in Enzymology" vol. **126** (1986) p. 402
[19] *B. Neidhart, K. P. Kringe, C. Lippmann, P. Deutschmann.* Vorträge anläßlich der Königsteiner Chromatographie-Tagung, 6. Diskussion Tagung über Hochleistungs-Flüssigkeit-Chromatographie. October 4–6, 1982, Travenünde Waters GmbH. Königstein. 1982, p. 151
[20] *A. Yamatodani, H. Wada*, Clin. Chem. **27**, 183 (1981).
[21] *D. D. Koch, P. T. Kissinger*, Anal. Chem. **52**, 27 (1980).
[22] *C. Lucarelli, P. Betto, G. Ricciarello*: "Picogram level determination of biogenic amines in plasma by Ion Pair HPLC with high sensitivity electrochemical detection." (poster). Presented at Eighth International Symposium on Column Liquid Chromatography. New York City, NY, USA May 20–25, 1984.
[23] *C. Lucarelli, P. Betto, G. Ricciarello, F. Sciarra, C. Tosti Croce*, Giornale Italiano di Chimica Clinica (in press).
[24] *L. Hansson, M. Glad, C. Hansson*, J. Chromatog. **265**, 37 (1983).
[25] *K. Kemper, E. Hegemeier, K. S. Boos, E. Schlimme*, J. Chromatog. **336**, 374 (1984).
[26] *F. Degel, P. Zuman, P. Sandik, G. Gilch*, Clin. Chem. **33**, 108 (1987).
[27] "Ion Exchange Chromatography" Pharmacia Fine Chemicals
[28] K. Oka, K. Kojima, A. Togari, T. Nagatsu, J. Chromatog. **308**, 43 (1984).
[29] *N. C. Parker, C. B. Levtzow, P. W. Wright, L. L. Woodard, J. F. Chapman*, Clin. Chem. **32**, 1473 (1986).
[30] *J. Joune, J. Martineau, N. Mariotte, C. Barthelemy, J. P. Muh, G. Lelord*, J. Chromatog. **378**, 437 (1986).
[31] *J. Odink, H. Sandman, W. H. P. Schreurs*, J. Chromatog. **377**, 145 (1986).
[32] *B. H. C. Westerink, N. Tenkate*, J. Clin. Chem. Clin. Biochem. **24**, 513 (1986).
[33] *A. H. Anton, D. F. Sayre*, J. Pharmacol. Exp. Ther. **138**, 360 (1962).

Received: June 30, 1987
Accepted: Aug. 5, 1987
F

Study on Optimal Packing Materials for High-Performance Hydrophobic-Interaction Chromatography of Proteins

T. Ueda* / Y. Yasui / Y. Ishida

R/D Engineering Department, Analytical Instruments Division, Shimadzu Corporation, 1 Nishinokyo-kuwabaracho,
Nakagyo-ku, Kyoto 604, Japan

Key Words

Hydrophobic-interaction chromatography
Silica-based packings
Protein retention
Thermal behavior

Summary

The nature and effects of bonded phases and analytical conditions on protein retention in high-performance hydrophobic-interaction chromatography (HIC) were investigated. Silica-based packing materials with different surface hydrophobicity were prepared and evaluated with respect to protein retention. The contact of proteins with the hydrophobic stationary phases caused conformational changes of proteins to some extent, but the extent of these changes was dependent on the hydrophobicity of the stationary phases, column temperature and the proteins themselves. Thermal behavior of some proteins in HIC on these phases is also shown.

Introduction

Hydrophobic-interaction chromatography (HIC) is a useful technique for analyzing proteins, enzymes, and nucleic acids, which complements ion-exchange, gel filtration, and reversed-phase chromatography. In HIC, the separation of sample components is based on the differences in the hydrophobic interaction between the packing material and sample molecules. An alternative method which separates proteins according to their hydrophobicity is reversed-phase chromatography (RPC), but in RPC most proteins elute in a denatured state due to the use of organic solvents containing acidic eluents. In contrast with RPC, HIC is based on a mild separation process which employs salt gradients of decreasing ionic strength. Therefore, HIC is expected to be suitable for preparative protein purification. Support materials for HIC were first synthesized by linking alkylamines to agarose gels in the early 1970's [1]. Much work has been carried out on the fractionation of protein mixtures by means of HIC ever since.

HIC in the high-performance mode is rapidly advancing aspect of HPLC separation of biopolymers. Recently, some packing materials have been developed specifically for high-performance HIC [2–10]. It should be recognized, however, that protein structural changes can occur even in HIC, depending on the nature of the bonded phase, analytical conditions (i.e., the mobile phase composition and pH or the column temperature, etc.) and the proteins themselves. Goheen and Engelhorn [11] demonstrated the band broadening of some protein peaks with the Bio-Gel TSK Phenyl-5PW column. They attributed the results to the influence of the eluent on protein structure. Ingraham et al. [12] also found the Bio-Gel TSK Phenyl-5PW column could promote denaturation of protein structure despite the relatively gentle hydrophobic packing material. They noted that the possibility of protein denaturation has to always be taken into consideration when a hydrophobic column is used, because the higher-order structures of most proteins are stabilized by internal hydrophobic interaction which can be destabilized by competitive hydrophobic interaction with the support materials. Therefore, it must be realized that chromatographic conditions in HIC may affect conformational changes of some proteins during the separation process.

This report examines the nature and effects of the bonded phase and analytical conditions on retention and protein denaturation. Support materials were prepared by chemically bonding alkyl moeties to hydrophilic polymer which was covalently bonded to mesoporous silica. The influence of ligand length and ligand density on retention and protein denaturation is discussed. Thermal behavior of some proteins on these phases is also shown.

Experimental

Preparation of Packing Materials

The preparation of silica-based packing materials for HIC consisted of a two-step procedure. First, hydrophilic polymer layers were chemically bonded to the silica surface to

0009-5893/87 0427-06 $03.00/0 © 1987 Friedr. Vieweg & Sohn Verlagsgesellschaft mbH

cover the silanol groups and to stabilize the silica material in the aqueous mobile phase as described previously [14]. Secondly, alkyl ligands were chemically bonded to this stabilized silica surface under controlled reaction conditions. All materials were packed into 50 × 4-mm i.d. stainless-steel tubes. Spherical silica gel used in this study had a particle size of 5μm and pore size of 300 Å.

Table I lists the different alkyl phases used in this study. The hydrophobicity of these bonded phases was evaluated with the capacity factor (k'_A) of anthracene. The values of k'_A were determined under the isocratic conditions of 60% methanol in water as a mobile phase at 40°C. A hold-up time (t_0) was measured with the retention time of uracil. Since an increased k'_A value represents the more hydrophobic surface, the surface hydrophobicity of these phases can be characterized with these k'_A values. A systematic increase in k'_A value from C1 to C3-1 (Table I) indicates an increase in ligand hydrophobicity from methyl to n-propyl groups. A gradual increase in k'_A value from C3-1 to C3-4 is caused by an increase in ligand density. In contrast with RPC materials, the ligand density of packing material in HIC is too low to quantify it precisely with elemental analysis. (Assuming that the ligand density is 0.1 μmole/m^2 and the specific surface area of 300 Å-pore size silica is approximately 100 m^2/g, an increase in C% caused by the introduction of n-propyl group leads to only 0.04%.) Therefore, these values of k'_A were used as the indices of hydrophobicity of these HIC materials. The C2 and C3-1 columns are now commercially available from Shimadzu Corporation (Kyoto, Japan) under the tradename of Shim-pack HPC-C2 and HPC-C3, respectively.

Instrumentation

HIC columns were tested on an LC-6A liquid chromatograph system (Shimadzu Corporation, Kyoto, Japan), consisting of two Model LC-6A solvent delivery pumps, an SCL-6A system controller, a SIL-6A autoinjector, a CTO-6A column oven, an SPD-6A spectrophotometric detector, and a C-R3A data processor. A precolumn (50 × 4 mm i.d.) containing 10-μm DIOL material was connected between the pumping system and autoinjector for HIC separation. A gradient delay volume of 2.5 ml was observed for this system.

Chemicals

All reagents were of the highest purity available. Mobile phases were prepared by adding the correct weight of salt and buffer to a volumetric flask, containing HPLC-grade water. All buffers for HIC were passed through 0.22-μm filters. All proteins were purchased from Sigma (St. Louis, MO, U.S.A.). :cytochrome C (type IV, from horse heart), myoglobin (type II, from sperm whale skeletal muscle), β-lactoglobulin (from bovine milk), α-lactalbumin (from bovine milk), lysozyme (from chicken egg white), ovalbumin, transferrin (human), α-chymotrypsinogen A (from bovine pancreas), ribonuclease A (from bovine pancreas), carbonic anhydrase (from bovine erythrocytes), and trypsin inhibitor (from soybean).

Table I. Characteristics of alkyl-bonded phases

Phase	Alkyl group	k'_A
C1	Methyl	0.95
C2	Ethyl	1.25
C3-1	n-Propyl	1.53
C3-2	n-Propyl	1.91
C3-3	n-Propyl	2.40
C3-4	n-Propyl	2.71

* k'_A is measured by injecting 0.01 % solution of anthracene under isocratic conditions. See experimental section.

Results and Discussion

The surface stabilized silica-based materials used in this experiment were quite stable as described previously [14] and no changes were observed during this study with respect to sample retention and peak shapes. Packing material pore size may affect protein retention. It should be noted that the specific surface area of silica gel decreases as the pore size increases. Protein penetration into the pore structure of silica gel is enhanced with increasing pore size, but it is difficult to control the ligand density of the stationary phase due to the concomitant reduction in surface area. A silica gel of 300-Å pore size proved to be an acceptable compromise with regard to protein penetration vs. specific surface area in this study.

Effect of the Hydrophobicity of the Stationary Phases on Protein Retention

The hydrophobicity of the stationary phases influenced protein retention. Alkyl groups of different chain lengths were introduced to the silica surface (under controlled reaction conditions), because the surface hydrophobicity of packing material depends not only on ligand density but on alkyl chain length as well. As seen in Fig. 1, the retention time and resolution of proteins increased as the alkyl chain length increased in agreement with other results [3, 15]. However, considerable negative effects were observed in the retention of α-lactalbumin and in the mass recovery of lactate dehydrogenase with the longer alkyl chain lengths. First, α-lactalbumin was not eluted from the column packed with n-propyl or longer materials at 35°C. Similar results were reported by Kato et al. [6] regarding the chromatographic profiles of α-lactalbumin and they pointed to the differences between Ether-5PW and Phenyl-5PW materials in HIC. Karger et al. [13, 16] have studied the thermal behavior of α-lactalbumin on the C1-ether phase in HIC and noted that chromatographic behavior of this protein was a sensitive function of column conditions because it is relatively labile and the thermal denaturation transition temperature is approximately 40°C. Consequently, as the stationary phase became more hydrophobic, α-lactalbumin was more likely to unfold and to be adsorbed to the stationary phase irreversibly. Second, separate experiments revealed that the mass recoveries of lactate dehydrogenase from the C2 and C3-1 columns were 100% and 82%, respectively. Although the better resolution of a mixture of proteins is achieved

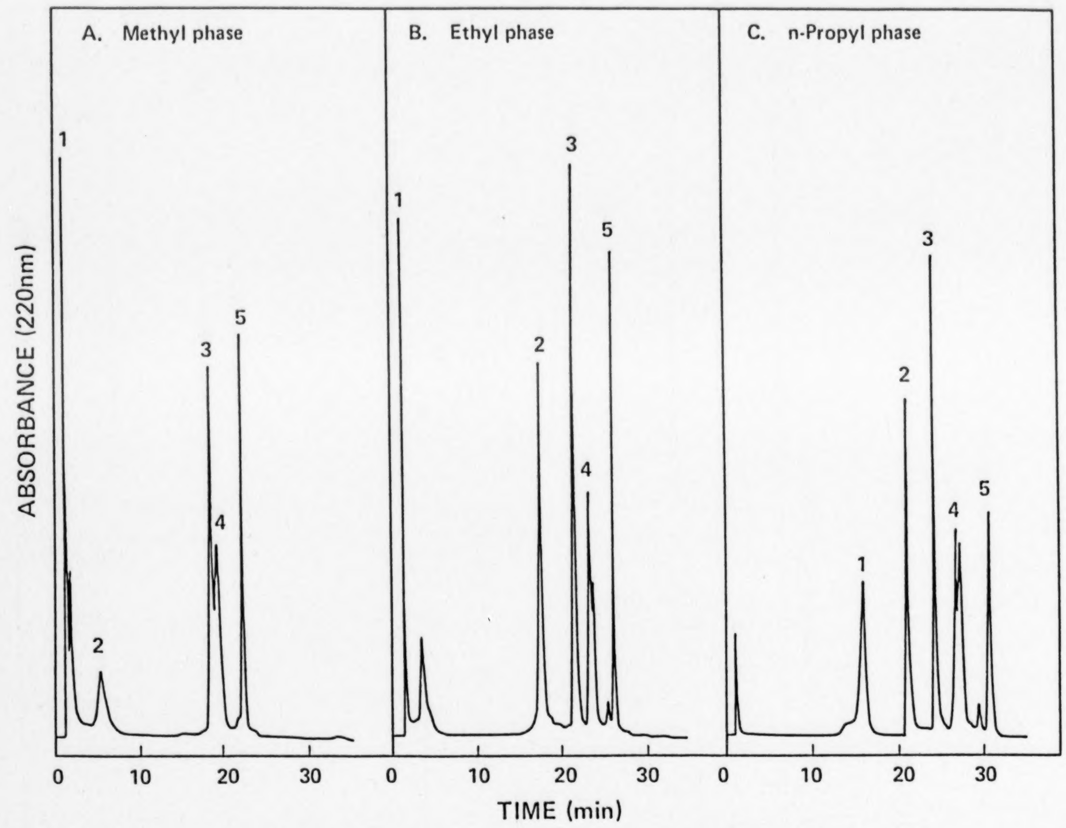

Fig. 1

Effect of alkyl chain length on protein retention.

The proteins were separated in a 20-min linear gradient from 2.5M ammonium sulfate in 0.1M phosphate buffer (pH 7.0) to 0.1M phosphate buffer (pH 7.0) at 35°C and a flow-rate of 0.5ml/min. Standard proteins: **1** = cytochrome C; **2** = myoglobin; **3** = lysozyme; **4** = ovalbumin; **5** = α-chymotrypsinogen A.

In chromatogram A, the alkyl chain on the stationary phase is methyl, in B it is ethyl, and in C it is n-propyl.

on the C3-1 column than the C2 column, some proteins may be adsorbed irreversibly on the C3-1 phase and this will result in poor mass recovery.

Ligand density of packing material also influenced protein retention. Four packing materials with different n-propyl ligand densities were prepared and evaluated chromatographically. The values of k'_A on the C3-1, C3-2, C3-3 and C3-4 columns were 1.53, 1.91, 2.40 and 2.71, respectively (Table I). As mentioned, an increase in the retention of anthracene indicates an increase in n-propyl ligand density. Protein retention on these columns was investigated to clarify the effect of ligand density on chromatographic profiles of proteins in HIC. Protein retention also increased as the ligand density of the packing material increased, as shown in Fig. 2. It is interesting to note that transferrin was eluted earlier than carbonic anhydrase from the C3-1 and C3-2 columns of lower ligand densities but the elution order of these proteins was reversed on the C3-4 column of higher ligand density. These phenomena may reflect the differences in the extent of conformational changes of these proteins. When protein molecules come into contact with the hydrophobic stationary phase, they may become unfolded to some extent. The extent of this conformational change will be dependent on the lability of the protein and the hydrophobicity of the stationary phase. The inversion of elution order between transferrin and carbonic anhydrase at higher ligand density may be ascribed to the difference in the lability of the proteins themselves, which are in contact with the hydrophobic stationary phase.

Fig. 3 shows the chromatographic profiles of β-lactoglobulin on the n-propyl phases with different ligand densities. β-Lactoglobulin was not eluted from the C3-3 and C3-4 columns with excessive ligand densities during the HIC gradient. The band broadening of this protein may be attributed to its conformational lability even at the lower ligand density. Alpert [10] has referred to a single broad peak caused by the average of the forms in equilibrium between the native and denatured forms of protein. Similar phenomena with respect to the influence of phenyl ligand density on protein retention were observed by Regnier et al. [17]. They noted that the peaks of proteins became somewhat sharper as the phenyl ligand density decreased,

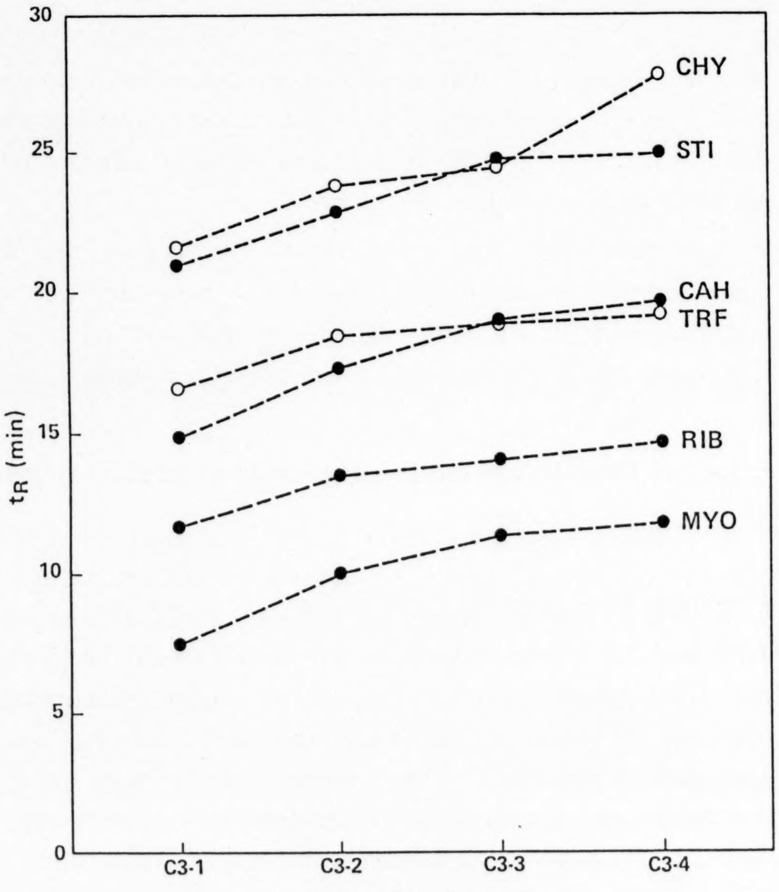

Fig. 2

Effect of n-propyl ligand density on protein retention.

Proteins were eluted in a 20-min linear gradient from 2.0M ammonium sulfate in 0.1M phosphate buffer (pH 7.0) to 0.1M phosphate buffer (pH 7.0) at 35°C and a flow-rate of 1.0ml/min. Abbreviations: MYO = myoglobin; RIB = ribonuclease A; TRF = transferrin; CAH = carbonic anhydrase ; STI = soybean trypsin inhibitor; CHY = α-chymotrypsinogen A.

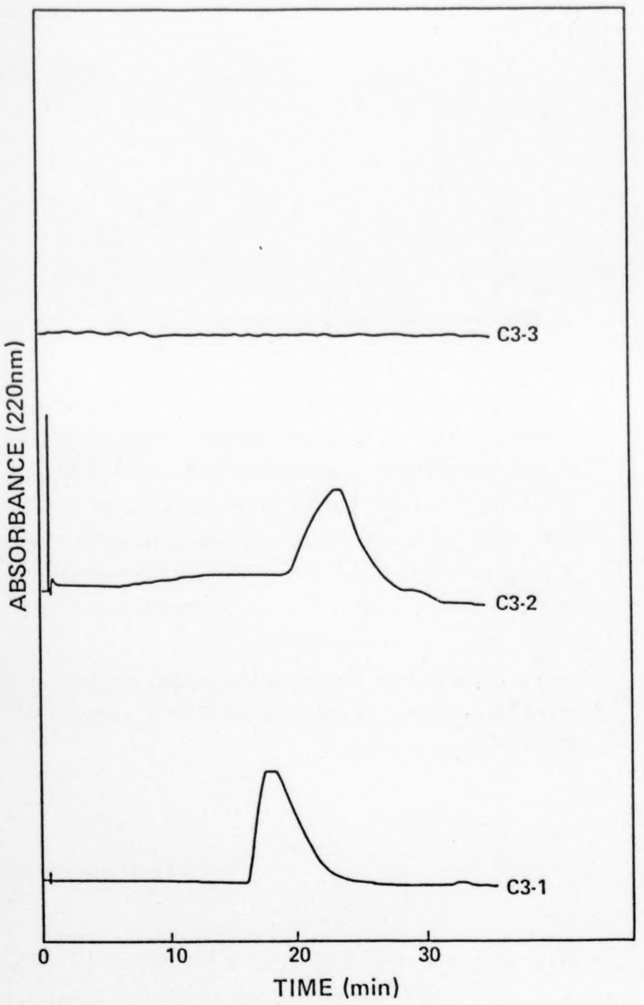

Fig. 3

Effect of n-propyl ligand density on the chromatographic profiles of β-lactoglobulin.

Chromatographic conditions are as in Fig. 2. Column numbers are indicated to the right of each profile.

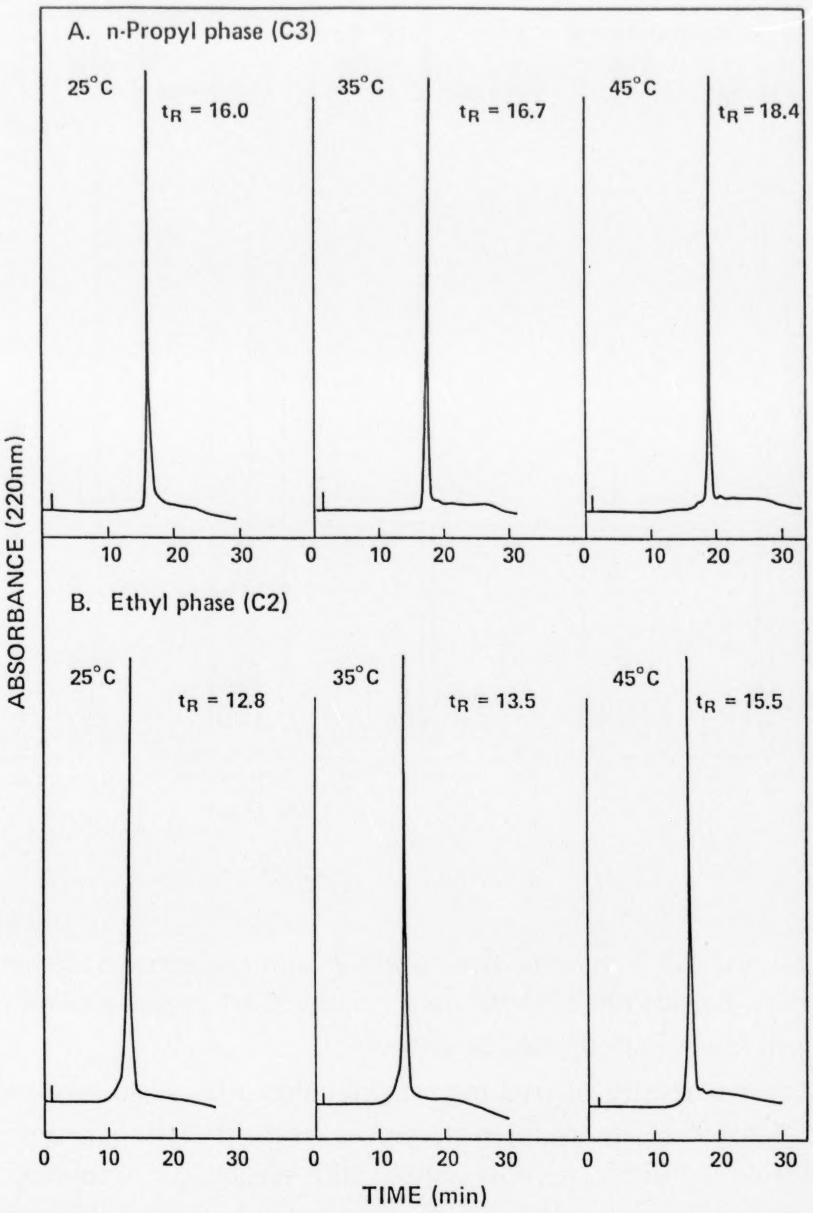

Fig. 4

Effects of temperature and stationary phase on the HIC elution profiles of cytochrome C.

A 20-min linear gradient was run from 3.0M ammonium sulfate in 0.1M phosphate buffer (pH 7.0) to 0.1M phosphate buffer (pH 7.0) at a flow-rate of 0.5ml/min. Column temperatures are indicated to the left of each profile.

but the resolution was lost due to decreased retention and/or loss of selectivity. These results indicate that partial denaturation of sample proteins can occur in contact with packings of higher ligand densities.

It was concluded that both ligand hydrophobicity and ligand density must be optimized so as to prepare packing materials suitable for HIC, taking into account the type of stationary phase applicable to practical separations.

Effect of Temperature on the Elution Profiles of Proteins

The effect of temperature on the retention of several proteins on the C2 and C3-1 columns is shown in Figs. 4, 5, 6, and 7. The k'_A values on the C2 and C3 phases were 1.25 and 1.53, respectively, as listed in Table I. Therefore, the C3-1 phase can be considered more hydrophobic than the C2 phase in this experiment, reflecting the ligand hydrophobicity itself. The retention of proteins in HIC was found to increase with an increase in column temperature [5, 13, 16], in contrast with the effects found in RPC. As can be seen in these figures, thermal behavior of proteins in HIC on these phases was classified into four types, as defined in the following.

The retention of cytochrome C on both phases increased as the column temperature increased, holding a sharp peak (Fig. 4). Compared with the other proteins, cytochrome C has a hydrophilic exterior and interacts weakly with the hydrophobic surface of each phase. Although the retention can be increased with an increase in the salt concentration of the initial buffer, thermal effect is not critical with regard to band broadening.

Fig. 5 shows the thermal behavior of β-lactoglobulin. It is interesting that the retention times of this protein at the three temperatures are almost the same on the C2 phase and the protein was eluted as a sharp peak. On the other hand, considerable changes were observed in both retention time and peak shape on the C3-1 phase. As shown in Fig. 5A, there is a slight increase in retention time from 25°C to 35°C, followed by a considerable change in retention from 35°C to 45°C. This trend on the C3-1 phase is suggestive of some conformational change of β-lactoglobulin at higher temperatures [13].

The thermal behavior of myoglobin is shown in Fig. 6. In this case, two peaks were observed at higher temperatures on the C3-1 phase. The first peak, which is seen at 35°C in Fig. 6A, may be ascribed to the native form of myoglobin and the latter peak to the denatured form. The native and denatured forms can be resolved if conformational equilibrium is slow relative to the time scale of migration through the column [10]. The difference in the retention times

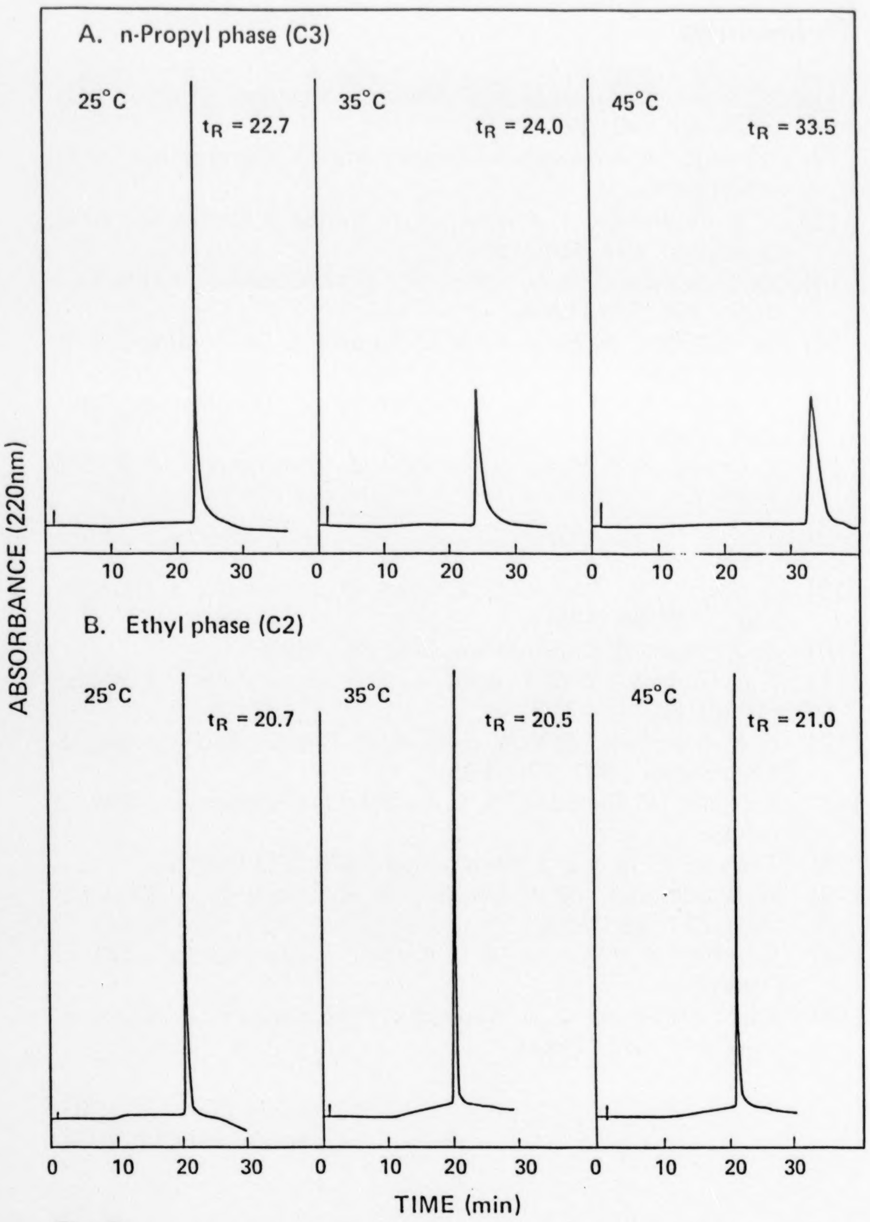

Fig. 5

Effects of temperature and stationary phase on the HIC elution profiles of β-lactoglobulin.

Chromatographic conditions are as in Fig. 4.

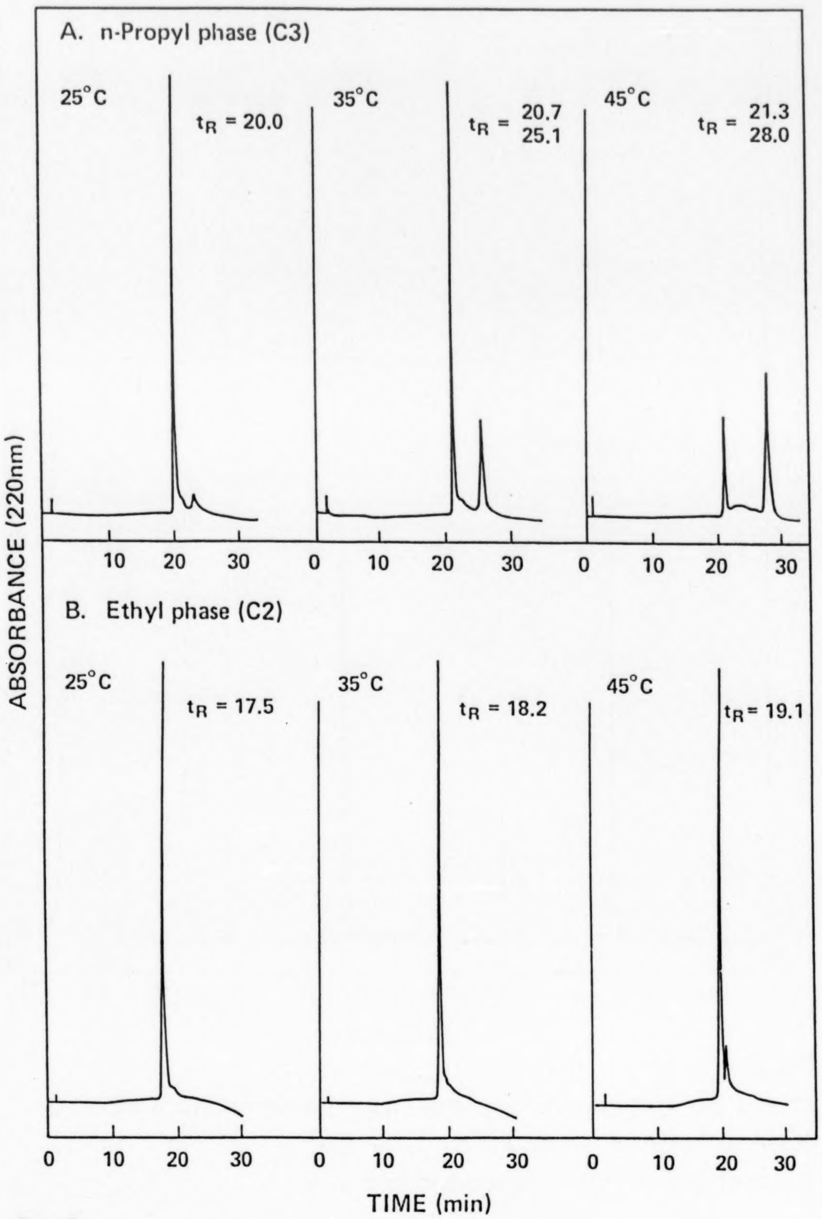

Fig. 6

Effects of temperature and stationary phase on the HIC elution profiles of myoglobin.

Chromatographic conditions are as in Fig. 4.

between two peaks increased as the column temperature increased. Moreover, the latter peak became taller than the first peak concomitantly with an increase in temperature. These results indicate that the conformational changes are induced by the elevated temperature and the contact with the more hydrophobic stationary phase. Nevertheless, the chromatographic profiles were almost identical from 25°C to 45°C on the ethyl phase, although a small shoulder peak was observed at 45°C.

Conspicuous effects of temperature and stationary phase were observed on the elution profiles of α-lactalbumin (Fig. 7). α-Lactalbumin was eluted in sharp peaks from the C2 phase at 25°C and 35°C, but in a broad peak at 45°C. Since the thermal denaturation transition temperature is approximately 40°C for α-lactalbumin in aqueous solution at pH 7 [10], the band broadening observed at 45°C on the C2 phase is most likely due to the partial conformational change of the protein. In contrast with the result on the C2 phase, α-lactalbumin was eluted in a heavily tailing peak from the C3-1 column at 25°C, but not eluted above 35°C. This behavior suggests that the contact of the protein with the more hydrophobic stationary phase will lead to the partial denaturation of the protein even at room temperature.

Since higher-order structures of most proteins are stabilized by hydrophobic interaction, the extent of hydrophobic interaction between the proteins and the surface of the packing material may weaken the structural stability of the proteins. It is apparent from these figures that an increase in the column temperature enhances the binding of the proteins to the hydrophobic matrices. Therefore, the utilization of lower column temperature can significantly suppress protein denaturation in HIC on the C3-1 phase. It was concluded that the thermal behavior of protein in HIC depended on both the stationary phase and the proteins themselves.

Conclusion

It is important to select optimal packing material for HIC separation, because the hydrophobicity of stationary phase influences protein retention regarding the retention time and peak shape. Optimal packing material for a given HIC separation is highly dependent on external hydrophobicity and conformational lability of proteins. Effect of column temperature on protein retention has proven critical on more hydrophobic packing materials.

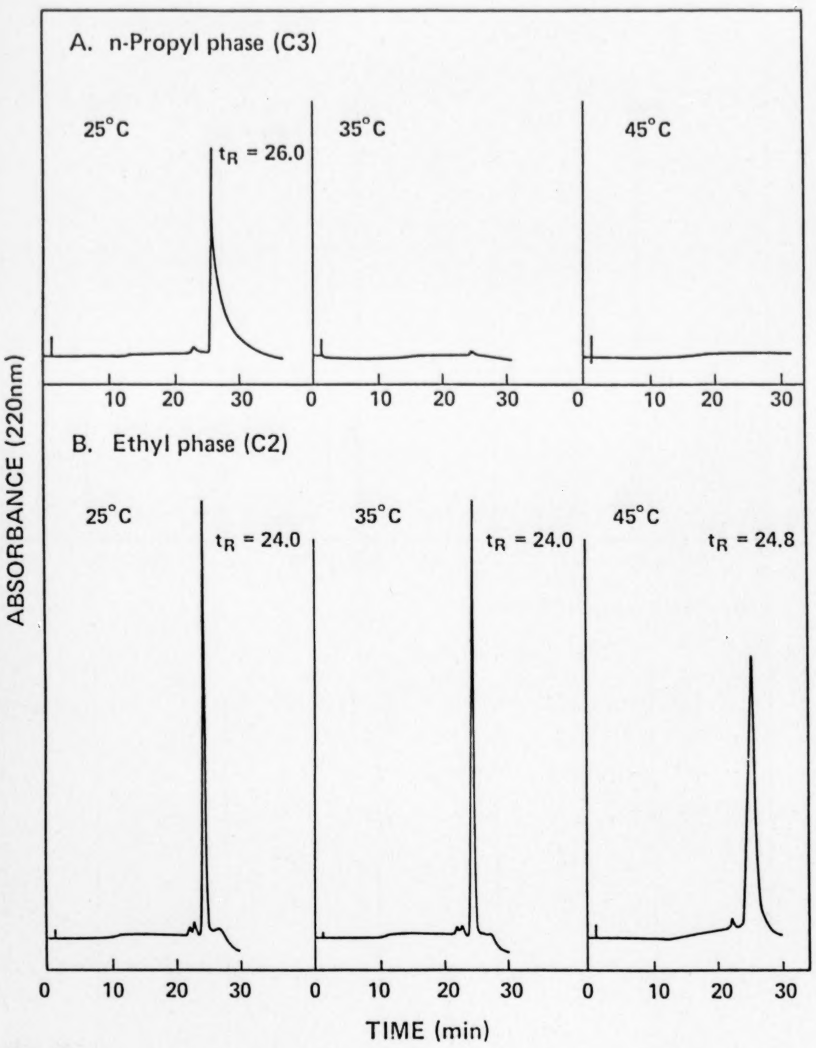

Fig. 7

Effects of temperature and stationary phase on the HIC elution profiles of α-lactalbumin.

Chromatographic conditions are as in Fig. 4.

References

[1] *Z. Er-el, Y. Zaidenzaig, S. Shaltiel*, Biochem. Biophys. Res. Commun., **49**, 383 (1972).
[2] *Y. Kato, T. Kitamura, T. Hashimoto*, J. Chromatogr., **292**, 418 (1984).
[3] *J. L. Fausnaugh, E. Pfannkoch, S. Gupta, F. E. Regnier*, Anal. Biochem., **137**, 464 (1984).
[4] *D. L. Gooding, M. N. Schmuck, K. M. Gooding*, J. Chromatogr., **296**, 107 (1984).
[5] *M. T. Miller, B. Feibush, B. L. Karger*, J. Chromatogr., **316**, 519 (1985).
[6] *Y. Kato, T. Kitamura, T. Hashimoto*, J. Chromatogr., **360**, 260 (1986).
[7] *J. Chang, Z. E. Rassi, C. Horváth*, J. Chromatogr., **319**, 396 (1985).
[8] *H. Engelhardt, U. Schön*, J. Liq. Chromatogr., **9**, 3225 (1986).
[9] *S. Hjerten, K. Yao, K. O. Erikson, B. Johansson*, J. Chromatogr., **359**, 99 (1986).
[10] *A. J. Alpert*, J. Chromatogr., **359**, 85 (1986).
[11] *S. C. Goheen, S. C. Engelhorn*, J. Chromatogr., **317**, 55 (1984).
[12] *R. H. Ingraham, S. Y. M. Lau, A. K. Taneja, R. S. Hodges*, J. Chromatogr., **327**, 77 (1985).
[13] *S. L. Wu, K. Benedek, B. L. Karger*, J. Chromatogr., **359**, 3 (1986).
[14] *T. Ueda, Y. Ishida*, J. Chromatogr., **386**, 273 (1987).
[15] *M. N. Schmuck, M. P. Nowlan, K. M. Gooding*, J. Chromatogr., **371**, 55 (1986).
[16] *S. L. Wu, A. Figueroa, B. L. Karger*, J. Chromatogr., **371**, 3 (1986).
[17] *J. L. Fausnaugh, L. A. Kennedy, F. E. Regnier*, J. Chromatogr., **317**, 141 (1984).

Received: July 2, 1987
Accepted: July 17, 1987
F

Separation of Polypeptide Antibiotics by Reversed-Phase High-Performance Liquid Chromatography

H.-P. Fiedler* / T. Hörner / A. Wörn

Universität Tübingen, Institut für Biologie II, Lehrstuhl Mikrobiologie I,
Auf der Morgenstelle 28, D-7400 Tübingen, FRG

Key Words

Column liquid chromatography
Adsorption effects
Polypeptide antibiotics
Quantitative determination

Summary

The influence of different reversed-phase packings and the addition of acidic modifiers to the mobile phase was observed on the separation of basic and neutral polypeptide antibiotics by gradient elution. A dependence of pore size, coverage, reaction type and endcapping of the packings was not observed. Nevertheless, not all reversed-phase packings were suitable for the separation of polypeptides, especially of basic molecules. The addition of phosphoric or perchloric acid to the mobile phase prevented adsorption of the basic polypeptide antibiotics on the stationary phase.

Introduction

The 22-peptide epidermin belongs to the polycyclic heterodetic class of peptide antibiotics [1] and is related to nisin [2] and subtilin [3]. The presence of two molecules of lysine cause the basic properties of epidermin. The substance is soluble in water, moderately soluble in methanol and has a molecular weight of 2136. Epidermin is produced by *Staphylococcus epidermidis* TÜ 3298 and can be isolated from the culture filtrate of the fermentation broth. The substance is antibiotically active against Gram-positive bacteria, especially against the anaerobic pathogen *Propionibacterium acnes* occuring in acne disease.

The quantification of substances during the fermentative production process demands a sensitive, selective, reproducible and rapid determination method. Reversed-phase high-performance liquid chromatography seemed to be a suitable method, but the HPLC analysis of epidermin by gradient elution with water/acetonitrile failed due to total adsorption of the substance on the stationary phases. Addition of the acidic modifier phosphoric acid in a concentration of 0.1% achieved a convenient separation of epidermin, but failed in the batch-to-batch reproducibility of some packing materials. This effect was probably caused by adsorption of the basic molecule on residual silanol groups of the stationary phase or by complexation on the reversed-phase packings. The HPLC separation on amino bonded phases resulted in a good retention behaviour, but was unsatisfactory due to tailing of the epidermin peak. Polystyrene packings were not efficient, because of the rapid elution of the antibiotic.

Basic compounds often show an unfavourable adsorption on the stationary phase [4–6]. In this paper we describe the adsorption of polypeptides depending on endcapping and surface treatment of different reversed-phase packings, as well as on the addition of acidic modifiers to the mobile phase. The influence of the sample was tested by comparing the separation of epidermin with other polypeptide antibiotics. Herbicolin A [7], which contains 1 molecule arginine, ist a basic compound like epidermin, whereas alamethicin [8] and suzukacillin [9] are neutral polypeptides. The structures of the antibiotics investigated are shown in Fig. 1.

Experimental

Columns

Hyperchrome HPLC columns (125 mm × 4.6 mm I.D.) filled with Nucleosil-100 C-18 (7 μm), Nucleosil-300 C-18 (7 μm), Spherisorb ODS II (5 μm) and Shandon Hypersil ODS (5 μm) were obtained from Grom (Ammerbuch, FRG). All columns were fitted with a pre-column (20 mm × 4.6 mm I.D., Grom). A LiChroCART HPLC cartridge (125 mm × 4 mm I.D.), filled with LiChrosorb RP Select B (7 μm) fitted with a pre-column (4 mm × 4 mm I.D.) was obtained from Merck (Darmstadt, FRG).

0009-5893/87 0433-06 $03.00/0

© 1987 Friedr. Vieweg & Sohn Verlagsgesellschaft mbH

Eluents

The polypeptide antibiotics were separated by gradient elution, using water, 0.1% aqueous phosphoric acid, 0.05% aqueous perchloric acid, respectively, as solvent A and acetonitrile as solvent B, from 0% to 100% solvent B in 10 minutes and a flow-rate of 2 ml/min.

HPLC Equipment

An HP 1090A liquid chromatograph (Hewlett-Packard, Waldbronn, FRG) was used with a DR5 solvent delivery system, variable autoinjector and autosampler. 10 µl of standards and centrifuged biological samples were injected. The substances were monitored by means of an HP 1040A diode array detection system. A detection wavelength of 225 nm and a bandwidth of 4 nm was used, with 550 nm and a bandwidth of 100 nm as referecne. Detector signals were processed and recorded on an HP 3092A integrator.

Chemicals

Acetonitrile (HPLC grade), phosphoric acid and perchloric acid (analytical grade) were obtained from Merck. Water was purified by means of a Milli-Q system (Millipore, Eschborn, FRG). Herbicolin A, alamethicin and suzukacillin were a generous gift of Prof. G. Jung (Universtiy of Tübingen).

Results

The Effects of Different Stationary Phases and Mobile Phases on the Separation of Epidermin

Fig. 2 shows the separation of epidermin on a commercial column filled with the endcapped reversed-phase material Nucleosil-100 C-18 by gradient elution from water to acetonitrile compared with gradient elution from phosphoric

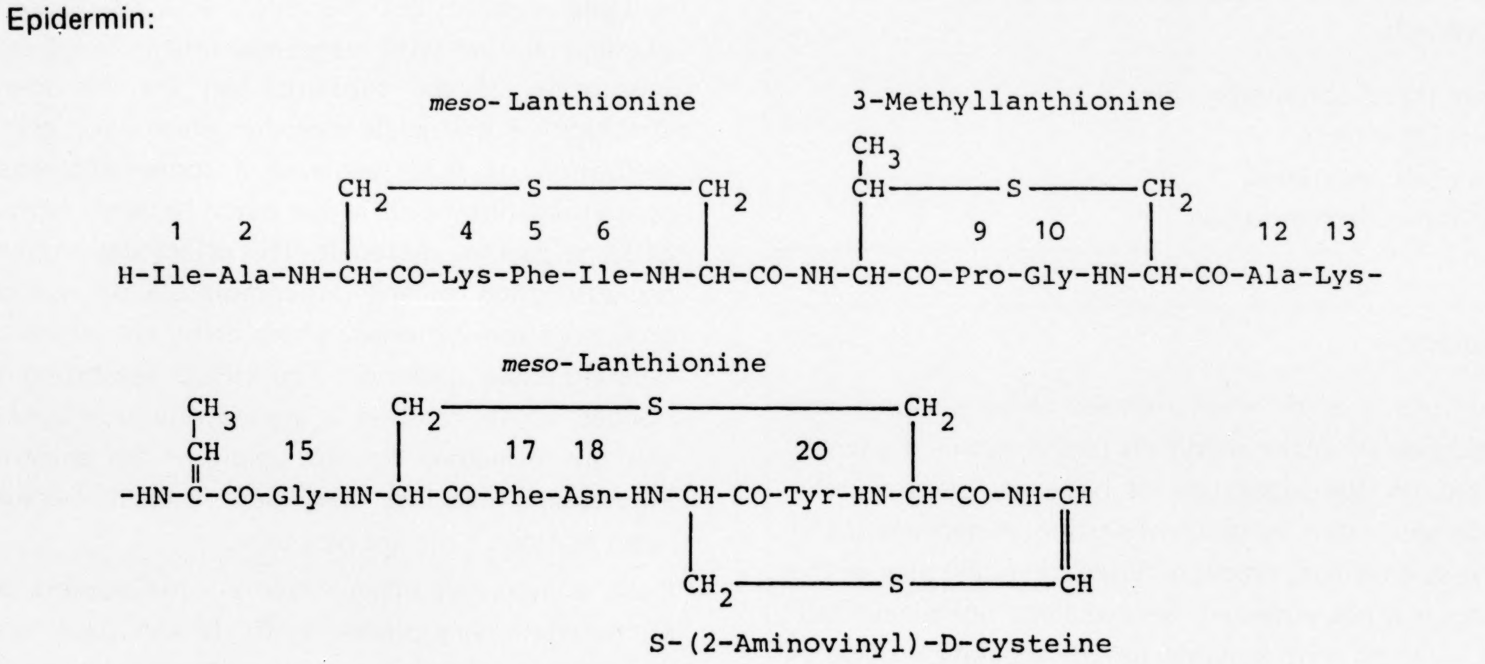
Epidermin:
meso-Lanthionine
3-Methyllanthionine
H-Ile-Ala-NH-CH-CO-Lys-Phe-Ile-NH-CH-CO-NH-CH-CO-Pro-Gly-HN-CH-CO-Ala-Lys-
meso-Lanthionine
-HN-C-CO-Gly-HN-CH-CO-Phe-Asn-HN-CH-CO-Tyr-HN-CH-CO-NH-CH
S-(2-Aminovinyl)-D-cysteine
Herbicolin A:
α-D-Glc-Abu-L-Thr-D-aThr-D-Leu-Gly-D-Gln-Gly-N-Me-L-aThr-L-Arg
Alamethicin:
Ac-Aib-Pro-Aib-Ala-Aib-Ala-Gln-Aib-Val-Aib-Gly-Leu-Aib-Pro-Val-Aib-Aib-Glu-Gln-Pheol
(Aib)
(Gln)
Suzukacillin:
Ac-Aib-Ala-Aib-Ala-Aib-Ala-Gln-Aib-Aib-Aib-Gly-Leu-Aib-Pro-Val-Aib-Iva-Gln-Gln-Pheol
(Aib)
(Leu)
(Aib)

Fig. 1

Structures of the polypeptide antibiotics epidermin, herbicolin A, alamethicin and suzukacillin.

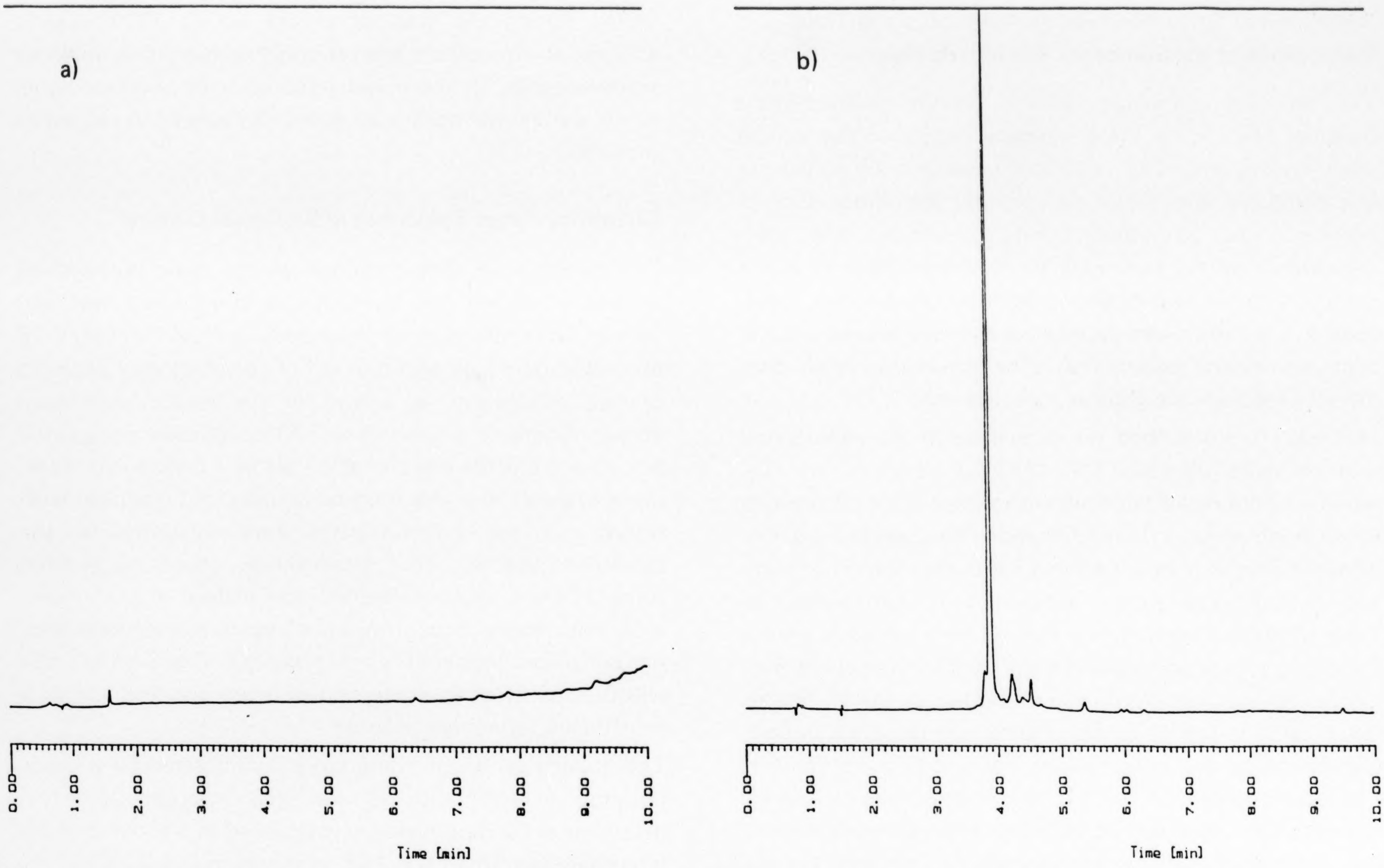

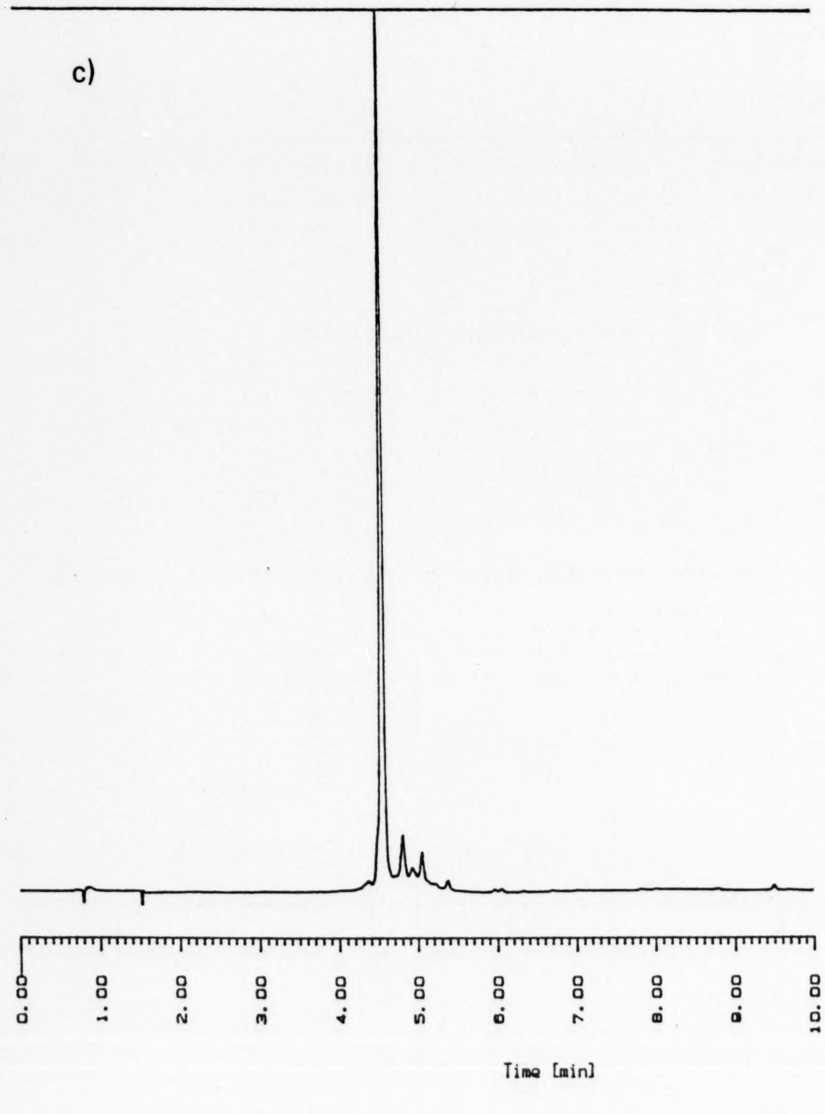

Fig. 2

Separation of epidermin on Nucleosil-100 C-18, with different mobile phases.

a) Gradient elution from water to 100% acetonitrile.

b) Gradient elution from 0.1% phosphoric acid to acetonitrile.

c) Gradient elution from 0.05% perchloric acid to acetonitrile.

acid and perchloric acid, respectively, to acetonitrile. The data show that the basic compound is totally adsorbed on the packing when gradient chromatography was performed with water/acetonitrile. No peaks were eluted during the gradient profile up to 100% acetonitrile. On the other hand, a successful separation was obtained by adding phosphoric acid or perchloric acid in a concentration of 0.1% or 0.05%, respectively, to solvent A.

The same selectivity could be achieved using the wide-pore endcapped packing Nucleosil-300 C-18 or the non-endcapped reversed-phase material LiChrosorb RP Select B with a pore size of 60 Å. These results indicate, that the separation of the basic polypeptide epidermin is neither affected by non-endcapping of the packings nor by the pore size of 60 Å.

In contrast to these results, no separation of epidermin could be achieved with the endcapped packing Spherisorb ODS II and the non-endcapped material Hypersil ODS. Addition of acidic modifiers to solvent A could not prevent adsorption on the stationary phase. No peaks were eluted by linear gradient elution from 0% to 100% acetonitrile.

Separation of Other Polypeptide Antibiotics and Their Dependence of the Stationary and Mobile Phase

The observed adsorption effects on the reversed-phase packings relating to the chemically nature of the sample were investigated. The retention behaviour of epidermin was compared with other polypeptide antibiotics, such as herbicolin A, alamethicin and suzukacillin and their dependence on the stationary phase and addition of acidic modifiers to the mobile phase. As mentioned above, herbicolin A is a basic molecule, whereas alamethicin and suzukacillin are neutral compounds. The chromatographic conditions used were the same as for epidermin.

In Table I are described the properties of the investigated reversed-phase packings [10, 11]. All packings are C_{18} modified silica-based materials with exception of LiChrosorb Select B which has a C_8 modification. The selectivity of the different reversed-phase packings for the separation of basic and neutral polypeptide antibiotics is summarized in Table II. Neutral compounds showed no adsorption on the stationary phases and a convenient separation could be performed without addition of any modifier to the eluents to restric peak tailing using Spherisorb and Hypersil. In contrast to the neutral polypeptides, basic compounds showed a strong adsorption on the different reversed-phase packing. A separation could not be achieved when gradient elution was performed with water/acetonitrile, no peaks were eluted during the gradient profile up to 100% organic solvent. A convenient separation of herbicolin A could be achieved with all the investigated reversed-phase packings when perchloric acid was added to solvent A as acidic modifier.

Quantification of Epidermin in Biological Cultures

The quantitative determination of the basic polypeptide epidermin during the fermentative production was performed with the reversed-phase packing Nucleosil-100 C-18 and addition of an acidic modifier to the mobile phase to prevent adsorption, as shown in the results mentioned above. Gradient elution from 0.1% aqueous phosphoric acid to acetonitrile was characterized by a convenient separation of epidermin in biological samples, but was poor with respect to the batch-to-batch reproducibility of the Nucleosil packing. This disadvantage could be avoided using 0.05% aqueous perchloric acid instead of phosphoric acid. With those concentrations of aqueous perchloric acid, no corrosion problems were observed. Fig. 3 shows the HPLC analysis of an epidermin standard solution and of a centrifuged fermentation broth.

The quantification of compounds is facilitated by a linear response in the range of analytical interest. With UV detection at 225 nm, linearity is achieved in a concentration range between 5 mg/l and 1 g/l, as shown in Fig. 4.

Table I. Properties of the investigated reversed-phase packings.

	Nucleosil-100 C-18	Nucleosil-300 C-18	Spherisorb ODS II	Hypersil ODS	LiChrosorb RP Select B
Pore size (Å)	100	300	80	100	60
Coverage	14% C	6% C	7% C	9% C	12% C
Reaction type	trifunctional	trifunctional	trifunctional	monofunctional	bifunctional
Endcapping	+	+	+	—	—)*

)*special treated to give homogeneity of the silica surface.

Table II. Selectivity of reversed-phase packings and their dependence on the mobile phase for separation of the polypeptide antibiotics epidermin, herbicolin A, alamethicin and suzukacillin.

Gradient	Antibiotic	Nucleosil-100 C-18	Nucleosil-300 C-18	Spherisorb ODS II	Hypersil ODS	LiChrosorb RP Select B
A	Epidermin	—	—	—	—	—
	Herbicolin A	—	—	—	—	—
	Alamethicin	+	+	+)*	+	+
	Suzukacillin	+	+	+)*	+	+
B	Epidermin	+	+	—	—	+
	Herbicolin A	+	+	+	—	+
	Alamathicin	+	+	+)*	+)*	+
	Suzukacillin	+	+	+	+	+
C	Epidermin	+	+	—	—	+
	Herbicolin A	+	+	+	+	+
	Alamethicin	+	+	+)*	+)*	+
	Suzukacillin	+	+	+)*	+	+

— adsorption; + convenient separation; +)* peak tailing

Gradient A: water to 100% acetonitrile; Gradient B: 0.1% aqueous phosphoric acid to 100% acetonitrile
Gradient C: 0.05% aqueous perchloric acid to 100% acetonitrile.

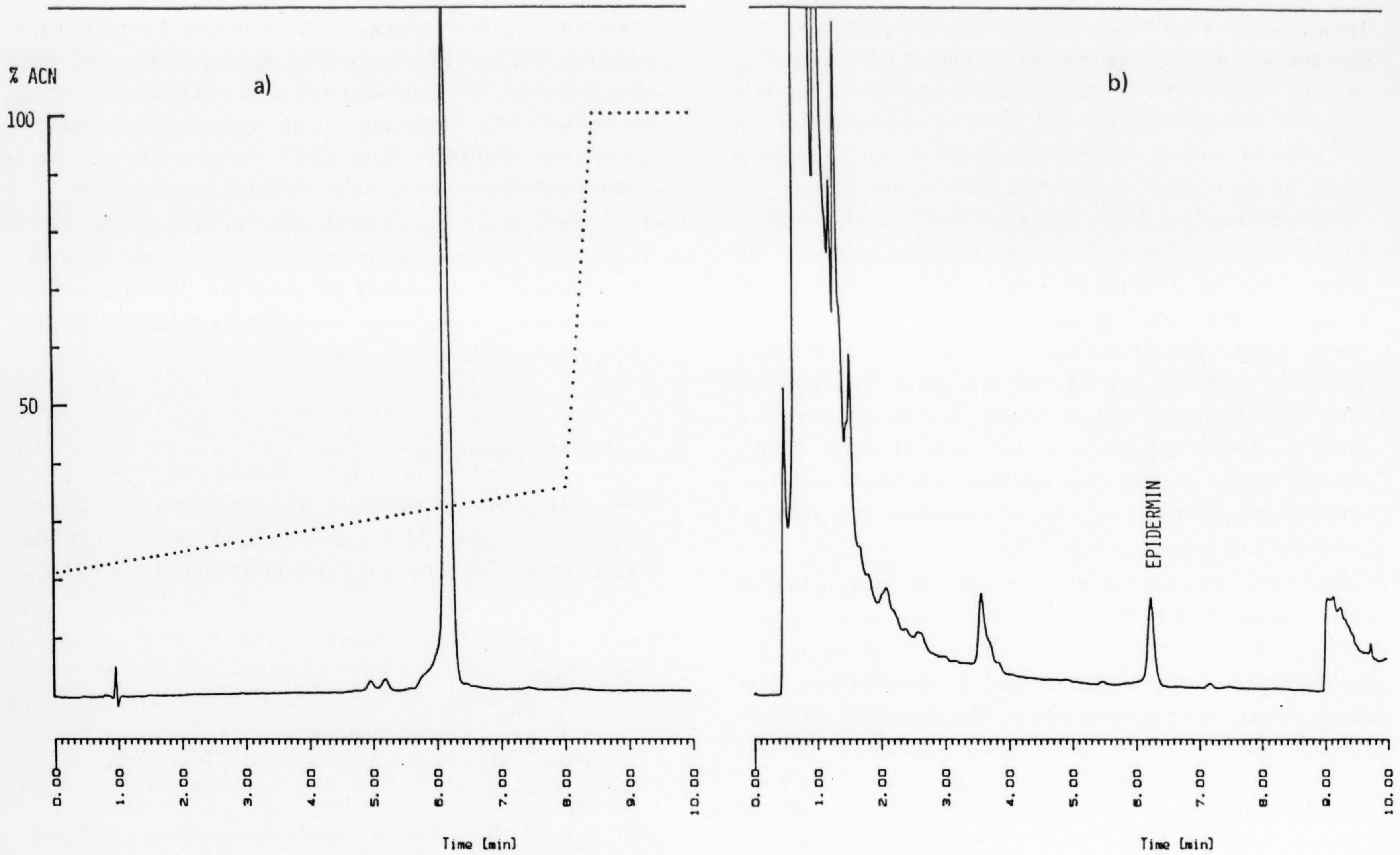

Fig. 3

HPLC analysis of epidermin on Nucleosil-100 C-18 by gradient elution with 0.05% perchloric acid and acetonitrile; gradient from 22.5% to 37% acetonitrile in 8 minutes, monitored at 225nm.

a) Epidermin standard (0.5mg/ml).

b) Centrifuged fermentation broth.

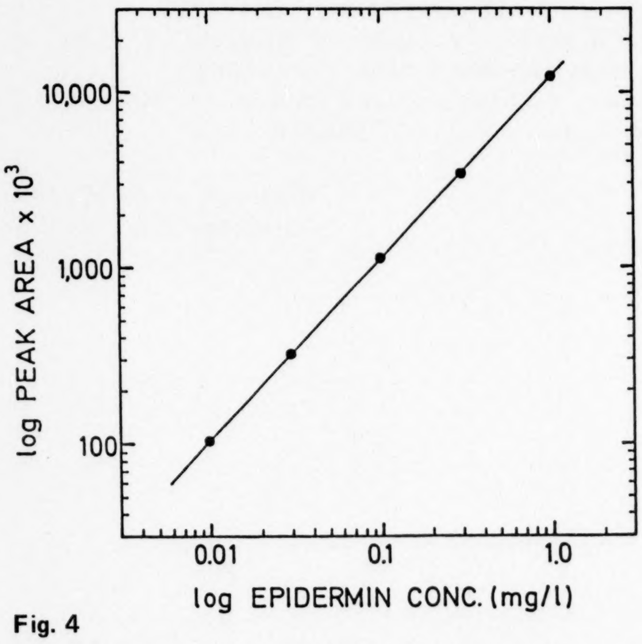

Fig. 4

Linear dynamic range of epidermin determination.

Table III. Precision of retention times and peak areas.

	Relative standard deviation (%)*	
	Retention time	Peak area
Epidermin, standard (0.5mg/ml)	0.2	1.3
Epidermin, culture filtrate	0.2	2.2

*based on twenty replicate analyses.

The precision of the method was tested by assaying the antibiotic standard and biological samples twenty times, as shown in Table III. The reproducibility of both the retention time and the peak area proved the system to be suitable for routine analysis.

Discussion

Undesired adsorption, especially of basic compounds, and the low hydrolytic stability of alkyl bonded-phase ligands have been intensivly studied by other workers [4–6]. Often the surface of the silica support used for reversed-phase packings is not homogeneous. The support contains unevenly distributed residual silanol groups as well as trace impurities, such as metal ions, which are able to interact with the sample. Such deleterious interactions can be observed mainly with polar, basic solutes [4]. It has been shown, that aqueous-organic solvent systems at low pH are deleterious to bonded-phase stability. Hydrolysis of the alkyl ligands is observed using aqueous phosphoric acid, trifluoroacetic acid or other acids in the range of about pH 2 [5]. But in contrast to the frequently-held opinion it was proved, that a fully bonded packing is not required to prevent deleterious interaction of basic compounds, proteins or other macromolecules with residual silanol groups on the packing surface. A good separation of certain proteins could be performed, even when 50% of the original covalently bonded stationary phase was lost from the packing. Undesired adsorption of basic compounds could be strongly affected by the presence of highly acidic, isolated silanol groups on the packings, which are not associated [6]. Those authors subdivided the silica supports in relatively adsorptive materials, e.g. Hypersil and Spherisorb, and less adsorptive materials, e.g. Nucleosil. The more adsorptive packings exhibit a higher concentration of highly acidic, isolated silanol groups than the less adsorptive packings, which are characterized by a higher content of associated or bonded silanol groups.

In the light of these results, adsorption or peak tailing of our investigated polypeptide antibiotics on reversed-phase packings like Hypersil and Spherisorb can be explained by the existence of highly acidic, isolated silanol groups. The basic compound epidermin was totally adsorbed on these packings and adsorption could not be prevented by addition of acidic modifiers to the mobile phase, in contrast to the less adsorptive reversed-phase materials Nucleosil and LiChrosorb RP Select B.

Conclusions

The separation behaviour of polypeptides on reversed-phase packings is mainly influenced by the presence of basic amino acids. Neutral molecules showed no separation problems, on the other hand the basic compounds were adsorbed on to the stationary phase.

Not all reversed-phase packings proved to be suitable for the separation of basic polypeptides. Pore size, coverage and type of material bonded to the packings had no effect on selectivity and resolution of the investigated compounds. Endcapping is not essential for the separation of basic molecules. Undesired adsorption is caused by the presence of highly acidic, isolated silanol groups on the packings and not by the content of associated or bonded silanol groups. The separation of basic polypeptides can be performed more favourable using reversed-phase packings of the less adsorptive type, which are characterized by a smaller content of highly acidic, isolated silanol groups.

The mobile phase has to be acidified to prevent adsorption of the basic polypeptides on the stationary phase. Addition of perchloric acid seemed to be more favourable than phosphoric acid, regarding the batch-to-batch reproducibility of the reversed-phase packings.

Acknowledgements

This work was supported by the Deutsche Forschungsgemeinschaft (SFB 323) and the Bundesministerium für Forschung und Technologie (Förderkennzeichen 03 8759).

References

[1] *H. Allgaier, G. Jung, R. G. Werner, U. Schneider, H. Zähner,* Angew. Chem. Int. Ed. Engl. **24,** 1051–1053 (1985).

[2] *E. Gross, J. L. Morell,* J. Am. Chem. Soc. **93,** 4634–4635 (1971).

[3] *E. Gross, H. H. Kiltz, E. Nebelin,* Hoppe-Seyler's Z. Physiol. Chem. **354,** 810–812 (1973).

[4] *J. Köhler, D.B. Chase, R.D. Farlee, A.J. Vega, J.J. Kirkland,* J. Chromatogr. **352,** 275–305 (1986).

[5] *J. L. Glajch, J. J. Kirkland, J. Köhler,* J. Chromatogr. **384,** 81–90 (1987).

[6] *J. Köhler, J. J. Kirkland,* J. Chromatogr. **385,** 125–150 (1987).

[7] *M. Aydin, N. Lucht, W. A. König, R. Lupp, G. Jung, G. Winkelmann,* Liebigs Ann. Chem. **1985,** 2285–2300.

[8] *G. Jung, N. Dubischar, D. Leibfritz, M. Ottnad, H. Probst, C. Stumpf* in: *Y. Wolman* (Ed.), "Peptides 1974", North-Holland Publ., Amsterdam, 1975, pp. 347–366.

[9] *E. Katz, M. Aydin, N. Lucht, W. A. König, T. Ooka, G. Jung,* Liebigs Ann. Chem. **1985,** 1041–1062.

[10] *R. E. Majors,* J. Chromatogr. Sci. **18,** 488–511 (1980).

[11] E. Merck Product Bulletin, RP Select B.

Received: June 29, 1987
Accepted: July 26, 1987
F

HPLC Assay of Enzymatic Activities

P. Pietta*/P. Mauri/M. Pace

Dipartimento di Scienze e Tecnologie Biomediche, Sezione Chimica Organica, Via Celoria, 2, I-20133, Milano Italy

Key Words

Column liquid chromatography
Enzyme assay
Urokinase

Summary

Instead of traditional methods, high-performance liquid chromatography can be used for the determination of enzymatic activities. Assays can be performed once the reaction mixture have been injected in the HPLC apparatus. The elution of the samples is carried out with suitable buffers, and the product(s) formed and left oven substrate(s) are quantitatively determined by means of an internal standard. HPLC assay is rapid, selective and comparable with traditional methods. Enzymatic activity can be easily measured in international units and the whole assay performed within 10–20 minutes. The results obtained for the urokinase asssay are provided as a detailed example in the text

Introduction

Enzyme assays are usually performed by measuring the increase of the product and/or the decrease of the substrate and relating these measurements to the amount of enzyme present. A number of methods have been employed in enzyme assays. Some of the most commonly used techniques include: spectroscopy, fluorescence, colorimetry, potentiometry, high-voltage electrophoresis and chromatography [1–5].

In recent years, high-performance liquid chromatography (HPLC) has played a key role in multicomponent analysis. The usefulness of HPLC stems not only from its power as a separation technique, but also from its versatility. The modes available, such as ion-exchange and reversed- and normal-phase, permit separation and measurement of the most complex samples. Therefore, HPLC has a tremendous potential for enzyme assays and has been employed in assays of diverse enzyme systems [6–8]. One outstanding feature of the technique, in terms of its use for enzyme analysis, is that the change in both substrate and product concentration can be measured concurrently.

In our laboratory, isocratic reverse-phase HPLC has been applied for the assay of various enzymes [9–12]. The purpose of this paper is to present our approach and to discuss the variables that are important in enzyme assays, using urokinase as an enzyme model.

Experimental

Materials

Gly-Arg-4-Nitroanilide and 4-Nitroaniline (pNA) were obtained from Novabiochem (Laufelfingen, Switzerland), urokinase from Protogen (Laufelfingen, Switzerland) and umbelliferone (7-Hydroxycoumarin) was obtained from Fluka (Buchs, Switzerland). Acetonitrile was of HPLC grade (Chromasolv; Riedel-de Häen, Hannover, FRG). Water was distilled twice and filtered through a 0.45 μm membrane (Type HA, Millipore). All other chemicals were of analytical grade.

Chromatographic Conditions

The HPLC system consisted of a Model 510 pump equipped with a Model U6K Universal injector, a Lambda-Max Model 480 variable ultraviolet detector and a Model 730 Data Module (Waters Ass., Milford, MA, USA). The eluent was 0.01 M sodium dihydrogen phosphate buffer, pH 3.1: acetonitrile (72:28) at a flow-rate of 1.5 ml/min. Samples were chromatographed on a μBondapak C_{18} (Waters Ass.) and the column effluent was monitored at 230 nm (0.05 a.u.f.s.).

Calibration Curves

Known volumes (10–100 μl) of 0.045 mM pNA dissolved in the eluent solution were pipetted into individual test tubes. Then 200 μl of the internal standard solution (0.003 mM in Water) were added to each tube and the volume was brought to 1 ml with the eluent buffer. Replicate injections of 20 μl were made for each sample.

Assay of Urokinase Activity

The reaction was carried out in a final volume of 2 ml in the presence of 1 mM Gly-Arg-pNA (60 mM phosphate buffer-0.6% NaCl, pH 7.8) at 37 °C and was started by the addition of 10–100 μl of urokinase stock solution (0.25 mg protein/

0009-5893/87 0439-03 $03.00/0

© 1987 Friedr. Vieweg & Sohn Verlagsgesellschaft mbH

ml). At fixed intervals, 20 µl were acidified by a three-fold dilution in the internal standard solution (0.4 mM umbelliferone in 15 mM hydrochloric acid pH 3.1), and replicate injections of 20 µl were made in the HPLC apparatus.

Results and Discussion

In order to establish a protocol for the determination of the activities of various enzymes, we standardized a procedure that can be generally used.

The procedure involves (Fig. 1):

a) the assessment of the chromatographic conditions for the separation of substrate, product and internal standard;
b) the standardization of each component, i.e. the linear relationship between moles of substrate and/or product and the detector response;
c) the study of the enzyme kinetics in order to determine the conditions for the one-point assay;
d) the routine measurement by one-point determination;
e) the comparison of the results with those obtained by traditional methods (spectrophotometric, potentiometric, etc.).

As an example, the results obtained for the urokinase assay are reported here.

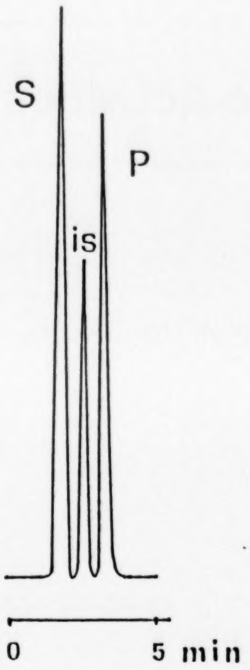

Fig. 2
Typical chromatogram of Gly-Arg-pNA(S), Umbelliferone(is) and pNA (P).
Chromatographic conditions: column, µBondapak C_{18} (300 × 3.9 mm); eluent, 10 mM sodium monohydrogen phosphate buffer pH 3.1 : acetonitrile (72:28); flowrate, 1.5 ml/min; detection, UV 230 nm.

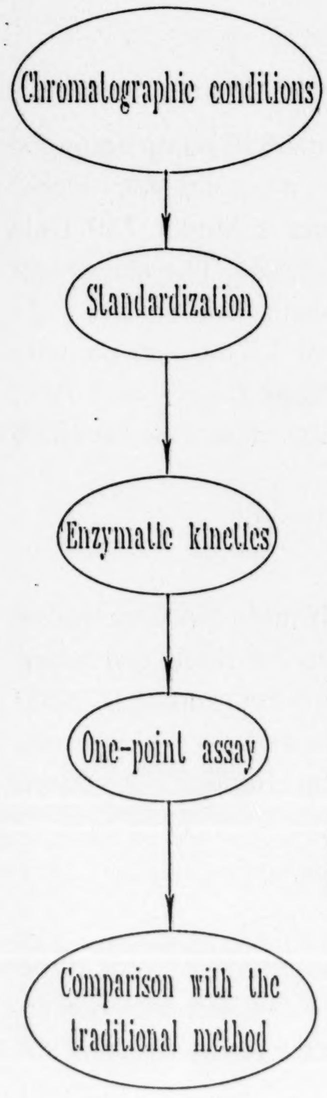
Chromatographic conditions
Standardization
Enzymatic kinetics
One-point assay
Comparison with the traditional method

Fig. 1
Procedure for the enzyme assay by HPLC.

Isocratic elution with acid buffers was studied, and the best separation was achieved on a µBondapak C_{18} column (Fig. 2). The pH of the incubation mixture was lowered to 3.1 from 7.8 by a three-fold dilution, with the elution buffer containing umbelliferone as the internal standard. At this pH value no change in the sample components was detected within 24 hrs.

A linear relationship between the peak-area ratios (product/internal standard) and the amount of injected product was found in the range of 0.1–2.0 nmol:

$$A = 0.69B - 0.0009;\ r = 1.000$$

where:

A = peak-area ratio: product/internal standard,
B = nmol of product.

The enzymatic reaction caused a significant amount of 4-nitroaniline to be produced, which was therefore chosen for the quantitative determination of the enzyme activity (Fig. 3). As shown in Fig. 4, the amount of 4-nitroaniline produced was linearly dependent on the urokinase activity. For these reasons, routineary assays were performed where the reaction was arrested after 20 min, and the activity of urokinase was determined in international units (µmol

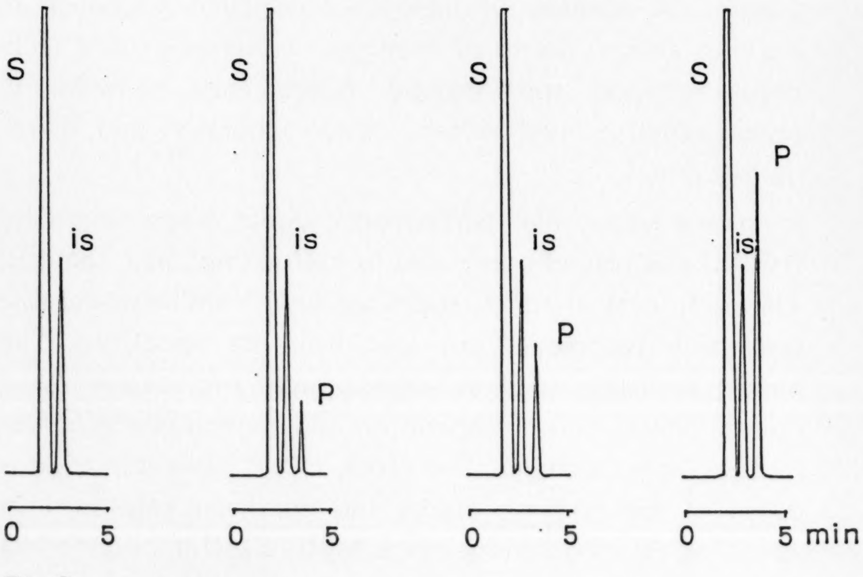

Fig. 3
Chromatograms of the reaction mixture after increasing incubation times. Chromatographic conditions as in Fig. 1.

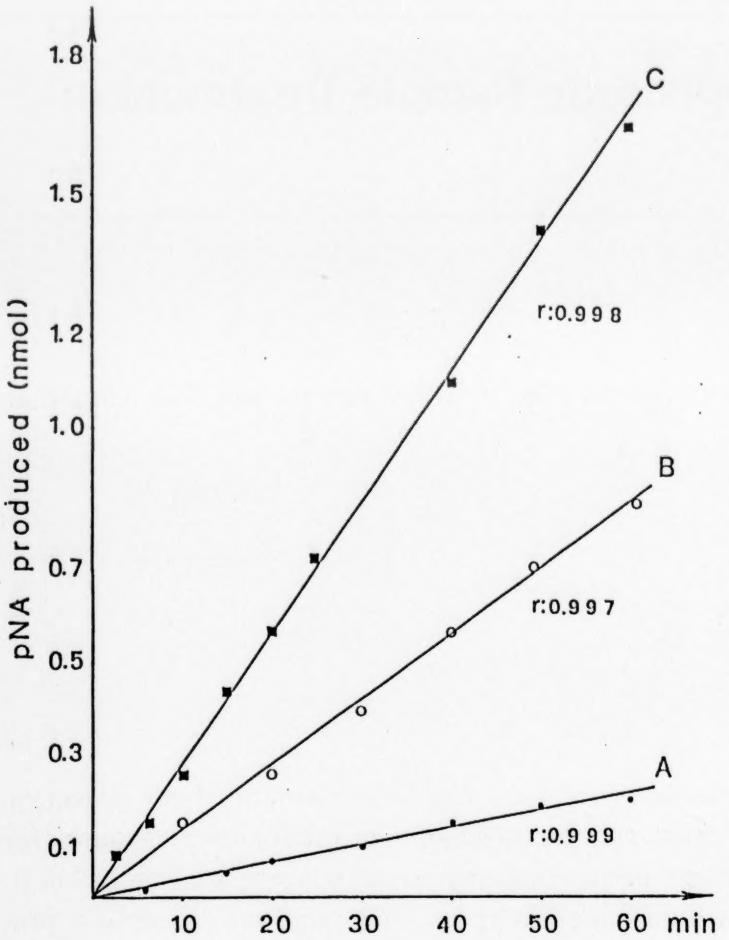

Fig. 4

Correlation of the amount of pNA produced with the volume of urokinase employed.

A = 10 μl, **B** = 40 μl, **C** = 100 μl of stock solution (0.25 mg/ml).

product/min). The results obtained from the analysis of different samples of urokinase were in good agreement with those obtained by the spectrophotometric method [13]. The correlation coefficient was + 4%.

The described procedure has been extended to several other enzymes [9–12, 14]; and the results confirmed the suitability of HPLC in the enzyme assays.

The main advantages of the HPLC method are the following:

1. Both substrate and product can be simultaneously and rapidly separated by an isocratic eluent mode.
2. Errors due to the interferences of competing enzymes or buffers are abolished.
3. Coupled reaction requiring more enzymes or cofactors can be avoided.

It can thus be concluded that the HPLC approach represents a valuable alternative to traditional methods.

References

[1] "Methods of Enzymatic Analysis", *Bergmeyer, H.U.*, Ed., Verlag Chemie, Weinheim; III edition, vol. I, 1983, p. 280.

[2] *M. Zimmermann, J.P. Quigley, B. Ashe, C. Dorn, R. Goldfarb, W. Troll,* Natl. Acad. Sci. USA **75,** 750–753 (1978).

[3] *R. Ruyssen, A. Lauwers,* Editors, "Pharmaceutical Enzymes", E. Story-Scientia, Gent, 1978, p. 33.

[4] *U. Hamber, M.L. Savolainen,* Acta Chem. Scand. **22,** 1452 (1968).

[5] *D.A. Vost, B.M. Anderson,* Anal. Biochem. **116,** 97 (1981).

[6] *S. Soeda, K. Abe, N. Nagamatsu,* J. Liq. Chromatogr. **4,** 713 (1981).

[7] *M. Zakaria, P.R. Brown,* J. Chromatogr. **226,** 267 (1981).

[8] *P.R. Brown, A.M. Krustulovic,* Anal. Biochem. **99,** 1 (1979).

[9] *P.G. Pietta, A. Calatroni, M. Pace,* J. Chromatogr. **241,** 409 (1982).

[10] *P.G. Pietta, A. Calatroni, R. Colombo,* J. Chromatogr. **243,** 123 (1982).

[11] *P.G. Pietta, P.L. Mauri, M. Pace,* J. Chromatogr. **367,** 223 (1986).

[12] *P.G. Pietta, P.L. Mauri, M. Pace,* J. Chromatogr. **390,** 458 (1987).

[13] *T. Morita, H. Kato, S. Iwanaga, K. Takada, T. Kimura, S. Sakakibara,* J. Biochem. **82,** 1495 (1977).

[14] *P.G. Pietta, P.L. Mauri, M. Pace,* in course of submission.

Received: July 1, 1987
Accepted: Aug. 6, 1987
F

Theoretical Considerations for Zone Electrophoretic Sample Treatment in Liquid Chromatography

W. Th. Kok

Laboratory for Analytical Chemistry, University of Amsterdam, Nieuwe Achtergracht 166, 1018 WV Amsterdam, The Netherlands

Key Words

Liquid chromatography
Sample treatment
Zone electrophoresis

Summary

In this paper a concept is proposed for the selective isolation of ionogenic, low-molecular weight compounds from biological samples prior to a determination by liquid chromatography. The basis for this sample treatment method is free zone electrophoresis in a system of capillaries connected by switching valves. The influence of various parameters (the geometry of the capillaries, the conductivity of the sample and the buffers used, protein binding) on the selectivity of the method is discussed. A strategy to study reversible protein binding of ionogenic compounds is indicated.

Calculations have been performed to estimate the temperature increase of the solutions during the electrophoretic process. It is shown that for a given amount of sample to be introduced and a maximum time allowed for the procedure, the temperature increase is the smallest when wide capillaries are used.

Equations are given describing the zone broadening caused by diffusion, by differences in temperature and by unequal migration path lengths in bent capillaries. It is shown that in this respect the use of narrow capillaries is usually preferable. A compromise has to be found starting from the boundary conditions on loadability and speed imposed by the chromatographic determination.

Introduction

With the improvements in separation speed and efficiency and detection sensitivity in high performance liquid chromatography (HPLC) accomplished in the last decade, a new emphasis has been laid on the importance of the sample preparation procedure. The improvement of the detection limits that can be reached has provoked a demand for ultra-trace determinations in very complex matrices. In such a determination it is often required to apply a prepurification procedure before the sample is injected onto the column. This is not only necessary to remove components which are harmful to the separation system, e.g. proteins in biological samples, but also to reduce the vast number of interfering compounds present in trace amounts in the samples. The sample treatment procedure should provide a group separation of the sample constituents.

Considerable work has been invested in the improvement of HPLC packings and instrumentation. This work has resulted in the possibility of performing efficient separations in a short time. In the present situation conventional sample treatment methods (precipitation, liquid-liquid extraction) would be the bottle-neck in the analysis. This explains the increased interest in techniques such as solid-phase extraction, which are more easy to automate ([1] and references therein). Solid-phase extraction coupled with HPLC constitutes a two-step separation system in which the first step brings about a group separation of the sample components. In principle however, for this group separation any separation technique may be applied.

In this work the feasibility of zone electrophoresis as a sample treatment technique is investigated. The intention is to develop a system by which low-molecular weight ionogenic compounds can be isolated from other sample components, i.e. from uncharged or oppositely charged species and high-molecular weight compounds (proteins) with a relatively low electrophoretic mobility, and to incorporate this system into an automated liquid chromatograph.

Theory on electrophoresis goes back to the previous century [2]. However, the application of zone electrophoresis to the purpose described above, under the boundary conditions imposed by the chromatographic procedure, requires a different outlook on well-established theory.

This study is meant to provide a theoretical basis for the experimental development of zone electrophoretic sample treatment (ZEST) for liquid chromatography.

0009-5893/87 0442-07 $03.00/0

© 1987 Friedr. Vieweg & Sohn Verlagsgesellschaft mbH

Principle and Boundary Conditions

When a ZEST system is to be coupled directly to a liquid chromatograph, the compounds of interest should be transferred to a medium suitable for injection onto the column. Therefore, anti-convective supporting media such as often used in electrophoretic techniques can not be used here, and some sort of capillary electrophoresis in free solution has to be applied.

In Fig. 1 a possible configuration of non-conducting capillaries is shown by which ZEST can be performed. Four stages can be descerned in the process. In the first stage (PREP) the capillaries are filled with an appropriate electrolyte solution. Since the compounds of interest will often be weak acids or bases, it is obvious to use a buffered solution. In the second stage (LOAD), a part of the capillary system is filled with the sample. The transition of the first stage to the second and subsequently to the next stages can be performed by the switching of liquid valves. In the third stage (PHOR) an electric field is applied between two electrodes in contact with the solutions in the capillaries. Zones of ionic compounds migrate through the system, the direction and speed determined by their charge and mobility. After a given time of electrophoresis, the electric power source is switched off, and in the fourth stage (ELUT) a part of the content of the capillaries, containing the compounds of interest, is flushed by the mobile phase toward the chromatographic column. By flushing the remainder of the sample out of the system with fresh buffer solution, the next cycle starts.

The occurrence of electro-osmotic flow does not make the described system inapplicable a priori. However, it is desirable to suppress this pehnomenon. Electro-osmotic flow is more difficult to control than electrophoretic migration, especially when components of biological samples adsorb on the capillary walls. Electro-osmosis can be suppressed by using inert material for the capillaries and by inserting physical barriers (membranes) in the electrophoretic pathway.

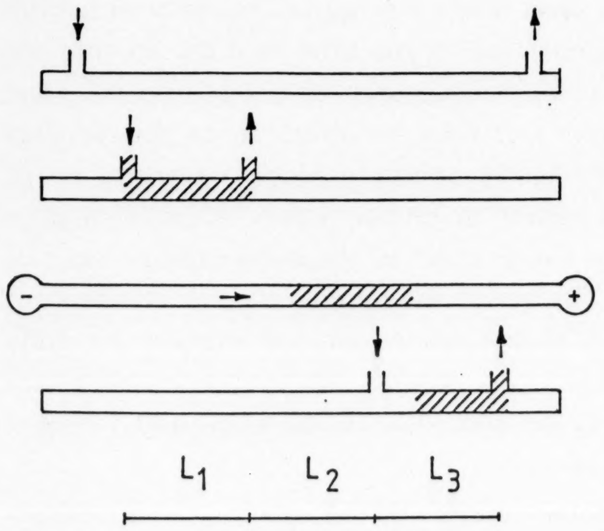

Fig. 1

Schematic set-up for zone-electrophoretic sample treatment. L_1: sample capillary; L_2: transfer capillary; L_3: injection capillary.

When electrophoresis is applied as the principal separation mechanism, it is essential to obtain narrow and sharp zones. In ZEST, however, zone broadness is of less importance. In fact, it is often desirable to collect a number of (overlapping) compound zones in the ELUT stage of the process. In many real determinations one is not interested in just one compound, but rather in a number of related compounds which may differ slightly in electrophoretic mobility. The group separation which is intended in the ZEST process does not require a high separation efficiency.

The amount of sample that can be loaded is of critical importance, since the detection limits that are obtained in the chromatographic determination are directly related to it. In a chromatographic procedure with a conventional (4.6 mm I.D.) column, sample size is usually between 5 and 100 μl. In this work a minimum sample size of 10 μl is taken as a boundary condition.

When ZEST can be performed simultaneously with the chromatographic elution of the previous sample and does not require more time, the time of analysis will not be extended. In this work we will take as a boundary condition that the electrophoresis time does not exceed 1000 s.

The original sample zone occupies a considerable part of the electrophoretic pathway. As will be shown, the conductivity of the sample has an influence on the obtainable speed of the process. Here, it is taken as a boundary condition that samples with a conductivity of 0.01 Ω^{-1} cm^{-1} and less can be handled. This implies that human serum samples can be introduced without dilution [3].

Selectivity

The migration velocity u of an ion is proportional with the strength of the applied electric field E:

$$u = u_0 E \quad (1)$$

The mobility u_0 of an ion is determined by its charge, its effective radius and the viscosity of the solution. Also, it depends to some extend on the ionic strength of the solution [4]. Of course, the mobility of weak acids and bases can be manipulated through the pH of the solution, and complexation with other sample or buffer components can influence the mobility. The usefulness of ZEST for the clean-up of biological samples is based on the difference in mobility between low-molecular weight compounds and proteins. Mobilities of proteins present in human serum or plasma do not exceed 10^{-4} cm^2 V^{-1} s^{-1} [5], while small ions have mobilities of 2–3.10^{-4} in buffered solutions. Therefore, small ions will be completely separated from the proteins when they have migrated over a distance twice the original zone length.

To evaluate the selectivity of the procedure in more detail, it can be derived how the recovery of a compound depends on its mobility. The system itself is characterized by the relative lengths of the sample, transfer and injection capillaries (L_1, L_2 and L_3, respectively). At first, it is assumed that sample and buffer contain the same supporting electrolyte in the same concentration, so that E is constant throughout the system. The applied voltage and the time of electrophoresis t_f can be tuned in such a way that the centre of some reference compound with mobility $u_{0,ref}$ coincides with the centre of the injection capillary:

$$t_f = \left(\frac{1}{2}L_1 + L_2 + \frac{1}{2}L_3\right)/u_{0,ref}\,E \qquad (2)$$

As long as $L_3 \geqq L_1$, the recoverey of this reference compound is complete. The recovery R of compounds with a lower mobility than the reference compound is then given by:

$$R = \frac{u_0}{u_{0,ref}}\left(\frac{1}{2} + \frac{L_2}{L_1} + \frac{1}{2}\frac{L_3}{L_1}\right) - \frac{L_2}{L_1}\ (0 \leqq R \leqq 1) \qquad (3a)$$

For compounds with a higher mobility:

$$R = 1 + \frac{L_2}{L_1} + \frac{L_3}{L_1} - \frac{u_0}{u_{0,ref}}\left(\frac{1}{2} + \frac{L_2}{L_1} + \frac{1}{2}\frac{L_3}{L_1}\right)(0 \leqq R \leqq 1) \qquad (3b)$$

In Fig. 2 the influence of the lengths of the capillaries on the selectivity is shown. By increasing the length of the injection capillary a wider range of compounds can be recovered completely. Increasing the length of the transfer capillary gives a sharper transition from complete recovery to complete rejection, at the expense of a higher applied voltage or a longer time of electrophoresis.

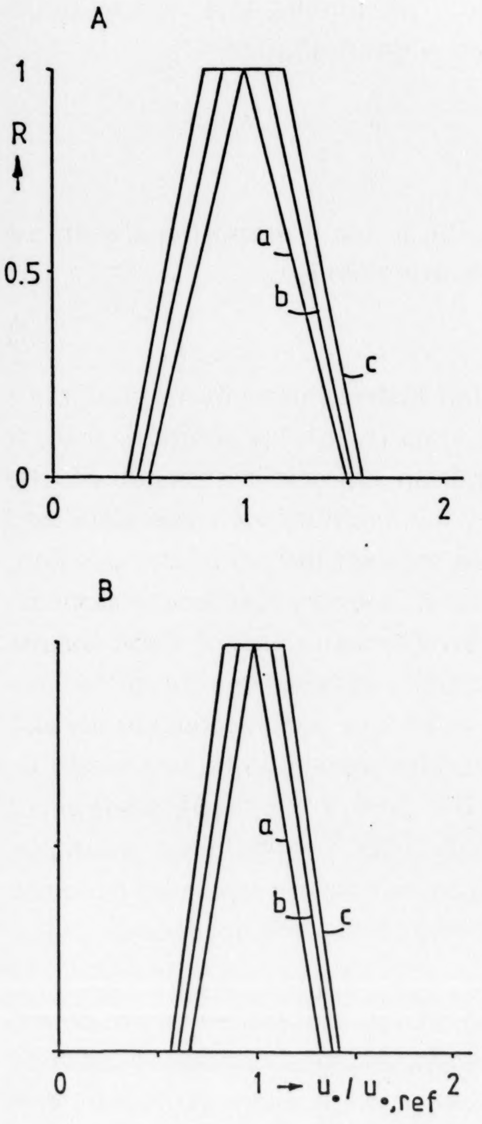

Fig. 2
Calculated dependency of the recovery on the ion mobility. Field strength and time of electrophoresis are tuned for a compound with $u_{0,ref}$. $L_2/L_1 = 1$ (A) and 2 (B). $L_3/L_1 = 1$ (a), 1.5 (b) and 2 (c).

Fig. 2 shows, as stated before, that complete isolation of monovalent ions ($u_0 > 2.10^{-4}$) from proteins ($u_0 < 10^{-4}$) present in biological samples is possible with $L_1 = L_2 = L_3$. This will be referred to as the critical geometry. In the critical geometry the zone of an ion has to migrate over a distance twice its length. From this the field strength can be calculated required to meet the boundary conditions on speed and loading capacity described in the previous section:

$$E = \frac{2\,V_s}{\pi r_{in}^2\, u_0\, t_f} \qquad (4)$$

In reality the situation may be more complex, since recoveries are also influenced by the ratio of conductivities γ of the sample and the buffer solution. When sample and buffer contain the same supporting electrolyte, a discontinuity of conductivity at the boundary of the solutions remains at the same place during electrophoresis according to the Kohlrausch theory [2]. Only the sharpness of the conductivity jump decreases due to ordinary diffusion. The field strength changes over the boundary. Since the current density is the same at both sides:

$$\gamma_s E_s = \gamma_b E_b \qquad (5)$$

If the change of mobilities with the ionic strength can be neglected, ion velocities change accordingly, so that the length of a zone z_b when it has migrated to the buffer containing capillaries is different from tis original length L_1:

$$z_b = \gamma_s/\gamma_b \cdot L_1 \qquad (6)$$

To calculate recoveries in this case, eqns (3a) and (3b) can still be used when L_2 and L_3 are substituted by $\gamma_b/\gamma_s \cdot L_2$ and $\gamma_b/\gamma_s \cdot L_3$, respectively.

Eq. (6) shows that sample compounds can be concentrated into a smaller volume by using a buffer with a higher conductivity than the sample. This phenomenon can be utilized to increase the loading capacity of the system.

Control of Operating Parameters

The development of a ZEST procedure for a particular compound will start with a series of measurements with variation of the electrophoresis time in order to find the conditions for complete recovery of the compound. Most of the parameters that have an influence on the recovery can be kept sufficiently constant. Modern electrophoretic power supplies deliver at choice a very stable voltage or current, and the composition of the buffer solution can be kept constant. The pH of the sample solution is often not critical, as long as the compounds of interest are fully ionized. However, two sources of irreproducibility are more difficult to control: the temperature and the conductivity of the sample.

Variation of the temperature of the solution can arise from variation of the ambient temperature, or from long-term heating of insufficiently thermostatted parts of the equipment during a series of measurements. For a small temperis decreased. When it is assumed that the mobility of the protein-bound ion is virtually zero, the apparent mobility u_0' of a compound which is bound for a fraction b is:

$$u_0' = u_0\,(1-b) \tag{12}$$

Since the mobility is back to its normal value as soon as an ion has left the protein containing sample capillary, the zone width in the buffer solution is increased.

The effect of irreversible and reversible binding on the recovery is shown in Fig. 4. With a critical geometry, optimized for complete recovery from a solution without proteins, a determination will yield the free compound only. If a series of measurements is performed with variation of the time of electrophoresis, conclusions may be drawn on the reversibility of the binding. If the binding is reversible, the total concentration (free and bound) of the compound of interest can be determined from the area under the curve of % recovery vs. electrophoresis time. With this method in fact the length of the compound zone is measured. However, when the binding of the compound is too strong, the risk exists that proteins reach the injection capillary.

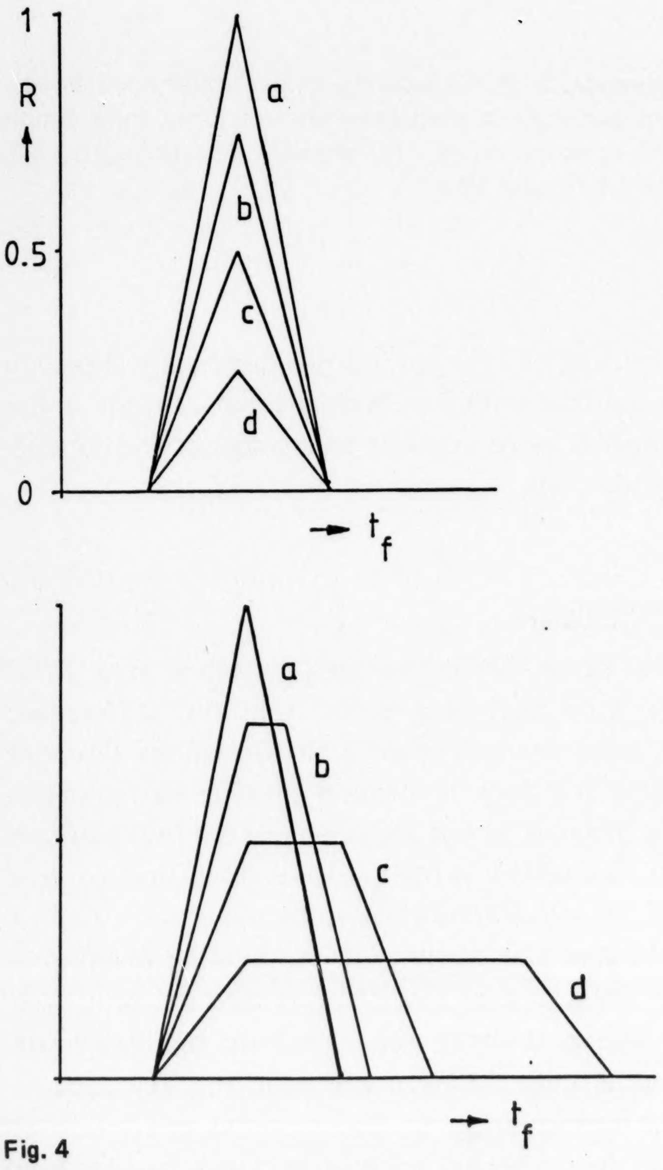

Fig. 4

Calculated dependency of the recovery on protein binding. (A) Irreversible binding. (B) Reversible binding. Percentage bound: 0 (a), 25 (b), 50 (c) and 75 (d). $L_2/L_1 = 1$. $L_3/L_1 = 1$.

Heat Production

The passage of current through the capillary system during electrophoresis is attended with a considerable evolution of heat. The rise of the temperature of the solutions is in practice the limiting factor for the speed of the procedure. Several harmful events may occur when the heat production is too high: decomposition of compounds of interest, clogging of capillaries by denaturation of proteins, bubble formation from dissolved gasses and even boiling of the solutions. Therefore, optimization of the system in respect to the temperature increase is important.

The heat production per unit length P in a capillary is given by:

$$P = \pi r_{in}^2\,\gamma E^2 \tag{13}$$

After switching on the voltage or current source the temperature of the solution rises rapidly, but when the outside of the capillary is cooled sufficiently (e.g. by forced air), a steady state temperature is reached after a short time. The steady state temperature difference over the capillary wall is given by [6]:

$$T_{in} - T_{out} = \frac{P}{2\pi K_c} \ln\left(\frac{r_{out}}{r_{in}}\right) \tag{14}$$

In this equation K_c is the thermal conductivity of the capillary wall.

For insulating polymer materials K_c is in the order of 2.10^{-3} J s^{-1} K^{-1}. The field strength necessary to meet the boundary conditions is given in eq. (4). Substitution of eqns. (4) and (13) into eqn. (14) gives:

$$T_{in} - T_{out} = \frac{2}{\pi^2}\,\frac{1}{K_c}\,\frac{\gamma \cdot V_s^2}{u_0^2\,t_f^2} \cdot \frac{1}{r_{in}^2} \ln\left(\frac{r_{out}}{r_{in}}\right) \tag{15}$$

The temperature increase in the capillaries can be made small by using a sufficiently thin capillary wall; then the logarithmic term in the right-hand side of eqn. (15) approaches zero. However, the heat conduction in the switching valves necessary to operate the system is the limiting factor, and calculations have to be performed using an "equivalent outer radius" representing the dimensions of the valves used. In Table I calculated values of the temperature increase are given for different capillary radii. An equivalent outer radius of 0.5 cm for the valves is taken, and an ion mobility of 2.10^{-4} cm^2 V^{-1} s^{-1}. Other values are as described in the boundary conditions.

It is clear from Table I that 0.25 mm I.D. capillaries can not be used without serious experimental problems. Both in respect to the temperature increase and to the required voltage the capillaries should be as wide and short a possible.

Table I. Required voltage and temperature increase at critical points for different capillary radii. For conditions see text.

r [cm]	L_1 [cm]	e_{app} [V]	$T_{in}-T_{out}$ [K]
0.0125	20	12.500	60
0.025	5	800	12
0.05	1.3	50	2

ature change the dependence of the mobility of an ion on the temperature can be approximated as:

$$\frac{\Delta u_0}{u_0} = p\,\Delta T \tag{7}$$

The temperature coefficient p is in the order of 0.02 K^{-1} for small ions. When the electrophoresis is carried out under constant-voltage conditions, the distance migrated will change accordingly. When the time of electrophoresis is tuned for some reference temperature T_{ref}, the recovery for a critical geometry as a function of the temperature is given by:

$$R = 1 - 2p\,|T - T_{ref}| \tag{8}$$

With a change in temperature the conductivity of the buffer and sample will also change. Under constant-current conditions the field strength will be lower when the conductivity is increased. When the temperature coefficients of the mobility of the supporting electrolyte and the compound of interest are approximately equal, these two effects cancel each other. This implies that under constant-current control the recovery is practically independent of the temperature.

The influence of the sample conductivity on the recovery when the voltage is kept constant is not the same as when the current is kept constant. When the voltage is controlled, the field strength in the buffer solution is:

$$E_b = \frac{e}{\gamma_b/\gamma_s \cdot L_1 + L_2 + L_3} \tag{9a}$$

while in the sample solution the field strength is given by:

$$E_s = \frac{e}{L_1 + \gamma_s/\gamma_b \cdot (L_2 + L_3)} \tag{9b}$$

With these equations recoveries can be deduced for cases when the sample conductivity differs from the value for which the system was tuned. For instance, when in a critical geometry the electrophoresis time is tuned using a standard solution with the same conductivity as the buffer, the recovery for samples with $\gamma_s < \gamma_b$ is:

$$R = \frac{4 \cdot \gamma_s/\gamma_b - 1}{2\,(\gamma_s/\gamma_b)^2 + \gamma_s/\gamma_b} \quad (0 \leqq R \leqq 1) \tag{10}$$

For samples with $\gamma_s > \gamma_b$:

$$R = \gamma_b/\gamma_s \tag{11}$$

Results of calculations for this and other geometries are shown in Fig. 3a. When the conductivity of a sample is too high, recovery may not be complete. However, a large variation of the conductivity to the low side is allowed, even for the critical geometry. This can be attributed to the effect of zone compression.

Under constant-current conditions, only the field strength in the sample solution is influenced by changes in the sample conductivity (cf. eqn. 5). Samples with a lower conductivity than the reference sample will always be recovered completely, due to the zone compression. Limits will be imposed only by the maximum voltage the constant-current supply is capable of delivering. For the critical geometry the recovery from samples with $\gamma_s > \gamma_b$ is given by eq. (11).

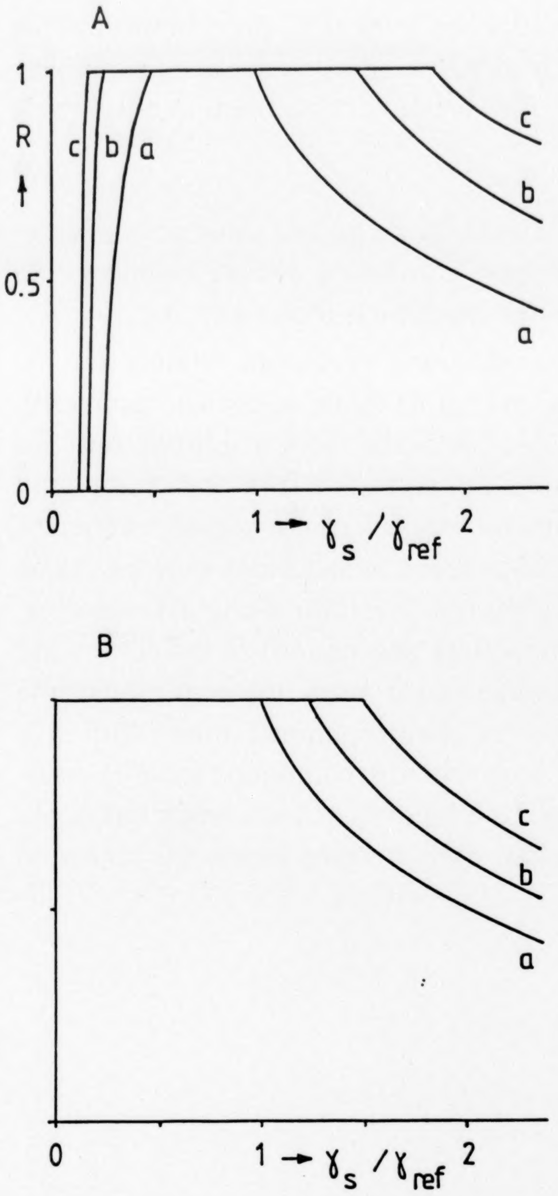

Fig. 3

Calculated dependency of the recovery on the sample conductivity. Field strength and time of electrophoresis are tuned for a sample with γ_{ref}. (A) constant voltage. (B) constant current. $L_2/L_1 = 1$. $L_3/L_1 = 1$ (a), 1.5 (b) and 2 (c).

Results of calculations for various geometries are shown in Fig. 3b. Comparison with Fig. 3a shows that a system under current control is more sensitive to changes of the conductivity to the high side.

Protein Binding

The mobility of an ion in the sample matrix may differ considerably from that in a buffer solution. Differences in viscosity, ionic strength or pH are trivial causes. Of more interest is the influence in protein binding in biological samples. For instance, drugs are often present in blood to a large extent bound to proteins. In a discussion of this effect on ZEST a distinction has to be made according to the reversibility of the binding. If the binding reaction is slow on the time-scale of the ZEST procedure, only free ions will migrate towards the injection capillary. The chromatographic determination will yield the free concentration of the compound.

On the other hand, if the binding is a fast equilibrium process, eventually all ions will be transferred to the buffer solution, but the apparent mobility in the sample solution

Eq. (15) can also be used to calculate a maximum injection volume or a minimum time of electrophoresis when from experimental data a maximum temperature increase as a boundary condition has to be imposed. Problems with excessive heat production can be decreased by loosening the demands made on loading capacity or speed.

The temperature increase during electrophoresis is proportional to the conductivity of the solutions. However, dilution of samples (and buffer) with water is not the answer. When the sample is diluted x times ($x > 1$), the conductivity is approximately 1/x times its original value, but the volume of the sample capillary should be increased x times to obtain the same sensitivity in chromatography. When the volume is increased by increasing the length of the injection capillary, the result is that the temperature increase is $1/x \cdot x^2 = x$ times higher. When the colume is increased by using wider capillaries (r_{in}^2 increased x times), the power per unit length stays the same. Only the logarithmic term in eq. (15) changes. A very small improvement is obtained resulting from the improved heat conduction in the valves.

The conclusion of the previous was that the capillaries should be as wide and short as possible. In practice, limits will be set by the size of the valves and connections to them. Eq. (15) was derived for the case that the transfer and injection capillaries have the same length as the sample capillary. However, in many applications the sample capillary should be shorter than the others to obtain complete recovery of a range of compounds and a sharply defined selectivity (see Fig. 2). The same effect can be obtained by increasing the buffer concentration. Though it can be shown that this does not improve the temperature increase in the sample capillary or the speed of the process, the same performance can be obtained with a lower applied voltage.

Zone Broadening

Several factors cause an increase of the lengths of zones of compounds of interest during the electrophoretic process. This zone broadening has to be taken into account in the development of the system to ensure complete recovery.

The first cause is ordinary axial diffusion. The contribution to the second moment of the zone is:

$$\sigma_z^2 = 2Dt_f \tag{16}$$

If the increase of the zone length Δz is defined as 4σ, this factor causes a Δz of 0.4 cm (with $t_f = 10^3$ and $D = 5.10^{-6}$), independent of the capillary radius.

A second cause of zone broadening is the temperature gradient developed in the radial direction within the capillary. Assuming uniform current density, the steady state temperature at a distance r from the axis of the capillary is [7]:

$$T(r) = T_{in} + \frac{P}{4\pi K_s}\left(1 - \frac{r^2}{r_{in}^2}\right) \tag{17}$$

where K_s is the thermal conductivity of the solution. For water K_s is 6.10^{-3} J s^{-1} cm^{-1} K^{-1}. The dependency of the mobility on the temperature was given in eq. (7). Combining eq. (1), (7), (13) and (17) gives the ion velocity as a function of r:

$$u(r) = u_{in} + \frac{p\gamma}{4K_s} \cdot u_0 E^3 \cdot (r_{in}^2 - r^2) \tag{18}$$

Superimposed on the velocity u_{in} determined by the temperature at the inner wall is a parabolic velocity profile, giving a mean extra velocity $\bar{u}_T$ of:

$$\bar{u}_T = \frac{p\gamma\, u_0 E^3\, r_{in}^2}{8K_s} \tag{19}$$

The zone broadening caused by the temperature gradient, counteracted by radial diffusion, can be treated in exactly the same way as Taylor [8] did for the parabolic velocity profile in laminar flow. The contribution to the second moment is then:

$$\sigma_z^2 = \frac{r_{in}^2\, \bar{u}_T^2\, t_f}{24\,D} \tag{20}$$

Using eq. (4), (19) and (20) this contribution to zone broadening was calculated for different capillary radii under the usual boundary conditions, assuming $p = 0.02$ K^{-1}. Results are presented in Table II. Surprisingly, only for the narrowest capillaries the temperature gradient contributes significantly to zone broadening.

Performing ZEST in a straight tube as shown schematically in Fig. 1, would require at least six independent switching valves. As will be shown in Part II of this study [9], it is possible to use only three conventional six-port valves if bending of the capillaries is allowed. This bending contributes to zone broadening. For a rigorous treatment of this phenomenon the exact geometry of the system should be known. However, the order of magnitude of the effect can be estimated from assumptions on the geometry and an analogy to the zone broadening caused by the temperature gradient. If a capillary is bent, ions following field lines in the outer curve will lag behind ions taking the inner curve; first, because the distance to be travelled is longer, secondly because the field strength in the outer curve is lower. For a capillary of length L forming a 180° loop, it is easy to show that ions appear at the end of the capillary with an apparent difference in velocity Δu:

$$\Delta u = u \cdot \frac{4\pi r}{L} \tag{21}$$

In this equation u is the velocity along the axis of the capillary. This distribution of ions over the length of the capillary is counteracted by diffusion over the width of the capillary. The resulting zone broadening will be comparable to that caused by a parabolic velocity profile with a mean velocity of $\Delta u/2$ and a diffusion distance of $2\,r_{in}$. Substitution of these values and eq. (1) and (21) in the Taylor-equation gives as estimate of the zone broadening:

$$\sigma_z^2 = \frac{2\pi^2\, u_0 E\, r_{in}^4}{3\,D\,L} \tag{22}$$

Calculations have been performed on the assumption that two equal 180° loops are passed, with independent contributions to zone broadening, under the usual boundary

Table II. Contributions to zone broadening in ZEST

r_{in} [cm]	σ_z^2 contribution [cm^2]				Δz [cm]	$\frac{\Delta z}{L_1}$
	axial diffusion	temperature gradient	bending	total		
0.0125	0.0100	0.0016	0.0001	0.0117	0.43	0.02
0.025	0.0100	0.0000	0.0012	0.0112	0.42	0.08
0.05	0.0100	0.0000	0.0186	0.0286	0.68	0.53

conditions. Results are included in Table II. Though the figures have only an indicative value, it is clear that this contribution can be a major problem when short, wide capillaries are used.

A fourth and last cause of zone broadening to be discussed is convection due to density differences. There may be a difference in density between sample and buffer, and differences may arise from temperature differences within one solution. Though it is difficult to treat this effect quantitatively, it is clear that convection is of more importance with wide capillaries than with narrow ones.

Conclusions

From a theoretical point of view it seems possible to develop a system for the selective separation of low-molecular weight ionogenic compounds from protein containing samples by zone electrophoresis, to be used as sample treatment technique for HPLC, with acceptable loading capacity and speed. The selectivity of the procedure can be controlled by the lengths of the capillaries used in the system or, alternatively, by manipulation of the conductivities of the solutions used. Current control during the electrophoretic process is to be preferred when large variations of the ambient temperature or of the conductivity of the samples to the low side are expected. When a large variation of the sample conductivity to the high side may occur, it is better to keep the voltage constant.

The loading capacity and speed of the procedure are limited by the heat production during electrophoresis. From boundary conditions imposed by the chromatographic procedure the geometry of the ZEST system can be optimized. In respect to heat development and required voltage it is preferable to use short, wide capillaries, but in respect to zone broadening long, narrow capillaries have to be used. With the boundary conditions assumed in this work (V_s = 10 μl, t_f = 1000 s) it seems a reasonable compromise to use 0.5 mm I.D. capillaries.

In part II of this study the experimental development of a ZEST system, its implementation in an automated chromatograph, and its characterization and evaluation will be described.

List of Symbols

symbol	unit	dimension	value used in calculations
γ	conductivity	Ω^{-1} cm^{-1}	0.01
D	diffusion coefficient	cm^2 s^{-1}	5.10^{-6}
e	applied voltage	V	
E	field strength	V cm^{-1}	
K_c	thermal conductivity of capillary	J s^{-1} cm^{-1} K^{-1}	2.10^{-3}
K_s	thermal conductivity of solution	J s^{-1} cm^{-1} K^{-1}	6.10^{-3}
L	length of capillary	cm	
L_1	length of sample capillary	cm	
L_2	length of transfer capillary	cm	
L_3	length of injection capillary	cm	
p	temperature coefficient of mobility	K^{-1}	0.02
P	power per unit length	j s^{-1} cm^{-1}	
r	radius, distance from axis	cm	
R	recovery		
σ_z^2	second moment of zone length	cm^2	
t_f	time of electrophoresis	s	10^3
T	temperature	K	
u	ion velocity	cm s^{-1}	
u_0	ion mobility	cm^2 V^{-1} s^{-1}	2.10^{-4}
u_0'	apparent ion mobility	cm^2 V^{-1} s^{-1}	
$\bar{u}_T$	mean extra velocity by temperature gradient	cm s^{-1}	
V_s	sample volume	cm^3	0.01
z	zone length	cm	
suffix b	refers to buffer solution		
suffix s	refers to sample solution		
suffix in	refers to inner capillary wall		
suffix out	refers to outer wall of capillary or valve		
suffix ref	refers to standard compound or conditions		

References

[1] *M. W. F. Nielen,* "Selective on-line precolumn sample handling and trace enrichment in liquid chromatography", thesis, Free University, Amsterdam, The Netherlands, 1987.

[2] *F. Kohlraush,* Ann. Physik., **62**, 209 (1897).

[3] *F. W. Sunderman,* Amer. J. Clin. Path., **15**, 219 (1945).

[4] *R. J. Wieme,* in "Chromatography", E. Heftman (Ed.), Van Nostrand Reinhold, New York, 3rd ed., Ch. 10 (1975).

[5] *D. H. Moore,* in "Electrophoresis, Theory, Methods and Applications", M. Bier (Ed.), Academic Press, New York, Ch. 9 (1959).

[6] *H. S. Carslaw, J. C. Jaeger,* "Conduction of Heat in Solids", Oxford Univ. Press, Oxford (U.K.), pp 188–190 (1959).

[7] ibid, pp. 191–192.

[8] *G. Taylor,* Proc. R. Soc. London, Ser. A, **219**, 186 (1953).

[9] *W. Th. Kok, K. P. Hupe, R. W. Frei,* in preparation.

Received: Juli 2, 1987
Accepted: Juli 22, 1987
F

A Micropreparative Chromatographic Strategy for the Purification and Sequence Analysis of Murine Granulocyte-Colony Stimulating Factor (mG-CSF)

E. C. Nice[1]*/R. J. Simpson[2]/N. A. Nicola[3]

[1]Melbourne Tumour Biology Branch, Ludwig Institute for Cancer Research, Australia 3050.
[2]Joint Protein Structure Laboratory, Ludwig Institute for Cancer Research and the Walter and Eliza Hall Institute, Australia 3050.
[3]Walter & Eliza Hall Institute of Medical Research, P0 Royal Melbourne Hospital, Victoria 3050, Australia.

Key Words

Microbore-HPLC
Micropreparative-HPLC
Microsequencing
Colony stimulating factors

Summary

A micropreparative chromatographic strategy using short (< 5 cm) 1 and 2 mm ID HPLC columns for preparing pure mG-CSF and its peptide fragments is described. The proteins and peptides are used to obtain both N-terminal and internal amino acid sequence data for the purpose of constructing sequence specific oligonucleotide probes for use in the isolation of the gene coding for the protein of interest, thereby ultimately enabling amplified amounts of protein to be generated using prokaryotic expression systems.

Introduction

Recent understanding of the biological, and possible clinical, significance of a number of the hemopoietic colony stimulating factors has highlighted the need to produce large quantities of these materials for detailed structure-function studies. Since they are only present in biological material in very small amounts [1] this goal will be most readily achieved using recombinant DNA based techniques. Two broad approaches are currently employed to isolate a specific gene (or cDNA) of interest. One makes use of synthetic oligonucleotide probes, constructed from a knowledge of the amino acid sequence (determined by Edman degradation of the isolated protein or generated peptide fragments) [2], whilst the other employs expression vectors and screening for biological activities, or reaction with specific antisera directed towards the purified protein of interest [3]. Now that protein sequencing technology [4] permits sequence data to be obtained at the 5–10 picomole level [5], the ability to purify and micromanipulate subnanomole amounts of protein and peptide fragments in a form suitable for microsequence analysis is the rate limiting step in a setting up the appropriate expression system.

In this report we will describe the protocol devised for obtaining both N-terminal and internal sequence data from approximately 300 picomoles of murine G-CSF isolated from 6 litres of mouse lung conditioned medium [6].

Materials and Methods

Reagents

Sodium chloride and hydrochloric acid (Aristar grade) were purchased from BDH (Poole, Dorset, UK). Trifluoroacetic acid (99% pure grade) and Tween 20 (10% solution in water) were from Pierce Chemical Co. (Rockford, Illinois, USA). Iodoacetic acid (Puriss grade) was obtained from Fluka (Buchs, Switzerland) and was recrystallised prior to use. Dithiothreitol was from Calbiochem (California, USA). All other chemicals were of the highest grade available commercially.

All organic solvents were HPLC grade. Deionised water, obtained from a tandem Milli-RO and Milli-Q system (Millipore Inc., Massachusetts, USA) was used for all buffers.

Preparation of Mouse Lung Conditioned Medium (MLCM)

Conditioned medium was prepared from the lungs of 3–4 month male and female mice of the C57BL/61/j/WEHI strain which had been injected intravenously with 5 μg of endotoxin (Difco) 3 h before sacrifice as described previously [6].

0009-5893/87 0449-06 $03.00/0

© 1987 Friedr. Vieweg & Sohn Verlagsgesellschaft mbH

High-Performance Liquid Chromatography Instrumentation

All high-performance separations were performed on a Hewlett Packard Model 1090 liquid chromatograph fitted with a Model 1040 diode array detector and a Model 3392A recording integrator. Chromatographic and spectral data were stored on disc (Hewlett Packard Model 9121) for subsequent analysis using the EVALU 1 and 2 software packages. Samples were injected using a Rheodyne Model 7125 valve equipped with a 2 ml injection loop installed in the column oven compartment. Large samples were loaded by repetitive injection. The elution profile was monitored in real rime at 215 nm and eluent peaks were recovered manually, allowance being made for the dead volume between the detector flow cell and the collection port.

Column Supports

The following supports were used in the final stages of the purification of the native protein, and in the generation of peptide fragments for microsequence analysis: (a) Beckman Ultrapore RPSC (75 x 4.6 mm ID), (b) Beckman Ultrapore RPSC (50 x 1 mm ID), (c) TSK 2000 SW (600 x 7.6 mm ID), (d) Pharmacia Superose 12, (e) Brownlee BU-300 (30 x 2.1 mm ID). The chromatographic conditions use are given in the ensuing text or the respective figure legends.

SDS-Polyacrylamide Gel Electrophoresis: (SDS-PAGE)

SDS-PAGE was performed on a Phast System (Pharmacia, Sweden) using Phast Gel Gradient 10—15 under standard conditions. Proteins were visualised by silver staining.

Amino Acid Sequence Analysis

Automated amino acid sequence analysis of purified proteins and polypeptides was performed using an Applied Biosystems Model 470A sequencer. Polybrene [7] was used as the carrier. Amino acid phenylthiohydantoin derivatives were analysed using the HPLC system described elsewhere [8].

Results and Discussion

The Purification, Analysis and N-Terminal Sequence of mG-CSF From Mouse Lung Conditioned Medium

The initial stages of the purification were essentially as described previously [6]. However in order to obtain homogeneous material, as evaluated by SDS-PAGE and N-terminal sequence analysis, material from the final size exclusion HPLC stage was further purified by chromatography on a Beckman Ultrapore RPSC column (300 Å pore size, 5 μ particle size, C3 funtionality, 75 x 4.6 mm ID). Proteins were recovered by a linear 60 min gradient (at a flow rate of 1 ml/min) between 30 and 60% acetonitrile containing 0.9% (w/v) sodium chloride (adjusted to pH 2.1 with concentrated HCl) (Fig. 1a). Column temperature was 25°C. Biological assay [6] of recovered fractions, (trapped at 0.5 min intervals into tubes containing Tween 20 final concentration 0.02% [6] to prevent losses by non-specific adsorption) indicated a single peak of biological activity, corresponding to the major UV absorbing material.

However the sodium chloride mobile phase, whilst having excellent absorption properties at 215 nm, thus facilitating

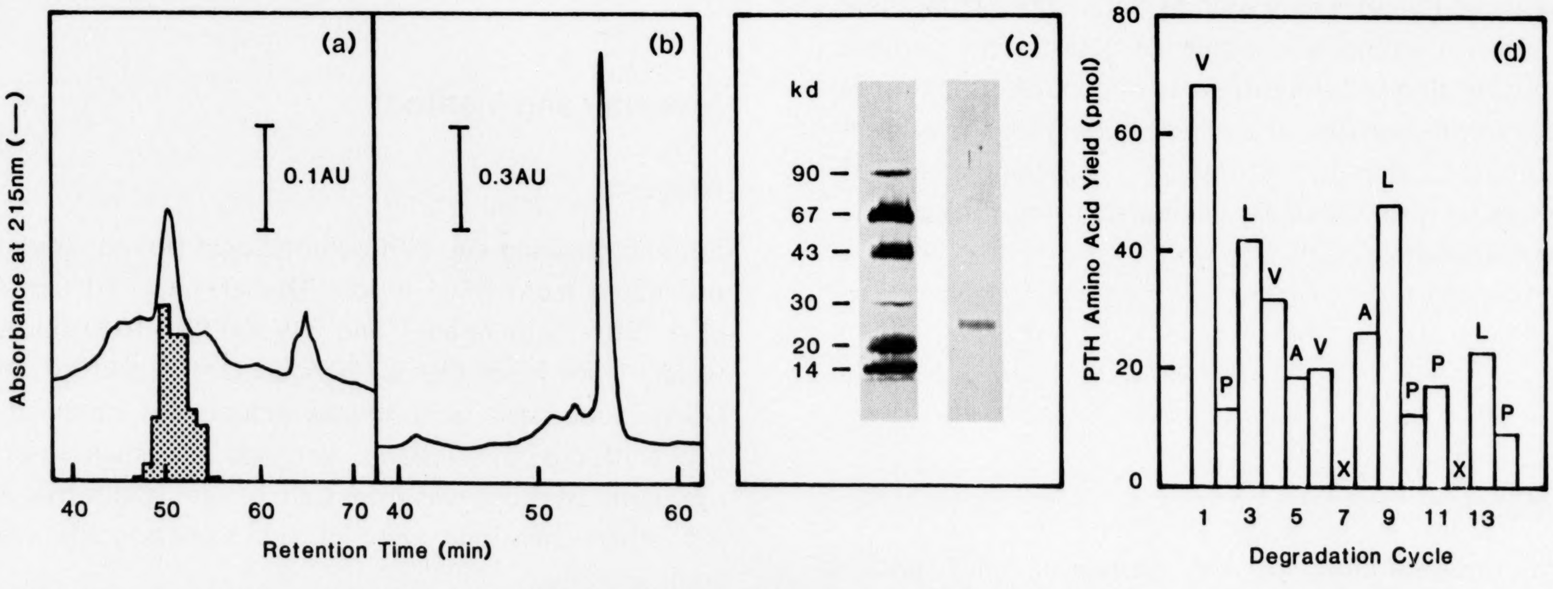

Fig. 1 The preparation of mG-CSF for N-terminal sequence analysis.

a: Conventional RP-HPLC. Column: Beckman Ultrapore RPSC, 75 x 4.6 mm ID. Primary solvent: 30% aqueous CH_3CN/0.9% (w/v) NaCl (pH 2.1). Secondary solvent: 60% aqueous CH_3CN/0.9% (w/v) NaCl (pH 2.1). Linear 60 min gradient. Flow 1 ml/min. Temp 25°C. Sample: mG-CSF from TSK3000SW (Table I, Step 6). The shaded area represents the biological activity in 0.5 min fractions. The 3 fractions corresponding to the major uv absorbing peak were pooled for further studies.

b: Microbore trace enrichment and buffer exchange. Column: Beckman Ultrapore RPSC, 50 x 1 mm ID. Primary solvent: 0.15% (v/v) aqueous TFA. Secondary solvent: 60% aqueous CH_3CN/0.125% (v/v) TFA. Linear 60 min gradient. Flow 50 μl/min. Temp 45°C. Sample: mG-CSF (500 μl aliquot) from **(a)** was diluted 1:1 with 0.02% (v/v) aqueous Tween 20. The sample was loaded at a flow rate of 1 ml/min (not shown). After 2 min the flow rate was reduced to 50 μl/min and the gradient initiated.

c: SDS-Polyacrylamide gel electrophoresis on Pharmacia Phast Sep gel 10—15% L. H. lane M. Wt markers. R. H. lane. 1 μl aliquot mG-CSF from (b).

d: N-terminal sequence analysis of mG-CSF. Material from **(b)** was applied directly to the sample disc of the gas phase sequencer. The PTH amino acids generated at each cycle were analysed by HPLC [8].

detection of small amounts of material and also being compatible with subsequent bioassay [9] is not compatible with direct N-terminal sequence analysis. The active fractions corresponding to the major UV absorbing peak were therefore pooled (1.5 ml), and an aliquot (500 μl) taken and diluted 1:1 with 0.02% aqueous Tween 20, for concentration and buffer exchange [10, 11] into a volatile TFA/CH_3CN solvent using the short microbore Ultrapore RPSC column (50 x 1 mm ID). The relatively large volume of the diluted aliquot from the conventional column ($\simeq$1 ml) can be readily loaded onto the microbore column at high flow rate (1 ml/min) because of the lower operating back pressures observed with short columns (back pressure being directly proportioned to column length). Following loading of the sample the flow rate was reduced to 50μ/min and the protein recovered using a linear 60 min gradient between a primary solvent of 0.15% (v/v) aqueous TFA and a secondary solvent of 60% CH_3CN/40% H_20/0.125% (v/v) TFA. (The slight variance in TFA concentration minimises baseline rise during the gradient.) The protein was recovered manually in an eluant volume of $\simeq$50 μl (Fig. 1b). The overall yields and purification factors are given in Table 1. It can be seen that an overall purification factor of $\simeq$500,000 was achieved. The additional stages reported herein give an apparent 10% increase in specific activity from those previously reported [6]. A small aliquot (1 μl) was taken for SDS-PAGE analysis (Fig. 1c) and the remainder applied directly to the Polybrene coated disc of the gas phase sequenator. A unique N-terminal sequence was obtained which permitted the assignment of the first 14 amino acid residues (Fig. 1d). The remainder of the material from the conventional (4.6 mm ID) column was purified (2 x 500 μl aliquots) for the generation of peptide fragments.

Enzymic Fragmentation of the Native Protein

In this instance the N-terminal sequence obtained proved unsuitable for the construction of oligonucleotide probes of limited degeneracy. Internal sequence was generated following enzymic digestion of the native protein. Whilst it is more common to reduce and alkylate prior to digestion this procedure necessitates a number of further manipulations with possible losses at each stage. Moreover it has been noted [12, 13] when investigating the disulphide bond assignment of recombinant proteins by enzymic mapping (when reduction of the disulphide bonds is to be avoided), that digestion of the native protein often leads of the generation of a number of peptide fragments.

Native mG-CSF, recovered from the 1 mm ID microbore column (step 8, Table I: approximately 33% of the total sample) was diluted 10 fold with 1% ammonium bicarbonate (pH 7.8), reducing the concentration of acetonitrile to $\simeq$5%, and incubated for 16 h at 37°C with 1 μg of *Staphylococcus aureus* protease V8. For comparative purposes an enzymic blank was also set up using a similar volume of HPLC solvent. Following digestion samples were fractionated on a Brownlee BU-300 column (30 x 2.1 mm ID) using the chromatographic conditions detailed in Fig. 2. Although only limited digestion had occurred one unique peak (VI) was recovered for subsequent amino acid sequence analysis. Sequence data was obtained at the 15 pmole level which permitted assignment of 18 amino acid residues.

Enzymic Fragmentation Following Succinylation(S) and Reduction-Carboxymethylation (RCM) of the Native Protein

To obtain further internal sequence the native protein was succinylated, reduced and carboxymethylated prior to digestion. The protocol used for this is detailed in Fig. 3. Succinylation was chosen for two reasons: – firstly it was hoped that the succinylated derivatives would be less hydrophobic and hence easier to recover in good yield from reversed phase (RP) supports: – secondly the succinylation would restrict the subsequent tryptic digestion to arginine residues, therefore potentially giving a smaller number of longer fragments for sequence analysis.

A ^{125}I-G-CSF tracer, prepared by the gas phase radioiodination procedure described previously [14], purified by microbore RP-HPLC, and characterised by size exclusion HPLC (Fig. 4) was added prior to the chemical derivatisation to facilitate both the identification of the protein and calculation of recovery during subsequent chromatographic desalting. Although the sensitivity associated with the use of microbore columns readily permits the detection of proteins at the low nanogram level [10], a radioactive tracer was added since the presence of artifactual

Table I. Purification of murine granulocyte-colony stimulating factor (mG-CSF)

Step	Volume ML	Protein MG/ML	Activity Units/ML	Activity Units/MGX10^{-3}	Purification -fold	Yield %
1. MLCM	3,000	1.76	2,500	1.42	1	100
2. Salting out chromatography	91	6.7	60,000	8.96	6.3	73
3. Phenyl-sepharose chromatography	41	3.9	185,000	47.4	33.4	100
4. Bio-gel P-60 chromatography	31	1.7	223,000	131.2	92.4	96
5. RP-HPLC phenyl-silica (x 2)	4	0.0013	750,000	577,000	406,000	40
6. TSK gel Filtration HPLC	1.5	0.0027	1,700,000	630,000	443,000	34
7. RP-HPLC C3 (300 Å) 4.6 MM ID	1.6	0.0024	1,616,000	679,000	471,126	33
8. RP-HPLC C3 (300 Å) 1 MM ID	0.05*	0.075*	53,738,000	713,000	495,000	33

* These values are extrapolated from data obtained with 1/3 of the sample

peaks from the relatively large quantities of reagents used during the derivatisation (eg. 6 M guanadinium hydrochloride) can interfere with the interpretation of chromatograms at these low peptide concentrations. It should be remembered however that, in some instances, the active and radiolabelled moieties can themselves be resolved by RP-HPLC [15].

Analytical microbore RP-HPLC indicated that although the native protein could be recovered essentially quantitatively from such supports (Table I) severe losses (> 75%) were experienced with the S-RCM material even if n-propanol was used as the organic modifier. We have noted previously [16] that RCM proteins can exhibit pronounced increased retention on RP-supports. The native G-CSF being already of very hydrophobic nature (eluting at $\simeq$50% CH_3CH) any increased retention on RP-columns would undoubtedly lead to the losses observed.

Size exclusion HPLC using Superose 12 was therefore chosen to desalt the S-RCM material. This support was chosen since, being based on a non-silica matrix, it is stable in solvent systems compatible with subsequent tryptic digestion (eg 100 mM NH_4HCO_3, pH 7.8). Although the detergent Tween 20 (0.02% v/v) had been used routinely to prevent losses during the purification of the native protein [6] it was omitted during the succinylation/reduction/alkylation stage since it was assumed that the presence of 6 M guanidinium hydrochloride would obviate this precaution. It was however included in the chromatigraphic solvents used for desalting to prevent possible losses due to non-specific absorption.

Whilst size exclusion chromatography has the advantage of being generally applicable to the chromatographic desalting of a wide range of proteins, peak volumes are invariably relatively large (500 μl – 1 ml). In this instance although protein standards chromatographed with acceptable efficiency (Fig. 5a) both the ultraviolet absorption profile (Fig. 5b) and the associated radioactivity (Fig. 5c) indicated that the S-RCM-G-CSF was recovered as a much broader

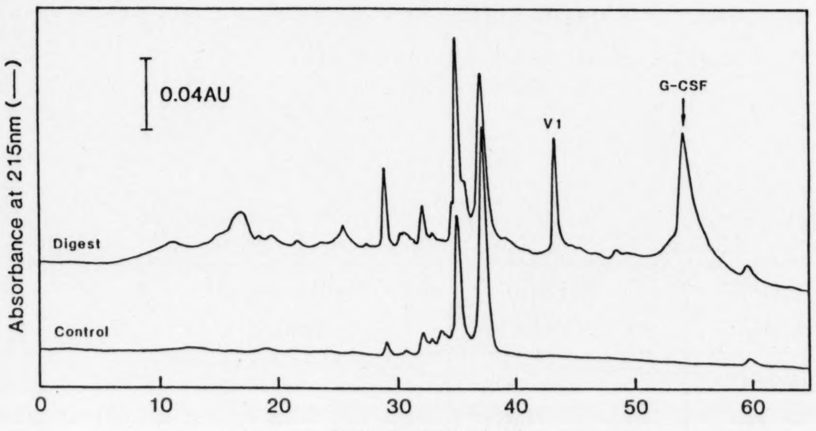

Fig. 2

The separation of a V8 digest of native mG-CSF column: Brownlee BU-300, 30 x 2.1 mm ID. Primary solvent: 0.15% (v/v) aqueous CH_3CN/0.125% (v/v) TFA. Flow 100 μl/min. Temp 45°C.

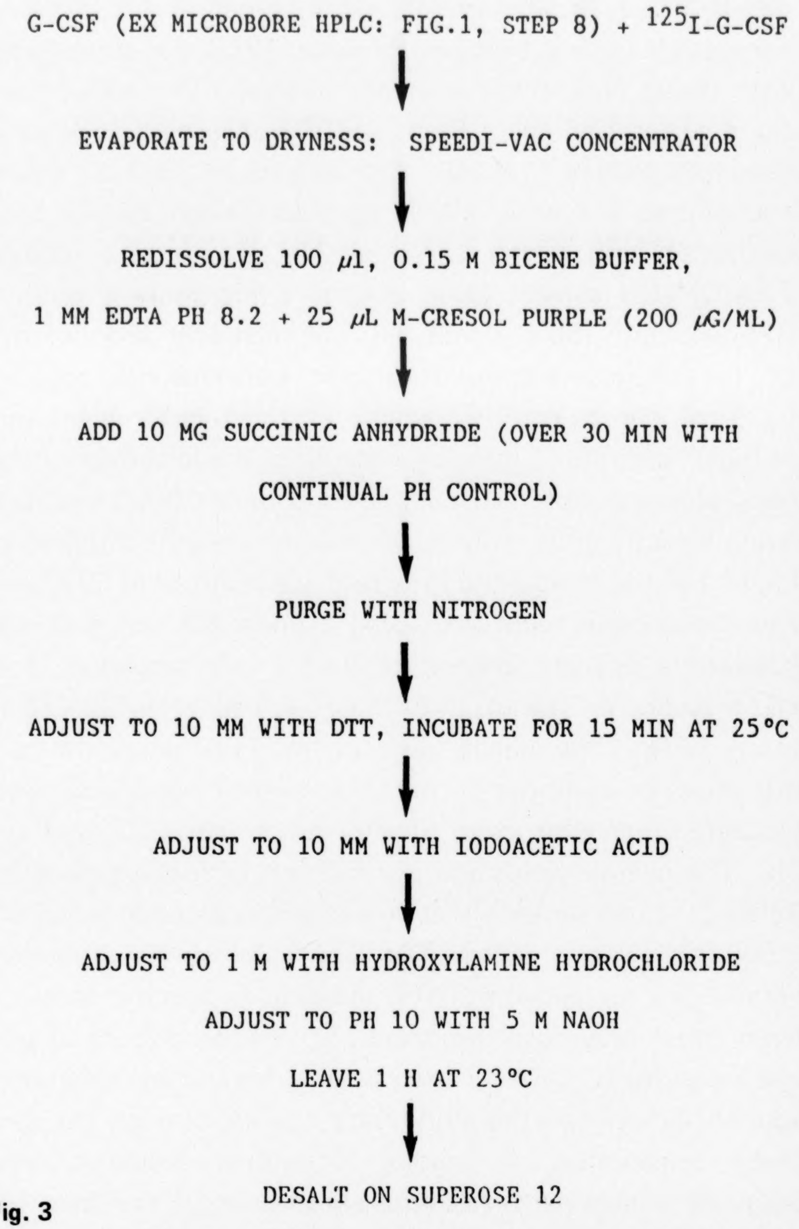
G-CSF (EX MICROBORE HPLC: FIG.1, STEP 8) + ^{125}I-G-CSF
EVAPORATE TO DRYNESS: SPEEDI-VAC CONCENTRATOR
REDISSOLVE 100 μl, 0.15 M BICENE BUFFER,
1 MM EDTA PH 8.2 + 25 μL M-CRESOL PURPLE (200 μG/ML)
ADD 10 MG SUCCINIC ANHYDRIDE (OVER 30 MIN WITH
CONTINUAL PH CONTROL)
PURGE WITH NITROGEN
ADJUST TO 10 MM WITH DTT, INCUBATE FOR 15 MIN AT 25°C
ADJUST TO 10 MM WITH IODOACETIC ACID
ADJUST TO 1 M WITH HYDROXYLAMINE HYDROCHLORIDE
ADJUST TO PH 10 WITH 5 M NAOH
LEAVE 1 H AT 23°C
DESALT ON SUPEROSE 12

Fig. 3

Protocol for the succinylation and reduction-carboxymethylation of mG-CSF.

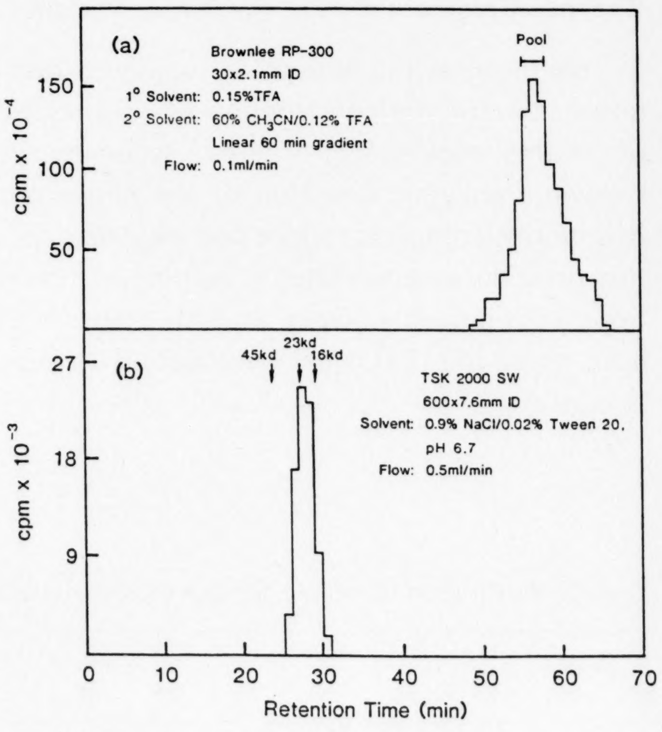

Fig. 4

The purification and characterisation of ^{125}I-mG-CSF.

a: RP-HPLC purification. Column Brownlee RP-300, 30 x 2.1 mm ID. Mobile phase conditions as detailed in Fig. 2. The fractions indicated (—) were pooled.

b: SEC-HPLC characterisation Column TSK 2000 SW. Sample: an aliquot (5 μl) of the pooled fractions from (**a**).

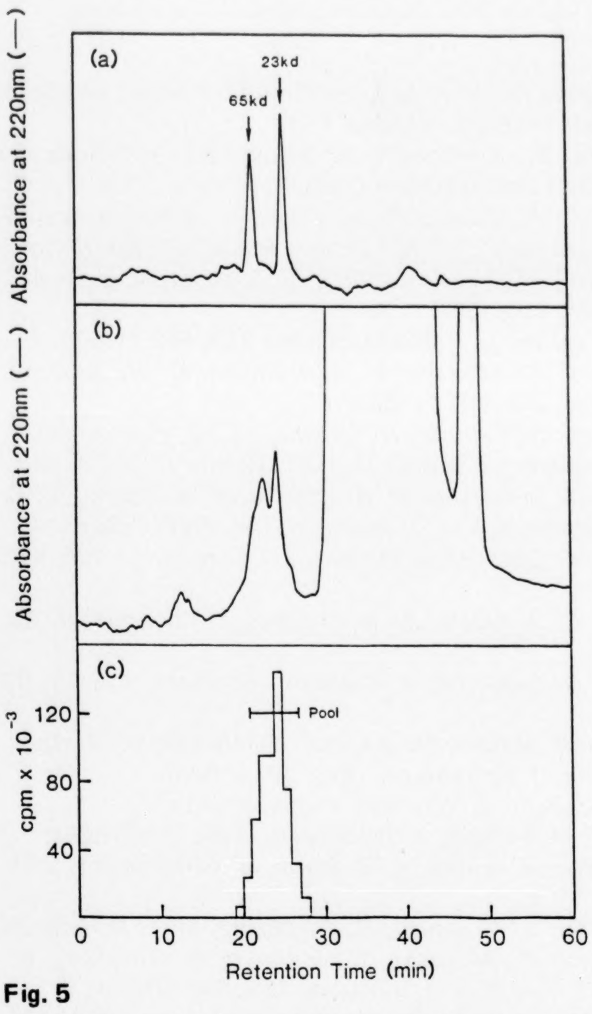

Fig. 5

Desalting of S-RCM-mG-CSF by SEC-HPLC on Superose 12. Mobile phase 100 mM NH_4HCO_3 (pH 7.8) containing 0.02% (v/v) Tween 20. Flow 0.5 ml/min.

a: Protein standards: Bovine serum albumin (65 kd), trypsin inhibitor (23 kd).

b: Succinylated and reduced-carboxymethylated mG-CSF: see Fig. 3. Material was recovered in 0.5 min fractions across the profile.

c: Radioactivity associated with (**b**).

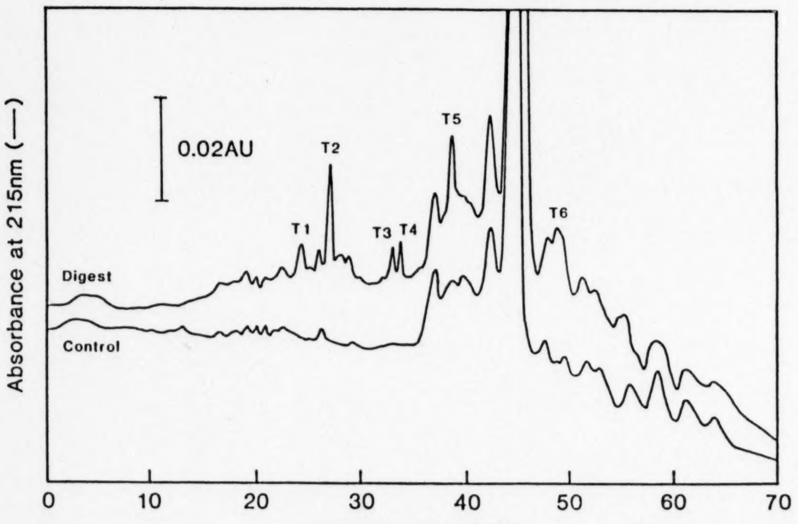

Fig. 6

The separation of tryptic peptides of S-RCM-mG-CSF. Column Brownlee BU-300, 30 x 2.1 mm ID. Chromatographic conditions as described in Fig. 2.

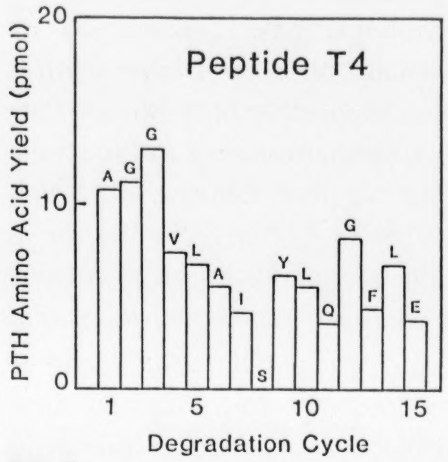

Fig. 7

Sequence analysis of tryptic peptide T_4 from Fig. 6.

peak. The fractions indicated were pooled and incubated with TPCK-trypsin (0.5 μg) overnight at 37 °C. A control containing all the reagents except the protein was chromatographed under identical conditions and a "blank" fraction of equivalent volume and elution position to the pooled protein sample was recovered and incubated overnight with 0.5 μg trypsin to enable the subsequent identification of solvent (eg. Tween 20) and enzyme related artefacts. The sample (volume $\simeq$3 ml) was then trace enriched onto the Brownlee BU-300 column (30 x 2.1 mm ID) at a flow rate of 2 ml/min before recovering the tryptic peptides with a linear 60 min gradient between 0.15% TFA and 60% CH_3CH/0.125% TFA at a flow rate of 100 μl/min (Fig. 6). The "blank" was chromatographed under identical conditions. Six peaks (T_1–T_6), which appeared unique to the protein digest, were chosen for sequence analysis. Peaks T_1–T_4 were sequenced directly. Peaks T_5 and T_6 were further purified by rechromatography on the same column, but using a linear 50 min gradient between 0.9% (w/v) aqueous NaCl (pH 6.5) and 50% CH_3CN at a flow rate of 100 μl/min (data not shown). These salt containing samples were exchanged into TFA/CH_3CN for loading onto the sequencer using the 1 mm ID microbore column as described earlier. No sequence data was obtained with peaks T_1 and T_5. The remaining peptides yielded 44 residues of unique sequence with initial yields ranging between 5 and 15 picomoles. Typical data, obtained with peptide T_4, is shown in Fig. 7. The remaining sequence data and its homology with the recently derived amino acid sequence for human GSF, determined from a cDNA clone [17], will be presented elsewhere [18].

Conclusion

All recovery problems become more acute when manipulating small (subnanomole) amounts of material. In an attempt to maximise recovery the following points in the protocol presented herein warrant specific mention:

(1) Previous studies [6] have shown that mG-CSF is extremely susceptible to losses by non-specific adsorption. The detergent Tween 20 was therefore used routinely to obviate such losses, except where it was deemed that the presence of other reagents (e.g. 6 M guanidinium hydrochloride, 50% CH_3CN) would prevent this. A significant disadvantage of any additive

when working at high sensitivity is that they, or impurities they may contain, often contribute significantly to the overall chromatographic background. Care was therefore taken to either chromatograph precisely prepared reagent blanks so that background peaks could be clearly identified (e.g. Fig. 2, Fig. 6), or in the case of the desalting by size exclusion to include a chromatographically defined radiolabelled marker (Fig. 5).

(2) It is now generally accepted that concentration steps such as lyophilisation or evaporation are to be studiously avoided when working with low (subnanomole) levels of protein [5, 8, 19]. To this end the protocol presented makes use of short (50 or 30 mm) narrow bore (1 or 2 mm ID) RP-HPLC columns for concentration and buffer exchange. Using these columns large sample volumes (up to 3 ml in this instance) could be rapidly trace enriched at high flow rate (1–2 ml/min) onto the column before recovering proteins or polypeptides, by gradient elution at flow rates of 50–100 μl/min, in peak volumes of 50–80 μl. Such volumes are ideally suited for direct application to the sample disc of the gas phase sequenator.

The method described has permitted the sequence assignment of 77 amino acid residues of murine G-CSF (≃50% of the molecule). This was obtained from approximately 300 picomoles of purified protein.

Acknowledgements

The authors thank Mr. L. Fabri for excellent technical assistance and Mr. M. Rubira for operation of the gas phase sequencer. We are indebted to Dr. A. W. Burgess for his continued support and encouragement and helpful discussions.

References

[1] *A. W. Burgess, N. A. Nicola,* in "Growth Factors and Stem Cells", Academic Press, Sydney, 1983.

[2] *T. Maniatis, E. F. Fritsch, J. Sembrook*, in "Molecular Cloning", Cold Spring Harbor Press, New York, 1982.

[3] *T. Huynh, R. A. Young, R. W. Davis,* in "DNA cloning: A Practical Approach", D. M. Glover, ed., IRL Press, Oxford.

[4] *R. M. Hewick, M. W. Hunkapiller, L. E. Hood, W. J. Dreyer,* J. Biol. Chem. **256**, 7990 (1981).

[5] *M. W. Hunkapiller, L. E. Hood,* Science **219**, 650 (1983).

[6] *N. A. Nicola, D. Metcalf, M. Matsumoto, G. R. Johnson,* J. Biol. Chem. **258**, 9017 (1983).

[7] *J. M. Bower, R. Camble, H. Gregory, E. L. Gerring, I. R. Willshire,* Experientia (Basel) **31**, 825 (1975).

[8] *B. Grego, I. R. Van Driel, P. A. Stearne, J. W. Goding, E. C. Nice, R. J. Simpson,* Eur. J. Biochem. **148**, 485 (1985).

[9] *E. C. Nice, M. Capp, M. J. O'Hare,* J. Chromatogr. **185**, 413 (1979).

[10] *E. C. Nice, C. J. Lloyd, A. W. Burgess,* J. Chromatogr. **29**, 153 (1984).

[11] *E. C. Nice, B. Grego, R. J. Simpson,* Biochem. Int. **11**, 87 (1985).

[12] *M. Kunitani, P. Hirtzer, D. Johnson, R. Halenbeck, A. Boosman, K. Koths,* J. Chromatogr. **359**, 391 (1986).

[13] *E. C. Nice, L. Fabri, L. Sparrow,* In preparation.

[14] *N. A. Nicola, D. Metcalf,* J. Cell Physiol. **124**, 313 (1985).

[15] *B. S. Welinder, S. Linde, J. S. Brush,* J. Chromatogr. **257**, 162 (1983).

[16] *R. J. Simpson, J. A. Smith, R. L. Moritz, M. J. O'Hare, P. S. Rudland, J. R. Morrison, C. J. Lloyd, B. Grego, A. W. Burgess, E. C. Nice,* Eur. J. Biochem. **153**, 629 (1985).

[17] *S. Nagata, M. Tsuchiya, S. Asano* et al., Nature, **319**, 415 (1986).

[18] *R. J. Simpson, N. Nicola, E. C. Nice,* Submitted to "Protein Sequences and Data Analysis".

[19] *F. S. Esch,* Anal. Biochem. **136**, 39 (1984).

Received: June 30, 1987
Accepted: July 17, 1987
F

Assessment of Semi-Automated Catecholamine Assay by HPLC: Choice of Reverse Phase C18 or Cation-Exchange Columns

M. Beschi* / M. Castellano / E. Agabiti-Rosei / D. Rizzoni / P. Rossini / G. Muiesan

Clinica Medica, Università degli Studi di Brescia, Spedali Civili Brescia, Italy

Key Words

Column liquid chromatography
Reverse phase
Cation exchange
Catecholamines

Summary

HPLC with electrochemical detection is useful in the assay of catecholamines in biological samples. Two types of chromatographic column are currently employed by most investigators: reverse phase C-18 (RPC-18) or strong cation-exchange (SCX) columns. Our aim was to evaluate the specificity, sensitivity and reproducibility of plasma and urinary catecholamine assay by these two columns.

Our study indicates that both columns give very good performance for clinical purposes but sensitivity, precision at low concentration and specificity seem to be better with ion-exchange columns which are therefore preferred at the present time.

Introduction

Measurement of catecholamines (noradrenaline -NA-, adrenaline -A- and dopamine -DA-) in biological samples is clinically useful for the diagnosis of phaeocromocytoma [1] and neural crest tumors; in addition, quantitation of catecholamines provides a well accepted index for assessing adrenergic activity [2, 3]. Several techniques have been proposed for measurement of plasma and urinary catecholamines.

In the past, fluorimetric [4] and radioenzymatic [5, 6, 7, 8] methods have been widely used. The older fluorimetric methods, that in human plasma samples give results similar to those obtained with enzymatic techniques, are practical and inexpensive but can be used only with relatively large samples owing to their comparatively low sensitivity. Radioenzymatic methods are highly sensitive but are also expensive and time consuming, so their routine use is not practical.

Recently, methods for determination of catecholamines based on high-performance liquid chromatography (HPLC) with electrochemical (ED) or coulometric (CD) detection have been proposed [9, 10, 11, 12]. These methods are as sensitive and accurate as the enzymatic techniques; in addition, they are inexpensive in materials and do not involve radioactive substances but as a manual technique they are rather time consuming.

For HPLC the choice of appropriate columns for optimum separation of catecholamines is crucial. We describe here a semi-automated assay for plasma catecholamines that enables an increased number of samples to be evaluated. In this study we have also assessed the performance of two most commonly used chromatographic columns: reverse phase C-18 (RP-C18) [13] and cation-exchange (SCX) [14].

Materials and Methods

Reagents

L-adrenaline, L-noradrenaline, dopamine and dihydroxybenzylamine (DHBA) were obtained from Sigma; aluminium oxide 90 active neutral and sodium-octansulfonate from Merck; Amberlite CG-50 from BDH. All the other reagents were of analytically pure grade and supplied from commercial sources. Only deionized and double-distilled water was used.

Mobile Phase

For RP-C18 columns mobile phase optimization was critical. The mobile phase was usually a citric-phosphate buffer 50 mMol, pH 5, containing Na^+EDTA 75 mg L^{-1}, and sodium 1-octansulfonate 60 mg L^{-1}; this buffer was mixed with methanol 95/5 (v/v).

For SCX columns, the best results were obtained with a citric-acetate buffer 100 mMol, pH 5.

In both cases solutions were filtered (0.45μ Millipore) and degassed (aspiration under vacuum and sonic treatment).

We installed an on-line degasser (ERMA model ERC 3310, Japan) in order to avoid bubble trap in pump heads and to obtain a less noisy baseline.

0009-5893/87 0455-05 $ 03.00/0 © 1987 Friedr. Vieweg & Sohn Verlagsgesellschaft mbH

Pump

The pump used in this study was a Waters model 590A equipped with an additional pulse damper. With this apparatus we had some problems related to both the accumulation of microbubbles in the pump heads and the rapid deterioration of piston seals. These problems were overcome by the connection of an on-line degasser apparatus (see above), and by the installation of a new type of seal, supplied by Millipore Waters S.p.A., Milan. With these adjustments, the pump has the stable flow necessary for a low noise baseline.

Automatic Sample Injector

A Waters WISP 710B automatic injector was used. It was shown to give high reproducible injections volumes (CV $<$ 1% for multiple injections of the same 50–80μl standard samples) as well as no detectable contamination between multiple consecutive samples.

With repeated injections of the same plasma or urine extracts, a noteworthy stability at room temperature (20–24°C) for up to 24 hours, with only a minimal reduction of endogenous catecholamines and DHBA ($<$ 2–3%), was observed.

Chromatographic Columns

The best results were obtained with an Altex Ultrasphere ODS (250 × 4.6mm, 5μ spherical packing) and an HPLC Technology Nucleosil 5SA (250 × 4.6mm, 5μ spherical packing), for RP-C18 and SCX respectively.

Detector

The apparatus used in this study was an ESA Coulochem detector model 5100A with an analytical cell model 5011. Detection was performed in conventional mode, with electrode 1 in "check" position and electrode 2 maintained at an oxidation potential of 0.30V.

Sample Handling

a) For plasma catecholamines assay.

Blood samples (4–5ml) were drawn from an antecubital vein into heparinized syringes, transferred immediately into ice-chilled polyethylene tubes and centrifuged, within 10 minutes, at 2000g for 10min at 4°C; 1mg sodium metabisulphite was added for each ml of plasma.

Step 1: to 2ml plasma were added 50μl internal standard (DHBA 0.1pM/μl), 50μl 5mM sodium metabisulphite, 500μl 1.5M Tris buffer pH 8.6 containing EDTA, and 20mg activated alumina. Standards were also run in each batch of extractions, where the plasma was replaced by 2ml 0.1M buffer phosphate, pH 7, with 50μl of a solution containing NA, A, DHBA, DA, 0.1pMμl^{-1} each.

Step 2: The tubes were mixed for 10min, washed twice with double distilled water and transferred into microfilters (Bioanalytical Service). Step 3: After centrifugation at 1000g for 30sec, alumina was added with 100μl 0.1M perchloric acid, containing 0.1mM sodium metabisulphite; then, after mixing for 3min and centrifugation at 1000g for 1min, the eluates were transferred into vials for automatic injection.

b) For urinary catecholamines assay.

With the SCX method there are no major changes in the extraction procedure in respect to plasma, except for the amount of both the biological sample (urine 0.5ml) and the internal standard (200μl 0.1pMμl^{-1}).

With RP-C18, due to the large number of interfering substances that can be found after alumina extraction, a further extraction with ion-exchange resin is essential.

Modifications in sample handling in respect to plasma are as follows:

- In step 1: urine 2ml, internal standard 200μl 1pM μl^{-1}, standards 200μl 1pMμl^{-1}.
- In step 3: add 200μl of perchloric acid then add 1M phosphate buffer, pH 6.2, and 0.1ml Amberlite CG-50 to the eluate.

Repeat the steps 2 and 3 using 2/3M boric acid instead of perchloric acid.

Integrator

The detector output was connected to a graphic integrator (Shimadzu C-R3A equipped with a FDD-1A double floppy disk drive); this integrator could directly calculate the amounts of various compounds and, at the same time, memorize the raw chromatographic data. This allows a subsequent reanalysis of the signal, with the possibility of settling the integration parameters in order to obtain the best performance.

Results

The extraction procedure for 30 samples needed about 3 hours. The chromatographic separation time (run time) for plasma assay was shorter than 20min with the SCX and shorter than 30min with for RP-C18.

For urine assay, due to the presence of interfering peaks, the run time was longer than 40min for both columns.

Linearity

Linearity was assessed for NA, A, DA in standard solutions, as well as in biological samples, which were submitted to the entire extraction procedure for amounts in the range 0.05 to 10pMol. The correlation coefficient was $r = 0.99$ (amounts injected vs. detector response).

Sensitivity

The detection limit of the assay was evaluated at a signal-to-noise ratio of 2, considering a mean recovery = 50%.

Results were as follows: noise = 10–20fMol; minimum detectable amount injected = 20–40fMol; minimum detectable concentration in plasma (extracting 2ml of plasma and injecting 80μl of the final eluate) = 25–50fMol/L; Minimal detectable concentration in urine (extracting 0.5ml of urine and injecting 20μl of the final eluate) = 400–800fMol/L.

In comparison with SCX columns, RP-C18 gave a slightly higher sensitivity for NA but lower sensitivity for A and mainly for DA. DA was often undetectable in plasma samples with RP-C18.

Reproducibility

The reproducibility was tested by repeated assay of pooled samples of human plasma with progressively increasing concentrations of NA, A and DA. For both RP-C18 and SCX column we performed 5 separate runs of 24 plasma samples (6 for each of four different concentrations).

The within-run and between-run variation coefficients were less than 10% for each amine with concentrations higher than 0.2–0.5 nMol, but they could rise to 25–35% with concentrations at the lower limit of sensitivity. SCX seems to give slightly better precision, particularly for DA and A at low concentrations (Fig. 1).

Specificity

High specificity was assessed on the basis of lack of significant interference with several compounds possessing a chemical structure similar to that of catecholamines. A further assessment of specificity was performed by adding to plasma samples of known catecholamine concentration scalar amounts of standard catecholamine solution and showing that the regression line was superimposible on that obtained with standard solutions alone.

On the other hand with RP-C18 but not with SCX we observed peaks of unknown origin which could interfere with catecholamines and with DHBA (Fig. 2). In addition,

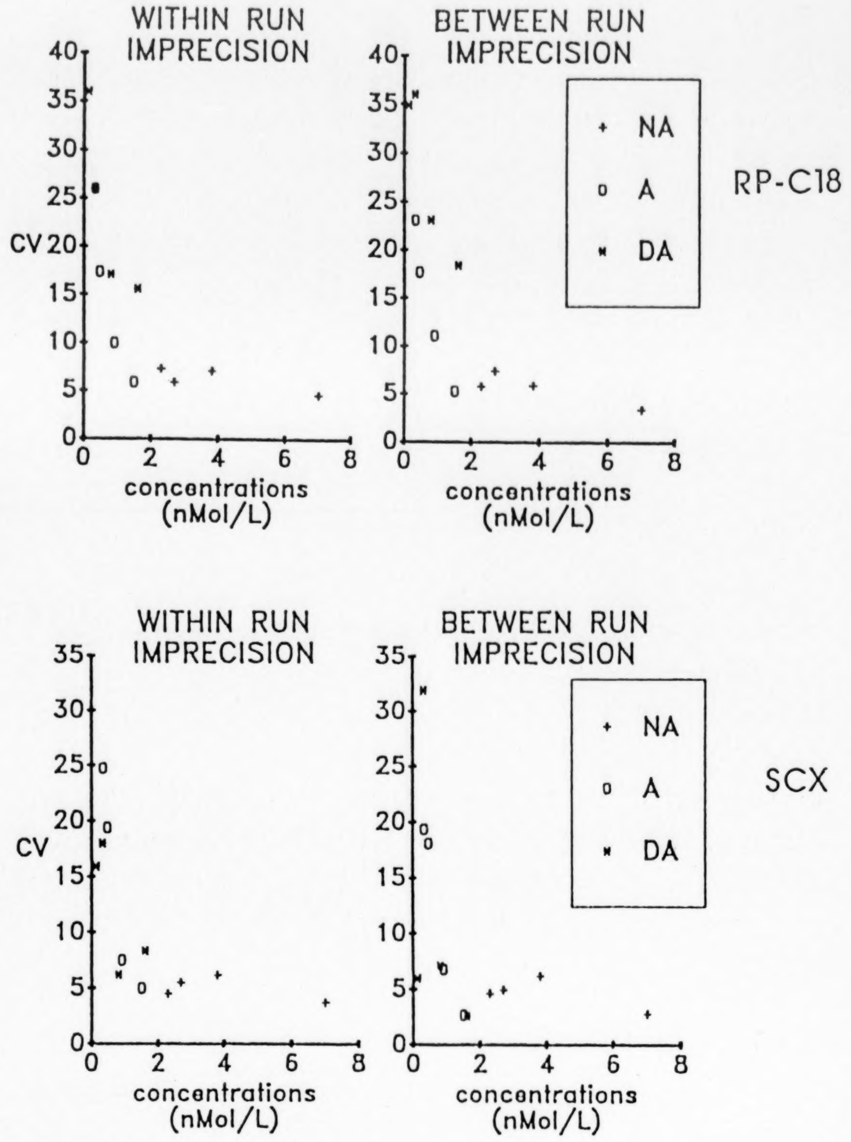

Fig. 2

Within-run and between-run imprecision using RP-C18 or SCX columns at different catecholamine concentrations.

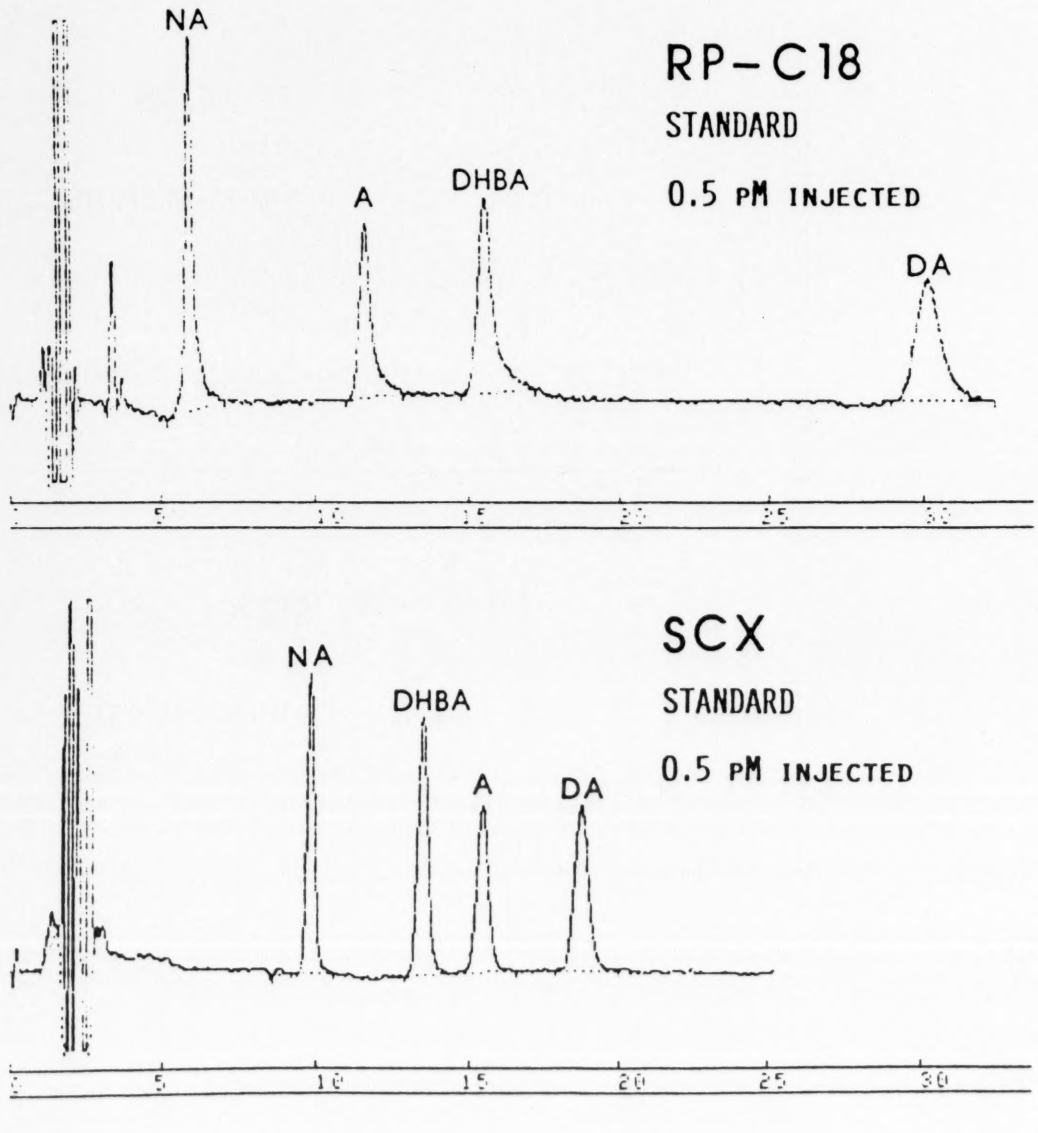

Fig. 1

Typical chromatograms of standard solution with RP-C18 and SCX columns.

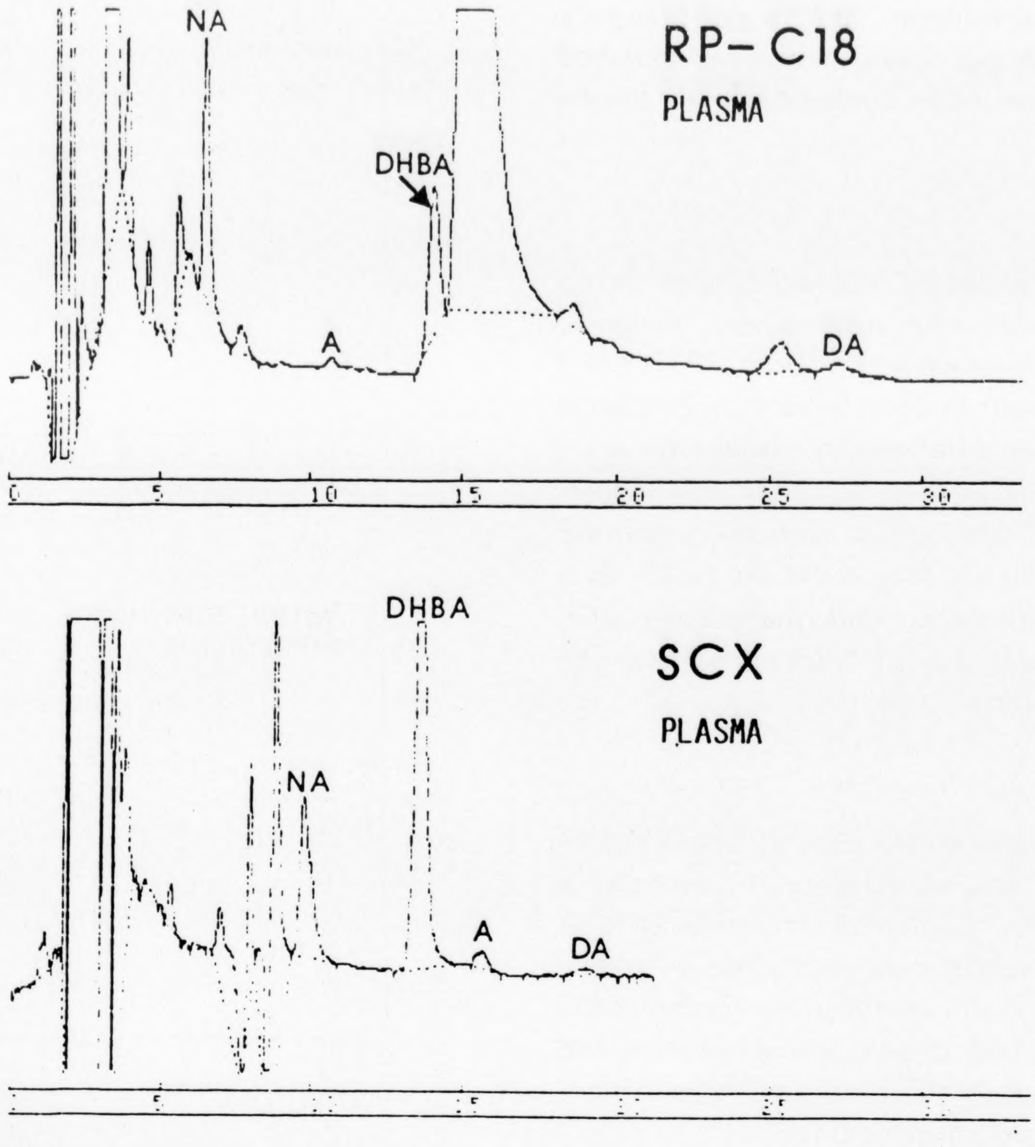

Fig. 3

Chromatograms of the same plasma sample obtained using RP-C18 or SCX columns.

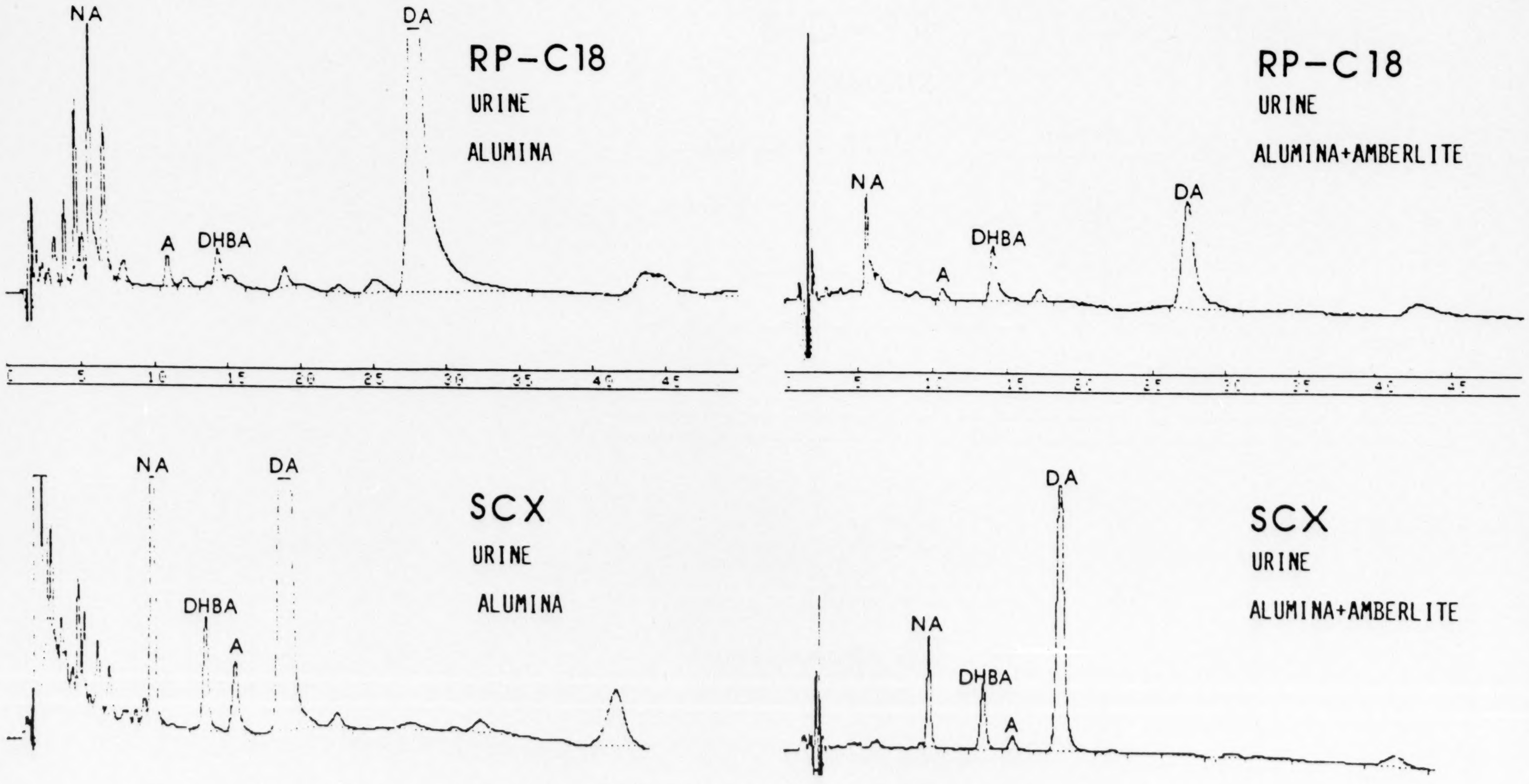

Fig. 4

Chromatograms of the same urine sample obtained using RP-C18 or SCX columns and different extraction procedure (see text).

while for the RP-C18 method it is necessary to perform two subsequent extractions in order to eliminate most interfering substances from the sample, for SCX one extraction is sufficient for an adequate chromatographic separation.

Conclusions

Our study indicates that a semi-automated technique for measuring catecholamines in biological samples, using HPLC with CD, gives results as good as those obtained in previous studies using normal techniques. In addition, our results are comparable to those obtained with radioenzymatic techniques by ourselves and others.

Our semi-automated technique offers the possibility of greatly increasing the number of samples that may be analyzed in a working day — in fact a technician may process up to 60 sample per day while with manual injection only 10–12 samples per day could be assayed.

The stability of the plasma extract at room temperature allows semi-automation of the procedure.

Our study indicates that both RP-C18 and SCX columns give very good performance for clinical purposes but sensitivity, precision at low concentration and specificity seem to be better with ion-exchange columns that are therefore preferred at present.

In comparison with radioenzymatic techniques, our method, that does not involve the use of radioactive material, is as sensitive, specific and reproducible, but it is also more economical and less time-consuming.

Acknowledgement

We thank Miss Alessandra Panarotto for her precious collaboration.

References

[1] *E. Agabiti-Rosei, C. Alicandri, M. Beschi, M. Castellano, R. Fariello, M. L. Muiesan, G. Romanelli, G. Muiesan*, in: "Endocrinology of Hypertension, *Mantero, F., Biglieri, E. G., Edwards, C. R. W.* eds., Academic Press, London and New York, 1982; p. 387.

[2] *C. R. Lake, M. G. Ziegler, I. J. Kopin*, Life Sci. **18**, 1315 (1976).

[3] *R. E. Cryer*, New Eng. J. Med. **303**, 436 (1980).

[4] *V. Renzini, C. A. Brunori, C. Valori*, Clin. Chim. Acta **30**, 587 (1970).

[5] *E. Agabiti-Rosei, M. Beschi, M. Castellano, S. Tosoni, C. Signorini*, J. Clin. Chem. Clin. Biochem. **22**, 539 (1984).

[6] *W. J. Raum*, Am. J. Physiol. **247**, E4 (1984).

[7] *J. D. Peuler, G. A. Johnson*, Life Sci. **21**, 625 (1977).

[8] *M. Da Prada, G. Zurcher*, Life Sci. **19**, 1161 (1976).

[9] *H. Hallman, L. O. Farnebo, B. Hamberger, G. Jonsson*, Life Sci. **23**, 1049 (1978).

[10] *P. Hjemdahl, M. Daleskog, T. Kahan*, Life Sci. **25**, 131 (1979).

[11] *D. S. Goldstein, G. Feuerstein, J. L. Izzo, I. J. Opire, H. R. Keiser*, Life Sci. **28**, 467 (1981).

[12] *R. C. Causon, M. E. Carruthers, R. Rodnight*, Anal. Biochem. **116**, 223 (1981).

[13] *V. A. Hammond, D. G. Johnston*, Clin. Chim. Acta **137**, 8 (1984).

[14] *B. E. Eriksson, S. Gustafsson, B. A. Persson*, J. Chromatogr. **278**, 255 (1983).

[15] *P. Hjemdahl*, Am. J. Phisiol. **247**, E13–E20 (1984).

[16] *A. M. Krstulovic*, J. Chromatogr. **229**, 1 (1982).

[17] *P. Hjemdahl*, Acta Physiol. Scand. (suppl.) **527**, 17 (1984).

[18] *J. S. Krouwer, R. Rabinowitz*, Clin. Chem. **30**(2), 290 (1984).

Received: June 30, 1987
Accepted: Aug. 5, 1987
F

Indirect Detection in Reversed-Phase Liquid Chromatography: Ion-Pair Retention Models for Cations on Polystyrene Polymers

E. Arvidsson[1]/J. Crommen[2]/G. Schill/D. Westerlund[1]*

[1] Department of Analytical Pharmaceutical Chemistry, Uppsala University, Biomedical Center,
P.O. Box 574, S-751 23 Uppsala, Sweden

[2] Institute of Pharmacy, University of Liège, Rue Fusch 5, 4000 Liège, Belgium

Key Words

Column liquid chromatography
Polystyrene polymers
Ion-pair retention model
Indirect detection

Summary

The distribution equilibria of cationic compounds in reversed-phase chromatographic systems (ion-pair chromatography) have been studied on the basis of their effect on a detectable mobile phase component. The solid phase was a polystyrene-divinylbenzene copolymer and the detectable component, a quaternary ammonium ion, 1-methylpyridine. The solutes were mono- and divalent amines and quaternary ammonium ions.

The cations can be retained by ion-pair adsorption and ion exchange. Expressions for the ion-pair retention of the solutes and the mobile phase cation (system peak) have been developed assuming Langmuir distribution of ion pairs to a solid phase with one kind of binding site. The validity of the expressions has been tested by evaluation of ion-pair distribution constants using non-linear curve fitting techniques. Good agreement for the constants of common ion pairs was obtained from different kinds of capacity ratio expressions.

Ion exchange retention can appear beside ion-pair retention, and it has been observed in the pH range 1.6–6.1. The effect depends not only on cations in the mobile phase, but also on the nature of the buffering systems.

Introduction

Ion-pair distribution is widely used in liquid chromatographic separations of ionized organic compounds. The principles were initially applied to liquid-liquid systems [1, 2], but the technique is now mainly used in reversed-phase systems with hydrophobic adsorbents as the solid phases. The retention can be regulated by the properties and the concentration of the counter ion as well as, in reversed-phase systems, by a competing ion with the same charge as the analyte [3, 4].

The components in the mobile phase can also be used for detection purposes; it is possible to follow the retention of compounds without inherent detectable properties [5, 6]. A detectable ion is then incorporated in the mobile phase and distributed to the solid phase. Injection of a sample causes equilibrium disturbances in the injection zone and two kinds of migrating zones are formed, one for each of the sample components and one for each of the mobile phase components, except the main solvent. The mobile phase in these zones has a composition that deviates from the bulk, and a chromatogram is obtained that comprises not only peaks for the injected compounds (solute peaks), but also peaks with constant retention that are typical for the composition of the chromatographic system (system peaks) [7]. The capacity ratios of these two kinds of peaks can be used in the calculation of distribution equilibria in the chromatographic system.

The purpose of this investigation was to study the distribution equilibria of cationic organic compounds in ion-pair chromatographic systems, using a polystyrene-divinylbenzene copolymer as the solid phase. A detectable cation was present in the mobile phase, and the retentions of both the injected solutes and the fairly hydrophobic detectable mobile phase cation were followed. Retention models were proposed, and their validity was tested by the calculation of equilibrium constants, using linear and non-linear curve fitting techniques. The capacity ratios of solutes and mobile phase components follow different expressions, creating possibilities for the critical testing of retention models and equilibrium constants.

Previous studies on reversed-phase ion-pair chromatography have mainly been performed on alkyl- or aryl-bonded silica, and the adsorption has been found to follow a Langmuir expression only under the assumption that the solid phase has two kinds of binding sites with different binding abilities and capacities [4, 8]. The heterogeneity of the surface is supposedly due to the presence of residual silanol groups beside the hydrophobic carbon chains. The present studies were made with a polystyrene adsorbent, PRP-1, which was earlier assumed to act as a homogeneous ad-

0009-5893/87 0460-09 $03.00/0

© 1987 Friedr. Vieweg & Sohn Verlagsgesellschaft mbH

sorbent. However, Stuurman et al. [9] found indications of ion-exchange effects on PRP-1 at pH 4–7 when it was used in reversed-phase ion-pair chromatography.

The studies were performed with variations of pH and of the nature and the concentration of the mobile phase ions. The results have shown that PRP-1 can act as single site adsorbent, but cation-exchange effects also seem to appear under certain chromatographic conditions. The ion-exchange properties might not be due to permanent charged groups on the solid phase, but may instead be caused by adsorbed buffering components.

Experimental

Apparatus

The detector was an LDC Spectromonitor III with variable wavelength. The pump was an Altex model 100 A. The injector was a Rheodyne 71-25 with a 24.6 μl loop. A HETO waterbath (Birkerφd, Denmark) Type 02 PT 923 was used for thermostating the chromatographic system. The pH measurements were made with a Beckman pHI 71 pH meter.

Chemicals

Butylamine HCl, pentylamine HCl, triethylmethylammonium HSO_4, 1-methylpyridinium HSO_4 and sodium octanesulfonate were recrystallized from water before use. All other chemicals were of analytical or similar grade and used without further purification.

Column Preparation and Chromatographic System

The columns (100 × 4.6 mm I.D.) were packed with PRP-I 10 μm (Hamilton Bonaduz AG, Switzerland), using a slurry medium containing 2.5% NaCl, 10% of glycerol and a minor amount of acetone in water. The columns were washed with 200 ml slurry medium and 100 ml water. Part of the study was performed with PLRP-S 5 μm (prepacked column, 150 × 4.6 mm I.D., from Polymer Laboratories Ltd, Amherst, MA, USA). The column performance was tested with acetonitrile as eluent and toluene, naphthalene and anthracene as solutes.

The eluent reservoir, injector, column and connecting tubes were thermostated at 25.0 ± 0.1 °C in a waterbath. The samples injected were dissolved in the mobile phase. The flow rate was 0.5 ml per min. No recirculation of the mobile phase was used.

The mobile phases contained 1-methylpyridine as the detectable component. It was added as HSO_4^--salt. Cyclamate or octanesulfonate (sodium-salts) were added as counter ions to some of the phases. The buffers contained phosphate or acetate, and the solvent was water with 4% methanol. The composition of the phases is given in Table I. The concentrations of H^+, $H_2PO_4^-$, and acetate were calculated from the total concentration of the acids, using the stoichiometric dissociation constants at the mean ionic strength 0.01 for phosphoric acid $pK_1 = 2.10$ and for acetic acid $pK_a = 4.85$. The volume of the mobile phase in the column, V_m, was obtained from the front peak (i.e. the first system peak) in the chromatogram. The retention of the solute peak, V_r, was measured at the peak maximum. The capacity ratios were calculated from $k' = (V_r - V_m)/V_m$.

Non-Linear Curve Fitting

The non-linear regression (NLR) analyses were performed by use of the Minuit program, version D 506 from Cern. It contains the minimizing procedures Simplex and Migrad [10]. Only k'-values that were independent of the solute concentration were used in the calculations.

Retention Models

The injection of a solute in a chromatographic system causes disturbances in the injection zone which affect a series of distribution equilibria coupled by a common interaction term. The effects of disturbances by solutes have been extensively treated by Helfferich [11] and the theoretical background has been elucidated by Riedo and Kovats [12]. The concentration changes can be described, as demonstrated in the following example, where $\Delta C_{i,s}$ is the change for a compound i in the stationary phase and $\Delta C_{i,m}$ is the change in the mobile phase. C° represents the initial concentration.

$$\Delta C_{i,s} = C_{i,s} - C^\circ_{i,s} = a_{i,1}\,\Delta C_{1,m} + a_{i,2}\,\Delta C_{2,m} + \dots + a_{i,n}\,\Delta C_{n,m} \qquad (1)$$

Table I. Composition of mobile phases. Solvent: water + methanol (96 + 4).

Phase No.	Solid phase	$[Q^+]\cdot10^4$	Counter ion		Buffer ions			
			type	conc. 10^3	$[H^+]\cdot10^3$	$[H_2PO_4^-]\cdot10^3$	$[Na^+]\cdot10^2$	$[Ac^-]\cdot10^2$
1	PRP-1	1.0	–		5.7–25	5.7–25	–	–
2	PRP-1	0.15	–		5.7–25	5.7–25	–	–
3	PRP-1	1.0	Cyclamate	5–30	5.7	5.7	0.5–3.0	–
4	PRP-1	1.0	Cyclamate	10	5.7–25	5.7–25	1.0	–
5	PRP-1	1.0	Cyclamate	5	< 0.05	5.0–20	1.0–2.5	–
6	PRP-1	1.0	Octanesulfonate	5	5.7–25	5.7–25	0.5	–
7	PLRP-S	1.0	Cyclamate	10	0.001–0.1	–	0–5.8	0–4.8

Concentrations in moles per liter. Q^+: methylpyridine.

where 1, 2, ..., n represents the different compounds in the mobile phase and

$$a_{i,j} = \frac{\delta C_{i,s}}{\delta C_{j,m}} . \qquad (2)$$

In this discussion $C_{i,s}$ is defined as the quotient of the amount of i in the stationary phase to the volume of mobile phase in the column.

The concentration disturbances caused by the injection of a solute are very small in analytical applications. It is possible to linearize the description of the distribution behaviour for the starting concentration in the mobile phase reservoir, which is 0 for a solute and $\neq 0$ for a mobile phase component.

Competition for the binding capacity of the solid phase is the most common interaction effect in reversed-phase chromatography. If an injected solute ion, HA^+, and a mobile phase ion, Q^+, are distributed to the solid phase as ion pairs with a counter ion X^-, and compete for its binding capacity according to a Langmuir expression; then the following expressions are valid [8, 13]:

$$C_{HAX,s} = \frac{A \cdot K_{HAX} \cdot [HA^+] \cdot [X^-]}{1 + K_{HAX} \cdot [HA^+] \cdot [X^-] + K_{QX} \cdot [Q^+] \cdot [X^-]} \qquad (3)$$

$$C_{QX,s} = \frac{A \cdot K_{QX} \cdot [Q^+] \cdot [X^-]}{1 + K_{QX} \cdot [Q^+] \cdot [X^-] + K_{HAX} \cdot [HA^+] \cdot [X^-]} \qquad (4)$$

$[HA^+]$, $[X^-]$ and $[Q^+]$ represent molar concentrations in the mobile phase. $A = K^0 \cdot W_s/V_m$, i.e., the product of the binding capacity of the solid phase and the phase volume ratio in the column. K_{HAX} and K_{QX} are the ion pair distribution constants defined by

$$K_{HAX} = \frac{C_{HAX,s}}{[HA^+] \cdot [X^-] \cdot [A_s]} \qquad (5)$$

$$K_{QX} = \frac{C_{QX,s}}{[Q^+] \cdot [X^-] \cdot [A_s]} . \qquad (6)$$

A_s represents available binding sites in the solid phase in moles/L.

The ion-pair distribution constants of divalent cations are defined as

$$K_{H_2AX_2} = \frac{C_{H_2AX_2,s}}{[H_2A^{+2}] \cdot [X^-]^2 \cdot [A_s]^2} . \qquad (7)$$

The distribution behaviour of HA^+ and Q^+ can be expressed in analogy with eqs. (1) and (2) by partial derivatives: $a_{HA,HA}$ and $a_{Q,Q}$, corresponding to the capacity ratios of HA^+ and Q^+, respectively. The partial derivatives should be evaluated for the starting concentrations, which for the injected solute HA^+ is zero and, for Q^+, equal to the concentration in the mobile phase reservoir.

$$\frac{\delta C_{HAX,s}}{\delta [HA^+]} = \frac{A \cdot K_{HAX} \cdot [X^-]}{1 + K_{QX} \cdot [Q^+] \cdot [X^-]} = k'_{HA} \qquad (8)$$

$$\frac{\delta C_{QX,s}}{\delta [Q^+]} = \frac{A \cdot K_{QX} \cdot [X^-]}{(1 + K_{QX} \cdot [Q^+] \cdot [X^-])^2} = k'_Q . \qquad (9)$$

If the mobile phase contains a further cation, HB^+, which is also distributed to the solid phase as ion pair with X^-, the following k' expressions are obtained:

$$k'_{HA} = \frac{A \cdot K_{HAX} \cdot [X^-]}{1 + K_{QX} \cdot [Q^+] \cdot [X^-] + K_{HBX} \cdot [HB^+] \cdot [X^-]} \qquad (10)$$

$$k'_Q = \frac{A \cdot K_{QX} \cdot [X^-] \cdot (1 + K_{HBX} \cdot [HB^+] \cdot [X^-])}{(1 + K_{QX} \cdot [Q^+] \cdot [X^-] + K_{HBX} \cdot [HB^+] \cdot [X^-])^2} . \qquad (11)$$

It should be noted that the partial derivative for the injected solute has such a form that the capacity ratio is directly proportional to the distribution ratio (cf. eq. (3)).

Results and Discussion

The validity of the retention models given above was tested by the calculation of distribution constants from k'-values after a systematic change of the composition of the mobile phase.

Approach to Constant Determination

The main part of the calculations was made with phases which contain methylpyridine (Q^+) as the detectable component, phosphoric acid (HP), dihydrogenphosphate (P^-) and H^+ as the buffering components and cyclamate (Cy^-) as an additional counter ion (see Table I). This means that the distribution can include no less than four ion pairs, QCy, QP, HCy, and NaCy and one uncharged component, HP, neglecting the highly hydrophilic NaP and the minor component HSO_4^- (maximum concentration of 10^{-4} M). Owing to the large number of constants, the determination had to be based on a stepwise approach.

Retention with Dihydrogenphosphate as Counter Ion

Cationic solutes and mobile phase components are significantly retained as ion pairs with dihydrogenphosphate, as shown in Table II. The retained system peak was well defined in all the systems, and injections in excess of the different mobile phase components indicated that it was given by Q^+. The solutes gave symmetrical peaks in phase 1, whereas the peaks were somewhat deformed in phase 2. This indicates that phase 2 is more easily overloaded, probably due to the fact that the concentration of Q^+ is only $1.5 \cdot 10^{-5}$ M, i.e. seven times lower than in phase 1.

The capacity ratios of the cationic solutes and the system peak decrease with increasing concentration of $H_2PO_4^-$ and H^+. Such effects can be obtained if the retention is governed by expressions analogous to eqs. (10) and (11), assuming that $K_{HP} \cdot [H^+] \cdot [P^-]$ is substituted for $K_{HBX} \cdot [HB^+] \cdot [X^-]$. However, calculation by non-linear regression for butylamine and for the system peak did not confirm the validity of these equations.

Inverting and introducing the proper symbols for the ionic components produces the following:

$$\frac{1}{k'_{HA}} = \frac{1 + K_{HP} \cdot [H^+] \cdot [P^-]}{A \cdot K_{HAP} \cdot [P^-]} + \frac{K_{QP} \cdot [Q^+]}{A \cdot K_{HAP}} . \qquad (12)$$

Table II. Retention with $H_2PO_4^-$ as the counter ion. Mobile phase: No. 1 + 2 (Table I)

		k'				
$[H^+]\cdot 10^3$*	$[Q^+]\cdot 10^4$	Butylamine	Triethylammonium	Pentamethonium	Diaminobutane	System peak
5.78	0.148	4.15	2.90	7.67	4.57	1.36
16.3	0.148	2.90	1.90	3.02	1.52	0.81
24.5	0.163	2.09	1.51	1.55	0.88	0.59
5.78	1.00	2.76	2.09	1.90	1.19	0.84
16.3	1.00	1.36	1.10	0.43	0.19	0.43
24.5	1.00	1.10	0.90	0.24	0.12	0.37

*) $[H_2PO_4^-] = [H^+]$.

If the model is valid, a plot of $1/k'_{HA}$ versus $[Q^+]$ at constants $[H^+]$ and $[P^-]$ should give a straight line with a slope equal to $K_{QP}/A\cdot K_{HAP}$. However, plots at different $[H^+]$ and $[P^-]$ values showed a change of not only the intercept but the slope as well, which indicates that eq. (12) does not include all the factors responsible for the retention.

Ion-Exchange Effects

The assumption of an additional retaining effect is supported by the change of the k'-quotients on the variation of the mobile phase composition shown in Table III. If eq. (10) is valid, the quotients between the capacity ratios of two amines with the same charge should be constant and independent of $[Q^+]$, $[H^+]$, and $[H_2PO_4^-]$. However, the quotient changes indicate that the proportions between $[Q^+]$ and $[H^+]$ have a significant influence on the retention. Such effects may appear when the retention is influenced by ion-exchange effects, as can be seen from the following.

When a cation exchanger is in contact with a mobile phase containing the mobile phase ions H^+ and Q^+ and the solute HA^+, an expression for its total binding capacity, C_R, has the following form:

$$C_R = [R^-H^+] + [R^-Q^+] + [R^-HA^+] \ , \tag{13}$$

where R^- represents anionic sites in the stationary phase. The exchange of H^+ for Q^+ can be expressed by an equilibrium constant, K_Q, defined by:

$$\frac{[R^-Q^+]\cdot[H^+]}{[R^-H^+]\cdot[Q^+]} = K_Q \tag{14}$$

and an analogous constant, K_{HA}, will express the exchange of H^+ for HA^+. Introduction of these parameters in eq. (13) gives the following expression for the concentration of HA^+ in the stationary phase:

$$[R^-HA^+] = \frac{q\cdot C_R\cdot K_{HA}\cdot[HA^+]}{[H^+] + K_Q\cdot[Q^+] + K_{HA}\cdot[HA^+]} \ , \tag{15}$$

where q is the phase volume ratio. The capacity ratio of the solute HA^+ owing to ion exchange, $k'_{HA,ie}$, is then given by:

$$k'_{HA,ie} = \frac{q\cdot C_R\cdot K_{HA}}{[H^+] + K_Q\cdot[Q^+]} \ . \tag{16}$$

The capacity ratio of the system peak given by Q^+, $k'_{Q,ie}$, can be obtained by an analogous deduction which gives:

$$k'_{Q,ie} = \frac{q\cdot C_R\cdot K_Q\cdot[H^+]}{([H^+] + K_Q\cdot[Q^+])^2} \ . \tag{17}$$

$[H^+]$ is much larger than $[Q^+]$, and it is possible that $K_Q\cdot[Q^+]$ can be smaller than $[H^+]$. The relationship between $k'_{HA,ie}$ and $1/[H^+]$ in eq. (16) should then approach linearity. A plot of the experimentally obtained k'_{HA} in phase 1 versus $1/[H^+]$ is given in Fig. 1. The linear relationship with an

Table III. Influence of Q^+ concentration on capacity ratio quotients. System: No. 1 and 2 (see Table I).

$[Q^+]\cdot 10^4$	$[H_2PO_4^-]\cdot 10^3$*	k'_{Tr}/k'_{BA}	k'_{PM}/k'_{DH}
1.00	5.8	0.76	0.63
1.00	16.3	0.81	0.50
1.00	24.5	0.82	0.50
0.148	5.8	0.70	0.60
0.148	16.3	0.66	0.50
0.163	24.5	0.72	0.57

*) $[H^+] = [H_2PO_4^-]$; BA = butylamine; Tr = triethylmethylammonium; PM = pentamethonium; DH = diaminohexane.

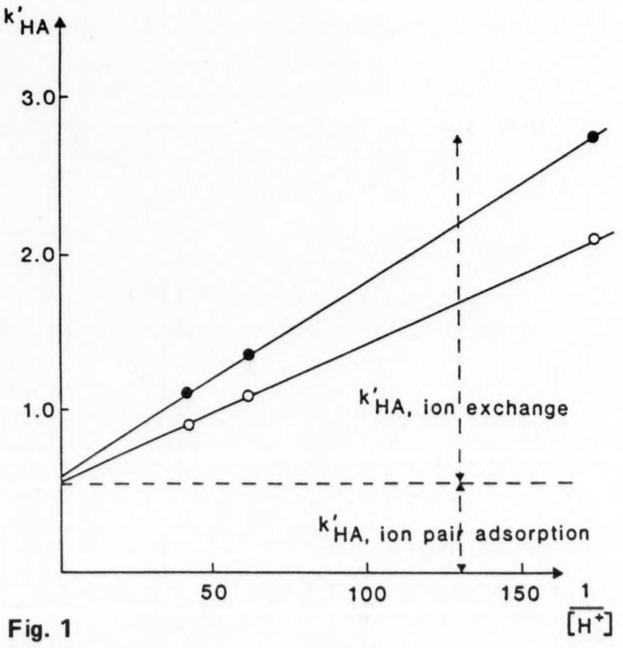

Fig. 1

Evaluation of ion-exchange effects.

Mobile phase: 1-methylpyridine 10^{-4} M in phosphoric acid 0.01–0.10 M. Solutes: ● butylamine ○ triethylmethylammonium.

intercept seems to indicate two retaining effects, one ion exchange effect as outlined above and one further effect that is independent of changes in $[H^+]$ or $[P^-]$.

The total retention is not independent of Q^+, as can be seen from Table II, and it might be that Q^+ influences only the second of the two retention effects. The results given by the amines in the phase with $[Q^+] = 1.5 \cdot 10^{-5}$ (phase 2) show no linear relationship between k'_{HA} and $1/[H^+]$, which would be the case if the second retention effect is not constant at the lower Q^+ concentration.

It is likely that the second retention effect is an ion-pair adsorption process, and the capacity ratio for HA^+ should then be given by a combination of eqs. (10) and (16). A retention model for the system peak based on the same principle is obtained by a combination of eqs. (11) and (17). Values of the constants obtained from these expressions by non-linear computations are given in Table IV.

The calculations based on k'_{HA} and k'_Q give two common constants, K_{HP} and K_{QP}. The resulting values are in acceptable agreement, considering the uncertainty of k' of the amines in phase 2. The ion-pair constants are high, in spite of the hydrophilic character of the anionic component, dihydrogenphosphate. $A = K^0 \cdot W_s/V_m$ (i.e., the product of the binding capacity and the phase volume ratio, calculated from the constants) has, on the other hand, a value of only 10^{-4} mole/L, which is very low compared with the values found for alkylbonded silica [13]. It shows that the binding site has a rather special character with low capacity, but high binding ability for hydrophilic compounds.

The ion-exchange retention constitutes a significant part of the total retention, as demonstrated by Fig. 1. The studies have been performed in the pH-range 1.6–2.2, and a retention effect of this magnitude can only be obtained if the binding groups belong to a fairly strong acid or a weak acid with high total binding capacity. It is unlikely that the ion-exchange effects are given by carboxylic groups with pK_a of 4–5, and sulfonic groups can hardly appear on the surface.

The high value of K_{HP} shows that the solid phase has a strong tendency to bind phosphoric acid, and it is possible that the ion-exchange effect is given by bound phosphoric acid molecules. Studies on indirect detection effects in reversed-phase systems [14] have shown that uncharged components and ion-pairs are bound to an adsorbing surface by different mechanisms with low mutual competition for the binding surface. The value of K_{HP} given above indicates a high degree of binding of phosphoric acid, but it may still be an underestimation, since the constant only expresses its competitive effect towards ion-pairs, and it is quite possible that almost all sites that can bind phosphoric acid are in fact occupied under the conditions used in phases 1 and 2. The ion-exchange binding capacity, C_R, will then be constant which is in accordance with the results presented above.

Cyclamate as Counter Ion

Addition of cyclamate to the mobile phase produces a large increase in the capacity ratios of the cationic solutes and the system peak as illustrated in Table V.

Table IV. Constants evaluated from capacity ratios of solutes and system peaks.

Phase	Anion	Constant	Triethylmethylammonium	Butylamine	System peak
1 + 2	$H_2PO_4^-$ (P)	K_{QP}	$5 \cdot 10^6$	–	$3.3 \cdot 10^6$
		K_{HP}	$1 \cdot 10^4$	–	$2.1 \cdot 10^4$
		$A \cdot K_{HAP}$	$8 \cdot 10^2$	$4 \cdot 10^2$	–
		$A \cdot K_{QP}$	–	–	$3.0 \cdot 10^2$
		$K^0 \cdot W_s/V_m$ (=A)	–	–	$0.9 \cdot 10^{-4}$
		$q \cdot C_R \cdot K_{HA}$	$1.1 \cdot 10^{-2}$	$0.9 \cdot 10^{-2}$	$0.4 \cdot 10^{-2}$

Non linear computations using eqs. (10) – (16) (solutes) and eqs. (11) – (17) (system peak).

Table V. Capacity ratios with cyclamate in the mobile phase.

Phase	k'_T	k'_{PM}	k'_Q	$[Cy^-] \cdot 10^3$	$[H^+] \cdot 10^3$	$[H_2PO_4^-] \cdot 10^3$
3	6.57	15.0	2.62	5.04	5.78	5.78
	8.23	23.0	3.24	10.0	5.78	5.78
	9.52	36.6	3.76	20.1	5.78	5.78
	9.81	34.7	4.00	30.1	5.78	5.78
4	5.86	13.0	2.38	10.0	12.0	12.0
	4.81	10.0	1.95	10.0	16.3	16.3
	4.12	7.19	1.86	10.0	19.9	19.9
	3.71	5.62	1.52	10.0	24.5	24.5
5	11.2	14.0	4.10	5.06	0.055	5.00
	9.62	12.3	3.48	5.04	0.035	10.0
	7.81	8.57	2.90	4.99	0.023	20.0

k'_T, k'_{PM}, and k'_Q are the capacity ratios of triethylmethylammonium, pentamethonium and the system peak, respectively.

When the mobile phase contains sodium cyclamate in addition to phosphoric acid, the capacity ratio expression for the ion-pair adsorption contains no less than seven distribution constants, neglecting the distribution of sodium dihydrogenphosphate. The validity of the capacity ratio models can only be tested after certain simplifications.

Change of sodium cyclamate concentration: In phase 3, the concentration of sodium cyclamate changes, whereas $[H^+]$ and $[P^-]$ are constant. The retention due to ion-pair adsorption, $k'_{HA,ip}$, is given by the following expression:

$$k'_{HA,ip} = \frac{A \cdot K_{HACy} \cdot [Cy^-] + A \cdot K_{HAP} \cdot [P^-]}{1 + [Cy^-] \cdot (K_{QCy} \cdot [Q^+] + K_{HCy} \cdot [H^+] + K_{NaCy} \cdot [Na^+]) + [P^-] \cdot (K_{QP} \cdot [Q^+] + K_{HP} \cdot [H^+])} . \quad (18)$$

$[Q^+]$, $[H^+]'$, and $[P^-]$ are constant. If $K_{NaCy} \cdot [Na^+]$ is negligible, eq. (18) can be transformed to:

$$k'_{HA,ip} = \frac{M1 \cdot [Cy^-]}{1 + K1 \cdot [Cy^-] + K2} , \quad (19)$$

where

$$M1 = A \cdot K_{HACy} + A \cdot K_{HAP} \cdot \frac{[P^-]}{[Cy^-]} \quad (20)$$

$$K1 = K_{QCy} \cdot [Q^+] + K_{HCy} \cdot [H^+] \quad (21)$$

and

$$K2 = (K_{QP} \cdot [Q^+] + K_{HP} \cdot [H^+]) \cdot [P^-] . \quad (22)$$

An expression for the retention of the system peak due to ion-pair adsorption, $k'_{Q,ip}$, can be based on eq. (11) and can be transformed to the following form:

$$k'_{Q,ip} = \frac{M2 \cdot [Cy^-]^2 \cdot D}{(1 + K1 \cdot [Cy^-] + K2)^2} , \quad (23)$$

where

$$D = K_{HCy} \cdot [H^+] + \frac{1 + K_{HP} \cdot [H^+] \cdot [P^-]}{[Cy^-]} , \quad (24)$$

whereas M2 is analogous to M1 with Q^+ substituted for HA^+.

$[Cy^-]$ and $[P^-]$ are of the same magnitude. Assuming that cyclamate produces significantly larger constants than dihydrogenphosphate M1, K1 and K2 can be evaluated from non-linear computation of the relationship between $[Cy^-]$ and the capacity ratios for ion-pair adsorption ($k'_{HA,ip}$ and $k'_{Q,ip}$).

The ion-exchange effects are difficult to estimate since the mobile phase contains not only H^+, but Na^+ as well in the same or higher concentration. However, the k'-values found showed good agreement with a non-linear plot based on the assumption of negligible ion-exchange. The constants found are given in Table VI. The agreement between the values of the common constant, K1, is excellent.

The very low values of K2 and the agreement between the found K1 indicate the absence of competition between cyclamate and phosphate ion-pairs. The assumption of negligible adsorption of NaCy is also supported. The constants for the phosphate ion-pairs found in phases 1 and 2 are obviously not valid in the presence of cyclamate.

Change of the phosphoric acid concentration: In phase 4, the concentration of sodium cyclamate is constant, whereas the concentration of phosphoric acid changes. Since $[H^+] = [P^-]$, eq. (18) can be given the following form:

$$k'_{HA,ip} = \frac{M1 \cdot [Cy^-]}{1 + K3 + K4 \cdot [H^+]} , \quad (25)$$

where

$$K3 = K_{QCy} \cdot [Cy^-] \cdot [Q^+] \quad (26)$$

and

$$K4 = K_{HCy} \cdot [Cy^-] + K_{QP} \cdot [Q^+] + K_{HP} \cdot [P^-] \quad (27)$$

($K_{NaCy} \cdot [Na^+]$ neglected).

Table VI. Ion-pair adsorption constants evaluated from capacity ratios of solute and system peaks: cyclamate as the main counter ion.

Phase	Counter ion	Constant	Triethylmethylammonium	Butylamine	System peak
3	Cyclamate	$A \cdot K_{HACy}$	$3.3 \cdot 10^3$	$4.0 \cdot 10^3$	–
	+	$A \cdot K_{QCy}$	–	–	$1.2 \cdot 10^3$
	$H_2PO_4^-$	$(K_{QCy}[Q^+] + K_{HCy}[H^+])^{a)}$	$3.0 \cdot 10^2$	$2.5 \cdot 10^2$	$2.8 \cdot 10^2$
		K_{HCy}	–	–	$4.8 \cdot 10^4$
		$(K_{QP}[Q^+] + K_{HP}[H^+]) \cdot [P]^{b)}$	$\ll 1$	$\ll 1$	
4	cyclamate	$A \cdot K_{HACy}$	$1.3 \cdot 10^3$	$2.3 \cdot 10^3$	–
	+	$A \cdot K_{QCy}$	–	–	$0.8 \cdot 10^3$
	$H_2PO_4^-$	K_{QCy}	$1.1 \cdot 10^6$	$1.2 \cdot 10^6$	–*
		K_{HCy}	$1.0 \cdot 10^4$	$1.4 \cdot 10^4$	$1.4 \cdot 10^4$
		$K^0 \cdot W_s/V_m$ (= A)	–	–	$6 \cdot 10^{-3}$

a) = K1; b) = K2; *) Acceptable precision could not be achieved.

The equation for the system peak is under the same conditions:

$$k'_{Q,ip} = \frac{M2 \cdot [Cy^-] \cdot E}{(1 + K3 + K4 \cdot [H^+])^2}, \quad (28)$$

where

$$E = K_{HCy} \cdot [Cy^-] \cdot [H^+] + K_{HP} \cdot [H^+] \cdot [P^-] + 1 . \quad (29)$$

The constants were evaluated by a non-linear regression technique, assuming that the ion exchange effects and adsorption of the phosphate ion-pairs are negligible. A plot for a monovalent amine is shown in Fig. 2, whereas a plot for the system peak is shown in Fig. 3. The constants are given in Table VI. The agreement between the common constants (K_{HCy} and K_{QCy}) is good.

The values of $A \cdot K_{HACy}$ obtained from phase 3 and phase 4 show acceptable agreement, and it is particularly noteworthy that calculations with K_{QCy} and K_{HCy} found in phase 4 give $K1 = (1.7 - 2.0) \cdot 10^2$, i.e., a value rather close to the values obtained in phase 3.

It is furthermore possible to calculate $A = K^0 W_s/V_m$, and the value, $6 \cdot 10^{-3}$, is about 70 times higher than the A value found for the phosphate ion-pairs. This lends support to the view that the retention as phosphate ion-pairs in phase 1 and 2 is due to a binding site that has a negligible influence in the presence of cyclamate.

Changes of $[H_2PO_4^-]$ and $[Na^+]$ at higher pH: The influence of changes in the dihydrogenphosphate and sodium concentrations in the pH range 4.2–4.6 was studied in a phase with constant cyclamate concentration (phase 5).

The retention changes in phase 5 (see Table V) are probably due to ion-exchange effects, since the studies in phases 3 and 4 indicate that the ion-pair retention is unaffected by adsorption of ion-pairs containing Na^+ and $H_2PO_4^-$. The influence of $[H^+]$ is negligible owing to its very low concentration, and in the expression for ion-exchange retention (eq. 16)), Na^+ should be substituted for H^+, as it is the main cation in the mobile phase.

A plot of k'_{HA} versus $1/[Na^+]$ did not show a linear relationship, in contrast to the relationship between k'_{HA} and $1/[H^+]$ (Fig. 1). This might be due to the influence of Q^+ on the ion-exchange retention, i.e. $K_Q \cdot [Q^+]$ not being much smaller than $[Na^+]$ (cf. eq. (16)). A test of this possibility was made for triethylmethylammonium.

$k'_{HA,ip}$ was calculated by eq. (25), using the constants obtained in phase 4 (Table VI) and assuming a negligible influence of $K4 \cdot [H^+]$. The ion-exchange retention can then be calculated by:

$$k'_{HA,ie} = k'_{HA} - k'_{HA,ip} . \quad (30)$$

The assumption of ion-exchange was tested by plotting according to the following relationship deduced from eq. (16):

$$\frac{1}{k'_{HA,ie}} = \frac{K_Q \cdot [Q^+]}{B} + \frac{[Na^+]}{B}, \quad (31)$$

where $B = q \cdot C_R \cdot K_{HA}$. The relationship between $1/k'_{HA,ie}$ and $[Na^+]$ was straight linear.

A further test according to the same principle was made for the system peak retention. $k'_{Q,ip}$ was calculated from the values in Table VI, phase 4, using eq. (28). It was applied in a linearized expression for the ion-exchange effect deduced from eq. (17):

$$\sqrt{\frac{[Na^+]}{k'_{Q,ie}}} = \frac{\sqrt{K_Q} \cdot [Q^+]}{\sqrt{q \cdot C_R}} + \frac{[Na^+]}{\sqrt{q \cdot C_R \cdot K_Q}} . \quad (32)$$

The plot of $\sqrt{[Na^+]/k'_{Q,ie}}$ versus $[Na^+]$ showed good linearity.

The tests give support to the suggestion that the observed changes in retention in phase 5 are due to ion-exchange regulated by $[Na^+]$.

Octanesulfonate as Counter Ion

A mobile phase with octanesulfonate as the main counter ion produces a retention of the cationic solutes that is considerably higher than that obtained with the same

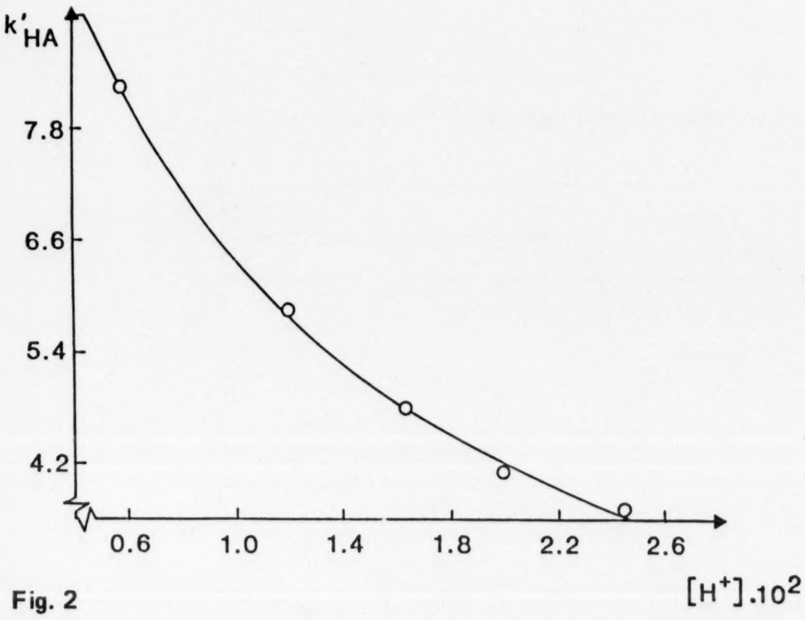

Fig. 2

Evaluation of ion-pair retention effects: monovalent cation.
Mobile phase: 1-methylpyridine 10^{-4} M + sodium cyclamate 0.01 M in phosphoric acid 0.01–0.10M. Solute: triethylmethylammonium.

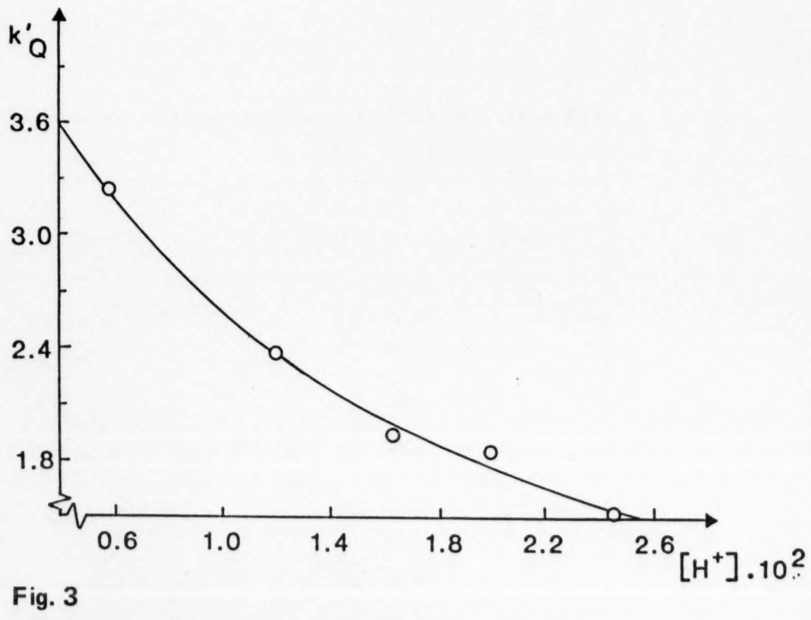

Fig. 3

Evaluation of ion-pair retention effects: system peak.
Mobile phase: 1-methylpyridine 10^{-4} M + sodium cyclamate 0.01 M in phosphoric acid 0.01–0.10M.

concentration of cyclamate. Phase 6 had a constant concentration of octanesulfonate and a varying concentration of phosphoric acid. The testing of the retention model and the evaluation of the distribution constants were based on eq. (25) for the solutes and eq. (28) for the system peak, octanesulfonate being substituted for cyclamate. The constants calculated from non-linear regression analysis are given in Table VII.

The results are based on retention measurements at five different phosphoric acid concentrations. The agreement is good between the K_{QSu} values, whereas K_{HSu}, calculated from the system peak, shows a somewhat higher deviation. The calculated value of $A = K^0 \cdot W_s/V_m$ is of the same magnitude as that obtained with cyclamate as counter ion.

Divalent Solutes

The divalent solutes were retained as ion-pairs with monovalent counter ions, and the capacity ratio expressions were deduced with two sites for monovalent ions (A_s) as the standard unit (cf. eq. (7)). When a divalent cationic solute H_2A^{+2} is retained in a mobile phase containing the monovalent ions Q^+, HB^+, and X^-, its ion-pair retention is given by:

$$k'_{H_2A,ip} = \frac{A' \cdot K_{H_2AX_2} \cdot [X^-]^2}{1 + (K_{QX} \cdot [Q^+] \cdot [X^-])^2 + (K_{HBX} \cdot [HB^+] \cdot [X^-])^2} \tag{33}$$

(where $A' = A/2$).

Studies of retention models were made with cyclamate and dihydrogenphosphate as counter ions in phases 1–5, using the principles for the computation of ion-pair constants shown above for monovalent solutes. The determinations were made with the divalent cations diaminohexane and pentamethonium.

In phases 1 and 2, constants could be evaluated with acceptable precision for pentamethonium, whereas the capacity ratios for diaminohexane were too low at higher $[H^+]$ and $[P^-]$. The values of K_{QP} and K_{HP} given in Table VIII agree fairly well with those obtained from the monovalent cations and the system peak (cf. Table IV).

Constants were also evaluated for diaminohexane and pentamethonium with cyclamate as the main counter ion in phases 3 and 4 using non-linear regression. A plot for pentamethonium is shown in Fig. 4. The constants are given in Table VIII. The values of K_{QCy} and K_{HCy} obtained with the divalent solutes are in good agreement with constants calculated from the capacity ratios of the monovalent cations (cf. Table VI). Calculations of $(K_{QCy} \cdot [Q^+])^2 + (K_{HCy} \cdot [H^+])^2$, using the constants obtained in phase 4, produced $1.4 \cdot 10^4$ and $1.1 \cdot 10^4$ for pentamethonium and diaminohexane, respectively, which is rather close to the results obtained in phase 3. The results provide good confirmation of the validity of the retention models used and support the observation that $H_2PO_4^-$ does not compete significantly with cyclamate for the binding to the adsorbent.

The results obtained at low $[H^+]$ in phase 5 did not contradict the conclusions based on the results with monovalent cations in the same phase. However, the constants in Table VIII did not allow such a precise calculation of $k'_{H_2A,ip}$; to achieve this, more experimental data are necessary.

Table VII. Ion-pair adsorption constants evaluated from capacity ratios of solute and system peaks: octanesulfonate as the main counter ion.

Phase	Counter ion	Constant	Methylamine	Tetra-methylammonium	System peak
6	Octanesulfonate (Su)	$A \cdot K_{HASu}$	$9.8 \cdot 10^3$	$11 \cdot 10^3$	–
	+	$A \cdot K_{QSu}$	–	–	$6.4 \cdot 10^4$
	H_2PO_4	K_{QSu}	$5.8 \cdot 10^6$	$4.2 \cdot 10^6$	$6.2 \cdot 10^6$
		K_{HSu}	$9.7 \cdot 10^4$	$7.7 \cdot 10^4$	$17 \cdot 10^4$
		$K^0 \cdot W_s/V_m$ (=A)	–	–	$1 \cdot 10^{-2}$

Table VIII. Constants evaluated from capacity ratios of divalent cations.

Phase	Counter ion	Constant	Pentamethonium	Diaminohexane
1 + 2	$H_2PO_4^-$ (P)	$A'^* \cdot K_{H_2AP_2}$	$9 \circ 10^6$	–
		K_{QP}	$2 \cdot 10^6$	–
		K_{HP}	$3 \cdot 10^4$	–
		$q \cdot C'^{**}_R \circ K_{H_2A}$	$6 \cdot 10^{-5}$	–
3	cyclamate	$A'^* \cdot K_{H_2ACy_2}$	$8.1 \cdot 10^5$	$3.9 \cdot 10^5$
	+			
	$H_2PO_4^-$	$(K_{QCy} \circ [Q^+])^2 + (K_{HCy} \cdot [H^+])^2$	$2.1 \cdot 10^4$	$1.8 \cdot 10^4$
4	cyclamate	$A'^* \circ K_{H_2ACy_2}$	$5.9 \cdot 10^5$	$3.3 \cdot 10^5$
	+			
	$H_2PO_4^-$	K_{QCY}	$1.0 \cdot 10^6$	$0.9 \cdot 10^6$
		K_{HCy}	$1.2 \cdot 10^4$	$1.5 \circ 10^4$

$^*A' = A/2$ $\quad$ $^{**}C'_R = C_R/2$

Table IX. Retention of cations with cyclamate in acetate buffer. Solid phase: PLRP-S (5 μm); Mobile phase: 0.01 M sodium cyclamate, 10^{-4} M methylpyridine and 4 % methanol in 0.05 m acetate buffer.

$[H^+]\cdot10^5$	$[Na^+]\cdot10^2$	$[HAc]\cdot10^2$	$[HAc]/[Na^+]$	k′				
				Propylamine	Tetramethyl-ammonium	Trimethylethyl-ammonium	Diaminobutane	System peak
7.1	2.0	4.0	2.0	4.36	1.70	2.91	6.24	3.75
1.0	4.2	1.8	0.43	3.52	1.18	2.42	3.58	2.92
0.08	5.8	0.2	0.034	3.64	1.12	2.30	3.24	2.82

Retention in Acetate Buffer

The studies with phosphate buffers in the mobile phase have shown that ion-exchange processes have influence on retention, and it was suggested that they might be due to adsorbed components of the buffer system. An illustration of the influence of an acetate buffer in a mobile phase with cyclamate as the main counter ion is shown in Table IX. The experiments were performed on PLRP-S, which is a styrene-divinylbenzene adsorbent similar to PRP-1 used in the previous studies.

A pH change from 4.15 to 5.00 gives rise to a strong decrease in the capacity ratio for all the cationic compounds, whereas a further change to pH 6.12 has a very slight effect. Ion-pair adsorption expressions analogous to eq. (10) can hardly explain this retention behaviour, and the reason cannot be a simple exchange process regulated by the main mobile phase cation, Na^+, since there is no linear relationship between the capacity ratios of the monovalent cations, k'_{HA}, and $1/[Na^+]$.

The retention change seems to be coupled with acetic acid and its $pK_a = 4.8$. If the ion-exchange is due to adsorbed acetic acid on the solid phase, the binding capacity will be approximately proportional to the concentration of unprotolyzed acetic acid (HAc) in the mobile phase. The relationship between k'_{HA} and $[HAc]/[Na^+]$ should then be approximately linear, whereas a divalent cation should have a similar relationship between k'_{H_2A} and $([HAc]/[Na^+])^2$. The results in Table IX seem to give some support to this suggestion.

Conclusions

The studies have shown that ionic compounds can be retained on a polystyrene-divinylbenzene copolymer by ion-pair adsorption and ion-exchange.

The ion-pair retention follows single site Langmuir models. Distribution constants have been evaluated by non-linear regression for monovalent and divalent cationic solutes as well as mobile phase cations. The validity of the retention expressions is confirmed by the agreement between the common constants found for the mobile phase ion-pairs.

The cations are retained as ion-pairs with hydrophobic counter ions, like cyclamate and octanesulfonate, as well as with buffer anions, like dihydrogenphosphate. The hydrophobic counter ions and the phosphate ions seem to cause binding to sites of different character, and there is no competition for the binding surface between the two kinds of ion-pairs.

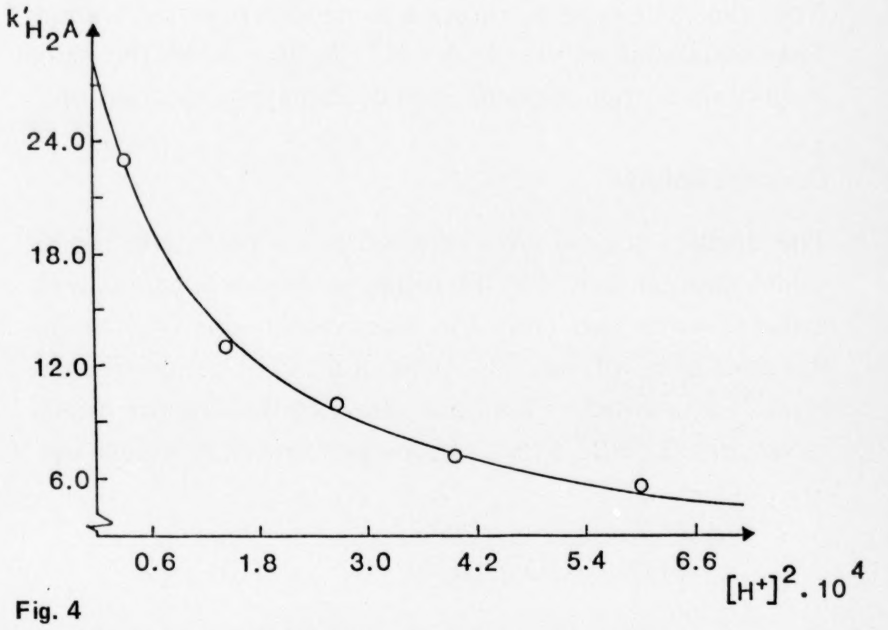

Fig. 4

Evaluation of ion-pair retention effects: divalent cation.
Mobile phase: 1-methylpyridine 10^{-4} M + sodium cyclamate 0.01 M in phosphoric acid 0.01–0.10 M. Solute: pentamethonium.

Cation exchange effects have been observed in the pH range 1.6–6.1. The effect depends not only on the cationic components in the mobile phase, but also on the nature of the buffer system.

References

[1] *S. Eksborg, P. O. Lagerström, R. Modin, G. Schill,* J. Chromatogr. **83,** 99 (1973).
[2] *S. Eksborg, G. Schill,* Anal. Chem. **45,** 2092 (1973).
[3] *A. Tilly-Melin, Y. Askemark, K. G. Wahlund, G. Schill,* Anal. Chem. **51,** 976 (1979).
[4] *A. Sokolowski, K. G. Wahlund,* J. Chromatogr. **189,** 299 (1980).
[5] *M. Denkert, L. Hackzell, G. Schill, E. Sjögren,* J. Chromatogr. **218,** 31 (1981).
[6] *L. Hackzell, G. Schill,* Chromatographia **15,** 437 (1982).
[7] *G. Schill, J. Crommen,* TrAC **6,** 111 (1987).
[8] *A. Tilly-Melin, M. Ljungcrantz, G. Schill,* J. Chromatogr. **185,** 225 (1979).
[9] *H. Stuurman, J. Köhler, S.-O. Jansson, A. Litzen,* Chromatographia **23,** 341 (1987).
[10] *M. Schröder-Nielsen,* Acta Pharm. Suec. **13,** 439 (1976).
[11] *F. Helfferich, G. Klein,* Multicomponent Chromatography, Dekker, New York, 1970.
[12] *F. Riedo, E. Kovats,* J. Chromatogr. **239,** 1 (1982).
[13] *S. O. Jansson, I. Andersson, B. A. Persson,* J. Chromatogr. **203,** 93 (1981).
[14] *J. Crommen, G. Schill, L. Hackzell, D. Westerlund,* Chromatographia **24,** 252 (1987).

Received: June 30, 1987
Accepted: July 23, 1987
F

Improved Cleanup Method for the Multiresidue Analysis of N-Methylcarbamates in Grains, Fruits and Vegetables by Means of HPLC with Postcolumn Reaction and Fluorescence Detection

A. de Kok*/M. Hiemstra/C. P. Vreeker

Governmental Food Inspection Service, Pesticide Analysis Department, Burgpoelwaard 6, 1824 DW Alkmaar, The Netherlands

Key Words

Column liquid chromatography
Postcolumn reaction detection
N-methylcarbamate pesticides
Solid phase extraction cleanup
Fruits and vegetables

Summary

An improved and quick cleanup method has been developed for the liquid chromatographic determination of 21 N-methylcarbamate pesticides and 10 of their metabolites in grains, fruits and vegetables. Various types of solid phase extraction columns have been tested for the cleanup step in order to replace the time-consuming cleanup method found in the literature. Aminopropyl-bonded silica columns proved to be superior to unbonded silica or octyl, octadecyl, cyanopropyl and diol-bonded silica. For all 16 types of matrices tested, a single column cleanup step appeared to be satisfactory.

The final determination was performed by separation of the N-methylcarbamates via high-performance liquid chromatography followed by postcolumn reaction, fluorogenic labelling of the hydrolytically formed methylamine with the orthophthalaldehyde/2-mercaptoethanol reagent, and fluorescence detection. Recovery data for 256 carbamate/commodity combinations will be given. The results of the routine analysis of real samples will also be presented. Finally, possibilities for confirming positive samples by an independent, second method will be discussed.

Introduction

The use of N-methylcarbamate pesticides in agriculture has increased considerably during the past decades. More and more applications have been found, e. g. as a more acceptable alternative for organochlorine pesticides. Besides, new members are continuously introduced in the group of N-methylcarbamates. For their analysis in routine food control, e. g. in crops, a multiresidue approach is required.

Traditionally, gas chromatography (GC) was chosen for analysis. However, due to their thermal instability, direct GC analysis of all N-methylcarbamates was impossible. Derivatization of the parent compounds or their hydrolysis products had to be applied. Because chemical and physicochemical properties of the carbamates are very different, most of the older publications deal with the analysis of a single carbamate or of a group of compounds which are rather similar.

In 1977 Moye et al. [1] introduced high-performance liquid chromatography (HPLC) with postcolumn reaction detection as a very promising alternative for GC analysis. After chromatographic separation, the N-methylcarbamates were hydrolysed on line with NaOH to methylamine, which was subsequently derivatised with the orthophthalaldehyde (OPA)/2-mercaptoethanol reagent. The fluorophore was then detected very selectively and sensitively with a fluorescence detector.

Much valuable work on refinement and application of the method on food samples was done by Krause [2, 3]. Engelhardt and Lillig [4] further improved the reaction detection system, but unfortunately, optimization was done for only a limited number of carbamate standards. The Krause method has been collaboratively studied in the USA [5] and its application in routine analysis is now increasing continuously [6–8]. The weakest part of the method in crop analysis is definitively the lengthy and time-consuming cleanup with liquid-liquid partitioning and column chromatography steps.

The aim of our study was to develop a simple, fast and cheap cleanup method which can be applied for all types of crop samples, including as many N-methylcarbamates and metabolites as possible in the multiresidue analysis. This has been achieved by the application of solid phase extraction columns with chemically-bonded silica sorbents.

0009-5893/87 0469-08 $03.00/0 © 1987 Friedr. Vieweg & Sohn Verlagsgesellschaft mbH

Experimental

Reagents

Methanol and dichloromethane (both HPLC grade), and acetone and petroleum ether at 40–60 °C (both pesticide grade), were obtained from Fisons plc (Loughborough, England). HPLC grade acetonitrile was from Rathburn (Walkerburn, Scotland). Water used for the HPLC was purified with an Elgastat UHQ water purification system (Elga, High Wycombe Bucks, England), obtained through Lameris (Breukelen, The Netherlands).

Sodium hydroxide (Baker analysed reagent) was purchased from Baker (Deventer, The Netherlands), di-sodiumtetraborate (anhydrous), orthophthalaldehyde (for fluorescence analysis) and 2-mercaptoethanol (pro analysi) from Merck (Darmstadt, FRG).

Bond Elut solid phase extraction columns (silica, octyl, octadecyl, diol, aminopropyl, cyanopropyl-bonded silica) from Analytichem (Harbor City, CA, USA), obtained through Betron Scientific (Rotterdam, The Netherlands), were used for cleanup. All columns contained 100 mg sorbent. The OPA reagent was prepared as follows: 10.6 g di-sodiumtetraborate was added to a 1-L volume flask and dissolved in purified water (ca. 500 ml) under heating. 250 mg orthophthalaldehyde was weighed and dissolved in 2 ml acetonitrile and then added to the 1-L volume flask. Subsequently, 0.5 ml 2-mercaptoethanol was also added and the flask was made up to volume with water.

Apparatus

The HPLC system consisted of a Kratos (Ramsey, NJ, USA) Model SF 400 pump, a Rheodyne (Berkeley, CA, USA) Model 7125 injection valve, provided with a 100-μl loop, and a Merck-Hitachi (Tokyo, Japan) Model F1000 double monochromator fluorescence detector. Chromatographic separations were carried out on a Merck LiChroCart 250 × 4.0 mm i.d. cartridge column, packed with LiChrosphere 100 RP-18 (5 μm), in conjunction with a 4.0 × 4.0 mm i.d. guard column, packed with LiChrosorb 100 RP-18. Isocratic analysis was performed with an acetonitrile-water (28:72) mobile phase at a flow-rate of 1.0 ml. min^{-1}.

The postcolumn reaction system consisted of a Kratos PCRS 520 postcolumn reactor and two Kratos SF 400 reagent delivery pumps, each provided with a membrane pulse dampener. The first pump added a 0.05 M NaOH solution via a Vortex mixing chamber (1.2 μl volume) to the column eluent. The hydrolysis took place in a PTFE knitted tube (5.1 m × 0.25 mm i. d.; 1.0 ml volume), kept at a temperature of 100 °C. After the hydrolysis reaction coil the OPA-reagent (0.05 M) was added via the second mixing chamber. The flow-rate of both reaction solutions was 0.5 ml.min^{-1}. All connecting tubing was of stainless steel with an internal diameter of 0.25 mm, except the capillary tubing from the second mixing chamber to the fluorescence detector, which was a 60 cm × 0.10 mm i. d. PTFE capillary. After the detector, a Beckman (San Ramon, CA, USA) back pressure regulator was installed to minimize detector noise due to possible bubble formation in the heated reaction stream.

The excitation and emission wavelengths for fluorescence detection were 340 nm and 455 nm, respectively. Chromatograms were recorded on a Kipp (Delft, The Netherlands) BD 41 recorder.

Sample preparation experiments with the solid phase extraction columns were executed by means of an Analytichem Vac Elut system. A Polytron (Kinematica, Luzern, Switzerland) Model PT 10-35 homogenizer was used for the extraction of crops.

Methods

Extraction

Fruits and vegetables: 15 g of chopped crop sample were weighed and transferred to a centrifuge tube. 30 ml of acetone were added and the sample was homogenized in 30 s by means of a Polytron. 30-ml of both dichloromethane and petroleumether were then added, and while mixing 60 s with the Polytron, extraction took place. After 2 min. of centrifugation at 4000 rpm, the organic phase was decanted and an aliquot of 2 ml was transferred to a calibrated test tube. The extract was evaporated to nearly dryness with a waterbath (65 °C), while the remaining solvent was allowed to evaporate in the air. The residue was redissolved in 1 ml dichloromethane.

Grains: 25 g of grain sample were weighed in an Erlenmeyer flask and extracted with 100 ml dichloromethane/acetone (1:1) by allowing it to stand overnight (16 h). An aliquot of 2 ml was taken to evaporate and redissolve in the same way as described above for fruits and vegetables.

Sample Cleanup

An aminopropyl-bonded silica column was preconditioned by rinsing it with 1 ml of dichloromethane. The 1-ml dichloromethane sample extract was applied, followed by another 0.5 ml dichloromethane which was used for rinsing the sample test tube. Directly from the start of applying the sample extract, the eluate from the column was collected in a test tube. The elution of the carbamates was proceeded with 1 ml dichloromethane:methanol (99:1). The combined eluate fractions were evaporated with a waterbath (50 °C) to nearly dry and, subsequently, the remaining solvent was allowed to dry in the air. The residue was then redissolved in 1 ml of acetonitrile/water mixture, equivalent to the HPLC mobile phase solvent with the help of an ultrasonic bath (1 min).

Results and Discussion

HPLC System

The chromatography and postcolumn reaction system for the carbamate analysis were based on the work of Krause [4]. As an important improvement, however, a PTFE knitted open tube (similar to that introduced by Engelhardt and Lillig [4] for this same method) was used as the hydrolysis chamber in the postcolumn reactor instead of a coiled stainless steel tube. In this way, band broadening of the eluted peaks was limited to a minimum. For recovery studies, isocratic analyses were run. In Table I, retention data and detection limits are given for 21 N-methylcarbamates and 10 of their metabolites. Within 60 min, 26 compounds were chromatographed. For the late-eluting carbamates methiocarb, promecarb, bufencarb, mexacarbate and aminocarb, a separate mobile phase composition is required to obtain a reasonable analysis time. In Fig. 1, chromatograms of 25 of the carbamates studied, divided over 3 mixtures, are shown. Good separation is achieved, although coelution of some carbamates can evidently not be avoided.

From Table I it can be seen that the sensitivity is excellent. Detection limits vary over the range 0.02–0.1 ng. As an exception, thiofanox shows a 10-fold lower sensitivity. The selectivity of this technique, relative to other pesticides, has already been described extensively by Krause [9].

We refrained from further optimization of the postcolumn reaction parameters because critical comparison of the optimization studies of Krause [2] and Engelhardt [4] reveals that further improvements are hardly possible if such a great number of compounds, as studied by us, are included in the analysis.

The only improvement left would be the application of a solid phase reactor [10], in which the hydrolysis is performed catalytically. The influence of pump pulse could be decreased, and even excluded if a real plus-free pump is used for the OPA reagent delivery. Future studies will be undertaken in this direction, with the emphasis on system stability evaluation during long term application in routine sample analysis.

Cleanup Experiments

Due to the wide variety of crop products which have to be analyzed in daily routine analysis, the development of a simple and uniform cleanup method is a very difficult task to achieve. This especially holds true when one tries to include as many carbamates and metabolites in one multiresidue method as possible. In order to eliminate the very lengthy and time-consuming cleanup steps which are used in the official AOAC multiresidue method for N-methylcarbamates [5, 6], a totally different approach was evaluated, viz. solid phase extraction (SPE) columns.

First, we studied the elution pattern of the carbamates and matrix interferences of some crops on various bonded silica columns in the reversed phase mode, viz. octyl, octadecyl, aminopropyl, cyanopropyl and diol-bonded silica, using methanol-water mixtures as eluant. As might have been expected, the similarity of the cleanup mode with the ultimate HPLC reversed phase separation caused the cleanup to be insufficient, i. e. early eluting interferences in the HPLC analysis could not be eliminated completely and/or early eluting carbamates were only partially recovered.

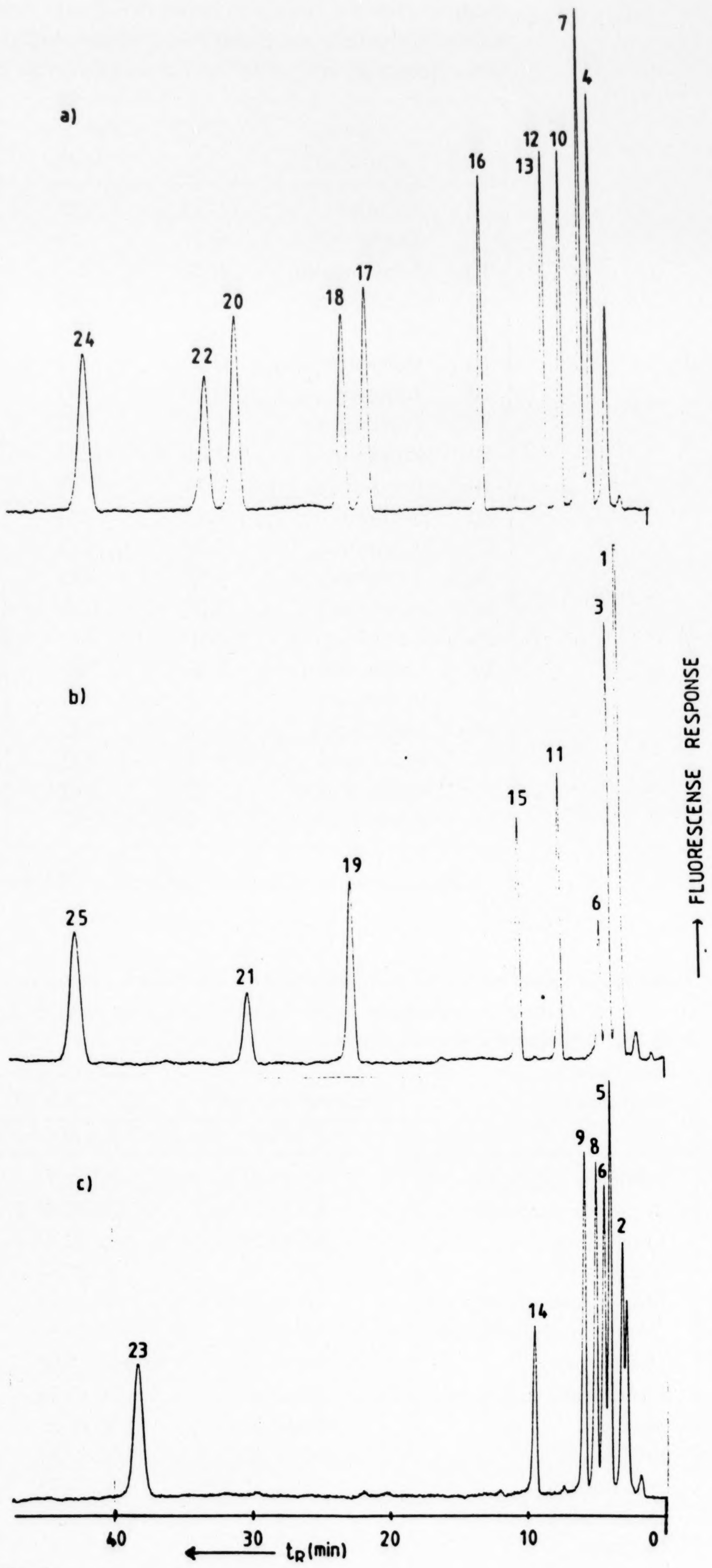

Fig. 1

HPLC chromatograms of 25 N-methylcarbamates in the system LiChrosphere 100 RP-18/acetonitrile-water (28:72). Fluorescence detection at excitation and emission wavelengths of 340 and 455 nm, respectively. Absolute injected amount: 2 ng of each carbamate, except thiofanox (20 ng), ethidimuron (10 ng) and butocarboxim (4 ng). Numbers above the peaks correspond with those given in table 1.

Therefore, it seemed a viable way to examine some normal phase cleanup modes. Unbonded silica, and aminopropyl, cyanopropyl and diol-bonded silica were tested. Sample extracts in dichloromethane were applied onto the SPE cartridges, whereby many carbamates already started to elute. The elution was completed with a dichloromethane/methanol mixture, with the percentage of methanol required for complete recovery dependent on the type of sorbent.

Table I. Relative retention times (RRT) and detection limits of 21 N-methylcarbamates and 10 of their metabolites in the reversed phase HPLC system LiChrosphere 100 RP-18 (5 μm)/acetonitrile-water, 28:72. Fluorescence detection was performed at an excitation and emission wavelength of 340 nm and 455 nm, respectively

No	Parent compounds	RRT	det. lim. (in pg)	No	Metabolites	RRT	det. lim. (in pg)
4	Oxamyl	0.19	25	1	Butocarboxim sulphoxide	0.15	25
7	Methomyl	0.23	25	2	Aldicarb sulphoxide	0.16	50
10	Ethidimuron	0.30	100	3	Butocarboxim sulphone	0.19	25
12	Dioxacarb	0.37	50	5	Aldicarb sulphone	0.21	25
13	Tranid	0.37	50	6	Thiofanox sulphoxide	0.23	50
15	Butocarboxim	0.51	50	8	Methiocarb sulphoxide	0.26	50
16	Aldicarb	0.58	50	9	3-Hydroxycarbofuran	0.30	50
17	Carbofuran	1.00*	50	11	Thiofanox sulphone	0.37	50
18	Propoxur	1.09	50	14	Methiocarb sulphone	0.48	50
19	Bendiocarb	1.12	50	23	1-Naphthol	1.89	100
20	Carbaryl	1.47	50				
21	Thiofanox	1.49	500				
22	Ethiofencarb	1.57	100				
24	Isoprocarb	2.01	100				
25	Landrin	2.10	100				
26	Carbanolate	2.49	100				
27	Promecarb	> 3	100				
28	Methiocarb	> 3	100				
29	Bufencarb	> 3	200				
30	Mexacarbate	> 3	200				
31	Aminocarb	> 3	200				

* Absolute retention time of carbofuran: 21 min.

Table II. Recoveries (in %) and repeatability coefficients of variation (C. V.) of N-methylcarbamates from fortified grain samples at the 0.05 and 0.5 ppm fortification level

Carbamate	Average recovery (C.V., n = 5) 0.05 ppm	0.5 ppm
Aldicarb sulphoxide	99 (1.1)	102 (0.7)
Aldicarb sulphone	99 (1.2)	102 (0.6)
Oxamyl	98 (1.2)	102 (0.4)
Methomyl	98 (1.4)	101 (1.4)
Methiocarb sulphoxide	96 (3.8)	96 (1.4)
3-Hydroxycarbofuran	98 (1.8)	100 (1.6)
Dioxacarb	98 (1.3)	101 (1.0)
Methiocarb sulphone	92 (2.4)	95 (1.1)
Aldicarb	100 (2.5)	100 (1.5)
Propoxur	98 (1.3)	100 (2.4)
Bendiocarb	97 (1.1)	100 (1.7)
Carbofuran	100 (2.1)	100 (1.7)
Carbaryl	95 (2.6)	98 (2.4)
Ethiofencarb	85 (2.1)	84 (2.4)
1-Naphthol	73 (1.7)	80 (2.5)
Isoprocarb	98 (1.0)	98 (2.4)
Landrin	98 (1.1)	98 (1.6)
Methiocarb	99 (1.8)	99 (1.8)

The sorbents tested provided a much better cleanup when used in the normal phase mode, as compared with the reversed phase mode, while recoveries were also satisfactory. The aminopropyl columns clearly surpassed the others, so this sorbent type was chosen for more extensive recovery studies. The dichloromethane (1 ml) in which the sample extract was applied, plus an additional 0.5 ml, directly eluted most of the parent carbamates quantitatively. The more polar compounds, e.g. aldicarb sulphoxide, 3-hydroxy-carbofuran and 1-naphthol, were subsequently eluted in the dichloromethane/1% methanol fraction, which was combined with the first fraction. Because the carbamates elute directly in a small volume while the interferences are kept on the SPE column, this normal phase cleanup step, with a minimal number of elutions, is very fast and attractive.

Recovery Studies for Crops

Initial recovery studies were executed with grain samples, which were fortified at the 0.05 and 0.5 ppm level with 18 carbamates and metabolites. These 18 compounds were divided over two mixtures in such a way so as to avoid problems with co-eluting carbamates during HPLC analysis. Following the procedure described in the experimental section, the recovery data, as depicted in Table II, were obtained. For all compounds, except ethiofencarb and 1-naphthol, recoveries exceeded the 90% level at both fortification levels, with good repeatability (C. V., 0.4–3.8%, n = 5).

After the positive results with the grain samples, the recovery studies were extended with 19 carbamates and metabolites on 12 different crops. Each crop type was chosen so as to represent a certain class of fruits and vegetables. The extraction method used in the first instance was taken from the routine method for the determination or organophosphorus and organochlorine pesticides in crops, thereby trying to make the extraction step uniform in the multiresidue analysis of the various pesticide classes. This approach automatically implies that the N-methylcarbamates are not necessarily extracted with an optimal recovery.

The recovery data are shown in Table III. Almost invariably, recoveries for all carbamate/commodity combinations were

Table III. Recoveries (in %) of N-methylcarbamates from 12 crop samples at the 0.05 and 0.5 ppm fortfication level. Each result is the average of a duplicate determination.

Carbamate	Recoveries at 0.05 ppm level											
	apple	beans	carrot	cauliflower	celery	cucumber	leek	onion	orange	potato	spinach	strawberry
Butoxycarboxim	74	73	73	72	74	72	72	71	73	73	73	72
Oxamyl	73	68	68	66	66	66	65	67	81	67	68	77
Methomyl	88	77	77	81	76	77	77	80	80	80	80	83
Meth. sulphoxide	74	66	67	70	69	69	66	71	73	74	71	73
3-OH-carbofuran	90	90	89	85	92	89	91	87	91	92	89	90
Ethidimuron	91	95	94	83	*	96	95	88	89	98	96	94
Dioxacarb	97	95	87	88	94	90	86	94	93	90	95	95
Meth. Sulphone	74	75	73	71	72	72	66	72	74	72	75	73
Aldicarb	91	90	89	86	90	90	85	93	91	85	93	93
Butocarboxim	89	89	90	82	92	90	89	87	88	93	91	90
Carbofuran	96	95	92	93	92	91	90	96	87	91	96	94
Propoxur	94	93	86	89	95	88	88	93	90	91	95	91
Bendiocarb	88	92	91	86	94	92	93	90	94	95	94	92
Carbaryl	91	94	90	88	91	95	90	91	93	92	93	94
Thiofanox	83	88	87	76	89	88	84	87	80	87	88	82
Ethiofencarb	88	83	77	76	83	80	80	72	*	78	84	86
1-Naphthol	75	72	74	75	73	76	72	74	74	69	77	81
Isoprocarb	86	87	85	83	82	88	81	85	86	86	88	83
Landrin	87	89	90	84	94	90	91	83	83	90	87	94
Carbamate	Recoveries at 0.5 ppm level											
Butoxycarboxim	70	75	78	75	80	79	77	75	80	74	74	74
Oxamyl	77	76	70	73	73	69	71	77	86	75	73	77
Methomyl	88	86	80	76	84	82	86	82	86	77	81	85
Meth. sulphoxide	85	81	77	84	82	74	80	77	85	85	84	77
3-OH-carbofuran	91	88	85	88	86	84	88	89	97	93	88	84
Ethidimuron	95	96	97	96	94	97	96	98	93	97	95	94
Dioxacarb	92	97	87	93	97	90	89	93	95	95	92	86
Meth. sulphone	78	83	75	74	73	80	70	74	85	78	77	76
Aldicarb	90	94	88	92	94	93	90	97	94	90	95	87
Butocarboxim	97	95	96	91	95	96	97	97	97	93	97	91
Carbofuran	92	95	93	96	94	94	93	93	94	97	95	93
Propoxur	91	93	90	95	95	90	92	92	94	94	91	91
Bendiocarb	96	96	93	98	97	98	98	97	97	98	97	95
Carbaryl	94	98	91	91	98	94	91	94	97	92	95	93
Thiofanox	95	98	96	98	86	94	96	97	94	88	95	96
Ethiofencarb	83	85	84	82	75	85	78	85	*	84	85	81
1-Naphthol	72	81	70	73	83	72	71	78	75	75	75	75
Isoprocarb	86	89	87	85	83	86	89	91	93	87	90	87
Landrin	93	93	95	94	93	92	94	95	94	93	96	95

* = recovery could not be calculated, due to sample interference

in the 70–100% range. Differences in duplicate values sporadically exceeded 5%, even at the 0.05 ppm level. It may be concluded from Table III that, on the average, the more polar carbamates (which elute early in the HPLC analysis) show a 10–20% lower recovery than the less polar compounds. Knowing that the cleanup step is quantitative, it is consequent to conclude that losses occur in the extraction step where the polar carbamates partially stay in the aqueous phase. As an example, butocarboxim sulphoxide and aldicarb sulphoxide always showed a recovery lower than 60%.

The repeatability of the method was determined by analyzing, in five-fold, carrot and cauliflower samples, fortified with 11 carbamates at the 0.2 ppm level (see Table IV). For cauliflower, excellent coefficients of variation (1.3–2.8%) were obtained. With carrots, these amounted

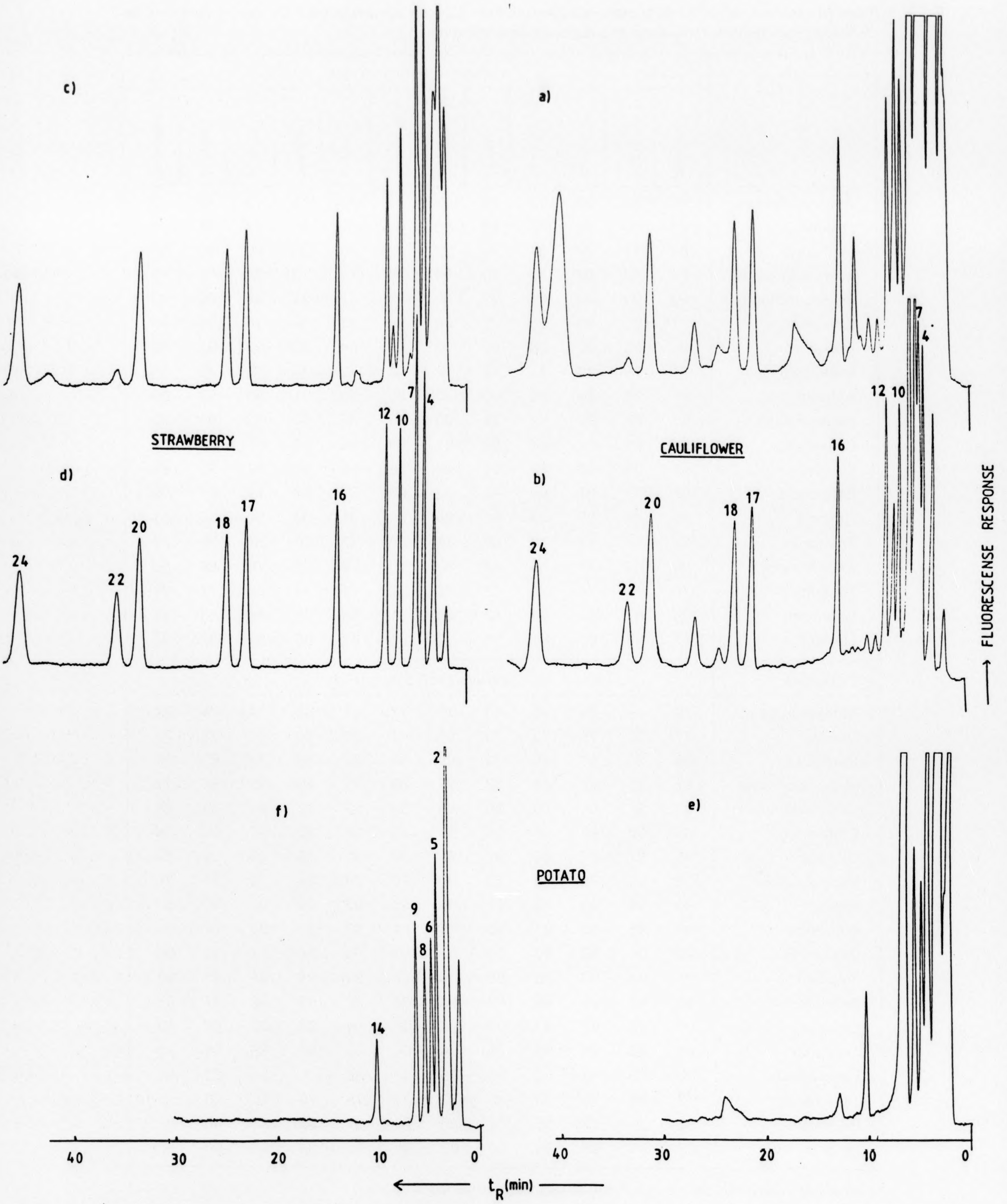

Fig. 2
HPLC chromatograms of sample extracts of cauliflower (a and b), strawberry (c and d), and potato (e and f), fortified with 0.05 ppm of N-methylcarbamates, before (a, c, and e) and after (b, d and f) cleanup on aminopropyl bonded silica SPE column. Injected amounts: 2 ng, which, is equivalent to 40 mg of original sample.

mostly to 2.1–2.8 %, but for aldicarb, aldicarb sulphoxide, oxamyl and methiocarb sulphone the figures were 6.4, 6.2, 5.4 and 3.4, respectively. This is still considered as acceptable in multiresidue analysis, keeping in mind that extraction efficiency for the latter-mentioned compounds was not maximal.

Table IV. Average recoveries (in %) and repeatability coefficients of variation (C.V.) for 11 N-methylcarbamates fortified to carrot and cauliflower at the 0.2 pp level

Carbamate pesticide	Average recovery carrot	(C.V., n = 5) cauliflower
Aldicarb sulphoxide	47 (6.2)	57 (2.7)
Oxamyl	73 (3.4)	73 (1.8)
Methomyl	87 (2.8)	80 (2.1)
3-Hydroxycarbofuran	93 (2.3)	91 (2.0)
Dioxacarb	92 (2.8)	93 (1.4)
Methiocarb sulphone	80 (5.4)	81 (2.8)
Aldicarb	84 (6.4)	82 (2.8)
Carbofuran	97 (2.5)	96 (2.3)
Propoxur	96 (2.8)	95 (2.4)
Carbaryl	97 (2.1)	97 (1.2)
Isoprocarb	94 (2.7)	90 (2.5)

Table V. Overview of real crop samples analysed for N-methylcarbamates

Sample type	No. of samples analysed	Samples with carbamate residues (in ppm)
Grains		
Wheat	92	–
Rye	10	–
Barley	20	–
Rice	50	3 (Carbaryl; 0.84, 0.21, 0.10)
Fruit/vegetables		
Potatoes	34	1 (Aldicarb sulphoxide; 0.01)
Chicory	19	–
Apple	18	1 (Oxamyl; 0.01)
Endive	4	–
Cauliflower	4	–
Beans	6	1 (Methomyl; 0.28)
Grapes	4	–
Tomatoes	4	–
Kiwi	3	–
Paprika	5	–
Cucumber	2	1 (Methomyl; 0.22)
Eggplant	1	1 (Methomyl; 0.01)
Bananas	3	–
Mandarins	5	1 (1-Naphthol; 0.6)
Grapefruit	6	–
Oranges	13	5 (1-Naphthol; 0.5, 0.9 Carbaryl; 0.01, 0.07 Carbofuran; 0.02)
Others	13	–

It is important to note here that in the extraction system used, viz. water/acetone-dichloromethane-petroleumether, the volume of the organic phase, after extraction and centrifugation, has decreased by an average of 10%. This is due to the partial miscibility of the organic phase with the aqueous matrix phase and/or to some evaporation losses which may occur during the centrifugation step. This can be corrected, which has been done with our data in the tables and which invariably caused recoveries to decrease below the 100% level.

Real Sample Analysis

The complete analysis method described in this paper was applied on a series of grain samples, which were analysed within a residue monitoring project in 1985/1986. The results are summarized in Table V. All wheat, rye and barley samples appeared to be negative. However, three out of fifty rice samples contained residues of carbaryl, at levels of 0.84, 0.21 and 0.10 ppm, respectively.

In Table V, results of the analysis of a variety of fruit and vegetable samples, which were purchased randomly on the market in the first quarter of 1987, are also included. Residues were generally low, and residue tolerances were exceeded only twice, viz. for methomyl in cucumber and beans, respectively. Limits of determination of the HPLC method in crop analysis are in the 5–10 ppb range, where an amount of extract equivalent to ca. 0.5 g of the sample is applied on the SPE column for cleanup. This is sufficient for residue work.

The HPLC analysis method for N-methylcarbamates has been working in routine analysis, uninterruptedly, in our laboratory for more than a year, to our entire satisfaction. In our future work, emphasis will be placed on the evaluation of various confirmation methods for positive residue containing samples. In the past, derivatization with pentafluorobenzyl bromide, directly [11] or after hydrolysis [12], followed by GC analysis, was a frequently applied method, which still may be used for confirmation purposes. However, recently some new developments have appeared in the literature. Krause [13] used, as an alternative to the HPLC fluorescence detection, an electrochemical technique to detect the phenol moiety, which is also formed by postcolumn hydrolysis of the carbamates. This provides a simple and selective confirmation. Besides HPLC, GC is now also gaining popularity again by the introduction of continously improved capillary columns. Wuest and Meier [14], and Braukhoff and Thier [15] analysed 9 and 15 N-methylcarbamates, respectively, via capillary GC with nitrogen specific thermionic detection. Applications on fruits and vegetables were shown. The sensitivity of the GC method is similar to that of HPLC with fluorescence detection.

In our laboratory, residues of carbamates were confirmed, amongst others, via capillary GC and Hall electrolytic conductivity detection, e.g. 0.1 ppm carbaryl in rice. Sometimes a less sensitive and selective HPLC method with UV detection may serve as a confirmation technique, as we have seen with the methomyl residues (0.2 ppm level) on beans and cucumbers.

A normal phase system (silica/dichloromethane) appeared to be very useful. It should be clear from the present paper and the cited literature that progress has been made in recent years in the analysis of carbamates in crops.

Conclusion

A simple and fast cleanup method, based on the principle of solid phase extraction columns, has been developed for the multiresidue HPLC analysis of 21 N-methylcarbamates and 10 of their metabolites in various crop samples. The use of a single sorbent type, aminopropyl-bonded silica, appeared to be sufficient for all 16 crop types studied, provided the normal phase mode, instead of the reversed phase mode, was chosen.

The carbamate pesticides can be detected down to the 5 ppb level, while an amount of sample extract, equivalent to only 0.5 g of the original sample, is taken for cleanup and subsequent HPLC analysis with postcolumn reaction detection and fluorescence detection. Recoveries for the large number of carbamate/crop combinations studied were almost invariably within the 70–100% range, and repeatability coefficients of variations, generally, did not exceed the 5% level. It has been demonstrated that the complete analysis method described allows succesful daily routine analysis. Positive carbamate residues in real samples were detected and confirmed with both capillary GC and HPLC-UV methods.

References

[1] *H. A. Moye, S. J. Sherer, P. A. St. John,* Anal. Lett. **10**, 1049 (1977).
[2] *R. T. Krause,* J. Chromatogr. Sci. **16**, 281 (1978).
[3] *R. T. Krause,* J. Assoc. Off. Anal. Chem. **63**, 1114 (1980).
[4] *H. Engelhardt, B. Lillig,* Chromatographia **21**, 136 (1986).
[5] *R. T. Krause,* J. Assoc. Off. Anal. Chem. **68**, 726 (1985).
[6] *R. T. Krause,* J. Assoc. Off. Anal. Chem. **68**, 734 (1985).
[7] *K. M. Hill, R. H. Hollowell, L. A. Dal Cortivo,* Anal. Chem. **56**, 2465 (1984).
[8] *K.-C. Ting, P. K. Kho, A. S. Musselman, G. C. Root, G. R. Tichelaar,* Bull. Environ. Contam. Toxicol. **33**, 538 (1984).
[9] *R. T. Krause,* J. Chromatogr. **185**, 615 (1979).
[10] *L. Nondek, R. W. Frei, U. A. Th. Brinkman,* J. Chromatogr. **282**, 141 (1983).
[11] *M. D. Jackson, S. D. Soileau,* Bull. Environ. Contam. Toxicol. **26**, 97 (1981).
[12] *J. A. Coburn, B. D. Ripley, A. S. Y. Chau,* J. Assoc. Off. Anal. Chem. **59**, 188 (1976).
[13] *R. T. Krause,* Paper presented at the 6th Int. Congr. Pestic. Chem., Ottawa, Canada (1986).
[14] *O. Wuest, W. Meier,* Z. Lebensm. Unters. Forsch. **177**, 25 (1983).
[15] *S. Brauckhoff, H.-P. Thier,* Z. Lebensm. Unters. Forsch. **184**, 91 (1987).

Received: June 30, 1987
Revised manuscript
received: July 29, 1987
Accepted: Aug. 5, 1987
F

Determination of the Enantiomeric Composition of Chiral Carboxylic Acids Using Chiral Derivatization and HPLC

L. Ladányi*/I. Sztruhár/P. Slégel/G. Vereczkey-Donáth

EGIS Pharmaceuticals, P.O. Box 100, H-1475 Budapest, Hungary

Key Words

Column liquid chromatography
Chiral carboxylic acid
Enentiomeric resolution
Chiral derivatization

Summary

The enantiomers of chiral carboxylic acids were separated as their diastereomeric amides with (1R,2R)-(-)-1-(4-nitrophenyl)-2-amino-1,3-propanediol ("levobase") and with "dextrobase" (the enantiomer of levobase) by high-performance liquid chromatography using a conventional C-18 column and various solvent systems containing acetonitrile, methanol, water, and phosphoric acid.

Introduction

For enantiomeric resolution of chiral carboxylic acids, direct high-performance liquid chromatographic (HPLC) techniques (using either chiral stationary phases [1–5] or chiral additives in the mobile phase [6–10] in conjunction with conventional columns) are widely applied.

Over recent years attention has increasingly focussed on the indirect methods in which derivatization reactions with optically active reagents are used and the covalently bound diastereomeric derivatives (amides, in most cases) are separated by conventional HPLC systems [11–22].

In our previous paper [22], we have described two new chiral derivatizing agents, "levobase" and "dextrobase" (I and II respectively in Fig. 2) for indirect enantiomeric separation of chiral carboxylic acids as their diastereomeric carboxamides by thin-layer chromatography (TLC). As coupling agents, dicyclohexylcarbodiimide (DDC) was used [23–24].

The present paper describes indirect HPLC methods for the determination of the enantiomeric composition of chiral carboxylic acids based on our previously reported derivatization technique for the formation of diastereomeric carboxamides.

Experimental

Apparatus

The HPLC system consisted of a Model 100 A pump (Altex, Berkeley, CA, USA) a 7125 loop injector (Rheodyne, Berkeley, CA, USA) with 10-μl loop, a 4020 variable wavelength UV detector (Pye Unicam, Cambridge, UK) and a 3390 A reporting integrator (Hewlett-Packard, Palo Alto, CA, USA).

Materials

All solvents used were of HPLC grade (LiChrosolve, Merck, Darmstadt, FRG). Water was double-distilled and stored in glass Levobase and dextrobase, manufactured by EGIS Pharmaceuticals (Budapest, Hungary) were available in high enantiomeric purity (m.p.: 163–165 °C for both enantiomers, $[\alpha]_D^{20} = -29.5$ and $+29.4$ (c = 1, 6M HCl) respectively. Cis-permethrinic acids (racemate, (+) and (–) enantiomer) were made available by CHINOIN Pharmacochemical Works Ltd. (Budapest, Hungary).

Other compounds obtained from commercial sources were: dicyclohexylcarbodiimide (DCC) 2-chloropropionic acid (racemate) from Fluka (Buchs, Switzerland), 3-bromo-2-methylpropionic acid from Toyosoda (Tokyo, Japan), N-carbobenzoxy-phenylalanine and α-methoxyphenylacetic acid from Sigma Chemie (Taufkirchen, FRG). 2-methoxy-3-benzoylpropionic acid [25], (2R)- and (2S)-2-chloropropionic acid [26], and 3-bromo-2-methylpropionic acid enantiomer mixture enriched in (2S)-form [27] were synthetized as described in the literature.

Chromatographic Conditions

The separations were carried out on a Partisil 10 ODS column (250 x 4.6 mm i.d.), (Whatman, NJ, USA) with different mobile phases (Table I) as follows:

Acetonitril – methanol – water – 85% phosphoric acid,

(A) 15:10:75:0.01,
(B) 5:15:80:0.01,
(C) 10:30:60:0,01,
(D) 30:15:55:0.01.

Isocratic elution was used at a flow rate of 1.3 cm^3/min.

0009-5893/87 0477-05 $03.00/0

© 1987 Friedr. Vieweg & Sohn Verlagsgesellschaft mbH

Table I. Enantiomeric resolution of chiral carboxylic acids, N-derivatized with levobase and dextrobase. Conditions: column, Partisil ODS (250 x 4.6 mm i.d.), 5 μm; mobile phase A, B, C, D (see Experimental), flow rate: 1.3 cm^3/min; detection UV at 278 nm.

Carboxylic acid (as in Fig. 1)	Derivatizing Agent						Mobile phase
	Levobase			Dextrobase			
	k'			k'			
	Peak 1*	Peak 2*	α	Peak 1*	Peak 2*	α	
1.	2.22 (R)	2.62 (S)	1.18	2.22 (S)	2.62 (R)	1.18	A
2.	3.24 (R)	3.72 (S)	1.16	3.24 (S)	3.72 (R)	1.16	B
3.	3.37 (R)	5.85 (S)	1.74	3.37 (S)	5.85 (R)	1.74	A
4.	5.57 (R)	6.44 (S)	1.16	5.57 (S)	6.44 (R)	1.16	C
5.	4.06 (1S, 2S)	4.81 (1R2R)	1.18	4.06 (1R2R)	4.81 (1S2S)	1.18	D
6.**	4.74	7.51	1.58	4.74	7.51	1.58	A

* Peaks numbered in order of elution
** Racemate

Derivatization Procedure

The carboxylic acid, ca. 0.05 mmol, is weighed in a 10 cm^3 volumetric flask, ca. 0.05 mmol of levobase (dextrobase) and 2 cm^3 of abs. methanol are added. After dissolution, 1.0 cm^3 of a 5 x 10^{-2} M DCC solution in abs. methanol is added. The reaction mixture is allowed to stand for 15 minutes, filled up to 10 cm^3 and homogenized, finally 10-μl portions are injected into the HPLC system.

Results and Discussion

Chiral carboxylic acids 1-6 (Fig. 1) were reacted with the derivatizing agent (I or II) in the presence of dicyclohexylcarbodiimide (DCC) as the coupling agent [22] (Fig. 2).

Typical chromatograms obtained for 3-bromo-2-methylpropionic acid are shown in Fig. 3.

The chromatographic behaviour of the investigated compounds following derivatization as described above is summarized in Table I.

As is evident from Table I, the resolution of enantiomers (as their diastereomeric carboxamides) is good, the separation factors ranging between 1.16 and 1.74.

When using shorter wavelengths (e.g. 220 nm) for UV detection, underivatized solutes, non-reacted reagents and intermediate III (see Fig. 2) could also be detected (Fig. 4).

Due to the diverse chemical structure of the investigated solutes, various mobile phases were used (see Table I) in order to achieve enhanced resolution.

Because of the different reactivity of the carboxylic acids toward DCC and the chiral derivatizing agent, the extent of conversion was time-dependent and always less than 100%. Therefore, derivatization reaction rates for the

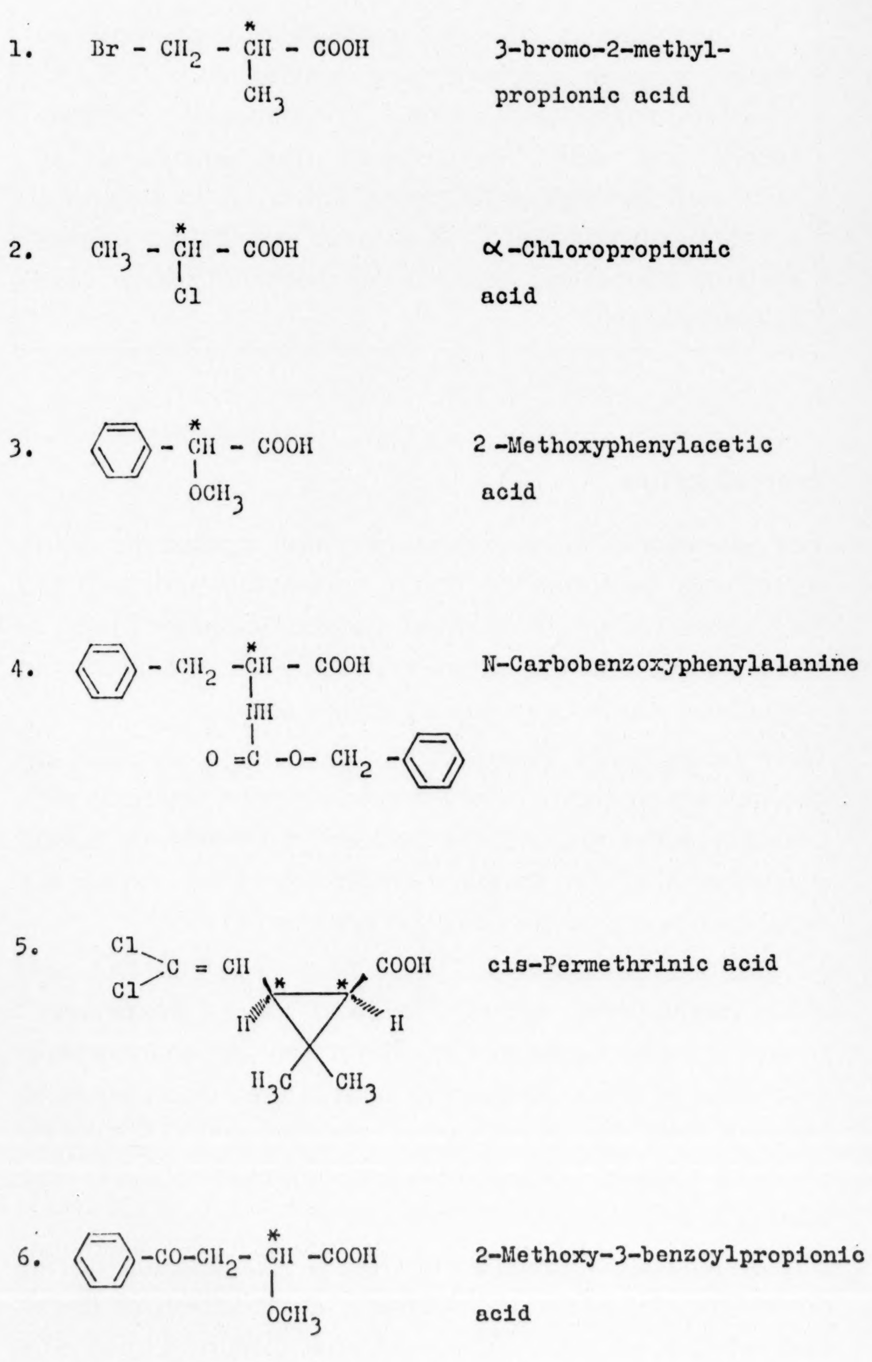
1.
3-bromo-2-methyl-propionic acid
2.
α-Chloropropionic acid
3.
2 -Methoxyphenylacetic acid
4.
N-Carbobenzoxyphenylalanine
5.
cis-Permethrinic acid
6.
2-Methoxy-3-benzoylpropionic acid

Fig. 1
Chemical structures of the carboxylic acids studies.

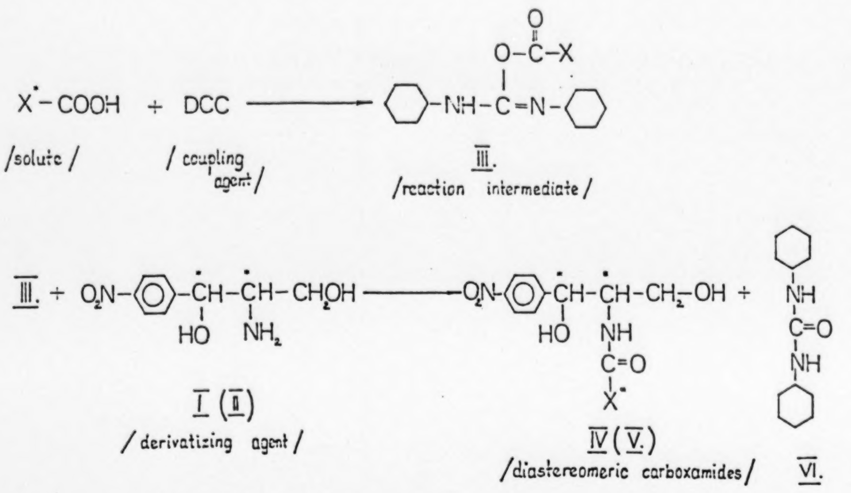

I : /1R,2R/-/-/-2-amino-1-/4-nitrophenyl/-1,3-propanediol /"levobase"/
II : /1S,2S/-/+/-2-amino-1-/4-nitrophenyl/-1,3-propanediol /"dextrobase"/

Fig. 2
The derivatization sequence.

corresponding antipodes should not differ. Otherwise, the obtained concentration ratio for the enantiomers, expressed as diastereomeric peak area ratio, is not correct ("kinetic resolution".) In model experiments (investigation of enantiomeric mixtures of given composition) were have found that the peak area ratio of the diastereomers was always constant (independently on the derivatization time) indicating that under the conditions employed there was no selective derivatization for the related enantiomers.

In fact, the obtained enantiomeric compositions were, in all cases, in a good agreement with the calculated compositions. This is shown in Table II for the enantiomers of 2-chloropropionic acid.

Similar results were reported for other DCC-catalyzed chiral derivatization reactions of N-protected amino acids [19]. Kinetic resolution, therefore, does not have to be taken into consideration.

In our previous paper [22], the description, chemistry, and the use of the new chiral derivatizing agents in TLC, as well as the spectrometric identification of the diastereomeric derivatives have been reported and discussed. I and II, as chiral key intermediate and side product respectively in the most commonly used manufacture of chloramphenicol [28], are stable, non-hazardous, low-cost and commercially available chemicals.

Both can be manufactured easily in very high enantiomeric excess (ee. ⩾ 99.8%).

In using either I or II as the derivatizing agent, reversed elution order was obtained for the corresponding enantiomers (see Table I).

This is the direct consequence of the fact that I and II are enantiomers of each other and that the retention times of the enantiomeric carboxamide derivatives formed (RRR/SSS and RSS/SRR in our cases) are the same in the used conventional ("non-chiral") chromatographic systems. Therefore, a proper selection between I and II always gives the possibility to elute an enantiomeric impurity before the corresponding enantiomer which is in excess, thus facilitating the accurate determination of the diastereomeric peak area ratio.

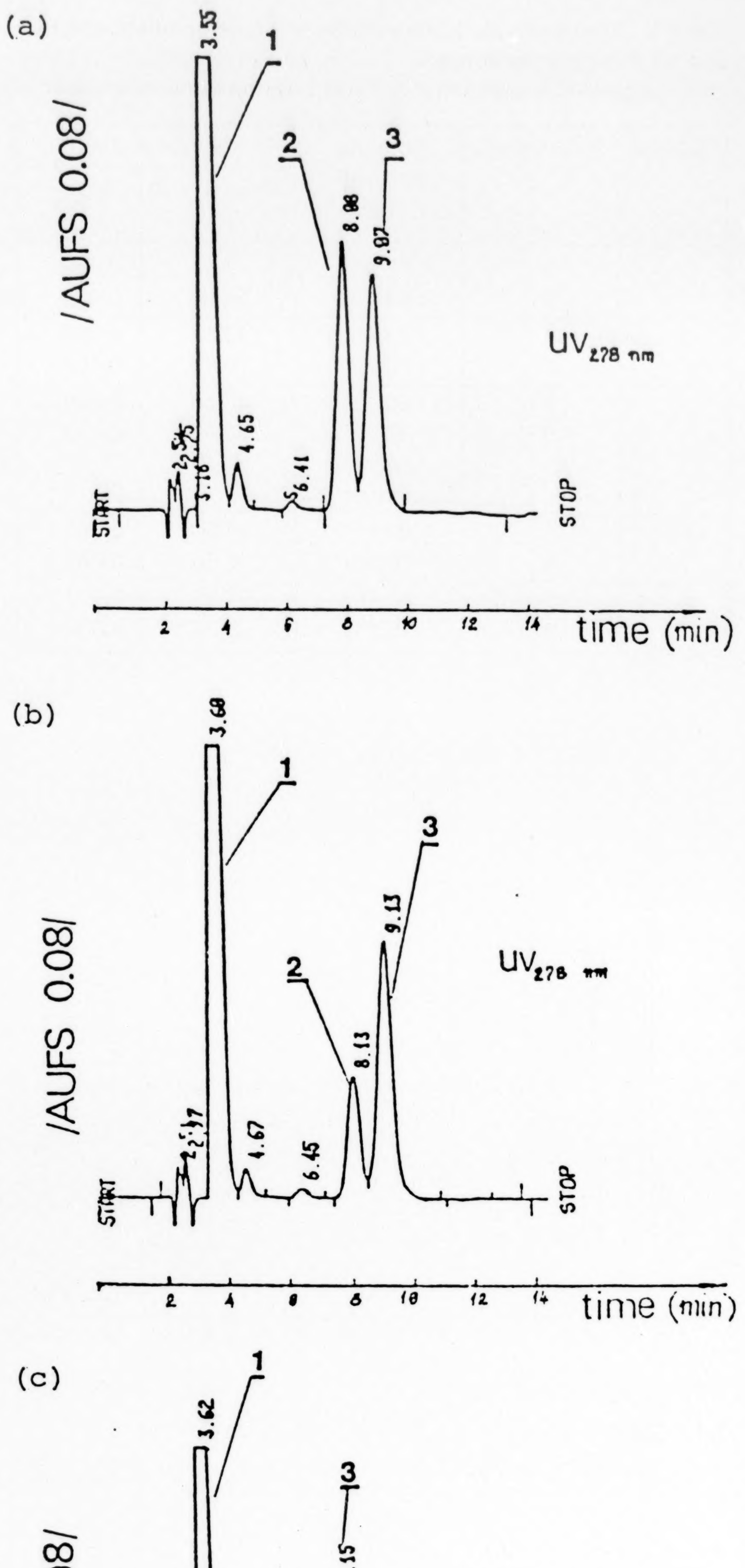

Fig. 3
HPLC resolution of enantiomers of 3-bromo-2-methylpropionic acid following derivatization with levobase (I) and dextrobase (II).
(a) racemate (derivatized with I.); (b) 1:2.45 R/S enantiomeric mixture (derivatized with I.); (c) 1:2.45 R/S enantiomeric mixture (derivatized with II.) (1) deriv. agent; (2) R-, (3) S-enantiomer. Chromatographic conditions: as in Table I.

Table II. Precision and accuracy of the HPLC determination of (R)- and (S)-2-chloropropionic acid
Chromtographic conditions as in Table I. Derivatizing agent: dextrobase

Sample	Enantiomer	Nominal Composition (%)	Found composition	
			Mean (n = 3) (%)	S.D.
1.	S R	5.30 94.70	5.41 94.56	0.066 0.075
2.	S R	23.68 76.32	23.52 76.03	0.026 0.153
3.	S R	50 50 (racemic mixture)	49.54 50.47	0.035 0.045
4.	S R	23.92 76.08	24.00 76.55	0.068 0.052
5.	S R	94.76 5.24	94.80 5.20	0.014 0.006

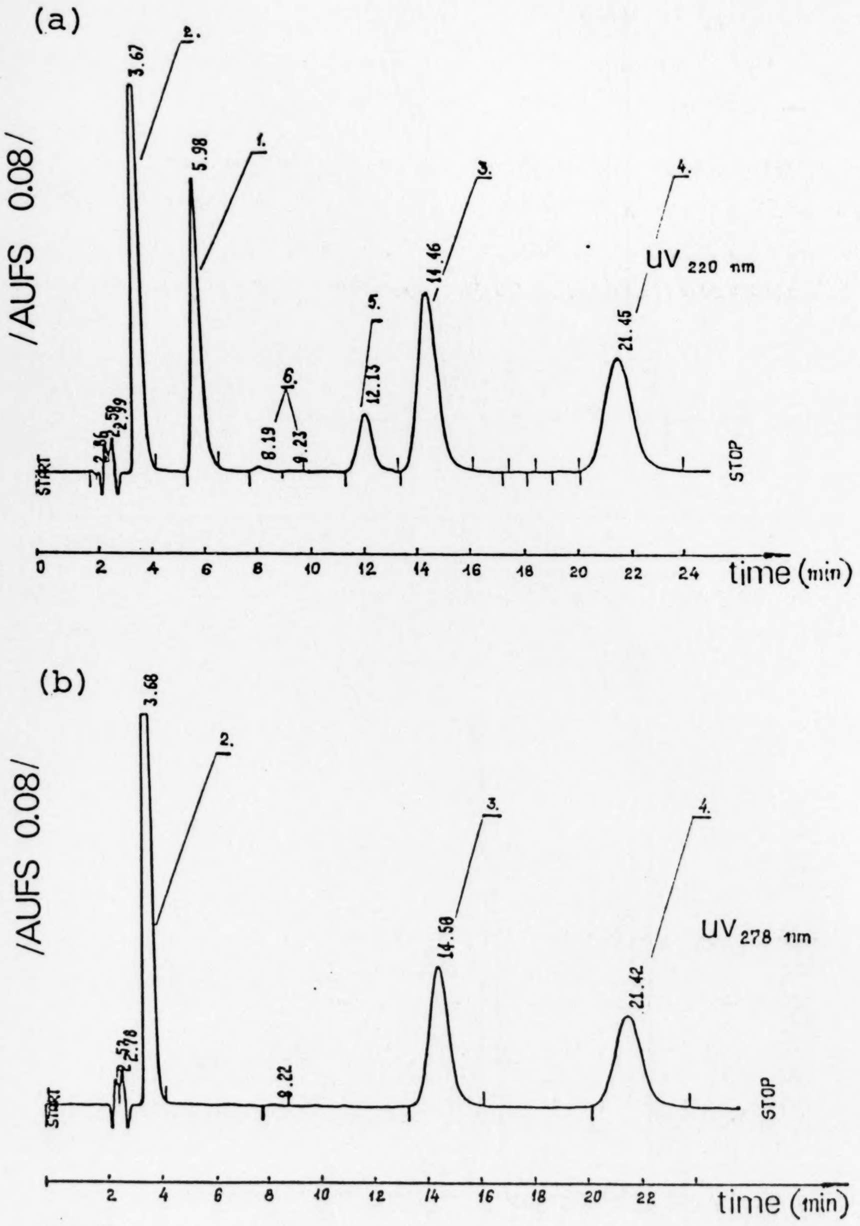

Fig. 4

HPLC separation of all species present in the reaction mixture obtained for racemic 2-methoxy-3-benzoylpropionic acid following derivatization with dextrobase. **(1)** underivatized acid; **(2)** dextrobase; **(3)** and **(4)** diastereomeric carboxamides; **(5)** intermadiate III (see Fig. 2); **(6)** unknown. Detection: (a) UV at 220 nm, (b) UV at 278 nm. Chromatographic conditions as in Table I.

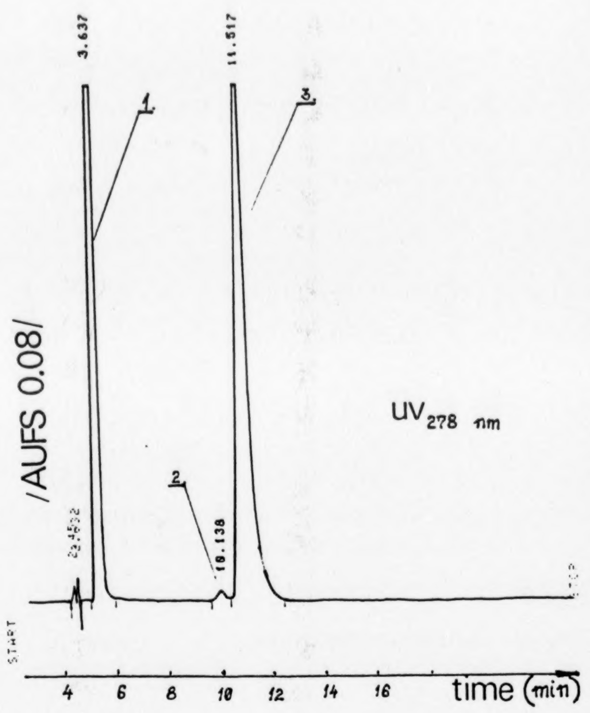

Fig. 5

Determination of the enantiomeric impurity in (–)-cis-permethrinic acid.
(1) dextrobase; **(2)** (+)-enantiomer; **(3)** (–)-enantiomer. Chromatographic conditions as in Table I.

The separation of an impurity of about 1.5% of (+)-cis-permethrinic acid in (–)-cis-permethrinic acid is shown in Fig. 5.

It can be seen that lower concentrations of enantiomeric impurities can easily be determined as well.

Acknowledgements

The authors are grateful to Dr. I. Beck for his valuable help in preparing the 2-chloropropionic acid enantiomers.

References

[1] *I. W. Wainer, T. D. Doyle,* J. Chromatogr. **284**, 177 (1984).
[2] *W. L. Hinze, T. E. Riel, D. W. Armstrong, W. De Mond, A. Alak, T. Ward,* Anal. Chem. **57**, 237 (1985).
[3] *S. Allenmark,* J. Liq. Chromatogr. **9** (2 & 3), 425 (1986).
[4] *G. Gübitz,* J. Liq. Chromatogr. **9** (2 & 3), 519 (1986).
[5] *J. Hermansson, M. Eriksson,* J. Liq. Chromatogr. **9** (2 & 3), 621 (1986).
[6] *N. Nimura, A. Toyoma, Y. Kasahava, T. Kinoshita,* J. Chromatogr. **238**, 671 (1982).
[7] *L. R. Gelber, J. L. Neumeyer,* J. Chromatogr. **257**, 317 (1983).
[8] *J. Debovski, J. Jurczak, D. Sybilska,* J. Chromatogr. **282**, 83 (1983).
[9] *C. Petterson,* J. Chromatogr. **316**, 553 (1984).
[10] *R. Wernicke,* J. Chromatogr. Sci. **23**, 39 (1985).
[11] *S. W. Mc. Kay, D. N. B. Malen, P. R. Shrubsall, B. P. Swann, W. R. N. Williams,* J. Chromatogr. **170**, 482 (1979).
[12] *I. W. Wainer,* J. Chromatogr. **202**, 478 (1980).
[13] *M. Jiang, D. M. Soderlund,* J. Chromatogr. **248**, 143 (1982).
[14] *J. Goto, N. Goto, T. Nambara,* J. Chromatogr. **239**, 559 (1982).
[15] *M. M. Maitre, G. Boss, B. Testa,* J. Chromatogr. **299**, 379 (1984).
[16] *T. M. Chen, J. I. Contario,* J. Chromatogr. **314**, 495 (1984).

[17] *H. Nagashima, Y. Tanaka, H. Watanabe, R. Hayaski* and *K. Kawada,* Chem. Pharm. Bull. **32**, No. 1, 251 (1984).

[18] *E. J. D. Lee, M. K. Williams, G. G. Graham, R. O. Day, G. D. Champion,* J. Pharm. Sci. **73**, 1542 (1984).

[19] *S. Görög, B. Herényi, M. Löw,* J. Chromatogr. **353**, 417 (1986).

[20] *S. Pedrazzini, W. Zanaboni-Muciaccia, C. Sacchi, A. Forgione,* J. Chromatogr. **415**, 214 (1985).

[21] *A. J. Hutt, S. Fourmed, J. Caldwell,* J. Chromatogr. **378**, 409 (1986).

[22] *P. Slégel, G. Vereczekey-Donáth, L. Ladányi, M. Tóth-Lauritz,* J. Biomed. Pharm. Anal., under publication.

[23] *J. C. Sheehan, G. P. Hess,* J. Amer. Chem. Soc. **77**, 1067 (1955).

[24] *Y. Klausner, M. Bodansky,* Synthesis. 453 (1972).

[25] Austrian Patent 333, 774 (10 December 1986); Chem. Abstr. **86**, P 171483 q.

[26] *J. S. C. Fu, S. M. Birnbaum, J. P. Greenstein,* J. Am. Chem. Soc. **76**, 6054 (1987).

[27] Hungarian Patent HU 30, 347, 28 March 1984. Chem. Abstr. **101**, p 130245y (1984).

[28] *L. M. Long, H. D. Trautmann,* J. Am. Chem. Soc. **71**, 2473 (1949).

Received: June 30, 1987
Accepted: July 28, 1987
F

Improved High Performance Liquid Chromatographic Determination of Amanitins with Electrochemical Detection

F. Tagliaro* /S. Chiminazzo/S. Maschio/F. Alberton/M. Marigo

Institute of Forensic Medicine, University of Verona, Verona, Italy

Key Words

Column liquid chromatography
Electrochemical detection
Butyl silica
Amanitins from fungi

Summary

The determination of amanitins, the main toxins of the poisonous fungus Amanita Phalloides, through an improved HPLC method with electrochemical detection is presented. It uses an improved reverse phase separation on a wide pore butyl column and amperometric detection in oxidizing mode at + 0.6 V. Compared to the previously reported methods employing narrow pore C18 packings and UV detectors, the described method gives a much lower detection limit (40, 80 and 70 pg ca. for alpha-, beta- and gamma-amanitin, respectively), and a better chromatographic efficiency. Coupled with a sample preparation procedure using disposable cartridges packed with C18 and underivatized silica (recovery of alpha-amanitin = 65 %, RSD 4.1 at 20 ng/ml), the method permits the quantitative determination of alpha-amanitin in serum at low concentrations (10–20 ng/ml). A tentative immuno-extraction of urine samples, by means of a solid phase antiserum, bound to nylon nets, allowing the detection of few nanograms of toxin per milliliter is also briefly described.

Introduction

Lethal poisoning due to the ingestion of poisonous fungi is still a problem in Italy (about 200 cases per year), with a mortality rate of 10–15 % of the hospitalized patients.

Most of fatal cases are caused by fungi of genus Amanita, and mainly by Amanita Phalloides. This fungus contains quite different toxic compounds such as phallotoxins, phallolysins, virotoxins and amatoxins, but the last ones, bicyclic octapeptides highly potent blockers of RNA polymerase II, could be considered the almost only causes of the lethal pathology.

Unluckily, the long latency (6 to 12 hours) and the non specificity both of the clinical symptoms and of the changes of clinical chemistry parameters hamper early diagnosis and therapy, that are essential for any clinical success. Therefore clinician's decisions must almost always be taken on the ground of anamnestic data of recent mushroom intake and of non specific gastrointestinal symptoms, with real possibilities of errors.

An even greater burden of responsibility, in case someone is charged with poisoning by fungi, is put on the forensic medicine investigator, that often lacks objective evidences to answer the court whether or not the cause of death is related to poisonous mushroom ingestion.

On this basis, several analytical methods have been developed for the identification of amatoxins in the fungal matrix and in biological fluids and tissues. Attention was particularly focussed on alpha-, and beta-amanitins, because of their high pharmacological potency (DL50 0.1 and 0.4 mg/kg, respectively) and their relatively high content in Amanita Phalloides (8 and 5 mg/100 g, respectively).

Radioimmunoassays (RIA) for amatoxins, with sensitivity in the range of nanograms per milliliter, were developed in 1975 by Faulstich [1] and Fiume [2]. But, because of the existence of specific and non specific interferences causing false positive or negative results, it has been widely accepted that, for forensic purposes, RIA results should be confirmed by alternative techniques, if an acceptable degree of certainty is to be gained.

Methods based on thin layer chromatography (TLC, HPTLC) have also been reported by several authors [3, 4], but though useful for the investigation of amanitin-containing fungi, they are not sensitive enough for the analysis of biological fluids.

More recently high performance liquid chromatography (HPLC) has been proposed in order to meet both the needs of high sensitivity and of chromatographic reliability. Most of the papers published in the leading journals, though quite different as far as sample preparation is concerned, report rather similar separation and detection techniques and methods [5–9]. Amanitin separations are generally carried out in reversed phase modes, through columns packed with C 18 silicas with narrow pores (ca. 60 Å). Either isocratic [5–7, 9] or gradient elutions [8] have been used. Detection is always by UV at 280–303 nm

0009-5893/87 0482-05 $ 03.00/0

© 1987 Friedr. Vieweg & Sohn Verlagsgesellschaft mbH

giving a lower limit of measurement of 5–10 ng ca. of injected alpha-amanitin. These limits, though much lower than that ones typical of TLC, are still poor compared to the amanitin levels present in intoxicated patients, which are in the range of few nanograms per milliliter of serum.

We report the results obtained in our laboratory by adopting a different approach to the problem, in order to improve both chromatographic efficiency and sensitivity. The separation of amanitins has been carried out through a reversed phase, "wide pore" butyl column with electrochemical detection (ED), in an oxidation mode. Preliminary qualitative data obtained by coupling an immunoaffinity based extraction with HPLC-ED are also described.

Experimental

Chemicals and Samples

Alpha-, beta- and gamma-amanitins were purchased from Serva (Heidelberg, FRG). Stock solutions of 500 μg/ml were prepared in methanol and stored at − 20 °C protected from light.

Water and acetonitrile used for HPLC were "HPLC grade", provided by Carlo Erba (Milan, Italy). The same firm furnished also all the other "analytical grade" chemicals used for buffer preparation and sample extraction procedures.

Disposable micro-columns filled with C18 coated silica and with underivatized silica particles (Sep-Pak C18 and Silica, respectively) were from Millipore (Milford, MS, USA).

All solvents and samples were filtered through 0.45 or 0.20 μm membranes furnished by Millipore, before being used for HPLC.

Sera from normal subjects served as blank samples. Negative samples, spiked with different amounts of amanitins were used as "positive" controls. A urine sample collected from a patient, that had been intoxicated by Amanita Phalloides 4 days before sampling and who subsequently died from hepatic and renal insufficiency, was also assayed. In this case, the sample was stored at − 20 °C, until analyzed.

Apparatus

The isocratic HPLC system used was composed of a Gilson (Villiers-le-Bel, France) model 302 pump, a Rheodyne (Cotati, CA, USA) injector model 7125 (with a 50 μl loop), a Violet (Rome, Italy) Clar 055 column oven and a Bio-Rad (Richmond, CA, USA) model 1340 amperometric detector with a glassy carbon electrode. When required a Jasco (Tokyo, Japan) 875 UV detector, set at 303 nm wavelength, was also used.

In the early part of the work, we used a column (250 × 4.6 mm) packed with 5 μm Spherisorb ODS2 (Phase Separatons, Queensferry, UK), but afterwards we adopted a Hypersil WP300 Butyl 5 μm (Shandon, Sewickley, PA, USA) with the same column size.

Peak areas were determined with a Gilson Data Module model 620.

Chromatographic Conditions

Preliminary experiments were performed using a mobile phase composed of 0.05 M sodium dihydrogen phosphate with 12 % acetonitrile.

The final mobile phase adopted for the assay of biological fluids was a mixture of 0.02 M ammonium acetate aqueous solution and acetonitrile (92 : 8, v : v), containing EDTA 0.5 mM, brought to pH 5 with acetic acid. Higher percentages of acetonitrile (up to 11 %) were used when retention times had to be shortened. Separations were carried out at 37 °C, and at a flow rate of 1 ml/min. Except for particular tests, the potential of the cell was set at + 0.60 V versus a reference electrode (Ag/AgCl).

Sample Preparation

Up to 2 ml of serum were loaded onto a Sep-Pak C18 cartridge, previously activated with 2 ml of acetonitrile and rinsed with 6 ml of water. After washing with 5 ml of water, amanitins were eluted with 2 ml of methanol: water (40 : 60, v : v). The eluate was extracted with a 2 x volume of a mixture of methanol : chloroform (50 : 50, v : v), by mixing in a vortex mixer for 3 min. The organic phase was dried under a stream of air, and the residue dissolved in 400 μl of chloroform: methanol: acetic acid (80 : 50 : 4.5, v : v : v). It was then loaded onto a Sep-Pak Silica cartridge, previously conditioned with 4 ml of the same mixture in which the extract had been redissolved, that served also for a first washing (2 ml) of the cartridge, after having loaded the sample. After a second washing with 0.5 ml of dichloromethane : methanol (70 : 30, v : v), the analytes were eluted with 1.2 X 2 ml of dichloromethane : methanol (50 : 50; v : v). The eluate was dried, redissolved in the chromatographic eluent and finally injected into the chromatograph.

A tentative immuno-extraction of amanitins from urine was performed using an anti-amatoxin antiserum chemically bound to nylon nets (0.56 cm^2), furnished as a component of a RIA kit by H. Faulstich (Max Planck Institute, Heidelberg, FRG). This antiserum, raised in rabbits against alpha-amanitin, is said to give a complete cross-reaction with gamma-amanitin and a 50 % cross-reaction with beta-amanitin [10]. The binding capacity of the nylon pieces for tritiated alpha-amanitins is about 3 ng. Since the nets were furnished already equilibrated with a solution of tritiated alpha-amanitin (the RIA tracer), it was necessary to wash it away with 20 ml of 0.05 M phosphate buffer pH 5 containing 30 % methanol. After equilibrating with 0.05 M phosphate buffer pH 7.5, the nets were incubated overnight, under gentle mixing, with 1 ml of urine, buffered at pH 7.5, by adding 1 ml of 0.1 M phosphate buffer. The nets were then washed with 2 × 3 ml of 0.9 % saline and finally amatoxins were eluted by incubating for 5 min with 200 μl of 0.05 M phosphate buffer pH 5 containing 30 % methanol. The eluate was directly injected into the chromatograph.

The same urine sample was also assayed by using the RIA kit purchased from H. Faulstich, according to the enclosed instructions.

Results and Discussion

Chromatographic Separation

The chromatographic method allowed a fairly good separation of alpha-, beta- and gamma-amanitin. Under the final conditions the three compounds eluted in the order beta, alpha and gamma, with retention times of ca. 12.00, 16.50 and 34.10 min respectively (Fig. 1). The capacity factors (k′) were, in the same order, 2.7, 4.1 and 9.6. The choice of high retention times was grounded on the need of achieving the maximum of resolution of amanitins from interferent peaks related to the matrix. The gamma-amanitin retention is out of the normally acceptable range of k′, but this compound is of minor toxicological interest, because of its lower content in Amanita Phalloides and its lower potency (DL50 = 0.8 mg/kg), compared to alpha- and beta-amanitin.

Retention times were sometimes changed, slightly modifying the acetonitrile percentage in the eluent, to meet particular needs of quickness or "cleanness" of the chromatograms or to determine gamma-amanitin more quickly.

Selectivity factors were always greater than 1.6, allowing a good resolution of the three amanitins.

The efficiency of the butyl wide pore column employed was about 20,000 plates/m, better than the 10,000 plates/m which we obtained with the ODS narrow pore column. The peak sharpness was also better, compared to the chromatograms published by those using narrow pore packings [5–9]. The reasons of this phenomenon are not yet clear since many, even bigger, peptides (i.e. endorphins, calcitonin) can be efficiently chromatographed through narrow pore C18 columns [11]. We could tentatively suggest that the interactions of these bicyclic octapeptides with the bonded phase were improved, when larger pores were used, thanks to a more efficient and homogeneous permeation of the packing particles, and perhaps to a more efficient and homogeneous deactivation of the silanol groups.

Electrochemical Detection

The presence of a 6-hydroxytryptophan residue in the molecules of alpha-, beta- and gamma-amanitin suggested to us the possibility of detecting these compounds through an electrochemical detector operating in an oxidative mode. The main advantages of this kind of detection, compared to UV absorbance measurement, are an higher sensitivity and the possibility of introducing a greater degree of selectivity.

The hydrodynamic voltammograms of the three amanitins (and of the mobile phase alone) are shown in Fig. 2. Half wave potentials of alpha- and gamma-amanitin (+ 0.44 V) are quite similar, but slightly different from beta-amanitin's one (+ 0.53 V). For this reason, it was impossible to meet simultaneously the best oxidizing potentials for detecting the three compounds. We chose the potential (+ 0.6 V) most suitable for alpha-amanitin, that is the most toxic of the three and, in Italy, the greatest amount of lethal toxin in Amanita Phalloides.

Under these conditions, the background current was quite acceptable, being in the range 1.8–2.5 nA, by using 0.02 M ammonium acetate buffer in the mobile phase. A previously tested mobile phase containing 0.05 M phosphate buffer gave poorer results, as far as the signal/background ratio was concerned, because of a shift towards higher potentials of the potential-current curves of amanitins. In this case the plateau region of alpha-amanitin began at + 0.8 V, with a 40 nA background current.

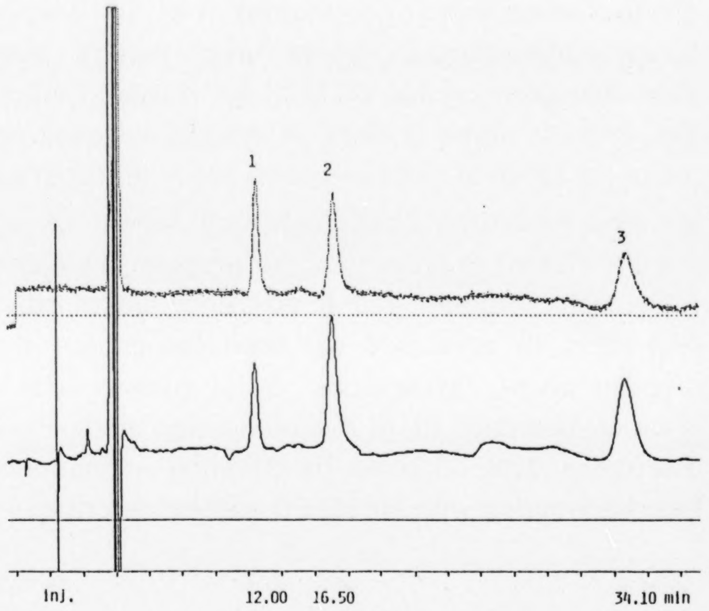

Fig. 1
HPLC chromatogram of an aqueous solution of 250 ng/ml of beta- (1), alpha- (2) and gamma-amanitin (3) carried out by the standard conditions described in the text. Detection was accomplished both by UV (303 nm wavelength, 0.001 AUFS) (dotted line) and by amperometry (+ 0.6 V, 10 nA FS) (solid line). Chart speed: 0.5 cm/min.

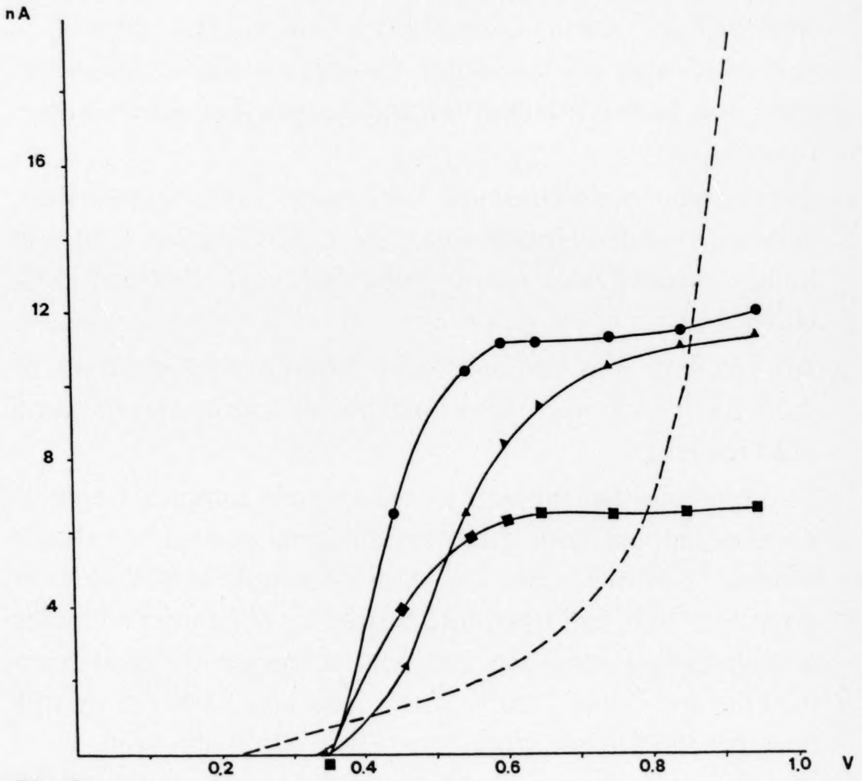

Fig. 2
Hydrodynamic voltammograms of alpha- (●), beta- (▲) and gamma-amanitin (■) and of the mobile phase alone (dashed line). Mobile phase: 0.02 M ammonium acetate : acetonitrile (90 : 10), brought to pH 5 with acetic acid. 50 ng of each amanitin was injected.

The detection limits, evaluated with standard solutions, were quite interesting, as compared to that ones reported with UV detectors [5–9]. They were ≈ 40 pg of injected compound for alpha-amanitin, 80 pg for beta-amanitin and 70 pg for gamma-amanitin (eluted in a rather broad peak), with a signal-to-noise ratio of 5. Beta-amanitin, though eluted in the sharpest peak, suffered from the low oxidizing potential (+ 0.6 V), below the plateau region (see Fig. 2).

The linearity of response was evaluated by injecting standard solutions of the three toxins, at serial dilutions; the corresponding regression equations demonstrated a fairly good linearity in the range 1 ng — 1 μg/ml (Table I).

Sample Preparation

So far our attempts have not yet been focussed on the optimization of sample preparation. The previously described extraction procedure for serum samples, using Sep-Pak C18 and Silica cartridges, was reported by Fenoil et al. [9]. Only minor changes were made, in order to shorten the extraction steps which are extremely time-consuming if performed on aqueous mixtures, as in this paper. An additional extraction step with methanol : chloroform (50 : 50, v : v) of the aqueous eluate from the first cartridge allowed the organic phase to be brought to dryness in a few minutes.

The procedure of sample clean up, though a little complex, achieved a fairly good elimination of interferent peaks at the retention times of alpha- and gamma-amanitins (Fig. 3). On the other hand the beta-amanitin peak was partially overlapped by a peak from the matrix, that in practice hampered the identification of this compound at levels below 100 ng/ml. Some attempts to improve the resolution of the two peaks by reducing the percentage of acetonitrile in the mobile phase, did give better separation but also resulted in too great an increase of alpha-amanitin retention time, and were judged not worthwhile since our main aim, was the determination of alpha-amanitin.

Table II summarizes the overall recovery and the precision of the HPLC-ED assay of the three amanitins, at the levels of 20 and 200 ng/ml, by using the extraction procedure described. It is clear that the losses of beta- and gamma-amanitins were too large under the conditions that gave an acceptable recovery of alpha-amanitin. A separate elution of each compound from the cartridges, under specifically tailored conditions, as proposed by Jehl [7] would probably overcome this problem.

Although successful with serum, the described clean up procedure failed in purifying urine samples, giving quite complex chromatograms with peaks coeluting with each amanitin. Therefore, we developed an alternative procedure based on immuno-affinity, taking advantage of the solid phase anti-amanitin antiserum, provided as a part of the RIA kit (from H. Faulstich), used in our laboratory for routine amanitin assays. In short (more details are in the Methods section), after having washed away the tracer, the nets were incubated with urine and, after a new washing cycle, the amanitin-like material was eluted and injected directly into the chromatograph. The binding capacity of the nets was quite small (3 ng ca.) and they were rapidly saturated, even in the presence of low concentrations of toxins, giving a non-quantitative recovery. Consequently only qualitative results could be obtained but in the case

Table I. Linearity of amanitin HPLC-ED determination

Analyte	Regression equation	Correlation coefficient
alpha-amanitin	y = 10.34 X + 0.89	0.99999
beta-amanitin	y = 8.00 X − 0.96	0.99999
gamma-amanitin	y = 7.79 X + 0.24	0.99999

x = concentration in ng/ml; y = current response in pA.
8 points for each compound were assayed in the range 1 ng-1 μg/ml.

Table II. Analytical recovery and precision

	20 ng/ml		200 ng/ml	
	% Recovery	RSD	% Recovery	RSD
alpha-amanitin	65	4.1	53	3.1
beta-amanitin	–	–	36	5.8
gamma-amanitin	36	5.2	30	2.0

Recovery is relative to the assay of spiked sera.
RSD = relative standard deviation (n = 5).

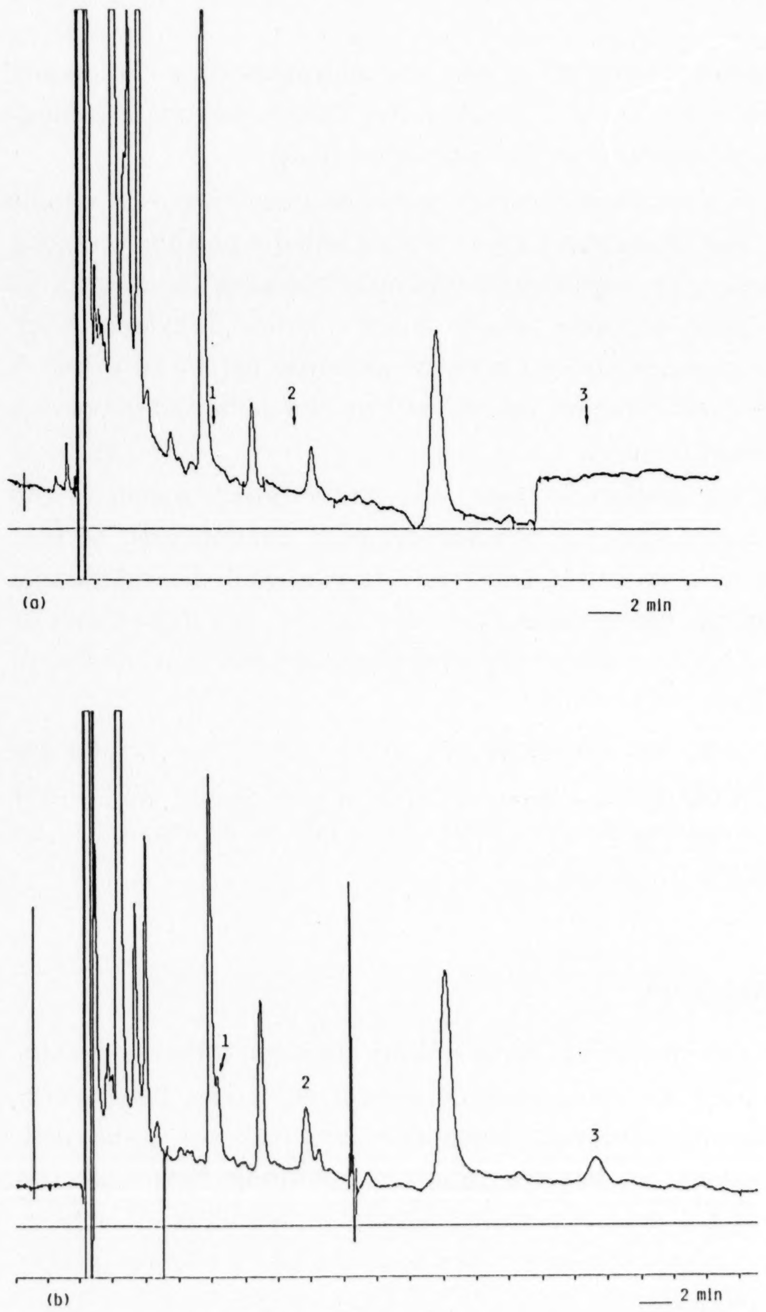

Fig. 3
HPLC chromatograms of a blank serum (a) and of a serum spiked with 20 ng/ml of alpha- (2), beta- (1) and gamma-amanitin (3) (b), extracted by Sep-Pak cartridges. Detector range: 2 nA.

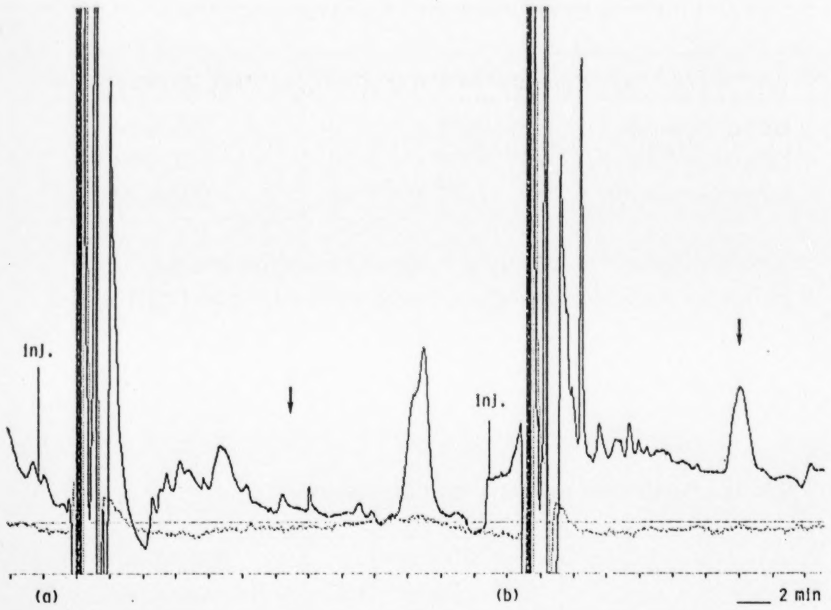

Fig. 4
HPLC chromatograms of a blank urine (a) and a urine sample from an intoxicated subject (b) containing 3 ng/ml ca. of alpha-amanitin, according to a RIA determination. Both were extracted with the described immuno-sorbent and directly injected. The arrow indicates the retention time of alpha-amanitin. Solid line: ED, range 2 nA FS; dotted line: UV detector at 303 nm, range: 0.01 AUFS.

of urine samples where concentrations are influenced mainly by diuresis, quantitative determinations are much less important than the qualitative data.

Fig. 4 shows the chromatograms of a negative urine sample (a), and of a sample taken from a lethally poisoned subject, 4 days after ingestion of Amanita Phalloides (b). A peak, at the same retention time of alpha amanitin, is evident, that, corresponded to ≈ 2.5 ng of amanitin per ml of urine. A RIA determination carried out on the same sample gave a result of 3 ng/ml.

The alpha-amanitin peak was rather broad, owing to the poor efficiency of the narrow pore column used at that time (Spherisorb ODS); yet, it was well distinguishable from the background from the matrix. No more cases of intoxication took place, after the assay was improved with the large pore column.

Although not definitive, we think that these results are encouraging for the use of immunoextraction procedures for preparing samples with low levels of amatoxins to be analyzed by HPLC.

Conclusion

The determination of amanitins through HPLC is greatly improved by using electrochemical detection, particularly as far as minimum detectable amounts are concerned. Compared to already reported methods based on UV detection, the minimum detectable amounts of alpha-, beta- and gamma-amanitin were reduced by a factor greater than, at least, ten by the HPLC-ED method.

Also the proposed use of a large pore butyl column, achieves some analytical improvements, particularly in the efficiency of amanitin separation, compared to that one obtained with normal pore, C18 columns, previously employed [5–9]. This fact allows the use of longer retention times, without excessive band broadening, in order to minimize interferences in the chromatograms by coeluting peaks.

According to our experience, it is almost impossible to obtain extraction, separation and detection conditions giving the best performances for the three amanitins at the same time. Therefore we focussed our efforts on alpha-amanitin, the most toxic and the most represented in Italian Amanita Phalloides.

Problems arising from the biological matrices still remain. Sample preparation based on disposable cartridges gives quite acceptable results when applied to sera, even with low amanitin concentrations, but not to urine: many spurious peaks related to the matrix cannot be eliminated from this sample. In order to overcome this problem, we tried the applicability of immuno-affinity, as a more specific tool for sample preparation before HPLC-ED. Lacking sufficient amounts of antisera, we have been forced to utilize immunosorbent nylon nets provided in a solid phase RIA kit for amanitins. Notwithstanding the low capacity of the immunoaffine nets with related saturation problems, we succeeded in identifying immuno-extracted material with the same retention time of alpha-amanitin in the urine of a subject intoxicated from Amanita Phalloides four days before sampling. On the ground of these quite tentative results, we belive that it is a quite promising way that should be pursued, going on towards the development of a highly sensitive HPLC method supporting the early diagnosis of intoxication from Amanita Phalloides.

Acknowledgements

The authors are thankful to Mrs. G. Carli and to Dr. F. Cristofori for skillful co-operation.

References

[1] *H. Faulstich, H. Trischmann, S. Zobeley,* FEBS Lett. **56,** 312 (1975).
[2] *L. Fiume, C. Busi, G. Campadelli-Fiume, C. Franceschi,* Experientia **31,** 1233 (1975).
[3] *H. Raanen,* J. Chromatogr. **38,** 403 (1968).
[4] *W. Palyza, V. Kulhanek,* J. Chromatogr. **53,** 545 (1970).
[5] *L. Pastorello, D. Tolentino, M. D'Alterio, R. Paladino, A. Frigerio, N. Bergamo, A. Valli,* J. Chromatogr. **233,** 398 (1982).
[6] *F. Belliardo, G. Massano,* J. Liquid Chromatogr. **6,** 551 (1983).
[7] *F. Jehl, C. Gallion, P. Birckel, A. Jaeger, F. Flesch, R. Minck,* Anal. Biochem. **149,** 35, (1985).
[8] *G. Caccialanza, C. Gandini, R. Ponci,* J. Pharm. Biomed. Anal. **3,** 179 (1985).
[9] *R. Fenoil, R. Alfieri, G. Weisz,* in "Developments in Analytical Methods in Pharmaceutical Biomedical and Forensic Sciences", G. Piemonte, F. Tagliaro, A. Frigerio and M. Marigo, eds., Plenum Publishing Co., New York, London, 1987; in press.
[10] *H. Faulstich, S. Zobeley, H. Trischmann,* Toxicon. **20,** 913 (1982).
[11] *M. Sbalzarini,* Giorn. It Chim. Clin. 8 (Suppl.), **29** (1983).

Received: June 29, 1987
Accepted: Juli 21, 1987
F

Approaches to the Liquid Chromatographic Determination of Carboxylic Acids Using Potentiometric Detection with a Metallic Copper Electrode

P. R. Haddad* / P. W. Alexander / M. Y. Croft / D. F. Hilton

Department of Analytical Chemistry, University of New South Wales, P. O. Box 1, Kensington, N.S.W. 2033, Australia

Key Words

Ion-exchange chromatography
Ion-exclusion chromatography
Potentiometric detection
Carboxylic acids
Metallic copper electrode

Summary

A metallic copper electrode is evaluated as a potentiometric detector for carboxylic acids. The application of this device to ion-exchange chromatography is illustrated by the determination of oxalate in urine. Oxalate was selectively detected in the presence of a 100-fold excess of sulphate after separation on a low-capacity methacrylate anion-exchange column using 0.7 mM potassium hydrogen phthalate at pH 7.1 as eluent. Calibration plots were linear up to 50 ppm of oxalate. Potentiometric detection has also been applied to ion-exclusion chromatography using 0.005% phosphoric acid as eluent. With this method detection limits of 0.2, 2.1, 5.0 and 5.3 μg were obtained for formic, acetic, propionic and iso-butyric acids, respectively.

Introduction

Carboxylic acids may be separated chromatographically using reversed-phase, ion-exchange or ion-exclusion techniques. In the reversed-phase approach, separation is achieved by buffering the mobile phase to an appropriate pH so that ionisation of the acids is suppressed [1], or by deliberately ionising the acids and then incorporating an ion-interaction reagent into the mobile phase [2]. In both of these approaches, separation of low molecular weight acids is difficult. The same is true of anion-exchange chromatography in which the acids are separated in their deprotonated forms [3].

A versatile approach is the use of ion-exclusion chromatography in which hydrophilic weak acids are separated on a high-capacity cation-exchange resin in the H^+ form, using an acidic eluent [4]. The solute acids are excluded from the anionic surface of the ion-exchange resin to an extent dependent on their degree of ionisation. Provided that the solutes in a mixture have sufficiently different pKa values, then excellent separation is possible.

Several detection modes have been coupled with the above chromatographic methods of separation. Direct UV absorbance measurements at short wavelengths (typically 200–215 nm) provide adequate response even for low molecular weight aliphatic acids and is the method of choice for reversed-phase and ion-exclusion chromatography. The use of this method imposes severe restrictions on the choice of eluent. Conductivity detection has also been employed, particularly after anion-exchange separation with strongly [5] or weakly [6] conducting eluents. It has been recently demonstrated that conductivity detection may also be employed successfully with ion-exclusion chromatography provided a weak acid, such as benzoic acid, is used as eluent [7].

Electrochemical detection has found little application in these areas. One example however is the use of a glass pH electrode for the indirect detection of eluted carboxylic acids [8]. We have developed a potentiometric method of detection based on the potential changes occurring at the surface of a metallic copper electrode. This electrode can provide a direct response to solutes which complex copper more strongly than eluent components, since passage of such a solute past the electrode causes a localised decrease in the concentration of copper ion (cuprous or cupric) at the electrode surface, and hence a change in potential. Alternatively, indirect detection of solutes which complex copper less strongly than the eluent components can be achieved by a localised increase in copper ion concentration at the electrode surface. These detection techniques have been applied in the determinations of inorganic anions and cations [9, 10]. In this paper, we illustrate the versatility of the potentiometric copper electrode detector by reporting its application to the selective detection of oxalate in urine after ion-exchange separation, and the detection of low molecular weight carboxylic acids after ion-exclusion separation.

0009-5893/87 0487-05 $03.00/0

© 1987 Friedr. Vieweg & Sohn Verlagsgesellschaft mbH

Experimental

Instrumentation

The liquid chromatograph comprised a Waters Associates (Milford, MA, USA) M6000 pump and U6K injector. Various detectors were used including a Waters M450 variable wavelength UV absorbance detector, a Waters M430 conductivity detector and a homemade potentiometric flow-through detector incorporating a copper wire indicator electrode. The design of the latter detector has been reported previously [11] and in this work, the detector was connected to a Radiometer (Copenhagen, Denmark) pH M62 millivolt/pH meter and interfaced to a Houston Instruments (Austin, TX, USA) model 5271 10 mV strip chart recorder. Chromatograms obtained with the UV and conductivity detectors were recorded with a Waters M730 data module.

Columns

The three anion-exchange columns used were a Hamilton (Reno, NV, USA) PRP X-100 ion-chromatography column, 250 × 4.1 mm i.d., a Waters Associates IC PAK A anion-chromatography column, 50 × 4.1 mm i.d. and a Vydac (The Separations Group, Hesperia, CA, USA) 300 IC anion-chromatography column, 50 × 4.1 mm i.d.. A Waters anion-concentrator column, 6.0 × 5.0 mm i.d. was used as a guard column and was housed in the appropriate Guard-Pak pre-column module.

The ion-exclusion column used was a Waters Fast Fruit Juice column 150 × 7.8 mm i.d., packed with 10 μm fully sulphonated polystyrene divinylbenzene resin. This column was operated at 55 °C using a Waters column heater.

Procedures

Standard solutions (1000 ppm) of the carboxylic acid solutes were prepared from Analytical Grade reagents in doubly distilled water. Eluents were prepared from Analytical Grade reagents dissolved in water treated by passage through a Millipore (Bedford, MA, USA) Milli Q water purification system. All eluents were filtered through 0.45 μm membrane filters and degassed in an ultrasonic bath prior to use. Urine samples were freshly collected prior to analysis, diluted five times, treated ultrasonically for five minutes and then passed through a Waters Associates C18 Sep-Pak cartridge which had previously been flushed with methanol. For studies involving acidified urine samples, 2 ml of either 1.0 M hydrochloric or nitric acid were added to a 2 ml aliquot of urine and the sample was allowed to stand for 30 min, after which time the sample was diluted to 10 ml with water and filtered through a 0.45 μm Millex filter (Millipore).

Results and Discussion

Electrode Response to Carboxylic Acids

In previous studies [12–14] on the potential changes exhibited by a metallic copper electrode, we have shown that under conditions where a single copper complex species with the injected ligand predominates, a Nernstian relationship exists between the potential of the copper electrode and the concentration of the injected ligand. Under conditions where the concentration of the injected ligand is very low, the above relationship becomes linear [9]. The direction of the measured potential change occurring when eluted species pass through the detection flow-cell is dependent on the relative extents to which the eluent components and the eluted solutes complex copper. We have adopted a convention where the peak is displayed as *positive* in situations where the solute complexes copper *more strongly* than the eluent, despite the fact that a negative potential change occurs due to the localised decrease in copper ion concentration at the electrode surface.

In the examples to be discussed, it is possible to predict the approximate magnitude and direction of the solute peaks by considering the side-reaction coefficients (α values) of the solutes and eluent components with copper. This calculation requires a knowledge of the eluent composition, together with an estimate of the solute concentration at the surface of the copper electrode. Table I lists values of $\alpha_{\mathrm{Cu(II)(L)}}$ for the eluents and solutes used in this study, based on the assumption that the ligands are present at 1 mM at the electrode surface.

Determination of Oxalate in Urine

In the diagnosis and treatment of certain pathological conditions such as kidney stone disease and hyperoxaluria, the determination of urinary oxalate levels plays an important role. Several methods have been developed for this determination, including colorimetry [15], enzymatic techniques [16], isotope dilution analysis [17] and gas chromatography [18]. The complexity of the sample matrix is such that many of these methods require either extensive sample clean-up procedures or isolation of the oxalate from the sample prior to quantitation. Such processes are usually time consuming and can lead to errors in the analysis. Liquid chromatography has also been applied to the analysis of urinary oxalate. Examples include pre-column derivatisation followed by reversed-phase sep-

Table I. Side-reaction coefficients, $\alpha_{\mathrm{Cu(II)(L)}}$, for eluents and carboxylic acids studied. In the case of carboxylic acids, α values were calculated at 1 mM.

Ligand	$\alpha_{\mathrm{Cu(II)(L)}}$	
	pH 3.3	pH 7.1
Phthalate (0.7 mM)	–	1.34
Phosphate (0.5 mM)	1.0	–
Acetic acid	1.02	1.05
Iso-butyric acid	1.01	1.06
Citric acid	58.9	736
Formic acid	1.01	1.04
Maleic acid	1.02	3.46
Oxalic acid	17.6	70.2
Propionic acid	1.01	1.05
Succinic acid	1.02	1.39
Tartaric acid	1.47	3.45
Sulphate	–	1.0

aration [19], ion-interaction chromatography with UV absorption [20] or amperometric [21] detection and suppressed ion chromatography with conductivity or electrochemical detection [22]. In each of these procedures, interference effects or poor correlation with alternative methods were observed.

The use of ion chromatography for the analysis of oxalate in urine is complicated by the difficulty in resolving oxalate from the large excess (typically 100 fold) of sulphate present. In addition, the regular practice of acidification of urine samples (usually with hydrochloric acid) in order to ensure dissolution of microcrystalline particles of calcium oxalate creates the possibility of further detection interferences for those methods which detect chloride ion. We have investigated the utility of non-suppressed ion chromatography for oxalate determinations by systematically evaluating a wide range of eluent-column combinations for the resolution of oxalate and sulphate. Three anion-exchange columns of different selectivities were examined using direct UV absorption, indirect or "vacancy" UV absorption and conductivity as detection methods. The first of these detection methods can be classified as selective because it shows response for only a limited number of solute ions, whereas the other two are universal detection modes and respond to all ions. Whilst some of the systems evaluated provided adequate separation and detection of oxalate in standard solutions, interference effects encountered in the analysis of urine samples forced the conclusion that no method was suitable for this application. These interferences showed as swamping of the oxalate peak by sulphate, insensitive response towards oxalate and severe baseline disturbances resulting from the acidity or chloride content of acid treated samples. It was clear that the ideal detection method should have high selectivity for oxalate over sulphate.

In the ion-exchange process, the elution of a solute ion must be accompanied by a localised deficiency of the eluent ion in order to preserve electroneutrality. Detection of the solute therefore relies on a difference in a measureable property between the solute and eluent ions. In the case of the metallic copper electrode, detection will be dependent on differences in the degrees of copper complexation exhibited by the eluent and solute ions, as indicated by their side-reaction coefficients. The data given in Table I suggest that when phthalate is used as eluent, the copper electrode detector should provide good sensitivity for oxalate. On the other hand, sulphate ion does not significantly complex copper and therefore little or no electrode response would be expected for this ion.

When the copper electrode detector was applied to the determination of oxalate excellent response to oxalate was observed, with linear calibration plots being obtained over the range 0–50ppm oxalate. Application of the method to the analysis of urine is illustrated in Fig. 1 which shows the chromatograms obtained with a phthalate eluent using potentiometric and indirect UV absorption detection. The chromatogram recorded with the UV absorption detector (Fig. 1(a)) shows a large sulphate peak which is barely resolved from the small oxalate peak. In contrast, the chromatogram recorded with the potentiometric detector (Fig. 1(b)) shows a clear oxalate peak, with no response for sulphate.

It may be noted that the sample illustrated in Fig. 1 was obtained with diluted urine which had not been acidified. Samples acidified with hydrochloric acid presented a problem in that the high chloride level caused destabilisa-

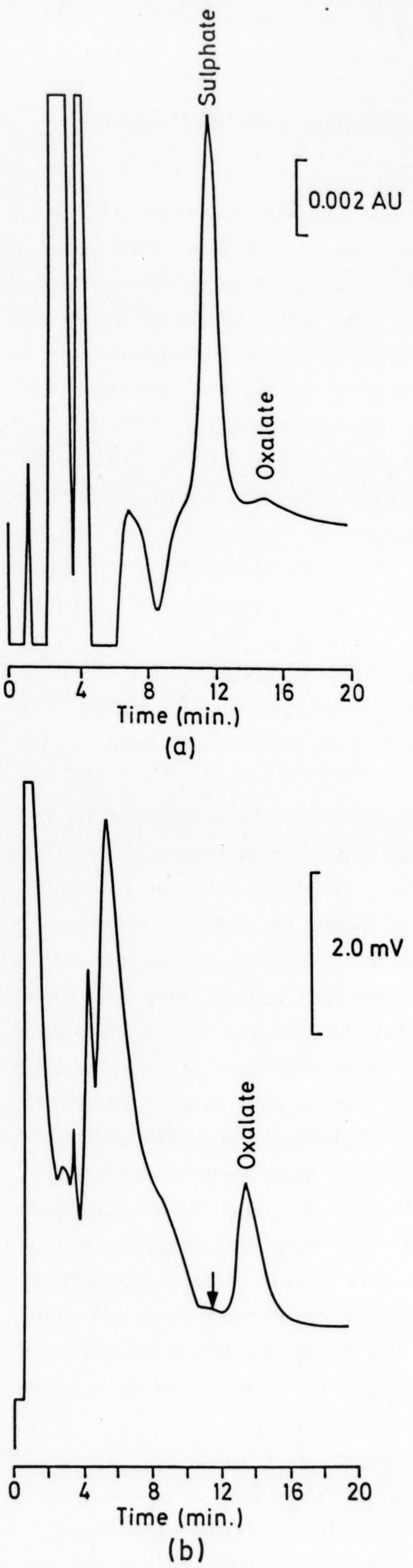

Fig. 1

Determination of oxalate in urine with ion-exchange separation, detection by indirect UV absorption at 280nm (a) and direct potentiometry using metallic copper indicator electrode (b). Arrow in (b) indicates retention time of sulphate.

Conditions. Column: Waters Associates IC Pak A, 50 × 4.6mm i.d. anion-exchanger. Eluent: 0.7mM potassium hydrogen phthalate pH 7.1. Flow-rate: 1.0ml min^{-1}. Sample: 10μl of 5-times diluted urine sample.

tion of the electrode, presumably due to precipitation of cuprous chloride at the electrode surface. This problem could be avoided by using a switching valve to divert the column effluent away from the potentiometric detector during the elution of chloride and then restoring flow through the detector prior to the elution of oxalate. However, it was better to use nitric acid for sample acidification in preference to hydrochloric acid, since high concentrations of nitrate ion in the samples did not lead to loss of electrode response or interference with oxalate.

Potentiometric Detection Coupled with Ion-Exclusion Separation

In view of the utility of ion-exclusion chromatography for the separation of carboxylic acids, this was investigated in order to determine whether it could be successfully coupled with potentiometric detection using a copper electrode. In ion-exclusion chromatography, the replacement of eluent ions by solute ions does not occur in the same manner as for ion-exchange chromatography. Retention of solutes is governed by a combination of the Donnan exclusion effect, size exclusion from the pores of the stationary phase and reversed-phase interaction with the unfunctionalised regions of the resin. Detection is therefore based solely on the difference in copper complexation between the eluent and solute ions but the indirect detection mode wherein the eluent is more strongly complexing than the solute is no longer applicable. Hence it is necessary to use eluents which are moderately weak in their complexation of copper.

Eluents which have been used for the separation of carboxylic acids by ion-exclusion chromatography include dilute solutions of sulphuric, phosphoric or benzoic acids. These acids vary in their ability to complex copper and would therefore provide differing background potentials when equilibrated with a metallic copper electrode. From the viewpoint of detection sensitivity this background potential should be as low as possible, yet at the same time it is desirable that the eluent show weak copper complexation in order to provide a stable baseline potential for the detector. For these reasons, we have selected phosphoric acid as the most appropriate eluent and this decision was further reinforced by the knowledge that phosphoric acid was the preferred eluent for the particular ion-exclusion column used in this work. The side reaction coefficients listed in Table I suggest that potentiometric detection of many carboxylic acids should be possible using a phosphoric acid eluent.

The retention times obtained for a range of carboxylic acids using 0.005% orthophosphoric acid as eluent with a Waters Associates Fast Fruit Juice column are listed in Table II. This Table also shows the pKa values for the acids considered. It is clear that the eluent used permits the separation of only a small number of the acids listed in Table II. All of the dicarboxylic acids are ionised at the pH of the eluent and therefore elute at the column void volume. Resolution of these acids could be achieved by increasing the eluent concentration in order to suppress partially their ionisation. Since the purpose of this work was to assess the feasibility of potentiometric detection rather than to maximise the separation of the carboxylic acids, four simple monocarboxylic acids were selected as the test mixture. Separation of this mixture is shown in Fig. 2, for which the potentiometric metallic copper electrode detector was used. Calibration plots obtained under the same chromatographic conditions are shown in Fig. 3.

It is fair to say that slow electrode response has been one of the major limitations of potentiometric detection in liquid chromatography. However, examination of Fig. 2

Table II. Retention times and pKa values for carboxylic acids obtained under chromatographic conditions in Fig. 2.

Carboxylic acid	Retention time (min)	pKa values
Tartaric	4.5	2.98, 4.34
Oxalic	4.5	1.23, 4.19
Citric	4.5	3.14, 4.77, 6.39
Maleic	5.6	1.83, 6.07
Succinic	6.6	4.16, 5.61
Formic	7.0	3.75
Acetic	8.0	4.75
Propionic	10.0	4.87
Iso-butyric	11.8	4.84
Heptanoic	45.0	4.89

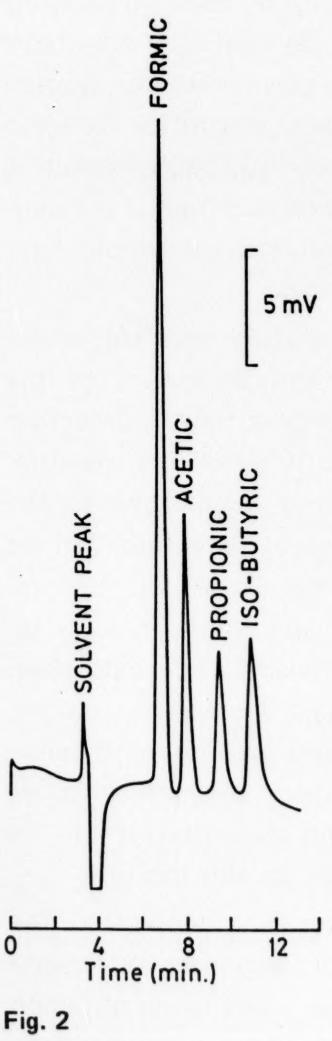

Fig. 2

Chromatogram for carboxylic acids using ion-exclusion separation and potentiometric detection with metallic copper indicator electrode.

Conditions. Column: Waters Associates Fast Fruit Juice column, 150 × 7.8mm i.d. Eluent: 0.005% (v/v) orthophosphoric acid. Column temperature: 55°C. Flow-rate: 0.6 ml min^{-1}. Injected amounts: 12, 70, 70 and 100 μg of formic, acetic, propionic and iso-butyric acids, respectively.

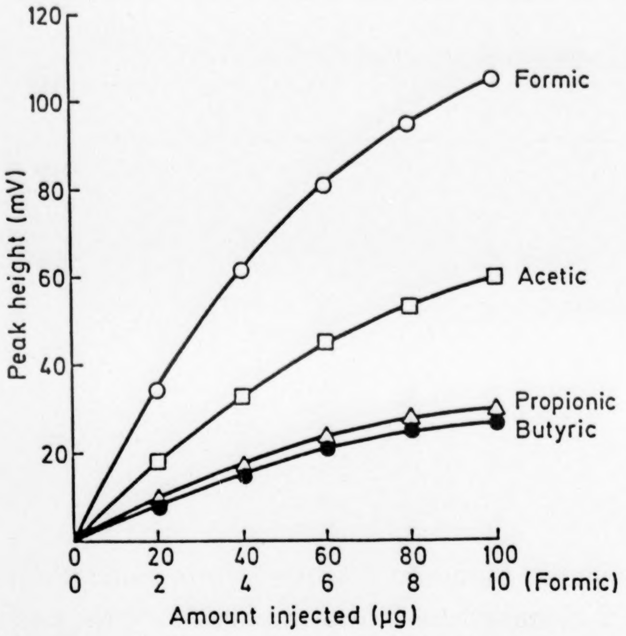

Fig. 3

Calibration plots obtained under chromatographic conditions in Fig. 2.

shows that excellent peak shape was obtained with the metallic copper electrode, which in turn suggests that this electrode gave rapid response to the elution of solute acids. The calibration plots given in Fig. 3 show the expected Nernstian behaviour where the electrode potential begins to level off at higher solute concentrations; a plot of electrode potential *versus* log[solute] was linear over the same concentration range shown in Fig. 3. Detection limits obtained for the components of the test mixture are listed in Table III; these values are superior to those achievable with refractive index detection and comparable to those for UV absorption at low wavelengths.

Table III. Detection limits obtained with potentiometric detection. Chromatographic conditions as Fig. 2. Detection limit calculated as amount of solute giving signal-to-noise ratio of 2.

Solute	Detection limit (µg)
Formic acid	0.2
Acetic acid	2.1
Propionic acid	5.0
Iso-butyric acid	5.3

Conclusions

Potentiometric detection of carboxylic acids using a metallic copper indicator electrode has been shown to be feasible in ion-exchange and ion-exclusion chromatography. Different constraints on selection of a suitable eluent exist for each system, however there is a wide range of eluent species compatible with the copper electrode detector. The result is that detection can be selective or universal, direct or indirect, which provides versatility in adapting potentiometric detection for specific applications.

References

[1] *B. B. Wheals*, J. Chromatogr., **122**, 85 (1976).
[2] *B. Fransson, K.-G. Wahlund, G. Schill*, J. Chromatogr., **125**, 327 (1976).
[3] *J. Aurenge*, J. Chromatogr., **84**, 285 (1973).
[4] *R. Wood, L. Cummings, T. Jupille*, J. Chromatogr. Sci. **18**, 551 (1980).
[5] *P. R. Haddad, A. L. Heckenberg*, J. Chromatogr. **300**, 357 (1984).
[6] *T. Okada, T. Kuwamoto*, Anal. Chem. **55**, 1001 (1983).
[7] *K. Tanaka, J. S. Fritz*, J. Chromatogr., **361**, 151 (1986).
[8] *S. Egashira*, J. Chromatogr. **202**, 37 (1981).
[9] *P. R. Haddad, P. W. Alexander, M. Trojanowicz*, J. Chromatogr. **321**, 363 (1985).
[10] *P. R. Haddad, P. W. Alexander, M. Trojanowicz*, J. Chromatogr. **324**, 319 (1985).
[11] *P. W. Alexander, M. Trojanowicz, P. R. Haddad*, Anal. Lett. **17**, 309 (1984).
[12] *P. W. Alexander, P. R. Haddad, M. Trojanowicz*, Anal. Chem. **56**, 2417 (1984).
[13] *P. R. Haddad, P. W. Alexander, M. Trojanowicz*, J. Chromatogr. **315**, 261 (1984).
[14] *P. W. Alexander, P. R. Haddad, M. Trojanowicz*, Anal. Chim. Acta **171**, 151 (1985).
[15] *A. Hodgkinson, A. Williams*, Clin. Chim. Acta **36**, 127 (1972).
[16] *N. Potezny, R. Bais, P. D. O'Loughlin, J. B. Edwards, A. M. Role, R. A. J. Conyers*, Clin. Chem. **29**, 16 (1983).
[17] *D. E. Duggal, R. W. Walker, R. M. Moll, W. Z. A. van der Huevel*, Anal. Biochem. **94**, 477 (1979).
[18] *H. A. Moye, M. H. Malagodi, D. H. Clarke, C. J. Miles*, Clin. Chim. Acta **114**, 173 (1981).
[19] *H. Hughes, L. Hagen, R. A. L. Hutton*, Anal. Biochem. **119**, 1 (1982).
[20] *L. Larson, B. Libert, M. Asperud*, Clin. Chem. **28**, 2272 (1982).
[21] *W. L. Mayer, J. P. McCarthy, M. S. Greenburg*, J. Chromatogr. Sci. **17**, 656 (1979).
[22] *W. G. Robertson, D. S. Scurr, A. Smith, R. T. Orwell*, Clin. Chim. Acta **126**, 91 (1982).

Received: June 28, 1987
Accepted: July 20, 1987
F

Tests for Liquid Chromatographs

M. J. Rehman*/K. P. Evans/A. J. Handley/P. R. Massey

Imperial Chemical Industries PLC, Plant Protection Division, Yalding, Kent, ME18 6HN, UK

Key Words

Liquid chromatography
Gradient analysis
Diode array

Summary

The paper describes tests for liquid chromatographs to assess the autosampler and pump flow rate precision; suitability of the instrument for normal phase chromatography; UV detector performance; and external band broadening characteristics. Tests for mixing and proportioning characteristics of solvent pumps and performance of diode array detectors are also considered. These tests are designed to evaluate the performance of both newly released liquid chromatography equipment and equipment already in operation. Data from evaluations carried out by instrument manufacturer's and suppliers is reported and discussed. This data offers specifications to a common format for initial selection of instruments prior to purchase.

Introduction

These tests were devised by the Liquid Chromatography Panel of ICI [1], representing the different Division of the Company. The tests are used to evaluate, under conventional chromatographic conditions, the performance of both newly released equipment, and equipment already operating within the Company. The objectives of the tests are to assess;

A. Autosampler and pump flow rate precision.
B. Suitability of instrument for normal phase chromatography.
C. UV detector performance;
    (1) refractive index sensitivity;
    (2) short/long term noise and drift;
    (3) linear range at high and low wavelengths.
D. Band broadening characteristics of the instrument.
E. Characteristics of gradient pumps:
    (1) Mixing and proportioning accuracy
    (2) Hold-up and equilibration volume
    (3) Repeatability of gradient analysis.
F. Performance of diode array detectors.

The test data is reported and discussed from evaluations performed on 6 manufacturer's instruments during the past 18 months. All the reported data was generated by the manufacturers themselves. However, additional evaluations on the same and other instruments have been carried out within the Company to confirm the manufacturers data as well as providing additional data to the existing data base.

Experimental

These test procedures have been written for a conventional liquid chromatography system (with detector cell of volume 8 μl, 1 cm path length, and injection volume of 10 μl), using columns 250 mm in length by 4.5 mm internal diameter packed with 5 μm packings. All solvents used should be of HPLC grade, and chemicals of the purest quality commercially available. Solutions should be prepared in the appropriate eluent of that test. Suitable integration parameters must be selected for each test based on the chromatograms obtained.

Test A.

The test is designed to obtain information on the precision of the autosampler and the delivery rate of the pump. The use of wash samples provides information on any 'carry-over' characteristics of the injection system. Repeated injections of a solution containing anisole and phenol (1.6 mg/ml and 3.0 mg/ml respectively) are performed under the conditions set out in Table I. The detector absorbance is 10 times offscale to allow visual inspection of wash chromatograms for 'carry-over' down to 0.1 %. After system equilibration, 30 injections of the solution are performed with a 'wash injection' (eluent) between every 2 solution injections. All retention times and peak areas are recorded.

Test B.

The test is designed to obtain information on the suitability of a liquid chromatograph for normal phase (adsorption) chromatography. Repeated injections of a solute containing phenol (2.3 mg/ml) are performed under the conditions set out in Table I. Once the system has been equilibrated, injections of the solute are made at 30 minute intervals for a period of 24 hours. All retention times and peak areas are recorded. Should the instrument under evaluation fail to

0009-5893/87 0492-09 $03.00/0

© 1987 Friedr. Vieweg & Sohn Verlagsgesellschaft mbH

Table I. HPLC conditions used for reported tests and chromatograms.

Test	Column		Eluent		UV Detector	
	Type	Temp (°C)	Composition (% v/v)	Flow (ml/min)	nm	AU
A	Spherisorb S5 ODS-1	40	MeOH : H_2O (60 : 40)	2	254	0.04
B	Partisil 5-Silica	35	Methylene Chloride	2	254	0.04
C(1)	Spherisorb S5 ODS-2	40	MeOH : H_2O (40 : 60)	1	280	0.25
C(2)	Spherisorb S5 ODS-1	40	MeOH : H_2O (60 : 40)	2	210	0.25
D	Spherisorb S5 ODS-1	40	MeOH : H_2O (60 : 40)	1	254	0.16
E	Spherisorb S5 ODS-1	40	MeOH : H_2O (gradient)	1	280	0.32
F	Spherisorb S5 ODS-1	40	MeCN : H_2O (80 : 20)	2	230 to 330	0.005 to 0.1

(1) = for dihydropyridone; (2) = for phenetole; MeOH = methanol; H_2O = water; MeCN = acetonitrile; nm = wavelength; AU = absorbance units. For the gradient programme (test E) see Table III.

perform this test, the test is repeated with an eluent of hexane/tetrahydrofuran (70 : 30), at a flow rate of 1 ml/min. The conditions/parameters and solute remain as stated above.

Test C.

These tests are designed to obtain information on the performance of variable wavelength UV detectors and are detailed in three parts.

1. Refractive Index (RI) Sensitivity. Ideally to minimise changes in baseline when running gradient analysis, UV detectors should be insensitive to changes in RI of the mobile phase. The sensitivity to RI effect is determined by measuring the change in baseline of the detector when the cell is filled with methanol (η = 1.329) and then with cyclohexane (η = 1.427). The detector is set at 270 nm and 0.01 AUFS; and the base line change is measured and expressed in AU.

2. Noise, Drift, and Flow Sensitivity. The procedures used for these tests are similar to those defined by T Wolf et al. [2]. All measurements are carried out at 254 nm, 210 nm and 390 nm (or 10 nm below the maximum selectable wavelength), at a detector time constant of 100 milliseconds (or fastest selectable), both in the static and dynamic mode.

3. Linear Range of the Detector. Two test compounds are used to obtain information on the linear range of variable UV detectors. The tests are carried out dynamically with a proven/reliable pump and injection system. A stock solution of each test compound is prepared individually (dihydropyridone and phenetole at 0.65 mg/ml) in two 100-ml volumetric flasks. Serial dilution of stock Solution A are used to prepare Solutions B-F, Table II. All solutions are prepared accurately.

The test solution C, corresponding to an absorbance of around 0.3 AU, is taken as the calibration solution, to which solutions of lower and higher absorbance values are compared. The solutions are chromatographed under the conditions outlined in Table I, with the injection being performed in the order C,B,B,C,D,D,C,A,A,C,E,E,C,F,F and C. Areas and absorbance of each injection are recorded.

Table II. Test solutions as used for detector linearity tests.

Solution	Concentration (approx. mg/ml)	Absorbance (approx. AU)	Dilution Factor (relative to solution C)
A	0.65	1.0	4
B	0.325	0.5	2
C	0.16	0.25	1
D	0.08	0.125	0.5
E	0.04	0.063	0.25
F	0.02	0.031	0.125

AU = absorbance units.

Test D.

Chromatographically well-behaved solutes should exhibit approximately the same number of theoretical plates irrespective of their relative retention. In practice the number of theoretical plates increase with relative retention due to the instrumental contribution (cell volume, connecting tubing volume, etc.) to the observed peak width. This test is designed to give an indication of the band broadening contribution of the instrument. Whilst this test provides information on the Extra-Column Band Broadening produced with conventional 4.5 mm i. d. columns, if the chromatograph is to be used or evaluated for microbore capability the test procedure detailed below should be repeated using an appropriate high efficiency 25 cm column, (2 mm and 1 mm i. d. etc., N $\geqslant$ 15,000 plates), operated at the optimum flow rate.

Repeated injections of a solute mixture containing 10 mg/ml acetone; 0.26 mg/ml phenol; 0.72 mg/ml 2,4-xylenol; 0.08 mg/ml p-nitrotoluene; and 0.8 mg/ml phenetole, are made under the conditions outlined in Table I, until constant retention times and peak widths at half height are obtained. Retention times and peak widths at half height for each peak are measured and recorded, Fig. 1.

Test E.

The test is designed to obtain quantitative information on the repeatability and accuracy of proportioning of the HPLC pump and provides information on the system delay to effect a change in composition. In the first two parts, the HPLC column is replaced with a short length of stainless steel tubing (25 cm length; 1/16" O.D. and 0.01 mm I.D.) crimped to give approximately 1000 psi back pressure, or alternatively a constant back pressure valve/restrictor may be used, however this may increase the hold up volume.

1. Mixing and Proportioning Accuracy. The four reservoirs are filled with either degassed water or degassed water containing 0.01 % w/v phenol. The solvent programme is run in two separate stages, 0–10 % proportions and 0–100 % proportions, each performed six times to assess repeatability. Provision is made for ternary and binary solvent systems. A flow rate of 1.5 ml/min, detection at 254 nm and a chart speed of 1 cm/min are used with the absorbance and recorder zero adjusted such that almost full width deflection is achieved for the range 0–10 % (or 0–100 %).

A solvent programme of 7 (or 9) incremental step changes at 5 min. intervals in eluent composition is used to examine solvent proportions in the range 0–10 % (or 0–100 %) of solvent B in A (A is water, B is 0.01 % phenol). A further 7 (or 9) decremental step changes at 5 min. intervals in eluent composition is used to examine the range 10–0 % (or 100–0 %) of solvent C in D (C is 0.01 % phenol in water, D is water). The concomitant changes in absorbance are recorded on a chart recorder such that a full scale deflection is achieved for either the 10 % or 100 % solvent proportion. Thereby a series of ascending and descending steps are recorded, from which the proportioning accuracy and repeatability are calculated.

2. Hold-up and Equilibration Volume. The hold up volume is defined as the volume of solvent pumped between initiating a solvent composition change and arrival of the solvent change at the detector. The equilibration volume is defined as the volume of solvent pumped between initiating a solvent change and 98 % completion of the change at the detector.

The hold up volume and equilibration volumes are defined and calculated from an incremental and a decremental step change in solvent composition of 10 %, with 60 min. equilibration times. The baseline is 100 % A (water), and full scale deflection is achieved with 10 % B (0.01 % phenol).

3. Repeatability of Gradient Analysis. The test is designed to obtain information on the repeatability of gradients generated by the pump. The test involves 20 replicate injections of a solute mixture containing 10 mg/ml acetone, 0.26 mg/ml phenol, 0.72 mg/ml 2,4-xylenol, 0.08 mg/ml p-nitrotoluene and 0.8 mg/ml phenetole (as used in test D) under the conditions set out in Table I and Table III. All peak areas and retention times are recorded, Fig. 2.

Table III. Gradient LC conditions for test E.

Time (min.)	% A	% B
0.0	30	70
10.0	100	0
15.0	100	0
17.0	30	70
30.0	30	70

A = methanol; B = water

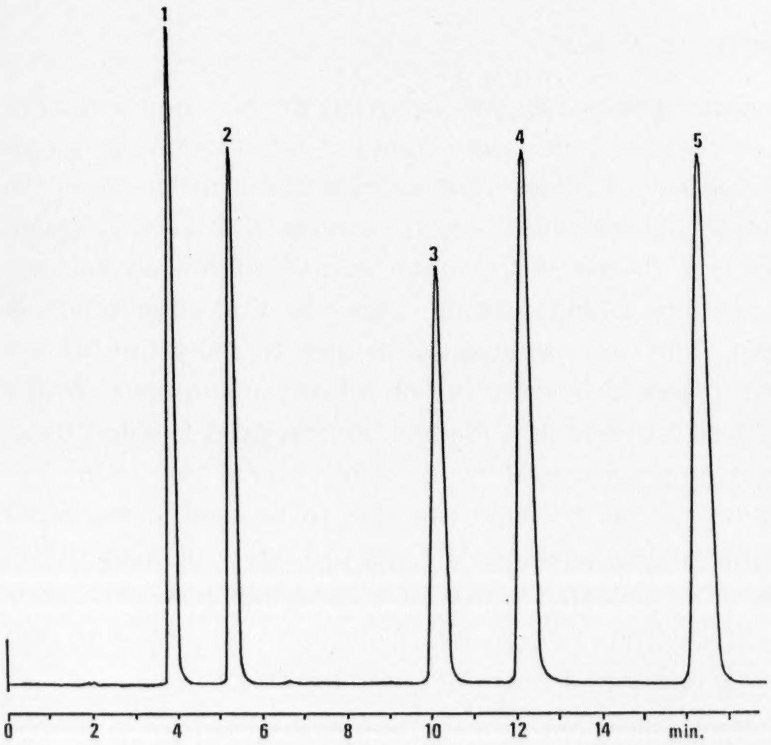

Fig. 1

Chromatogram from test D, showing **1** = acetone, **2** = phenol, **3** = 2,4-xylenol, **4** = p-nitrotoluene, **5** = phenetole.

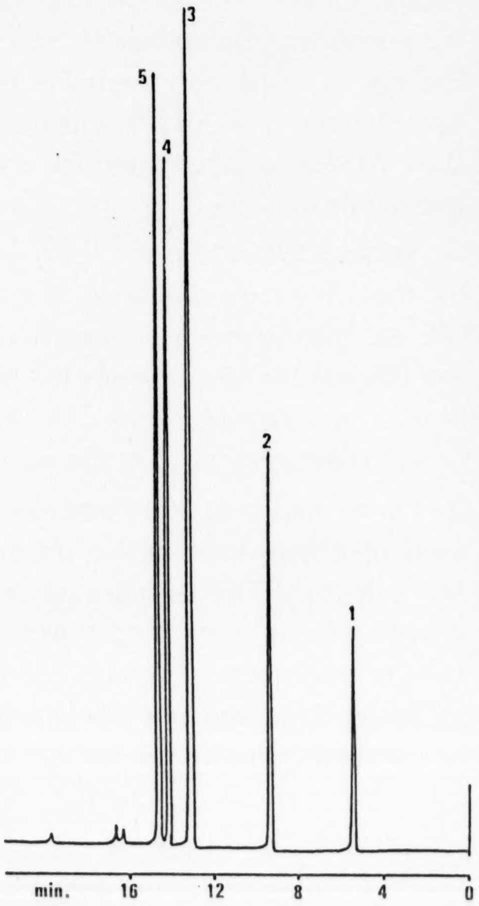

Fig. 2

Chromatogram from gradient Test F, showing **1** = acetone, **2** = phenol, **3** = 2,4-xylenol, **4** = p-nitrotoluene, **5** = phenetole.

Test F.

Apart from its use as a variable wavelength detector, diode array/scanning detectors are able to give spectral and peak purity information for a peak. The test is designed to assess the quality of spectral information although at present no satisfactory procedure has been devised to examine peak purity. A checklist (Table IV), has been included as many facilities reflect the software and handling capabilities of the system. This test is to be used in addition to test C.

A solution of napthalene is prepared in mobile phase to produce an absorbance of 0.06–0.07 AU (approximately 1 mg/ml). Serial dilutions are made to give solutions in the following ranges; 0.05–0.02 AU; 0.02–0.01 AU; 0.01–0.005 AU; 0.005–0.001 AU. Five injections of each solution are performed using the conditions set out in Table I. Each chromatogram, its apex spectra, and a reference spectra taken between 4–5 min. is recorded and stored. The hardware and software revisions used are also recorded.

Results and Discussion

Original data for six manufacturer's instruments is reported and discussed. This data was generated by the individual instrument manufacturers and instrument suppliers themselves. Where the evaluations were repeated, the best data has been reported.

Test A.

From the data provided, the Relative Standard Deviation (RSD) from 30 injections is calculated for the anisole, phenol retention times (RT) and peak areas (PA). To correct for 'drift' in the chromatographic system the

Table IV. Checklist for Diode Array detectors.

1 Wavelength range?
2 Full wavelength range with 1 lamp?
3 No. of diodes/wavelength range (e.g. HP1040A 200/400 nm)
4 Wavelength accuracy?
5 Minimum bandwidth?
6 Maximum bandwidth?
7 Flow cell; length; volume; max back pressure?
8 No. of recorder outputs?
9 No. of separate wavelengths selectable per sample?
10 If wavelength selected does not exactly coincide with a diode what wavelength is used?
11 How can spectra be saved, upslope, apex, downslope, set times?
12 Can spectra be overlaid, how many?
13 Can spectra from different chromatograms be overlaid?
14 Can spectra be normalised using wavelength of maximum absorption or user selected wavelength?
15 Can spectra be smoothed, are spectra smoothed?
16 Can spectra be substracted?
17 First and second derivative spectra?
18 Can spectra be labelled, names and structures?
19 3-D plots?
20 Isograms?
21 Plots on A4 non thermal paper?
22 Signal ratios, how presented?
23 Can chromatograms be replotted at different attentuation or normalised?
24 Can chromatograms from two different injections be overlaid or plotted on the same paper?
25 Can a 10 minute and a 20 minute chromatogram both be plotted on one sheet with a 20 minute axis?
26 Are chromatograms produced on A4 non thermal paper?
27 Can chromatograms be labelled with names and structures?
28 Self-diagnostic wavelength calibration?
29 Lamp energy output, minimum level?
30 Memory available for storing raw data?
31 What is the max acquisition rate of spectra (full range spectra and including diode resetting time)?
32 Do different wavelengths have to be specified pre-run or extracted post-run from spectral data?
33 Does the data sampling rate; (1) Affect the maximum run time, (2) Limit the no. spectra or wavelengths used?
34 Fore/back ground processing: Receive and process data at the same time?
35 Are sample filenames user selectable for automated runs?
36 How easy is quantitative analysis to set up?
37 Full instrument diagnostics and print-out?
38 Can spectral/chromatographic data be accessed by. (1) Other data systems, (2) Other manufactures data systems?
39 Can the method/instrument parameters be printed out?
40 Does it assess peak purity, how?
41 Parameter to identify peaks or confirm peak identity?
42 Can it perform internal standard, external standard, height and area calculations?
43 Can it simultaneously control the associated HPLC system?

Table V. Data for test A. Relative standard deviation (n = 30).

Instrument Manufacturer	1	2	3	4	5	6
RT Phenol	0.17	0.13	0.31	0.28	0.52	0.12
PA Phenol	0.42	0.27	0.66	0.61	0.65	2.25
RT Anisole	0.11	0.12	0.16	0.41	0.84	0.09
PA Anisole	0.48	0.29	0.95	0.71	0.86	1.48
Corrected Phenol PA	0.40	0.12	0.78	0.19	0.84	0.49
Corrected Anisole PA	0.35	0.12	1.05	0.23	1.40	0.43
Anisole PA/Phenol PA	0.38	0.13	0.72	0.34	0.73	2.06
% Carry over	< 0.1	< 0.1	< 0.1	< 0.1	0.76	< 0.1

RT = retention times; PA = peak areas

Table VI. Data for test B. Relative standard deviation (n = 48).

Instrument Manufacturer	1*	2	3	4	5	6
RT Phenol	0.06	0.05	0.17	0.30	0.36	0.45
PA Phenol	0.43	0.19	1.24	0.59	0.85	3.89
Corrected Phenol PA	0.55	0.22	1.51	0.53	1.02	4.12

*test carried out with hexane: tetrahydrofuran (70 : 30) as eluent.
RT = retention times; PA = peak areas

PA's of second injection of each pair is divided by the PA's of the first injection of the same pair, and RSD calculated for the 15 corrected results of anisole and phenol PA's. To eliminate any errors from variations in autosampler injection or integration, the ratio of anisole/phenol PA's is also calculated and thus the RSD from the resulting 30 PA ratios. The wash chromatograms are inspected for signs of carry-over. This visual inspection is necessary even though a minimum area low enough to detect 0.1 % carry-over has been used to distinguish between spuriouse noise and genuine carry-over. Table V lists the calculated RSD's of data from test A provided by various instrument manufacturers (IM).

Satisfactory data was provided by most manufacturers in general. Three of the IM's had to repeat their evaluations because of instrument/operational faults during their initial evaluations. IM6 performed the evaluations on three separate occasions by three different analysts. It is quite evident that IM6 has problems with their autosampler or their ability to use their own instruments. The tests are being repeated by the IM again, using different instruments of the same model.

The sample carry-over between injections can be reduced to a minimum (< 0.1 %) by including a wash injection. The IM5 data for sample carry-over was excessive, (0.76 %) but was reduced to < 0.1 % with wash procedures between sample injections. IM5 have included in their autosampler manual the importance of wash procedures to reduce sample carry-over. One must remember, that wash procedure from a central bottle/vial is better than wash injections from vials dispersed between samples, resulting in the reduction of the actual samples in the sample tray.

Test B.

From the data, the RSD of 48 injections is calculated for phenol RT's and PA's. To correct for 'drift', it is assumed that alternative injections are calibration standard solutions. Thus RSD of the 24 results obtained by dividing the PA obtained for the 'sample solution' by the PA obtained for the preceding 'standard solution' is also calculated. Table VI lists the RSD's of data from this test.

The IM1 markets an expensive and complex instrument. However, this instrument was found to be unsuitable for applications which employed methylene chloride (this is used routinely within the Company for process monitoring/control as well as routine quality control where instruments are kept running for long periods of time). Several attempts in using methylene chloride by the IM as well as in the Company produced RSD's for corrected phenol PA in the range 1.5–4, mostly at the upper end. The IM eventually indicated that their instrument was primarily designed for reversed-phase applications, although they did indicate problems with the autosampler when used with methylene chloride. During discussions with the IM1 it was indicated that they were to incorporate a thermostated sample compartment for use with volatile solvents. Similarly, IM4 was able to improve their data (for both tests A and B) when evaluations were repeated employing a thermostated sample tray in their autosampler. Again, unsatisfactory data from IM6.

Most autosamplers are designed with their sample tray locating directly above all the electronics. Thus, the heat generated from the electronics affects the volatile samples, especially when performing more than one injection from the same sample vial. Therefore, the problem seems to be the temperature of the sample compartment area, coupled with the accuracy of variable volume injectors.

Test C.

Table VII shows the data from the detector performance tests. The definitions and the units of the terms used are as defined by T Wolf et al. [2].

Table VII. Data for test C.

Instrument Manufacturer	1	2	3	4	5	6
RI Sensitivity (10^{-3} AU)	1.5	3.5	NIL	9.0	1.0	3.0
Static short term noise (10^{-4} AU/cm)	0.5	1.4	0.4	0.7	0.5	0.5
Static long term noise (10^{-4} AU/cm)	0.6	0.2	0.6	0.5	0.2	0.6
Static Drift (10^{-4} AU/hr)	4.2	0.4	1.8	2.0	0.6	1.9
Dynamic short term noise (10^{-4} AU/cm)	0.5	1.4	0.5	0.6	0.5	0.3
Dynamic long term noise (10^{-4} AU/cm)	0.6	0.2	0.8	0.5	0.2	0.8
Dynamic drift (10^{-4} AU/hr)	4.3	0.4	1.0	3.5	0.3	3.8
Flow sensitivity (10^{-4} AU min/ml)	A	A	1.0	5.5	0.9	0.1
Dihydropyridone linearity (1)	0.93	0.78	3.13	2.37	2.37	B
Dihydropyridone linearity (2)	1.10	0.77	3.41	2.37	2.39	B
Phenetole linearity (1)	1.74	0.53	1.83	2.11	2.27	B
Phenetole linearity (2)	1.60	0.88	1.90	2.11	2.36	B

AU = absorbance units
(1) Normal external standard calculation
(2) Bracketing of standard either side of samples
A – Not measurable B – Completely non-linear, possible injector problems
Noise, Drift and Flow Sensitivity data at 254 nm listed.
RSD's for linearity given from 8 results in each case.

As expected, the noise, drift and flow sensitivity at 390 nm were found to be comparable to the values listed in Table VII, but considerably higher at 210 nm. In some cases the flow sensitivity measurements were difficult to carry out as negative as well as positive values were obtained with increased flow. In summary, the generation of this type of data prevents misleading or erroneous comparisons amongst different types of detectors, yet provides useful information of selection of the most suitable detector. Presently, additional tests to evaluate (i) minimum detection level, and (ii) wavelength accuracy for detectors are also being investigated within the Company.

From the data provided in linearity tests, the peak areas (PA's) of injection (inj) of each solution (sol) can be treated in two different ways.

1. *Normal external standard type calculation;*

$$\text{(a)}\quad \frac{\text{PA of 1st inj of sol B}}{\text{PA of 1st inj of sol C}} \times \frac{100}{\text{dilution factor for B}}$$

similarly for solution D, E, A and F, using preceeding injection of solution C in each case (producing 10 results in total).

2. *Bracketing of 'standard' either side of 'sample';*

$$\text{(a)}\quad \frac{\text{PA of 1st inj of sol B}}{\left(\text{PA of 1st inj of sol C}) + (\text{PA of 2nd inj of sol C}\right)/2} \times \frac{100}{\text{dilution factor for B}}$$

$$\text{(b)}\quad \frac{\text{PA of 2nd inj of sol B}}{\left(\text{PA of 1st inj of sol C} + (\text{PA of 2nd inj of sol C}\right)/2} \quad \frac{100}{\text{dilution factor for B}}$$

similarly for solution D, E, A and F, using injections of solution C either side of the other injections (producing 10 results in total).

The RSD of the data resulting from both types of treatment (n = 10) is calculated for both dihydropyridone and phenetole. As all solutions were prepared from the same stock solution, making allowance for their respective dilution factors, means that all calculated results should be around 100. Any deviation from the value of 100 indicates a deviation from linear detector response and would be apparent in the resulting RSD (Table VII).

The chemical dihydropyridone was chosen as it exhibited non-linearity with some detectors. These detectors indicated non-linearity at the upper end of the absorbance scale (1 AUFS). Detectors from IM4 and IM5 have shown to be non-linear at either end of the absorbance scale for both chemicals. The data from IM6 defied explanation, and the authors of the paper were surprised that IM6 were able to report such data – highlighting again their inability to interpret their own data and to use liquid chromatographs.

Test D.

The theory for Extra Column Band Broadening (ECBB) was stated in a paper by Lauer and Rozing [3]. The total variance of a chromatographic peak was expressed as

$$0^2 t = 0^2\ \text{column} + 0^2\ \text{external} \qquad (1)$$

where 0^2 column and 0^2 external are the peak variance due to the column and instrumental (extra-column) factors respectively. In terms of the peak width at half height, which is the easiest parameter to measure experimentally, this gives:

$$(W\ 0.5)^2\ \text{total} = (W\ 0.5)^2\ \text{column} + (W\ 0.5)^2\ \text{external} \qquad (2)$$

The theoretical efficiency of a column (N) is given by:

$$N\ \text{column} = \frac{5.54\ Vr^2}{(W\ 0.5)^2\ \text{column}}$$

$$\text{i.e.}\ (W\ 0.5)^2\ \text{column} = \frac{5.54\ Vr^2}{N\ \text{column}}$$

substituting this value for $(W\ 0.5)^2$ column into eq. 2

$$(W\ 0.5)^2\ \text{total} = \frac{5.54\ Vr^2}{N\ \text{column}} + (W\ 0.5)^2\ \text{external}$$

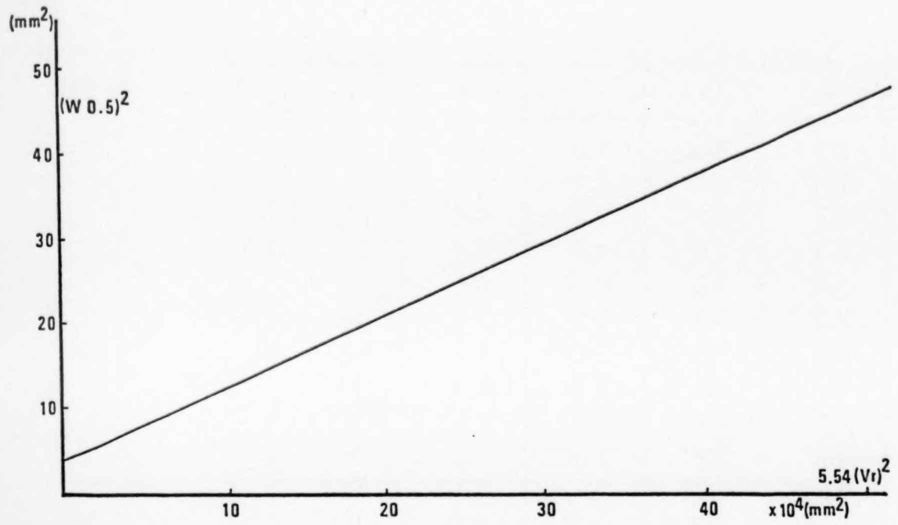

Fig. 3
Extra column band broadening extrapolation in Test D.

Thus a plot of (W 0.5)^2 total against 5.54 Vr^2 should yield a linear relationship of intercept (W 0.5)^2 external and slope of 1/N column. Therefore, from the measurements of retention time (Vr, mm) and width of half-height (W 0.5, mm) for each peak, a graph is plotted of (W 0.5)^2 against 5.54 (Vr)^2 for the five peaks (Fig. 3). A least squares analysis is carried out to determine the intercept and hence the extra column dispersion (in μl).

The ECBB obtained from IM's evaluations is listed in Table VIII. However, as stated in the experimental section, this test only provides information with conventional 4.5 mm i.d. columns. Ideally, for such a system, the ECBB should be no greater than 40 μl. Values considerable higher than 40 μl would highlight the poor dispersion characteristics of an instrument configuration. Table VIII also lists extra column dispersion (using narrow bore columns at different flow rates) for instrument configuration from IM1, which is marketed as having minimum system dispersion.

Table VIII. Data for test D.

A

Instrument Manufacturer	1	2	3	4	5	6
Extra column dispersion (μl)	38	76	34	36	?	30

B

Column i.d. (mm)	Eluent Flow (ml/min)	N (per meter)	Column Dispersion (μl)
4.5	1.00	74,600	38
2.0	0.39	60,400	27
2.0	0.19	64.800	23
2.0	0.10	69,800	18
1.0	0.08	41,600	10
1.0	0.04	50,300	7
1.0	0.01	34,400	3

Data from the instrument manufacturer 1 on narrow bore columns at different flow rates (B).
i. d. = internal diameter; N = theoretical plates

Test E.

This test has only recently been released after extended inhouse evaluations. Therefore, no data as yet is available from instrument manufacturers. However, data and experience from our in-house evaluation is discussed.

1. From the series of step changes recorded (Fig. 4), the distance $X_1 - X_{12}$ and $Y_1 - Y_{16}$ are measured. The repeatability of the instrument to generate specific solvent composition is then indicated by the mean deflection and its standard deviation calculated for each solvent composition change for the six replicate traces of each programme.

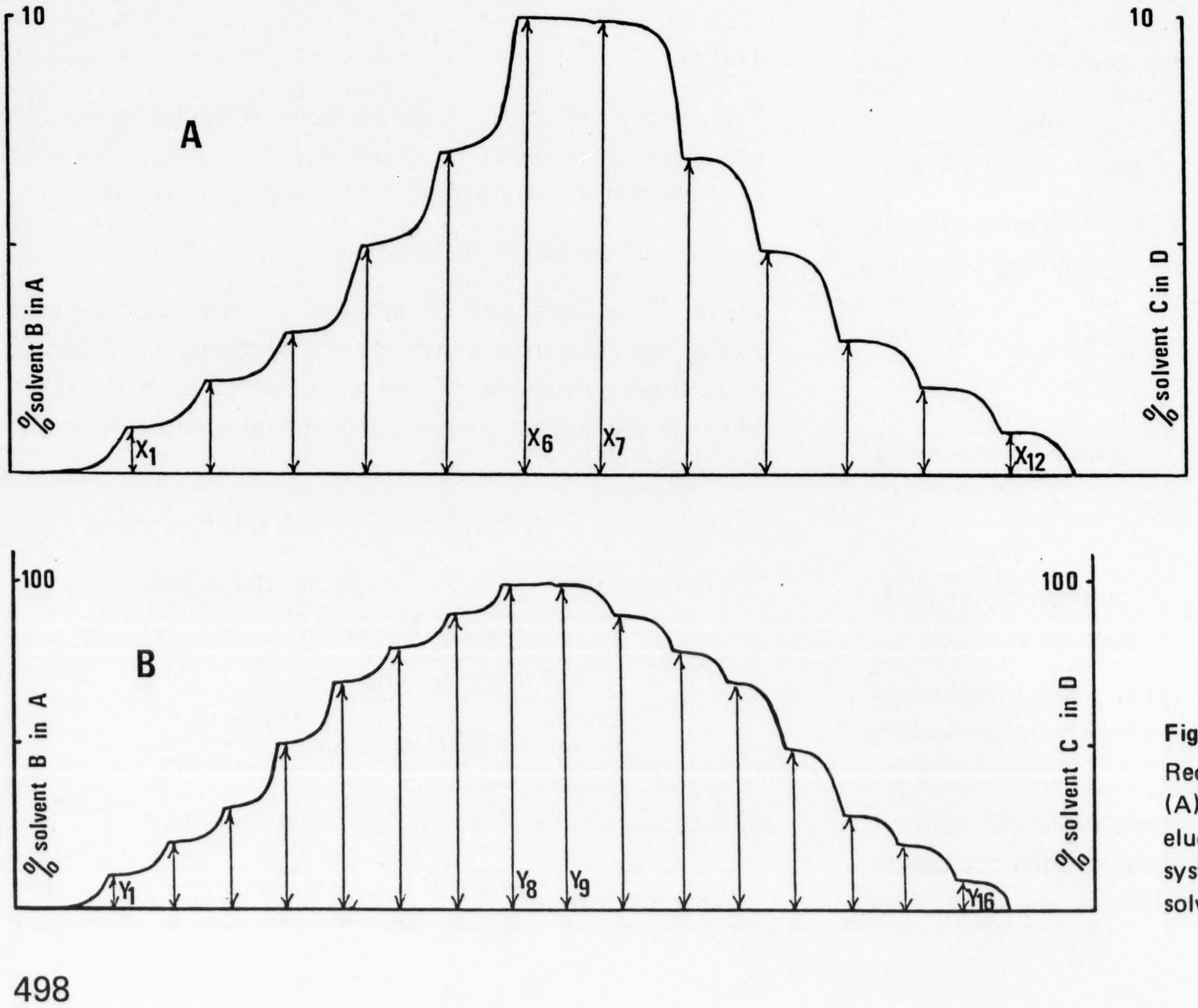

Fig. 4
Recorder trace for test E, showing 0–10 % (A), and 0–100 % (B) step changes in eluent composition. For binary solvent systems, reservoir C = A; and for ternary solvent systems reservoir D = A.

Table IX. Data for Test E (1)

A.

	MD (mm)	RSD	T (mm)	% EP
X_1	19.5	2.81	17.5	11.7
X_2	37	1.80	34.9	6.0
X_3	54	1.27	52.4	3.2
X_4	87.4	0.96	87.3	0.3
X_5	122	0.56	122.2	−0.1
X_6	174	0.63	174.5	−0.3
X_7	175	0.54	174.5	0.3
X_8	125	0.97	122.2	2.3
X_9	91	1.18	87.3	4.3
X_{10}	56.5	2.24	52.4	7.9
X_{11}	39	2.20	34.9	11.7
X_{12}	22	2.77	17.5	26.1

MD = Mean deflection
T = theoretical base line shift
% EP = % error in composition
0–10 % composition change (A)
0–100 % composition change (B)

B.

	MD (mm)	RSD	T (mm)	% EP
Y_1	16	2.57	16.5	−3.0
Y_2	33	0.62	33	0.0
Y_3	49	0.83	49.5	−1.0
Y_4	81.5	0.50	82.5	−1.2
Y_5	116	0.35	115.5	0.4
Y_6	132	0.28	132	0.0
Y_7	149.5	0.25	148.5	0.7
Y_8	165	0.0	165	0.0
Y_9	165	0.12	165	0.0
Y_{10}	149	0.17	148.5	0.3
Y_{11}	134	0.15	132	1.5
Y_{12}	116.5	0.42	115.5	0.9
Y_{13}	84.5	0.61	82.5	2.4
Y_{14}	51.5	0.96	49.5	4.0
Y_{15}	33.5	1.13	33	1.5
Y_{16}	18	0.0	16.5	6.6

The proportioning accuracy is calculated assuming that the correct values were obtained for the 10 % and 100 % change which produced full scale deflections. The theoretical baseline shift (T) for a solvent change whose minor solvent proportion is % B, is calculated from:

$$T_{\%B} = [X_6 + X_7)/20] \ \times B\,\% \quad \text{for } 0\text{–}\ 10\,\% \text{ range}$$

and

$$T_{\%B} = [Y_8 + Y_9)/200] \times B\,\% \quad \text{for } 0\text{–}100\,\% \text{ range}$$

The percentage error in composition (% EP) for each solvent proportion step is then calculated from:

$$\%\ EP \text{ for } \%\ B = (\text{mean deflection for } \%\ B - T_{\%B})/T_{\%B}$$

where $T_{\%B}$ is the theoretical value derived above.

Table IX shows data obtained from our instrument. Large RSD's were obtained for solvent composition change in the range 1–3 % ($X_1 - X_3$ and $X_{10} - X_{12}$), reflecting the difficulty in reliably generating solvents with very small proportions of the minor solvent. Most of the variation is due to error in measuring the small distances X_1, X_{12}, Y_1 and Y_{16}. However, comparison of Y_2 with X_2, both having similar sized deflection, indicates that it is considerably more reliable to generate a mobile phase whose minor solvent proportion is 10 % (RSD = 0.62), than a 1 % (RSD = 1.80). The % EP data reflects the errors in composition, but in addition shows that incremental step changes are likely to have errors due to the deficiency of the minor solvent proportion, indicated by the negative values. The decremental steps in composition all have errors due to an excessive proportion of the minor solvent. The data indicates that this instrument should not be used to generate mobile phase where the minor solvent proportion is less than 5 %.

2. From the chromatographic trace obtained, a baseline between the start and end, and a parallel line extending the 10 % B deflection are drawn. The perpendicular distance (Z) is measured; a further parallel baselines at 0.02Z and 0.98Z are drawn. The distance A, B, C, D (Fig. 5) are measured and converted to volume where;

A = Hold up time for an incremental step
B = Equilibration time for an incremental step
C = Hold up time for a decremental step
D = Equlibration time for a decremental step

Data was obtained from an HPLC system used in a routine environment during the test evaluation. Both the incremental and decremental steps had hold up volumes of 0.05 ml; and as expected from the % EP data, the equlibration volume for the incremental step (0.17 ml) was less than the equilibration volume for the decremental step (0.19 ml).

3. From the data, the RSD from 20 injections is calculated. Table X shows the data obtained during the test evaluations on our instrument. Although, the retention times show ex-

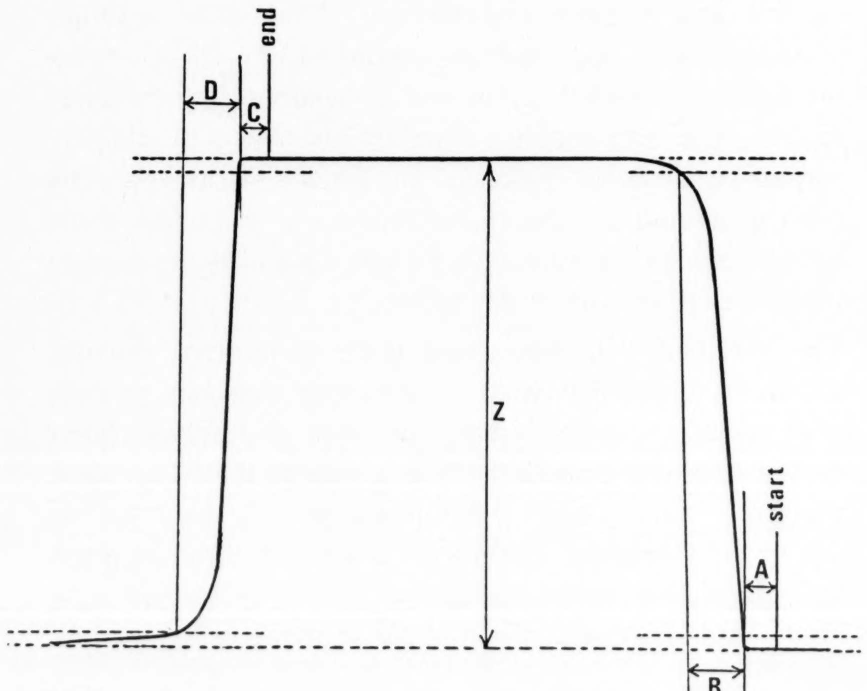

Fig. 5
Recorder trace for test E (2).

cellent precision, the peak areas of phenol and phenetole are less precise than the others. The variation in peak area precision may be due to integration problems, although a wavelength of 280 nm was chosen to reduce the baseline upset caused during gradient analysis.

Many HPLC systems, capable of running gradients, are bought instead for their ability to run isocratic analysis by generating the mobile phase. This is an important consideration for method development and eventual instrument control for automated method development.

Test F.

Plot is obtained by overlaying, the five apex spectra from each solution, using the reference spectra to correct for background drift. The spectra should be normalised at 230 nm, and the number of data scans averaged to obtain the apex spectra specified. The compiled spectra from the most concentrated solution is used to assess the resolution factor (R). The distance H and h at 265 nm and 270 nm respectively (Fig. 6), is measured to calculate R from; R = h/H.

This test is still under evaluation within the Company. The evaluations to date have shown the complexity of devising a test which examines the data storage, software and presentation of information in conjunction with the ability of the detector. The simple test outlined, examines spectral quality, repeatability, and the lowest concentration at which an acceptable repeatable spectrum was obtained. At present it has been difficult to find a suitable means of quantifying the data because of the range of ways in which data is or may not be presented.

A potential purchaser must first clearly define the instruments intended use and software needs for which the extensive though not exhaustive check list, Table IV, has been found to be helpful.

Conclusions

These tests were derived from procedure used in a number of ICI Divisions. Instruments are assessed in the manner in which they would be used within the Company both in a routine and research environment. They offer a simple semi-automated approach to evaluating any HPLC instrumentation. Provided these test procedures are followed exactly, the tests enable a standardised means of comparison across different makes of equipment. All the data has been generated by the manufacturers or suppliers themselves, thereby demonstrating their capability to support the release of new instrumentation.

The resultant data base from these evaluations provides LC users within ICI with information that can simplify their initial choice of equipment prior to purchase. Some of the data was unacceptable and outside the ICI criteria, therefore making such instruments of only very limited use to the Company. Evaluation of a liquid chromatograph for a particular user's application is then performed separately using methods which relate to that specific application.

Table X. Data for test E (3).

Peak	RSD of RT	RSD of PA
Acetone	0.18	0.24
Phenol	0.18	0.64
2,4-Xylenol	0.30	0.36
p-Nitrotoluene	0.30	0.27
Phenetole	0.30	0.91

RT = retention times; PA = peak areas

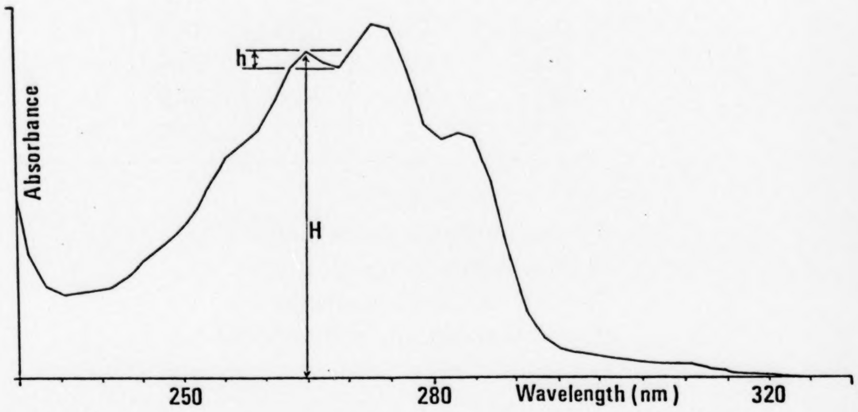

Fig. 6

Spectra from test G, used to assess quality of spectral information, and resolution factor (R).

It is evident that IM6 (an instrument supplier and not a manufacturer) was unable to provide satisfactory data even after several attempts. Their interpretation of the test data was against the requirements of the everyday analyst working in an LC laboratory. However, further discussion with this particular supplier confirmed that they did not have adequate technical applications chemists or support. Their main priority was on the sales side, although the evaluations are now being performed at their research laboratories sited alongside their main production facility.

Instrument manufacturers should quote practical and realistic specifications that are useful to an analyst. The specifications quoted by the manufacturers are of little practical use, nor do they offer data that can be compared to another manufacturer. It is hoped that all manufacturers will in future quote specifications based on widely accepted test procedures. This paper offers a first step to such a goal.

Acknowledgement

The authors wish to thank Dr. F. McLennan and Mr. D. A. Warwick of ICI for their contributions, and the members of the ICI LC Panel for their support and contributions.

References

[1] LC Panel of ICI, Internal report TMY 320A (1985).
[2] *T. Wolf, G. T. Fritz, L. R. Palmer,* J. Chromatog. Sci. **19**, 387 (1981).
[3] *H. H. Lauer, G. P. Rozing,* Chromatographia, **14**, 11 (1981).

Received: June 29, 1987
Accepted: July 29, 1987
F

Simultaneous Determination of CGP 22 848 and its Major Metabolite (Free Carboxylic Acid) CGP 35 652 in Plasma by HPLC

A. Sioufi* / F. Leroux / J. P. Dubois

Laboratoires Ciba-Geigy, Biopharmaceutical Research Center, B. P. 308, F-92506 Rueil-Malmaison, France.

C. Mondadori / W. Froestl

Ciba-Geigy Pharma, Research and Development, Basle, Switzerland.

Key Words

Column liquid chromatography
Liquid-solid extraction
CGP 22 848 and its metabolite

Summary

A specific method for the quantitative determination of CGP 22 848 (a basic compound) and its major metabolite CGP 35 652 (a free carboxylic acid metabolite) in plasma using CGP 17 582 as internal standard is described. Separation of components is by reversed-phase chromatography using a mobile phase consisting of pH 3 phosphate buffer-acetonitrile (76 : 24, v/v) at a flow-rate of 1 ml/min in conjunction with a Radialpak C18 cartridge combined with a radial compression separation system or by using a mobile phase consisting of pH 3 phosphate buffer-acetonitrile (80 : 20, v/v) at a flow-rate of 0.8 ml/min in conjunction with a Novapak C18 column. Rapid extraction of CGP 22 848 and CGP 35 652 from plasma is achieved using reversed-phase C18 columns (Bond-Elut or Supelco). With 250 μl of plasma, concentrations down to 0.078 μM (25 ng/ml) of CGP 22 848 B and 0.326 μM (100 ng/ml) of CGP 35 652 A can be determined. A wavelength of 221 nm was used to monitor CGP 22 848, 280 nm for CGP 35 652 and 320 nm for the internal standard.

Introduction

CGP 22 848 B, [1, 2, 5, 6-tetrahydro-1-[2-(1H-indol-3-yl) ethyl]-3-pyridine carboxylic acid methyl ester hydrochloride] was selected as a new nootropic agent. It is extensively metabolized in plasma, the major metabolite being the free carboxylic acid, CGP 35 652. The chemical structures of the drug, of its metabolite and of the internal standard used are given in Fig. 1.

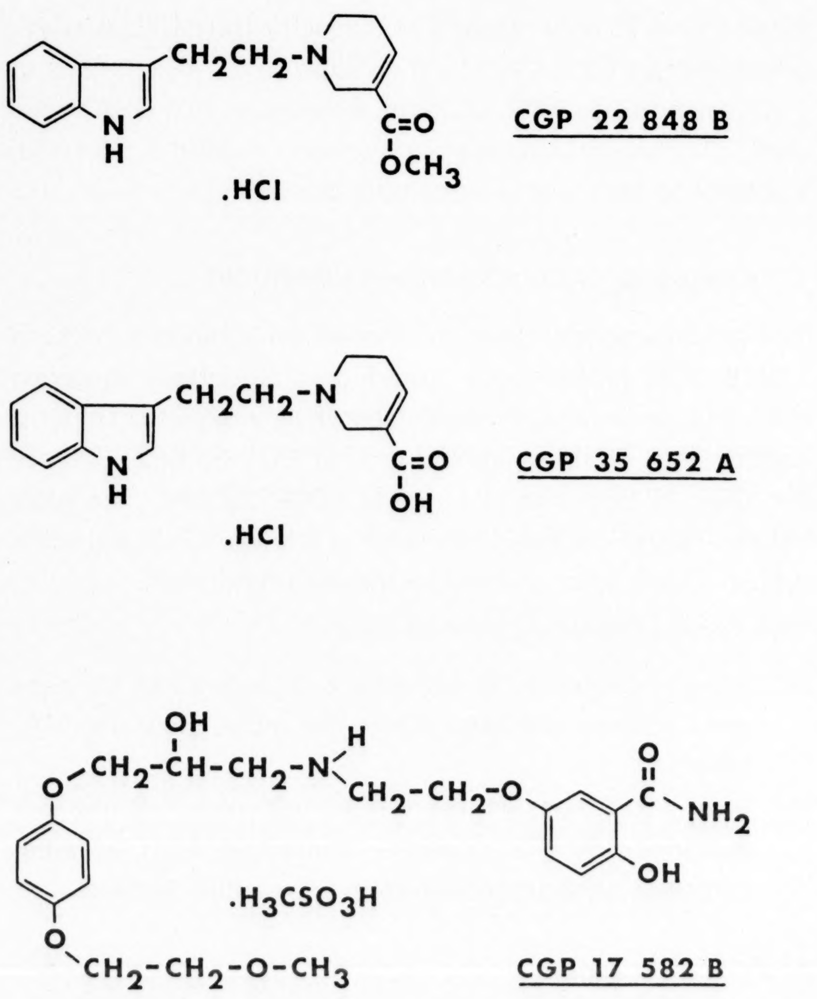

Fig. 1
Chemical structures of CGP 22 848 B, CGP 35 652 A and of the internal standard CGP 17 582 B.

0009-5893/87 0501-04 $03.00/0

© 1987 Friedr. Vieweg & Sohn Verlagsgesellschaft mbH

CGP 22 848, a basic compound, and CGP 35 652, an acidic compound cannot be simultaneously extracted from plasma using liquid-liquid extraction. The extension of the use of silica with a bonded organic phase from liquid chromatography to sample preparation, now offers a viable alternative to liquid-liquid extraction [1]. This paper describes a new extraction method based on the use of short columns of reversed-phase silica (C18 Bond-Elut or LC-18 Supelco) which quantitatively extracts CGP 22 848, CGP 35 652 and the internal standard. The method is rapid, technically simple and leads to a sensitive, accurate and reproducible assay for CGP 22 848 and its major metabolite in plasma.

Experimental

Solvents and Reagents

The synthetic reference compounds CGP 22 848 B, CGP 35 652 A and CGP 17 582 B (Fig. 1) were provided by Ciba-Geigy Limited (Basle, Switzerland).

The solvents used were acetonitrile (412411, Carlo Erba, Milano, Italia), methanol (20847, Prolabo, Paris, France), and deionized water. The 0.1 M sodium acetate solution was prepared by dissolving 0.82 g anhydrous sodium acetate (Merck 6264, Darmstadt, FRG) in water and making up to a final volume of 100 ml. pH 3 phosphate buffer was prepared by dissolving 2.72 g potassium dihydrogen phosphate (Merck 4873) in water and making up to a final volume of 2000 ml. Ten drops of orthophosphoric acid (Merck 573) were then added to the solution.

Extraction Columns and Vacuum Apparatus

Bond-Elut C18 columns of 1 ml capacity (607 101, Analytichem, Harbor City, CA, USA) or Supelco LC-18 columns of 1 ml capacity (5-7002, Supelco, Bellefonte, PA, USA) were used in conjunction with a vacuum manifold (5-7030, Supelco) to facilitate rapid sample processing.

Chromatographic Equipment and Conditions

The chromatography was performed on a Hewlett-Packard 1081B high performance liquid chromatograph equipped with a variable programmable absorbance detector (Kratos, Spectroflow 783) set at 280 nm for CGP 35 652, 320 nm for CGP 17 582 and 221 nm for CGP 22 848. The peak heights were obtained through a Hewlett-Packard data system (3388 A) connected to the chromatograph.

Two types of columns were be used:

(a) 4 μm, Novapak C18 150 mm X 3·9 mm I.D, stainless steel column (86 344, Waters-Millipore, Bedford, MA, USA).

(b) 4 μm, Radialpak Novapak C18 100 mm X 8 mm I.D cartridge (86 342, Waters) combined with a radial compression separation system (Z-module, Waters).

Analytical Procedure

Sample preparation: Sample preparation is done with Bond-Elut C18 columns or with Supelco LC-18 columns. The column is positioned in the luer fitting in the vacuum manifold. Twelve columns can be used at a time. A vacuum of 25–50 cm Hg is applied to the manifold to elute the different washes. The column is conditioned by passing 2 X 1 ml 0.01 M HCl, 2 X 1 ml acetonitrile, 2 X 1 ml H_2O. The vacuum is turned off as soon as the water is run through to prevent the tubes from drying out. 50 μl internal standard methanolic solution (0.97 nmol) are introduced in a 5 ml polypropylene tube and evaporated to dryness under a nitrogen stream at room temperature. 250 μl plasma, 250 μl 0.1 M CH_3COONa are added, the mixture is shaken on a Vortex mixer and the solution is run through the column by applying the vacuum to the manifold. Each column is then washed with 2 X 1 ml H_2O.

Following the last wash, the vacuum is maintained until the column is dry. The cover of the manifold is then removed and the stainless steel needles of the cover are wiped with a tissue to remove drops of washing solution. Glass conical tubes are then positioned under each column. 2 X 500 μl methanol are run through to the column by applying the vacuum to the manifold. The eluent is evaporated to dryness at 50 °C under nitrogen, reconstituted in 500 μl of mobile phase and 70 μl are injected onto the column of the liquid chromatograph.

Chromatography: A degassed mobile phase pH 3 (10^{-2} M) phosphate buffer solution-acetonitrile (76 : 24, v/v) was used at a flow-rate of 1 ml/min when the analytical column was a Radialpak cartridge in combination with the Z-module. The pressure at the top of the column was 40 bar.

A degassed mobile phase pH 3 (10^{-2} M) phosphate buffer solution-acetonitrile (80 : 20, v/v) was used at a flow-rate of 0.8 ml/min when the analytical column was a stainless steel column. The pressure at the top of the column was 80 bar. The mobile phases and the columns were at room temperature. For both types of columns, the retention times were around 5.6 min or CGP 35 652, 9.8 min for CGP 17 582 and 12.4 min for CGP 22 848.

Calibration: The concentration of the internal standard solution in methanol was 19.4 μM (10 mg/l). Methanolic calibration solutions contained 0.390 to 15.6 μM (0.125 to 5 mg/l) of CGP 22 848 B and 1.63 to 65.2 μM (0.5 to 20 mg/l) of CGP 35 652 A.

Calibration samples were prepared by introducing 50 μl of each of three methanolic solutions containing either CGP 22 848 B, CGP 35 652 A or CGP 17 582 B into a 5 ml polypropylene tube. Methanol was evaporated under nitrogen at room temperature and 250 μl plasma were added to obtain the reference samples ranging from 0.078 to 3.12 μM (25 to 1000 ng/ml) for CGP 22 848 B and from 0.326 to 13 μM (0.1 to 4.0 μg/ml) for CGP 35 652 B.

The calibration curves were obtained from the ln-ln plot of the peak-height ratios versus the plasma concentrations. The equations of the curves were estimated by the least-squares method using ln-ln regression:

$$\ln y = \ln a + b \ln x$$

In normal coordinates this equation becomes $y = ax^b$.

Results and Discussion

Choice of the Analytical Column

The best separation was obtained with C18 columns, especially 4 μm Novapak C18. 4 μm Radialpak Novapak C18 cartridges combined with the Z-module exhibited properties similar to those of the Novapak stainless steel column. They can be operated at a lower inlet pressure and are less expensive. Around 800 injections can be done on the same column.

Sample Preparation, Clean-up Procedure

The yield of the extraction and analytical procedure was found to be 60 % for CGP 35 652, 80 % for CGP 17 582 and 95 % for CGP 22 848 by comparing the detector response after direct injection and after extraction. The Bond-Elut columns and Supelco columns may be used twice without affecting their performance. Regeneration is effected by simply washing with twice the column volume (1 ml) of methanol immediately following use.

Plasma Interference

CGP 35 652, CGP 17 582 and CGP 22 848 are conveniently separated from plasma components as can be shown in Fig. 2. An endogenous peak at a retention time of 60 min was present in the chromatograms of all plasma tested. Several column clean-up washings were studied in an attempt to eliminate this peak but were unsuccessful because they affected the yield of the analytical procedure for CGP 35 652.

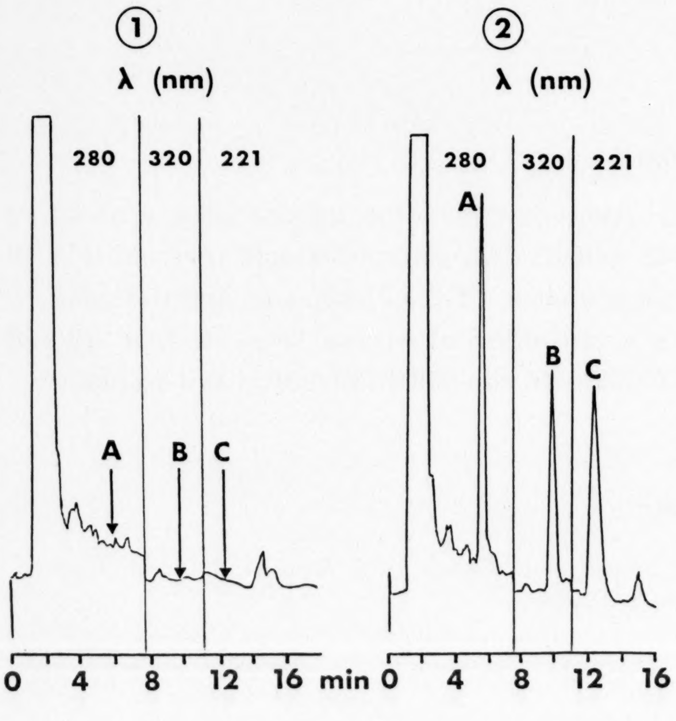

Fig. 2

Examples of chromatograms. (1) human plasma blank (extract of 250 μl of plasma); (2) the same plasma spiked with 815 nmol of CGP 35 652 A (A), 4.85 μmol of internal standard (B), and 156 nmol of CGP 22 848 B (C).

Standard Curves

Some variation in the standard curves obtained on separate days was noticed, which is the reason why they were obtained daily. Fig. 3 shows a calibration curve obtained for CGP 22 848 and Fig. 4 a calibration curve obtained for CGP 35 652.

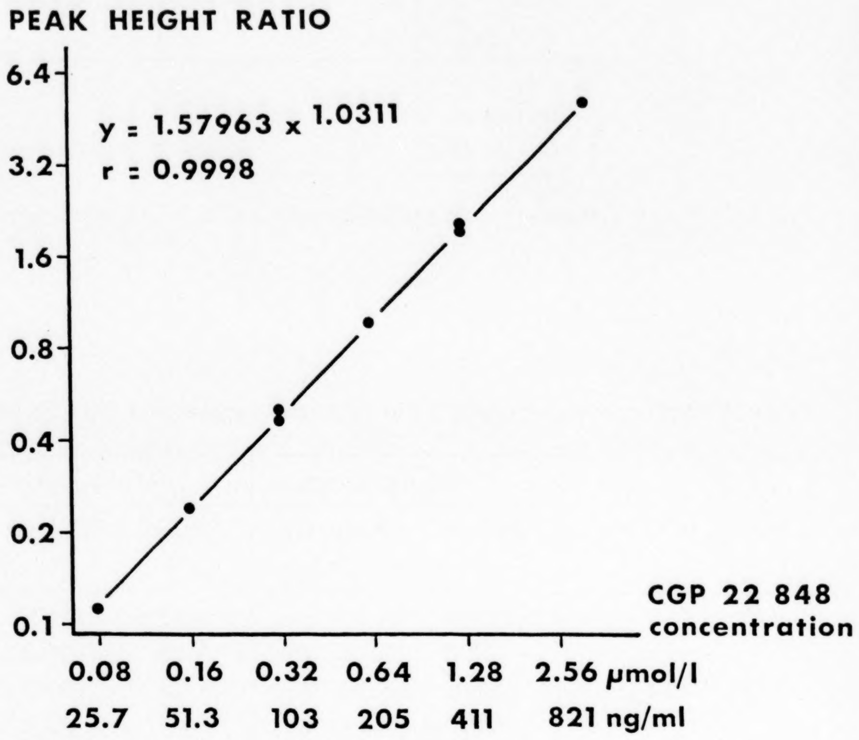

Fig. 3

Calibration curve of CGP 22 848 in plasma.

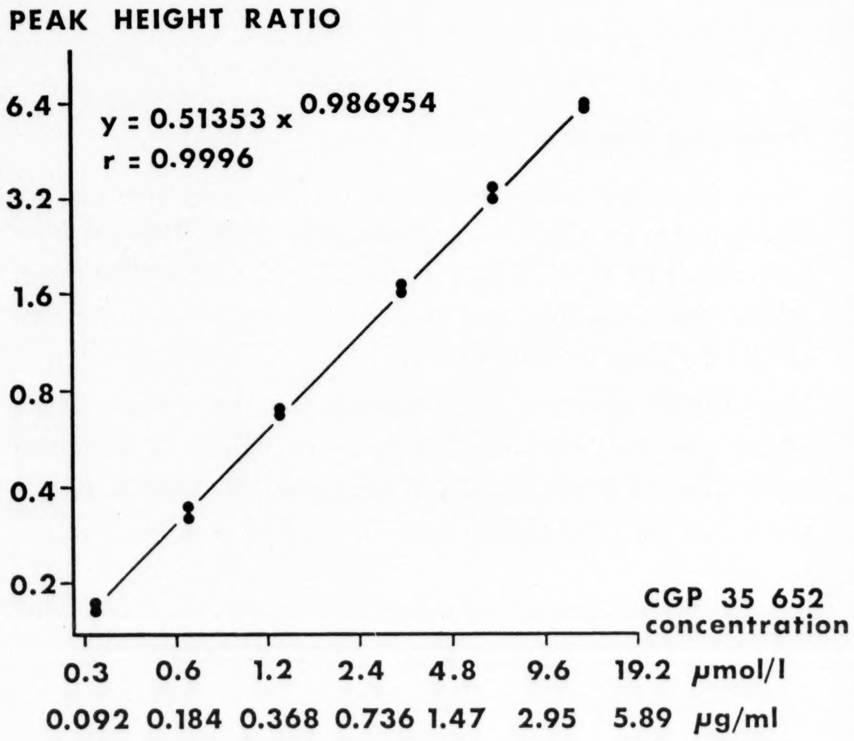

Fig. 4

Calibration curve of CGP 35 652 in plasma.

Table I. Within day precision of the assay and recovery of CGP 22 848 in spiked plasma samples. (To convert into μg/ml, multiply by 0.3208)

	0.078 μM added		0.212 μM added		1.50 μM added		3.12 μM added	
	Found μM	Recovery %	Found μM	Recovery %	Found μM	Recovery %	Found μM	Recovery %
	0.078	100.0	0.218	102.8	1.45	96.7	3.15	101.9
	0.075	96.2	0.243	114.6	1.51	100.7	3.21	102.9
	0.072	92.3	0.215	101.4	1.51	100.7	3.08	98.7
	0.069	88.5	0.218	102.8	1.50	100.0	3.10	99.4
	0.069	88.5	0.203	95.8	1.51	100.7	3.24	103.8
	0.078	100.0	0.228	107.5	1.51	100.7	3.10	99.4
Mean	0.074	94.3	0.221	104.2	1.50	99.9	3.15	100.9
C.V. (%)	5.6		6.1		1.6		2.1	
Mean recovery +/– SD (%)	99.9 +/– 5.4							

Recovery: (Added/Found) .100 %. S.D.: standard deviation. C.V.: (S.D./Mean) .100 %.

Table II. Within day precision of the assay and recovery of CGP 35 652 in spiked plasma samples. (To convert into μg/ml, multiply by 0.3068).

	0.326 μM added		1.69 μM added		2.61 μM added		6.52 μM added		13.0 μM added	
	Found μM	Recovery %	Found μM	Recovery %	Found μM	Recovery %	Found μM	Recovery %	Found μM	Recovery %
	0.332	101.8	1.72	101.8	2.62	100.4	6.68	102.5	13.0	100.0
	0.306	93.9	1.73	102.4	2.56	98.1	6.70	102.8	13.7	105.4
	0.326	100.0	1.69	100.0	2.92	111.9	6.53	100.2	13.5	103.8
	0.365	112.0	1.63	96.4	2.76	105.7	7.48	114.7	12.7	97.7
	0.365	112.0	1.62	95.9	2.86	109.6	6.84	104.9	12.7	97.7
	0.319	97.9	1.72	101.8	2.62	100.4	6.54	100.3	13.5	103.8
Mean	0.336	102.9	1.69	99.7	2.76	104.4	6.80	104.2	13.2	101.4
CV (%)	7.3		2.9		5.4		5.2		3.3	
Mean recovery +/– SD (%)	102.5 +/– 5.2									

Recovery: (Added/Found) .100 %. S.D.: standard deviation. C.V.: (S.D./Mean) .100 %.

Within Day Precision

The within day precision of the method was checked by determining six plasma samples spiked with different concentrations of CGP 22 848 B and CGP 35 652 A. The mean values, the recoveries and the coefficients of variation obtained are given in Tables I and II.

The limit of quantitation, established as the concentration which can be determined with a coefficient of variation lower than 10 % was 0.078 μM (25 ng/ml) for CGP 22 848 B and 0.326 μM (100 ng/ml) for CGP 35 652 A.

Conclusion

The HPLC assay described for simultaneous analysis of CGP 22 848 and its free carboxylic acid metabolite CGP 35 652 in plasma using CGP 17 582 as an internal standard permits the quantitation of plasma levels of CGP 22 848 and CGP 35 652 with convenient precision and accuracy.

Reference

[1] *R. D. McDowall, J. C. Pearce, G. S. Murkitt,* J. Pharm. Biomed. Anal., **4**, 3 (1986).

Received: June 28, 1987
Accepted: July 23, 1987
F

New HPLC-Chiral Stationary Phases for Enantiomeric Resolution of Sulfoxides and Selenoxides

G. Gargaro[1)]/F. Gasparrini[1)]/D. Misiti[1)]*/G. Palmieri[2)]/M. Pierini[1)]/C. Villani[1)]

[1)] Istituto di Chimica Organica, Facoltà di Farmacia, Università degli Studi "La Sapienza", P. le A. Moro 5, 00185 Roma, Italy
[2)] Dipartimento di Scienze Chimiche, Università degli Studi, Via S. Agostino 1, 62032 Camerino, Italy

Key Words

Column liquid chromatography
Optical resolution of sulfoxides and selenoxides
Chiral bonded phases

Summary

Enantiomers of several sulfoxides and some selenoxides can be easily separated by using a new chiral stationary phase (CSP-DACH-DNB) containing the 3,5-dinitrobenzoyl derivative of R,R-(−)1,2-diamino-cyclohexane as selector, covalently bonded to the siliceous matrix. The easy operative conditions and the high enantioselectivity values (α) allow a direct transfer of the analytical separations to a semi-preparative and preparative scale.

Introduction

General methods for the direct chromatographic separation of enantiomers are rapidly evolving, and significant progress in HPLC enantiomeric resolution has been achieved in recent years. The most promising methods are those based upon direct enantiomeric resolution by chiral stationary phases, and several interesting approaches to the design of sufficiently enantioselective chiral phases have been reported [1–6].

Such separation processes, whether those on an analytical scale or those on a semipreparative or preparative one, are widely applied to several areas of chemical, biochemical, pharmacological and medical research.

As regards the type of the stationary phase, we have previously reported [7–9] on the design and preparation, as well as have made a preliminary evaluation, of some chiral stationary phases (CSP) for the separation of enantiomers of many compounds of different classes.

Chiral sulfoxides and selenoxides were selected since they are gaining considerable importance in asymmetric organic synthesis [10]. Moreover, several drugs are chiral by virtue of their sulfoxide moiety and they metabolize *via* sulfoxide-reduction. Therefore, rapid and sensitive methods for the resolution and quantification of individual optically pure enantiomers, either on a preparative or analytical scale, are of great importance.

A general method for resolving sulfoxides and selenoxides efficiently and conveniently would facilitate a variety of stereochemical studies. It is very difficult, indeed, to realize diastereoisomeric derivatives through the sulfoxide or selenoxide functions.

Experimental

Chemicals

LiChrosorb Si100 (particle size 5μ), LiChroprep Si60, 15–25μ, and HPLC grade chromatography solvents were purchased from Merck (Darmstadt, FRG).

3-Glycidoxypropyl-trimethoxysilane was from Janssen (Belgium), R,R(−)1,2-diamino-cyclohexane (DACH) was from Strem Chemical Inc., the S,S(+)-enantiomer was prepared as reported [11] and the racemate was from Aldrich-Chemie (FRG).

3,5-Dinitrobenzoylchloride, triethylamine, THF and DMF were from Farmitalia Carlo Erba (Milano, Italy).

The racemic sulfoxides have been obtained following the described procedure [12–14]; the selenoxides, whether as a racemic mixture or as an enriched mixture in one of the two enantiomers, have been prepared as reported [15].

The remaining chemicals were reagent grade and used as purchased.

Chiral Stationary Phase

The chiral stationary phase (CSP-DACH-DNB) was prepared as shown in Scheme I by the same procedure previously described by us in the literature [9].

Apparatus and Chromatographic Procedures

a) Analytical liquid chromatography was performed using a Waters HPLC apparatus (Waters Assoc., Milford, MA, USA), consisting of two 510 Mod. Delivery systems, a U6K Mod. Injector, a 490 Mod. Programmable multiwavelength detector, a 410 Mod. Refractive index detector and a Waters™ 840 data and chromatography control station.

The column was stainless-steel (15cm × 4.0mm i.d.), packed with LiChrosorb Si100 DACH-DNB, 5μ, by following the slurry packing procedure: grafted silica (1.5g) was dispersed in CCl_4 (50ml) and then treated by ultra-

0009-5893/87 0505-05 $03.00/0

© 1987 Friedr. Vieweg & Sohn Verlagsgesellschaft mbH

sounds for 5′. The slurry thus obtained was packed with a Haskel pump Mod. DSTV-122, using n-hexane as the pressurizing solvent.

b) Semipreparative liquid chromatography was performed by using a Miniprep LC (Jobin Yvon, Longjumeau, France) equipped with a 2.0cm i.d. column and R.I. detector.

The preparative column was packed as follows: a suspension of the desired amount of packing material (LiChroprep Si60 DACH-DNB, 15–25μm, 45g in n-hexane/IPA, 80:20, v/v, 110ml) was maintained in an ultrasonic bath for 5min, poured into the column, axially compressed until a selected packing pressure was reached (12Bar), and finally conditioned by passing 2–3 times the interstitial volume of eluent (60ml). The same column can be used successfully for several injections and can be easily regenerated by passing 2–3 times the interstitial volume of 60ml.

In order to recover the packing material, the injector was removed from the column and the piston was allowed to push out the compressed adsorbent.

Generally, the loading capacities for 2cm i.d. columns lie in the range 10–500mg, depending on the enantioselectivity factor (α) of the separation.

Results and Discussion

The present paper addresses the utilization of new chiral stationary phases for the resolution of sulfoxides and selenoxides within the frame of our research on the HPLC enantiomeric resolution, and on the chemistry of sulfoxides [12–14].

The above-mentioned phases [9] have been obtained by first reacting the glycidoxypropyl silica gel (GPSG) with (R,R)(−) 1,2-diamino-cyclohexane, or, when necessary, with both the (S,S)-enantiomer or the racemate, and then by derivatizing the thus-prepared matrix with 3,5-dinitrobenzoyl chloride according to the following scheme:

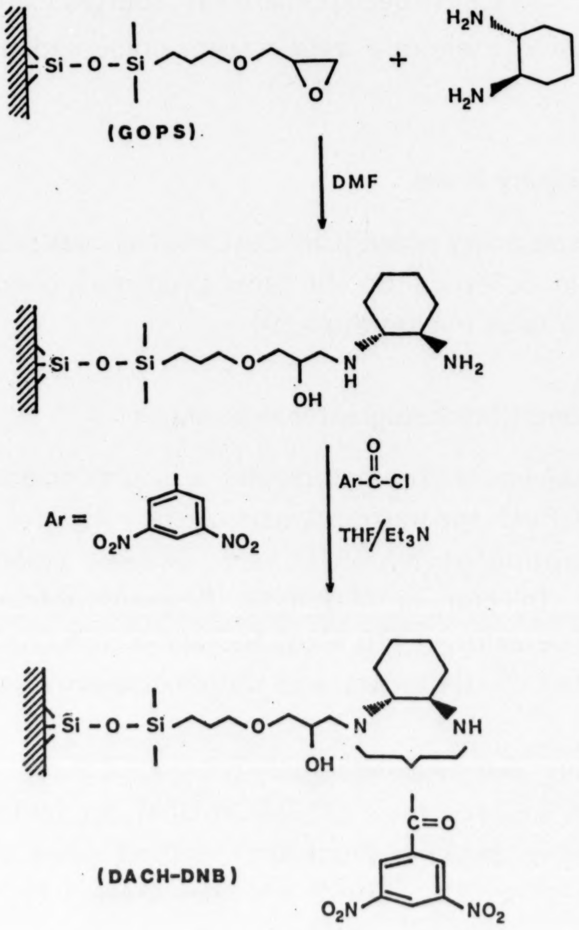

Scheme I

The results obtained are reported in Tables I, II and III; they show how easily racemic mixtures of sulfoxides (*1–20*) and selenoxides (*21–23*) can be resolved by using CSP-DACH-DNB, and they show that the enantioselectivity factor (α) closely depends on the composition of the mobile phase. For this reason different mobile phases such as n-hexane/CH_2Cl_2, n-hexane/dioxane, and n-hexane/IPA were utilized.

The best results in terms of the symmetry of the chromatographic peaks and of the enantioselectivity factor in the case of aryl-alkyl-sulfoxides were obtained by using the n-hexane/dioxane mixture. Figs. 1 and 2 show the results related to two different substrates.

The molecular recognition mechanism generally supposes the formation of at least three points of interaction, one of these (interactions) being dependent upon the stereochemistry of the solute enantiomer. In the present instance, they are essentially represented by the π-π interaction between the dinitrobenzoyl group (or groups) of the selector and the aromatic ring (or rings) of the selectand, by hydrogen bonds between the sulfoxide or selenoxide group and the –NH–DNB group of the selector, and finally by steric interactions.

In the case of the several alkyl-aryl-sulfoxides examined in the present paper, the influence of the type of substituent on the aromatic ring, together with the effect of the steric hindrance of the alkyl substituent, support the above hypothesis.

The results reported in Table I generally show an increased value of both the capacity factor (K′) and the enantioselectivity factor (α) for the sulfoxides bearing electron-drawing substituents on the aromatic part, in agreement with a stronger π-π interaction between the 3,5-dinitrobenzoyl group (or groups) of the selector and the π-basic part of the selectand.

Moreover, for the above-mentioned sulfoxides, the enantioselectivity factor (α) is closely related to the nature of the alkyl-group. In Fig. 3, indeed, we can observe that the α value goes up by increasing the steric hindrance of the *R*-group.

On this subject, it is noteworthy that compound *6* shows the highest value of α within the examined sulfoxides. This shift from the general trend can be justified by the double π-π interaction with the selector produced by the two aromatic systems present in the structure of the sulfoxide *6*. Thus, the increased retention of one of two enantiomers produces a high value of the α factor.

Further, in order to optimize the experimental conditions, the relation between the α value and the capacity factor K′ was analyzed. The results of this analysis are shown in Fig. 4. The reported graph clearly shows no changes for the α up to a value of K′ of about 30.

The above-reported analytical data were obtained by using an analytical column of 4.0mm i.d. and 15cm length. Such a column allows the separation of samples in a range between milligrams and nanograms, whereas larger amounts of sample need semi-preparative or preparative columns. The good analytical results obtained can be easily transferred to semi-preparative or preparative scale.

Table I. Resolution of sulfoxides.

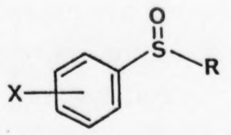

Compound					
R	X	K'	α	% IPA % Dioxane % CH_2Cl_2 (in hexane)	T (°C)
1) CH_3	H	9.32	1.10	20	25
		20.00	1.21	30	25
		19.88	1.06	50	25
2) $(CH_3)_2CH$	H	4.38	1.25	20	25
		8.50	1.38	30	25
		12.55	1.16	50	25
3) cyclohexyl	H	4.91	1.28	20	25
		10.75	1.36	30	25
		11.00	1.16	50	25
4) $n-C_{10}H_{21}$	H	3.71	1.22	20	25
		6.56	1.39	30	25
		5.78	1.19	50	25
5) $n-C_{18}H_{37}$	H	3.09	1.24	20	25
		5.00	1.45	30	25
		4.11	1.22	50	25
6) $C_6H_5-CH_2$	H	8.74	1.57	20	25
		14.40	1.82	30	25
		10.55	1.42	50	25
7) $C_6H_5(CH_2)_2$	H	5.89	1.21	20	25
		9.00	1.33	30	25
		8.78	1.16	50	25
8) $C_6H_5-S-CH_2$	H	9.72	1.16	20	25
		13.37	1.27	30	25
		8.67	1.11	50	25
9) CH_3	$p-CH_3O$	18.12	1.10	20	25
		39.12	1.23	30	25
		37.89	1.06	50	25
10) CH_3	$o-CH_3O$	11.26	1.28	20	25
		28.50	1.40	30	25
		21.67	1.21	50	25
11) CH_3	$m-CH_3O$	13.21	1.08	20	25
		22.87	1.22	30	25
		29.55	1.04	50	25
12) CH_3	$p-CH_3$	9.18	1.20	20	25
		18.75	1.35	30	25
		25.44	1.10	50	25
13) CH_3	$p-CH_3COO$	26.38	1.00	20	25
		22.25	1.07	30	50
		54.50	1.00	50	25
14) CH_3	$p-CH_3OCO$	14.19	1.07	20	25
		12.00	1.19	30	25
		20.78	1.04	50	25
15) CH_3	$p-Cl$	6.62	1.05	20	25
		7.00	1.18	30	25
		15.11	1.03	50	25
16) CH_3-CH_2	$p-NO_2$	8.00	1.07	20	25
		6.25	1.14	30	25
		14.50	1.03	50	25
17) CH_3	$X-C_6H_4$ = 2-naphthyl	25.98	1.04	10	50
		20.50	1.15	30	25
		28.75	1.03	50	25
18) $p-CH_3-C_6H_4-SCH_2$	$p-CH_3$	11.94	1.25	20	25
		19.63	1.32	30	25
		10.67	1.17	50	25

An example of a quite difficult semi-preparative separation is reported in Fig. 5. Racemic phenyl-benzyl-sulfoxide *6* with an α value of 1.57 (elution with n-hexane/*i*-propanol, 80:20 v/v) was separated by an axially-compressed column (2.0cm i.d., 21cm length), packed with LiChroprep Si60 DACH-DNB 15–25μ (45g), and prepared according to the aforementioned Scheme I.

The load was acceptable and the e.e. of the separated fractions was quite high; further, better results for these two parameters can be achieved by using the recycle technique.

Conclusions

The ability to resolve a wide selection of sulfoxides and selenoxides upon CSP, such as DACH-DNB, is very helpful in asymmetric synthesis and in pharmaceutical and pharmacological research. The present approach represents a quick and reliable method for the purification of small amounts of optically high pure samples.

Table II. Resolution of sulfoxides.

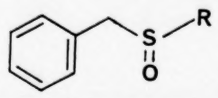

	R	K'	α	% IPA % Dioxane (in hexane)	T (°C)
19)	$CH_2CH{=}CH_2$	6.01	1.07	20	25
		14.75	1.08	30	25
20)	$(CH_2)_3S{-}C_6H_5$	10.12	1.03	20	25
		16.54	1.06	30	25

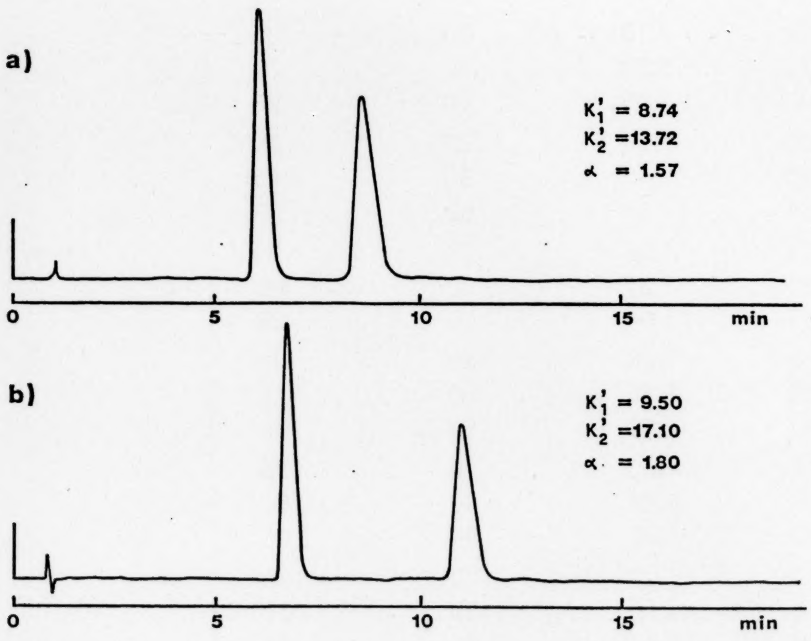

Fig. 1

Resolution of racemic benzyl-phenyl-sulfoxide (*6*).

Conditions: a) flow rate: 2ml/min; eluent: n-hexane/*i*-propanol, 80:20, v/v; U.V. detector: 254nm; T = 25°C.
b) flow rate: 2ml/min; eluent: n-hexane/dioxane, 60:40, v/v; U.V. detector: 254nm; T = 25°C.

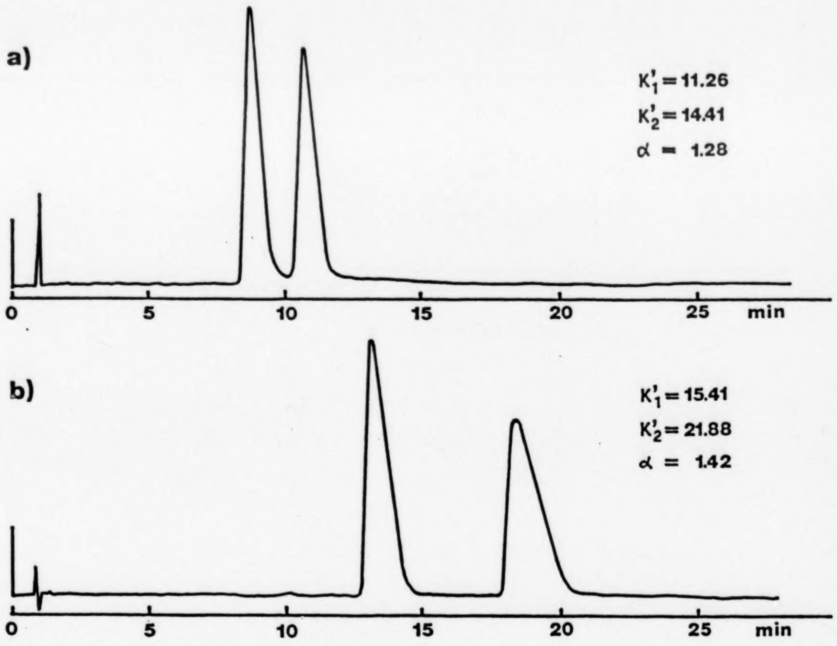

Fig. 2

Resolution of racemic 2-methoxyphenyl-methyl-sulfoxide (*10*).

Conditions: a) flow rate: 2ml/min; eluent: n-hexane/*i*-propanol, 80:20, v/v; U.V. detector: 254nm; T = 25°C.
b) flow rate: 2ml/min; eluent: n-hexane/dioxane, 60:40, v/v; U.V. detector: 254nm; T = 25°C.

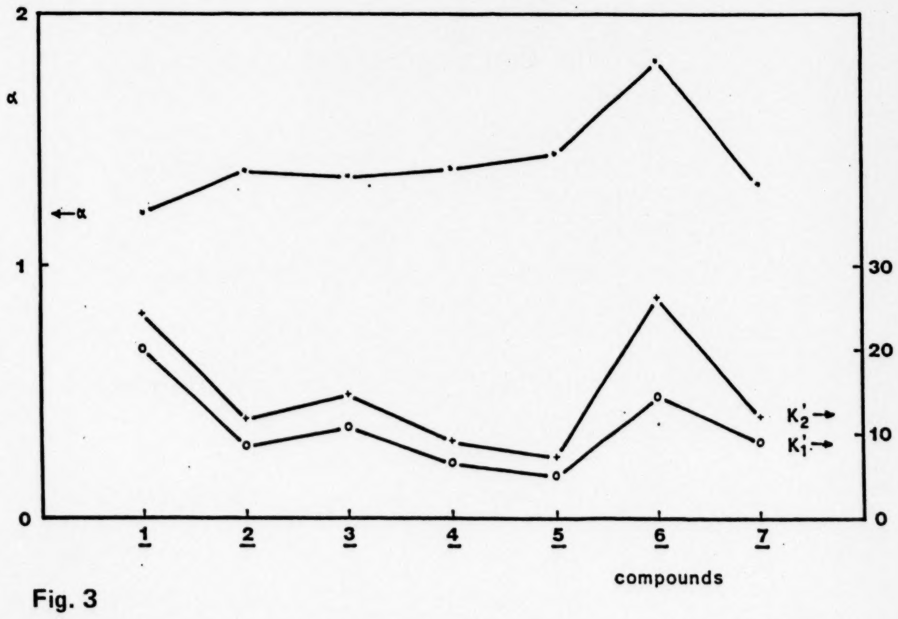

Fig. 3

Relation between enantioselectivity (α) or capacity factors (K'_1 and K'_2) and steric hindrance of the alkyl group (R) for a series of aryl-alkyl-sulfoxides (ArSOR) (Eluent: n-hexane/dioxane, 70/30, v/v; see table I).

Table III. Resolution of selenoxides.

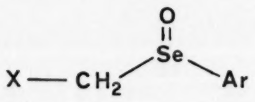

	Compound		K'	α	IPA/CH_2Cl_2/Hexane (v/v/v)	T (°C)
	Ar	X				
21)	C_6H_5	C_6H_5	6.83	1.72	20/20/60	25
22)	C_6H_5	$C(C_6H_5)_2OCH_3$	15.6	1.09	6/14/80	25
23)	$o{-}CH_3OC_6H_4$	$C(C_6H_5)_2OCH_3$	17.9	1.19	6/14/80	25

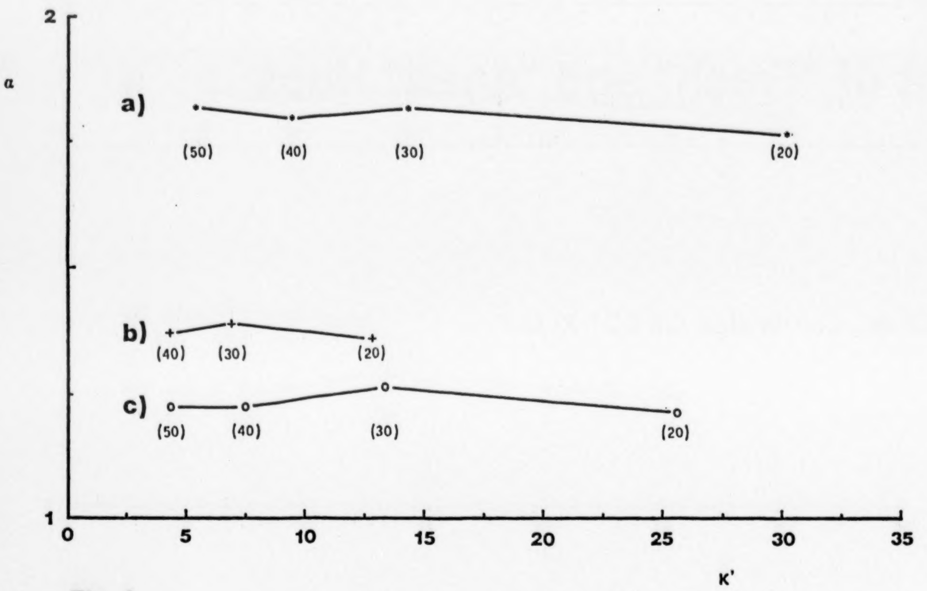

Fig. 4

Relation between enantioselectivity (α) and capacity factor (K') for: a) benzyl-phenyl-sulfoxide (*6*); b) n-decyl-phenyl-sulfoxide (*4*); c) phenylthiomethyl-methyl-sulfoxide (*8*).

Conditions: flow rate: 2ml/min; eluent: Figures in brackets represent % dioxane in n-hexane; U.V. detector: 254nm.

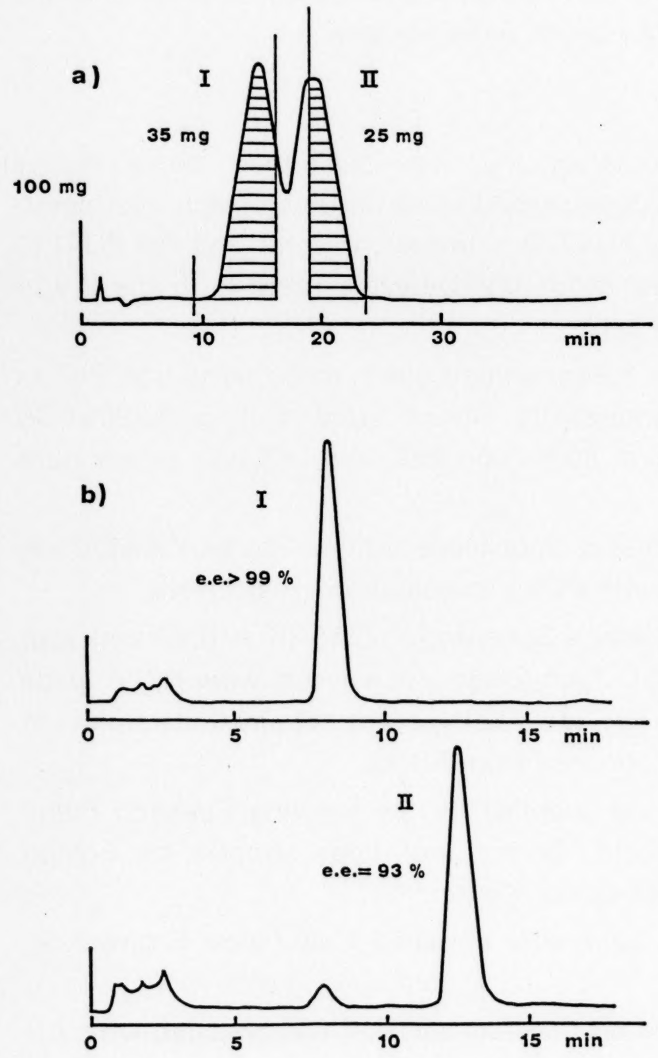

Fig. 5

a) Preparative separation of a racemic benzyl-phenyl-sulfoxide (*6*). (α = 1.57)

Column: 210 X 20mm, LiChroprep Si60 DACH-DNB, 15–25μm, 45g (axial compression)

Conditions: flow rate: 27ml/min; eluent: n-hexane/*i*-propanol, 80:20, v/v; detector: R.I.

b) Purity control of fractions.

Column: 150 X 4mm, LiChrosorb Si100 DACH-DNB, 5μm,

Conditions: flow rate: 2.0ml/min; eluent: n-hexane/*i*-propanol, 80:20, v/v; U.V. detector: 254nm

Indeed, the chiral column not only provides an initial means for resolving such compounds, but also provides a micro method for following rates of racemization.

An additional advantage is represented by the fact that it is possible to prepare columns with the two trans-enantiomers and with the racemic form. This possibility allows the discrimination of chiral compounds from achiral ones in complex mixtures.

It is noteworthy that the above-mentioned phase is easy to prepare, reproducible and quite cheap; it is also absolutely stable and no racemization or hydrolysis, also in polar solvents, was observed. Finally, it can be utilized to resolve (on a preparative scale) mixtures of enantiomers obtained during organic syntheses.

Acknowledgements

Work supported by M.P.I. Italy and by the National Research Council (CNR, Italy), under the "Progetto Finalizzato Chimica Fine e Secondaria". The authors wish to thank Prof. M. Tiecco, University of Perugia, Italy, for supplying the selenoxides described in the present paper.

References

[1] *W. H. Pirkle, J. M. Finn*, in "Asymmetric Synthesis" (*J. D. Morrison*, ed.), Academic Press, New York, 1983, p. 87–124.
[2] *V. A. Davankov, A. A. Kurganov, A. S. Bochkov*, Advan. Chromatogr. **22**, 71 (1984).
[3] *S. Cacchi, G. Gargaro, F. Gasparrini, D. Misiti*, Chimica Oggi, 1984(12), 11.
[4] *E. Gil-Av*, in "The Science of Chromatography" (*F. Bruner*, ed.), J. Chromatography Library, Elsevier, Amsterdam, vol. 31, p. 111–130 (1985).
[5] *R. Dennis*, Pharmacy International, 1986(10), 246.
[6] *D. W. Armstrong*, Analytical Chemistry **59**, 84A (1987).
[7] *G. Gargaro, F. Gasparrini, D. Misiti, C. Villani*, Italian-Israeli Symposium on "Modern Trends in Organic Chemistry", Rehovot, Israel, 1985.
[8] *G. Gargaro, F. Gasparrini, D. Misiti, C. Villani*, 10th Symposium on Column Liquid Chromatography, San Francisco, California 1986.
[9] *F. Gasparrini, D. Misiti, G. Palmieri, C. Villani, M. Sinibaldi*, J. Am. Chem. Soc., sent for publication.
[10] *M. Madesclaire*, Tetrahedron, **42**, 5459, 1986.
[11] *F. Galsbol, P. Steembol, B. S. Sorensen*, Acta Chem. Scand., **26**, 3605 (1972).
[12] *F. Gasparrini, M. Giovannoli, D. Misiti, G. Natile, G. Palmieri*, Tetrahedron, **39**, 3181 (1983).
[13] *F. Gasparrini, M. Giovannoli, D. Misiti, G. Natile, G. Palmieri*, Tetrahedron, **40**, 165 (1984).
[14] *F. Gasparrini, M. Giovannoli, L. Maresca, G. Natile, G. Palmieri*, Synth. Commun. **14**, 1111 (1984).
[15] *M. Tiecco, M. Tingoli, L. Testaferri, D. Bartoli*, Tetrahedron Lett., **28**, 3849 (1987).

Received: Aug. 3, 1987
Accepted: Sep. 10, 1987
F

Fast LC Analysis of the α-Acid Content of "Fresh" and "Aged" Hops

J. T. Hann

Philips Analytical, Applications Laboratory, Pye Unicam, York Street, Cambridge, CB1 2PX, U.K.

Key Words

Liquid chromatography
Conductivity
Hops
Humulones
Lupulones

Summary

A quaternary mobile phase was optimized in conjunction with Fast LC techniques to separate α and β acids extracted from hops in less than 4 minutes. The method is proposed for automated analysis of large numbers of hop samples and its usefulness is demonstrated by comparing α-acid levels obtained by liquid chromatographic and conductometric techniques. Both assays provided similar values for "fresh" hops but in "aged" hops liquid chromatography showed a lower level of α-acids.

Introduction

The usefulness of hops in brewing is principally a consequence of their α-acid content. During the brewing process α-acid are isomerized to iso-α-acids which provide the subtle bitter taste.

Obviously, high α-acid content hops are useful to both the harvester and brewer and a quick, easy means of assay to assess the quality of hops is required. A range of non-specific methods have been developed including polarimetry [1] and spectrophotometry [2], but conductometric methods [3] have become generally accepted.

In recent years the brewing industry has begun to use extracted hop oils in preference to raw hops and interest has focussed on the relative contribution to quality and taste of the bitter components such as α-acids, β-acids and other minor constituents. Non specific measurements of quality such as the Lead Conductance Value (LCV) [4] can be replaced by HPLC (LC) to give specific information about the age and condition of hops and the relative contribution of important bitter components. In addition the utilization of α-acids in brewing processes can be followed and optimized for economy and taste.

At harvest, many thousands of samples must be assayed quickly and accurately. Methods based on binary mobile phases [5–7] in LC do not always offer sufficient selectivity to separate closely related compounds in a short time and consequently analysis times are long.

Materials

Liquid chromatography was performed on a Philips PU4100/42 Quaternary Liquid Chromatograph incorporating an oven, PU4700 automatic injector and the PU4110 Variable Wavelength UV Detector fitted with the 2.5 μl Fast LC flow cell.

Conductance measurements were made using the Philips PW9527 Conductivity Meter fitted with a PW9551/60 glass Platinum immersion cell with PT100 temperature sensor.

pH measurements were made using a Philips PW9420 pH meter fitted with a CE1 combination pH electrode.

The column was a Spherisorb-3-ODS (6 X 0.46 cm) supplied by HPLC Technology. All solvents were HPLC grade from BDH. The ion pairing agent tetramethylammonium chloride was obtained from Fisons.

Pure α-acid was supplied by the Brewing Research Foundation, Nutfield, Surrey and hops samples by English Hops, Paddock Wood, Kent.

The ceramic balls were obtained from Pascal Engineering, Crawley.

The 4 % W/V lead acetate solution was prepared with AR grade crystals in methanol with 5 drops of glacial acetic acid in each 100 ml. The solution was standardized against a methanolic solution of 0.1 N Sulphuric Acid (4 ml in 40 ml methanol). All reagents were obtained from BDH.

Methods

Lead Conductance. Almost 100 years ago hop bitter compounds were divided into a lead precipitable fraction (α-acids) and another fraction (β-acids) [8]. This separation forms the basis of the accepted method of analysis of

0009-5893/87 0510-03 $03.00/0

© 1987 Friedr. Vieweg & Sohn Verlagsgesellschaft mbH

α-acids. The method is not specific for α-acids and results are quoted as lead conductance value for hops.

The method described here is consistent with the Hop Marketing Board's Laboratory [4] 15 g of thoroughly broken hops were shaken vigourously for six minutes in a 750 ml polythene bottle with three ceramic balls (25 mm diam.) and 100 ml toluene. The extract was decanted and filtered before a 10 ml aliquot was diluted with 40 ml methanol. The conductivity of this solution was monitored during successive 0.2 ml additions of the 4 % lead acetate solution. The conductivity readings were plotted graphically as ordinates against the volume of lead acetate solution as abscissa (Fig. 1). The end point was taken as the intercept of the initial static and final rising trend.

Liquid Chromatography. A quaternary mobile phase was developed in conjunction with Fast LC techniques to separate α and β acids into five peaks in less than four minutes.

Fast LC is a technique developed to increase sample turnover in automated analysis. Short, efficient columns packed with 3 μm material are coupled to instruments optimized for low dispersion (low dead volume, low flow cell volume and fast detector response times) to provide resolution of 5–10 components in 3–4 minutes.

A 1 ml aliquot of the extract obtained for lead conductance measurement was made up to 25 ml with methanol. 5 μl of this solution was injected into the chromatograph.

The mobile phase was 57 % 50 mM phosphate buffer at pH 6.5 containing 0.03 M tetramethylammonium chloride, 15 % methanol, 18 % Acetonitrile and 10 % tetrahydrofuran.

This quaternary mixture was delivered across the column at 2.5 ml/min with an oven temperature of 40 °C. Detection was at 330 nm with a 0.12 second time constant.

Cohumulone was resolved from the co-eluting humulone and adhumulone (Fig. 2). The response of these compounds was assumed equal and total area was plotted against an abscissa adjusted to give % weight for weight α acid in hop sample (Fig. 3).

Estimation of α-Acids in Hops. Six varieties of hops from the 1986 harvest were assayed by lead conductance and LC in June 1987. At the time of assay six identical hop samples

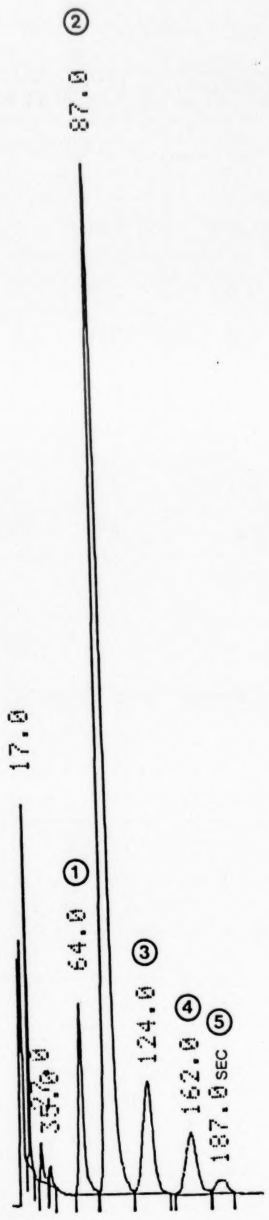

Fig. 2

Chromatogram showing separation of α and β acids. **1** = Cohumulone, **2** = Humulone/Adhumulone, **3** = Colupolone, **4** = Lupulone, **5** = Adlupulone.
Column: Spherisorb 30DS (6 X 0.46 cm)
Mobile Phase: 57 % 50 mM phosphate buffer at pH 6.5 containing 0.03 M tetramethylammonium chloride, 15 % methanol, 18 % acetonitrile and 10 % tetrahydrofuran.
Flow Rate: 2.5 ml/min.
Detection: 330 nm.

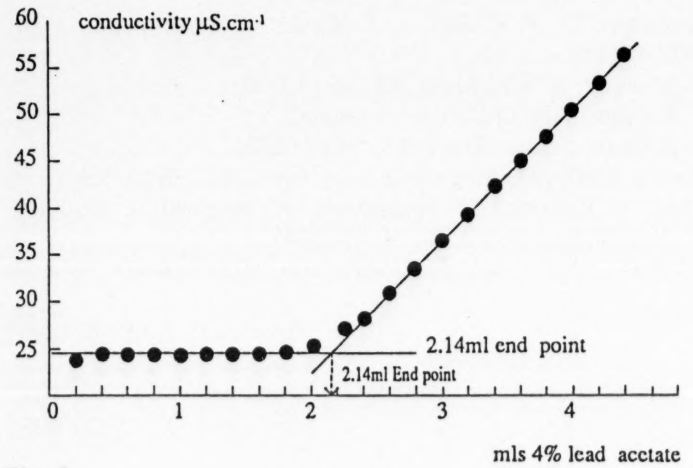

Fig. 1
Titration curve for sample of hops.

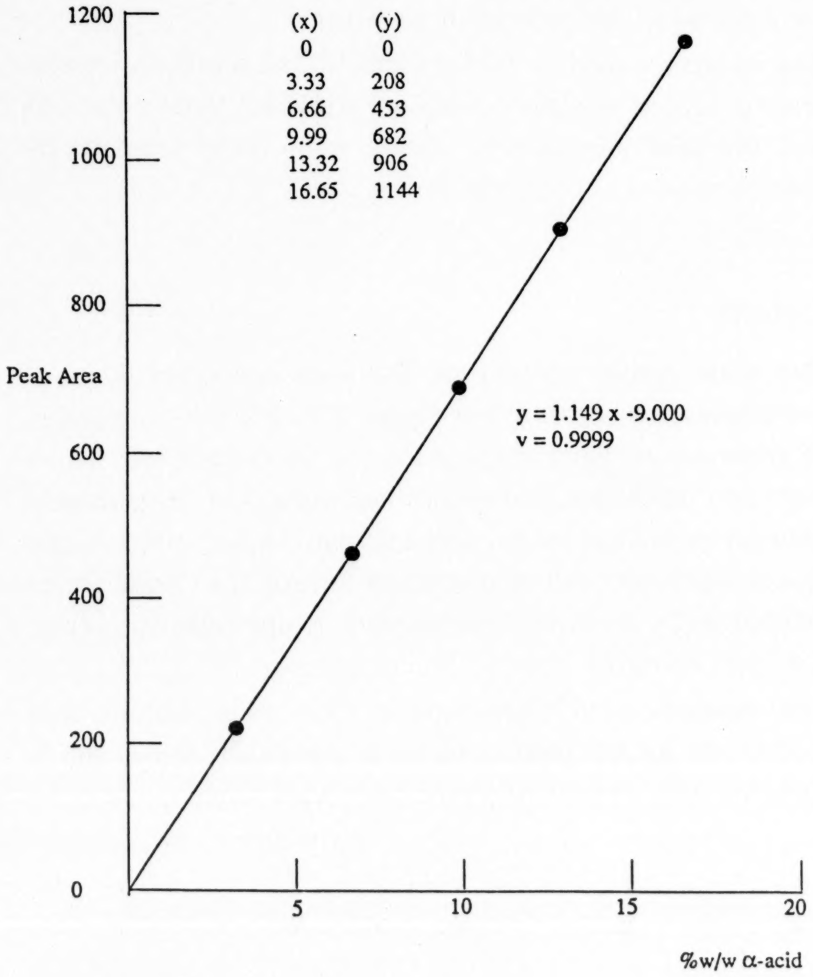

Fig. 3
LC Calibration Curve for Combined α-acid Peaks.

Table I. Comparison of α-acid Content of "Fresh" and "Aged" Hops using Liquid Chromatography.

Hop Variety	% W/W α-acid Content						% Cohumulone	
	Cohumulone		Adhumulone Humulone		Total			
	"Fresh"	"Aged"	"Fresh"	"Aged"	"Fresh"	"Aged"	"Fresh"	"Aged"
Challenger	1.0	0.8	3.4	3.1	4.4	3.9	22.7	20.5
North Down	1.5	1.3	3.1	3.0	4.6	4.3	32.6	30.2
Yeoman	2.5	1.7	6.2	4.4	8.7	6.1	28.7	27.9
Target	2.6	1.7	4.9	3.5	7.5	5.2	34.7	32.7
Fuggle	1.0	0.5	2.4	1.4	3.4	1.9	29.4	26.3
Goldings	1.6	1.0	3.9	2.6	5.5	3.6	29.1	27.8

Table II. Comparison of α-acid Content of "Fresh" and "Aged" Hops using Lead Conductance Value.

Hop Variety	% W/W α-acid Content	
	"Fresh"	"Aged"
Challenger	4.7	3.9
North Down	4.5	4.2
Yeoman	8.9	6.7
Target	7.8	6.1
Fuggle	3.4	2.5
Goldings	5.4	3.9

were placed under Infra-Red irradiation (8 hours per day) for a period of ten days prior to assay.

The results are given in Tables I and II. The liquid chromatographic results are the average of triplicate determinations and the lead conductance reults were taken from single determinations of each hop variety.

Results

The total α-acid content of the hops estimated by both techniques was within the range 3.4–8.9 %. Comparison of these results were made using the Students t test. There was no significant difference between the total α-acid content estimated by LC and LCV on "fresh" hops. There was a significant fall in α-acid content of the "aged" hops estimated by both techniques with a significantly greater fall revealed by LC than LCV.

The resolution of Cohumulone from Adhumulone and Humulone by LC demonstrated a significant fall in the % Cohumulone content when the hops were "aged".

Conclusions

The estimation of α-acid content of hops using lead conductance remains a viable method provided the hops are ideally stored. However, hops exposed to raised temperature and possibly humidity will lose α-acids and lead conductance values will no longer reflect the true level. Liquid chromatography is a more specific means of assay and not only reflects the true α-acid content but also provides information about the relative concentration of individual α-acids. The relative Cohumulone content was reduced by the ageing process in this experiment showing this α-acid to be less stable than Humulone and/or Adhumulone.

Fast LC techniques can be applied to the separation of the α and β acids to give an assay which involves less operations, increases sample turnover and is less subjective than lead conductance methods.

Further Work

The change in α-acid content may be more significant immediately following harvest. Conductivity and liquid chromatography will be applied to fresh hops on a weekly basis immediately following harvest. The absolute and relative concentrations of α and β acids will be compared and the merits of HPLC and LCV assessed.

References

[1] *W. Gough,* J. Inst. Brew. **62,** 9 (1956).
[2] *G. Alderton, G. F. Bailey, J. C. Lewis, F. Stitt,* Anal. Chem. **26,** 983 (1954).
[3] *G. A. Howard,* J. Inst. Brew. **77,** 18 (1971).
[4] *G. K. Buckee,* Private Communication.
[5] *G. K. Buckee,* J. Inst. Brew. **91,** 143 (1985).
[6] *N. Van de Velde, M. Verzele,* J. Inst. Brew. **92,** 584 (1986).
[7] *M. One, Y. Kakudo, Y. Yamamoto, K. Nagami, J. Kumada,* Amer. Soc. Brew. Chem. **42,** 167 (1984).
[8] *F. Hayduck,* Wochenschrift für Brauerei, p937 (1888).

Received: July 10, 1987
Revised manuscript
received: Oct. 5, 1987
Accepted: Oct. 13, 1987
F

The System Evaluation Strategy in Practice, Allowing Direct Estimation of Peak Heights and Limits of Detection in HPLC

Pamela J. Naish[1] * / M. J. Keesman[2]

[1] Philips Analytical, Cambridge
[2] Philips Research Laboratories, Eindhoven, Netherlands

Key Words

System evaluation strategy
Peak heights
Peak dilutions
Limits of detection

Summary

The novel system evaluation strategy recently developed describes an HPLC system in terms of two parameters, that ideally are independent of the test conditions. These describe the peak height response, or dilution, occurring in the column and the system. Limits of detection (LOD's) can thus also be calculated. System parameters, (e.g. cell length, external dispersion), chromatographic parameters (e.g. retention, column length, flow-rate), and sample parameters (e.g. sample volume & absorptivity), are all included. Consequently this approach is applicable to the chromatographer and LC system designer alike.

The system evaluation strategy was previously demonstrated under typical chromatographic conditions, on two HPLC systems, and systematic changes were studied. In principle this is applicable to any compound under any chromatographic conditions, on any column. This is now to be investigated further, under a wide range of conditions, and applied to the calculation of an LOD in a real LC analysis.

Introduction

The system evaluation strategy [1] was designed to allow prediction of the peak height and peak dilution, and thus the sensitivity and limit of detection, combining system, chromatographic and sample parameters. It was originally conceived to allow a systematic understanding of the combined effects of external dispersion and cell dimensions, on the chromatographic result, to aid LC system design. However, it has real potential in the full optimization of LC analyses, when matching the sensitivity required with that achievable, in manual or automated running.

This approach regards the dilution that occurs during chromatography as composed of dilution within the column and within the system: analogous to the total dispersion being composed of column and external dispersions. Thus simple expressions for the apparent dilution (A'/p) were derived [1], that have two terms relating to the column and external dispersions, (eq. (1));

$$\left(\frac{A'}{p}\right)^2 = \alpha \frac{t_r^2}{L} + \beta, \qquad (1)$$

where $\alpha = \dfrac{v^2 H \alpha'}{\mathrm{Vinj}^2}$ and $\beta = \dfrac{v^2 \beta'}{\mathrm{Vinj}^2}$

$$\text{i.e.} \quad \left(\frac{A'}{p}\right)^2 = \frac{v^2 H \alpha'}{\mathrm{Vinj}^2}\,\frac{t_r^2}{L} + \frac{v^2 \beta'}{\mathrm{Vinj}^2} \qquad (2)$$

(where A' = absorbance of each component per cm of pathlength at original concentrations, p = peak-height (A.U.) of each peak in the chromatogram, v = flow-rate (µl/sec), H = plate-height (mm), Vinj = volume of injection (µl), t_r = retention time (sec), L = column length, and α' and β' are the system parameters).

Now a system can be evaluated in terms of α' and β', from a single chromatographic run and thus dilutions or peak-heights can be calculated for the conditions of interest.

This theory [1] also allows calculation of limits of detection (LOD), by comparison of the peak-height p, with the noise-level n, (eq. (3)).

$$\mathrm{LOD}^2 = \gamma \frac{t_r^2}{L} + \phi \qquad (3)$$

where $\gamma = \dfrac{9n^2 H v^2 \alpha'}{a^2}$ and $\phi = \dfrac{9n^2 \cdot v^2 \beta'}{a^2}$

(and a = component absorptivity.)

Previously [1], variations in 1. the column plate height from changes in column lengths and the size of packing, 2. sample volumes, and 3. column dimensions were studied. This showed that α' was independent of H, Vinj, column length and diameter, and system dispersion, and that β' was independent of column dimensions, but dependent on the system dispersion. (The errors on β' values were greater than α' due to the extrapolation, as β' is derived from the intercept.) Calculated and empirical LOD values on a test compound agreed well.

0009-5893/87 0513-04 $03.00/0

© 1987 Friedr. Vieweg & Sohn Verlagsgesellschaft mbH

As the eluent viscosity affects H, (column plate-count) [2], through the diffusion coefficient, changes in eluents and temperature should affect α, but should leave α' unaffected. H is also a function of flow-rate [3], so similarly α should be affected, and α' should remain unaffected. As σ_{EXT} is composed of diffusion components, σ_{EXT} can be predicted to be affected by solvent viscosity, and thus affected by eluent and temperature. The dependence of σ_{EXT} on flow-rate is already well-known [4]. Approximate values of H from FWHH (full width half-height) measurements of the last peak ($k' \sim 10$) were employed here.

In this paper, the effects of typical chromatographic variations are investigated, viz. eluent, isoeluotropic solvents and temperature; the effects on α' and β' being studied.

The calculated and experimental LOD in a real analysis, (for salbutamol) is compared.

Experimental

Equipment

The HPLC system was a PU4100 composed of a 4 solvent-mixing system, column oven, and variable-wavelength detector fitted with the 8μl analytical flow-cell and a 7125 Rheodyne valve. The columns used were 10 and 22 cm long by 4.6 mm i.d. cartridges packed with 5μm RP-18 packing.

Data handling was achieved on a PU4810 integrator providing peak-height information. All equipment from Philips Analytical, Cambridge, UK.

Chromatography

The sample (working mixture) contained acetophenone (19.68μg/ml), propiophenone (19.84μg/ml), butyrophenone (34.64μg/ml), valerophenone (49.52μg/ml), hexanophenone (58.00μg/ml), octanophenone (80.00μg/ml), in methanol : acetonitrile : water 28 : 22 : 50. Detection was at 243 nm, response time 0.5 sec. Eluents were acetonitrile/water 62 : 38, 58 : 42, 54 : 46, methanol/water 72 : 28, THF/water 44 : 56. Temperatures used were 35, 40, and 45°C. Flow-rates employed were 2, 1.5, 0.8 ml/min.

Nominal values of the column efficiencies were taken from the FWHH measurements of the octanophenone peak, ($k' \sim 10$), where $\sigma_{COL} \gg \sigma_{EXT}$. The sample was characterized by measuring the absorbances of six individual working solutions, with the same concentrations as each component in the working mixture. (All measurements on a Philips PU8800 UV spectrophotometer in 0.2 cm cell at 243 nm providing the A$'$ values.)

The sample loop was calibrated using accurate injection volumes (5μl to 35μl) of the working mixture and comparing the peak areas with those from the sample loop (nominally 20μl). This gave Vinj = 27.0μl (RSD = 0.81%).

For the LOD determination of salbutamol, the sample contained 21.1 mg salbutamol sulphate in 100 ml water. Chromatographic conditions [5] were propan-2-ol/acetate buffer (0.015M Ammonium acetate, pH 4.5 adjusted with glacial acetic acid) 8.0 : 92.0, flow 2 ml/min, at 35°C on 5μm Hypersil Cyano (20 cm × 4.6 mm i.d.), with detection at λ276 nm, response time 0.5 sec, and sample volume 27.0μl. Diluted sample contained 570 ng/ml salbutamol sulphate in water.

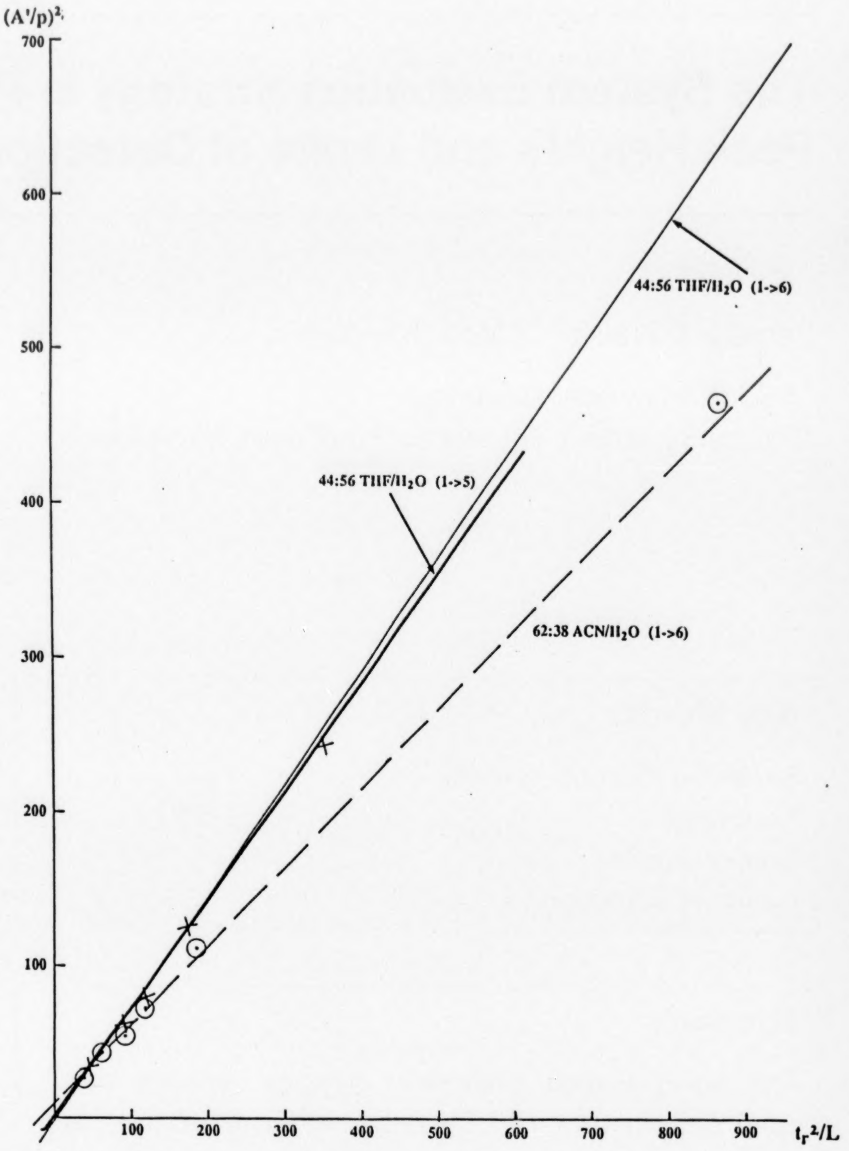

Fig. 1
Correlation of $(A'/p)^2$ and (t_r^2/L)
for 44 : 56 THF/Water, peaks 1 → 6 and 1 → 5,
for 62 : 38 ACN/Water, peaks 1 → 6.

Results and Discussion

For each set of conditions, comparisons were made with the reference conditions of acetonitrile : water 62 : 38, flow-rate of 2 ml/min ($v = 33.33\mu l/sec$), at 40°C. The $(A'/p)^2$ and t_r^2/L values were correlated for each run, and the values for α and β, & the correlation coefficients, r$'$, listed (Table Ia–d) along with the H values (from FWHH of final peak), and α/H or α'/H values.

The variations in α and α/H are listed as percentages in Table II, for changes in eluent, isoeluotropic solvents and temperature. Although the changes in α and H are highly significant, changes in α/H and thus α' are much reduced and will be close to the experimental error. In all runs variation in β values are much greater, and although the errors here will be greater (as intercept values from extrapolations), previous [1] β values from repeat determinations, (from different columns in same system for ex-

Table I. Listing of system evaluation parameters (α, β), correlation coefficient r′, plate-height H, and α/H, with eluent, isoeluotropic solvent, temperature and flow-rate changes

	Temp. °C	Flow μl/sec	α	β	r′	H mm	α/H
(a) Eluent							
62:38 ACN:H_2O	40	33.33	0.563	7.38	0.99994	0.0129	43.6
58:42 ACN:H_2O	40	33.33	0.577	5.88	0.99995	0.0131	44.1
54:46 ACN:H_2O	40	33.33	0.584	2.25	0.99993	0.0133	43.8
(b) Isoeluotropic solvents							
62:38 ACN:H_2O	40	33.33	0.563	7.38	0.99994	0.0129	43.6
44:56 THF:H_2O	40	33.33	0.728	− 1.71*	0.99994	0.0172	42.3
72:28** MeOH:H_2O	40	33.33	0.613	8.98	0.99994	0.0139	44.1
(c) Temperature							
62:38 ACN:H_2O	35	33.33	0.578	9.12	0.99994	0.0133	43.5
62:38 ACN:H_2O	40	33.33	0.563	7.38	0.99994	0.0129	43.6
62:38 ACN:H_2O	45	33.33	0.555	6.26	0.99995	0.0129	43.0
(d) Flow-rate							α/v^2H
62:38 ACN:H_2O	40	33.33	0.563	7.38	0.99994	0.0129	0.0393
62:38 ACN:H_2O	40	25.0	0.305	8.83	0.99992	0.0128	0.0380
62:38 ACN:H_2O	40	13.3	0.095	0.838	0.99987	0.0139	0.0385

* Correlation gives negative intercept
** Only one run available.

Table II. Listing of percentage changes in α and α/H, with change in k′, caused by eluent, isoeluotropic solvents, and temperature effects.

Variation in	α	k′	α/H
(a) Eluent	3.6%	0.4–8.1 to 0.7–16.3	0.9%
(b) Isoeluotropic solvents	26%	0.4–8.1 ACN 0.7–8.7 THF 0.5–9.9 MeOH	4.2%
(c) Temperature	4.1%	0.4–8.3 35°C 0.4–7.6 45°C	1.4%

ample), showed less variation. One negative intercept was observed, for the THF:water run, but this correlation (see Fig. 1), shows the extent of the extrapolation, and the consequent large effect of the last peak. Also the relative sizes of β and $(A'/p)^2$ values, only allow a small error in the slope before β becomes negative. The large value of H observed here, due to the high eluent viscosity, causes the increased α, and imparts a high gradient to this correlation increasing the effects of errors. If this is not due to errors this negative intercept indicates a problem with our simple model (see below).

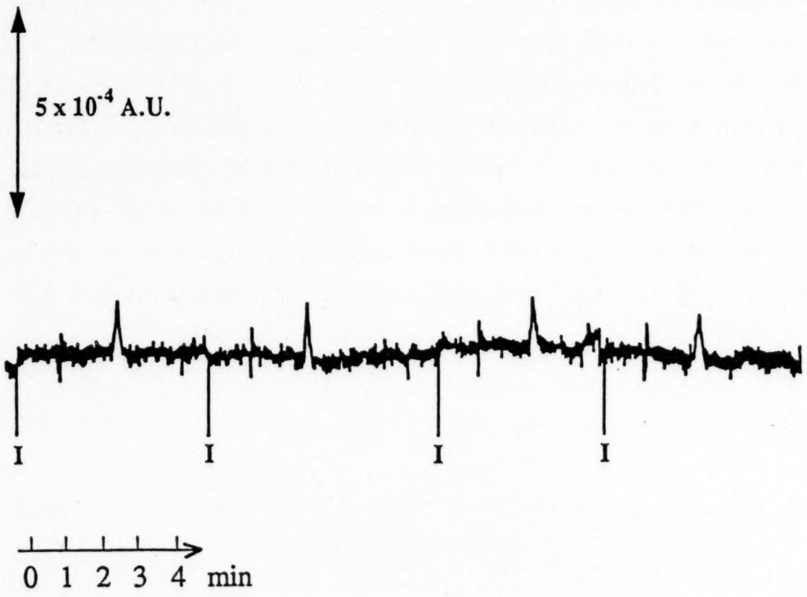

Fig. 2

Repeat chromatograms of salbutamol (for conditions see text); amount injected = 15.3ng.

P/N = 3.4, So Experimental LOD = 13.5ng, calculated LOD = 14.8ng (see text), I = injection.

For changes in flow-rate the variation in α/v^2H values, and thus α', are at a similar level, ~ 3%.

The value determined for α', 28.4 cm^{-2}, RSD = 1.7%, (n = 9), agrees reasonably with the previous value $\alpha' = 29.9$ cm^{-2} (single determination), on the PU4100 system. As β' appears to be dependent on chromatographic parameters, the use of reference conditions need consideration. (It should be noted that in well designed LC systems, where $\sigma_{EXT} < 0.5\sigma_{COL}$ [6], then the β term becomes insignificant relative to the contribution from the α term).

The LOD was calculated (from eq. (3)), for salbutamol under these conditions (with noise = 4.4×10^{-5} A.U., H = 0.084 mm, from FWHH measurement, absorptivity = 5.68 μg^{-1} cm^{-1} ml, with $t_r = 174$ sec and using $\alpha' = 28.4$ cm^{-2}, $\beta' = 5.3$ cm^{-2} sec^2).

Calculated LOD is 14.8 ng.

Experimental LOD is 13.5 ng (see Fig. 2, where 15.3 ng gives P/N of 3.4, average of 5 injections).

This approach assumes a constant H value for all 6 peaks in the calibration run. This is the same assumption as in the extrapolation method [6] for separation of σ_{COL} and σ_{EXT} from σ_{TOT} data. Recent discussions [7] question this assumption, but no empirical data was shown to support their findings. If H varied across the calibration set of peaks in a systematic way, this can be built into our model, as suggested for the extrapolation method originally [8].

Conclusions

The system evaluation strategy testing has now covered eluent mixtures, isoeluotropic solvents, temperatures, and flow. Employing our model, then α' values appear independent of chromatographic conditions. The FWHH data on the last peak for estimating H, appears sufficient for these calibrations over k' range (~ 0.5–10). The large variation in H, with chromatographic conditions, is potentially the largest problem to using this strategy as a predictive tool and methods for estimating H, with varying experimental conditions now need investigation. However peak heights, dilutions and LOD's are dependent on $\sqrt{H}$, so the dependence is lower than most other factors. β' values show significant variations between differing conditions. If σ_{EXT} is dependent on eluent viscosity, then this behaviour is expected, and reference conditions may be necessary.

To validate this model, an independent method for determination of H and σ_{EXT} is essential; the FWHH estimates for H and the extrapolation method [6] employ very similar assumptions to this work, and thus this method is not independent.

Thus an efficient method to characterize peak-profiles is needed. Approximations to exponentially modified Gaussians have been used with some success [9], but examples have been found where this model is believed to be inadequate [10]. Second statistical moments (SSM) assumes no peak shape, but determination of the end-points is a serious problem.

Clearly this type of approach, evaluating systems and predicting peak heights and limits of detection, should see an increasing usage to achieve optimum performance from particular column and system combinations, either in manual or automated operation.

References

[1] *P. J. Naish, R. J. Dolphin, D. P. Goulder*, J. Chromatogr., **395**, 55 (1987).
[2] *C. R. Wilke, P. Chang*, A. I. Ch. E. J., **1**, 264 (1955).
[3] *L. R. Snyder, J. J. Kirkland* in "Introduction to Modern Liquid Chromatography", 2nd. edition, Wiley Interscience, New York and London, 1979.
[4] *K. W. Freebairn, J. H. Knox*, Chromatographia, **19**, 37 (1984).
[5] *M. Mulholland, P. J. Naish, J. Waterhouse*, HPLC '87, poster #Tu-P-28.
[6] *P. J. Naish, R. J. Dolphin, C. V. Perkins*, Chromatographia, **20**, 335 (1985).
[7] *H. A. Claessens, C. A. Cramers, M. A. J. Kuyken*, Chromatographia, **23**, 189 (1987).
[8] *W. Th. Kok, U. A. Th. Brinkman, R. W. Frei, H. B. Kanekamp, F. Nooitgedacht, H. Poppe*, J. Chromatogr., **237**, 357 (1982).
[9] *J. P. Foley, J. G. Dorsey*, Anal. Chem., **55**, 730 (1983).
[10] *J. Doehl, T. Greibokk*, J. Chromatogr. Sci., **25**, 99 (1987).

Received: July 27, 1987
Accepted: Oct. 22, 1987
F

High-Performance Liquid Chromatographic Analysis of Ginsenosides in *Panax Ginseng* Extracts Using Glass-ODS Column

H. Kanazawa[1]/Y. Nagata[1]/Y. Matsushima[1]*/M. Tomoda[1]/N. Takai[2]

[1]Kyoritsu College of Pharmacy, Shibakoen 1-5-30, Minato-ku, Tokyo, 105 Japan
[2]Institute of Industrial Science, University of Tokyo, Roppongi 7-22-1, Minato-ku,
Tokyo 106, Japan

Key-Words

Column liquid chromatography
Octadecylsilyl-porous glass
Ginsenosides
Panax ginseng

Summary

Octadecyl-porous glass was prepared and used as the packing for reversed-phase high-performance liquid chromatography. A mixture of ginsenosides, saponins of ginseng was analyzed with detection at 203 nm. Ginsenosides Rf, Rg_2, Rb_1, Rc, Rb_2, and Rd were separated with acetonitrile-water (27.5 : 72.5) as the mobile phase. A well-resoluted chromatogram of ginsenosides Ro, Rg_1 and Re was also obtained with acetonitrile-water (16.5 : 83.5). The whole separation was achieved in 12 min with a flowrate of 1 ml/min. Calibration curves of ginsenosides Rb_1, Rc, Rb_2, Rd, Rg_1 and Re were linear up to 5 μg. It can be concluded that the rapid and accurate analysis of ginsenosides is possible by the described method.

Introduction

A high-performance liquid chromatographic (HPLC) method using a column containing octadecylsilyl porous glass (glass-ODS) achieved rapid and excellent separation of antipyretic drugs [1]. As a part of our interest in the HPLC analysis of biological and medical materials, we applied the method for analysis of ginsenosides. Ginsenosides are saponins of ginseng, the roots of *Panax ginseng,* which has long been used as a folk medicine, and many studies suggest that its pharmacological effects are due to the saponins [2–4].

HPLC analysis of ginsenosides have been reported by a number of researchers [5–9]. The present method using glass-ODS column has an advantage in the rapid separation of ginsenosides and will find its place among other analytical methods which are in routine use.

Experimental

Material

Acetonitrile used as the mobile phase was of HPLC grade (Wako, Tokyo, Japan). Water was deionized and distilled. Other chemicals were of reagent grade.

Samples of ginseng were obtained from different commercial sources. The standard samples of ginsenosides were kindly supplied by Prof. J. Shoji of Showa University, Tokyo.

Glass-ODS

Borosilicate glass prepared from SiO_2, Al_2O_3 and B_2O_3 was reheated and treated with acid. Porous glass thus obtained was chemically modified by the reaction with octadecylchlorosilane according to the general procedure described previously [1]. The elemental analysis showed that the prepared glass-ODS contained Si, B and Al in the molar ratio of 89, 0.6 and 1.5, respectively. It contained 12 % ODS and its pore size was 550 Å. Glass-ODS with a particle size of 8–10 μm was packed into a 150 X 4 mm I.D. stainless-steel column by the high-pressure slurry technique.

Chromatographic Conditions

The HPLC system used consisted of a Toyo Soda Model CCPM multi pump, a Rheodyne Model 7125 valve, a Toyo Soda Model UV-8000 monitor and a Hitachi Model 833A data-processor. The system was operated at room temperature. The flow-rate was 1 ml/min and the peaks were monitored at 203 nm.

0009-5893/87 0517-03 $ 03.00/0

© 1987 Friedr. Vieweg & Sohn Verlagsgesellschaft mbH

Ginseng was extracted with methanol and the extract was filtered, dried and refrigerated. Immediately before analysis, the extract was dissolved in water and applied to a Sep-Pak C_{18} cartridge (Waters) pretreated with water and methanol. After washing the column with water and 30 % methanol, the ginsenosides were eluted with methanol and the eluate was evaporated to dryness under reduced pressure. The residue was dissolved in the HPLC solvent and injected into the HPLC system. The column was washed with 30–40 ml of methanol with a flow-rate of 2–3 ml/min before and after analysis.

HPLC fractions of the extracts were analyzed by means of thin-layer chromatography (TLC). TLC-plate Silica gel 60 (E. Merck) was used and the solvent was the lower layer of a mixture of chloroform, methanol and water (13 : 7 : 2). Spots of ginsenosides were detected with coloration by spraying with 10 % sulfuric acid and heating.

Results and Discussion

Acetonitrile-water was used as the mobile phase. The retention times of ginsenosides were greatly affected by the composition of the mobile phase. Fig. 1 shows the effect of the water content on the k' values measured for the standard samples of seven ginsenosides with a flow-rate of 1 ml/min. Chromatograms of mixtures of ginsenosides are shown in Fig. 2. Ginsenosides Rf, Rg_2, Rb_1, Rc, Rb_2, and Rd were separated with acetonitrile-water (27.5 : 72.5). A well-resoluted chromatogram of ginsenosides Ro, Rg_1 and Re was also obtained with acetonitrile-water (16.5 : 83.5). The whole separation was achieved in 12 min with a flow-rate of 1 ml/min.

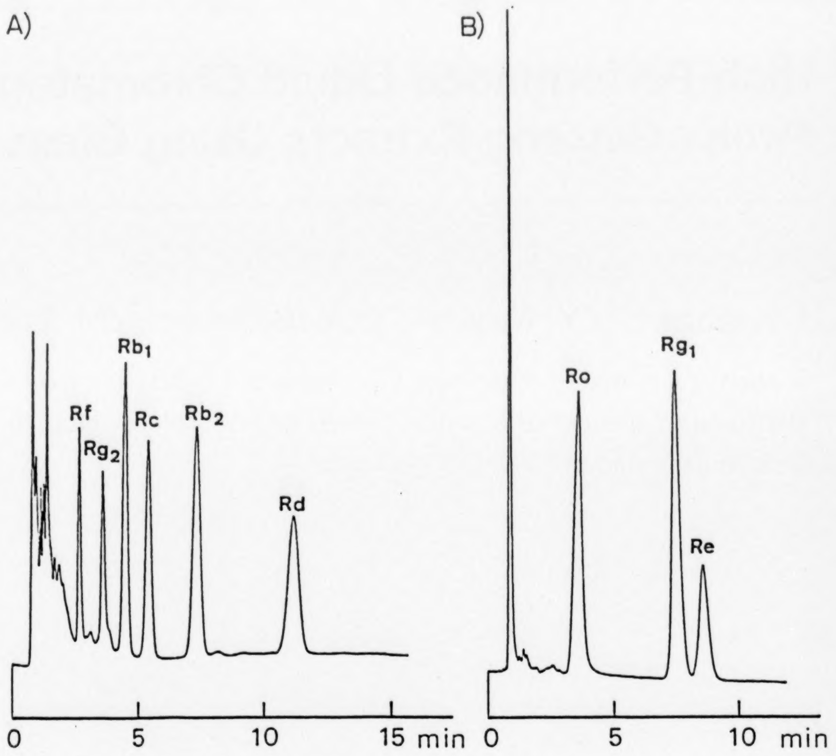

Fig. 2

HPLC-chromatograms of a mixture of ginsenosides.
Eluent: A, acetonitrile-water (27.5 : 72.5);
B, acetonitrile-water (16.5 : 83.5)
Column: Glass-ODS (4 mm I.D. X 150 mm).
Flow-rate: 1.0 ml/min. Detection at 203 nm.

The solutions containing 0–5 µg of ginsenoside were injected and the corresponding peak areas integrated. The calibration curves had a correlation coefficient very near to unity as shown in Figs. 3 and 4. The curves were reproducible and the limit of detection of each ginsenosides was about 300 ng.

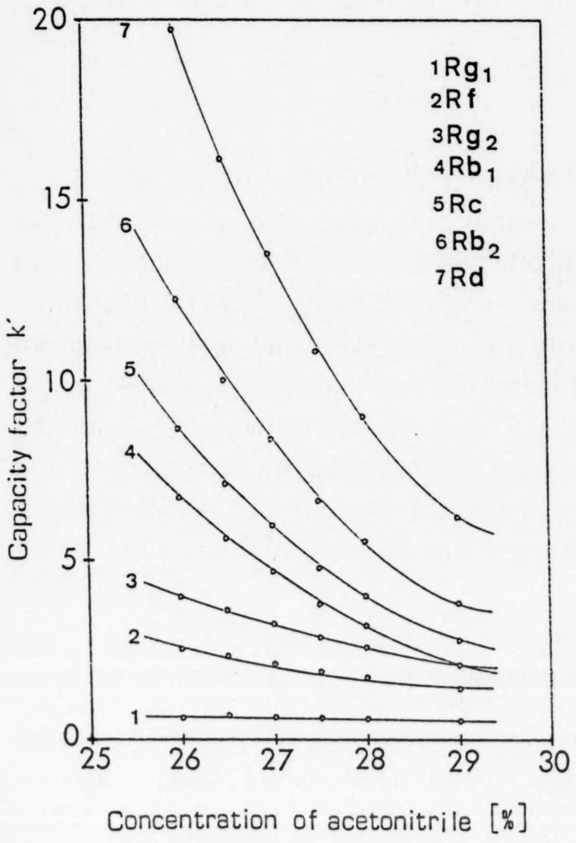

Fig. 1

Effect of acetonitrile concentration in the mobile phase on the capacity factor (k') of ginsenosides.

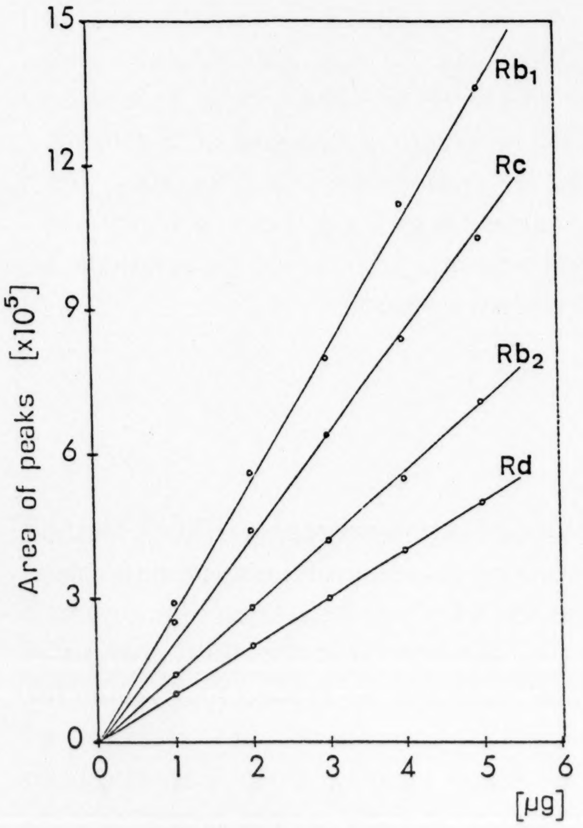

Fig. 3

Calibration curves of ginsenosides.
Eluent: acetonitrile-water (27.5 : 72.5).

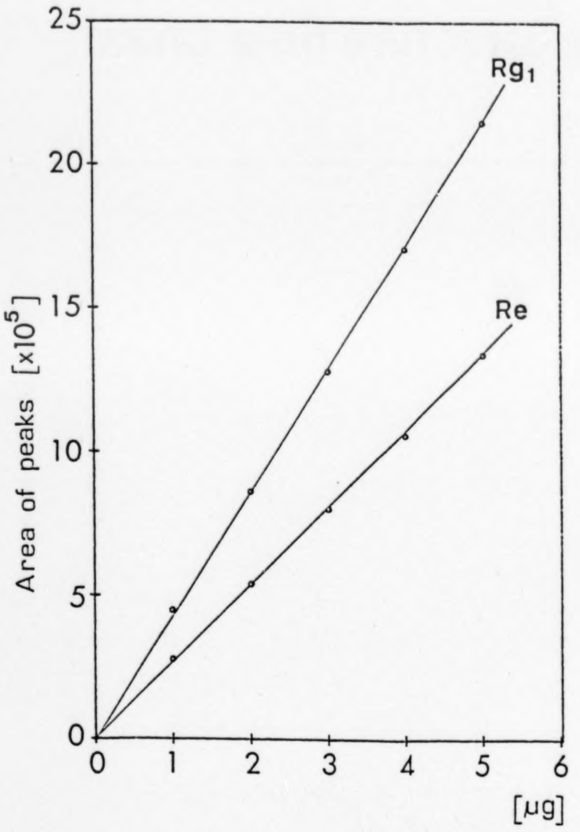

Fig. 4

Calibration curves of ginsenosides.
Eluent: acetonitrile-water (16 :84).

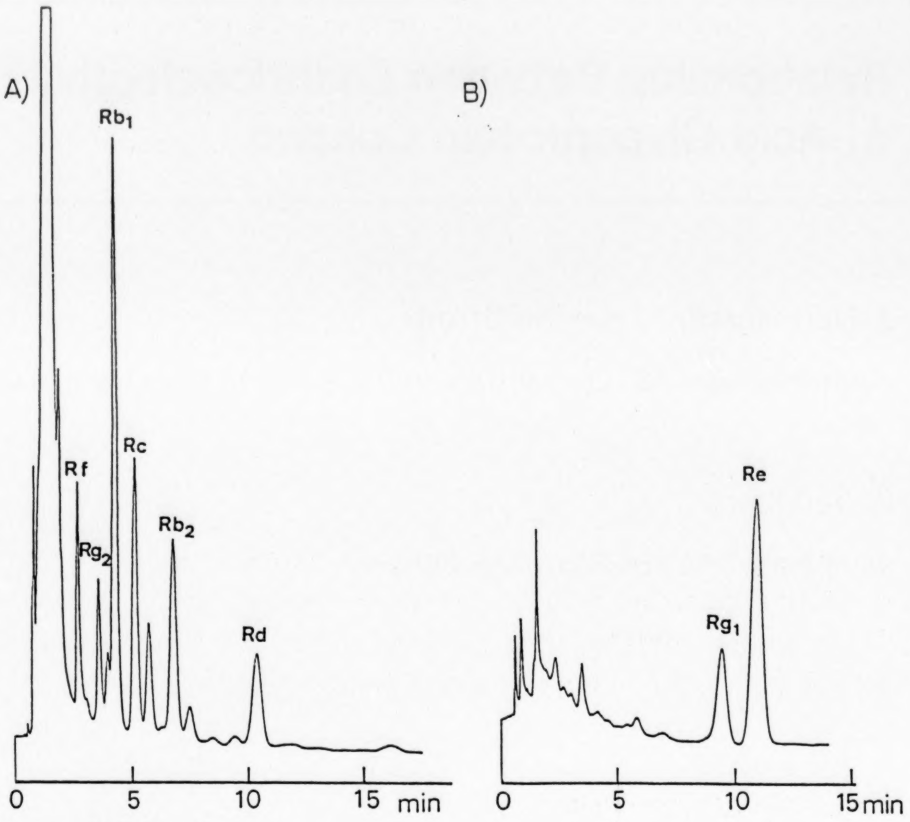

Fig. 5

HPLC-chromatograms of a ginseng extract.
Eluent: A, acetonitrile-water (27.5 : 72.5);
B, acetonitrile-water (16 : 84)
Column: Glass-ODS (4 mm I.D. X 150 mm).
Flow-rate: 1.0 ml/min. Detection at 203 nm.

Chromatograms of a ginsenoside extract are shown in Fig. 5. Separation of the ginsenoside peaks were quite satisfactory. The ginsenoside fractions were taken and subjected to the HPLC analysis. Each fraction gave a single chromatographic peak. The fractions were also analyzed by means of TLC. They gave single spots and showed the same R_F values as the standard samples of the assigned peaks.

Known amounts of the ginsenosides were added to ginseng and the crude drug was extracted as described. Ginsenosides in the extracts were determined by the calibration curves. Recoveries of the amounts added were in the range of 97 to 101 % as shown in Table I. The table also lists the coefficients of variation in the determination of known amounts of each ginsenoside.

Table I. Recoveries and coefficients of variation (C.V.)

Ginsenoside	Recovery % (n = 3)	C. V. % (n = 4)
Rg$_1$	97	2.0
Re	101	2.1
Rb$_1$	98	2.1
Rc	96	3.1
Rb$_2$	96	2.4
Rd	100	2.4

We conclude from the results mentioned above that the rapid and accurate analysis of ginsenosides is possible by the present method. Analysis of ginsenosides in crude drugs and various pharmaceutical preparations are in progress in our laboratories.

References

[1] *Y. Matsushima, Y. Nagata, K. Takakusagi, M. Niyomura, N. Takai,* J. Chromatogr. **332,** 265 (1985).
[2] *K. Takagi, H. Saito, H. Nabata,* Japan J. Pharmacol. **22,** 245 (1972).
[3] *K. Takagi, H. Saito, M. Tsuchiya,* Japan J. Pharmacol. **22,** 339 (1972).
[4] *H. Oura, A. Kumagai, S. Shibata, K. Takagi,* ed., "Ginseng" Kyoritsu Pub., Tokyo, 1981.
[5] *F. Soldati, O. Sticher,* Planta Medica **39,** 348 (1980).
[6] *H. R. Schulten, F. Soldati,* J. Chromatogr. **212,** 37 (1981).
[7] *T. Nagasawa, T. Yokozawa, Y. Nishino, H. Oura,* Chem. Pharm. Bull., **28,** 2059 (1980).
[8] *P. Pietta, P. Mauri, A. Rava,* J. Chromatogr. **356,** 212 (1986).
[9] *N. Nishimoto, S. Masaki, S. Hayashi, T. Takemoto, T. Hayashi, T. Tsuji,* Shoyakugaku Zasshi **40,** 345 (1986).

Received: July 1, 1987
Accepted: July 28, 1987
F

Relationship Between Enantioselectivity and Solute Structure on a Chiral α_1-Acid Glycoprotein Column

J. Hermansson* / Kerstin Ström

Apoteksbolaget AB, Central Laboratory, S-105 14 Stockholm, Sweden

R. Sandberg

Astra Alab, S-151 85 Södertälje, Sweden

Key Words

Column liquid chromatography
α-acid glycoprotein column
EnantioPac column
N-aminoalkylsuccinimide enantiomers
1-alkyl-2',6'-pipecoloxylidide enantiomers

Summary

The relationship between the enantioselectivity, the retention and the solute structure for N-aminoalkylsuccinimides and 1-alkyl-2',6'-pipecoloxylidides have been studied using α_1-acid glycoprotein as the chiral stationary phase. Both the enantioselectivity and the retention are highly affected by small changes of the solute structure in series of homologous compounds. For example, increasing the steric bulk on a basic aliphatic nitrogen improves the enantioselectivity. It was also demonstrated for the succinimides that the magnitude of the separation factor was highly affected by the distance between the basic nitrogen and the chiral center. The chiral selectivity was not lost for the succinimides despite the fact that the basic nitrogen was separated from the chiral center with seven atoms, which may be an effect of that these compounds contain more than one strong hydrogen bonding group. Substitution in the aromatic ring of the succinimides also influences both the retention and the chiral selectivity to a large extent. Electronegative substituents can increase the separation factor but introduction of an alkyl or an alkoxy group in the aromatic ring decreases the enantioselectivity for the succinimides.

Introduction

Chiral selectivity can be obtained when two enantiomers form complexes with different stability with a chiral selector. α_1-acid glycoprotein (α_1-AGP), a human plasma protein, has been demonstrated to be a chiral selector with an extremely broad applicability. Hermansson developed the first chiral phase based on α_1-AGP in 1983 [1]. In a series of papers the properties and the utility of the α_1-AGP column have been studied [1–9].

α_1-AGP is a glycoprotein with a molecular weight of about 40000. It consists of a single peptide chain, containing 181 amino acids, to which 5 carbohydrate units are linked. The peptide chain constitutes about 55% of the molecular weight. The isoelectric point of the protein is 2.7 in phosphate buffer [10]. This is the result of the high content of sialic acid in α_1-AGP, 14 terminal sialic acid residues per protein molecule [10]. The mechanism behind the stereoselective binding of enantiomers to α_1-AGP is complex. However, it can be assumed that the α_1-AGP molecule contains a main binding domain ("binding site"), probably an area of the α_1-AGP molecule which is especially rich in hydrophobic amino acids. Since this domain is built up of the peptide chain there are numerous different chiral binding groups present in this domain, beside the hydrophobic groups, like hydrogen bonding amides, anionic and cationic groups. It can not be excluded that other "binding sites" also can exist and it can be assumed that the carbohydrate moiety of the protein is involved in the stereoselective retention of enantiomers. The carbohydrate moiety is built up of sialic acid, hexosamine and neutral hexoses all containing chiral carbons.

The previous studies have described the effects of different mobile phase additives on the retention and the enantioselectivity with the purpose to characterize basic requirements for obtaining high separation factors [1–9]. The present study describes the relationship between the chiral selectivity, the retention and the molecular structure for closely related compounds of 1-alkyl-2',6'-pipecoloxylidide and N-aminoalkylsuccinimide type in an attempt to reach a deeper understanding of the complex nature of the chiral recognition mechanism and to define structural features of the solutes important for the chiral resolution.

0009-5893/87 0520-07 $03.00/0

© 1987 Friedr. Vieweg & Sohn Verlagsgesellschaft mbH

Experimental

Apparatus

The liquid chromatographic system consisted of a Waters M 6000 A pump, a Waters Model U6K injector and a Shimadzu SPD-2A variable wavelength UV detector operated at 215 nm. The α_1-AGP silica (5 μm) was prepared as described previously [11]. α_1-AGP was immobilized on an amino silica, which was prepared by reacting epoxide-silica with 1,3-diaminopropane. The α_1-AGP silica was packed in a column (100 × 4.0 mm) at 4200 psi using a mixture of 2-propanol and water (1 + 1) as slurry medium and driving liquid. A Haskel pump was used for the column packing. The commercially available α_1-AGP column, EnantioPac, was kindly supplied by LKB Produkter AB, Bromma, Sweden.

Chemicals

The model compounds used in this study were kindly supplied by Dr. R. Sandberg, Astra Alab, Södertälje, Sweden, or synthesized in our laboratory. The structures of the model compounds are given in Table I and II.

Results and Discussion

Influence of Molecular Structure on Retention and Enantioselectivity

A) 1-alkyl-2′,6′-pipecoloxylidides and related compounds (PPX series). The structures of the local anaesthetic drugs mepivacaine and bupivacaine and homologues (1-alkyl-2′,6′-pipecoloxylidides, the PPX series) are given in Table I. Fig. 1A demonstrates the logarithm of the capacity factors obtained for the eight compounds in the PPX series, using the EnantioPac column. The capacity factors for the alkyl substituted compounds increase with increasing length of the alkyl chain. It is very interesting to compare the capacity factors obtained for the enantiomers of mepivacaine, with a methyl group on the piperidine nitrogen, with PPX with a hydrogen atom on the nitrogen. Loss of a methyl group from the (S)-isomer of mepivacaine resulted in a strong increase of the capacity factor for the corresponding PPX enantiomer, whereas a loss of a methyl group from (R)-mepivacaine resulted in a very strong decrease of the capacity factor. The capacity factors for the (R)-forms of the compounds in the homologues series increase with increasing hydrophobicity with about 0.25 log units per carbon atom. However, a smaller increase

Table I. Structures of compounds in the PPX series

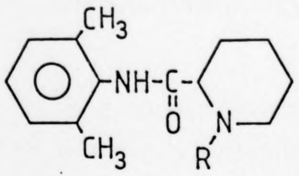

Compound	R
PPX	H
Mepivacaine	CH_3
RAD 201	C_2H_5
RAD 239	C_3H_7
Bupivacaine	C_4H_9
RAD 393	C_5H_{11}
PPX-Hexyl	C_6H_{13}

Table II. Structures of compounds in the RAC series.

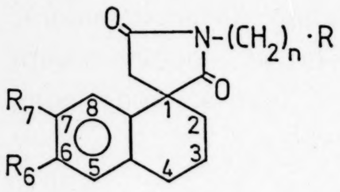

R_7	H	H	H	H	H	H	H	CH_3	CH_3	OH	OH	CH_3O
R_6	H	H	H	H	H	H	H	H	H	H	H	H
R / n	$N{<}^{CH_3}_{CH_3}$	$N{<}^{C_2H_5}_{C_4H_5}$	$N{<}^{H}_{CH_3}$	$N{<}^{H}_{C_2H_5}$	$N{<}^{H}_{C_3H_7}$	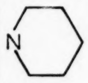	$N{<}^{CH_3}_{(CH_2)_2OH}$	$N{<}^{CH_3}_{CH_3}$	$N{<}^{C_2H_5}_{C_2H_5}$	$N{<}^{C_2H_5}_{C_2H_5}$	$N{<}^{CH_3}_{CH_3}$	$N{<}^{CH_3}_{CH_3}$
2	RAC 102	RAC DEAEA	RAC 112				RAC 157			RAC 800		
3	RAC DAMPA	RAC 109		RAC 216		RAC 314	RAC 392	RAC 269	RAC 268	RAC 288		
4	RAC 308	RAC 309	RAC 310		RAC 312	RAC 214	RAC 322			RAC 290	RAC 289	RAC 294
5	RAC 127	RAC 126					RAC 811					

R_7	$(CH_3)_2HCO$	$(CH_3)_2HCO$	F	F	Cl	H	H	H
R_6	H	H	H	H	H	CH_3O	CH_3O	CH_3O
R / n	N $^{CH_3}_{CH_3}$	N $^{C_2H_5}_{C_2H_5}$	N $^{CH_3}_{CH_3}$	N $^{C_2H_5}_{C_2H_5}$	N $^{C_2H_5}_{C_2H_5}$	N $^{CH_3}_{CH_3}$	N $^{C_2H_5}_{C_2H_5}$	N $^{CH_3}_{(CH_2)_2OH}$
2						RAC 160		RAC 272
3	RAC 241	RAC 242	RAC 518	RAC 519	RAC 354	RAC 158	RAC 159	RAC 223
4							RAC 803	RAC 224

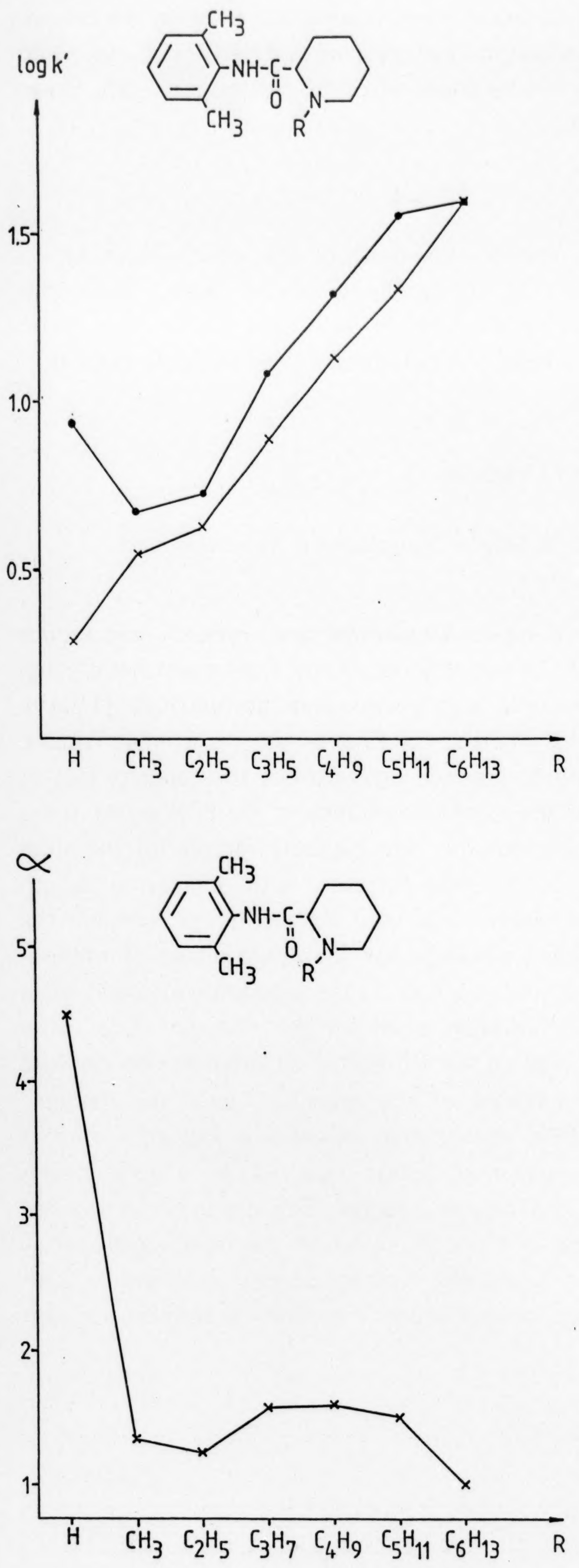

Figs. 1A and B

Influence of alkylchain length on the capacity factors and the enantioselectivity for a series of mepivacaine homologous. The R-form is eluted first.

Column: EnantioPac (100 X 4.0 mm)

Mobile phase: 6% (v/v) 2-propanol in 0.01 M phosphate buffer pH 7.26.

was observed between the methyl and ethyl homologues for both enantiomers. The strong difference in the binding affinity for the PPX enantiomers resulted in an α-value of 4.5 which is demonstrated in Fig. 1B. The separation of the PPX enantiomers is shown in Fig. 2. An increase of the length of the alkyl substituent on the piperidine nitrogen increases the chiral selectivity and a broad maximum was obtained with propyl, butyl and pentyl groups on the piperidine nitrogen. A further increase of the size of the alkyl group resulted in a total loss of the chiral selectivity.

B) N-aminoalkylsuccinimides. The general formula of the N-aminoalkylsuccinimide is given in Table II together with the structures of the homologues used in this study. In the study of the N-aminoalkylsuccinimides we have characterized the effects of three principally different changes of the solute structure:

- Variation of the length between the chiral carbon and the basic nitrogen atom.
- Changing the kind of substitution at the basic nitrogen atom.
- Substitution in the aromatic ring.

Influence of Distance between the Chiral Carbon and the Basic Nitrogen Atom

Variation of the distance between the chiral carbon and the basic nitrogen influences the enantioselectivity and the retention to a large extent as demonstrated in Figs. 3A and B. The distance between the basic nitrogen and the chiral center was varied by variation of the length of the carbon chain between the imide nitrogen and the basic nitrogen atom. From Fig. 3A can be seen that for the dimethylamino, diethylamino as well as for the aminoalcohol compound the highest retention was obtained with a distance of 2 or 5 carbons between the nitrogen atoms. This means that the hydrophobicity of the compound is of minor importance for the retention of these compounds compared to more specific interactions with the chiral phase. A reasonable explanation to the variation of the capacity factors with the distance between the chiral carbon and the basic nitrogen is that there are many potential binding groups in the binding site including different anionic groups as well as many different hydrogen bonding groups like amides. For the cationic solutes used as model com-

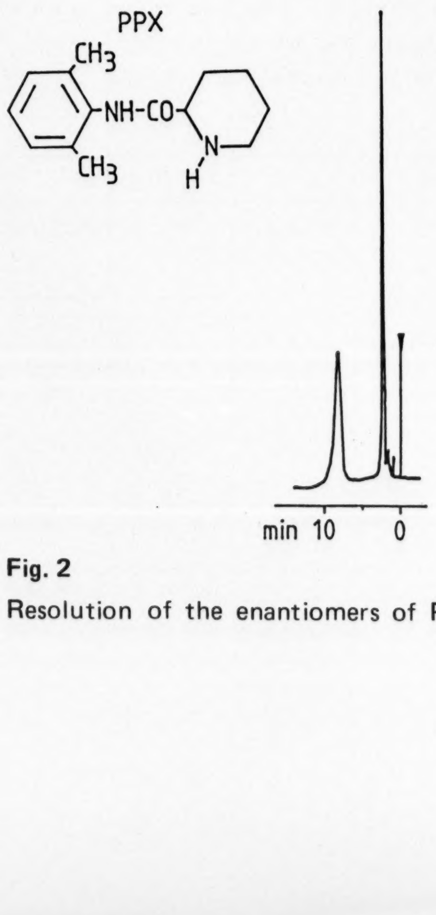

Fig. 2

Resolution of the enantiomers of PPX. Conditions: As in Fig. 1.

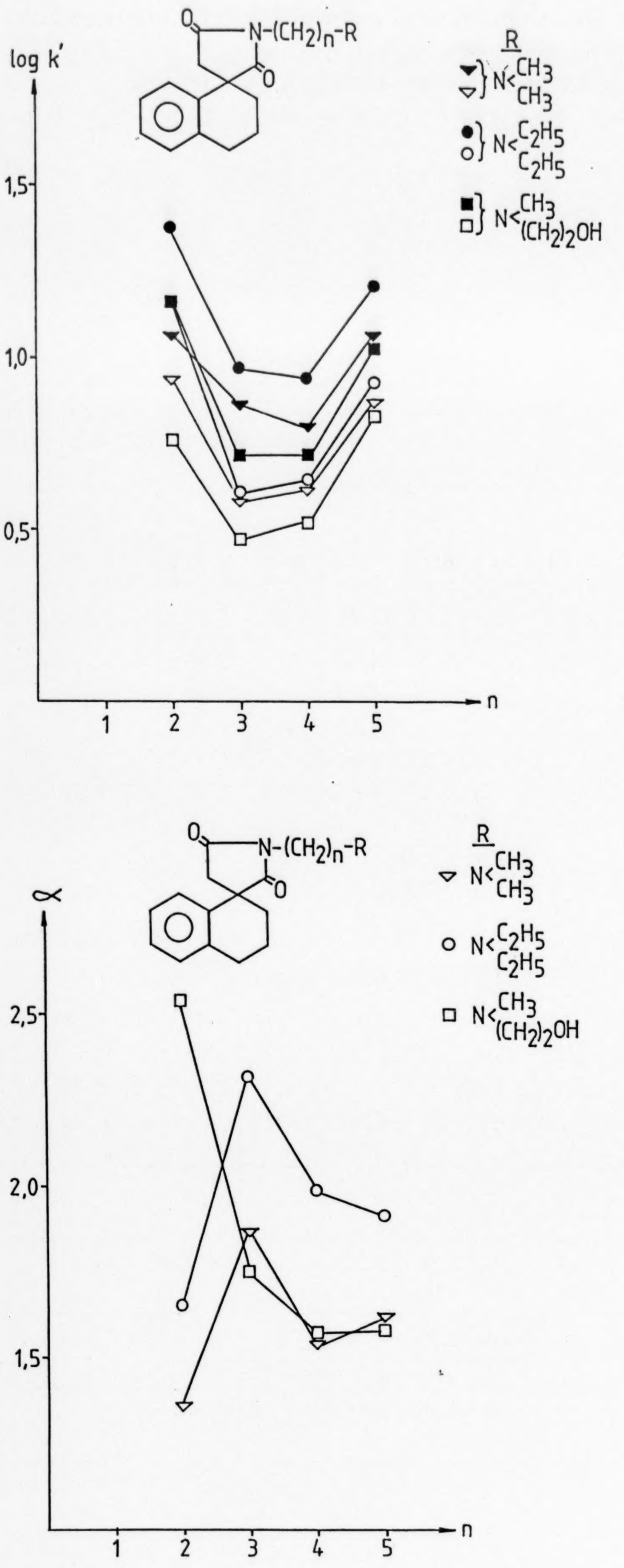

Figs. 3A and B

Influence of the distance between the imide and basic nitrogen atoms on the capacity factors and the enantioselectivity.

Column: α_1-AGP column (100 X 4.0 mm) 80 mg α_1-AGP/gram.
Mobile phase: As in Fig. 1.

pounds in this study the anionic binding groups are probably of special importance. It can be assumed that the different binding groups are more or less accessible for the basic nitrogen of the solute depending on the length of the aminoalkyl chain of the succinimides. We have also considered the possibility that the effect on the retention was related to differences in the pk_a-values. For example, the pk_a-values for the dimethylamino compounds (Fig. 3A) increases from 7.8 to 9.8 when increasing the length of the carbon chain from n = 2 to 5. This means that the charge on the nitrogen increases when the length of the carbon chain increases (pH of the mobile phase ~ 7.2). However, there is no simple relationship between the retention of these compounds and the degree of charge on the basic nitrogen. Lower retention was obtained for the compounds with n = 3 than for the compounds with n = 5 and 2.

The enantioselectivity is also highly affected by the distance between the chiral center and the basic nitrogen which is demonstrated in Fig. 3B. The enantioselectivity for the aminoalcohol compounds decreases from $\alpha = 2.54$ to 1.58 by increasing the distance between the basic nitrogen and the chiral carbon. The dimethyl- and diethylamine compounds demonstrate a different behaviour compared to the amino-alcohol compounds as demonstrated in Fig. 3B. Maximum enantioselectivity for these compounds was obtained when n = 3. A further shortening of the carbon chain to n = 2 resulted in decreasing chiral selectivity. Furthermore, the diethylamino compounds gave higher separation factors than the corresponding dimethylamino compounds.

Substitution at the Basic Nitrogen

It has been demonstrated that the kind of substitution at basic nitrogen atoms influences the enantioselectivity to a large extent [1, 7]. However, only a few short series of compounds have been investigated which means that the knowledge is very limited. The influence of different substituents on the basic nitrogen atom on the chiral selectivity is demonstrated in Fig. 4 for two different series of N-aminoalkylsuccinimide compounds, one with 3 carbons and the other with 4 carbons between the nitrogen atoms. The result of this study indicates that a monoalkyl on the nitrogen atom gives a lower enantioselectivity than the corresponding disubstituted compound, independently of the distance between the nitrogens. Moreover, an increase of the steric bulk from monomethyl to piperidine increases the chiral selectivity when n = 4. However, the highest separation factor for the other series of compounds (n = 3) was obtained with a diethylamino group, whereas the piperidine group reduces the separation factor for this series of compounds.

The retention of the first eluted enantiomer of the compounds presented in Fig. 4 are influenced to a rather limited extent by the kind of substitution at the basic nitrogen atom. A change from a monomethyl amino group to a piperidine ring (n = 4) increases the capacity factor from 4.4 to 5.6. Fig. 5 demonstrates the separation of the enantiomers of RAC 518.

Influence of Ring Substitution on Capacity Factors and Stereoselectivity

Substitution in the aromatic ring influences both the enantioselectivity and the capacity factors to a large extent for the compounds demonstrated in Table III. The enantioselectivity for the diethylamino compounds with n = 3 increases by introduction of electronegative substituents

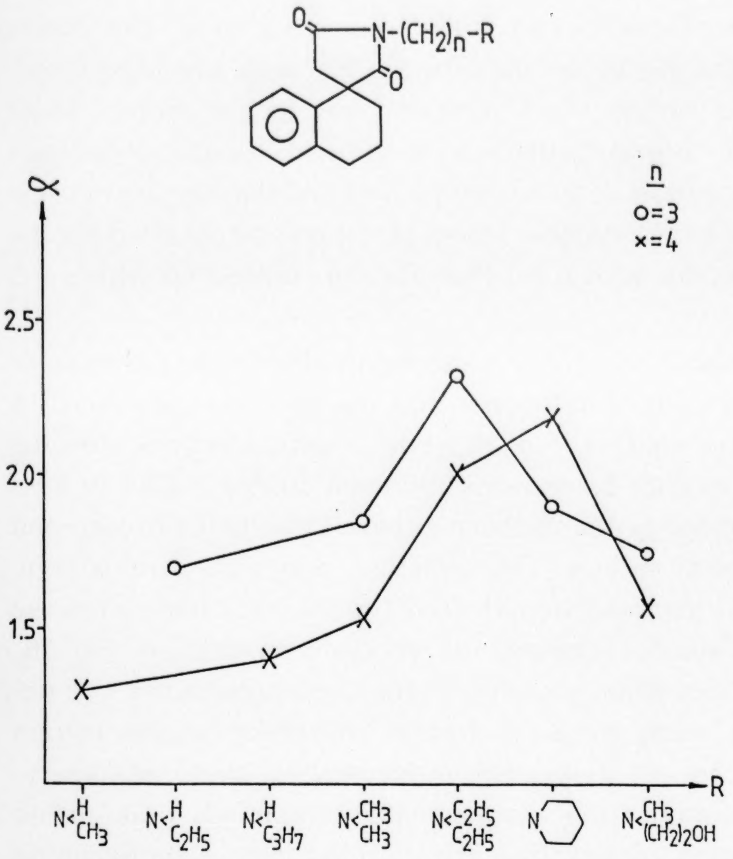

Fig. 4

Influence of the kind of substitution on the basic nitrogen atom on the enantioselectivity.

Conditions: As in Fig. 3.

Table III. Capacity factors and stereoselectivity for ring substituted N-aminoalkylsuccinimides.

Column: α_1-AGP 4 X 100 mm (80 mg prot/g solid phase)

Mobile phase: 6% 2-propanol phosphate buffer. pH = 7.25. μ = 0.02.

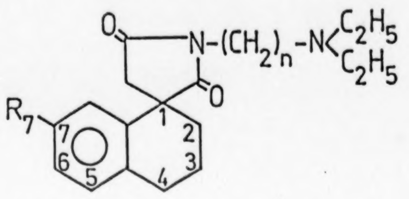

n	R7	F	Cl	OH	H	CH_3	OCH_3	$OCH(CH_3)_2$
2	k'_1			16.9	14.4			
	α			1.12	1.65			
3	k'_1	4.47	8.34	5.02	3.98	10.6		12.6
	α	2.33	3.35	2.61	2.32	2.12		1.52
4	k'_1			6.35	4.33		9.84	
	α			1.65	1.99		1.08	
5	k'_1				8.40			
	α				1.91			

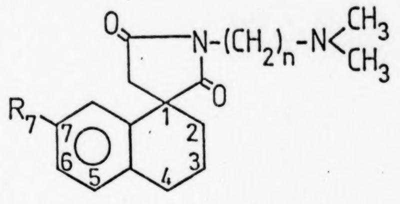

n	R7	F	OH	H	CH_3	OCH_3	$OCH(CH_3)_2$
2	k'_1			8.53			
	α			1.35			
3	k'_1	3.54		3.86	8.33		8.03
	α	1.74		1.86	1.49		1.50
4	k'_1		5.28	4.06		6.52	
	α		1.46	1.53		1.14	
5	k'_1			7.18			
	α			1.61			

in position 7 of the aromatic ring. However, this is not a general phenomenon for the N-aminoalkylsuccinimides which can be seen if the α-values obtained for the hydroxy compounds are compared with the α-values obtained for the corresponding unsubstituted compounds. Furthermore, introduction of an alkyl or an alkoxy substituent in position 7 of the aromatic ring decreases the enantioselectivity. Moreover, lower chiral selectivities were obtained for the dimethylamino compounds which is mainly due to the smaller steric bulk at the basic nitrogen.

The retention is highly affected by the nature of the group introducted in the aromatic ring as demonstrated in Table III. Introduction of a methyl group or a chlorine atom in position 7 increases the retention drastically. It is also interesting to note that introduction of fluorine in position 7 has a very limited influence on the capacity factor and the enantioselectivity compared to the effects obtained with chlorine.

Effect of pH on Enantioselectivity and Retention

It has been observed previously for basic, acidic as well as for uncharged solutes that both the retention and the enantioselectivity are strongly affected by the pH of the mobile phase [1, 6].

The capacity factors and the separation factors obtained for all the compounds in the RAC series at pH 6.02 and 7.26 are summarized in Table IV. From these data it can be seen that the capacity factors decrease between 3–10 times by decreasing pH from 7.26 to 6.02, whereas the chiral selectivity in most cases are influenced to a rather limited extent. For some of the compounds, RAC 310, RAC 120B, RAC 800, RAC 289, RAC 268 and RAC 269 even higher α-values were obtained at pH 6.02. This means that it is preferable to use a pH around 6 in order to obtain a fast separation of the N-aminoalkylsuccinimide enantiomers.

Compounds with Two Chiral Carbons

Introduction of an ethyl group in the aminoalkyl chain of RAC 102 and RAC DEAEA, respectively, creates a new chiral center in the molecules resulting in two diastereomeric pairs (RAC 120A and B, RAC 210A and B). The structures are presented in Table V. Introduction of the ethyl group in the aminoalkyl chain of RAC 102

Table IV. Effect of pH on enantioselectivity and retention

Column: as in Fig. 3

Solute	6% 2-propanol FB pH = 6.02 k'_1	 $\mu = 0.02$ α	6% 2-propanol FB pH = 7.26 k'_1	 $\mu = 0.02$ α
RAC 102	1.39	1.30	8.53	1.35
RAC DAMPA	0.84	1.62	3.86	1.86
RAC 308	0.90	1.48	4.06	1.53
RAC 127	1.40	1.58	7.18	1.61
RAC DEAEA	2.15	1.61	14.40	1.65
RAC 109	0.94	1.93	3.98	2.32
RAC 309	1.05	1.71	4.33	1.99
RAC 126	1.72	1.84	8.40	1.91
RAC 157	1.16	2.04	5.75	2.54
RAC 392	0.73	1.62	2.97	1.75
RAC 322	0.82	1.47	3.31	1.57
RAC 112	0.87	1.27	3.74	1.34
RAC 310	0.97	1.35	4.44	1.30
RAC 216	0.83	1.55	3.42	1.69
RAC 312	1.18	1.40	5.90	1.39
RAC 314	1.05	1.70	4.44	1.89
RAC 214	1.32	1.97	5.59	2.18
RAC 120A	4.98	1.11	32.5	1.20
RAC 120B	4.82	1.70	36.0	1.59
RAC 210A	3.97	2.31		
RAC 210B	3.10	2.46		
RAC 800	2.64	1.22	16.9	1.12
RAC 288	1.14	2.33	5.02	2.61
RAC 290	1.40	1.63	6.35	1.65
RAC 289	1.22	1.50	5.28	1.46
RAC 294	1.68	1	6.52	1.14
RAC 272	0.82	1.35	1.89	2.11
RAC 223	0.72	1.18	2.29	1.37
RAC 224	0.82	1.40	2.75	1.71
RAC 269	1.57	2.02	8.33	1.49
RAC 268	2.09	2.34	10.6	2.12
RAC 518	0.85	1.67	3.54	1.74
RAC 519	1.03	2.05	4.47	2.33
RAC 354	1.94	3.20	8.34	3.35
RAC 241	1.84	1.47	8.03	1.50
RAC 242	2.71	1.50	12.6	1.52
RAC 160	0.80	1.39	2.84	1.87
RAC 158	0.75	1.15	2.90	1.23
RAC 159	0.90	1.17	3.65	1.20
RAC 803	1.09	1.69	4.30	1.82
RAC 811	1.36	1.54	6.78	1.58

Table V. Structures of compounds with two chiral atoms

RAC 120A	RAC 120B	RAC 210A	RAC 210B
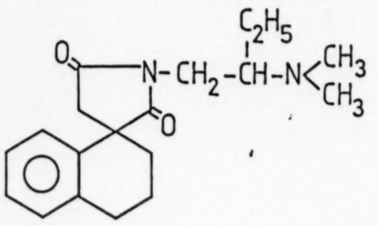		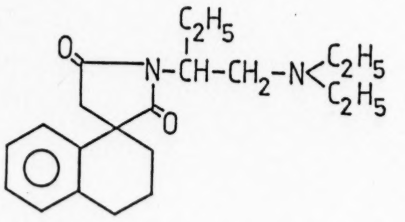	

and RAC DEAEA, respectively, improves the chiral selectivity for three of the compounds (RAC 120B, RAC 210A and RAC 210B), whereas the separation factor for the enantiomers of RAC 120A decreases. It can also be noted that higher chiral selectivity was obtained for RAC 120A and B with a diethylamino group, than for RAC 210A and B with a dimethylamino group. This is consistent with the results obtained for other compounds in the RAC series, cf. Figs. 3B and 4. Almost the same capacity factor was obtained for the first eluted enantiomer of RAC 120A and B, but RAC 120B demonstrated a much higher enantioselectivity (see Table IV).

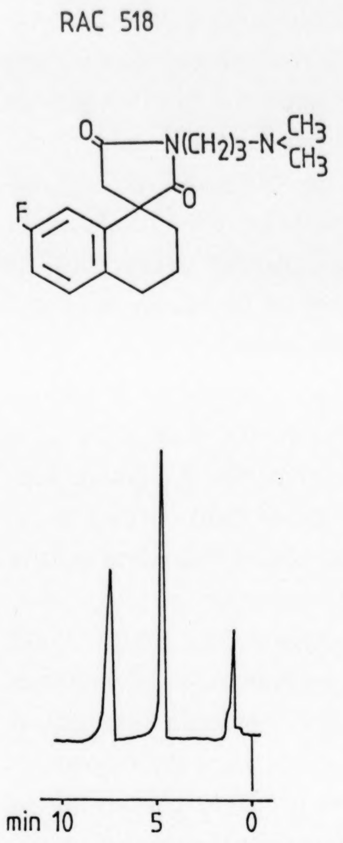

Fig. 5
Resolution of the enantiomers of RAC 518.
Conditions: As in Fig. 3.

Chiral Selectivity – Solute Structure

Enantioselective separations can be obtained when enantiomers form complexes with different stability with the chiral selector. It is generally assumed that interaction between the solutes and the chiral selector in at least three points is a prerequisite for obtaining chiral selectivity.

The lack of information concerning the tertiary structure of α_1-AGP and the groups involved in the binding of the solutes means that no general rules can be given about the structural features required for obtaining enantioselective separations. However, based on our experience from the resolution of many different chiral compounds, empirical conclusions can be drawn about the structural features needed for obtaining chiral resolution [12]. The studies performed so far have indicated that chiral resolution can be obtained if the solutes have two binding groups and a ring structure in the vicinity of these groups. It has been observed that it is favourable if the ring structure is coupled directly to the chiral atom or hydrogen bonding group, or if the ring structure comprising the chiral center.

The binding groups can be hydrogen bonding groups like alcohols and amides or groups participating in ionic binding like ammonium groups (A^+) or anionic groups like carboxylic acids. Previous studies [7], and the present study have also indicated that the distance between the binding groups and the chiral center influences the chiral selectivity. Chiral resolution can normally be obtained if the A^+ group has a distance of $\leqslant 3$ atoms from the chiral center and the hydrogen bonding group should preferably be coupled directly to the chiral center or be separated from the chiral center with maximally two atoms.

The results presented in Fig. 3B for a series of N-aminoalkylsuccinimide homologues demonstrate that it is possible to resolve chiral compounds with the A^+ group separated from the chiral center with more than three atoms. However, these compounds contain more than one strong hydrogen bonding group which gives other prerequisites for obtaining enantioselective separations. Additional hydrogen bonding groups in the molecule seem to decrease the importance of a short distance between the chiral center and the A^+ group in order to achieve enantioselectivity. As can be seen for the compounds presented in Fig. 3B the A^+ group is located between four and seven atoms from the chiral center but high separation factors were obtained for all compounds.

It has also been demonstrated, using the aminoalcohols metoprolol and homologues, that the chiral selectivity can be completely lost by changing the distance between A^+ and the chiral center [7]. Metoprolol has an alcohol group coupled directly to the chiral center and one secondary amino group separated from the chiral carbon with one methylene group. The enantiomers of metoprolol are separated with an α-value of 1.5. However, lengthening of the distance between the amino group and the chiral carbon to two alkyl carbons decreases the separation factor and the chiral selectivity was completely lost by increasing the distance to three carbons.

Beside the above mentioned empirical conclusions that can be drawn about the structural features of the solutes needed for chiral selectivity, the present study supports the earlier made observations that increasing steric bulk on a basic aliphatic nitrogen improves the chiral selectivity in most cases which is demonstrated in Fig. 4.

In conclusion, the present study has demonstrated that small changes of the solute structure influences the retention and the enantioselectivity to a large extent. Series of structurally related compounds behave in many cases in a unique way, with respect to the enantioselectivity, for a certain change of the solute structure. The understanding of such effects on a molecular level is not yet possible due to the lack of a detailed knowledge of the character of the binding groups involved in the stereoselective binding of the solutes. This means that more specific rules for the relationship between the solute structure and the enantioselectivity can be given only for groups of closely related compounds.

However, based on the experience from the resolution of many different chiral compounds, empirical conclusions can be drawn concerning the structural features of the solute required for chiral separation.

References

[1] *J. Hermansson*, J. Chromatogr., **269**, 71 (1983).

[2] *J. Hermansson*, J. Chromatogr., **298**, 67 (1984).

[3] *J. Hermansson, M. Eriksson, O. Nyquist*, J. Chromatogr., **336**, 321 (1984).

[4] *J. L. G. Nilsson, J. Hermansson U. Hacksell, S. Sundell*, Acta Pharm. Suec., **21**, 309 (1984).

[5] *J. Hermansson*, J. Chromatogr., **325**, 379 (1985).

[6] *J. Hermansson, M. Eriksson*, J. Liq. Chromatogr., **9**, 621 (1986).

[7] *G. Schill, I. Wainer, S. Barkan*, J. Liq. Chromatogr., **9**, 641 (1986).

[8] *G. Schill, I. Wainer, S. Barkan*, J. Chromatogr., **365**, 73 (1986).

[9] *D. Ofori Adjei, Ö. Eriksson, B. Lindström, J. Hermansson, K. Adjepon-Yamoah, F. Sjöqvist*, Therapeutic Drug Monitoring, **8**, 457 (1986).

[10] *K. Schmid*, in: *F. Putman* (Editor), The Plasma Proteins: Structure Function and Genetic Control. Vol. I, Academic Press, New York, 1975, p. 184.

[11] *J. Hermansson*, US patent no. 4.612.121.

[12] *J. Hermansson, G. Schill*, in: *P. R. Brown* and *R. Hartwick* (Editors), High Performance Liquid Chromatography, in press.

Received: June 28, 1987
Revised manuscript
received: Sept. 7, 1987
Accepted: Sept. 11, 1987
F

High Voltage Capillary Zone Electrophoresis: Operating Parameters Effects on Electroendosmotic Flows and Electrophoretic Mobilities

K. D. Altria / C. F. Simpson

Analytical Science Group, Department of Chemistry, Birkbeck College, University of London, 20 Gordon St.,
London WC 1H OAJ, UK

Key Words

Zone electrophoresis
Electrophoresis in capillaries
High voltage fields
Electroendosmosis

Summary

In High Voltage Capillary Zone Electrophoresis a field is applied across a narrow bore capillary filled with electrolyte solution. An electroendosmotic (EEO) flow is generated within this capillary which sweeps solutes along the tube.

An absolute method of flow estimation is described, along with some operating parameter effects on the solute mobility. System parameters enabling flow direction reversal and a zero flow are described. The use of several capillaries simultaneously and the effect of pH on EEO flow rates are also shown. Effects of various operating parameters on solute resolution are also detailed.

Introduction

High Voltage Capillary Zone Electrophoresis (HVCZE) is a rapidly developing, highly efficient separation technique in which a large potential drop is applied across a narrow bore capillary. Charged species will migrate electrophoretically towards the appropriate electrode and are separated by differences in their electrophoretic mobilities. In addition, under the influence of the applied field, electroendosmotic (EEO) flow is generated in the capillary which transports solutes molecules towards the detecting system independent of their individual charge. The characteristics of the EEO flow is such that minimal zone broadening occurs [1], as the solute travels along the capillary, which keeps zones sharp. Efficiencies of up to one million theoretical plates have been reported [2].

Solute migration times are dependent upon both EEO flow rate and solute electrophoretic mobility. Clearly, a precise measure of EEO flow rate would enable accurate determination of electrophoretic mobilities. Previous work in this area [2] has largely depended upon measurement of uncharged marker solute elution times, which are carried through the system under EEO flow only. Whilst this method is satisfactory, problems may arise due to adsorption or conductivity effects. Here we describe a method of estimating the EEO flow, which is free from any anomalous effects.

Theory

The hydrated surface of silica consists of ionized silicic acid groups which are neutralised by hydronium ions (hydrated cations). These cations arrange themselves into two layers. There is a closely bound layer held by electrostatic forces which is termed the "compact layer". Thermal motion causes some of the hydronium ions to diffuse away from the compact layer and form a loosely held layer termed the "diffuse layer".

If an electric field is imposed tangentially to the surface, the ions in the diffuse layer migrate towards the oppositely charged electrode entraining the water of solvation resulting in a flow of the solution [3]. This movement of solution is known as electroendosmosis (EEO) and its direction and magnitude depends upon both the substance of the containing capillary and the nature of the solvent used [4]. If the bulk solution flows tangentially to the surface a "plane of shear" is established at, or just above, the interface between the compact and diffuse layers. The potential at this plane of shear is termed the zeta potential (ζ) and is affected by the nature of any added electrolyte, in terms of its concentration and valency, i.e. the composition of the solvent used and the material used to construct the capillary.

The flow profile observed for EEO is virtually "plug" flow compared with that observed with "normal" laminar flow in capillaries. This plug flow profile reduces the band broadening processes that occurs as a solute travels along the tube; thereby minimizing zone broadening due to kinetic effects. Electroendosmotic flow has been exploited for both electrophoretic and chromatographic separations [1].

0009-5893/87 0527-06 $03.00/0

©1987 Friedr. Vieweg & Sohn Verlagsgesellschaft mbH

The velocity of the EEO flow (U_{EEO}) is given by:

$$U_{EEO} = (D/4\pi\eta)E\zeta = \mu_{EEO}E \tag{1}$$

where:

E = Electric field gradient (V/cm)
D = Dielectric constant
η = Viscosity of the medium
ζ = Zeta potential
μ_{EEO} = Coefficient of electroendosmotic flow, (may be taken to be analogous to electrophoretic mobility)

The electrophoretic migration velocity of an ion (U_{EP}) is given by:

$$U_{EP} = \mu_{EP}V \tag{2}$$

V = Applied voltage
μ_{EP} = Electrophoretic mobility ($cm^2 sec^{-1} V^{-1}$)

And the net migration velocity of an ion (U_{net}) in the presence of EEO flow may be obtained from:

$$U_{net} = (\mu_{EP} + \mu_{EEO})V \tag{3}$$

remembering that mobilities are signed quantities.

Migration time data may be used in order to ascertain μ_{EP} values if precise μ_{EEO} measurements have been made.

$$T = L^2/V(\mu_{EP} + \mu_{EEO}) \tag{4}$$

L = Length of capillary to optical centre of detector (cm)
T = Migration time (sec)

Experimental

A dual polarity 0–60kV power supply (Brandenburg, Croydon, Surrey, Model No. 2928) was used. Fused silica capillary was supplied by Scientific Glass Engineering, Milton Keynes. A modified Perkin Elmer Model No. PE-2000 fluorimeter detector was used throughout. A diagram of the experimental system is shown in Fig. 1. Sample injection was by the "electromigration" technique as described elsewhere [1]. EEO flows were measured by weighing the mass of buffer transferred from the anode to the cathode (or vice versa) over a timed period using a Mettler Digital balance Model No. AE160, as previously described [5]. Data presented here are the means of duplicate measurements.

All the reagents used were analytical grade and supplied by British Drug Houses, Poole, Dorset, England. Solutions were prepared by weight in degassed, near conductivity water obtained from a Elgastat Spectrum Still, Model No. SC1, High Wycombe, Bucks, England.

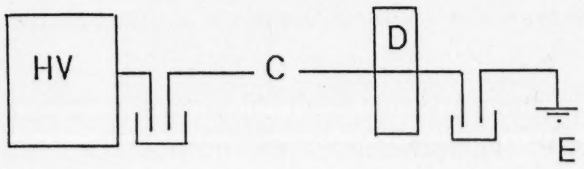

C = Capillary
D = Detector
E = Earth

Fig. 1
Diagram of system apparatus

Results and Discussion

An absolute method of estimating electroendosmotic flows has been developed [5] based on weight measurements. Precisions of 1.3% R.S.D. have been obtained from 10 replicate measurements; which compares favourably with previously described methods of EEO flow estimation.

Weights of solvent transferred per second were transformed into EEO flow rates ($cm\,sec^{-1}$) using eq. (5):

$$\text{EEO flow rate} = cm\,sec^{-1} = \{(m/\rho)/t\}/CSA \tag{5}$$

ρ = Density
CSA = Capillary cross sectional area (cm^2)
t = time of weight transfer (sec)
m = mass transferred (g)

The coefficient of EEO flow, μ_{EEO}, is calculated from eq. (6).

$$\mu_{EEO} = cm^2\,sec^{-1}\,V^{-1} = \text{EEO flow rate}/E \tag{6}$$

Previous methods used to estimate EEO flow rates include the use of migration time data from neutral solutes. These solutes, possessing a zero mobility, are swept to the detector solely by the EEO flow. Migration times are obtained subject to there being no ionization of the solute in the solvent, or any adsorption onto the capillary walls. Flow rate measurements obtained using neutral species may be time consuming as the migration times tend to be long.

Problems of solute adsorption can be pronounced in HVCZE [2] which have led to attempts to deactivate the walls by silanization. However, silanization affects the zeta potential [1, 7] and therefore alters the EEO flow rate. High solute concentrations have been shown to severely distort the conductivity profile [2]. Therefore, careful consideration must be taken when selecting an appropriate "neutral" marker solute.

Another method adopted for flow rate estimation has been to place a u.v. absorbing species into the high voltage buffer reservoir and then monitor the u.v. absorption of the earth reservoir [3]. This involved periodic stopping of the voltage and taking sample for testing. This method gave precisions in the order of 6% R.S.D. Apparent problems with this technique include molecular diffusion of the solute occurring whilst the voltage is switched off. Additional errors will occur due to the intervals between absorbance checks. Monitoring the time required for the level in one of the reservoir to be raised a specific height has also been used [4] to estimate EEO flows.

Solute migration time is related to both solute mobility and EEO flow rate (eq. (4)). Good reproducibility (1.5% R.S.D.) of migration times has been observed from 10 replicate runs. Reproducibility is often poor in conventional forms of electrophoresis; largely due to problems of gel to gel variation. However, in HVCZE the system parameters are more readily controlled leading to good precision. These results are in accordance with those recently published (8) concerning reproducibility in electrokinetic chromatography; an associated technique.

The electrophoretic mobility of an ion can be found directly from eq. (4) if the exact EEO flow rate for a particular capillary, under certain conditions, is first established.

Conditions for Zero EEO Flow

Use of a 0.02 M s-benzyl thiouronium chloride (BTC) solution (pH 4.5) in HVCZE has been found to produce a zero EEO flow. Under these conditions mobilities may be directly calculated from migration times using eq. (4), as the U_{EEO} term is zero i.e.

$$T = L^2/V(\mu_{EP}) \tag{7}$$

This property of zero flow is an advantage when studying parameter effects on mobilities; as there is no EEO flow term.

A decrease in BTC concentration from 0.02 M resulted in a concentration dependent increase in flow rate (Table I). It was impossible to operate at higher concentrations than 0.02 M due to problems of joule heating.

Application of a negative potential to a capillary containing 0.02 M s-benzyl thiouronium chloride also resulted in a zero flow. Therefore this electrolyte can be used for the analysis of either anions or cations by a simple reversal of the power supply polarity.

Relationship Between Applied Voltage and Mobility

Mobilities of two fluorescent solutes, quinine and quinacrine, were monitored, with respect to applied voltage. The results are shown in Fig. 2 below. Results were obtained applying voltages across a 75 μm wide, 100 cm long capillary filled with 0.02 M phosphate buffer.

Table II shows that mobilities were found to be effectively constant below 15 KV, but above this level increased linearily with applied voltage. At these higher voltages the capillary was unable to dissipate efficiently all the joule heat evolved; thus leading to a rise in temperature. Solvent viscosity decreases with rise in temperature, and since electrophoretic mobilities are inversely proportional to viscosity this decrease in viscosity above 15 KV leads to higher mobilities. This explains the deviation from linearity with increase in applied voltage.

Table I. Flow rate dependence on BTC concentration

Concentration (M)	Flow rate (cm sec^{-1})
0.02	0
0.002	0.049

Table II. Relationships of mobility with applied voltage

Solute	Equation of the line	Correlation
Quinine	y = 2.10E-4 + 7.14e-6x	1.00
Quinacrine	y = 2.73E-4 + 7.98e-6x	1.00

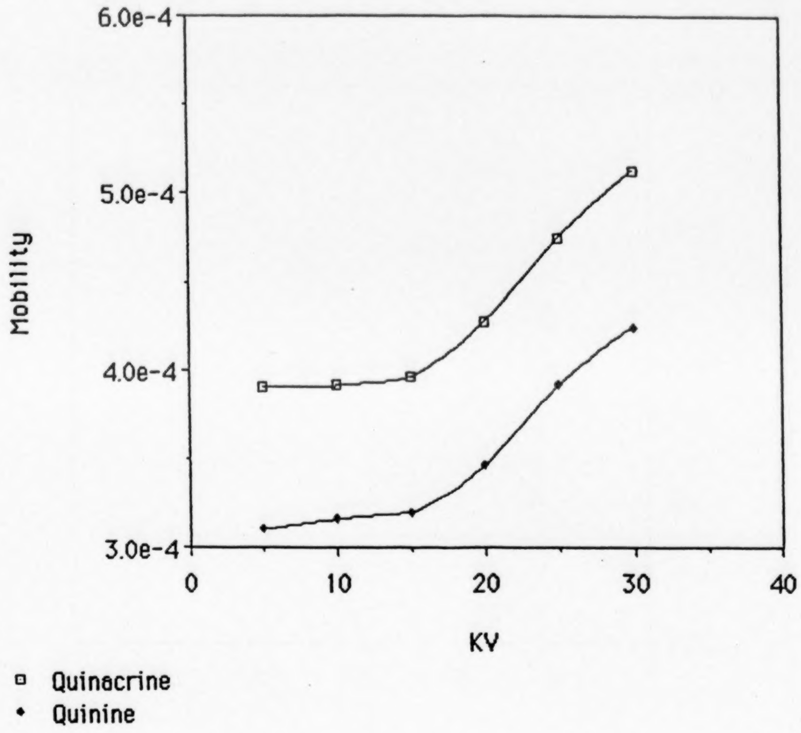

Fig. 2
μE ($cm^2 sec^{-1} V^{-1}$) versus applied voltage

Effect of pH on EEO Flow Rate

It has been previously shown [3] that EEO flow rates were linearily dependent on pH. However, this work covered only a limited range of pH from 5 to 8. It has been found that with a high pH, fast flows are observed but as pH conditions are varied through neutral and then acidic, the flow is greatly reduced, ceases and then reverses its direction (Fig. 3). These results may be explained as occurring due to neutralisation of surface anions, such as siloxy ions, by hydrogen ions from within the bulk solution. The positive flow values observed using acidic solutions may be explained by some protonation of surface silanols which would result in a positively charged surface.

The solutions used to produce actual pH conditions are shown in Table III and were all 0.02 M concentration. All measurements were made applying + 30 KV across a 75 μm bore, 100 cm long capillary.

Effect of pH on Mobility

The mobility of quinine has been studied over a range of pH values. Mobilities were calculated using eq. (4). The EEO flow rates varied as in Fig. 3. The pH dependency of quinine is shown in Fig. 4.

Quinine is known to have pKa values of 4.11 and 8.00. Thus effect of pH variation is that at low (acidic) pH's, below the first pKa, quinine exists as a doubly charged

Table III. Electrolyte solutions used in EEO versus pH experiment

pH	0.02 M solution	pH	0.02 M solution
12.1	NaOH	4.5	s-Benzylthiouronium Chloride
11.05	$NaHCO_3$	2.8	Thiodiglycollic Acid
6.8	Phosphate buffer		

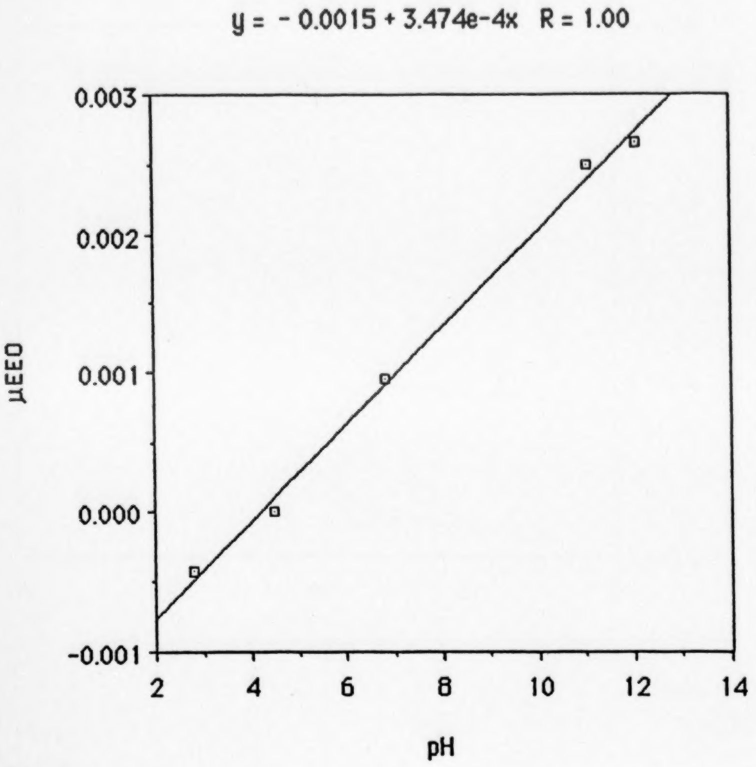

Fig. 3
μEEO (cm^{2}sec^{-1}V^{-1}) versus pH

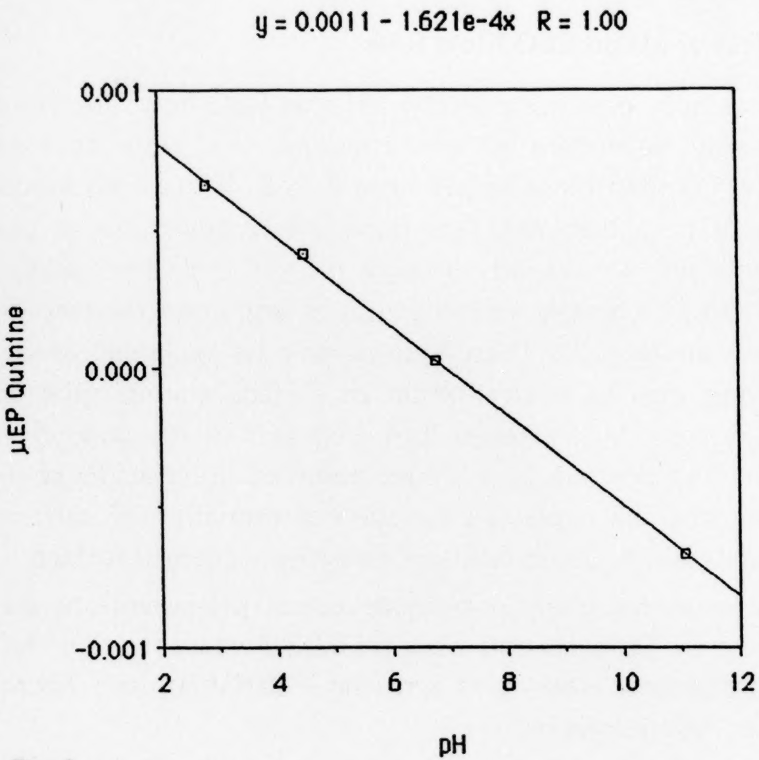

Fig. 4
μEP (cm^{2}sec^{-1}V^{-1}) of quinine versus pH
30KV applied across a 75μm × 100cm capillary

cation with an associated strongly positive mobility. When operating at a pH between the two Pka's, quinine will exist as a singly charged cation; with a diminished positive mobility. Above pH 8.00 quinine exists in the anionic form with a negative mobility.

Reversal of EEO Flow Direction

A reversal in the direction of "normal" EEO flow (i.e. towards the earth electrode) may be produced using solutions of cetyltrimethylammonium bromide (CTMAB). The flow rate became more positive as the CTMAB concentration was reduced; as shown in Fig. 5. Due to limited water solubility, concentrations in excess of 0.002M were not used. The graph was extrapolated back to include a flow rate measurement performed on pure distilled water.

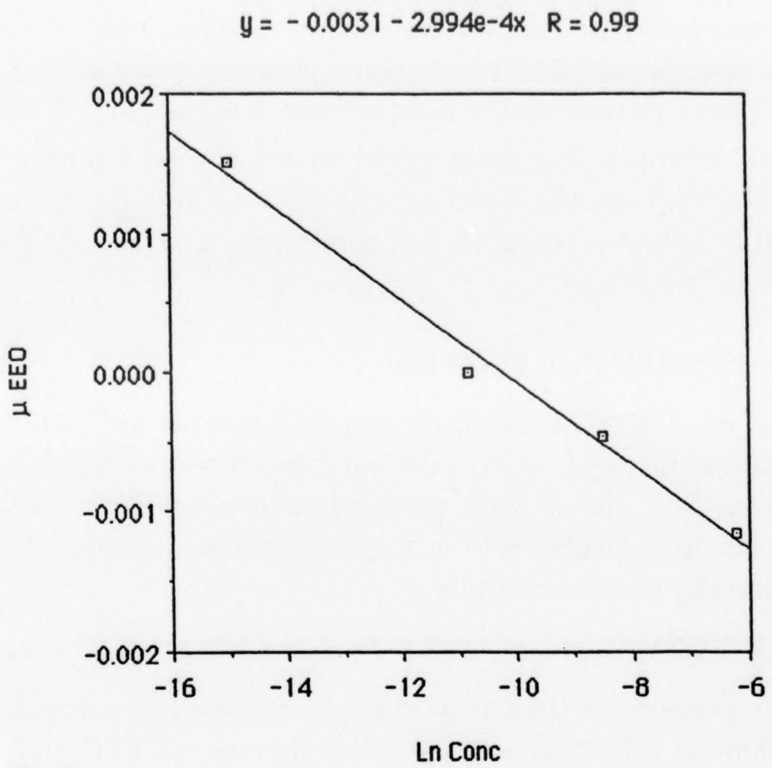

Fig. 5
μEEO (cm^{2}sec^{-1}V^{-1}) versus Ln CTMAB concentration (M)
30KV applied across a 75μm × 100cm capillary

A "normal" flow direction is produced when applying a negative potential to a solution of CTMAB. This combination of both negative applied potential and solutions of CTMAB may be useful for anion analysis. Migration of anions would, under these operating conditions, be in the flow direction, instead of against it; as is normally the case.

The magnitude of flows produced using CTMAB solutions has been shown to be pH independent over the range pH 4.5 to 11.0. This affords a means whereby it may be possible to operate at pH extremes whilst still maintaining a constant flow rate. It may be beneficial to operate at pH extremes when attempting analysis of components with high or low pKa values. Increasing the ionic strength of a 0.002M CTMAB solution by the addition of sufficient potassium chloride, to make the solution 0.02M in KCl, had no effect on the EEO flow rate. The zeta potential should be influenced by the addition of any added electrolyte. However, the current carried by the solutions increased due to the increased conductivity of the carrier electrolyte.

These findings are currently under investigation [9].

Flow Rate Manipulation by pH Control

The elution order usually obtained in HVCZE, when applying a positive potential, is that of cations (migrating by EEO and their electrophoretic mobilities), neutrals and lastly anions. Cations are eluted rapidly allowing little time for separation to occur. However, anions have long elution times as their electrophoretic migration direction is against the EEO flow. It is not possible to slow down the flow rate sufficiently to allow separation of cations

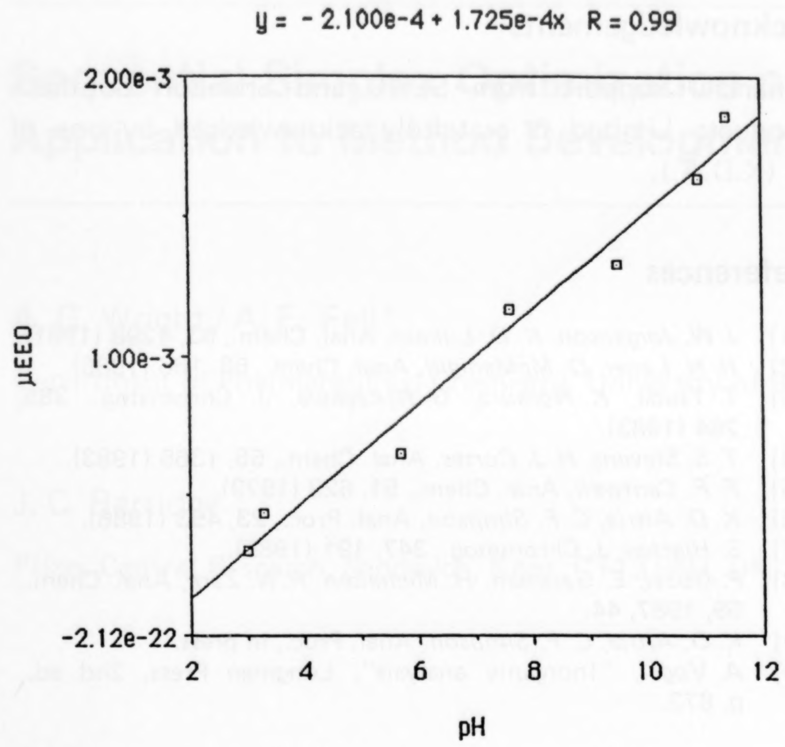

Fig. 6

μEEO (cm^2 sec^{-1} V^{-1}) versus pH

30 KV applied across a 75 μm × 100 cm capillary

Table IV. Effect of NaOH additions to buffer solutions on pH and EEO flow rate

Addition of NaOH (ml)	pH	EEO flow rate
0	3.0	3.02e-4
0.2	3.3	4.44e-4
1.55	5.7	6.54e-4
3.18	7.6	11.73e-4
4.35	9.5	13.33e-4
5.06	10.9	16.34e-4
5.86	11.4	18.61e-4

without excessively extending anion migration times. This problem may be solved by pH manipulation of EEO flow rates. Aliquots of 0.02 M NaOH were added to several 100 ml portions of a universal buffer [10] which had an initial pH of 3.0 (Table IV). Flow rate measurements were performed on these solutions. These alkali additions caused the flow rate to increase proportionately as shown in Fig. 6.

A graph of addition of NaOH (ml) versus μEEO gave an linear relationship with a correlation factor of 0.99.

At the initial, low pH values, the minimal flow rates observed would allow time for separations of cations to occur. However, an increase in pH would raise the flow rate in order to elute the neutral species. At higher pH values i.e. in excess of pH 7, the fast flow would be suffice to sweep the anions to the detector within manageable lengths of time.

Computer control of alkali addition to the buffer reservoir may present a method that may be of considerable use for the separation of complex mixtures of anions, neutrals and cations. This will be reported subsequently.

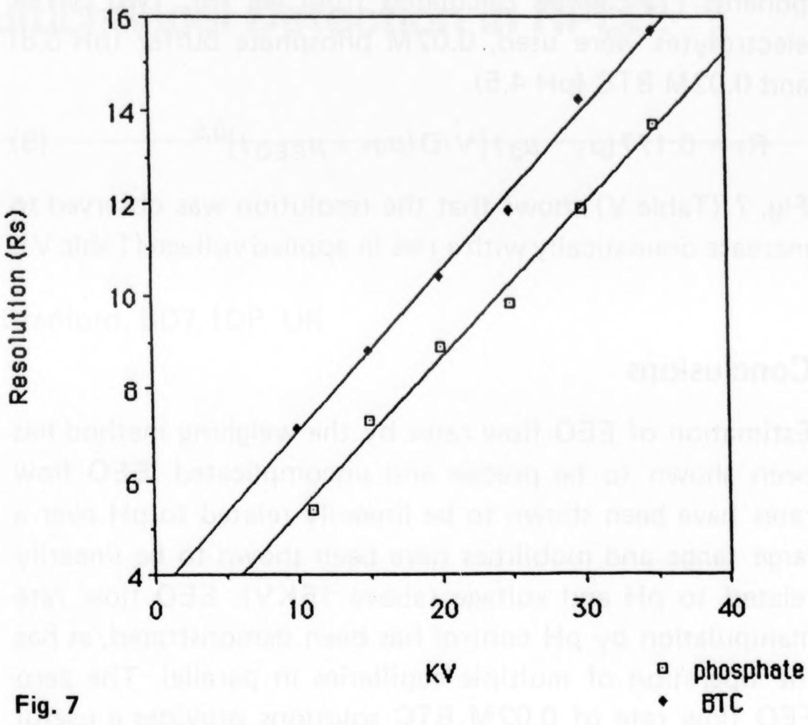

Fig. 7

Resolution (Rs) versus applied voltage

Voltage applied across 75 μm × 100 cm capillary

Table V. Resolution and migration time dependency on applied voltage

i) Migration times (mins) using 0.02 M BTC

Applied voltage	Quinine	Quinacrine	ΔT
10 KV	34.6	28.0	6.6
30 KV	8.8	7.1	1.7

ii) Relationships between Rs and applied voltage

Electrolyte	Equation of the line	Correlation
0.02 M BTC	y = 3.55 + 0.346x	1.00
0.02 M phosphate	y = 2.00 + 0.330x	1.00

Multiple Capillary Applications

Use of a single power supply for simultaneous multiple separations has also been demonstrated. Two or more capillaries have been operated in parallel from the same buffer reservoir. The current doubled as the current carrying capacity of the system doubled. Flow rates were found to be identical when voltage was applied across several identical capillaries at the same time. Thus it may be possible to construct a device capable of performing several electrophoretic separations simultaneously with the resultant saving in analysis time and, in addition, this facility could enable preparative separations to be undertaken, without overloading any one of the capillaries with loss in resolution. Individual capillaries would have to be separately loaded with sample.

Effect of Applied Voltage upon Resolution

The effect of varying the applied voltage upon solute resolution has been studied and the results are shown in Fig. 7 and Table V. The solutes used were quinine and quinacrine. The quinacrine was eluted first in all electro-

The various optimisation procedures require the extraction of different types of information from separations. Thus simultaneous procedures require the recognition of individual peaks, because the regression equations used rely upon measurement of retention for each peak. Simultaneous procedures are therefore best suited to the separation optimisation of samples of known composition, where standards can be injected for identification.

Sequential procedures require that the quality of a separation be expressed as a single numerical value using a chromatographic response function (CRF). This is often a complex function incorporating resolution and other factors, such as the number of peaks and analysis time [7]. Sequential approaches are less dependent upon solute recognition, but require detection of all peaks and have often been applied to samples where established UV spectra for the components have indicated an appropriate detection wavelength. The sequential simplex optimisation procedure for HPLC method development [6–10] does have its limitations, leading to uncertainty regarding:

a) the elution of all components from the column;
b) the resolution of all peaks;
c) the location of the global optimum, as opposed to adequate separations.

The conventional mode of detection in HPLC exploits UV absorbance at a single wavelength to detect all UV-active peaks, reveal incomplete resolution and provide sufficient information to identify separated components by their retention times. The limited information available means that it is not possible to fulfil all these requirements.

The recent advent of rapid-scanning linear photodiode array UV detectors capable of simultaneously monitoring chromatographic signals at multiple detection wavelengths and of acquiring spectral information at sequential elution times [21], has added a new dimension to the chromatographic data available to the analyst. This increased information content has already been exploited to interrogate peak homogeneity in optimising separations [22, 23].

The present studies investigate the utility of multi-wavelength diode array detection as a means of enhancing the application of sequential simplex to automated HPLC method development. A number of on-board data processing routines implemented in a commercial liquid chromatograph are extended by addition of software for multi-channel simplex optimisation, for a new 'stop' criterion and a new method for peak correlation. The theoretical basis for a new peak purity parameter is proposed and these techniques utilised in the practical optimisation of a six-component model system.

Theory

Assessment of Extent of Elution

In optimisation procedures it is necessary to introduce a 'stop criterion' whereby optimisation is stopped when the separation can be shown to be completed. For a chromatographic separation the completeness of elution can be assessed in two ways. With a well-characterised sample the correct number of UV-active peaks present will be known and can be verified in the chromatogram. While this is not possible for an unknown sample, a parameter which expresses the extent of elution of all UV-active peaks can nevertheless be calculated.

Several situations can give rise to fewer chromatographic peaks being detected than the number of components actually present in the sample. For example, two or more peaks within the chromatogram may overlap; one or more peaks may remain to be eluted from the column; or, peak overlap and incomplete elution may both occur. Thus it is necessary to distinguish incomplete elution from peak overlap. Moreover, these situations should be distinguished from that where one or more peaks are not observed at the detection wavelength selected.

Any method for assessing completeness of elution should incorporate a contribution from each individual UV-active solute and yield a calculated value representing complete elution of all the solute peaks.

In the present work it is proposed that a measure of the total chromatographic integral for all peaks at a defined detection wavelength can be predicted by measuring the *static* UV absorbance for the solute mixture at that wavelength. The extent of elution is then established by direct comparison between observed and predicted values for the total chromatographic integral. In making this comparison, it is assumed that both the spectrophotometer and the HPLC detector are operated under identical conditions of wavelength, bandwidth, temperature and solvent. It is also assumed that chromatographic band broadening does not significantly affect the absolute value of the observed chromatographic integral.

The total spectrophotometric absorbance (A_s^λ) at wavelength λ for all UV-absorbing components is defined as:

$$A_s^\lambda = \sum^{i} \epsilon_i^\lambda c_i l_s \tag{1}$$

where:

ϵ_i^λ is the absorptivity ($l \cdot mol^{-1} \cdot cm^{-1}$) of solute i at wavelength λ;

c_i is the concentration ($mol \cdot l^{-1}$) of solute i; and l_s is the pathlength (cm) of the spectrophotometer cell

In the proposed procedure, the sample solute mixture is studied both chromatographically and spectrophotometrically. For spectrophotometric measurement the sample is usually diluted to a concentration c_i' defined as:

$$c_i' = \frac{V}{V_d} \cdot c_i \tag{2}$$

where: V is the sample volume (ml) taken, and V_d is the volume (ml) to which it is diluted.

The total absorbance observed, A_s^λ, for this diluted concentration and at a specified wavelength therefore becomes:

$$A_s^\lambda = \frac{\sum_{i=1}^{n} \epsilon_i^\lambda \cdot c_i \cdot l_s \cdot V}{V_d} \tag{3}$$

The chromatographic integral for any component i, I_i^λ, at any wavelength λ is expressed as absorbance unit · seconds

(A · s); thus the total integral, I^λ, for all components is defined as:

$$I^\lambda = \sum_{i=1}^{n} I_i^\lambda \tag{4}$$

In HPLC each component is eluted in a defined volume of mobile phase and the time taken for this volume to pass through the detector cell is inversely proportional to the flow rate. Since the chromatographic integral, I^λ, is an inverse function of the flow rate, the predicted chromatographic integral, I_p^λ, may be estimated from:

$$I_p^\lambda = \frac{\sum_{i=1}^{n} \epsilon_i^\lambda \cdot c_i \cdot l_c \cdot V'}{f_v} \tag{5}$$

where: l_c is the pathlength (cm) of the HPLC detector cell, V' is the volume injected (ml) and f_v is the flow rate ($ml \cdot min^{-1}$)

Expressing flow rate as $ml \cdot s^{-1}$ and substituting (3) in (5) yields:

$$I_p^\lambda = \frac{A_s \cdot V_d \cdot l_c \cdot V' \cdot 60}{V \cdot I_s \cdot f_v} \tag{6}$$

This relationship provides a tool for estimating the completeness of elution at any wavelength, λ, by comparing the observed chromatographic integral, I^λ, with that predicted, I_p^λ. Further discrimination can be achieved by utilising data acquired simultaneously at a number of wavelengths.

Recognition of Peak Overlap

The use of a CRF [6] with sequential simplex necessitates an assessment of peak homogeneity for each peak in the chromatogram. The incorporation of multichannel detection into the simplex procedure allows a number of peak homogeneity tests to be performed [21, 23, 24]. A new peak homogeneity algorithm is included in the operating software for the commercial instrument used in the present studies.

At a defined wavelength the absorbance of a single chromatographic peak arising from two overlapping components is the sum of each individual absorbance at all points throughout the peak profile [25], provided that the Beer-Lambert law applies to both components.

In cases where some separation occurs without any observed resolution, the relative contributions of the two components will change throughout the peak profile. If there is a sufficient difference between the spectra of the components, this would be expected to lead to changes in the peak shape and apparent peak retention time when observed at different wavelengths. Careful definition of the limits of the shift in apparent retention time for the composite peak would detect the occurrence of peak overlap in such cases.

The detectability of such shifts in observed retention time as a function of wavelength will depend upon a number of factors, including: the relative values of the molar absorptivities at the wavelengths selected; the relative concentrations of the two components; the digitisation rate (i.e. the number of points per second used to describe the peak profile); and the absolute value of the displacement between two overlapping peaks, Δt.

At any instant in time, t, and at any specified wavelength, λ, the total absorbance of the composite peak, $A_T^\lambda(t)$, is defined as:

$$A_T^\lambda(t) = A_1^\lambda(t) + A_2^\lambda(t) \tag{7}$$

where: $A_1^\lambda(t)$ and $A_2^\lambda(t)$ are the individual absorbances of peaks 1 and 2 at time t, respectively.

For a typical, chromatographic peak, concentration is ideally described by a Gaussian function (strictly, a skewed Gaussian). Thus, the peak absorbance at λ for component i at any time t is defined as:

$$A_i^\lambda(t) = \epsilon_i^\lambda \cdot l_c \cdot c_{max,i} \cdot \exp[-(t - t_{R,i})^2/2\sigma_i^2] \tag{8}$$

where:

ϵ_i^λ is the molar absorptivity of component i at wavelength λ

$c_{max,i}$ is the concentration of component i at the peak maximum

t is observation time

t_R is the retention time for component i

σ_i, the standard deviation for peak i, is a measure of peak dispersion

l_c is the pathlength for the HPLC detector cell.

Combining (7) and (8) enables the composite peak absorbance, $A_T^\lambda(t)$, to be defined as:

$$\begin{aligned} A_T^\lambda(t) = {} & \epsilon_1^\lambda \cdot l_c \cdot c_{max,1} \exp[-(t - t_{R,1})^2/2\sigma_1^2] + \\ & \epsilon_2^\lambda \cdot l_c \cdot c_{max,2} \exp[-(t - t_{R,2})^2/2\sigma_2^2] \end{aligned} \tag{9}$$

Differentiating this function with respect to time describes the gradient of the peak profile; when this function has a value of zero it corresponds to the *composite* peak maximum observed at t_{max}:

$$\begin{aligned} & \epsilon_1^\lambda \cdot l_c \cdot c_{max,1} \frac{d}{dt}[\exp[-(t_{max} - t_{R,1})^2/2\sigma_1^2]] + \\ & \epsilon_2^\lambda \cdot l_c \cdot c_{max,2} \frac{d}{dt}[\exp[-(t_{max} - t_{R,2})^2/2\sigma_2^2]] = 0 \end{aligned} \tag{10}$$

Simplification yields:

$$\begin{aligned} & -A_{max,1}^\lambda \frac{(t_{max} - t_{R,1})}{\sigma_2} \exp[f_1(t)] = \\ & A_{max,2}^\lambda \frac{(t_{max} - t_{R,2})}{\sigma_2} \exp[f_2(t)] \end{aligned} \tag{11}$$

where:

t_{max} is now the observed retention time of the composite peak

$A_{max,1}^\lambda$ and $A_{max,2}^\lambda$ are the absorbances at the individual peak maxima for components 1 and 2, respectively

$\exp[f_1(t)]$ and $\exp[f_2(t)]$ represent the exponential term of the Gaussian time functions defined in (10)

If $A_{max,1}^\lambda \gg A_{max,2}^\lambda$ then $(t_{max} - t_{R,1}) \rightarrow 0$ and $t_{max} \rightarrow t_{R,1}$. Conversely, if $A_{max,2}^\lambda \gg A_{max,1}^\lambda$ then $t_{max} \rightarrow t_{R,2}$. For the situation where $A_{max,1}^\lambda = A_{max,2}^\lambda$ then $t_{max} = (t_{R,1} + t_{R,2})/2$, the mean value.

Any change in the amplitude of $A^{\lambda}_{max,1}$ relative to $A^{\lambda}_{max,2}$ due to a change in wavelength, would lead to a change in the apparent peak retention time, t_{max} [26]. Recognition of this relationship of t_{max} with wavelength depends upon the intrinsic spectral profiles of the overlapping components, the instrumental settings and the inherent errors due to noise (electronic, flow). In cases where spectra are very similar, then little change in the value of t_{max} would be detected as a function of wavelength. Indeed, the test would be expected to function most sensitively at wavelengths identified as the maximum and minimum from the graph of the absorbance ratio (A_1/A_2) versus λ, as discussed in earlier work [24].

Determination of Chromatographic Separation Quality

As described earlier the simplex optimisation procedure requires the quality of a chromatographic separation to be described as a single numerical value by a chromatographic response function (CRF). The CRF developed for these studies incorporates the summated resolution values, the number of peaks and a target retention time for the last peak, T_A. However, the program ensures that any retention time for the last peak, T_L, that occurs within ± 1 minute of the target time, T_A, is equally acceptable, since the last term in the function is only included if it exceeds 1 minute. The CRF expression used is:

$$\mathrm{CRF} = \sum_{i=1}^{n-1} R_i + n - |T_A - T_L|$$

where:

R_i is the resolution between adjacent peak pairs, (R_i is limited to a maximum value of 1).

n is the number of peaks detected.

The target retention time used in the present work was 5 minutes.

The CRF utilised in this study is designed to give a maximum response when the separation fulfils or exceeds the pre-determined development requirements. Thus, if the maximum value, CRF_{max}, is reached during the course of optimisation, then the simplex can be halted. CRF_{max} depends upon the number of peaks present. Clearly, for an unknown sample, the prediction of CRF_{max} at the start of optimisation is not possible. However, the use of multi-channel detection enables detection of all UV-active peaks eluted, and in some cases it can enable recognition of peak overlap. As the simplex procedure progresses, updated estimates of the number of peaks present are calculated until the 'stop criterion' described above is satisfied i.e. the total integral observed at each of three wavelengths is equal to that predicted spectroscopically. Eventually the estimate reaches its highest value, which may be less than the actual value of the number of UV-active components present, if one or more peaks are retained on column, or, if irresolvable peak overlap occurs.

A routine (Fig. 1) has been incorporated into the simplex software [7] which halts the procedure, and switches the chromatograph to standby mode, if the CRF_{max} is reached on three (not necessarily consecutive) occasions. This number is selected to ensure that the simplex is not halted by noise artefacts.

Simplex optimisation incorporating single channel detection is conventionally halted either by reaching a pre-set 25-injection limit, or by the simplex size failing below a pre-specified value. Thus, the quality of separation has no direct influence on the termination of the procedure. In the present work, the proposed modifications retain the 25-injection limit, but also permit the criterion for terminating the optimisation to be directly related to the quality of the separation as expressed by CRF_{max}.

Determination of Elution Order

For efficient optimisation it is helpful to establish a tool which detects peak cross-over. Changes in elution order can be detected by tracking individual peaks within the chromatograms. Unequivocal recognition of peaks can generally be obtained by injecting the individual components, where these are available. Another property that can be used for solute recognition is the spectrum of the component itself. However, closely related components generally display similar spectra. Thus spectra alone do not provide discrimination between structually

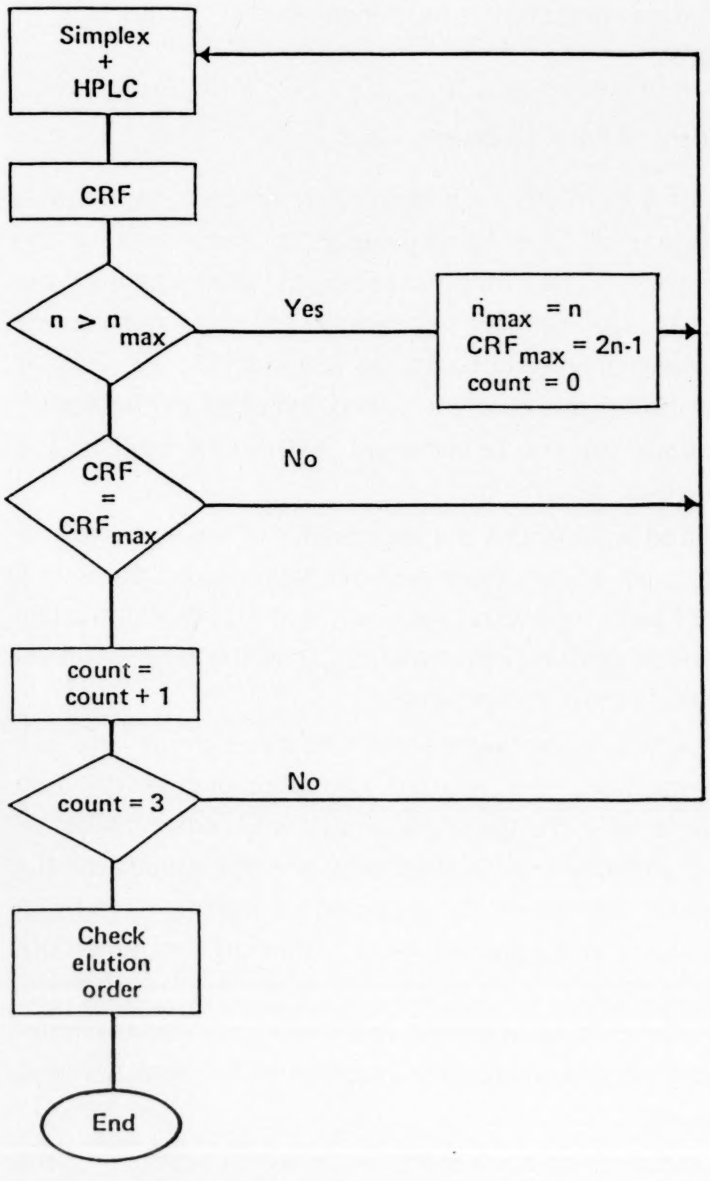

Fig. 1

Flow diagram for the stop criterion incorporated into the sequential simplex procedure.

similar compounds, although they can be valuable tools for recognition in some cases.

The peak area can be characteristic for a particular component, since it is dependent on both absorptivity at the detection wavelength and concentration. However, peak area determined at a single wavelength would not be expected to give positive identification, since several components could in principle have similar areas at the wavelength selected [27]. Multi-channel detection enables peak area to be measured at several wavelengths, and this can provide sufficient information for peak recognition. It is even possible to distinguish between two spectrally similar components, provided that they differ in concentration. The method would break down if two peaks in a chromatogram had a spectrum-concentration combination that yielded similar peak areas at the particular wavelengths selected.

Where a CRF is used to assess the quality of a separation it attains its maximum value when the separation fulfils the criteria specified for maximum and minimum retention times and for minimum resolution. However, this may not be the global optimum. A number of circumstances can arise that lead to more than one eluent composition being found for an acceptable separation. For example, different pairs of peaks may produce the limiting resolution utilised in the CRF; alternatively, comparable separations may be obtained for systems with different peak elution order. Since the maximum value of the resolution is constrained to 1, the maximum CRF (CRF_{max}) may reflect separations which are less good than the global optimum separation; in other words, a number of acceptable points could, in principle, be found which fulfil (in essence, exceed) the CRF criterion adopted.

Thus during the course of the sequential simplex procedure several separations fulfilling the development criteria, and producing CRF_{max}, may be located. These practical solutions to the development problem, which can be described as 'development solutions', can be further investigated in order to establish whether they are attributable to one or more changes in elution order, or to other factors. The first 'development solution' located can be used to provide a reference set of peak area-wavelength data for each peak detected in the chromatogram. These characteristic data can allow recognition of the peaks in the 'development solutions' subsequently observed.

Peak areas at the detection wavelengths selected, for the chromatogram that meets the CRF_{max} criterion for the first time, are used as reference data. The algorithm developed compares the similarity between area data for peaks in the reference chromatogram, and peaks in subsequent chromatograms that fulfil the development criteria. A best fit value ranging between 0 and 100, is then calculated in the following way. The integral, at wavelength $\lambda 1$ for each reference (initial) chromatographic peak, $I_R^{\lambda 1}$, is compared in turn with the integrals for every chromatographic peak in subsequent chromatograms, $I_2^{\lambda 1}$, at the same wavelength. The relative degree of fit, $S^{\lambda 2}$, at wavelength $\lambda 1$ is defined as:

$$S^{\lambda 2} = I_2^{\lambda 2}/I_R^{\lambda 2} \qquad (12)$$

If the ratio exceeds 1 then for convenience the reciprocal is taken:

$$S^{\lambda 1} = I_R^{\lambda 1}/I_2^{\lambda 1} \qquad (12a)$$

The procedure is repeated for each detection wavelength selected and the ratio summated to give a total degree of fit value, S_T, defined as:

$$S_T = \sum_{i=1}^{n} S^{\lambda i} \qquad (13)$$

The final best fit value, S_F, is obtained by dividing S_T by the number of detection wavelengths and scaling to 100:

$$S_F = (S_T/n) \cdot 100 \qquad (14)$$

where: n is the number of detection wavelengths used.

The closer the best fit value approaches 100, the greater the correlation between the two peaks. Small variations in peak areas do occur with changes in mobile phase composition, due to solvochromic effects on the spectra. In the Author's experience such variations for the solutes used are not significant over a range of compositions of acetonitrile, tetrahydrofuran (THF) and methanol with water.

Experimental

Apparatus and Materials

The system used was a Hewlett-Packard 1090A chromatograph (Hewlett-Packard Ltd., Wokingham, UK) comprising an HP 1040A diode array detector, a DR5 ternary pumping system and a 100-position autosampler. The system was controlled by an HP85B computer. Separations were performed on a 125 × 4.6mm Partisphere-C18 5-μm column (Whatman).

Mobile phases consisted of different ternary mixtures of acetonitrile, THF and water (Rathburn Chemicals, Peebles, UK). A model system of: 3-hydroxybenzaldehyde (HBA), phenol (Phen), propyl-p-hydroxybenzoate (PHB), butyl-p-hydroxybenzoate (BHB), diethyl phthalate (DP) and toluene (Tol) was used throughout. A Pye-Unicam PU8600 spectrophotometer operating at the same wavelength, bandwidth and temperature as the HPLC detector was used to obtain absorbance data for the solute mixture.

Software

Programs for the sequential simplex optimisation procedure were written in BASIC as a series of 'hook' programs on the HP85B. The quality of separation was assessed using a chromatographic response function (CRF). The simplex procedure was limited to a maximum of 25 injections before optimisation was halted.

Results and Discussion

In this study emphasis was placed upon exploiting the on-board facilities of the commercial LC system. The applicability and practical simplicity of this approach to LC method development was exemplified for a model six-component solute mixture, treated as an unknown sample during these studies. It was assumed that no information concerning the number of peaks or their spectra was available.

To determine a suitable detection wavelength for a single channel sequential simplex procedure, the UV profile for the solute mixture was recorded (Fig. 2). The region below 230nm was ignored to avoid possible solvent cut-off effects. Since the UV profile does not have any clearly defined maximum between 230 and 300nm, 240nm was selected as being representative of the absorbances over this range.

A sequential simplex procedure was carried out at this wavelength, with a maximum run time of 7 minutes and no constraints on the acetonitrile and THF concentrations (Fig. 3). A 'development solution' mobile phase composition was identified for the separation as MeCN-THF-Water (6.8:31.4:61.8, v/v). However, only four clearly defined peaks were detected (Fig. 4).

This 'development solution' separation was further investigated using simultaneous monitoring at three detection wavelengths (240, 260 and 280nm) (Fig. 4). The completeness of elution was also evaluated using the algorithm proposed at each wavelength for a 7 minute response. From Table I it can be seen that the predicted integral at 260nm does not accord with the observed value, indicating incomplete elution. The run time was extended to 10 minutes and good agreement was observed between the predicted and observed integrals for every wavelength selected (Table II).

The proposed algorithm for assessment of completeness of elution relative to predicted values has been demonstrated, in the present study, to be useful, so long as any non-

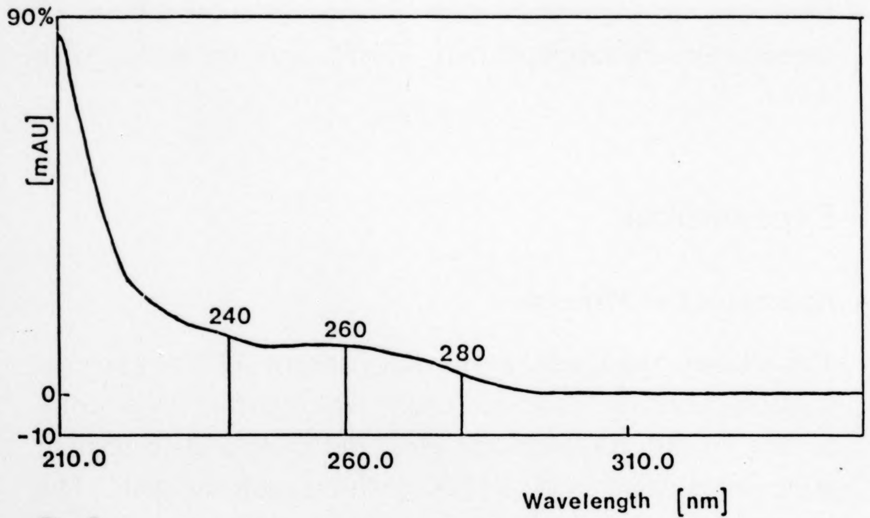

Fig. 2
Off-line UV spectrum for the complete solute mixture.

Table I. Agreement between predicted total chromatogram integral and that observed for 7- and 10-minute run times at three wavelengths (240, 260 and 280nm).

Wave-length nm	Expected Integral A·s	Summated Integral for 7 min run time A·s	Agree-ment %	Summated Integral for 10 min run time A·s	Agree-ment %
240	22.95	22.73	99	23.36	102
260	19.17	17.01	89	19.78	103
280	9.86	9.85	100	9.85	100

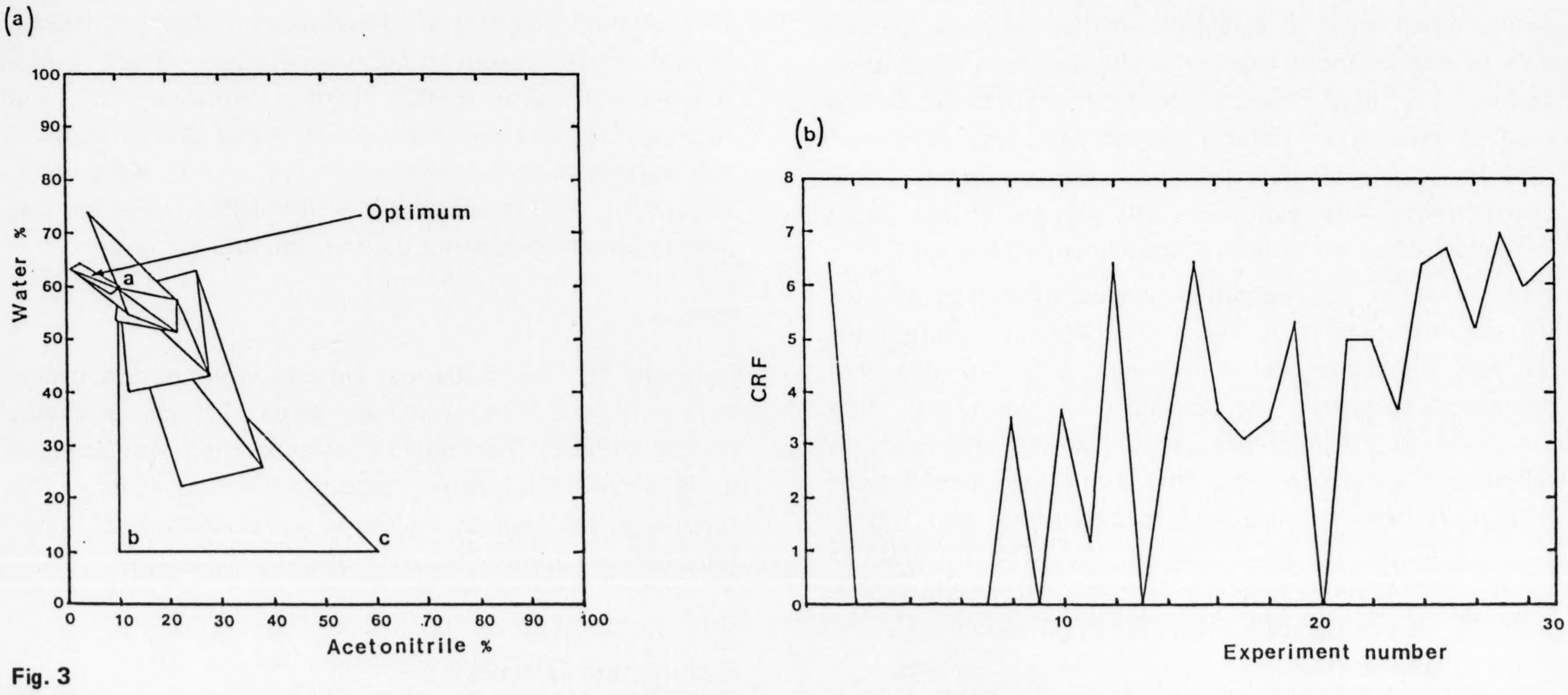

Fig. 3

(a) Movements of the sequential simplex procedure with a detection wavelength of 240nm; a, b and c are the three starting points. Optimum separation conditions: acetonitrile-THF-water (6.8:31.4:61.8, % v/v); CRF = 7.

(b) Plot of CRF with experiment number; $CRF_{max} = 7$ for four peaks.

Table II. Best fit values (calculated by proposed algorithm) between peaks in the three 'development solutions' located. Detection wavelengths used: 240, 260 and 280 nm.

First Optimum peak number	Second Optimum peak number						Third Optimum peak number					
	1	2	3	4	5	6	1	2	3	4	5	6
1	98	35	34	22	28	75	97	38	34	23	30	75
2	35	98	34	46	33	38	34	93	34	48	33	39
3	33	34	98	40	86	32	32	34	96	39	91	31
4	21	45	40	97	40	29	20	42	41	96	40	28
5	28	33	83	40	98	27	27	34	81	39	92	26
6	75	37	33	30	28	98	74	36	34	31	30	96

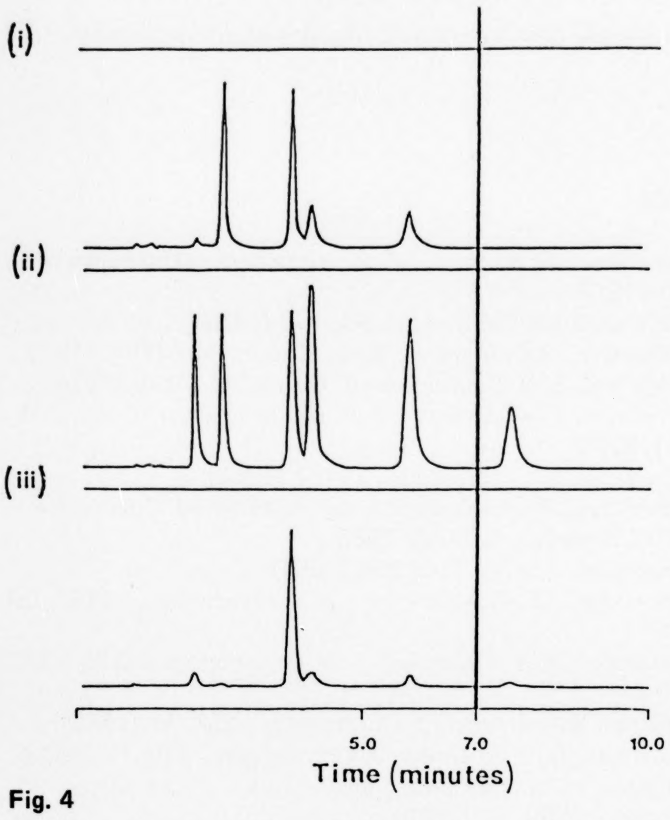

Fig. 4

Optimum separation conditions run for detection wavelengths i) 280 nm, ii) 260 nm and iii) 240 nm showing 7 and 10 minute cut-off times.

eluted components make a contribution to sample spectrophotometric UV absorbance at the wavelength or wavelengths selected. If any non-eluted component has no significant UV absorbance at the detection wavelength, elution will appear, wrongly, to be complete. Diode array detection can reveal the presence of all eluted components by multi-wavelength monitoring. Moreover this detector can assist in establishing that one or more components has failed to be eluted from the column through comparison of predicted and observed chromatographic integrals at several wavelengths. Although the proposed algorithm currently requires an off-line determination which necessitates a solvent that closely approximates to that for the development solution, this procedure could, in principle, be automated.

The use of multi-wavelength detection enabled an accurate assessment of CRF_{max} and the incorporation of the stop criterion proposed earlier. When the sequential simplex was halted earlier than the pre-set 25-injection limit, three 'development solutions' were located. The elution order of components in these separations was

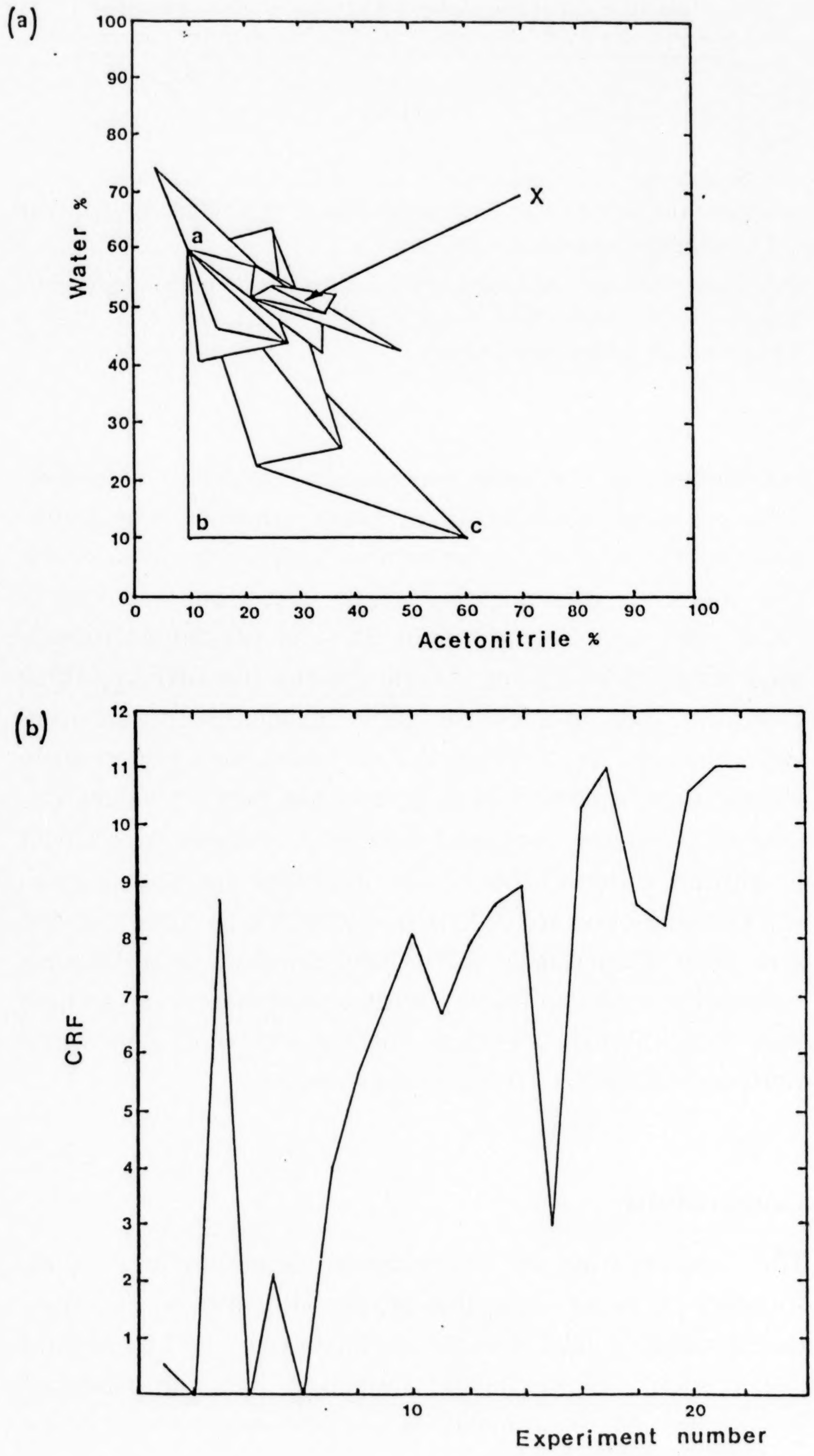

Fig. 5

(a) Movements of the sequential simplex procedure with detection wavelengths of 240, 260 and 280 nm; a, b and c are the three starting points. X = 'development solutions' i), ii) and iii). Separation conditions for 'development solutions':

i) and ii) acetonitrile-THF-water (34.3 : 17.1 : 48.6, % v/v);
iii) acetonitrile-THF-water (37.5 : 11.4 : 51.1, % v/v);
$CRF = CRF_{max} = 11$.

(b) Plot of CRF with experiment number, $CRF_{max} = 11$ for six peaks.

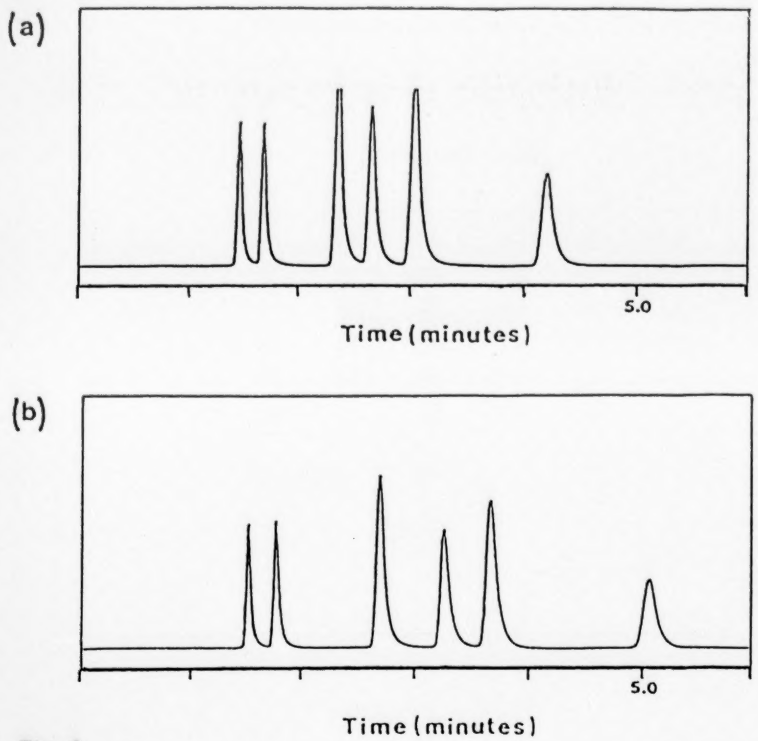

Fig. 6

(a) Separation for 'development solutions' i) and ii); mobile phase composition: acetonitrile-THF-water (34.3 : 17.1 : 48.6, % v/v); CRF = 11; detection wavelength 260 nm.

(b) Separation for 'development solution' iii); mobile phase composition: acetonitrile-THF-water (37.5 : 11.4 : 51.1, % v/v); CRF = 11; detection wavelength 260 nm.

established by the peak recognition algorithm described. The practical application of these routines was implemented by running a sequential simplex procedure for the mixture, incorporating three detection wavelengths (240, 260 and 280nm) (Fig. 5). The procedure terminated after 19 injections, having located the CRF_{max} three times. In this instance the three 'development solutions' were close in factor-space. All six peaks were eluted within the time specified (Fig. 6) and the best fit values calculated using the proposed algorithm revealed no changes in elution order (Table II), as indicated by the diagonal values being close to 100. It is interesting to note that the area ratio technique is sufficiently selective to distinguish between propyl and butyl p-hydroxybenzoate, even though they have almost identical spectra and their concentrations only differ by 10% in this instance.

Conclusions

The incorporation of multichannel detection and its associated software into the sequential simplex optimisation procedure improves its application to HPLC method development. Multi-channel detection has a number of features which recommend its use with sequential simplex optimisation:

a) all UV-active peaks can be detected;

b) partially overlapping peaks can be detected, provided their spectra are sufficiently different, from changes in the apparent retention time when recorded at different wavelengths;

c) peak tracking can be implemented by measuring peak areas at different wavelengths to ascertain elution order;

d) completeness of elution can be more effectively determined when applying the algorithm at several wavelengths.

The combination of multi-channel detection with the sequential simplex optimisation procedure can lead to more efficient method development with consequent savings in time and development costs. This can be implemented in a fully automated procedure requiring no prior information on the number of components, their spectral characteristics or retention behaviour.

Acknowledgement

One of the authors (AGW) would like to thank Pfizer Central Research UK for providing the studentship for this research.

References

[1] *W. Spendley, G. R. Hext, F. R. Hinsworth*, Technometrics, **4**, 441 (1962).
[2] *D. E. Long*, Anal. Chim. Acta, **46**, 193 (1969).
[3] *S. N. Deming, S. L. Morgan*, Anal. Chem., **45**, 278A (1973).
[4] *S. L. Morgan, S. N. Deming*, Anal. Chem., **46**, 1170 (1974).
[5] *M. W. Routh, P. A. Swartz, M. B. Denton*, Anal. Chem., **49**, 1422 (1977).
[6] *J. C. Berridge*, J. Chromatogr., **244**, 1 (1982).
[7] *J. C. Berridge*, Techniques for the Automated Optimization of HPLC Separations, Wiley 1985.
[8] *J. C. Berridge*, Analyst **109**, 291 (1984).
[9] *J. C. Berridge, E. G. Morrissey*, J. Chromatogr., **316**, 69 (1984).
[10] *A. S. Kester, R. E. Thompson*, J. Chromatogr., **310**, 372 (1984).
[11] *M. Otto, W. Wegschieder*, J. Chromatogr., **258**, 11 (1983).
[12] *M. L. Cotton, G. R. B. Down*, J. Chromatogr., **259**, 17 (1983).
[13] *J. L. Glajch, J. J. Kirkland K. M. Squire, J. M. Minor*, J. Chromatogr. **199**, 57 (1980).
[14] *J. L. Glajch, J. J. Kirkland, L. R. Snyder*, J. Chromatogr., **238**, 269 (1982).
[15] *J. L. Glajch, J. L. Gluckman, J. G. Charikofsky, J. M. Minor, J. J. Kirkland*, J. Chromatogr., **318**, 23 (1985).
[16] *P. J. Schoenmakers, A. C. J. H. Drouen, H. A. H. Billiet, L. De Galan*, Chromatographia **15**, 688 (1982).
[17] *A. C. J. H. Drouen, H. A. H. Billiet, P. J. Schoenmakers, L. De Galan*, Chromatographia **16**, 48 (1982).
[18] *P. R. Haddad, A. C. J. H. Drouen, H. A. H. Billiet, L. De Galan*, J. Chromatogr., **282**, 71 (1983).
[19] *H. A. H. Billiet, A. C. J. H. Drouen, L. De Galan*, J. Chromatogr., **316**, 231 (1984).
[20] *H. A. Cooper, R. J. Hurtubise*, J. Chromatogr., **324**, 1 (1985).
[21] *B. J. Clark, A. F. Fell, H. P. Scott, D. Westerlund*, J. Chromatogr., **286**, 271 (1984).
[22] *J. K. Strasters, H. A. H. Billiet, L. de Galan, B. G. M. Vandeginste, G. Kateman*, J. Chromatogr., **385**, 181 (1987).
[23] *T. P. Bridge, M. H. Williams, G. G. R. Seaton, A. F. Fell*, Chromatographia **24**, 691 (1987).
[24] *A. F. Fell, H. P. Scott, R. Gill, A. C. Moffat*, J. Chromatogr., **282**, 123 (1983).
[25] *A. H. Anderson, T. C. Gibb, A. B. Littlewood*, Anal. Chem., **42**, 440 (1970).
[26] *J. M. Vandenbelt, C. Henrich*, Appl. Spectroscopy **7**, 171 (1953).
[27] *H. J. Issaq, K. L. McNitt*, J. Liq. Chromatogr. **5**, 1771 (1982).

Received: June 30, 1987
Revised manuscript
received: Oct. 9, 1987
Accepted: Oct. 20, 1987
F

Group Separation of PCDDs, PCDFs, PACs and Aliphatic Compounds on an Amino Bonded Stationary Phase for HPLC

A. L. Colmsjö*

National Institute of Occupational Health, Analytical Division, S-171 84 Solna, Sweden

Y. U. Zebühr/Conny E. Östman

Department of Analytical Chemistry, University of Stockholm, S-106 91 Stockholm, Sweden

Key Words

Column liquid chromatogrpahy
Amino bonded phase
PCDD
PCDF
Backflush

Summary

A HPLC method for the clean up of PCDD and PCDF samples is presented. The method utilizes the possibility of separating compounds according to the number of double bonds by using an amino bonded stationary phase. Aliphatics as well as compounds with higher aromaticity than PCDD/PCDF are removed. In addition, the latter can be collected as one fraction. The fractionation in fast, done in one step and automated.

Introduction

Polynuclear aromatic compounds (PAC) constitute a group of compounds, a number of which posses strong carcinogenic, mutagenic and/or toxic properties (for example benzo(a)-pyrene (BaP) and 3,4,7,8-tetrachlorodibenzo-p-dioxine). During the last decade, the development of new and better quantitative and qualitative methods for chemical analysis of PACs has been a subject of intensive investigation [1–5].

In 1977 Wise et al. [8] introduced the use of uBondapak NH_2 for the separation of polynuclear aromatic hydrocarbons (PAHs) into fractions according to the number of condensed aromatic rings. In particular the authors observed that "A GC-MS analysis performed on the fraction between naphthalene and anthracene fraction was found to consist primarily of three ring compounds containing a five-member ring (i. e., dibenzothiophenes, dibenzofurans and fluorenes)". Following this, a number of authors have made attempts to explain the retention mechanisms of the NH_2 phase in the straight phase mode. In 1980 Liphard [9] concluded that "The separation is controlled only by the number of double bonds in a given hydrocarbon molecule. It is essentially independent of the molecular mass for a large variety of compounds investigated. (shown on partially hydrogenated PAHs)". Snyder and Schunk summarized in 1982 [10] that "The mechanism of retention in these liquid chromatographic systems involves monolayer coverage of the adsorbent surface by mobile phase molecules and displacement of solvent molecules by adsorbing solute molecules." and finally in 1983 Karlesky et al. [11] concluded that "the mechanism of separation is mainly due to a charge transfer interaction between the lone pair electrons on the stationary phase nitrogen and the pi-electron cloud of the solute PNAs. Elution order seems to depend upon a combination of pi-energy, and type of ring condensation of the solute".

This paper demonstrates the possibility of separating polychlorinated dibenzodioxines (PCDDs) and dibenzofuranes (PCDFs) from aliphatic compounds and compounds of higher aromaticity, i. e. PACs with three condensed rings or more, by using a uBondapak NH_2 column in straight phase mode utilizing backflush technique.

Experimental

A soot sample from the electrostatic filters of an municipal incineration plant in surburban Stockholm was Soxhlet extracted during 14 hours, using toluene as extractant. Strongly polar compounds were removed from the sample by filtration on a short silica column, 0.3 g silica deactivated with 10% water, using hexane as mobile phase. This yielded a raw extract to be further cleaned up using HPLC.

The HPLC system (Fig. 1) consisted of a Waters 590 Programmable Solvent Delivery Module (PSDM), a Waters Automatic Valve Station (WAVS), a Waters Automatic Switching Valve (WASV) and a Hitachi 655A-22 UV-absorbance detector. The WAVS module was used for heart cutting of the dioxine fraction followed by backflushing. The PAC fraction, eluting as one narrow backflush peak,

0009-5893/87 0541-04 $03.00/0

© 1987 Friedr. Vieweg & Sohn Verlagsgesellschaft mbH

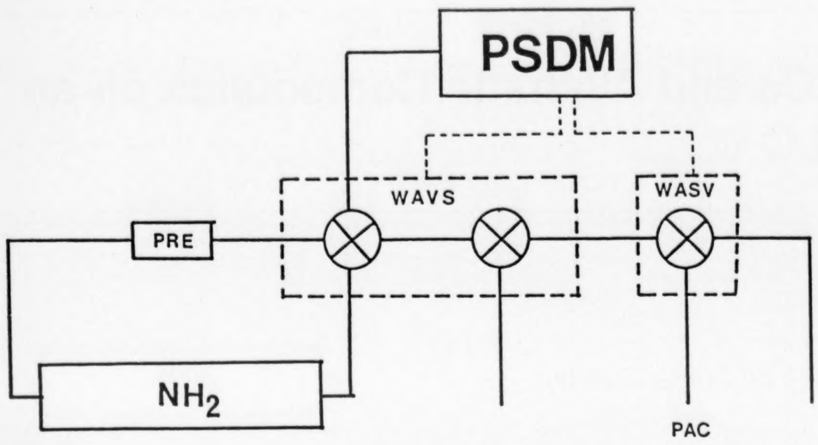

Fig. 1

Schematice of the backflush system with the amino column. PSDM: Programmable Solvent Delivery Module. WAVS: Waters Automatic Valve Station.

was collected using the WASV. Rathburn HPLC grade hexane was used as mobile phase without further purification. Flow was kept at 3 ml/min during forward elution. During backflush, a flow of 5 ml/min was used to increase speed of the fractionation procedure. Valve switching was controlled by the PSDM, making possible a completely automated fractionation procedure. Anthracene was used as standard compound for the setting of the backflush time and a standard mixture containing compounds with 3–6 aromatic rings was used for setting the time for collection interval for the backflush peak.

Gas chromatography with different detection techniques was used for analysis of the fractions. Analysis of dioxines was performed using a Varian 3300 equipped with a split/splitless injector, an electron capture detector and a SE-54 column. PAC fractions were analyzed with a Varian 3700 equipped with split/splitless injector, a CPSil-8/CB 24 m X 0.32 mm column, and flame ionization and thermal ionization detectors. A Hewlett Packard 5790A with a SE-54 column, interfaced with a Jeol JMS-D300 mass spectrometer was used for mass spectrometric analysis. Multiple ion detection (MID) technique was used for detection and identification of dioxines, while ordinary scanning technique were utilized for the PAC fractions.

Results

According to the theory of primary retention for a normal phase system applied to an n-alkyl amino bonded stationary phase, solutes consisting of two condensed rings should exhibit approximately the same retention characteristics. Nevertheless, secondary retention effects, possibly affecting the charge transfer interaction between the pi-electrons of the solute and the amino group of the stationary phase, must be taken into account if the separation technique is to be applied on samples with a wide variety of isomers. I. e. if polychlorinated dibenzodioxines and polychlorinated dibenzofuranes (including 210 compounds) are to be separated from compounds with higher aromaticity, good retention characteristics must be available or registered. Due to lack of standard compounds this is difficult to perform. This problem was solved by using a cleaned-up extract containing PCDDs and PCDFs, derived from a municipal incineration plant. The sample was analysed utilizing a uBondapak NH_2 column with hexane as mobile phase and monitoring the effluent at an absorption wavelength of 238 nm. In Fig. 2, the chromatogram is shown. Retention times of toluene, naphthalene, anthracene and phenanthrene are indicated with dashed lines in the chromatogram. Additional retention characteristics were obtained from selected PCDD, PCDF and polychlorinated biphenyls (PCB) standard compounds.

Among the secondary retention effects which can be anticipated from a polychlorinated two aromatic ring system, shielding is probably the most significant. I. e., chlorine atoms shield parts of the pi-electron system of the solutes. This gives rise to a weaker retention probably due to steric effects caused by the solute. This is demonstrated by decachlorobiphenyl having the same retention as toluene (Table I). Another important retention mechanism is probably charge transfer interactions between the lone pair electrons of the hetero atoms, like oxygen and nitrogen, of the solute molecules and the lone pair electrons of the amino group of the stationary phase. This could be the explanation for octachlorodibenzo-p-dioxin having stronger retention than decachlorobiphenyl (Table I).

Using retention data from HPLC of standard compounds and the PCDD/PCDF raw extract and further, GC-ECD and GC-MS analysis of the HPLC fraction of the raw extract eluting between toluene and anthracene, it was confirmed that all major PCDDs and PCDFs elute in this fraction with the HPLC system used. This fact was used to construct a simple backflush routine, which made possible collection of compounds with two aromatic rings in one fraction and further, by reversing the solvent flow in the column, collect all higher aromatic compounds in one peak, figure 4. Aliphatic compounds (up to C_{35}

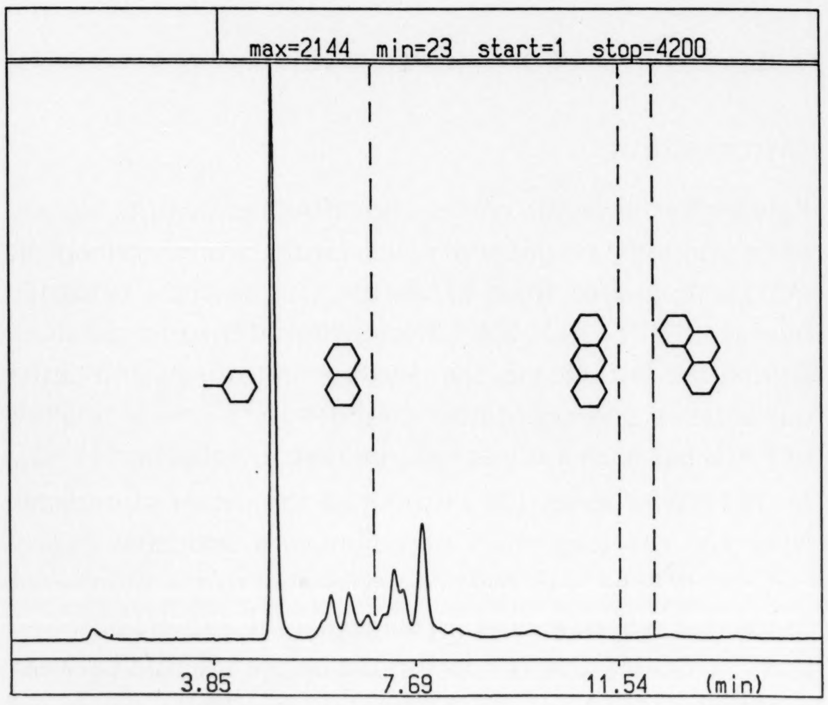

Fig. 2

HPLC-Chromatogram of a PCDD/PCDF sample. The retention times of toluene, naphthalene, anthracene and phenanthrene are indicated. Flow rate: 3 ml/min. Column: Waters uBondapak NH_2 250 X 10 mm. Mobile phase: n-hexane. Detector UV 238 nm.

Table I. Retention times, relative to anthracene, of some compounds on a uBondapak NH_2 column. Mobile phase: n-hexane.

Compound	Relative retention time
Toluene	0.42
Decachlorobiphenyl	0.44
1,2,4-TCDD	0.57
1,2,3,4-TCDD	0.60
OCDD	0.69
Anthracene	1.00
Phenanthrene	1.05
Pyrene	1.33
Chrysene	2.15
Benzo(a)pyrene	2.87

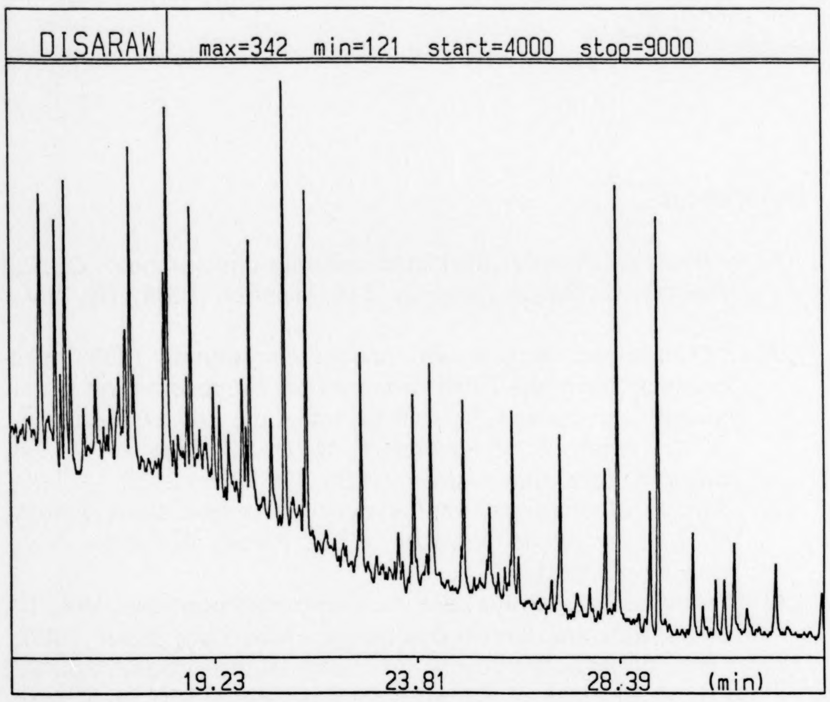

Fig. 3

GC-FID chromatogram of the raw extract. Column: CPSil-8/CB 24 m X 0.32 mm. Temperature programmed from 70 °C to 275 °C with 7 °C/min.

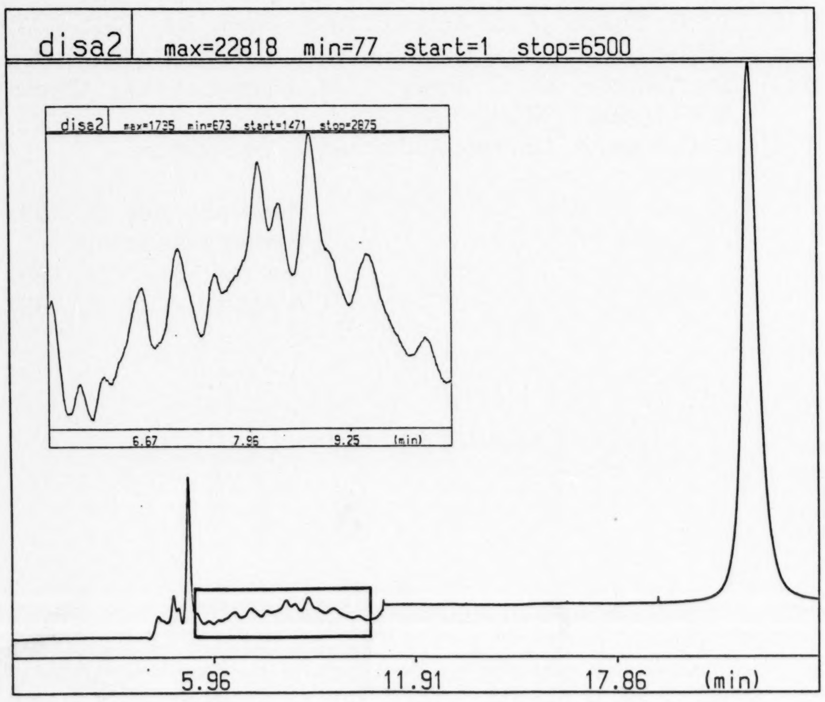

Fig. 4

HPLC-chromatogram derived from the sample in Fig. 3. Flow rate: 3 ml/min (which was reversed at the retention time of anthracene and increased to 5 ml/min). Column: Waters uBondapak NH_2. Detector UV 238 nm.

n-alkanes) eluted prior to the two ring fraction. The time for reversing the flow was set to the start of elution of anthracene. This yielded a complete recovery of phenanthrene and phenanthrene derivatives. This was done because phenanthrene and methylated phenanthrenes are some of the most abundant PAHs in combustion processes. Some loss of alkylated anthracene derivatives is possible [12]. Anthracene is detected as a minor constituent in most samples, giving low quantitative loss of information if data for anthracene derivatives are left out.

The qualitative result of this separation (or clean-up) technique is demonstrated on a sample derived from particulate matter, collected from an electrostatic filter of a municipal incineration plant. Fig. 3 shows the GC-FID chromatogram of the raw extract. The main peaks occurring in a homologous series are aliphatic hydrocarbons. The chromatogram obtained from the raw extract from the HPLC separation described above is shown in Fig. 4, with an enlargement of the part of the chromatogram containing the PCDDs and PCDFs. When injected on a gas chromatograph equipped with an electron capture detector, this fraction yields the chromatogram shown in Fig. 5. A multi-step open column clean up system [6, 7], including the use of Al_2O_3, active charcoal and different modified silica adsorbents, was applied as an alternative clean up of the raw extract. Fingerprints of the GC-ECD traces from the raw extract, the HPLC fraction and the PCDD/PCDF fraction obtained with the multi step method, were compared, showing an almost identical distribution of PCDD/PCDF between raw extract and the HPLC fraction. When

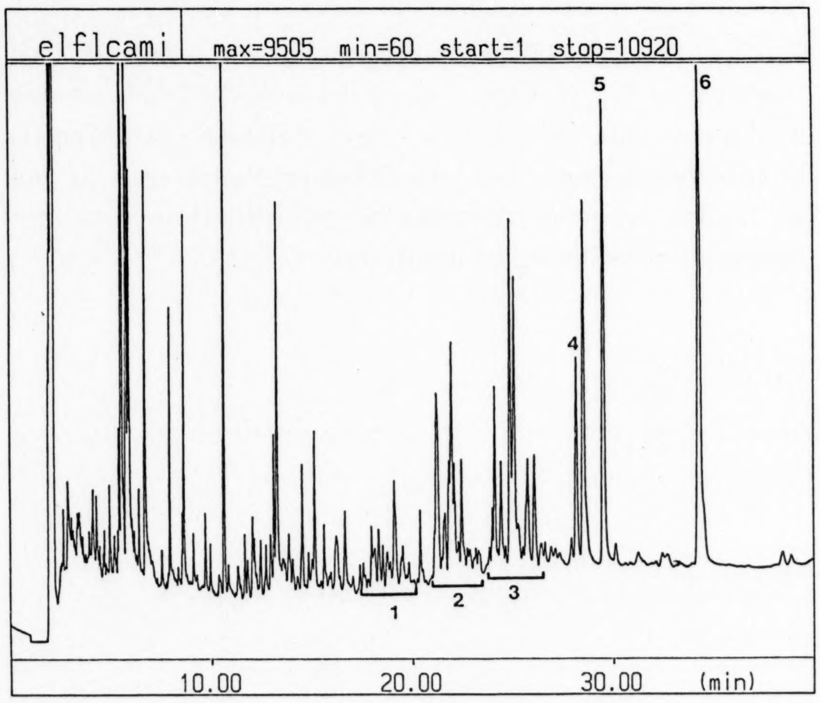

Fig. 5

GC-ECD chromatogram of the HPLC-separated two aromatic ring compounds. Column: SE-54. Initial temp: 110 °C. Temp. programmed to 200 °C with 20 °C/min and further programmed to 290 °C with 5 °C/min.

Identification of a few peaks: **1** = Tetrachlorodibenzo-p-dioxines and furanes; **2** = Pentachlorodibenzo-p-dioxines and furanes; **3** = Hexachlorodibenzo-pdioxines and furanes; **4** = 1,2,3,4,6,7,8-heptachlorodibenzofurane; **5** = 1,2,3,4,6,7,8-heptachlorodibenzo-p-dioxine; **6** = Octachlorodibenzodioxine.

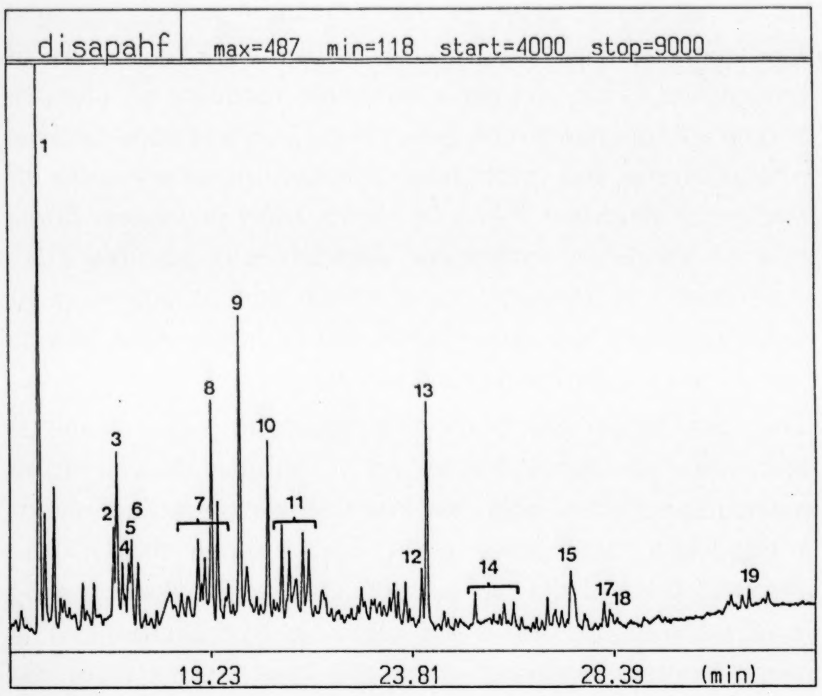

Fig. 6

GC-FID Chromatogram of the DMF cleaned-up backflush peak of Fig. 4. GC conditions as in Fig. 3.

Identification of some peaks: **1** = Phenanthrene, **2** = 3-methylphenanthrene, **3** = 2-methylphenanthrene, **4** = 4H-cyclopenta(def)-phenanthrene, **5** = 4 + 9-methylphenanthrene, **6** = 1-methylphenanthrene, **7** = Dimethylphenanthrenes, **8** = Fluoranthene, **9** = Pyrene, **10** = Benzo(a)fluorene, **11** = Methyl-202s, **12** = Benzo(a)anthracene, **13** = Chrysene, **14** = Methyl-228s, **15** = Benzofluoranthenes, **17** Benzo(e)pyrene, **18** = Benzo(a)pyrene, **19** = Indeno(1,2,3-cd)pyrene.

comparing the PCDD/PCDF fraction obtained with the multi step method with the raw extract, indications of selective (e.g., adsorption or evaporation) losses of several PCDD and PCDF isomers in the former case were observed. This will be further discussed in a separate paper.

Finally, the GC-FID chromatogram of the backflush peak is shown in Fig. 6. Even though the levels of PAHs are low, a number of compounds were detected. Anthracene, phenanthrene and polymethylated phenanthrenes as well as higher aromatic compounds as benzo(e)pyrene and benzo(a)pyrene could be identified.

Conclusion

The usefulness of an amino bonded stationary phase in the normal phase mode for the separation of PCDDs and PCDFs, from compounds with higher aromaticity (for example PAHs) has clearly been demonstrated. This clean-up procedure can replace open column clean up multi step procedure in the analysis of PCDDs and PCDFs. The method further gives the possibility of collecting the PAH fraction from the sample. Since the fractionation is readily automated and is completed within 25 minutes, it strongly decreases both time for the clean up of samples and the active presence of personnel. Other two aromatic ring compounds are not separated from the PCDDs and PCDFs. This emphasises the necessity of an additional separation step when samples containing high amounts of PCBs are to be analysed.

References

[1] "Analysis of polychlorinated dioxines and furanes", Critical Review, *C. Rappe,* Environ. Sci. Technol. 1984, 18, 78A–90A.

[2] "Chlorinated dioxins and related compounds 1985", proceedings from the Fifth International Symposium on Chlorinated Dioxins and Related Compounds; Eds. *O. Hutzinger, W. Crummett, F. W. Karasek, E. Merian, G. Reggiani, M. Ressinger, S. Safe,* Chemosphere 1986, 15, 1085–2132.

[3] Analytical Chemistry of Polycyclic Aromatic Compounds", *M. L. Lee, M. V. Novotny, K. D. Bartle,* Academic Press, New York, 1981.

[4] "Handbook of Polycyclic Aromatic Hydrocarbons, Vol. 1", Ed. *A. Björseth,* Marcel Dekker Inc., New York, Basel, 1983.

[5] "Handbook of Polycyclic Aromatic Hydrocarbons, Vol. 2", Eds. *A. Björseth, T. Ramdahl,* Marcel Dekker Inc., New York, Basel, 1985.

[6] *L. M. Smith, D. L. Stalling, L. L. Johnson,* Anal. Chem. **56,** 1830–1842 (1984).

[7] *L. L. Lamparksi, T. J. Nestrick,* Anal. Chem. **52,** 2045–2054 (1980).

[8] *S. A. Wise, S. N. Chesler, H. S. Hertz, L. R. Hilpert, W. E. May,* Anal. Chem. **49,** 2306–2310 (1977).

[9] *K. G. Liphard,* Chromatographia **13,** 603–606 (1980).

[10] *L. R. Snyder, T. C. Schunk,* Anal. Chem. **54,** 1764–1772 (1982).

[11] *D. Karlesky, D. C. Shelly, I. M. Warner,* J. Liq. Chrom. **6,** 471–495 (1983).

[12] *C. Östman, A. Colmsjö,* Submitted for publication.

Received: July 3, 1987
Revised manuscript
received: Sept. 22, 1987
Accepted: Oct. 4, 1987
F

Liquid Chromatographic Characterization of the Deoxyribonucleoside-5'-Phosphates and Deoxyribonucleoside-3',5'-Bisphosphates Obtained by ^{32}P-Postlabeling of DNA

M. W. Dietrich / W. E. Hopkins II / Karen J. Asbury / W. P. Ridley

Environmental Health Laboratory, Monsanto Company, 645 S. Newstead, St. Louis, Mo 63110, USA

Key Words

Reversed-phase HPLC
Nucleotides
DNA adducts
DNA binding

Summary

The use of high-performance liquid chromatography (HPLC) for the characterization of the adducts formed by the ^{32}P-postlabeling of DNA is described. Adducts formed from the reaction of DNA with small molecules are characterized as deoxyribonucleoside-5′-monophosphates. Adducts formed from the reaction of DNA with larger molecules are characterized as 3′,5′-bisphosphates. In either case, good separations are obtained for adducts, other than methyl, by conventional reversed-phase chromatography using a C_{18} column. Ion-exchange chromatography can be used in selected circumstances where reversed-phase techniques are not successful. Using sample concentration techniques, sensitivities are achievable which make this technique applicable to *in vivo* situations.

Introduction

Covalent binding to DNA is thought to be an essential step in the mode of action of many chemical carcinogens. The study of the adducts formed by these materials has been very difficult because of the low level of adduct formation. Most studies to date have involved the use of a radiolabeled form of the test chemical, usually based on carbon 14 or tritium incorporation. This approach had provided useful information in some cases but is limited in applicability by the availability of the radiolabeled test compound and the difficulty in establishing that the observed low level radiolabeled products are adducts. Impurities formed by tritium exchange can occur as well as the normal trace level impurities encountered in such analyses. A derivatization approach with electrophores followed by electron capture gc or gc/ms has been reported for pyrimidine bases such as cytosine [1, 2]. Potentially this approach has high sensitivity but is not applicable to all the types of adducts expected. Labeling of DNA with ^{32}P after modification (postlabeling) is an attractive alternative for adduct characterization with potentially wide applicability. The use of high specific activity ATP for incorporation of the label can provide high sensitivity. This approach has been studied extensively by Randerath [3–7]. His approach involves the reaction of DNA with the chemical under study followed by enzymatic hydrolysis of the resulting modified DNA to form deoxyribonucleoside-3′-phosphates. This is followed by reaction with [^{32}P]-ATP of high specific activity to form 3′,5′-bisphosphates labeled in the 5′ position. These products are then analyzed by TLC. Haseltine [8] has attempted to modify this technique by the enzymatic hydrolyses of the 3′,5′-bisphosphates resulting from the reaction of DNA with dimethyl sulphate to the corresponding radiolabeled deoxyribonucleoside-5′-phosphates. The resulting products were analysed by HPLC. The series of reactions involved is shown schematically in Fig. 1. We have studied the ^{32}P-postlabeling approach at both the 3′,5′-bisphosphate and 5′-monophosphate stages with analyses by HPLC. The nature of the reaction products formed from both small and large electrophiles has been studied together with the HPLC conditions necessary to resolve the adducts formed. The potential sensitivity of this approach has been investigated and compared to the TLC approach of Randerath [3–7].

Experimental

Reagents and Chemicals

Type I DNA from calf thymus, micrococcal nuclease, apyrase, nuclease P1 from *Penicillium citrinum*, 2′-deoxyguanosine-3′-monophosphate and 2′-deoxyguanosine-5′-monophosphate were obtained from Sigma Chemical Co., St. Louis, MO, USA. Dimethyl sulfate (DMS) (99+%), di-

0009-5893/87 0545-07 $03.00/0

© 1987 Friedr. Vieweg & Sohn Verlagsgesellschaft mbH

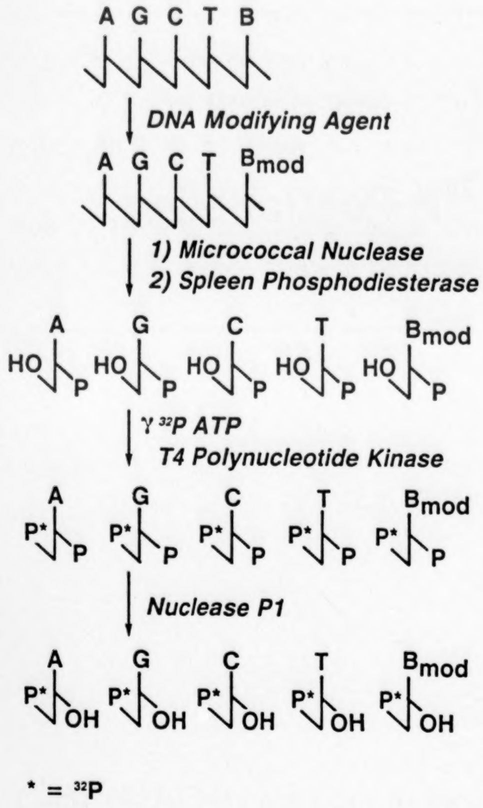

Fig. 1
Outline of the DNA postlabeling method.

ethyl sulfate (DES) (98%) and methyl methanesulfonate (MMS) (98%) were the products of Aldrich (Milwaukee, WI, USA). Spleen phosphodiesterase (Boehringer-Mannheim, Indianapolis, IN, USA), T4 polynucleotide kinase (Amersham, Arlington Heights, IL, USA) and [^{32}P]-adenosine-5′-triphosphate-tetra(triethylammonium) salt at 3000 Ci/mmol (New England Nuclear, Boston, MA, USA) were purchased from the companies indicated. Benzo(a)-pyrene-trans-7,8-dihydrodiol-9,10-epoxy(anti) (BPDE) (99+%) was obtained from the NCI Chemical Carcinogen Repository at Midwest Research Institute (Kansas City, MO, USA).

Micrococcal nuclease, obtained as a solid, was dissolved in distilled water (0.21 U/μl) and dialyzed against distilled water at room temperature for 30 min using a 0.025μm "V" Series Membrane (Millipore, Bedford, MA, USA). Spleen phosphodiesterase, obtained as an ammonium sulfate suspension, was dialyzed in the same manner as micrococcal nuclease. The volume of the spleen phosphodiesterase solution doubled during dialysis. Other materials were used in the form received from the supplier. Potassium phosphate (monobasic) and sodium phosphate (monobasic) were obtained from Fischer Scientific (Fair Lawn NJ, USA). Methanol was purchased from American Burdick and Jackson (Muskegon, MI, USA). All buffers for HPLC were prepared using water distilled from a Nanopure Ultrapure System from Sybrum/Barnstead (Boston, MA, USA). All mobile phase solutions were filtered through a Micronsep Magna Nylon 66 0.22 micron filter from MSI (Honeoye Falls, NY, USA).

Chemistry and Enzymology

Modification of deoxyguanosine-3′-phosphate (3′-dGMP). 3′dGMP was allowed to react for 30 minutes with an excess of DMS or MMS or for 90 minutes with DES in Tris-HCl at pH 8.0 at 37 deg. C. An equimolar amount of β-mercaptoethanol was then added and the sample was incubated for an additional 30 or 90 minutes. 3′-dGMP (1 mg) in water was allowed to react with BPDE (1 mg) in acetone for 22 hours at 37 deg. C. The mixture was extracted with ethyl acetate for 6–9 times to remove unreacted BPDE.

Modification of DNA. DNA was reacted for 0.5 hours with an excess of DMS or MMS or for 2.5 hours with DES in Tris-HCl pH 8.0 at 37 deg. C. The DNA was purified by dialysis against Tris-HCl for 15 hours at 4 deg. C or by precipitation with 0.1 volume of sodium acetate (2.5M) and 2 volumes of ethanol. DNA (1 mg) was incubated with BPDE (1 mg) in acetone:water (1:1) at 37 deg. C for 15 hours. The mixture was extracted with ethyl acetate followed by ethyl acetate/1-butanol (1:1) and then the DNA was precipitated by the addition of sodium acetate and ethanol.

Hydrolysis of DNA and labeling of the digest. DNA, control and modified, was hydrolyzed with micrococcal nuclease and spleen phosphodiesterase for 2 hours at 37 deg. C and diluted 1:10 with distilled water [4]. A portion of the diluted digest was added to buffer (pH 9.6) and reacted with [^{32}P]-ATP in the presence of T4 polynucleotide kinase for 1 hour at 37 deg. C as described by Gupta et al. [4] to form the bisphosphates.

Hydrolysis of the bisphosphates. The bisphosphates were converted to 5′-monophosphates using nuclease P1 [4]. Immediately before analysis, apyrase (10 mU) was added and the digest was incubated for 10 minutes.

Nuclease P1 pretreatment. Hydrolyzed DNA was incubated with nuclease P1 in buffer at pH 5.0 for 40 minutes at 37 deg. C as described by Reddy and Randerath [7].

Acid hydrolysis. The products of the reaction of DMS or DES with 3′-dGMP were hydrolyzed with 0.2 N HCl at 70 deg. C for 20 minutes.

Apparatus

The HPLC system consisted of a Model 5500 liquid chromatograph with a UV-200 variable wavelength detector set at 260 nm (both from Varian Associates, Sunnyvale, CA, USA). Samples were injected with a Rheodyne (Cotati, CA, USA) 7125 500-μl injection loop. For radioactive samples, a Berthold LB 503 HPLC radioactivity monitor (Pittsburg, PA, USA) with a 600μl flow cell was used. A FMI (Oyster Bay, NY, USA) RP-G50 lap pump maintained a flow of 5.0 ml/min of Atomlight (NEN, Boston, MA, USA) scintillation cocktail through the radioactivity monitor. For reversed-phase chromatography, a Chromanetics (Malaga, NJ, USA) 5μm Spherisorb ODS-2, 25.0 cm × 4.6 mm i.d. analytical column was used protected by a Brownlee cartridge C18 guard column (Brownlee labs, Santa Clara, CA, USA). For ion-exchange chromatography, a Vydac 303NT405 (Hesperia, CA, USA) 5 cm × 4.6 mm i.d. nucleotide analysis column was used. The output from both detectors was monitored and plotted by a Spectra-Physics (San Jose, CA, USA) 4270 integrator.

Chromatographic Procedures

For reversed-phase chromatography of the monophosphates and bisphosphates, two eluants were used; eluant A was 0.075M potassium phosphate adjusted to a pH of 3.0 with concentrated phosphoric acid and eluant B was methanol. Most separations were performed with 100% A held for 15 minutes followed by a 15 minute linear gradient to 40% B. The flow rate was 1.0ml/min. For separating the bulky adducts, an additional 15 minute linear gradient to 100% B was added. For reversed-phase chromatography of the bases, eluant A was 0.025M potassium phosphate adjusted to pH 5.6 with 1.0N sodium hydroxide and eluant B was 3:2 methanol/water. A linear gradient over 18 minutes from 100% A to 20% B was used. The flow rate was 1.5ml/min. The mobile phase used for ion-exchange chromatography was 0.04M sodium phosphate adjusted to a pH of 3.0 with concentrated phosphoric acid. The flow rate was 0.5ml/min.

Results and Discussion

Chromatography of Deoxyribonucleoside-5′-phosphates and 3′,5′-bisphosphates

The separation of deoxyribonucleoside monophosphates has been studied extensively by both reversed-phase and ion-exchange chromatography [9–13]. Most of these studies have been based on the 3′ products. We have found the 5′ materials give similar separations under reversed-phase conditions with a C_{18} column. Fig. 3 shows a chromatogram obtained from a synthetic mixture of the four deoxyribonucleoside-5′-phosphates corresponding to the major components of DNA. At a pH of 4.5, a well resolved chromatographic peak is obtained for each component. The most common modification to DNA by electrophiles involves reactions of nucleotides containing a purine base. The resulting modified nucleotides in most cases would be expected to be less polar than the corresponding unmodified nucleotide and thus would have longer retention times under reversed-phase conditions. We thus attempted to identify chromatographic conditions under which the adducts of the purine containing nucleotides would elute free of interference from the high levels of unmodified nucleotides normally present. The conditions shown in Figure 2A meet these criteria for adducts of deoxyadenosine-5′-phosphate (5′dAMP). The observation of low level adducts of deoxyguanosine-5′-phosphate would be difficult however, because of the presence of the large peak of 5′-dAMP.

Conditions were sought in which the 5′-dGMP would be the last eluting of the unmodified nucleotides. Neither changing the ionic concentration of the buffer or the early methanol gradient had a substantial effect on the relative elution of the deoxyribonucleoside-5′-phosphates. Changes in pH however, were found to have a substantial effect as is shown in Table I. At a pH of 3.0, see Fig. 2B, 5′-dGMP was found to be the last eluting nucleotide. Although the unmodified nucleotides are not as well resolved under these conditions, adducts of 5′-dGMP would be expected to elute in a chromatographically clean region. Should it be desirable, lowering the pH to 2.0 should be useful when attempting to identify adducts of dTMP. Ion-exchange chromatography was found to give separations similar to those of reversed-phase chromatography and may prove useful if an alternate separations mode is

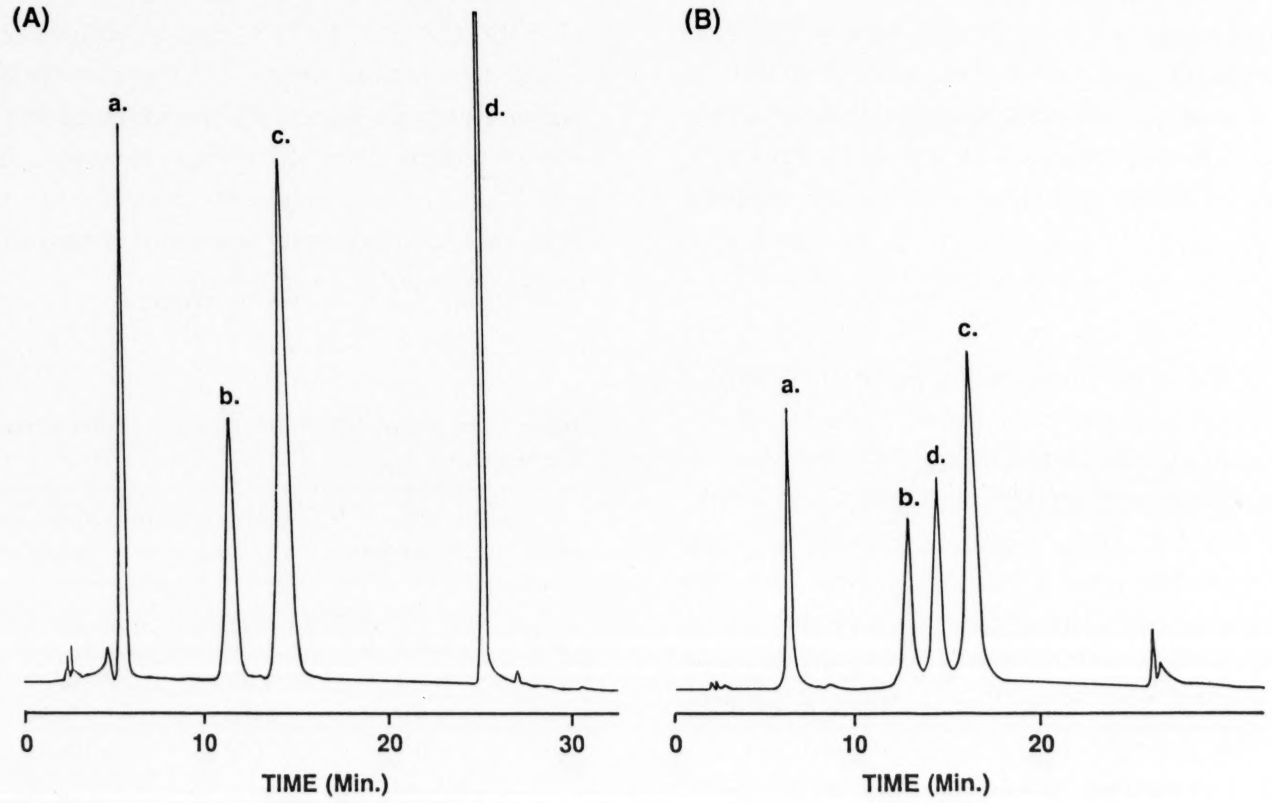

Fig. 2

Chromatograms of the principle deoxyribonucleoside -5′-phosphates of DNA (A) At pH = 4.5. (B) At pH = 3.0. Peaks: a = 5′-dCMP; b = 5′-dTMP; c = 5′-dGMP; d = 5′-dAMP. Reversed-phase chromatography on C_{18}, 100% buffer for 15min followed by a 15min linear gradient to 40% methanol with UV detection.

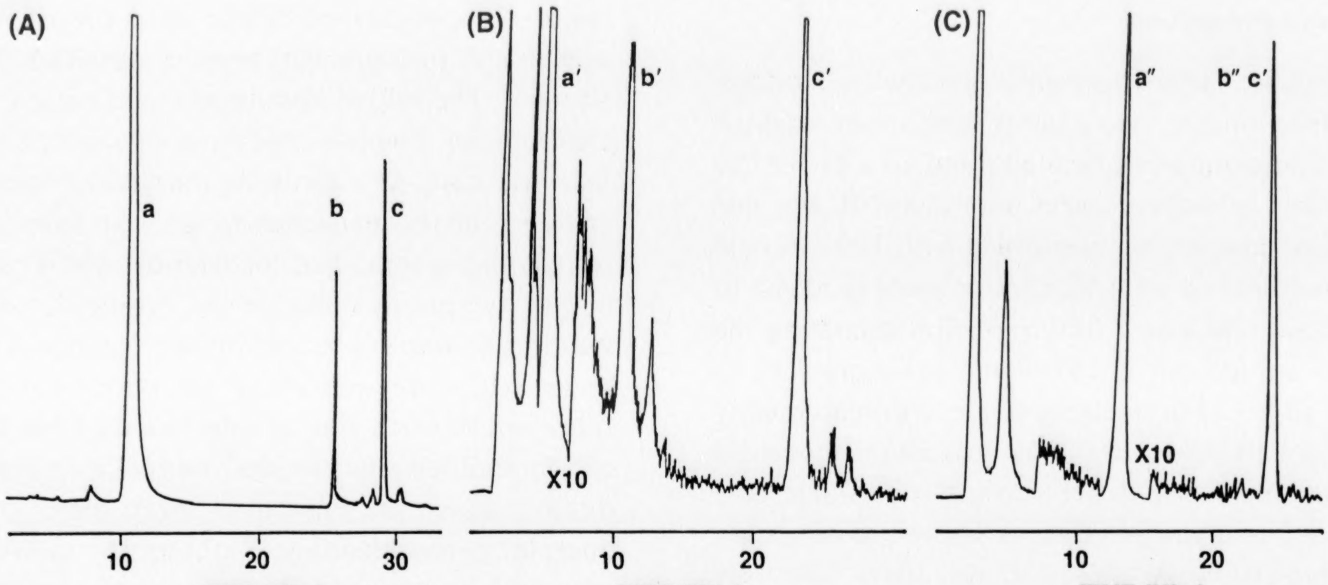

Fig. 3

Chromatograms from the reaction of dGMP with DES. (A) As deoxyribonucleoside-3′-phosphates. (B) As deoxyribonucleoside-3′-,5′-bisphosphates. (C) As deoxyribonucleoside-5′-phosphates. Peaks: a = 3′-dGMP, a′ = 3′,5′-dGbisP; a″ = 5′-dGMP; b = N-7 ethyl-3′-dGMP; b′ = N-7 ethyl-3′,5′-dGbisP; b″ = N-7 ethyl-5′-dGMP; c = ethyl ester of 3′-dGMP; c′ = ethyl ester of 3,5′-dGbisP. The chromatographic conditions are as described in Fig. 2B except that detection in B and C are by radioactivity monitor.

required. Unmodified 3′,5′-bisphosphates were found to be poorly retained under the reversed-phase conditions used in this study. Counter ions may be employed [12] to increase the retention time of such materials. As will be discussed later the early elution of unmodified bisphosphates can be useful when attempting to identify adducts.

To evaluate the applicability of this approach to the identification of DNA adducts, investigations were undertaken *in vitro* with direct acting electrophiles. Examples were chosen that would give adducts expected to have differing chromatographic mobilities. Examples of methylating agents, ethylating agents and a molecule expected to give a large bulky adduct were chosen. Attempts were made to identify the adducts formed and to obtain an estimate of the potential detection limit for this type of adduct. Some experimentation was conducted with 3′-dGMP as representative of one of the most reactive sites in DNA. Invariably, when this was followed by a study with DNA, similar, although at times a smaller number of, adducts were observed.

Methyl Adducts

The reaction of DNA with methylating agents is reported to occur primarily at guanine with the N-7 methyl derivative being the primary product formed [14]. We have investigated the reaction of 3′-dGMP with DMS and MMS. The reaction of both of these materials showed a single product with a retention time 3 minutes greater than 3′-dGMP. This sample was labeled with [^{32}P]-ATP and enzymatically hydrolyzed to give 5′-dGMP and a single product with a retention time 3 minutes greater than 5′-dGMP. To verify that the product formed was indeed the expected N-7 methyl derivative, the HPLC peak of 3′-dGMP and the HPLC peak of the product formed from the reaction with DMS were separately collected and acid hydrolyzed. As expected, 3′-dGMP was quantitatively converted to the corresponding base guanine. The reaction product was quantitatively converted to a compound which co-eluted with a sample of authentic N-7-methylguanine.

Calf thymus DNA was reacted with DMS and carried through the same reaction sequence to yield the 5′-monophosphates. A small peak was observed at the same retention time as that from the reaction of 3′-dGMP with DMS and is presumed to be that of the N-7 methyl derivative of 5′-dGMP. An identical peak although at lower levels was observed with MMS. These observations are inconsistent with those of Haseltine [8] who studied the reaction of DNA with DMS and reports a much later retention time for the peak attributed to this derivative.

The small difference in retention time between the peaks of 5′-dGMP and its N-7 methyl adduct (ca 3 minute) preclude the measurement of these methyl adducts unless present at high levels. We investigated the effect of pH on the retention time difference between these components and found little change over the pH range shown in Table I. The two components were not resolved under the ion-exchange conditions reported.

Table I. Effect of pH on the retention time of deoxyribonucleoside-5′-phosphates (a).

pH	Retention Time (Minutes) 5′-dCMP	5′-dTMP	5′-dGMP	5′-dAMP
2.0	7.3 ± .2 (b)	20.3 ± .3	18.7 ± .4	15.0 ± .2
3.0	6.8 ± .4	13.6 ± .5	17.0 ± .7	15.5 ± .4
3.5	6.7 ± .1	13.2 ± .2	16.9 ± .3	19.7 ± .2
4.0	6.4 ± 0	12.8 ± 0	16.2 ± .3	24.5 ± .2
6.0	4.4 ± .1	10.0 ± .3	13.1 ± .3	25.3 ± .1

(a) Abbreviations used: deoxycytosine-5′-phosphate, 5′-dCMP; deoxythymidine-5′-phosphate, 5′-dTMP; deoxyguanosine-5′-phosphate, 5′-dGMP; deoxyadenosine-5′-phosphate, 5′-dAMP.

(b) Mean ± Standard Deviation

Ethyl Adducts

The reaction of DNA with ethylating agents is reported to give primarily reaction at guanine [14]. The primary products have been identified as containing the N-7 ethylguanine or 3′-ethylphosphate ester moieties [14]. We have investigated the reaction of 3′-dGMP with DES. Fig. 3A shows the chromatogram obtained from the products of the reaction of 3′-dGMP with DES. Two products identified as b (25.0 minute) and c (28.7 minute) together with unreacted 3′-dGMP (9.9 minute) were observed. Fig. 3B shows the chromatogram obtained from the products of the reaction of this sample with [^{32}P]-ATP. The peak labeled a′ is deoxyguanosine-3′,5′-bisphosphate (5.7 minute). The identity of the minor peaks identified as b′ (11.6 minute) and c′ (24.6 minutes) will be discussed later. This mixture of bisphosphates was enzymatically hydrolyzed to yield ^{32}P labeled 5′-monophosphates with the results shown in Fig. 3C. The peak labeled a″ has an identical retention time to authentic 5′-dGMP. The identity of the single minor component observed, identified as b″c′ (25.2 minutes) is discussed below.

To help interpret the results reported above, components b and c were collected as separate fractions, concentrated and carried through the same reactions as the above sample. Using this approach component b was shown to be converted to b′ and subsequently to b″. This behavior, by comparison to the results obtained for the methylated adducts, suggests these components contain the N-7 ethyl moiety (as 3′,5′-bisphosphate and 5′-monophosphate, respectively). This was subsequently confirmed by the acid hydrolysis of component b which yielded a compound with retention time consistent with that expected for 7-ethylguanine. In a similar manner, component c was found to be converted to c′. Further hydrolysis of this compound was incomplete leaving residual c (ca 40%) and resulted in the formation of a component (ca 60%) with an identical retention time to authentic 5′-dGMP. These observations are consistent with c and c′ containing the 3′-ethylphosphate ester moiety. Upon hydrolysis of c′ by nuclease P1 the ethyl moiety would be lost forming the unmodified 5′-dGMP. This was confirmed by acid hydrolysis of peak c which yielded only a compound with identical retention time to guanine.

Bulky Adducts

Many of the aromatic carcinogens which have been studied react with DNA to give adducts which are much larger than those obtained from simple aliphatic alkylating agents. The chromatographic properties of these adducts are expected to be different from those described previously. We have studied this type adduct using benzo(a)pyrene diol epoxide (BPDE). This material is purported to be the active intermediate responsible for the carcinogenicity of benzo(a)pyrene [15, 16]. Two principle adducts, both with deoxyguanosine, have been reported [15] when BPDE is reacted with undenatured DNA.

Fig. 4A shows the chromatogram obtained from control DNA carried through the procedures leading to deoxyribonucleoside-5′-phosphates. The chromatographic conditions have been modified to elute substantially less polar adducts. The peaks observed from about 13 to 18 minutes are due to 5′-dTMP, 5′-dAMP and 5′-dGMP. The earlier eluting peaks are due to 5′-dCMP, impurities related to ATP and what appears to be 3′,5′-bisphosphates which would indicate incomplete hydrolyses to the 5′-monophosphates. No peaks are observed in the chromatographic region expected for a bulky adduct. In Fig. 4B is shown the chromatogram obtained when DNA is reacted with BPDE and carried through the same procedure. In addition to the peaks observed in the control sample, two peaks are observed with retention times between 40 and 50 minutes. These peaks are consistent in appearance with those observed from the reaction of tritiated BPDE with DNA [15] and are in a chromatographic region indicating considerable non-polar character requiring a very high methanol content for elution.

Randerath [7] has reported that bulky adducts such as those from BPDE can not be converted from 3′,5′-bisphosphates to 5′-monophosphates by reaction with nuclease P1. To clarify the nature of the adducts observed in Fig. 4B, the reaction sequence was repeated with samples

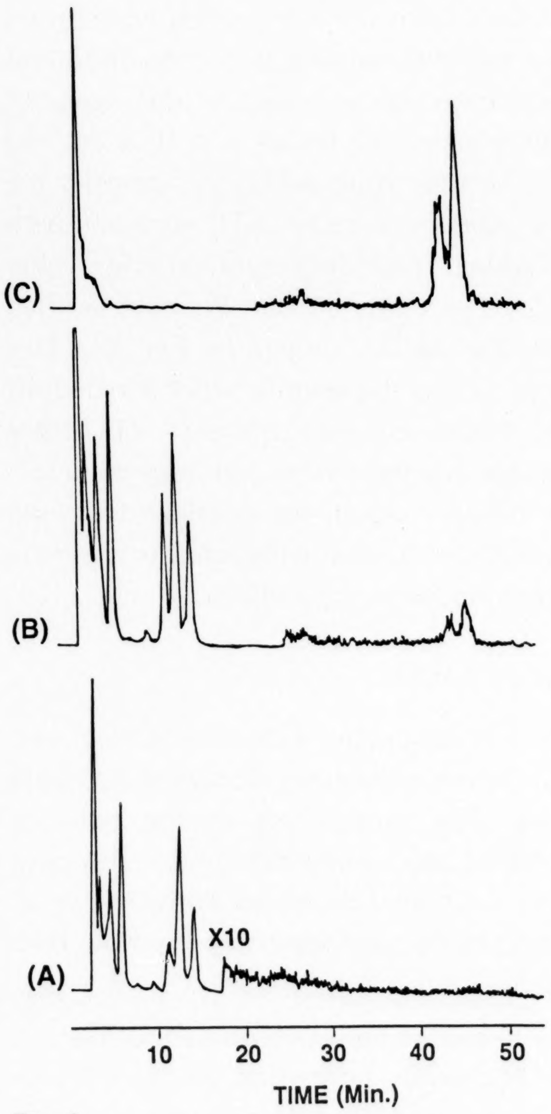

Fig. 4

Chromatograms from the reaction of BPDE with DNA. (A) Control. (B) Reaction from BPDE. (C) Reaction with BPDE including nuclease P1 pretreatment. Peaks: bisphosphates and impurities (0–10 minute); unmodified phosphates (11–20 minute); adducts (40–50 minute). The chromatographic conditions are identical to those of Fig. 2B except that an additional 15 minute linear gradient to 100% methanol was added and detection was by radioactivity monitor.

taken before and after reaction with nuclease P1. This data clearly showed the conversion of the unmodified 3′-monophosphates to 3′,5′-bisphosphates with subsequent conversion to 5′-monophosphates. The two peaks with retention times between 45 and 50 minutes were present at identical retention times in both samples. The presence of ^{32}P and the lack of a change in retention times confirms Randeraths' observation that the conversion of this type of bulky adduct from bis to monophosphate can not be carried out enzymatically with nuclease P1. This does not restrict the applicability of the HPLC approach since these adducts are well retained on C_{18} without an ion pairing reagent and can be studied as bisphosphates. The difference in behavior of ethyl and BPDE adducts suggests that some intermediate size adducts may be partially hydrolyzed by nuclease P1 and be present as both the bis and 5′-monophosphate. This must be taken into account before interpreting the chromatograms obtained from such materials.

Increased Sensitivity With Bulky Adducts

To increase the sensitivity of the ^{32}P-postlabeling technique for bulky adducts, Reddy and Randerath [7] have utilized this differing reactivity to nuclease P1. Before reaction with ATP to form bisphosphates, the sample at the 3′-monophosphate stage, is treated with nuclease P1. This removes the 3′-phosphate moiety from the unmodified nucleotides yielding nucleosides but has no effect on the modified nucleotides. The resulting nucleosides do not serve as substrates for T4 polynucleotide kinase and thus are not radiolabeled by ^{32}P transfer from ATP. This permits the use of much higher specific activity ATP to react with the low level of adduct providing considerably higher sensitivity for this type of bulky adduct. We have verified this approach with the results shown in Fig. 4C. This sample was processed as was the sample which yielded 4B except that it was pretreated with nuclease P1 before reaction with ATP. No unmodified nucleotides were observed and a much stronger signal was obtained from the adducts. This approach was subsequently used to estimate the sensitivity of detection for bulky adducts.

Estimation of Detection Limits

The use of the flow thru radioactivity monitor is much less time consuming than fraction collection followed by liquid scintillation counting. The sensitivities of the two approaches were found to be comparable under the conditions of this study. Estimated detection limits shown in Table II are based on results obtained using the flow thru radioactivity monitor.

Methyl adducts. The detection limit determined for methyl adducts by HPLC was severely limited by our inability to find chromatographic conditions under which these adducts were well resolved from the unmodified nucleotides. An estimate of lower detection limit was made by adding successively larger amounts of 5′-dGMP to a sample containing methyl adduct until the peak for the methyl adduct, which appeared as a shoulder of the 5′-dGMP peak, was barely detectable. The HPLC fraction representing this region, the dGMP peak and appropriate background samples were collected and counted by liquid scintillation counting. The results shown in Table II indicate an ability to detect a level of one adduct formed per 1000 nucleotides. This compares unfavorably with the data reported by Randerath [5] and indicates the approach reported therein to be the method of choice when utilizing ^{32}P-postlabeling for the study of methyl adducts.

Table II. Detection limits of DNA adduct formation utilizing ^{32}P post-labeling.

Adduct Type	Approximate Detection Limit this study	 Randerath et al.
Methyl	1 in 10^3	1 in 6 X 10^5 (5)
Ethyl	1 in 10^4	
Benzo(a)Pyrene Diol Epoxide		
direct measurement	1 in 10^4	1 in 10^7–10^8 (4)
after nuclease P1 pretreatment	1 in 10^6	ca 1 in 10^{10} (7)

Bulky (non-polar) adducts. These are defined as adducts for which the modification is so great that the chromatography on C_{18} is dominated by the adduct portion of the modified 5′-monophosphate or 3′,5′-bisphosphate. These adducts will exhibit a long retention time requiring a substantial level of strong solvent (methanol) to elute. The results obtained for BPDE are considered typical for this type of adduct. They are considered as a separate class when exploring detection limits since both the nuclease P1 pretreatment procedure reported by Randerath [7] and the butanol extraction procedure of Gupta [17] are expected to the applicable for this type of adduct. An estimate of lower detection limit was made by reacting DNA with BDPE, hydrolyzing to the 3′-monophosphates, pretreating with nuclease P1 to remove unmodified nucleotides and reaction with high specific activity ATP. The resulting sample was diluted with the bisphosphates obtained from control DNA. At a level equivalent to approximately one adduct per one million nucleotides, interference by unidentified ^{32}P containing impurities limited further measurement. Efforts are underway to lower the detection limit for this type of adduct by finding techniques which will remove these impurities.

Intermediate size (polarity) adducts. These are defined empirically as adducts of sufficient size to somewhat modify the polarity of the resulting modified 5′-monophosphate (or 3′,5′-bisphosphate if the latter is not hydrolyzed by nuclease P1). Such adducts will yield chromatographic peaks with intermediate retention times under reversed-phase conditions reflecting both the polar nature of the phosphate moiety and the non-polar nature of the adduct moiety. The concentration approaches used to obtain high sensitivity for bulky adducts may not be applicable with these materials. The lower detection limits of these adducts will be effected both by presence of the unmodified nucleotides and by interference from the ^{32}P impurities observed with BPDE. The latter elute in the same chromatographic region as the adducts of DES. The unmodified nucleotides can be removed at the 3′-monophosphate stage by collecting the HPLC fraction of the adducts for subsequent analyses or possibly by clean up via solid phase extraction procedures. We are currently exploring means to remove the ^{32}P containing impurities. Until they can be removed, the lower detection limit for this type of adduct, as represented by the adducts of DES, is limited to approximately 1 adduct per 10,000 nucleotides.

The HPLC approach presented here is an attractive alternative to the thin layer chromatographic approaches previously investigated. It allows the versatility of HPLC separations and excellent quantitation capabilities to be applied to studies of this type. Although the detection limits obtained to-date are not as low as those obtained by TLC, approaches are under investigation which may reduce this difference.

References

[1] *A. Nazareth, M. Joppich, S. Abdel-Baky, Kathleen O'Connell, A. Sentissi, R. W. Giese*, J. Chromatogr. **314**, 201–210 (1984).

[2] *G. B. Mohamed, A. Nazareth, M. J. Hayes, R. W. Giese, P. Vouros*, J. Chromatogr. **314**, 211–217 (1984).

[3] *K. Randerath, M. Vijayaraj Reddy, R. C. Gupta*, Proc. Natl. Acad. Sci USA **78**, 6126–6129 (1981).

[4] *R. C. Gupta, M. Vijayaraj Reddy, K. Randerath*, Carcinogenesis **3**, 1081–1092 (1982).

[5] *M. Vijayaraj Reddy, R. C. Gupta, Erika Randerath, K. Randerath*, Carcinogenesis **5**, 231–243 (1984).

[6] *K. Randerath, Erika Randerath, H. P. Agrawal, R. C. Gupta, M. E. Schurdak, M. Vijayaraj Reddy*, Environ. Health Per. **62**, 57–65 (1985).

[7] *M. Vijayaraj Reddy, K. Randerath*, Carcinogenesis **7**, 1543–1551 (1986).

[8] *W. A. Haseltine, W. Franklin, Judith A. Lippke*, Environ. Health Per. **48**, 29–41 (1983).

[9] *E. Nissinen*, Analyt. Biochem. **106**, 497–505 (1980).

[10] *Phyllis R. Brown, A. M. Krstulovic, R. A. Hartwick*, in *Giddings, Gruska, Cazes* and *Brown* (Editors), Advances in Chromatography, Dekker, New York, 1980, p. 101–138.

[11] *M. Zakaria, P. R. Brown*, J. Chromatogr. **226**, 267–290 (1981).

[12] *A. M. Krstulovic, Phyllis R. Brown*, "Reversed-Phase High-Performance Liquid Chromatography", J. Wiley and Sons, Inc., New York, 1982.

[13] *Charlotte Yu Ip, D. Ha, P. W. Morris, M. L. Puttemans, D. L. Venton*, Analytical Biochemistry **147**, 180–185 (1985).

[14] *D. T. Beranek, Constance C. Weis, D. H. Swenson*, Carcinogenesis **1**, 595–606 (1980).

[15] *T. Meehan, K. Straub, M. Calvin*, Nature **269**, 725–727 (1977).

[16] *T. Meehan, K. Straub*, Nature **277**, 410–412 (1979).

[17] *R. C. Gupta*, Cancer Res. **45**, 5656–5662 (1985).

Received: July 2, 1987
Revised manuscript
received: Nov. 2, 1987
Accepted: Nov. 4, 1987
F

Hysteretic Effect of the Coating Solvent on Chiral Recognition by Cellulose Derivative

T. Shibata* / T. Sei / H. Nishimura

Daicel Chemical Industries Ltd., Research Center, 1239 Shinzaike, Himeji, 671-12, Japan

K. Deguchi

JEOL Ltd. 1418 Nakagami, Akishima, Tokyo, 196, Japan

Key Words

Chromatography
Cellulose derivatives
Optical resolution
Phenol
Solid state NMR

Summary

The solvent used to dissolve cellulose ester and prepare the composite of the cellulosic and a support as a chiral stationary phase was found to give a profound hysteretic effect on the chiral recognition ability of the stationary phase.

Introduction

In 1973 Hesse and Hagel reported the successful chromatographic optical resolution on a so-called microcrystalline cellulose triacetate [1]. Subsequently, it had been generally accepted that the microcrystalline nature is a crucial condition for chiral recognition. We recently showed that crystallites exhibit only little contribution to the chiral adsorption of cellulose triacetate (both I and II polymorphes). That lead us [2, 3] to the successful development of novel chiral stationary phases i.e., cellulose esters coated on a support (see also Okamoto et al.) [4, 5]. We now wish to report a profound hysteretic effect of the solvent with which the cellulosic has been coated on the support, on the adsorptive behavior.

Experimental

General Procedure

Preparation of a stationary phase; One portion of a cellulose ester was dissolved in the solvent and mixed with four portions of silica gel (for example, Lichrospher Si-1000 treated with diphenylsilanizing agent). Solvent removal under vacuum gave a powderous composite, which was slurry-packed into a stainless steel column (25cm × 4.6mm i.d.).

Chromatograms were taken under the following conditions: mobile phase, a 9:1 mixture of hexane and 2-propanol; flow rate, 0.5ml/min; temperature, 20–25°C; sample amount, ca. 50μg of an aromatic compound and ca. 0.1mg of a nonaromatic compound. Apparatus: pump, Toyo Soda 803D; UV detector, Shimadzu Instruments SPD-6A. The separation factors (α) were calculated assuming that the dead volume, Vo = 2.5ml. The chromatograms of some racemates on cellulose triacetate and cellulose tribenzoate are shown in Figs. 1, 2, and 3.

Results

Figs. 1–3 indicate that a coating solvent gives a profound hysteretic effect on the adsorptive characteristics of cellulose triacetate (CTA). The effects of trifluoroacetic acid (chiral stationary phase (CSP) *2* and phenol (CSP *3*) showed the same tendency, that is, increased separation factors were given to some compounds including *trans*-2,3-diphenyloxirane, 4-phenyl-1,3-dioxane, and 2-phenylcyclohexanone and similar or reduced ones to Tröger's base, etc. But the magnitude of the effect of phenol is much larger than that of trifluoroacetic acid and that given to a completely acetylated cellulose (CSP *5*) is much larger than that given to an incompletely acetylated cellulose (the degree of substitution, DS = 2.85, CSP *3*) (Fig. 1). Similar hysteretic effect was also observed on cellulose tribenzoate although not so dramatic as on CTA (Fig. 3).

Discussion

Origins of the hysteretic effect. The opportunity of studying the effect of phenol was available in the course of solid state NMR study to explore the interaction between a molecule and solid cellulose triacetate (CTA) impregnated with the molecule. We measured the solid-state high resolu-

0009-5893/87 0552-03 $03.00/0

© 1987 Friedr. Vieweg & Sohn Verlagsgesellschaft mbH

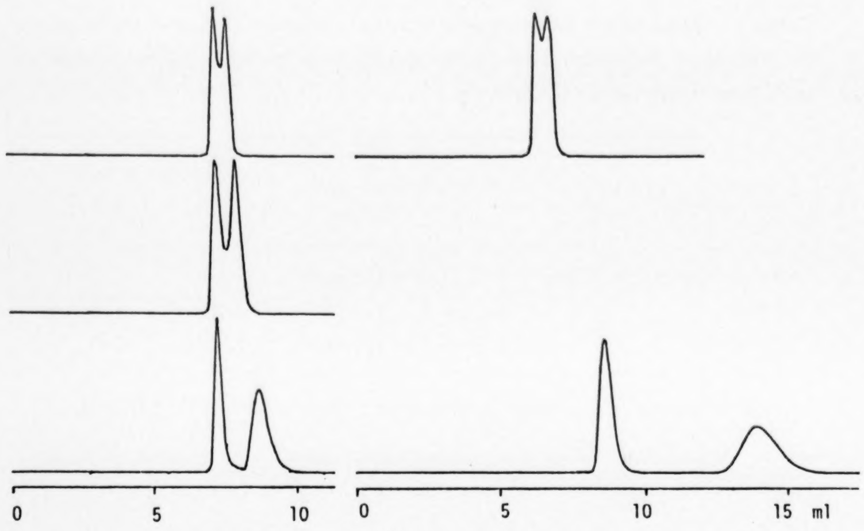

Fig. 1

Chromatograms of 2-phenylcyclohexanone obtained on cellulose triacetates (CTAs) coated on silicagel. Those on the left were obtained on CTA of DS (degree of substitution) = 2.85 and $\overline{M}w$ (weight-averaged molecular weight) = 9900 coated with dichloromethane only (chiral stationary phase (CSP) *1*, upper), with a 9:5 mixture of dichloromethane and trifluoroacetic acid (CSP *2*, middle), and a 8:1 mixture of dichloromethane and phenol (CSP *3*, lower) respectively. Those on the right, on CTA of DS = 3.0 and $\overline{M}w$ = 9960 coated with dichloromethane only (CSP *4*, upper) and with a 8:1 mixture of dichloromethane and phenol (CSP *5*, lower). The molecular weights were determined by GPC in chloroform with polystyrene as the standard.

tion ^{13}C NMR spectra of CTAs solidified from dichloromethane only, from dichloromethane-trifluoroacetic acid, and from dichloromethane-phenol [6]. The most outstanding difference among those spectra was that the polymer obtained from the latter solvent system showed considerably smaller width of the C-1 resonance line (370 Hz, 230 Hz, 160 Hz, respectively). Considering the results of the measurement of spin-lattice relaxation time, the sharpness of the resonance peak is rationalized in terms of some structural regularity, conceivably a smaller deviation of the conformation of the glycosidic linkages. Thus the tendency of the latter solvent system to give larger separation factors in chromatography can be attributed to the higher structural regularity. The rationalization is supported by the fact that the hysteretic effect observed in the case of incompletely acetylated cellulose (CSP *3*), which has an intrinsic irregularity, is much less apparent.

Crystallinity and crystalline lattice. The X-ray diffractograms of the cellulose triacetates (CTAs) solidified from the solvent systems are shown in Fig. 4. These show that every CTA is essentially amorphous and the results of ^{13}C solid state NMR study are therefore regarded as representative of the amorphous region.

It is very interesting that the CTA obtained from the phenolic solution showed an X-ray diffractogram (powder

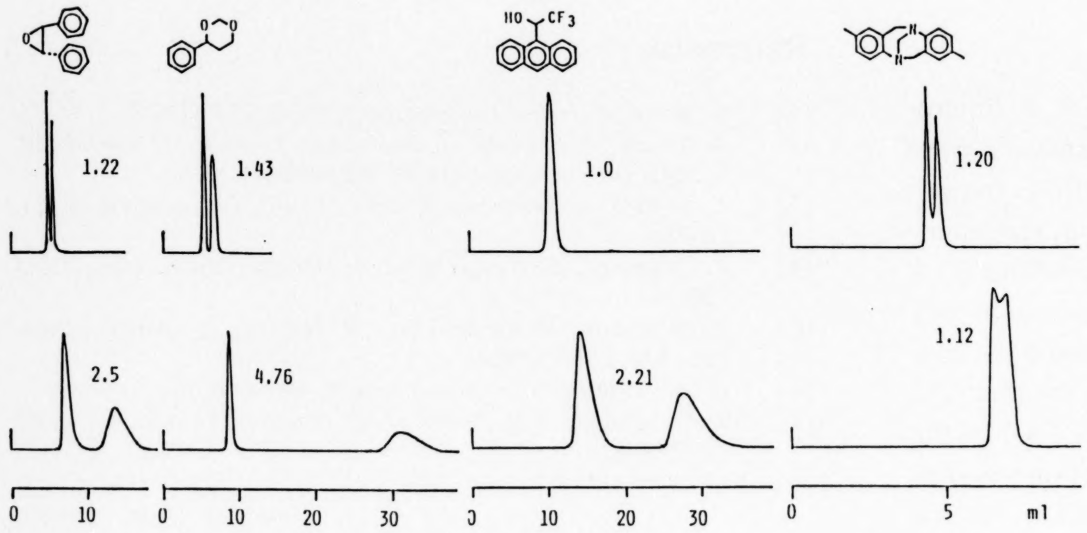

Fig. 2

Chromatograms of some racemates obtained on CSP *4* (upper) and an CSP *5* (lower). Separation factors are given above each chromatogram.

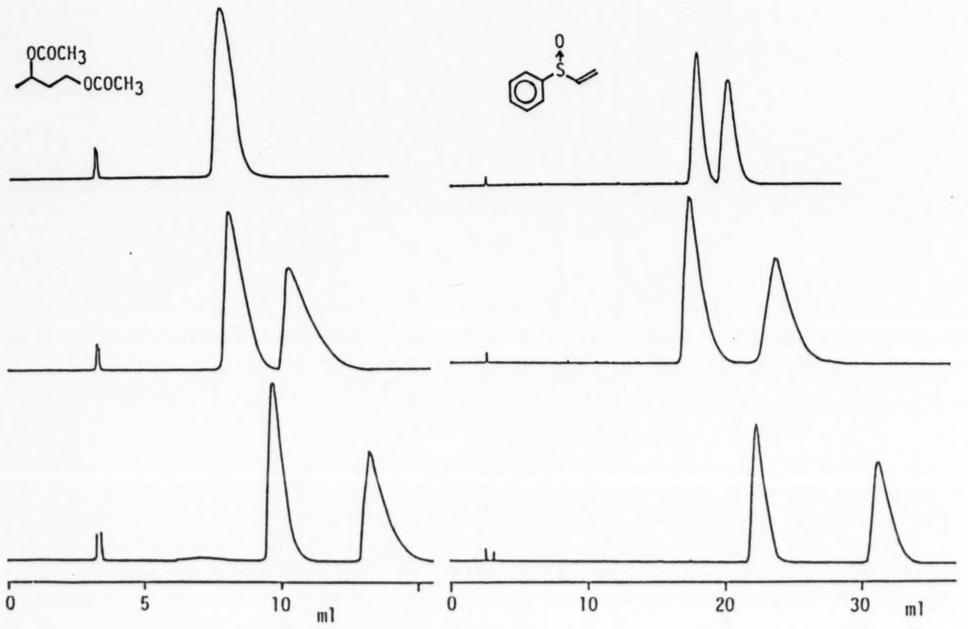

Fig. 3

Chromatograms of 1,3-diacetoxybutane (left) and phenyl vinyl sulfoxide (right) obtained on cellulose tribenzoate coated on silica gel with dichloromethane only (CSP *6*, upper), with a 10:3 mixture of dichloromethane and benzene (CSP *7*, middle), and with a 10:1 mixture of dichloromethane and nitrobenzene (CSP *8*, lower) respectively.

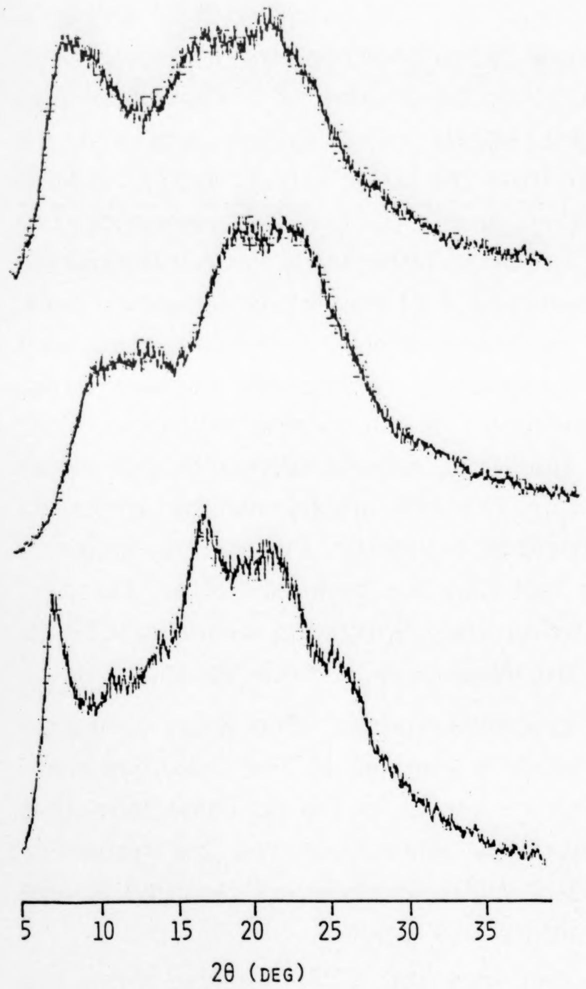

Fig. 4

X-ray diffractograms of powderous cellulose triacetates solidified from the similar solvent systems to those of Fig. 1. Dichloromethane only (upper), dichloromethane-trifluoroacetic acid (middle), and dichloromethane-phenol (lower).

method) closely resembling to that of CTA I (microcrystalline CTA) rather than CTA II which recovery from a CTA solution results as a rule [7]. Therefore, the adsorptive characteristics of the corresponding stationary phase (CSP *5*) were compared with microcrystalline CTA and CTA coated on silica gel with dichloromethane only (CSP *4*) (Table I). Although it is difficult to give a definite conclusion, the behavior of CTA resulted from the phenolic solution is apparently different from that of CTA-I in the point that the former exhibits a better performance with hexane (containing a small amount of a modifier) as the mobile phase, whereas the latter with an alcoholic liquid. Detailed study on the structure and the adsorptive behavior of the CTA is under progress.

Table I. Separation factors and optical rotation in the mobile phase of the first elute on the chiral stationary phases (CSPs) made of cellulose triacetates (CTAs).

Stationary phase	*trans*-1,2-diphenyloxirane A*	B*	Tröger's base A*	B*
Microcrystalline CTA	1.0	1.75(+)	1.0	1.97(–)
CSP *4*	1.22(–)	1.18(–)	1.20(+)	1.18(+)
CSP *5*	2.5 (–)	1.0 (–)	1.12(–)	1.0

* mobile phase A: hexane-2-propanol; mobile phase B: ethanol.

Conclusion

This study showed that by means of an artificial control of the higher-order structure, cellulose triacetate (CTA) recovered from a solution can be endowed with an ability of chiral recognition (i.e., separation factor) even larger than the CTA keeping a naturally occurring higher-order structure, that is, so-called microcrystalline CTA. However, the adsorption characteristics of such a CTA are quite different from microcrystalline cellulose triacetate. The hysteretic effect of a coating solvent is not only practically useful but also informative from the viewpoint of polymer morphology.

References

[1] *G. Hesse, R. Hagel*, Chromatographia **6**, 277 (1973).
[2] *A. Ichida, T. Shibata, I. Okamoto, Y. Yuki, H. Namikoshi, I. Toga*, Chromatographia **19**, 280 (1984).
[3] *T. Shibata, I. Okamoto, K. Ishii*, J. Liq. Chromatogr. **9**, 313 (1986).
[4] *Y. Okamoto, M. Kawashima, K. Hatada*, Chem. Lett. 1984, 739.
[5] *Y. Okamoto, M. Kawashima, K. Hatada*, J. Amer. Chem. Soc. **106**, 5357 (1984).
[6] *T. Sei, T. Shibata, H. Nishimura, K. Deguchi*, in preparation.
[7] *B. B. Sprague, J. L. Riley, H. D. Noether*, Textile Res. J. **28**, 275 (1958).

Received: Aug. 4, 1987
Revised manuscript
received: Sep. 14, 1987
Accepted: Sep. 21, 1987
F

Fluorescence Enhancement for Aflatoxins in HPLC by Post-Column Split-Flow Iodine Addition from a Solid-Phase Iodine Reservoir

H. Jansen* / R. Jansen / U. A. Th. Brinkman / R. W. Frei

Department of Analytical Chemistry, Free University, De Boelelaan 1083, NL-1081 HV Amsterdam, The Netherlands

Key Words

Column liquid chromatography
Fluorescence detection
Post-column derivatization with I_2
Aflatoxins

Summary

A method for post-column derivatization of the highly carcinogenic aflatoxins with iodine has been developed. It involves splitting of the mobile phase used for the reversed phase HPLC separation. One part flows through the injection valve and the C_{18} analytical column to achieve the separation. The other part flows through a column packed with solid iodine. The iodine-containing solution is recombined with the flow coming from the analytical column. The derivatization reaction takes place in a knitted open tubular reactor maintained at 60 °C. Detection is done by fluorescence measurement. Due to the low solubility of iodine in the mobile phase, the iodine solid-phase column can be used for very long periods of time before refilling is necessary. The analytical system consists of only one pump and therefore gives the opportunity to carry out low-cost post-column reaction detection. The method yields reproducible results, a linear response over at least two orders of magnitude and detection limits of about 1 ppb, both for standard solutions and for peanut butter samples.

Introduction

Aflatoxins are highly carcinogenic compounds produced by the fungi Aspergillus flavus and A. parasiticus. The aflatoxin (Af), B_1, B_2, G_1 and G_2 are potential contaminants of certain foodstuffs such as peanut and maize products. They can also be found in milk when cows are fed with contaminated products. Because of their high toxicity, there is a demand for the determination of minute amounts of aflatoxins. HPLC with fluorescence detection is often the method of choice. Zimmerli [1] used a silica-packed flow cell. A higher sensitivity is then obtained by the adsorption of the aflatoxins on the silica thereby stabilizing the molecule and permitting a higher fluorescence yield. The phenomenon is known from thin-layer chromatography [2, 3]. A similar effect can be obtained by making use of derivatization techniques to enhance detectability. AfB_2 and AfG_2 have a high native fluorescence, whereas the fluorescence of AfB_1 and AfG_1 is strongly solvent dependent [4]. When using aqueous solvents, as in reversed-phase HPLC, AfB_1 and AfG_1 can be derivatized to increase their fluorescence intensity by iodine attachment to the double bond (Fig. 1). The resulting derivatives are about as fluorescent as AfB_2 in aqueous solvents [5]. A number of minor additional products are formed. However, for post-column derivatization, this is not a drawback and several HPLC methods with post-column iodination have been published [4, 6, 7]. A saturated solution of iodine in water is added to the column effluent for the derivatization. Although good results are reported, there are several disadvantages: the reagent addition causes dilution, the reagent solution must be prepared daily for stability reasons and an additional pump is needed. These disadvantages can be overcome by the on-line electrochemical production of the reagent [8] or by adding the reagent from a parallel column. A similar approach has been described in a previous paper for post-column pH-adaptation for the determination of barbiturates [9]. An elevated pH was created by the use of an anion exchanger packed in a column parallel to the separation column. The addition of bis (2,4,6-trichlorophenyl)oxalate to the mobile phase via a parallel column has been studied for chemiluminescence detection in HPLC [10]. In the present paper, the reagent addition approach is investigated for the determination of aflatoxins.

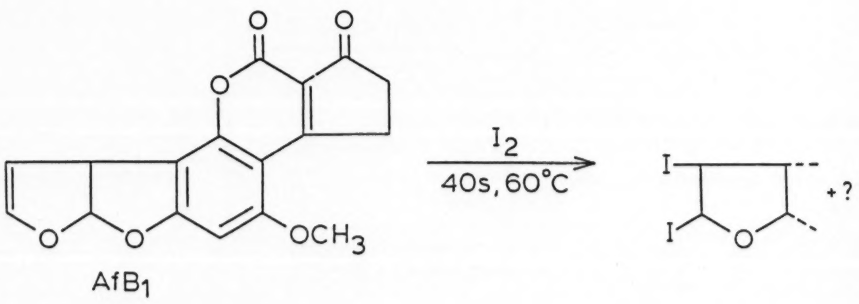

Fig. 1
Derivatization of Aflatoxin B_1 with iodine.

0009-5893/87 0555-05 $03.00/0
© 1987 Friedr. Vieweg & Sohn Verlagsgesellschaft mbH

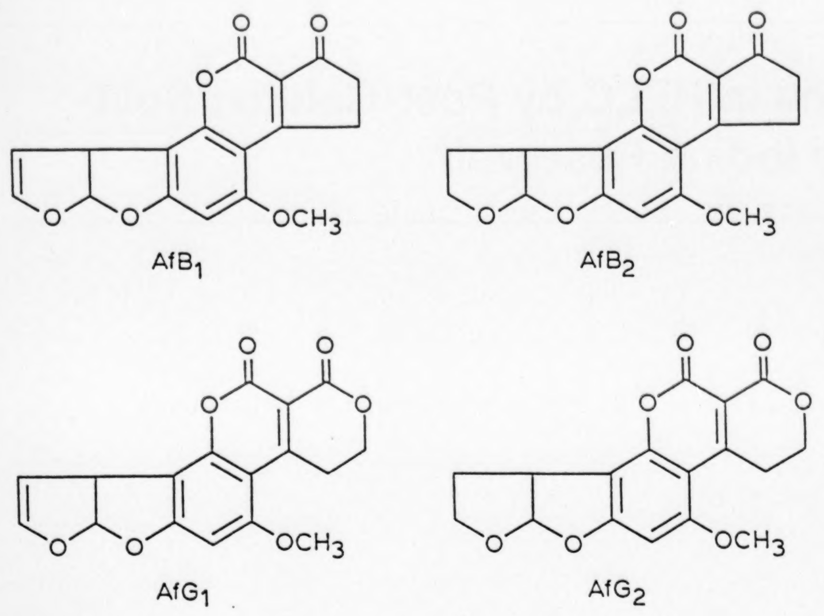

Fig. 2
Structures of the aflatoxins used.

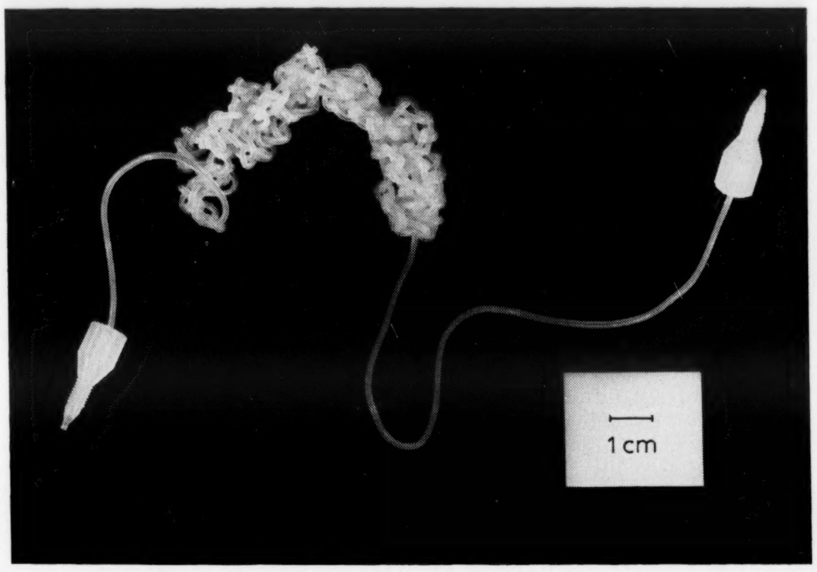

Fig. 4
Knitted PTFE reactor (3.5 m X 0.5 mm I.D., 0.69 ml) with laboratory-built 'hand-tight' Kel-F nut/ferrule combinations.

Experimental

Chemicals

HPLC-grade water was produced in a Milli-Q system (Millipore, Bedford, MA, USA) and was used throughout this work. The eluent was made by mixing water, HPLC-grade methanol (J. T. Baker, Deventer, The Netherlands) and HPLC-grade acetonitrile (J. T. Baker) in a 60:24:16 (v/v/v) ratio, and was degassed in vacuo in an ultrasonic bath prior to use. Stock solutions of each of the aflatoxins used, i.e., aflatoxin B$_1$, B$_2$, G$_1$ and G$_2$ (Fig. 2) (10 μg/ml in chloroform) were a gift from Rikilt (Wageningen, The Netherlands). These stock solutions were diluted with methanol to the desired concentration level prior to analysis. Once diluted, the solutions were kept in the dark at 4 °C. Iodine (p.a. quality) was purchased from J. T. Baker. A sodium thiosulphate titration solution was made from a Titrisol ampule (E. Merck, Darmstadt, FRG). All solvents used were of pro analysi quality.

Apparatus

The experimental set-up is shown in Fig. 3. The system was built from a reciprocating high-pressure pump (Model 302; Gilson, Villiers-le-Bel, France) equipped with a laboratory-constructed membrane-type pulse dampener, an injection valve with a 10 μl sample loop, a wide-bore splitting T-piece (Valco, Houston, TX, USA) and a small-bore low-volume mixing T-piece (Valco). The splitting ratio was controlled by a flow restrictor made from a narrow-bore packed column together with a needle valve. The 200 mm X 4.6 mm I.D. analytical column was laboratory-packed with 5 μm LiChrosorb RP-18 (Merck). The iodine column was made by dry packing a 100 mm X 4.6 mm I.D. stainless-steel column with ground solid iodine particles (ca. 0.8 g). The reaction capillary (PTFE, 3.5 m X 0.5 mm I.D., 0.69 ml volume) was knitted as described by Engelhardt and Neue [11] (Fig. 4) in order to enhance radial mass transfer which results in lower axial dispersion. The temperature of the reactor was kept constant using a thermostatted water bath. The fluorescence detector (SFM 23; Kontron, Zürich, Switzerland) was operated at 365 nm excitation wavelength and 440 nm emission wavelength. All chromatograms were registered by a strip-chart recorder (BD-40; Kipp & Zonen, Delft, The Netherlands). The fluorescence detector was interfaced with a microcomputer (IIe; Apple, Cupertino, CA, USA). A chromatography software package (Chromatochart, Heyden & Sons, London, UK) and a dot-matrix printer (NL-10; Star MFG Co. Ltd., Japan) were used with the computer. All connections in the experimental set-up were made from stainless-steel capillary tubing fitted with laboratory-constructed 'hand-tight' Kel-F nut/ferrule combinations.

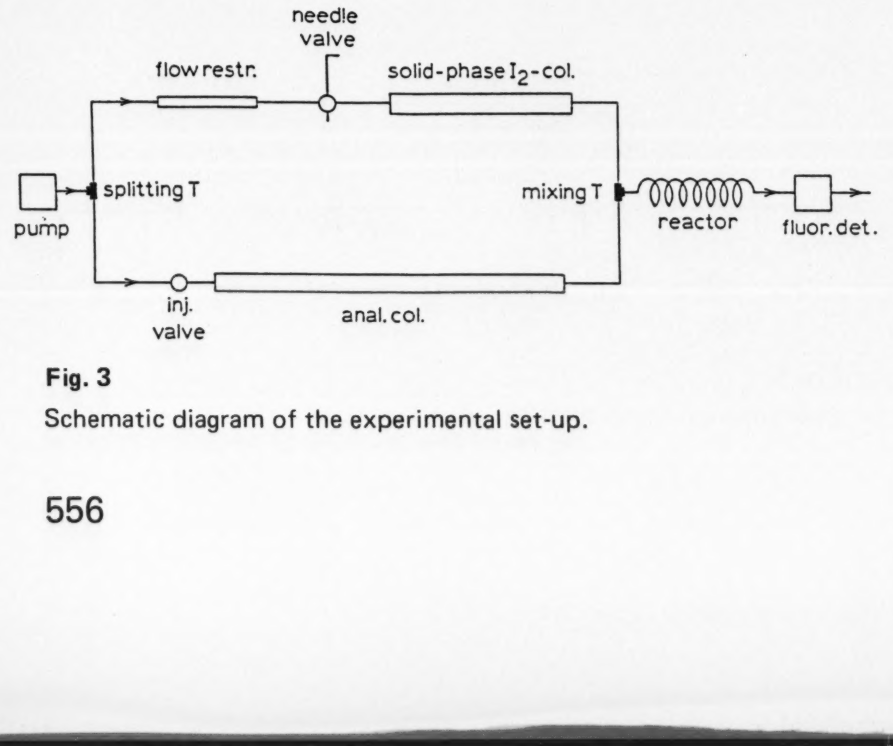

Fig. 3
Schematic diagram of the experimental set-up.

In part of the optimization studies, the solid-phase iodine column was connected to a second high-pressure pump.

Extraction Procedure for Peanut Butter Samples

The sample preparation method for peanut butter used in this work was based on the method as described in ref. [12]. In a 500 ml separatory funnel, 50 g peanut butter, either non-spiked or spiked with a known volume of an aflatoxin stock solution, was extracted with 250 ml of water-methanol (55:45, v/v) and 100 ml of n-hexane. After ca. 30 min, 25 ml of the water-methanol phase was pipetted into a 100 ml separatory funnel. Then, the water-methanol phase was extracted for 5 min with 25 ml of chloroform. The chloroform phase was evaporated with nitrogen and the residue dissolved in 1 ml of methanol. 10 μl aliquots of this methanol solution were injected into the analytical system.

Results and Discussion

Optimization of the Experimental Conditions

In the initial series of experiments, the system shown in Fig. 3 was equipped with an additional pump as described under 'Apparatus', in order to allow for easy flow-rate regulation, i.e., optimization, in the iodine column. In this set-up, the solvent mixture entering the iodine column was invariably the same as the mobile phase. The flow-rate through the analytical column was kept constant at 1 ml/min. A sample solution was prepared containing 40 μg/l of AfB$_1$ and AfG$_1$ each, and 20 μg/l of AfB$_2$ and AfG$_2$ each. Peak heights of all four aflatoxins in the chromatogram were measured as a function of the flow-rate through the solid-phase iodine column. The temperature of the PTFE reactor was kept constant at 60 °C. The results obtained are shown in Fig. 5. For both AfB$_1$ and AfG$_1$ an optimum is observed at a flow-rate of ca. 30 μl/min through the iodine column. At lower flow-rates, the iodine concentration obviously is too low for successful derivatization. The decreasing fluorescence intensity with increasing iodine flow-rate is caused by the quenching effect of iodine, the (relatively small) dilution of mobile phase with iodine solution and the decreased reaction time for AfB$_1$ and AfG$_1$. From Fig. 5 one can calculate that, compared with the measurement of their native fluorescence, about a 20-fold increase for AfB$_1$ and AfG$_1$ is obtained at the optimal flow-rate (ca. 30 μl/min). This flow-rate was adjusted by using the needle valve, the outlet of the solid-phase iodine column being connected to a 100 μl pipette for accurate flow-rate measurements.

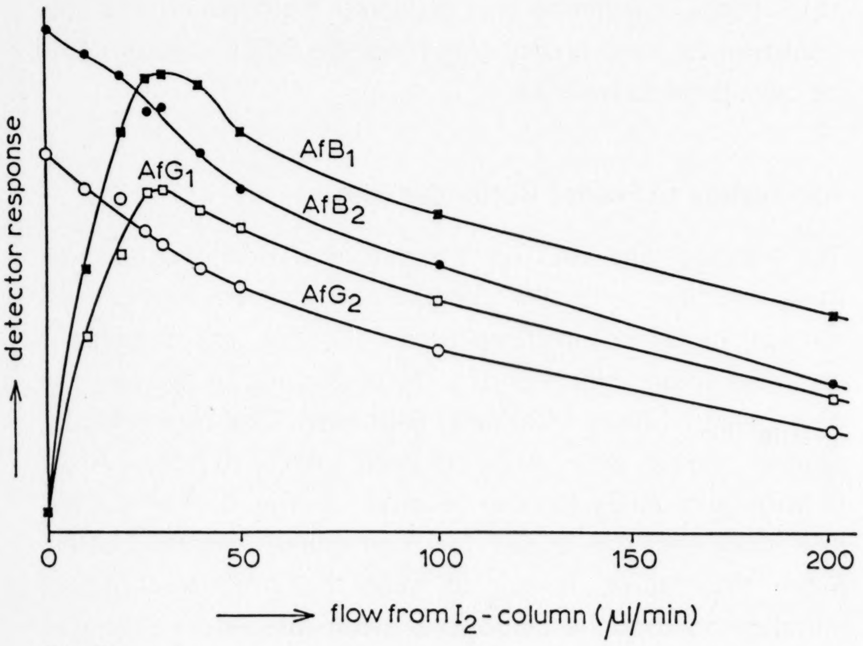

Fig. 5

Peak heights of aflatoxins in the chromatogram as a function of the flow-rate through the solid-phase iodine column. Conditions: flow-rate of mobile phase (water-methanol-acetonitrile, 60 : 24 : 16 (v/v/v)) through analytical column (200 mm × 4.6 mm I.D., packed with 5 μm LiChrosorb RP-18) kept constant at 1.0 ml/min; flow-rate of mobile phase through solid-phase iodine column (100 mm × 4.6 mm I.D.) controlled by a laboratory-constructed syringe pump; injection volume, 10 μl; AfB$_1$ and AfG$_1$, 40 μg/l, AfB$_2$ and AfG$_2$, 20 μg/l; derivatization in knitted PTFE reactor (3.5 m × 0.5 mm I.D.) maintained at 60 °C; fluoresence detection at 365 (ex) and 440 (em) nm.

At a total flow-rate of 1 ml/min, i.e., 0.97 ml/min through the analytical column and 30 μl/min through the solid-phase iodine column, the iodine concentration in the PTFE reactor, i.e., in the derivatization medium, was determined by titration of the mobile phase with sodium thiosulphate using starch as the indicator. An iodine concentration of 0.063 g/l was found. This means that the iodine concentration in the fluid directly downstream from the solid-phase iodine column was 2.1 g/l. The very low flow-rate through the solid-phase iodine column has two distinct advantages, viz. a long lifetime of the column (ca. 25 days when used for 8 hours per day) and only negligible dilution of the mobile phase.

The responses of all four aflatoxins in the analytical system as a function of the PTFE reactor temperature were studied over the 20–60 °C range (Fig. 6). A flow-rate of 1 ml/min was maintained through this reactor which resulted in a 41 s hold-up time. For both AfB$_1$ and AfG$_1$ an increase in response with increasing reactor temperature was observed; according to expectation, for the two other, non-reacting, aflatoxins the responses were hardly affected by temperature. In all further experiments, a reaction temperature of 60 °C was used. Without modification of the present set-up, temperatures higher than 60 °C could not be maintained because of the formation of gas bubbles in the mobile phase.

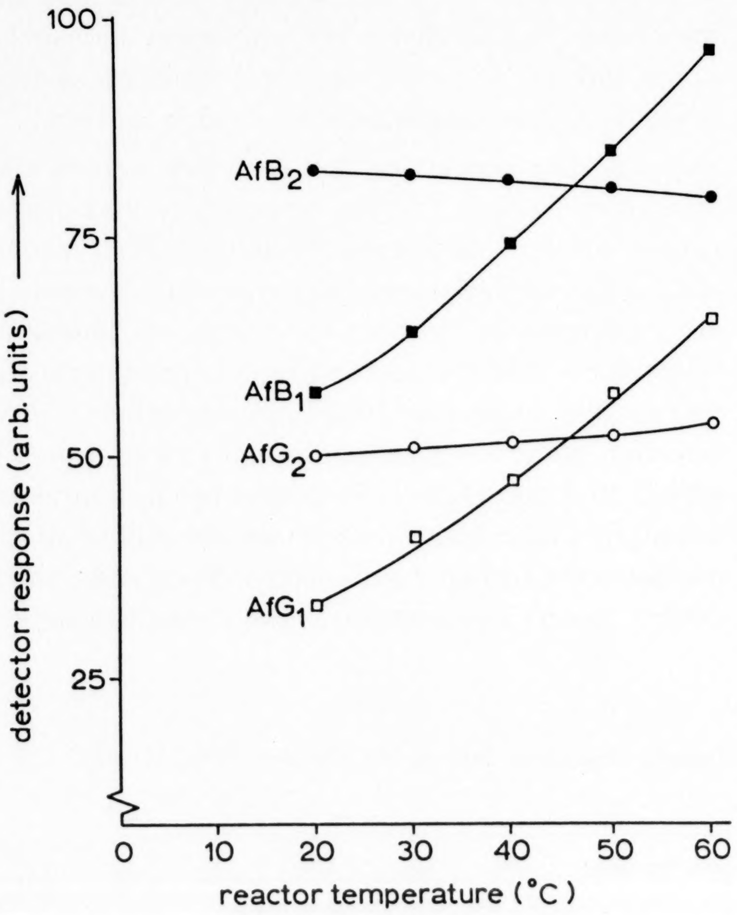

Fig. 6

Peak heights for aflatoxins in the chromatogram as a function of PTFE reactor temperature. AfB$_1$ and AfG$_1$, 40 μg/l, AfB$_2$ and AfG$_2$, 20 μg/l. Conditions: flow-rate of mobile phase, 1.0 ml/min; 0.97 ml/min through the analytical column and 30 μl/min through the solid-phase iodine column; injection volume, 10 μl; derivatization in knitted PTFE reactor; fluorescence detection at 365 (ex) and 440 (em) nm.

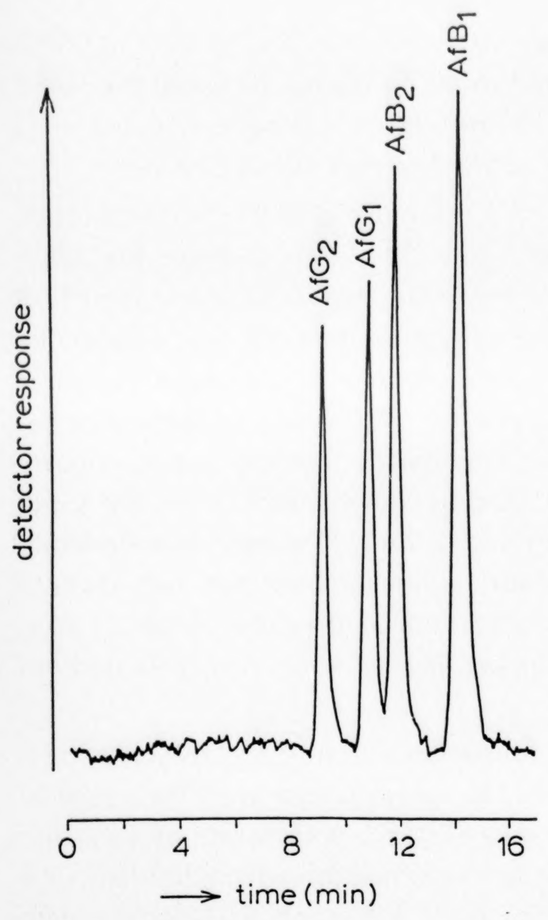

Fig. 7

Chromatogram of a test mixture of AfB_1 and AfG_1 (each 40 μg/l), AfB_2 and AfG_2 (each 20 μg/l). Conditions: PTFE reactor temperature, 60 °C. All other conditions as in Fig. 6.

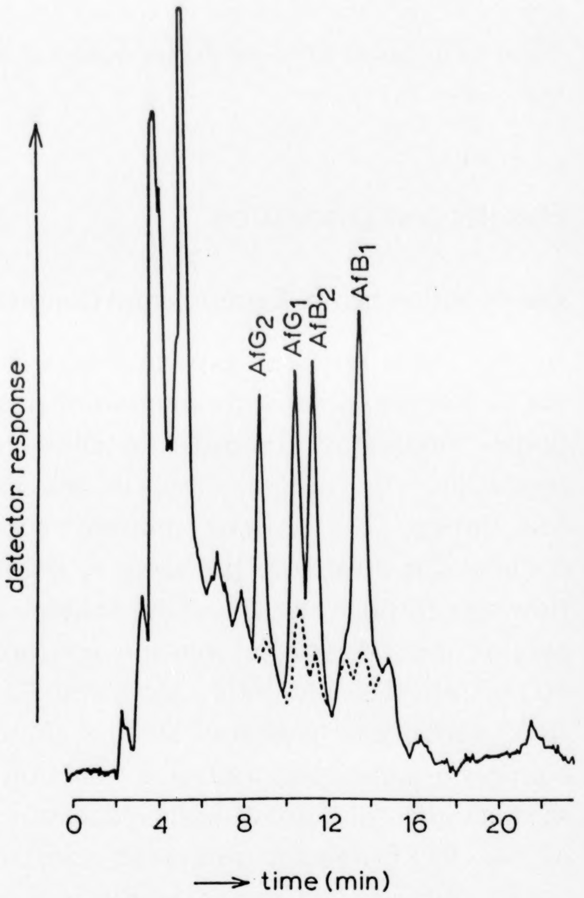

Fig. 8

——— Chromatogram of an extract of peanut butter spiked with AfB_1 (8 ppb), AfG_1 (8 ppb), AfB_2 (4 ppb) and AfG_2 (4 ppb). Sample pretreatment, cf. text. – – – –, Chromatogram of an extract of non-spiked peanut butter. Conditions as in Fig. 7.

Analysis of Standard Solutions

A chromatogram of a test mixture of four aflatoxins in the system C_{18}-bonded silica with water-methanol-acetonitrile (60 : 24 : 16 (v/v/v)) as the mobile phase is shown in Fig. 7. A good separation is achieved in ca. 15 min.

Relevant data concerning the analytical system are summarized in Table I. For the repeatability measurements a sample solution containing 40 μg/l of AfB_1 and AfG_1, and 20 μg/l of AfB_2 and AfG_2 was used. The within-one-day repeatabilities for both total residence time and peak height show that the splitting ratio is not subject to large fluctuations. With the 10 μl injection volume used the detection limits in concentration units range from 0.8 ppb (AfB_2) to 2 ppb (AfG_1). Responses for all four aflatoxins investigated were linear from the detection limit up to 1 ng, this being the highest mass injected. Since AfB_2 and AfG_2 exhibit good fluorescence without derivatization, the contribution to band broadening caused by the PTFE reactor could be measured by injecting AfB_2 and AfG_2 in the analytical system as described above and in the same system but without the PTFE reactor, while keeping all other conditions unchanged. Only a slight difference in total band broadening was observed from which the contribution to band broadening from the PTFE reactor could be calculated to be 3.5 s.

Table I. Analytical data for the aflatoxin HPLC system*

Compound	t_R (min)	Repeatability (% R.S.D., n = 10)		Detection limit**	
		t_R	peak height	(pg)	(fmol)
AfG_2	9.3	1.2	2.7	10	32
AfG_1	11.0	0.7	2.8	20	63
AfB_2	12.0	0.6	3.9	8	28
AfB_1	14.5	0.8	4.7	15	52

* Conditions as in Fig. 7; t_R, total residence time.

** S/N = 3 : 1.

Application to Peanut Butter Samples

The method was used for the determination of aflatoxins in spiked peanut butter. Sample pretreatment was carried out as described in 'Experimental'. The chromatogram obtained upon injection of a 10 μl aliquot of the extract of a peanut butter (Markant, Bilthoven, The Netherlands) sample spiked with AfB_1 (8 ppb), AfG_1 (8 ppb), AfB_2 (4 ppb) and AfG_2 (4 ppb) is given in Fig. 8. The dotted line indicates the signal for non-spiked peanut butter. From this figure, it can be seen that trace-level determination down to the 1-ppb level is possible before chemical interferences start to intervene. The maximum allowed concentration for aflatoxins in peanut butter is 5 ppb (Food and Drugs Act). It can be concluded that the peanut butter analyzed contains a much lower concentration of aflatoxins. Sample pretreatment recoveries were measured by comparing peak heights in chromatograms of extracts from spiked peanut butter (spiking level as in Fig. 8) and mean peak heights obtained upon injection of a standard mixture (concentrations as in Fig. 6). The results are summarized in Table II.

Table II. Recovery of the aflatoxin pretreatment procedure*

Compound	Recovery (%)	Rel. S.D. in recovery
AfG_2	100	4
AfG_1	74	13
AfB_2	85	9
AfB_1	80	6

* Conditions as in Fig. 7, n = 5.

Conclusions

The post-column addition of iodine to an HPLC mobile phase by the use of a solid-phase iodine column mounted parallel to the analytical column allows low-cost reaction detection of aflatoxins, because only one pump is needed for both separation and reagent addition. The reaction with iodine effects an approximately 20-fold increase in the fluorescence intensity of the aflatoxins B_1 and G_1. The system is simple and gives satisfactory results in all respects; its performance is comparable with that of other methods [4, 6–8]. The method has been shown to be suitable for the quality control of peanut butter.

The present method has the advantage that it can be used for long periods of time before refilling the solid-phase iodine column is needed. When post-column addition of iodine is made in the usual way, i.e., when a saturated solution of iodine in water is added by means of a second pump, daily preparation of the solution is needed for stability reasons and the dilution factor is higher. In principle, this dilution factor can be diminished by adding a more concentrated solution of iodine in some organic solvent; however, then, the reagent pump must be able to make accurate solvent delivery at very low flow-rates. The only other post-column derivatization with iodine without the need for a reagent pump described up to now [8] yields results comparable to those described in the present paper, but more hardware is required.

The present method shows one further application of the split-flow principle for post-column reagent addition from a parallel column. The applications include addition of an oxidant (this paper), pH-adaptation [9] and oxalate ester addition for peroxyoxalate chemiluminescence detection [10]. A further increase of the range of applications is to be expected in the near future.

Acknowledgements

This work was supported by the Dutch Foundation for Technical Sciences, grant No. VCH 33.0436. Mr. W. A. Traag (Rikilt, Wageningen, The Netherlands) is thanked for providing the aflatoxin stock solutions.

References

[1] *B. Zimmerli,* J. Chromatogr. **131,** 458 (1977).
[2] *A. Weissbach, Z. Hurwitz,* J. Biol. Chem. **234,** 705 (1959).
[3] *V. S. Waravdekar, L. D. Saslaw,* J. Biol. Chem. **234,** 1945 (1959).
[4] *M. J. Shepherd, J. Gilbert,* Food Additives and Contaminants **1,** 325 (1984).
[5] *N. D. Davis, U. L. Diener,* J. Ass. Offic. Anal. Chem. **63,** 107 (1980).
[6] *L. G. M. Th. Tuinstra, W. Haasnoot,* J. Chromatogr. **282,** 457 (1983).
[7] *P. G. Thiel, S. Stockenström, P. S. Gathercole,* J. Liq. Chromatogr. **9,** 103 (1986).
[8] *W. Th. Kok, Th. C. H. van Neer, W. A. Traag, L. G. M. Th. Tuinstra,* J. Chromatogr. **367,** 231 (1986).
[9] *H. Jansen, C. J. M. Vermunt, U. A. Th. Brinkman, R. W. Frei,* J. Chromatogr. **366,** 135 (1986).
[10] *J. R. Poulsen, J. W. Birks, P. van Zoonen, C. Gooijer, N. H. Velthorst, R. W. Frei,* Chromatographia **21,** 587 (1986).
[11] *H. Engelhardt, U. D. Neue,* Chromatographia **15,** 403 (1982).
[12] Official Methods of Analysis of the Association of Official Analytical Chemists, 13th Edition, p. 420 (ed. *W. Horwitz,* A.O.A.C., Washington 1980).

Received: July 24, 1987
Accepted: Aug. 4, 1987
F

Determination of Chlorproguanil and Metabolites in Biological Fluids

R. B. Taylor* / R. R. Moody / N. A. Ochekepe

School of Pharmacy, Robert Gordon's Institute of Technology, Schoolhill, Aberdeen AB9 IFR, UK

B. Law

Imperial Chemical Industries, Pharmaceuticals Division, Alderley Park, Macclesfield, SK10 4TG, UK

Key Words

Column liquid chromatography
Chlorproguanil
Metabolites
Biological fluids

Summary

The retention behaviour of chlorproguanil and its putative metabolites chlorcycloguanil and 3,4-dichlorophenylbiguanide has been studied on a reversed phase chromatographic system incorporating sodium lauryl sulphate as hydrophobic pairing ion. On the basis of data obtained and comparison of standard compounds with components present in urine following the administration of chlorproguanil, the identity of the metabolites have been confirmed chromatographically. A third unidentified metabolite is also observed. The retention study allows selection of a solvent system which, when used with a small volume, 100 × 2 mm, 3 μm ODS column, enables chlorproguanil and its two major metabolites to be determined in plasma, whole blood and urine. The analytical characteristics of the method are reported and the usefullness of the method in obtaining pharmacokinetic data on the drug and its metabolites is discussed.

Introduction

As a result of resistance and toxicity to many of the drugs used prophylactically against malaria there has been a resurgence of interest in the biguanides proguanil (Paludrine[1]) and chlorproguanil (Lapudrine[1]) [1–3]. Although both of these compounds have been used as antimalarials for many years their pharmacokinetics have not been extensively studied. This has been due in part to the lack of analytical methods adequately specific and sensitive for the determination of these drugs and their metabolites in biological fluids. Very early work on proguanil in 1946 [4] involved colorimetric analysis and allowed limited pharmacokinetic data to be obtained following large dosages of the parent drug. More recently several analytical methods based on high performance liquid chromatography have appeared in the literature [5–8] and these have been applied to more detailed studies of the disposition of this compound following single and multiple 200 mg doses; this being the accepted prophylactic dosage. Of particular interest in such investigations has been the levels of the metabolite, cycloguanil which is thought to be the species active against the malaria parasite [9, 10].

For chlorproguanil almost no pharmacokinetic data exists in the literature. While there is now a need for such data, the analysis of this compound in limited volumes of biological fluids is more difficult. The accepted prophylactic dose is 20 mg once a week, which imposes lower detection limit requirements than in the case of proguanil. Also the metabolites have not been identified, although it has been tacitly assumed that metabolism will be analogous to that of proguanil. A very recent communication has reported a method based on reverse phase HPLC which while it can detect the parent drug, is not adequate to detect any metabolites in plasma following an oral dose of 80 mg [11].

It was the purpose of the present work to investigate the chromatographic behaviour of chlorproguanil and its putative metabolites chlorcycloguanil and 3,4-dichlorophenylbiguanide in the reversed phase hydrophobic pairing ion situation and to verify the identities of the metabolites observed in urine chromatographically. From this it was intended to describe an assay method for chlorproguanil and its two major metabolites, to report the analytical characteristics of the assay and to discuss its suitability for use in pharmacokinetic studies. Although plasma and urine are the usual biological matrices for the study of pharmacokinetic parameters, in the case of the anti-malarials, binding to erythrocytes is considered to be of importance. Hence, the applicability of the method to whole blood was also evaluated. Recently, there have been advances in chromatography which improve detection limits for analytes

---

[1] Paludrine and Lapudrine are the property of Imperial Chemical Industries plc.

0009-5893/87 0560-05 $ 03.00/0

© 1987 Friedr. Vieweg & Sohn Verlagsgesellschaft mbH

present in limited quantities of sample. These include solid phase extraction which allows a high degree of pre-column sample "clean-up" and also the use of narrow or microbore columns with conventional injection and detection systems [12]. This latter approach has been applied to the determination of endogenous steroids and shown to reduce detection limits appreciably [13]. These advances, together with the selectivity obtainable by hydrophobic pairing ion separations, are employed in the analytical methods reported.

Experimental

Materials and equipment: A Waters Associates M6000A pump and M440 fixed wavelength (254 nm) ultraviolet detector fitted with a nominal 18 μl flowcell were used. A Rheodyne 7125 valve fitted with a 20 μl loop was used for injection and columns were 100 × 2 mm slurry packed in the laboratory with 3 μm ODS Hypersil. Solid phase extraction of the samples and standards was by Bond-elut C-18 cartridge fitted to a Vac-elut, 10 cartridge manifold. Column dead time was determined by measuring the time of elution of the aqueous solvent used for injection. The volumetric flow rate used was 0.3 ml/min. All biguanide samples used as standards were made available by ICI plc. Acetonitrile and methanol were of HPLC grade and water was purified by a Millipore Milli-Q system. All other reagents were of AnalaR or equivalent grade.

Sample pretreatment and extraction: Pretreatment of plasma, blood and urine was as described previously [6]. Plasma and blood samples were extracted using C-18 Bond-elut cartridges previously wetted with methanol (2 ml) and conditioned with water (2 ml). After application of the sample (1 ml) the cartridge was washed with water (2 ml) and methanol (2 ml). The biguanides were eluted in methanol (1 ml) containing 0.01% perchloric acid. After evaporation of the methanol the sample was redissolved in 50 μl water with vortex mixing immediately before chromatography. Urine samples were treated similarly except that after application of sample the cartridge was washed with water (3 ml) and 40% methanol in water (1 ml) as a pure methanol wash resulted in loss of biguanides.

Identification of metabolites: The extract of a urine sample obtained following ingestion of 20 mg chlorproguanil was chromatographed in various concentrations of sodium lauryl sulphate in acetonitrile: 10 mM phosphate buffer (40:60) as was an aqueous mixture containing standards of chlorproguanil, chlorcycloguanil and 3,4-dichlorophenylbiguanide. Standards of proguanil and its metabolites were also included. The urine extract was also compared with standard compounds in eluant containing a fixed concentration of sodium lauryl sulphate with varying concentrations of tetrabutylammonium bromide as organic counter ion.

Quantitative procedures: Subsequent to measurements of the effects of organic modifier and pairing ion concentrations a solvent of acetonitrile: 10 mM phosphate buffer (50:50) containing 200 mM sodium lauryl sulphate was used for quantitative determinations.

For plasma and blood determinations calibration curves were prepared by spiking blank plasma or whole blood with four concentrations of chlorproguanil, chlorcycloguanil and 3,4-dichlorophenylbiguanide. Proguanil was also included as the internal standard. Concentrations varied according to the drug levels anticipated and were typically in the range 2 to 10 ng/ml. Blank urine samples were similarly spiked to provide drug and metabolite levels up to 1 μg/ml. Standards and biological samples were subjected to the same extraction and chromatographic procedures. Peak height measurements were made at 0.0025 to 0.005 AUFS for plasma and blood and 0.1 to 0.2 for urine. Blank plasma and urine samples were included in all calibration procedures and calibration equations were obtained by regression of peak height ratio on concentration.

The recoveries of chlorproguanil at 10 ng/ml and metabolites at 5 ng/ml were determined by comparing peak heights obtained after extraction of spiked plasma and urine with those obtained by direct injection of the appropriate concentration of aqueous standards of each of the compounds. The precision of the overall method including extraction and chromatography was assessed by the constancy of the calibration lines for sets of standards run over a period of several weeks. Detection limits were estimated in plasma by injecting successively lower concentrations until a signal to noise ratio of approximately 3 was obtained.

Results and Discussion

While capacity factors can be taken as an indication of identity, the complex variation observed when a hydrophobic pairing ion is added to the eluent [14] can provide additional confirmation of identity. Fig. 1 shows the variation of capacity factor with sodium lauryl sulphate concentration for proguanil, chlorproguanil and their respective metabolites. Superimposed on these plots are the capacity factors obtained for the characteristic peaks found in the urine extract of a subject after a single 20 mg dose of chlorproguanil. To obtain increased resolution among the compounds for identification a solvent of acetonitrile: buffer (40:60) was used. A representative chromatogram of the urine extract is shown in Fig. 2A. In Fig. 1, all of the standard compounds exhibit the complex behaviour observed previously for ionic compounds [14]. Peak number 6 in the urine sample is seen to correspond with plot number 6 and thus represents the parent chlorproguanil. The correspondence of peaks 2 and 4 in Fig. 2A with plots 2 and 4 in Fig. 1 confirms the identities of two of the metabolites found as chlorcycloguanil and 3,4-dichlorophenylbiguanide. The presence of chlorcycloguanil and 3,4-dichlorophenylbiguanide is further confirmed by the information in Fig. 3. Identical behaviour for urinary metabolites and standard compounds is shown following addition of cationic organic counter ion, tetrabutylammonium bromide, to the eluent. Similar behaviour was observed when tetraethylammonium bromide was used in place of the tetrabutylammonium. Fig. 2B shows a

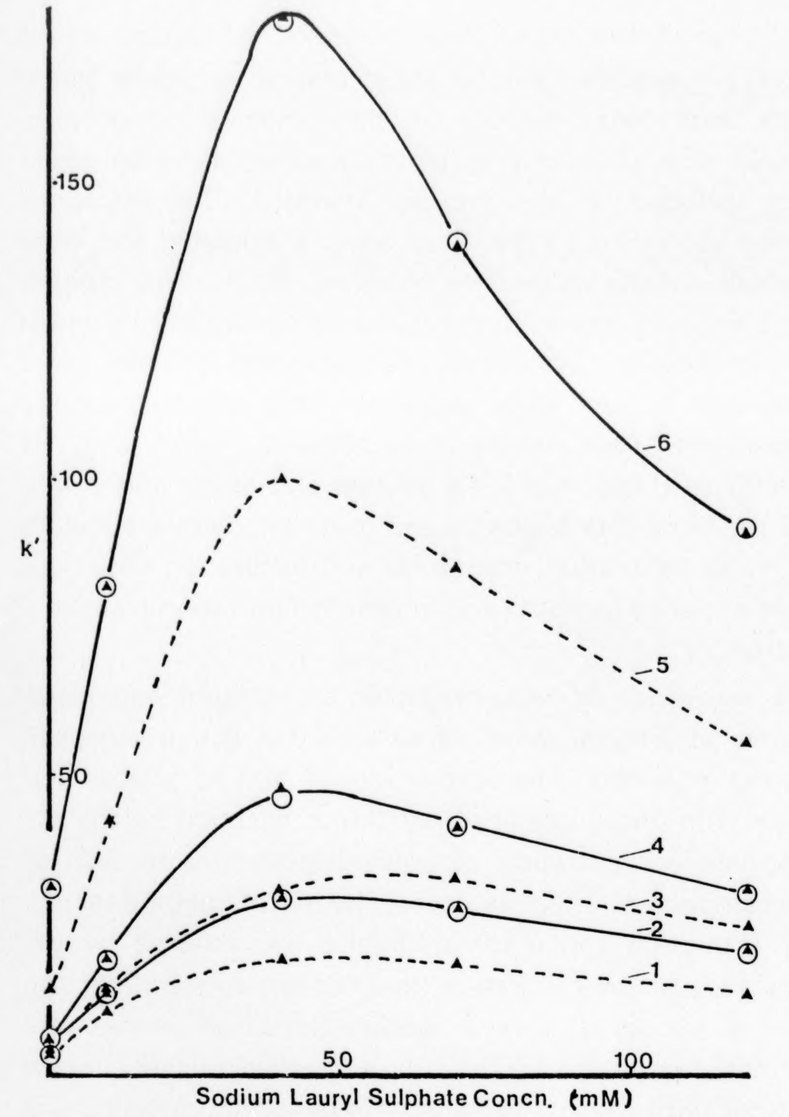

Fig. 1

Variation of capacity factors of the biguanides with sodium lauryl sulphate concentration. Solvent acetonitrile: 10 mM phosphate buffer (40:60).

Standard compound identification: **1** = cycloguanil, **2** = chlorcycloguanil, **3** = 4-phenylbiguanide, **4** = 3,4-dichlorophenylbiguanide, **5** = proguanil, **6** = chlorproguanil.

Experimental points marked as circles represent capacity factors of compounds found to be present in urine extract.

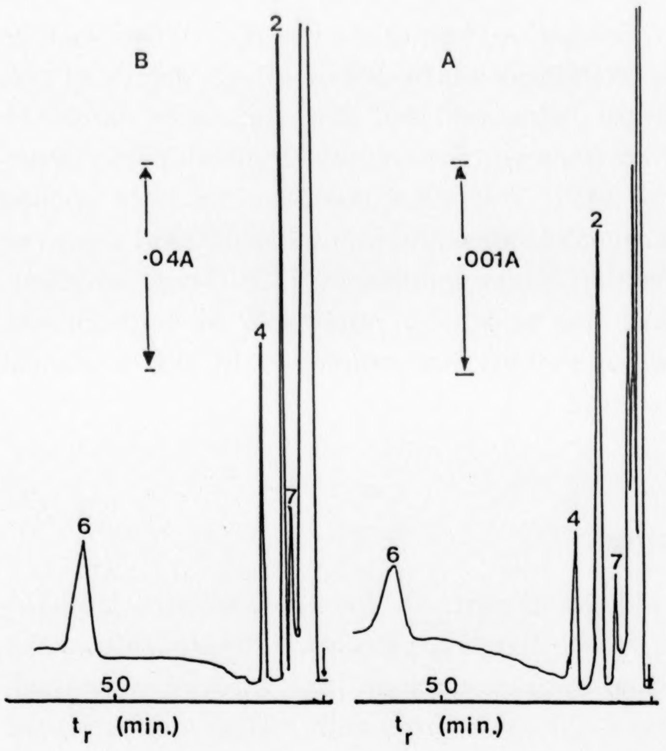

Fig. 2

Representative chromatograms of urine extracts following a 20 mg oral dose of chlorproguanil in a solvent of acetonitrile: 10 mM phosphate buffer (40:60) containing (A) 40 mM sodium lauryl sulphate (B) 40 mM sodium lauryl sulphate and 20 mM tetraethylammonium bromide. Peak identification as in Fig. 1.

representative chromatogram of the urine extract in presence of tetraethylammonium bromide and sodium lauryl sulphate. Addition of such organic counter ion has been shown to be capable of producing marked changes in selectivity among mixtures of other organic bases such as the tricyclic anti-depressants [15]. In the case of the biguanides hydrophobicity differences among the compounds are so marked that retention order is maintained. Similar behaviour, with no marked differences in retention order was observed when other pairing ions were used unlike a previous investigation where changes in the retention order of acidic species were observed with different ion pairing agents [16]. These data are taken as good evidence that the metabolites formed from chlorproguanil are analogous to those formed by proguanil. Fig. 2A and 2B also show the presence of a third unidentified metabolite of chlorproguanil (peak 7).

Fig. 1 also illustrates the very marked increase in capacity factor of chlorproguanil over proguanil while a corresponding increase is not seen for the respective cyclo-metabolites.

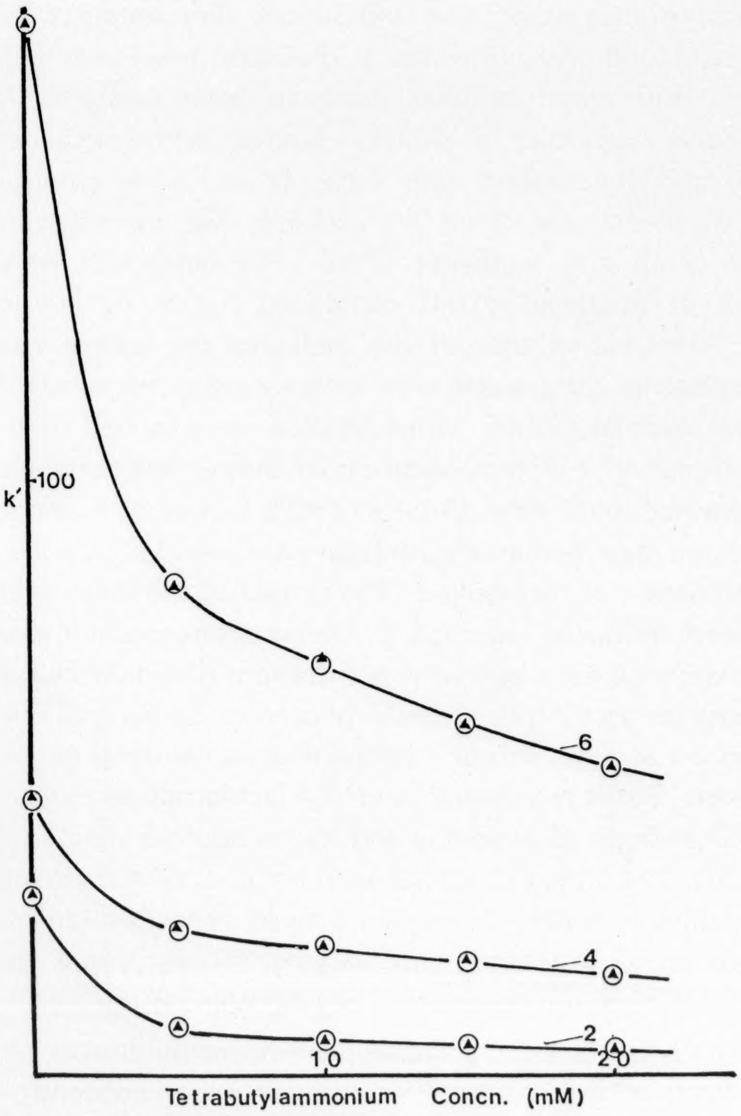

Fig. 3

Variation of capacity factors with tetrabutylammonium bromide concentration at a sodium lauryl sulphate concentration of 40 mM. Solvent and compound identification as in Fig. 1.

Thus, since the purpose of this analytical method is to determine chlorproguanil at maximum sensitivity while maintaining an adequate separation of chlorcycloguanil from the solvent front, the solvent of acetonitrile: 10 mM phosphate buffer (50:50) containing 200 mM sodium lauryl sulphate represents the optimum solvent found. This results in appreciably longer analysis times than in the case of proguanil. Fig. 4 shows representative chromatograms of plasma, blood and urine following administration of chlorcycloguanil.

The analytical characteristics of the method for assay of chlorproguanil and its two major metabolites are summarised in Tab. I. The somewhat lower recoveries from urine compared with plasma may reflect the ease with which the biguanides can be removed from the Bond-elut cartridge when analysing urine in contrast to plasma samples. Hence it is likely that some of the biguanides are being removed in the 40% methanol wash. Detection limits are quoted only for plasma. These are comparable with those quoted previously for the proguanil system [6]. In the case of the cyclo-metabolite this limit is more variable than the others since the quality of the extraction step is critical for this compound. The precision of the analytical method is reported in terms of the mean of slopes and correlation coefficients for the regression lines obtained on different days over a period of weeks for different concentration ranges of standard used.

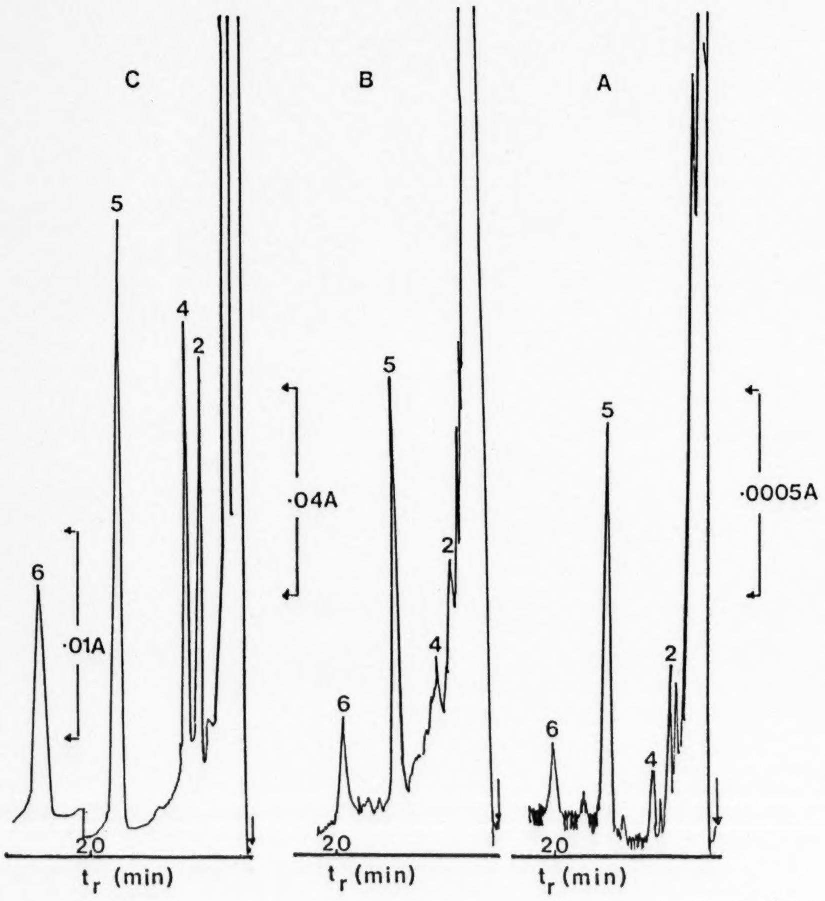

Fig. 4

Representative chromatograms of (A)-plasma, (B)-whole blood, (C)-urine following ingestion of a 20 mg dose of chlorproguanil in a solvent of 200 mM sodium lauryl sulphate in acetonitrile: 10 mM phosphate buffer (50:50). Peak identification as in Fig. 1.

Table I. Characteristics of the analytical method.

Compound	2	4	5	6
Parameter				
Plasma recovery at 5 ng/ml (%) (Std. Dev.) n=6	100 (3)	98 (6)	102 (5)	101 (11)
Urine recovery at 500 ng/ml (%) (Std. Dev.) n=8	99 (3)	96 (5)	97 (6)	86 (5)
Mean slope of plasma calibration line (Std. Dev. X 10^3) n = 6	28.0 (10.0)	36.1 (12.8)	–	11.1 (3.1)
Mean correlation coefft. plasma calibration line (Std. Dev. X 10^3) n=6	0.998 (2)	0.995 (4)	–	0.989 (8)
Mean slope of urine calibration line n=2	1.61	2.35	–	5.58
Mean correlation coefft. urine calibration line n=2	0.996	0.999	–	0.998
Detection limit plasma and whole blood (ng/ml)	0.5–1	0.5–1	–	0.8–2

* 2-chlorcycloguanil; 4-3,4-dichlorophenylbiguanide; 5-proguanil; 6-chlorproguanil

The method reported highlights the usefullness of hydrophobic pairing ions in the analysis of such basic drugs. There is a marked improvement in peak shape and thus resolution on addition of pairing ion. Also the capacity factors are increased so that the most polar metabolite of interest chlorcycloguanil can be resolved from the solvent front. In this case the very wide differences in hydrophobicity between this metabolite and the parent drug results in a very large retention time for chlorproguanil compared with the cyclo metabolite. In this situation the small column volume used is a considerable advantage in minimising dilution of the parent drug by the column [17]. The observed efficiency of 2500 to 3000 obtained for chlorproguanil shows that, at such capacity factors column efficiency is not adversely affected by the use of 20 μl sample injection volumes and conventional path length detectors. The method presented here may be modified by altering the organic modifier concentration according to the needs of a particular analytical situation. If a lower detection limit for the parent drug is required its capacity factor can be reduced by increasing the proportion of acetonitrile concentration and choosing an appropriate concentration of pairing ion but the metabolites will not be adequately retained. Alternatively, reduction of solvent strength will allow increased retention of the metabolites which will be of advantage in the determination of chlorcycloguanil. The method described has been shown to be reliable in practice and is currently being applied to a pharmacokinetic study of chlorproguanil involving several dosage levels and the results of this study will be published at a later time.

Acknowledgements

The authors gratefully acknowledge the expert help of Mrs. A. S. Low and the gift of blood from the Grampian Blood Transfusion Service for calibration purposes.

References

[1] Bull. W. H. O. **62**, (Suppl.), 123 (1984).

[2] *A. Bjorkman, J. Brokult, M. Willcox, P. O. Pehrson, L. Rombo, P. Hedman, G. Hetland, E. Kollie, A. P. Hanson, E. Bengtsson*, Ann. Trop. Med. Parasitol. **79**, 597 (1985).

[3] *A. Henderson, J. A. Rixom*, Trans. Roy. Soc. Trop. Med. Hygiene **81**, 981 (1986).

[4] *B. G. Maegraith, M. M. Tottey, A. R. D. Adams, W. H. Andrews, J. D. King*, Ann. Trop. Med. Parisitol. **40**, 493 (1946).

[5] *R. R. Moody, A. B. Selkirk, R. B. Taylor*, J. Chromatogr. **182**, 359 (1980).

[6] *R. B. Taylor, R. R. Moody, N. A. Ochekpe*, J. Chromatogr. **416**, 394 (1987).

[7] *M. D. Edstein*, J. Chromatogr. **380**, 184 (1986).

[8] *J. A. Kelly, K. A. Fletcher*, J. Chromatogr. **381**, 464 (1986).

[9] *N. N. Crounse*, J. Org. Chem. **16**, 493 (1951).

[10] *A. F. Crowther, A. A. Levi*, Brit. J. Pharmacol. **8**, 93 (1953).

[11] *M. D. Edstein, J. R. Veenendaal*, Trans. Roy. Soc. Trop. Med. Hyg. **81**, 136 (1987).

[12] *R. Gill, B. Law*, J. Chromatogr. **354**, 185 (1986).

[13] *R. B. Taylor, K. E. Kendle, R. G. Reid*, J. Chromatogr. **385**, 383 (1987).

[14] *R. Gloor, E. L. Johnson*, J. Chromatogr. Sci. **15**, 413 (1977).

[15] *C. T. Hung, R. B. Taylor*, J. Chromatogr. **240**, 61 (1982).

[16] *D. G. Durham, C. T. Hung, R. B. Taylor*, Intl. J. Pharmaceut. **11**, 31 (1982).

[17] *J. H. Knox*, J. Chromatogr. Sci. **15**, 352 (1977).

Received: June 30, 1987
Accepted: Aug. 10, 1987
F

Optimization of Peptide Separations in Reversed-Phase HPLC: Isocratic Versus Gradient Elution

C. T. Mant / T. W. Lorne Burke / R. S. Hodges*

Department of Biochemistry and the Medical Research Council of Canada Group in Protein Structure and Function, University of Alberta, Edmonton, Alberta, T6G 2H7, Canada

Key Words

Preparative reversed-phase chromatography
Peptides
Isocratic and gradient elution
Analytical columns

Summary

We have determined the interaction behaviour of peptides with hydrophobic stationary phases on analytical columns using isocratic or shallow gradient elution for the purpose of developing procedures for rapid optimization of conditions for preparative reversed-phase chromatography of peptides. From our investigation of the separation of two closely related decapeptides (differing by one methyl group), in a 1:1 molar ratio on an analytical C8 column, we have found that shallow gradients of 0.1% acetonitrile/min appeared to be the best compromise between resolution and a practical run time for preparative peptide separations. Up to 20 mg of the two-peptide mixture was efficiently resolved on the analytical column, with > 97% recovery of homogeneous peptides.

Introduction

The excellent resolving power and versatility of reversed-phase chromatography (RPC) has led to its becoming the dominant mode of high-performance liquid chromatography for both analytical and preparative separations of peptides in recent years [1]. Preparative chromatography is defined not by the quantity of material injected, but by the purpose of the separation. Thus, the purification of micrograms of a peptide for subsequent testing may be termed preparative as much as a separation of gram quantities [2, 3]. However, the levels of homogeneous product(s) required per single injection and/or the complexity of the sample mixture will have a bearing on the type and size of columns and instrumentation necessary to carry out the desired separation. Most researchers would probably desire to carry out both analytical and preparative peptide separations on analytical equipment and columns, taking advantage of the powerful resolving capability of small particle size (5–10 μm) reversed-phase packings [3–6]. In addition, for purification of substantial levels of a desired peptide, researchers would ideally prefer to be able to optimize a separation based upon the retention time of the peptide(s) in an initial analytical elution profile to obtain maximum loading and resolution in the shortest time for preparative chromatography [4–7].

In this study, we have clearly demonstrated that the interaction behaviour of peptides with hydrophobic stationary phases is quite different to that of small organic molecules such as alkylphenones under the conditions commonly required to optimize preparative separations i.e., isocratic [8] or shallow gradient elution [4–6]. Having determined the behaviour of peptides under these conditions, we have been able to achieve both maximum resolution and maximum loading of two closely related decapeptides (differing by one methyl group), in a 1:1 molar ratio, on an analytical column. This ratio was chosen to represent the most difficult separation that would be encountered by researchers in the preparative purification of peptides.

Experimental

Materials

HPLC-grade water and acetonitrile were obtained from Fisher Scientific (Fairlawn, NJ, USA). HPLC-grade TFA and alkylphenone HPLC standards were obtained from Pierce Chemical (Rockford, IL, USA).

Peptides

Peptides 1–5 were synthesized on a Beckman Model 990 peptide synthesizer (Beckman Instruments, Berkeley, CA, USA) using the general procedure for solid-phase synthesis described by Parker and Hodges [9]. The composition of the peptides varied as follows: peptide 2, -Gly^3-Gly^4-; peptide 3, -Ala^3-Gly^4-; peptide 4, -Val^3-Gly^4-; peptide 5, -Val^4-Val^5-. All peptides contained a N$^\alpha$-acetylated N-

0009-5893/87 0565-08 $03.00/0 © 1987 Friedr. Vieweg & Sohn Verlagsgesellschaft mbH

terminal and a C-terminal amide, except peptide 1, which was identical to peptide 3 but had a free α-amino group. These peptides were obtained from the Alberta Peptide Institute, Department of Biochemistry, University of Alberta, Edmonton, Alberta, Canada, T6G 2H7.

Apparatus

The HPLC instrument consisted of a Varian Vista Series 5000 liquid chromatograph (Varian, Walnut Creek, CA, USA) coupled to a Hewlett-Packard (Avondale, PA, USA) HP1040A detection system, HP85B computer, HP9121 disc drive, HP2225A Thinkjet printer and HP7470 plotter. Samples were injected with a 2.0ml injection loop (Model 7125, Rheodyne, Cotati, CA, USA).

Columns

Separations were carried out on an Aquapore RP-300 C_8 analytical reversed-phase column, 220 x 4.6mm i.d., 7μm particle size, 300Å pore size (Brownlee Labs. Santa Clara, CA, USA).

Gradient delay time (t_g)

Gradient delay time is defined in this work as the time for the gradient to reach the detector from the proportioning valve via pump, injection loop and column.

Results and Discussion

Nature of the Interactions of Peptides with Hydrophobic Stationary Phases

Before conditions can be optimized for analytical or preparative reversed-phase separations of peptides, it is important to understand their mechanism of interaction with the hydrophobic stationary phase. Figure 1 illustrates the effect of isocratic elution on the retention of a series of five decapeptides and four alkylphenones on an analytical Aquapore C_8 column (220 x 4.6mm i.d.). Peptides P2 and P3 differ by only a methyl group; peptides P3 and P4 differ by two carbon atoms; peptides P4 and P5 differ by three carbon atoms (see Experimental). The alkylphenones, A1–A4 – denoting propiophenone, butyrophenone, valerophenone and hexanophenone, respectively differ by a methylene group from each other. Mixtures of the peptides or alkylphenones were chromatographed isocratically at a flow-rate of 1ml/min in 0.05% aqueous trifluoroacetic acid (TFA) containing various percentage concentrations (v/v) of acetonitrile. The retention values of the solutes were expressed as $R_t - t_0$, where R_t was the observed retention time and t_0 was the time for elution of unretained compounds. This value (t_0) was determined by injecting a 1μl aliquot of TFA. A dramatic change in peptide retention times with small changes in isocratic concentrations of acetonitrile in the isocratic solvent was observed, reflecting the results obtained in previous studies [10–15]. In fact, the range of acetonitrile concentration over which each peptide was eluted was only ~ 14% ± 2% (the upper limit of acetonitrile concentration was taken as that just required to elute the peptide at t_0 and the lower limit was taken as that required to elute the peptide within 2h). In contrast, the range for each alkylphenone was ~ 55% ± 5%. Under conditions where solutes are partitioning with the hydrophobic stationary phase, the logarithm of their capacity factor (k′) values should show a linear dependence with concentration of organic modifier in the mobile phase [14–16]. Figure 2 shows such a dependence between $\log_{10} k'$ of the peptides and alkylphenones with isocratic concentration of acetonitrile. The capacity factor (k′) was calculated using the equation: $k' = (R_t - t_0)/t_0$, where R_t is the retention time of the peptide or alkylphenone and t_0 is the retention time of unretained compounds (uracil). Retention time values become less accurate as they ap-

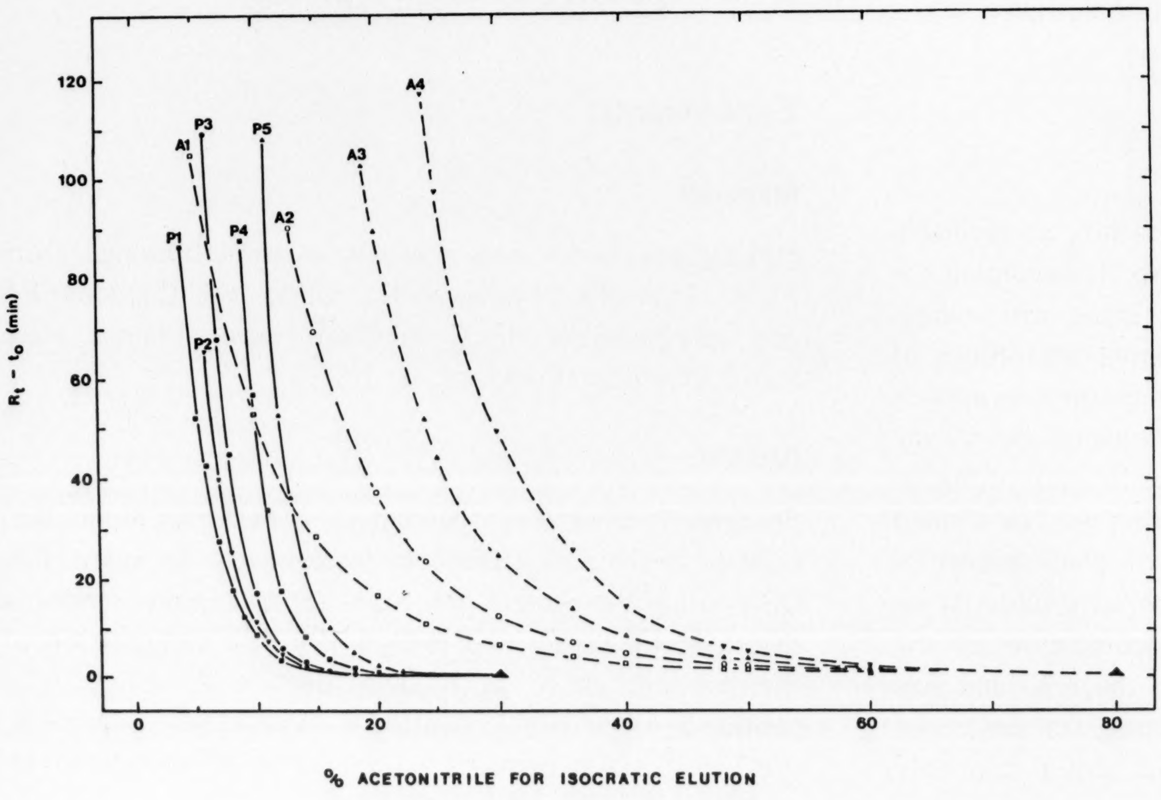

Fig. 1

Plot of retention times of peptides and alkylphenones *versus* the concentration of acetonitrile used for isocratic elution. Column: Aquapore C_8 (220 X 4.6mm i.d.). Conditions: isocratic elution with 0.05% aqueous TFA containing various percentage concentrations (v/v) of acetonitrile; flow-rate, 1ml/min; 26°C; absorbance at 210nm. Retention times are expressed as observed retention times (R_t) minus the time taken for elution of unretained compounds (t_0). P1–P5 denote decapeptides 1–5, respectively (see Experimental). A1–A4 denote propiophenone, butyrophenone, valerophenone and hexanophenone, respectively.

proach t_0 and values which were $< 2t_0$ were not included in the plot shown in Fig. 2. The plots for the five peptides formed a series of essentially parallel lines, as did the plots for the alkylphenones. However, the slopes for the peptides were markedly steeper than for those of the alkylphenones. Thus, a 5% (v/v) increase in the acetonitrile concentration caused a seven-fold decrease in the k' values of the peptides; in contrast, the k' values of the alkylphenones changed only by a factor of 1.7. The partitioning rate of the alkylphenones with the hydrophobic stationary phase is much greater than the partitioning rate of peptides. The peptides partition only to a very limited extent [17] and approach an adsorption/desorption mechanism of interaction. This slow partitioning rate of the peptides is reflected by the sensitivity of their retention time values to small changes in isocratic acetonitrile concentration (Fig. 1) and the steepness of the peptide semilogarithmic plots demonstrated in Fig. 2. As the slopes approach the vertical, the interaction mechanism approaches 100% adsorption/desorption.

The results demonstrated in Figs. 1 and 2 indicate that the acetonitrile concentration range available for practical isocratic separations of the peptides to baseline resolution is very narrow. This is clearly illustrated by comparing the effect of isocratic elution at 1 ml/min on the elution profiles of four alkylphenones (A1–A4) (Fig. 3, top) with peptides 2–4 (P2–P4) (Fig. 3, bottom). Above 50% or 13% concentrations (v/v) of acetonitrile in the 0.05% aqueous

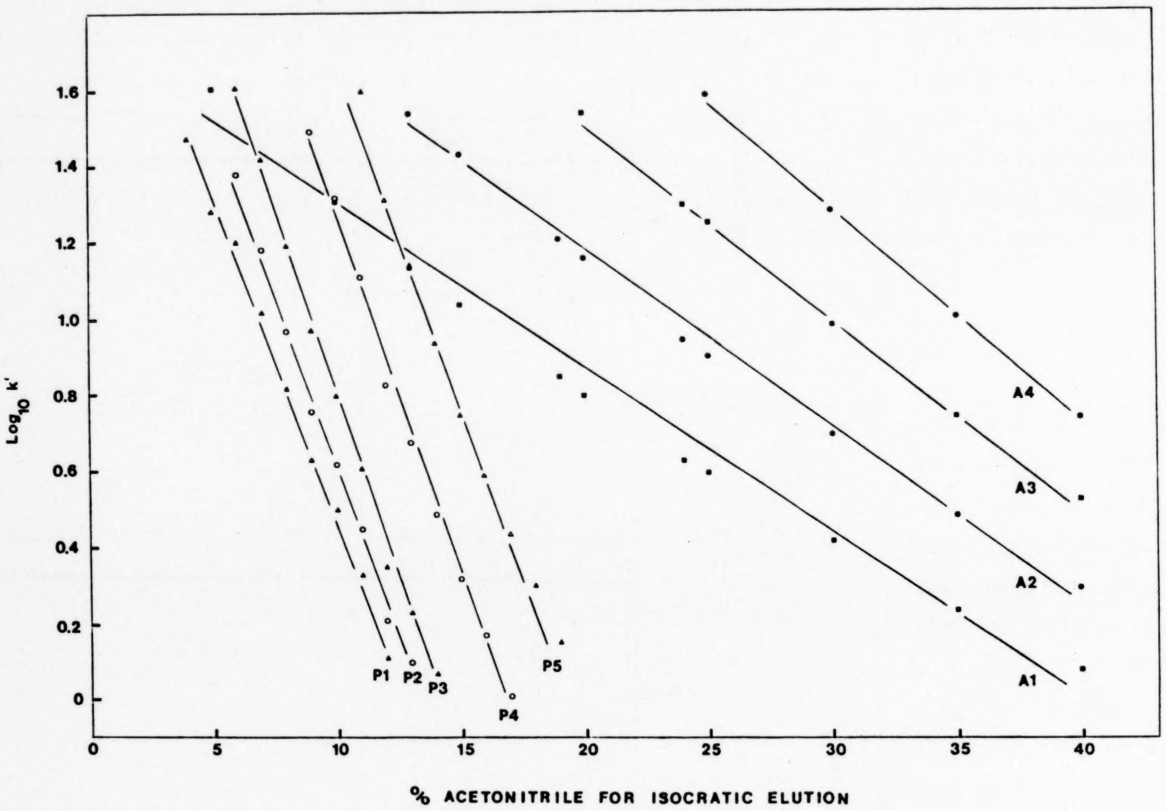

Fig. 2

Effect of acetonitrile concentration on the $\log_{10}k'$ (capacity factor) values of peptides and alkylphenones during isocratic elution. Column: Aquapore C_8 (220 X 4.6 mm i.d.). Conditions: isocratic elution with 0.05% aqueous TFA containing various percentage concentrations (v/v) of acetonitrile; flow-rate, 1 ml/min; 26°C; absorbance at 210 nm. P1–P5 denote decapeptides 1–5, respectively (see Experimental). A1–A4 denote propiophenone, butyrophenone, valerophenone and hexanophenone, respectively. The capacity factor (k') was calculated using the equation: $k' = (R_t - t_0)/t_0$, where R_t is the retention time of the peptide or alkylphenone and t_0 is the retention time of unretained compounds (uracil).

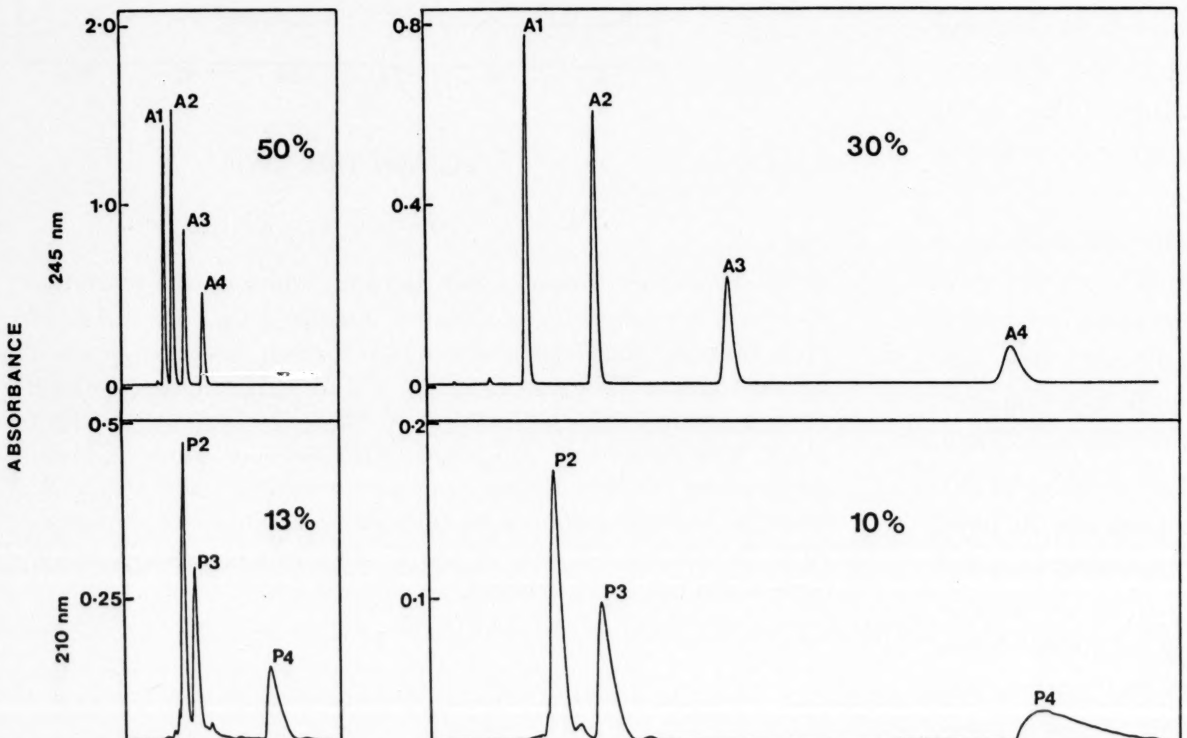

Fig. 3

Effect of isocratic elution on resolution of peptides and alkylphenones. Column: Aquapore C_8 (220 X 4.6 mm i.d.). Conditions: mixtures of peptides or alkylphenones were subjected to isocratic elution in 0.05% aqueous TFA containing various percentage concentrations (v/v) of acetonitrile labelled in each panel; flow-rate, 1 ml/min; 26°C. P2–P4 denote decapeptides 2–4, respectively (see Experimental). A1–A4 denote propiophenone, butyrophenone, valerophenone and hexanophenone, respectively.

mobile phase, the components of the alkylphenone or peptide mixtures, respectively, are no longer baseline resolved. Below 30% or 10% acetonitrile concentrations, all the alkylphenone and peptide components, respectively, are no longer eluted within a 60 min time period. Thus, the alkylphenones can be separated isocratically within a reasonable time over a wide range of acetonitrile concentrations (30–50%); in contrast, the peptides can be separated isocratically within a reasonable time only over a very narrow range of acetonitrile concentrations (10–13%). In other words, the partitioning range, or partitioning window, allowable for efficient peptide separation is very narrow compared to the alkylphenones. We have defined the partitioning window of a particular sample component as the range of isocratic organic solvent concentration available to separate the peptide (baseline resolution) from its nearest impurities. Since this window is very narrow for peptides, optimizing isocratic conditions for practical and reproducible peptide separations can prove difficult. In addition, although the alkylphenone peaks broaden as the isocratic concentrations are decreased, the peaks remain symmetrical. In contrast, the peptide peaks not only broaden with decreasing acetonitrile concentrations, but also tail severely.

Isocratic versus Gradient Elution of Peptides

The most difficult type of peptide separation problem encountered by researchers generally involves the resolution of two closely related peptides, particularly if these peptides are present in similar quantities. Separation of small analytical samples of such peptide mixtures may be relatively simple to achieve by linear gradient elution. In fact, the most common analytical method for analytical peptide separations involves a linear AB gradient (1% B/min at a flow-rate of 1 ml/min), where solvent A is 0.05%–0.1% aqueous TFA and solvent B is 0.05%–0.1% TFA in acetonitrile. However, in order to increase the sample loading potential for peptides of close hydrophobicity, the separation of the peptides must be optimized. This is generally achieved by shallowing the linear gradient to improve resolution around the peak(s) of interest [4–6]. The shallower the gradient, the better the separation. Taken to its logical conclusion, isocratic elution should maximize the separation of two closely-related peptides.

Fig. 4 demonstrates the effect on the analytical separation of decapeptides 2 and 3 (denoted S2 and S3, respectively) as the linear gradient steepness was decreased from 1% acetonitrile/min (Panel A; starting conditions, 0% acetonitrile) to 0.1% acetonitrile/min (Panel B; starting conditions, 7% acetonitrile), to 0.05% acetonitrile/min (Panel C; starting conditions, 7% acetonitrile) and, finally, to isocratic elution with 7% acetonitrile. The peptides differed by only a single methyl group and were present in a 1:1 molar ratio, representing a particularly difficult separation problem for sample loads exceeding analytical levels (> 1 mg). The presence of acetonitrile in the starting solvent for the two shallow gradients (Panels B and C) was necessary to ensure elution of both peptides within a reasonable time. The peptides exhibited increasing separation, and subsequent peak broadening, with decreasing

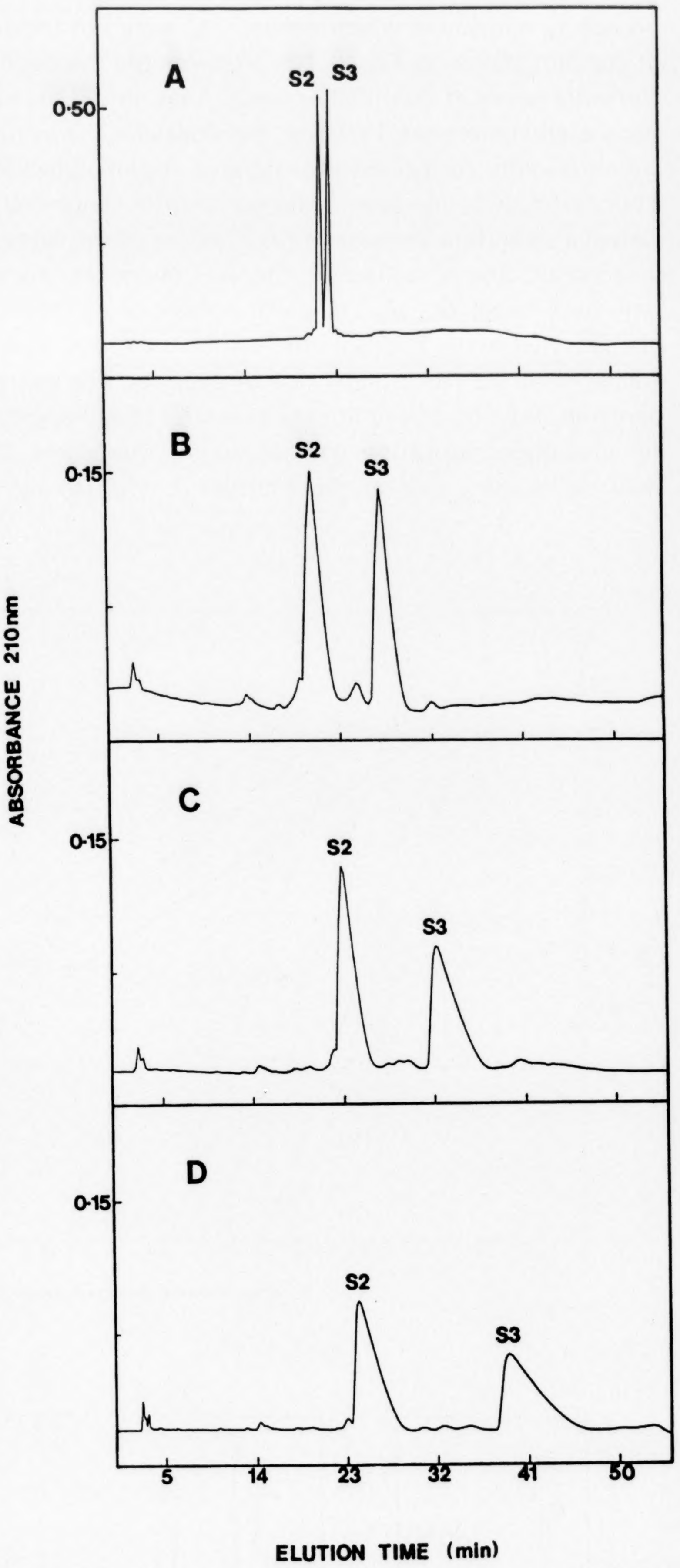

Fig. 4

Effect of gradient steepness and isocratic elution on the separation of closely related peptides. Column: Aquapore C_8 (220 × 4.6 mm i.d.). Panel A: linear AB gradient (1% B/min), where solvent A is 0.05% aqueous TFA and solvent B is 0.05% TFA in acetonitrile; starting conditions, 100% solvent A. Panel B: linear AB gradient (0.1% B/min); starting conditions, 93% A/7% B. Panel C: linear AB gradient (0.05% B/min; starting conditions, 93% A/7% B. Panel D: isocratic elution with 93% A/7% B. Flow-rate, 1 ml/min; 26°C. Sample load, 0.1 mg. S2 and S3 denote decapeptides 2 and 3, respectively (see Experimental).

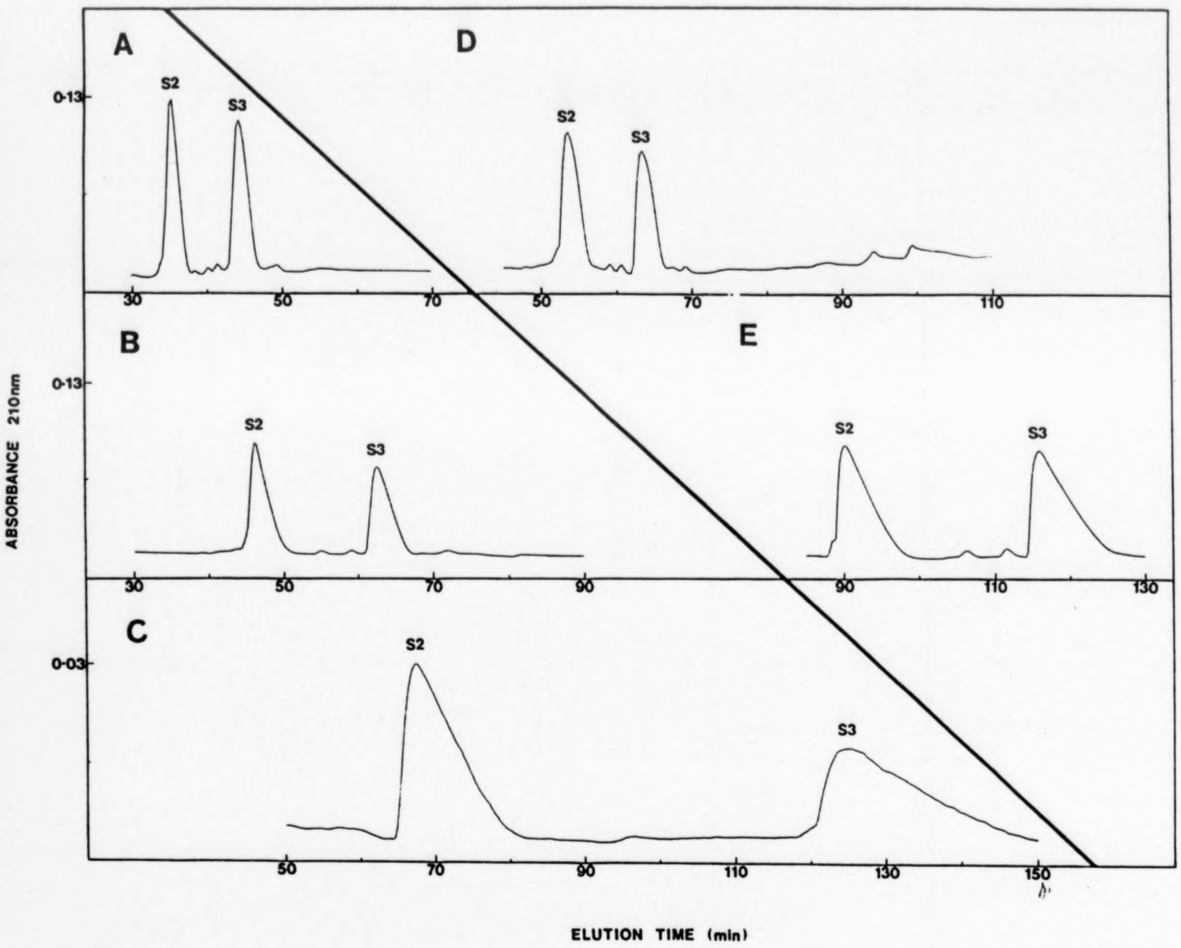

Fig. 5

Effect of starting conditions on the separation of closely related peptides by gradient or isocratic elution. Column: Aquapore C_8 (220 × 4.6 mm i.d.). Panel A: linear AB gradient elution (0.1% B/min), where solvent A is 0.05% aqueous TFA and solvent B is 0.05% TFA in acetonitrile; starting conditions, 95% A/5% B. Panel B: linear AB gradient (0.05% B/min); starting conditions, 95% A/5% B; panel C: isocratic elution with 95% A/5% B. Panel D: linear AB gradient (0.1% B/min); starting conditions, 97% A/3% B. Panel E: linear AB gradient (0.05% B/min); starting conditions, 97% A/3% B. Flowrate, 1 ml/min; 26°C. Sample load, 0.1 mg. S2 and S3 denote decapeptides 2 and 3, respectively (see Experimental).

gradient steepness, with maximum separation being achieved under isocratic elution conditions.

In Fig. 5, the same shallow gradients have been applied to the separation of the two peptides, but the initial concentration of acetonitrile in the mobile phase has been varied. Comparison of Panels A (0.1% acetonitrile/min; starting conditions, 5% acetonitrile), B (0.05% acetonitrile/min; starting conditions, 5% acetonitrile) and C (isocratic elution with 5% acetonitrile) again demonstrate that decreasing gradient steepness improves peptide separation. Similarly, increased separation resulted from decreasing the gradient steepness from 0.1% acetonitrile/min (Panel D) to 0.05% acetonitrile/min (Panel E) under starting conditions of 3% acetonitrile in the mobile phase. Maximum separation of the peptides was again achieved by isocratic elution (Panel C). However, as discussed previously (Fig. 1–3), optimum isocratic conditions are extremely difficult to predict, due to the very narrow partitioning window for peptides. In addition, isocratic conditions tend to produce very broad peaks. The results also demonstrate that, if a very shallow gradient is used (0.05% acetonitrile/min), separation of the two peptides can be maximized (compare Panels C [Fig. 4], B [Fig. 5] and E [Fig. 5]). However, this may also cause a considerable extension of the run time. Thus, to decrease the run time, the starting conditions of acetonitrile concentration can be varied while maintaining the same steepness of the gradient. This is shown by comparing Panels A (0.1% acetonitrile/min; starting conditions, 5% acetonitrile) and D (0.1% acetonitrile/min; starting conditions, 3% acetonitrile) or Panels B (0.05% acetonitrile/min; starting conditions, 5% acetonitrile) and E (0.05% acetonitrile/min; starting conditions, 3% acetonitrile).

Figure 6 graphically summarises the effect of acetonitrile concentration on isocratic elution *or* the effect of acetonitrile concentration used in the starting conditions for shallow gradient elution on the separation (ΔR_t, where R_t denotes retention time) of peptides S2 and S3 (top panel) and the retention time of S3 (bottom panel). The small change in starting acetonitrile concentrations for the 0.1% B/min gradient does not have the same dramatic effect on peptide retention times observed for the 0.05% B/min gradient and the isocratic elution separations. Hence, it is easier to optimize preparative separations using 0.1% B/min gradients. Figs. 4–6 demonstrate that, depending on the difficulty of a separation and the desired run time, shallow gradients of 0.1% acetonitrile/min appear to be the best compromise between resolution and a practical run time for peptide separations.

Effect of Sample Load on Peptide Resolution

The optimum conditions determined above for analytical separation of S2 and S3 now served as the basis for a scale-up to higher sample loading. Increasing the sample load eventually leads to reduced component retention times during isocratic or gradient elution. During the present investigation of the effects of increased sample loading on peptide retention and resolution, the starting solvent for linear gradient elution (0.1% acetonitrile/min) did not contain acetonitrile. Thus, any tendency for the peptides to elute earlier with increasing sample load would not be amplified by the presence of acetonitrile in the starting solvent.

Figure 7 demonstrates the effect of increased sample load of peptides S2 and S3 on the analytical Aquapore C_8 column. The sample mixture again contained a 1:1 molar ratio of the two peptides, which were eluted at 1 ml/min by a linear AB gradient (0.1% B/min), where solvent A was 0.05% aqueous TFA and solvent B was 0.05% TFA in acetonitrile. At small sample loads (0.1 mg and 1 mg total),

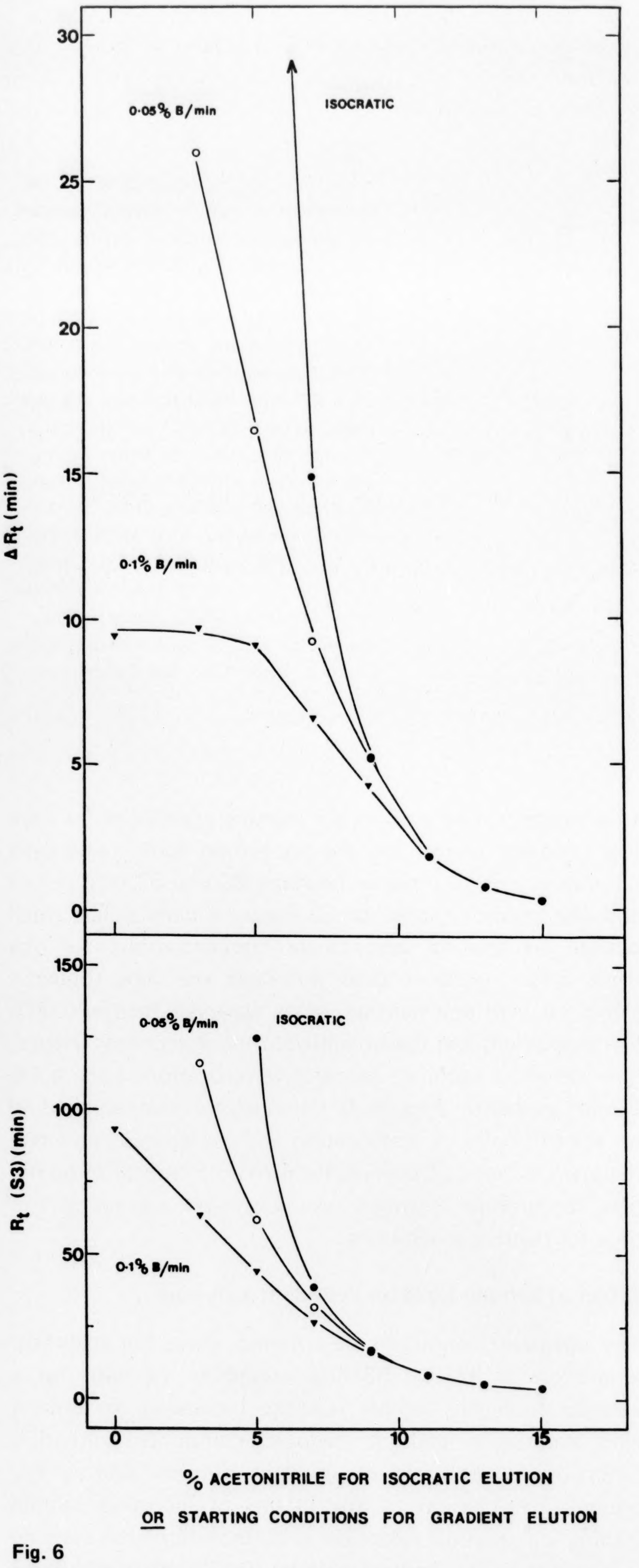

Fig. 6

Graphical profiles showing effect of acetonitrile concentration for isocratic elution *or* the acetonitrile concentration used in the starting conditions for gradient elution on peptide retention and resolution. Column: Aquapore C_8 (220 X 4.6 mm i.d.). Gradient elution: peptides were subjected to linear AB gradient elution at 0.05% B/min or 0.1% B/min, where solvent A is 0.05% aqueous TFA and solvent B is 0.05% TFA in acetonitrile, with various starting concentrations of acetonitrile in the initial mobile phase. Isocratic elution: peptides were eluted with varying concentrations of acetonitrile in 0.05% aqueous TFA. Flow-rate, 1 ml/min; 26°C; absorbance at 210 nm. Sample load, 0.1 mg. Top panel: ΔR_t denotes the difference in retention times (min) of S2 and S3 (denoting decapeptides 2 and 3, respectively; see Experimental). Bottom panel: R_t denotes retention time (min) of S3.

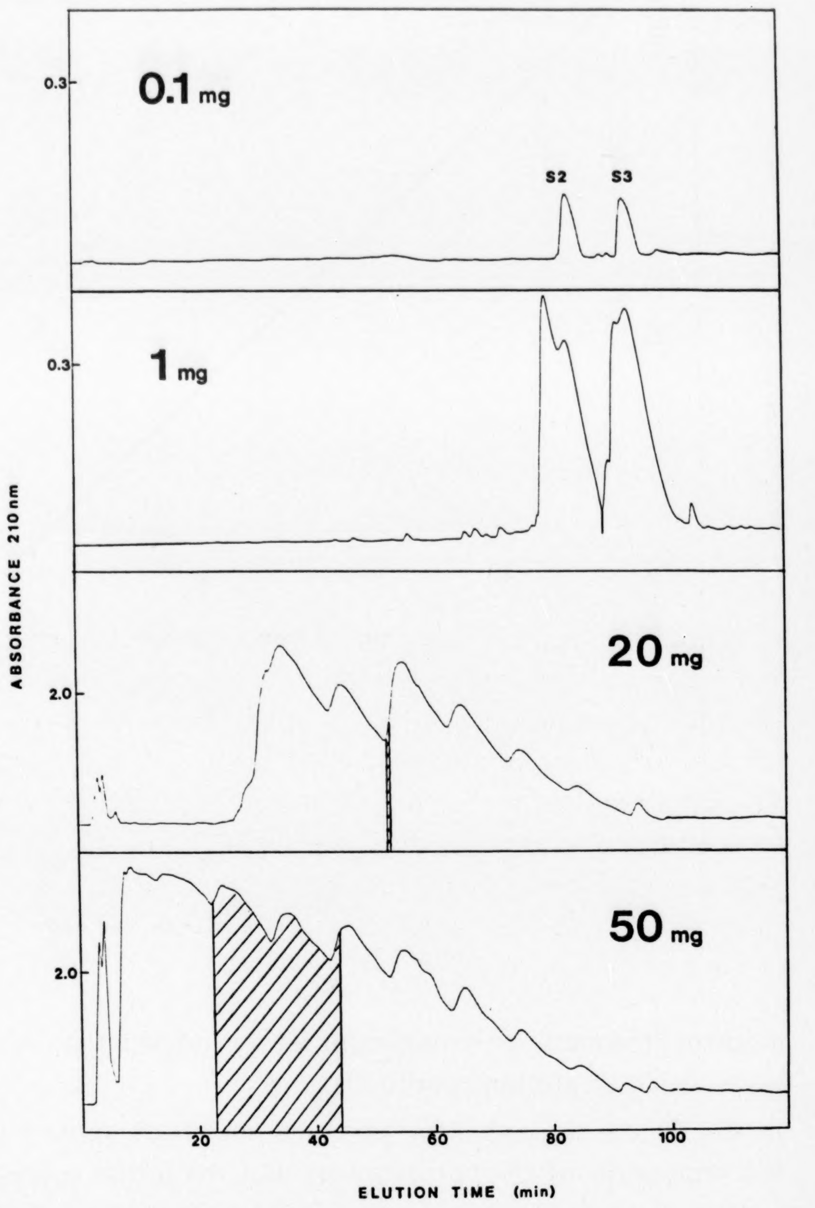

Fig. 7

Effect of sample load on the peptide elution profiles. Column: Aquapore C_8 (220 X 4.6 mm i.d.). Conditions: linear AB gradient (0.1% B/min), where solvent A is 0.05% aqueous TFA and solvent B is 0.05% B in acetonitrile; flow-rate, 1 ml/min; 26°C. Sample loads: 0.1 mg, 1 mg, 20 mg in, respectively, 5 μl, 50 μl and 1000 μl of solvent A from a 20 mg/ml solution and 50 mg in 300 μl of solvent A. Peptides S2 and S3, denoting, respectively, decapeptides 2 and 3 (see Experimental) were present at all sample loads in a 1:1 molar ratio. Hatched areas indicate cross-contamination observed from the isocratic fraction analysis described in text.

S2 and S3 were resolved with 100% relative recovery of both peptides (Table 1). As one can see from the 20 mg and 50 mg injections, the point of separation between S2 and S3 can no longer be seen and fraction analysis must be carried out in order to make pools of pure components. Isocratic analyses were carried out as this enables rapid analysis of fractions without the need for column regeneration between analyses [1]. At a sample loading of 20 mg, 99% of recovered S2 and 98% of recovered S3 were isolated as pure fractions. Only one fraction (1 ml) was cross-contaminated. Thus, despite the gross skewing of the peptide peaks, the shallow acetonitrile gradient produced an impressively efficient separation of a high peptide sample load on the analytical column. However, at a loading of 50 mg, and although neither S2 nor S3 was detected in the breakthrough peak (t_0), there was considerable cross-contamination. This resulted in reduced relative recoveries of 87% and 61% of S2 and S3, respectively (Table I), indicating that the column had been overloaded in terms of

Table I. Effect of sample loading on peptide recovery

Sample No.	Quantity Injected (mg)			Total Recovery (%)	Relative Recovery[b] (%)	
	S2[a]	S3[a]	Total		S2	S3
1	0.05	0.05	0.1	–	100	100
2	0.5	0.5	1	–	100	100
3	5.1	4.9	10	89.0	98	98
4	10.2	9.8	20	89.5	99	98
5	24.4	25.6	50	93.5	87	61

[a] S2 and S3 denote decapeptides 2 and 3, respectively, with S3 containing an additional methyl group (see Experimental).

[b] Fraction of a pure peptide recovered from the total of that peptide recovered.

efficient recovery of pure components under the conditions used. Thus, the practical limit for this analytical column to achieve this difficult separation (expressed as amount of decapeptide injected) is approximately 30 mg. The time required to completely elute both peptides from the column was identical for all sample loads, i.e., at this gradient steepness (0.1% acetonitrile/min), total sample elution time was independent of sample load. Figure 8 demonstrates the effect of variation of sample load (S2 plus S3) on the retention time of S2 during shallow gradient elution (Fig. 7). The retention time of S2 decreased rapidly (82 min to 6 min) as the sample load increased from 0.1 mg to 50 mg.

The results demonstrated in Figs. 7 and 8 indicate the difficulties in predicting the chromatographic behaviour of preparative peptide sample loads from run conditions optimized for analytical separations. However, they also demonstrate how these optimized conditions may still produce excellent separation, in high yield and purity, of desired closely-related peptide components on analytical columns. Thus, a researcher would not need to know with any great accuracy either the peptide sample load or levels of individual peptide components applied to an analytical column and subjected to shallow gradient elution. If the loading was too low, the peptides may take some time to elute, but the separation would be very efficient. If the loading was too high, the resolution of the peptides may suffer, but high yields of homogeneous product(s) may still be achieved. From Table I, total peptide recovery (S2 plus S3) was 89.0%, 89.5% and 93.5% for 10 mg, 20 mg and 50 mg loads, respectively, indicating that, whatever the sample load, efficient recovery of peptides is possible. Hence, if the load was too high for a single chromatographic run, unresolved components may simply be pooled, lyophilized, and subjected to a repeat run, highlighting the versatility of this system.

Optimization Procedure for Preparative Purification of Peptides on Analytical Columns

(i) Perform an analytical separation using a linear AB gradient at a flow-rate of 1 ml/min and a gradient steepness of 1% B/min starting from 0% B at time 0 min. The sample load should be sufficient to give a full-scale absorbance deflection of about 0.5 AU at 210 nm with flow cells of 0.6–1.0 cm path length.

(ii) Repeat the above run, changing only the gradient steepness to 0.1% B/min. Though the run time will be extended considerably, the baseline separation (distance between the peaks) will be greatly improved while still maintaining a relatively good peak shape. The time for elution of the components at this gradient steepness can be easily estimated:

$$\frac{1\%}{0.1\%} \times (R_t - t_g) + t_g \, ,$$

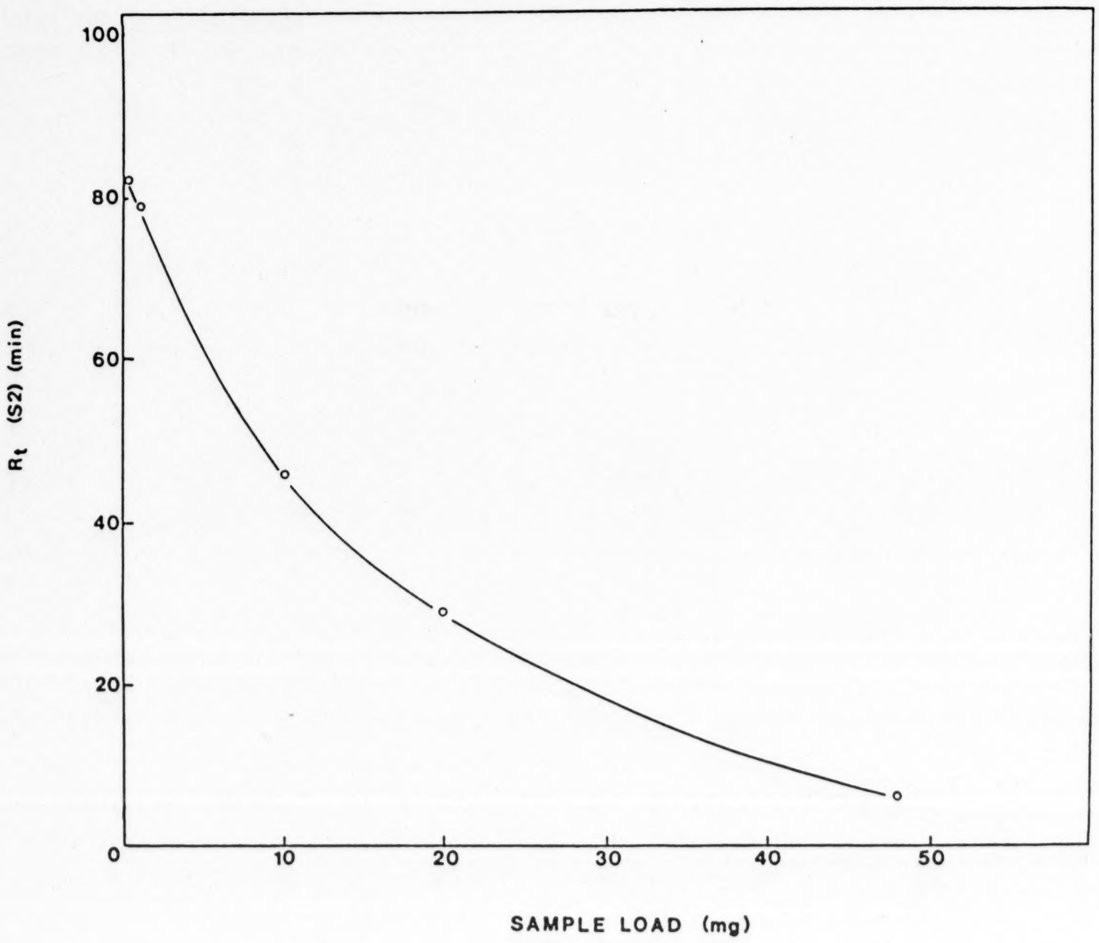

Fig. 8

Plot of sample load *versus* peptide retention. Column: Aquapore C_8 (220 × 4.6 mm i.d.). Conditions: linear AB gradient (0.1% B/min) starting from 0% B at time 0 min, where solvent A is 0.05% aqueous TFA and solvent B is 0.05% B in acetonitrile; flow-rate, 1 ml/min; 26°C. Sample loads: 0.1 mg, 1 mg, 10 mg, 20 mg and 50 mg of S2 plus S3 in a 1:1 molar ratio. R_t denotes retention time (min) of S2. S2 denotes decapeptide 2 (see Experimental).

where 1%/0.1% is the ratio in the change of gradient steepness, R_t is the retention time of the component of interest using the 1% B/min gradient, and t_g is the gradient delay time (see Experimental). In this study, t_g was 10.5 min and the retention time of S3 was 22.5 min (Fig. 4, Panel A). Thus, the estimated time for elution of S3 using a gradient steepness of 0.1% B/min would be 130 min. Observed retention times are always less than this estimate (Fig. 7, top panel). This analytical run thus establishes the run time for the preparative run described below.

(iii) Perform a preparative run at a gradient steepness of 0.1% B/min with a 100-fold increase in sample load. Collect fractions at convenient intervals (1 ml fractions are recommended for flow-rates of 1 ml/min). The time required to completely elute all components of interest at this gradient steepness is identical to that observed for the analytical load described in (i).

(iv) Perform fraction analysis on the same analytical column. These fractions can be quickly analysed by using isocratic elution. The recommended conditions for isocratic elution are determined as follows:

$$\text{isocratic concentration of acetonitrile} = R_t - t_g,$$

where R_t and t_g are defined above (ii).

(v) If subsequent preparative runs are required, the investigator may wish to increase further the sample load, depending on the results of the first preparative run and the amount of sample still to be purified.

Conclusions

These experiments suggest that if one desires to maximize sample load on any given column, one must start the gradient at 0% acetonitrile independent of the hydrophobicity of the peptides of interest. In addition, the 0.1% B/min gradient ensures maximum resolution with minimum tailing and reasonable run times over a wide range of sample load (loads differing by at least 100-fold). If a researcher wants to decrease run times, he can increase the gradient steepness (e.g., to 0.2% B/min), with the likely sacrifice of yield of homogeneous product(s) at any given sample load.

Work is in progress to apply the results of this study in the scale up to 1 cm and 2.5 cm columns.

Acknowledgements

This work was supported by the Medical Research Council of Canada and equipment grants from the Alberta Heritage Foundation for Medical Research.

References

[1] *J. Rivier, R. McClintock, R. Galyean, H. Anderson*, J. Chromatogr. **288**, 303 (1984).
[2] *R. E. Majors*, LC.GC Magazine of Liquid and Gas Chromatography **3**, 862 (1984).
[3] *K. Harrison, C. D. Carr, W. Beckham Jr., T. Yates*, Presented at the 10th International Symposium on Column Liquid Chromatography, San Francisco, 1986.
[4] *P. Böhlen, G. Kleeman*, J. Chromatogr. **205**, 65 (1981).
[5] *W. S. Hancock, J. T. Sparrow*, J. Chromatogr. **206**, 71 (1981).
[6] *S. James, H. P. J. Bennett*, J. Chromatogr. **326**, 329 (1985).
[7] *R. Sitrin*, LC.GC Magazine of Liquid and Gas Chromatography **4**, 530 (1985).
[8] *S. Linde, B. S. Welinder, B. Hansen, O. Sonne*, J. Chromatogr. **369**, 327 (1986).
[9] *J. M. R. Parker, R. S. Hodges*, J. Prot. Chem. **3**, 465 (1985).
[10] *H. P. J. Bennett, A. M. Hudson, C. McMartin, G. Purdon*, Biochem. J. **168**, 9 (1977).
[11] *K. Krummen, R. W. Frei*, J. Chromatogr. **132**, 27 (1977).
[12] *J. E. Rivier*, J. Liq. Chromatogr. **1**, 343 (1978).
[13] *M. J. O'Hara, E. C. Nice*, J. Chromatogr. **171**, 209 (1979).
[14] *M. Abrahamsson, K. Gröningsson*, J. Liq. Chromatogr. **3**, 495 (1980).
[15] *Gy. Vigh, Z. Varga-Puchony, J. Hlavay, E. Papp-Hites*, J. Chromatogr. **236**, 51 (1982).
[16] *K. E. Bij, Cs. Horváth, W. R. Melander, A. Nahum*, J. Chromatogr. **203**, 65 (1981).
[17] *D. Guo, C. T. Mant, A. K. Taneja, J. M. R. Parker, R. S. Hodges*, J. Chromatogr. **359**, 499 (1986).

Received: June 28, 1987
Accepted: Oct. 19, 1987
F

Study on the Structure of Chemically Bonded C_{18} Phase for HPLC

B. Buszewski*/Z. Suprynowicz

Department of Chemical Physics, Institute of Chemistry, Maria Curie Skłodowska University, 20-031 Lublin, Poland

Key Words

Packings for column liquid chromatography
High coverage density
Test of residual silanols
Model of chemical bonded phase

Summary

The use of monofunctional organosilanes for the preparation of packings with chemically bonded phases guarantees to obtain a defined monomeric structures of bonded alkylsilyl groups. The effect of hydrophobization of the surface of silica gel support modified with methyloctadecylchlorosilane in the presence of an activator has been investigated. A dense coverage of the surface ($> 4\,\mu$moles/m^2) with the C_{18} groups is obtained at $pK_a \approx 8$. By changing the nature and concentration of the activator packings with controlled surface density can be prepared, when the structure of the starting silica gel support are properly selected. On the basis of a simplified cylindrical model of the support's pores and the geometrical structure of the C_{18} molecules the maximum value of surface coverage as well as the dimensions of the chains of chemically bonded phases could be estimated.

Introduction

A significant progress in the preparation of packings for high-performance liquid chromatography (HPLC) has taken place in the past years. Packings characterized by a dense surface coverage of the silica gel support with the chemically bonded alkylsilyl ligande ($\alpha_{RP} \geqslant 4\,\mu$moles/m^2) have been prepared [1–5]. These packings can be used in either normal (NP-LC) or reversed-phase (RP-HPLC) systems [1].

They can be widely used especially for the determination of substances isolated from biological materials using ion-pair RP-HPLC [3, 4]. Kováts et al. [2] have proposed for the first time the synthesis of packings densely covered with C_{18} phase. These packings were produced on the basis of Cab-O-Sils using N.N-dimethylaminoalkylsilane as the modifier. The packings prepared in this way had a coverage of about 4.3 μmoles/m^2.

Similar results [3, 5] were obtained with silica gel (specific surface area: 360 m^2/g; pore volume: 2.1 ml/g; pore diameter: 20 nm) but in this case monochlorooctadecylsilane (ODMCS) was used as the modifier. The reaction was carried out in the presence of an activator which has guaranted basic conditions for the reaction ($pK_a = 8.3$). It should be pointed out that the modification reactions occured under conditions completely different than those described by Kováts et al.

It is known from earlier papers [1, 6–9] that the use of monofunctional modifiers leads to the formation of purely "monomeric" and defined structures of the chemically bonded phase. The use of di- and trifunctional modifiers leads to the formation of cross linked polymeric structures and as a consequence an irregular lattice screening of unblocked silanols can be formed [1, 3, 6, 9, 10–12]. Thus it can be concluded among others the stereochemistry of the surface reaction depends on the functionality of the modifier. On the other hand, it is known, that the geometry and chemical nature of the support also influence the density and homogenity of the surface coverage [3, 6, 11, 13–15].

Investigations carried out by many investigators showed that apart of the silanol and siloxane groups small amounts of strong adsorption centers having higher reactivity can also exist on the surface of silica [6, 11, 17–21]. Moreover, Verzele et al. [20, 21] showed, that surface heterogenity may be caused by the existence of many different metal ions which can significantly influence the crystallographic structure of the support as well as its chemical character. From this reason production of reproducible lots of packings can encounter significant difficulties; preparation of such packings has not been described in details.

From the same reasons the data of Berendsen et al. [7, 13], based on the number of bonded ligands as well as on the geometrical model of the surface constructed on the basis of dimensions of C_{18} molecules cannot be accepted.

This hypothetical brush model proposed by these authors significantly differs from the drop model proposed by Lochmüller et al. [11, 15]. According to the theory of

0009-5893/87 0573-06 $03.00/0

© 1987 Friedr. Vieweg & Sohn Verlagsgesellschaft mbH

hydrophobility the surface of prepared packing shows a dynamic character and under synthesis conditions the alkylsilyl molecules have such a conformation of the hydrocarbon chain which differs from that predicted theoretically.

We have carried out investigations related to the effect of blocking the surface of silica gel supports by octadecylsilyl molecules. On the basis of the known physico-chemical parameters of the support the percent carbon content after modification and of the determination of residual silanols we have evaluated the density and homogenity of surface coverage.

Experimental

Materials

Spherical silica gel (SG) produced by Polymer Institute, Bratislava, Czechoslovakia [23, 24] was used as the support of the chemically bonded phase. Surface characteristics of this support are given in Table I.

The support's surface was modified using dimethylchlorooctadecylsilane (ODMCS) (Petrarch Systems, Levittown, PA, USA) in the presence of an activator (A-morpholine) (Reachim Moscow, USSR). The following solvents were used; toluene, benzene, acetone, methanol, chloroform, diethyl ether (POCh, Gliwice, Poland), tetrahydrofuran (THF) and n-hexane (Reachim, Moscow, USSR). Although all solvents were of analytical grade they were additionally purified and dried using the method described previously [25].

Silanization Procedure

Silanization of the spherical silica gel was carried out according to the procedure described in previous publications [3, 5]. The reaction can be illustrated by the following scheme:

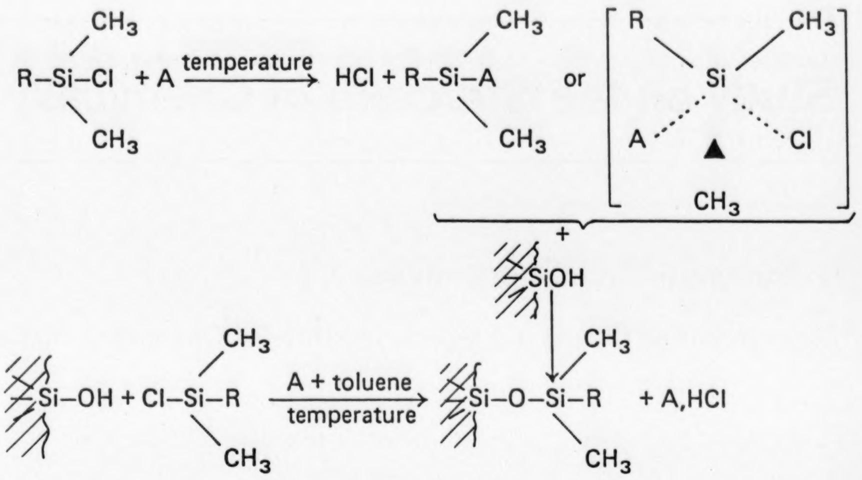

where: R = $C_{18}H_{37}$ and A = activator (organic base, i. a., heterocyclic amine protecting the reaction medium at $pK_a = 6–8.5$).

Before chemical modification the silica gel surface was purified using HCl [26], in order to remove trace amounts of metal ions.

The synthesis is carried out in dry toluene containing 4 ppm of water in a special vacuum reactor having the shape of an ampule [3]. Depending on the nature and concentration of the activator a series of packings with different densities of surface coverage were obtained [3–5] (packings 1–5). SG was also modified with ODMCS, without the activator (packing 6). The characteristics of the packings prepared are given in Table I.

Physico-Chemical and Chromatographic Properties of the Column Packings

The specific surface area (S_{BET}), pore diameter (D) and pore volume (V_p) were measured before and after modification using a Sorptomatic Model 1800 of Carlo Erba, Milano, Italy.

Table I. General characteristics of the prepared packing materials

Packing No	Type of packings	Porosity			α_{SiOH} µmoles/m^2	Coverage density		
		V_p cm^3/g	D nm	S_{BET} m^2/g		% C	α_{RP} µmoles/m^2	α_{nRP} nm^{-1}
—	Bare SG	2.1	20.0	360	5.20	—	—	3.13^a
1	SG-C$_{18}$ "monomeric"	1.92	18.28	338	4.53	5.08	0.72	0.38
2		1.85	17.62	262	3.05	10.36	1.86	0.84
3		1.75	16.66	226	2.07	15.54	2.88	1.36
4		1.65	15.71	198	1.18	20.36	3.66	1.93
5		1.50	14.28	175	0.12	25.52	4.24	2.65
6^b		1.86	17.60	273	3.12	16.71	2.62	1.48

SG = silica gel
V_p = pore volume, D = mean pore diameter, S_{BET} = specific surface area
α_{SiOH} = concentration of the accessible silanol groups
α_{RP} = concentration of chemically bonded C_{18} phase
α_{nRP} = the number of alkyl groups per one nm^2
a = the number of accessible surface silanol groups per one nm^2
b = material synthesized without the use of an activator.

The surface silanol concentration (α_{SiOH}) was determined by means of their reaction with a dimethylzinc-tetrahydrofuran complex [27, 28]. This reaction permits the determination of the amount of accessible surface $\geqslant$SiOH groups. The density of octadecyl ligands (α_{RP} and α_{nRP}) was calculated according to Berendsen et al. [7]. The carbon content was determined using the Model 240 elemental analyzer of the Perkin-Elmer Corp., Norwalk, CT, USA.

The effectivity of solvent purification was evaluated by spectrophotometric measurements carried out using a Specord UV-VIS spectrophotometer of Carl Zeiss (Jena, GDR) equipped with 1-cm quartz cuvettes. The amount of contained water was determined with help of the Model E-457 automatic Carl Fisher titrator manufactured by Methrom AG, Harisau, Switzerland.

Stainless-steel columns. 100 × 4 mm i.d. purchased from the Chemical Reagents Factory (ZOCh, Lublin, Poland) were used in the chromatographic measurements. A 8% (w/w) slurry of the silica in tetrachloromethanemethonol-mixture was charged into the columns under 450 atm pressure using a homemade packing apparatus [29]. A Pye Unicam LC 20 liquid chromatograph equipped with a UV detector operating at 254 nm (Pye Unicam, Cambridge, United Kingdom) was used. The samples were injected by a Rheodyne 7120 injector (Rheodyne, Berkeley, CA, USA) using a 10-μl sample loop.

Dead-volume in NP-HPLC was determined by the injection of carbon tetrachloride according to Unger's recommendations [6] whereas in RP-HPLC systems this value was determined on the basis of the solvent peaks, according to Buszewski [3].

Results and Discussion

In our previous papers [3, 5, 30] we have shown that in order to obtain a high and homogeneous coverage of the support surface by chemically bonded C_{18} or dimethylaminosilane the reaction should be carried out in the presence of an activator, according to the suggestion of Kováts et al. [2]. The role of activator is very different and has been discussed in detail [3–5]. Some differences in the surface concentration of the C_{18} groups caused by a different carbon percentage can be observed as a function of the pK_a of the activator (see Fig. 1). The dotted line corresponds to coverage obtained for the spherical silica gel in the absence of an activator (packing 6), i.e., when the support was modified with ODMCS in the presence of toluene only. The continous curve illustrates the effect of the acticator's action according to scheme 1. By changing the nature and concentration of the activator packings with controlled coverage can be prepared. Maximal α_{RP} values are obtained at pK_a = 8.33, i.e., at the pK_a value of morpholine used as the activator during synthesis.

This amine was used in the preparation of the investigated packings. Changing the molar ratio of morpholine and ODMCS permits to produce packings with different characteristics (Table I) [3, 5].

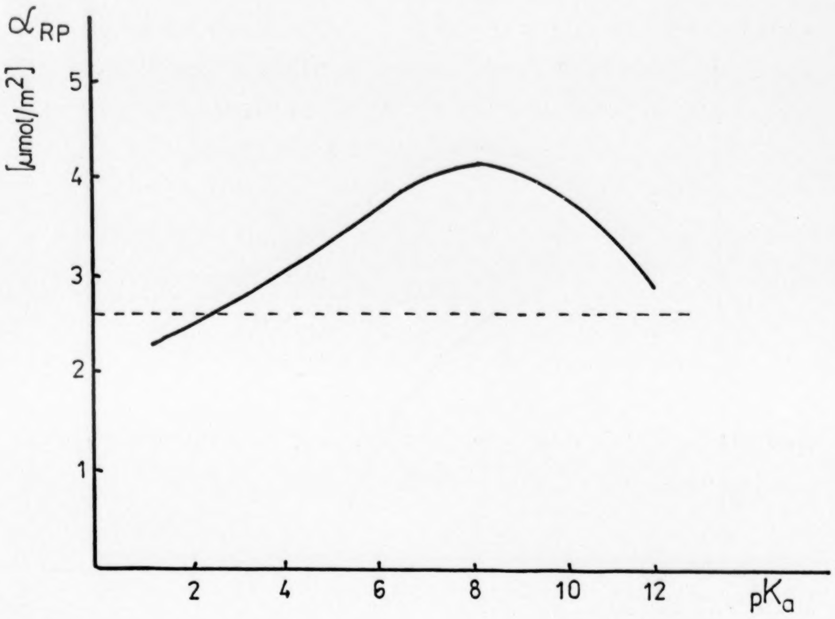

Fig. 1

Effect of the activatoris action on the coverage of the supports surface by C_{18} groups. α_{RP} = concentration of the chemically bonded C_{18} phase, μmol/m^2. Continous line = in the presence of the activator; dotted line = without the activator.

Data listed in Table I and literature dats show that highest surface coverages are obtained for packing No 5 containing 25,52% of carbon, which corresponds to α_{RP} = 4.24 μmoles/m^2. The molar ratio of A and ODMCS was equal to 1.5 : 1 [3, 5]. This indicates that during the synthesis reaction about 85% of accessible silanol groups have been blocked. Change in the molar ratio leads to a change in the α_{RP} value of packings; as a consequence of α_{SiOH} values of another materials increase proportionally. The parameters characterizing the porosity of the support also change with an increase in the amount of alkylsilyl surface groups.

One can conclude from the porosimetric data that in spite of the dense coverage of packing No 5 the pores are not completely blocked by alkyl chains. Therefore we can conclude that this material would have a relatively high selectivity in gel-permeation chromatography (GPC). We have investigated this using tetrahydrofuran as the mobile phase, at a flow rate of 0.5 ml/min. Polystyrene standards (PS) with molecular weights of 600–650,000 were used as the solutes. Typical GPC calibration curves for unmodified spherical silica gel and for packing 5 are presented in Fig. 2.

The course of the curves presented in this figure are in good agreement with sorptomatic data (see Table I). Chemical modification of the surface causes a decrease in the exclusion limit in comparison to the starting material as well as a decrease in the elution volume (V_e) value.

From these considerations one can conclude that in spite of using a strongly polar mobile phase the C_{18} molecules occupy different surface area than suggested by Berendsen et al. [7]. Similarly the length of the alkyl chain under dynamic conditions, i.e., during the contact of the packing with the eluent also differs from one suggested by these authors, postulating that the maximum attainable coverage for C_{18} phase is approximately equal to 2.0 alkylsilyl ligands per nm^2 which corresponds approximately to

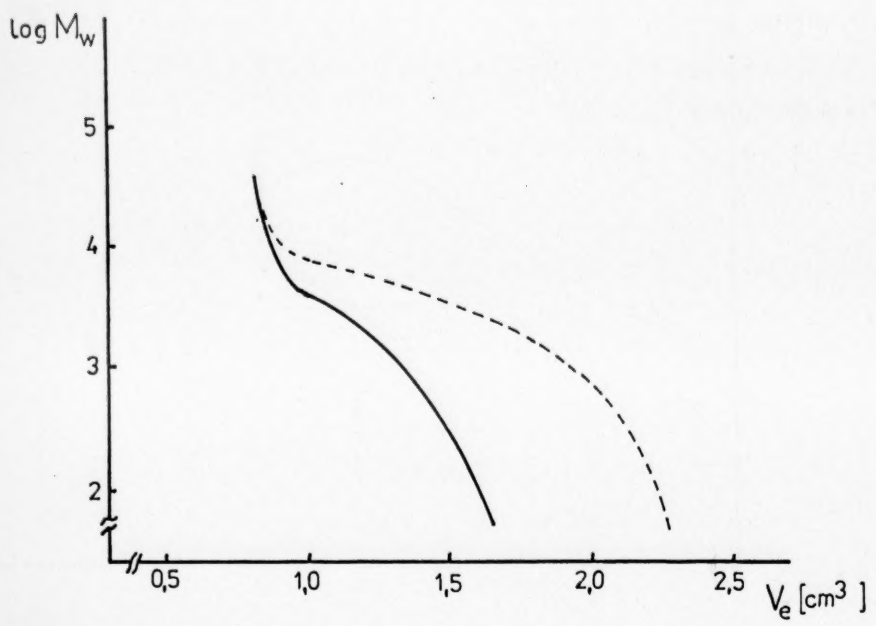

Fig. 2
Plot of log mol. wt against the elution volume (V_e) for the unmodified support (dotted line) and for packing No 5 (continous line; α_{RP} = 4.24 μmoles/m^2). For conditions see the text.

3.3 μmoles/m^2 and the legnth of the alkyl chain is equal to 2.43 nm [7].

We cannot accept this concept because from the data listed in Table I one can conclude that the maximum α_{RP} and α_{nRP} values differ by 75% from the data presented by Berendsen et al. [7].

It is clear that the density and homogenity of surface coverage will be strongly dependent on porosity (diameter and shape of the pores). Accepting the cylindrical model of pores proposed by de Boer we have used in our experiments a support having a mean pore diameter (D) equal to 20 nm, which permits to minimize the interactions between the individual C_{18} ligands and thus restrict the mutual interactions between the alkyl groups. We have stated that silica gel contains 5.20 μmoles/m^2 of $\geqslant$SiOH groups which can be easily blocked by alkylsilyl molecules. Such a content of $\geqslant$SiOH groups corresponds to 3.13 OH groups/nm^2.

According to the theory of hydrophibility [1, 11, 12, 22] and to Lox's data [31] in a polar medium C_{18} chains can attain a configuration different than the one predicted theoretically, and the length of these chains can be reduced by one-third, (from 2.45 nm to 1.8–1.9 nm).

If we now assume that the angle formed between Si–O–Si bonds is equal to 130° and that parts of the molecules have characteristic values as given in Table II, then it is very probable that the alkylsilyl group (i) does not have cylindrical shape, (ii) the surface occupied by one alkylsilyl molecule is 0.6 nm^2 and (iii) the length of a C_{18} unit including the CH_3–Si–CH_3 group is approximately equal to 1.9 nm. The reason for this may be that solvation processes occur on the packing surface and, depending on the chemical nature of the mobile phase, these processess can influence the shape of the solvated alkylsilyl ligand. In this connection we should mention, that in the case of dense surface coverage [$\alpha_{RP} > 4$ μmoles/m^2] the chains can attain a form similar to "drops" of solvated stationary phase. A model surface densely covered by C_{18} ligands may be illustrated by the scheme presented in Fig. 3. The data obtained permit to conclude that 85% of accessible OH groups are blocked by alkylsilyl ligands (Table I).

This suggestion may be confirmed by the relationship between α_{RP} and α_{SiOH} presented in Fig. 4 where differences between theoretical (from the silica network) and experimental coverage values appear at $\alpha_{RP} \approx 3.7$ μmoles/m^2. Starting from the very probable model of the support surface covered with a chemically bonded liquid phase we have examined the retention of the components of a test mixture in systems containing a nonpolar mobile phase [12]. As it is evident from Fig. 5 a fairly linear

Table II. Physical characteristics of the bonded C_{18} chains*

van der Waals radii nm		Covalent bond length nm		Bond angle degree
O	0.140	C–C	: 0.154	112
Si	0.195	C–H	: 0.106	120
H	0.100	Si–C	: 0.189	
C		Si–CL	: 0.183	
CH_3 group				

* According to ref. [32].

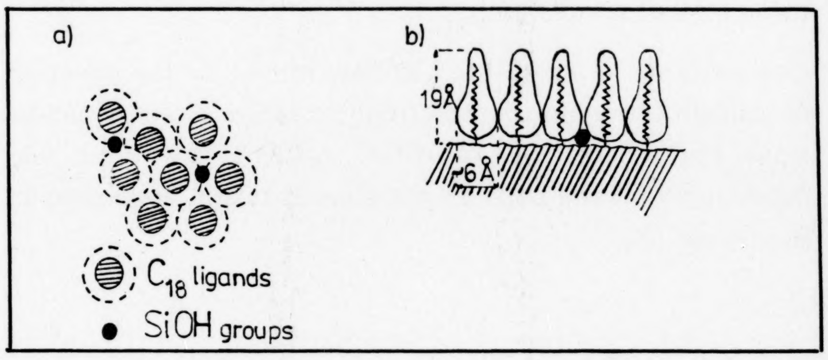

Fig. 3
Model of the chemically bonded C_{18} phase; (a) scheme of the homogenity of surface coverage with C_{18} and SiOH groups; (b) scheme illustrating a conformation of C_{18} lingands on the support's surface.

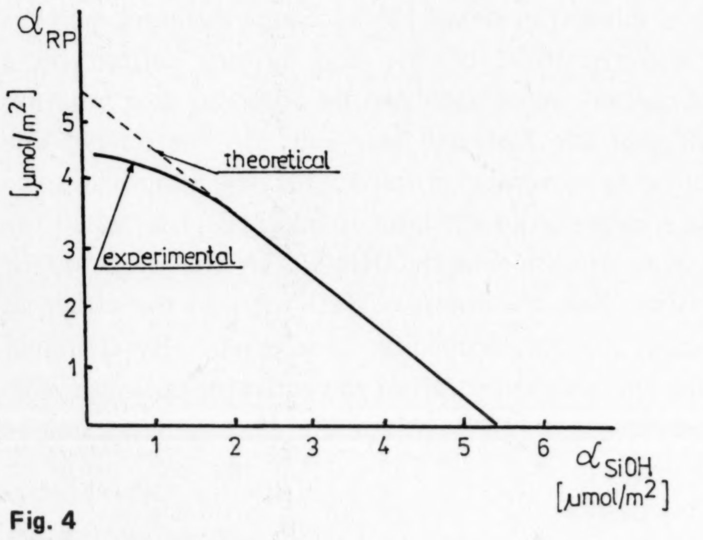

Fig. 4
Effect of blocking of the accessible surface OH groups by alkylsilyl molecules. Dotted line corresponds to the number of accessible silanol groups which can be theoretically blocked. Continous line corresponds to the number of SiOH groups blocked by alkylsilyl molecules.

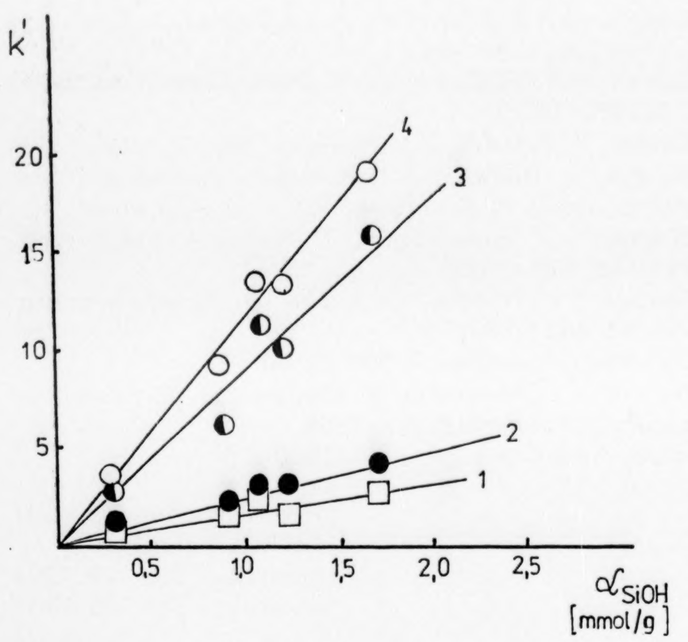

Fig. 5

Dependence of the capacity factor (k') values on the concentration of residual silanol groups (α_{SiOH}, mmol/g) for the packings listed in Table I (packings No 1–5).

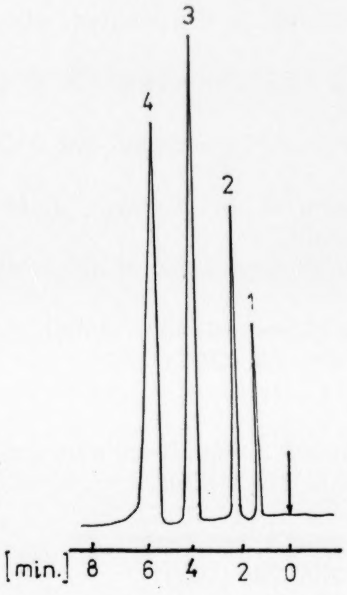

Fig. 6

Separation of a test mixture on the column containing packing No 5 (α_{RP} = 4.24 μmoles/m^2). Chromatographic conditions: mobile phase, 75–25% (v/v) n-hexane-chloroform flow rate, 1 ml/min; detector, UV operating at 254 nm.

Peaks: **1** = nitrobenzene, **2** = acetone, **3** = 2,6-dimethylpyridine, **4** = pyridine.

relationship is observed between the retention of polar solutes and the silanol concentration under normal-phase LC conditions.

From Fig. 5 it results that the retention of pyridine and 2,6-dimethylpyridine (basic substances) is more dependent on the concentration of the silanol groups than the retention of acetone and nitrobenzene. Benesi [33] expected an increased specifity of sterically hindered pyridines, e.g., 2,6-dimethylpyridine to interact with the surface silanol groups, due to the relative flexibility of the hydroxyl group in the hydrogen-bonding interaction with the hindered free electron pair of nitrogen. Moreover it results from this dependence that if the more dense and homogenous coverage is present than is more difficult the access of solute molecules to the unblocked and screened SiOH groups.

This suggestion may be confirmed by the results of separation of the test mixture on the column packed with packing No 5 (Table I) for which α_{RP} = 4.24 μmoles/m^2. Recently this separation has been proposed as a test for ligand layer homogenity [3, 12].

Fig. 6 suggest that, due to the dense coverage with the monomeric C_{18} phase strong silanophobic interactions between polar (mainly basic) solutes and the silanized surface are near completely eliminated. This fact is reflected in the increase of the symmetry of the peaks as well as in an improvement of the resolution of individual peaks.

Conclusions

It can be concluded in general that hydrophobization of the surface with the chemically bonded alkylsilane in the presence of an activator results in good and reproducible HPLC column packings. A high density of reversed-phase was obtained in which 85% of the available surface are blocked.

Application of the method described here make possible the control of the coverage density.

"Brush" structures having the form of a "drop" appear to be very probable in the case of dense coverages. These structures correlate strictly the geometrical dimensions of C_{18} ligands. The application of spectroscopic methods e.g., cross polarization – magic angle spin – nuclear magnetic resonance (CP-MAS-NMR) or FTIR should give more reliable information about the structures obtained and should permit a more precise evaluation of the experimental results.

Acknowledgements

The authors thank to Drs. Dr. Berek and L. Nondek for valuable remarks and for the realization of some physicochemical measurements.

Reference

[1] *C. F. Poole, S. A. Schuette,* "Contemporary Practice of Chromatography", Elsevier, Amsterdam 1984.
[2] *K. Szabó, N. Le Ha, Ph. Schneider, P. Zeltmer, E. sz. Kováts,* Helv. Chim. Acta **67**, 2128 (1984).
[3] *B. Buszewski, Ph. D. Thesis,* Slovak Technical University, Bratislava 1986.
[4] *B. Buszewski, K. Šebeková, P. Božek, D. Berek,* J. Chromatogr. **367**, 171 (1986).
[5] *B. Buszewski, A. Jurášek, J. Garaj, L. Nondek, I. Novák, D. Berek,* J. Liq. Chromatogr. in press (1987).
[6] *K. K. Unger,* Porous silica, Elsevier, Amsterdam 1979.
[7] *G. E. Berendsen, K. A. Pikaart, L. de Galan,* J. Liq. Chromatogr. **3**, 1437 (1980).
[8] *H. Engelhardt, B. Dreyer, H. Schmidt,* Chromatographia **16**, 11 (1982).
[9] *L. C. Sander, S. A. Wise,* J. Chromatogr. **316**, 163 (1983).
[10] *E. Bayer, K. Albert, J. Reiners, H. Nider, D. Müller,* J. Chromatogr. **281**, 197 (1983).
[11] *R. L. Gilpin,* J. Chromatogr. Sci. **22**, 371 (1984).

[12] *L. Nondek, B. Buszewski, D. Berek,* J. Chromatogr. **360**, 241 (1986).
[13] *E. Berendsen, L. de Galan,* J. Liq. Chromatogr. **1**, 403 (1978).
[14] *B. W. Sands, Y. S. Kim, J. L. Bass,* J. Chromatogr. **360**, 353 (1986).
[15] *C. H. Lochmüller, A. S. Colborn, M. L. Hunnicut, J. M. Harris,* Anal. Chem. **55**, 1344 (1983).
[16] *D. B. Marshall, K. A. Snyder, C. H. Lochmüller,* J. Chromatogr. Sci. **22**, 217 (1984).
[17] *L. R. Snyder, J. W. Ward,* J. Phys. Chem. **70**, 3941 (1966).
[18] *M. L. Hair, W. Hertl,* J. Phys. Chem., **72**, 4269 (1969).
[19] *M. L. Miller, R. W. Linton, G. E. Maciel, B. L. Hawkinds,* J. Chromatogr. **319**, 9 (1985).
[20] *M. Verzele, M. De Potter, J. Ghysels,* J. High Resolution and Chromatography Communication **2**, 151 (1979).
[21] *M. Verzele,* LC and HPLC Magazine, **1**, 217 (1983).
[22] *Cs. Horváth,* LC and HPLC Magazine, **1**, 552 (1983).
[23] *D. Berek, I. Novák,* U.S. Pat., **4**, 255, 286 (1981).
[24] *I. Novák, D. Berek*, U.S. Pat., **4**, 382, 070 (1983).
[25] *Z. Suprynowicz, B. Buszewski, R. Lodkowski, J. Trocewicz,* Polish Pat. 125, 388 (1984).
[26] *Z. Suprynowicz, B. Buszewski, E. Tracz,* Chem. Anal. (Warsaw) **23**, 985 (1978).
[27] *L. Nondek, V. Vyskočil,* J. Chromatogr. **206**, 581 (1981).
[28] *L. Nondek, A. Reissová*, J. High Resol. Chromatogr./Chromatogr. Commun. **7**, 153 (1984).
[29] *B. Buszewski, Z. Suprynowicz, T. Pastuszak,* Chem. Anal. (Warsaw) **28**, 527 (1983).
[30] *B. Buszewski, L. Nondek, A. Jurášek, D. Berek,* Chromatographia, **23**, 442 (1987).
[31] *M. Lox,* Marcromolecules, **7**, 660 (1974).
[32] *V. Bažant, V. Chvalovskiý, J. Rathovskiý*, "Organosilicon Compounds" Academia Prague 1965.
[33] *H. Benesi,* Anal. Chem. **32**, 1410 (1960).

Received: Aug. 3, 1987
Revised manuscript
received: Sep. 12, 1987
Accepted: Sep. 20, 1987
F

Criteria for Judging the Quality of Separation in Chromatograms Containing Solvent Peaks

P. J. Schoenmakers[1]* /P. J. Naish[2]/R. J. Hunt[2]

Philips Research Laboratories, P.O. Box 80000, 5600 JA Eindhoven, The Netherlands[1], and [2]Philips Analytical, York Street, Cambridge CB 1 2 PX, UK.

Key Words

Optimization criteria
Selectivity optimization
Resolution
Solvent peaks
Matrix peaks

Summary

Formal procedures used for optimizing chromatographic selectivity require objective, numerical functions to assess the quality of each chromatogram obtained during the process. Many of such optimization criteria have been suggested for chromatograms in which all or a number of well-shaped peaks need to be separated.

This paper describes a method by which resolution can be measured in chromatograms in which very large, highly non-symmetrical background peaks, *e.g.* typical solvent peaks, are present. Using this method, various optimization criteria can be calculated. The method is evaluated using a simulation program which constructs chromatograms from the recorded profiles of individual experimental peaks. It is also demonstrated for use in an experimental optimization procedure in reversed-phase liquid chromatography.

Introduction

Separation in chromatography is determined by three factors: retention, selectivity, and efficiency. Of these, the efficiency is largely independent for the other two. It is determined mainly by the dimensions of the column, and it is affected by the operating conditions (*e.g.* solvent composition, temperature), and possibly the instrument [1, 2].

Retention (capacity factors) and selectivity (differences in capacity factors) are by definition not independent of each other. If all capacity factors remain unaltered, so does the selectivity. Nevertheless, it is common to optimize retention first, and then to "fine-tune" the selectivity. A reasonable estimate for conditions that yield optimum retention (*e.g.* capacity factors in the range $1 < k < 10$) can often be made on the basis of knowledge and experience, or on the basis of single "scanning" experiment (see ref. [3], section 5.4.2).

The selectivity of the system for two solutes i and j (in order of elution) can be defined as the relative retention $\alpha_{ji} = k_j/k_i$. Unfortunately, α cannot usually be predicted, unless very extensive knowledge is available on the chromatographic behaviour of the compounds to be separated. Therefore, in order to optimize the selectivity it is required to record chromatograms and to use the information contained therein. Optimization procedures (ref. [3] chapter 5) can be used to locate the best possible conditions. In order to be able to decide which conditions are best, we need to define what is the best chromatogram, in other words we need objective optimization criteria.

A variety of different optimization criteria have been suggested in the literature (for a review see ref. [3], chapter 4) and applied in different procedures. Different criteria will be required in different situations, and criteria can be defined that correspond to the lowest possible analysis time, the best distribution of peaks, the minimum required number of plates, *etc.* [4]. However, there has been a strong emphasis on criteria for the so-called general case, *i. e.,* the situation in which all peaks in the chromatogram are relevant solutes which need to be separated and all are considered to be of equal importance.

In this paper, we will be discussing the situation in which a very large, highly non-symmetrical peak is present in the chromatogram. This may typically be a solvent or matrix peak. In this paper, we refer to a solvent peak as a broad peak with a sharp front, which is not retained on the column. All other large, non-symmetrical signals are referred to as matrix peaks. Hence, a solvent peak is a special case of a matrix peak.

The solvent (or matrix) peak itself is not considered to be of interest, but it is important to separate it from the

0009-5893/87 0579-09 $ 03.00/0

© 1987 Friedr. Vieweg & Sohn Verlagsgesellschaft mbH

(much smaller) relevant solute peaks. A simple method is described to deal with this problem in optimization criteria. The method is tested using simulated chromatograms [5] and its applicability is demonstrated experimentally in reversed-phase liquid chromatography (RPLC).

Theory

Solvent Peaks

Fig. 1 shows a typical profile of a solvent peak, followed by a (very) well separated smaller peak. The peak height of the smaller peak (h) and its peak width at 13.5% of its height (corresponding to 4 times the standard deviation, σ, in case of a Gaussian peak) are indicated in the figure. The resolution between two successive peaks in a chromatogram is usually defined as

$$R_{s,ji} = \frac{t_j - t_i}{w_i/2 + w_j/2} \simeq \frac{\Delta t_{ji}}{2\sigma_i + 2\sigma_j} , \tag{1}$$

where t is the retention time and w the peakwidth. Hence, a second small (Gaussian) peak would be separated from the one shown in Fig. 1 with $R_s = 1$, if the location of its peak maximum was approximately 4σ away. Clearly, the situation for the separation between the solvent peak in Fig. 1 and the small peak is very different. The reason for this is the excessive width of the solvent peak in comparison to the solute peak.

In Fig. 1 the width of the solvent peak (w_{sp}) is indicated at the same height at which the width of the small peak corresponds to 4σ, *i. e.* at 13.5% of the height of the small peak. It is obvious that $w_{sp} \gg 4\sigma$, but also that w_{sp} will be a strong function of the height of the solute peak. Generally, it is unattractive if optimization criteria are affected by the quantitative composition of the sample (ref. [3], p. 129). However, in the case of a small solute peak on the flank of a large solvent peak, the difference in area between the two peaks is the very reason why a special optimization criterion needs to be defined. In other words, the relevant width of the solvent peak is determined by the relative height of the solute peak.

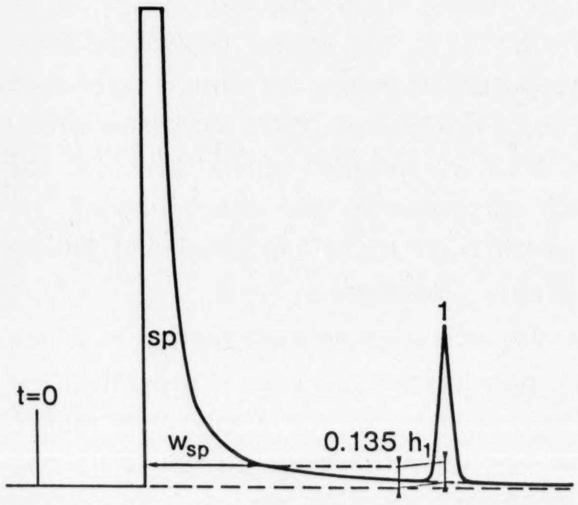

Fig. 1

Schematic chromatogram showing a solvent peak followed by a small solute peak. The measurement of the solvent-peak width (w_{sp}) at 13.5% of the peak height of the solute peak is illustrated in the figure.

Having defined w_{sp}, we may next define a weighting factor w_f for a solvent peak eluting at $t = t_0$ as follows

$$w_f = \frac{w_{sp}}{w_0} \simeq \frac{w_{sp}}{4\sigma_0} = \frac{w_{sp}\sqrt{N}}{4t_0} . \tag{2}$$

In eq. (2) N is the number of theoretical plates of the column and the subscript 0 refers to an ideal (*i. e.* very small) peak at $t = t_0$. If the solvent peak was such an ideal peak, then the weighting factor w_f would equal 1. Typical solvent peaks are much broader, so that $w_f > 1$.

For the solvent peak in Fig. 1, the peak width on the left-hand side (front) of the peak is clearly different from that on the right-hand side (tail). If we assume that the front of the peak is steep (corresponding to an ideal peak), then we may assume that the peak width on the right-hand side is $w_{sp} - w_0/2$, and we may calculate the resolution between the solvent peak and the solute peak from

$$R_s^{sp} = \frac{\Delta t}{w_{sp} - w_0/2 + w_1/2} , \tag{3}$$

where 1 denotes the solute peak. If the solvent peak was an ideal (small) peak at $t = t_0$, then we would have

$$R_s^0 = \frac{\Delta t}{w_0/2 + w_1/2} , \tag{4}$$

so that the ratio between the two resolution values is given by

$$\frac{R_s^{sp}}{R_s^0} = \frac{w_0/2 + w_1/2}{w_{sp} - w_0/2 + w_1/2} = \frac{w_0 + w_1}{2w_{sp} - w_0 + w_1} = \frac{w_0 + w_1}{w_0(2w_f - 1) + w_1} . \tag{5}$$

If we introduce

$$w_0 = 4\sigma_0 = \frac{4t_0}{\sqrt{N}} \tag{6}$$

and

$$w_1 = 4\sigma_1 = \frac{4t_0(1 + k_1)}{\sqrt{N}} , \tag{7}$$

then we find

$$\frac{R_s^{sp}}{R_s^0} = \frac{1 + (1 + k_1)}{(2w_f - 1) + (1 + k_1)} = \frac{2 + k_1}{2w_f + k_1} . \tag{8}$$

We see from eq. 8 that R_s^{sp} approaches R_s^0 if w_f approaches 1, *i. e.* if the solvent peaks approaches a small peak of ideal width. If w_f becomes very large, then the ratio approaches $(2 + k_1)/2w_f$.

We may use eq. (8) as a correction factor for resolution values calculated simply on the basis of retention times. For example, the separation factor S between the solutes i and j is defined ref. [3], p. 126) as

$$S_{ji} = R_{s,ji}\,\frac{2}{\sqrt{N}} = \frac{k_j - k_i}{2 + k_i + k_j}\,. \tag{9}$$

For the separation between a solute with $k_1 = 1$ and an ideal peak at $t = t_0$ ($k = 0$) we find a separation factor (S^0) of 1/3. If the same solute peak is to be separated from a solvent peak with $w_f = 20$, then, because eq. (9) shows S to be proportional to R_s, we may use eq. (8) to find

$$S^{\mathrm{sp}} = \frac{2 + k_1}{2w_f + k_1}\,S^0, \tag{10}$$

from which we find $S^0 = 3/41.1/3 = 1/41$. This value may subsequently be used in optimization criteria instead of the ideal value of 1/3. The validity of this simple approach will be investigated below.

Matrix Peaks

Matrix peaks, as opposed to solvent peaks, may appear anywhere in the chromatogram, *i.e.* not necessarily at $t = t_0$. Also, matrix peaks do not necessarily show a sharp front and a shallow tail as does the typical solvent peak in Fig. 1. Two examples of matrix peaks are schematically illustrated in Fig. 2.

Fig. 2a shows a broad, non-symmetrical matrix peak, preceded by a small peak and with another small peak on its decending flank. A change in the detector attenuation has been suggested to locate the position of the peak top. To the left of the peak maximum, the matrix-peak width on the beginning of the matrix peak (w_b) can be measured at 13.5 % of the height of the preceding peak (h_b). Following the peak maximum, the height corresponding to 13.5 % of the peak height of the small peak (h_e) first needs to be estimated, as is indicated in the figure. At this height, the value of (w_e) may then be measured.

Fig. 2b shows a matrix peak which is partly below the baseline, w_e may now be measured from the reflection point (where the signal passes through zero) to the end of the peak at a distance h_e below the baseline, as indicated in the figure.

It is clear that matrix peaks of many different forms occuring anywhere in the chromatogram may be characterized by two parameters: (w_b) and (w_e). If t_{mp} is the retention time of the maximum (or as in Fig. 2b the reflection point) of the matrix peak, then we may define weighting factors for both the front ($w_{f,b}$) and the tail ($w_{f,e}$) of the matrix peak:

$$w_{f,b} = \frac{w_b}{2\sigma} = \frac{w_b\sqrt{N}}{2t_{\mathrm{mp}}}\,, \tag{11}$$

and

$$w_{f,e} = \frac{w_e}{2\sigma} = \frac{w_e\sqrt{N}}{2t_{\mathrm{mp}}}\,, \tag{12}$$

If we indicate the solute peak before the matrix peak with 1 (capacity factor k_1), the peak after the matrix peak by 2 and the matrix peak by mp ($k_{\mathrm{mp}} = t_{\mathrm{mp}}/t_0 - 1$), then we find in a manner analogous to the situation for solvent peaks

$$\frac{R_{s,b}}{R_s^0} = \frac{S_b}{S^0} = \frac{2 + k_1 + k_{\mathrm{mp}}}{1 + w_{f,b} + k_{\mathrm{mp}}w_{f,b} + k_1}\,, \tag{13}$$

and

$$\frac{R_{s,e}}{R_s^0} = \frac{S_e}{S^0} = \frac{2 + k_2 + k_{\mathrm{mp}}}{1 + w_{f,e} + k_{\mathrm{mp}}w_{f,e} + k_2}\,. \tag{14}$$

Eq. (14) does not reduce to eq. (8) for $k_{\mathrm{mp}} = 0$, because in the solvent-peak situation we found it convenient to measure the peak width over the entire peak (see Fig. 1) rather than on the tail alone (as in Fig. 2).

Eq. (13) and (14) are general equations, which allow us to deal with any kind of matrix peak at any position in the chromatogram for which the respective widths on the beginning (w_b) and on the end (w_e) can be measured. If a solvent peak occurs in the chromatogram at $t \simeq t_0$, but if the front of this peak is not ideally steep, than the solvent peak may be treated as a matrix peak and eq. (14) may be used instead of eq. (8).

Experimental

Simulated Chromatograms

The procedure used to simulate chromatograms using recorded experimental peak profiles has been described elsewhere [5]. The solvent peak used in the simulated chromatograms was obtained by gas chromatography

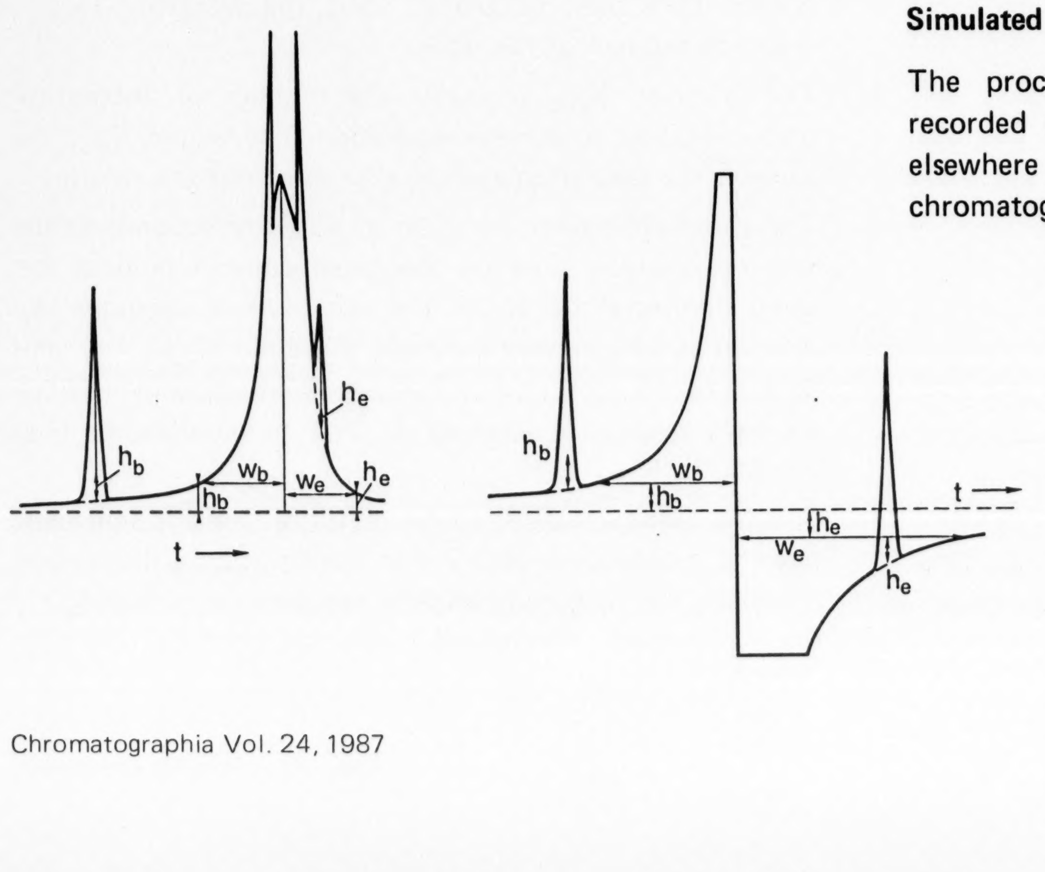

Fig. 2
Two schematic examples of matrix peaks, illustrating the measurement of the relevant parameters.

(GC). The simulation program allows the respective widths of the rising and descending parts of peaks to be varied independently. The solvent peak was given a steep rising flank (zero width). The solute peaks were also recorded (GC) peak profiles, with equal width factors applied to the two sides of the peaks (*i. e.* peaks were reproduced as they appeared in GC). The peak width of the solutes was taken proportional to the retention time so as to keep the apparent number of plates constant.

Liquid Chromatography

RPLC experiments were carried out on a PU4100 liquid chromatograph from Philips Analytical. Acetophenone and propiophenone were selected as test solutes. The sample solvent contained acetone and methanol. Injection of 20-μl samples caused a large solvent peak to be observed at the detection wavelength of 243 nm. A 10 cm by 4.6 mm i.d. ODS column was used at a flow rate of 2 ml/min. The detector response time was set at 0.5 s.

A number of experimental chromatograms were recorded with different mixtures of methanol and water as the mobile phase. Duplicate measurements were performed at most compositions (see Table IV below). The number of plates was measured from the peak width of the second solute peak at half the maximum height.

Results and Discussion

Simulated Chromatograms

Fig. 3 shows a typical example of a simulated chromatogram. During the simulations the locations of the solute peaks, the (relative) peak heights of the solute and solvent peaks, and the width of the solvent peak have been varied.

Fig. 3 shows the measured solvent-peak width (at 0.135 h_1 = 13.7 mm above the baseline) to be 267 mm. With a t_0 value of 50 mm and with N = 5500 (as measured from the peak width of the second solute peak at half the maximum height) we find for the separation between the solvent peak and the first solute peak (for which $k_1 = 2$) in this chromatogram a weighting factor of $w_f = (267/200)\sqrt{5500} = 99$. If the solvent peak would have been very small, then we would have found from eq. (9) $S^0_{1,0} = 1/2$ and $R^0_s = (1/4)\sqrt{5500} = 18.5$. In the present case, with $w_f = 99$, we find from eq. (8) $R^{sp}_s = 18.5/4/200) = 0.37$.

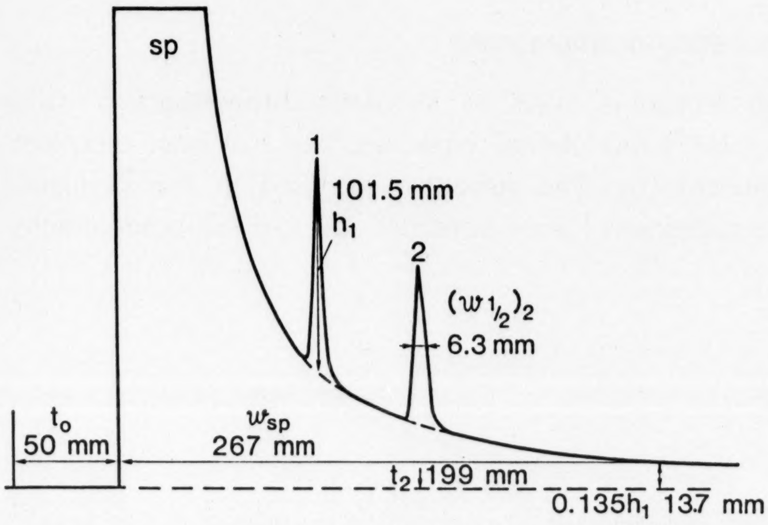

Fig. 3

Simulated chromatogram with two solute peak on the flank of a solvent peak. $k_1 = 2$, $k_2 = 3$, $N \simeq 5500$. Relative peak height: $h_{sp}/h_1 \simeq 20$.

Since the second solute peak is of similar size as the first one, its separation from the solvent peak is not critical (although it may easily be measured from the chromatogram). The separation factor between the two solute peaks ($S_{2,1}$) is 1/7 ($k_2 = 3$), and the resolution between these two peaks is 5.3. These figures show that the two solute peaks are more than adequately separated, but that they are not sufficiently removed from the solvent peak. Other simulated chromatograms have been evaluated in a similar manner.

Effect of peak positions: Table I summarizes the results of a series of simulations in which the solvent peak was maintained constant, but the positions of the two solute peaks (*i. e.* k_1 and k_2) were varied. w_{sp} and hence w_f vary upon changing the location of the first solute peak. When k_1 increases, h_1 decreases, and w_{sp}, which is now measured at a smaller distance above the baseline, increases. However, although w_f increases, the ratio $S^{sp}_{1,0}/S^0_{1,0}$ which according to eq. (8) is equal to $(2 + k_1)/2w_f + k_1)$, remains virtually constant. The particular (GC) solvent peak used for the simulations shows a hyperbolic decay, due to which w_{sp} and w_f increase roughly proportionally to k_1.

Fig. 4 shows the variation of $S^0_{1,0}$ and $S^{sp}_{1,0}$ with k. For constructing this figure, additional points were obtained by using the proportionality between h_1 and $1/(1 + k_1)$, and by measuring w_{sp} at the appropriate height above the baseline in an arbitrary chromatogram. It is seen that the variation of the two separation factors is qualitatively similar. However, there are separate vertical axis for the two curves, which differ by a factor of 20. Whereas $S^0_{1,0}$ equals 1/3 at $k_1 = 1$ and the number of plates required to achieve $R^0_s = 1.5$ is about 80 (eq. 9), $S^{sp}_{1,0}$ is only 0.0175 and $N_{ne} \simeq 30{,}000$. On the present column, with $N = 5500$ and the solvent peak left unaltered, $k_1 \geqslant 6$ is required to realize $R^{sp}_s > 1.5$ (*i. e.* $S^{sp}_{1,0} > 0.04$).

In the second part of Table I, a number of optimization criteria have been calculated using the weighting factors from the top half of the table.

The criterion S_{min} indicates the number of theoretical plates required to achieve separation. The heigher S_{min}, the easier is the separation and the shorter can be the column.

The threshold separation criterion (S_k) corresponds to the shortest analysis time on the given column (and at the given flow rate) for which the resolution is adequate. S_k is equal to $1/k_\omega$ above a certain threshold ($S_{min} > \epsilon$), and $S_k = 0$ for ($S_{min} < \epsilon$). For the present situation ($N = 5500$) we have assumed a value of $R_s > 1$ to be adequate (*i. e.* $\epsilon = 0.027$).

$\bar{S}$ is the average separation factor for all (in this case two) pairs of successive peaks. $\bar{S}$ is in itself not an optimization criterion, but its computation is required for obtaining r^*, the (calibrated) normalized resolution product (ref. [3],

Table I. Evaluation of a series of simulated chromatograms with varying capacity factors of the solute peaks. Peak areas were kept constant. The solvent-peak width (w_{sp}) was measured at a height of 0.135 h_1 above the baseline. $N \simeq 5500$. Relative peak height for $k_1 = 2$: $h_{sp}/h_1 \simeq 5$. $t_0 = 50$ mm. All figures in the table except w_{sp} (mm) are dimensionless

a. Characterization of chromatograms

nr.	k_1	k_2	w_{sp}	w_f	$S^0_{1,0}$	$S^{sp}_{1,0}/S^0_{1,0}$	$S^{sp}_{1,0}$	$S_{2,1}$
2.1	1	2	76.6	28	1/3	0.053	0.0175	0.200
2.2	2	6	103	38	1/2	0.051	0.026	0.400
2.3	5	6	176	65	5/7	0.052	0.038	0.077
2.4	10	11	266	99	5/6	0.057	0.048	0.043
2.5	2	3	103	38	1/2	0.051	0.026	0.143

b. Optimization criteria

nr.	S_{min}	S_k [1]	$\bar{S}$	r*	$(r_{nt})_{f,d}$	$(t_{ne})^{-1}_{f,d}$
2.1	0.0175	0	0.109	0.29	$5.50\ 10^{-5}$	$1.02\ 10^{-4}$
2.2	0.026	0	0.213	0.23	$4.63\ 10^{-5}$	$9.66\ 10^{-5}$
2.3	0.038	0.17	0.0575	0.88	$1.93\ 10^{-4}$	$2.06\ 10^{-4}$
2.4	0.043	0.09	0.0455	1.00	$1.54\ 10^{-4}$	$1.54\ 10^{-4}$
2.5	0.026	0	0.084	0.53	$1.23\ 10^{-4}$	$1.69\ 10^{-4}$

1 For $\epsilon = 0.027$.

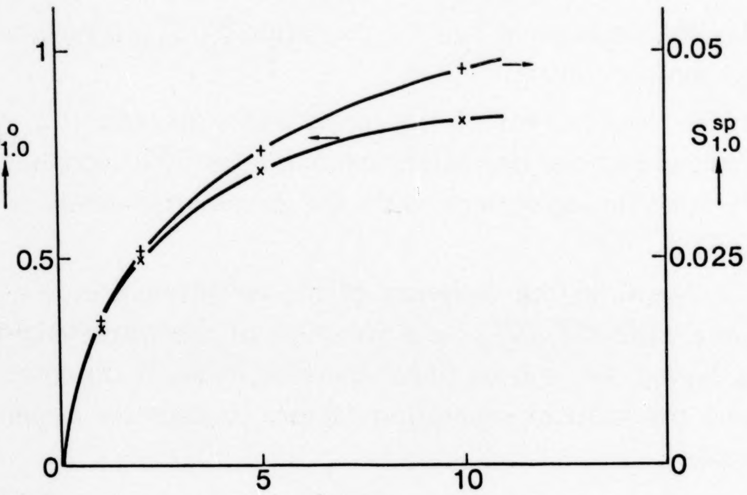

Fig. 4

Variation of $S^0_{1,0}$ and $S^{sp}_{1,0}$ with solute capacity factor for the simulated chromatograms described in Table I.

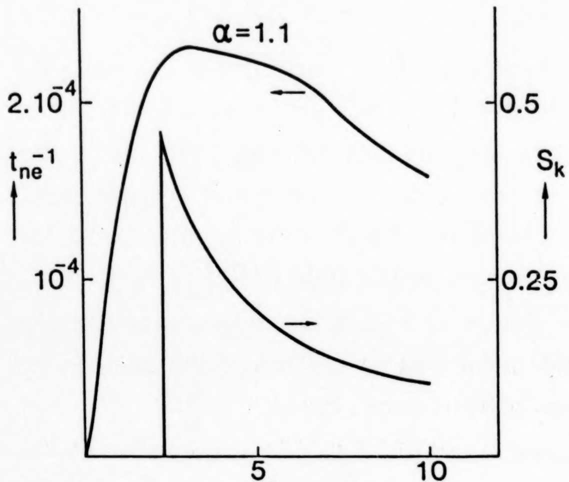

Fig. 5

Two response surfaces for the simulated optimization of the separation of two solutes with $\alpha = 1.1$ from a solvent peak. The capacity factor of the first solute peak is varied. S_k ist shown for $\epsilon = 0.027$.

p. 139). This criterion aims at the best possible distribution of the peaks over the chromatogram. r^* is equal to 1 if the peaks are ideally spread over the chromatogram (all separation factors equal). It has been demonstrated that r^* is not a suitable criterion if the capacity factor of the last peak in the chromatogram (k_ω) varies significantly [4].

The next criterion in the table, $(r^*_{nt})_{f,d}$, is a time-corrected resolution product, the main focus of which is to minimize the required analysis time using a column similar to the present one (same column characteristics and flow rate), but the length of which is defined by the results of the optimization process. This criterion has a secondary contribution from the distribution of peaks in the chromatogram.

Finally, the required analysis time, $(t_{ne})_{f,d}$, which (in arbitrary units) corresponds to

$$(t_{ne})_{f,d} = \frac{1 + k_\omega}{S^2_{min}} \quad , \tag{15}$$

strictly corresponds to the minimum time required for the analysis, with the column length variable. The reciprocal value (t^{-1}_{ne}) is listed in the table, because this is a criterion to be maximized. In most practical situations $(r^*_{nt})_{f,d}$ and $(t^{-1}_{ne})_{f,d}$ turn out to yield comparable results (*i. e.* the same location for the optimum).

From Table Ib we find that out of the five chromatograms characterized, chromatogram 2.4 would require the lowest number of theoretical plates ($N_{ne} \simeq 2000$ for $R_s = 1$). However, on the present column the separation is fastest (*i. e.* S_k is highest) for chromatogram 2.3, for which the resolution is adequate with $N = 5500$ and the capacity factors are much lower. Chromatogram 2.3 is also favoured if we allow the column length to vary (highest value for t^{-1}_{ne}).

Using the variation of $S^{sp}_{1,0}$ with k shown in Fig. 4, we can simulate various optimization problems. For example, Fig. 5 concerns the separation of two solutes for which $\alpha_{2,1} = 1.1$ from the solvent peak. The criteria S_k (for $\epsilon = 0.027$) and t^{-1}_{ne} are plotted as a function of the capacity factor of the first solute peak (k_1). It is seen that optimum separation may be anticipated around $k_1 \simeq 3$. Fig. 6 shows a simulation of the most rapid separation, which may be achieved on a

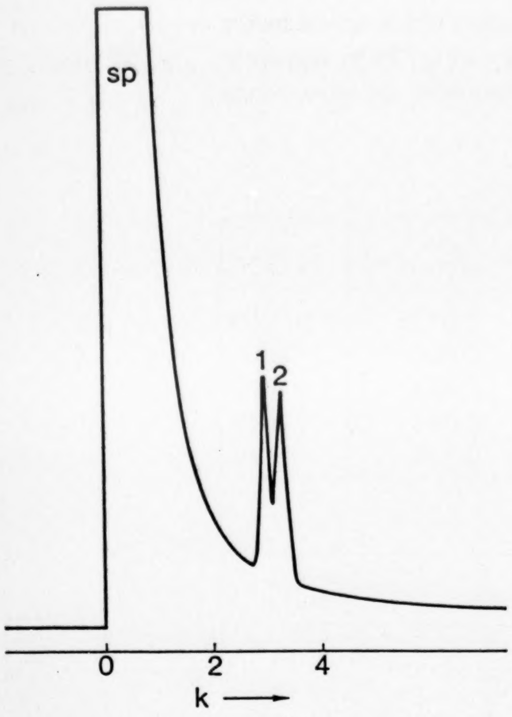

Fig. 6

Simulated optimum chromatogram for the separation of two solutes for which $\alpha = 1.1$. The capacity factor of the first solute has been optimized (see Fig. 5). $N = 3600$. Other conditions as in Table I.

column with 3600 plates with optimum k values. By definition, the resolution if Fig. 6 is just adequate, but with only 3600 plates, the analysis may be very fast. Using the present method, the resolution between the solvent peak and the first solute peak is judged to be equally good (or bad) as that between the two solute peaks ($R_s^{sp} \simeq R_{s,21} \simeq 1$). The chromatogram shown in Fig. 6 illustrates that the use of weighting factors allows us to optimize the selectivity in situations in which solvent peaks occur.

Effect of relative peak heights: Table II shows the results of the evaluation of a series of simulated chromatograms in which the peak-height ratio between the solvent peak and the first solute peak was varied, while the peak positions were kept constant.

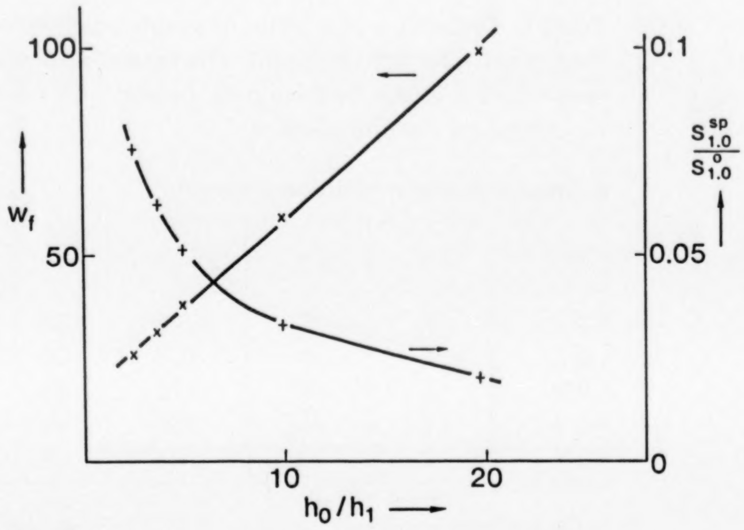

Fig. 7

Variation of the weighting factor w_f and the ratio $S^{sp}_{1,0}/S^{0}_{1,0}$ with the relative height of the solute peak for the simulated chromatograms described in Table II.

Unlike the situation in Table I, the ratio $S^{sp}_{1,0}/S^{0}_{1,0}$ is now no longer almost constant.

If the relative heights of the solute peaks decrease (*i. e.* if the concentrations decrease), the value for $S^{sp}_{1,0}$ decreases, very much in agreement with the chromatographers intuition.

Fig. 7 illustrates the variation of the weighting factor w_f and the ratio $S^{sp}_{1,0}/S^{0}_{1,0}$ as a function of the peak height ratio h_0/h_1. An almost linear increase in w_f is observed, causing the ratio of separation factors to decrease hyperbolically.

The optimization criteria shown in Table IIb show that the effect of the peak-height ratio is correctly reflected in all

Table II. Evaluation of a series of simulated chromatograms with varying peak-height ratios. The solvent-peak width (w_{sp}) was measured at a height of 0.135 h_1 above the baseline. $N \simeq 5500$. $k_1 = 2, k_2 = 3$. $t_0 = 50$ mm. All figures in the table except w_{sp} (mm) are dimensionless

a. Characterization of chromatograms

nr.	h_{sp}/h_1	w_{sp}	w_f	$S^0_{1,0}$	$S^{sp}_{1,0}/S^0_{1,0}$	$S^{sp}_{1,0}$	$S_{2,1}$
3.0 = 2.5	4.91	103	38	1/2	0.051	0.026	0.143
3.1	2.46	69	26	1/2	0.075	0.038	0.143
3.2	3.68	84.5	31	1/2	0.062	0.031	0.143
3.3	9.82	159	59	1/2	0.033	0.017	0.143
3.4	19.65	267	99	1/2	0.020	0.010	0.143

b. Optimization criteria

nr.	S_{min}	$1/k_\omega$ [1]	$\overline{S}$	r^*	$(r^*_{nt})_{f,d}$	$(t_{ne})^{-1}_{f,d}$
3.0	0.026	0	0.084	0.53	$1.23\ 10^{-4}$	$1.69\ 10^{-4}$
3.1	0.038	0.33	0.090	0.67	$2.95\ 10^{-4}$	$3.61\ 10^{-4}$
3.2	0.031	0.33	0.087	0.59	$1.84\ 10^{-4}$	$2.40\ 10^{-4}$
3.3	0.017	0	0.080	0.38	$4.45\ 10^{-5}$	$7.23\ 10^{-5}$
3.4	0.010	0	0.0765	0.24	$1.22\ 10^{-5}$	$2.50\ 10^{-5}$

[1] For $\epsilon = 0.027$.

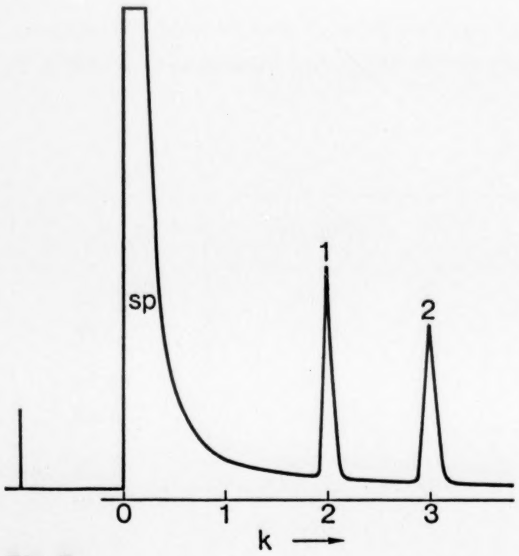

Fig. 8

Best of the simulated chromatograms, selected on the basis of the $(t_{ne})^{-1}_{f,d}$ criterion. Further details in Table III (chromatogram 4.3).

optimization criteria. The higher the peak-height ratio, the higher is the required number of plates for the separation, the longer the required column and the longer the analysis time.

Effect of solvent-peak width: Table III shows the results of the evaluation of a series of chromatograms in which the peak heights and positions were kept constant, but in which the width of the solvent peak was varied. It is seen from the table that an exact proportionality was obtained between the set value for the solvent peak width (in arbitrary units) and the value measured from the chromatogram (in mm). This confirms that w_{sp} can be accurately measured from the chromatogram.

The weighting factor w_f is seen to increase rapidly with increasing width of the solvent peak. Again, the trend is accurately reflected in the calculated optimization criteria.

Optimum chromatogram: On the present column, there are several chromatograms (3.1, 3.2 and 4.3) which yielded adequate resolution ($R_s \geqslant 1$) all with equal analysis times ($k_2 = 3$). The S_k criterion does not differentiate between the different chromatograms. The t^{-1}_{ne} criterion yields chromatogram 4.3 as the unique optimum. The corresponding chromatogram obtained with $N = 5500$ is shown as Fig. 8. Because $S_{min} = 0.050$ for this chromatogram, only 3600 plates are required to achieve $R_s = 1.5$, and 1600 plates to achieve $R_s = 1$.

Liquid Chromatography

The chromatograms were evaluated as shown in Fig. 3. The results are collected in Table IV.

Fig. 9 shows the observed variation of the weighting factor w_f and the number ot theoretical plates (N_2) as a function of the mobile phase composition. w_f is seen to be relatively constant over a wide range in composition ($0.5 < \phi < 0.8$). At low methanol concentrations w_f increases sharply, because minor contaminants start to be resolved from the solvent peak at these compositions, and because the height of the first solute peak becomes low. Because of the irregular shape of the solvent peak, the ratio $S^{sp}_{1,0}/S^{0}_{1,0}$ is seen in Table IV to vary considerably with varying composition. This is in contrast to the situation in Table I and Fig. 4 and it illustrates the ability of the present method to deal with solvent peaks of irregular shapes.

The values of N_2 show both systematic and random variations. The higher values at lower methanol concentrations may be due to a peak compression effect (2), the sample solvent (containing water, methanol and acetone in 40:30:30 ratio) being weaker than the mobile phase. Because there was more than 30% difference between the lowest (4330) and the highest value (6420) observed for N_2, it was decided to modify the calculations of the optimization

Table III. Evaluation of a series of simulated chromatograms with varying solvent-peak width. The actual solvent-peak width (w_{sp}) was measured at a height of $0.135\,h_1$ above the baseline. $N \simeq 5500$. $k_1 = 2, k_2 = 3$. $t_0 = 50$ mm. Relative peak height: $h_{sp}/h_1 \simeq 5$. All figures in the table except w_{sp} (mm) are dimensionless

a. Characterization of chromatograms

nr.	w_{sp} set	w_{sp} measured	w_f	$S^0_{1,0}$	$S^{sp}_{1,0}/S^0_{1,0}$	$S^{sp}_{1,0}$	$S_{2,1}$
4.0 = 2.5	120	103	38	1/2	0.051	0.026	0.143
4.1	240	202	75	1/2	0.026	0.013	0.143
4.2	180	154	57	1/2	0.034	0.017	0.143
4.3	60	51.1	19	1/2	0.100	0.050	0.143

b. Optimization criteria

nr.	S_{min}	$1/k_\omega$[1]	$\overline{S}$	r^*	$(r^*_{nt})_{f,d}$	$(t_{ne})^{-1}_{f,d}$
4.0	0.026	0	0.084	0.53	$1.23\ 10^{-4}$	$1.69\ 10^{-4}$
4.1	0.013	0	0.078	0.31	$2.35\ 10^{-5}$	$4.23\ 10^{-5}$
4.2	0.017	0	0.080	0.38	$4.45\ 10^{-5}$	$7.23\ 10^{-5}$
4.3	0.050	0.33	0.0965	0.77	$5.48\ 10^{-4}$	$6.25\ 10^{-4}$

1 For $\epsilon = 0.027$.

Table IV. Evaluation of a series of experimental (RPLC) chromatograms with varying mobile phase composition (ϕ is volume fraction of methanol in water). Sample: acetophenone and propiophenone in a solvent containing acetone. The solvent-peak width (w_{sp}) was measured at a height of 0.135 h_1 above the baseline. t_0 = 31.4 s. All the figures in the table are dimensionless

a. Characterization of chromatograms

ϕ	k_1	k_2	N_2	w_f	$S^0_{1,0}\sqrt{N_2}$	$S^{sp}_{1,0}/S^0_{1,0}$	$S^{sp}_{1,0}\sqrt{N_2}$	$S_{2,1}\sqrt{N_2}$
0.85	0.21	0.31	4510	5.95	6.26	0.182	1.14	2.74
0.85	0.20	0.31	4330	5.94	6.08	0.181	1.10	2.76
0.80	0.29	0.45	4930	4.09	8.88	0.270	2.40	4.18
0.80	0.29	0.46	5600	4.15	9.56	0.268	2.56	4.46
0.75	0.39	0.62	4880	4.02	11.30	0.283	3.20	5.34
0.75	0.35	0.58	4840	3.96	10.48	0.284	2.98	5.38
0.70	0.51	0.86	4970	4.12	14.32	0.286	4.10	7.32
0.70	0.51	0.86	5120	4.14	14.52	0.285	4.14	7.42
0.65	0.70	1.23	4840	4.24	18.04	0.295	5.32	9.38
0.65	0.70	1.23	4710	4.00	17.78	0.310	5.52	9.22
0.60	0.93	1.69	6230	4.56	25.04	0.292	7.30	12.98
0.60	0.93	1.69	5920	4.41	24.34	0.300	7.30	12.68
0.60	0.93	1.70	6250	4.57	25.16	0.291	7.32	13.02
0.55	1.32	2.50	5720	4.62	30.14	0.315	9.48	15.26
0.55	1.29	2.40	5600	4.65	29.36	0.311	9.12	14.62
0.50	2.03	4.08	5550	5.02	37.54	0.334	12.54	18.82
0.40	4.05	9.01	6100	12.31	52.30	0.211	11.04	25.70
0.40	4.09	9.02	6420	12.02	53.84	0.217	11.66	26.12

Table IV.

b. Optimization criteria

ϕ	$S_{min}\sqrt{N_2}$	$S_{k,N}$[1]	$(t_{ne,N})^{-1}_{f,d}$
0.85	1.14	0	0.99
0.85	1.10	0	0.92
0.80	2.40	0	3.97
0.80	2.56	0	4.49
0.75	3.20	1.61	6.32
0.75	2.98	1.72	5.62
0.70	4.10	1.16	9.04
0.70	4.14	1.16	9.21
0.65	5.32	0.81	12.69
0.65	5.52	0.81	13.66
0.60	7.30	0.59	19.81
0.60	7.30	0.59	19.81
0.60	7.32	0.59	19.85
0.55	9.48	0.40	25.68
0.55	9.12	0.42	24.46
0.50	12.54	0.25	30.96
0.40	11.04	0.11	12.18
0.40	11.66	0.11	13.57

[1] For ϵ_N = 2.95.

criteria, in such a way that the actual number of plates was taken into account.

If N cannot be considered constant, then the factor determining the minimum resolution in the chromatogram is not S_{min}, but $S_{min}\sqrt{N}$ *(see eq. 9). This* factor is listed in Table IV. Likewise, a threshold criterion for sufficient separation on the present column in the shortest possible time may by defined as $S_{k,N} = 1/k_\omega$ for $S_{min}\sqrt{N} > \epsilon_N$, and $S_{k,N} = 0$ for $S_{min}\sqrt{N} < \epsilon_N$. The difference between ϵ_N and R_s is a factor of 2. By using ϵ_N = 2.95 in Table IV, we accept chromatograms for which $R_{s,\,min} \geqslant 1.5$.

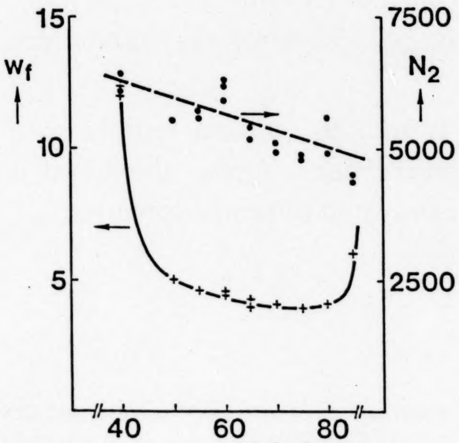

Fig. 9

Variation of the weighting factor w_f and number of plates of the second peak (N_2) for the experimental RPLC chromatograms described in Table IV.

The required analysis time is proportional to the plate height, and therefore inversely proportional to the observed number of plates on a column of a given length. Hence, we calculated a modified required analysis time criterion $(t_{ne,N})^{-1}_{f,d}$ from

$$(t_{ne,N})^{-1}_{f,d} = \frac{S^2_{min} N_2}{1 + k_\omega} \quad . \qquad (16)$$

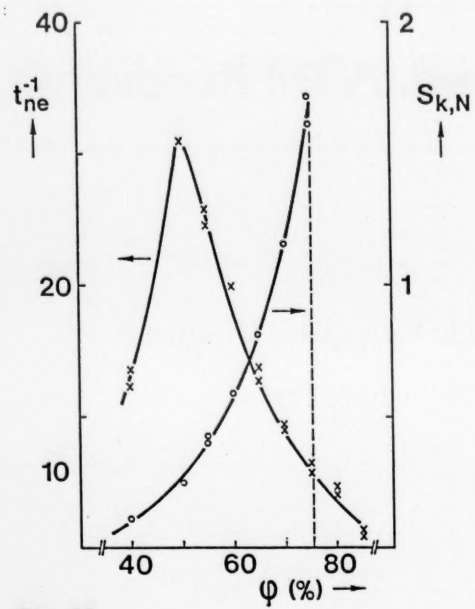

Fig. 10

Response surfaces for the optimization of the mobile phase composition in RPLC for a sample containing a solvent peak. Data were taken from Table IV.

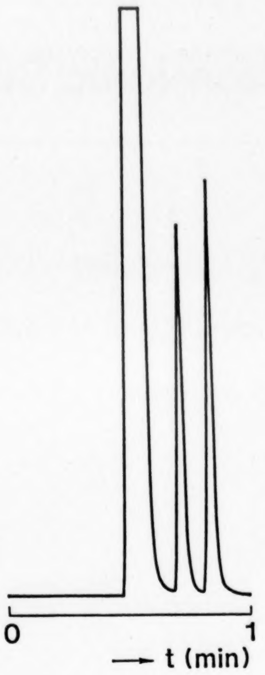

Fig. 11

Optimum chromatogram, selected from the chromatograms in Table IV, using the same column ($S_{k,N}$ criterion).

Fig. 10 shows the response surfaces obtained from the data in Table IV for the criteria $S_{k,N}$ and $(t_{\mathrm{ne},N})^{-1}_{\mathrm{f,d}}$. It can be seen from this figure that the $S_{k,N}$ criterion (for $\epsilon_N = 2{,}95$) suggests that $\phi \simeq 0.75$ provides adequate separation in the shortest possible time on the present column. This chromatogram is shown as Fig. 11. If the column length can be varied, $\phi = 0.5$ may be used. At this composition the minimum resolution on the present column is about 6. If this is reduced to 1,5 then the number of plates (and therefore the column length) may be reduced by a factor $4^2 = 16$. Allowing for the higher capacity factors at $\phi = 0.5$, this separation could be about 5 times faster than the one shown in Fig. 11.

The present example illustrates the posibility of measuring the resolution and of calculating optimization criteria in real chromatograms, in which large, irregularily shaped background peaks are present. The results of the optimization procedure illustrated in Figs. 10 and 11 show that the present method may be of help for the application of selectivity optimization procedures to real samples.

Conclusions

1. A simple method has been described to measure the resolution between small (solute) peaks and large, highly non-symmetrical (solvent or matrix) peaks in a chromatogram.
2. The method has been tested on simulated chromatograms containing typical solvent peaks. Variations in peak position, (relative) peak height, and solvent-peak width all appear to be correctly reflected in the corrected resolution values.
3. The corrected resolution values (or separation factors) may be used in various optimization criteria. A simulated example has been demonstrated.
4. The method has also been applied to an experimental optimization procedure in RPLC. Using different optimization criteria, sensible optima were found.
5. The present work should be significant for the application of formal optimization procedures to *real* samples.

References

[1] *P. J. Naish,* J. Chromatogr., **395**, 55 (1987).
[2] *P. J. Naish, D. P. Goulder, C. V. Perkins,* Chromatographia, **20**, 335 (1985).
[3] *P. J. Schoenmakers,* The Optimization of Chromatographic Selectivity, A Guide to Method Development, Elsevier, Amsterdam, 1986.
[4] *P. J. Schoenmakers,* J. Liq. Chromatogr., in print.
[5] *R. J. Hunt,* J. High Resol. Chromatogr. and Chromatogr. Comm. **8**, 347 (1985).

Received: June 29, 1987
Accepted: Aug. 18, 1987
F

HPLC Determination of Non-Ionic Surfactants Used in Tertiary Oil Recovery

P. L. Desbène*[1]/B. Desmazières[1]/J. J. Basselier[1]/L. Minssieux[2]

[1] Laboratory of Structural Organic Chemistry, P. and M. Curie University, 4 place Jussieu, 75230 Paris Cedex 05, France

[2] Oil Field Department, Petroleum French Institute, 1–4 Avenue de Bois Préau, 92500 Rueil-Malmaison, France

Key Words

Column liquid chromatography
Determination of surfactants in brine and oil
Tertiary oil recovery.

Summary

Having developed a chromatographic technique with a diol bonded phase for the study of the distribution versus ethylene oxide number (E.O.) for various non-ionic polyoxyethylated surfactants used in enhanced oil recovery (KL 6, $\bar{n}$ = 6 E.O.; KM 11, $\bar{n}$ = 11 E.O. and KM 20, $\bar{n}$ = 20 E.O.) we report here the titration of one of these surfactants (KL 6) in the presence of an ionic surfactant (S 385, sulfonated petroleum fraction) and other non-ionic surfactants (KM 11 and/or KM 20) which are the conditions found in enhanced oil recovery.

This work has been carried out in brine and in n-decane, as a model for the petroleum phase.

Obviously in the case of aqueous phases it was necessary to carry out a thorough dehydration before the chromatographic analyses.

We have shown that it is possible, under these conditions, to determine the KL 6 surfactant in the concentration range 500 to 6000 ppm with a precision of 70 ppm without experiencing interference from KM 11 or KM 20 non-ionic surfactants or S 385 ionic surfactant. Furthermore, from some of the samples studied which were in contact with the rock shale, we showed that strong adsorption of the KL 6 occurs. Chromatographic analyses show that this surfactant is only desorbed from the rock shale when employing a non-ionic surfactant such as KM 25 which is much more polar than the KL 6.

Introduction

Enhanced oil recovery (or tertiary oil recovery) was introduced some years ago because of the necessity to thoroughly recover oil from the rock shale.

Among the different processes of enhanced oil recovery the chemical processes, which are based on the injection of water and chemical additives (polymers, alkaline compounds, surfactants), are rapidly developing by reason of the soaring costs of prospecting and drilling (as in offshore oil fields for instance).

Mixtures of surfactants are used in order to modify interfacial tension between hydrocarbons and the rock. In fact, in the oil field, crude oil is stored in rock pores where it is more or less trapped. The theory of oil trapping is well known [1–3] and interfacial phenomena play a fundamental part in this mechanism. In a medium preferentially wettable by water oil is trapped in the form of small drops in the biggest pores. A decrease in the interfacial tension or an increase of the pumping rate is necessary. In the conditions encountered in the oil field it is difficult to increase the pumping rate. Accordingly enhanced recovery is obtained by chemical additives which decrease the interfacial tension, modifying the wettability or increasing the viscosity of the water.

The mechanisms encountered in enhanced oil recovery by the chemical method are very complex and it is thus very important to analyse and quantify the surfactants present in the different liquid phases obtained in the exploitation of this method.

We have recently developed a chromatographic technique allowing a satisfactory analysis, as a function of the ethylene oxide number, of non-ionic surfactants used for enhanced oil recovery. These surfactants are obtained from the condensation of natural C_{16} and C_{18} fatty alcohols and ethylene oxide [4]. Thus we have undertaken the qualitative and quantitative sutdy of one of these surfactants (KL 6) under the conditions of enhanced oil recovery, that is to say, in the presence of other non-ionic surfactants (KM 11 and/or KM 20) and in the presence of ionic surfactants (for instance S 385 resulting from the sulfonation of oil aromatic fractions).

The analysis must be performed in various media such as briny water containing Cl^-, SO_4^{--}, Ca^{++}, Mg^{++} ions, with a maximum total concentration of 30 g/l and in n-decane, modelling oil.

0009-5893/87 0588-05 $03.00/0

© 1987 Friedr. Vieweg & Sohn Verlagsgesellschaft mbH

It must be noted that, in these conditions, the KL 6 concentration varies in the range 1000 to 10000 ppm.

Experimental

Apparatus

The chromatographic analyses were carried out using a low pressure gradient liquid chromatograph (Hewlett Packard 1090) controlled by a micro computer HP 85 with a Rheodyne Model 7010 injector (10 to 100 μl loop). The detector was a Philips PU 4020 at 235 nm. A Hewlett Packard terminal 1 level 4 integrator from an HP 5880 A GC was used to handle the data.

Solvents

All the solvents used (n-heptane, dichloromethane, methanol) were HPLC grade (Merck, BDH or SDS).

Reagents

The non-ionic (KL 6, KM 11 and KM 20) and ionic (S 385) surfactants were of technical grade.

The water used to prepare the brine solutions was purified using a Millipore system (Milli Q and Milli RO).

The sodium, calcium and magnesium chlorides and the sodium sulfate were purchased from Prolabo (analytic grade).

HPLC Analyses of KL 6 Solutions

Column: diol bonded silica (Lichrospher, Merck); 25 cm × 0.46 cm; $d_p = 5$ μm.
Mobile phase: n-heptane/dichloromethane/methanol 92/5/3.
Flow rate: 1 ml/min.
Temperature: 25 °C.
U.V. detection: $\lambda = 235$ nm.

Brine Water Preparation

17 grams of NaCl were added to 1 litre of demineralised water. After complete dissolution were added successively and in this order: 2.4 g of $MgCl_2$, 6 H_2O); 4.8 g of $CaCl_2$ and 5.9 g of Na_2SO_4.

Example of the Determination of KL 6 Solution in Brine

A sample of 4 ml of brine was submitted to an azeotropic dehydration in a Dean-Stark tube. After benzene evaporation a precipitate appeared in the bottom of the flask. This precipitate was washed down with 2 ml of mobile phase to give a concentration of the KL 6 surfactant in the organic phase, ready to be injected, twice that of the initial brine solution.

Determination of Samples Resulting from a Dynamic Contact with the Rock Shale

9.6 ml of saline aqueous solution containing KL 6, KM 11 and/or KM 20 and S 385 corresponding to 0.4 pore volume was injected in a rock shale. They were displaced by one pore volume (24 ml) of a polymer solution (polyacrylamide). The rock shale was then washed by several pore volumes and successive fractions of eluent were collected. After washing KM 25 was injected in order to desorb the non-ionic surfactants which would otherwise irreversible interact with the rock shale while the eluent was still collected when leaving the rock. Each fraction was then lyophilized. 3 ml of mobile phase was added before proceeding to the HPLC analysis under the reported conditions.

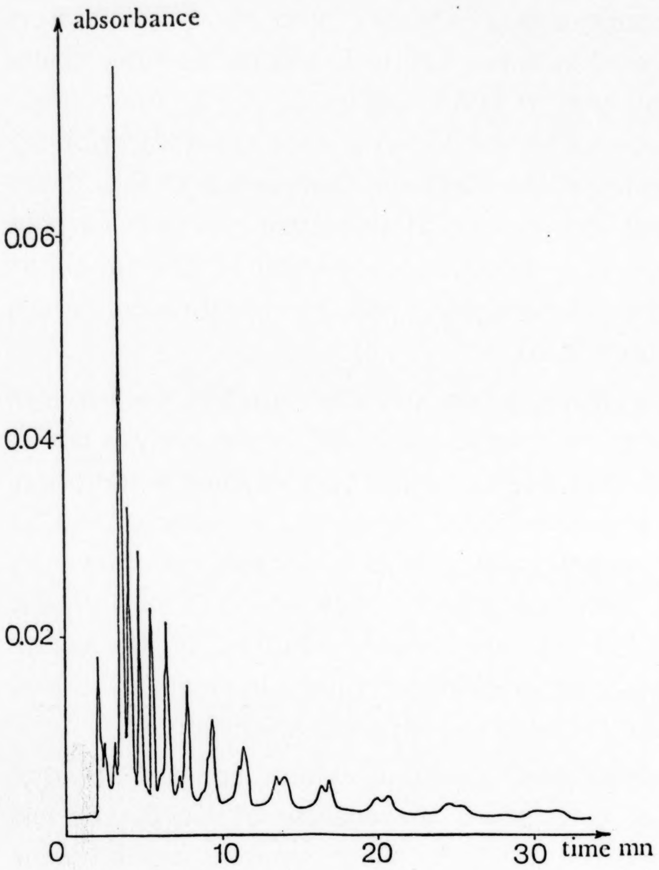

Fig. 1

Fractionating of KL6 obtained by normal phase partition chromatography on bonded silica (stationary phase: Lichrospher diol, $d_p = 5$ μm; mobile phase: n-heptane/CH_2Cl_2MeOH 90/5/5).

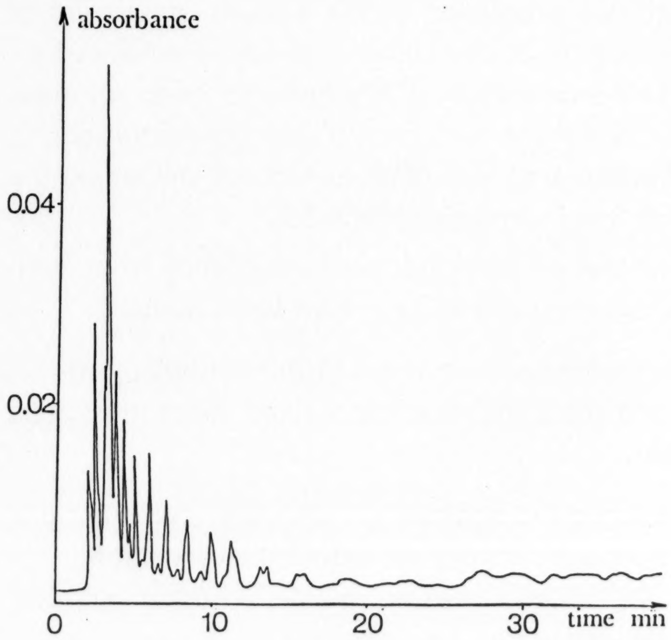

Fig. 2

Fractionating of a mixture of KL6 and KM20 obtained by normal phase partition chromatography on diol bonded silica (operating conditions as in Fig. 1).

Results and Discussion

First of all we checked that in the conditions previously defined for the analysis of KL 6 [4], there was no interference with the other non-ionic (KM 11, KM 20) and ionic (S 385) surfactants found in the mixtures used for enhanced oil recovery.

Without any derivatisation, it is easy to avoid the interferences which should take place if the surfactants were analysed after esterification by the 3,5-dinitrobenzoylchloride. In fact, the KL 6 is the only surfactant among the three non-ionic surfactants used in enhanced oil recovery (KL 6, KM 11 and KM 20) which naturally possesses a chromophoric group. The UV absorption results from the presence of an unsaturation in one of the fatty chains as shown by the ^{1}H NMR spectra of KL 6. Accordingly this non-ionic surfactant shows a weak UV adsorption for wavelengths lower than 240 nm. Comparison of Figs. 1 and 2 shows that the analysis of surfactant mixtures without derivatisation at a detection wavelength of 235 nm allows a very satisfactory detection of KL 6 in mixtures containing KM 11 and/or KM 20.

Furthermore there is no possible interference between KL 6 and the ionic sufactant S 385 in the analysis conditions selcted, that is to say, a diol bonded silica as stationary phase and a mobile phase containing n-heptane/CH_2Cl_2/MeOH in the proportions 90/5/5. In fact, as shown by Fig. 3, the ionic surfactant S 385 which is an aromatic sulphonated oil fraction remains adsorbed (in the conditions previously defined) at the column inlet while the non-sulphonated material in the sample is totally eluted.

This non-sulphonated fraction, which appears at total elution, does not disturb the analysis of KL 6. The less polar component of KL 6, which contains one ethylene oxide group, has a capacity fractor differing from zero (see Fig. 4).

Thus it is reasonable to think of successfully analyzing the KL 6 in mixtures containing non-ionic surfactants (KL 11 and/or KM 20) and an ionic surfactant (S 384) as proven by the comparison of Figs. 1 and 2.

Subsequently we proceeded to the analysis of samples of KL 6 orginating from the aqueous phase of enhanced oil recovery. This aqueous phase is a complex brine solution. In addition to mineral salts, in variable concentrations, it contains a mixture of non-ionic surfactants (including the KL 6) and an ionic surfactant (the S 385).

At first a calibration curve has been established from standard solutions containing at least three surfactants:

- KL 6 in variable concentrations (1000 to 6000 ppm)
- KM 11 and the S 385 (each at a fixed concentration of 5000 ppm).

The chromatographic analysis of such aqueous solutions requires a thorough dehydration before their injection.

From five independent analyses of each standard solution, that is to say from 20 measures, we have obtained the following calibration curve:

KL 6 concentration (ppm) = 1.89 10^{-2} x Detector response + 60.5 (with an excellent correlation coefficient, r = 0.997).

From five independent analyses of brine solution containing 1000 ppm of KL 6 and 5000 ppm of KM 11 and of S 385 we have obtained using the calibration curve a concentra-

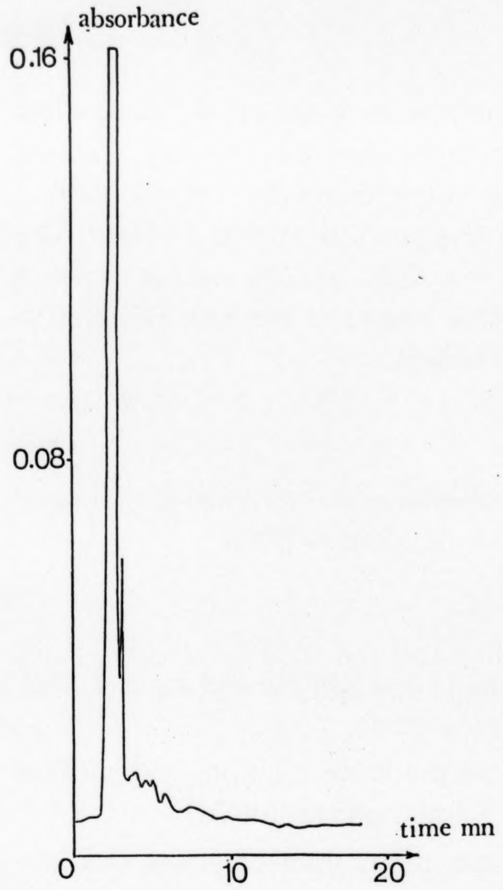

Fig. 3

Chromatogram of the ionic surfactant S 385 obtained by normal phase partition on diol bonded silica (operating conditions as in Fig. 1).

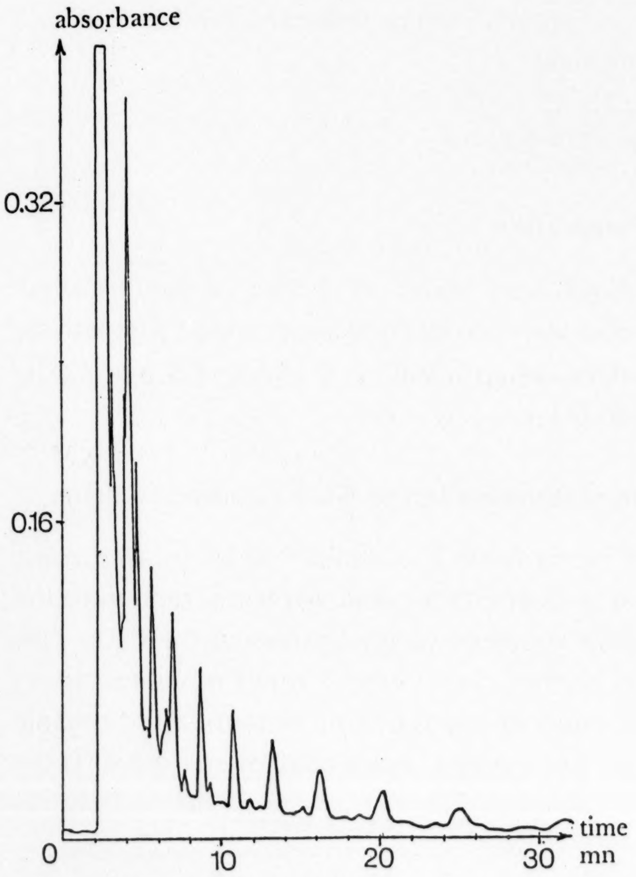

Fig. 4

Chromatogram of a mixture of ionic and non-ionic surfactants (KL 6 + KM 11 + S 385: 6000, 5000 and 5000 ppm) obtained by normal phase partition chromatography on diol bonded silica (operating conditions as in Fig. 1).

tion value of 960 ppm for KL 6 (standard deviation = 72 ppm). The threshold of this method is estimated to be less than 500 ppm.

This method is equally clearly adapted to the analysis of the organic phase (n-decane) modelizing oil. In fact in the same way a linear regression has allowed the computation of a calibration curve from the analysis of organic standard solutions of KL 6 (concentration range of 1000 ppm to 5000 ppm) in the presence of KM 11 (5000 ppm) and S 385 (5000 ppm). The following relation is obtained:

KL 6 concentration (ppm) = $2.61\ 10^{-2} \times$ Detector response + 23.9

Once more the correlation coefficient is excellent (r = 0.998). From seven independent analyses of a solution containing 2750 ppm of KL 6, 5000 ppm of KM 11 and 5000 ppm of S 385 in n-decane, an experimental concentration of 2700 ppm of KL 6 is found. The standard deviation is 70 ppm. So the validity of our analytical method for brine and organic solutions is confirmed by the satisfactory agreement between experimental and theoretical values.

After testing the viability and the validity of our method we have applied it to study the behaviour of KL 6 in brine solutions in dynamic contact with the rock shale.

The principle of this experiment is the following. A brine containg a mixture of non-ionic surfactants (KL 6 and KM 11) and ionic surfactant (S 385) is injected into a core of rock shale previously equilibrated with brine. This injection and the controlled movement of the sample band through the core are obtained by means of a polymer piston. After percolation of the rock by the sample band the rock is washed with pure water. The aqueous phase percolating from the rock is collected. 40 fractions are obtained (fractions 1 to 40). Afterwards the KM 25 surfactant is used to help the eventual desorption of KL 6. Fractions are continuously collected during this desorption (fractions 41 to 50). At the end of the experiment fifty fractions are qualitatively and quantitatively analysed according to our chromatographic method. Between collection and analysis each fraction is lyophilized for preservation purposes.

Figs. 5 and 6 show the chromatograms obtained firstly from fractions collected during the washing (Fig. 5a: fraction 16 and Fig. 5b: fraction 24) and secondly from fractions collected during the desorption of KL 6 by KM 25 (Fig. 6a: fraction 43 and Fig. 6b: fraction 46).

From these analyses the following points are deduced:

The large excess of KL 6 used during dynamic equilibration is eluted at the beginning of the washing phase (the solution injected presents a high concentration of 20 g/l and the rock possesses a low specific surface of about 1 m^2/g). The comparison between Fig. 5a and Fig. 1 (sample of KL 6 at 1500 ppm) clearly indicates that the fraction shown in Fig. 5a does not contain any trace of KL 6.

Moreover, if KL 6 is adsorbed on the sandstone used in this experiment, this adsorption is irreversible. A thorough washing does not produce desorption as clearly proven by the chromatogram of the 24th fraction shown in Fig. 5b.

Finally a notable result is that the injection of a more polar surfactant than KL 6 (KM 25) results in a desorption of the KL 6 components. This is revealed by the Fig. 6 which gives the chromatograms of fractions collected after

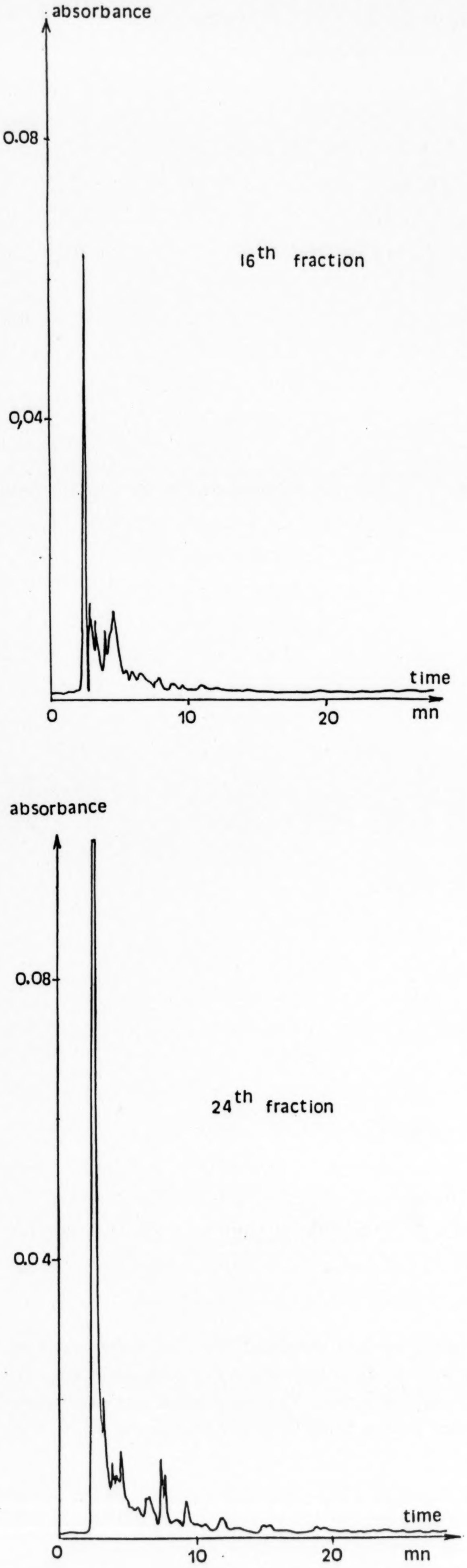

Fig. 5

Chromatograms of two fractions collected during the washing after dynamic contact with the rock shale of a brine solution containing KL 6, KM 11 and S 385 (operating conditions as in Fig. 1); a) 16th fraction, b) 24th fraction.

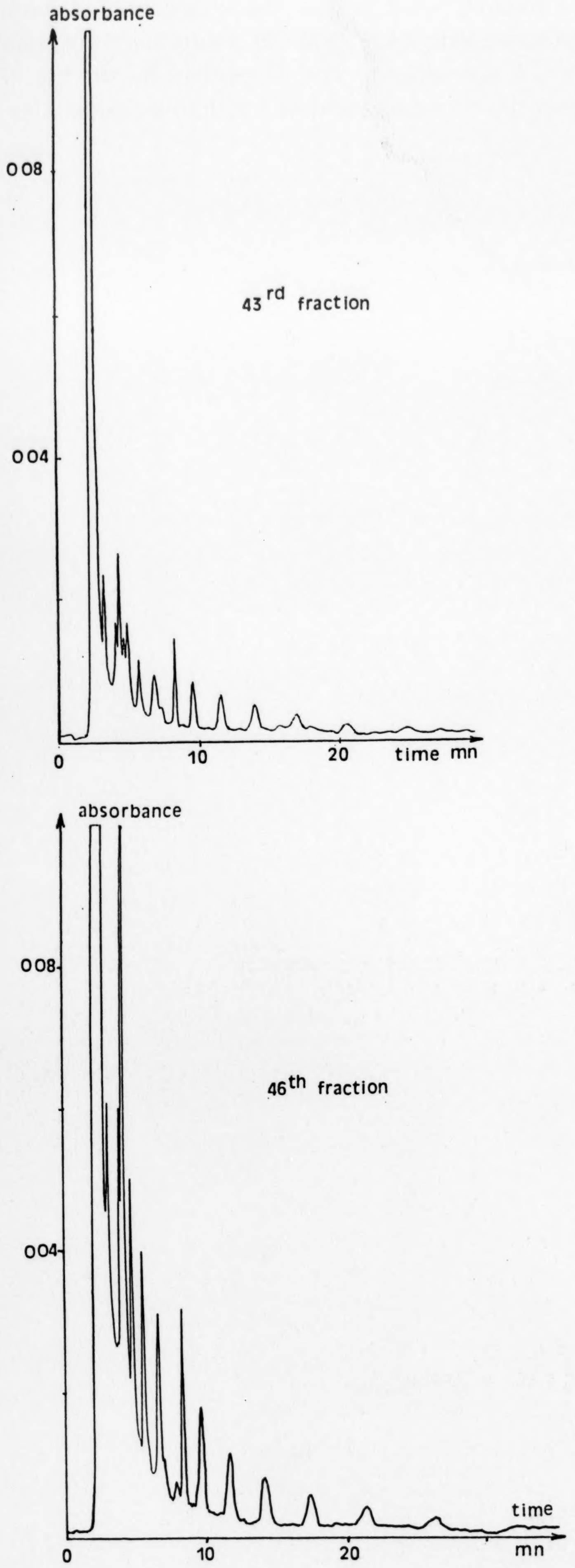

Fig. 6

Chromatograms of two fractions collected after an experiment of desoprtion of KL 6 by KM 25 (operating conditions as in Fig. 1); a) 43rd fractions; b) 46th fraction. The rock shale was previously put in dynamic contact with a brine solution containing KL 6, KM 11 and S 385.

percolation of KM 25 through the whole rock. The components of these two last fractions are clearly identified as the components of KL 6 by comparison of Figs. 1 and 6.

It is possible by means of peak integration and by using the calibration curve previously reported to quantify the KL 6 in each fraction. For instance the 43rd and 46th fractions shown in Figs. 6a and 6b contain 3.8 mg/l and 41 mg/l of KL 6 respectively.

Conclusions

We have established that it is possible to study and to determine KL 6 in the presence of other ionic and non-ionic surfactants in various phases obtained during enhanced oil recovery.

Under these conditions it is possible to study the partitioning of this non-ionic surfactant in more or less complex biphasic and triphasic equilibria encountered during enhanced oil recovery.

Finally after an experiment of dynamic contact of a brine solution of this surfactant with a sandstone, used as a model of rock shale, the analytical method that we report has allowed us to establish the irreversible adsorption of KL 6 and the possibility of its desorption by means of a more polar surfactant, KM 25, without modification of the distribution of KL 6 as a function of its ethylene oxide number.

After these very encouraging first results we intend to extend this study to the other non-ionic surfactants used in enhanced oil recovery.

References

[1] *J. Briant,* Sciences et Techniques, **4**, 27 (1977).
[2] *J. Labrid,* Colloques Nationaux du C.N.R.S., **938**, 321 (1977).
[3] *B. Larde,* Revue Institut Français du Pétrole, **20**, 253 (1965).
[4] *P. L. Desbène, B. Desmazieres, V. Even, J. J. Basselier, L. Minssieux*, Chromatographia **24**, 857 (1987).

Received: June 30, 1987
Revised manuscript
received: Sept. 30, 1987
Accepted: Oct. 5, 1987
F

Automated Preparative HPLC of Prostanoids

J. Veisserik* / T. Somer

Special Design Office, Academy of Sciences of Estonian SSR, Tallinn, USSR.

M. Lohmus / Y. Lille

Institute of Chemistry, Academy of Sciences of Estonian SSR, Tallinn, USSR.

Key Words

Preparative column liquid chromatography
Prostanoids
Water-saturated silica
Automated separation

Summary

The separation of prostaglandins (PG) PGE_1, PGE_2, $PGF_{1\alpha}$, $PGF_{2\alpha}$ and $PGF_{2\beta}$ on Silasorb 600 columns with a water-containing mobile phases is described. A flexible, automated, preparative liquid-chromatographic (PLC) system has been used involving column switching, column temperature control, solvent selection and automated fraction collection.

Introduction

Reversed-phase liquid chromatography is a conventional method for analytical, high-performance liquid chromatographic (HPLC) separations of PGs [1–4], but on a preparative scale there are some difficulties in recovering product fractions from aqueous and acidic mobile phases. Among numerous normal-phase column packings for HPLC silica gel is the cheapest and possesses quite a high selectivity for the separation of particular isomers. As reported earlier in [5], and shown here, in analytical HPLC and preparative separations, respectively, significant peak tailing of PGs as carboxylic acids on silica gel should be overcome by using a water-containing mobile phase (up to saturation). Hence it is possible to carry out preparative separations on silica gel columns satisfactorily. The mobile phases used for normal-phase separation on silica gel are easily removable by vacuum rotary evaporators and this method is superior to reversed-phase preparative separation.

We also report that difficulties in fractionating PGs with a very low selectivity (α) may be overcome by using a flexible PLC system and a column switching technique.

Experimental

Materials and Supplies

All solvents (analytical grade) were purchased from Reakhim (USSR). Hexane was used without purification. Isopropanol was redistilled. The ternary eluting solutions used were clear and there were no water droplets on the reservoir walls.

PGs were purchased from the Pilot Production Plant of Organic Synthesis and Biopreparations (Institute of Chemistry, Tallinn). A previously purified biosynthetic mixture of PGE_2 (62.1 %) and PGE_1 (36.8 %) was used. The mixture of PGFs was synthesized chemically from PGEs with the following composition: $PGF_{3\alpha}$ – 1 %, $PGF_{2\alpha}$ – 44.2 %, $PGF_{1\alpha}$ – 6.3 %, $PGF_{3\beta}$ – 1.3 %, $PGF_{2\beta}$ – 39.0 %, $PGF_{1\beta}$ – 8.1 %.

Apparatus

The PLC system PVK-31 (Speical Design Office, Academy of Sciences of the Estonian SSR) was used at a column oven temperature of 35 °C and coupled to a double-beam microspectrophotometer [6].

Column switching and an automated fraction collection system with peak detection and peak sub-fractionation by timing modes were used. Stainless steel columns packed with Silasorb 600 (5 μm, 7.5 μm, and 20 μm; Lachema) were used (Table I). The loop mixture sampling-system with loop volumes of 2 and 9 ml was used for manual and automated sampling. Cuts were taken from the PVK-31 separation and analysed by HPLC.

Results and Discussion

As reported earlier, the use of water-containing mobile phases permits separation of PGs with high efficiency on silica gel [5]. In this paper, complete resolution of PGE_2 and PGE_1 using the hexane-isopropanol-water mobile phase and Zorbax SIL column is shown. We have achieved resolution on a semipreparative scale using Silasorb 600 columns (Fig. 1 and 2). This, however, needed relatively

0009-5893/87 0593-04 $03.00/0

© 1987 Friedr. Vieweg & Sohn Verlagsgesellschaft mbH

high capacity factors (K′ = 8 to 12) and small sample sizes (20 and 150 mg, for columns 10 mm i.d. and 30 mm i.d. respectively, being limiting values for complete resolution). We have established that the quantity of pure PGE_2 recovered (99.9 %) per unit time could be significantly increased by using a higher percentage of isopropanol and higher column loadings. On the preparative scale, using a column loading of 300 mg, 1.45 g of PGE_2 (99.5 %) was obtained with 10 injections (Fig. 3) (recovery 80 % from the initial PGE_2).

This method also proved to be useful in the separation of PGs of the F-series. As shown in Fig. 4, injecting a 40 mg sample onto the column (30 × 1 cm i.d.) allowed complete separation of $PGF_{2\alpha}$ and $PGF_{1\alpha}$ from each other and from other PGs of the F-series. If the column loading is increased and eluting peaks are fractionated, we can

Table I. Columns

Fig.	Column dimensions i.d. X length, mm	packing, particle size µm	Efficiency* theoretical plates
1	300 X 10	5	10000
2	300 X 30	5	4300
3	300 X 30	5	4300
4	300 X 10	7.5	6000
5	300 X 10	7.5	6000
6	300 X 10	7.5 and 5	6000, 10000

* Column efficiency was measured from naphthalene eluted by hexane.

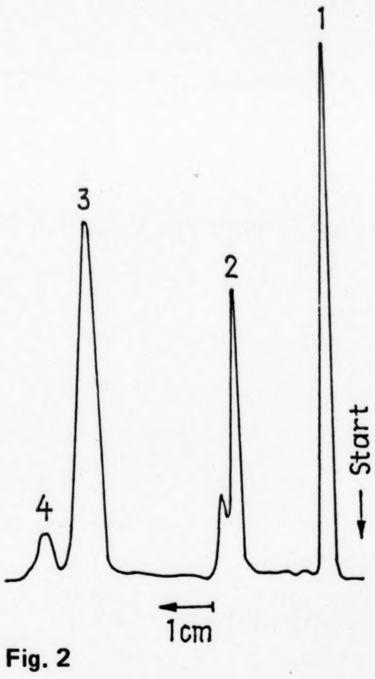

Fig. 2

Separation of PGE_2 and PGE_1 on 300 × 30 mm id column, non-overloaded. Conditions: Silasorb 600 5 µm; mobile phase; hexane/isopropanol/water (88 : 11.5 : 0.5) 40 ml min^{-1}; UV 224 nm at 1 AUFS; chart speed 10 cm h^{-1}; column temperature 35 °C, sample size 150 mg; peaks **1** = solvent, **2** = PGA, **3** = PGE_2, **4** = PGE_1.

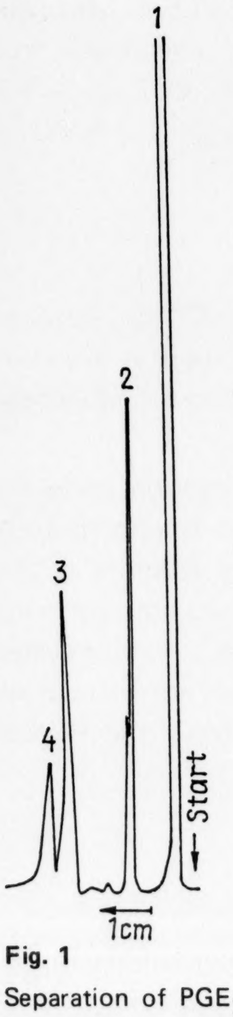

Fig. 1

Separation of PGE_2 and PGE_1 on 300 × 10 mm id column, non-overloaded. Conditions: Silasorb 600 5 µm; mobile phase: hexane/isopropanol/water (88 : 11.5 : 0.5) 10 ml min^{-1}; UV 218 nm at 0.5 AUFS; chart speed 10 cm h^{-1}; column temperature 35 °C, sample size 20 mg; peaks: **1** = solvent, **2** = PGA, **3** = PGE_2, **4** = PGE_1.

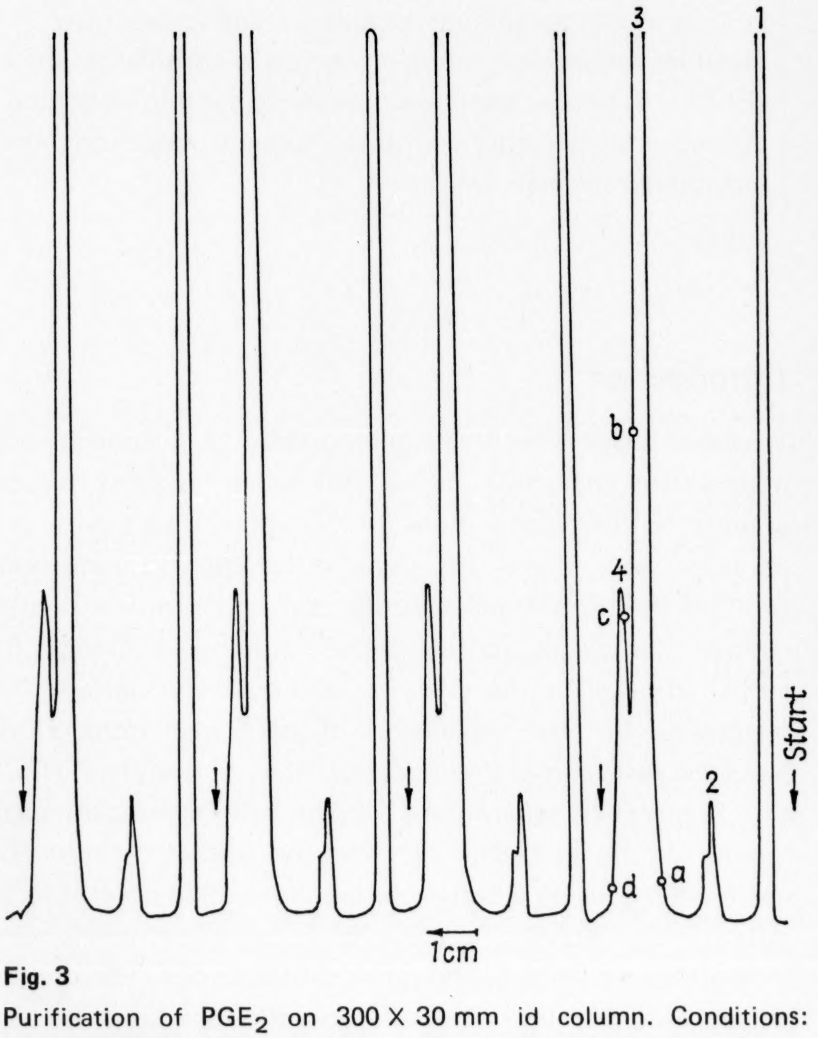

Fig. 3

Purification of PGE_2 on 300 × 30 mm id column. Conditions: Silasorb 600 5 µm; mobile phase; hexane/isopropanol/water (85 : 14.4 : 0.6) at 45 ml min^{-1}; UV 224 nm at 1 AUFS; chart speed 10 cm h^{-1}; column temperature 35 °C, sample size 300 mg; peaks: **1** solvent, **2** = PGA, **3** = PGE_2, **4** = PGE_1 Automated peak level fraction collection: **a** = start for PGE_2, **b** = end for PGE_2, **c** = start for PGE_1, **d** = end for PGE_1.

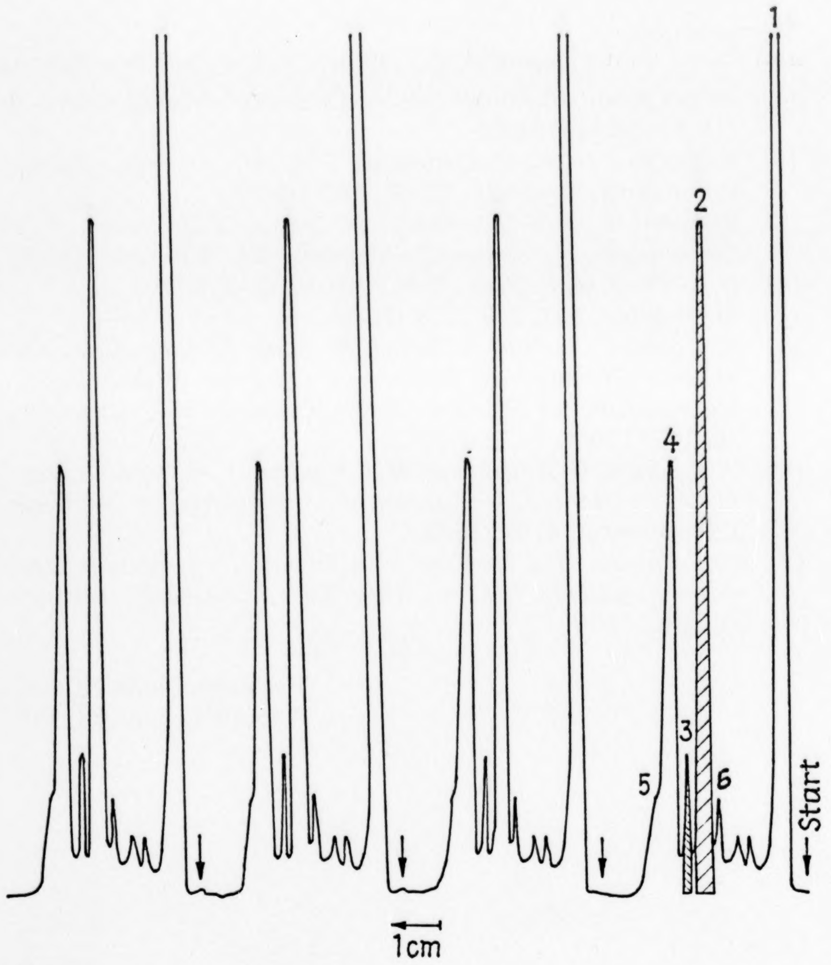

Fig. 4

Separation PGFs. Conditions: Silasorb 600 7.5 μm. 300 X 10 mm id; mobile phase: hexane/isopropanol/water (80 : 19.2 : 0.8) 8 ml min^{-1}; UV 218 nm at 0.5 mm AUFS; chart speed 10 cm h^{-1}; column temperature 35 °C; sample size 40 mg; peaks: **1** = solvent, **2** = $PGF_{2\alpha}$, **3** = $PGF_{1\alpha}$, **4** = $PGF_{2\beta}$, **5** = $PGF_{1\beta}$; automated peak sub-fractionation by timing collection, **6** = signal peak for collecting time start. Collected peaks: 2 (purity 99 %) and 3 (purity 85 %).

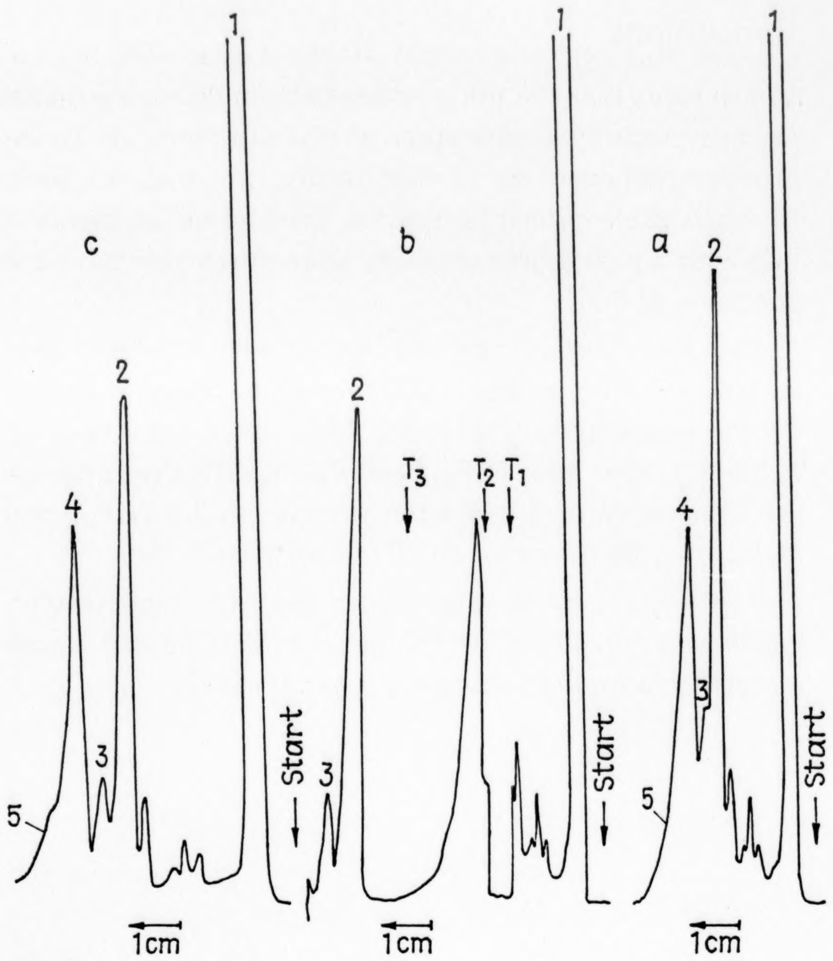

Fig. 5

Separation of $PGF_{2\alpha}$ and $PGF_{1\alpha}$, using column switching. Conditions: Silasorb 600 7.5 and 5 μm, 300 X 10 mm id; mobile phase: hexane/isopropanol/water (80 : 19.2 : 0.8) 8 ml min^{-1}. UV 220 nm at 1 AUFS; chart speed 10 cm h^{-1}; columns temperature 35 °C; sample size 150 mg; peaks: **1** = solvent, **2** = $PGF_{2\alpha}$, **3** = $PGF_{1\alpha}$, **4** = $PGF_{2\beta}$, **5** = $PGF_{1\beta}$. Fig. a: resolution on 7.5 μm column only; Fig. b: $T_1 \rightarrow T_2 - PGF_{1\alpha} + PGF_{2\alpha}$ cutting, T_3- end resolution $PGF_{1\alpha}$ and $PGF_{2\alpha}$ in second column, 5 μm; Fig. c: resolution on 7.5 and 5 μm columns, connected on-line.

expect an increased throughput but in this case, the column switching technique is also useful. If the column loading is increased to 150 mg, this results in loss of resolution of $PGF_{2\alpha}$ and $PGF_{1\alpha}$ (Fig. 5a). Coupling two columns in series allowed separation of this pair of compounds (Fig. 5c), but resolution of the compounds could be improved by reducing the loading of the second column and by-passing the unwanted part of the PG mixture (Fig. 5b).

It was found that the use of Silasorb 600 with a particle size of at least 5 or 7.5 μm was needed for separation of PGs of series 1 and 2, but $PGF_{2\alpha}$ and $PGF_{2\beta}$ could also be separated on the column packed with 20 μm particles (Fig. 6). As we found, this separation may be improved by using the hexane-ethyl acetate-water mobile phase as a more selective one for the separation of this pair of PG isomers (but this method is less selective for separating PGs of a different degree of saturation).

We suppose, therefore that this method is also useful for laboratory scale separation of synthetic PGs and their analogues where the presence of various isomeric mixtures is often unavoidable (as a rule, silica gel shows higher selectivity in the separation of isomers than bonded-phase packings [7]).

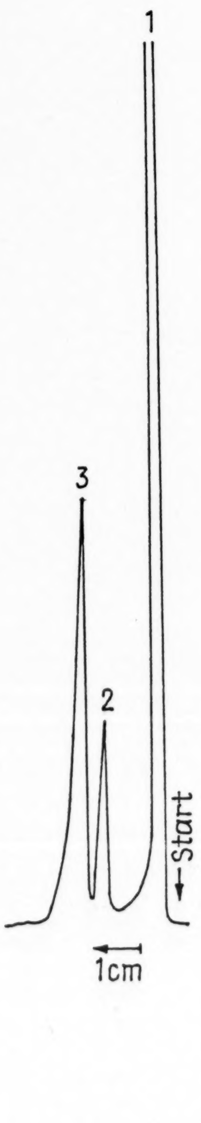

Fig. 6

Resolution of $PGF_{2\alpha}$ and $PGF_{2\beta}$. Conditions: Silasorb 600 20 μm, 300 X 10 mm id mobile phase: hexane/isopropanol/water (80 : 19.2 : 0.8) at 10 ml min^{-1}; UV 220 nm at 0.5 AUFS; chart speed 10 cm h^{-1}; column temperature 35 °C; sample size 20 mg; peaks: **1** = solvent, **2** = $PGF_{2\alpha}$, **3** = $PGF_{2\beta}$.

Conclusions

It is evident that the use of water-containing mobile phases permits preparative separation of PGs satisfactorily. As the products obtained are of high purity, this method seems to be suitable primarily for the production of standard PGs with a high degree of purity (including stable synthetic analogues of PG).

It has been shown that the use of high-efficiency preparative columns (at least 4000 theoretical plates) is needed for the separation of PGE_2 and PGE_1 (with a purity of up to 99.5 %) and also $PGF_{2\alpha}$ and $PGF_{1\alpha}$. This requires the use of packings of 5 or 7.5 μm particle size but $PGF_{2\alpha}$ and $PGF_{2\beta}$ may be separated on 20 μm particles as well.

This method permits the use of relatively high column loadings (5 to 10 mg of PG per 1 g of silica gel) which is acceptable for high-efficiency separation.

References

[1] *A. Terragno, R. Rudzik, N. A. Terragno,* Prostaglandins. **21** (1), 101–112 (1981).

[2] *R. Freixa, J. Casas, J. Rosello, E. Gelpi,* J. High, Resolut. Chromatogr. Commun. **7,** 156–157 (1984).

[3] *S. P. Peters, E. S. Schulman, M. C. Liu, E. C. Hayes, L. M. Lichtenstein,* J. Immunol. Methods. **64,** 335–343 (1983).

[4] *D. L. Theis, M. L. Rusk, S. M. Plaisted, B. G. Snider,* J. Chromatogr. **321,** 209–215 (1985).

[5] *M. Lohmus, A. Paju, N. Samel, M. Lopp, U. Lille,* Eesti NSV Teaduste Akadeemia Toimetised, Keemia (Proceedings of the Academy of Sciences of the Estonian SSR, Chemistry. **35,** 142 (1986).

[6] *G. I. Baram, N. A. Grachev, N. I. Komarova, M. P. Perelroyzen, Yu. A. Bolvanov, S. V. Kuzmin, V. V. Korgattsey, E. A. Kuper,* J. Chromatogr. **4,** 69 (1983).

[7] *L. R. Snyder, J. J. Kirkland,* Introduction to modern liquid chromatography. 2nd ed., New York, Chichester, Brisbane, Toronto, 1979.

Received: June 28, 1987
Accepted: July 23, 1987
F

High-Performance Liquid Chromatographic Analysis of Isoxazolylpenicillins in Plasma and Urine Samples

U. R. Tjaden / H. Lingeman* / R. A. M. van der Hoeven / J. A. C. Bierman / H. J. E. M. Reeuwijk / J. van der Greef

Division of Analytical Chemistry, Center for Bio-Pharmaceutical Sciences, Leiden University, P.O. Box 9502, 2300 RA Leiden, The Netherlands

Key Words

Column liquid chromatography
Absorbance detection
Isoxazolylpenicillins
Plasma and urine samples

Summary

A simple and fast liquid chromatographic method is described, applicable to the routine analysis of isoxazolylpenicillins (cloxacillin, dicloxacillin, flucloxacillin) in biological fluids (plasma, urine). The method is based on a simple dilution step employed to destroy the protein binding, which is over 95%, and allows the detection of concentrations down to 10μg/ml. In order to analyze concentrations of less than 10μg/ml, a liquid-liquid extraction with dichloromethane must be executed prior to the reversed-phase analysis with absorbance detection at 206nm. The minimum detectable amounts of the isoxazolylpenicillins with this procedure are between 2.5 and 5.1ng in 100μl plasma samples. The stability of the penicillin samples in aqueous solutions (stock solutions, eluents) was investigated and no significant degradation was observed during the storage and analysis of the samples. Furthermore, the degree of protein binding was established by using a suitable ultrafiltration technique, and the usefulness of the developed procedures in pharmacokinetic studies was demonstrated.

Introduction

The isoxazolylpenicillins (IXP), cloxacillin (C), dicloxacillin (D), and flucloxacillin (F), are semisynthetic penicillins (Fig. 1) presently used in clinical therapies for the treatment of, and the prophylaxis against, staphylococcal infections [1].

C [2], D[3], and F [2] are normally analyzed using a microbiological assay. However, the described assays possess disadvantages such as cross-reactivity, most of the IXP metabolites react as well, and the sensitivity of the assay is not the same for the different IXPs. The IXP metabolites possess antibacterial activity, are present in urine and in plasma, the amounts in plasma are relatively low, and 10% to 15% of the excreted IXP represents the metabolites [4]. Therefore, it is advisable to analyze the plasma and urine samples not only with a microbiological assay, but also with a selective and sensitive liquid chromatographic (LC) assay.

For the analysis of penicillins, a number of LC procedures have been described, including reversed-phase (RP) chromatography, RP-ion-pair (RP-IP) chromatography, and the use of post-chromatographic derivatization techniques [5–11]. Detection of the analytes is performed with ultra-violet (UV) absorbance detection at 254nm or at wavelengths near 200nm.

The described sample pretreatment procedures depend on the required sensitivity of the method. For the relatively high concentrations (more than 10μg/ml), a simple dilution of the sample with a suitable buffer or water-methanol mixture is sufficient for the analysis of the analytes in urine samples [1, 5]. For the relatively low concentrations (less than 10μg/ml), a liquid-liquid extraction with chloroform or dichloromethane is described for the analysis of the analytes in plasma or serum samples [8, 11]. A protein precipitation procedure with trichloroacetic acid, acidic methanol or with acidic acetonitrile mixtures is also possible, but in this case direct analysis of the sample is necessary due to the instability of the solutes in aqueous acidic solvents [5, 10, 11].

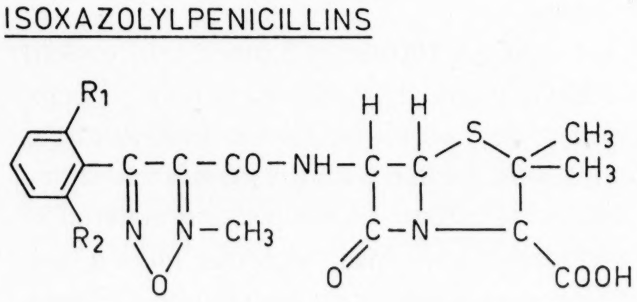

compound	R1	R2
CLOXACILLIN	Cl	H
DICLOXACILLIN	Cl	Cl
FLUCLOXACCILLIN	Cl	F

Fig. 1
Structures of isoxazolylpenicillins.

0009-5893/87 0597-05 $03.00/0

© 1987 Friedr. Vieweg & Sohn Verlagsgesellschaft mbH

In most of the described procedures, nafcillin (N) is used as the internal standard. However, precautions should be taken due to the instability of N, and naturally of the other penicillins as well, in aqueous solutions.

The solutes (C, D, F, and N) are soluble to freely soluble in water, and the pH of an aqueous solution is between 4.5 and 7.5. However, the maximum stability is obtained at pH 6.5 [11]. IXPs rapidly lose their activity in aqueous solutions, especially in acidic solutions [12], and there is a tendency towards accelerated degradation in concentrated solutions. Furthermore, the samples should be stored in airtight containers at temperatures below 277 K and without exposure to daylight because except for a hydrolytic degradation, photochemical and oxidation reactions also influence the stability of the analytes.

The applied procedure is a combination of several of the published studies [4, 11] in order to obtain the required sensitivity, accuracy and reproducibility, as well as to allow automation of the procedure. An octyl modified silica is used as the stationary phase with low wavelength absorbance detection (206nm) in combination with a dilution procedure or an adapted dichloromethane extraction technique.

The degree of protein binding of the analytes is established by convective filtration of free microsolute through an anisotropic, hydrolytic ultrafiltration membrane and subsequent analysis of the supernatant.

The presented method allows the bioanalysis of IXPs in human plasma and urine samples after administration of C, D and F.

Experimental

Chromatography

The automated LC system consisted of a LKB (Bromma, Sweden) model 2150 solvent delivery system. Injections, with a fixed 100μl loop, were executed with a Promis (Spark Holland, Emmen, The Netherlands) autosampler. UV absorbance detection at 206nm was applied using a LKB model 2151 variable wavelength detector. The measurements of the peak height and peak height ratios were made with a computing integrating recorder C-R3A (Shimadzu, Kyoto, Japan).

Stainless steel columns of 100mm × 3.0mm i.d., packed with Nucleosil 100 C_8 material (Macherey & Nagel, Düren, FRG) with 5μm particles, were used for the analysis of the IXPs. The columns were packed with the pressurized slurry technique by dispersing 500mg of the packing material in 4ml of 1,1,1-trichloroethane. After vigorous mixing, the resulting suspension was poured into a pre-column (250mm × 4.6mm i.d.), which was connected to the empty analytical column. Subsequently the column was packed with an air amplifier booster pump (Model 122, Haskel Inc., Burbank, CA, USA) by pumping 50ml of methanol through the columns at a pressure of 60MPa. A flow-rate of 1.0ml/min was maintained and the chromatography was performed at ambient temperatures.

The applied mobile phases consisted of 35% (v/v) methanol and 65% (v/v) 0.02M sodium acetate buffer. For the analysis of the urine and the plasma samples, the pH of this buffer was 4.9 and 4.6, respectively.

In the analysis of the plasma samples, N was used as an internal standard for the analysis of samples containing C and F, and F was used as the internal standard for the analysis of the samples containing D.

Ultrafiltration

The ultrafiltration experiments, to establish the non-protein bounded fractions, were performed with a Sorvall (DuPont instr., Newtown, Conn., USA) RC-2 superspeed centrifuge with a fixed rotor angle of 34° at 2000g. The micro-partition system (MPS-1) was equipped with YMT membranes of 14mm (Amicon, Oosterhout, The Netherlands).

Materials and Solutions

Sodium salts of C (batch nr. 114) and F (batch nr. 124) were kindly donated by Astra (Södertälje, Sweden). The sodium salt of D (I, batch nr. B.5684; II, batch nr. 10800) came from Bristol-Myers (Weesp, The Netherlands) and the sodium salt of N was purchased from Gist-Brocades (Delft, The Netherlands). All other compounds and organic solvents came from various sources, were of analytical reagent grade and were used as such.

Throughout the study, deionized water (Milli Q water purification system, Millipore, Bedford, MA, USA) was used.

Stock solutions of C, D, F, and N (1μg/μl) were prepared freshly every week in a physiological salt solution and stored in the dark at 253K. The physiological salt was prepared by dissolving 0.9% (w/v) sodium chloride in water. The applied acetate buffers consisted of different mixtures of 0.02M acetic acid and 0.02M sodium acetate. Alkaline dichloromethane solutions were achieved by vigorous mixing of equal volumes of dichloromethane and 1M ammonium hydroxide solution. After phase separation, the organic phase was stored in carefully closed airtight containers.

Sample Preparation and Storage

All of the urine and plasma samples were stored at 253K in the dark and were analyzed immediately after thawing.

Urine samples. After defrosting, the urine samples were diluted with the physiological salt solution of 99 to 9999 volumes, depending on the concentration of the samples, and 100μl aliquots were analyzed with the described LC system.

Plasma samples containing more than 10μg/ml of the analytes. After defrosting, the plasma samples were diluted with 99 volumes of the physiological salt solution after the addition of 20μl of the diluted stock solution (0.05μg/μl) of the internal standard. 100μl aliquots were subsequently analyzed with the LC system.

Plasma samples containing less than 10μg/ml of C and F. A 100μl plasma sample was mixed with 20μl of a diluted stock solution (0.05µg/µl) of the internal standard, 20µl 0.5M hydrochloric acid and 100µl 0.5M citric acid. After the addition of 2.5ml of dichloromethane, which was saturated with water, the resulting solution was mixed for 5min in a rotating mixing device (60rpm). After centrifugation for 5min (2500g), the organic phase was diluted with 0.5ml of alkaline dichloromethane and evaporated to dryness under a stream of dry nitrogen. The residue was dissolved in 250µl of the physiological salt solution, and a 100µl aliquot was injected onto the chromatographic system.

Plasma samples containing less than 10µg/ml of D. After thawing of the sample, a 500µl aliquot was mixed with 100µl of the diluted stock solution (0.05µg/µl) of the internal standard, 100µl 0.5M hydrochloric acid, and 500µl 0.5M citric acid. After the addition of 5ml of dichloromethane, the mixture was treated in the same way as described for the analysis of the plasma samples containing C and F.

Plasma samples for protein binding studies. Plasma samples of 1ml were spiked with 50µg/ml of the analytes and incubated for 16 hours at 310K in the dark. After the incubation, 800µl fractions were transferred to the sample reservoir of the MPS-1 system containing the YMT membrane, and the reservoir was carefully capped. The whole device was centrifuged for 15min at 298K in the fixed-angle centrifuge. 25µl of the filtrate was subsequently analyzed chromatographically.

Results and Discussion

Stability

Because of the reported limited stability of IXP derivatives in aqueous solutions [5, 10, 11], first of all the stability of the stock solutions (stored at 253K) was investigated 3 times a week by peak height comparisons with freshly prepared solutions. Normally IXPs are stored at temperatures of 203K, but in this study no significant degradation (less than 2%) was observed after 1 week of storing the samples at 253K. The stability of the solid material was tested by comparising the 2 different batches of D at the end of the study. The first batch (Batch I) was received at the beginning of the study and the second batch (Batch II) was received at the end of the study. The solid material was stored at 253K and after 3 months of storage, no significant degradation was observed. Contrary to the data given in the literature, it can be concluded that it is not necessary to store the solid samples or the stock solutions at temperatures below 253K.

However, at room temperature the degradation of the IXP is faster. The maximum stability, the aqueous solutions, is obtained at a pH of 6.5, but the pH of the stock solutions of the analytes in the physiological salt solution varies from 4.5 to 7.5. The result was that the stock solutions, and the more diluted solutions, could only be stored for 6 hours (Fig. 2).

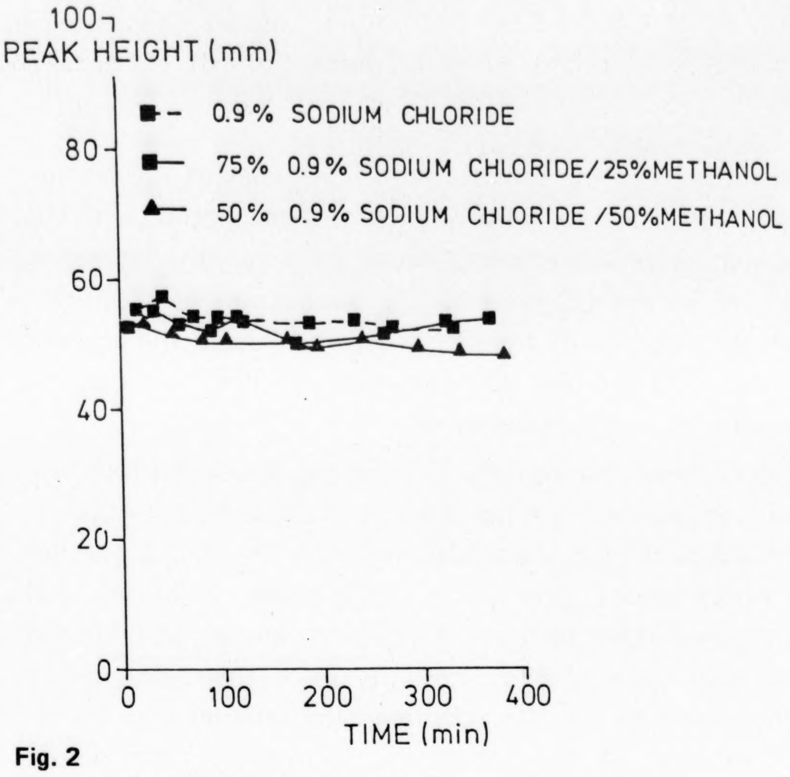

Fig. 2

Peak height-time curves of cloxacillin in aqueous solutions.

Furthermore, the stability of the analytes was studied in mixtures of 0.9% sodium chloride and methanol, and no significant degradation was seen within 6 hours at room temperature (Fig. 2). The stability of the analytes after the extraction with the acidic dichloromethane and mixing with the alkaline dichloromethane, which resulted in a pH of about 6.5, was tested and again no significant degradation was observed. However, whenever the addition of the alkaline dichloromethane was omitted, the IXPs, and especially N, were not stable during the rest of the pretreatment procedure or during the subsequent analysis with the autosampler-equipped chromatographic system.

For the internal standard N, a limited solubility is described in the literature. In aqueous solutions with a pH of about 5.6 or at lower pH values, the free acid can be precipitated. However, during the sample pretreatment procedure no precipitation of this compound was observed because of the relatively low concentration of the solute.

Sample Pretreatment Procedures

The described protein precipitation procedures cannot be used as such because of the stability of the IXP, the relatively low concentrations, and because of the automated LC procedure [8, 10, 11]. Therefore, and to improve the throughput, samples containing 10µg/ml or more were only diluted with the physiological salt solution. Because of the relatively high concentrations of the analytes in urine samples, all samples could be analyzed with this dilution procedure. Regarding the concentrations in the plasma samples, only a limited number of the samples could be analyzed by this method.

To insure that this simple dilution step did not influence the accuracy of the method, the calibration curves obtained with the diluted plasma samples were compared with the calibration curves obtained with the extracted plasma samples. The result was that dilution of the plasma samples with 9, 24, or 99 volumes of physiological salt solution produced calibration curves (slope and intercept) comparable to the extracted samples. From these experiments it can be concluded that, although the IXPs are bound to serum proteins, a simple dilution with at least 9 volumes of the 0.9% sodium chloride and the subsequent chromatographic analysis was sufficient to eliminate errors due to the protein binding of the analysis.

The dilution of the samples with 9 volumes of the physiological salt solution, however, was not compatible with the chromatographic system because of a rapidly increasing pressure in the LC system. The application of a dilution with 99 volumes of the salt solution allowed the analysis of over 500 samples per analytical column, without the necessity of using pre-columns.

As previously mentioned, this simple dilution procedure could not be used for the analysis of the samples with concentrations of less than 10μg/ml. After testing a number of pretreatment procedures (solid-phase isolations and continuous flow techniques [13]), a simple liquid-liquid extraction with dichloromethane gave the best results with respect to the throughput of the samples and the reproducibility of the procedure. Extraction from acidic solvents was necessary to achieve acceptable blank chromatograms and high recoveries. The addition of citric acid was necessary to stabilize the IXP during the extraction procedure.

The extraction recoveries after the analysis of 5 plasma samples that were spiked with 1, 2, 5, and 10μg/ml of C, D, or F were 94.3% ± 4.1%, 91.5% ± 3.8%, and 77.5% ± 4.5%, respectively. The somewhat lower recovery for D is caused by the different phase-volume ratio that must be applied because the plasma levels of D are much lower in comparison with the C and F levels. These low concentrations necessitate the use of the extraction procedure for all of the plasma samples containing D.

Chromatography and Detection

In order to achieve the required selectivity, an octyl-modified silica column produced better results in comparison with the more generally applied octadecyl-modified silica columns (Fig. 3). The result of the higher co-solvent (methanol or acetonitrile) concentrations, when using C_{18} columns, was a co-elution of the IXP with some matrix components.

Methanol was applied as the organic modifier because it gave a somewhat better compromise between the selectivity and the detectability of the system in comparison with the use of acetonitrile.

For the chromatography of the samples, two mobile phases were applied with different pH. Regarding the stability of the analytes, the pH of the mobile phase should be about 6.5. However, at this pH the selectivity of the chromatographic system was not sufficient to separate the IXP from the matrix peaks. Therefore, the pH was lowered to 4.9 for the analysis of the urine samples and to 4.6 for the analysis of the IXP in the plasma samples. The capacity ratios of the 3 analytes and the internal standard were not markedly influenced by changing the pH from 4.9 to 4.6 (Fig. 4).

The internal standard for the determination of D was F, and N was applied as the internal standard for the determination of C and F (Fig. 5). For the analysis of D, it was also possible to use C as an internal standard.

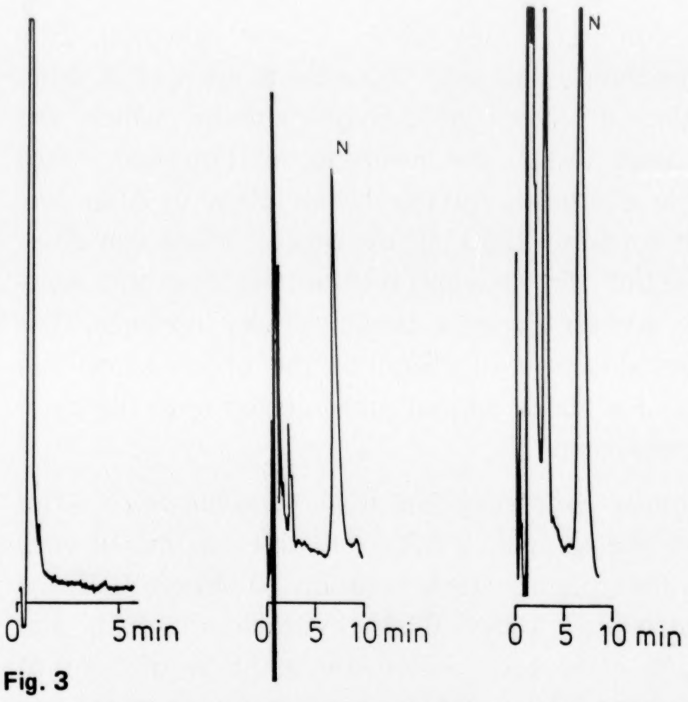

Fig. 3

Urine and plasma blank chromatograms. A, urine blank chromatogram treated for analysis of D (dilution); B, plasma blank chromatogram treated for analysis of C (dilution); C, plasma blank chromatogram treated for analysis of F (extraction).

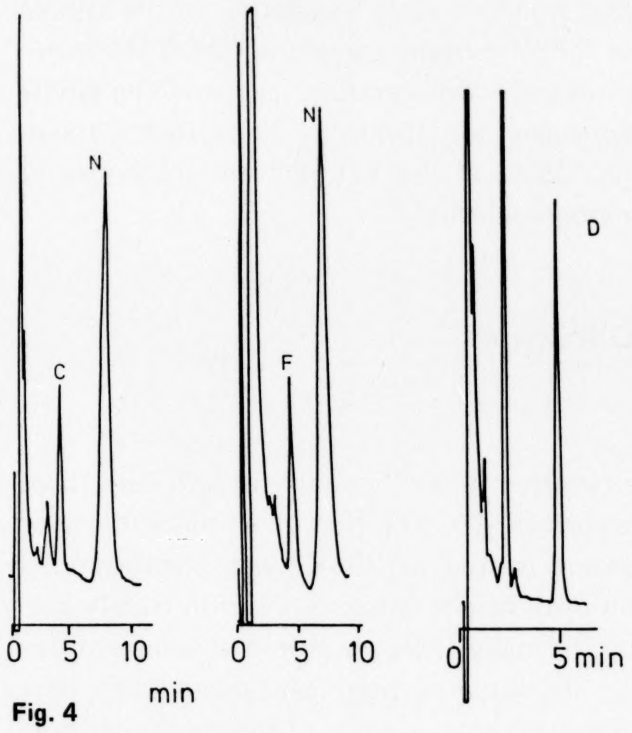

Fig. 4

Diluted plasma and urine samples containing isoxazolylpenicillins. A, diluted plasma sample containing 27.3μg/ml cloxacillin; B, diluted plasma sample containing 17.1μg/ml flucloxacillin; C, diluted urine sample containing 225.0μg/ml dicloxacillin (C, cloxacillin; D, dicloxacillin; F, flucloxacillin; N, nafcillin).

The detection of the IXP was executed with a variable wavelength detection near the absorbance maximum of the analytes at 206nm. The combination of automated LC analysis and the relatively low pH of the eluent allows the detection of the solutes without interferences from endogenous compounds.

Analytical Variables

Linearity. In order to investigate the linearity of the procedure, blank plasma samples (n = 12) were spiked with

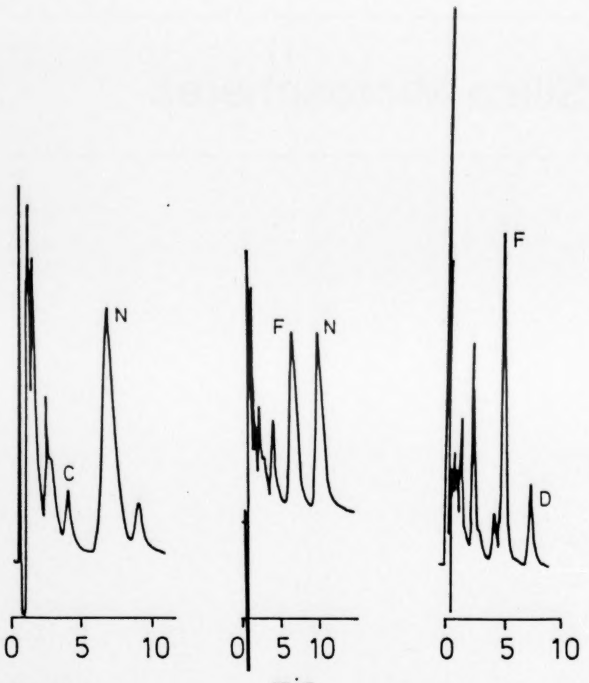

Fig. 5

Extracted plasma samples containing isoxazolylpenicillins. A, analysis of cloxacillin (2.21 μg/ml); B, analysis of flucloxacillin (2.02 μg/ml); C, analysis of dicloxacillin (3.42 μg/ml) (C, cloxacillin; D, dicloxacillin; F, flucloxacillin; N, nafcillin).

either 0.2 to 10 μg/ml or 5 to 200 μg/ml of the 3 IXPs and analyzed with the dilution and the extraction procedure, respectively. For instance, for C, the equation for the calibration curve after dilution of the samples was $y = 1.74\ (\pm 0.01)\ x - 0.09\ (\pm 1.02)$ $(r = 0.9999)$, and after extraction of the samples it was $y = 0.94\ (\pm 0.02)\ x + 0.08\ (\pm 0.06)$ $(r = 0.9995)$. In the equations for the calibration curves, x and y are the peak height of the IXP and the IXP concentration (μg/ml), respectively. The numbers in parentheses are the standard deviations and the correlation coefficient. The calibration curves showed about the same linearity for all 3 analytes, and the linear dynamic range was over 3 orders of magnitude.

Detectability. The minimum detectable amount, with a signal to noise ratio of three, from the described procedure was 2.5 ng for C, 3.5 ng for F, and 5.1 ng for D, after the analysis of 5 spiked plasma samples. The detection limits in urine samples were comparable to the plasma samples.

Precision. An indication of the within-day and day-to-day reproducibility is given by the correlation plot of the analyzed quality control samples (samples with exactly known concentrations). For instance, after the analysis of 170 plasma samples, spiked with 1 to 100 μg/ml of C, D, or F, the slope of the correlation plot is 1.003 (± 0.003), with a correlation coefficient of 0.994. Y and x are the real and the calculated concentrations, respectively. The within-day precision of the procedure was established by comparing the slopes of the calibration curves, which were measured every day. For instance, for D, the mean slopes of 5 calibration curves of extracted plasma samples, was 0.66, with a standard deviation of 0.02. The within-day precision of the other analytes, of the dilution procedure, and of the urine samples were about the same or even better.

Protein Binding

In order to accurately calculate the binding percentages, the separation of the free IXP fraction from the protein bound analyte fraction was executed with an ultrafiltration system. The principle of this micropartition technique is based on a filtering of the free analyte through an anisotropic, hydrophilic ultrafiltration membrane [14]. A fixed angle rotor centrifuge was applied because this type of centrifuge produces more filtrate per unit time in comparison with, for instance, the swinging bucket rotor-based centrifuges. The ultrafiltrate, with the free analyte, was collected in the filtrate cup and separated from the protein bound analyte and the other macromolecular components. The standard YMT membrane used enables the ultrafiltration of solutes with a molecular mass up to 30.000. The possibility of irreversible adsorption of the analytes to the ultrafiltration membrane was checked by addition of the free analyte (50 μg/ml) to the system and subsequent analysis of the ultrafiltrate. Incubation for 16 hours was executed because no reliable data were present about the speed of the protein binding of the IXP.

The degree of protein binding was 97.4 ± 0.7% for C, 98.6 ± 1.1% for D, and 98.1 ± 0.3% for F, based on the analysis of 24 samples. No adsorption of the analytes onto the membrane was detected. Except for the plasma samples spiked with 50 μg/ml, some samples spiked with 25 and 100 μg/ml were analyzed and the calculated degree of protein binding did not differ significantly. This means that the degree of protein binding is probably analyte concentration independent, in the investigated concentration area.

References

[1] *Y. Murai, T. Nakagawa, K. Yamaoka, T. Uno*, Chem. Pharm. Bull., **31**, 3292 (1983).
[2] *T. Bergan, B. Oydvin*, Acta Path. Microbiol. Scand., **808**, 101 (1972).
[3] *S. Löfgren, G. Bucht, B. Hermansson, S. E. Holm, B. Winblad, S. R. Norrby*, Scand. J. Infect. Dis., **18**, 365 (1986).
[4] *H. H. W. Thijssen, H. Mattie*, Antimicrob. Agents Chemother., **10**, 441 (1976).
[5] *J. Sjövall, G. Alvan, D. Westerlund*, Clin. Pharmacol. Ther., **38**, 241 (1985).
[6] *J. Carlqvist, D. Westerlund*, J. Chromatogr., **344**, 285 (1985).
[7] *D. Westerlund, J. Carlqvist, A. Theodorsen*, Acta Pharm. Suec., **16**, 187 (1979).
[8] *S. J. Soldin, A. M. Tesoro, S. M. MacLeod*, Ther. Drug Monitoring, **2**, 417 (1980).
[9] *Y. Murai, T. Nakagawa, K. Yamaoka, T. Uno*, Int. J. Pharm., **15**, 309 (1983).
[10] *H. H. W. Thijssen*, J. Chromatogr., **183**, 339 (1980).
[11] *F. W. Teare, R. H. Kwan, M. Spino, S. M. MacLeod*, J. Pharm. Sci., **71**, 938 (1982).
[12] *T. Bergan, B. Oydvin*, Chemother., **20**, 263 (1974).
[13] *U. R. Tjaden, E. A. de Bruijn, R. A. M. van der Hoeven, C. Jol, J. van der Greef, H. Lingeman*, J. Chromatogr. **420**, 53 (1987).
[14] *J. A. Sophianopoulos, S. J. Durham, A. J. Sophianopoulos, H. L. Ragsdale, W. O. Cropper*, Arch. Biochem. Biophys., **187**, 132 (1978).

Received: July 22, 1987
Accepted: Aug. 5, 1987
F

Surface Treatment and Porosity Control of Porous Silica Microspheres

R. W. Stout* / G. B. Cox / T. J. Odiorne

E. I. du Pont de Nemours & Co., Inc., Glasgow Site, Wilmington, DE 19898, USA

Key Words

High performance liquid chromatography
Porosity silica microspheres
Ammonium bifluoride
Pore size surface acidity

Summary

Porous silica microspheres (PSM) have been treated with ammonium bifluoride to adjust porosity, pore size, remove surface impurities, and minimize surface acidity. The porosities of four silicas having mean pore diameters ranging from 150 to 750 Å have been altered from initial values to the point at which the mechanical strength is insufficient to allow packed columns with acceptable performance. It is shown that a linear relationship exists between a change in porosity and the relative amount of ammonium bifluoride used to treat the silica. This reagent removes silica homogeneously from all pores in a given microsphere in a controllable and predictable manner. This treatment increases the peak capacity and improves chromatographic performance. The surfaces of treated silicas were probed with thiamine in the ion-exchange chromatographic mode. The slopes and intercepts of plots in which retention is plotted against the reciprocal of buffer concentration were both significantly reduced indicating that surface acidity is minimized by this treatment.

Introduction

R. K. Iler [1] developed a process for producing uniform-sized spherical microspheres from a variety of metal oxides. In this process, urea and formaldehyde are polymerized at low pH in the presence of colloidal particles. Coacervated liquid droplets are formed having spherical shape which settle from the reaction medium and are subsequently harvested and dried. These spherical materials are fired at elevated temperature to burn out the polymer binder leaving porous inorganic microspheres which are well suited for high performance liquid chromatography (HPLC). When silica is selected as the metal oxide, then porous silica microspheres (PSM) are produced. PSM packing materials have been prepared with various bonded phase ligands using molecular monolayer chemical bonding techniques and have been sold under the trade name "Zorbax®" for more than a decade. Numerous chromatographic experiments have been performed using these packings and the results of several of these have been reported [2–6].

The PSM materials have many physical properties which directly relate to their utility as chromatographic supports. The microsphere mean diameter is determined by process variables. The process produces a narrow mean size distribution and the mean pore diameter can be controlled independently by selecting different sizes of silica sol in the range of 50 to 4000 Å. The naturally spherical shape allows the materials to be packed in close random geometrical arrangement in column blanks. This yields a very stable packed bed which has minimal tendencies toward settling, collapse or channeling. PSM packings are quite rigid and can withstand large inlet operating pressures up to 350 bar, in most cases. The strength of the materials appears to be related to how many sol particles comprise the aggregate and also on the degree of sintering. The high temperature firing step of the process produces "necks" among the sol particles which are in mutual contact. The relative size or thickness of the neck depends on the degree of sintering which is proportional to temperature and time of the firing step. The actual size is a function of temperature, time, impurities, and sol size. The resultant pore structure is an open network effectively devoid of closed pores or "ink bottles" and small molecules may explore the entire pore region.

Studies on porosity have indicated that the number of contact points per sol particle is about 5 for PSM materials [2]. Thus, each particle is sintered to five of its nearest neighbors. If the degree of sintering remains constant, then the absolute strength of the microsphere is proportional to the number of particles in the aggregate at constant volume

0009-5893/87 0602-11 $03.00/0

© 1987 Friedr. Vieweg & Sohn Verlagsgesellschaft mbH

and thus depends on the sol size. As the sol size is increased to vary mean pore diameter, the strength of the microsphere decreases. To compensate for this effect and maintain minimum crush resistence levels, the larger pore size materials (500–4000 Å) are processed at a higher temperature to increase the degree of sintering. A direct consequence of this measure is a sacrifice of specific pore volume (σ).

The porosity of PSM and other chromatogrpahic packings has been well studied [1–12]. Knox and McLennan [10] have investigated highly porous silica gels in the size-exclusion chromatographic (SEC) mode and compared their findings with several other silicas. Unger et al. [11] have investigated the influence of pore size, surface area, and porosity on chromatographic performance and suggested that the values of these parameters should be adjusted depending on the intended chromatographic mode of operation. Englehardt and Muller [2] studied the physical properties of various silicas and also reported on the pH of the silica surfaces. Surface pH directly influences the retention and peak shape of ionizable solutes. Zorbax® was found to have the lowest pH of all silicas examined. Surface acidity and its effect on basic solutes have been studied by Köhler et al. [13, 14] and methods have been devised to minimize the isolated acidic silanols believed to be present on the surface.

To summarize the findings above: it is apparent that Zorbax® PSM chromatographic packing materials generally yield the lowest specific pore volume and often have more acidic surface character when compared to other materials. Measures to enhance the porosity and minimize the surface acidity form the basis of this paper.

Theory

Porosity Control

Consider an empty cylindrical chromatographic column blank. The total volume inside, neglecting the volume of the frits and fittings, is:

$$V_c = \pi \left(\frac{d}{2}\right)^2 L \qquad (1)$$

where d is the inside diameter (mm) and L is the column length (mm).

When the tube is filled with porous silica microspheres in a random close-packed arrangement, then all volumes inside the tube can be accounted for by:

$$V_c = V_0 + V_s + V_p + V_1 \qquad (2)$$

where V_0 is the total volume in the interstitial space around the spheres, V_s is the volume occupied by the solid silica support, V_p is the pore volume and V_1 is the volume occupied by any bonded phase ligand. When the column is optimally packed, $V_0 \simeq 0.4\,V_c$. Let θ be defined as the volume fraction ($\simeq$ 0.6 V_c) occupied by the spheres and V_m the total volume accessible to a small molecular probe and let $V_1 = 0$, since bonded phases are not considered in this case. Then the following relationships are apparent:

$$V_0 = (1-\theta)\,V_c \qquad (3)$$

$$V_m = V_0 + V_p \qquad (4)$$

$$V_m = V_c[1-\theta\,(1-\Phi)] \qquad (5)$$

Φ is defined as the ratio of the pore volume V_p to the total volume occupied by the solid chromatographic support.

$$\Phi = \frac{V_p}{V_s + V_p} \qquad (6)$$

If silica is used as the solid support and has a density δ, then the specific pore volume $\boldsymbol{\sigma}$ can be expressed as:

$$\sigma = \frac{V_p}{V_s \delta} \qquad (7)$$

also,

$$V_p = \theta\,\Phi\,V_c \qquad (8)$$

Superscripts (^{0}) can be used to denote the initial state of a sample of porous substrate before treatment with reagents which will influence V_s and V_p. The initial state of the porous fraction can be expressed as:

$$\Phi^0 = \frac{V_p^0}{V_s^0 + V_p^0} \qquad (9)$$

A reagent which dissolves the substrate will remove some quantity of silica, V_x in volume units, and V_p will increase at the expense of V_s. Then the new porous fraction will be:

$$\Phi = \frac{V_p^0 + V_x}{(V_p^0 + V_x) + (V_s^0 - V_x)} = \frac{V_p^0 + V_x}{V_p^0 + V_s^0} \qquad (10)$$

If the volume of silica removed is a linear function of reagent, then a plot of V_x against the quantity of reagent would yield a straight line of positive slope passing through the origin. The function should be of the form:

$$V_x = m\beta\,V_s^0 \qquad (11)$$

where m is a constant and β is the weight ratio of the quantities of reagent to silica.

Eqs. (9–11) may be combined to give:

$$\Phi = \Phi^0 + m\beta\,[1-\Phi^0] \qquad (12)$$

and the slope "s" of this becomes

$$s = \frac{\partial \Phi}{\partial \beta} = m\,(1-\Phi^0) \qquad (13)$$

Eq. (12) predicts that any desired value of Φ can be obtained if the initial porous fraction Φ^0 and the slope s are known. As the weight ratio β is increased, there will be some value where $\Phi = 1$ which implies that all silica has been removed. At this limit, $m\beta = 1$ or $\beta_{max} = 1/m$. Eqs. (12, 13) will be experimentally examined in the next section to verify the assumptions implicit in their derivation.

Peak Capacity

The resolving power of a chromatographic column can be estimated by the use of a peak capacity parameter, Υ. This is defined as the number of peaks that can be separated without overlap in a given elution volume. Consequently, the peak width, as determined by theoretical plate efficiency, and a specified volume are important factors. In SEC, the separation must be accomplished within a volume equal to V_p. An expression may be derived which relates Υ and Φ.

Peak capacity, Υ, is given by Giddings [17] and Knox [10] for the size-exclusion mode:

$$\Upsilon = 1 + 0.6\, N^{1/2} \log_{10} \frac{V_p + V_0}{V_0} \qquad (14)$$

This can be combined with eqs (3) and (8) to give:

$$\Upsilon = 1 + 0.6\, N^{1/2} \log_{10} \frac{\theta\,\Phi + (1-\theta)}{(1-\theta)}$$

and for $\theta = 0.6$

$$\Upsilon = 1 + 0.6\, N^{1/2} \log_{10} [1.5\,\Phi + 1] \qquad (15)$$

It should be noted that there are several simplifying assumptions inherent in eq. (14), such that the prediction of an increase in Υ with inreasing Φ is correct in direction but only approximate in magnitude.

Surface Acidity

Retention in liquid chromatography is given by:

$$k' = \phi K \qquad (16)$$

where

$$k' = \frac{V_r - V_m}{V_m} \qquad (17)$$

and ϕ is the phase ratio while K is the distribution constant.

The distribution constant is the ratio of the concentrations of solute in the stationary phase to the mobile phase. The phase ratio may have several definitions and the choice depends on the chromatographic mode of operation [16]. For purposes of acidity measurement, ϕ is assumed to be proportional to fixed properties of the column and is not related to the concentration of ionogenic sites present on the silica surface. Such an assumption is necessary since ϕ and K cannot be separated mathematically or independently determined by any known experimental techniques. This assumption must be extended to include comparison of silica surfaces in which the surface area, specific pore volume, and other parameters are significantly altered.

For a cation exchange separation on silica, two main equilibria are important. These are ionization of the silanol groups:

$$SiOH = SiO^- + H^+;\ K_{SiOH} = [SiO^-][H^+]/[SiOH]$$

and exchange of ions:

$$SiO^-M + NR_4^+ \quad SiO^-NR_4^+ + M^+$$

The ion-exchange equilibrium constant is given by:

$$K_{ix} = [SiO^-NR_4^+][M^+]/[SiO^-M^+][NR_4^+]$$

Under normal chromatographic conditions, the concentration of metal ions in the buffer is well in excess over both the concentration of hydrogen ions and of the solute. Thus, it may be assumed that all ionized silanol groups are associated with a metal ion and, therefore:

$$[SiO^-] = [SiO^-M^+]$$

Then the ion-exchange equilibrium constant can be expressed in terms of the silica ionization:

$$K_{ix} = \frac{[SiO^-NR_4^+][M^+][H^+]}{[NR_4^+]\, K_{SiOH}\ [SiOH]}$$

The distribution coefficient (K) for the chromatographic process is given by the ratio of the concentration of the solute in the stationary phase to that in the mobile phase:

$$K = [SiO^-NR_4^+]/[NR_4^+]$$

$$= K_{ix} \cdot K_{SiOH} \cdot \frac{[SiOH]}{[M^+][H^+]}$$

The capacity factor of a chromatographic peak is given by the product of the distribution coefficient for the retention process and the phase ratio (ϕ). Hence:

$$k'_{ix} = \phi \cdot K_{ix} \cdot K_{SiOH} \frac{[SiOH]}{[M^+][H^+]} \qquad (18)$$

At constant hydrogen ion concentration, k′ is predicted to be a function of $1/[M^+]$. If the ionic strength is varied, a plot of k′ versus the reciprocal of concentration of the competing ion should yield a straight line graph which passes through the origin. The slope of the line is a function of the concentration of silanol groups – related to the degree of hydroxylation of the surface – and to the product of the ion-exchange equilibrium constant and the silanol ionization constant. Changes in any one of these parameters will cause a change in the slope of the plot. An increase in the degree of hydroxylation of the surface of the silica can influence both the concentration of the groups and their acidity [13]. In addition, the techniques employed to achieve this may change the surface and thus the phase ratio within the system area of the silica. The plot is also expected to pass through the origin of the graph, at which the concentration of the competing ion is infinite. An intercept is due to a process or processes not involving ion-exchange chromatography occurring during the separation. These processes can be non-ionic, such as adsorption or can also involve "salting-out" (hydrophobic interaction) chromatography, in which case, there will be an increase in retention with increasing salt concentration, as has been reported for caffeine under similar conditions [15]. In the latter case, a marked deviation from linearity is expected, as the ion-exchange and salting out occur at opposite ends of the concentration range.

The capacity factor is also predicted to be a function of hydrogen ion concentration. The slope of the k′ versus $1/[M^+]$ plots is given by:

$$\text{Slope} = \phi \cdot K_{ix} \cdot K_{SiOH} [SiOH]/[H^+] \qquad (19)$$

and a plot of the logarithm of the slope against pH should yield a straight line graph.

Experimental

Silica Packing Materials

Silicas of different pore size, mean particle diameter, and specific surface area were obtained from E. I. du Pont de Nemours & Co., Inc. (Wilmington, DE, USA) and had been produced according to the method of Iler [1].

Chemicals and Reagents

Tetrahydrofuran and methanol, HPLC grade, were obtained from J. T. Baker Chemical Co. (Phillipsburg, NJ, USA) and used as received. Deionized water was produced from a Continental Water System Unit (North Wales, PA, USA). Monobasic sodium phosphate was from J. T. Baker. Thiamine was obtained from Sigma Chemical (St. Louis, MO, USA). Ammonium bifluoride was from Aldrich (Milwaukee, WI, USA). Polystyrene Molecular Weight Standards were from E. I. du Pont de Nemours & Co., Inc. (Wilmington, DE, USA).

A Du Pont Model 8800 HPLC System (Wilmington, DE, USA) was used for all SEC (size-exclusion) experiments. Acidity measurements were conducted on either a LKB GTI HPLC System (Gaithersburg, MD, USA) or a Hewlett Packard 1090 HPLC System. All detector analog data were digitized, processed, and archived using a Nelson Model 761 Interface Unit (Cupertino, CA, USA), and a Hewlett Packard 200 Series Computer System (Fort Collins, CO, USA).

Treatment of Silicas With $(NH_4)HF_2$

10g of a given silica was slurried in 50 mL H_2O in a plastic beaker with magnetic stirring. A quantity of $(NH_4)HF_2$ was dissolved in 50 mL H_2 in a different plastic beaker. The salt solution was rapidly added to the silica slurry and stirred for some known time (0.25 to 72 hours). The product was filtered using a sintered glass funnel and washed extensively with water, methanol, and Freon® 113. The silica was then oven dried at 110° and 24″ Hg vacuum for approximately one hour.

Column Filling

Columns were filled at inlet pressures of 3000 or 6000 psi using proprietary procedures.

Results and Discussion

Porosity and Peak Capacity

Iler [2] and Unger [11] have compiled data on the porosity of particle aggregates which differ in spatial geometries.

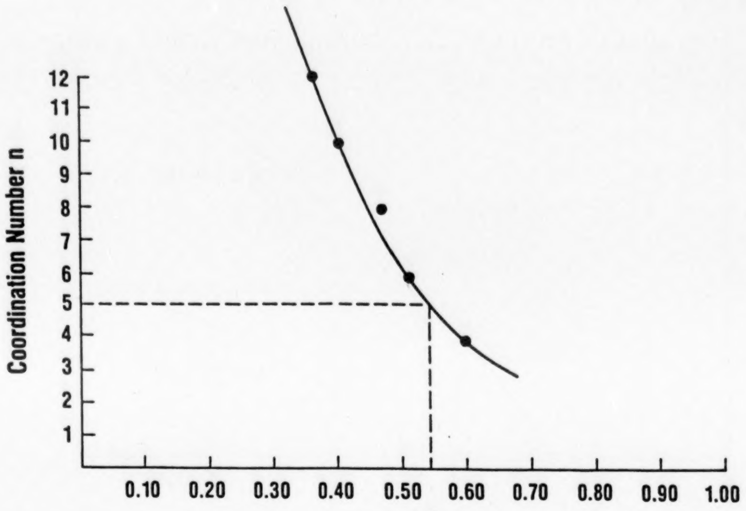

Fig. 1

Plot of coordination n versus porous fraction Φ. Data taken from Ref. [2].

Depending on the coordination number, n, the porosity of the aggregate varies with n and is independent of particle diameter. The average coordination number for Zorbax® is 5. This is illustrated in Fig. 1 which shows how the porous fraction Φ varies with n.

Knox and McLennan [10] have studied highly porous silicas along with other commercially available packing materials. Table I, compiled from their findings, illustrates the relationships among various geometrical parameters of the silicas examined. The specific pore volume σ is highest for an experimental silica SG60F and lowest for PSM (1.70 versus 0.45 $cm^3 g^{-1}$). The ratio V_0/V_c, which is equal to $1-\theta$, is nearly constant (0.4) for all silicas except the highly porous material. A significant deviation from this value is impossible to attain without crushing the packing material or underfilling the tube during column filling. The calculated value of Φ of 0.79 appears to be too large for the SG60F. All silicas listed in Table I have Φ values exceeding 0.6, except for the PSM silica which has a value of 0.51. Thus, PSM packings have ample mechanical strength, but the chromatographic parameters indicate that these materials are not optimized in terms of porosity.

This effect may be illustrated by examining Fig. 2, which was constructed from numerical data generated by eq. (15). The peak capacity (ϒ) increases for an increase in either theoretical plate efficiency N or porous fraction Φ or both. For a column with N = 10,000, ϒ will increase from 13.3 to 17.7 when Φ is independently increased from 0.4 to 0.6.

Table I. Geometrical parameters of porous silicas*.

Packing	$\frac{V_p}{V_0}$	$\frac{V_s}{V_0}$	$\frac{V_0}{V_c}$	$\frac{V_p}{V_c}$	$\frac{V_s}{V_c}$	$\frac{V_s}{V_s+V_p}$	β	Φ	σ cm^3g^{-1}
Hypersil®	0.81	0.52	0.43	0.35	0.22	0.39	NA	0.61	0.71
SG60F	1.53	0.41	0.34	0.52	0.14	0.21	NA	0.79	1.70
PSM	0.70	0.70	0.42	0.29	0.29	0.50	NA	0.51	0.45
LiChrosphere®	0.96	0.55	0.40	0.38	0.22	0.37	NA	0.64	0.79
Porasil®D	1.00	0.50	0.40	0.40	0.25	0.38	NA	0.67	0.91

*Data from Ref. [10]

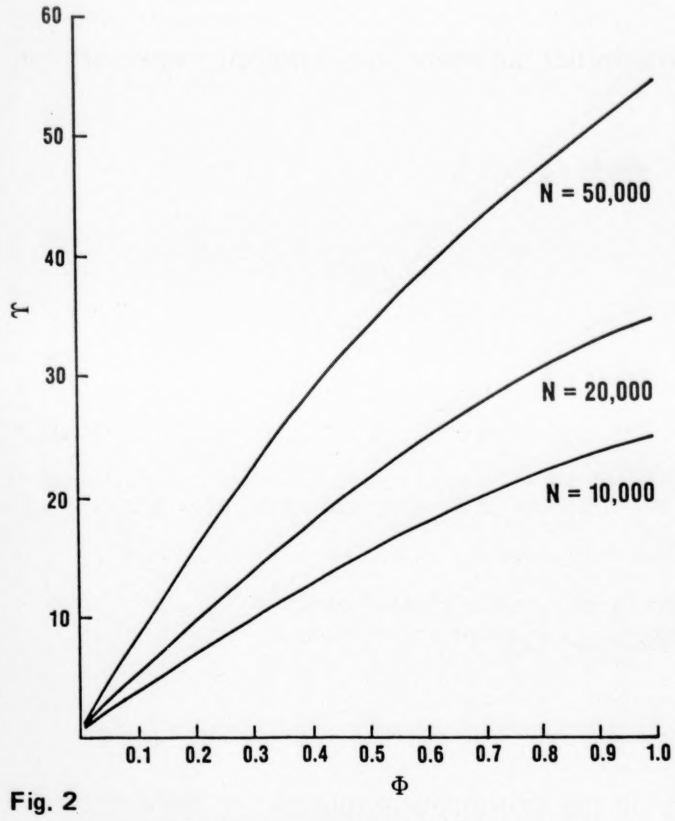

Fig. 2

Plot of peak capacity ϒ versus porous fraction Φ. Numerical data generated by eq. (15).

Thus, the resolving power of columns used in size-exclusion or gel filtration modes of operation may be significantly enhanced by adjusting Φ up to a suitable limit commensurate with mechanical strength which directly influences packed bed stability. This limit is approximately 0.65.

The first experiment was conducted using Zorbax® PSM 150. The reagent weight ratio β and reaction times t were varied within wide limits. The resulting silicas were packed in 9.4 mm i.d. × 250 mm length columns ($V_c = 17.34 cm^3$) and subjected to chromatographic measurements. Samples of each silica were submitted for specific surface area measurements (S_{BET}). Size-exclusion chromatography (SEC) was used to measure essential chromatographic geometrical parameters using THF (tetrahydrofuran) as mobile phase. Samples were prepared from contrived mixtures of polystyrene molecular weight standards (PS MW).

Effect of $(NH_4)HF_2$ on Porous Silica Microspheres

Ammonium bifluoride, $(NH_4)HF_2$, was selected as a reagent to homogeneously dissolve SiO_2 from the surface of porous silica microspheres. Other salts have been used in experiments employing hydrothermal methods [18], however, no clear mechanism describing changes in geometrical parameters were found when fluoride and other anions were used at neutral pH. Indeed, only the use of phosphate resulted in changes in specific pore volume.

Results of the preliminary experiments on PSM 150 (150 Å pore diameter) are given in Table II. These results describe the effect of removing silica from the microsphere surface. For a reaction time of 1 hour, V_m is observed to increase from 12.40 to 13.54 cm^3, as β is increased from 0 to 1.01. A corresponding decrease in the weight of silica inside the column, W, is observed. When the reaction time was extended to 72 hours, similar results are observed, but the additional reaction time causes another effect in which some silica is slowly redeposited. This effect was not studied in detail.

Results from B.E.T. measurements must agree with these obtained by SEC methods. Reasonable agreement is found by noting that the pore volumes obtained by B.E.T. (Table II V,N_2 e.g. mL liquid per gram) follow those corresponding values measured by SEC methods within experimental error. If eq. (7) is rearranged to solve for the density of silica, then with the data from Table II, the value obtained is $\delta = 2.21$ (range 2.19 to 2.39), which is very close to the accepted value of 2.20. Vespalec et al. [18] and Verzele et al. [19] find different values of δ ranging from 1.6 to 2.4 gcm which are explained by postulating the existence of micropores. The Zorbax® process uses pure SiO_2 with the accepted value (2.20 gcm^{-3}) and is devoid of micropores [8].

Fig. 3A shows a plot of the average pore diameter D_p versus the ratio β for PSM silicas 150 A, B, C from data in Table II. A linear relationship ($R^2 = 0.9998$) with limited data is observed which implies that the $(NH_4)HF_2$ removes silica in some homogeneous manner. The results also suggest that this method may be used to select any desired average pore diameter commensurate with porosity or stability limitations.

Table II. Chromatographic and nitrogen desorption results for PSM 150 treated with $(NH_4)HF_2$.

Silica Designation	$(NH_4)HF_2$ Treatment		Nitrogen Desorption Measurements			SEC Results						
			Surface area	Pore Dia.	Pore Vol.							
	β	t (hr)	S_{BET} (m^2g^{-1})	D_p (Å)	V, N_2 (cm^3g^{-1})	V_0[1] (cm^3)	V_m[2] (cm^3)	V_p (cm^3)	V_s (cm^3)	W[3] (g)	σ[4] (cm^3g^{-1})	Φ
150 A	0	0	121	160	0.49	7.18	12.40	5.22	4.94	11.01	0.47	0.514
150 B	0.335	1	120	179	0.58	7.24	12.76	5.52	4.58	9.76	0.57	0.547
150 C	1.01	1	155	215	0.84	6.98	13.54	6.55	3.81	8.46	0.77	0.633
150 D	0.335	72	141	178	0.62	7.05	12.63	5.58	4.71	10.07	0.55	0.542
150 E	1.01	72	159	220	0.87	6.70	13.44	6.74	3.90	8.50	0.79	0.633

1) V_0 measured by elution volume (V_R) of 1.8×10^{-6} MW Polystyrene Standard. 2) Vm measured by elution volume of toluene.

3) W determined by weighing the contents of the column after chromatographic experiments. 4) Calculated from the ratio V_p/W.

Since it is generally accepted that HF reacts with SiO_2 to form SiF_4 and subsequently hydrolyzes, it appears that four moles of $(NH_4)HF_2$ will react with one mole of silica quantitatively under these conditions. The formula weight of silica is taken as 60.1 and 57.04 for the reagent. Thus from eq. (12) when all silica is dissolved, β_{max} must have a value of 3.8 and $m\beta = 1$. Substituting this into eq. (12) gives the result that $\Phi = 1$ indicating total porosity which, of course, has no physical meaning. The theoretical value of m must then be 0.263.

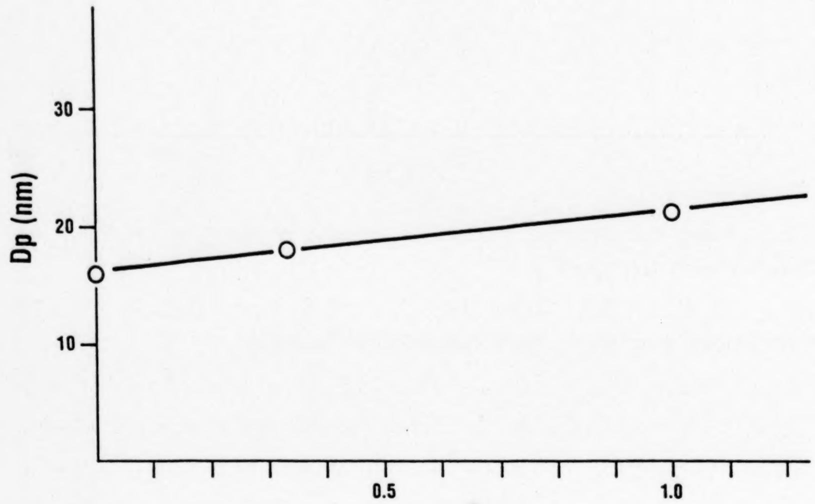

Fig. 3A

Plot of average pore diameter D_p versus β for PSM 150. Data taken from Table II for t = 1 hour.

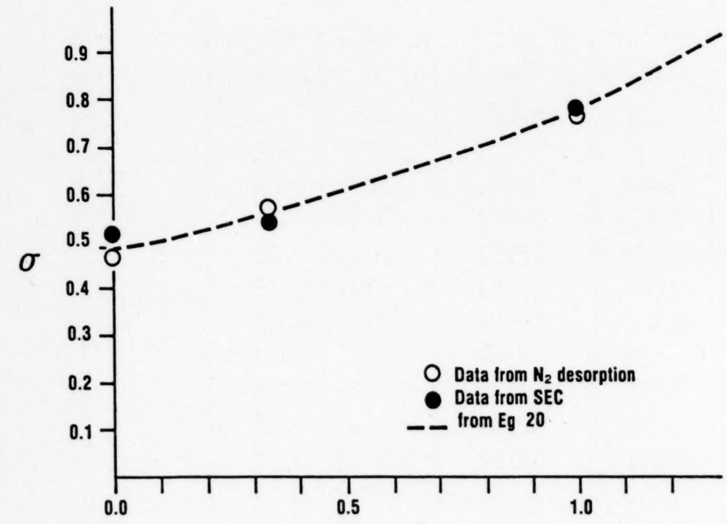

Fig. 3B

Plot of specific pore volume σ versus β for PSM 150.
(●), experimental points taken from Table II for t = 1 hour
(○), values calculated from eq. (7).
(– – –) is the theoretical function generated by eq. (20).

If eqs. (6), (7), and (12) are combined using the superscripts (^{0}) to denote initial parameter states before treatment with the reagent then:

$$\sigma = \frac{\sigma^0 \delta + m\beta}{\delta(1 - m\beta)} \tag{20}$$

Experiments were devised to investigate this relation of σ and β. σ was determined both by direct physical measurement using nitrogen desorption and by a combination of chromatographic measurements and a knowledge of the weight of silica with the column. Fig. 3B shows a plot of σ values determined by both procedures against β. The dashed line is the theoretical curve derived from eq. (20). There is obviously a good fit between the two experimental determinations and the theoretical relation which prompted us to widen the scope of the experiments.

Effect of $(NH_4)HF_2$ on Pore Structure

More elaborate experiments were designed based on the results obtained above to examine the effect of $(NH_4)HF_2$ on silicas of different values of Φ^0, σ^0, and S^0_{BET}. PSM 300 was selected and the column dimensions were reduced to 6.2 mm i.d. × 250 mm (V_c = 7.55 cm). β was varied from 0 to 1.2, while the reaction time was reduced to 15 min. The results are given in Table III. Since smaller column volumes (V_c) are used, the data must be less precise. Constant column filling parameters were employed for all silicas. In our experience, optimal theoretical plate efficiency of packed columns requires adjustments in filling parameters for each silica so the apparent increase in N and lowering of skew may not be taken as clear evidence of improved chromatographic performance in this case, although Vespalec et al. [18] observed such effects.

The effects of the ammonium bifluoride on pore structure were examined for PSM 300 (300 Å) Table VIII gives the elution volumes, V_R, for several PS MW standards. Fig. 4 shows a plot of log PS MW against V_R. It is observed that the incremental increase in V_R for any selected PS is roughly proportional to the amount of reagent used in the PS MW range 9000 to 50,000. For larger PS MW standards, the difference in V_R becomes smaller. This trend is expected since the reagent should remove SiO_2 from the surface of all pores to the same extent, but the change in pore diameter will be greater for the smaller pores. Fig. 4 clearly indicates that the reagent homogeneously removes SiO_2 from the microspheres.

Table III. Chromatographic results for PSM 300 treated with $(NH_4)HF_2$.

Silica Designation	V_0 (cm^3)	V_m (cm^3)	V_p (cm^3)	V_s (cm^3)	β	Φ	σ (cm^3g^{-1})	N	Skew
300 A	3.50	5.76	2.26	1.78	0.00	0.558	0.573	9622	0.45
300 B	3.50	5.77	2.27	1.78	0.20	0.560	0.580	14275	0.48
300 C	3.39	5.94	2.55	1.61	0.40	0.613	0.720	16178	0.62
300 D	3.28	5.99	2.71	1.56	0.60	0.635	0.790	18651	0.31
300 E	3.31	6.13	2.82	1.42	0.80	0.665	0.902	21322	0.35
300 F	3.25	6.33	3.08	1.22	1.20	0.716	1.148	19399	0.09

Similar studies were conducted on PSM 500 (500 Å and the results are given in Table IV. In this case, the column filling inlet pressure was reduced from 6000 psi to 3000 psi for $\beta > 0.8$. This reduction was necessary to avoid crushing the microspheres. Stable columns were produced at this level (500 K. L) with acceptable efficiency. Similar results are tabulated for PSM 1000 (750 Å) and listed in Table V. The columns were all loaded at inlet pressures of 3000 psi to avoid crushing as above. When $\beta = 1.2$, a skew of 1.43 was noticed and further attempts to increase Φ were abandoned. The PSM 1000 Å silica had $\Phi^0 = 0.437$, the lowest of the silicas studied and this was increased to $\Phi = 0.58$ (PSM 1000 F) when $\beta = 1.0$.

Detailed experiments on column bed stability were not conducted since the focus of these experiments was on Φ and surface acidity.

From the Theory Section, eq. (12) predicts that Φ will be a linear function of β and that the slope would be dependent on the initial porous fraction Φ^0. Table VI shows the slopes from experimental results and Fig. 5 shows a plot of data obtained from Tables II–V. The expected linearity is observed. Given the initial porous fraction of any silica, the desired new porous fraction Φ can be conveniently estimated by this method. V_0 and V_m, from eq. (5), may be calculated in advance.

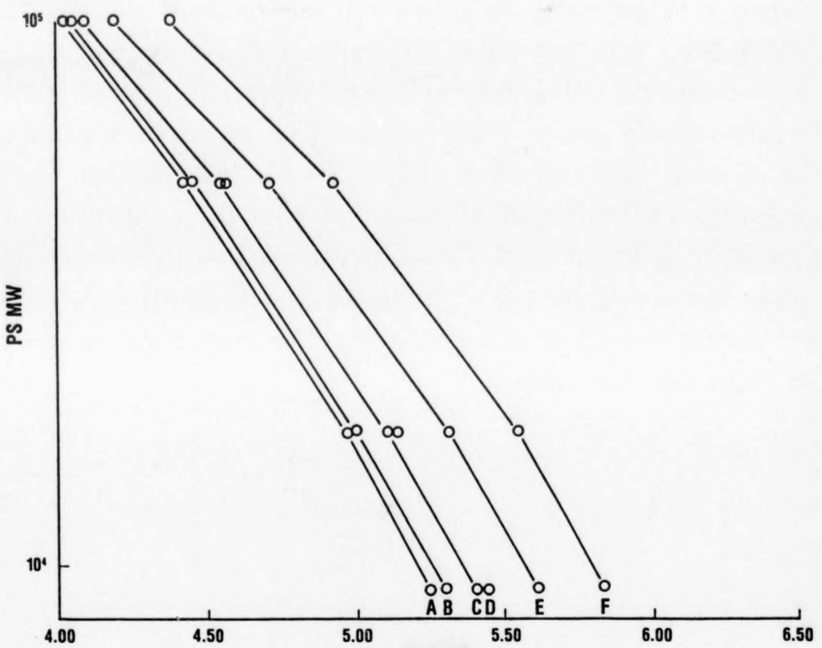

Fig. 4

Plot of log Polystyrene molecular weight versus V_R for PSM 300 treated with $(NH_4)HF_2$.

A: $\beta = 0$; B: $\beta = 0.2$; C: $\beta = 0.4$; D: $\beta = 0.6$; E: $\beta = 0.8$; F: $\beta = 1.20$. Conditions as given in the Experimental Section.

Table IV. Chromatographic results for PSM 500 treated with $(NH_4)HF_2$.

Silica Designation	V_0[3) (cm^3)	V_m[4) (cm^3)	V_p (cm^3)	V_s (cm^3)	β	Φ	σ (cm^{3}g^{-1})	N	Skew
500 A[1)	3.34	5.43	2.09	2.10	0.00	0.496	0.448	19378	0.64
500 B[1)	3.31	5.51	2.20	2.04	0.10	0.531	0.490	15881	1.04
500 C[1)	3.33	5.56	2.23	1.99	0.12	0.528	0.509	19010	0.88
500 D[1)	3.31	5.57	2.26	1.98	0.14	0.533	0.519	21727	0.93
500 E[1)	3.29	5.55	2.26	2.00	0.16	0.531	0.513	21686	0.64
500 F[1)	3.25	5.54	2.29	2.01	0.18	0.533	0.518	19386	0.92
500 G[1)	3.28	5.54	2.26	2.01	0.20	0.529	0.511	19715	0.75
500 H[1)	3.30	5.62	2.32	1.93	0.40	0.546	0.546	15481	0.90
500 I[1)	3.38	5.80	2.42	1.75	0.60	0.580	0.629	13409	0.52
500 J[1)	3.19	5.85	2.26	1.70	0.80	0.610	0.711	17133	0.43
500 K[2)	3.10	6.05	2.95	1.50	1.20	0.663	0.893	17467	0.80
500 L[2)	3.14	6.25	3.11	1.30	1.40	0.705	1.087	17993	0.80

[1)]Columns filled using constant inlet pressure of 6000 psi. [2)]Inlet pressure of 3000 psi. [3)]V_0 measured with 9 X 10^{6}MW polystyrene standards. [4)]V_m measured with toluene.

Table V. Chromatographic results for PSM 1000 treated with $(NH_4)HF_2$.

Silica Designation	V_0 (cm^3)	V_m (cm^3)	V_p (cm^3	V_s (cm^3)	β	Φ	σ (cm^{3}g^{-1})	N	Skew
1000 A	3.43	5.23	1.80	2.32	0.00	0.437	0.353	25025	0.38
1000 B	3.32	5.38	2.06	2.17	0.20	0.487	0.432	20024	0.24
1000 C	3.34	5.40	2.06	2.15	0.40	0.489	0.436	23443	0.58
1000 D	3.40	5.56	2.16	1.99	0.60	0.520	0.493	25723	0.54
1000 E	3.33	5.49	2.16	2.06	0.80	0.511	0.477	24563	0.47
1000 F	3.34	5.78	2.44	1.77	1.00	0.580	0.626	24704	0.42
1000 G	–	–	–	–	1.20	–	–		1.43

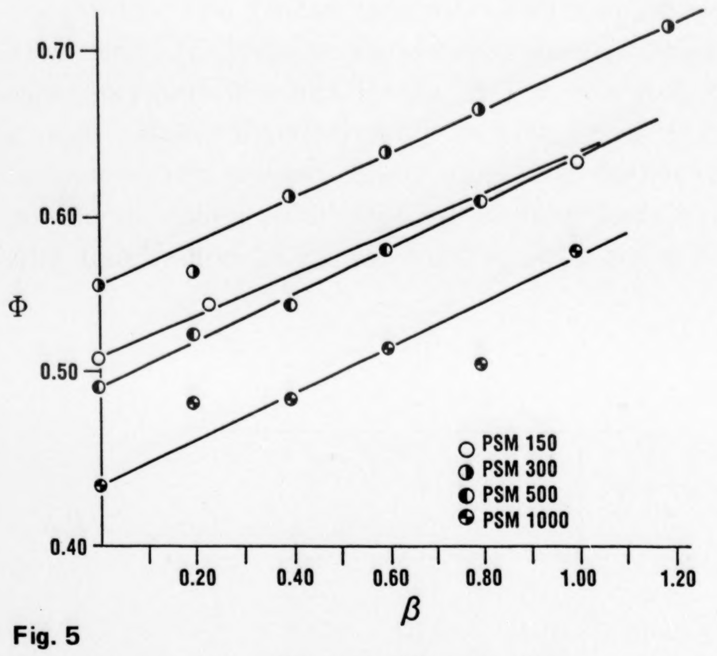

Fig. 5

Plot of Φ versus β for PSM 150, 300, 500, 1000.

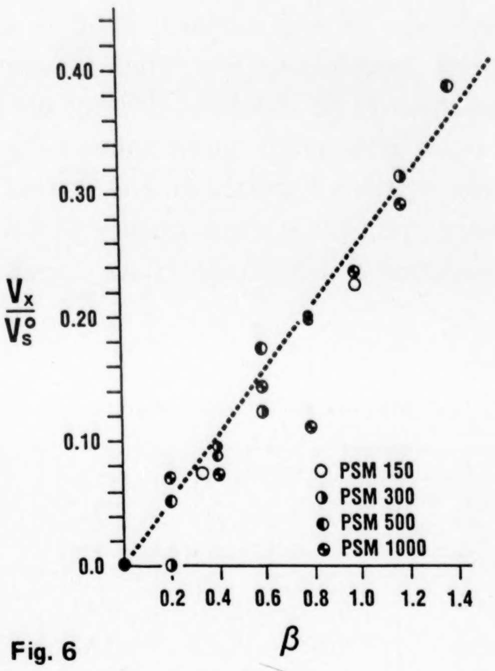

Fig. 6

Plot of $\frac{V_x}{V_s^0}$ versus β.

Table VI. Results of linear least squares regression fit to data.

PSM	Φ°	Slope, S	Correlation Coefficient	m*
150	0.511	0.1201	0.99859	0.246
300	0.560	0.1236	0.99007	0.281
500	0.494	0.1455	0.99756	0.288
1000	0.446	0.1167	0.92866	0.211

*Calculated from eq. (13)

Since $V_x = m\beta V_s^0$, the V_x values may be calculated from Tables II–V for all values of β. If (V_x/V_s^0) is then plotted against mβ, a straight line of slope 0.263 should result which passes through the origin. Such a plot is shown in Fig. 6, and indicates good correlation with theory.

The fit to theory might well be improved if the purity of the reagent is taken into account, but this area was not investigated. The use of larger columns would reduce errors in V_R, but it was not anticipated that this measure would give results sufficiently different from those reported to justify the effort.

Figs. 7A, B show the chromatographic effects of enhanced resolution by adjusting Φ. Fig. 7A shows the separation of PS MW standards on PSM 1000 using SEC. Fig. 7B shows the improvement in resolution where β = 1.20. A similar effect can be seen by comparing Figs. 8A, B for PSM 300. V_R data and peak identities for Figs. 7A, B and Figs. 8A, B are given in Table VIII. Treatment of the silicas with $(NH_4)HF_2$ results in an increase in resolution for all peaks.

Surface Acidity Experiments

As outlined in the Theory Section, the slope of a plot of k′ against reciprocal metal ion concentration for a solute which undergoes ion-exchange chromatography on silica has a number of components. Of these, the ion-exchange equilibrium constant is not expected to be a strong function of small changes in the acidity of the silanol groups or

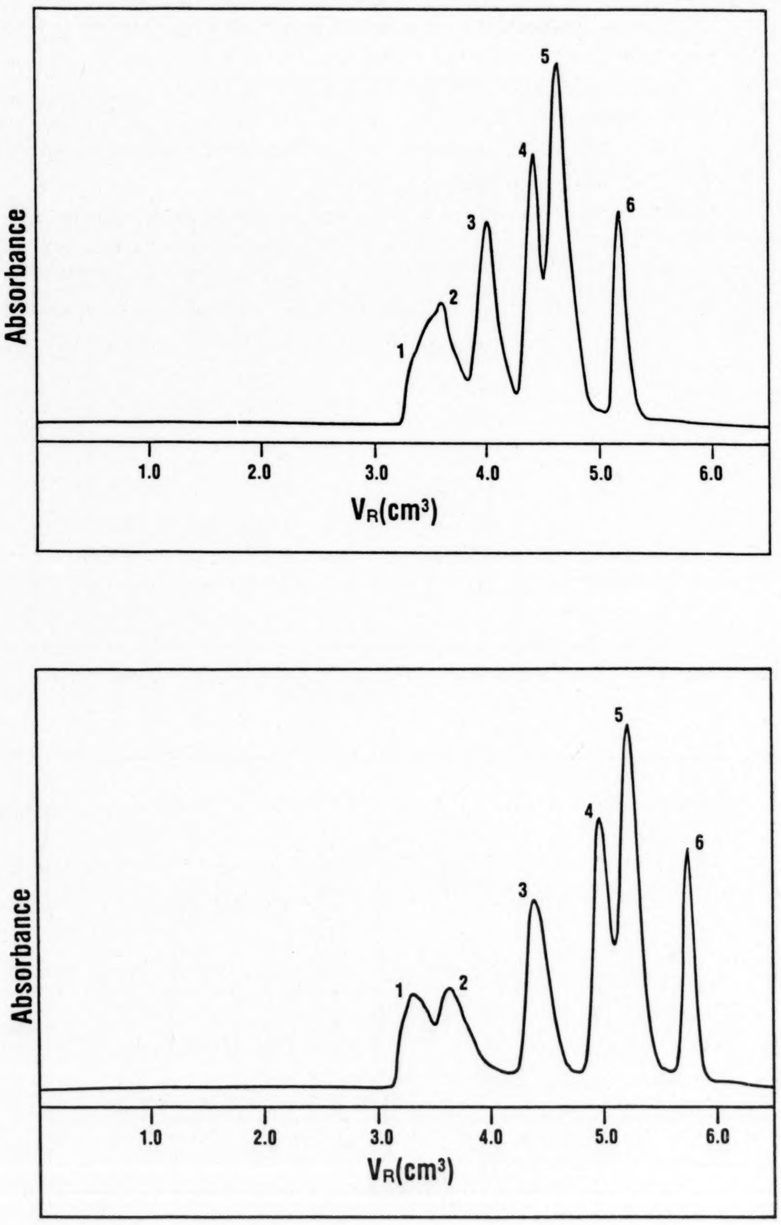

Fig. 7A, B

Comparison of chromatographic results of the separation of polystyrene molecular weight standards on treated and untreated PSM 1000.

7A: β = 0; 7B: β = 1.2; flow rate: 1.00 $cm^3 min^{-1}$; mobile phase: THF, peak identities given in Table VIII.

the degree of hydroxylation of the surface as it is a property of the ionized hydroxyls. For the present purposes, this will be assumed to be constant. The remaining factors are much more dependent upon these parameters. The concentration of silanol groups on the surface of silica can vary depending upon the thermal history of the material. Thermal analytical techniques have been employed to measure this for heat-treated, non heat-treated, and rehydroxylated heat-treated silicas [13]. This work suggests that the surface silanol concentration can range between 5 and 8 μmol m^{-2} for different silicas. Thus, a rehydroxylation procedure could increase the concentration of surface silanols by some 60% which should be reflected in the slope of the k′ versus 1/[sodium] plot. It is

Table VII. Geometrical parameters of porous silicas.

Packing	$\frac{V_p}{V_0}$	$\frac{V_s}{V_0}$	$\frac{V_0}{V_c}$	$\frac{V_p}{V_c}$	$\frac{V_s}{V_c}$	$\frac{V_s}{V_p+V_s}$	β	Φ	σ cm^{3}g^{-1}
PSM 150	0.73	0.69	0.41	0.30	0.28	0.49	0.00	0.51	0.48
PSM 150	0.76	0.63	0.42	0.32	0.26	0.45	0.33	0.53	0.55
PSM 150	0.94	0.55	0.40	0.38	0.22	0.37	1.01	0.63	0.78
PSM 300	0.72	0.54	0.44	0.32	0.24	0.43	0.00	0.57	0.61
PSM 300	1.01	0.41	0.41	0.42	0.17	0.29	1.20	0.70	1.10
PSM 500	0.63	0.63	0.44	0.28	0.28	0.50	0.00	0.50	0.45
PSM 500	0.99	0.41	0.42	0.41	0.17	0.29	1.40	0.70	1.10
PSM 1000	0.52	0.68	0.45	0.24	0.31	0.56	0.00	0.43	0.35
PSM 1000	0.73	0.53	0.44	0.32	0.23	0.42	1.00	0.57	0.75

Table VIII. Retention volumes of $(NH_4)HF_2$ treated and untreated Zorbax®.

Polystyrene MW (Daltons)	PSM 300 Retention volume and Peak Identity V_R (cm^3)			PSM 1000 Retention Volume and Peak Identity V_R (cm^3)		
	V_R $\beta = 0$	V_R $\beta = 1.20$	Peak Number	V_R $\beta = 0$	V_R $\beta = 1.20$	Peak Number
9,000,000	—	—		∿ 3.60	3.31	1
1,800,000	3.33	3.12	1			
900,000	—	—		∿ 3.60	3.64	2
233,000	3.56	3.54	2	4.02	4.41	3
100,000	4.03	4.38	3	4.43	4.98	4
50,000	4.43	4.94	4	4.64	5.24	5
17,500	4.97	5.55	5	—	—	
9,000	5.25	5.84	6	—	—	
92	5.74	6.28	7	5.18	5.75	6

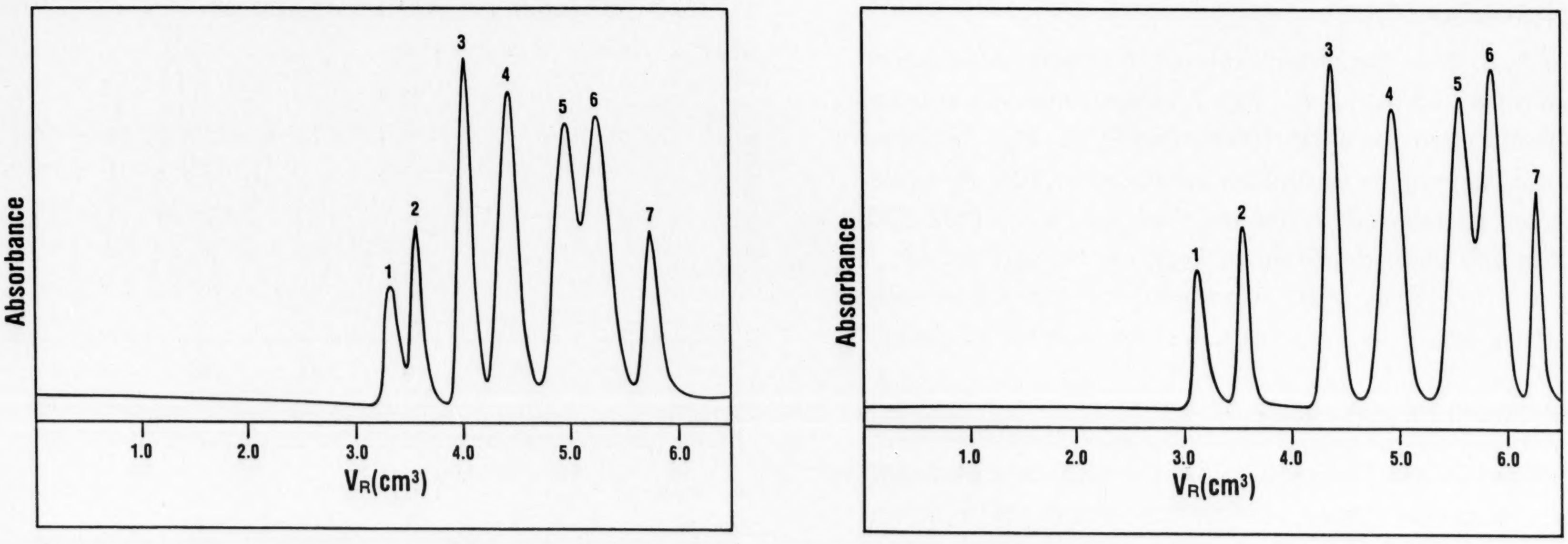

Fig. 8 A, B

Comparison of chromatographic results of the separation of polystyrene molecular weight standards on treated and untreated PSM 300.

8A: $\beta = 0$; 8B: $\beta = 1.2$; chromatogrpahic conditions: same as Fig. 7A, 7B; peak identities given in Table VIII.

Table IX. Surface acidity of PSM 300 and 500 treated with ammonium bifluoride.

Silica	β	k^1 (0.2M)	k^1 (0.02M)	Slope	Intercept
PSM 500	0	0.57	0.84	0.0032	0 651
	0.12	0.24	0.25	0.0001	0.242
	0.14	0.21	0.22	0.0001	0.218
	0.16	0.23	0.22	−0.0002	0.231
	0.20	0.19	0.21	0.0003	0.191
	0.40	0.22	0.31	0.0018	0.207
	0.60	0.19	0.22	0.0005	0.190
PSM 300	0	0.86	1.35	0.0091	0.814
	0.2	0.25	0.42	0.0033	0.227
	0.4	0.26	0.35	0.0017	0.247
	0.6	0.27	0.37	0.0020	0.256
	0.8	0.25	0.36	0.0020	0.244
	1.2	0.25	0.34	0.0017	0.240

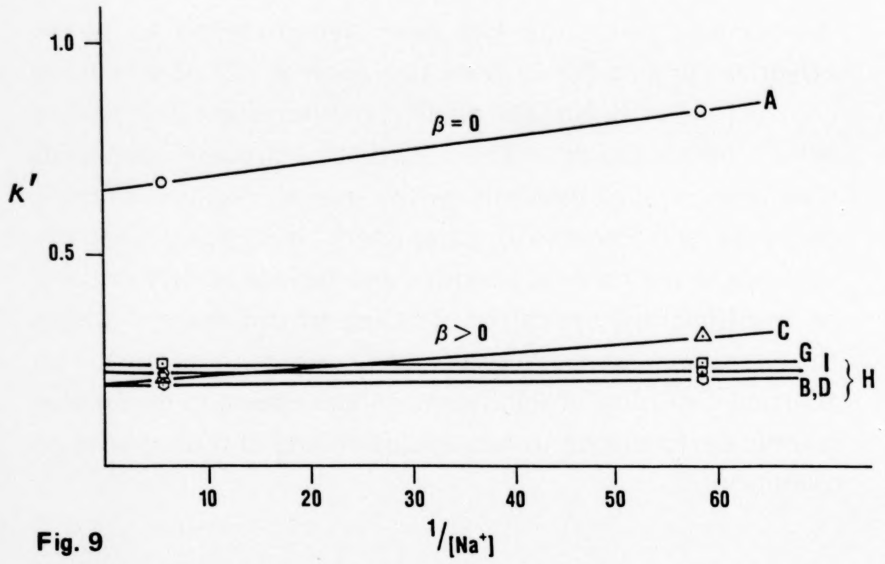

Fig. 9

Plot of k' of Thiamine versus 1/[Na$^+$] for PSM 500.

A: $\beta = 0$; B: $\beta = 0.1$; C: $\beta = 0.12$; D: $\beta = 0.14$; G: $\beta = 0.2$; H: $\beta = 0.4$; I: $\beta = 0.6$.

Conditions: Column: 25 cm × 6.2 mm. Mobile Phase: 15% Methanol in phosphate buffer pH 4.6. Flow Rate: 3.6 ml/min. Temperature: Ambient.

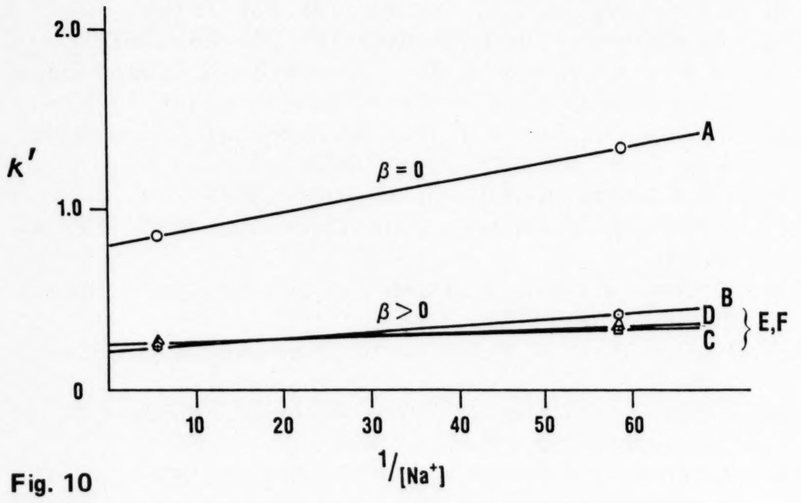

Fig. 10

Plot of k' of Thiamine versus 1/[Na$^+$] for PSM 300.

A: $\beta = 0$; B: $\beta = 0.2$; C: $\beta = 0.4$; D: $\beta = 0.6$; E: $\beta = 0.8$; F: $\beta = 1.2$. Chromatographic conditions as Fig. 9.

also claimed by the same authors (Ref. [13]) that the rehydroxylation procedure reduces the acidity of the silica surface. This should be shown as a reduction in the dissociation constant of the surface silanols and this in turn should result in a reduction in slope.

Experiments were designed to remove successive layers of silica from the surface of heat-treated silica particles in order to investigate if the effects of the dehydration occurred only at the surface or if they resulted in a deeper, more fundamental modification of the silica matrix. Chromatographic testing was carried out as detailed earlier [15] using thiamine as test solute in a methanol:phosphate buffer mobile phase. Capacity factors were measured at two sodium ion concentrations and the slopes and intercepts of the k' vs. 1/[buffer] plots were calculated. The results of experiments treating PSM 300 and 500 silicas with varying proportions of ammonium bifluoride are shown in Table IX and the corresponding graphs are plotted in Figs. 9 and 10. These data show clearly that the slope of the k' vs. 1/[buffer] plot reduces to a constant level after treatment with any of the concentrations of ammonium bifluoride, all of which correspond to removal of more than one surface layer of silica. This constancy in performance indicates clearly that the interior of the silica is uniform in structure and in these cases, at least, is quite different from its surface which is presumably most affected by dehydration processes occurring during the sintering of the particle. The data also show that any effect on the slope from an increase in surface silanol concentration by removal of the original surface is more than offset by the reduction in acidity. It is also of interest to note that the intercept is reduced approximately three-fold by the treatment and this too is independent of the quantity of ammonium bifluoride used. This implies that a considerable part of the secondary non-ionic retention mechanism is influenced either by the surface acidity or by the degree of hydroxylation.

Experiments were also carried out with smaller pore silicas. These were expected to allow more accurate measurement of the effects because of the larger surface area, higher phase ratio and, therefore, larger k' values expected for the thiamine. A measurement of slope and intercept was made for a PSM 100 (100 Å) packing (which had received only an acid treatment) at each of pH values of 2.1, 4.6 and 7.0. According to the earlier discussion, the value of the slopes were expected to be a log-normal function of pH. The data are shown in Table X and the plot of logarithm of the slope vs pH is shown in Fig. 11. This plot is linear, as predicted, although the value of its slope is not unity as would be expected from the equation.

The values of slope and intercept for some PSM 150 silicas were also determined. These were materials which had been both acid and bifluoride treated. These data are shown in Table X. The ammonium bifluoride treatment showed a clear effect for the PSM 150 samples labelled (a) and (d).

Because the slope and intercept data contain the phase ratio as part of their value, in principle, it should be possible to normalize them with respect to the surface area of the silicas. Table X also shows values for the slopes and intercepts obtained by division by the nominal surface area of the packing materials. These values are all the same order of magnitude which suggests that although this is broadly the right approach, other factors exist which influence the ultimate values obtained. There may be impurities within the silica which influence its ion-exchange properties. For comparison, data from a PSM 60 (72 Å) which was

Table X.

Silica	S_{BET} ($m^2 g^{-1}$)	Nitric acid treatment				Ammonium bifluoride Treatment			
		Slope	Intercept	Slope/S_{BET} × 10^4	Intercept/S_{BET} × 10^2	Slope	Intercept	Slope/S_{BET} × 10^4	Intercept/S_{BET} × 10^2
PSM 300	50	0.009	0.814	1.8	1.6	0.0021	0.243	0.42	0.49
PSM 500	20	0.0032	0.65	1.6	3.3	0.0003	0.213	0.15	1.06
PSM 150(a)	140	0.137	2.12	9.8	1.5	0.034	1.09	2.4	0.78
PSM 250(b)	140	0.088	1.75	6.3	1.3	0.032	1.10	2.3	0.79
PSM 150(c)	140	0.099	2.51	7.1	1.8	0.038	1.28	2.5	0.91
PSM 150(d)	140	0.089	2.03	6.4	1.5	0.053	1.49	3.8	1.06
PSM 150(e)	150	0.025	2.27	1.7	1.5	0.026	1.37	1.7	0.91
PSM 100	260	0.018*	1.17*	–	–	–	–	–	–
PSM 100	260	0.197	4.12	7.5	1.6	–	–	–	–
PSM 100	260	2.04**	8.00**	–	–	–	–	–	–
PSM 60	380	–	–	–	–	0.023	2.22	0.6	0.58

*at pH 2.1 **at pH 7.0

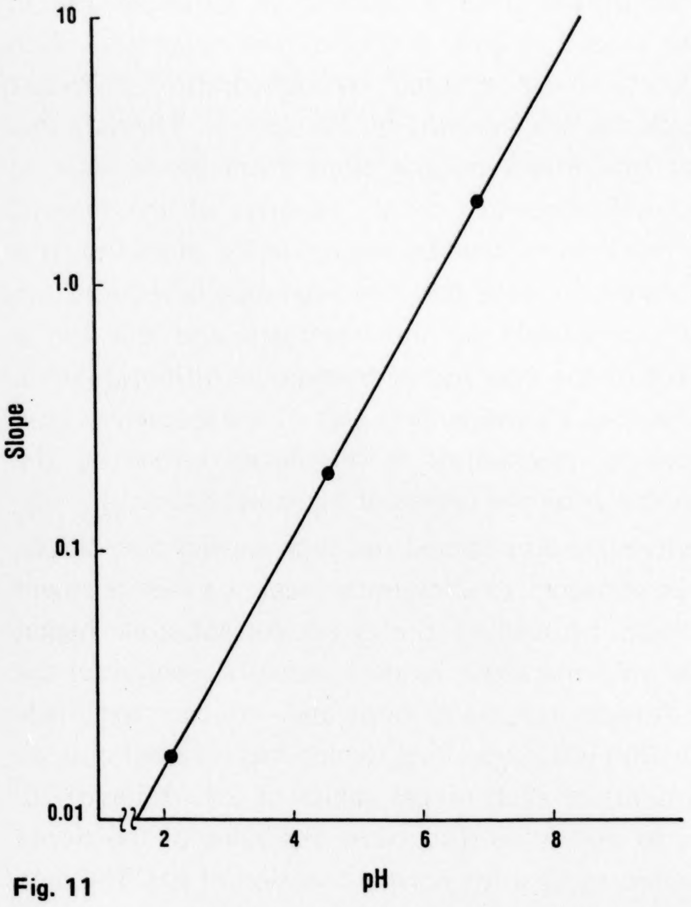

Fig. 11

Plot of slope of k' versus 1/[Na^+] graphs against pH for PSM 100. Column: 15cm × 4.6mm. Mobile Phase: 15% Methanol in phosphate buffer adjusted to pH 2.1, 4.6 and 7.0. All other conditions as Fig. 9.

prepared according to the method of Kirkland & Köhler [14] is included in the table. This fits within the spread of data observed for the materials tested here which implies that the two processes give materials of broadly equivalent surface acidity.

Acknowledgements

The authors are indebted to many people who contributed significantly to this effort: P.C. Cain slurry loaded the numerous columns. S.K. Leung performed the wet chemistry and obtained SEC data. B.J. Permar conducted the surface acidity experiments. P.K. Young typed the manuscripts. We are also indebted to L.R. Snyder for stimulating discussions, suggestions, and review of the results.

Conclusions

Ammonium bifluoride has been demonstrated to be an effective reagent for 1) pore size control, 2) pore volume control and 3) surface acidity minimization for porous silica microspheres. The Zorbax® process produces chromatographic packings with several highly desirable chemical and geometric parameters, but due to factors inherent in the process, porosity and surface acidity remained insufficiently optimized. The use of this reagent allows the porosity, pore volume, and surface acidity to be adjusted resulting in significant enhancement in chromatographic performance in size-exclusion and elution modes of operation.

References

[1] *R.K. Iler, H.J. McQueston,* U.S. Pat. 4,010,242 (1974).
[2] *R.K. Iler,* "The Chemistry of Silica", Wiley-Interscience, New York, 1979.
[3] *J.J. Kirkland,* J. of Chromatogr. **83,** 149–167 (1973).
[4] *W. Yau, C. Ginnard, J.J. Kirkland,* J. of Chromatogr. **149,** 465–487 (1978).
[5] *J.J. Kirkland,* J. of Chromatogr. **125,** 231 (1976).
[6] *J.J. Kirkland,* J. of Chromatogr. **185,** 273–288 (1979).
[7] *W. Yau, J. Kirkland, D. Bly,* "Modern Size-Exclusion Liquid Chromatography", Wiley-Interscience, New York, 1979.
[8] *C. Glinka, L. Sander, S. Wise, M. Hunnicutt, C. Lochmuller,* Anal. Chem. **57,** 2079–2084 (1985).
[9] *J.C. Giddings,* Anal. Chem. **39,** 1027 (1967)
[10] *J. Knox, F. McLennan,* J. of Chromatogr. **185,** 289–304 (1979).
[11] *K. Unger, J. Kinkel, B. Anspach, H. Giesche,* J. of Chromatogr. **296,** 3–14 (1984).
[12] *H. Engelhardt, H. Muller,* J. of Chromatogr. **218,** 395–407 (1981).
[13] *J. Köhler, D. Chase, R. Farlee, A. Vega, J. Kirkland,* J. of Chromatogr. **352,** 275–305 (1986).
[14] *J. Köhler, J. Kirkland,* J. of Chromatogr. **385,** 125–150 (1987).
[15] *G.B. Cox, R.W. Stout,* J. of Chromatogr. **384,** 315 (1986).
[16] *P. Jandera, H. Colin, G. Guiochon,* Anal. Chem. **54,** 435–441 (1982).
[17] *J.C. Giddings,* Anal. Chem. **39,** 1027 (1967).
[18] *R. Vespalec, M. Cigankova, J. Viska,* J. of Chromatogr. **354,** 129–143 (1986).
[19] *M. Verzele, C. Dewaele, D. Duquet,* J. of Chromatogr. **329,** 351–357 (1985).

Received: June 29, 1987
Accepted: Aug 1, 1987
F

Determination of Priority Pollutant Phenols by Isocratic HPLC

P. Alarcón* / A. Bustos

Centro de Investigaciones del Agua, C.S.I.C., Arganda del Rey, 28500 Madrid, Spain

B. Cañas / M. D. Andrés / L. M. Polo

Facultad de CC.Químicas, Dep. Q.Analítica, U.Complutense de Madrid, 28040 Madrid, Spain

Key Words

Liquid chromatography
Isocratic HPLC
Phenols in water
Priority pollutants

Summary

An isocratic high performance liquid chromatographic method, able to determine ng/l of Priority Pollutant Phenols (PPP) in water, is proposed. A Nucleosil 5 C18 column and an 30 mM ammonium acetate (pH 5.0): acetonitrile : methanol (56 : 34 : 10) eluent are used. Linearity ranges from 5–50 ppm of phenols; variation coefficients are about 4% (n = 7) at the 30 ppm level with a 5 μl injection. Dual UV detection helps to identify different phenols. The use of an anionic exchanger column and of methanol : hydrochloric acid (9 : 1) as eluent allows selective preconcentration of priority phenols and recoveries in the range 79–105%.

Introduction

Phenols are common water pollutants because they are extensively used as pesticides, and they may be produced during the chlorination process of water supplies [1]. The U.S. Environmental Protection Agency (EPA) has included eleven phenols on the list of priority pollutants [2], due to their toxic properties.

The 4-aminoantipyrine spectrophotometric method is the most widely used for the determination of total phenols [3]. In order to quantify the individual phenols, chromatographic methods are needed. Due to their high polarity and low vapour pressure [4], GC methods with derivatization are required [5]. HPLC is quite suitable for the separation of chloro, nitro and methyl phenols, but the differences in their chromatographic behaviour are such that ionization suppression and gradient techniques are needed to achieve good resolution in short analysis times [4].

The aim of this work is to develop an isocratic HPLC method for the determination of trace amounts of phenols specified by EPA (PPP) in waters, using analysis times shorter than those employed by gradient techniques. For this purpose ternary mobile phase systems were employed.

Experimental

Chemicals

Priority Pollutant Phenols (PPP) were purchased from Supelco, Inc. (Bellefonte, PA, USA) and were of chromatographic standard grade. HPLC grade methanol and acetonitrile were obtained from Mallinckrodt (Paris, KY, USA). Water was obtained from a Milli-Q (Millipore, Bedford, MA, USA) purification system. All reagents were of analytical grade. The strongly alkaline anion exchanger, Lewatit M 5080 (Merck, Darmstadt, FRG), was used for preconcentration purposes. The anionic exchanger was purified before packing by the following steps: 1) wash successively with 2M sodium hydroxide, then water and then 4M hydrochloric acid, 2) wash with acetone, 3) repeat step 1 and finally 4) wash with methanol: 4M hydrochloric acid (9:1).

The mobile phase was the ternary system 30 mM ammonium acetate pH 5.0 : acetonitrile : methanol (56 : 34 : 10), unless otherwise indicated. Before use, this eluent was degassed under vacuum and filtered with an all-glass apparatus through 0.45 μm filters (Millipore).

Apparatus and Column

Analyses were performed with a Waters (Milford, USA) Liquid Chromatograph consisting of a WISP automatic injector, a model 590 solvent-delivery pump and a model 481 variable wavelength detector, set at 280 nm; a model 440 fixed wavelength detector was used at 254 nm as an auxiliary detector. Outputs were monitored with a model 730 data module Waters. A pH-meter equipped with a combined electrode was used for pH adjusments (PHM 82, Radiometer, Copenhague, Denmark).

The analytical column was a pre-packed 120 × 4 mm i.d. Nucleosil 5 C18 column (Knauer, Berlin, FRG).

0009-5893/87 0613-04 $03.00/0

© 1987 Friedr. Vieweg & Sohn Verlagsgesellschaft mbH

Procedure

Preconcentration was carried out using a home-made 9 mm i.d. borosilicate glass column packed with 1.3 g of exchanger, added as a water slurry.

A 500 ml volume of the water sample was adjusted to pH 11 with 0.1 M sodium hydroxide using a pH-meter. This volume was drawn through the column, previously conditioned with purified water at the same pH. After successively washing with 10 ml of methanol, water and 0.1 M hydrochloric acid, phenols were eluted with 15 ml of methanol:hydrochloric acid (9:1). Five microlitres of the eluate were injected into the chromatograph. Retention times were measured at room temperature, and were used without correction. Potassium nitrate was used to establish the dead time.

Results and Discussion

Choice of Mobile Phase

According to the literature, the capacity factor (k') of PPP may be changed by adjusting the pH within the working pH interval of the silica-based columns. Using a mobile phase consisting of pH 5.0 buffer: acetonitrile (85:15), it is possible to get k' values smaller than 10 for some PPP [6]. On the basis of these data, 30 mM of ammonium acetate was chosen as the most versatile buffer to control the pH of the mobile phase.

In our previous experiments using buffer: acetonitrile binary eluents, we found k' values smaller than 10 for all PPP when a ratio of 58:42 was employed. However, the couple 2-NP; 2,4-DMP did not give complete resolution. In order to improve resolution for this couple, a buffer-acetonitrile-methanol ternary mixture was tested. According to Parris' criterion [8] the eluotropic strength of the initial binary mobile phase was 1.35. In order to maintain this eluotropic strength in the ternary eluent, the methanol and acetonitrile percentages must obey the following equation:

$$y = 0.42 - 0.81\,x$$

where 100 y = % acetonitrile and 100 x = % methanol. The values of k' obtained for the different ratios studied are shown in Fig. 1.

As can be seen, small deviations from isoeluotropic conditions are observed for most of the phenols, the same as in previous results [7]. Large discrepancies for PCP and 2,4,6-TCP may mainly be attributed to the effect of pH on dissociation of these two phenols when the nature of the solvent changes. Regarding selectivity, important conclusions may be drawn from this figure; for example, resolution of the couple 2-NP; 2,4-DMP increases with increasing percentage of methanol.

However, resolution of the couple DNOC; Phenol decreases when the mobile phase contains more than 20% methanol. Best results can be expected using percentages of methanol between 10–20%. A very promising eluant to separate 2-NP; 2,4-DMP contains 10% methanol because Rs = 3.36; moreover k' (PCP) = 7.86. Nevertheless for 20% methanol,

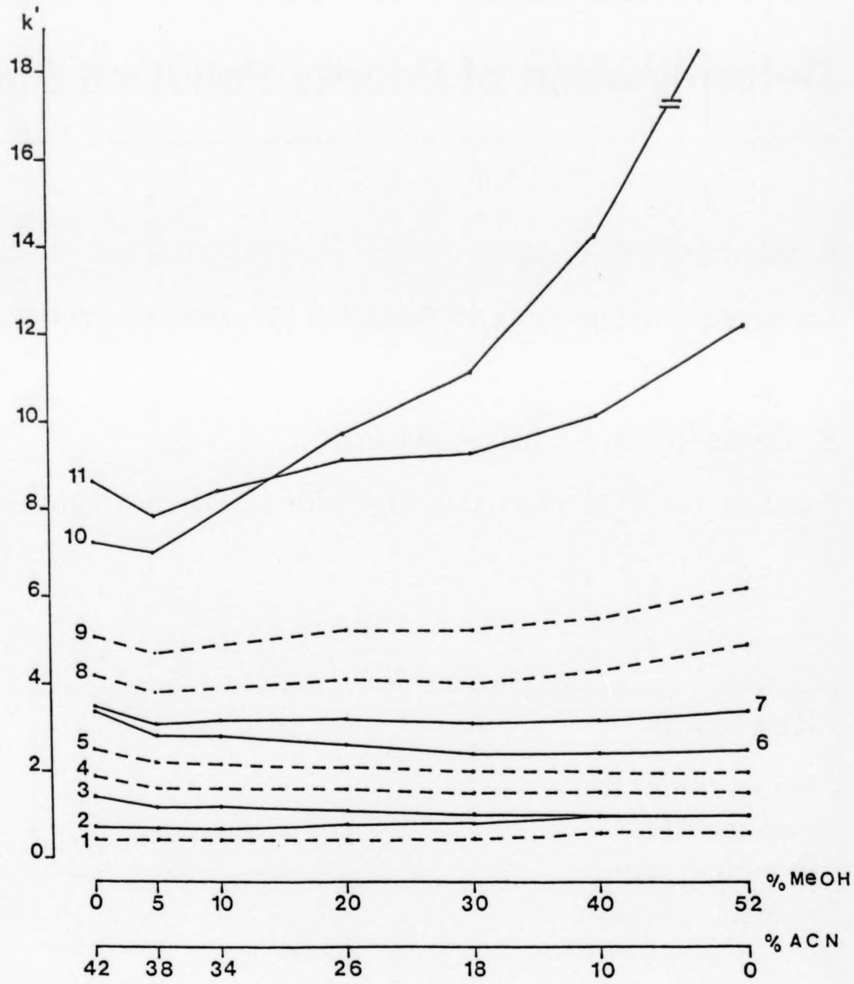

Fig. 1

Variation in the capacity factor, k', with mobile phase methanol (MeOH): acetonitrile (ACN) ratios. Mobile phase compositions maintain the eluotropic strength.

Conditions: identical with Fig. 3 except for MeOH: ACN ratio variation. For peak identification, see Table III.

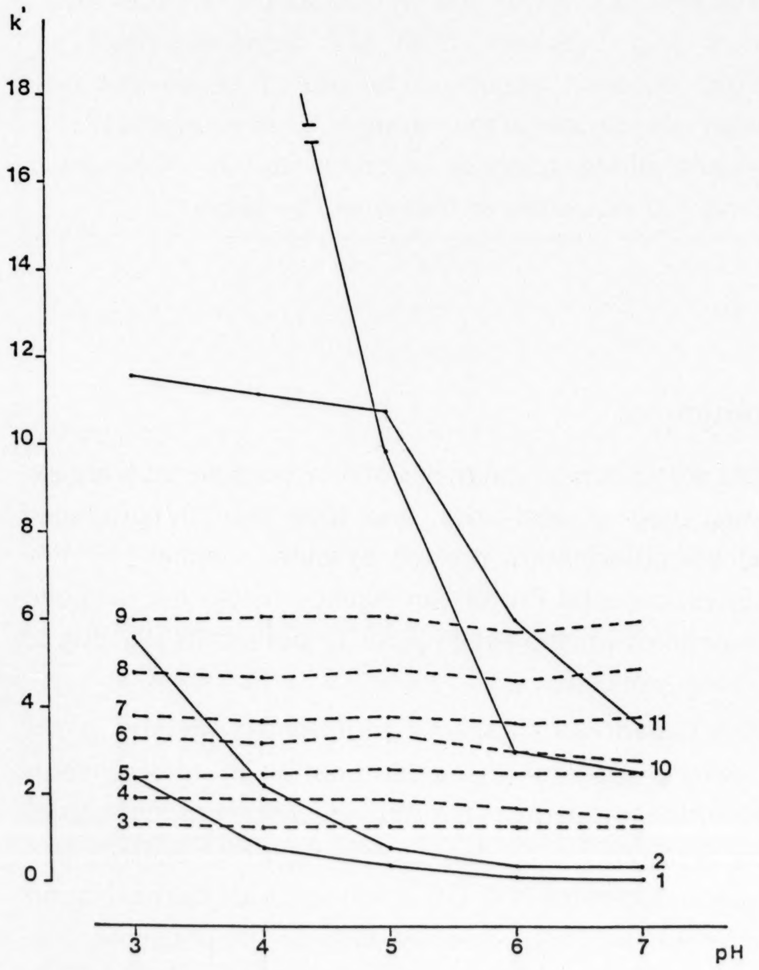

Fig. 2

Variation in the capacity factor, k', with buffer pH.

Conditions: identical with Fig. 3 except for pH variation. For peak identification, see Table III.

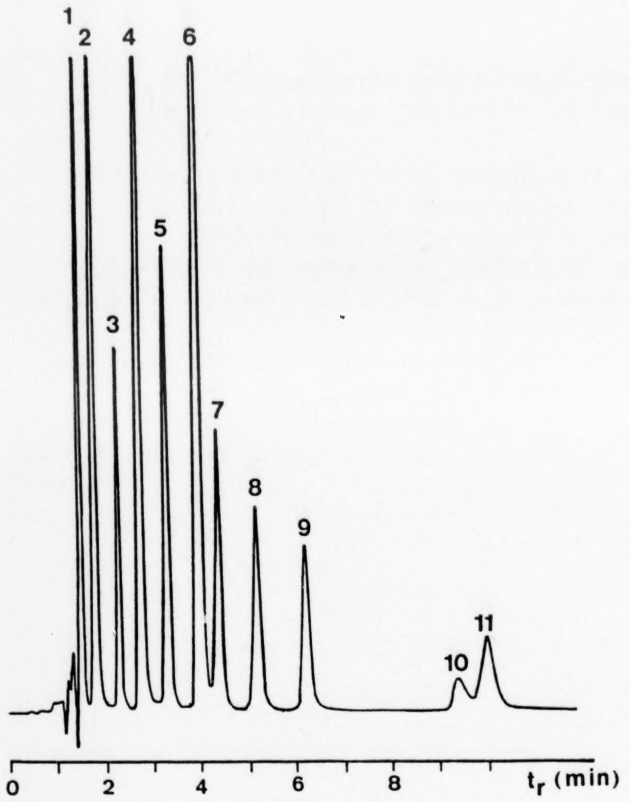

Fig. 3

Isocratic separation of priority pollutants phenols.

Instrument: HPLC Waters system; column: Nucleosil 5 C18, 4 × 120 mm; flow rate: 1.0 ml/min; eluent 30 mM ammonium acetate pH 5.00 : acetonitrile : methanol (56 : 34 : 10); detection: 280 nm at 0.05 AUFS; injection volume: 5 µl; sample: approximately 0.15 µg each phenol. For peak identification, see Table III.

k' (PCP) = 9.69 is higher and analysis time for all PPPs is increased.

pH Optimization

The pH effect of acetic acid-ammonium acetate buffer on k' values of PPP is shown in Fig. 2. The pH was adjusted in all cases with acetic acid, except for pH 3 in which hydrochloric acid was used.

As can be seen, the effect of pH on k' is greater for 2,4-DNP; DNOC; 2,4,6-TCP and PCP; according to the literature these are the most acidic phenols, their pKa values being 3.9, 4.35, 6.0, and 5.25, respectively. In particular, the k' value of PCP changes drastically below pH 6, as could be expected from its ionization equilibrium. It is suggested that the best pH for resolution of PCP is close to five; for pH values higher than 5, overlapping with 2-NP (pH 6) and 2-CP (pH 7) is appreciable. At pH values lower than 5, the effect of k' diminishes and overlapping of DNOC and 2,4-DNP with other phenols occurs.

Table I. General chromatographic performance.

Criterion	Parameter	Level	Range
Area repeatability	C.V. (n = 7)	30 ppm	0.41–5.9 %
t_r repeatability	C.V. (n = 7)	30 ppm	0.16–1.08%
Linearity	r^2	5–50 ppm	0.9914–0.9995
Detection limit	Heigh S/N = 3/1		0.5–8.0 ng 0.1–0.8 ppm

Table II. A280/A254 ratios for priority pollutants phenols.

Compound	A (counts)		A280/A254
	270 nm	254 nm	
2,4-Dinitrophenol	10938	27083	0.40
4,6-Dinitro-2-methylphenol	19767	26588	0.74
Phenol	6609	4061	1.63
4-Nitrophenol	20555	6141	3.35
2-Chlorophenol	8727	2061	4.23
2-Nitrophenol	21515	10275	2.09
2,4-Dimethylphenol	6870	1124	6.11
4-Chloro-3-methylphenol	4296	721	5.96
2,4-Dichlorophenol	3897	466	8.36
Pentachlorophenol	845	6173	0.14
2,4,6-Trichlorophenol	1750	1429	1.22

Conditions identical with Fig. 3.

No significant changes in k' were found with varying buffer concentrations within the concentration range 30–100 mM. Thus a 30 mM concentration was chosen.

After optimizing methanol percentage and pH, the best experimental conditions were 30 mM ammonium acetate pH 5.0 : acetonitrile : methanol (56 : 34 : 10).

General Chromatographic Performance

Table I summarizes the analytical data obtained by the proposed procedure, using the chromatographic conditions specified in Fig. 3.

In general, good linearity and repeatability were found for all PPPs. Under working conditions, most trouble was given by PCP, but even for this pollutant, linearity and reproducibility were similar to those of the other phenols.

The good resolution of the peaks attained allowed identification of phenols on the basis of height ratios at two different wavelenghts. Results are shown at Table II. It can be seen that PCP; 2,4-DNP and DNOC give better responses at 254 nm, unlike the other PPPs that give higher responses at 280 nm.

Table III. Recovery of priority pollutants phenols from water.

Peak	Compound	Symbol	Recovery
1	2,4-Dinitrophenol	2,4-DNP	105
2	4,6-Dinitro-2-methylphenol	DNOC	93
3	Phenol	Phenol	91
4	4-Nitrophenol	4-NP	79
5	2-Chlorophenol	2-CP	85
6	2-Nitrophenol	2-NP	95
7	2,4-Dimethylphenol	2,4-DMP	86
8	4-Chloro-3-methylphenol	4,3-CMP	102
9	2,4-Dichlorophenol	2,4-DCP	79
10	Pentachlorophenol	PCP	93
11	2,4,6-Trichlorophenol	2,4,6-TCP	95

Spike level: 200 ppb. Recovery in %.

Recovery Studies

Recovery experiments were carried out on a pure water sample spiked with 200 ppb of different PPPs, applying the procedure specified in the experimental section of this paper. Recoveries were in the range of 79–105% and the results are shown in Table III. Best recoveries were found for 2,4-DNP (105%) and 4,3-CMP (102%), and the worst recoveries were found for 4-NP (79%) and 2-CP (85%).

Acknowledgement

The financial support of the Spanish C.A.I.C.Y.T. project 2251/83, and the I.G.M.E. is gratefully acknowledged.

References

[1] *L. W. Condie,* J. Am. Waters Works Assoc. **78,** 73 (1986).
[2] *L. H. Keith, W. A. Telliard,* Environ. Sci. Technol. **13,** 416 (1979).
[3] *G. Norwitz, P. N. Keliher,* Anal. Chim. Acta. **144,** 273 (1982).
[4] *P. A. Realini,* J. Chromatogr. Sci. **19,** 124 (1981).
[5] *G. Bengtsson,* J. Chromatogr. Sci. **23,** 397 (1985).
[6] *R. E. Shoup, G. S. Mayer,* Anal. Chem. **54,** 1164 (1982).
[7] *P. J. Shoenmakers, H. A. Billiet, L. De Galan,* J. Chromatogr. **218,** 261 (1981).
[8] *N. A. Parris:* in "Instrumental Liquid Chromatography", Elsevier Sci. Publishers, B.V. 1984, p. 397.

Received: June 29, 1987
Accepted: Aug. 5, 1987
F

The Application of Porous Silica Layers in Open Tubular Columns for Liquid Chromatography

P. P. H. Tock[1]* /G. Stegeman[1] /R. Peerboom[1] /H. Poppe[1] /J. C. Kraak[1] /K. K. Unger[2]

[1] Laboratory for Analytical Chemistry, University of Amsterdam, Nieuwe Achtergracht 166, 1018 WV Amsterdam, The Netherlands

[2] Institut für Anorganische und Analytische Chemie, Johannes Gutenberg-Universität, 6500 Mainz, FRG

Key Words

Liquid-liquid chromatography
Porous silica layers
Open tubular columns
Capillary columns

Summary

Two methods to realize a porous retentive silica layer on the inner wall of 10–25 μm fused silica capillaries for OTLC, etching and precipitation of silica from solution, have been investigated. Etching of the fused silica capillaries with 1M KOH, creates an activated surface, but the capacity of the silica layer is too small to serve as retentive layer in OTLC. Better prospects are offered by the precipitation of silica from a solution of polyethoxysiloxane, dynamically coated on the inner wall of the fused silica capillary. It appears to be possible to deposite a porous silica layer up to 0.8 μm thick (in a 25 μm capillary) by this method, which seems to be suitable for liquid-solid an dynamically generated liquid-liquid chromatography in open tubular columns. The performance of these columns are demonstrated by means of efficient separations of test mixtures using on-column fluorescence detection.

Introduction

The favourable prospects of liquid chromatography in open tubular columns (OTLC) with respect to separation speed and the realization of large plate numbers has been extensively discussed by various authors [1–5]. However, the full exploration of OTLC requires column diameters in the order of 5 μm and smaller. These dimensions put severe demands on the magnitude of the external peak broadening caused by the detection and injection system. Knox et al. [2] calculated that in order to make OTLC superior to LC in packed columns the external peak broadening must be kept below 10 nanoliter. It has been shown that these stringent requirements put on the external peak broadening can be met in practice, when applying on-column optical detection methods [6–8] or electrochemical detection [9] and split flow injection techniques as commonly applied in GC [10, 11].

Besides the experimental requirements also a stable retentive layer of about 1 μm must be present on the wall of the capillary to obtain an acceptable phase ratio necessary to retain the solutes and to avoid stationary phase overload [12]. Until now the preparation of a suitable retentive layer hampers mostly the exploration of OTLC.

In the developments of capillary gas chromatography (GC) the same problem, i. e. that of obtaining a stable retentive layer, has played a predominant role and a large amount of research has been devoted to this. It therefore lies at hand to consider the various experimental methods used in GC in the past for their suitability to treat 5–25 μm tubes and indeed the next discussion will follow this line.

Films of simple stationary liquids are well applicate in GC, although the phase ratio is generally low (high in GC nomenclature). The application in LC does not seem to be attractive, because of the expected dissolution of the phase in the eluent.

Later developed immobilized liquids do not present this problem and can be applied in thicker films. Indeed successful applications in OTLC of the immobilized silicones has been reported, using static coating [13, 14]. However, although this approach deserves further research, especially because it can be used with fused silica tubes, the layer thickness is limited a diffusion coefficients in the applied cross linked phases are low [14].

Quite another approach, clearly described by Golay [15] and since then also extensively investigated in GC, is that of applying on the tube wall porous layers or particles, that can either act as an adsorbent, or as a support for a stationary liquid. In the latter case the higher liquid loadings are distributed over a large surface and stationary phase mass transfer can remain fast.

0009-5893/87 0617-08 $03.00/0

© 1987 Friedr. Vieweg & Sohn Verlagsgesellschaft mbH

This basic concept, Porus Layer Open Tubular (PLOT) and Support Coated Open Tubular (SCOT) columns, has been implicated in GC in the past in a number of ways [16]:

1. chemical treatment of the inside wall of glass columns with alkaline [17, 18] and acid solutions [19]. Partial dissolution of the glass material leads to a porous structure.
2. Coating particles on the inside wall with dynamic [15, 20] or static coating [21–24].
3. Embedding porous particles in the tube wall by drawing an open capillary from a large diameter tube filled with particles, while a tungsten wire presses the particles to the wall at the position of fusion [25].

The first way has been used for preparing OTLC columns from soda-lime or borosilicate glass tubes and good results have been obtained [26–28]. However, this approach does not work for fused silica tubes which from the point of view of optical on-column detection and mechanical strength are superior to the normal glass columns [29].

The two other ways may be valuable, but their realization for OTLC fused silica tubes presents some large experimental problems, connected with the smaller diameters (5–25 μm) involved and/or the necessity of high temperature treatments.

In this paper we report the results of an investigation to create a thick porous silica layer on the inner wall of 10–25 μm fused silica capillaries by precipitation of silica from a solution of polyethoxysiloxane, dynamically coated on the inner wall of the capillary. The practical aspects of the etching and precipitation technique and its utility to realize a rigid porous layer of fused silica capillaries suitable for liquid-solid and dynamically generated liquid-liquid chromatography in OTLC will be discussed. Efficient separations of test mixtures will be shown.

Experimental

Materials and Chemicals

Solvents used were analytical grade cyclohexane and ethanol (Merck Darmstadt, FRG), methylene chloride and γ-butyrolacton, purchased from Janssen (Beerse, Belgium) and BDH (Poole, UK) respectively. Destilled water was firstly deionized through a PSC filter assembly (Barnstead, Boston MA, USA). Prior to use all solvents were filtered by vacuum suction over 0.5 μm filters (Type FH, Millipore, Bedford, MA, USA). The mobile phase applied for the liquid-liquid system was cyclohexane, saturated with γ-butyrolacton at 20 °C. The polycyclic aromatics used as test compounds were obtained from Janssen (Beerse, Belgium). Stock solutions of the test compounds were prepared in cyclohexane. Fused silica capillaries of different lengths and internal diameter were obtained from SGE (Ringwood, Victoria, Australia).

Apparatus

Figure 1 schematically shows the experimental set-up of the OTLC system, which consisted of a thermostatted solvent reservoir (volume = 400 ml), which could be pressurized with helium and served as a constant pressure pump; a 0.5 μl injection valve (model 7520, Rheodyne, Berkely, CA, USA) equipped with a home made double splitting device (see figure 1b). The columns were fitted in a home made thermostatted jacket connected to a thermostat (Haake, Type F, Berlin, FRG). A Shimadzu RF-530 fluorescence detector (Kyoto, Japan) modified according to Folestad [30] or a helium-cadmium laser (Liconix, model 4207 NB, Sunnyvale, CA, USA) combined with a modified Zeiss M4Q III fluorimeter (Jena, GDR) were used for on-column fluorescence detection. In both systems the protective layer was burned off at the end of the capillary over a lenght of 2 cm. The signal was recorded with a Kipp & Zonen micrograph BD5 (Delft, The Netherlands). The SEM-pictures were taken with a dual scanning electron microscope (ISI-D 130, Japan). ^{1}H NMR spectra were run on a Bruker AC 100 instrument.

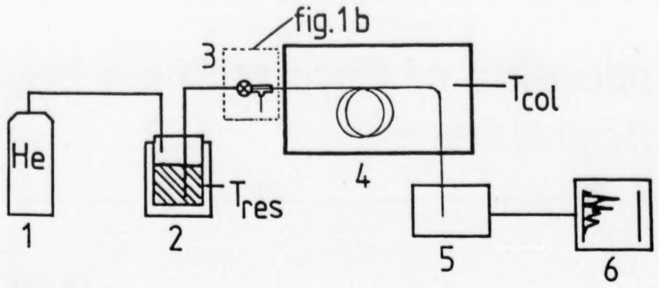

Fig. 1a

The chromatographic set-up.

1: helium-bomb; 2: thermostatted solvent reservoir; 3: injector equipped with a splitting device; 4: capillary column in thermostatted jacket; 5: modified fluorescence or laser induced fluorescence detector; 6: recorder.

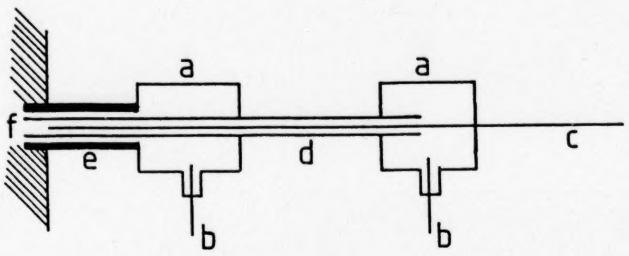

Fig. 1b

The double splitting device.

a: 1/16" swagelok union tee; b: waste capillaries; c: capillary column; d: fused silica capillary, ID = 500 μm; e: stainless steel tubing; f: injector.

Procedures

Determination of the Internal Diameter of the Capillaries

The average internal diameter (ID) of the capillaries were determined in advance by two methods, both based on the Hagen-Poisseuille law [31]. Figure 2 shows schematically the experimental set-up used in both methods. With the first method the pressure decline of a reservoir filled with helium (volume = 2.89 ml) with the capillary as outlet is measured as a function of time. The Hagen-Poisseuille law

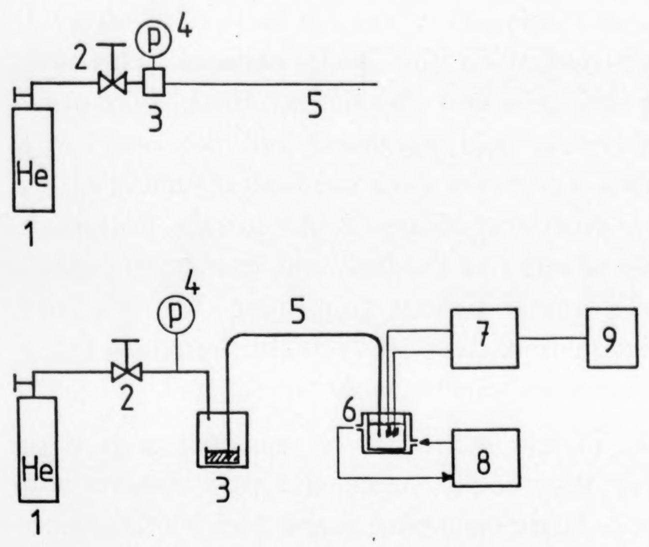

Fig. 2

The experimental set-up for ID-measurements.
a. Aerodynamic method.
1: helium-bomb; 2: pressure valve; 3: reservoir; 4: pressure-gauge; 5: capillary.
b. Method based on conductivity.
1: helium-bomb; 2: pressure valve; 3: reservoir containing KCl-solution; 4: pressure-gauge; 5: capillary; 6: thermostatted conductivity cel; 7: conductometer equipped with Pt-electrodes; 8: thermostat; 9: recorder.

and the Boyle law, and integration lead to the following relation between the unknown diameter and the observed parameters. From the pressures p_1 and p_2 observed at times t_1 and t_2 ($t_2 = t_1 + \Delta t$) one can calculate the inner diameter as

$$d_c^4 = \frac{128\,\eta\, l_c\, V}{\pi\, p_0\, \Delta t} \times \ln\left(\frac{p_2 + p_0}{p_1 + p_0} \times \frac{p_1 - p_0}{p_2 - p_0}\right)$$

where η is the viscosity of helium,
l_c the length of the capillary,
V the volume of the vessel and
p_0 the atmospheric pressure.

In the second method a 1M KCl-solution is pressed through the capillary and comes out in a vessel containing 10 ml water. The increase in conductivity can be measured as a function of time. This yields the flow rate of the KCl-solution, which in turn can be used to calculate the diameter with the Hagen-Poisseuille law.

$$d_c^4 = \frac{128\,\eta\, l_c\, V}{\pi\, c\, \Delta p} \times \frac{dG/dt}{dG/dc}$$

where dG/dt is the change in conductivity in time, dG/dc is the slope of the conductivity versus concentration curve of the KCl-solution, η is the viscosity of the KCl-solution, l_c the length of the capillary, V the volume of the water in the vessel. c the concentration of KCl in the capillary and Δp the pressure difference on the capillary.

Etching Method

Fused silica capillaries are drawn at 2000 °C [32], which results in a very low density of surface silanolgroups. Wright [33] measured 0.35 μmole OH/m^2 in fused silica tubing. Therefore the surface must be etched with alkaline solution to convert siloxane groups into silanol groups [34]. A solution of potassium hydroxide was pumped through the fused silica column for several hours, using the reservoir as shown in Fig. 3. The column and reservoir were placed in an oven to control the temperature. The column outlet has to end under water to avoid blockage at that point by the formation of a precipitate, probably silica. After etching the column was rinsed at room temperature, first with water, then with 0.03M HCl for 2 hours and finally with water until the effluent became neutral. Next the column was dried at 200 °C under a stream of helium for at least 2 hours.

The Preparation of a Porous Silica Layer from PES

The deposition of a stable porous silica layer on the inner wall of fused silica capillaries was performed by precipitation of silica from a solution of polyethoxysiloxane (PES). The PES was prepared by hydrolytic polycondensation of tetraethoxysilane (TES) according to Unger et al. [35, 36]. To 50 ml of TES (0.22 mole) dissolved in 30 ml of dry ethanol, 5.7 ml water (0.32 mole) containing 60 μmole HCl was added. This solution was vigorously stirred for 1 hour and then refluxed for 6 hours. Next ethanol and HCl were evaporated in vacuo. The purity of the obtained PES was controlled by NMR- and IR-measurements. ^{1}H NMR (CD_2Cl_2): δ 4.0–3.7 (2H, several q, J = 6.9 Hz, $-Si-O-CH_2-C$), δ 1.3–1.1 (3H, several t, J = 6.9 Hz, $-Si-O-C-CH_3$). IR (cell path NaCl, CH_2CL_2) (cm^{-1}): 2975, 2930, 2900, 1480, 1420, 1395, 1300, 1165, 1120–1060, 980, 820–660.

The dried capillaries, treated with 1M KOH at room temperature for 2 hours and rinsed with HCl, were dynamically coated with PES by fitting the capillary with a 25 cm long plug of pure PES. The plug was pressed through the column with helium with a linear velocity of 30 cm/hr. The PES-layer was converted into silica by treatment with gaseous ammonia in a helium stream for one day at room temperature. Next the capillary was flushed with 0.01 M ammonia for half an hour, rinsed with water for 3 hours and finally dried for at least two hours at 200–250 °C while purging with helium.

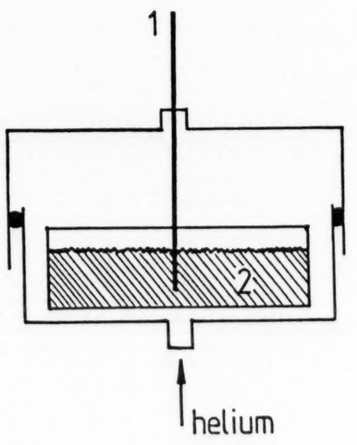

Fig. 3

Coating reservoir for filling capillaries.
1: capillary column; 2: glass bottle filled with coating or etching solution.

Chromatography

The dynamically generated liquid-liquid system applied in this study consisted of cyclohexane as mobile phase and γ-butyrolacton as stationary phase [38]. The stationary phase was generated on an etched or PES-treated fused silica capillary by pumping through of cyclohexane saturated at 20 °C with γ-butyrolacton. The solvent reservoir and the column were kept at 20 °C. The loading of the capillary with γ-butyrolacton can be enhanced by injecting, a few times, small amounts of pure γ-butyrolacton. It must be noticed that the saturation of cyclohexane with γ-butyrolacton requires at least 12 hours of intensive stirring of both phases mixed in a ratio of cyclohexane/γ-butyrolacton 10 : 1 (v/v).

Preparation of the SEM-Samples

A 10 cm long capillary was cut from an untreated or a treated column and fixed on a 5 mm thick glass plate (5 cm x 5 cm) with beeswax. Next the capillary was polished with very fine polishing paper (P800,WETORDRY TRI-M-ITE PAPER, silicon carbide, 3M) until the inner tube was open. The capillary was removed from the plate by dissolving the beeswax in methylene chloride and then the capillary was cleaned by ultrasonic treatment in methylene chloride. A 5 mm piece of the capillary was fixed on a specimen mount (ϕ = 8 mm) and sputtered with gold.

Results and Discussion

Liquid-Solid Chromatography

– *on etched surfaces.* It is well known that by chemical treatment of the surface of glass capillaries with acids or bases, the surface may obtain a more porous structure for use as an adsorbent (eventually after chemical modification). For soda-lime or borosilicate glass such a porous structure can be obtained by treatment with an acid. These types of glass contain other metals then silica in their crystal structure (f.i. alkali metals) which can be leached out with acids, without destroying the Si–O network. However, fused silica is very pure and contains less then 1 ppm other metals and therefore acid treatment will not result in a porous structure. For fused silica capillaries, etching with a base is the only possibility to modify the surface. Potassium hydroxide was selected as the base and its etching capabilities was tested under various conditions. The influence of a washing step with 0.03 M HCl was also tested. In Fig. 4 the treatment steps are schematically represented.

The retention of the etched layer was measured with cyclohexane as the mobile phase and fluoranthene and 2-naphtol, or 9, 10-diphenylanthracene and 9-anthracenecarbonitril as solutes. The results of these measurements are compiled in Table I. From this table it can been that the retention of the etched layer increases with increasing KOH concentration. KOH concentration > 1M could not be used, because these solutions were too viscous to pump through the capillaries. It can also be seen that the etching improves when raising the temperature from 45 °C to 90 °C, but becomes worser at 130 °C. In this latter case serious blockage occured during the etching procedure. From the observed small retention of 2-naphtol, under all etching conditions, it must be concluded that no real porous structure is formed due to the etching. It seems that just silica is dissolved from the surface, which lead to a very small increase of the surface area. From measurements of the inner diameter, before and after etching, it was indeed found that about 1 μm silica was removed from the surface of the capillaries. This indicates that it is not possible to create a thick porous layer on fused silica capillaries by etching.

From table 1 it can also been seen that the best results were obtained under very mild conditions, 2 hours at 20 °C (Fig. 5a and 5b). This observation can be explained by assuming that under these conditions only the surface siloxane groups are attacked and converted into silanol-groups. It was found that a washing step with HCl was necessary, because after etching with KOH and washing

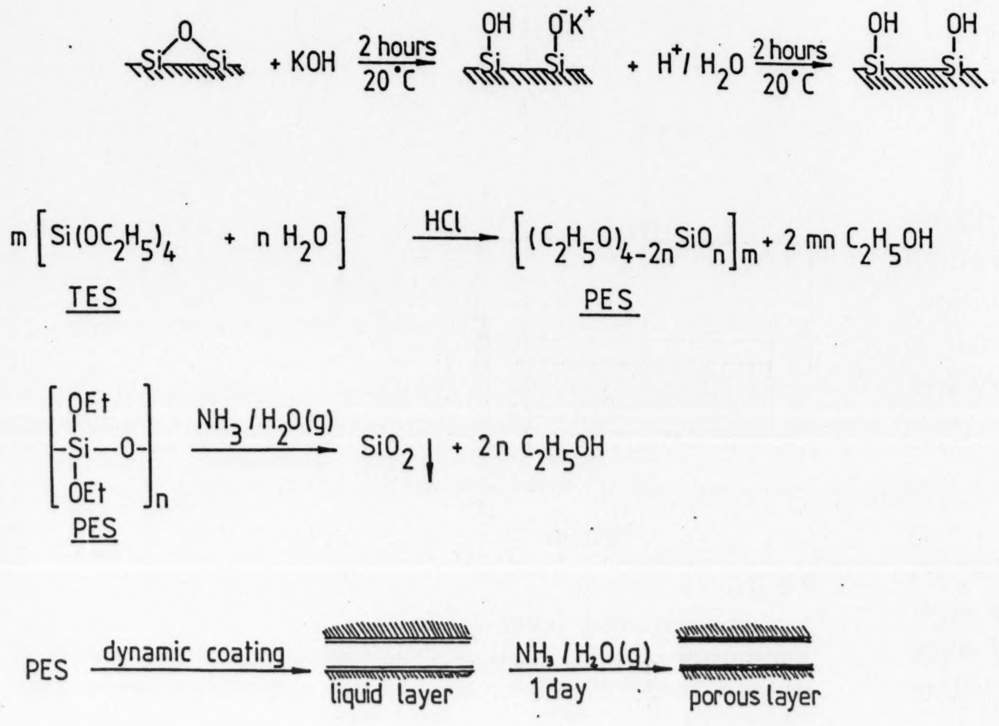

Fig. 4

Schematically representation of etching and PES procedure.

Table I. Retention of 2-naphtol (1) or 9-anthracenecarbonitril (2) on fused silica capillaries etched with potassium hydroxide or treated with polyethoxysiloxane (PES). Mobile phase: cyclohexane; unretained = anthracene or 9,10-diphenylanthracene

ID_{cap}	time	[KOH]	[HCl]	Temp.	PES	k′ (1)	k′ (2)
μm	hr	M	M	°C			
25	–	–	–	–	–	0.01	0.01
10	–	–	–	–	–	0.04	0.04
25	17.0	0.01	–	90	–	0.04	–
25	17.5	0.1	–	90	–	0.05	–
25	6.0	1.0	–	90	–	0.10	–
25	6.0	1.0	–	45	–	0.06	–
25	6.0	1.0	–	90	–	0.10	–
25	6.0	1.0	–	130	–	0.07	–
25	16.0	1.0	–	20	–	0.45	–
25	2.0	1.0	–	20	–	0.45	–
10	2.0	1.0	–	20	–	1.00	–
25	2.0	1.0	0.03	20	–	0.30	0.11
10	2.0	1.0	0.03	20	–	0.75	0.28
25	2.0	1.0	0.03	20	1 x	2.70	–
10	2.0	1.0	0.03	20	1 x	> 6.0	0.90
25	2.0	1.0	0.03	20	3 x	> 14.0	–

with water the retention is different. We assume that the surface is still covered with potassium-ions (see Fig. 4), which cannot be removed from the surface by water, but had to be removed with acid to get silanolgroups on the surface.

– *on PES-treated capillaries.* The treatment of fused silica capillaries with KOH does not result in a porous silica surface, it would be better to deposite a porous silica layer on the surface. The method, originally used for preparation of spherical porous silica particles by precipitation of silica from a solution of polyethoxysiloxane (PES) [35], was used with some slight modifications. PES, dynamically coated on the wall, was converted into silica by treatment wit gaseous ammonia in a helium stream for 1 day and finally rinsed with 0.01 M ammonia for half an hour and with water for several hours. It turned out to be impossible to treat the capillary with aqueous ammonia immediately after coating, because PES was stripped from the wall into the solvent front where it polymerized and finally blocked the capillary.

The use of static coating is preferable to dynamic coating, because thicker films can be obtained. However, we were not able to apply static coating, probably because the PES available was of insufficient viscosity. Therefore the preparation of a thick silica layer had to be done by carrying out the procedure with dynamic coating several times in succession. The retention of the porous layer was measured with cyclohexane as mobile phase and fluoranthene and 2-naphtol, or 9,10-diphenylanthracene and 9-anthracenecarbonitril as solutes.

The results of these measurements are compiled in Table 1. From these data it can be seen that the retention of the retained solutes for a capillary, which had been coated once is increased by a factor 9 against the retention on an etched capillary. For a capillary treated three times this factor is 20. In Fig. 6 a chromatogram of a PES-treated capillary is shown. The thickness of the porous layer couldn't be determined under a light microscope, because

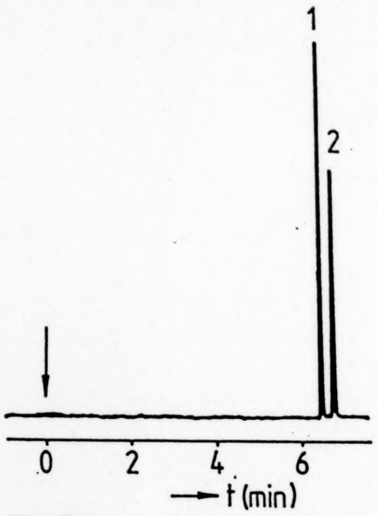

Fig. 5a

LSC-chromatogram of an untreated capillary.
Column 3 m X 10 μm, mobile phase: cyclohexane. Injection volume 40 pl. Fluorescence detector, λ_{ex} = 260 nm and λ_{em} = 420 nm. Linear velocity of the mobile phase 8.3 mm/s. **1** = 9–10 diphenylanthracene; **2** = anthracenecarbonitril k′ = 0.04.

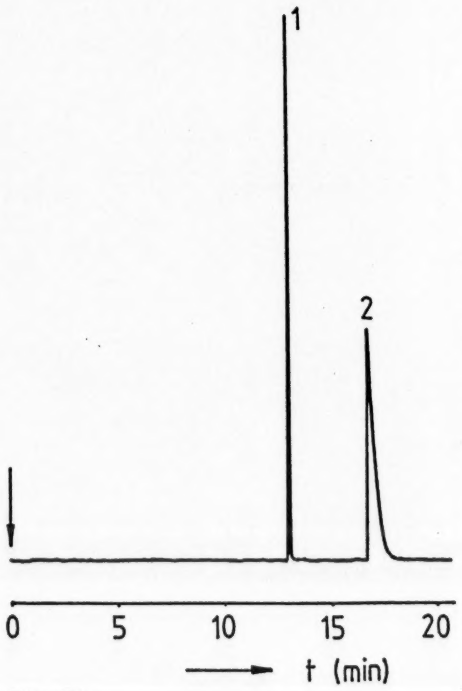

Fig. 5b

LSC-chromatogram of an etched capillary.
Column 2.75 m X 10 μm. Linear velocity of mobile phase 3.7 mm/s. **2** = 9-anthracenecarbonitril k′ = 0.28. Other details as in Fig. 5a.

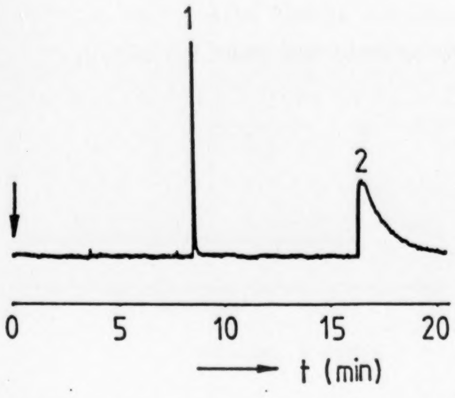

Fig. 6

LSC-chromatogram of a capillary treated one time with PES. Column 2.25 m × 10 μm. Linear velocity of mobile phase 4.3 mm/s. **2** = 9-anthracenecarbonitril k′ = 0.9. Other details as in Fig. 5a.

the layer wasn't visible. Therefore we had to use an electron microscope for examining the film thickness and the pore structure of the layer. In Fig. 7 some SEM pictures are shown. From these pictures it can be seen that the thickness of the silica layer, in a several times treated 25 μm capillary, is about 0.8 μm. The pore structure is very regular and the pore diameter is about 20 nm. The silica layer seems to be well attached on the wall and proved to be stable during the course of the experiments (at least several weeks).

Solvent Generated Liquid-Liquid Systems (LLC)

When using a liquid stationary phase in OTLC the liquid has to be immobilized in order to avoid dissolution of this liquid in the mobile phase. This immobilization step has serious consequences with respect to the allowable film

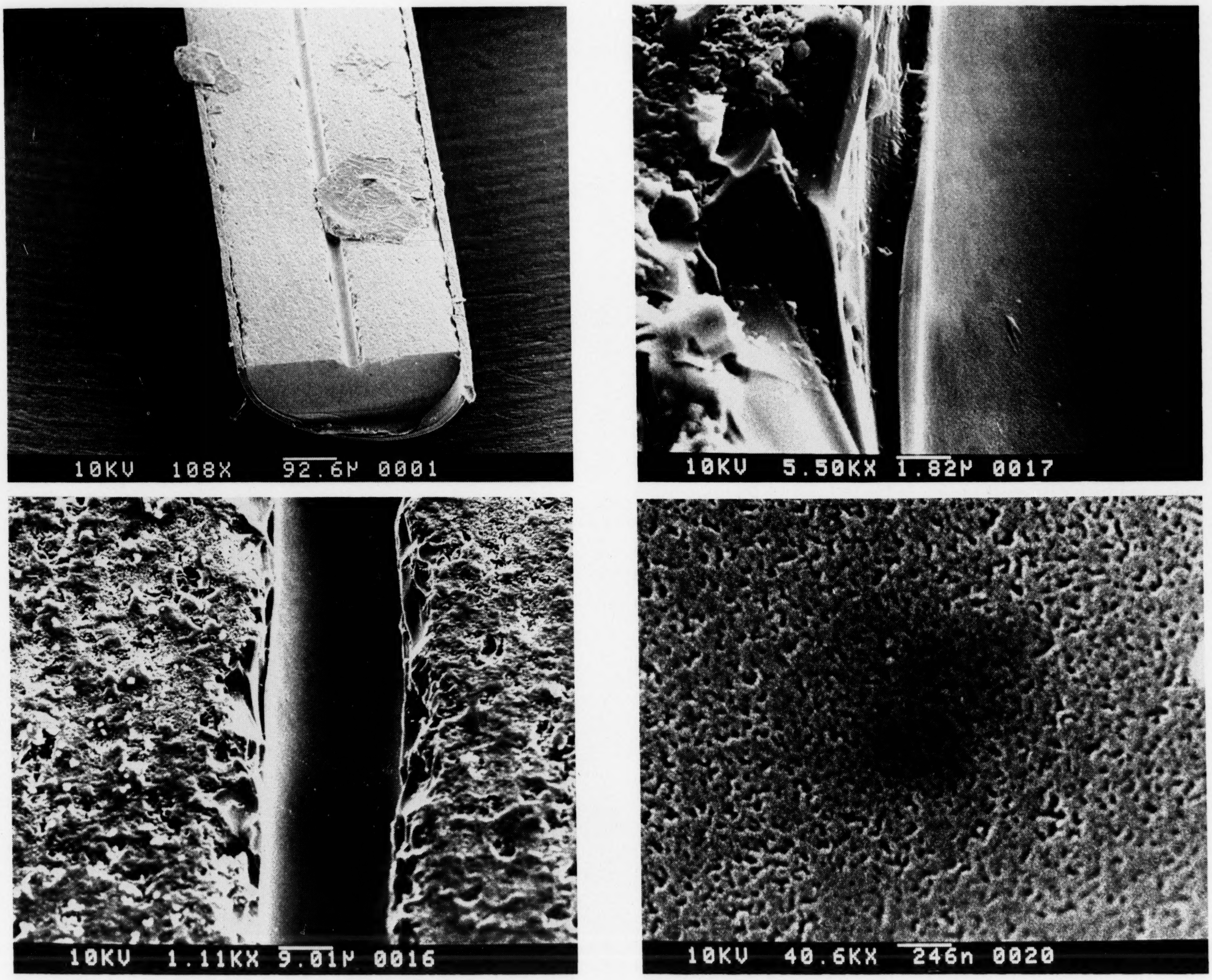

Fig. 7

SEM-pictures of a capillary treated several times with PES.

a. A view of the open capillary, d_c = 25 μm, magnification 108 x.

b. The capillary tube, on the left side of the inner tube the porous silica layer can be seen, magnification 1.11 kx.

c. The porous silica layer, d_f about 0.8 μm, magnification 5.50 kx.

d. The pore structure of the porous silica layer, the pore diameter is about 20 nm, magnification 40.6 kx.

thickness, because of the small diffusion coefficients in such immobilized phases [14]. The film thickness and thus the loadability can be significantly larger when less viscous liquids are used as stationary phase [37]. It has been shown that a non viscous polar liquid can be generated in the pores of bare silica, by pumping through of a non-polar liquid saturated with this polar liquid [38]. This technique was applied to etched an porous layer 10 μm ID fused silica capillaries, with a phase system of γ-butyrolacton/ cyclohexane. It appeared possible to generate γ-butyrolacton on the surfaces, on which polycyclic aromatics are retained. The same polycyclic aromatics did not show retention in the adsorption mode using pure cyclohexane as mobile phase. From known partition coefficients of the polycyclic aromatics in the γ-butyrolacton/ cyclohexane system, the phase ratios (V_s/V_m) at the same linear velocity could be calculated on the capillary. They were found to be 0.020 for an etched. 0.025 for an acid treated etched and 0.038 for a porous layer (1 time treated) capillary. It appeared that a precise thermostatting of the liquid-liquid system in the stock reservoir and column was necessary to obtain a stable system. Fig. 8 shows chromatograms of mixtures of polycyclic aromatics obtained on 10 μm liquid-liquid capillaries. In Table 3 it can be seen that numbers of 390 000 and 180 000 were found for respectively anthracene and beno(a)pyrene, at linear velocity of 1.8 mm/s, which is 17 and 36 % less then the theoretical values using D values, as tabulated in Table 2, calculated with the Wilke Chang equation [39, 40]. This illustrates the potential of OTLC in the liquid-liquid mode.

Conclusion

The use of low viscosity stationary phases in OTLC is very attractive, because the high diffusivities allow for large film thickness, with high loadabilities that partially will abate detection problems. For that purpose a porous wall layer for immobilization of such phases by capillary forces is needed. It has been shown that such porous layers cannot the obtained by etching of fused silica tubes. However, an in situ polymerization of PES to silica leads to porous layers, with suitable pore diameters, on which dynamically coated liquid-liquid systems can be implemented. The results for 10 and 25 μm tubes display only slight deviations from the theoretical expectations for efficiency, which probably can be attributed to external peak broadening.

The procedure is carried out at mild temperatures, thus avoiding disruption of the outer protective polyimide layer of fused silica capillaries. This advantage is of great practical importance, in comparison to other routes to porous silica that could be applied in OTLC tubes, such as e. g. the agglomeration of very fine silica spheres as suggested by Kirkland [42].

Table II. Partition coefficient and diffusion coefficients of some polycyclic aromatics in phase system: cyclohexane/γ-butyrolacton

Compund	K_p	D_m 10^{-9} m^2/s	D_s 10^{-9} m^2/s
Anthracene	5.09	0.94	0.47
Pyrene	6.58	0.90	0.46
Fluoranthene	7.49	0.88	0.45
Benzo(a)pyrene	14.03	0.83	0.43

K_p : distribution coefficient, taken from ref [41];
D_m: diffusion coefficient in the mobile phase, cyclohexane;
D_s : diffusion coefficient in the stationary phase, γ-butyrolacton; both calculated at 295 K, using the Wilke Chang equation.

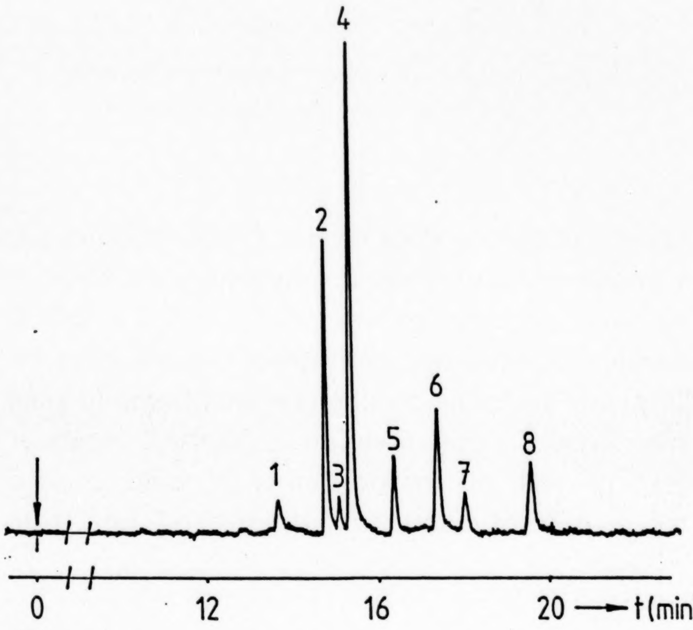

Fig. 8a

LLC-chromatogram of an etched capillary.
Column 2.9 m X 10 μm, mobile phase: cyclohexane, saturated with γ-butyrolacton, stationary phase: γ-butyrolacton. Linear velocity of mobile phase 3.6 mm/s. **1** = unknown; **2** = anthracene; **3** = nafthalene; **4** = fluoranthene; **5** = chrysene; **6** = benzo(b)fluoranthene; **7** = benzo(ghi)perylene; **8** = 1,2,5,6-dibenzanthracene. Other details as in Fig. 5a.

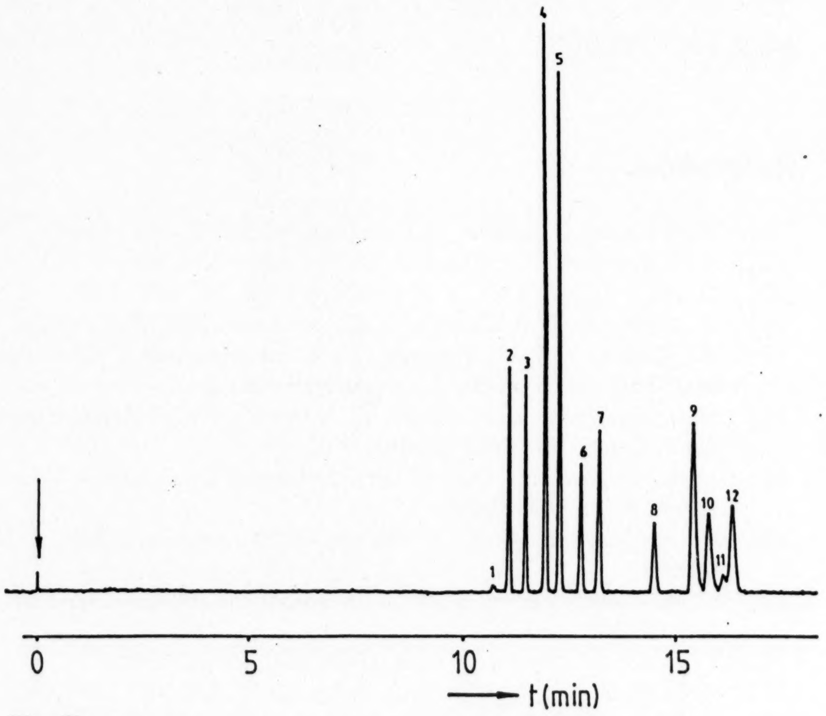

Fig. 8b

LLC-chromatogram of a capillary treated one time with PES.
Column 2 m X 10 μm, mobile phase: cyclohexane, saturated with γ-butyrolacton, stationary phase: γ-butyrolacton. Linear velocity of mobile phase 3.6 mm/s. **1** = unknown; **2** = 9-10 diphenylanthracene; **3** = 9-phenylanthracene; **4** = 9-methylanthracene; **5** = anthracene; **6** = pyrene; **7** = fluoranthene; **8** = 1,2-benzanthracene; **9** = benzo(a)-pyrene; **10** = benzo(k)fluoranthene; **11** = benzo(b)fluoranthene; **12** = 9-anthracenecarbonitril. Other details as in Fig. 5a.

Table III. Observed and calculated plate heights in open tubular liquid liquid chromatography using a 2 m X 10 μm I.D. column

	linear velocity, mm/s								
	1.8			3.2			4.5		
Compound	k'	H_{exp} μm	H_g μm	k'	H_{exp} μm	H_g μm	k'	H_{exp} μm	H_g μm
Anthracene	0.12	5.1	4.3	0.16	8.5	7.0	0.20	11.8	10.4
Pyrene	0.16	6.6	4.8	0.21	11.3	8.1	0.25	15.7	12.0
Fluoranthene	0.19	6.3	5.2	0.25	11.4	8.9	0.30	16.2	13.5
Benzo(a)pyrene	0.35	11.0	7.0	0.46	23.2	12.7	0.55	30.7	20.0
V_s/V_m	0.025			0.032			0.038		

D_m and D_s values were taken from Table II;
H_g calculated using the Golay equation;
H_{exp} is the average of at least 2 measurements;
k' is the average of at least 2 measurements.

The availability of porous silica layered OTLC columns also opens up immense possibilities to implement all kinds of chemistries developped for packed column HPLC in OTLC, such as chemical bonding of substituted and non-substituted alkyl chains, ion exchange groups and enantiomeric selectors. Further work in this direction is planned. However, most urgent is work on the possibility of static coating, and on the relation of reaction conditions and pore structure of the layer.

Acknowledgement

The authors wish to thank Mr. F. Knipscheer for preparing the SEM-samples, Mr. W. Takkenberg for monitoring the SEM-samples and Mr. B. Eray for teaching the preparation of polyethoxysiloxane. Support for this work was provided by the Netherlands Foundation for Chemical Research (SON) with financial aid from the Netherlands Organization for the Advancement of Pure Research (ZWO) under grant 700-344-003.

References

[1] *J. H. Knox, M. Saleem,* J. Chromatogr. Sci. **7**, 614 (1969).
[2] *J. H. Knox, M. T. Gilbert,* J. Chromatogr. **186**, 405 (1979).
[3] *D. Ishii, T. Takeuchi,* J. Chromatogr. Sci. **18**, 462 (1980).
[4] *J. Jorgenson, E. J. Guthrie,* J. Chromatogr. **255**, 335 (1983).
[5] *R. Tijssen, J. P. A. Bleumer, M. E. van Kreveld,* J. Chromatogr. **260**, 297 (1983).
[6] *M. J. Sepaniak, J. D. Vargo, C. N. Kettler, M. P. Maskarinec,* Anal. Chem. **56**, 1252 (1984).
[7] *J. B. Phillips, D. Luu, J. B. Pawliszyn, G. C. Carle,* Anal. Chem. **57**, 2779 (1985).
[8] *H. P. M. van Vliet, H. Poppe,* J. Chromatogr. **346**, 149 (1985).
[9] *L. A. Knecht, E. J. Guthrie, J. Jorgenson,* Anal. Chem. **56**, 479 (1984).
[10] *T. Tsuda, M. Novotny,* Anal. Chem. **50**, 271 (1978).
[11] *V. L. McGuffin, M. Novotny,* Anal. Chem. **55**, 580 (1983).
[12] *H. Poppe, J. C. Kraak,* J. Chromatogr. **255**, 395 (1983).
[13] *A. Farbrot, S. Folestadt, M. Larsson,* J. High Resol. Chromatogr. Commun. **9**, 117 (1986).
[14] *O. van Berkel, J. C. Kraak, H. Poppe,* in preparation.
[15] *M. J. E. Golay,* in: Gas Chromatography 1960 (*R. P. W. Scott,* ed.), Butterworths, London, 1960, pp 139–143.
[16] *L. S. Ettre, J. E. Purcell,* Porous-Layer Open-Tubular Columns – Theory, Practice and Applications. In: Advances in Chromatography, vol. 10, *J. C. Giddings* and *R. A. Keller,* eds. M. Dekker Inc., New York, 1974, pp 1–97.
[17] *M. Mohnke, W. Saffert,* in: Gas Chromatography 1962 (*M. van Swaay*, ed.) Butterworths, London, 1962, pp 216–224.
[18] *F. A. Bruner, G. P. Cartoni*, Anal. Chem. **36**, 1522 (1964).
[19] *A. V. Kiselev,* in: Gas Chromatography 1962 (*M. van Swaay,* ed.), Butterworths, London, 1962, pp xxxiv-liii.
[20] *R. Kaiser,* Chromatographia **1**, 34 (1968).
[21] *C. Horváth,* Trennsäulen mit dünnen porosen Schichten für die Gaschromatographie, Inaugural Dissertation, J. W. Goethe University, Frankfurt am Main, West Germany, 1963.
[22] *I. Halász, C. Horváth,* Nature (London) **197**, 71 (1963).
[23] *I. Halász, C. Horváth,* Anal. Chem. **35**, 499 (1963).
[24] *C. Vidal-Madjar, J. Ganansia, G. Guiochon,* in: Gaschromatography 1970 (*N. Stock*, ed.), Inst. of Petroleum, London, 1971, pp 20–34.
[25] *D. W. Grant,* J. Gas Chromatogr. **6**, 18 (1968).
[26] *D. Ishii, T. Tsuda, T. Takeuchi,* J. Chromatogr. **185**, 73 (1979).
[27] *T. Tsuda, K. Hibi, T. Nakanishi, T. Takeuchi, D. Ishii,* J. Chromatogr. **158**, 227 (1978).
[28] *D. Ishii, T. Takeuchi,* J. Chromat. Sci. **22**, 400 (1984).
[29] *W. Jennings,* J. High Resol. Chromatogr. Chromatogr. Commun. **3**, 601 (1980).
[30] *S. Einarsson, S. Folestad, B. Josefsson, S. Lagerkvist,* Anal. Chem. **58**, 1638 (1986).
[31] *S. Coffa, P. P. H. Tock, F. Nooitgedacht,* unpublished results.
[32] *S. R. Lipsky, W. J. McMurray, M. Hernandez, J. E. Purcell, K. A. Billeb,* J. Chromat. Sci. **18**, 1 (1980).
[33] *B. W. Wright, P. A. Peaden, M. L. Lee, G. M. Booth,* Chromatographia **15**, 584 (1982).
[34] *A. M. Filbert, M. L. Hair,* Adv. Corros. Sci. Technol. **5**, 1 (1976).
[35] *K. K. Unger, J. Schick-Kalb, K. F. Krebs,* J. Chromatogr. **83**, 5 (1973).
[36] *K. K. Unger, J. Schick-Kalb, B. Straube,* Colloid & Polymer Science **253**, 658 (1975).
[37] *H. Poppe*, CLC symposium Edinburgh, 1984.
[38] *J. P. Crombeen, S. Heemstra, J. C. Kraak,* Chromatographia **19**, 219 (1984).
[39] *C. P. Wilke, P. Chang,* Am. Inst. Chem. Eng. J. **1**, 264 (1955).
[40] *S. Bretsznajder,* Prediction of Transport and Other Physical Properties of Fluids, Pergamon Press, Oxford, 1971, pp. 33–39, 358–383.
[41] *J. P. Crombeen, S. Heemstra, J. C. Kraak,* Chromatographia **19**, 219 (1984).
[42] *J. J. Kirkland,* personal communication.

Received: Aug. 3, 1987
Revised manuscript
received: Oct. 8, 1987
Accepted: Oct. 13, 1987
F

New Detection Modes for the Determination of Cephalosporins and Their Decomposition Products

M. D. Blanchin[1] * / W. Th. Kok[2] / H. Fabre[1]

1 Laboratoire de Chimie Analytique, Faculté de Pharmacie, F-34060 Montpellier Cedex, France
2 Laboratory for Analytical Chemistry, University of Amsterdam, NL-1018 WV Amsterdam, The Netherlands

Key Words

Column liquid chromatography
Cephalosporins electrochemical detection
Cephalosporins fluorescence detection
Cephalosporins comparison detection modes

Summary

The feasibility of using fluorescence and electrochemical detection after high performance liquid chromatography separation is investigated for a sensitive and selective determination of cephalosporins and their decomposition products. The sensitivity and detectability of fluorescence and electrochemical detection are compared to those of UV absorption detection.

The methods have been validated for the determination of cephalosporins in biological fluids and for stability studies *in vitro*.

Introduction

Cephalosporins are a widely used class of antibiotics from the β-lactam family.

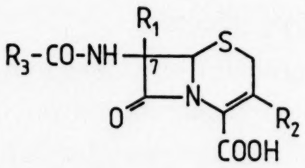

These compounds are generally monitored by HPLC with UV absorption detection in biological fluids and pharmaceutical formulations. However, this detection mode lacks specificity for the determination of cephalosporins in biological fluids and it does not allow the detection of non UV absorbing decomposition products for stability studies *in vitro*. In the search for selective and/or sensitive methods for the determination of cephalosporins, the possibility of using fluorescence and electrochemical detection as complementary or alternative detection modes to UV absorption detection has been investigated.

The methods discussed are based:

- on the properties presented by some substituents (R_3) on the side-chain in the 7-position of the β-lactam nucleus: when a primary amino group is present, fluorescence detection can be used after post-column derivatization with fluorescamine; when an aminothiazole group is present, anodic amperometric detection can be used.
- on the possibility that the β-lactam ring is oxidized by bromine; this is used for indirect electrochemical detection.

The sensitivity and detectability of the proposed methods have been compared to those of UV absorption detection.

The methods have been validated for the determination of caphalosporins in biological fluids and for stability studies *in vitro*.

Fluorescence Detection

Principle

Cefaclor, cefalexin, cefadroxil, cephradine, cefaloglycine and cefroxadine (which have a primary amino group on their side-chain) give fluorescent derivatives with fluorescamine. The reaction is fast and can be used for a post-column derivatization of these compounds.

Optimized Operating Conditions (Scheme 1)

Results

Linearity: 0–1000 ng injected.
Repeatability: 3.5%
Sensitivity: equivalent to that of UV absorption detection.
Detectability: 5 ng injected.

This method is reliable for the determination of cephalosporins in serum and urine. Its selectivity is better than that obtained using UV absorption detection as shown on the chromatograms of a urine sample spiked with cefroxadine (Fig. 1).

0009-5893/87 0625-03 $03.00/0

© 1987 Friedr. Vieweg & Sohn Verlagsgesellschaft mbH

Scheme 1

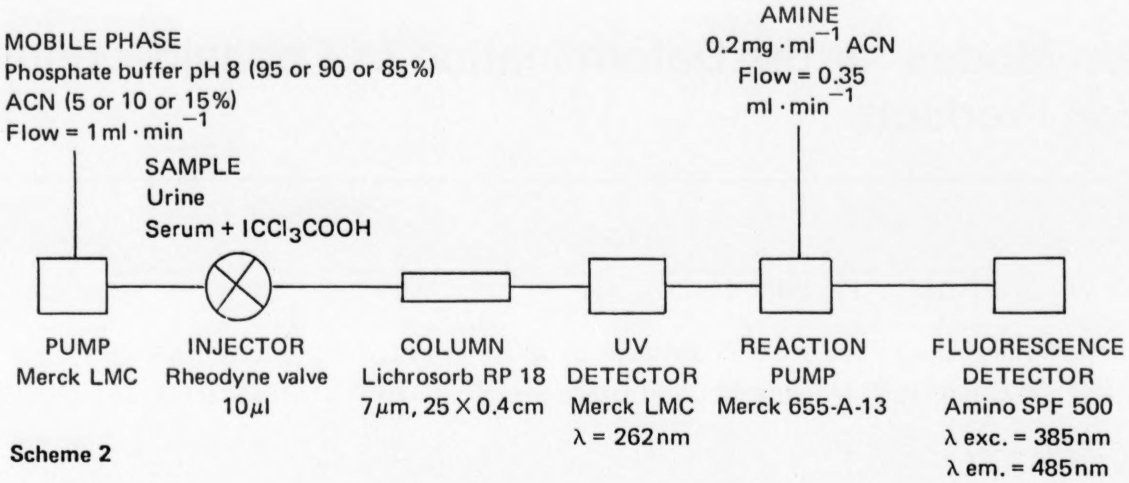
MOBILE PHASE
Phosphate buffer pH 8 (95 or 90 or 85%)
ACN (5 or 10 or 15%)
Flow = 1 ml · min^{-1}
SAMPLE
Urine
Serum + $ICCl_3COOH$
FLUORESC-AMINE
0.2 mg · ml^{-1} ACN
Flow = 0.35 ml · min^{-1}
PUMP
Merck LMC
INJECTOR
Rheodyne valve
10 μl
COLUMN
Lichrosorb RP 18
7 μm, 25 X 0.4 cm
UV DETECTOR
Merck LMC
λ = 262 nm
REACTION PUMP
Merck 655-A-13
FLUORESCENCE DETECTOR
Amino SPF 500
λ exc. = 385 nm
λ em. = 485 nm

Scheme 2

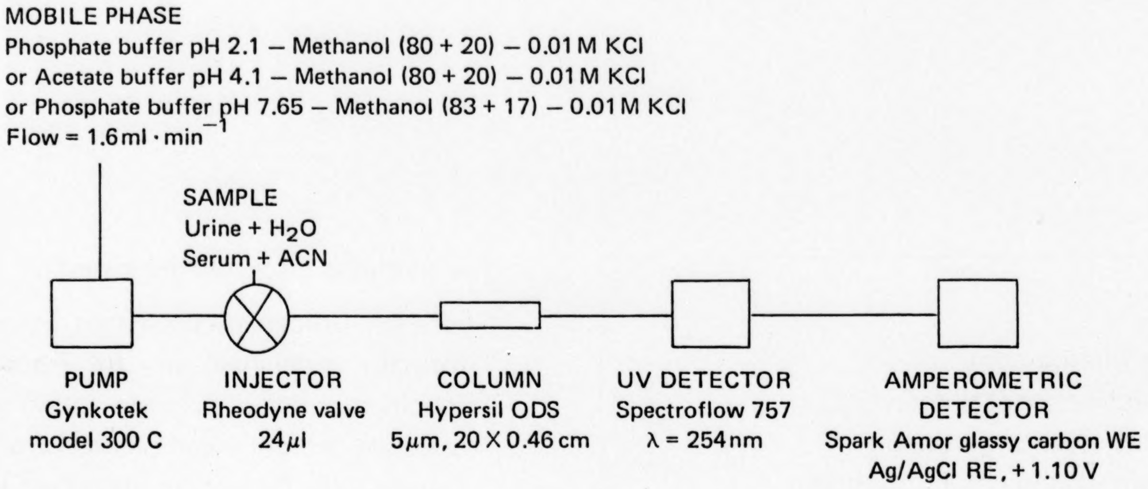
MOBILE PHASE
Phosphate buffer pH 2.1 – Methanol (80 + 20) – 0.01 M KCl
or Acetate buffer pH 4.1 – Methanol (80 + 20) – 0.01 M KCl
or Phosphate buffer pH 7.65 – Methanol (83 + 17) – 0.01 M KCl
Flow = 1.6 ml · min^{-1}
SAMPLE
Urine + H_2O
Serum + ACN
PUMP
Gynkotek
model 300 C
INJECTOR
Rheodyne valve
24 μl
COLUMN
Hypersil ODS
5 μm, 20 X 0.46 cm
UV DETECTOR
Spectroflow 757
λ = 254 nm
AMPEROMETRIC DETECTOR
Spark Amor glassy carbon WE
Ag/AgCl RE, + 1.10 V

Direct Electrochemical Detection

Principle

Cefotaxime and its main decomposition products, ceftizoxime, cefmenoxime, ceftazidime and ceftriaxone (which have an aminothiazole substituent on their side-chain) can be oxidized at a glassy carbon electrode with a potential of + 1.1. V (vs Ag/AgCl). Characteristic hydrodynamic voltammograms have been obtained at pH 2.1, 4.1 and 7.6.

Optimized Operating Conditions (Scheme 2)

Results

Linearity: 0–500 ng injected.
Repeatability: 3.5%.
Sensitivity: better than that obtained with UV absorption detection (× 5 to 8).
Detectability: 0.5 ng injected.

This method is reliable for the determination of cephalosporins in serum and urine. Moreover, in drug stability studies *in vitro*, it allows the detection of more decomposition products than in UV absorption detection, as shown on the chromatograms on a cefmenoxime aqueous solution (Fig. 2).

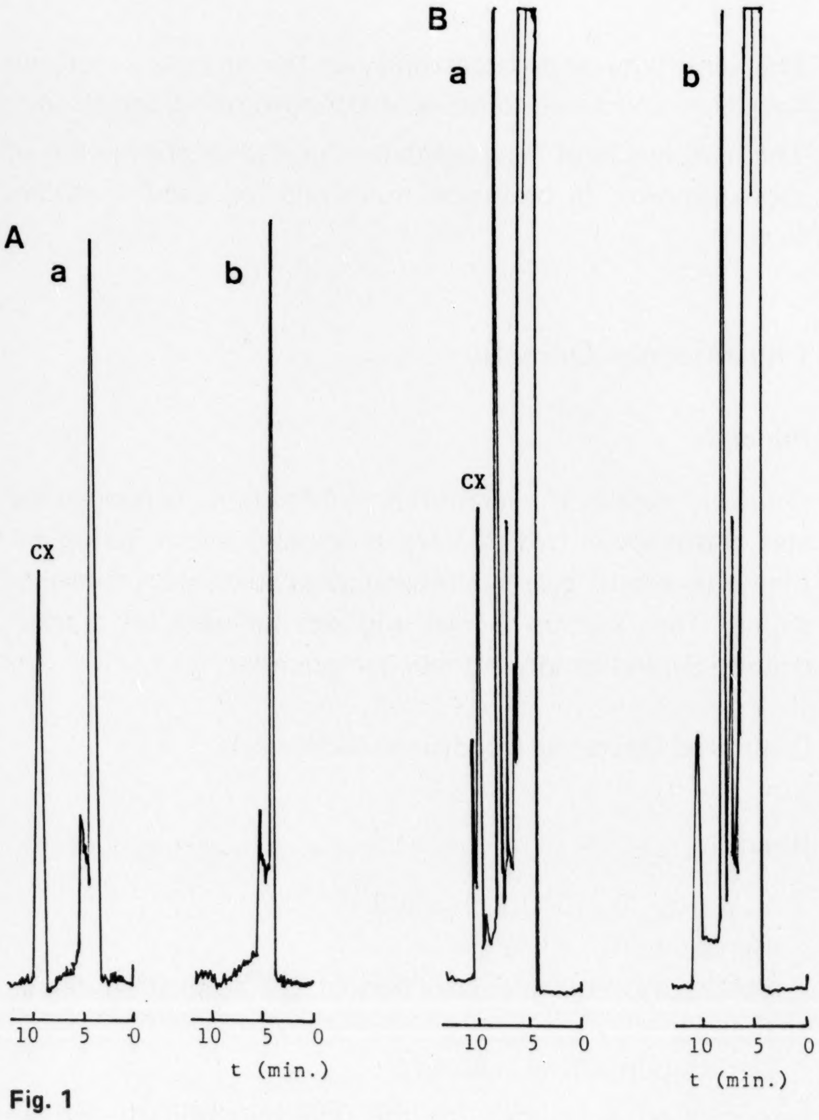

Fig. 1
Chromatograms of cefroxadine (CX) in urine
A – Fluorescence detection.
B – UV absorption detection.
a – Urine spiked with 5.5 μg · ml^{-1} CX
b – Blank urine

Indirect Electrochemical Detection

Principle

In this in-line coulometric titration technique, the bromine is electrochemically produced in the column effluent from a precursor (Br^-) added in the mobile phase. After reaction

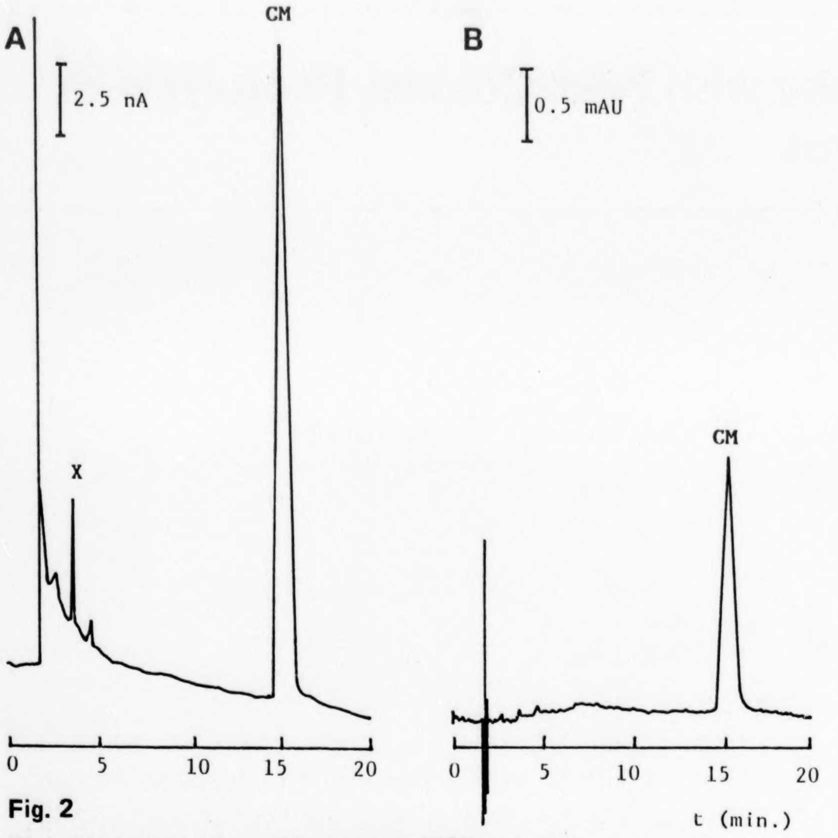

Fig. 2

Chromatograms of a cefmenoxime (CM) solution

A — Electrochemical detection.

B — UV absorption detection.

Injected amount 76.3 ng.

Mobile phase: 0.05 M phosphate buffer pH 2.1–CH_3OH (80 + 20).

Flow = 1.6 ml · min^{-1}.

X = unknown degradation product.

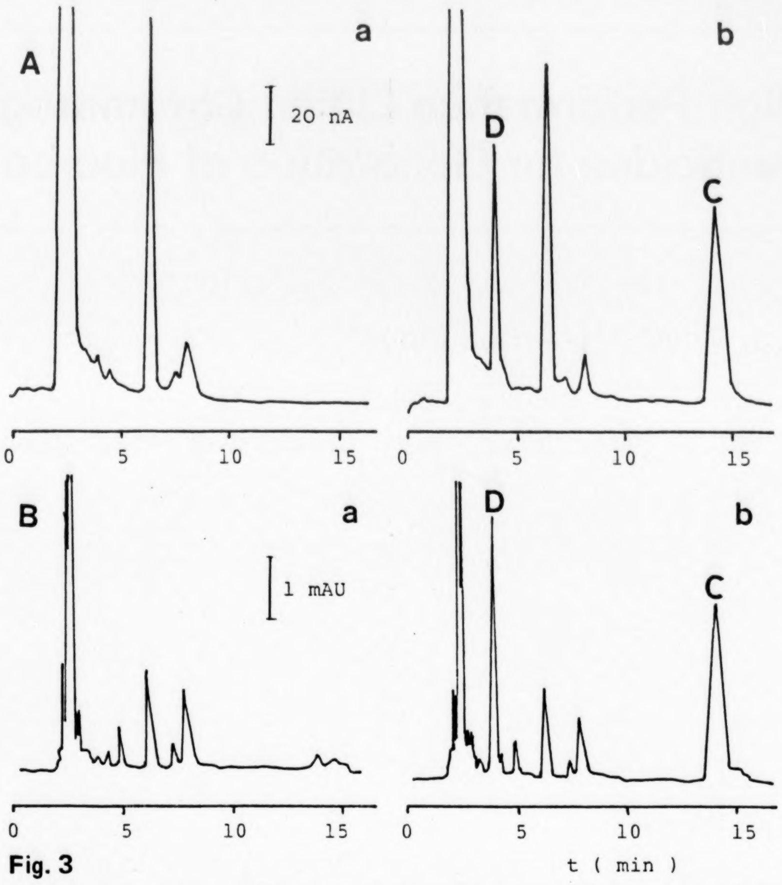

Fig. 3

Chromatograms of cefotaxime (C) and desacetylcefotaxime (D) in serum

A — Indirect electrochemical detection, $i_G = 25 \mu A$

B — UV absorption detection

a — Blank urine

b — Serum spiked with 26.7 μg · ml^{-1} C and 11.5 μg · ml^{-1} D. Sample diluted with water (1 + 4) before injection.

Scheme 3

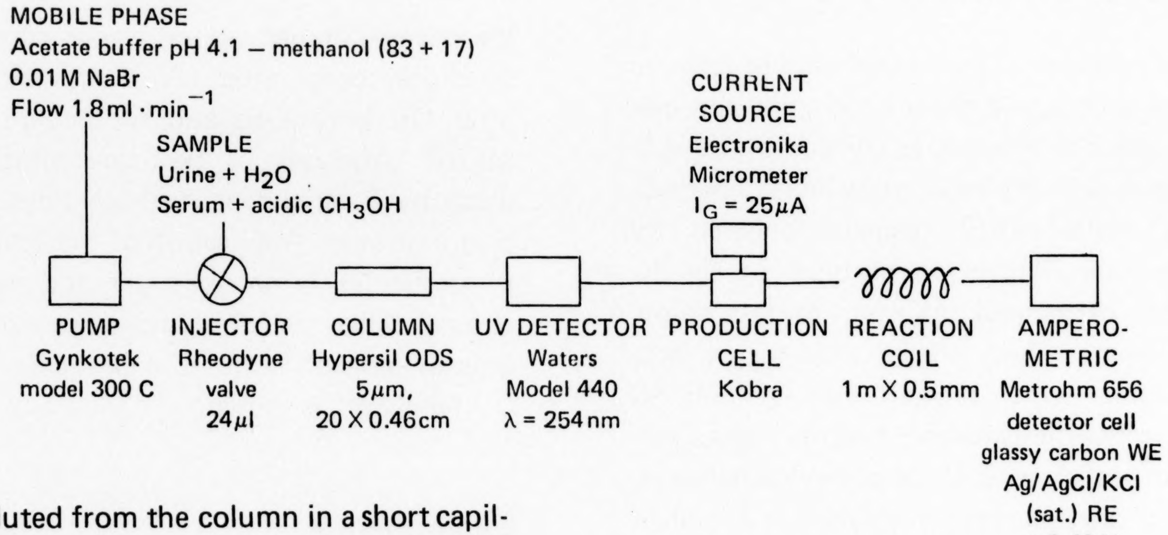
MOBILE PHASE
Acetate buffer pH 4.1 — methanol (83 + 17)
0.01 M NaBr
Flow 1.8 ml · min⁻¹
SAMPLE
Urine + H₂O
Serum + acidic CH₃OH
CURRENT SOURCE
Electronika
Micrometer
I_G = 25 μA
PUMP
Gynkotek
model 300 C
INJECTOR
Rheodyne
valve
24 μl
COLUMN
Hypersil ODS
5 μm,
20 X 0.46 cm
UV DETECTOR
Waters
Model 440
λ = 254 nm
PRODUCTION CELL
Kobra
REACTION COIL
1 m X 0.5 mm
AMPERO-METRIC
Metrohm 656
detector cell
glassy carbon WE
Ag/AgCl/KCl
(sat.) RE
+ 0.40 V

with cephalosporins eluted from the column in a short capillary coil, the bromine excess is determined with an amperometric detector, in a reductive mode. This method has particularly been studied on cefotaxime and its decomposition products, but it has also been extended to cephalosporins bearing various substituents (ceftizoxime, cefmenoxime, ceftazidime, cefotiam, cefoxitin, cefadroxil, cefsulodin and cefazolin). It can be applied to all the cephalosporins since it is based on the property of the β-lactam ring to be oxidized by bromine.

Optimized Operating Conditions (Scheme 3)

Results

Linearity: 0–350 ng injected.

Repeatability: 3%

Sensitivity: equivalent to that obtained with UV absorption detection.

Detectability: 3 ng injected.

This method is reliable for the determination of cephalosporins in serum and urine. Its selectivity is better than that obtained with UV absorption detection, as shown on the chromatograms of a serum sample spiked with desacetylcefotaxime and cefotaxime (Fig. 3). Moreover, it allows the detection of decomposition products which do not absorb in UV for drug stability studies *in vitro*.

Conclusion

The developed methods are reliable and have been validated for the determination of cephalosporins in serum and urine.

Electrochemical and fluorescence detection are more specific or sensitive detection modes than UV absorption detection.

Electrochemical and fluorescence detection can be used as alternative or complementary detection modes to UV absorption detection in therapeutic monitoring, pharmacokinetic studies and in drug stability studies *in vitro*.

Received: July 20, 1987
Accepted: Aug. 5, 1987
F

High Performance Liquid Chromatography with Post-Column Photolysis of Pesticides for Generation of Fluorophores

C. J. Miles* / H. Anson Moye[1]

Department of Agricultural Biochemistry, University of Hawaii at Manoa, Honolulu, Hawaii 96822
[1] Pesticide Research Laboratory, University of Florida, Gainesville, FL 32611, USA

Key Words

Column liquid chromatography
Photolysis
Pesticide analysis
Fluorescence

Summary

Several classes of pesticides have been found to respond to a high performance liquid chromatography post-column reaction detector that employs UV photolysis with an optional reaction with o-phthalicdicarboxaldehyde-2-mercaptoethanol (OPA-MERC) reagent followed by fluorescence detection. Photolysis of most of the N-methylcarbamates, carbamoyl oximes, carbamothioic acids, dithiocarbamates, and phenylureas tested produced primary amines which reacted with OPA-MERC to form the respective derivatives. In some cases, substituted aromatic pesticides such as phenylcarbamates, phenylamides, and phenylureas photolyzed to chemical species which had native fluorescence. This technique was successfully applied to a method for pesticide analyses in groundwater and vegetation. For aldicarb sulfone, a pesticide that did not absorb UV light, use of acetone as a photosensitizer enhanced detection.

Introduction

Occurrence of pesticides in groundwater has aroused the interest of scientists and the public alike. Information concerning contamination of water has been lacking, consequently there are current efforts by the USEPA to examine approximately 1500 well water samples from the 50 states for about 120 pesticides [1]. Studies of this type need methods that can rapidly and sensitively determine several pesticides in a single analysis.

Currently, EPA Method 531 can sensitively and selectively determine N-methylcarbamates and carbamoyl oxime pesticides by HPLC with a post-column reaction detector [2]. After separation the pesticides are hydrolyzed with hot base to form methylamine which condenses with o-phthalicdicarboxaldehyde (OPA) and 2-mercaptoethanol (MERC) to produce a highly fluorescent isoindole [3]. Luchtefeld [4] demonstrated that phenylurea herbicides could be sensitively determined by HPLC with post-column photolysis and labelling with OPA-MERC to form fluorescent products.

We have examined several classes of nitrogenous pesticides for fluorescence after UV photolysis and for fluorescence after UV photolysis and subsequent reaction with OPA-MERC. Analyses of pesticide phototransformation products by independent methods have revealed partial reaction pathways. Application of this technique to the analysis of pesticides in groundwater and vegetation are demonstrated. Also, use of a photosensitizer to enhance photolysis of aldicarb sulfone, a pesticide that does not absorb UV light well, is shown.

Experimental

An illustration of the instrument used is shown in Fig. 1 and details of the equipment used can be found elsewhere [5]. Linuron, monuron, and methomyl were obtained from DuPont (Wilmington, DE) while the remainder of the standard pesticides came from the U.S. Environmental Protection Agency, Pesticides and Industrial Chemicals Repository (Research Triangle Park, NC). One mg/mL solutions of each pesticide were prepared in acetonitrile. (Caution: All pesticides are potentially harmful and should be handled with care!).

Groundwater was obtained from a well in Collier County, Florida, and was fortified by adding selected pesticides. Fortified groundwaters were analyzed without any sample pretreatment. Vegetation samples were obtained from the IR-4 project in our laboratory. Samples were fortified with thiobencarb (Bolero®; Chevron Chem. Co.) and analyzed by the method described by the manufacturer. The method consists of blending chopped sample with ethyl acetate in triplicate, filtration, and concentration by rotary evapora-

0009-5893/87 0628-05 $03.00/0

© 1987 Friedr. Vieweg & Sohn Verlagsgesellschaft mbH

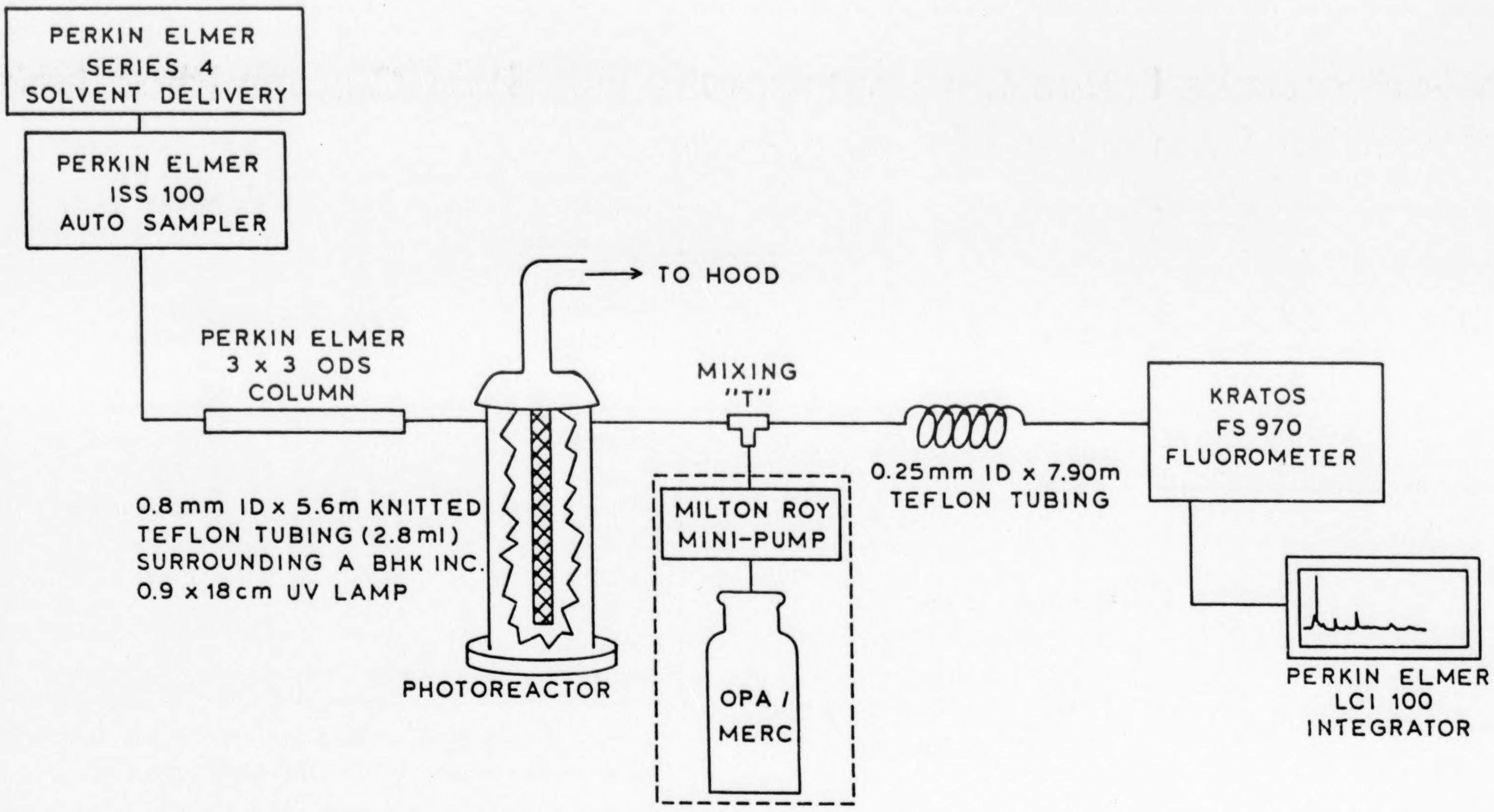

Fig. 1

Configuration of the HPLC post-column UV photolysis/OPA-MERC instrumental system. Optional equipment is enclosed by dashed lines.

tion. This concentrate is fractionated on an alumina column with 15% ether in hexane and concentrated again before determination by GC/NPD. The above extracts were dried and reconstituted in acetonitrile for analysis by the HPLC instrument shown in Fig. 1. Fortified vegetation samples that were prepared as described above except not fractionated on the alumina column were also analyzed by the same HPLC instrument.

Photodegraded pesticide solutions were obtained by irradiating 200μg of each pesticide in acetonitrile in the photoreactor at 0.5 mL/min. Controls were prepared identically with the UV light off. Primary amines in these mixtures were determined by cation exchange HPLC with post-column fluorogenic labeling with OPA-MERC (see ref. [5] for details). Photodegraded and control pesticide mixtures were acylated with trifluoroacetic anhydride (1 hour @ 100°C) and analyzed by gas chromatography/mass spectrometry on a Finnigan 4500 system.

Results and Discussion

Several of the pesticides tested showed fluorescence (Ex 235nm; Em > 418nm) after photolysis and all of these compounds had aromatic character suggesting that phototransformation of this moiety results in fluorescent species. Phenylureas, phenylcarbamates, and phenylamides are pesticides that respond this way. Examination of structures and several experiments indicated that these fluorescent species were hydroxy-substituted anilines and mass spectra are consistent with this identification [5].

Photolysis of most of the N-methylcarbamates, carbamoyl oximes, carbamothioic acids, dithiocarbamates, and phenylureas tested produced primary amines which fluoresced when reacted with OPA-MERC. Exceptions were (a) pesticides that did not absorb UV light well, such as aldicarb sulfone, (b) phenylureas that did not have at least one methyl group attached to the nitrogen atom opposite the ring, and (c) dithiocarbamates without the N,N-dimethyl group. Although most of these pesticides which reacted with OPA-MERC to give fluorophores produced methylamine upon photolysis, carbamothioic acids produced primary amines corresponding to the alkyl groups attached to the nitrogen atom. Fig. 2 summarizes the photolysis reactions observed in this study.

Application of this technique to a method for the determination of pesticides in groundwater showed that several classes of pesticides could be separated and detected at ppb concentrations (see Fig. 3). These pesticides are from lists of pesticides that the USEPA has recognized as potential groundwater pollutants and are part of a National Pesticide Survey of Ground Water [1]. Currently, this HPLC/photolysis/fluorescence method can determine 25 pesticides from the USEPA lists; those compounds and their detection limits are listed in Table I. This method allows rapid, selective and sensitive analysis of groundwater samples with no sample preparation other than filtration.

Recoveries of thiobencarb from fortified celery, lettuce, and carrot vegetation using GC/NPD and HPLC/photolysis/fluorescence were comparable (see Table II). Analysis of the same vegetation without the alumina column cleanup

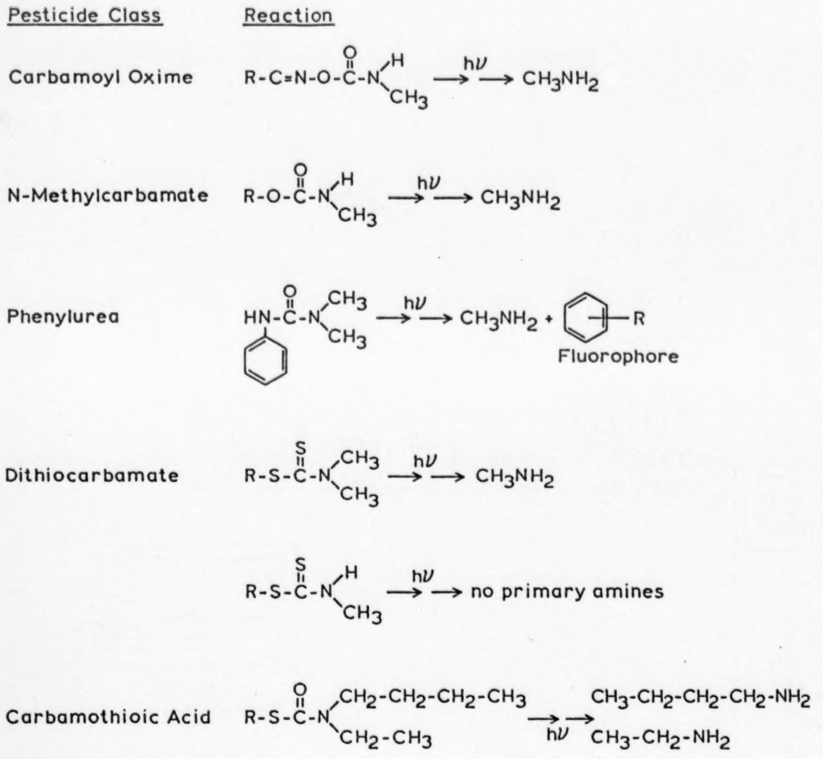

Fig. 2
Photolysis reactions observed in this work.

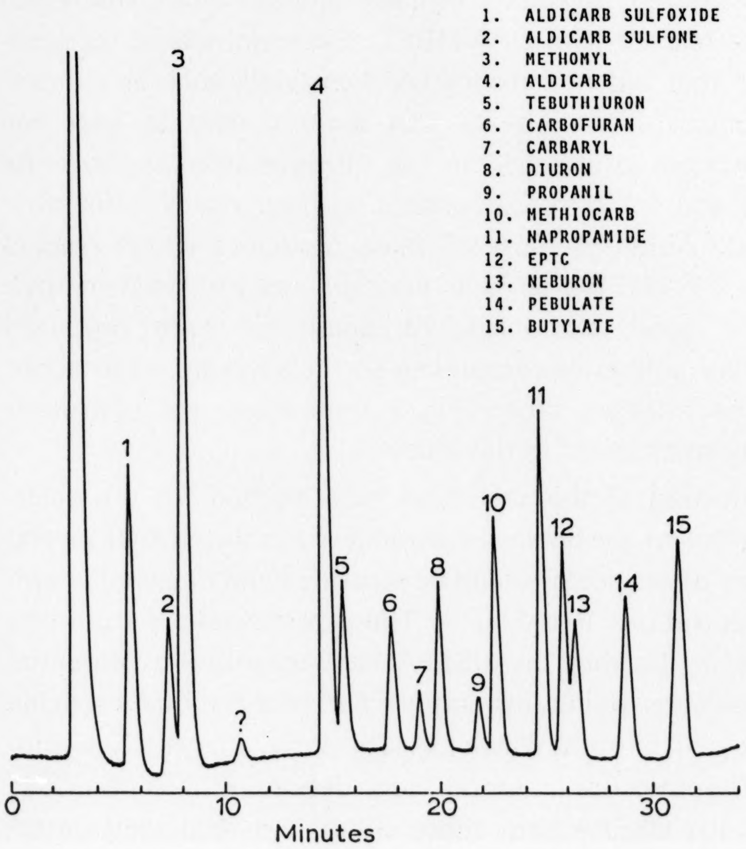

Fig. 3
Chromatogram of 15 pesticides from the USEPA National Pesticide Survey in Ground Water lists analyzed by the instrument in Fig. 1 (with OPA-MERC). Conditions: Perkin-Elmer 3 X 3 C_{18} column; 1.0mL/min, linear gradient of 95% water/5% acetonitrile to 50% water/50% acetonitrile in 20min, hold at 50/50 for 10min; 8min equilibration at 95/5; about 100ng each except 1000ng for aldicarb sulfone and tebuthiuron.

Table I. Pesticides from the USEPA National Pesticide Survey in Ground Water lists that can be analyzed with the instrument shown in Fig. 1 and limits of detection (ng)*.

List 1		List 2	
Aldicarb	0.9	Barban	(4.9)
Aldicarb sulfoxide	1.0	Chlorpropham	(5.0)
Baygon	1.3	Linuron	(4.7)
Butylate	1.0	Neburon	0.8
Cycloate	1.8	Pebulate	1.1
Diuron	4.6	Propanil	(0.7)
Fluometuron	(1.4)	Vernolate	1.1
Propachlor	(88)	Methiocarb	3.4
Propham	(5.0)	EPTC	3.9
Aldicarb sulfone	26	Napropamide	2.2
Carbaryl	13		
Carbofuran	4.7		
Methomyl	0.7		
Oxamyl	ca. 1		
Tebuthiuron	26		

* Limit of detection criteria is S/N = 3; all detection limits in parenthesis are without the OPA-MERC reagent.

Table II. Percent recoveries (avg of duplicates) of Bolero (thiobencarb) from fortified vegetation samples using two methods.

GC/NPD	0.5ppm	1.0ppm	1.0ppm[a]
celery	88	83	[b]
lettuce	104	84	[b]
carrots	84	98	[b]
HPLC/photolysis/fluorescence			
celery	107	87	102
lettuce	140	104	105
carrots	104	87	58

[a] no alumina column clean-up step
[b] interference prevented measurement.

by GC/NPD was not possible because of crop interferences but thiobencarb was resolved from crop coextracts by the HPLC/photolysis/fluorescence system (see Fig. 4). Elimination of the alumina column cleanup step significantly decreases sample analysis time and should increase precision by minimizing sample manipulation.

Aldicarb sulfone did not produce high fluorescence with this system whereas aldicarb and aldicarb sulfoxide did [5]. This failure is apparently caused by the weak absorption of 254nm radiation from the photolysis lamp by aldicarb sulfone. A means of circumventing this problem is to cause indirect photolysis of the analyte by using a photosensitizer, such as acetone. Acetone absorbs the UV radiation and transfers the energy to aldicarb sulfone to achieve photolysis.

After acetone was added to the mobile phase (95% water/5% methanol) in varying amounts, the reaction detector response of aldicarb sulfone increased more than 10-fold with 0.3% acetone (see Fig. 5). Chromatograms of aldicarb sulfoxide and aldicarb sulfone standards and fortified and control groundwater in the presence and absence of acetone show the effect of photosensitizer (Fig. 6). These results

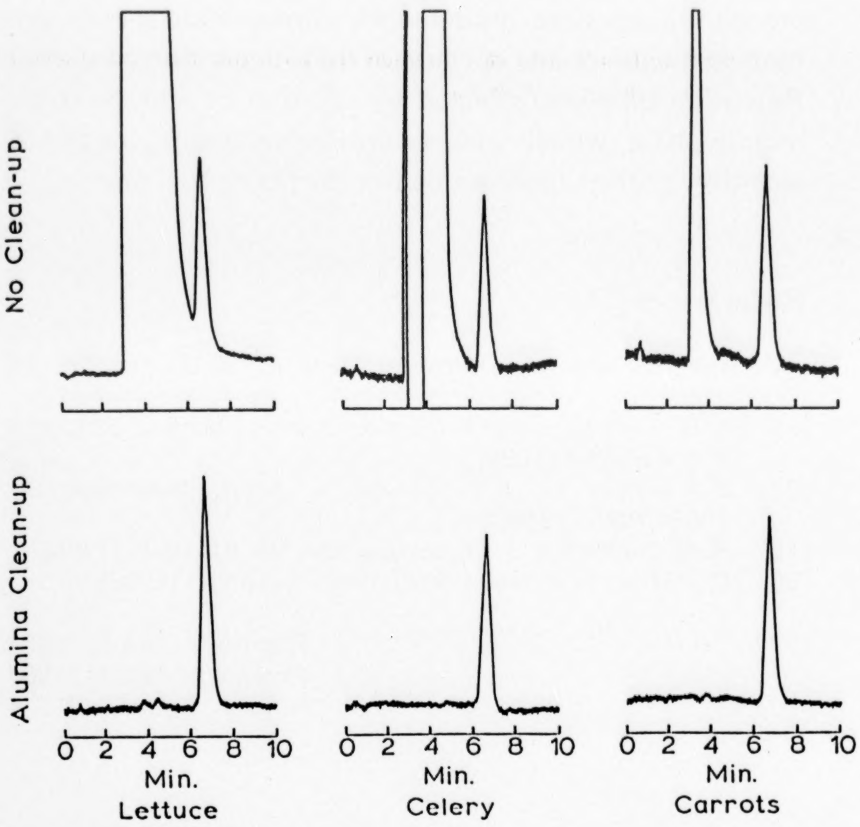

Fig. 4

Chromatograms of crop extracts fortified with thiobencarb (6.5 min) with and without alumina column clean-up step analyzed by the instrument in Fig. 1 (with OPA-MERC). Conditions: Perkin-Elmer 3 X 3 C_{18} column; 1.0 mL/min of 50% water/50% acetonitrile.

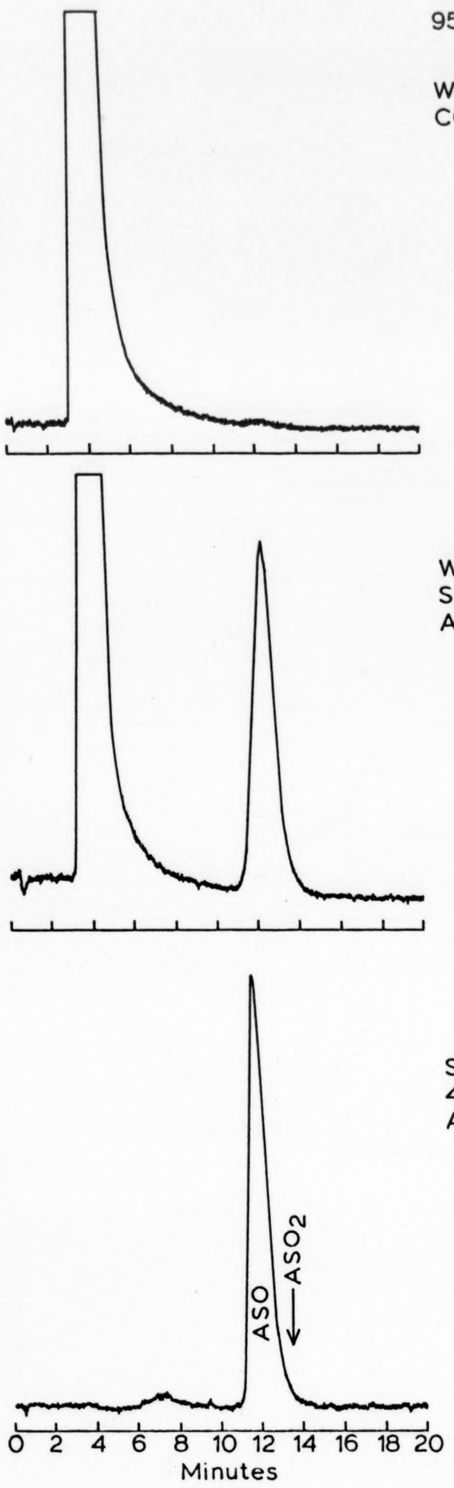

Fig. 6

Chromatograms of well water, well water fortified with 100 ppb aldicarb sulfoxide (ASO) and aldicarb sulfone (ASO_2), and ASO and ASO_2 standards analyzed by the instrument in Fig. 1 (Perkin-Elmer 3 X 3 C_{18} column, 1.0 mL/min of 95% water/5% methanol).

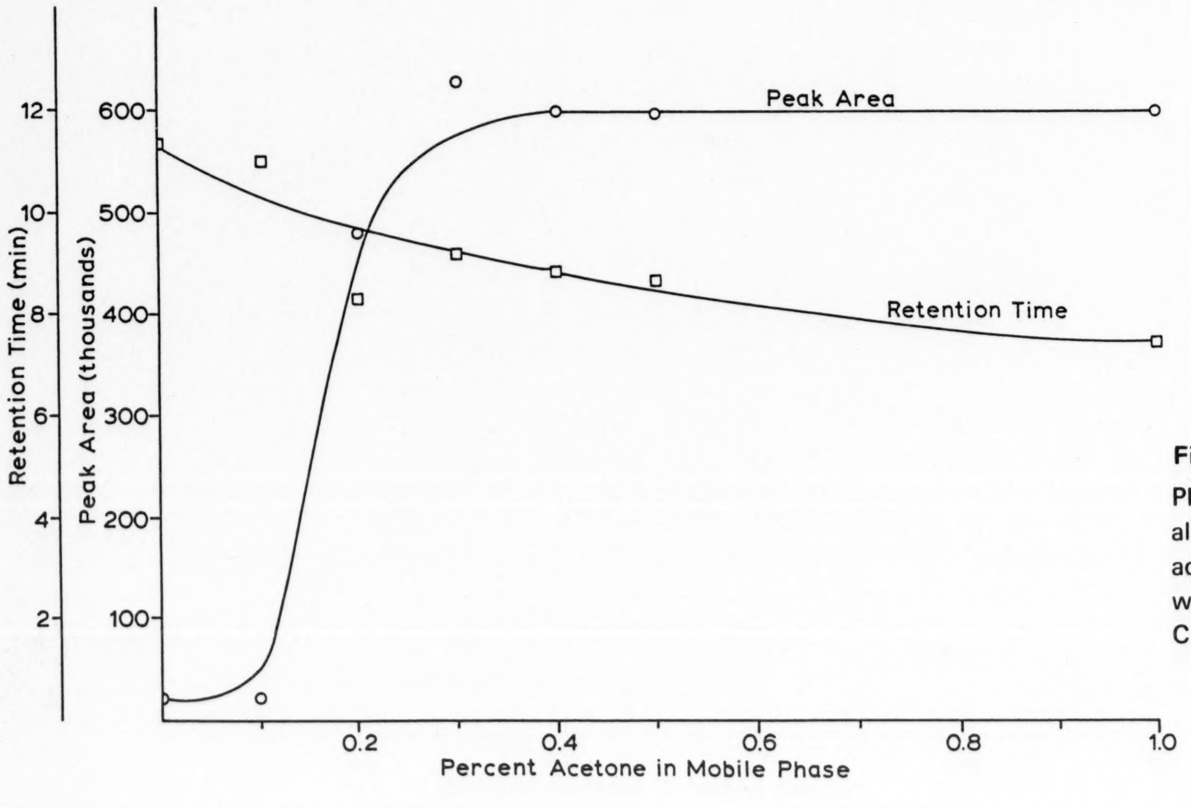

Fig. 5

Plots of the retention time and peak area of aldicarb sulfone as a function of the percent of acetone added to the mobile phase of 95% water/5% methanol (Perkin-Elmer 3 X 3 C_{18}).

are significant since groundwater contamination with aldicarb pesticide usually consists of these two oxidized species. Retention time was affected by addition of acetone to the mobile phase, which could be avoided by adding the photosensitizer post-column but before the photolysis reactor.

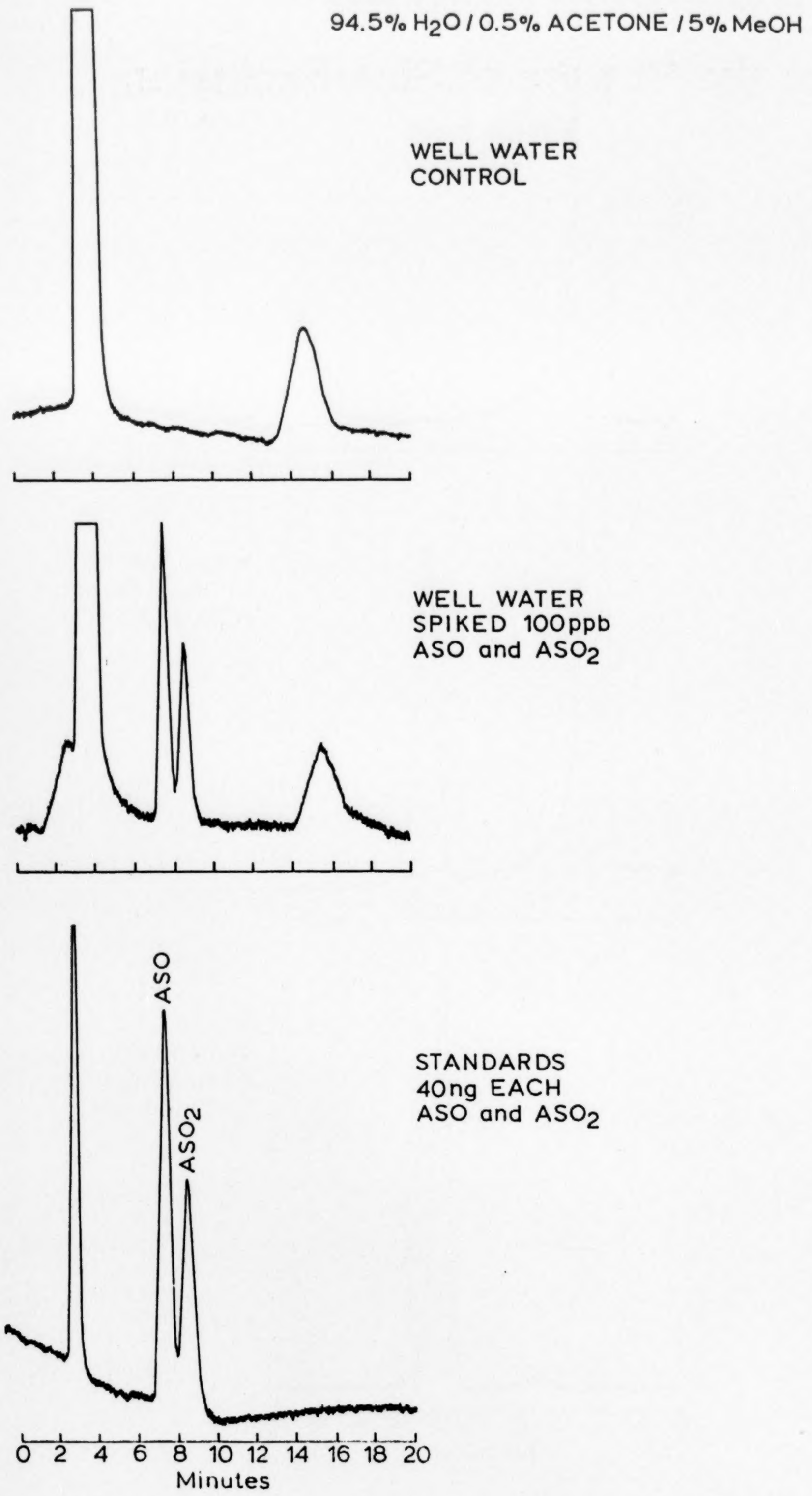

Fig. 7

Same as Fig. 6 except 0.5% acetone added to the mobile phase.

References

[1] Pesticide and Toxic Chemicals News, p. 19–20, February 11, 1987.
[2] U.S. Environmental Protection Agency, Method 531, EPA 600/4-85/054 (1985).
[3] *S. S. Simons Jr., D. F. Johnson*, J. Amer. Chem. Soc. **98**, 7098–7099 (1976).
[4] *R. G. Luchtefeld*, J. Chromatogr. Sci. **23**, 516–520 (1985).
[5] *C. J. Miles, H. A. Moye*, Anal. Chem. (in press) (1988).

Received: June 30, 1987
Accepted: Aug. 11, 1987
F

Effect of Draining of Macromolecules on the Results of Size-Exclusion Chromatography Measurements

L. Z. Vilenchik* / T. P. Zhmakina / V. P. Sklizkova / V. V. Kudriavtsev / T. B. Tennikova / N. G. Belnikevich / B. G. Belenkii / S. Ya. Frenkel / M. M. Koton

Institute of Macromolecular Compounds, Academy of Sciences of the USSR, Leningrad, USSR

Key Words

Size-exclusion chromatography
Macromolecules
Polymers
Draining

Summary

Using chromatographic analysis and viscometric investigations of polyamic acids, it has been shown that the linear relationship of the logarithm of intrinsic viscosity and the logarithm of molecular weight of flexible-chain macromolecules exhibits a break on passing from the oligomeric to the polymeric range. Simultaneously, the Huggins constant also changes.

These changes result from a decrease in the draining of macromolecules with increasing number of statistical segments. In particular, draining affects the hydrodynamic dimensions determining the SEC-behavior of macromolecules.

Semi-empirical expressions have been obtained for the Flory constant Φ and the constants in the Mark-Kuhn-Houwink equation as functions of the draining of macromolecules, the number of their statistical segments and the parameter of volume interaction characterizing the thermodynamic strength of solvent. For this purpose the solution of an integral equation for eigen-functions in the Zimm theory found by Tschoegl was applied.

Introduction

Size-exclusion chromatography (SEC) is one of the most reliable physico-chemical methods for the determination of the hydrodynamic size of macromolecules $R \equiv (M[\eta])^{1/3}$. This size is a universal (general) characteristic of all macromolecules and solvents uniquely determining the retention time of macromolecules in a chromatographic experiment [1–3]. To our opinion all the attempts to choose another universal characteristic have failed just because only the R value takes into account both the average size of the macromolecules and the density of the macromolecular coil as well as its partial draining determined by the value of the hydrodynamic interaction between the segments. It is precisely these factors that determine the behaviour of macromolecules in the SEC process.

Theoretical

The effect of draining of the molecular coils on R can easily be followed from the corresponding changes in the Flory parameter Φ representing in the Flory-Fox equation the coefficient of proportionality between the hydrodynamic volume and the cube of the mean-square size of macromolecules $(\overline{S^2})^{1/2}$

$$M[\eta] = \Phi(\epsilon, N, \kappa)\, 6(\overline{S^2})^{3/2} \qquad (1)$$

where $(\overline{S^2})^{1/2} = A\,N^{(1+\epsilon)/2}/(6 + 5\epsilon + \epsilon^2)^{1/2}$.

Here the Flory parameter $\Phi(\epsilon, N, \kappa)$ is written as a function of different variables. One of them, ϵ, characterizes the solvent capacity. The value of ϵ varies from 0 for poor solvents to 0.33 for good solvents [4]. Another value, N, also being the argument of the function $\Phi(\epsilon, N, \kappa)$ is the number of statistical segments in the macromolecular chain. κ characterizes the degree of draining of macromolecules. It is independent on N and is determined as a function of the length of the statistical segments A, their friction coefficient f_0, the solvent capacity ϵ, and viscosity η_0 [5]

$$\kappa = 1 - \frac{4 \cdot 2^{\epsilon/2} f_0}{(12\pi^3)^{1/2} A \eta_0 (1-\epsilon)} \qquad (2)$$

The draining coefficient determined in this manner increases with increasing A and decreasing f_0. It ranges from $\kappa = 1$ when the hydrodynamic interaction between the segments is completely absent (as in Rouse's theory [6]) to $\kappa = 0$ when the coils are non-draining (as in Zimm's theory [7]) but the hydrodynamic interaction is not necessarily very strong. Many theoretical approaches are known

0009-5893/87 0633-04 $03.00/0

© 1987 Friedr. Vieweg & Sohn Verlagsgesellschaft mbH

in which the type of function $\Phi(\epsilon, N, \kappa)$ is derived and its values are estimated. Most of them are presented, for example, in Yamakawa's monograph [8]. However, chromatography requires the function $\Phi(\epsilon, N, \kappa)$ to be as simple as possible for the convenience of the calculation of the value of R in actual experiments.

We propose to use as this dependence the following equation:

$$\Phi(\epsilon, N, \kappa) = \Phi(\epsilon)(1-\kappa)\left[1+\left(\frac{N-N_0}{N}\right)^k \kappa\right] \qquad (3)$$

where $k = 1$ at $N \leqslant N_0$, $k = 3$ at $N > N_0$, $N_0 = 13$, $\Phi(\epsilon) = \Phi(0) \times (1 - 2.63\epsilon + 2.86\epsilon^2)$, $\Phi(0) = 2.86 \times 10^{21}$ l/M.

Eq. (3) is based on the model approach which does not take into account the transverse dimensions of chain units.

This equation employs the solution of the integral equation written for eigenfunctions in the framework of Zimm's theory [7]. Unlike other known solutions this solution was found by Tschoegl [5] taking into account the correction proposed by Osaki [9] extending the solution to the range of low values of $N < 10$.

The family of curves reflecting the relationship in eq. (2) is shown in Fig. 1. Here the value Φ is a function of κ at various values of the parameter ϵ and of the number of statistical segments N. A specific feature of this family of curves is the occurrence of three types of curves: convex curves at $N > N_0$, concave curves at $N < N_0$ and almost linear curves at $N = N_0 = 13$.

The function $\Phi(\epsilon, N, \kappa)$ changes over a wide range from the value of $\Phi(0)$ to zero depending on the draining of the molecules. As a result, the value of R and hence the behaviour of macromolecules in the SEC-experiment also changes with $\Phi(\epsilon, N, \kappa)$. With increasing draining, the hydrodynamic size of molecules decreases and the chromatographic retention increases whereas the size of the coils (average according to conformation) remains invariable. Since the researchers are most often interested in the molecular weights of the polymer samples and molecular-weight distributions rather than in the values of R, it follows that in the interpretation of experimental data partial draining of macromolecules should be taken into account.

The transition from R to M is usually made with the aid of the Mark-Kuhn-Houwink equation:

$$[\eta] = K_\eta M^a \qquad (4)$$

which may be considered as an empirical relationship between the sizes R and the molecular weights M of the macromolecules

$$M = (R^3/K_\eta)^{1/(a+1)} \qquad (5)$$

The constants K_η and a contained in eq. (5) are usually found from the reference literature or determined from the data of special measurements, for example, viscometric and chromatographic measurements [10]. However, the dependence of the Flory parameter Φ on the draining of macromolecules requires a change in the K_η and a values occurring with a change in N. This can easily be seen if an expression R from eq. (1) is substituted into eq. (5) and eq. (2) is applied:

$$K_\eta = \left(\frac{\lambda}{M_0}\right)^{a+1} A^{2-a}[6/(6+5\epsilon+\epsilon^2)]^{3/2}\Phi(\epsilon)(1-\kappa) \qquad (6)$$

$$a = \frac{1+3\epsilon}{2} + \ln\left[1+\left(\frac{\bar{N}-N_0}{\bar{N}}\right)^k \kappa\right] / \ln \bar{N} \qquad (7)$$

where M_0 is the molecular weight of the repeat unit of the macromolecule and λ is the length of the projection of this unit on the chain direction.

Eqs. (6) and (7) are obtained with the assumption that the coefficients K_η and a are independent on the number of statistical segments over a relatively wide range of changes in N. It is reasonable to single out at least three of these ranges: the oligomer ($N < N_0$), the polymer ($N_0 < N < N_1 \geqslant 10 \cdot N_0$) and the high polymer ($N > N_1$) ranges.

This division is tentative. It is caused by the considerations of convenience. $\bar{N}$ is an average value of N characteristic of each of the three above ranges. For these ranges it is possible to write approximately:

$$\begin{array}{ll} a \cong \dfrac{1+3\epsilon}{2} - \dfrac{\kappa}{\ln \bar{N}} & \text{at } N < N_0,\ 0 < \bar{N} < N_0 \\ a \cong \dfrac{1+3\epsilon}{2} + \dfrac{\kappa}{\ln \bar{N}} & \begin{array}{l}\text{at } N \geqslant N_0,\ N_0 < \bar{N} < N_1 \\ \text{and at } N > N_1,\ \bar{N} > N_1\end{array} \end{array} \qquad (8)$$

Eq. (8) corresponds to the dependence of $\ln[\eta]$ on $\ln M$ shown in Fig. 2. It is clear that at the boundary between the oligomers and the polymer ranges (at $N = N_0$) the value a is equal to $a = (1+3\epsilon)/2$. In the limiting case of nondraining molecules, the parameter a acquires the same value in any of the three ranges. In the oligomer range in which the ratio $(N - N_0)/N$ is negative, the value of a is less than $(1+3\epsilon)/2$. In the polymer range $(N - N_0)/N$ it is positive and the value of a is greater than $(1+3\epsilon)/2$. In the high polymer range (at very high N) the value of a

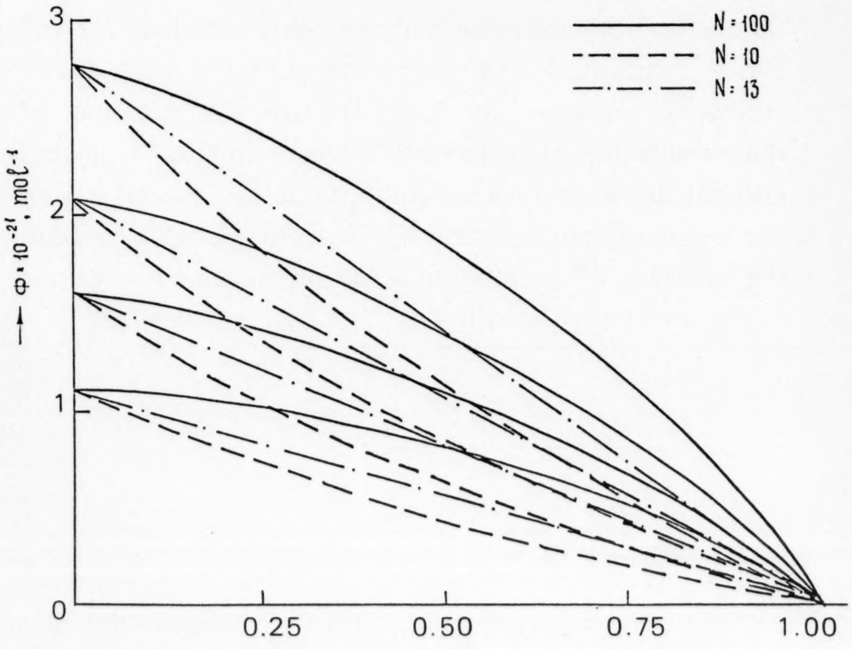

Fig. 1

Flory's parameter Φ vs. degree of the draining of macromolecules at various values of ϵ and N: 1 – $\epsilon = 0$; 2 – $\epsilon = 0.1$; 3 – $\epsilon = 0.2$; 4 – $\epsilon = 0.33$. Solid lines correspond to N = 100; broken lines correspond to N = 10; dashed lines correspond to $N = N_0 = 13$.

decreases again. This behaviour of the parameter a corresponds to Kuhn's concepts [11], and eq. (8) provides a convenient method for the calculation of the a value in each of the ranges of variation in N.

The results presented in this paper caution against a rough averaging of the experimental dependences of $\ln[\eta]$ on $\ln M$ over the entire range of molecular weight values. In the case of draining coils, this averaging can lead to serious errors in the determination of molecular weights.

Experimental

As an example, we are going to report our results obtained in the investigation of polyamic acid [12]. The work with this polymer, a polyelectrolyte, was carried out under the conditions of complete suppression of polyelectrolytic swelling. It was possible to obtain agreement between the data on average molecular weights of the polyamic acid, M_n, M_w and on M_z, determined by SEC, viscometry, light scattering and osmometry only because the draining of macromolecules and the related break in the dependence of $\ln[\eta]$ on $\ln M$ were taken into account. Moreover, a jump in the value of the constant K′ from the Huggins equation was also observed:

$$\eta_{sp}/C = [\eta] + K'C[\eta]^2 \qquad (9)$$

where η_{sp} is the specific viscosity and C is the concentration of the solute. These data are given in Figs. 3 and 4.

It should be noted that the conclusion confirming partial draining of polyamic acid molecules has also been drawn in ref. [13] in which a change in the value of the fundamental hydrodynamic constant at varying molecular weight has also been detected for these molecules:

$$I = R D \eta_0/T \qquad (10)$$

where D is the diffusion coefficient of the macromolecules and T is the absolute temperature.

Results

The draining of macromolecules is an important factor leading to a change in the parameters of the Mark-Kuhn-Houwink equation on passing from the oligomer to the polymer range and subsequently to the high polymer range [14]. This factor should be taken into account in the interpretation of the data of a SEC measurement on passing from the universal calibration dependence of the retention time to the molecular weight dependence.

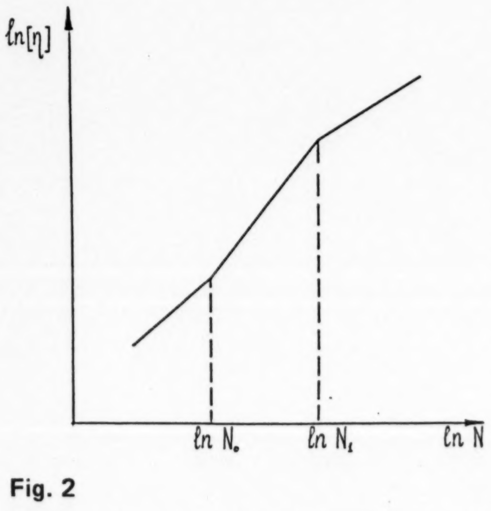

Fig. 2

General shape of the relationship of ln M and ln M over a wide range of changes in M.

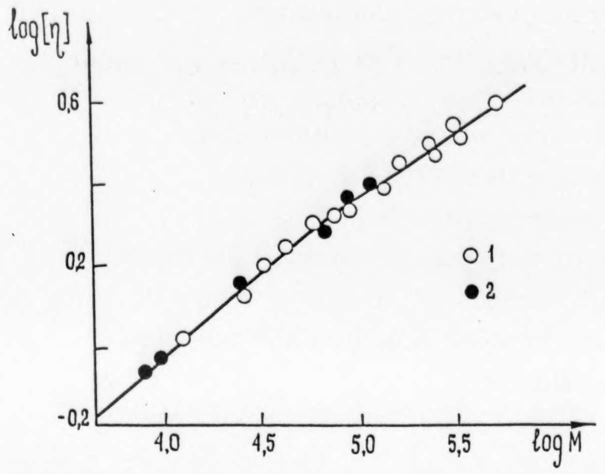

Fig. 3

Experimental relationship of $\log[\eta]$ and $\log M$ for the solutions of polyamic acid in dimethyl formamide (DMF) with additives: 1 – data of light scattering, 2 – data of SEC.

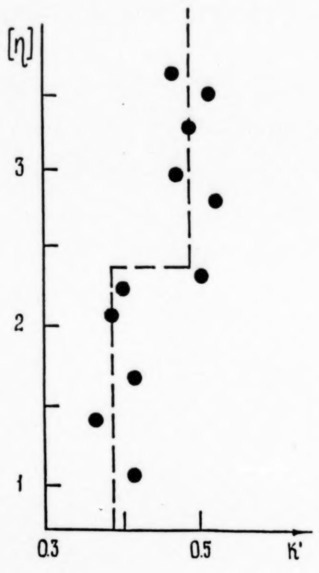

Fig. 4

Stepwise type of the relationship of Huggins constant K′ and $[\eta]$ with changing molecular weight of the molecules of polyamic acid in DMF with additives.

List of Symbols

A	length of a statistical segment
C	concentration of the solute
D	diffusion coefficient of the macromolecule
f_0	friction coefficient of a statistical segment of the macromolecule
I	fundamental hydrodynamic constant
k	auxiliary parameter equal 1 or 3
K′	constant in Higgins equation
K_η	constant in Mark-Kuhn-Houwink equation
M	molecular weight
M_0	molecular weight of the repeat unit in the macromolecule

M_n	number-average molecular weight
M_w	weight-average molecular weight
M_z	z-average molecular weight
R	hydrodynamic size of macromolecules
$(\overline{S^2})^{1/2}$	mean-square size of macromolecules
T	absolute temperature
N	number of statistical segments in the chain
N_0	value of number of statistical segments being a boundary between oligomers and polymers
$\overline{N}$	average value of N
ϵ	parameter characterizing the solvent capacity
η_0	viscosity
$[\eta]$	intrinsic viscosity
η_{sp}	specific viscosity
λ	length of the projection of the repeat unit in the macromolecule on the chain direction
π	3.14
Φ	Flory parameter
κ	parameter characterizing the degree of the draining of macromolecules

References

[1] *Z. Grubisic, P. Rempp, H. Benoit*, J. Polym. Sci., **135**, 753 (1967).

[2] *E.P. Otocka, M.J. Hellman*, Polymer letters, **12**, 331 (1974).

[3] *L.Z. Vilenchik, T.P. Zhmakina, B.G. Belenkii, B.I. Venzel*, Visokomol. Soed., **26A**, 2457 (1984).

[4] *O.B. Pticin, Yu. Ye. Eyzner*, Visokomol. Soed., **3**, 1863 (1961).

[5] *N.W. Tschoegl*, J. Chem. Phys., **39**, 149 (1963); **40**, 473 (1964).

[6] *P.E. Rouse*, J. Chem. Phys., **21**, 1272 (1953).

[7] *B.H. Zimm*, J. Chem. Phys., **24**, 269 (1956).

[8] *H. Yamakawa*, Modern Theory of polymer Solutions, Harper and Row, New York, 1971.

[9] *K. Osaki*, Macromolecules, **5**, 142 (1972).

[10] *B.G. Belenkii, L.Z. Vilenchik*, Modern Liquid Chromatography of Macromolecules, Elsevier, Amsterdam, 1983.

[11] *W. Kuhn, H. Kuhn*, Helv. Chim. Acta, **28**, 97 (1945).

[12] *L.Z. Vilenchik, V.P. Sklizkova, T.B. Tennikova, N.G. Belnikevich, V.V. Nesterov, V.V. Kudriavtsev, B.G. Belenkii, S.Ya. Frenkel*, Visokomol. Soed., **27A**, 927 (1985).

[13] *O.V. Kallistov, Yu.E. Svetlov, T.A. Startseva, V.P. Sklizkova, V.V. Kudriavtsev, M.M. Koton*, Dokl. Akad. Nauk. SSSR, **244**, 396 (1979).

[14] *L.Z. Vilenchik, T.P. Zhmakina, B.G. Belenkii, S.Ya. Frenkel*, Acta Polymerica, **36**, 125 (1985).

Received: June 29, 1987
Revised manuscript
received: Sep. 24, 1987
Accepted: Sep. 29, 1987
F

Solid Phase Extraction and Direct HPLC Separation of Bilirubin and its Conjugates in Plasma

Fami Li/C. K. Lim*/T. J. Peters

Division of Clinical Cell Biology, MRC Clinical Research Centre, Watford Road, Harrow, Middlesex
HAI 3UJ, UK.

Key Words

Column liquid chromatography
Solid phase extraction
Bilirubin

Summary

A semi-automatic reversed-phase HPLC system is described for the direct determination of conjugated and unconjugated bilirubin in human plasma. An Advanced Automated Sample Processor (AASP) is used for sample preparation, and for controlling sample injection and elution. The method is highly sensitive, requiring only 10–50 μl of plasma per assay.

Introduction

The determination of conjugated and unconjugated bilirubin in plasma is important for the differential diagnosis of the various types of jaundice. A major problem in the analysis of conjugated and unconjugated bilirubin in plasma is that while unconjugated bilirubin can be quantitatively extracted, recovery of the conjugates is low and variable due to strong binding to proteins. This problem may be overcome by converting the mono- and di-conjugate (Fig. 1) into the corresponding mono- and di-methyl ester by transmethylation with 2 % KOH in methanol [1]. The methyl esters and unconjugated bilirubin can then be extracted with chloroform for separation by TLC [1] or HPLC [2, 3]. The method, however, is unable to measure the covalently bonded bilirubin-albumin complex (δ-bilirubin or biliprotein) which co-precipitated with the plasma protein. Biliprotein is present in patients with heptobiliary disease and is believed to be related to the duration of cholestasis [4]. Several methods have been described for assaying biliprotein [5–8]. The procedure of McKavanagh and Billing [8], which employed a disposable cartridge to extract conjugated and unconjugated bilirubin but allowed biliprotein to pass straight through the column for subsequent assay by a standard diazo reaction method [9], is the most promising because of its speed and simplicity. Based on the solid phase extraction technique we describe here a semi-automatic HPLC assay for conjugated and unconjugated bilirubin in plasma.

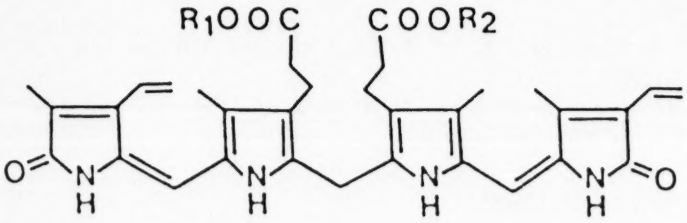

Fig. 1

Structures of bilirubin and its conjugates. Bilirubin: $R_1 = R_2 = H$; Bilirubin C-8 monoglucuronide: R_1 = glucuronic acid, R_2 = H; Bilirubin C-12 monoglucuronide: R_1 = H, R_2 = glucuronic acid; Bilirubin diglucuronide: $R_1 = R_2$ = glucuronic acid.

Experimental

Materials and Reagents

Bilirubin was from Sigma Chemical Co. (Poole, Dorset, UK). Mesobilirubin was prepared by hydrogenation of bilirubin in 0.1 M NaOH with palladium on charcoal as catalyst [10]. Caffeine, sodium benzoate, ammonium acetate, sodium acetate, acetic acid and dimethyl sulphoxide (DMSO) were AnalaR grade from BDH Chemicals (Poole, Dorst, UK). Caffeine-sodium benzoate solution was prepared by adding caffeine (37.5 g), sodium benzoate (57.0 g) and sodium acetate (94.5 g) to water (500 ml) at 60 °C. The mixture was stirred until completely dossolved. It was cooled to room temperature and made up to 1 litre with water.

Sample Preparation with AASP Cartridges

All sample manipulation were carried out in dim light. An Advanced Automated Sample Processor (AASP) Vac-Elut system (Varian, Walnut Creek, CA, USA) was used. The extraction cartridges were C-8 bonded phase. The solutions were driven through the cartridges by positive nitrogen pressure. The extraction procedure was as follows:

(i) Condition the cartridge with methanol (0.5 ml) followed by caffeine-sodium benzoate solution (1 ml).
(ii) Mix plasma (10–50 μl) with caffeine-sodium benzoate solution (0.5 ml). Load mixture onto cartridge and collect the eluate.

0009-5893/87 0637-02 $03.00/0
© 1987 Friedr. Vieweg & Sohn Verlagsgesellschaft mbH

(iii) Wash cartridge with caffeine-sodium benzoate solution (1 ml) and collect the eluate. Combine eluates from (ii) and (iii) for measurement of biliprotein if required.

(iv) Wash cartridge with water (1 ml) followed by 20 % (v/v) methanol in 0.1 M ammonium acetate, pH 5.16 (1 ml).

The cartridge containing the extracted pigments was then placed in the AASP machine for automatic injection and HPLC separation. The run time, cycle time and valve reset time were all set for 13 min.

HPLC

A Varian model 5000 liquid chromatograph with a UV-100 variable-wavelength detector set at 454 nm was used. The separation was carried out on 5 μm ODS-Hypersil (25 cm X 5 mm) from Shandon Southern (Runcorn, Cheshire, UK). The eluents were 0.5 M ammonium acetate adjusted to pH 5.16 with acetic acid (solvent A) and 1 : 1 (v/v) acetonitrile-DMSO (solvent B). The elution program, at a flow rate of 1 ml/min, was as follow:

time 0 to 5 min: linear gradient from 55 to 80 % B;
time 5 to 8 min: isocratic elution at 80 % B;
time 8.1 min: reset to 55 % B;
time 13 min: program complete, automatic injection of second sample, reset to time 0 and restart elution program.

Bilirubin diglucuronide, the two monoglucuronide isomers and unconjugated bilirubin were clearly resolved. Mesobilirubin was used as the internal standard.

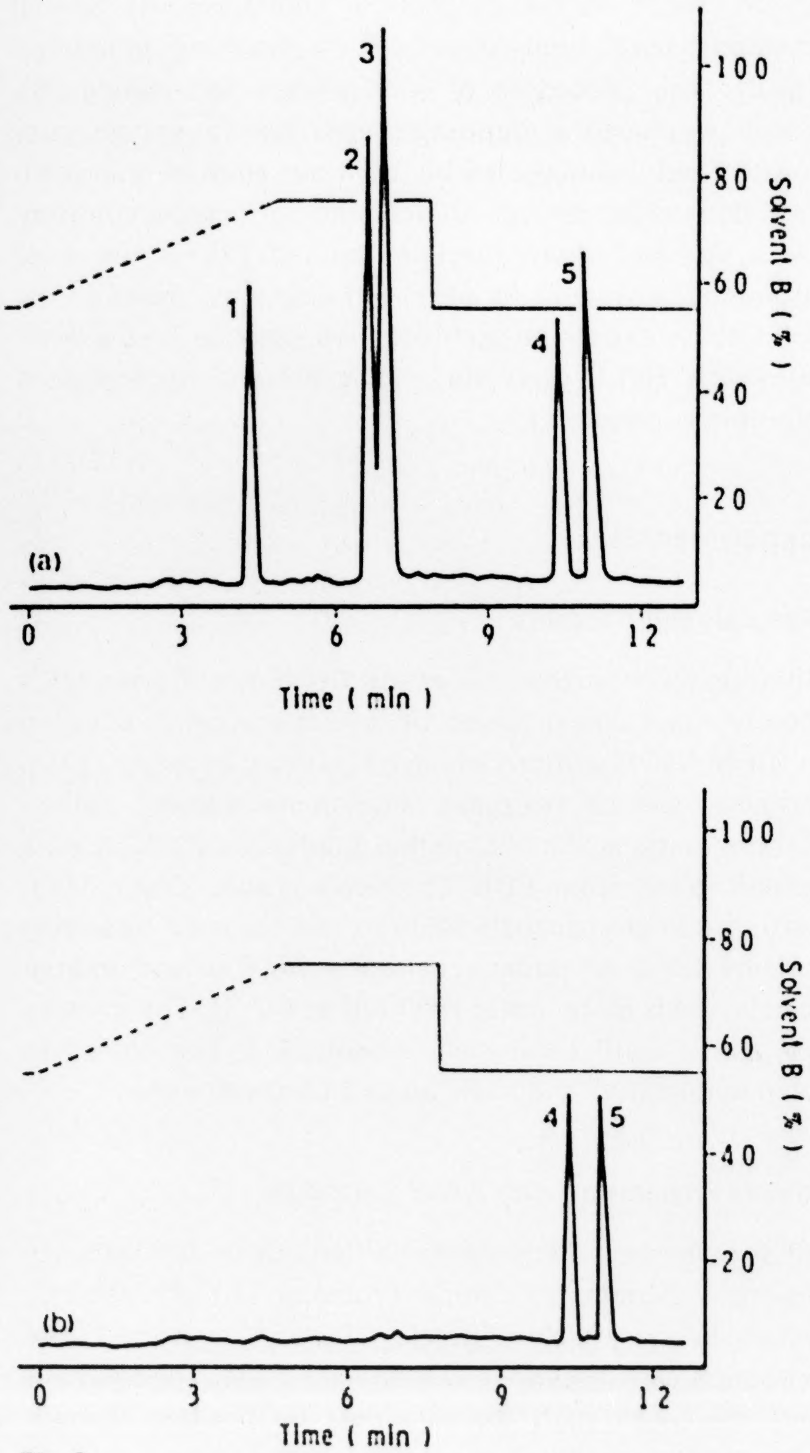

Fig. 2

Separation of conjugated and unconjugated bilirubin in plasma. (a) 10 μl plasma from a patient with hyperbilirubinaemia; (b) 50 μl plasma from a normal subject. HPLC conditions are as described in the Experimental section. Peaks: **1** = bilirubin diglucuronide; **2** = bilirubin C-8 monoglucuronide; **3** = bilirubin C-12 monoglucuronide; **4** = mesobilirubin (internal standard); **5** = bilirubin.

Results and Discussion

Caffeine-sodium benzoate solution [11] and certain drugs [12] are able to displace conjugated and unconjugated bilirubin from their protein-binding sites. The released pigments can be effectively extracted onto reversed-phase cartridges with virtually 100 % recovery. Solid-phase extraction of bilirubins is superior to the transmethylation – solvent extraction method [2] as no derivatization is needed. Another advantage is that bilirubins immobilized on the solid phase are more stable than in solution. A large number of cartridges can thus be processed for automated injection and separation. Typical separations are shown in Fig. 2.

Using the on-line AASP-HPLC system, the extracted bilirubins are totally injected. The method is highly sensitive and requiring only 10–50 μl of plasma per assay. It is therefore especially useful for the differential diagnosis of neonatal jaundice.

The present method does not allow the direct determination of biliprotein. However, since this fraction can be collected from the eluates of the cartridge, it can be measured separately using a standard diazo procedure [9].

References

[1] *N. Blanckaert,* Biochem. J. **185**, 115 (1980).
[2] *N. Blanckaert, P. M. Kabra, F. A. Farina, B. E. Stafford, L. J. Marton, R. Schmid,* J. Lab. Clin. Med. **96,** 198 (1980).
[3] *F. Li, C. K. Lim, T. J. Peters,* J. Chromatogr. **353,** 19 (1986).
[4] *J. S. Weiss, A. Gautman, J. J. Lauff, M. W. Sundlerg, P. Tatlow, J. J. Boyers, D. Seligson,* New Engl. J. Med. **309,** 147 (1983).
[5] *J. J. Lauff, M. E. Kasper, R. T. Ambrose,* Clin. Chem. **29,** 800 (1983).
[6] *N. Blanckaert, G. d'Argenio,* Gastroenterology **82,** 1222 (1982).
[7] *N. Blanckaert, R. Servaes, P. Leroy,* J. Lab. Clin. Med. **108,** 77 (1986).
[8] *S. M. McKavanagh, B. H. Billing,* Biomed. Chromatogr., in press (1987).
[9] *B. T. Doumas, B. W. Perry, E. A. Sasse, J. V. Straumfjord Jr.,* Clin. Chem. **19,** 984 (1973).
[10] *H. Fischer, H. W. Haberland,* Hoppe-Seyler's Z. Physiol. Chem. **232,** 236 (1935).
[11] *K. L. J. Vink, W. Schuurman, R. van Gansewinkel,* Clin. Chem. **32,** 1389 (1986).
[12] *B. E. Davies,* Br. J. Clin. Pharmac. **20,** 345 (1985).

Received: June 30, 1987
Accepted: July 28, 1987
F

Some Aspects of the Preparative Separation of Enantiomers on Chiral Stationary Phases

Veronika R. Meyer

Institute of Organic Chemistry, University of Bern, Freiestraße 3, CH-3012 Bern, Switzerland

Key Words

Column liquid chromatography
Chiral stationary phase
Preparative separation
Polarimeter detector

Summary

In preparative column liquid chromatography, it is necessary to work with conditions of mass overload to obtain high throughput per unit time. The influence of sample mass and of eluent composition on the separation of R,S-1-(1-naphthylethyl)propylamide on chiral 3,5-dinitrobenzoylphenylglycine-silica (Pirkle type stationary phase) was investigated. At a sample load of 200μg of racemate per gram of stationary phase, the column becomes overloaded. At higher sample loads the peaks become triangular; therefore the first peak is always pure up to loads of 10mgg^{-1}, although resolution is low. The purity of the second peak depends on sample mass, but not on the strength (polarity) of the mobile phase. This is due to the effect that peak width, as well as resolution, decrease as the polarity of the eluent increases. In certain cases the polarimeter, used as a detector, can give more information on peak purity than the UV detector.

Introduction

Direct gas [1] and liquid [2] chromatographic separation of enantiomers on chiral stationary phases have become more and more important in the last few years. In column liquid chromatography, an increasing number of chiral stationary phases are commercially available [3], allowing the analytical and preparative separation of a large number of enantiomers without the need for the formation of diastereomers. It can be expected that the direct chromatographic separation of enantiomers on a preparative scale will gain increasing importance, in spite of the eminent progress in asymmetric synthesis [4, 5]. This can be seen from the growing number of papers dealing with preparative separations on chiral stationary phases of different type: on "brush-type" phases [6–11], on cyclodextrin [12], on chiral polyacrylamide derivative [13, 14] or on protein phase [15].

For the occasional separation of small amounts of a mixture of enantiomers, it is not necessary to optimize the chromatographic conditions. However, if larger amounts need to be separated, it would be of interest to know the conditions needed to obtain maximum throughput per unit time. It is obvious that it is necessary to search for conditions under which as high a separation factor α as possible can be obtained. For this purpose, a variety of stationary and mobile phases should be tested. It should not be overlooked that ternary mobile phases may yield higher separation factors than binary ones [16]. This problem solved, the question will arise how many milligrams or grams of enantiomeric (or racemic) mixture can be loaded onto the column per injection without loss of chiral separation.

This paper attempts to find answers to the following questions:

- What happens if the sample amount injected onto a column with chiral stationary phase is increased?
- Which conditions allow maximum sample throughput?
- What information can be obtained when the polarimeter is used as a detector?

Experimental

Chiral Stationary Phases

Two different columns with chiral N-3,5-dinitrobenzoylphenylglycine bonded on microparticulate silica (Pirkle type) as the stationary phase, both from Serva Feinbiochemica GmbH & Co. (Heidelberg, FRG) have been used:

- Preparative column 9.5mm i.d. × 25cm length with Chiral L-DPG=Daltosil 100 4μm. This stationary phase is the (S)-antipode. From earlier investigations with columns of this dimension, we found that it comprises rather exactly 10g of stationary phase.
- Analytical column 4.6mm i.d. × 25cm length with Chiral DNBPG-C=Si100Polyol 5μm. This stationary phase is the (R)-antipode.

0009-5893/87 0639-07 $03.00/0

©1987 Friedr. Vieweg & Sohn Verlagsgesellschaft mbH

Mobile Phase

Various mixtures of hexane fraction (solvent for HPLC, Romil Chemicals Ltd., Shepshed, England) and isopropanol (for HPLC, Fluka AG, Buchs, Switzerland) were used. Flow rates were 7 ml min^{-1} for the preparative column and 2 ml min^{-1} for the analytical one.

Chiral Sample

Racemic 1-(1-naphthylethyl)propylamide was used as the test compound. This compound can be easily prepared from cheap starting materials, and is nontoxic. The chiral recognition mechanism of this type of compound on Pirkle-type stationary phases is known [17, 18]. Synthesis was as follows [19]: Propionic acid chloride (purum, Fluka) was dissolved in anhydrous dioxane, and a solution of (±)-1-(1-naphthyl)ethylamine (purum, Fluka) and propylene oxide (puriss. p.a., Fluka) in anhydrous dioxane was added dropwise. After one hour of stirring, the mixture was poured into ice-water that had been acidified with diluted hydrochlorid acid. After filtration, the product was washed with water to neutrality and dried at 60°C and 0.1 mbar. The white powder had an excellent melting point interval (118–119°C) and did not show any by-product by thin-layer chromatography; therefore it was not recrystallized. A small amount of R(+)-1-(1-naphthylethyl)-propylamide was synthesized by the same procedure, starting from R(+)-1-(1-naphthyl)ethylamine (99%+, Aldrich-Chemie, Steinheim, FRG). $[\alpha]_D^{21} = +61.8°$ (c = 2 in methanol).

Using this compound it was found that on the preparative column the S(−)-enantiomer of naphthylethyl-propylamide is eluted first, whereas on the analytical column this is the R(+)-enantiomer.

UV Detectors

For preparative separations, a Uvikon LCD 725 UV detector with a cell path length of 10 mm, or a Uvikon 720 LC UV detector with 1 mm path length (both from Kontron, Zürich, Switzerland), were used, depending on sample mass. For high sample loads it was necessary to use the 1 mm cell. Detection wavelength was varied between 254 nm and 315 nm, higher wavelengths were used for high sample loads. For analytical separations, a Hitachi 100-10 Spectrophotometer with 10 mm flow cell (Kontron) was used at 254 nm.

Polarimeter

A Perkin-Elmer 241 Polarimeter (Perkin-Elmer, Überlingen, FRG) with a cell volume of 40 μl was used at the Hg wavelength 436 nm. Recorder range was ± 5 degrees, integration time was 0.5 s.

Injector

A Rheodyne 7120 syringe loading sample injector (Rheodyne, Berkeley, USA) with interchangeable loops with volumes of 20 μl, 100 μl, 200 μl, 500 μl, 1 ml and 2 ml was used.

Calculations

Indices 1 and 2 refer to the first and second eluted enantiomer, respectively.

Capacity factor:

$$k' = \frac{t_R - t_0}{t_0}$$

t_R: retention time of the peak maximum. For strongly asymmetric peaks, as they are obtained at mass overload conditions, the peak maximum markedly differs from the center of gravity of the peak.

t_0: retention time of a nonretained solute.

Separation factor:

$$\alpha = \frac{k'_2}{k'_1}$$

Resolution:

$$R_S = 1.198\frac{t_{R(2)} - t_{R(1)}}{w_{\frac{1}{2}(1)} + w_{\frac{1}{2}(2)}}$$

$w_{\frac{1}{2}}$: peak width at half height

Kaiser's resolution [20]:

$$\frac{f}{g} \quad \text{(see Fig. 1a)}$$

For strongly overlapping peaks, R_S cannot be calculated, but $\frac{f}{g}$ gives a good definition of peak overlap ($\frac{f}{g} = 1$ means baseline separation).

Tailing:

$$T = \frac{b_{0.1}}{a_{0.1}} \quad \text{(see Fig. 1b)}$$

Plate number:

$$N = 41.7\,\frac{(t_R/w_{0.1})^2}{T + 1.25}$$

$w_{0.1}$: peak width at 0.1 height.

This equation produces good results for peaks with tailing [21]. In the case of mass overload, it is not possible to calculate correct plate numbers [22], but this equation was used as a pragmatic criterion for the efficiency of the column.

The Influence of Increasing Sample Mass on the Separation

Various sample amounts from 2 μg up to 100 mg of racemate were injected onto the preparative column. This corresponds to loads of 0.2 μg g^{-1} to 10 mg g^{-1} (sample mass per gram of stationary phase). Sample volume was always kept low enough to avoid volume overload, i.e. the sample volume was only a small fraction of the width of the first

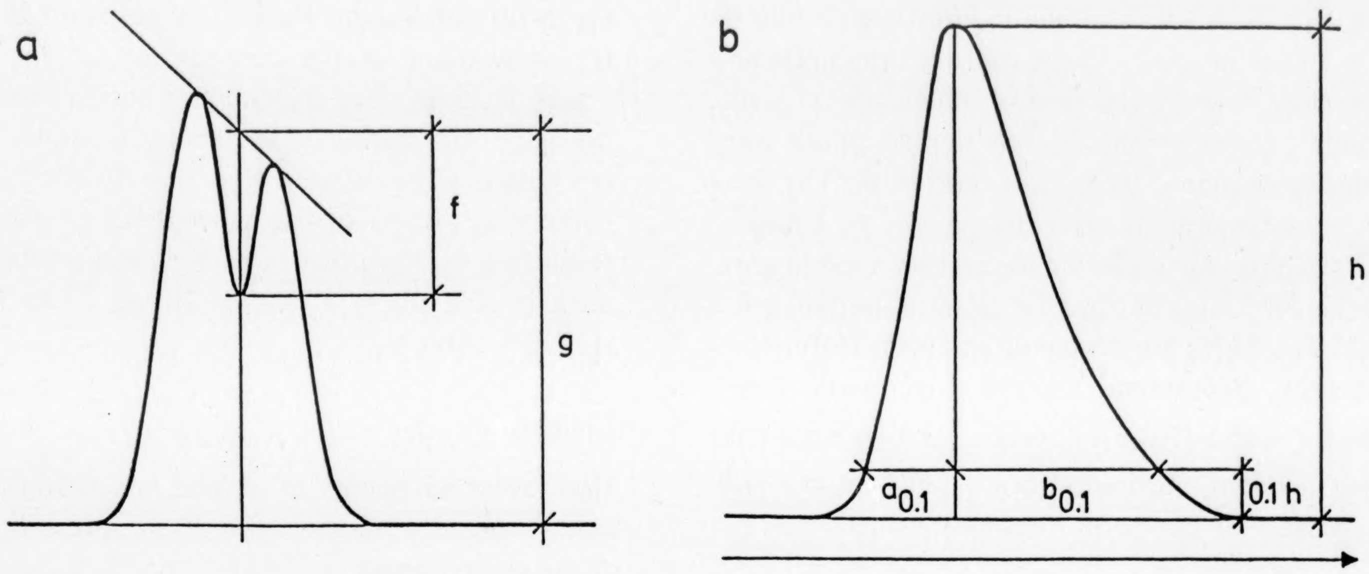

Fig. 1
Definition of the resolution function $\frac{f}{g}$ (a) and of tailing (b).

Table I. Effect of increasing sample mass on chromatographic performance. The 9.5mm × 25cm column contains approx. 10g of chiral stationary phase. Mobile phase: hexane/isopropanol 6:4. Other conditions see text.

Mass racemate	Load	Peak shape	k'_1	α	R_S	$\frac{f}{g}$	T_1	N_1	Purity first peak	Purity second peak
2 μg	0.2 μg g^{-1}	Gauss*	2.13	1.52	3.9		1.97	1520	100 %	100 %
20 μg	2 μg g^{-1}	Gauss*	2.06	1.50	4.0		1.86	1760	100 %	100 %
200 μg	20 μg g^{-1}	Gauss*	2.00	1.47	3.5		2.24	1630	100 %	100 %
2 mg	200 μg g^{-1}	Triangle	1.66	1.42	2.5		3.56	790	100 %	100 %
20 mg	2 mg g^{-1}	Triangle	1.42	1.34	1.1	0.96	3.75	290	100 %	97.3 %
50 mg	5 mg g^{-1}	Triangle	1.20	1.26		0.62	6.58	105	100 %	88.6 %
100 mg	10 mg g^{-1}	Triangle	1.03	1.22		0.36	9.25	50	100 %	77.5 %

* with tailing

Table II. Effect of increasing sample mass on chromatographic performance. The 9.5mm × 25cm column contains approx. 10g of chiral stationary phase. Mobile phase: hexane/isopropanol 1:1. Other conditions see text.

Mass racemate	Load	Peak shape	k'_1	α	R_S	$\frac{f}{g}$	T_1	N_1	Purity first peak	Purity second peak
2 μg	0.2 μg g^{-1}	Gauss*	1.53	1.51	3.3		1.90	1320	100 %	100 %
20 μg	2 μg g^{-1}	Gauss*	1.46	1.50	3.7		2.44	1510	100 %	100 %
200 μg	20 μg g^{-1}	Gauss*	1.44	1.45	3.4		2.58	1580	100 %	100 %
2 mg	200 μg g^{-1}	Triangle	1.12	1.44	2.3		2.70	1100	100 %	100 %
20 mg	2 mg g^{-1}	Triangle	0.92	1.36	1.1	0.92	4.52	305	>99.9 %	98.0 %
50 mg	5 mg g^{-1}	Triangle	0.84	1.30		0.61	6.39	140	>99.9 %	87.3 %
100 mg	10 mg g^{-1}	Triangle	0.79	1.19		0.33	6.90	74	100 %	72.5 %

* with tailing

Table III. Effect of increasing sample mass on chromatographic performance. The 9.5mm × 25cm column contains approx. 10g of chiral stationary phase. Mobile phase: hexane/isopropanol 4:6. Other conditions see text.

Mass racemate	Load	Peak shape	k'_1	α	R_S	$\frac{f}{g}$	T_1	N_1	Purity first peak	Purity second peak
2 μg	0.2 μg g^{-1}	Gauss*	1.06	1.53	3.3		1.86	1750	100 %	100 %
20 μg	2 μg g^{-1}	Gauss*	1.05	1.50	3.3		1.95	1920	100 %	100 %
200 μg	20 μg g^{-1}	Gauss*	1.00	1.48	3.1		2.20	1840	100 %	100 %
2 mg	200 μg g^{-1}	Triangle	0.71	1.42	2.0		2.11	1400	100 %	100 %
20 mg	2 mg g^{-1}	Triangle	0.61	1.34	0.9	0.86	3.02	495	100 %	95.5 %
50 mg	5 mg g^{-1}	Triangle	0.55	1.32		0.62	4.51	220	>99.9 %	88.0 %
100 mg	10 mg g^{-1}	Triangle	0.50	1.22		0.23	4.37	150	>99.9 %	77.3 %

* with tailing

eluted peak (the peak width in volume units can easily be calculated if the base width of the peak in time units and the volume flow rate of the mobile phase are known). Three different compositions of the mobile phase were used: hexane/isopropanol 6:4, 1:1, and 4:6. The corresponding chromatographic data are shown in Tables I, II, and III. All data are mean values of two experiments. k_1' is the capacity factor of the first peak, determined for the peak pair. T_1 and N_1 are the tailing and the plate number of the first peak, determined for the single peak. Overlapping peaks $\left(\frac{f}{g}<1\right)$ were collected as two fractions, fractionation made at the lowest point between the two peaks, and checked for purity on the analytical column.

Discussion

The term "mass overload" (also called "concentration overload") means that the chromatographic separation takes place in the nonlinear part of the adsorption isotherm. Capacity factors and peak widths are not independent of sample mass, as this is the case at analytical conditions (i.e. without mass overload).

Peak Shape: Under conditions of mass overload, the peak shape is no longer gaussian (of course, in most cases distorted, i.e. with tailing), but triangular [23, 24]. Peak shapes were judged by eye and the transition from distorted Gauss to Triangle is continuous, therefore the statements given in the tables are not free from subjectivity. Nevertheless, it can be said that mass overload seems to occur at sample loads of $200 \mu g\, g^{-1}$ and more.

Capacity Factor: On this type of stationary phase, k_1' decreases with increasing sample load, and at $10 mg\, g^{-1}$ reaches a value which is approx. 50% of the value under analytical conditions. According to the definition that mass overload begins if k' is lowered by 10% [25], the column is overloaded at a load of $200 \mu g\, g^{-1}$.

Separation Factor: α is independent of the composition of the mobile phase (at least in the range investigated). It decreases markedly with increasing sample load.

Resolution: It is difficult to measure R_S exactly at low sample loads, due to an adverse signal-to-noise level. It can be clearly seen that the resolution rapidly decreases at sample loads of $200 \mu g\, g^{-1}$ and higher. The resolution decreases with increasing polarity of the mobile phase.

Tailing: T_1 increases with increasing sample mass (the peaks become triangular) and decreases with increasing polarity of the mobile phase.

Plate Number: For the determination of N_1, the same is true as discussed above for R_S. But it is obvious that the column rapidly loses performance if the sample load is $200 \mu g\, g^{-1}$ or more. N_1 decreases with increasing tailing; therefore under these conditions, i.e. with mass overload, N_1 is higher for more polar mobile phases. This effect compensates for the lower resolution in these cases.

Purity of the First Peak: The first peak is always pure, even at a load of $10 mg\, g^{-1}$. This is due to the triangular peak shapes and the steep front of the second peak.

Purity of the Second Peak: The purity of the second peak is independent of the composition of the mobile phase (there is some error in manual fraction collection and the precision of purity determinations must not be overestimated). The reasons for this surprising fact are the competing effects of the dependence of plate number and resolution on the polarity of the mobile phase. The second peak is pure up to a load of $200 \mu g^{-1}$. At $10 mg^{-1}$, it is still 75% pure.

Conclusions

Mass overload occurs at a load of $200 \mu g\, g^{-1}$ (see peak shape, capacity factor, resolution, plate number, purity of the second peak).

The first peak is always pure. In cases where only one of the enantiomers is needed in pure form, it would be of interest to buy the column in this optical form which elutes this enantiomer first. Few chiral stationary phases are available in both forms, but dinitrobenzoylphenylglycine silica is.

The purity of the second peak is not influenced by the composition of the mobile phase. It only depends on sample mass.

Up to loads of $10 mg\, g^{-1}$, no breakdown in the chiral recognition mechanism can be observed. The loadability of this type of chiral stationary phase seems not to differ from those of silica columns.

Remark: The results obtained in this study are only valid for this sample and this stationary phase. It can be assumed that it is not absolutely valid for Pirkle-type stationary phases from other manufacturers because loadability depends on the amount of chiral moiety per gram of stationary phase. This amount on its side depends on the specific surface area, the pore width of the silica used and on the yield of the bonding reaction. The results may have little or no validity for other types of chiral stationary phases, e.g. protein phases.

Conditions for Maximum Sample Throughput

The "best" mobile phase is hexane/isopropanol 4:6 because separation times are shortest with this eluent. The peak purities are not injured by this high polarity and therefore the strength of the mobile phase.

Because the first peak is pure under all conditions investigated here, it could be assumed it would be best to work at as high a load as possible if only the first peak needs to be collected. This is not true because under these conditions a remarkable amount of the first eluted enantiomer is "lost" in the second peak. (The second peak, which then would not be pure, of course can be reinjected.) The *yield per injection* is calculated as follows:

injection of 100 mg of racemate
the second peak has a purity of 77% (see Tables)
77% = 50 mg of R(+)
23% = 14.9 mg of S(−)
therefore the first peak contains 35.1 mg of S(−)

If only 50mg of racemate is injected, the second peak has a purity of 88%, therefore the first peak consists of 21.6mg of pure S(–). Although the injection was only 50% of the amount mentioned above, the yield is 62% of the former one.

If 20mg are injected, the second peak has a purity of 95% and the yield of the first enantiomer will be 9.5mg.

Similar considerations can be found in the paper of Tambute et al. [11].

The *throughput per unit time* is highest with the highest sample load. But it must be taken into consideration that the influence of the sample mass on the moment of chromatogram completion is negligibly low, as can be seen in Fig. 2. Under conditions of mass overload, the retention time decreases with increasing sample load, but the peak end is independent therefrom; this effect is clearly demonstrated in Fig. 2 of the paper of Eisenbeiss et al. [24]. The width of the 100mg sample peak pair can be determined to be 1.65min (Fig. 2). Therefore every 1.65 min a new sample could be injected, giving a yield of 35mg of pure S(–)-enantiomer. Throughput is 21mg min^{-1}. The same calculation for the 50mg sample (peak width 1.48min, yield 21.6mg) gives a throughput of 14.6mg min^{-1}.

The Information Given by the Polarimeter Used as a Detector

If specific rotation or sample mass is high enough, the polarimeter can be used as a detector for liquid chromatography of optically active compounds [9, 15, 26–30]. In preparative separations, sample mass is high, so polarimetric detection is possible in any case [9, 15]. However, some points need attention:

- A flow-through polarimeter cell of low internal volume is needed. The polarimeter must be equipped with a recorder output or a computer interface.
- Specific rotation is dependent on wavelength, and usually increases with decreasing wavelength [26, 27]. For maximum sensitivity it would be necessary to choose the lowest possible wavelength at which the eluate (i.e. the solute or the mobile phase itself) does not absorb. For preparative applications it will most often not be necessary to take this point into consideration.
- As in UV detection, in principle polarimetric signals are dependent on sample mass. But if peaks of opposite optical rotation are overlapping, their signals will cancel each other out to a higher or lower degree, depending on the amount of overlapping. Quantitative interpretation of polarimeter signals is therefore of minor interest.

This latter point helps to answer the question of whether the polarimeter signal is more helpful for the fractionation of the eluate than is the UV absorbance signal. If peaks are well resolved, fractionation produces no problem: The two peaks will both be positive in the UV trace and have opposite signs in the polarimeter trace. Both enantiomers can be collected in pure form. But if peaks are overlapping, the question arises as to whether it is possible to interpret the detector signals in such a manner that pure fractions can be obtained. Let us inspect Fig. 3.

In this simplified drawing the peaks are exactly triangular and have no tailing. (The triangular shape is due to mass overload; "no tailing" means that the peak does not end in the baseline little by little, but by a well-defined intersect of two straight lines.) Moreover, and this is a simplification as well, the two peaks of a racemic sample are exactly the

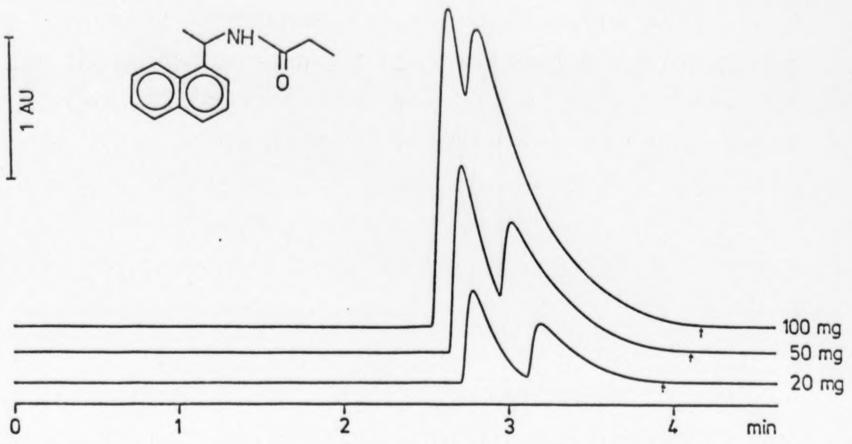

Fig. 2

Influence of sample mass on peak shape. Arrows show the peak ends. Column: 9.5mm X 25cm. Stationary phase: Chiral L-DPG= Daltosil 100 4μm. Mobile phase: hexane/isopropanol 4:6, 7ml min^{-1}. UV detector: 310nm.

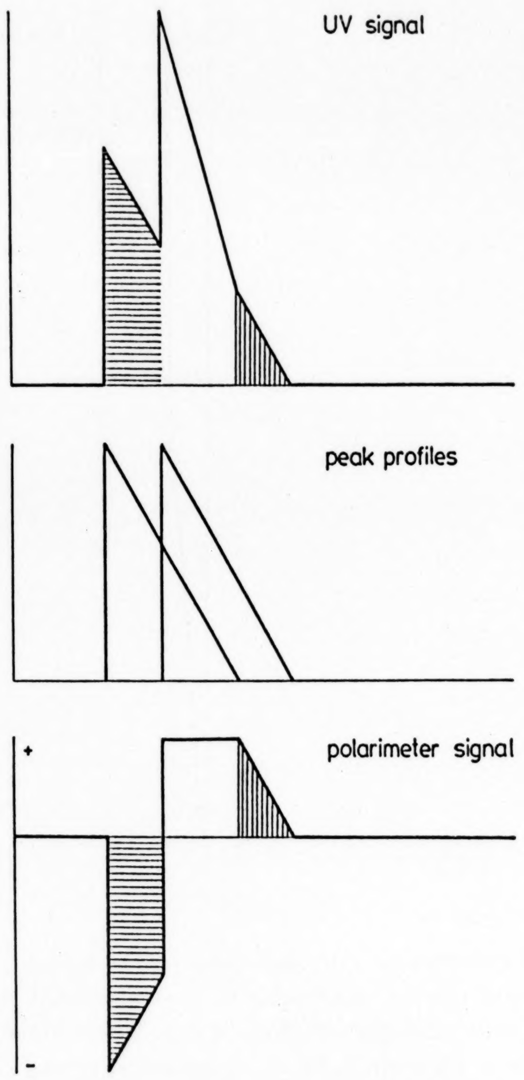

Fig. 3

Theoretical UV and polarimeter signals of a partially resolved racemate under conditions of mass overload. Peak shapes have been simplified. The first peak is the (–)-enantiomer. Shaded areas are pure.

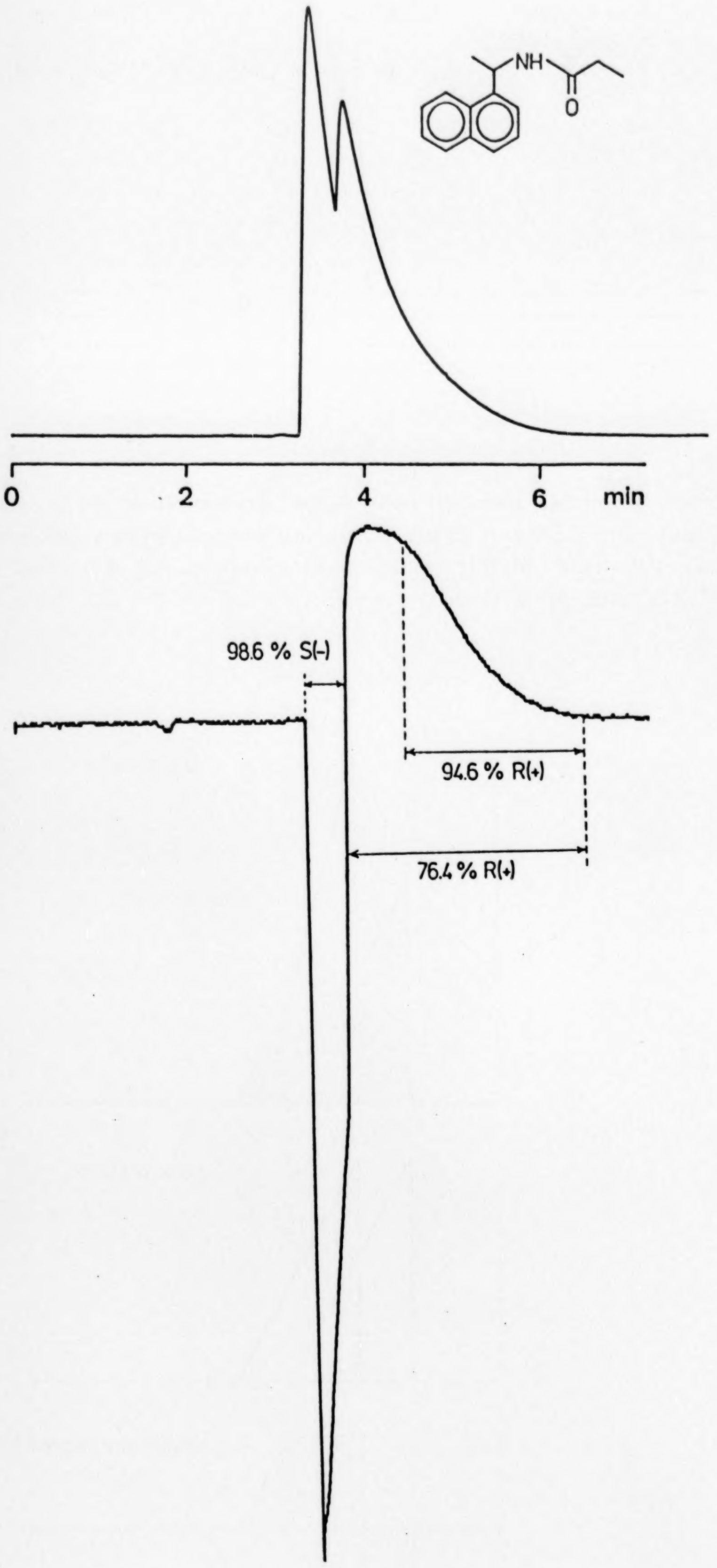

Fig. 4

Experimental UV and polarimeter signals of a partially resolved racemate on conditions of mass overload (two independent injections). Sample: 100 mg R,S-1-(1-naphthylethyl)propylamide. Column: 9.5 mm × 25 cm. Stationary phase: Chiral L-DPG=Daltosil 100 4 μm. Mobile phase: hexane/isopropanol 6:4, 7 ml min^{-1}. UV detector: 310 nm. Polarimeter: Hg lamp 436 nm. The purity of collected fractions was determined by analytical HPLC on a chiral stationary phase.

same width, and therefore have the same height. The resulting UV signal is the sum of the peak areas, but the polarimeter trace is the difference between them in the region of peak overlap. Therefore, the polarimeter shows an abrupt change in sign when the second peak becomes eluted followed by a horizontal plateau. The fractions in advance of the sign change and after the plateau are optically pure. It can be clearly seen that concerning the second pure fraction, the polarimeter signal is easier to interprete than the UV signal.

In practice the peaks show tailing, and therefore judgement of the signals is more difficult. It is obvious that the bend in the UV trace, which indicates the second pure fraction, cannot be observed under these circumstances. The plateau of the polarimeter trace becomes less pronounced or even disappears. These facts are confirmed by the experimental chromatogram of Fig. 4. Although the polarimeter signal is difficult to interprete, the end of the plateau can be estimated, and it was possible to obtain a fraction of 94.6% optical purity.

Conclusion

Under favourable circumstances the polarimeter signal can be a better aid for peak fractionation than the UV detector signal.

Acknowledgement

The two columns with chiral stationary phase used for this work are a gift from Serva Feinbiochemica GmbH & Co., Heidelberg, FRG.

References

[1] *V. Schurig*, Kontakte (Darmstadt) **1986** (1), 3.
[2] *W. Lindner, C. Pettersson*, in: "Liquid Chromatography in Pharmaceutical Development, An Introduction", *I. W. Wainer*, ed., Aster Publishing Corp., Springfield, 1985; p. 63.
[3] *R. Däppen, H. Arm, V. R. Meyer*, J. Chromatogr. **373**, 1 (1986).
[4] *J. D. Morrison*, ed., "Asymmetric Synthesis", Vol. 1–5, Academic Press Inc., Orlando, 1983–1986.
[5] *R. Scheffold*, ed., "Modern Synthetic Methods", Vol. **4**, Springer-Verlag, Berlin, 1986.
[6] *W. H. Pirkle, J. M. Finn*, J. Org. Chem. **47**, 4037 (1982).
[7] *W. H. Pirkle, J. M. Finn*, in "Asymmetric Synthesis", *J. D. Morrison*, ed., Vol. 1, Academic Press Inc., Orlando 1983; p. 116–119.
[8] *S. A. Matlin, R. Zhou*, Journal of HRC & CC **7**, 629 (1984).
[9] *W. H. Pirkle, A. Tsipouras, T. J. Sowin*, J. Chromatogr. **319**, 392 (1985).
[10] *J. A. Perry, J. D. Rateike, T. J. Szczerba*, J. Liquid Chromatogr. **9**, 3297 (1986).
[11] *A. Tambute, P. Gareil, M. Caude, R. Rosset*, J. Chromatogr. **363**, 81 (1986).
[12] *B. Zsadon, M. Szilasi, L. Décsei, A. Ujházi, J. Szejtli*, J. Chromatogr. **356**, 428 (1986).
[13] *G. Blaschke, J. Maibaum*, J. Chromatogr. **366**, 329 (1986).
[14] *H. J. Schmahl*, Fresenius Z. Anal. Chem. **326**, 150 (1987).
[15] *P. Erlandsson, L. Hansson, R. Isaksson*, J. Chromatogr. **370**, 475 (1986).
[16] *P. Pescher, M. Caude, R. Rosset, A. Tambute*, J. Chromatogr. **371**, 159 (1986).
[17] *W. H. Pirkle, C. J. Welch*, J. Org. Chem. **49**, 138 (1984).
[18] *J. W. Wainer, M. C. Alembik*, J. Chromatogr. **367**, 59 (1986).

[19] *P. A. Ongley*, ed., "Organicum", Addison-Wesley Publishing Comp., Reading, 1973; p. 432.

[20] *R. E. Kaiser*, "Gaschromatographie", Geest & Portig, Leipzig, 1960; p. 33.

[21] *J. P. Fooley, J. G. Dorsey*, Anal. Chem. **55**, 730 (1983).

[22] *A. M. Lenhoff*, J. Chromatogr. **384**, 285 (1987).

[23] *P. Gareil, C. Durieux, R. Rosset*, Sep. Sci. Technol. **18**, 441 (1983).

[24] *F. Eisenbeiss, S. Ehlerding, A. Wehrli, J. F. K. Huber*, Chromatographia **20**, 657 (1985).

[25] *L. R. Snyder*, "Principles of Adsorption Chromatography", Marcel Dekker, New York, 1986; p. 78.

[26] *J. L. DiCesare, L. S. Ettre*, J. Chromatogr. **251**, 1 (1982).

[27] *A. Mannschreck, A. Eiglsperger, G. Stühler*, Chem. Ber. **115**, 1568 (1982).

[28] *W. Boehme, H. Stenz, O. Bonsignori*, Int. Lab. **13** (5, June), 28 (1983).

[29] *C. Meinard, P. Bruneau, J. Perronnet*, J. Chromatogr. **349**, 109 (1985).

[30] *E. S. Yeung*, in: "Detectors for Liquid Chromatography", *E. S. Yeung*, ed., John Wiley & Sons, New York, 1986; p. 204–228.

Received: June 29, 1987
Accepted: July 23, 1987
F

Protein Surface Area and Retention in Hydrophobic Interaction Chromatography

A. Katti[1)] / Y.-F. Maa / Cs. Horváth*

Department of Chemical Engineering, Yale University, New Haven, CT 06520, USA

Key Words

Column liquid chromatography
Hydrophobic interactions
Proteins
Surface tension
Salt effect

Summary

Molecular surface areas accessible to a 4 Å diameter spherical probe were calculated from crystallographic data for five proteins: α-chymotrypsinogen A, lysozyme, trypsinogen, ribonuclease A and ribonuclease S. The retention factors of various proteins were measured on stationary phases having polyether- and phenyl-ligates and with aqueous eluents containing $(NH_4)_2SO_4$, Na_2SO_4 or NaCl at pH 7.0. The logarithmic retention factors were plotted against the salt molality and the hydrophobic interaction parameters evaluated from the limiting slopes of the plots at high salt concentrations for the proteins in the chromatographic systems investigated. The hydrophobic interaction parameters thus obtained were linear in both the molecular surface areas of the proteins and the molal surface tension increments of the salts. The experimental results obtained with these relatively simple proteins of known molecular structure, which were available in high purity, support earlier theoretical predictions for the dependence of the hydrophobic interaction parameter on the surface area of the protein and the surface tension raising effect of the salt.

Introduction

Hydrophobic interaction chromatography (HIC) is increasingly used for protein separations mainly because it offers a selectivity different from that of the traditional electrostatic interaction (ion-exchange) chromatography. The stationary phase in HIC contains weakly hydrophobic ligates covalently bound to the "soft" hydrophilic surface of the support and most commonly gradient elution from high to low salt concentrations is used to separate the components of a protein mixture. The technique originates from Tiselius' concept of "salting-out" chromatography [1] and has found wide applications with polysaccharide based stationary phases in classical column chromatography of proteins [2, 3]. Recently, sorbents prepared from macroporous, microparticular supports with appropriate surface properties have been introduced for use in HIC under conditions employed in HPLC [4–9]. The functional groups of such stationary phases include polyether-, phenyl- and various alkyl-ligates. The effect of the stationary phase and the operational variables [4, 6, 8–11] as well as changes in protein conformation [12–14] during the chromatographic process in HIC have been extensively investigated. Most studies were aimed at a phenomenological analysis of the retention data obtained under different elution conditions and the effect of stationary phase properties on the retention of various proteins is still largely unexplored.

A decade ago a simple theory [15, 29] has been put forward to explicate the role of neutral salts in hydrophobic interactions of proteins, such as those that govern their retention in HIC. According to that extended version of the solvophobic theory [16, 17], which was successfully used for the treatment of reversed-phase chromatography [18, 19], the change in the free energy in HIC with the salt concentration in the eluent is determined mainly by the contact surface area upon binding of the protein molecule by the nonpolar ligates of the stationary phase and the nature of the salt as measured by its propensity to increase the surface tension of aqueous solutions [20]. The complexity of the process under consideration [21], however, is likely to involve a number of other phenomena e.g. specific salt effects, that are not treated by the simple theory.

On the other hand, the results of a recent systematic study [22] on the retention of lysozymes from various

---

[1)] Present Address: Oak Ridge National Laboratory, Analytical Chemistry Division, Oak Ridge, TN 37831, USA

0009-5893/87 0646-05 $ 03.00/0

© 1987 Friedr. Vieweg & Sohn Verlagsgesellschaft mbH

bird species in HIC lend support to the key features of the above theory. For instance at sufficiently high salt concentrations plots of $\ln k'$ versus salt molality in the eluent yielded straight lines that were parallel for the proteins believed to have similar hydrophobic surface areas. Furthermore, the increase in the logarithmic retention factor paralleled the salt mediated increase in the surface tension of the aqueous eluent. Both observations support the predictions of the extended solvophobic theory [15].

The availability of crystallographic data and computer programs for the calculation of the molecular surface areas of proteins prompted us to examine the relationship between the surface area and retention behavior in HIC. The surface areas were calculated by using the algorithm of Lee and Richards [23] and the retention of the proteins was measured under conditions usually employed in HIC at high salt concentrations. The proteins of known atomic coordinates that were available in pure form for the experiments had similar molecular sizes and isoelectric points. The results were analyzed within the hermeneutics of the above theory in order to relate the experimental hydrophobic interaction parameters [24] to both the surface areas of the proteins and the surface tension increments of the salts used in the eluent.

Experimental

Instruments and Columns

The liquid chromatograph was assembled from an LDC (Riviera Beach, FL, USA) Constametric IIIG and a Constametric I metering pumps with a Model 1601 Gradient Master controller and mixer. Samples were injected with a Rheodyne (Cotati, CA, USA) Model 7010 sampling valve having a 20 microliter sample loop. An LDC SpectroMonitor D variable-wavelength UV detector was used at 220nm and chromatograms were obtained with a Model BD41 Kipp and Zonen [Delft, The Netherlands] strip chart recorder. The column and solvent reservoir were kept at 30°C by using a Neslab (Portsmouth, NJ, USA) Model RTT-4DD constant temperature bath.

The polyether type stationary phase was prepared by covalent attachment of polyethylene glycol, MW 1000 daltons, to 5 micron, Vydac 300 Å silica gel as described previously [26] and a 100 × 4.6mm column was slurry packed with methanol at 8000 psi. The other column was a 750 × 7.5mm Bio-Gel TSK-Phenyl 5-PW column generously donated by Bio-Rad (Richmond, CA, USA).

Materials

Trypsinogen (TRY), crystallized, was purchased from US Biochemical Corp. (Cleveland, OH, USA). α-Chymotrypsinogen A (α-CHY), type II, 6X crystallized and lyophilized, ribonuclease A (RNase A), type II-A, chromatographically purified, and ribonuclease S (RNase S), type XII-A, all from bovine pancreas as well as lysozyme (LYS) from chicken egg white, grade I, 3X crystallized dialyzed and lyophilized, were supplied by Sigma (St. Louis, MO, USA). Reagent grade ammonium sulfate, sodium chloride, sodium sulfate decahydrate and mono and dibasic sodium phosphates were obtained from J. T. Baker (Phillipsburg, NJ, USA). Distilled water was prepared with a Barnstead unit (Barnstead, MA, USA).

Procedures

Mobile phases of various salt concentrations were made by diluting the appropriate stock solution containing either 3M $(NH_4)_2SO_4$, 5M NaCl, or 1.3 M Na_2SO_4 in 50 mM phosphate buffer, pH 7.0, with the same phosphate buffer. Protein samples were prepared *ad hoc* by dissolving about 1 mg of protein in 1 ml of the mobile phase prior to injection. Each protein was chromatographed at least three times under isocratic elution conditions at flow rates ranging from 1.0 to 3.0ml/min. Retention times were measured at the intersection of the tangents drawn to the two inflection points of the peaks. The retention time of $NaNO_3$, which was added to the sample, was taken as the mobile phase hold-up time. The retention factor of the protein was calculated [26] from each chromatographic run and an average value was taken. The reproducibility of the measurements was within 1%. The range of salt concentration used is listed in Table I that also shows that only a limited set of data were measured with the two ribonucleases.

The logarithmic retention factors were plotted against the molal salt concentration in the mobile phase and typical results are shown in Fig. 1. The limiting slopes of the plots at high salt concentrations were taken as the straight line obtained by a least square fit of the five highest data points. Statistical analysis was done using the programming language APL.

Calculation of the Protein Surface Area

The algorithms developed by Lee and Richards [23] and the atomic coordinates of the proteins from the Brookhaven National Laboratory Protein Data Bank, Upton, New York, were used to calculate the surface area of the proteins. The file numbers were BNL143, BNL345, BNL313, BNL312, and BNL260 for α-CHY, TRY, RNase S, RNase A, and LYS; respectively. The program calculated the "accessible" surface area, i.e., the area traced out by the center of a spherical probe representing a solvent molecule as it is rolled over the surface of the protein molecule of interest [27].

Table I. Range of salt molality in measurements of the hydrophobic interaction parameters.

Protein	$(NH_4)_2SO_4$		Na_2SO_4	NaCl
	Polyether	Phenyl	Phenyl	Phenyl
Ribonuclease S	2.42–2.9	–	–	–
Ribonuclease A	2.42–2.9	1.9 –2.15	–	–
Lysozyme	1.6 –1.9	1.4 –1.65	0.95–1.1	2.8–3.7
Trypsinogen	1.6 –1.85	1.0 –1.24	0.7 –0.85	2.1–2.9
α-Chymotrypsinogen A	1.3 –1.4	0.65–0.85	0.5 –0.6	1.1–1.9

Results and Discussion

Properties of the proteins under investigation are presented in Table II. It is seen that their molecular weight ranges between 13.7 and 25.7 kD and their isoelectric points vary between 8.7 and 11.0. The protein surface areas computed from atomic coordinates with a probe diameter of 4.0 Å are listed. In addition, the surface areas of equivalent spheres estimated from the molecular weight of the proteins by using a value of 0.74 cm^3/g for the specific volume are also included for reference. It is seen that the range of protein surface area is relatively small and there is only a rough correlation between the molecular weights and surface areas calculated by the computer program. The surface area of the proteins increases in the order of RNase S < LYS < RNase A < TRY < α-CHY.

In HIC the dependence of the logarithmic retention factor, ln k′, on the molality of the salt, m, in the eluent has been [20] expressed as

$$RT \ln k' = \text{const.} - (\alpha m^{0.5}/(1+\beta m^{0.5})) - (\tau+\delta) m + N \Delta A \sigma m \quad (1)$$

where α and β are constants for a given protein in the Debye term, τ is a function of the dipole moment of the protein and the dielectric constant of the medium and the parameter δ is related to the net free energy change due to van der Waals interactions and is expected to be constant for a given protein and chromatographic system. In the last term on the RHS of eq. (1), N is Avogadro's number, ΔA is the contact area between the protein and the nonpolar ligates of the stationary phase upon binding and σ is the molal surface tension increment of the salt.

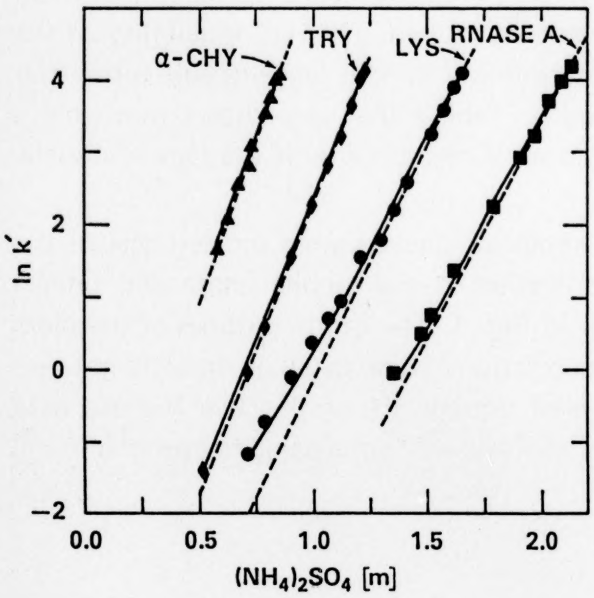

Fig. 1

Typical experimental results illustrated by the plot of ln k′ vs salt molality. Column, TSK-phenyl; eluent 50 mM phosphate buffer, pH 7.0, containing $(NH_4)_2SO_4$ at different concentrations; flow rate, 3 ml/min; temperature, 30°C, detector wavelength, 220 nm. Symbols are: ▲ α-chymotrypsinogen, ◆ trypsinogen, ■ ribonuclease A, ● lysozyme.

At sufficiently high salt concentrations the Debye term becomes negligible and the plot of the logarithmic retention factor against the molal salt concentration reaches a limiting value given by

$$d \ln k'/dm = C = (-(\tau+\delta) + N A\sigma)/RT \quad (2)$$

The limiting slope of the ln k′ vs m plot at high salt as illustrated in Fig. 1 has been termed the hydrophobic interaction parameter, C, and has been discussed in previous treatments [24, 25] of the effect of salt concentration on retention in biopolymer chromatography. If for the proteins under investigation which have similar surface properties and net charges, the molecular contact area upon bindling to the nonpolar ligates of the stationary phase, ΔA, would be proportional to the accessible surface area, S, so that for each protein

$$\Delta A = aS \quad (3)$$

where a is a proportionality constant. Furthermore, if under conditions of the experiments the conformation of the proteins is similar to that in the crystalline state [28], then S can be represented by the surface areas calculated from the atomic coordinates. By combining eq. (2) and (3) we obtain

$$C = -(\tau+\delta)/RT + aNS\sigma/RT \quad (4)$$

Since with proteins of similar size, net charge and charge distribution the term $(\tau+\delta)$ is expected to be similar in a

Table II. Properties of the proteins under investigation.

Protein	Symbol	Molecular Weight	pI	Net Charge[c]	Surface Area Å^2 Computed Accessible[d]	Surface Area Å^2 Equivalent Sphere[e]
Ribonuclease S	X	13,700	9.4[b]	–	7070	3177
Ribonuclease A	■	13,700	9.4[b]	4.9	7706	3177
Lysozyme	●	14,410	11.0[b]	6.9	7684	3286
Trypsinogen	◆	23,900	8.7[a]	6.3	9494	4604
α-Chymotrypsinogen A	▲	25,700	9.6[a]	5.0	9687	4834

[a] [30]

[b] [31]

[c] J. Warwicker and F. M. Richards personal communication. Calculation at pH 7.0 and 0.1 M ionic strength.

[d] Computed from atomic coordinates with a probe diameter of 4.0 Å.

[e] Calculated from the specific volume and molecular weight.

particular chromatographic system, with these assumptions we expect the following relationship to hold:

$$C = \text{const.} + aNS\sigma/RT \qquad (5)$$

Eq. (5) predicts that the hydrophobic interaction parameter is a linear function of the protein surface area calculated from crystallographic data. In order to test the validity of eq. (5) for the set of proteins under investigation, the hydrophobic interaction parameters were evaluated from retention data obtained with two kinds of stationary phases and eluents containing ammonium sulfate. As shown by the plots of the hydrophobic interaction parameter against the surface area of the proteins in Fig. 2 a linear dependence according to eq. (5) does indeed exist. The correlation coefficients for the data obtained on the phenyl and the polyether stationary phases were 0.963 and 0.988, respectively.

According to the theory the intercepts in Fig. 2 represent the net electrostatic and van der Waals interactions and they are significantly different for the data obtained with the two stationary phases. The value of the intercept of the line for the data obtained with the polyether column is 2.2 times greater than that with the phenyl column.

Another test of eq. (5) was made by plotting the hydrophobic interaction parameters calculated from data obtained using the phenyl column with eluents containing different salts against the protein surface area. The results are illustrated in Fig. 3 and the limited set of data suggests the existence of a linear relationship.

From eq. (5) it follows that the slopes of the straight lines in Figs. 2 and 3 are proportional to the molal surface tension increment since

$$dC/dS = aN\sigma/RT \qquad (6)$$

On the other hand, eq. (5) also predicts that the hydrophobic interaction parameter linearly depends on the molal surface tension increments of the salts with a slope given by

$$dC/d\sigma = aNS/RT \qquad (7)$$

In order to examine the consistency of the above relationships the hydrophobic interaction parameters were also plotted against the molal surface tension increment and the results are illustrated in Fig. 4.

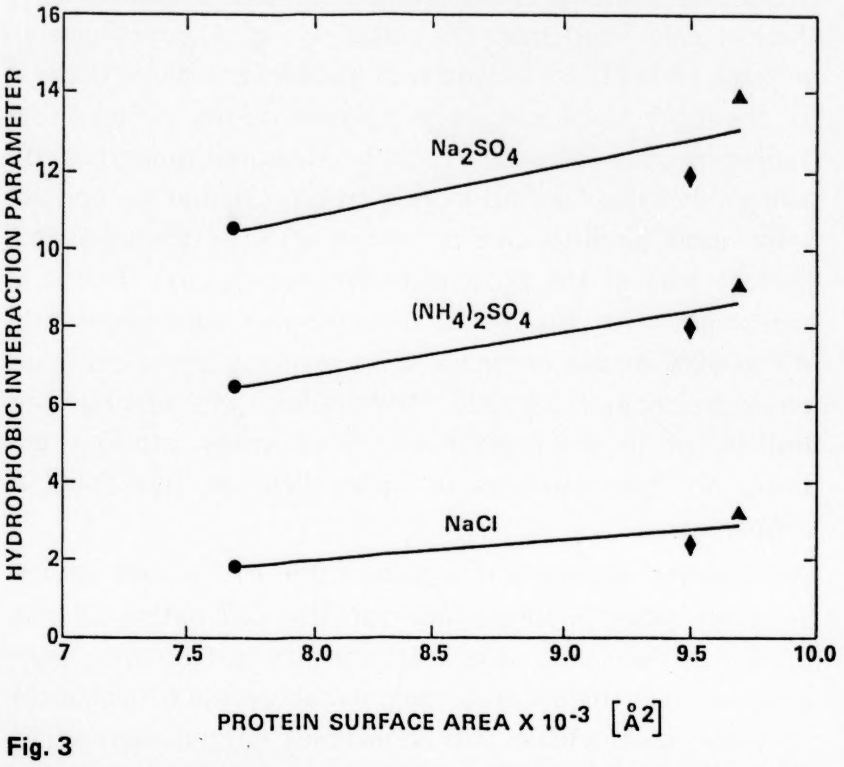

Fig. 3

Plot of the hydrophobic interaction parameter measured on the phenyl stationary phase with various salts in the eluent against the surface area of the proteins calculated with a 4.0 Å diameter probe. The symbols are as in Fig. 1.

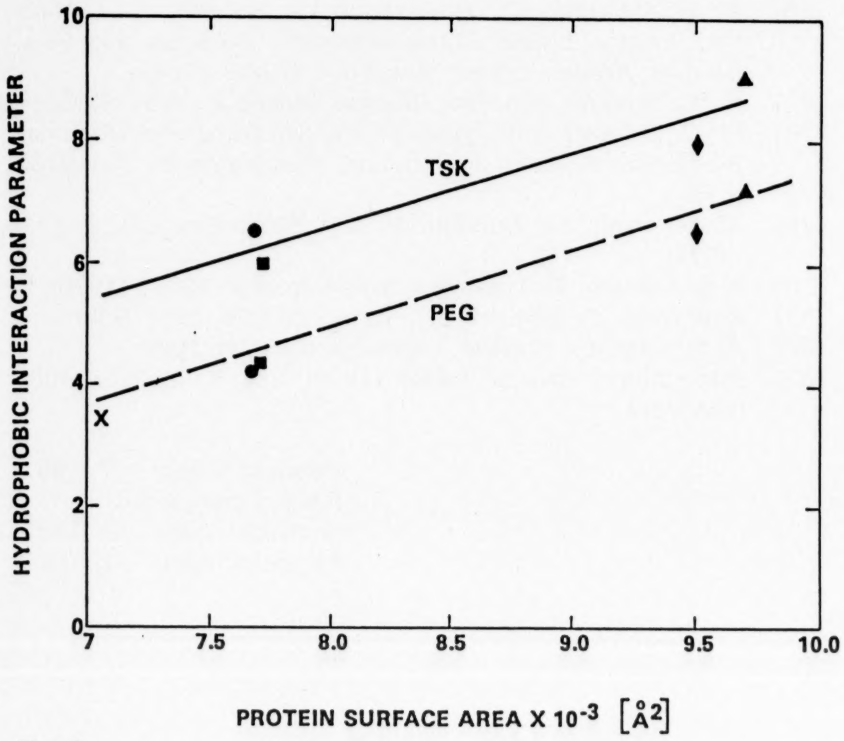

Fig. 2

Plots of the hydrophobic interaction parameters measured on stationary phases containing polyether (dashed line) or phenyl (solid line) ligates and with (NH$_4$)$_2$SO$_4$ in the eluent against the surface area of proteins calculated with a 4.0 Å diameter probe. The symbols are as in Table II.

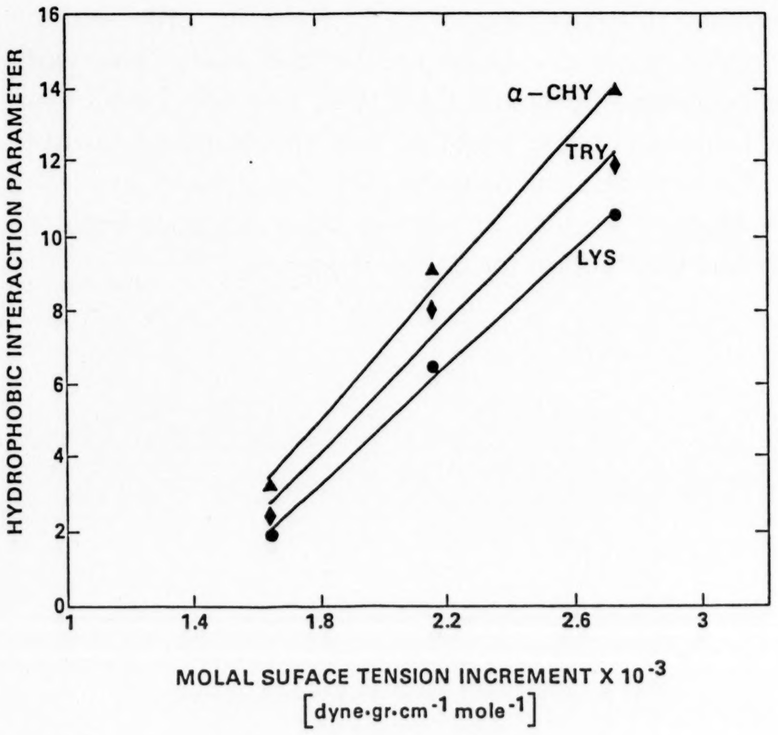

Fig. 4

Plot of the hydrophobic interaction parameter of proteins measured on the phenyl stationary phase against the molal surface tension increment of the salts in the eluent. The symbols are as in Fig. 1.

From the slopes in Fig. 4 and the protein surface areas, we have calculated according to eq. (7) the value of the proportionality factor 'a' and found it to be 0.43, 0.38 and 0.42 for LYS, TRY, and α-CHY, respectively. On the other hand, from the data presented in Figs. 2 and 3, the respective a values were 0.20, 0.21 and 0.14 for Na_2SO_4, $(NH_4)_2SO_4$ and NaCl, by using the pertinent molal surface tension increments [33] in the calculation according to eq. (6). Thus, the proportionality factors calculated from plots of the hydrophobic interaction parameter against the surface area are consistently the double of those obtained from the plots of C against the σ. The proportionality factors calculated from the slopes in Fig. 4, which give an average of 0.41, are viewed with greater confidence because of the more equal spacing of the data points in Fig. 4 that represent plots of experimentally measured quantities. By using this value we find in view of eq. (3) that the contact area upon binding involves about 40% of the accessible surface area of the proteins under investigation. This is in agreement with the results of computer calculations that 40 to 60% of the surface of these proteins can be considered hydrophobic [23, 32]. Nevertheless, this finding may not be of general significance since other proteins are likely to have surfaces of quite different hydrophobic properties.

An attempt was made to employ other probe sizes as well as other possible algorithms for the calculation of the protein surface area (e.g. total contact surface area, nonpolar contact surface area, nonpolar accessible surface area) in order to elucidate the importance of the method of calculation of the surface area, but essentially the same results have been obtained.

Acknowledgements

The authors are indebted to J. Warwicker and F. M. Richards for valuable discussions and access to the data base and computer programs and to Z. El Rassi for providing the polyether stationary phase used in this study. This work was supported by grants CA 21948 and GM 20993 from the National Cancer Institute and the National Institute for General Medical Sciences, US Department of Health and Human Services, as well as by a contract from the National Foundation for Cancer Research.

References

[1] *A. Tiselius*, in Chromatographic Analysis, Discussion of the Faraday Society, No. 7, Hazell, Watson and Winey, Ltd., London, 1949, p. 9.

[2] *S. Shaltiel*, Meth. Enzymol. **34**, 126 (1974) and **104**, 69 (1984).

[3] *S. Hjerten*, in N. Catsimpoolas (Ed.), Methods of Protein Separation, Vol. 2, Plenum Press, New York, 1976, p. 233.

[4] *J. D. Pearson, M. Mitchell, F. E. Regnier*, J. Liq. Chromatogr. **6**, 1441 (1983).

[5] *Y. Kato, T. Kitamura, T. Hashimoto*, J. Chromatogr. **266**, 49 (1983).

[6] *D. L. Gooding, M. N. Schmuck, K. M. Gooding*, J. Chromatogr. **296**, 107 (1984).

[7] *N. T. Miller, B. Feibush, B. L. Karger*, J. Chromatogr. **316**, 202 (1985).

[8] *J.-P. Chang, Z. El Rassi, Cs. Horváth*, J. Chromatogr. **396**, 399 (1985).

[9] *Z. El Rassi, Cs. Horváth*, J. Liq. Chromatogr. **9**, 3245 (1986).

[10] *J. L. Fausnaugh, L. A. Kennedy, F. E. Regnier*, J. Chromatogr. **165**, 3 (1979).

[11] *A. J. Alpert*, J. Chromatogr. **359**, 85 (1986).

[12] *S. L. Wu, A. Benedek, B. L. Karger*, J. Chromatogr. **359**, 3 (1986).

[13] *K. Benedek, S. Dong, B. L. Karger*, J. Chromatogr. **317**, 227 (1984).

[14] *S. L. Wu, A. Figuera, B. L. Karger*, J. Chromatogr. **371**, 3 (1986).

[15] *W. Melander, Cs. Horváth*, Arch. Biochem. Biophys. **183**, 200 (1977).

[16] *O. Sinanoǧlu*, in B. Pullman (Ed.) Molecular Associations in Biology, Academic Press, New York, 1968, pp. 427–415.

[17] *O. Sinanoǧlu, S. Abdulnur*, Fed. Proc. **24**, 12 (1965).

[18] *Cs. Horváth, W. R. Melander, I. Molnár*, J. Chromatogr. **125**, 129 (1976).

[19] *Cs. Horváth, W. R. Melander*, J. Chromatogr. Sci. **15**, 393 (1977).

[20] *W. R. Melander, D. Corradini, Cs. Horváth*, J. Chromatogr. **317**, 67 (1984).

[21] *T. Arakawa, S. N. Timasheff*, Biochemistry **21**, 6545 (1982).

[22] *J. L. Fausnaugh, F. E. Regnier*, J. Chromatogr. **359**, 131 (1986).

[23] *B. Lee, F. M. Richards*, J. Mol. Biol. **55**, 379 (1971).

[24] *Cs. Horváth, W. R. Melander, Z. El Rassi*, presented at the 9th International Symposium on Column Liquid Chromatography, Edinburgh, July 1–5, 1985, Lecture PL 3.3.

[25] *Cs. Horváth, Z. El Rassi*, Chromatogr. For., Sept./Oct., 49 (1986).

[26] *W. R. Melander, Cs. Horváth*, in Cs. Horváth (Ed.), High Performance Liquid Chromatography: Advances and Perspectives, Academic Press, New York, (1980) p. 113.

[27] *F. M. Richards*, Ann. Rev. Biophys. Bioeng. **6**, 151 (1977).

[28] *M. O. Dayhoff* (Ed.), Atlas of Preotein Structures, National Biomedical Research Foundation, Washington D. C. (1973) p. 60.

[29] *W. Melander, Cs. Horváth*, J. Solid Phase Biochem. **2**, 141 (1977).

[30] *P. G. Righetti, T. Caravaggio*, J. Chromatogr. **127**, 1 (1976).

[31] *Z. El Rassi, Cs. Horváth*, J. Chromatogr. **359**, 258 (1986).

[32] *A. M. Katti, Cs. Horváth*, unpublished results, 1986.

[33] International Critical Tables (1929) Vol. 4, McGraw Hill, New York.

Received: July 2, 1987
Revised manuscript
received: Sep. 28, 1987
Accepted: Oct. 1, 1987
F

Biomonitoring of Workers Exposed to Aromatic Amines in Rubber Vulcanization

I. Pavan[1] / F. Belliardo[2]* / E. Buglione[1] / M. M. Massiccio[1]

[1] Istituto di Medicina del Lavoro, [2] Dipartimento di Scienza e Tecnologia del Farmaco, Universita di Torino, Corso Raffaello 31, I-10125 Torino, Italy

Key Words

N-(1-methylethyl)-N'-phenyl-1,4-Benzendiamine (IPPD)
N-(2,3-dimethylpropyl)-N'-phenyl-1,4-benzendiamine (6PPD)
Rubber vulcanizers
Biomonitoring

Summary

A method based on solid phase extraction and reversed phase LC for quantitation of IPPD (N-(1-methylethyl)-N'-phenyl-1,4-Benzendiamine) and 6PPD (N-(2,3-dimethylpropyl)-N'-phenyl-1,4-Benzendiamine) in the urine of rubber vulcanization workers is described. The method provided a 91.8 +/− 1.45 % mean recovery of IPPD and 93.8 +/− 1.65 % mean recovery of 6PPD from fortified urines in the 10.0 to 250.0 $\mu g\ l^{-1}$ range. Standard curves bracketing this concentration range had linear coefficients greater than 0.9989. The average relative standard deviation for the entire concentration range was 1.93 % for IPPD and 2.3 % for 6PPD. The method has been applied successfully to biomonitoring IPPD in the nanomole range in the urine of rubber vulcanization workers.

Introduction

Aromatic amines derived from p-phenylendiamine are widely used as anti-oxidants in rubber compounding. Normal concentrations are between 1 and 2 % of the rubber. N-(1-methylethyl)-N'-phenyl-1,4-Benzendiamine (IPPD, CAS Reg. No. 101-72-4) and N-(2,3-dimethylpropyl)-N'-phenyl-1,4-Benzendiamine (6PPD, CAS Reg. No. 739-24-8) are the rubber anti-oxidants most commonly used in Italy. In humans, IPPD and 6PPD are suspected caricinogens [1], moreover IPPD is a potent skin sensitizer [2]. IPPD and 6PPD are excreted in urine mainly as the parent compounds [3].

Since the introduction in Italy in the late 1970s of stringent regulations on the production and use of aromatic amines, ambient air as well as biological monitoring for rubber antioxidants has become mandatory.

In 1981 [4] we developed a method for separation and quantitation of IPPD in urine based on a liquid-liquid extraction procedure and LC analysis. Although this technique was adequate for the analysis of urines containing exogenous aromatic amines, a modification of the liquid-liquid extractive procedure was required to eliminate the most critical point in the proposed method, that is, the formation of emulsions. The introduction of solid-phase extraction allowed us to simplify sample handling and to save time in sample preparation and consequently to increase the speed of routine control analyses. The method was applied to monitoring the presence of IPPD in the urine of sixteen rubber vulcanizers during two consecutive working weeks.

Experimental

Standards, Solvents and Reagents

IPPD and 6PPD standards of known purity (greater than 98 %) were supplied by Bayer (FRG) and were used without further purification. For all operations HPLC grade solvents (J. T. Baker Chemicals B. V., Deventer, The Netherlands) were used. SPE prepacked octadecyl (C18) disposable columns from J. T. Baker (Phillipsburg, NJ, USA) were employed.

Standard solutions of IPPD and 6PPD were prepared by dissolving 2 mg of each standard, exactly weighed on a Cahn electrobalance mod .G2, in distilled water further purified by a Water-I apparatus (Gelman Sciences, Michigan, USA), and diluting to volume in a 1000 ml volumetric, dark-glass flask. Standard fortified urine samples were prepared by adding IPPD and 6PPD stock solutions to obtain final concentrations of 10.0, 20.0, 30.0, 50.0, 100.0, 150.0, 200.0 and 250.0 micrograms of IPPD and 6PPD per liter of urine.

0009-5893/87 0651-04 $ 03.00/0

© 1987 Friedr. Vieweg & Sohn Verlagsgesellschaft mbH

Urine Samples

Urine samples were collected during two working weeks in a rubber-curing workshop on a group of 16 workers (rubber vulcanizers). Samples were collected for every worker, starting from the end-shift on Friday, followed up with two consecutive series of five working days (before-shift and end-shift), and ending with before-shift on Monday. Dark glass containers were used, and urine samples were kept in a refrigerator (4 °C) to retard amine oxidation and analyzed within 24 h according to the procedure described below.

Extraction Procedure

100 ml urine, adjusted to pH 7, were drawn through the SPE prepacked column, assembled on a home-made rack operating under light vacuum. Columns were pre-conditioned with two column volumes of methanol, followed by two column volumes of distilled water. The elution of aromatic amines from the SPE column was performed with 5 ml of methanol. The methanol collected was evaporated to dryness in a Rotavapor at 45 °C. The residues were redissolved in 200 μl methanol; 10 μl were injected into the LC.

Chromatography System

The analyses were performed on a Perkin-Elmer Series 410 liquid chromatograph equipped with a Rheodyne 7125 injection valve and a Perkin-Elmer LC-100 Column Oven. Component elution was monitored with a Perkin-Elmer LC-95 variable wavelength detector equipped with a flow cell of 4.5 μl. A PartiSpere C18, 5 μm (125 × 4.6 mm I.D., Whatman, New Jersey, USA) column was used. The separations were achieved under the following conditions: mobile phase, methanol: water (78:12) adjusted to pH 6.7 with ammonium hydroxide, 0.02 M in ammonium acetate; flow rate, 2 ml min^{-1}; temperature, 35 °C; wavelength, 290 nm. Peak areas were measured by Laboratory Computing Integrator LCI-100 Perkin-Elmer.

Method of Calculation

All determinations were related to the IPPD and 6PPD external standard solutions. Results were calculated using the response ratios computed from the electronically integrated peak areas of the calibration standards.

Results and Discussions

Baseline separation was achieved under the experimental conditions; over a period of three weeks mean retention times were 253 and 375 sec, with coefficients of variation of 0.82 and 0.95 % for IPPD and 6PPD respectively. Co-extracted compounds from human urine caused no interference at the retention times of IPPD and 6PPD peaks. Fig. 1 is an LC chromatogram of IPPD and 6PPD standards. Some typical results for the LC analysis of the two aromatic amines in human urine of exposed workers are illustrated in Fig. 2.

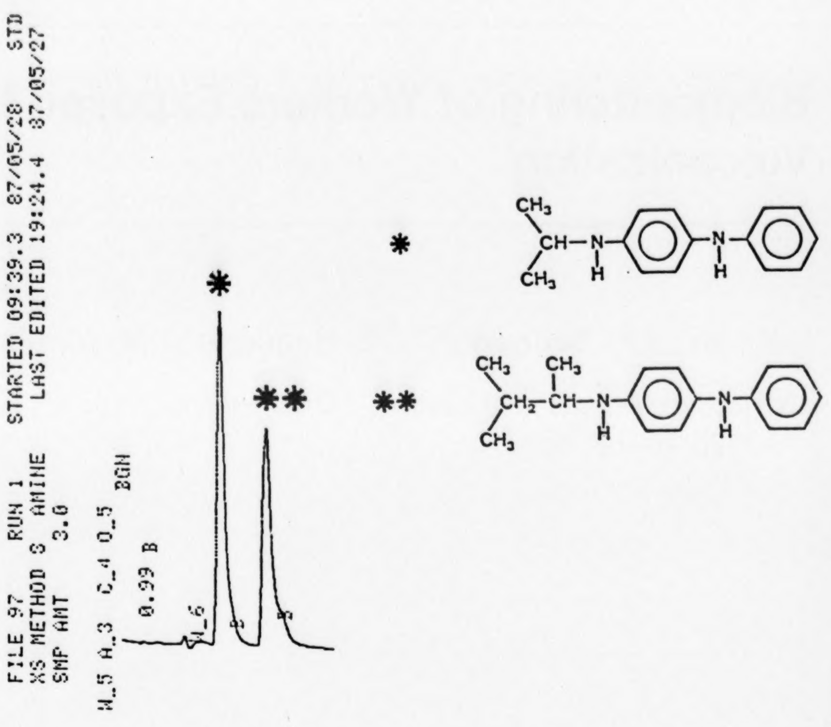

```
FILE 97     RUN 1     STARTED 09:39.3  87/05/28    STD
XS METHOD 3  AMINE      LAST EDITED 19:24.4  87/05/27
SMP AMT     3.0

W_5 A_3  C_4 O_5
                  BGN
     0.99 B
```

Fig. 1

LC chromatogram of IPPD and 6PPD standards.

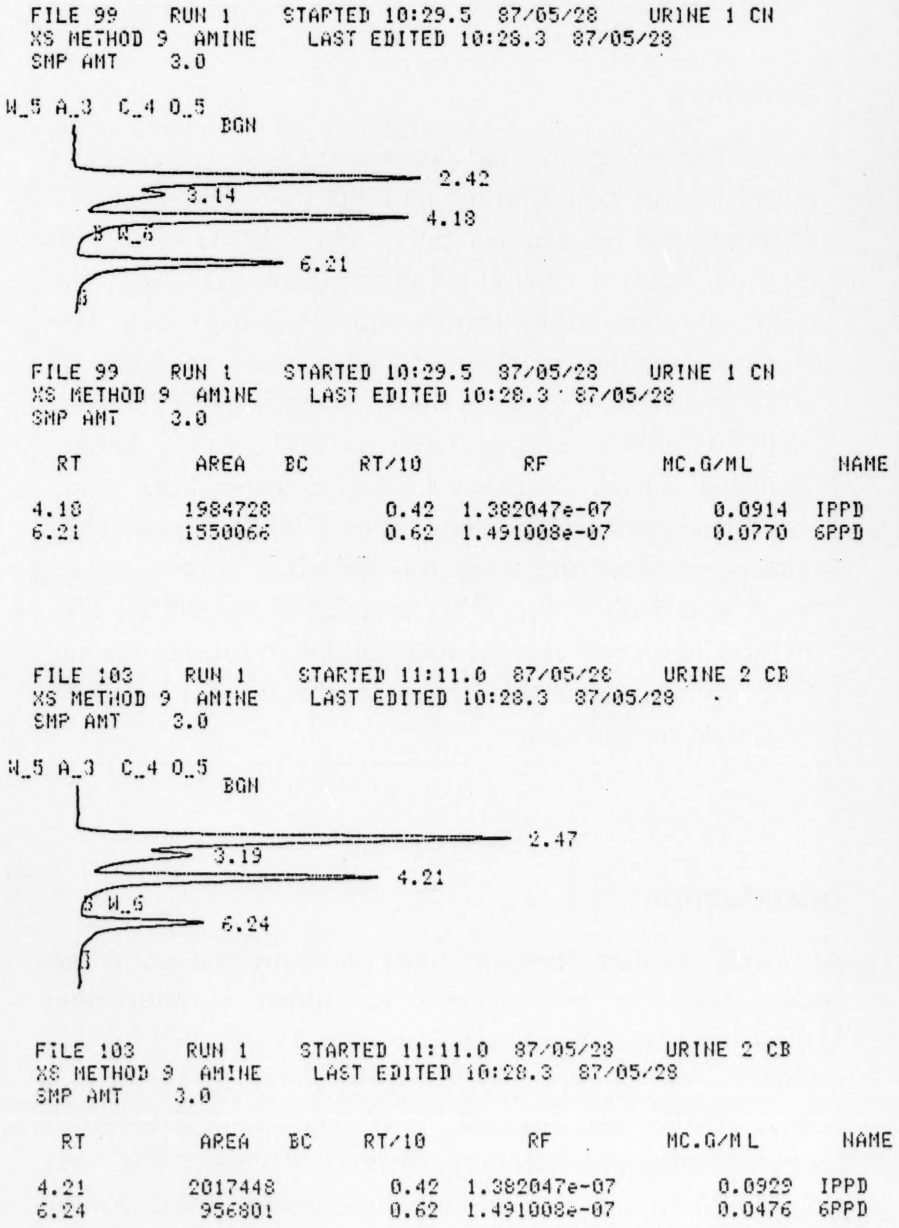

```
FILE 99     RUN 1     STAPTED 10:29.5  87/05/28     URINE 1 CN
XS METHOD 9  AMINE     LAST EDITED 10:28.3  87/05/28
SMP AMT     3.0
```

```
FILE 99     RUN 1     STARTED 10:29.5  87/05/28     URINE 1 CN
XS METHOD 9  AMINE     LAST EDITED 10:28.3 · 87/05/28
SMP AMT     3.0

  RT          AREA   BC    RT/10         RF           MC.G/ML      NAME

4.18         1984728           0.42  1.382047e-07          0.0914  IPPD
6.21         1550066           0.62  1.491008e-07          0.0770  6PPD
```

```
FILE 103    RUN 1     STARTED 11:11.0  87/05/28     URINE 2 CB
XS METHOD 9  AMINE     LAST EDITED 10:28.3  87/05/28    ·
SMP AMT     3.0
```

```
FILE 103    RUN 1     STARTED 11:11.0  87/05/28     URINE 2 CB
XS METHOD 9  AMINE     LAST EDITED 10:28.3  87/05/28
SMP AMT     3.0

  RT          AREA   BC    RT/10         RF           MC.G/ML      NAME

4.21         2017448           0.42  1.382047e-07          0.0929  IPPD
6.24          956801           0.62  1.491008e-07          0.0476  6PPD
```

Fig. 2

LC chromatograms of urine samples of two rubber workers exposed to IPPD and 6PPD.

A calibration curve consisting of a blank and eight single standards, as indicated, above were prepared for each aromatic amine (Fig. 3 and Fig. 4; Table I and Table II). The correlation coefficients for the peak area ratio against the IPPD and 6PPD concentrations (by linear regression) were usually 0.999 or better, indicating a high degree of linearity in the calibration curves over the concentration range studied. Under the experimental conditions this procedure can be used in routine quantitation of IPPD and 6PPD concentrations in urine as low as 10 ppb with 100 ml sample. Concentrations lower than 5 ppb can be detected but quantitation was not exact.

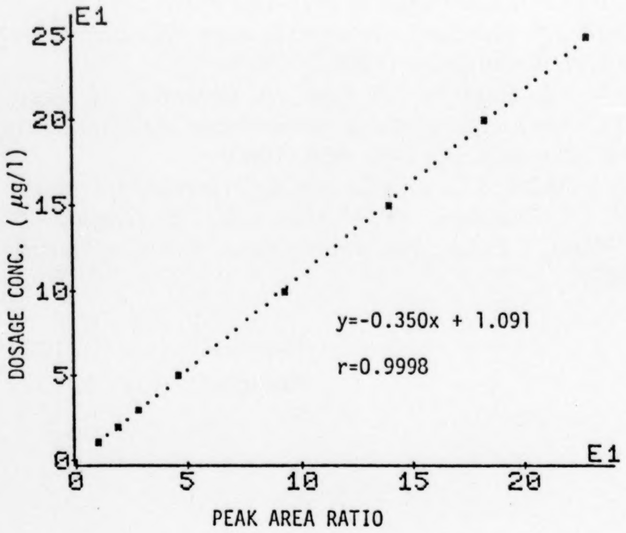

Fig. 3
Linear regression analysis of IPPD in fortified urine samples.

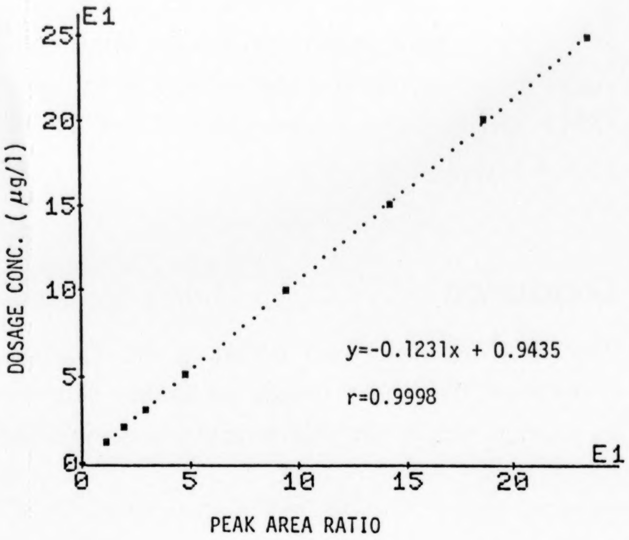

Fig. 4
Linear regression analysis of 6PPD in fortified urine samples.

Table I. Recovery and accurancy of IPPD in urine samples (n = 5)

Fortified dose level (μg/l)	Mean IPPD found in urine (μg/l)	Mean Recovery (%)	Standard Deviation	Relative Standard Deviation (%)
Blanck	–	–	–	–
10.00	9.2	92.0	0.39	4.20
20.00	18.3	91.5	0.66	3.60
30.00	27.3	91.0	0.49	1.79
50.00	45.3	90.6	0.43	0.94
100.00	93.5	93.5	1.15	1.23
150.00	140.2	93.4	1.05	1.12
200.00	182.6	91.3	1.18	1.29
250.00	228.2	91.3	1.25	1.36
		91.8 +/− 1.45		1.93

Table II. Recovery and accurancy of 6PPD in urine samples (n = 5)

Fortified dose level (μg/l)	Mean 6PPD found in urine (μg/l)	Mean Recovery (%)	Standard Deviation	Relative Standard Deviation (%)
Blank	–	–	–	–
10.00	9.4	94.0	0.60	6.3
20.00	18.6	91.5	1.03	5.5
30.00	28.2	94.0	0.87	3.1
50.00	47.2	94.4	0.85	1.8
100.00	93.7	93.7	0.71	0.7
150.00	142.2	94.8	0.80	0.5
200.00	186.8	93.4	0.50	0.2
250.00	236.7	94.6	0.90	0.3
		93.8 +/− 1.65		2.3

The outlined method was applied to monitoring the presence of unchanged IPPD in urine samples, during two consecutive working weeks, of sixteen rubber vulcanizers [5]. The excretion of absorbed IPPD, especially in the curing, where skin contact become important for the absorption of aromatic amines, starts during the working day. Under experimental conditions, it attains 20 % of its maximum 5 h after initial skin contact; the excretion peak is obtained 6 h later. IPPD concentrations in the urine were always significantly higher in the end-shift than in the before-shift sample (means 83.57 versus 19.55 $\mu g\,l^{-1}$; $P < 0.001$, two tailed; Wilcoxon matched pairs, signed-ranks test). Altogether the sample with less-than-detectable IPPD concentration decreased from 28.7 % before-shift to 4.4 % end-shift.

Conclusion

The method described offers a rapid, easy, and accurate technique for the analysis of exogenous aromatic amines in human urine. In this study we concluded that the use of disposable SEP columns for the clean-up technique has significant advantages of speed and simplicity for the assay. Work is under way employing these analytical methods to monitor exposed rubber industry workers.

References

[1] IARC Monographs on the evaluation of the carcinogenic risk of chemicals to humans. "The rubber industry", vol. 28. ISRC, Lyon, pp. 252 (1982).

[2] BRMA Toxicity and safe handling of rubber chemicals. "BRMA Code of practice". British Rubber Manufacturers' Association Ltd. Birmingham (1985).

[3] *E. Capodaglio, L. Pozzoli, V. Foa, A. Colombi, C. Sassi, A. Fantuzzi,* "Rischi, patologia e prevenzione nell' industria della gomma", Acireale, pp. 549–556 (1983).

[4] *F. Belliardo, I. Pavan,* J. Liquid Chrom. **4**, 279 (1981).

[5] *G. Scansetti, E. Buglione, M. M. Massiccio, D. Greghi, L. Inglese, W. Pisani, I. Pavan,* Int. Arch. Occup. Environ. Health, in press (1987).

Received: July 23, 1987
Accepted: Aug. 4, 1987
F

L-N-(3,5-Dimethoxybenzoyl)isoleucine Chiral Stationary Phase for Separation of Enantiomers by HPLC

W. J. Vloon / C. Siekerman / J. C. Kraak*

Laboratory for Analytical Chemistry, University of Amsterdam, Nieuwe Achtergracht 166, 1018 WV Amsterdam,
The Netherlands

Key Words

Column liquid chromatography
Chiral separation
HPLC
Benzoin

Summary

L-N-(3,5-dimethoxybenzoyl)isoleucine, ionically bonded to γ-aminopropyl silica, has been tested as a chiral stationary phase for the separation of racemates by HPLC. The phase shows good selectivity towards different types of racemates and in particular for those having an electron-poor aromatic group in their molecule. The separation of benzoin racemate can be achieved on the developed chiral phase with an α value of 1.10.

Introduction

The application of chiral stationary phases for the separation of enantiomers by HPLC has become increasingly successful nowadays, in particular the contribution of Pirkle et al. [1–4] and of Ôi et al. [5, 6] has advanced the development of several types of selective chiral stationary phases.

One of the most successful is R-N-(3,5-dinitrobenzoyl)-phenylglycine, developed by Pirkle et al. [3] some years ago. In a previous paper [7] we reported a variant of this phase, the R-N-(pentafluorobenzoyl)phenylglycine phase which shows a somewhat different selectivity towards various types of solutes compared with R-N-(3,5-dinitrobenzoyl)phenylglycine. The difference between these two phases indicates that the enantioselectivity of the chiral phase can be influenced by the type of functional groups attached to the benzoyl ring.

In the present paper we report the results of another variant of the Pirkle phase, L-N-(3,5-dimethoxybenzoyl)-isoleucine, ionically bonded to γ-aminopropyl silica, for the separation of enantiomers by HPLC.

Experimental

Apparatus

The liquid chromatograph consisted of a constant flow pump (Gynkotek, model 300C); a high-pressure sampling valve (Rheodyne, model 7125, Berkeley, USA), equipped with a 20μl sample loop and an UV spectrophotometer (Kratos Spectroflow 757, Kipp en Zonen, The Netherlands). The wavelength of the latter was usually set at 254nm. The columns were 316 stainless steel (150 × 4.6mm i.d.).

IR spectra were recorded on a Perkin-Elmer 1310, the absorptions are given in cm^{-1}. The ^1H NMR spectra were run on a Bruker WM-250 instrument. The mass spectra were obtained with a Varian MAT-711 instrument.

Materials

All solvents were of analytical grade (Merck, Darmstadt, FRG). Tetrahydrofuran (THF) was freshly distilled over $LiAlH_4$. The solutes were from Janssen Chimica (Beerse, Belgium) or synthesized by ourselves. l-isoleucine was from Janssen Chimica and R-N-(3,5-dinitrobenzoyl)phenylglycine from Sigma Chemicals (St. Louis, MO, USA). γ-aminopropyl silica was LiChrosorb NH_2 5μm (Merck, Darmstadt, FRG). N-hydroxysuccinimide and 3,5-dimethoxybenzoic acid were from Janssen Chimica.

Procedures

Synthesis of the N-hydroxysuccinimide ester of 3,5-dimethoxybenzoic acid: A mixture of 2.18g 3,5-dimethoxybenzoic acid, 1.38g N-hydroxysuccinimide and 2.70g N,N′-dicyclohexylcarbodiimide, dissolved in 30ml dry 1,4-dioxane, was stirred for 20 hours at 20°C, under nitrogen. The precipitate was filtered off and the filtrate was evaporated to dryness in vacuo. The residue was stirred for 30min with 50ml of a mixture of n-pentane/diethylether (1:1 v/v) and then filtered. The filtrate was evaporated to dryness *in vacuo* and the crude residue of the N-hydroxysuccinimide ester of 3,5-dimethoxybenzoic acid was directly used for the reaction with l-isoleucine. IR ($CHCl_3$)

0009-5893/87 0655-04 $03.00/0

© 1987 Friedr. Vieweg & Sohn Verlagsgesellschaft mbH

(cm^{-1}): 3000, 2960, 2940, 2860, 1810, 1780, 1740, 1605, 1595, 1460, 1160.

Synthesis of L-N-(3,5-dimethoxybenzoyl)isoleucine: To the crude residue of the N-hydroxysuccinimide ester of benzoic acid prepared before, 1.70g l-isoleucine, 4ml triethylamine and 10ml dry dimethylformamide was added and this mixture was stirred for 48 hours at 20°C. Then 100ml water was added and the mixture stirred for two hours at 20°C. Next the mixture was adjusted to pH = 2 with concentrated hydrochloric acid and extracted 3 times with 50ml CH_2Cl_2. The collected organic layers were dried over Na_2SO_4, filtered and evaporated *in vacuo*. The crude residue was purified by flash chromatography on silica gel by successive elution with 100ml of a mixture of ethylacetate/petroleum ether (1:1 v/v), 100ml ethylacetate and 100ml of a mixture of ethylacetate/ethanol (9:1 v/v). The fractions of the elution with pure ethylacetate and with the mixture of ethylacetate/ethanol were collected and evaporated *in vacuo* [8]. The pure chiral product obtained is a colourless oil. The yield was 1.62g (46%).

IR ($CHCl_3$) (cm^{-1}): 3430, 2960, 2940, 1720, 1655, 1590, 1510, 1455, 1420, 1350, 1155.

^1H NMR ($CDCl_3$): δ 8.3 (1H, broad, COOH); 6.90 (2H, d, J = 2.1 Hz, ArH); 6.77 (1H, d, J = 8.3 Hz, NH); 6.56 (1H, t, J = 2.1 Hz, ArH); 4.77 (1H, dd, J = 8.3 Hz, J = 4.7 Hz, NCHC); 3.79 (6H, s, CH_3O); 2.1–1.9 (1H, m, CCHC); 1.65–1.45 (1H, m, ABM system, CCH_2C); 1.40–1.10 (1H, m, ABM system, CCH_2C); 0.97 (3H, d, J = 6.8 Hz, CH_3C); 0.93 (3H, t, J = 7.3 Hz, CH_3C). High resolution mass spectrum: calculated for $C_{15}H_{21}NO_5$, 295.1420; found, 295.1428.

Column preparation: The coating of the chiral phase on the γ-aminopropyl silica was performed in a pre-packed column, which was packed with the slurry technique, using isopropanol as slurry liquid and methanol as displacer liquid up to a maximum pressure of 500 bar. The column was successively washed with 50ml methanol, 50ml dry tetrahydrofuran (THF), 40ml of a 5% (v/v) solution of triethylamine in dry THF, 20ml dry THF and finally with 20ml dry CH_2Cl_2. Next the column was coated with the chiral phase by recycling a solution of 870mg of the chiral acid in 25ml of CH_2Cl_2 for 17 hours at a flowrate of 1 ml/min. Then the column was washed with 50ml of CH_2Cl_2 and finally with hexane/isopropanol (19:1 v/v) until a stable baseline was achieved.

Results and Discussion

As mentioned before the L-N-(3,5-dimethoxybenzoyl)-isoleucine (DMI) phase is a modification of the R-N-(3,5-dinitrobenzoyl)phenylglycine (DNP) phase as developed by Pirkle et al. [3]. We decided to use the isoleucine derivative instead of the phenylglycine because with isoleucine there is less risk of racemization during the synthesis of the chiral phase and the determination of the optical purity by NMR is easier because of the presence of two chiral centers. Although the replacement of phenylglycine by isoleucine has some small effects on the enantioselectivity as shown by Pirkle et al. [3], the change of the type of functional groups in the benzoyl ring will have a more pronounced effect on the α values.

In order to investigate the effect of the replacement of the type of functional groups in the benzoyl ring on the enantioselectivity, the capacity factors and selectivity factors (α values) of racemates were measured on the DMI and DNP phase. The results of these measurements are given in Table I. For comparison also the capacity factors and α values on the R-N-(pentafluorobenzoyl)phenylglycine (PFP) phase, as measured previously [7], are included in this table.

Significant differences in retention and selectivity between these three chiral phases can be observed from this table. The capacity factors of all solutes decrease in the order DMI $\leqslant$ PFP $<$ DNP. Because the amount of stationary phase loading was not found to differ significantly (70–80mg/g packing), these differences in the magnitude of retention must be attributed to non-stereoselective interactions of the solutes with the functional groups in the benzoyl ring.

The variation of the type of functional groups in the benzoyl ring also significantly influences the α values of the test racemates. The NO_2 and F groups are strongly electron withdrawing which causes the benzoyl ring to become very electron deficient (π-acid). This favours the interaction with solutes with an electron rich aromatic part (π-base) via π-π interactions, from which it has been proved to play a role in the chiral recognition [9]. From Table I it can indeed be seen that solutes with electron rich aromatic groups have the largest value on the DNP and PFP phase.

Besides the π-π interaction the presence of a dipole moment in the benzoyl ring also seems to play a role in the extent of chiral recognition as can be seen when comparing the α values on the DNP phase, which has a large dipole moment in the benzoyl ring, with the PFP phase where a dipole moment is absent. The effect of the presence of methoxy groups on the nature of the benzoyl ring is opposite to that caused by the NO_2 and F groups. Methoxy groups are electron donating groups and this makes the benzoyl ring electron rich (that is, more π-base like). This favours π-π interactions with solutes with electron poor aromatic groups (π-acids). Moreover, the two methoxy groups in DMI also produce a dipole moment in the benzoyl ring, which is favourable for chiral recognition. The different π-π interaction abilities of the DMI phase compared to the DNP and PFP phase can be judged from the α values of some of the test racemates. For instance, the α value of the ethyl ester of the DNP phase used as a solute, of which the benzoyl ring is a strong π-acid, is considerably larger on the DMI phase ($\alpha = 1.45$) than on the DNP phase ($\alpha = 1.11$), while on the PFP phase $\alpha = 1.00$.

The opposite is found for 2,2,2-trifluoro-1-(9-anthryl)-ethanol, which is a strong π-base. The α values decrease in the order DNP $>$ PFP $>$ DMI. As the methoxy as well as the NO_2 groups introduce a dipole moment in the benzoyl ring of the chiral phase, the difference in the α values may be attributed to the difference in the nature of the π-π interaction of both chiral phases, providing

Table I. Capacity factors, k′, and selectivity factors, α, of some racemates on DNP, PFP and DMI chiral stationary phases.

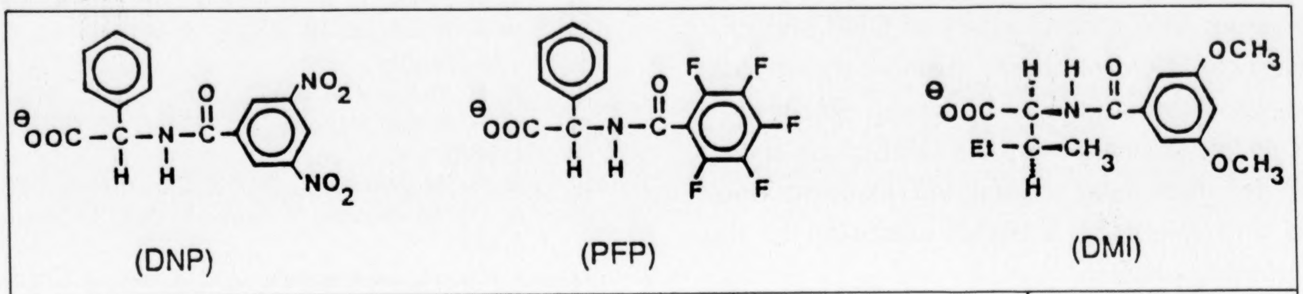
(DNP)

(PFP)

(DMI)

Compound	DNP		PFP		DMI	
	k′	α	k′	α	k′	α
1) 2,2,2-Trifluoro-1-(9-anthryl)ethanol	1.67	1.49Δ	0.80	1.13Δ	2.15	1.00∇
2) 3-Phenylsuccinimide	10.6	1.13Δ	7.12	1.19Δ	11.3	1.09∇
3) 1,1′-Bi-2-naphtol	5.93	1.41Δ	3.61	1.10Δ	7.22	1.07∇
4) 3-Phenylphthalide	2.80	1.04Δ	2.33	1.00∇	1.95	1.00○
5) RS/SR-1-phenylsulphinyl 2-methyl-3-buten-2-ol	22.8	1.08Φ	14.4	1.05Φ	2.32	1.00∇
6) RR/SS-1-phenylsulphinyl 2-methyl-3-buten-2-ol	17.8	1.10Φ	11.8	1.12Φ	2.92	1.00∇
7) Methyl mandelate	2.15	1.08Δ	5.32	1.08Φ	1.83	1.16∇
8) Mandelamide	15.1	1.05Δ	11.4	1.12Δ	9.83	1.25∇
9) Benzoin	4.03	1.03∇	3.08	1.00∇	2.66	1.10○
10) 5-Methyl-5-phenylhydantoin	17.9	1.18Δ	8.74	1.27Δ	15.7	1.11∇
11) Ethyl N-(pentafluorobenzoyl)phenylglycinate	4.10	1.00Δ	3.14	1.14Δ	0.96	1.06Δ
12) Ethyl N-(3,5-dinitrobenzoyl)phenylglycinate	12.6	1.11Δ	4.90	1.00Δ	4.39	1.45Δ

○ hexane + 1% isopropanol
Φ hexane + 2.5% isopropanol
∇ hexane + 5% isopropanol
Δ hexane + 10% isopropanol

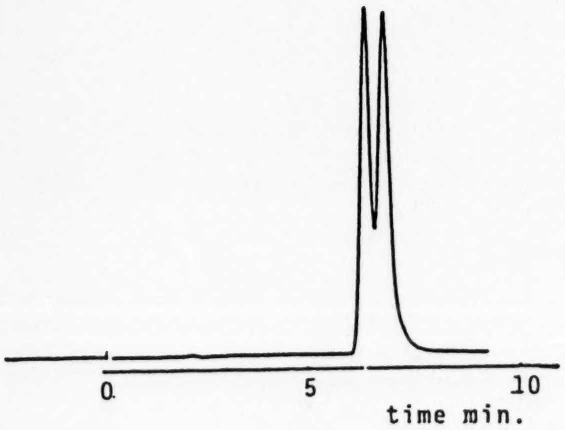

Fig. 1

Separation of enantiomers of benzoin on DMI phase. Mobile phase: n-hexane + 1% (v/v) isopropanol

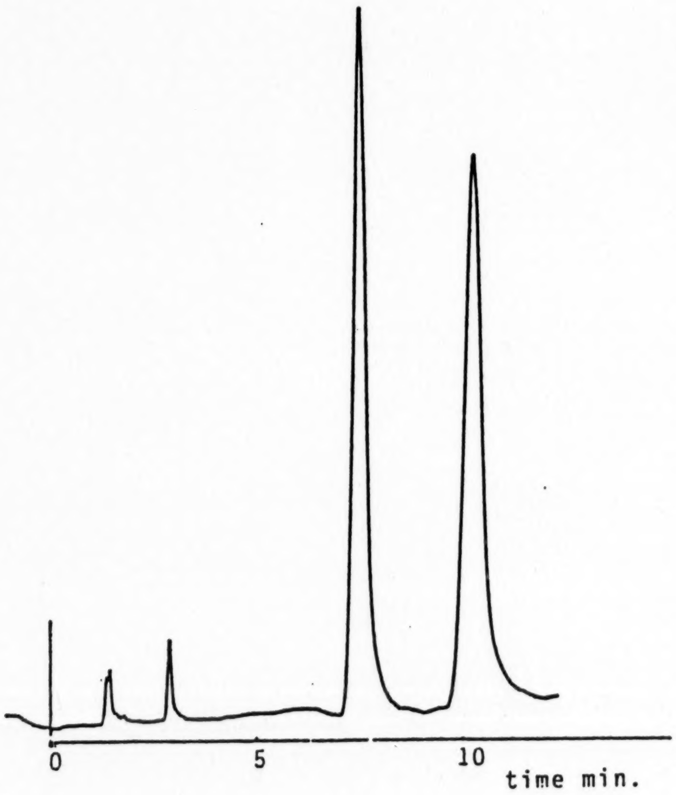

Fig. 2

Separation of enantiomers of ethyl ester of R-N-(3,5-dinitrobenzoyl)-phenylglycine on DMI phase. Mobile phase: n-hexane + 10% (v/v) isopropanol the influence of the type of amino acid is indeed insignificant. This is now under investigation.

The different α values of the ethyl esters of DNP and PFP on the three investigated chiral phases, support the importance of dipole-dipole interactions in chiral recognition [9]. The results so far indicate that the DMI phase shows good selectivity for racemates containing electron poor aromatic groups and might be a useful extension of the known chiral stationary phases.

Some typical chromatograms of benzoin racemate and of the DNP-ethylester on the DMI column are shown in Fig. 1 and 2.

References

[1] *W. H. Pirkle, D. W. House*, J. Org. Chem., **44**, 1957 (1979).
[2] *W. H. Pirkle, D. W. House, J. M. Finn*, J. Chromatogr., **192**, 143 (1980).
[3] *W. H. Pirkle, J. M. Finn*, J. Org. Chem., **46**, 2935 (1981).
[4] *W. H. Pirkle, Myung Ho Hyun*, J. Chromatogr., **322**, 295 (1985).
[5] *N. Ôi, M. Nagase, T. Doi*, J. Chromatogr., **257**, 111 (1983).
[6] *N. Ôi, M. Nagase, Y. Inda, T. Doi*, J. Chromatogr., **259**, 487 (1983).
[7] *J. Kip, P. van Haperen, J. C. Kraak*, J. Chromatogr., **356**, 423 (1986).
[8] *W. C. Still, M. Kahn, A. Mitra*, J. Org. Chem., **43**, 2923 (1978).
[9] *W. H. Pirkle, Myung Ho Hyun*, J. Chromatogr., **328**, 1 (1985).

Received: July 30, 1987
Accepted: Aug. 12, 1987
F

Recognizing Chromatographic Peaks with Pattern Recognition Methods III. Application of the Algorithm for Peak Recognition in Trace Analysis

G. Reich

Institute for Analytical Chemistry, University of Vienna, Währingerstr. 38, A-1090 Vienna, Austria

Key Words

Peak recognition
Chromatographic data system
Pattern recognition

Summary

The application of a newly developed peak recognition algorithm is shown. This algorith is based on the KNN method, one of the pattern recognition methods. It is shown that peaks with a S/N-ratio down to one can be safely recognized. This is also possible if the baseline has not only detector noise, but has other disturbances, e.g., noise signals which are generated by a reaction detector. The recognition ability of the algorithm is demonstrated by a standard chromatogram with three different concentrations and with two different sampling rates. The improvement against the classical algorithm is demonstrated. Some properties of the algorithm are discussed.

Introduction

A new method has been recently proposed for the recognition step in the automated processing of chromatograms [1, 2]. This method uses an algorithm selected from the pattern recognition methods, namely the k-nearest neighbor (KNN) method. The great advantages of this algorithm is its low sensitivity to high noise levels and that the recognition ability is not changed by increasing the sampling rate.

A short description of this algorithm will be given; for a more detailed discussion see our previous papers [1, 2]. The algorithm starts with the definition of a peak profile function. The shape of this profile has to be the shape of the chromatographic peak, which is searched for. But the profile function can also be a more complex peak shape, like a tailing peak or a pair of poorly separated peaks. If this algorithm is used in a "learning" mode, then the profile function can be determined from the actual chromatogram at hand. Baseline drift and noise signals can also be included in the definition of the profile function.

The profile function is defined by a number of amplitude values at equidistant points. With n values given this profile function can be represented by a point in the n dimensional pattern space: n consecutive digitized values from the chromatogram represent a second point in the pattern space. The distance between these two points gives the value of the peak recognition function (PRF). The smaller the distance between the points is, the more similar are the shape of the profile function and the shape of the part of the chromatogram in the comparison window. With the moving window method different parts of the chromatogram are selected. The window is moved over the chromatogram and if the chromatogram shows a peak at a given position the value of the PRF goes through a minimum at this position. The lower the value of this minimum is, the more similar are the shape of the profile function and the shape of the chromatographic peak. The distance between these points can be calculated by different distance measures [2]. The calculation of the distance of the two points in the pattern space is done by summations, therefore, in contrast to the classical algorithm, the integration and not the differentiation is used for the recognition process. This fact results in an S/N improvement in the recognition process and not in an S/N reduction like in the classical algorithm.

To show the recognition capability of the new algorithm a phenol solution at three different concentrations is chromatographed, where the lowest concentration gives peaks with an S/N-ratio of approximately one. The position of any peak can be verified by the chromatograms at the other concentrations. The sampling rate is set at 10 samples per second (10 Hz). This high sampling rate is selected to show the independence of the algorithm from the sampling rate. Increasing the sampling rate to get a better noise suppression by the recognition process is possible. To show the properties of the algorithm with a more common sampling rate a program was written to change the sampling rate of the data file. This program calculates the mean of a given number of sample values (bunching). A second set of data files with a sampling rate of 1 Hz has been created with this program. A program supplied with the data system has been modified to convert the binary data file of the data system to an ASCII data file. The ASCII data file can be processed by the programs of the new algorithm.

0009-5893/87 0659-07 $ 03.00/0

© 1987 Friedr. Vieweg & Sohn Verlagsgesellschaft mbH

The distance measure used in this evaluation is the correlation coefficient, or more correct the negative value of the correlation coefficient. A description of this and other distance measures is given in ref. [2]. A new algorithm for recognizing the minimas in the PRF is used. In the first publication [1] simply each minimum after a given number of points with a negative difference to the preceding point is taken as a peak position. On real signals this algorithm finds too many peak positions. If the distance between two peaks is approximately four to six times the width of the profile an additional minimum between the two peaks is generated by the algorithm. The size and the shape of this additional minimum can be influenced by the selection of the profile function. A strategy to select the real peak positions from all peak position which are found will therefore be necessary. A possible selection criterium is the width of the minimum valley of the PRF compared with the profile width and the width of safely identified peaks. Another criterium is the symmetry of the PRF minimum valley. The new method for determining all relevant peak positions collects all the minimas found with the algorithm described above, sorts them according to their values of the minimum and selects a given number of them with the lowest values. It can be seen easily that the value of the minimum for a noise peak is larger than the minimum for a real peak. It is evident that it is not easy to decide if a certain minimum corresponds actually to a peak or if it is only a noise peak. Additional information, e. g., the analysis of the noise itself, has to be incorporated in the algorithm to reach a correct decision. In our case the decision is easy because only a standard solution is used and the number and positions of all peaks are known.

Experimental

Eight phenols in three different concentrations are used as standard solutions for the chromatograms. Solution 1 is the most concentrated sample. Solution 2 is Solution 1 diluted by a factor of 5 and Solution 3 is Solution 2 diluted by a factor of 10. The names of the solutes and their concentrations are given in Table I. The phenols were separated by gradient elution. The Detection was done by fluorescence detection after an oxidation by cerate. The chromatographics conditions and the reaction detection method are taken from the literature [3]. The chromatographic system consisted of a Varian LC 5000 (Varian, Walnut Creek, California, USA), the reagent delivery system Merck 655A-13 (Merck, Darmstadt, FRG), the fluorescence detector Merck F1000 and the data system 3000 (Nelson Analytical, Cupertino, California, USA) based on an IBM-AT computer (IBM, Boca Raton, Florida, USA). The new programs were written in FORTRAN, BASIC and Turbo-Pascal. The calculations were done on the PC and on the Mainframe computer (IBM 3083) of the computing center at the University of Vienna. The graphic output was plotted on a HP 7550 plotter (Hewlett-Packard, Palo Alto, California, USA).

Table I. Solutes and sample amounts (ng/injection volume) used in the solutions

Peak number	Solute	Amount [ng]		
		Solution		
		1 (1:1)	2 (1:5)	3 (1:50)
1	Phenol	25	5	0.5
2	4-Nitrophenol	125	25	2.5
3	2-Chlorophenol	25	5	0.5
4	2-Nitrophenol	25	5	0.5
5	2,4-Dimethylphenol	25	5	0.5
6	4-Cl-3-methylphenol	125	25	2.5
7	2,4-Dichlorophenol	25	5	0.5
8	2,4,6-Trichlorophenol	75	15	1.5

Results and Discussion

All figures are laid out in the same way. The chromatogram is shown on top and the peak recognition fuction (PRF) is shown below at the same time scale. The profile function used is shown at the beginning of the chromatogram. All chromatograms with the same sampling rate are grouped together. Part a) shows the chromatogram for Solution 1 (1:1), part b) for Solution 2 (1:5) and c) for Solution 3 (1:50). The large marks at the bottom of the chromatogram show the position of recognized peaks.

Fig. 1 shows the chromatograms for the sampling rate of 10 Hz. The noise seen on these chromatograms is noise from the reagent pump and not detector noise. A closer look on peak 5 in Solution 2 given in Fig. 2 shows this. The peaks at the beginning of the chromatogram (first ten minutes) are the results of the starting gradient in conjunction with the reagent for the reaction detection and an insufficient reequilibration time. The objective of this study is to show the capabilities of this algorithm in real practice and not to show perfect chromatograms.

The number of dimensions of the pattern space used with this sampling rate is 991 and the profile function is a gaussian peak with a peak width of 10 sec. In the chromatograms of Solution 1 and Solution 2 all eight peaks can be seen very easily and at all eight peak locations the minimum in the PRF is clearly expressed. The chromatogram of Solution 3 shows visible peaks for solute 2 and 6, which are the largest peaks in the chromatograms. Peak 1 is on a large and broad baseline peak and can, like all the other remaining peaks, be recognized only because its location is known. The look on the PRF shows clear minimas for all peaks except peak 5. This peak is nearly lost in the rough baseline, but a minimum can be seen at approximately the right location. The retention times for all solutes on all chromatograms with a sampling rate of 10 Hz are given in Table II. The corresponding minimum value of the PRF is included. The value of the PRF for a perfect recognition is -1 because the correlation coefficient, as is known, can only take values between 1 and -1.

Fig. 3 shows the results for a sampling rate of 1 Hz. In this case the number of dimensions of the pattern space used is 99. The width of the profile peak is again 10 sec. It can be seen that the result is nearly identical with the first example.

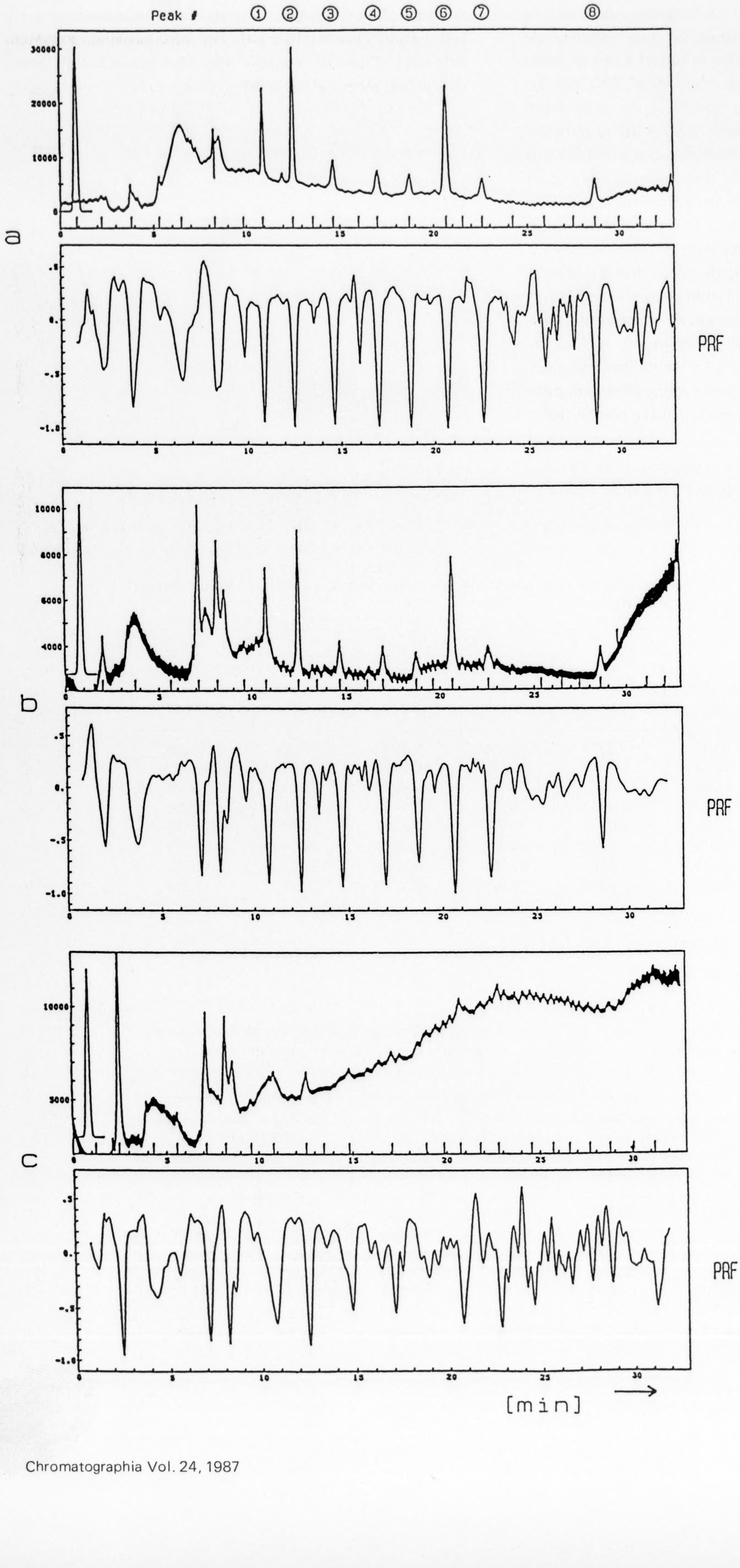

Fig. 1

Chromatogram and peak recognition function (PRF) acquired with a sampling rate of 10 Hz. a) for Solution 1 (1:1), b) for Solution 2 (1:5) and c) for Solution 3 (1:50). In each case the chromatogram is on the top and the corresponding PRF is shown below. The profile function used is given at the beginning of the chromatogram.

Table III gives the retention times and the values of the minimum of the PRF. The values of the minimas are slightly smaller (the absolute value is larger) by most peaks than those with the higher sampling rate. This can be expected, because the pumping noise is a deviation from the profile function and, therefore, the similarity between the profile function and the chromatographic peaks is reduced. It should be mentioned that no bunching occurs with this algorithm and a greater sampling rate results in a more exact definition of the signal. This has the advantage that certain signal characteristics can be more accurately reproduced, but it also has the disadvantage that if a general useful profile is used, the similarity between the profile and the chromatogram is slightly reduced. Another very useful property of the algorithm is the possibility to include an optimization of the profile function in the recognition step. By adjusting the profile function to the actual chromatogram a kind of deconvolution can be included in the recognition.

Fig. 4 shows the result for the classical recognition algorithm. Solution 1 and 2 show perfectly recognized peaks. A recognized peak is indicated by plotting the peak baseline. With Solution 3 however only the larger peaks are correctly recognized. This result can be expected because of the low S/N-level. Table IV lists the retention times for all peaks recognized by the classical algorithm.

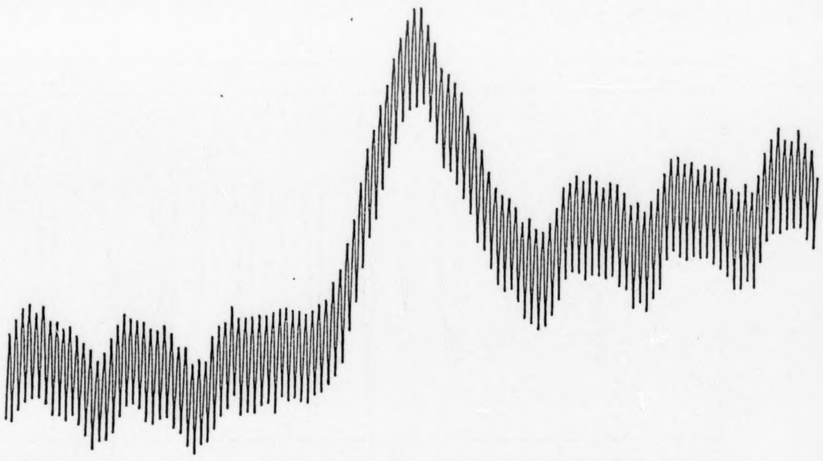

Fig. 2
Magnification of Peak # 5 from Solution 2 in Fig. 1.

Table II. Retention times and values of the minimum of the peak recognition function (PRF) for the chromatograms with a sampling rate of 10 Hz

Peak number	Solution					
	#1 (1:1)		#1 (1:5)		#3 (1:50)	
	t_R	MV	t_R	MV	t_R	MV
1	10.90	−0.9374	10.77	−0.8933	10.80	−0.6406
2	12.52	−0.9811	12.50	−0.9783	12.56	−0.8432
3	14.65	−0.9581	14.68	−0.9280	14.82	−0.5084
4	16.99	−0.9757	16.95	−0.9102	17.08	−0.5357
5	18.69	−0.9865	18.72	−0.6997	18.91	−0.2149
6	20.66	−0.9948	20.64	−0.9924	20.74	−0.6415
7	22.58	−0.9481	22.55	−0.8384	22.76	−0.6728
8	28.66	−0.9669	28.57	−0.5726	28.75	−0.2640

t_R = Retention time in minutes.
MV = Minimum value of the PRF.

Table III. Retention times and values of the minimum of the peak recognition function for the chromatograms with a sampling rate of 1 Hz

Peak number	Solution					
	#1 (1:1)		#1 (1:5)		#3 (1:50)	
	t_R	MV	t_R	MV	t_R	MV
1	10.90	−0.9369	10.78	−0.8980	10.80	−0.6512
2	12.52	−0.9791	12.52	−0.9782	12.57	−0.8645
3	14.67	−0.9584	14.70	−0.9647	14.83	−0.5394
4	17.00	−0.9764	16.97	−0.9459	17.08	−0.5839
5	18.70	−0.9892	18.73	−0.7376	18.92	−0.2174
6	20.67	−0.9931	20.65	−0.9953	20.75	−0.6552
7	22.58	−0.9500	22.55	−0.9168	22.77	−0.6953
8	28.67	−0.9690	28.58	−0.6033	28.77	−0.2962

t_R = Retention time in minutes.
MV = Minimum value of the PRF.

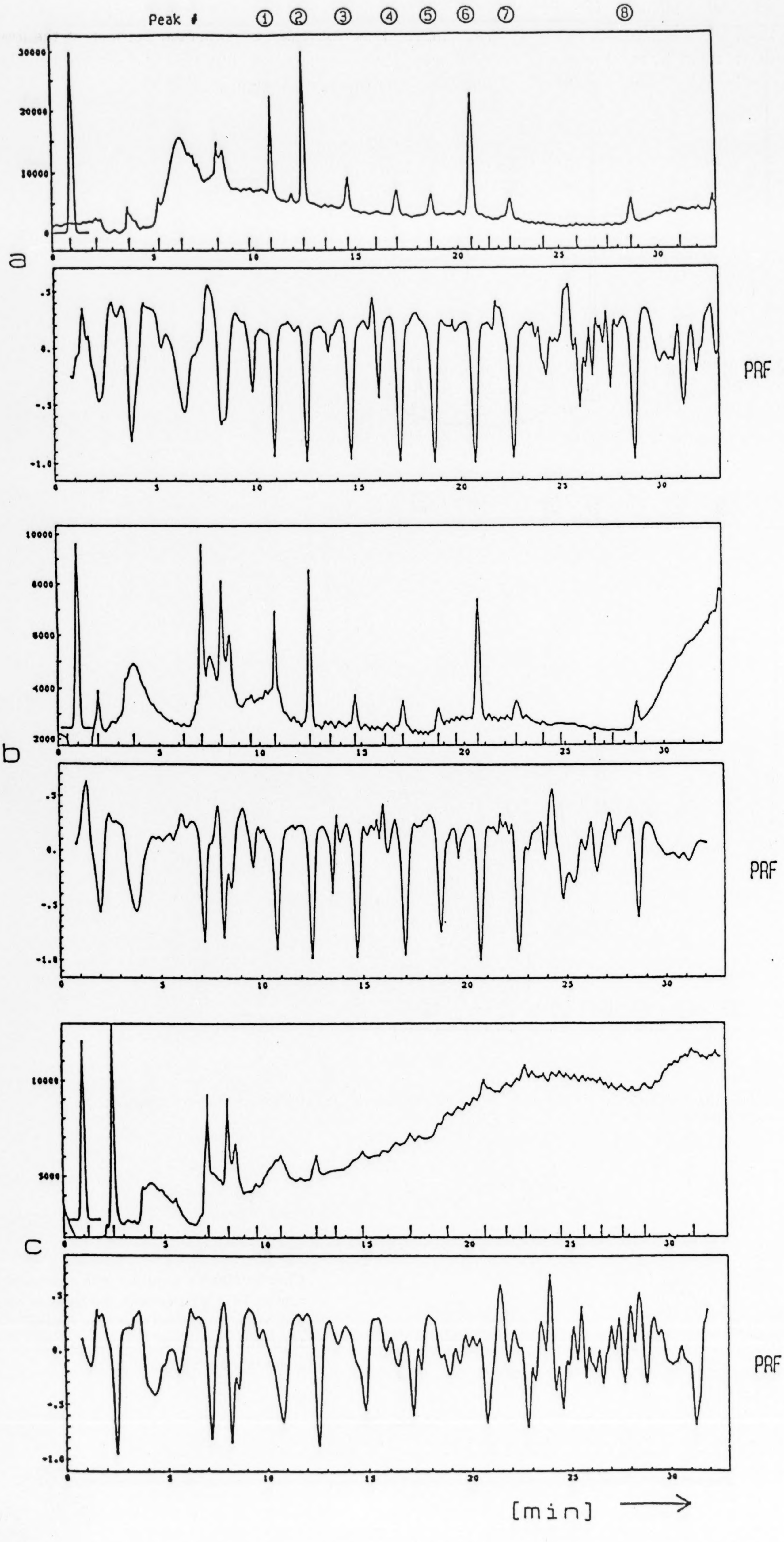

Fig. 3
Chromatogram and peak recognition function (PRF) acquired with a sampling rate of 1 Hz. Other parameters as in Fig. 1.

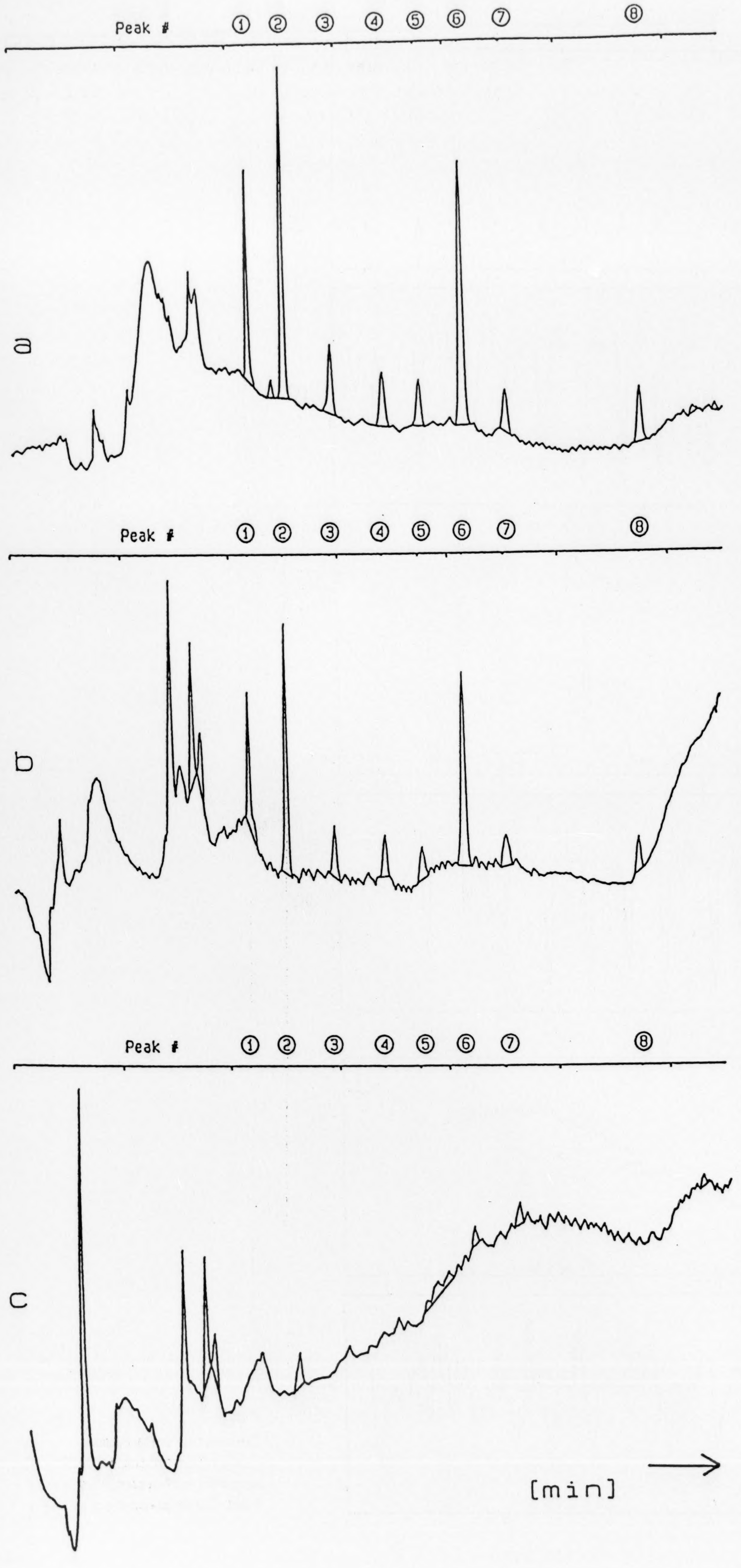

Fig. 4

Chromatograms, acquired with a sampling rate of 1 Hz, plotted with the baseline for each peak recognized with the classical algorithm. The order of the chromatograms is the same as in Fig. 1.

Table IV. Retention times [min] for the chromatograms calculated with the classical algorithm

Peak number	Solution		
	# 1 (1:1)	# 2 (1:5)	# 3 (1:50)
1	10.92	10.81	–
2	12.54	12.54	12.61
3	14.70	14.73	–
4	17.03	16.99	–
5	18.74	18.76	–
6	20.71	20.69	20.76
7	22.65	22.60	22.83
8	28.72	28.64	–

Conclusion

It has been proven that this new algorithm has superior recognition abilities. Peaks with S/N-ratios down to approximately one and below can be recognized with this algorithm. In fact more information on the noise has to be used to decide if a certain minimum corresponds to an actual peak or if it is only a noise peak. The quantitation of the peaks needs also a new algorithm because this algorithm gives only the peak position and a rough approximation of the peak shape. Both can be used to calculate an estimate of the peak area, and to calculate, more accurately, the peak height. The classical algorithm has the advantage to give the peak start and the peak end and, although they are often wrong, they can be used to calculate the peak area.

Acknowledgement

The autor thanks M. Maurer and G. Lamprecht for their help by measuring the chromatograms and using their chromatographic methods. Special thanks must be given to Prof. J. F. K. Huber for the encouragement to proceed with this work. Thanks also go to Nelson Analytical for their donation of the data system software and the AD-converter.

References

[1] *G. Reich,* Anal. Chim. Acta in print (1987).
[2] *G. Reich,* Anal. Chim. Acta in print (1987).
[3] *A. W. Wolkoff, R. H. Laroes,* J. Chrom. **99** 731 (1974).

Received: Aug. 4, 1987
Accepted: Aug. 15, 1987
F

Analysis of Enhanced Oil Recovery Formulations

Y. L. Hofman*/H. P. Angstadt

Sun Refining and Marketing Co., P. O. Box 1135, Marcus Hook, PA 19061, USA

Key Words

Column liquid chromatography
Ion-exchange chromatography
Surfactants analysis
Produced fluids analysis

Summary

Methods for the determination of low levels of surfactants in produced oil field brines have been developed. Alkylbenzene sulfonates (ABS) and alkylether sulfates can be quantified at very low levels by high-performance liquid chromatography (HPLC) and mobile-phase ion chromatography (MPIC), respectively. These methods proved to be rapid, selective, and gave results in excellent agreement with traditional low-phase titration techniques. Although this paper records the use of these methods for analysis of oil field produced fluids, they should be easily adaptable to other situations wherein the analysis of these two classes of surfactants is required.

Introduction

This paper describes a combination of methods used for the analysis of surfactant mixtures which are frequently used in various oil field processes such as drilling operations, clean-up procedures, and various enhanced oil recovery processes. Frequently, the surfactants used in these processes are not single substances but are instead complex mixtures of two or more principle surfactants and other additives, the composition of the mixture being constructed so as to achieve some particularly desirable property as required by the reservoir being treated or the process being used. This work describes the analysis of a surfactant mixture containing alkylaromatic sulfonates and alkylether sulfates, two general classes of surfactants frequently used in oil field operations.

High-performance liquid chromatoraphy (HPLC) is rapidly becoming a powerful tool in the analysis of surfactants used in the oil field. The separation of petroleum sulfonates according to their degree of sulfonation by anion-exchange chromatography is documented in the literature [1]. Nakae et al. [2] reported a procedure than uses simple reversed-phase chromatography to resolve mixtures of C_{10} to C_{13} alkylbenzene sulfonates. J. Larson [3] used indirect photometric liquid chromatography (IPC) for the determination of alkyl sulfonates. The IPC approach improves peak shape and increases linear range. All of these procedures had typical analysis times of twenty to thirty minutes.

We developed a rapid quantitative technique for the analysis of an alkylbenzene sulfonate surfactant (ABS) in produced well brines by means of reversed phase HPLC using UV detection. Surfactants of this type are usually complex mixtures of many isomers and the techniques and conditions required to obtain good reproducibilities with high sensitivity will be described. The system used including a diode-array detector was capable of detecting less than 5 ppm of surfactant in produced brine samples.

Surfactants used in oil field processes are usually complex formulations of more than one type surfactant, and often contain other compounds used as co-surfactants, bacteriostats, tracers, etc. The surfactant package used in this investigation contained an alkylether sulfate, in addition to the sulfonate, which does not contain a significant ultraviolet active chromophore, thus rendering diode-array detection ineffective. Refractive index (RI) detection was insufficiently sensitive for the surfactant concentration levels expected in the produced water.

Mobile-phase ion chromatography (MPIC) was introduced for the analysis of aliphatic anionic surfactants by J. Weiss [4]. The adaptation of this technique for the detection of very low concentrations of alkylether sulfates (AES) in brine solutions containing 2–10 % salt concentration is described. This procedure is applicable to the routine laboratory analysis of organic sulfates.

The combination of these two techniques allowed the progress of the surfactants to be monitored as they moved through a typical reservoir from an injector to an producing well. Furthermore, the determination of the relative concentrations of each surfactant in the produced water provided additional insight into the relative mobility of these surface active agents within the formation.

0009-5893/87 0666-05 $03.00/0

© 1987 Friedr. Vieweg & Sohn Verlagsgesellschaft mbH

Experimental

The analysis of low level components of the surfactant formulation was accomplished by using a combination of a Hewlett-Packard HPLC system equipped with a diode-array UV spectrophotometric detector and the Dionex 4000i Ion Chromatograph with Micro Membrane Suppressor (MMS). For the HPLC analyses the column selected was a LIChrosorb RP-8 (4.6 mm X 20 cm, particle size 10 μm) having the C_8 bonded to a silica surface. This column was found to give the greatest response among these tested. With the ion chromatograph a column having a stationary phase derived from non-derivatized, high specific area divinylbenzene was used. This column is only slightly polar and essentially hydrophobic. Operating conditions for both instruments are given in Table I.

Results and Discussion

One of the most difficult tasks in the application of chemicals to solve subsurface problems is to adequately characterize the reservoir in which a particular technique is to be used. Reservoir characterization is frequently aided by the use of tracer molecules: compounds which are placed into the formation in known concentrations via an injection well and can be readily detected in the fluids from the production wells. Data such as the length of time it takes for the tracer to appear in the fluids from the producing wells, the concentration of the tracer in these fluids, and the dispersion of the tracer over time are then combined with other well data to generate a limited description of the formation through which the fluids have passed. Frequently after reservoir characterization efforts, chemicals are then added to the injection water which are expected to facilitate the removal of additional oil, oil that cannot be recovered by water flooding alone. In other techniques chemicals are added via an injection well and then recovered via production from the same well and their rate of recovery is used to obtain information concerning depth of penetration into the formation or other characteristics about near well bore conditions. Determining the fate of these chemicals presents a significant analytical challenge; however, the more effectively this can be done, the more accurate and valuable will be the evaluation of the formation and of the performance of the chemicals under test.

A field test was carried out to evaluate the performance of several chemicals in a typical reservoir. Prior to the addition of the chemical package sodium thiocyanate was injected into the formation as a tracer and two weeks later the injection of the chemicals was begun. At this point samples of the produced fluids, oil and water were obtained from the wells surrounding the injection well. The produced water was analyzed for the presence of thiocyanate, sulfonate and sulfate using the techniques described herein.

One of the surfactants in the chemical package used to treat the reservoir was an alkylbenzene sulfonate (ABS) and its UV absorbance curve is shown in Fig. 1. Fig. 2 is the UV

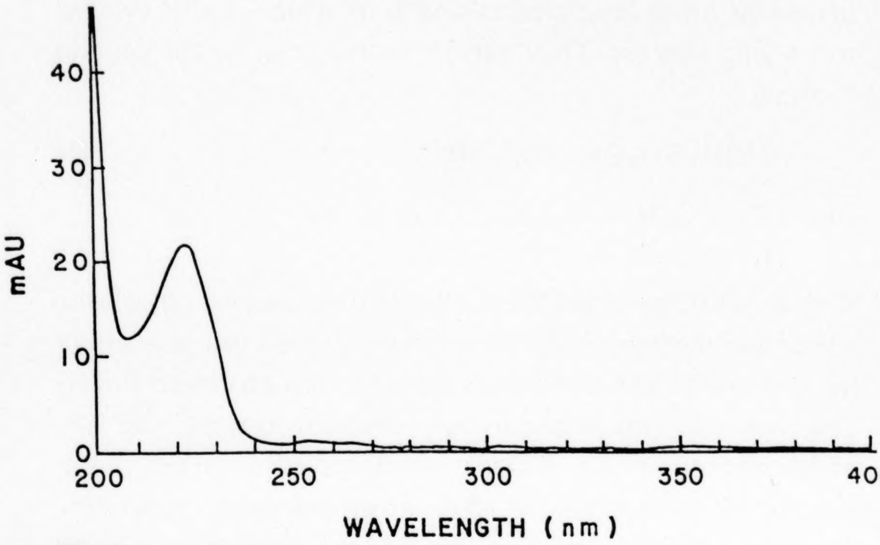

Fig. 1
Absorbance spectrum of alkylbenzene sulfonate.

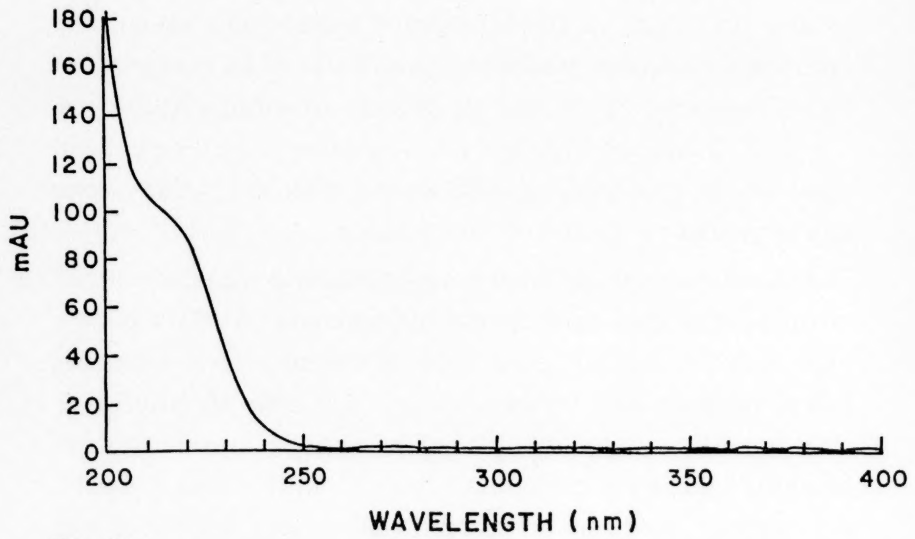

Fig. 2
Absorbance spectrum of NaSCN.

Table I. Instrumental operating conditions

HPLC	Ion-Chromatograph
Column: RP-8	Detector: Suppressed Conductivity
λ: 225 nm	Fibre Suppressor: Type AFS-2
Loop: 20 μl	Regerant: 0.025 M. sulfuric acid
Attenuation: 2 X 4	Column: MPIC – NS1 (250 X 4.6 mm I.D.)
Chart Speed: 0.5 cm/min.	Eluent: 0.01 M Ammonium hydroxide in 28.5 % CH_3CN
Flow of Mobile Phase: 0.65 ml/min.	Attenuation: 3uS
% B: 30 % Acetonitrile	Flow rate: 1.2 ml/min.
% A: 70 % Water	Loop: 50 μl

absorbance surve of sodium thiocyanate. Consideration of these two curves led to a selection of λ = 225 nm for the detector. The elution parameters listed in Table I provided sufficient resolution of these two compounds; a typical chromatogram is shown in Fig. 3. Calibration curves (Fig. 4) for both thiocyanate and ABS were independently prepared using standard solutions. Each point represents the average of triplicate analyses; the response is see to be linear over the concentration range investigated; and response factors were calculated based on the resultant straight lines.

In addition to the ABS, an alkylether sulfate (AES) was used as a co-surfactant. Normal commercial AES preparations are not pure isomeric species but are instead a mixture of one or more base alcohols each of which is ethoxylated to varying degrees. They can be represented by the generic formula

$$R_1O(CH_2CH_2O)_n - SO_3^-Na^+ \qquad (I)$$

where $R_1 = C_8H_{17}, C_{10}H_{21}, C_{12}H_{25}$, etc.
$n = 1, 2, 3, 4, \ldots$

With aliphatic alcohols the molecule possesses no significant UV active chromophore; RI detection proved too insensitive for the low concentrations expected in the produced fluids. The use of mobile-phase ion chromatography (MPIC), which combines the classical elements of reversed phase ion-pair chromatography with a suppressed-conductivity detector, allowed the analysis of the alkylether sulfate component of the surfactant package at concentration as low as 10–20 ppm. Fig. 5 illustrates a typical AES chromatogram; independent GC-MS analysis allowed the assignment of the first peak as unethoxylated parent alcohol sulfate, and the subsequent peaks as the sulfates of an homologous series representing increasing degrees of ethoxylation (i. e. n = 1, 2, 3, etc. of I). The individual ether-sulfates were not resolved. In this analysis ABS eluted after the sulfate series and provided no source of interference.

The stationary phase of the column was a non-derivatized porous resin, derived from divinyl benzene (DVB), having a high specific surface area. Due to its structural elements (alkyl residues and benzene rings), it is only slightly polar and essentilly hydrophobic. The mobile phase was an aqueous solution of an ion-pair reagent, in this case NH_4OH. An organic modifier – acetonitrile – was added to the mobile phase to support ion-pair formation and, by adjusting its concentration, to obtain the necessary degree of compound separation.

The analysis of actual field produced brine solutions (a typical chromatogram is shown in Fig. 6) indicated that the inorganic ions in the water eluted with the first few peaks of the AES. We, therefore, selected six peaks with a retention time of 4.28 to 6.35 minutes appearing beyond the interfering ions for the analysis. The calibration curve resulting from standard samples prepared with synthetic field brine using those peaks is shown in Fig. 7. Again each standard was analyzed in triplicate and the average values were used to construct the curve. The response is seen to be linear over the range investigated.

The analysis of water produced from a reservoir presents some unusual analytical challenges in that the water will normally contain a significant concentration (perhaps to 20 wt. %) of inorganic ions, and once the surfactant reaches the producing well, emulsified crude oil will also be present.

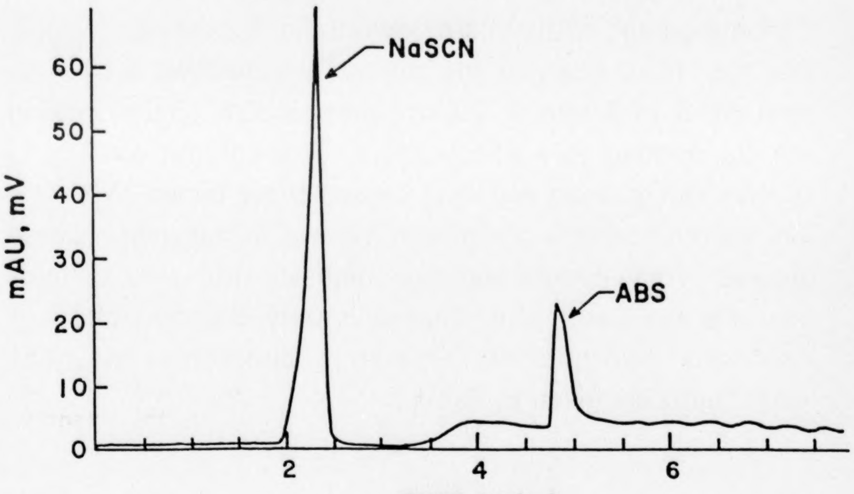

Fig. 3
HPLC chromatogram of ABS and NaSCN.

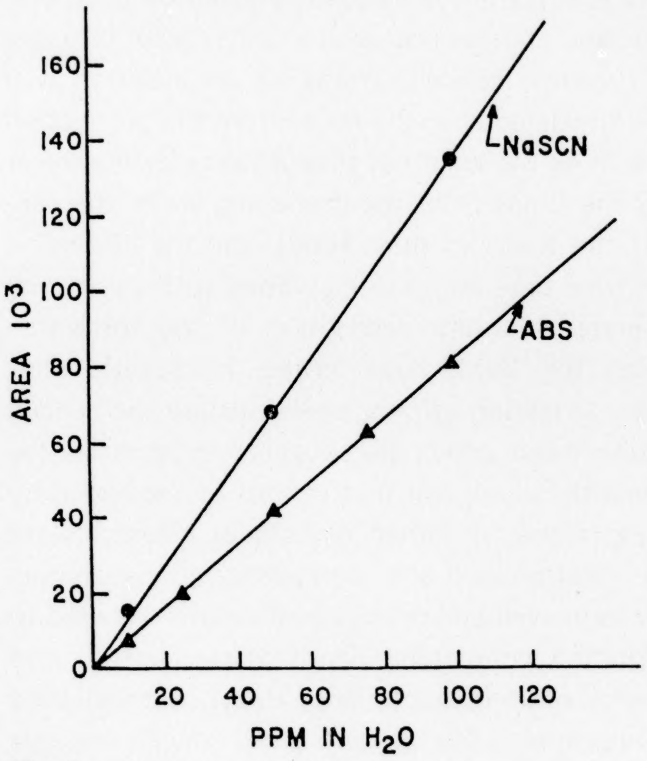

Fig. 4
Calibration curves for ABS and NaSCN.

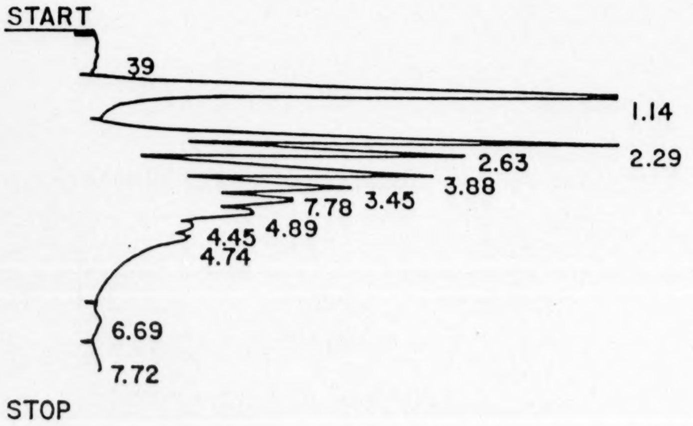

Fig. 5
Chromatogram of an alkylether sulfate obtained by ion chromatography. The numbers over the peaks give the retention times.

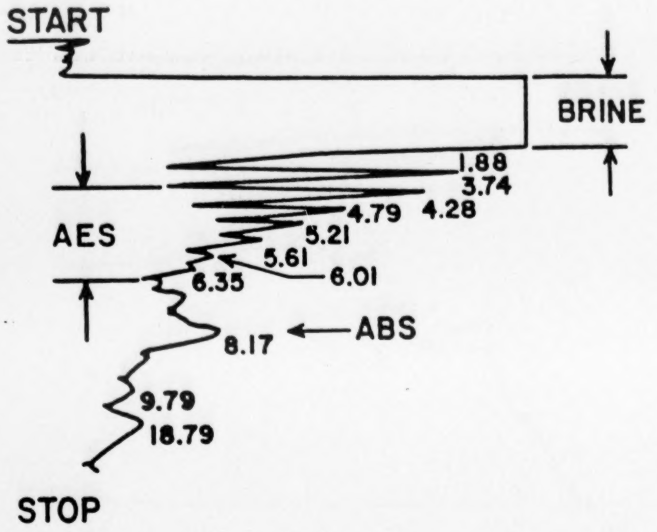

Fig. 6

Typical chromatogram of the produced brine, obtained by ion chromatography. The numbers over the peaks give the retention times.

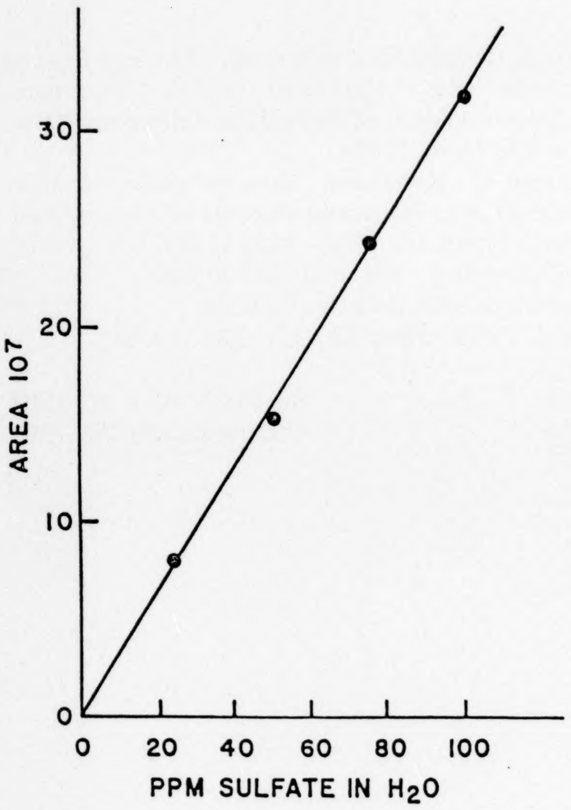

Fig. 7

Calibration curve of alkylether sulfate.

In this particular study, an alternate colorimetric method for SCN$^-$ soon established that components of the emulsified crude oil possessed UV chromophores that overlapped with the SCN$^-$ absorption and these compounds could not be resolved by the column under any reasonable HPLC operating conditions. Thus, although the HPLC method herein described for SCN$^-$ tracer analysis is highly accurate and precise, we were unable to successfully apply it in this case.

During oil field operations, the mixture of chemicals introduced into a reservoir is a carefully constructed blend of various compounds the function of which is often to lower the interfacial tension (IFT) between the crude oil and the connate water. To do this it is desirable that the chemical blend retain its integrity as it moves though the oil bearing formation. On the other hand to get from the injector to the producing well the chemical package must travel several hundred feet though clay-bearing sandstone, the net effect of which is to simulate a large and long chromatographic column. "Chromatographic separation"' of the blend components would greatly reduced their efficacy at oil/water IFT reduction and hence reduce the amount of recoverable oil. Thus, the ability to determine when and in what concentration each component of the surfactant package arrives at the producing wells would be very valuable in assessing the performance of the particular blend of chemicals used.

In Fig. 8 are displayed the results obtained from the analysis of the produced water from a well located about 1,000 ft. from the point of injection. From these results, it can be determined that both surfactants appeared in the produced water about 150 days after injection. Their simultaneous arrival indicates an absence of significant reservoir chromatographic separation, a very important finding. The ABS/AES injected ratio was 3.0 and Fig. 9 shows how this ratio changed with time in the reservoir. That this ratio does not remain constant may be attributable to a number of factors such as the relative adsorptive characteristics of the two different surfactants, the relative amount of precipitation caused by multi-valent ions, and different relative oil solubilities.

Since the concentration of aniocially active surfactants (but not the individual surfactants) can be determined by means of a two-phase colorimetric titration (5) a method existed for estimating the accuracy of our combined methods. The titration method suffers from the fault that it will titrate any *in-situ* generated anionically active compounds arising from contact of the crude oil with basic connate or flood water. The agreement between the two-phase titration method and the sum of the HPLC and ion-chromatographic methods for total surfactants is shown on Fig. 10. Considering the diversity of the types of analysis and the potential for instrumental interferences from the contaminants in reservoir produced waters we believe the agreement is quite good.

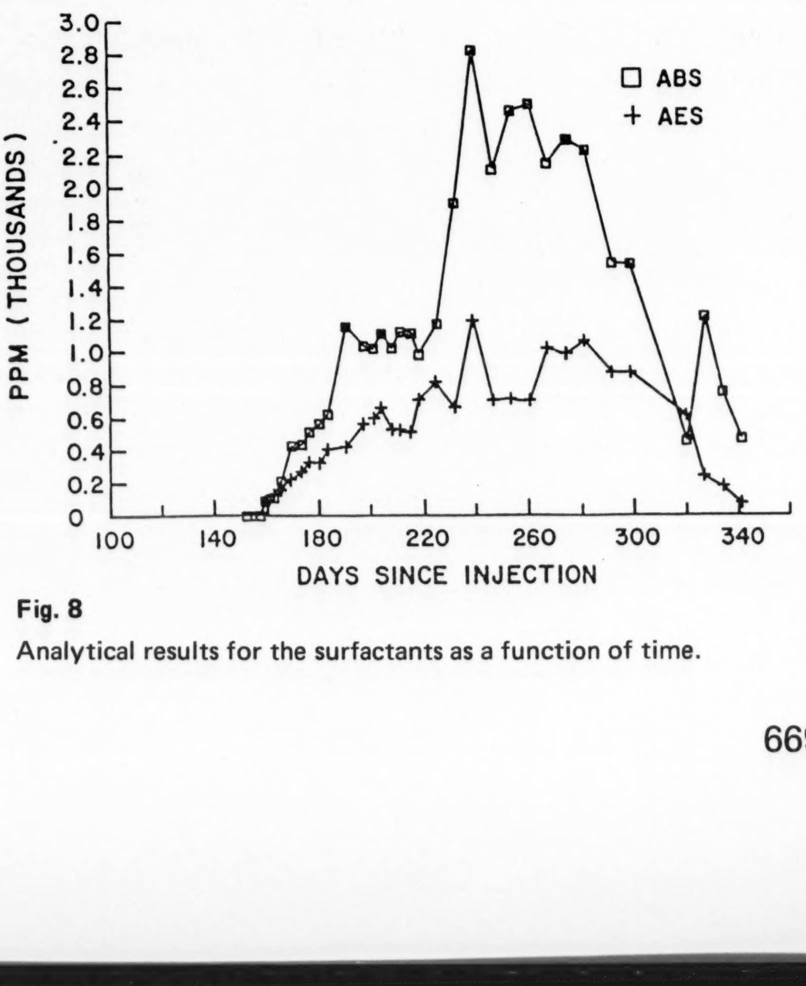

Fig. 8

Analytical results for the surfactants as a function of time.

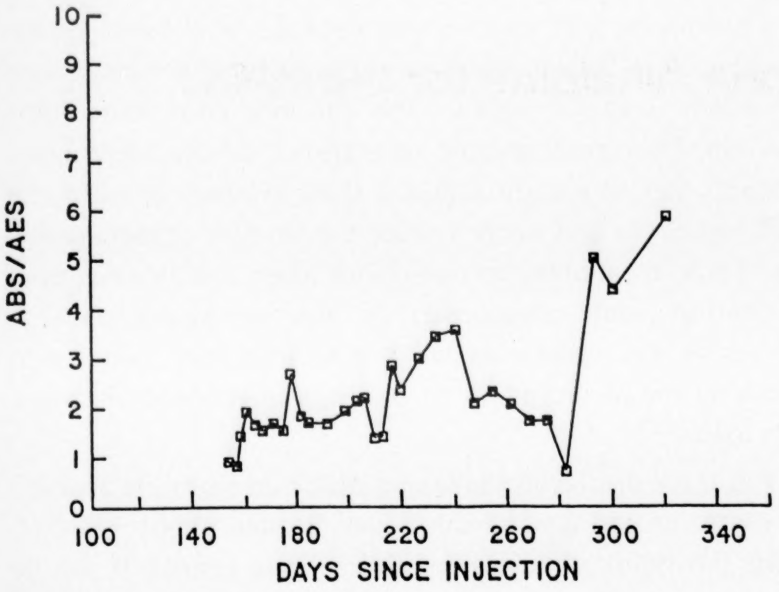

Fig. 9

The determined ABS/AES ratio as a function of time.

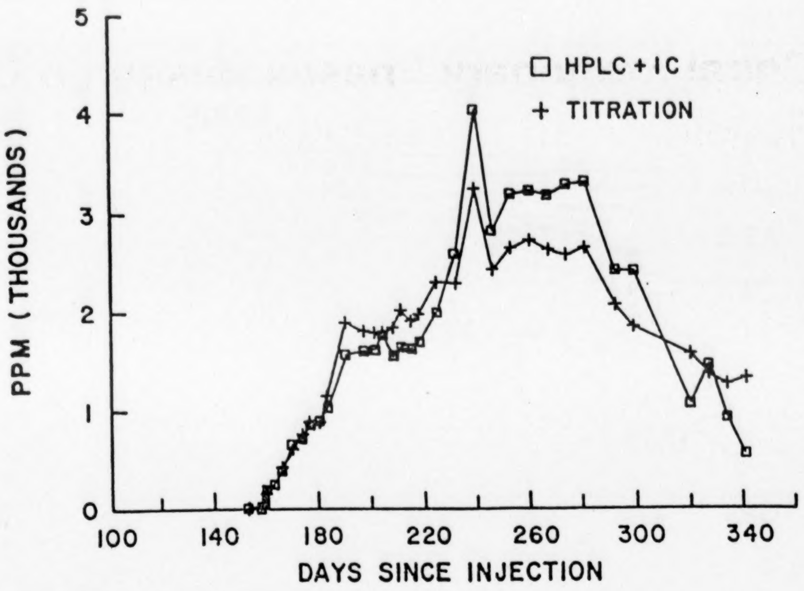

Fig. 10

Total surfactant concentration as a function of time.

The data obtained from the analysis of produced fluids for injected chemicals can provide significant information about the characteristics of a reservoir. The absence of injected chemicals can also provide evidence for a lack of communication between injector and producing wells. The changes in relative, as well as absolute, concentration of simultaneously injected surfactants can lead to important conclusions relative to chromatographic phenomena, adsorption characteristics, and other subterranean processes. The above described analytical techniques have resulted in information being obtained that has increased our knowledge about the movement of chemicals and fluids through a reservoir.

References

[1] *D. R. Zornes, G. P. Wilhite, M. J. Michnick,* "An Experimental Investigation Into the Use of High-Pressure Liquid Chromatography for the Determination of Petroleum Sulfonates." Soc. Pet. Eng. T. 207–218 (June 1978).

[2] *A. Nakae, K. Tsuji, M. Yamanaka,* "Determination of Alkyl Chain Distribution of Alkylbenzenesulfonates by Liquid Chromatography." Anal. Chem. **53**, 1818–1821 (1981).

[3] *J. R. Larson,* J. Chromatogr. **356**, 379–381 (1986).

[4] *J. Weiss,* J. Chromatogr. **353**, 303–307 (1986).

[5] *S. R. Epton,* Trans. Faraday Soc. **44**, 226–230 (1948).

Received: June 28, 1987
Accepted: July 28, 1987
F

Chiral Stationary Phases Based on Cinchona Alkaloids for the HPLC Resolution of Racemates

C. Rosini/C. Bertucci/D. Pini/P. Altemura/P. Salvadori*

Centro di studio del CNR per le Macromolecole Stereordinate ed Otticamente Attive, Dipartimento di Chimica e Chimica Industriale, via Risorgimento 35, I-56100 Pisa, Italy

Key Words

Column liquid chromatography
Chiral stationary phases
Cinchona alkaloids

Summary

The employment of three chiral stationary phases (CSPs) obtained by derivatizing γ-mercaptopropylsilanized silica gel with quinine, quinidine and N-methylquinium iodide, for the separation of organic racemates, is presented. They are quite useful in the resolution of alkylarylcarbinols, binaphthyl derivatives, amides and other substances of pharmaceutical interest.

Introduction

A new family of chiral stationary phases (CSPs) derived from Cinchona alkaloids has been recently introduced [1–4]. The alkaloid residue can be anchored to a chromatographic support of γ-mercaptopropylsilica gel by means of an anti-Markovnikov attack of the thiol group, to the vinylic double bond of the alkaloid. Chiral phases derived from quinine, quinidine and cinchonidine have been prepared and their ability to resolve some organic racemates discussed. An interesting feature of the above alkaloids is that they can form several derivatives by simple chemical manipulations and such derivatives, in turn, can be very useful in preparing some new and effective CSPs. For instance, by alkylating quinine with methyl iodide, N-methylquininium iodide can be obtained, and the usefulness of this compound in preparing a CSP for the resolution of pharmaceutical substances has been shown in preliminary experiments [5].

In this paper, therefore, the general applicability to the resolution of racemates of the Cinchona-alkaloid based chiral CSPs obtained from quinine, SiSQuin, *I,* quinidine, SiSQuind, *II* and N-methylquininium iodide, SiSQuinmei, *III,* will be presented and discussed.

Experimental

Chromatographic Separations

The chromatographic separations were carried out by means of a JASCO Twinkle apparatus connected to a JASCO Uvidec-100 V detector. The circular dichroism (CD) detection was provided by a JASCO J500C spectrometer equipped with a micro HPLC cell.

Preparation of the Chiral Stationary Phases

The chiral stationary phases *I* and *II* were prepared by a procedure already described [1, 2]. The alkaloid content, evaluated as previously reported [1, 2], was about 10% by weight. The CSP *III,* SiSQuinmei, was prepared as follows: to a solution of 3.3 g (7.02 mmol) of N-methylquininium iodide in 50 ml DMF, were added 0.115 g (0.7 mmol) α, α'-azoisobutironitrile and 5.28 g γ-mercaptopropylsilanized silica, obtained starting from LiChrosorb Si 60 (Merck, 5 μ), as described previously [1, 2]. The slurry was maintained at about 90 °C for 24 h, with stirring. After centrifugation, the solid was washed extensively with DMF until disappearance of the alkaloid absorption in the washings and, after that, with methanol, ether and pentane. The alkaloid content of the modified silica obtained, evaluated as described previously [1, 2], was about 11 % by weight.

Preparation of the Compounds

Compounds *1* and *2* were prepared as previously reported [1–4]. Compounds *3, 4* and *5* were obtained by reacting the amine with the appropriate acid chloride in ether in the presence of excess Et_3N. Ibuprofen and pirprofen were obtained by acetone extraction from commercial samples; the anilides were prepared from the acid chloride in the case of ibuprofen whilst, for pirprofen, direct reaction between the acid and the amine was performed in the presence of EEDQ [6]. Compound *8a* was a commercial sample from Aldrich, USA and used without further purification, *8b* and *8c* were synthetized from racemic phenylglicine and phenylalanine, respectively, by a known procedure [7]. Compounds *9a–c*

0009-5893/87 0671-06 $ 03.00/0

© 1987 Friedr. Vieweg & Sohn Verlagsgesellschaft mbH

and *10* were obtained by acetone extraction of commercial preparations.

Results and Discussion

Chart 1 shows the structures of the CSPs studied in the present investigation. As is well known, quinine and quinidine differ only in the absolute configuration at C(8) and C(9) and, in practice, they behave as a "quasi-enantiomeric" pair, when they act as classical resolving agents [8] or chiral auxiliaries for asymmetric synthesis [9]. The third CSP reported in the present work, SiSQuinmei, possesses the same stereochemical features as SiSQuin, the only difference with respect to *I* being the presence of a quaternary nitrogen atom in the quinuclidine group. In Chart 2 are shown the structures of the racemates studied, representative of some classes of substances under investigation: the CSPs *I, II* and *III* are found to be quite efficient in separating alkylarylcarbinols, *1,* binaphthyl derivatives, *2,* as well as aromatic amides derived from amines, *3, 4* and *5.* Some pharmaceutical compounds can be separated after a simple derivatization, such as two widely employed non-steroidal antinflammatory agents (ibuprofen and pirprofen) separable as anilides (compounds *6* and *7*), whilst others can be resolved directly as substituted hydantoines, *8,* benzo-

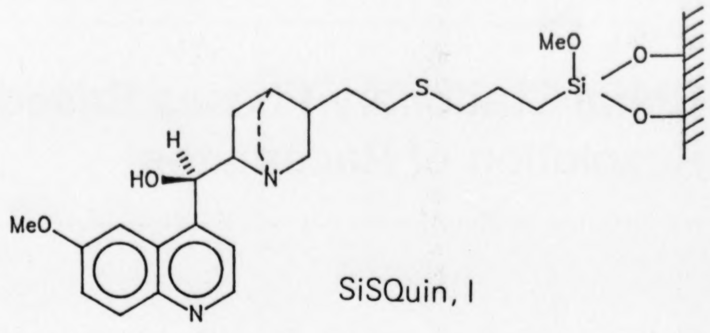
MeO
Si
O
O
S
H
HO
N
MeO
N
SiSQuin, I

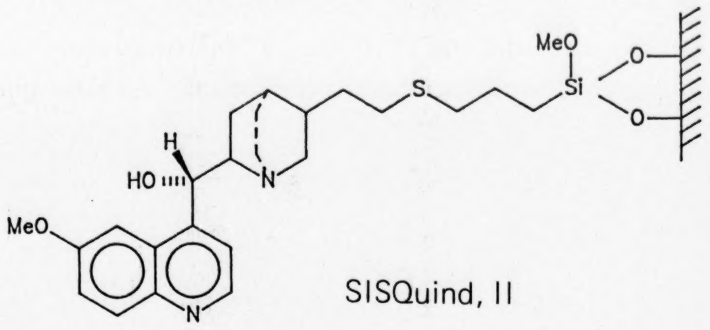
MeO
Si
O
O
S
H
HO
N
MeO
N
SISQuind, II

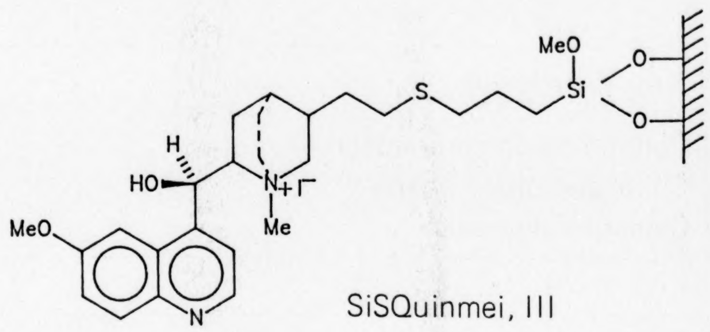
MeO
Si
O
O
S
H
HO
N+ I−
Me
MeO
N
SiSQuinmei, III

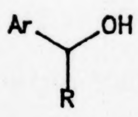

1

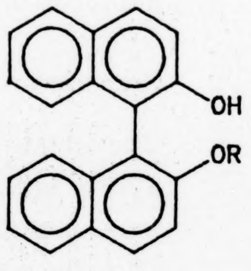

2

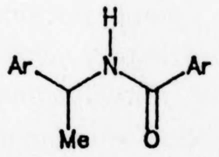

3

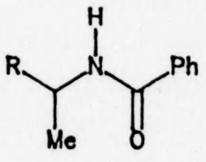

4

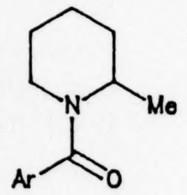

5

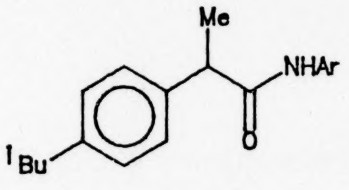
Me
NHAr
O
ᵗBu
6

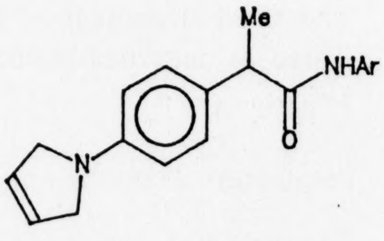

7

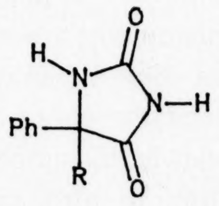

8

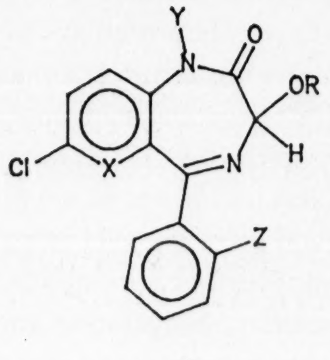
Y
N
O
OR
H
N
Cl
X
Z
9

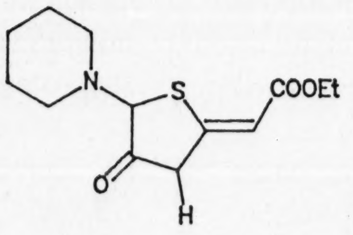

10

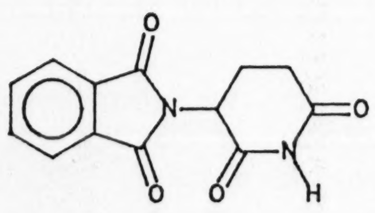

11

diazepinones, *9,* the diuretic etozoline *10,* and the notorious sedative thalidomide *11*.

Table I shows the results obtained in the resolution of several alkylarylcarbinols on the three CSPs *I, II* and *III*. The separation of compounds *1a, c–h* on the CSP *I* (SiSQuin) has been already presented [1, 3]. It has been noticed that the S antipode is eluted first on this CSP and the steric hindrance of the R group is important to obtain a good separation factor α [10], whilst, from this point of view, the nature of the substituent in the para position of the Ar ring is not relevant, affecting only the overall retention, that is, the capacity factor, k [10]. When the resolution of compounds of general formula *1* has been attempted on the "quasi-enantiomeric" phase *II,* the elution order is reversed, the R enantiomer being eluted first. This inversion confirms the importance of the –OH at C (9) for chiral recognition [4]. The results obtained on the CSP *III* SiSQuinmei, deserve a few comments. First of all, this last CSP seems to be generally less effective in the separation of this class of compounds, in fact, separability factors α of about 1 can be measured and only the CD detection indicates a very small extent of separation. It is noteworthy that only the carbinols having a strong electron-donating group in the para position show a separation factor which is different from unity and the elution order is the same as observed in the case of CSP I. Reasonably, in the case of *III,* a chiral discrimination mechanism is operating which is different from that operating in the case *I* and *II.* In particular, the presence on the phenyl ring, of an electron-donating or withdrawing group can give rise to the presence of a dipole on the aromatic moiety. Then an electrostatic interaction can originate between the above described dipole and that present on the CSP ($R_3N^+I^-$ group). The importance of dipole-dipole interactions in determining chiral discrimination mechanisms, has been clearly pointed out in recent papers [11, 12].

The resolution of some binaphthyl derivatives is reported in Table II: this subject has been discussed in detail, as far as the CSPs *I* and *II* are concerned, in a previous work [4]. By means of an accurate analysis of the NMR spectra of compound *2d* in the presence of quinine (as a soluble model of the CSP) it has been possible to establish that the discrimination of the two antipodes by the CSPs goes through the formation of diastereoisomeric adducts by hydrogen bonding [the –OH at C (9) of the CSP and the free hydroxyl group of the substrate]. The relative stability of the adducts is determined by the extent of steric interactions between the –OR group of the substrate and the –OMe moiety of the CSP and the R enantiomer of *2d* gives rise, in the above adduct, to larger repulsive interaction than does the S antipode. The CSP SiSQuinmei gives values of the separation factor, α, which are not too different from those obtained with the CSPs *I* and *II,* and the first eluted enantiomer is S, that is, the same antipode which is less retained on SiSQuin, *I*.

Table I. Resolution of some alkylarylcarbinols of general formula *1*.a)

No	Ar	R	SiSQuin				SiSQuind				SiSQuinmei			
			K_1	α	CD	AC	K_1	α	CD	AC	K_1	α	CD	AC
1a	phenyl	Me	7.3	1.	+	S	5.6	1.	–	R	8.0	1.	+	S
1b	phenyl	Et	4.7	1.	+	S	4.1	1.	–	R	7.7	1.	+	S
1c	phenyl	Pr^i	4.8	1.08	+	S	2.5	1.	–	R	5.	1.	+	S
1d	phenyl	Bu^t	3.1	1.10	+	S	2.2	1.07	–	R	4.	1.	+	S
1e	p.tolyl	Bu^t	2.3	1.07	+	S	2.2	1.03	–	R	2.7	1.	+	S
1f	p.CF_3-C_6H_4	Bu^t	6.5	1.06	+	S	2.8	1.05	–	R	4.5	1.	+	S
1g	p.NMe_2-C_6H_4	Bu^t	5.4	1.05	+	S	2.7	1.	–	R	6.2	1.12	+	S
1h	p.NMe_2-C_6H_4	C_6H_{11}	7.3	1.	nd	/	7.	1.	nd	/	10.8	1.08	nd	/

a) Eluent hexane/2-propanol 99/1; flow 1 ml/min; in all cases studied CD detection at 270 nm.

Table II. Resolution of some binaphthylderivatives of general formula *2*.

No	R	SiSQuin				SiSQuind				SiSQuinmei			
		K_1 a)	α	CD b)	AC	K_1 a)	α	CD b)	AC	K_1	α	CD	AC
2a	H	3.8	1.10	+	S	3.8	1.	–	R	13. a)	1.05	+ b)	S
2b	Me	1.0	1.08	+	S	1.3	1.07	–	R	2.7 c)	1.09	– d)	S
2c	Bu^n	0.9	1.11	+	S	0.9	1.06	–	R	3.7 c)	1.07	– d)	S
2d	Pr^i	0.7	1.16	+	S	1.1	1.17	–	R	2.4 c)	1.07	– d)	S
2e	$COCH_3$	1.	1.	+	S	1.1	1.08	–	R	14.8 c)	1.	+ d)	/
2f	$COBu^t$	0.7	1.	+	S	1.1	1.17	–	R	5.8 c)	1.06	– d)	/

a) Eluent acetonitrile; flow 1ml/min

b) CD detection at 235 nm

c) Eluent hexane/2-propanol/methylene chloride 90/5/5; flow 1 ml/min

d) CD detection at 280 nm

Table III shows the results obtained in the separation of some amides having general formulas *3, 4* and *5.* It can be seen that:

i) CSPs *I* and *II*, while providing separation factors which are quite similar, invert elution orders, that is, the more retained antipode on CSP *I* is the less retained on CSP *II;*

ii) CSP *III* seems to give rise to better resolution than the previous CSPs (see for instance compound *3d*). For this CSP also it is interesting to note that on passing from *3a* to *3d* the α value increases from 1.12 to 1.31, that is, the steric hindrance of the groups linked to the chiral center seems to play an important role;

iii) the effect of the structure of the aroyl moiety of the amide on the α value cannot be accounted for in a straightforward manner;

iv) benzamides of simple, open-chain aliphatic amides (*4a* and *4b*) are completely unresolved on these phases, only the aromatic amide of 2-methylpiperidine *5b* giving rise to a small but definite separation, at least on CSP *III*.

In Table IV are listed the resolution of some amides derived from ibuprofen *6* and pirprofen *7,* together with three aryl substituted hydantoins *8.* As far as the ibuprofen amides *6* are concerned, it may be noted that they are separable on all the present phases with the only exception of the aliphatic derivative *6e*. Also for compounds *6–8* the two CSPs SiSQuin and SiSQuind provide inverted elution orders, as can be seen from the signs of the CD at a fixed wavelength. In the case of *6a* the elution order has been fully established by means of an enriched sample of ibuprofen: the S enantiomer is the less retained on *I* whilst it is the more retained on

Table III. Resolution* of some amides of general formula *3, 4, 5.*

No	Ar	R	Ar′	SiSQuin				SiSQuind				SiSQuinmei			
				K_1	α	CD	AC	K_1	α	CD	AC	K_1	α	CD	AC
3a	phenyl		phenyl	2.5a)	1.06	+	R	2.3	1.10	–	S	12.9d)	1.12	+	R
3b	phenyl		α-napht	4.0a)	1.05	nd	/	4.6	1.09	nd	/	9.5	1.10	nd	/
3c	phenyl		β-napht	3.8a)	1.10	nd	/	3.6	1.11	nd	/	5.5	1.06	–	/
3d	α-napht		phenyl	1.7b)	1.10	–	R	2.3	1.06	+	S	9.3e)	1.31	–	R
3e	α-napht		α-napht	2.6b)	1.04	nd	/	2.5	1.10	nd	/	13.4e)	1.12	nd	/
3f	α-napht		β-napht	2.5b)	1.10	–	/	2.2	1.11	+	/	13.5e)	1.15	–	/
4a		Et		5.7c)	1.	nd	/	8.3	1.	nd	/	10.7	1.	+	/
4b		Bu^t		2.4c)	1.	+	/	2.3	1.	nd	/	5.	1.	+	/
5a	phenyl			3.4c)	1.	+	/	3.2	1.	–	/	5.5	1.	+	/
5b	α-napht			6.2c)	1.	nd	/	5.1	1.	nd	/	14.4	1.05	nd	/

*In all cases CD detection at 254 nm and flow 1 ml/min.

a) Eluent hexane/2-propanol/methylene chloride 90/10/5
b) Eluent hexane/2-propanol/methylene chloride 70/20/2.5
c) Eluent hexane/2-propanol/methylene chloride 94/1/5
d) Eluent hexane/2-propanol 90/10
e) Eluent hexane/2-propanol 80/20

Table IV. Resolution* of some derivatives of general formula *6, 7, 8.*

No	Ar	R	SiSQuin				SiSQuind				SiSQuinmei			
			K_1	α	CD	AC	K_1	α	CD	AC	K_1	α	CD	AC
6a	phenyl		1.9a)	1.	+	S	2.3a)	1.05	–	R	6.6a)	1.09	+	S
6b	p.MeO-C_6H_4		3.8a)	1.07	+	/	4.3a)	1.12	–	/	13. a)	1.13	+	/
6c	p.NO_2-C_6H_4		8. b)	1.06	+	/	6.4b)	1.07	–	/	13. b)	1.06	+	/
6d	α-napht		2.3a)	1.	–	/	2.7a)	1.	+	/	9.3a)	1.11	–	/
6e	n.C_5H_{11}		1. a)	1.	nd	/	0.8a)	1.	–	/	2.3a)	1.	nd	/
7a	p.MeO-C_6H_4		4.4c)	1.	+	/	7. c)	1.	–	/	10. d)	1.08	+	/
7b	α-napht		3.8c)	1.	–	/	6.1c)	1.	+	/	10.7d)	1.11	–	/
8a	phenyl	H	2.4c)	1.	–	/	2.7c)	1.	+	/	6.7c)	1.16	–	/
8b	phenyl	Me	2. c)	1.	–	/	5.4c)	1.	+	/	4.1c)	1.18	–	/
8c	benzyl	H	5. c)	1.	+	/	3. c)	1.	–	/	5. c)	1.	+	/

*In all cases CD detection at 254 nm and flow 1 ml/min.

a) Eluent hexane/2-propanol 90/10;
b) Eluent hexane/2-propanol/methylene chloride 95/5/5;
c) Eluent hexane/2-propanol 80/20;
d) Eluent hexane/2-propanol/methylene chloride 100/20/10

II. The α values obtained on phase *III* for compounds *6* and *7* are larger than those obtained on *I* and *II* indicating an increased discrimination capability of the support derived from the quinine salt. In particular, it is interesting to compare the elution orders obtained on *III*, for compounds *3a* and *6a*:

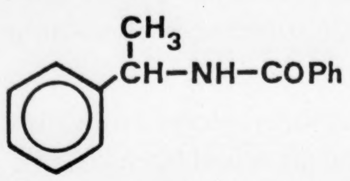

3a

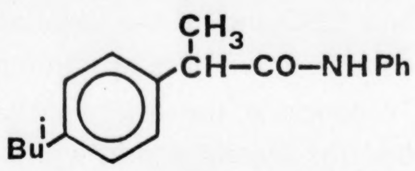

6a

In the case of *3a* the R enantiomer is eluted first on the CSP *III* whilst in the case of *6a* the same enantiomer is the more retained one. This fact has been reliably established by enantiomeric enriched samples of α-phenyl-ethylamine and ibuprofen. The structures of the two compounds are very similar; disregarding the presence of the alkyl substituent in the para position of *6a*, the main difference between them is that in *3a* the amide group is linked to the chiral center through the nitrogen atom whilst in *6a* it is the carboxyl moiety that forms the bond to the chiral center. A phenomenon of this kind has also been observed during the resolution of amides on a Pirkle CSP [12]; there is an inversion of the elution order for amides derived from racemic amines compared with that obtained in the case of amides derived from racemic acids. This observation suggests that the interaction between the amide dipole on the substrate and the amide dipole on the CSP was mainly responsible of the formation of the adduct between the solute and CSP and that the interaction has a directional character, orienting the two molecules in the adduct. A similar situation could also be present in the case of the resolution of amides on the CSP *III;* here the interacting dipoles could be the amide dipole of the analyte and $CH_3N^+I^-$ dipole of the CSP. Such an interpretation is also consistent with previous observations in the case of the resolution of alkylarylcarbinols on *III*. In the last Table the resolution of some other substances of pharmaceutical interest are reported and in Fig. 1 the resolution of *9c* (lormetazepam) is shown. The benzodiazepinones *9* are quite well resolved on all the present CSPs and, in the case of SiSQuinmei, α values ranging from 1.2 to 1.6 are obtained. Again, the quasi-enantiomeric relationship between *I* and *II* has a consequence an opposite elution order in the

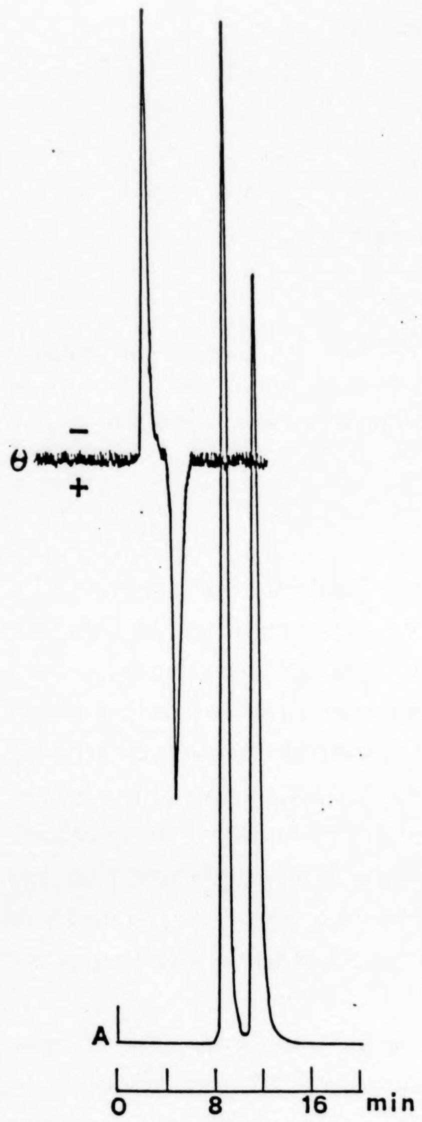

Fig. 1

Resolution of lormetazepam *9c* on CSP *III*, SiSQuinmei. Eluent: hexane/2-propanol/methylene chloride (100:28:24; v/v/v), flow 1 ml/min. Absorption (A) and CD (θ) detection carried out at 254 nm.

Table V. Resolution* of some derivatives of general formula *9, 10, 11.*

No	R	X	Y	Z	SiSQuin				SiSQuind				SiSQuinmei			
					K_1	α	CD	AC	K_1	α	CD	AC	K_1	α	CD	AC
9a	H	CH	H	H	2.6[a)]	1.09	–	R	3.5[a)]	1.08	+	S	4. [a)]	1.18	–	R
9b	H	CH	H	Cl	2.7[a)]	1.18	–	R	3.8[a)]	1.25	+	S	5.6[a)]	1.59	–	R
9c	H	CH	CH_3	Cl	1.4[a)]	1.12	–	R	2.1[a)]	1.10	+	S	3. [a)]	1.40	–	R
9d	Ac	CH	H	H	1.4[a)]	1.	+	S	0.6[a)]	1.	–	R	3.1[a)]	1.	–	R
10					3.5[b)]	1.	nd	/	2.8[b)]	1.	nd	/	3.7[b)]	1.13	–	/
11					4. [c)]	1.		/	5.7[c)]	1.09	+	/	8.1[c)]	1.06	–	/

*In all cases CD detection at 254 nm; flow 1 ml/min

a) Eluent hexane/2-propanol/methylene chloride 100/28/24

b) Eluent hexane/2-propanol/methylene chloride 90/2/8

c) Eluent hexane/2-propanol/methylene chloride 70/20/5

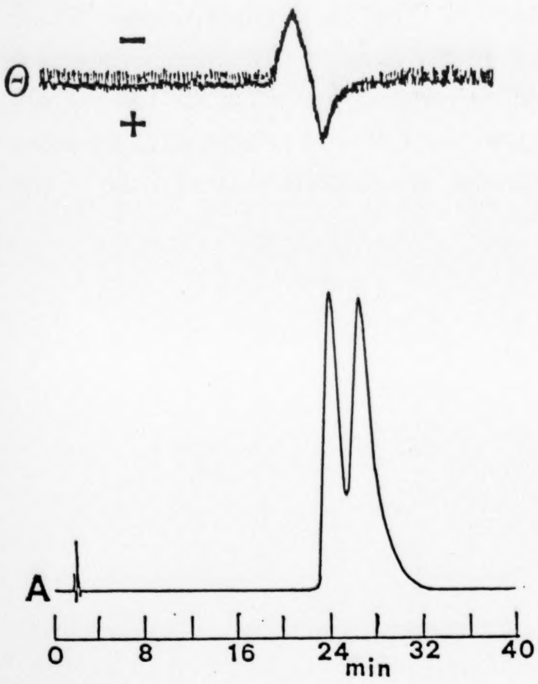

Fig. 2

Resolution of thalidomide *11* on CSP *III*, SiSQuinmei. Eluent: hexane/2-propanol/acetonitrile (70/20/5; v/v/v), flow 1 ml/min. Absorption (A) and CD (θ) detection carried out at 254 nm.

two cases. As can be seen from Table V, the presence of a hydroxyl function at C (3) is fundamental for an efficient separation: in fact the C (3)-acetylated derivative *9d* is only partially separated (the uv detector provides only a single peak, the slight extent of the resolution being indicated by the CD detector). Furthermore the alkylation of the amide nitrogen reduces (although to a minor extent) the α values: a N-methylated benzodiazepinone is less separated than the corresponding N–H compound (see *9b* vs. *9c*). Therefore all the hydroxyamide portion of *9* has to be involved in the chiral discrimination process.

Lastly, the data of Table V show that only CSP *III* can satisfactorily separate both etozoline *10* and thalidomide *11* (Fig. 2). In this respect it is noteworthy that, to the best of our knowledge, the only separation of the latter compound reported in the literature has been carried out by Blaschke [13]; the present results show that CSP III can constitute an alternative tool to obtain *11* in optically active form.

Conclusions

The results presented in this paper clearly show that a new group of CSPs for the chromatographic resolution of racemates can be obtained from the alkaloids of the Cinchona family. Interestingly, the CSPs derived from quinine and quinidine afford, at least for the classes of compounds presently studied, similar separations with the remarkable feature that the elution order is inverted on passing from CSP *I* to CSP *II*. This fact confirms the general trend observed when these two alkaloids are used as chiral auxiliaries in organic chemistry: the products obtained with the former are enantiomeric to those provided by the latter. Furthermore, the third CSP, SiSQuinmei, gives better results with respect to the separation obtained on SiSQuin and SiSQuind in the resolution of substances containing polar functions like an amide group.

To conclude, the variety of the structures resolved indicates that the present phases are quite versatile and hence can be usefully employed in those fields of chemistry (like pharmacology and biochemistry) where enantiomeric separations have become key steps.

Acknowledgements

The authors wish to thank Prof. W. H. Pirkle, University of Illinois, Urbana, USA, for providing them with samples of compounds *5b* and *9d*, Prof. G. Blaschke, Universitaet Munster, FRG, for *11* and Prof. R. Menicagli, Università di Pisa, for the enriched sample of ibuprofen.

References and Notes

[1] *C. Rosini, C. Bertucci, D. Pini, P. Altemura, P. Salvadori,* Tetrahedron Letters, **26**, 3361 (1985).
[2] *C. Rosini, P. Altemura, D. Pini, C. Bertucci, G. Zullino, P. Salvadori,* J. Chromatogr., **348**, 79 (1985).
[3] *D. Pini, C. Rosini, C. Bertucci, P. Altemura, P. Salvadori,* Gazz. Chrim. Ital., **116**, 603 (1986).
[4] *P. Salvadori, C. Rosini, D. Pini, C. Bertucci, P. Altemura, G. Uccello-Barretta, A. Raffaelli,* Tetrahedron, in press.
[5] *C. Bertucci, C. Rosini, D. Pini, P. Salvadori,* J. Pharm. Biom. Anal., **5**, 171 (1987).
[6] *B. Belleau, G. Malek,* J. Am. Chem. Soc., **90**, 1651 (1966).
[7] *T. Suzuki, K. Igarasi, K. Hase, K. Tuzimura,* Agr. Biol. Chem., **37**, 411 (1973).
[8] see, for instance, *J. Jacques, A. Collet, S. H. Wilen,* "Enantiomers, Racemates, and Resolutions", J. Wiley & Sons, New York, 1981; *P. Newman,* "Optical Resolution Procedures for Chemical Compounds", Optical Resolution Information Center, Manhattan College, Riverdale, New York, 1981.
[9] *H. Wynberg,* Topics in Stereochem., **16**, 87 (1986).
[10] The chromatographic parameters k and α have been defined as follows: k is the capacity factor = (retention time of the enantiomer-retention time of an unretained sample/retention time of an unretained sample) and α is the ratio between the k's of the enantiomers. This definition follows, for instance, from: *W. H. Pirkle* and *J. M. Finn,* in "Asymmetric Synthesis", *J. D. Morrison,* ed., Academic Press, New York, 1983, p; 87.
[11] *I. W. Wainer, T. D. Doyle, F. S. Fry, Jr., Z. Hamidzadeh,* J. Chromatogr., **355**, 149 (1986).
[12] *I. W. Wainer, M. C. Alembik,* J. Chromatogr., **367**, 59 (1986).
[13] *G. Blaschke,* Angew. Chem. Int. Ed. Engl., **19**, 13 (1980).

Received: June 28, 1987
Accepted: July 24, 1987
F

Attempts for the Chromatographic Separation of D- and L-Penicillamine Enantiomers

Katalin Kovács-Hadady* / Ilona T. Kiss

BIOGAL Pharmaceutical Works, Debrecen, Hungary

Key Words

Separation of enantiomers
Penicillamine
Optical isomers
Thiazolidine carboxylic acid derivatives

Summary

The chromatographic characteristics of the thiazolidine carboxylic acids formed by the reaction of D- and L-penicillamine with various substituted benzaldehydes and heterocyclic aldehydes have been studied on Chiralplate layers. It has been found that the nature and position of substituents strongly affect the R_F values and resolution factors (R_S) of the isomers. An unambigous relationship has been established between the R_S values of the L- and D-enantiomers and the dipole moment of the aldehydes. The transformation to thiazolidine carboxylic acids with benzaldehyde and substituted benzaldehydes, however, is not complete, thus the reaction with formaldehyde is still more suitable for quantitative determination of penicillamine isomers.

Introduction

Chromatographic separation of optical isomers of various compounds, among others different drugs, are in the centre of interest. Many reports have been published in this field especially for amino acid enantiomers. Thus, for example HPLC [1–4] and TLC [5] methods were used for the separation of D- and L-penicillamine. The optical isomers of penicillamine can be separated on silica gel plates containing the copper (II) complex of (2S,4R,2′RS)-4-hydroxy-1-(2′-hydroxy-dodecil)proline via their 5,5-dimethylthiazolidine carboxylic acid derivatives formed only with formaldehyde [5]. This reaction is fast, easily realizable and results in complete separation. However, the penicillamine also readily reacts with other aldehydes forming different thiazolidine carboxylic acids.

In this work the results obtained for the chromatographic separation of penicillamine isomers with various benzaldehyde derivatives and heterocyclic aldehydes are reported.

Experimental

Chemicals

The D- and L-penicillamine used were Fluka products of the highest purity. The benzaldehyde derivatives and heterocyclic aldehydes were prepared at the Lajos Kossuth University, Debrecen, Hungary. Solvents used for the chromatography were of HPLC quality. Bi-distilled water was used for the preparation of the samples. The Chiralplate chromatographic plates used were manufactured by Macherey Nagel, FRG.

Sample Preparation

0.1 mmol of penicillamine was dissolved in 0.1 ml of water, then 0.5 ml aldehyde solution of 0.1 mmol · dm^{-3} concentration in methanol was added into it. After sealing the mixture was kept at 60–65 °C for 8 hours. 2 μl portions of the samples were applied onto the plate, and the spots were dried with cold air.

Chromatographic Conditions

The pre-treatment of the plates, the chromatographic development and visualization of the spots were performed by the method of Günther et al. [5] at 25 °C. The solvent system used was methanol-water-acetonitrile (50:50:200). R_F and R_S values were calculated from the results of three parallel measurements.

$$R_S = 2\left[\frac{Z_{s1} - Z_{s2}}{w_{b1} - w_{b2}}\right]$$

Z_{s1} = migration distance of compound 1 with base width w_{b1}

Z_{s2} = migration distance of compound 2 with base width w_{b2}

0009-5893/87 0677-03 $03.00/0

© 1987 Friedr. Vieweg & Sohn Verlagsgesellschaft mbH

Table I. Reproducibility of the R_F and R_S values

Derivative	R_F ± r.s.d., (%)		
	Chamber 1	Chamber 2	Chamber 3
D-5,5-dimethylthiazolidine carboxylic acid	0.54 ± 1.7	0.55 ± 1.6	0.56 ± 1.5
L-5,5-dimethylthiazolidine carboxylic acid	0.67 ± 1.7	0.70 ± 1.9	0.71 ± 1.6
D-2-phenyl-5,5-dimethyl-thiazolidine carboxylic acid	0.58 ± 1.7	0.59 ± 2.2	0.60 ± 1.1
L-2-phenyl-5,5-dimethyl-thiazolidine carboxylic acid	0.65 ± 1.4	0.67 ± 2.3	0.68 ± 1.5
$R_{S,\ L/D}$ (formaldehyde)	3.19 ± 7.8	3.37 ± 12.8	3.33 ± 7.2
$R_{S,\ L/D}$ (benzaldehyde)	2.04 ± 7.5	2.16 ± 12.2	2.31 ± 7.3

Table II. R_F and R_S values of the thiazolidine carboxylic acids

Aldehyde	$R_{F,D}$	$R_{F,L}$	R_S	μ[6]
4-dimethylaminobenzaldehyde	0.56	0.71	4.08	5.60
indol-3-carboxaldehyde	0.54	0.69	3.98	–
2-nitrobenzaldehyde	0.65	0.77	3.18	4.30
4-hydroxybenzaldehyde	0.65	0.76	3.14	4.22
5-nitrofuraldehyde	0.72	0.82	2.88	3.45
benzaldehyde	0.59	0.67	2.19	2.81
3-methoxy-4-hydroxybenzaldehyde	0.63	0.71	2.17	2.87
4-cyanobenzaldehyde	0.68	0.78	2.13	–
4-carboxybenzaldehyde	0.63	0.70	2.04	2.37
2,3-dimethoxybenzaldehyde	0.58	0.65	1.95	–
4-bromobenzaldehyde	0.54	0.61	1.93	2.22
4-nitrobenzaldehyde	0.62	0.72	1.75	2.49
4-hydroxy-5-chlorobenzaldehyde	0.54	0.70	1.65	–
4-chlorobenzaldehyde	0.57	0.62	1.31	2.05
2,5-dimethoxybenzaldehyde	0.56	0.60	1.22	–

Results and Discussion

Formation of Thiazolidine Carboxylic Acids with Substitued Benzaldehydes

Penicillamine and formaldehyde form 5,5-dimethylthiazolidine carboxylic acid in aqueous solution. The conversion is complete in two hours at 50°C. The reaction also takes place with benzaldehyde and substitued benzaldehydes – with the only exception of 2-carboxybenzaldehyde – however, the transformation is slower. From the aldehydes studied only 5-nitrofuraldehyde reacts completely at 60–65°C in 8 hours. In some cases (4-chlorobenzaldehyde, 2,5-dimethoxybenzaldehyde) fine precipitate occured in the solution after cooling, although it redissolved after gently heating. On the other hand, with 4-hydroxybenzaldehyde fine crystals appeared during heating.

Reproducibility of R_F and R_S Values

The thiazolidine carboxylic acid derivatives of D- and L-penicillamine formed with substitued benzaldehydes and heterocyclic aldehydes were applied on three plates. The plates were developed simultaneously in Desaga-type chambers. D- and L-thiazolidine carboxylic acids formed with formaldehyde and benzaldehyde were also applied on the plates. The results obtained for the last four compounds on 15 plates are listed in Table I; R_F and R_S values are shown for each chamber.

The relative standard deviations (in percentage) of the R_F values are within 2.5%, however, the reproducibility of the R_S values are smaller, since the error of measuring the spot diameter is also included in these values.

When the penicillamine isomers are reacted with benzaldehyde derivatives a second asymetric centre is formed in the thiazolidine carboxylic acids. The diastereomer pairs, however, cannot be detectable on the chromatographic plate.

Effect of the Structure of the Aldehydes on the R_F and R_S

The R_F and R_S values determined for the different penicillamine-aldehyde derivatives are summarized in Table II. As can be seen from the table, the resolution factor is higher than unity for all benzaldehyde derivatives studied.

If electron-withdrawing substituents (nitro, cyano, carboxyl) are on the aromatic ring, the R_F values of the D-thiazolidine carboxylic acids are higher than that of the benzaldehyde derivative itself. In the case of electron-releasing substituents (dimethylamino, halogens, methoxy, except hydroxy), however, the R_F values of the D-isomers decrease while those of the L-isomers do not change or only slightly decrease compairing to that of the benzaldehyde derivative.

In Fig. 1 the values of the resolution factors (R_S) are plotted as a function of the dipole moment of the benzaldehyde and the studied heterocyclic aldehyde derivatives. The figure shows that the relationship between them is near to linear. This means that the complex-forming capability of the thiazolidine carboxylic acids is strongly influenced by the nature and position of the substituents on the phenyl group.

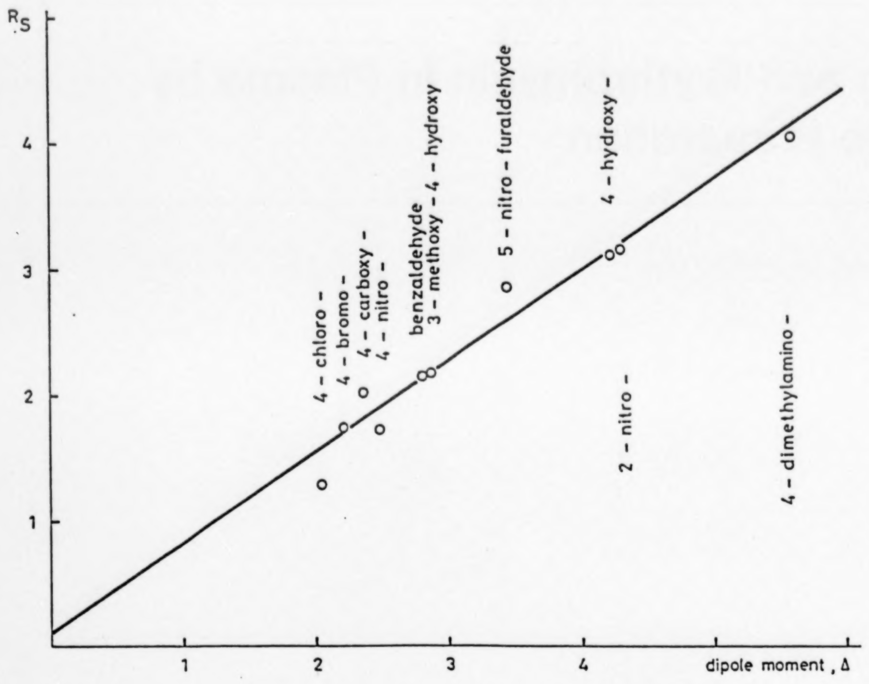

Fig. 1

Relationship between the R_S values of D- and L-thiazolidine carboxylic acids and the dipole moments of the aldehydes

References

[1] *F. Nachtmann*, Int. J. Pharm. **4**, 337 (1980).

[2] *N. Büyüktimkin*, Microchim. Acta (Wien) I. 29 (1985).

[3] *E. Busker, K. Günther, J. Martens*, J. Chromatogr. **350**, 179 (1985).

[4] *S. Lam, A. Karmen*, J. Liq. Chrom. **9**, 291 (1986).

[5] *J. Martens, K. Günther, M. Schickedanz*, Arch. Pharm. (Weinheim) **319**, 461 (1986).

[6] *A. L. McClellan*, "Tables of Experimental Dipole Moments", W. H. Freeman and Comp., San Francisco—London, 1963.

Received: June 30, 1987
Accepted: Aug. 3, 1987
F

Determination of 2'-Acetyl Erythromycin and Erythromycin in Plasma by HPLC Using Manual and Robotic Sample Preparation

P. Kokkonen*/H. Haataja/S. Välttilä

Orion Corporation Ltd., Orion Pharmaceutica, P.O. Box 65, SF-02101 Espoo, Finland

Key Words

Column liquid chromatography
Coulometric detection
Robotic sample preparation
2′-acetyl erythromycin
Erythromycin

Summary

A simple and specific HPLC method with coulometric detection was developed for the determination of 2′-acetyl erythromycin and erythromycin in human plasma. Methyl tert-butyl ether was used as the extraction solvent after alkalization of plasma samples. The plasma extracts were chromatographed on a reverse phase column using 4-component mobile phase. The manual sample preparation procedure was modified so that it could also be applied to the robotic system (Zymate™ Laboratory Automation System). The linear range was 0.25–7.0 µg/ml. The quantitation limit for 2′-acetyl erythromycin and erythromycin was 0.05 µg/ml. Equivalent manual and robotic sample preparation methods were used to analyze a large number of plasma samples.

Introduction

Erythromycin is a macrolide antibiotic. The stearate salt of 2′-acetyl erythromycin (erythromycin acistrate) is a new pro-drug of erythromycin. It is partly hydrolyzed to erythromycin in plasma and body fluids. The structures of 2′-acetyl erythromycin and erythromycin are presented in Fig. 1.

Few HPLC methods have been published for the determination of erythromycin [1–5], erythromycin propionyl ester [1] and erythromycin ethylsuccinate [2] in biological fluids. These methods include HPLC with coulometric [1, 4, 5], fluorescence [2] and UV detection [3]. The aim of this study was to develop a simple and sensitive HPLC method for the determination of 2′-acetyl erythromycin and erythromycin in human plasma for a large number of samples. The method had to involve separation of anhydro-2′-acetyl erythromycin and anhydroerythromycin, which are possible acidic degradation products of analytes in the stomach. The manual sample preparation procedure was modified to that it could also be applied to the robotic system (Zymate™ Laboratory Automation System).

Materials and Methods

Reagents

Erythromycin base and 2′-acetyl erythromycin base were obtained from the Research Center of Orion Pharmaceutica (Espoo, Finland). Tetrahydrofuran and methyl tert-butyl ether (HPLC grade) were obtained from Rathburn (Walkerburn, Scotland). Acetonitrile (LiChrosolv for chromatography), glacial acetic acid 100% (p.a. grade) and sodium acetate trihydrate (p.a. grade) were purchased from E. Merck (Darmstadt, FRG). Methanol (Neskrom) and sodium hydroxide were supplied by Orion Pharmaceutica. Water was distilled and purified by a Milli-Q system (Millipore, Bedford, MA, USA).

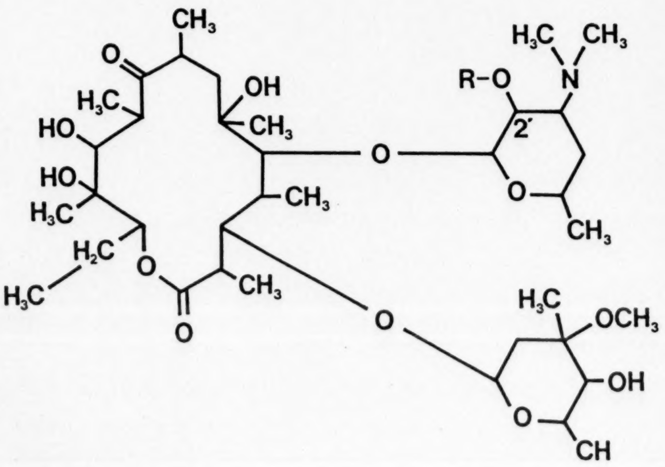

Fig. 1

Chemical structures of 2′-acetyl erythromycin (R = $COCH_3$) and erythromycin (R = H).

0009-5893/87 0680-03 $03.00/0

© 1987 Friedr. Vieweg & Sohn Verlagsgesellschaft mbH

HPLC Instrumentation

The analyses were performed with a high-performance liquid chromatographic system consisting of a LKB 2150 HLPC dual piston pump (LKB-Produkter, Bromma, Sweden), a WISP 710B automatic injector (Waters Associates, Milford, MA, USA) and an HP 3392A integrator (Hewlett-Packard, Avondale, PA, USA). A coulometric detector, ESA Model 5100A Coulochem (Environmental Sciences Associates, Bedford, MA, USA) in the oxidative screen mode with ESA Model 5020 guard cell, was used. The potentials of the analytical cells were + 0.70 V (I) and + 0.85 V (II). The guard cell potential was + 0.90 V. Response time was 10 s. Carbon filters (0.5 μm) were installed before a guard and an analytical cell. The 10 μm Techopak T-15 reverse phase C-18 column (15 cm × 4 mm, i.d.) was supplied by HPLC Technology (Cheshire, UK).

Mobile Phase

The mobile phase consisted of 86% acetonitrile, 3% methanol, 3% tetrahydrofuran and 8% 0.075 M sodium acetate buffer, which was adjusted to pH 4.1 with glacial acetic acid. Tetrahydrofuran was distilled. The mobile phase was filtered with 0.2 μm polyvinylidene difluoride Durapore filter (Millipore, Bedford, MA, USA). The flow rate of the mobile phase was 1.5 ml/min.

Robotic System

The Zymate^{TM} Laboratory Automation System (Zymark Corporation, Hopkinton, MA, USA) consisted of a Zymate Laboratory Robot, a Zymate Laboratory Controller and Zymate Laboratory Stations, which were Z510 Master Laboratory Station, Z410 Capping Station, Z620 Vortex Station, Z710 Centrifuge, Z310 HPLC Injector Station, Z900 general Purpose Hand, Z905 Dual Function Hand, Z910 Precision Microliter Syringe Hand and Z830 Power and Event Controller. Additional laboratory stations were freezer (Elektro Helios) with automatic computer controlled door mechanism (Oy Chroma-Lab Ab, Östersundom, Finland). Pierce Reacti-Therm Heating Module and Reacti-Vap Evaporator (Pierce Chemical Company, Oud-Beijerland, Holland). The schematic bench layout is illustrated in Fig. 2.

Sample Preparation (manual/robotic)

400 μl of 0.1 N sodium hydroxide was added to 1.0 ml of human plasma to adjust pH to 10. The sample was mixed for 30 s and vortexed with 5.0 ml/4.0 ml of methyl tert-butyl ether for 1 min/2 min. After 5 min of centrifugation (3000 rpm), 4.0 ml/2.8 ml of organic layer was evaporated to dryness in a gentle stream of nitrogen at + 40 °C. The residue was dissolved in 150 μl/250 μl of the mobile phase and vortexed for 2 min. An aliquot of 10 μl/20 μl was injected.

The robotic sample preparation procedure was programmed to operate in a serial fashion, where batches of two samples were interleaved. The manual sample preparation procedure was performed as a small batch analysis. The number of samples processed at a time was limited to avoid degradation of the analytes.

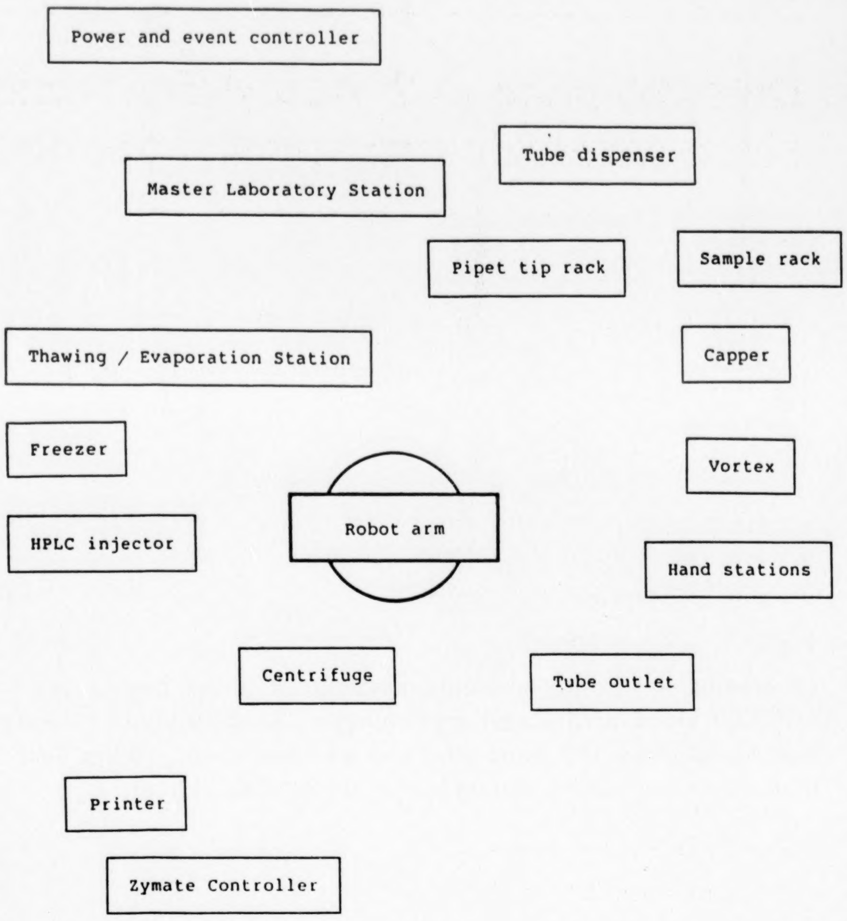

Fig. 2
Schematic bench layout of the robotic sample preparation system.

Calibration Sample Preparation

The stock solutions containing 10 mg of 2′-acetyl erythromycin and erythromycin were prepared in 10 ml of acetonitrile. Further dilutions were made in acetonitrile. Calibration plasma samples were prepared manually by adding 2′-acetyl erythromycin and erythromycin in 50 μl of acetonitrile to 1.0 ml of blank human plasma. After mixing, the calibration samples were frozen at − 20 °C for the robotic procedure and transferred to the freezer of the robot (− 5 °C). In the manual procedure the calibration samples were processed immediately without freezing.

Results and Discussion

The manual procedure involving single extraction was transferred to the robotic system with minor modifications. The lowest detectable amount injected was 300 pg of 2′-acetylerythromycin and 600 pg of erythromycin (S/N = 3). The limit of quantitation (with c.v. less than 20%) was 0.05 μg/ml for the analytes. 2′-acetyl erythromycin and erythromycin were quantitated using linear regression calibration curves, which were obtained by plotting the peak heights against the concentrations. The calibration curves were constructed daily after analyzing calibration samples containing 2′-acetyl erythromycin and erythromycin 0.25, 0.50, 1.00, 2.00, 3.00 and 5.00 μg/ml. If necessary, a calibration sample of 7.00 μg/ml was used. The curves for manual and robotic calibration samples were linear (typically r = 0.999) over the range 0.25–7.00 μg/ml and passed close to the origin.

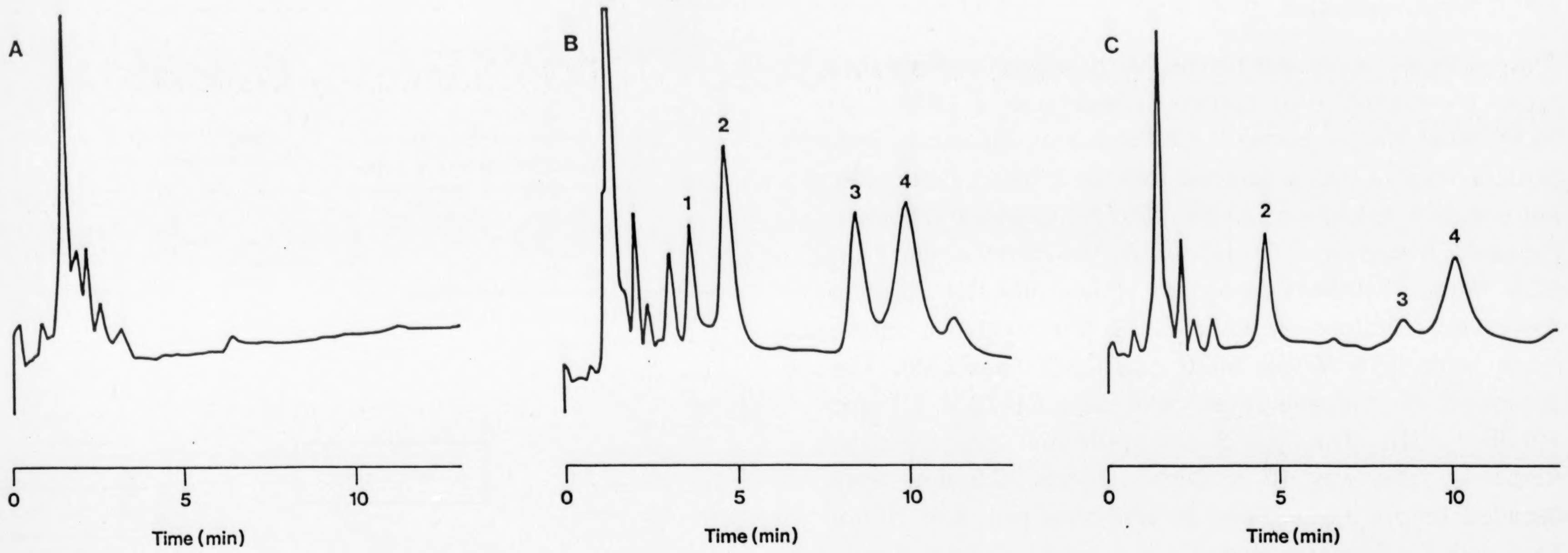

Fig. 3

Chromatograms of human plasma extracts. (A) Blank plasma, (B) Calibration sample containing 0.50 μg/ml of anhydro-2′-acetyl erythromycin (1), 1.00 μg/ml of 2′-acetyl erythromycin (2), 0.50 μg/ml of anhydroerythromycin (3) and 1.00 μg/ml of erythromycin (4). (C) Sample of healthy volunteer (12 hours after oral administration). 10 μm Techopak C-18 column, mobile phase composed of acetonitrile, methanol, tetrahydrofuran and sodium acetate buffer, pH 4.1 (86:3:3:8).

Table I. Recovery (mean % ± s.d.) and precision (c.v.) of the method for determination of 2′-acetyl erythromycin and erythromycin in human plasma using manual and robotic sample preparation. Means of 6 samples

	Manual		Robotic	
	recovery %	c.v. %	recovery %	c.v. %
2′-acetyl erythromycin	103.6 ± 3.4	3.3	92.1 ± 3.8	4.2
Erythromycin	99.6 ± 3.5	4.4	104.4 ± 4.1	4.0

Manual: calibration sample 1.00 μg/ml plasma
Robotic: calibration sample 2.00 μg/ml plasma

Table II. Accuracy of calibration samples for determination of 2′-acetyl erythromycin and erythromycin in human plasma using manual and robotic sample preparation. Means of 20 samples

	added μg/ml	Manual found μg/ml	Robotic found μg/ml
2′-Acetyl erythromycin	5.00	4.95 ± 0.20	4.95 ± 0.12
	3.00	3.04 ± 0.09	2.97 ± 0.34
	2.00	2.00 ± 0.04	2.04 ± 0.25
	1.00	0.99 ± 0.04	0.98 ± 0.09
	0.50	0.49 ± 0.02	0.47 ± 0.06
	0.25	0.25 ± 0.02	0.24 ± 0.07
Erythromycin	5.00	5.05 ± 0.17	5.08 ± 0.32
	3.00	3.08 ± 0.08	2.98 ± 0.23
	2.00	1.92 ± 0.07	2.01 ± 0.22
	1.00	0.98 ± 0.03	0.98 ± 0.04
	0.50	0.51 ± 0.02	0.50 ± 0.06
	0.25	0.29 ± 0.04	0.27 ± 0.06

Within-run precision was studied by analyzing spiked plasma samples. Recovery was studied by comparing peak heights from extracted spiked plasma samples with those obtained from stock solutions diluted with the mobile phase. Good recovery and sufficient precision were achieved both in the manual and robotic methods. The results are summarized in Table I. The accuracy was examined with the calibration plasma samples over the whole calibration range. The two sample preparation systems were comparable. The results are summarized in Table II.

Chromatograms of human plasma extracts are illustrated in Fig. 3. Anhydro-2′-acetyl erythromycin and anhydroerythromycin, possible acidic degradation products in the stomach, could be separated from the analytes as shown in Fig. 3. None of the drugs tested, i.e., nitrazepam, atropine, lidocaine, adrenaline, and ketoprofen, disturbed the chromatographic analysis. Erythromycin B and C could be separated from 2′-acetyl erythromycin and erythromycin.

The manual and robotic sample preparation methods were equivalent for the determination of 2′-acetyl erythromycin and erythromycin in human plasma. The two sample preparation methods were suitable for a large number of samples. In routine work, the yield of one week was 150 manually-and 150 robotically-prepared plasma samples. In total 1500 plasma samples were analyzed.

References

[1] *C. Stubbs, I. Kanfer,* Tenth International Symposium on Column Liquid Chromatography, San Francisco, California, USA, 1986.
[2] *K. Tsuji,* J. Chromatogr., **158**, 337 (1978).
[3] *C. Stubbs, J. M. Haigh, I. Kanfer,* J. Pharm. Sci., **74**, 1126 (1985).
[4] *M.-L. Chen, W. L. Chiou,* J. Chromatogr., **278**, 91 (1983).
[5] G. S. Duthu, J. Liq. Chromatogr., **7**, 1023 (1984).

Received: June 30, 1987
Revised manuscript
received: Aug. 31, 1987
Accepted: Sep. 3, 1987
F

Chromatographic Properties of Mixed Cyano/ODS Chemically Bonded Phases for HPLC

A. Colmsjö[1] / Monica W. Ericsson*

Department of Analytical Chemistry, University of Stockholm, 106 91 Stockholm, Sweden
[1] National Institute of Occupational Health Analytical Division, Stockholm, Sweden

Key Words

Column liquid chromatography
Bonded phases
Cyano/ODS phases
Specific selectivity

Summary

A number of different cyano/ODS polymeric modified silica gel phases were prepared by simultaneous bonding of cyanoalkylsilanes and octadecylsilane. Cyano contents between 10–80 % were obtained. High surface coverage (above 4 μmole/m^2), as well as low hydroxyl content, characterised all phases. The modified silica was suitable for separations in both straight and reversed phase mode. Significantly reduced retention times were obtained in the reversed phase mode for high molecular weight polyaromatic compounds (Mw above 300).

Introduction

In recent years new types of selective bonded phases with mixed functional groups have been introduced [1–5]. Through the bonding of polar and non-polar groups on the same stationary phase, it is possible to obtain the separation of sample components, depending on both adsorption and partition chromatography. Phases with mixed functional groups can be achieved by various modification methods, such as through the bonding of a multifunctional reagent [1–2], by multistep modification of the silica gel (where different functional groups are bonded in each step) [3–4], or by modification using mixtures of reagents [5]. The cyanogroup has been found to be very useful, due to its versatility both in reversed and normal phase chromatography [6–8]. An increased polarity is obtained when cyanoalkylsilane is mixed with ODS, and a decrease in polarity can be registered when the cyanosilane is combined with aminosilane. Cyano columns can also be an alternative to a two column series (a polar and a nonpolar column) when eluted with a gradient of wide polarity differences [9].

In all syntheses of bonded phase material, it is important to minimize the amount of unreacted hydroxyl groups. Several different methods are proposed in the literature [10–19]. Modification of silica gel through polymeric bonding of a silane reagent represents one of the suggested methods. Low hydroxyl content, as well as high surface coverage, are characteristic of a polymeric phase [20, 21]. In a previous paper, various polymeric CN/ODS columns were tested in reversed phase systems [5]. The investigation was extended further in this work to include straight phase systems. The possibility of influencing the content of bonded cyano groups was also studied.

Experimental

Chemicals

Octadecyltrichlorosilane (Merck) and cyanodecyltrichlorosilane (Silar) were used without further treatment. Before use cyanopropyltrichlorosilane (Petrarc) was distilled under reduced pressure. Carbon tetrachloride, analytical grade (Merck), was distilled and stored over molecular sieves 4 A. Tetrahydrofuran, methanol, dichloromethane and acetone were all of analytical grade (Merck) and were used as received. HPLC-grade acetonitrile and hexane (Rathburn) were used without further purification. Water used for HPLC was deionized and redistilled at the laboratory. The silica gel used for modification was Nucleosil 5 u, 300 A (Macherey & Nagel). Acid resistant stainless stell tubing and fittings (Valco or Swagelock) were used throughout the whole HPLC-column system.

Modification of Silica Gel

The same batch of silica gel was used for all columns. The silica gel was refluxed with 0.1 M HCl for 1 hour and washed to neutral with deionized water prior to use. Silica gel modified with a polymeric layer of organosilane was prepared according to Sander and Wise [22]. To 100 ml dry carbon tetrachloride and 10 ml silane reagent, slightly heated in a 500 ml round bottomed glass vessel, 2 g dry silica gel was added with careful mixing followed by 0.5 ml destilled water. The reaction mixture was then refluxed for 4 hours, after which the silica gel was transferred to a glass bottle fitted with a teflon seal. The various solvents were carefully mixed by shaking the sealed bottle by hand and then centrifuged to facilitate the removal of solvent.

0009-5893/87 0683-04 $ 03.00/0

© 1987 Friedr. Vieweg & Sohn Verlagsgesellschaft mbH

Finally, the material was dried to free flow under a stream of nitrogen and with careful heating. Six different packing materials were prepared. Three contained mixtures of octadecyltrichlorosilane/cyanopropyl trichlorosilanes, and the other three were mixtures of octadecyltrichlorosilane and cyanodecyltrichlorosilane. In table 1, the added quantities of the various silane reagents are listed. Carbon and nitrogen contents of the modified phases were determined by elementar analysis at NOVO Analytical Laboratory (Denmark).

Column Packing

Columns of dimensions 150 x 3 mm were packed by the slurry method. Modified silica was mixed with carbon tetrachloride by ultrasonification for 30 seconds, yielding a uniform and relatively stable slurry. 250 ml of acetone was pumped through the packing bomb, followed by 250 ml methanol. Each column was mounted in the HPLC instrument and equilibrated over night with acetonitrile.

Instrumentation

The HPLC separations were carried out on a Shimadzu Spectrophotometric LC-4A with an 8 μl variable UV-adsorption detector SPD-2AS. Column packing was effected by use of a Haskel pump. The detector signals from both instruments were A/D converted and registered by an ABC-800 microcomputer system, with which all other signal treatment and plotting were also performed.

Standard Solutions

Compound	concentration	solvent
Parabene standard:		
methylparabene	0.1 μg/μl	hexane
ethylparabene	0.1 μg/μl	
propylparabene	0.1 μg/μl	
OH test mixture:		
anisole	0.005 μg/μl	hexane
methylbenzoate	0.005 μg/μl	
acetophenone	0.005 μg/μl	
PAC:		
cyanoanthracene	14.40 ng/μl	hexane
anthracene	11.80 ng/μl	

Result and Discussion

Influence of Reaction Conditions on the Amount of Cyano in the Bonded Phases

In Table I, the six different column materials are listed. The surface coverage was calculated using the following formula [23]:

$$\text{Coverage} = \frac{\%\text{C} \times 10^6}{((1200 \times \text{N}) - \%\text{C}\,(\text{Mw} - 1))\,S_{BET}}$$

$N = 18$, $Mw = 331$ ($CH_3(CH_2)_{17}Si(HO)_2O-$)

$N = 11$, $Mw = 244$ ($CN(CH_2)_{10}Si(HO)_2O-$)

$N = 4$, $Mw = 146$ ($CN(CH_2)_3Si(HO)_2O-$)

$S_{BET} = 100\ m^2/g$ (according to the manucaturer)

Columns with significantly different CN content were only obtained when cyanopropyltrichlorosilane was used as the reagent (column no 1–3). Increased amounts of cyano reagent resulted in increased CN concentration, as well as higher surface coverage. On the other hand, when various amounts of cyanodecyltrichlorsilane were added, the CN concentration and the coverage remained unaffected. Due to this result, only columns 1 to 3 were further investigated.

Properties of CN/ODS Columns in a Reversed Phase System

Good separations of polyaromatic compounds (PAC) have been obtained on polymeric-bonded C_{18} phases [21, 24, 25]. However, these materials are less fitted for the separation of higher molecular weight PACs. The high retention times of PACs (MW over 300) can be decreased by the addition of dichloromethane to the mobile phase, but this can result in peak-splitting [26]. Polymeric CN/ODS columns were found to be an alternative to dichloromethane modification of the mobile phase on polymeric C_{18} columns. On the CN/ODS-bonded phase, low k′ values and gaussian peaks were obtained for the high molecular weight PAHs. The decrease in the k′ value on the mixed phases was exemplified with coronene. This compound has a retention time of several hours (k′ value > 20) on a polymeric C_{18} column with acetonitrile as mobile phase. On the CN/ODS material, the k′ values decreased depending on the amount bonded cyanogroups to 1.8 (column no 1), 2.5 (column no 2) and 3.9 (column no 3). Some other PACs

Table I. Type and quality of silane reagents added during synthesis of modified silica gel for various columns.

Column no	ODS ml	Cyanopropylsilane ml	Cyanodecylsilane ml	Coverage μmol/m^2	% CN-alkyl bonded
1	9.5	0.5	–	12.81	72
2	9.9	0.1	–	6.74	49
3	9.95	0.05	–	4.57	14
4	9.5	–	0.5	4.22	37
5	9.9	–	0.1	4.68	27
6	9.95	–	0.05	4.18	22

(Mw 328) could also be eluted and will be further investigated.

Properties of CN/ODS Columns in Normal Phase Systems

Residual hydroxyls: A mixture of anisole, methylbenzoate and acetophenone, according to [27], was injected on the columns with hexane as the mobile phase. Obtained k' values are listed in Table II, and corresponding values for a polymeric C_{18} phase prepared on the same silica material were included. Only slight variations were obtained for the four columns tested independent of surface coverage. The results indicate low residual OH content.

Separation of cyanoanthracene and anthracene: In Fig. 1, the k'-value for the two compounds are plotted versus % CN of the bonded phase. The four curves represent the separation in hexane and hexane/dichloromethane (90:10), respectively. Capacity factors, as well as resolution, remained constant in the more polar mobile phase. However, with hexane as the mobile phase, an increase in the retention time for cyanoanthracene versus cyano content of the bonded phase was obtained. This result suggests a larger influence of bonded cyano groups on the retention time when a nonpolar mobile phases is used.

Separation of parabenes: Massart et al. [9] studied the separation of food perservatives on cyano columns and suggested hexane/dichloromethane (60:40) as the mobile phase for isocratic elution. A mixture of methyl-, ethyl- and propylparabene was analysed with the same mobile phase on the CN/ODS columns. The result is presented in Fig. 2. Compared to Massart et al., the k'-values decreased on the mixed phase. Massart obtained k'values of 3.2 (propylparabene), 3.4 (ethylparabene) and 3.8 (methylparabene) compared to 1.08, 1.34 and 1.8, respectively, on the 72 % CN column.

Conclusion

Polymeric-bonded CN/ODS columns with variable cyano content can be obtained by chemical bonding of a mixture of cyanopropyltrichlorosilane and octadecyltrichlorosilane. Bonded phase material prepared in this way was found suitable for separations both in reversed and normal phase chromatography. A significant decrease in the retention time for high molecular weight PACs (Mw above 300) was obtained compared to polymeric ODS phases. Selectivity differences in the straight phase mode of CN/ODS, compared to commercial cyano columns in the separation of food preservatives, were also demonstrated.

Table II. k'-values for anisole, methylbenzoate and acetophenone on the CN/ODS and ODS column. System: hexane.

Column no	% CN bonded	coverage µmol/m^2	anisole	methylbenzoate	acetophenone
1	72	12.81	0.16	0.44	1.21
2	49	6.74	0.14	0.40	1.18
3	14	4.57	0.13	0.44	1.25
ODS	0	6.23	0.09	0.34	0.93

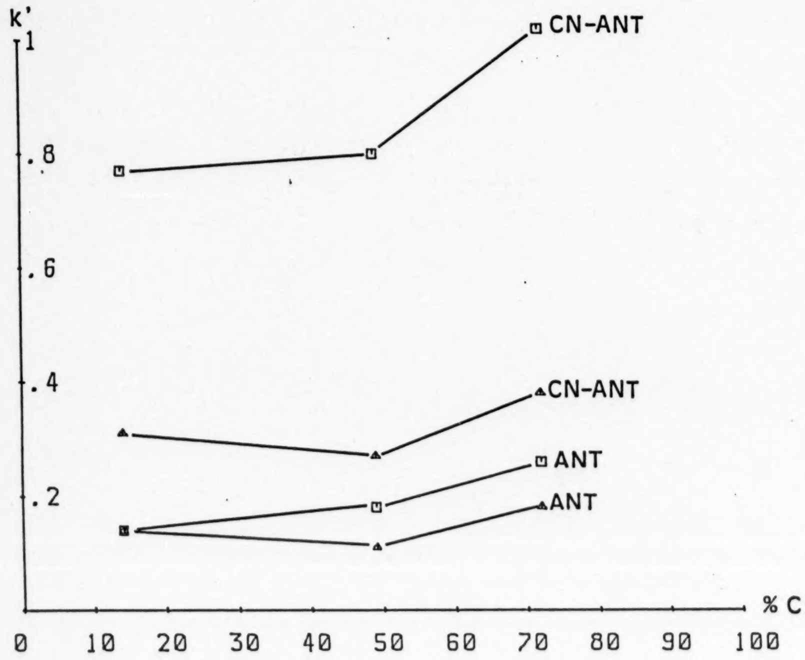

Fig. 1

k'-values for cyanoanthracene and anthracene versus % CN in the bonded phases. The k'-values were measured for isocratic elution in hexane (□) and hexane/dichlormethan 90/10 (△) at a flow rate of 0.6 ml/min.

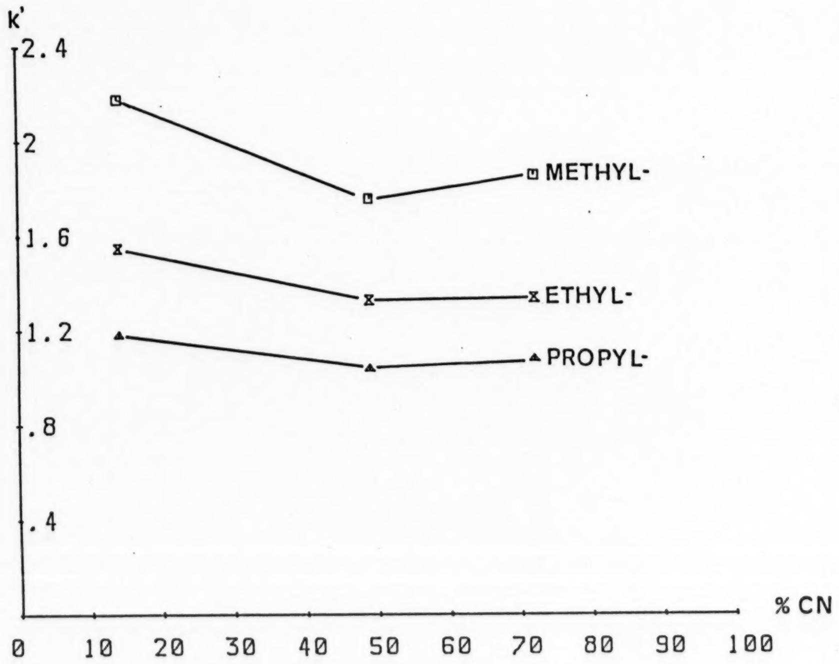

Fig. 2

k'-values for methyl-, ethyl- and propylparabene versus % CN in the bonded phases. The k' values were measured for isocratic elution in hexane/dichloromethane (60/40) at a flow rate of 0.6 ml/min.

References

[1] *J. B. Crowther, R. A. Hartwick*, Chromatographia, **16**, 349 (1982).

[2] *W. E. Hammers, A. G. M. Theeuwes, W. K. Brederode, C. L. De Ligny*, J. Chromatogr., **234**, 321 (1982).

[3] *C. H. Loesch, W. Simon*, Chromatographia, **17**, 669 (1983).

[4] *H. Frigge, A. Deege, J. Köhler, G. Schomburg*, J. Chromatogr., **351**, 393 (1986).

[5] *A. L. Colmsjö, M. W. Ericsson*, Chromatographia, **21**, 392 (1986).

[6] *M. Gazdag, G. Szepesi, L. Huszaé*, J. Chromatogr., **371**, 277 (1986).

[7] *E. L. Weiser, A. W. Salotto, S. M. Flach, L. R. Snyder*, J. of Chromatogr., **303**, 1 (1984).

[8] *W. T. Cooper, P. L. Smith*, J. Chromatogr., **355**, 57 (1986).

[9] *M. De Smet, G. Hoogewijs, M. Puttemans, D. L. Massart*, Anal. Chem., **56**, 2662 (1984).

[10] *H. Engelhardt, B. Dreyer, H. Schmidt*, Chromatographia, **16**, 11 (1982).

[11] *C. Dewaele, P. Mussche, M. J. Verzele*, J. High Res. Chromatogr. Comm., **5**, 616 (1982).

[12] *G. E. Berendsen, L. de Galan*, J. Liq. Chromatogr., **1**, 430 (1978).

[13] *H. Hemetsberg, P. Behresmeyer, J. Henning, H. Ricken*, Chromatographia, **12**, 71 (1979).

[14] *T. Welsch, H. Frank*, J. Chromatogr., **267**, 39 (1983).

[15] *W. Maasfeld, H. Richen*, Chromatographia **9**, 303 (1976).

[16] *C. J. Little, A. D. Dale, M. B. Evans*, J. Chromatogr., **153**, 543 (1978).

[17] *K. Takamayama, H. C. Jordi, F. Benson*, J. Liq. Chromatogr., **3**, 61 (1980).

[18] *C. Gonneyt, D. Morel, E. Ramamonjinina, J. Serptinet, P. Claudy, J. M. Letoffe*, J. Chromatogr., **330**, 227 (1985).

[19] *S. A. Wise, L. C. Sander, W. E. May*, J. Liq. Chromatogr., **14**, 2709 (1983).

[20] *L. C. Sander, S. A. Wise*, Advances in Chromatogr. Giddings, Brown and Grushka Eds., 26 (1986).

[21] *A. Colmsjö, M. Ericsson*, J. Liq. Chromatogr., **9**, 2825 (1986).

[22] *L. C. Sander, S. A. Wise*, Anal. Chem., **56**, 504 (1984).

[23] *G. E. Berendsen, K. A. Pikaart, L. de Galan*, J. Liq. Chromatogr., **3**, 1437 (1980).

[24] *E. Katz, K. Ogan*, J. Liq. Chromatogr., **3**, 115 (1980).

[25] *A. Colmsjö, J. MacDonald*, Chromatographia, **14**, 227 (1980).

[26] *J. C. Fetzer, W. R. Biggs*, J. Chromatogr., **386**, 87 (1987).

[27] *N. Tanaka, H. Godell, B. L. Karger*, J. Chromatogr., **158**, 233 (1978).

Received: June 30, 1987
Revised manuscript
received: Sep. 7, 1987
Accepted: Sep. 12, 1987
F

Measurement of Polyunsaturated Fatty Acids of Myocardial Lipids by High Performance Liquid Chromatography

G. A. Cordis[1] / M. Renuka Prasad[1] / H. Otani[1] / R.M. Engelman[2)] / D.K. Das*[1)]

Department of Surgery, [1)] University of Connecticut School of Medicine, Farmington, CT 06032, USA,
[2)] Baystate Medical Center, Springfield, MA 01107, USA

Key Words

Column liquid chromatography
Polyunsaturated fatty acids
Heart
Myocardial ischemia

Summary

This report describes a modified method for the separation and analysis of polyunsaturated fatty acids such as 20:4, 20:5, and 22:6, using HPLC. The results show that these fatty acids are well separated from the saturated acids. Since the unsaturated fatty acids elute earlier than saturated acids, and this method does not require the fractionation of free fatty acids using thin layer chromatography, a necessary step for the gas chromatographic analysis, the recoveries of polyunsaturated fatty acids were significantly higher as compared to those from gas chromatography. Furthermore, HPLC and gas chromatographic methods gave identical results for the acyl chain composition of phosphatidylserine. The advantages of using HPLC over gas chromatography in determining the acyl chain composition of free fatty acids and phospholipids are also discussed.

Introduction

The physiological importance of polyunsaturated fatty acids such as arachidonic acid (20:4), eicosapentenoic acid (20:5), and docosahexenoic acid (22:6) in heart is well established [1, 2]. The acyl chain composition of free fatty acids and phospholipids are routinely measured in several laboratories employing gas chromatography (GC). Recently, Chien and his co-workers employed high pressure liquid chromatography (HPLC) method to analyze free fatty acid profiles of phosphatidylcholine and lysophosphatidylcholine of myocardial tissue [3]. However, these studies have not focused on other polyunsaturated fatty acids such as 22:6, which comprises 10–15% of the total fatty acids in phosphatidylethanolamine, phosphatidylserine and phosphatidylinositol [4]. In this report, we have modified the methods of Chien et al. [3] and Wood and Lee [5] to analyze standard polyunsaturates like 20:4, 20:5, and 20:6. The modified method has been used to analyze the acyl chain composition of free fatty acids and phosphatidylserine isolated from rat heart and the results compared with GC method. The advantage of HPLC over GC for the study is also discussed. These measurements of free fatty acids and phospholipids are important in the clinical studies of myocardial infarction.

Materials and Methods

All reagents were highest purity available. Fatty acid standards were obtained from Nu-Chek-Prep, Inc. (Elysian, MN, USA). HPLC grade methanol, acetonitrile, chloroform and hexane were obtained from Burdick & Jackson Laboratories, Inc. (Muskegon, MI, USA). Silica SEP-PAK™ columns were purchased from Waters Associates (Milford, MA, USA). All other chemicals including petroleum ether, ether and acetic acid were of ACS-certified grade. TLC plates (Silica Gel GF and Silica Gel K6) were purchased from Anal Tech. Inc. (Newark, DE, USA) and Whatman Chemical Separation Inc. (Clifton, NJ, USA), respectively.

Lipid Extraction

Lipids were extracted from the hearts of properly anesthetized rats according to the method described by Bligh and Dyer [6]. In short, heart biopsies of about 230 mg weight were homogenized in 3 ml of methanol:chloroform mixture (2:1, v/v) using a Polytron homogenizer (Brinkman, NY, USA), and lipids were extracted. Ten nanomoles of 17:0 fatty acid were added to each homogenate as internal standards. The extracted lipids were divided into three parts: (1) HPLC Analysis: To the first part acetic acid (100 parts extract/0.01 part of acetic acid) was added and then passed

0009-5893/87 0687-04 $03.00/0 © 1987 Friedr. Vieweg & Sohn Verlagsgesellschaft mbH

through silica gel SEP-PAK™ columns. The columns were washed with 14 ml of a solvent containing $CHCL_3$:acetic acid:butylated hydroxytoluene (BHT) (100:10:0.01, v/v/w) [7].

The free fatty acids in the extract were processed to synthesize derivatives of phenacyl esters for subsequent analysis by HPLC. (2) GC Analysis: The second portion of the lipid extract was subjected to thin layer chromatography to separate FFAs from glycerides and cholesterol for subsequent GC analysis as described later. (3) Assay for Phosphatidylserine: The third portion of the lipid extract was used to isolate phosphatidylserine employing thin layer chromatography using silica gel K6 plate and $CHCL_3$: CH_3OH: petroleum ether:acetic acid:boric acid (40:10:30:10:1.8, v/v/v/v/w) as the solvent system. The phosphatidylserine spot was scraped off, and methyl esters were prepared as described by Culp et al. [8].

HPLC

The neutral lipids were evaporated under nitrogen at 40 °C, and then they were derivatized to phenacyl esters of free fatty acids (FFAs) according to previously described method [5]. A Waters Associates (Milford, MA, USA) chromatograph consisting of WISP model 710B injector, Model 720 system controller, Model 730 and 740 Data Modules, Model 490 Programmable Multiwavelength UV detector, Model 6000A and 45 pumps were used in our study. For separation of fatty acids, a uBondapak™ C_{18} Guard-PAK™ precolumn, Z-Module, a NOVA-PAK™ C_{18} radial compression cartridge were used. Twentyfive microliters of the phenacyl derivatives of FFA were injected at a flow rate of 2 ml/min and monitored at an absorbance of 242 nm. Mobile phase A consisted of 65% acetonitrile and 10% methanol, while phase B consisted of 100% acetonitrile. The esters were eluted with an initial mobile phase consisting of 72% acetonitrile, 8% methanol for 48 minutes followed by a 10 minutes linear gradient with 79.5% acetonitrile, 3% methanol, 7 minutes of isocratic gradient with 79.5% acetonitrile, 3% methanol, 5 minutes linear gradient to 95% acetonitrile, 1.5% methanol, 11 minutes of isocratic with 95% acetonitrile, 1.5% methanol and finally completed by equilibrating with the initial mobile phase for 10 minutes. Baseline subtractions was used with the model 490 detector.

GC

The extracted lipids (second part of the lipid extract) were evaporated to dryness under nitrogen at 40 °C, and ten nanomoles of C20:0 fatty acid was added as internal standard. 100 μl of $CHCL_3$:methanol (2:1, v/v) was added to each extract, and 50 μl was spotted on activated silica GF TLC plates. The FFAs were separated from the triglycerides, diglycerides and cholesterol using a solvent system consisting of petroleum ether:ether:acetic acid (80:20:1, v/v/v) [8]. The FFAs spots were scraped off the TLC plates, and methanol and sulfuric acid were added to them, heated at 70 °C for 45 minutes followed by extraction of methyl esters with hexane and saturated sodium chloride [8]. The hexane extracts were evaporated under N_2 at 40 °C. Twentyfive microliters of hexane were added to the extract, and 2 μl were injected onto a 5% DEGS-PS column in a Hewlet-Packard Model 5890 gas chromatograph. A linear temperature program from 150 °C to 180 °C, at a rate of 10 °C/min, and final temperature of 180 °C for 45 min were employed.

Results and Discussion

The retention times of phenacyl esters and methyl esters of standard free fatty acids analyzed by HPLC and GC, respectively, are given in Table I. In both methods the free fatty acid derivatives of increasing chain length and double bonds were well separated. In the gas chromatographic method, the unsaturated fatty acid always eluted after the corresponding saturated fatty acid, while in HPLC the fatty acid ester of unsaturated fatty acid eluted earlier than the corresponding saturated acid. Thus the noticeable advantage in the HPLC method is the earlier elution of polyunsaturates viz; 22:6, 20:5 and 20:4, which are of physiological importance. This earlier elution always gives symmetrical peaks with smaller peak widths and larger peak heights (Fig. 1). Such peak characteristics are essential for the analysis of polyunsaturates where the mole percents are only 5–15% either in free fatty acids or in phospholipids of myocardial tissue [4].

During myocardial ischemia and reperfusion, the membrane phospholipids are degraded, while the free fatty acid concentration increases [9]. Such increases in free fatty acids and their derivatives have been suggested to be one of the several reasons for the tissue damage during ischemia and reperfusion. Furthermore, Chien et al. [3] have shown that it is the unsaturated fatty acids, i.e., 18:1, 18:2 and 20:4 which increase during ischemia. However, both Chien et al. [3] and our laboratory [9] have shown that phosphatidylinositol and phosphatidylethanolamine are also degraded during ischemia. As mentioned earlier, the studies of Chien et al. [3] did not detect 22:6 fatty acid either in

Table I. Retention times of the elutions of methyl esters of fatty acids by Gas Chromatography and phenacyl esters by High Perfomrnace Liquid Chromatography.

	Retention Times (minutes)	
Fatty Acids	GC	HPLC
12:0	–	8.25
14:0	–	17.20
15:0	–	25.20
16:0	10.078	37.10
17:0	11.356	53.65
18:0	12.993	60.40
18:1	13.679	39.60
18:2	15.185	22.15
18.3	–	13.70
20:0	–	70.10
20:4	26.185	18.65
20:5	30.378	11.80
22:6	41.845	15.50

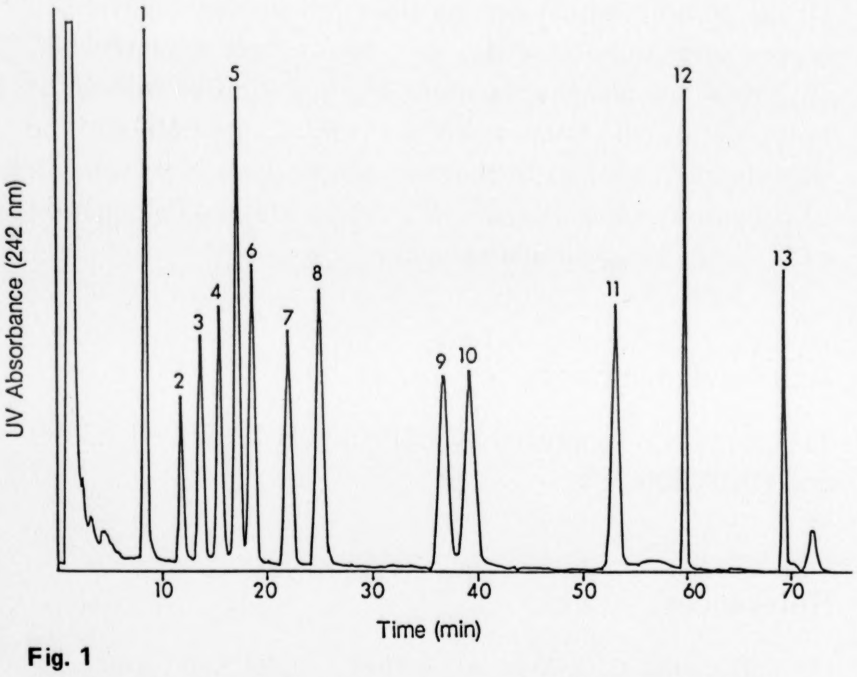

Fig. 1

HPLC separation of phenacyl esters of standard free fatty acids. Column: NOVA-PAK^{TM} C_{18} radial compression cartridge; flow rate: 2.0ml/min; detection: 0.1 A.U.F.S. at 242nm; mobile phase: 72% acetonitrile, 8% methanol for 48 min, 10 min linear gradient to 79.5% acetonitrile, 3% methanol, 79.5%acetonitrile, 3% methanol for 7 min, 5 min linear gradient to 95% acetonitrile, 1.5% methanol, and 95% acetonitrile, 1.5% methanol for 11 min.

Standard compounds (3.8 nmoles): 1. 12:0, 2. 20:5, 3. 18:3, 4. 22:6, 5. 14:0, 6. 20:4, 7. 18:2, 8. 15:0, 9. 16:0, 10. 18:1, 11. 17:0, 12. 18:0, 13. 20:0.

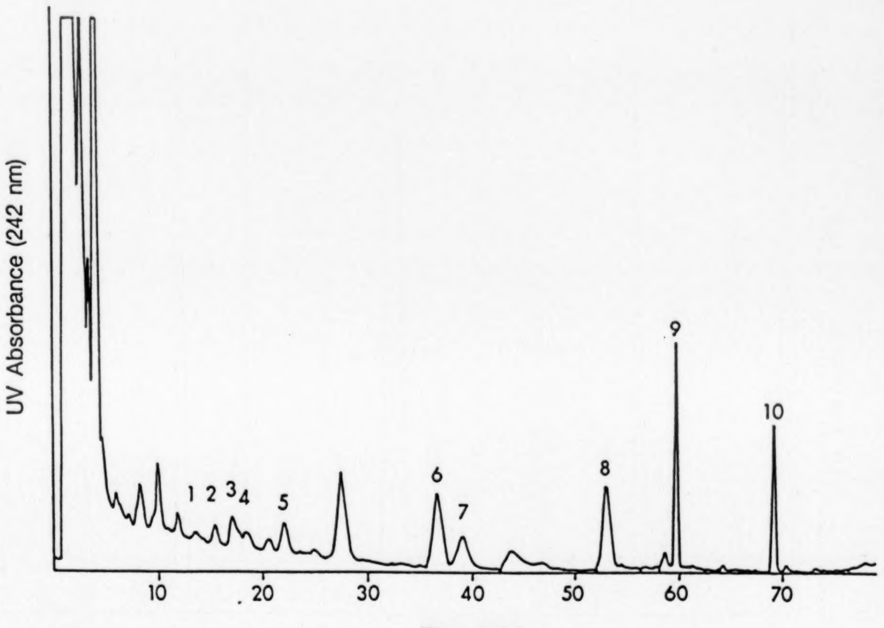

Fig. 2

HPLC separation of phenacyl esters of rat myocardial free fatty acids. Analytical conditions same as Fig. 1. Peak identity: 1. 18:3, 2. 22:6, 3. 14:0, 4. 20:4, 5. 18:2, 6. 16:0, 7. 18:1, 8. 17:0, 9. 18:0, 10. 20:0.

phospholipids and/or in free fatty acid fraction. In this study, we have analyzed the myocardial free fatty acids by HPLC and GC chromatographic techniques (Table II). The 20:4 and 22:6 acids were detected and quantitated only by HPLC (20:4 = 4.19 nmoles/g wet wt and 22.6 = 2.99 n moles/g wet wt), (Fig. 2), while no peaks corresponding to these fatty acids were detected by the GC method. This discrepancy can be easily attributed to the differences in methodology of preparation of fatty acid derivatives. For the HPLC method, the neutral lipids were eluted from SEP-PAK^{TM} columns, and the phenacyl esters were prepared without separating the triglyceride or cholesterol on TLC plates. However, for the GC method the free fatty acids have to be separated from triglyceride and cholesterol before derivatizing to methyl esters. Although butylated hydroxytolnene was always included during extraction and subsequent procedures, the polyunsaturated fatty acids are likely to get oxidized during isolation of free fatty acids as well as during the TLC separation procedure. However, in the HPLC method the triglyceride and cholesterol fraction will not interfere, for the analysis of phenacyl esters of free fatty acids, since the guard column absorbs all of the triglyceride and cholesterol fraction.

The acyl chain composition of phosphatidylserine isolated from rat heart using both HPLC and GC methods are shown in Table III. It can be easily seen that both methods yielded similar results. However, compared to FFA analysis by GC, the FFA profiles of phosphatidylserine fraction analyzed by HPLC showed two additional peaks for the unsaturates 20:4 and 22:6 (Fig. 3). These differences can be attributed to the fact that during TLC the fatty acids always remained esterified to the hydroxyl group of glycerol, and hence lesser oxidation of polyunsaturated fatty acids.

Table II. Comparison of acyl chain composition of myocardial free fatty acids by Gas Chromatography and High Performance Liquid Chromatography.

	Acyl Chain Composition (nmol/gm wet wt)[a]	
Fatty Acids	GC	HPLC
14:0	N.D.[b]	10.45 ± 1.20
16:0	36.77 ± 3.47	43.00 ± 6.88
18:0	32.44 ± 9.85	30.16 ± 2.59
18:1	27.55 ± 0.72	22.69 ± 4.53
18:2	6.79 ± 0.96	6.63 ± 1.04
18:3	N.D.	3.68 ± 0.62
20:4	N.D.	4.19 ± 0.67
22:6	N.D.	2.99 ± 0.86

[a] Mean ± standard deviation. n = 3. [b] N.D. = Peak not detected.

Table III. Comparison of acyl chain composition of isolated phosphatidylserine by Gas Chromatography and High Performance Liquid Chromatography.

	Acyl Chain Composition (nmoles FFA)[a]	
Fatty Acid	GC	HPLC
14:0	N.D.[b]	N.D.
16:0	12	12
18:0	687	684
18:1	450	390
18:2	3	1
18:3	N.D.	2
20:4	3	7
22:6	63	70

[a] Average for two independent determinations.
[b] N.D. = Peak not detected.

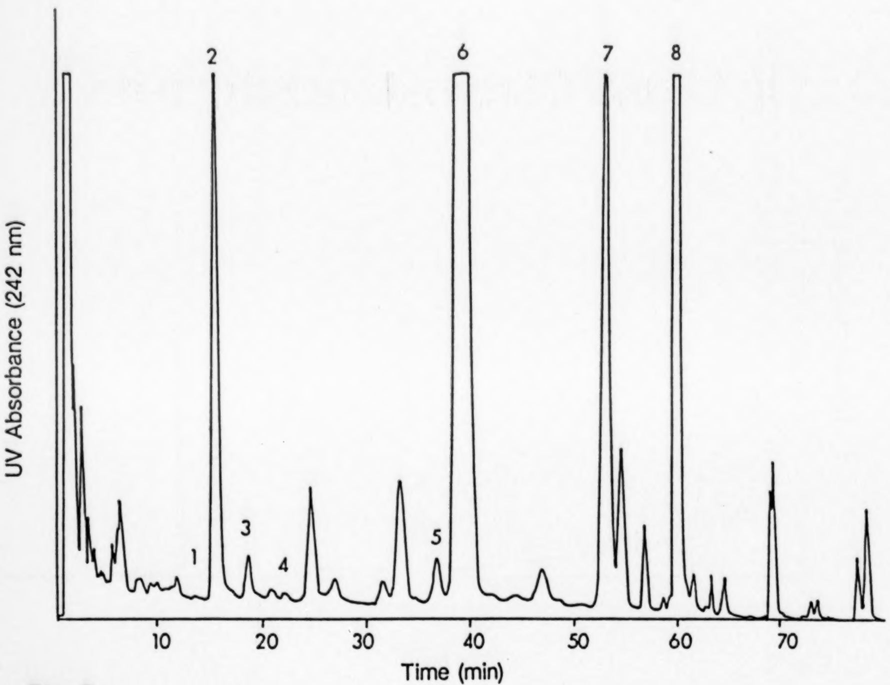

Fig. 3

HPLC separation of phenacyl esters of fatty acid from the acyl chain of isolated rat myocardial phosphatidylserine.

Analytical conditions same as Fig. 1. Peak identity: 1. 18:3, 2. 22:6, 3. 20:4, 4. 18:2, 5. 16:0, 6. 18:1, 7. 17:0, 8. 18:0.

In summary the HPLC method gave the complete separation and analysis of polyunsaturates like 20:5 and 22:6. The minute quantities of these acids from myocardial tissue was better detected employing the HPLC method. Thus HPLC method appears to be a better choice for measuring FFA of heart or any other tissue. In addition, this method can also be used to measure the acyl chain composition of other phospholipids. At this juncture, it is noteworthy to mention that not only the free fatty acids can be analyzed by HPLC, they may be isolated from the HPLC column which can be used for further analysis by mass spectrophotometry or for other biomolecular structural studies. Furhtermore, the quantitative analysis of polyunsaturated fatty acids by HPLC method can be conveniently applied to measure the enzymatic conversion of polyunsaturates like Δ^6, Δ^5, desaturates, and elongation of 6, 9, 12, γ-trans-linolenic acid.

Acknowledgements

This study was supported by USPHS NIH 22559, HL 33889 and HL 34360.

References

[1] *T. Victor, C. la Cock, A. Lochner,* J. Mol. Cell Cardiol. **16**, 709 (1984).

[2] *K.R. Chien, L.M. Buja, J.T. Willerson,* in "Myocardial Ischemia and Lipid Metabolism", R. Ferrari, A.M. Katz, A. Shug, O. Visioli, eds., Plenum Press, New York, 1984; p. 243.

[3] *K.R. Chien, A. Han, A. Sen, L.M. Buja, J.T. Willerson,* Circ. Res. **54**, 313 (1984).

[4] *R. Wood,* in "Geometrical and Positional Fatty Acid Isomers", E.A. Emken, H.J. Dutton, eds., American Oil Chemists' Society, Champaign IL, 1979, p. 213.

[5] *R. Wood, T. Lee,* J. Chromatog. **254**, 237 (1983).

[6] *E.G. Bligh, W.J. Dyer,* Can. J. Biochem. Physiol. **37**, 911 (1959).

[7] *J.G. Hamilton, K. Comai,* J. Lipid Res. **25**, 1142 (1984).

[8] *B.R. Culp, W.E.M. Lands, B.R. Lucchesi, B. Pitt, J. Romson,* Prostaglandins **20**, 1021 (1980).

[9] *H. Otani, R.M. Engelman, J.J. Rousou R.H. Breyer, D.K. Das,* J. Mol. Cardiol. **18**, 953 (1986).

Received June 29, 1987
Revised manuscript
received: Sep 3, 1987
Accepted: Sep 9, 1987
F

An Expert System for Eluent Optimisation in Liquid Chromatography with Photodiode Array Detection

T. P. Bridge*[1]/M. H. Williams[1]/G. G. R. Seaton[2]/A. F. Fell[2]

[1] Department of Computer Science, Heriot-Watt University, 79 Grassmarket, Edinburgh EH1 2 HJ, UK

[2] Department of Pharmaceutical Chemistry, University of Bradford, Bradford BD7 1DP, UK

Key Words

Expert system
Reversed-phase liquid chromatography
Mobile phase optimisation
Peak homogeneity validation
Photodiode array detection

Summary

The problem of eluent optimisation in reversed-phase liquid chromatography is a complex diagnostic situation, amenable to an expert system approach. Such a system has been developed in microProlog, which uses a gradient elution experiment to determine the appropriate initial solvent strength for a given separation, followed by response-surface modelling using an iterative lattice method to determine the mobile phase composition for optimum resolution. Spectral information from a diode array detector is used to track the retention position of each component as the mobile phase composition is varied. Peak homogeneity is assessed by a number of independent modules, the output from which is utilised by the expert system to validate the model constructed by the optimisation procedure.

Introduction

The determination of the mobile phase composition that gives the best possible resolution of the components of a given sample within an acceptable analysis time, is a complex task requiring the adjustment of a number of interacting variables. The identity and concentration of the organic modifier(s), the pH of the mobile phase, the identity of the buffer used, if any, and the identity and concentration of any added components in the mobile phase are amongst the parameters available to the analyst. The adjustment of these parameters to achieve the desired separation is a time consuming operation, requiring a combination of methodological experimentation and knowledge of the probable behaviour of the analyte.

Automated optimisation strategies have been suggested before [1], but most implementations rely upon a search of the parameter space to locate the optimum conditions. The system described in this paper has the capacity to use information derived during the initial stages of the optimisation procedure to predict an optimum composition of the mobile phase for resolution of each separately identifiable solute in an unknown mixture. This prediction is iteratively refined until a true optimum mobile phase composition is established.

Optimisation Strategy

The strategy adopted for use in the expert system is to establish the initial solvent strength required for the separation by means of a water-methanol gradient elution experiment, and then to construct a model of the response surface over the solvent triangle bounded by isoelutropic water-modifier mixtures of equivalent eluting power to that of the initial mixture [2]. A flow-chart of this strategy is reproduced as Fig. 1. The modifiers employed for this stage are methanol, acetonitrile and tetrahydrofuran.

The model construction process is based on an iterative lattice approach [3], whereby a logarithmic relationship is assumed between mobile phase composition and the phase capacity ratio of each component. This allows a prediction to be made of the separation between all pairs of solutes at all points within the solvent triangle, and hence permit selection of the conditions predicted to give the optimum separation. The data provided by the separation performed using this predicted mobile phase composition allow the model to be refined and a new optimum mobile phase predicted. The cycle of prediction, experimentation and refinement continues iteratively until no further improvement in resolution is achieved.

0009-5893/87 0691-05 $03.00/0

© 1987 Friedr. Vieweg & Sohn Verlagsgesellschaft mbH

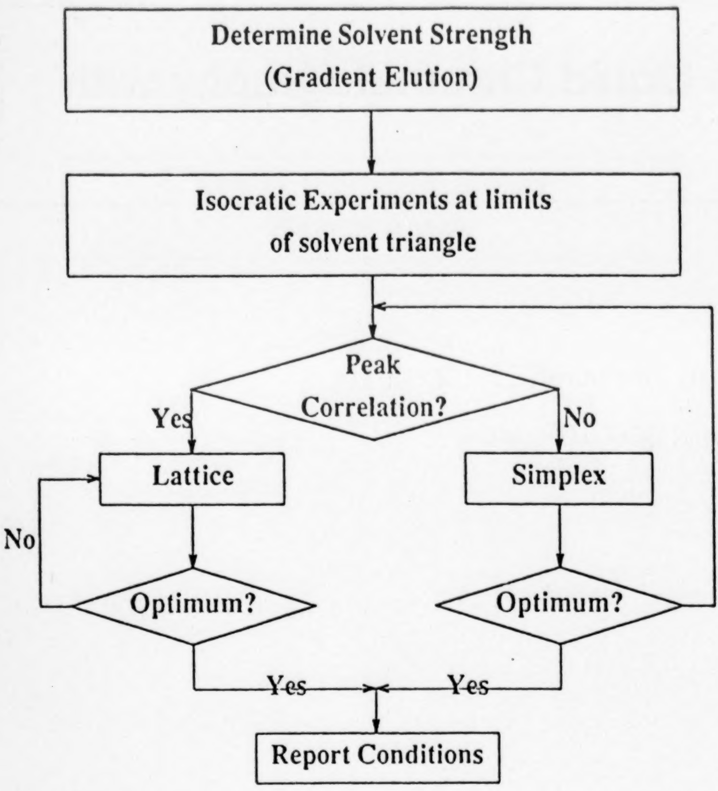

Fig. 1
The optimisation strategy employed by the expert system.

The iterative lattice approach to mobile phase optimisation relies upon the correct and unambiguous identification of each solute in each of the chromatograms. Despite the array of tests for peak homogeneity available to the system, as described below, the situation may still arise in which the unambiguous assignment of a retention time for each component may not be possible. For example the difference between the spectra for a pair of peaks may be so small as to be below the discrimination limit of the system. Ambiguity may also arise in cases of isoelution that are not detected by the peak homogeneity tests currently available to the system.

Under these conditions the system may call on a modified Simplex procedure [4] to enable the optimisation to continue. To utilise the Simplex method the overall quality of each chromatogram is described by a numerical value, calculated according to an appropriate response function [5]. The optimisation proceeds by discarding the mobile phase conditions giving the least favourable value for the response function. A new composition for the mobile phase is predicted by reflecting this discarded point about the line connecting the two remaining data points.

After each new experiment carried out under the control of the Simplex optimisation strategy, the component spectra are examined in an attempt to acquire sufficient spectral information for unambiguous assignation to be made. This then enables the iterative lattice method to continue the overall optimisation process.

Peak Homogeneity Assessment

The construction of the response surface model requires that the retention time of each solute be established for each of the mobile phases used. To assist in this, spectral information is acquired for each peak by means of a photodiode array detector [6]. This allows each eluting peak to be characterised by a spectral profile, which should enable it to be associated with a particular component in the mixture. The assignment of spectral profiles is staightforward for peaks containing only one component unless two or more components exhibit similar spectra. However the process is more complicated in cases of co-elution, when estimates of the true spectral profiles of the contributing components must be produced by a suitable deconvolution of the matrix of (A, λ, t) data. As such a deconvolution process may require the expenditure of a significant amount of computing time, the expert system is provided with a number of tools to assess the homogeneity of each detected peak. The use of deconvolution can therefore be restricted to cases where the chromatographic peak is found to be heterogeneous.

The tests for assessing peak homogeneity currently available to the system are:

(a) Comparison of the normalised spectral profiles recorded on the upslope and the downslope of the peak. The difference between the two curves is indicative of the extent of heterogeneity in the peak.

(b) Evaluation of the derivative total-absorbance chromatogram. For an homogeneous peak the first derivative with respect to time of the total-absorbance chromatogram would be expected to exhibit one zero-crossing, with two zero-crossings present in the second derivative chromatogram. An increase in the number of zero-crossings indicates the presence of two or more components in the peak.

(c) Determination of the apparent retention time as a function of detector wavelength. For an homogeneous peak the apparent retention time determined at any wavelength, will vary only due to noise in the signal. If two or more components are present, with different spectral profiles, then the apparent retention time of the peak will depend upon the detection wavelength [7].

(d) Examination of the absorbance-ratio chromatogram. The ratio of the absorbance detected at two wavelengths will be essentially invariant with time across a pure peak. The presence of a second co-eluting component with a different spectral profile to the first, will result in a variation in the value of the absorbance ratio across the chromatographic peak.

Since the accuracy of the above tests is affected to different degrees by a number of factors (e.g. changes in the peak profile, the signal-to-noise ratio of the detector and the degree of similarity between the component spectra) the interpretation of the information provided by the tests requires consideration of these factors, when they can be determined. To improve the reliability of the system for detecting co-eluting solutes, rules to direct the interpretation of these test results are being progressively developed for inclusion in the system. The modular nature of the expert system will facilitate the incorporation of additional homogeneity tests at a later stage.

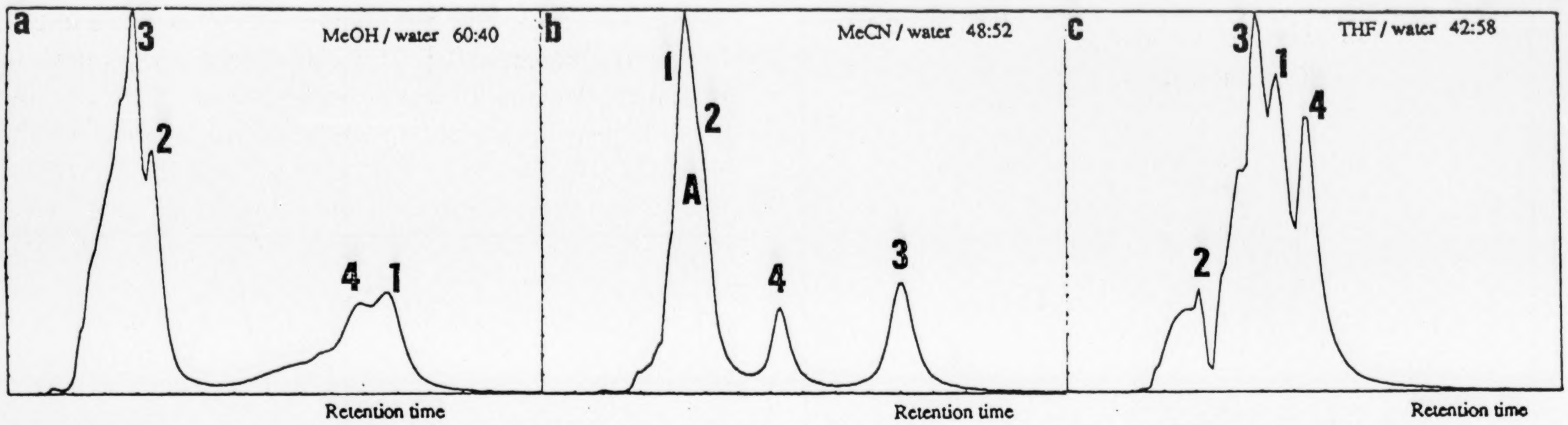

Fig. 2

Initial isoelutropic chromatograms.

(a) Mobile phase methanol-water 60:40 v/v
(b) Mobile phase acetonitrile-water 48:52 v/v
(c) Mobile phase tetrahydrofuran-water 42:58 v/v

Solutes: 1: 3-hydroxybenzaldehyde; 2: phenol; 3: diethyl phthalate; 4: n-propyl-p-hydroxybenzoate. Peak A: Peak for which homogeneity tests are illustrated in Fig. 5.

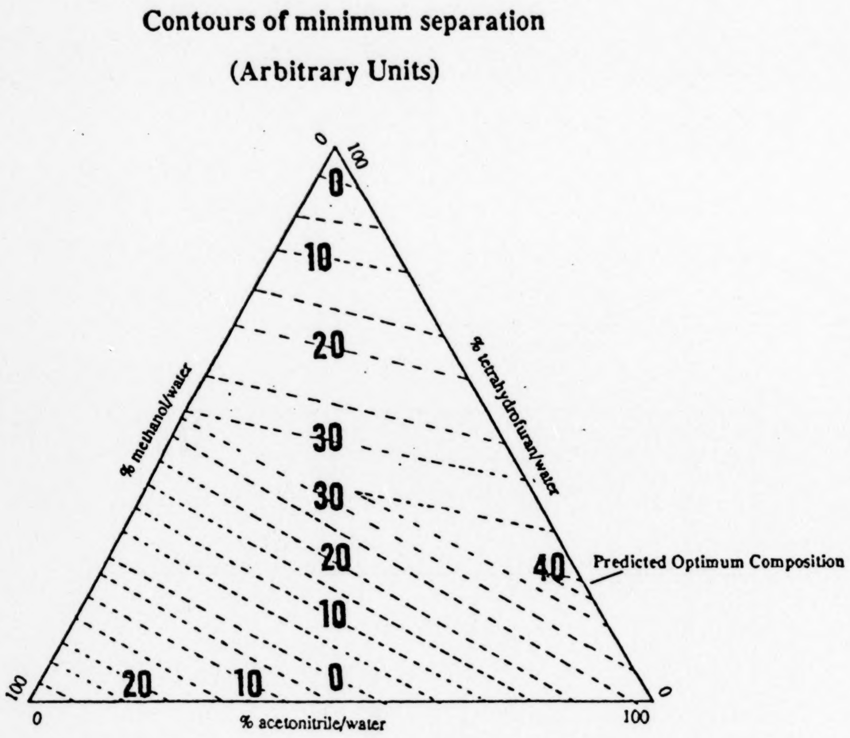

Fig. 3

Response surface predicted by iterative lattice modelling from the chromatograms in Fig. 2.

Implementation

The expert system consists of a number of modular routines, the internal operation of each module being independent of the rest of the system. The decision-making modules are written in microProlog [8] to which an extension has been provided [9] enabling it to call numerical processing modules written in other languages such as Pascal and Basic. The system is hosted on an IBM PC-XT microcomputer, with data from the photodiode array detector passed to the computer via an RS232C serial data link. The present system requires an operator to prepare the mobile phases, operate the pumps and perform the injections. It is intended to bring these tasks under direct control at a later stage in the development of the overall system.

Materials

HPLC-grade methanol, acetonitrile and tetrahydrofuran (Rathburn Chemicals, Walkerburn, UK) were used as received. All eluents were filtered through Millipore® 0.45 μm filters in all-glass apparatus and degassed under reduced pressure in an ultrasonic bath for 10 minutes. 3-hydroxybenzaldehyde, n-propyl-p-hydroxybenzoate, diethyl phthalate and phenol (BDH, Poole, UK) were used without further purification.

Equipment

Eluent delivery was achieved by the use of two PU4010 pumps under the control of a PU 4850 chromatography data station (Pye Unicam Ltd., Cambridge, UK). The 100 × 5 mm column was packed with 5-μm Hypersil ODS; solute detection was achieved using a Pye Unicam PU4021 diode array detector.

Optimisation of the Separation of a Four Component Mixture

The operation of the expert system has been demonstrated for the optimisation of a synthetic mixture. The test mixture contained 3-hydroxybenzaldehyde, n-propyl-p-hydroxybenzoate, diethyl phthalate and phenol dissolved in methanol at a concentration of 20 mg/ml.

The initial gradient elution experiment indicated that the required elutropic strength would be provided by a binary mixture of water and methanol (40:60 v/v). Equivalent combinations of water-acetonitrile (48:52 v/v) and water-tetrahydrofuran (58:42 v/v) were also prepared. The sample was injected onto the chromatograph using these three isoelutropic mobile phases; the chromatograms are presented as Fig. 2. After determining the homogeneity of the detected peaks, spectra were extracted for the four components from each of the chromatograms and a model of the response surface constructed. Here the resolution

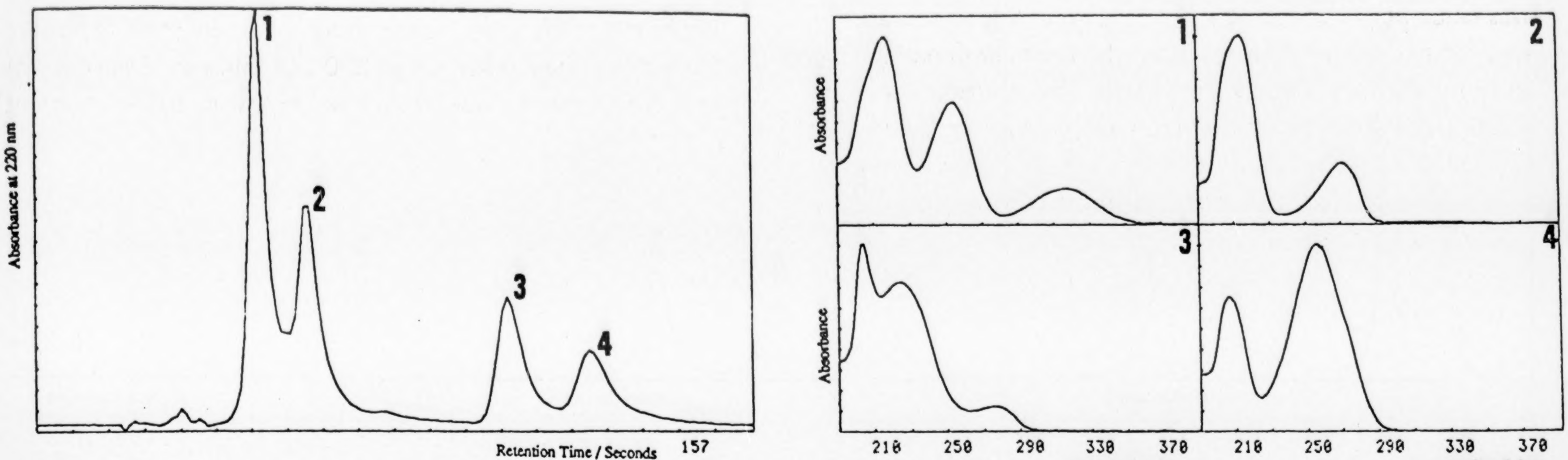

Fig. 4

Chromatogram produced under the optimum conditions predicted by the expert system. Mobile phase methanol-acetonitrile-tetrahydrofuran-water 24:5:21:50 v/v. Solute identities as for Fig. 2.

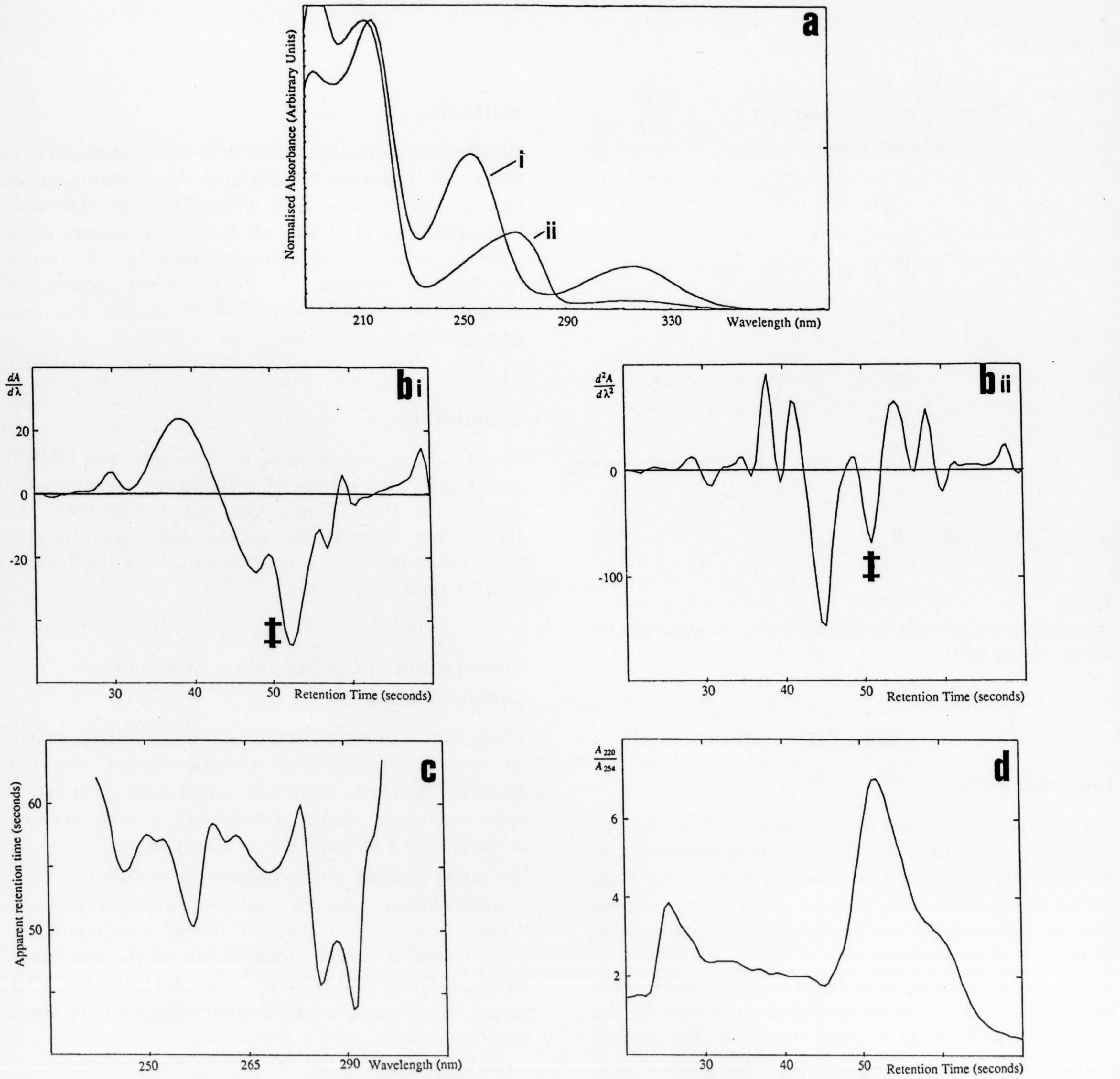

Fig. 5

Homogeneity tests applied to peak A in Fig. 2b.

(a) Comparison of spectral profiles. (i) Spectrum from upslope. (ii) Spectrum from downslope.

(b) First (i) and second (ii) derivative total absorbance chromatograms. Features marked ‡ are indicative of heterogeneity.

(c) Variation of apparent retention time with detector wavelength.

(d) Absorbance ratio chromatogram.

was calculated for each pair of solutes at 2% increments in each of the three solvents, within the limits bounded by the solvent triangle. Fig. 3 represents the contour lines of equal separation for the worst resolved pair of solutes at each eluent combination. The figure depicts the first stage of the search for the true optimum composition. The response surface produced at this stage may be visualised as a set of adjacent planes, tilted relative to one another. In addition to the predicted global optimum composition, with a separation of over 40 arbitrary units, the system predicts the existence of two local optima: one located at the apex representing 100% methanol-water, with a separation of 32 arbitrary units; the other is located at the apex for 100% THF-water and has a separation of under 5 arbitrary units. A chromatogram was then carried out under the conditions predicted by this model and the data produced subsequently included in the model to allow an improved optimum to be established. At this stage the solvent triangle was subdivided by a line (or lines) connecting the latest experimental point with each of the apexes of the triangle surrounding that point, thereby producing up to three new, smaller, triangles. A resolution model was produced for each of these subsets of the solvent triangle and a new optimum composition established. The process of continual refinement was continued until no further improvement in the resolution was indicated. The final optimum chromatogram is shown in Fig. 4.

Assessment of Peak Homogeneity

The operation of the homogeneity assessment tool described above is illustrated in Fig. 5, when applied to the composite peak A in Fig. 2b.

Fig. 5a demonstrates the difference in spectral profiles obtained from the leading and trailing edges of the peak. For an homogeneous peak these normalised spectral profiles should only differ by an amount related to the noise of the detector.

Fig. 5b shows the profiles of the first and second derivative chromatograms, with the presence of a second component indicated by the features marked ‡ and the number of zero crossing points in the second derivative profile.

Fig. 5c is a plot of the apparent retention time as a function of detector wavelength. The variation indicated in this plot again suggests that more than one component is present.

Fig. 5d ist the absorbance ratio chromatogram produced from the signals detected at 220 and 254 nm. The ratio for an homogeneous peak would be expected to be invariant with time.

Conclusions

The system presented here is still in the early stages of development, but it illustrates some of the potential of a knowledge based approach to the problem of eluent optimisation in reversed-phase liquid chromatography. A number of enhancements are proposed, including the development of a series of rules to allow more intelligent use of the homogeneity data, an independent module to assist in the selection of the column and initial solvent selection, and direct control of the chromatographic hardware.

Acknowledgements

The Authors acknowledge receipt of a Post-Doctoral Assistantship from the SERC for one of us (TPB), a studentship from the Royal Society of Chemistry Analytical Trust (GGRS) and the generous loan of equipment by Pye Unicam Ltd., Cambridge.

References

[1] *J. C. Berridge,* "Techniques for the Automated Optimisation of HPLC Separations", Wiley, Chichester, (1985).

[2] *P. J. Schoenmakers, H. A. H. Billiet, L. de Galan,* J. Chromatogr., **205**, 13 (1981).

[3] *A. C. J. H. Drouen,* "Computerised Optimisation and Solute Recognition in Liquid Chromatographic Separations", PhD Thesis, Technical University Delft, (1985).

[4] *J. C. Berridge,* Analyst, **109**, 291 (1984).

[5] *J. C. Berridge,* J. Chromatogr., **244**, 1 (1982).

[6] *A. F. Fell, H. P. Scott, R. Gill, A. C. Moffat,* Chromatographia, **16**, 69 (1982).

[7] *A. G. Wright, A. F. Fell, J. C. Berridge*, Chromatographia **24**, 533 (1987).

[8] *K. L. Clark, F. G. McCabe,* "micro-PROLOG: Programming in Logic", Prentice-Hall International, London, 1984.

[9] *K. T. Milne, M. H. Williams, B. J. Clark, A. F. Fell,* Anal. Proc., **23**, 157 (1986).

Received: July 31, 1987
Accepted: Aug 14, 1987
F

Automated Two-Dimensional HPLC Residue Procedure for Glyphosate on Cereals and Vegetables with Postcolumn Fluoregenic Labelling

L. G. M. Th. Tuinstra* / P. G. M. Kienhuis

State Institute for Quality Control of Agricultural Products, P.O. Box 230, 6700 AE Wageningen, The Netherlands

Key Words

Glyphosate
Agricultural products
Automated determination

Summary

A procedure for glyphosate in cereals and vegetables is described in which a 250-μl extract in water is injected on an AX/Corasil Bondapack pre-column. After washing with water the retarded glyphosate is forward eluted on an Ionosphere A anion-exchange column with the buffered eluent. The pre-column is backflushed and regenerated with acetic acid. Recovery experiments with barley, wheat and rye (tolerance 5–20 mg/kg) at the 1 mg/kg level showed recoveries of 80 % (C.V. = 10 %).

For potatoes, strawberries and asparagus, with a tolerance of 0.05 mg/kg, experiments at the 1 mg/kg level indicated promising results suitable for working at residu levels with these products.

Introduction

The nonselective herbicide glyphosate [N-(phosphonomethyl)glycine] (Fig. 1) has wide application, not only post-harvest, but also up to seven days before harvest (e.g. cereals, potatoes, asparagus), only when the plants are completely ripened. Maximum residue limits (MRL's) differ widely. For wheat 5 mg/kg and barley 20 mg/kg is permitted while for potatoes, asparagus and strawberries only 0.05 mg/kg is permitted. In the Netherlands the MRL concerns only glyphosate and not the main metabolite (aminomethyl)phosphonic acid (AMPA) (Fig. 1). Many ways of extraction and determination have been pusblished. Generally they have one thing in common: they are time consuming. As glyphosate is very polar, extraction can only be carried out with water [1], some times in combination with a non-mixing organic solvent [2–4]. Because of the low MRL the extract should be concentrated several (up to six) times [4]. For clean-up purposes cation... [1, 2, 5], anion-exchange [4–6] and gel-permeation columns [1, 4] have been used, very often in combination.

Detection is carried out, either with gas chromatography after derivatization [1, 4, 7, 8] or with HPLC as such with

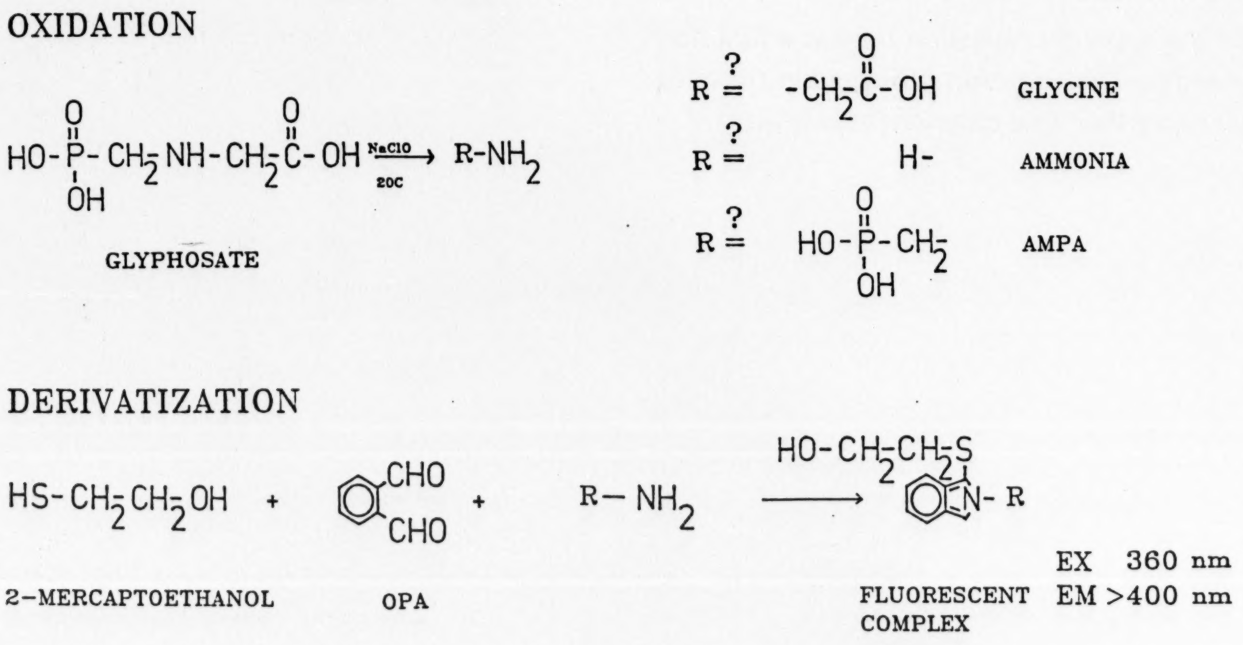

Fig. 1

Reaction of glyphosate with hypochloride and the OPA-mercaptoethanol reagent.

0009-5893/87 0696-05 $ 03.00/0

© 1987 Friedr. Vieweg & Sohn Verlagsgesellschaft mbH

UV [9], or differential pulse polarography [10] detection or with HPLC and fluorescense detection where pre-column [3, 11] or postcolumn (PC) derivatization [2, 5, 6] has been carried out. The PC oxidation with hypochlorite and derivatization with o-phthalaldehyde (OPA) is given in Fig. 1.

Though literature indicates HPLC separations of glyphosate on anion- or cation-exchange columns, we preferred anion exchange columns, because amino acids, well available in the matrix, react with OPA and should therefore not be retained on the analytical column. This can be realized by working at low pH values were the amino acids behave like neutrals. As the pkl value of glyphosate is 2.3 [5] this pH value was chosen for the separation of glyphosate on an anion-exchange column with quaternary ammonium functional groups attached to silica.

In a neutral environment (pH = 7) glyphosate is trivalent negative and shows a good retention on an anion-exchange column [5, 11]. Therefore it was investigated to use this type of columns as a pre-concentration column to overcome evaporating several times large volumes of water. This report describes the combination of a concentrating and cleaning pre-column and an analytical column by way of two six-port valves, resulting in an HPLC method for the determination of glyphosate at residue levels using postcolumn fluoregenic labelling.

Materials and Methods

Equipment

Wisp 710 B (Waters, Milford, MA 01757, USA) injection volume 50–2000 µl; 2 M-45 pumps (Waters); System Controller 720 (Waters); two six-port valves (Valco Instrument Co., Houston, Texas, USA): Solvent switch (Valco); Skalar tubing pump (Skalar Analytical BV, Breda, Netherlands); two glass coils (Skalar), inner diameter 2 mm, residence time 210 sec for the oxidation and 30 sec for the derivatization reaction; debubbler; tees.

Pre-column: AX/Corasil Bondapack (Waters) quarternary ammonium group attached to silica; 0.3 x 10 cm; 37–50 µm. Analytical column: Ionosphere A; quarternary ammonium group attached to silica 0.3 x 10 cm, 10 µm (Chrompack, Middelburg, Netherlands). Aminco fluorescence detector (AMINCO, Silver Spring, Maryland 20910, USA) excitation wavelength 360 nm, emission wavelength above 400 nm.

The whole system (Fig. 2) worked at room temperature.

Reagents

Pre-column regeneration: acetic acid 1 M.

HPLC eluent: Dissolve 0.34 g KH_2PO_4 in 1 l deionized water and add 1 ml H_3PO_4 (85 %). The pH should be 2.1. Degass eluent. Flow rate: 0.6 ml/min. Oxidizing reagent: from a domestic product such a volume was taken that it contained 0.08 g of active chlorine. This was added to 1 liter buffer solution in deionized water containing 8.7 g $K_2HPO_4 \cdot 3\,H_2O$; 5.8 g NaCl and 1 ml Brij-35 (Merck). The pH should be 9.1. Flow 0.42 ml/min. Fluoregenic reagent: dissolve 0.9 g o-phthalaldehyde and 1 ml 2-mercaptoethanol in 10 ml methanol and add this to 250 ml from a concentrated buffer solution containing 12.4 g H_3BO_3 and 12.4 g NaOH (solid) per 1 l deionized water and fill this up to 1 l with deionized water. The pH should be 9.2. Flow rate: 0.42 ml/min.

The glyphosate standard contains 1 µg/ml deionized water.

Switching Procedure

With the described equipment, reagents and method the following time events were programmed into the system controller:

time min	flow rate ml/min	action
0	1	Start Wisp, injecting on the pre-column.
4	1	Activating column switch valve to bring pre-column in line with the analytical column. Analysis on analytical column starts.
8	1	Activate column switching valve. Pre-column goes back to original (load) position.
10	3	Activate backflush valve.
10.01	3	Increase flow rate of pump 1 and activate the solvent switching valve to backflush pre-column with 1 M acetic acid.
16	3	Activate solvent switching valve to backflush the pre-column with water.
26	1	Activate backflush valve (original position).
30	1	New analysis can start.

Residue Procedure

Weigh 10 g of grinded cereals or vegetable, add 100 ml deionized water and 50 ml chloroform in a 250 ml-glass centrifuge bottle. Shake for 30 min. Centrifuge at 3000 g for 10 min. Take 3–4 ml from the supernatant for filling the vials of the Wisp. In a series of unknown samples, standard solutions and recovery experiments are included.

Results and Discussion

By combining the analytical column with a UV (195 nm) detector [9] it was possible to find the best eluent composition (see reagents) with respect to peak width (at half height: 0.4 min) and retention time (7 min). The PC procedure as described in the literature [2, 5] was used as starting point for our experiments. Since Archer and Stokes [5] indicated that a too low hypochlorite flow caused a noisy baseline, we choose a flow of 0.42 ml/min. The buffer solution concentration given by Moye et al. [2] was halved. For the derivatization we took the concentrations from work of Archer and Stokes [5] and the pH from Moye et al. [2]. The pH should be around 9. By addition of NaOH or

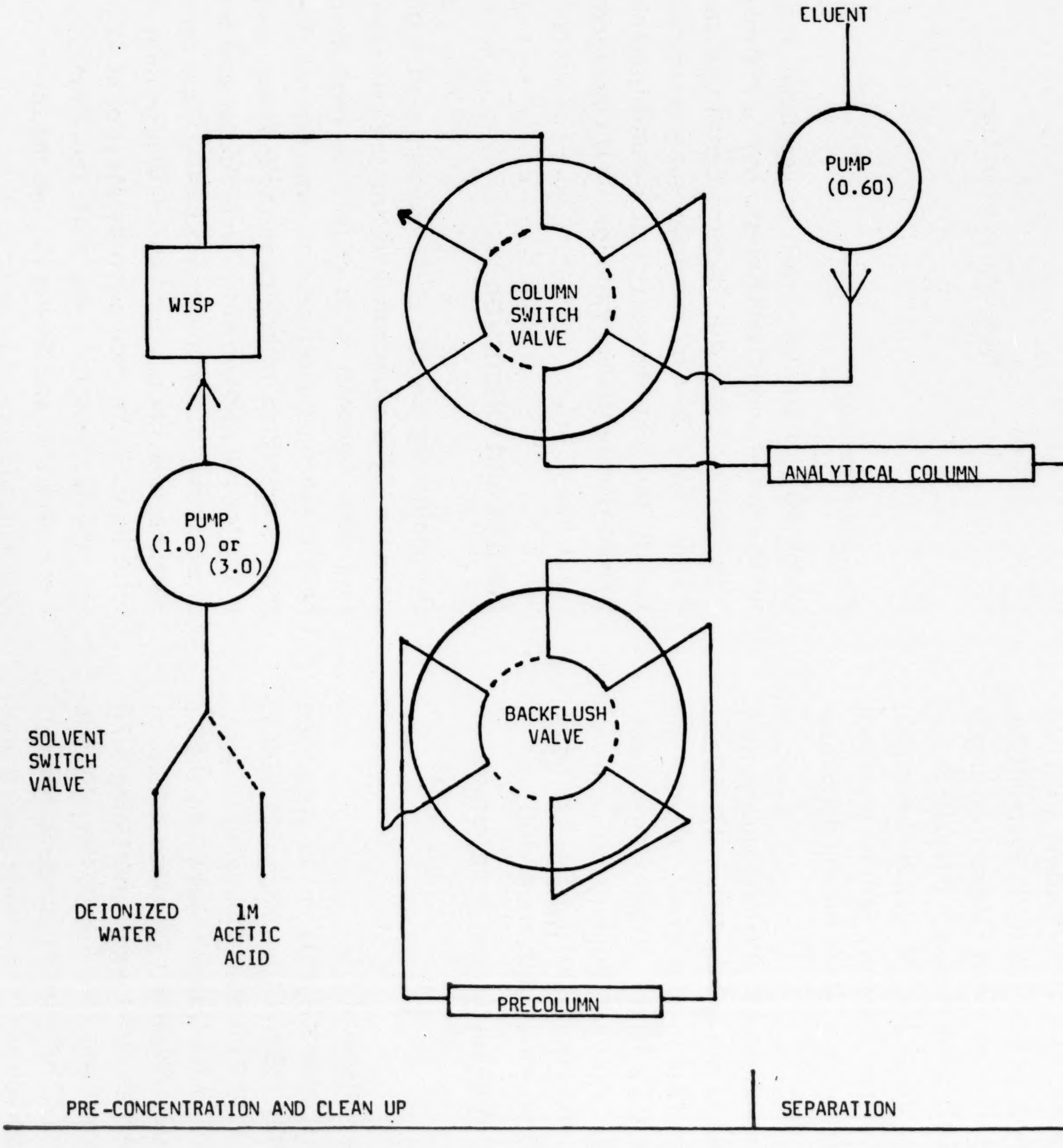
ELUENT
PUMP
(0.60)
WISP
COLUMN
SWITCH
VALVE
ANALYTICAL COLUMN
PUMP
(1.0) or
(3.0)
BACKFLUSH
VALVE
SOLVENT
SWITCH
VALVE
DEIONIZED
WATER
1M
ACETIC
ACID
PRECOLUMN
PRE-CONCENTRATION AND CLEAN UP
SEPARATION

Fig. 2

HPLC system for the glyphosate procedure. The three valves are in the t = 0 position. Flow in ml/

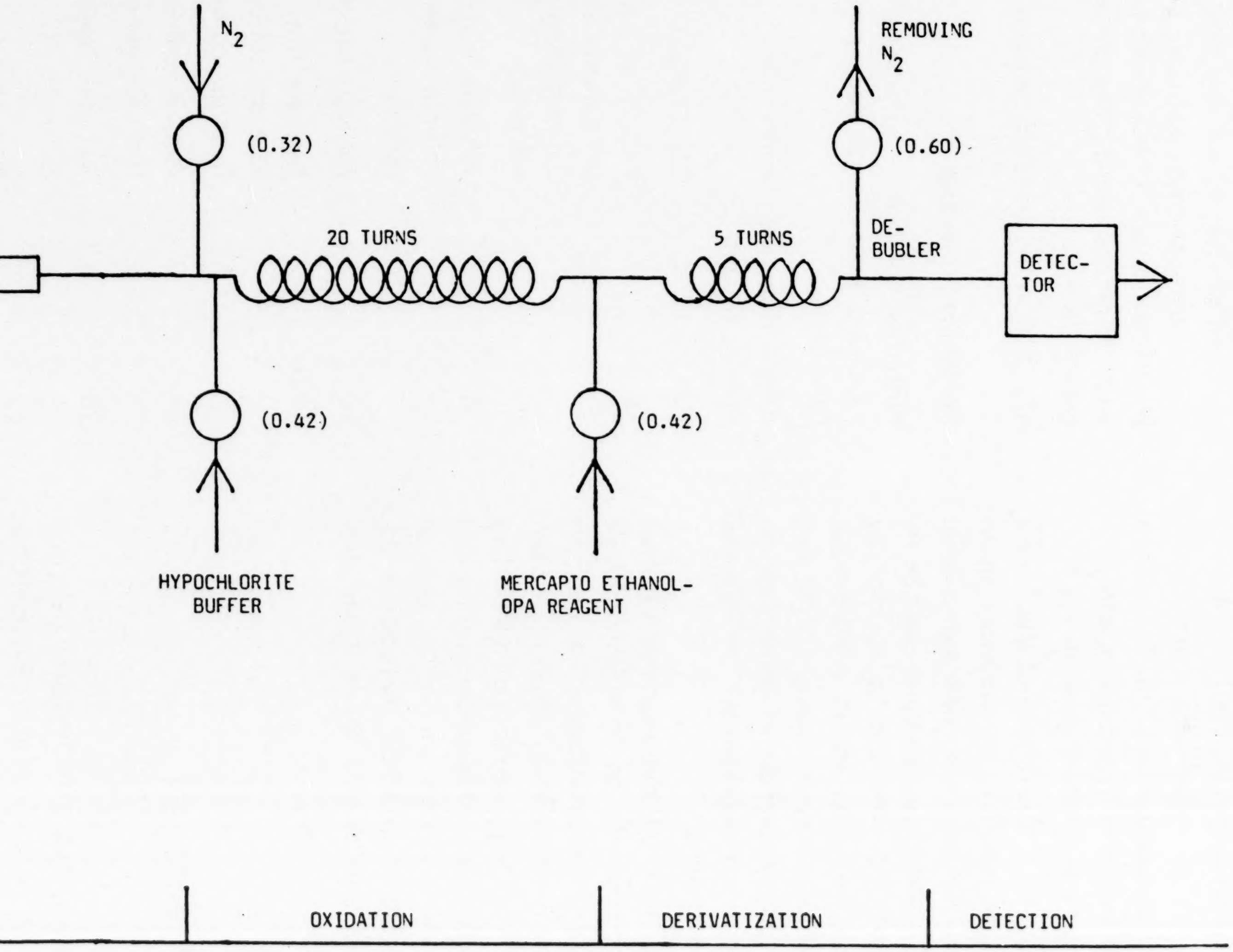

N2
REMOVING N2
(0.32)
(0.60)
20 TURNS
5 TURNS
DE-BUBLER
DETECTOR
(0.42)
(0.42)
HYPOCHLORITE BUFFER
MERCAPTO ETHANOL-OPA REAGENT
OXIDATION
DERIVATIZATION
DETECTION

in ml/min in brackets.

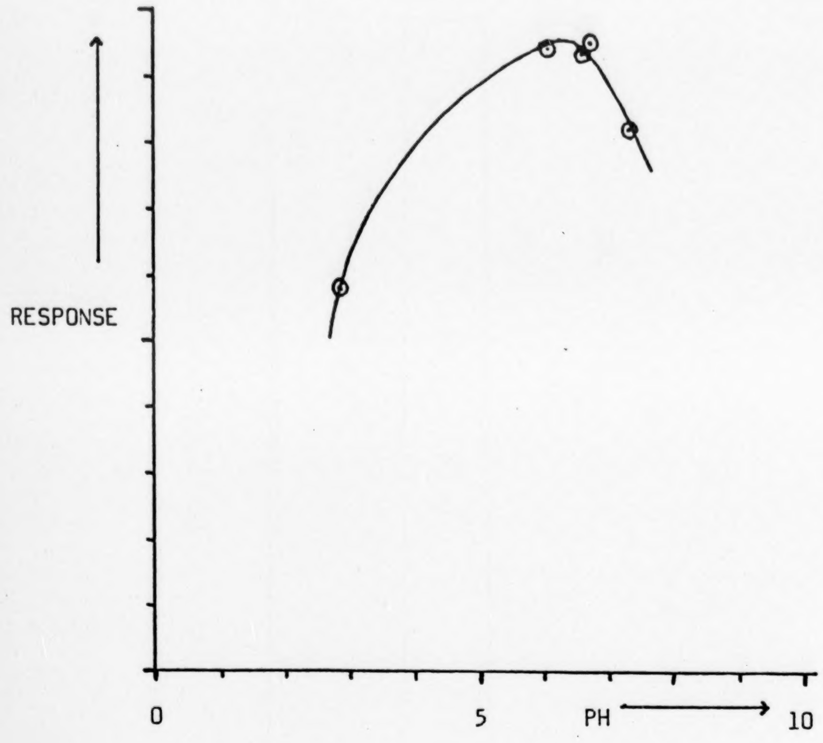

Fig. 3
Influence of pH on the oxidation reaction. Other reaction conditions are as indicated under reagents.

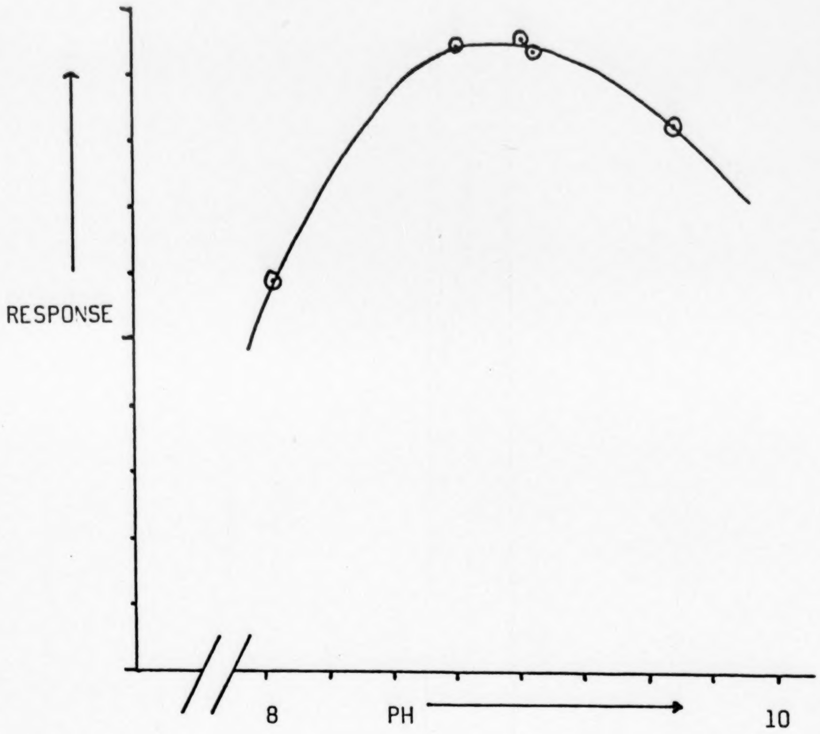

Fig. 4
Influence of pH on the derivatization reaction. Other reaction conditions are as indicated under reagents.

HCl the pH for the oxidation as well as for the derivatization reaction was optimized and controlled (Fig. 3 and 4).

To restrict peak broadening in the reaction coils, nitrogen segmentation, excluding ammonia and oxygen from the air, was included in the transport of reagents and eluents. With the PC set up, retention for glyphosate increased from 7 to 12–13 min and the peakwidth at half height to 0.5 min under the final conditions.

In neutral environment (pH = 7) glyphosate shows a stronger retention behaviour on anion-exchange columns than on cation-exchange columns [5, 11]. First experiments with a pre-column (length 10 mm, i.d. 2.5 mm) filled with AX/Corasil (35–50 μm) showed indeed a good retention for glyphosate dissolved in deionized water. However when the (cereal) samples, extracted with deionized water, were injected (at 1 ml/min), the capacity and therefore the retention was decreased, probably due to the presence of many other extra ions from the matrix. Decreasing the injection flow rate did not improve the situation. Therefore the pre-column length was increased to 10 cm. After application of the sample extract on the pre-column at 1 ml/min this column was flushed forwards with deionized water to wash away less retarded compounds. This increase in column length and washing with water did not result in a broader peak.

The retention behaviour of the pre-column was also tested with cereal sample extracts spiked at 1 mg/kg with glyphosate in relation to the injection volumes of the extract. Varying the volume from 125 to 1000 μl (containing 12.5 ng –100 ng glyphosate), on the column we have learned that injection volumes of 250 μl did not result in lower recoveries. When injecting 1000 μl extract of barley, wheat or rye (grinded to less than 2 mm) recoveries of glyphosate were about 50 %. When the particles were larger than 2 mm, even 1000 μl spiked sample extract could be injected without loss.

It should be noted that injecting only standard glyphosate, even with large injection volumes, showed a good linear response.

As the MRL's for most cereals is in the mg/kg range there is no need to inject volumes larger than 50 μl. At 250 μl injection volumes and a spike level of 1 mg/kg the mean recovery for the tested cereals was 80 % with a coefficient of variation (CV) of 10 %. The use of a Seppak C_{18} reversed-phase column or a 0.45 μm disposable filter for removing very fine sample particles in the extract were not succesful either for removing these particles or for improving the recovery when injecting larger volumes of the extract. As the pre-column is backflushed each time after forward flushing the sample on the analytical column, no problems of clogging of the pre-column or analytical column were met.

For agricultural products, others than cereals, an MRL of 0.05 mg/kg exists. A few experiments were carried out to see if the method, in principle, could be applicable at these low MRL's. Potatoes, asparagus and strawberries were, after homogenization, spiked with 1 mg/kg glyphosate, extracted as described and injected in the system with increasing volumes e.g., 250 μl (= 25 mg sample) 500 μl and 1000 μl. It appeared again that at 250 μl the recoveries were acceptable (> 70 %) while at higher volumes the recoveries strongly decreased. In the blank sample extract as such no response was observed at the appropriate retention time (Figs. 5a and b). The extrapolated detection limit is in the order of 0.04 mg/kg, just below the MRL. Either a better pre-column with a higher capacity should be used, or the sensitivity of the detection system should be improved to quantify glyphosate at the MRL of 0.05 mg/kg. The latter seems to be no problem with present-day fluorescence detection.

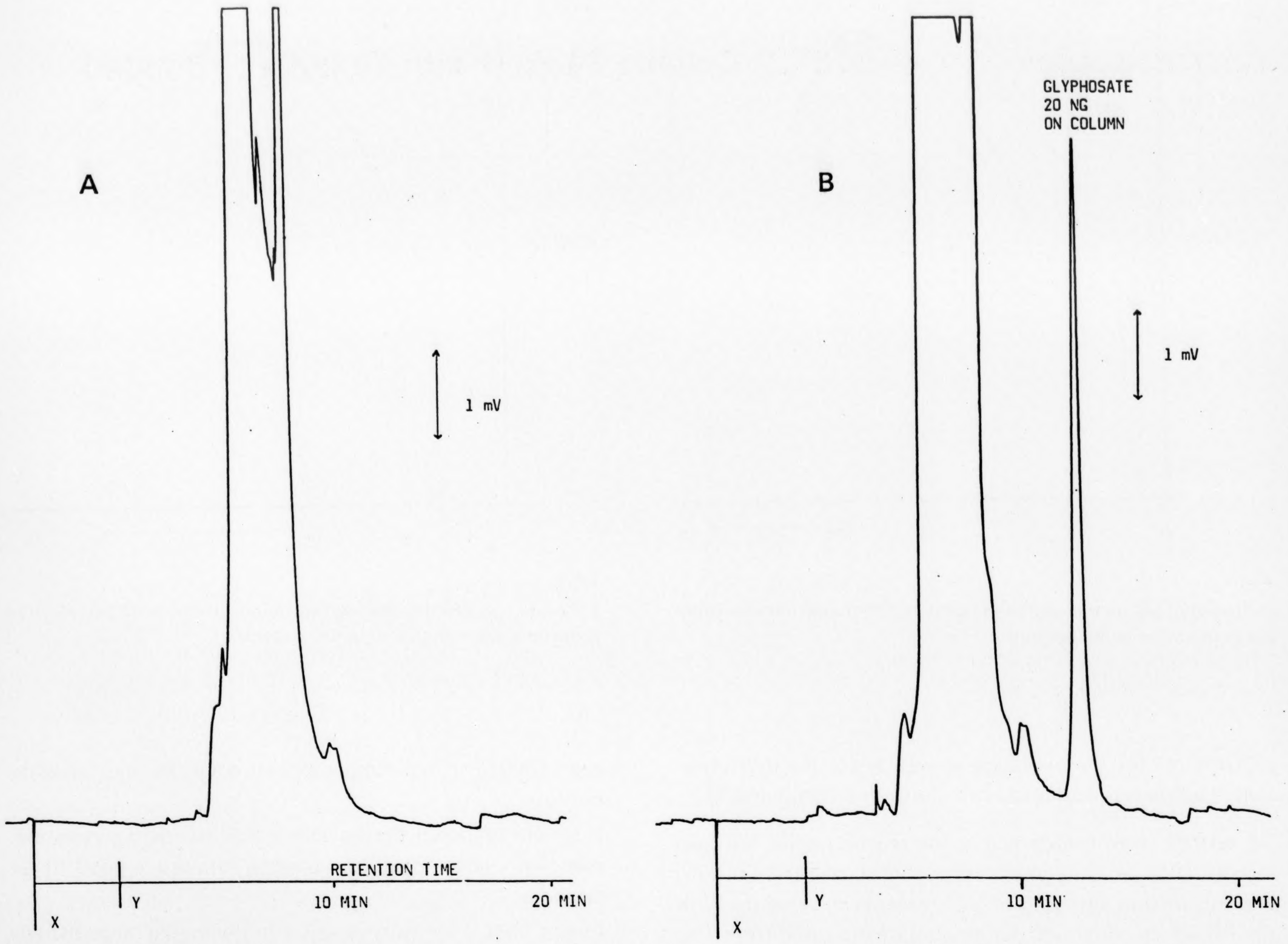

Fig. 5

Glyphosate chromatograms: A: potato blank extract; b: potato spiked with 1 mg/kg; X: injection on pre-column; Y: injection from pre-column on analytical column.

Conclusion

The described procedure is applicable in different types of agricultural products with a detection limit of 0.2 mg/kg for glyphosate and a recovery of about 80 %. The method is very promising at lower levels and probably applicable immediately with more sensitive fluorescence detection. One technician can handle about 45 samples a day.

References

[1] *R. A. Guinivan, N. P. Thompson, W. B. Wheeler*, J. Ass. Offic. Anal. Chem., **65**, 35–39 (1982).
[2] *H. A. Moye, C. J. Miles, S. J. Scherer*, J. Agric. Food Chem., **31**, 69–72 (1983).
[3] *H. Roseboom, C. J. Berkhoff*, Anal. Chim. Acta, **135**, 373–377 (1982).
[4] *J. N. Seiber, M. M. McChesney, R. Kon, R. A. Leavitt*, J. Agric. Food Chem., **32**, 681–683 (1984).
[5] *T. E. Archer, J. D. Stokes*, J. Agric. Food Chem., **32**, 586–588 (1984).
[6] *J. E. Cowell, J. L. Kunstman, P. J. Nord, J. R. Steinmetz, G. R. Wilson*, J. Agric. Food Chem., **34**, 955–960 (1986).
[7] *H. A. Moye, C. L. Deyrup*, J. Agric. Food Chem., **32**, 192–195 (1984).
[8] *C. L. Deyrup, S. Chang, R. A. Weintraub, H. A. Moye*, J. Agric. Food Chem., **33**, 944–947 (1985).
[9] *A. J. Burns*, J. Chromatogr. Sci., **17**, 333–335 (1979).
[10] *R. L. Glass*, J. Agric. Food Chem., **32**, 1249–1253 (1984).
[11] *R. L. Glass*, J. Agric. Food Chem., **31**, 280–282 (1983).

Received: July 1, 1987
Accepted: Sep. 3, 1987
F

Characteristics of a New HPLC Column Packed with Octadecyl-Bonded Polymer Gel

Y. Yanagihara*/K. Yasukawa/U. Tamura/T. Uchida/K. Noguchi

GS Development Dept., Asahi Chemical Ind. Co., Ltd., 1-3-2 Yakoo, Kawasaki-ku, Kawasaki-shi, 210 Japan

Key Words

Reversed phase liquid chromatography
Octadecyl-bonded polymer gel
ODP
Asahipak

Summary

The chromatographic efficiency and stability of a new octadecyl-bonded polymer (ODP) gel, developed for reversed phase liquid chromatography (RPLC) by substitution of stearate ester groups for the hydroxyl groups of vinyl alcohol copolymer particles, were investigated and compared with those of conventional gels. The efficiency of the column packed with the ODP gel was practically unaffected by repeated alternating passages of distilled water and acetonitrile, apparently because the gel volume was affected similarly by both solvents. Like conventional ODS columns, the ODP column demonstrated a close correlation between log k' (capacity factor) and carbon atom number in alkyl alcohols in accordance with Martin's rule and H ~4dp, thus indicating a high column efficiency for these alcohols. The capacity factor of the ODP column for pyridine with acidic eluent was smaller than that of ODS columns, and the pyridine peak was sharp and symmetrical.

Introduction

Reversed phase chromatography is the most commonly employed form of high performance liquid chromatography (HPLC), particularly because of its high efficiency in the separation of many substances of low molecular weight.

Traditionally, the packing materials for RPLC have broadly involved a silica base, chemically bonded with octadecyl silane (ODS). ODS gels, however, can only be used for a rather restricted range of solvents and analysates. This restriction is directly related to the characteristics of silica. ODS columns decline sharply in efficiency with carriers which are alkaline or contain buffers, ruling out their use in the mobile phase. They also tend to absorb or display asymmetrical peaks for many basic substances.

Column packed with polymer gels are also commercially available for RPLC. They allow the use of eluents in a broader range, as they are chemically stable in alkaline and buffered solutions. Their utilization has been relatively limited, however, because they generally display low separation efficiency and also because their gel volumes vary widely with eluent polarity.

An octadecyl-bonded polymer (ODP) gel packing, consisting essentially of hydrophilic vinylalcohol copolymers bearing chemically bonded C18 groups, was developed to eliminate the limitations imposed by the conventional ODS and polymer gels. As described here, the characteristics and performance of this gel were investigated and compared with those of commercial ODS and polymer gels.

Experimental

ODP gel containing many stearate-ester C18 groups was obtained by reacting stearyl chloride with the hydroxyl groups of vinylalcohol copolymer. The C18 carbon content of the resulting gel was estimated from gel weights before and after the reaction.

The influence of various solvents on gel volume was determined on the basis of solvent regain (S_R). Dry gel was dispersed in the solvent, and the dispersion was centrifuged to remove excess solvent. The weight W_1 of the wet gel was then measured. The gel was next dried, and again weighed, to obtain W_2. S_R, in ml solvent/g gel, was calculated by the equation $S_R = [(W_1 - W_2)/d]/W_2$, with d as the solvent density.

Titration curves were obtained by washing the gel with diluted aqu. hydrochloric acid and then distilled water, dispersing the gel in aqu. 0.1 N NaCl, and titrating the dispersion with aqu. 0.02 N NaOH.

0009-5893/87 0701-04 $03.00/0

© 1987 Friedr. Vieweg & Sohn Verlagsgesellschaft mbH

Table I. Characteristics of ODP, ODS and ACT-1 gels

		ODP	ODS	ACT-1
Average particle diamter (μm)		5.0	10.2	15.5
Solvent regain (S_R) (ml/g)	Distilled water	0.69	0.87	1.07
	Acetonitrile	0.76	0.86	1.66
C18 carbon content (%)		17	10	

Gel particle diameter was measured by a Coulter Counter (Coulter Electronics Co.).

The ODP gel packing column was stainless steel, of 6mm inner diameter and 150 mm length.

A comparison was made between the commercially availably μBondapak 4.1 mm × 150 mm (Waters) and ACT-1 4.6 mm × 100 mm (Interaction Chemicals) columns and their gels, which were obtained by removal from the packed columns.

Chromatography equipment included LC4A (Shimadzu) and 880PU (JASCO) pumps, a Shodex SE-51 (Showa Denko) RI detector, a UVIDEC-IV (JASCO) UV detector, and a 7125 (Rheodyne) injector.

Reagents and solvents were from Wako.

Results and Discussion

Gel Characteristics

Table I shows the gel characteristics as observed for the ODP gel and the gels from the two commercial columns. The μBondapak column, as an ODS column for RPLC, is widely employed throughout the world. The ACT-1 is packed with a polymer gel, consisting of stryrene-divinylbenzene copolymer with C18 groups bonded to its benzene rings, and is recognized for its amenability to a wide range of pH.

As shown in terms of S_R in the table, the ODP gel volumes were similar in distilled water and in acetonitrile. The difference in volume for the ODP gel was comparable to that of the ODS gel, which was least affected by the change in solvents, and far smaller than that of the ACT-1 gel.

S_R is an indirect expression of gel pore volume in a given solvent. In general, changes in the volume are dependent on the solvent polarity. They generally correspond with changes in S_R, and can therefore be estimated on this basis. For any gel, large differences among S_R values in solvents of differing polarity are undesirable, as this means the gel will undergo marked swelling and shrinkage when exposed to different solvents in succession, and thus decline in column efficiency due to a loss of packing uniformity within the column.

The titration curves in Fig. 1 show the ODP gel to be practically free from acidic groups such as those found in ODS gels. The rapid initial rise in the pH of the ODP gel dispersion indicates few or no acid groups were present in the gel. In contrast, the slow initial rise in the pH of the ODS gel dispersion indicates the presence of a weakly acidic group in the ODS gel, which may be identified as silanol.

The silanol groups in ODS gels generally tend to interact with basic compounds such as amines, thus preventing their elution from the HPLC column or resulting in asymmetrical peaks for these compounds. The results indicate that this problem will not occur with the ODP column, as the ODP gel contains practically no acidic functional groups.

Retention of Column Efficiency with Differing Solvents

As shown in Table II, the ODP column suffered no loss in column efficiency after repeated passage of water and acetonitrile in succession through the column. In a number of theoretical plates (NTP) and elution volumes for creatinine and benzoate ester compounds, the ODP column performance was the same before and after this passage. The results indicate that the column efficiency will be completely retained under exposure to these two solvents either in succession or in combination.

It is generally desirable in RPLC to utilize various organic solvents such as acetonitrile, methanol and tetrahydrofuran as eluents, in addition to water. Conventional polymer columns, however, pose restrictions on their use. One example of this is the note in the instruction manual for the ACT-1 column, made against the use of aqueous acetonitrile in concentrations of less than 30%. This limitation may be attributed to the markedly smaller S_R value of the gel in water than in acetonitrile, and a resulting tendency for loss of packing uniformity and column efficiency in acetonitrile solutions of lower concentrations.

The retention of column efficiency with the ODP gel may be attributed to the small difference between its S_R values in water and in acetonitrile. The results of the present study indicate that it can be used effectively with aqueous acetonitrile solutions well below 30% in concentration, and thus with far less restriction on eluent composition than conventional polymer gels.

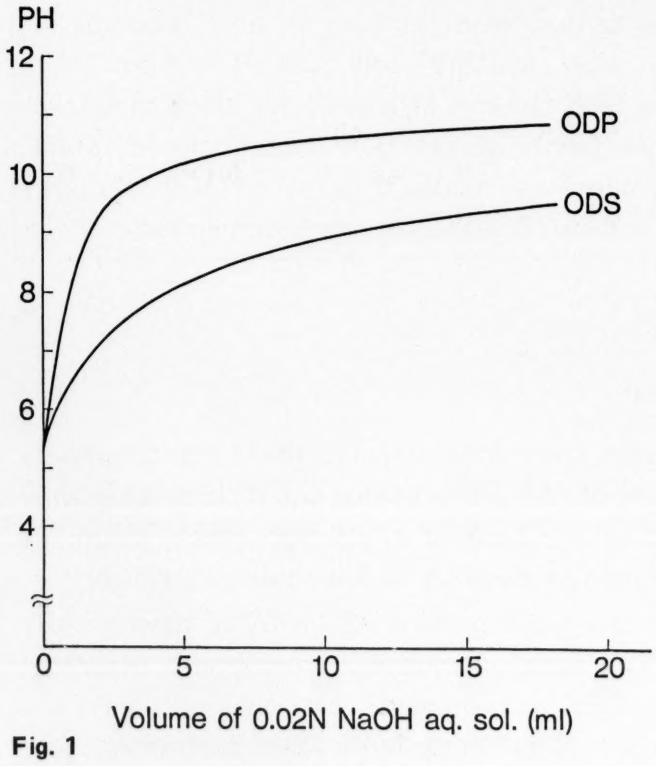

Fig. 1

Titration curves of the ODP and ODS gels.

Table II. Influence of repeated eluent exchange on ODP column efficiency.

Sample	Before passage		After passage	
	Elution volume V_E (ml)	Number of theoretical plates NTP	Elution volume V_E (ml)	Number of theoretical plates NTP
Creatinine	2.45	5,900	2.45	5,900
Methylbenzoate	4.82	6,100	4,82	6 100
n-Butylbenzoate	7.84	7,000	7.84	6,700
n-Hexylbenzoate	12.70	7,100	12.70	7,100

Eluent exchange conditions: 5 cycles of distilled water and then acetonitrile passages through the column each at 0.5 ml/min for 1 hr. Measurement conditions of column efficiency: Eluent, acetonitrile/distilled water (70/30, v/v); flow rate, 1.0 ml/min; detector, UV 254 nm; temperature 30 °C.

Capacity Factor and NTP for Alkyl Alcohols

In the analysis of the series of alkyl alcohols, the ODP column showed a close correlation between log k' (capacity factor) and the number of carbon atoms in the analysate, as shown in Fig. 2. This is in accordance with Martin's rule, and is an essential characteristic of RPLC. The slope of this correlation line represents the selectivity of the column for the analysates.

As shown, the capacity factor and selectivity of the ODP column for these alkyl alcohols are almost the same as those of the ODS column, but lower than those of the ACT-1 column.

As a rule, the capacity factor of a gel tends to rise with increasing carbon content in the gel. On this basis the ODP column, with its higher carbon content, might be expected to be considerably higher than that of the ODS column [1]. The observed similarity in the capacity factors of these two columns can be explained, however, by the lower specific gravity of the ODP gel, which translates to a relatively low level of carbon content per unit volume of gel.

Fig. 3 shows the relationship between NTP and capacity factor as observed in all three columns with alkyl alcohols. The ODS column exhibited high NTP values at k' of 1 to 8. This indicated a high efficiency in separation of substances with long, as well as short, elution times. The NTP of the ACT-1 column is generally less than 1/4 that of the ODS column, and declines significantly with increasing k'. The curve of the ODP column is roughly similar to that of the ODS column, but at a considerably higher NTP of 7,000 or more throughout the k' range of 1 to 8. It must be noted, however, that a precise comparison between the three gels would require the same particle size for all three, which was not the case in this study.

Analysis of Pyridine

As indicated by chromatogram b in Fig. 4, ODS columns are not entirely satisfactory for the analysis of basic substances, such as compounds containing nitrogen atoms, because of interactions other than hydrophobic, which tend to occur between the compounds and the silanol in the gel.

In this study, a mixture of pyridine and phenol was separated with the ODS and the ODP columns. Pyridine carries a

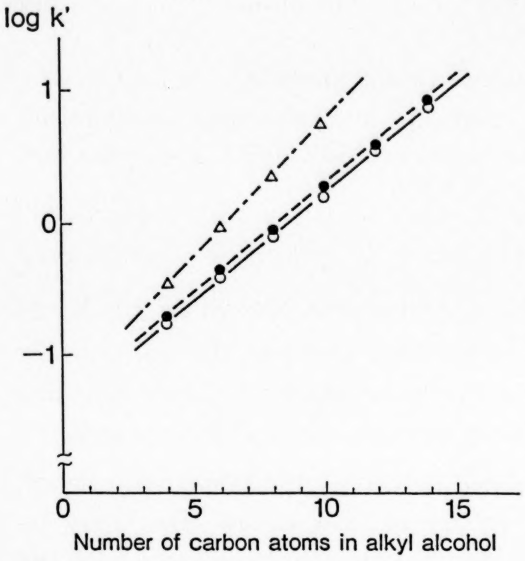

Fig. 2

Relationship between the logarithm of capacity factor and carbon number in alkyl alcohol.

Columns: (-○-) Asahipak ODP-50, 6.0 × 150 mm; (-●-) μBondapak ODS, 3.9 × 150 mm; (-△-) ACT-1, 4.6 × 100 mm. Sample: n-alkyl alcohol (n = 4, 6, 8, 10, 12, and 14). Eluent: Methanol/distilled water (80/20 v/v). Flow rate: 1.0 ml/min (ODP), 0.4 ml/min (ODS), 0.5 ml/min (ACT-1).

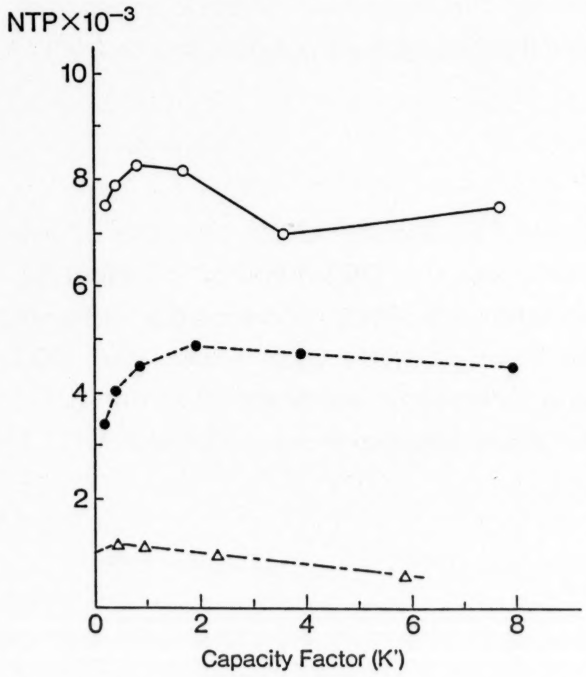

Fig. 3

Relationship between number of theoretical plates and capacity factor.

Columns: (-○-) Asahipak ODP-50, 6.0 × 150 mm; (-●-) μBondapak ODS, 3.9 × 150 mm; (-△-) ACT-1, 4.6 × 100 mm. Other conditions as in Fig. 2.

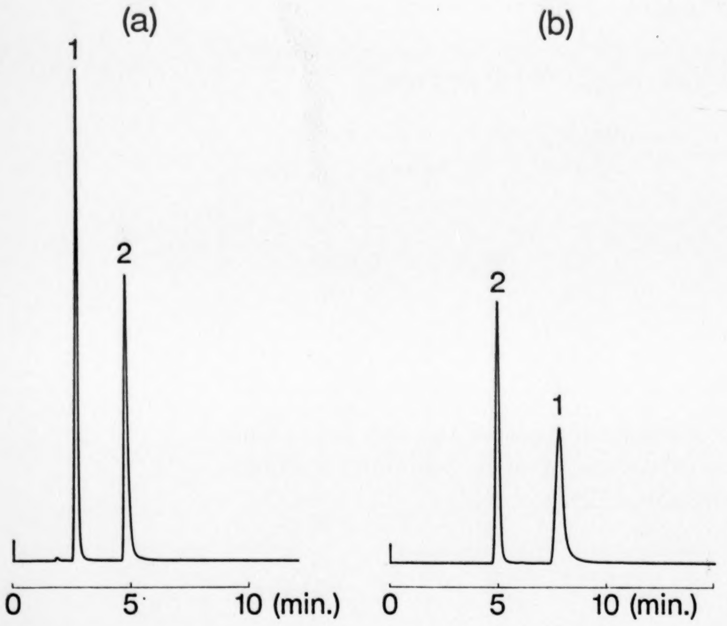

Fig. 4
Analysis of mixture of pyridine (1) and phenol (2).
Columns: (a) Asahipak ODP-50, (b) μBondapak ODS. Eluent: Acetonitrile/distilled water/acetic acid (60/40/0.1, v/v). Flow rate: 1.0 ml/min (ODP), 0.4 ml/min (ODS).

charge, and is more hydrophilic than phenol in this acidic solution. If the only interaction between the gel and the analysates is a hydrophobic interaction, then pyridine should first be eluted from the column, and phenol later.

On the ODS column, pyridine was eluted later than phenol, with a larger tailing in its elution curve. This may be attributed to interactions other than hydrophobic with the ODS gel, and most probably an acid-base interaction between the pyridine and the weakly acidic silanol groups in the gel.

On the ODP column, in contrast, pyridine was eluted earlier than phenol with a better elution curve symmetry than that obtained on the ODS column, as shown in chromatogram a of Fig. 4. This indicates that the absence of silanol or other acidic functional groups in the ODP gel makes it highly appropriate for the separation of basic substances, such as pyridine, solely through hydrophobic interaction.

Conclusion

The ODP column may be considered, on the basis of this study, to equal or excel the ODS column in retention, selectivity, and column efficiency. Commercial columns with polymer gels have generally been lower than ODS columns in separation efficiency, and the NTP of the ACT-1 column used in this study was also shown to be low. The low NTP of the ACT-1 column may be attributed to a hydrophobic effect of the benzene ring in its matrix, acting in addition to that of its C18 groups and thus resulting in a low equilibrium rate in the interaction between the gel matrix and the analysates. The matrix of the ODP gel, in contrast, is composed of hydrophilic vinylalcohol copolymer. Thus, as with the ODS gel matrix, the only hydrophobic interaction occurring in the matrix is that between the C18 groups and the analysates. This may be presumed to result in a high mass transfer rate, and thus in a high NTP.

It may further be concluded that the ODP column will retain its efficiency under gradual or even abrupt changes in the eluent being used. This was shown by chromatograms obtained on the same column before and after alternating passages of water and acetonitrile, as well as the small difference between ODP gel volumes in these two solvents. As shown in a previous study with a different hydrophilic vinylalcohol gel, the efficiency of the packed column can be expected to remain practically unaffected by the passage of organic solvent if the ratio of the gel volume in water to that in the solvent is 0.95 or more [2]. In the present study, the ratio with acetonitrile as the solvent was about 0.96, as calculated from S_R and gel density (1.23). These results, taken togehter, show the ODP column to be highly amenable to both water and acetonitrile in the mobile phase.

The ODP column is the first column packed with octadecyl-bonded polymer gel that offers high separation efficiency, similar to that of ODS column, and amenability to aqueous acetonitrile without restrictions on its concentration. This high separation efficiency also applies to basic compounds, which are often difficult to separate on ODS columns, because the ODP gel contains practically no acidic functional groups.

ODS columns have been broadly used for HPLC analysis because of their high separation efficiency for many compounds. The ODP column may be expected to further broaden the range of RPLC applications.

References

[1] *A. M. Krstulovic, P. R. Brown,* Reversed Phase High Performance Liquid Chromatography, John Wiley & Sons, Inc., New York, 1982.
[2] *N. Hirata, M. Kasai, Y. Yanagihara, K. Noguchi,* J. Chromatogr. **396**, 115 (1987).

Received: June 29, 1987
Revised manuscript
received: July 23, 1987
Accepted: Aug. 1, 1987
F

On-Line Extraction of Metal Ions Using Liquid-Liquid Segmentation and a Membrane Type Phase Separator for Fluorescence Detection

B. D. Karcher* / I. S. Krull

Barnett Institute and Department of Chemistry, Northeastern University, Boston MA, 02115, USA

R. G. Schleicher / S. B. Smith, Jr.

Thermo Jarrell Ash, 8 East Forge Parkway, Box 9101, Franklin, MA 02038, USA

Key Words

Oxine
Membrane phase separator
Diamagnetic metal ions
Post-column extraction
Fluorescence
Segmented flow reactor

Summary

A liquid segmented post-column reaction system has been used to extract metal ions from an aqueous eluent into an organic solvent for fluorescence detection. The metals Zr(IV), Ga(III), Sc(III), Y(III), In(III), Al(III), La(III), Zn(II), Cd(II), Ca(II) and Mg(II) have been isocratically separated on a C_{18} column by virtue of the secondary chemical equilibrium established by an eluent containing n-octanesulfonate, tartaric acid, and hydroxyisobutyric acid. The chelating reagent 8-hydroxyquinoline dissolved in methylisobutyl ketone (MIBK) was used to extract the metals and a membrane type phase separator was effective at separating the phases and directing the organic stream to the detector. The response for this detection approach was linear for metal ion concentrations spanning the range of the detector, and detection limits for most metals were low parts-per-billion (ppb). Band broadening for the extraction system was examined and compared to a direct post-column reaction using oxine dissolved in acetone.

Introduction

In recent years, use of two-phase segmented flow through narrow tubing has been used for liquid-liquid solvent extraction for a variety of on-line applications including sample clean-up [1], preconcentration of analytes [2], enhancement in compatibility between analyte and detector [3–6], and post-column reaction [7, 8]. In most systems, the analyte is extracted from the aqueous phase into an organic phase, a portion of the organic phase is separated from the two-phase system using a phase separator, and the organic phase is directed to the detector for quantitation.

Several different types of phase separators have been employed, including systems based on density differences between phases [9, 10], those with phase guide inserts which are preferentially wetted by either the organic or aqueous phase [5], and systems based upon selective permeability of a porous membrane to the phase which wets the membrane material [2, 4, 11–13]. Based upon separation efficiency, band broadening characteristics, and range of carrier-extractant combinations, membrane separators have proven superior to the other types [14, 15].

In this paper, a liquid-liquid flow segmented system is presented for on-line extraction of diamagnetic metal ions for fluorescence detection. The chelating agent 8-hydroxyquinoline (oxine) dissolved in methylisobutyl ketone (MIBK) was used to extract injected sample for flow injection analysis (FIA) or HPLC detection, and aqueous and organic phases were efficiently separated using a membrane-type phase separator, which directed 100% of the organic phase to the fluorimeter.

The system was developed as a straightforward adaptation of the manual procedure for extracting metals [16]. Two post-column reagents solutions were required, oxine dissolved in organic, and a solution for aqueous pH adjustment. Extractions of this type are characterized by several intermediate processes occurring within either the delay or extraction tubing [17]. In reference to the reagent used in this study, the first step is a distribution of oxine between phases at each aqueous-organic interface. Because the aqueous reagent solution is highly basic, the oxine entering the aqueous phase undergoes acid dissociation to the quinolinolate ion. Once formed, quinolinolate ions may react with metal cations to form hydrophobic species which preferentially distribute into the organic phase.

0009-5893/87 0705-08 $03.00/0 © 1987 Friedr. Vieweg & Sohn Verlagsgesellschaft mbH

The extraction reaction may be summarized by the following general equation which assumes that no side-reactions occur in either the aqueous or organic phase:

$$M^{+n} + n\,HOx_{(o)} \rightleftharpoons M(Ox)_{n\,(o)} + n\,H^+$$

where M^{+n} is the metal ion, HOx is oxine, H^+ is a proton, $M(Ox)_n$ is the complex, and the subscript (o) refers to the organic phase. The equilibrium constant for the extraction reaction is

$$K_{ex} = \frac{[M(Ox)_n]_o[H^+]^n}{[M^{+n}][HOx]_o{}^n} \qquad (1)$$

If no intermediate metal-oxinate complexes are formed, and assuming no other reagents in the aqueous phase react with the metal ions, the ratio $[M(Ox)_{n\,(o)}]/[M^{+n}]$ is equal to the distribution coefficient D. Then

$$D = \frac{K_{DC}K_F(K_a)^n}{(K_{DR})^n}\,\frac{[HOx]_o{}^n}{[H^+]^n} = K_{ex}\,\frac{[HOx]_o{}^n}{[H^+]^n} \qquad (2)$$

where K_{DR} is the distribution constant of the oxine reagent between phases, K_a is the acid dissociation constant for oxine, K_F is the formation constant of a metal oxinate complex, K_{DC} is the distribution constant of the complex between phases, and K_{ex} is the extraction constant.

It follows from this simplified model of an extraction reaction that the amount of metal in the organic versus aqueous phase increases with two experimentally controllable variables; the concentration of reagent in the organic phase, and the pH of the aqueous phase. The on-line reaction has been optimized with respect to pH, oxine concentration, extraction time and flow rates for eleven different metals. The sensitivity and overall performance of extraction has been critically compared to a similar post-column reaction using oxine and fluorescence detection, but not requiring phase separation [18]. And finally, the technique has been applied to the analysis of a soil sample.

Experimental

Apparatus

A schematic diagram of the HPLC instrumentation is shown in Fig. 1. A Waters 501 high pressure pump (Waters Chromatography Division, Millipore Co., Milford, MA) was used for solvent delivery. Samples were injected by means of a liquid sampling valve (Rheodyne Model 7120, Berkeley, CA) containing a 20μl loop volume. A 6.0cm length of 0.25mm i.d. stainless steel tubing (Analabs, North Haven, CT) was used to connect the injector and a C_{18}, 125 × 4.0 mm, 5μm Lichrospher column (EM Science, Cherry Hill, NJ). Teflon tubing (50 × 0.3mm i.d. Supelco, Bellefonte, PA) and gripper fittings (Anspec, Ann Arbor, MI) were used to connect the column to the post-column reaction pump (PCR). All wetted components within the PCR (Hitachi/EM) Science, Cherry Hill, NJ) were made of Teflon or Kel-F. Two pumps of the PCR were used to deliver reagent solutions. Both reagents were initially mixed in a 0.3mm i.d. Kel-F Tee, and allowed to react in a 55cm length of half inch coiled 0.5mm i.d. Teflon tubing before mixing with the column effluent. Metals were extracted within knitted open tubular (KOT) 0.5mm i.d. Teflon tubing of various lengths.

The phase separator was made in-house from a Bioanalytical Systems (BAS, West Lafayette, IN) electrochemical cell and the essential components of gasket (BAS), hydrophobic membrane (0.5μm FH, Millipore), and borosilicate pad (Millipore) are illustrated in Fig. 2. The actual construction of the separator consisted of gasket, membrane, gasket, membrane, gasket, borosilicate pad, and gasket (listed from the segmented flow inlet). The overall dead volume was calculated to be approximately 60μl. In order to achieve 100% separation of the organic and aqueous streams, the pressure across the membrane surface was adjusted using flow regulators (Rainin, Emeryville, CA, #02–0175) placed at the aqueous waste stream and immediately after

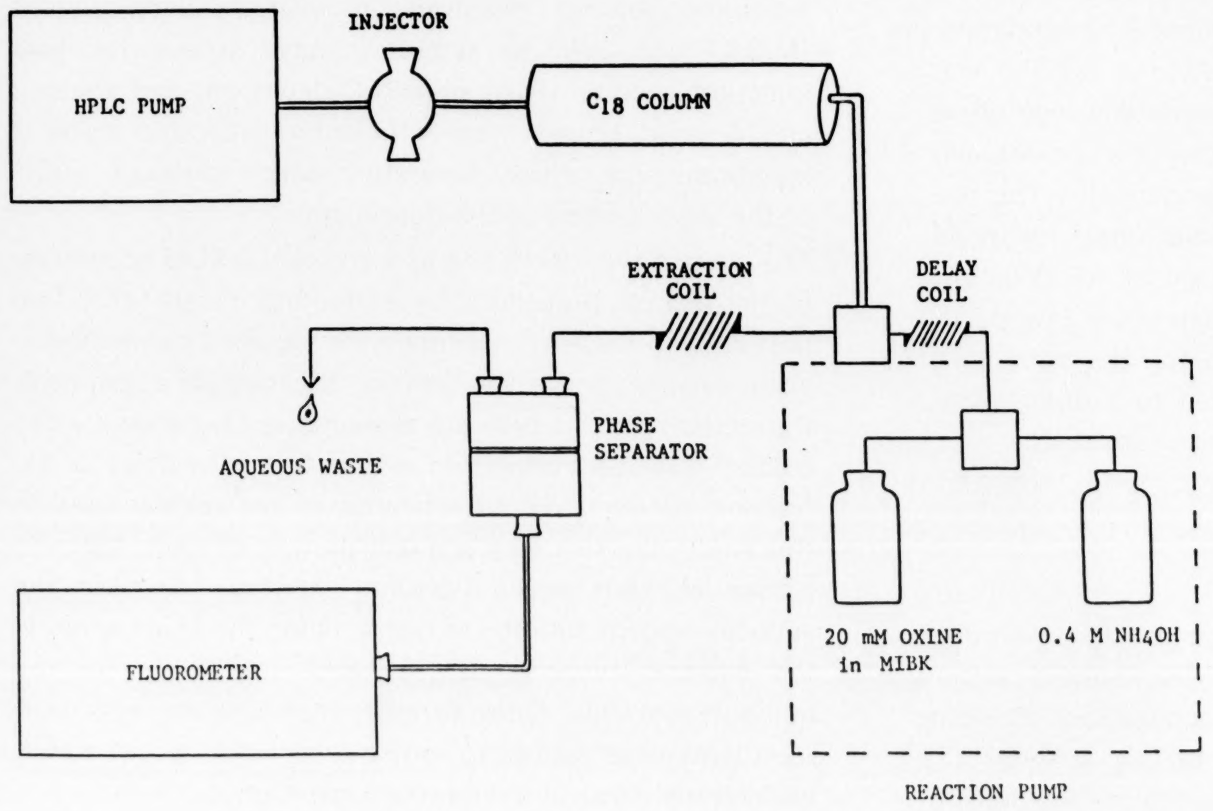

Fig. 1

Schematic of HPLC and liquid-liquid post-column extractor.

the detector. The membranes were initially wetted with the organic solvent at the beginning of experimentation, and approximately 10min were required after flow initiation to adjust the regulators and allow the system to reach a steady state. All plastic tubing connections to the PCR and phase separator were made with gripper fittings.

The chromatographic detector was a Waters 420 filter fluorimeter with a phosphor coated mercury lamp (F4T5/BL) and a 8μl flow cell. The excitation and emission filters were 360nm bandpass and 455nm longpass, respectively. An Omniscribe series D5000 (Houston Instruments, Bellaire, TX) strip chart recorder was used for data collection. Finger tight fittings (Anspec) were used to connect the separator and detector.

Reagents and Chemicals

All chemicals were analytical reagent grade quality or better and used without further purification. The aqueous metal standards used for the optimization studies were either 5 or 50ppm metal stock solutions were prepared from chlorides of magnesium and aluminum (J. T. Baker, Phillipsburg, NJ), scandium (III) and zirconium (IV) from (Aldrich, Milwaukee, WI), calcium (Sigma, St. Louis, MO) and indium (III) from (Alfa, Danvers, MA). Solutions of yttrium (III) (Aldrich), lanthanum (III) (Matheson, Coleman and Bell, Norwood, OH), zinc (J. T. Baker), and gallium (III) (Alfa) were prepared from nitrate salts. The cadmium stock (Mallinckrodt, Paris, KY) was prepared from the acetate salt. Distilled deionized water (Corning Mega-Pure, Corning, NY) was used for all metal standards and mobile phases.

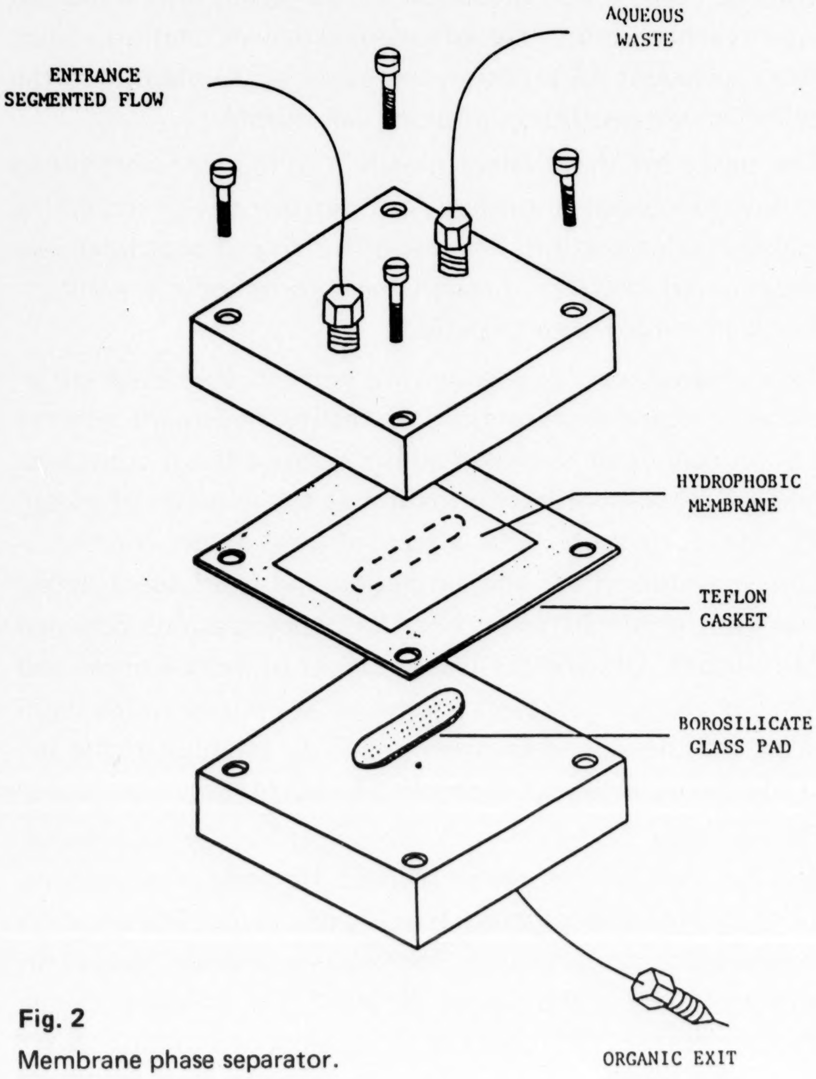

Fig. 2
Membrane phase separator.

The two reagent solutions consisted of 8-hydroxyquinoline (oxine, MCB, Cincinnati, OH) prepared in methylisobutyl ketone (MIBK, EM Science), and an aqueous solution of NH_4OH.

Extraction Optimization

Flow injection analysis (FIA) was used for all reaction optimization studies. Reagent solutions containing 10mM oxine dissolved in the solvents hexane (EM Science), toluene (Burdick and Jackson Muskegon, MI), n-nonane (Burdick and Jackson), chloroform (EM Science), and MIBK (EM Science) were used to study the effect of solvent on extraction. A 100mM stock solution of oxine was prepared in neat ethanol (Florida Distillers) and 5ml aliquots taken to prepare each reagent. The NH_4OH reagent was 0.5M, and a 25cm length of 0.3mm i.d. Teflon tubing was used for the extractor.

Reaction time optimization was examined using two sets of reagent concentrations; 16.7mM oxine and 0.2 M NH_4OH, and 20.0mM oxine and 0.4 M NH_4OH. Ammonium hydroxide concentration was optimized using a 340cm extractor and an oxine solution of 10mM. Oxine concentration was optimized using 0.4 M NH_4OH and a 340cm extractor. The reagent flows were 1.0ml/min oxine and 0.7ml/min NH_4OH, and the mobile phase was used as carrier (0.8ml/min) for all studies.

Peak Dispersion

FIA was used to study the effect of extractor length on band broadening. The extractors tested ranged from 85cm to 510cm, and were 0.5mm i.d. KOT. The reagents were 20mM oxine and 0.4mM NH_4OH, at flows of 0.6ml/min and 0.4ml/min, respectively.

Variances for the total chromatographic-extraction system were determined using the same post-column reagents as in FIA, along with a 340cm KOT extractor.

For detection without extraction, one reagent solution was used and consisted of 5.4mM oxine and 0.2m NH_4OH, prepared in 1:1 water:methanol, and delivered at 0.6ml/min. A chart speed of 25cm/min was used for all variances, and the reported value represents an average of at least three measurements.

Chromatography

The mobile phase contained 2.27mM n-octanesulfonic acid as the sodium salt (Aldrich), 8.18mM tartaric acid (Alfa), 52.9mM 2-hydroxy-2-methylpropanoic acid (2-hydroxyisobutyric acid, HIBA, Aldrich), and 10.7% v/v methanol (EM Science, Omnisolv, Cherry Hill, NJ). The pH was adjusted with ammonium hydroxide (MCB, Gibbstown, NJ) to 4.1 prior to the addition of methanol. A Chemtrix type 40E pH meter (Hillsboro, OR) was used for pH measurements. The mobile phase was filtered with 0.22μm Durapore filters (GVWP, Millipore) and degassed prior to use. The mobile phase was delivered at 0.8ml/min.

The extraction chromatograms were recorded using reagent solutions containing 20mM oxine in MIBK and 0.4M NH_4OH, at flow rates of 0.6 and 0.4ml/min, respectively.

The extractors used were Teflon (KOT) reactors of various lengths, with an internal diameter of 0.5 mm.

Chromatograms for the direct post-column reaction of oxine (no extraction) were recorded using a reagent containing 5.4 mM oxine and 0.2 M NH_4OH, prepared in 1 : 1 water : methanol (Omnisolv, EM Science). The reagent was delivered at 0.6 ml/min, and the reactor was a 30 cm length of 0.3 mm i.d. Teflon tubing.

Soil Sample

Soil samples were carefully weighed and transferred to pyrex crucibles. Ten mLs of concentrated nitric acid was added and the mixture heated for 1 hour. The contents were then filtered into a 100 ml volumetric flask, and diluted to volume. The blank contained no soil extract.

Results and Discussion

Extraction Optimization

Flow injection was used to investigate the effects of organic solvent, extractor length, reagent concentrations and flow rates on the fluorescence derived from on-line extracted metal ions. The extraction capability of oxine prepared in hexane, toluene, n-nonane, chloroform and MIBK was determined for the metals Zr(IV), Ga(III), Sc(III), Y(III), In(III), Al(III), La(III), Zn(II), Cd(II), Ca(II) and Mg(II).

Hexane and nonane were not amenable for solvent extraction of the complexes, as the fluorescence measured was very weak for each metal tested. In addition, peak widths were generally four times wider for the hexane and nonane extractions compared to the other solvents. Table I lists the averaged relative peak height for each metal extracted into MIBK, $CHCl_3$ and toluene.

The coordinating ability of MIBK permitted more efficient cadmium and magnesium extraction than the other oxine-solvent combinations studied. As a result, plus the future intent to use flame atomic absorption (FAAS) and/or inductively coupled plasma (ICP) detection in conjunction with the extractor and separator, further experimentation and optimizations were done using oxine dissolved in MIBK. Zirconium and calcium fluorescence was weak for all oxine-solvent reagent solutions, and neither metals were included in the remaining studies.

Table I. Relative fluorescence intensity of metals extracted using oxine-solvent reagent solutions

Metal	MIBK	$CHCl_3$	Toluene
Al	1.57	1.00	3.14
Ca	1.00	2.16	8.08
Cd	9.85	1.00	0.00
In	1.00	1.06	1.02
Ga	1.03	1.00	1.31
La	4.23	6.40	1.00
Mg	16.00	1.30	1.00
Sc	1.00	1.04	1.77
Y	1.00	1.14	1.59
Zn	3.55	4.07	1.00
Zr	1.66	1.00	0.00

Oxine reagent was 10 mM prepared in each organic solvent, and delivered at 1.0 ml/min. NH_4OH reagent was 0.5 M, and delivered at 0.7 ml/min. The extraction coil was 25 cm of 0.3 mm i.d. Teflon tubing. All instrumentation as in Fig. 1, without the column.

The influence of the extractor length on fluorescence intensity was studied up to 510 cm, using 85 cm length increments. The oxine and NH_4OH reagents were 20.0 mM and 0.4 M, respectively. Peak height maxima were observed for all metals except aluminum, whose response increased with increasing extractor length. Peak widths were found to increase with extractor length for all metals, due to mixing between segments of similar phases in the extractor [19, 20]. The optimal extractor length was chosen to be 340 cm.

The oxinate fluorescence of the divalent metals (Cd, Mg, Zn) was greatest using either an 85 or 170 cm length extractor, and decreased dramatically with further increase in extractor length. This behavior is explained by the formation of coordinatively unsaturated oxinates, and characteristic of metals cations with +n charge and coordination number greater than 2n whose free coordination sites have been filled by water molecules [21]. Although this type of chelate is fairly insoluble in water, continued extraction elimits transfer back to the aqueous phase.

The effect of oxine concentration was studied by measuring the peak heights for extracted metals using reagent concentrations of 1, 5, 10, 20 and 30 mM. At 1.0 mM, zero response was recorded for the metals Y, Mg, Al, and La. Using 5.0 mM oxine, the fluorescence had developed to 76%, 5%, 5%, and 11%, respectively, of the maximum observed for each metal. As expected, fluorescence increased with increasing reagent concentration for all metals until a plateau was reached, indicative of quantitative extraction. Since the coefficient of variation increased at 30 mM oxine, the optimum concentration of oxine was 20 mM.

The peaks for the divalent metals (Cd, Mg, Zn) were broad at low oxine concentrations, but narrowed with increasing reagent concentration. The low diffusivity of coordinatively unsaturated chelates through the hydrophobic membrane was believed to cause this effect.

As indicated, eq. (2) was derived without consideration of metal or ligand side-reactions. In reality, hydroxide concentration cannot be increased ad infinitum without consideration of metal-hydroxo formation at the expense of metal-oxinate formation. The effect of hydroxide concentration was studied for the extraction and fluorescent detection of the metals using NH_4OH concentrations between 0.05–0.6 M. Off-line pH measurement of mobile phase and NH_4OH reagent mixtures, prepared at volume ratios equivalent to the flow rates used in HPLC, established the pH of the mixtures to lie between 9.17–10.74.

Fluorescence increased with increasing NH_4OH concentration for most of the metals studied. However, the response for aluminum and cadmium steadily decreased. The trivalent metals share similar values for their hydroxide formation constants, while the values between the divalent metals are also similar [22]. Likewise, an analogous situation exists for the formation constants of oxine [23]. The hydroxides of aluminium and cadmium, appear to be less labile than the other metals examined. As a result, the response for Al and Cd might be expected to increase with increasing extractor length at high oxine:NH_4OH ratios. This was not observed using 20 mM oxine and 0.4 M NH_4OH reagents, but became apparent upon lowering NH_4OH concentration to 0.2 M. Despite the incomplete extraction of Al and Cd at these conditions, the best NH_4OH concentration was determined to be 0.4 M NH_4OH.

Reagent flow rate was optimized by measuring the fluorescence for extracted Ga, Zn, Sc, Y and Mg at total reagent flows between 0.5–2.0 ml/min. Solvent delivery from the PCR was controlled by a single mechanism, making it impossible to set individual reagent flow rates. Due to physicochemical differences between MIBK and water, the oxine reagent was pumped approximately 1.4 times faster than the NH_4OH solution. The response for each metal initially increased with reagent flow rate, passed through a maximum, then decreased as the flow rate was further increased. The optimum for most metals was realized at a total flow of 1.0 ml/min, 0.6 ml/min of which was organic and 0.4 ml/min aqueous.

Analytical figures of merit were determined for post-column extraction with fluorescence detection of metals using the optimized reaction conditions (Table II). The range of metal concentrations used for linear regression calculations are indicated, and span the entire operational range of the fluorimeter. Detection limits were determined by injecting progressively more dilute metal standards until a signal three times the background noise was measured. The y-intercepts may be indicative of a slightly higher extraction efficiency at higher metal concentrations, although none of the intercepts differed significantly from zero at the 95% level of confidence.

Peak Dispersion

The entire contribution of the FIA apparatus to peak variance was calculated for different length KOT extractors.

The Foley and Dorsey method was used because of its sensitivity to asymmetric peak shapes [24]. In addition to system variance, asymmetry factors (B/A) and peak widths at 10% peak height ($W_{.1}$), are also presented in Table III. Variances calculated by this method are accurate for $1.0 \leqslant B/A \leqslant 2.76$, and those variances falling outside this range have been excluded from Table III.

In general, peak width and variance increased with extractor length. The values of B and A also increase with extractor length, but B/A decreased, indicating an increase in the peak centroid. Increased broadness and centroid with extractor length is illustrative of mixing between segments of similar phase inside the extraction tubing, and is due to a thin sheath of organic solvent wetting the interior wall of the Teflon extractor. In this regard, the use of extractors made of glass may be superior to the Teflon used in this study. The glass coils available in our laboratory were approximately 0.3 mm i.d., but would not elicit 100% separation of phases. Pressures across the membrane were adjust-

Table II. Figures of merit for extraction and fluorescence detection of metals

Metal	Concentration Range (ppm)	Slope	Intercept	Correlation Coefficient	Detection Limit (ppb)
Y(III)	2.0–.009	829.2	−27.7	0.9989	6
Al(III)	3.0–.009	816.4	−48.4	0.9986	3
Sc(III)	3.0–.019	328.4	−25.6	0.9974	18
In(III)	22.7–.138	154.6	−81.4	0.9989	30
Mg(II)	6.4–.020	149.1	−10.4	0.9991	10
Zn(II)	25.0–.138	70.2	− 3.0	0.9999	40
Cd(II)	50.0–.110	56.1	− 6.9	0.9999	50
Ga(III)	10.0–.384	50.9	−22.4	0.9981	90
La(III)	50.0–.096	26.8	+39.7	0.9978	40

Reagent solutions were 20 mM oxine in MIBK and 0.4 M NH_4OH, delivered at 0.6 and 0.4 ml/min, respectively. The extractor was a 340 cm length of KOT Teflon, 0.5 mm i.d.

Table III. Effect of extractor length on metal ion peak shape

Metal	Extractor Length (cm)	$W_{.1}$ (cm)	B/A	Variance (sec^2)
Ga	85	7.01	2.85	–
	170	8.25	1.93	29.8
	340	8.77	1.62	30.4
	510	10.89	1.58	46.1
Sc	85	6.92	2.93	–
	170	7.38	2.30	26.8
	340	9.32	1.77	36.3
	510	9.43	1.64	35.4
Y	85	7.02	3.02	–
	170	7.85	1.81	26.1
	340	9.35	1.64	34.8
	510	9.09	1.69	33.6
Al	85	7.73	3.17	–
	170	6.90	1.96	21.2
	340	9.61	1.67	37.3
	510	10.36	1.35	38.2
In	85	7.17	2.88	–
	170	7.77	2.31	29.8
	340	7.14	1.97	22.7
	510	10.31	2.05	48.7
Zn	85	8.57	2.96	–
	170	8.42	3.38	–
	340	11.01	2.56	63.2
	510	11.74	2.36	69.8
La	85	10.24	4.22	–
	170	9.87	2.58	51.1
	340	10.92	1.88	52.2
	510	15.41	2.02	108.2
Cd	85	5.65	2.39	16.0
	170	7.28	2.28	25.8
	340	8.48	2.17	34.4
	510	10.02	2.06	46.2
Mg	85	19.48	6.16	–
	170	13.17	5.34	–
	340	12.79	4.18	–
	510	15.21	5.75	–

The extractors were 0.5 mm i.d. KOT Teflon, the reagents 20 mM oxine and 0.4 m NH_4OH at flow rates of 0.6 and 0.4 ml/min, respectively. A mobile phase carrier was used at 0.8 ml/min.

ed using the flow regulators, but in spite of countless attempts, the separation efficiency could not be improved for any of the glass coils. Teflon tubing of 0.3mm i.d. was also tested, and found to be equally uneffective at separating the phases.

The total peak variance for the optimized flow injection extraction system was compared to a flow injection approach utilizing a direct post-column reaction of oxine (Table IV). An oxine reagent solution prepared in an alcohol:water solvent mixture was used in the direct reaction, and the entire flow of carrier plus reagent was directed to the fluorimeter without need of phase separation. Peak variances for extracted metals were between three and nine times larger than variances measured for the direct reaction. Because the lanthanum peak was severely tailed, its variance for the direct reaction was calculated using peak width at half height. Its actual variance was much greater than reported in Table IV.

It might be expected that the direct reaction variances be similar for all metals, however, this was not observed. In addition to the injector, mixing tee, connection tubing, and detector, several other variables that factor into the calculated variances are mixing noise of the PCR, and kinetics of formation of metal complexes with the mobile phase components and/or oxine, and the adsorption effects of these species onto surfaces, i.e., the KOT Teflon reactor. Mixing noise was most troublesome at high detector gain as exemplified by the metals Sc, Y, and Zn which were recorded at a higher sensitivity than the other metals. Adsorption of metal-ligand species onto the Teflon reactor was manifested by tailed peaks and large asymmetry factors. The adsorption phenomenon is not a critical aspect for direct detection of metals because of the short reactor lengths used, however, improvements in peak shape might be realized using a glass reactor.

Peak variances were also determined for metals separated using both direct and extraction detection (Table IV). The largest variances were recorded for cadmium and magnesium, due to broad peak shape and lower diffusivity of the coordinatively unsaturated chelates through the hydrophobic membrane of the phase separator. A direct result of a separation based upon secondary chemical equilibria is the fact that neither peak width nor variance increased predictably with increased retention.

Table IV. Total FIA and HPLC system variances for direct and extraction detection using oxine

Metal	Retention time (min)	FIA variance (sec^2) Direct	FIA variance (sec^2) Extr.	HPLC variance (sec^2) Direct	HPLC variance (sec^2) Extr.
Zr	0.97	8.7	NE	18.9	NE
Ga	1.68	9.6	30.4	167.4	128.7
Sc	2.13	12.9	36.4	36.5	45.1
Y	2.60	10.9	34.8	12.5	47.0
Al	3.23	7.2	37.3	82.1	165.0
In	3.25	8.6	22.7	61.4	89.2
Zn	4.32	10.7	63.3	20.2	63.3
La	6.88	3.9	52.8	29.7	243.8
Cd	10.22	8.3	34.4	114.8	379.3
Ca	12.33	5.0	NE	366.2	NE
Mg	14.87	8.2	77.1	178.5	1951.8

Extraction conditions were 340cm KOT, 20mM oxine in MIBK at 0.6ml/min, and 0.4 M NH_4OH delivered at 0.4ml/min. A 30cm length of 0.3mm i.d. Teflon tubing was used for the direct reaction. The reagent was 5.4mM oxine dissolved in 1:1 water:methanol and 0.2 M NH_4OH, delivered at 0.6ml/min. NE = not extractable.

The column variance was calculated for both direct and extraction detection by subtracting the FIA variances from the HPLC results. The column variances obtained from the extraction and direct reactions, however, were not within experimental error of each other, and suggest an interdependence of peak dispersion with the rate of formation and the nature of each complex formed. That is, using FIA, metals do not have sufficient contact time (seconds) with mobile phase components to permit a close approach to equilibrium. This results in the formation of species unlike those formed in HPLC, where metals reside within the mobile phase in excess of minutes. As a consequence, the adsorption effects in the FIA and HPLC post-column reaction tubing are significantly different.

Chromatography

Fig. 3a–c are chromatograms of a ten metal mixture (indium not included because it co-eluted with aluminum) and illustrate the overall performance of the direct and extraction detection systems. Fig. 3a was recorded using the direct post-column reaction and a 30cm reactor, while Figs. 3b and 3c have been extracted using 3cm and 340cm length KOT extractors, respectively. Metal concentrations were different for the direct and extracted chromatograms, and are indicated in the figure caption. Calcium and zirconium were not included in the extracted sample because of their low fluorescent intensities following extraction.

Figs. 3b and 3c illustrate the dependence of fluorescence on extractor length. For most metals, fluorescence increased with extractor length. The signal for magnesium, on the other hand, decreased with increased extractor length as a consequence of coordinated water and its effect on chelate solubility.

A soil sample was collected from a Boston construction site and analyzed using extraction detection (Fig. 4). The soil was found to contain 7.8mg/g Al and 3.1mg/g Mg.

Conclusions

On-line extraction with fluorescence detection has been shown to be a viable detection approach for the metals Ga(III), Sc(III), Y(III), Al(III), In(III), La(III), Zn(II), Cd(II), and Mg(II). The calibration curves for all metals were linear across the range of detector sensitivities, and detection limits have been improved by at least a factor of ten for all metals compared to a direct reaction approach. The improvement in detection limits result from lower system noise (mixing noise) and enhanced fluorescence from an organic media. Peak dispersion is larger for extraction detection than direct reaction detection, and has been attributed to mixing between solvent segments of similar phase in the extractor.

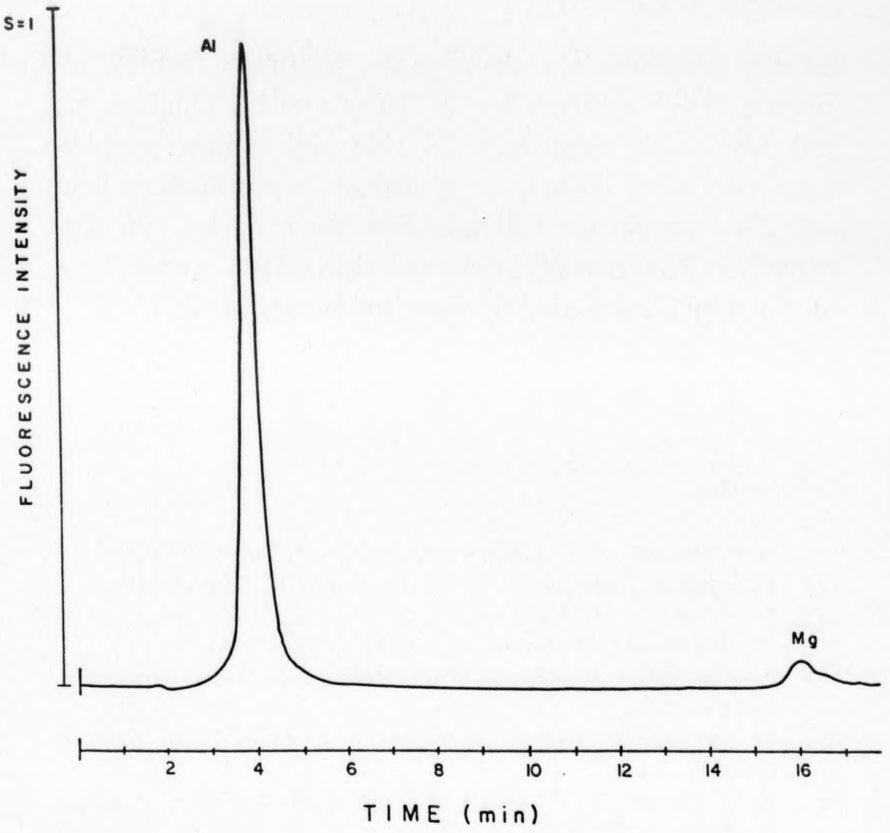

Fig. 4

Analysis of soil sample. Reaction conditions same as Fig. 3c.

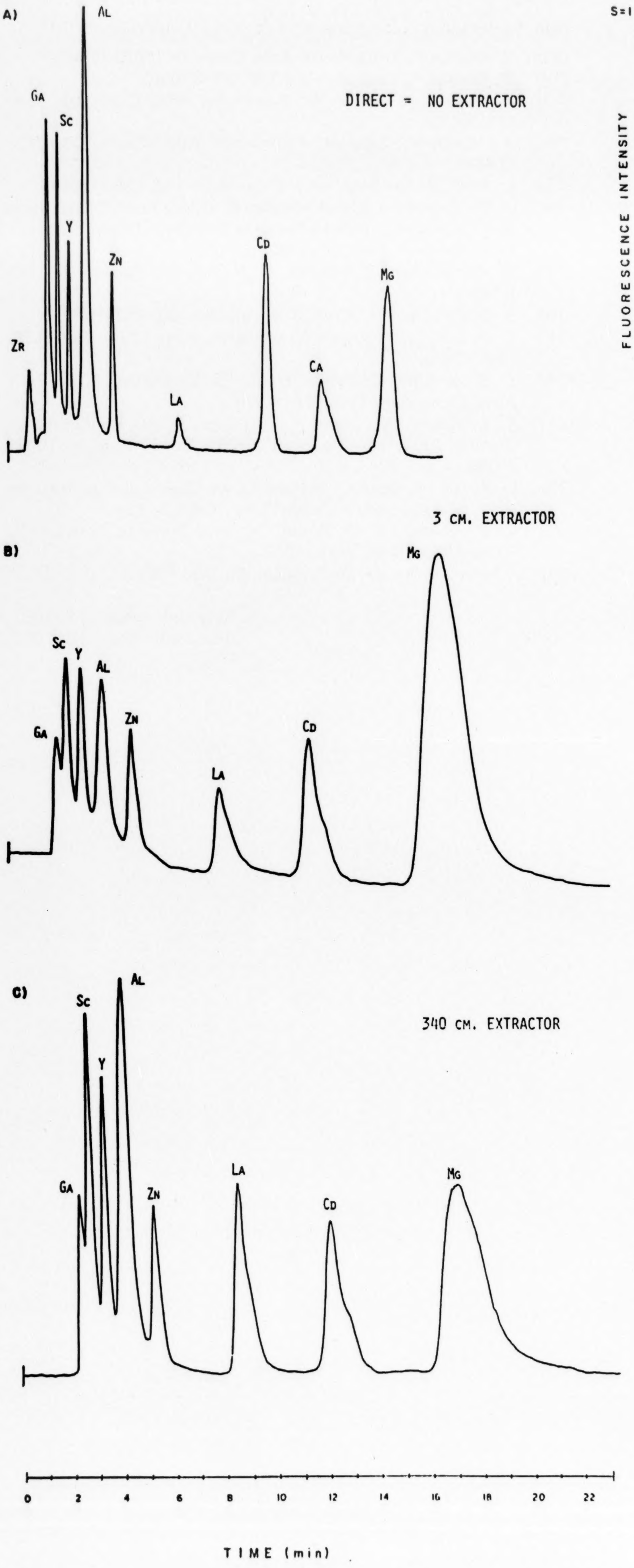

Fig. 3

Direct and extraction fluorescence detection of separated metals. Fig. (3a) the reagent was 5.44mM oxine in 1:1 water:methanol and 0.2M NH_4OH, flow rate 0.6ml/min, the reactor was 30cm length of 0.3mm i.d. Teflon tubing. The sample contained 11.6ppm Zr, 4.2ppm Ga, 5.0ppm Sc, 2.5ppm Y, 2.5ppm Al, 6.0ppm Zn, 3.5 ppm La, 16.0ppm Cd, 40.6ppm Ca, and 2.5ppm Mg. Sensitivity = 8. Fig. (3b–c) recorded using two reagent solutions; 20mM oxine in MIBK, and aqueous 0.4M NH_4OH, flow rates 0.6 and 0.4ml/min, resp. Metal sample contained 4.2ppm Ga, 1.5ppm Sc, 0.5ppm Y, 2.0ppm Al, 4.8ppm Zn, 9.0ppm La, 13.8ppm Cd, and 14.5ppm Mg. Sensitivity = 4. A 3cm extractor was used to record Fig. 3b and a 340cm length for Fig. 3c.

Acknowledgements

We very gratefully acknowledge the continued interest and support of G. Desotelle and M. Gurkin at EM Science, Inc. This work was supported, in part, by grants, graduate student support, chemical and instrumental donations from both Thermo/Jarrell Ash and EM Science, Inc. We also thank Ron Shoup at BAS for the halves of the electrochemical cell which were used to make the separator.

References

[1] *J. A. Sweilsh, F. F. Cantwell*, Anal. Chem. **57**, 420 (1985).
[2] *L. Nord, B. Karlberg*, Anal. Chim. Acta **125**, 199 (1981).
[3] *F. A. Maris, M. Nijenhuis, R. W. Frei, G. J. De Jong, U. A. Th. Brinkman*, Chromatographia **22**, 235 (1986).
[4] *E. Fogelqvist, M. Krysell, L.-G. Danielsson*, Anal. Chem. **58**, 1516 (1986).
[5] *M. Gallego, M. Silva, M. Valcarcel*, F. Z. Anal. Chem. **323**, 50 (1986).
[6] *B. L. Karger, D. P. Kirby, P. Vouros, R. L. Foltz, B. Hidy*, Anal. Chem. **51**, *2324 (1979).*
[7] *J. A. Apffel, U. A. Th. Brinkman, R. W. Frei*, Chromatographia **18**, 5 (1984).
[8] *K. Tsuji*, J. Chrom. **158**, 337 (1978).
[9] *H. Bergamin, J. X. Medeiros, B. F. Reis, E. A. G. Zagatto*, Anal. Chim. Acta **101**, 9 (1978).
[10] *M. J. Whitaker*, Anal. Chim. Acta **179**, 459 (1986).
[11] *L. Fossey, F. F. Cantwell*, Anal. Chem. **54**, 1693 (1982).
[12] *M. Maeda, A. Tsuji*, Analyst **110**, 665 (1985).
[13] *J. Kawase, A. Nakae, M. Yamanaka*, Anal. Chem. **51**, 1640 (1979).
[14] *K. Ogata, K. Taguchi, T. Imanari*, Anal. Chem. **54**, 2127 (1982).
[15] *L. Nord, B. Karlberg*, Anal. Chim. Acta **118**, 285 (1980).
[16] *J. Minczewski, J. Chwastowska, R. Dybczynski*, "Separation and Preconcentration Methods in Inorganic Trace Analysis", Ellis Horwood, England, 1982; p. 106.
[17] *O. Klinghoffer, J. Ruzicka, E. H. Hansen*, Talanta **27**, 169 (1980).
[18] *B. D. Karcher, I. S. Krull*, J. Chrom. Sci. **25**, 472, 1987.
[19] *T. Imasaka, T. Harada, N. Ishibashi*, Anal. Chim. Acta **129**, 195 (1981).
[20] *C. E. Werkhoven-Goewie, U. A. Th. Brinkman, R. W. Frei*, Anal. Chim. Acta **114**, 147 (1980).
[21] *K. L. Chang, K. Ueno, T. Imamura*, "CRC Handbook of Organic Analytical Reagents", CRC Press, Florida, 1982; p. 255.
[22] *S. Kotrly, L. Sucha*, "Handbook of Chemical Equilibria in Analytical Chemistry", John Wiley, 1985; p. 124.
[23] *A. E. Martell, R. M. Smith*, "Critical Stability Constants", Plenum Press, New York, 1976.
[24] *J. Foley, J. Dorsey*, Anal. Chem. **55**, 730 (1983).

Received: Aug. 24, 1987
Accepted: Sept. 18, 1987
F

Use of Unmodified Silica with Buffered Aqueous Mobile Phase Mixtures for Selective Chromatography of Basic Drugs

R. W. Schmid* / Ch. Wolf

Laboratory of Psychoactive Drug Analysis, Psychiatric University Hospital of Vienna, Währinger Gürtel 18–20,
A-1090 Wien, Austria

Key Words

Liquid chromatography
Unmodified silica
Buffered aqueous mobile phase mixtures
Basic drugs

Summary

The characteristic selectivity of unmodified silica using mixed aqueous-methanolic mobile phase systems for the separation of basic drugs was studied. It was found that low buffer concentration-high methanol eluents show increased chromatographic performance over mobile phase systems lower in methanol and higher in ion strength. Regarding an assumed ion-exchanger retention mechanism, the capacity factors of an amino group containing drugs is primarily dependent on the concentration of the cation and the pH-value of the eluent. By increasing the pH-value of the eluent, elution order of primary and secondary to tertiary amines is reversed. By only using eluents with buffering capability, a very high stability and reproducibility of retention of the basic drugs could be observed. Comparing three different brands of unmodified silica materials, with different pore size and specific surface area, only small differences in the selectivity for the tested drugs could be found.

Introduction

Although reversed-phase chromatography has developed in the recent past in to an universal separation system for trace analysis of basic drugs in biological fluids, the selectivity of reversed-phase separations is insufficient for many problems. Severe peak tailing and poor column efficiencies are commonly encountered problems, and a range of different counter-measures have been reported to keep such problems at a minimum. This chromatographic behavior shows that basic compounds are retained on modified silica by more than just lipophilic retention mechanisms. It has been attributed to polar interactions of the amino-functionality in the solute to "active sites", notable to unreacted silanols groups on the modified silica surface [1, 2].

Systematic investigation of this polar retention for use in chromatography was first undertaken by Jane et al. [3], who chose unmodified silica with an aqueous methanol eluent for the analysis of basic drugs of abuse, and who pointed to the potential of such a separation system for the analysis of aminogroup containing drugs. Although retention mechanisms of such polar separations on unmodified silica with aqueous eluents have not yet been fully explained and seem to be multifunctional, they have been described by ion-exchange interactions with silanol groups on the silica surface [4–6].

Since then, different separation systems describing the chromatography of organic amines on unmodified silica with aqueous-organic eluents have been published [4, 6–10].

Only limited general information is available from the literature about systematic studies on how the selectivity of the separation of basic amino-group containing compounds on unmodified silica is influenced by mobile phase composition. In a recent publication [12], structure retention relationships for the separation of basic organic compounds on silica was studied, but only for constant chromatographic conditions.

The aim of the study in this paper was to determine how to control retention of different substituted amino-group containing drugs on unmodified silica by variing different chromatographic conditions. To further a study by Sudgen et al. [6], the influence of buffer ions, ion strength, pH-value and temperature on the retention of a group of test drugs was determined for eluents systems with low ion-strength and high methanolic content. The final results should provide additional information toward a better understanding of retention mechanisms of basic drugs on unmodified silica and about its practical application in the analysis of basic drugs in biological samples.

0009-5893/87 0713-07 $ 03.00/0

© 1987 Friedr. Vieweg & Sohn Verlagsgesellschaft mbH

Experimental

The chromatographic equipment used in this study consisted of a Gilson Mod. 302 HPLC pump, a Hitachi 655A UV-detector, a Gynkotek NZ 190 injection valve equipped with a 10μl sample loop and a LDC CI 10 integrator. Temperature of the columns was controlled by a thermostated water-bath.

Silica materials and mobile phase systems: The main part of the separations were done on a 11 cm × 4.6 mm i.d. cartridge packed with spherical silica Partisphere Si (5μm particle size, 120A pore size and 160 m^2/g average surface area) (Whatman Inc., NJ, USA). In some experiments a 12.5 cm × 4 mm i.d. cartridge, packed with spherical silica Supersphere Si (4μm particle size, 60A pore size and 650 m^2/g average surface area) (Merck, Darmstadt, FRG) and a 12.5 cm × 4 mm i.d. column, packed with spherical silica Nucleosil Si (5μm particle size, 100A pore size and 350 m^2/g average surface area) (Macherey & Nagel, Düren, FRG) were used.

Because commercially obtained silica columns are commonly supplied in hexane for use in normal phase chromatography, they have to be conditioned for aqueous eluents by a subsequent washing cycle with chloroform, methanol and the mixed buffer/methanol eluent.

If not specifically noted, chromatographic runs were performed at a temperature of 25°C. Buffer salts, acids and bases were obtained from different suppliers at the highest quality commercially available.

Methanol and water were HPLC-grade, obtained from Rathburn Chemicals (Scotland, UK). Mobile phase mixtures were prepared by adding a concentrated aqueous buffer solution to an appropriate amount of water and organic modifier. The pH-adjustment of buffers was done in the aqueous part of the mobile phase prior to mixing. Drugs for test samples were gifts from different pharmaceutical manufacturers. Stock solutions of the drugs were obtained by dissolving them in methanol. Individual drug test mixtures were prepared from these stock solutions and diluted with mobile phase. Generally 10μl of the test mixtures were injected onto the chromatographic system. The drugs were detected at 254 nm.

For analysis of blood samples, sample preparation was done using a 20 × 2.5 mm precolumn, which was mounted on the injector in place of the injection loop and packed with Sepralyte C-2 40μm (Analytichem Intl., Harbor City, CA, USA). After prewashing with 1 ml methanol and 1 ml water, 1 ml of plasma was applied onto the precolumn. After washing with 1 ml water and 10% methanolic solution, the precolumn was switched into the HPLC-stream.

Results and Discussion

Selection of Test Substances

Homologue polycyclic basic drugs with different degrees of substitution at the amino function were chosen as test substances: desmethylnortriptyline (DM-NOR) as the primary amine, nortriptyline (NOR) as the secondary amine and amitrityline (AMI), 3-chlor-amitriptyline (Cl-AMI) and imipramine (IMI) as tertiary amines (Fig. 1). The reason for selecting these specific types of tricyclic drugs was that one amino functionality in the solutes is located on an aliphatic side chain and not in the ring system, so that a possible steric influence on the amine-silica interaction is reduced.

Experiments were started by comparing a mobile phase system low in ion-strength and high in methanol content (3 mM Na-acetate pH 7.9, 80% methanol) with an eluent higher in salt concentration and lower in methanol (15 mM Na-acetate buffer pH 7.9, 50% methanol). While both mobile phase systems show comparable capacity factors for the test compounds, dramatic differences in their chromatographic results can be seen: broad and tailing peaks

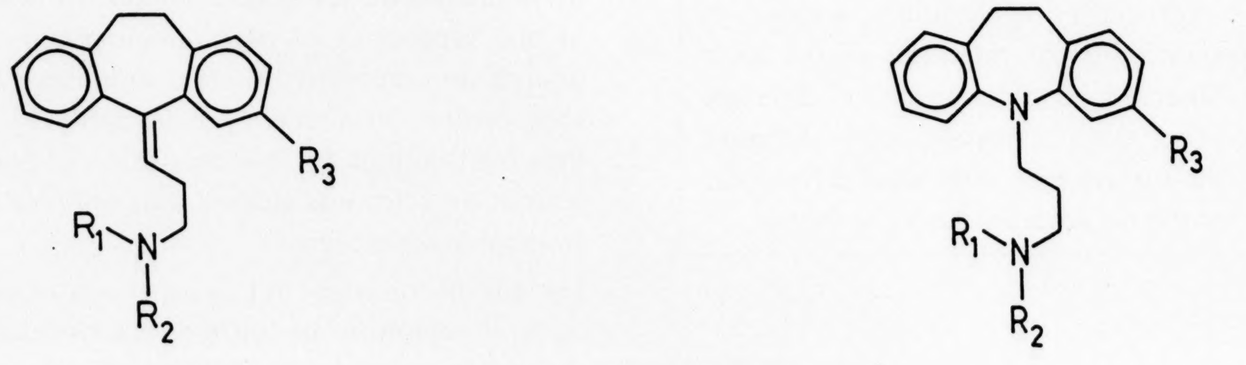

	R_1	R_2	R_3
AMITRIPTYLINE (AMI)	CH_3	CH_3	H
NORTRIPTYLINE (NOR)	CH_3	H	H
DESMETHYLNORTRIPTYLINE (DMNOR)	H	H	H
3-CHLOR AMITRIPTYLINE (CL-AMI)	CH_3	CH_3	CL

	R_1	R_2
IMIPRAMINE (IMI)	CH_3	CH_3
DESMETHYLIMIPRAMINE (DIMI)	CH_3	H
CLOMIPRAMINE (CL)	CH_3	CH_3
DESMETHYLCLOMIPRAMINE (DCL)	CH_3	H

Fig. 1

Structures of test drugs used in the experiments.

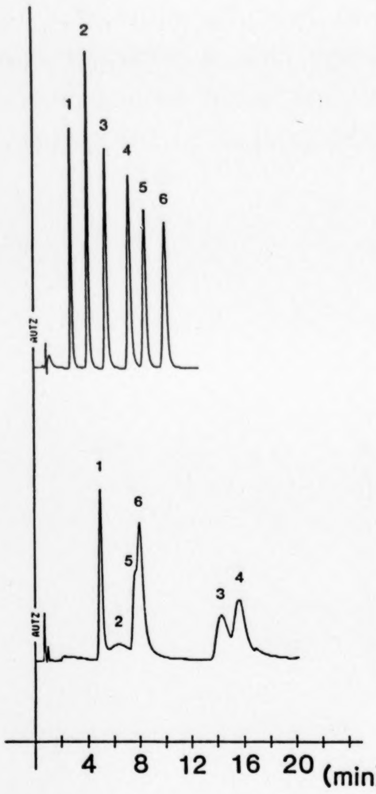

Fig. 2

Separation of basic drugs on 11 cm × 4.6 mm Partisphere Si. Chromatographic conditions:

Upper chromatogram: 80% MeOH, 3 mM Na-acetate buffer pH = 7.9.

Lower chromatogram: 50% MeOH, 15 mM Na-acetate buffer pH = 7.9.

Flow: 1.4 ml/min.

1 = fluvoxamine, **2** = tamoxifen, **3** = clomipramine, **4** imipramine, **5** = desmethyl-clomipramine, **6** desmethyl-imipramine.

Table I. Difference in column performance for methanol-lean and methanol-rich eluents.

Eluent Composition	Plate Numbers (plates/m)					
	FLU	TAM	DMCI	DIMI	CI	IMI
50% MeOH/ 15 mM Na-acetate	28050	534	10330	10400	9360	13400
80% MeOH/ 3 mM Na-acetate	33380	40815	44470	51380	58520	64321

found in the methanol-lean eluent indicate that besides polar amine-silanol interactions, other mechanisms, such as hydrophobic interactions with the silica surface [13] or solubility effects, might additionally influence the retention of basic drugs (Fig. 2). In contrast, in the mobile phase mixture low in ion-strength and high in organic modifier content, chromatograms with excellent peak symmetry and column efficiency were obtained and maximal plate number could be calculated (Table I). Because of these practical aspects, in all further experiments only mobile phase systems low in ionic concentration and high in organic modifier were examined.

Influence of Ion-Strength on the Retention of Basic Drugs on Silica

When ion-exchange is assumed as the main type of retention mechanism for the amino drugs on unmodified silica, k′-values should be strongly dependent on the concentration of cations in the eluent, due to a competitive displacement from the ion-exchange sites [14]. In order to reduce a possible specific influence of certain kinds of anions on the displacement equilibrium, the dependence was studied with NH_4OH as ionic species in the aqueous methanol eluent, thus leaving only hydroxy-ions as the weak ion-pair forming anion in the solution.

An increase in the concentration of ammonia in the mobile phase led to an exponential decrease in the retention of the basic drugs (Fig. 3), a result that is in accordance with ion-exchange theory [4–6]. While with eluents very low in ion-strength, high k′-values can be achieved, such mobile phase systems are limited in their practical application because chromatographic separations using eluents with very low salt concentrations will easily be destablized by even the smallest amount of salt introduced by injection of samples. Therefore, in all further experiments, the eluent buffer was fixed at a concentration of 3 mM, which can be regarded as a compromise between available buffering capability and sufficient resolution in the separation of the test drugs. Nevertheless, this buffer concentration is generally lower than that reported for silica separations systems in the literature.

Importance of Buffered Eluents for Chromatography on Unmodified Silica with Aqueous Eluents

A defined and stable ionic environment on the silica surface must be considered as a precondition for reproducible separations on the basis of ion-exchange retention. Thus, before chromatographic separations are started on un-

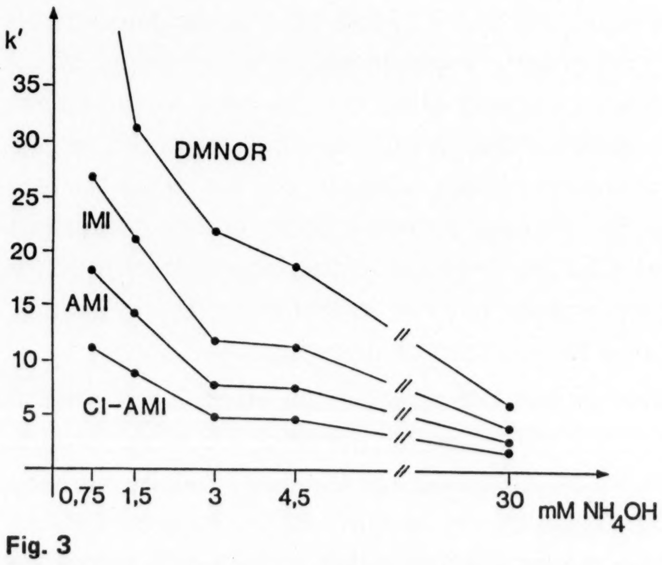

Fig. 3

Dependence of k′-values of the tricyclic drugs on cation concentration.

NH_4OH in 80% methanol, 1.4 ml/min.

Column: 11 cm × 4.6 mm Partishere Si.

modified silica with aqueous eluents, conditioning of the silica is of extreme importance until ionic concentration and pH-value on the silica surface are in equilibrium with the mobile phase. A defined and equilibrated silica surface will only be obtained when eluents with buffering capacity are used, a fact that is of special importance for eluents with low ionic strength, as in this study.

According to the results of this study, by using buffering eluents, retention times and selectivity of separations will be stable and highly reproducible. Due to the high percentage of organic modifier in the used mobile phase systems, the choice of the type of buffer salts in the eluent is limited by their solubility: e.g. phosphate salts, exhibiting a broad buffering range, have to be avoided because of their insolubility even at low concentration ranges in eluent systems high in methanol.

Influence of pH-Value on the Retention of Basic Drugs

In cation-exchange chromatography on organic resins, retention of solutes is strongly controlled by the pH-value of the eluent [14]. A similar dependence must be expected in the chromatography of basic drugs on unmodified silica. When retention of the test drugs on unmodified silica is compared for two mobile phase systems similar in ion-strength but one of low pH-value (Na-acetate/acetic acid 4 mM, pH = 4.73, measured in the aqueous part, 80% methanol) and one of high pH-value (NH_4NO_3/NH_4OH 0.5 mM/2.5 mM, pH = 10.0, measured in the aqueous part, 80% methanol), a general increase of k′-values for all drugs is observed (Fig. 4). Interestingly, the increase in the retention of primary and secondary amino drugs is higher than for the tertiary amines. To gain more complete information about this interesting chromatographic behavior, a detailed study in the pH-dependence became necessary. Careful considerations about the eluent mixtures for such an experiment revealed that an independent variation of the pH-value in the eluent, keeping the type and concentration of the cation constant and still obtaining a buffering system, is only possible when the type of anion in the buffer is varied.

Observing these limitations, a set of different eluent buffers was selected for the study of pH-dependence, covering the pH-range between pH 6–12 (Table II). As was demonstrated in the preliminary experiments, the retention of all tricyclic amines increased when the pH-value in the eluent changed to basic values, which can be attributed to the increasing charging of the silanols on the silica surface [4, 5] (Fig. 5). Moving to more basic eluent conditions will result in a further increase in the retention of primary and secondary amines but not in tertiary tricyclic amines, where retention factors start to decrease.

For pH-values in the eluent above a pH of 10, a general decrease of the k′-values of all the tricyclic drugs occurs. These data can be explained by the fact that by shifting from acidic to basic eluent conditions, the increased charging of silanol groups on the silica surface will lead to a general increase of the k′-values of the amino-drugs. In the pH-range between pH 8.5 and 10, differences in the degree of dissociation in the amino-functionalities of the differently substituted amines, according to their pK_a-values, start to play the major role for retention. This is reflected in a reversal of the elution order of the more basic primary (DM-NOR) and secondary (NOR) amines to the tertiary

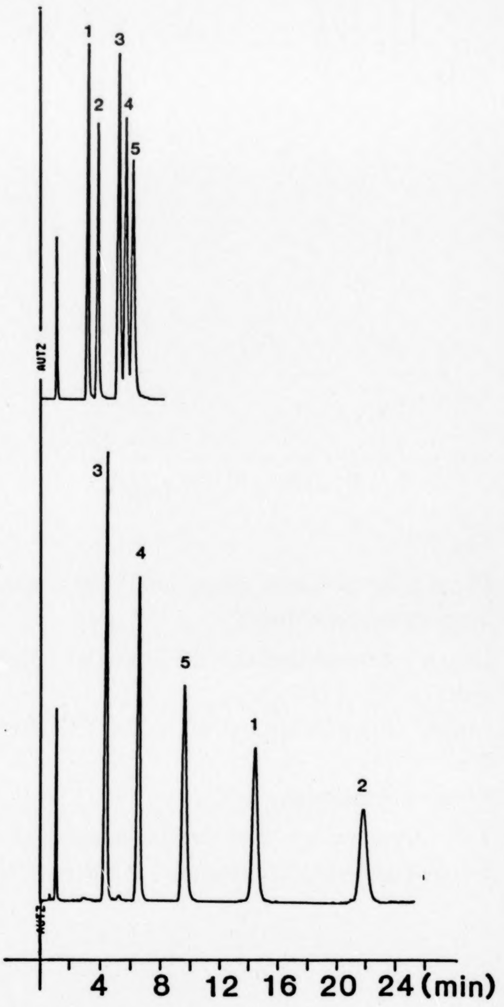

Fig. 4

Influence of pH-values of the eluent on retention of tricyclic drugs.

Chromatographic conditions:

Upper chromatogram: 80% MeOH, 2 mM Na-acetate/2 mM acetic acid, pH = 4.6.

Lower chromatogram: 80% MeOH, 0.5 mM NH_4NO_3/2.5 mM NH_4OH, pH = 10.0.

Column: 11 cm X 4.6 mm Partispere Si, flow: 1.4 ml/min.

1 = DM-NOR, **2** = NOR, **3** Cl-AMI, **4** = AMI, **5** = IMI.

Table II. Buffer eluent composition used in the study of pH-dependence of k′-values.

Cation	Conc.	Anion	Conc.	pH-Values of the Aqueous Solution	% MeOH
NH_4	3 mM	Cl	2.9 mM	6.4*	80%
NH_4	3 mM	Cl	2.5 mM	7.2*	80%
NH_4	3 mM	Cl	2.3 mM	8.2*	80%
NH_4	3 mM	Cl	1.5 mM	8.8	80%
NH_4	3 mM	NO_3	1.5 mM	9.2	80%
NH_4	3 mM	NO_3	0.5 mM	10.0	80%
diethyl-amine	3 mM	Cl	1.5 mM	11.0	80%
diethyl-amine	3 mM	–	–	11.6	80%

* Low buffering capability of the eluent, long equilibration time of silica column is necessary.

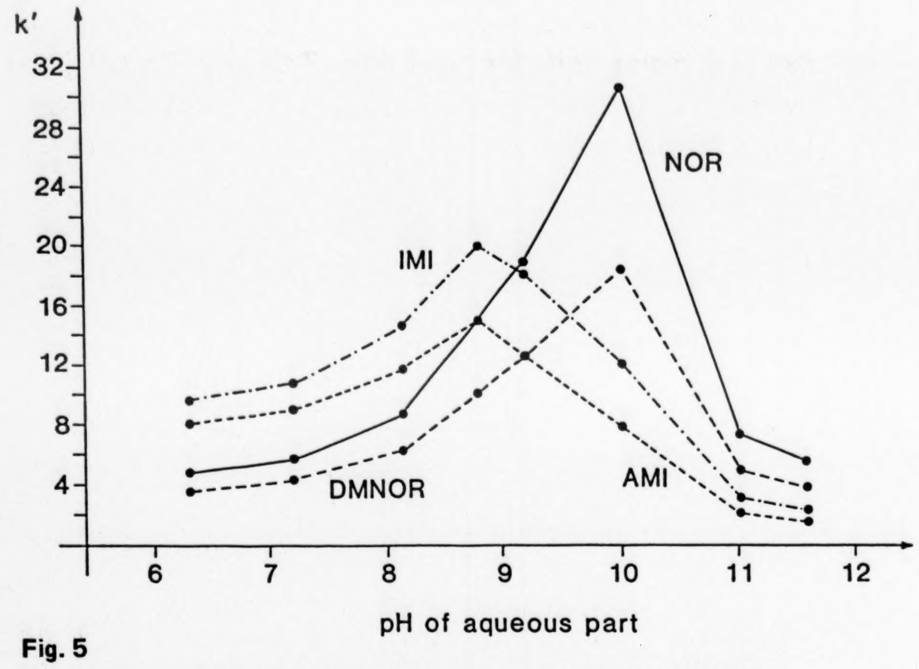

Fig. 5

Dependence of k'-values of tricyclic drugs on pH-value in eluent.
Composition of eluents used as in Table I.
Column: 11 cm × 4.6 mm Partisphere Si, flow: 1.4 ml/min.

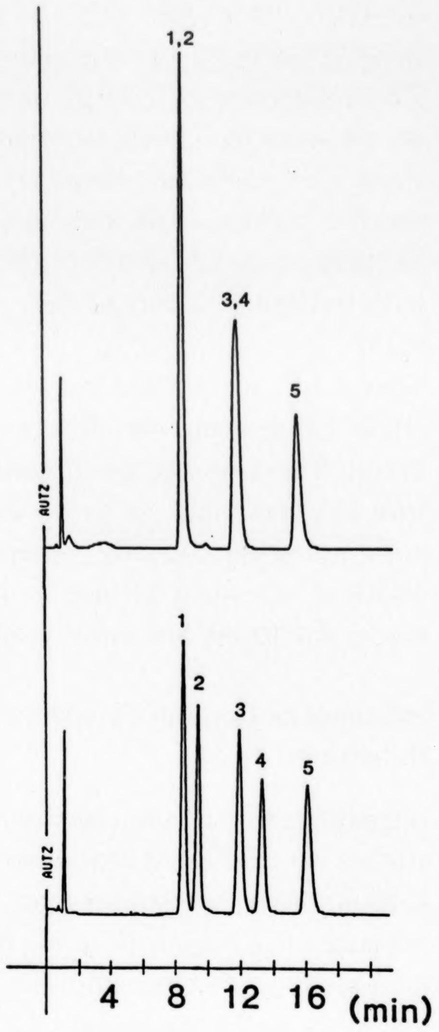

Fig. 6

Influence of type of anion on retention of tricyclic drugs.

Lower chromatogram: 80% MeOH, 1.5 mM perchloric acid/3 mM NH_4OH, pH = 8.9.

Upper chromatogram: 80% MeOH, 1.5 mM hydrochloric acid/3 mM NH_4OH, pH = 8.9.

Column: 11 cm × 4.6 mm Partisphere Si, flow: 1.4 ml/min.

1 = Cl-AMI, **2** = DM-NOR, **3** = AMI, **4** = NOR, **5** = IMI.

amines (IMI, AMI). At pH-values above 10, the general suppression of ionisation of the amino-groups is reflected in a decreasing retention of all tricyclic amines.

The shift in elution order between primary and secondary over tertiary amines offers great potential for the chromatography of differently substituted amino containing drugs, and it indicates that separation systems can be tuned according to the basicity of the drugs and to the variation of the pH-value in the eluent. This is of particular interest for the analysis of basic drugs, together with their metabolites, in biological samples.

Influence of the Nature of the Buffer Anion

Similarly, ion-pair formation in the mobile phase should have an influence on the selectivity and the degree of retention of the amino-group containing drugs on unmodified silica. But, as was the case in studying the pH-dependence, the nature and concentration of the anion in a buffer system cannot deliberately be changed without drastically influencing the pH-value. For this reason, while keeping the concentration of the NH_4-cation constant at 3 mM, only two different anions in the same concentration were found where the pH-value in the buffer was constant.

Exchanging the anion perchlorate for the weak ion-pairing anion chloride at a buffer pH of 8.9 will increase the retention of primary and secondary amine relative to that of tertiary amines; an effect similar to a small increase in the pH-value in the pH-range between 8.5–9.5 (Fig. 6).

Stability of Columns Using Basic Eluents

Because the high selectivity achieved in the separation of the test drugs can be found at basic pH-values of the mobile phase system, considerable concern can be raised about the stability of silica columns under these eluent conditions. Experience in continuously employing silica columns for routine analysis over a period of weeks under basic pH-conditions showed that unmodified silica has a surprising stability even in eluents with pH up to a value of 11. This might be explained by the low solubility of unmodified silica in eluents with low buffer concentration and high content of organic modifier and by the use of ammonium salts (in which silica is known to be less soluble) instead of sodium salts for buffer systems, a fact that has been reported in detail by Wehrli et al. [15].

Retention times and selectivity of silica columns used over long periods with buffered aqueous eluents are remarkably stable and no baseline drift should be observed [12], as long as preparation of the mobile phase is reproducible and accurate.

Comparison of Different Silica Packings

Because ion-exchange mechanisms are directly associated with the physical-chemical properties of the silica surface, a possible influence from the type of silica materials and their origins could be exspected. Few reports have been published in the literature about differences found in various brands of silica packings. To the contrary, the constant use of one special brand of silica was repeatedly recommended by Gill et al. [8, 9].

Three different brands of unmodified spherical silica materials were compared in this study (Fig. 7). Although the silica from different manufacturers differ strongly in their specific surface areas and pore sizes, remarkable little differences in elution order or relative k′-values were observed with buffering eluents as they were commonly used in this study.

Similarily, no differences in chromatographic behavior could be detected for different batches of the same silica brand. These results are in contrast to reports in the literature [4], and might partly be the result of the use of eluents with buffering capacity, where differences in basic properties of the silica surface might be eliminated, as well as partly due to the low ion-strength of the eluents used.

Influence of Column Temperature on the Selectivity of Retention

Increasing the column temperature from ambient temperature to 55°C has no significant effect on the relative elution order of the tricyclic drugs, but causes a general decrease in k′-values (Fig. 8). Because mass transfer of the ion-exchange mechanism is increased, increased chromatographic performance will be observed at elevated temperatures (Table III).

Analysis of Basic Drugs in Biological Samples by Using Unmodified Silica Columns

Because of good chromatographic performance and the unique selectivity for basic compounds, unmodified silica in buffered aqueous eluents can be regarded as the first choice in the analysis of basic amino-group containing compounds in biological samples. Based on the above results, several routine methods for the measurement of different drugs and their metabolites in blood (e.g. the determination of tamoxifen and metabolites in blood [16]) have been developed and routinely used in the authors' laboratory.

As an example of high specificity, the separation of different tricyclic drugs in blood on unmodified silica with a buffered aqueous mobile phase after one-step extraction using a C-2 pre-column is shown in Fig. 9. It should be noted that no peaks with k′-values higher than one, originating from the blood plasma matrix, can be observed in the chromatogram of the blank plasma sample.

Conclusions

Through the use of aqueous mobile phase mixtures with low buffer concentrations, a marked increase in column performance in the chromatography of basic drugs on unmodified silica can be found. The retention of the basic drugs seems to follow an assumed ion-exchange mechanism and is strongly influenced by the concentration of cations and the pH-value in the eluent. Under acid pH-eluent conditions, capacity factors and selectivity for the tested drugs are low, but increase when shifting to basic values.

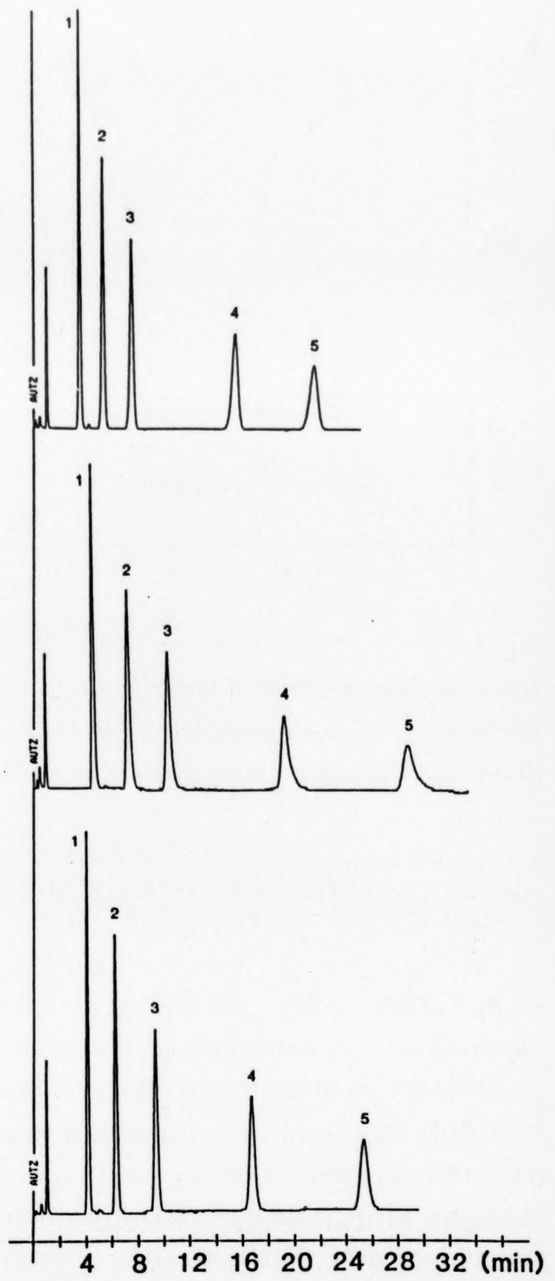

Fig. 7

Selectivity of different silica materials.

Upper chromatogram: 12.5cm X 4mm Nucleosil Si 100, 5μm.
Middle chromatogram: 12.5cm X 4mm Lichrosphere Si 60, 4μm.
Lower chromatogram: 11cm X 4.6mm Partisphere Si 120, 5μm.

Chromatographic conditions: 80% MeOH, 3mM NH_4OH, pH = 10.7, flow: 1.4ml/min.

1 = Cl-AMI, **2** = AMI, **3** = IMI, **4** = DM-NOR, **5** = NOR.

Table III. Column efficiencies at different column temperatures.

	Plate Numbers (plates/m)				
Col. Temp. in °C	Cl-AMI	AMI	IMI	DM-NOR	NOR
25°C	30160	53230	55750	84470	93130
35°C	45230	59520	67870	87410	94950
45°C	61550	75330	80760	92060	97940
55°C	64050	90120	94260	95330	99450

A selectivity change in the retention of primary and secondary over tertiary amino-compounds in the pH-range between 8.5–10 can be observed, which can be explained by differences in degree of ionisation, according to the basicity of the compounds. A similar, but not so marked effect can be seen when strong ion-pair forming anions are included in the mobile phase.

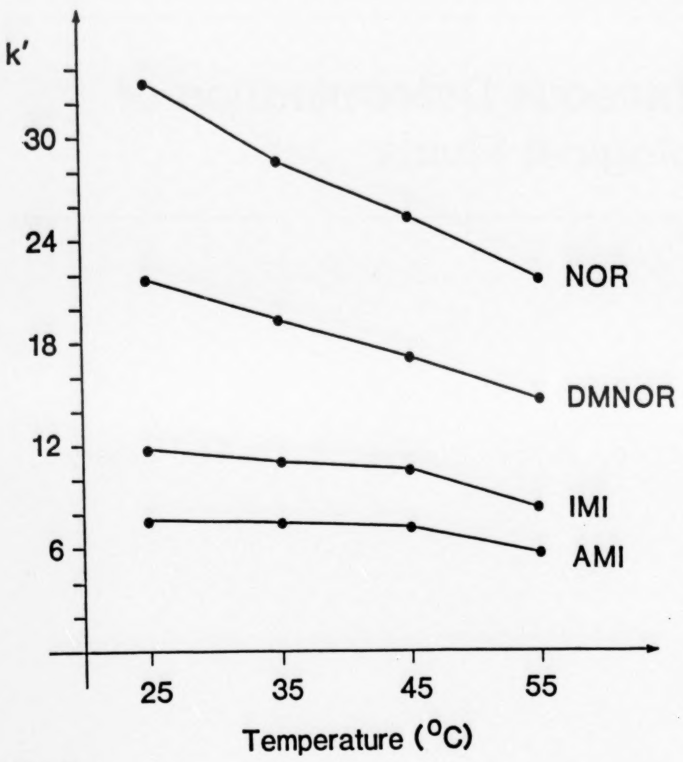

Fig. 8
Dependence of k'-values of tricyclic drugs on column temperature.
Chromatographic conditions: 80% MeOH, 3 mM NH_4OH pH = 10.7.
Column: 11 cm × 4.6 mm Partisphere Si, flow: 1.4 ml/min.

Although mobile phase mixtures at rather high pH-values were used, column stability was high and differences between various brands of unmodified silica were found to be small, which might be due to the low ion strength of the chosen mobile phase system. For reproducible ion-exchange chromatography, the use of eluents with buffering capability becomes an absolute necessity, especially when the eluent is low in ion strength.

Under the precondition that the silica system is buffered by the mobile phase, a chromatographic system with unique separation power for basic drugs as well as very high stability and reproducibility can be obtained, where selectivity can be adjusted by the modification of the pH-conditions.

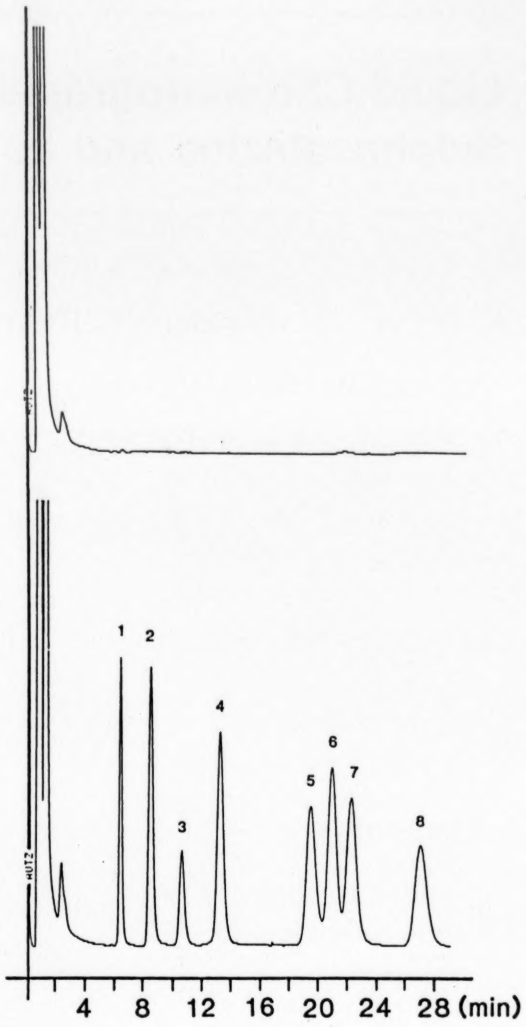

Fig. 9
Separation of a spiked and blank blood plasma sample on Partisphere Si after on-line precolumn sample preparation.
Chromatographic conditions: 80% MeOH, 5 mM NH_4OH, pH = 10.7, flow: 1.4 ml/min.
Lower chromatogram: spiked blood plasma sample.
1 = CLOMI, **2** = IMI, **3** = thioridazine, **4** = DM-NOR, **5** = NOR, **6** = E-10-OH-NOR, **7** = Z-10-OH-NOR, **8** = DIMI (100 ng each).
Upper chromatogram: blank blood plasma sample.

References

[1] *E. Papp, G. Vigh*, J. Chromatogr. **259**, 49 (1983).
[2] *E. Papp, G. Vigh*, J. Chromatogr. **282**, 59 (1983).
[3] *I. Jane*, J. Chromatogr. **111**, 227 (1975).
[4] *R. J. Flanagan, I. Jane*, J. Chromatogr. **323**, 173 (1985).
[5] *G. B. Cox, R. W. Stout*, J. Chromatogr. **384**, 315 (1987).
[6] *K. Sudgen, G. B. Cox, C. R. Loscombe*, J. Chromatogr. **149**, 377 (1978).
[7] *B. A. Bidlingmeyer, J. K. Del Rios, J. Korpi*, Anal. Chem. **54**, 442 (1982).
[8] *R. Gill, M. D. Osselton, R. M. Smith, T. D. Hurdley*, J. Chromatogr. **386**, 65 (1987).
[9] *B. Law, R. Gill, A. C. Moffat*, J. Chromatogr. **302**, 165 (1984).
[10] *J. Crommen*, J. Chromatogr. **186**, 705 (1979).
[11] *B. B. Wheals*, J. Chromatogr. **187**, 65 (1980).
[12] *B. Law*, J. Chromatogr. in press (1987).
[13] *K. E. Bij, Cs. Horvath, W. R. Melander, A. Nahum*, J. Chromatogr. **203**, 65 (1981).
[14] *J. C. Kraak* in: C. F. Simpson (Ed.), Techniques in Liquid Chromatography, Wiley Heyden 304 (1982).
[15] *A. Wehrli, J. C. Hildenbrand, H. P. Keller, R. Stampfli, R. W. Frei*, J. Chromatogr. **149**, 199 (1978).
[16] *Ch. Kikuta, R. W. Schmid*, J. Pharmaceut. Biomed. Anal. in press.

Received: Aug. 12, 1987
Revised manuscript:
received: Sep. 7, 1987
Accepted: Sep. 10, 1987
F

Liquid Chromatographic Method for the Simultaneous Determination of Sulphasalazine and its Main Metabolites in Biological Fluids

K. Róna*[1]/V. Winkler[2]/T. Riesz[1]/B. Gachályi[1]

[1]Postgraduate Medical University, I. Department of Medicine, H-1389 Budapest, P.O.B. 112, Hungary

[2]National Institute of Rheumatological Disease, "A" Department of Rheumatology, H-1525 Budapest, P.O.B. 54, Hungary

Key Words

Salicylazosulphapyridine
5-aminosalicylic acid
Sulphapyridine
Rheumatoid arthritis
HPLC

Summary

An HPLC procedure was developed for the simultaneous determination of salicylazosulphapyridine, and its main metabolites 5-aminosalicylic acid and sulphapyridine, in human serum and synovial fluid. The analytical procedure consisted of a single ion-pair extraction step for an Extrelut column with methylene chloride. The investigated compounds and the added sulphadimidine internal standard were eluted from a Hypersil-MOS reversed-phase column by stepwise gradient; mobile phase was methanol-0.01 M potassium dihydrogenphosphate (3:7, 0.0–2.0 min and 8:2, 2.1–6.5 min).

Introduction

Salicylazosulphapyridine (SASP) has been used succesfully for many years in the treatment of patients with Crohn's disease and ulcerative colitis. More recent studies have demonstrated that SASP is also effective in rheumatoid arthritis (RA) in doses of 2 to 4 g daily [1–3].

When SASP reaches the large bowels it is metabolized by gut bacterial azoreductase to biologically active moieties; 5-aminosalicylic acid (5-ASA) and sulphapyridine (SP). 5-ASA is eliminated mainly in acetylated form (Ac-5-ASA), SP is metabolized both by acetylation and hydroxylation to N-acetylsulphapyridine (AcSP), 5-hydroxysulphapyridine (5-OHSP) and N-acetyl-5-hydroxysulphapyridine (Ac-5-OHSP). The metabolites are conjugated with glucuronic acid to their corresponding glucuronides and are excreted in the urine (Fig. 1) [4–6].

Although generally effective, clinical response to SASP in RA is unpredictable, and in some cases therapy is not sufficiently effective. In addition, some patients have difficulties in tolerating the drug [7–9].

According to our knowledge, the difference in the individual reactions to the drug can be explained by the different metabolical capabilitites of the patients which reflect their genetic differences. It has been proven that the capability of both acetylation and hydroxylation, as drug metabolizing enzyme-reactions, is determined by genetic factors. Thus studies related to populations show polymorphism in the metabolizm of numerous drugs [10].

In Fig. 1 where the metabolizm of SASP is shown, it can be seen that the two active metabolites of SASP (5-ASA and SP) are further acetylated and hydroxylated. The proportion of acetylated and hydroxylated SP in serum and urine depends on the genetically determined acetylation and hydroxylation phenotypes [8, 9]. (In the normal population, about 50% of the people are rapid and 50% slow acetylators and 10% are poor and 90% extensive hydroxylators.)

The aim of our study was to define a connection between the patients' reactions to SASP and the concentration of SASP and its main metabolites in biological fluids, as well as between the reaction of the acetylator and hydroxylator phenotypes of the patients to their response to the drug.

A number of assays are available for the determination of plasma concentrations of SP or 5-ASA and its metabolites using high-performance liquid chromatography (HPLC). SP has been determined using a UV monitor, while 5-ASA has been measured fluorimetrically or by HPLC with a fluorimetric detector [5, 11, 12, 13]. Here we report on an HPLC method for the simultaneous determination of SASP and its main metabolites, SP and 5-ASA, detected by coupling a fluorimetric detector to a UV monitor [14, 15]. Sulphadimidine (SUD) is used as an internal standard. The selectivity of the method is good and its sensitivity is sufficient for therapeutic drug monitoring in serum and synovial fluid.

0009-5893/87 0720-05 $03.00/0

© 1987 Friedr. Vieweg & Sohn Verlagsgesellschaft mbH

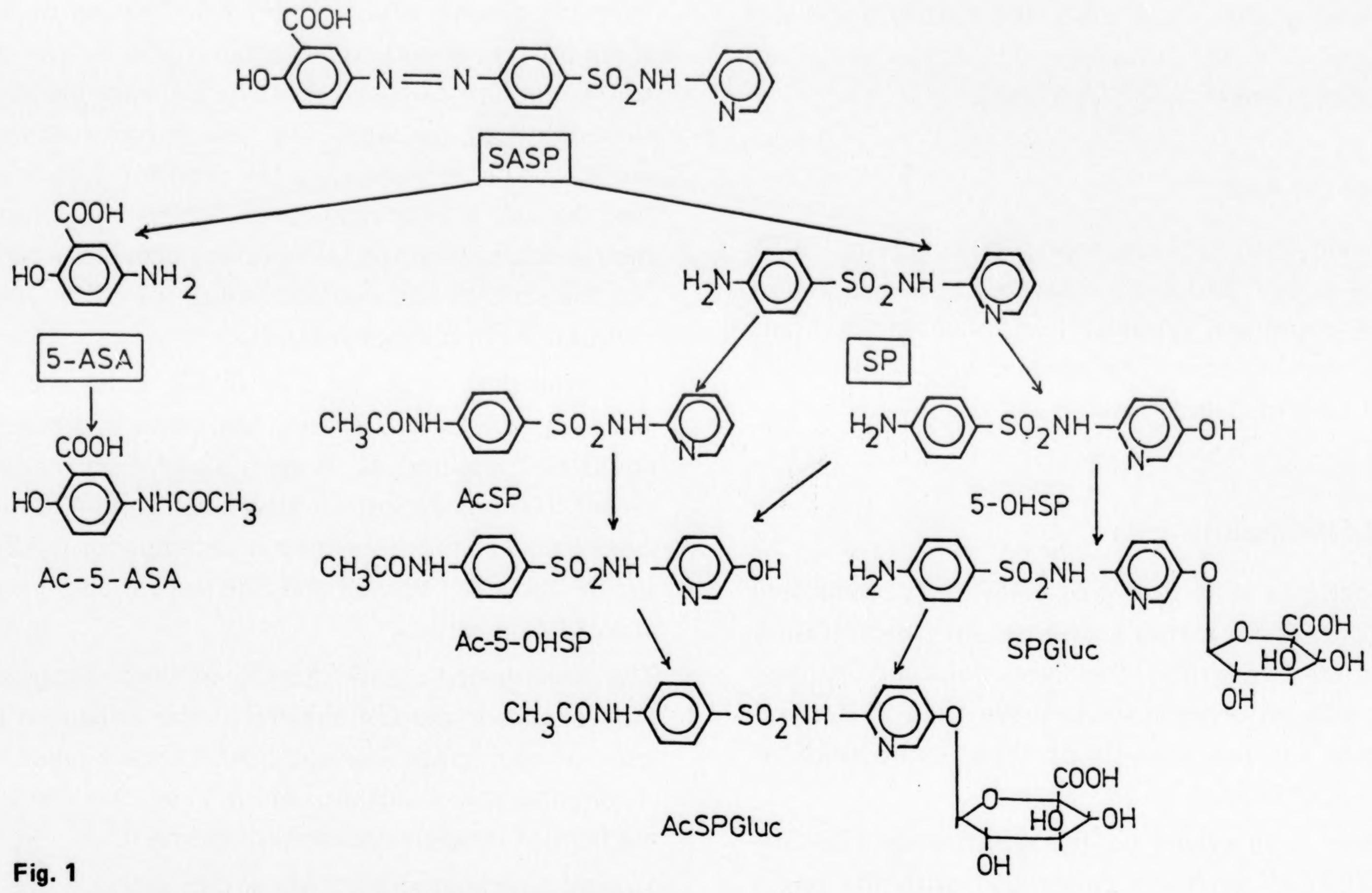

Fig. 1
The main metabolic pathway of salicylazosulphapyridine.

Experimental

Reagents

Salicylazosulphapyridine (trade name Salazopyrin) (SASP), sulphapyridine (SP) and 5-aminosalicyl acid (5-ASA) were gifts of Pharmacia (Uppsala, Sweden). The internal standard sulphadimidine (SUD) was purchased from Alkaloida (Tiszavasvári, Hungary). Methanol and Extrelut were obtained from E. Merck (Darmstadt, FRG). Tetrabutyl ammonium hydroxid (TBAOH) was purchased from Jansen (Beerse, Belgium). All other chemicals used were the products of Reanal (Budapest, Hungary) and were of analytical grade.

Stock Solutions

Stock solution of SASP, SP, 5-ASA and SUD (0.2 mg/ml) were prepared in a methanol-1/15 M, pH 8.3 disodium hydrogenphosphate (1:1) mixture and stored at 4 °C. Work solutions were made by appropriate dilution with methanol-water (1:1) for the calibration curves daily.

Analytical Procedure

Human serum or synovial fluid were prepared by centrifugation (3000 g, 10 min) and kept frozen at − 20 °C until analysis. To 1.0 ml of serum or synovial fluid, 10 μg of SUD internal standard in 50 μl of methanol-1/15, pH 8.3 disodium hydrogenphosphate (1:1) solution, 0.5 ml of double -distilled water, 0.5 ml of 0.5 M, pH 7.4 phosphate buffer and 0.1 ml of 40% tetrabutylammonium hydroxide were added. After shaking for 5 sec in a shaker, the samples were poured onto a chromatographic column (250 × 5 mm I.D.) filled with 1.5 g Extrelut and were eluted with 3 × 5 ml of methylene chloride after 15 min. The methylene chloride eluate was evaporated to dryness in a nitrogen stream, the dry residue was dissolved in 100 μl of methanol-water (1:1) solution by shaking for 30 s, and 5 μl aliquots were injected onto the analytical column.

Preparation of Calibration Curves

The straight-line calibration graphs were obtained for SASP, 5-ASA and SP by adding 10 μg SUD (internal standard) and SASP, SP in amounts of 0.1–40.0 μg (0.1, 0.5, 1.0, 5.0, 10.0, 15.0, 20.0, 30.0, 40.0) and 5-ASA in amounts of 0.1–3.0 μg (0.1, 0.5, 1.0, 1.5, 2.0, 3.0) to 1.0 ml control serum and synovial fluid, free of any drugs. The samples were assayed according to the analytical procedure. The ratios of the peak areas of investigated drug and internal standard were plotted.

Chromatographic Conditions

HPLC was performed on a Hewlett-Packard 1090 chromatograph equipped with a 5 μl loop and a HP 85B System master (with a HP 9121 dual disc drive). Detection of 5-ASA was achived by coupling a fluorimetric detector (Shimadzu RF-530, excitation wavelength 310 nm, emission wavelength 430 nm) to the diode-array detector of HP 1090 chromatograph (254 and 360 nm). Area integrations, calculations and plotting of the chromatogram were carried out by a Hewlett-Packard 3390A integrator, 7470 plotter for UV monitor and a OH-827 recorder (Radelkis, Hungary) for fluorescence detector. A MOS-Hypersyl (RP-8) prepacked column (100 × 2.1 mm I.D.; 5 μm particle size) (Hewlett-Packard) was used at room temperature for the separation of the compounds. The flow-rate was 0.2 ml/

min. A stepwise gradient was used, the mobile phase was biner; methanol-0.01 M potassium dihydrogenphosphate (3:7, 0.0–2.0 min and 8:2, 2.1–6.5 min).

Application of the Assay

The investigated RA patients receiving long-term SASP therapy (2–4 g per day) were assayed for SASP, 5-ASA and SP in the serum and synovial fluid collected two hours after the last morning dose. The samples were immediately centrifugated, decanted and frozen – 20 °C until analysis.

Results and Discussion

On treating patients with 2–4 g of SASP daily, according to the literature 5-ASA shows a peak serum concentration of about 1 μg/ml. In addition, the highly polar 5-ASA must be extracted into an organic solvent. We tried to develop an assay usable for the analysis of these compounds in serum and synovial fluid.

These problems were solved by the addition of TBAOH, so that the TBAOH can form an ion-pair with the acidic salycilate. The associated 5-ASA complex was extracted into the organic phase at pH 7.4. The use of Extrelut for clean-up was found to be a rapid and simple method for the extraction of SASP, 5-ASA, SP from blood serum and synovial fluid, as well. The low concentration of 5-ASA could not be detected by a UV monitor. For this reason we had to use a fluorescence detector. The coupled fluorimetric detector to the UV monitor provides a rapid method for the simultaneous determination of SASP and its major metabolites in biological fluids.

The retention times for 5-ASA, SP, SUD and SASP were 1.8, 2.3, 3.2 and 5.2 min, respectively. Each compound could be measured at its own absorption maximum. This meant 310 nm excitation wavelength and 430 nm emission wavelength at the fluorimetric detector for 5-ASA, 254 nm for SP and SUD as well and 360 nm for SASP at the diode-array UV detector.

The homogeneity and identity of chromatographic peaks were checked: the UV spectra of the inflection points and apex of each peak (except 5-ASA) were taken during the chromatographic elution, and UV spectra were drawn by the help of Hewlett-Packard equippment.

Typical chromatograms of serum extracts are shown in Fig. 2. As we mentioned above, the analytical procedure

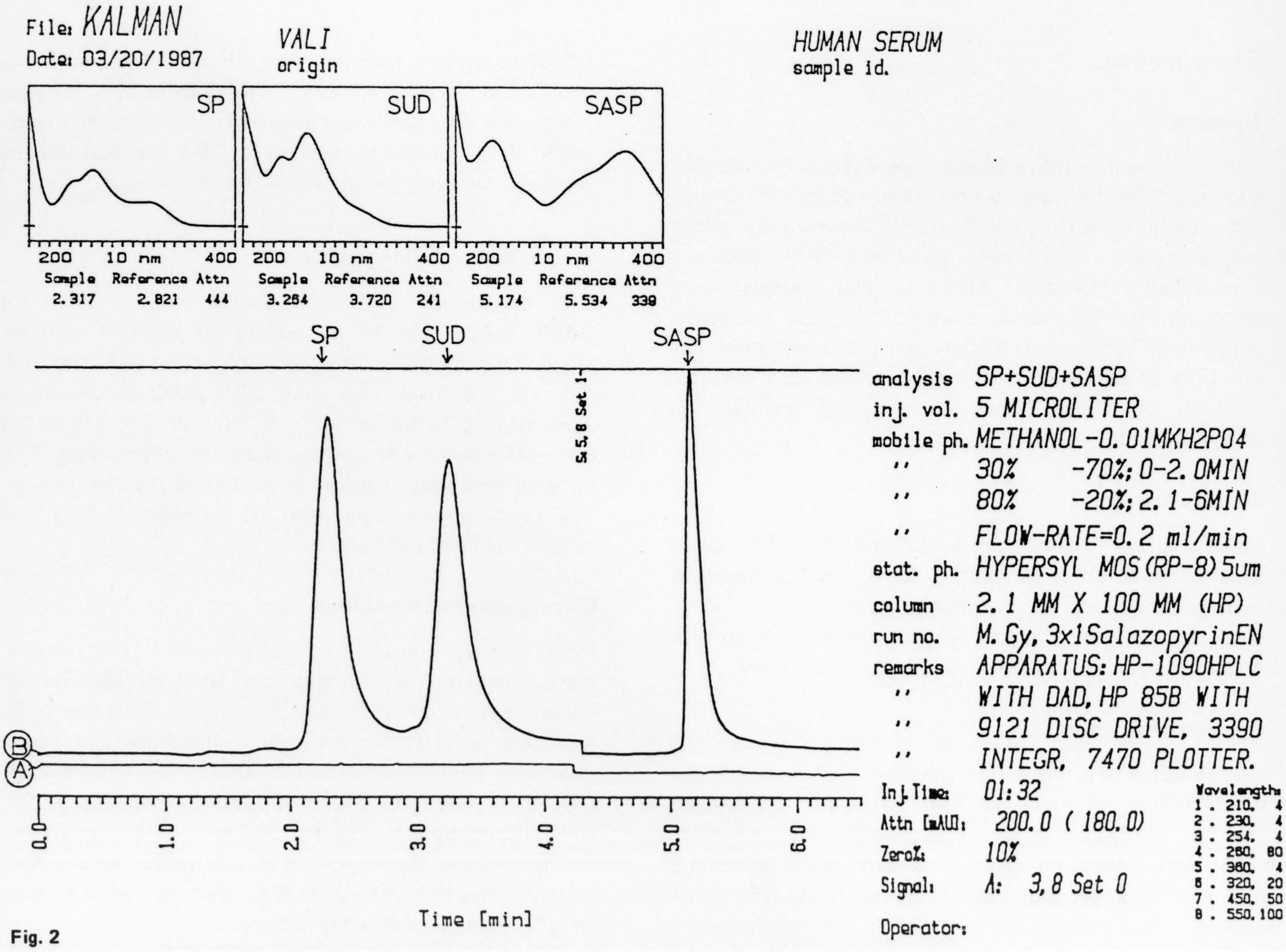

analysis SP+SUD+SASP
inj. vol. 5 MICROLITER
mobile ph. METHANOL-0.01MKH2PO4
'' 30% -70%; 0-2.0MIN
'' 80% -20%; 2.1-6MIN
'' FLOW-RATE=0.2 ml/min
stat. ph. HYPERSYL MOS (RP-8) 5um
column 2.1 MM X 100 MM (HP)
run no. M. Gy, 3x1SalazopyrinEN
remarks APPARATUS: HP-1090HPLC
'' WITH DAD, HP 85B WITH
'' 9121 DISC DRIVE, 3390
'' INTEGR, 7470 PLOTTER.
Inj. Time: 01:32
Attn [mAU]: 200.0 (180.0)
Zero%: 10%
Signal: A: 3,8 Set 0
Operator:

Wavelength:
1 . 210, 4
2 . 230, 4
3 . 254, 4
4 . 280, 80
5 . 360, 4
6 . 320, 20
7 . 450, 50
8 . 550, 100

Fig. 2

Separation of human serum extracts.

Top: UV spectra of the peaks of serum extract. Bottom: chromatograms of serum extracts; (A) blank serum extract; (B) serum extract of a patient treated chronically with 3 g salicylazosulphapyridine (SalazopyrinEN) per day. Serum containing 15 μg/ml of SP, 10 μg/ml of SUD and 12 μg/ml of SASP.

from serum and synovial fluid is one and the same thing and the chromatograms are very similar as well (Fig. 3). Under the HPLC conditions used, no interference by endogeneous compounds has been observed, and the SP, SUD and SASP showed well resorved peaks. The chromatograms were obtained at the fluorimetric detector from the determination of 5-ASA in serum and synovial fluid and are presented in Fig. 4. Extraction of blanks indicated that no interference from endogenous compounds occurred.

The calibration curves of area ratios versus 5-ASA, SP and SASP concentrations were linear over the range 0.1–3 μg/ml for 5-ASA and 0.1–40.0 μg/ml for SP and SASP from serum and synovial fluid, respectively. The mean correlation coefficients for 5-ASA, SP and SASP calibrations obtained from 10 analytical runs were 0.990, 0.995 and 0.994, respectively. The day-to-day coefficient of variation of the slope of calibration curves was 3.6% for 5-ASA, 3.4% for SP and 3.5% for SASP (n = 10). The detection limits were found to be 0.1 μg of 5-ASA, SP and SASP per ml of serum or synovial fluid. Table I shows the accuracy and the coefficients of variation for identical samples in the concentration range of interest.

The assay has been applied to various biological (serum and synovial) fluids obtained from RA patients receiving orally 2–4 g SASP daily (2–4 × 1 g). Details of the clinical experiment are published elsewhere [16], here we present only the analytical results.

Steady-state concentrations of up to 18 μg/ml SASP, up to 40 μg/ml SP and up to 1.0 μg/ml 5-ASA were found and were dependent on pharmacogenetic status, the biological fluids (serum or synovial) and, of course, the daily dose.

The advantage of the described assay over other HPLC assays is that it can measure the SASP and its main metabolites simultaneously. In addition, each chromatographic run is complete within 6 min, providing a rapid method for the routine analysis. In conclusion, the described method can be used for therapeutic drug level monitoring of SASP, 5-ASA and SP, which can be helpful in the therapy of RA.

Acknowledgement

We are grateful to Pharmacia Ltd. for supplies of salicylazosulphapyridine, 5-aminosalicylic acid and sulphapyridine, and we thank Beckman Ltd for access to the Shimadzu RF-530 fluorescence detector.

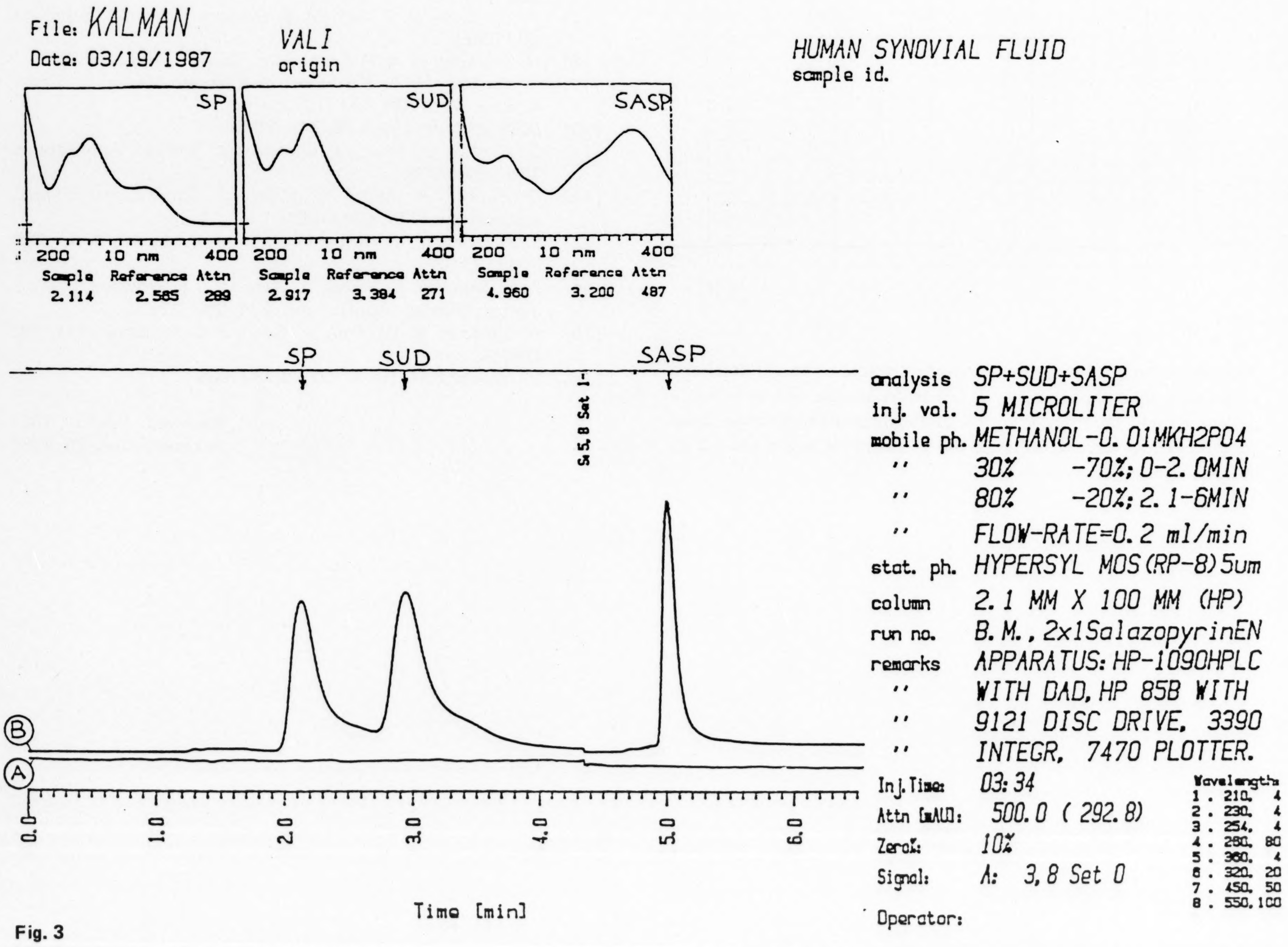

```
analysis    SP+SUD+SASP
inj. vol.   5 MICROLITER
mobile ph.  METHANOL-0. 01MKH2PO4
  ''        30%      -70%; 0-2. 0MIN
  ''        80%      -20%; 2. 1-6MIN
  ''        FLOW-RATE=0. 2 ml/min
stat. ph.   HYPERSYL MOS (RP-8) 5um
column      2. 1 MM X 100 MM (HP)
run no.     B. M., 2x1SalazopyrinEN
remarks     APPARATUS: HP-1090HPLC
  ''        WITH DAD, HP 85B WITH
  ''        9121 DISC DRIVE. 3390
  ''        INTEGR. 7470 PLOTTER.
Inj. Time:   03: 34                       Wavelength
Attn [mAU]:   500. 0 ( 292. 8)            1 . 210.   4
                                          2 . 230.   4
ZeroX:       10%                          3 . 254.   4
                                          4 . 280.  80
Signal:      A:  3, 8 Set 0               5 . 360.   4
                                          6 . 320.  20
                                          7 . 450.  50
                                          8 . 550. 100
Operator:
```

Fig. 3

Separation of human synovial fluid extracts.

Top: UV spectra of the peaks of synovial fluid extract. Bottom: chromatograms of synovial fluid ectracts; (A) blank synovial fluid ectract; (B) synovial fluid extract of a patient treated chronically with 2 g salicylazosulphapyridine (SalazopyrinEN) per day. Synovial fluid containing 7 μg/ml of SP, 10 μg/ml of SUD and 6 μg/ml of SASP.

Table I. Accuracy, precision and recoveries for 5-ASA, SP and SASP n = 5 at each concentration

Amount added (μg/ml of serum)	Amount found (μg/ml of serum)			Coefficient of variation (%)		
	5-ASA	SP	SASP	5-ASA	SP	SASP
0.1	0.045	0.086	0.089	6.6	6.2	6.0
0.5	0.25	–	–	6.0	–	–
1.0	0.49	0.90	0.93	5.0	4.9	4.9
2.0	1.00	–	–	3.7	–	–
5.0	–	4.50	4.50	–	4.6	4.7
10.0	–	9.20	9.10	–	3.1	3.3
20.0	–	18.20	18.40	–	1.8	1.8

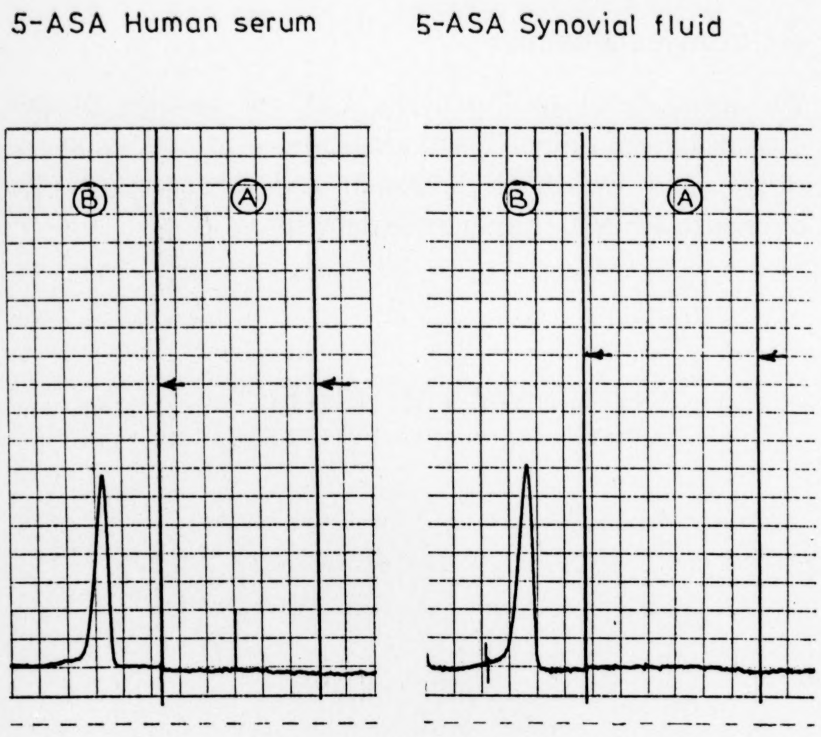

Fig. 4

Typical chromatograms of 5-aminosalicylic acid of serum (left) and of synovial fluid (right) extracts. (A) blank sample, (B) sample of a patient treated chronically with 4 g salicylazosulphapyridine (SalazopyrinEN) per day, (0.65 μg of 5-ASA per ml of serum and 0.8 μg of 5-ASA per ml of synovial fluid).

References

[1] *D. E. Bax, M. S. Greaves, R. S. Amos,* Br. J. of Rheumatology **25**, 282 (1986).

[2] *V. C. Neumann, A. J. Taggart, P. LeGallez, C. Astbury, J. Hill, H. A. Bird,* J. Rheumatol. **13**, 285 (1986).

[3] *J. Taggart, V. C. Neumann, J. Hill, C. Astbury, P. LeGallez, J. S. Dixon,* Drugs **32** (Suppl. 1), 27 (1986).

[4] *N. O. Ahnfelt, R. Modin, M. L. Odell, U. Ohlson,* J. of Pharmaceutical and Biomedical Analysis **4**, 261 (1986).

[5] *C. Fischer, U. Klotz,* J. Chromatogr. Biomed. Applications, **162**, 237 (1979).

[6] *A. K. Azad Kahn, H. H. Johnston, S. C. Truelove,* Gut **16**, 832 (1975).

[7] *R. S. Amos, D. E. Bax, M. S. Greaves,* Drugs **32** (Suppl. 1), 58 (1986).

[8] *H. Schröder, D. A. P. Evans,* Med. Genet **9**, 168 (1972).

[9] *K. M. Das, M. A. Eastwood, J. P. A. Mc Manus, W. Sircus,* N. Engl. Med. **289**, 491 (1973).

[10] *D. W. J. Clark,* Drugs **29**, 342 (1985).

[11] *C. Fischer, U. Klotz,* J. Chromatogr. Biomed. Applications, **146**, 157 (1978).

[12] *C. Fischer, K. Maier, U. Klotz,* J. Chromatogr. Biomed. Applications, **225**, 498 (1981).

[13] *S. H. Hansen,* J. Chromatogr. Biomed. Applications, **226**, 504 (1981).

[14] *P. N. Shaw, A. L. Sivner, L. Aarons, J. B. Houston,* J. Chromatogr. Biomed. Applications, **274**, 393 (1983).

[15] *W. Lindner, R. W. Frei, W. Santi,* J. Chromatogr. **111**, 365 (1975).

[16] *V. Winkler,* Orv. Hetil. **127**, 2073 (1986).

Received: June 30, 1987
Accepted: July 25, 1987
F

Enantiomeric Resolution of N-Methyl-α-Amino Acids and α-Alkyl-α-Amino Acids by Ligand-Exchange Chromatography

H. Brückner

Institute of Food Technology, University of Hohenheim, D-7000 Stuttgart 70, FRG

Key Words

Ligand-exchange chromatography
Chiral separation
N-methyl-DL-α-amino acids
DL-α-alkyl-α-amino acids
Polarimeter detector

Summary

The enantiomeric resolution of N-methyl-DL-α-amino acids (NMe-AA) and DL-α-alkyl-α-amino acids (AAA) was achieved by ligand-exchange (LE) high performance liquid chromatography (HPLC) using silica bonded L-amino acids as the chiral selector (Chiral ProCu, Chiral HyproCu, Chiral ValCu, Nucleosil Chiral-1). Using aqueous solutions of copper sulfate or acetate adjusted to pH 4–6 and the addition of acetonitrile (10–20%) or methanol (10–40%), baseline resolution occurred in many cases. By comparison with enantiomers of known optical configuration, the elution order of a number of NMe-AA and AAA could be determined and on-line polarimeter detection enabled the assignment of the optical rotation, elution order and configuration of AAA enantiomers. Using a preparative column (300mm × 20mm i.d.) packed with Chiral ProCu, a baseline resolution of 60mg DL-α-methylphenylalanine was achieved. Further, LE-TLC, using a chiral stationary phase ("Chiralplate"), enabled the chiral separation of very hydrophobic AAA, characterized by increasingly large alkyl side chains, *viz.* the homologous series α-ethylalanine to α-nonylalanine and α-propyl-α-amino-*n*-butyric acid to α-hexyl-α-amino-*n*-butyric acid.

Introduction

The separation of amino acids and their enantiomers without the need of prior derivatization and sensitive quantitative determination is still a challenge to be tackled by chromatographers [1–6]. Ideally, this method should be extendable to the great variety of non-protein and synthetic amino acids [7] and should also be accessible for scaling-up, enabling the preparative isolation of these compounds.

One promising approach in this direction which has attracted much attention and effort in recent years is a methodology referred to as ligand-exchange chromatography (LEC), which takes advantage of the varying stability of mixed, diastereomeric metal complexes of amino acids. The various approaches and methodologies have been reviewed in detail [8–16]. Although LEC does not yet entirely fulfill the above requirements, the acceptance and anticipation of this technique is not only demonstrated by the numerous contributions to the subject, but also by the fact that very recently several companies started supplying chiral LE-phases based on silica bonded L-amino acids[1]. Among the non-protein amino acids, N-methyl-α-amino acids (NMe-AA) and α-alkyl-α-amino acids (AAA) are of considerable interest. NMe-AA occur in plants [17–19] and are also frequently constituents of peptide antibiotics [20–23]. The most simple AAA, *viz.*, α-methylalanine (Aib), is the specific marker amino acid of a particular group of "peptaibol antibiotics"[2] [24–26]. Further, members of the above groups of amino acids have been found as constituents in carbonaceous meteorites [27], the investigation of which contributed much to the methodology of amino acid trace analysis [28–30] and enantiomeric resolution [31, 32]. Interest in this research is ongoing, as shown by the controversial discussion on the ratio of enantiomers of α-ethylalanine (isovaline, Iva) found in the Murchison meteorite [33]. Moreover, much is anticipated from the incorporation of the sterically highly constrained amino acids mentioned above into synthetic peptide hormones [34–37].

As a result of the difficulties encountered in the scale-up synthesis of optically pure, or the enantiomeric resolution of AAA, with very few exceptions [38, 39] exclusively non-chiral AAA have been used in peptide drug design. Analogously, the use of NMe-AA in peptide synthesis is hampered by the steric hindrance of the imino group, as well as by the easy racemization of the compounds [40, 41] under the drastic conditions of the activation of their carboxy group.

Presented at the Eleventh International Symposium on Column Liquid Chromatography, June 28–July 3, 1987, Amsterdam, The Netherlands. Parts of the results have also been presented at ANAKON '87, May 11–14, Baden-Baden, FRG, and the Tenth American Peptide Symposium, May 23–28, 1987, St. Louis, MO, USA.

---

1) Chiral ProCu, Chiral HyproCu, Chiral ValCu, Serva, Heidelberg, FRG; Nucleosil Chiral-1, Macherey-Nagel, Düren, FRG; Chiral Pak WH and WM, Daicel, Tokyo, Japan

2) Standards of peptaibol antibiotics are supplied by BACHEM AG, Hauptstr. 144, CH-4416, Bubendorf, Switzerland

0009-5893/87 0725-14 $ 03.00/0

© 1987 Friedr. Vieweg & Sohn Verlagsgesellschaft mbH

In continuation of our work concerning the analysis and enantiomeric resolution of AAA [42–45], and their utilization in synthetic peptide chemistry [46–49], we now show that LE-HPLC, using various silica bonded L-amino acids and Cu^{2+} as the complexing ion, is capable of separating a large number of racemic NMe-AA and AAA. Further, chiral phase LE-TLC was used for the comparison of a homologous series of hydrophobic AAA, characterized by increasingly large alkyl side chains.

Experimental

Sources and abbreviations of N-methyl-α-amino acids and α-alkyl-α-amino acids:

N-methyl-DL-alanine and N-methyl-L-alanine (NMe-Ala), N-methyl-DL-valine and N-methyl-L-valine (NMe-Val), N-methyl-DL-glutamic acid (NMe-Glu), N-methyl-L-phenylalanine (NMe-Phe) were purchased from Serva (Heidelberg, FRG), N-methyl-DL-aspartic acid, N-methyl-L-aspartic acid, N-methyl-L-glutamic acid (NMe-Glu), N-methyl-D-phenylalanine (NMe-Phe), N-methyl-DL-leucine and N-methyl-L-leucine (NMe-Leu) from Sigma (St. Louis, USA).

The following α-alkylated amino acids are formally derived by the substitution of the C^{α} hydrogen atom of the respective α-amino acid (abbreviated according to the three letter nomenclature, cf. Eur. J. Biochem. **138**, 9 (1984)) by a methyl (Me) group and were of commercial grade: DL-α-methylaspartic acid (α-Me-Asp), DL-α-methylglutamic acid · $0.5H_2O$ (α-Me-Glu), DL-α-methylhistidine (α-Me-His), DL-α-methylornithine (α-Me-Orn), DL-α-methylserine (α-Me-Ser), DL-α-methylmethionine (α-Me-Met), DL-α-methylphenylalanine (α-Me-Phe), DL-α-methyl-*meta*-methoxyphenylalanine (α-Me-PheOMe), DL- and L-α-methyltyrosine (α-Me-Tyr), DL- and L-α-methyl-3-(3,4-dihydroxyphenyl)-alanine (α-Me-Dopa), DL-α-methyltryptophane (α-Me-Trp) were purchased from Sigma, DL-α-methylleucine (α-Me-Leu) was from Bachem (Bubendorf, Switzerland), DL-α-ethylphenylglycine (α-Et-Phg) from EMKA Chemie (Markgröningen-Talhausen, FRG), and α-methylalanine (α-Me-Ala or α-aminoisobutyric acid, Aib) from Fluka (Buchs, Switzerland).

The α-alkylated α-amino acids listed below are not commercially available, and thus they have been synthesized in our laboratory according to the Strecker procedure by reaction of the respective ketones (Fluka) with sodium cyanide and hydrolysis of the nitriles formed by hydrochloric acid. The amino acids were liberated from the hydrochlorides by addition of tributylamine [50] and purified by crystallization. In the cases described below, the amino acids were formally derived from alanine (Ala) by C^{α} hydrogen substitution by alkyl groups or, with second priority, from α-amino-*n*-butyric acid (Abu). In addition, the rational nomenclature of these compounds is given (abbreviations of *n*-alkyl groups: Me, methyl; Et, ethyl; Prop, propyl; But, butyl; Pent, pentyl; Hex, hexyl; Hept, heptyl; Oct, octyl; Non, nonyl). DL-α-Ethylalanine (α-Et-Ala, 2-methyl-2-amino-*n*-butanoic acid), DL-α-propylalanine (α-Prop-Ala, 2-methyl-2-aminopentanoic acid), DL-α-butylalanine (α-But-Ala, 2-methyl-2-aminohexanoic acid), DL-α-pentylalanine (α-Pent-Ala, 2-methyl-2-aminoheptanoic acid), DL-α-hexylalalanine (α-Hex-Ala, 2-methyl-2-aminooctanoic acid), DL-α-heptylalanine (α-Hept-Ala, 2-methyl-2-aminononanoic acid), DL-α-octylalanine (α-Oct-Ala, 2-methyl-2-aminodecanoic acid), DL-α-nonylalanine (α-Non-Ala, 2-methyl-2-aminoundecanoic acid), DL-α-propyl-α-amino-*n*-butyric acid (α-Et-Abu, 2-ethyl-2-aminopentanoic acid), DL-α-butyl-α-amino-*n*-butyric acid (α-But-Abu, 2-ethyl-2-aminohexanoic acid), DL-α-pentyl-α-amino-*n*-butyric acid (α-Pent-Abu, 2-ethyl-2-amino-*n*-butyric acid), DL-α-hexyl amino-*n*-butyric acid (α-Hex-Abu, 2-ethyl-2-aminoheptanoic acid).

Pure enantiomers of α-Et-Ala to α-Pent-Ala were obtained by digestion of the N-chloroacetyl or N-trifluoroacetyl derivatives with acylase I or carboxypeptidase A [49, 51, 52] (for formulae see also Fig. 1).

In the case of pure enantiomers (not racemates) in the series α-Et-Ala to α-Pent-Ala the R, S nomenclature has been used to avoid ambiguities, since the respective AAA can be derived from either a D- or L-amino acid [42, 74, 75]; cf. also Table II.

High-Performance Liquid Chromatography

Columns

Analytical separations were carried out using Hyperchrome columns (250 mm × 4 mm i.d., Manufit system, Bischoff Analysentechnik, Leonberg, FRG) equipped with pre-columns (cartridges, 20 mm × 4 mm i.d.) and packed with the chiral phases Chiral ProCu = Daltosil 100, Chiral HyproCu = Daltosil 100 and Chiral ValCu = Daltosil 100, 5 μm (Serva, Heidelberg, FRG). For another series of experiments, a column (250 mm × 4.6 mm i.d., no pre-column) packed with Nucleosil Chiral-1 (Macherey-Nagel, Düren, FRG) was used. For preparative separations, a Hyperchrome column (250 mm × 20 mm i.d., pre-column 50 mm × 20 mm i.d.) packed with Chiral ProCu = Daltosil 100, 5 μm, was employed. The analytical columns were kept at suitable temperatures by a water-jacket (Knaur, Bad Homburg, FRG) and a thermostat (Haake, Karlsruhe, FRG). The preparative column was put into a large waterbath equipped with a magnetic stirrer (Köttermann, Uetze-Henigsen, FRG). Fig. 1 also shows the structures of the stationary phases.

Instrumental

Analytical and preparative HPLC using UV-detection was carried out using a Perkin-Elmer Liquid Chromatograph Series 3B composed of two dual-head reciprocating pumps, a variable-wavelength spectrophotometric detector LC-75, a recorder 561 and a Model D-2000 chromatointegrator (Merck-Hitachi, Darmstadt, FRG). HPLC for the polarimeter detection was performed with a Perkin-Elmer Series 10 isocratic pump, a variable-wavelength spectrophotometric detector LC 90 UV and a LCI-100 laboratory computing integrator (Perkin-Elmer). Samples were injected automatically using a Perkin-Elmer ISS 100 or ISS 101 autosampler. For preparative injections, a Rheodyne Modell 7125 valve (Rheodyne, Cotati, CA, USA) equipped

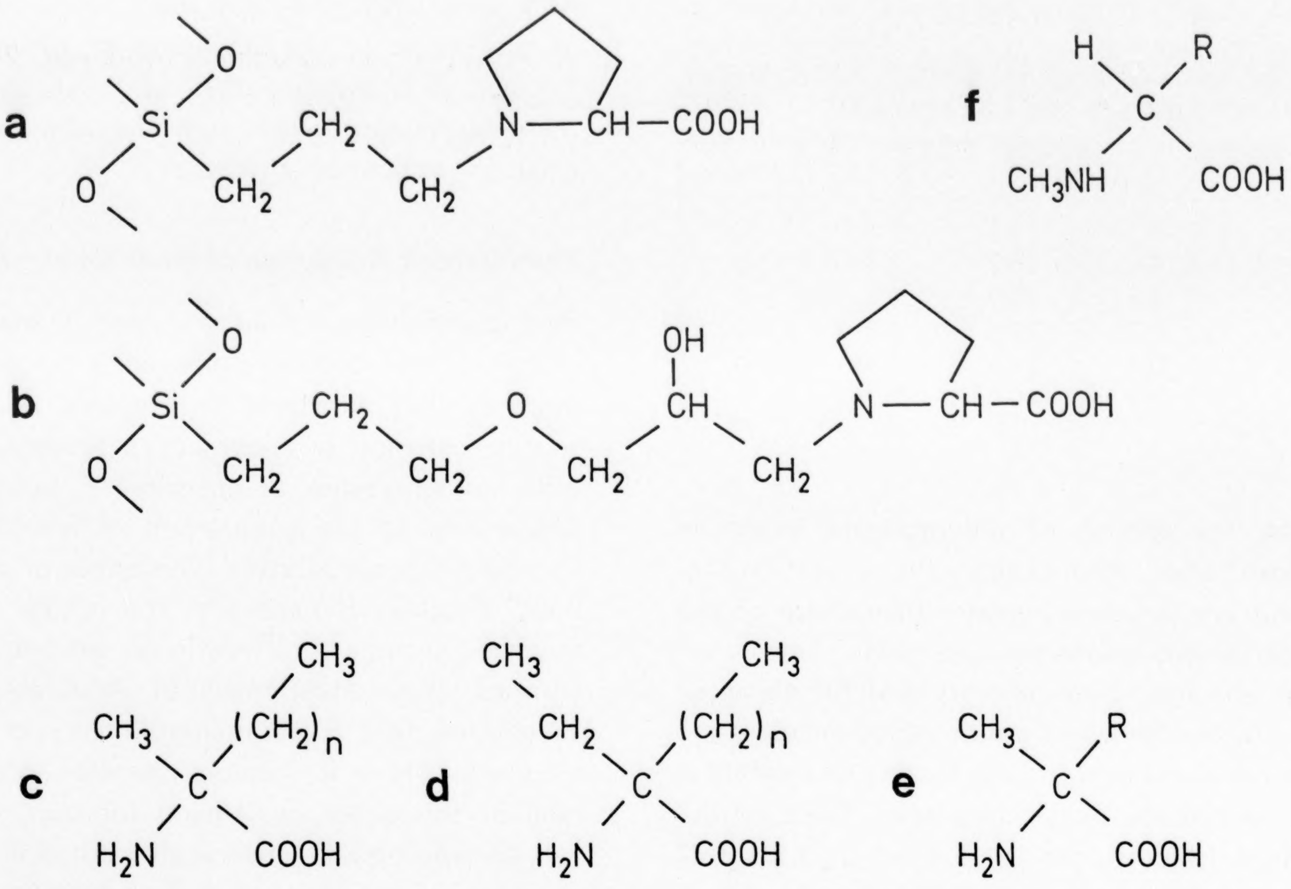

Fig. 1

Structures of the chiral stationary phases (a), Nucleosil Chiral-1; (b), Chiral ProCu; and formulae of (c), α-alkyl-alanins (n = 1–8); (d), α-alkyl-α-amino-*n*-butyric acids (n = 3–6); (e), α-methyl-α-amino acids; and (f), N-methyl-α-amino acids (R = protein amino acid side chain).

with a 1-ml sample loop was used, and suitable fractions were collected manually. After concentration *in vacuo*, Cu^{2+} could be removed as CuS by bubbling H_2S gas through the solution or by liberating H_2S *in situ* from thioacetamide (Merck, Darmstadt, FRG). Cu^{2+} could also be removed by passing the neutralized solution through a column packed with Chelite C ion-exchanger (Serva).

For determining the optical rotation, a polarimeter detector Model 241 LC, designed for use in a liquid chromatography system, equipped with a flow cell of a nominal volume of 80μl and having a path length of 100mm, was used. This detector is suitable for measurements at various wavelengths within the UV-VIS range by the individual choice of six interference filters as standards for the filter turrent (Na 589nm and Hg 578nm, 546nm, 365nm, 302nm). Polarimeter detection was, in general, carried out at 578nm, with the exception of α-Me-Val at 435nm, and integration times of 2sec were used.

Sample Preparation

For analytical runs 5–10μl, for polarimeter detection 40–100μl, of 0.1–0.5% samples in the eluent employed were used. Amino acids having a low solubility in the eluent were dissolved in a suitable amount of 6N HCl and adjusted to a slightly acidic pH (4–5) by the addition of ca. 12% aqueous NH_3 (proved by spotting samples taken by a capillary onto pH papers). To avoid crystallisation, the respective solution was warmed and/or immediately injected onto the column if necessary.

Eluents

The following eluents were degassed by sonification prior to use. If given, the pH was adjusted with 2N HCl or 2N NaOH, with the exception of 10mmol $CuSO_4$ having pH 4.7 without adjustment. This eluent designation has been used in the text throughout.

A, 1mmol Cu(II)acetate in 10% methanol, pH 4.5;
B, 1mmol Cu(II)sulfate in 40% methanol;
C, 1mmol Cu(II)acetate in 10% acetonitrile, pH 4.0;
D, 1mmol Cu(II)acetate in 10% acetonitrile, pH 5.0;
E, 1mmol Cu(II)acetate in 10% acetonitrile, pH 6.0;
F, 10mmol Cu(II)sulfate in 10% acetonitrile;
G, 10mmol Cu(II)sulfate;
H, 1mmol Cu(II)acetate in 20% acetonitrile, pH 4.0;
I, 10mmol Cu(II)sulfate in 10% methanol.

Copper(II)sulfate · $5H_2O$ and copper(II)acetate were from Sigma, methanol and acetonitrile of HPLC grade from Merck.

Resolution of N-Methyl-DL-α-Amino Acids

The schematic structures of the chiral stationary phases and compounds employed in the following analysis are shown in Fig. 1, and the enantiomeric resolution of selected N-methyl-DL-α-amino acids (NMe-AA) by LE-HPLC is shown in Fig. 2. The respective adjusted retention times $t'_{D,L}$ and separation factors α ($\alpha = t'_L/t'_D$) are compiled in Table I. In the examples shown, baseline resolution was achieved using proline as the chemically bonded ligand. In all cases, the D-enantiomer elutes before the L-enantio-

Table I. Adjusted retention times t'_D and t'_L of D- and L-enantiomers and separation factors α ($\alpha = t'_L/t'_D$) of N-methyl-α-amino acids separated by ligand-exchange (LE) HPLC (Chiral ProCu). For conditions see Fig. 2 (NMe-DL-AA $\hat{=}$ DL-NMe-AA).

Amino Acid	t'_D	t'_L	α	Eluent
(a) NMe-DL-Ala	4.7	8.3	1.8	D
(b) NMe-DL-Val	4.6	16.7	3.6	D
(c) NMe-DL-Phe	7.9	32.9	4.2	D
(d) NMe-DL-Leu	7.7	13.6	1.8	D
(e) NMe-DL-Asp	10.1	24.4	2.4	D
(f) NMe-DL-Glu	3.2	5.5	1.7	C

mer, proven by the spiking of the racemates with the respective L-enantiomer. Remarkably, the separation factors of NMe-AA are in general greater than those of the respective underivatized protein amino acids. This is attributed to the enhanced hydrophobity and the electron-donating effect of the N-methyl group, which increases the basicity of the nitrogen electron pair, leading to a stabilization of the mixed ligand metal complexes. These results suggest that most NMe-AA can be resolved by LE-HPLC into enantiomers using the given or slightly modified conditions. The excellent resolution is of interest because the enantiomeric resolution of NMe-AA is in general more difficult to achieve than that of protein amino acids [53]. LE-HPLC, therefore, might be very useful in peptide chemistry where NMe-AA have been found to racemize easily in the course of the activation of carboxy groups [54]. Further, it is assumed that LE-HPLC should also enable the determination of the optical configuration of NMe-AA occurring in peptide antibiotics.

Enantiomeric Resolution of DL-α-Alkyl-α-Amino Acids

Pure enantiomers of all free and numerous derivatized protein or non-protein amino acids having a C^{α} hydrogen atom can be purchased or prepared relatively easily by routine chemical or enzymatic procedures. Therefore, the order of emergence of enantiomers by LE-HPLC can be determined by the comparison of retention times or by spiking a racemic mixture with either of the pure enantiomers. Further, if necessary, the optical rotation can be measured using a conventional off-line polarimeter. In contrast, pure enantiomers of AAA are, with very few exceptions (see Experimental), not yet available commercially. There is, however, as mentioned at the beginning of this paper, a demand for pure enantiomers and for an appropriate analytical methodology for the determination of their optical purity. Despite difficulties due to severe steric constraints [55], gas-liquid chromatography employing chiral and non-chiral stationary phases has been shown to be a very suitable technique for the enantiomeric resolution of AAA [43, 45, 49, 56, 57].

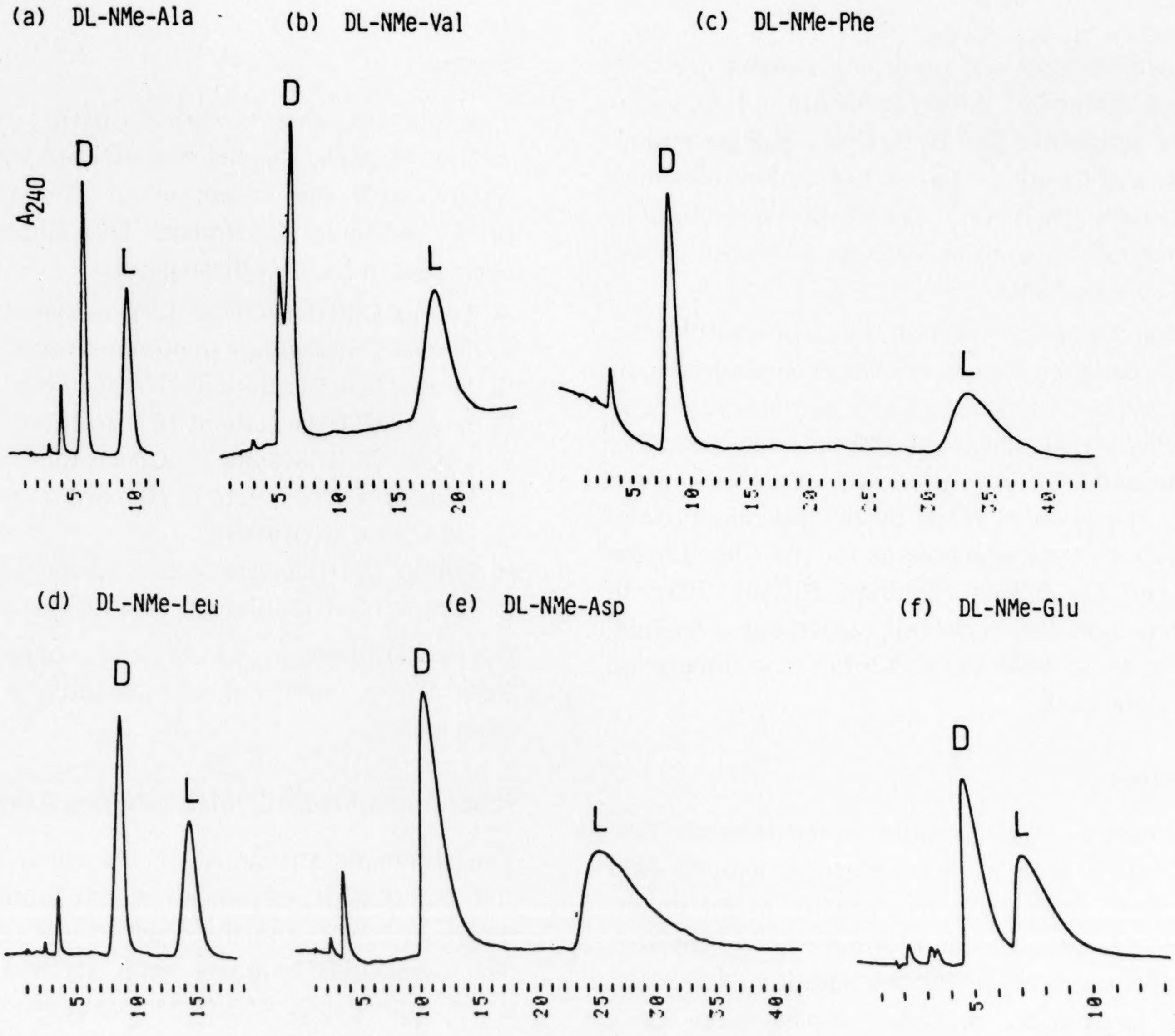

Fig. 2

Enantiomeric resolution of N-methyl-α-amino acids by LE-HPLC. Conditions: column, 270 mm × 4 mm i.d.; stationary phase, Chiral ProCu, 5 μm; a, b, c, d, e, eluent **D**; f, eluent **C**; flow rate, 2 ml/min; absorbance, 240 nm; temperature, 40°C.

With regard to LEC, the majority of investigations focused on α-amino acids and, in particular, protein amino acids. However, Davankov et al. [8, 58, 59] already included Iva and non-protein amino acids in systematic investigations for elucidating resolution mechanisms. Engel and Nagy [32] were successful in separating DL-Iva occurring in a carbonaceous meteorite with extremely high resolution factor by employing ion-exchange chromatography and L-Pro as chiral solute [2, 60]. Weinstein and Grinberg [61] separated a number of AAA by LE-HPLC by forming mixed copper complexes with N,N-dimethyl-L-valine and N,N-dipropyl-L-alanine, detected by post-column derivatization with o-phthaldialdehyde and 2-mercaptoethanol (OPA–2-Me) at elevated temperatures to increase the fluorescence yield, a phenomenon which had been already recognized by Cronin et al. [29, 30] and also investigated in our study on AAA and α-amino alcohols [43]. Keller and Dick [62] failed in the resolution of DL-Iva by LE-HPLC, but could resolve several fluorinated analogs, and Florance et al. [63] separated a number of AAA on silica-bonded Pro (Chiral Pak WH). DL-α-Me-Dopa was resolved by Oelrich et al. [64], Gübitz et al. [65, 66] using LE-HPLC, and by LE-TLC by Günther and Martens et al. using "Chiralplate" [67–71].

In order to develop methods for the optimized enantiomeric resolution of DL-AAA capable of extension to preparative separations, we investigated comparatively the commercially available chiral LEC phases Chiral ProCu, Chiral HyproCu and Chiral ValCu [65, 66] and Nucleosil Chiral-1 [72] (Fig. 1). As shown in Figs 3 to 6 and quantified in Table II, chiral phases are in general capable of separating all AAA used in this study and give, in most cases, baseline resolution, providing that a suitable composition, pH, and temperature of the respective eluent are chosen. It is remarkable to note, in analogy to protein amino acids, and in striking contrast to GLC determinations or HPLC methods using derivatized AAA, the sometimes extremely large separation factors of enantiomers, in particular for aromatic side chain AAA (cf. Figures).

AAA that have exclusively alkyl side chains show approximately equal separation factors towards all stationary phases. Chiral ValCu gives much lower separation factors and retention times for aromatic side chain AAA, although baseline resolution occurred in every case (Fig. 5). The enantiomers of α-Me-Asp and α-Me-Glu show a difference in their separation behaviour on Chiral HyproCu (Fig. 4). In contrast to the former, where almost baseline separation occurs, the latter shows just an indication of separation under identical conditions. α-Me-Glu, however, is baseline resolved on Chiral ProCu, while α-Me-Asp is less resolved in this case (Fig. 3). In addition, α-Me-Asp shows baseline resolution on Nucleosil Chiral-1 (Fig. 6), while α-Me-Glu is less well separated (not shown in Fig.). Although the trifunctional acidic and basic amino acids are most sensitive with regard to their chiral resolution on the experimental conditions (in particular, composition of eluent and pH), this is also valid for neutral amino acids, as demonstrated by α-Me-Leu, which on Nucleosil Chiral-1 has the best resolution at pH 5 (Fig. 6).

The homologous series α-Et-Ala to α-Oct-Ala shows, in all cases, baseline separation of enantiomers and about equal separation factors (1.4 to 1.7) on Chiral ProCu. Further, the retention times of the first and second eluted enantiomers of α-But-Ala to α-Oct-Ala are about equal, with the exception of α-Hept-Ala (cf. Table II and Fig. 3). This suggests that, although the growing alkyl side chain contributes much to the increasing hydrophobity of the respective AAA, it has little influence on retention times and separation factors.

In comparison, the resolution of enantiomers of Asp, Leu and Phe, as examples for acidic, neutral and aromatic side

Table II. Chiral separation of DL-α-alkyl-α-amino acids by ligand-exchange chromatography and assignment of the elution order and optical rotation of enantiomers.

Amino acid	A			B				C				D				E			
	Peak 1	Peak 2	El.	t'_{R_1}	t'_{R_2}	α	El.	t'_{R_1}	t'_{R_2}	α	El.	t'_{R_1}	t'_{R_2}	α	El.	t'_{R_1}	t'_{R_2}	α	El.
DL-α-Et-Ala	R(–)	S(+)	A	9.5	13.3	1.4	D	2.2	3.6	1.6	F	8.8	5.3	1.4	C	5.4	6.8	1.3	D
DL-α-Prop-Ala	R(–)	S(+)	A	4.0	6.1	1.5	H	3.0	4.1	1.4	F	5.2	6.9	1.3	H	6.6	8.8	1.3	D
DL-α-But-Ala	R(–)	S(+)	A	6.0	9.1	1.5	H	3.9	5.3	1.4	F	5.0	7.9	1.4	H	6.8	9.0	1.3	D
DL-α-Pent-Ala	R(–)	S(+)	A	6.5	10.9	1.7	A	n.	n.	n.	n.	n.	n.	n.	n.	n.	n.	n.	n.
DL-α-Hex-Ala	(–)	(+)	A	7.2	12.2	1.7	A	n.	n.	n.	n.	n.	n.	n.	n.	n.	n.	n.	n.
DL-α-Hept-Ala	(–)	(+)	B	14.2	20.2	1.4	A	n.	n.	n.	n.	n.	n.	n.	n.	n.	n.	n.	n.
DL-α-Oct-Ala	(–)	(+)	G	6.5	10.7	1.6	A	n.	n.	n.	n.	n.	n.	n.	n.	n.	n.	n.	n.
DL-α-Me-Val	D(+)	L(–)	A	3.4	5.8	1.7	H	2.1	4.1	2.0	F	5.5	7.2	1.3	H	6.0	7.8	1.3	D
DL-α-Me-Leu	D(–)	L(+)	A	4.5	7.6	1.7	H	3.3	5.0	1.5	F	4.9	7.1	1.5	H	1.5 (5.8; 8.0)	1.9 (8.4; 9.8)	1.3 (1.5; 1.2)	C (D; F)
DL-α-Me-Met	D(–)	L(+)	A	9.7	13.3	1.4	F	3.2	4.4	1.4	F	4.0	5.0	1.3	H	n.	n.	n.	n.
DL-α-Me-Ser	D(–)	L(+)	A	2.0	5.1	2.6	H	1.7	5.0	2.9	F	2.9	3.8	1.3	H	n.	n.	n.	Fig. 6
DL-α-Me-Asp	D(–)	L(+)	H	6.2	7.2	1.2	C	19.0	24.2	1.3	F	n.	n.	n.	n.	4.7	5.9	1.3	C
DL-α-Me-Glu	n.	n.	n.	5.9	7.5	1.3	C	18.2	18.2	1.0	F	n.	n.	n.	n.	n.	n.	n.	n.
DL-α-Me-Orn	(+)	(–)	H	3.4	4.5	1.3	F	0.7	1.5	2.1	F	n.	n.	n.	n.	n.	n.	n.	n.
DL-α-Me-His	D(+)	L(–)	A	4.0	8.2	2.1	H	5.6	10.2	1.8	F	10.3	18.4	1.8	H	n.	n.	n.	Fig. 6
DL-α-Me-Phe	D(–)	L(+)	A	5.7	19.7	3.5	H	2.8	24.6	8.8	F	7.9	13.4	1.7	C	n.	n.	n.	n.
DL-α-Et-Phg	D(–)	L(+)	A	21.3	39.1	1.8	F	n.	n.	n.	n.	12.5	16.5	1.3	C	n.	n.	n.	n.
DL-α-Me-PheOMe	(–)	(+)	B	7.7	32.1	4.2	H	n.	n.	n.	n.	10.7	20.0	1.9	C	n.	n.	n.	n.
DL-α-Me-Tyr	D(–)	L(+)	B	4.4	26.3	6.0	H	2.8	24.6	8.8	F	6.1	13.1	2.1	C	n.	n.	n.	n.
DL-α-Me-Trp	(–)	(+)	B	13.2	59.5	4.5	H	7.6	50.8	6.7	F	n.	n.	n.	n.	n.	n.	n.	n.
DL-α-Me-Dopa	D(–)	L(+)	B	22.1	94.2	4.3	B	n.	n.	n.	n.	n.	n.	n.	n.	n.	n.	n.	n.

A, assignment of the configuration and optical rotation [(–), *levorotatory*; (+), *dextrorotatory*] of the first (peak 1) and second (peak 2) eluted enantiomer of α-alkyl-α-amino acids (AAA) determined by a polarimeter detector and LE-HPLC; **B–E**, adjusted retention times t'_R [$t'_R = t_R - t_M$; t'_R, retention time of the first (R_1) and second (R_2) eluted enantiomer; t_M, retention time of methanol] of the first (t'_{R_1}) and second (t'_{R_2}) eluted enantiomers, and separation factors α ($\alpha = t'_{R_2}/t'_{R_1}$) of the enantiomers. Stationary phases (conditions are given in the respective figure legends): **A**, Chiral ProCu (Fig. 7); **B**, Chiral ProCu (Fig. 3); **C**, Chiral HyproCu (Fig. 4); **D**, Chiral ValCu (Fig. 5); **E**, Nucleosil Chiral-1 (Fig. 6); El., eluent (for composition see Experimental); n., not determined. For DL and RS see Experimental; cf. also Fig. 7.

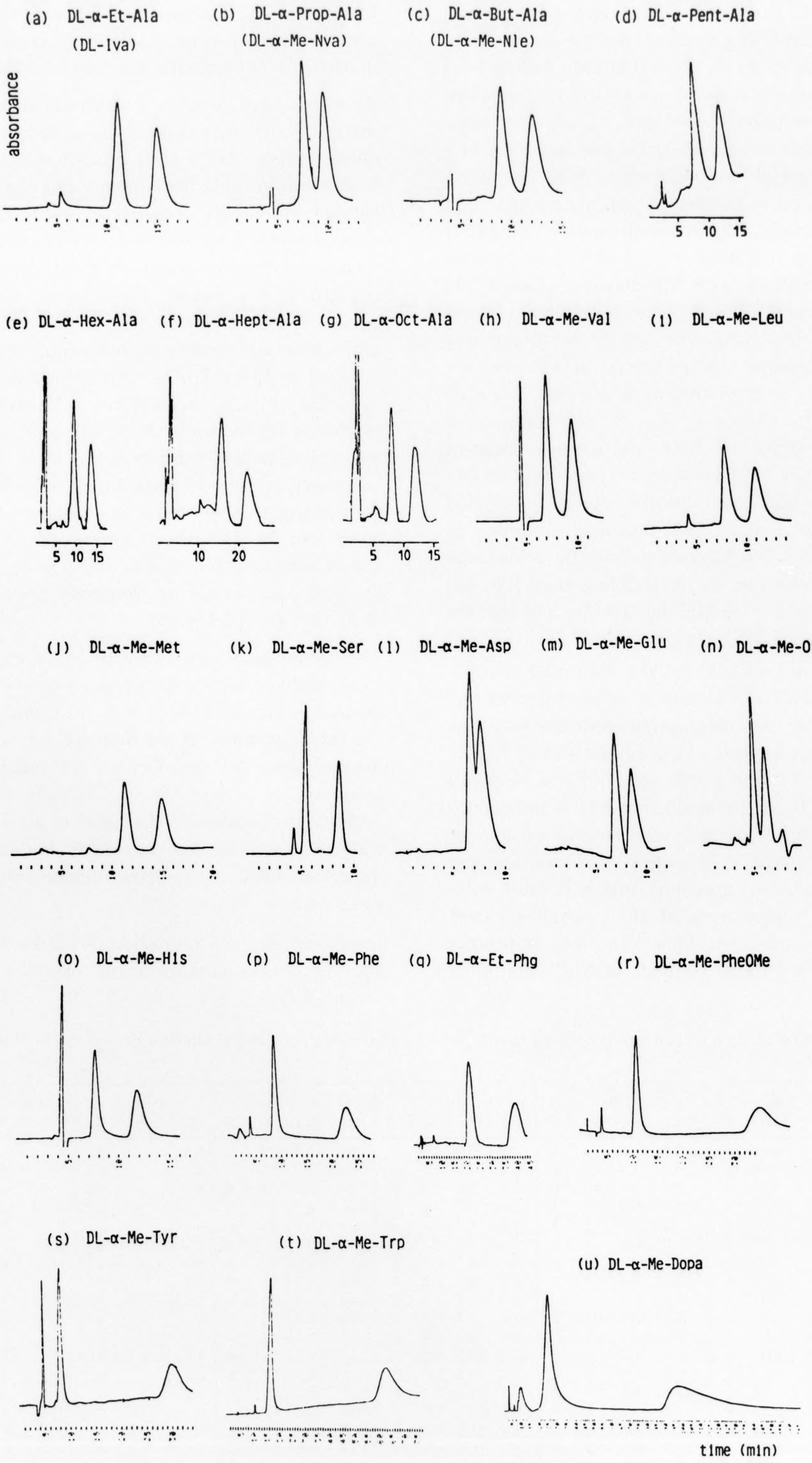

Fig. 3

Enantiomeric resolution of α-alkyl-α-amino acids by LE-HPLC. Conditions: column, 270 mm × 4 mm i.d.; stationary phase, Chiral ProCu, 5 μm; a, eluent **D**; b, c, h, i, k, o, p, r, s, t, eluent **H**; j, n, eluent **F**; l, m, eluent **C**; q, eluent **G**; d, e, f, g, eluent **A**; u, eluent **B**; a, flow rate, 1.5 ml/min; b, c, h, i, k, j, n, o, p, q, r, s, t, u, flow rate, 1.0 ml/min; d, e, f, g, flow rate, 2 ml/min; m, l, flow rate, 3 ml/min; a, b, j, k, l, m, n, o, p, q, r, s, t, absorbance 240 nm; d, e, f, g, absorbance 245 nm; temperature, 40 °C, with the exception of l, m, 60 °C and u, at ambient temperature.

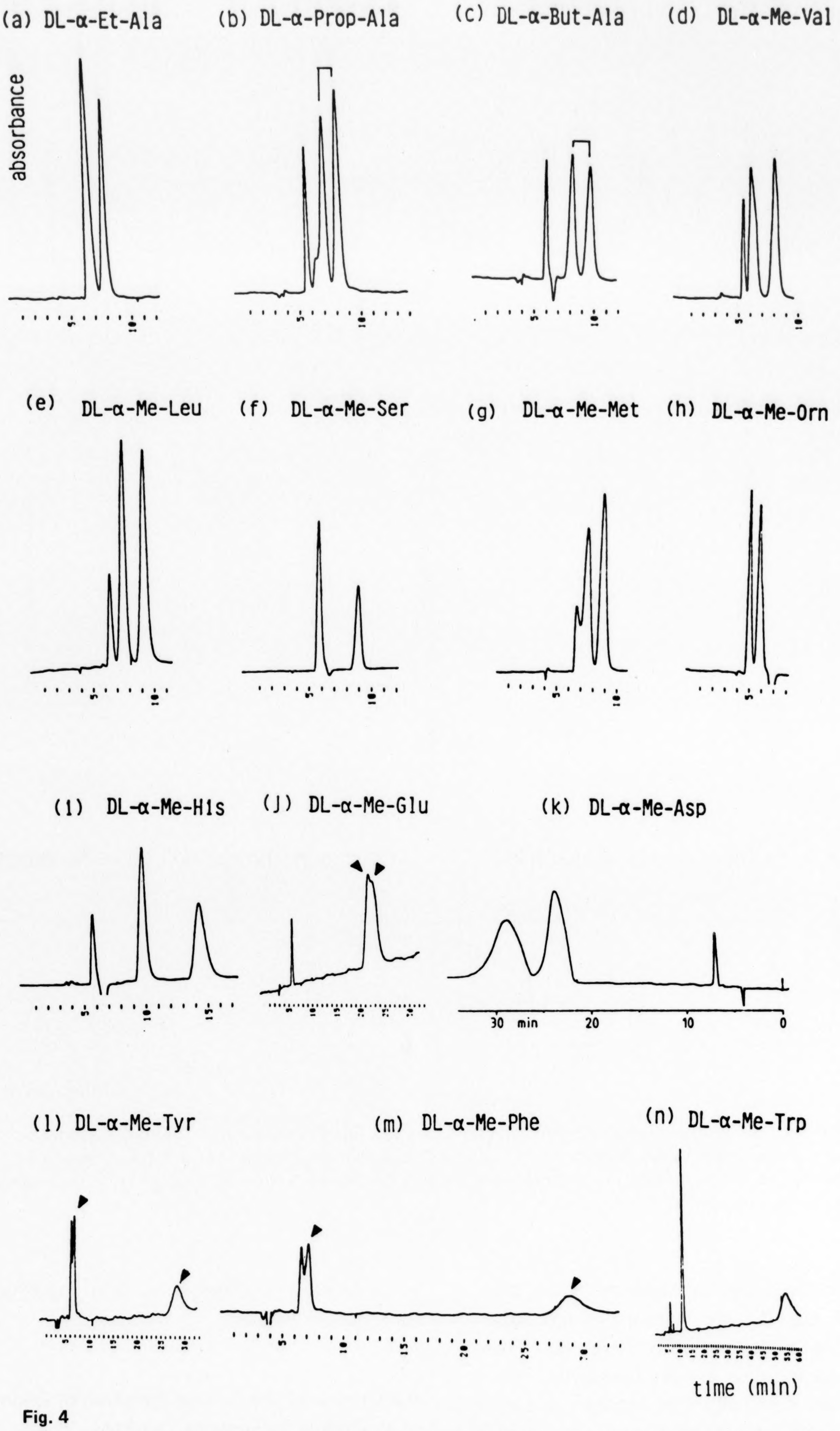

Fig. 4

Enantiomeric resolution of α-alkyl-α-amino acids by LE-HPLC. Conditions: column, 270 mm × 4 mm i.d.; stationary phase, Chiral HyproCu, 5 μm; eluent **G**, flow rate, 0.9 ml/min; absorbance 235 nm; temperature, 40 °C.

chain amino acids, respectively, their N-methylated derivatives (NMe-Asp, NMe-Leu and NMe-Phe) and C^{α} methylated analogues (α-Me-Asp, α-Me-Leu and α-Me-Phe) were investigated (Table III). Under the conditions used, the enantiomers of α-Me-Asp show just the beginning of a separation, whereas NMe-Asp is baseline resolved. That this is solely attributable to the electron-donating effect of the N-methyl group, increasing the basicity and stability of the mixed ligand complex, is not supported when compared with Asp, which is equally well resolved.

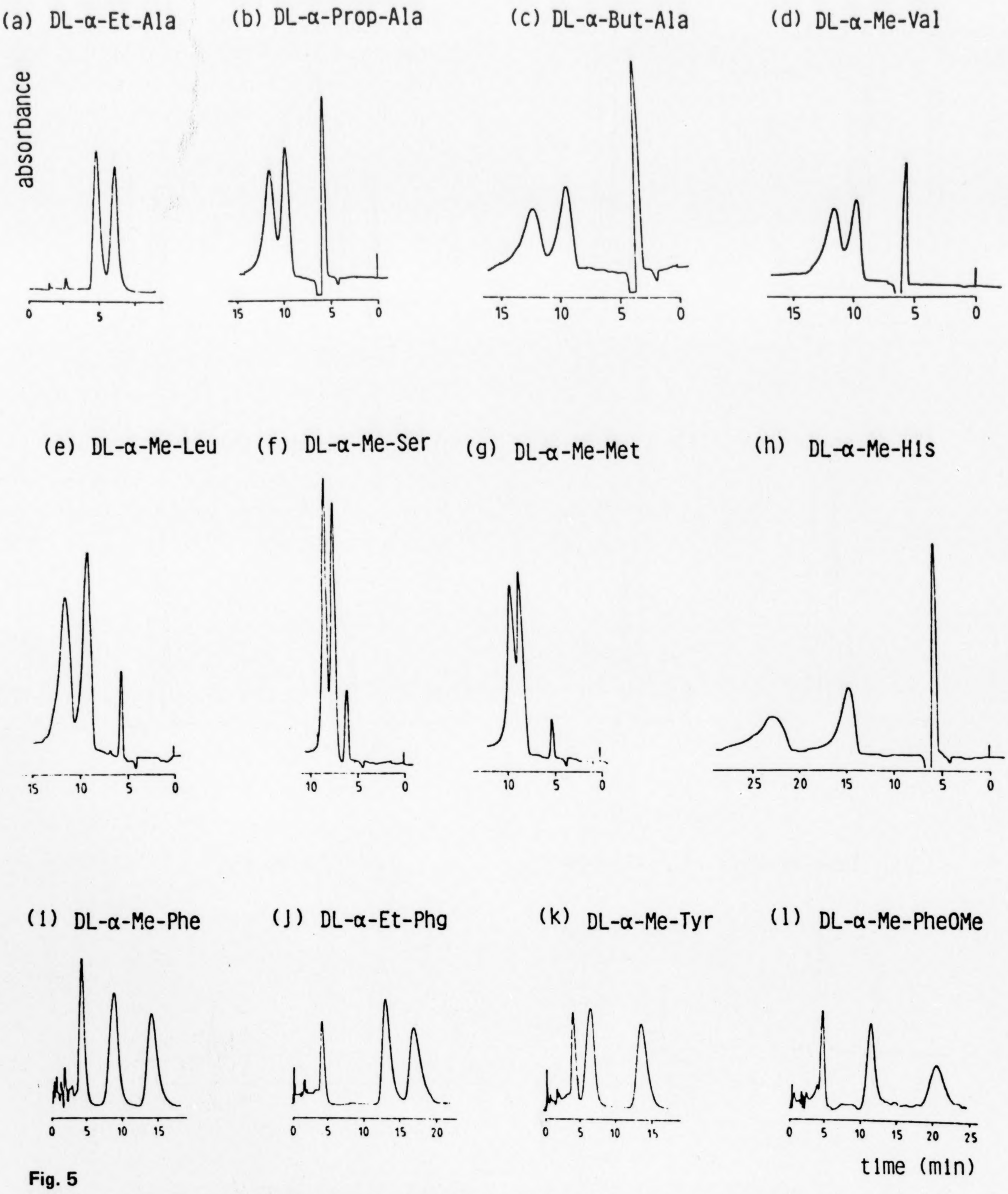

Fig. 5

Enantiomeric resolution of α-alkyl-α-amino acids by LE-HPLC. Conditions: column, 250mm X 4mm i.d.; stationary phase, Chiral ValCu, 5μm; a, i, j, k, l, eluent **C**; b, c, d, e, f, g, h, eluent **H**; a, i, j, k, l, flow rate, 2ml/min; b, c, d, e, f, g, h, flow rate, 0.9ml/min; a, i, j, k, l, absorbance 245nm; b, c, d, e, f, g, h, absorbance 235nm; temperature, 40°C.

The existence of pronounced sterical constraints on the complex formation of the C^α alkyl groups is not supported when comparing α-Me-Leu with NMe-Leu. The enantiomers of these compounds are well resolved, producing nearly equal resolution factors in contrast to Leu, which is not resolved under these conditions. The small effect of steric hindrance is also supported when comparing retention times and separation factors of the series α-Et-Ala to α-Oct-Ala (cf. Table II). α-Me-Phe and NMe-Phe show roughly equal retention times of the first and second eluted enantiomers; DL-Phe is well resolved, but has a significantly lower separation factor.

In summary, N-methylation of an α-amino acid leads to an, in part drastic, increase of the separation factors of enantiomers (as shown for Leu, Asp and Phe), and C^α methylation can lead to a decrease (as shown for Asp) or an increase (as shown for Leu and Phe) of the factors for these derivatives.

Assignment of the Optical Rotation of Enantiomers by Use of an On-line Polarimeter Detector

As shown in Table II and Fig. 7, this correlation could be made for all AAA used in this study, with the exception of DL-α-Me-Glu. As a result of the much lower sensitivity of the polarimeter detector as compared to the UV-detector and the low optical rotations of AAA in general, the analytical column employed (Chiral ProCu) had to be overloaded. However, even in this case the polarimeter detector worked satisfactorily. For example, in the case of DL-α-Me-Asp, the polarimeter detector revealed a negative optical rotation at the increasing slope and a positive optical rota-

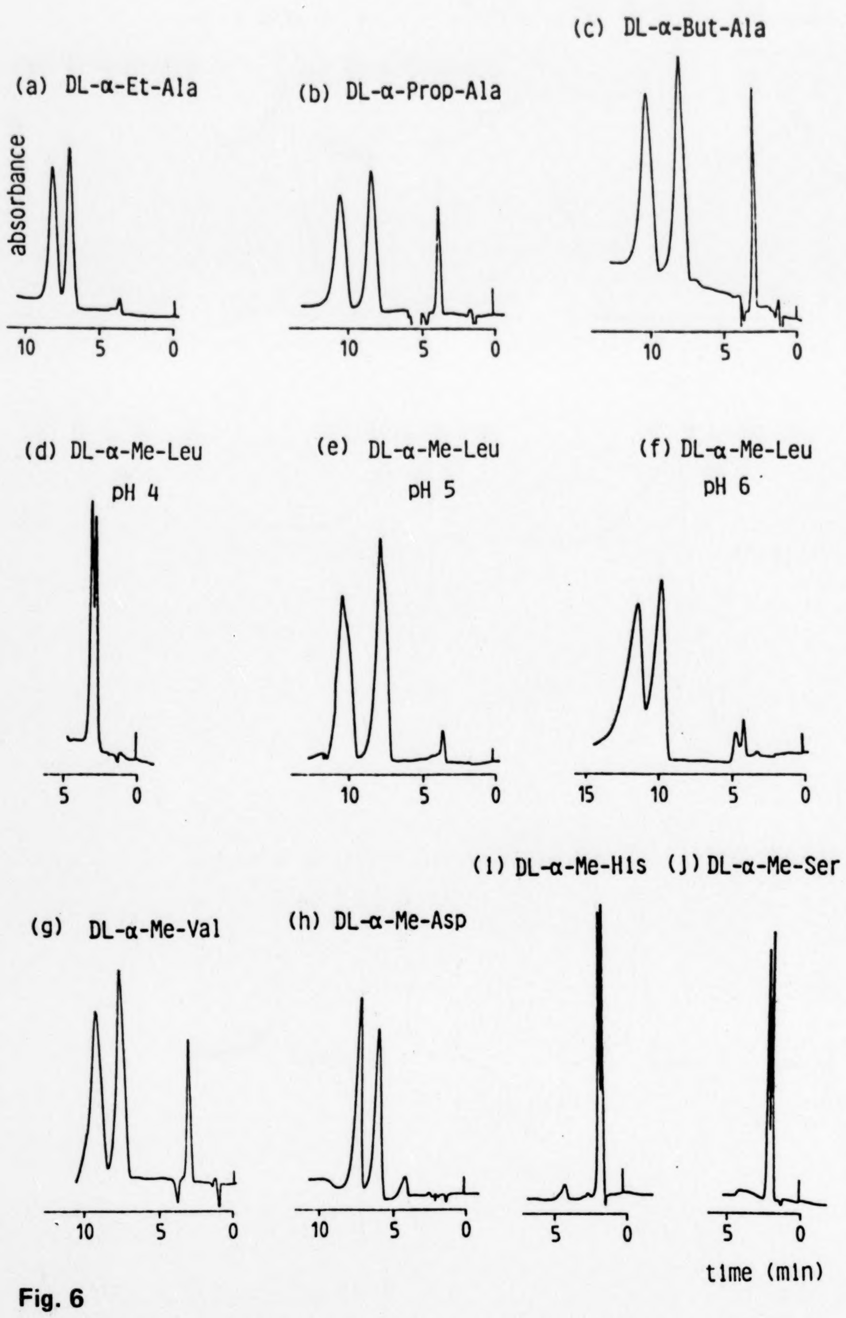

Fig. 6

Enantiomeric resolution of α-alkyl-α-amino acids by **LE-HPLC**. Conditions: column, 250 mm X 4 mm i.d.; stationary phase, Nucleosil Chiral-1, 5 μm; a, b, c, e, g, eluent **D**; d, h, i, j, eluent **C**; f, eluent **E**; flow rate, 1.5 ml/min; absorbance, 240 nm; temperature, 60 °C.

tion at the decreasing slope, although UV detection gave a single peak. Under the experimental conditions used, this was not the case for DL-α-Me-Glu.

The experiments were carried out at 578 nm, with the exception of α-Me-Val measured at 435 nm, and performed at ambient temperature (with the exception of α-Oct-Ala, the resolution of which was carried out at 45 °C to overcome the very low solubility). The conditions for the on-line polarimeter determination of the optical rotations are given in Fig. 7, and the conditions for the analytical enantiomeric resolutions in Fig. 3. Although they are not completely identical, it is not assumed (but see discussion below) that the limited variations of the eluent composition and temperature, as indicated in Figures and Table II, will change the order of emergence of the enantiomers or the sign of the optical rotation.

Within the homologous series α-Et-Ala to α-Oct-Ala, the (−)-enantiomer elutes before the (+)-enantiomer in all cases, as was also found for α-Me-Met, α-Me-Ser and for the aromatic side chain AAA. Exceptions are the basic amino acids α-Me-Orn and α-Me-His, where the (+)-enantiomer elutes before the (−)-enantiomer. The branched side chain AAA, α-Me-Val and α-Me-Leu, show the reversed optical rotation of the enantiomers eluted first and second, respectively (cf. Fig. 7). This corresponds to the chiroptical behaviour of L(+)-Val and L(−)-Leu, where the L-enantiomers in aqueous solutions have the opposite sign of the optical rotation. In many cases, where the pure enantiomers of AAA were available, assignment of the order of emergence, optical rotation and absolute configuration under the experimental conditions used could be made. It should be mentioned in this connection that Weinges and Stemmle [73] concluded from the optical rotation dispersion (ORD) spectra of aliphatic AAA obtained by asymmetric Strecker synthesis that those having an even number of carbon atoms in the longer side chain (*viz.* α-Et-Ala to α-But-Ala) belong to the S(+)-series, and those having odd numbers (*viz.* α-Prop-Ala and α-Pent-Ala) belong to the R(−)-series. Although it was suggested by Neuberger [74] that the designation D and L should not be applied to AAA, Greenstein and Winitz [75] pointed out that the biological behaviour, e.g. stereoselective digestion by enzymes, should be taken into account. Chiral enzymatic recognition was even found to be valid for the series of unusual AAA, α-Et-Ala to α-Pent-Ala [49], where the R(−)-enantiomers elute before the S(+)-enantiomers. Since in the cases of the higher homologues, α-Hex-Ala to α-Oct-Ala, the (−)-enantiomers also elute before the (+)-enantiomers, this suggests that in the whole series the R-enantiomers elute before the S-enantiomers. In conclusion, AAA, under similar conditions, show the same order of emergence (R before S, with the exception of Pro) as α-amino acids [65, 66]. With regard to strongly deviating conditions it should be emphasized, however, that the sign of the optical rotation and the order of emergence of enantiomers depend on the composition and pH of the eluent and the type of the chiral stationary phase. In particular, the sign of the optical rotation of copper complexes of amino acids depends, according to the Pfeiffer-Christeleit rule, on the wavelength

Table III. Comparison of the adjusted retention times t'_1 and t'_2 and separation factors α of selected DL-α-amino acids and their N-methylated and C^α methylated analogs.

Amino Acid	t'_1	t'_2	α	Eluent
DL-Asp	5.21	7.23	1.39	C
NMe-DL-Asp	3.61	9.00	2.49	C
DL-α-Me-Asp	6.53	7.57	1.16	C
DL-Leu	7.57 (n.r.)			C
NMe-DL-Leu	5.87	10.62	1.81	C
DL-α-Me-Leu	6.94	11.88	1.71	C
DL-Phe	10.01	22.03	2.20	D
NMe-DL-Phe	7.67	33.58	4.38	D
DL-α-Me-Phe	9.09	31.24	3.44	D

The R-enantiomers elute before the S-enantiomers; n.r., not resolved. Conditions: Column, 250 mm X 4 mm i.d., Chiral ProCu, 5 μm, flow rate, 2 ml/min; absorbance, 240 nm; temperature, ambient.

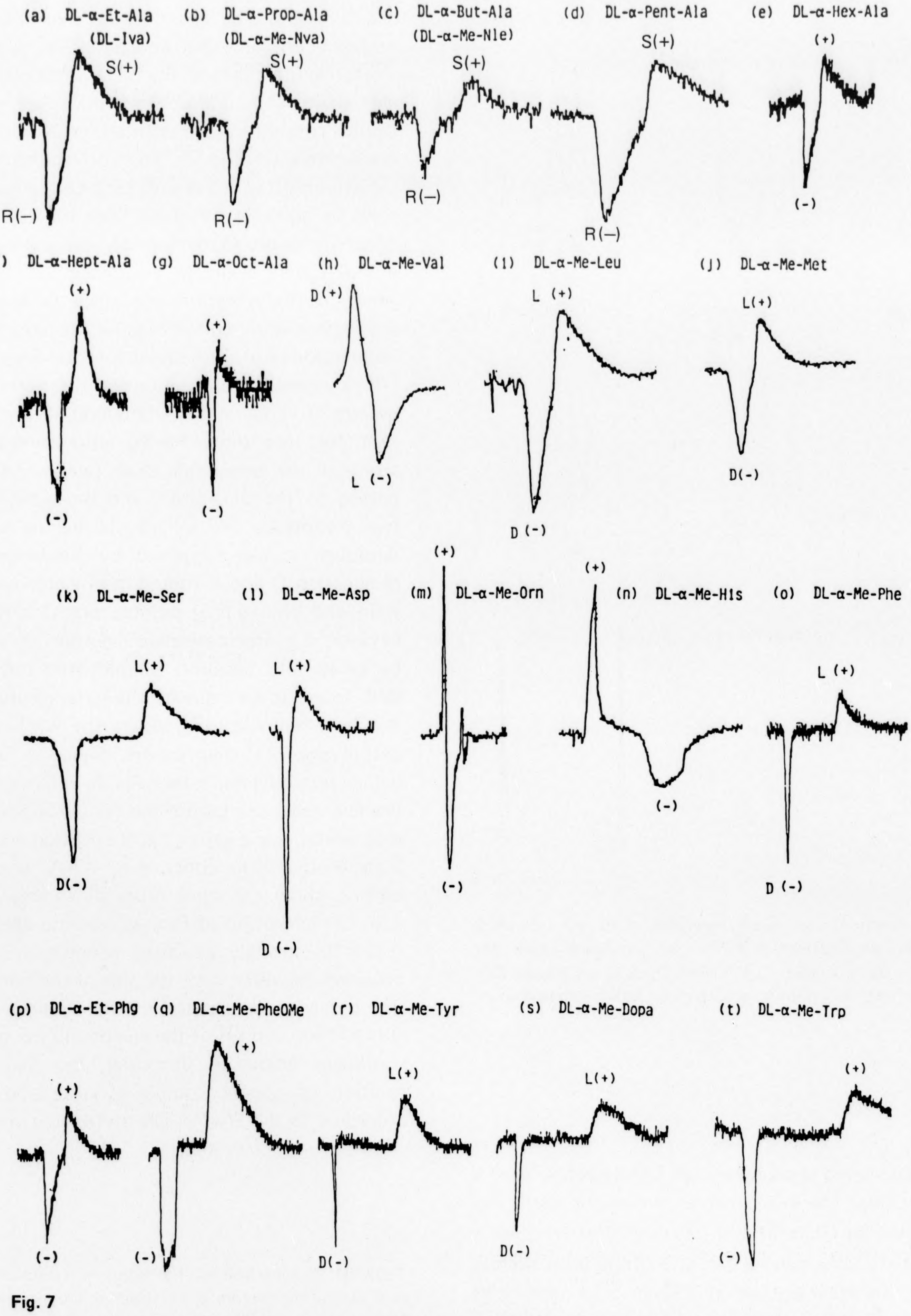

Fig. 7

On-line polarimeter determination of the sign of the optical rotation of enantiomers of α-alkyl-α-amino acids. Conditions: column, 270 mm × 4 mm i.d.; stationary phase, Chiral ProCu, 5 μm; a, b, c, d, e, h, i, j, k, n, o, p, eluent **A**; f, eluent **B**; g, l, m, eluent **H**; detection, polarimeter detector; integration time, 2 sec; absorbance, Hg 578 nm, with the exception of h, 435 nm; temperature, ambient, with the exception of g, 45°C; flow rate, 1 ml/min; chart speed, 1 mm/min and 5 mm/min respectively; relevant sections of the chromatograms are shown. In cases where the pure enantiomers were available, the order of emergence and optical rotation could be assigned (cf. also Table II and Experimental).

and might even change in ORD from *levorotatory* to *dextrorotatory* and *vice versa* [76–78]. Concerning the chiral stationary phase, it was found that replacement of L-Pro by L-Phe, for example, gives just the reversed elution order of α-amino acids [65].

Semipreparative Separation of Racemic α-Alkyl-α-Amino Acids

One promising aspect of LEC is the possibility to scale up analytical separations without any need for previous derivatization. Semipreparative separations for selected AAA

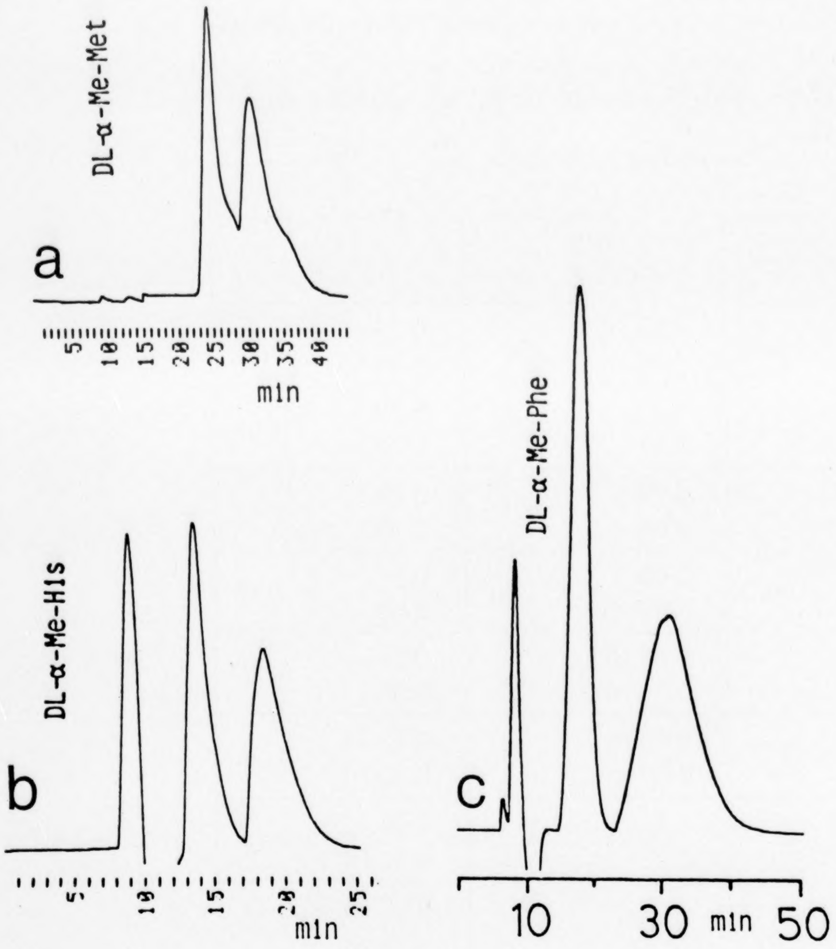

Fig. 8

Semipreparative separation of (a), DL-α-Me-Met (8mg in 300μl eluent); (b), DL-α-Me-His (10mg in 500μl eluent); (c), DL-α-Me-Phe (60mg in 1ml eluent). Conditions: column, 300mm X 20mm i.d. (inclusive 50mm pre-column); Chiral ProCu, 5μm; eluent, (a), **G**; (b), **C**; (d), **I**; flow rate, 10ml/min; temperature, 60°C; absorbance, a, b, 250nm, c, 270nm; pressure, 13—14MPa.

are shown in Fig. 8. Using a 300mm × 20mm i.d. column (inclusive pre-column), packed with Chiral ProCu, 60mg DL-α-Me-Phe could be baseline resolved in a single run. DL-α-Me-His and DL-α-Me-Met, having much lower separation factors compared to aromatic side chain AAA, could be resolved in 8mg and 10mg amounts in single runs. One limitation of the method is the relatively low solubility of amino acids, like α-Me-Tyr, in neutral aqueous eluents. Applications of strong acidic or basic solutions to the column will destroy the copper complex. However, dissolving the amino acid in hot solvents, adding an organic modifier, and resolving the solute at elevated temperatures, or preparing an acidic solution of the amino acid, back-titrating to about neutral, as well as immediately injecting it onto the column to avoid crystallization, may overcome these difficulties in part. Further, chiral phases of the types used under the conditions employed lead to a much faster leaching out of the columns as compared to the reversed-phase materials normally used. Therefore, use of a pre-column and the occasional addition of stationary phase are recommended.

Ligand-exchange Thin-layer Chromatography

An interesting approach in the enantiomeric separation of chiral compounds by LEC is the development of TLC plates coated with a chiral selector, available under the trade name "Chiralplate" [69]. We were interested as to whether this methodology is applicable for separating a homologous series of very hydrophobic DL-AAA having long, unbranched alkyl side chains, namely the series α-Et-Ala to α-Non-Ala and α-Prop-Abu to α-Hex-Abu (Fig. 9, Table IV). These compounds are sufficiently soluble in methanol-chloroform 4:1 to prepare, even in the case of α-Non-Ala, about 1% solutions.

Among the series α-Et-Ala to α-Non-Ala, the first amino acid could not be resolved over a distance of 7.5cm, but when run over 13cm just a separation occurred. In the cases of α-Et-Ala to α-Pent-Ala, where pure enantiomers were available [49], the respective S-enantiomers show the higher R_F-values. This behaviour, therefore, is assumed to be valid for the whole series. The enantiomers of α-Prop-Abu to α-Hex-Abu are well resolved in system I, showing increasing resolution factors. Interestingly, the R_F-values

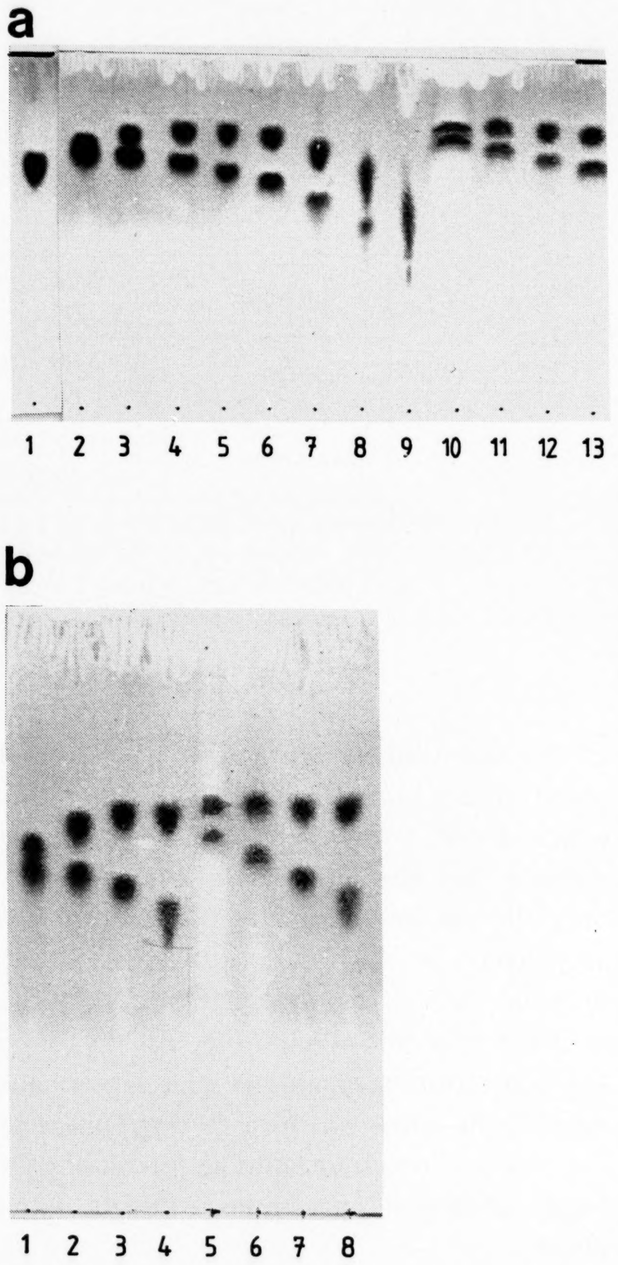

Fig. 9

Ligand-exchange TLC of homologous series of DL-α-alkyl-α-amino acids on Chiralplate. (a), 1, Aib, non-chiral standard; 2, α-Et-Ala; 3, α-Prop-Ala; 4, α-But-Ala; 5, α-Pent-Ala; 6, α-Hex-Ala; 7, α-Hept-Ala; 8, α-Oct-Ala; 9, α-Non-Ala; 10, α-Prop-Abu; 11, α-But-Abu; 12, α-Pent-Abu; 13, α-Hex-Abu; (b), 1, α-Et-Ala; 2, α-Prop-Ala; 3, α-But-Ala; 4, α-Pent-Ala; 5, α-Prop-Abu; 6, α-But-Abu; 7, α-Pent-Abu; 8, α-Hex-Abu. Application of (a), 3-μl and (b), 2.5-μl aliquots of 1% solutions of amino acids in methanol-chloroform (4:1); solvent system (a), acetonitrile-1-propanol-water (2:2:1), (b), acetronitrile-methanol-water (4:1:1); distance start to front, (a), 7.5cm, (b), 13cm; detection with 0.1% ninhydrin in ethanol.

Table IV. Comparison of R_F-values* and resolution factors α of α-alkyl-α-amino acids by TLC on Chiralplate (α = higher R_F/lower R_F).

Solvent systems: **I**, acetonitrile-methanol-water (4:1:1); **II**, acetonitrile-water (4:1); **III**, acetonitrile-1-propanol-water (4:1:1); **IV**, acetonitrile-1-propanol-water (2:2:1).

Amino acid	Solvent system							
	I		II		III		IV	
	R_F	α	R_F	α	R_F	α	R_F	α
(α-Et-Ala)	0.61 0.55	1.11	0.70 0.70	1.00	0.59 (t) 0.55 (t)	1.07	0.74 (t) 0.72 (t)	1.03
α-Prop-Ala	0.63 0.55	1.15	0.69 0.62	1.11	0.67 0.57	1.18	0.78 0.72	1.08
α-But-Ala	0.63 0.51	1.24	0.65 0.57	1.14	0.69 0.54	1.28	0.79 0.70	1.13
α-Pent-Ala	0.62 0.46	1.35	0.59 0.41 (t)	1.44	0.68 0.49 (t)	1.39	0.78 0.68	1.15
α-Hex-Ala	0.59 (t) 0.34 (t)	1.74	(nd)	–	0.62 (t) 0.34 (t)	1.82	0.77 0.65	1.18
α-Hept-Ala	0.46 0.16	2.88	(nd)	–	0.53 (t) 0.30 (t)	1.77	0.73 (t) 0.59 (t)	1.24
α-Oct-Ala	(s)	–	(s)	–	(nd)	–	0.66 (t) 0.51 (t)	1.29
α-Non-Ala	(s)	–	(s)	–	(s)	–	0.52 (t) 0.39 (t)	1.33
α-Prop-Abu	0.66 0.62	1.06	0.66 0.61	1.08	0.63 (t) 0.60 (t)	1.05	0.80 0.77	1.04
α-But-Abu	0.66 0.58	1.14	0.65 0.57	1.14	0.70 0.59	1.19	0.81 0.74	1.09
α-Pent-Abu	0.66 0.54	1.22	0.59 0.46 (t)	1.28	0.68 0.54	1.26	0.80 0.72	1.11
α-Hex-Abu	0.62 0.49 (t)	1.27	(nd)	–	0.65 0.47 (t)	1.38	0.79 0.69	1.14
α-Me-Ala** (Aib)	0.55 (t)		0.68		0.51 (t)		0.69 (t)	

* distance start to front 7.5 cm (13 cm)
** internal, non-chiral standard

(t) spot tailing
(nd) not determinable
(s) substance remains at the start

of the enantiomers running to the front of the plate are about equal, in contrast to their more retained antipodes, which show strongly decreasing R_F-values. This would indicate that the retention of one series of enantiomers is only slightly influenced by the increasing size of the side alkyl chain in contrast to the other. A similar tendency, although less pronounced, is also observed in the series α-Et-Ala to α-Non-Ala (cf. Fig. 9b). As found in a model on the separation mechanisms of α-amino acids using N-dodecyl-L-His adsorbed on a reversed-phase [59], this would indicate a strong hydrophobic interaction of the side chain length of the respective enantiomers with the stationary phase.

When using solvent systems I–III, α-Oct-Ala and α-Non-Ala remained at the start, however, they showed migration and resolution when solvent system IV was used.

Conclusions

LE-HPLC was found to be a very suitable technique for the enantiomeric resolution of NMe-AA and AAA, and it has the advantage that no derivatization is required. All chiral phases investigated were capable of separating racemic AAA, and slight differences in separation factors might be overcome by using an optimized eluent. A weakly acidic pH (4–6), the addition of organic modifiers (methanol, acetonitrile), appropriate concentrations of the complexing copper ion, and elevated temperatures all improve the chiral resolution and peak symmetry and shorten analysis time. Employing L-Val as the chiral selector gave rise to lower separation factors in most cases when compared to Pro and Hypro, although baseline resolution for many AAA was achieved, and the shortened retention times might be advantageous in the case of aromatic side chain amino acids.

Semi-preparative separations of racemic AAA by LE-HPLC using the method described will easily provide pure or enriched enantiomers useful for further investigations, such as the assignment of the order of emergence of enantiomers using other conditions or resolution techniques. Use of a polarimeter detector enables the on-line determination of the optical rotation of AAA enantiomers and might make possible the assignment of the absolute configuration. LE-TLC using a chiral phase is also a suitable technique for the enantiomeric resolution of AAA, but it has limitations with regard to the solubility and variability of the solvent systems used. With regard to the evaluation of theories that explain and predict resolution mechanisms and the elution order of enantiomers of amino acids by chiral phase LEC, we suggest the inclusion of both N-methylated (alkylated) and C^{α} methylated (alkylated) analogs in experiments, as a satisfactory and comprehensive theory has to explain the unexpected behaviour observed in some cases. Investigation of these compounds, therefore, may also contribute to models for chiral recognition.

Acknowledgements

The author is obliged to Mr. R. Jöster, Perkin-Elmer Analytic, Vaihingen, F.R.G., for placing the polarimeter detector at his disposal and for technical instructions. Thanks are due to Misses S. Sorsche, B. Single, and D. Mauch for valuable technical assistance in various parts of the work and Miss R. Fischer and Mr. M. Currle for the synthesis of several α-alkyl-α-amino acids. I also want to express my gratitude to Prof. D. Seebach, Institut für Organische Chemie der ETH Zürich, Switzerland, and Dr. J. Kamphuis, DSM Research, Geleen, The Netherlands, for several standards of enantiomerically pure α-alkylated amino acids [79, 80] and thank warmly Dr. T. Graser, who carried out several initial experiments on the subject.

This work was partially supported by the Deutsche Forschungsgemeinschaft (Br 880/3-1 and 880/3-3).

References

[1] *I. Molnár, C. Horváth*, J. Chromatogr. **142**, 623 (1977).
[2] *P. E. Hare, E. Gil-Av*, Science (Washington, DC), **204**, 1226 (1979).
[3] *R. Schuster*, An. Chem. **52**, 617 (1980).
[4] *E. Gil-Av, A. Tishbee, P. E. Hare*, J. Am. Chem. Soc. **102**, 5115 (1980).
[5] *B. H. Reitsma, E. S. Yeung*, J. Chrom. **362**, 353 (1986).
[6] *J. Haginaka, J. Wakai*, J. Chrom. **396**, 297 (1987).
[7] "Amino Acids, Peptides and Proteins", Specialist Periodical Reports, Chem. Soc., London, vol. 1 (1969) – vol. 18 (1987); continuing series.
[8] *V. A. Davankov, A. V. Semechkin*, J. Chromatogr. **141**, 313 (1977).
[9] *V. A. Davankov*, in "Advances in Chromatography", *J. C. Giddings, S. Grushka, J. Cazes, P. R. Brown*, eds., vol. 18, Marcel Dekker, New York, 1980; p. 139.
[10] *W. Lindner*, Chimia, **35**, 294 (1981).
[11] *R. F. Pfeifer, D. W. Hill*, in "Advances in Chromatography", *J. C. Giddings, S. Grushka, J. Cazes, P. R. Brown*, eds., vol. 22, Marcel Dekker, New York, 1983; p. 37.
[12] *V. A. Davankov, A. A. Kurganov, A. S. Bochov*, in "Advances in Chromatography", *J. C. Giddings, S. Grushka, J. Cazes, P. R. Brown*, eds., vol. 22, Marcel Dekker, New York, 1983; p. 71.
[13] *V. A. Davankov*, in "Handbook of HPLC for the Separation of Amino Acids, Peptides and Proteins", *W. S. Hancock*, ed., vol. 1, CRC Press, Boca Raton, USA, 1984; p. 393.
[14] *M. H. Caude, A. P. Jardy, R. H. Rossedt*, in "Handbook of HPLC for the Separation of Amino Acids, Peptides and Proteins", *W. S. Hancock*, ed., vol. 1, CRC Press, Boca Raton, USA, 1984; p. 141.
[15] *E. Gil-Av, S. Weinstein*, in "Handbook of HPLC for the Separation of Amino Acids, Peptides and Proteins", *W. S. Hancock*, ed., vol. 1, CRC Press, Boca Raton, USA, 1984; p. 429.
[16] *R. Däppen, H. Arm, V. R. Meyer*, J. Chromatogr. **373**, 1 (1986).
[17] *T. Hoshino*, Liebigs Ann. Chem. **520**, 31 (1935).
[18] *W. M. Cahill, R. W. Jackson*, J. Biol. Chem. **126**, 29 (1938).
[19] *K. Mwauluka, E. A. Bell, B. V. Charlwood, J. M. Briggs*, Phytochemistry **14**, 1657 (1975).
[20] *R. Traber, H. R. Loosli, H. Hofmann, M. Kuhn, A. von Wartburg*, Helv. Chim. Acta **65**, 1655 (1982).
[21] *J. C. Sheehan, H. G. Zachau, W. B. Lawson*, J. Am. Chem. Soc. **80**, 3349 (1958).
[22] *T. K. Audhya, D. W. Russell*, J. Chem. Soc. Perkin Trans. I, **1974**, 743.
[23] *M. Aydin, N. Lucht, W. A. König, R. Lupp, G. Jung, G. Winkelmann*, Liebigs Ann. Chem. **1985**, 2285.
[24] *H. Brückner, M. Przybylski*, Chromatographia **19**, 188 (1984).
[25] *H. Brückner, C. Kussin, T. Kripp*, in "Peptides: Chemistry and Biology, Proceedings of the Tenth American Peptide Symposium", *G. R. Marshall*, ed., ESCOM Science Publishers, Leiden, The Netherlands, 1988; in press.
[26] *M. El Hajji, S. Rebuffat, D. Lecommandeur, B. Bodo*, Int. J. Peptide Protein Res. **29**, 207 (1987).
[27] *J. R. Cronin, W. E. Gandy, S. Pizzarello*, in "Biogeochemistry of Amino Acids", *P. E. Hare, T. C. Hoering, K. King*, eds., Wiley, London, 1980; p. 153.
[28] *J. G. Lawless*, Geochim. Cosmochim. Acta **37**, 2207 (1973).
[29] *J. R. Cronin, P. E. Hare*, Analyt. Biochem. **81**, 151 (1977).
[30] *J. R. Cronin, S. Pizzarello, W. E. Gandy*, Anal. Biochem. **93**, 174 (1979).
[31] *G. E. Pollock*, An. Chem. **44**, 2368 (1972); erratum **46**, 614 (1974).
[32] *M. H. Engel, B. Nagy*, Nature, **296**, 837 (1982).
[33] *C. T. Pillinger*, Nature **296**, 802 (1982).
[34] *M. C. Koshla, H. Munoz-Ramirez, M. M. Hall, P. A. Khairallah, F. M. Bumpus*, J. Med. Chem. **20**, 1051 (1977).
[35] *P. Cordopatis, D. Theodoropoulos*, Experientia **39**, 106 (1983).
[36] *K. Inouye, K. Watanabe, K. Namba, H Otsuka*, Bull. Chem. Soc., Jap. **43**, 3873 (1970).
[37] *R. Cotton, P. M. Hardy, A. E. Langran-Goldsmith*, Int. J. Peptide Protein Res. **28**, 245 (1986).
[38] *M. C. Koshla, K. Stachowiak, R. R. Smeby, F. M. Bumpus, F. Piriou, K. Lintner, S. Fermandjian*, Proc. Natl. Acad. Sci. USA **78**, 757 (1981).
[39] *M. L. Moore, W. F. Huffman, W. M. Bryan, J. Silvestri, H.-L. Chang, G. R. Marshall, F. Stassen, J. Stefankiewicz, L. Sulat, D. Schmidt, L. Kinter, J. McDonald, D. Ashton-Shue*, in "Peptides: Structure and Function, Proceedings of the Ninth American Peptide Symposium", *C. M. Deber, V. J. Hruby, K. D. Kopple*, eds., Pierce Chemical Company, Rockford, IL, USA, 1985; p. 607.
[40] *J. R. McDermott, N. L. Benoiton*, Can. J. Chem. **51**, 1915 (1973).
[41] *J. R. McDermott, N. L. Benoiton*, Can. J. Chem. **51**, 2562 (1973).
[42] *H. Brückner, G. J. Nicholson, G. Jung, K. Kruse, W. A. König*, Chromatographia **13**, 209 (1980) and 516.
[43] *H. Brückner, I. Bosch, T. Graser, P. Fürst*, J. Chromatogr. **386**, 251 (1987).
[44] *H. Brückner*, Fresenius Z. Anal. Chem. **327**, 32 (1987).
[45] *H. Brückner, I. Bosch, S. Kühne, S. Zivny*, in "Peptides: Chemistry and Biology, Proceedings of the Tenth American Peptide Symposium", *G. R. Marshall*, ed., ESCOM Science Publishers, Leiden, The Netherlands, 1988; in press.
[46] *H. Brückner, G. Jung*, Liebigs Ann. Chem. **1982**, 1677.
[47] *M. Kokkinidis, D. Tsernoglou, H. Brückner*, in "Peptides 1986, Proceedings of the 19th European Peptide Symposium", *D. Theodoropoulos*, ed., de Gruyter, Berlin, 1987; p. 319.
[48] *H. Brückner*, in "Peptides 1986, Proceedings of the 19th European Peptide Symposium", *D. Theodoropoulos*, ed., de Gruyter, Berlin, 1987; p. 231.
[49] *H. Brückner, S. Kühne, S. Zivny, M. Currle*, in "Peptide Chemistry 1987", *T. Shiba, S. Sakakibara*, eds., Protein Research Foundation, Minoh Osaka, 1988, in press.
[50] Autorenkollektiv, in "Organikum", VEB Deutscher Verlag der Wissenschaften, Berlin, 1986, p. 447.
[51] *S. M. Birnbaum, L. Levintow, R. B. Kingsley, J. P. Greenstein*, J. Biol. Chem. **194**, 455 (1952).
[52] *J. Turk, G. T. Panse, G. R. Marshall*, J. Org. Chem. **40**, 953 (1975).
[53] *W. A. König, I. Benecke, N. Lucht, E. Schmidt, J. Schulze, S. Sievers*, J. Chromatogr. **279**, 555 (1983).

[54] *C. van der Auwera, M. J. O. Anteunis*, Int. J. Peptide Protein Res. **29**, 574 (1987).

[55] *H. Brückner, I. Bosch, T. Graser, P. Fürst*, J. Chromatogr. **395**, 569 (1987).

[56] *N. Frydman, T. Tamari, B. Feibush, E. Gil-Av*, Proc. Isr. Chem. Soc., 42nd Meeting, Dec. 1972, p. 11 (1973).

[57] *S.-C. Chang, R. Charles, E. Gil-Av*, J. Chromatogr. **238**, 29 (1982).

[58] *V. A. Davankov, A. S. Bochkov, Y. P. Belov*, J. Chromatogr. **218**, 547 (1981).

[59] *V. A. Davankov, A. S. Bochkov, A. A. Kurganov, P. Roumeliotis, K. K. Unger*, Chromatographia **13**, 677 (1980).

[60] *M. H. Engel, P. E. Hare*, Yearbook Carnegie Institution, Washington, **80**, 394 (1981).

[61] *S. Weinstein, N. Grinberg*, J. Chromatogr. **318**, 117 (1985).

[62] *J. W. Keller, K. O. Dick*, J. Chromatogr. **367**, 187 (1986).

[63] *J. Florance, A. Galdes, Z. Konteatis, Z. Kosarych, K. Langer, C. Martucci*, J. Chromatogr. **414**, 313 (1987).

[64] *E. Oelrich, H. Preusch, E. Wilhelm*, J. High Resol. Chromatogr./Chromatogr. Commun. **3**, 269 (1980).

[65] *G. Gübitz, F. Juffmann, W. Jellenz*, Chromatographia **16**, 103 (1982).

[66] *G. Gübitz*, J. Liquid Chromatogr. **9**, 519 (1986).

[67] *J. Martens, K. Günther, M. Schickedanz*, Arch. Pharm. (Weinheim), **319**, 572 (1986).

[68] *K. Günther, M. Schickedanz, K. Drauz, J. Martens*, Fresenius Z. Anal. Chem. **325**, 298 (1986).

[69] *K. Günther, M. Schickedanz, J. Martens*, Naturwissenschaften **72**, 149 (1985).

[70] *K. Günther, J. Martens, M. Schickedanz*, Angew. Chem. **25**, 284 (1986); Angew. Chem. Int. Ed. Engl. **25**, 278 (1986).

[71] *K. Günther*, GIT Supplement **3**, 6 (1986).

[72] *R. Roumeliotis, K. K. Unger, A. A. Kurganov, V. A. Davankow*, J. Chromatogr. **255**, 51 (1983).

[73] *K. Weinges, B. Stemmle*, Chem. Ber. **106**, 2291 (1973).

[74] *A. Neuberger*, in "Advances in Protein Chemistry", *M. L. Anson, J. T. Edsall*, eds., Academic Press, New York, 1948; p. 297.

[75] *J. P. Greenstein, W. Winitz*, "Chemistry of the Amino Acids", vol. 1, Wiley, New York, 1961; p. 88.

[76] *P. Pfeiffer, W. Christeleit*, Z. Physiol. Chem. **245**, 197 (1937).

[77] *J. P. Greenstein, M. Winitz*, "Chemistry of the Amino Acids", vol. 1, Wiley, New York, 1961; p. 118.

[78] *F. Kerek, G. Snatzke*, Angew. Chem. **87**, 133 (1975); Angew. Chem. Int. Ed. Engl. **14**, 109 (1975).

[79] *D. Seebach, A. Fadel*, Helv. Chim. Acta **68**, 1243 (1985).

[80] *W. Kruizing, R. Kellogg, J. Kamphuis, W. H. J. Boesten, E. E. Schoemaker, E. M. Meijer*, J. Org. Chem. (1987), submitted for publication.

Received: Aug. 21, 1987
Revised manuscript
received: Oct. 27, 1987
Accepted: Oct. 30, 1987
F

The Application of Immobilized Liquids for Open Tubular Liquid Chromatography

O. van Berkel* / H. Poppe / J. C. Kraak

Laboratory for Analytical Chemistry, University of Amsterdam, Nieuwe Achtergracht 166, 1018 WV Amsterdam,
The Netherlands

Key Words

Column liquid chromatography
Open tubular columns
Determination of diffusion coefficients
Immobilization

Summary

The applicability of immobilized silicone phases, as reversed phase retentive layers in 5–25μm fused silica capillaries for open tubular liquid chromatography (OTLC) has been investigated. Various types of silicone phases have been tested, of which vinyl containing gums show the most promising features, to create a stable retentive layer in fused silica capillaries.

Diffusion coefficients of solutes in the immobilized silicone phases were determined by static measurement and found to be in the order of $5\text{–}27 \cdot 10^{-12}\,m^2/s$. These relatively small diffusion coefficients form the main drawback of the immobilized silicone phases, because this seriously hinders the use of thick layers of the stationary phase which is preferred in OTLC to avoid mass overload.

Introduction

It has been theoretically derived that liquid chromatography in open tubular columns can be competitive or superior to LC in packed columns, when the inner diameter of the tube is in the range of 5–25μm and the volume standard deviation of the external peak broadening is kept at about 1 nanoliter. A uniform, stable 0.5–1μm thick retentive layer is also necessary on the inner wall of the tube [1, 2].

Glass and fused silica capillaries with an i.d. of 5–25μm are now available and it has been shown that the requirements put on the magnitude of the external peak broadening can be met by applying on-column detection and split injection techniques [3–6]. However, less progress has been made in the application of a suitable retentive layer on the inner wall of such tubes. Up till now the best results were obtained with soda lime or borosilicate glass capillaries [7]. However, these soft glass capillaries are very brittle and less suited for on-column optical detection techniques. In this respect fused silica capillaries offer better mechanical and optical properties and have a relatively inert and well defined surface.

Despite the large experience in preparing capillary fused silica columns for GC, these techniques have been only rarely successfully applied to 5–25μm i.d. columns for LC [5, 8]. Recently Larsson et al. [9] reported very impressive results on the application of swollen crosslinked siloxane phases in small i.d. fused silica columns for OTLC.

In the present study we report the results of an investigation into the use of crosslinked siloxane phases as reversed retentive layers on 5–25μm i.d. fused silica capillaries for OTLC. The study includes the static measurement of diffusion coefficients of some test solutes in crosslinked siloxane phases.

Experimental

The OTLC set up is schematically shown in Fig. 1. It consisted of a metal reservoir (500ml) which could be pressurized with helium, acting as a constant pressure pump; an injection valve (0.5μl Rheodyne model 7120, Berkeley, USA) combined with a homemade splitting device, allowing injections at the nano to pico liter level. The capillary columns were mounted to the injection valve in such a way that the inlet of the capillary is as close as possible to the rotor. The polyimide layer of the fused silica capillaries was burned off from the end of the column over a length of about 3cm to allow on-column laser induced fluorescence detection with a He/Cd laser as excitation source (λ_{ex} = 325nm) or an argon ion laser (λ_{ex} = 365nm) and a modified fluorimeter (Zeiss M4QIII, Jena, GDR) as photodetector [3].

0009-5893/87 0739-06 $ 03.00/0

© 1987 Friedr. Vieweg & Sohn Verlagsgesellschaft mbH

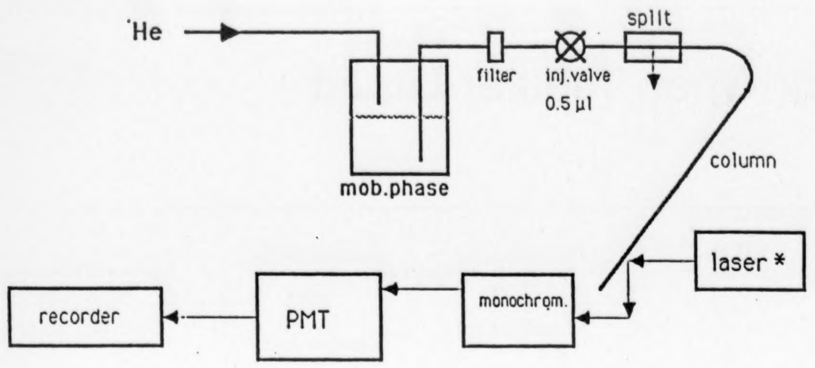

* He/Cd laser (Liconix), wavelength 325 nm
argon-ion laser (Innova), wavelength 365 nm

Fig. 1

Schematic representation of the chromatographic OTLC setup.

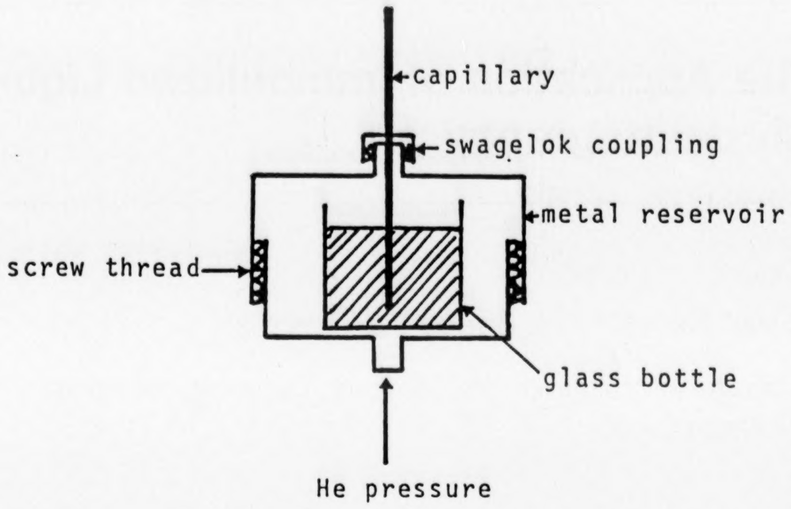

Fig. 2

Schematic representation of the reservoir to fill the fused silica columns.

Materials

All solvents were of spectroscopic quality (J.T. Baker, Deventer, The Netherlands) and were filtered through a 0.2μm millipore filter prior to use. The fused silica columns were obtained from SGE (Ringwood, Australia); the inner diameter of the columns, as specified by the manufacturer, was always checked by our own aerodynamic measurement based on the Hagen-Poiseuille relation. The siloxane phases OV-101, OV-1, SE-30 were from Chrompack (Middelburg, Holland), PS-255 was from Fluka (Switzerland) and poly-methylhydrosilane and dicumylperoxide from Merck (Darmstadt, FRG).

Procedures

Fig. 2 shows the reservoir used to fill or wash the fused silica capillaries with solutions.

The coating procedure involved four steps: hydrothermal treatment, deactivation, static coating and crosslinking.

For the hydrothermal treatment the capillary was filled for 95% of its length with a solution of 10% (v/v) of hydrochloric acid and both ends of the capillary were closed by melting. The column was heated for 90 min at 120°C and washed with water then methanol and dried under a stream of He at 140°C for one hour. Next the column was deactivated by filling it with 10% (v/v) solution of polymethylhydrosilane in **n**-pentane and forcing out this solution with He at a rate of 1.5 cm/min. After sealing both ends of the column by melting, the column was heated for two hours at 260°C and then washed with **n**-pentane. The hydrothermally treated and deactivated column was coated by the static method by filling it with a solution of the stationary phase in butane or pentane, containing dicumylperoxide in the ratio: stationary phase/dicumylperoxide = 20:1 (w/w). Then both ends of the column were connected to a vacuum pump and evacuated, at 10°C above the boiling point of the applied solvent (e.g. 10°C resp. 45°C), for one day (butane) or several days (n-pentane)/meter column length. Next the column was flushed with He in order to remove oxygen and then heated for 1 hour at 160°C to realize the cross-linking. Finally the column was conditioned for 30 min at 200°C under a stream of He.

Results and Discussion

Techniques used in GC to deposit a liquid layer on fused silica capillaries (i.e. static and dynamic coating from solutions of a real liquid in a volatile solvent) [10–12] have been adapted for LC capillaries. However, in liquid chromatography the liquid phases have to be immobilized in order to avoid their dissolution in the mobile phase. Unfortunately the common immobilization procedures (e.g. crosslinking) lead to a considerable increase in the viscosity of the stationary liquid and thus to smaller diffusion coefficients, which will result in a slower mass transfer. This means that the thickness of the immobilized liquid cannot be too large in order to avoid a too great loss in efficiency.

The maximum film thickness of the retentive layer ($d_{f,max}$) to give a 20% contribution to mass transfer in the liquid phase can be calculated with the Golay equation. For a solute with $k' = 3$ the maximum film thickness permissible is equal to a $d_{f,max} = 0.3 \cdot d_c \cdot (D_{is}/D_{im})^{1/2}$ where d_c = column diameter and D_{is} and D_{im} are the diffusion coefficients of the solute in the stationary and mobile phases respectively. For common liquids the diffusion coefficients of solutes can be calculated with the Wilke-Chang equation but this equation fails for crosslinked phases because of their polymeric nature and the lack of the necessary chemical and physical data.

In order to calculate the maximum film thickness for the applied immobilized crosslinked silicone phases, we decided to determine experimentally the diffusion coefficients of some test solutes in these phases by a method described in principle by Crank et al. [13] and Skelland et al. [14]. For that purpose a set up shown in Fig. 3 was used. It consisted of a glass vessel with a flat bottom, on which a thick film of a silicone phase was immobilized in the same way as applied for the fused silica capillaries (see procedures). A solution of the test solute was brought into the vessel and well stirred. By means of a pump a small part of this solution was recycled through a fluorimetric detector. This allows the measurement of the concentration of the test solute in the solution at any time after bringing the solute solution in contact with the silicone layer. Fig. 4 shows a

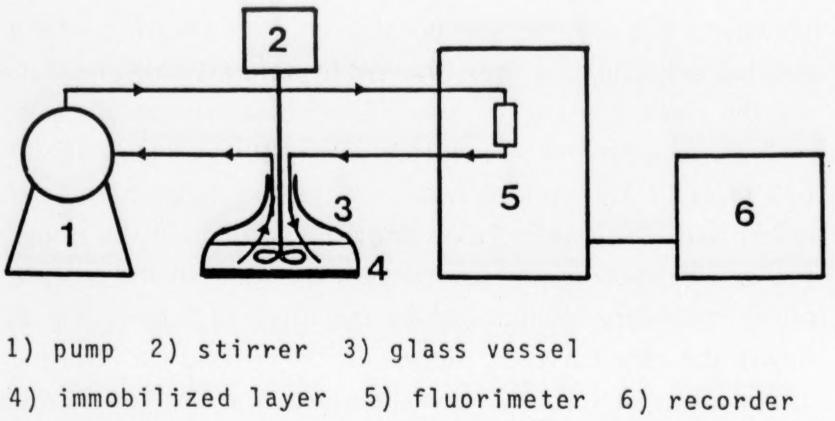
2
1
3
4
5
6
1) pump 2) stirrer 3) glass vessel
4) immobilized layer 5) fluorimeter 6) recorder

Fig. 3

Schematic representation of the experimental set-up for the measurement of diffusion coefficients in immobilized methylsilicone films.

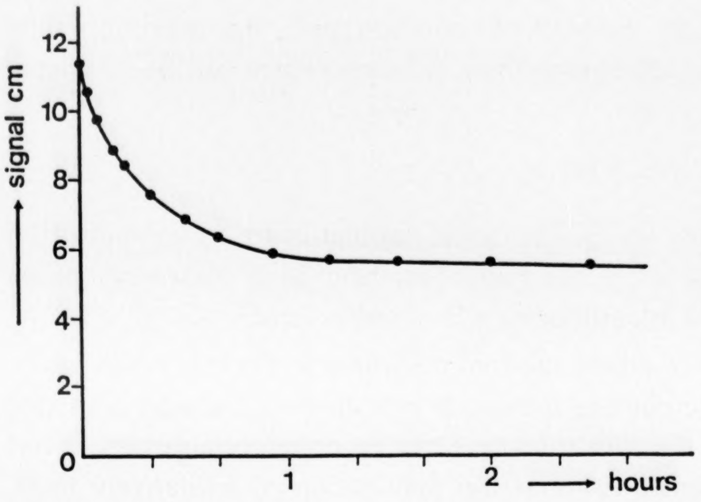

Fig. 4

Time course of the concentration of a solute in solution in contact with an immobilized methylsilicone film.

typical example of the decrease of the concentration of a solute in the circulated solution with time. According to Crank et al. [13] the fractional uptake of a solute from a stirred solution into a flat sheet, completely surrounded by the solvent, by diffusion is given by the following expression:

$$\frac{M_t}{M_\infty} = 1 - \sum_{n=1}^{\infty} \frac{2\alpha(1+\alpha)}{1+\alpha+q_n^2\alpha^2} e^{-D_{is}q_n^2 t/l^2} \qquad (1)$$

where:

M_t = total quantity of solute in the sheet at time t

M_∞ = total quantity of solute in the sheet at infinite time.

α = $C_0/M_\infty - 1$, where C_0 = initial solute concentration

D_{is} = diffusion coefficient of the solute in the sheet

l = thickness of the sheet

q_n = the non zero positive roots of the equation: $\tan(q) + \alpha * q + q = 0$

Skelland et al. [14] have shown that the solution of Crank is also valid if one side of the flat sheet is impermeable, as is the case in our experimental set up.

The value of M_t, M_x and α can be obtained from the measurement of the concentration change of the solute in the solution with time as is shown in Fig. 4. With these values, D_{is} can be calculated for a given α value by eq. 1.

The method described was applied to the measurement of the diffusion coefficient of two solutes in three immobilized silicone films from two different solvent compositions. The results of these measurements are given in Table I.

The spread in the value of the diffusion coefficient, calculated at different times intervals (i.e. different M_t/M_∞ values) was found to be less than 10%, which indicates the reliability of the method. From Table I it can be seen that the diffusion coefficients of anthracene and pyrene range from 5 to $8 \cdot 10^{-12} m^2/s$ for the OV-101 phase and from 16 to $27 \cdot 10^{-12} m^2/s$ for the mixed OV-101/OV-1 phase. These found D_{is} values are significantly smaller then those assumed by Knox et al. [1] and Cramers et al. [15], but agree very well with the D_{is} value of salicylic acid in crosslinked ethylmethacrylate ($7 \cdot 10^{-12} m^2/s$), as determined by Woods et al. [16].

Table I. Experimental data of the batch diffusion coefficient measurements in immobilized polymethylsilicone phases.

solute	anthracene		pyrene	
stationary phase	OV-101	OV-101	OV-101	OV-101
film thickness (μm)	0.185	0.185	0.236	0.236
% immobilization yield	75.9	75.9	92.7	92.7
solute conc. (ng/ml)	0.95	0.57	0.65	1.00
acetonitrile/water	1:1	1:1	3:7	3:7
phase ratio	0.012	0.012	0.014	0.014
diffusion coeff. ($10^{-12} m^2/s$)	5.2 ± 0.3	8.5 ± 0.7	5.0 ± 0.4	6.1 ± 0.9
solute	**anthracene**		**pyrene**	**anthracene***
stationary phase	OV-101	OV-101	OV-101/OV-1	OV-101/OV-1
film thickness (μm)	0.236	0.236	0.241	0.241
% immobilization yield	92.7	92.7	92.5	92.5
solute conc. (ng/ml)	0.93	0.62	1.33	0.62
acetonitrile/water	3:7	3:7	3:7	1:1
phase ratio	0.014	0.014	0.015	0.020
diffusion coeff. ($10^{-12} m^2/s$)	6.4 ± 0.6	7.0 ± 0.5	16 ± 2	27 ± 2

* the ratio of OV-101/OV-1 was 3:1 (w/w)

The D_{is} value of pyrene is always somewhat smaller than that of anthracene, in agreement with the difference of the molar volumes of these solutes. The significant difference in D_{is} values between the pure OV-101 and the mixed OV-101/OV-1 phase must be attributed to the difference in the extent of crosslinking. The OV-1 has a longer molecular skeleton than OV-101 and thus less active sites, per unit volume, available for crosslinking. This will result in a more open structure of the OV-101/OV-1 phase, making it more accessible than the OV-101 phase with resulting easier diffusion. From Table I it can also be seen that the diffusion coefficients are, as expected, independent on the solute concentration and solvent composition.

With the measured D_{is} values of the test solutes and their D_{im} value in common liquids ($5-7 \cdot 10^{-10} m^2/s$), as calculated with the Wilke-Chang equation, the maximum film thickness of immobilized silicone phases can be estimated and becomes:

$$d_f = 0.03\text{—}0.06 \cdot d_c$$

This leads for 5—25μm i.d. capillaries to a maximum film thickness of 0.15—1μm, resulting in a maximum phase ratio of 0.14, still quite a favourable value.

In order to adjust the film thickness to the maximum value, the static coating technique was applied, because with this method the film thickness can be precisely adjusted. It has been found [10] that the application of a relatively thick film in capillaries, by the static coating technique, gives less blockage when a not too viscous solution of methylsilicone is used. For that reason we initially selected the fluid methylsilicone OV-101 instead of the gumlike methylsilicones OV-1, SE-30 and PS-255. However, the results with the OV-101 phase were disappointing for the following reasons: in most attempts plugs of stationary phase appeared along the whole capillary after the crosslinking and blocked the column. In those rare cases where no plug formation occurred, the capillary blocked at larger flowrates (7 mm/s), which indicates an insufficient immobilization of the phase on the surface of the fused silica column. In order to decrease the plug formation and to improve the immobilization, it was decided to mix the fluid OV-101 phase with 25% (w/w) of the methylsilicone gum OV-1. This ratio was selected to make the coating solution not too viscous. After the crosslinking the capillaries were washed with a mixture of acetone/dichloromethane 1:1 (v/v) to remove byproducts. However, it appeared that under these conditions the film swells considerably and blocked the column. Therefore in all further experiments the columns were washed with mobile phase.

The coating with the OV-101/OV-1 mixture went significantly better than with pure OV-101. In 50% of all attempts a visually uniform film was observed on 25μm i.d. capillaries. The phase was stable with acetonitrile/water 1:1 (v/v) as the mobile phase. With this phase system, polycyclic aromatics show small retention and were used to measure the theoretical plate height versus the linear velocity (H/v plot). The H/v plot of anthracene ($k' = 0.30$) is shown in Fig. 5. At small linear velocity the experimental values coincides very well with the theoretical values as calculated with the Golay-equation and using the experimentally determined diffusion coefficient. However, at larger linear velocities the experimental H values are significantly larger then the theoretically calculated values. These deviations point to an additional stationary phase mass transfer effect, probably caused by a non uniform film thickness. Attempts to increase the k' factors of the test solutes by increasing the water content of the mobile phase up to 70% (v/v) failed because under these conditions the OV-101/OV-1 columns blocked. This result indicates an insufficient immobilization of the crosslinked phase on the surface of the fused silica column.

It has been found that the immobilization of silicone phases on fused silica columns is better the more gumlike the methylsilicone [10]. Therefore increasing the OV-1 content in the OV-101/OV-1 mixture looks the obvious choice. However, this will increase considerably the viscosity of the coating solution and thus the risk of column plugging during the static coating. We therefore decided to mix the OV-101 phase with the less viscous methylsilicone gum SE-30 in a ratio of 1:1. Indeed with this mixture no problems occured with the coating and immobilization and the phase could withstand larger percentages of water in the mobile phase, necessary to increase the retention of solutes. Fig. 6 shows the H/v curve of pyrene ($k' = 1.11$) on a 25μm × 125 cm fused silica column coated with the OV-101/SE-30 phase. The experimental and theoretical values agree well at small linear velocities. However, at larger velocities the experimental values are larger than expected on basis of the theory, similar to the results found with the OV-101/OV-1 phase. Probably the non uniformity of the layer causes the deviations between theory and practice.

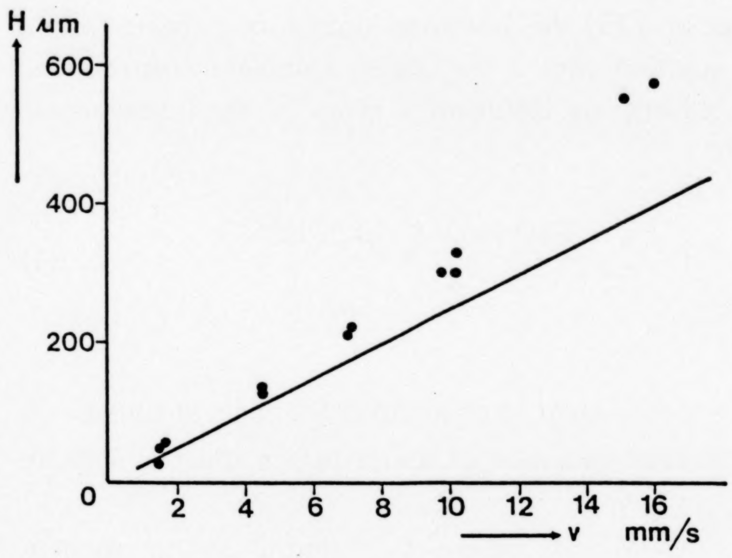

Fig. 5

H/v curve of anthracene as measured on a 25μm × 170 cm fused silica column, coated with OV-101/OV-1 (3:1 w/w). Experimental conditions: on column laser induced fluorescence detection. $k' = 0.30$; film thickness = 0.25μm mobile phase composition: water/acetonitrile (1:1 v/v); solid line = theoretical H value, $D_{im} = 0.6 \cdot 10^{-9} m^2/s$; $D_{is} = 27 \cdot 10^{-12} m^2/s$.

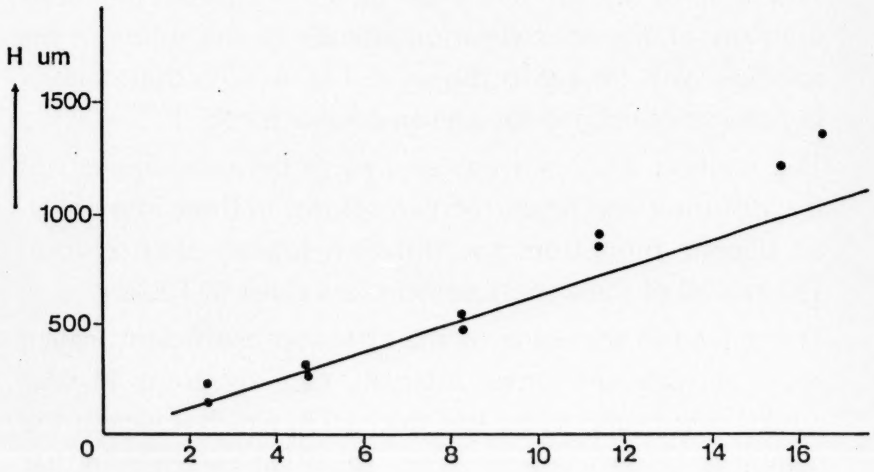

Fig. 6

H/v curve of pyrene ($k' = 1.11$) on a 25μm × 120 cm fused silica column, coated with OV-101/SE-30 (1:1 w/w). Experimental conditions: film thickness = 0.38μm; mobile phase: acetonitrile/water (4:6 v/v); solid line = theoretical calculated H value, $D_{im} = 0.55 \cdot 10^{-9} m^2/s$ and $D_{is} = 16 \cdot 10^{-12} m^2/s$.

It is known that the presence of a few percent of vinyl groups in the methylsilicones favours the crosslinking and immobilization of thick layers [10]. PS-255 is such a vinyl containing methylsilicone phase, and its succesful use in OTLC has been reported [8]. We therefore investigated also this phase, mixed with OV-101 and as such, as stationary phase. The results with the PS-255/OV-101 mixture as well as with the pure PS-255 phase were very good.

Relatively thick stationary layers could be easily realized on fused silica columns down to 5μm i.d. The phases appear to withstand water/acetonitrile mixtures in all ratios, which allows the adjustment of k' factors over a wide range. The good reproducibility of the coating method is reflected in Fig. 7, showing the relationship between the k' factors of some test solutes and the phase ratio on a number of fused silica columns with different diameters and film thickness.

The performance of columns coated with the PS-255/OV-101 mixture is demonstrated in Fig. 8 and 9, showing a chromatogram of a test mixture of polycyclic aromatics on a 25μm × 100cm column at moderate and large linear velocity.

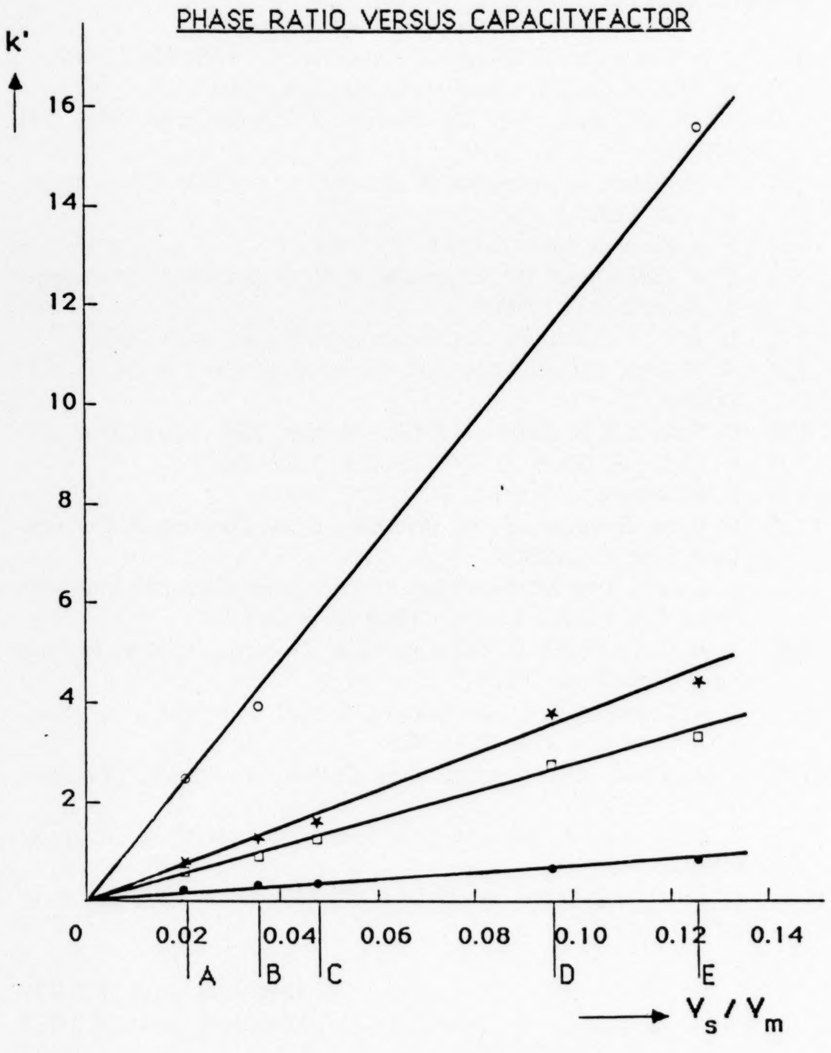

Fig. 7

The capacity factor of some test solutes versus the phase ratio on different fused silica columns with different film thickness.

● = anthracene-CN; □ = anthracene; ★ = 9-methylanthacene; ○ = 9-phenyl-anthracene.

mobile phase: acetonitrile/water (4:6 v/v)
column A: 5μm i.d., coated with 0.028μm PS-255
column B: 5μm i.d., coated with 0.045μm PS-255
column C: 26.1μm i.d., coated with 0.29μm PS-255
column D: 26.1μm i.d., coated with 0.57μm PS-255
column E: 25.1μm i.d., coated with 0.70μm PS-255/OV-101 (1:1 w/w)

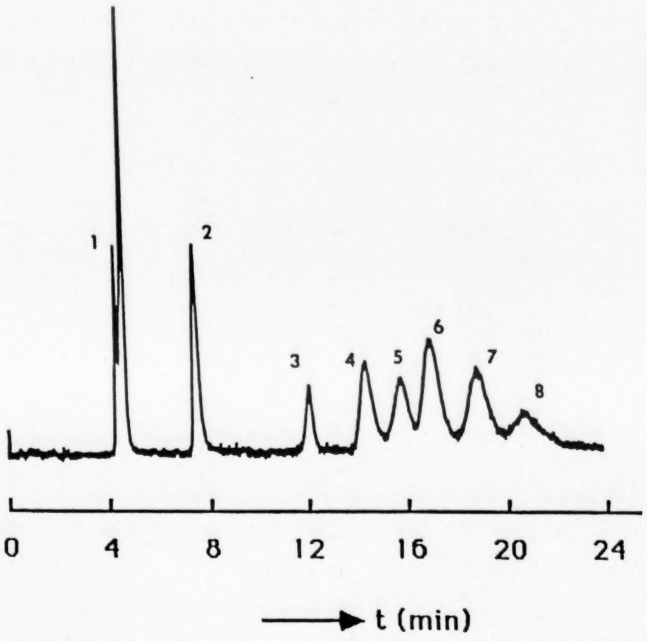

Fig. 8

Chromatogram of a test mixture of polycyclic aromatics on a 25.1 × 94 cm fused silica column, coated with PS-255/OV-101 (1:1 w/w).

Experimental conditions: film thickness = 0.70 μm; mobile phase: acetonitrile/water (4:6 v/v); linear velocity = 3.9 mm/s; on column laser detection $\lambda_{ex} = 325$nm; $\lambda_{em} = 420$nm; (1) anthranilic acid; (2) 9-cyano-anthracene; (3) acenaphtylene; (4) phenanthrene; (5) fluoranthene; (6) pyrene; (7) acenaphtene; (8) benzo (b) fluoranthene.

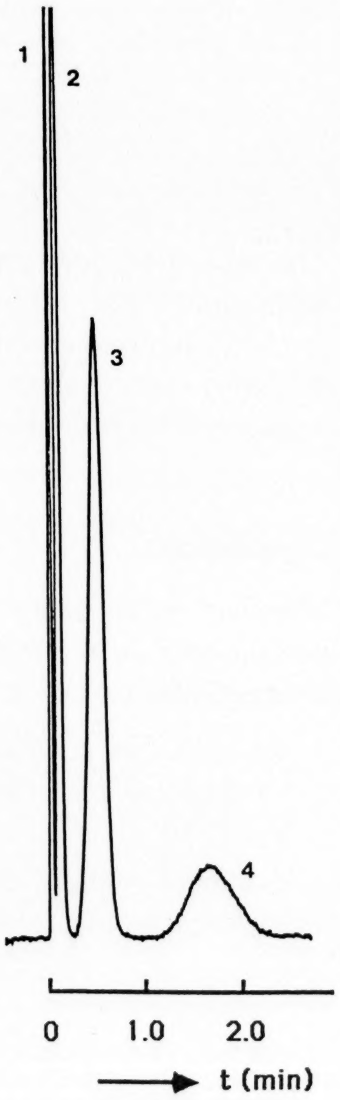

Fig. 9

High speed separation of polycyclic aromatics on a 25.1μm × 94cm fused silica column, coated with PS-255/OV-101 (1:1 w/w).

Experimental conditions: Linear velocity = 140mm/s; on column laser detection $\lambda_{ex} = 365$nm; (1) anthranilic acid; (2) 9-cyano-anthracene; (3) anthracene and 9-methyl-anthracene; (4) 9-phenyl-anthracene. Other conditions as in Fig. 8.

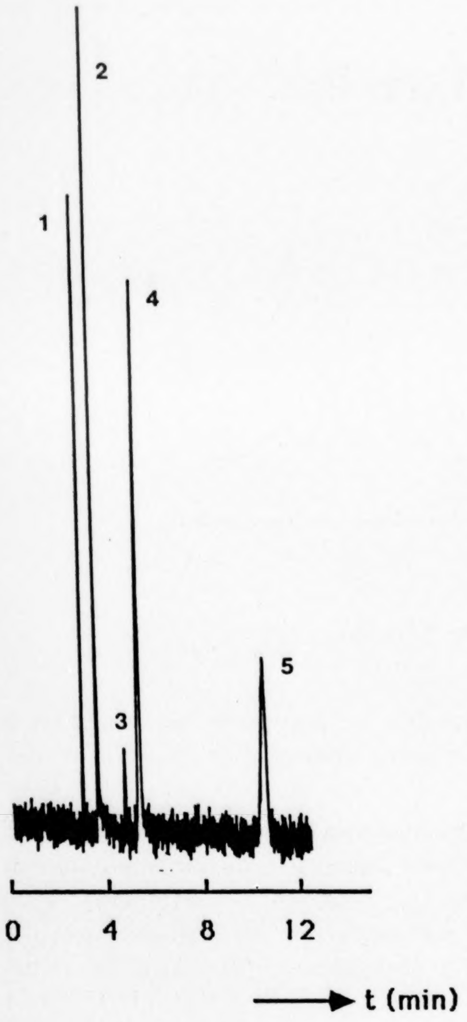

Fig. 10
Chromatogram of a test mixture of polycyclic aromatics on a $5\mu m \times 100 cm$ fused silica column, coated with PS-255. Experimental conditions: film thickness = $0.028\mu m$; other conditions as in Fig. 9.

The separation power of a $5\mu m \times 100 cm$ column, coated with pure PS-255, is shown in Fig. 10. The plate number of 9-methyl-anthracene with a $k' = 0.8$, at the linear velocity of 0.57 cm/s used, is about 66.000 which is 20% less than the value expected from theory.

Conclusions

The main results of the investigation to apply immobilized polysilicones as reversed phase retentive layers on fused silica columns for OTLC can be summarized as follows:

- the diffusion coefficient of solutes in the crosslinked immobilized methylsilicone phases are in the order of $5–27 \cdot 10^{-12} m^2/s$.
- the liquid methylsilicone OV-101 is unsuitable for giving a stable retentive layer on fused silica capillaries.
- mixtures of the liquid methylsilicone OV-101 with the gumlike methylsilicones OV-1 and SE-30 give better results but are not well able to withstand high water contents in the mobile phase.
- Excellent results were obtained with the vinyl containing PS-255 methylsilicone phase, which allows the deposition of stationary layers $0.03–0.7\mu m$ thick on $5–25\mu m$ i.d. fused silica columns up to 2 ml length. The PS-255 and mixtures of PS-255/OV-101 phase can withstand all ratios of water/acetonitrile mixtures.
- the performance of the fused silica capillary columns coated with an immobilized stationary phase comes close to the theoretical expectations.
- since the coating with n-butane as coating solvent is less time consuming than with n-pentane; this solvent is favoured for producing thick films [17, 18].

Acknowledgement

Part of this work was possible due to a grant of Pye Unicam Limited, Cambridge, UK to one the authors (O.v.B.).

References

[1] *J. H. Knox, M. T. Gilbert*, J. Chromatogr. **186**, 405 (1979).
[2] *H. Poppe*, CLC Symposium Edinburgh, 1984.
[3] *H. P. M. van Vliet, H. Poppe*, J. Chromatogr. **346**, 149 (1985).
[4] *S. Folestad, L. Johnson, B. Josefsson, B. Galle*, Anal. Chem. **54**, 925 (1982).
[5] *F. J. Yang*, J. HRC & CC **4**, 83 (1981).
[6] *E. J. Guthrie, J. W. Jorgenson, P. R. Oluzneski*, J. Chromatogr. Sci. **22**, 171 (1984).
[7] *D. Ishi, T. Takeuchi*, J. Chromatogr. Sci. **22**, 400 (1984).
[8] *A. Fabrot, S. Folestad, M. Larsson*, J. HRC & CC **9**, 117 (1986).
[9] *S. Folestad, M. Larsson*, J. Chromatogr. **394**, 455 (1987).
[10] *K. Grob, G. Grob*, J. HRC & CC **6**, 133 (1983).
[11] *L. Blomberg*, J. HRC & CC **7**, 232 (1984).
[12] *C. P. M. Schutjes, E. A. Vermeer, C. A. Cramers*, J. Chromatogr. **279**, 49 (1983).
[13] *J. Crank*, The Mathematics of Diffusion, Oxford University Press, Elly House, London 1964 formula 4.37.
[14] *A. H. P. Skelland*, Diffusional Mass Transfer, John Wiley and Sons, New York, 1974.
[15] *C. A. Cramers, C. E. van Tilburg, C. P. M. Schutjes, J. A. Rijks*, J. Chromatogr. **279**, 83 (1983).
[16] *J. M. Wood, D. Attwood, J. H. Collett*, J. Pharm. Pharmac. **34**, 1 (1982).
[17] *T. Wännman, L. Blomberg, S. Schmidt*, J. HRC & CC **8**, 32 (1985).
[18] *K. Janák, V. Kahle, K. Tesařík, M. Morká*, J. HRC & CC **8**, 843 (1985).

Received: Aug. 3, 1987
Accepted: Sept. 7, 1987
F

Analytical and Preparative Methods for β-Exotoxin from *Bacillus Thuringensis*

T. Suortti[1]*/L. Ylinen[2]/P. Kärppä[2]

[1]Technical Research Centre of Finland, Food Research Laboratory, Biologinkuja 1, SF-02150 Espoo, Finland

[2]Farmos-Group Ltd./Agrochemical Division, P.O. Box 425, SF-20101 Turku, Finland

Key-Words

β-exotoxin
Analytical liquid chromatography
Ion pairing liquid chromatography
Preparative liquid chromatography

Summary

The *β*-exotoxin from *Bacillus thuringensis* is a well known insecticide. The bioassay usually employed for its analysis is time-consuming and subject to many disturbances. The previously reported HPLC analysis has been shown to give erroneous results in some cases.

A new analysis system has how been designed. The system is based on separation of *β*-exotoxin from the culture broth, and from various preparations containing *β*-exotoxin by ion-pairing. For sample preparation in more complex matrices an method employing solid phase extraction was developed.

In order to obtain a standard for quantitative analysis a preparative method for the isolation of *β*-exotoxin from concentrated culture broth after successive precipitations was also developed.

Introduction

Bacillus thuringensis produces several insecticidal toxins. *β*-Exotoxin is a nucleotide (Fig. 1) which is capable of inhibiting RNA biosynthesis [1]. The most frequently employed method for the determination of *β*-exotoxin has been fly bioassay, which measures inhibition in the development of houseflies from larvae to adults [2]. This assay requires several days and is unspecific and subject to many variables. The other methods previously suggested have been the isotope dilution method [3] and microbiological assay [4].

In recent years three high performance liquid chromatography (HPLC) methods for exotoxin have been published. One of these [5] is based on ion-exchange and requires long analysis times and gradient elution. The first reverse-phase (RP) HPLC method [6] was shown to be non-specific [7]. The second reverse-phase method, which was published after we had completed our studies [8], is said to have been made more specific simply by using a somewhat higher pH in the eluating buffer. This method is also incapable of analyzing *β*-exotoxin in preparations containing complex fillers. We have studies ion-pairing RP-HPLC of *β*-exotoxin and applied it for the determination after suitable sample preparation.

As we were not able to obtain *β*-exotoxin standard from commercial or non-commercial sources, we also developed an RP-HPLC system for the preparative isolation of *β*-exotoxin.

Experimental

Apparatus

For analytical separation an HPLC instrument consisting of the following components was employed: M-6000A pump, M-710B automatic injector, Nova-pak C_{18} column

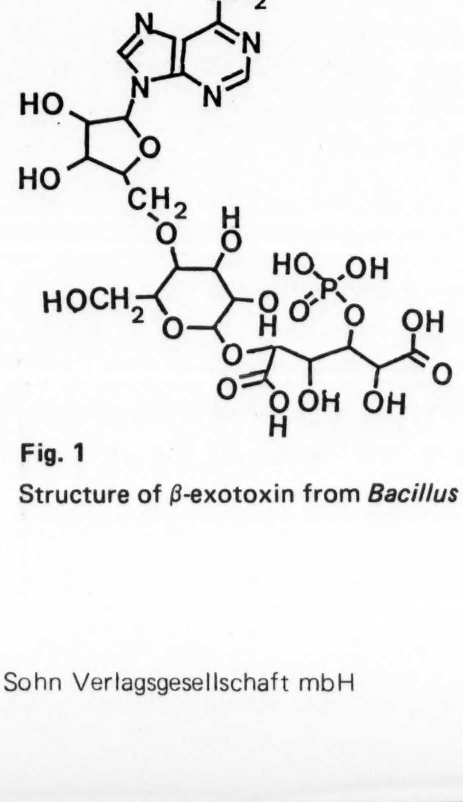

Fig. 1
Structure of *β*-exotoxin from *Bacillus thuringensis*.

0009-5893/87 0745-03 $ 03.00/0

© 1987 Friedr. Vieweg & Sohn Verlagsgesellschaft mbH

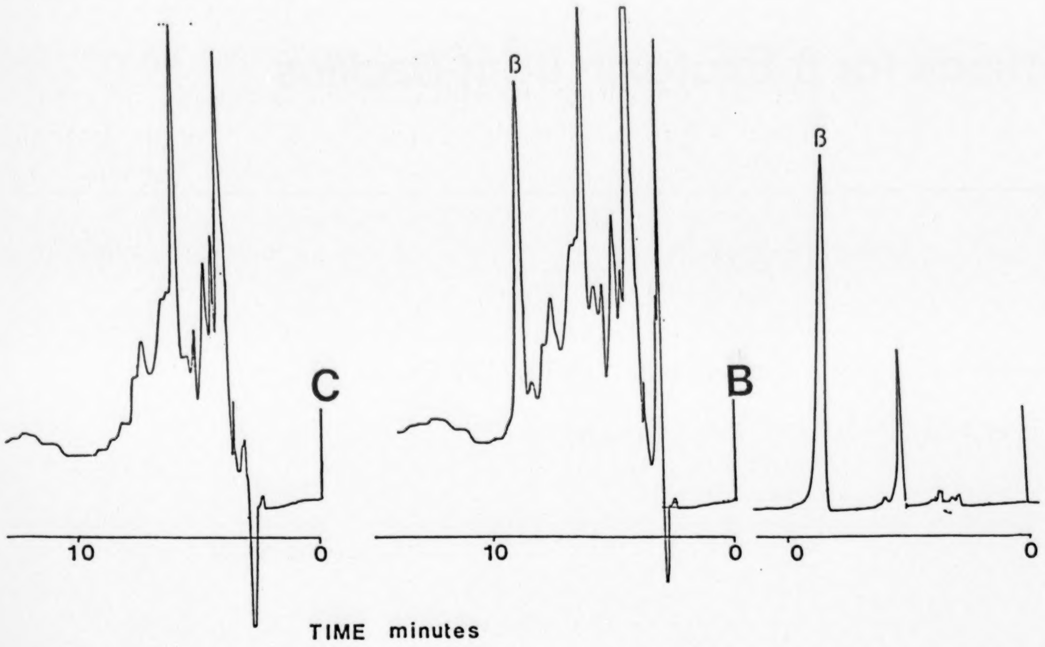

Fig. 2
Ion-pairing RP-HPLC of β-exotoxin
A. 5 mg/l standard sensitivity 0.01 aufs
B. β-exotoxin sample preparel as described
C. Sample if filler without β-exotoxin. Sensitivity 0.005 aufs at 254 nm. Nova-Pak C_{18} column (8 × 100 mm), mobile phase 45/55 MeOH/20 mM TBA-phosphate at a flow-rate of 1 ml/min. Injection volume 50 μl.

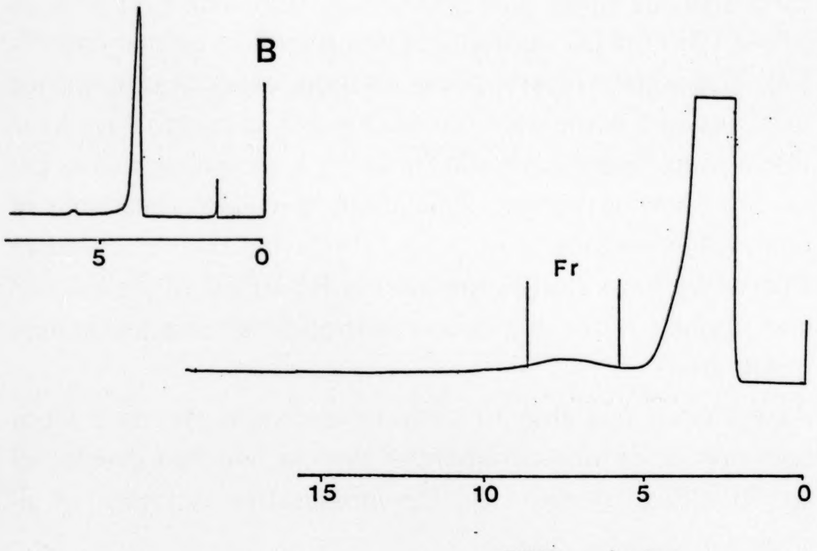

Fig. 3
A. Preparative HPLC of β-exotoxin precipitate. Prep-pak C_{18} (57 × 300 mm), mobile phase: 5/95 methanol/NH_4Ac-TEA-buffer (pH 4.0) 150 ml/min. RI 5 ×
b. Rechromatography of the collected fraction marked in chromatogram A. 15 μl injection, mobile phase 5%95 methanol/20 mM Na-phosphate (pH 4.5) 2 ml/min on Novapak C_{18} (8 × 100 mm). Detection at 254 nm, 02. aufs.

in RCM-100 column chamber, M-440 UV-detector monitoring at 254 nm and M-401 (all from Millipore/Waters Div.). For development of the preparative system an 8 × 300 mm column hand-packed with PrepPak 500 C_{18} (the same packing as in 57 × 300 mm preparative columns) was used.

For preparative separation a Waters M-500A preparative liquid chromatograph equipped with a Prep PAK C_{18} cartridge (57 × 300 mm) was employed.

Eluents

Eluents were prepared using analytical grade reagents and chromatographic grade organic solvents and Milli-Q water (Millipore). Tebrabutylammonium (TBA) phosphate solutions were prepared by diluting 0.4 M tetrabutyl ammonium hydroxide solution with water and adjusting the pH with phosphoric acid before addition of methanol.

Buffer for preparative separations was made up from acetic acid, ammonium hydroxide and freshly distilled triethylamine.

Sample preparation for analytical separations: Preparations to be analysed were diluted 1:100 with 20 mM Sodium phosphate buffer (pH 4.0). 1 ml sample was applied to the activated Sep-Pak C_{18} cartridge (activation by 10 ml methanol followed by 20 ml 20 mμ Na-phosphate buffer (pH 4.0)). The cartridge was washed with 1 ml phosphate buffer and the fraction containing β-exotoxin was eluted with 4 ml 30/70 methanol/Na-phosphate buffer solution. 100 μl 0.4 N TBA-OH solution was added to the sample and made up to 5 ml with water. 50 μl sample of this solution was injected into the HPLC instrument. The analytical separations were varried out 45/55 methanol/20 mM TBA-phosphate buffer (pH 6.5) at a flow rate of 1 ml/min (Fig. 2).

Preparative separations: β-exotoxin was precipitated from culture broth of *B. thuringensis* by the method of Benz [9] with gradual addition of ethanol. The dried crude preparation was dissolved in 1% ammonium acetate/triethylamine buffer (pH 4.5) as a 25% solution. 25 ml injection of this solutions was chromatographed with the same buffer modified with 5% methanol at a flow rate of 150 ml/min (Fig. 3). The collected fractions were analyzed with analytical HPLC and the fractions containing β-exotoxin was lyophilized. The activity of the preparation was also determined with fly bioassay.

Results and discussion: Chromatography with 20 mM sodium phosphate buffers showed that the highest k′-value was obtained at pH 4, which was chosen as the pH of the buffer for the first step in sample preparation. The retention of β-exotoxin is strongly dependent on the methanol concentration in RP-HPLC (Fig. 4) and ion-pairing RP-HPLC (Fig. 5), which means that careful adjustment of the organic modifier concentration is a key factor for a succesful analysis both in analytical and preparative separations. In contrast to other nucleotides, β-exotoxin gave strongly deformed peaks with eluent of pH < 6. The concentration of counter-ion when chromatographed in the

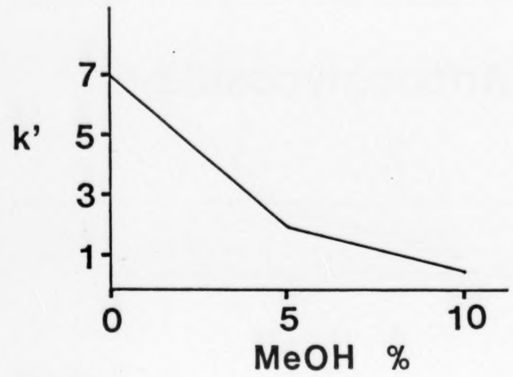

Fig. 4

Effect of the methanol concentration on k′ of β-exotoxin in RP-HPLC.

Buffer: 20 mM Na-phosphate (pH 4.0).

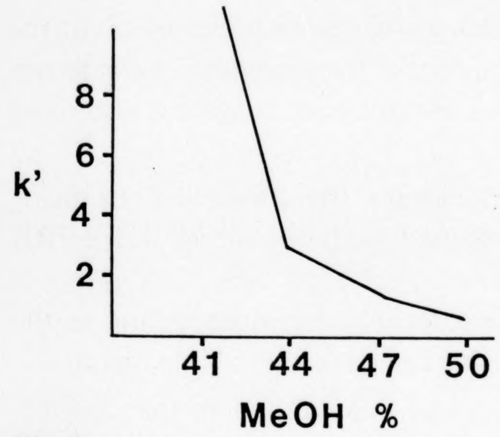

Fig. 5

Effect of methanol concentration on k′ of β-exotoxin in ion-pairing RP-HPLC.

Buffer: 20 mM TBA-phosphate (pH 6.5) diluted with varying amounts of methanol.

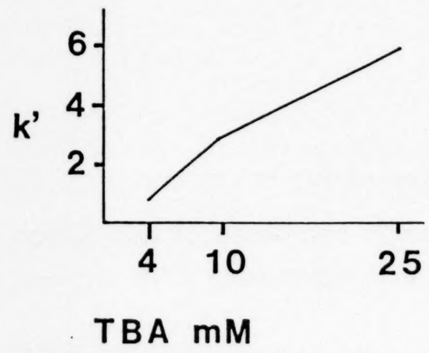

Fig. 6

Effect of TBA-phosphate concentration on k′ of β-exotoxin in ion-pairing RP-HPLC. Methanol concentration 44 %.

ion-pairing mode also has a profound influence on the k′-value (Fig. 6). When these variables were adjusted correctly, ion-pairing RP-HPLC connected with RP-sample preparation resulted in selectivity which made possible the analysis of β-exotoxin in very complex matrices. The standard curves war linear in the concentration range studied (5 ... 500 mg/l) and passed through origin. The sensitivity of the determination was of the order of 0.1 mg/l. The relative standard deviation was ± 1 % and the recovery of β-exotoxin additions was 90—103 %.

The yield from one preparative run was about 50 mg β-exotoxin. The purity of β-exotoxin was calculated on the basis of spectrophotometric measurement and the extinction coefficient reported for adenine nucleotides and nucleosides (ϵ_{260} = 14200 in 0.1 N HCl) to be 88 % and the concentration of the major impurity to be about 3 %.

References

[1] *J. Vankova,* Folia Microbiol. **23**, 162 (1978).
[2] *C. M. Ignoffo, I. Card,* J. Econ. Entomol. **63**, 1987 (1970).
[3] *K. Sebesta, K. Horska, J. Vanova,* Coll. Czech. Chem. Commun. **38**, 298 (1973).
[4] *G. Rosenburg, G. Carlberg, H. G. Gyllenberg,* J. Appl. Bacteriol. **34**, 417 (1971).
[5] *E. B. Danilova, E. B. Kruglyak,* J. Invertebr. Potal. **42**, 334 (1983).
[6] *D. D. Oehler, R. E. Gingrich, M. Haufler,* J. Agric. Food Chem. **30**, 407 (1982).
[7] *D. E. Johnson, R. E. Peterson,* Eur. J. Appl. Microbiol. Biotechnol. **17**, 231 (1983).
[8] *D. P. Campbell, D. E. Dieball, J. M. Brackett,* J. Agric. Food Chem. **35**, 156 (1987).
[9] *G. Benz,* Experientia **22**, 81 (1966).

Received: June 30, 1987
Accepted: Aug. 5, 1987
F

Multidimensional Ion-Pair HPLC for the Purification of Aminoglycoside Antibiotics with Refractive Index Detection

D. Samain*/P. Dupin/P. Delrieu/G. Inchauspe

Laboratoire de Biochimie Microbienne, Centre de Transfert en Microbiologie-Biotechnologie
(INSA), 126 Avenue de Rangueil, F-31077 Toulouse Cedex, France

Key Words

Ion-pair HPLC
Gradient conditions
Refractive index
Aminoglycoside
Perfluorinated carboxylic acids

Summary

Gradient chromatographic conditions with refractive index detection are defined for the ion-pair separation of the non-UV-absorbing aminoglycoside antibiotics. The method was applied with an off-line ion-pair prepurification step to the separation and characterization of unknown aminoglycoside starting from filtered broths. An on-line prepurification process has also be designed.

Introduction

In our previous work, we had shown that ionic compounds such as aminoglycoside antibiotics (AG) could be satisfactorily separated by ion-pair reversed-phase HPLC using the volatile perfluorinated ion-pairing agents [1] which had so far been mainly used for the separation of peptides and proteins [2, 3].

Besides the possibility of easy recovery of pure AG by simple lyophilisation of the eluate, we have shown that the use of these ion pairing agents could lead to special selectivity effects involving a concerted mechanism between ionic and hydrophobic interactions [4].

We have also demonstrated that these ion-pairing agents could be adequately mixed to provide non-expensive aqueous mobile phases leading to the satisfactory ion-pair preparative chromatography of AG [5, 6].

These results were, however, obtained with isocratic chromatographic conditions. In the case of unknown chromatographic behaviour, these conditions have to be ascertained by trial and error and this may rapidly become a tedious and time-consuming task. Gradient elution would thus seem appropriate but is not practicable with non-UV-absorbing compounds such as AG. Since preservation of the antimicrobial activity is essential for antibiotic characterization, derivatisation with a chromogenic reagent is also ruled out.

In this paper, we demonstrate the possibility of using gradient conditions combined with refractive index (RI) detection for the chromatography of AG. This result is achieved by varying the solvent strength according to the ratio of different ion-pairing agents in the mobile phase.

We also report applications of this method to the purification of unknown AG starting from filtered broths [7]. Due to the complexicity of the initial mixture, we have also developed an on-line extraction procedure which allows further satisfactory processing by gradient chromatographic analysis with RI detection.

Experimental

Apparatus

The following instruments were used in this study:

- a high-pressure chromatograph composed of two Gilson 302 pump (Gilson Medical Electronics, Villiers-le-Bel, France
- a Gilson 302 pump to pump the HFBA solution of AG through the precolumn.
- a Rheodyne 7060 6-port two-position valve used with a Rheodyne 7001 pneumatic actuator (Cotati, USA).
- a Rheodyne 5308 three-way slider valve with its 5300 pneumatic actuator to provide solvent selection
- an Apple IIe computer (Apple Computer, France) with a Gilson 603 software, to achieve full automation of the apparatus.
- a Gilson refractive index detector
- Waters C_{18} disposable cartridge
- SEP PAK (Millipore, USA)
- an analytical PRP-1 Hamilton (250 X 4.6 mm, 10 μm) column (Reno Nevada)
- a PRP1 Brownlee (30 X 4.6 mm, 10 μm) Guard column
- a Varian 311 A (Bremen, FRG) mass spectrometer
- emitters purchased from Linden Chromaspec (Bremen, FRG).

0009-5893/87 0748-05 $03.00/0

© 1987 Friedr. Vieweg & Sohn Verlagsgesellschaft mbH

Reagents

Heptafluorobutyric (HFBA) and trifluoroacetic (TFA) acid were purchased from Fluka (CH-9470 Buchs, Switzerland) and used without further purification. Methanol and water were HPLC grade. AG antibiotics were kindly provided by G. Etienne (Toulouse University, France). Kanamycin was obtained from Rhône-Poulenc Laboratories (Vitry, France), gentamicins from Roger Bellon Laboratories. Apramycin was obtained from Eli Lilly France (St. Cloud).

Microorganisms, Antibacterial Activity and Antibiotic Production

Assay Bacteria: *Bacillus subtilis* ATCC 6633. The strain was grown for 2 days at 37 °C on a sporulation medium consisting of Nutrient broth (Difco) 8 g, yeast extract 4 g, $MnCl_2$, $4H_2O$ 10 mg, agar 15 g, distilled water 1 liter, adjusted to pH 7.2 before autoclaving. The spores were collected in physiologic water, heated at 70 °C for 30 minutes and stored at 4 °C. The assay medium consisted of Polypeptone (Biokar) 5 g, beef extract (Difco) 3 g, TAPS (Sigma) 3 g, agar 20 g, distilled water 1 liter. The medium was adjusted to pH 9 before autoclaving then inoculated with 1,000 cfu/ml of *B. subtilis* and incubated for 18 hours at 37 °C.

Aminoglycoside-producing strains: These strains were provided by C. Deshayes (Sanofi, Elf Bio Recherche, Toulouse, France).

The following procedure on liquid medium is representative. Spores grown for 10 to 15 days at 28 °C on ATCC medium 172 are inoculated in a seed medium (M 221) consisting of starch 1 %, glucose 1 %, peptone 0.5 %, beef extract 0.2 %, yeast extract 0.3 %, soybean meal 0.2 %, $CaCO_3$ 0.2 %, distilled water for 1 liter. After 2–3 days at 28 °C on a rotary shaker (220 rpm) one of the following two media are inoculated with the seed medium in the ratio: 5 %: Medium 254; starch 4 %, soy peptone 0.5 %, yeast extract 4 %, K_2HPO_4O, 0.2 %, NaCl 0.2 %, $MgSO_4$, 7 H_2O 0.2 %, $CaCO_3$ 0.1 %. Medium M 222; same as M 151 without agar. After 3 to 5 days at 28 °C on a rotary shaker (220 rpm) the broths are collected. The cultures are then tested for antimicrobial activity.

Extraction and Purification of the Antibiotics

The following procedures are representative:

Off-line purification process: 50 ml of fermentation broth are adjusted to 50 mM HFBA. The mixture is homogenized for 1 hour at ambient temperature, centrifuged and the supernatant collected and adsorbed on a C_{18} SEP PAK cartridge. The cartridge is washed with 6 mL 50 mM aqueous HFBA 75 % – MeOH 25 % solvent, reequilibrated with 6 ml 50 mM aqueous HFBA mobile phase and eluted with 5 ml aqueous 50 mM TFA; 1 mL fraction is collected and tested for antimicrobial activity against *Bacillus subtilis*. The active fractions are concentrated to dryness under reduced pressure and submitted to ion-pair gradient HPLC.

On-line purification process: After equilibration of the precolumn with 6 ml of a 50 mM aqueous HFBA solution, 200 μg of the gentamicin complex in 10 mL of an 50 mM aqueous HFBA solution are pumped through the precolumn (flow rate 1.5 ml/min). The precolumn is then washed with 4 ml of pure 50 mM aqueous HFBA (flow rate 1.5 ml/min) and the six-port two-position valve is switched to elute the gentamicin complex onto the analytical column.

Results and Discussion

Design of Gradient Chromatographic Conditions with RI Detection

Although other detection systems have been described to insure universal detection (mass detector [8], mass spectrometer [9]), the differential refractive index detector remains so far the only widely available non-destructive detector for non-UV-absorbing compounds.

The major liability of RI detection is, of course, its inability to be used with gradient elution.

Any change in the refractive index of the mobile phase will be interpreted as signal by the detector usually erasing any other informations. To design gradient conditions with RI detection, one must then consider mobile phases of different solvent strength but having similar refractive index values. Solvent strength is usually varied by modification of the concentration of the organic modifier, or, in ionpair chromatography, by modification of the concentration and the nature of the ion-pairing agent. In a previous work [5], we had shown that the strength of the mobile phase could be adjusted by using mixed ion pairing agents (IPA).

Indeed the results shown in Table I indicate that large k′ variations are achieved will small changes in IPA composition. Aqueous 50 mM trifluoracetic acid appears to be a strong mobile phase, able to elute all the AG, while addition of small amounts of heptafluorobutyric acid considerably weakens the eluting power of the mobile phase. Gradient conditions may then be defined between these class of mobile phases. From a RI point of view, the mobile phases used in the experiment should be almost identical since their global molarity remains constant (50 mM).

Direct measurement of the ΔRI of mobile phases I/II and I/III (Table I) proved this assumption to be accurate. Some

Table I. k′ and RI variations of AG with increased HFBA

Aminoglycoside antibiotics	Mobile phases 50 mM TFA/50 mM HFBA		
	50 : 0	48 : 2	47 : 3
	ΔRI X 10^{-4}		
	0	0.02	0.03
	Capacity factors (k′)		
Kanamycin	0.1	2	3
Apramycin	0.3	5	7
Butirosine	0.2	4	6
Gentamicins	2.1	> 10	> 10
	4.2	> 10	> 10
	8.9	> 10	> 10

care must, however, by exercised in the preparation of the mobile phases.

In particular, all the mobile phases used in a set of experiments should be derived from the same mother liquor (aqueous 50 mM TFA.) prepared beforehand.

The mobile phases prepared herewith typically exibit ΔRI values less than 0.03 10^{-4} URI. This value is compatible with the highest practicable sensitivity of most common RI detectors.

If need be, ΔRI can be easily reduced by addition of a small amount of organic modifier, i. e., methanol. Such small amounts of an organic modifier have negligible chromatographic effects but they induce large variations in RI (Table II).

We further test the RI compatibility of these mobile phases by running a blank gradient from 6 % 50 mM HFBA/94 % 50 mM TFA to 100 % 50 mM TFA.

To lessen even more the residual ΔRI between the mobile phases, the gradient was actually run with the following set of solvents:

– pump A: 10 % 50 mM HFBA/90 % 50 mM TFA;
– pump B: 100 % 50 mM TFA.

The initial mobile phase was then 60 % A – 40 % B and the final mobile phase: 100 % B. The resulting base line is shown in Fig. 1.

As expected, the ΔRI between the beginning and the end of the gradient is quite acceptable. During the course of the gradient, however, a hump is observed. The slope of the hump is steeper at the beginning of the gradient suggesting that it is produced by elution of HFBA anchored on the stationary phase surface. In addition, actual return to the base line is only observed 45 minutes after the end of the gradient suggesting the lasting presence of HFBA in the mobile phase.

The magnitude of this phenomenon suggests that the chromatographic behaviour of AG should be significantly affected.

The chromatographic behaviour of some aminoglycosides was then investigated using this gradient. These AG were chosen according to their inability to be separated adequately with isocratic conditions. The chromatographic profile for kanamycin, apramycin and the gentamicin complex is shown in Fig. 2.

This chromatogram indicates that the presence of the hump does not hinder the RI detection of AG. We observe also that indeed, all the AG injected are eluted and separated very satisfactorily within the gradient run. Considering the large k's, resolution and peaks symmetry factor appear to be excellent.

As expected, HFBA contribution to the chromatographic process is important at the beginning of the gradient run allowing good separation between kanamycin and apramycin.

A lasting effect of HFBA is also observed at the end of the run with a large k′ increase of the various components of the gentamicin complex. Interestingly, the retention effect of HFBA on gentamicins does not affect the selectivity of TFA which induces the separation of the individual components of the gentamicin complex (1, 3). This lasting effect of HFBA is in good agreement with the slow return to equilibrium of the base line after the end of the gradient run observed above.

Application to the Analysis of Unknown AG from Filtered Broths

This separation process was then applied to the analysis of unknown AG produced by wild microorganisms. In our previous work [7] we had shown that crude AG extracts could not be analysed directly by HPLC and had to be prepurified using conventional technics such as ion exchange. These technics, however, perform often poorly and we have found that they could be advantageously

Table II. Dependence of the RI of an aqueous solution as a function of MeOH concentration

Methanol ml/l	U.RI X 10^6
0.1	2.4
0.2	7.5
0.5	13.0

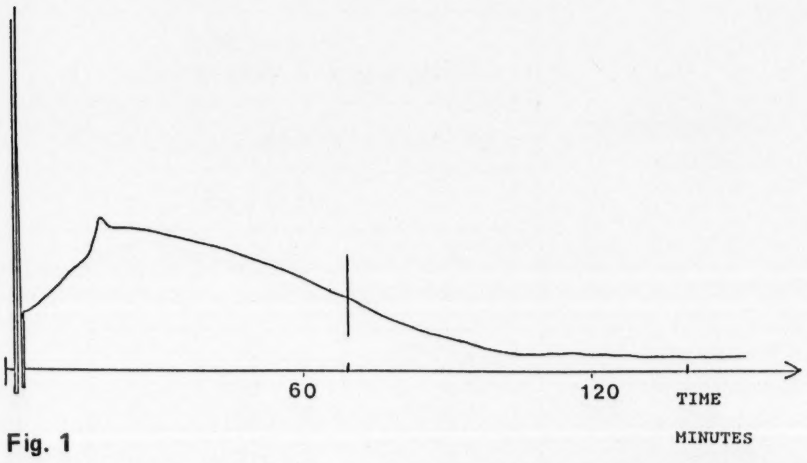

Fig. 1

Chromatographic profile obtained with a blank gradient: 6 % 50 mM HFBA/94 % 50 mM TFA → 100 % TFA (50 mn); 1 mL/min; RI detection.

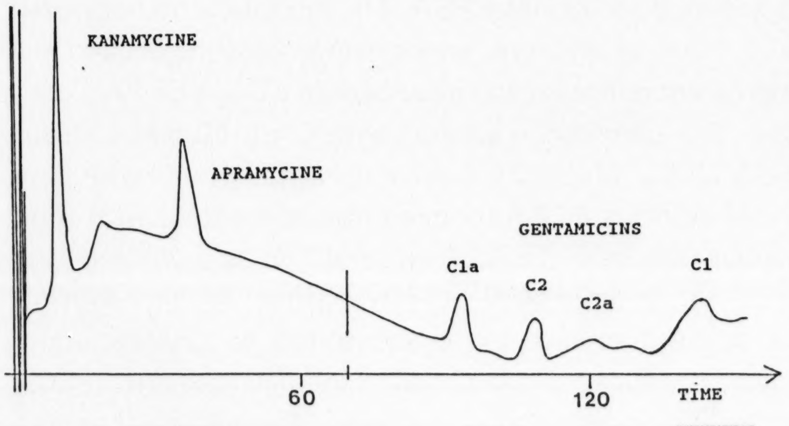

Fig. 2

Ion-pair gradient chromatogram of kanamycin (100 μg), apramycin (100 μg) and gentamicins (200 μg): 6 % 50 mM HFBA/94 % 50 mM TFA → 100 % TFA (50 mn); 1 mL/min; RI detection.

replaced by the ion pair reversed-phase extraction procedure summarized below. This prepurification procedure is based on the large difference in retention power between HFBA and TFA and can be conveniently and quickly performed on a disposable reversed-phase cartridge such as Waters C18 SEP PAK [10].

1. Ion pair adsorption of the AG from a 50 mM HFBA solution of the filtered fermentation broth on a C18 SEP PAK cartridge.
2. Elution of the non-polar, ionic contaminants from the cartridge with an 50 mM aqueous HFBA 75 %-MeOH 25 % mobile phase.
3. Return to an 50 mM aqueous HFBA mobile phase.
4. Selective elution of the AG with an aqueous 50 mM TFA mobile phase.
5. Testing of the different fractions for antimicrobial activity.

The prepurified AG obtained herein are then analyzed by gradient ion-pair HPLC. The different components separated were again tested for antimicrobial activity against *Bacillus subtilis.*

The fractions containing the antimicrobial activity were concentrated and submitted to field-desorption mass spectrometry (FDMS) [7, 11].

Three distinct wild strains (A-854, A-855 and A-1294) producing AG were studied. The results obtained are presented in Table III and a representative ion-pair gradient chromatogram of the active fraction of strain 855 is shown in Fig. 3.

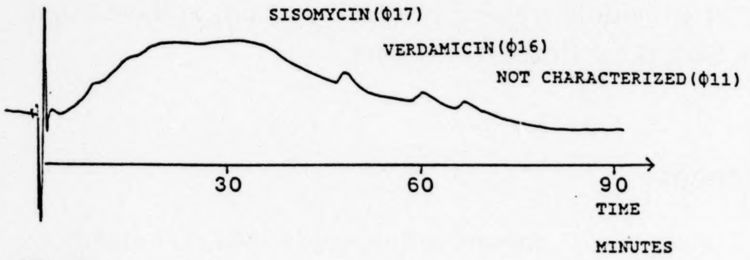

Fig. 3

Ion-pair gradient chromatogram of the active fraction of strain A 855: 5 % 50 mM HFBA/95 % 50 mM TFA → 100 mM TFA (30 min); 1 mL/min; RI detection. Inhibition diameters corresponding to the respective peaks are given between brackets.

These results show that excellent separation, purification and subsequent characterization of micro-amounts of unknown AG can be rapidly achieved with this process.

The presence of sisomicin and verdamicin [12] was detected in the active fraction of strain A-855. The presence of fortimicin A and B [13] was detected in the active fraction of strain A-854 and strain A-1294 was found to produce a mixture of fortimicin B and of dactimicin [14].

Design of an On-Line Purification Process

Although effective, the purification process described above still relies on an off-line prepurification step. In an attempt to increase the overall effectiveness, we set up to design an on-line process [15] which could analyze and purify AG directly from filtered broths.

This new procedure takes advantage of the programming capabilities of present-day HPLC equipment to achieve full automation.

The sequence of events (Fig. 4) is analogous to a precolumn trace enrichment procedure using a six-port, two-position valve to provide the adequate connections to the column and the precolumn.

From a chromatographic point of view, the on-line process is identical to the off-line process described above.

The AG, in a 50 mM aqueous HFBA solution, are pumped through the precolumn which ion pair extracts them from the surrounding medium. After various washing steps, the six-port, two-position valve is switched and the AG are eluted onto the analytical colum by the initial mobile phase of the gradient run. Detection is achieved as previously with the RI detector.

The chromatographic profile obtained for the gentamicin complex with a conventional injection is shown in trace b of Fig. 6. Trace a was obtained by ion pair extraction with the precolumn of the same amount of gentamicins from a 10 ml 50 mM aqueous HFBA solution, followed by a 4 ml wash of pure 50 mM aqueous HFBA.

These results show that although the extraction and washing steps have somewhat modified the retention time and slightly broadened the gentamicin peaks, separation remains very satisfactory. The RI detection is not altered, except for the very first minutes of the gradient run when the

Table III. Characterization by ion-pair gradient HPLC/FDMS of AG produced by wild organisms. Gradient conditions: 5 % 50 mM HFBA/95 % 50 mM TFA → 100 % TFA; 1 mL/min; RI detection.

AG producing strains	Gradient time (minutes)	Retention time (minutes)	FDMS $(M+H)^+$	Theoretical molecular weight	Identified AG
A-855	30	48 64	448 462	447 461	Sisomicin Verdamicin Not characterized
A-854	50	80 87	350 406	349 405	Fortimicin B Fortimicin A
A-1294	30	47 60	350 433	349 432	Fortimicin B Dactimicin

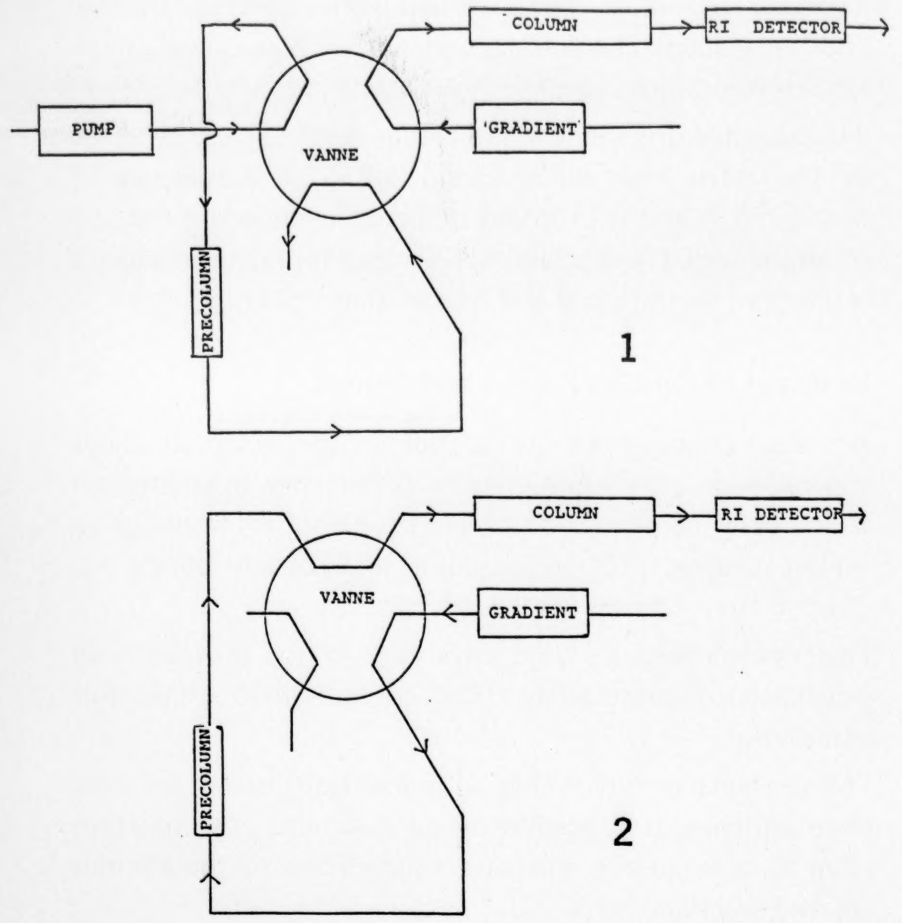

Fig. 4

Flow sheet of the on-line prepurification process.
Position I: Loading and washing steps.
Position II: Injection step.

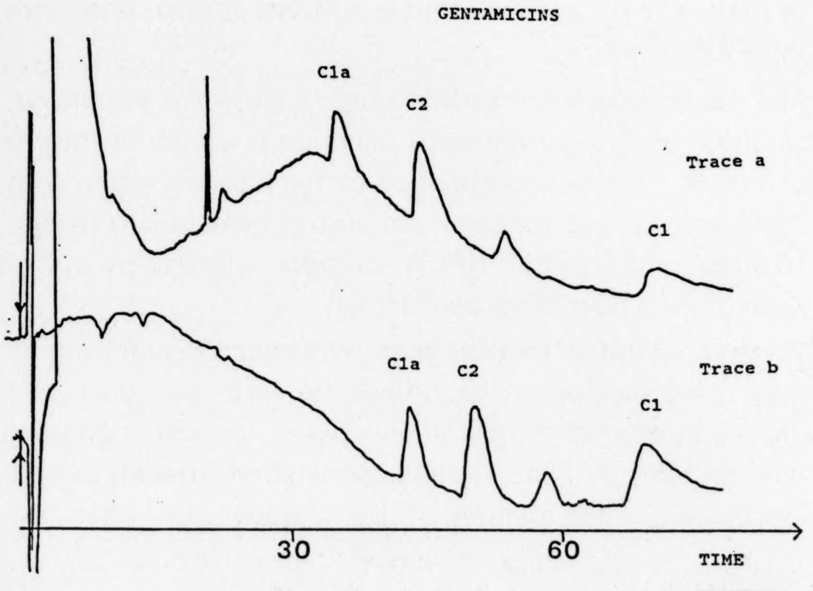

Fig. 5

Ion-pair gradient chromatogram of gentamicins: a) precolumn injection; b) conventional injection. Gradient conditions: 6 % 50 mM HFBA/94 % 50 mM TFA → 100 % TFA (30 min); 1 mL/min; RI detection.

HFBA adsorbed on the precolumn desorbs and creates a short-lasting saturating peak. Most important, the recovery yield of gentamicins after the ion-pair extraction steps appears almost quantitative (80 %).

In another experiment, however, we have found that the addition of another washing step with 50 mM aqueous HFBA 85 % – MeOH 15 % decreases the recovery yield to only 10 %.

This procedure has thus clearly a great potential for the on-line purification of AG from filtered broths.

Care must, however, be exercised in order to optimize the results, particularly in extrapolating the results from the off-line study.

Conclusion

In this work, we have shown that gradient conditions could be defined in ion-pair chromatography for the satisfactory separation of non-UV-absorbing compounds such as aminoglycoside antibiotics with RI detection. We have shown that this method could be applied to the separation and characterization of unknown AG starting from filtered broths.

The scope of utilization of RI detection has been previously hindered by its inability to be used in gradient conditions. The results presented here show that careful planning of the chromatographic process can permit actual RI detection in gradient conditions, even with a complex sequence of chromatographic events.

Further work is in progress in our laboratory to extend the scope of the RI-detected gradient to other class of non-UV-absorbing compounds such as sugars.

Acknowledgement

This work was supported by grants from the Ministère de la Recherche et de la Technologie, from the Fondation pour la Recherche Médicale and from the Centre National de la Recherche Scientifique. We are also grateful to C. Deshayes for providing the AG producing strains and we thank the Sté Sanofi for financial support.

References

[1] *G. Inchauspe, D. Samain,* J. Chromatogr. **303,** 277 (1984).
[2] *C. Olieman, D. Voskamp,* „CRC Handbook of HPLC for the Separation of Amino Acids, Peptides and Proteins, vol 1", W. S. Hancock ed. Massey University, Palmerton North, New Zealand 1984, p 161.
[3] *H. P. J. Bennet, J. Browne, P. L. Brubaker, S. Salomon,* J. Chromatogr. Sci. **19,** 197 (1981).
[4] *G. Inchauspe, P. Delrieu, P. Dupin, M. Laurent, D. Samain,* J. Chromatogr. (1987) in press.
[5] *I. De Miguel, E. Puech-Costes, D. Samain,* J. Chromatogr. (1987) in press.
[6] *S. G. Costanzo,* J. Chromatogr. **314,** 402 (1984).
[7] *G. Inchauspe, C. Deshayes, D. Samain,* J. Antibiot. **38,** 1526 (1985).
[8] *T. H. Mourey, L. E. Oppenheimer,* Anal. Chem. **56,** 2427 (1984).
[9] *P. J. Arpino,* Mass. Spectrometry Advances A. 161 (1982).
[10] *H. Terada, M. Asanoma, Y. Sakate,* J. Chromatogr. **318,** 299 (1985).
[11] *H. R. Schulten,* J. Chromatogr. **251,** 105 (1982).
[12] *G. H. Wagman, R. T. Testa, J. A. Marquez,* J. Antibiot. **23,** 555 (1970).
[13] *M. J. Weinstein, G. M. Leudemann, E. M. Oden, G. H. Wagman,* Antimicrob. Agents Chemother. **1963,** 1 (1964).
[14] *K. Ohba, T. Tsuruoka, K. Mizutani, N. Kato, S. Omoto, N. Esaki, S. Inouye, T. Niida,* J. Antibiot, **34,** 1090, (1981).
[15] *K. Oka, K. Minagawa, S. Hora,* Anal. Chem. **56,** 24, (1984).

Received: July 2, 1987
Accepted: July 28, 1987
F

Effects of Modifiers on the Chromatographic Behaviour of Propafenone and its Major Metabolites

B. Marchesini*/L. Tomasi

Servizio di Farmacologia clinica e terapia, Policlinico S. Orsola, Via Massarenti, 9, I-40138 Bologna, Italy

Key Words

Antiarrhythmic agents
Propafenone determination
Propafenone metabolites
Amine modifiers

Summary

Propafenone (PPF) is a new antiarrhythmic agent with structural features in common with the class of beta-blocking drugs (phenoxypropanolamines). Because of its high lipophilicity, the drug is strongly retained in reverse phase (RP) columns and simultaneous determination with the main polar metabolites 5-OH-PPF, N-depropyl-PPF and 5-OH-4-methoxy-PPF requires long run times (up to 50 min.)

Oxidative metabolism in vivo often produces derivatives whose higher polarity results from the addition of a polar group and/or the subtraction of an apolar one. These metabolites show similar chromatographic behaviour in RP mode and the trade-off between their separation and the sensitivity of the parent compound must be investigated. In an effort to shorten the run time we examined the retention of these early eluting substances as a function of different amine additives, pH and organic content in mobile phase using C8 and C-18 columns from different sources, previously characterized for their free silanophilic and hydrophobic activities. Under optimal conditions the run time was reduced to 14 minutes and an application of the optimized method to the determination in plasma samples of the drug and its main metabolites after chronic therapy with PPF is presented. To investigate possible coelution of other yet undiscovered metabolites which could accumulate in some patients under chronic treatment, the analysis was carried out using an electrochemical detection in parallel with the UV. Agreement was found between the two detection procedures and suggest no interference.

Introduction

Competing-ion chromatography has been often used for the analysis of basic drugs and their metabolites in reverse phase mode [1, 2]. In this case an ionic compound of charge similar to that of the solute to be determined is added to the mobile phase. The fate of this additive is to mask unreacted residual silanol groups and to be adsorbed onto the alkyl moiety of the solid phase [3]. This leads to a dramatic improvement of the symmetry and efficiency of otherwise badly tailing peaks. This technique was applied to the determination of the new antiarrhythmic drug Propafenone 2′-[3-(propylamino)-2-hydroxy-propoxy]-3-phenylpropiophenone and its major metabolites (Fig. 1) in plasma [4]. However, this method requires long run tumes (up to 50 min.) and thus is neither technically nor economically feasible for routine use in most clinical laboratories. The reason for these extreme conditions lies in the difficulty of separating polar metabolites keeping on sufficient sensitivity in the detection of the late eluting parent compound.

In an effort to shorten the run time we reexamined the retention of these early eluting metabolites as a function of some common alkylammonium ions as tail reducers.

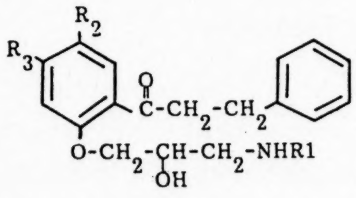

	R_1	R_2	R_3
Propafenone (PPF)	CH_2 CH_2CH_3	H	H
5-OH-Propafenone	$CH_2CH_2CH_3$	OH	H
5-OH-4OMe-Propafenone	$CH_2CH_2CH_3$	OH	OCH_3
N-depropyl-Propafenone	H	H	H

Fig. 1
Structural formula of Propafenone and its major metabolites.

0009-5893/87 0753-06 $03.00/0

© 1987 Friedr. Vieweg & Sohn Verlagsgesellschaft mbH

Moreover, since the hydroxylated derivative is claimed to be the most important contributor to antiarrhythmic activity besides Propafenone [5], a parallel detection was carried out to establish the peak purity of this compound.

Experimental

Chemicals

Propafenone, its metabolites and the internal standards (LU 41616 = 2′-[3-(3″-hydroxy-3″-methylbutilamino)-2-hydroxypropoxy]-3-phenyl-propiophenone and Li1115 = 2′-[3-(ethylamino)-2-hydroxy-propoxy]-3-phenyl-propiophenone were obtained from Knoll (Ludwigshafen, Rhein, FRG). Analytical-grade diethylether with B.H.T. as preservative was used (C. Erba, Milan, Italy). Acetonitrile Lichrosolv® was from Merck (Darmstadt, FRG). Tetrabutylammonium bisulfate (TBA), Triethylamine (TEA) and Hexadecyltrimethylammonium bromide (CTAB) from different sources were used without purification. All other substances were of analytical or reagent grade.

Apparatus

HPLC separations were carried out using a Perkin-Elmer Series 3B pump and a Perkin-Elmer LC-75 spectrophotometer set at 215 or 254 nm. In some experiments with phenolic derivatives we used an ESA Model 5100A coulometric detector (ESA Inc., Bedford, USA) equipped with a Model 5010 double electrode cell in series with a guard cell Model 5020. The potentials used for the assay were + 0.65 V for the guard cell, 0.00 V for the upstream electrode and − 0.20 V for the downstream electrode (E. Brode, personal communication [6]).

Samples (20 μl) were injected using Rheodyne valves (Mod. 7010/7125) onto a Merck Lichrosorb RP-18 10 μm column (25 x 0.46) or a 10 μm (25 x 0.46) Partisil ODS (Whatman, Clifton, USA). In some experiments a 5 μm (25 x 0.46) RP-Select B (Merck, Darmstadt, FRG) was also employed. The column temperature was controlled by recirculating water through a glass-jacket from a thermostatted bath. The pH was monitored with a Beckman digital meter equipped with standard electrodes.

Chromatographic Technique

Columns were tested for the hydrophobic (HP) and silanophilic (SiOH) character before and after beeing in contact with mobile phase containing alkylammonium ions [7]. The solutes used for the testing were uracil, benzene and anthracene (HP Index) and N,N-diethyltoluamide (SiOH Index). The hold up volume (V_0) used to measure capacity factors (k′) was determined from the peak obtained after the injection of fructose. Sodium nitrate was used as qualitative marker of the amine adsorption onto the alkyl moiety of the stationary phase.

Phosphate buffer (PB) 50 mM, pH = 2.60 was used to prepare the eluents. Since pH meter readouts change with the addition of amines to the mobile phase, phosphoric acid was added to re-establish the original pH reading of the mixture. Per cent acetonitrile varied from 25 to 35. The flow rate was 1 ml/min in each case.

Analytical Procedure

Extraction of Propafenone, its metabolites and internal standards from plasma samples was performed as described by Kates [4] with the following modifications. Plasma samples (1 ml) were alkalinized (pH = 9.5) with diluted ammonia and a first extraction was performed with diethylether. After removement of plasma the organic phase was shaken with 250 μl of phosphoric acid 0.5 N and, after centrifugation, the organic layer was discarded. The acqueous phase was then alkalinized as in the first step, and the extraction procedure repeated. The organic layer was finally separated and dried under a stream of nitrogen at 37 °C. The residue was reconstituted in 100 μl of mobile phase and a fixed amount of the final solution injected onto the column. The UV detection was accomplished at 215 nm.

For the analysis of the plasma extract with the electrochemical detection a third internal standard was introduced (LU46532 = 5′-(hydroxy)-2′-[3-(ethylamino)-2-hydroxy-metoxy-propoxy]-3-phenyl-propiophenone.

Results and Discussion

Silanol Masking Effect of Different Amines

The existence of at least two mechanisms for the retention of protonated amines in reverse-phase chromatography is recognized [3]. The first binding mechanism is believed to be due to an ion-exchange process with the acidic silanols and the second one is assumed to be based on the hydrophobic interaction with the stationary phase. Bij et al. [8] described a procedure for the evaluation of the potency of the masking agent in reducing the silanophilic interaction. According to this approach the retention factor k of an analyte obtained at a certain concentration A of the amine additive in the mobile phase can be subtracted from the retention factor k_0, obtained in the absence of the additive to yield the following expression for the equilibrium constant, K_A, of the silanol masking agent

$$\frac{[A]}{k_0 - k} = \frac{1}{k_2 K_A} + \frac{[A]}{k_2}$$

where k_2 is the retention factor for the binding to silanols in absence of the amine additive. This relationship was derived assuming that the amount of the binding sites available for the hydrophobic interaction did not change after the addition of the amine to the mobile phase. Experiments to calculate the silanophilic binding constants and to compare the masking effects of TEA, NA (at different concentrations of CH_3CN), TBA and CTAB were performed by measuring the retention of 5-OH-PPF at different concentrations of the modifiers. The data relative to the Lichrosorb RP-18 phase (Fig. 2) suggest the validity of the adopted model and that the efficacy in reducing silanophilic interaction increase with carbon number and linearity of the chain. In the figure the data relative to CTAB are

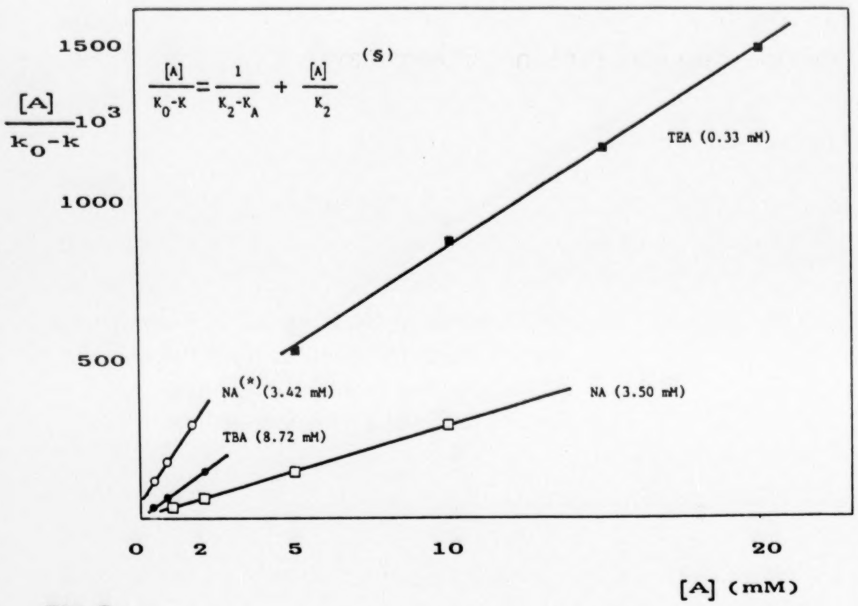

Fig. 2

Silanophilic binding constants (§) of different amines. Eluent: 25% CH_3CN and 75% mM PB pH 2.6 (* = 35% CH_3CN). Solid phase: Lichrosorb RP-18. (§) K. Bij et al. "J. Chromatogr." **203**, 65 (1981).

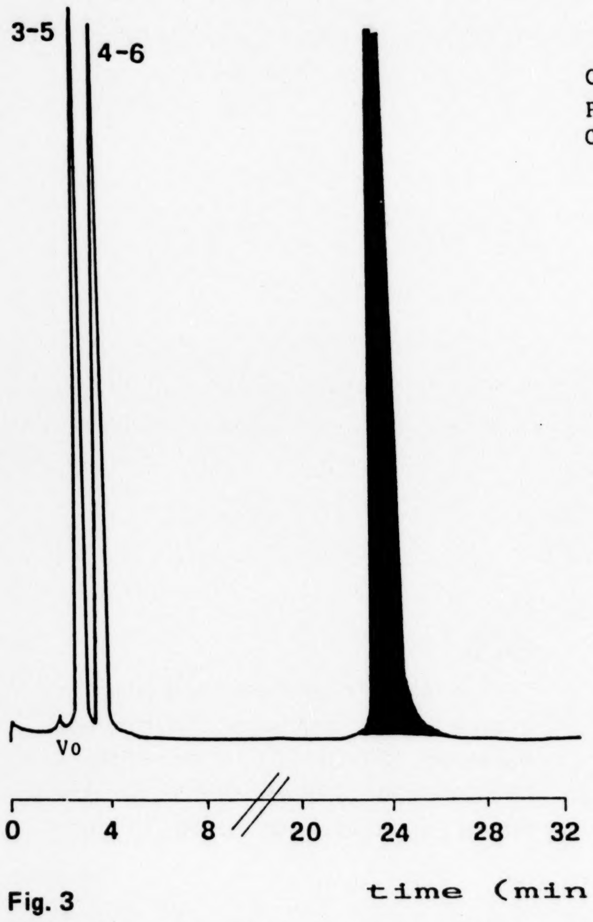

Fig. 3

Retention of Propafenone, its metabolites and nitrate ion (solid peak) in presence of 1 mM CTAB added to the mobile phase. 3) 5-OH-PPF, 4) Nor-PPF, 5) 5-OH-4-OMe-PPF and 6) PPF. Solid phase: Lichrosorb RP-18.

not reported. The reason is that the effect on the chromatographic behaviour was so abnormal that even at a concentration of 1 mM the compounds of interest were unretained (Fig. 3). The retention of nitrate ion is conform with the observation that a very large amount of the amine had to be absorbed onto the solid phase. This effect was not evidenced by other Authors [8] probably because of the much higher content of CH_3CN in the mobile phase they used.

The silanophilic binding constants relative to the Partisil ODS phase could not be calculated because the plot of $[A]/k_0 - k$ vs $[A]$ was not linear. The reason of this behaviour can be due to the change of the silanolic character we observed after the treatment with mobile phases containing nonylamine. This was evidenced by the redetermination of the SiOH index which passed from 6.786 to 4.64 with a great improvement of the peak symmetry. The change was found to be irreversible.

This behaviour was totally different from that of the Lichrosorb RP-18 phase and suggests that the environment in which acidic silanols are located may play an important role. In a recent study where these effects were taken into account for the characterization of sorbents for solid phase extractions Blevins has found an irreversible absorption for the polar analyte aniline [9]. Moreover, other workers [3] reported on the difficulty of removing all alkylammonium ions from the stationary phase suggesting that some of the silanol groups can bind very tightly.

Of the alkylamines tested, nonylamine was found to be the most effective masking agent considering that bulk additive such as TBA give little improvement of the simmetry, as also observed by other Authors [10]. An amine concentration which reduces the silanol effect by 90% has been recommended [8]; in this case 2.86 mM for NA with the Lichrosorb RP-18 phase. With these conditions, however, a strong overlapping was evidenced between Nor-PPF and 5-OH-4-OMe-PPF peaks with an inversion of the retention times with respect to those obtained without the amine added. We thus decided to investigate the effect of increasing the concentration of the amine modifier over the silanol saturating value on the selectivity using both the octadecyl phases. Fig. 4 summarizes the data of these experiments. At zero concentration of NA the elution profile of the compounds is different in the two systems. This was expected because of the very low carbon coverage of the Partisil phase which makes it to resemble to an octylsilica. The elution profile obtained by Kates et al. [4] who used an octyl-silica is in fact very similar. This characteristic behaviour was used at the beginning of the experiments to confirm the presence of an N-dealkylated metabolite in the plasma of patients undergoing chronic therapy with Propafenone.

While with the Partisil-ODS phase the separation of the metabolites gets worse with increasing the amine content in the mobile phase, an improvement is obtained with the other phase. In particular the separation between Nor-PPF and 5-OH-PPF increases with increasing the efficiency and the simmetry of the peaks. The 5-OH-4-OMe-PPF peak is also separated from the others. This last metabolite is however virtually absent in the plasma of patients on chronic treatment [4].

This behaviour was not obtained just increasing the CH_3CN content of the mobile phase and we suggest that an increase of the amount of modifier onto the alkyl moiety of the solid phase may be of benefit when a separation of early eluting polar metabolites on a RF column is attempted. The overall improved effect of adding NA to the mobile phase is illustrated in Fig. 5. The result of increasing pH of the

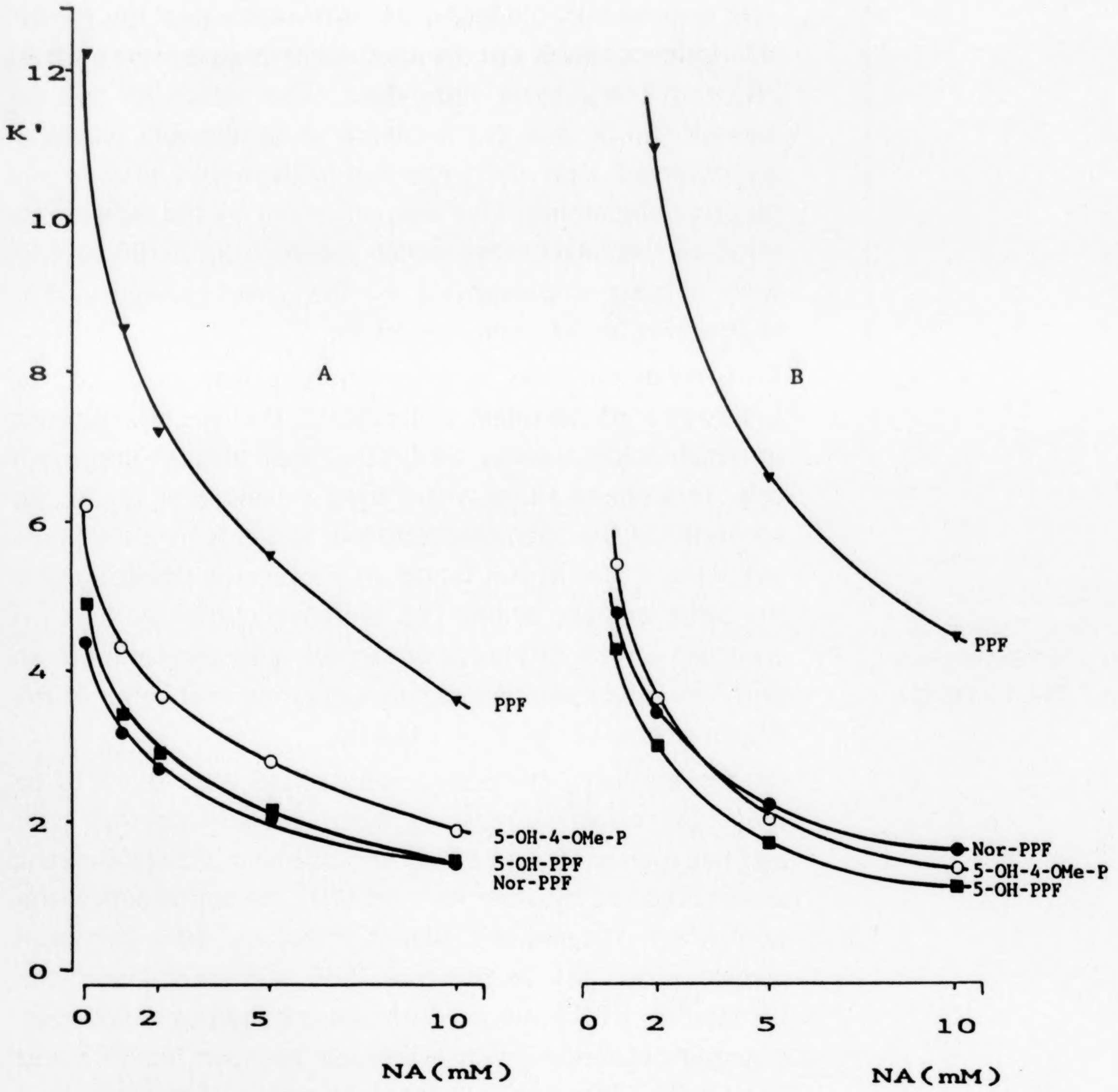

Fig. 4

Dependence of the k′ values of Propafenone and its major metabolites from the content of nonylamine in the mobile phase. A) Partisil ODS, B) Lichrosorb RP-18.

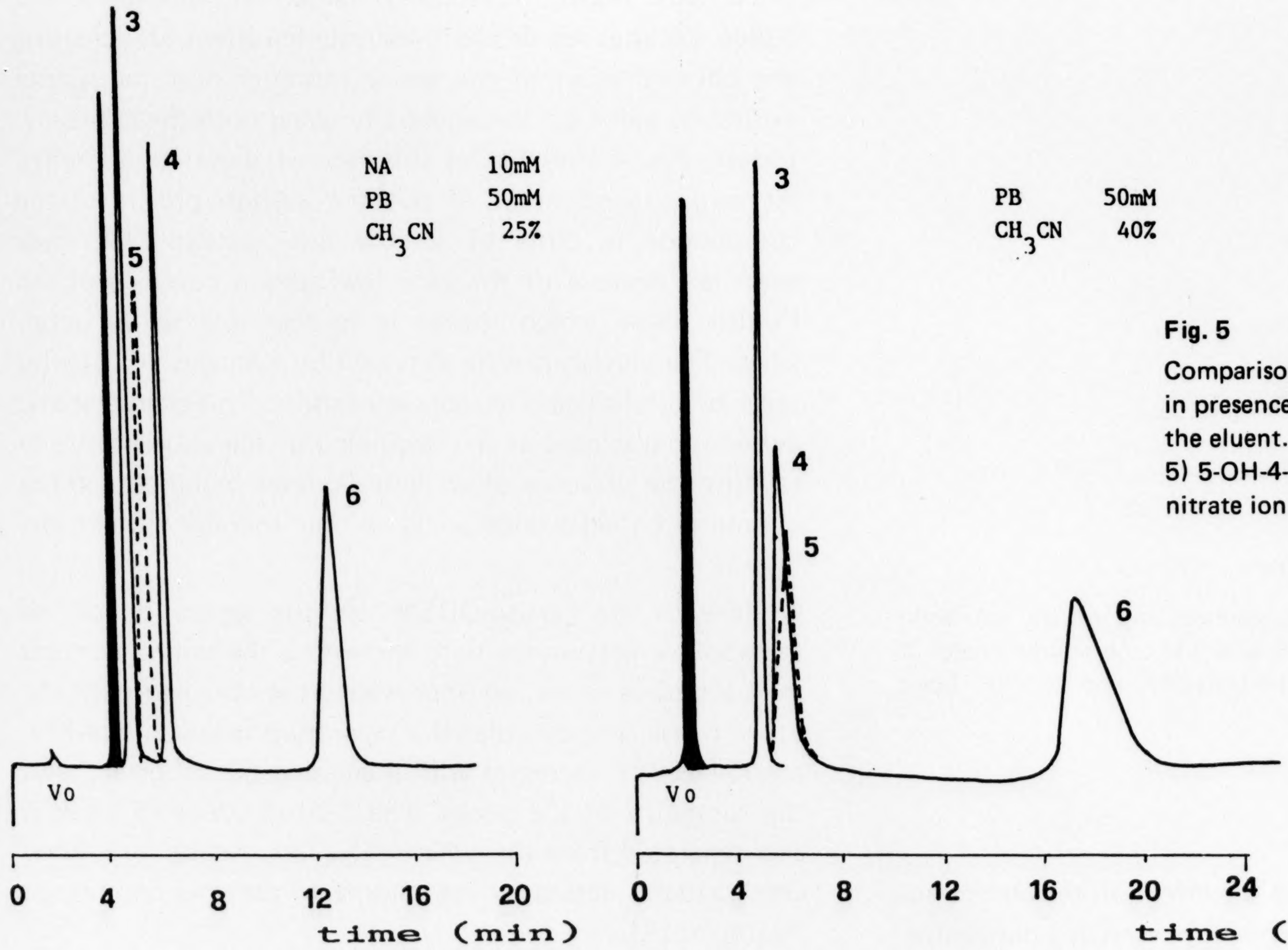

Fig. 5

Comparison of peak shapes and selectivity in presence and absence of nonylamine in the eluent. 3) 5-OH-PPF, 4) Nor-PPF, 5) 5-OH-4-OMe-PPF and 6) PPF. Solid peak: nitrate ion. Solid phase: RP-18, 10 μm.

mobile phase was investigated with the RP-Select B column for which the chromatographic behaviour is claimed to be unaffected by unreacted silanols. The behaviour of Propafenone and its metabolites was found as expected i. e., k′ values increased with pH. Irrelevant was the effect on the selectivity (Fig. 6).

Application in Pharmakokinetics

Fig. 7 shows the plasma concentrations of PPF and its major metabolites in plasma over a period of 24 hours from a patient given 300 mg t.i.d. after discontinuation of the morning dose. In this assay 1 ml of plasma was used and the

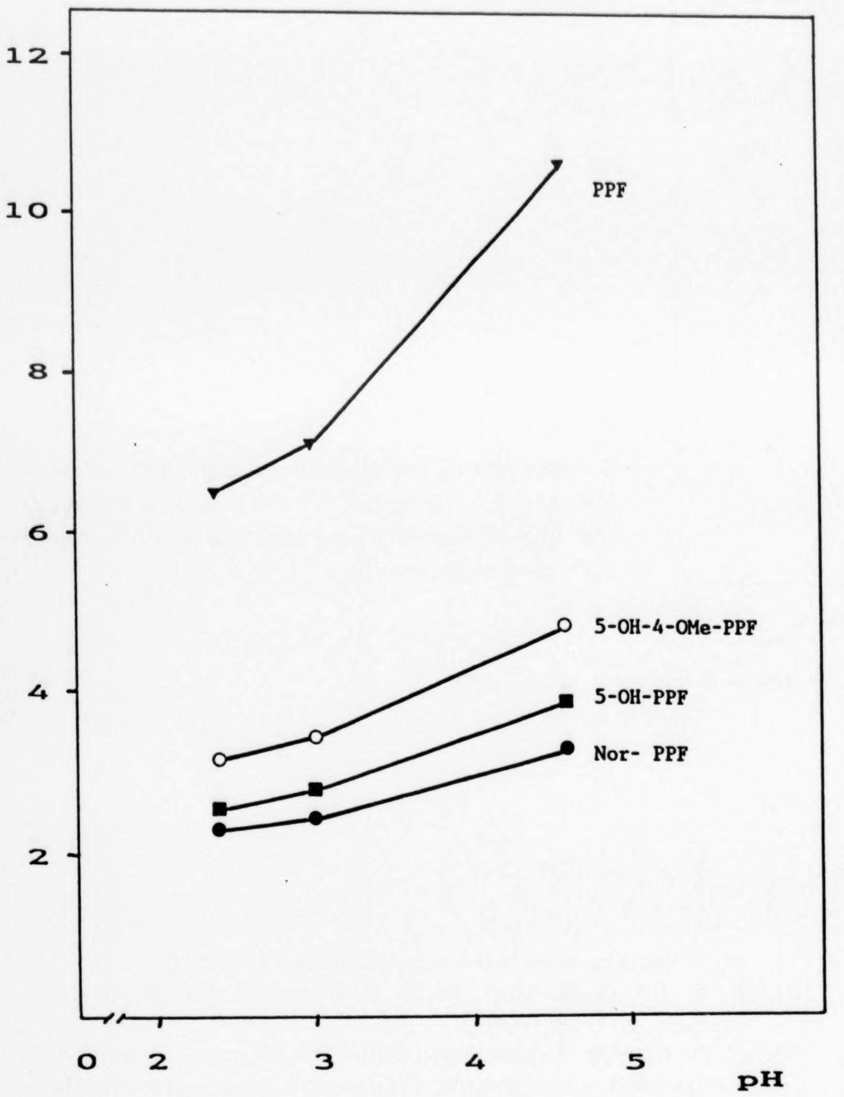

Fig. 6
Dependence of K′ on pH. Mobile phase without any amine added. Solid phase: RP-Select B, 5 μm.

results expressed in ng/ml. It is well evident that N-dealkylation oxidative pathway is not saturated in this patient recognized as a slow hydroxylator.

The method proposed by Kates et al. [4] has thus been subtantially improved although its low sensitivity restricts pharmacokinetic studies to patients under chronic treatment.

The investigate possible coelution of other yet undiscovered metabolites and the peak purity of 5-OH-PPF (claimed to be the most important contributor to antiarrhythmic activity besides PPF), the analysis was carried out using an electrochemical detection in parallel with the UV. The comparison of the two detection procedures is shown in Fig. 8.

UV on average was 2.03 ng/ml higher than EC, with a 95 % confidence interval of 4.10 to − 0.04. The difference between the two procedures was not significantly different from zero and its SD was 4.78.

This agreement suggests that no interference arising from both accumulated metabolites or endogenous compounds is to be expected when the analysis is carried out using either of the detection systems.

Acknowledgment

The Authors wish to acknowledge Drs. M. Hollmann and E. Brode, Knoll AG Ludwigshafen/Rhein (FRG) for the gift of pure standard samples and Mrs. A. Candi (USL 28, Bologna, Italy) for the technical assistance.

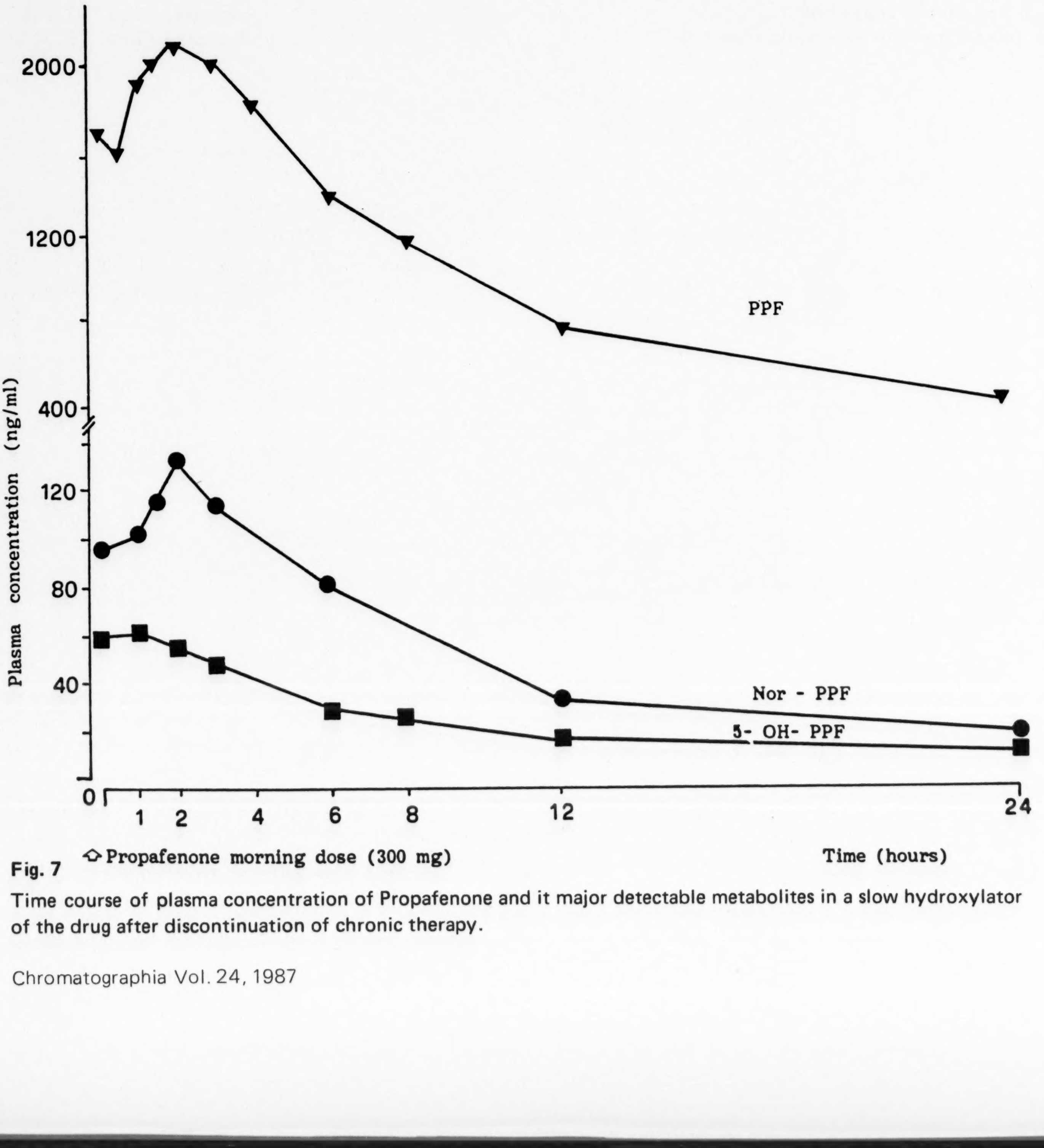

Fig. 7
Time course of plasma concentration of Propafenone and it major detectable metabolites in a slow hydroxylator of the drug after discontinuation of chronic therapy.

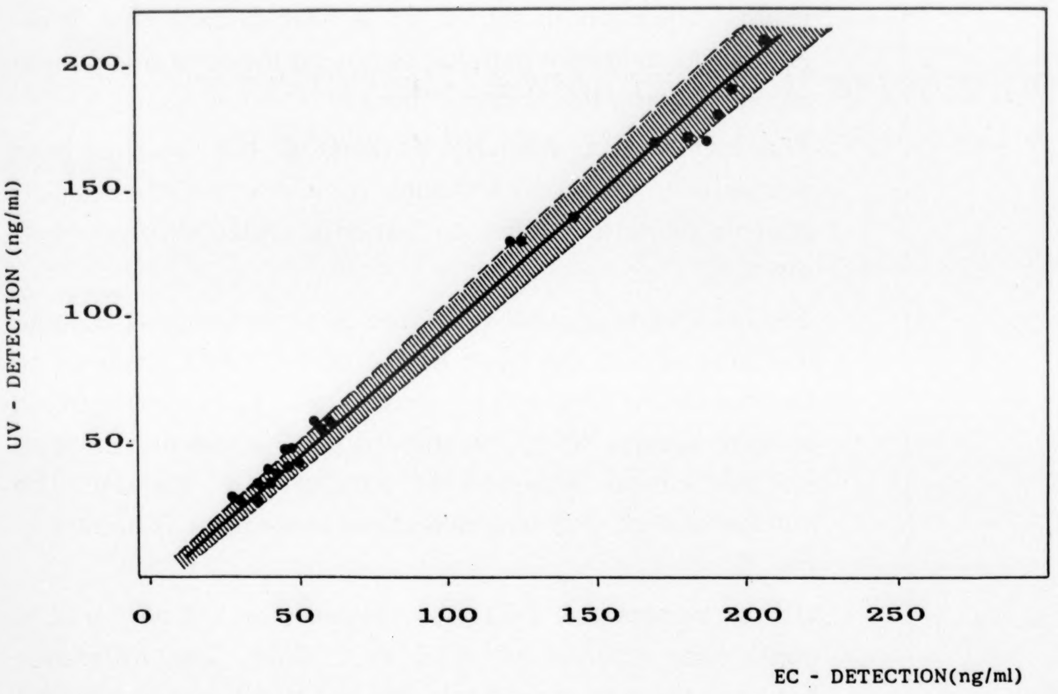

Fig. 8

Comparison of the analyses of 5-OH-PPF using the UV and EC detectors. The heavy line represents the line of identity and the dashed lines delimit 10 % deviation from it.

References

[1] *R. P. Koshakji, A. J. J. Wood,* J. Pharm. Sci., **75** 87 (1986).

[2] *H. F. Proeiss, T. B. Townsend,* Clin. Chem., **32**, 1311 (1986).

[3] *O. A. G. J. Van Der Houwen, R. H. A. Sorel, H. Hilshoff, J. Teewsen, A. W. M. Indemans,* J. Chromatogr., **209**, 393 (1981).

[4] *R. E. Kates, Y. G. Yee, R. A. Winkle,* Clin. Pharmacol. Ther. **37**, 610 (1985).

[5] *G. von Philipsborn, J. Gries, H. P. Hofman, H. Kreiskott, R. Kretzshmar, C. D. Muller, M. Raschak, J. Teschendorf,* Arzneimittel-forsch/Drug. Res. **34** (II), 1489 (1984).

[6] *E. Brode,* Knoll Internal Reports (personal communication).

[7] *M. J. Walters,* accepted for publication in JAOAC.

[8] *K. E. Bij, C. Horvath, W. R. Melander, A. Nahum,* J. Chromatogr., **201**, 65 (1981).

[9] *D. D. Blevins,* Proceedings of the Third Annual International Symposium on "Sample Preparation and Isolation Using Bonded Silicas", Cherry Hill, May 5–6 (1986).

[10] *A. Sokolowski, K. G. Wahlund,* J. Chromatogr., **189**, 299 (1980).

Received: June 30, 1987
Revised manuscript
received: Sep. 7, 1987
Accepted: Sep. 9, 1987
F

Narrow-Bore Liquid Chromatography with Multichannel Detection in Paediatric Biochemistry: Analysis of Phenylalanine and Tyrosine in Phenylketonuria

Elaine M. Kirk / B. J. Clark / A. F. Fell*

Department of Pharmaceutical Chemistry, University of Bradford, Richmond Road, Bradford, BD7 1DP, UK

Key Words

Narrow-bore liquid chromatography
Linear diode array (LDA)
Phenylalanine (Phe)
Tyrosine (Tyr)
Phenylketonuria (PKU)

Summary

In paediatric biochemistry, the analysis of drugs and endogenous compounds in preterm or low-birth weight neonates presents particular analytical problems. Sensitive techniques with small sample capacity are essential and in this context, narrow-bore (1–2mm) LC columns, coupled with appropriate low-volume detector cells and connections to reduce band dispersion, have been shown to offer significant advantages. By comparison with conventional columns an increase in sensitivity by a factor of *ca.* 2 can be achieved. The combination of narrow-bore columns and rapid-scanning UV detectors in reversed-phase LC enables the spectral information to be used for both peak recognition and homogeneity validation. Furthermore, "diode bunching" in the wavelength domain leads to a further two-fold increase in sensitivity. This combination of column and detector technology has been utilised in the design of a sensitive serum micro-assay of the essential aromatic amino acids in paediatric samples, capable of being used with 500nl sample, sensitive to 13pg phenylalanine and 9pg tyrosine and linear over the requisite therapeutic range.

Introduction

Phenylketonuria (PKU) is an inherited disorder of amino acid metabolism. It is characterized principally by elevated serum levels of the essential aromatic amino acid phenylalanine, normally 50–120μM; a rise to greater than 1000 μM is not unusual. Abnormal metabolites of phenylalanine are also excreted in the urine, principally phenylpyruvic acid and orthohydroxyphenylacetic acid. The patient is unable to metabolise phenylalanine normally, the fundamental defect being a lack, or inactivity, of the hepatic enzyme phenylalanine *p*-hydroxylase which converts phenylalanine to tyrosine:

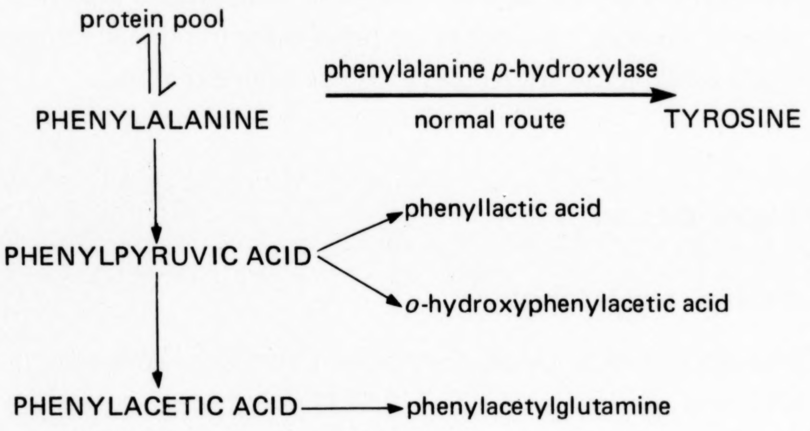

(from ref. [1])

PKU is a fairly uncommon condition, the incidence being 1 in 10,000–20,000 births, but if unrecognized and untreated, irreversible moderate to severe retardation with schizoid tendencies becomes apparent by the end of the child's first year.

To minimise brain damage, the earliest possible recognition and commencement of dietary restriction of phenylalanine is essential. However this treatment should be monitored throughout since deficiencies of essential amino acids, such as phenylalanine and tyrosine, can also be damaging, as they are involved in the synthesis of neurotransmitters and hormones.

Of the several methods proposed for the analysis of amino acids and peptides in biological materials, most rely on pre- or post-column derivatisation to generate the phenylthiohydantoin [2], dansyl [3], *o*-phthaldialdehyde [4, 5] or other derivatives which can be detected by conventional UV- or fluorescence spectrometers with high sensitivity. Lindroth and Mopper [5] were in fact able to detect less than 1 picomole of a number of amino acids using the fluorogenic reagent *o*-phthaldialdehyde. Hancock et al. [6] used an ion-pair system with reversed-phase HPLC and

0009-5893/87 0759-07 $03.00/0

© 1987 Friedr. Vieweg & Sohn Verlagsgesellschaft mbH

detection at 190–200nm to detect nanogram levels of free amino acids. More recent methods include high-resolution proton-Fourier transform NMR-spectrometry [7] or HPLC of blood spots on filter paper [8, 9].

One of the most important characteristics of an LC system is its sensitivity. As shown by Scott [10], for a peak having a height equivalent to twice the noise level, the minimum detectable mass is proportional to the square of the column radius. Thus a 2.1mm i.d. column should enable the detection of almost one fifth of the mass detected when using the regular 4.6mm i.d. column, assuming that band dispersion resulting from the injection, connection tubing, column and detection system are equal in both cases. In practice these increases in sensitivity are difficult to realise because of the stringent demands small columns make on the chromatographic apparatus with which they are employed.

Narrow-bore LC (column 1–2mm i.d.) is gaining acceptance as a reasonable compromise between the advantages (eg. sensitivity enhancement) and disadvantages (eg. instrumentation demands) of small column technology. Other benefits, including their suitability for small sample sizes, have been well documented in the literature [10–12].

In screening serum samples for endogenous analytes, it is often helpful to have additional information of a qualitative nature in order to confirm the peak assignations assumed. In this context, the utility of rapid-scanning linear photodiode array (LDA) detectors [13] has been examined.

Experimental

Reagents and Materials

Methanol (HPLC grade, Rathburn Chemicals, Walkerburn, UK) was used as received. A 0.05M solution of potassium dihydrogen orthophosphate (AnalaR grade, BDH, Poole, UK) was prepared with glass-distilled water and filtered under vacuum by Millipore 0.45μm MA filters using an all-glass apparatus. The pH was then adjusted. Degassing was effected by a continuous stream of helium at 180ml/min. Sodium hydroxide and zinc sulphate were used as received from BDH.

The amino acids tyrosine (Tyr), phenylalanine (Phe), tryptophan (Trp) and the internal reference standard β-2-thienyl-DL-alanine (IS) were obtained from Sigma (St. Louis, Mo., USA). Paediatric serum samples were kindly supplied by the Royal Hospital For Sick Children (Edinburgh, Scotland, UK).

Standard Solutions

For quantitative analysis, phenylalanine (75–1507μM) and tyrosine (15–307μM) were prepared by dilution in glass-distilled water after weighing on a Cahn C-31 microbalance (California, USA). Serum standards were prepared by spiked dilutions vortex-mixed in human serum.

Equipment

The analytical columns were 100 × 2.1mm i.d. (narrow-bore) and 100 × 4.6mm i.d. (regular) both packed with the monofunctional 5-μm Spherisorb RP-18 OD-102 (Brownlee, Santa Clara, CA, USA). The optimised solvent system employed was methanol – 0.05M potassium dihydrogen orthophosphate (13:87, v/v) adjusted to pH 4.0, at optimised flow rates of 0.08ml/min for narrow-bore work and 1.20ml/min for regular bore separations. Chromatography in both cases was effected at ambient temperature.

Using the narrow-bore column, a 0.5μl Rheodyne injection valve (Model 7520, Rheodyne, Berkeley, CA, USA) and an LKB 2150 pump (LKB-Produkter, AB, Bromma, Sweden) three types of detection system were investigated.

Detection system IA comprised the single-channel variable-wavelength LDC SpectroMonitor 3000 Detector (LDC/Milton Roy, Stone, Staffordshire, UK) fitted with a 1-μl flow cell, 3mm pathlength. This was employed at the optimised detection wavelength of 210nm (Fig. 1).

The Pye-Unicam PU 4021 multichannel detector (Cambridge, UK), used in conjunction with the PU 4895 LC interface and PU 4850 computer, comprised detection system IB. The detector was again fitted with a 1-μl flow cell, 3mm pathlength. Spectral resolution was 4nm per diode in the range 189–390nm (Fig. 2).

System IC utilised the same detection system as IB but exploited the fact that using the PU 4021 adjacent diode resolution elements could be combined systematically ("diode bunching") to enhance sensitivity.

The regular column, a 20-μl Rheodyne injection valve (Model 7125), and LKB 2150 pump were employed with detection system II. This system comprised the single-channel variable wavelength LDC SpectroMonitor 3000 detection system fitted with a 14-μl flow cell, 10mm pathlength. This was again employed at the optimised detection wavelength of 210nm.

In an effort to reduce extra-band dispersion, all connecting tubes were kept as short and as narrow as possible (0.13mm i.d.).

In-line filters were connected in-series to both columns for all detection configurations.

Methodology

Validation

The narrow-bore HPLC method developed, using system IA, was compared with an automated version of the fluorimetric method proposed by McCaman and Robins [14, 15], as modified by the Royal Hospital For Sick Children, Edinburgh [16]. Twenty-one clinical samples from phenylketonuric patients were analysed for phenylalanine by the respective methods and the concentrations plotted against each other (see Fig. 3).

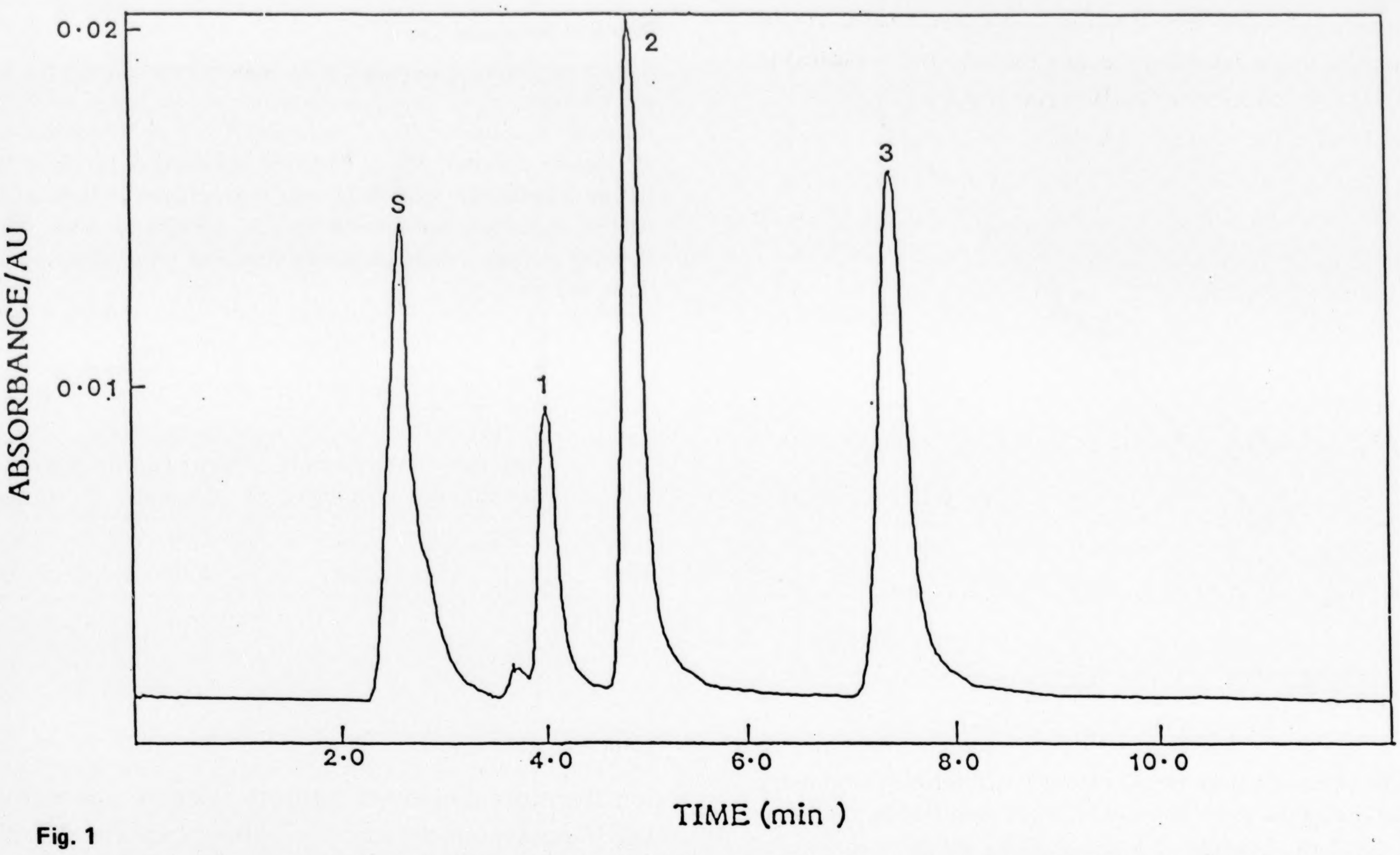

Fig. 1

Chromatogram of clinical sample from phenylketonuric patient (sample code no. 8, see Table II). For chromatographic conditions, see text; narrow-bore column used with detection system IA; parameters: sensitivity 0.02 AUFS; injection volume 0.5μl; wavelength of detection 210nm. Peak identification: S, polar endogenous components from serum; 1, Tyr; 2, internal standard; 3, Phe.

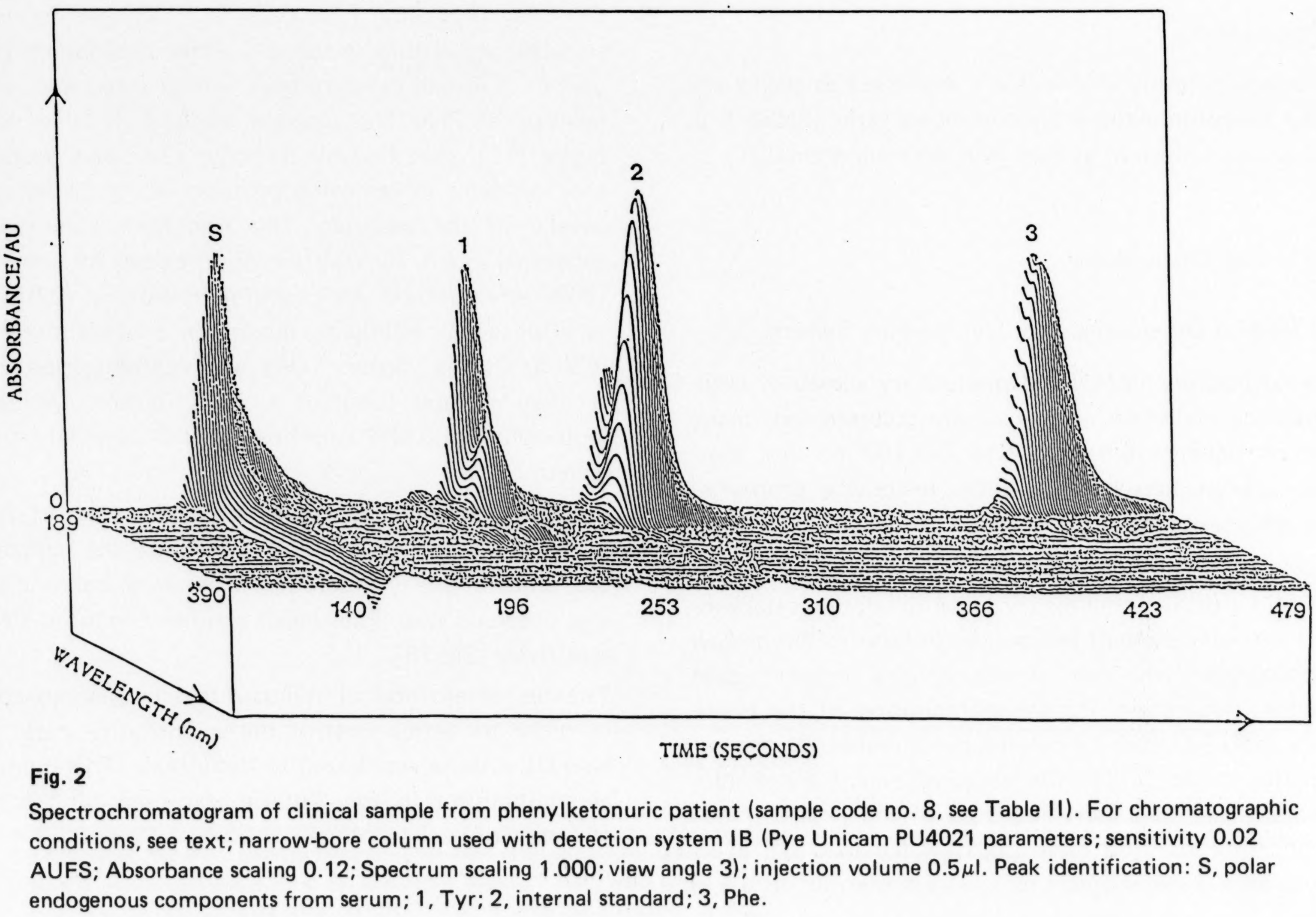

Fig. 2

Spectrochromatogram of clinical sample from phenylketonuric patient (sample code no. 8, see Table II). For chromatographic conditions, see text; narrow-bore column used with detection system IB (Pye Unicam PU4021 parameters; sensitivity 0.02 AUFS; Absorbance scaling 0.12; Spectrum scaling 1.000; view angle 3); injection volume 0.5μl. Peak identification: S, polar endogenous components from serum; 1, Tyr; 2, internal standard; 3, Phe.

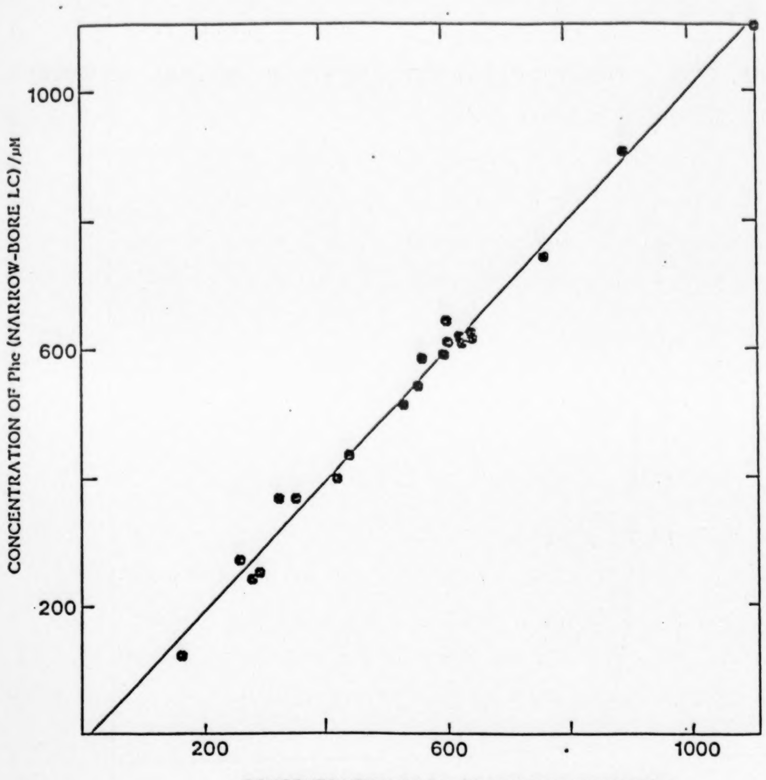

Fig. 3

Correlation of narrow-bore HPLC method with referee fluorimetric method of McCaman and Robins [14, 15], as modified by the Royal Hospital for Sick Children, Edinburgh [16], for clinical samples from phenylketonuric patients. Correlation coefficient r = 0.9946 (n = 21). Narrow-bore LC method utilised detection system IA, parameters as Fig. 1.

Table I. Detection limits.

Detection limits, expressed as pg injected on-column for SNR = 2, are the mean of at least four determinations. Injection volume of a solution in water of Phe 1.5μM and Tyr 0.3μM: narrow-bore, 0.5 μl; regular column, 20μl. Nominal wavelength for each detector, 210nm. Detection system IA and II employed at sensitivity 0.001 AUFS, detection systems IB and IC sensitivity 0.01 AUFS and nominal default values of bandwidth. For chromatographic conditions, see text.

Compound	Detection Limit (pg)			
	Single Channel		Linear Diode Array	
	II Regular Column	IA Narrow-bore Column	IB Narrow-bore Column	IC Narrow-bore Column
Phe	83	31	24	13
Tyr	31	24	19	9

Detection Limits

The detection limits (Table I) are expressed as picograms injected on-column for a signal-to-noise ratio (SNR) = 2. All values are a mean of at least four determinations.

Results and Discussion

HPLC Method Development for Narrow-bore System

Choice of packing material: A preliminary survey of available packing materials in narrow-bore columns led to the choice of Spherisorb-5μm RP-18 OD-102 on the basis of the superior base silica and the selectivity properties for the analytes of interest.

Optimization of mobile phase and flow rate: For clinical amino acid analysis, preliminary experimentation established that a mobile phase of methanol – potassium dihydrogen orthophosphate with an octadecylsilane column gave satisfactory separation. Parallel optimisation of the phase capacity ratio (k′) and the column performance (N, theoretical plates metre^{-1}) for the principal eluent parameters was performed. Progressive increases of the organic modifier concentration from 0 to 20% v/v led to a fall in k′ and improved peak shape; this was optimum at 13% v/v methanol for both systems. Variation of the eluent pH from 2.5–5.0 produced only a small effect on the k′ value, as did adjustment of buffer molarity from 50 to 200mM. However, pH exerted a marked effect on N, the optimum being observed at pH 4.0. The optimum eluent composition therefore employed for both systems was methanol – 0.05M potassium dihydrogen orthophosphate (13:87, v/v) adjusted to pH 4.0. For narrow-bore work this gave acceptable resolution of Tyr (k′ = 0.78), internal standard (k′ = 1.14) and Phe (k′ = 2.28), eluted the polar components at the solvent front, and resulted in a total analysis time of 8.5 minutes (Fig. 2).

Choice of protein precipitant and pretreatment process: Six protein precipitation procedures were examined [17–24]. Of these only zinc hydroxide [17, 18] was found to be suitable at 210nm, since the other procedures [19–24] yielded a broad reagent peak which interfered with the analysis of Phe. The classical method of Hiller and Van Slyke [17], modified by Somogyi [18], was found to be very efficient in removing proteins whilst giving good recovery of the analytes. The zinc hydroxide reagent is generated *in situ* by addition of an excess of zinc sulphate (10% w/v; 100μl) and sodium hydroxide (0.5M; 50μl) to 50μl serum. Following mixing on a vortex mixer (Spiramix 5, Denley, Sussex, UK) and centrifugation at 120g for five minutes (Centaur 1, MSE, Sussex, UK) a filled-loop volume of 500 nanolitres of the supernatant was injected.

Previous work had established that an excess of zinc sulphate was required in order to stabilise the sample pH at 6.6, since at pH 8 and above, an unusual baseline artefact was observed near Phe which seriously reduced detection sensitivity [25, 26].

The use of an internal standard was considered advisable in order to better control the quantitative data. β-2-thienyl-DL-alanine was found to be suitable. This is employed as an inhibitor in the Guthrie test used for the routine screening of neonates for PKU.

Quantitative Evaluation

The method developed for analysis of the aromatic amino acids phenylalanine and tyrosine in paediatric samples was designed to require a very small sample volume and was found to be rapid, sensitive and precise. Peak height response ratios for Tyr: IS and for Phe: IS in spiked human serum were linear with concentration over the clinical ranges of interest (Tyr, 15–304µM; Phe, 75–1500µM): Tyr, $y = 0.0043x - 0.0381$ ($r = 0.9971$; $n = 6$); Phe, $y = 0.0028x - 0.0260$ ($r = 0.9996$; $n = 6$). By comparison with aqueous standards, the recovery data for Phe at normal and elevated levels were: 80.5% (70µM) and 94.7% (1120µM), respectively. At 62µM recovery of Tyr was 90.5%. The within-batch relative standard deviation (RSD) was: Phe, 1.25% at 1010µM (n = 6); Tyr, 1.44% at 257µM (n = 6).

For the determination of phenylalanine levels, this narrow-bore method correlated well with the results of an established fluorimetric referee procedure [14, 15] run by an independent paediatric biochemistry laboratory [16]. The range of the twenty-one clinical samples was such that the levels of phenylalanine varied from near normal (162µM) to elevated levels of greater than 1000µM as illustrated in Fig. 3, for which the regression equation is: $y = 1.0167x - 13.32$ (correlation coefficient, $r = 0.9946$; $n = 21$).

In Table II the results of the two procedures are compared. By both the paired t-test and F-test no significant difference could be found between the set of results obtained by the McCaman and Robins procedure and the set of results obtained by the narrow-bore LC method. This reinforces the good correlation stated above.

Whilst high mass sensitivity may not be of critical importance when assaying high serum phenylalanine levels in PKU, it is an important parameter in the assay of Tyr and in small-sample forensic work and in other areas of paediatric biochemistry. In evaluating the detection limits of both columns with various detector configurations, the conventional definition of on-column sensitivity was adopted for SNR = 2.

Comparing the single-channel system IA and II with the narrow-bore column and regular column respectively, an interesting and significant difference is seen between these two results (Table I). Under optimum conditions for both columns, an increase in mass sensitivity is observed, approximately 2.5 times in the case of Phe and 1.3 for Tyr. This would indicate that the extra band-dispersion problems discussed previously have limited the sensitivity increase expected.

The narrow-bore column was then coupled to the multichannel Pye-Unicam linear diode array (System IB) to investigate whether a further increase in sensitivity could be effected. Comparing the sensitivity data achieved with this system with that obtained using System IA it can be seen that the linear diode array displays similar sensitivity to that of the single-channel system (Table I).

The effect on sensitivity using System IB together with a technique known as "diode bunching" (System IC) was then examined. The outputs of adjacent diode resolution elements are added together about a median wavelength to increase the effective detector bandwidth (DBW) at that wavelength (Fig. 4).

With progressive increases of the DBW from the default value of 4nm to 20nm, the signal-to-noise ratio (SNR) shows an increase up to an optimum, and then falls progressively (Fig. 5). The DBW corresponding to the maximum SNR yields the maximum sensitivity. The ratio of this optimum DBW to the spectral bandwidth, SBW, of the analyte (*ca* 0.5 in the case of both Phe and Tyr) will vary according to the dispersion ratio across the diode

Table II. Comparison of narrow-bore LC and referee (McCaman and Robins) procedures.

Concentrations of Phe (µM) found in 21 paediatric serum samples by both methods. Narrow-bore column used with detection system IA (parameters as Fig. 1); injection volume 0.5µl; wavelength of detection, 210nm. Each figure represents the mean of two independent measurements. For chromatographic conditions, see text.

Sample Code	1	2	3	4	5	6	7	8	9	10	11
Referee Method (µM)	162	258	278	290	323	351	419	440	528	553	560
Narrow-bore LC Method (µM)	121	271	241	251	366	366	398	434	513	542	585
Sample Code	12	13	14	15	16	17	18	19	20	21	
Referee Method (µM)	596	600	603	621	625	640	642	761	891	1110	
Narrow-bore LC Method (µM)	592	644	611	620	610	626	617	743	906	1102	

Group mean ± S.D. (n = 21): Referee Method 535.8 ± 224.0µM
Narrow-bore LC method 531.4 ± 228.9µM

Paired t test at P = 0.01 (n = 40), $t_{calc.} = 0.061$, $t_{tab} = 2.704$. No significant difference.

Variance ratio F-test at P = 0.01 (n = 40)

$F_{calc} = 3.93 \times 10^{-3}$, $F_{tab} = 7.31$. No significant difference.

array, which is a function of the instrument. In the present work, the optimum detector bandwidth was found to be 10nm (Fig. 5). Diode bunching led to a further increase in sensitivity by a factor of two for both analytes (Table I).

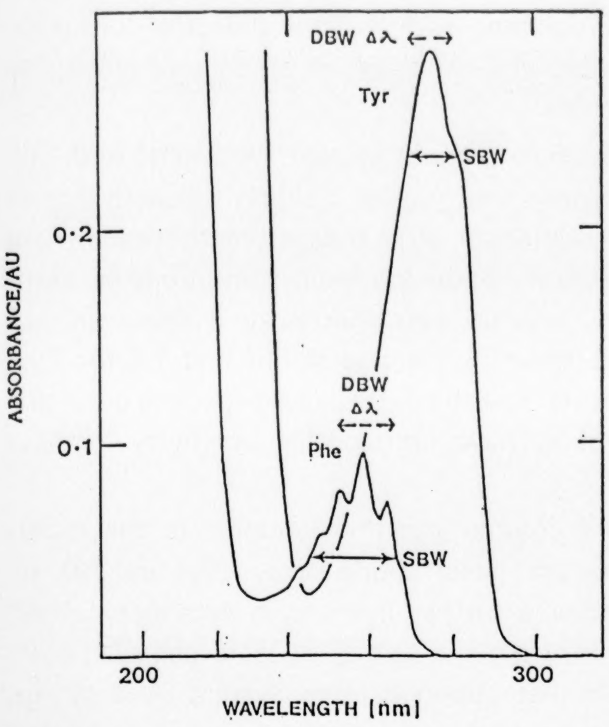

Fig. 4
UV-absorption spectra of Phe and Tyr in 0.05M phosphate buffer. SBW, spectral bandwidth; DBW, detector bandwidth, adjustable from default value of 4nm.

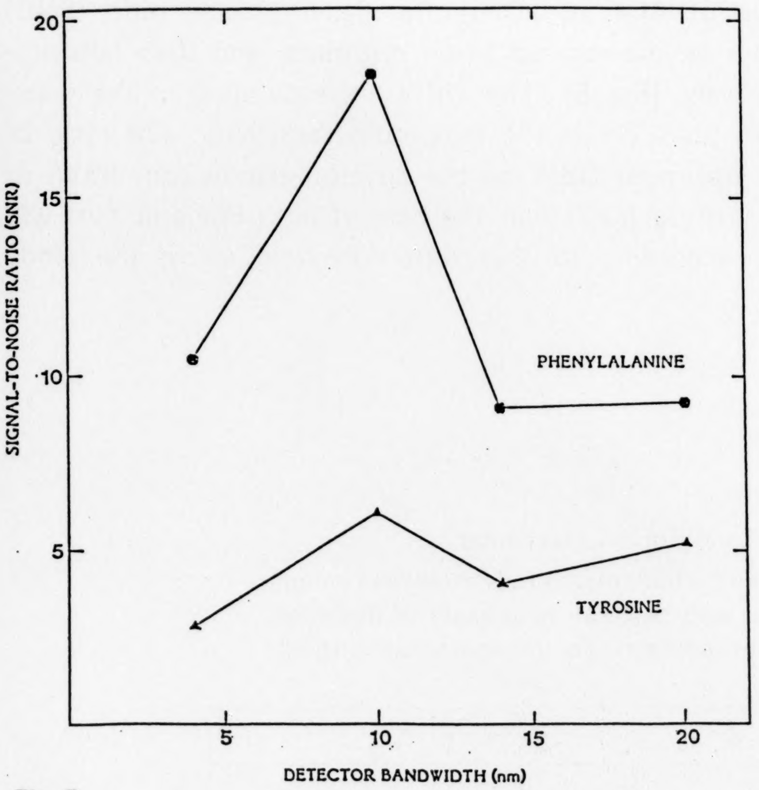

Fig. 5
Relationship of signal-to-noise ratio (SNR) with detector bandwidth for Phe and Tyr at an observation wavelength of 210nm. For chromatographic conditions, see text. Instrumental conditions for detection system IC: PU 4021 used in the "Summed Absorbance" mode; sensitivity 0.01 AUFS; injection volume 0.5μl.

In conclusion, both the narrow-bore/single-channel system and the narrow-bore coupled with the linear diode array, with or without additional digital enhancement, have been shown to be more sensitive than system II with the regular column. This has been achieved with commercially available equipment, and the narrow-bore and regular columns have been compared under strictly comparable and individually optimised conditions.

The simple deproteinisation procedure was shown to be very effective in reducing serious interference in the assay (Fig. 1). Build up of endogenous materials on the column system is apparent in some earlier HPLC methods reported for the analysis of Phe and Tyr in serum [4], where breakthrough of endogenous material appears to compromise the early-eluting Tyr and Phe peaks.

Future Developments

Other amino acid abnormalities can be assessed whilst screening/monitoring PKU by this rapid chromatographic method. High tyrosine levels in tyrosinaemia can be detected, the defect here being in tyrosine metabolism with secondary build up of Phe. It is clearly of clinical significance not to confuse this with PKU.

Tryptophan levels are also relevant to studies on brain serotonin metabolism and have been investigated in chronic schizophrenia and a number of other disease states [27, 28]. Although not the primary objective of this work, it was found that tryptophan could be detected quantitatively using these procedures, eluting at 14.6 minutes ($k' = 4.84$).

The method can also be used for measuring Phe:Tyr ratios in loading tests for the determination of heterozygote parents in genetic counselling.

In forensic toxicology and in areas of paediatric biochemistry where sensitivity and sample size are particular problems, the combination of narrow-bore HPLC with linear diode array detection clearly has significant potential.

Acknowledgements

The authors would like to thank the following people for their help and interest: Dr. J.M. Rattenbury, Dr. R.J. Dolphin and Pye Unicam Limited for the loan of the multichannel detector and 1-μl flow cell, and Mr A.L. Holmes for technical assistance.

References

[1] *W.E. Knox*, in "The Metabolic Basis of Inherited Disease", J.B. Stanbury, J.B. Wyngaarden and D.S. Fredrickson, eds., McGraw-Hill Book Co., New York, USA, 1972; p. 279.
[2] *C.L. Zimmerman, E. Appella, J.J. Pisano*, Anal. Biochem., **77**, 569 (1977).
[3] *T. Yamabe, N. Takai, H. Nakamura*, J. Chromatogr., **104**, 359 (1975).
[4] *L.M. Neckers, L.E. Delisi, R.J. Wyatt*, Clin Chem., **27**, 146 (1981).
[5] *P. Lindroth, K. Mopper*, Anal. Chem., **51**, 1667 (1979).
[6] *W.S. Hancock, C.A. Bishop, M.T.W. Hearn*, Anal. Biochem., **92**, 170 (1979).
[7] *W. Lehnert, D. Hunkler*, Eur. J. Pediatr., **145** (4), 260 (1986).

[8] *R. A. Roesel, P. R. Blankenship, F. A. Hommes*, Clin. Chim. Acta., **156** (1), 91 (1986).
[9] *Y. Watanabe, K. Imai*, J. Chromatogr., **309** (2), 279 (1984).
[10] *R. P. W. Scott*, in "Small Bore Liquid Chromatography Columns", R. P. W. Scott, ed., Wiley, Chichester, UK, 1984; p. 17.
[11] *M. V. Novotny, D. Ishii*, in "Microcolumn Separations", M. V. Novotny and D. Ishii, eds., Elsevier, Amsterdam, Netherlands, 1984; preface, p. XI.
[12] *P. Kucera*, in "Microcolumn High-performance Liquid Chromatography", P. Kucera, ed., Elsevier, Amsterdam, Netherlands, 1984; p. 39.
[13] *A. F. Fell, H. P. Scott, R. Gill, A. C. Moffat*, Chromatographia, **16**, 69 (1982).
[14] *M. W. McCaman, E. Robins*, J. Lab. Clin. Med., **59**, 885 (1962).
[15] *P. W. K. Wong, M. E. O'Flynn, T. Inoue*, Clin. Chem., **10**, 1098 (1964).
[16] *J. M. Rattenbury*; unpublished observations, Royal Hospital for Sick Children, Edinburgh, 1980.
[17] *A. Hiller, D. D. van Slyke*, J. Biol. Chem., **53**, 253 (1922).
[18] *M. Somogyi*, J. Biol. Chem., **86**, 655 (1930).
[19] *R. Guthrie*, J. Amer. Med. Assoc., **178**, 863 (1961).
[20] From, "Techniques In Clinical Chemistry", *P. L. Wolf, D. Williams, T. Tsudaka, L. Acosta*, eds., Wiley, New York, 1972.
[21] *R. C. Baselt*, in "Analytical Procedures For Therapeutic Drug Monitoring And Emergency Toxicology", Biomedical Publications Inc., Davis, California, USA, 1980.
[22] *P. B. Hamilton*, Ann. N. Y. Acad. Sci., **102**, 55 (1962).
[23] *K. Diem*, in "Documenta Geigy", K. Diem, ed., Geigy, Manchester, 1963.
[24] *P. B. Hamilton, D. D. van Slyke*, J. Biol. Chem., **150**, 231 (1943).
[25] *B. J. Clark*; unpublished data, Heriot-Watt University, Edinburgh, 1981.
[26] *A. F. Fell, B. J. Clark, H. P. Scott*, J. Chromatogr., **297**, 203 (1984).
[27] *E. F. Domino, R. R. Krause*, Biol. Psychiatry, **8**, 265 (1974).
[28] *J. D. Fernstrom, R. J. Wurtman*, Science, **173**, 139 (1971).

Received: Aug. 3, 1987
Revised manuscript
received: Sep. 4, 1987
Accepted: Sep. 8, 1987
F

A Rapid Method for the Determination of an Unstable Metabolic Intermediate.
The Metabolic Formation of Benzamide and Benzoic Acid via Diacyl Amine Intermediate

M. Pálfi-Ledniczky*/I. Weisz, G. Dénes

Central Research Institute for Chemistry of the Hungarian Academy of Sciences, P. O. Box 17, H-1525
Budapest, Hungary

K. Ujszászy

Spectroscopic Department, EGIS Pharmaceutical Factory, P. O. Box 100, H-1475 Budapest, Hungary

Key Words

Column liquid chromatography
Beclamide
Benzamide
Diacyl amine

Summary

In order to elucidate the formation of benzamide and benzoic acid as rat urine metabolites of beclamide (N-benzyl-3-chloropropionic acid amide) we studied in vitro metabolism by rat liver and brain homogenates. Beclamide is oxidized on benzyl carbon atom into diacyl amine, which is a mild acylating agent and is unstable. Therefore it hydrolyses into benzamide or benzoic acid (considering only the transformation of the benzyl group). Our rapid method consisting of the extraction of the homogenates with chloroform, separation on a short column and HPLC analysis was able to identify beclamide, benzamide and diacyl amine in one chromatogram on a silica column (Hypersil 5 μm) eluted with hexane-ethyl acetate (1 : 1, v/v), and detected by UV absorbance monitoring at 264 nm.

Introduction

The metabolism of beclamide (N-benzyl-3-chloropropionic acid amide), one of the anticonvulsive drugs used in human therapy has been investigated in human subjects [1]. Nicholls et al. [1] reported that beclamide was metabolized mainly via aromatic hydroxylation. Besides other minor metabolites the amount (one fourth of the radioactivity excreted in the urine) of hippuric and benzoic acids was striking and puts forward suggestion for another oxidative metabolic pathway.

In order to elucidate the possible biological transformation of N-benzyl derivatives of acidic amides into benzamide and benzoic acid, we have studied in vitro metabolism of beclamide. The investigated in vitro experiments proved the formation of benzamide through the intermediate N-benzoyl-3-chloropropionic acid amide (diacyl amine), as far as both products were detected in liver and brain homogenates.

Materials and Methods

Materials

Beclamide in 0.33 g dragees (Posedrine) was from Laboratoires Aron (Suresnes, France). The pure crystalline solid was extracted with dichloromethane from the dragees dissolved in water; its purity was more than 99 %.

N-benzyl-3-chloropropionic acid amide (diacyl amine) was synthesized in our laboratory.

Biological Sample

For liver and brain homogenization the liver (10 g) and brain (2 g) of RG-Wistar male rats, weighing 200 g, were used. After mixing with threefold volume of physiological saline solution and centrifuged at 10000 g at 4 °C, the supernatants were incubated with 0.5 μM of Beclamide pro gram of liver or brain for 10, 20, 30 and 60 min, at 37 °C.

Isolation of Beclamide and its Metabolites

The biological reactions were terminated by the addition of three portions of 10 ml cold chloroform. The beclamide and its metabolites were separated on a short Lichroprep Si 60 (Merck) column (4 cm × 1 cm ID), eluted successively with 5–5 ml hexane, 5 : 1 (v/v) and 1 : 1(v/v) mixtures of hexane-ethyl acetate and ethyl acetate; subsequently they were analyzed by liquid chromatography. Liquopump 312

0009-5893/87 0766-03 $03.00/0

© 1987 Friedr. Vieweg & Sohn Verlagsgesellschaft mbH

(Labor MIM) was used to deliver the solvent at 1.0 ml/min. The eluent was monitored at 264 nm with a Labor MIM variable wavelength ultraviolet detector. The column was 25 cm × 4.6 mm ID packed with Hypersil silica 5 μm (Shandon). Samples were introduced with a Negretti and Zambra injection system incorporating a 20-μl loop. Hexane-ethyl acetate mixture (1 : 1, v/v) was used as the mobile phase.

The structure of the metabolites was determined by electron impact mass spectra using AEI MS 902 double focusing mass spectrometer with a field strength of 7 kV and a wire current between 0–20 mA.

Results and Discussion

Based on the work of our and other laboratories [1, 2] considerable interest has been focused on the minor metabolites of beclamide, namely benzamide and the intermediate diacyl amine.

The separation and identification of beclamide and its metabolites were performed by the procedure described in Fig. 1. Fig. 2 shows a chromatogram obtained when analyzing the mixture of beclamide and its metabolites. The presence of the unstable metabolite was determined by means of mass spectral analysis of the eluted sample (Fig. 3). Table I presents the measured amount of beclamide and the estimated quantities of the metabolites in each incubation mixture.

Benzamide is formed as a metabolite of acidic N-benzyl amides via the scheme shown in Fig. 4. Recently Gorrod et al. [3] reported on a similar in vitro oxidative route of N-benzyl-4-substituted-anilines to N-benzoyl-derivatives.

This paper reports on a technique requiring no special equipment and can be easily performed in a short time. This was important because of the rapid conversion of the intermediate. This method may give an example for solving the problem of unstable compounds avoiding reactive conditions.

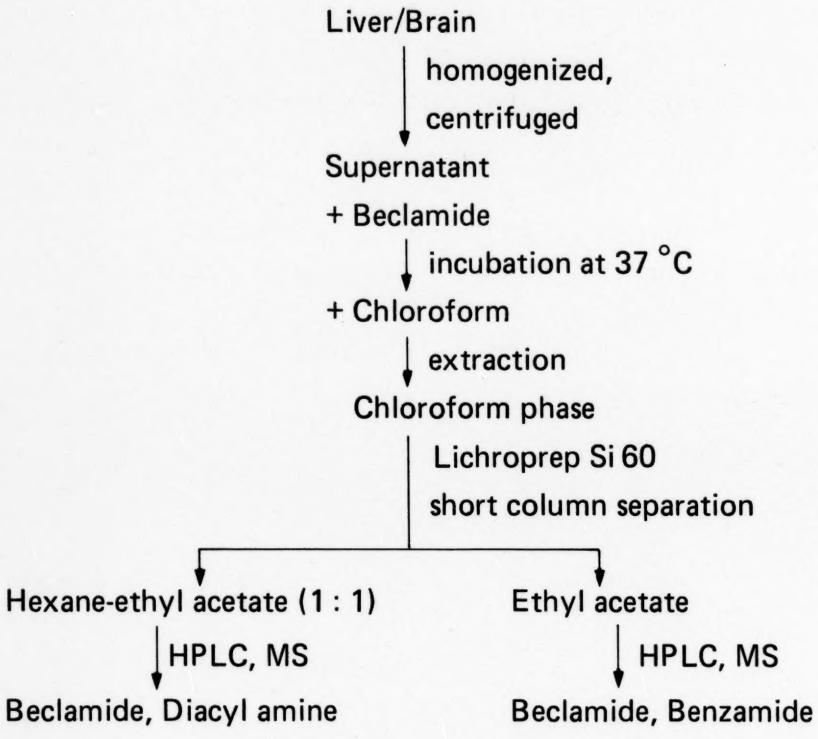

Fig. 1
Investigation of in vitro metabolism of beclamide.

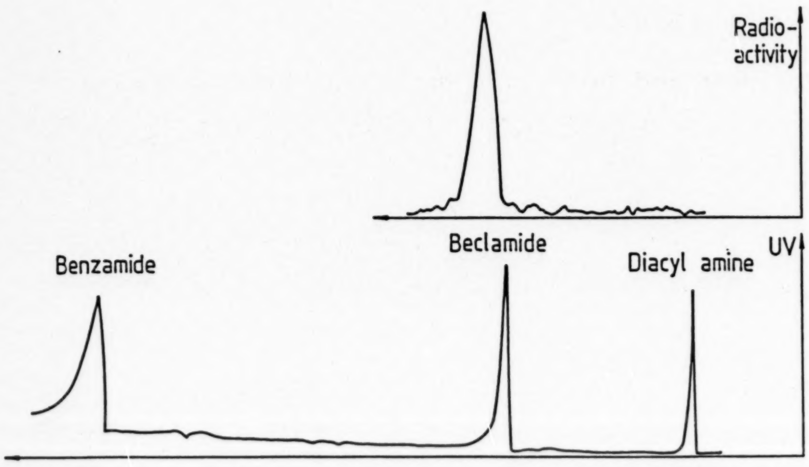

Fig. 2
Chromatography of beclamide and its metabolites, diacyl amine and benzamide. Column: 25 cm X 4.6 mm ID, packed with Hypersil silica 5 μm. Mobile phase: hexane-ethyl acetate, 1 : 1 (v/v); flow rate: 1 ml/min. UV detection at 264 nm. Retention times: diacyl amine, 263 sec; beclamide, 716 sec; benzamide, 1693 sec.

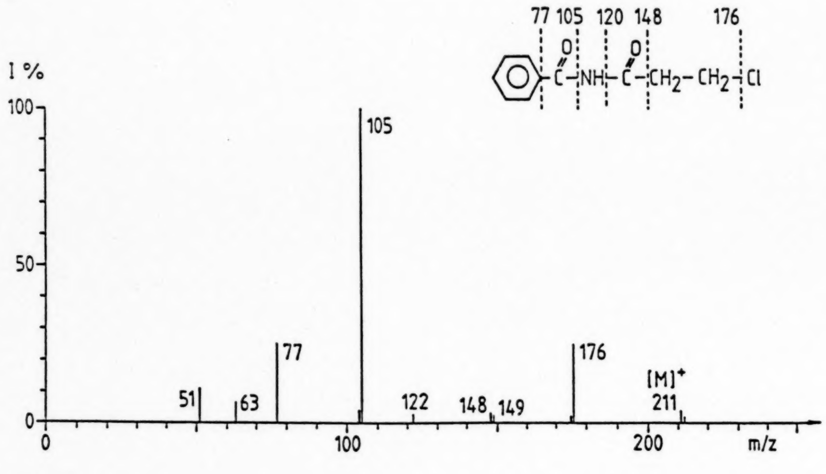

Fig. 3
Mass spectrum of diacyl amine.

Table I. The conversion of beclamide into diacyl amine and benzamide in the supernatant of rat liver and brain.

Time of incubation (min)	Beclamide % of dose	Diacyl amine*	Benzamide
with liver			
10	96.0	+	+
20	92.0	–	+
30	78.0	–	++
60	53.0	–	+++
with brain			
10	98.0	+	–
20	98.0	+	+
30	90.4	+	+
60	79.4	+	+

* N-benzoyl-3-chloropropionic acid amide

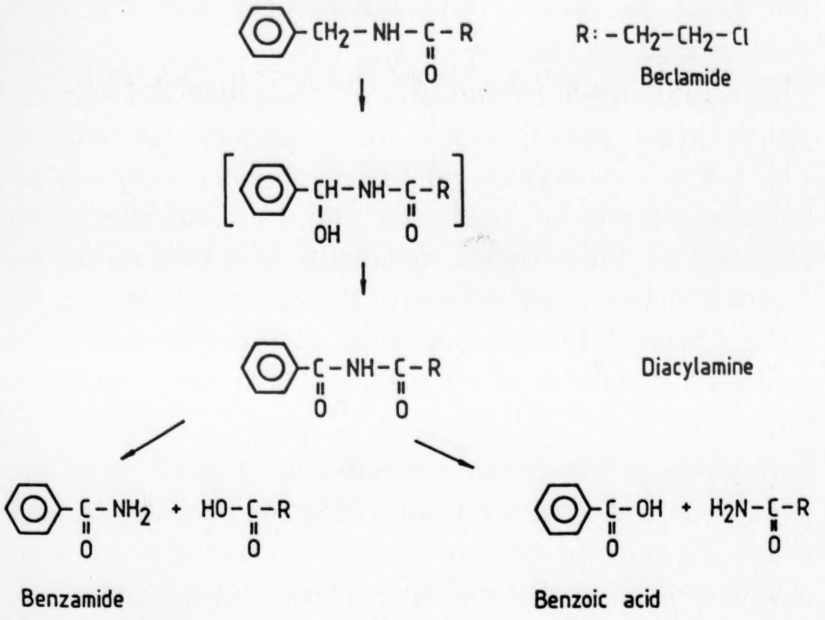
R: –CH₂–CH₂–Cl
Beclamide
Diacylamine
Benzamide
Benzoic acid

Fig. 4

Scheme of the biotransformation of acidic N-benzyl amides.

References

[1] *P. J. Nicholls, M. S. F. Ross, D. K. Luscombe,* Xenobiotica **9**, 129–40 (1979).

[2] *M. Pálfi-Ledniczky, I. Szinai, K. Ujszászy, S. Holly, I. Weisz, V. Kemény, H. Tüdös, M. Horváth, L. Ötvös,* in "Bio-Organic Heterocycles", H. C. Van der Paas, L. Ötvös and M. Simonyi (Eds.) Akadémiai Kiadó, Budapest 1984; pp. 329–333.

[3] *J. W. Gorrod, N. J. Gooderham,* Xenobiotica **17**, 165–77 (1987).

Received: June 30, 1987
Revised manuscript
received: Sep. 25, 1987
Accepted: Sep. 28, 1987
F

High-Performance Liquid Chromatography of Amino Acid Peptides and Proteins

Part: LXXXIII[1]

Evaluation of Retention and Bandwidth Relationships for Proteins Separated by Isocratic Anion-Exchange Chromatography

M.T.W. Hearn*/A.N. Hodder/P.G. Stanton/M.I. Aguilar

Department of Biochemistry, Monash University, Clayton, Victoria 3168, Australia

Key Words

Anion-exchange chromatography
Proteins
Retention and bandwidth relationship

Summary

The retention behaviour of seven globular proteins ranging in molecular weight from 12,000 to 69,000 was investigated using Mono-Q anion-exchange resin as the stationary phase and sodium chloride as the displacer salt. In particular the influence of changes in ionic strength and mobile phase pH on the isocratic retention properties was assessed. Several proteins were found to have significant retention when the pH of the mobile phase was below the reported pI values of the proteins. This behaviour results from the non-uniform charge distribution on the protein surface, which allows interaction with the charged stationary phase even though the protein net charge is equal to or greater than zero. The influence of pH and ionic strength on experimentally observed bandwidths was also investigated. The dependence of the effective reduced plate height on solute capacity factor was found to vary significantly with the mobile phase pH, a behaviour consistent with the interplay of complex multisite binding kinetics. These results provide a basis for further detailed investigations into the mechanism of interaction of proteins not only with charged surfaces associated with adsorptive chromatographic media but also with other macromolecules.

Introduction

Ion-exchange (IEX) and reversed-phase high-performance liquid chromatography (RP-HPLC) are now both extensively used for the high-resolution analysis and purification of peptides, proteins and other biological macromolecules. As part of this widespread application the development of optimisation models for the reversed-phase separation of peptides and proteins on micro-particulate stationary phases has attracted considerable attention in recent years [1–4]. These models have provided a useful basis for assessing the retention and bandwidth behaviour of peptides and proteins allowing more detailed investigations on the physicochemical phenomena associated with the interaction of biomacromolecules with hydrophobic surfaces.

Although a large amount of work has been carried out with conventional ion-exchange supports [5–9], there have been relatively few detailed systematic studies on the retention phenomena on modern high-performance ion-exchange materials. Protein retention on ion-exchange surfaces arises from electrostatic interactions between the protein surface and the charged stationary phase. The 'net-charge' concept has been widely used [5, 6] as a predictive basis to anticipate the retention characteristics of proteins with both anion- and cation-exchange resins. Commercially available materials are often characterised and marketed on the basis of this principle. According to this model, a protein will be retained on a cation-exchange column if the solvent pH is lower than the known pI-value of the protein due to the protein carrying net positive charges $Z_n \geqslant +1$. Conversely, a protein will be retained on an anion-exchange resin when the eluant is above the protein pI, i.e., $Z_n \leqslant -1$. A codicil to this model is that with mobile phases operating at a pH equal to the protein's pI, the surface of the protein is considered to be overall electrostatically neutral, i.e., $Z_n = 0$, and under these conditions the protein should not be retained on either cation or anion ion-exchange columns. Clearly this model represents a simplistic approach to describing peptide and

---

[1] For Part LXXXII, see ref. [27].

0009-5893/87 0769-08 $03.00/0

© 1987 Friedr. Vieweg & Sohn Verlagsgesellschaft mbH

protein retention in IEX. In a changing mobile phase environment, the coulombic surface of a protein can manifest a dynamic distribution of charged groups which, due to point site interactions, may result in retention with ion-exchangers even though the pH of the bulk mobile phase corresponds to the protein's pI value. Furthermore, the influence of mobile phase constituents, such as buffer salts and displacer ions on the secondary and tertiary structure of protein solutes has largely not been addressed in the development of such retention models in IEX. For example, the existence of localised Donnan potentials, due to dynamic buffer-mediated dielectric or polarised environments, and even incremental pH changes due to protic equilibrium within the pore structure of the stationary phase which differs from that at the exterior surface or in the bulk phase, is disregarded in the 'net-charge' retention concept. The interplay of these dynamic buffer effects forms the basis of the chromatofocusing technique and underlies the change in the double layer structure when different ion or organic solvent combinations are used as eluents in IEX. The present paper, the first in a series of studies in which we investigate mechanistic details of protein retention in IEX, examines the chromatographic behaviour of a series of globular proteins of varying pI and molecular weight eluted from the strong anion-exchange Mono-Q column under isocratic conditions.

Materials and Methods

Apparatus

All chromatographic experiments were performed with a Pharmacia (Uppsala, Sweden) fast protein liquid chromatography (FPLC) system consisting of two P-500 syringe pumps, a V-7 injector and a 278 nm fixed-wavelength single-path UV monitor, coupled to a two channel REC 482 pen recorder and a Perkin-Elmer (Norwalk, CT, USA) LCI-100 integrator.

Isocratic elution was controlled with a Pharmacia GP-250 solvent programmer. Mono-Q prepacked strong anion-exchange columns (HR 5/5,50 × 5 mm I.D.) were used throughout. The pH measurements were performed with an Orion (MA, USA) SA 520 meter, equipped with a combination glass electrode. All chromatographic separations were carried out at ambient temperatures of 20 °C.

Chemicals and Reagents

Bovine erythrocyte carbonic anhydrase, sperm whale skeletal muscle myoglobin (type iii), hen egg white lysozyme (grade 1), hen egg ovalbumin (grade v), horse heart cytochrome C (type iv), human serum albumin, bovine haemoglobin (type 1), bis-tris, triethanolamine and piperazine were all purchased from Sigma (St. Louis, MO, USA). Sodium chloride (AnalR grade) was obtained from BDH (Port Fairy, Australia). Quartz distilled water was further purified on a Milli-Q system (Millipore, Bedford, MA, USA), Hydrochloric acid (spec. gravity 1.16, AnalR grade) was purchased from BDH.

Chromatographic Procedures

Eluent A was a 0.02 mole/l solution of a suitable buffering ion. The buffers used were piperazine (pH 5.50 and 9.60), bis-tris (pH 6.50) and triethanolamine (pH 7.50). For all cases, eluent B contained 0.02 M of the appropriate buffer and 0.3 M sodium chloride as the displacer salt. Eluent A and B were filtered (0.45 μm cellulose acetate HAWP 04700 Millipore Corp, Bedford MD, USA) and degassed under vacuum. Protein solutions were prepared by dissolving the protein in eluent A at a concentration of 5 mg/ml unless otherwise specified. Protein solutions were filtered before use through 0.22 μm ACROLC13 filters (Gelman Sciences, Sydney, Australia). Protein sample sizes ranged from 5 to 1000 μg with injection volumes between 10 and 200 μl. At each pH, samples were eluted isocratically, starting at 100% eluent B and repeated, at decreasing concentrations of B, until the protein elution volume was greater than 25 column volumes.

At each solution pH, log k' and log (1/c) data were collected for each protein and subjected to an iterative regression analysis to determine the y-intercept (log K), slope (Z) and correlation coefficient. Column efficiency or the effective reduced plate height (h_{eff}), was determined from peak width at half height measurements and second moments. The column dead time, t_0, was calculated from the retention time of a salt breakthrough peak following a 50 μl injection of 1M sodium chloride in 100% eluent B (0.3 M sodium chloride).

Results and Discussion

Retention Relationships

Retention in IEX is largely dependent on the degree of electrostatic interaction between the solute molecules and the stationary phase surface. In the simplest case the magnitude of the electrostatic force, F, betwen two point charges, Q_1 and Q_2, separated by distance, r, is given by

$$F = \frac{Q_1 Q_2}{\epsilon_m r^2} \tag{1}$$

where ϵ_m is the dielectric constant of the medium. However, in the IEX of peptides and proteins the stationary phase and solute cannot be represented as point interacting charges. In particular, the amphoteric nature of proteins significantly complicates their treatment as a single charged species. In high-performance anion-exchange chromatography, for example, it is assumed that protein solutes interact with the stationary phase exclusively through the surface anionic groups. In this case the magnitude of the electrostatic interaction depends on several factors. These include (i) the number of charged sites on the solute molecule that interact simultaneously with the packing; (ii) the charge density of the packing, i.e. its ζ potential; and (iii) the mobile phase composition. A non-mechanistic, stoichiometric equation can be written for the mass distribution of a solute molecule, P^{+-a}, in IEX as follows:

$$(P^{+-a})_m + (a/b)\,(D^{+-b})_s \rightleftharpoons (P^{+-a})_s + (a/b)\,(D^{+-b})_m \tag{2}$$

where D^{+-b} is the displacer counter ion and subscripts m and s represent the mobile and stationary phases. The equilibrium constant for the ion-exchange process may be represented as

$$K_b = \frac{[P^{+-a}]_s \, [D^{+-b}]_m^{Z_t}}{[P^{+-a}]_m \, [D^{+-b}]_s^{Z_t}} \qquad (3)$$

for large molecules, such as proteins, Z_t represents the ratio (a/b), of the effective charge on the solute to that on the displacer counter ion [10]. If it is assumed that the near-equilibrium conditions for chromatographic processes apply, i.e., that both the phase ratio and the distribution coefficient are constant and the adsorption isotherm is linear, the above distribution model can be rewritten in terms of non-mechanistic expressions which describe the relationship between solute retention and the displacer ion concentration. For monovalent salts, the following general linearised expression can be obtained [11, 12]:

$$k' = Kc^{-Z} \qquad (4)$$

which can be expressed logarithmically as

$$\log k' = \log K + Z \log (1/c) \qquad (5)$$

where k' is the capacity factor, c is the concentration of the displacer ion and K is a constant which incorporates the binding constant K_b, the phase ratio, Φ, the stationary phase ligand concentration D_b, and the constants a and b which adjust for solute and salt valancy according to the following relationship,

$$K = K_b \Phi \frac{[D_b]Z_t}{ab} . \qquad (6)$$

The tangent Z to the curve obtained in a plot of log k' versus log (1/c) can be determined at any value of k' and the value of log K can be obtained by extrapolation using regression analysis. According to eq. (5) with a fixed mobile phase pH, the logarithmic capacity factor corresponding to protein retention in ion-exchange should be linearly related to the inverse of the logarithm of the concentration of displacer ion. Furthermore, Z is considered to be equal to the number of charged interactive sites involved with the binding established between the protein solute and the stationary phase. However, in physicochemical terms, this interpretation of Z may not be equivalent to the definition of Z_t as the ratio of the charge on the protein to that on the displacer ion. In the idealised case of all charges interacting with the stationary phase surface Z becomes equal to Z_t but generally Z will be less than Z_t.

An assumption inherent in the net charge hypothesis is that similar dependences of Z on pH should be obsered for all proteins. Such an assumption does not account for variation in protein structural topography due to the unique amino acid composition or structural hierachy nor does it address the effect of mobile phase induced conformational changes. Systematic variation in solvent composition through manipulation of ionic strength, pH and the nature of the displacer ion will therefore reveal solute-specific changes in solute selectivity and provide a basis for the development of detailed data bases describing the influence of mobile phase conditions on the structure of protein solutes and their interaction with chromatographic and biological charged surfaces. In the current study, the effect of manipulating mobile phase ionic strength and pH were investigated. Isocratic retention data for seven globular proteins listed in Table I were obtained on a Mono-Q strong anion-exchange column. The proteins varied in molecular weight from 12,000 to 69,000 with pI-values in the range of 4.7 to 11.0. All proteins were chromatographed in the first instance using a constant buffer concentration (20 mM) at various pH values with the sodium chloride concentration varying between 0 and 300 mM at a flow rate of 1 ml/min.

Table I. Protein physical parameters.

No.	Protein (Source)	pI	MW	$D_m \times 10^{-10}$ (m^2/min)**	Z-Value pH 5.5	6.5	7.5	9.6
1.	Ovalbumin (egg white)	4.70	43,500	4.24	4.12	6.01	6.69	7.73
2.	Albumin (human serum)	5.85	69,000	3.64	2.34	5.57	4.81	11.14
3.	Carbonic anhydrase (bovine erythrocytes)	5.89	30,000	4.80	0.33	0.92	1.37	2.16
4.	Haemoglobin (bovine blood)	6.80	64,500	3.72	–	–	–	5.04
5.	Myoglobin (sperm whale muscle)	7.68 8.18	17,500	5.74	0.00	0.16	–0.062	2.76
6.	Cytochrome C (horse heart)	9.4	12,400	6.42	–	–	–	–
7.	Lysozyme (hen egg white)	11.0	14,300	6.12	–	–	–	–

**Calculated from Stokes-Einstein equation [26].

Fig. 1 represents plots of retention of each protein as a function of the salt concentration for the proteins listed in Table I, with the data fitted by iterative curve fitting approaches. The well documented rapid increase in k' with decreasing salt concentration is clearly evident from Fig. 1. In common with similar multisite interaction processes found in the reversed-phase chromatography of proteins, curvi-linear plots of log k' versus log 1/[NaCl] were observed with little correlation evident for a simple dependency of the slope Z on molecular weight. Even within the range $0 < \log k' < 1$, proteins with an overall net negative charge (pI ≪ mobile phase pH) do not exhibit linear retention plots predicted by eq. (5). These plots become increasingly curved at higher salt concentrations and eventually approach asymptotic values at very low log k' values. This corresponds to the protein having minimal interaction with the support surface at high ionic concentration.

From Fig. 1 it is also evident that mixed mode retention processes can occur with specific proteins when separated on this strong anion-exchanger. For example, cytochrome C and lysozyme are both basic proteins (high pI values) and under the elution conditions of pH 9.6, these proteins would be expected to have little interaction with the positively charged functional groups on the stationary phase. The downward curving plots observed for lysozyme and cytochrome C at low salt concentrations probably result from these proteins interacting via van der Waals and Lifshitz force effects with the stationary phase as the major retention process. An increase in ionic strength reduces the protein solubility in the mobile phase and the proteins are 'salted out' through hydrophobic effects, onto the stationary phase surface. As a result, the capacity factors of the basic proteins are seen to increase with increasing ionic strength, under some pH conditions. The fact that this effect was not evident with the low pH mobile phase conditions or with the acidic proteins may simply reflect comparative differences in hydrophobicity between amino- and carboxyl-groups, a property previously exploited in isoelectric point pH precipitation techniques [13].

Proteins are amphoteric in nature. Their titration curves reveal that at a unique pH value, zero net charge is manifested where the ratio of anionic to cationic groups reaches unity. This pH value is characteristic for each protein and is referred to in a electrokinetic system as the isoelectric point, pI. As the mobile phase pH is decreased below the protein pI, the protein gains increasing cationic character due to protonation of accessible amino groups. Similarly as pH is increased the proteins acquire more anionic character through carboxyl group ionisation. Manipulation of mobile phase pH therefore presents an attractive method for regulating the degree of protein interaction with the stationary phase in IEX, and has formed the basis of numerous applications with conventional and high performance chromatographic media [14, 15].

Fig. 1–4 represent plots of protein retention as a function of the salt concentration at four different mobile phase pH values. As is evident from these data protein retention decreased with the Mono-Q, a strong anion-exchanger, as the pH was lowered. With this support, increased sup-

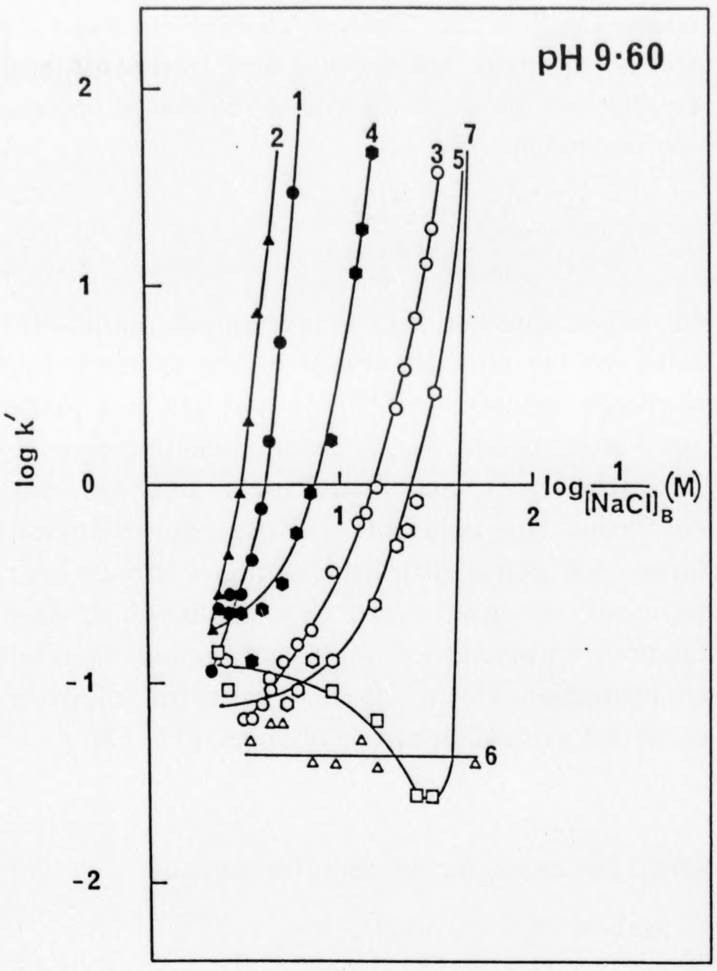

Fig. 1

Plots of log k' versus log 1/[NaCl] for the seven proteins listed in Table I. The plots were derived from data obtained in isocratic elution experiments with varied sodium chloride concentrations at pH 9.6 and a flow rate of 1 ml/min.

Other chromatographic conditions are given in Materials and Methods. See Table I for the code to protein solutes and for the derived Z values.

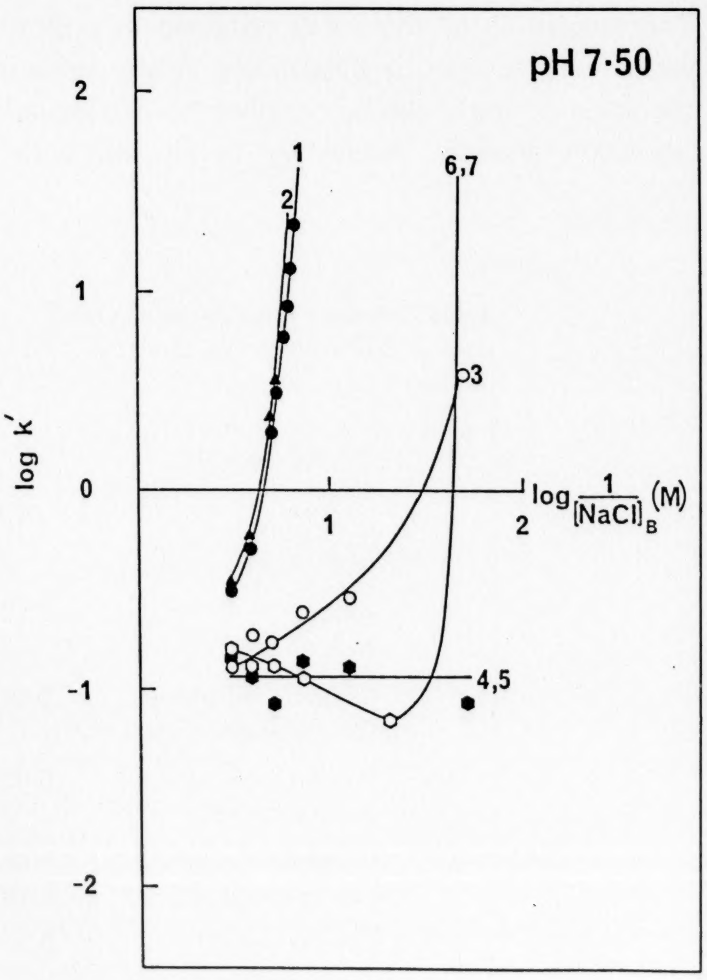

Fig. 2

Plots of log k' versus log 1/[NaCl] for proteins 1–7. The plots were derived from isocratic elution data as in Fig. 1 at pH 7.5.

See legend to Fig. 1 for other details.

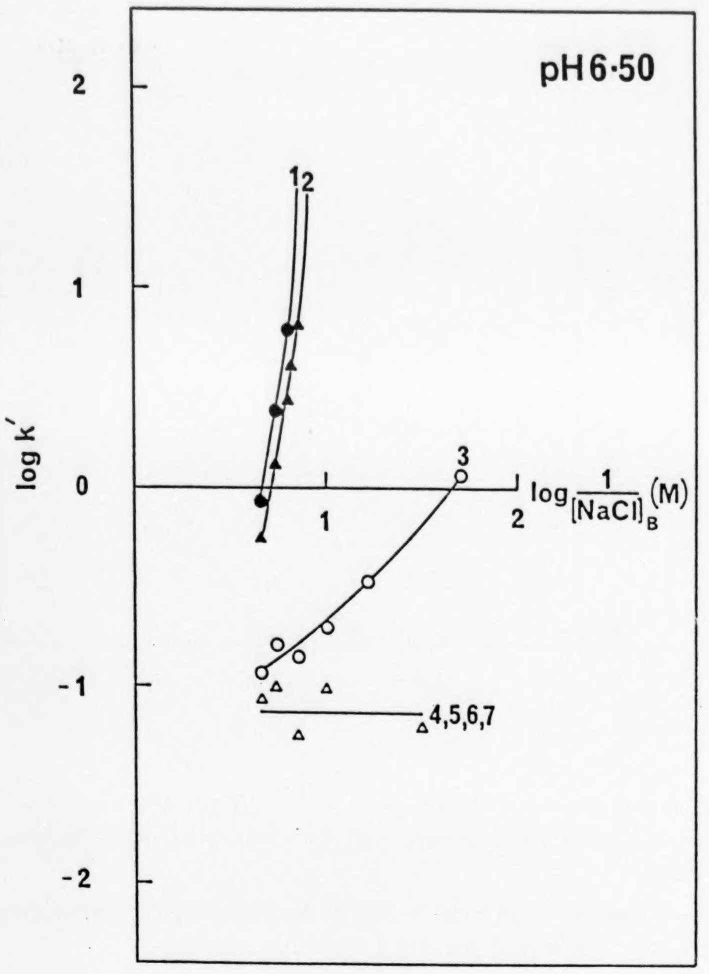

Fig. 3
Plots of log k′ versus log 1/[NaCl] as in Fig. 1 at pH 6.5.
See legend to Fig. 1 for other details.

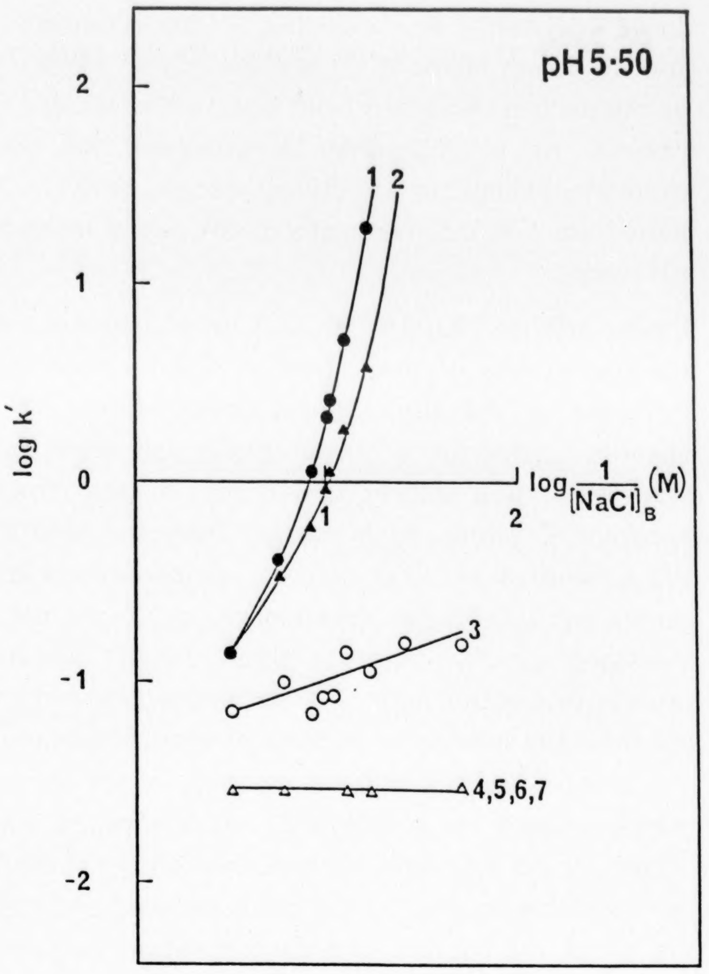

Fig. 4
Plots of log k′ versus log 1/[NaCl] as in Fig. 1 at pH 5.5.
See legend to Fig. 1 for other details.

pression of carboxyl group ionisation leads to the lowering of the Z value for each protein and concommitant faster elution times. At this stage, the precise physicochemical significance of Z remains to be determined. It has been shown [2, 16, 17] that the corresponding S-value in reversed-phase chromatography not only relates to the hydrophobic contact area established between the protein solute and the stationary phase, but is also dependent on the polarity and disposition of surface amino acids. Clearly, the experimental Z-values observed in IEX will be a result of a complex interplay between the relative distribution of charged groups on the protein with varying affinities for the stationary phase and the displacing properties of the mobile phase constituents. In this context, Z may thus reflect the coulombic contact area more germanely rather than the total number of surface charges on a protein in free solution of identical pH, buffer and ionic composition.

A variety of arguments have been advanced by other investigators [18, 19] to interpret protein separations on ion-exchange resins in terms of a close predictive relationship between protein retention and its corresponding titration curve. It has been assumed in some studies that a protein would not be retained with ion-exchange supports when the mobile phase pH equals the protein's pI value. Recent studies [12, 15] have however demonstrated that significant deviations from the expected retention behaviour based on this assumption, can occur. From the majority of proteins studied to date some degree of retention at their pI can be ascertained.

As far as protein-stationary phase interactions are concerned the vectorial sum of all interacting charge potentials for a highly curved porous coulombic surface will be different to that generated by an infinitely flat surface. An incremental Donnan potential can then exist between surface charges located inside and outside the pores. As a consequence of this phenomenon, the pH of the solvent contained within the pores will be different to that of the bulk mobile phase. These small differences in pH may be sufficient to allow significant protein retention even though the pH of the mobile phase is equivalent to the protein pI value. In addition, the dynamic three dimensional structure of the proteins can also give rise to anomalous retention behaviour. The heterogeneous distribution of charged groups on the protein surface are capable of generating localised electrostatic potentials, allowing specific site or domain interactions with the stationary phase even when the bulk ionisation state of the protein corresponds to the pI condition. Steric restrictions imposed by the protein structure can also reduce the potential number of interactions between the protein and stationary phase. Such anomalies which may be attributed to charge asymetry are evident in the data shown in Fig. 2. For example, human serum albumin (2) and to a lesser extent carbonic anhydrase (3) both show retention to the Mono-Q protein support with mobile phase pH's well below their pI values.

Manipulationn of mobile phase pH can have a dramatic effect on chromatographic selectivity of protein mixtures in IEX systems. For example, if the retention plots for human serum albumin (2) and ovalbumin (1) are followed as the pH was decreased from high to low values a complete reversal of elution order is observed. An even more dramatic change in selectivity occurs between carbonic anhydrase (3) and haemoglobin (4) over a much narrower pH range.

Earlier studies [10, 15, 20, 21] have attempted to clarify the significance of the Z term in IEX by investigating the influence of the displacer salt composition. The physicochemical properties of the displacer salt were thought to contribute in a poorly understood manner towards the apparent Z values. As is evident from the data shown in Fig. 5, with a Mono-Q column, Z increases with pH. A generalised sigmoidal dependence of Z on pH can be envisaged which represents three distinct situations for protein interaction with the stationary phase. In the first instance, the maximum number of charged binding sites on the protein surface will be reached at pH values which greatly exceed the protein's pI. At this point, further increases in pH will have no influence on the retention properties of the solute. As the pH is reduced and approaches the pI of the protein, the concommitant decrease in the number of interactive surface charges will result in a marked dependence of Z on pH. Finally, at pH's well below the pI of the protein, replusion between the positively-charged stationary phase and the fully protonated protein would lead to minimal binding where Z values approach zero over a certain pH range.

In Fig. 5 plots of protein Z values as a function of eluent pH for ovalbumin, human serum albumin, carbonic anhydrase and myoglobin are shown using sodium chloride as the displacer salt. The trends observed show solute specific effects both in terms of the magnitude of the experimentally determined Z-values and the pH range over which these Z-values are seen to vary. These results presumably arise as a consequence of the amino acid composition and tertiary structure of the solutes which impart a unique surface charge distribution that determine the interactive properties of particular pH conditions.

We were consequently interested to compare the effect of buffer composition on the Z-dependencies. With ovalbumin for example, a three to four fold difference in the magnitude of the Z-parameter was found using the same chromatographic support and similar pH range to that used by other workers [20]. The buffers used were piperazine versus sodium acetate (pH 4.0–5.5), bis-tris versus hydroxylamine HCl (pH 6.0–7.0) and triethanolamine versus tris (pH 7.5–8.0). All constituents of the mobile phase, that is, pH, displacer salt and buffer ions, may synergistically participate in the retention process which result in the experimentally observed k' values through their effects on the nature of the solvated double layer. Clearly the nature of the buffer species also contribute to retention behaviour in IEX of proteins and peptides. It is noteworthy that changes from sodium chloride to magnesium chloride with constant buffer species showed [20] much less dependence of Z on pH, for ovalbumin, than did changes in the buffer constituents with the same displacer salt.

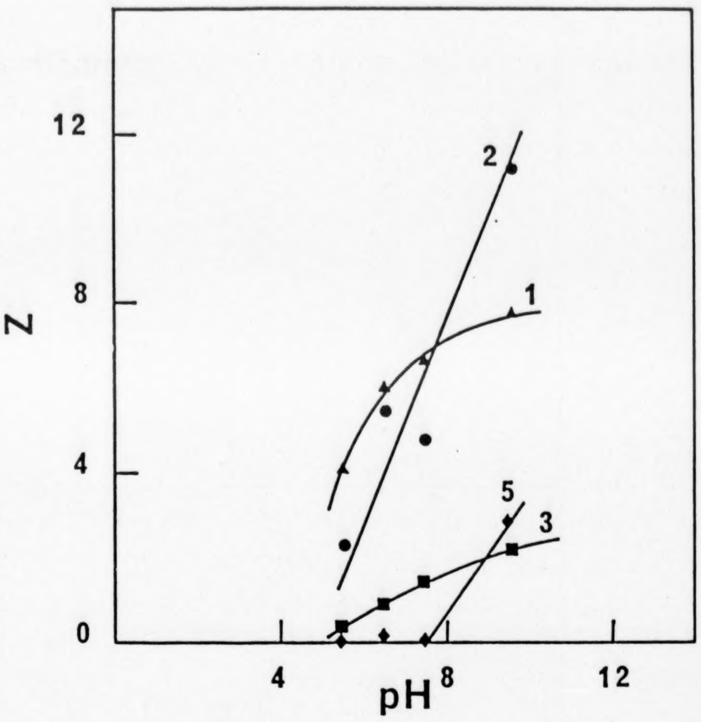

Fig. 5

Plot of Z versus pH for proteins 1, 2, 3, and 5, chromatographed isocratically on a Mono-Q column at 1 ml/min with NaCl as the displacer salt.

The data was derived from Figs. 1–4 and the calculated Z-values are listed in Table I. See legend for Fig. 1 for other details.

Bandwidth Relationships

Studies on the kinetics of protein adsorption and desorption at charged stationary phase surfaces, such as quarternary amines, potentially offer much more useful information about the mechanism of protein retention. Although the accumulation and analysis of kinetic data is often complex, it can be obtained through analysis of band broadening effects directly from digitised chromatographic data.

When conditions of linear elution chromatography apply, and in the absence of slow secondary equilibria, the rate of dispersion of a solute band as it migrates through a column can be defined in terms of the Knox equation [22], such that

$$h_{eff} = A\nu^{0.33} + \frac{B}{\nu} + C\nu \qquad (7)$$

where ν is the reduced velocity and h_{eff} is the effective reduced plate height, which can be related to the peak variance, as

$$\sigma_{\nu}^{2} = \frac{h_{eff}\, d_p\, t_R^2}{L} \qquad (8)$$

where d_p is the particle diameter, L is the column length and t_R is the retention at the centre of gravity for a peak, which for gaussian peaks is equivalent to the retention time at the peak apex. Thus changes in bandwidth (as $4\sigma_t$ or $4\sigma_{\nu}$) of an eluted solute at time t_R, from a particular column, will be directly translated into h_{eff} values by utilising peak width or second moment data.

The A term of the Knox equation accommodates solute diffusional effects due to eddy diffusion and non-uniform linear velocities of the solute zone and mobile phase resulting from irregularities in the column packing.

The B term of the Knox equation arises from dispersion contributions of the solute zone in both the mobile and stationary phases and accounts for the rate at which the solute diffuses in the column with well packed high performance ion-exchange columns operating at high flow rate conditions, i.e. when $\nu \geqslant 100$, the dependency of the reduced plate height on the reduced velocity can be approximated to

$$h_{eff} = C\nu \, . \tag{9}$$

Under these conditions, h_{eff} becomes insensitive to changes in both the $A\nu^{1/3}$ and B/ν terms. The C term accounts for resistance to mass transfer at the stationary phase surface inside the pores of the column packing and consequently varies significantly with the separation conditions. According to Giddings [23] the dependence of C on the separation conditions for a column of well-packed spheres can be represented by

$$C = \frac{1}{30} \left[\frac{k''}{(1 + k'')^2}\right] \left[\frac{D_m}{D_{sz}}\right] \tag{10}$$

where D_m and D_{sz} represented the distribution coefficients for the mobile phase and the stationary zone respectively and k'' is the zone capacity factor equivalent to

$$k'' = \frac{\text{mass of solute in the stationary phase}}{\text{mass of solute in the mobile phase}} \, . \tag{11}$$

In Fig. 6 the dependency of h_{eff} for haemoglobin on the salt concentration at four different solvent pH values is shown. Haemoglobin was isocratically eluted, using sodium chloride as the displacer salt at a constant flow rate of 1 ml/min. As the solvent pH was decreased the dependence on the salt concentration progressively diminished. Increased protonation of the carboxyl groups at lower solvent pH values decreases the interaction between solute and stationary phase, decreasing the retention time.

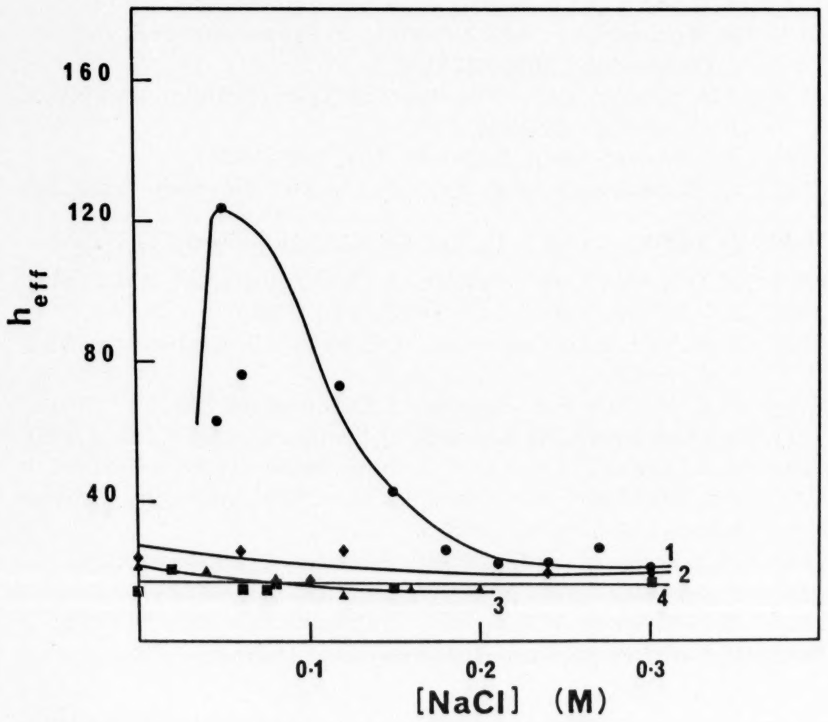

Fig. 6

Plots of h_{eff} versus [NaCl] for haemoglobin (4) at (1) pH 9.6 (2) pH 7.5, (3) pH 6.5 and (4) pH 5.5. Values of h_{eff} were determined from measurements of peak width at peak half height.

If it assumed that ratios of D_m and D_{sz} under these various pH conditions remained essentially constant then the contribution of diffusion processes associated with mass transfer of the solute to the overall kinetics of the separation would be diminished through the dependence of the C-term on the zone capacity factor. Furthermore, if experimental capacity factors are dependent on the concentration of the displacer ion exclusively, and the kinetics of solute migration are independent of the mobile phase composition, superimposable plots of h_{eff} versus k' at different pH values for a particular protein would be anticipated on the basis of the relationships expressed in eqs. (9) and (10). Figs. 7 and 8 illustrate the dependencies of h_{eff} on k' for ovalbumin and human serum albumin respectively, where a marked variation in the h_{eff}-values over the pH range for both proteins is observed. For example, in both cases, at $k' = 4$, there was approximately a two-fold difference in the magnitude of the experimentally-observed h_{eff}-values. The discrepancy between the values at pH 9.60 and 5.50 is particularly significant as piperazine was the buffer salt used for both solvent systems.

The degree of protein ionisation and the exposure to different salt concentrations has clearly influenced the diffusional properties and binding kinetics of these solutes, through, for example, the existence of multiple interactive sites, on either a conformationally invariant or interconverting species, with different affinities for the stationary phase surface. The retention and bandwidth data clearly indicate that the mechanism of protein retention in ion-exchange chromatography is a complex interaction between the protein solute, the mobile phase constituents and the charged stationary phase surface. The effect of salts on the stability, solubility and biological activity of several small globular proteins has been well-characterised [24, 25]. It has been established that preferential interactions of proteins with solvent components can result in either stabilisation or denaturation of the protein. Furthermore, while the primary influence of mobile phase pH is to change the electrostatic properties of proteins in terms of the overall net charge, the contribution of localised ionisation changes to kinetic aspects of protein-salt interactions clearly has significant practical consequences. With IEX supports for example, the application of tandem columns operating at different mobile phase pH's in the analysis and purification of protein mixtures offers a simple and rapid method to efficiently separate proteins through manipulation of the interactive properties of the protein via subtle changes in the surface charge distribution. Furthermore, the current study demonstrates the capability of IEX in the isocratic mode as a viable alternative in the final stages of an isolation procedure. The potential now exists to separate charged isoforms of a target protein by isocratic elution at an appropriate pH. However, the retention behaviour of peptides and proteins is also strongly influenced by the nature of the displacer ion through the relative affinity of the anions for the stationary phase and their effect on protein structure.

The next paper in the series, therefore, will describe the results of detailed investigations on the influence of the

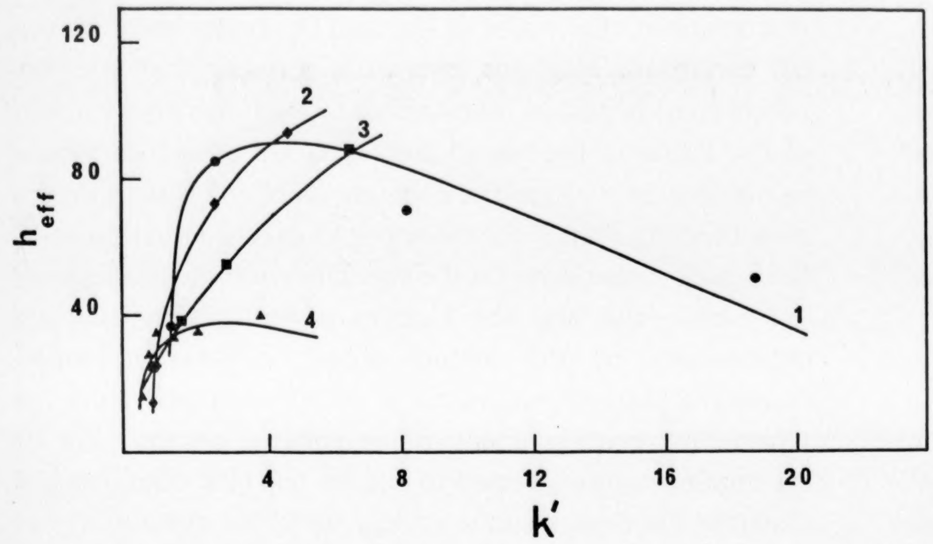

Fig. 7

Plot of h_{eff} versus k' for ovalbumin. The measurements were carried out at pH = (1) 9.60, (2) 7.5, (3) 6.5 and (4) 5.5.

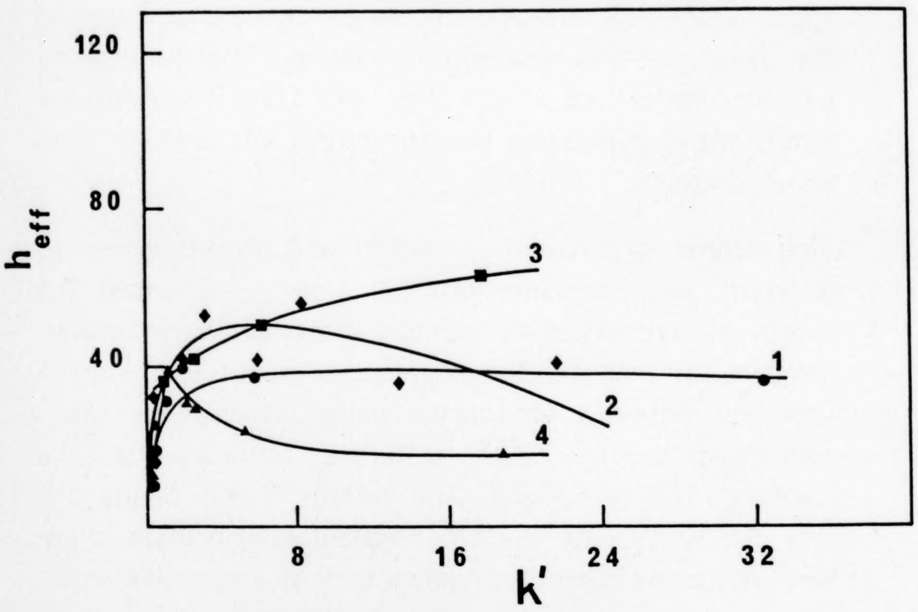

Fig. 8

Plot of h_{eff} versus k' for human serum albumin. The measurements carried out at pH values indicated in Fig. 7.

various displacer salts, selected from the lyotrophic series, on isocratic retention and bandwidth properties of several globular proteins.

Acknowledgement

The support of the National Health and Medical Research Council of Australia, Australian Research Grants Committee and Monash University Special Research Fund Committee is gratefully acknowledged. M.I.A. is a recipient of a Monash University Postdoctoral Fellowship.

References

[1] *L.R. Snyder,* in High Performance Liquid Chromatography. Advances and Perspectives, Academic Press (Cs. Horváth, ed.), 1980, Vol. 1, 207.

[2] *M.I. Aguilar, A.N. Hodder, M.T.W. Hearn,* J. Chromatogr. **327,** 115 (1985).

[3] *M.A. Stadalius, H.S. Gold, L.R. Snyder,* J. Chromatogr. **296,** 31 (1984).

[4] *M.T.W. Hearn,* in Chemical Separations (C.J. King, J.D. Navratil, eds.), Litarvan Press, 1986, Vol. 1, 77.

[5] *N.K. Boardman, S.M. Partridge,* Biochem. J. **59,** 543 (1955).

[6] *S.R. Himmelhoch,* Meth. Enzymol. **22,** 273 (1971).

[7] *H. Schwab, W. Rieman III, P.A. Vaughan,* Anal. Chem. **29,** 1357 (1957).

[8] *E.C. Freiling,* J. Am. Chem. Soc. **77,** 2067 (1955).

[9] *H.F. Walton,* Anal. Chem. Rev. **52,** 15R (1980).

[10] *M.A. Quarry, R.L. Grob, L.R. Snyder,* Anal. Chem. **58,** 907 (1986).

[11] *P. Jandera, J. Churacek,* J. Chromatogr. **91,** 207 (1974).

[12] *W. Kopaciewicz, M.A. Rounds, J. Fausnaugh, F.E. Regnier,* J. Chromatogr. **266,** 3 (1983).

[13] *J.M. Curling* (ed.). Separation of Plasma Proteins, Pharmacia, A.B., Uppsala, Sweden, 1983.

[14] *J.S. Richey,* Meth. Enzymol. **104,** 223 (1984).

[15] *W. Kopaciewicz, F.E. Regnier,* Anal. Biochem. **133,** 251 (1983).

[16] *M.T.W. Hearn, M.I. Aguilar,* J. Chromatogr. **359,** 31 (1986).

[17] *M.T.W. Hearn, M.I. Aguilar,* J. Chromatogr. **397,** 371 (1987).

[18] *J.S. Richey,* Amer. Lab. **14 (2),** 104 (1982).

[19] *L.A. Haff, L.G. Fagerstam, A.R. Barry,* J. Chromatogr. **266,** 409 (1983).

[20] *M.A. Rounds, F.E. Regnier,* J. Chromatogr. **283,** 37 (1984).

[21] *A. Velayudhan, Cs. Horváth,* J. Chromatogr. **367,** 160 (1986).

[22] *G.J. Kennedy, J.H. Knox,* J. Chromatogr. Sci. **10,** 549 (1972).

[23] *J.C. Giddings,* in Dynamics of Chromatography, Marcel Dekker, New York, 1965.

[24] *T. Arakawa, S.N. Timasheff,* Biochem. **21,** 6545 (1982).

[25] *T. Arakawa, S.N. Timasheff,* Biochem. **23,** 5912 (1984).

[26] *M.T.W. Hearn, M.I. Aguilar,* J. Chromatogr. **352,** 35 (1986).

[27] *M.T.W. Hearn,* Proc. Aus. Acad. Sci., in press.

Received: June 31, 1987
Accepted: Aug 29, 1987
F

Determination of Hydrophobic Parameters by Reversed-Phase High-Performance Liquid Chromatography. Effect of Stationary Phase

Th. Braumann*[1)]/H.-G. Genieser[2)]/C. Lüllmann[2)]/B. Jastorff[2)]

1) GAT Gamma Analysentechnik GmbH, Dionysiusstraße 6, 2850 Bremerhaven, FRG
2) University of Bremen, Dept. of Biology/Chemistry, 2800 Bremen 33, FRG

Key Words

Hydrophobic parameters
Stationary phase
Quantitative structure-activity relationships

Summary

The utility of reversed-phase liquid chromatographic retention data as hydrophobic parameters has been studied. Using methanol/water eluents, the retention behaviour of neutral benzene derivatives was measured on six different alkyl-bonded stationary phases. Analysis of (i) the functionality of the silane reagent, (ii) possible endcapping, (iii) the surface area of the bonded phase, (iv) the carbon content, and (v) the amount of residual silanol groups revealed that the different columns covered a broad spectrum of stationary phase properties representative for many currently available bonded phases.

Measurement of the capacity factors at different mobile phase compositions indicated homoenergetic retention behaviour on all columns, although the structure of the bonded phases and the amounts of accessible silanol groups were very different. However, absolute retention varied by 20–30 % so that the capacity factors were column-specific and hence had little significance as general hydrophobic parameters.

Upon extrapolation of retention data from the binary methanol/water eluents to a pure aqueous eluent, the resulting log k_w values derived by linear regression analysis were practically independent from the particular column used to measure retention. Thus, log k_w can be used directly as a hydrophobic parameter in studies on Quantitative Structure-Activity Relationships.

Introduction

The retention of a solute in reversed-phase HPLC (RPLC), i. e. its distribution between the non-polar stationary phase and the polar, water-containing mobile phase, has been successfully described by applying the solvophobic theory [1] to RPLC [2]. Accordingly, the driving force for retention is the unfavourable interaction of a solute with the surrounding water molecules of the mobile phase, giving rise to a net-free energy change upon the inclusion of the solute to the nonpolar ligands of the support. This picture implies that the interaction of the solute with, e. g., the octadecylsilylated surface, is weak and non-selective [2, 3]. Thus, retention in RPLC is basically governed by the solvophobic (hydrophobic) effect which plays an important part in phenomena of physicochemical, pharmacological and biological interest [4].

Indeed, many studies have shown ([5–12] and references cited therein) that RPLC retention data of a large variety of solutes are strongly related to their n-octanol/water distribution coefficient, log P, which is routinely used to quantitatively describe the hydrophobic nature of compounds and to relate biological activity to molecular structure [13]. In view of the fact that retention measurements in RPLC have a great number of practical advantages over log P determinations by the shake-flask technique, it has been proposed that RPLC may be a better alternative for the determination of hydrophobic parameters for compounds of biological interest [9–12, 14–16].

However, an important barrier for the general acceptance of RPLC in this rapidly growing field seems to be the lack of standardization of reversed-phase packing material [17]. Due to differences in the pore size distribution and the surface area of the silica gel, the bonding procedures, and the functionalities of octyl- or octadecylchlorosilanes coupled to the silanol groups, retention data obtained with differ-

0009-5893/87 0777-06 $03.00/0

© 1987 Friedr. Vieweg & Sohn Verlagsgesellschaft mbH

ent columns under identical mobile phase conditions are hardly comparable [18, 19]. Thus, the assessment of a solute's hydrophobic parameter by RPLC requires a reference system in which solute retention is related to that of standard compounds with known log P values. However, the reported relationship between retention parameter and log P hold only for a given compound class and a given chromatographic system and are of little general significance [6, 9, 10, 11].

We have previously shown [6, 9, 11] that selectivity differences arising from specific interactions between mobile phase and solute can be eliminated by using log k_w as a descriptor for solute hydrophobicity. Log k_w is obtained by extrapolation of retention data from binary solvent systems to aqueous eluents [20]. Provided that ODS packings in combination with methanol/water eluents are used, the calculated log k_w values are practically identical with log P measured in the standard n-octanol/water distribution system [7, 9, 12]. In the present study, we examined the influence of stationary phase properties on the magnitude and variability of log k_w. We selected six different reversed-phase packings, showing different bonded phase structures and different amounts of unreacted silanol groups, which are representative for the range of stationary phase material currently available.

The results indicate that the stationary phase-induced variance of log k_w of chemically distinct solutes is small, and in most cases equal or better than the variance of published log P values. In view of the fact that both hydrophobic parameters are related by a Collander-type eqn. with a slope of 1.0 and an intercept close to zero, log k_w may be regarded as a useful substitute for log P in studies on quantitative structure-activity relationships for neutral compounds.

Experimental

The liquid chromatograph consisted of a GAT-ICI Model 235 gradient-system (GAT Gamma Analysentechnik, Bremerhaven, FRG), a Model GAT-LCD-501 variable wavelength detector (GAT) and a Model C-R3A integrator (GAT). A volume of 5-μl of a 0.1 mM methanolic sample solution was injected via a Valco Model C6W sample valve (GAT), and the retention times were measured with a stopwatch. The reproducibility of retention time measurement was better than 1 % (n = 6), so that in all experiments two independent runs were made.

The mobile phase was prepared by the gradient former of the chromatograph and consisted of different volume fractions of methanol (Baker HPLC reagent) in doubly distilled water. The flow rate was 1.5 ml/min at room temperature. The column dead volume was determined as previously described [9].

All benzene derivatives, obtained from Merck (Darmstadt, FRG), were of the highest purity available. Pre-packed columns of Bio-Sil 5S RP-18 and LiChrosorb RP-select B were from Biorad (Richmond, CA, USA) and Merck, respectively. The other stationary phases (Table I) were packed into a column (25 cm X 4.6 mm I.D.) (Merck) by the slurry technique, using tetrachloroethylene as the suspending medium [9]. Different batches of LiChrosorb RP-18 were from Merck, and Kieselgel 60 C_{18} was from Riedel-de Haen (Seelze, FRG). A monomeric 10-μm RP-18 phase was synthesized from Polygosil 60 (Machery-Nagel, Düren, FRG) and chlorodimethyloctadecylsilane (Petrarch Systems, Bristol, PA, USA), as has been previously described [21].

The structure of the ligand and its functionality were determined by gas chromatographic analysis of the reaction products of a potassium hydroxide fusion of the stationary phases [22]. Trifunctional silicas yielded mainly n-octadecane, difunctional material produced cyclic tri- and tetrasiloxanes, and from monofunctional silicas trialkylsilanols and hexaalkyldisiloxanes were obtained after alkali fusion [23]. Column packings which had been endcapped could be identified by the appearance of hexamethyldisiloxane under the same reaction conditions [24].

The surface area of the stationary phases was determined by the BET method [25] using nitrogen as the adsorbate. The carbon content of the packings was measured by the Mikroanalytisches Laboratorium Beller (Göttingen, FRG).

The amount of unreacted silanol groups was determined chromatographically by a procedure proposed by Karch et al. [18]. The columns were extensively washed with dioxane and then equilibrated with n-heptane. It turned out to be necessary to wash each column for at least 24 h with n-heptane at 1 ml/min in order to measure reproducible retention times. Benzene and nitrobenzene were injected as 1 % (v/v) heptane solutions, and the retention times were measured with a stop-watch at a flow rate of 1 ml/min. The capacity factors were calculated as described above.

Data processing and regression analysis were carried out using a standard computer program for multivariate data analysis.

Table I. Properties of reversed-phase stationary phases.

Column No.	Column type	Batch	Particle size (μm)	Specific surface (m^2/g)	Carbon loading (% w/w)	Ligand conc. (μmol/m^2)	Silane functionality	Ligand type	End-capping	Structure
1	LiChrosorb RP-18	VV2249	10	128	17.8	6.1	difunctional	RP-18	No	Polymeric
2	LiChrosorb RP-18	VV1106	10	135	21.2	6.8	difunctional	RP-18	No	Polymeric
3	LiChrosorb RP-Select B	430083	5	213	11.9	5.2	difunctional	RP-8	No	
4	Kieselgel 60 C_{18}	B 2288	10	82	19.7	11.1	trifunctional	RP-18	Yes	Polymeric
5	Bio-Sil 55 RP-18	30363	5	85	9.3	4.6	monofunctional	RP-18	No	Monomeric
6	Polygosil 60 RP-18	homemade	10	110	11.9	4.5	monofunctional	RP-18	No	Monomeric

Results and Discussion

Detailed studies on the preparation and properties of reversed phases have revealed that differences in the chromatographic performance may depend on many support characteristics [18, 19]. Among the most important are the structure of the bonded phase and the amount of unreacted silanol group, both of which are responsible for selectivity differences observed between columns of nominally the same composition [26–29].

Structure of the Bonded Phase

Monomeric phases result from the reaction of monofunctional silane reagents with silanol groups at the silica gel surface. Since only one bond is formed per silane molecule, the resulting surface modification has been described as brush-type [18]. Monomeric phases may also be produced with di- and trifunctional silane reagents in the complete absence of water during synthesis; in the presence of water, however, silane hydrolysis and polymerization lead to the formation of polymeric phases which may be regarded as "liquid-like" [30], but whose structure is not exactly known [28]. Selectivity differences among monomeric and polymeric phases have been traced back to steric effects [28] and to differences in the solvation of the bonded surface [29].

The ligand functionality of six different packings was analysed by gas chromatography of the alkali fusion products [11, 23] and is indicated in Table I. Besides the home-made packing (column 6), only Biosil 5S was synthesized with a monofunctional silane reagent, so that both columns certainly contain a monomeric brush-type surface. This is also evident from the carbon loadings presented in Table I.

To discriminate between a monomeric and polymeric structure of the other packings, the carbon loading and the surface area have been determined (Table I). It should be noted that surface area measurements by the BET method have not been performed with the "naked" silica gel, but with the bonded phases, so that the resulting data are about 50–60 % lower due to the reduction of the accessible surface area upon silanization of the silica gel matrix [27, 31]. Therefore, the data for the surface coverage, calculated according to [27], are correspondingly higher and are only useful for comparison purposes [31]. Despite this restriction it is clear from the data presented in Table I that columns 1, 2, and 4 contain a polymeric phase, as carbon loading, as well as surface coverage, largely exceed the maximum 10–11 % carbon loading and 3 μmol/m^2 surface coverage which are accepted criteria for monomeric phases [18, 27, 28].

Residual Silanol Groups.

For sterical reasons it is impossible to react all silanol groups of the silica gel surface. Depending on the conditions of the bonding procedure [18], a variable amount of hydroxyl group remains accessible to solute-stationary phase interactions with particularly polar and positively charged compounds [32], giving rise to selectivity differences among reversed-phase packings.

The first evidence for the amount of residual silanol group can be obtained by an examination of whether the bonded phases have been endcapped with a small silane reagent. Although the effect of endcapping on the number of accessible silanol sites has been questioned [18, 31], many authors recommend a vigorous silylation in order to minimize "silanophilic" interactions between solute and stationary phase. According to a gas chromatographic analysis of the alkali fusion products [24], only one packing has been endcapped by the manufacturer (Table I). Since this phase contained the highest amount of residual silanol groups (see below), endcapping is obviously very ineffective. Rather, highly reactive monofunctional silanization reagents should be used to obtain phases with low potential for silanophilic interactions, as has been recently suggested [33, 34].

A chromatographic analysis of the contribution of silanol groups to retention has been performed by measuring the capacity factors of benzene and nitrobenzene with n-heptane as the mobile phase [18]. The results presented in Table II indicate that, according to the quality criteria for reversed-phase material as defined by Karch et al. [18], column 1 and 2 contain a low, column 3 and 6 a medium, and column 4 and 5 a high amount of silanol sites, which may contribute to selectivity differences among the various columns. Interestingly, the endcapped phase shows the highes amount of residual hydroxyl group, which may be explained by hydroxilation of unreached chlorine atoms of the trifunctional silane reagent during chromatography in aqueous eluents [31]. It should be mentioned that Schomburg et al. [35] have presented a more sensitive chromatographic procedure for the evaluation of silanophilic interaction, using strongly basic compounds such as octyl pyridine.

In summary, the reversed phases used in this study to evaluate the utility of retention parameters as descriptors for the hydrophobicity of neutral solutes represent a broad sprectrum of stationary phase characteristics which are meaningful in practice for many commercially available columns (i. e., monomeric phases with medium (column 6) and high (column 5), as well as polymeric phases with low (column 1, 2) and high (column 4), residual silanol content). Also included is the possibility of compairing the effect of batch-to-batch variations of columns obtained from the same manufacturer (column 1, 2). Finally, the effect of chain length can be studied with an octylsilica column, which has been developed for the chromatography of basic compounds known to interact with residual silanol groups (column 3).

Table II. Capacity factors, k′, of benzene and nitrobenzene measured on different columns using n-heptane as the mobile phase

Column No.	Column type	capacity factor k′ Benzene	Nitrobenzene
1	LiChrosorb RP-18	0.035	0.597
2	LiChrosorb RP-18	0.031	0.512
3	LiChrosorb RP-Select B	0.056	0.937
4	Kieselgel 60 C^{18}	0.057	1.336
5	Bio-Sil 5S RP-18	0.104	1.664
6	Polygosil 60 RP-18	0.049	0.895

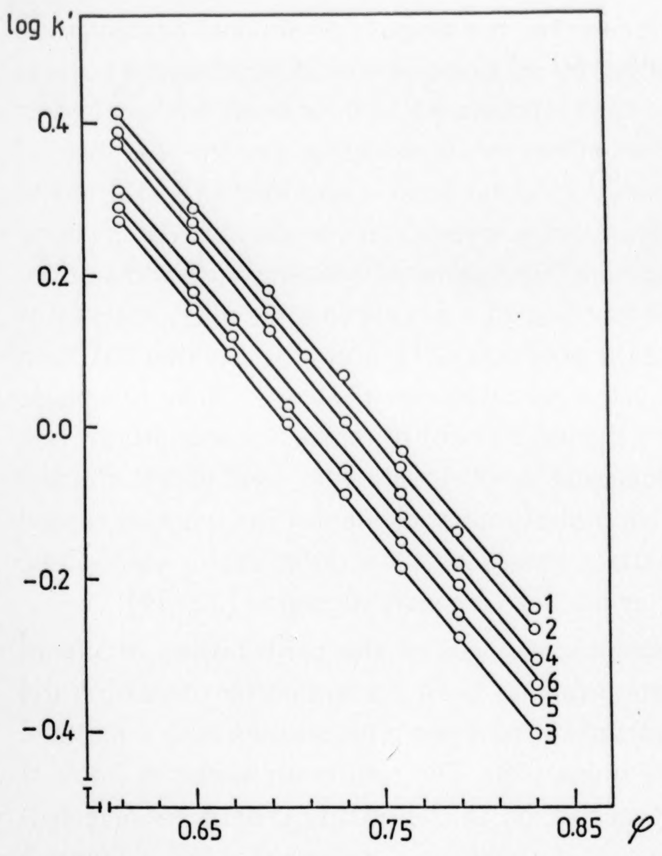

Fig. 1
Plot of log k' *versus* volume fraction of methanol in the aqueous eluent, φ, for benzene on different columns. Column numbers are identified in Table I.

Retention Parameter as Descriptors for Solute Hydrophobicity

Retention in RPLC is described by the solute capacity factor, k', calculated as the normalized solute retention, *viz.*, $k' = (t_R - t_0)/t_0$, where t_R is the solute retention time and t_0 is the mobile phase hold-up time. Fig. 1 shows a plot of log k' *versus* φ, the volume fraction of methanol in the aqueous eluent, for benzene on different columns. Similar plots can also be obtained for the other solutes used in this study (data not shown). Large variations of log k' values are observed at any mobile phase composition, which are least pronounced for k' measured on different batches of the same packing material (column 1, 2). These variations in absolute retention are mainly caused by differences in the phase ratios of mobile and stationary phase [36], and are only small when the same silica gel and the same bonding procedure are used. Thus, the (logarithmic) capacity factor is unsuitable as a general hydrophobic parameter due to its strong dependence on stationary phase properties.

The data presented in Fig. 1 on the dependence of log k' on the volume fraction of methanol, φ, can be used to calculate the slope S and the intercept with the ordinate, log k_w, by linear regression analysis [20]. Table III collects the relevant data for 7 polar and non-polar benzene derivatives. The magnitude of S depends on the structure of the solute, the organic modifier, and, according to Dolan et al., also on stationary phase properties [20, 38]. Indeed, column 3 generally shows the highest values for S, which may be due to the presence of octyl- instead of octadecyl-ligands (Table I). For the other columns, no correlation between any stationary phase property and S is apparent, in accordance with the recent work of Lehtonen [38].

The extrapolated solute capacity factor for an aqueous eluent, log k_w, has been used to quantitatively describe the hydrophobic nature of a wide variety of solutes [5–12]. Inspection of Table III reveals that log k_w, unlike the capacity factor k' measured at a certain mobile phase composition, is not affected by the different stationary phase properties showing a standard deviation of 2–4 % for the mean log k_w. Thus, we conclude that log k_w is indeed a solute property and is not affected by the specific reversed phase used to measure the capacity factors in methanol water eluents. Since this conclusion is based on the retention behaviour of only 7 different solutes, we have collected retention data from the literature which have been measured on additional ODS packings under similar mobile phase conditions (Table IV). Considering the great diversity of chemical structures of, e. g., alkylbenzenes and phenols, and thus the varying potential of specific interactions between solute, mobile phase and stationary phase, the log k_w values are remarkably consistent. The standard deviation of the mean from up to 6 different log k_w values does not exceed 10 %, and is for most solutes much lower (Table IV). These data strongly support our conclusion that capacity factors obtained by extrapolation of retention data from methanol/water to 100 % water are insensitive to variations of stationary phase properties. It would be of interest to test whether this conclusion also holds for the new reversed-phase packings which have been synthesized by polymer coating of trimethylsilylated silica gel [39].

Table III. Regression analysis of the relationship between the volume fraction of methanol in water (φ) and log k' according to $\log k' = S\varphi + \log k_w$. The standard deviations of the regression coefficients were always better than ± 0.15, and the regression correlation coefficient was always ⩾ 0.999.

Solute	log k_w on column No.						Mean ± S.D.	S on column No.						Mean ± S.D.
	1	2	3	4	5	6		1	2	3	4	5	6	
Toluene	2.78	2.71	2.83	2.77	2.62	2.62	2.72 ± 0.09	3.41	3.36	3.72	3.49	3.38	3.34	3.45 ± 0.14
Chlorobenzene	2.84	2.78	2.87	2.85	2.70	2.68	2.79 ± 0.08	3.52	3.48	3.82	3.62	3.52	3.44	3.57 ± 0.14
Fluorobenzene	2.38	2.32	2.34	2.31	2.24	2.28	2.31 ± 0.05	3.21	3.20	3.37	3.19	3.19	3.16	3.22 ± 0.08
Benzene	2.23	2.20	2.18	2.24	2.10	2.10	2.18 ± 0.06	2.97	2.97	3.12	3.07	2.97	2.92	3.00 ± 0.08
Nitrobenzene	1.99	1.93	1.96	1.93	1.99	1.86	1.94 ± 0.05	2.88	2.85	3.04	2.88	2.99	2.80	2.91 ± 0.09
Benzylalcohol	1.33	1.31	1.21	1.29	1.24	1.25	1.27 ± 0.05	2.53	2.57	2.52	2.52	2.53	2.48	2.53 ± 0.02
Phenol	1.33	1.32	1.28	1.30	1.20	1.25	1.28 ± 0.05	2.55	2.54	2.66	2.55	2.55	2.50	2.56 ± 0.05

Table IV. Literature log k_w values for benzene derivatives and fused arenes. log k_w values were either directly taken or calculated from retention data given for different methanol/water compositions. Measured log P values were taken from Ref. [13].

Solute	Stationary phase							
	Nucleosil RP-18 Ref. [40]	Hypersil RP-18 Ref. [7]	LiChrosorb RP-18 Ref. [8]	LiChrosorb RP-18 Ref. [12]	Miscellaneous Refs. [41–43]	This study (Table III)	Mean ± S.D.	log P
Benzene	2.16	2.05	2.11	1.99	2.08	2.18	2.08 ± 0.06	2.13
Chlorobenzene	2.80	2.71	2.80	2.70		2.79	2.76 ± 0.05	2.81
Fluorobenzene			2.28			2.31	2.30	2.27
p-Dichlorobenzene	3.26	3.33	3.43	3.32			3.34 ± 0.07	3.39
1,3,5-Trichlorobenzene		4.51	4.26				4.39	4.49
p-Chlorotoluene	3.37	3.32		3.34			3.34 ± 0.07	3.39
Toluene	2.72	2.59	2.74	2.60	2.71	2.72	2.68 ± 0.07	2.73
Ethylbenzene	3.18	3.25	3.27				3.23 ± 0.05	3.15
n-Propylbenzene	3.82	3.99	3.97				3.93 ± 0.09	3.70
n-Butylbenzene	4.32		4.57				4.45	4.26
p-Xylene		3.18	3.29	3.20	3.29		3.24 ± 0.06	3.15
Naphthalene	3.22	3.28	3.48				3.33 ± 0.14	3.36
Phenanthrene		4.30	4.54				4.42	4.46
Anthracene		4.46	4.73				4.60	4.45
Pyrene		4.89	5.10				5.00	4.88
Biphenyl	3.89	4.03	4.17				4.03 ± 0.14	4.06
Phenol	1.34	1.37	1.27	1.27		1.28	1.31 ± 0.05	1.46
p-Chlorophenol	2.15	2.21	2.27	2.33			2.24 ± 0.08	2.39
p-Nitrophenol	1.77	1.77		2.00	1.68		1.81 ± 0.14	1.92
Nitrobenzene	2.03	1.93	1.91	1.81	1.91	1.94	1.92 ± 0.07	1.84
p-Nitrotoluene		2.42		2.31	2.33		2.35 ± 0.06	2.39
p-Dinitrobenzene	1.81	1.72		1.48	1.86		1.72 ± 0.17	1.48
Aniline	1.21	0.98	1.05	0.98	1.11		1.07 ± 0.10	0.90
Benzaldehyde	1.80		1.74		1.65		1.73 ± 0.08	1.45
Benzylalcohol	1.47	1.29				1.27	1.33 ± 0.10	1.10

These phases have been shown to contain extremely low numbers of unreacted silanol groups [33–35] and thus possesss a highly hydrophobic surface.

It has recently been summarized [11] that an excellent mutual agreement exists between log k_w and log P derived from the standard n-octanol/water distribution system. A slope very close to unity and an intercept near zero indicated identical thermodynamic behaviour of the solutes in the static liquid-liquid distribution system and the dynamic chromatographic systems. Thus, log k_w appears to be equivalent to log P in its ability to model the hydrophobic nature of neutral compounds.

Precise log P values, however, are difficult to determine by the conventional shake-flask technique. Solute impurities, instabilities, dissociation and volatility greatly affect measured distribution coefficients, which are, furthermore, only measurable up to log P = 4 (10, 40, 41). For example, reported log P values for benzene varied from 1.56 to as high as 2.34 [10, 13, 43, 44, 45], and even larger discrepancies have been noted for very hydrophobic compounds [44]. In view of the fact that retention time measurements can also be performed with high precision for impure, unstable and volatile compounds covering a much wider range of hydrophobicity, and considering the insensitivity of log k_w on column-to-column variance, we conclude that log k_w may substitute log P as a convenient hydrophobic parameter for neutral compounds.

Acknowledgements

This work was supported by grants from the Deutsche Forschungsgemeinschaft (Ja 246/4-3) and the Fonds der Chemischen Industrie. We are grateful to Karl-Heinz Burgard for performing the statistics, to Ulrike Bottin for drawing the figure, and to Sabine Schockert for preparing the tables.

References

[1] *O. Sinanoglu,* in "Molecular Associations in Biology", B. Pullman, ed., Academic Press, New York, 1968, pp. 427.

[2] *Cs. Horvath, W. Melander, I. Molnar,* J. Chromatogr. **125,** 129 (1976).

[3] *B. L. Karger, J. R. Gant, A. Hartkopf, P. H. Weiner,* J. Chromatogr., **128,** 65 (1976).

[4] *C. Tanford,* "The hydrophobic Effect", Wiley, New York, 1980.

[5] *A. Hulshoff, J. H. Perrin,* J. Chromatogr., **129,** 263 (1976).

[6] *Th. Braumann, L. H. Grimme,* J. Chromatogr., **206,** 7 (1981).

[7] *T. L. Hafkenscheid, E. Tomlinson,* J. Chromatogr., **218,** 409 (1981).

[8] *W. E. Hammers, G. J. Meurs, C. L. de Ligny,* J. Chromatogr., **247,** 1 (1982).

[9] *Th. Braumann, G. Weber, L. H. Grimme,* J. Chromatogr., **261,** 329, (1983).

[10] *M. Harnisch, M. J. Möckel, G. Schulze,* J. Chromatogr., **282,** 315 (1983).

[11] *Th. Braumann,* J. Chromatogr., **373,** 191 (1986).

[12] *N. El Tayar, H. van de Waterbeemd, B. Testa,* Quant. Struct.-Act. Relat., **4,** 69 (1985).

[13] *C. Hansch, A. Leo,* "Subsituent Constants for Correlation Analysis in Chemistry and Biology", Wiley, New York, 1979.

[14] *S. H. Unger, C. H. Chiang,* J. Med. Chem., **24,** 262 (1981).

[15] *D. A. Brent, J. J. Sabatka, D. J. Minick, D. W. Henry,* J. Med. Chem., **26,** 1014 (1983).

[16] *R. Kaliszan,* J. Chromatogr., **220,** 71 (1981).

[17] *R. E. Majors,* J. Chromatogr. Sci., **18,** 488 (1980).

[18] *K. Karch, I. Sebestian, I. Halasz,* J. Chromatogr., **122,** 3 (1976).

[19] *P. E. Antle, A. P. Goldberg, L. R. Snyder,* J. Chromatogr., **321,** 1 (1985).

[20] *L. R. Snyder, J. W. Dolan, J. R. Gant,* J. Chromatogr., **165,** 3 (1979).

[21] *H. Hemetsberger, M. Kellermann, H. Ricken,* Chromatographia, **10,** 726 (1977).

[22] *H.-G. Genieser, D. Gabel, B. Jastorff,* J. Chromatogr., **264,** 127 (1983).

[23] *C. Lüllmann, H.-G. Genieser, B. Jastorff,* J. Chromatogr., **323,** 273 1985.

[24] *C. Lüllmann, H.-G. Genieser, B. Jastorff,* J. Chromatogr., **354,** 434 (1986).

[25] *S. Brunauer, P. Emmett, E. J. Teller,* J. Amer. Chem. Soc., **60,** 303 (1983).

[26] *H. Colin, A. Krstulovic, G. Guiochon,* J. Chromatogr., **255,** 295 (1983).

[27] *S. A. Wise, W. E. May,* Anal. Chem., **55,** 1479 (1983).

[28] *L. C. Sander, S. A. Wise,* Anal. Chem., **56,** 504 (1984).

[29] *R. P. W. Scott, C. F. Simpson,* J. Chromatogr., **197,** 11 (1980).

[30] *L. C. Sander, J. B. Callis, L. R. Field,* Anal. Chem., **55,** 1068 (1983).

[31] *G. E. Berendsen, L. de Galan,* J. Liquid Chromatogr., **1,** 561 (1978).

[32] *K. E. Bij, Cs. Horvath, W. Melander, A. Nahum,* J. Chromatogr., **203,** 65 (1981).

[33] *G. Schomburg, A. Deege, J. Köhler, U. Bien-Vogelsang,* J. Chromatogr., **282,** 27 (1983).

[34] *G. Schomburg, J. Köhler, H. Figge, A. Deege, U. Bien-Vogelsang,* Chromatographia, **18,** 265 (1984).

[36] *W. R. Melander, J. Stoveken, Cs. Horvath,* J. Chromatogr., **199,** 35 (1980).

[37] *J. W. Dolan, J. R. Gant, L. R. Snyder,* J. Chromatogr., **165,** 31 (1979).

[38] *P. Lehtonen,* J. Chromatogr., **330,** 243 (1985).

[39] *H. Figge, A. Deege, J. Köhler, G. Schomburg,* J. Chromatogr., **351,** 393 (1986).

[40] *P. J. Schoenmakers, H. A. H. Billiet, L. de Galan,* J. Chromatogr., **218,** 261 (1981).

[41] *N. El Tayar, H. van de Waterbeemd, M. Gryllaki, B. Testa, W. F. Trager,* Int. J. Pharm., **19,** 271 (1984).

[42] *M. Bieganowska, E. Soczewinski,* J. Chromatogr., **205,** 451 (1981).

[43] *R. M. Smith,* J. Chromatogr., **236,** 313 (1982).

[44] *L. P. Sarna, P. E. Hodge, G. R. B. Webster,* Chemosphere, **13,** 975 (1984).

[45] "Log P and parameter database: a tool for the quantitative prediction of bio-activity", Pomona College Medicinal Chemistry Project, Comtex Sci. Corp., New York, 1983.

Received: July 2, 1987
Revised manuscript
received: Sep. 16, 1987
Accepted: Oct. 5, 1987
F

An Experimental Verification of the Electrostatic Theory for Ion Pair Chromatography

J. Ståhlberg*[1] / A. Furängen

Astra Pharmaceutical Production AB, Quality Control, S-151 85 Södertälje, Sweden

Key Words

Ion pair chromatography
Retention mechanism
Electrostatic theory, experimental verification

Summary

The purpose of this paper is to present experimental results in order to test the electrostatic theory. The experimental results for a number of different analytes and amphiphilic modifiers are compared with the theory. It is found that the experimental results are in good agreement with the predictions from the electrostatic theory.

Introduction

Liquid chromatographic analysis of organic ions is often carried out with a non-polar stationary phase and a polar mobile phase containing an amphiphilic ion. A number of different names have been given to this analytical technique [1] and some of these are: ion pair chromatography, soap-chromatography, dynamic ion-exchange chromatography, ion interaction chromatography. etc. The name ion pair chromatography seems to be the most widely used and will therefore be used in this paper.

The variety of names reflects the uncertainty that exists about the physico-chemical interpretation of the experimental data. A great number of models for ion pair chromatography have been published and some of these are found in references [1–11]. Chromatographic data are usually interpreted according to the ion pair model or the dynamic ion-exchange model. It has recently been claimed that the controversy between the various models has been settled in favour of the latter model but it is also stated that a number of different equilibria exist in the system [12].

The Gouy-Chapman-theory in combination with a modified Langmuir isotherm has been applied to ion pair chromatography [11] and it was found that it qualitatively and semiquantitatively describes the behavior of such systems. In the present paper experimental results are presented and analysed in order to test the electrostatic theory. The experiments are performed with a number of different analytes and amphiphilic modifiers. Also different compositions of the mobile phase are used.

The electrostatic theory gives consistent equations for cases where the sign of the charges of the analyte ion and amphiphilic modifier are the same and opposite, respectively. The experimental results are also used to verify these relations.

It is found that the experimental results are in good agreement with the predictions from the electrostatic theory.

Theory

The electrostatic theory for ion pair chromatography based on the Gouy-Chapman equation and a modified Langmuir isotherm has been presented in ref. [11]. The hypothesis of the electrostatic theory is that the equilibrium distribution of an analyte ion, B, is primarly determined by a chemical energy term, ΔG_B^0, and an electrostatic energy term, $-z_B F \Delta\Psi_0$. Specific effects such as ion-ion correlation are thus neglected. The following equation for the capacity factor is then easily derived.

$$k'_{c,B} = \phi \exp \frac{-\Delta G_B^0 - z_B F \Delta\Psi_0}{RT} \qquad (1)$$

where $k'_{c,B}$ is the capacity factor for B when the concentration of amphiphilic modifier in the mobile phase is c and ϕ is the phase ratio.

According to this theory $\Delta\Psi_0$ is primarily dependent on the concentration of amphiphilic modifier, A, on the surface, the dielectricity constant and ionic-strength of the mobile phase [11]. The presence of other charged species on the surface must also be considered e.g. dissociated silanol-groups.

---

[1] Affiliated to the Institute of Physical Chemistry, University of Uppsala, Sweden

0009-5893/87 0783-07 $03.00/0

© 1987 Friedr. Vieweg & Sohn Verlagsgesellschaft mbH

It is usually found that, when varying the concentration of amphiphilic modifier in the mobile phase, the change in capacity factor for an uncharged molecule is small compared to the change for a charged molecule. As an approximation eq. (1) can therefore be written

$$k'_{c,B} = k'_{0,B} \exp\left(-\frac{z_B F \psi_0}{RT}\right) \qquad (2)$$

where $k'_{0,B}$ is the capacity factor for B at some reference composition of the mobile phase for which the electrostatic potential is set to zero. In this paper $k'_{0,B}$ refers to the case where there is no amphiphilic modifier present in the mobile phase. The second term in eq. (2) is the change in the electrostatic potential, relative to the reference state, caused by the change in concentration of amphiphilic modifier on the surface.

Despite its simple form, eq. (2) has important and easily tested consequences for the behavior of the capacity factor of different ions. Consider the case where two different negatively charged analyte ions, B_1^- and B_2^-, are chromatographed using a mobile phase containing a positively charged amphiphilic modifier with concentration c_A. The capacity factor for these two molecules is according to eq. (2):

$$k'_{c,B_1^-} = k'_{0,B_1^-} \exp\left(\frac{F\psi_0}{RT}\right) \qquad (3)$$

$$k'_{c,B_2^-} = k'_{0,B_2^-} \exp\left(\frac{F\psi_0}{RT}\right) \qquad (4)$$

Taking the ratio of these equations one obtaines:

$$\frac{k'_{c,B_1^-}}{k'_{0,B_1^-}} = \frac{k'_{c,B_2^-}}{k'_{0,B_2^-}} \qquad (5)$$

Thus if the approximative form of the electrostatic theory is correct, the ratio $k'_{c,B^-}/k'_{0,B^-}$ as a function of the concentration c_A is the same for different analytes with charge -1. If both the analyte ions and the amphiphilic modifier are positively charged then eq. (2) gives that the ratio

$$\frac{k'_{0,B_1^+}}{k'_{c,B_1^+}} = \frac{k'_{0,B_2^+}}{k'_{c,B_2^+}} \qquad (6)$$

Analogous discussion gives that eq. (5) is valid for two positive and eq. (6) for two negative charged analytes when the amphiphilic modifier is negative.

If the analyte ions have charge -2 and the amphiphilic modifier is positively charged, eq. (2) gives that:

$$\frac{k'_{c,B_1^{2-}}}{k'_{0,B_1^{2-}}} = \frac{k'_{c,B_2^{2-}}}{k'_{0,B_2^{2-}}} \qquad (7)$$

The approximative form of the electrostatic theory, i.e. eq. (2), predicts that the ratios in eq. (5) and (6) are identical functions of the concentration of amphiphilic modifier in the mobile phase. Eq. (8) gives a general expression for eqs. (5)–(7) which is independent of B.

$$\frac{{k'_{c,B}}^{-\frac{z_A}{z_B}}}{k'_{0,B}} = f(c_A);\ /z_A/ = 1 \qquad (8)$$

The validity of eq. (8) is discussed in the Result Section by use of experimental data presented in this paper.

Experimental

Apparatus

A Varian 5000 liquid chromatograph was used (with puls dampener) and the detector was a LDC Spectro Monitor III measuring at 255 nm. The injector was a Rheodyne Model 7126 with a 5 μl loop.

The column was a C_{18} μBondapak (15 cm X 3,9 mm I.D.; Waters Assoc.).

A water-bath, HETO type 01 T 640 (Birkerod, Denmark) was used to thermostat solvent reservoir.

The pH measurements were performed with a Radiometer PHM 82 standard pH-meter, equipped with a Radiometer combined electrode.

Chemicals and Reagents

As analyte ions (B) the following substances were used; bupivacaine (dl-1-Butyl-2′, 6′-pipecoloxylidide), lidocaine (2-(Diethylamino)-N-(2,6-dimethylphenyl)acetamide) and etidocaine (N-(2,6-Dimethylphenyl)-2-(ethylpropylamino)-butane-amide) of pharmacopoeial grade, supplied by Astra Pharmaceutical Production AB, Södertälje, Sweden, benzyltrimethylammonium chloride, benzyltriethylammonium chloride, benzyltri-n-butylammonium bromide (Merck, Schuchardt), benzenesulfonic acid sodium salt, naphthalene-2-sulfonic acid sodium salt, anthraquinone-2-sulfonic acid sodium salt, 1-naphtol-3,6-disulfonic acid disodium salt (Fluka AG, Buchs), 1.5-naphthalenedisulfonic acid disodium salt (Aldrich-Chemie, Steinham) and phenol from Merck, Darmstadt. The amphiphilic modifiers (A) were obtained from Fluka (tetraethylammonium chloride and tetrabutylammonium chloride), Aldrich Chemie (tetrapentylammoniumchloride) and Eastman Kodak (octyl sodiumsulfate and 1-hexanesulfonic acid sodium salt).

All other substances were of analytical or reagent grade and used without further purification.

Chromatographic Technique

The mobile phase consisted of phosphate buffer and acetonitrile in various volume ratios, (q + l or 8 + 2). The pH of the buffer was 2.1 (I = 0.05 M) when the positive modifiers were used and 3.4 (I = 0.09 M) for the negative. The modifiers were added to the mobile phase and the analyte ions were injected after dissolution in the mobile phase. The injected amount of analyte was always $< 10^{-8}$ mol. After passage of 100 ml mobile phase, the system was arranged for recirculation with 500 ml of mobile phase in the reservoir.

The flowrate was 0.70 ml/min throughout all of the studies and the mobile phase reservoir was thermostated in a water-bath at 300 K.

Retention time t_R was converted to capacity factor k' via the relationship

$$k' = (t_R - t_0)/t_0 \qquad (16)$$

where t_0 is the retention time of an unretained component, i.e. water. All k' values below 0.40 were neglected. All chromatographic results reported are the means of duplicate or triplicate injections.

Results and Discussion

The purpose of this work is to test the validity of eq. (8) and this is done by measuring the capacity factor for a number of analyte ions, B. These ions have different charge z_B where the sulfonates are negatively charged, phenol uncharged, the tertiary (lidocaine, bupivacaine, etidocaine) and the quaternary ammonium ions positively charged at the pH used. Also a number of amphiphilic modifiers, A, with different charge, z_A are used.

Monovalent Ions.

In Tables I–VI the experimental data as capacity factors are listed. Amphiphilic modifiers of different hydrophobicity and charge, as well as different compositions of the mobile phase are presented. The capacity factors in Table I are plotted *vs* the concentration of tetraethylammonium in Fig. 1. This kind of plots are used in most chromatographic papers. It shows the decrease in retention for positive analyte ions and the increase of the negative analyte ions, when a positive modifier like a quaternary ammonium ion is used in different concentrations. The uncharged compound, phenol, is very little affected in the system.

In the Theory section it was shown that according to the electrostatic theory the quotient $(-z_A/z_B)\log(k'_{c,B}/k'_{0,B})$ is the same for different B as a function of $\log c_A$, eq. (8).

The quotient in the Figures are calculated from data in Tables I–VI. In Fig. 2–7 this quotient is plotted as a function of $\log c_A$ for a number of analyte ions with different sign of charge. Each figure differs in the choice of amphi-

Table I. The capacity factor for different analytes with tetraethylammonium (A^+) as amphilic modifier. Experimental conditions: mobile phase, acetonitrile-water (10 + 90); phosphate buffer pH = 2.1.

A^+ (mM)	phenol ◭	benzene-sulfonate ■	naphtalene-2-sulfonate ●	bupivacaine △	etidocaine ⊗	bensyltriethyl ammonium □	1.5-naphtalene disulfonate ◑	1-naphtol-3.6-disulfonate ◨
0	5.94	0.82	10.0	42.7	28.8	5.88	–	–
10	5.56	1.05	12.7	30.9	20.8	3.72	–	–
20	5.50	1.24	14.4	27.3	18.6	3.21	0.42	0.62
40	5.30	1.34	15.8	24.2	16.6	2.68	0.62	0.82
80	5.29	1.52	17.7	22.1	15.2	2.30	0.81	1.03
120	5.00	1.60	17.2	20.5	14.1	2.06	0.86	1.05

Table II. The capacity factor for different analytes with tetrabutylammonium (A^+) as amphilic modifier. Experimental conditions: mobile phase, acetonitrile-water (10 + 90); phosphate buffer pH = 2.1.

A^+ (mM)	phenol ◭	benzene-sulfonate ■	naphtalene-2-sulfonate ●	bupivacaine △	etidocaine ⊗	bensyltriethyl ammonium □	1.5-naphtalene disulfonate ◑	1-naphtol-3.6-disulfonate ◨
0	5.94	0.82	10.0	42.7	28.8	5.88	–	–
0.10	5.45	1.58	19.8	20.1	13.9	3.03	0.79	1.13
0.25	5.55	2.08	27.2	15.4	10.7	2.32	1.45	2.05
0.50	5.41	2.70	36.5	11.2	7.8	1.66	2.75	3.86
1.00	6.28	4.39	57.2	–	–	1.43	6.37	8.79
2.00	6.05	5.75	78.7	6.7	4.4	0.96	13.1	17.5
4.00	5.76	7.16	99.5	4.3	3.1	0.53	24.2	31.7

Table III. The capacity factor for different analytes with tetrabutylammonium (A^+) as amphilic modifier. Experimental conditions: mobile phase, acetonitrile-water (20 + 80); phosphate buffer pH = 2.2.

A^+ (mM)	phenol ◭	naphtalene-2-sulfonate ●	anthraquinone 2-sulfonate ▲	bupivacaine △	etidocaine ⊗	bensyltriethyl ammonium □	benzyltri-n-butylammonium X	1.5-naphtalene sulfonate ◑	1-naphtol-3.6-disulfonate ◨
0	2.60	1.66	4.61	6.54	4.88	1.70	43.6	–	–
0.20	2.61	2.51	7.03	4.46	3.39	1.14	33.2	–	–
0.50	2.70	3.92	11.2	3.43	2.59	0.83	24.1	0.42	0.45
1.00	2.74	5.62	15.6	2.62	2.00	0.61	17.5	0.78	0.88
1.50	2.72	6.65	18.9	2.18	1.69	0.50	14.2	1.15	1.26
3.00	2.78	9.32	26.5	1.61	1.23	–	9.78	2.19	2.46
5.00	2.78	12.7	36.1	1.14	0.91	–	6.57	4.01	4.16

Table IV. The capacity factor for different analytes with tetraethylammonium (A^+) as amphilic modifier. Experimental conditions: mobile phase, acetonitrile-water (20 + 80); phosphate buffer pH = 2.2.

A^+ (mM)	phenol ◭	naphtalene 2-sulfonate ●	anthraquinone 2-sulfonate ▲	bupivacaine △	etidocaine ⊗	bensyltri-n-butyl-ammonium X	1.5-naphtalene disulfonate ◑	1-naphtol-disulfonate ◨
0	2.60	1.66	4.61	6.54	4.88	43.6	–	–
0.03	2.66	3.97	11.2	3.22	2.43	19.6	0.42	0.43
0.06	2.70	5.77	16.5	2.47	1.88	15.1	0.84	0.90
0.10	2.68	6.32	17.8	2.03	1.54	12.9	1.15	1.24
0.15	2.86	9.64	27.5	1.65	1.24	9.38	2.43	2.65
0.20	2.82	10.7	30.8	1.41	1.05	7.97	2.86	3.16
0.30	3.04	13.8	40.3	1.36	1.03	7.43	4.40	4.74
1.00	3.00	26.7	79.8	0.62	0.46	3.16	15.9	15.9

Table V. The capacity factor for different analytes with octylsodiumsulfate (A^-) as amphilic modifier. Experimental conditions: mobile phase, acetonitrile-water (10 + 90); phosphate buffer pH = 3.4.

A^- (mM)	phenol ◭	naphtalene-2-sulfonate ●	anthraquinone 2-sulfonate ▲	lidocaine ⊠	bensyltrimethyl ammonium ○	benzyltriethyl-ammonium □
0	4.99	7.98	42.6	6.10	2.03	5.79
0.10	5.06	5.73	31.2	12.7	3.63	10.6
0.20	4.96	4.70	25.2	17.6	4.92	14.2
0.40	4.77	3.69	19.7	24.6	6.42	17.6
0.80	4.70	2.71	14.0	37.9	9.20	27.0
1.2	4.72	2.20	11.3	49.8	11.8	33.3
2.0	4.66	1.73	8.76	66.8	18.5	46.3

Table IV. The capacity factor for different analytes with tetrapentylammonium (A^+) as amphilic modifier. Experimental conditions: mobile phase, acetonitrile-water (20 + 80); phosphate buffer pH = 2.2.

A^- (mM)	phenol ◭	naphtalene-2-sulfonate ●	anthraquinone 2-sulfonate ▲	lidocaine ⊠	bensyltrimethyl ammonium ○	benzyltriethyl-ammonium □
0	4.99	7.98	42.6	6.10	2.03	5.79
0.50	4.90	6.92	36.5	7.14	2.20	6.33
1.5	5.01	6.26	33.9	9.69	2.75	8.07
5.0	4.92	4.57	24.2	15.6	4.19	11.8
10	4.93	3.61	19.0	23.1	6.14	15.5
20	4.85	2.68	13.7	32.6	7.84	21.2
50	4.68	1.77	8.55	48.5	11.7	30.2

philic modifier, the sign of charge of the modifier as well as the composition of the mobile phase.

From the figures the following features may be noted: The quotient $(-z_A/z_B)\log(k'_{c,B}/k'_{0,B})$ as a function of c_A is almost the same for analyte ions with different structure and charge, e. g. cf. Fig. 3. The same conclusion is still valid when the composition of the mobile phase is changed, (cf. Fig. 3 and 4), when another positively charged modifier is used, (cf. Figs. 4 and 5) and when modifiers with different sign of charges are used, e. g. Figs. 3 and 7. In conclusion the figures show that the prediction made by the electrostatic theory is basically correct, cf. eq. (8).

According to the electrostatic theory eq. (8) should be valid for any analyte ion. However, it must be remembered that there are a number of assumptions and approximations inherent in this equation. A discussion of these assumptions and how they influence the capacity factor is found in ref. [11] and [13]. Thus eq. (8) can not be expected to hold exactly and it is difficult to theoretically estimate how large the deviations are.

From the figures it is seen that eq. (8) generally holds very well for analyte ions of the same charge. Small systematic deviations are found between tertiary and quaternary amines in Figs. 2, 6 and 7. A general trend in the experimental results is that when c_A increases, the relative increase in the capacity factor of an ion B with charge opposite to that of the amphiphilic modifier is larger than the relative decrease in capacity factor of a B with the same charge. An exception is when tetraethylammonium ion is used as amphiphilic modifier.

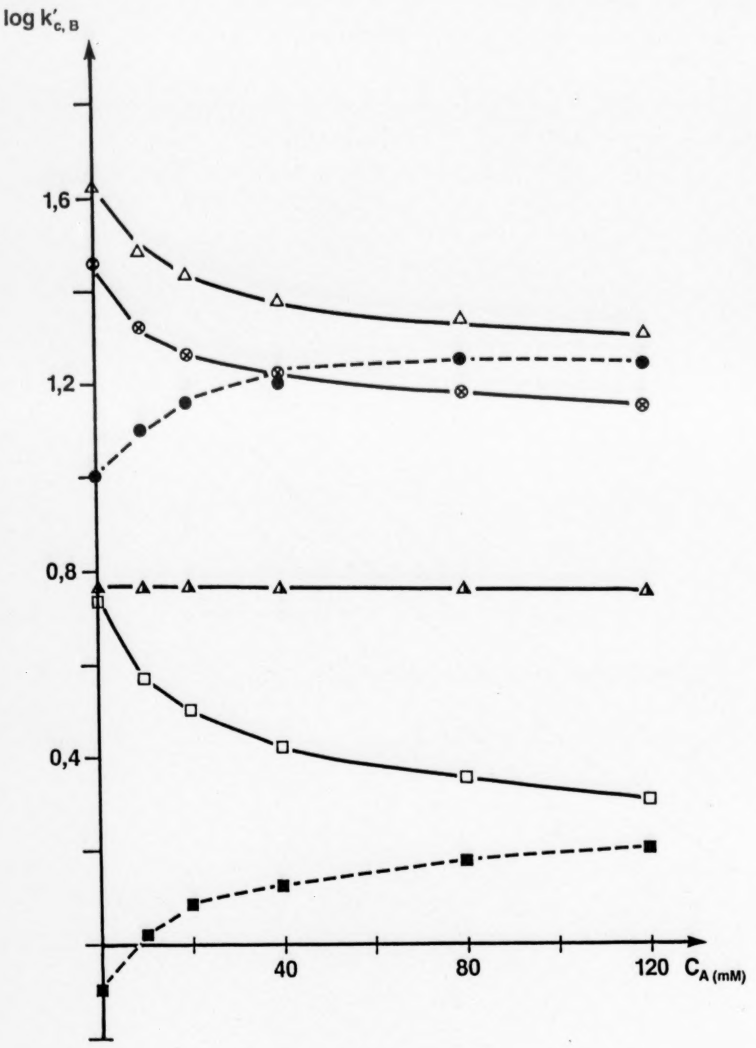

Fig. 1

The capacity factor for different analytes *vs* the mobilde phase concentration of tetraethylammonium ion.

Experimental conditions and symbols in Table I.

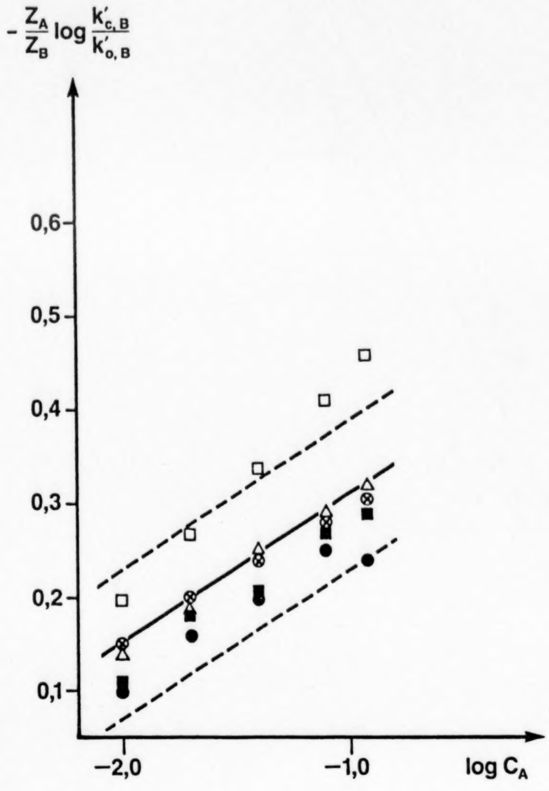

Fig. 2

$(-\ z_A/z_B)\ \log(k'_{c,B}/k'_{0,B})$ *vs* log concentration of tetraethylammonium ion in the mobile phase.

Experimental conditions and symbols in Table I.

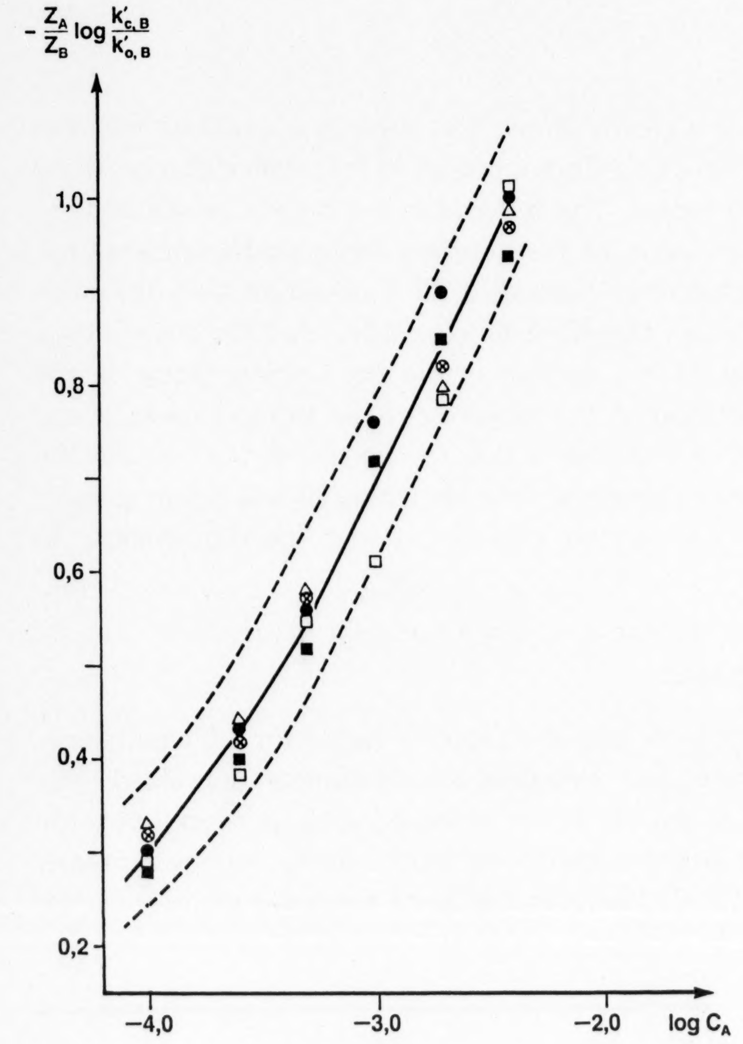

Fig. 3

$(-\ z_A/z_B)\ \log(k'_{c,B}/k'_{0,B})$ *vs* log concentration of tetrabutylammonium ion in the mobile phase.

Experimental conditions and symbols in Table II.

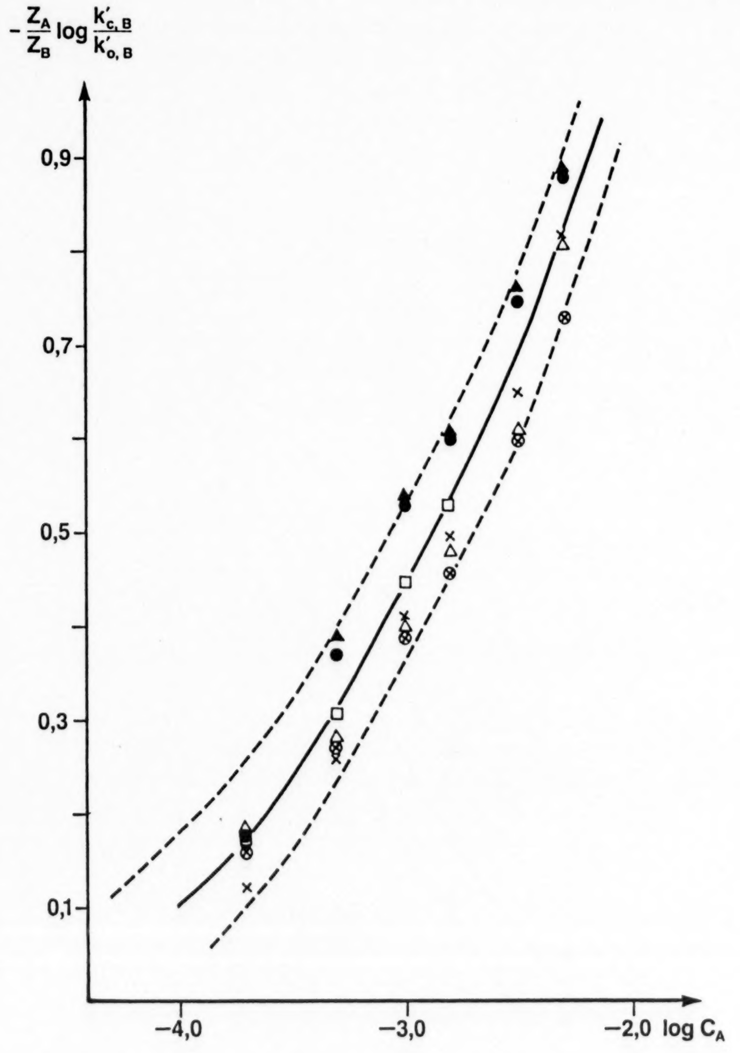

Fig. 4

$(-\ z_A/z_B)\ \log(k'_{c,B}/k'_{0,B})$ *vs* log concentration of tetrabutylammonium ion in the mobile phase.

Experimental conditions and symbols in Table III.

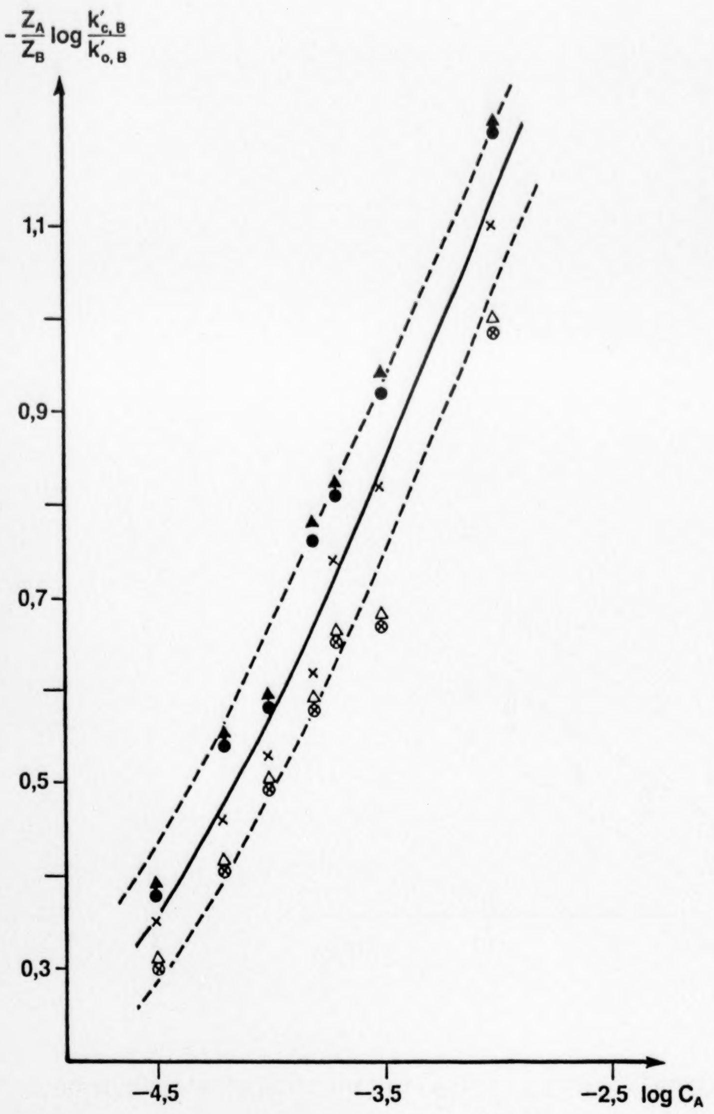

Fig. 5

($-z_A/z_B$) log ($k'_{c,B}/k'_{0,B}$) *vs* log concentration of tetrapentylammonium ion in the mobile phase.

Experimental conditions and symbols in Table IV.

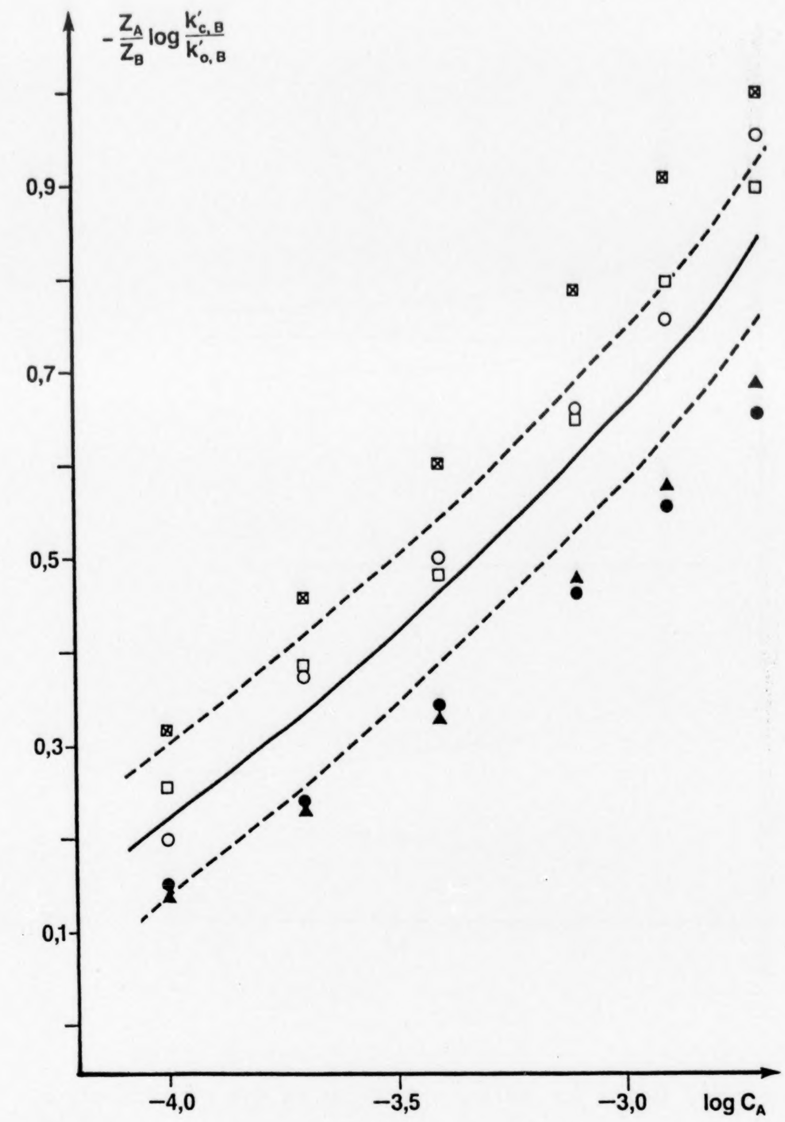

Fig. 6

($-z_A/z_B$) log ($k'_{c,B}/k'_{0,B}$) *vs* log concentration of octylsodiumsulfate in the mobile phase.

Experimental conditions and symbols in Table V.

The figures clearly show, that there is a similarity between analyte ions of different charge in the relative change of the capacity factor. The full line in the figures corresponds to the mean value of the quotient for the different analytes. The dotted lines illustrate a 20 % deviation from the mean value. It can therefore be concluded that the electrostatic potential of the surface is the dominating factor in the determination of this relative change. In most cases, about 80 % of this change is due to changes in the non-specific electrostatic potential. The remaining 20 % is due to specific effects, i. e. ion-ion correlation and specific changes in $-\Delta G^0_B$.

Divalent Ions

In Tables I–IV also the capacity factor for 1.5-naphtalenedisulfonate and 1-naphtol-3.6-disulfonate are listed. According to eq. (8) a plot of $\log (k'_{c,B}/k'_{0,B})^{1/2}$ *vs* $\log c_A$ for divalent ions is equal to the plots used for monovalent ions in Figs. 2–7. However the acids are hydrophilic and thus

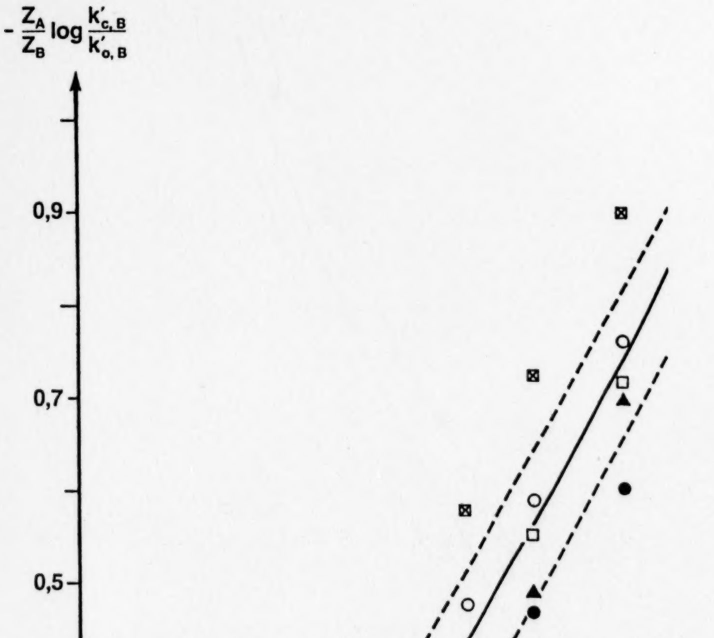

Fig. 7

($-z_A/z_B$) log ($k'_{c,B}/k'_{0,B}$) *vs* log concentration of 1-hexanesulphonate in the mobile phase.

Experimental conditions and symbols in Table VI.

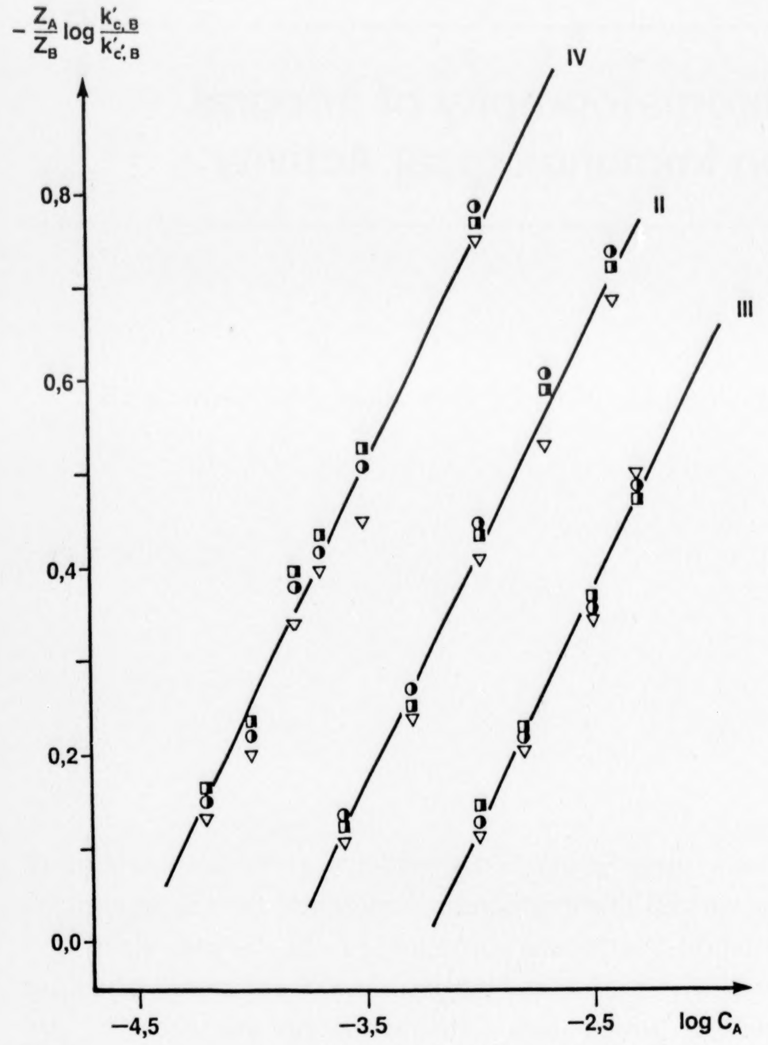

Fig. 8

(− z_A/z_B) log ($k'_{c,B}/k'_{0,B}$) *vs* log concentration of amphiphilic modifier for divalent analytes and a number of modifiers. In each system the corresponding mean value for the monovalent ions is also represented (▽).

Experimental condition and symbols: Line IV as Table IV, line II as Table II, line III as Table III, drawn as the mean values of the monovalent ions examined.

k'_0 could not be measured with any good precision. Instead the plot log $(k'_{c,B}/k'_{c',B})^{1/2}$ is used where $k'_{c',B}$ is the smallest capacity factor for the disulfonate listed in each table, (e. g. just above 0.4). Fig. 8 shows plots for the two divalent ions and the corresponding mean values for the monovalent ions. No difference is found between the divalent sulphonates, and there is no deviation between the mean value for the monocharged analytes and the divalent sulphonates.

It can thus be concluded that eq. (8) holds for monovalent ions as well as for divalent ions and that specific forces between B and A due to the molecular structure of these species are small.

Practical Consequences

The electrostatic theory claims that the quotients $k'_{c,B}/k'_{0,B}$ and $k'_{0,B}/k'_{c,B}$ as a function of the concentration c_A are the same for different analytes with the charge − 1 and + 1 respectively, cf. eqs. (5) and (6). This is verified with the results listed in e. g. Table II. The known quotients for e. g. etidocaine at different concentrations of tetrabutylammonium ion can be used to calculate $k'_{c,B}$ for benzenesulfonate and benzyltriethylammonium just by knowing their $k'_{0,B}$ values. The results are plotted in Fig. 9, showing calculated and found data. The calculated and found lines are almost identical, illustrating a very useful consequence of the electrostatic theory in practical work with ion pair chromatography.

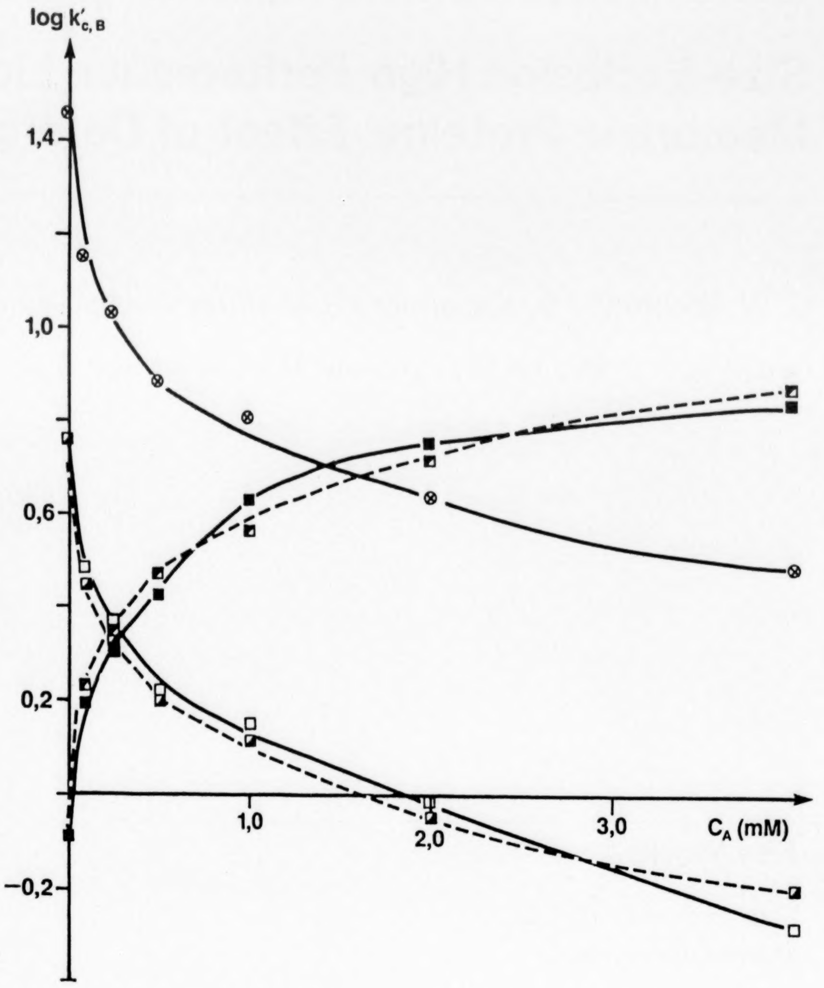

Fig. 9

Calculated (dotted lines) and found (full line) capacity factors *vs* the mobile phase concentration of tetrabutylammonium ion.

Experimental conditions and symbols in Table II.

Acknowledgements

We thank Professor Mats Almgren for valuable discussion of the manuscript, Miss Ingela Hägglund for her skillful technical assistance and Mrs. Anne Olsen for typing the manuscript.

References

[1] *W. R. Melander, Cs. Horváth,* Chromatogr. Sci. **31**, 27 (1985).
[2] *A. Tilly-Melin, Y. Askemark, K. G. Wahlund, G. Schill,* Anal. Chem. **51**, 976 (1979).
[3] *B. A. Bidlingmeyer, S. N. Deming, W. P. Price Jr., B. Sachok, M. Petrusek,* J. Chromatog. **186**, 419 (1979).
[4] *C. T. Hung, R. B. Taylor,* J. Chromatog. **202**, 333 (1980).
[5] *P. T. Kissinger,* Anal. Chem. **49**, 883 (1977).
[6] *W. R. Melander, Cs. Horváth,* J. Chromatog. **202**, 221 (1980).
[7] *J. H. Knox, R. A. Hartwick,* J. Chromatog. **204**, 3 (1981).
[8] *S. Afrashtehfar, F. C. Cantwell,* Anal. Chem. **54**, 2422 (1982).*S.*
[9] *J. J. Stranahan, S. N. Deming,* Anal. Chem. **54**, 2251 (1982).
[10] *J. H. Knox, G. R. Laird,* J. Chromatog. **122**, 17 (1976).
[11] *J. Ståhlberg,* J. Chromatog. **356**, 231 (1986).
[12] *H. G. Barth, W. E. Barber, C. H. Lochmüller, R. E. Majors, F. E. Regnier,* Anal. Chem. **58**, 211R (1986).
[13] *J. Ståhlberg*, Chromatographia **24**, 820 (1987).

Received: June 28, 1987
Revised manuscript
received: Sept. 15, 1987
Accepted: Oct. 6, 1987
F

Size-Exclusion High-Performance Liquid Chromatography of Integral Membrane Proteins; Effect of Detergents on Immunological Activity

G. W. Welling* / B. Kazemier / S. Welling-Wester

Department of Medical Microbiology, Rijksuniversiteit Groningen, Oostersingel 59, 9713 EZ Groningen, The Netherlands

Key Words

Size-exclusion HPLC
Membrane proteins
Detergents
Sendai virus

Summary

A mixture of integral membrane proteins from Sendai virus was used as a model to study the effect of various detergents and organic solvent on the purification by size-exclusion high-performance liquid chromatography (HPLC) on two tandemly linked Superose-6 columns. The best separations were obtained with either 0.1% sodium dodecyl sulphate, 0.05% sarkosyl or 0.1% lauryldimethylamineoxide in the eluent. In addition, the effect of the eluent on the immunological activity as a measure of intact structure was studied. A considerable part of the protein structure remained intact after HPLC and was able to react with antibodies directed against the intact virus proteins.

Introduction

Integral membrane proteins cross the lipid bilayer of the membrane once or several times and detergents or organic solvents have to be used to extract the proteins from the bilayer [1]. Integral membrane proteins are often more hydrophobic than an average protein, since a significant part of the polypeptide chain interacts with the hydrophobic tails of the phospholipid molecules in the lipid bilayer. The percentage of large hydrophobic amino acids can be considered as an indicator of the hydrophobicity of a protein [1, 2]. This percentage is 20.2% in an average protein and 30.3% in a number of membrane proteins. Because of this hydrophobicity, integral membrane proteins show a strong tendency to aggregate, which results in difficulties during purification.

We have used Sendai virus proteins as model proteins to study various chromatographic methods for the separation of integral membrane proteins [1–3]. Sendai virus is a paramyxovirus of mice. Its envelope is composed of a lipid bilayer in which two integral membrane proteins are embedded, the fusion protein F ($M_r = 65,000$) and the hemagglutinin-neuraminidase protein HN ($M_r = 68,000$). The F protein consists of two components F_1 ($M_r = 50,000$) and F_2 ($M_r = 13–15,000$) which are connected by disulfide bridges. The HN protein is found in a monomeric, a dimeric and a tetrameric form, HN, HN_2 and HN_4, respectively. HN_2 and HN_4 can be converted to the monomeric form by treatment with a reducing agent. Presumably due to limited proteolysis, a truncated form (without the transmembrane spanning region) is sometimes present in detergent extracts e.g. in a dimeric form (HN_{2-}). Intact multimeric forms of the HN and F protein appear as spikes on the outside of the virus particle extending into the solution.

The strategy to purify integral membrane proteins generally involves extraction of the integral membrane proteins from the lipid bilayer followed by chromatography. During chromatography e.g. size-exclusion chromatography, a denaturant, a detergent or an organic solvent has to be present in the eluent to prevent aggregation. A wide variety of additives has been used for size-exclusion high-performance liquid chromatography (HPLC) of membrane proteins, sodium dodecyl sulphate (SDS) [4–6], sarkosyl [7], triethylamine-Triton X-100 [8], Brij 35 [9], (3-((3-cholamidopropyl)dimethylammonio)-1-propanesulfonate (CHAPS) [10], Tween-20 [10], octylglucoside [11], guanidine-HCl [5, 12] and deoxycholate [13]. However, eluents containing these compounds have not been used to purify one model mixture on one type of column. In the present study, Sendai virus membrane proteins are used as a model mixture to investigate the usefulness of these eluents for size-exclusion HPLC of integral membrane proteins on two coupled columns of Superose-6. In addition, the intactness of the structure of the proteins is investigated by determination of the reaction of the proteins with an antiserum directed against the intact virus.

0009-5893/87 0790-05 $03.00/0

©1987 Friedr. Vieweg & Sohn Verlagsgesellschaft mbH

Materials and Methods

Virus; Detergent Extraction

Sendai virus was grown in 10-day-old embryonated chicken eggs. Allantoic fluid was collected after 72h at 36°C. Debris was pelleted at 2000g (20min) and virus was pelleted at 22,000rpm (70,000g) for 90min. The virus pellet was resuspended in 5mM Tris-HCl (pH 7.2) containing 10% (w/v) sucrose and stored at − 80°C. Virions (20mg/ml) were extracted by adding an equal volume of 4% (w/w) Triton X-100 (BDH, Poole, UK) for 15min at room temperature. After centrifugation at 100,000g for 90min, the supernatant was stored at − 80°C.

Removal of Triton X-100

Amberlite XAD-2 resin was washed several times with methanol. 500mg dry resin was added per ml of detergent extract. The mixture was rotated for 30min at room temperature and the resin was removed by centrifugation over a 2μm column frit mounted in a 1ml Eppendorf tip.

Size-Exclusion HPLC

Chromatography was performed with an LKB 2150 pump (LKB, Bromma, Sweden), a Rheodyne 7125 injector (Inacom, Veenendaal, The Netherlands) an LKB 2151 UV-monitor and two tandemly-linked columns of Superose 6HR 10/30 (300 x 10mm i.d.) (Pharmacia, Uppsala, Sweden). Prior to HPLC, the detergent-free extract was incubated for 20min in an equal volume of the concentrated (2x) buffers used for elution (Table I).

385μg of the Sendai virus membrane protein mixture in 200μl of eluent was injected. The flow-rate was 0.5ml/min and the absorbance was monitored at 280nm.

Determination of Critical Micelle Concentration (CMC)

The CMC of decylpolyethyleneglycol-300 was determined with the pinacyanol chloride method [14, 15]. To 1ml of a detergent solution, 1ml of a 10^{-5}M solution of pinacyanolchloride (Janssen, Beerse, Belgium) was added. The spectrum between 500–600nm was recorded and the height of the maximum at 600–610nm was plotted against the detergent concentration. At the CMC, the absorbance starts to increase.

Table I. Eluents used for size-exclusion HPLC and the critical micelle concentration (CMC) of detergents.

eluent	ref. (eluent)	CMC (%)	ref. (CMC)
0.1% SDS	4–6	0.07	19
0.05% sarkosyl	7		
20% acetonitrile			
0.1% Brij 35	9	0.01	19
0.03% Tween-20	10	0.006	20
0.1% octylglucoside	11	0.73	21
0.1% LDAO		0.048	22
0.1% decylpolyethylene-glycol-300	18	< 0.025	this study
0.25% CHAPS	10	0.49	21

Detergents were from the following manufacturers: SDS (Bio Rad, Richmond, USA); sarkosyl, LDAO and CHAPS (Fluka, Buchs, Switzerland); octylglucoside (Boehringer, Mannheim, FRG); Brij 35, Tween-20 (Merck, Darmstadt, FRG); decylpolyethyleneglycol (Kwant-Hoog vacolie Recycling and Synthese, Bedum, The Netherlands). Detergents were used in 50mM sodium phosphate, pH 6.5 except for CHAPS in 100mM sodium phosphate, pH 6.5 and sarkosyl in 10mM Tris-HCl, pH 7.5 with 0.6M NaCl.

SDS-Polyacrylamide Gel Electrophoresis (SDS-PAGE)

The column eluates were analyzed with an LKB-midget system on 8% SDS-gels [16] without reduction of the samples. Polypeptide bands were visualized with a silver-staining method [17].

Enzyme-Linked Immunosorbent Assay (ELISA)

The ELISA was carried out as described [6] with some modifications. Polystyrene microtiterplates (Dynatech, Denkendorf, FRG) were coated with 5μg of protein (based on A_{280} values) per well in 100μl 50mM sodium carbonate, pH 9.6 overnight at 4°C. The proteins were allowed to react with a 1:100 (v/v) dilution of antiserum from Sendai virus-infected mice (100μl/well). Subsequently, a 1:1000 dilution of peroxidase-labeled anti IgG (ShaM/IgG/PO-Pasteur) was added. Peroxidase activity was visualized by adding 100μl 50mM sodium potassium phosphate, pH 5.6 containing 0.2mg/ml ortho-phenylenediamine-dihydrochloride (Eastman Kodak, Rochester, USA) and 0.006% H_2O_2. The reaction was terminated by adding 50μl 2M H_2SO_4 and the optical density at 492nm was read in a microplate photometer. Optical density values below 0.2 were considered as negative.

Results and Discussion

Specific Resolution of Reference Proteins

The specific resolution (R_s) (ref. [18]) between two pairs of reference proteins, bovine serumalbumin (BSA) and ovalbumin (OVA); OVA and trypsin-inhibitor (TI) was determined after elution of these proteins from the two coupled Superose-6 columns with the eluents listed in Table I. Because of its high viscosity, it was not possible to use 6M guanidine-HCl in 50mM sodium phosphate, pH 6.5 [5] under the same elution conditions (0.5ml/min) and it was not subjected to further study. The R_s of BSA-OVA and OVA-TI was 5.1 and 5.8, respectively in 50mM sodium phosphate, pH 6.5 containing 0.1% SDS. A similar performance for the BSA-OVA pair was obtained with the only other eluent containing an anionic detergent, sarkosyl (sodium dodecyl sarcosinate). The R_s of the OVA-TI pair was lower (33%) with this detergent. The R_s values obtained with the other eluents were considerably lower. They were 15–48% lower for the BSA-OVA pair and 37–55% for the OVA-TI pair.

Size-Exclusion-HPLC of Sendai Virus Proteins

The elution patterns obtained after chromatography of the mixture of Sendai virus proteins are shown in Fig. 1–4. Fig. 1 shows the separation obtained with an extract that

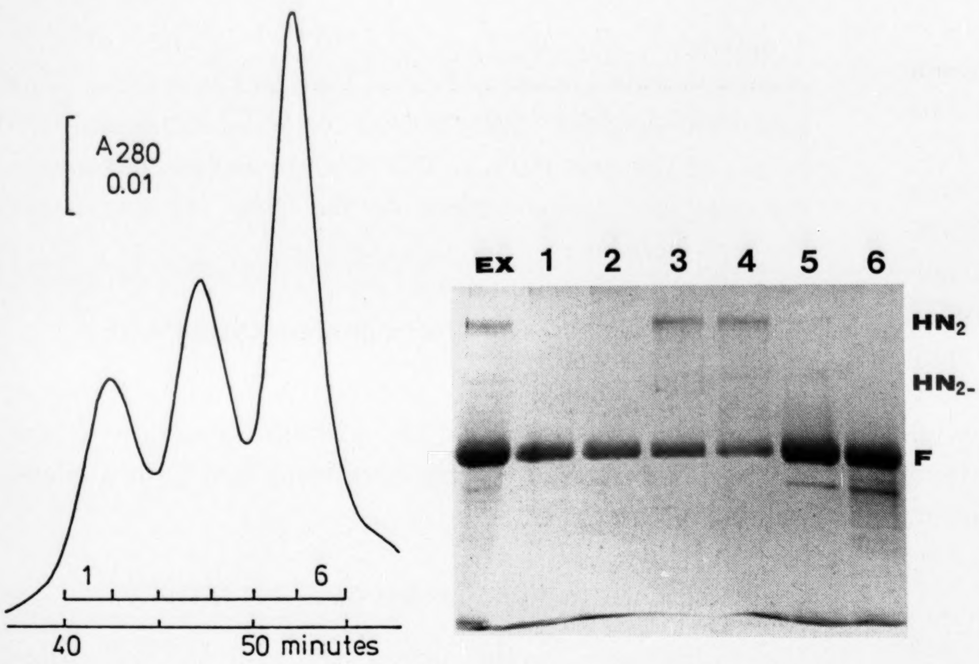

Fig. 1

Size-exclusion HPLC of Sendai virus membrane proteins on two tandemly-linked Superose-6 (300 X 10 mm i.d.) columns. The column was eluted with 0.1% SDS in 50 mM sodium phosphate, pH 6.5 at a flow-rate of 0.5 ml/min. The absorbance was monitored at 280 nm. Fractions (1–6) were analyzed on 8% SDS-gels. EX, the Sendai virus extract. The positions of the HN$_2$, HN$_2$– and the F protein are indicated.

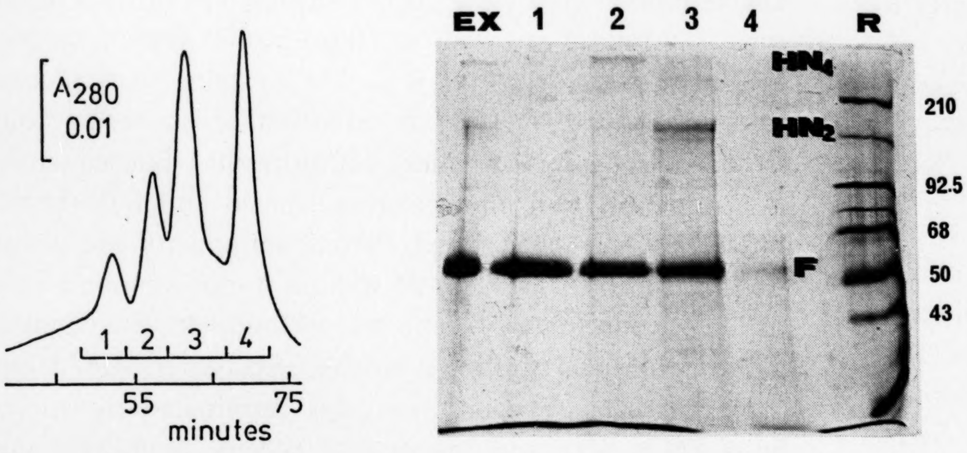

Fig. 2

Size-exclusion HPLC of Sendai virus membrane proteins on two tandemly-linked Superose-6 (300 X 10 mm i.d.) columns. The column was eluted with 0.05% sarkosyl in 10 mM Tris-HCl, pH 7.5 containing 0.6 M NaCl at a flow-rate of 0.5 ml/min. The absorbance was monitored at 280 nm. Fractions (1–4) were analyzed on 8% SDS-gels. EX, the Sendai virus extract. The positions of the HN$_4$, HN$_2$, and the F protein are indicated. R, reference proteins, of which the molecular weight is indicated in kilodaltons.

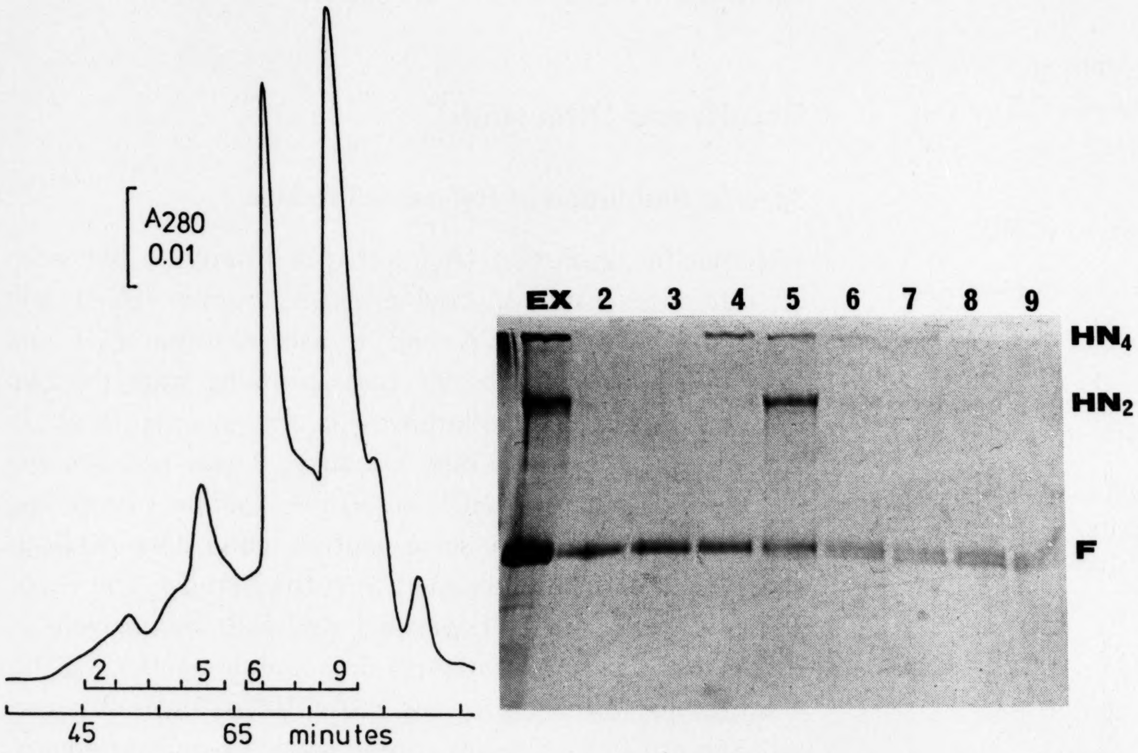

Fig. 3

Size-exclusion HPLC of Sendai virus membrane proteins on two tandemly-linked Superose-6 (300 X 10 mm i.d.) columns. The column was eluted with 0.1% LDAO in 50 mM sodium phosphate, pH 6.5 at a flow-rate of 0.5 ml/min. The absorbance was monitored at 280 nm. Fractions (2–9) were analyzed on 8% SDS-gels. EX, the Sendai virus extract. The positions of the HN$_4$, HN$_2$ and the F protein are indicated.

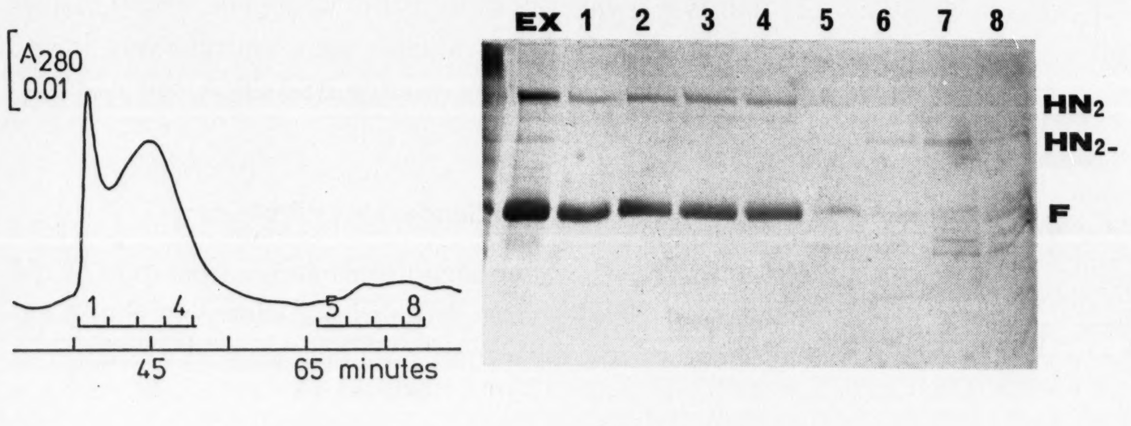

Fig. 4

Size-exclusion HPLC of Sendai virus membrane proteins on two tandemly-linked Superose-6 (300 X 10 mm i.d.) columns. The column was eluted with 0.1% octylglucoside in 50 mM sodium phosphate, pH 6.5 at a flow-rate of 0.5 ml/min. The absorbance was monitored at 280 nm. Fractions (1–8) were analyzed on 8% SDS-gels. EX, the Sendai virus extract. The positions of the HN$_2$, HN$_2$– and the F protein are indicated.

was eluted with 0.1% SDS in 50 mM sodium phosphate, pH 6.5. This extract and that with 0.1% octylglucoside (Fig. 4, EX) contain less HN_4 protein than those containing 0.05% sarkosyl and 0.1% LDAO (Fig. 2, 3, EX). The reason for this is not entirely clear, although conversion to the HN_{2-} form (see below) by limited proteolysis during pretreatment prior to injection may play a role. Fractions 3 and 4 contain the HN_2 protein and starting from fraction 4, a small amount of HN_{2-} is found. All fractions do contain the F protein, suggesting that large micellar complexes containing the F protein were separated on the column. When 0.05% sarkosyl is used in the eluent, the elution pattern shown in Fig. 2 is obtained. The profile consists of 4 relatively sharp peaks which all contained the F protein. In peak 2 and 3, the HN_4 and HN_2 proteins were present, respectively. This means that peaks 1 and 4 contain relatively pure F protein. Lauryldimethylamineoxide (LDAO) is a detergent with some special features. It is a non-ionic detergent above neutral pH and below pH 3 it is in its cationic form [22]. We have used this detergent at pH 6.5, where it will be largely non-ionic. The elution pattern is shown in Fig. 3. Relatively sharp peaks were obtained, most of which contained F protein, while the HN_4 protein was present in peaks 4 and 5 and the HN_2 protein in peak 5 only.

Elution with buffers containing the other additives, 0.1% Brij 35, 0.03% Tween-20, 0.1% octylglucoside, 0.1% decylpolyethyleneglycol-300, 0.25% CHAPS and 20% acetonitrile did not give satisfactory results. With CHAPS and acetonitrile in the eluent, only one peak in the void volume of the column was obtained and SDS-PAGE showed that the mixture of Sendai virus proteins eluted as one large complex (not shown). Fig. 4 shows the elution pattern obtained when 0.1% octylglucoside is present in the eluent. The pattern obtained with decylpolyethyleneglycol-300, Brij 35 and Tween-20 was similar. The mixture of proteins was eluted from the column in 2 peaks and the fractions 1–4 had almost the same composition as the starting mixture except for a polypeptide with a molecular weight of 110 kilodaltons, which was eluted as a broad peak (fractions 6–8) with a retention time of 70–80 min. In a separate experiment, a protein of the same molecular weight was purified by ion-exchange HPLC that strongly reacted with a monoclonal antibody directed against HN (unpublished results). Presumably, this polypeptide is a dimer of a truncated form i.e. without the hydrophobic transmembrane spanning region. Without this region, the protein is less hydrophobic and is not present in large micelles composed of detergent and protein molecules.

Table II. Immunological activity of Sendai virus membrane protein fractions after size-exclusion HPLC in different eluents.

0.1% SDS in 50 mM sodium phosphate, pH 6.5 (Fig. 1)	
fraction	optical density at 492 nm
1	0.50
2	0.57
3	0.51
4	0.40
5	0.98
6	1.06
0.05% sarkosyl in 10 mM Tris-HCl, pH 7.5 with 0.6 M NaCl (Fig. 2)	
1	1.54
2	0.86
3	1.16
4	< 0.2
0.1% LDAO in 50 mM sodium phosphate, pH 6.5 (Fig. 3)	
2 + 3	< 0.2
4	< 0.2
5	< 0.2
6	< 0.2
7	< 0.2
9	< 0.2
0.1% octylglucoside in 50 mM sodium phosphate, pH 6.5 (Fig. 4)	
1	> 2.0
2	> 2.0
3	> 2.0
4	> 2.0

Immunological Activity

Antibodies directed against intact protein can be used to probe intactness of protein structure after chemical modification or exposure to harsh elution conditions or pretreatment. Table II shows data on the reactivity of antibodies directed against intact Sendai virus proteins after size-exclusion HPLC with the eluents listed in Table I. SDS does affect the immunological activity to some extent, but a considerable part of the proteins remains intact and still reacts with the antiserum. This is even more so when the proteins are eluted with a buffer containing sarkosyl. This anionic detergent differs only from SDS with respect to the hydrophilic part of the molecule, methylglycine instead of sulphate in SDS. It has been noted before that in contrast to SDS, sarkosyl does not denature certain membrane proteins [23]. LDAO appears to affect the immunological activity, although it is a non-ionic detergent and this group of detergents is commonly found to be mild [19, 20]. When an eluent with octylglucoside is used, the immunological activity is not affected. One of the reasons is almost certainly that this detergent did not disrupt the micellar aggregate of membrane proteins and detergent molecules thereby maintaining a conformation resembling that in the native structure. Residual LDAO present in freeze-dried peak fractions may have interfered with the immunological procedure. Fractions were dialyzed overnight against water, lyophilized and the residue was dissolved in ELISA coating buffer (5 μg protein per 100 μl). Depending on the volume and the amount of protein in the fraction, this will result in relatively high concentrations of detergent in the sample for the ELISA. Except for octylglucoside, most detergents will then have concentrations above the CMC and will be concentrated together with the protein. This means that the fractions may contain up to 0.14% SDS, 0.25% sarkosyl and 0.5% LDAO. In a separate experiment we incubated the mixture of Sendai virus proteins (56 μg/100 μl) for 20 min in the eluent i.e. in 0.1% SDS, 0.05% sarkosyl, 0.1% LDAO and 0.1% octylglucoside. The samples were serially diluted in coating buffer and investigated in the ELISA. The immunological activity (optical density at 492 nm) of 15 ng of Sendai virus protein mixture in SDS, sarkosyl, LDAO and octylglucoside, was 0.30, 0.45, 0.31 and 0.41, respectively. Apparently the high concentration of LDAO in the fractions prevented coating in the ELISA, resulting in optical density values below 0.2. These results show that depending on the ultimate use of the protein, various eluents may be useful for a size-exclusion HPLC step in a purification procedure. An anionic detergent precludes subsequent use of ion-exchange HPLC. Proteins are still immunologically active indicating that a considerable part of the conformation of the protein remains intact. Sarkosyl is a relatively mild ionic detergent. Immunological activity is not affected but only the F protein can be purified in this way (Fig. 2). Many of the other eluents may be combined with subsequent ion-exchange HPLC and especially LDAO is promising in this respect (Fig. 3), although the effect of this detergent on the immunological activity needs further investigation.

Finally, the results show that the best separations were obtained with eluents containing the detergent at a concentration above the CMC (Table I). However, this does not necessarily mean that efficient separations are always obtained when the detergent is used at such a concentration, as was shown by the results obtained with 0.1% Brij 35 and 0.1% decylpolyethyleneglycol in the eluent.

References

[1] *G. W. Welling, R. van der Zee, S. Welling-Wester*, J. Chromatogr. **418**, 223 (1987).

[2] *G. W. Welling, K. Slopsema, S. Welling-Wester*, J. Chromatogr. **397**, 165 (1987).

[3] *G. W. Welling, R. van der Zee, S. Welling-Wester*, Trends Anal. Chem. **5**, 225 (1986).

[4] *G. Winkler, F. X. Heinz, C. Kunz*, J. Chromatogr. **297**, 63 (1984).

[5] *R. C. Montelaro, M. West, C. J. Issel*, Anal. Biochem. **114**, 398 (1981).

[6] *G. W. Welling, J. R. J. Nijmeijer, R. van der Zee, G. Groen, J. B. Wilterdink, S. Welling-Wester*, J. Chromatogr. **297**, 101 (1984).

[7] *K. Kita, H. Murakami, H. Oya, Y. Anraka*, Biochem. Int. **10**, 319 (1985).

[8] *D. J. McKean, M. Bell*, Protides Biol. Fluids **30**, 709 (1982).

[9] *D. H. Calam, J. Davidson*, J. Chromatogr. **296**, 285 (1984).

[10] *R. S. Matson, S. C. Goheen*, J. Chromatogr. **359**, 285 (1986).

[11] *L. J. DeLucas, D. D. Muccio*, J. Chromatogr. **296**, 121 (1984).

[12] *P. Tempst, D. D.-L. Woo, D. B. Teplow, R. Aebersold, L. Hood, S. B. H. Kent*, J. Chromatogr. **359**, 403 (1986).

[13] *P. Lambotte, J. Van Snick, T. Boon*, J. Chromatogr. **297**, 139 (1984).

[14] *T. Nakagawa, K. Shinoda*, in "Colloidal Surfactants", *E. Hutchinson* and *P. van Rysselberghe*, eds., Academic Press, New York, 1963; p. 97.

[15] *M. Grabo*, Thesis, University Basel, 1982.

[16] *U. K. Laemmli*, Nature (London), **227**, 680 (1970).

[17] *W. Wray, T. Boulikas, V. P. Wray, R. Hancock*, Anal. Biochem. **118**, 197 (1981).

[18] *G. W. Welling, K. Slopsema, S. Welling-Wester*, J. Chromatogr. **359**, 307 (1986).

[19] *A. Helenius, D. R. McCaslin, E. Fries, C. Tanford*, Meth. Enzymol. **56**, 734 (1979).

[20] *A. Helenius, K. Simons*, Biochim. Biophys. Acta **415**, 29 (1975).

[21] *L. M. Hjelmeland, A. Crambach*, Meth. Enzymol. **104**, 305 (1984).

[22] *K. W. Herrmann*, J. Phys. Chem. **66**, 295 (1962).

[23] *H. Wroblewski, R. Burlot, K.-E. Johansson*, Biochimie **60**, 389 (1978).

Received: June 29, 1987
Accepted: July 23, 1987
F

HPLC of 9-Fluorenylmethylchloroformate-Polyamine Derivatives with Fluorescence Detection

J. R. Price/P. A. Metz[1]/H. Veening*

Department of Chemistry, Bucknell University, Lewisburg, PA 17837, USA

[1] Lonza Inc., 3500 Trenton Avenue, Williamsport, PA 17701, USA

Key Words

Pre-column derivatization
9-Fluorenylmethylchloroformate (FMOC)
Fluorescence detection
Hydrolyzed serum

Summary

There are a number of reagents available for fluorescent labelling of primary amines. These include dansyl chloride, o-phthalaldehyde, fluorescamine, and a new reagent, 9-fluorenylmethylchloroformate (FMOC), reported recently. This paper describes a reversed-phase HPLC procedure for the separation and fluorescence detection of polyamines following pre-column derivatization with FMOC. The polyamines studied by this method include putrescine, cadaverine, spermidine, and spermine. Experiments were carried out to determine maximum fluorescence excitation and emission wavelengths, optimum reaction pH, linear ranges, and minimum detection limits for each of the polyamines. The HPLC method includes a gradient program which provides complete separation from serum hydrolysate components and specificity for the four polyamines with detection limits ranging from 2 to 9 pg. This procedure was applied to hydrolyzed serum samples.

Introduction

During recent years there has been much interest in the physiological and clinical significance of certain polyamines. Although the exact biological role of these compounds has not been fully elucidated, elevated levels of polyamines are associated with rapid regeneration or regrowth of tissue [1]. High levels of polyamines in urine of diagnosed cancer patients have been reported [2, 3]. Polyamines have also been reported in synovial fluid [3], serum [3, 4], and various tissues [5].

Methods of analysis for biogenic amines include enzymatic assay [6], thin-layer chromatography [7], gas chromatography [8], ion-exchange [9, 10], and more recently, reversed-phase high-performance liquid chromatography (HPLC) including pre-column [4, 5, 11, 12] and post-column [3] derivatization.

A new pre-column derivatizing reagent, 9-fluorenylmethylchloroformate (FMOC) has been used successfully for HPLC separations and assay of amino acids using fluorescence detection [13–15]. FMOC reacts with both primary and secondary amines under basic conditions to produce a highly fluorescent derivative. Einarsson et al., report the fluorescence excitation and emission maxima of the derivatives to be 260 and 310 nm, respectively [13–15].

This paper describes a sensitive and specific reversed-phase HPLC separation of FMOC derivatives of the clinically important polyamines, putrescine (PUT), cadaverine (CAD), spermidine (SPD) and spermine (SPM). The structures of these compounds in their unprotonated forms are shown in Table I.

Table I. Polyamine structures

Name	(Abbreviation)	Structures
Putrescine	(PUT)	$H_2N(CH_2)_4NH_2$
Cadaverine	(CAD)	$H_2N(CH_2)_5NH_2$
Spermidine	(SPD)	$H_2N(CH_2)_3NH(CH_2)_4NH_2$
Spermine	(SPM)	$H_2N(CH_2)_3NH(CH_2)_4NH(CH_2)_3NH_2$

0009-5893/87 0795-05 $03.00/0

© 1987 Friedr. Vieweg & Sohn Verlagsgesellschaft mbH

Experimental

Reagents and Chemicals

Polyamines were obtained as the hydrochloride salts from Sigma Chemical Company (St. Louis, MO 63178, USA) and were used without further purification. The derivatizing reagent, 9-fluorenylmethylchloroformate (FMOC), was purchased from Fluka AG (Buchs, Switzerland). Reagent-grade sodium bicarbonate and HPLC-grade acetonitrile were purchased from J. T. Baker (Phillipsburg, NJ 08865, USA), HPLC-grade water was produced in-house and was used in all experiments.

Apparatus

The binary chromatographic system consisted of two Model 6000A pumps (Waters Associates, Milford, MA 01757, USA) with a model 660 solvent programmer (Waters). The sample injector was a model 7010 (Rheodyne Inc., Cotati, CA 94928, USA) with a 20-μL loop. The analytical column was 15 x 0.46 cm (I.D.) packed with 5 μm particles of end-capped C_{18} (Varian, Inc., Walnut Creek, CA 94598, USA). Fluorescence detection was achieved with a Model FS-970 (Schoeffel, Division of Kratos, Westwood, NJ 07675, USA). The wavelength of excitation was set at 265 nm and fluorescence emission was monitored through either 340 or 440 nm cut-off filters (Kratos).

Chromatograms were recorded with a Spectra-Physics Model SP4270 integrator (Spectra-Physics, Santa Clara, CA 95051, USA).

Separation of the polyamine-FMOC derivatives was achieved with an aqueous (pH 6.1)/acetonitrile gradient of 60% to 100% in 20 min at a flow rate of 1.0 mL min^{-1}.

Pre-Column Derivatization

To 400 μL of polyamine-containing sample was added 100 μL of bicarbonate/carbonate buffer (pH 8.5) and 500 μL of 5.8 mM FMOC in HPLC-grade acetonitrile. The mixture was gently swirled for 30 seconds prior to injection.

In certain instances the effluent from the column containing the desired fraction was collected for further spectral studies. This was done by derivatizing 1.0 μg of polyamine with excess FMOC and collecting the eluted derivative in six successive runs, for the duration of full-scale detector response.

Preparation of Serum Samples

Serum samples (taken from healthy patients) were hydrolyzed in 6 M HCl for 14 h following a procedure published previously [10]. This was done to ensure the release of protein-bound polyamines prior to analysis [16]. The resulting hydrolysate was evaporated to dryness under vacuum at a temperature of 60 °C. The residue was neutralized with dilute KOH, re-evaporated and diluted with HPLC-grade water. A 100-μL aliquot of this solution was added to 400 μL of bicarbonate buffer. The mixture was centrifuged for 10 min at 3200 RPM and filtered through an LID/X 0.45-μm filter (Xydex Corp., Bedford, MA 01730, USA) prior to derivatization. Spiked serum samples were prepared by adding known amounts of each polyamine prior to hydrolysis.

Results and Discussion

Fig. 1 shows the fluorescence excitation and emission spectra obtained for six collected fractions of the PUT–FMOC derivative. Similar spectra were recorded for the CAD, SPD, and SPM derivatives. While the excitation and emission wavelength maxima for the polyamine-FMOC derivatives are in agreement with those previously reported for the amino acid derivatives these compounds display a unique secondary emission band from 580 to 680 nm. This previously unreported emission permits the choice of an additional (optional) HPLC fluorescence detection wavelength and adds a distinct selectivity advantage to this method.

The reaction of FMOC with polyamines was found to be pH dependent. The optimum reaction pH was determined for each eluted polyamine derivative by measuring the fluorescence intensity (using the HPLC detector) as a function of reaction pH (Fig. 2). These experiments were carried out at λ_{exc} = 265 nm and $\lambda_{em} > 440$ nm. From this study, a reaction pH of 8.5 was chosen for analytical work. At higher pH values it is possible that the hydrolysis of FMOC is favored; whereas, in more acidic solutions, excessive polyamine protonation may prevent complete derivatization.

Chromatograms for the separation of standard mixtures of the four polyamines are shown in Fig. 3 and 4. Fluorescence emission was monitored with 440 and 340 nm cut-off filters, respectively. Under the gradient conditions used, the four polyamine derivatives are completely resolved, with the PUT and CAD derivatives exhibiting a resolution of 0.98 or greater. The analyte derivatives are also separated from hydrolyzed FMOC and other reaction by-products. It can be seen from Fig. 4 that many more unknown peaks appear at $\lambda_{em} > 340$ nm.

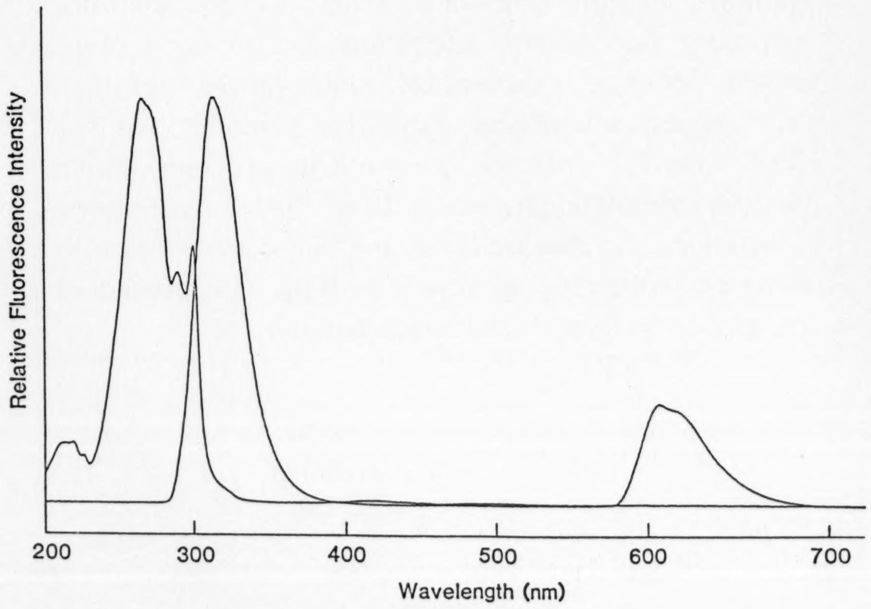

Fig. 1

Fluorescence excitation and emission spectra of eluted PUT-FMOC. (6.0 μg PUT with excess FMOC injected).

A study of average peak height as a function of the amount of each polyamine used was performed. Fig. 5 and 6 show excellent linear response from 800 to well below 1 ng at emission cut-off wavelengths of 440 and 340 nm, respectively. In each case, linear regression plots are presented with r^2 values ranging from 0.994 to 0.999.

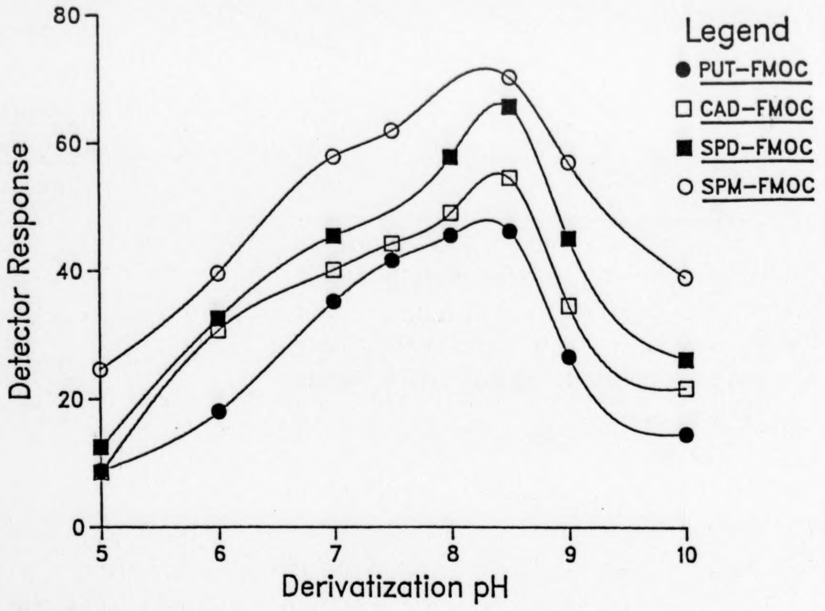

Fig. 2

Detector response vs. pH for eluted polyamine-FMOC derivatives. (CAD, SPD and SPM curves are off-set.)

λ_{exc} = 265 nm
$\lambda_{em} > 440$ nm.

Fig. 7A and 7B represent chromatograms of hydrolyzed serum samples, one of which (B) is spiked with known amounts of each polyamine. Fig. 7B shows the polyamine derivatives completely resolved from FMOC and FMOC-derivatized amino acids residues. It was found, however, that fluorescence detection at $\lambda_{em} > 440$ nm (Fig. 3) is more selective than at $\lambda_{em} > 340$ nm (Fig. 4). Interference from natively fluorescing compounds or other FMOC-derivatized products is minimized at the former wavelength.

Detection of polyamine-FMOC derivatives space at $\lambda_{em} >$ 440 nm, while offering greater selectivity, is inherently less sensitive. Table II and III list the limits of detection for the derivatives at emission cut-off wavelengths of 440 nm and 340 nm, respectively. Relative precision data are also reported. The picogram detection limits found are comparable to those previously reported for amino acid-FMOC derivatives [13–15] and are adequate for clinical purposes [17].

Since FMOC has been reported to react with both primary and secondary amines [18], it is possible that single or multiple derivatizations may occur with polyamines. It is yet to be determined if the current reaction conditions lead to multiple derivatization. Experiments are currently under way to isolate, identify and characterize polyamine-FMOC derivatives.

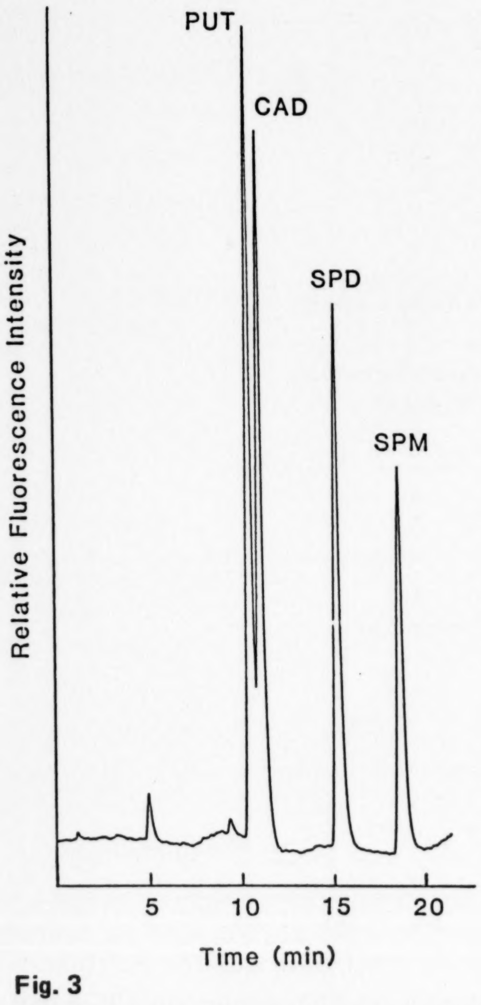

Fig. 3

Chromatogram for FMOC derivatives of PUT, CAD, SPD and SPM. (0.5 μg of each polyamine.)

Flow rate: 1.0 mL $\min^{-1}$; Column: 15 × 0.46 cm C_{18} (end capped); Gradient: 60 to 100 % water-acetonitrile in 20 min.

λ_{exc} = 265 nm
$\lambda_{em} > 440$ nm.

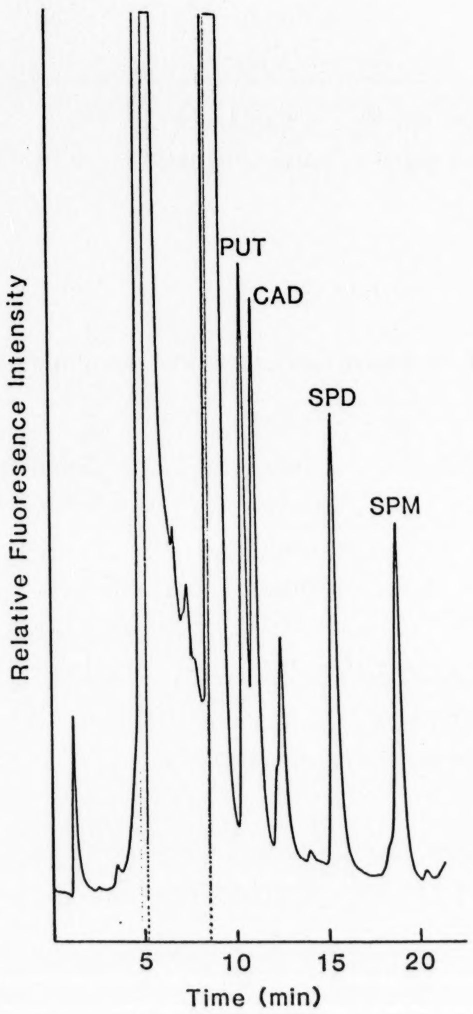

Fig. 4

Chromatogram for FMOC derivatives of PUT, CAD, SPD and SPM. (10 ng of each polyamine.)

λ_{exc} = 265 nm
$\lambda_{em} > 340$ nm

All other conditions the same as in Fig. 3.

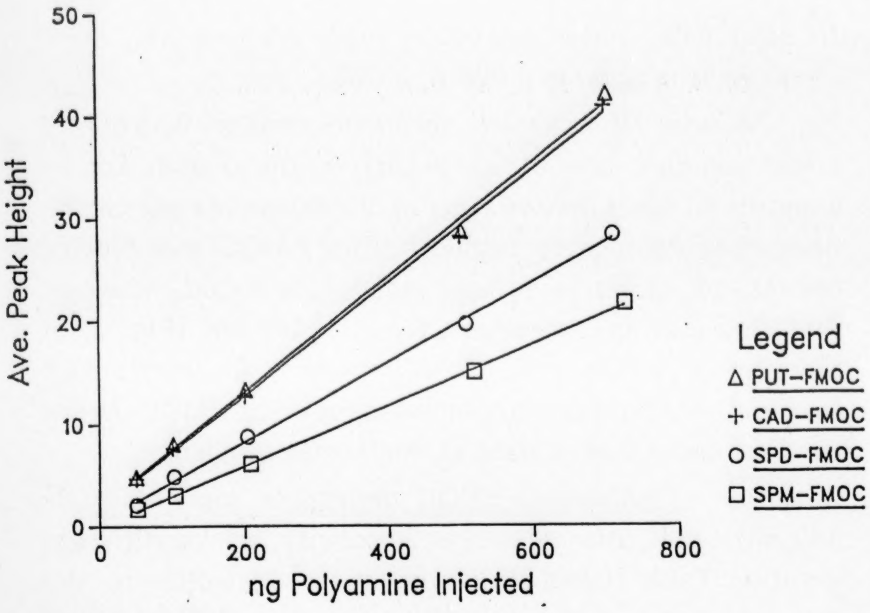

Fig. 5

Average peak height vs. ng polyamine injected.
$\lambda_{exc} = 265$ nm
$\lambda_{em} > 440$ nm.

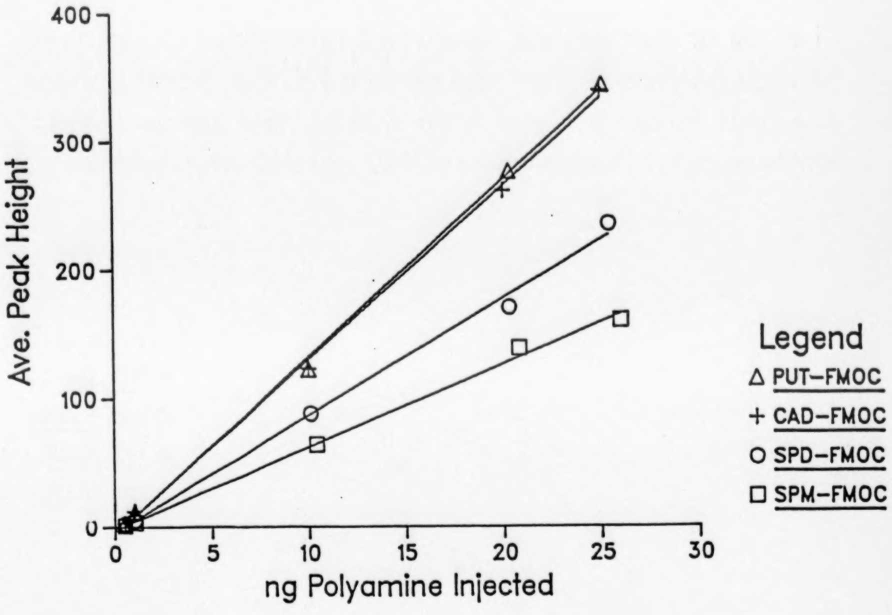

Fig. 6

Average peak height vs. ng polyamine injected.
$\lambda_{exc} = 265$ nm
$\lambda_{em} > 340$ nm.

Table II. Quantitative reproducibility and minimum detection limits for polyamine FMOC-derivatives*

Compound	Amount Injected (ng)	Number of Samples Analyzed	Coefficient of Variation Peak height	Minimum Detection Limit** (ng)
PUT	502	5	0.9	2
CAD	500	5	1.1	2
SPD	508	5	0.8	3
SPM	519	5	2.0	4

* $\lambda_{exc} = 265$ nm; $\lambda_{em} > 440$ nm
** Based on a signal-to-noise ratio of 3:1

Table III. Quantitative reproducibility and minimum detection limits for polyamine-FMOC derivatives*

Compound	Amount Injected (ng)	Number of Samples Analyzed	Coefficient of Variation Peak height	Minimum Detection Limit** (pg)
PUT	5.02	7	0.7	4
CAD	5.00	7	0.6	9
SPD	5.08	7	0.7	7
SPM	5.19	7	1.4	7

* $\lambda_{exc} = 265$ nm; $\lambda_{em} > 340$ nm
** Based on a signal to noise ratio of 3:1

Conclusions

HPLC analysis of FMOC-polyamine derivatives with fluorescence detection is highly sensitive and selective. The limits of detection and linear ranges of the polyamine derivatives reported in this paper compare favorably with previously published data. The derivatization procedure is rapid and simple and HPLC analysis time is less than 30 min, making this method attractive for biomedical studies.

Acknowledgment

Acknowledgment is made to the Donors of the Petroleum Research Fund, administered by the American Chemical Society, for the support of this research. The authors are grateful to American Home Foods Products, Inc. (Milton, PA, USA) for technical assistance and support, and to Dr. Richard C. Simpson of Merck Sharp and Dohme Laboratories for running fluorescence spectra.

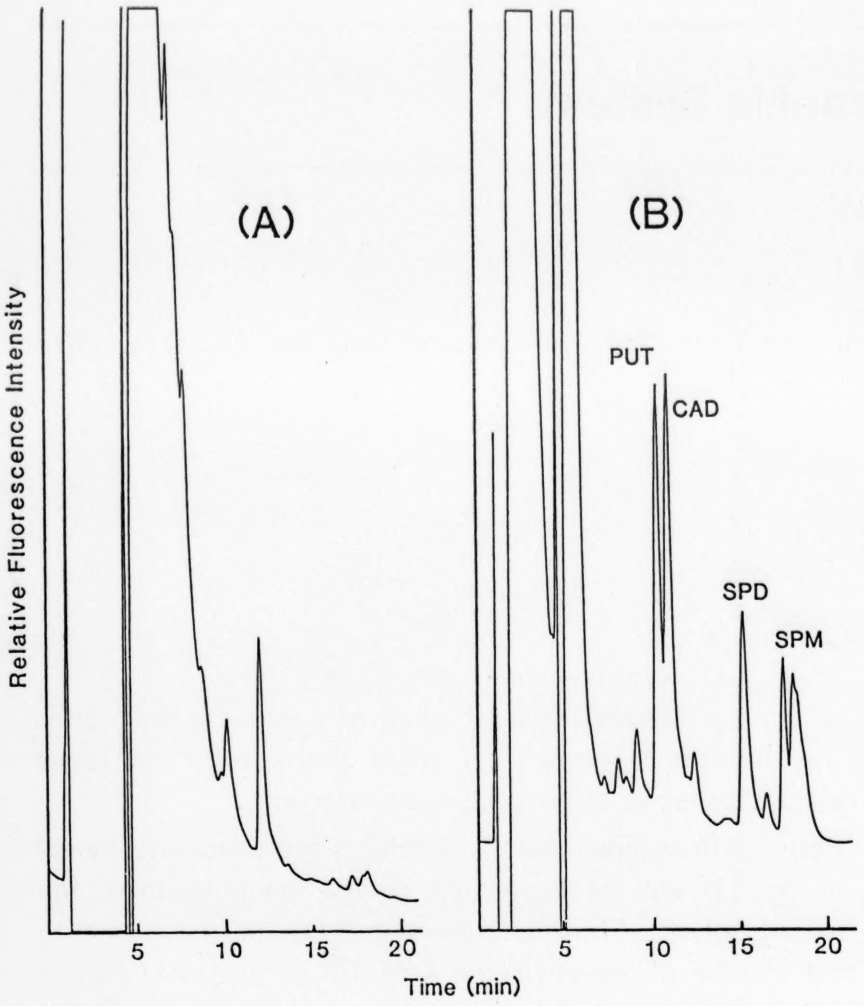

Fig. 7

(A) Chromatogram for hydrolyzed serum.

(B) Chromatogram for hydrolyzed serum spiked with 30 ng of each polyamine

$\lambda_{exc} = 265$ nm

$\lambda_{em} > 340$ nm .

All other conditions the same as in Fig. 3.

Reference

[1] *D. H. Russell, B. G. M. Durie,* Progress in Cancer Research and Therapy, Vol. 8, Polyamines as Biochemical Markers of Normal and Malignant Growth, Raven Press, New York 1978, p. 170.

[2] *D. H. Russell,* Nature New Biology, **233**, 144–145 (1971).

[3] *R. C. Simpson, H. Y. Mohammed, H. Veening,* J. Liq. Chromatogr., **5**, 245–264 (1982).

[4] *N. D. Brown, M. P. Strickler, J. M. Whaun,* J. Chromatogr., **245**, 101–108 (1982).

[5] *R. F. Minchin, G. R. Hanau,* J. Liq. Chromatogr., **7** 2605–2610 (1984).

[6] *J. M. Tiller, D. L. Bloxam,* Anal. Biochem., **131**, 426–429 (1983).

[7] *T. Kremmer, L. Holczinger, M. Boldizsár, L. Selmeci, S. Bardócz,* J. Chromatogr., **286**, 371–379 (1984).

[8] *M. Dalene, T. Lundh, L. Mathiasson,* J. Chromatogr., **322**, 169–176 (1985).

[9] *N. Sayem-el-Daher, R. E. Simard, L. L'Heureux, A. G. Roberge,* J. Chromatogr., **256**, 313–321 (1983).

[10] *H. Veening, W. W. Pitt, G. Jones,* Jr., J. Chromatogr., **90**, 129–139 (1974).

[11] *T. Skaaden, T. Greibokk,* J. Chromatogr., **247**, 111–122 (1982).

[12] *K. Samejima,* J. Chromatogr., **96**, 250–254 (1974).

[13] *S. Einarsson, B. Josefsson, S. Lagerkvist,* J. Chromatogr., **282**, 609–618 (1983).

[14] *S. Einarsson, B. Josefsson, P. Möller, D. Sanchez,* Anal. Chem., **59**, 1191–1195 (1987).

[15] *S. Einarsson, S. Folestad, B. Josefsson, S. Lagerkvist,* Anal. Chem., **58**, 1638–1643 (1986).

[16] *D. H. Russell, S. D. Russell,* Clin. Chem., **21**, 860–863 (1975).

[17] *D. H. Russell, B. G. M. Durie,* Progress in Cancer Research and Therapy, Vol. 8, Polyamines as Biochemical Markers of Normal and Malignant Growth, Raven Press, New York 1978, pp. 128–134.

[18] *L. A. Carpino, G. Y. Han,* J. Org. Chem., **37**, 3404–3409 (1972).

Received: June 30, 1987
Accepted: Aug 28, 1987
F

Selectivity in a Liquid-Solid Chromatographic System

S. M. Petrović*/S. Lomić/I. Šefer

Institute of Microbiological Processes and Applied Chemistry, Faculty of Technology, University of Novi Sad, 21000 Novi Sad, Yugoslavia

Key Words

Column liquid-solid chromatography
Selectivity
Mobile phase
Stationary phase

Summary

Utilizing experimentally determined capacity ratios and "a priori" calculated activity coefficients of the solutes the selectivity of separation in a liquid-solid chromatographic system is studied. Both the experimentally determined selectivity factor (α) and the calculated selectivity factor in the mobile phase (α^m) of a solute pair fit a quadratic function of the concentration of eluting solvent components. Comparing these factors it is shown that the selectivity in the stationary phase (α^s) is fairly constant when the composition of the mobile phase is changed.

Introduction

The selectivity of a separation system is an irreplaceable factor for the calculation of the chromatographic resolution in liquid chromatography (LC). The prime intention in changing the separation system is to encrease the selectivity. The important variables for changing selectivity in liquid-solid chromatography (LSC) are the adsorbent type and the composition of the eluting solvent. As in LSC only two effective adsorbent types exist, silica and alumina, satisfactory separation is mostly achieved by changing the mobile phase composition. Selectivity factor, α, in LC for a certain support and mobile phase composition is defined as the ratio of the capacity factors, k, of two solutes. As the capacity factor of a solute in LSC has been expressed in terms of activity coefficients [1–3], the selectivity can be characterized in the following way:

$$\alpha = \frac{k_2}{k_1} = \frac{\gamma_2^m \gamma_1^s}{\gamma_1^m \gamma_2^s} = \frac{\alpha^m}{\alpha^s} \quad (1)$$

where γ is the activity coefficient of a solute in the mobile (m) and the stationary (s) phase and α is the respective selectivity factor. Solute 2 is more retained.

For a defined adsorbent and solutes the selectivity factor of eq. (1) will be dependent on the composition of the eluting solvent. There are several expressions characterizing the change of selectivity in LSC by varying the mobile phase composition. Snyder [4] defines the selectivity factor as

$$\log \frac{k_2}{k_1} = \log \alpha = a\,(\Delta S_0 - \Delta A_s \epsilon) \quad (2)$$

where a = parameter for the activity of the adsorbent, S_0 = dimensionless free energy of adsorption of a solute on an adsorbent of standard activity (a = 1), A_s = the solute molecular area occupied on the surface and ϵ = solvent strength parameter. For a binary solvent system of different component concentrations I and II the selectivity difference is

$$\log \frac{\alpha_{II}}{\alpha_I} = a\,\Delta A_s\,(\epsilon_{II} - \epsilon_I) = a\,\Delta A_s \Delta\epsilon \quad (3)$$

Subsequently, Soczewinski [5–7] derived the relationship which can be written in the following form:

$$\log k = \log k^0 - n \log \varphi \quad (4)$$

where φ = volume fraction of the more polar component in a binary solvent system, k^0 = capacity factor of a solute when φ = 1 and n = constant. The selectivity factor is then related to φ by

$$\log \frac{k_2}{k_1} = \log \alpha = \log \frac{k_2^0}{k_1^0} - (n_2 - n_1) \log \varphi = = \log \alpha^0 - \Delta n \log \varphi \quad (5)$$

Combining eqs. (2–5) Perry [8] derived an equation relating α_{II}/α_I to both Δn and $\Delta\epsilon$.

Eq. (1) offers us a possibility to examine the selectivity in the stationary phase when selectivity in the mobile phase is determined or calculated. Previously [3] activity coefficients of a solute in the mobile phase for some monofunctional benzene derivatives (benzyl acetate, acetophenone, benzyl alcohol and 1-phenylethanol) and various

0009-5893/87 0800-05 $03.00/0

© 1987 Friedr. Vieweg & Sohn Verlagsgesellschaft mbH

mobile phase compositions were calculated using the functional group contribution method (UNIFAC method [9–11]). Also, applying high-performance liquid chromatography on silica and using binary mobile phases (heptane mixed with ethyl acetate, tetrahydrofuran or 2-propanol in various proportions) the capacity factors of the mentioned solutes were determined [3]. On the basis of these data we now compare in this work the selectivity factor α of a solute pair with the selectivity factor in the mobile phase α^m, in order to examine the selectivity of separation in the stationary phase.

Experimental

All experiments and calculations of activity coefficients were performed in our previous work [3].

Results and Discussion

The respective selectivities of eq. (1) for various mobile phase compositions are presented in Table I. Selectivity factors α and α^m are calculated as k_2/k_1 and γ_2^m/γ_1^m, respectively, using data of Ref. [3]. Selectivity in the stationary phase α^s is calculated as α^m/α.

When other conditions are defined the selectivity in LSC can be controlled either by altering concentration of the eluent components or by substituting eluent components. Both approaches should lead to the change of α and α^m. As it is seen from Table I both factors α and α^m for all examined mobile phases decrease with increasing the concentration φ of the polar component in the eluent. Also, the replacement of ethyl acetate or tetrahydrofuran with the more polar solvent 2-propanol leads to the decrease of these two factors. These observations considering α have

Table I. Respective selectivity factors (α, α^m and α^s) of solute pairs for different concentrations (φ%) of the polar moderator in the binary mobile phase (Eq. 1)

φ%	Solute pair*																	
	AP/BA			BAI/BA			1-PE/BA			BAI/AP			1-PE/AP			BAI/1-PE		
	α	α^m	α^s	α	α^m	α^s	α	α^m	α^s	α	α^m	α^s	α	α^m	α^s	α	α^m	α^s
	Heptane – ethyl acetate																	
0.1	2.13	1.58	0.74															
0.3	2.10	1.58	0.75															
0.5	2.10	1.58	0.75				10.07	3.12	0.31				4.78	1.98	0.41			
1.0	2.02	1.57	0.78	14.50	4.06	0.28	9.81	3.04	0.31	7.19	2.58	0.36	4.86	1.93	0.40	1.48	1.34	0.91
2.0	1.89	1.56	0.83	13.34	3.87	0.29	9.02	2.89	0.32	7.08	2.47	0.35	4.80	1.85	0.39	1.48	1.34	0.91
4.0	1.91	1.55	0.81	11.80	3.54	0.30	8.55	2.65	0.31	6.18	2.29	0.37	4.48	1.71	0.38	1.38	1.34	0.97
6.0	1.91	1.53	0.80	11.71	3.28	0.28	8.19	2.46	0.30	6.12	2.14	0.35	4.28	1.61	0.38	1.43	1.33	0.93
8.0	1.82	1.51	0.83	10.23	3.07	0.30	6.97	2.30	0.33	5.61	2.03	0.36	3.82	1.52	0.40	1.47	1.33	0.91
10.0	1.89	1.50	0.79	9.96	2.89	0.29	6.79	2.17	0.32	5.27	1.93	0.37	3.59	1.45	0.40	1.47	1.33	0.91
12.0	1.81	1.48	0.82	9.79	2.74	0.28	6.66	2.07	0.31	5.41	1.85	0.34	3.68	1.39	0.38	1.47	1.33	0.91
14.0	1.81	1.47	0.81	9.36	2.62	0.28	6.37	1.98	0.31	5.17	1.78	0.34	3.52	1.35	0.38	1.47	1.33	0.91
	Heptane – tetrahydrofuran																	
0.1	2.22	1.58	0.71															
0.3	1.93	1.58	0.82															
0.5	2.02	1.58	0.79				10.26	3.15	0.31				5.99	1.99	0.39			
1.0	1.98	1.59	0.80	14.00	4.13	0.30	9.09	3.09	0.34	7.06	2.61	0.37	4.58	1.95	0.43	1.54	1.34	0.87
2.0	1.91	1.59	0.83	12.09	3.99	0.33	7.51	2.98	0.40	6.32	2.51	0.40	3.93	1.88	0.48	1.61	1.34	0.83
4.0	1.92	1.59	0.83	11.39	3.75	0.33	8.25	2.80	0.34	5.93	2.36	0.40	4.30	1.77	0.41	1.38	1.34	0.97
6.0	1.91	1.59	0.83	11.47	3.55	0.31	8.03	2.65	0.33	6.02	2.23	0.37	4.22	1.67	0.39	1.43	1.34	0.94
8.0	1.91	1.60	0.84	10.89	3.38	0.31	7.63	2.52	0.33	5.71	2.12	0.37	4.00	1.58	0.39	1.43	1.34	0.94
10.0	1.90	1.60	0.84	10.71	3.24	0.30	7.19	2.41	0.33	5.64	2.03	0.36	3.79	1.51	0.40	1.49	1.34	0.90
12.0	1.92	1.60	0.83	10.47	3.12	0.30	7.16	2.32	0.32	5.46	1.93	0.36	3.74	1.45	0.39	1.46	1.34	0.92
14.0	1.93	1.60	0.83	10.45	3.01	0.29	7.03	2.24	0.32	5.41	1.88	0.35	3.64	1.39	0.38	1.49	1.34	0.90
	Heptane – 2-propanol																	
0.1	1.92	1.58	0.82	13.54	4.20	0.31	11.22	3.14	0.28	7.07	2.66	0.38	5.85	1.99	0.34	1.21	1.34	1.11
0.3	1.95	1.57	0.81	12.97	4.02	0.31	10.71	3.00	0.28	6.64	2.56	0.39	5.49	1.91	0.35	1.21	1.34	1.11
0.5	2.06	1.56	0.76	12.42	3.85	0.31	10.29	2.88	0.28	6.02	2.46	0.41	4.99	1.84	0.37	1.21	1.34	1.11
1.0	1.79	1.55	0.86	9.97	3.49	0.35	7.94	2.61	0.33	5.57	2.26	0.41	4.44	1.69	0.38	1.26	1.34	1.06
2.0	1.68	1.51	0.90	8.33	2.92	0.35	6.62	2.19	0.33	4.95	1.93	0.39	3.94	1.45	0.37	1.26	1.33	1.06
4.0	1.55	1.45	0.94	7.07	2.19	0.31	5.89	1.65	0.28	4.57	1.51	0.33	3.80	1.14	0.30	1.20	1.33	1.11
6.0	1.32	1.40	1.07	5.61	1.74	0.31	4.71	1.32	0.28	4.26	1.24	0.29	3.58	0.93	0.26	1.19	1.32	1.11
8.0	1.30	1.36	1.04	5.21	1.44	0.28	4.18	1.10	0.26	4.00	1.06	0.27	3.21	0.81	0.25	1.25	1.31	1.05
10.0	1.25	1.32	1.05	4.93	1.23	0.25	4.00	0.94	0.24	3.94	0.93	0.24	3.20	0.71	0.22	1.23	1.31	1.07
12.0	1.25	1.28	1.03	4.58	1.07	0.23	4.17	0.82	0.20	3.67	0.83	0.23	3.33	0.74	0.19	1.10	1.30	1.18
14.0	1.32	1.25	0.95	4.32	0.94	0.22	3.91	0.73	0.19	3.28	0.75	0.23	2.96	0.58	0.20	1.10	1.29	1.17

* Abbreviations of the solutes: AP – acetophenone, BA – benzyl acetate, BAI – benzyl alcohol, 1-PE – 1-phenylethanol

been already stated in numerous papers (e. g. Refs. [4, 8, 12]).

For solute pairs containing the same polar functional group or functional groups of similar polarity, i. e., for the solute pairs benzyl alcohol/1-phenylethanol and acetophenone/benzyl acetate both α and α^m did not vary or varied only slightly with φ, so that they can be considered constant. In accordance with this the α^s values for these solute pairs are also constant. However, for other solute pairs (Table I) α^s is also fairly constant when φ is varied. Thus, according to eq. (1), α^m should be linearly related to α with a slope equal to α^s. Representative plots of such relationship are shown in Fig. 1. An approximately linear dependence is obtained between α^m and α. The slopes, as well as the average α^s values from Table I for each solute-pair and eluent used are presented in Table II.

Two classes of polar solvents were examined in this work: ethyl acetate and tetrahydrofuran of class P and 2-propanol of class AB [13]. The effect of the polar solvent on α^m, and consequently on α, is evident from Table I. Namely, for solvent systems containing ethyl acetate or tetrahydrofuran and for solute pairs alcohol/ester or ketone α^m at $\varphi = 0.01$ is higher by a factor of about 1.5 than at $\varphi = 0.14$. For the heptane — 2-propanol system and the same solute pairs this factor is about 3.5. In other words, the variation of the selectivity in the mobile phase with φ is more expressive in solvents of class AB than in solvents of class P, while the selectivity factor α^m of the same solute pair is higher in solvents of class P. On the other hand, it seems that the nature of the polar solvent does not affect the selectivity in the stationary phase. The selectivity factors α^s of corresponding solute pairs in systems containing solvents of class P and AB have very similar average values (Table II). Thus, the alteration of the polar solvent concentration or the change of the polar solvent or the polar solvent class will influence only the selectivity in the mobile phase. Consequently, the change of selectivity α in LSC is only the result of selectivity changes in the mobile phase.

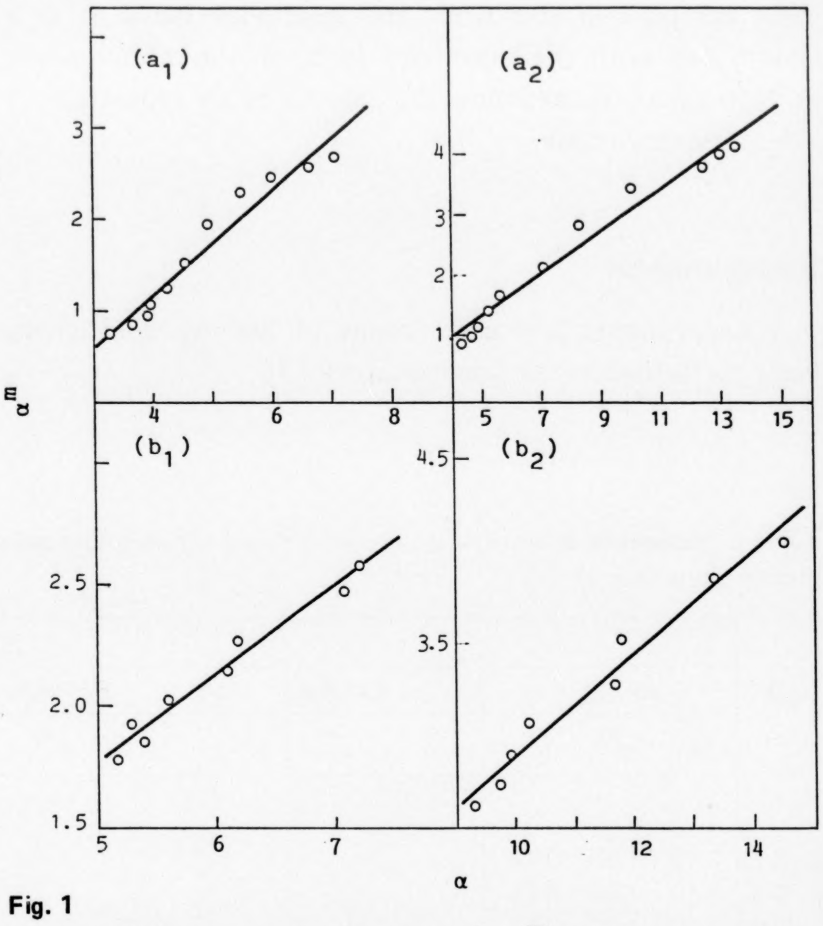

Fig. 1

Plots of the linear relationship between α^m and α values for the solute pairs benzyl alcohol/acetophenone (1) and benzyl alcohol/benzyl acetate (2) in solvent systems heptane — 2-propanol (a) and heptane — ethyl acetate (b).

Table II. Calculated α^s values for the solute pairs and mobile phases listed in Table I

	α^s					
	AP/BA	BAl/BA	1-PE/BA	BAl/AP	1-PE/AP	BAl/1-PE
	Heptane — ethyl acetate					
Mean value*	0.79 ± 0.033	0.29 ± 0.009	0.31 ± 0.009	0.36 ± 0.012	0.39 ± 0.012	0.92 ± 0.021
Slope**		0.28	0.30	0.36	0.41	
$(Q-Q')_q$***	0.76	0.28	0.31	0.35	0.40	0.91
$(Q-Q')_l$****	0.77	0.29	0.31	0.36	0.40	0.92
	Heptane — tetrahydrofuran					
Mean value	0.81 ± 0.038	0.31 ± 0.015	0.34 ± 0.026	0.37 ± 0.018	0.41 ± 0.031	0.91 ± 0.044
Slope		0.31	0.27	0.46	0.40	
$(Q-Q')_q$	0.78	0.31	0.34	0.39	0.43	0.84
$(Q-Q')_l$	0.80	0.32	0.34	0.39	0.43	0.89
	Heptane — 2-propanol					
Mean value	0.93 ± 0.11	0.29 ± 0.044	0.27 ± 0.045	0.32 ± 0.074	0.29 ± 0.072	1.10 ± 0.043
Slope		0.35	0.32	0.58	0.53	
$(Q-Q')_q$	0.79	0.32	0.29	0.41	0.37	1.11
$(Q-Q')_l$	0.95	0.34	0.31	0.40	0.37	1.11

* Mean value ± standard deviation of α^s data of Table I.

** Values calculated as the slope of Eq. 1.

*** Data calculated as Q—Q′ differences of Eqs. 7 and 9; q = quadratic

**** Data calculated as Q—Q′ differences of Eqs. 8 and 10; l = linear

Let us now consider the function between α^m and the composition of the mobile phase. It should be noted here that although α values fit rather well eq. (5) $\log \alpha^m$ is not linearly related to $\log \varphi$. Formerly, it has been argued [3] that the activity coefficient of a solute in the mobile phase is best related to φ by the following expression:

$$\ln \gamma_i^m = m\varphi^2 + p\varphi + q \tag{6}$$

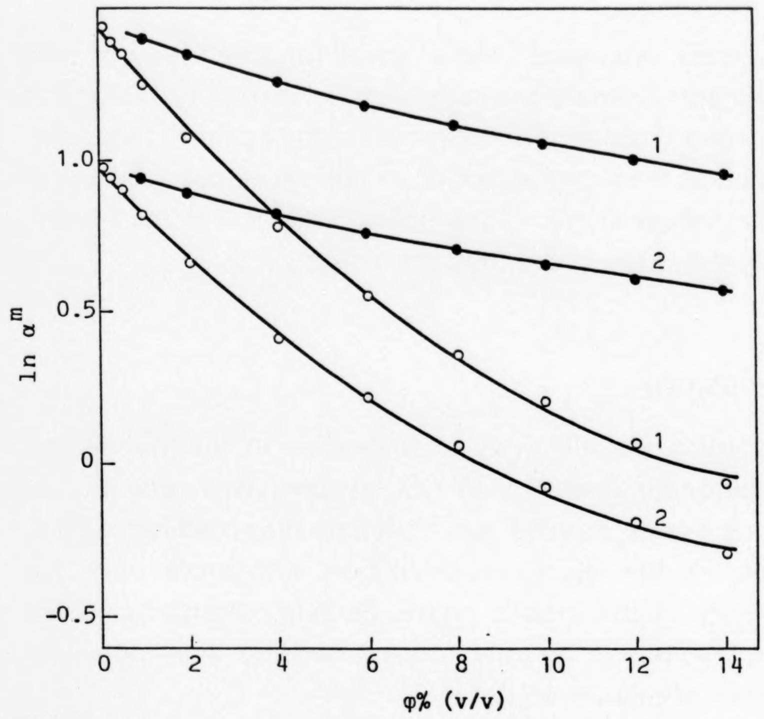

Fig. 2

Plots of the quadratic relationship between $\ln \alpha^m$ and φ (eq. 7) for the solute pairs benzyl alcohol/benzyl acetate (1) and benzyl alcohol/acetophenone (2) in solvent systems heptane – ethyl acetate (●) and heptane – 2-propanol (○).

where m, p and q are constants. Applying eq. 6 on the selectivity in the mobile phase the following relationship is obtained:

$$\ln \alpha^m = \ln \frac{\gamma_2^m}{\gamma_1^m} = (m_2 - m_1)\varphi^2 + (p_2 - p_1)\varphi + q_2 - q_1 = $$

$$= M\varphi^2 + P\varphi + Q \tag{7}$$

Values of α^m from Table I fit very well eq. (7) (Fig. 2). With a rather good approximation eq. (7) can be written in the following form:

$$\ln \alpha^m = P\varphi + Q \tag{8}$$

Combining eqs. (7) and (1) the selectivity factor in LSC can be expressed as

$$\ln \alpha = \ln \alpha^m - \ln \alpha^s = M\varphi^2 + P\varphi + Q - \ln \alpha^s = M\varphi^2 + P\varphi + Q' \tag{9}$$

and in simpler form we have

$$\ln \alpha = P\varphi + Q' \tag{10}$$

Coefficients of eqs. (7–10) are presented in Table III. Representative plots of eq. (9) are depicted in Fig. 3. Eq. (9), derived from the solubility parameter theory [14], describes well the relationship between α and φ. At the same time the accuracy of eq. (10) is approximately of the same magnitude as of eq. (5), derived from the competition theory [4–7, 13].

Eqs. (7) and (9) predict the same coefficients M and P in both relationships. Only several respective values in Table III can be considered similar, however, the prediction of α on the basis of the M and P coefficients of eq. (7) is not bad for polar solvents of class P (see Fig. 3, the dashed lines).

Table III. Coefficients of Eqs. 7–10 for the solute pairs and mobile phases listed in Table I

Solute	Eq. 7			Eq. 9			Eq. 8		Eq. 10	
pair	M	P	Q	M	P	Q′	P	Q	P	Q′
				Heptane – ethyl acetate						
AP/BA	0.75	– 0.62	0.46	9.77	– 2.33	0.74	– 0.52	0.46	– 1.07	0.72
BAI/BA	10.33	– 4.89	1.45	20.05	– 6.14	2.71	– 3.37	1.14	– 3.19	2.65
1-PE/BA	12.31	– 5.12	1.16	14.85	– 5.51	2.33	– 3.42	1.13	– 3.45	2.29
BAI/AP	10.23	– 4.31	0.99	18.24	– 5.29	2.03	– 2.82	0.67	– 2.61	1.97
1-PE/AP	10.95	– 4.41	0.70	7.67	– 3.68	1.61	– 2.89	0.67	– 2.62	1.59
BAI/!-PE	0	0	0.29	3.69	– 0.39	0.38	0	0.29	0.15	0.37
				Heptane – tetrahydrofuran						
AP/BA	0.10	0.08	0.46	11.17	– 1.89	0.71	0.01	0.46	– 0.04	0.68
BAI/BA	6.30	– 3.34	1.45	20.14	– 4.74	2.63	– 2.42	1.43	– 1.78	2.56
1-PE/BA	8.92	– 3.79	1.17	17.05	– 4.46	2.25	– 2.50	1.14	– 2.10	2.21
BAI/AP	7.26	– 3.61	0.99	13.34	– 3.61	1.94	– 2.54	0.97	– 1.65	1.90
1-PE/AP	7.06	– 3.66	0.71	7.98	– 2.95	1.56	– 2.68	0.69	– 1.85	1.53
BAI/!-PE	0	0	0.29	16.90	– 2.76	0.47	0	0.29	– 0.28	0.41
				Heptane – 2-propanol						
AP/BA	3.71	– 2.12	0.46	42.98	– 9.05	0.70	– 1.45	0.43	– 0.27	0.48
BAI/BA	51.37	– 17.65	1.43	73.45	– 17.71	2.56	– 11.00	1.34	– 8.20	2.43
1-PE/BA	50.27	– 17.23	1.14	85.47	– 18.63	2.36	– 10.50	1.05	– 7.58	2.22
BAI/AP	45.23	– 15.20	0.97	31.17	– 8.72	1.86	– 9.35	0.90	– 4.69	1.81
1-PE/AP	46.84	– 15.13	0.68	42.34	– 9.58	1.67	– 9.07	0.60	– 4.10	1.60
BAI/1-PE	– 1.58	– 0.07	0.29	– 11.17	0.85	0.19	– 0.28	0.29	– 0.59	0.21

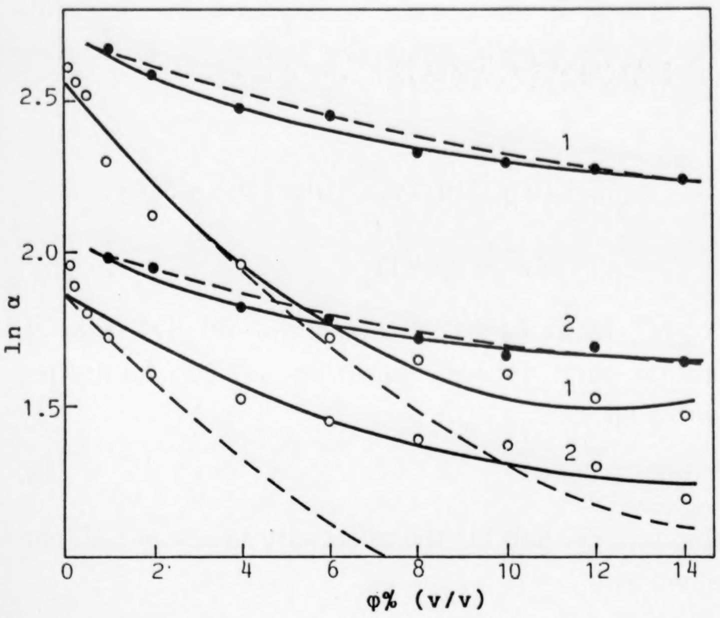

Fig. 3

Plots of the quadratic relationship between ln α and φ (eq. 9) for the solute pairs and solvent systems indicated in Fig. 2. Dashed lines are constructed by using the coefficients of eq. 7 listed in Table III.

On the other hand, predicted α values for mobile phases containing 2-propanol deviate significantly from the experimental data, especially for higher φ values, as a consequence of significant variation in the α^s values around the mean value (12–25%) in comparison with variations obtained for systems containing solvents of class P (2.6–7.6%). However, the $Q-Q'$ differences of both eqs. (7) and (9) and eqs. (8) and (10), presented also in Table II, accurately predict the mean α^s values, much better than the slope of eq. (1).

Thus, on the basis of data presented in Table II it may be concluded that selectivity in the stationary phase of a LSC system depends merely on the nature of the compared solutes. For example, the examined alcohols possess the same functional group in different positions, thus the polarity difference between them is small and α^s is approximately equal to unity. For the acetophenone/benzyl acetate pair the polarity difference is not high and α^s is approximately equal to 0.8. For the other examined pairs the polarity difference increases and α^s decreases; e.g., for the benzyl alcohol/benzyl acetate and benzyl alcohol/acetophenone pairs the α^s values are about 0.3 and 0.4, respectively. Generally, it can be concluded that for a more polar solute/less polar solute pair α^s will vary between zero and unity. As the polarity difference between two solutes increases α^s will approach zero. This assumption has been also checked by data from the literature [15] (adsorbent: silica, mobile phase: 2,2,4-trimethylpentane-1-butanol). Comparing experimental α and calculated α^m values for the solute pairs phenol/benzyl alcohol, benzyl alcohol/acetophenone, acetophenone/anthracene, phenol/acetophenone, benzyl alcohol/anthracene and phenol/anthracene the respective mean α^s values were: 0.63, 0.38, 0.35, 0.21, 0.15 and 0.08. These data affirm the above assumption that α^s decreases as the polarity difference between solutes increases. Also, the α^s value for the benzyl alcohol/acetophenone pair lies between the limiting values for this pair in Table II confirming the conclusion that the mobile phase composition does not affect selectivity in the stationary phase.

Thus, once determined tha α^s value for a pair may be used for the approximate prediction of the selectivity factor α in other solvent systems combining it with "a priori" calculated α^m values. Predicted selectivities will be rather accurate at lower concentrations of the polar moderator in the system, i. e., in the range where they are highest.

Conclusions

Considering the selectivity of separation in the mobile and the stationary phase of an LSC system, two general conclusions can be pointed out from data discussed here. First, change in the eluent composition influences only the selectivity in the mobile phase. Second, selectivity in the stationary phase is only determined by the molecular structure of related solutes.

References

[1] *E. H. Slaats, J. C. Kraak, W. J. T. Brugman, H. Poppe,* J. Chromatogr. **149**, 255 (1978).
[2] *A. Rizzi,* J. Chromatogr. **348**, 1 (1985).
[3] *S. M. Petrović, S. Lomić, I. Šefer,* Chromatographia, in press.
[4] *L. R. Snyder,* "Principles of Adsorption Chromatography, Marcel Dekker, New York, 1968.
[5] *E. Soczewinski,* Anal. Chem. **41**, 179 (1969).
[6] *E. Soczewinski, W. Golkiewicz,* Chromatographia **4**, 501 (1971).
[7] *E. Soczewinski,* J. Chromatogr. **130**, 23 (1977).
[8] *J. A. Perry,* J. Chromatogr. **165**, 117 (1979).
[9] *A. Fredenslund, R. L. Jones, J. M. Prausnitz,* AIChE J. **21**, 1086 (1975).
[10] *A. Fredenslund, J. Gmehling, M. L. Michelsen, P. Rasmussen, J. M. Prausnitz,* Ind. Eng. Chem., Process Des. Dev. **16**, 450 (1977).
[11] *J. Gmehling, P. Rasmussen, A. Fredenslund,* Ind. Eng. Chem., Process Des. Dev. **21**, 118 (1982).
[12] *E. Soczewinski, W. Golkiewicz, W. Markowski,* Chromatographia **8**, 13 (1975).
[13] *L. R. Snyder, H. Poppe,* J. Chromatogr. **184**, 363 (1980).
[14] *J. H. Hildebrand, J. M. Prausnitz, R. L. Scott,* "Regular and Related Solutions", Van Nostrand-Reinhold, New York, 1970.
[15] *J. E. Paanakker, J. C. Kraak, H. Poppe,* J. Chromatogr. **149**, 111 (1978).

Received: June 29, 1987
Accepted: Sept 21, 1987
F

Monitoring Free Silanols on Reversed-Phase Supports with Peptide Standards

C. T. Mant/R. S. Hodges*

Department of Biochemistry and the Medical Research Council of Canada Group in Protein Structure and Function, University of Alberta, Edmonton, Alberta, Canada T6G 2H7

Key Words

Reversed-phase chromatography
Peptide standards
Monitoring free silanols

Summary

A series of synthetic peptide HPLC standards has been designed for use in monitoring free silanols on silica-based reversed-phase supports. The four standards (+ 1 to + 4 net charge) showed great versatility in monitoring silanol activity over a pH range of 2.0 to 7.0. We have developed a silanol monitoring system based on the sensitivity of the standards to ionic interactions with reversed-phase packings at pH 7.0. This monitoring procedure involves chromatographing the peptides at pH 7.0 with a combined acetonitrile and sodium perchlorate linear AB gradient and is generally applicable to reversed-phase packings exhibiting a wide range of silanol concentrations. These standards not only demonstrate the presence and extent of free silanols, they also allow the researcher to determine what changes must be made to the mobile phase compositon to minimize ionic interactions. In addition, the standards, in conjunction with the double gradient monitoring system at pH 7.0, will aid researchers and manufacturers in the improvement and development of reversed-phase matrices.

Introduction

The powerful resolving capability of reversed-phase chromatography (RPC) has resulted in its becoming the predominant mode of high-performance liquid chromatography (HPLC) for a wide range of compounds in recent years. The majority of reversed-phase separations are still performed on silica-based supports, chemically modified by the reaction of chloroalkylsilanes with silanols present on the surface of the silica. Residual silanol groups present on the surface of silanized silica can influence the reversed-phase chromatographic behaviour of polar solutes, particularly basic compounds, often producing undesirable effects such as peak tailing and non-reproducible solute retention times [1–4]. A deterioration in column performance also becomes apparent after extensive use of a silica-based reversed-phase column, due to the gradual removal of hydrophobic ligands from the silica, resulting in an increased concentration of underivatized silanols [5, 6]. Researchers wishing to monitor silanol activity on reversed-phase columns would undoubtedly desire a method that is fast, simple, non-destructive to the reversed-phase packing and compatible with commonly available HPLC instrumentation [4, 7]. To this end, several empirical procedures have been proposed, generally employing normal- or reversed-phase separations of polar organic solutes [4, 8–11]. A method involving isotopic exchange of silanol protons with deuterium has also been reported [7].

The above methods of silanol monitoring have all proved useful to varying degrees. However, researchers would likely prefer not only to assess the level of silanol activity on a particular reversed-phase column, but also gauge the effect this activity may have on their particular compound(s) of interest. It is often preferable to use compounds that are structurally similar to the sample of interest, and that presumably interact with the reversed-phase support in a similar manner, to achieve the most precise and accurate analysis of solute and stationary phase interaction. Hence, peptide standards are best suited for monitoring peptide/protein interactions with reversed-phase packings [12].

In this study, we describe the design and application of a mixture of four synthetic peptide HPLC standards for monitoring free silanols on reversed-phase silica-based packings. The standards showed great versatility in monitoring silanol activity (over a pH range of 2.0 to 7.0) on commercial columns and columns prepared in the laboratory.

0009-5893/87 0805-10 $03.00/0 © 1987 Friedr. Vieweg & Sohn Verlagsgesellschaft mbH

Experimental

Materials

SynChropak silica (6.5 μm particle size, 300 Å pore size) was obtained from SynChrom (Linden, IN, USA).

HPLC-grade water, acetonitrile and isopropanol were obtained from Fisher Scientific (Fairlawn, NJ, USA). HPLC-grade TFA was obtained from Pierce Chemical (Rockford, IL, USA). Reagent grade orthophosphoric acid and triethylamine were obtained from J. T. Baker (Phllipsburg, NJ, USA). Reagent grade dichloromethane and pyridine were redistilled prior to use. Chlorodimethyloctylsilane was obtained from Aldrich Chemical (Milwaukee, WI, USA). Alkylphenone standards were obtained from Pierce Chemical. Molecular Sieves (Type 4A, Grade 514, 8-12 mesh beads, 4 A pore size) were obtained from Fisher Scientific. Membrane filters (47 mm diameter discs; 0.45 μm pore size), resistant to organic solvents, were obtained from S.P.E. Ltd. (Rexdale, Ontario, Canada).

Synthetic Peptide Standards

The peptide standards described were synthesized on a Beckman Model 990 peptide synthesizer (Beckman Instruments, Berkeley, CA, USA) using the general procedure for solid-phase synthesis described by Parker and Hodges [13]. The standards are available from Synthetic Peptides Incorporated, Department of Biochemistry, University of Alberta, Edmonton, Alberta, Canada, T6G 2H7.

Apparatus

Columns were packed using a Shandon HPLC packing pump (Sewickley, PA, USA). The HPLC apparatus consisted of a Spectra-Physics (Autolab Division, San Jose, CA, USA) SP8700 solvent delivery system and SP8750 organizer module coupled to a Hewlett-Packard (Avondale, PA, USA) HP1040A detection system, HP3390A integrator, HP85 computer, HP9121 disc drive and HP7470A plotter. Samples were injected with a 2.0 ml injection loop (Model 7125, Rheodyne, Cotati, CA, USA).

Silanization procedure: The silanization solution consisted of 1%–10% (v/v) chlorodimethyloctylsilane and 0.8 M pyridine in dichloromethane (previously dried over molecular sieves and filtered through a 0.45 μm membrane filter). Silica (lg) was suspended in 20 ml of silanization solution and stirred gently at room temperature (26 °C) for 90 min. The dichloromethane was then removed by filtration through a 0.45 μm membrane filter and the modified silica washed successively with 50 ml of dichloromethane and isopropanol. The silica was then ready for packing. This procedure was originally reported by Mant and Hodges [6].

Column packing: The freshly-prepared reversed-phase packing (850 mg) was suspended in 15 ml of isopropanol and degassed in an ultrasonic bath for 5 min. The silica slurry was then packed vertically at 6000 p.s.i. into a 75 x 4.6 mm I.D. stainless steel column, with isopropanol as packing solvent and nitrogen as the pressurizing gas. After 30 ml of isopropanol had passed through the column, it was inverted and a further 30 ml of isopropanol passed through. The column was then reinverted and a final 30 ml of isopropanol passed through the column. These inversions were carried out on the Shandon packing apparatus to remove any trapped air and did not change the direction of solvent flow through the column.

Results and Discussion

Design of Peptide Standards

Four synthetic undecapeptide standards (1–4) were prepared, with each peptide containing an N^{α}-acetylated N-terminal and a C-terminal amide. Peptides 1 and 2 were based on the sequence, X^1-X^2-Gly-Leu-Gly-Gly-Ala-Gly-Gly-Leu-Lys, where X^1-X^2- were substituted with G^1-G^2- (peptide 1) or Lys^1-Tyr^2 (peptide 2); peptides 3 and 4 were based on the sequence, X^1-X^2-Ala-Leu-Lys-Ala-Leu-Lys-Gly-Leu-Lys, where X^1-X^2- were substituted with G^1-G^2 (peptide 3) or Lys^1-Tyr^2- (peptide 4). RPC is often used during peptide mapping of proteins, and the 11-residue length of the standards was designed to approximate the average size of cleavage fragments from proteolytic (e.g. tryptic) digests of proteins. Peptides 1-4 contained, respectively, 1-4 basic residues (lysine residues) with no acidic residues present. Thus, over the pH range used for the majority of reversed-phase separations (pH 2 to 7), the net charge of + 1 to + 4, for peptides 1-4, respectively, did not change. The basic character of the peptides ensured their sensitivity to any ionic as opposed to hydrophobic stationary phase characteristics; this sensitivity increased with increasing basic character (peptide 1 to peptide 4) of the standards. The hydrophobicity of the standards also increased from peptide 1 to peptide 4.

The optimum resolution of peptides is usually achieved between 15% and 40% of the organic solvent in the gradient [14] and, through the use of amino acid residue coefficients developed by Guo et al. [15], the peptide standards were also designed to enable precise assessment of column selectivity at the limits of this range. Thus, standards 1 and 2 (+ 1 and + 2 net charge, respectively) formed a peptide pair, closely related in hydrophobicity, at the lower limit of the optimum organic solvent concentration range; standards 3 and 4 (+ 3 and + 4, respectively) formed a closely related peptide pair at the upper limit. Peptides 2 and 4 contained tyrosine residues, enabling detection of these standards at 280 nm, and simplifying peak identification of the closely-related peptide pairs. In addition, the sequence of the standards was chosen to ensure the peptides would lack conformation on binding to the support since the non-polar environment of the matrix may induce α-helical structure in potentially α-helical molecules [16, 17].

Effect of Alkylsilane Concentration on Carbon Content and Performance Characteristics of Reversed-Phase Packings

The silanization procedure described in the experimental section was designed to produce a series of C_8 reversed-

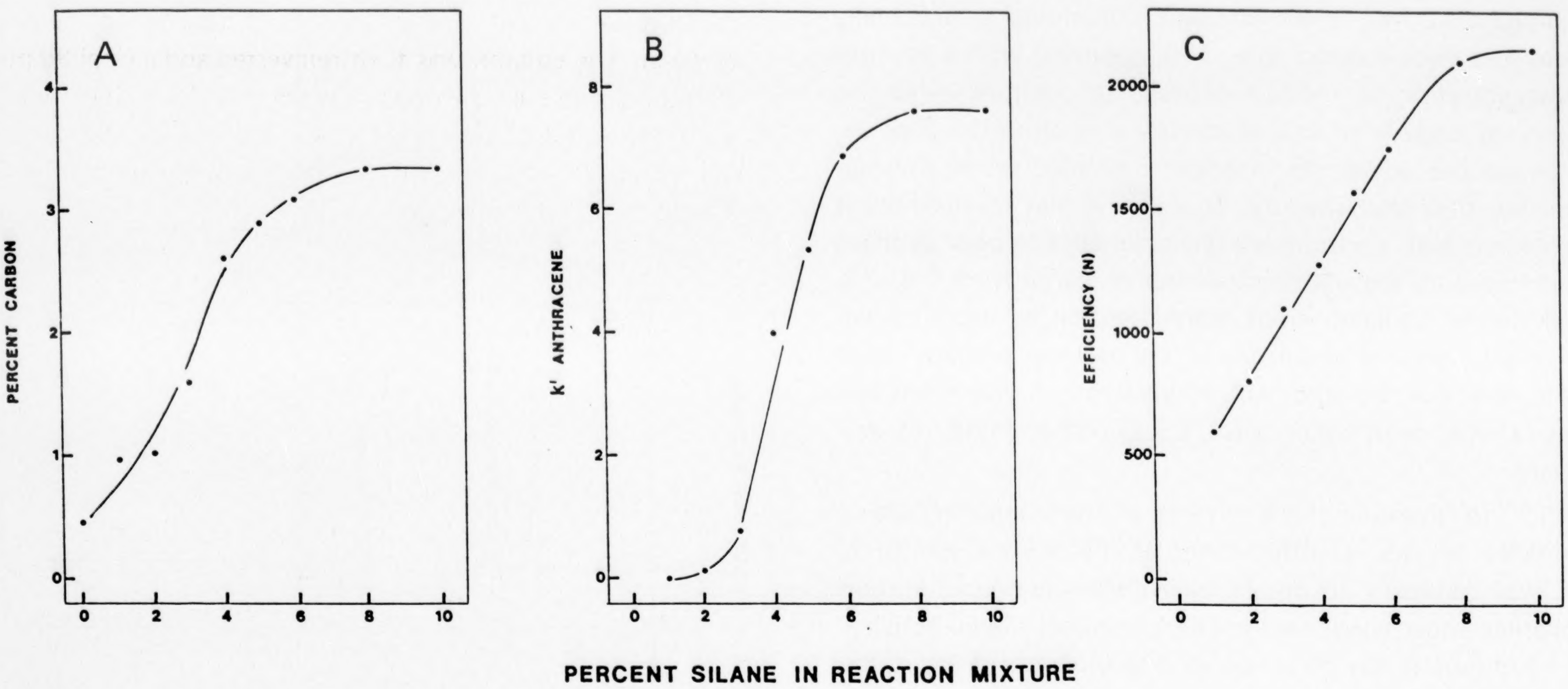

Fig. 1

Effect of concentration of monochloroalkylsilane during silanization of a silica support on the carbon content and performance characteristics of reversed-phase packings. Columns: analytical columns (75 × 4.6 mm I.D.) containing SynChropak silica (6.5 µm particle size, 300 Å pore size) chemically modified by a silanization reaction mixture containing 1 % to 10 % (v/v) of monochlorodimethyloctylsilane (see Experimental). Panel A: effect of alkylsilane concentration on carbon content (%, w/w) of reversed-phase packing. Panel B: effect on capacity factor (k') of anthracene; k' was calculated using the equation: $k' = R_t - t_0/t_0$, where R_t is the retention time of anthracene and t_0 is the retention time of unretained compounds (uracil). Panel C: effect on number of theoretical plates (N); theoretical plates were calculated using the equation: $N = 5.5\ (R_t/W_{1/2})$, where R_t is the retention time of anthracene and $W_{1/2}$ is the peak width at half height. For the purposes of this study, the packings prepared from 4 %, 5 %, 6 %, 8 % and 10 % alkylsilane concentrations were referred to as columns C4, C5, C6, C8 and C10, respectively.

phase silica-based columns (75 x 4.6 mm I.D.), containing packings with a range of bonded phase coverage and, hence, a range of concentrations of underivatized silanols present on the silica surface. The columns all contained SynChropak silica of 6.5 µm particle size and 300 Å pore size. Since pore diameter has little effect on peptide separations [18] and most researchers who separate peptides also separate proteins, the 300 Å support appeared to be a good choice for the present study. The use of a monofunctional (monochloro) alkylsilane reagent simplified the derivatization procedure and ensured a uniform monomeric coverage of the silica support.

Fig. 1 demonstrates the effect of increasing concentration (%, v/v) of chlorodimethyloctylsilane in the silanization reaction mixture (see Experimental) on carbon content (determined by elemental analysis) and performance characteristics of the resultant reversed-phase packings. Prior to silanization, the silica contained 0.45 % carbon (w/w). Panel A demonstrates an increase in carbon content (%, w/w) of the silica with increasing concentration of alkylsilane in the silanization solution, up to a maximum of ~3.4 % carbon at an alkylsilane concentration of 8 %. Higher concentrations of alkylsilane had negligible further effect on carbon content, reflecting the results of previous workers [19, 20], and suggesting that a minimum alkylsilane concentration is required to ensure maximum and reproducible surface coverage of silica beyond which higher concentrations have little or no effect [19, 20]. Panel B demonstrates the effect of alkylsilane concentration on the capacity factor (k') of anthracene (eluted with 45 % aqueous acetonitrile at a flow-rate of 1 ml/min). After an initial slow increase in k' at low levels of alkylsilane concentration (1–3 %), the capacity factor values increased more rapidly until, at an alkylsilane concentration of 8 %, a maximum k' value of 7.6 min was obtained. No further increase in k' was observed at higher concentrations of alkylsilane. The observed increase in k' values reflected the increasing carbon content of the reversed-phase columns as the alkylsilane concentration increased from 1 % to 8 % (Panel A) in the reaction mixture. This dependence of solute k' values on the carbon content of reversed-phase packings is well recognized [10, 21–23]. Panel C demonstrates a similar increase in the number of theoretical plates (N) of the reversed-phase packings with increasing alkylsilane concentration used in the derivatization mixture and, hence, increasing carbon content (Panel A), up to a maximum value of ~2200 for 8 % and 10 % concentrations of alkylsilane.

Development of Silanol Monitoring Procedure

From the results presented in Fig. 1, we chose several columns, containing reversed-phase packings with a useful range of bonded phase coverage (and, hence, residual silanol concentrations), for assessing the silanol monitoring capability of the peptide standards. The packings prepared with 4 %, 5 %, 6 %, 8 % and 10 % alkylsilane concentrations in the silanization reaction mixture (see Experimental) were deemed most suitable for this purpose. The columns containing these packings represented columns typically encountered during reversed-phase separations in the laboratory, i.e., from columns containing a maximally covered silica support (8%, 10% columns) with a minimal concentration of residual silanols, to columns exhibiting varying degrees of silanol activity due either to their extensive use and/or to incomplete bonded phase coverage during their manufacture. It was felt that reversed-phase packings with performance characteristics as poor as those exhibited by the stationary phases prepared from 1%–3% alkylsilane concentrations would seldom be encountered. For the purposes of this study, the packings prepared from 4%, 5%, 6%, 8% and 10% alkylsilane concentrations will be referred to as columns C4, C5, C6, C8 and C10, respectively.

Prior to examining the effects of variations in silanol activity on the retention times of the peptide standards, it was necessary to obtain their chromatographic elution profiles under conditions ensuring minimal silanol activity. In addition, it was important to determine the utility of the peptide standards over the entire pH range available to researchers for reversed-phase separations on silica-based columns (pH 2-7). Fig. 2 demonstrates the elution profiles of the peptide standards on column C4 at pH 2.0 (Panel A), pH 4.5 (Panel B) and pH 7.0 (Panel C). The profile demonstrated in Panel A was obtained by linear AB gradient elution (1% B/min) at a flow-rate of 1 ml/min, where solvent A was 0.05% aqueous TFA and solvent B was 0.05% TFA in acetonitrile. The profile demonstrated in Panel B was obtained by linear AB gradient elution (2% B/min, equivalent to 1% acetonitrile/min) at a flow-rate of 1 ml/min, where solvent A was aqueous 250 mM triethylammonium phosphate (TEAP), pH 4,5, and solvent B was 50% solvent A and 50% acetonitrile. Solvent A was prepared by adding sufficient triethylamine to 250 mM orthophosphoric acid until the desired pH was obtained. The profile demonstrated in Panel C was obtained by linear AB gradient elution (1.67% B/min, equivalent to 1% acetonitrile/min) at a flow-rate of 1 ml/min, where solvent A was aqueous 10 mM $(NH_4)_2HPO_4$, pH 7.0, and solvent B was 60% aqueous acetonitrile, both solvents containing 100 mM sodium perchlorate ($NaClO_4$). Prior to use, solvent A for the pH 4.5 and pH 7.0 systems and the aqueous component of solvent B for the pH 7.0 system were passed through a preparative C_{18} column to remove impurities. At pH 2.0, silanol ionization is suppressed and, hence, ionic interaction of the hydrophobic stationary phase with basic peptide residues is minimized. It should be noted, however, that a low pH does not necessarily completely eliminate silanol effects, since this effect as a function of pH will be dependent on the type of silica used. Thus, although at pH 2.0 silanol ionization was suppressed on the SynChropak silica (Fig. 2, Panel A), this was not the case with a commercial packing described later in this study (Fig. 7, Column A, top panel). Acting as weak acids, silanols are negatively charged above pH 3.5–4.0, resulting in strong ionic interactions with basic peptide residues. The silanol masking properties of amines are well known [3, 24] and sodium perchlorate is a chaotropic reagent capable of suppressing ionic interaction between the peptides and packing material [5, 25].

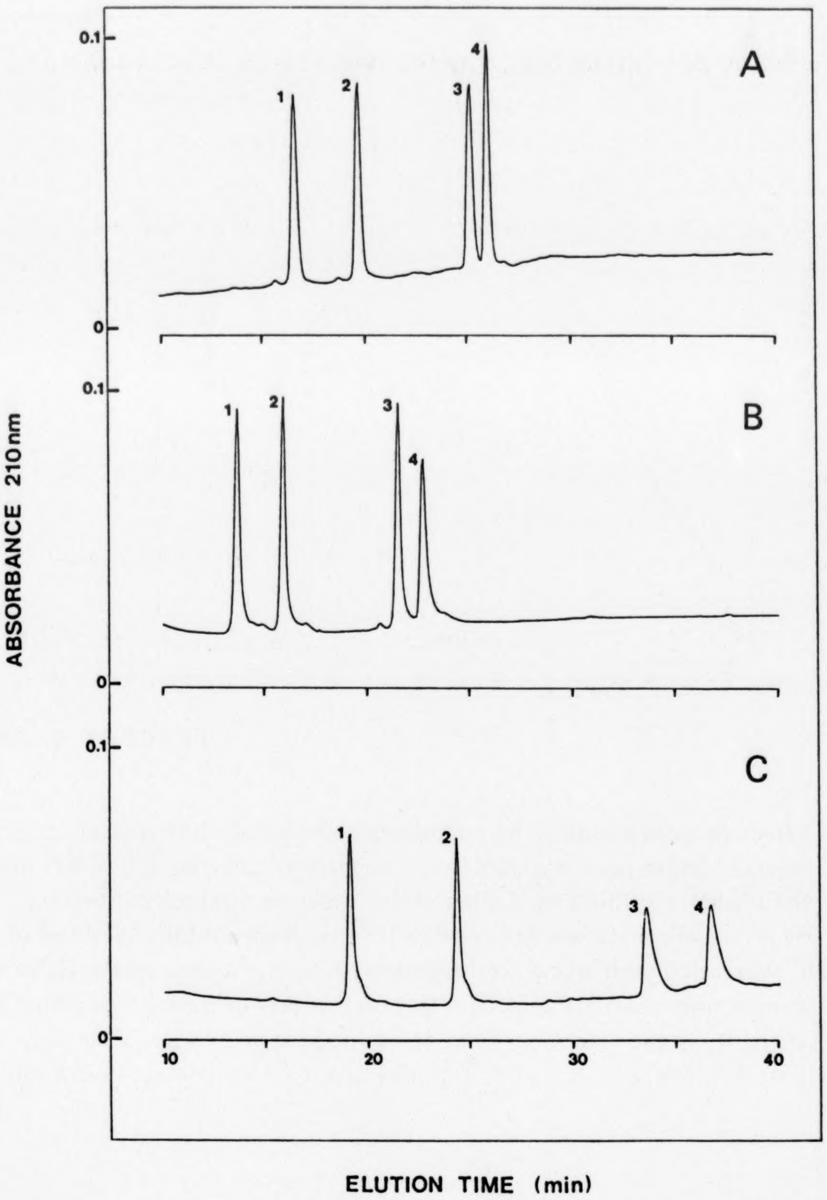

Fig. 2

Reversed-phase elution profiles of peptide standards on an incompletely derivatized reversed-phase column. Column: analytical column (75 × 4.6 mm I.D.) containing a silica support derivatized with a silanization reaction mixture containing 4% (v/v) of chlorodimethyloctylsilane. Column referred to as C4 in text. Panel A: elution profile at pH 2.0; linear AB gradient (1% B/min), where solvent A is 0.05% aqueous TFA and solvent B is 0.05% TFA in acetonitrile. Panel B: elution profile at pH 4.5; linear AB gradient (2% B/min, equivalent to 1% acetonitrile/min), where solvent A is aqueous 250 mM TEAP, pH 4.5, and solvent B is 50% solvent A and 50% acetonitrile. Panel C: elution profile at pH 7.0; linear AB gradient (1.67% B/min, equivalent to 1% acetonitrile/min), where solvent A is aqueous 10 mM $(NH_4)_2HPO_4$, pH 7.0, and solvent B is 60% aqueous acetonitrile, both solvents containing 100 mM $NaClO_4$. Flow-rate, 1 ml/min; 26°C. The numbers 1–4 denote peptide standards 1–4, respectively.

Thus, all three solvent systems producing the peptide elution profiles shown in Fig. 2 were designed to minimize ionic interactions between the peptide standards and the stationary phase. The separation of the four standards in all three solvent systems was excellent. The profiles obtained with the pH 2.0 (Panel A) and pH 4.5 (Panel B) systems were very similar. The slightly longer retention times of the peptides in the pH 2.0 mobile phase compared to the pH 4.5 system was probably due to the more hydrophobic nature of the TFA anionic counterion compared to the phosphate ion. The significantly longer retention times of the peptides at pH 7.0 (Panel C) compared to the pH 2.0 and pH 4.5 profiles, together with some peak broadening of the standards, suggested some ionic interaction of the peptides with column C4 due to incomplete suppression of silanol activity at neutral pH. The results demonstrated that even on a column with significant silanol activity, satisfactory resolution of the basic standards may be achieved at pH 2.0 to pH 7.0 through the proper choice of solvent components.

For maximum practical value to the researcher, any method for monitoring free silanols on reversed-phase packings should be generally applicable to a wide range of columns exhibiting a wide range of silanol activities. Hence, for the development of the present method, chromatographic conditions were sought which would allow significant, but controllable, ionic interactions of the peptide standards with the hydrophobic stationary phase. The effective suppression of silanol ionization at pH 2.0 precludes the use of the gradient elution conditions demonstrated in Fig. 2, Panel A, for our method development. At pH 4.5 (Fig. 2, Panel B), a pH value only slightly higher than the characteristic pKa range of free silanols (pH 3.5–4.0), there is a possibility that not all silanols will be ionized. However, at neutral pH (Fig. 2, Panel C), all free silanols should be completely ionized. Adjustment of the sodium perchlorate concentration in the pH 7.0 mobile phase should then enable control of the level of ionic interaction between the basic peptide standards and the negatively charged silanols. The effect of a gradual decrease in sodium perchlorate levels in the pH 7.0 mobile phase from 100 mM to 50 mM, 25 mM, 10 mM, 5 mM and, finally, 0 mM $NaClO_4$ on the elution profiles of the peptide standards was examined. A general increase in peptide retention times with decreasing salt concentration was observed, this effect being more and more pronounced with decreasing carbon content of the reversed-phase packings (Fig. 1, Panel A) and increasing net positive charge of peptides 1–4 (+ 1 to + 4 net charge, respectively) (data not shown). However, a single set of chromatographic conditions which would enable a convenient monitoring of the effect of silanol activity over the entire range of columns was elusive. Peptides 3 and 4 (+ 3 and + 4 net charge, respectively) proved to be extremely sensitive to ionic interactions with the hydrophobic stationary phase. Peptide 4, particularly, very rapidly showed significant peak broadening and long retention times even at relatively high levels of salt concentration on columns C4, C5 and C6. In the absence of perchlorate at pH 7.0, this peptide was so strongly retained by all five columns, including the maximally covered columns (C8 and C10) that even isocratic elution with 100% acetonitrile failed to elute it from the reversed-phase packings. In contrast, changes in retention times and peak shapes of peptides 1 and 2 (+1 and +2 net charge, respectively) were much less dramatic on all the columns.

The greatest extent of this limited ionic interaction of peptides 1 and 2 with the reversed-phase packings was observed at low salt concentrations on columns C4 and C5. These results suggested that a gradient of increasing salt concentration from 0 mM $NaClO_4$ in solvent A, concurrent with the acetonitrile gradient, had the best potential for a general silanol monitoring system applicable to a wide range of columns. An initial attempt at such a double gradient system involved a linear AB gradient (1.67% B/min, equivalent to 1% acetonitrile/min and 1.67 mM $NaClO_4$/min) at a flow-rate of 1 ml/min, where solvent A was aqueous 10 mM $(NH_4)_2HPO_4$, pH 7.0, and solvent B was 60% aqueous acetonitrile containing 100 mM $NaClO_4$. Despite the promise shown by the subsequent peptide elution profiles, particularly in the changes in the retention behaviour of peptides 3 and 4 with variations in silanol activity, it was felt that a further shallowing of the salt gradient was necessary to affect more strongly the retention times of the more weakly basic standards (peptides 1 and 2). Hence, subsequent reversed-phase separations of the peptide standards were carried out by applying a linear AB gradient (2% B/min, equivalent to 1% acetonitrile/min and 1 mM $NaClO_4$/min) at a flow-rate of 1 ml/min, where solvent A was aqueous 10 mM $(NH_4)_2HPO_4$, pH 7.0, and solvent B was 50% aqueous acetonitrile containing 50 mM $NaClO_4$. The effect of this double gradient system on the retention times of the peptide standards and a mixture of alkylphenone standards is demonstrated graphically in Fig. 3. The retention times of the peptide standards (Panel A) increased with decreasing ligand coverage of the silica support (and, hence, with increasing free silanol concentration). In contrast, the retention times of the alkylphenones increased with increasing ligand coverage (Panel B). The neutral nature of alkylphenone standards makes them insensitive to any ionic, as opposed to hydrophobic, interactions with reversed-phase packings. Thus, although they are useful for monitoring hydrophobic ligand density on a silica support, they are unsuitable for monitoring silanol activity. The effect of the gradient elution system on the peptide elution profiles became more pronounced with increasing net positive charge of the standards (peptide 1 to peptide 4) and increasing silanol concentrations (columns C10 to C4), resulting in a series of non-parallel curves (Panel A). In contrast, the alkylphenone plots formed a series of parallel curves (Panel B), again reflecting the neutral nature of these compounds. Fig. 4 demonstrates representative peptide elution profiles of the peptide standards at pH 7.0. Panel A shows the profiles of the standards on the maximally covered C8 following linear AB gradient elution under conditions where any potential ionic interactions are suppressed by having 100 mM $NaClO_4$ in both solvent A and B (see Fig. 2, Panel C for details). All four peptide standards were well resolved, exhibited good peak shape and were eluted within a reasonable run time ($<$ 40 min). Panel B shows the profiles of the peptide standards on the same column, obtained with the double gradient system (1 mM sodium perchlorate/min) described above (Fig. 3). A comparison of Panels A and B demonstrates significant peak broadening of peptides 3 and 4, and a slight decrease in the peak height of peptide 2. The effect of the double gradient on the retention behaviour of peptide 1 was negligible. The retention times of the peptides in both gradient elution systems were very similar. Panel C demonstrates the elution profile of the peptide standards, obtained with the same double gradient elution system (Fig. 3), on column C4. The contrast

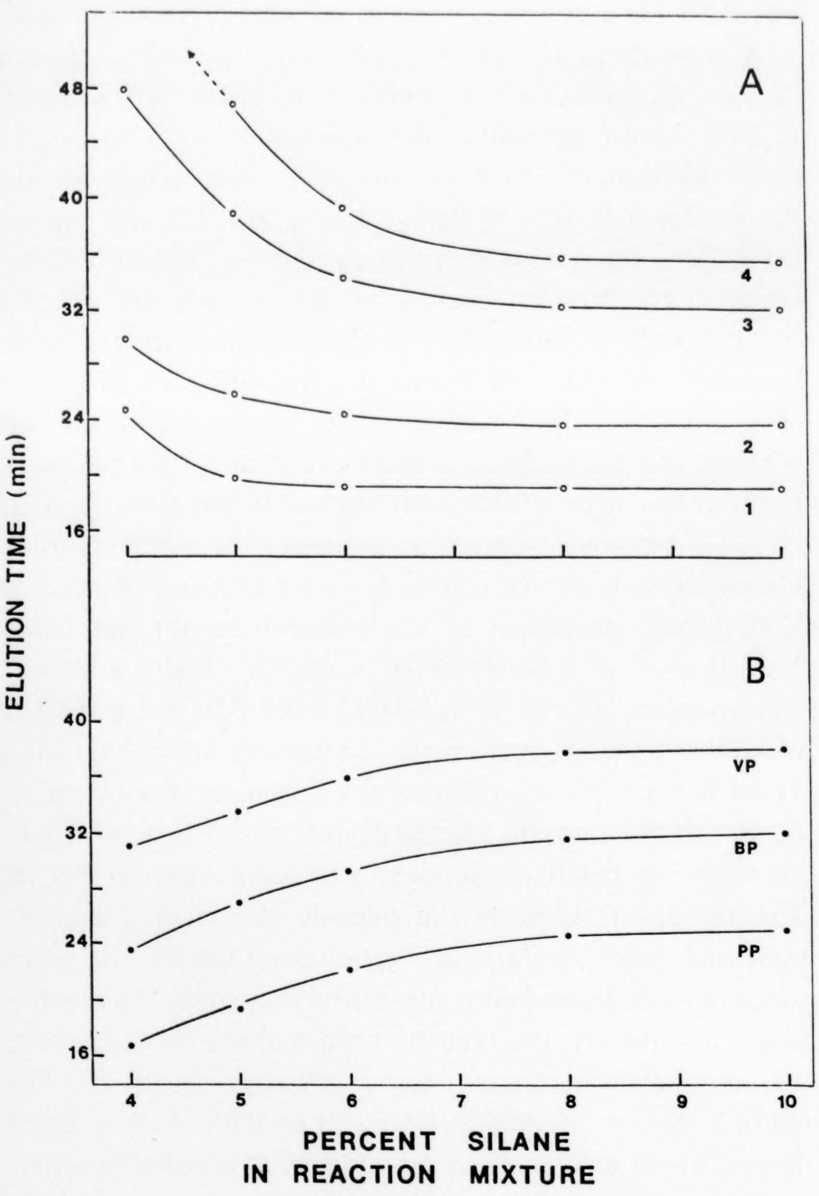

Fig. 3

Effect of silanol concentration on retention times of peptide and alkylphenone reversed-phase HPLC-standards. Columns: analytical columns (75 X 4.6 mm I.D.) containing a silica support derivatized with varying concentrations (1–10%, v/v) of chlorodimethyloctylsilane in the silanization reaction mixture. Chromatographic conditions: linear AB gradient (2% B/min, equivalent to 1% acetonitrile/min and 1 mM $NaClO_4$/min), where solvent A is aqueous 10 mM $(NH_4)_2HPO_4$, pH 7.0, and solvent B is 50% aqueous acetonitrile containing 50 mM $NaClO_4$; flow-rate, 1 ml/min; 26°C. Panel A: peptide standards 1–4 (+1 to +4 net charge, respectively). Panel B: alkylphenone standards; PP, BP, VP denote propiophenone, butyrophenone and valerophenone, respectively.

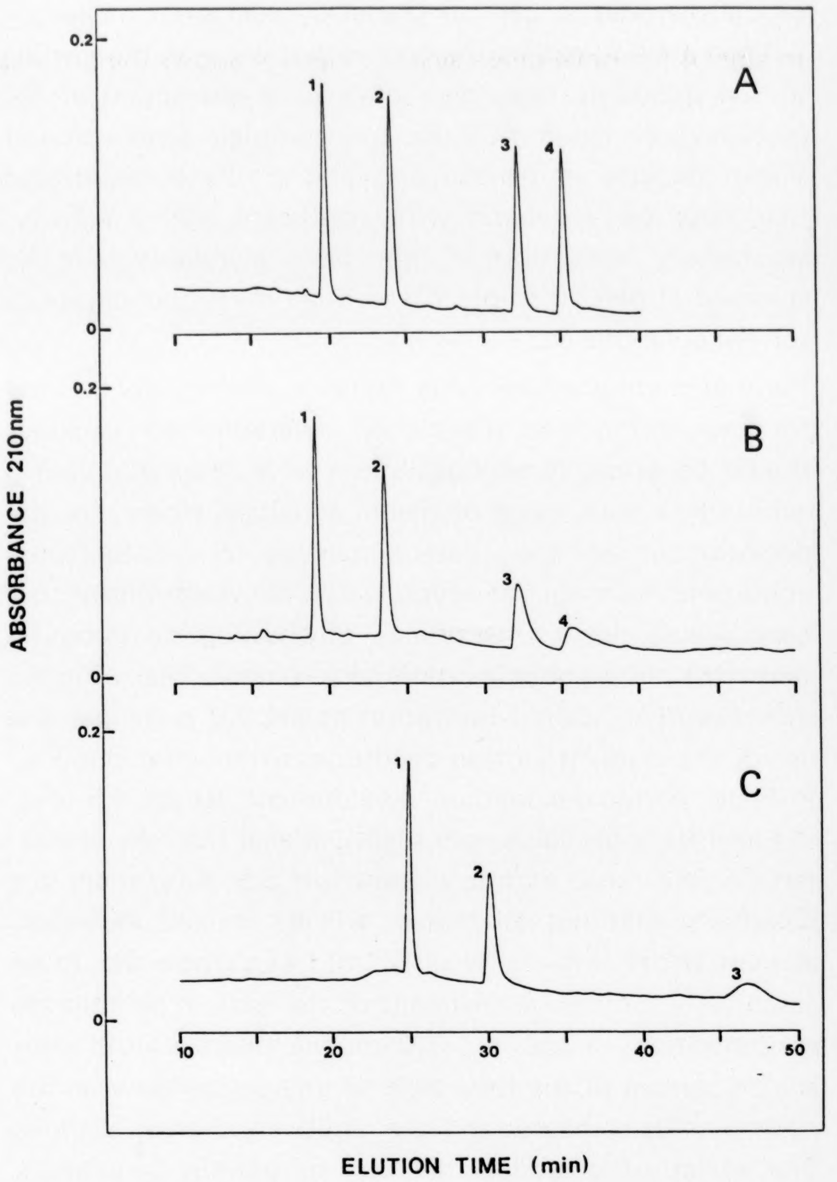

Fig. 4

Monitoring of free silanols with peptide standards at pH 7.0. Panel A: column, C8; conditions, linear AB gradient (1.67% B/min, equivalent to 1% acetonitrile/min), where solvent A is aqueous 10 mM $(NH_4)_2HPO_4$, pH 7.0, and solvent B is 60% aqueous acetonitrile, both solvents containing 100 mM $NaClO_4$. Panel B: column, C8; conditions, linear AB gradient (2% B/min, equivalent to 1% acetonitrile/min and 1 mM $NaClO_4$/min), where solvent A is aqueous 10 mM $(NH_4)_2HPO_4$, pH 7.0, and solvent B is 50% aqueous acetonitrile containing 50 mM $NaClO_4$. Panel C: column, C4; conditions, same as for Panel B. Flow-rate, 1 ml/min; 26°C. See Fig. 1 for descriptions of columns. The numbers 1–4 denote peptide standards 1–4, respectively.

between this profile and that obtained on column C8 (Panel B) is quite dramatic. All four peptides are retained longer on column C4 compared to column C8, the change in retention times becoming increasingly more pronounced with increasing net positive charge of the peptide standards. The most highly charged peptide (peptide 4; + 4 net charge) was, in fact, never observed to elute from the column. There was also a further deterioration in peak shape of peptides 2 and 3 on column C4 (Panel C) compared to C8 (Panel B). It was interesting to note that, even on a column considered to have maximum possible ligand coverage (C8), ionic interactions were detected by the peptide standards (Fig. 4, Panel B). Steric effects preclude derivatization of 100% of available silanols during silanization [26]. Although the remaining free silanols are effectively shielded by the hydrophobic ligands on the silica support, some ionic interactions are inevitable, particularly at neutral pH. Even on a well-covered column (C8, C10), peptide standards 3 and 4 were extremely sensitive to the presence of residual free silanols. In contrast, the retention behaviour of peptides 1 and 2 was only seriously affected by the presence of high concentrations of free silanols. Thus, the results presented in Figs. 3 and 4 demonstrate the general appicability of these standards combined with the double gradient silanol monitoring system to measure a wide range of silanol activity. The goal of manufacturers should be to prepare columns lacking interactions with, in particular, peptides 3 and 4 using this pH 7.0 silanol monitoring system.

Fig. 5 demonstrates elution profiles of the peptide standards in a pH 4.5 mobile phase system. Panel A shows the profiles obtained on column C8 following linear AB gradient elution under the conditions described previously in Fig. 2, Panel B (250 mM TEAP in solvent A). These conditions were designed to minimize any ionic interactions between the peptides and the hydrophobic stationary phase. Panel B shows the profile obtained on the same column when subjected to a similar double gradient system to that developed at pH 7.0 (Fig. 4, Panels B and C). In this case, the peptides were subjected to linear gradient elution (2% B/min, equivalent to 1% acetonitrile/min and 1 mM TEAP/min) at a flow-rate of 1 ml/min, where solvent A was aqueous 10 mM TEAP, pH 4.5 and solvent B was 50% aqueous acetonitrile containing a total concentration of 60 mM TEAP. Solvent B was prepared by mixing equal volumes of acetonitrile and aqueous 120 mM TEAP solution, pH 4.5. The elution profiles demonstrated in Panels A and B of Fig. 5 were very similar, with all four peptides exhibiting excellent peak shape and reasonable run times. Panel C demonstrates the effect of the double gradient system at pH 4.5 on the elution profiles of the peptides on column C4. Although the peak shapes of the four standards have deteriorated compared to column C8 (Panel B), their retention times have actually decreased from those obtained on the maximally covered column. Although the deterioration in peak shape is indicative of ionic interactions with the C4 stationary phase (compare Fig. 5, Panel C [shallow gradient of TEAP from 10 mM to 60 mM] with Fig. 2, Panel B [starting with 250 mM TEAP in solvent A]), the decrease in retention times of this column compared with the more hydrophobic C8 suggests that these interactions had been effectively suppressed even by the relatively low levels of TEAP used in the double gradient system. The much reduced sensitivity of the double gradient system at pH 4.5 (Fig. 5, Panels B and C) compared to that obtained at pH 7.0 (Fig. 4, Panels B and C) probably reflected a higher degree of silanol ionization (and, hence, a greater potential for ionic interaction) at the higher pH value. These results confirmed that a pH 7.0 double gradient systen, due to its excellent sensitivity to the presence of free silanols, had the best potential as a generally applicable monitoring procedure.

Monitoring of Free Silanols on Commercial Reversed-Phase Packings

We now applied our pH 7.0 double gradient procedure to brand new analytical reversed-phase columns obtained from different manufacturers. Column B contained a C_8 reversed-phase packing of 7 μm particle size and 300 Å pore size; Column A contained a C_{18} reversed-phase packing of 5 μm particle size and 300 Å pore size. Fig. 6 demonstrates elution profiles of the four peptide standards at pH 7.0 on Column B. Panel A shows the profile obtained under conditions designed to minimize any ionic interactions, (100 mM $NaClO_4$ in solvents A and B, see Fig. 2, Panel C for conditions). Panels B and C illustrate the effect of shallowing the sodium perchlorate gradient (while maintaining the same acetonitrile gradient) on the peptide elution profiles obtained on this column. Panel B shows the peptide elution profiles obtained by linear AB gradient elution (1.67% B/min, equivalent to 1% acetonitrile/min and 1.67 mM $NaClO_4$/min) at a flow-rate of 1 ml/min, where solvent A was aqueous 10 mM $(NH_4)_2HPO_4$, pH 7.0, and solvent B was 60% aqueous acetonitrile containing 100 mM $NaClO_4$. Panel C shows the profiles obtained by linear AB gradient elution (2% B/min, equivalent to 1% acetonitrile/min and 1 mM $NaClO_4$/min) at a flow-rate of

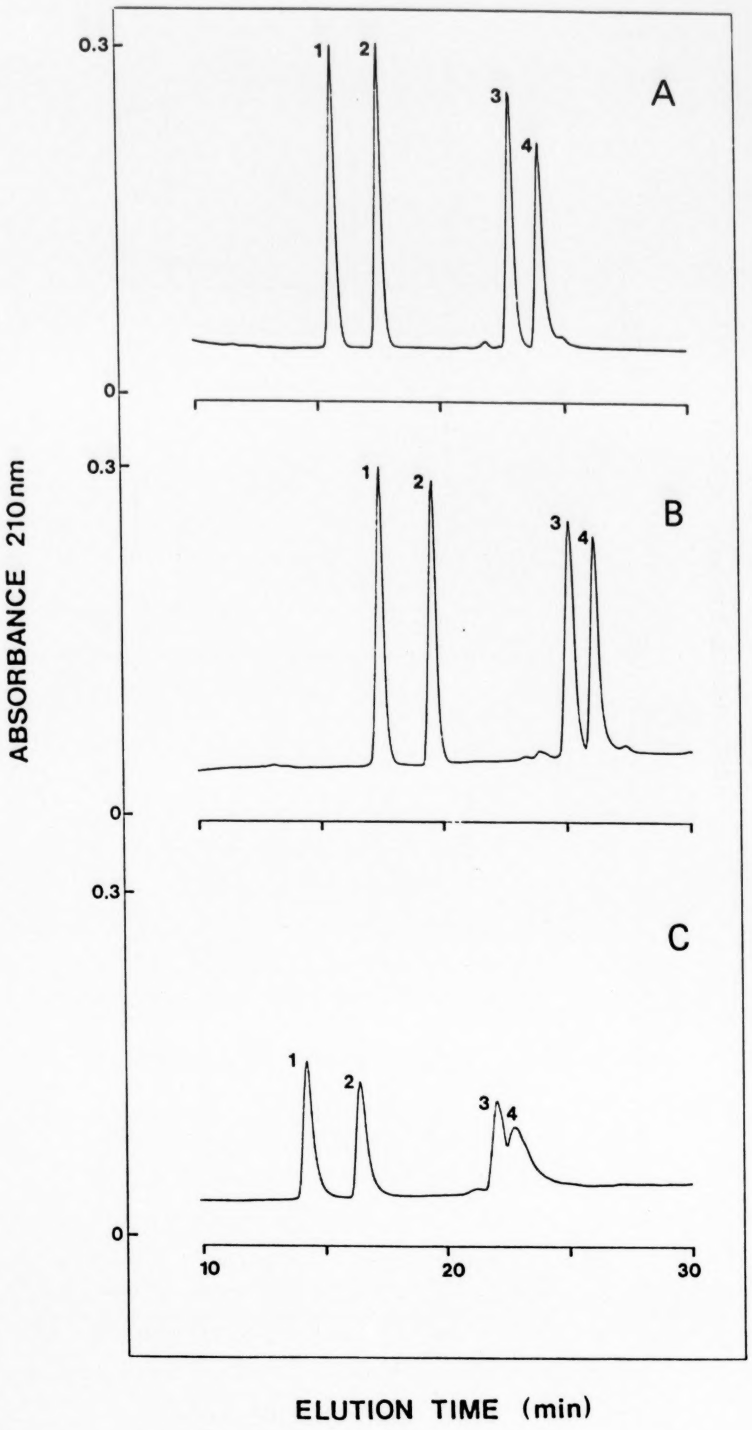

Fig. 5

Monitoring of free silanols with peptide standards at pH 4.5. Panel A: column, C8; conditions, linear AB gradient (2% B/min, equivalent to 1% acetonitrile/min), where solvent A is aqueous 250 mM TEAP, pH 4.5, and solvent B is 50% A and 50% acetonitrile. Panel B: column, C8; conditions, linear AB gradient (2% B/min, equivalent to 1% acetonitrile/min and 1 mM TEAP/min), where solvent A is aqueous 10 mM TEAP, pH 4.5, and solvent B is 50% aqueous acetonitrile containing 60 mM TEAP (solvent B was prepared by mixing equal volumes of acetonitrile and an aqueous 120 mM solution of TEAP, pH 4.5). Panel C: column, C4; conditions, same as for Panel B. Flow-rate, 1 ml/min; 26°C. See Fig. 1 for descriptions of columns. The numbers 1–4 denote peptide standards 1–4, respectively.

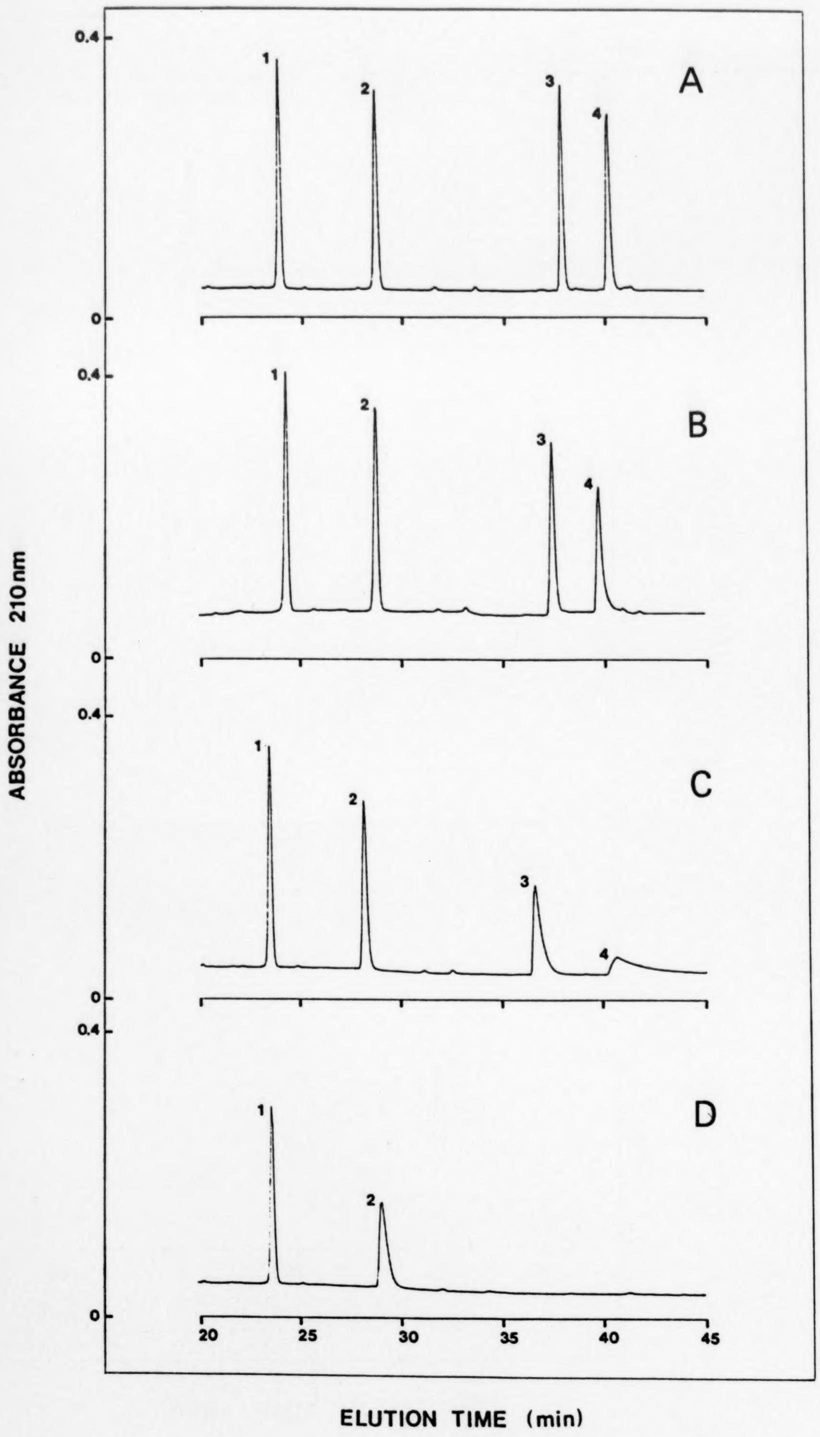

Fig. 6

Monitoring of free silanols on a commercial reversed-phase column with peptide standards. Column B: analytical C_8 column (220 × 4.6 mm I.D.) with a 7 μm particle size and 300 Å pore size. Conditions: Panel A, linear AB gradient (1.67% B/min, equivalent to 1% acetonitrile/min), where solvent A was aqueous 10 mM $(NH_4)_2HPO_4$, pH 7.0, and solvent B was 60% aqueous acetonitrile, both solvents containing 100 mM $NaClO_4$; Panel B, linear AB gradient (1.67% B/min, equivalent to 1% acetonitrile/min and 1.67 mM $NaClO_4$/ min), where solvent A is aqueous 10 mM $(NH_4)_2HPO_4$, pH 7.0, and solvent B is 60% aqueous acetonitrile containing 100 mM $NaClO_4$; Panel C, linear AB gradient (2% B/min, equivalent to 1% acetonitrile/min and 1 mM $NaClO_4$/min), where solvent A is aqueous 10 mM $(NH_4)_2HPO_4$, pH 7.0, and solvent B is 50% aqueous acetonitrile containing 50 mM $NaClO_4$; Panel D, linear AB gradient (1.67% B/min, equivalent to 1% acetonitrile/min), where solvent A is aqueous 10 mM $(NH_4)_2HPO_4$, pH 7.0, and solvent B is 60% aqueous acetonitrile. Flow-rate, 1 ml/min; 26°C. The numbers 1–4 denote peptide standards 1–4, respectively.

1 ml/min, where solvent A was aqueous 10 mM $(NH_4)_2HPO_4$, pH 7.0, and solvent B was 50% acetonitrile containing 50 mM $NaClO_4$. Panel D shows the profiles obtained in the absence of perchlorate. The peptides were eluted by a linear AB gradient (1.67% B/min, equivalent to 1% acetonitrile/min) at a flow-rate of 1 ml/min, where solvent A was aqueous 10 mM $(NH_4)_2HPO_4$, pH 7.0, and solvent B was 60% aqueous acetonitrile. The retention times of the four peptides in the elution profiles shown in Panels A–C were very similar. However, both of the double gradient profiles (Panels B and C) exhibited peak deterioration of peptides 3 and 4, particularly with the shallower (1 mM salt/min) salt gradient (Panel C), compared to the excellent elution profile of the standards obtained with a pH 7.0 system designed to suppress ionic interactions (Panel A; 100 mM $NaClO_4$ in solvents A and B). Peptide 2 also showed a slight decrease in peak height in the 1 mM salt/min profile (Panel C). In the absence of sodium perchlorate (Panel D), peptides 3 and 4 were never observed to elute from the column. In addition, the retention time of the more weakly basic peptide 2 increased, and peak shapes visibly deteriorated for peptides 1 and 2, compared to the profiles shown in Panels A–C. These results clearly demonstrated the effectiveness of the basic peptide standards in monitoring silanol activity on what is known to be a maximally covered column with high ligand density.

Fig. 7 compares the elution profiles of the peptide standards on Columns A and B at pH 2.0, pH 4.5 and pH 7.0. The top panels demonstrate the elution profiles obtained at pH 2.0 with a linear AB gradient (1% acetonitrile/min) at a flow-rate of 1 ml/min, where solvent A was 0.05% aqueous TFA and solvent B was 0.05% TFA in acetonitrile. The middle panels demonstrate the profiles obtained at pH 4.5 with a linear AB gradient (2% B/min, equivalent to 1% acetonitrile/min and 1 mM TEAP/min) at a flow-rate of 1 ml/min, where solvent A was aqueous 10 mM TEAP, pH 4.5, and solvent B was 50% aqueous acetonitrile containing 60 mM TEAP. Solvent B for this system was prepared as described previously (Fig. 5, Panels B and C). The bottom panels demonstrate the profiles obtained at pH 7.0 with a linear AB gradient (1.67% B/min, equivalent to 1% acetonitrile/min and 1.67% $NaClO_4$/min) at a flow-rate of 1 ml/min, where solvent A was aqueous 10 mM $(NH_4)_2HPO_4$, pH 7.0, and solvent B was 60% aqueous acetonitrile containing a total concentration of 100 mM $NaClO_4$. The contrast in the performances of the two columns was striking. Column A exhibited significant ionic interactions with the basic peptide standards (apparent mainly from the retention behaviour and peak deterioration of peptides 3 and 4) over the entire pH range (pH 2–7) available to chromatographers on silica-based reversed-phase packings. Column A exhibited considerable silanol activity at pH 7.0 even in the presence of 100 mM $NaClO_4$ in both mobile phase solvents (data not shown). In fact, the silanols were not completely suppressed with a concentration of 200 mM $NaClO_4$ in both solvents (data not shown), the elution profile of the standards resembling that obtained on Column B when applying a shallow (1 mM salt/min) sodium perchlorate gradient (Fig. 6, Panel C). A satisfactory peptide elution profile was not even obtained at pH 2.0, where silanol ionization is usually effectively suppressed. It should be noted that other peptides of lower hydrophobicity and net positive charge than peptides 3 and 4 gave no indication of silanol interaction at pH 2.0. In contrast, the elution profiles obtained on Column B were excellent at all three pH values, although some ionic interaction was apparent in the double gradient

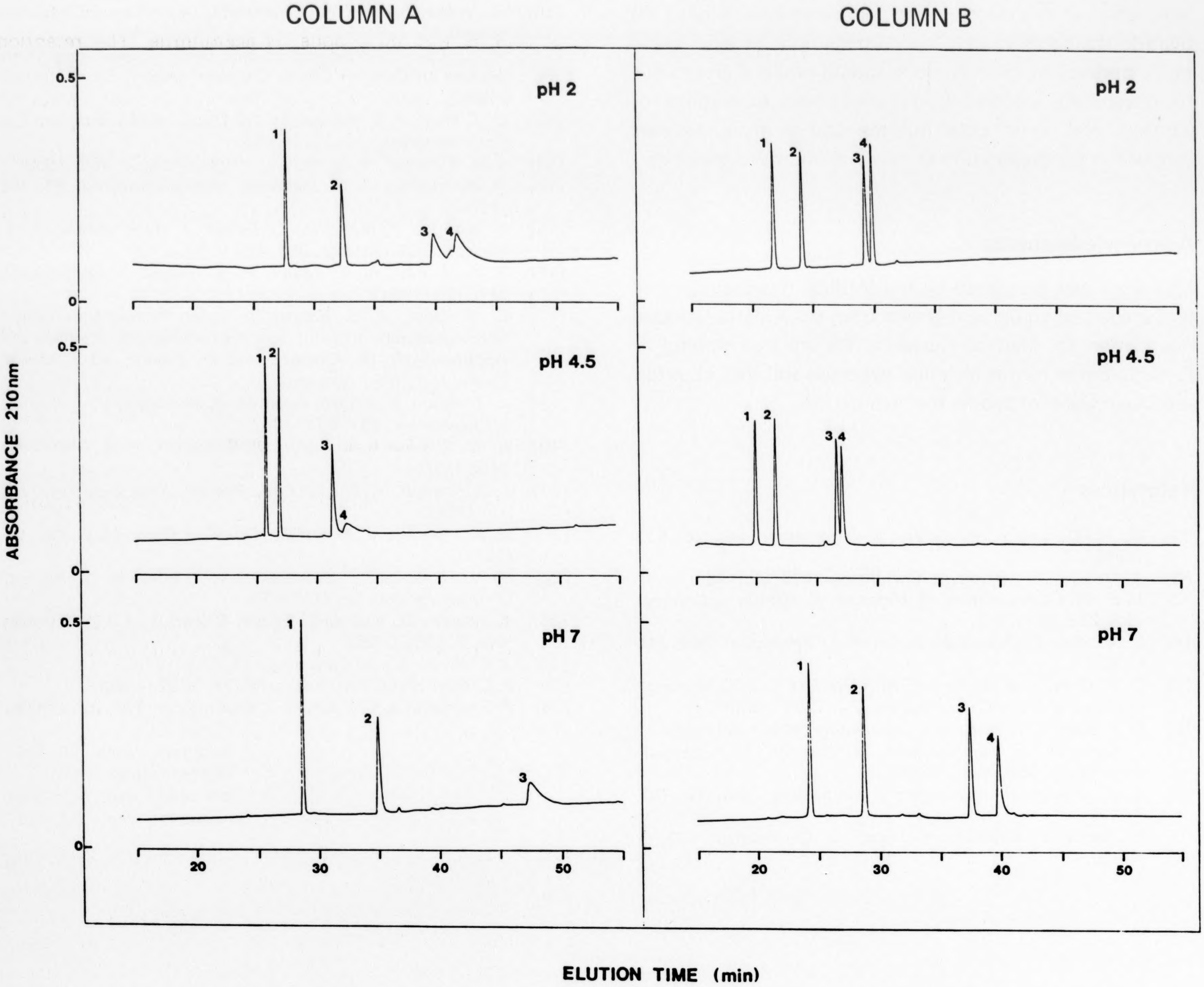

Fig. 7
Monitoring of free silanols on commercial reversed-phase columns with peptide standards. Column A: analytical C_{18} column (250 × 4.6 mm I.D.) with a 5 μm particle size and a 300 Å pore size. Column B; analytical C_8 column (220 × 4.6 mm I.D.) with a 7 μm particle and a 300 Å pore size. Conditions: pH 2.0, linear AB gradient (1 % B/min), where solvent A is 0.05 % aqueous TFA and solvent B is 0.05 % TFA in acetonitrile; pH 4.5, linear AB gradient (2 % B/min, equivalent to 1 % acetonitrile/min and 1 mM TEAP/min), where solvent A is aqueous 10 mM TEAP, pH 4.5, and solvent B is 50 % acetonitrile containing 60 mM TEAP (solvent B was prepared by mixing equal volumes of acetonitrile and an aqueous 120 mM solution of TEAP, pH 4.5); pH 7.0, linear AB gradient (1.67 % B/min, equivalent to 1 % acetonitrile/min and 1.67 mM $NaClO_4$/min), where solvent A is aqueous 10 mM $(NH_4)_2HPO_4$, pH 7.0, and solvent B is 60 % aqueous acetonitrile containing 100 mM $NaClO_4$. Flow-rate, 1 ml/min; 26 °C. The numbers 1–4 denote peptide standards 1–4, respectively.

pH 7.0 system as noted previously (Fig. 6, Panel B). For both columns, ionic interaction was more pronounced at pH 7.0 than at pH 4.5, stressing again the greater utility of a double gradient silanol monitoring system at neutral pH than at pH levels closer to the pKa values of silanols. Peptides with charges of + 3 and + 4 are not uncommon, and researchers can now demonstrate with our standards whether interactions are occurring and how the buffer system must be changed to suppress these interactions if they are observed in our monitoring system.

Conclusions

We have developed a silanol monitoring system based on the sensitivity of a mixture of four basic peptide standards (+ 1 to + 4 net charge) to ionic interactions with reversed-phase packings. The monitoring procedure involves chromatographing the peptides at pH 7.0 with a combined acetonitrile (1 % acetonitrile/min) and sodium perchlorate (1–2 mM salt/min) linear AB gradient. We suggest a salt gradient of 1 mM sodium perchlorate/min for general application of this method. The impressive sensitivity of the peptide standards toward ionic interactions on even maximally derivatized silica supports should prove of great value to researchers involved in reversed-phase separations of peptides and other polar solutes, and to manufacturers involved in the preparation of new and improved packings.

Acknowledgements

This work was supported by the Medical Research Council of Canada and equipment grants from the Alberta Heritage Foundation for Medical Research. We are also grateful to T. W. L. Burke for his technical expertise and Vicki Luxton and Dawn Oare for typing the manuscript.

References

[1] *N. H. C. Cooke, K. Olsen,* J. Chromatogr. Sci. **18**, 512 (1980).

[2] *A. Nahum, Cs. Horva*th, J. Chromatogr. **203**, 53 (1981).

[3] *K. E. Bij, Cs. Horváth, W. R. Melander, A. Nahum*, J. Chromatogr. **203**, 65 (1981).

[4] *L. Nondek, B. Buszewski, D. Berek*, J. Chromatogr. **360**, 241 (1986).

[5] *C. T. Mant, J. M. R. Parker, R. S. Hodges*, LC.GC Magazine of Liquid and Gas Chromatography **4**, 1004 (1986).

[6] *C. T. Mant, R. S. Hodges*, J. Chromatogr. **409**, 155 (1987).

[7] *J. Goworek, F. Nooitgedacht, M. Rijkhof, H. Poppe*, J. Chromatogr. **352**, 399 (1986).

[8] *R. E. Majors, H. J. Hopper*, J. Chromatogr. Sci. **12**, 767 (1974).

[9] *K. Karch, I. Sebestian, I. Halász*, J. Chromatogr. **122**, 3 (1976).

[10] *H. Hemetsberger, M. Kellermann, H. Ricken*, Chromatographia **10**, 726 (1977).

[11] *M. J. Walters*, Presented at the Tenth International Symposium on Column Liquid Chromatography, San Francisco (1986).

[12] *C. T. Mant, R. S. Hodges*, LC.GC Magazine of Liquid and Gas Chromatography, **4**, 250 (1986).

[13] *J. M. R. Parker, R. S. Hodges*, J. Prot. Chem. **3**, 465 (1985).

[14] *M. Hermodson, W. C. Mahoney*, Methods Enzymol. **91**, 352 (1983).

[15] *D. Guo, C. T. Mant, A. K. Taneja, J. M. R. Parker, R. S. Hodges*, J. Chromatogr. **359**, 499 (1986).

[16] *S. Y. M. Lau, A. K. Taneja, R. S. Hodges*, J. Chromatogr. **317**, 129 (1984).

[17] *C. T. Mant, R. S. Hodges*, in "High Performance Liquid Chromatography of Biological Macromolecules: Methods and Applications", (K. Gooding and F. Regnier, eds.), Marcel Decker Inc., 1987 (in press).

[18] *K. J. Wilson, E. van Wieringen, M. W. Berchtold, G. J. Hughes*, J. Chromatogr. **237**, 407 (1982).

[19] *R. K. Gilpin, J. A. Korpi, C. A. Janicki*, Anal. Chem. **47**, 1498 (1975).

[20] *J. D. Pearson, N. T. Lin, F. E. Regnier*, Anal. Biochem. **124**, 217 (1982).

[21] *M. C. Hennion, C. Picard, M. Caude*, J. Chromatogr. **166**, 21 (1978).

[22] *H. Hemetsberger, P. Behrensmeyer, J. Henning, H. Ricken*, Chromatographia **12**, 71 (1979).

[23] *P. Spacek, M. Kubin, S. Vozka, B. Porsch*, J. Liq. Chromatogr. **3**, 1465 (1980).

[24] *J. E. Rivier*, J. Liq. Chromatogr. **1**, 343 (1978).

[25] *J. L. Meek*, Proc. Nat. Acad. U.S. **77**, 1632 (1980).

[26] *P. Roumeliotis, K. K. Unger*, J. Chromatogr. **149**, 211 (1978).

Received: June 29, 1987
Revised manuscript
received: Sep. 15, 1987
Accepted: Sep. 18, 1987
F

Synthesis of an N-butylpyrrolidine Phase Using the Allyl Bonded Stationary Phase as an Intermediate

J. J. Pesek*/ E. L. Tarver/ A. Lange

Department of Chemistry, San Jose State University, San Jose, CA 95192, USA

Key Words

Column liquid chromatography
Allyl bonded phase
Aminomethylation reaction
Synthesis of new bonded phases

Summary

The versatility of the allyl phase is exploited by using it as an intermediate in the production of a weak anion exchange material that would be difficult to synthesize directly using organochlorosilane reagents. The stability of the allyl phase under the severe reaction conditions (170° and 140 atm of CO) of aminomethylation also is demonstrated. The product N-butylpyrrolidine phase is characterized spectroscopically by ESCA and DRIFT which also indicate a high conversion (greater than 90%) of the allyl phase. In addition, the carbon-nitrogen ratio of the product phase supports a high yield. Chromatographic characterization is done by the retention indices of the alkylarylketone homologous series and by capacity factor (k') determinations for inorganic anions and amino acids.

Introduction

In a recent report [1] we have shown that chlorination of a silica surface followed by reaction with a Grignard reagent offers a viable alternative to organochlorosilane reagents for the synthesis of chemically bonded stationary phases. Early studies used the chlorination/Grignard reaction scheme for bonding organic moities to glass [2] and to silica surfaces for gas chromatography [3, 4]. Previous problems with residual salts have been overcome by an acid:base clean-up process [1]. It should now be possible to produce phases which might be difficult or impossible to synthesize via organochlorosilane reagents.

In addition to the chlorination/Grignard synthetic pathway, it was suggested that the allyl phase might be a useful intermediate in the synthesis of new phases [1]. Subsequent reports have shown that the allyl phase could indeed serve such a function in making new phases for gas chromatography [5] as well as a cation exchange material for HPLC [6]. The possibility of *in situ* conversions was shown as another practical feature of the allyl phase for HPLC [6].

To be fully exploited as a viable intermediate in bonded phase synthesis, the allyl phase must be able to withstand extreme reaction conditions. If the allyl phase does not degrade easily, then it becomes a more useful intermediate in possible synthetic routes. Because olefin chemistry is so varied and the possible reaction products so numerous, the desirability of using such an intermediate is obvious.

One possible reaction for testing the durability of the allyl phase involves the aminomethylation of the double bond [7].

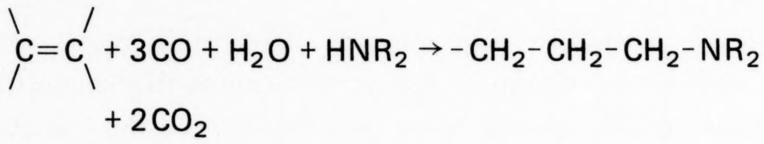

$$>C=C< + 3CO + H_2O + HNR_2 \rightarrow -CH_2-CH_2-CH_2-NR_2 + 2CO_2$$

This reaction utilizes a temperature of about 170° and a pressure of 140 atm of CO. In the presence of Rh_2O_3 as a catalyst, the reaction proceeds via formation of a rhodium carbonyl [8]. Such an *in situ* generation of a toxic carbonyl is much more satisfactory than a previous procedure which directly utilized $Fe(CO)_5$. In addition, the rhodium oxide powder is converted to a material which can be easily removed from the system after the reaction is complete without contaminating the silica. Yields in normal solution reactions have been about 80% with Rh_2O_3 alone and over 90% with the addition of some $Fe(CO)_5$. Therefore this reaction seems to be a good choice for checking the durability of the allyl phase as well as producing a useful product phase in reasonably good yield.

Experimental

Materials

The columns used were 25.0 cm × 4.6 mm ID or 10 cm × 4.6 mm ID and contained a packing of 10 μm

0009-5893/87 0815-05 $03.00/0

© 1987 Friedr. Vieweg & Sohn Verlagsgesellschaft mbH

Partisil (Whatman, Clifton, NJ) having a surface area of 350 m^2/g. The allyl phase was prepared according to a previously described procedure [1].

However, the apparatus was modified so that all reactions and washings up to the clean-up of the final product were done in a single closed system under 5 psi of nitrogen. Transfers of silica and reagents between vessels were done through glass tubing instead of a cannula [1] by using nitrogen pressure.

The alkylarylketone samples (Eastman, Rochester, NY, USA) for retention index measurements were used as received. All solutes in the test mixtures of inorganic anions and amino acids consisted of reagent grade chemicals. Chromatographic grade solvents were used as received and water was prepared by filtration through a Milli-Q (Millipore, Bedford, MA, USA) apparatus. The rhodium oxide catalyst (Morton Thiokol, Danvers, MA, USA) for the aminomethylation reaction was added in the form of an anhydrous powder. All of the other chemicals for the aminomethylation of the allyl phase were reagent grade.

Conversion of the allyl phase to the N-butylpyrrolidine phase was accomplished by adding 10g of the allyl bonded material to a Parr Model 4052 pressure reactor containing 60 mL of N-methylpyrrolidine, 5×10^{-4} moles of Rh_2O_3, 0.5 moles of pyrrolidine, and 0.5 moles of water. The reactor was closed and the pressure was raised to 140 atm with CO and the temperature was brought to 170°. The mixture was allowed to react for three hours. After the reaction period, the vapors were vented and the solid was collected by filtration. The product was washed with 100 mL of methanol, followed by 100 mL of DI Water, and then dried for 12h at 110°.

Apparatus

Carbon, hydrogen, and nitrogen elemental analyses were performed by Chemical Analytical Services (Berkeley, CA, USA). ESCA spectra were provided by Surface Science Laboratories (Mountain View, CA, USA). The results for each of these analyses are shown in Table I.

Infrared spectra were recorded on a Perkin-Elmer Model 1800 spectrometer operated in the diffuse reflectance (DRIFT) mode. The sample was prepared by making a mixture of 15% bonded phase in dry KBr. A difference spectrum was obtained by subtracting the spectrum of a 15% mixture of bare silica in dry KBr from the sample spectrum.

The HPLC system consisted of a Waters 6000A solvent delivery system and a Waters Model 440 absorbance detector. The ion chromatograph was a Waters Model ILC-1.

Chromatography

The retention index determinations were made according to the procedure of Smith [9] using 10% aqueous methanol as the mobile phase. Inorganic anions were separated using 5 mM phosphate buffer at several pH's, and amino acids k' values were determined in 5 mM phosphate buffer at pH = 8.0. Void volumes were determined by injection of nitrate in the HPLC system.

Results and Discussion

Previous studies [5, 6] on the allyl phase have shown that modifications can be easily monitored by the use of DRIFT difference spectra. Fig. 1 shows the two most important features of the IR spectrum for this purpose: the carbon-hydrogen stretching region and the carbon-carbon double bond stretch. In the spectrum of the allyl starting phase,

Table I. Elemental analyses of bonded phases.

	Allyl	N-butylpyrrolidine
ESCA (Atom %)		
C	9.7	14.0
N	a	1.2
O	59.0	56.0
Si	31.0	29.0
Microanalytical (Weight %)		
C	2.80	5.82
H	b	1.09
N	b	1.19

a = not detected, b = not determined

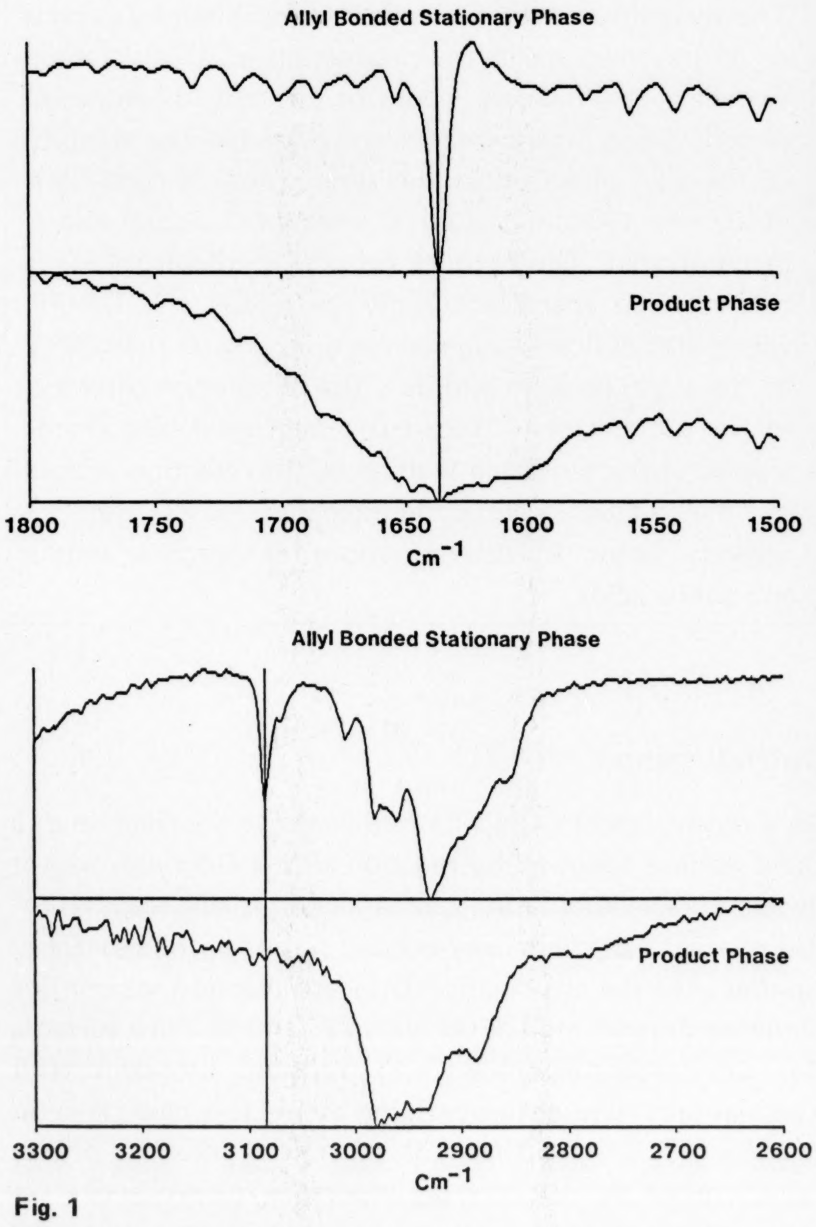

Fig. 1

DRIFT spectra of carbon-hydrogen stretching region (bottom) and carbon-carbon double bond stretching region (top) for both the allyl phase and the product from the aminomethylation of the allyl phase.

the carbon-hydrogen olefinic stretch at 3080 cm^{-1} and the carbon-carbon double bond stretch at 1630 cm^{-1} are easily identified. The spectrum of the product of the aminomethylation reaction is also presented in Fig. 1 and clearly shows that both of these peaks have disappeared. The complete absence of both of these peaks indicates that the reaction has proceeded in high yield, probably greater than 90%, although no exact quantitation can be arrived at from these results. Further evidence for the success of the reaction is seen in the marked change of the saturated carbon-hydrogen stretching region between 3000 and 2800 cm^{-1}.

Fig. 2 shows the ESCA spectrum of the product formed from the aminomethylation reaction. As expected, the spectrum consists of peaks for Si, O, and C as well as the N 1s peak at 398 eV. This is direct evidence that the nitrogen has been incorporated into the bonded phase. Also shown in Fig. 2 is the expanded spectrum between 298 and 318 eV where two rhodium peaks occur: the Rh (3d5/2) at 307 eV and the Rh (3d7/2) at 312 eV. No evidence of either peak is seen which corresponds to less than 0.4 atom % Rh indicating successful removal of most of the residual catalyst. Table I gives the atom percentage determinations from ESCA measurements on both the starting allyl phase and the reaction product. These values are useful as indicators and are not a true quantitative determination since the system has not been calibrated. What can be noted is an increase in the atom percent of carbon as the amount of organic material increases upon reaction with the pyrrolidine and the appearance of measureable nitrogen indicating a successful addition to the allyl bonded phase. As the surface becomes more densely coated with organic material the corresponding percentages of silicon and oxygen detected by ESCA decrease.

Table I also shows the carbon, hydrogen, and nitrogen elemental analyses. The carbon:hydrogen ratio (~5.3:1) based on weight % is close to the expected value (~6.0:1) for the $C_8H_{16}N$ formula of the N-butylpyrrolidine phase. The carbon:nitrogen ratio (~4.9:1) based on weight % is somewhat lower than the expected value of 6.8:1. This may be due to inaccuraccies in the analysis (a small error, particularly in nitrogen, will cause a large change in the ratio), some other bonding of pyrrolidine to the silica, or a combination of both. Bonding of pyrrolidine alone would give a carbon:nitrogen ratio of 3.4:1. It seems unlikely that cleavage of the allyl phase has occured because subjecting the material to similar conditions without the catalyst and pyrrolidine resulted in no loss of the allyl phase as determined by elemental analysis. The only reported [7] side product from this reaction is a ketone which would have the formula $C_8H_{14}NO$. This seems unlikely to be a significant fraction of the material since the ESCA analysis shows a decrease in oxygen upon reaction and there is no carbonyl stretch observed in the DRIFT spectrum. In contrast to the elemental analysis ESCA gives a result for the carbon:nitrogen ratio that is too high. The number based on the atom percent (see Table I) is 14.2/1.2 or ~11:1 instead of the 8:1 value expected. Because ESCA is a surface tecnique the detection efficiency for N may be lower since it is somewhat buried by the carbons in the pyrrolidine ring. This would lead to a higher carbon:nitrogen ratio. It appears that the discrepancies between the two methods are probably within experimental error and the conversion to the N-butylpyrrolidine phase has been successful. The extent of conversion is probably better than 90% because no evidence of the starting allyl phase is seen in the DRIFT spectrum. It should be noted that the 90% yield for the heterogeneous reaction in this study is better than the 80% reported for the normal homogeneous solution aminomethylation using rhodium oxide and carbon monoxide [7].

Fig. 3 is a plot of log k' vs. carbon number × 100 for the alkylarylketone homologous series on an N-butylpyrrolidine

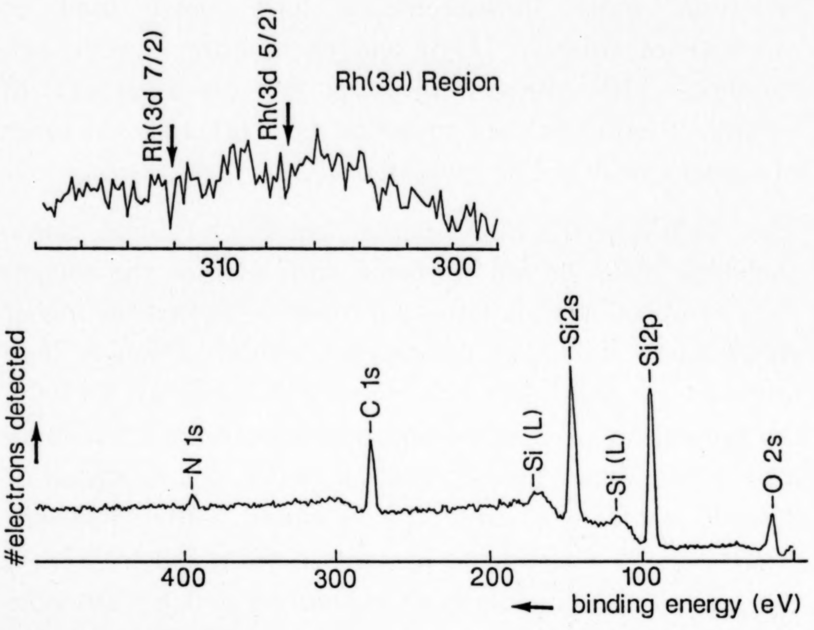

Fig. 2

Complete ESCA spectrum (top) and expanded ESCA spectrum of the rhodium region (bottom) of product from the aminomethylation of the allyl phase.

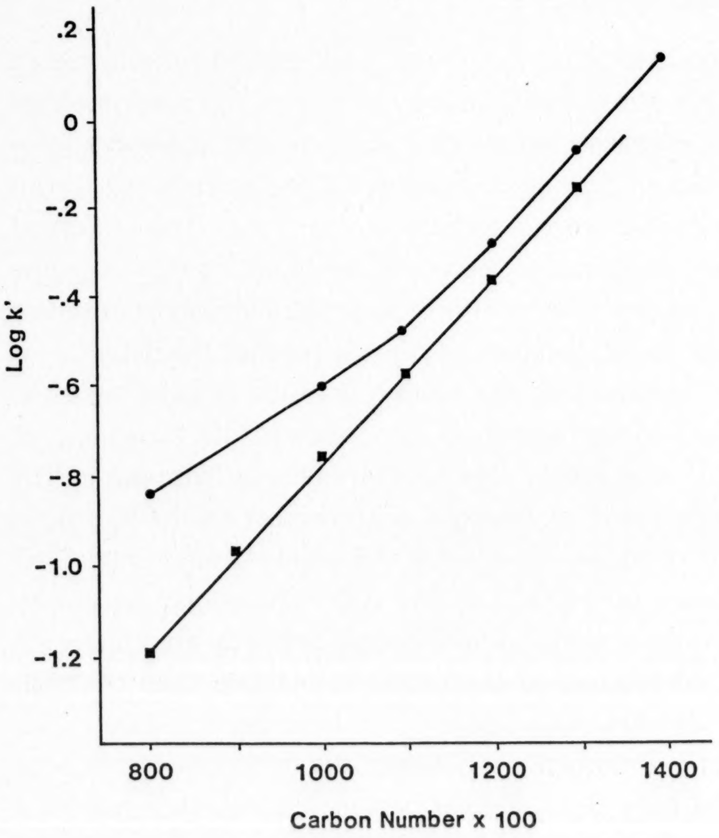

Fig. 3

Log k' vs. carbon number × 100 for alkylarylketones on N-butylpyrrolidine phase.

column as well as an allyl column [1]. It has been shown previously [6] that modification of the allyl phase will cause a shift in the retention indicies of the alkylarylketones. The figure clearly shows that such a shift has occured for the conversion of allyl to N-butylpyrrolidine. As expected, the retention volume of each of the compounds in the series increases after this conversion due to the higher carbon loading (Table I). It is not a uniform increase in retention index which would occur for simple lenthening of a normal hydrocarbon chain. In this case the increase in carbon loading involves the addition of the bulky pyrrolidine group. A greater increase in retention is observed for the smaller members of the homologous series. Steric hindrance may prevent the higher molecular weight homologs from completely interacting with all of the bonded phase. While retention index measurements have been used to characterize columns [1, 6] and to monitor column performance [10], further investigations on a variety of columns need to be done to define more precisely the types of curves that might be generated.

The N-butylpyrrolidine phase exhibits typical anion exchange behavior for inorganic samples. For the solvent peak a reversal in conductivity is observed as first the higher conductance excluded cations are eluted which is then followed by the lower conductance solvent. At pH = 6.5 the separation of fluoride and bicarbonate occurs with an α of $\sim$9.5. When the pH is raised to 7.5, the retention of fluoride is shortened so that it is eluted with the solvent and the k' of bicarbonate is reduced from 3.3 to 1.7. At this pH it is also possible tu elute chloride with a reasonable retention time. When the pH is raised further to 8.2, the chloride k' is reduced from 6.3 to 2.1, while the bicarbonate k' becomes 0.4. The elution profiles observed in this study are consistent with other anion exchange materials [11a, 12a] and along with the solvent peak behavior are further chromatographic indications of the success of the aminomethylation reaction.

It was observed that the solvent peak elution time decreased as the pH was raised. This may be due to aggregation of the bonded material which may exclude the solvent and/or a decrease in hydrogen bonding of the solvent as protons are removed from the tertiary amine group. The effects of hydrogen bonding can be tested by injecting H_2O into the system. In this case an almost symmetrical peak is observed when the lower conductivity water reaches the detector. If D_2O is injected into the system, a much broader two-step peak with longer retention is observed. The broadness of the peak is probably due to the increased strength of the deuterium bond to nitrogen with respect to the hydrogen bond to nitrogen. Eventually the more strongly held D_2O is displaced by H_2O. The two-step feature may be due to the presence of both protonated and unprotonated nitrogen. If a 50:50 mixture of D_2O/H_2O is injected, then the peak retains the two-step feature but becomes narrower. This behavior is intermediate between the two extremes of pure H_2O and pure D_2O. Similar behavior is not observed for a commerical strong anion exchange material. Symmetrical peaks are obtained for both D_2O and H_2O when injected into an identical 5 mM phosphate buffer.

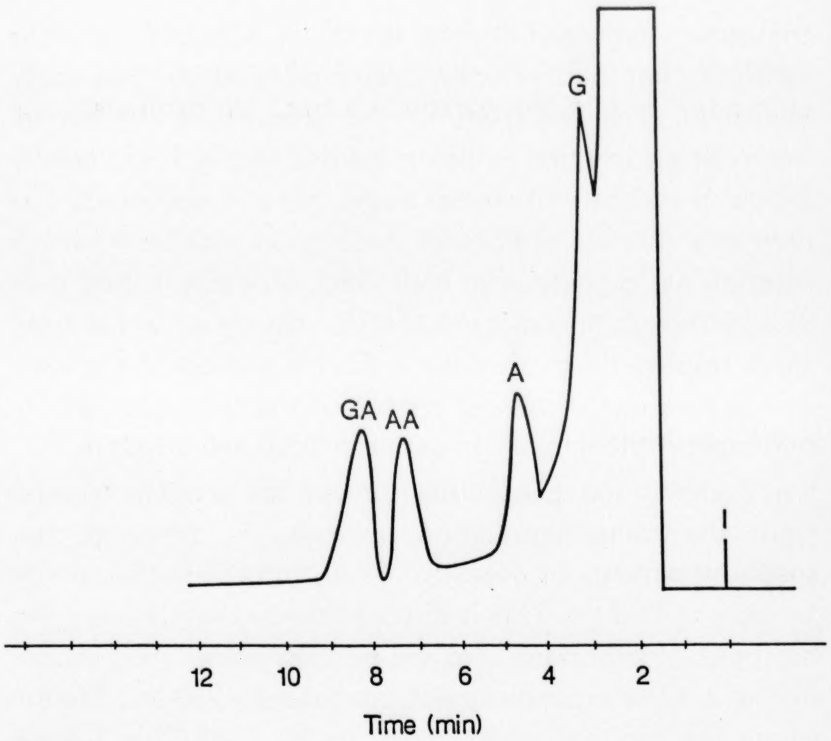

Fig. 4

Separation of some amino acids on the N-butylpyrroldine phase.
I = injection.
Sample: G = Glycine, A = Alanine, AA = Aspartic Acid, GA = Glutamic Acid. Mobile Phase: 5 mM phosphate, pH = 8.0.

Table II. Capacity factors (k') for amino acids^{a}

Amino Acid	k'
Glycine	0.4^{b}
Alanine	1.2
Leucine	2.9 (3.1)^{b}
Phenylalanine	2.8
Aspartic acid	2.6
Glutamic acid	3.0

a = solvent is 5 mM phosphate, pH = 8.0; column 10.0 cm X 4.6 mm ID
b = column 25.0 cm X 4.6 mm ID

Fig. 4 illustrates the separation of several amino acids on the N-butylpyrrolidine phase. Capacity factors for these and several other amino acids are given in Table II. While the results are not identical to those obtained for other commercial anion exchangers [11b, 12b], the difference may be due to a mixture of retention mechanisms. At the pH used for this measurement (8.0) the bonded phase is probably a mixture of protonated (charged) and unprotonated (uncharged) pyrrolidine groups. Such evidence already exists from both the solvent peak elution behavior as a function of pH and as a function of deuterium substitution. Therefore it is quite likely that retention of the amino acids is a mixture of anion exchange effects as well as reverse phase effects. Kohler [13] has synthesized a somewhat similar polymeric phase that seems to possess mixed retention characteristics. The heterocylic ring in that study was a pyrrolidone which has one carbonyl group instead of the totally nonfunctionalized four carbon atoms that are in the pyrrolidine ring. Unfortunately the anion exchange properties of this material were not investigated although the protein separations reported might indicate such behavior. More detailed studies of both the retention and solvent peak characteristics of the N-butylpyrrolidine phase are currently underway.

Acknowledgement

The Partisil silica used for stationary phase preparation in this study was obtained from the substrate collection established at Duke University by a gift from Whatman Inc.

References

[1] *J.J. Pesek, S.A. Swedberg,* J. Chromatogr. **361,** 83 (1986).
[2] *J. Wartmann, H. Duel,* Helv. Chim. Acta **42,** 1166 (1959).
[3] *D. Locke, J. Schmerund, B. Banner,* Anal. Chem. **44,** 90 (1972).
[4] *J.J. Pesek, J.A. Graham,* Anal. Chem. **49,** 133 (1977).
[5] *J.J. Pesek, P. Mahabadi, S.J. Chan,* Chromatographia **23,** 3 (1987).
[6] *J.J. Pesek, G. Guiochon,* J. Chromatogr. **395,** 1 (1987).
[7] *A.F.M. Iqbal,* Helv. Chim. Acta **54,** 1440 (1971).
[8] *P. Chini, S. Martinengo,* Chem. Commun. 1092 (1969).
[9] *R.M. Smith,* J. Chromatogr. **236,** 313 (1982).
[10] *S.A. Swedberg, P.M. Bassett, J.J. Pesek, A. Fink,* J. Chromatogr. **393,** 317 (1987).
[11] "Waters Sourcebook for Chromatography Columns and Supplies", 1986, a) p. 88; b) p. 34.
[12] "Chromatography Catalog No. 100", Alltech Associates, 1987, a) pp. 385, 387; b) p. 349.
[13] *J. Kohler,* Chromatographia **21,** 573 (1986).

Received: June 30, 1987
Revised manuscript
received: Sep 22, 1987
Accepted: Sep 29, 1987
F

A Quantitative Evaluation of the Electrostatic Theory for Ion Pair Chromatography

J. Ståhlberg[1]

Astra Pharmaceutical Production AB, Quality Control, S-151 85 Södertälje, Sweden

Key Words

Ion-pair chromatography
Retention mechanism
Electrostatic theory, quantitative evaluation

Summary

A quantitative model for ion pair chromatography based on the electrostatic theory is described. The model is based on the solution of the linearised Poisson-Boltzmann equation in a cylinder. The obtained equations are compared with experimental data from a number of different systems. The agreement between theory and experiments is satisfactorily. Systematic deviations due to the use of the linearised equation and ion correlation effects are discussed.

Introduction

Liquid chromatographic analysis of organic ions is often carried out with a non-polar stationary phase and a polar mobile phase containing an amphiphilic ion. The name ion-pair chromatography seems to be the most widely used for this technique and will be used also in this paper. A great number of models of the so-called "mechanism" of ion-pair chromatography have been published and some of these are found in references [1–11].

A majority of the proposed models, including the ion-pair-model [1] and the dynamic ion-exchange mode [1, 5, 7] are stoichiometric, i.e. they construct a reaction scheme and the corresponding equilibrium constants express the interaction between the oppositely charged amphiphilic modifier and analyte ions in the system. By combining theese constants with the Langmuir-isotherm equations are obtained for the capacity factor as a function of different variables.

From a physical point of view, the presence of long range forces (i.e. the coulombic-interactions) makes all the stoichiometric models incapable to give a correct description of the different processes of ion-pair chromatography. This is due to the fact that the used equilibrium constants are not constants when the electrostatic field varies, e.g. at a charged surface with varying surface charge density.

The effect of coulombic interactions on ionic systems are usually obtained by solving the Poisson-Boltzmann equation. This equation has a rigorous solution for a charged planar surface in contact with an electrolyte, i.e. the well known Gouy-Chapman theory [12,13]. The Gouy-Chapman theory in combination with a modified Langmuir isotherm was recently applied to ion-pair chromatography [11] and it was found that it qualitatively and semiquantitatively describes the behavior of such systems.

It is important in this context to comment on the physical background of the electrostatic theory for ion-pair chromatography. Consider a system composed of a surface and a solvent containing different ions. If it is assumed that the different ions have different affinity to the surface, the ions will be differently distributed between the surface and the solvent. So, if the system is composed of e.g. a RP-18 surface and sodium octylsulfate dissolved in polar solvent, the octylsulfate ions have a higher affinity to the surface than the Na^+-ions. This means that the concentration of octylsulfate in the surface layer will be higher than the concentration of sodium ions. An electrical double layer is therefore formed and a difference in electrostatic potential between the bulk solvent and the surface exists. So, in ion-pair chromatography, it is the different solubility in the stationary phase of the amphiphile and its counter ion that creates the surface potential. This difference is usually such that the surface potential has a strong influence on the distribution of analyte ions between the stationary and mobile phase. A theory for ion-pair chromatography must therefore include a treatment of the surface potential.

The basic assumption of the electrostatic theory is that the changes in capacity factor for an ionic analyte, when varying the concentration of amphiphilic, is governed by the surface potential. It has recently been shown that this basic assumption holds well for a number of amphiphiles and analytes [14].

---

[1] Affiliated to the Institute of Physical Chemistry, University of Uppsala, Sweden.

0009-5893/87 0820-07 $03.00/0

© 1987 Friedr. Vieweg & Sohn Verlagsgesellschaft mbH

It is important to note that a number of secondary effects are neglected in this theory e.g. specific interactions between the ions, monopole-dipole interactions, changes in the properties of the surface layer and mobile phase when varying the concentration of amphiphile, image forces etc. Dependent on the chromatographic system these secondary effects can be expected to be more or less important. A quantitative theory including all secondary effeects are, for a number of reasons, out of reach. However, since the surface potential dominates in most cases, it is important to investigate if existing theories for calculation of this potential is applicable to ion-pair chromatography.

In this paper a linear isotherm is used in combination with the electrostatic theory. The expression obtained from solving the linearised Poisson-Boltzmann equation for a cylinder is used to calculate the surface potential. The purpose is to investigate how such a simplified theory compares with experimental results and to analyse the deviations in order to improve the theory. It is found that this simplified electrostatic model in general agrees well with the experimental results.

Theory

The electrostatic theory for ion-pair chromatography is developed in ref. [11]. The hypothesis of this theory is that the capacity factor of an analyte ion B is expressed by eq. (1).

$$k'_{c,B} = \phi\ \exp\left(\frac{-\Delta G_B^0}{RT} - \frac{z_B F \Delta\psi_0}{RT}\right) = k'_{0,B}\exp\left(-\frac{z_B F \Delta\psi_0}{RT}\right) \qquad (1)$$

where ΔG_B^0 is the free energy of adsorption of B and $\Delta\psi_0$ is the difference in electrostatic potential between the surface of the stationary phase and the mobile phase. ϕ is the phase ratio of the column and $k'_{0,B}$ is the capacity factor for B when $\Delta\psi_0 = 0$. The electrostatic potential of the bulk mobile phase can to a first approximation be considered to be a constant which in the following is set to zero. It is usually found that when varying the concentration of amphiphilic modifier the change in capacity factor for an uncharged molecule is small compared to the change for a charged molecule. As an approximation we therefore assume that $-\Delta G_B^0$ is independent of the electrostatic potential of the surface, ψ_0. This approximation is not strictly true since the changes in ψ_0 are obtained by varying the concentration of amphiphilic modifier at the surface, and will therefore be coupled to slight changes of the properties of the surface layer. An important feature of eq. (1), even with this approximation, is that it gives a simple and consistent explanation for the retention of analyte ions with different values of z_B. When the charge of the analyte ion is of opposite (same) sign as the charge of the amphiphilic modifier, the analyte experiences an electrostatic attraction (repulsion) to (from) the surface and the retention increases (decreases).

It is clear from the foregoing discussion that the calculation of ψ_0 is of outmost importance for a quantitative description of ion-pair chromatography. The general relation between ψ_0, and the surface concentration of amphiphilic modifier, n_A, for a planar surface is obtained with the Gouy-Chapman equation. The basic assumptions of this equation are: 1) the charged surface is impenetrable for the ions in the electrolyte, 2) the charge is uniformly spread over the surface, 3) the electrolyte ions behave as point charges, 4) the mobile phase is a continuum up to the surface and with a constant dielectricity constant [12, 13]. Despite all of these limitations it is well known that the theory is in good agreement with real systems containing monovalent electrolyte ions.

It has been found that the Gouy-Chapman theory correctly describes the behavior of mono-valent electrolyte ions in non-homogenous systems for high concentration (~ 10 M) of the electrolyte near the surface [15] and for a concentration of surface charges $< 3 \cdot 10^{-6}$ mol/m^2 in contact with 0.1 M electrolyte solution [16]. However, due to the neglect of ion-ion correlation the agreement is poorer for electrolytes containing ions with higher charge [16, 17]. Deviations from the theory are also expected when the electrolyte contains ions with high polarizability. The fact that the Gouy-Chapman theory is successful, despite its assumptions, is discussed in ref. [13].

The Influence of Pores on the Electrostatic Theory

The solution of the Poisson-Boltzmann equation is dependent on the geometry of the system. In liquid chromatography the system usually consists of porous particles packed in a column. An explicit relation between ψ_0 and the concentration of surface charge, n_A, at a cylindrical surface has been obtained from the linearised Poisson-Boltzmann equation [18]. The equation is:

$$\psi_0 = \frac{z_A n_A F}{\kappa \epsilon_0 D} \cdot \frac{I_0(\kappa r)}{I_1(\kappa r)}. \qquad (2)$$

Here I_0 and I_1 are modified Bessel functions of the first kind of order zero and one, respectively. D is the dielectricity constant of the mobile phase and ϵ_0 is the permittivity of vacuum. The pore radius is r and κ is the reciprocal Debye-length and is defined as

$$\kappa = F\,\Big(\sum_i z_i^2 \bar{c}_i / \epsilon_0 DRT\Big)^{1/2} \qquad (3)$$

where $\bar{c}_i$ is the bulk concentration of ions (mol/m^3) with charge z_i. So κ^2 is proportional to the ion-strength of the mobile phase.

By comparing eq. (2) with the solution for a planar surface it is seen that the potential on the cylindrical surface is a factor $I_0(\kappa r)/I_1(\kappa r)$ higher for equal surface charge densities. In Fig. 1 the quotient $I_0(\kappa r)/I_1(\kappa r)$ is plotted as a function of κr, calculated from values in ref. [19]. It can be concluded that in real chromatographic systems with an unknown distribution of pore radii the relation between ψ_0 and ionic-strength is complicated.

The theories for ion-pair chromatography usually relates the retention of the analyte to the concentration of the amphiphilic modifier in the mobile phase. In order to calculate ψ_0 an expression for the isotherm of the amphiphilic modifier is therefore required and most of the proposed models use a Langmuir isotherm. The interface between the polar mobile phase and the hydrophobic

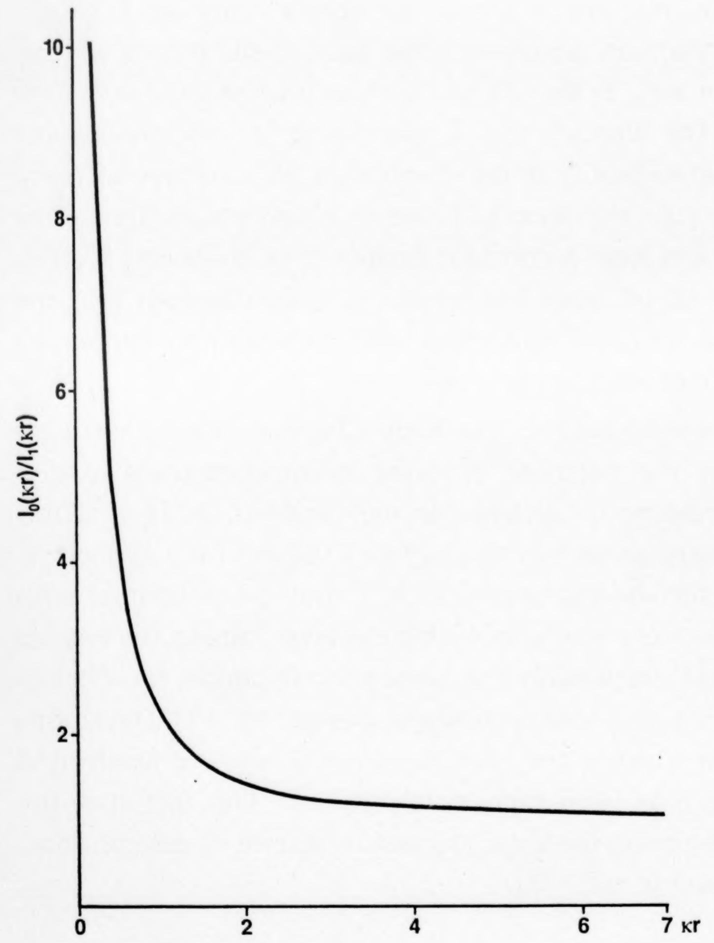

Fig. 1
$I_0(\kappa r)/I_1(\kappa r)$ as a function of κr.

RP-surface has the same characteristics in many respects as the oil-water interface. For the isotherm of amphiphilic molecules at this latter interface Davies and Rideal writes [13]:

> "For the adsorption of ions (such as laurysulphate, $C_{12}H_{25}SO_4^-$) the Langmuir equation no longer holds: such adsorption equations are necessarily invalid because they contain no term for the energy of the electrical double layer which is constituted by the charged surface and the underlying counter-ions."

It is therefore not surprising that measured isotherms on RP-18 do not fit the Langmuir equation [20, 21]. Davies and Rideal kinetically derived a modified Langmuir isotherm where the electrostatic potential of the surface was included [13]. This isotherm has recently been used to derive equations for retention of analytes in ion-pair chromatography [11].

A Simplified Electrostatic Theory for Ion-Pair Chromatography

In ref. [11] the theory for ion-pair chromatography was developed from the rigorous solution of the Poisson-Boltzmann equation for a planar surface and a modified Langmuir isotherm. Due to the complicated mathematical form of these equations they are difficult to use in practice. A more practical expression is obtained if two assumptions are made:

1. The solution of the linearised Poisson-Boltzmann is used, i.e. eq. (2).
2. The concentration of amphiphilic modifier at the surface is much lower than the mono-layer capacity.

The latter assumption means that the isotherm for an amphiphilic modifer (A) can be written as:

$$n_A = B \cdot c_A \cdot \exp\left(-\frac{\Delta G_A^0}{RT} - \frac{z_A F \psi_0}{RT}\right) \tag{4}$$

where ΔG_A^0 is the free energy of adsorption for A when $\psi_0 = 0$ and B is a measure of the thickness of the surface layer. Substituting eq. (2) into eq. (4) one obtains

$$\psi_0 \cdot \exp\left(\frac{F\psi_0}{RT}\right) = \frac{B \cdot I_0(\kappa r) \cdot F \cdot \exp\left(-\frac{\Delta G_A^0}{RT}\right) z_A}{\kappa \epsilon_0 D I_1(\kappa r)} \cdot c_A \,. \tag{5}$$

When the ionic-strength is constant the left hand side of the equation is proportional to the concentration of amphiphilic modifier in the mobile phase. According to eq. (1) the changes in the capacity factor are due to changes in ψ_0. Substituting eq. (1) into eq. (5) and taking the logarithm, eq. (6) is obtained.

$$-\frac{z_A}{z_B} \ell n\left(\frac{k'_{c,B}}{k'_{0,B}}\right) + \ell n\left(-\frac{RT}{z_A z_B F} \ell n\left(\frac{k'_{c,B}}{k'_{0,B}}\right)\right) = \ell n c_A + \ell n K \tag{6}$$

where

$$K = \frac{B \cdot I_0(\kappa r) F \cdot \exp\left(-\frac{\Delta G_A^0}{RT}\right)}{\kappa \epsilon_0 D I_1(\kappa r)} \,. \tag{7}$$

When the capacity factor is expressed as a function of the concentration of a monocharged amphiphilic modifier in the mobile phase the following equation is obtained:

$$\left(\frac{k'_c}{k'_0}\right)^{-\frac{z_A}{z_B}} = \exp\Bigg(\frac{FK}{RT} c_A \exp\Bigg(-\frac{FK}{RT} c_A \exp\Bigg(-\frac{FK}{RT} c_A \exp \Bigg(-\frac{FK}{RT} c_A \exp \ldots\Bigg)\Bigg)\Bigg)\Bigg) \ldots \tag{8}$$

Since this equation is of an infinite form it is of no practical use. Eq. (6) will therefore be used when this simplified electrostatic theory is compared with experimental results, i.e. Figs. 2–6.

Results and Discussion

According to the simplified electrostatic theory the left hand side of eq. (6) as a function of $\ell n c_A$ is a straight line with slope 1. The electrostatic theory also predicts that all analyte ions fall on the same straight line for a given amphiphilic modifier and mobile phase. These predictions are tested in this paper by using experimental results from ref. [14]. The result is presented in Figs. 2–6 for different amphiphilic modifiers and for each amphiphile a number of analyte ions. The full line in each figure is the theoretical line with slope 1. There is a corresponding table to each figure presenting numerical information for each analyte ion. For analytes with charge −2, the $k'_{0,B}$ value is estimated from eq. (6) and the mean value of the monocharged analytes. In the experiments performed with hexanesulphonate as amphiphilic modifier (Table V) the variation

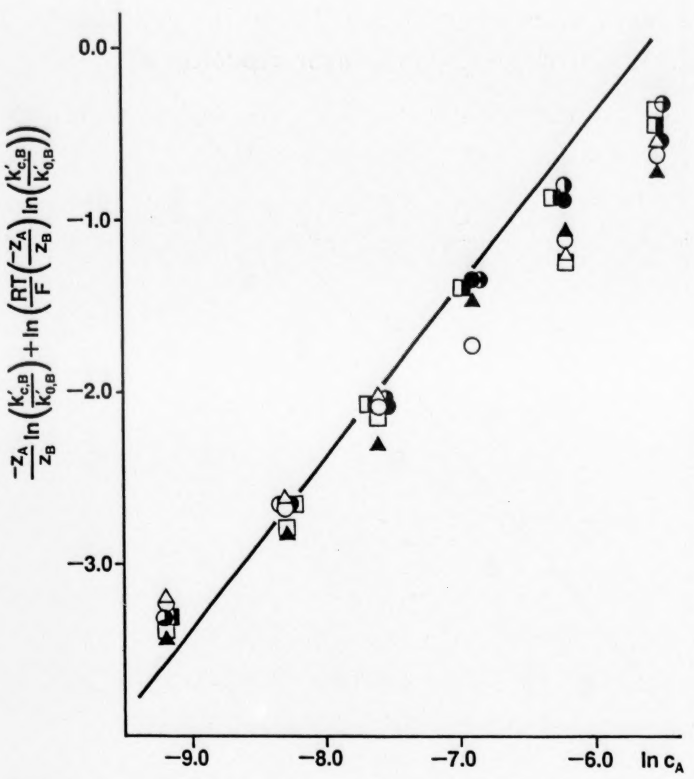

Fig. 2

$-\frac{z_A}{z_B}\ln\left(\frac{k'_c}{k'_0}\right)+\ln\left(-\frac{z_A}{z_B}\cdot\frac{RT}{F}\ln\left(\frac{k'_c}{k'_0}\right)\right)$ as a function of $\ln c_A$.

(See eq. (6).)

A = tetrabutylammonium ion. Mobile phase: CH_3CN/H_2O (10:90), pH = 2.1. Full line is the theoretical line with slope = 1. Symbols for the analytes are found in Table I.

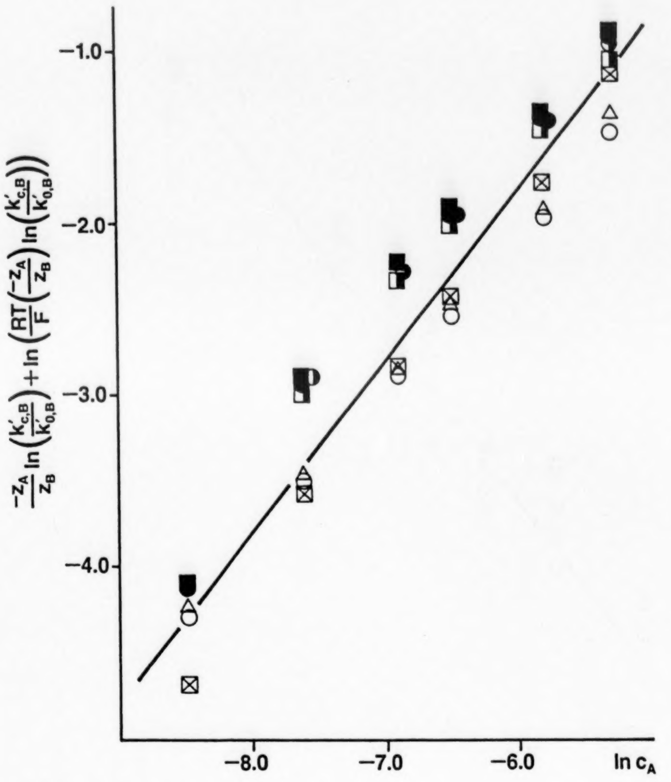

Fig. 3

$-\frac{z_A}{z_B}\ln\left(\frac{k'_c}{k'_0}\right)+\ln\left(-\frac{z_A}{z_B}\cdot\frac{RT}{F}\ln\left(\frac{k'_c}{k'_0}\right)\right)$ as a function of $\ln c_A$.

(See eq. (6).)

A = tetrabutylammonium ion. Mobile phase: CH_3CN/H_2O (20:80), pH = 2.1. Full line is the theoretical line with slope 1. Symbols for the analytes are found in Table II.

Table I. Numerical data for the fit of straight lines to experimental data in Fig. 2. Amphiphilic modifier: tetra butylammonium chloride. Mobile phase: acetonitrile/water (10:90), pH = 2.1.

Analyte, symbol	Charge of the analyte	Intercept	Slope	Correlation coefficient
Etidocaine, ○	+ 1	3.33	0.72	0.999
Bupivacaine, △	+ 1	3.29	0.71	0.998
Bensyltriethylammonium, □	+ 1	3.89	0.80	0.995
Naphtalene-2-sulfonate, ●	− 1	4.00	0.80	0.996
Bensylsulfonate, ▲	− 1	3.67	0.77	0.993
Naphtalene-1,5-disulfonate, ◑	− 2	4.26	0.83	0.998
1-Naphtol-3,6-di-sulfonate, ◨	− 2	4.10	0.81	0.998

Table II. Numerical data for the fit of straight lines to experimental data in Fig. 3 Amphiphilic modifier: tetra butylammonium chloride. Mobile phase: acetonitrile/water (20:80), pH = 2.1.

Analyte, symbol	Charge of the analyte	Intercept	Slope	Correlation coefficient
Etidocaine, ○	+ 1	3.14	0.87	1.000
Bupivacaine, △	+ 1	3.27	0.88	0.999
Bensyltributylammonium ⊠	+ 1	4.62	1.08	0.999
Naphtalene-2-sulfonate, ●	− 1	4 33	0.97	0.994
Anthraquinone-2-sulfonate, ■	− 1	4.38	0.98	0.994
Naphtalene-1,5-disulfonate, ◑	− 2	4.44	0.99	0.989
1-Naphtol-3,6-disulfonate, ◨	− 2	4.26	0.98	0.992

of κ is not negligible. The reported values has therefore been corrected for this according to eq. (2) assuming that the $I_0(\kappa r)/I_1(\kappa r)$ is constant.

From the tables it is seen that the linearity is very good in all cases but the slope is in general somewhat lower than what is predicted from eq. (6). This equation is, however, based on a linear relationship between the potential and the concentration of A on the surface. This is a good approximation for a limited potential range i.e. $\Delta\psi^0 < 30$ mV. In these cases the potential range is usually ≈ 60 mV so the condition for linearity is not strictly fulfilled.

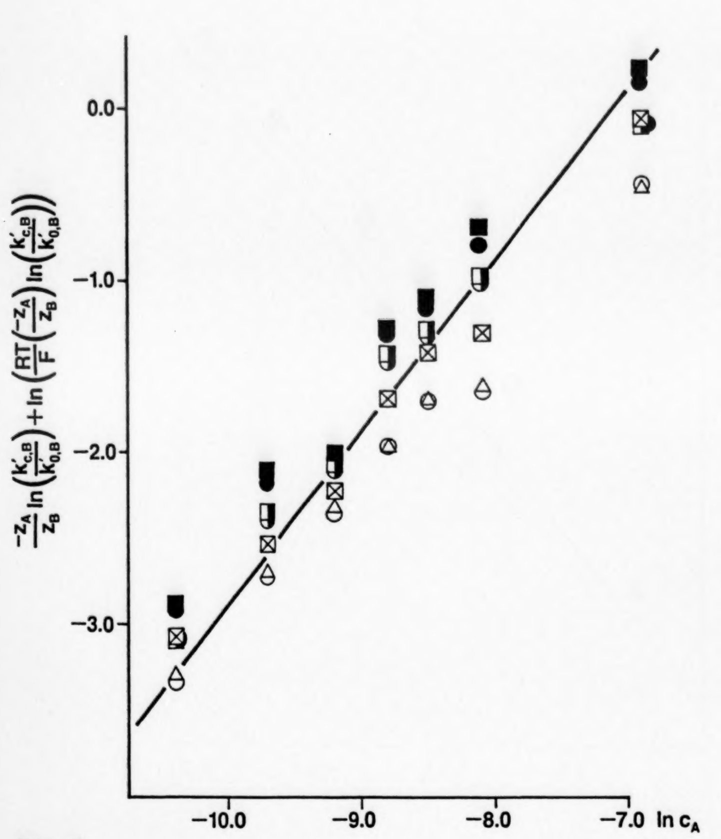

Fig. 4

$-\frac{z_A}{z_B}\ln\left(\frac{k'_c}{k'_0}\right)+\ln\left(-\frac{z_A}{z_B}\cdot\frac{RT}{F}\ln\left(\frac{k'_c}{k'_0}\right)\right)$ as a function of $\ln c_A$.

(See eq. (6).)

A = tetrapentylammonium ion. Mobile phase: CH_3CN/H_2O (20:80), pH = 2.1. Full line is the theoretical line with slope 1. Symbols for the analytes are found in Table III.

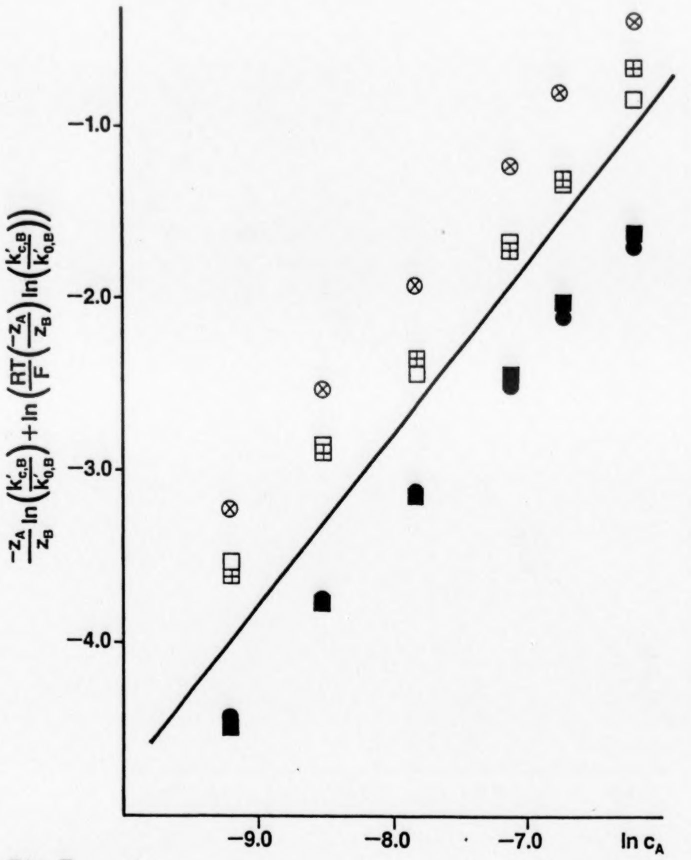

Fig. 5

$-\frac{z_A}{z_B}\ln\left(\frac{k'_c}{k'_0}\right)+\ln\left(-\frac{z_A}{z_B}\cdot\frac{RT}{F}\ln\left(\frac{k'_c}{k'_0}\right)\right)$ as a function of $\ln c_A$.

(See eq. (6).)

A = octylsulphate. Mobile phase: CH_3CN/H_2O (10:90), pH = 3.4. Full line is the theoretical line with slope 1. Symbols for the analytes are found in Table IV.

Table III. Numerical data for the fit of straight lines to experimental data in Fig. 4 Amphiphilic modifier: tetra pentylammonium chloride. Mobile phase: acetonitrile/water (20:80), pH = 2.1.

Analyte, symbol	Charge of the analyte	Intercept	Slope	Correlation coefficient
Etidocaine, ○	+ 1	5.10	0.81	0.994
Bupivacaine, △	+ 1	5.01	0.80	0.995
Bensyltributylammonium, ⊠	+ 1	5.80	0 86	0.995
Naphtalene-2-sulfonate, ●	− 1	6.33	0.88	0.994
Anthraquinone-2-sulfonate, ■	− 1	6.52	0.90	0.993
Naphtalene-1,5-disulfonate, ◑	− 2	5.96	0.86	0.995
1-Naphtol-3,6-disulfonate, ◨	− 2	5.95	0.86	0.993

Table IV. Numerical data for the fit of straight lines to experimental data in Fig. 5. Amphiphilic modifier: octylsulfate. Mobile phase: acetonitrile/water (10:90), pH = 3.4.

Analyte, symbol	Charge of the analyte	Intercept	Slope	Correlation
Lidocaine, ⊗	+ 1	5.59	0.96	1.000
Bensyltriethylammonium, □	+ 1	4.65	0.89	0.998
Bensyltrimethylammonium, ⊞	+ 1	5.14	0.95	0.997
Naphtalene-2-sulfonate, ●	− 1	4.01	0.91	1.000
Anthraquinone-2-sulfonate, ■	− 1	4.44	0.97	0.999

By comparing the general solution for a plane surface with the corresponding linearised Poisson-Boltzmann equation, the slope is estimated to $\simeq 0.82$ for a potential range of 60 mV. So, the small deviations between theory and experimental results are in part due to non-linearities in the rigorous equations. There is also a variation in slope mainly between the different systems that have been studied, e.g. the slope for tetrabutylammonium ion is in the range 0.87–1.08 in one system and in the range 0.71–0.83 in another system. These differences may be caused by e.g. differences in the solvation of the tetrabutylammonium ion on the surface. This difference gives a difference in the

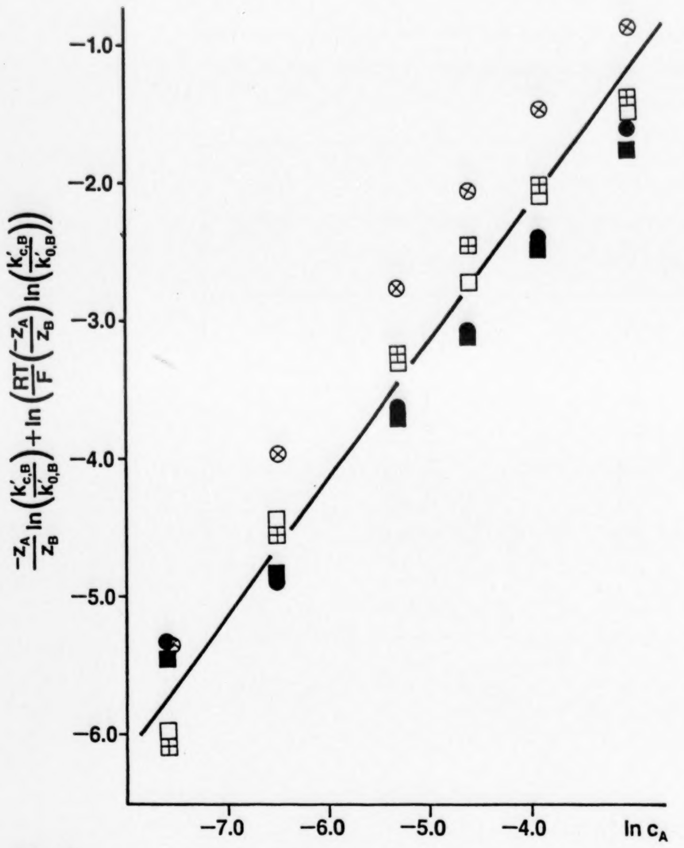

Fig. 6

$-\frac{z_A}{z_B}\ln\left(\frac{k'_c}{k'_0}\right)+\ln\left(-\frac{z_A}{z_B}\cdot\frac{RT}{F}\ln\left(\frac{k'_c}{k'_0}\right)\right)$ as a function of $\ln c_A$.

(See eq. (6).)

A = hexylsulphonate. Mobile phase: CH_3CN/H_2O (10:90), pH = 3.4. Full line is the theoretical line with slope 1. Symbols for the analytes are found in Table V.

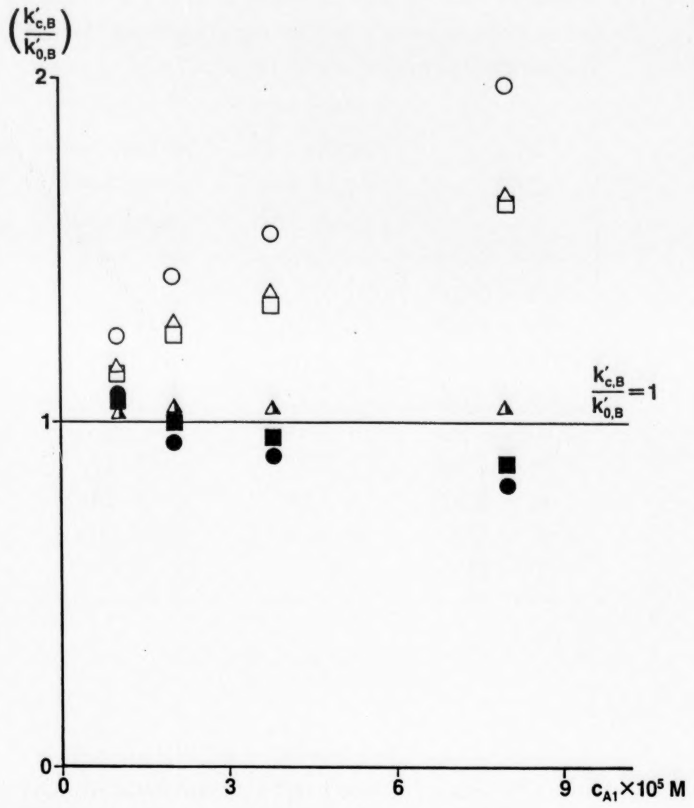

Fig. 7

$k'_{c,B}/k'_{0,B}$ as a function of concentration of octylsulfate (A) at low concentrations.

Analytes are: ○ = lidocaine, □ = bensyltriethylammonium ion, △ = bensyltrimethylammonium ion, ■ = Anthraquinone-2-sulfate, ● = Naphtalene-2-sulfonate, ▲ = Phenol.

Experimental conditions as in Fig. 5.

Table V. Numerical data for the fit of straight lines to experimental data in Fig. 6. Amphiphilic modifier: hexanesulfonate. Mobile phase: acetonitrile/water (10:90), pH = 3.4.

Analyte, symbol	Charge of the analyte	Intercept	Slope	Correlation
Lidocaine, ⊗	+ 1	2.60	1.02	0.997
Bensyltriethylammonium, □	+ 1	1.91	1.00	0.994
Bensyltrimethylammonium, ⊞	+ 1	2.45	1.04	0.982
Naphtalene-2-sulfonate, ●	− 1	1.01	0.87	0.997
Anthraquinone-2-sulfonate, ■	− 1	1.10	0.88	0.995

interaction between the adsorbed amphiphilic modifier, the charged analyte ions and the electrolyte counter-ions in the mobile phase.

From the tables and the figures it is seen that there are systematic differences between analytes with the same sign of charge as the amphiphilic modifier and analytes with opposite sign of charge. The general trend is that the slope is lower for analytes with the same sign of charge as the amphiphilic modifer, than when they are of opposite sign. The figures also show that there is generally a small difference in the value at the ordinate between analytes with different sign of charge. When the sign of the analyte is opposite to the sign of the amphiphilic modifier the value at the ordinate is generally higher than when they are of the same sign.

However, the differences between analytes of the same charge are generally negligible. According to eqs. (5) and (6) the value of the ordinate in the figures is related to the potential experienced by the analyte and the slope of the straight line is related to the change in this potential when c_A changes. The results show that analytes with the same sign as the amphiphile generally experience a lower potential than analytes with opposite sign. The slope is also lower for analytes with the same sign as the amphiphile i.e. these ions experience a lower increase in potential than analyte ions with opposite sign.

The interaction between analyte and amphiphile is to some extent dependent on their relative sign of charges specific to the analyte's sign of charge and to a lesser extent to its molecular strucutre. These experimental results indicate that these specificities generally contribute with less than 20% of the total change in interaction [14].

It can be concluded that the apparent electrostatic potential created by the adsorbed amphiphile is somewhat dependent on the analyte's sign of charge. This relatively small deviation from the electrostatic theory is probably due to ion-correlation and the fact that the charges at the surface are discrete and not smeared out. Consider e.g. a negatively

Table VI. The change of the apparent electrostatic potential ($\Delta\psi_0$) calculated from eq. (1) for various analytes when the concentration of octylsulphate changes, ΔC_A. Mobile phase: acetonitrile/water (10:90), pH = 3.4. Experimental procedure as in ref. [14].

ΔC_{A^-} mM	Naphtalene-2-sulfonate $\Delta\psi_0$, mV	Anthraquinone-2-sulfonate $\Delta\psi_0$, mV	Lidocaine $\Delta\psi_0$, mV	Bensyltriethylammonium $\Delta\psi_0$, mV	Bensyltrimethylammonium $\Delta\psi_0$, mV	$\frac{\Delta\psi_+}{\Delta\psi_-}$
0.00 → 0.01	0	0	– 5.75	– 3.90	– 3.33	∞
0.01 → 0.02	– 1.66	– 0.18	– 3.31	– 2.41	– 2.04	2.81
0.02 → 0.04	– 1.03	– 1.25	– 2.26	– 1.96	– 1.87	1.78
0.04 → 0.08	– 2.28	– 1.95	– 6.29	– 4.91	– 5.25	2.59
0.10 → 0.20	– 5.12	– 5.53	– 8.47	– 7.45	– 7.86	1.49
0.20 → 0.40	– 6.25	– 6.29	– 8.67	– 5.59	– 6.88	1.12
0.40 → 0.80	– 7.98	– 8.94	– 11.08	– 11.03	– 9.30	1.24
0.80 → 1.20	– 5.39	– 5.56	– 7.17	– 5.44	– 6.39	1.16
1.20 → 2.00	– 6.21	– 6.49	– 7.59	– 8.53	(– 11.64)	1.27

charged amphiphile that is adsorbed on the surface at low concentrations. Since the charges are discrete and on the average far apart the assumptions made in the presented theory are not strictly fulfilled. When a positively charged analyte adsorbs on the surface it will on the average be closer to the negative amphiphile than a negatively charged analyte will be. This is a ion-correlation effect which makes the positive analyte experience a higher surface potential than a negative analyte. It is thus expected that the relative difference between positive and negative analytes decreases when the concentration of amphiphilic modifier increases at the surface. From the figures it is seen that the charge dependent specificity is largest when octylsulphate is used as amphiphile, this system is therefore used to test this hypothesis. In Table VI is shown how the apparent electrostatic potential for the different analyte ions decreases when the concentration of A in the mobile phase increases. (So, e.g. when c_A increases from 0.10 to 0.20 mM the change in capacity factor for bensyltriethylamonium ion corresponds to a change in the electrostatic potential of −7.45 mV).) The column to the right shows the quotient between the mean potentials for positive and negative analyte ions. The general trend is that this quotient decreases when the concentration of A^- increases i.e. in accordance with the suggested hypothesis. However, more investigations are needed to understand why ion-correlation effects are much more important with octylsulphate than with the other amphiphilic modifiers.

Acknowledgement

The author is greatful to Professor M. Almgren for valuable discussions of the manuscript.

References

[1] *W.R. Melander, Cs. Horvàth,* Chromatogr. Sci. **31,** 27 (1985).

[2] *A. Tilly-Melin, Y. Askemark, K.G. Wahlund, G. Schill,* Anal. Chem. **51,** 976 (1979).

[3] *B.A. Bidlingmeyer, S.N. Deming, W.P. Price Jr., B. Sachok, M. Petrusek,* J. Chrom. **186,** 419 (1979).

[4] *C.T. Hung, R.B. Tylor,* J. Chrom. **202,** 333 (1980).

[5] *P.T. Kissinger,* Anal. Chem. **49,** 883 (1977).

[6] *W.R. Melander, Cs. Horvàth,* J. Chrom. **201,** 211 (1980).

[7] *J.H. Knox, R.A. Hartwick,* J. Chrom. **204,** 3 (1981).

[8] *S. Afrashtehfar, F.C. Cantwell,* Anal. Chem. **54,** 2422 (1982).

[9] *J.J. Stranahan, S.N. Deming,* Anal. Chem. **54,** 2251 (1982).

[10] *J.H. Knox, G.R. Laird,* J. Chrom. **122,** 17 (1976).

[11] *J. Ståhlberg,* J. Chrom. **356,** 231 (1986).

[12] *A.W. Adamson,* "Physical Chemistry of Surfaces", Wiley, New York, 4th ed., 1982.

[13] *J. T. Davies, E. K. Rideal,* "Interfacial Phenomena", Academic Press, New York, 2nd ed. 1963.

[14] *J. Ståhlberg, A. Furängen,* Chromatographia **24,** 783 (1987).

[15] *B. Jönsson, H. Wennerström, B. Halle,* J. Phys. Chem. **84,** 2179 (1980).

[16] *G.M. Torrie, J.P. Valleau,* J. Phys. Chem. **86,** 3251 (1982).

[17] *P. Linse, G. Gunnarsson, B. Jönsson,* J. Phys. Chem. **86,** 413 (1982).

[18] *R.E. Rice, F.H. Horne,* J. Colloid Interface Sci. **105,** 172 (1985).

[19] Standard Mathematical Tables CRC Press, Cleveland, 19th ed. (1971).

[20] *A. Bartha, Gy. Vigh, H.A.H. Billiet, L. de Galan,* J. Chrom. **303,** 29 (1984).

[21] *A. Bartha, Gy. Vigh, H.A.H. Billiet, L. de Galan,* Chromatographia **20,** 587 (1985).

Received: June 28, 1987
Revised manuscript
received: Sep 15, 1987
Accepted: Oct 6, 1987
F

Determination of Acetylcholine and Choline in the Femtomole Range by Means of HPLC, a Post-Column Enzyme Reactor, and Electrochemical Detection

G. Damsma[1] * / D. Lammerts van Bueren[2] / B. H. C. Westerink[1] / A. S. Horn[1]

1 Department of Medicinal Chemistry, University of Groningen, A. Deusinglaan 2, 9713 AW Groningen, The Netherlands
2 Chrompack International, Middelburg, The Netherlands

Key Words

Column liquid chromatography
Acetylcholine
Choline
Enzyme reactor
Electrochemical detection

Summary

The measurement of choline and acetylcholine by means of HPLC, a post-column enzyme reactor, and electrochemical detection has been simplified and optimised. The use of a cation exchanger and enzyme reactor fitted in a cartridge holder appeared to result in reproducible, sensitive, and selective measurement of endogenous choline and acetylcholine with a lower detection limit of 50 fmole.

Introduction

Acetylcholine (ACh) was the first molecule to which a chemical transmission function in biological systems was ascribed. It has only recently become possible to determine ACh by the use of HPLC methods, the latter being now so familiar for the determination of other biologically neuroactive compounds, such as monoamines and amino acids. The main reason for the delay in the introduction of a HPLC-method for ACh was the lack of a sensitive and specific detection principle. This problem has been overcome by the isolation [1] and subsequent commercial availability of choline oxidase. This enzyme catalyses the oxidation of choline (Ch), thereby producing betaine and hydrogen peroxide. The latter compound can be oxidised by a platinum electrode at relatively low potentials. The prior conversion of acetylcholine to choline and acetate is achieved by acetylcholine esterase (Fig. 1).

Israel and Lesbats [2] used choline oxidase for the measurement of ACh by means of a direct assay without chromatographical separation. Potter et al. [3] reported the determination of ACh and Ch by means of HPLC. ACh and Ch were first separated on a reversed phase column, the column-effluent was mixed on-line with an enzyme reagent in order to produce hydrogen peroxide, which was detected electrochemically with a platinum electrode. The enzyme reagent contained acetylcholine esterase and choline oxidase buffered to pH 8.0, thereby increasing the pH of the column effluent (pH 5.0) in order to achieve more optimal enzyme activity conditions (pH 7.8).

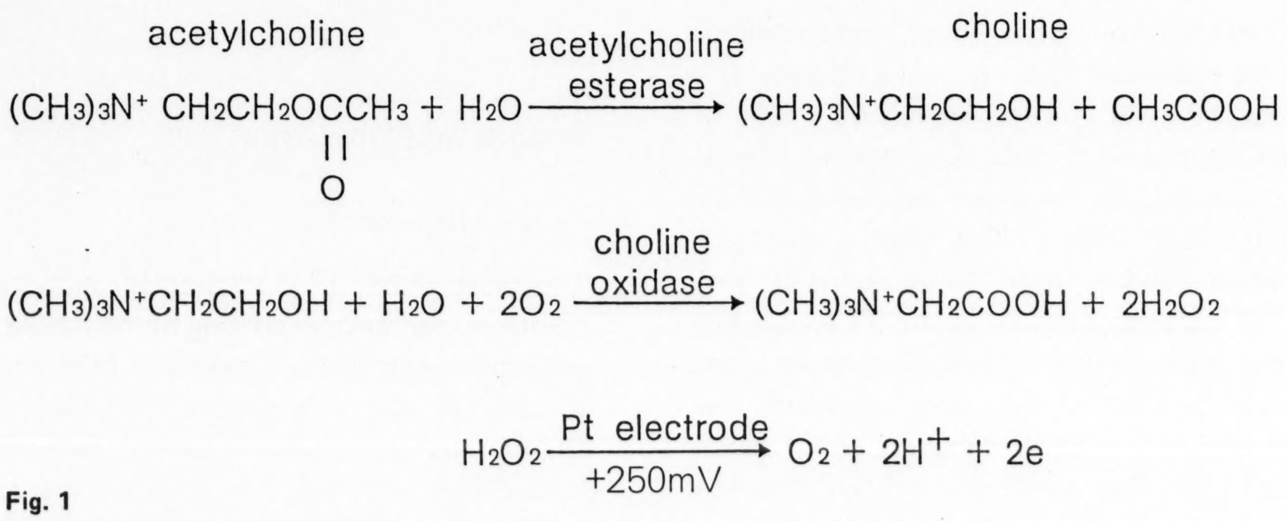

$$(CH_3)_3N^+CH_2CH_2O\underset{\underset{O}{\|}}{C}CH_3 + H_2O \xrightarrow[\text{esterase}]{\text{acetylcholine}} (CH_3)_3N^+CH_2CH_2OH + CH_3COOH$$

$$(CH_3)_3N^+CH_2CH_2OH + H_2O + 2O_2 \xrightarrow[\text{oxidase}]{\text{choline}} (CH_3)_3N^+CH_2COOH + 2H_2O_2$$

$$H_2O_2 \xrightarrow[+250\text{mV}]{\text{Pt electrode}} O_2 + 2H^+ + 2e$$

Fig. 1

Enzymatic conversion of acetylcholine and choline and subsequent electrochemical oxidation of produced hydrogen peroxide.

0009-5893/87 0827-05 $03.00/0

© 1987 Friedr. Vieweg & Sohn Verlagsgesellschaft mbH

The approach of Potter and coworkers was soon followed by others [4]. A major improvement involved the immobilisation of enzymes, thereby reducing the waste of expensive enzymes and making the post-column enzyme injection superfluous. The enzymes were either physically absorbed to an anion exchanger [5] or alternatively chemically bound to glutaraldehyde activated silica [6], cyanogen bromide activated Sepharose [7] or glutaraldehyde activated alkylamino glass beads [8].

To avoid the necessity of the addition of post-column reagents, a mobile phase had to be developed which was not only suitable for the chromatographic separation but also for the subsequent enzymatic reaction, which is optimal between pH 8.0–8.5 [1]. This necessitates separations at an alkaline pH, which may give rise to stability problems with the widely used silica columns. The use of a mobile phase of pH 7.0–7.2 was accompanied by a decrease of the column life [10] due to dissolution of the silica [7]. When a mobile phase at pH 7.4 was used, the analytical column had to be repacked weekly [10].

We now report an improved assay for Ch and ACh using a cation exchanger which is stable at pH 8.0 and a mini enzyme reactor in which the enzymes are covalently bound to glutaraldehyde activated silica.

Materials and Methods

Materials

Acetylcholine chloride, choline chloride, acetylcholine esterase (EC 3.1.1.7, type VI-S from electric eel, 260 IU/mg), choline oxidase (EC 1.1.3.17., from Alcaligenes sp., 12.7 IU/mg), and sodium laurylsulphate were obtained from Sigma Chemical Co. (St. Louis, MO, USA)). All other chemicals were of analytical grade and purchased from Merck (Darmstadt, FGR). Water, purified by a Milli-Q system (super-C cartridge, ion-Ex cartridges, organex-Q cartridge, 0.2 uM filter; Millipore, Bedford, MA, USA) was used for all aqueous solutions.

Stock solutions of Ch and ACh were prepared in 0.01% acetic acid; fresh standards were prepared weekly by appropriate dilution of the stock solution in 0.01% acetic acid; stock and standard solutions were stored at 4°C.

The Analytical System

The analytical system comprises a liquid chromatograph (LKB 2150; LKB-Produkter AB, Bromma, Sweden), a pulse damper (SSI, 12-0125), a precolumn (100 × 3.0mm, reversed phase, Chromspher 5 C18; Chrompack, Middelburg, The Netherlands), an injector (Rheodyne 7125; Rheodyne, Cotati, USA) with a 20μl loop, a guard column (reversed phase, 10 × 2.1mm; Chrompack), an analytical column (100 × 3.0mm, reversed phase 5 C18; Chrompack), an enzyme reactor (10 × 2.1mm; Chrompack), and an electrochemical detector (Amor; Spark Holland, Emmen, The Netherlands; or alternatively a home made detector was used [7]). The guard column, the analytical column, and the enzyme reactor are all fitted in one cartridge holder (Chrompack).

The mobile phase consisted of 0.2 M potassium phosphate (pH 8.0) to which 0.005 M potassium chloride was added. The mobile phase was filtered at 0.45μm and degassed by ultrasonic vacuuming. The system flow was set at 0.6ml/min.

The Amor detector was equipped with a platinum working electrode, an in situ Ag/AgCl reference electrode, a carbon composite auxillary electrode, and a cell volume of 2μl. Using this detector, hydrogen peroxide was maximally oxidised at +250 mV.

Preparation of the Analytical Column

ACh and Ch were separated on a cation exchange column. This column was prepared by loading a reversed phase Chromspher C18 column with laurylsulphate resulting in a functional cation exchanger. The loading procedure was performed using the HPLC-pump, by the following subsequent steps (each step is maintained for 20 minutes at a flow rate of 1ml/min): washing with methanol (100%), methanol/water (1:1), water (100%), loading with sodium laurylsulphate dissolved in water (5mg/ml). Then the pump is thoroughly washed with water (column off-line). Subsequently, the column is washed with water (5min) and finally equilibrated (60min) with mobile phase. During the preparation of the analytical column the reactor and guard column are removed or replaced by dummy columns, and the column outlet is disconnected from the detector.

Preparation of the Enzyme Reactor

ACh is hydrolysed by acetylcholine esterase and the resulting choline is subsequently oxidised by choline oxidase to betaine and hydrogen peroxide (Fig. 1). These two enzymes were immobilized as follows: a Hypersil APS-2 column, activated with glutaraldehyde (Chrompack, 10 × 2.1mm) is connected to the HPLC and equilibrated with mobile phase (20min). An enzyme solution, containing 80 U acetylcholine esterase and 40 U choline oxidase dissolved in 500μl mobile phase, is carefully injected onto an empty column (3 × 100mm; Chrompack), placed before the reactor. Subsequently, the enzyme solution is pumped through the glutaraldehyde activated reactor with mobile phase (0.05ml/min, 20min).

Results and Discussion

Enzyme Reactor

The most widely used method for enzyme immobilisation employs aminopropyl coating of the support and subsequent activation with glutaric aldehyde [11]. In the present case a commercially available silica column modified with aminopropyl groups and activated with glutardialdehyde is loaded with enzymes. The enzymes are covalently bound, on-line, through Schiff base formation in a simple one step procedure.

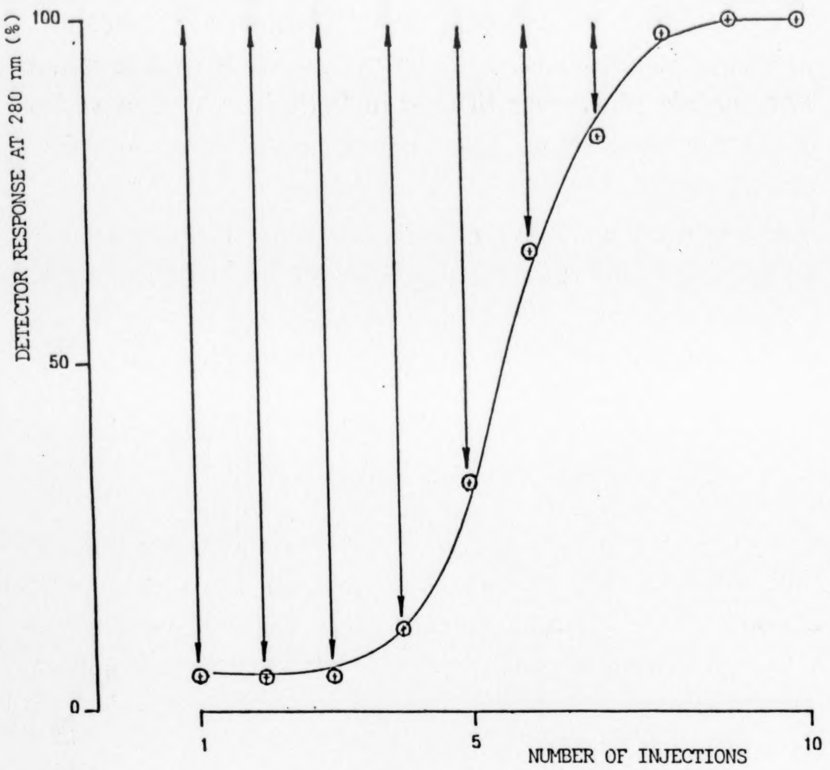

Fig. 2

Loading of glutaraldehyde activated Hypersil APS-2 column with enzymes via the sample loop (20μl).

Each injection contains 1.5 U acetylcholine esterase and 0.75 U choline oxidase.

Arrows indicate amount of enzyme retained in the reactor.

To determine the amount of enzyme bound by the reactor, the outlet of a glutaraldehyde activated reactor is connected to a spectrophotometer monitoring proteins at 280 nm. We repeatedly injected 20μl enzyme solution containing 1.5 unit acetylcholine esterase and 0.75 units choline oxidase dissolved in the mobile phase (Fig. 2).

The amount of enzyme bound in the reactor can be estimated from this figure by integration of the complementary surface of the injections showing less than maximal response (indicated by arrows, Fig. 2). The estimated 360μg protein which remained in the glutaraldehyde activated reactor is covalently bound to 34.6μl glutaraldehyde activated Hypersil APS-2, i.e. 10μg protein per μl column volume. These amounts of protein correspond to about 4 U choline oxidase and 8 U acetylcholine esterase per reactor.

Mobile Phase Conditions

Two mobile phase parameters were investigated: the ionic strength and the pH (Fig. 3).

It is obvious that an increase in the ionic strength of the mobile phase will cause a corresponding decrease in the capacity factors for Ch and ACh, while the detector response increases accordingly.

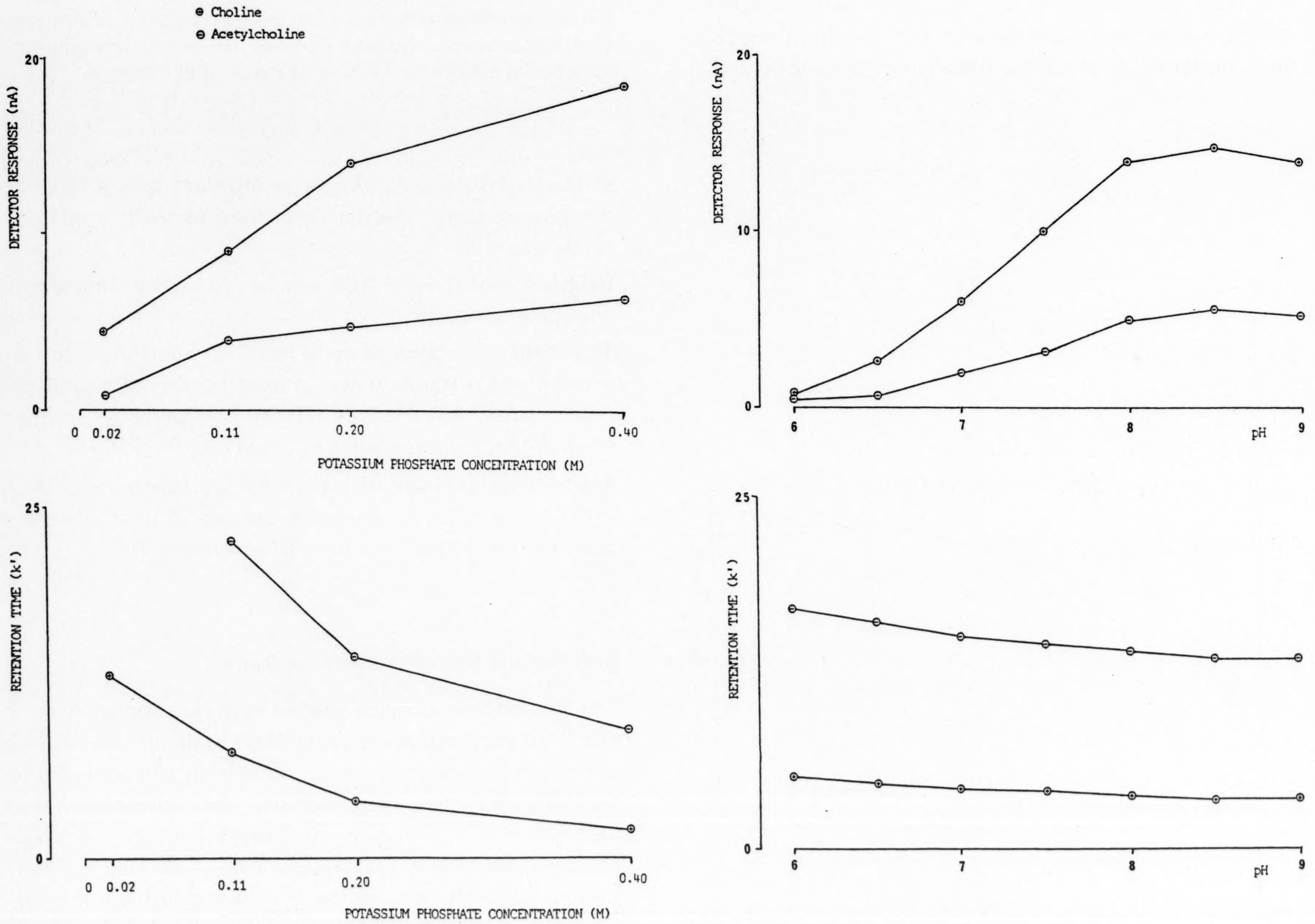

Fig. 3

Effect of ionic strength and the pH of the mobile phase on retention times and detector responses of Ch (○) and ACh (●).

Each point represents the average of at least three standard injections (20 pmol/20μl).

An increase of the pH of the mobile phase from 6.0 to 9.0 causes a minor decrease in capacity factors for Ch and ACh. The effects of the pH on the detector response of Ch and ACh are maximal between pH 8.0–8.5, confirming previously reported data [6, 8]. No significant difference was observed in the base line noise when the ionic strength or pH of the mobile phase was varied.

To discriminate between the enzymatic conversion efficiency of the reactor and detector efficiency we injected ACh, Ch and hydrogen peroxide (200 pmol/20 μl) while the guard column and analytical column were removed from the system (Fig. 4). The hydrogen peroxide detection efficiency was attenuated by an increase in the pH of the mobile phase, while the enzymatic conversion of Ch and ACh was optimal between pH 0.0 and pH 0.5. The enzyme conversion curves for Ch and ACh completely overlap, indicating that choline oxidase and not acetylcholine esterase is the limiting enzyme step.

Most importantly, the enzymatic conversion is maximal from pH 8–8.5, corresponding to an 100% enzymatic conversion of ACh and Ch (since their detector responses are twice the equimolar hydrogen peroxide detector responses, as can be expected from the stoichiometry of the enzymatic conversions (Fig. 1)).

Chromatography and Performance of the Analytical System

Fig. 5 shows a chromatogram which is obtained after in vivo brain dialysis of the rat [12]. These samples contain very low amounts of endogenous ACh, while up to 1000 times higher levels of Ch are found in these samples. Fig. 5 shows that such samples can be analysed satisfactorily by the present assay. The detection limit for ACh is 50 fmole (S/N ratio = 2).

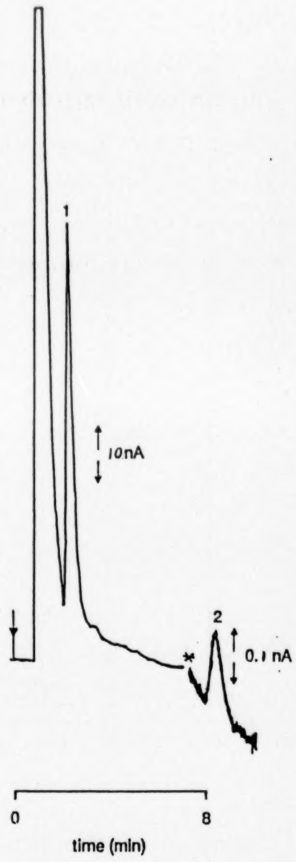

Fig. 5

Chromatogram of micro dialysis sample from the rat brain directly injected in a 100 μl loop.

The choline peak (1) represents 58 pmole and the acetylcholine peak (2) 250 femtomole.

The asterisk indicates a change in sensitivity of the recorder.

Conditions: flow rate, 0.6 ml/min; mobile phase, 0.2 M potassium phosphate pH 8.0; column, cation exchanger (modified Chromspher 5 C18); post-colum enzyme reactor, glutaraldehyde activated Hypersil APS-2 producing hydrogen peroxide; detection, electrochemical detection at 500 mV by means of oxidation at Pt electrode.

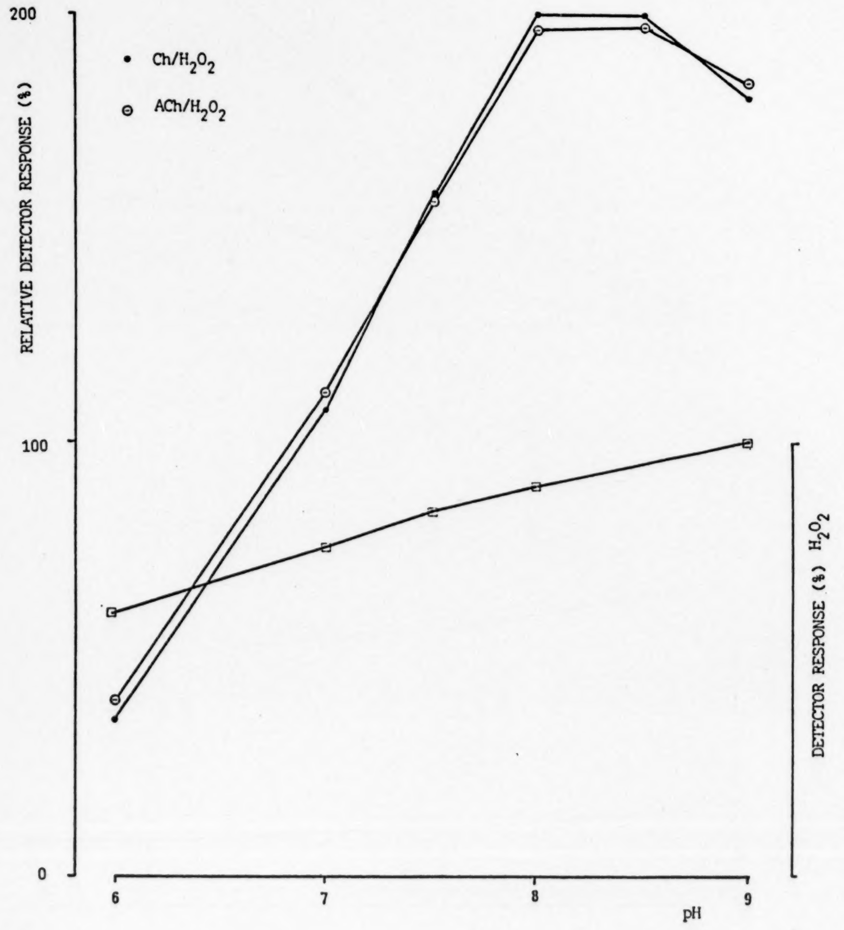

Fig. 4

Effect of pH on enzyme conversion efficiency (left), corrected for the detector response, and on the detector response (right). Each point represents the average of at least three injections (200 pmol/20 μl).

Calibration of Ch and ACh was carried out by comparisons with pure standards.

The detector response is directly proportional to the amount of Ch and ACh over at least 4 orders of magnitude, ranging from 100 fmole – 1000 pmole per 20 μl injected (data not shown, previously reported by others [6–8]).

The relative standard deviation for 23 injections of ACh and Ch was 1.3% for 2 pmoles injected. Similar low intra-assay variances have been reported previously [8].

Stability and Maintenance of the System

The immobilised enzyme reactor was very stable: After 1 month of continuous use (over 1000 brain dialysis samples were analysed) the enzymatic conversion still appeared to be 100%. With respect to stability, the present reactor is superior to the previously described cyanogen bromide activated Sepharose reactor [7, 10] which was replaced weekly; probably because the agarose support is not a sufficiently rigid matrix for HPLC applications [11].

The analytical column showed an increase in back pressure and peak width after 1 month of continous use, causing a decrease of peak height of about 50%. These column deterioriations can be virtually eliminated by reloading the column with laurylsulphate. When no samples were run the pH of the mobile phase could be lowered and the flow was set at 0.03 ml/min to increase the life time of the system. Alternatively the reactor may be stored at 4°C, provided that it is protected against drying. In addition when less sensitive measurements of Ch and ACh are required (e.g. brain tissue levels, [7]), the pH may be lowered to 7.0; at this pH the assay still has sufficient sensitivity to record subpicomole amounts.

Conclusion

In summary, the present report describes a simple enzyme immobilisation procedure on a commercially available glutaraldehyde activated Hypersil APS-2 minicolumn. The enzyme conversion was 100% for at least 4 orders of magnitude. The cation exchanger, which is easy to prepare, was sufficiently stable at pH 8.0. The cation exchanger and the reactor are fitted in one cartridge holder, thereby reducing dead volumes to a minimum.

The measurement of Ch and ACh by means of LC-ED using a post-column enzyme conversion as originally described [3] has been simplified and optimized with a detection limit of about 50 fmole. The method is sensitive enough to record endogenous release of ACh sampled by micro dialysis from the rat brain [12].

Acknowledgements

Mrs. F. van Putten, Mr. W. E. B. van den Dool, and Drs. F. Flentge, H. Rollema, and W. H. Kuhr are acknowledged for their help.

References

[1] *S. Ikuta, S. Imamura, H. Misaki, Y. Horiuti*, J. Biochem. **82**, 1741 (1977).
[2] *M. Israel, B. Lesbats*, Neurochem. Int. **3**, 01 (1981).
[3] *P. E. Potter, J. L. Meek, N. H. Neff*, J. Neurochem. **41**, 188 (1983).
[4] *Y. Maruyama, Y. Ikarashi, C. L. Blank*, Trends Pharmacol. Sci. **8**, 84 (1987).
[5] *J. L. Meek, C. Eva*, J. Chromatog. **317**, 343 (1984).
[6] *T. Yao, M. Sato*, Anal. Chim. Acta **172**, 371 (1985).
[7] *G. Damsma, B. H. C. Westerink, A. S. Horn*, J. Neurochem. **45**, 1649 (1985).
[8] *M. Asano, T. Miyauchi, T. Kato, K. Fujimori, K. Yamamoto*, J. Liq. Chromatogr. **9**, 199 (1986).
[9] *C. Eva, M. Hadjiconstantinou, N. H. Neff, J. L. Meek*, Anal. Biochem. **143**, 320 (1984).
[10] *G. Damsma, B. H. C. Westerink, J. B. de Vries, C. J. van den Berg, A. S. Horn*, J. Neurochem. **40**, 1523 (1987).
[11] *L. Dalgaard*, Trends in Anal. Chemistry **5**, 185 (1986).
[12] *G. Damsma, B. H. C. Westerink, A. Imperato, H. Rollema, J. B. De Vries, A. S. Horn*, Life Sci. **41**, 873 (1987).

Received: July 2, 1987
Accepted: Aug. 11, 1987
F

A Practical Approach to the Preparative Purification of Peptides using Analytical Instrumentation with Analytical and Semipreparative Columns

J. M. Robert Parker / C. T. Mant / R. S. Hodges*

Department of Biochemistry and the Medical Research Council of Canada Group in Protein Structure and Function, University of Alberta, Edmonton, Alberta, Canada T6G 2H7

Key Words

Preparative reversed-phase chromatography
Peptides
Shallow gradient elution
Analytical and semipreparative columns

Summary

We have examined the effect of particle size of silica-based reversed-phase packings and column packing techniques on the reversed-phase analytical separation of a peptide mixture. A C_{18} packing of 15–20 μm average particle size produced satisfactory peptide resolution, allowing a relatively inexpensive scale up to the preparative purification of peptides. A shallow gradient (0.1% acetonitrile/min) elution procedure was developed for the preparative purification of closely related decapeptides (differing by one methyl group) on analytical (250 × 4.1 mm I.D.) and semipreparative (250 × 10 mm I.D.) columns. Up to 30 mg and 225 mg of the two-peptide mixture was efficiently resolved, with high yields of homogeneous peptides, on analytical and semipreparative columns, respectively, containing the 15–20 μm packing. We have also demonstrated the potential of our purification procedure for resolving more complex multicomponent mixtures by efficiently separating a total of 22 mg of three closely-related peptides on analytical columns containing 7 μm or 15–20 μm particle size reversed-phase packings. The use of the inexpensive 15–20 μm packing, coupled with the ability to pack efficient columns with analytical HPLC instrumentation, offers great cost saving potential.

Introduction

We have developed an optimization procedure for the preparative reversed-phase chromatographic separation of peptides on HPLC columns and instrumentation designed primarily for analytical work [1]. The procedure involved the use of a shallow, linear AB gradient elution system (0.1% B/min), where solvent A was 0.05% aqueous trifluoroacetic acid (TFA) and solvent B was 0.05% aqueous TFA in acetonitrile. This shallow gradient system enabled maximum resolution on an analytical column (220 × 4.6 mm I.D.), within a resaonable run time, of up to 30 mg of a mixture of two closely related peptides differing by only one methyl group and present in a 1:1 molar ratio. Homogeneous yields of recovered peptides were consistently $>97\%$ for this peptide mixture, designed to represent the most difficult separation problem which would be encountered by reseachers in the preparative purification of peptides.

The optimization procedure, developed on a 7 μm particle size stationary phase, took full advantage of the powerful resolving capability of small particle size (5–10 μm) reversed-phase packings. Scale up to higher sample loading would require either a further shallowing of the gradient steepness ($<0.1\%$ B/min) or the use of wider columns in order to maintain similar yields of homogeneous product(s). Decreasing the gradient steepness will lead to increasingly longer and, eventually, impractical run times. In addition, the loading capacity of the analytical column will eventually limit the amount of peptide sample mixture which can be separated to a satisfactory degree. Although higher sample loads are possible with increasing column size, the concommitant use of expensive small particle size packings in these columns may soon become prohibitively costly. An alternative is to use less costly, larger particle size packings [2]. Some peptide resolution is lost with increasing particle size [3, 4]. However, if good resolution can be achieved on a small particle size analytical column, then use of a larger particle, wider-bore column is warranted for larger loads [5].

In the present study, we have examined the effect of particle size and packing technique on the analytical reversed-phase separation of peptide mixtures. Having demonstrated the utility of a 15–20 μm reversed-phase packing, we proceeded to scale up our preparative reversed-phase procedure, achieving significantly higher peptide sample loadings of

0009-5893/87 0832-07 $03.00/0

© 1987 Friedr. Vieweg & Sohn Verlagsgesellschaft mbH

two closely related peptides, while maintaining good resolution, on semi-preparative (250 x 10 mm I.D.) compared to analytical (250 x 4.1 mm I.D.) columns. In addition, we have also demonstrated the potential for extending our preparative purification procedure to more complex multicomponent peptide mixtures.

Experimental

Materials

SynChropak C_{18} reversed-phase packings (6.5 μm or 30 μm spherical particle size, 300 Å pore size) were obtained from SynChrom (Linden, IN, USA). Vydac C_{18} reversed-phase packings (15–20 μm or 20–30 μm average spherical particle size, 300 Å pore size) were obtained from Vydac The Separations Group (Hesperia, CA, USA). All packings were silica-based.

HPLC-grade water, acetonitrile and isopropanol were obtained from Fisher Scientific (Fairlawn, NJ, USA). HPLC-grade TFA was obtained from Pierce Chemical (Rockford, IL, USA).

Peptides

Peptides S1–S5 were synthesized on a Beckman Model 990 peptide synthesizer (Beckman Instruments, Berkeley, CA, USA) using the general procedure for solid-phase synthesis described by Parker and Hodges [6]. The peptides were based on the sequence, Arg-Gly-X^3-X^4-Gly-Leu-Gly-Leu-Gly-Lys, where -X^3-X^4- were substituted as follows: peptide S2, -Gly^3-Gly^4-; peptide S3, -Ala^3-Gly^4-; peptide S4, -Val^3-Gly^4-; peptide S5, -Val^3-Val^4-. All peptides contained a N^{α}-acetylated N-terminal and a C-terminal amide, except peptide S1, which was identical to peptide S3 but had a free α-amino group. These peptides were obtained from the Alberta Peptide Institute, Department of Biochemistry, University of Alberta, Edmonton, Alberta, Canada, T6G 2H7.

Apparatus

Several columns were packed using a Shandon HPLC packing pump (Sewickley, PA, USA). The HPLC instrument consisted of a Spectra-Physics (Autolab Division, San Jose, CA, USA) SP8700 solvent delivery system and SP8750 organizer module coupled to a Hewlett-Packard (Avondale, PA, USA) HP1040A detection system, HP3390A integrator, HP85 computer, HP9121 disc drive and HP7470A plotter. Samples were injected with a 2.0 ml injection loop (Model 7125, Rheodyne, Cotati, CA, USA).

Column Packing Procedures

(i) Dry packing: columns fitted with a reservoir were filled with the desired material. This apparatus was then tapped in a vertical direction until the reversed-phase bed had settled.

(ii) Slurry packing with an HPLC pump: the silica packing was suspended in isopropanol to a slurry concentration of ~5% (w/v) and degassed under vacuum for 5 min. The packing was then allowed to settle and most of the isopropanol decanted off. The resultant thick slurry was then poured into a stainless steel column reservoir (350 x 7.5 mm I.D.) attached to the desired stainless steel HPLC column (250 x 4.1 mm or 10 mm I.D.). Having filled the reservoir with isopropanol, the top of the reservoir was attached to the Spectra-Physics HPLC pump. With the column bypass valve open, the pump was initialized into 'purge' mode. Once the isopropanol flow-rate had reached maximum (~10 ml/min), the bypass valve was closed, forcing the solvent to flow downward and vertically through the reservoir/HPLC column system (the pressure was not allowed to exceed 5000 p.s.i.). After 100 ml of isopropanol had passed through the column, the pump was turned off.

(iii) Slurry packing with a Shandon HPLC packing pump: the slurry was prepared as described in (ii). The slurry was then packed downward and vertically at 5000 p.s.i. into a 250 x 4.1 mm I.D. or 250 x 10 mm I.D. stainless steel HPLC column, via a 350 x 7.5 mm I.D. stainless steel column reservoir, with isopropanol as packing solvent and nitrogen as the pressurizing gas. The solvent flow was allowed to continue until 100 ml of isopropanol had passed through the column.

Results and Discussion

Effect of Packing Procedure and Stationary Phase Particle Size on Peptide Resolution

Determining the effect of particle size on peptide resolution required a series of columns with a range of reversed-phase packings. Since commercially-available columns are somewhat costly, and vary in column dimensions, we decided to pack our own columns. This study was designed to develop preparative reversed-phase chromatographic methods which may be applied to instrumentation commonly available to most laboratories. It was felt that the option of being able to pack columns on commonly available instrumentation, i.e., without the necessity of a commercial column packer, would also be an advantage.

Fig. 1 demonstrates the elution profiles of a mixture of five synthetic decapeptide standards, S1–S5, on analytical columns (250 x 4.1 mm I.D.) containing reversed-phase packings with particle sizes of 6.5 μm, 15–20 μm, 20–30 μm and 30 μm (Panels A–D, respectively). The top run of each panel shows the results for a dry packed column; the middle run shows the results for a slurry packed column using an HPLC pump; the bottom run shows the results for a slurry packed column using a commerical column packer. The five peptide standards are closely-related in hydrophobicity – between S2 and S3 there is an increase of only one carbon atom, between peptides S3 and S4 there is an increase of two carbon atoms, and between S4 and S5 there is an increase of three carbon atoms – enabling a precise assessment of the peptide resolving capability of the reversed-phase packings. There was a general progressive deterioration of peptide resolution with increasing particle

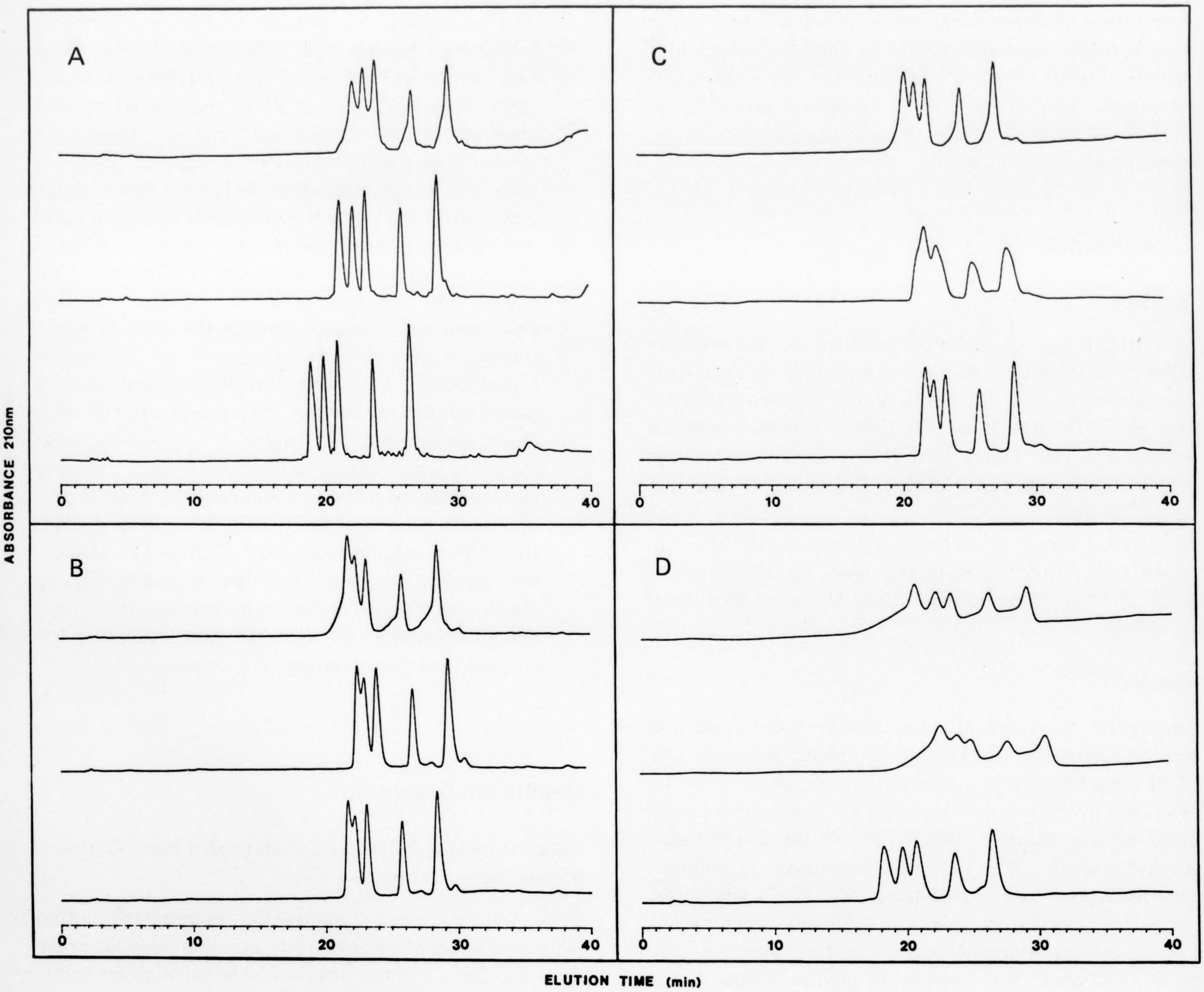

Fig. 1

Effect of reversed-phase packing particle size on analytical resolution of a synthetic peptide mixture.

Column dimensions: 250 × 4.1 mm I.D. Conditions: linear AB gradient (1% B/min), where solvent A is 0.05% aqueous TFA and solvent B is 0.05% TFA in acetonitrile; flow-rate, 1 ml/min; 26 °C; 0.15 AUFS.

Panel A: SynChropak C_{18} reversed-phase packing, 6.5 µm particle size. Panel B: Vydac C_{18}, 15–20 µm. Panel C: Vydac C_{18}, 20–30 µm. Panel D: SynChropak C_{18}, 30 µm.

All packings had a pore size of 300 Å. For each panel, the top elution profile shows the result for a dry-packed column; the middle elution profile shows the results for a slurry-packed column using an HPLC pump; the bottom elution profile shows the result for a slurry-packed column using a commercial column packing apparatus. Sequence variations of decapeptides S1–S5 are described under Experimental.

size of the hydrophobic stationary phase, independent of the procedure used to pack the columns. The commercial high-pressure column packer overall produced the best columns. In fact, the 6.5 µm packing, packed in this manner, gave identical results to those obtained with columns purchased commercially and containing the same packing. Both the 15–20 µm (Panel B) and the 20–30 µm (Panel C) average particle size packings also produced reasonable peptide elution profiles when slurry packed on the column packer (bottom profiles). Columns containing 6.5 µm, 20–30 µm and 30 µm particle size materials were slurry packed with the HPLC pump in duplicate, while the procedure was carried out four times for the 15–20 µm material. In all cases, performance reproducibility of the columns was excellent. What is most interesting is that the 6.5 µm and 15–20 µm packings, when slurry packed with the HPLC pump, produced very similar elution profiles to those produced by these stationary phases when slurry packed by a commercial high-pressure column packer. These results were even more gratifying considering that packing columns with satisfactory chromatographic characteristics becomes increasingly difficult with decreasing particle size [7]. In contrast, the HPLC-packed column with 20–30 µm average particle size did not produce a satisfactory peptide elution profile. None of the dry-packed columns or any of the 30 µm particle size columns produced peptide elution profiles satisfactory enough for the purposes of the present study.

From these results, the Vydac C_{18}, 15–20 μm packing was chosen as the most acceptable for scale up to higher peptide sample loads. Apart from its being relatively inexpensive compared to smaller particle size packings [2–5], the good peptide resolving capability of this packing when slurry packed with either an HPLC pump or a commercial packer made it eminently suitable for preparative work. The relatively low cost and excellent resolutive qualities of 15–20 μm average particle size packings have, in fact, led to their increasing use for preparative peptide separations in recent years [2–5].

Effect of Sample Load on Resolution of a Two-Component Peptide Mixture

The performance of a reversed-phase packing in preparative purification should first be tested in an analytical column to determine whether scale up to higher diameter columns, containing significantly higher amounts of packing material, is viable. The effect of sample load on the resolution of closely related peptides was examined on an analytical column (250 × 4.1 mm I.D.) containing Vydac C_{18}, 15–20 μm particle size reversed-phase packing. The column was slurry packed by using the HPLC pump. Fig. 2 demonstrates the effect of increasing sample load on the elution profiles of peptides S2 and S3 (differing by only a single methyl group) on this analytical column. The sample mixture contained a 1:1 molar ratio of the two peptides, which were eluted at 1 ml/min by a linear AB gradient (0.1% B/min), where solvent A was 0.05% aqueous TFA and solvent B was 0.05% TFA in acetonitrile. At small sample loads (0.075 mg and 0.75 mg total), S2 and S3 were resolved with no overlap between the peaks. However, the point of separation between S2 and S3 can no longer be seen for the 7.5 mg, 15 mg and 30 mg injections, and fraction analysis had to be carried out in order to make pools of pure components. Isocratic analyses were carried out as this enabled rapid analysis of fractions without the need for column regeneration between analyses [3]. At a sample loading of 7.5 mg, 95% and 96% of recovered S2 and S3, respectively, were isolated as pure fractions; at a sample loading of 15 mg, 94% and 88% of recovered S2 and S3, respectively, were isolated as pure fractions; at a sample loading of 30 mg, 90% and 86% of recovered S2 and S3, respectively, were isolated as pure fractions (Table I). For the 7.5 mg, 15 mg and 30 mg injections, total peptide recovery was 100% (Table I). Although the amount of cross-contamination between the peptides increased with increasing sample load (7.5 mg to 30 mg), relative recoveries of pure peptides were always > 86%. In addition, neither S2 and S3 was detected in the breakthrough peak (t_0) at any sample load. Thus, despite skewing of the peptide peaks, the shallow acetonitrile gradient produced impressively efficient separations of

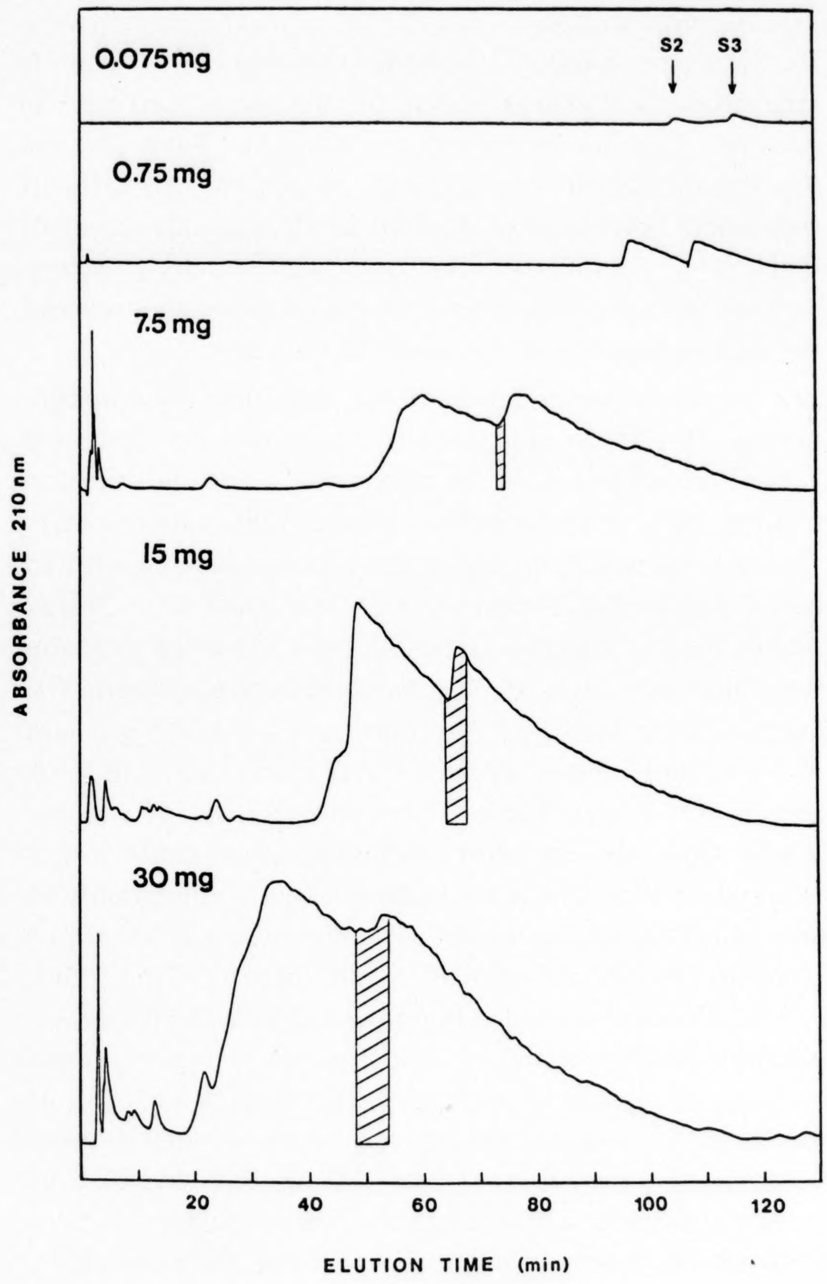

Fig. 2

Effect of sample load on the peptide elution profiles.

Column: analytical column (250 × 4.1 mm I.D.) containing Vydac C_{18} reversed-phase packing (15–20 μm average particle size; 300 Å pore size).

Conditions: linear AB gradient (0.1% B/min), where solvent A is 0.05% aqueous TFA and solvent B is 0.05% TFA in acetonitrile; flow-rate, 1 ml/min; 26 °C; 3.0 AUFS.

Sample loads: 0.075 mg, 0.75 mg, 7.5 mg, 15 mg and 30 mg in 10 μl–200 μl solvent A.

Decapeptides S2 and S3 (see Experimental) were present at all sample loads in a 1:1 molar ratio. Hatched areas indicate cross-contamination observed from the isocratic fraction analysis described in text.

Table I. Effect of sample loading on peptide recovery from an analytical reversed-phase column (250 × 4.1 mm I.D.).

Sample No.	Quantity Injected (mg)			Total Recovery (%)	Relative Recovery[b] %)	
	S2[a]	S3[a]	Total		S2	S3
1	0.036	0.039	0.075	–	–	–
2	0.36	0.39	0.75	–	–	–
3	3.6	3.9	7.5	100	95	96
4	7.6	7.9	15.0	100	94	88
5	14.3	15.7	30.0	100	90	86

[a] S2 and S3 are decapeptides with S3 containing an additional methyl group (see Experimental).

[b] Fraction of a pure peptide recovered from the total of that peptide recovered.

these closely related peptides at high sample loads on this 15–20 μm particle size packing. In fact, the elution profiles demonstrated in Fig. 2 compared favourably with those obtained previously [1] under similar conditions on an analytical column (220 × 4.6 mm I.D.) containing a 7 μm particle size C_8 packing. Although the peptide peaks on the 15–20 μm packing were somewhat broader at low sample loads (< 1 mg) compared to the 7 μm packing, this is not important at higher sample loads. The peak shape on the larger particle size packing was significantly smoother at higher sample loads compared to the 7 μm packing, where the absorbance profile displayed multiple peaks even though the eluted component was homogeneous. Relative recoveries of pure peptides were a little higher on the 7 μm column at high sample load (99% and 98% of S2 and S3, respectively, for a 20 mg sample injection) compared to the 15–20 μm packing (94% and 88% of S2 and S3, respectively, for a 15 mg sample injection). However, total peptide recoveries were always higher on the larger particle size packing. The practical limit for both the 7 μm [1] and 15–20 μm particle size packings to achieve this difficult separation (expressed as amount of decapeptide injected) under the conditions used was approximately 30 mg. Further increases in sample load would likely soon exceed the loading capacity of the analytical columns.

The excellent performance of the analytical column containing 15–20 μm C_{18} packing, described in Fig. 2 and Table I, prompted scale up of our preparative purification method to a semipreparative column (250 × 10 mm I.D.). This column was again prepared by slurry packing with an HPLC pump. Fig. 3 demonstrates the effect of increased sample load of peptides S2 and S3, in a 1:1 molar ratio, on their elution profiles on the semipreparative column. The peptides were eluted at 5 ml/min by a linear AB gradient (0.1% B/min), where solvent A was 0.05% aqueous TFA and solvent B was 0.05% TFA in acetonitrile. The higher eluent flow-rate for this semipreparative column was required to maintain a linear flow velocity comparable to that obtained on the analytical column at a flow-rate of 1 ml/min (Fig. 2). At a small sample load (0.75 mg total), S2 and S3 were resolved with no overlap between the peaks. Isocratic fraction analyses were required at higher sample loadings. At a sample loading of 15 mg, 77% and 73% of recovered S2 and S3, respectively, were isolated as pure fractions; at a sample loading of 150 mg, 86% and 92% of recovered S2 and S3, respectively, were recovered as pure fractions; at a sample loading of 225 mg, 89% and 85%, respectively, were recovered as pure fractions (Table II). Total peptide recoveries were 100%, 87% and 83% for the 15 mg, 150 mg and 225 mg sample loadings, respectively (Table II). Although, as seen previously for the analytical column (Fig. 2), the number of cross-contaminated fractions increased with increasing peptide load, relative recoveries of the two peptides were always good. In fact, the relative recoveries of pure S2 and S3 were somewhat higher for the 150 mg and 225 mg loadings compared to the 15 mg loading, although total recoveries for these two higher peptide loads were a little smaller compared to the 15 mg injection. The time required to completely elute both peptides from the column was identical for all sample loads (Fig. 3), i.e., at

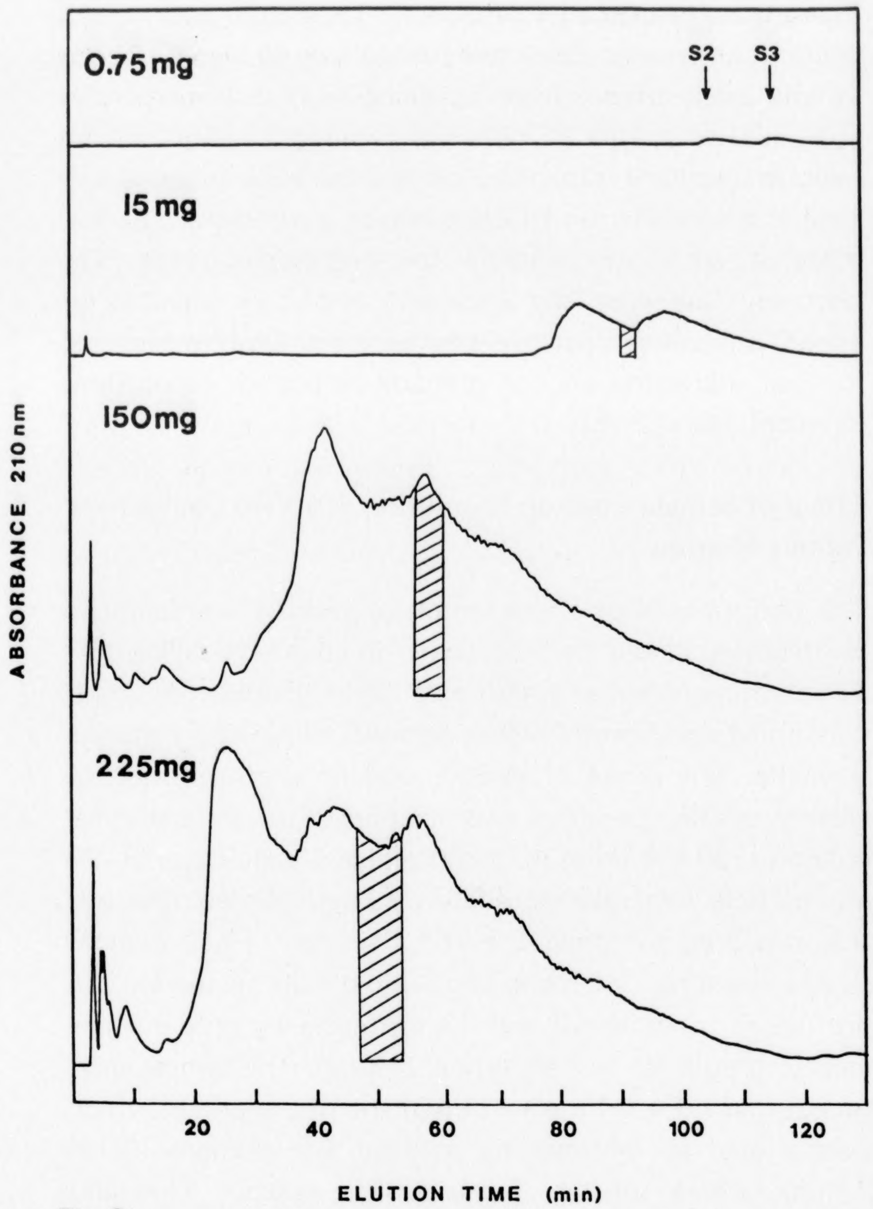

Fig. 3

Effect of sample load on the peptide elution profiles.

Column: semi-preparative column (250 × 10mm I.D.) containing Vydac C_{18} reversed-phase packing (15–20 μm average particle size; 300 Å pore size).

Conditions: linear AB gradient (0.1% B/min), where solvent A is 0.05% aqueous TFA and solvent B is 0.05% TFA in acetonitrile; flow-rate, 5 ml/min; 26 °C; 3.5 AUFS.

Sample loads: 0.75mg, 15mg, 150mg and 225 mg in 100 μl–1500 μl solvent A.

Decapeptides 2 and 3 (see Experimental) were present at all sample loads in a 1:1 molar ratio. Hatched areas indicate cross-contamination observed from the isocratic fraction analysis described in text.

Table II. Effect of sample loading on peptide recovery from a semi-preparative reversed-phase column (250 × 10 mm I.D.).

Sample No.	Quantity Injected (mg)			Total Recovery (%)	Relative Recovery[b] (%)	
	S2[a]	S3[a]	Total		S2	S3
1	0.36	0.39	0.75	–	–	–
2	7.1	7.9	15.0	100	77	73
3	71	89	150	87	86	92
4	107	118	225	83	89	85

[a] S2 and S3 are decapeptides with S3 containing an additional methyl group (see Experimental).

[b] Fraction of a pure peptide recovered from the total of that peptide recovered.

this gradient steepness (0.1% acetonitrile/min), total sample elution time was independent of sample load. Similar results were observed for the analytical column (Fig. 2). The 225 mg peptide injection probably represents the practical limit for this semipreparative column under the conditions used to achieve the separation of the two closely related peptides with satisfactory homogenous peptide yields. Thus, the practical limit for this semipreparative column was 7 to 8-fold greater than that of the analytical column which is in agreement with the 6-fold increase in column volume. These impressive results demonstrated both the effectiveness of the shallow gradient preparative procedure and the utility of the 15–20 μm reversed-phase C_{18} packing in enabling scale up of the procedure to high sample loads at relatively low cost.

Fig. 4 demonstrates the effect of variation of sample load (S2 plus S3) on the elution time of S2 on the analytical (Fig. 2) and semipreparative (Fig. 3) reversed-phase columns during shallow gradient elution. The retention time of S2 decreased rapidly (93 min to 5 min) on the analytical column as the sample load increased from 0.75 mg to 75 mg. A similar effect was apparent for the semipreparative column, where the peptide retention time decreased (107 min to 25 min) as the sample load increased from 0.75 mg to 225 mg. As expected this decrease in retention time was not as rapid as that obtained on the analytical column.

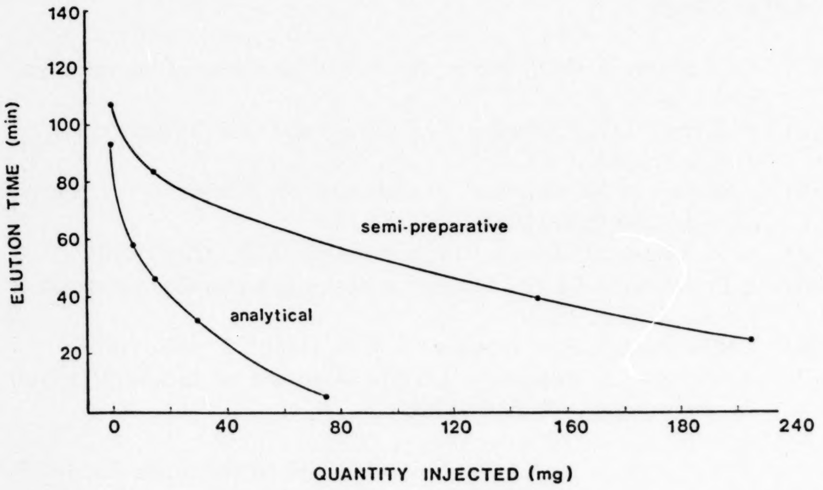

Fig. 4

Plot of sample load *versus* retention.

Columns: analytical column (250 × 4.1 mm I.D.) containing Vydac C_{18} (average particle size 15–20 μm; pore size 300 Å) reversed-phase packing; semi-preparative column (250 × 10 mm I.D.) containing the same packing material as the analytical column.

Conditions: linear AB gradient (0.1% B/min), where solvent A is 0.05% aqueous TFA and solvent B is 0.05% TFA in acetonitrile; flow-rate, 1 ml/min (analytical column) or 5 ml/min (semi-preparative column); 26 °C.

Sample loads: analytical column, 0.075 mg, 0.75 mg, 7.5 mg, 15 mg and 30 mg of S2 plus S3 in 10 μl–200 μl solvent A; semi-preparative column, 0.75 mg, 15 mg, 150 mg and 225 mg of S2 plus S3 in 100 μl–1500 μl solvent A; S2 and S3 were present in a 1:1 molar ratio.

Results show elution time for S2. Decapeptides S2 and S3 differ by one methyl group (see Experimental).

Effect of Sample Load on Resolution of a Three-Component Peptide Mixture

Having successfully demonstrated how our preparative purification procedure, using a 15–20 μm particle packing, could efficiently resolve a two-component mixture of closely related peptides, we then wished to determine how well this procedure would extend to a more complex three-component peptide mixture at high sample loadings. Fig. 5 compares the elution profiles of a three peptide mixture at the same sample loading (7.8 mg S2 + 9.1 mg S3 + 5.9 mg S4 = 22.8 mg total) on analytical columns (250 × 4.1 mm I.D.) packed with a 7 μm (Panel A) or 15–20 μm (Panel B) C_8 or C_{18} reversed-phase packing, respectively. The decapeptides S2 and S3 differed by a single carbon atom; the decapeptides S3 and S4 differed by two carbon atoms. The peptides were eluted at a flow-rate of 1 ml/min with a linear AB gradient (0.1% B/min), where solvent A was 0.05% aqueous TFA and solvent B was 0.05% TFA in acetonitrile.

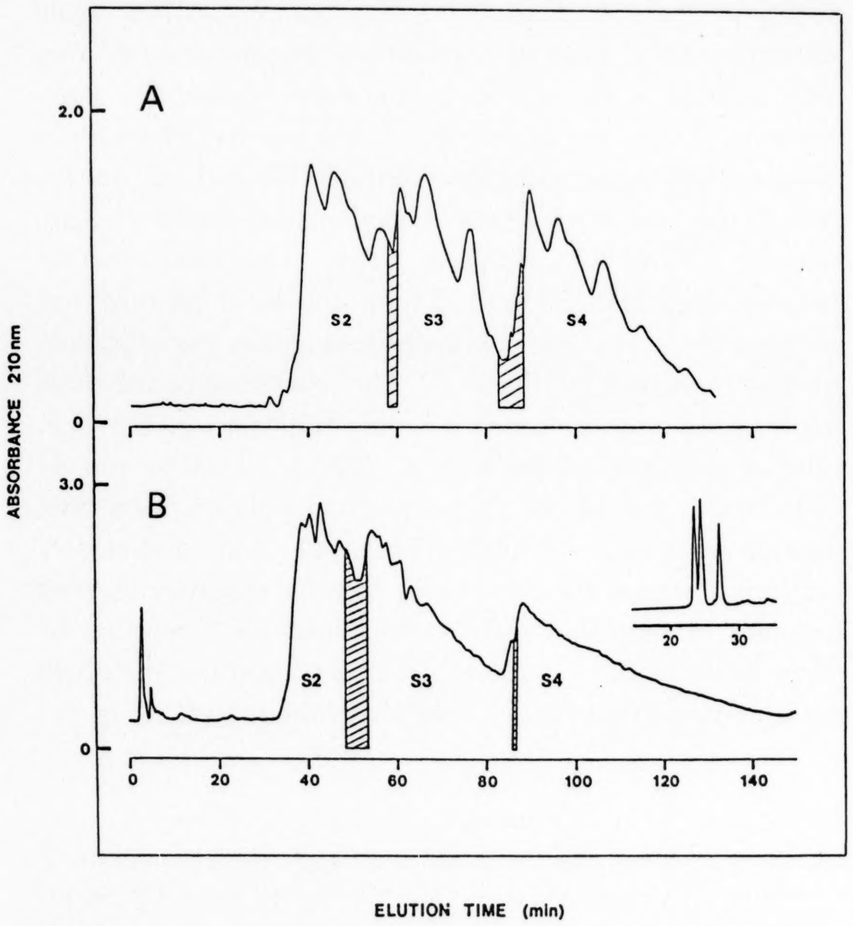

Fig. 5

Effect of sample load on the peptide elution profiles.

Columns: Panel A, Aquapore C_8 analytical column (220 × 4.6 mm I.D.; particle size 7 μm; pore size, 300 Å); Panel B, analytical column (250 × 4.1 mm I.D.) containing Vydac C_{18} reversed-phase packing (average particle size, 15–20 μm; pore size, 300 Å).

Conditions: linear AB gradient (0.1% B/min), where solvent A is 0.05% aqueous TFA and solvent B is 0.05% TFA in acetonitrile; flow-rate, 1 ml/min; 26 °C; 2.0 (Panel A) and 3.0 (Panel B) AUFS.

Sample load: 22.8 mg, incorporating 7.8 mg, 9.1 mg and 5.9 mg of peptides S2, S3 and S4, respectively in 150 μl solvent A.

The inset elution profile in Panel B shows the analytical separation (1% B/min) of the three peptides on the analytical column containing the 15–20 μm particle size packing. Sequence variations of decapeptides S2, S3 and S4 are described in Experimental. Hatched areas indicate cross-contamination observed from the isocratic fraction analysis described in text.

Table III. Recovery of peptides following preparative purification on an analytical reversed-phase column.

Quantity Injected (mg)				Total Recovery (%)	Relative Recovery[b] (%)		
S2[a]	S3[a]	S4[a]	Total		S2	S3	S4
7.8	9.1	5.9	22.8	96	82	90	98

[a] S2, S3 and S4 are synthetic decapeptides (see Experimental).
[b] Fraction of a pure peptide recovered from the total of that peptide recovered.

The inset elution profile in Panel B shows the analytical separation (1% B/min) of the three peptides on the analytical column containing the 15–20 μm particle size packing. The elution profiles of the peptides on both columns were similar, with peak shapes again being somewhat superior on the larger particle size packing (Panel B) compared to the 7 μm packing (Panel A), although deterioration of peak shape was apparent on both columns. Isocratic fraction analysis of the elution profiles again determined the levels of cross-contamination (indicated by the hatched areas in Fig. 5) between the peptide components. There was an increase in the number of fractions cross-contaminated between peptides S2 and S3 on the 15–20 μm packing (Panel B) compared to the 7 μm packing (Panel A). However, the cross-contamination between peptides S3 and S4 on the large particle size packing (Panel B) was markedly lower than that observed on the 7 μm packing (Panel A). The separation of the three peptides on both columns was very satisfactory. The high relative recoveries of peptides S2 (82%), S3 (90%) and S4 (98%) from the 15–20 μm particle size column, for a total peptide recovery of 96% (Table III), was particularly gratifying. It was also interesting to note that the observed decrease in retention time at this load for a mixture of three peptides (22.8 mg) was predicted using the analytical curve of sample load *versus* retention time shown in Fig. 4.

Conclusions

The excellent resolving capability of a 15–20 μm average particle size reversed-phase packing has enabled the successful scale up of our shallow gradient purification procedure to significant sample loadings (225 mg) of a two-component mixture containing peptides differing by only a methyl group. These results suggest there is a maximum load to achieve efficient separation of two peptides closely related in retention time (~ 1 min apart on an analytical run using a gradient steepness of 1% B/min). This maximum is 30 mg and 225 mg total weight of peptide mixture for analytical and semipreparative columns, respectively, under the conditions used in this study. Although some resolution is lost with larger particle size during analytical chromatography, this loss is relatively unimportant for preparative runs. The extension of this procedure to more complex peptide mixtures of closely related peptides, is currently being investigated. The results of this study also indicate that 15–20 μm particle size packings are very suitable for general analytical and preparative reversed-phase applications in the laboratory. The use of this inexpensive packing, coupled with the ability to pack efficient columns with analytical HPLC instrumentation, offers great cost saving potential.

Acknowledgements

This work was supported by the Medical Research Council of Canada and equipment grants from the Alberta Heritage Foundation for Medical Research.

References

[1] *C. T. Mant, T. W. L. Burke, R. S. Hodges*, Chromatographia **24**, 565 (1987).
[2] *R. Sitrin,* LC.GC Magazine of Liquid and Gas Chromatography **4,** 530 (1986).
[3] *J. Rivier, R. McClintock, R. Galyean, H. Anderson,* J. Chromatogr. **288,** 303 (1984).
[4] *K. K. Unger, R. Janzen,* J. Chromatogr. **373,** 227 (1986).
[5] *R. E. Majors,* LC.GC Magazine of Liquid and Gas Chromatography **3,** 862 (1985).
[6] *J. M. R. Parker, R. S. Hodges,* J. Prot. Chem. **3,** 465 (1985).
[7] *M. Verzele, C. Dewaele,* LC.GC Magazine of Liquid and Gas Chromatography **4,** 614 (1986).

Received: June 29, 1987
Revised manuscript
received: Sep. 15, 1987
Accepted: Sep 18, 1987
F

RP-HPLC Assay for 1,2-5,6-Dianhydro-3,4-Disuccinyl-Galactitol and Its Metabolites in Blood Plasma and Liver

Gy. Szókán*[1] / I. Elekes[2] / E. Táborhegyi[1] / Gy. Csanádi[3] / J. Bencze[4]

[1] Institute of Organic Chemistry, Eötvös University, Muzeum krt. 4/B, H-1088 Budapest, Hungary

[2] Research Group for Peptide Chemistry, Hungarian Academy of Sciences, Muzeum krt. 4/B, H-1088 Budapest, Hungary

[3] Central Research Institute of Chemistry, Hungarian Academy of Sciences, Pusztaszeri ut 11, H-1525 Budapest, Hungary

[4] Research Institute of Oncopathology, H-1525 Budapest, Hungary

Key Words

Column liquid chromatography
Sample preparation
Plasma and liver
Epoxides

Summary

A method involving pre-column derivatization and HPLC assay is described for measuring submicrogram quantities of 1,2-5,6-dianhydro-3,4-disuccinyl-galactitol (1,2-5,6-dianhydro-3,4-bis(carboxypropionyl)-galactitol), an effective cytostatic drug and its metabolites in blood plasma and liver homogenate. The substance and its metabolites were derivatized with sodium pentamethylene-dithiocarbamate to form different bis(dithiocarbamoyl) esters, which can be detected by UV absorbance at 254 and 280 nm. The directly derivatized products were then extracted into $CHCl_3$, and after sample preparation resolved by RP-HPLC on SAS-Hypersil column.

Introduction

1,2-5,6-dianhydrogalactitol (DAG) (I), like other bifunctional alkylating agents, has a marked cytostatic effect [1], but its applicability is limited in medicine by its toxicity [2]. To decrease toxicity and increase selectivity, the 3,4-diacyl-derivatives (II and III) were synthesized [3, 4].

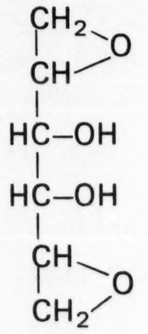

I

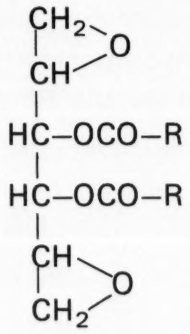

II R = CH_3

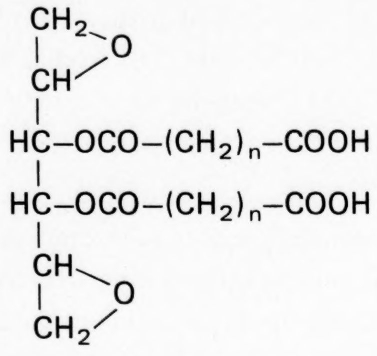

III n = 1, 2, 3

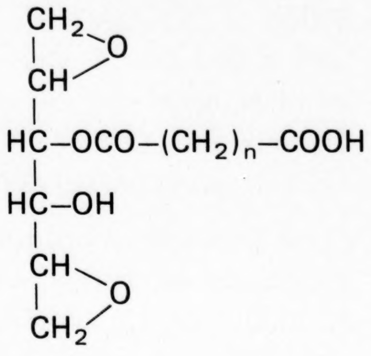

IV

Of the DAG-derivatives, the 1,2-5,6-dianhydro-3,4-bis-(carboxypropionyl)-galactitol, DiSuDAG (III, n = 2) has the best pharmacological properties [5].

Unfortunately, the high reactivity of epoxides towards nucleophiles, and their lack of chromophoric intensity in the UV region (failing to absorb light above 210 nm), considerably limit the analytical methodology available for their determination at therapeutic levels in biological samples.

Several gas chromatographic and HPLC methods have been developed for DAG (I) and DiAcDAG (II) determination in biological fluids [6–9]. Munger [8] elaborated a normal phase HPLC method, in which pre-column derivatization of DAG (I) with diethyl-dithiocarbamic acid (DDTC) was carried out directly in biological fluids. Because of free carboxyl groups in compounds III, this method should be further improved.

Experimental

Apparatus

HPLC separations were performed on a laboratory-assembled instrument consisting of a reciprocating piston pump (Type 1515; Orlita, Giessen, FRG), a variable-wavelength UV monitor fitted to an 8 μl flowcell (Model 212; Cecil, Cambridge, UK) and a sample injector (Model 7011 loop injectior; Rheodyne, Berkeley, CA, USA). Column effluents were monitored at 254 and 280 nm. The chromatograph was operated isocratically at ambient temperature. Peaks were recorded on a Type OH-814/1 chart recorder (Radelkis, Hungary).

0009-5893/87 0839-03 $03.00/0

© 1987 Friedr. Vieweg & Sohn Verlagsgesellschaft mbH

Materials

Sodium penta-methylene-dithiocarbamate (Na-PMDTC) was synthesized according to Livshits and Preobrazhenskii [10]. All chromatographic solvents used were of the highest reagent grade. The HPLC column packing materials were Hypersil ODS and Hypersil SAS (Shandon Southern Products, Runcorn, UK).

Details of the synthetic procedure of 1,6-bis(pentamethylene-dithiocarbamoyl)-2,5-dihydroxy-3,4-bis(β-carboxypropionyl)hexane (DiSuDAG-PMDTC adduct), as well as PMDTC adduct of different DAG derivatives (II, III) and DDTC adduct of DiSuDAG (III, n = 2) and MonoSuDAG (IV, n = 2), will be published elsewhere.

Derivatization

1 ml of plasma serum or liver homogenate, containing 3–500 μg of DiSuDAG (III, n = 2) was placed into a 20 ml centrifuge tube, to which 0.5 ml buffer (pH 7.0) and 0.5 ml of aqueous solution of NaPMDTC reagent were added. The mixture was allowed to stand at room temperature for 1 hr and was extracted as follows:

Extraction with chloroform. The mixture was extracted at pH 4.5 and centrifuged with 3.0 volumes (6 ml) chloroform at 3000g for 10 min. The chloroform layer was washed with 40% NaCl solution. The washed chloroform solution was evaporated to dryness in vacuo, and the residue was dissolved in methanol, diluted ten times with eluent and directly injected into the column. The extraction yields were determined by standards, using HPLC.

Solid phase extraction with SEP-PAK C_{18} cartridge (Waters Ltd). At first the cartridge was washed with 5 ml water, 3 ml methanol then again with 3 × 5 ml water. The sample was injected by syringe. The superfluous material was washed off from the cartridge with 3 × 5 ml water and the product was eluted by 3 ml methanol. Its aliquot was used for HPLC.

Chromatography

In each run, 10 μl of methanol eluent solution containing the derivatized DiSuDAG (III, n = 2) and its metabolites was injected. The mobile phases were methanol – water mixtures with flow rates between 1.0 and 1.4 cm^3/min.

Results and Discussion

According to Munger [8], dithiocarbamate is a suitable reagent for the direct derivatization of epoxides in biological fluids to form compounds having intensive UV absorbance at 254 and 280 nm.

In order to achieve a better extraction, a new reagent with higher hydrophobicity, the sodium pentamethylene-dithiocarbamate (V) [10], was introduced for the derivatization of DiSuDAG (III, n = 2) and its metabolites and analogues. It is also a water soluble substance that reacts readily with epoxides to give dithiocarbamoyl esters:

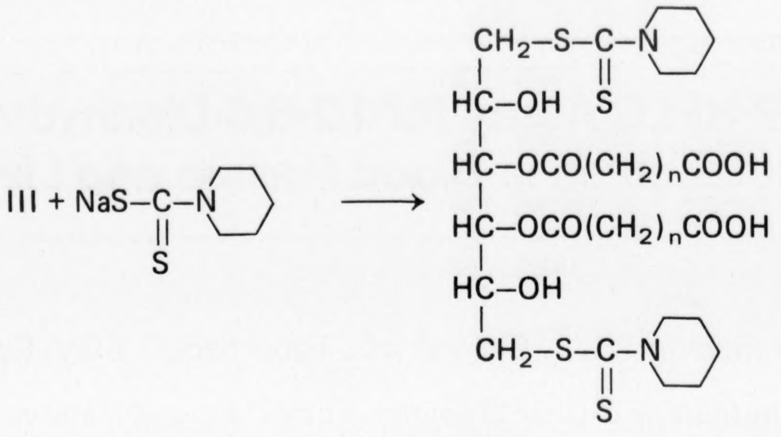

V VI

The derivatives of different galactitols and their hypothetic metabolites (VI, VII and VIII) were synthesized as standard control substances for calibration, t_R determination and peak identification in the measurements. Their structures were identified and characterized by UV, IR and NMR measurements. They showed very high UV absorbance at 254 and 280 nm with molar extinction coefficients between 18,000–22,000.

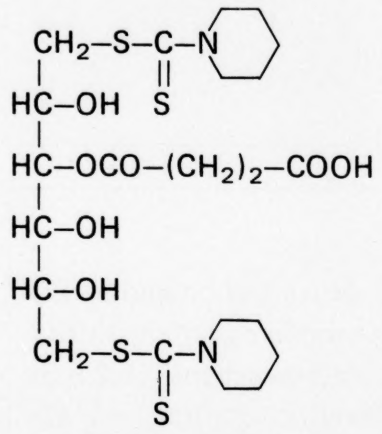

MonoSuDAG-PMDTC

VII

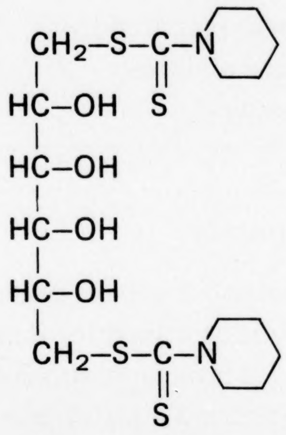

DAG-PMDTC

VIII

After optimization of RP-HPLC conditions, baseline separations were achieved for the different glactitol derivatives (Fig. 1).

The detection limit for the derivatives in our chromatographic system is between 100 pmol and 1 nmol.

The peaks of derivatives (VI, VII) containing succinyl groups showed a tailing because of the free dissociable COOH group. Applying an acidic eluent system (pH 4–5) the peak symmetry was improved, but the t_R became higher.

As the succinyl group decreased, the hydrophobic character of the dithio-carbamoyl derivatives t_R of VI and VII were lower than that of VIII. When the OH groups of compound I were acetylated (II, R = CH_3), the opposite effect was achieved in t_R: the DiAcDAG (II)-DDTC had the highest hydrophobicity and the greatest t_R as well.

Comparing the chromatographic properties of PMDTC and DDTC derivatives, it seems that the PMDTC derivatives are more retarded by the RP column than the DDTC derivatives, due to increased hydrophobicities.

The baseline separations of derivatives (VI, VII, VIII) of DiSuDAG (III, n = 2) and their two chief metabolites (I, IV) are demonstrated in Fig. 1 (chromatographic data see in Table I).

Table I. Chromatographic data of DDTC and PMDTC derivatives

Epoxides	Derivatives	k'
DiMalDAG (III, N = 1)	PMDTC	0.63
DiSuDAG (III, n = 2)	PMDTC	2.44
	DDTC	1.05
MonosuDAG (IV)	PMDTC	5.13
DiGluDAG (III, n = 3)	PMDTC	5.88
DAG (I)	PMDTC	9.80
	DDTC	6.10
DiAcDAG (II)	DDTC	22.52

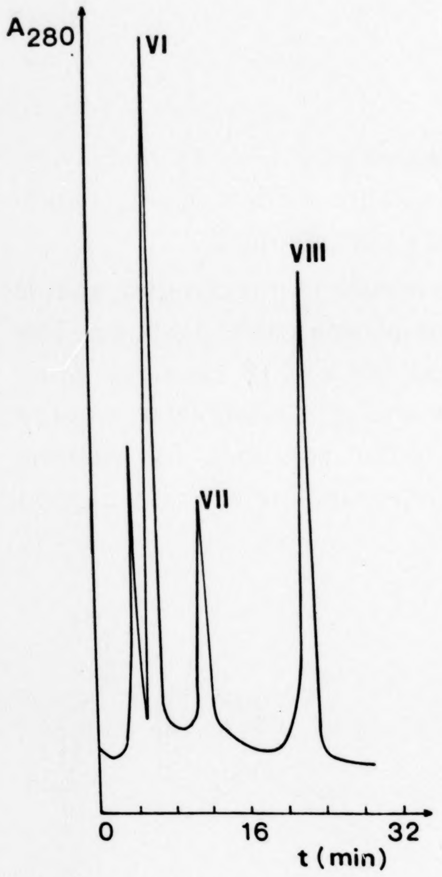

Fig. 1

Chromatographic pattern of separation of different galactitol derivatives. Conditions (see optima). Peaks from the start: DiSuDAG-PMDTC, (**VI**, n = 2), MonoSuDAG-PMDTC (**VII**) and DAG-PMDTC (**VIII**).

The increase in length of the carbon chain of the acyl group (III, n = 1, 2, 3) changes the t_R as expected (see Table I).

In conclusion, the following optimal conditions were found for the measurements: SAS-Hypersil packing material, MeOH:0.02 M phosphate buffer (pH 5.1) 45:55 or 40:60 (v/v) eluents, 1–1.2 cm^3/min flow rate and UV detection at 280 nm.

Plasma and liver samples could be derivatized without prior extraction of the drug (III, n = 2). A great excess of the reagent was used to achieve a high yield of derivatization. The recoveries from different sources were controlled with the help of standards. It was found that the extraction rate was most effective at pH 4.5. The best conditions in sample preparation were found when the liquid and solid phase extraction methods were combined to remove the undesired components of biological fluids (proteins, excess NaPMDTC solution, etc.) prior to HPLC determination.

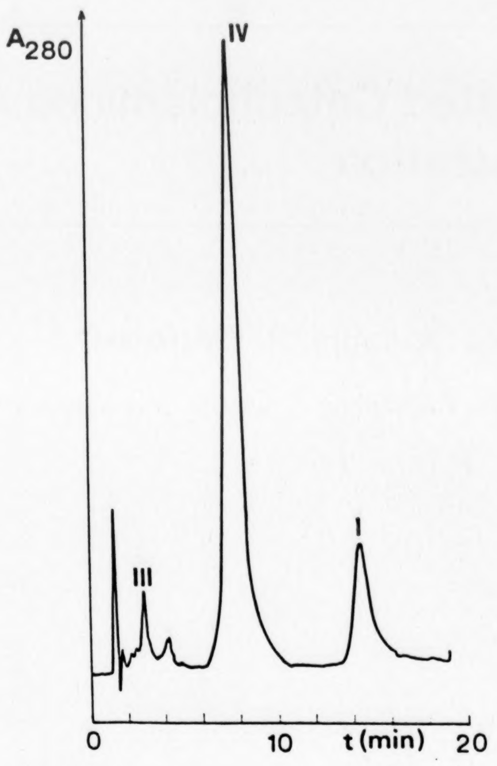

Fig. 2

RP-HPLC separation of hydrolysate of DiSuDAG using rat liver homogenate. Conditions: PMDTC derivatization, sample preparation (see in the text), SAS-Hypersil column, 1.2 cm^3/min, 40:60 (v/v) methanol – 0.02 M phosphate buffer pH 5.1, UV detection at 280 nm. Identified peaks: DiSuDAG (**III**, n = 2), MonoSuDAG (**IV**) and DAG (**I**).

The PMDTC adduct of DiSuDAG and its metabolites can be washed from the cartridge quantitatively by using methanol.

The half-time of decomposition of DiSuDAG was measured in vivo in rat plasma fluid, using this new derivatization method followed by RP-HPLC. The metabolites were identified as MonoSuDAG and DAG.

Investigations on the rate of ester hydrolysis of DiSuDAG, using rat liver homogenate as an aspecific esterase enzyme source, showed that the main metabolite was MonoSuDAG (IV) with quite a small quantity of DAG (I) (Fig. 2).

References

[1] *L. Németh, L. Institoris, S. Somfai, F. Gál, S. Pályi, J. Sugár, O. Csuka, Z. Szentirmay, B. Kellner*, Cancer Chemother. Rep. **56**, 593 (1972).

[2] *R. T. Eagen, N. J. Ingle, S. Fritak, J. Rubin, L. K. Kvols, D. T. Carr, D. T. Coles, J. R. O'Fallon*, Cancer Treatment Rep. **61**, 1339 (1971).

[3] *L. Ötvös* and coworkers, C. A. **85** 108938F (1976) CAS Registry Number: 57.230-48-5 Patent.

[4] *I. Elekes* et al., Hungarian Patent 2649/80.

[5] *S. Somfai-Relle*, in "14th International Cancer Congress" Abstract of Papers, *S. Eckhardt*, ed., Karger/Akadémiai Kiadó, Basel/Budapest, 1986; p. 18.

[6] *T. Kimura, L. A. Sternson, T. Higuchi*, Clin. Chem. **22**, 1639 (1976).

[7] *V. Erdély-Tóth, S. Kerpel-Fronius, B. Kanyár, S. Eckhardt*, Cancer Chemother. Pharm. **16**, 257 (1986).

[8] *D. Munger, L. A. Sternson, A. J. Repta, T. Higuchi*, J. Chromatography **143**, 375 (1977).

[9] *W. D. Henner, E. A. Furlong, S. L. Kelley, A. Rosavsky*, J. Pharm. Sci. **74**, 983 (1985).

[10] *S. S. Livshits, N. A. Preobrazhenskii*, J. Gen. Chem. USSR, **16**, 925 (1945); C. A. **40**, 6872 (1946).

Received: July 1, 1987
Revised manuscript
received: Sept. 15, 1987
Accepted: Sept. 23, 1987
F

A Fully Automated Catecholamines Analyzer Based on Cartridge Extraction and HPLC Separation

G. Grossi*/A. Bargossi/A. Lippi/R. Battistoni

Laboratorio Centralizzato, Policlinico S. Orsola, Via Massarenti 9, 40138 Bologna, Italy

Key Words

Column liquid chromatography
Automated analysis
Catecholamines in plasma and urine

Summary

A fully automated analyzer is described for the HPLC analysis of catecholamines.

Firstly urinary and plasma catecholamines are reacted with diphenylboronic acid giving a complex without requiring a pH-meter step. This complex is strongly retained on a C 18 cartridge and elution with acetic acid solutions shows recoveries higher than 90 %. The catecholamines are eluted also by the mobile phase employed for the HPLC' analysis.

An intelligent autosampler makes the complex and fills a loop with all the solvents necessary for the sample cleanup. It then inverts the flow and pumps the sample and the solvents throught the cartridge.

In the elution step the disposable extraction cartridge is positioned on stream with the HPLC analytical column by an automatic sampler.

The separation is performed by ion-pair reversed-phase high-performance liquid chromatography, with sodium dodecyl sulphate as pairing ion, a short analytical column and electrochemical detection.

The HPLC analysis time is 3 min and the total sample turnover time is 8 min.

The recoveries and the precision of the analyzer are given together with correlation with manual HPLC.

Introduction

Urinary catecholamines are not retained on reversed-phase cartridges and are usually extracted on cation-exchange columns after a careful pH adjustment [1]. A liquid-liquid extraction, not requiring a pH-meter step, has been reported in the literature [2].

Urinary and plasma catecholamines (Fig. 1) react with diphenylboronic acid in an alkaline medium giving a complex the structure of which is shown in Fig. 2.

In our method the first step is making this complex, that is more stable than the parent plasma catecholamines. The complex is strongly retained on a C 18 cartridge when operating in alkaline media and it is possible to employ buffer and also methanol-buffer solutions for washing steps, without loss of the compounds of interest. Elution

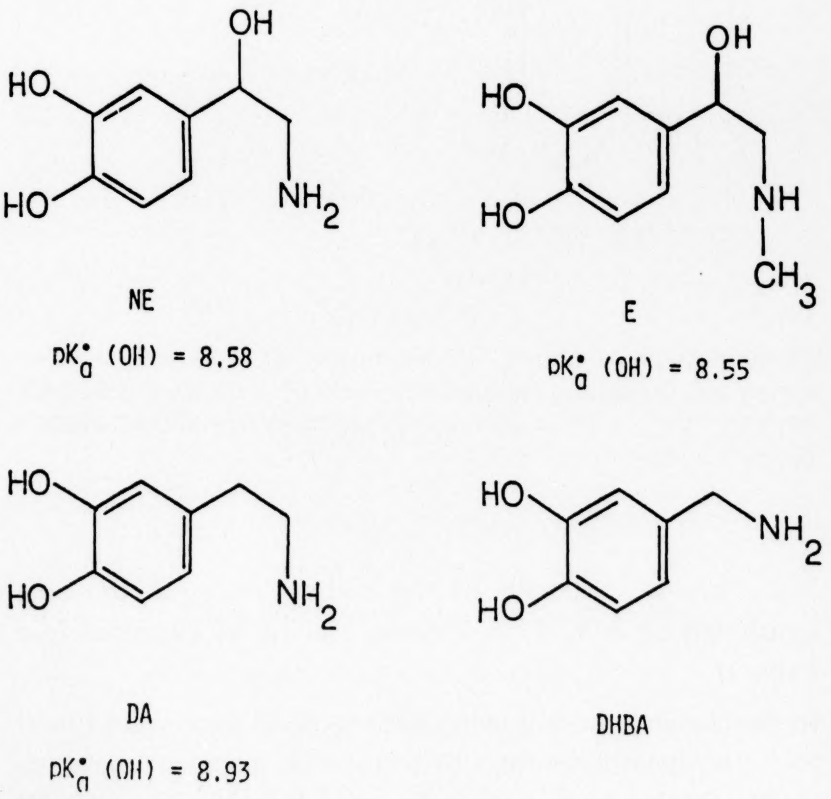

Fig. 1

Catecholamines structure. **NE** = Norepinephrine, **E** = epinephrine, **DA** = dopamine, DHBA = Dihydroxybenzylamine (Internal Standard).

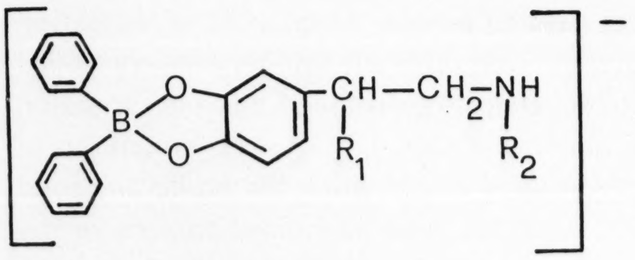

Fig. 2

Diphenylborate-catecholamine complex structure.

0009-5893/87 0842-05 $03.00/0

© 1987 Friedr. Vieweg & Sohn Verlagsgesellschaft mbH

with acetic acid solutions shows recoveries higher than 90 % and the catecholamines are eluted by the mobile phase employed for the HPLC analysis.

As the complex is negatively charged, we studied the effect of ion-pairing with tetrabutylammonium ion in the reversed-phase extraction, testing many sorbents.

The separation is performed by ion-pair reversed-phase HPLC, with sodium dodecyl sulphate as pairing ion, a fast C 18 (3 μm, 3 cm) analytical column and electrochemical detection.

Full automation is obtained by coupling two devices: a solid phase automatic sampler (AASP, Varian) and an intelligent autosampler (Gilson). In this way all the sample clean-up steps are performed automatically and we can define the technique as a column-switching with disposable precolumns. The HPLC analysis is 3 min (fast HPLC); the sample turnover time is 8 min. Samples can be kept for many hours before analysis because of the stability of the complex.

Materials

Norepinephrine (NE), epinephrine (E), dopamine (D) and the internal standard dihydroxybenzylamine (DHBA) were obtained from Sigma (St. Louis, Mo, USA); diphenylborate-ethanolamine (DPBEA) and tetrabutylammonium bromide (TBA) from Aldrich (Milwaukee, Wi, USA); sodium dodecyl sulphate from BDH (Poole, Dorset, UK).

The extraction cartridges, silica bonded with octadecyl (C 18), octyl (C 8), ethyl (C 2), cyclohexyl (CH) and phenyl (PH) groups, in the two versions (Bond Elut 100 mg and AASP cassette) were from Analytichem International (Harbor City, Ca, USA); the HPLC pump model 2010, the solid-phase automatic sampler model AASP, the ten-port Valco injection valve and the recorder model 1201 were from Varian, USA.

The sample preparator model 222, the dilutor model 401 and the interface model Anachem were from Gilson, France. The column effluent was monitored with a dual-electrode coulometric electrochemical ESA detector (model 5100 A Coulochem with a 5021 conditioning cell and a 5011 high-sensitivity cell, Environmental Sciences Assoc., Bedford, Ma, USA).

The optimized HPLC system for catecholamines was assembled as follows: solvent reservoir → HPLC pump → saturation column (125 X 4 mm, Sepralite C 18 40 μm, Analytichem Int.) → ten-port valve → AASP extraction cartridge → ten-port valve → filter (model 7315, Rheodyne, USA) → analytical column (30 X 4 mm, HS-3 C 18, 3 μm, Perkin-Elmer) → conditioning cell (set at + 0.45 V) → high-sensitivity cell (set at: det. 1, + 0.10 V; det. 2, − 0.30 V) → recorder. The mobile phase was methanol − acetonitrile − 50 mM phosphate buffer, pH 2.8 15 : 8 : 77, containing 200 mg/l of sodium dodecyl sulphate.

The urine samples were preserved with 0.1 M HCl.

Methods

Table I shows the method for manual clean-up of urine samples. For automated extraction, we employed the AASP solid phase autosampler, connected with the intelligent autosampler (Fig. 3).

The extraction micro-columns (50 mg of sorbent) are assembled in cassette of ten (Fig. 4) and are substituted

Table I. Urinary catecholamines C 18 Bond Elut extraction.

Extraction column: Bond Elut C 18, 100 mg (Analytichem Int.)
Sample: 0.5 ml of urine + 10 μl of I.S. (DHBA, 15 μg/ml) + 1 ml of 2.0 M NH_4Cl-NH_4OH (pH 8.5) buffer containing 0.2 % (W/V) of diphenylborate-ethanolamine complex (Aldrich) and 0.5 % (W/V) of EDTA.

- activate with 2 X 1 ml of methanol;
- equilibrate with 2 X 1 ml of 0.2 M NH_4Cl-NH_4OH buffer, pH 8.5 containing 0.05 % of EDTA;
- apply 1 ml of sample;
- wash with 2 X 1 ml of buffer;
- wash with 1 ml of methanol-buffer pH 8.5 20 : 80;
- elute with 2 ml of 0.08 M acetic acid.

Inject 50 μl into HPLC
HPLC flow: 2 ml/min
Detector: response 2, gain 10 X 10
Recorder chart: 5 mm/min.

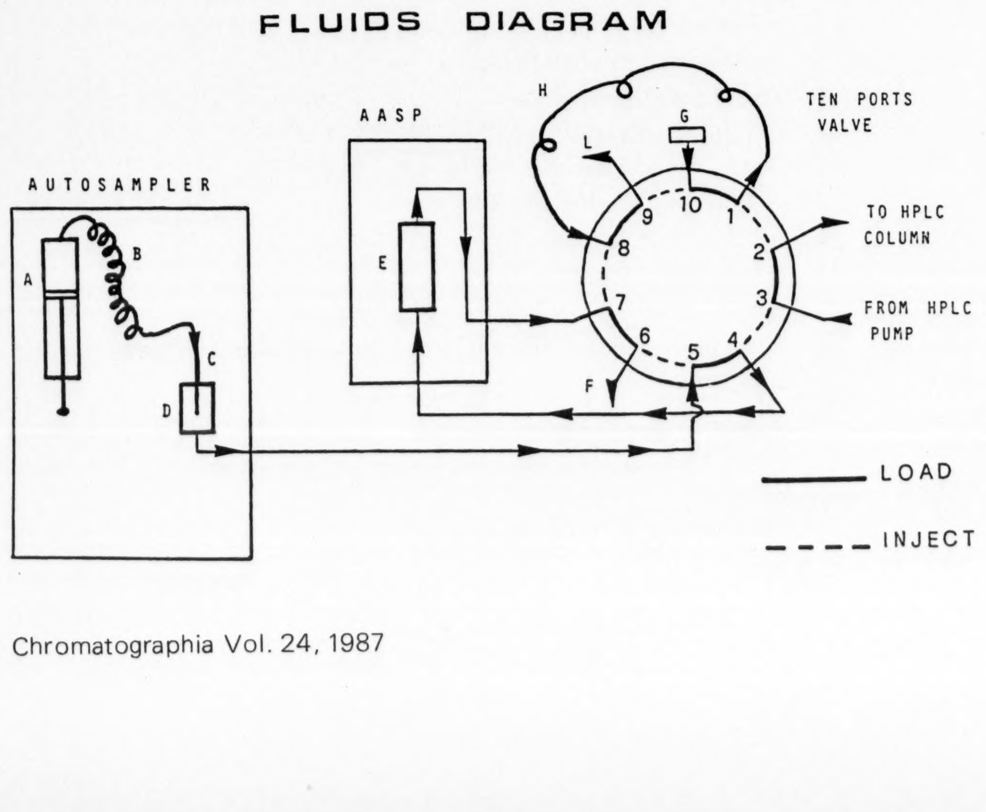

Fig. 3
AASP fluids diagram
A — Low-cost syringe pump (dilutor Mod. 401, Gilson)
B — 5 ml loop
C — Needle of the autosampler
D — Injection port
E — AASP extraction cartridge
F — Purge solvent drain
G — Septum for manual injection
H — Manual injection loop
L — Manual injection drain

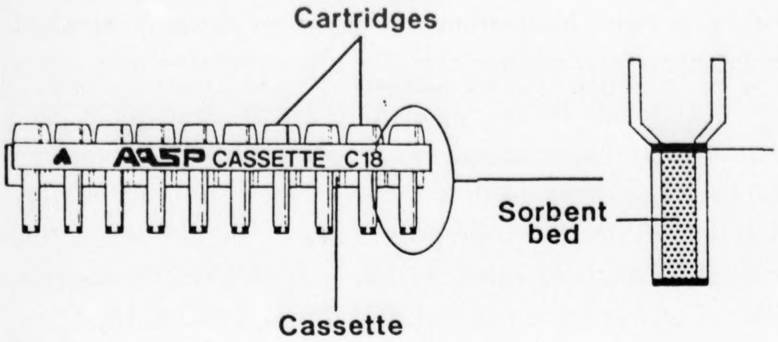

Fig. 4
Disposable extraction cartridges.

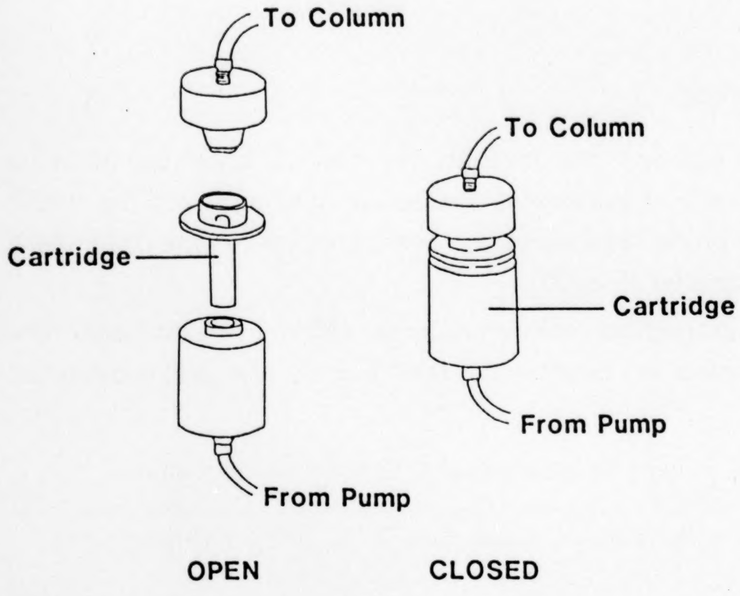

Fig. 5
AASP compression chamber in open and closed positions.

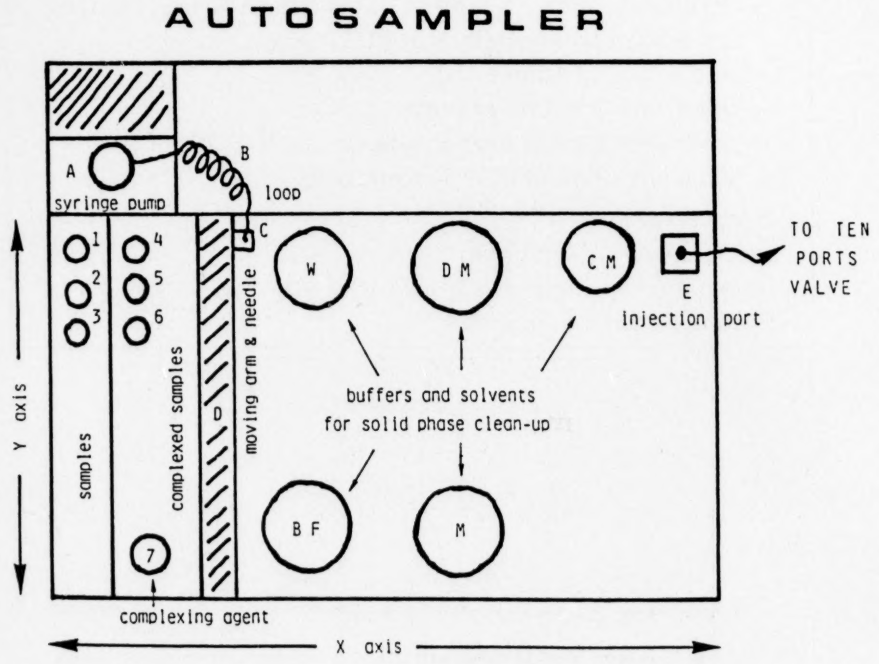

Fig. 6
Intelligent autosampler. The arm (D) moves the needle (C) along the axes X and Y on a tray containing the samples (up to 40) and the buffers necessary for the column switching clean-up.

A syringe pump (A) and a 5 ml loop (B) are connected to the needle, which moves in the sequence: needle washing step; internal standard solution in buffer with diphenylborate (7); void tube for making the complex (4); sample (1); void tube (4); needle washing step; water (W); methanol-buffer solution (DM, diluted; or CM, concentrated, only for ion-pairing technique); buffer (BF); complexed sample (4); buffer (BF); methanol (M); injection port (E).

for the autosampler vials. The disposable extraction cartridge is pneumatically positioned on stream with the HPLC analytical column (Fig. 5). The intelligent autosampler (Fig. 6) dilutes the urine or plasma sample, making the complex and then co-operates on stream with the AASP, filling firstly a 5 ml loop with all the solvents necessary for the sample clean-up, then inverting the flow, pumps these solvents through the cartridge positioned on the AASP.

For the elution, a ten-port time commanded valve connects the cartridge on stream with the analytical column, and the catecholamines are eluted by the HPLC mobile phase. Then the AASP changes the cartridge to a new one, the Gilson washes the 5 ml loop and the system is ready for the next sample.

Table II shows the catecholamine extraction method for urine samples by LC column switching.

For manual extraction of plasma samples we used the ion-pairing technique, by adding tetrabutylammonium bromide to the sample and to the buffers employed (Table III). For plasma catecholamine column switching extraction we do not use ion-pairing, but the separation is obtained using two fast HPLC analytical columns (Table IV).

Results and Discussion

Fig. 7 shows the chromatograms obtained from urine samples. When injecting pure mixture no difference in efficiency was noted for 5 μl injection, 50 μl injection of the extracted solutions and AASP injection. This is probably due to the small amount of stationary phase in the analytical column, so that the injection of 50 μl of 0.08 % acetic acid modifies the equilibrium and the k^1 of the catecholamines is near 0, so that they are concentrated at the top of the column, till the mobile phase turns again to that supplied by the pump. For the column switching technique the water used for the last washing step reaches the analytical column before the catecholamines and the HPLC mobile phase in which they are eluted from the extraction cartridge. The result is a mini-gradient, and the efficiency for the catecholamines is improved.

Table II. Urinary catecholamines, C 18 column switching extraction.

Extraction column: AASP cassette C 18 (Analytichem Int.)

The autsampler makes the complex by mixing 0.25 ml of urine, 5 μl of I.S. (DHBA, 15 μg/ml) and 0.5 ml buffer pH 8.5 containing diphenylborate.

Then sucks in sequence:
- 1.25 ml of water;
- 0.5 ml of methanol-buffer pH 8.5 20 : 80;
- 1.0 ml of buffer pH 8.5;
- 0.15 ml of sample;
- 0.5 ml of buffer;
- 0.5 ml of methanol.

Then pumps in the reverse order these solutions through the cartridge.

Valve reset: 0.1 min;
HPLC flow: 2 ml/min;
Detector: response 2, gain 10 X 10;
Recorder: 5 mm/min.

Table III. Plasma catecholamines, C 18 Bond Elut extraction.

Extraction column: Bond Elut C 18, 100 mg (Analytichem Int.)

Sample: 2 ml of plasma + 25 μl of I.S. (DHBA, 100 ng/ml) + 1 ml of 2.0 M NH_4Cl-NH_4OH (pH 8.5) buffer containing 0.2 % of diphenylborate, 1.2 % (W/V) of tetrabutylammonium bromide (TBA, Aldrich) and 0.5 % of EDTA.

- activate with 2 X 1 ml of methanol;
- equilibrate with 3 X 1 ml of 0.2 M NH_4Cl-NH_4OH buffer, pH 8.5, containing 0.05 % of EDTA and 0.4 % of TBA;
- apply the sample;
- wash with 2 X 1 ml of buffer;
- wash with 2 X 1 ml of methanol-buffer 1 : 1 solution, containing 0.4 % of TBA;
- wash with 1 ml of water;
- wash with 0.25 ml of HPLC mobile phase;
- elute with 0.25 ml HPLC mobile phase.

Inject 50 μl into HPLC;
HPLC flow rate: 2 ml/min
Detector: response 2, gain 100 X 10
Recorder chart: 5 mm/min.

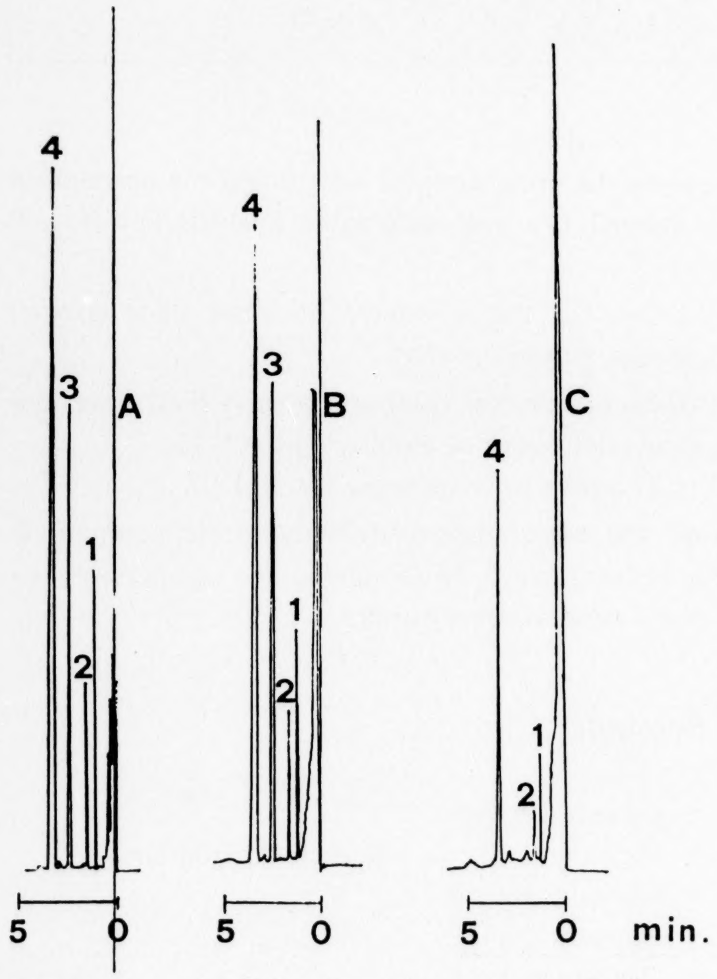

Fig. 7

Urine analytical profile. A, Bond Elut extraction; B and C, column switching Peaks: 1, NE; 2, E; 3, I.S.; 4, D.
A and B: urine containing NE, 160 μg/l; E, 125 μg/l; D, 700 μg/l;
C: urine blank without I.S.: NE, 60 μg/l; E, 25 μg/l; D, 300 μg/l.
Analytical conditions:
mobile phase: methanol-acetonitrile-50 mM phosphate buffer, pH 2.8, 15 : 8 : 77, containing 200 mg/l of sodium dodecylsulphate. Flow rate 2 ml/min – analytical column 30 X 4 mm, HS-3 C 18, 3 μm (P.E.). Detector: guard cell, + 0.45 V; detector 1, + 0.10 V; detector 2, – 0.30 V, gain 10 X 10, response 2.

Fig. 8 shows the chromatograms obtained from plasma samples. For manual extraction, ion-pairing was used in order to remove some artefacts appearing between E and the internal standard (dihydroxybenzylamine).

Table IV. Plasma catecholamines, C 18 column switching extraction

Extraction column: AASP cassette C 18 (Analytichem Int.) The autosampler makes the complex by mixing 0.6 ml of plasma, 7,5 μl of I.S. (DHBA, 100 ng/ml) and 0.3 ml of buffer pH 8.5, containing diphenylborate. Treat all the samples at once.

Then sucks in sequence:
1.25 ml of water;
0.5 ml of methanol-buffer pH 8.5 20 : 80;
1.0 ml of buffer pH 8.5;
0.6 ml of sample;
0.5 ml of buffer;
0.5 ml of methanol.

Then pumps in reverse order these solutions through the cartridge.

Valve reset: 0.2 min
HPLC flow rate: 1.5 ml/min
2 analytical columns (30 X 4 mm, HS-3 C 18, 3 μm, P.E.)
Detector: response 2, gain 100 X 10
Recorder: 5 mm/min.

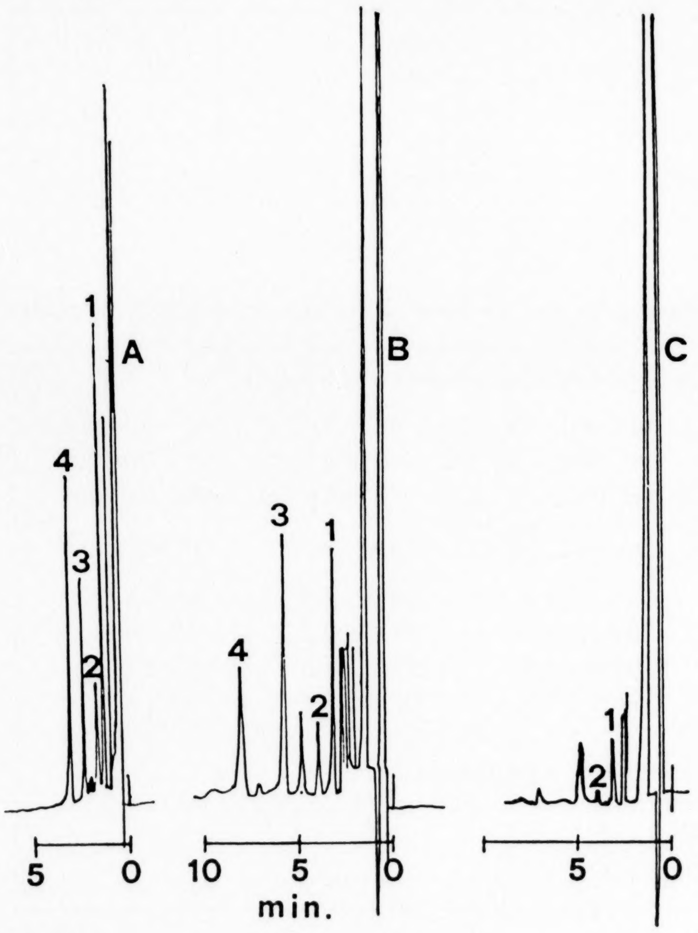

Fig. 8

Plasma analytical profile. A, Bond Elut extraction; B and C, column switching.
Peaks: 1, NE; 2, E; 3, I.S.; 4, D.
A and B: plasma spiked containing: NE, 500 pg/ml;
E, 250 pg/ml; D, 500 pg/ml.
C: real plasma sample extracted without I.S.: NE, 122 pg/ml; E, 48 pg/ml.
Analytical conditions:
mobile phase: methanol – acetonitrile – 50 mM phosphate buffer, pH 2.8, 15 : 8 : 77, containing 200 mg/l of sodium dodecylsulphate; flow rate: A, 2 ml/min; B (and C), 1.5 ml/min; analytical column: A, 30 X 4 mm, HS-3 C 18, 3 μm; B, 2 of these columns; detector: guard cell, + 0.45 V; detector 1, + 0.10 V; detector 2, – 0.30 V; gain 100 X 10, response 2.

With the ion-pairing the complex is more retained on the reversed-phase so that it is possible to wash the column with solutions of methanol-buffer (1 : 1) to remove the artefacts. One analytical column is enough to obtain a good separation.

For column switching we obtained a large solvent peak when using one analytical column; it is impossible to employ the ion-pairing technique, because the retention times decrease injection after injection, as the amount of TBA reaching the analytical column increases.

For these reasons the best choice was to increase the column separation by doubling the column length.

Table V shows the retention times and the turnover times. The recoveries and the precision of the column switching method are summarized in Table VI.

The normal range of catecholamines concentrations were calculated for 40 urine and 10 plasma samples obtained from healthy adults (Table VII).

Table V. Retention times.

	Urine samples	Plasma samples
NE	1.2 min	2.8 min
E	1.6 min	3.6 min
I.S.	2.2 min	5.2 min
D	3.2 min	7.2 min
turnover:	8 min	12 min

Table VI. Recoveries and precision of the column switching methods.

% Absolute recovery for a urine containing (μg/1):

Low:	NE, 60;	E, 25;	IS, 500;	D, 300	(n = 20)
Medium:	NE, 160;	E, 125;	IS, 500;	D, 700	(n = 20)
High:	NE, 560;	E, 525;	IS, 500;	D, 2300	(n = 20)

	low	medium	high
NE	95.2 ± 2.6	97.3 ± 2.1	99.9 ± 1.7
E	93.1 ± 3.2	97.4 ± 2.2	99.7 ± 1.8
IS	97.0 ± 1.8	97.1 ± 1.8	97.3 ± 1.9
D	96.4 ± 1.9	97.6 ± 1.9	99.8 ± 1.4

% Absolute recovery from plasma,
for a plasma containing NE, 500 pg/ml; E, 250 pg/ml (n = 20)
NE = 92.3 ± 3.2
E = 95.1 ± 3.5

Table VII. C. normal ranges.

Urinary normal values;
7 hours urine collection, n = 40 (20 males, 20 females);
age: 25–45 years.

NE		8.4 ÷ 48.6	μg/g of urinary creatinine
	$\bar{X}$	= 24.4 ± 13.10	μg/g of urinary creatinine
E		1.0 ÷ 7.2	μg/g of urinary creatinine
	$\bar{X}$	= 4.8 ± 5.21	μg/g of urinary creatinine
D		111 ÷ 267	μg/g of urinary creatinine
	$\bar{X}$	= 190 ± 58.1	μg/g of urinary creatinine

Plasma catecholamines normal range (n = 10).

NE = 80 ÷ 260 pg/ml
E = 8 ÷ 40 pg/ml

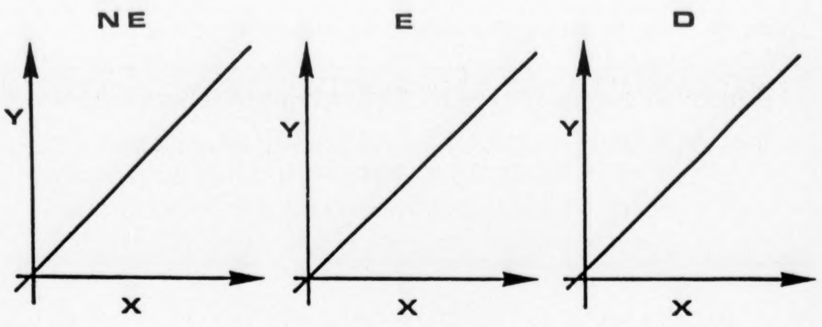

Fig. 9
Urinary catecholamines correlation study.
X = Bond Elut extraction; Y = column switching extraction.

Table VIII. Urinary catecholamines correlation study.

X = C 18 Bond Elut extraction
Y = column switching extraction
n = 40

NE	Y	= 0.9950 X + 0.1575
	r	= 0.9983
E	Y	= 1.0145 X − 0.0596
	r	= 0.9988
D	Y	= 0.9875 X + 2.3475
	r	= 0.9991

For the same 40 urine samples we studied the correlation between manual (X) and automated analysis (Y) (Fig. 9 and Table VIII).

We tested also for the reliability of other silica bonded reversed-phases, and found that:

- octyl (C8), cyclohexyl (CH) and phenyl (PH) show the same recoveries obtained employing the C 18;
- ethyl (C2) gives a poor recovery for NE).

In plasma, the catecholamine-diphenylborate complex is stable for more than 5 hours, giving the opportunity to analyze many samples every batch.

List of Symbols

C = Catecholamines
HPLC = High-performance liquid chromatography
NE = Norepinephrine
E = Epinephrine
D = Dopamine
DHBA = Dihydroxybenzylamine
DPBEA = Diphenylborate-ethanolamine complex
TBA = Tetrabutylammonium bromide
EDTA = Ethylendiaminotetraacetic acid

References

[1] *G. M. Anderson, J. G. Young, P. I. Jatlow, D. J. Cohen,* Clin. Chem., **27,** 2060 (1981).

[2] *F. Smedes, J. C. Kraak, H. Poppe,* J. Chromatogr., **231,** 25 (1982).

Received: Sept. 3, 1987
Revised Manuscript
received: Oct. 22, 1987
Accepted: Nov. 9, 1987
F

Separation of Urea and other Polar Compounds by HPLC

M. Pálfi-Ledniczky*/G. Dénes

Central Research Institute for Chemistry of the Hungarian Academy of Sciences, P. O. Box 17,
H-1525 Budapest, Hungary

K. Ujszászy

Spectroscopic Department, EGIS Pharmaceutical Factory, P. O. Box 100,
H-1475 Budapest, Hungary

Key Words

Column liquid chromatography
Urea
Silica phase

Summary

Urea, glycolic and aminoxyacetic acid amides are the polar metabolites of 2-acetyl-3-phenyl-tetrahydro-1,2,4-oxadiazin-5-one (RGH 4615). They cannot be separated on octadecyl-, cyanosilyl- or amino-phase columns, but silica, used with C_3-C_4 alcohol and water mixtures as the eluent permits their separation. Besides refractive index detection and on-line radioactivity measurement the metabolic formation of ^{14}C-urea was proved by enzymatic cleavage into $^{14}CO_2$.

Introduction

Studying the metabolism of 2-acetyl-3-phenyl-tetrahydro-1,2,4-oxydiazin-5-one (RGH 4615) [1, 2] in rat water-soluble metabolites containing ^{14}C-labelled carbon atom were also found in the urine. These minor components were separated on Florisil column and eluted with methanol-water solvents, together with urea.

Besides the analytical separation of the assumed metabolic compounds the large amount of urea present also represents a problem. The use of octadecyl-, cyanosilyl- or amino-phase columns was not as successful for the separation as silica, using alcohol-water mixtures as the eluent.

Experimental

Apparatus

Liquopump 312 (Labor MIM) delivering solvent at 1.0 ml/min. The eluent was monitored by a differential refractometer (Waters Associates) and on-line LB 503 radioactivity monitor (Berthold). 25 cm X 4.6 mm ID columns packed with Hypersil C_{18} 10 μm, Hypersil AOS 5 μm, Hypersil CPS 5 μm, Chromsil silica 10 μm and Hypersil silica 5 μm were used. Samples were introduced with a Negretti and Zambra injection system incorporating a 20-μl loop. Distillated water, methanol, n-butanol and isopropanol were used as eluents. All solvents were of HPLC grade (Merck).

Materials

Urea was a product of Reanal, ^{14}C-urea, aminoxyacetic and glycolic acid amides were prepared in our laboratory. Urease was obtained from E. Merck.

Enzymatic Hydrolysis

0.5 ml of the aqueous ^{14}C-urea solution was added to 3.5 ml of urease (500 E/ml) dissolved in 0.1 M (pH 6) sodium acetate buffer, and the mixture was incubated at 50 °C for 20 min in nitrogen atmosphere. The reaction was stopped by the addition of 0.5 ml of 1 N H_2SO_4 to pH 2, nitrogen was passed through the solution at 5 ml/min for 10 min in order to purge $^{14}CO_2$ into the absorber fluid, for radioactivity measurement.

0009-5893/87 0847-02 $03.00/0 © 1987 Friedr. Vieweg & Sohn Verlagsgesellschaft mbH

Results and Discussion

The tested HPLC methods (phases and eluents) and the retention times obtained are summarized in Table I. In order to get successful preparative separation of the metabolites from the large amount of urea it was useful to convert some part of the urea into CO_2 (Fig. 1). The enzymatic hydrolysis of urea was performed in an apparatus shown in Fig. 2. The converted radioactive CO_2 proves that urea is one of metabolites of RGH 4615. Fig. 3 shows the water-soluble metabolites; their structures were determined by mass and infrared spectral data.

Table I. Separation of polar compounds by different HPLC methods

Stationary phase/ Eluents	Retention time of Urea (min)	Aminoxyacetic acid amide (min)	Glycolic acid amide (min)
Hypersil C_{18} 10 µm			
Water	3.6	3.5	3.5
Water-Methanol (9 : 1)	2.5	2.5	2.5
Isopropanol	3.0–3.5	3.0–3.5	3.5
Hypersil AOS 5 µm			
Water	2.9	2.9	3.2
Water-Methanol (7 : 3)	3.0	3.0	3.4
Hypersil CPS 5 µm			
Water	2.9	3.0	2.9
Methanol-Water (7 : 3)	2.8	2.8	2.8
Methanol	2.9	3.0	2.9
Chromsil silica 10 µm			
n-Propanol	5.0	4.5	4.6
Water-n-Propanol (1:9)	5.1	4.5–5.2	4.5
Water-n-Butanol (1:9)	4.5–5.1	8.3	5.4
Water-n-Butanol (5:95)	6.8	7.5	5.2
Hypersil silica 5 µm			
Water-n-Butanol (1:9)	5.8	7.2	4.5
Water-Isopropanol-n-Butanol (5 : 2 : 93)	6.2	7.8	4.8

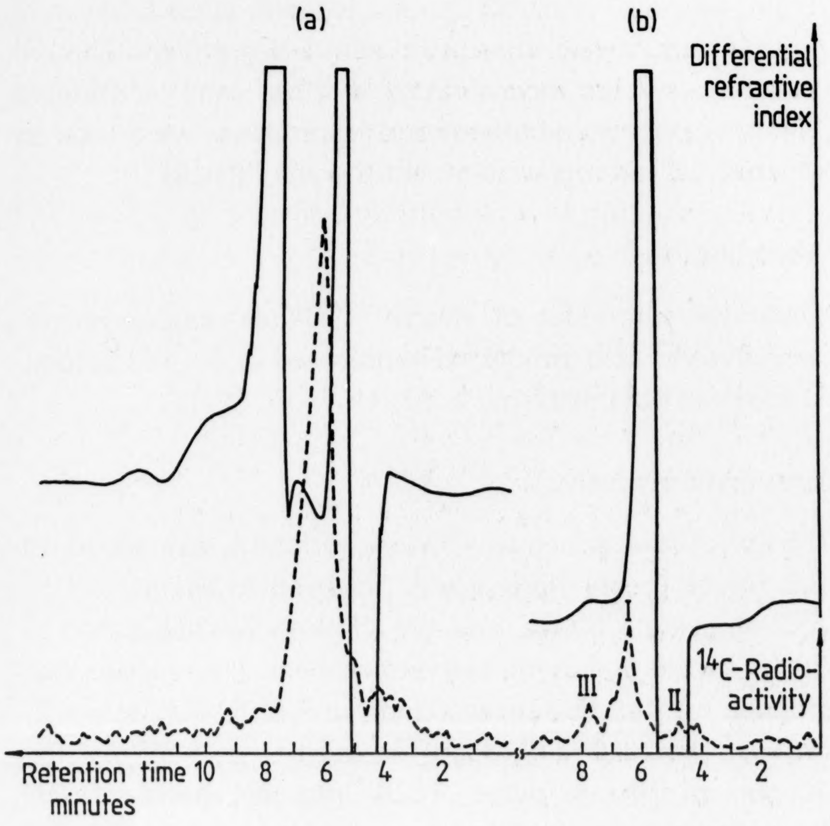

Fig. 1

HPLC Separation of a biological sample (a) before and (b) after urease enzymatic hydrolysis. Hypersil silica 5 µm column. Eluent: water-isopropanol-n-butanol (5 : 2 : 93). Detectors: (a) differential refractometer (on-line); (b) ^{14}C radiodetector (on-line).

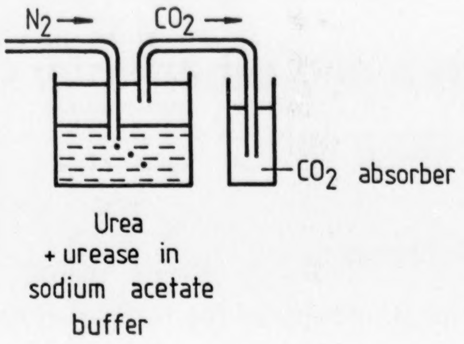

Fig. 2

Apparatus for the enzymatic cleavage of urea into CO_2.

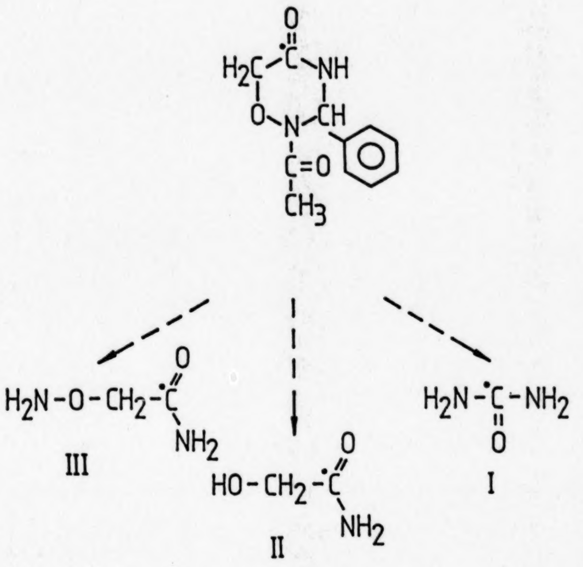

Fig. 3

Polar metabolites of RGH 4615 (2-acetyl-3-phenyl-tetrahydro-1,2,4-oxadiazin-5-one). I = urea, II = glycolic acid amide, III = aminoxyacetic acid amide.

This paper confirms that modified silica phase can improve the separation of non-ionic polar compounds from each other, even if one of them is excreted in much greater amount than the others.

References

[1] *L. Kisfaludy, L. Ürögdi, A. Patthy, L. Dancsi, J. Szilbereky, E. Moravcsik, H. Tüdös, L. Ötvös, Zs. Tegyei:* "Tetrahydro-1,2,4-oxadiazin-5-one derivatives, and medicines containing these compounds". Eur. Pat. Appl.: EP 55490 Al/1982.

[2] *M. Pálfi-Ledniczky, I. Szinai, K. Ujszászy, S. Holly, I. Weisz, V. Kemény, H. Tüdös, M. Horváth, L. Ötvös* in "Bio-Organic Heterocycles", H. C. Van der Plas, L. Ötvös, M. Simonyi (Eds.), Akadémiai Kiadó, Budapest, pp. 329–333 (1984).

Received: June 30, 1987
Revised manuscript
received: Sep. 25, 1987
Accepted: Sep. 28, 1987
F

Study of the Selective Retention of Fluorinated Compounds on Perfluorinated Stationary Phases

I. de Miguel/S. Exbrayat/D. Samain*

Centre de Transfert en Biotechnologie-Microbiologie (INSA/UPS), 126, Av. de Rangueil, 31077 Toulouse Cedex, France

Key Words

Segregation
Perfluorinated
Column liquid chromatography

Summary

The basis of the selective retention of perfluorinated compounds on perfluorinated bonded phases is examined. It is shown that the selective retention increases dramatically by increasing chain length and strand multiplicity.

Introduction

Segregation between perfluorinated (PF) and perhydrogenated (PH) compounds is a well known phenomenon. Studies by Mukerjee et al. [1] on the physical behaviour of PF and PH mixed oils and surfactants showed a segregation at micellar formation level.

Theoretical studies carried out by Kruger et al. [2] indicate that the internal rotation energetic barrier is much higher for PF linear compounds than for PH ones. It means that mobility on PF chains is lower than on PH ones and this seems to be a determining factor in the reciprocal non solubility.

In chromatography, de Galan [3] had demonstrated that fluorocarbon bonded phases exhibit specific fluorine-fluorine interaction and show enhanced retention for fluorine containing compounds. HPLC seems than to be a convenient tool to study segregation phenomenon in detail.

We thus sought to investigate the influence of the chain length on the chromatographic segregation of linear (PH and PF) compounds by using a PF HPLC bonded phase. We studied also the cooperative effect induced by the presence of several PF chains on the same compound.

The first parameter is studied by comparison of the retention of comercially available linear alcohols. For the second one, we have synthetized double- and tetra-strand compounds with various PH and PF chain lengths and studied their respective retention.

Experimental

General Data

Material: A Gilson M 302 pump, a Gilson M 803 C Manometric Module, a Gilson M 131 Refractive Index Detector (Gilson Med. Int., Villiers le bel, France), a Shimazdu U.V. adsorption Detector (Shimazdu Co., Kyoto, Japan) and a Rheodyne HPLC Injector (Rheodyne, Cotati, CA, USA) were used as the HPLC system. The column was a heptadecafluorodecyl (FD) Chromegabond 5 μm, 25 cm x 4.6 mm purchased from Interchim (Monluçon, France).

Unless otherwise specified the HPLC flow rate was 1 ml/min.

Thin Layer Chromatography (TLC) was performed on DC-Alurolle Kiesselgel 60 F254 (Merck, Darmstadt, FRG).

An Infra-red Spectrometer Acculab 4 (Beckman, Berkeley, CA, USA) was used for product characterization.

Sep-pack Silica Cartridges (Waters Ass., Milford, MA, USA) were used for fast product purification.

Products: Methanol, acetonitrile, chloroform and Freon 113 were HPLC grade. Pyridine and dichloromethane were analytical grade and purchased from Prolabo (Paris, France).

1,2 Butanediol, phenyl β-D glucopyranoside, decanoyl chloride, butyric anhydride and linear hydrocarbon alcohols were purchased from Fluka (Buchs, Switzerland) and were used without further purification.

Linear perfluorinated alcohols were kindly provided by I. Rico (Laboratoire des IMRCP, University of Toulouse) and can be obtained from Fluorochem Ltd. (Glossop, UK).

Heptafluorobutyric anhydride and (Perfluorohexyl) acetyl chloride were purchased from Riedel de Häen (Hannover, FRG) and were used without further purification.

Preparation of Tetra ((Perfluorohexyl) Acetoxy) Phenyl β-D Glucopyranoside ($PF_{4\times6}$)

The following procedure is representative. Phenyl β-D glucopyranoside (PG) (10 mg, 0.039 mM) is suspended in 0.5 ml of dry acetonitrile containing 24 μl of pyridine. (Perfluorohexyl) acetyl chloride (PAC) (117 mg, 0.3 mM) is added and the reaction mixture is placed in a well stoppered vial and heated for 12 hours at 70°C.

0009-5893/87 0849-05 $ 03.00/0

© 1987 Friedr. Vieweg & Sohn Verlagsgesellschaft mbH

After completion of the reaction, the excess PAC is quenched with a few drops of cold water. Chloroform (2 ml) is then added and the resulting solution is washed with a cold solution of 0.01 M HCl followed by a wash with brine.

The organic layer is dreid on anhydrous Na_2SO_4, filtered and concentrated to a 200 µl volume under a stream of nitrogen.

The reaction products are then applied on top of a Sep-pak silica cartridge previously equilibrated with chloroform/hexane (50/50) and the column is developped with a gradient from chloroform/hexane (50/50) to 100 % chloroform. 1 ml fractions are collected and tested by TLC ($CHCl_3$). The fractions containing $PF_{4\times6}$ are collected and concentrated under a stream of nitrogen to give 36 mg (yield 55 %) of pure compound.

Analytical: TLC (SiO_2, $CHCl_3$): one spot, RF: 0.85 (detected by U.V. activity and H_2SO_4, 50 %); U.V. max. 240 nm; I.R. ester C=O band 1750 cm^{-1} (s) and $-CF_2-$ $-CF_3$ at 1250–1110 cm^{-1} (s).

Preparation of Tetra(decanoyl-oxy) Phenyl β-D Glucopyranoside ($PH_{4\times10}$)

The procedure used is similar to that for $PF_{4\times6}$. PG (10 mg, 0.039 mMO is treated with a 0.5 ml solution of decanoyl chloride (57 mg, 0.3 mM) in pyridine/CH_2Cl_2 (1/20). After purification, 28 mg of pure compound are obtained (yield 70 %).

Analytical: TLC (SiO_2, $CHCl_3$): one spot, Rf: 0.85 (detected by U.V. activity and H_2SO_4, 50 %); U.V.: max. 240 nm; I.R.: ester C=O band 1735 cm^{-1} (s) and $-CH_2-$ $-CH_3$ band 2850–2960 cm^{-1} (s).

Preparation of Tetra (Butanoyl-oxy) Phenyl B-D Glucopyranoside $PH_{4\times3}$

The procedure used is similar to that for $PF_{4\times6}$. PG (10 mg, 0.039 mMO is treated with a 0.5 ml solution of butyric anhydride (123 mg, 0.3 mM) in pyridine/Cl_2CH_2 (1/20). After purification 17 mg of pure product are obtained (yield 80 %).

Analytical: TLC (SiO_2, $CHCl_3$): one spot, Rf: 0.57 (detected by U.V. activity and H_2SO_4); U.V.: max. 240 nm; I.R.: ester C=O band 1735 cm^{-1} (s) and $-CH_2-$ $-CH_3$ band 2850–2960 cm^{-1} (m).

Preparation of Bis 1,2 (butynoyl-oxy) Butane ($PH_{2\times3}$)

The reaction procedure is the same as that for $PF_{4\times6}$.

Butanediol (10 mg, 0.22 mM) is treated with 0.5 ml of dry dichloromethane containg 70 µl of pyridine and 126 mg (0.88 mM) of butyric anhydride.

After extraction, the chloroform layer is concentrated under a stream of nitrogen to give 38 mg of crude $PH_{2\times3}$. 5 mg of crude $PH_{2\times3}$ are further purified by HPLC (mobile phase: methanol/water 60/40, k': 3). The fractions corresponding to the product are collected and concentrated under reduced pressure to give 4 mg of pure $PH_{2\times3}$.

Analytical: U.V.: end absorption; I.R.: ester C=O band 1735 cm^{-1} (s) and $-CH_2-$ $-CH_3$ band 2960–2850 cm^{-1} (m).

Preparation of Tetra (heptafluorobutanoyl-oxy) Phenyl β-D Glucopyranoside ($PF_{4\times3}$)

This procedure is representative. PG (10 mg, 0.039 mM) is placed into a reaction vial containing 100 µl (0.4 mM) of pure Heptafluorobutyric anhydride (HFBAA). The reaction vial is well stoppered and heated at 70 °C.

After 16 hours the reaction mixture is cooled and then freeze dried under high vacuum to give 38 mg of pure $PF_{4\times3}$ (yield 95 %).

Analytical: TLC (SiO_2, $CHCl_3$): one spot, Rf: 0.8 (detected by U.V. activity and H_2SO_4, 50 %); U.V.: max. 240 nm; I.R.: ester C=O band 1790 cm^{-1} (s) and $-CF_2-$ $-CF_3$ band 1250–1110 cm^{-1} (m).

Preparation of Bis 1,2 (heptafluorobutanoyl-oxy) Butane ($PF_{2\times3}$)

The procedure is similar to that for $PF_{4\times3}$. Butanediol (10 mg, 0.22 mM) is placed in a reaction vial containing 200 µl (0.88 mM) of pure HFBAA. After lyophilisation, product recovery is 63 mg (yield 60 %).

Analytical: U.V.: end absorption; I.R.: ester C=O band 1790 cm^{-1} (s) and $-CF_2-$ $-CF_3$ band 1250–1110 cm^{-1} (m).

Results and Discussion

In the course of his work, de Galan [4] had shown that highly fluorinated stationary phases appeared to show a remarkably specific fluorine-fluorine interaction. He had also suggested that the extremely low polarity of the perfluorinated stationary phases could result in a higher overall selectivity.

We believe that this selective fluorine-fluorine interaction may have an interesting potential in chromatographic applications, particularly for dynamic ligand anchoring. We thus sought to investigate the basis of this phenomenon in order to achieve maximal selectivity.

Interesting studies were carried out by Mukerjee et al. [1, 5] on the critical micellar concentration (CMC) of PF and PH mixed surfactants. These works show that, when the CMC is measured as a function of the PF surfactant mojar fraction, deviations in the ideal behaviour indicate that segregation between these two families takes place, giving rise to the formation of distinct PF and PH micelles.

In addition, theoretical studies from Kruger et al. [2] on PF and PH moleculares and its response to paramagnetic relaxing agents, indicate that the Zig-Zag structure is more stabilized in PF linear compounds. In fact, the internal rotation energy barrier in perfluoroethane is much higher than in ethane. In other words, internal mobility is higher for PH linear compounds than for PF ones, and this seems to be a determining factor in the reciprocal non solubility.

The segregation phenomenon appears then to be closely dependent upon the molecular structure.

Accordingly, we postulate that the selective chromatographic retention of PF linear compounds on perfluoroalkyl bonded phases should vary in a non linear way with increasing chain length.

Comparison of the Respective Retentions of PF and PH Linear Compounds

In order to study the influence of the number of carbons upon the selective retention of PF linear compounds, we undertook a systematic study of the chromatographic behaviour of two series of linear alcohols (PF and PH) on a perfluorinated HPLC bonded phase.

The segregation value was defined quantitatively as the capacity factors ratio (k'_F/k'_H) between PF and PH homologuous compounds.

Results are given in Fig. 1. The logarithm of the segregation value ($\log k'_F/k'_H$) is plotted as a function of the number of carbons in the linear chain for various mobile phases.

Selective retention of PF alcohols compared to their PH homologues grows exponentially with increasing alkyl chain length. According to these results, the segregation value between linear PF and PH alcohols can be defined, for methanol/water mobile phase systems, by the following exponential equation:

$$k'_F/k'_H = (100\,\%\ \mathrm{MeOH})^{0.75\ C}$$

where % MeOH is the methanol percentage in the mobile phase and C is the number of carbons of the alkyl chain.

The results of this study suggest that a cooperative effect in retention is exhibited in fluoroalkyl chains when increasing the chain length. This effect appears to be in direct relation with the structure stabilization of the perfluoroalkyl chain brought about by its interaction with the PF stationary phase.

However interesting, the selective retention effect observed with linear PF compounds, cannot be expected to compete with conventional covalent ligand inmobilization.

We thus sought to investigate the possible retention gain brought about by the presence of several linear PF chains within the same compound. Such spider like multi-strand compounds are widely found in nature. One of the best known examples [6] is the Lipid A component of the Lipopolysaccharides of Gram-bacteria. Gram-bacteria, such as *Escherichia coli*, live in aggressive environments. Protection is achieved by tough anchoring of an extended polysaccharide chain in the outer bacterial membrane by the multistrand Lipid A.

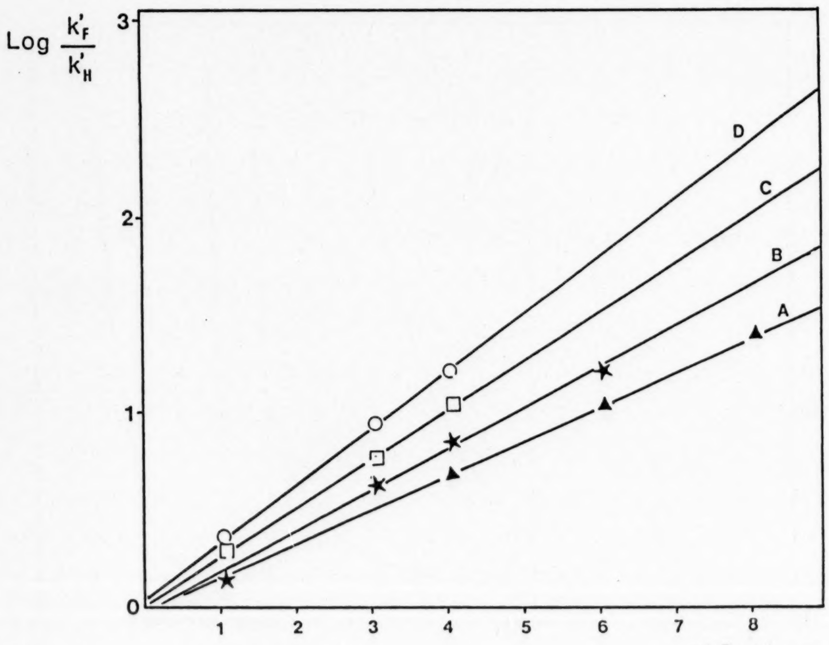

Fig. 1

The logarithm of the segregation value (expressed as k'_F/k'_H) in linear alcohols, is plotted in function of the chain length for different MeOH/H_2O mobile phases (A: 90/10, B: 80/20, C: 70/30, D: 60/40).

Column: Chromegabond FD 5 μm, 25 cm x 4.6 mm.

We suggest that in the case of multi-strand PF compounds, preferential orientation should be likewise favored and even reinforced by the specific fluorine-fluorine interaction.

A two dimensional retention cooperativity could then be expected with increase of the chain length and of the number of PF strands.

Synthesis of Multi-Strand Compounds

In order to check whether our hypothesis was valid, we synthesized a number of PH and PF multi-strand compounds.

Double-strand compounds were prepared by esterification of butanediol with PF and PH anhydrides (Fig. 2).

Tetra-strand compounds were prepared by esterification of phenyl β-D glucopyranoside (Fig. 2). The phenyl derivative was selected to provide convenient U.V. detection.

It is interesting to note that different reaction conditions have to be used since the reactivity of PF anhydrides and acid chlorides is altered by the presence of strongly electronegative fluorine atoms.

In case of HFBAA, the reaction has to be carried out in neat HFBAA [8] since pyridine proved to be an inhibitor of the reaction.

The positive charge density created on the carbonyl group ba adjacent fluorine atoms also induces an increased instability of the ester bond in alkaline conditions.

We observed that the intercalation of a CH_2 unit between the carbonyl group and the PF chain gives rise to increased stability allowing better handling of the product.

The Retention as a Function of the Strand Multiplicity

In order to study the retention effect of several PF chains within the same compound, retention of the double-strand

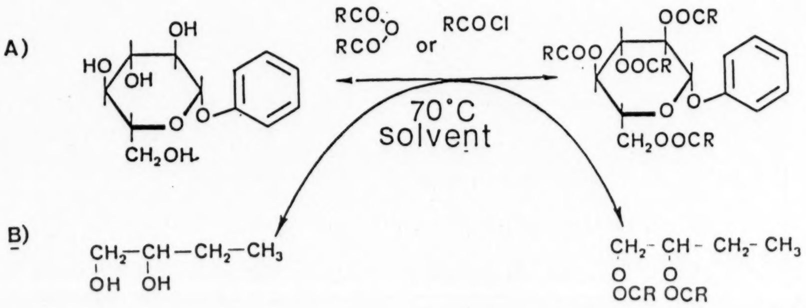

Fig. 2

Esterification reactions schema. Differents compounds are prepared depending on R as follows:

A) $PF_{4\times6}$ R= $CF_3(CF_2)_5CH_2-$
$PF_{4\times3}$ R= $CF_3CF_2CF_2-$
$PH_{4\times9}$ R= $CH_3(CH_2)_8-$
$PH_{4\times3}$ R= $CH_3CH_2CH_2-$

B) $PF_{2\times3}$ R= $CF_3CF_2CF_2-$
$PH_{2\times3}$ R= $CH_3CH_2CH_2-$

$PF_{2\times3}$ was compared to a six carbons (PF_6) linear alcohol. In this case, both compounds contain an equal number of carbons but with different distribution.

The results presented in Fig. 3 show that, with the same number of fluorinated carbons, the double strand $PF_{2\times3}$ is more retained than the single strand PF_6.

This result is worth noticing since a single PF_3 chain exhibits only 1/10 of the retentive power of the PF_6 chain. A strong cooperative effect is thus observed in the case of multistrand compounds.

We then investigated the dependence of the segregation according to the strand multiplicity of the compound. This dependence was precisely studied by the comparison of the segregation value of double-strand compounds with the segregation value of mono-strand compounds.

The results presented in Fig. 4 indicate that segregation is indeed larger with double-strand compounds than with single ones.

$$k'PF_{2\times3}/K'PH_{2\times3} \gg k'PF_6/k'PH_6$$

Selective retention of PF compounds is then more efficiently achieved with double-strand compounds than with linear ones.

In the case of tetra-strand compounds (Fig. 5), a huge difference in retention is observed between PF and PH compounds In fact, PH and PF analogues cannot be eluted with the same solvent system, and the large segregation increase can only be expressed qualitatively.

Conclusion

In this work we have shown that specific retention of PF compounds on PF stationary phases is closely dependent upon compound structure.

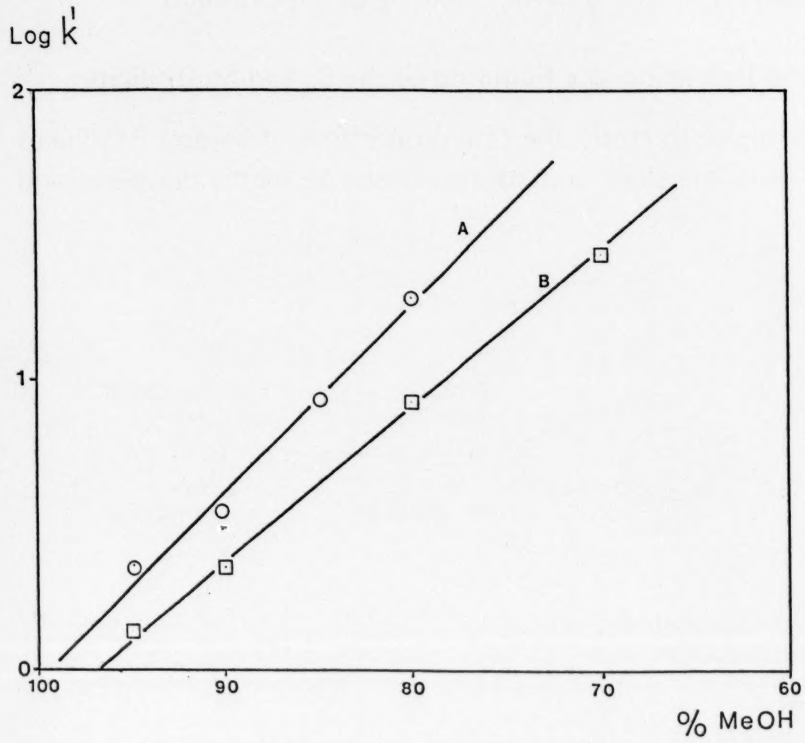

Fig. 3

Retention, expressed as k' of $PF_{2\times3}$ (A) and of PF_6 (B) in function of the mobile phase composition. Mobile phase: MeOH/H_2O. Column: Chromegabond FD 5 μm, 25 cm x 4.6 mm.

Segregation is particulary noticeable with linear compounds and grows exponentially by increasing the chain length and the number of chains within the same compound.

In the case of multi-strand compounds, segregation values can reach truly astonishing levels. The tremendous retention power introduced by these multi-strand compounds should allow a number of interesting applications such as, for instance, the dynamic anchoring of biomolecules.

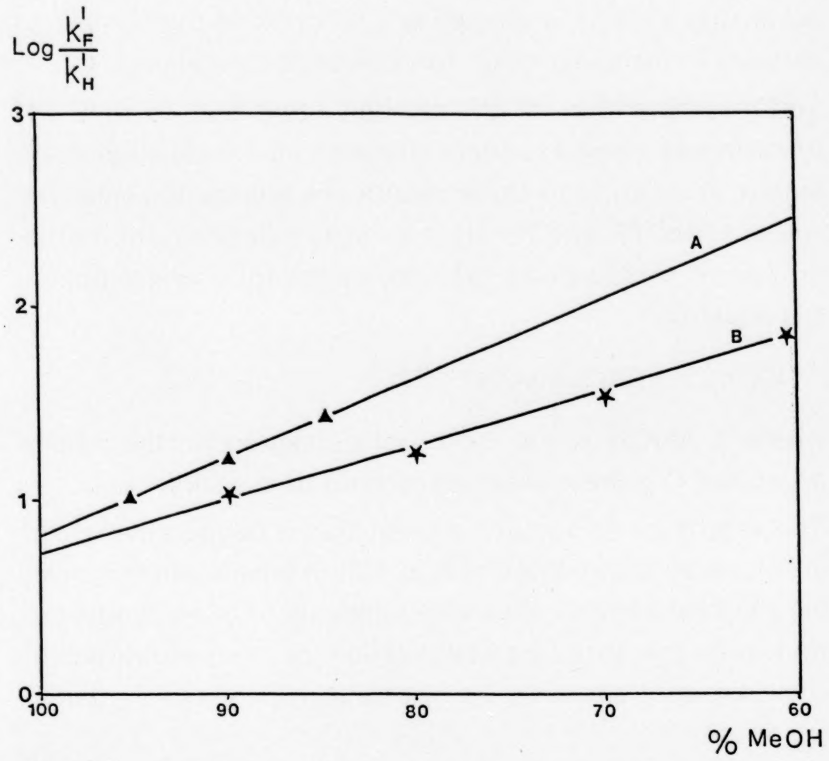

Fig. 4

Logarithm of segregation values (expressed as k'_F/k'_H) in function of the mobile phase for double-strand ($PF_{2\times3}/PH_{2\times3}$) compounds (A) and for linear monostrand (PF_6/PH_6) compounds (B). Mobile phase: MeOH/H_2O. Column: Chromegabond FD 5 μm, 25 cm x 4.6 mm.

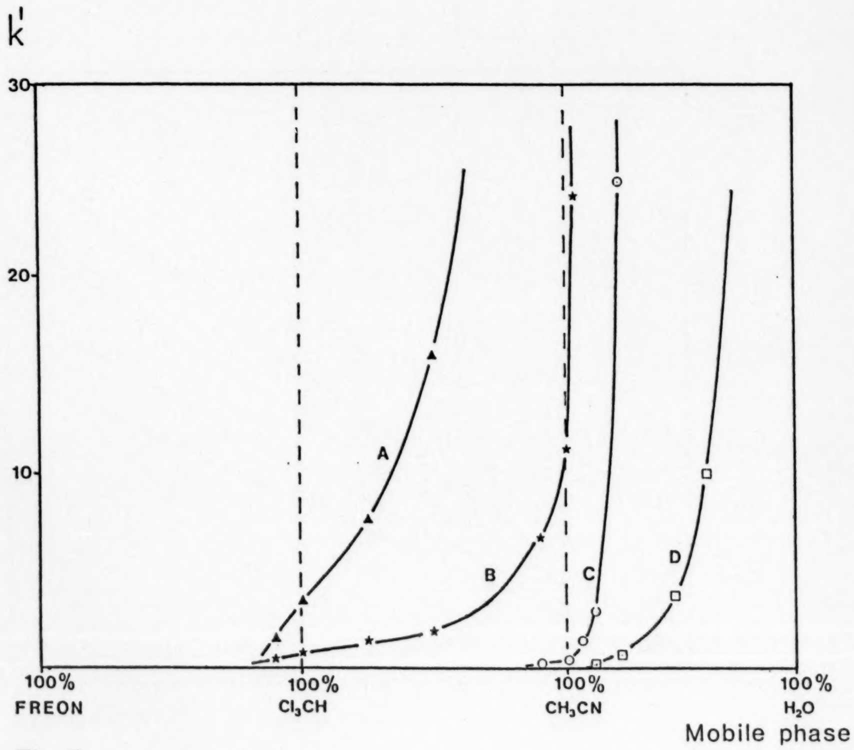

Fig. 5

Study of the retention, espressed as k', of tetra-strand compounds for differents mobile phase systems.

A: $PF_{4\times6}$, B: $PF_{4\times3}$, C: $PH_{4\times9}$, D: $PH_{4\times3}$.

Column: Chromegabond FD 5 μm, 25 cm x 4.6 mm.

Acknowledgements

We are very grateful to Dr. I. Rico (University of Toulouse) for interesting disucssion.

This work was supported by grants from the Réseau International des Biotechnologies, the Fondation pour la Recherche Médicale and the Centre National de la Recherche Scientifique.

References

[1] *P. Mukerjee, A. Y. S. Yang*, The J. of Phys. Chem. **80** (12), 1383 (1976).

[2] *D. G. Kruger, S. Rajan, C. A. Kingsbury*, J. of Solution Chemistry, **11** (10), 719 (1982).

[3] *G. E. Berendsen, K. A. Pikaart, L. De Galan*, Anal. Chem., **52**, 1990–1993 (1980).

[4] *H. A. H. Billiet, P. J. Schoenmakers, L. De Galan*, Journal of Chrom., **218**, 443–454 (1981).

[5] *P. Mukerjee*, J.A. O.C.S., **59** (12), 573 (1982).

[6] *O. Luderitz, C. Galanos, E. T. Rietschel*, Pharmac. Theor. **15**, 383–402 (1982).

[7] *E. T. Rietschel, H. W. Wollenweber, H. Brade* in "Handbook of endotoxin, Vol. I". Ed: R. A. Proctor, University of Wisconsin Medical Schook, Madison, Wisconsin, USA (1984), p. 187.

[8] *G. Eklund, B. Josefsson, C. Roos*, Journal of Chrom., **142**, 575–585 (1977).

Received: July 2, 1987
Accepted: Sep. 8, 1987
F

HPLC and RIA Procedure for Cyclosporine A Determination Compared with Clinical Background

J. Klima*/R. Petrásek/V. Kočandrle/J. Kašlik

Institute for Clinical and Experimental Medicine, Videňska 800, 140 00 Prague 4 – Krč (Czechoslovakia)

Key Words

Cyclosporine A
Column liquid chromatography
RIA
Clinical interpretation

Summary

The aim of our study was to monitor Cyclosporine A (CA) during a long-term period and to determine whether the whole-blood levels, estimated by HPLC and radioimmunoassay (RIA), provide a relevant indicator of the toxic effect of CA, of the interference of endogenous substances with CA and of interactions of erythromycin and ketoconazole with CA metabolims. The ratios of CA concentrations, estimated by RIA and by HPLC were calculated in order to analyse changes in CA metabolism. A decrease in this ratio was observed in these patients during periods of erythromycin and ketoconazole therapy deteriorating hepatic function. We observed unusual higher CA concentrations measured by HPLC compared with RIA in heart transplant patient with marked renal insiffuciency after one-year follow-up period of treatment of CA. The comparison of CA whole-blood levels estimated using HPLC and RIA makes it possible to analyse the individual biotransformation of CA to its metabolites, and interference of endogenous substance in special clinical situations.

Introduction

The measurement of Cyclosporine A (CA) is fraught with difficulties, and an appreciation of the very considerable problems involved is essential to any rational interpretation of the results [1].

Two analytical techniques are available for the analysis: high-performance liquid chromatography (HPLC) and radioimmunoassay (RIA).

The aim of our study was to monitor CA during a long-term period and to determine whether the whole-blood levels, estimated by HPLC and RIA, provide a relevant indicator of the toxic effect of CA, of the interference of endogenoues substances with CA and of interactions of erythromycin and ketokonazole with CA metabolism.

However, the plasma and serum concentrations are an inconstant measure of CA in the blood, because redistribution of the drug between erythrocytes and plasma or serum occurs in vitro during storage and processing of blood specimens [2]. We used for the CA measurement whole blood.

Patients and Treatment

Five heart-transplant patients were studied. They were treated with CA for between ten and fifteen months. Perioperatively, the drug was administered by continous infusion at a rate of 6 mg/kg per 24 h. After 48 h, CA was given orally, twice daily in a total dose ranging from 75 to 650 mg. The CA solution was taken before the morning meal (fasting state) and after the evening meal. The total daily dose was reduced over the course of three months, according to the CA blood levels and the helper/suppressor cell ratios in the peripheral blood. In addition to CA, all patients received prednisone (70 mg/day, decreased stepwise to 20 mg/day). Erythromycin and ketoconazole were used by three patients to prevent infections. The daily dose of erythromycin was 2 g/day and of ketoconazole, 200 mg/day. The administration of diuretic and antiarrythmic drugs was dependent on the clinical status of the patients.

Determination of Cyclosporine

Blood samples for CA assay were drawn into heparinized tubes before the morning dose of CA and stored at 4 °C. The CA levels in whole blood were measured depending on the patients' clinical status, using RIA and HPLC. The blood samples for the two types of determination were collected at the same time. Conventional RIA for whole

0009-5893/87 0854-03 $03.00/0

© 1987 Friedr. Vieweg & Sohn Verlagsgesellschaft mbH

blood was carried out according to the manufacturer's instructions using the kit supplied by Sandoz (Basle, Switzerland). The simple, accurate and specific isocratic HPLC procedure developed by Kabra et al. [3] was adapted by Klima et al. [4] for use with Czechoslovak extraction and analytical columns. The CA was extracted from whole blood by the C_{18} solid-phase extraction procedure, and an aliquot of the eluate was analysed on a glass column.

Acetonitrile and tetrahydrofuran, both of HPLC grade, were obtained from Fluka (Ulm, FRG). Dimethyl sulphoxide (for gas chromatography) and hexane (for gas chromatography) were obtained from Merck (Darmstadt, FRG). Absolute ethanol (190 proof) was obtained from Lachema (Brno, Czechoslovakia). Cyclosporine A and cyclosporine D were obtained from Sandoz (Basle, Switzerland). Water was redestilled in glass and filtered through 0.45-μm poly(tetrafluoroethylene) membrane filters (Sartorius, Göttingen, FRG).

Vac Elut™ vacuum chamber and Bond-Elut™ C_{18}, 100 mg/(1 ml), extraction columns were obtained from Analytichem International (Harbour City, CA, USA).

Glass column (15 cm x 3.3 mm) packed with Separon SGX CN and Pre-Sep C-18 extraction cartridges, were obtained from Tessek Ltd. (Aarhus, Denmark, Prague, Czechoslovakia).

A SP 8100 XR liquid chromatograph, equipped with a column oven, a Model SP 8440 XR variable-wavelength detector and a Data System SP 4200 (all from Spectra-Physics, San Jose, CA, USA), was employed. The column was mounted in an oven. The samples were injected into a Valco valve with a 100-μl sample loop, mounted on the chromatograph. For the chromatographic separation, a mixture of 430 ml acetonitrile and 570 ml of 19 mM phosphate buffer (pH 7.0) was used. The mobile-phase flow rate was 0.5 ml/min. The wavelength for analysis was set at 210 nm and the sensitivity at 0.01 a.u.f.s.. The separation on the cyanoethyl column was achieved at a temperature of 50 °C.

The CN-glass columns (Tessek Ltd.) required only half as much acetonitrile as in the original method. This inexpensive column was replaced after every 100–150 analyses.

Cyclosporine D (CD), was used as internal standard. For calibration, standards of 250 and 500 μg/l of CA in whole blood were used, both for HPLC and RIA. The quantitative analysis of CA was based on the peak-area ratio of CA and CD. The sensitivity, the recovery, the intra-assay precision of the HPLC method was described by Klima et al. [4].

Calculation of RIA/HPLC Ratio

The ratios of CA concentrations, estimated by RIA and by HPLC, were calculated. The RIA/HPLC ratios were calculated in order to analyse changes in CA metabolism. While the HPLC method selectively detecs the parent CA compounds, the non-specific RIA kit measures several cross-reacting metabolites, due to the low specifity of the polyclonal antibody reagent.

As a consequence of the cross-reactivity of the polyclonal antibody supplied with RIA kit, the results for patient samples are typically higher than those produced by HPLC. This ratio gives an idea of the proportions of the parent CA and its metabolites [5].

Results

Blood levels of CA were measured by HPLC and RIA in 125 specimens during a one-year following-up period. The mean ± standard deviations (S.D.) of four patients after heart transplant are shown in Table I, for the period without application of erythromycin and ketoconazole and for the period of therapy. In all cases described above, the statistical analysis consisted of a paired t-test. In all clinical situations, there were statistically significant differences between the concentrations estimated by HPLC and RIA.

The influence of erythromycin and ketoconazole was tested in three patients which were treated with these drugs. For the statistical analysis a non-pairing t-test was used. One hundred one CA blood levels measured during a one-year follow up period were divided into two groups. The first group consisted of CA blood levels in patients without erythromycin and ketoconazole therapy and second group in those given therapeutic doses of both drugs. Both HPLC and RIA were used for the determination of CA and its metabolites. The RIA/HPLC ratios were calculated in order to analyse changes in CA metabolism. The results are shown in Table I.

The mean CA concentrations were significantly lower in the patient group without erythromycin and ketoconazole therapy, and the RIA/HPLC values were higher. Erythromycin and ketoconazole therapy increased the mean CA concentration estimated by the HPLC and RIA methods, and the RIA/HPLC ratio decreased. This fact demonstrates that erythromycin and ketoconazole inhibit the biotransformation of CA.

Differences between the results given by RIA and HPLC may be very large; RIA results up tp 12.3 higher than HPLC have been noted by patients with normal hepatic function during the one-year follow-up period. A decrease in this ratio was observed in these patients during periods of erythromycin and ketoconazole therapy deteriorating hepatic function.

These findings suggest that it would be unwise to rely on RIA measurements of CA as a guide to therapy in patients who have showen signs of deteriorating hepatic function. A selective measurement of the drug would be more appropriate in these patients, although valuable clinical data on hepatic function may accrue by recording changes in the RIA/HPLC ratio.

Determination of Cyclosporine and Interference of Endogenous Substance

The major advantage attributed to HPLC methods is a selective measurement of the drug. We observed the unusual higher CA concentrations measured by HPLC compared with RIA in heart transplant patient with marked renal insufficiency after one-year follow-up period of treatment of CA. The results are shown in Table II.

Table I. Concentrations (μg/l) of cyclosporine a in whole blood in heart-transplant patients during a one-year follow-up period

Statistical analyses: I, paired t-test; II, non-paired t-test									
	Period without therapy			Period with therapy			one-year period		
	HPLC	RIA	RIA/HPLC	HPLC	RIA	RIA/HPLC	HPLC	RIA	RIA/HPLC
(I) Four patients, one without therapy and three with erythromycin and ketoconazole therapy									
No. of blood samples	113	113	113	12	12	12	125	125	125
Mean concentration	144.4	577.1^{+}	5	8.12.9	1637.5^{+}	3.4	208.6	679.0^{+}	4.8
± S.D.	± 96.9	± 287.4	± 2.5	± 864.5	± 940.0	± 2.0	± 337.5	± 501.3	± 2.5
Min. concentration	35	170	1.4	125	600	1.1	35	170	1.1
Max. concentration	490	2900	12.3	2685	3200	7.5	2685	3200	12.3
(II) Three patients with erythromycin and ketoconazole therapy									
No. of blood samples	89	89	89	12	12	12			
Mean concentration	136.3	561.5	4.9	812.9^{+}	1637.5^{+}	3.4^{+}			
± S.D.	± 82.8	± 299.6	± 2.3	± 864.5	± 940.0	± 2.0			
Min. concentration	50	170	1.4	125	600	1.1			
Max. concentration	455	2900	11.5	2685	3200	7.7			

$^{+}$ $p < 0.001$

Table II. Concentrations (μg/l) of cyclosporine a in whole blood

	HPLC	RIA	RIA/HPLC
I. Usual cyclosporine A concentrations			
No. of blood samples	19	19	19
Mean concentration	162.4	531.1	3.9
± S.D.	± 68.8	± 87.7	± 2.3
II. Unusual cyclosporine A concentrations			
No. of blood samples	4	4	4
Mean concentration	1531.3	553.7	0.4
± S.D.	± 515.7	± 214.6	± 0.2
III. Cyclosporine A concentrations after more effective chromatographic separation			
No. of blood samples	4	4	4
Mean concentration	125.0	553.7	4.7
± S.D.	± 52.6	± 214.6	± 1.2

We have highlighted these difficulties by using more effective chromatographic separation. For the chromatographic separation the CN column was used with a higher efficiency (number of theoretical plates). The symmetrical peak that had been identified as CA alone could be resolved into two peaks. The more effective chromatographic separation decreased the mean CA concentration estimated by the HPLC and adjusted the mean RIA/HPLC ratio; see Table II.

Discussion

Our HPLC method estimated CA concentrations in whole blood and therefore the concentrations of CA were not altered by temperature-dependent redistribution between erythrocytes and plasma. The RIA method also used whole blood samples. The analytical conditions for HPLC and RIA were comparable. The results of this study confirm that the RIA method overestimates the concentration of CA. Variations in the CA blood concentrations between individual patients were observed. Within the same patient, the RIA/HPLC ratio between the two results is not constant since the relative difference between the concentrations of CA and its metabolites does not remain the same throughout a dosage interval.

Interference of endogenous substance suggest that the HPLC measurement of CA is not without its own problems. The HPLC technique has many potential advantages compared with currently available RIAs, especially for definitive pharmacokinetic studies, since RIAs are known to overestimate the actual concentrations in patient samples.

Clinically, this implies that in most cases the CA dose can be recuded and the dosage intervals lengthened during application of drugs that interact with the biotransformation of CA in the liver. Since the biotransformation parameters differ widely per individual, changes in dosage should be guided by the whole blood levels. The comparison of CA whole blood levels estimated using HPLC and RIA makes it possible to analyse tthe individual biotransformation of CA to its metabolites, and interference of endogenous substance in special clinical situations.

References

[1] *D. W. Holt, J. T. Marsden, A. Johnston,* Transplantation Proceedings, Vol. XVIII, No. 6, Supp. 5 (December), 1986; p. 101.

[2] *S. M. Fayonor, T. P. Moyer, S. Sterioff,* Mayo Clin. Proc. **59**, 571 (1984).

[3] *P. M. Kabra, J. H. Wall, N. Blackaert,* Clin. Chem. **31**, 1717 (1985).

[4] *J. Klima, R. Petrásek, V. Kočandrle,* J. Chromatogr. **385**, 357 (1987).

[5] *Z. Varghese, M. K. Chan, L. V. Steele, P. Sweny, O. N. Fernado, J. F. Moorhead,* Lancet, i, 1407 (1984).

Received: June 29, 1987
Accepted: Aug 29, 1987
F

Analysis of Non-Ionic Surfactants Used in Tertiary Oil Recovery. Optimisation of Stationary Phase in Normal Phase Partition Chromatography

P. L. Desbène*[1] / B. Desmazières[1] / V. Even[1] / J. J. Basselier[1] / L. Minssieux[2]

[1] Laboratory of Structural Organic Chemistry, P. and M. Curie University, 4 Place Jussieu, 75230 Paris Cedex 05, France
[2] Oil Field Department, Petroleum French Institute, 1–4 Avenue de Bois Préau, 92500 Rueil-Malmaison, France

Key Words

Column liquid chromatography
Diol bonded phase
Analysis of non-ionic surfactants
Derivatisation

Summary

Non-ionic surfactants, made from ethylene oxide units of various lengths condensed with long chain aliphatic alcohols, which are used extensively in enhanced crude oil recovery have been analysed in the past by both adsorption and normal phase partition chromatography. These methods work satisfactorily for narrow range polymers but are of no use for wide range higher molecular weight materials.

We have investigated the performance of a new silica diol bonded phase and compared its chromatographic behaviour with amino and cyano bonded phases for the separation of non-ionic surfactants. After derivatisation with 3,5-dinitrobenzoyl chloride it was found that only the diol phase gave a good evaluation of the distribution versus the number of ethylene oxide units for three surfactants KL 6, KM 11 and KM 20 (the number represent the average number of ethylene oxide units in the molecule). Isocratic elution was used in the case of KL 6 and KM 11 and gradient elution for KM 20. In spite of the presence of over 40 peaks in the chromatogram of KM 20, analysis was accomplished in about 45 minutes. Identification of peaks was achieved by the coelution of a pure standard.

Introduction

Enhanced oil recovery has been employed for a number of years to increase the amount of crude oil recovered from reservoir rocks. One of the main methods of enhanced recovery is the use of water injection with the addition of various additives to the water (polymers, alkaline compounds and surfactants). Mixtures of surfactants are used in order to modify the interfacial tension between the hydrocarbons and the reservoir rocks. The oil is trapped within the pores of the rock and increasing the wettability and viscosity of the water helps it to displace the crude oil from the pores.

The materials used represent a considerable cost to the oil industry and it is, therefore, of importance to be able to analyse and quantify the compounds used as surfactants.

Gas chromatography can be used after derivatisation [1–4] provided that there are no more than 14 ethylene oxide units in the molecule. HPLC has been widely used for the analysis of ionic [5, 6] and non-ionic surfactants [7, 8]. From the literature it would appear that adsorption chromatography will not give a satisfactory analysis of surfactants having a wide distribution of polyethylene oxide units [9–12] and only C_2 bonded silica seems to be suitable for reversed-phase chromatography [8, 13–18] but the batch to batch reproducibility of this material is poor.

Steric exclusion chromatography is unsatisfactory since Bombaugh showed that recycling was necessary to obtain a good separation with an effective column length of 50 m, resulting in an analysis time of 20 hours [19].

The only HPLC technique which appears to offer promise for the analysis of surfactants in terms of their ethylene oxide distribution is normal phase partition chromatography with amino bonded silica [20, 21] and cyano bonded material [20]. A new diol bonded silica has recently become available and this paper describes a comparative study of amino, cyano and diol bonded phases using three different surfactants KL 6, KM 11 and KM 20.

Experimental

Apparatus

The apparatus comprised a Philips PU 4003 dual piston pump and associated controler, a Rheodyne 7010 injector with a 10–100 µl sample loop, a Philips PU 4025 UV/visible detector and an Iota differential refractometer. The signals from the detectors were displayed on a Kipp and Zonen

0009-5893/87 0857-05 $ 03.00/0

© 1987 Friedr. Vieweg & Sohn Verlagsgesellschaft mbH

recorder. The UV/visible spectra were also recorded with a Hewlett Packard 8450A photodiode array spectrophotometer.

Columns

All the columns used were 250 mm × 4.6 mm i.d. The first was a 7 μm Zorbax amino column (DuPont), the second was a 7 μm Zorbax cyano column and the third was a 5 μm Lichrospher (Merck) diol column packed in our laboratory by the method reported by Rocca [22].

Solvents and Reagents

All the solvents were HPLC grade from Merck, BDH and SDS. The surfactant standards with six ethylene oxide units and either a C_{16} or a C_{18} moiety were purchased from Nikko and the surfactants studied (KL 6, KM 11 and KM 20) were of technical grade. The 3,5-dinitrobenzoyl chloride derivatising reagent (DNB) was purchased from Prolabo (RP grade).

Derivatisation

The water present in each sample was removed by Dean and Stark distillation with benzene. DNB was added in stoichiometric quantity together with magnesium shavings to remove HCl formed in the reaction. KL 6 and KM 11 required refluxing for 30 minutes; KM 20 required 60 minutes. After refluxing the solution was cooled and filtered and the benzene evaporated. The resultant ester was suitable for analysis by HPLC without further preparation.

Mobile Phases

For the amino and cyano columns mixtures of n-heptane, dichloromethane and methanol were used in various proportions. For the diol phase the same solvent mixture was used for isocratic elution and gradient elution was carried out with the following program:

Solvent A	97.5%	n-heptane/dichloromethane (95/5 v/v)
	2.5%	propan-2-ol
Solvent B	70%	n heptane/dichloromethane (95/5 v/v)
	30%	propan-2-ol

Analysis time (min)	%B
0	0
40	100
65	0

Results and Discussion

The non-ionic surfactants KL 6, KM 11 and KM 20 used in this work are obtained from the condensation of ethylene oxide with C_{16}–C_{18} natural fatty alcohols. Two of these surfactants (KM 11 and KM 20) have no chromophore and do not allow a satisfactory detection in the ultraviolet. Refractometry is unsuitable for quantitative analysis of these compounds (see Fig. 1) and cannot be used with an gradient elution.

We have therefore derivatised the surfactants with 3,5-dinitrobenzoyl chloride (DNB) by the method of Nozawa et al. [8] to obtain absorption at 254 nm (Fig. 2).

We then undertook a comparative study of the three polar bonded phases in order to optimize the separation of the polyoxyethylenic chains of the surfactants.

Amino bonded silica. The most suitable mobile phase for separating the non-ionic surfactants KL 6 and KM 11 as a function of their ethylene oxide number is a ternary eluent containing n-heptane/CH_2Cl_2/MeOH 90/5/5. The chromatograms of KL 6 and KM 11 are shown in Figs. 2 and 3.

It is interesting to note that normal phase partition chromatography allows separation simultaneously as a function of the ethylene oxide numbers and as a function of the nature of the fatty alcohol chains.

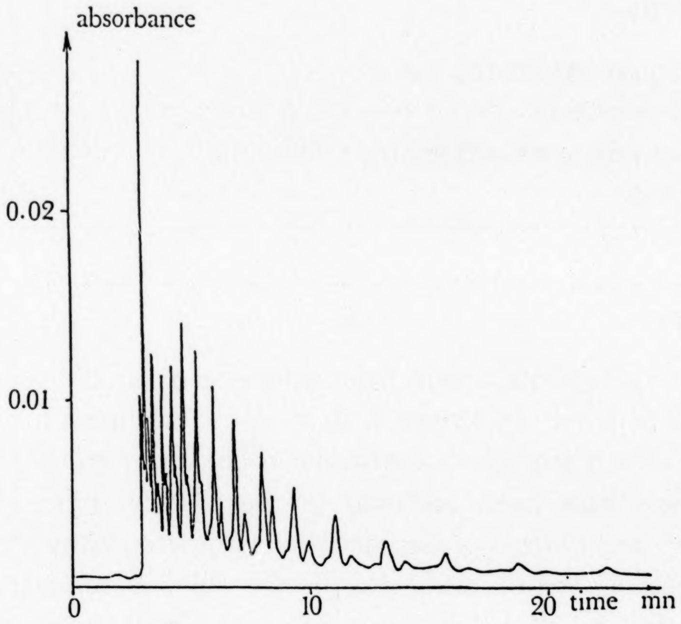

Fig. 2

Chromatogram of KL 6, derivatised in the form of its dinitrobenzoyl-ester, obtained with a UV detector (stationary phase: Zorbax NH_2, d_p = 7 μm, column 25 × 0.46 cm, bobile phase: n-heptane/CH_2Cl_2/MeOH 90/5/5, flow rate: 1 ml/min, $\lambda_{detection}$ = 254 nm).

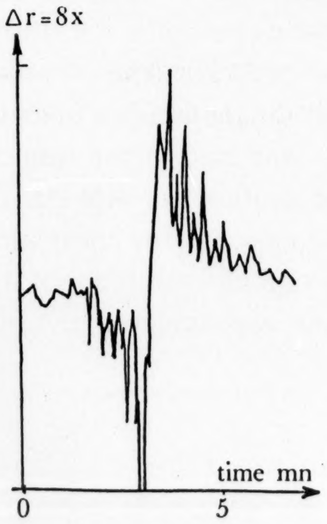

Fig. 1

Detection by means of a differential refractometric detector of KL 6 (stationary phase: Zorbax NH_2, d_p = 7 μm, column: 25 × 0.46 cm, mobile phase: n-heptane/CH_2Cl_2/MeOH, 80/10/10, flow rate: 1 ml/min).

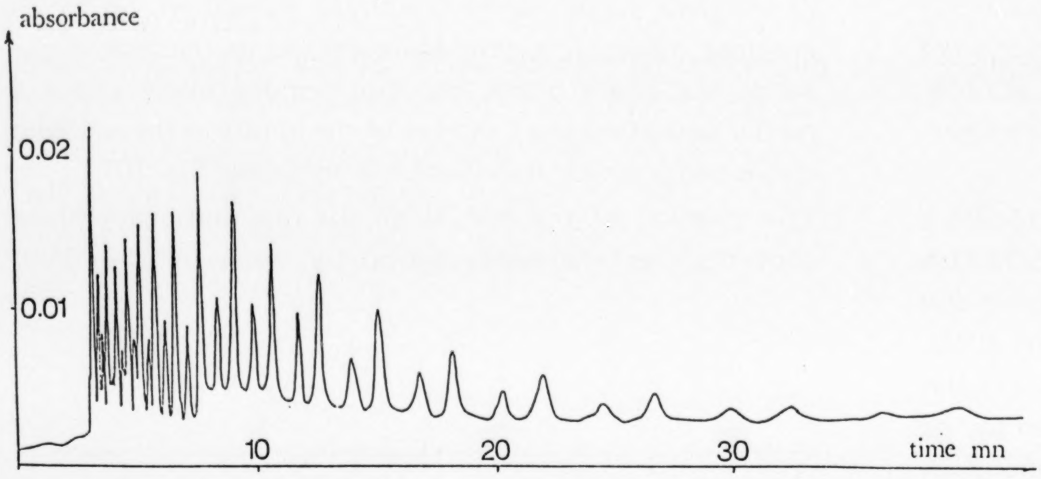

Fig. 3

Chromatogram of the KM 11 DNB ester obtained with an amino phase (stationary phase: Zorbax NH$_2$, d_p = 7 µm, column 25 × 0.46 cm, mobile phase: n-heptane/CH$_2$Cl$_2$/MeOH 90/5/5, flow rate: 1 ml/min, $\lambda_{detection}$ = 254 nm).

The presence of a double distribution is in fact the indication of a further separation of the aliphatic chains.

In order to have a correct attribution of the number of ethylene oxide units for each peak, we have used two commercial standards. These two compounds have both a polyoxyethylenic chain of 6 ethylene oxide units but one has a C_{16} aliphatic chain and the other a C_{18} chain. The compound with the longer aliphatic chain is the first eluted.

The chromatographic analysis of the KL 6 derivative in the presence of the DNB ester of the C_{18} standard with 6 E.O. units is shown in Fig. 4.

The coelution method allows a precise attribution of the ethylene oxide number for the chromatographic peak of each component of the surfactant. It is then possible to study the distribution of each surfactant as a function of the ethylene oxide number and to compute its mean ethylene oxide number ($\bar{n}$).

Because of the widening of chromatographic peaks when retention time increases, chromatograms such as those given in Figs. 3 and 4 for KL 6 and KM 11 give a distorted picture of the distribution of ethylene oxide numbers in these surfactants. To avoid this distortion, we give the histograms of distribution of the two surfactants KL 6 and KM 11 in Figs. 5 and 6. All further chromatograms of the surfactants are presented in the form of histograms.

The mean length of polyoxyethylenic chains is easily computed or deduced from the histograms. The following values are found:

$\bar{n}$ = 6.5 E.O. for the KL 6 surfactant
$\bar{n}$ = 9.5 E.O. for the KM 11 surfactant.

The latter value is lower than the expected value of 11 E.O. The drift observed in the baseline does not explain the discrepancy between the experimental and the expected values. It is likely that, because of the strong polarity of the amino phase, the mobile phase does not give a sufficient elution of the most polar components of KM 11. In isocratic elution it is impossible to use a significantly more polar mobile phase because the resolution of the components of KM 11 having a low number of E.O. would be insufficient.

A partial demixing is observed for eluents containing more than 8% of methanol, and gradient elution with more than this amount of methanol cannot be used.

The amino phase, which gives good results for the distribution of KL 6, is not suitable for KM 11 and the results are still worse in the case of KM 20 which contains the most polar components.

Cyano bonded silica. This stationary phase, beeing less polar, is slightly better than the amino phase for the study

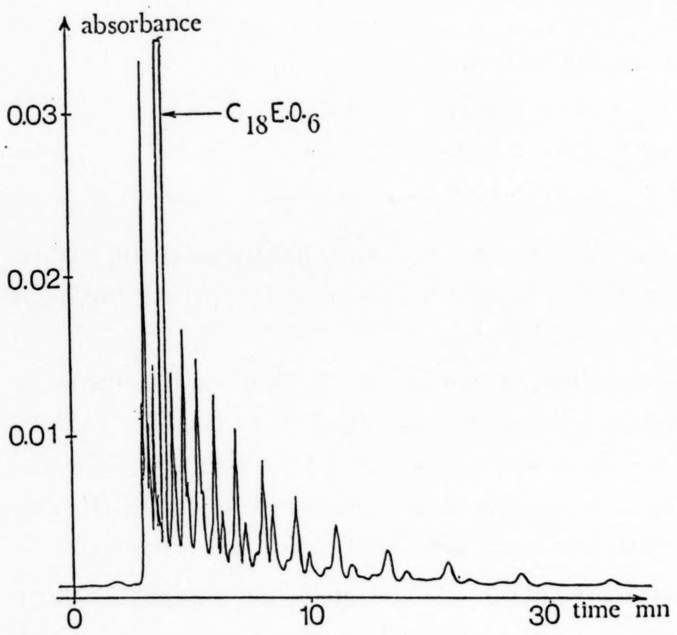

Fig. 4

Coelution of the DNB esters of the KL 6 and the standard surfactant C_{18} EO$_6$ (same conditions as those given in Fig. 2).

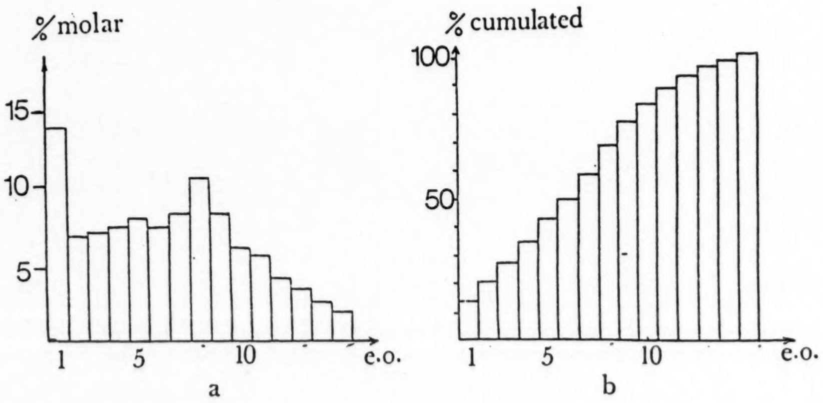

Fig. 5

Distribution histograms of KL 6 determined from the data of chromatography using amino bonded silica as stationary phase; a) distribution as a function of ethylene oxide number; b) cumulated retention as a function of ethylene oxide number.

of the polyoxyethylenic surfactants. After optimisation of the mobile phase it is possible to obtain the distribution of KL 6 (mobile phase: n-heptane/CH_2Cl_2/MeOH, 90/7/3), and the distribution of KM 11 (mobile phase: n-heptane/CH_2Cl_2/MeOH, 90/5/5).

The mean number of ethylene oxide is 6.1 E.O. for KL 6 and 10.2 E.O. for KM 11. The value obtained for KM 11 is greater than in the case of the amino column but is still lower than the expected value of 11 E.O. units. The difference is likely to come from the retention of the most polar components of KM 11. This hypothesis is confirmed by the partition histogram which is truncated for the higher E.O. numbers. The demixing of methanol at concentrations greater than 8% does not permit a gradient elution to improve the separation. The result for KM 11 indicates clearly that a good analysis of KM 20 cannot be expected since this surfactant has even more polar chains than KM 11 retained on the column. After optimisation of the mobile phase, an experimental value of $\bar{n} = 12$ E.O. is found instead of the expected value of $\bar{n} = 20$ E.O.

Diol bonded silica. We have obtained satisfactory distribution analysis for each of the three surfactants with this stationary phase. Figs. 7 to 9 give the histograms and the computed values of mean ethylene oxyde numbers of KL 6, KM 11 and KM 20

The results are the following:

KL 6 $\bar{n}_{exp} = 6.1$ E.O.
KM 11 $\bar{n}_{exp} = 10.8$ E.O.
KM 20 $\bar{n}_{exp} = 20.1$ E.O.

Stet KL 6 and KM 11 correctly analyzed by isocratic elution when using this stationary phase but KM 20 must be analyzed by gradient elution.

In isocratic elution a better result than with amino or cyano bonded phases is obtained for KM 20 analysis ($\bar{n}_{exp} = 15.4$ E.O. versus respectively 10.4 E.O. and 12 E.O.) after optimisation of the mobile phase (n-heptane/CH_2Cl_2/MeOH 91/5/4) but a correct value is still not obtained.

The use of isopropanol combined with gradient elution gives a satisfactory elution of the compounds having a high number of E.O. (Fig. 9). Under these conditions of analysis it is possible to obtain a distribution of KM 20 as a function of ethylene oxide number, without truncation, up to 39 ethylene oxides (Fig. 9b). Moreover, as in the case of the amino stationary phase, the diol bonded phase allows a partial separation as a function of the nature of the aliphatic chains and a double distribution is obtained (Fig. 10).

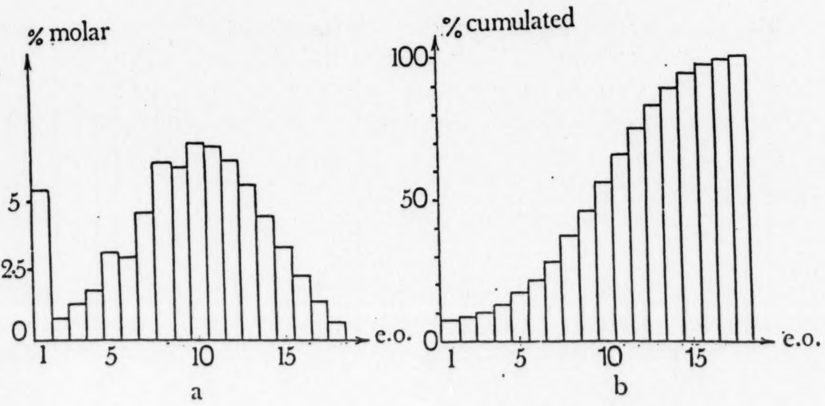

Fig. 6

Distribution histograms of KM 11 obtained from the data of chromatography using amino bonded silica as stationary phase; a) distribution as a function of ethylene oxide number; b) cumulated retention as a function of ethylene oxide number.

This analysis of the KM 20 on the diol stationary phase confirms that the derivatisation by means of the DNB,

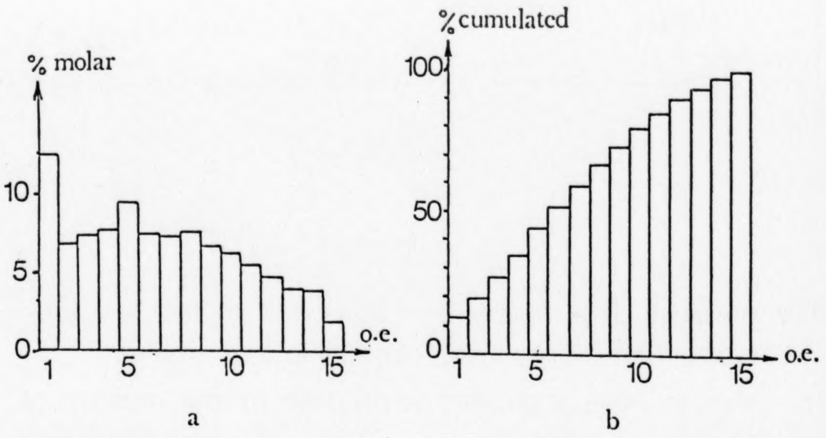

Fig. 7

Distribution histograms of KL 6 determined from the data of chromatography using diol bonded silica as stationary phase (mobile phase: n-heptane/CH_2Cl_2/MeOH 90/8.5/1.5); a) retention as a function of E.O. number; b) cumulated retention as a function of E.O. number.

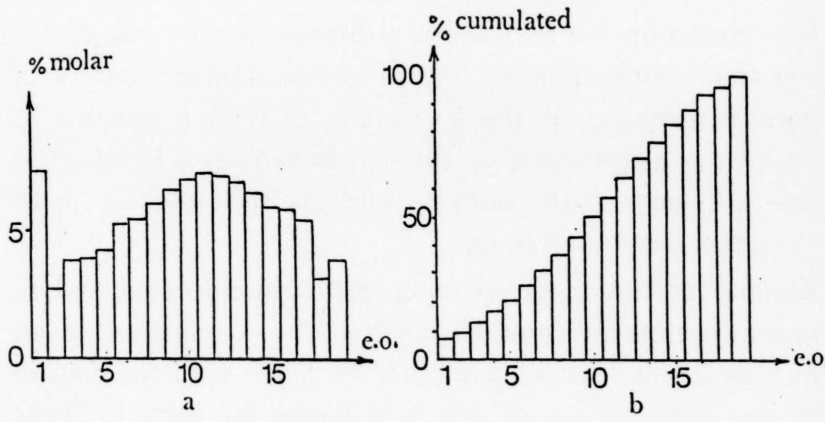

Fig. 8

Distribution histograms of KM 11 obtained from chromatographic data using diol bonded silica as stationary phase (mobile phase: n-heptane/CH_2Cl_2/MeOH 90/6/4); a) retention as a function of E.O. number; b) cumulated retention as a function of E.O. number.

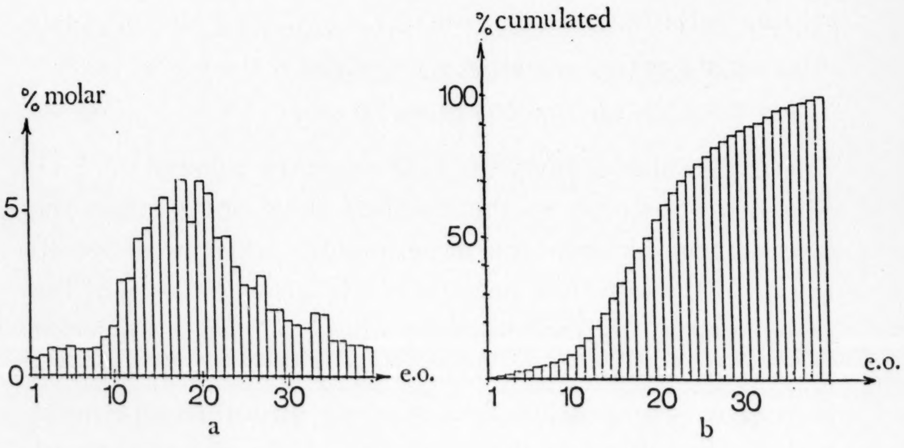

Fig. 9

Distribution histograms of KM 20 obtained from chromatographic data using diol bonded silica as stationary phase (gradient elution given in experimental part); a) retention as a function of E.O. number; b) cumulated retention as a function of E.O. number.

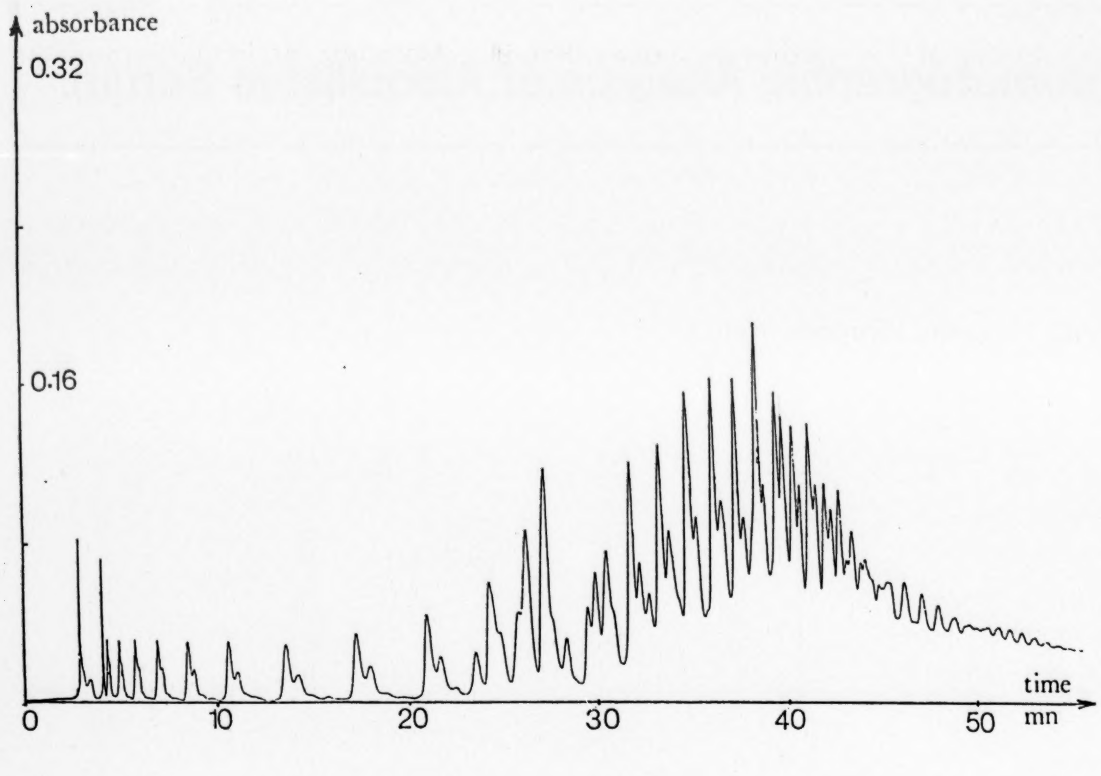

Fig. 10

Chromatogram of the DNB ester of KM 20 using a diol bonded silica as stationary phase and a gradient elution (see experimental part). Column: Lichrospher diol, $d_p = 5\ \mu m$, flow rate: 1 ml/min, $\lambda_{detection} = 254$ nm.

which allows a good detection of the surfactants by U.V., is perfectly suitable. The esterification reaction is obviously quantitative whatever the length of the ethoxylated chain.

Conclusions

From this study of the chromatographic analysis of non-ionic surfactants used in enhanced oil recovery the following points emerge.

The analysis of the non-ionic surfactants as a function of their number of ethylene oxide units is possible only after derivatisation with 3,5-dinitrobenzoyl chloride. The analysis can then be effected in a single run, in a simple and reproducible way, by normal phase partition chromatography on bonded silica.

Among the different commercially available bonded silica phases the diol phase is the only one well suited to the analysis of the distribution of non-ionic surfactants containing a high number of ethylene oxide units. With this phase it is possible to determine the distributions of KL 6 and KM 11 as a function of their E.O. numbers by isocratic elution. In the case of KM 20 gradient elution is necessary to obtain the whole distribution.

Finally it must be noted that when using the diol bonded silica a partial separation as a function of the nature of the aliphatic chains is superimposed on the main separation as a function of ethylene oxide number. The resolution as a function of aliphatic chain length is not sufficient and we are investigating how modification of the silica grafting, particularly of the spacer length, might improve the separation in order to simultaneously obtain both the ethylene oxide distribution and information on the aliphatic chains.

References

[1] *J.L. Iverson, A.I. Sheppard,* J. Chromatogr. Sci. **13,** 505 (1975).

[2] *J. Pollerberg,* Fet. Sei. Ans. **60,** 179 (1967).

[3] *T.H. Liddicoet, L.H. Smithson,* J. Amer. Oil Chemists Soc. **42,** 1097 (1965)

[4] *B.G. Luke,* J. Chromatogr. **84,** 43 (1973).

[5] *D.R. Zornes, G.P. Willhite, M.J. Michnick,* Soc. Pet. Eng. J. **18,** 207 (1978).

[6] *W.D. MacMillan, H.V. Wright,* J. Amer. Oil Chemists Soc. **54,** 1963 (1977).

[7] *A.J. Van Welly, H.J. Vonk, L.G.J. Van der Ven, A.J.J. de Breet, F.P.B. Vandermaeden, M.E.F. Biemond, A. Venema, W.B.G. Huysmans,* Tr. Mezhdunar. Kongr. Poverkhn. Akt. Verhestvam 7th **1,** 435 (1977).

[8] *A. Nozawa, T. Ohuna,* J. Chromatogr. **187,** 261 (1980).

[9] *K. Nakamura, I. Matsumoto,* Bull. Chem. Soc. Japan **8,** 1342 (1975).

[10] *J.D. McClure,* J. Amer. Oil Chemists Soc. **59,** 8 (1982).

[11] *M.C. Allen, D.E. Linder,* J. Amer. Oil Chemists Soc. **58,** 950 (1981).

[12] *A. Aserin, M. Frenkel, N. Garte,* J. Amer. Oil Chemists Soc. **61,** 805 (1984).

[13] *D. Thomas, J.L. Rocca,* Analusis **7,** 836 (1979).

[14] *K. Nakamura, Y. Morikawa, I. Matsumoto,* J. Amer. Oil Chemists Soc. **58,** 72 (1981).

[15] *K. Nakamura, Y. Morikawa,* J. Amer. Oil Chemists Soc. **59,** 64 (1982).

[16] *C. Demange,* Revue Franc. Corps Gras, 211 (1982).

[17] *N. Parris,* J. Liquid Chromatogr. **3,** 1743 (1980).

[18] *N. Parris, W.M. Linfield, R.A. Barford,* Anal. Chem. **49,** 2228 (1977).

[19] *K.J. Bombaugh,* J. Chromatogr. **53,** 27 (1970).

[20] *A.M. Rothman,* J. Chromatogr. **253,** 283 (1982).

[21] *F. Bogatski, H. Lippmann,* Acta Polymerica **34,** 219 (1983).

[22] *B. Coq, C. Gonnet, J.L. Rocca,* J. Chromatogr. **106,** 249 (1975).

Received: June 30, 1987
Revised manuscript
received: Sep 30, 1987
Accepted: Oct 5, 1987
F

High-Performance Liquid Chromatographic Analysis of Azlocillin in Serum.

T. Valenza*/P. Rosselli

Clinical Laboratory Analysis, U.S.L. 10/D, Careggi Hospital, Florence, Italy

Key Words

Column liquid chromatography
Azlocillin in serum

Summary

A rapid and sensitive high performance liquid chromatographic method is described for the determination of azlocillin in serum.

This method involves a short manual protein precipitation of the sample followed by an injection into a PR 18 column for separation and quantitation.

The mobile phase was a 22% (V/V) solution acetonitrile in phosphate buffer pH 4.8 at a flow rate of 2,5 ml/min. The spectrophotometer detector was set at 220 nm with a sensitivity of 0.08 AUFS.

Introduction

Azlocillin (Securopen) is an antibiotic with a broad spectrum of antimicrobial activity, particularly against Pseudomonas aeruginosa. It's chemical structure is shown in Fig. 1.

Untill now concentrations of azlocillin have been determined by microbiological procedures [1, 4]. An HPLC method has been published for the determination of azlocillin in urine [5].

We report a rapid, simple, accurate and sensitive HPLC method for the determination of azlocillin in serum.

Materials and Methods

The analysis was performed on a 2B liquid chromatograph (Perkin Elmer, Monza Italy) equipped with a Perkin Elmer LC 85 variable wavelength detector. A Rheodyne model 7125 (Supelchem, Milan, Italy) injector with a 20 μl sample loop was used.

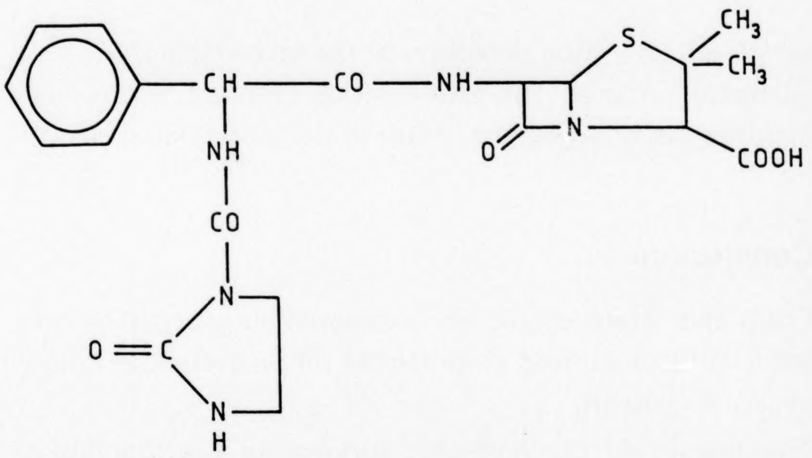

Fig. 1
Structural formula of azlocillin.

Reagents

Chemicals used were: azlocillin (Securopen, Bayer, Milan, Italy), mezlocillin (Baypen, Bayer, Milan, Italy), disodium hydrogen phosphate and potassium diyidrogen phosphate (Merck, Bracco, Milan, Italy) and acetonitrile (Lichcrosolv). Stock solutions (1200 μg/ml) of azlocillin and mezlocillin as internal standard were prepared by dissolving 131.0 mg of azlocillin sodium and 126.7 mg of mezlocillin sodium in 100 ml phosphate buffer 0.1 M pH 6. Further dilutions of the stock solution of azlocillin were made in free human serum to prepare the standard curves.

Chromatographic Conditions

A 10 μm RP 18, 250 × 4 mm column (Merck, Bracco, Milan, Italy) was used. The mobile phase was a 22% (V/V) solution of acetonitrile in phosphate buffer 0.01 M, pH 4.8. The mobile phase was prepared daily and filtered/degassed using a vacuum filter system. The flow rate was 2.5 ml/min; the detector was set at 220 nm with a sensitivity of 0.08 AUFS.

0009-5893/87 0862-03 $03.00/0

© 1987 Friedr. Vieweg & Sohn Verlagsgesellschaft mbH

Analytical Procedure

Into micro-conical centrifuge tubes (1 × 4 cm) were pipetted 300 µl of serum, 50 µl of working internal standard and 300 µl of acetonitrile as precipitation solution. The tubes were briefly vortex-mixed an centrifuged at 10.000 g for 4 minutes. 5 µl of the supernatant were injected into the liquid chromatograph.

Results

Fig. 2 shows chromatograms of a blank serum and of a serum of a subject treated with azlocillin. Fig. 3 shows azlocillin concentrations in serum versus time for one patient receiving a dose of 100 mg/Kg.

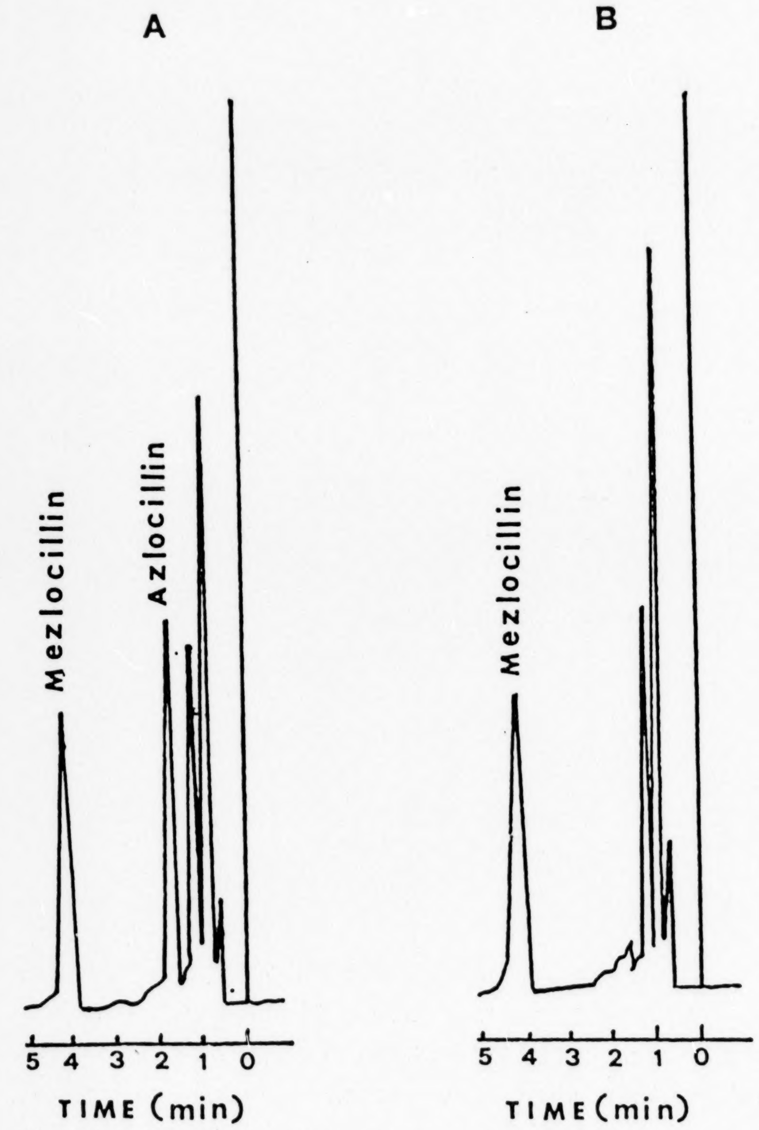

Fig. 2

Chromatograms of serum extracts from a patient treated with azlocillin (mezlocillin as internal standard) (A) and of a blank sample from the same patient before the beginning of the treatment (B).

The calibration plot was linear for serum concentrations ranging between 12,5 to 400 µg/ml. The regression equation and linear regression coefficient were $y = 0.1879 + 0.114x$, $r = 0.9994$, respectively.

The lowest detection limit was 5 µg/ml.

The precision (within assay variability) and reproducibility (between assay variability) of the method were established by analysing drug free samples spiked with three different concentrations of azlocillin (30, 150 and 300 µg/ml). The coefficients of variations (V.V. %) are listed in Table I.

Discussion

The wavelength (220 nm) was chosen as a compromise between a high sensitivity range (190–220 nm) but with high interferences and a low sensitivity range (240–250 nm) with low interferences.

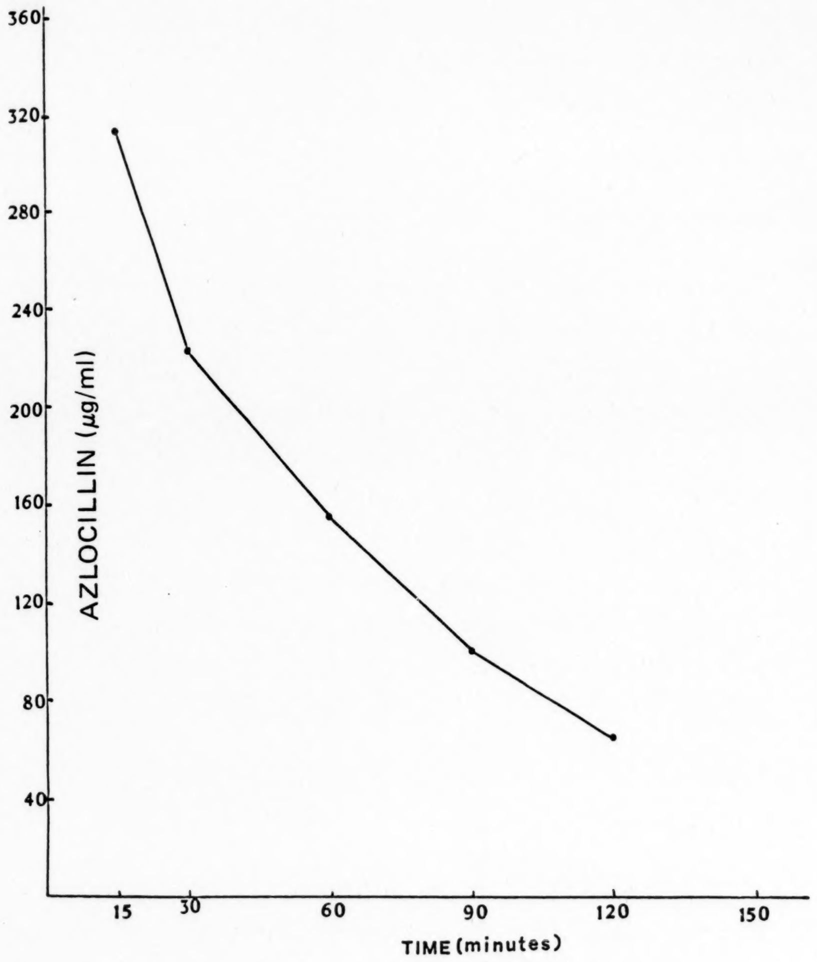

Fig. 3

Azlocillin concentrations in serum versus time foroone patient receiving azlocillin 100 mg/kg by intravenous infusion over 30 minutes.

Table I. Precision of the analysis of plasma samples spiked with azlocillin. n° = 15

Amount of AZL in plasma (µg/ml)	Within assay Quantity found (µg/ml)	C.V. (%)	Between assay Quantity found (µg/ml)	C.V. (%)
30.0	30.2	4.1	29.1	10.7
150.0	146.9	2.9	150.5	2.7
300.0	316.5	4.1	308.0	3.6

Acetonitrile was chosen as a simple and efficient purification medium. No interfering peaks from endogenous compounds were detected in 50 serum samples from different patients.

The total analysis time for 10 samples was 10 minutes for sample preparation and 6 minutes for chromatographic separation.

The method is simple, rapid and accurate and an alternative to microbiological procedures.

References

[1] *N. E. Moller, K. R. Eriksen, C. Feddersen, E. W. Flensborg, N. Hoiby, S. Norn, K. Rosendal, P. O. Schiotz, P. Stahlskov,* Chemiotherapy against Pseudomonas aeruginosa in cystic fibrosis, Eur. J. Respir. Dis., **63**, 130 (1982).

[2] *J. V. Bennett, J. L. Brodie, E. J. Benner, W. M. M. Kirby,* simplified, accurate method of antibiotic assay of clinical specimens, Appl. Microbiol., **14**, 170 (1966).

[3] *J. A. Bosso, B. A. Saxon, J. J. Herbst, J. M. Matsen,* Azlocillin pharmacokinetics in patients with cystic fibrosis, Antimicrob. Agents Chemother. **25**, 630 (1984).

[4] *U. Sitka, L. Weingartner, R. Patsch, I. Richter,* Pharmacokinetic and clinical studies of azlocillin in pediatrics, Abstract of international symposium on acylureido penicillins, Vienna 1979: 105.

[5] *V. W. Gau, F. A. Horster,* Hochdruckflüssigkeitschromatographische Analyse von Azlocillin und seinem Penicilloat im Urin, Drug Res. 29, 1941 (1979).

Received: Sep. 16, 1987
Accepted: Sep. 28, 1987
F

Determination of Organic Colorants in Cosmetic Products by High-Performance Liquid Chromatography

J. W. Wegener[1]*/J. C. Klamer[1]/H. Govers[1]/U. A. Th. Brinkman[2]

[1] Institute for Environmental Studies, Free University, P.O. Box 7161, 1007 MC Amsterdam, The Netherlands
[2] Department of Analytical Chemistry, Free University, De Boelelaan 1083, 1081 HV Amsterdam, The Netherlands

Key Words

Column liquid chromatography
Organic colorants
Cosmetics
Diode array detector

Summary

High-performance liquid chromatography (HPLC) with UV-vis detection was used for the determination of organic colorants in cosmetic products. 126 colorants were characterized by their retention times in an ion-pair reversed-phase HPLC system with gradient elution, and by their UV-vis spectra, recorded with a diode array detector (DAD). The method is rapid and efficient, as is demonstrated by the analysis of 45 cosmetic samples.

Introduction

As part of a programme to unite the legislation on cosmetics in its member states, the Council of the European Commission has listed, either definitively or provisionally, 143 organic colorants in its Directives that are allowed to be used in cosmetic products. In order to verify the observance of the directive, a rapid and efficient method for the determination of organic colorants in cosmetics is required.

In the field of food-dye analysis, where the colorants generally used are water-soluble ionic compounds, a number of high-performance liquid chromatographic (HPLC) methods have been developed [1, 2]. In the cosmetics industry, both ionic and non-ionic colorants are used. In our previous paper [3], the development of an ion-pair reversed-phase HPLC system was described; this method allowed the determination of both types of colorants. Sample pretreatment was derived from thin-layer chromatographic (TLC) methods for the determination of colorants in cosmetics, described elsewhere [4].

In our previous work, 21 synthetic organic colorants were included and 8 samples of finished cosmetic products were analyzed. In the present work, the number of colorants has been increased to 126 (including 13 natural colorants), which compelled us to use a more sophisticated method of identification viz. via diode array detection. In addition, the original sample pretreatment and HPLC procedure have been optimized in order to increase the stability of the chromatographic system, to improve the limits of detection and to reduce the time of analysis. With regard to the latter aspect, the replacement of a conventional variable-wavelength detector by a rapid-scanning diode array detector (DAD) has been very beneficial, because it allows for the collection of all relevant spectral data of the colorants in a single chromatographic run.

Similar methods, using a DAD as well, have been published in the literature recently; one deals with readily soluble dyes only [5], while the other is intended for the analysis of disperse dyes in polyester fibres [6].

Experimental

Chromatography

A Hewlett-Packard (Waldbronn, FRG) 1090M liquid chromatograph was employed, comprised of a PV5 ternary solvent delivery system, an injector of variable loop volume (adjusted to 10 μl) and a DAD covering the UV-vis range from 200 to 600 nm. Separations were carried out on a 100 × 4.6 mm I.D. stainless steel column, prepacked with 3 μm Micropher C-18 (Chrompack, Middelburg, The Netherlands) and thermostated at 30 °C. The analytical column was protected by a 2 × 4.6 mm I.D. stainless-steel guard column, home-packed with 3 μm Microspher C-18. This guard column is identical to the short precolumn recently developed at our University for rapid on-line trace enrichment [7]; a similarly designed cartridge-type precolumn system is commercially available from Chrompack.

The solvents for the mobile phase were (A) distilled water, and (B) a 0.005 M tetrabutylammonium (TBA) solution in

0009-5893/87 0865-11 $03.00/0

© 1987 Friedr. Vieweg & Sohn Verlagsgesellschaft mbH

methanol. (B) was prepared from a 0.5M TBA solution which contained 0.385 mole of tetrabutylammonium hydroxide and 0.385 mole of potassium hydroxide, dissolved in 770 ml of distilled water, and adjusted to pH 7.0 with phosphoric acid. A linear gradient was run from A:B = 75:25 to A:B = 0:100 in 25 min, at a flow-rate of 1 ml/min; the final composition was maintained for 15 min, followed by a reverse gradient of 5 min, and re-equilibration of the column by maintaining the initial composition for 10 min.

Detection

In the proposed HPLC procedure, detection is, for obvious reasons, carried out by means of absorption measurement in the visible range. For some of the colorants, however, the spectra in this range are closely similar, which could hamper unambiguous identification. Spectra were, therefore, recorded over the 200–600 nm range. The upper limit of 600 nm is imposed by the technical specifications of the DAD, although for blue and green colorants an upper limit of 700 nm would have been more optimal. All spectra were stored on diskette and plotted on paper, to be compiled in the form of a spectral atlas.

Chemicals

The sample extraction solvent was dimethylformamide, containing 5% concentrated phosphoric acid (DMF/H^+). For sample pretreatment, n-hexane, chloroform, distilled water and an aqueous 0.1 M TBA solution made by 5-fold dilution of the 0.5 M TBA solution (cf. above) were used. Methanol, distilled water, tetrabutylammonium hydroxide, potassium hydroxide and concentrated phosphoric acid were used to prepare the HPLC solvents described above. All chemicals were of normal analytical grade quality.

Colorants

Reference samples of colorants were obtained from various suppliers. Table I lists all 126 colorants studied in numerical order according to their Colour Index Constitution number [8]. In addition, their generic names according to the Colour Index, the European Commission, the U.S. Food and Drug Administration [9] and the German Research Society [10] – the institutes that have classified colorants – are given.

Sample Preparation

The general procedure for sample preparation was as follows: Add 10 ml of DMF/H^+ to 0.5 g of the cosmetic sample, and heat the mixture for 60 min at 60 °C. Filter the mixture, add 50 ml of an aqueous 0.1 M TBA solution to the filtrate, extract the mixture twice with 10 ml of chloroform, concentrate the combined chloroform extracts by gentle evaporation until a sufficiently intensely coloured solution is obtained. If the results of the latter step are not satisfactory, 50 ml of the 0.1 M TBA solution should be added to the concentrate, followed by extraction with chloroform and concentration of the combined chloroform extracts.

Depending on the type of sample, minor modifications in the general procedure are required. Fatty solids, such as lipsticks, have to be defatted by extraction of the DMF/H^+ mixture with n-hexane, prior to filtration. Emulsions such as creams do not require the heating and filtration steps. Finally, aqueous and alcoholic samples that are sufficiently coloured (e.g. shampoos and lotions) can be injected directly, using an injection volume of 60 μl instead of 10 μl.

Results and Discussion

HPLC

Stationary and Mobile Phase. In our previous paper, the separation of 21 colorants was described, using a 250 × 4.6 mm I.D. stainless-steel column, packed with 8 μm CP-Spher C-18 (Chrompack) and a 45 min linear gradient from A:B = 50:50 to A:B = 0:100. For the present study (in which 126 colorants were screened), essentially the same chromatographic system was used. In order to optimize the separation and, at the same time, reduce the time of analysis, various columns were tested: 250 × 4.6 mm I.D. columns packed with 8 μm Hypersil ODS (Shandon, Runcorn, Cheshire, UK), 10 μm Vydac TP-RP (Varian, Palo Alto, CA, USA) or 8 μm CP-Spher (Chrompack) and a 100 × 4.6 mm I.D. column packed with 3 μm Microspher (Chrompack). Using a test mixture containing 9 colorants, it was observed that the Microspher column offered the best performance; the time of analysis was about half that of the other columns, without loss in peak shapes and overall resolution. Using this column, the linear gradient elution program finally adopted, from A:B = 75:25 to A:B = 0:100, took a mere 25 min.

Precolumn. There are three parameters which, in the present study, may cause a considerable shortening of the lifetime of the analytical column: the use of a gradient (changing solvent composition), the use of ion-pair reagent (quaternary ammonium salts, relatively high pH values) and the injection of crude samples.

In order to protect the analytical column, a 2 × 4.6 mm I.D. stainless-steel precolumn, manually packed with a methanolic slurry of 3 μm Microspher C-18 was inserted between the injector and the analytical column. This did not noticeably affect the retention times, nor did it cause additional band broadening. After 2 days of continuous analysis of cosmetic samples, a 50% increase in back-pressure was observed, indicating serious contamination of the precolumn. Upon repacking the precolumn – which is only a matter of minutes – the back-pressure was restored to its initital value. If no precolumn was used, the contamination would have deteriorated the analytical column. When using this type of precolumn, the lifetime of the analytical column was as high as 3 to 6 months.

Colorants

Retention. Using the HPLC system described in the previous sections, retention times were measured for all 126 colorants. These are reported in Table II. The majority of

Table I Colorants under investigation in the present study, in numerical order according to the Colour Index constitution number.

CI number	Colour Index generic name	EC number	GRC name	FDA name
10006	Pigment Green B		C-WR Grün 6	
10020	Acid Green 1		C-ext Grün 6	
	Pigment Green 12*			
10316	Acid Yellow 1		C-ext Gelb 1	Ext. D&C Yellow 7
11680	Pigment Yellow 1		C-ext Gelb 2	
11710	Pigment Yellow 3		C-ext Gelb 3	
11725	Pigment Orange 1		C-WR Gelb 7	
11920	Solvent Orange 1		C Orange 1	
	Food Orange 3			
12010	Solvent Red 3		C-ext Braun 3	
12075	Pigment Orange 5		C Orange 18	D&C Orange 17
12085	Pigment Red 4		C Rot 1	D&C Red 36
12120	Pigment Red 3			
12150	Solvent Red 1		C Rot 2	
12370	Pigment Red 112		C—WR Rot 19	
12420	Pigment Red 7			
12480	Pigment Brown 1			
12490	Pigment Red 5		C-ext Rot 58	
12700	Solvent Yellow 16			
	Disperse Yellow 16			
13015	Acid Yellow 9	E 105	C Gelb 9	
	Food Yellow 2			
13065	Acid Yellow 36		C-ext Gelb 10	
14270	Acid Orange 6	E 103	C Gelb 12	
	Food Yellow 8			
14700	Food Red 1		C Rot 57	FD&C Red 4
14720	Acid Red 14	E 121	C Rot 54	
	Food Red 3			
	Mordant Blue 79			
14815		E 125	C Rot 49	
15510	Acid Orange 7		C-ext Orange 8	D&C Orange 4
	Pigment Orange 17*			
	Solvent Orange 49*			
15525	Pigment Red 68		C-ext Rot 59	
15580	Pigment Red 51			
15585	Pigment Red 53		C Rot 55	D&C Red 8, 9
15620	Acid Red 88		C-WR Rot 13	
15630	Pigment Red 49		C Rot 56	
15800	Pigment Red 64		C-ext Rot 57	D&C Red 31
	Pigment Brown 5*			
15850	Pigment Red 57		C Rot 12	D&C Red 6, 7
15865	Pigment Red 48		C-ext Rot 60	
15880	Pigment Red 63		C-ext Rot 61	D&C Red 34
15980	Food Orange 2	E 111	C Orange 9	
15985	Food Yellow 3	E 110	C Orange 10	FD&C Yellow 6
	Pigment Yellow 104*			
16035	Food Red 17		C Rot 60	FD&C Red 40
16185	Acid Red 27	E 123	C Rot 46	FD&C Red 2
	Food Red 9			
	Pigment Red 193*			
16230	Acid Orange 10		C-ext Orange 11	
	Food Orange 4			
16255	Acid Red 18	E 124	C Rot 47	
	Food Red 7			
16290	Acid Red 41	E 126	C Rot 48	
	Food Red 8			
17200	Acid Red 33		C Rot 58	D&C Red 33
	Food Red 12			
18050	Acid Red 1		C Rot 63	
	Food Red 10			
18130	Acid Red 155		C-WR Rot 4	
18690	Acid Yellow 121		C-WR Orange 9	
	Solvent Yellow 21			
18736	Acid Red 180		C-WR Orange 8	
	Solvent Orange 6*			
18820	Acid Yellow 11		C-WR Gelb 9	

Table I (continued)

CI number	Colour Index generic name	EC number	GRC name	FDA name
18965	Acid Yellow 17 Food Yellow 5			
19120	Acid Yellow 13 Solvent Yellow 15		C-ext Gelb 20	
19140	Acid Yellow 23 Food Yellow 4 Pigment Yellow 100*	E 102	C Gelb 10	FD&C Yellow 5
20040	Pigment Yellow 16			
20170	Acid Orange 24		C-ext Braun 4	D&C Brown 1
20470	Acid Black 1		C-WR Schwarz 1	
21100	Pigment Yellow 13			
21110	Pigment Orange 13			
21115	Pigment Orange 34			
24790	Acid Red 63		C-WR Rot 18	
26100	Solvent Red 23		C-ext Rot 56	D&C Red 17
27290	Acid Red 73			
27306	Solvent Red 31		C-WR Rot 14	
27755	Food Black 2	E 152	C Schwarz 7	
28160	Direct Red 81		C-WR Rot 6	
28440	Food Black 1	E 151	C Schwarz 6	
40215	Direct Orange 34, 39, 44, Direct Orange 46, 60		C-WR Orange 1	
40800	Food Orange 5			
40820	Food Orange 6	E 160e	C Orange 16	
40825	Food Orange 7	E 160f	C Orange 17	
40850	Food Orange 8			
42045	Acid Blue 1 Food Blue 3		C-ext Blau 13	
42051	Acid Blue 3 Food Blue 5	E 131	C Blau 20	
42053	Food Green 3		C Grün 12	FD&C Green 3
42080	Acid Blue 7		C-WR Blau 11	
42090	Acid Blue 9 Food Blue 2 Pigment Blue 24*		C Blau 21	D&C Blue 4 FD&C Blue 1
42100	Acid Green 9		C-WR Grün 5	
42170	Acid Green 22		C-ext Grün 10	
42510	Basic Violet 41 Solvent Red 41* Pigment Violet 4*		C-WR Violett 8	
42520	Basic Violet 2			
42535	Basic Violet 1 Solvent Violet 8* Pigment Violet 3, 27*		C-ext Violett 5	
42640	Acid Violet 49 Food Violet 2		C Violett 10	FD&C Violet 1
42735	Acid Blue 104		C-ext Blau 14	
44045	Basic Blue 26 Solvent Blue 4* Pigment Blue 2*		C-WR Blau 8	
44090	Basic Blue 15	E 142	C Grün 4	
45100	Acid Red 52			
45170	Basic Violet 10 Solvent Red 49* Pigment Violet 1, Red 173		C Rot 59	D&C Red 19, 37
45190	Acid Violet 9 Solvent Violet 10		C-WR Violett 5	
45220	Acid Red 50		C-WR Rot 16	
45350	Acid Yellow 73 Solvent Yellow 94*		C-ext Gelb 16	D&C Yellow 7, 8
45370	Acid Orange 11 Solvent Red 72* Pigment Orange 39*		C Rot 27	D&C Orange 5
45380	Acid Red 87 Pigment Red 90* Solvent Red 43*		C Rot 30	D&C Red 21, 22

Table I (continued)

CI number	Colour Index generic name	EC number	GRC name	FDA name
45396	Solvent Orange 16			
45405	Acid Red 98			
45410	Acid Red 92		C Rot 34	D&C Red 27, 28
	Solvent Red 98*			
	Pigment Red 174*			
45425	Acid Red 95		C Rot 35	D&C Orange 10, 11
	Solvent Red 73*			
	Pigment Red 191*			
45430	Acid Red 51	E 127	C Rot 38	FD&C Red 3
	Food Red 14			
	Pigment Red 172*			
	Solvent Red 140*			
47000	Solvent Yellow 33		C-ext Gelb 23	D&C Yellow 11
47005	Acid Yellow 3	E 104	C Gelb 11	D&C Yellow 10
	Food Yellow 13			
	Pigment Yellow 115*			
50325	Acid Violet 50		C-WR Violett 10	
50420	Acid Black 2			
58000	Mordant Red 11		C-ext Rot 62	
	Pigment Red 83*			
59040	Solvent Green 7		C-ext Gelb 24	D&C Green 8
60725	Solvent Violet 13		C-ext Violett 18	D&C Violet 2
60730	Acid Violet 43		C-ext Violett 21	Ext. D&C Violet 2
61554	Solvent Blue 35		C-ext Blau 12	
61565	Solvent Green 3		C Grün 10	D&C Green 6
61570	Acid Green 25		C Grün 11	D&C Green 5
61585	Acid Blue 80		C-WR Blau 10	
62045	Acid Blue 62			
73000	Pigment Blue 66		C Blau 22	D&C Blue 6
	Vat Blue 1			
73015	Acid Blue 74	E 132	C Blau 19	FD&C Blue 2
	Food Blue 1			
	Pigment Blue 63*			
73360	Vat Red 1		C Rot 28	D&C Red 30
73385	Pigment Violet 36		C-ext Violett 20	
	Vat Violet 2			
73915	Pigment Red 122			
74180	Direct Blue 86		C-WR Blau 12	
	Pigment Blue 17*			
75100	Natural Yellow 6, 19			
	Natural Red 1			
75120	Natural Orange 4	E 160b	C Orange 12	
75130	Natural Yellow 26	E 160a	C Orange 11	
	Natural Brown 5			
75135	Natural Yellow 27	E 161c,d,e	C Orange 15	
75300	Natural Yellow 3	E 100	C Gelb 15	
75470	Natural Red 4	E 120	C Rot 50	
75660	Natural Yellow 8, 11		C-WR Gelb 15	
75810	Natural Green 3	E 140	C Grün 7, 8	
		E 101		
		E 160c		
		E 162		
		E 163		
Bromothylmolblue				
Bromocresolgreen				

*: derivative of the parent colorant, having different counter-ions or complexing agents.

Table II Retention times (min) of 126 organic colorants.[+]

Colorant	Retention time (min)			
10006	19.3			
10020	13.2			
10316	13.0			
11680	24.3			
11710	24.1			
11725	23.1			
11920	15.7			
12010	22.1	25.5	27.0	28.2
12075	23.0			
12085	25.8			
12120	26.1			
12150	24.7			
12370	26.2			
12420	27.5			
12480	27.1			
12490	24.7			
12700	21.6			
13015	8.5			
13065	18.1			
14270	8.9			
14700	16.8			
14720	16.0			
14815	15.0			
15510	17.4			
15525	13.9			
15580	16.4			
15585	20.6			
15620	17.8			
15630	20.2			
15800	19.4			
15850	17.7			
15865	16.4			
15880	18.8			
15980	13.0			
15985	12.4			
16035	13.1			
16185	12.2			
16230	11.5			
16255	14.2			
16290	10.9			
17200	13.7			
18050	12.0			
18130	20.2			
18690	21.6	19.9		
18736	19.6	14.7		
18820	16.2			
18965	11.3			
19120	9.9			
19140	11.8			
20040	26.1			
20170	13.3	20.1	19.8	
20470	15.9			
21100	34.7			
21110	25.2	23.5		
21115	25.2	25.9		
24790	20.4	20.1		
26100	28.4			
27290	15.9			
27306	14.9	12.2		
27755	11.2			
28160	22.1	20.3		
28440	11.7			
40215	15.2	15.6		
40800	29.4	25.8		
40820	28.4	34.4		
40825	30.0			
40850	28.5	27.7		
42045	13.9	14.9		
42051	16.3			
42053	14.1			
42080	18.5	16.2	16.5	17.8
42090	14.4			
42100	14.7	14.4		
42170	15.3			
42510	14.1			
42520	14.1			
42535	20.0	22.2	16.6	
42640	17.7	16.2	17.5	
42735	19.6			
44045	25.2			
44090	10.2	12.1		
45100	13.9			
45170	20.4			
45190	18.1	14.8		
45220	13.3			
45350	14.7			
45370	15.1			
45380	17.7			
45396	14.7			
45405	18.9	15.6		
45410	20.8			
45425	15.8			
45430	18.8			
47000	19.5			
47005	14.8	14.2	12.7	11.3
50325	13.8			
50420	19.1	12.5	24.6	
58000	20.8			
59040	12.2			
60725	27.5			
60730	20.0			
61554	26.9			
61565	29.8			
61570	19.0	23.4		
61585	19.6			
62045	19.3			
73000	18.0			
73015	10.2			
73360	31.9	29.8	27.8	
73385	30.9			
73915	26.8			
74180	19.3			
75100	11.6	12.9	17.0	
75120	38.3			
75130	39.0	38.3		
75135	39.0			
75300	38.4			
75470	12.6			
75660	37.8			
75810	38.0			
E 101	22.2	5.2		
E 160c	37.5			
E 162	37.9			
E 163	27.0			
BTB*	18.2			
BCG*	15.2			

* BTB: Bromothymolblue; BCG: Bromocresolgreen

[+] If more than one peak is present, retention times of the peaks are given in order of descending peak height.

the analytes displayed a single peak only. Among the exceptions were most of the natural colorants (extracts of plants or insects) which contain a variety of coloured chemical compounds, synthetic colorants that are essentially mixtures and synthetic colorants that contain coloured impurities. Chromatograms of representative examples of such colorants are shown in Figs. 1–3.

Unsatisfactory peak shapes in the selected HPLC system were found for a few colorants only. Cationic colorants cannot be expected to be retained in a fully reproducible way in an ion-pair system developed for the separation of anionic colorants; (ion-exchange) interaction with the residual silanol groups and hydrophobic interaction with the chemically bonded phase may easily play a predominant role, with the former mechanism readily effecting peak broadening and/or tailing. Only 6 of the colorants under investigation were cationic (described as basic colorants in Table I). Highly unpolar colorants, which tended to elute late, often showed broad peaks because of the absence of sufficient peak compression effected by the gradient. This effect can be expected to occur at retention times exceding 24 minutes. Once the retention data had been compiled, several mixtures were prepared, each containing 5–10 colorants having retention times sufficiently far apart to avoid identification problems. These mixtures were used for rapid checks of the repeatability of the retention times and checks of the efficiency of the HPLC system (repeatability was very good thanks to the thermostated column compartment; retention times varied only a few percent). Chromatograms of such mixture are shown in Figs. 4–6.

Detection. In view of the large number of colorants to be determined, the diode array detection principle should be used in order to capitalize on the combined potential of spectral and retention characteristics for successful identification. If economic reasons, however, dictate that work should be carried out with a conventional variable-wavelength detector, four detection-wavelengths should be selected to achieve some selectivity and near-to-optimum sensitivity: 400 nm for the yellow colorants, 475 nm for the orange-red colorants, 525 nm for the purple-red colorants (red colorants make up about 50% of all the colorants considered, which calls for an additional means of discrimination between the different hues of the red colorants), and 600 nm for the blue and green colorants. In this case, actually described in our previous paper, the analysis of a cosmetic sample requires at least four injections [3].

When using a DAD, the detection wavelength can, in principle, be time-programmed, in order to have the detection wavelength set at the value of maximum absorption for each individual colorant. Although this would lead to the lowest detection limits possible, the extremely large number of colorants under investigation prohibits such an approach. Fortunately, the rather broad peaks of the absorption spectra of the colorants in the visible range permit the use of the 400–600 nm bunching principle without a considerable increase in the detection limits.

For 50 colorants (representative for the whole collection), the detection limits were actually determined; values of 0.3 to 3 ng were recorded for a large majority of all colorants

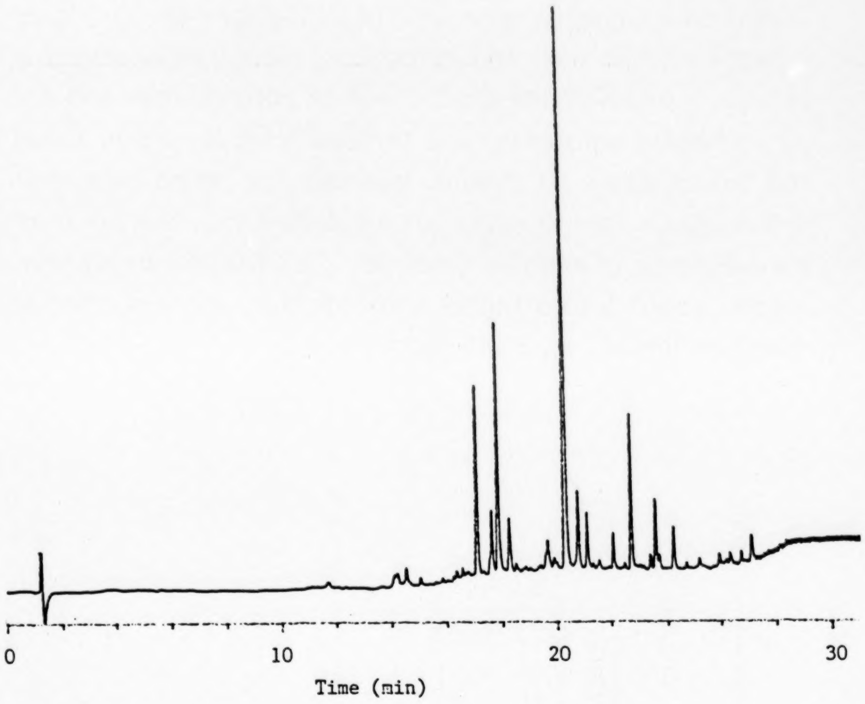

Fig. 1

Chromatogram of CI 75810 (chlorophyll), a natural colorant containing different compounds absorbing in the visible region.

Chromatographic conditions: 100 × 4.6 mm I.D. 3 μm Microspher C-18 column; 25 min linear gradient 25 to 100% methanol + 0.005M TBA in water; flow-rate, 1 ml/min; injection volume, 10 μl; detection wavelength, 400–600 nm.

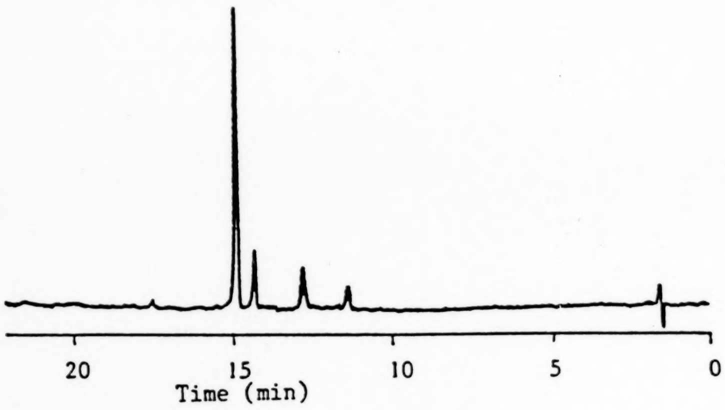

Fig. 2

Chromatogram of CI 47005, essentially a mixture of colorants, differing from each other by the number and positions of methyl and sulphonic acid groups.

Chromatographic conditions: see Fig. 1, except for detection wavelength, 425 nm.

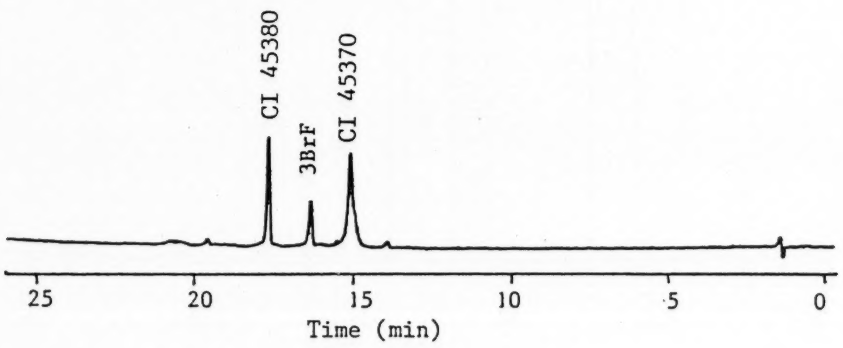

Fig. 3

Chromatogram of a mixture of CI 45370 and CI 45380 (di- and tetrabromofluorescein, respectively), revealing the presence of their common impurity, tribromofluorescein.

Chromatographic conditions: see Fig. 1, except for detection wavelength, 500 nm.

(based on a signal-to-noise ratio of 3:1). Significantly higher detection limits were found for most natural colorants, due to their generally low coefficient of absorptivity, and for very unpolar colorants, due to their long retention times and broad peaks. It should, however, be noted here that unambiguous identification of a colorant may well require the recording of a whole spectrum. This will, on an average, require about 5-fold higher amounts than those quoted as detection limits, i.e., 2–15 ng.

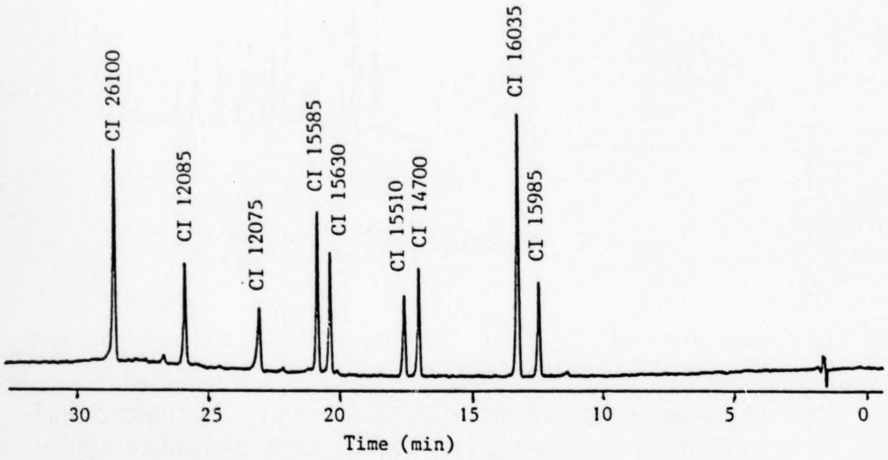

Fig. 4

Chromatogram of a mixture of 9 red colorants.

Chromatographic conditions: see Fig. 1, except for detection wavelength, 500 nm.

Applications

A total of 45 cosmetic samples were analyzed, which included lipsticks, nail-varnishes, eyeshadows, liquid make-ups, face-powders, creams, lotions, shampoos, foam-bath concentrates, soap-bars, hair-gels and after-sun creams. The samples were obtained from different suppliers, together with the disclosure. A number of the analyses were carried out in the framework of an interlaboratory comparison test, organized by the EC. The results are summarized in Table III. In 37 out of the 45 samples, a total of 74 organic colorants were identified representing only 31 different colorants; only 8 colorants were not identified for reasons to be mentioned below. The remaining 8 samples did not contain any organic colorant at all (mostly eye-shadows). Their colour is due to the presence of inorganic colorants, which can as a matter of course not be identified by the present method.

As for the colorants which were not identified, in one case a colorant could not be detected because it did not belong to the group of colorants under investigation. With one sample, a lotion, two peaks were observed but – compared with the colorants disclosed by the supplier – they had distinctly longer retention times. The analysis was repeated twice, and in both cases the same phenomenon was observed. The presence of sample constituents that interfere with the chromatographic analysis appears to be the most logical

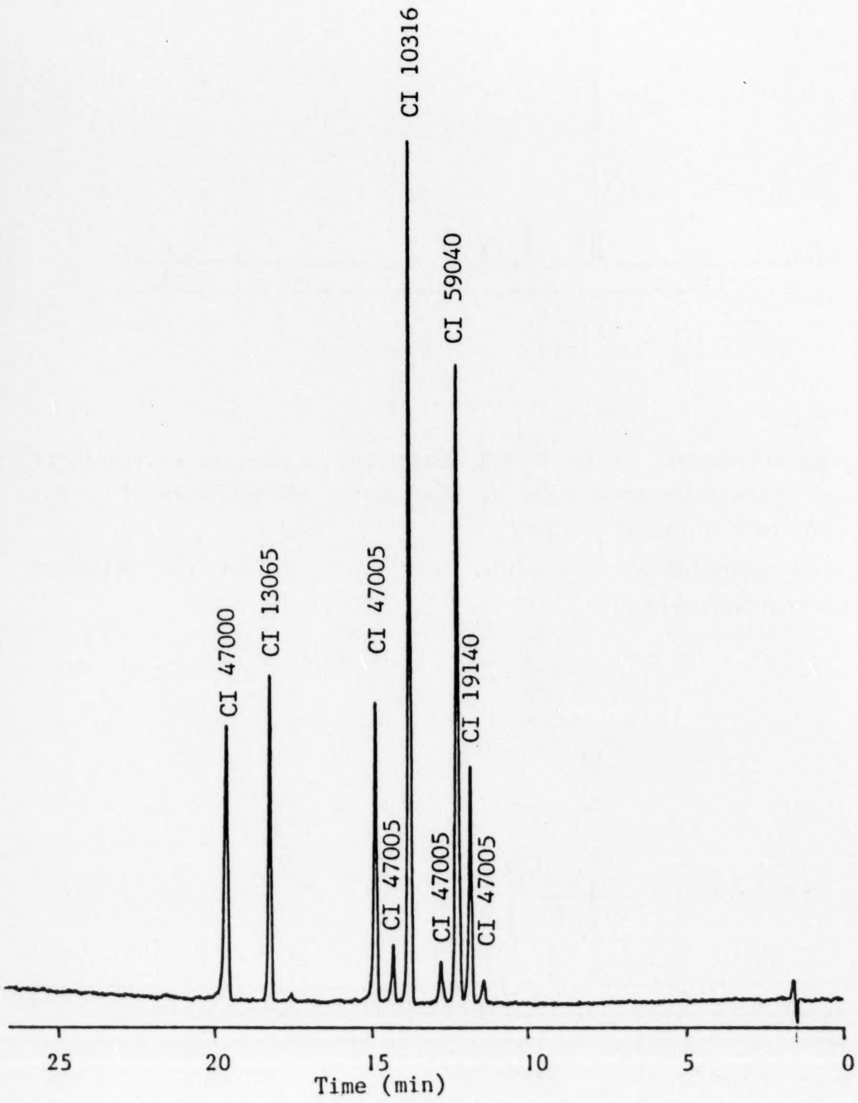

Fig. 5

Chromatogram of a mixture of 6 yellow colorants. As one of the colorants (CI 47005) is essentially a mixture of colorants (see Fig. 2), 9 peaks are present.

Chromatographic conditions: see Fig. 1, except for detection wavelength, 425 nm.

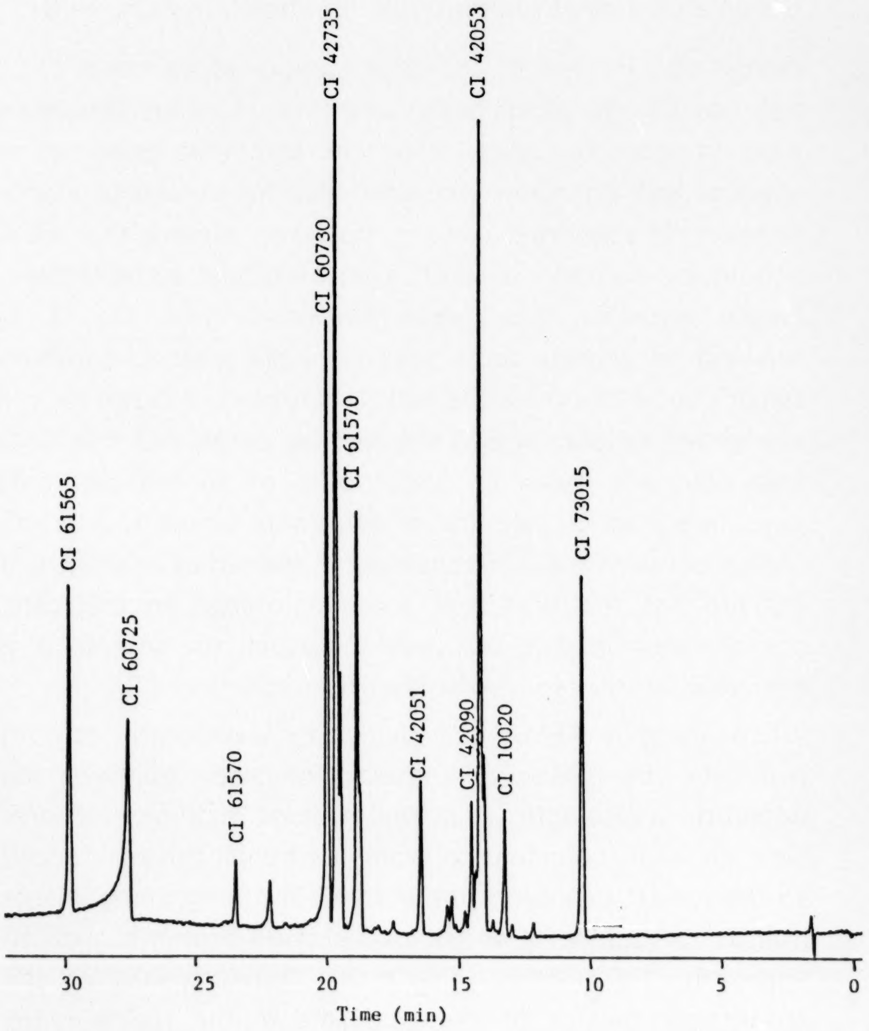

Fig. 6

Chromatogram of a mixture of 11 blue colorants.

Chromatographic conditions: see Fig. 1, except for detection wavelength, 600 nm.

Table III Analyses of 45 cosmetic samples.

Sample type	Disclosed colorants					Results of analysis*
Lipstick	19140					
	12085					
	45396					
	12085	15850	45370	45380		15850 not detected
	15585	45430				
	15585	15850	45370	45380		
	12085	15850	19140			
	15630					
	12085	15850	45370	45380	45410	
	15585	15630	45380			
	15850	15880				15880 not identified
	12085	12490	15850			12490 not detected
	15525	15865	47005			unknow red detected**
Nail-varnish	15850	19140				
	15880	19140				
Shampoo	75580					75580 not identified
	45430					
	45170					
Foam-bath	15985	16035	19140	42090		42090 not detected
	13065	42051	45350			
Cream	14700	15510	19140			
	19140					
Lotion	16255	19140				2 unknown colorants
	14720					
	14700	19140				
	14700	19140	42090			
After-sun cream	42090	45170				
Hair-gel	42090					
Face-power	19140	45410	73360			45410 not detected
	no organic colorants					
Liquid make-up	no organic colorants					
Make-up powder	15585	45410				***
	no organic colorants					
	73360					
Eye-shadow	15850					
	12075					
	15850					
	15585					
	75470					
	no organic colorants					
	no organic colorants					
	no organic colorants					
	no organic colorants					
	no organic colorants					
Soap-bar	12490					

*: if no remarks are given, the results of analysis are in agreement with the disclosure

**: see Fig. 7

***: see Fig. 8

explanation. In one case, an unidentifiable colorant was detected that was not disclosed by the supplier (see Fig. 7). Finally, in 5 cases, a colorant that should have been present according to the supplier's specifications simply was not detected. Insufficient detector sensitivity of the present HPLC system is probably the main cause of this negative result. A more sensitive detector, however, would be of the variable wavelength principle, requiring the time-consuming repeated analyses at different detection-wavelengths.

As an illustration, HPLC chromatograms for two analyses are shown in Figs. 7 and 8.

Conclusions

Ion-pair reversed-phase HPLC on octadecyl-modified silica with gradient elution, based on the use of a dilute solution of TBA in aqueous methanol, provides a rapid means for the determination of both ionic and non-ionic organic colorants in cosmetic products. In all probability, separation of the ionic colorants proceeds via an ion-pair mechanism, while separation of the non-ionic analytes is based on hydrophobic interaction with the alkylmodified silica.

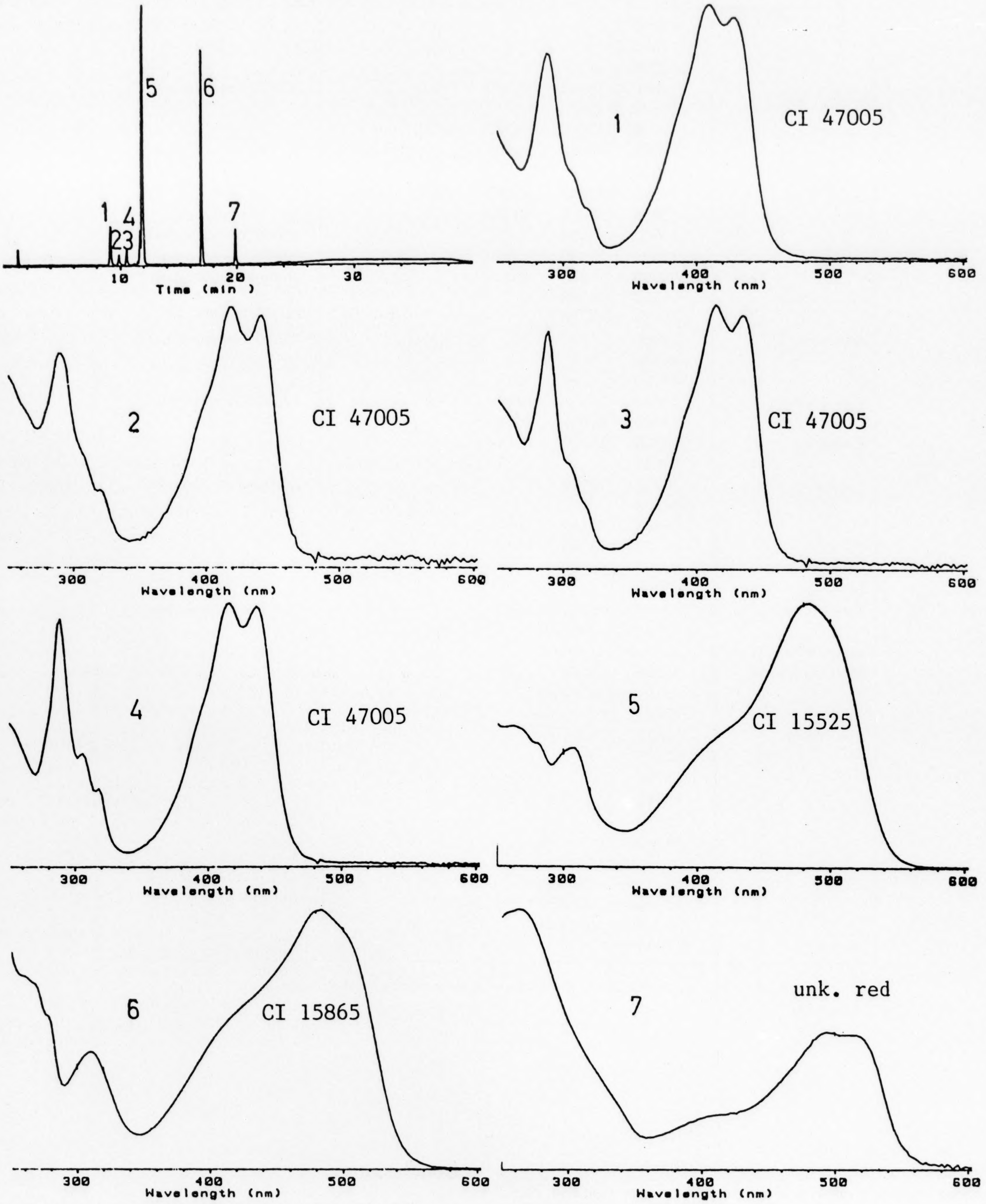

Fig. 7

Chromatogram of an extract of a lipstick, with UV-vis spectra of the peaks. Note the spectral ressemblance of the various constituents of CI 47005 and the presence of an unidentifiable compound, possibly a contamination of one of the identified red colorants. Chromatographic conditions: see Fig. 1.

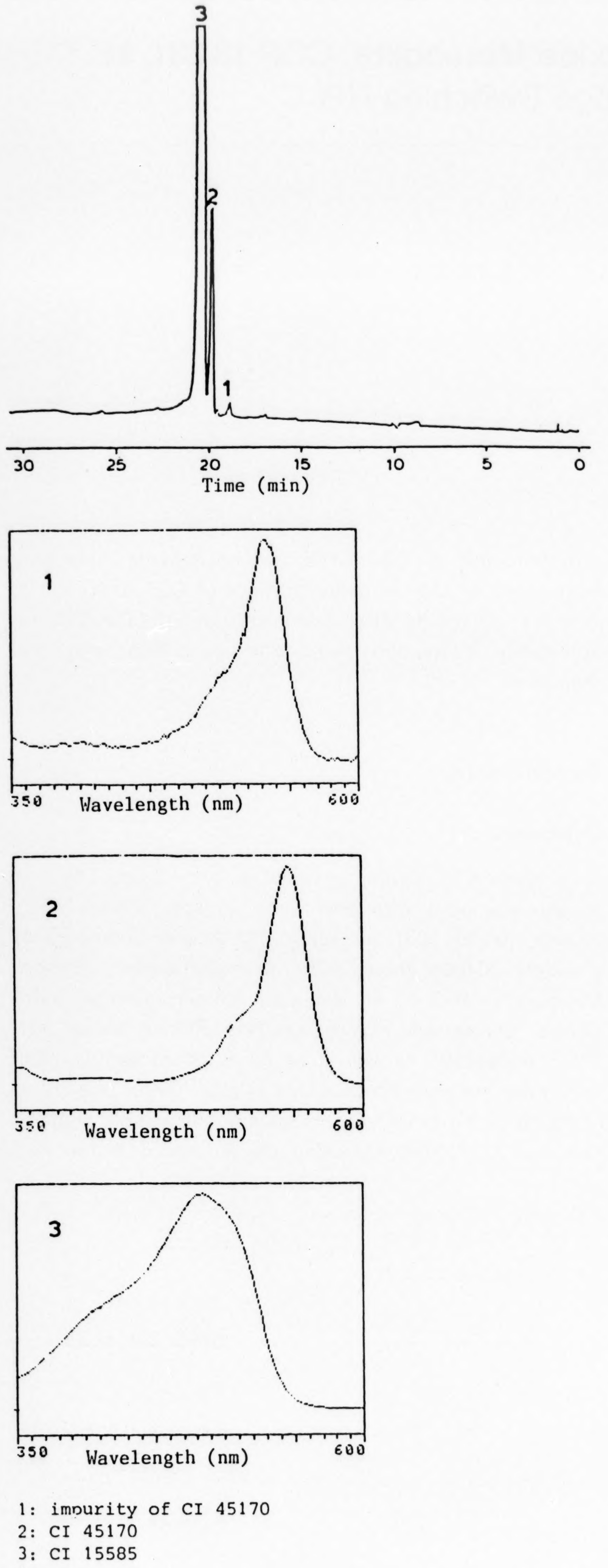

Fig. 8

Chromatogram of an extract of a make-up, with UV-vis spectra of the peaks.

Chromatographic conditions: see Fig. 1.

In principle, detection can be carried out with a conventional variable-wavelength detector. The presence of a large number – i.e., 126 in the present study – of colorants, with colours ranging from yellow to blue, justifies the incorporation of a DAD. In the present study, this system has been used for the determination of organic colorants in 45 cosmetic products. In a large majority of all cases, the analysis was completely successful even though sample pretreatment was kept to a minimum.

Acknowledgements

This work was carried out under contract to the Commission of the European Communities, Directorate XI (Protection of the Environment, Consumer and Nuclear Safety), contract numbers V/82/587, V/83/260, 84-B-6673-11-006-11S and 85-B-6673-11-006-11S. The experimental work was carried out in the laboratories of the Joint Research Centre of the European Communities, Petten Establishment (Petten, The Netherlands), of the Free University, Department of Analytical Chemistry (Amsterdam, The Netherlands) and of the Institute for Environmental Studies, Free University (Amsterdam, The Netherlands). Thanks are due to Mr. R. J. Fordham and Dr. W. Karcher of the JRC, Petten Establishment, for valuable advice and discussions.

References

[1] *J. F. Lawrence, F. E. Lancaster, H. B. S. Conacher,* J. Chromatogr. **218,** 168 (1981).
[2] *M. L. Puttemans, L. Dryon, D. L. Massart,* J. Assoc. Off. Anal. Chem. **64,** 1 (1981).
[3] *J. W. M. Wegener, H. J. M. Grünbauer, R. J. Fordham, W. Karcher,* J. Liq. Chrom. **7,** 809 (1984).
[4] *A. Perdih,* Fres. Z. Anal. Chem. **260,** 278 (1972).
[5] *K. M. Weaver, M. E. Neale,* J. Chromatogr. **354,** 486 (1986).
[6] *B. B. Wheals, P. C. White, M. D. Paterson,* J. Chromatogr. **350,** 205 (1985).
[7] *C. E. Goewie, M. W. F. Nielen, R. E. Frei, U. K. Th. Brinkman,* J. Chromatogr. **301,** 325 (1984).
[8] Colour Index, third edition, Society of Dyers and Colorists, Bradford, 1971.
[9] Handbook of U.S. Colorants for Foods, Drugs and Cosmetics, D.M. Marmion, John Wiley and Sons, New York, 1979.
[10] Kosmetische Färbemittel, Deutsche Forschungsgemeinschaft, Harald Boldt Verlag, Boppard, 1977.

Received: July 1, 1987
Accepted: Aug. 14, 1987
F

Determination of CGP 6140 and its N-Oxide Metabolite, CGP 13 231, in Plasma and Urine by Columns or Cartridge Switching HPLC

J. B. Lecaillon* / A. Sioufi / C. Souppart / J. P. Dubois

Laboratoires CIBA-GEIGY, Biopharmaceutical Research Center, B. P. 308, F-92506 Rueil-Malmaison, France

Key Words

Antiparasitic compound
Metabolites
Column-switching method
Cartridge-switching method
Method comparison

Summary

Two methods were developed for the determination of CGP 6140 and its N-oxide metabolite. The first method was based on trace enrichment, rinsing on a first column (LiChroprep RP-2) and *backflush* on the analytical column (Spherisorb ODS 1). The second method was based on trace enrichment onto a cartridge and *forwardflush* on the analytical column using the Advanced Automated Sample Processor (AASP). CGP 6140 and its N-oxide metabolite are spectrophotometrically detected at 405 nm. The reproducibility and accuracy of the methods were convenient. The limits of quantitation (50 nmol/l in plasma and 250 nmol/l in urine) were sufficient to follow the concentrations of CGP 6140 and its N-oxide metabolite after a 100 mg single oral dose of CGP 6140 to volunteers.

Introduction

CGP 6140, 4-nitro-4′-(N-methyl-piperazinyl-thiocarbonyl-amido)-diphenylamine, was selected as a potent antiparasitic compound possessing a macrofilaricidal activity in the treatment of onchocerciasis. The chemical structures of the drug, of its N-oxide metabolite, CGP 13 231, of other metabolites detected in urine of rats and of the internal standard used in the analytical methods, CGP 10 631, are given in Fig. 1. A previous less sensitive HPLC method for the determination of CGP 6140 and of metabolites by direct injection of diluted biological medium has been submitted for publication [1]. Two methods (column and cartridge switching) were developed for the determination of CGP 6140 and its N-oxide metabolite in order to follow the concentrations of CGP 6140 and its N-oxide metabolite after administration of CGP 6140 to volunteers. These two methods are described below and compared.

Experimental

Equipment

Two systems of sample preparation were used. The first system was built with one pump (Gilson, Villiers-le-Bel, France, model 303), an automatic sampler composed of a sampler (Gilson, model SC6), a peristaltic pump (Gilson, Minipuls II) and an air actuated sample injection valve (Valco, Chrompack France, Les Ulis, France, model AH-CV-6-UHPa-N60), as well as an air actuated sample injection valve for column-switching (Valco, model AH-CV-6-UHPa-N60). With the second system, the sample preparation was performed by using the Advanced Automated

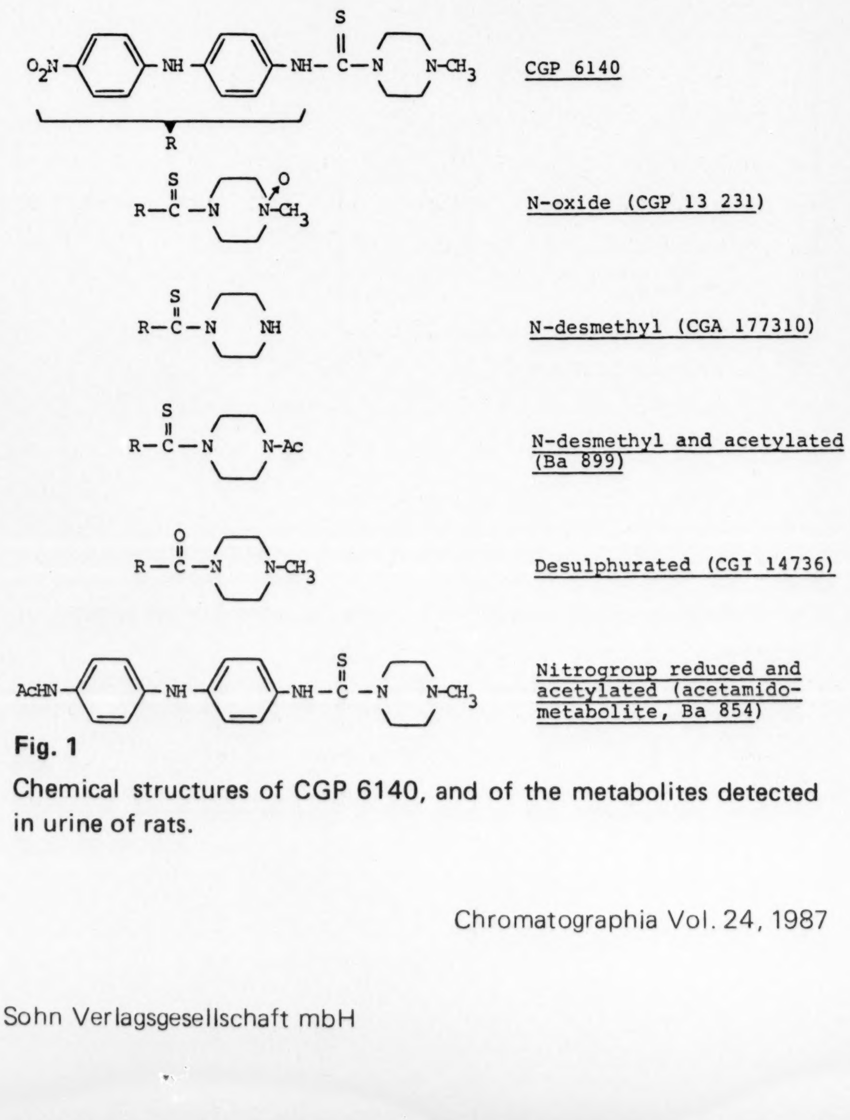
O_2N
NH
NH
S
C
N
N-CH$_3$
CGP 6140
R
N-oxide (CGP 13 231)
N-desmethyl (CGA 177310)
N-desmethyl and acetylated (Ba 899)
Desulphurated (CGI 14736)
AcHN
Nitrogroup reduced and acetylated (acetamido-metabolite, Ba 854)

Fig. 1
Chemical structures of CGP 6140, and of the metabolites detected in urine of rats.

0009-5893/87 0876-05 $03.00/0

© 1987 Friedr. Vieweg & Sohn Verlagsgesellschaft mbH

Sample Processor (Varian, Les Ulis, France, model AASP + AASP PrepStation). Further equipment was the same in the two methods: a pump (Gilson, model 303), a spectrophotometer set at 405nm (Kratos, Paris, France, model Spectroflow 783) and a computing integrator (Spectra-Physics, Les Ulis, France, model 4100) which actuates the valves, the sampler or the AASP, records the chromatogram and gives the area of the chromatographic peaks.

Stationary Phases and Columns

The following columns and cartridges were used:

1. 25cm long, 4.7mm i.d. column dry-packed with LiChroprep RP-2, 25–40μm reversed-phase material (Art. 9304, Merck France, Nogent-sur-Marne, France).
2. 25cm long, 4.7mm i.d. analytical column slurry-packed with Spherisorb ODS 1, 5μm (Art. SB 2251, SFCC, Gagny, France).
3. C2 reversed-phase cassette (Art. 8831000200, Varian France). Each cassette comprised 10 sorbent extraction cartridges filled with C2 bonded silica sorbent.

Solvents and Reagents

The synthetic reference compounds (see Fig. 1) CGP 6140, CGP 13 231, CGA 177310 and CGP 10 631 were provided by Ciba-Geigy Limited (Basel, Switzerland). N-acetyl derivative of N-desmethyl CGP 6140 (BA 899), desulphurated metabolite (CGI 14736) and the acetamido metabolite (BA 854) were provided by Hindustan Ciba-Geigy Limited, Research Centre (Bombay, India). All solvents and reagents were of analytical grade (Merck France), acetonitrile was of HPLC quality (Art. 412412, Carlo Erba France, Puteaux, France) and methanol was of RPE-ACS quality (Art. 414816, Carlo Erba France).

Column-Switching Procedure

A flow diagram of the column switching arrangement is shown in Fig. 2. Samples of diluted and centrifuged plasma (450μl plasma + 1.8ml H_2O-MeOH (70:30, v/v) + 45μl internal standard solution) or diluted urine (120μl urine + 1.1ml H_2O-MeOH (70:30, v/v) + 60μl internal standard solution) are loaded on the sampler. The samples are carried by the peristaltic pump into the injection valve equipped with a 2ml loop (for plasma) or 1ml loop (for urine). The samples are then injected on the RP2 column. The three compounds (CGP 6140, CGP 13 231, CGP 10 631) are retained on the sorbent and the column is rinsed during five minutes with degassed distilled water-MeOH (90:10, v/v) at a flow-rate of 5ml/min. The compounds are then back-eluted from the RP2 column, loaded and eluted on the analytical column with the mobile phase: acetonitrile-methanol-ammonia aqueous solution $4 \cdot 10^{-3}$mol/l (54.5:5:40.5, v/v/v) at a flow-rate of 1ml/min.

Cartridge-Switching (AASP) Procedure

The schematic outline of the AASP/HPLC method [2] is shown in Fig. 3. The bonded phase in each cartridge of the cassette is solvated with 0.5ml of methanol passing through the cartridge. The sorbent is then conditioned further with 0.5ml of water. Samples of diluted and centrifuged plasma (400μl plasma + 1ml H_2O + 40μl internal standard solution or calibration solution) or diluted urine (100μl urine + 1ml H_2O + 50μl internal standard solution or calibration solution) are loaded on the cartridge. The solute retained on the cartridge is rinsed with 1.5ml of K_2HPO_4 solution, 10^{-2} mol/l. All solutions passed through the sorbent cassette using a pneumatic manifold (AASP PrepStation). The cassettes are put on the AASP and the compounds are then eluted from each cartridge and loaded on the analytical column with the mobile phase: acetonitrile-methanol-ammonia aqueous solution $4 \cdot 10^{-3}$mol/l (54.5:5:40.5, v/v/v).

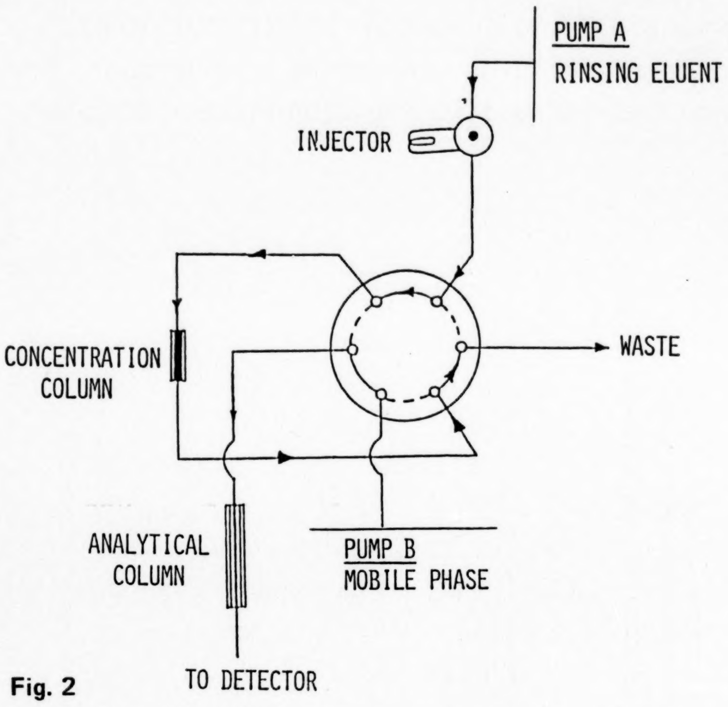

Fig. 2

Schematic outline of the sample analysis used in the column-switching HPLC method. Injection and concentration of the sample on the concentration column. Rinsing for 5min at 5ml/min with water-methanol (90:10, v/v). Backflush elution with the mobile mobile phase and loading on the column.

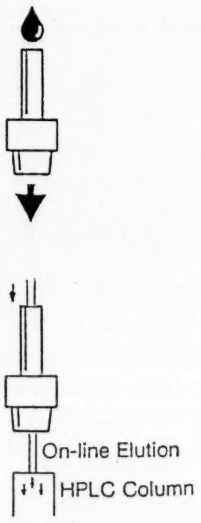

1. WASH THE CARTRIDGE WITH 0.5 ML OF METHANOL AND WITH 0.5 ML OF WATER.
2. ADD THE SAMPLE : 400 μL PLASMA OR 100 μL URINE + 1 ML H_2O + 40 μL INTERNAL STANDARD SOLUTION.
3. RINSE WITH 1.5 ML OF K_2HPO_4, 10^{-2} MOL/L.
4. PUT THE CASSETTE INTO THE AASP AND LOAD THE COMPOUNDS FROM THE CARTRIDGE ONTO THE COLUMN WITH THE MOBILE PHASE.

Fig. 3

Schematic outline of the sample analysis used in the AASP/HPLC method.

Calibration and Internal Standard

The internal standard stock solution is prepared by dissolving 4 mg of CGP 10 631 in 100 ml of methanol. Two tenfold dilutions are then prepared: one in methanol and the other in distilled water-methanol (80:20, v/v). The water-methanol solution serves as the internal standard solution. The final concentration obtained for the two dilutions is 14.8 μmol/l. All these solutions are prepared in glass flasks.

The calibration stock solution is prepared by dissolving 5 mg of CGP 6140 and 5 mg of CGP 13 231 monohydrate compound, in 50 ml of the diluted methanolic solution of CGP 10 631 in a polypropylene flask. Calibration solutions are prepared by dilution of the calibration stock solution by the internal standard solution in polypropylene flasks.

Four to five plasma or urine calibration samples are worked up according to the described procedure. The ratios of peak areas of CGP 6140 (or CGP 13 231)/CGP 10 631 are plotted as a function of the sample concentration. The regression method used for the determination of calibration curves is the weighted linear least squares regression with a weighting factor of $1/C^2$, where C is the concentration of the compound in the calibration sample [3].

Results and Discussion

The chromatograms of a plasma blank, a plasma sample of a patient at 4 h postdosing after a 800 mg dose, a urine blank and a urine sample of a patient for the 18–24 h collection period after a 100 mg dose are shown in Fig. 4 and 5. No N-desmethyl metabolite (CGA 177310), N-acetyl derivative of N-desmethyl CGP 6140 (BA 899) and desulphurated metabolite (CGI 14736), which were previously recorded in the urine of rats, were detected in the plasma or urine of humans. These compounds, whose retention times were measured after injection of a synthetic mixture, were separated from plasma and urine compounds, the unchanged drug, the N-oxide metabolite and the internal standard (see Fig. 4 and 5). They might be quantitated with the described method without modification of the chromatographic conditions.

Figs. 6 and 7 show calibration curves obtained for CGP 6140 and CGP 13 231. The precision and the reproducibility of the methods were studied by the determination of plasma or urine samples spiked with known amounts of CGP 6140

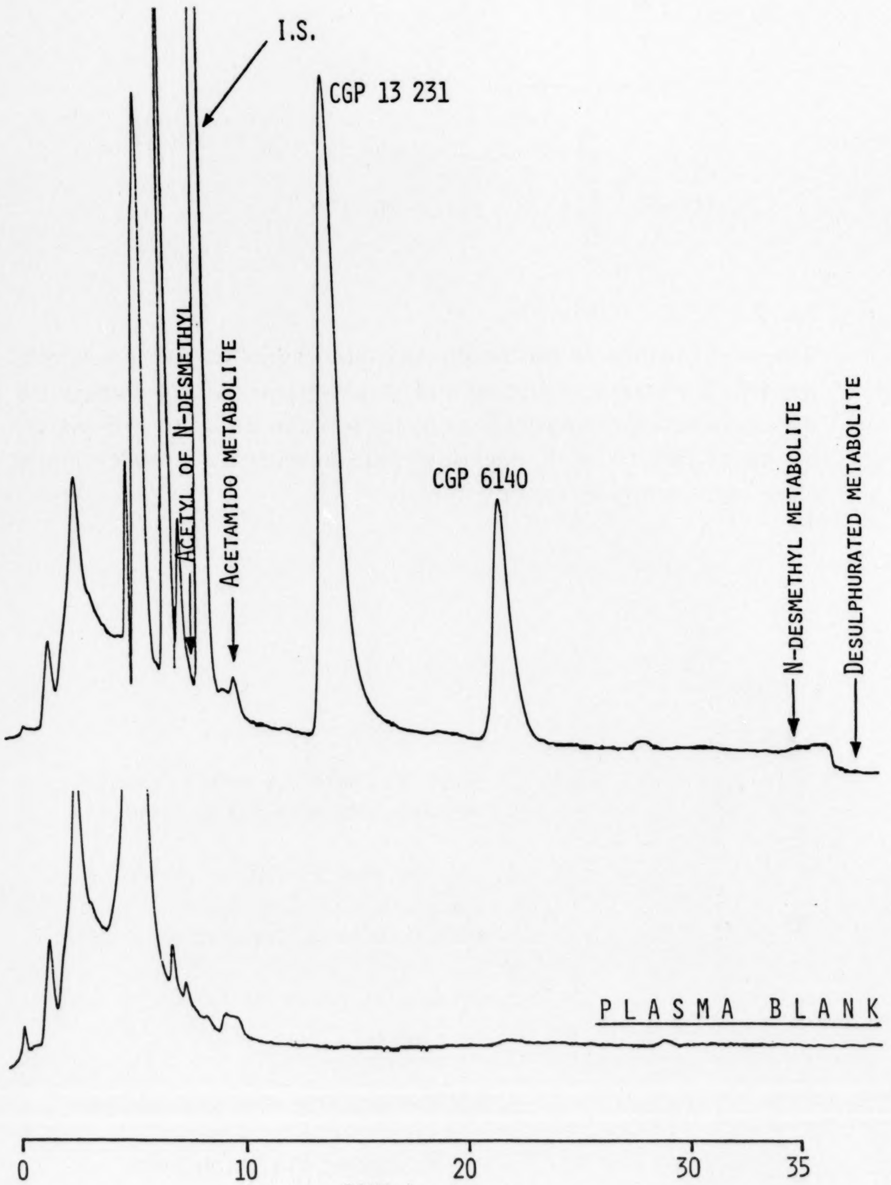

Fig. 4

Chromatograms of a plasma blank and a plasma sample of patient at 4 h postdosing after a 800 mg dose (column-switching HPLC method). Measured concentrations: CGP 6140 = 802 nmol/l, CGP 13 231 = 2110 nmol/l.

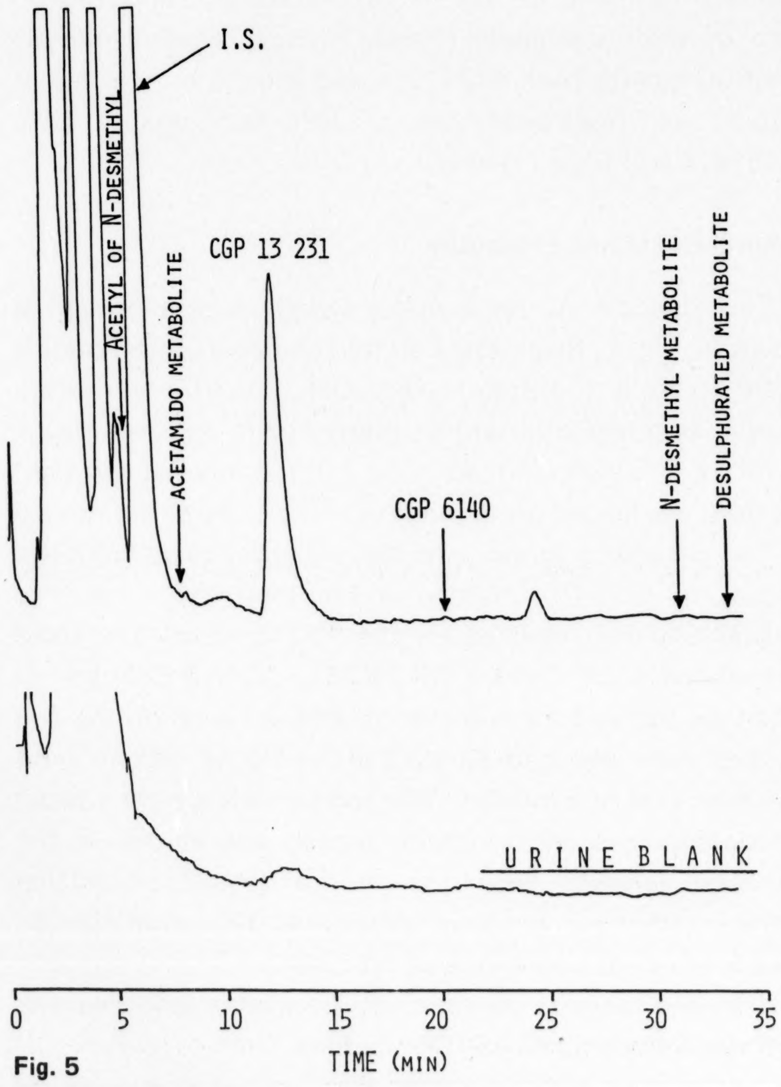

Fig. 5

Chromatograms of a urine blank and a urine sample of a patient for the 18–24 h collection period after a 100 mg dose of CGP 6140 (AASP/HPLC method). Measured concentrations: CGP 6140 = not detected, CGP 13 231 = 775 nmol/l.

Table I. Validation of the column-switching HPLC method obtained with day to day determination of spiked samples.

Compound: CGP 6140

Fluid	Introduced (nmol/l)*	Number of assays	Mean recovery ± SD (%)	Overall recovery ± SD (%)
Plasma	135	23	98.8 ± 9.9	101.8 ± 8.2 n = 98
	269	17	100.2 ± 9.4	
	539	14	100.2 ± 6.6	
	673	6	95.9 ± 9.6	
	1346	19	104.3 ± 4.6	
	2693	19	107.2 ± 4.3	
Urine	673	7	98.6 ± 13.5	99.6 ± 10.1 n = 35
	1346	6	93.0 ± 9.5	
	2692	7	95.4 ± 9.5	
	6730	9	105.2 ± 6.1	
	13460	6	104.0 ± 8.1	

Compound: CGP 13 231

Plasma	123	22	97.9 ± 12.1	100.3 ± 8.0 n = 104
	247	19	102.1 ± 9.0	
	493	14	106.5 ± 6.0	
	617	10	99.8 ± 6.3	
	1233	19	97.9 ± 3.1	
	2467	20	99.5 ± 3.3	
Urine	617	28	103.7 ± 8.9	102.5 ± 6.9 n = 105
	1233	17	100.9 ± 5.8	
	2466	19	100.8 ± 7.3	
	6166	22	103.7 ± 5.3	
	12332	19	102.6 ± 5.2	

Recovery = (found/introduced concentration) X 100.

* To convert into ng/ml of CGP 6140, multiply the concentrations by 0.3715 and to convert into ng/ml of CGP 13 231, multiply by 0.3875.

Table II. Validation of the cartridge-column switching method (AASP system) obtained with day to day determination of spiked samples.

Compound: CGP 6140

Fluid	Introduced (nmol/l)*	Number of assays	Mean recovery ± SD (%)	Overall recovery ± SD (%)
Plasma	53.9	5	97.2 ± 8.0	97.0 ± 8.2 n = 17
	135	1	89.4	
	269	4	96.9 ± 6.8	
	539	3	88.9 ± 0.6	
	1346	2	109.7	
	2693	2	108.1	
Urine	269	4	90.4 ± 8.1	94.8 ± 6.2 n = 12
	1346	3	92.8 ± 1.0	
	6730	3	99.6 ± 3.7	
	13460	2	99.4	

Compound: CGP 13 231

Plasma	49.3	5	96.3 ± 8.1	99.9 ± 7.8 n = 17
	123	1	95.9	
	247	4	104.2 ± 8.2	
	493	3	104.2 ± 5.6	
	1233	2	106.5	
	2467	2	92.4	
Urine	247	4	107.4 ± 10.9	103.7 ± 7.0 n = 16
	1233	5	102.8 ± 6.5	
	6166	3	103.8 ± 1.8	
	12232	3	99.9 ± 7.0	
	41103	1	104.0	

Recovery = (found/introduced concentration) X 100.

* To convert into ng/ml of CGP 6140, multiply the concentrations by 0.3715 and to convert into ng/ml of CGP 13 231, multiply by 0.3875.

and CGP 13 231 during several weeks of use, concurrently with the determination of clinical samples. The recoveries and coefficients of variation are given in Tables I and II. The limits of quantitation were 50nmol (about 20ng/ml) of CGP 6140 or of CGP 13 231 per liter of plasma and 250nmol (about 100ng/ml) of CGP 6140 or of CGP 13 231 per liter of urine. The limits of detection were about 5 times less than the limits of quantitation.

Comparison of the Column-Switching and AASP Procedures

With the column-switching method, the RP 2 column was replaced every 40 injections to allow good chromatographic purification of the sample and a protection of the analytical column from endogenous plasma and urine components. The analytical column could be used for the determination of 150–200 samples and gave peak shoulders after such a series of determinations. With the cartridge-switching method (AASP), the life of the analytical column appeared longer than with the first system and more than 200 sample determinations could be performed. The solvent consumption was higher with the first system due to the rinsing step. This was balanced with the cost of the cassettes with the AASP system. The reproducibility and accuracy of the methods were convenient and similar (Tables I and II).

The two methods appeared sensitive enough to follow the plasma concentrations of CGP 6140 and of its N-oxide metabolite, CGP 13 231, after a single oral dose of 100mg of CGP 6140 given to volunteers (Fig. 8).

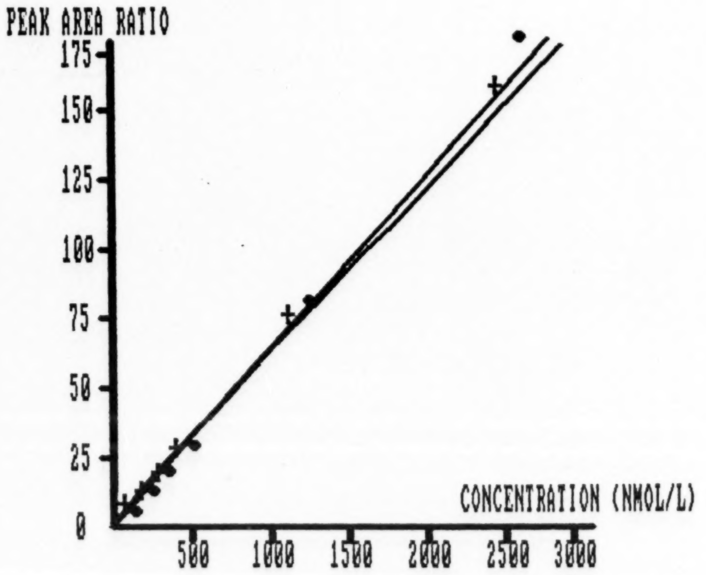

Fig. 6

Calibration curves of CGP 6140 and CGP 13 231 in plasma (column-switching HPLC method): ●—● CGP 6140, +—+ CGP 13 231.

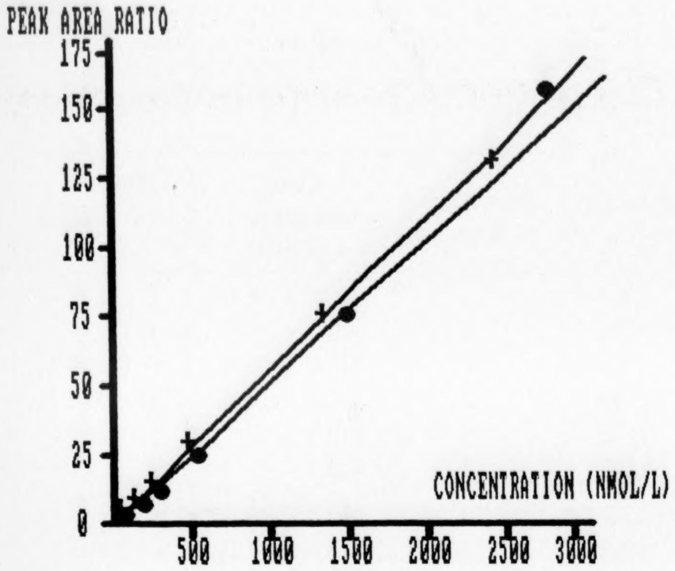

Fig. 7

Calibration curves of CGP 6140 and CGP 13 231 in urine (AASP/HPLC method): ●—● CGP 6140, +—+ CGP 13 231.

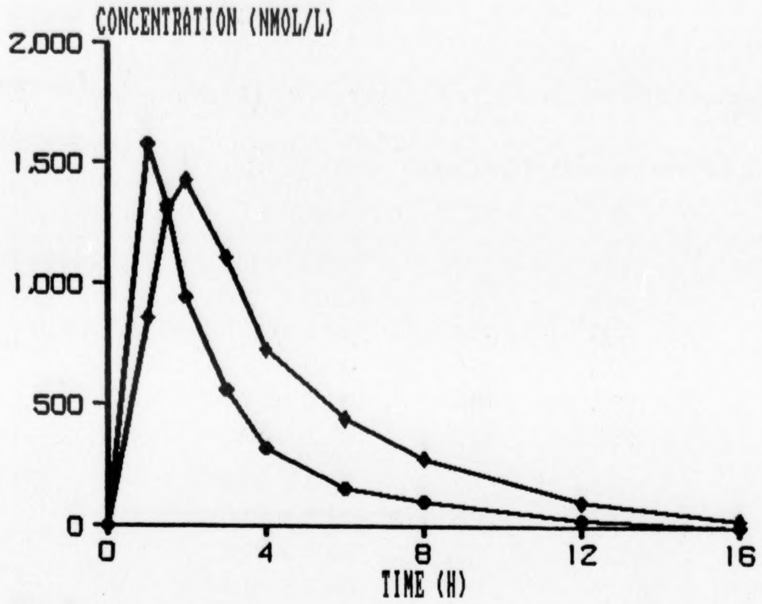

Fig. 8

Curves of CGP 6140 and CGP 13 231 in plasma after a single oral administration of 100 mg of CGP 6140 (column-switching method): ●—● CGP 6140, ♦—♦ CGP 13 231.

References

[1] *S. C. Bhatia, S. N. Revankar, B. Anjaneyulu, N. D. Desai, M. M. Banavalikar, D. Subrahmanyan*, submitted for publication in J. Chromatogr.

[2] *L. Yago*, Int'l. Lab. **18** (9), 40 (1985).

[3] *D. A. Schoeller*, Biomed. Mass Spectrometry **3**, 265 (1976).

Received: June 30, 1987
Accepted: Oct. 19, 1987
F

High Performance Displacement Chromatography of Proteins: Separation of β-Lactoglobulins A and B

A.W. Liao[1] / Z. El Rassi[1] / D.M. LeMaster[2] / Cs. Horváth[1] *

[1] Department of Chemical Engineering and [2] Department of Molecular Biophysics and Biochemistry, Yale University, New Haven, Connecticut 06520, USA

Key Words

Preparative column liquid chromatography
Displacement chromatography
Chondroitin sulfate
Polygalacturonic acid
Ion exchange
β-Lactoglobulins

Summary

β-Lactoglobulins A and B were separated by high performance displacement chromatography on an anion-exchanger column with chondroitin sulfate as the displacer. A sample of 100 mg containing a mixture of the two *β*-lactoglobulins was separated on a column of 75 x 7.5 mm in a single chromatographic run. The separation process followed the rules of the classical displacement development: the two proteins formed contiguous rectangular bands and their concentrations were dependent on the displacer concentration. The results demonstrate that high performance displacement chromatography is a useful technique for the separation of proteins in preparative amounts with columns and instrumentation typically used in analytical HPLC. Furthermore, it has the potential to become the method of choice in large scale separation of proteins.

Introduction

Previous results from our laboratory have shown that in preparative scale chromatography the displacement mode offers significant advantage over the conventional linear elution mode. Displacement chromatography of aromatic compounds [1], nucleic acid fragments [2], corticosteroids [3], amino acids [4], peptides [5] and antibiotics [6] has been carried out with columns and instrumentation generally used in analytical HPLC.

Displacement development is a nonlinear chromatographic technique that is suitable for the separation of multicomponent mixtures containing closely related substances. Its essential features have been established more than four decades ago [7]; the fundamentals and applications of the technique in HPLC were reviewed recently [8]. In displacement chromatography the column is first equilibrated with the carrier, also called presaturant, and then loaded with the feed mixture to be separated so that the components are adsorbed by the stationary phase. Thereafter a sufficiently concentrated solution of a displacer, also called desorber, which binds to the stationary phase more strongly than any of the feed components, is introduced. The sample components are displaced from the stationary phase by the displacer front moving down the column. The components become separated as a result of their competition for the binding sites at the stationary phase surface during the displacement process. Ultimately they form adjacent rectangular bands that move with the same velocity as the displacer front. For displacement to take place the concentrations of the displacer and the feed components must be in the nonlinear region of their respective adsorption isotherms and therefore are much higher than those in linear elution chromatography.

So far high performance displacement chromatography was used only for the separation of relative low molecular weight substances and separation of proteins with the use of a single displacer has not been successful. Nevertheless, the word 'displacement' was employed in conjunction with protein chroamtography. An ampholyte mixture was used in the mobile phase for the separation of proteins on an ion exchange column and the method was called carrier displacement chromatography [9]. Since the proteins are eluted by the ampholyte mixture and a pH gradient was set up in the column that also contributes to the separation, the mechanism of the process resembles that of chromatofocusing [10, 11]. A mixture of carboxymethyldextrans of different degrees of substitution was successfully employed as the displacer for protein separation on anion exchanger column [12–16]. The carboxymethyldextrans which served as spacers between the proteins were also mixed with the proteins separated and the mechanism of the process involved possibly both displacement and elution with the polydisperse displacer solution.

0009-5893/87 0881-05 $03.00/0

© 1987 Friedr. Vieweg & Sohn Verlagsgesellschaft mbH

The goal of the present work is to demonstrate that the process of displacement chromatography as described theoretically [17] and demonstrated experimentally for small molecules [1–6] is also applicable to the separation of proteins. A mixture of two closely related proteins, β-lactoglobulins A and B, was separated by high performance displacement chromatography on an analytical DEAE column and with chondroitin sulfate as the displacer. The results have established that proteins can indeed be separated by classical displacement chromatography and the technique has a potential in the preparative and process scale purification of biopolymers.

Experimental

Equipment

The flow sheet of the displacement chromatograph is shown in Fig. 1. Displacement chromatography and HPLC analysis were performed by using two Model 100A pumps and a Model 420 controller (Beckman Instrument, Fullerton, CA, USA) as well as a Model 7010 sample injector (Rheodyne, Berkeley, CA, USA) with a 4 ml and 20 μl sample loop, respectively. Column effluent was monitored by a Model GM 770 variable wavelength UV detector (Kratos, Ramsey, NJ, USA) and a Model CI-10 integrator (LDC, Riviera Beach, FL, USA) whereas a Model 7000 Ultrorac fraction collector (LKB, Gaithersburg, MD, USA) was used to collect fractions.

Columns

A TSK DEAE 5-PW (75 x 7.5 mm) column was used for displacement chromatography. Diethylaminoethyl (DEAE) derivative of 5 μm Vydac macroporous silica (The Separation Group, Hesperia, CA, USA) was packed from methanol slurry into a 30 x 4.6 mm stainless steel tubing at 8000 psi.

Reagents

Pure β-lactoglobulins A and B (LAC-A and -B) from bovine milk and their mixture (LAC), as well as a mixture of chondroitin-4-sulfate and chondroitin-6-sulfate from shark cartilage and polygalacturonic acid from oranges were purchased from Sigma (St. Lous, MO, USA). Toluidine blue 0 was from Aldrich (Milwaukee, WI, USA) and polyacrylic acids having different mean molecular weights were obtained from Polysciences (Warrington, PA, USA). Acrylamide, N,N'-bis-methyleneacrylamide, tetramethylethylenediamine, ammonium persulfate and Coomassie blue were from Bio-Rad (Richmond, CA, USA). All the other chemicals were of reagent grade from J. T. Baker (Philipsburg, NJ, USA). Distilled water was made by a Barnstead Nanopure unit.

Procedures

Displacement development: The TSK DEAE 5-PW column was first equilibrated with 25 mM sodium phosphate, pH 7.0, the carrier, before each displacement run.

The mixture of the two β-lactoglobulins was dissolved in the carrier and the solution was filtered by a 0.45 μm HA membrane (Millipore, Bedford, MA, USA). The feed solution was first loaded into the 4-ml sample loop and from there onto the column. Then the weakly sorbed components of the sample were removed from the column by washing it with 15 ml of the carrier.

Solutions of chondroitin sulfate in the carrier at different concentrations were used for displacement at a flow-rate of 0.1 ml/min. The column effluent was monitored at 315 nm and fractions were collected in 2 min intervals. The displacement run was completed upon appearance of the displacer in the effluent as tested by the metachromasia reaction of chondroitin sulfate with toluidine blue 0 [18, 19]. In all cases the front fraction with positive metachromasia reaction corresponded to the disappearance of the detection signal of the proteins at 315 nm.

After each run the column was washed with 50 ml of 500 mM sodium phosphate, pH 7.0, and 100 ml of 900 mM NaCl in 10 mM Tris, pH 9.8 at 1 ml/min. Five 1.5 ml pulses of 0.16 M sodium hydroxide in 3 min intervals were injected into the column during perfusion with the latter regenerant. The column was then reequilibrated with 100 ml of the carrier before starting the next displacement run. The lengthy regeneration protocol is likely to be too conservative, but no attempt was made to reduce the time of this step.

Analysis of the fractions: The fractions were analyzed by isocratic HPLC with the DEAE-silica column and 91 mM sodium phosphate, pH 7.0, as the eluent at a flow rate of 1 ml/min. An aliquot of 25 μl from each fraction was injected. The column effluent was monitored at 278 nm and the peak areas were measured in order to calculate the concentrations of LAC-A and LAC-B in the fractions. The calibration curve was prepared by using 9.6 as the specific absorbance for a 1 % solution of either lactoglobulins at 278 nm [20]. The purity of the fractions was confirmed by disc polyacrylamide gel electrophoresis. A native gel system of Laemmli [21] was used with a 6 % stacking gel and 15 % separating gel. From each fraction an aliquot of 5-μl was mixed with 15 μl of 20 % (w/v) sucrose and 2 μl of the mixture was applied to the slot in the slab gel. The gel was subjected to electrophoresis at 200 V (3 mA) for 4 hr and the proteins were stained with Coomassie blue.

Results and Discussion

β-Lactoglobulins

β-Lactoglobulins are the major whey proteins of cow's milk and have been studied extensively [22, 23]. Among the five genetic variants identified so far LAC-A and -B are the most prevalent. Each of them has 165 amino acid residue, two disulphide bridges and a free cysteine. At pH 7.0 they are present as dimers having molecular weight of 36,000 Da. LAC-A and -B differ in two amino acid residues: instead of Asp 64 and Val 118 in A, there are Gly and Ala in B. Thus LAC-A has one more negative charge than LAC-B and the isoelectric point of the two proteins is 5.13 and 5.23, respectively [24].

Selection of the Displacer

In preliminary experiments the use of polyacrylic acid as the displacer was investigated. The polyacrylic acids at our disposal had a very wide molecular weight distribution [25] and for this reason they did not form a sharp displacer front. In displacement experiments the LAC-A and -B bands were found to be contaminated by polyacrylic acid and some fraction of the polyacrylic acids may have acted as a spacer because the two protein bands were not contiguous.

Chondroitin sulfate, which is reportedly monodisperse or nearly so with a molecular weight of 50,000 [26], was found to be a suitable displacer. As a carbohydrate it is highly hydrophilic and furthermore strongly acidic due to the abundance of carboxylic and sulfate groups in the molecule. For this reason it binds stronger to the anion exchanger than the proteins under investigation. The displacement process was not altered by any untoward interaction between chondroitin sulfate and LAC's and the results suggest that chondroitin sulfate, which has a narrow molecular weight distribution, may be a generally useful displacer in separations on anion exchanger columns.

In some experiments polygalacturonic acid was also used as displacer and its effects in displacement development (data not shown) were found to be similar of chondroitin sulfate. It is likely that various other carboxylated polysaccharides of appropriate molecular weight and molecular weight distribution that are readily available in pure form can also be used as suitable displacers in chromatography with anion exchanger columns.

Effect of Protein Loading

Fig. 2A illustrates a displacement chromatogram of 100 mg of a protein mixture containing LAC-A and -B. It was obtained on a 75 x 7.5 mm DEAE column with chondroitin sulfate as the displacer and shows that satisfactory separation of the two β-lactoglobulins was chieved. Chondroitin sulfate acted as a true displacer; its front butted the rectangular band of the second component, LAC-A, and no chondroitin sulfate was found in any of the two contiguous proteins bands. With such sample load and the given column, the final pattern was not reached as seen from the shape of the LAC-B band in Fig. 2A and a longer column would have been needed for full development under the conditions of the experiment. Upon reducing the feed to 78 mg, however, the displacement train was fully or almost fully developed as shown by the quasi-rectangular bands in Fig. 2B. The plateau concentration of the second band was about 20 mg/ml in both cases suggesting that the conditions for LAC-A were isotachic at the fixed displacer concentration employed.

Effect of Displacer Concentration

Figs. 3A and 3B show the effect of changing the displacer concentration. A decrease in the concentration of chondroitin sulfate from 20 mg/ml to 3 mg/ml effected a corresponding decrease in the plateau concentration of the LAC bands as expected from the theory of displacement chromatography [17]. A quantitative interpretation of the approximately fivefold decrease in protein concentration, however, would require knowledge of the pertinent adsorption isotherms.

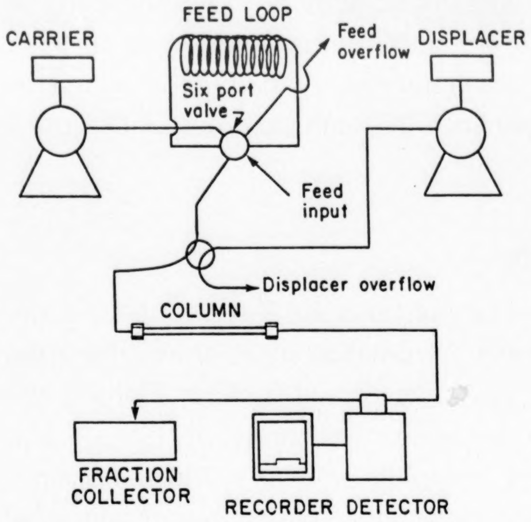

Fig. 1

Flow sheet of the displacement chromatograph.

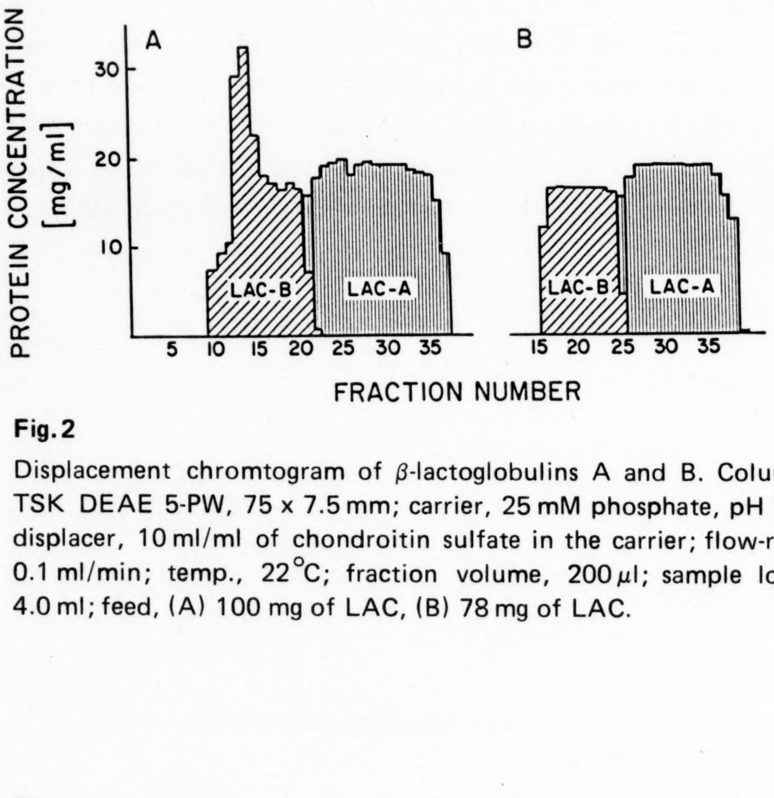

Fig. 2

Displacement chromtogram of β-lactoglobulins A and B. Column, TSK DEAE 5-PW, 75 x 7.5 mm; carrier, 25 mM phosphate, pH 7.0; displacer, 10 ml/ml of chondroitin sulfate in the carrier; flow-rate, 0.1 ml/min; temp., 22°C; fraction volume, 200 μl; sample loop, 4.0 ml; feed, (A) 100 mg of LAC, (B) 78 mg of LAC.

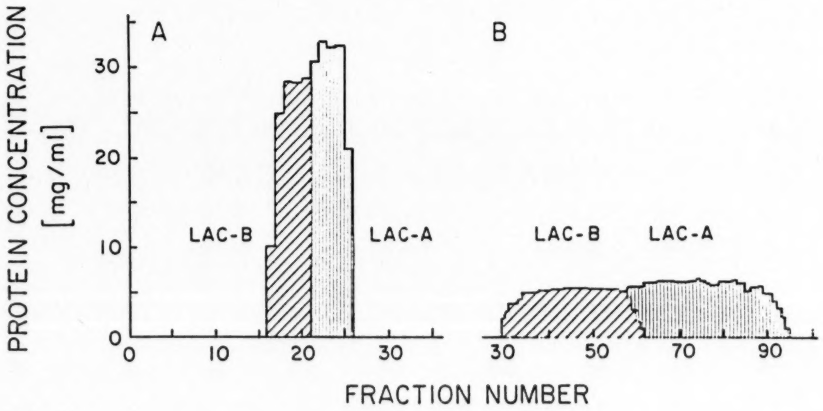

Fig. 3

Displacement chromatogram of β-lactoglobulins A and B. Conditions as in Fig. 2 except (A) 20 mg/ml of chondroitin sulfate was the displacer and the feed was 62 mg of LAC, (B) 3 mg/ml of chondroitin sulfate and the feed was 70 mg of LAC.

Mass Recovery of β-Lactoglobulins

In each chromatographic run the total amount of the LAC present in the fractions collected was evaluated and expressed as the percentage of the LAC content of the feed as the measure of mass recovery. In all displacement experiments it was found to be higher than 95 % for either β-lactoglobulins. This is in agreement with the findings by others [27] that the recovery of enzymatic activity in elution chromatography on TSK DEAE 5-PW column was close to 95 %. Thus, displacement development yielded mass recoveries similar to those retained with such columns under other chromatographic conditions.

Purity of the Products

According to HPLC analysis both LAC-A and LAC-B obtained by displacement chromatography from the LAC mixture were highly pure. As shown in Figs. 2 and 3 the line of demarcation between the bands of LAC-A and LAC-B was sharp and occupied only one 200 μl fraction. Additional information on product purity was obtained by disc electrophoresis. Electrophoretic patterns such as shown in Fig. 4 were in excellent agreement with the results of HPLC analysis but also revealed the presence of another species in the last LAC-A fraction, collected just before the breakthrough of the displacer front. This trace contaminant which could be an aggregate of LAC-A or other genetic variant [22] was probably too strongly retained on the column under analytical conditions but was enriched and recovered by displacement development. This finding also suggests that displacement chromatography could be a suitable tool to concentrate trace contaminants in proteinaceous drugs and other similar products.

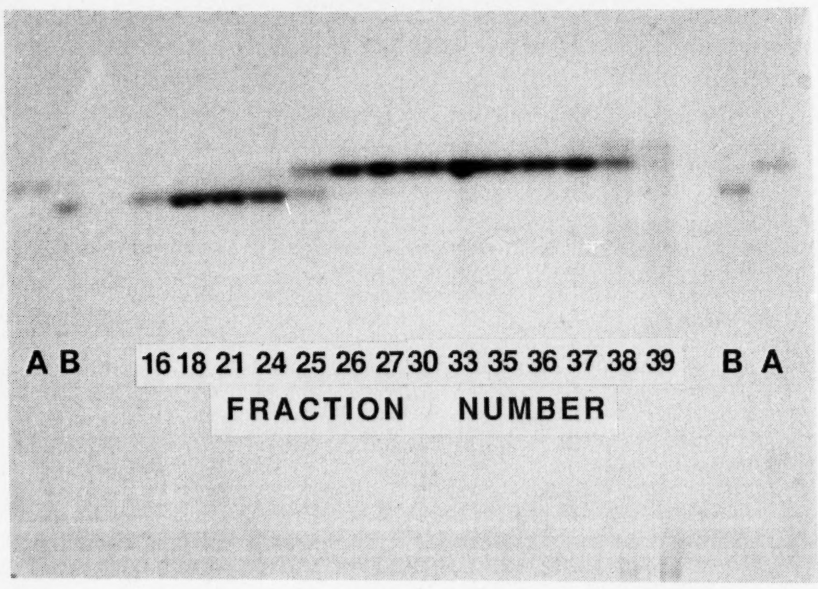

Fig. 4

Electrophoretic pattern of the fractions obtained in displacement chromatography of β-lactoglobulins A and B. The samples were obtained under conditions shown in Fig. 2B. A is LAC-A standard and B is LAC-B standard.

Comparison of Displacement and Elution

The separation efficiency of the column operated in the elution mode rapidly decreases with increasing sample load as illustrated in Fig. 5 and 6. As illustrated in Fig. 5 not more than 20 mg of LAC mixture could be separated with the 75 x 7.5 mm TSK DEAE 5-PW column by isocratic elution. On the other hand as shown in Fig. 2A the separation of 100 mg of LAC mixture was readily carried out on the same column in the displacement mode. Since the column loading capacity with gradient elution is greater than

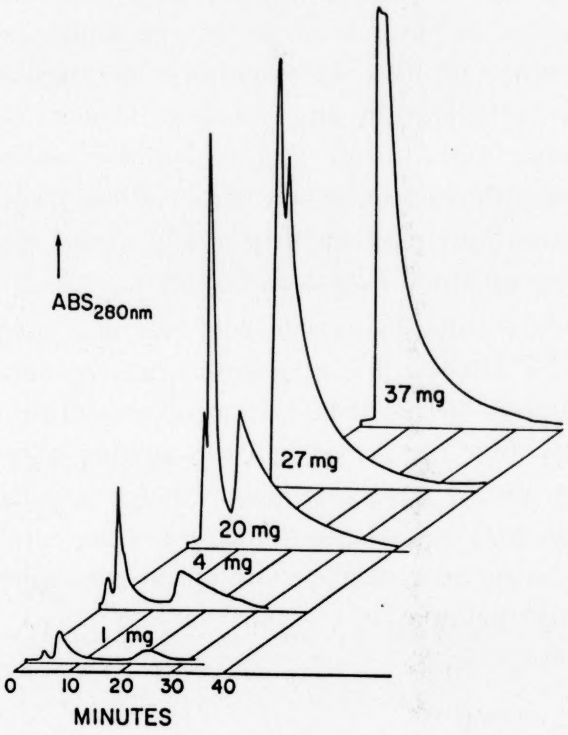

Fig. 5

Effect of sample load on the separation of β-lactoglobulins A and B by isocratic elution. Column, TSK DEAE 5-PW, 75 x 7.5 mm; eluent, 130 mM phosphate buffer, pH 7.0; flow rate, 1 ml/min; temp., 22 °C; sample loop, 0.5 ml.

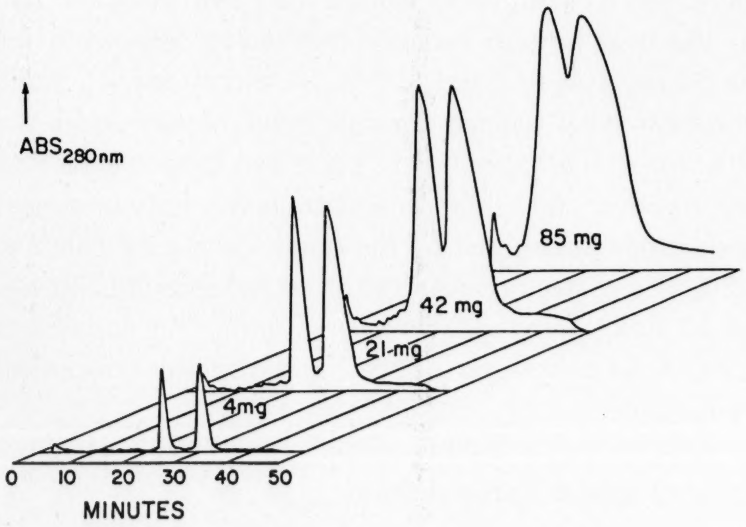

Fig. 6

Effect of sample load on the separation of β-lactoglobulins A and B obtained by gradient elution. Column, TSK DEAE 5-PW, 75 x 7.5 mm; gradient elution from 25 mM to 263 mM phosphate buffer, pH 7.0, in 40 min followed by isocratic elution for 5 min; flow-rate, 1 ml/min; temp., 22 °C; sample loop, 0.5 ml.

with isocratic elution, experiments were carried out with the same column by gradient elution and the results are shown in Fig. 6. The amount of LAC that could be separated by gradient elution was not greater than 40 mg, i.e., less than half of the amount separated by displacement. Because of the high loading capacity and concomitantly higher throughput with fast column regeneration, displacement has the potential to become the dominant mode in preparative chromatography.

Longevity of Column

Since LAC's and chondroitin sulfate as negatively charged macroions interact strongly with the DEAE stationary phase, a small fraction of both remains firmly bound to the column after completion of the displacement development and can be removed only by using sodium hydroxide solution in the regeneration step.

The longevity of the TSK DEAE 5-PW column [27], which has a polymeric matrix and can sustain wash with alkaline solution in the regeneration step, was quite satisfactory. Column performance was monitored constantly by measuring the isocratic retention of LAC, using 130 mM phosphate buffer at pH 7.0 as eluent. No appreciable change in the column retentivity was observed after 20 cycles of combined displacement runs and regeneration steps.

On the other hand, several siliceous DEAE columns were also employed for displacement but their useful life was short for lack of a suitable regeneration protocol. The employment of typical regeneration methods [28], such as washing with formic acid, 0.1 % aqueous trifluoroacetic acid-propanol gradient, 6 M guanidine hydrochloride, 8 M urea with 1 M sodium chloride, potassium thiocyanate in dimethylsulfoxide, was not successful. Evidently proteins and/or the displacer remained bound to the stationary phase surface. In fact after three cycles siliceous anion exchangers generally lost their retentivity for acidic proteins and exhibited the properties of a cation exchanger so that they could be used to separate basic proteins. Since siliceous stationary phases could not be regenerated by using sodium hydroxide, their usefulness in displacement chromatography or in preparative chromatography with high sample loads at large may be limited.

Conclusion

As shown by the separation of β-lactoglobulins A and B the process of displacement chromatography is applicable not only to small molecules but also to proteins in an essentially identical fashion. Chondroitin sulfate or possibly other acidic polysaccharides appear to be generally useful displacers for the separation of acidic proteins on anion exchanger columns. As the amount of sample that can be separated on a given column by displacement is much larger than that by elution, displacement chromatography is a promising technique for preparative of micropreparative biopolymer separations.

Acknowledgements

We thank Y. Kato for the gift of the TSK DEAE 5-PW column. This work was supported by Grants Nos. GM 20993 and CA 21948 from National Institutes of Health, U.S. Department of Health and Human Resources.

References

[1] *Cs. Horváth, A. Nahum, J. Frenz*, J. Chromatogr. **218**, 365 (1981).
[2] *Z. El Rassi, Cs. Horváth*, J. Chromatogr. **266**, 319 (1983).
[3] *H. Kalász, Cs. Horváth*, J. Chromatogr. **239**, 423 (1982).
[4] *Cs. Horváth, J. Frenz, Z. El Rassi*, J. Chromatogr. **255**, 273 (1983).
[5] *S. M. Cramer, Z. El Rassi, Cs. Horváth*, J. Chromatogr. **394**, 305 (1987).
[6] *H. Kalász, Cs. Horváth*, J. Chromatogr. **215**, 295 (1981).
[7] *A. Tiselius,* Arkiv Kemi, Mineralogi Geologi 16: 18,1 (1943).
[8] *Cs. Horváth*, in 'The Science of Chromatography', Journal of Chromatography Library Vol. 32, F. Brunner, ed., Elsevier, New York, 1985; pp. 179–203.
[9] *D. H. Leaback, H. K. Robinson*, Biochem. Biophys. Res. Commun. **67**, 248 (1975).
[10] *L. A. Sluylerman, O. Elgersma*, J. Chromatogr. **150**, 17 (1978).
[11] *L. A. Sluylerman, J. Wijdenes*, J. Chromatogr. **150**, 31 (1978).
[12] *A. R. Torres, S. C. Edberg, E. A. Peterson*, J. Chromatogr. **389**, 177 (1987).
[13] *A. R. Torres, B. E. Dunn, S. C. Edberg, E. A. Peterson*, J. Chromatogr. **316**, 125 (1984).
[14] *E. A. Peterson, A. R. Torres*, Methods Enzymol. **104**, 113 (1984).
[15] *A. R. Torres, E. A. Peterson*, Anal. Biochem. **98**, 353 (1979).
[16] *A. R. Torres, E. A. Peterson*, J. Biochem. Biophys. Methods, **1**, 349 (1979).
[17] *J. Frenz, Cs. Horváth*, AIChE J. **31**, 400 (1985).
[18] *K. Walton, C. Ricketts*, British J. Exp. Pathology **35**, 427 (1954).
[19] *H. Kramer, G. Windrum*, J. Histochem Cytochem **3**, 227 (1955).
[20] *S. N. Timasheff, R. Townend*, J. Am. Chem. Soc. **83**, 464 (1960).
[21] *U. K. Laemmli*, Nature **227**, 680 (1970).
[22] *H. A. McKenzie*, in 'Milk Proteins: Chemistry and Molecular Biology', H. A. McKenzie, ed., Academic Press, New York, 1971; pp. 257–330.
[23] *R. L. J. Lyster*, J. Dairy Res. **39**, 279 (1972).
[24] *S. Fredriksson*, Anal. Biochem. **50**, 575 (1972).
[25] *J. C. Giddings, G. C. Lin, M. N. Myers*, J. Liq. Chromatogr. **1**, 1 (1978).
[26] *M. Mathews*, Arch. Biochem. Biophys. **61**, 367 (1956).
[27] *Y. Kato, K. Nakamura, T. Hashimoto*, J. Chromatogr. **266**, 385 (1984).
[28] *C. T. Wehr*, J. Chromatogr. **418**, 27 (1987).

Received: Sep. 7, 1987
Accepted: Sep. 11, 1987
F

Sensitive and Selective Bioanalytical Assay for the Determination of Dobutamine in Rat Plasma Samples

H. Lingeman* / J. A. Haverhals / H. J. E. M. Reeuwijk / U. R. Tjaden / J. van der Greef

Division of Analytical Chemistry, Center for Bio-Pharmaceutical Sciences, Leiden University, P. O. Box 9502, 2300 RA Leiden, The Netherlands

Key Words

Column liquid chromatography
Fluorescence detection
Dobutamine
Plasma samples
Liquid-liquid extraction

Summary

Dobutamine is one of the synthetic catecholamines acting directly on β_1-receptors. For the analysis of dobutamine in rat plasma samples, a selective and sensitive liquid chromatographic method is described. After a simple liquid-liquid extraction, separation of the analyte was performed using a reversed-phase ion-pair system with an octyl modified silica column. The solute was detected by fluorescence detection, applying an excitation wavelength of 285nm and an emission wavelength of 313nm. The (im)possibilities of the application of the normally used assays for the isolation, concentration and quantitation of catecholamines are discussed. By the addition of a minimum amount of modifier to the mobile phase, the selectivity of the system was increased significantly. With this method the detection limit is 9ng/ml in 0.2ml plasma samples. The application of the method is shown in rat plasma samples by measuring the concentration-time curves to establish plasma level-effect relationships for this drug.

Introduction

Dobutamine (DBT) (Fig. 1) is a synthetic catecholamine, chemically related to dopamine, but possessing a bulky aromatic substituent on the amino function [1]. The analyte acts directly on the β_1-receptors and shows a strong inotropic and weak chronotropic effect. Contrary to dopamine, DBT does not effect the dopaminergic receptors in the renal vasculature, and therefore does not produce renal vasodilatation. Side effects of the solute, which are unpredictable in some cases, are hypertrophy and necrosis of the heart cell [2]. In order to investigate these effects, it is necessary to develop a rapid, selective and sensitive method for the routine analysis of DBT in plasma and myocard tissue homogenates.

Murphy et al. [3] described an enzymatic procedure utilizing ^{3}H-methyl-S-adenosylmethionine. In this procedure DBT is converted into the labelled methyl derivative in the presence of catechol-O-methyl transferase, but due to the limitations inherent in enzymatic assays, modern chromatographic methods are to be preferred.

Although some gas chromatographic assays have been described, these procedures will not be the method of first choice because the analyte must be derivatized, silylated or acetylated before quantitation can be performed [3]. On the contrary, liquid chromatographic (LC) methods can be executed without a derivatization procedure.

Because of the structural relationship between DBT and the endogenous catecholamines (e.g. adrenaline, dopamine, noradrenaline), the application of the chromatographic [4–6] and sample pretreatment [5, 7] procedures described for these catecholamines were first investigated.

Electrochemical detection of the analyte after reversed-phase (RP) LC analysis is described, but a gradient technique [8] is needed or the sensitivity of the method is not acceptable [9]. Fluorometric detection of DBT is also applied [10, 11], but the detection conditions are not chosen in the optimum (the maximum). The necessary sample pretreatment is executed either by a simple liquid-liquid extraction [10] or by a solid-phase isolation procedure, applying the relatively polar cyano cartridges [11], the apolar C_{18} cartridges [9] or aluminum oxide columns [8]. The actual analysis of the drug is performed on a RP

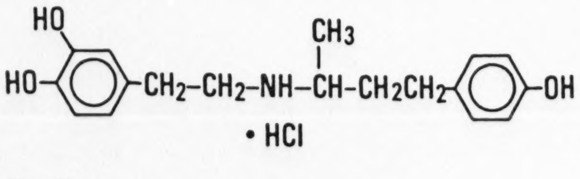

Fig. 1
Chemical structure of dobutamine

0009-5893/87 0886-05 $ 03.00/0

© 1987 Friedr. Vieweg & Sohn Verlagsgesellschaft mbH

octadecyl stationary phase. The corresponding mobile phase exists of an acidic aqueous methanol or acetonitrile buffer [8–11].

In this study a simple and relatively fast LC procedure is described for the analysis of DBT in plasma samples, without the need for derivatization or laborious sample pretreatment. Isolation of the analyte from the matrix was performed by a liquid-liquid extraction with ethyl acetate from an alkaline solution. DBT was subsequently analyzed with a RP-ion-pair (IP) octyl modified silica gel system and detected, selectively, by fluorometric detection. In this procedure no internal standard was applied to check the variability in the extraction efficiency.

Experimental

Materials

DBT hydrochloride was obtained from Eli Lilly (Amsterdam, The Netherlands). Methanol and all other organic solvents were of analytical reagent grade, obtained from Baker (Deventer, The Netherlands), and used without further purification. Ethyl acetate (Baker, reagent grade) was distilled from glass and saturated with water before use. Tributylphosphate [11], diphenylborate, ethanolamine and tetraoctylammonium chloride [7], aluminum oxide [5], Polygosil C_8 (40–63μm) and all other chemicals came from various sources and were used as received.

Throughout the study deionized water (Milli Q Water Purification System, Millipore, Bedford, MA, USA) was used. A solution of 5M dipotassium hydrogenphosphate (Merck, Darmstadt, FRG), and an 0.015M heptanesulfonic acid sodium salt solution (Janssen Chimica, Beerse, Belgium) adjusted to pH 2.0 with concentrated sulphuric acid, were applied for the extraction and chromatography of the analyte.

Chromatography

The LC system consisted of a reciprocating pump (Orlita, Gießen, FRG) equipped with a bourdon spring and a bourdon-type manometer. A Rheodyne (Berkeley, CA, USA) fixed volume (0.1ml) manual injector was used to load and inject the samples. The analytical column was a 100 × 3.0mm i.d. stainless steel column packed with 5μm spherical Nucleosil C_8 particles (Macherey & Nagel, Düren, FRG). Detection was accomplished, unless stated otherwise, by a fluorescence detector model SFM 23 (Kontron, Zurich, Switzerland), operating at excitation and emission wavelengths of 285nm and 313nm, respectively. In special cases a Perkin-Elmer LS-4 (Beaconsfield, UK) fluorescence detector was applied using the same conditions, but applying slit widths of 10nm. Data were plotted using a Shimadzu C-R3A chromatopack integrator (Kyoto, Japan).

The mobile phase consisted of 75% (v/v) of the 0.015M heptanesulfonate solution (pH 2.0) and 25% (v/v) of methanol. Chromatography was performed at ambient temperatures and a flow rate of 1.1ml/min was maintained.

Sample Preparation and Storage

Arterial rat plasma samples were prepared in heparinized polyethylene tubes and centrifuged immediately (4000g) for 3min at ambient temperature. The supernatant was directly mixed with 50μl of a solution of 60mg glutathione per ml of plasma and 0.5mg ethyleneglycol-N,N,N′,N′-tetraacetic acid (EGTA) per ml of plasma, frozen in ice, and stored at 250K in 1.5ml polypropylene tubes until the actual analysis took place.

Assay Procedures

Spiked blank plasma samples or aqueous solutions of 0.2ml were mixed with 65μl of an aqueous solution of 0.25M ethylenediaminetetraacetic acid (EDTA), 75μl of a solution of 0.25M L-ascorbic acid and 0.1ml of a 5M dipotassium hydrogenphosphate buffer. The defrosted rat plasma samples were mixed with 0.1ml of the phosphate buffer and 0.14ml water. The final pH of all of these solutions was about 9. The resulting solutions were extracted twice with 3.0ml of the distilled ethyl acetate. The combined organic layers were evaporated to dryness under a stream of dry nitrogen. The residues were dissolved in 0.2ml of the mobile phase, and 50μl portions were subsequently injected into the chromatographic system.

Results and Discussion

Degradation and Metabolism

The primary non-conjugated metabolite of DBT is the 3-methoxy derivative, which is produced by a catechol-O-methyl-transferase and which is very rapidly conjugated with glucuronic acid [3]. Because the half-life time of the solute in plasma samples is less than 5min, it is necessary that the samples are stored at 250K until the actual analysis takes place. Under these conditions the samples could be stored for several weeks.

The stability of DBT in alkaline solutions is limited. The half-life of the analyte is 30–45min under such conditions [1]. Therefore, chromatography should be performed in acidic eluents, as the solute is relatively stable below pH 5 [5].

EDTA or EGTA were added to the plasma samples in order to complexate metal ions, and ascorbic acid or glutathione were added to prevent oxidation of the analyte. No significant differences were found between the addition of EDTA or EGTA, or between ascorbic acid or glutathione.

Sample Pretreatment

To avoid time-consuming and laborious sample pretreatment procedures, two solid-phase isolations were investigated for their ability to selectively clean-up and concentrate the sample in one step. The reported procedures applying C_{18} [9] or cyano [11] cartridges were not the methods of first choice because of their limited selectivity or low recoveries.

To eliminate these limitations, the use of home-made Polygosil C_8 columns was investigated. The columns were packed in teflon tubing, applying about 300mg of the Polygosil material for each column. The stationary phase was wetted with methanol and conditioned with water. Subsequently, the sample was adjusted to the column, washed with water and eluted with methanol. The C_8 material was chosen because its polarity was between the polarities of the cyano and the C-18 columns. However, the recovery of this method was very disappointing in comparison with the reported systems [9, 11].

Another selective sample pretreatment procedure for catecholamines is described by Anton and Sayre [12]. The solutes are adsorbed at a relatively high pH (pH 8.6) onto aluminum oxide and are desorbed at a relatively low pH (pH 3.0). The recovery for the endogenous catecholamines is over 95% [5], but for DBT the recovery was only 63.1 ± 10.9% (n = 8) for plasma samples spiked with 500ng/ml DBT. This low recovery is probably due to steric hindrance of the bulky substituent on the nitrogen.

One of the liquid-liquid extractions described for endogenous catecholamines is based on complexation (in alkaline solution) of diphenylborate with the catechol function, followed by an IP extraction [7]. The hydrophobic diphenylborate forms a negatively charged stable complex with the analyte, which can be extracted, with heptane, as an IP, using tetraoctylammonium as the counter-ion. The reproducibility of this procedure, for DBT, was good. The recovery was, in contrast to the endogenous catecholamines, very low. After the analysis of 6 plasma samples spiked with 500ng/ml DBT, the calculated recovery was 14.9% ± 2.1%.

Since the solid-phase isolations and the diphenylborate system were not successful, a liquid-liquid extraction was investigated. Due to the amphoteric character of DBT, liquid-liquid extractions are only possible if a suitable counter-ion is added to the plasma sample. In this study, extraction of the solute was performed at a pH of 9, with the described phosphate buffer. However, the use of a pH 9 borate buffer or a 1 M bicarbonate buffer resulted in very low recoveries [10]. The explanation is probably that the bicarbonate and the borate anions do not complex sufficiently with the analyte to allow IP extraction of DBT.

Furthermore, the extraction of the solute is only possible with relatively polar solvents, such as ethyl acetate and diethyl ether. The use of less polar solvents (e.g. dichloromethane, chloroform, toluene, hexane) resulted in a dramatically decreased extraction efficiency. However, pre-extraction of the plasma samples with hexane was a suitable method to remove some late-eluting endogenous matrix components in the chromatogram, which shortens the total analysis time.

Chromatography

For the analysis of DBT, different chromatographic systems have been described. Using the more polar cyano columns in the RP mode, the capacity ratios (k′) are markedly increased in comparison with the apolar C_{18} modified systems. However, because of the limited selectivity on the latter systems, in this study C_8 modified silica gel systems were applied.

The possibility of using C_8 columns in the RP mode was first investigated. The mobile phase consisted of a 0.05M dipotassium phosphate buffer (pH 3.0), containing 10% (v/v) or 15% (v/v) of methanol. The k′ values for DBT in these systems were 8.71 and 5.53, respectively. The endogenous catecholamines were not retained at all in these systems. However, the selectivity was not sufficient if plasma samples were analyzed; some endogenous interferences co-eluted with the analyte.

For the analysis of endogenous catecholamines, an RP-IP system is described [13]. In this system an organic liquid, tributylphosphate, is adsorbed onto an C_8 modified silica gel column. Protonated amines, including DBT, are chromatographed as an IP on this system, consisting of an acidic aqueous buffer (saturated with tributylphosphate) and containing the perchlorate anion as the IP reagent [12]. The k′ values of adrenaline and dopamine varied between 1.80 and 4.22 when a concentration of 0.15M perchloric acid was applied. However, the k′ of DBT in this system was over 25. Even by decreasing the perchlorate concentration, by lowering the pH, by increasing the temperature, or by adding methanol, no acceptable k′ value for the analyte could be achieved. An explanation for the different behavior of DBT is the bulky substituent on the nitrogen atom.

The final chromatographic system was a combination of the two described methods. Without the addition of an IP reagent to the mobile phase, some endogenous co-eluting peaks with DBT were observed. Therefore, an acidic mobile phase was applied, and by using a counter-ion, it was possible to retain the analyte selectively. Because of the relative hydrophobic character of the analyte, counter-ions such as chloride, perchlorate, phosphate, sulphate, heptanesulfonate, and octanesulfonate were investigated (Table I). The use of the hydrophobic counter-ion heptanesulfonate gave the best compromise between the required selectivity and the total analysis time. By varying the concentration of the counter-ion, almost any desirable k′ value for DBT could be achieved. Interferences from endogenous compounds were further diminished in this system by optimizing the concentration of the IP reagent and the concentration of the modifier in the eluent, since the majority of the interfering compounds are not retained by an IP

Table I. Capacity ratios of dobutamine in reversed-phase ion-pair systems.

Ion-Pairing Reagent and Concentration	Capacity Ratio
0.05 M Sulphuric acid	6.72
0.05 M Phosphoric acid	7.53
0.05 M Perchloric acid	9.79
0.005M Heptanesulfonic acid	15.8
0.005M Octanesulfonic acid	> 25

Stationary phase: Nucleosil C_8 (5µm particles). Mobile phase: 75% (v/v) 0.015M heptanesulfonic acid (pH 2.0) and 25% methanol mechanism. The selectivity of the system could not be improved by using acetonitrile instead of methanol in the mobile phase.

The combination of pH 9 for the sample pretreatment and pH 2 for the chromatographic separation offers a high degree of selectivity in the developed procedure.

In the developed procedure the following eluting solvent was used: a mixture of 0.015M heptanesulfonate in a phosphate buffer of pH 2.0 containing 25% (v/v) of methanol. As can be seen in Fig. 2, the addition of 25% of methanol was sufficient to elute the interfering compounds at the beginning of the chromatogram. In the chromatograms shown, the retention time of DBT is about 9min. But by increasing the concentration of methanol the retention time could be shortened, which was very helpful when other matrices (e.g. myocard homogenates, urine) were studied.

Analytical Variables

Linearity. In order to investigate the linearity of the procedure, blank rat plasma samples were spiked with different amounts of DBT to obtain concentrations of 10, 50, 100, 200, 300, 400, 500 and 600ng/ml. The calibration curves showed good linearity; e.g. $y = 0.024\ (\pm 0.001)\ x + 0.004\ (\pm 0.175)$ $(r = 0.998)$ was the equation for the calibration line after analyzing 16 samples, where y and x are the peak height of the DBT peak and the DBT concentration (ng/ml), respectively. The numbers in parentheses are the standard deviations and the correlation coefficient, respectively. The linear dynamic range of this procedure was three decades, but in the concentration range of 500ng/ml to 1000ng/ml, it was necessary to dissolve the residue in 1ml of the eluent instead of in 0.2ml of the mobile phase, due to solubility problems of the analyte.

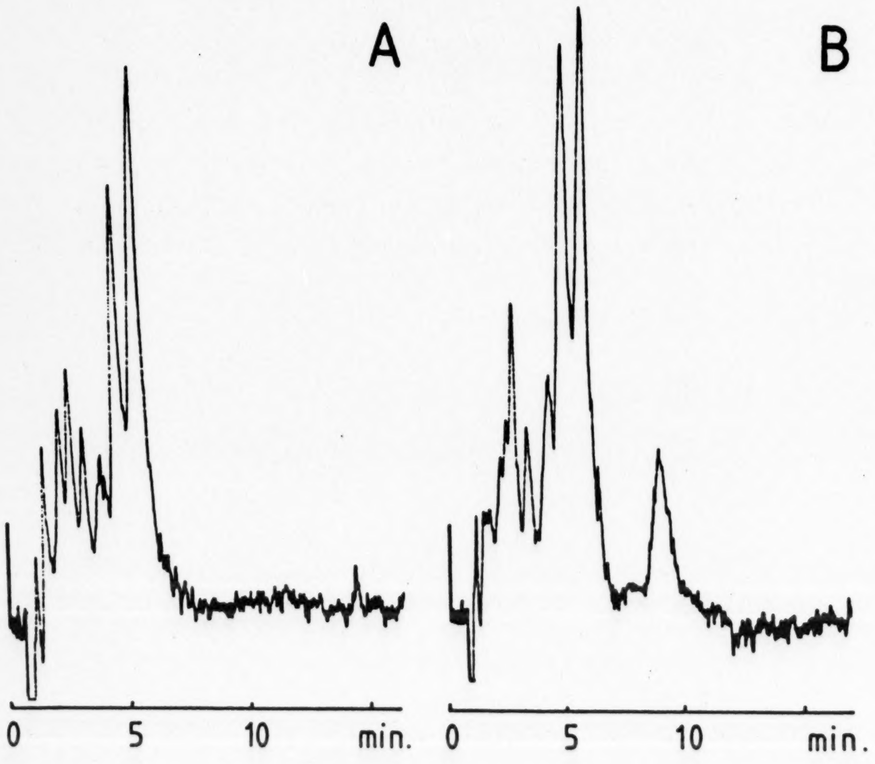

Fig. 2

Chromatograms of extracted plasma samples of 200μl (A, blank; B, plasma spiked with 150ng/ml dobutamine)

Precision. The within-run (within-day) precision was established for 10 samples at a concentration of 500ng/ml DBT in rat plasma samples. The 10 samples were analyzed within a period of 24 hours. The within-day standard deviation was 3.4%.

The described internal standards [9–11] for the analysis of DBT could not be used because the differences in k' values of these compounds and the analyte itself were too large in the developed system. Furthermore, the use of an internal standard did not increase the precision of the method significantly, but the total analysis time almost doubled when the described internal standards were applied.

Recovery. The absolute recovery of the liquid-liquid extraction procedure was 81.1% with a standard deviation of 4.9% after the analysis of 12 samples spiked with 50ng/ml of the analyte and comparison of the peak height with the peak height obtained after the analysis of non-extracted samples. Furthermore, no indications were found that the recovery was concentration-dependent.

Sensitivity and determination limit. The emission spectrum of DBT indicated a fluorescence maximum near 313nm. The maximum excitation wavelength is 285nm. For an optimal detection it is necessary to adjust the fluorescence detector to these wavelengths. Therefore, the method is more sensitive and selective in comparison with the study of McKennon and Kates [10], in which excitation is performed at 195nm. The influence of the pH on the fluorescence sensitivity of DBT was not investigated because of the limited stability of the analyte in alkaline solutions.

The minimum amount of DBT that could be analyzed in aqueous samples with a signal to noise ratio of 3 was 2.3ng/ml. The corresponding determination limit in 0.2ml plasma samples was 14.5ng/ml. However, whenever the Perkin Elmer LS-4 detection system was applied instead of the described Kontron fluorescence detector, the determination limit could be lowered to 9.1ng/ml. This determination limit could even be lowered to about 1ng/ml through the combination of a larger sample volume, a larger injection loop and a smaller final dilution volume.

Interferences

Several drugs, such as adrenaline, noradrenaline, dopamine, epinine, 5,5-dihydroxybenzylamine (the internal standard for the endogenous catecholamines), caffeine, and buphenine, were screened for their possible interference with the described procedure, but none of the listed compounds interfered with the DBT analysis. As can be seen in the chromatogram of a blank plasma sample (Fig. 2), no interfering matrix peaks in this concentration range were eluted with the same k' value as DBT.

Application of Chromatographic Procedure

The described procedure was applied for the analysis of DBT in rat plasma samples after the intravenous administration of a 0.75mg bolus injection in a rat weighing 350g. Because of the short plasma half-life of the solute, intravenous administration is the most important dosage form for the analyte. The results are shown in Fig. 3. The DBT

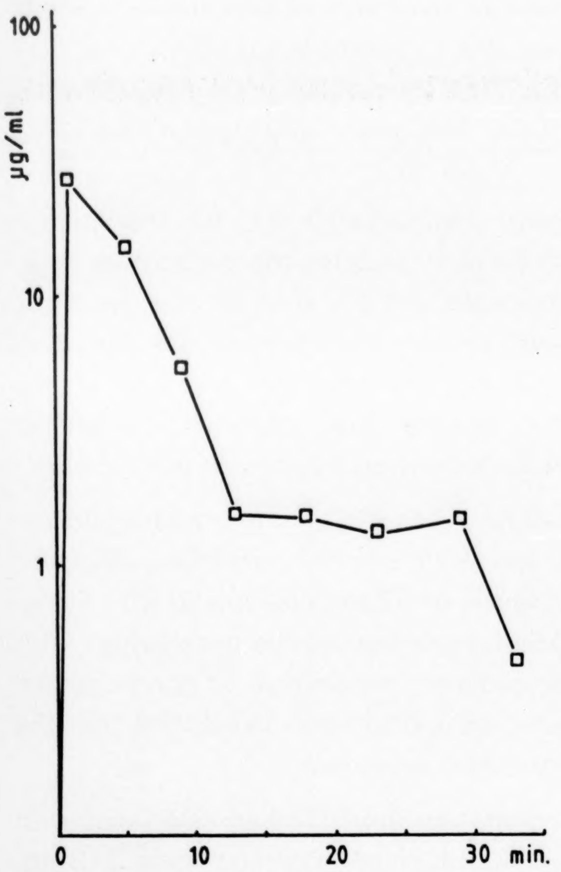

Fig. 3

Concentration-time curve after intravenous injection of 0.75 mg of dobutamine

concentration in the concentration-time curve could be calculated with the following equation:

$$\text{concentration DBT } (\mu g/ml) = 52.271 \times e^{-0.264t}.$$

The half-life time, calculated from the first 5 data points (0–15 min), was 2.63 min. The concentration of the solute after 35 min was about 0.44 µg/ml, indicating that the sensitivity of the method was sufficient to allow pharmacokinetic experiments. However, if 7.5 mg of the analyte was administered, the half-life time was shortened to 1.71 min, probably due to a different distribution of the analyte in the tissues.

Acknowledgements

The authors are indebted to the following persons for the execution of the practical analytical research: J. Bouman, C. M. van der Meulen and to L. Hollaar, A. van der Laar and A. C. M. Zoet (Academical Hospital, Leiden, The Netherlands) for the pharmacokinetic experiments.

References

[1] *R. H. Bishara, H. B. Long*, Analytical Profiles of Drug Substances, **8**, 139 (1979).
[2] *M. Brandl, T. Pasch, H.-D. Kamp, J. Grimm*, Int. Care Med., **9**, 61 (1983).
[3] *P. J. Murphy, T. L. Williams, D. L. Kau*, J. Pharmacol. Exp. Ther., **199**, 423 (1976).
[4] *H. Lingeman, W. J. M. Underberg, A. Takadate, A. Hulshoff*, J. Liq. Chromatogr., **8**, 789 (1985).
[5] *H. J. E. M. Reeuwijk, H. Lingeman, J. de Jong, U. R. Tjaden, J. van der Greef*, Analyst, in press.
[6] *M. Goto, G. Zou, D. Ishii*, J. Chromatogr., **275**, 271 (1983).
[7] *F. Smedes, J. C. Kraak, H. Poppe*, J. Chromatogr., **231**, 25 (1982).
[8] *P. H. Schwartz, S. W. Hutchins, M. H. Cheng, E. L. Arcinue, A. I. Lipsey*, Clin. Chem., **30**, 1031 (1984).
[9] *G. E. Hardee, J. W. Lai*, Anal. Lett., **16**, 69 (1983).
[10] *D. W. McKennon, R. E. Kates*, J. Pharm. Sci., **67**, 1756 (1978).
[11] *R. Knoll, M. Brandl*, J. Chromatogr., **345**, 425 (1985).
[12] *A. H. Anton, D. F. A. Sayre*, J. Pharmacol. Exp. Ther., **138**, 360 (1962).
[13] *H. J. L. Janssen, U. R. Tjaden, H. J. de Jong, K.-G. Wahlund*, J. Chromatogr., **202**, 223 (1980).

Received: July 22, 1987
Accepted: Aug. 5, 1987
F

Classification of Chromatographic Data Using Multidimensional Polynomials

M. E. Cohen*

Department of Mathematics, California State University Fresno, Fresno, CA, 93740, USA

D. L. Hudson

Section on Medical Information Science, University of California San Francisco,
2615 East Clinton Avenue, Fresno, CA 93703, USA

Key Words

Ascitic fluid
Hypersurfaces
Liver disorders
New orthogonal polynomials
Pattern recognition

Summary

A pattern recognition methodology has been developed for analysis of chromatographic data. The method uses a new class of multidimensional orthogonal polynomials developed by Cohen in conjunction with a supervised learning technique. The method is applicable to any chromatographic data for which classification into two or more categories is desired. The algorithm analyzes both elution times and peak areas. An application is shown for the analysis of organic acids in ascitic fluid obtained from patients with liver disorders. Classification of these patients for presence or absence of bacterial infection shows over ninety percent correct classification.

Introduction

Automated pattern recognition for analysis of chromatograms has been a topic of continuing interest. Albano et al. [1] and Wold and Johansson [2] approached this problem using a technique, denoted the SIMCA method, which involves fitting a hyerplane to each class. This method has been used in a number of applications [3, 4]. Other pattern recognition techniques also exist. Surveys of these techniques show a wide variety of applications [5, 6]. Other chemical applications of pattern recognition include work by Coomans et al. [7, 8]. These techniques also have wide applications in the field of medicine [9–12].

In previous work of the authors [13], a new pattern recognition technique was applied to chromatographic analysis. Unlike the SIMCA method, this technique does not restrict itself to hyperplanes in n-dimensional space, but rather utilizes non-linear surfaces for category division using non-statistical methods [14–16]. In this method, a new class of one-dimensional orthogonal polynomials developed by Cohen was utilized. From these one-dimensional expressions functions of higher dimensionality were generated by taking advantage of multiplicative properties of orthogonal functions. In this paper, a new multidimensional orthogonal function developed by Cohen is utilized in a pattern recognition algorithm. This new function allows direct calculation of multidimensional dividing hypersurfaces, thus significantly reducing computational complexity, and providing an exact solution rather than an approximation. In addition, the data were processed to account for variability among runs. Due to these variations, the actual time of occurrence for a particular peak may fluctuate, and the peak area may also vary. In order to account for this fuzziness in the data, short time intervals were considered which were centered at the most likely occurrence for each particular peak. The areas were then grouped into three categories, since the actual concentrations were imprecise.

In this paper, the new method utilizing the multidimensional orthogonal function, as well as methods for incorporation of fuzzy data, is illustrated on the same application as the one-dimensional case: analysis of chromatograms obtained from ascitic fluid withdrawn from patients with liver disorders.

Ascitic fluid often accumulates in the abdomen of patients with liver disorders. A spontaneous infection may occur in these patients, a condition know as spontaneous bacterial peritonitis (SBP). Previous studies have shown that the pH of the ascitic fluid is useful in diagnosing this condition at an early stage, with a lowered pH indicative of the presence of the condition [17, 18]. A study was undertaken using high performance liquid chromatography (HPLC) as a means for determining the organic acids responsible for the lowered pH.

0009-5893/87 0891-04 $03.00/0

© 1987 Friedr. Vieweg & Sohn Verlagsgesellschaft mbH

The pattern classification method utilizes a supervised learning approach, consisting of a number of phases: feature extraction, iterative development of a separating hypersurface, and testing of the resulting hypersurface for accuracy. The method is applicable to the analysis of chromatographic data where combinations of either the occurrence of a peak at certain retention times or the magnitude of the peak is of importance in classifying the chromatogram into two or more categories.

Methodology

A sample of ascites fluid was withdrawn by paracentesis from the abdomen of a patient, usually in the course of his treatment. The ascitic fluid was routinely cultures to ascertain the presence of infection, and if positive, the identity of the pathogen. A portion of the ascites fluid was frozen for future study and served as the source of the samples analyzed in this study [13].

Prior to attempting to determine the organic acid profile of a particular sample using high-performance liquid chromatography (HPLC), it was necessary to isolate the acids from other potentially interfering constituents typically present in ascitic fluid. The following extraction procedure was developed for this project:

To 1.0 ml of sample was added 0.2 ml of saturated K_2HPO_4 to achieve a slightly basic pH and the resulting solution thoroughly mixed with 3 ml of an organic solvent consisting of tert. butyl ether-isopropyl alcohol (95 : 5). Following centrifugation, the overlying organic layer containing many of the interfering constituents was suctioned off and discarded. The pH of the aqueous phase was then lowered by the addition of 0.2 ml of 18 N H_2SO_4 and the undissociated organic acids extracted by thorough agitation into 5.0 ml of the tert. butyl ether-isopropyl alcohol solvent. Following centrifugation to enhance complete separation of the two phases, 4.5 ml of the overlying organic layer was pipetted off and retained; the remainder, as well as the aqueous phase, were discarded. 2.0 ml of 0.1 M NaOH was added to the organic phase and the organic acids back-extracted into the aqueous phase via thorough mixing. Following centrifugation, the overlying organic acids in the aqueous phase, the water was removed via freeze-drying under vacuum. Finally, an aqueous solution of the organic acids was reconstituted by dissolving the freeze-dried residue in 0.5 ml of H_2O and 0l1 ml of 2 N H_2SO_4. A water blank was simultaneously carried through the extraction procedure so that any artifacts introduced by the extraction could subsequently be identified and eliminated from consideration.

Separation of the organic acids in the extracted and reconstituted sample of ascites fluid was performed with HPLC, primarily via the ion-exclusion mode, on a 220 X 4.6 mm Brownlee Labs, Inc. column, packed with Polypore H, a 10-micron, macroporous styrene divinyl benzene resin. The column was maintained at a uniform temperature of 39 °C. The mobile phase or eluent consisted of 0.01 M H_2SO_4, prepared from deionized water, deaerated and filtered through a 0.45 μm filter before use. Eluent was delivered to the column by a Consta Metric III metering pump from Laboratory Data Control at a rate of 0.6 ml per minute. Samples were introduced with a 50 μl syringe, via a Rheodyne injection valve, into a 20 μl loop in the eluent flow. Effluent from the HPLC column passed into the flow cell of a Laboratory Data Control Spectro Monitor III spectrophotometer, where the organic acids were detected in the UV at the carboxyl absorption band of 210 nm. Detector output was recorded on a SpectraPhysics SP4270 Chromatography Integrator, which subsequently analyzed the individual organic acid peaks for retention time and area. The water blank was also subjected to HPLC and the areas of the peaks that appeared were subtracted from the areas of the corresponding peaks in the sample chromatogram.

It was presumed that an organic acid could be identified by the retention time of its chromatographic peak. Individual standard solutions of known concentrations of biologically important short-chained mono-, di- and tri-protic organic acids were prepared and the retention time of each determined by HPLC under the aforementioned experimental conditions. Retention times for the following organic acids were identified in this manner: oxalic, oxaloacetic, citric, iso-citric, -hetoglutaric, tartaric, pyruvic, ascorbic, malic, succinic, lactic, 3-hydroxy-butyric, formic, glutaric, acetic, fumaric, propionic, iso-butyric, n-butyric, 3-methyl-butyric, 2-methyl-butyric, valeric and caproic acids.

Ascitic fluid was analyzed by the above method. In addition, some of the fluid was cultured for the presence of bacteria for 72 h. Chromatographic analysis and pattern recognition took approximately 3 h.

Although the automatically integrated chromatogram contained continuous analog data, two aspects of these time series data are of significance: 1) the area under each peak; 2) the elution time of each peak. In each chromatogram as many as 47 separate areas and elution times may be present. Thus there are potentially 94 distinct elements which are of significance for analysis of the chromatogram.

Once the data base was completed, pattern classification was begun. In the first phase, feature extraction, parameters were identified which could prove useful in separating data into categories. In the case of the ascitic fluid, the objective was to divide the samples into two categories: those from patients with SBP, and those from patients without SBP, by analyzing the pattern of organic acids which occurred in the patients with liver disorders for whom prompt diagnosis is crucial. Peaks were identified by establishing time intervals, denoted buckets, which consisted of the most likely occurrence of a peak ± a fixed interval adjustment. The 47 possible peaks were treated both qualitatively as the presence or absence of a peak at a designated time, and quantitatively as the area under each peak. Three categories were used for peak areas: little or no acid (less than 100 units), moderate amount of acid (between 100 units and the mean value for all samples for that peak), or a large amount of acid (more than the mean value).

Available data of known classification were divided into two groups: a training set and a test set. Actual diagnosis was made by bacterial culture, a process which takes 72 hours or more. The training set was then used, in conjunction with the othogonal function, to obtain weighting factors for each feature. The data set contained 45 samples, of which 25 were positive for SBP. A training set of 20 was selected, with 10 positives. A separating hypersurface was then obtained using the following method.

The classification method is based on the potential function approach to decision function generation. The multivariate potential function is defined as

$$P(\bar{x}, \bar{y}) = \sum_{i=1}^{\infty} \lambda_i^2 f_i(\bar{x})\, f_i(\bar{y})$$

where $f_i(\bar{x})$ are orthonormal functions, $\bar{x}, \bar{y}$ are n-dimensional feature vectors, and λ_i, i 1,2 ... are real numbers. The equation which represents the decision hypersurface is then

$$D(\bar{x}) = \sum_{i=1}^{\infty} c_i f_i(\bar{x})$$

where c_i, i = 1,2 ... are unknown and determined iteratively from the feature vectors in the training set. For a two-class problem, the decision is made according to

$D(x) > 0$ class 1
$D(x) < 0$ class 2
$D(x) = 0$ indeterminant

In practice, the orthonormal functions $f_i(\bar{x})$ may be replaced by orthogonal functions, since all comparisons are made to zero, so all equations may be considered to be multiplied by the normalizing constant.

The orthogonal function to be used is the new multidimensional Cohen orthogonal polynomial

$$C_n(x_1, x_2, \ldots x_\ell) =$$

$$\frac{\ell!}{n!\,(\ell-n)!} + \sum_{k=1}^{n} \frac{(-1)^k (\ell-k)!}{(n-k)!\,(\ell-n)!} \cdot \sum_{i_k=k}^{\ell} \; \sum_{i_{k-1}=k-1}^{i_k-1} \cdots \sum_{i_2=2}^{i_2-1}$$

$$\prod_{p=1}^{k} x_i^{a(n,i_p)} \frac{[a(n, ip) + v_{ip}]}{v_{i_p}}$$

$$\int_0^1 \int_0^1 \cdots \int_0^1 C_n C_m\, x_1^{v_1-1} x_2^{v_1-1} \ldots x_\ell^{v_\ell-1} \ldots dx_1 \ldots dx_\ell = 0 \quad n \neq m$$
$$= A \quad n = m$$

where ℓ is the dimensionality of the data, v_i, i = 1, ..., ℓ are parameters which may be arbitrarily selected and A is the normalization constant. v_i, i = 1, ... ℓ are assigned values corresponding to the components of the first feature vector.

In this paper, we make the assumption $a(n, i_p) = 1$. $P(\bar{x}, \bar{x}_k)$ is then defined by

$$P(\bar{x}, \bar{x}_k) = \sum_{i=1}^{\infty} \theta_i(\bar{x})\, \theta_i(\bar{x}_k)$$

where $\theta_i(\bar{x})$ are the components of the Cohen polynomials, which themselves form an orthogonal set

$$\int_{-1}^{1} \cdots \int_{-1}^{1} \theta_n(x_i \ldots, x_\ell)\, \theta_m(x_1, \ldots, x_\ell)\, dx_1 \ldots dx_\ell \quad \begin{array}{l} = 0 \quad n \neq m \\ = B \quad n = m \end{array}$$

where B is the normalization constant.

Once the hypersurface was obtained, it was tested for accuracy on the remaining data which made up the test set. Results are summarized below.

Results

The results for the multidimensional pattern classification are shown in Table I. The column denoted $C_n(x)$ is the multidimensional Cohen polynomial. Note that only two samples were misclassified, one positive for presence of SBP, and the other negative. As a means of comparison, the results for the single-dimensional Cohen polynomial are shown in the column $g_n^{1,2}(x)$. In addition, nonlinear statistical discriminant analysis was run. These results are in the third column. Table II shows specificity, sensitivity, and accuracy. The equations for these measures are:

Sensitivity:	(Total classified positive)/(Total true positives)
Specificity:	(Total classified negative)/(Total true negatives)
Accuracy:	(Total correctly classified)/(Total)

These measurements are important in medical studies in that sensitivity gives a measure of false negatives, while specificity measure false positives. The equation of the hypersurface is:

$$\begin{aligned} D_C = & -76 + 84x_1 - 8x_3 - 34x_4 - 15x_5 + 29x_1x_2 \\ & + 27x_1x_3 + 16x_1x_4 + 23x_1x_5 + 5x_2x_3 + 5x_2x_4 \\ & + 2x_2x_5 + 6x_3x_4 + 5x_3x_5 + 4x_4x_5 \end{aligned}$$

where

x_1: concentration of lactic acid
x_2: degree of presence at time x (22)
x_3: degree of presence at time x (32)
x_4: degree of presence at time x (58)
x_5: degree of presence at time x (74)

Table I: Number of misclassified samples

	$C_n(x)$*	$g_n^{1,2}(x)$**	nonlinear discriminant analysis***	# in training Set	Total #
Class 1 (positive)	1	2	4	10	25
Class 2 (negative)	1	1	2	10	20
Overall	2	3	6	20	45

*Multidimensional Cohen polynomial
**Special case of one-dimensional Cohen polynomial
***Run using BMDP statistical package

Table II: Sensitivity, Specificity, and Accuracy

	$C_n(x)$	$g_n^{1,2}(x)$	Nonlinear discriminant analysis
Sensitivity	96	92	84
Specificity	95	95	90
Accuracy	95.5	93.3	86.7

The new method is seen to be extremely accurate, with high levels of both sensitivity and specificity. The techniques described here can be used on any chromatographic data which requires classification of results into two or more categories. The use of flexible time intervals and categoric grouping of peak areas also broadens the applicability of the technique. Work is continuing in applying this methodology to new data sets.

References

[1] *C. Albano, W. Dunn, U. Edland, E. Johansson, B. Worden, M. Sjostrom, S. Wold,* Analytica Chimica Acta, **103**, 429 (1978).

[2] *S. Wold, E. Johansson,* Analytica Chimica Acta, **133**, 251 (1981).

[3] *G. Blomquist, E. Johansson, B. Soderstrom, S. Wold,* J. Chromatog., **173**, 19 (1979).

[4] *E. Jellum, I. Bjornson, R. Nesbakken, E. Johannson, S. Wold,* J. Chromatog., **217**, 231 (1981).

[5] *E. A. Patrick,* Syst., Man, Cybern. Rev., **6**, 4 (1977).

[6] *E. H. Shortliffe, B. G. Buchanan, E. A. Feigenbaum,* Proc. IEEE, **67**, 1207 (1979).

[7] *D. Coomans, I. Boeckaert, A. Tassin, et al.,* Anal. Chem. Acta CTO, **133**, 215 (1981).

[8] *D. Coomans, I. Boeckaert, A. Tassin, et al.,* Anal. Chem. Acta, **134**, 139 (1982).

[9] *M. Ben-Bassat, R. W. Carlson, et al.,* IEEE Trans. on Pattern Analysis and Machine Intelligence, PAMI-**2**, 1481 (1980).

[10] *M. Ben-Bassat, D. B. Campbell, et al.,* IEEE Trans of Pattern Analysis and Machine Intelligence, PAMI-**5**, 225 (1983).

[11] *E. A. Patrick,* System., Man, Cybern. Rev., **6**, 4 (1977).

[12] *E. A. Patrick, F. Stelmock, L. Shen,* IEEE Trans. on Systems, Man, and Cybernetics, **SMC4**, 1 (1974).

[13] *M. E. Cohen, D. L. Hudson,* J. Chrom., **384**, 145 (1987).

[14] *M. E. Cohen, D. L. Hudson, C. P. Deedwania,* Use of pattern recognition techniques to classify exercise testing data, Park City, Utah, September 1984, IEEE, New York, 1984.

[15] *M. E. Cohen, D. L. Hudson, P. C. Deedwania, N. Gitlin,* Pattern recognition using new orthogonal functions to classify medical data, Proc., Microcomputers in Medicine, New York, 1984, ISMM, New York, 1984.

[16] *M. E. Cohen, D. L. Hudson,* in: *M. Gupta* (editor), Approximate Reasoning in Expert Systems, North Holland, 1985, p. 435.

[17] *M. E. Cohen, D. L. Hudson, N. Gitlin,* Pattern classification using a new orthogonal function for recognition of SBP, Proc., American Association of Medical Systems and Informatics, San Francisco, May, 1984, IEEE, New York, 1984.

[18] *D. L. Hudson, M. E. Cohen, N. Gitlin,* Pattern classification of patients with spontaneous bacterial peritonitis using new orthogonal functions with extensions to higher dimensions, Proc., Symposium on Computer Applications in Medical Care, Washington, D. C., November, 1984, IEEE, New York, 1984.

Received: June 30, 1987
Accepted: Aug. 27, 1987
F

Quantitative Determination of Terbutaline in Human Plasma After Administration of Bambuterol Using Coupled Columns and Electrochemical Detection

B.-M. Kennedy/A. Blomgren/L.-E. Edholm/C. Roos*

Pharmacokinetics Laboratory (Bioanalysis), AB Draco[1], P.O. Box 34, S-221 00 Lund, Sweden.

Key Words

Bambuterol
Terbutaline
Coupled columns
Human plasma
Electrochemical detection

Summary

A method is presented for quantitative determination of terbutaline after administration of its prodrug Bambuterol. Terbutaline is extracted from plasma by liquid-solid extraction on small C_{18}-cartridges. The extract is then analysed by coupled column liquid chromatography with amperometric detection.

To inhibit the esterase catalyzed hydrolysis of bambuterol to terbutaline an analogue of bambuterol is added to the plasma sampling tubes.

The within-day variation on spiked samples were 2.1 % and 2.4 % at 8.0 and 40.0 nmol/L respectively. The between-day variation on spiked samples (8.0 nmol/L) was 3.6 % and on authentic samples 5.9 % at the 11 nmol/L level.

The absolute recovery was in the range 83–94 % for terbutaline and the internal standard. The limit of quantitation was set at 4.0 nmol/L (C_v = 3.4 %, n = 46).

Introduction

Bambuterol (Fig. 1a) is a carbamate prodrug of terbutaline (Fig. 1b) (Bricanyl®), a β_2-receptoragonist widely used in the treatment of asthma. Bambuterol has been developed with the aim of producing a prodrug of terbutaline with prolonged duration of effect and lower incidence of side effects. For the pharmacokinetic evaluation of terbutaline generated in vivo from bambuterol it is necessary to measure plasma concentrations down to about 4 nmol/L.

In early pharmacokinetic studies of bambuterol terbutaline was determined with a method based on GC-MS [1]. However, irreproducible results were obtained.

Parallel investigations on the metabolic fate of bambuterol showed that a number of metabolites were formed [2]. It is likely that some of these metabolites were transformed to terbutaline during the derivatization step and/or the GC-MS analysis [1].

It has previously been shown that a method based on coupled column liquid chromatography with amperometric detection, can be used for quantitation of terbutaline in

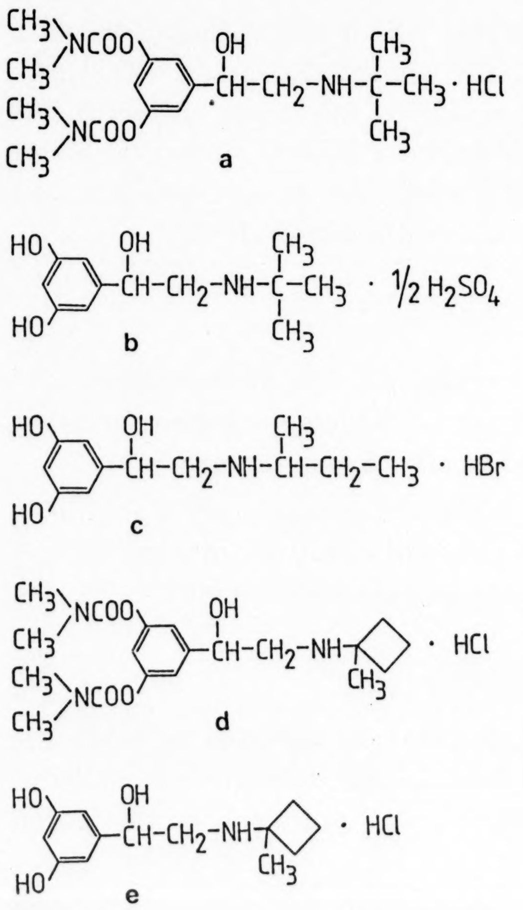

Fig. 1

Structures of bambuterol (a), terbutaline (b), the internal standard, KWD 2030 (c), the inhibitor, D2456 (d) and the hydrolysis product of the inhibitor, D2136 (e).

---

[1] Subsidiary of AB Astra.

0009-5893/87 0895-05 $03.00/0

© 1987 Friedr. Vieweg & Sohn Verlagsgesellschaft mbH

plasma after administration of Bricanyl® [3]. This method provides mild conditions during sample work-up and chromatography. And as different modes of chromatography (reversed-phase, ion-exchange) are combined with a heart-cut technique [4] and amperometric detection, excellent selectivity is obtained. In this paper, a modification of this method is described for quantitative analysis of terbutaline after administration of bambuterol. The method has now been used in routine work for a couple of years.

As bambuterol and some of its metabolites are hydrolysed by blood enzymes, special care has to be taken to inhibit further hydrolysis to terbutaline in a drawn blood sample. This is done by adding an esterase inhibitor of a similar structure (Fig. 1d) to bambuterol to the tubes used for collection of the blood samples.

Experimental

Chemicals

Bambuterol (5-[2-(tert-butylamino)-1-hydroxyethyl]-m-phenylene bis (dimethylcarbamate)hydrochloride), terbutaline (5-[2-(tert-butylamino)-1-hydroxyethyl]-m phenylenediol sulphate), the internal standard (see Fig. 1c). (5-[2-(sec-butylamino)-1-hydroxyethyl]-m-phenylenediol nydrobromide) and the inhibitor (D2456) (5-[2-(1-methylcyclobutylamino)-1-hydroxyethyl]-m-phenylene bis (dimethylcarbamate) hydrochloride) were of internal supply.

Acetonitrile and methanol were HPLC-grade (Rathburn Chemicals, Walkerburn, Great Britain), ethanol (absolute, 99.5%, Kemetylprodukter AB, Bromma, Sweden), glutathione (Sigma Chemical Company, St. Louis, MO, USA), sodium hydroxide p.a. (EKA AB, Surte, Sweden). All water used was purified with a Milli Q system (Millipore Corp., Bedford, Mass., USA). All other chemicals were of analytical grade (E. Merck, Darmstadt, FRG).

Buffers

Phosphate buffer 10 mmol/L pH 7.5: Sodium dihydrogen phosphate (10 mmol/L) and di-Sodium hydrogen phosphate (10 mmol/L) are mixed to pH 7.5 (approximately 1 + 3).

Ammonium chloride buffer 50 mmol/L pH 8.5: 1.34 g ammonium chloride is dissolved in 500 mL of water and pH is adjusted to pH 8.5 with ammonia 500 mmol/L.

Mobile Phases

Mobile phase 1 (Sodium acetate 50 mmol/L) for column 1. 20.5 g of anhydrous sodium acetate is dissolved in 5000 mL of water. pH is adjusted to 4.7 with concentrated acetic acid.

Mobile phase 2 for column 3. 10.5 g of sodium hydroxide and 20.5 g of anhydrous sodium acetate and 21.0 g of citric acid monohydrate are dissolved in 5000 mL of water (yields pH 6.0). 3400 mL of this buffer is mixed with 600 mL of acetonitrile and 400 mL of methanol. The mobile phases are degassed by purging with helium for five minutes.

Standard Solutions and Calibration Curve

Stock solution for terbutaline and internal standard are prepared in water. Working standards of terbutaline are prepared by diluting the stock solution with water. The working solution of the internal standard is prepared by diluting the stock solution with phosphate buffer 10 mmol/L pH 7.5.

Calibration curves are prepared by adding working standards (100 μL) for terbutaline and for the internal standard (1.00 mL) to 2.00 mL of plasma (containing inhibitor), giving concentrations in the range 4.0–50 nmol/L for terbutaline and 25 nmol/L for the internal standard.

Blood Sampling and Storage

Blood samples are collected into Na-heparinized Venoject® tubes (10 mL) containing 100 μL of esterase inhibitor solution (1 mmol/L). The tube is turned upside down 7 times and then immediately centrifuged for 10 minutes at 1400 g. Plasma samples were stored at − 18 °C.

Sample Work-Up

2.00 mL of plasma and 1.00 mL internal standard solution are mixed in a 10 mL glass tube. The sample is then concentrated on a Bond Elut® C_{18} cartridge previously conditioned by washing with 2 x 3 mL of ethanol, 2 x 3 mL of water and 2 mL of phosphate buffer pH 7.5. The column is then washed with 2 x 2 mL of water and then eluted with 1 mL of the ethanol/ammonium chloride buffer (95/5), into a glass tube containing 50 μL of glutatione solution (50 mmol/L). The eluate is evaporated to dryness in a vacuum at 50 °C. The residue is dissolved in 250 μL of mobile phase 1 and 80 μL is injected into the LC-system.

To process a large number of samples simultaneously, a home-made vacuum box with room for up to 50 Bond Elut cartridges is used.

A detailed description of the working principles for the coupled column system is given elsewhere [3, 4]. Fig. 2 illustrates the modified system. In Table I technical details are given.

The pretreated sample is injected into the LC-system and preseparated on column 1. A microprocessor controlled column switching valve is used to transfer the part of eluate

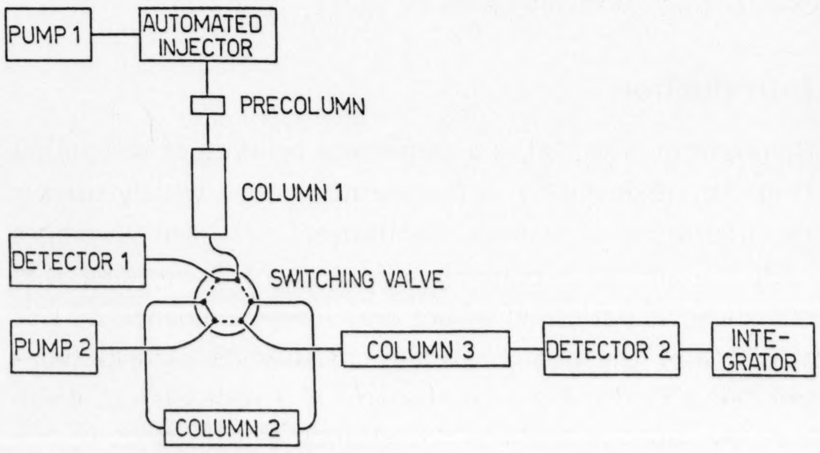

Fig. 2

The chromatographic system. The working principle is explained in the text and conditions are given in Table I.

Table I. Experimental details for quantitative determination of terbutaline in human plasma after administration of Bambuterol.

Automatic injecton: WISP 710B (Waters)
Pumps: Waters model 590 (pump 1) and LKB 2150 (pump 2).
Flow rates: 0.8 mL/min. for both pumps.
Detector: LC-4B amperometric detector from Bioanalytical Systems with a TL-5 glassy carbon electrode and an Ag/AgCl (NaCl, 3 mol/L) reference electrode. Working potential 0.90 V.
Column switching valve: Valco model CV-6-UHPa-N60, electrically operated.
Integrator: Hewlett Packard, model 3388A.

Column	Dimensions (mm)	Packing material	Manufacturer
Precolumn	4 x 6.8	Guard PAK CN	Waters Assoc., Milford, Mass., USA
Column 1	150 x 3	Nucleosil C_6H_5 (7 μm)	Macherey-Nagel & Co., Düren, FRG
Column 2	23 x 4	Sep PAK® C_{18}	Waters Assoc.
Column 3	200 x 3	Nucleosil 10 SA	Macherey-Nagel & Co.

containing terbutaline and internal standard from column 1 to column 2. On column 2 the band leaving column 1 is compressed [4]. From column 2 the sample is backflushed onto column 3 by means of mobile phase 2.

Quantitation

For quantitation, the peak height ratio between terbutaline and the internal standard is calculated and plotted against concentration. Least square linear regression of the data is used to establish the calibration curve. Data presented in this work was obtained using the programmable HP 3388A integrator.

Linearity

The linearity of the method was investigated by analysing spiked plasma samples (containing inhibitor) with concentrations of 4.0, 8.0, 16.0, 32.0, 48.0, 64.0 and 128 nmol/L. The peak height ratio between terbutaline and the internal standard was plotted against the concentration.

Recovery

The absolute recovery was tested on spiked plasma samples, that were taken through the entire analytical procedure. Comparison was made with directly injected aqueous samples.

Results and Discussion

Sampling and Storage

As bambuterol is enzymatically hydrolysed in blood to the monocarbamate of terbutaline and terbutaline [2], it is essential that the inhibitor (D2456) is added to the plasma sampling tubes prior to sampling. Studies of the inhibitory effect of D2456 show that sufficient protection against hydrolysis in blood is obtained with the recommended amounts added to the sampling tubes. No degradation has been observed during storage, thawing or sample work-up. Plasma samples stored at − 18°C are stable for at least two hundred days.

Sample Work-Up

Solid phase extraction on disposable cartridge columns offers a convenient way of handling a large number of samples. However, in our experience and as is well known there can be large batch to batch variations for silica based packing materials used in these type of columns. This might effect recovery, and therefore the recovery of terbutaline and the internal standard should be checked for every new batch. Similarly, it is necessary to run blank plasma samples to exclude interferences due to these variations.

Liquid Chromatography

By using coupled column liquid chromatography, high selectivity is achieved which increases the possibility of quantifying low concentrations of the drug in biological samples. This selectivity gain reduces the effort that otherwise has to be spent on a more complicated sample work-up. Typical chromatograms obtained from authentic plasma samples are shown in Fig. 3.

During routine work the precolumn insert is changed daily and the overall chromatographic performance checked. Differences in batches of the column packing materials used for column 1 and column 3 (e.g. Nucleosil C_6H_5, 10SA) have also been found.

Therefore, control of new batches are made so that no background peaks will occur in blank plasma samples, that the necessary resolution is achieved, that the retention times are reasonable and that the stability of the packing materials allows the columns to be used for several weeks.

The influence of pH, ionic strength and organic modifier on the retention for terbutaline and the internal standard on an hydrophobic phase as well as on an strongly acidic ion-exchange have been discussed elsewhere [3].

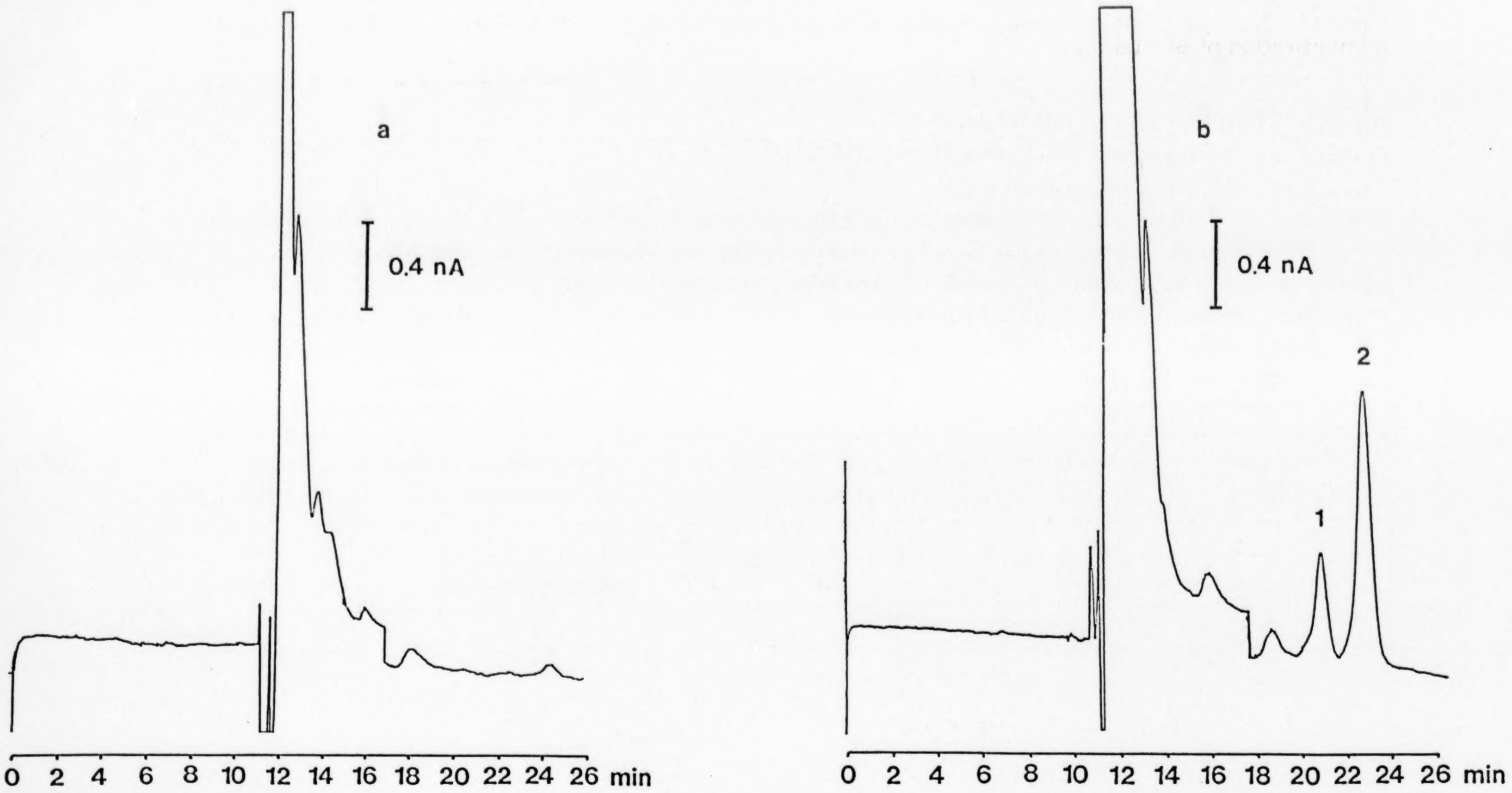

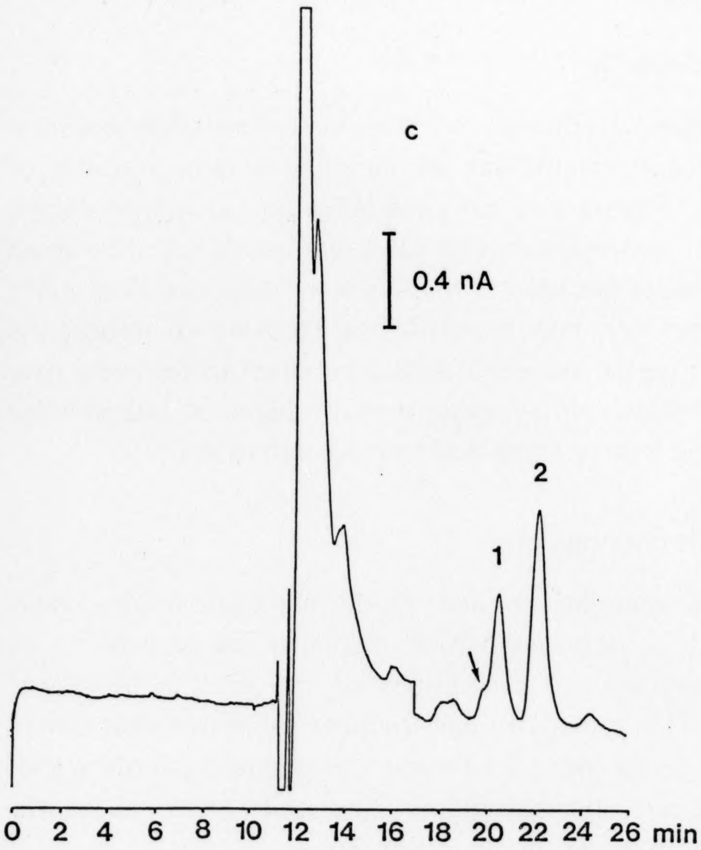

Fig. 3

Chromatograms from blank plasma (a), authentic sample, 8.0 nmol/L, (b) and authentic sample with interference (arrow, see text) (c), **1** = terbutaline, **2** = internal standard.

Electrochemical Detection

The internal standard used is chemically very similar to terbutaline and its electrochemical properties are similar.

The choice of mobile phase, pH and oxidation potential with respect to detector response, has previously been studied [5].

Selectivity

A chromatogram of a typical blank plasma sample is shown in Fig. 3a.

Test of potentially interfering compounds showed that the drug salbutamol nearly overlapped with the terbutaline peak. Thus, if salbutamol is present in a plasma sample no value can be given for terbutaline. The following drugs were found not to interfere: isoprenaline, orciprenaline, fenoterol, rimiterol and theophylline. To minimize the risk for interference by other compounds blank plasma samples should always be taken before dosing in clinical studies to check that there are no interfering peaks.

Of the hitherto identified metabolites of bambuterol [2], none have retention characteristics such that they could interfere. However, sometimes a peak of unknown identity occurs, which is only partially resolved from the terbutaline peak (see Fig. 3c). As this has been seen only from samples obtained after administration of bambuterol and not of terbutaline, it may be a metabolite of bambuterol.

Furthermore, the inhibitor D2456 and its hydrolysis product (Fig. 1d and e) do not interfere.

Performance Characteristics

Linearity: The method was linear over the range (4.0–128 nmol/L) studied (r = 0.9996).

Recovery: The absolute recoveries of terbutaline in spiked samples at levels of 8.0 and 40.0 nmol/L were typically 83% and 90% respectively. For the internal standard it was 94% for a concentration of 25 nmol/L.

Table II. Analytical characteristics for quantitative determination of terbutaline in human plasma after administration of Bambuterol.

Within-day variation						
Control sample	Concentration (nmol/L)	Concentration found (nmol/L) (mean ± SD)	C.V. (%)	Bias (range) (%)	n	
Spiked	8.0	8.2 ± 0.17	2.1	+ 0.4 to 4.6	10	
Spiked	40.0	40.2 ± 0.95	2.4	− 1.9 to + 2.9	10	
Between-day variation						
Control sample	Concentration (nmol/L)	Concentration found (mean ± SD)	C.V. (%)	Bias (range) (%)	n	Time of storage (days)
Spiked	8.0	8.0 ± 0.29	3.6	− 3.6 to + 3.6	91	94
Authentic	–	11.5 ± 0.68	5.9	–	54	233

Precision and accuracy: The within-day and between-day variations for spiked and authentic control samples are presented in Table II. The accuracy of the method for the spiked blank plasma samples is also shown.

Limit of quantitation: The limit of quantitation was set to 4.0 nmol/L, limited by plasma background peaks. The between-day variation (C_v) for such spiked samples was typically 3.4% (n = 46).

References

[1] *S.-E. Jacobsson, S. Jönsson, C. Lindberg, L.-Å.Svensson,* Biomed. Mass Spectrom. **7**, 265 (1980).

[2] *L.-Å. Svensson, A. Tunek,* Drug Metab. Rev. In Press.

[3] *L.-E. Edholm, B.-M. Kennedy, S. Bergqvist,* Chromatographia, **16**, 341 (1982).

[4] *L.-E. Edholm, L. Ögren,* in "Liquid Chromatography in Pharmaceutical Development", I. Wainer, ed., Aster, Springfield, Oregon, 1986; p. 323.

[5] *S. Bergqvist, L.-E. Edholm,* J. Liq. Chromatogr., **6** (3), 559 (1983).

Received: June 30, 1987
Accepted: Aug. 10, 1987
F

Bitte zurück an:
Please return to:

Direkte Durchwahl
☎
(0 61 21) 30 80 21

Friedr. Vieweg & Sohn
Verlagsgesellschaft mbH
– Anzeigenverkauf –
Postfach 58 29
6200 Wiesbaden 1

Chromatographia

Einkaufsnachweis – Purchasing Information

Hiermit bestellen wir ab sofort bis auf Widerruf unten stehende Eintragungen zum Preis von DM 6,30 pro Zeile. Stichworte sind kostenlos. Abrechnung erfolgt halbjährlich mit Beleg. Für Klischeeanzeigen werden DM 2,70 pro mm berechnet.

Herewith we order immediately until recalled the undermentioned entries at the cost of DM 6,30 per line. Index free of charge. Settlement will be made halfyearly by voucher. Advertising-blocks will be charged with DM 2,70 per mm.

Rabattstaffel/Discounts:

3 Eintragungen/entries	5%
6 Eintragungen/entries	10%
12 Eintragungen/entries	15%
24 Eintragungen/entries	20%

Stichworte/Index

Firmeneintragungen/entries

Stempel/Stamp

Unterschrift/Signature

Purchasing Information
Chromatographia-Einkaufsnachweis

Alu-Oxide für die Chromatographie

ICN
ICN BIOMEDICALS
D-3440 Eschwege
Teletex 5 65 18 18 = icn
(früher **Woelm**-Adsorbentien)

Chromatographische Datensysteme

Nelson Analytical GmbH
Stefansbecke 42, Postfach 92 20 45
4322 Strockhövel
Tel. 02339/6037, Telex 8239115 afa d

Chromatographs Liquid

Dr. Herbert Knauer
Wissenschaftl. Geräte KG
Heuchelheimer Str. 9
6380 Bad Homburg

Columns for Liquid Chromatography

ZINSSER
ANALYTIC
P. O. Box 50 11 51
D-6000 Frankfurt 50

Detectors for Liquid Chromatography, HPLC-Systems

Dr. Herbert Knauer
Wissenschaftl. Geräte KG
Heuchelheimer Str. 9
6380 Bad Homburg

Dosiermembranpumpen

LEWA Herbert Ott GmbH + Co.
Ulmer Straße 10, D-7250 Leonberg
Tel. 0 71 52 / 14-0, Telex 7 24153

HPLC

BRUKER
Bruker · Franzen Analytik GmbH
Kattenturmer Heerstr. 122
D-2800 Bremen, Tel. 0421 · 870080

Kieselgele für die Chromatographie

ICN
ICN BIOMEDICALS
D-3440 Eschwege
Teletex 5 65 18 18 = icn
(früher **Woelm**-Adsorbentien)

Markierte Verbindungen für die Autoradiographie

ICN
ICN BIOMEDICALS
D-3440 Eschwege
Teletex 5 65 18 18 = icn
(früher **Woelm**-Adsorbentien)

Massen-Spektrometrie

BRUKER
Bruker · Franzen Analytik GmbH
Kattenturmer Heerstr. 122
D-2800 Bremen, Tel. 0421 · 870080

NMR Lösungsmittel und NMR Reagenzien

ICN
ICN BIOMEDICALS
D-3440 Eschwege
Teletex 5 65 18 18 = icn

Reversed Phase Kieselgele

ICN
ICN BIOMEDICALS
D-3440 Eschwege
Teletex 5 65 18 18 = icn
(früher **Woelm**-Adsorbentien)

Solvents

ZINSSER
ANALYTIC
P. O. Box 50 11 51
D-6000 Frankfurt 50

Better than Silica

The backbone of a PRP column is a macroporous styrene divinylbenzene copolymer in the form of spherical particles. It stands for outstanding stability. From pH 1 to pH 12. In any aqueous or organic eluent. With perfect selectivity. The chromatographic properties are determined by the physical and chemical structure of the polymer. No surface coating of the particles would interfere with your chromatographic phase.

A full set of finger-tight guard cartridges saves your column from fouling.
Ask for comprehensive application literature.

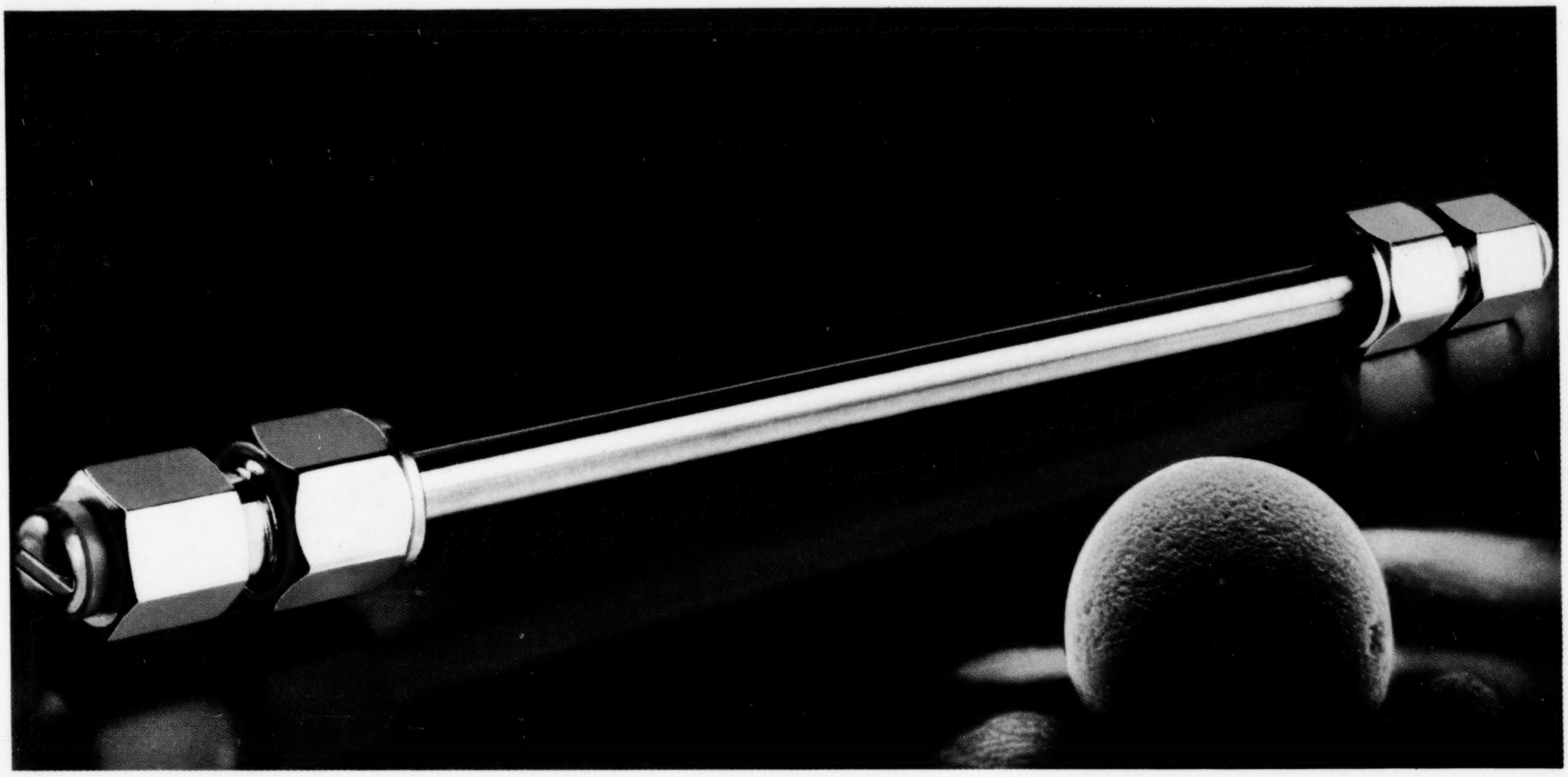

PRP-1

A long lasting column for reversed phase chromatography.
Exceptional stability in ion-pair chromatography work. High affinity to aromatic and polycyclic compounds. Particle size 5 and 10 µm. Preparative columns for efficient protein fractionation free of silica residues.

PRP-X100

An inexpensive column for ion chromatography of anions. F^-, $C1^-$, Br^-, $N02^-$, $N03^-$, $P04^{3-}$, $S04^{2-}$. Use it in single column or suppressor systems with a wide range of eluents. With any detector system. The sensitivity ranges from ppb to ppm by selection of corresponding injection volumes. No need of sample enrichment or column switching.

PRP-X200

An inexpensive column for ion chromatography of cations. Na^+, K^+, Mg^{2+}, Ca^{2+}, $NH4^+$. Rely on improved consistency and equality of column packing. Perform rapid routine analysis of common inorganic species with a new analytical method. The separation conditions are adjusted according to the relative peak height of all components via eluent modification.

HAMILTON

Hamilton Bonaduz AG
P. O. Box 26
CH-7402 Bonaduz, Switzerland
Telephone 081 37 01 01
Telefax 081 37 25 63
Telex 74206 cham ch
New Tx. No. w.e.f. Oct. 87: 85 13 11